INDUSTRIAL VENTILATION

Design Guidebook

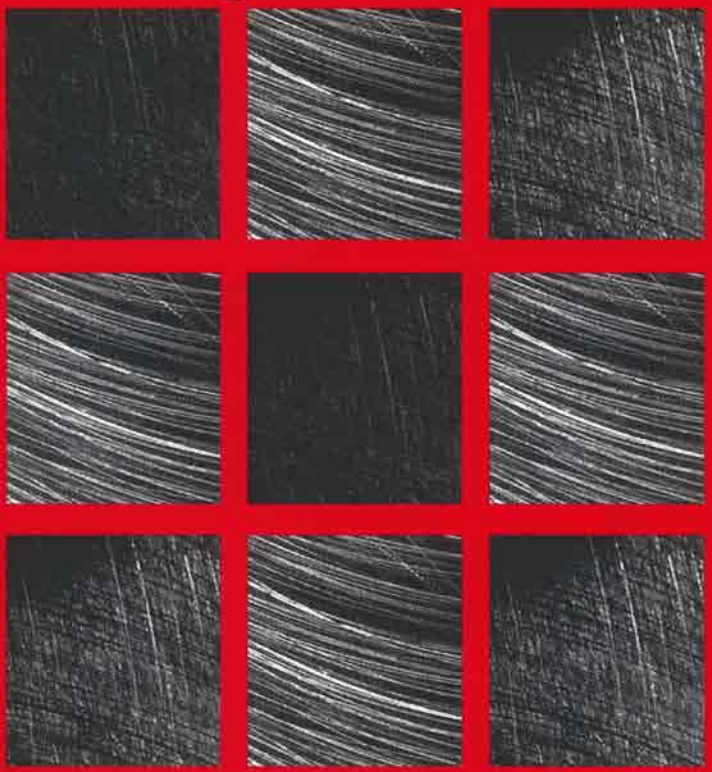

EDITED BY

Howard Goodfellow

Esko Tähti

INDUSTRIAL VENTILATION DESIGN GUIDEBOOK

This page intentionally left blank

INDUSTRIAL VENTILATION DESIGN GUIDEBOOK

Edited by

Howard Goodfellow

Stantec Global Technologies, Ltd.
Mississauga, Ontario L5N 7G2
Canada

Esko Tähti

Finnish Development Centre for Building Services, Ltd
FIN-00120 Helsinki
Finland

and

Department of Chemical Engineering and Applied Chemistry
University of Toronto
Toronto, Ontario M5S 3E5
Canada

ACADEMIC PRESS

A Harcourt Science and Technology Company

San Diego San Francisco New York Boston London Sydney Tokyo

This book is printed on acid-free paper. ∞

Academic Press
A Harcourt Science and Technology Company
525 B Street, Suite 1900, San Diego, California 92101-4495, USA
http://www.academicpress.com

Academic Press
Harcourt Place, 32 Jamestown Road, London NW1 7BY, UK
http://www.academicpress.com

Library of Congress Catalog Card Number: 00-111522

International Standard Book Number: 0-12-289676-9

PRINTED IN THE UNITED STATES OF AMERICA
01 02 03 04 05 06 MM 9 8 7 6 5 4 3 2 1

CONTENTS

5 Physiological and Toxicological Considerations 173

6 Target Levels 355

This page intentionally left blank

CONTRIBUTORS

Numbers in parentheses indicate the chapter(s) containing the author's contribution(s).

Larry G. Berglund (5) Department of Architecture, Faculty of Engineering, Tohoku University, Sendai 980-77 AOBA Japan

Bernhard Biegert (1, 2, 10) University of Stuttgart IKE-LHR, Stuttgart, D-70550, Germany

Lorraine Conroy (10) Environmental & Occupational Health Sciences, University of Illinois at Chicago, Chicago, Illinois 60612

Vincenzo Corrado (11) Dipartimento di Energetica del Politecnico di Torino, Facoltà di Architettura, Torino I-10100, Italy

Eric F. Curd (4, 9, Appendix) Liverpool - John Moores University, West Kirby Wirral L48 8BJ, UK

Lars Davidson (11) Chalmers University of Technology, Gothenburg, Sweden

Viktor Dorer (11) Section 175, EMPA, Dübendorf CH-8600, Switzerland

Antonio Dumas (10) Dipartimento di Ingegneria Energetica, Nucleare e del Controllo Ambientale, Universitá di Bologna, Bologna I-40136, Italy

Mamdouh El Haj Assad (4, 8, 9) Laboratory of Applied Thermodynamics, Helsinki University of Technology, Espoo FIN-02015 HUT, Finland

Michael Ellenbecker (10) Department of Work Environment, University of Massachusetts, Lowell, Massachusetts 01854

Jan Emilsen (9) Johnson Controls Norden AS, Tiller N-7075, Norway

Bernard Fletcher (10) Health and Safety Laboratory, Sheffield S3 7HQ, Great Britain

Richard P. Garrison (10) Department of Environmental Health Sciences, School of Public Health, University of Michigan, Ann Arbor, Michigan 48109

Howard D. Goodfellow (10, 13) Department of Chemical Engineering and Applied Chemistry, University of Toronto, Toronto, Ontario, Canada M5S 3E5

Mario Grau-Rios (6) Instituto Nacional de Higiene y Seguridad en el Trabajo, Madrid E-28071, Spain

Jan Gustavsson (9) Camfil Ab, Trosa S-61933, Sweden

Kim Hagström (3, 6, 8) Faculty of Mechanical Engineering, Helsinki University of Technology, Espoo FIN-02015 HUT, Finland

Timo Hautalampi (8) Turku Regional Institute of Occupational Health, Turku FIN-20520, Finland

Jaap Hogeling (9) ISSO, 3000 BV Rotterdam, The Netherlands

Derek Ingham (10, 13) Department of Applied Mathematics, University of Leeds, Leeds LS2 9JT, United Kingdom

Pentti Kalliokoski (5) Department of Environmental Sciences, University of Kuopio, Kuopio FIN-70211, Finland

Jonathan W. Kaufman (5) Naval Air Warfare Center, Patuxent River, Maryland 20670

Markus Koschenz (11) Section 175, EMPA, Dübendorf CH-8600, Switzerland

Hannu Koskela (8) Turku Regional Institute of Occupational Health, Turku FIN-20520, Finland

Ilpo Kulmala (10) VTT Automation, Tampere FIN-33101, Finland

Markku Lampinen (4, 14) Laboratory of Applied Thermodynamics, Helsinki University of Technology, Espoo FIN-02015 HUT, Finland

Ulf Landström (5) National Institute for Working Life, Umeå S-907 13, Sweden

Matti Lehtimäki (13) VTT Automation, Tampere FIN-33101, Finland

Bengt Ljungqvist (10) Building Services Engineering, KTH, Stockholm S-10044, Sweden

Albrecht Lommel (10) Wald, Switzerland (formerly of Swiss Federal Laboratories for Materials Testing and Research, EMPA)

Sante Mazzacane (9) Department of Architecture, Università di Ferrara, Ferrara 44100, Italy

Domingo Moreno-Beltrán (6) Escuela Tecnica Superior de Ingenieros Industriales, Universidad Politecnica de Madrid, Madrid E-28006, Spain

Alfred Moser (11) Swiss Federal Institute of Technology ETH, Department of Architecture, Air and Climate Group, Zurich, Switzerland

Elisabeth Mundt (7) KTH, Royal Institute of Technology, Stockholm S-10044, Sweden

Peter V. Nielsen (12) Department of Building Technology, Aalborg University, Aalborg DK-9000, Denmark

Raimo Niemelä (6) Department of Physics, Finnish Institute of Occupational Health, Vantaa FIN-01620, Finland

Lars Olander (6, 8, 10) Building Services Engineering, KTH, Royal Institute of Technology, Stockholm S-10044, Sweden

Bjarne W. Olesen (6) Wirsbo-Velta GmbH, D-22851 Norderstedt, Germany

Leena Perttu-Roiha (13) Fortum Oil and Gas Oy, Porvoo, Finland

Vladimir Posokhin (7) Kazan State Architechtural-Construction Academy, Tatarstan, Russia

Jorma Railio (1, 2, 9) Association of Finnish Manufacturers of Air-Handling Equipment, AFMAHE, Helsinki FIN-00130, Finland

Mike Ratcliff (7) Rowan Williams Davies & Irvin Inc., Guelph, Ontario, Canada

Berit Reinmüller (10) Building Services Engineering, KTH, Stockholm S-10044, Sweden

Michael Robinson (10) Division of Mathematics, School of Science and Mathematics, Sheffield Hallam University, UK

Gunnar Rosén (10, 12) Department of Work Organisation Research, National Institute for Working Life, Solna S-171 84, Sweden

Sakari Sainio (16) Espoo-Vantaa Institute of Technology, Espoo, Finland

Esa Sandberg (8) Satakunta Polytechnic, Pori FIN-28600, Finland

Kai Savolainen (5) Department of Industrial Hygiene and Toxicology, Finnish Institute of Public Health, Helsinki FIN-01620, Finland; and Department of Environmental Medicine, National Public Health Institute, Kuopio FIN-70701, Finland

Alois Schälin (11) Air Flow Consulting Alois Schälin, afc, CH-8092 Zurich, Switzerland

Eugene Shilkrot (7) TSN II Promsdanii, Thermec, Moscow 127238, Russia

Kai Siren (12) Helsinki University of Technology, HVAC Laboratory, Espoo FIN-02015 HUT, Finland

Petri Sjöholm (13) Laboratory of Energy Economics and Power Plant Engineering, Helsinki University of Technology, Espoo FIN-02015 HUT, Finland

Håkon Skistad (7, 8) SINTEF Energy Research, Refrigeration, and Air Conditioning, Trondheim N-7034, Norway

Bengt Steen (15) Department of Environmental Systems Analysis, Chalmers University of Technology, Gothenburg, Sweden

Andrey Strongin (7) TSN II Promsdanii, Thermec, Moscow 127238, Russia

Esko Tähti (6) Finnish Development Centre for Building Services LTD, Helsinki FIN-00120, Finland

Per Olaf Tjelflaat (8) Department of Refrigeration and Air Conditioning, NTNU, Norwegian University of Science and Technology, Trondheim N-7034, Norway

Heikki Torvela (13) Centre for Environmental Technology, Meri-Lappl Institute, University of Oulu, Oulu, Finland

Katsuhiko Tsuji (10) College of Integrated Arts & Sciences, Osaka Prefecture University, Sakai, Osaka 599-8531, Japan

János Vad (12) Department of Fluid Mechanics, Technical University of Budapest, Budapest, Hungary

Irma Welling (10) Lappeenranta Regional Institute of Occupational Health, Lappeenranta FIN-53850, Finland

Xianyun Wen (10) School of the Environment, University of Leeds, UK

Ralf Wiksten (8, 9) Laboratory of Applied Thermodynamics, Helsinki University of Technology, Espoo FIN-02015 HUT, Finland

Alexander Zhivov (7, 8) University of Illinois, Champaign, Illinois 61820

ACKNOWLEDGMENTS

The editors express their appreciation to the many international authors and reviewers who contributed to the *Design Guidebook*. It is clearly the volunteer efforts of these dedicated individuals that have made the publication of this first edition of the *Industrial Ventilation Design Guidebook* a reality. We have enjoyed working with this truly outstanding team of scientists and researchers who have been committed to our vision to produce an international handbook of the highest quality in the field of industrial ventilation.

Special thanks are due to the patience and determination of the contributors who tirelessly prepared drafts and redrafts, attended meetings and more meetings, and reviewed proofs, more proofs, and then the final proofs. It has been a pleasure to work with all members of the professional team at Academic Press toward the common goal of publishing this book on schedule.

The editors acknowledge the significant contributions by Esko Virtanen of TEKES during all stages of this project. Also, we would like to acknowledge the exceptional work and long hours by Kalevi Pöntinen at the Helsinki University of Technology, who has been the overall coordinator for the communications between the editors, contributors, and the publishing team.

Two organizations that have supplied the fundamental building blocks and supporting organizations for this vision of publishing the first edition of the *Design Guidebook* are the Helsinki University of Technology and COST. Special thanks are due to these organizations. A brief introduction to these two organizations is presented below.

TEKNILLINEN KORKEAKOULU
TEKNISKA HÖGSKOLAN
HELSINKI UNIVERSITY OF TECHNOLOGY

Helsinki University of Technology

The Helsinki University of Technology (HUT) is the oldest and largest university of technology in Finland, dating back to the nineteenth century. In 1849, the Helsinki Technical School was founded, marking the beginning of organized technical education in Finland. In 1872 the school became the Helsinki Polytechnic School and in 1879 the Helsinki Polytechnical Institute. In 1908 the name was changed to the Helsinki University of Technology, and thus the teaching of technology at the university level began in Finland. In the 1950s and 1960s new premises were built to house the University of Technology in Otaniemi and the university moved from Helsinki to the neighboring city of Espoo. HUT includes 12 faculties, 9 separate institutes, and 15 degree programs.

The Laboratory of Applied Thermodynamics has had a significant involvement in industrial ventilation activities since the inception of the national Finnish industrial ventilation technology program INVENT 1988. One of the first projects was the Design and Dimensioning Criteria for Industrial Ventilation. The laboratory is a proposer and coordinator for the European COST Action G3, "Industrial Ventilation" (1996–2003), and the Network of Industrial Ventilation, INVENTNET (2000–2002). The main interests of the laboratory are new technical solutions for energy conversion and equipment and to provide comprehensive education in the field of thermal engineering. The present research areas of the Laboratory of Applied Thermodynamics are fuel cells and hydrogen technology, experimental fluid dynamics using laser Doppler anemometry, new and innovative energy production methods, technical and chemical thermodynamics, modern heat pumps and heat exchangers, low-emission combustion technologies, industrial ventilation (INVENT), and computational fluid dynamics (FINFLO).

The Laboratory of Applied Thermodynamics provides comprehensive education in the field of energy engineering. The students, mostly in applied thermodynamics, have profound theoretical and practical bases in energy conversion processes and equipment. They master the basic mathematical and physical principles of energy physics and are then capable of specializing in a wide range of different technical applications of energy engineering. The main fields of education cover technical and chemical thermodynamics, heat and power generation processes and equipment, renewable energy production methods, heat and mass transfer, heat exchangers, and fluid mechanics. Some of the research project results are also included in subsequent education. The calculation of thermodynamic equilibrium of thermochemical systems can be done using computer programs such as ELCHEM and HSC, which are based on the laboratory's own research work. The education of computational fluid dynamics is strongly connected with the FINFLO research project team.

COST

Founded in 1971, COST is an intergovernmental framework for European cooperation in the field of scientific and technical research, allowing the coordination of nationally funded research on a European level. COST actions cover basic and precompetitive research as well as activities of public utility.

The goal of COST is to ensure that Europe holds a strong position in the field of scientific and technical research for peaceful purposes, by increasing European cooperation and interaction in this field. Ease of access for institutions from nonmember countries also makes COST a successful tool for tackling topics of a truly global nature.

To emphasize that the initiative came from the scientists and technical experts themselves and from those with a direct interest in furthering international collaboration, the founding fathers of COST opted for a flexible and pragmatic approach. COST activities have in the past paved the way for community activities, and its flexibility allows COST actions to be used as a testing and exploratory field for emerging topics.

The member countries participate on an "à la carte" principle, and activities are launched using a "bottom-up" approach. One of its main features is its built-in flexibility. This concept clearly meets a growing demand, and in addition, it complements the community programs.

COST has a geographical scope beyond the EU, and most of the Central and Eastern European countries are members. COST also welcomes the participation of interested institutions from non-COST-member states without any geographical restriction.

COST has developed into one of the largest frameworks for research cooperation in Europe and is a valuable mechanism for coordinating national research activities in Europe. Today it has almost 200 actions and involves nearly 30,000 scientists from 32 European member countries and more than 50 participating institutions from 11 nonmember countries.

Among these is COST Action G3 on industrial ventilation. This action *was launched in 1996 and comprises to date more than 60 experts from fourteen* COST countries and from institutions of four nonmember countries. Its main objective, as stipulated in the Memorandum of Understanding of the action, is to "produce a basis for a Design Guidebook by a multidisciplinary approach based on gathering the expert knowledge which exists internationally, further developing it and making it available for the designers."

tion, is to "produce a basis for a Design Guidebook by a multidisciplinary approach based on gathering the expert knowledge which exists internationally, further developing it and making it available for the designers."

The present volume is tangible proof of the success of COST Action G3. Thanks to the early fulfillment of this objective, possible further developments, and the quality of the team of experts gathered throughout Europe and beyond, this action, initially scheduled to terminate by the end of 2001, was prolonged until April 2003 by the Committee of Senior Officials of COST.

ABOUT THE EDITORS

Howard D. Goodfellow, Ph.D., P.Eng.

Howard D. Goodfellow is Vice President of Stantec Global Technologies Ltd. Stantec is a Canadian professional services firm providing knowledge-based solutions for infrastructure and facilities. Stantec sells and markets Goodfellow EFSOP™ (*E*xpert *F*urnace *S*ystem *O*ptimization *P*rocess), an award-winning software and hardware technology system. Goodfellow EFSOP™ uses online off-gas chemistry measurements from industrial combustion processes for closed-loop control for process optimization.

The company he founded in 1986, Goodfellow Consultants Inc., received the 1992 Canada Award for Business Excellence (CABE) in the environment field for the development of a computer program for the design of specialized industrial ventilation systems. Dr. Goodfellow is a recognized expert in the ventilation, air pollution control, and air quality areas.

He graduated with a Ph.D. from the Department of Chemical Engineering and Applied Chemistry at the University of Toronto and has been responsible for specialized consulting and engineering design services for over 1000 industrial and government clients in the environmental field.

He is an Adjunct Associate Professor in the Department of Chemical Engineering and Applied Chemistry at the University of Toronto, where he teaches a graduate course in ventilation and conducts research and development in the ventilation and indoor air quality field. Dr. Goodfellow was awarded the 2T5 Meritorious Service Medal of the Engineering Alumni Association of the University of Toronto. The award was for his outstanding contributions as an engineer, teacher, researcher, author, and administrator in the field of ventilation and occupational health at the University of Toronto, with global recognition for achievements in the advancement of environmental consulting. Professor Goodfellow also teaches a Mine Ventilation and Occupational Health course at the University of Toronto in the Lassonde Mineral Engineering Programme. Dr. Goodfellow has presented numerous courses internationally in the clean air technology field, both for industrial clients and at conferences and seminars, and he has presented and/or published over 100 technical papers.

Goodfellow has presented numerous courses internationally in the clean air technology field, both for industrial clients and at conferences and seminars, and he has presented and/or published over 100 technical papers.

Dr. Goodfellow has worked with TEKES and the INVENT team in Finland since 1993. He spent three months (April–June 1997) lecturing at the Helsinki University of Technology, initiating research projects in the ventilation field, and working with Finnish experts in the planning stages of the *Design Guidebook*.

Esko Tähti, Ms, S. Eng.

Esko Tähti is Managing Director of Suomen Talotekniikan Kehityskeskus Oy (TAKE, Finnish Development Centre for Building Services, Ltd.). The company is owned by Finnish associations and companies in the business area of building services. The company is established to accomplish R&D projects in the field of building services.

The company was founded in 1991 and started its activities in 1996 when Esko Tähti became its managing director. TAKE's scope of activities includes the whole area of building services. Its other major projects have been in the area of energy use in buildings, life cycle economy, water services, indoor air control, clustering, and IT technologies and automation.

One of the first projects has been the *Design Guidebook*, the "bible" of industrial ventilation. The project has been administrated by the COST secretariat. Esko Tähti has been Chairman of the Management Committee together with Helsinki University of Technology Professor Markku Lampinen and researcher Kalevi Pöntinen.

Esko Tähti graduated in 1967 from the Helsinki University of Technology Laboratory of Applied Thermodymanics. He has been working in different positions in the Finnish companies Metso (Valmet Paper Machines), ABB, and Nokia and also in the Ministry of Environment and Helsinki University of Technology. He has held various positions within Finnish organizations in the area of building services, acting as teacher, researcher, author, and administrator. One important role has been in international projects, especially at the European level and as a contact person for Russian scientists in the area of industrial ventilation. Esko Tähti was also the coordinator of the Finnish technology program INVENT for the period 1991–1996. This program initiated this handbook during an international brainstorming session at Zurich in 1995.

PREFACE

The primary goal of the *Industrial Ventilation Design Guidebook* is to develop a systematic approach to the design of air technology systems based on current scientific research and engineering knowledge on a global basis. There is no internationally accepted handbook available that describes the basic theories and science behind the technical solutions for industrial air technology. Our objective has been to develop a much-needed scientific reference book that covers the whole field of industrial air technology based on validated and updated technology from leading scientists, engineers, and researchers worldwide. This preface outlines why there is a need for a reference handbook, how this goal has been achieved, what has been achieved, and the intended audience for this book.

Rapid changes in process and manufacturing industries and demands for improved workplace environments have placed new demands on the design of advanced industrial ventilation systems. These systems must be more tightly integrated with processes and building service systems. The optimization step requires new design tools and technological innovations. The challenges are not only for technical solutions but also for new technical standards and policy actions to support the technological progress. In many industries the objective is not only to comply with legal standards, but to minimize health risks as much as possible. These objectives require the design team to work closely with the end users to specify target levels or energy consumption levels. The *Industrial Ventilation Design Guidebook* is a compilation of the current knowledge base in the industrial air technology field into a systematic and integrated handbook.

The question may be asked, "How has the goal of publishing the handbook been achieved?" Many factors have contributed to this goal. For those of us who have worked in the industrial ventilation field for several years, there was a recognition that an international guidebook based on the best scientific knowledge on the subject of industrial ventilation would be an essential first step to raise the level of industrial ventilation worldwide. An important step was the organizing of the first International Conference on Ventilation for Contaminant Control in Toronto in 1985. This conference was attended by over 300 delegates. Over 80 scientific papers in the field of industrial ventilation (research and development and applications) were presented at the

conference. Subsequent international conferences have been held every three years. The complete list follows:

Ventilation '85	Toronto, Canada
Ventilation '88	London, UK
Ventilation '91	Cincinnati, Ohio, USA
Ventilation '94	Stockholm, Sweden
Ventilation '97	Ottawa, Canada
Ventilation 2000	Helsinki, Finland
Ventilation 2003	Sapporo, Japan

To date, there have been more than 1500 attendees and more than 500 technical papers or presentations delivered at these conferences. A critical mass of researchers, engineers, and scientists developed through the INVENT program in Finland, which started in 1991. These activities have expanded to include scientists, engineers, and practitioners from some 18 countries as part of the COST Action Program.

The *Industrial Ventilation Design Guidebook* is the first comprehensive, definitive handbook to cover all aspects of air technology on a worldwide basis. The structure of the 16 chapters is as follows:

1. Industrial Air Technology—Description
2. Terminology
3. Design Methodology of Industrial Air Technology
4. Physical Fundamentals
5. Physiological and Toxicological Considerations
6. Target Levels
7. Principles of Air and Contaminant Movement Inside and Around Buildings
8. Room Air Conditioning
9. Air Handling Processes
10. Local Ventilation
11. Design with Modeling Techniques
12. Experimental Techniques
13. Gas Cleaning Technology
14. Pneumatic Conveying
15. Environmental Assessment Tools
16. Economic Aspects

The book is intended for engineers, scientists, seniors at the university level, and graduate students who have a fundamental understanding of the concept of fluid flow, thermodynamics, and heat transfer. The handbook bridges the disciplines of engineering and occupational health and safety (industrial hygiene). The book can be used as a textbook, a scientific reference for researchers, and a fundamental handbook for practitioners in the industrial air technology field.

This international handbook will be updated regularly in order to meet our objective of including the most current scientific knowledge on a global basis. The plan is to also publish additional volumes to cover systems and

equipment and guidelines for specific industrial applications based on leading-edge concepts of design methodology and target levels.

In closing, we are reminded of a statement by the renowned Albert Einstein: "If we did all the things that we are capable of doing, we would literally astound ourselves." The publication of this first edition of *Industrial Ventilation Design Guidebook* is an astounding event. The opportunity to be editors of this handbook has been a truly exciting and satisfying experience. It has been a unique opportunity and a pleasure to collaborate with our international friends on this journey.

H. D. Goodfellow
E. Tähti

This page intentionally left blank

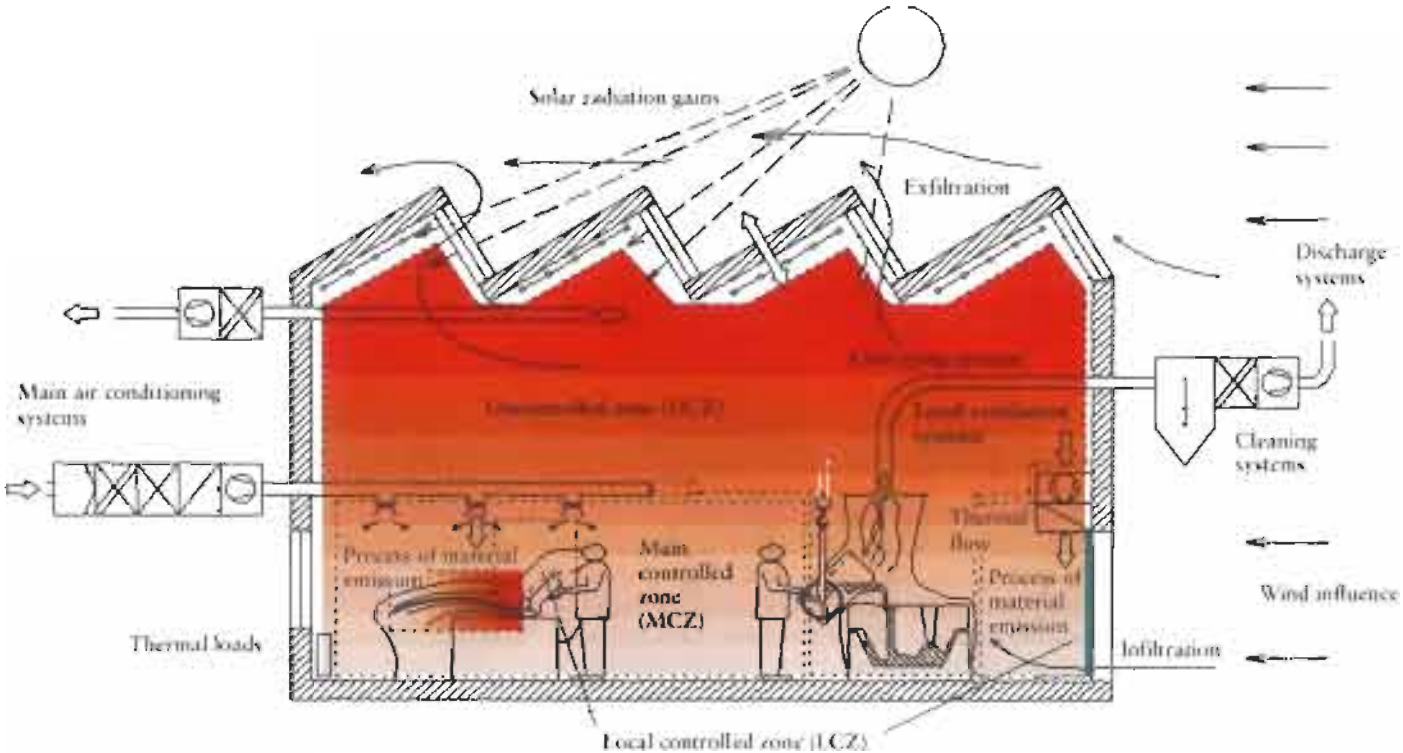

FIGURE 1.1 Industrial Air Technology

1 INDUSTRIAL AIR TECHNOLOGY—DESCRIPTION

BERNHARD BIEGERT

University of Stuttgart, IKE-LHR, Stuttgart, Germany

JORMA RAILIO

Association of Finnish Manufacturers of Air-Handling Equipment, Helsinki, Finland

1.1 INTRODUCTION—WHY ATTENTION TO INDUSTRIAL AIR TECHNOLOGY?

A young scientist said, "I have never seen a complex scientific area such as industrial ventilation, where so little scientific research and brain power has been applied." This is one of the major reasons activities in the industrial ventilation field at the global level were started. The young scientist was right. The challenges faced by designers and practitioners in the industrial ventilation field, compared to comfort ventilation, are much more complex. In industrial ventilation, it is essential to have an in-depth knowledge of modern computational fluid dynamics (CFD), three-dimensional heat flow, complex fluid flows, steady state and transient conditions, operator issues, contaminants inside and outside the facility, etc.

In all ventilation, the condition of the indoor environment, called indoor air quality (IAQ), and the exposures for the occupants are important. In industrial facilities, the contaminant emission rates may be 10–100 times higher than in nonindustrial facilities, but for many contaminants the IAQ levels may

Industrial Ventilation Design Guidebook

be the same. The first priority is to consider the process, but other important issues, such as occupants, energy, environment, and corporate image, must also be considered.

Energy is a key issue and is closely associated with the environment. Global environmental issues must be addressed, where the energy chain from resources to end users is of vital importance.

It is recognized that some countries are leaders in the area of scientific research and experimental development. It is also known that Scandinavian countries have been in the forefront of implementing leading-edge technology for good environmental practice and energy-efficient plants in the 1980s and 1990s. The challenge is the implementation of the best industrial ventilation technology and practice to all workplaces on a global basis.

The objectives of new innovations, procedures, systems, and equipment to fulfill the end user's needs must be included as a part of the ongoing development program. Significant advances in technology presented in this book are target levels, systematic design methodology, indoor air quality strategies, and control of flow in facilities. The objective is to make them work in practice and to continue the development process.

It will be critical to update publications such as the *Design Guide Book* in the industrial ventilation field on a regular basis. Never stop the developing process; study, develop, and update everything, taking into account life-cycle ecological issues.

When we compare industrial air technology (IAT) with comfort ventilation, we can see that technologically our task is very challenging. To fulfill all the needs of the end user is often impossible. If the IAQ is fulfilled, the amount of air may be so large that draftiness is too high. We must also have the courage to say what is possible and what is not. We also have to create tools to validate this.

The benefits of advanced industrial air technology are:

- Improved health of workers and reduced absenteeism as a result of better IAQ
- Improved work satisfaction, higher productivity, and reduced production failures as a result of improved indoor air quality
- Reduction in maintenance costs for the building fabrics, machinery, and products
- Reduction in energy consumption as a result of improved usage patterns and reduced air flow rates
- Increased awareness, and therefore improved selection, of new energy-efficient systems in ventilation design, also leading to reduced energy consumption
- Cleaner surroundings, and thus an improved image of the company, resulting from improved systems and equipment
- Reduction in environmental pollution due to lower energy usage and lower emissions to the surroundings
- Improved life cycle economy resulting from the use of high-level industrial air technology systems and equipment

Field studies have revealed a significant potential for energy saving by modern industrial air technology. For example, one study revealed great varia-

tion in energy consumption (a ratio of 5:1) in technically similar welding halls; this study showed the best indoor air quality was achieved in the hall with the lowest energy consumption. With commercially available high-level design concepts it is possible to decrease the contaminant load by about 90% and the heat load by about 60% compared with medium-level applications.

The above results show the need to increase the level of knowledge from "rules of thumb" to a more rigorous scientific procedure based on validated data and design methods.

1.2 DEFINITION AND PURPOSE OF INDUSTRIAL AIR TECHNOLOGY

Figure 1.1 (see color insert) is a schematic representation of the principles of IAT. Industrial air technology (IAT) can be defined as

> Air flow technologies that control workplace indoor environment and emissions

A longer definition is

1. Air flow technologies that achieve and maintain a safe, healthy, productive and comfortable indoor environment in premises and occupied enclosures where this need is determined not only by human occupancy, normal human activities, and construction and finishing materials but also, and often primarily, by other factors, for example, production processes
2. Process air technology, such as air and gas purification, drying, or pneumatic conveying
3. Safety air technology, including risk assessment, that minimizes damages and hazards caused by accidents, fire, and explosion

It is typical for industrial premises to have, in one space, **zones** with different target levels. The target levels may be determined for the whole area or locally. Often only a part of the space requires controlling of the indoor environment parameters. In addition to the main controlled zone, there may be one or more local controlled zones with target levels different from those in the main controlled zone.

In addition to measures to control the indoor environment, industrial air technology also includes measures to prevent harmful emissions from industrial processes from being discharged outdoors, such as conveying and cleaning technologies and controlled discharge of exhaust air. Other systems include, drying (pulp drying, milk drying, crisp-bread drying, etc.), process ventilation, and safety air systems.

The scope of IAT includes premises other than traditional industrial process buildings, such as hospitals; underground car parks; mining, railroad, and vehicle tunnels; livestock buildings; and other premises and processes.

1.3 AIR TECHNOLOGY SYSTEMS

Industrial air technology systems can be classified into two categories: industrial ventilation and process air technology. A brief description of each type of system follows. More details are presented in Chapter 2.

1. Industrial Ventilation

Air Conditioning Systems

Air conditioning systems control air quality and thermal environment for both human occupancy and processes.

General Ventilation Systems

In general ventilation systems some indoor air parameters are controlled only partially. Target levels are usually lower than for air conditioning.

Local Ventilation Systems

Local ventilation systems are used for local controlled zones. These systems are based on local capture of contaminants.

Process Ventilation Systems

In process ventilation the target is to maintain defined conditions to ensure process performance (e.g., paper machine hoods).

2. Process Air Technology

Cleaning Systems

Cleaning systems are used to remove contaminants, clean the resulting fluid flows, and collect materials before discharge of exhaust air.

Pneumatic Conveying Systems

Conveying systems are used to transport captured pollutants from processes to a collection point.

Drying System

Drying systems are used to remove moisture, gases, and vapors from a product.

Safety Air Technology Systems

Air technology systems may be designed for control of smoke during fires or to reduce risks of explosions.

1.4 DESIGN GUIDEBOOK (DGB)

1.4.1 History and State of the Art

A group of international specialists in the area of industrial ventilation have decided to write a handbook (the "Bible") of industrial air technology. The book, *Industrial Ventilation Design Guidebook* (DGB), will be written as a major cooperation effort. People and organizations from the following countries participate in the work of one or more international actions within the scope: Belgium, Canada, Czech Republic, Denmark, Finland, France, Germany, Hungary, Italy, Japan, the Netherlands, Norway, Russia, Sweden, Spain, Switzerland, the U.K., and the U.S.A. Australia and Poland are also interested.

The available systematic information regarding industrial air technology is scarce. There are some handbooks, such as those of Hemeon (USA),[1] Baturin (1972),[2] Heinsohn (USA),[3] Goodfellow (Canada),[4] and ACGIH (USA),[5] but they do not cover the whole field of industrial air technology. There is no internationally accepted handbook available, and the designer has no validated solutions at his disposal. According to the present state of the art, both capturing and ventilating systems are designed based on know-how rules (e.g., air exchange rate) and rarely achieve the targeted heat and contaminant load removal without overdimensioning and excessive costs. This expertise is not generated by systematic investigations but by experience with various plants under construction and in operation. This is obviously due to a total lack of approved design criteria and a lack of international or European standardization, which make effective ventilation design impossible.

Another main reason to write a handbook for industrial air technology was that there are large gaps and inaccuracies in the technical literature. Goodfellow and Klus[6] outlined specific needs for a Design Guide Book in the industrial ventilation field in an evaluation report for the Finnish INVENT Technology program.[7]

The project will be carried out in phases including the *Fundamentals*, *Systems and Equipment,* and *Applications*. The main target of the DGB project is to write an internationally accepted handbook, a much needed scientific reference, covering the whole field of industrial air technology with validated and updated knowledge, and through it to raise the level of industrial air technology worldwide.

The *Fundamentals* book describes the basic theories and science behind the technical solutions for industrial air technology. Equipment-specific theories will be completed in the *Systems and Equipment* book. The *Applications* book will describe technical solutions for specific industrial sectors and technology areas, including design and construction methodology.

1.4.2 Structure of the DGB *Fundamentals*

This volume, *Fundamentals,* is structured in 16 chapters, as follows:

1. Industrial Air Technology—Description

The introductory chapter to the *Design Guidebook* describes why more attention should be paid to industrial air technology, the definition and purpose of industrial air technology, and the basic system principles.

2. Terminology

This chapter describes the set approach dealing with units, symbols, and definitions, which are essential for providing texts that do not cause confusion by having various chapters that use different symbols relating to the same unit. This chapter provides the common language that is used throughout the book.

3. Design Methodology

Design methodology is the systematic description of the technical design process of industrial air technology as an elementary part of the whole life cycle of the industrial plant.

4. Physical Fundamentals

This chapter introduces the important topics of fluid flow, properties of gases, heat and mass transfer, and physical/chemical characteristics of contaminants. The aim is to assist all engaged in industrial air technology in understanding the physical background of the issues involved.

5. Physiological and Toxicological Considerations

This chapter introduces fundamentals of human physiology and health requirements relevant to the control of indoor environment within industrial buildings.

6. Target Levels

The chapter presents a new concept called target levels. It outlines the role of target levels in the systematic design methodology, the scientific and technical grounds for assessing target levels for key parameters of industrial air technology, and the hierarchy of different target levels, as well as some examples of quantitative targets.

7. Principles of Air and Contaminant Movement inside and around Buildings

This chapter presents the basic processes of air and contaminant movement, such as jets, plumes, and boundary flows.

8. Room Air Conditioning

This chapter describes the room air conditioning process, including the interaction of different flow elements: room air distribution, heating and cooling methods, process sources, and disturbances. Air handling equipment, including room air heaters, is discussed in the form of "black boxes" as far as possible.

9. Air Handling Processes

This chapter describes the fundamentals of air handling processes and equipment and gives answers to questions relating to the theoretical background of air handling unit and ductwork dimensioning and building energy systems optimization.

10. Local Ventilation

This chapter describes the aerodynamic principles, models, and equations that govern the flow and the contaminant presence and transport in a designated volume of a work room. The purpose of local ventilation is to control the transport of contaminants at or near the source of emission, thus minimizing the contaminants in the workplace air.

11. Modeling Techniques

This chapter describes calculation models for building energy demand and air flow in and around industrial buildings. Special attention is paid to simulation of airborne contaminant control.

Four methods for industrial air technology design are presented: computational fluid dynamics (CFD), thermal building dynamics simulation, multizone

airflow models, and integrated airflow and thermal modeling. In addition to the basic physics of the problem, the purpose of the methods, recommended applications, limitations, cost and effort, and examples are provided.

12. Experimental Techniques

This chapter covers a description of conventional measurement techniques used in ventilation as well as other, related topics such as flow visualization, laser-based measurement techniques, and scale model experiments.

13. Gas Cleaning Technology

This chapter describes the fundamentals of gas cleaning technology in branches of removal of particulates and gaseous compounds. This chapter also includes the fundamentals of particulate and gaseous measurements technology.

14. Pneumatic Conveying

Basic principles of pneumatic conveying and equations are presented. A new pressure loss equation is presented with examples.

15. Environmental Life Cycle Assessment

Life cycle assessment (LCA) is a compilation and evaluation of inputs, outputs, and the potential environmental impacts of a product system throughout its life cycle. The LCA methodology is comprehensively described based on the ISO 14000 series standards. References are also given to LCA information sources.

16. Economic Aspects

Life cycle cost (LCC) calculations are made to make sure that both the purchase price and the operating costs for life cycle are considered in investment decisions. In the chapter the basic calculation methods and sensitivity analysis are introduced. Examples of calculation results and references to LCC information sources are given.

REFERENCES

1. Hemeon, W.C.L. *Plant and Process Ventilation*, 2nd ed., Industrial Press, New York, 1963.
2. Baturin, V. V. *Fundamentals of Industrial Ventilation*, 3rd ed., Pergamon Press, Oxford, UK, 1972.
3. Heinsohn, Robert Jennings. *Industrial Ventilation Engineering Principles*, John Wiley & Sons, New York, NY, 1991.
4. Goodfellow, Howard D. *Advanced Design of Ventilation Systems for Contaminant Control*, Elsevier, Amsterdam, 1985.
5. *Industrial Ventilation, A Manual of Recommended Practice*, 23rd ed., Committee on Industrial Ventilation, American Conference of Governmental Industrial Hygienists, Cincinnati, OH, 1998.
6. Goodfellow, Howard D., and John Klus. *Evaluation Report of the INVENT Technology Programme*, TEKES (Technology Development Centre), Finland, February 1997.
7. INVENT Technology Programme, 1991–1996, Finland, FIMET.

This page intentionally left blank

2 TERMINOLOGY

BERNHARD BIEGERT

University of Stuttgart, IKE-LHR, Stuttgart, Germany

JORMA RAILIO

Association of Finnish Manufacturers of Air-Handling Equipment, Helsinki, Finland

2.1 MAIN DEFINITIONS

Figures 1.1, 2.1, 2.2, and 2.3 will explain the main terminology. These technologies and systems are described in technical details in Chapters 7 and 8.

2.1.1 Zones

Typically, industrial premises have, in one space, zones with different activities, which require different target levels for the indoor environment and its control. These target levels may be determined for the whole area or locally. Also, often only a part of the space needs to be controlled. In addition to the main controlled zone, there may be one or more local controlled zones with targets different from those in the main controlled zone. For example, machines equipped with electrical components require a very clean and accurately controlled indoor environment, while the unoccupied zone near the ceiling needs only roughly controlled protection against structural damages.

In industrial premises the target levels of indoor air quality, as well as other targets (e.g. emissions), shall be specified zone by zone.

Industrial Ventilation Design Guidebook

A *controlled zone* is a zone in which the thermal and air purity (quality) conditions are controlled to their specified levels. The two categories of controlled zones are as follows:

- The *main controlled zone* is normally a large area, which is often the same as the occupied zone.
- A *local controlled zone* is an area where the air is controlled locally; the control requirements may be for worker protection and comfort, for process control, or for production protection.

An *uncontrolled zone* is a zone in which the thermal and air purity (quality) conditions are not specified or controlled.

Note: There may also be uncontrolled zones near to the processes inside the main controlled zone.

Capture zones are zones in which source emissions will be captured by a source-capturing system, and where the capture efficiency is determined and shall be maintained over the working period. From the pollutant concentration point of view, the capture zone is uncontrolled (e.g., workers shall not enter a capture zone without additional protection).

2.1.2 Industrial Air Conditioning Systems

According to Chapter 1, industrial air technology includes measures for indoor environments (general and local); measures to prevent harmful emissions from industrial processes from being discharged outdoors, such as conveying and cleaning technologies; and measures to prevent or minimize damages caused by accidents, fire, or explosion.

2.1.2.1 Air Conditioning Systems

Room air conditioning (see Fig. 2.1) systems are used to control the main controlled zone. Systems can be divided into subsystems, e.g.:

- Air-handling systems
- Air distribution systems (ductwork)
- Room air distribution systems
- Ventilation systems
- Room heating and cooling systems
- Main exhaust systems
- Discharge systems: stacks, environmental dispersion

Note: Air distribution systems are not ventilation or air conditioning systems. For example, mixing air distribution and displacement air distribution are methods to bring the supply air to the treated space.

Discharge systems are used to discharge exhaust air to the outdoors in such a way that harmful spreading of pollutants to the environment and back indoors is avoided.

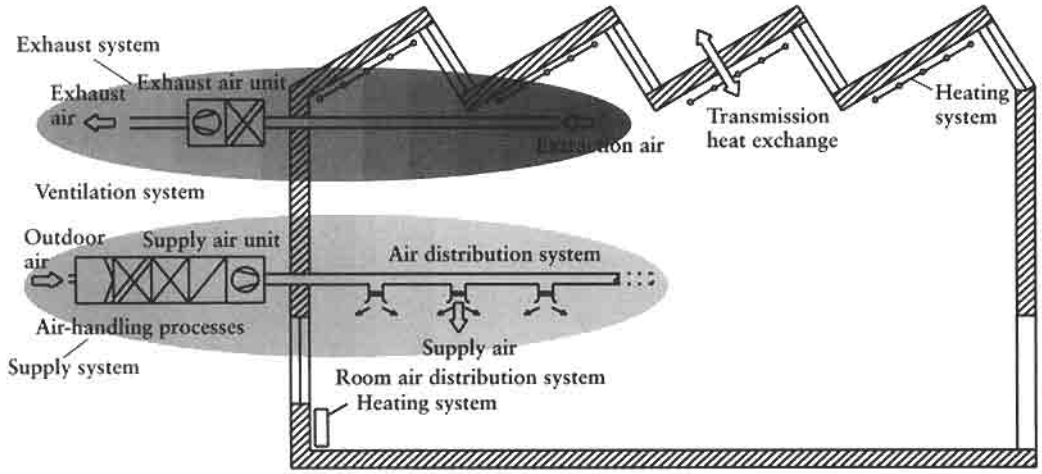

FIGURE 2.1 Main air conditioning systems.

2.1.2.2 Local Ventilation Systems

Local ventilation systems (see Fig. 2.2) are used for local controlled zones. These systems are air technological methods for local protection. Primarily, local protection should be made using process methods such as encapsulation or process modification (see "Design Methodology," Chapter 3). Another use for local ventilation systems is source capturing.

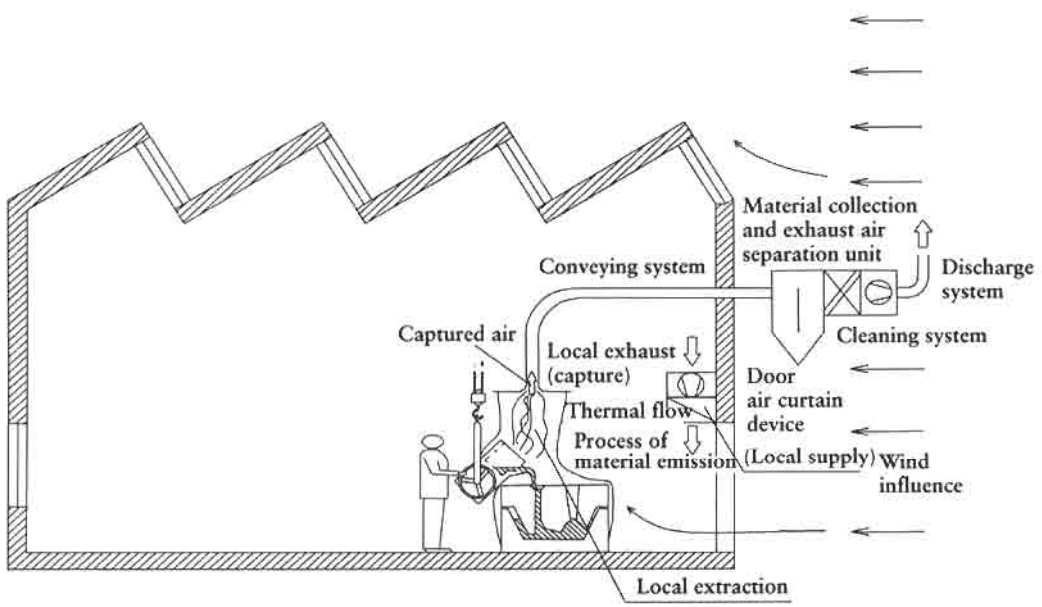

FIGURE 2.2 Local ventilation systems.

TABLE 2.1 Ideal Room Air Conditioning Strategies

	Strategy			
	Piston	**Stratification**	**Zoning**	**Mixing**
Description	To create unidirectional airflow field over the room area by supply air	To support flow field created by density differences by replacing the airflow out from the room area with supply air	To control air conditions within selected zone in the room by the supply air and allow stratification of heat and contaminants in the other room areas	To provide uniform conditions throughout the ventilated space
Heat, humidity, and contaminant distribution*	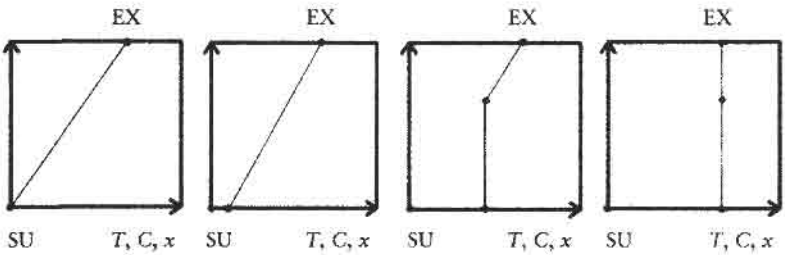			
Main characteristics	Room airflow patterns controlled by low-momentum unidirectional supply airflow, strong enough to overcome disturbances	Room airflow patterns controlled mainly by buoyancy; supply air distribution with low momentum	Room airflow patterns controlled partly by supply and partly by buoyancy	Room airflow patterns controlled typically by high-momentum supply airflow
Ideal contaminant and heat removal efficiency				
Typical application (example of a general room air distribution method)	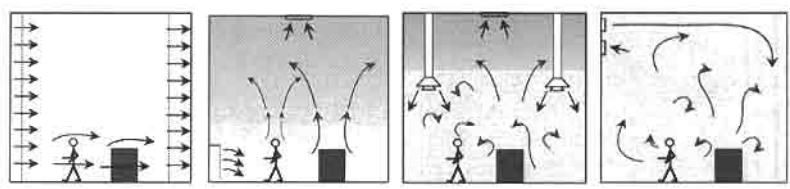			

*x-axis: °C, mg/m^3, g/kg; y-axis: room dim. (e.g., height); SU = supply, EX = exhaust

Local ventilation systems can be divided into the following subsystems:

- Local exhaust
- Local supply, including air curtains (i.e., control of air flow using jets)
- Combined local supply and exhausts

Parts of subsystems include fans, ducts, and filters.

2.1.2.3 Methods for Room Air Conditioning: Basic Strategies

A detailed description of the methods for room air conditioning is presented in Chapter 8. Table 2.1 summarizes the strategies.

2.1.3 Process Air Technology Systems

2.1.3.1 Cleaning Systems

These include equipment for supply air and equipment for exhaust air and gases. Cleaning of supply air is normally called air filtering, when the contaminant concentration upstream from the air filter is less than, e.g. 1–2 mg/m^3. Also, chemical filtration can be applied for supply air.

There are many types of cleaning systems and equipment, for example:

- Dynamic separators
- Wet separators
- Electric filters
- Desulfurization equipment (SO_x control)
- Denitrification equipment (NO_x control)

2.1.3.2 Conveying Systems

These are mainly pneumatic conveying systems, in which impurities and solid waste, but also materials or goods, are transported by air flows. The systems categories are low-pressure, medium-pressure and high-pressure systems, depending on how heavy the impurities are that the system will transport.

2.1.3.3 Drying Systems

These systems and equipment are used, e.g., in paper machines, using air or radiant drying.

2.1.4 Safety Air Technology Systems

These include, for example, smoke extraction systems. In ventilation and air conditioning systems certain equipment can also require special safety measures (e.g., due to explosion risks).

2.1.5 Definitions of Types of Air

The definitions of the types of air are presented in Fig. 2.3.

- Supply air
- Exhaust air

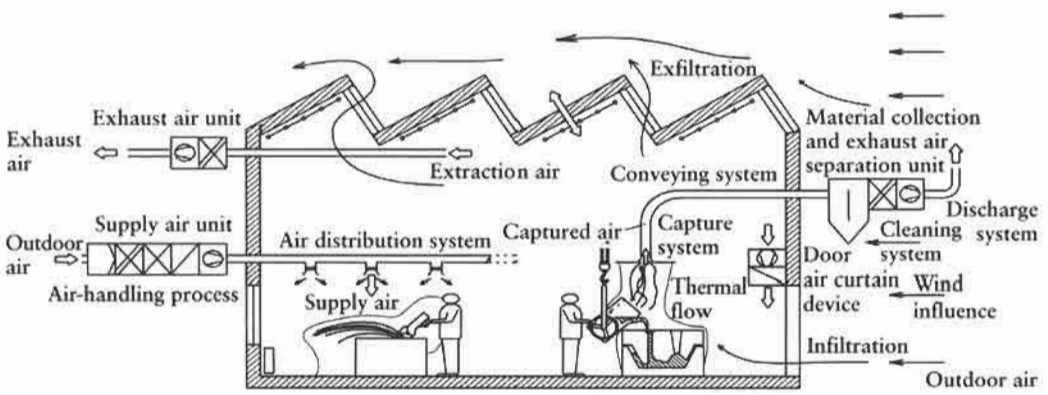

FIGURE 2.3 Definitions of air.

- Extract (main, local) air
- Recirculated air
- Outdoor air
- Transferred air (two types—direct or via an air-handling system)
- Infiltration
- Exfiltration
- Indoor air

Transferred air can be intentionally or unintentionally transferred. Exhaust air is air leaving the building. Extract air is air leaving the room (it may be partly returned into the room).

3

DESIGN METHODOLOGY OF INDUSTRIAL AIR TECHNOLOGY

KIM HAGSTRÖM

Faculty of Mechanical Engineering,
Helsinki University of Technology,
Espoo, Finland

3.1 INTRODUCTION

Environmental issues are being addressed more and more heavily in today's and future society. Thus, it is natural that in industrial processes and in their design, environmental effects are also considered over the whole life cycle. The life cycle of the production process can be divided into four parts: design, construction, operation, and end of the process. Each part consists of different tasks. Design methodology is a part of the whole process from starting point to "grave." The life

Industrial Ventilation Design Guidebook

cycle of the production process is illustrated in Fig. 3.1. Also, in Table 3.1 short descriptions and lists of tools for different tasks are given. Some of the tools are already in use, even if some of them are still missing from the engineer's tool case.

It is important to understand that the results of the design process are what mainly determine the ventilation system performance with all its consequences. Thus, it is necessary to build all the life cycle targets into plans. In order to ensure the transfer of these targets from the plan to the actual product, commissioning, operations, and maintenance plans should always be included in the design work. The value of proper design and commissioning will be paid back when process modifications are made during the operation period. One essential item in efforts toward optimal industrial ventilation is a common understanding of the design: *design methodology.*

The design methodology is a description of a technical design process that covers the whole lifetime of the production process. Most decisions concerning industrial ventilation are made at the design stage, and are reflected in construction, operation, maintenance, service, etc.

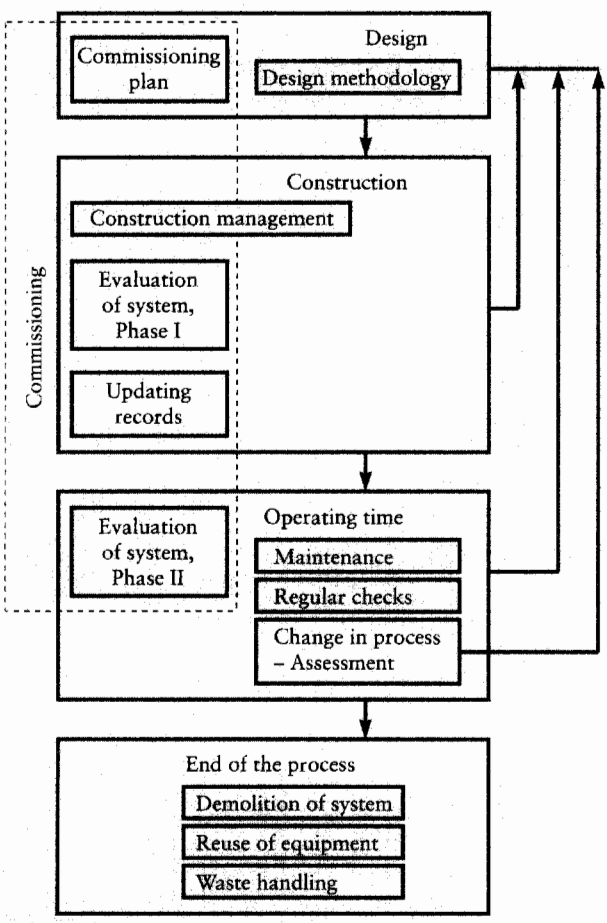

FIGURE 3.1 Design methodology process.

The first and most important aim of design methodology is to produce, by systematic analysis, a description of the design procedure that is commonly accepted and used in every process in different markets. The idea is to make a description of the technical process of design; in other words, to answer two questions:

- What is to be made clear and done during the design procedure?
- In which order are the tasks to be done?

The design methodology *does not* take a position on who does this or that task. That is part of administrative or commercial flow, which varies in different parts of the world and even in different projects in one country.

Once described, the design methodology can be applied for several usages. The need of the design methodology description was identified at an early stage of the *Design Guide Book* project. As such, it serves as a clue for this book. As design methodology vigorously describes the connections and correlation of different tasks, it could also be utilized as a skeleton of computerized design tools, such as expert systems, and as a tool for systematic analyses. It can be, and already has been, applied in research projects in order to identify gaps in knowledge or by financiers when assessing the need for proposed research.

3.2 DESIGN METHODOLOGY DESCRIPTION

Basic elements in the methodology can be presented in several ways. Table 3.1 gives an idea of the whole contents. In addition, decision trees are needed, because the design process requires many back couplings which cannot be illustrated in table form. The decision tree technique is a tool for dividing a process, here Design Methodology, into subtasks, which have their accurate inputs and outputs. The order of the tasks is chosen so that the data needed to do a task are given or calculated before that task to minimize the number of back couplings. Thus, the tree guides the right execution order of the subtasks. It also serves as an internal quality guidance tool for design process, because the quality of the preceding subtasks' results will be assessed in the next task, where they are used as input data.

In real projects the number of back couplings is much higher because of the administrative process, where the accuracy of the input data will improve during design. In early stages of the design one has to work with very preliminary and inaccurate information to produce preliminary results, such as cost estimates and space reservations, which have to be given in spite of missing data. Nevertheless even in such cases the whole decision tree must be gone through; the only difference is that missing data are replaced with an estimate. When missing data become available, the process is gone through again in order to review the plans. Such descriptions that cover all possible back couplings cannot be made, because completion of the projects varies among the different countries, branches, and partners that are involved. As a matter of fact, the nature of targeted design emphasizes the core idea of the design methodology. To achieve the optimal solution and all the original targets, one has to redesign all the tasks following the point at which a change, such as new input information, was made.

TABLE 3.1 Design Methodology and Associated Tools

Administrative Flow—Quality Assurance: Prestudies, Design, Construction, Maintenance

Design Criteria		Tools
Given data	Data dependent only on the site location and do not change during design process.	Database Weather model
Process description	Purpose: Identification of possible emission sources, occupational areas, effects of environmental parameters to production, needs for enclosure and ventilation. Division of process into such parts that their inputs and outputs can be defined.	Expert systems Databases
Building layout and construction	Collection of properties of building layout, constructions, windows as basic values for load calculations.	Databases
Target level assessment	Prediction of target levels for indoor and outdoor conditions based on requirements of laws and orders, human health, production processes and equipment, and type of premises and construction. Needed as a standard to which system solutions are compared.	Classifications Regulations
Source description	Characteristics of sources and calculations methods for load calculation.	Calculation models
Calculation of local loads	Calculation of loads from different subprocesses.	Building model
System Performance		
Local protection	Examination of subprocesses in order to provide proper working conditions by it or to reduce emissions to environment. In case use of local protection system effect on exposure of the process, load calculations shall be revised.	Calculation models Prefabricated products
Calculation of total loads	Calculation of total loads from different subprocesses and environment.	
System selection	Based on technical calculations, conditions achievable by different systems are compared to target levels to identify acceptable systems, which are compared to each other and the most suitable system is selected on the basis of different parameters: Power and energy consumption and investment and life cycle costs.	System description and characterization Heat, mass, and energy balances
Equipment selection	Based on technical specification, acceptable equipment is identified. Final selection is made on the same basis as in selection of system.	Equipment selection programs and diagrams
Detailed design	Includes the following subtasks: detailed design of ventilation systems, design of adjustment and control system, commissioning plan.	Duct design programs and diagrams CAD solutions (Drawing tools)

Common items (built into tools):
–Energy consumption
–Ecological issues
–Costs (construction, life cycle)

(*continues*)

TABLE 3.1 *(continued)*

Administrative Flow—Quality Assurance: Prestudies, Design, Construction, Maintenance		
Construction/Commissioning		**Tools**
Construction management		Mounting design Materials handling Commissioning plan
Evaluation of system, Phase 1	Inspections and startup and functional performance tests.	Performance tests Checks Measurements
Updating records	System descriptions User instructions	CAD programs (Drawing tools)
User training	Training of operating and maintenance people	Lectures Practical training Participating in the evaluation
Operating Time (Use)		
Evaluation of system, Phase 2	Functional performance tests in different situations	Performance tests
Maintenance	Measures to keep ventilation system operating at the specified level economically.	Maintenance plan Monitoring Health surveillance
Regular checks	Measures to secure that system and equipment performance are unchanged. Additionally, evaluation of the system toward new requirements.	Energy audits Environment audits Assessment (COSSH)
Process changes	Adoption of the process changes by evaluating influences to ventilation system and to conditions. When needed, renewing of ventilation system to meet targets.	Assessment (COSSH) System simulation
End of Process		
Demolition of system	Design and completion of demolition, taking into account possible risks. (e.g., asbestos)	Assessment of the risk to health Special working methods
Reuse of equipment	Evaluation of the value and usefulness of the equipment and components.	Condition analysis of the equipment
Waste handling	Separation of different types of waste. Handling of problem waste. Recycling materials.	Records of materials used Marking of components
Common items (built into tools): –Energy consumption –Ecological issues –Costs (construction, life cycle)		

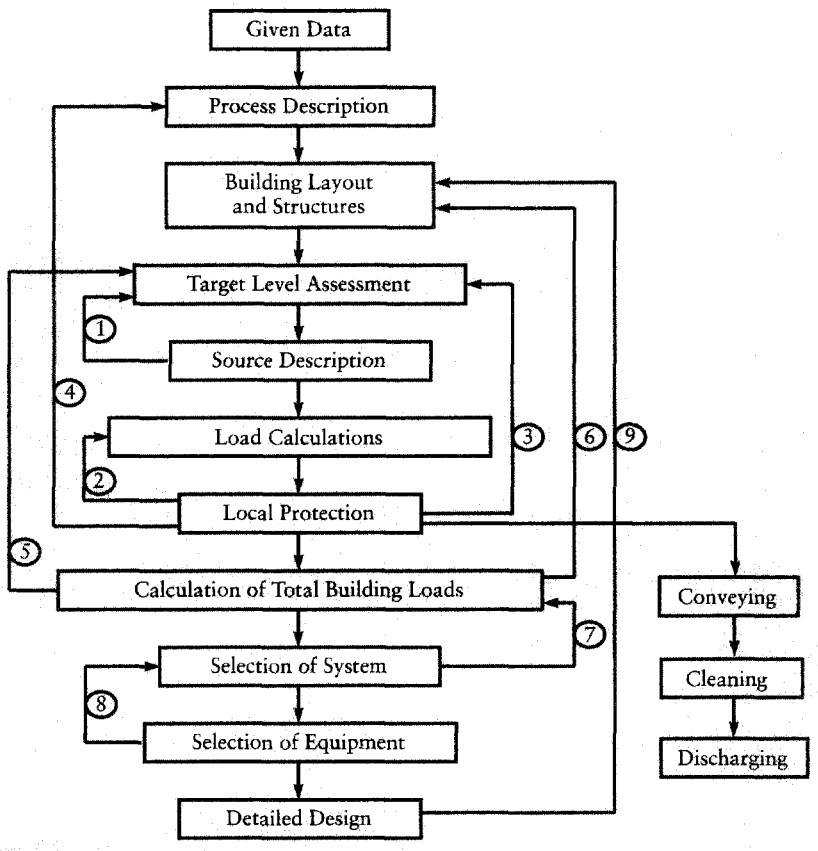

FIGURE 3.2 Decision tree of design process.

Correspondingly, when an existing industrial process is to be renewed, it is sufficient to redesign only such subtasks of the design methodology that are influenced by the change made. Naturally, this kind of procedure requires that the original design and previous changes have been documented properly.

A decision tree for Design Methodology is illustrated in Fig. 3.2. Each step in the tree is explained briefly below. The steps have also their own subtrees, which are described separately.

Explanations of Fig. 3.2

Step 1: Given Data

Identify and collect data that depend only on the site location and that do not change during the design process, such as outdoor conditions.

Step 2: Process Description

- Identify the industrial process and subprocesses.
- Identify possible emission sources, occupational areas, effects of environmental parameters, needs for enclosure and ventilation equipment.

- Divide process into parts such that their inputs from and outputs to the environment can be defined.
- When the process or subprocess is not well defined during the initial period of design, obtain the data from similar processes based on recent successful practices. Obtain and use more precise data as soon as possible.

Step 3: Building Layout and Construction

- Collect properties of building layout, structures, and openings and their properties as basic values for load calculations.
- Complete zoning of building based on division of the process and building layout.
- Make space reservations and add structures needed for ventilation equipment.

Step 4: Target Level Assessment

- Define target levels for indoor (zones) and outdoor (exhaust) conditions.
- Specify design conditions in which the target levels are to be met.
- Define target levels for the ventilation system, such as reliability, energy consumption, investment, life cycle costs, etc.

Step 5: Source Description

Clarify characteristics of the sources and calculation methods for calculation of local loads.

Step 6: Calculation of Local Loads

Calculate loads from individual sources to the environment.

Step 7: Local Protection

Examine subprocesses (sources) in order to provide proper working conditions near them (local zones) or to reduce emissions to the environment.

Step 8: Calculation of Total Building Loads

- Calculate total loads (heat, humidity, contaminants) from different subprocesses and environment (building) to ventilated enclosure (zones).
- Take into account that loads are usually time dependent.

Step 9: Selection of the System

- Select acceptable systems based on target levels.
- Compare acceptable systems in order to choose the most desirable one.
- Use systems that allow maximum flexibility in air flow rates and control strategies when selection of systems is based on inaccurate (preliminary) data on production processes, volumes, and raw materials to be used in the building. Emission rates from these processes and total loads might be changed during the detailed design step.
- Consider constraints on the system selection, if some equipment has been already selected and installed in the earlier design period.

Step 10: Selection of Equipment

- Work out performance characteristics to the equipment.
- Select acceptable equipment based on performance characteristics.
- Compare acceptable equipment in order to choose the most desirable one.
- Make a technical specification of selected equipment.

Step 11: Detailed Design

- Do detailed layout and dimensioning design.
- Design adjustment and control system.
- Consider special issues such as thermal insulation, condensation risks, fire protection, and sound and vibration damping.
- Make commissioning plan.

Steps 12–14: Design of Conveying, Cleaning and Discharge of the Pollutants

See details in Chapters 13 and 14.

Explanations of Back Couplings

BC 1: Source Description → Target Level Assessment

If some new agent is identified, the target level has to be defined for that agent too.

BC 2: Local Protection → Calculation of Local Loads

If the local protection has an effect on the exposure of the source, recalculate the load.

BC 3: Local Protection → Target Level Assessment

If defined target levels cannot be reached, reconsider target levels.

BC 4: Local Protection → Process Description

Consider whether there is some process method to protect source/environment. In that case, return to process description. For example, if thermal insulation is needed to reduce loads, consider what influence that has on the process itself (Insulation may, e.g., lead to a need to change material of equipment).

BC 5: Calculation of Total Building Loads → Target Level Assessment

- Consider whether some source has governing role to total loads. At least, if returned from Selection of System, choose one of the two actions below.
- If some source has governing role over total loads, reconsider the target level of that local zone in order to reduce loads.
- If there is no source that governs total loads, reconsider the target level of main zones in order to reduce loads.

BC 6: Calculation of Total Building Loads → Building Layout and Structures

If building loads have governing role over total loads, reconsider whether there is something that can be done with constructions (e.g., thermal insulation) to reduce loads.

BC 7: Selection of System → Calculation of Total Building Loads

If target levels cannot be achieved with any system or it is not economically possible, check whether something can be done with loads.

BC 8: Selection of Equipment → Selection of System

If no acceptable equipment exists, reconsider Selection of System with available equipment.

BC 9: Detailed Design → Building Layout and Structures

- Identify openings needed in structures.
- Identify additional space and structure needs for ventilation installations.

3.3 GIVEN DATA

In this description given data, such as outdoor conditions, depend only on the site location and do not change during the design process. Naturally it is possible that given values may be corrected during the design process, but that is due to missing information, not because conditions have changed.

The division of the data is shown in Fig. 3.3.

The *tools* for this task are:

- Databases
- Weather models

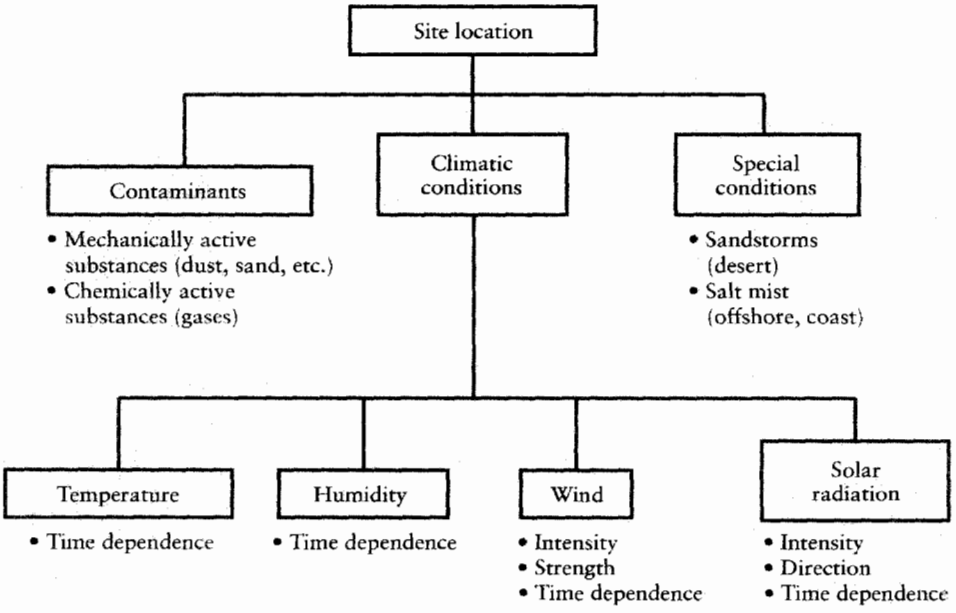

FIGURE 3.3 Given data.

3.4 PROCESS DESCRIPTION

Understanding of the technological process and identification of subprocesses are essential for proper ventilation design, especially when designing process ventilation but also in enclosure air technology. The purpose of process description is to identify possible emission sources, occupational areas, the effects of environmental parameters on production, needs for enclosure and ventilation equipment, etc. One purpose is to divide the process into parts such that their inputs and outputs (e.g., process, piping and duct connections, electricity, exposure) to environment can be defined. Parts here can be different departments, and inside them, subprocesses. See Fig. 3.4.

Also, possible specific secondary sources of energy should be studied at this stage.

Tools for this task could include databases and further expert systems.

3.5 BUILDING LAYOUT AND CONSTRUCTION

This task considers the effect of building and construction properties to indoor environment. It requires the collection of properties of building layout, construction, openings and their properties as basic values for load calculations. See Fig. 3.5.

The *output* of this task could, in addition to the list of properties, also include a more sophisticated building model, in which collected properties are built in: infiltration model, thermal model, etc.

Tools for this task include:

- Architect designs
- Databases

3.6 TARGET LEVEL ASSESSMENT

This task consists of defining target levels for indoor and outdoor conditions based on requirements for laws and regulations, human health, production processes and equipment, and type of premises and construction. Target levels should also be defined for the ventilation system. For the decision tree, see Fig. 3.6.

Target levels are needed as a standard to which system solutions are compared. During comparison it may become evident that target levels cannot be achieved with any solution or that they lead to very expensive solutions. In such cases target levels have to be reconsidered (back coupling).

Explanations of Fig. 3.6

Step 1: Musts

Clarify requirements due to laws, regulations, standards related to legislation, processes, and equipment.

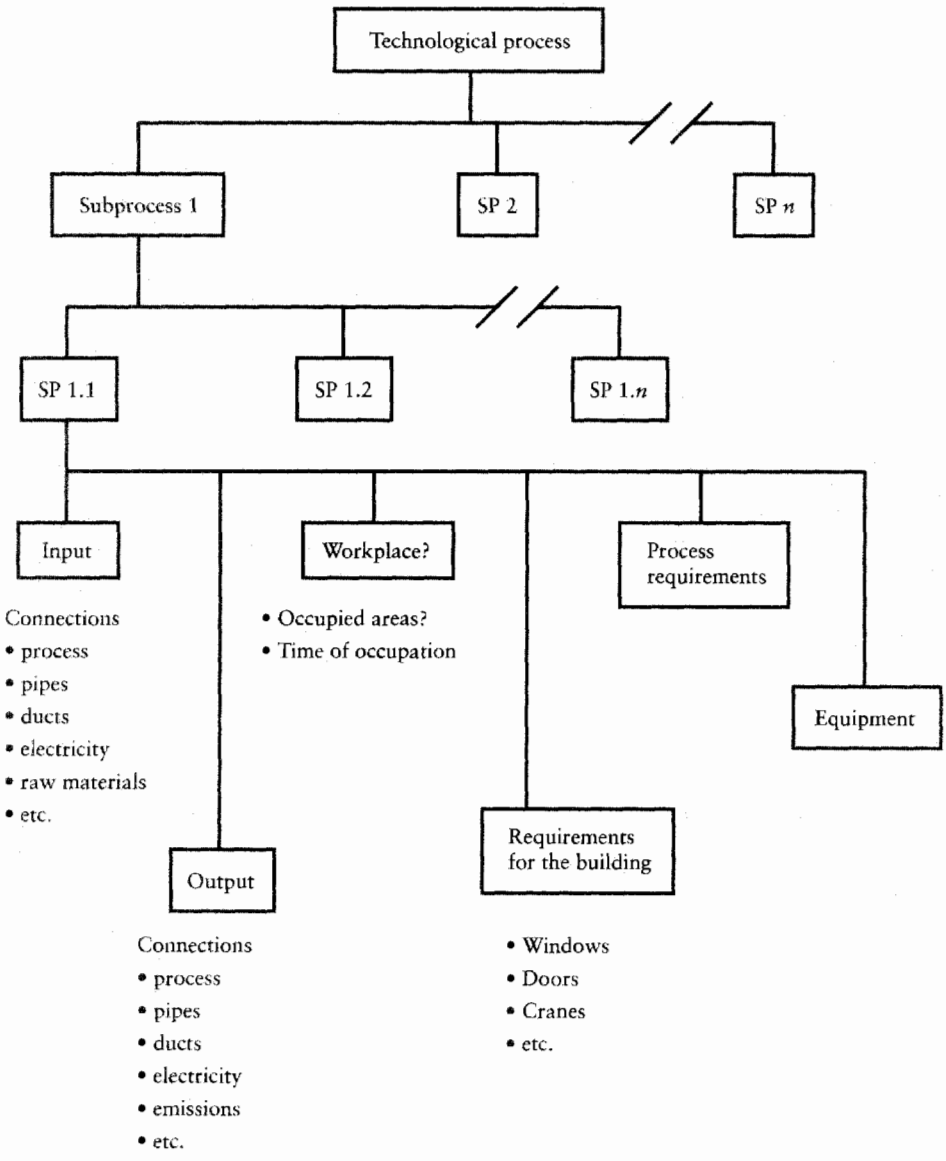

FIGURE 3.4 Process description. Division of process into such parts that their inputs, outputs, and target levels can be specified. A subprocess can be source or separate area/room that is to be protected from its environment.

Step 2: Needs

Clarify standards not related to legislation, such as those related to human comfort, guidelines, codes of practice, and custom needs.

Step 3: Target Levels

Decide target levels based on musts and needs.

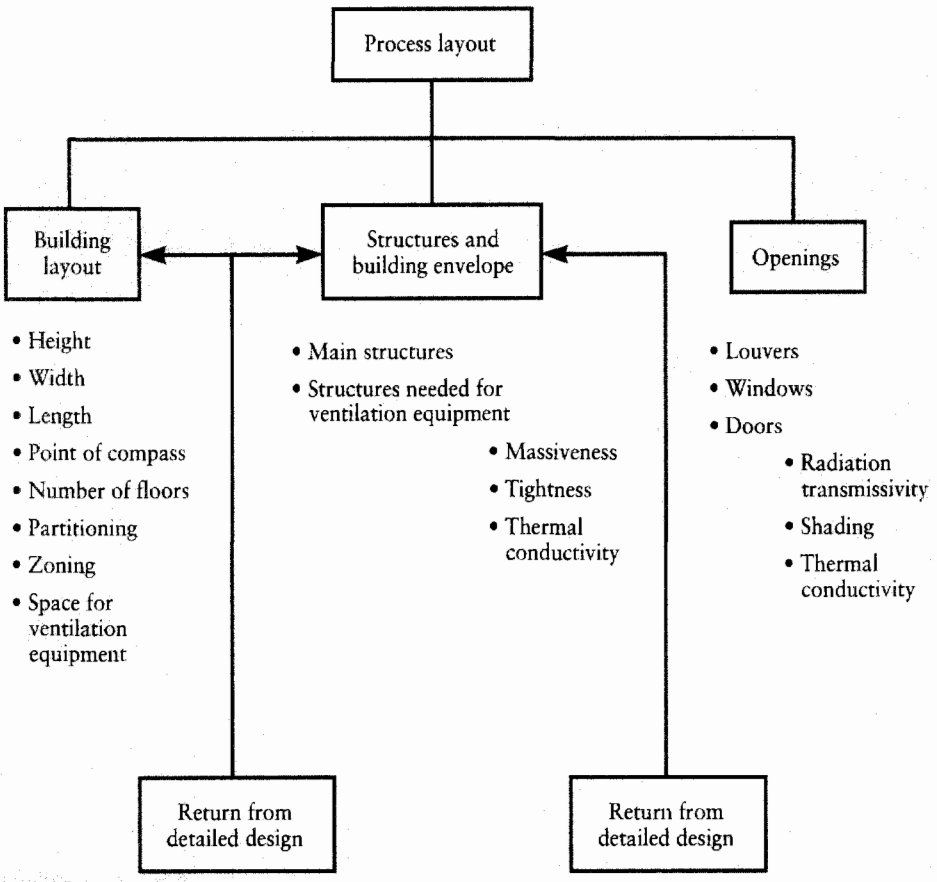

FIGURE 3.5 Building layout and structures.

Step 4: Design Conditions

Suggest and agree with customer on the outdoor conditions within which the target levels have to be met, e.g., absolute maximum temperature versus 95% temperature.

Step 5: Reliability

- Study the reliability requirements of the process with the customer.
- Define and get the customer's acceptance of the needs for ventilation system reliability, e.g., what is the allowed break-off time.

The *tools* for this task include:

- Laws, regulations
- Standards
- Guidelines, codes of practice

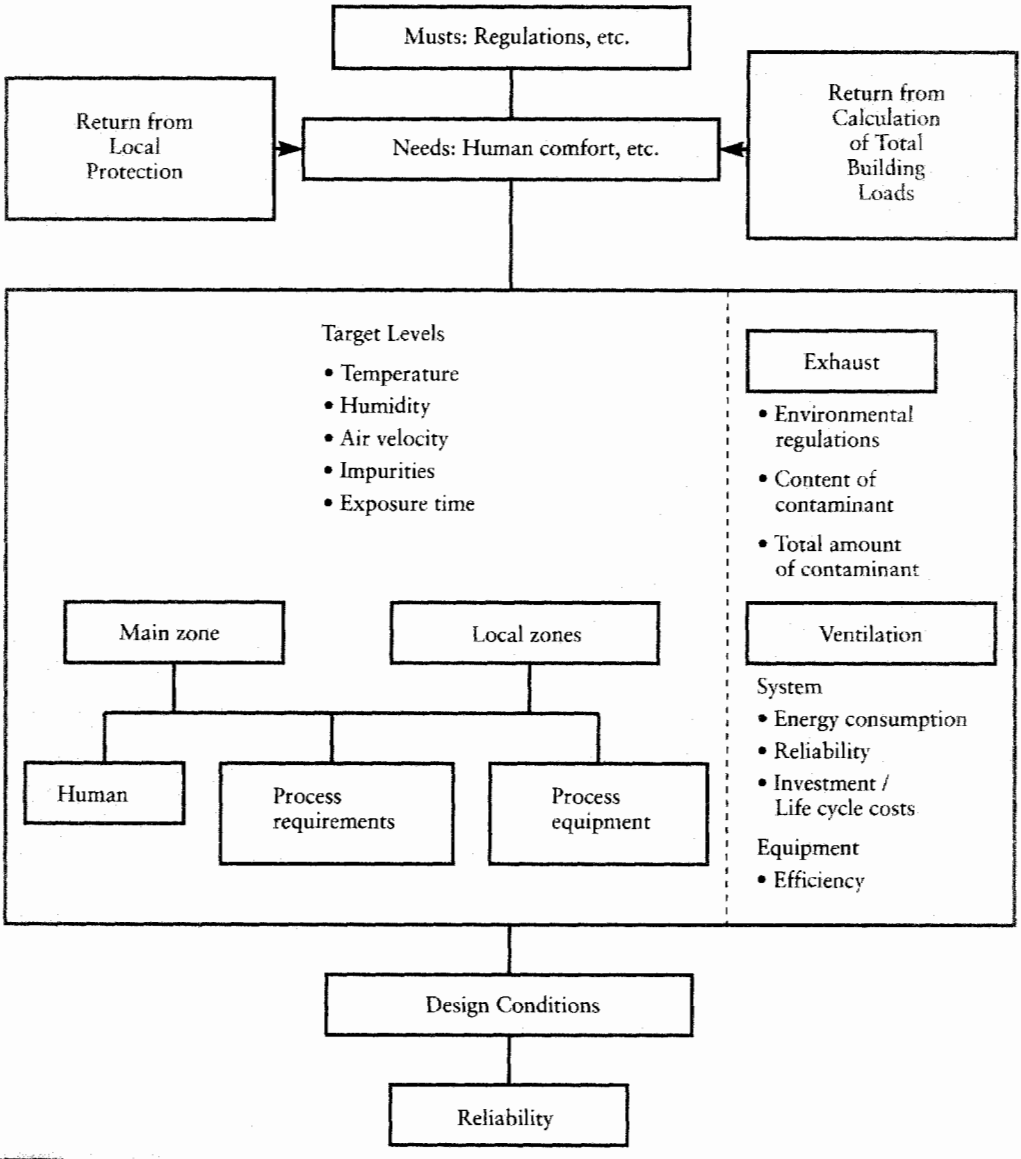

FIGURE 3.6 Target level assessment.

3.7 SOURCE DESCRIPTION

This task identifies characteristics of each source and calculation methods for load calculation. See Fig. 3.7.

The *tools* for this task include:

- Standard tests
- Physical modeling
- Databases
- Guidelines

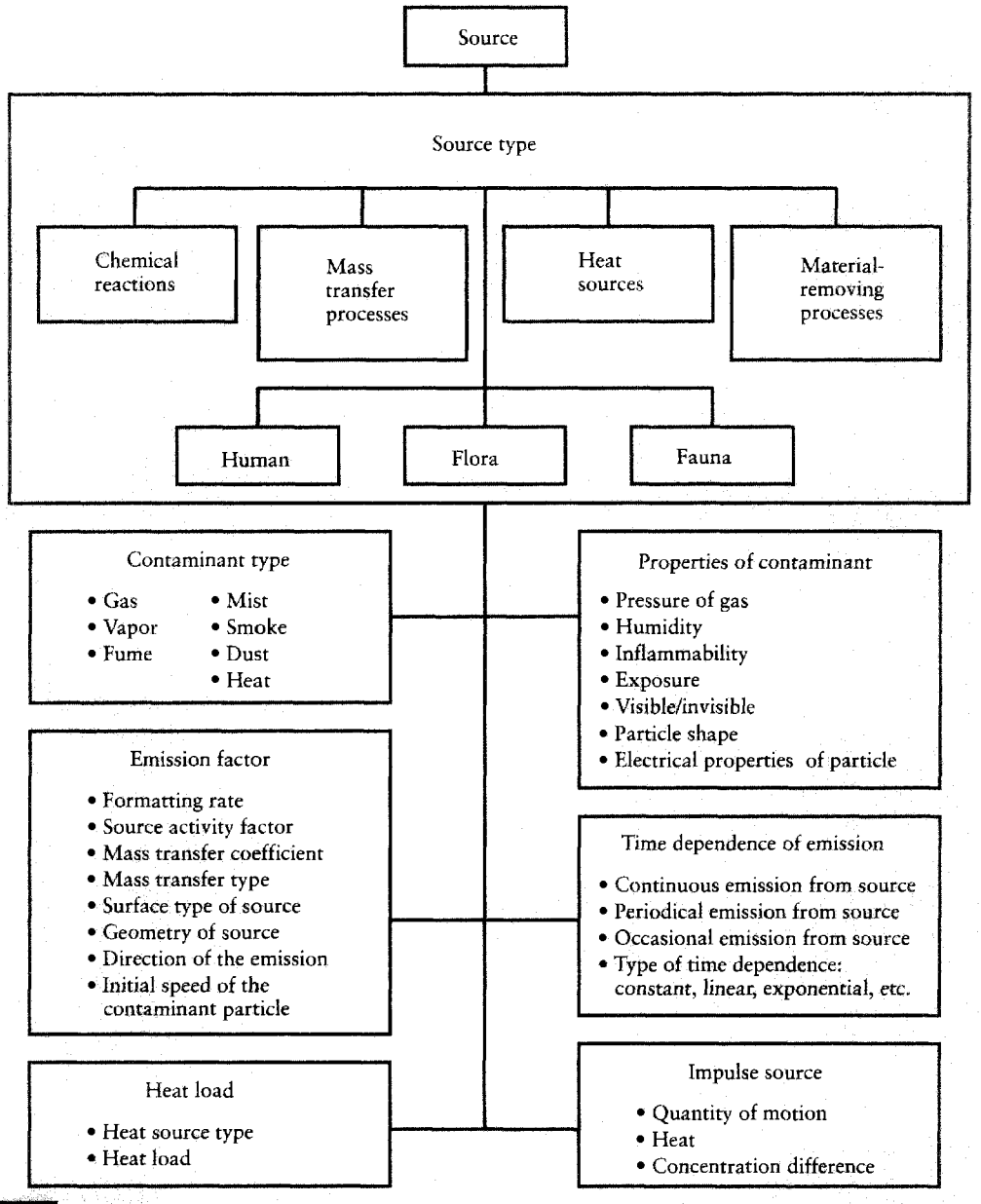

FIGURE 3.7 Source description, characteristics of the source and calculation methods for load calculation.

3.8 CALCULATION OF LOCAL LOADS

This task involves calculation of loads from different subprocesses (heat, humidity, contaminants). Loads are usually time dependent, which has to be taken into account. See Fig. 3.8.

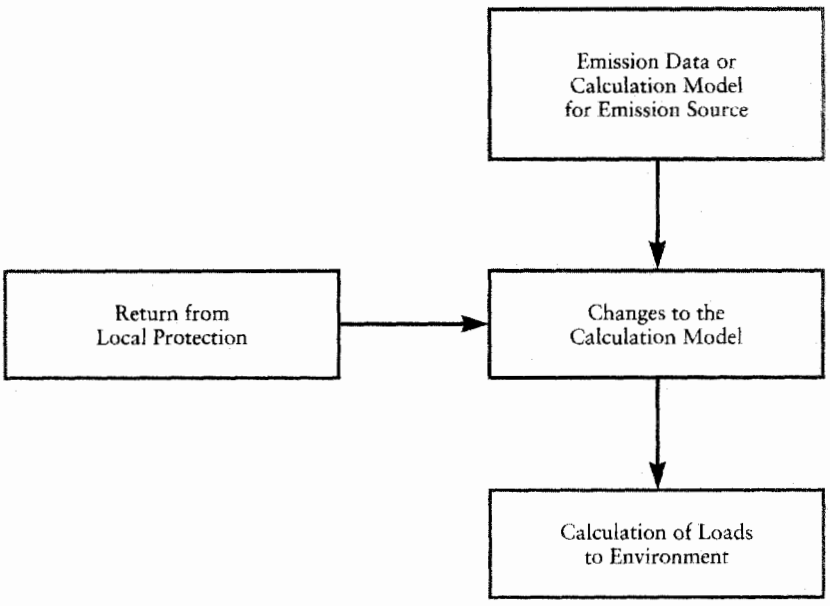

FIGURE 3.8 Calculation of local loads.

Explanations of Fig. 3.8

Step 1: Emission Data/Calculation Model

Obtain data from Source Description.

Step 2: Changes to the Calculation Model

- Derive modifications on the case
- Make additional modifications, if returned from Local Protection

Step 3: Calculation of Loads to Environment

Calculate emissions from the source to the environment.

The *tools* for this task include design tools for calculation (models) and measured data of emissions in different processes, which are defined in Source Description.

3.9 LOCAL PROTECTION

Subprocesses are examined in order to provide proper working conditions locally or to reduce emissions to environment (see Fig. 3.9).

Before considering ventilation, technical measures applied to process methods must be considered.

The last method in protection of the worker is respiratory protective equipment.

In case use of a local protection system has an effect on exposure of the process, load calculations shall be revised.

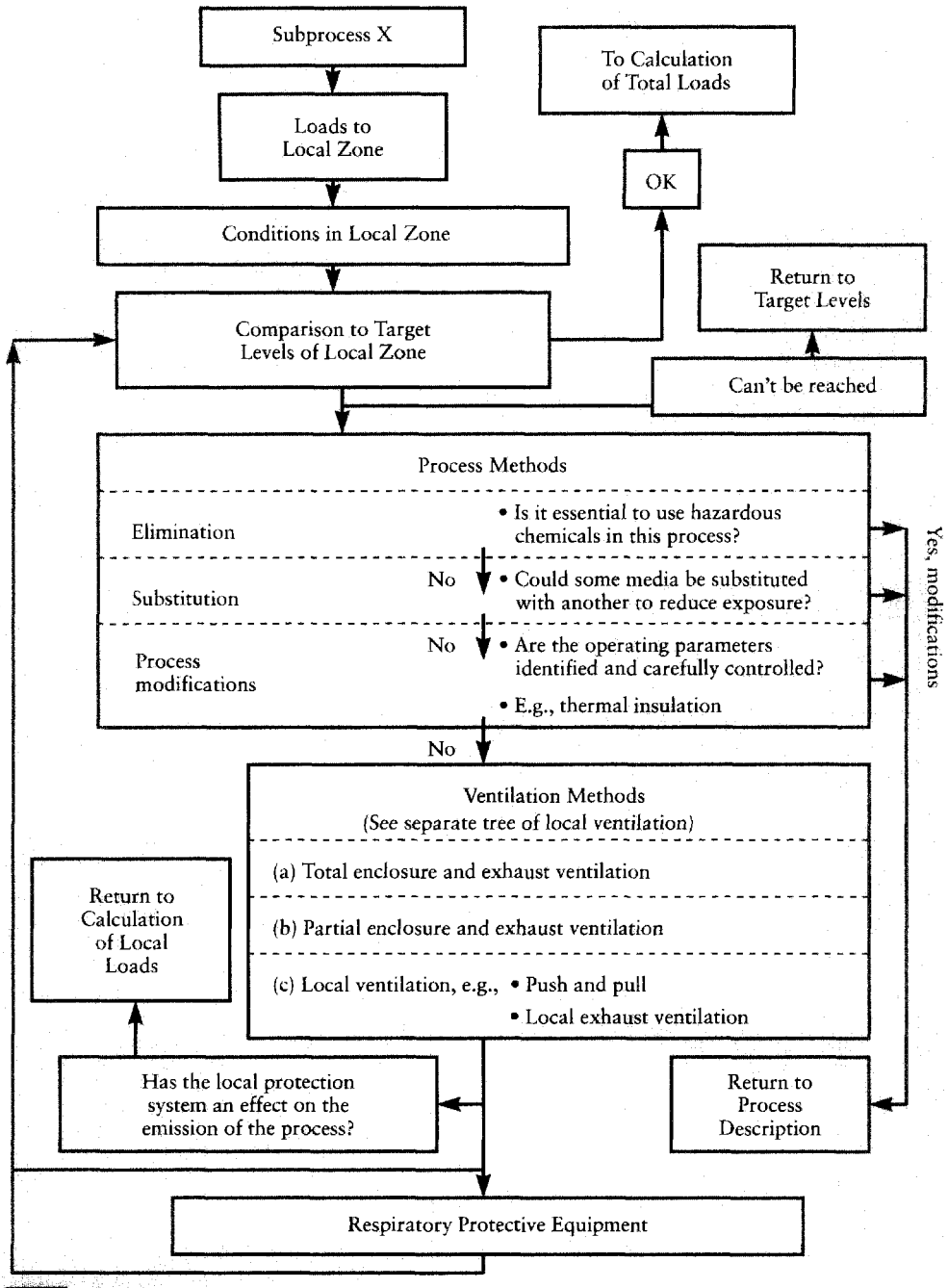

FIGURE 3.9 Local protection.

Explanations of Fig. 3.9

Step 1: Loads to Local Zone

Clarify loads that influence the local zone.

Step 2: Conditions in Local Zone

Calculate the conditions in the local zone.

Step 3: Comparison to Target Levels of Local Zone

Compare calculated conditions to the target levels of the zone.

Step 4: Process Methods

Consider whether there are any process methods to reduce loads.

Step 5: Ventilation Methods

Select the optimal ventilation method to reduce emissions and/or to protect workers. (For details, see the subtree Fig. 3.10.)

Step 6: Effect of Local Protection on the Emission of the Process

Consider whether the local protection influences the emission of the process. In that case, return to Calculation of Local Loads.

Step 7: Respiratory Protective Equipment

If no other method provides protection to the worker, design respiratory protective equipment. In the design phase, the minimum is to identify the need for personal protection.

The *tools* for this task include:

- Balances (heat, contaminants, etc.)
- Computational fluid dynamics (CFD)
- Empirical methods
- Process methods
- Ventilation methods (see the subtree in Fig. 3.10.)

Explanations of Fig. 3.10

Step 1: Source Characteristics

Characteristics are defined in Source Description.

Step 2: Alternative Prevention Methods

Select methods that could be used in this case.

Step 3: Calculation of Prevention Methods

Calculate performances of different methods and make them comparable.

Step 4: Selection of the Hood

- Select the method that is optimal in this case (efficiency, economy, etc.).
- After selection, return to Local Protection (design of general ventilation system).

Step 5: Design of Conveying System

Design conveying system to convey captured contaminants away (separate tree).

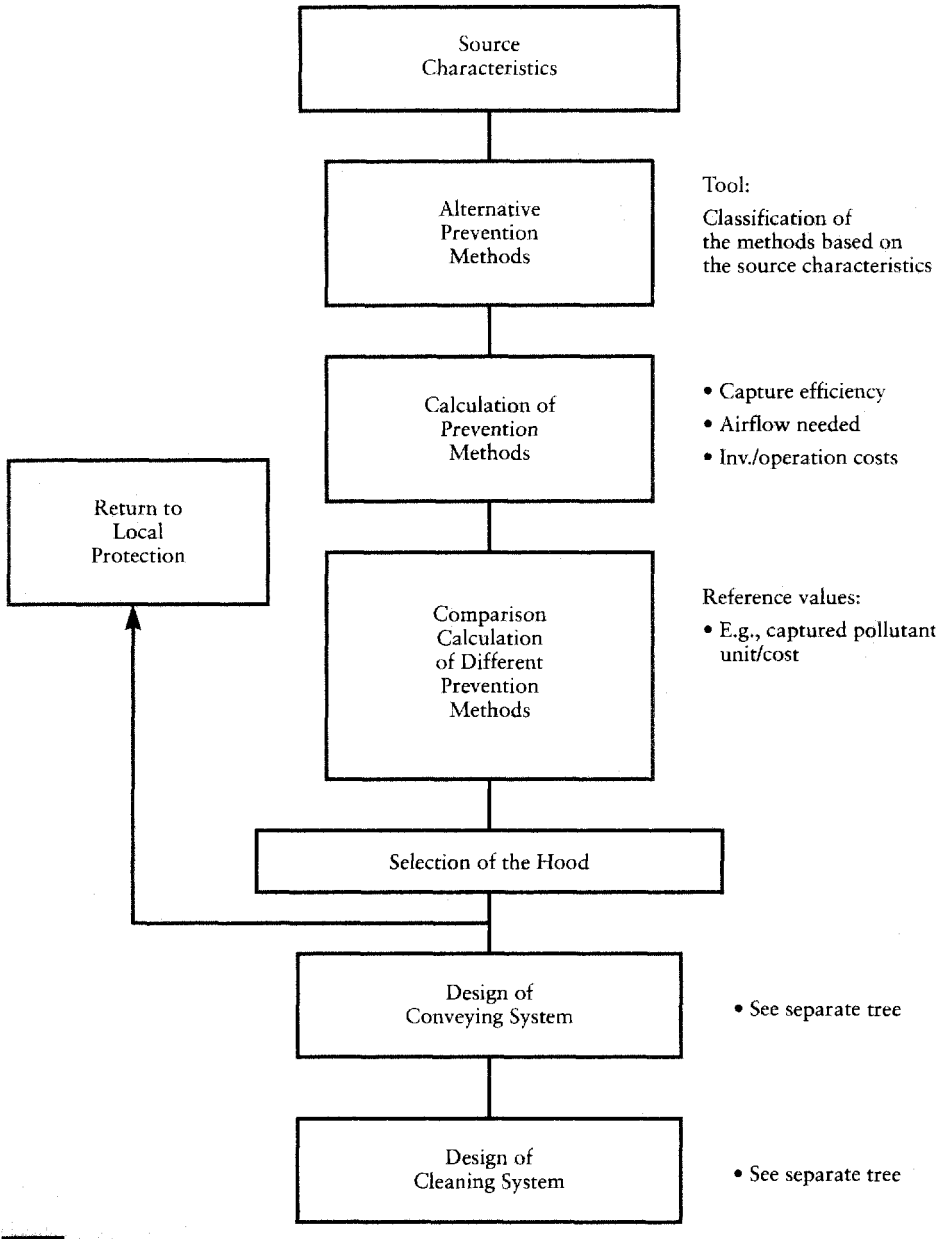

FIGURE 3.10 Local ventilation.

Step 6: Design of Cleaning System

Design cleaning system for contaminants, if needed; e.g., it may be necessary to clean extract air or to recover some valuable substance (separate tree).

3.10 CALCULATION OF TOTAL LOADS

Total loads from different subprocesses and environment (building) to the ventilated enclosure are calculated using design tools (heat, humidity, impuri-

ties). Loads usually are time dependent, which has to be taken into account. See Fig. 3.11.

Explanations of Fig. 3.11

Step 1: Loads to General Ventilation System

Loads from different sources to the general ventilation system are determined taking into account local protection.

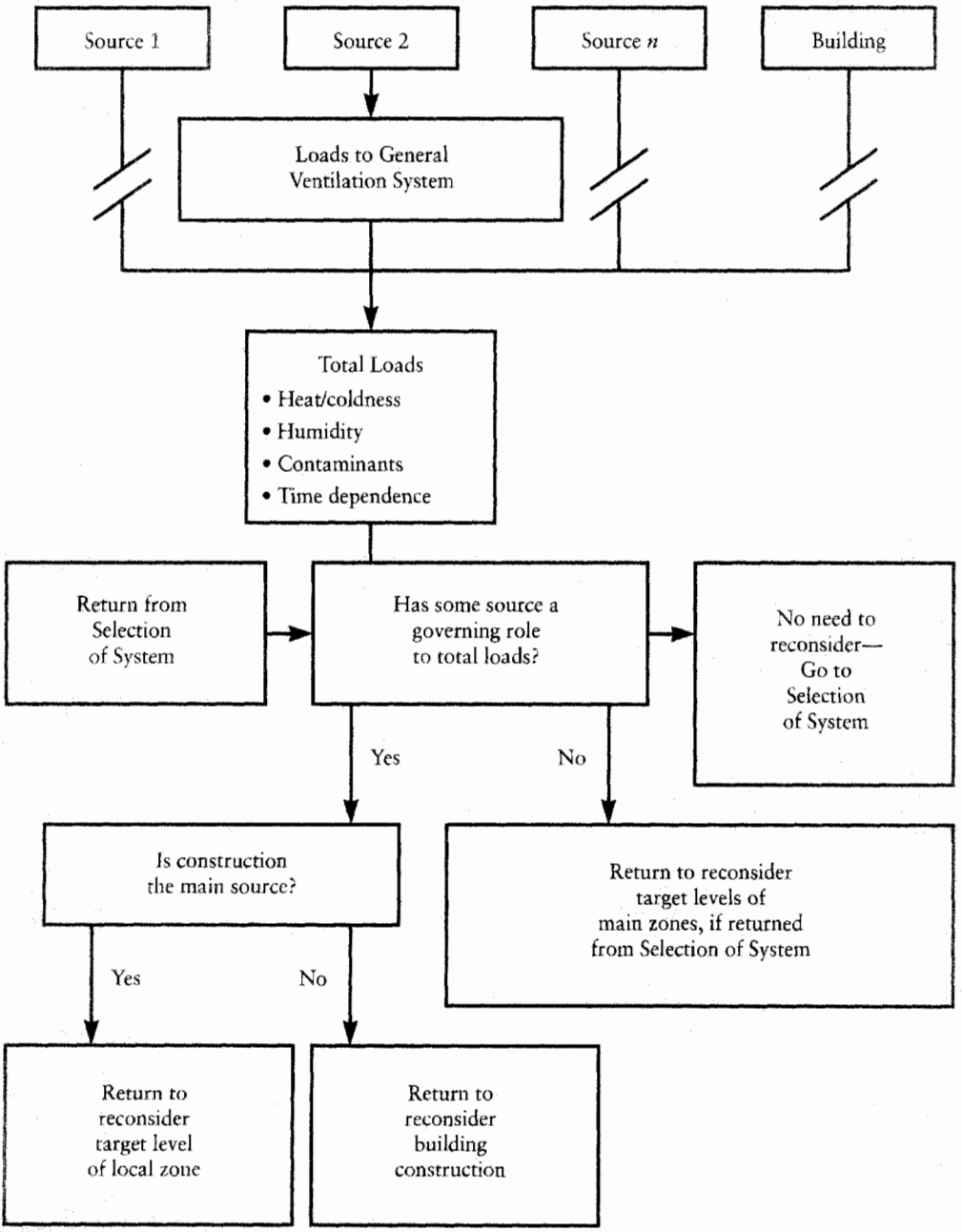

FIGURE 3.11 Calculation of total loads.

Step 2: Total Loads

Calculate total loads, taking into account the time dependence of the loads.

Step 3: Check for a Source That Has Governing Role to Total Loads

- Check whether there is some single source that alone produces most of the loads.
- If you are calculating the loads at first, there might not be a need to reconsider at this stage.
- If the answer is yes,
  - If construction is the main source, return to Building Layout and Construction and reconsider whether there is something that can be changed in building construction to reduce loads.
  - Reconsider the target levels of local zone to reduce emission of a single source.
- If the answer is no, reconsider the target levels of the main zone (general ventilation), if loads cannot be reduced.

3.11 SELECTION OF SYSTEM

There are two different tasks in system selection: acceptance of systems based on target levels, and comparison of acceptable systems in order to choose the most desirable one.

Based on technical calculations the conditions achievable by different systems (ventilation, cleaning, etc.) are compared to target levels to identify acceptable systems. Dimensioning properties could be:

- Mass and heat balances
- Room flow models

Acceptable systems are compared to each other and the most suitable system is selected on the basis of different parameters, such as power and energy consumption and investment and life cycle costs. See Fig. 3.12. Tools for comparison are energy balances and cost analyses.

Explanations of Fig. 3.12

Step 1: Alternative Ventilation/AC Systems

Select alternative ventilation systems for comparison.

Step 2: Alternative Air Distribution Systems

Select alternative air-distribution systems for comparison.

Step 3: Technical Calculations

Calculate the operation of different solutions.

Step 4: Comparison to Target Levels

- Compare conditions reached with different systems to target levels.

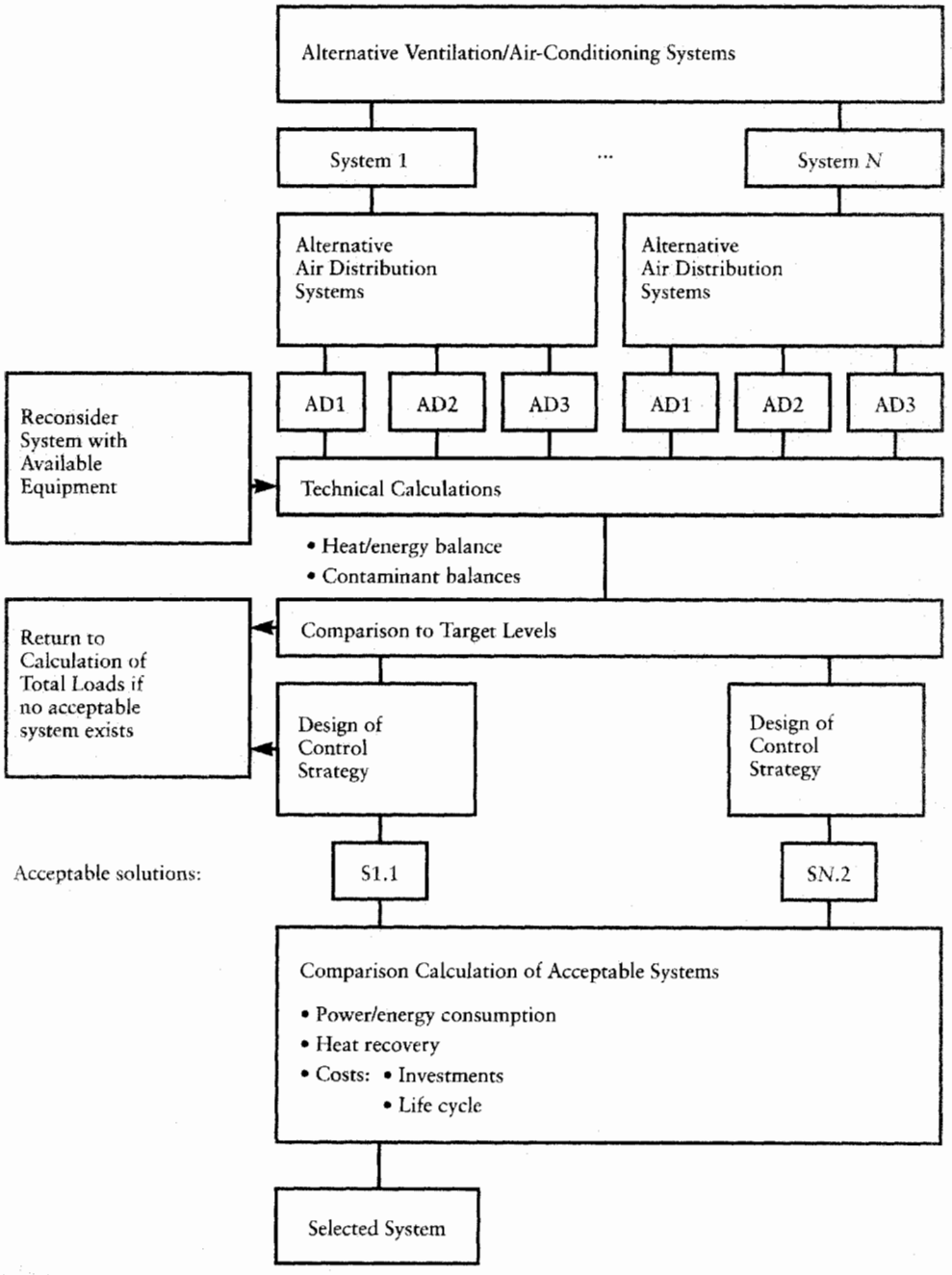

FIGURE 3.12 Selection of system.

- Accept systems that fulfill the targets for further comparison.
- If no acceptable system exists, return to calculation of Total Loads to consider whether there is something that can be done with the total loads.

Step 5: Design of Control Strategy

- Design control strategy for acceptable systems in order to handle different situations (seasonal, process variations).
- As in step 4, if none of the acceptable systems can handle different situations, return to calculation of Total Loads to consider whether there is something that can be done with the total loads.

Step 6: Comparison Calculation of Acceptable Systems

Calculate costs, consumption of goods (energy, electricity, etc.), and possible heat recovery of acceptable systems.

Step 7: Selected System

Select the optimal system based on the comparison calculations.
The *tools* include:

- Zone models
- CFD
- Energy simulation

3.12 SELECTION OF EQUIPMENT

Based on technical specifications, acceptable equipment is identified. The final selection is made on the same basis as in Selection of System. The decision tree is shown in Fig. 3.13.

Explanations of Fig. 3.13

Step 1: Performance Characteristics

Define performance characteristics based on system selection.

Step 2: Alternative Equipment

Select alternative equipment for comparison.

Step 3: Selection of Acceptable Equipment

- Compare different equipment to performance characteristics.
- Accept equipment that fulfills the characteristics for further comparison.
- If no acceptable equipment exists, return to selection of system to reconsider system selection with available equipment.

Step 4: Feasibility Comparison of Acceptable Equipment

Calculate costs, consumption of goods (energy, electricity, etc.), and possible heat recovery of acceptable systems.

Step 5: Selection of Equipment

Select the optimal equipment solution based on the comparison calculations.

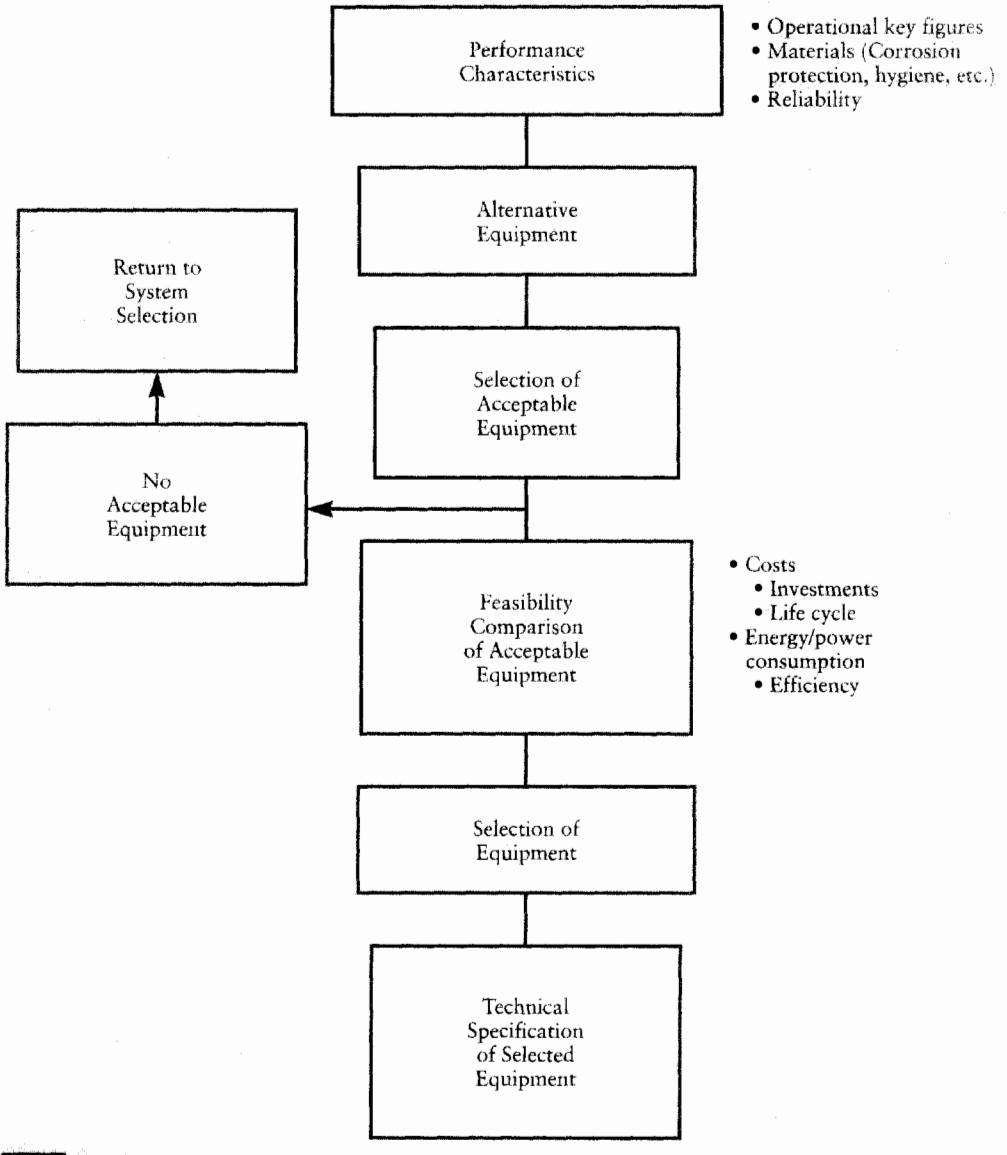

FIGURE 3.13 Selection of equipment.

Step 6: Technical Specification for Selected Equipment

Develop a technical specification for selected equipment. The *tools* include:

- Computer programs
- Diagrams for manual use

3.13 DETAILED DESIGN (ENGINEERING)

The decision tree for this step is shown in Fig. 3.14.

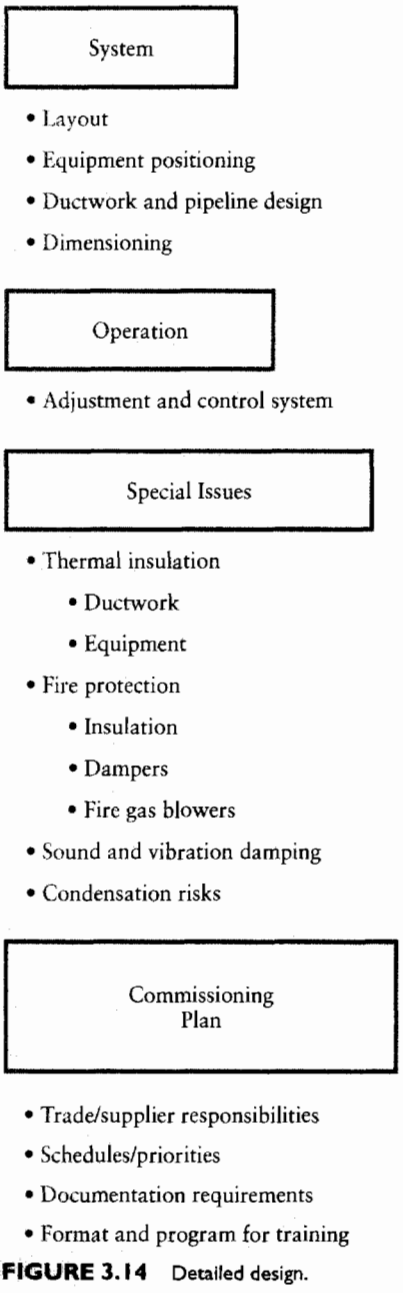

FIGURE 3.14 Detailed design.

3.13.1 Subtask 1: Ventilation System

- Lay out design (location of ductwork and pipelines) in detail.
- Size the system.
- Locate equipment and components, taking into account access for cleaning and maintenance and maintenance routes to components

that may require changing (or removal or replacement) such as filters.
- Design and dimension the ductwork and pipelines.

The *tools* for this subtask include:

- Duct design and dimensioning programs and diagrams
- Computer-aided design (CAD) solutions (drawing tools)

3.13.2 Subtask 2: Operation

Design of the adjustment and control system.
The *tools* for this subtask include:

- Simulation programs
- Manufacturers' recommendations and prefabricated systems

3.13.3 Subtask 3: Special Issues

- Design thermal insulation for ductwork and equipment.
- Design to prevent condensation risks.
- Design fire protection:
  - Insulation
  - Fire dampers
  - Fire gas blowers
- Design sound and vibration damping.

The *tools* for this subtask include:

- Regulations
- Standards
- Manufacturers' guidelines

3.13.4 Subtask 4: Commissioning Plan

- Specify the responsibility of each trade, system installer, or equipment supplier.
- Plan the construction schedules and priorities.
- Specify the documentation requirements and format, such as checklists for recording inspections, startup, and functional performance tests.
- Develop the format and program for training operating and maintenance personnel.

The *tools* for this subtask include the standards.

BIBLIOGRAPHY

Bach, H. et al. *Gezielte Belüftung der Arbeitsbereiche in Produktionshallen zum Abbau der Schadstoffbelastung*. Forschungsbericht HLK-1-92, 2nd ed., Verein der Förderer der Forschung im Bereich Heizung, Lüftung, Klimatechnik, Stuttgart, September 1993.

Buonicore, A.J. and Davis, W.T., ed. *Air Pollution Engineering Manual*, Van Nostrand Reinhold, New York, 1992.

A Step by Step Guide to COSHH Assessment. Health and Safety Series Booklet HS(G) 97. Health and Safety Executive, UK. 1993.

Biegert, B., and Dittes, W. *Katalog technischer Maßnahmen zur Luftreinhaltung am Arbeitsplatz—Lufttechnische Maßnahmen. Band I: Konzeption, Auswahl und Auslegung von Einrichtungen zur Luftreinhaltung am Arbeitsplatz*. Wirtschaftsverlag Bremerhaven, 2000. (Schriftenreihe der Bundesanstalt für Arbeitschutz und Arbeitsmedizin: Forschung, Fb 834)

Goodfellow, H. D. *Advanced Design of Ventilation Systems for Contaminant Control*, Elsevier, Amsterdam, 1985.

Hagström, K., Holmberg, R., Lehtimäki, M., Niemelä, R., Railio, J., and Siitonen, E. "Design Criteria for Air Filtration in General Industrial Ventilation." *Proceedings of Ventilation '97*, Ottawa, Canada, 1997, p. 59–65.

Heikkinen, M., "Study of Contaminant Sources in the Manufacturing Industry," *Proceedings of the 4th International Symposium on Ventilation for Contaminant Control, Stockholm, Sept 5–9, 1994.*

Richtlinie VDI 3802, Dezember 1998. Raumlufttechnische Anlagen für Fertigungsstätten (Air Conditioning Systems for Factories).

VDI 2262/ Blatt 1, April 1993. Luftbeschaffenheit am Arbeitsplatz, Minderung der Exposition durch luftfremde Stoffe; Allgemeine Anforderungen (Workplace Air, Reduction of Exposure to Air Pollutants—General Requirements).

VDI 2262/ Blatt 2, August 1997. Luftbeschaffenheit am Arbeitsplatz, Minderung der Exposition durch luftfremde Stoffe; Verfahrenstechnische und organisatorische Maßnahmen. Entwurf. (Workplace Air, Reduction of Exposure to Air Pollutants — Process Technological Measures).

Richtlinie VDI 2262, Blatt 3, Mai 1994. Luftbeschaffenheit am Arbeitsplatz, Minderung der Exposition durch luftfremde Stoffe: (Lufttechnische Maßnahmen (Workplace Air, Reduction of Exposure to Air Pollutants—Ventilation Technical Measures).

4
PHYSICAL FUNDAMENTALS

MARKKU LAMPINEN AND MAMDOUH EL HAJ ASSAD

Laboratory of Applied Thermodynamics, Helsinki University of Technology, Helsinki, Finland

ERIC F. CURD

West Kirby Wirral, United Kingdom

Industrial Ventilation Design Guidebook

4.1 FLUID FLOW

It is essential that the engineer involved in industrial ventilation have a good foundation in the subject of fluid mechanics, which involves the study of fluids at rest or in motion.

The fields of application are wide involving computational fluid dynamics (CFD), flow in ducts and pipes, pumps, fans, collection devices, pollution dispersal, and many other applications.

4.1.1 Fluid Properties

4.1.1.1 Fluid Classification

Matter is considered to exist in three states

- Solid
- Liquid
- Gaseous

The term *fluid* applies to both liquids and gases, including liquids and gases containing particulate matter of various sizes.

When a shearing stress is imposed on a solid, deformation occurs, until a point is reached when the internal stresses produced balance the shearing stresses. Provided the elastic limit for the material is not exceeded the solid will return to its original shape when the load is removed.

A fluid, on the other hand, flows under the action of a shearing stress no matter how small this stress is. A fluid at rest has no shearing stresses, and all forces are at right angles to the surrounding surfaces. Materials such as glass and solid bitumen are fluids and, if stressed for a period of time, will tend to flow.

Ideal Fluid

A theoretical ideal fluid situation, "a perfect fluid" having a constant density and no viscosity, is often used in a theoretical analysis.

Real Fluid

A real fluid will have a velocity gradient when flowing due to the viscosity of the fluid.

Incompressible Fluid

An incompressible fluid is a fluid whose density remains constant during flow. Liquids are normally treated as being incompressible, as a gas can be when only slight pressure variation occurs.

Compressible Fluid

A compressible fluid is a fluid in which significant density variations that occur during its flow have to be considered, as is usually the case with vapors and gases.

Flow Classification

Flows may be subdivided into steady and unsteady, uniform and nonuniform, laminar and turbulent, and rotational and irrotational flows.

Steady Flow

A flow is steady when the conditions at any point remain constant with respect to time.

Unsteady Flow

An unsteady flow is one in which the conditions at any point vary with time; such a flow is also called a transient flow.

Uniform Flow

A flow is uniform when the velocity of flow is the same at any given instant at every point in the fluid. This state of affairs can exist only with an ideal fluid. However, steady flow (uniform flow) is assumed to take place in a duct with the velocity constant along a streamline.

Nonuniform Flow

In a nonuniform flow the velocity varies from point to point along a streamline.

Laminar Flow

Laminar flow occurs at low flow rates, in which all particles of a fluid move parallel to the walls of the duct.

Transitional Flow

The flow region between laminar and turbulent flow is called transitional flow. It is three dimensional and varies with time.

Turbulent Flow

Turbulent flow occurs at higher flow rates. The particles of the fluid have velocity components perpendicular to the general direction of flow.

Rotational Flow

Rotational flow occurs in an element of a fluid that rotates about its axis, in addition to having translational motion (e.g., water passing through a paddle wheel).

Irrotational Flow

Irrotational flow occurs when the fluid motion rotates about its axis (e.g., water flowing in a bend in a pipe).

Other definitions to consider are:

Path Line

A path line is the path traced by a single particle of fluid over a period of time.

Streamline

A streamline shows the direction of a number of particles of fluid at the same instant in time. Flow cannot take place across a streamline. Path lines and streamlines will be identical for steady flow.

Stream Tube

A number of streamlines form a stream tube. Flows can enter and leave a stream tube only through the ends.

Stream Surface

A stream surface is the surface of a stream tube.

Streak Line

When a dye is injected into a fluid, the resulting streak lines provide flow visualization of fluid particles that have passed the same density of the fluid.

One-, Two-, or Three-Dimensional Flow

Flow may be steady but have a variation of velocity, pressure, etc., with position. If one optional coordinate is used to describe the flow it is one-dimensional, a typical case being uniform flow in a constant-area duct.

Two-dimensional flow is in the x and y directions, while three-dimensional flow is in the x, y, and z directions.

A fluid can be considered as being liquid, which is incompressible, or a gas, which is easily compressible. When a force of sufficient magnitude is applied to a fluid, motion will occur provided the frictional resistance within an open system is overcome.

A gas expands in an enclosure to fill up the entire space, while a liquid presents a free surface in contact with the gas boundary above it.

Once a fluid starts to move in a conduit, shearing forces are set up, the maximum being at the wall of the conduit. At this surface the velocity is at the lowest, while in adjacent layers above this surface the velocity increases as the shearing stresses decrease.

It is the dynamic viscosity μ of the gas/fluid that determines its ability for free flow. Very viscous fluids require a large energy input to overcome the frictional forces.

4.1.1.2 Properties of Fluids

Density

Density is the mass per unit volume kg m^{-3}. The density of a fluid depends on temperature and on atmospheric pressure or a static imposed head. At standard conditions 20 °C and 101.325 kPa (atmospheric pressure at sea level)

$$\rho_{water} = 998.2 \text{ kg m}^{-3}$$
$$\rho_{air} = 1.2 \text{ kg m}^{-3}$$

From these differences it will be seen that water is 832 times as heavy per unit volume as air.

Water at 100 °C at atmospheric pressure has a density of 958 kg m^{-3}. For data at other temperatures and pressures for water and other fluids, full use has to be made of various reference tables.

The relationship that exists between liquid density and temperature is expressed by

$$\Delta\rho = \frac{\Delta\theta^2}{A}. \tag{4.1}$$

where

$\Delta\rho = \rho_0 - \rho$
$\Delta\theta = \theta - \theta_0$

$$\rho = \rho_0 - \frac{(\theta - \theta_0)^2}{A}, \tag{4.2}$$

where

ρ is the density at the temperature θ
ρ_0 is the density at the temperature θ_0
A is a constant, specific to the fluid

The relation of liquid density to pressure is

$$\frac{\Delta\rho}{\rho_0} = \frac{\Delta p}{E}, \tag{4.3}$$

where E is the modulus of elasticity.

The density of an ideal gas is dependent on the pressure and temperature as

$$p = \rho R T, \tag{4.4}$$

where R is the gas constant of the gas in question, J kg^{-1} K^{-1}. It is calculated by dividing the general gas constant $R = 8314.3$ J $kmol^{-1}$ K^{-1} by the molecular weight of the gas. If the composition of the ideal gas is unknown, but its pressure, temperature, and density are known, the value of the gas constant can be calculated from

$$R = \frac{p_0}{\rho_0 T_0}. \tag{4.5}$$

The equation can also be expressed as

$$\frac{\rho}{\rho_0} = \frac{pT_0}{p_0 T}. \tag{4.6}$$

The state equation of an ideal gas such as steam is

$$pv = ah + b, \tag{4.7}$$

where

v is the specific volume, $v = 1/\rho$,
h is enthalpy,
a and b are constants.

This equation is seldom used, because the tables of the thermodynamic properties of fluids (steam tables) allow the values of the fluid/gas vapor to be accurately obtained.

Specific Weight

Specific weight is the weight per unit volume and is equal to $\rho \cdot g$, where g is the acceleration due to gravity. In the case of water of density 1000 kg m^{-3} the specific weight is 9.81×10^3 N m^{-3}.

Specific Gravity

Sometimes called relative density, specific gravity is the ratio of the fluid density with respect to a reference substance at a specified temperature.

Mercury has a density of 13600 kg m^{-3} and is 13.6 times as heavy as water, or 11333 times as heavy as the same volume of air.

Water is taken to have a specific gravity of 1.0 at 4 °C, where it has its maximum density, with other liquids having a value either greater or less than this.

In the case of air, the specific gravity is taken as 1.0, with all other gases having specific gravity greater or less than this value.

Plastic Fluids

Various types of fluids, known as plastic fluids, may be encountered, which do not start to flow until a certain minimum shear stress is reached. The relationship between shear stress and the rate of shear strain may or may not take a linear form.

If linear, the plastic is known as a Bingham plastic, a typical case being sewage sludge.

Pseudo-plastic Fluids

With this type of fluid the viscosity decreases as the shear strain increases, typical cases being mud and liquid cement.

Dilatant Fluids

Quicksand is included in this category. The viscosity increases as the rate of shear strain increases.

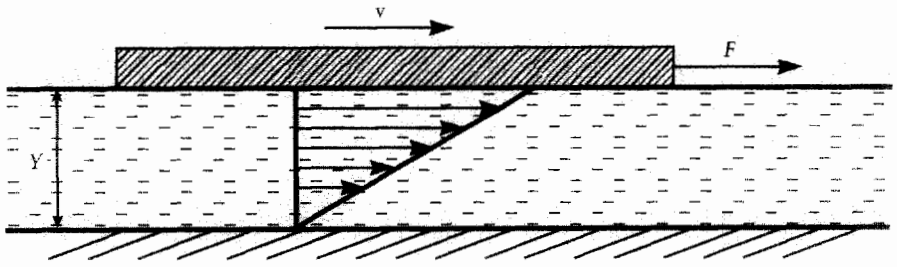

FIGURE 4.1 Viscosity

Surface Tension

Surface tension is the property of a fluid that produces capillary action, the rise and fall in a tube.

Water in a tube wets the glass, and the liquid rises, producing a cup. In the case of mercury, the glass is not wetted and the liquid falls, producing an inverted cup.

Viscosity

Viscosity is the shear resistance between adjacent fluid layers. Consider in Fig. 4.1 the shearing action between two parallel planes, each of area A, separated by a distance Y. The tangential force F for a given area required to slide one plate over the other at a velocity (v) parallel to each other is

$$F = \mu \frac{\mathrm{v}}{\mathrm{Y}} A. \tag{4.8}$$

The proportionality factor μ is the dynamic viscosity of the fluid, its units being force × time/length^2 and is expressed as N s m^{-2} or Pa s.

Examination of the thermodynamic properties of fluid tables shows how the viscosity varies with temperature. In order to obtain a general impression of this, consider the data in the thermal properties of fluid tables and the various values at different temperatures.

Another viscosity unit is the kinematic viscosity ν. This is the ratio of viscosity to density. Common units used for this are the stoke (1 cm^2 s^{-1}) and the centistoke (1 mm^2 s^{-1}).

Because the velocity change in the y direction is linear, Eq. (4.8) can be written as

$$F = \mu \frac{d\mathrm{v}}{dy} A. \tag{4.9}$$

When the shearing stress $\tau = F/A$,

$$\tau = \mu \frac{d\mathrm{v}}{dy}. \tag{4.10}$$

With most fluids the shearing stress τ is linearly proportional to the change of velocity; hence viscosity μ is not a function of dv/dy. A fluid having these characteristics is called a Newtonian fluid.

If the viscosity is a function of dv/dy, the fluid is classed as a non-Newtonian fluid. Fluids of this type are outside the scope of this chapter.

A special case of a Newtonian fluid is that of an ideal fluid, in which the viscosity $\mu = 0$. Ideal fluids do not exist; however, in many noncritical applications, the friction can be ignored to simplify calculations.

Thus viscosity is not a function of dv/dy, and it is independent of pressure. However, it is a function of the temperature.

The viscosity of noncompressible fluids depends on the temperature as

$$\frac{\mu}{\mu_0} = \exp\left(\frac{B}{C+T} + \frac{B}{C+T_0}\right), \tag{4.11}$$

where

μ is the viscosity at any temperature T,
μ_0 is the viscosity at any temperature T_0,
B and C are constants, depending on the nature of the fluid.

The viscosity of a gas depends on the temperature according to

$$\frac{\mu}{\mu_0} = \frac{S+T_0}{S+T}\left(\frac{T}{T_0}\right)^{2/3}, \tag{4.12}$$

where S is a constant specific for the gas. A simplified version sometimes used is

$$\frac{\mu}{\mu_0} = \left(\frac{T}{T_0}\right)^n. \tag{4.13}$$

The kinematic viscosity ν is the ratio of the dynamic viscosity μ and density ρ:

$$\nu = \frac{\mu}{\rho}. \tag{4.14}$$

The kinematic viscosity of a gas is a function of the pressure, and its dimension is the square of length divided by the time, its unit being $m^2\ s^{-1}$.

In old literature the cgs system is found, in which the dynamic viscosity is measured in centipoise = 0.1 poise = 0.001 dyne s cm^{-2}:

$$1\ \text{cP} = 10^{-2}\ \text{g cm}^{-1}\text{s}^{-1} = 10^{-3}\ \text{kg m}^{-1}\text{s}^{-1}\ . \tag{4.15}$$

The non-SI unit of kinematic viscosity is the centistoke:

$$1\ \text{cSt} = 10^{-2}\ \text{cm}^2\text{s}^{-1} = 10^{-6}\ \text{m}^2\text{s}^{-1}\ . \tag{4.16}$$

4.1.2 Constants for Water

For water the values of the constants discussed in the previous section are given in Table 4.1. The value of the elasticity modulus increases as the pressure and temperature increase. At a pressure of 10 MPa and temperature 373 K, the elasticity modulus E is 2.7×10^9 Pa.

The equations do not give exact results, but the error is small and in many cases can be ignored.

TABLE 4.1 Constants for Water

Pressure	p_0 = kPa
Temperature	$T_0 = 273.15$ K
Density	$\rho_0 = 999.80$ kg m^{-3}
Constant A	$A = 225.30$ m^3 K^2 kg^{-1}
Velocity of sound	$c_0 = 1400$ m s^{-1}
Viscosity	$\mu_0 = 1.791 \times 10^{-3}$ kg s^{-1}m^{-1}
Kinematic viscosity	$\nu_0 = 1.791 \times 10^{-6}$m^2 s^{-1}
Constant B	$B = 511.6$ K
Constant C	$C = -149.4$ K
Specific heat	$c_p = 4182.6$ J kg^{-1}K^{-1}
Modulus of elasticity	$E_0 = 1.95 \times 10^9$ N m^{-2}

4.1.3 Constants for Gases

The constants for various gases are listed in Table 4.2, where

ρ_0 = density
c_0 = velocity of sound
R = gas constant
μ_0 = dynamic viscosity
κ = adiabatic constant

4.1.4 Properties of Air and Water Vapor

Air can be considered as an ideal gas, which has a definition

$$pv = RT, \tag{4.17}$$

or

$$p = \rho RT. \tag{4.18}$$

This is the state equation of an ideal gas, where p is pressure, v is specific volume, ρ is density, R is the gas constant, and T is absolute temperature. In an airflow there is a transfer of heat from one layer to another. This change of

TABLE 4.2 Constants for Gases

	ρ_0 (kg m^{-3})	c_0 (m s^{-1})	R (J kg^{-1} K^{-1})	μ_0 (kg s^{-1}m^{-1})	τ
Air	1.275	332	287.04	1.717×10^{-5}	1.402
O_2	1.409	315	259.78	1.928×10^{-5}	1.399
N_2	1.234	37	296.75	1.625×10^{-5}	1.400
H_2	0.0887	1260	4124.0	8.350×10^{-5}	1.409
CO_2	1.949	259	188.88	1.370×10^{-5}	1.301

$p_0 = 100$ kPa, $T_0 = 273.15$ K

state is adiabatic and reversible. Such an adiabatic reversible process is called an isentropic state change: one in which the entropy remains constant.

The thermodynamic equations to be considered at this stage are

$$T\,ds = dh - v\,dp, \tag{4.19}$$

where

s is the entropy, kJ kg^{-1} K^{-1}
h is the enthalpy, kJ kg^{-1}

For isentropic process we can write

$$dh = v\,dp. \tag{4.20}$$

The specific enthalpy change is defined as

$$dh = c_p\,dT. \tag{4.21}$$

The state equation gives

$$p\,dv + v\,dp = R\,dT. \tag{4.22}$$

When dT is eliminated from this equation, the following differential equation results:

$$\frac{dv}{v}\left(\frac{1}{\frac{R}{c_p} - 1}\right) = \frac{dp}{p}, \tag{4.23}$$

Solving,

$$pv^{c_p/(c_p - R)} = \text{constant}. \tag{4.24}$$

When c_p and R can be treated as constants, the equation is usually written as

$$pv^{\tau} = \text{constant}. \tag{4.25}$$

For a gas of one-atom molecules $\kappa = 5/3 = 1.67$. For a gas of two-atom molecules $\kappa = 7/5 = 1.4$. For gas of molecules containing three or more atoms $\kappa = 9/7 = 1.3$.

For air (mostly a mixture of N_2 and O_2) the following is valid:

$$pv^{1.4} = p_0 v_0^{1.4} = \text{constant}. \tag{4.26}$$

Water vapor is considered as an ideal gas and is defined by

$$pv = ah + b, \tag{4.27}$$

where a and b are constants. Converting,

$$p\,dv + v\,dp = a\,dh \tag{4.28}$$

and as

$$dh = v\,dp, \tag{4.29}$$

giving

$$pv^{1/(1-a)} = \text{constant}, \tag{4.30}$$

or

$$pv^k = \text{constant}, \tag{4.31}$$

where k is an empirically determined constant. For water vapor (H_2O) $k = 1.3$.

4.1.5 Liquid Flow

In this section incompressible liquid flow is dealt with, and the effect of compressibility is ignored.

4.1.5.1 Energy Equation

The energy equation of a continuing system can be presented by means of the first law of thermodynamics and the energy balance of a flow system as

$$\left.\begin{aligned} dh + g\,dz + d\left(\frac{v_m^2}{2}\right) &= 0 \\ dh = T\,ds + v\,dp &= T\,ds + \frac{dp}{\rho} \end{aligned}\right\} \Rightarrow T\,ds + \frac{dp}{\rho} + g\,dz + d\frac{v_m^2}{2} = 0 \quad . \tag{4.32}$$

As the potential energy term has an essential meaning in hydromechanics, the static head is selected as a comparison quantity. When the energy equation (4.32) is divided by g and integrated, it gives the Bernoulli flow tube equation

$$\frac{p_1}{\rho g} + z_1 + \frac{v_{m1}^2}{2g} = \frac{p_2}{\rho g} + z_2 + \frac{v_{m2}^2}{2g} + \int_1^2 \frac{T}{g} ds = H_1 \quad , \tag{4.33}$$

where

$$\begin{aligned} H_1 &= \text{hydraulic head} \\ \frac{v_m^2}{2g} &= \text{velocity head} \\ z &= \text{elevation head} \\ \frac{p}{\rho g} &= \text{pressure head} \end{aligned}$$

$$h_f = \int_1^2 \frac{T}{g} ds = \text{resistance head}$$

All flow losses are included in the term h_f, which in a flow system consists of two parts:

1. Friction resistance
2. Local resistance

4.1.5.2 Viscous Flow

When liquid flows along a solid surface (see Fig. 4.2) a shearing stress is set up (friction power/surface), which is expressed by

$$\tau = f\frac{\rho v_m^2}{2} \quad \text{for a plate} \tag{4.34}$$

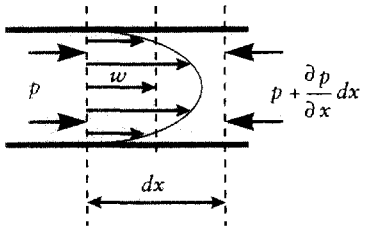

FIGURE 4.2 Tube flow velocity profile.

or

$$\tau = f \frac{\rho v_m^2}{2} = \xi \frac{\rho v_m^2}{8} \qquad \text{for a tube,} \tag{4.35}$$

where

v_m is mean velocity (velocity is zero at the surface)
f is a dimensionless friction factor
$\xi = 4f$; this is the Blasius friction factor

In some literature λ or β is used instead of ξ; it is essential to use ξ, because λ is used for thermal conductivity and β is used for cubic expansion of air or an angle.

In a tube, the pressure is constant in all radial directions perpendicular to the axis; it varies only in the flow direction x. The power balance of the element dx, denoting the sectional surface area as A and the periphery as C, gives

$$-\tau C\,dx - \frac{dp}{dx} dx A = 0 \qquad \text{and} \qquad -\frac{dp}{dx} = \frac{\tau C}{A} = \frac{\Delta p}{l} = f \frac{\rho v_m^2}{2} \frac{C}{A}.$$

Denoting the hydraulic diameter as $d_h = 4A/C$, we have

$$\frac{\Delta p}{l} = \frac{4f \rho v_m^2}{d_h \; 2} = \xi \frac{\rho v_m^2}{2 d_h} \tag{4.36}$$

and the friction resistance head corresponding to the pressure difference is

$$h_f = \frac{\Delta p}{\rho g} = \xi \frac{l}{d_h} \frac{v_m^2}{2g}. \tag{4.37}$$

The factor ξ depends on the Reynolds number, which is a dimensionless variable that denotes the nature of flow:

$$\mathrm{Re} = \frac{v_m d}{\nu} = \frac{\rho v_m d}{\eta} = \frac{4 q_m}{\pi d \eta}, \tag{4.38}$$

where

v_m is the mean velocity
d is the characteristic length of a surface; in the case of flow in a tube it is the tube diameter (note that d may be expressed by L in the case of a plate)
ν is the kinematic viscosity
η is the dynamic viscosity
q_m in the mass flow

Viscosity is defined by means of the equation

$$\tau = \eta \frac{dv}{dy}, \tag{4.39}$$

where dv/dy is the velocity gradient, τ is the shearing stress between two flow layers, and η is the dynamic viscosity.

4.1.5.3 Laminar and Turbulent Flow

Flow phenomena can be divided into three main types:

- Laminar (streamline)
- Transitional
- Turbulent

In laminar flow there are no disturbances, and therefore all flow particles move in the same direction. Transitional flow is the flow regime that takes place during the change from streamline to turbulent flow. In the case of turbulent flow the particles move in a given flow direction, but the flow is erratic and random.

Laminar Tube Flow

When the Reynolds number is under 2000, it is shown empirically that the flow in a smooth tube is laminar. This flow has a parabolic velocity profile, as shown in Fig. 4.3.

Now consider a cylindrical volume element in a flow stream. The radius of the element is r and its length is L. The force produced by the flow in this volume is due to the viscosity, which is

$$2\pi r L\tau = -2\pi r L\eta \frac{dv_m}{dr}, \qquad r = -\eta \frac{dv_m}{dr}.$$

The pressure difference (drop) between the ends of the element produces a force $\Delta p \pi r^2$, and considering the force balance,

$$\Delta p \pi r^2 = -2\pi r L\eta \frac{dv_m}{dr}.$$

Simplifying this gives

$$-\int_w^0 dv_m = \frac{\Delta p}{2\eta L}\int_0^R r dr.$$

Denoting w as v_{m1} at $r = 0$ and noting that $v_m = 0$ at $r = R$, the integration gives

$$w = v_{m1} = \frac{\Delta p}{4\eta L}R^2. \tag{4.40}$$

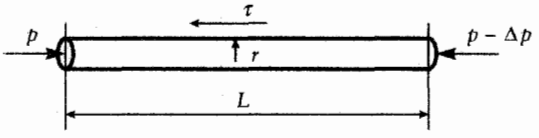

FIGURE 4.3 Cylindrical volume element.

For a parabolic velocity profile the velocity expression is

$$v_m = \frac{\Delta p}{4\eta L}(R^2 - r^2). \tag{4.41}$$

Volume flow is calculated by integrating the expression for the velocity over the surface:

$$q_v = \int_0^R 2\pi r v_m \, dr = \frac{\Delta p \pi}{2\eta L}\int_0^R (R^2 r - r^3)\, dr = \frac{\Delta p \pi}{2\eta L}\left(\frac{R^4}{2} - \frac{R^4}{4}\right)$$

Hence

$$q_v = \frac{\Delta p \pi R^4}{8\eta L}. \tag{4.42}$$

The mean velocity is

$$v_m = \frac{q_v}{\pi R^2} = \frac{\Delta p}{8\eta L}R^2. \tag{4.43}$$

The pressure difference is

$$\Delta p = \frac{8\eta v_m L}{R^2} = \frac{32\eta v_m L}{D^2}. \tag{4.44}$$

Equation (4.44) is the Hagen-Poiseuille law, which shows that the pressure loss during laminar flow is linearly proportional to the flow velocity.

The following equations show the relationship between the pressure loss and the friction factor:

$$\Delta p = \xi \frac{L}{D}\frac{\rho v_m^2}{2} = \frac{32\eta v_m L}{D^2} \tag{4.45}$$

$$\xi = 64\frac{\eta}{\rho D v_m} = \frac{64}{\mathrm{Re}} \tag{4.46}$$

This connection is valid for laminar flow, as $\mathrm{Re} < 2000$.

Turbulent Flow

Laminar flow after transition usually turns into turbulent flow when $\mathrm{Re} > 2000$. It has been shown that the pressure loss of a turbulent flow is caused by a friction factor with the magnitude of

$$f = 0.079\mathrm{Re}^{-1/4}, \qquad \text{when } \mathrm{Re} < 10^5. \tag{4.47}$$

This equation is the Blasius equation.

The shearing stress τ_0 on the surface of the flow duct and the pressure loss can now be solved from Eq. (4.48), given below:

$$\tau_0 = f\frac{1}{2}\rho v_m^2 = 0.0395\rho\nu^{1/4}D^{-1/4}v_m^{7/4}$$

$$\Delta p = 2f\frac{L}{D}\rho v_m^2 = 0.158L\rho\nu^{1/4}D^{-5/4}v_m^{7/4}. \tag{4.48}$$

Thus $\Delta p \sim v_m^{1.75}$.

When $\mathrm{Re} > 10^5$, the following equation, derived by means of the logarithmic velocity distribution by Prandtl and the empirical research results of Nikuradse, is valid:

$$\frac{1}{\sqrt{f}} = 4.01 \ln(\mathrm{Re}\sqrt{f}) - 0.4 . \tag{4.49}$$

Surface Roughness

In the previous section it was assumed that the surface of the flow duct was smooth. In reality duct surfaces are rough to varying degrees, which has an effect on the magnitude of friction. Thus Eqs. (4.47) and (4.49) represent the lowest possible levels of f; in other words, the effect of roughness is zero.

To allow for the effect of roughness one can use the results of empirical tests in ducts that have been artificially roughened with particles glued on the surface. This approach allows roughness levels to be determined as a function of the particle diameter k. The following friction factor equation has been derived for large Reynolds numbers:

$$\frac{1}{\sqrt{f}} = 4.0 \ln \frac{\mathrm{Re}}{k} + 3.48 . \tag{4.50}$$

This is an ultimate case, when the friction factor is no longer a function of the Reynolds number and is a function of roughness; the pressure loss is now $\Delta p \sim w^2$, where w is the fluid velocity in the duct. The surface roughness of typical manufactured ductworks varies between the values of a theoretically fully smooth duct and an artificially roughened one. Accordingly the pressure loss varies between $\Delta p \sim w^{1.75} - w^2$ and $\xi = f(\mathrm{Re}, \text{roughness})$.

With most forms of duct, the roughness given by the following Colebrook and White equation can be used (Eq. (4.51)). This equation has been determined by calculating an equivalent roughness, corresponding to the sand particle tests results and taking into account that with large Reynolds numbers the friction factor's dependency on the Re value is minimal.

$$\frac{1}{\sqrt{f}} = -\ln\left[\frac{5.04}{\mathrm{Re}\sqrt{f}} + \frac{k}{3.71 d}\right] \tag{4.51}$$

This equation represents the change-over section between a smooth tube and a fully developed rough flow.

In practice the friction factors are calculated either by integration of Eq. (4.51) or by reference to a Moody chart. This is based on Eq. (4.51) by using equivalent roughness values representing the sand particle roughness (see Table 4.3).

Figure 4.4 shows the Moody chart for tubes when $k = 0.03$ mm, which is the case for steel tubes. Friction factors for other values of k can be attained by using the following ratio:

$$\left(\frac{k}{d}\right) \text{curve} = \left(\frac{k}{d}\right) \text{case}$$

and determining the corresponding diameter from the Moody chart, which is derived from this equation.

TABLE 4.3 Equivalent Roughness Values for Various Materials

Material	k_{equiv}
Commercial or follower steel	0.046
Asphalted cast iron	0.120
Galvanized steel	0.150
Cast iron	0.26
Wooden surface	0.18–9
Concrete	0.3–3

4.1.5.4 Single Resistances in a Tube Flow

In addition to the friction factor, individual resistances in ducts have to be taken into account. These resistances are created by the velocity, through bends, branches, valves, and other obstructions in the duct.

The single resistance factor ζ is defined as

$$\frac{\Delta p}{\rho g} = \zeta \frac{v_m^2}{2g} \qquad \text{or} \qquad \Delta p = \zeta \frac{\rho v_m^2}{2}. \tag{4.52}$$

The ζ values for different types of resistances are available in hydraulics textbooks and also from the literature of pipe and valve manufacturers.

The pressure loss and the corresponding resistance height in Eq. (4.53) and Eq. (4.54), respectively, are the sum of the friction losses and individual resistances:

$$\Delta p_{loss} = \left(\zeta \frac{1}{d_h} + \sum \zeta \right) \frac{\rho v_m^2}{2} \tag{4.53}$$

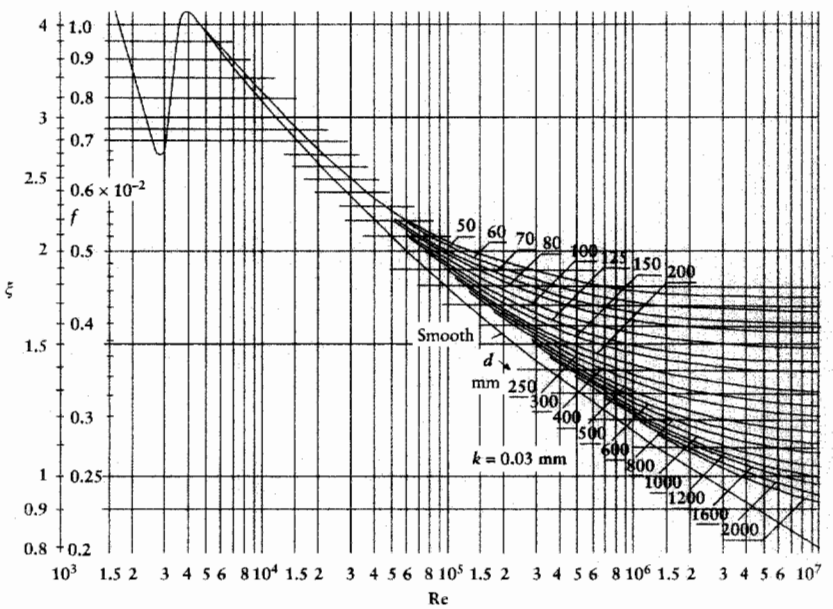

FIGURE 4.4 Moody chart, $k = 0.03$ mm.

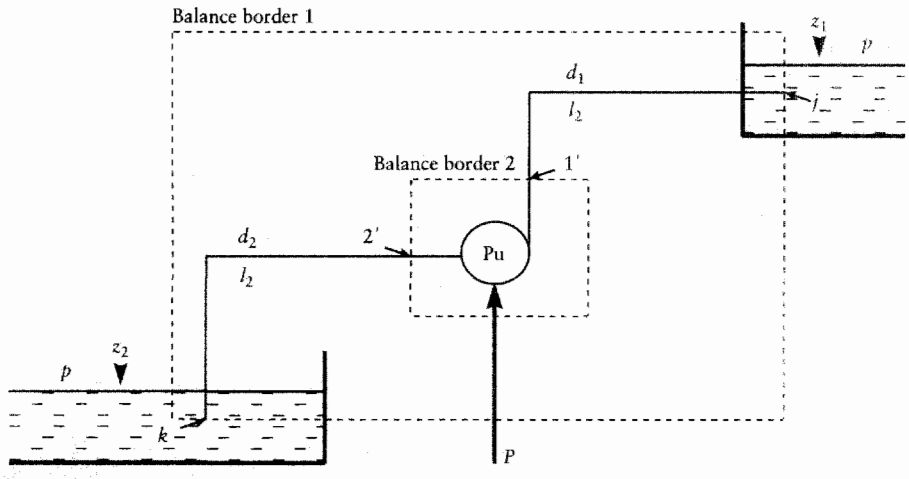

FIGURE 4.5 Pumping from one tank to another tank.

and

$$h_f = \frac{\Delta p_{\text{loss}}}{\rho g} = \left(\zeta \frac{1}{d_h} + \sum \zeta\right) \frac{v_m^2}{2g}. \tag{4.54}$$

Example 1

Find the power P required by the pump in the system shown in Fig. 4.5. The energy balance of a continuing system, when $q_m = q_v \rho$, gives q_m.

$$\frac{P}{q_v \rho g} = h_f + \frac{p_1 - p_2}{\rho g} + (z_1 - z_2) + \frac{v_{m1}^2 - v_{m2}^2}{2g}. \tag{4.55}$$

When $p_1 = p_2$ and $v_{m1} = v_{m2} = 0$, we obtain for the system defined by balance border 1:

$$\frac{P}{q_v \rho g} = h_f + (z_1 - z_2)\,, \tag{4.56}$$

where

$$h_f = \left(\xi_1 \frac{l_1}{d_1} + \sum\nolimits_1 \zeta\right) \frac{v_{m1}^2}{2g} + \left(\zeta_2 \frac{l_2}{d_2} + \sum\nolimits_2 \zeta\right) \frac{v_{m2}^2}{2g}\,.$$

Resistance factors ξ are taken from the Moody chart, when the Reynolds number and roughness are known.

$$\text{Re} = \frac{v_m d}{\nu}$$

and v_m is determined by the volume flow $q_v = A v_m$, where A is the cross-sectional area of the tube.

Single resistances ζ can be found from the literature. One of the single resistances is the outflow loss at point 1. The outflow loss is the kinetic energy representing v_{m1} and therefore $\zeta_{\text{outflow}} = 1$.

The form of Eq. (4.56) depends on the chosen balance border. The border can be chosen arbitrarily. When the balance space is chosen according to the balance border 2, the energy equation is

$$\frac{P}{q_v \rho g} = h_f' + \frac{P'_1 - P'_2}{\rho g} + z_{1'} - z_{2'} + \frac{v_{m1'}^2 - v_{m2'}^2}{2g}. \tag{4.57}$$

Using the values corresponding to the states 1′ and 2′, h_f' is the resistance height between 1′ and 2′, and $p_{1'}$ and $p_{2'}$ are determined by the pressure loss and initial pressure. Other quantities are determined correspondingly. It is worth noting that there are no outflow losses in this case. Generally, it is wise to use energy balances in calculations.

The above is valid for a liquid flow, when the effect of compressibility can be ignored when calculating gas flows with small pressure differences. For instance, in ventilating duct work, air is not compressed, so the density is considered as constant. In HVAC technology a unit of pressure frequently used for convenience is a water column millimeter, 1 mm $H_2O \approx 10$ Pa.

4.1.5.5 Pressure Loss in Gas and Steam Pipes

When the gas compressibility no longer can be bypassed, the pressure loss equation is written in a differential form

$$dp = \left(\xi \frac{dl}{D} + \sum \zeta\right) \frac{\rho v_m^2}{2}, \tag{4.58}$$

where dl is the differential pipe length and D is the diameter.

On the basis that $\rho v_m A = q_m$ or $v_m = q_m / \rho A$,

$$dp = \left(\xi \frac{dl}{D} + \sum \zeta\right) \frac{q_{m^2}}{2\rho A^2} = \left(\xi \frac{dl}{D} + \sum \zeta\right) \frac{8 q_{m^2}}{\rho D^4 \pi^2}. \tag{4.59}$$

When both sides of the equation are multiplied by p we have

$$p\, dp = \left(\xi dl + D \sum \zeta\right) \frac{8 q_{m^2}}{D^5 \pi^2} \cdot \frac{p}{\rho}. \tag{4.60}$$

For an ideal gas,

$$pV = NT \qquad \text{or} \qquad pv = p/\rho = T/M,$$

or when the gas follows the formula $pv = h^*/\zeta$, where ζ is the process factor and $h^* = h - h_0$, the deviation from the enthalpy of the reference state, Eq. (4.60), can easily be integrated, giving

$$\frac{p_1^2 - p_2^2}{2} = \frac{p}{\rho} \cdot \frac{8}{\pi^2} \cdot \frac{q_{m^2}}{D^5} \left(\xi L + D \sum \zeta\right), \tag{4.61}$$

where $p/\rho =$ constant.

If the pressures and densities are known we can solve for either q_m or D from this equation.

If either p_1 or p_2 is known, simplification of the left side of Eq. (4.61) gives

$$\frac{p_1^2 - p_2^2}{2} = \frac{p_1 + p_2}{2} \cdot (p_1 - p_2) = p\Delta p = p_1 \Delta p_1 = p_2 \Delta p_2, \tag{4.62}$$

where Δp_1 and Δp_2 are auxiliary quantities, which can be solved from Eqs. (4.61) and (4.62). The real pressure loss can then be solved with the equations

$$\frac{\Delta p}{\Delta p_1} = \frac{2}{1 + \sqrt{1 - 2\Delta p_1 / p_1}} \tag{4.63}$$

and

$$\frac{\Delta p}{\Delta p_2} = \frac{2}{1 + \sqrt{1 - 2\Delta p_2 / p_2}} . \tag{4.64}$$

These equations can be used when the Mach number is small, and the acceleration effect is ignored.

Example 2

Calculate the final pressure of air flowing in a 200 m long pipe, when the initial pressure of air is 800 kPa and the mass flow is 2.5 kg s^{-1}. The pipe diameter is 100 mm, the roughness is 0.03 mm, and the sum of the single resistances is 6.5. The air temperature is 300 K, the molar mass 28.96 kg $kmol^{-1}$, and the dynamic viscosity 1.85×10^{-5} kg $s^{-1}m^{-1}$.

First calculate

$$pv = \frac{TR}{M} = \frac{300 \cdot 8.314}{28.96} = 86.13 \text{ kJ kg}^{-1}.$$

Determination of friction factor ξ:

$$\mathrm{Re} = \frac{4 \cdot q_m}{\pi d \eta} = \frac{4 \cdot 2.5}{\pi \cdot 0.1 \cdot 1.85 \cdot 10^{-5}} = 1.72 \cdot 10^6$$

and

$$k = 0.03 \text{ mm} \quad \Rightarrow \quad \xi = 0.0154.$$

Equation (4.61) gives

$$\begin{aligned} \frac{p_1^2 - p_2^2}{2} &= pv \cdot \frac{8}{\pi^2} \cdot \frac{q_m^2}{D^5} \left(\xi L + D \sum \zeta \right) \\ &= 86.13 \times 10^3 \cdot 0.81 \cdot \frac{2.5^2}{0.1^5} (0.0154 \cdot 200 + 0.1 \cdot 6.5) \text{Pa}^2 \\ &= 1.626 \times 10^{11} \text{Pa}^2 \end{aligned}$$

Pressure loss from Eqs. (4.62) and (4.63):

$$\Delta p_1 = \frac{p_1^2 - p_2^2}{2 \cdot p_1} = \frac{1.626 \times 10^{11}}{2 \cdot 800 \times 10^3} = 101.7 \text{ kPa}$$

$$\frac{\Delta p_1}{p_1} = \frac{101.7}{800} = 0.127$$

$$\frac{\Delta p_1}{p_1} = \frac{2}{1 + \sqrt{1 - 2 \cdot \frac{\Delta p_1}{p_1}}} = \frac{2}{1 + \sqrt{1 - (2 \cdot 0.127)}} = 1.073$$

$$\Delta p = (1.073 \cdot 101.7)\ \text{kPa} = 109\ \text{kPa}$$

Final pressure is

$$p_2 = p_1 - \Delta p = (800 - 109) = 691\ \text{kPa}\ .$$

4.1.5.6 Dimensioning of a Duct with Liquid Flow

This example demonstrates the dimensioning of a duct with a frictional incompressible fluid flow. Now the Bernoulli equation can be written as

$$p_1 + \rho g z_1 + \frac{1}{2}\rho w_1^2 = p_2 + \rho g z_2 + \frac{1}{2}\rho w_2^2 + \Delta p\ , \tag{4.65}$$

where

$$\Delta p = \left(\xi \frac{L}{D} + \sum \zeta\right) \rho \frac{w^2}{2} = \text{pressure loss term},$$

$$\xi \frac{L}{D} \rho \frac{w^2}{2} = \text{the pressure loss due to the friction},$$

$$\sum \zeta \rho \frac{w^2}{2} = \text{the pressure loss due to the single resistances.}$$

To determine the pressure losses, we have to find out whether the flow is laminar or turbulent, because $\xi = f(\text{Re},\ k/d)$. In practical dimensioning, Eq. (4.66) and the Moody chart are used.

$$\frac{1}{\sqrt{\xi}} = -2 \ln\left[\frac{2.52}{\text{Re}\sqrt{\xi}} + \frac{k}{3.71 d}\right]\ . \tag{4.66}$$

Empirical tables are used to determine the value of the single resistances.

The determination of the desired volume flow $\dot{V}$ and the pressure difference $p_2 - p_1$ leads to an iterative procedure in a turbulent case, due to terms ξ and $\sum \zeta$. In a laminar flow

$$\xi = \frac{64}{\text{Re}},$$

so no iteration is needed. This is due to the fact that the pipe diameter d is reduced from its value in the formula for the pressure loss caused by friction, because $\text{Re} = 4 q_v / \pi\, d v$.

Example 3

A pipe of diameter d_0 conveys water at a volume flow rate q_v as shown in Fig. 4.6. The lateral branches 1-2 and 3-4 are each required to have volume flows of $q_v/6$. The pressures at points 0, 2, and 4 are known; the water leaves the system at points 2 and 4. Determine diameters d_4 and d_2.

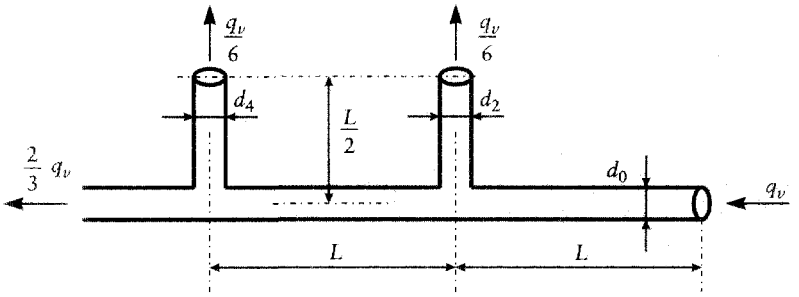

FIGURE 4.6 The system to be dimensioned.

The following values are known:

$$\text{Volume flow} = 10\ \text{m}^3\ \text{s}^{-1}$$

$$\text{Diameter } d_0 = 79.8\ \text{mm}$$

$$\text{Pressure } p_0 = 600\ \text{kPa}$$

$$p_2 = p_4 = 250\ \text{kPa}$$

$$\text{Temperature } T = 283\ \text{K}$$

$$\text{Length } L = 50\ \text{m}$$

$$\text{Roughness } k = 0.03\ \text{mm}$$

Water properties can be found from tables, such as the VDI-Wasserdampftafeln; The NBS/NRC Steam Tables; the ASHRAE and CIBSE Guides; or *Thermodynamic and Transport Properties of Fluids* by Mayhew and Rodgers.

First we dimension d_4, and now Eq. (4.65) is

$$p_0 + \rho g z + \frac{1}{2}\rho w_0^2 = p_4 + \rho g z_4 + \frac{1}{2}\rho w_4^2 + \Delta p_4\ . \tag{4.67}$$

Taking $z_0 = 0$, when $T = 283$ K, $\rho = 999.7$ kg/m^{-3}, $\nu = 1.3 \times 10^{-6}$ m^{2}s and $q_{v_0} = q_v = 10$ m^3 s^{-1}. Thus the flow velocity $w_0 = 2$ ms^{-1}. From Eq. (4.67) we receive

$$106\,823 = 499.85 w_4^2 + \Delta p_4\,. \tag{4.68}$$

The formula for the pressure loss is now

$$\begin{aligned}\Delta p_4 = &\left[\xi \frac{50}{79.8 \times 10^{-3}} + (-0.075)\right]\frac{999.7 \cdot 2^2}{2} + \xi_{13}\frac{50}{79.8 \times 10^{-3}} \\ &\times 999.7 \cdot \frac{1.666^2}{2} + \left[0.88 + \xi_{34}\frac{25}{d_4}\right]\frac{999.7 w_4^2}{2} + \frac{999.7 w_4^2}{2}\end{aligned} \tag{4.69}$$

The Reynolds number is

$$\text{Re}_{01} = \frac{4 q_v}{\pi d_0 \nu} = 1.227 \times 10^5\,.$$

Hence the flow is turbulent.

When $k = 0.03$ mm, the ratio $k/d = 0.000\,375$, and therefore the friction factor $\xi_{01} = 0.0193$. Correspondingly, $\mathrm{Re}_{13} = 10 \times 10^5$ and $\xi_{13} = 0.0196$.

The formula for pressure loss is

$$\Delta p_4 = 41\,080 + \left(989.7 + \xi_{34}\frac{12\,496.3}{d_4}\right) w_4^2 . \tag{4.70}$$

The dimensioning of pipe 3-4 happens by means of Eqs. (4.68) and (4.70). The iteration equation is now

$$d_4 = \left(9.854 \times 10^{-9} + \frac{8.554 \times 10^{-7}}{d_4}\xi_{34}\right)^{1/4} \tag{4.71}$$

Calculations are dealt with in the following stages

1. d_4 is chosen.
2. Re and k/d_4 are calculated.
3. ξ_{34} is read from the Moody chart as a function of Re and k/d_4.
4. A new d_4 is calculated with Eq. (4.71) until the d_4 value is suitable.

Calculations are best carried out in a tabular form. The value of d_4 is 29.7 mm. In practice the next larger standard pipe size would be selected.

The diameter d_2 is solved analogously. The Bernoulli equation at the interval 1-2 is

$$106\,823 = 499.85 w_2^2 + \Delta p_2 . \tag{4.72}$$

The pressure loss is

$$\begin{aligned} \Delta p_2 &= \frac{0.0193 \cdot 50 \cdot 999.7 \cdot 2^2}{79.8 \times 10^{-3} \cdot 2} + \left[0.88 + \xi_{12}\frac{25}{d_2} + 1\right]\frac{999.7 w_2^2}{2} \\ &= 24\,178.2 + \left(939.7 + 12\,496.25\frac{\xi_{12}}{d_2}\right) w_2^2 \end{aligned} \tag{4.73}$$

The iteration equation is

$$d_2 = \left(7.844 \times 10^{-8} + \frac{6.809 \times 10^{-7}}{d_2}\xi_{12}\right)^{1/4} \tag{4.74}$$

The diameter $d_2 = 28.8$ mm.

Example 4

A pump lifts water from a lake. At the pump suction entry a foot valve is fitted. Determine the maximum static delivery height the water can be raised without cavitation taking place. The saturation pressure of water is 1.23 kPa at 10 °C and the dynamic viscosity is 1.3×10^{-3} kg m^{-1} s^{-1}. The suction pipe water velocity is 2.0 m s^{-1}, the internal pipe diameter is 100 mm, and the pipe roughness is 0.03 mm. The resistance of the foot valve is 4.5.

Note: Cavitation occurs when the pressure at a point in a liquid flow field is equal or less than the vapor pressure of the liquid. At this point bubbles of vapor are formed, this is cavitation. It has serious effects such

as loss of duty, loss in efficiency, and serious erosion on the suction side of the pump impeller.

Pressure at the suction inlet p_t:

$$p_t = p_i - \rho g h_s - \rho g h_f \geq 1.23 \text{ kPa} \ . \tag{4.75}$$

Resistance head:

$$h_f = \left(\xi \frac{h_s}{d} + \sum \zeta \right) \frac{w^2}{2g} .$$

Friction factor:

$$\text{Re} = \frac{w d \rho}{\eta} = \frac{2.0 \cdot 0.1 \cdot 1000}{1.3 \times 10^{-3}} = 153\,850$$

$$k = 0.03 \text{ mm}, \quad d = 100 \text{ mm} \quad \Rightarrow \xi = 0.0185$$

By substituting the resistance head loss equation in Eq. (4.75) the suction head loss is determined from

$$p_i - \rho g h_s - \rho g \left(\xi \frac{h_s}{d} + \sum \zeta \right) \frac{w^2}{2g} = 1.23 \text{ kPa}$$

$$h_s = \frac{p_i - 1.23 - \rho g \sum \zeta \frac{w^2}{2g}}{\rho g \left(1 + \xi \frac{1}{d} \cdot \frac{w^2}{2g} \right)}$$

$$= \frac{100 - 1.23 - 1000 \cdot 9.81 \cdot 4.5 \cdot \frac{4.0}{2 \cdot 9.81}}{1000 \cdot 9.81 \left(1 + 0.0185 \cdot \frac{1}{0.1} \cdot \frac{4.0}{2 \cdot 9.81} \right)}$$

$$= 8.82 \text{ m}.$$

Bibliography

Bennett, C. D. and Myers, J. E., *Momentum, Heat and Mass Transfer.* McGraw-Hill, New York, 1962.

Buckingham, E., *Phys. Rev.* 4, 345, 1914.

Bridgman, P. W., *Dimensional Analysis.* 1931.

Eckert, E. R. G. and Drake, R. M. Jr., *Analysis of Heat and Mass Transfer.* McGraw-Hill, New York, 1972.

Fuller, E. N., Schettler, P. D., and Giddings, J. C., A New Method for Prediction of Binary Gas-Phase Diffusion Coefficients, *Ind.Eng.Chem.*, 58(5), 19–27, 1966.

Henley, E. J., and Rosen, E. M., *Material and Energy Balance Computations.* Wiley, New York, 1969.

Keey, R. B., *Drying Principles and Practice.* Pergamon Press, Oxford, 1972.

King, C.J., *Separation Processes.* McGraw-Hill, New York 1971.

Lampinen, M. J. and Toivonen, K., Application of a Thermodynamic Theory to Determine Capillary Pressure and Other Fundamental Material Properties Affecting the Drying Process, *DRYING'84*, Springer-Verlag, 228–244, 1984.

Luikov, A. V. and Mikhailov, Yu. A., *Theory of Energy and Mass Transfer.* Revised English ed. Pergamon Press, New York, 1965.

Lydersen, A. L., *Mass Transfer in Engineering Practice*. Wiley, New York, 1983.
Nyvlt, J., *Industrial Crystallisation from Solutions*. Butterworths, London 1971.
Oliver, E. D., *Diffusional Separation Processes: Theory, Design and Evaluation*. Wiley, New York, 1966.
Reid, R. C., Prausnitz, J. M., and Sherwood, T. K., *The Properties of Gases and Liquids*. McGraw-Hill, New York, 1977.
Sherwood, T. K., Pigford, R. L., and Wilke, C. R., *Mass Transfer*. McGraw-Hill, New York, 1975.
Sissom, L. E., and Pitts, D. R., *Elements of Transport Phenomena*. McGraw-Hill New York, 1972.
Treybal, R. E., *Mass Transfer Operations*. McGraw-Hill, New York, 1968.

4.2 STATE VALUES OF HUMID AIR; MOLLIER DIAGRAMS AND THEIR APPLICATIONS

4.2.1 Properties of Air and Other Gases

The analysis of dry atmospheric air varies with location, altitude, time of year, and other factors. Table 4.4 gives the molecular weights of the constituents and the volumetric and gravimetric analyses.

For general engineering work for altitudes up to 1500 m it is sufficiently accurate to use the following:

By volume:		By weight:	
$O_2 = 21\%$,	$N_2 = 79\%$	$O_2 = 23\%$,	$N_2 = 77\%$

The above values are based on the assumption that argon is combined with nitrogen, adjusting the molecular weight to 28.16. Other gases present in the atmosphere air are normally ignored, as these represent less than 0.003% (by volume, 27.99 ppm). Table 4.5 provides some basic information on these trace gases.

The gases also have other constituents mixed with them, typical ones being: dusts, pollens, bacteria, viruses, mold spores, smoke particles, and the products of industrial activity such as SO_2, H_2, and S. Volcanic activity also adds various gases and dusts to the atmosphere.

4.2.2 Fundamentals

Air is seldom dry; it normally contains varying amounts of moisture. Humid air is a mixture of dry air and water vapor. The term *dry air* denotes the mixture of all gases present in air (nitrogen, oxygen, carbon monoxide, and inert gases), except water vapor.

TABLE 4.4 Analysis of Air at Sea Level

Constituent	Symbol	Molecular weight (M)	Volumetric analysis %	Gravimetric analysis %
Nitrogen	N_2	28.016	78.09	75.55
Oxygen	O_2	32.00	20.95	23.13
Argon	Ar	39.944	0.93	1.27
Carbon dioxide	CO_2	44.01	0.03	0.05
Total			100	100

Source: R.B. Keey, *Drying Principles and Practice*, 1972

TABLE 4.5 Minor Constituents of Dry Air

			Parts per million	
Gas	**Symbol**	**Molecular weight**	**Volume**	**Weight**
Neon	Ne	20.183	18	12.9
Helium	He	4.003	5.2	0.74
Methane	CH_4	16.04	2.2	1.3
Krypton	Kr	83.8	1	3
Nitrous oxide	N_2O	44.01	1	1.6
Hydrogen	H_2	2.016	0.5	0.03
Xenon	Xe	131.3	0.08	0.37
Ozone	O_3	48.00	0.01	0.02
Radon	Rn	222	0.06×10^{-12}	—

The molar mass of dry air is dependent on the consistency of air, but for standard air it is $M_i = 0.028964$ kg/mol. In practical calculations we may use the rough value of 0.0290 kg/mol. The molar mass of water vapor is $M_h = 0.0180153$ kg/mol and the rough value used in practical calculations is 0.0180 kg/mol.

According to the state equation of ideal gas, the partial density of dry air in humid air is

$$\rho_i = \frac{p_i M_i}{RT}, \tag{4.76}$$

where p_i is the partial pressure of dry air and R is the gas constant. According to present knowledge, the best value for the gas constant is

$$R = (8.31441 \pm 0.00026)$$

In practical calculations we use the value of $R = 8.314$ J/mol K.

The partial density of water vapor in humid air is

$$\rho_h = \frac{p_h M_h}{RT}, \tag{4.77}$$

where p_h is the partial pressure of water vapor.

The density of humid air is the sum of the partial densities of dry air and water vapor,

$$\rho = \rho_i + \rho_h \tag{4.78}$$

and the total pressure of humid air is a sum of the partial pressures of dry air and water vapor:

$$p = p_i + p_h \tag{4.79}$$

The mass of dry air in a volume V is denoted as m_i ($\rho_i = m_i/V_i$) and the mass of water vapor in V is m_h ($\rho_h = m_h/V_h$). Humidity of air, meaning the ratio of water vapor mass to dry air mass, is defined as

$$x \equiv \frac{m_h}{m_i}. \tag{4.81}$$

Using partial pressures, this definition can be written as

$$x \equiv \frac{\rho_h}{\rho_i}. \tag{4.82}$$

Humidity x is thus a dimensionless number, but sometimes a "dimension" is added to it, as a reminder of its definition. We can, for instance, write $x = 0.05$ or $x = 0.05$ kg H_2O/kg d.a., where d.a. stands for dry air.

According to Eqs. (4.76), (4.78), and (4.80), humidity can be written as

$$x = \frac{M_h p_h}{M_i p_i} = 0.6220 \frac{p_h}{p_i} = 0.6220 \frac{p_h}{p - p_h}. \tag{4.83}$$

By solving the partial pressure of water vapor from the equation above, we receive

$$p_h = \frac{xp}{0.6220 + x}. \tag{4.84}$$

We denote again the mass of dry air in a volume V as m_i and the mass of water vapor as m_h. When humid air is treated as an ideal mixture of two components, dry air and water vapor, the enthalpy of this mixture is

$$H = m_i h_i + m_h h_h, \tag{4.85}$$

where h_i is the specific enthalpy of dry air (J/kg) and h_h is the specific enthalpy of water vapor.

Technical calculations dealing with humid air are reasonable to solve with dry air mass flow rates, because these remain constant in spite of changes in the amount of water vapor in the air. For that reason a definition for enthalpy,

$$h_k = \frac{H}{m_i}, \tag{4.86}$$

which is the enthalpy of humid air divided by the dry air mass, is made. The dimension of enthalpy h_k is J/kg, but it is often written as J/kg d.a. as a reminder that the total enthalpy of the mixture is calculated in terms of a kilogram of dry air.

Combining Eqs. (4.85) and (4.86), we get

$$m_i h_k = m_i h_i + m_h h_h,$$

and using Eq. (4.81) we have

$$h_k = h_i + x h_h. \tag{4.87}$$

In calculations with humid air, when the pressure is not high (usually the atmospheric pressure of 1 bar), water vapor and dry air can be handled as an ideal gas, as we have already done in Eqs. (4.76) and (4.78). For ideal gases the specific enthalpy is just a function of temperature:

$$h_i = h_i(T)$$

and

$$h_h = h_h(T).$$

When 0 °C dry air is chosen as the zero point of dry air enthalpy, and 0 °C water as the zero point of water vapor enthalpy, the enthalpies of dry air and water vapor can be calculated from the equations

$$h_i(T) = \int_{273.15\text{K}}^{T} c_{pi}(T)\, dT \tag{4.88}$$

$$h_h(T) = l_{ho} + \int_{273.15\text{K}}^{T} c_{ph}(T)\, dT \tag{4.89}$$

where $c_{pi}(T)$ is the specific heat of dry air (J/kg K), $c_{ph}(T)$ is the specific heat of water vapor, and l_{ho} is the heat of vaporization at 0 °C. Its numerical value is

$$l_{ho} = 2501 \text{ kJ/kg}$$

Specific heats c_{pi} and c_{ph} are somewhat dependent on temperature. In the temperature range of −10 to +40 °C, their average values are

$$c_{pi} = 1.006 \text{ kJ/kg °C}$$
$$c_{ph} = 1.85 \text{ kJ/kg °C}.$$

At the temperature of +50 °C, their values are $c_{pi} = 1.008$ kJ/kg °C and $c_{ph} = 1.87$ kJ/kg °C.

Using numerical values mentioned above, the enthalpy of humid air h_k (Eq. (4.87)) can be written as

$$h_k = 1.006\theta + x(2501 + 1.85\theta) \text{ kJ/kg}, \tag{4.90a}$$

where θ is the temperature in Celsius. Equation (4.90*a*) can also be written as

$$h = c_{pi}\theta + x(l_{ho} + c_{ph}\theta) \tag{4.90b}$$

We denoted the mass of dry air in a volume V as m_i, that is, $\rho_i = m_i/V_i$, and the mass of water vapor in V as m_h, that is, $\rho_h = m_h/V_h$. In practical calculations we usually handle volume flow $q_v(\text{m}^3/\text{s})$ instead of volume V. For instance, the value of volume flow is known in the suction inlet of a fan when the operating point of the fan is defined. Volume flow q_v, expressing the total air flow or the combined volume flow of water vapor and dry air, is not constant in various parts of the duct, because the pressure and temperature can vary. Therefore in technical calculations dealing with humid air, material flows are treated as mass flows. Also, while the humidity can vary, the basic quantity is dry air mass flow $\dot{m}_i$(kg d.a./s). If, for instance, we know the volume flow q_v of a fan, the dry air mass flow through the fan is

$$\dot{m}_i = p_i q_v \tag{4.91}$$

where p_i is the partial pressure of dry air in the suction inlet of the fan, in the same place where the total volume flow $\dot{V}$ is defined. Accordingly, the water vapor flow $\dot{m}_h$ (kg H_2O/s) along the volume flow is

$$\dot{m}_h = p_h q_v, \tag{4.92}$$

where p_h is the partial pressure of water vapor.

Due to the definition of humidity (4.87), on the basis of the Eqs. (4.91) and (4.92),

$$\dot{m}_h = x\dot{m}_i, \tag{4.93}$$

When an energy balance is written, an enthalpy flow of humid air $\dot{H}$ is needed. This can be written according to the Eqs. (4.85) and (4.93) as

$$\dot{H} = \dot{m}_i h_i + \dot{m}_h h_h = \dot{m}_i (h_i + x h_h)$$

or briefly, using definition (4.86),

$$\dot{H} = \dot{m}_i h_k . \tag{4.94}$$

In energy balance calculations, which we will handle later on, we use Eq. (4.94).

Example 1

A fan takes +15 °C humid air at 0.5 m³/s. What is the dry air mass flow $\dot{m}_i$ taken by the fan when the outdoor humidity is $x = 0.009$ and the outdoor pressure is $p = 1.0$ bar ?

Partial pressure of water vapor is calculated from Eq. (4.84):

$$p_h = \frac{0.009}{0.6220 + 0.009} \cdot 1.0 = 0.01426 \text{ bar} .$$

Dry air partial pressure is

$$p_i = p - p_h = 1.0 - 0.01426 = 0.986 \text{ bar} = 0.986 \cdot 10^5 \text{ Pa} .$$

Partial density of dry air is calculated from Eq. (4.76):

$$\rho_i = \frac{0.986 \cdot 10^5 \cdot 0.0290}{8.314 \cdot (273.15 + 15)} = 1.194 \text{ kg d.a./m}^3 .$$

Dry air mass flow is calculated from Eq. (4.91):

$$\dot{m}_i = 1.194 \cdot 0.5 = 0.597 \text{ kg d.a./s} .$$

Water vapor flow through the fan is

$$\dot{m}_h = x \dot{m}_i = 0.009 \cdot 0.597 = 0.005373 \text{ kg } H_2O/\text{s} .$$

4.2.3 Water Vapor Pressure in the Presence of Air

The equilibrium between water and water vapor in the case of humid air is illustrated in Fig. 4.7.

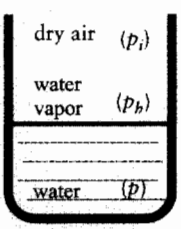

FIGURE 4.7 Equilibrium between water and vapor in the presence of air.

The state of equilibrium differs from the equilibrium between water and pure water vapor in that, in a gas phase, there is also inert gas (dry air) present. This means that the water pressure is equal to the total gas pressure, $p = p_i + p_h$, not to the water vapor pressure p_h.

In a state of equilibrium the chemical potentials of water and water vapor are equal:

$$\mu_v(T, p) = \mu_h(T, p_h), \tag{4.95}$$

where the subscript v refers to water and h to water vapor. Notice that $p = p_i + p_h$.

From Eq. (4.95) the partial pressure of water vapor p_h can be solved for, and we see that it is dependent on temperature and the partial pressure of dry air:

$$p_h = p_h(T, p_i). \tag{4.96}$$

Next we will show that the dependence of water vapor pressure on the partial pressure of dry air is very small, and consequently a good approximation is

$$p_h = p_h(T). \tag{4.97}$$

To show this, Eq. (4.95) is differentiated, and we get

$$\frac{\partial \mu_v}{\partial T} dT + \frac{\partial \mu_v}{\partial p} dp = \frac{\partial \mu_h}{\partial T} dT + \frac{\partial \mu_h}{\partial p_h} dp_h . \tag{4.98}$$

On the other hand,

$$\begin{aligned} \frac{\partial \mu_v}{\partial T} &= -s_v, & \frac{\partial \mu_h}{\partial T} &= -s_h, \\ \frac{\partial \mu_v}{\partial p} &= v_v, & \frac{\partial \mu_h}{\partial p_h} &= v_v, \end{aligned} \tag{4.99}$$

where s_v is the specific entropy of liquid water, s_h is the specific entropy of water vapor, v_v is the specific volume of water, and v_h is the specific volume of water vapor. Notice that $v_h = 1/\rho_h$. Substituting Eqs. (4.99) in Eq. (4.98), we obtain

$$-s_v\, dT + v_v\, dp = -s_h\, dT + v_h\, dp_h ,$$

and it follows that

$$dp_h = \frac{s_h - s_v}{v} dT + \frac{v_v}{v_h} dp . \tag{4.100}$$

On the other hand, while $\mu = h - Ts$, in accordance with the balance clause (4.95),

$$h_v - Ts_v = h_h - Ts_h ,$$

and it follows that

$$s_h - s_v = \frac{h_h - h_v}{T} .$$

Substituting this equation in Eq. (4.100), we obtain

$$dp_h = \frac{h_h - h_v}{T v_h} dT + \frac{v_v}{v_h} dp . \tag{4.101}$$

On the other hand, the differential of the total pressure is

$$dp = dp_i + dp_h,$$

which, substituted in Eq. (4.101), gives

$$dp_h = \frac{h_h - h_v}{T(v_h - v_v)} dT + \frac{v_v}{v_h - v_v} dp_i. \tag{4.102}$$

This differs from the water pressure equation of Clapeyron, which lacks the last term. If $p_i = 0$ or $dp_i = 0$, then Eq. (4.102) is identical to the Clapeyron equation, as it should be.

Considering that $v_h >> v_v$ and $v_h = 1/\rho_h$ and using Eq. (4.78), an approximation to Eq. (4.102) is obtained:

$$\frac{dp_h}{p_h} = \frac{M_h(h_h - h_v)}{RT^2} dT + \frac{M_h v_v}{RT} dp_i. \tag{4.103}$$

On the other hand,

$$\frac{dp_h}{p_h} = d(\ln p_h),$$

so according to Eq. (4.103) we can write

$$\left(\frac{\partial(\ln p_h)}{\partial T}\right)_{p_i} = \frac{M_h(h_h - h_v)}{RT^2} \tag{4.104}$$

$$\left(\frac{\partial(\ln p_h)}{\partial p_i}\right)_T = \frac{M_h v_v}{RT} \tag{4.105}$$

The specific volume of water is approximately $v_v = 10^{-3}$ m^3/kg, and an estimate of Eq. (4.105) at a temperature of 50 °C is

$$\left(\frac{\partial(\ln p_h)}{\partial p_i}\right)_T = \frac{0.0180 \cdot 10^{-3}}{8.314 \cdot 323.15} \frac{1}{\text{Pa}} = 6.70 \cdot 10^{9} \frac{1}{\text{Pa}}.$$

Integrating Eq. (4.105) with the help of this value we can examine the effect of air on the vapor pressure. When the partial pressure of air $p_i = 0$ and when the partial pressure of air is 10^5 Pa, a ratio of the vapor pressures corresponding to these situations at the temperature of 50 °C is obtained:

$$\ln \frac{p_h(50\ ^\circ\text{C}, p_i = 10^5\ \text{Pa})}{p_h(50\ ^\circ\text{C}, p_i = 0)} = 6.70 \cdot 10^{-9} \frac{1}{\text{Pa}} \cdot (10^5 - 0)\ \text{Pa} = 6.70 \cdot 10^{-4}$$

or

$$\frac{p_h(50\ ^\circ\text{C}, p_i = 10^5\ \text{Pa})}{p_h(50\ ^\circ\text{C}, p_i = 0)} = e^{6.70 \cdot 10^{-4}} = 1.0006702.$$

When $p_i = 0$, a situation is described where water and water vapor are in an equilibrium without the presence of dry air. The corresponding vapor pressure can be found in tables for vapor:

$$p_h(50\ ^\circ\text{C}, p_i = 0) = p'h(50\ ^\circ\text{C}) = 0.12335\ \text{bar}.$$

The difference between vapor pressures is $p_h(50\ °C,\ p_i = 10^5\ Pa) - p_h(50\ °C,\ p_i = 0) = 8\ Pa$.

This shows that the presence of air in the gas phase has a very small influence on the vapor pressure of water. Repeating the same calculation procedure for other temperatures, we can show that the vapor pressure of water can with good accuracy be taken from the vapor pressure tables for saturated water (water has the same pressure as water vapor when they are in equilibrium), as though there were no air in the gas phase. So the vapor pressure of water is with good accuracy also in this case just a function of temperature, and Eq. (4.97) is valid. New vapor pressure tables will not be needed for calculations with humid air.

4.2.4 Vapor Pressure of Water and Ice and Calculation of Humid Air State Values

The partial pressure of water vapor in air cannot be higher than the vapor pressure of saturated water $p'_h(T)$ corresponding to air temperature T. If it were higher, condensation of water vapor would occur until the equilibrium state corresponding to the saturated vapor pressure was achieved.

Saturated water vapor pressure is most accurately found from vapor tables or can be approximated with the following equation:

$$\log p'_h(\theta) = 28.59051 - 8.2\ \log(\theta + 273.16) + 0.0024804(\theta + 273.16) - \frac{3142.31}{\theta + 273.16} \tag{4.106}$$

The logarithm in Eq. (4.106) is Briggsian (a logarithm with 10 as the base), pressure is in units of bar, and the temperature is in Celsius.

A simpler approximation for the pressure of saturated water vapor is

$$ph'(T) = p_o \exp(11.78(T - 372.79)/(T - 43.15)), \tag{4.107}$$

where the constant $p_o = 10^5$ Pa and the temperature T is in degrees Kelvin.

When the temperature is under 0 °C, the saturation pressure p_h, is calculated using the vapor pressure of ice (ice turns into vapor directly, i.e., sublimates) and we can use the following empirical formula:

$$\log p'_h(\theta) = 10.5380997 - \frac{2663.91}{\theta + 273.16} \tag{4.108}$$

The logarithm in Eq. (4.108) is Briggsian, pressure has units of mbar, and the temperature is in Celsius.

For the vapor pressure of ice, the equation of Clapeyron can be obtained in the same way as for water:

$$dp_h = \frac{h_h - h_i}{T(v_h - v_i)} dT\ , \tag{4.109}$$

where h_i is the enthalpy of ice and v_i is the specific volume of ice.

The relative vapor pressure of air or the relative humidity is defined by the equation

$$\varphi = \frac{p_h}{p'_h(T)}, \tag{4.110}$$

where p_h is the partial pressure of water vapor in air and $p'_h(T)$ is the saturated water vapor pressure at temperature T. When φ is 1 or 100%, we say that the air is saturated.

Example 2a

Find the properties of saturated air and $\varphi = 50\%$ air, when the total pressure of air is $p = 1.0$ bar and the temperature of air is 20 °C.

(a) **Saturated air, $\varphi = 100\%$**

- Pressure of saturated vapor $p'_h(20\ °C)$ from Eq. (4.106):

$$\log p'_h(20\ °C) = 28.59051 - 8.2\ \log(20 + 273.16) + 0.0024804(20 + 273.16) - \frac{3142.31}{20 + 273.16} = 1.631$$

$$p'_h(20\ °C) = 10^{-1.631}\text{bar} = 0.0234\ \text{bar}$$

- Humidity x from Eq. (4.83):

$$x = 0.6220 \cdot \frac{0.0234}{1.0 - 0.0234} = 0.01490\ \text{kg}\ H_2O/\text{kg d.a.}$$

- Densities ρ_i, ρ_h, and ρ from Eqs. (4.76), (4.78), and (4.79):

$$\rho_h = \frac{0.0234 \cdot 10^5 \cdot 0.018053}{8.314 \cdot 293.15} = 0.01731\ \text{kg/m}^3$$

$$\rho_i = \frac{(1.0 - 0.0234) \cdot 10^5 \cdot 0.028964}{8.314 \cdot 293.15} = 1.1606\ \text{kg/m}^3 \left(= \frac{\rho_h}{x}\right)$$

$$\rho = 1.1606 + 0.01731 = 1.178\ \text{kg/m}^3$$

$$h_k = 1.006 \cdot 20 + 0.01490 \cdot (2501 + 1.85 \cdot 20) = 57.9\ \text{kJ/kg d.a.}$$

(b) **Humid air, $\varphi = 50\%$**

$$p'_h(20\ °C) = 0.0234\ \text{bar}$$

$$p'_h = 0.5 \cdot 0.0234 = 0.0117\ \text{bar}$$

$$x = 0.6220 \cdot \frac{0.0117}{1.0 - 0.0117} = 0.00736\ \text{kg}\ H_2O/\text{k.g. d.a.}$$

$$\rho_h = \frac{0.0117 \cdot 10^5 \cdot 0.018053}{8.314 \cdot 293.15} = 0.00865\ \text{kg/m}^3$$

$$\rho_i = \frac{(1.0 - 0.0117) \cdot 10^5 \cdot 0.028964}{8.314 \cdot 293.15} = 1.174\ \text{kg/m}^3 \left(= \frac{\rho h}{x} = \frac{0.00863}{0.00736}\right)$$

$$\rho = 1.174 + 0.00865 = 1.183\ \text{kg/m}^3$$

$$h_k = 1.006 \cdot 20 + 0.00736 \cdot (2501 + 1.85 \cdot 20) = 38.8\ \text{kJ/kg d.a.}$$

Example 2b

Find the properties of saturated air and $\varphi = 50\%$ air, when the total pressure of air is $\pi = 0.825$ bar and the temperature of air is 20 °C.

(a) Saturated air, $\varphi = 100\%$

$$p'_h\ (20\ ^\circ\text{C}) = 0.0234 \text{ bar}$$

$$x = 0.6220 \cdot \frac{0.0234}{0.825 - 0.0234} = 0.01816 \text{ kg } H_2O/\text{kg d.a.}$$

$$\rho_h = 0.01731 \text{ kg/m}^3$$

$$\rho_i = \frac{(0.825 - 0.0234) \cdot 10^5 \cdot 0.028964}{8.314 \cdot 293.15} = 0.953 \text{ kg/m}^3 \left(= \frac{\rho_h}{x} \right)$$

$$\rho = 0.970 \text{ kg/m}^3$$

$$h_k = 1.006 \cdot 20 + 0.01816 \cdot (2501 + 1.85 \cdot 20) = 66.2 \text{ kJ/kg d.a.}$$

(b) Humid air, $\varphi = 50\%$

$$p'_h(20\ ^\circ\text{C}) = 0.0234 \text{ bar}$$

$$p_h = 0.0117 \text{ bar}$$

$$x = 0.6220 \cdot \frac{0.0117}{0.825 - 0.0117} = 0.00895 \text{ kg } H_2O/\text{kg d.a.}$$

$$\rho_h = 0.0865 \text{ kg/m}^3$$

$$\rho_i = \frac{(0.825 - 0.0117) \cdot 10^5 \cdot 0.028964}{8.314 \cdot 293.15}$$

$$= 0.967 \text{ kg/m}^3 \left(= \frac{\rho_h}{x} = \frac{0.00863}{0.00736} \right)$$

$$h_k = 1.006 \cdot 20 + 0.00895 \cdot (2501 + 1.85 \cdot 20) = 42.8 \text{ kJ/kg d.a.}$$

Comparing Examples 2a and 2b we notice that the total air pressure has effects on the humidity x, partial density of dry air p_i, total pressure or pressure of humid air, and enthalpy h_k. Knowing the total pressure is therefore essential in calculations of the thermodynamic properties of humid air.

Pressure and humidity have also an effect on the mass flows. We continue Examples 2a and 2b by calculating the dry air mass flow in a fan when the humid air volume flow in the fan is 0.8 m^3/s. According to Eq. (4.91) and the calculations above, we obtain

$$\dot{m}_i = \rho_i q_v = 1.1606 \cdot 0.8 = 0.928 \text{ kg d.a./s}$$
$$\dot{m}_h = 0.01490 \cdot 0.928 = 0.01383 \text{ kg/s} \qquad \text{(Ex. 1a)}$$

$$\dot{m}_i = 1.174 \cdot 0.8 = 0.939 \text{ kg d.a./s}$$
$$\dot{m}_h = 0.00736 \cdot 0.939 = 0.00691 \text{ kg/s} \qquad \text{(Ex. 1b)}$$

$$\dot{m}_i = 0.953 \cdot 0.8 = 0.762 \text{ kg d.a./s}$$
$$\dot{m}_h = 0.01816 \cdot 0.762 = 0.01384 \text{ kg/s} \qquad \text{(Ex. 2a)}$$

$$\dot{m}_i = 0.967 \cdot 0.8 = 0.774 \text{ kg d.a./s}$$
$$\dot{m}_h = 0.00895 \cdot 0.774 = 0.00693 \text{ kg/s} \qquad \text{(Ex. 2b)}$$

Thus the total mass flows $\dot{m} = (\dot{m}_i + \dot{m}_h)$ differ in different cases. Water vapor flow $\dot{m}_h$ is obtained by multiplying the dry air mass flow by the corresponding humidity x (Eq. 4.93). As a basic quantity in humid air mass and energy balance calculations, we use dry air mass flow $\dot{m}_i$, and the effect of humidity on the energy balance is noted in the enthalpy h_k (Eq. 4.87).

4.2.5 Construction of a Mollier Diagram

Properties of humid air are usually described by means of the Mollier diagram. The Mollier diagram is constructed for a certain air pressure, normally for the value

$$p = 1.013 \text{ bar} = 760 \text{ mm Hg} = 1 \text{ atm},$$

which is the so-called standard atmosphere pressure. As suggested in Examples 1 and 2, a Mollier diagram can be used only when the total pressure is the same or almost the same as the pressure for which the diagram was constructed.

The abscissa of the Mollier diagram is humidity x. The axis is provided with a pitched scale. A straight line is drawn with a 45° angle to the abscissa, and it is provided with an enthalpy scale (h_k) according to the equation $h_k = l_{ho} \cdot x = 2501.6 \cdot x$, kJ/kg (Fig. 4.8). Consequently the enthalpic scale (h_k) is also pitched.

Now we construct this oblique-angled coordinate system with isotherms.

$$\theta = 0 \text{ °C}, \qquad h_k = c_{pi}\theta + x(c_{ph}\theta + l_{ho}) = xl_{ho} = 2501x, \text{ kJ/kg} .$$

While the h_k scale was constructed with the equation $h_k = 2501x$, it is noticed that the isotherm $\theta = 0$ °C joins the abscissa.

For $\theta = \theta_1 g \cdot h_k = c_{pi}\theta_1 + x(c_{ph}\theta_1 + l_{ho}) = 1.006\theta_1 + x(1.85\theta_1 + 2501)$.

The isotherm $\theta = \theta_1$ is a straight line in the $h_k - x$ coordinate system. The isotherms are not exactly parallel due to the term $c_{ph}\theta_1$. When $\theta_1 < 0$ °C, the isotherms go downward (relative to the abscissa), and when $\theta_1 > 0$ °C, the isotherms go upward.

The isotherms cut the y-axis at $x = 0$ or $h_k = c_{pi}\theta$. When c_{pi} is held constant, it follows that the temperature scale is pitched.

When the saturation curve ($\varphi = 100\%$) and other curves of relative humidity (φ) are added, the Mollier diagram is complete (Fig. 4.9).

Example 3

Construct a Mollier diagram for air, when the total pressure of air is 875 mbar.

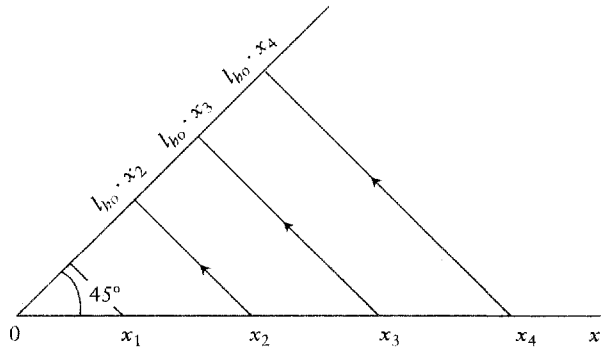

FIGURE 4.8 Constructing the enthalpy scale.

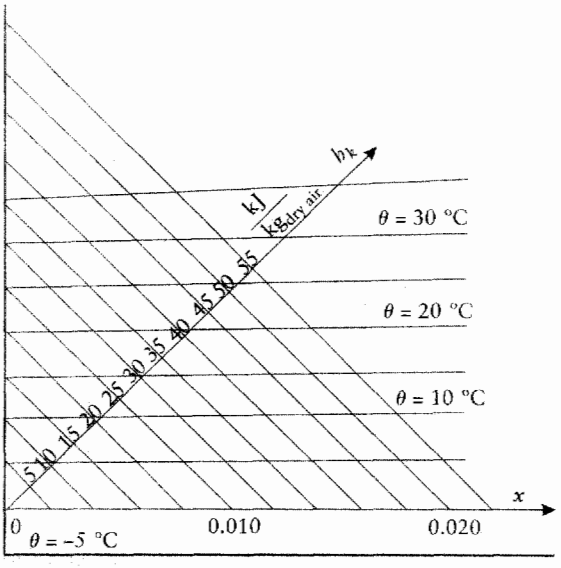

FIGURE 4.9 Fundamental scales of the Mollier diagram.

First we construct the $h_k - x$ coordinate system according to the instructions given above.

We provide the y-axis $x = 0$ with temperatures with the help of the equation

$$h_k = c_{pi}\theta + x(c_{ph}\theta + l_{ho}) = c_{pi}\theta = 1.006\theta, \text{ kJ/kg} .$$

When $\theta = -5$ °C, $h_k = -5.03$ kJ/kg, and when $\theta = +5$ °C, $h_k = +5.03$ kJ/kg, etc. Points where the isotherms cut the y-axis are located pitched.

Next we draw the saturation curve in the $h_k - x$ coordinate system. Vapor pressures can be calculated with Eqs. (4.106) and (4.108) or taken directly from the tables. The humidity x' corresponding to the saturation pressure $p'_h(t)$ is calculated with Eq. (4.83) noting that $p = 0.875$ bar. The enthalpy of humid saturated air is calculated with Eq. (4.94):

$$h'_k = 1.006\theta + x'(1.85\theta + 2501), \text{ kJ/kg} .$$

The saturation curve is drawn through points (x', h'_k), calculated for different temperatures. At the same time the other ends of isotherms are determined, and because they are straight lines, they can now be drawn.

The curves of relative humidity $\varphi_1, \varphi_2, \ldots$ can now be easily drawn with the help of the isotherms by just calculating the humidity corresponding to $\varphi_1, \varphi_2, \ldots$ and using the already constructed isotherms.

With high temperatures the x' values will not fit into the diagram. Then the h_k values have to be calculated with smaller x values in order to draw the isotherms. In Table 4.6 these values are calculated with values $x = x_{50\%}$ at various temperatures. Drawing the fundamental axes and isotherms with the instructions given above and the saturation curve with the help of Table 4.6 leads to the Mollier diagram in Fig 4.10*a*.

TABLE 4.6 Values Calculated for the Construction of the Mollier Diagram When the Total Pressure is $p = 0.875$ bar

		$\varphi = 100\ \%$		$\varphi = 50\ \%$	
θ (°C)	p'_h (bar)	x'	h'_k (kJ/kg)	$x_{50\%}$	h'_k (kJ/kg)
−10	0.00260	0.00185	−5.47	0.000925	
−5	0.00402	0.00287	+2.12	0.001432	
0	0.00611	0.00437	10.93	0.00218	
+5	0.00872	0.00626	20.7	0.00311	
10	0.01227	0.00885	32.4	0.00439	
15	0.01704	0.01235	46.3	0.00612	
20	0.0234	0.01709	63.5	0.00843	41.5
25	0.0317	0.0234	84.8	0.01147	54.4
30	0.0424	0.0317	111.2	0.01544	69.7
35	0.0562	0.0427	144.8	0.0206	88.1
40	0.0738	0.0573	187.8	0.0274	110.8

In Figs. 4.10*b–d* some commonly used Mollier diagrams are presented. The diagram in Fig. 4.10*b* is valid for the air pressure $p = 1$ bar and is used in conventional calculations of air conditioning technology. Figure 4.10*c* is an American version of Fig. 4.10*b*. It is a mirror image, and the direction of the scales is reversed. A diagram that covers a very wide temperature range and is therefore excellently suited to applications in the field of process technology is presented in Fig. 4.10*d*. This diagram is used, for example, in the technical design of the drying part of a paper machine. In Fig. 4.10*d* the enthalpy scale is on the abscissa and the curves of constant enthalpy are straight lines. The curves give the humidity relation, which is defined as $f = x/x'(\theta)$, where $x'(\theta)$ is the humidity of saturated air at temperature θ. Humidity relation f and relative humidity φ are different figures and should not be mixed.

4.2.6 Determination of Air Humidity

The humidity of air can be measured by either the dewpoint of the air or its wet bulb temperature.

Dewpoint means the temperature of saturated water vapor that has the same vapor pressure as the humid air in question. When the total pressure is constant, the constant vapor pressure means the same as the humidity x. In other words, dewpoint is the temperature of saturated air that has the same humidity as the air being considered.

By cooling a certain surface so cold that water starts condensing on it and measuring that temperature, the dewpoint can be measured. Combining this with the measurement of the dry bulb temperature, the state of air can be defined.

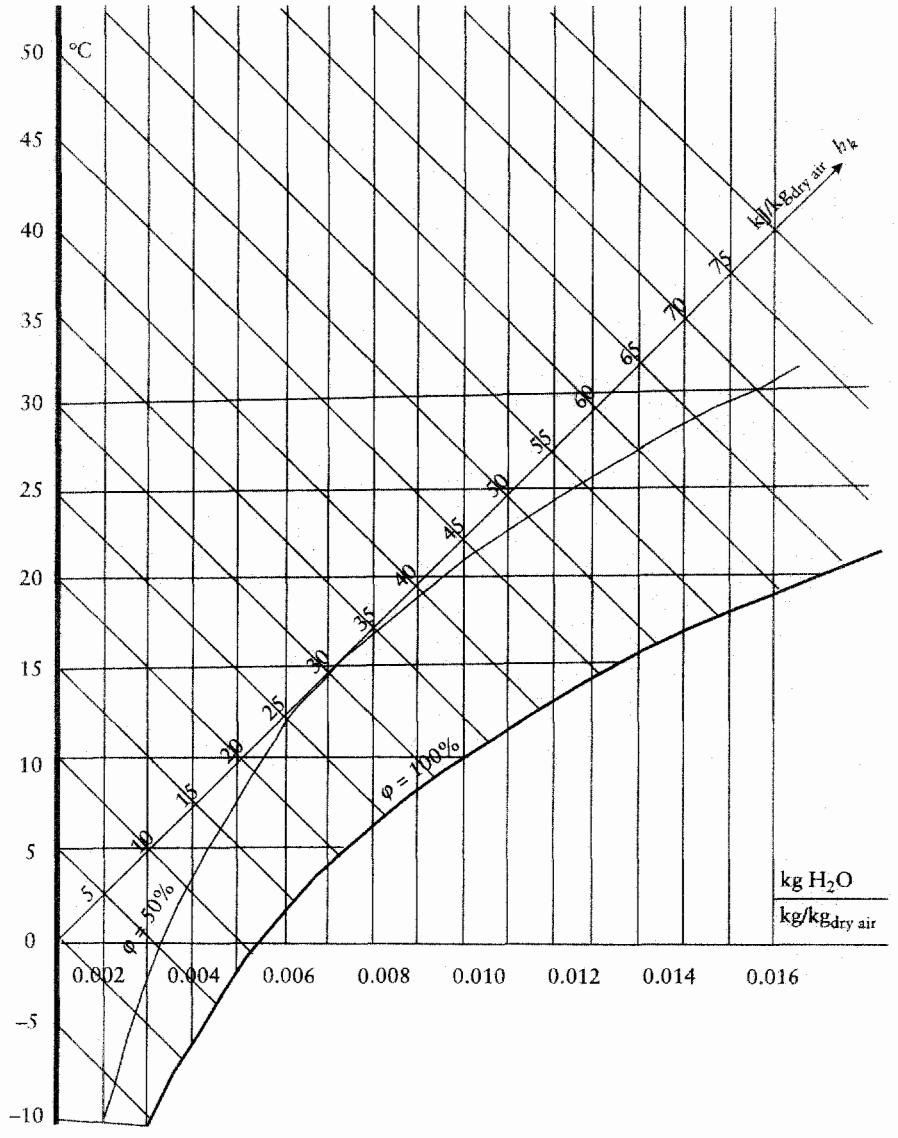

(*a*)

FIGURE 4.10a Mollier diagram, $p = 0.875$ bar.

Example 4

The dry bulb temperature of air is 20 °C and the dewpoint is 8 °C. What is the relative humidity?

$$h'_p\ (20\ °C) = 0.0234\ \text{bar} \qquad h'_p\ (8\ °C) = 0.01072\ \text{bar}$$

$$p_h\varphi = p'_h\ (20\ °C) = 0.01072/0.0234 = 0.458 = 45.8\%.$$

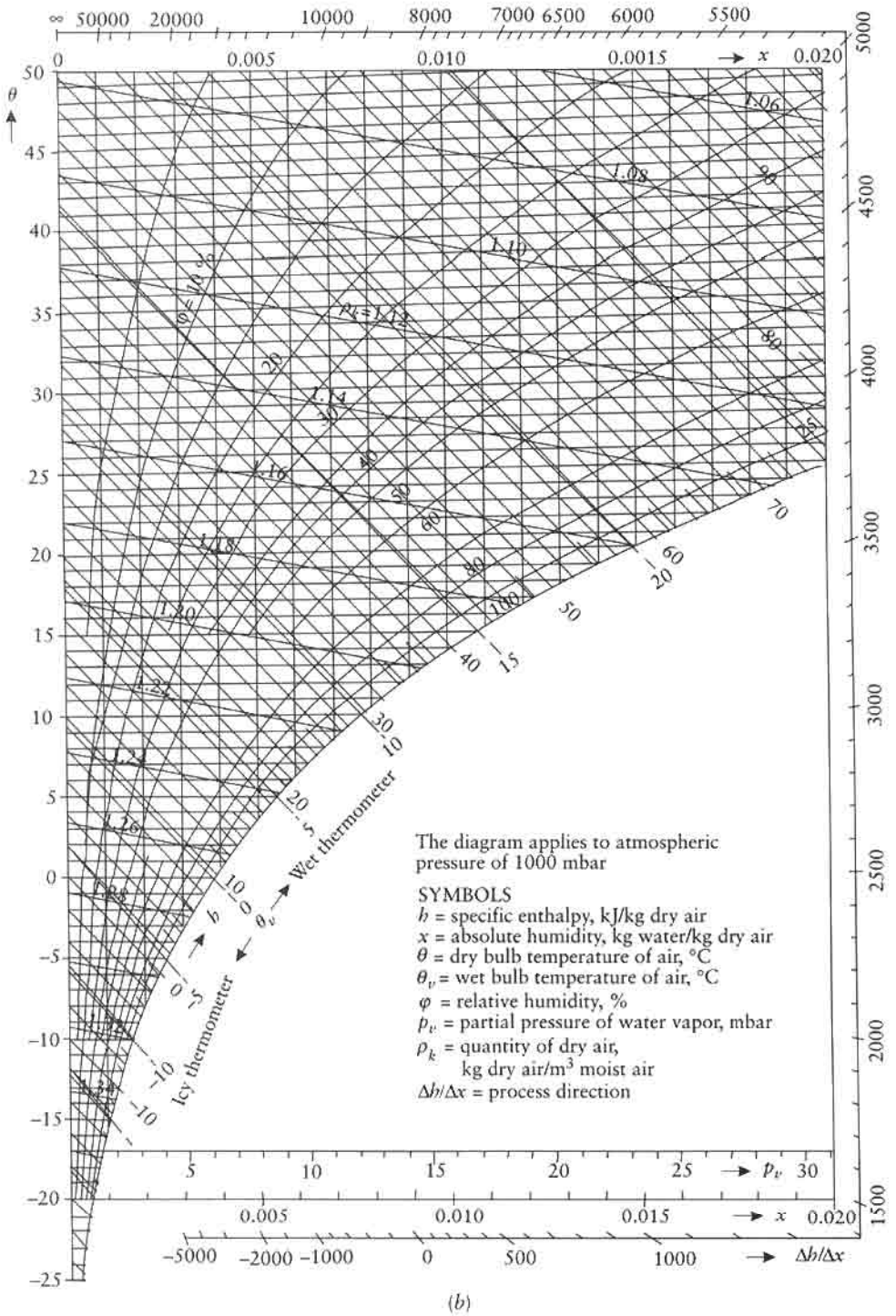

(b)

FIGURE 4.10b Mollier diagram.

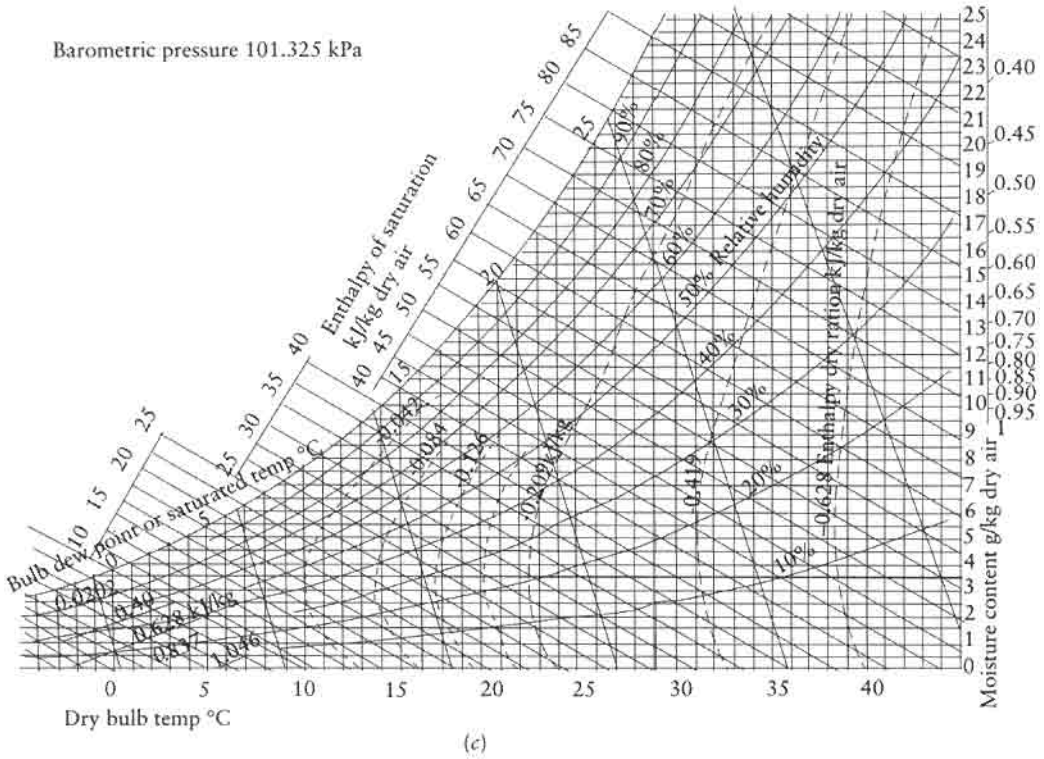

FIGURE 4.10c Mollier diagram.

Example 5

The air pressure in a room is 950 mbar, the temperature is 20 °C, and the relative humidity $\varphi = 40\%$. Define the dewpoint of the room.

$$h'_p(20\ ^\circ\text{C}) = 0.0234 \text{ bar} \qquad p_h = 0.4 \cdot 0.0234 \text{ bar} = 0.00936 \text{ bar}$$

θ_1 is found by using the tables; $h'_p\ (\theta_1) = 0.00936$ bar, and thus $\theta_1 = 6.0\ ^\circ\text{C}$.

The total pressure thus has no importance. If this result is sought from a Mollier diagram by finding the intersection of the humidity line (x = humidity of air = constant) and the saturation curve, which gives the dewpoint temperature, a diagram constructed for a pressure of 950 mbar should be used. A decent approximation can be found from a diagram constructed for pressure $p = 1$ bar.

When a damp cloth is laid in an air flow, it settles after a certain time to an equilibrium temperature, the so-called wet bulb temperature (θ_M), which is determined through heat and mass transfer. Negotiating the heat flow obtained by radiation and conduction, the heat balance of the wet cloth in a stationary situation can be expressed as

$$\alpha(\theta - \theta_M) = m''_h\ l(\theta_M), \tag{4.111}$$

where θ is the temperature of the air flow (°C), m''_h is the water flow vaporizing from the damp cloth (kg/m^2 s), $l(\theta_M)$ is the vaporization heat of water at temperature θ_M (J/kg), and α is the convective heat transfer coefficient (W/m^2 °C).

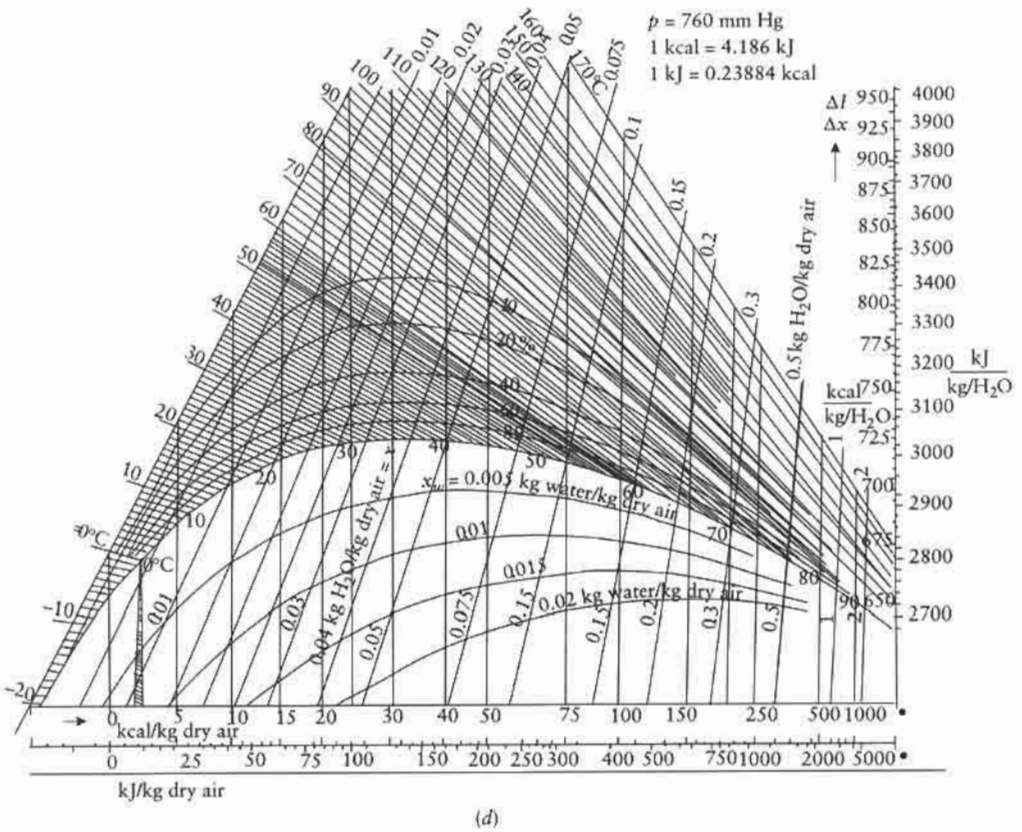

(*d*)

FIGURE 4.10d Mollier diagram for humid air with the perspective modification of Salin-Soininen.

An equation for the water flow vaporizing from the surface of the cloth can be obtained as

$$m_h'' = M_h \frac{p}{RT} k \ln \frac{p - p_h}{p - h_p'(\theta_M)}, \tag{4.112}$$

where k is the mass transfer coefficient (m/s). According to the analogy between heat and mass transfer coefficient,

$$k = \frac{\alpha}{\rho c_p} \mathrm{Le}^{1-n}, \tag{4.113}$$

where the power n varies between 0.33 and 0.5 and

$$\rho c_p = \rho_h c_{ph} + \rho_i c_{pi} \tag{4.114}$$

Also,

$$\mathrm{Le} = \frac{\rho c_p D}{\lambda}. \tag{4.115}$$

The dimensionless number Le is called the Lewis number (in Russian literature it is called the Luikov number). The Lewis number incorporates the specific heat capacity of humid air ρc_p (J/m^3 °C), the diffusion factor of water vapor in

air D (m²/s), and the heat conductivity of humid air λ (W/m °C). In Table 4.7 the thermodynamic properties of saturated air, including the diffusion factor and the heat conductivity are presented.

Substituting Eqs. (4.112) and (4.113) into Eq. (4.111), we obtain

$$\theta - \theta_M = \frac{M_h}{\rho c_p} \frac{p}{RT} \mathrm{Le}^{1-n} \, l(\theta_M) \ln \frac{(p - p_h)}{p - h'_p \, (\theta_M)}, \tag{4.116}$$

from which we observe that the heat transfer factor α has been reduced. The only factor in Eq. (4.116) depending on the airflow conditions of the measurement is the power n in the Lewis number. Because the value of the Lewis number is very close to 1, the effect of n is very small.

The wet bulb temperature θ_M can be solved for from Eq. (4.116) when the state of the air, the temperature t, and the partial pressure of water vapor p_h are known. Inversely, if the temperature t and the wet bulb temperature θ_M are known, the partial pressure and consequently the humidity of air can be found from Eq. (4.116).

Example 6

Given the temperature of air $\theta = °C$ and the wet bulb temperature $\theta_M = 10$ °C, calculate the humidity x, when the pressure of air is (a) $p = 1$ bar and (b) $p = 0.90$ bar.

By solving for the steam pressure ρ_h from Eq. (4.116), we obtain

$$p - p_h = (p - h'_p \, (\theta_M)) \exp\left[(\theta - \theta_M) \left(\frac{\rho c_p}{M_h} \frac{RT}{p} \frac{1}{\mathrm{Le}^{1-n}} \frac{1}{l(\theta_M)} \right) \right]. \tag{4.117}$$

The diffusion factor D, which is contained in the Lewis number, is inversely related to the total pressure:

$$D = \frac{1}{p} f(T). \tag{4.118}$$

From Table 4.7 we obtain the diffusion factor at the temperature of 10 °C and pressure $p = 1.0$ bar: $D(10\ °C, p = 1.0\ \text{bar}) = 23.3 \cdot 10^{-6} \text{m}^2/\text{s}$. The diffusion factor at the same temperature but a pressure $p = 0.9$ bar is, according to Eq. (4.118), $D(10\ °C, p(0.9\ \text{bar})) = 25.9 \cdot 10^{-6} \text{m}^2/\text{s}$.

For heat conductance there is a dependency on pressure almost like that of Eq. (4.118), so for good accuracy it is a valid approximation that $D/\lambda = g(T)$. From Table 4.7 we have $\lambda(10\ °C, p(1.0\ \text{bar})) = 0.02466$ W/m K, and so $D/\lambda = 9.45 \cdot 10^{-4} \text{m}^3$ K/J. Vaporization heat and the pressure of saturated steam are, from Table 4.7;

$$l(\theta_M) = l(10\ °C) = 2477 \cdot 10^3 \text{ J/kg},$$

$$p'_h(\theta_M) = p'_h(10\ °C) = 0.012271 \text{ bar}.$$

Temperature T is taken as a mean boundary layer temperature:

$$T = (20 + 10)/2 + 273.15 = 288.15 \text{ K}$$

Heat capacity,

$$\rho c_p = \rho_i c_{pi} + \rho_h c_{ph} = \rho_i (c_{pi} + x c_{ph}), \tag{4.119}$$

TABLE 4.7 Thermodynamic Characteristics of Saturated Air for a Total Pressure of 100 kN/m²

Temperature (°C)	Humidity (kg H_2O/kg dry air)	Water vapor partial pressure (kPa)	Water vapor partial density (kg/m³)	Water vaporization heat (kJ/kg)	Mixture enthalpy (kJ/kg dry air)	Dry air partial density (kg $_{dry\ air}$/m³)	Kinematic viscosity (10^4 m²/s)	Specific heat (kJ/K kg)	Heat conductivity (W/m K)	Diffusion factor water-air (10^4m²/s)	Temperature (°C)
0	0.003 821	0.6108	0.004 846	2 500.8	9.55	1.285	13.25	1.0108	0.023 80	22.2	0
2	0.004 418	0.705 4	0.005 557	2 495.9	13.06	1.275	13.43	1.012 0	0.024 13	22.4	2
4	0.005 100	0.812 9	0.006 358	2 491.3	16.39	1.264	13.61	1.013 4	0.024 27	22.6	4
6	0.005 868	0.934 6	0.007 257	2 486.6	20.77	1.254	13.79	1.014 9	0.024 40	22.8	6
8	0.006 749	1.072 1	0.008 267	2 481.9	25.00	1.243	13.97	1.016 7	0.024 54	23.1	8
10	0.007 733	1.227 1	0.009 396	2 477.2	29.52	1.232	14.15	1.018 6	0.024 66	23.3	10
12	0.008 849	1.401 5	0.010 66	2 472.5	34.37	1.221	14.34	1.020 8	0.024 78	23.6	12
14	0.010 105	1.597 4	0.012 06	2 467.8	39.57	1.211	14.52	1.023 3	0.024 90	23.9	14
16	0.011 513	1.816 8	0.013 63	2 463.1	45.18	1.199	14.71	1.026 0	0.025 00	24.2	16
18	0.013 108	2.062	0.015 36	2 458.4	51.29	1.188	14.89	1.029 1	0.025 11	24.5	18
20	0.014 895	2.337	0.017 29	2 453.1	57.86	1.177	15.08	1.032 5	0.025 20	24.8	20
22	0.016 892	2.642	0.019 42	2 449.0	65.02	1.175	15.27	1.036 4	0.025 29	25.2	22
24	0.019 131	2.982	0.021 77	2 442.0	72.60	1.154	15.46	1.040 7	0.025 37	25.5	24
26	0.021 635	3.360	0.024 37	2 439.5	81.22	1.141	15.65	1.045 5	0.025 44	25.9	26
28	0.024 435	3.775	0.027 23	2 434.8	90.48	1.129	15.84	1.050 9	0.025 08	26.3	28
30	0.027 558	4.241	0.030 36	2 430.0	100.57	1.116	16.03	1.056 9	0.025 56	26.6	30
32	0.031 050	4.753	0.033 80	2 425.3	111.58	1.103	16.22	1.063 5	0.025 61	27.0	32
34	0.034 950	5.318	0.037 58	2 420.5	123.72	1.090	16.41	1.071 0	0.025 65	27.4	34
36	0.039 289	5.940	0-041 71	2 415.8	136.99	1.076	16.61	1.079 3	0.025 67	27.8	36
38	0.044 136	6.624	0.046 22	2 411.0	151.60	1.061	16.80	1.088 5	0.025 69	28.3	38
40	0.049 532	7.375	0.051 14	2 406.2	167.64	1.046	17.00	1.098 9	0.025 69	29.7	40

42	0.055 560	8.198	0.056 50	2 401.4	185.40	1.030	17.20	1.110 3	0.025 68	29.1	42
44	0.062 278	9.010	0.062 33	2 396.6	204.94	1.014	17.39	1.123 2	0.026 66	29.6	44
46	0.069 778	10.085	0.068 67	2 391.8	226.55	0.9979	16.59	1.137 5	0.025 63	30.0	46
48	0.078 146	11.161	0.075 53	2 387.0	250.45	0.9791	17.79	1.153 4	0.025 58	30.5	48
50	0.087 516	12.335	0.082 98	2 382.1	277.04	0.9606	17.99	1.171 3	0.025 52	30.9	50
52	0.098 018	13.613	0.091 03	2 377.3	306.64	0.9411	18.19	1.191 3	0.025 45	31.4	52
54	0.109 76	15.002	0.099 74	2 372.4	339.51	0.9207	18.39	1.213 7	0.025 36	31.9	54
56	0.122 97	16.509	0.109 1	2 367.6	373.31	0.8999	18.59	1.238 9	0.025 26	32.4	56
58	0.137 90	18.146	0.119 3	2 362.7	417.72	0.8768	18.79	1.267 3	0.025 14	32.9	58
60	0.154 72	19.92	0.130 2	2 357.9	464.11	0.8532	18.99	1.299 4	0.025 01	33.4	60
62	0.173 80	21.84	0.141 9	2 353.0	516.57	0.8283	19.19	1.335 7	0.024 87	34.0	62
64	0.195 41	23.91	0.154 5	2 348.1	575.77	0.8021	19.38	1.377 0	0.024 71	34.5	64
66	0.220 21	26.14	0.168 0	2 343.1	643.51	0.7746	19.57	1.424 1	0.024 55	35.1	66
68	0.248 66	28.55	0.182 6	2 338.2	721.01	0.7456	19.76	1.478 2	0.024 37	35.7	68
70	0.281 54	31.16	0.198 1	2 333.3	810.36	0.7150	19.94	1.541 8	0.024 18	36.3	70
72	0.319 66	33.96	0.214 6	2 328.3	915.57	0.6829	20.01	1.613 2	0.023 99	36.9	72
74	0.364 68	36.96	0.232 4	2 323.3	1 035.60	0.6489	20.28	1.698 6	0.023 79	37.6	74
76	0.417 90	40.19	0.251 4	2 318.3	1 179.42	0.6132	20.44	1.799 4	0.023 60	38.3	76
78	0.480 48	43.65	0.271 7	2 313.3	1 348.40	0.5755	20.58	1.919 9	0.023 41	39.0	78
80	0.559 31	47.36	0.293 3	2 308.3	1 560.80	0.5358	20.71	2.066 4	0.023 23	39.8	80

(continues)

TABLE 4.7 *(continued)*

Temperature (°C)	Humidity (kg H_2O/kg dry air)	Water vapor partial pressure (kPa)	Water vapor partial density (kg/m³)	Water vaporization heat (kJ/kg)	Mixture enthalpy (kJ/kg dry air)	Dry air partial density ($kg_{dry\ air}/m^3$)	Kinematic viscosity (10^4 m³/s)	Specific heat (kJ/K kg)	Heat conductivity (W/m K)	Diffusion factor water-air (10^4m³/s)	Temperature (°C)
82	0.655 73	51.33	0.316 2	2 303.2	1 820.46	0.4939	20.81	2.247 7	0.023 07	40.7	82
84	0.777 81	55.57	0.340 6	2 298.1	2 148.92	0.4497	20.90	2.476 7	0.022 94	41.5	84
86	0.937 68	60.50	0.366 6	2 293.0	2 578.73	0.4031	20.96	2.773 9	0.022 85	42.5	86
88	1.152 44	64.95	0.394 2	2 287.9	3 155.67	0.3542	20.99	3.170 8	0.022 81	43.6	88
90	1.458 73	70.11	0.423 5	2 282.8	3 978.42	0.3026	20.99	3.730 4	0.02283	44.7	90
92	1.927 18	75.61	0.454 5	2 277.6	5 236.61	0.2482	20.94	4.574	0.022 95	46.0	92
94	2.731 70	81.46	0.487 3	2 272.4	7 395.49	0.1909	20.84	5.987	0.023 18	47.4	94
96	4.426 70	87.69	0.522 1	2 267.1	11 944.39	0.1305	20.69	8.820	0.023 55	49.0	96
98	10.303 06	94.30	0.558 8	2 261.9	27 711.34	0.06694	20.47	17.338	0.024 09	50.8	98
100	•	101.325	0.597 7	2 256.7	•	0	20.08	•	0.024 86	52.8	100

has to be iterated because steam pressure p_h and therefore humidity x are at this stage unknown. When humidity is low, as in this example, an approximation is $\rho c_p \cong \rho_i c_{pi}$. The calculation can be repeated when needed using the steam pressure from Eq. (4.117). In this example, we don't do that. For calculating the density and heat capacity, we will use an approximation $\rho_{cp} \cong \rho_i$, so $p \cong p_i$ and $cp \cong c_{pi}$. From this approximation it follows that

$$\frac{\rho c_p}{M_h}\frac{RT}{p} \cong \frac{M_i}{M_h}c_p \cong \frac{M_i}{M_h}c_{pi}, \tag{4.120}$$

whose value is

$$\frac{M_i}{M_h}c_{pi} = 1617 \text{ J/kg °C}.$$

From Eq. (4.76) we get the partial pressure of dry air:

$$\text{(a)}\quad \rho_i = \frac{p_i M_i}{RT} \cong \frac{pM_i}{RT} = \frac{10^5 \cdot 0.029}{8.314 \cdot 288.15} = 1.211 \text{ kg/m}^3,$$

$$\text{(b)}\quad \rho_i = \frac{p_i M_i}{RT} \cong \frac{pM_i}{RT} = \frac{0.9 \cdot 10^5 \cdot 0.029}{8.314 \cdot 288.15} = 1.089 \text{ kg/m}^3,$$

The Lewis number in cases a and b is as follows:

$$\text{(a)}\quad \text{Le} = \frac{\rho c_p D}{\lambda} \cong \rho_i c_{pi}\frac{D}{\lambda} = 1.211 \cdot 1006 \cdot 9.45 \cdot 10^{-4} = 1.151$$

It is assumed that $n = 0.5$, so $\text{Le}^{1-n} = \text{Le}^{1-0.5} = 1.073$

$$\text{(b)}\quad \text{Le} = \frac{\rho c_p D}{\lambda} \cong \rho_i c_{pi}\frac{D}{\lambda} = 1.089 \cdot 1006 \cdot 9.45 \cdot 10^{-4} = 1.035$$

Thus $\text{Le}^{1-n} = 1.017$. Substituting all values into Eq. (4.117), we obtain

(a) $p - p_h = (1.0 - 0.012271)$

$$\exp\left[(20-10)\cdot 1617 \cdot \frac{1}{1.073}\cdot\frac{1}{2477.2\cdot 10^3}\right] \text{bar} = 0.99376 \text{ bar}$$

$$p_h = (1.0 - 0.99376) \text{ bar} = 0.00624 \text{ bar} = 624 \text{ Pa}$$

$$x = 0.6220\,\frac{p_h}{p - p_h} = 0.6220 \cdot \frac{624}{10^5 - 624} = 0.00391$$

(b) $p - p_h = (0.9 - 0.012271)$

$$\exp\left[(20-10)\cdot 1617 \cdot \frac{1}{1.017}\cdot\frac{1}{2477.2\cdot 10^3}\right] \text{bar} = 0.89345 \text{ bar}$$

$$p_h = (0.9 - 0.89345) \text{ bar} = 0.00655 \text{ bar} = 655 \text{ Pa}$$

$$x = 0.6220\,\frac{p_h}{p - p_h} = 0.6220 \cdot \frac{655}{10^5 - 655} = 0.00456$$

Comparing the results for (a) and (b), we see that pressure has a considerable effect on the result. This is important to remember, especially in industrial ventilation and process measurements with notable underpressures and overpressures.

We will now derive an approximation for Eq. (4.116) that can be used when the partial pressure of water vapor in air is low compared with the total pressure.

First we note that with fairly good accuracy it is valid that

$$\ln\frac{p-p_h}{p-p'_h\,(\theta_M)} = \ln\left[1+\frac{p'_h\,(\theta_M)-p_h}{p-p'_h\,(\theta_M)}\right] \cong \frac{p'_h\,(\theta_M)-p_h}{p-p'_h\,(\theta_M)} \cong \frac{p'_h\,(\theta_M)}{p-p'_h\,(\theta_M)} - \frac{p_h}{p-p_h}$$

where using Eq. (4.83) leads to the approximation

$$\ln\frac{p-p_h}{p-p'_h\,(\theta_M)} \cong \frac{M_i}{M_h}(x'(\theta_M)-x)\ , \tag{4.121}$$

where $x'(\theta_M)$ is the humidity of saturated air at temperature θ_M when the total pressure of air is p.

Substituting approximations (4.120) and (4.121) to Eq. (4.116), we obtain

$$\frac{x'(\theta_M)-x}{t-\theta_M} = \frac{c_p}{l(\theta_M)}\cdot\frac{1}{\mathrm{Le}^{1-n}} \tag{4.122}$$

The Lewis number for air is approximately 1 (see Example 6), so with good accuracy $\mathrm{Le}^{1-n} \cong 1$, and we get an approximation from Eq. (4.122):

$$\frac{x'(\theta_M)-x}{t-\theta_M} = \frac{c_p}{l(\theta_M)}. \tag{4.123}$$

Above we considered the question of which temperature the damp cloth settles to when it is thermally insulated against all surroundings but the airflow, and when it can be assumed that there is no radiation heat transfer between the cloth and the airflow. In this consideration the state of the air has been constant.

If, instead, the air is damped adiabatically with the wet cloth, so that the state of the air varies, the cloth will settle to a slightly different temperature. Each state of air (θ, x) is represented by a certain wet bulb temperature θ_M, which can be calculated from Eq. (4.116) or its approximation (4.123), when the partial pressures of water vapor are low compared with the total pressure. When the state of air reaches the saturation curve, we have an interesting special case. Now the temperatures of the airflow and the cloth are identical. This equilibrium temperature is called the *adiabatic cooling border* or the *thermodynamic wet bulb temperature* (θ_{ad}).

When air is humidified with water flow $\dot{m}_v$ and when the incoming and outgoing humid airflows are denoted $\dot{m}_1$ and $\dot{m}_2$, the energy balance of the conditioning chamber can be written as

$$\dot{m}_2 h_2 - \dot{m}_1 h_1 = \dot{m}_v h_v\ . \tag{4.124}$$

Equation (4.124) is illustrated in Fig. 4.11.

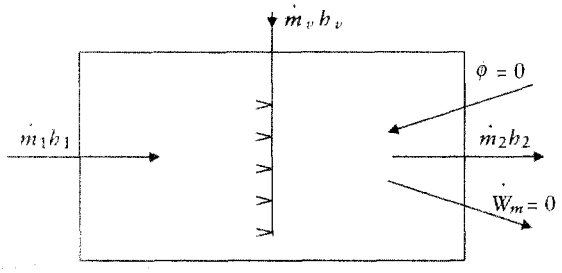

FIGURE 4.11 Energy balance for an adiabatic conditioning chamber.

In Eq. (4.124) the incoming enthalpy flow of humid air is

$$\dot{m}_1 h_1 = \dot{m}_{i1} h_{i1} + \dot{m}_{h1} h_{h1} \tag{4.125a}$$

and the outgoing enthalpy flow is

$$\dot{m}_2 h_2 = \dot{m}_{i2} h_{i2} + \dot{m}_{h2} h_{h2} . \tag{4.125b}$$

While the dry air flow stays constant, it can be written that

$$\dot{m}_i = \dot{m}_{i1} = \dot{m}_{i2} \tag{4.126}$$

and using Eq. (4.126) the enthalpy flows (4.125a–b) can be written as

$$\dot{m}_1 h_1 = \dot{m}_i h_{k1} \tag{4.127a}$$

$$\dot{m}_2 h_2 = \dot{m}_i h_{k2}, \tag{4.127b}$$

where according to Eq. (4.87)

$$h_{k1} = h_{i1} + x_1 h_{h1} \tag{4.128a}$$

$$h_{k2} = h_{i2} + x_2 h_{h2} . \tag{4.128b}$$

When all the water fed to the conditioning chamber vaporizes, the following humidity balance is valid:

$$\dot{m}_v = \dot{m}_{h2} - \dot{m}_{h1} = \dot{m}_i (x_2 - x_1) . \tag{4.129}$$

Substituting Eqs. (4.127a–b) and (4.129) into the energy balance (4.124), we obtain

$$\frac{\Delta h_k}{\Delta x} = h_v , \tag{4.130}$$

where $\Delta h_k = h_{k2} - h_{k1}$ and $\Delta x = x_2 - x_1$. When air is humidified adiabatically with water with temperature θ_{ad}, the enthalpy of water is now

$$h_v = c_{pv} \theta_{ad} \tag{4.131}$$

If, in addition, the air is humidified so that it reaches the saturation point, with the corresponding temperature θ_{ad}, we will now use the notations

$$\begin{aligned} h_{k2} &= h_{kad} \\ x_2 &= x_{ad} \end{aligned} \tag{4.132}$$

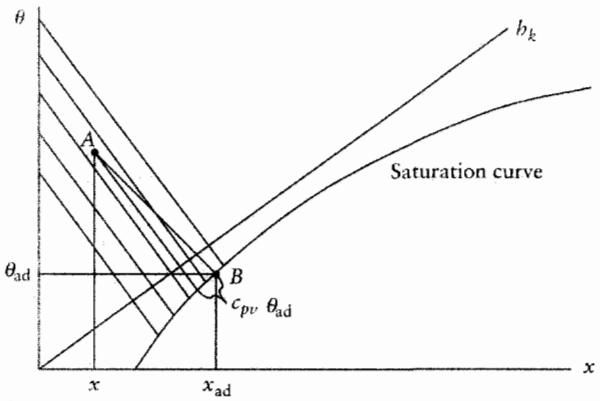

FIGURE 4.12 The state change of air in adiabatic humidification. *A* is the initial state and *B* is the saturated final I state.

Using the notations in (4.132) we can without danger of mix-up leave out the subscript 1 of the incoming point and write $x_1 = x$ and $h_{k1} = h_k$. Using these notations and Eq. (4.131), Eq. (4.130) can be written as

$$\frac{h_k - h_{kad}}{x - x_{ad}} = c_{pv}\theta_{ad}. \tag{4.133}$$

So the state point of air in the Mollier diagram is shifted in a direction where the dependency between the enthalpy and the humidity change according to the Eq. (4.133) is valid. This result is illustrated in Fig. 4.12.

Equation (4.133) can be formally written in a form resembling Eq. (4.123). To demonstrate this, we first write Eq. (4.133) as

$$h_k - h_{ad} - c_{pv}\theta_{ad}(x - x_{ad}) = 0$$

On the other hand,

$$h_k = c_{pi}\theta + x(c_{ph}\theta + l_{ho}) = 0$$

and

$$h_{kad} = c_{pi}\theta_{ad} + x_{ad}(c_{ph}\theta_{ad} + l_{ho})$$

Substituting these into the equation above, we obtain by grouping terms appropriately

$$\begin{aligned} &c_{pi}(\theta - \theta_{ad}) + x c_{ph}(\theta - \theta_{ad}) + x(l_{ho} + c_{ph}\theta_{ad} - c_{pv}\theta_{ad}) \\ &\quad - x_{ad}(l_{ho} + c_{ph}\theta_{ad} - c_{pv}\theta_{ad}) = 0 \end{aligned} \tag{4.134}$$

On the other hand, the vaporization heat of water at temperature θ_{ad} is

$$l(\theta_{ad}) = l_{ho} + c_{ph}\theta_{ad} - c_{pv}\theta_{ad} \tag{4.135}$$

and the specific heat of humid air per kilogram of dry air is

$$c_{pk} = c_{pi} + x c_{ph} \tag{4.136}$$

Substituting Eqs. (4.135) and (4.136) in Eq. (4.134), we get

$$\frac{x_{ad} - x}{\theta - \theta_{ad}} = \frac{c_{pk}}{l(\theta_{ad})}, \tag{4.137}$$

which is equivalent to Eq. (4.133).

Equation (4.137) is almost exactly the same as the approximation equation (4.123) derived for wet bulb temperature. When the partial pressure of water vapor is low compared with the total pressure—in other words when the humidity x is low—the specific heat of humid air per kilogram of humid air, c_p, and the specific heat of humid air per kilogram of dry air, c_{pk}, are almost the same: $c_p \cong c_{pk}$. Therefore, in a situation where the humidity is low and $\text{Le} \cong 1$, the thermodynamic wet bulb temperature is very nearly the same as the technical wet bulb temperature θ_M.

Example 7

(Table 4.7)Draw in the Mollier diagram at the 14 °C point of the saturation curve (a) the state change line of the adiabatic humidification and (b) an auxiliary line, associated with the wet bulb temperature measurement, by means of which the state can be defined. The pressure of air is $p = 1$ bar.

$$p'_b(14\ ^\circ\text{C}) = 0.01597 \text{ bar} \qquad \text{(Table 4.7)}$$

$$x_{ad} = 0.6220 \cdot \frac{0.01597}{1.0 - 0.01597} = 0.01009 = x'(\theta_M)$$

$$l(14\ ^\circ\text{C}) = 24678 \text{ kJ/kg} \qquad \text{(Table 4.7)}$$

$$\rho_i = 1.211 \text{ kg/m}^3 \qquad \text{(Table 4.7)}$$

$$\rho_b = 0.01206 \text{ kg/m}^3 \qquad \text{(Table 4.7)}$$

$$\rho = \rho_i + \rho_b = 1.223 \text{ kg/m}^3$$

$$\rho c_p = \rho_i c_{pi} + \rho_b c_{pb} = 1.211 \cdot 1.006 + 0.01206 \cdot 1.85 = 1.241 \text{ kJ/m}^3\ ^\circ\text{C}$$

$$c_p = 1.015 \text{ kJ/kg } ^\circ\text{C}$$

$$D = 23.9 \cdot 10^{-6} \text{ m}^2/\text{s} \qquad \text{(Table 4.7)}$$

$$\lambda = 0.0249 \text{ W/m/°C}$$

$$\text{Le} = \frac{D\rho c_p}{\lambda} = \frac{23.9 \cdot 10^{-6} \cdot 1241}{0.0249} = 1.191$$

$$n \cong 0.5$$

(a) We choose an auxiliary point on the isotherm $\theta = 25$ °C. According to Eq. (4.137),

$$x_{ad} - x = \frac{1.025}{2467.8} \cdot (25 - 14) = 0.00457\ ,$$

so it follows that the place of the auxiliary point is $x = 0.00552$.

(b) For the auxiliary point on the isotherm $\theta = 25$ °C, according to Eq. (4.122),

$$x'(\theta_M) - x = \frac{1.015}{2467.8} \cdot \frac{1}{1.191^{0.5}} \cdot (25 - 14) = 0.00415\ ,$$

and it follows that the place of the auxiliary point is $x = 0.00594$. The results are illustrated in Fig. 4.13.

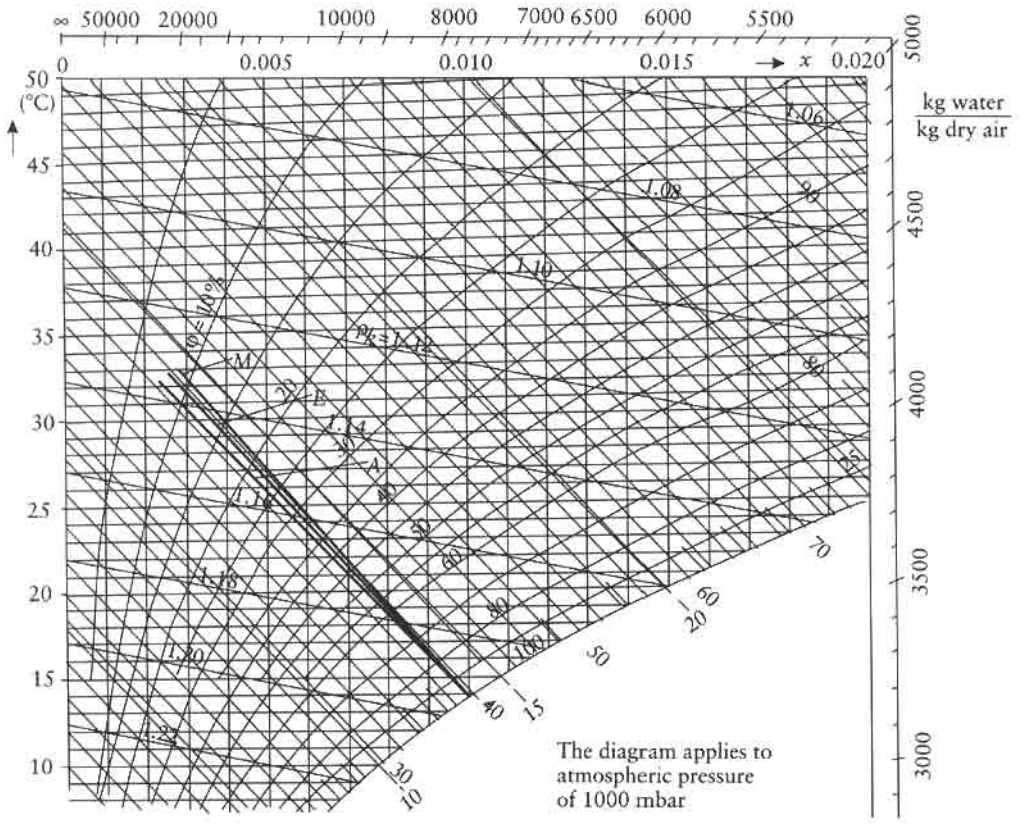

FIGURE 4.13 Determination lines for the state of air when $\theta_M = \theta_{ad}$14 °C.. M = determination line for wet bulb temperature, *E* = constant enthalpy, *A* adiabatic humidification line.

The enthalpy of humid air responding to the point 14 °C on the saturation curve is

$$h_{kad} = 1.0016 \cdot 14 + 0.01009 \cdot (1.85 \cdot 14 + 2501) = 39.58 \text{ kJ/kg} .$$

The humidity at the temperature of 25 °C corresponding to this enthalpy is determined from the equation

$$39.58 = 1.006 \cdot 25 + x(1.85 \cdot 25 + 2501) ,$$

and so $x = 0.00567$.

Comparing this value with the (*a*) and (*b*) point results of Example 7, we discover that the line of constant enthalpy lies between the determination line of wet bulb temperature and the adiabatic humidification line. The nearer the Lewis number is to 1, the nearer the wet bulb temperature is to the adiabatic humidification temperature.

In practical calculations the Mollier diagram's constant enthalpy line can be used as the auxiliary line for the wet bulb temperature line to a satisfactory

accuracy. The intersection of the constant enthalpy line with the isotherm responding to the temperature of air gives the humidity of air. For more accurate calculations Eq. (4.116) should be used, or its approximation (4.122) when the steam pressures (p_h and p'_h) are low compared to the total pressure of air (p).

As an example of using a Mollier diagram in defining the state of air, we can take a typical measurement from the local exhaust hood of a paper machine. The temperature of the exhaust air is 82 °C and its wet bulb temperature 60 °C. In Fig. 4.10*d* we move from the saturation curve at the point 60 °C straight up along the constant enthalpy line ($h_k = 460$ kJ/kg d.a.) until we reach the isotherm $\theta = 82$ °C. The intersection represents the state of air, and from Fig. 4.10*d* we see that to the accuracy of the diagram $x = 0.14$ and the corresponding humidity relation $f \equiv x/x'(82\ °C) = 0.20$. Based on the values $x = 0.14$ and $p = 1.0$ bar the relative vapor pressure φ can be calculated. From Eq. (4.84) we have $p_h = 0.183$ bar and from Table 4.7 p'_h (82 °C) = 0.5133 bar; then on the basis of definition (4.110) $\varphi = (p_h/p'_h) = 0.356 = 35.6\%$. We see that the values of f and φ clearly differ from each other.

According to Eq. (4.122) when $\mathrm{Le} \cong 1$, $l(\theta_M) \cong 2450$ kJ/kg and $c_p \cong 1.0$ kJ/kg °C:

$$p_h = p'_h\,(\theta_M) - 6.6 \cdot 10^{-4} \cdot p \cdot (\theta - \theta_M)\frac{1}{°C} \tag{4.138}$$

and by means of this the state of air can be approximately calculated. Often we call the temperature of air the dry bulb temperature to distinguish it from the wet bulb temperature.

It is important to emphasize that, especially in process measurements, radiation can have an essential influence on the wet bulb temperature, and therefore generally the wet bulb temperature is dependent on the measurement device and the method of measurement. If the airflow is very low, the radiation can have a remarkable contribution in addition to the convective heat transfer. Basically, an equation analogous to Eq. (4.138) can be empirically determined for each wet bulb temperature and method of measurement.

4.2.7 State Changes of Humid Air

Now we will consider a balance borderline of the system presented in Fig. 4.14. The system can be any part of the air surrounding the process device. If an air-handling application is considered, the balance can be calculated over the inner air of a room, an office, or an industrial hall, for example.

The energy balance of the system, consisting of the area inside the balance borderline, is in a stationary situation:

$$\begin{aligned}\phi - \dot{W}_m = {} & (\dot{m}_i h_{k2} - \dot{m}_i h_{k1}) + [(\dot{m}_{j2} h_{j2} - \dot{m}_{j1} h_{j1}) \\ & + (\dot{m}_{v2} h_{v2} - \dot{m}_{v1} h_{v1}) + (\dot{m}_{h2} h_{h2} - \dot{m}_{h1} h_{h1})]\end{aligned} \tag{4.139}$$

where ϕ is the net heat power received by the system, $\dot{W}_m$ is the net work power to the environment preferred by the system, $\dot{m}_v$ is the water flow (1 = inflow, 2 = outflow), $\dot{m}_j$ is the ice flow, and $\dot{m}_h$ is the separate clean steam flow not included in the air flows. The steam flows included in the

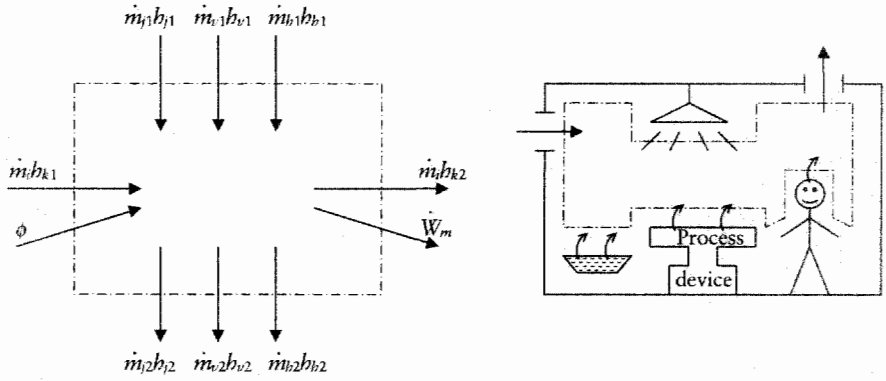

FIGURE 4.14 The energy-humidity borderline.

humid air flow are $\dot{m}x_1$ and $\dot{m}_i x_2$ and they have an effect on the energy balance through terms h_{k1} and h_{k2}.

Correspondingly, the humidity or water balance is

$$\dot{m}_i(x_2 - x_1) = (\dot{m}_{f1} - \dot{m}_{f2}) + (\dot{m}_{v1} - \dot{m}_{v2}) + (\dot{m}_{h1} - \dot{m}_{h2}) \tag{4.140}$$

In many cases the incoming and outgoing air flows can consist of various air flows in different states (temperature, humidity), which must be treated separately. This means that the air enthalpy flow must be divided into corresponding parts.

Example 8

Mixing of two air flows. As illustrated in Fig 4.15*a*, the energy balance is

$$\dot{m}_{i1}h_{k1} + \dot{m}_{i2}h_{k2} = \dot{m}_{i3}h_{k3} \tag{4.141}$$

and the humidity balance is

$$\dot{m}_{i1}x_1 + \dot{m}_{i2}x_2 = \dot{m}_{i3}x_3 \tag{4.142}$$

The dry air balance is

$$\dot{m}_{i1} + \dot{m}_{i2} = \dot{m}_{i3} \tag{4.143}$$

From Eqs. (4.141)–(4.143) it follows that

$$\frac{h_{k3} - h_{k2}}{h_{k1} - h_{k3}} = \frac{x_3 - x_2}{x_1 - x_3} = \frac{\dot{m}_{i1}}{\dot{m}_{i2}}, \tag{4.144}$$

which shows that the mixing point is on the line connecting points 1 and 2 in Fig 4.15*b*.

Example 9

Heating of an air flow. From Eq. (4.139) it follows that

$$\phi = \dot{m}_{i1}(h_{k2} - h_{k1}) \tag{4.145}$$

and from Eq. (4.140),

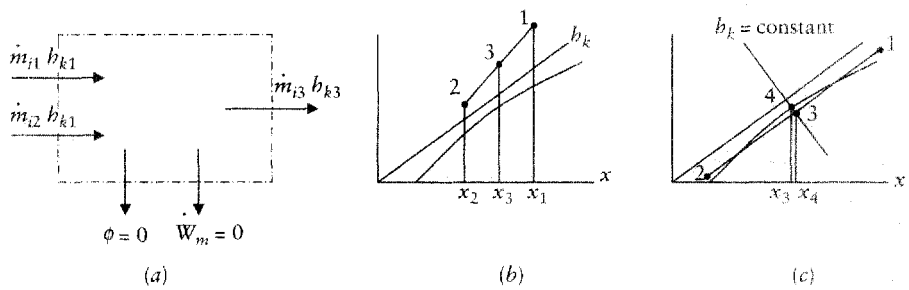

FIGURE 4.15 The mixing point in a Mollier diagram. If the supersaturated area (c) is considered, the state of the air is driven to point 4 and $(x_3 - x_4)$ kg H_2O/kg d.a. of water is condensed in the mixing chamber.

$$\dot{m}_i(x_2 - x_1) = 0,$$

so $x_2 = x_1$. When air is heated, the state point moves up along the constant humidity line.

Example 10

Cooling of an airflow. From Eq. (4.139) it follows that

$$\phi = \dot{m}_i(h_{k2} - h_{k1}) + \dot{m}_{v2}h_{v2}, \tag{4.146}$$

where now $\phi < 0$. When air is cooled, some water can be condensed. This depends on the surface temperature of the cooling coil, and therefore we have the term $\dot{m}_{v2}h_{v2}$ in the equation above. From Eq. (4.140) we obtain the water balance

$$\dot{m}_i(x_2 - x_1) = -\dot{m}_{v2},$$

so the final humidity $x_2 \leq x_1$. The air cooling process is illustrated in Fig. 4.16.

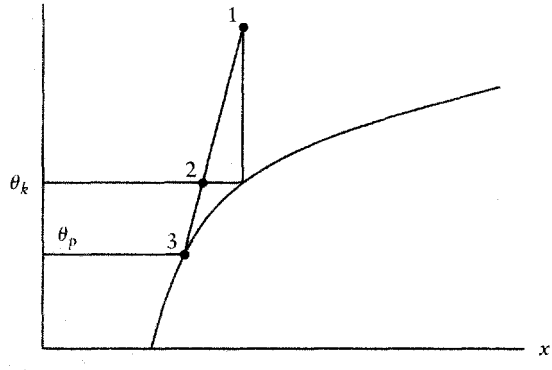

FIGURE 4.16 Air state change in a cooling coil. If the surface temperature θ_p is under the dew point θ_k, there will be condensation. If $\theta_p > \theta_k$ cooling takes place along the constant humidity line $x_1 = x_2$.

When the airflow meets a surface whose temperature is lower than the dewpoint, water vapor from the air condenses on the surface of the cooling coil. If all air comes into contact with the cold surface, the state of the air after the process will be at point 3. Some air always escapes the cold surface, and therefore the state of air after contact with the coil is a mixture of saturated air (3) and escaped air (1). The mixing point (2) lies on the line connecting points 1 and 3, as shown in Example 8. The nearer point 2 is to point 3, the more effective is the cooling coil.

Example 11

Adding steam to the air. From Eqs. (4.139) and (4.140) it follows that

$$\dot{m}_h h_h = \dot{m}_i (h_{k2} - h_{k1})$$

$$\dot{m}_h = \dot{m}_i (x_2 - x_1),$$

where $\dot{m}_h$ is the added steam flow and h_k its enthalpy. From these equations it follows that

$$\frac{h_{k2} - h_{k1}}{x_2 - x_1} = h_h. \tag{4.147}$$

In differential form Eq. (4.147) is

$$\frac{dh_k}{dx} = h_h. \tag{4.148}$$

On the other hand, differentiating Eq. (4.90b), $h_k = c_{pi}\theta + x(c_{ph}\theta + l_{ho})$, with respect to the variables θ and x, we obtain

$$dh_k = (c_{pi} + xc_{ph})d\theta + (\theta c_{ph} + l_{ho})dx\ ,$$

and substituting this in Eq. (4.148) we get

$$\frac{d\theta}{dx} = \frac{h_h - (l_{ho} + \theta c_{ph})}{c_{pi} + xc_{ph}} = \frac{h_h - h_h(\theta)}{c_{pi} + xc_{ph}}\ , \tag{4.149}$$

where $h_h(\theta) = l_{ho} + c_{ph}\theta$ is the steam enthalpy at air temperature θ.

From Eq. (4.149) we notice that if the temperature of the steam added to air is below the temperature of the air, the air will cool down and $d\theta/dx < 0$. If the steam temperature is higher than the air temperature, the temperature of air will rise ($(d\theta)/dx > 0$).

Example 12

The room temperature is required to be 20 °C and the relative humidity $\varphi = 50\%$. The net heat load developing in the room is 2.45 kW and the net steam flow $1.5 \cdot 10^{-3}$ kg/s. What should the inlet air temperature and humidity be when the inlet air is (a) $\dot{m}_i = 0.3$ kg/s and (b) $\dot{m}_i = 0.6$ kg/s

$$p'_h\ (20\ °C) = 0.02337 \qquad p_h = 0.5 \cdot 0.02337\ \text{bar} = 0.01169\ \text{bar},$$

$$\text{Room air humidity } x = 0.6220 \cdot \frac{0.01169}{1.0 - 0.01169} = 0.00736.$$

When the inlet air is well mixed with the room air, the humidity of the outlet air (2) is the same as the room air humidity, so $x_2 = 0.00736$, and its temperature is the same as the temperature of the room air, $\theta = 20\ ^\circ\text{C}$.

The enthalpy of the outlet air $h_{k2} = 1.006 \cdot 20 + 0.00736 \cdot 2501 + 1.85 \cdot 20 = 38.8$ kJ/kg. The enthalpy of inlet air h_{k1} and its humidity x_1 are determined by the energy and humidity balances:

$$\dot{m}_i(h_{k2} - h_{k1}) = \phi + \dot{m}_h h_h$$

$$\dot{m}_i(x_2 - x_1) = \dot{m}_h$$

The net heat power also includes the enthalpy flow, $\dot{m}_h h_h$. Then

$$\phi + \dot{m}_h h_h = 2.45 \text{ kW}$$

and therefore

(a) $$h_{k2} - h_{k1} = \frac{2.45}{0.3} = 8.2 \text{ kJ/kg} \longrightarrow h_{k1} = 38.8 - 8.2 = 30.6 \text{ kJ/kg}$$

(b) $$h_{k2} - h_{k1} = \frac{2.45}{0.6} = 4.1 \text{ kJ/kg} \longrightarrow h_{k1} = 38.8 - 4.1 = 34.7 \text{ kJ/kg}$$

The arising steam flow is $\dot{m}_h = 1.53 \cdot 10^{-3}$ kg/s, and thus

(a) $$x_2 - x_1 = \frac{1.53 \cdot 10^{-3}}{0.3} = 0.0051$$
$$x_1 = 0.00736 - 0.00255 = 0.00481$$

(b) $$x_2 - x_1 = \frac{1.53 \cdot 10^{-3}}{0.6} = 0.00255$$
$$x_1 = 0.00736 - 0.00255 = 0.00481$$

The corresponding air temperatures can be calculated with the equation

$$\theta = \frac{h_k - x l_{h0}}{c_{pi} + x c_{ph}} .$$

(a) $x = 0.00226 \qquad h_k = 30.6$ kJ/kg

$$\theta = \frac{30.6 - 0.00226 \cdot 2501}{1.006 + 0.00226 \cdot 1.85} = 24.4\ ^\circ\text{C}$$

(b) $x = 0.00481 \qquad h_k = 34.7$ kJ/kg $\qquad \theta = 22.2\ ^\circ\text{C}$

The result of Example 12 is illustrated in Fig. 4.17.

4.2.8 Example of Cooling Tower Dimensioning

Cooling towers are commonly used for water cooling, but they can also be used for heat recovery from outlet air. If the water temperature is higher than the dew-point of the air, water will cool in the tower. Cooling is caused by vaporization on the surface of the water drops. The vaporization energy comes from the inner energy of the water and in a certain phase, when the water temperature is lower than the dry bulb temperature of the air, also from the airflow. When the water temperature drops to near the air wet bulb temperature at the observation point,

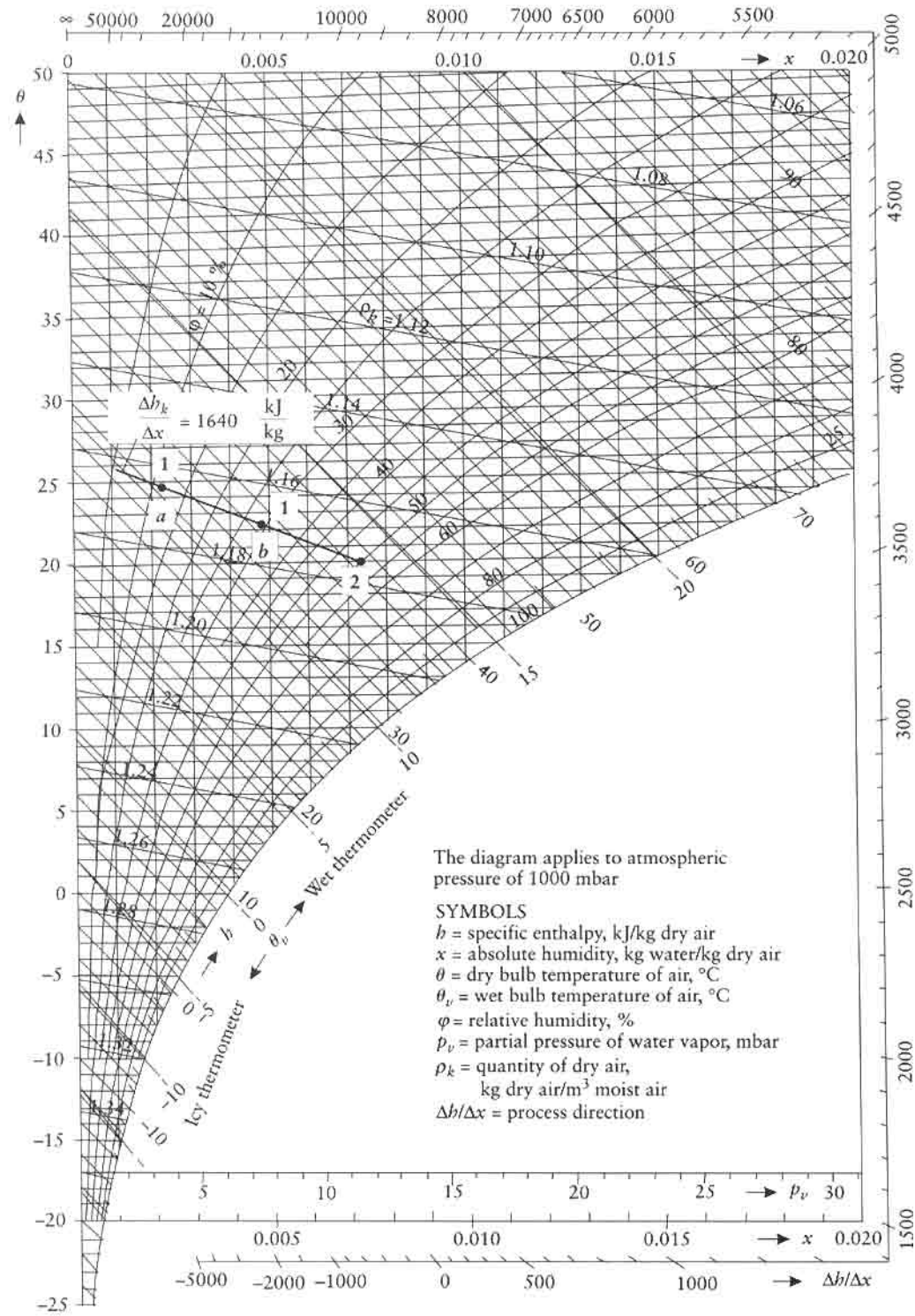

FIGURE 4.17 The state determination line for inlet air.

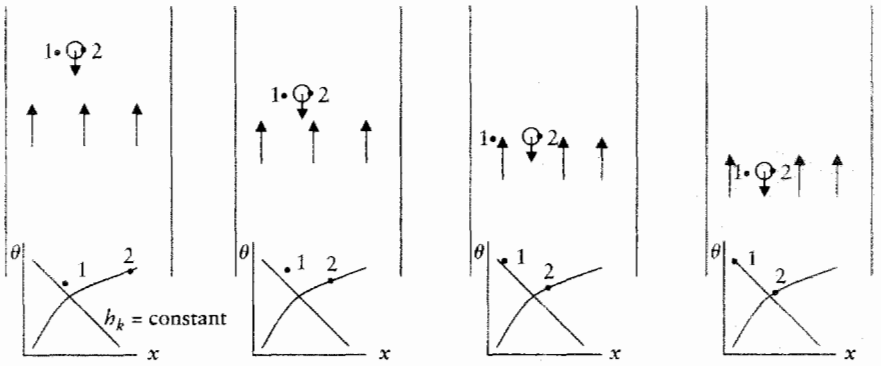

FIGURE 4.18 Water drop cooling in the air flow. Point (1) represents the air state surrounding the water drop (2).

water will not cool further even though there is still water vaporization from the drop surface. This is due to the fact that the temperature difference between the air dry bulb temperature and drop surface is so large that the energy needed for vaporization comes convectively from the air. This is illustrated in Fig. 4.18.

If the air dewpoint is higher than the water temperature (or more accurately, the surface temperature of the drops), water vapor condenses from the air on the surface of the water drops. Now the water warms up and the air cools down and at the same time dries up; in other words, the cooling tower recovers heat from the outlet air. We will now consider the operation of a cooling tower more closely with the notations of Fig. 4.19.

The energy balance for a distance dL is

$$-\dot{m}_v c_{pv}\, d\theta_v = \dot{m}_h''\, l(\theta_v)\, dA - \alpha(\theta - \theta_v)\, dA \quad .$$

From Eqs. (4.112), (4.113), and (4.121), we have, when $\mathrm{Le} \cong 1$, for vaporization $\dot{m}_h'' = (\alpha/c_p)(x'(\theta_v) - x)$, and substituting this in the equation above, we get

$$-\dot{m}_v\, c_{pv}\, \frac{c_p}{\alpha}\, d\theta_v = -[c_p(\theta - \theta_v) + (x - x'(\theta_v))l(\theta_v)]\, dA \quad .$$

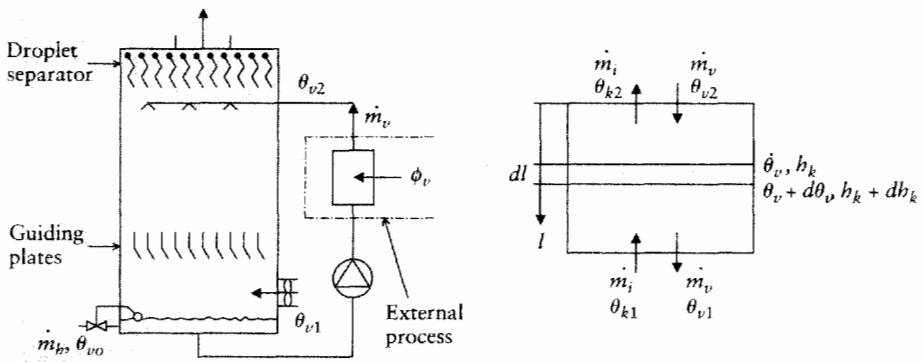

FIGURE 4.19 Mathematical approach for a cooling tower.

On the other hand, while [Eq. (4.119)] $c_p = (\rho_i/\rho)(c_{pi} + x c_{ph}) \cong c_{pi} + x c_{ph}$ and $l_0 \cong l(\theta_v)$, we obtain, according to the definition of h_k [Eq. (4.90b)], an approximate value of

$$c_p(\theta - \theta_v) + (x - x'(\theta_v))l(\theta_v) = h_k - h'_k(\theta_v) \ ,$$

and thus we have

$$d\phi = -\dot{m}_v c_{pv}\, d\theta_v = \frac{\alpha}{c_p}(h'_k(\theta_v) - h_k)\, dA \ . \tag{4.150}$$

Alternatively, we can write the energy balance with the help of the enthalpy flows as

$$-\dot{m}_i\, dh_k = \dot{m}_v c_{pv}\, dt_v - d\dot{m}_v c_{pv} t_v ,$$

where $d\dot{m}_v = \dot{m}_i\, dx$, where dx is the humidity change of the airflow. Then we can write

$$-\dot{m}_v c_{pv}\, d\theta_v = -\dot{m}_i(dh_k - c_{pv}\theta_v\, dx) .$$

While $dh_k = (c_{pi} + c_{ph})\, d\theta + l_0\, dx$ and $c_{pv}\theta_v \ll l_0$, to a good accuracy $dh_k - c_{pv}\theta_v\, dx \cong dh_k$ and therefore

$$d\phi = -m_v c_{pv}\, d\theta_v = -m_i\, dh_k$$

Considering Eq. (4.150), we have

$$\dot{m}_i\, dh_k = \frac{\alpha}{c_p}(h_k - h'_k(\theta_v))\, dA . \tag{4.151}$$

From Eq. (4.151) we see that in a dampening process the state of air tends to change toward the saturated air state corresponding to the surface temperature of the water. We will now solve the Eq. (4.151) approximately. First we state that

$$dh_k = d(h_k - h'_k(\theta_v)) + dh'_k(\theta_v) = d(h_k - h'_k(\theta_v)) + \frac{dh'_k(\theta_v)}{dh_k}\, dh_k$$

Using the approximation

$$\frac{dh'_k(\theta_v)}{dh_k} = \frac{h'_k(\theta_{v1}) - h'_k(\theta_{v2})}{h_{k1} - h_{k2}}$$

we get

$$dh_k = \frac{d(h_k - h'_k(\theta_v))}{1 - \dfrac{h'_k(\theta_{v1}) - h'_k(\theta_{v2})}{h_{k1} - h_{k2}}} = \frac{(h_{k1} - h_{k2})d(h_k - h'_k(\theta_v))}{(h_{k1} - h'_k(\theta_{v1})) - (h_{k2} - h'_k(\theta_{v2}))} ,$$

and substituting this in Eq. (4.151), we have

$$\frac{d(h_k - h'_k(\theta_v))}{h_k - h'_k(\theta_v)} = \frac{\alpha}{c_p m_i(h_{k1} - h_{k2})} \cdot [(h_{k1} - h'_k(\theta_{v1})) - (h_{k2} - h'_k(\theta_{v2}))] \cdot dA \ .$$

Integrating the equation above, we obtain

$$\dot{m}_i(h_{k1} - h_{k2}) = \frac{\alpha A}{c_p}\, \Delta h_{k\,\ln} , \tag{4.152}$$

where the definition $\Delta h_{k\,\ln}$ is

$$\Delta h_{k\,\ln} = \frac{(h_{k1} - h'_k\,(\theta_{v1})) - (h_{k2} - h'_k\,(\theta_{v2}))}{\ln \dfrac{h_{k1} - h'_k\,(\theta_{v1})}{h_{k2} - h'_k\,(\theta_{v2})}}$$

and

$$A = A_k A_p L$$

The quantity αA_p is defined separately for each type of cooling tower. It depends on many variables: jet pressure, jet division, airflow velocity, and others. The total energy balance for a cooling tower is (see Fig. 4.19)

$$\dot{m}_i(h_{k2} - h_{k1}) = \dot{m}_h c_{pv}\theta_{vo} + \dot{m}_h c_{pv}(\theta_{v2} - \theta_{v1}) \ ,$$

where θ_{vo} is the temperature of the excess feed water. The need for excess feed water represents the rate of vaporization $\dot{m}_h$. Usually the term $\dot{m}_h c_{pv}\theta_{vo}$ has minor significance (vaporization rate $\dot{m}_h$ corresponds usually to just a small percentage of the water flow $\dot{m}_v$), so on the basis of Eq. (4.152) we get an equation for the cooling power ϕ_v:

$$\phi_v = \dot{m}_i c_{pv}(\theta_{v2} - \theta_{v1}) = \frac{\alpha A}{c_p}\,\Delta h_{k\,\ln} \tag{4.153}$$

We can dimension a cooling tower according to the equation above.

Example 13

A paper industry's cooling tower recovers heat from the outlet air. This situation is represented by the following values:

- Inlet air enthalpy $h_{k1} = 293$ kJ/kg
- Outlet air enthalpy $h_{k2} = 208$ kJ/kg (saturated 44.3 °C air)
- Outlet water temperature $\theta_{v1} = 40$ °C
- Inlet water temperature $\theta_{v2} = 5.0$ °C
- Water flow $\dot{m}_v = 44$ kg/s
- Air flow $\dot{m}_i = 44 \cdot 4.186 \cdot (40 - 5)/(293 - 208) = 75.8$ kg/s
- Cross-sectional area of the cooling tower $A_k = 31$ m^2 and height $L = 3$ m

It is discovered that in the cooling tower the water moving downward from the jets changes its direction to upward after drop formation. There is an effective heat transfer process when the drops move upward: heat transfers from the outlet air to the drops through convection and condensation.

Drops collide with the drop separator and drain down to the lower part of the tower. These drops are large, so their total surface area is small and insignificant. The effective heat transfer process takes place when the drops move with the air flow, so this arrangement has to be treated as a parallel flow heat transfer.

(*a*) Calculate αAp. According to the parallel flow principle, the situation is as shown in Fig. 4.20.

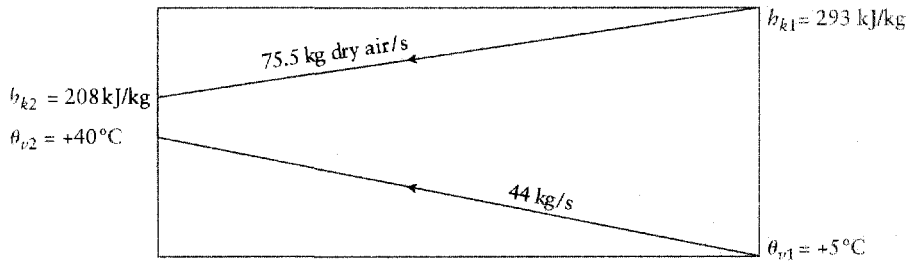

FIGURE 4.20 Heat transfer according to the parallel flow principle.

First we calculate the logarithmic enthalpy difference:

$$h'_k\,(\theta_{v1}) = h'_k\,(5°\text{C}) = 18\ \text{kJ/kg}$$
$$h'_k\,(\theta_{v2}) = h'_k\,(40°\text{C}) = 168\ \text{kJ/kg}$$

and

$$\Delta k_{\text{kln}} = \frac{(293-18)-(208-168)}{\ln\dfrac{293-18}{208-168}} = 121.9\ \text{kJ/kg}$$

The specific heat capacity of humid air calculated per kilogram of dry air is

$$c_{pK} = c_{pi} + x c_{pb} = 1.006 + 08 \cdot 1.85 = 1.154\ \text{kJ/kg °C}$$
$$c_p = \frac{\rho_i}{\rho} c_{pK} = 1.154(\ \text{kJ/kg °C})$$

From Eq. (4.153),

$$\alpha A = -\frac{c_p}{\Delta h_{\text{kln}}} \dot{m}_v c_{pv}(t_{v1} - t_{v2}) = -\frac{1.154}{121.9} \cdot 44.0 \cdot 4.186 \cdot (5-40)$$
$$= 61.0\ \text{kW/°C}$$

On the other hand, $AA_p\ A_k\ L$, and therefore

$$\alpha Ap = \frac{61.0\ \text{kW/°C}}{A_k - L} = \frac{61.0}{31.3} = 0.656\ \text{kW/°C m}^3$$

(*b*) The same cooling tower is to function as a water cooler. Let the outdoor air be 24 °C, φ = 50%, and the air flow 100 kg/s (dry air). The water inlet temperature is 24 °C and the water flow 30 kg/s. What is the cooling capacity if we assume that $\alpha \sim \sqrt{v_i}$ and $A_p \sim \dot{m}_v$, or $\alpha A_p = k\sqrt{v_i}\dot{m}_v$ and also that the active cooling process is parallel-flow heat transfer?

For case (a) was 44 kg/s and the air flow velocity = (75.5/1.0)/31 = 2.44 m/s. Therefore the heating capacity (or cooling capacity, depending on the sign) can be presented as

$$\phi = \frac{\alpha A_p A_k L}{c_p} \Delta h_{\text{kln}} = \frac{k\sqrt{v_i}\dot{m}_v}{c_p} A_k L \Delta h_{\text{kln}},$$

and solving factor k out of this equation,

$$k = \frac{c_p \phi}{\sqrt{v_i}\dot{m}_v A_k L \Delta h_{\text{kln}}} = \frac{1.154 \cdot (44.0 \cdot 4.186 \cdot (40-5))}{\sqrt{2.44} \cdot 44.0 \cdot 31.0 \cdot 3 \cdot 121.9} = 9.55 \cdot 10^{-3}.$$

Then the capacity ϕ is

$$\phi = \frac{k}{c_p} \cdot A_k L \cdot \sqrt{v_i}\dot{m}_v \Delta h_{kln} = \frac{9.55 \cdot 10^{-3}}{1.154} \cdot 31.3 \cdot \sqrt{v_i}\dot{m}_v \Delta h_{kln}$$

and after calculations,

$$\phi = 0.770 \cdot \sqrt{v_i} \cdot m_v \cdot \Delta h_{kln}$$

where v_i is in m/s, $\dot{m}_v$ in kg/s, Δh_{kln} in kJ/kg, and ϕ is in kW. It was found that $\dot{m}_v = 30$ kg/s and $\dot{m}_i = 100$ kg/s, and now $v_i \cong (100/1.2)/31 = 2.69$ m/s. Thus

$$\phi = 0.770 \cdot \sqrt{2.69} \cdot 30.0 \cdot \Delta h_{kln} = 37.9 \cdot \Delta h_{kln}$$

The cooling tower functioning in an air cooling situation is illustrated in Fig. 4.21. Because of the logarithmic enthalpy difference the solution must be iterated:

1. Guess: $\theta_{v2} = 20°C$; $h'_k\ (20°C) = 57.9$ kJ/kg

$$\phi = 30 \cdot 4.186 \cdot (24 - 20) = 502 \text{ kW}$$

$$h_{k2} - h_{k1} = 502/100 = 5.02 \text{ kJ/kg}; \quad h_{k2} = 53.3 \text{ kJ/kg}$$

$$\Delta h_{kln} = \frac{24.1 - (57.9 - 53.3)}{\ln \dfrac{24.1}{57.9 - 53.3}} = 11.8 \text{ kJ/kg}$$

$$\phi = 37.9 \cdot 11.8 = 446 \text{ kW}$$

$$h_{k2} = 24 - 446/30 \cdot 4.186 = 20.4°C$$

2. We choose $\theta_{v2} = (20.0 + 20.4)/2 = 20.2°C$; $h'_k\ (20.2\ °C) = 58.6$ kJ/kg.

$$\phi = 30 \cdot 4.186 \cdot (24 - 20.2) = 477 \text{ kW}$$

$$h_{k2} = 48.3 + 477/100 = 53.1 \text{ kJ/kg}$$

$$\Delta h_{kln} = \frac{24.1 - (58.6 - 53.1)}{\ln \dfrac{24.1}{58.6 - 53.1}} = 12.6 \text{ kJ/kg}$$

$$\phi = 37.9 \cdot 12.6 = 477 \text{ kW}$$

Now $\theta_{v2} = 20.2°C$ and cooling capacity $\phi = 477$ kW.

When the cooling tower was operating as a heat recovery device, its capacity was considerably higher because of the high temperatures and humidities. In case (a) we had

$$\phi = 44 \cdot (40 - 5) \cdot 4.186 = 6450 \text{ kW}\ .$$

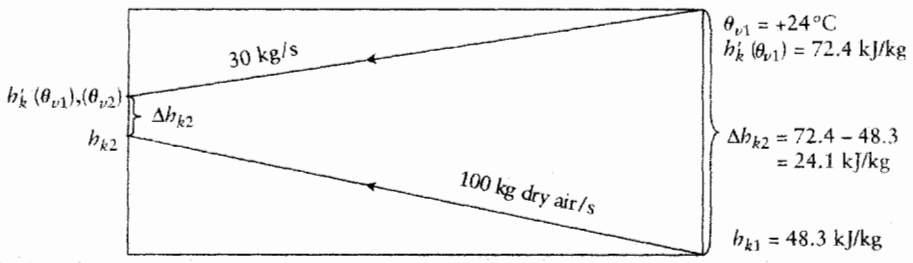

FIGURE 4.21 Water cooling in a cooling tower, which operates according to the parallel flow principle; in other words, the water spray turns in the direction of the air flow.

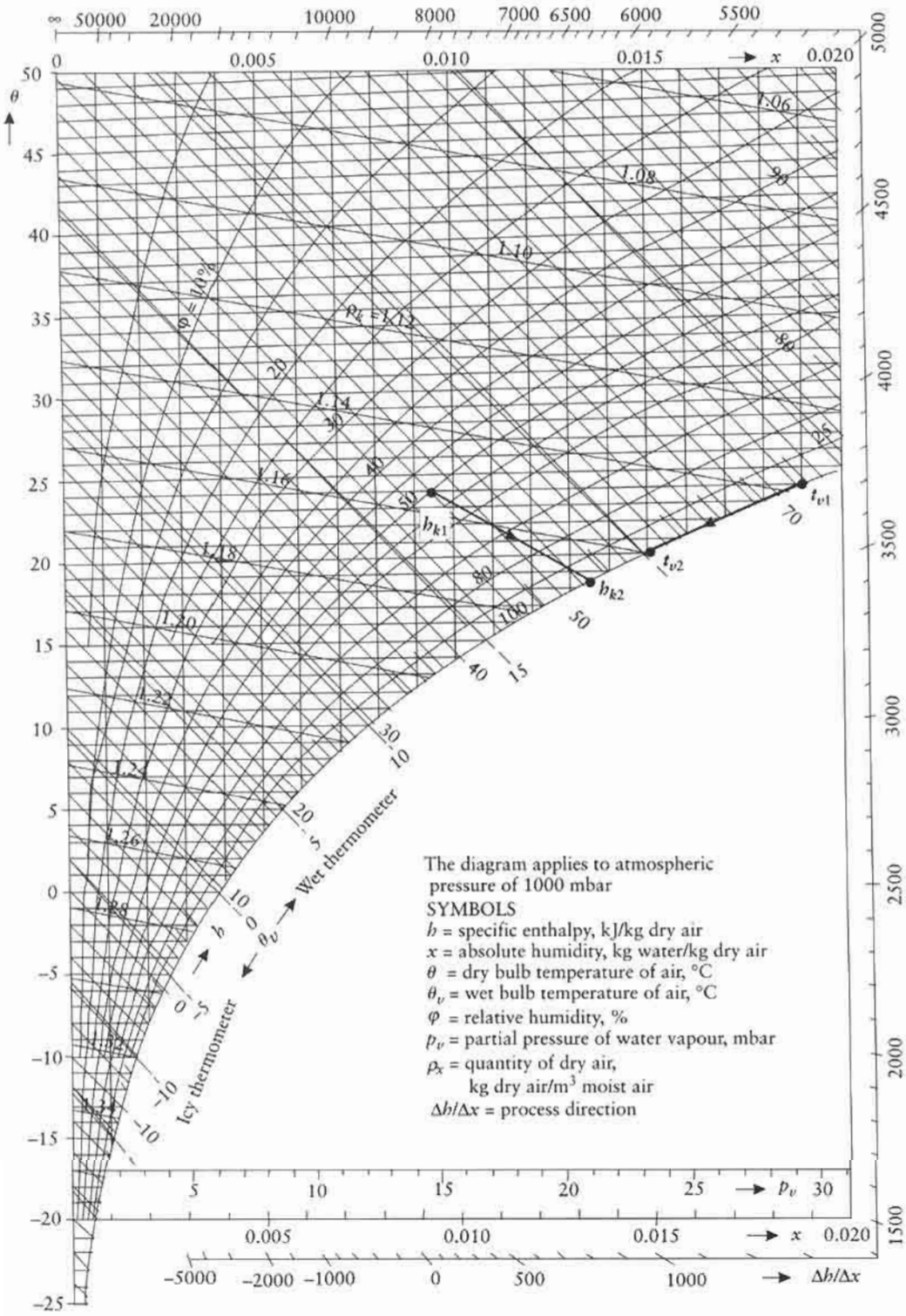

FIGURE 4.22 Water cooling in a cooling tower.

If we assume that the outlet air is saturated, the air state change process is as presented in Fig. 4.22. The exact determination of the air humidity at the end of the process would demand separate mass and heat transfer examinations.

4.3 HEAT AND MASS TRANSFER

This section introduces the important subject of heat and mass transfer to serve as a reference work to both the beginning engineer and the practicing industrial ventilation engineer.

4.3.1 Different Forms of Heat Transfer

For any method of heat transfer to take place, a temperature difference is necessary between two faces of a solid body, or at the boundaries of a gas or vapor. Heat transfer will take place only from a high-temperature source to a lower-temperature sink and is an irreversible process unless acted upon by another agency, as is the case with the refrigeration process.

Heat transfer may occur by one or more of three different modes:

- Conduction, which may be one-, two-, or three-dimensional or internally generated
- Convection, which may be natural or forced
- Radiation, which may be symmetrical or nonsymmetrical

4.3.1.1 Conduction

Conduction takes place at a solid, liquid, or vapor boundary through the collisions of molecules, without mass transfer taking place. The process of heat conduction is analogous to that of electrical conduction, and similar concepts and calculation methods apply. The thermal conductivity of matter is a physical property and is its ability to conduct heat. Thermal conduction is a function of both the temperature and the properties of the material. The system is often considered as being homogeneous, and the thermal conductivity is considered constant.

Thermal conductivity, λ, $\mathrm{W\ m^{-1}\ ^{\circ}C^{-1}}$, is defined using Fourier's law,

$$q_x = -\lambda \frac{\partial T}{\partial x} = \frac{\Phi_x}{A}, \tag{4.154}$$

where

$q = \Phi/A = \Phi''$ is the heat flow $(\mathrm{W\ m^{-2}})$
Φ_x is the heat flow in the x direction
$\partial T/\partial x$ is the temperature gradient

The minus sign in the equation denotes that the heat flow is positive in the direction of decreasing temperature.

Figure 4.23 represents a simple one-dimensional system with constant heat flow Φ through the plate. The plate thickness is Δx (m) and the area of the plate is A $(\mathrm{m^2})$.

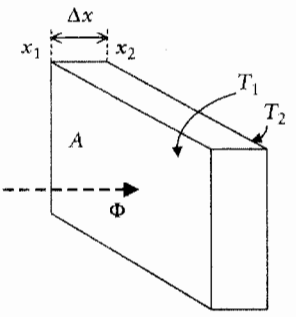

FIGURE 4.23 One-dimensional heat flow.

Integration of Eq. (4.154) with constant heat conductivity gives

$$\Phi \int_{x_1}^{x_2} dx = -\lambda A \int_{T_1}^{T_2} dT$$

$$\Phi = -\lambda A \frac{\Delta T}{\Delta x} . \tag{4.155}$$

One-dimensional heat conduction means that the heat flow is in one direction only, and one coordinate is required to represent the case. For example, in the case of a cylinder it is parallel with the radius.

4.3.1.2 Convection

Convection occurs in a moving fluid, generally from the fluid to a solid surface or vice versa. Although heat transfer between single particles is by conduction, it is the energy transfer with the matter that governs the heat transfer. The basic laws of heat and mass transfer have to be considered in order to describe convection mathematically.

Natural convection is self-induced and is created by the density differences, which are temperature related; the boiling of water in a kettle is an example of free convection. Forced convection is caused by an external force being applied by mechanical means such as a fan or pump; the cooling of a warm bottle in cool flowing water is an example of forced convection.

Convection is influenced by the fluid flow adjacent to the solid surface. To appreciate the mechanics of this mode of heat transfer, the nature of the fluid flow in relation to the particular flow process must be known. Consideration of the flow structure created by the passage of a turbulent fluid over a smooth solid surface shows (see Fig. 4.24)

1. The determining factor in convection is the flow boundary layer. Outside the boundary layer, the fluid is considered to have achieved a maximum velocity at an infinite distance from the surface.
2. In a laminar boundary layer, no mixing takes place and the flow is parallel. In this case the heat transfer occurs mainly by conduction through the boundary layer.

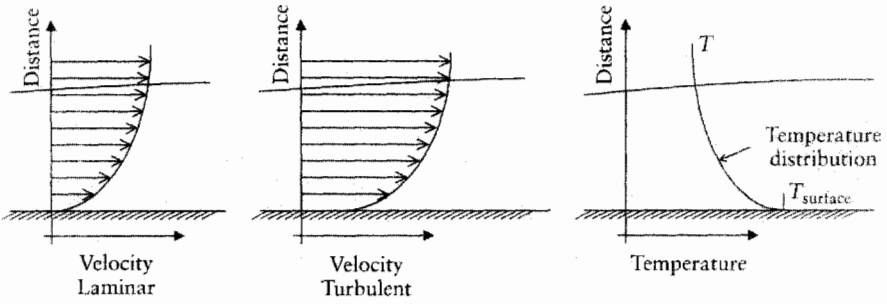

FIGURE 4.24 Laminar and turbulent boundary layers and temperature distribution inside the boundary layer.

3. In a turbulent boundary layer, flow takes place in the direction perpendicular to the surface over which the flow occurs.

A heat transfer factor (α) between the fluid and surface is defined as

$$q = \alpha\Theta = \frac{\Phi}{A} = \Phi'', \tag{4.156}$$

where Θ is the temperature difference between the surface and the fluid at a long distance from the surface.

When heat transfer occurs by conduction through the boundary layer,

$$\alpha \sim \frac{\lambda}{\delta}, \tag{4.157}$$

where δ is the thickness of the boundary layer, and the unit of α is $\mathrm{W\,m^{-2}\,K^{-1}}$. The heat transfer factor α thus decreases as the boundary layer thickness increases. The following discussion gives some indication of the range of the heat transfer values obtained due to the different modes of convective heat transfer.

Next we give some values of α to give an idea of the magnitude of the heat transfer:

	α, $\mathrm{W\,m^{-2}\,K^{-1}}$
Free convection	3.5–50
Forced convection, air	10–500
Forced convection, liquid	100–5000

A liquid has a higher rate of conductivity than a gas.

In boiling convection, liquid motion is created by steam bubbles breaking loose from the surface.

If steam condenses on a surface, there is no boundary layer; the resistance to heat flow is due to scale, metal thickness, and the condensed liquid layer, resulting in a high heat transfer factor. A thin layer of air or other noncondensing gas forms at the surface through which the steam diffuses. The heat transfer factor diminishes rapidly but is considerably higher than in dry convection.

4.3.1.3 Radiation

Heat radiation is electromagnetic radiation that all bodies emit due to their temperature. The wavelength of electromagnetic radiation is between 0.3 and 50 μm. This mode of heat transfer does not depend on an intermediate agent. When radiation falls on a body, part of the energy is absorbed, part is reflected, and the remainder is transmitted through the body. These components of the incoming radiation are the absorption ratio α, reflectance ratio ρ and transmission ratio τ. When a body is in a state of equilibrium, the incoming and outgoing radiation are equal. Hence, $\alpha + \rho + \tau = 1$.

A body having good electrical conductivity will absorb the incoming radiation on a distance of one wavelength. Now $\tau = 0$ and $\alpha + \rho = 1$.

A planar polished surface reflects heat radiation in a similar manner with which it reflects light. Rough surfaces reflect energy in a diffuse manner; hence radiation is reflected in all directions. A blackbody absorbs all incoming radiation and therefore has no reflection. A perfect blackbody does not exist; a near perfect blackbody surface such as soot reflects 5% of the radiation, making it the standard for an ideal radiator.

The radiant emittance of a blackbody is

$$M_m = \sigma T^4, \tag{4.158}$$

where σ is the Stefan-Boltzmann constant, 11.865 W m^{-2} (MJ/kmol)$^{-4}$.

The radiation emitted by a body due to its temperature is defined by the factor ϵ, the emissivity,

$$\epsilon M_m = \epsilon \sigma T^4. \tag{4.159}$$

This leads to Kirchhoff's law,

$$\epsilon(T, \vartheta, \nu) = \alpha(T, \vartheta, \nu), \tag{4.160}$$

for a given temperature, angle, and frequency. For approximate calculations the emissivity can be assumed constant over the whole frequency spectrum. In this case the body is classified as a gray body.

The net heat transfer between two surfaces according to Eq. (4.159) is proportional to the first or second power of the temperature difference; hence the radiation heat transfer dominates at a high temperature or for large temperature differences. When the temperature difference is small, a heat transfer factor is used similar to that used for convective heat transfer:

$$q = \alpha_s \Delta T. \tag{4.161}$$

4.3.2 Analogy with the Theory of Electricity

Equation (4.154) gives conduction for the one-dimensional case with constant thermal conductivity:

$$\Phi = \frac{\lambda A}{\delta} \Theta, \tag{4.162}$$

where δ is the distance corresponding to the temperature difference. For the three heat transfer forms,

- Conduction, Eq. (4.162)
- Convection, Eq. (4.156)
- Radiation, Eq. (4.161)

we have, respectively,

$$\Theta = \frac{\delta}{\lambda A}\Phi \tag{4.163}$$

$$\Theta = \frac{1}{\alpha_k A}\Phi \tag{4.164}$$

$$\Theta = \frac{1}{\alpha_s A}\Phi. \tag{4.165}$$

Following from Ohm's electrical law (theory of electricity), a heat resistance can be defined:

$$\text{potential difference} = \text{resistance} \cdot \text{current}$$

$$\text{temperature difference} = \text{heat resistance} \cdot \text{heat flow}$$

$$\Theta = R \cdot \Phi. \tag{4.166}$$

The conductance or the coefficient of heat transfer $U = 1/R$, or

$$\Phi = U\Theta. \tag{4.167}$$

For conduction the heat resistance is the distance divided by the heat conductivity, $R = \delta/\lambda A$, and the heat conductance is heat conductivity divided by distance, $U = \lambda A/\delta$. For convection and radiation the heat resistance is 1 divided by the heat transfer factor, $1/\alpha A$, and the heat conductance is the same as the heat transfer factor, $U = \alpha A$. A coefficient of heat flow is also used, the K value, which is the total conductance:

$$K = \frac{U}{A}\left[\frac{\mathrm{W}}{\mathrm{m^2K}}\right] \tag{4.168}$$

The following connecting rules are based on the above analogy:
heat resistance R in series connection

$$R = R_1 + R_2$$

and in parallel connection

$$\frac{1}{R} = \frac{1}{R_1} + \frac{1}{R_2}$$

heat conductance series connection

$$\frac{1}{U} = \frac{1}{U_1} + \frac{1}{U_2}$$

and in parallel connection

$$U = U_1 + U_2$$

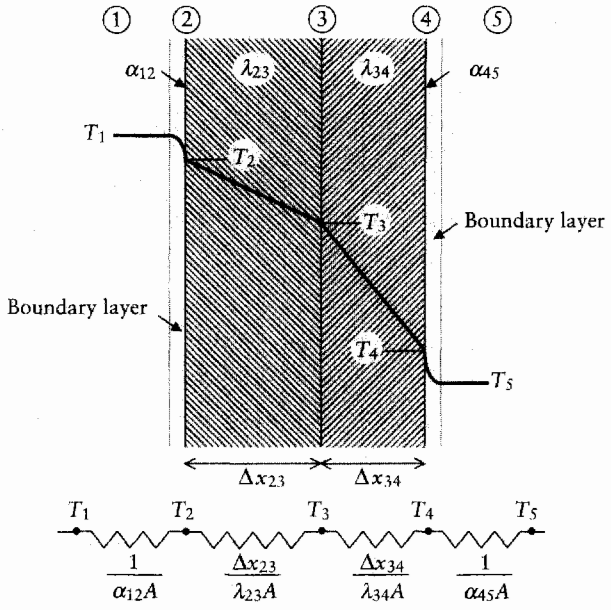

FIGURE 4.25 Heat transfer through a wall.

The heat resistance between the fluids on the two sides of the pipe wall in Fig. 4.25 is

$$R \cdot A = \frac{A}{U} = \frac{1}{K} = \frac{1}{\alpha_1} + \frac{1}{\alpha_2} + \sum \frac{\delta}{\lambda}, \tag{4.169}$$

where $\alpha = \alpha_{conv} + \alpha_{rad}$, and δ and λ are the thickness and heat conductivity of consecutive layers.

The resistance between the fluids on the inside and outside of the pipe is obtained by integrating with respect to the radius (Fig. 4.26):

$$R \cdot 1 = \frac{1}{U} = \frac{1}{\pi d_u \alpha_u} + \frac{1}{\pi d_s \alpha_s} + \sum \frac{\ln \frac{d_{ui}}{d_{si}}}{2\pi\lambda_i} \tag{4.170}$$

The sum includes concentric cylinder layers, such as the layer between the outer and inner diameters of the pipe or a possible thermal insulation layer. For each layer the corresponding heat conductivity λ_I is used. The outer heat transfer factor is the sum of the proportions of convection and radiation. (*Note:* Very thin pipes or wires should not be insulated. Because the outer diameter of the insulation is smaller than λ/α_u, the resistance is less than that without the insulation.)

The resistance between fluids separated by two coaxial spherical surfaces is

$$R = \frac{1}{\pi d_u^2 \alpha_u} + \frac{1}{\pi d_s^2 \alpha_s} + \frac{\delta}{\frac{1}{2\pi\lambda}\left(\frac{1}{d_u} - \frac{1}{d_s}\right)}. \tag{4.171}$$

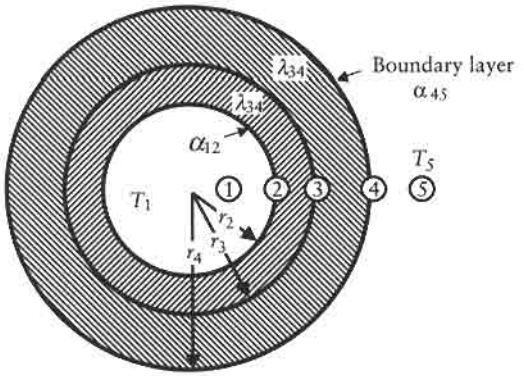

FIGURE 4.26 Heat flow through a pipe wall.

Example 1

Heat transfer through a pipe wall. A pipeline part 15 m long carries water. Its internal diameter d_i is 34 mm and its external diameter d_o is 42 mm. The thermal conductivity of the pipe λ is 40 W m^{-1} K^{-1}. The pipeline is located outdoors, where the outdoor temperature θ_{ao} is −8 °C. Determine the minimum flow velocity necessary in the pipe to prevent the pipe from freezing. The heat transfer coefficient inside the pipe is α_s = 1000 W m^{-2} K^{-1} and outside the pipe $\alpha_{u,\,conv}$ = 5 W m^{-2} K^{-1}and $\alpha_{u,rad}$ = 4 W m^{-2} K^{-1}. The specific heat capacity of water is c_p = 4.2 kJ kg^{-1} K^{-1}, and the initial temperature of water θ_i = 4 °C.

$$\alpha_u = \alpha_{u,\,conv} + \alpha_{u,\,rad} = (5+4)\ \mathrm{Wm^{-2}\ K^{-1}} = 9\ \mathrm{Wm^{-2}K^{-1}}$$

$$R' = \frac{1}{\pi d_u \alpha_u} + \frac{1}{\pi d_s \alpha_s} + \sum \frac{\ln \frac{d_u}{d_s}}{2\pi\lambda_i}$$

$$= \frac{1}{\pi \cdot 0.042\ \mathrm{m} \cdot 9(\mathrm{W/m})^2\ \mathrm{K}} + \frac{1}{\pi \cdot 0.034\ \mathrm{m} \cdot 1(\mathrm{W/m})^2\ \mathrm{K}}$$

$$+ \frac{\ln \frac{42}{34}}{2\pi \cdot 40 \mathrm{W/m\ K}} = 0.852(1)\mathrm{m^2\ K/W}$$

$$d\Phi = \dot{m} c_p\, d\Theta = -\frac{1}{R'}\Theta\, dx \quad \Rightarrow \quad \int_{\Theta_1}^{\Theta_2} \frac{d\Theta}{\Theta} = -\frac{1}{R'\dot{m}c_p}\int_0^1 dx$$

$$\Rightarrow \quad \ln\frac{\Theta_2}{\Theta_1} = -\frac{L}{R'\dot{m}c_p}$$

$$\dot{m} = \frac{L}{R' c_p \ln\frac{\Theta_1}{\Theta_2}}$$

$$w = \frac{q_v}{A} = \frac{\dot{m}/\rho}{\pi d_s^2/4} = \frac{4L}{R' c_p \ln\frac{\Theta_1}{\Theta_2} \rho \pi d_s^2}$$

$$= \frac{4 \cdot 15\mathrm{m}}{0.852 \cdot 4200 \cdot \ln(12/8) \cdot 1000 \cdot \pi \cdot 0.034^2}$$

$$= 0.011\ \mathrm{m/s}$$

4.3.3 Heat Conduction

The heat flow density q of a material depends on the local temperature gradient, according to Fourier's law:

$$q = -\lambda \frac{\partial T}{\partial x}. \tag{4.172}$$

In simple one-dimensional cases, it is easy to determine the temperature gradient and calculate the heat flow from Fourier's law.

The general case is that of steady-state flow, and the thermal conductivity factor is a function of the temperature. In the unsteady state the temperature of the system changes with time, and energy is stored in the system or released from the system reduced. The storage capacity is

$$\frac{dU}{dt} = \Phi = mc_p \frac{\partial T}{\partial t}$$

$$= \rho c_p V \frac{\partial T}{\partial t}. \tag{4.173}$$

4.3.3.1 General Heat Conduction Equation

Consider a small control volume $V = \delta x \delta y \delta z$ (Fig. 4.27), where the inner heat generation is $Q_g'''(T)$ (heat production/volume) and the heat conductivity is $\lambda(T)$. The material is assumed to be homogeneous and isotropic, and the internal heat generation and thermal conductivity are functions of temperature.

The heat flow to the control volume through area $\delta y \delta z$ at x is

$$\delta Q_x = -\delta y \delta z \lambda(T) \left(\frac{\partial T}{\partial x} \right) \delta t. \tag{4.174}$$

The outgoing heat at the point $x + \delta x$ is

$$\delta Q_x = -\delta y \delta z \left[\lambda(T) \frac{\partial T}{\partial x} + \frac{\partial}{\partial x} \left(\lambda(T) \frac{\partial T}{\partial x} \delta x \right) \delta t \right]. \tag{4.175}$$

Similar formulas can be derived for the other directions. The change of internal energy inside the control volume during time δt is

$$\delta U = \rho c_p \delta x \delta y \delta z \frac{\partial T}{\partial t} \delta t \tag{4.176}$$

and the heat generation inside the control volume is

$$\delta Q_g = Q_g''' (T)\, \delta x \delta y \delta z \delta_t. \tag{4.177}$$

From the first law of thermodynamics,

$$\delta Q_x + \delta Q_y + \delta Q_z + \delta Q_g = \delta Q_{x+\delta x} + \delta Q_{y+\delta y} + \delta Q_{z+\delta z} + \delta U. \tag{4.178}$$

Substituting Eq. (4.175) and the formulas for other directions into Eq. (4.178) gives

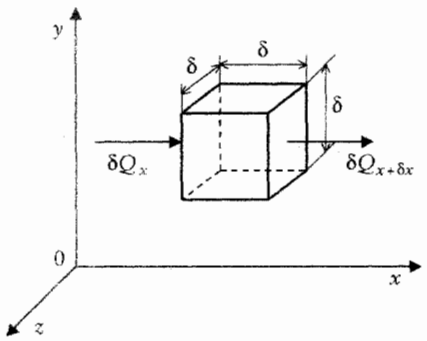

FIGURE 4.27 Control volume.

$$\frac{\partial}{\partial x}\left(\lambda(T)\frac{\partial T}{\partial x}\right)+\frac{\partial}{\partial y}\left(\lambda(T)\frac{\partial T}{\partial y}\right)+\frac{\partial}{\partial z}\left(\lambda(T)\frac{\partial T}{\partial z}\right)+Q_g'''(T)=\rho c_p\frac{\partial T}{\partial t}\ . \quad (4.179)$$

It is normal to assume that the thermal conductivity is constant; hence Eq. (4.179) gives

$$\frac{\partial^2 T}{\partial x^2}+\frac{\partial^2 T}{\partial y^2}+\frac{\partial^2 T}{\partial z^2}+\frac{Q_g'''}{\lambda}=\frac{1}{a}\frac{\partial T}{\partial t}\ , \quad (4.180)$$

or

$$\frac{\partial T}{\partial t}=a\nabla^2 T+H\ , \quad (4.181)$$

where

$\partial T/\partial t$ is the derivative of temperature as a function of time; in a steady-state case it is equal to zero

$a=\lambda/\rho c_p$, the heat conductivity or thermal diffusivity

$H=\Phi'''/C'''$ = heat generation inside a material; for example, for Joule's heat or a nuclear reaction, Φ''' = heat generation/volume and $C'''=c_p\rho$ = heat capacity/volume

For Cartesian coordinates

$$\nabla^2 T=\frac{\partial^2 T}{\partial x^2}+\frac{\partial^2 T}{\partial y^2}+\frac{\partial^2 T}{\partial z^2}\ ,$$

for cylindrical coordinates

$$\nabla^2 T=\frac{\partial^2 T}{\partial r^2}+\frac{1}{r}\frac{\partial^2 T}{\partial r}+\frac{1}{r^2}\frac{\partial^2 T}{\partial \phi^2}+\frac{\partial^2 T}{\partial z^2}\ ,$$

and for spherical coordinates

$$\nabla^2 T=\frac{1}{r}\frac{\partial^2 rT}{\partial r^2}+\frac{1}{r^2\sin\psi}\frac{\partial}{\partial\psi}\left(\sin\psi\frac{\partial T}{\partial\psi}\right)+\frac{1}{r^2\sin^2\psi}\frac{\partial^2 T}{\partial\phi^2}\ .$$

See Fig. 4.28.

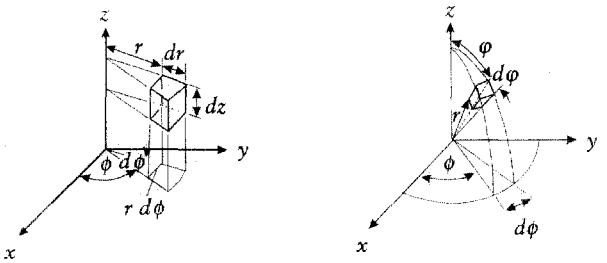

FIGURE 4.28 Cylindrical and spherical coordinates.

4.3.3.2 One-Dimensional Steady-State Heat Conduction

Infinite Plate

A simple case of heat conduction is a plate of finite thickness but infinite in other directions. If the temperature is constant around the plate, the material is assumed to have a constant thermal conductivity. In this case the linear temperature distribution and the heat flow through the plate is easy to determine from Fourier's law (Eq. (4.154)).

In a case similar to Fig. 4.23 the heat conduction equation (Eq. (4.180)) becomes

$$\frac{\partial^2 T}{\partial x^2} = 0. \tag{4.182}$$

In steady-state conditions the right side of Eq. (4.180) is zero, and no heat generation takes place; the thermal conductivity in the one-dimensional case is constant.

The solution of Eq. (4.182) is

$$T = C_1 x + C_2, \tag{4.183}$$

with boundary conditions

$$T = T_1 \quad \text{when } x = x_1$$
$$T = T_2 \quad \text{when } x = x_2$$

This gives the linear temperature distribution

$$T = T_1 + (T_2 - T_1)\frac{x - x_1}{x_2 - x_1} \tag{4.184}$$

Substituting the above equation into Eq. (4.154) gives the heat flow through the plate:

$$q = -\lambda \frac{\partial T}{\partial x} = \lambda \frac{T_1 - T_2}{x_2 - x_1} = \lambda \frac{T_1 - T_2}{\Delta x}. \tag{4.185}$$

Axial-Symmetric Case

For the axial-symmetric case the equation is

$$\nabla^2 T = \frac{\partial^2 T}{\partial r^2} + \frac{1}{r}\frac{\partial T}{\partial r} + \frac{1}{r^2}\frac{\partial^2 T}{\partial \phi^2} + \frac{\partial^2 T}{\partial z^2}. \tag{4.186}$$

In the one-dimensional case

$$\frac{d^2T}{dr^2} + \frac{1}{r}\frac{dT}{dr} = 0. \tag{4.187}$$

The solution of Eq. (4.187) is

$$T = C_1 \ln r + C_2, \tag{4.188}$$

with boundary conditions

$$T = T_1 \quad \text{when } r = r_1$$

$$T = T_2 \quad \text{when } r = r_2$$

The logarithmic temperature distribution is

$$T = T_1 + (T_2 - T_1)\frac{\ln\frac{r}{r_1}}{\ln\frac{r_2}{r_1}}. \tag{4.189}$$

Thus the heat flow per a unit of length Φ' is

$$\Phi' = -\lambda 2\pi r\frac{dT}{dr} = \lambda 2\pi\frac{T_1 - T_2}{\ln\frac{r_2}{r_1}}. \tag{4.190}$$

4.3.4 Heat Convection

The mathematical principles of convective heat transfer are complex and outside the scope of this section. The problems are often so complicated that theoretical handling is difficult, and full use is made of empirical correlation formulas. These formulas often use different variables depending on the research methods. Inaccuracy in defining material characteristics, experimental errors, and geometric deviations produce noticeable deviations between correlation formulas and practice. Near the validity boundaries of the equations, or in certain unfavorable cases, the errors can be excessive.

The general forms of the convection equations are given below in a simple form. More accurate equations can be found from the latest research results presented in technical journals.

The general equation for the case of forced convection is Nu $= f$(Re, Pr). In the case of free convection it is Nu $= f$(Gr, Pr).

$$\text{Nu} = \text{Nusselt number} = \frac{\alpha L}{\lambda}$$

$$\text{Gr} = \text{Grashof number} = \frac{g\vartheta L^3}{\nu^2}$$

$$\vartheta = \frac{\Delta v}{v_\infty} = \alpha_v \Theta \qquad \Theta = T_p - T_\infty$$

where T_p is the surface temperature.

$$\alpha_v = \frac{1}{v}\left(\frac{\partial V}{\partial T}\right)_p$$

$$\text{Pr} = \text{Prandtl number} = \frac{\nu}{a}\frac{\nu C_p \rho}{\lambda}$$

$$\text{Re} = \text{Reynolds number} = \frac{wL}{\nu}$$

The characteristic length L denotes the pipe diameter or the hydraulic diameter $d_{\text{hyd}} = 4A/P$ (A is the cross-sectional area and P is the wet periphery). If the cross-section is not circular, or in the case of a plane, the length is measured in the flow direction.

The temperature changes taking place through the surface of an exothermic body depend on the material characteristics and changes in the parameters. In formulas involving convection, either the solid surface temperature or the heat flow from the surface is assumed to be constant. The temperature θ defines the material characteristics (c, ρ, ν, etc.). Normally this temperature is the mixed temperature of the flowing fluid. The mean temperature of the boundary layer is the average temperature of the surface temperature and the undisturbed flow ($T_m = (T_p + T_\infty)/2$). Sometimes the boundary layer temperature, which is the average of the mixing temperature and the surface temperature, is used.

4.3.3.3 Calculation Using the Correlation Formulas

First the dimensionless characteristics such as Re and Pr in forced convection, or Gr and Pr in free convection, have to be determined. Depending on the range of validity of the equations, an appropriate correlation is chosen and the Nu value calculated. The equation defining the Nusselt number is

$$\text{Nu} = \frac{\alpha L}{\lambda} \tag{4.191}$$

given the heat transfer factor α. Using the equation

$$q = \frac{\Phi}{A} = \alpha\Theta, \tag{4.192}$$

the heat flow density is determined, which represents a certain temperature difference or the temperature difference between the wall and the fluid for a certain heat flow rate.

As an example, for free convective heat transfer from a vertical wall,

$$\text{Nu} = 0.13 \cdot (\text{Gr Pr})^{1/3} = 0.13 \cdot \left(\frac{g\vartheta L^3}{\nu^2}\text{Pr}\right)^{1/3}. \tag{4.193}$$

Equations (4.191), (4.192), and (4.193) give

$$q = 0.13\lambda\left(\frac{g\vartheta}{\nu^2}\text{Pr}\right)^{1/3}\Theta. \tag{4.194}$$

This equation does not incorporate the characteristic length L; hence the wall height has no influence on heat transfer.

In problems of forced convection, it is usually the cooling mass flow that has to be found to determine the temperature difference between the cooling substance and the wall for a given heat flow. In turbulent pipe flow, the following equation is valid:

$$\mathrm{Nu} = 0.0395\mathrm{Re}_d^{3/4}\mathrm{Pr}^{1/3} = \frac{qd}{\lambda\Theta}. \tag{4.195}$$

The mass flow is found using the continuity equation $\dot{m} = \rho w \pi d^2/4$ and the Reynolds number formula $\mathrm{Re} = 4\dot{m}/(\pi\rho\, d\nu)$:

$$\dot{m} = \frac{\pi\rho\, d\nu}{4}\left(\frac{qd}{0.0395\mathrm{Pr}^{1/3}\Theta\lambda}\right)^{4/3}. \tag{4.196}$$

In some convection equations, such as for turbulent pipe flow, a special correction factor is used. This factor relates to the heat transfer conditions at the flow inlet, where the flow has not reached its final velocity distribution and the boundary layer is not fully developed. In this region the heat transfer rate is better than at the region of fully developed flow.

The reason the heat transfer is improved can be seen from the equations $\mathrm{Nu} = \alpha s/\lambda$ (where s is the thickness of the boundary layer) and $q = \alpha\Theta$, giving

$$q = \frac{\mathrm{Nu}\lambda\Theta}{s} \tag{4.197}$$

Thin boundary layers provide the highest values of heat flow density. Because the boundary layer gradually develops upstream from the inlet point, the heat flow density is highest at the inlet point. Heat flow density decreases and achieves its final value in the region of fully developed flow. The correction is noted in the equations by means of the quotients d/L and d/x.

For some fluids, such as oils, the viscosity is temperature dependent. Here the correction factor $(\eta_F/\eta_w)^{0.14}$ is used, where η_F is the viscosity at the mean fluid temperature and η_w is the viscosity at the wall temperature.

4.3.3.4 Forced Convection

In this section the correlations used to determine the heat and mass transfer rates are presented. The convection process may be either free or forced convection. In free convection fluid motion is created by buoyancy forces within the fluid. In most industrial processes, forced convection is necessary in order to achieve the most economic heat exchange. The heat transfer correlations for forced convection in external and internal flows are given in Tables 4.8 and 4.9, respectively, for different conditions and geometries.

The mass transfer correlations are obtained by replacing Nu by Sh and Pr by Sc according to the heat and mass transfer analogy.

TABLE 4.8 Heat Transfer Correlations for External Flow

Geometry	Conditions	Correlation
Flat plate	Laminar, local, T_{av} $Pr \geq 0.6$, $Re_x < 10^5$	$Nu_x = 0.332\ Re_x^{1/2}\ Pr^{1/3}$
	Laminar, average, T_{av} $Pr \geq 0.6$, $Re_x < 10^5$	$\overline{Nu}_x = 0.664\ Re_x^{1/2}\ Pr^{1/3}$
	Turbulent, local, T_{av} $60 \geq Pr \geq 0.6$ $Re_x \leq 10^8$	$Nu_x = 0.0296\ Re_x^{1/2}\ Pr^{1/3}$
	Mixed, average, T_{av} $60 > Pr > 0.6$, $Re_x \leq 10^8$	$\overline{Nu}_x = (0.037\ Re_x^{4/5} - 871)\ Pr^{1/3}$
	Fully turbulent, average, T_{av} $5\times10^5 < Re_x < 10^8$	$\overline{Nu}_x = 0.037\ Re_x^{4/5}\ Pr^{1/3}$
Cylinder	Average, T_∞, $Pr > 0.7$ $0.4 < Re_d < 4\times10^5$	$\overline{Nu}_d = C\ Re_d^m\ Pr^{1/3}$ C and m are given in Table 4.10
	Average, T_∞, $500 > Pr > 0.7$ $1 < Re_d < 10^6$	$\overline{Nu}_d = C\ Re_d^m\ Pr^n \left(\frac{Pr_\infty}{Pr_s}\right)^{1/4}$ C and m are given in Table 4.11
	Average, T_{av} $Re_d\ Pr > 0.2$	$\overline{Nu}_d = 0.3 + \frac{0.62\ Re_d^{1/2}\ Pr^{1/3}}{\left[1+\left(\frac{0.4}{Pr}\right)^{2/3}\right]^{1/4}} \times \left[1+\left(\frac{Re_d}{28\ 200}\right)^{5/8}\right]^{4/5}$
Sphere	Average, T_∞, $380 > Pr > 0.71$ $3.5 < Re_d < 7.6\times10^4$ $1 < \frac{\mu_\infty}{\mu_S} < 3.2$	$\overline{Nu}_d = 2 + (0.4\ Re_d^{1/2} + 0.06\ Re_d^{2/3}) \times Pr^{0.4}\left(\frac{\mu_\infty}{\mu_s}\right)^{1/4}$
Falling drop	Average, T_∞	$\overline{Nu}_d = 2 + 0.6\ Re_d^{1/2}\ Pr^{1/3}\left[25\left(\frac{x}{d}\right)^{-0.7}\right]^{1/4}$

Note: $T_{av} = 0.5(T_\infty + T_s)$, where T_∞ is the free stream temperature and T_s is the surface temperature.

4.3.3.5 Free Convection

Flow up a Vertical Wall

$$Nu_l = \left\{0.825 + \frac{0.387(Gr\ Pr)^{1/6}}{\left(1+\left(\frac{0.492}{Pr}\right)^{9/16}\right)^{8/27}}\right\}^2, \tag{4.198}$$

valid for $Gr_l Pr < 10^{12}$

$$T_{st} = 0.5(T_\infty + T_p)$$

Flow Upward on a Horizontal Plane

$$\begin{aligned} Nu_l &= 0.70(Gr\ Pr)^{1/4} \quad Gr\ Pr < 4\times10^7 \\ Nu_l &= 0.155(Gr\ Pr)^{1/3} \quad Gr\ Pr > 4\times10^7 \end{aligned} \tag{4.199}$$

$$T_{st} = 0.5(T_\infty + T_p)$$

TABLE 4.9 Heat Transfer Correlations for Internal Flow

Conditions	Correlation
Laminar, fully developed, T_m, $q_s'' = cst$, $\text{Pr} > 0.6, \text{Re}_d < 2300$	$\text{Nu}_d = 4.36$
Laminar, fully developed, T_m, $T_s = cst$, $\text{Pr} > 0.6, \text{Re}_d < 2300$	$\text{Nu}_d = 3.66$
Laminar, thermal entry length $\overline{T}_m$, $T_s = cst$, $\text{Pr} >> 1$ or unheated starting length	$\overline{\text{Nu}}_d = 3.66 + \dfrac{0.0668\left(\dfrac{d}{L}\right)\text{Re}_d\text{Pr}}{1 + 0.04\left[\left(\dfrac{d}{L}\right)\text{Re}_d\text{Pr}\right]^{2/3}}$
Turbulent, fully developed, T_m, $160 > \text{Pr} > 0.6, \text{Re}_d > 2300, \dfrac{L}{d} > 10$	$\text{Nu}_d = 0.023\ \text{Re}_d^{4/5}\ \text{Pr}^{1/3}$
Turbulent, fully developed, T_m, $16\,700 > \text{Pr} > 0.7, \text{Re}_d > 10^4, \dfrac{L}{d} > 10$	$\overline{\text{Nu}}_d = 0.027\ \text{Re}_d^{4/5}\ \text{Pr}^{1/3}\left(\dfrac{\mu}{\mu_S}\right)^{0.14}$
Liquid metals, turbulent, fully developed, T_m, $q_s'' = cst$, $3.6 \times 10^3 < \text{Re}_d < 9.05 \times 10^5$, $10^2 < \text{Pe}_d < 10^4$	$\overline{\text{Nu}}_d = 4.82 + 0.0185(\text{Re}_d\ \text{Pr})^{0.827}$
Liquid metals, turbulent, fully developed, T_m, $T_s = cst$, $\text{Pe}_d > 100$	$\overline{\text{Nu}}_d = 5 + 0.025(\text{Re}_d\ \text{Pr})^{0.8}$

Note: T_m is the mean bulk temperature and $\overline{T}_m = 0.5(T_{m,\text{in}} + T_{m,\text{out}})$.

TABLE 4.10 Constants for External Flow Correlation

Re_d	C	m
0.4–4	0.989	0.33
4–400	0.911	0.385
40–4000	0.683	0.466
4000–40 000	0.193	0.618
40 000–400 000	0.027	0.805

TABLE 4.11 Constants for External Flow Correlation

Re_d	C	m
1–400	0.75	0.4
400–1000	0.51	0.5
10^3–2×10^5	0.26	0.6
2×10^5–10^6	0.076	0.7

Flow Past a Horizontal Pipe

$$\text{Nu}_d = \left\{0.825 + \frac{0.387(\text{Gr Pr})^{1/6}}{\left(1 + \left(\dfrac{0.492}{\text{Pr}}\right)^{9/16}\right)^{8/27}}\right\}^2, \tag{4.200}$$

valid for $\text{Gr}_d\text{Pr} < 10^{12}$

$$T_{\text{st}} = 0.5(T_\infty + T_p)$$

Example 2

Heat transfer coefficient between a pipe and a wall. Water flows in a pipe ($d_s = 15$ mm) with a velocity of $v = 1.0\ m\ s^{-1}$. The mean temperature of water is $\theta_m = 15\ °C$, and the wall temperature $\theta_s = 50\ °C$. Calculate the heat transfer coefficient away from the pipe inlet. For water the properties are $\eta_{15°C} = 1.14 \times 10^{-3}\ kg\ m^{-1}s^{-1}$, $\eta_{50°C} = 0.54 \times 10^{-3}\ kg\ m^{-1}s^{-1}$, $c_{p15°C} = 4.2\ kJ\ kg^{-1}K^{-1}$, and $\lambda_{15°C} = 0.60\ W\ m^{-1}K^{-1}$, with turbulent flow. The Nusselt number equation is

$$Nu_d = 0.037(Re^{0.75} - 180)Pr^{0.42}\left[1 + \left(\frac{d}{L}\right)^{2/3}\right]\left(\frac{\eta_F}{\eta_W}\right)^{0.14} \tag{4.201}$$

$$Re = \frac{vd}{\nu} = \frac{vd\rho}{\eta} = \frac{1.0\frac{m}{s} \times 0.015m \times 1000\ \frac{kg}{m^3}}{1.14 \cdot 10^{-3}\ \frac{kg}{ms}} = 1.32 \times 10^4$$

$$Pr = \frac{\eta c_p}{\lambda} = \frac{1.14 \times 10^{-3} \cdot 4200}{0.6\ \frac{W}{m\,K}} = 7.98$$

The flow is turbulent, $Re > 2300$, and thus the part of Eq. (4.201) that considers the inlet flow region ≈ 1 can be ignored.

$$Nu_d = 0.037(Re^{0.75} - 180)Pr^{0.42}\left(\frac{\eta_F}{\eta_W}\right)^{0.14}$$

$$= 0.037((1.32 \times 10^4) - 180) \times 7.98^{0.42}\left(\frac{1.14}{0.54}\right)^{0.14} = 103.3$$

$$Nu_d = \frac{\alpha d}{\lambda} \Rightarrow \alpha = \frac{Nu_d \lambda}{d} = \frac{103.3 \times 0.60\ \frac{W}{m\,K}}{0.015} = 4100\ \frac{W}{m^2\,K}$$

4.3.5 Thermal Radiation

4.3.5.1 Planck's Law of Radiation

Total heat transfer consists of radiation at different frequencies. The distribution of radiation energy in a spectrum and its dependency on temperature is determined from Planck's law of radiation. $M_{m\nu}$ and $M_{m\lambda}$ are the spectral radiation intensities for a blackbody:

$$M_{m\nu} = \frac{2\pi h \nu^3}{c^2\left(\exp\left(\frac{h\nu}{\lambda T}\right) - 1\right)} = f(\nu, T) \tag{4.202}$$

$$M_{m\lambda} = \frac{2\pi h c^2}{\left(\exp\left(\frac{hc}{\lambda T}\right) - 1\right)} = \frac{\frac{c_1}{\lambda^5}}{\exp\left(\frac{c_2}{\lambda T}\right) - 1} = f(\lambda, T) \tag{4.203}$$

where

h = Planck's constant = 3.99028×10^{-7} J s/kmol = 6.6252×10^{-34} J s

c = velocity of light = 2.9979×10^{8} m/s

c_1 = first radiation constant = $2\pi hc^2 = 3.7415 \times 10^{-16}$ W m^2

c_2 = second radiation constant = $hc = 119.626\ \mu\text{m}\dfrac{\text{MJ}}{\text{kmol}}$
= 14387.9 μm K

When these are derived with respect to the wavelength, and the wavelength value, with the maximum value of radiation intensity, is solved for, the result is Wien's law:

$$\begin{aligned}\lambda_{\max} \cdot T &= \text{constant} \\ &= 2898\ \mu\text{m K} \\ &= 24\ 093\ \mu\text{m kJ/kmol}\end{aligned} \tag{4.204}$$

According to Wien's law, the wavelength representing the maximum point decreases with increasing temperature (Fig. 4.29).

The visible region of the spectrum lies between the wavelengths of 0.4 and 0.7 μm. When the temperature of a body is increased, its color changes toward smaller wavelengths—in other words, from the red region of the spectrum to the blue region.

4.3.5.2 Emissivity and Absorption

Suppose two objects are in a hollow (Fig. 4.30): object A, which is black, and object B, which is gray (a body that does not absorb all the incoming radiation). The energy and mass are in balance when the temperatures of A, B, and C are equal. In the balanced state the radiation emitted by the bodies is equal to the radiation received.

The radiation density in C is in constant balance at all points and in all directions (for a given frequency). The radiation density is

$$L = \frac{d\Phi}{dA\ d\omega} \tag{4.205}$$

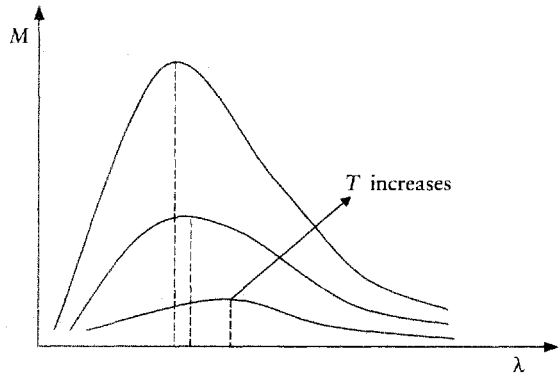

FIGURE 4.29 Radiation intensity of a blackbody as a function of wavelength (temperature parameter).

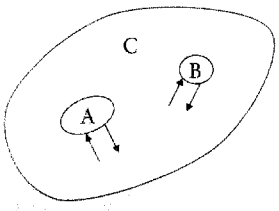

FIGURE 4.30 Radiative bodies.

when the radiant energy $d\Phi$ passes through a surface element dA in the direction of its normal vector, in a space angle element $d\omega$.

For a black object,

$$L_\nu \, d\nu = L_{m\nu} \, d\nu \Rightarrow L_\nu = L_{m\nu}. \tag{4.206}$$

A gray object absorbs only part of the incoming radiation: incoming $= \alpha L_\nu \, d_\nu =$ outgoing $= \epsilon L_{m\nu} \, d\nu$.

From Kirchhoff's law,

$$\alpha(\nu, T, \vartheta) = \epsilon(\nu, T, \vartheta) \tag{4.207}$$

absorption ratio = emissivity

ϑ = direction angle to the surface normal

The radiation intensity from a surface to a semispace is temperature dependent on

$$\varphi_{\text{emis}} = \epsilon M_m = \int e(\nu) M_{m\nu} \, d\nu \tag{4.208}$$

$$M_m = \sigma T^4$$

$$\sigma = 5.67032 \times 10^{-8} \frac{\text{W}}{\text{m}^2 \, \text{K}^4}, \text{ the Stefan-Boltzmann constant.}$$

The radiation intensity absorbed by the surface is

$$\varphi_{\text{abs}} = \alpha E = \int \alpha(\nu) E_\nu \, d\nu \tag{4.209}$$

E = radiation intensity = incoming Φ/A.

Emissivity is strongly dependent on the surface quality. The emissivity of a rough surface is greater than that of a smooth surface, increasing the rate of absorption. Emissivity values are found in textbooks. Care must be taken when using these values, as they usually denote total emissivities. The emissivity is considered constant in the spectrum, and this may be a poor approximation.

For example, the emissivity of white paper is high (≈ 0.93) at room temperature and, according to Kirchhoff's law, the absorption factor at the same temperature is also high. At relatively low temperature, as in this case, the radiation is concentrated in the long wavelengths, according to Wien's law. However, when the same paper receives radiation from the sun, at a radiation temperature of 6000 K, when the absorption factor is small, this radiation has a short wavelength. A white object is a good reflector; this is why white clothing is used in the tropics.

When a low-temperature heating radiator is painted, the color is selected according to heat radiation. At this relatively low temperature, the radiation lies almost outside the visible region. The color may be deceptive. Snow is a good reflector of visible radiation; still, its total emissivity and therefore its absorption in normal conditions is as high as 0.98. Visible radiation passes through glass; its emissivity at the temperature 20 °C is 0.98. Glass radiation lies within the 300–2800 nm range. An important feature of glass is that it is opaque to longwave radiation, which is produced by low-temperature emitters. It is this phenomenon that is termed the greenhouse effect.

The radiation emitted by the sun, due to its high temperature, has a short wavelength. Glass is transparent at this wavelength, allowing the radiation to pass through into the interior of the building. This energy is absorbed by the room surfaces, causing them to rise in temperature and to become low-temperature emitters. The radiation from these low-temperature surfaces is longwave, to which glass is opaque, and thus the radiation cannot escape through the glass to the outdoors, resulting in a rise in the space temperature. The transmission of radiation through the glass depends on the spectral characteristics of the nature of the glass.

Example 3

Silica glass transmits 92% of the radiation in the wavelength region of 0.3–2.7 μm, and it is impervious to other radiation. Determine the wavelength of the sun's radiation that the glass transmits when the sun is treated as a blackbody, $T = 5600$ K. What happens for a blackbody at a temperature of 295 K?

According to Eq. (4.204), at the median point of the spectral energy, λ_{50}, $T = 4107$ μm K, and therefore the median point of the spectral energy of the sun is

$$\lambda_{50} = 4107 \ \mu\text{m K}/5600 \ \text{K} = 0.733 \ \mu\text{m}$$

Calculations using Planck's radiation law show which part of the radiation energy remains in the wavelength range:

$$\lambda_{50}/\lambda_1 = 0.733/0.35 = 2.095 \longrightarrow \frac{1}{M}\int_0^{\lambda} M_\lambda d\lambda = 0.06$$

$$\lambda_{50}/\lambda_2 = 0.733/2.7 = 0.2716 \longrightarrow \frac{1}{M}\int_0^{\lambda} M_\lambda d\lambda = 0.97$$

Thus 97% – 6% = 91% of the radiation energy lies in the range, and the silica glass transmits 91% · 92% = 83.7% of the radiation energy.

4.3.5.3 Lambert's Cosine Law

The radiation power in the direction of the normal vector to the surface dA in a space angle $d\omega$ (see Fig. 4.31) is

$$d\Phi = L \, dA \, d\omega \tag{4.210}$$

and in the direction ϑ,

$$d\Phi = L \, dA \cos\vartheta \, d\omega, \tag{4.211}$$

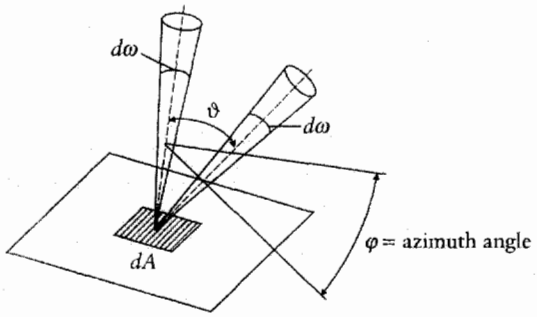

FIGURE 4.31 Direction and nature of incident radiation.

where $dA \cos \vartheta$ is the projection surface of the opening in the direction concerned. Thus the radiation power is distributed to different directions at a ratio of $\cos \vartheta$. This is the cosine law of Lambert. It is valid for a blackbody and approximately valid for insulating materials, but it cannot be used for bright metal surfaces.

Substituting in Eq. (4.211) gives

$$d\omega = d\varphi \sin\vartheta \, d\vartheta = d\varphi \, d(\cos\vartheta) \tag{4.212}$$

and integrating for the radiation intensity to the semispace by a blackbody gives

$$d\Phi = M_m \, dA = \pi L_m \, dA, \tag{4.213}$$

where $M_m = \pi L_m = \sigma T^4$.

4.3.5.4 Thermal Radiation inside a Vacuum (without Gas)

Surface element dA_j is located on the spatial surface A_j sending radiation to the surface A_i. The radiation power from the surface element dA_j to the element dA_i according to Eq. (4.211) is

$$d\Phi_{ji} = L_j(\omega_j) dA_j \cos \vartheta_j \, d\omega_j. \tag{4.214}$$

The solid angle $d\omega_j = dA_i \cos \vartheta_i / r^2$. Equation (4.211) gives

$$\frac{d\Phi_{ji}}{dA_i} = L(\omega_j) \frac{\cos \vartheta_i \, \vartheta_j}{r^2} = dA_i = dE_{ij}, \tag{4.215}$$

where E_{ij} is the proportion of the radiation from dA_j relative to the radiation intensity of dA_i. If Lambert's cosine law is valid, L is not dependent on direction and

$$\pi L_j = M_j. \tag{4.216}$$

Thus

$$dE_{ij} = M_j \frac{\cos \vartheta_i \cos \vartheta_j}{\pi r^2} \, dA_i \tag{4.217}$$

$$dE_{ij} = M_j \varphi_{ij} \, dA_j. \tag{4.218}$$

The visibility factor of the surface element φ_{ij} depends on the geometry and gives that part of the radiation intensity of dA_j that falls directly on the surface dA_i or vice versa.

The radiation intensity of a surface element is the sum of emission and reflection:

$$M_i = \epsilon_i M_{mi} + \rho_i E_i, \tag{4.219}$$

where ρ = reflectance and

$$E_i = \int_{A_j} \varphi_{ij} M_j \, dA_j, \tag{4.220}$$

giving an integral formula for the radiation intensity function,

$$M_i = \epsilon_i M_{mi} + \rho_i \int_{A_j} \varphi_{ij} M_j \, dA_j. \tag{4.221}$$

Equation (4.221) is difficult to solve, and for practical cases approximate methods are used.

Usually the surface is divided into zones, and with sufficient accuracy M is considered constant over this area, giving

$$M_i = \epsilon_i M_{mi} + \rho_i \sum M_k f_{ik}, \tag{4.222}$$

where

$$f_{ik} = \int_{A_k} \phi_{ik} \, dA_k \tag{4.223}$$

Also, by integration,

$$M_l A_l = \int_{A_l} M_l \, dA_l = \epsilon_i A_l M_{mi} + \rho_i \sum M_k A_l F_{kl}, \tag{4.224}$$

where

$$F_{kl} = \frac{1}{A_l} \int_{A_l} f_{lk} \, dA_l = \frac{1}{A_l} \int_{A_l} \int_{A_k} \varphi_{lk} \, dA_k \, dA_1 \tag{4.225}$$

F_{kl} is the visibility factor between two finite surfaces, and $A_l F_{kl} = A_{kl}$ is the geometrical radiation surface. Equation (4.225) shows that the geometrical radiation surface is symmetric and therefore

$$A_{kl} = A_{lk}. \tag{4.226}$$

Integrated over the semispace, the integrals (4.223) are 1. Thus in the hollow,

$$\sum F_{kl} = 1 \quad \text{and} \quad \sum A_{kl} = A_k. \tag{4.227}$$

This sum includes all the hollow surfaces and also the surface k, if it is concave, in which case the portion F_{kk} of the received radiation is reflected back.

The net radiation power falling the surface is the difference between the incoming and outgoing radiation and the difference between absorption and emission:

$$\frac{\Phi_{\text{net}}}{A} = q = E - M = \alpha E - \epsilon M_m. \tag{4.228}$$

Eliminating E when $\epsilon = \alpha$,

$$q = \left(M - \frac{M_m \epsilon}{\alpha} \right) \frac{\alpha}{\rho} = \frac{\epsilon}{\rho} (M - M_m) \, . \tag{4.229}$$

For direct net radiation between two blackbodies (from Eq. (4.220)),

$$\Phi_{12\text{net}} = (M_{m1} - M_{m2})A_{12} = A_{12}\sigma(T_1^4 - T_2^4) \,. \tag{4.230}$$

Radiation heat transfer in a hollow can be represented by electrical analogy as

$$\Phi_{\text{net}} = qA = \frac{\alpha}{\rho}A\left(M - \frac{\epsilon}{\alpha}M_m\right) = G(M - U) \tag{4.231}$$

$$\text{current} = \text{conductance} \times \text{potential difference}$$

where $(\epsilon/\alpha)M_m = U$ = radiation potential, which is dependent on the temperature; ϵ is dependent on the radiation properties of the surface and the temperature; and α is dependent on the spectrum of the incoming radiation. $(\alpha/\rho)A = G$ = radiation conductance between the potentials U and M.

For a gray body

$$\Phi = G(M - U)$$

When the surface is black, $G = \infty$ or $R = 0$, while $\alpha = 1$ and $\sigma = 0$; points U and M unite and the potential is M_m.

When the surface is thermally insulated, $\Phi_{\text{net}} = 0$. Points U and M unite and the potential is $M = (\epsilon/\alpha)M_m = UE = M$.

For two surfaces, $\Phi_{ij\,\text{net}} = E_{ij}A_i - E_{ji}A_j = A_{ji}(M_j - M_i)$, so by analogy A_{ij} is the radiation conductance between potentials M_i and M_j (see Fig. 4.32).

When there are only two surfaces in the hollow, the net thermal radiation is

$$\Phi_{12} = G(U_1 - U_2) = \frac{U_1 - U_2}{\frac{1}{G_1} + \frac{1}{A_{12}} + \frac{1}{G_2}} = \frac{\frac{\epsilon_1}{\alpha_1}M_{m1} - \frac{\epsilon_2}{\alpha_2}M_{m2}}{\frac{\rho_1}{\alpha_1 A_1} + \frac{1}{A_{12}} + \frac{\rho_2}{\alpha_2 A_2}} \,. \tag{4.232}$$

If surface 1 is convex or planar, all the incoming radiation is from surface 2, and $F_{12} = 1$, while the visibility factor expresses that part of radiation coming from this surface. If surface 2 is concave, a part of the radiation is also from this surface.

$$A_1F_{12} = A_{12} = A_{21} = A_2F_{21} = A_1$$

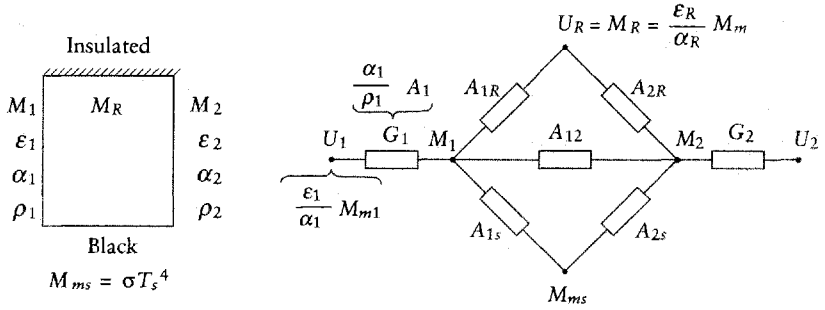

FIGURE 4.32 Radiation net for a hollow with four surfaces.

$$q_1 = \frac{\Phi_{12}}{A_1} = \frac{\frac{\epsilon_1}{\alpha_1} M_{m1} - \frac{\epsilon_2}{\alpha_2} M_{m2}}{\frac{\rho_1}{\alpha_1} + 1 + \frac{\rho_2}{\alpha_2}\frac{A_1}{A_2}}. \tag{4.233}$$

When $\rho_1 = 1 - \alpha_1$,

$$q_1 = \frac{\frac{\epsilon_1}{\alpha_1} M_{m1} - \frac{\epsilon_2}{\alpha_2} M_{m2}}{\frac{1}{\alpha_1} + \frac{\rho_2}{\alpha_2}\frac{A_1}{A_2}}. \tag{4.234}$$

Equation (4.234) is valid for two coaxial cylinders and spheres. If $A_2 >> A_1$, $\alpha_2 \approx \epsilon_2$, as almost all the radiation from surface 2 is reflected back to it.

$$q_1 = M_{m1}\epsilon_1 - M_{m2}\alpha_1. \tag{4.235}$$

For two planes whose dimensions are large compared with the distance between them,

$$F_{12} = F_{21} = 1 \qquad A_{12} = A_1 = A_2$$

$$q = \frac{\frac{\epsilon_1}{\alpha_1} M_{m1} - \frac{\epsilon_2}{\alpha_2} M_{m2}}{\frac{\rho_1}{\alpha_1} + 1 + \frac{\rho_2}{\alpha_2}} = \frac{\frac{\epsilon_1}{\alpha_1} M_{m1} - \frac{\epsilon_2}{\alpha_2} M_{m2}}{\frac{1-\alpha_1}{\alpha_1} + 1 + \frac{1-\alpha_2}{\alpha_2}} = \frac{\frac{\epsilon_1}{\alpha_1} M_{m1} - \frac{\epsilon_2}{\alpha_2} M_{m2}}{\frac{1}{\alpha_1} + \frac{1}{\alpha_2} - 1}. \tag{4.236}$$

It is difficult to estimate the absorption ratio. Approximately $\alpha_1 = \epsilon_1(T_2)$ and $\alpha_2 = \epsilon_2(T_1)$.

When the absorption relations are not dependent on temperature, the following approximations can be used ($\alpha = \epsilon =$ constant $= 1 - \rho$). For two coaxial cylinders and spheres,

$$q = \frac{M_{m1} - M_{m2}}{\frac{1-\epsilon_1}{\epsilon_1} + 1 + \frac{1-\epsilon_2}{\epsilon_2}\frac{A_1}{A_2}} = \frac{M_{m1} - M_{m2}}{\frac{1}{\epsilon_1} + \frac{A_1}{A_2}\left(\frac{1}{\epsilon_2} - 1\right)}. \tag{4.237}$$

For two parallel planes, $A_1 \approx A_2$,

$$q = \frac{M_{m1} - M_{m2}}{\frac{1}{\epsilon_1} + \frac{1}{\epsilon_2} - 1}. \tag{4.238}$$

When $A_2 >> A_1$,

$$q = \epsilon_1(M_{m1} - M_{m2}). \tag{4.239}$$

In HVAC technology the following formula is used for small temperature differences with sufficient accuracy (see Fig. 4.33):

$$q_t = \alpha_s \Delta T \approx \epsilon_1 \alpha_{mu} \Delta T. \tag{4.240}$$

Example 4

Radiation heat transfer. The radiation heat transfer between two parallel planes is reduced by placing a parallel aluminum sheet in the middle of the gap. The surface temperatures are $\theta_1 = 40$ °C and $\theta_2 = 5$ °C, respectively; the emissivities are $\epsilon_1 = \epsilon_2 = 0.85$. The emissivity of both sides of the aluminum

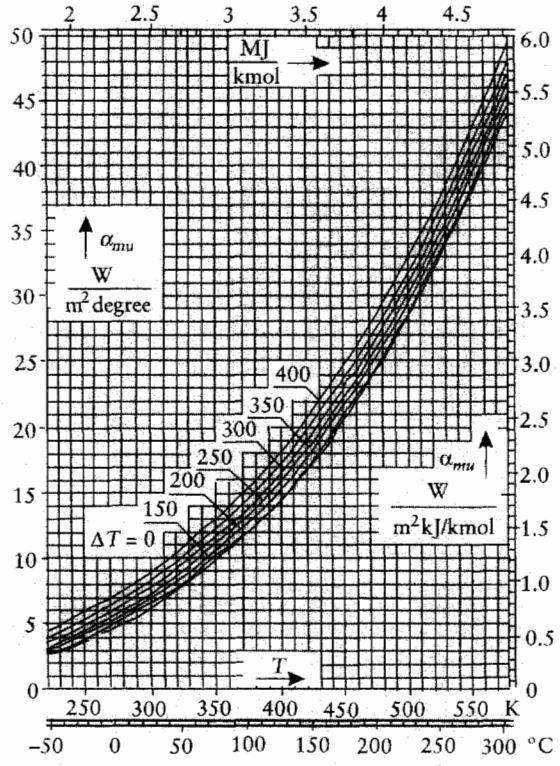

FIGURE 4.33 Heat transfer factor representing blackbody radiation for various mean temperatures and temperature differences.

is $\epsilon_a = 0.05$. Calculate by how much the radiation heat transfer is reduced due to the aluminum sheet; surface temperatures remain constant, and the surfaces are assumed to be gray.

Without the aluminum sheet,

$$q_{12} = \frac{M_{m1} - M_{m2}}{\frac{1}{\epsilon_1} + \frac{1}{\epsilon_2} - 1} = \frac{\sigma(T_1^4 - T_2^4)}{\frac{2}{\epsilon} - 1}$$

$$= \frac{5.27 \frac{\text{W}}{\text{m}^2 (100\ \text{K})^4} (3.13^4 - 2.78^4)(100\ \text{K})^4}{\frac{2}{0.85} - 1} = 151.9 \frac{\text{W}}{\text{m}^2}$$

$$A_{1a} = A_{a2} = \frac{1}{\frac{1}{\epsilon_1} + \frac{1}{\epsilon_a} - 1}.$$

With the aluminum,

$$q_{1a} = A_{1a}\sigma(T_1^4 - T_a^4) = q_{a2} = A_{a2}\sigma(T_a^4 - T_2^4) \quad \Rightarrow$$

$$T_a^4 = \frac{T_1^4 + T_2^4}{2} = \frac{313^4 + 278^4}{2} = 7.785 \times 10^9\ \text{K}^4\ .$$

Thus

$$q_{1a} = \frac{1}{\frac{1}{0.85} + \frac{1}{0.05} - 1} 5.67 \frac{\text{W}}{\text{m}^2(100\ \text{K})^4}(3.13^4 - 77.85)(100\ \text{K})^4 = 5.1 \frac{\text{W}}{\text{m}^2} .$$

Radiation heat transfer decreases by

$$1 - \frac{5.1}{151.9} \times 100\% = 96.6\% .$$

4.3.6 Mass Transfer Coefficient

Consider a binary mixture consisting of components A and B. If component A moves with a velocity of v_A and the component B with a velocity of v_B there is a force against the motion of component A that is proportional to the velocity difference $(v_A - v_B)$. This is the physical content of Fick's law in the steady-state condition.

$$j_A = -D_{AB} \frac{\partial c_A}{\partial z} , \tag{4.241}$$

where j_A is the molar flux density (mol/m^2 s), D_{AB} is the diffusion factor (m^2/s), c_A is the concentration of component A (mol/m^3), and z is a coordinate parallel to the flux (m). Note that $j_A = c_A v_A$. On the basis of the force and counterforce, $D_{AB} = D_{BA}$.

Note: Equation (4.241) characterizes diffusion when the mixture element is in steady state with no turbulence. Diffusion in a pipe can be represented by Eq. (4.241) in convective mass transfer; the flow and turbulence are important.

An important convective flow is created from vaporization alone, if no other component is absorbed from the gas and is replacing the vaporizing component. In drying technology, for example, the diffusion process is considered to be diffusion between water vapor (A) and dry air (B) (a mixture of nitrogen and oxygen), and only a small amount of dry air replaces the vaporized water, if the volume of the water in the form of liquid is very small. With good accuracy $j_B = 0$, and the diffusion caused by the concentration gradient $\partial c_B/\partial z$ is fulfilled with convective flow (Stefan flow) according to

$$j_B = -D_{BA} \frac{\partial c_B}{\partial z} + c_B v ,$$

where $c_B v$ represents the convective flow that cancels the diffusion. Therefore the Stefan flow is

$$v = \frac{D_{BA}}{c_B} \frac{\partial c_B}{\partial z} .$$

The net flow of component A with Stefan flow taken into consideration is

$$j_A = -D_{AB} \frac{\partial c_A}{\partial z} + c_A v = -D_{AB} \frac{\partial c_A}{\partial z} + \frac{c_A}{c_B} D_{BA} \frac{\partial c_B}{\partial z} .$$

With constant temperature $(c = c_A + c_B = \text{constant})$,

$$\frac{\partial c_A}{\partial z} + \frac{\partial c_B}{\partial z} = 0 \text{ and } D_{AB} = D_{BA}$$

giving

$$j_A = -D_{AB} \frac{c}{c - c_A} \frac{\partial c_A}{\partial z} . \tag{4.242}$$

Integrating Eq. (4.242) gives

$$j_A = \frac{D_{AB} \cdot c}{z} \ln \frac{c - c_{A2}}{c - c_{A1}} . \tag{4.243}$$

where z is the thickness of the diffusion layer, $c_{A2} = c_A(z = z)$, and $c_{A1} = c_A(z = 0)$.

By giving j_A a constant value, $c_A(z)$ can be calculated from Eq. (4.243) for different z values. The concentration c_B can then be calculated as $c_B(z) = c - c_A(z)$. The result is shown in Fig. 4.34.

Component A diffuses due to the concentration gradient $-\partial c_A / \partial_z$. Component B diffuses due to the mean molar velocity v, $v = (c_A v_A + c_B v_B)/c$, like a fish swimming upstream with the same velocity as the flowing water, $j_B = 0$, with regard to a fixed point.

In a distillation process the diffusion is nearer to the case $j_A = -j_B =$ constant or component B absorbs in place of the vaporizing component A, and now $j_B \neq 0$. If $j_A = -j_B$, the concentrations are similar to those presented in Fig. 4.35.

An integral equation consistent for this case is the integrated Eq. (4.21):

$$j_A = \frac{D_{AB}}{z}(c_{A1} - c_{A2}). \tag{4.244}$$

Figures 4.34 and 4.35 represent two extreme cases. Drying processes represent the case shown in Fig. 4.34 and distillation processes represent Fig. 4.35. Neither case represents a convective mass transfer case; while the gas flow is in the boundary layer, other flows are Stefan flow and turbulence. Thus Eqs. (4.243) and (4.244) can seldom be used in practice, but their forms are used in determining the mass transfer factor for different cases.

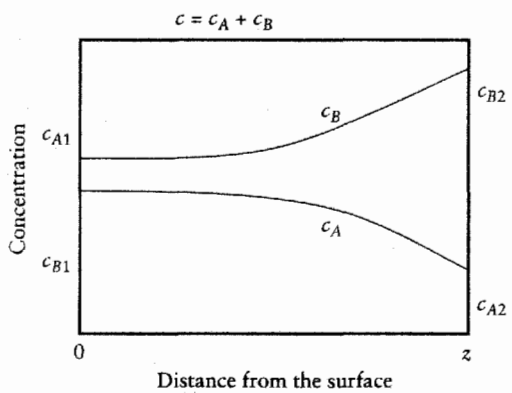

FIGURE 4.34 Diffusion of A through B when $j_B = 0$: semipermeable surface.

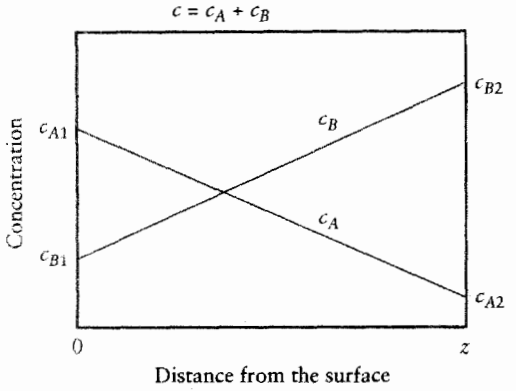

FIGURE 4.35 Diffusion with equal measures, $j_A = j_B$: fully permeable surface.

Considering the case of Eq. (4.244), it is normal to describe a real mass transfer case by taking into consideration the boundary layer flows and the turbulence by using a mass transfer factor k'_c, which is defined by

$$j_A = k'_c\,(c_{A1} - c_{A2})\,. \tag{4.245}$$

For Eq. (4.243), which can be written similar to Eq. (4.244) as

$$j_A = \frac{D_{AB}c}{z}\ln\frac{c_{B2}}{c_{B1}} = \frac{D_{AB}c\,\ln\frac{c_{B2}}{c_{B1}}}{z(c_{A1} - c_{A2})}\,(c_{A1} - c_{A2})$$

$$= \frac{D_{AB}c}{z}\,\frac{\ln\frac{c_{B2}}{c_{B1}}}{(c_{A1} - c_{A2})}\,(c_{A1} - c_{A2}),$$

it is seen that by defining a logarithmic concentration difference

$$c_{BM} = \frac{c_{B2} - c_{B1}}{\ln\frac{c_{B2}}{c_{B1}}}, \tag{4.246}$$

Eq. (4.243) can be written in an identical form:

$$j_A = \frac{D_{AB}c}{zc_{BM}}(c_{A1} - c_{A2})\,. \tag{4.247}$$

Based on this, it is normal to define a mass transfer factor consistent with this case, analogous with Eq. (4.245):

$$j_A = k_c(c_{A1} - c_{A2}) \tag{4.248}$$

Assuming that the relation of Eqs. (4.243) and (4.244) represents correctly the ratio of the real mass transfer flows, if it is valid that

$$\frac{j_A(j_B = 0)}{j_A(j_A = -j_B)} = \frac{j_A(\text{Eq. (4.243)})}{j_A(\text{Eq. (4.244)})},$$

with Eq. (4.237) and the equations defining the mass transfer factors, Eqs. (4.245) and (4.248) give

$$k_c = \frac{c}{c_{BM}} k_c'. \tag{4.249}$$

If the ideal gas law is used for the gases the concentrations can be shown by using partial pressures:

$$\frac{c_A}{c} = \frac{p_a}{p} = y_A, \tag{4.250}$$

where $p = p_A + p_B$ is the total pressure and y_A is the molar fraction of component A in the gas. The total concentration $c = c_A + c_B$ can be expressed in terms of pressure:

$$c = \frac{n}{V} = \frac{p}{RT}, \tag{4.251}$$

where $R = 8.314$ J/kmol and T is the temperature (K). Partial pressure ρ_A can be calculated from

$$\rho_A = \frac{p_A M_A}{RT} = M_A c_A, \tag{4.252}$$

where M_A and M_B are the molar masses of components A and B. Equation (4.246) can be expressed in a form using partial pressures:

$$p_{BM} = \frac{p_{B2} - p_{B1}}{\ln \frac{p_{B2}}{p_{B1}}} = \frac{p}{c} c_{BM}. \tag{4.253}$$

Equation (4.247) can then be written as

$$j_A = \frac{D_{AB} p}{RTz p_{BM}} (p_{A1} - p_{A2}). \tag{4.254}$$

By using different potential differences,

$$c_{A1} - c_{A2} = \frac{c}{p}(p_{A1} - p_{A2}) = c(y_{A1} - y_{A2}) = \frac{M_B}{M_A} c(\rho_{A1} - \rho_{A2}) \quad , \tag{4.255}$$

single-material flow can be written in various ways:

$$j_A = k_c(c_{A1} - c_{A2}) = k_G(p_{A1} - p_{A2}) = k_y(y_{A1} - y_{A2}) \quad . \tag{4.256a}$$

Instead of the molar flow, the mass flow can be used:

$$m_A'' = M_A j_A = k_\rho(\rho_{A1} - \rho_{A2}). \tag{4.256b}$$

With the use of Eqs. (4.255) and (4.256a), the following relationships between the mass transfer factors are obtained:

$$k_c = \frac{1}{c} k_y = \frac{RT}{p} k_y = \frac{p}{c} k_G = RT k_G. \tag{4.257a}$$

Correspondingly, using Eqs. (4.255) and (4.256b) the following is obtained:

$$k_c = \frac{k_\rho}{M_B c} = \frac{RT}{M_B p} k_\rho. \tag{4.257b}$$

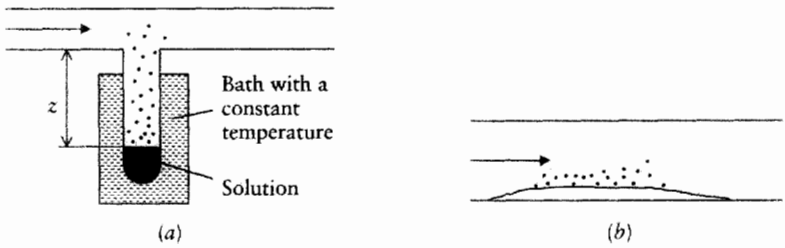

FIGURE 4.36

The equations are valid for the case $j_A = -j_B$:

$$k'_c = \frac{RT}{p}k'_y = RTk'_G = \frac{RT}{M_B p}k'_\rho. \tag{4.258}$$

By using Eq. (4.253), the approximation (4.249) becomes

$$k_c = \frac{p}{p_{BM}}k'_c. \tag{4.259}$$

In practice the mass transfer factors are often presented without stating the experimental assumptions by which $j_A = -j_B$ or $j_B = 0$ has been obtained. The designer has to decide on the suitability of the experiments from which the quantity k'_c or k_c, is measured.

An idea of the approximate nature of Eq. (4.249) or the equivalent Eq. (4.259) can be gained by comparing a pure-diffusion case (Fig. 4.36*a*) with the case involving a diffusion boundary layer (Fig. 4.36*b*).

4.3.7 Heat and Mass Transfer Differential Equations in the Boundary Layer and the Corresponding Analogy

We will consider flow through a solid element. Introducing the notations for molar flow density, partial density, and the reaction rate gives an equation for the mass balance:

$$M_A\left(\frac{\partial I_{Ax}}{\partial x} + \frac{\partial I_{Ay}}{\partial y} + \frac{\partial I_{Az}}{\partial z}\right) + \frac{\partial \rho_A}{\partial t} = M_A r_A \tag{4.260}$$

(outflow − inflow) + accumulation = generation

where

I_{Ax} is the molar flow density of component A (mol/m^2 s) in the x direction
M_A is the molar mass of component A (kg/mol)
ρ_A is the partial density of component A (kg/m^3)
r_A represents the formation rate of component A by chemical reactions (mol/m^3 s)

The corresponding equation for component B is

$$M_B\left(\frac{\partial I_{Bx}}{\partial x} + \frac{\partial I_{By}}{\partial y} + \frac{\partial I_{Bz}}{\partial z}\right) + \frac{\partial \rho_B}{\partial t} = M_B r_B\ . \tag{4.261}$$

The total mass balance is the sum of Eqs. (4.260) and (4.261):

$$\frac{\partial(M_A I_{Ax} + M_B I_{Bx})}{\partial x} + \frac{\partial(M_A I_{Ay} + M_B I_{By})}{\partial y} + \frac{\partial(M_A I_{Az} + M_B I_{Bz})}{\partial z} + \frac{\partial \rho}{\partial t} = 0, \tag{4.262}$$

where $\rho = \rho_A + \rho_B$. For a two-component or binary mixture, $M_A r_A + M_B r_B = 0$ is valid.

The mass flow density of the mixture in the x direction is defined by

$$\rho u_x = M_A I_{Ax} + M_B I_{Bx}, \tag{4.263}$$

with corresponding equations for other directions or velocities u_y and u_z. Using these notations, the mass balance of the mixture (Eq. (4.262)) is written as

$$\frac{\partial(\rho u_x)}{\partial x} + \frac{\partial(\rho u_y)}{\partial y} + \frac{\partial(\rho u_z)}{\partial z} + \frac{\partial \rho}{\partial t} = 0 \ . \tag{4.264}$$

For the mass balance of component A, diffusion velocity and the corresponding diffusion factor are defined with regard to the mean molar velocity v, defined by the equation

$$\mathrm{v}_x = \frac{c_A}{c}\mathrm{v}_{Ax} + \frac{c_B}{c}\mathrm{v}_{Bx}, \tag{4.265}$$

where v_{Ax} is the velocity of component A in the x direction, assuming a stable coordinate system. According to this the mass flow density is

$$M_A I_{Ax} = \rho_A \mathrm{v}_{Ax} = M_A c_A \mathrm{v}_{Ax}. \tag{4.266}$$

The velocity of the mass center of the system, u_x (Eq. (4.263)), can be written as

$$\rho u_{Ax} = \rho_A \mathrm{v}_{Ax} + \rho_B \mathrm{v}_{Bx} \tag{4.267}$$

using velocities v_{Ax} and v_{Bx}. The mass flow density may be written in the following ways:

$$\rho \mathrm{v}_{Ax} = \rho_A(\mathrm{v}_{Ax} - \mathrm{v}_x) + \rho_A \mathrm{v}_x \tag{4.268a}$$

$$= \rho_A(\mathrm{v}_{Ax} - u_x) + \rho_A u_x \tag{4.268b}$$

$$= \rho_A \frac{\mathrm{v}_{Ax} - u_x}{\mathrm{v}_{Ax} - \mathrm{v}_x}(\mathrm{v}_{Ax} - u_x) + \rho_A u_x \ . \tag{4.268c}$$

In a boundary layer equation the mass center is considered with the help of the velocity (u_x, u_y, u_z) and therefore a distribution of the velocity of the mass center is desirable. The diffusion velocity and diffusion factor are determined with regard to velocity v_x, giving a formula for $\mathrm{v}_{Ax} - \mathrm{v}_x$, but not for $\mathrm{v}_{Ax} - u_x$. A useful approach is offered by Eq. (4.268c), using the artificial multiplication factor $(\mathrm{v}_{Ax} - u_x)/(\mathrm{v}_{Ax} - \mathrm{v}_x)$.

From Eq. (4.267) and $\rho = \rho_A + \rho_B$, it is seen that the following equation is valid:

$$\rho_A(\mathrm{v}_{Ax} - u_x) = -\rho_B(\mathrm{v}_{Bx} - u_x) = \frac{\rho_A \rho_B}{\rho}(\mathrm{v}_{Ax} - \mathrm{v}_{Bx}) \ . \tag{4.269}$$

The last term is best understood by noting that

$$(v_{Ax} - v_{Bx}) = (v_{Ax} - u_x) - (v_{Bx} - u_x)$$

and then using the first part of Eq. (4.269).

Using Eq. (4.265) and $c = c_A + c_B$, the following connections result:

$$c_A(v_{Ax} - v_x) = -c_B(v_{Bx} - v_x) = \frac{c_A c_B}{c}(v_{Ax} - v_{Bx}) \quad . \tag{4.270}$$

According to Eqs. (4.269) and (4.270),

$$\frac{v_{Ax} - u_x}{v_{Ax} - v_x} = \frac{\left(\frac{\rho_B}{\rho}\right)(v_{Ax} - v_{Bx})}{\frac{c_B}{c}(v_{Ax} - v_{Bx})} = \frac{\rho_B c}{\rho c_B}$$

Because $\rho_A = M_A c_A$, $\rho_B = M_B c_B$, and $\rho = Mc$, where $M = (c_A/c)M_A + (c_B/c)M_B$,

$$\frac{v_{Ax} - u_x}{v_{Ax} - v_x} = \frac{M_B}{M} . \tag{4.271}$$

Substituting Eq. (4.271) in Eq. (4.268c) gives

$$\rho_A v_{Ax} = \frac{M_B \rho_A}{M}(v_{Ax} - v_x) + \rho_A u_x . \tag{4.272}$$

For diffusion flow, $\rho_A(v_{Ax} - v_x)$, Fick's model (Eq. (4.241)) gives

$$\rho_A(v_{Ax} - v_x) = M_A j_{Ax} = -M_A D_{AB} \frac{\partial c_A}{\partial x} . \tag{4.273}$$

Using important connections,

$$M_A I_{Ax} = \rho_A v_{Ax} = \frac{M_B}{M} M_A j_A + \rho_A u_x = -\frac{M_A M_B}{M} D_{AB} \frac{\partial c_A}{\partial x} + \rho_A u_x \quad . \tag{4.274}$$

To shorten the notations, the following definition is used:

$$D'_{AB} = \frac{M_B}{M} D_{AB} . \tag{4.275}$$

Using this, the mass flow density is represented as

$$M_A I_{Ax} = -M_A \, D'_{AB} \frac{\partial c_A}{\partial x} + \rho u_x \, , \tag{4.276}$$

and correspondingly for directions y and z. Substituting Eq. (4.276) into Eq. (4.260) and keeping D'_{AB} constant gives

$$\frac{\partial(\rho_A u_x)}{\partial x} + \frac{\partial(\rho_A u_y)}{\partial y} + \frac{\partial(\rho_A u_z)}{\partial z} - M_A \, D'_{AB} \left(\frac{\partial^2 c_A}{\partial x^2} + \frac{\partial^2 c_A}{\partial y^2} + \frac{\partial^2 c_A}{\partial z^2} \right) + \frac{\partial \rho_A}{\partial t} = M_A r_A \tag{4.277}$$

If the mixture density $\rho = \rho_A + \rho_B$ is held constant, Eq. (4.264) gives

$$\frac{\partial u_x}{\partial x} + \frac{\partial u_y}{\partial y} + \frac{\partial u_z}{\partial z} = 0 . \tag{4.278}$$

Dividing Eq. (4.277) by M_A and using Eq. (4.278) gives

$$u_x \frac{\partial c_A}{\partial x} + u_y \frac{\partial c_A}{\partial y} + u_z \frac{\partial c_A}{\partial z} + \frac{\partial c_A}{\partial t} = D'_{AB} \left(\frac{\partial^2 c_A}{\partial x^2} + \frac{\partial^2 c_A}{\partial y^2} + \frac{\partial^2 c_A}{\partial z^2} \right) + r_A \quad , \quad (4.279)$$

because $c_A = (\rho_A / M_A)$.

In a similar manner, the energy balance equation can be determined:

$$u_x \frac{\partial T}{\partial x} + u_y \frac{\partial T}{\partial y} + u_z \frac{\partial T}{\partial z} + \frac{\partial T}{\partial t} = a \left(\frac{\partial^2 T}{\partial x^2} + \frac{\partial^2 T}{\partial y^2} + \frac{\partial^2 T}{\partial z^2} \right) + \frac{\dot{Q}}{\rho c_p} \quad . \quad (4.280)$$

where $a = \lambda / \rho c_p$ and $\dot{Q}$ is the heat generation per unit volume due to the chemical reactions (W m^{-3}), or $\dot{Q} = r_A \Delta H$, where ΔH is the reaction heat (J/mol). The thermal conductivity of the mixture is λ (W m^{-1} K^{-1}), and c_p is the specific heat (J kg^{-1} K^{-1}), or $\rho c_p = \rho_A c_{pA} + \rho_B c_{pB}$.

Equations (4.279) and (4.280) are similar. Figure 4.37 shows a two-dimensional boundary layer flow over a plane. Ignoring any chemical reactions and considering steady-state conditions, Eqs. (4.279) and (4.280) give

$$u_x \frac{\partial c_A}{\partial x} + u_z \frac{\partial c_A}{\partial z} = D'_{AB} \left(\frac{\partial^2 c_A}{\partial x^2} + \frac{\partial^2 c_A}{\partial z^2} \right) \quad (4.281)$$

$$u_x \frac{\partial T}{\partial x} + u_z \frac{\partial T}{\partial z} = a \left(\frac{\partial^2 T}{\partial x^2} + \frac{\partial^2 T}{\partial z^2} \right). \quad (4.282)$$

Assuming laminar flow for a linear momentum equation in the x direction (an approximation from the Navier-Stokes equations) gives

$$u_x \frac{\partial u_x}{\partial z} + u_z \frac{\partial u_x}{\partial x} = \nu \left(\frac{\partial^2 u_x}{\partial x^2} + \frac{\partial^2 u_x}{\partial z^2} \right) \quad (4.283)$$

where ν is the kinematic viscosity (m^2/s).

Equations (4.281)–(4.283) have to be solved at the same time as the continuity equation (4.278). The following dimensionless variables are used:

$$w_x = \frac{u_x}{u_o} \quad (4.284a)$$

$$w_z = \frac{u_z}{u_o} \quad (4.284b)$$

$$z_A = \frac{c_A - c_{As}}{c_{Ao} - c_{As}} \quad (4.284c)$$

$$\theta = \frac{T - T_s}{T_o - T_s} \quad (4.284d)$$

$$\xi = \frac{x}{L} \quad (4.284e)$$

$$\eta = \frac{z}{L}, \quad (4.284f)$$

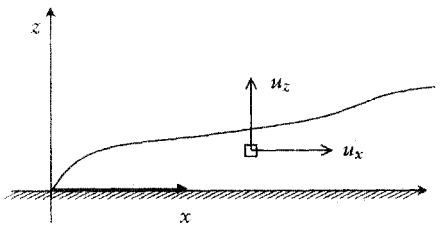

FIGURE 4.37 Boundary layer flow.

where u_o is the velocity outside the boundary layer or formally, $c_{As} = c_A(z = 0)$; c_{Ao} is the concentration of component A outside the boundary layer, $T_s = T(z = 0)$, and T_o is the temperature outside the boundary layer. The dimension L is the characteristic length. All dimensionless variables range between 0 and 1.

For example, $u_x(x, z) = u_o w_x(\xi(x), \eta(z))$. Using the chain rule,

$$\frac{\partial^2 u_x}{\partial x^2} = \frac{\partial}{\partial x}\left(\frac{\partial u_x}{\partial x}\right) = \frac{\partial}{\partial x}\left(u_o \frac{\partial w_x}{\partial \xi}\frac{d\xi}{dx}\right) = \frac{u_o}{L}\frac{\partial}{\partial x}\left(\frac{\partial w_x}{\partial \xi}\right)$$

$$= \frac{u_o}{L}\frac{\partial}{\partial \xi}\left(\frac{\partial w_x}{\partial \xi}\frac{d\xi}{dx}\right) = \frac{u_o}{L^2}\frac{\partial^2 w_x}{\partial \xi^2}$$

Treating the other terms in a similar manner, the linear momentum equation in a dimensionless form is obtained:

$$w_x\frac{\partial w_x}{\partial \eta} + w_z\frac{\partial w_x}{\partial \xi} = \frac{1}{\mathrm{Re}}\left(\frac{\partial^2 w_x}{\partial \xi^2} + \frac{\partial^2 w_x}{\partial \eta^2}\right), \tag{4.285}$$

where $\mathrm{Re} = (u_o L)/\nu$ is the Reynolds number.

The dimensionless form of the continuity equation (4.278) ($u_y = 0$) in two-dimensional boundary layer flow is

$$\frac{\partial w_x}{\partial \xi} + \frac{\partial w_z}{\partial \eta} = 0. \tag{4.286}$$

For the two equations (4.285) and (4.286) and two unknown variables $w_x(\xi, \eta), w_z(\xi, \eta)$, boundary conditions are $\eta = 0$; $w_x = 0$, $\eta = \infty$; $w_x = 1$, $w_z = 0$. The boundary condition $w_z(\eta = 0)$ is not given in a mass transfer case, as it depends on the vaporization.

The dimensionless form of Eq. (4.282) is

$$w_x\frac{\partial \theta}{\partial \xi} + w_z\frac{\partial \theta}{\partial \eta} = \frac{a}{Lu_o}\left(\frac{\partial^2 \theta}{\partial \xi^2} + \frac{\partial^2 \theta}{\partial \eta^2}\right)$$

$$\frac{a}{Lu_o} = \frac{\lambda/\rho c_p}{Lu_o} = \frac{1}{\mathrm{Re\,Pr}},$$

where $\mathrm{Pr} = (\mu c_p)/\lambda$ is the Prandtl number and μ is the dynamic viscosity, giving

$$w_x\frac{\partial \theta}{\partial \xi} + w_z\frac{\partial \theta}{\partial \eta} = \frac{1}{\mathrm{Re\,Pr}}\left(\frac{\partial^2 \theta}{\partial \xi^2} + \frac{\partial^2 \theta}{\partial \eta^2}\right). \tag{4.287}$$

Boundary conditions for the dimensionless temperature are

$$\begin{aligned} \theta &= 0 \text{ at } \eta = 0 \\ \eta &= \infty \text{ at } \theta = 1 \end{aligned} \tag{4.288}$$

From Eqs. (4.285)–(4.286) and (4.287)–(4.288),

$$\theta = F(\xi, \eta, \text{Re}, \text{Pr}). \tag{4.289}$$

Equation (4.289) is an approximation in the mass transfer case, as the boundary conditions cannot always set $w_z(z = 0) = 0$. For the case $j_A = -j_B$, we nearly have $w_z(z = 0) = 0$, and the analogy equation is based on this situation.

The dimensionless form of Eq. (4.281) is

$$w_x \frac{\partial z_A}{\partial \xi} + w_z \frac{\partial z_A}{\partial \eta} = \frac{D'_{AB}}{L u_o}\left(\frac{\partial^2 z_A}{\partial \xi^2} + \frac{\partial^2 z_A}{\partial \eta^2}\right)$$

$$\frac{D'_{AB}}{L u_o} = \frac{D'_{AB}/\nu}{L u_o/\nu} = \frac{1}{\text{Re Sc}}$$

where $\text{Sc} = \nu/D'_{AB}$ is the Schmidt number. We thus have

$$w_x \frac{\partial z_A}{\partial \xi} + w_z \frac{\partial z_A}{\partial \eta} = \frac{1}{\text{Re Sc}}\left(\frac{\partial^2 z_A}{\partial \xi^2} + \frac{\partial^2 z_A}{\partial \eta^2}\right) \tag{4.290}$$

Boundary conditions for the dimensionless concentration are

$$\begin{aligned} &\text{at } \eta = 0,\ z_A = 0 \\ &\text{at } \eta = \infty,\ z_A = 1. \end{aligned} \tag{4.291}$$

Equation (4.287) is in exactly the same form as Eq. (4.290), and the boundary conditions (4.288) and (4.291) are also similar.

If the solution to Eq. (4.289) is known, it is also valid for (4.290)–(4.291); hence

$$z_A = F(\xi, \eta, \text{Re}, \text{Sc}). \tag{4.292}$$

The function F is then the same in Eqs. (4.289) and (4.292). This is not strictly correct, however; see the comments after Eq. (4.289).

We can apply this result to determine the analogy between mass and heat transfer factors. Mass flow density j_A (mol/m^2 s) can be given as

$$j_A = -D_{AB}\left(\frac{\partial c_A}{\partial z}\right)_{z=0} = k'_c\,(c_{As} - c_{Ao})\,. \tag{4.293}$$

The mass transfer factor k'_c is used because Eqs. (4.289) and (4.292) demand the boundary condition $w_z(\eta = 0) = 0$, which represents the case $j_A = -j_B$. Strictly speaking, a new mass transfer factor should be defined that represents the situation $M_A j_A = -M_B j_B$ or $w_z = 0$.

Using the dimensionless quantities z_A and η, Eqs. (4.284c) and (4.284f), Eq. (4.293) can be written as

$$j_A = -D_{AB}(c_{Ao} - c_{As})\frac{1}{L}\left(\frac{\partial z_A}{\partial \eta}\right)_{\eta=0} = k'_c\,(c_{As} - c_{Ao})\,,$$

in which

$$\mathrm{Sh} = \frac{k_c' L}{D_{AB}} = \left(\frac{\partial z_A}{\partial \eta}\right)_{\eta = 0}. \tag{4.294}$$

The dimensionless quantity Sh is called the Sherwood number.

The heat transfer factor α is defined by

$$q = -\lambda \left(\frac{\partial T}{\partial z}\right)_{z = 0}, \tag{4.295}$$

where q is the heat flow density from the surface to the surroundings. Using dimensionless variables Θ and η from Eqs. (4.284d) and (4.284f), Eq. (4.295) gives

$$\mathrm{Nu} = \frac{\alpha L}{\lambda} = \left(\frac{\partial \theta}{\partial \eta}\right)_{\eta = 0}, \tag{4.296}$$

where the dimensionless quantity Nu is the Nusselt number.

According to Eqs. (4.289) and (4.292) it is seen that with constant ξ or x

$$\left(\frac{\partial z_A}{\partial \eta}\right)_{\eta = 0} = \frac{\partial F}{\partial \eta}(\xi, 0, \mathrm{Re}, \mathrm{Sc}) = G(\mathrm{Re}, \mathrm{Sc})$$

$$\left(\frac{\partial \theta}{\partial \eta}\right)_{\eta = 0} = \frac{\partial F}{\partial \eta}(\xi, 0, \mathrm{Re}, \mathrm{Pr}) = G(\mathrm{Re}, \mathrm{Pr}),$$

which leads to the important results

$$\mathrm{Sh} = G(\mathrm{Re}, \mathrm{Sc}) \tag{4.297}$$

$$\mathrm{Nu} = G(\mathrm{Re}, \mathrm{Pr}) \tag{4.298}$$

The above shows how the dimensionless numbers are used to provide the most accurate solution. Collecting these definitions together,

$$\mathrm{Sh} = \frac{k_c' L}{D_{AB}},\ \mathrm{Nu} = \frac{\alpha L}{\lambda},\ \mathrm{Re} = \frac{u_0 L}{\nu},\ \mathrm{Pr} = \frac{\mu c_p}{\lambda},\ \text{and}\ \mathrm{Sc} = \frac{\nu}{D_{AB}'}$$

Note the diffusion factor appearing in the Schmidt number, $D_{AB}' = (M_B/M)D_{AB}$ (Eq. (4.275)).

The preceding discussion has attempted to formulate the situation for laminar boundary layer flow as accurately as possible and to obtain precise correlation between the heat transfer and mass transfer factors.

It is not possible to translate the above reasoning to turbulent flow, as turbulent flow equations are not reliable. However, in practice it is typical to assume that the same analogy is also valid for turbulent flow. Because of this hypothesis level, it is quite futile to use the diffusion factor D_{AB}' in the Schmidt number; instead we will directly use the number D_{AB} as in the Sherwood number. Hence in practical calculations $\mathrm{Sc} = \nu/D_{AB}$.

Example 5

Heat transfer is defined by $\mathrm{Nu} = A\mathrm{R}^m\mathrm{Pr}^n$. The function $G(\cdot)$ is given as

$$G(\mathrm{Re}, \mathrm{Pr}) = A\mathrm{Re}^m\mathrm{Pr}^n.$$

According to the analogy model, it is valid that

$$\mathrm{Sh} = G(\mathrm{Re}, \mathrm{Sc}) = A\mathrm{Re}^m\mathrm{Sc}^n \tag{4.299}$$

This allows the mass transfer factor to be calculated. The above equation can be refined to

$$\mathrm{Sh} = G(\mathrm{Re}, \mathrm{Sc}) = A\mathrm{Re}^m\mathrm{Pr}^n\left(\frac{\mathrm{Sc}}{\mathrm{Pr}}\right)^n.$$

It follows that

$$\frac{k_c' L}{D_{AB}} = \frac{\alpha L}{\lambda}\left(\frac{\nu/D_{AB}}{\rho c_p/\lambda}\right)^n,$$

simplifying to

$$k_c' = \frac{\alpha}{\rho c_p}\mathrm{Le}^{1-n}, \tag{4.300}$$

where $\mathrm{Le} = (D_{AB}\rho c_p)/\lambda = \mathrm{Pr}/\mathrm{Sc}$ is the Lewis number (or Luikov's number in the Russian literature).

4.3.8 Diffusion through a Porous Material

In a steady-state situation when gas flows through a porous material at a low velocity (laminar flow), the following empirical formula, Darcy's model, is valid:

$$\rho u_x = -\frac{k}{\nu}\frac{\partial p}{\partial x}, \tag{4.301}$$

where k represents the permeability of the matter (m^2). The kinematic viscosity of the gas is denoted by ν (m^2/s), and ρ is the density of the gas for the total volume—or if the real density of the gas is d, $\rho = \phi d$, where ϕ is the volume percentage of the gas in the porous material. It is also seen that ϕ gives the percentage of the free cross-sectional area of the gas in the material:

$$\phi = \frac{\rho}{d} = \frac{m(g)/V}{m(g)/V(g)} = \frac{V(g)}{V} = \frac{A(g)L}{AL} = \frac{A(g)}{A}.$$

In Eq. (4.301) velocity u_x is the real velocity of the gas in the pores: $u_x = q_v/A(g) = q_v/(\phi)A$, where q_v is the volume flow.

From Darcy's equation we can determine a formula for the counterforce produced by the porous material to the flowing or diffusing component A. If this counterforce is found, it can be added to the diffusion resistance force caused by component B to component A; hence the sum of these two forces represents the total diffusion resistance.

For a porous material the linear momentum equation can be written as

$$\rho\frac{\partial u_x}{\partial t} = -\phi\frac{\partial p}{\partial x} + f_{mx}, \tag{4.302}$$

where f_{mx} represents the resistance force between the gas and the material, the flow friction. The term ϕ is important in Eq. (4.302). It comes from the fact that while ρ appears on the left side of Eq. (4.302), the balance is constructed

for the mixture of the material and the gas, and therefore the pressure must be calculated for the surface area of the total material ϕp. When ϕ is held constant, independent of x, Eq. (4.302) is obtained.

In a steady-state case, Eq. (4.302) is simplified to

$$f_{mx} = \phi \frac{\partial p}{\partial x},$$

and with Eq. (4.301),

$$f_{mx} = -\frac{\eta}{k}\phi^2 u_x, \tag{4.303}$$

with $\nu = \eta/d = \eta\phi/\rho$. If the flow velocity is zero, Eq. (4.303) can be interpreted as saying that the resistance force is linearly proportional to the velocity difference between the gas and the material and also linearly proportional to the dynamic viscosity of the gas.

Equation (4.303) is valid but it is lacking something. The resistance force $f_{mx}^{(A)}$ that applies to the component A has to be found, and not that for the whole mixture. The force applying to the whole mixture f_{mx} is the sum of the partial forces $f_{mx}^{(A)}$ and $f_{mx}^{(B)}$:

$$f_{mx} = f_{mx}^{(A)} + f_{mx}^{(B)}. \tag{4.304}$$

Assuming that the force is divided along the ratio of the mass flows, Eq. (4.303) gives

$$f_{mx}^{(A)} = -\frac{\rho_A}{\rho}\frac{\eta}{k}\phi^2 \mathrm{v}_{Ax} \tag{4.305a}$$

$$f_{mx}^{(B)} = -\frac{\rho_B}{\rho}\frac{\eta}{k}\phi^2 \mathrm{v}_{Bx}. \tag{4.305b}$$

Summing (4.305a) and (4.305b), f_{mx} is obtained for Eq. (4.303). This is due to the fact that $\rho_A \mathrm{v}_{Ax} + \rho_B \mathrm{v}_{Bx} = \rho u_x$.

We now consider the resistance force $f_{mx}^{(A)}$ caused by the diffusion. This force resists the diffusion flow in a porous material together with $f_{mx}^{(A)}$. Writing the linear momentum equation for component A in accordance with Eq. (4.302),

$$\rho_A \frac{d\mathrm{v}_{Ax}}{dt} = -\phi \frac{dp_A}{dx} + f_{dx}^{(A)} + f_{dx}^{(B)}. \tag{4.306}$$

This gives a model for $f_{mx}^{(A)}$, Eq. (4.305b), but not a model for force $f_{dx}^{(A)}$. While force f_{mx} gives the flow force caused by the material, it is normal to represent this fact so that $f_{dx}^{(A)}$ gives the pure diffusion resistance force that is not caused by the material. This requires treating $f_{dx}^{(A)}$ independently from the material or porosity.

For $\phi = 1$ or $k = \infty$, where $f_{mx}^{(A)} = 0$, Eq. (4.306) gives

$$\rho_A \frac{d\mathrm{v}_{Ax}}{dt} = -\frac{\partial p_A}{\partial x} + f_{dx}^{(A)}. \tag{4.307}$$

In a steady-state case the results are

$$f_{dx}^{(A)} = \frac{\partial p_A}{\partial x}. \tag{4.308}$$

In a steady-state case at constant pressure ($p = p_A + p_B = \text{constant}$), Fick's law (Eq. (4.273)) is valid:

$$\rho_A(v_{Ax} - v_x) = -M_A D_{AB} \frac{1}{RT} \frac{\partial p_A}{\partial x} ,$$

with $c_A = p_A/(RT)$.

Instead of the mean velocity v_x weighted with the molar fractions, a velocity weighted with the mass fractions—the mass center velocity u_x—can be used. Using Eq. (4.271), the above equation becomes

$$\rho_A(v_{Ax} - u_x) = -\frac{M_A M_B}{M} \frac{D_{AB}}{RT} \frac{\partial p_A}{\partial x} , \tag{4.309}$$

Equations (4.308) and (4.309) give a formula for the diffusion resistance force $f_{dx}^{(A)}$:

$$f_{dx}^{(A)} = -\frac{M}{M_A M_B} \frac{RT}{D_{AB}} \rho_A(v_{Ax} - u_x) . \tag{4.310}$$

Substituting the formulas for forces $f_{dx}^{(A)}$ and $f_{mx}^{(A)}$ (Eqs. (4.310) and (4.305a)) in Eq. (4.306) gives

$$\rho_A \frac{dv_{Ax}}{dt} = -\phi \frac{\partial p_A}{\partial x} - \frac{M}{M_A M_B} \frac{RT}{D_{AB}} \rho_A(v_{Ax} - u_x) - \frac{\eta_A \phi^2}{k} v_{Ax} . \tag{4.311}$$

In the steady-state case Eq. (4.311) is simplified to

$$\frac{M}{M_A M_B} \frac{RT}{D_{AB}} \rho_A(v_{Ax} - u_x) + \frac{\rho_A \eta \phi^2}{\rho k} v_{Ax} = -\phi \frac{\partial p_A}{\partial x} . \tag{4.312}$$

The aim is to solve this equation for the term v_{Ax}, or actually $\rho_A v_{Ax}$, which is the diffusion flow density of component A.

An important case is

$$v_{Bx} = 0. \tag{4.313}$$

This case applies to drying processes (B = dry air), condensation, and absorption, such as the diffusion of sulfur dioxide gas through a calcium oxide.

When Eq. (4.313) is valid, $\rho u_x = \rho_A v_{Ax} + \rho_B v_{Bx} = \rho_A v_{Ax}$, and $u_x = (\rho_A/\rho) v_{Ax}$ $(\rho = \rho_A + \rho_B)$. Therefore, in this case

$$v_{Ax} - u_x = \left(1 - \frac{\rho_A}{\rho}\right) v_{Ax} = \frac{p_B}{p} v_{Ax} . \tag{4.314}$$

Substituting Eq. (4.314) in Eq. (4.312) and solving for the mass flow density gives

$$\rho_A v_{Ax} = -\frac{\phi}{\frac{M}{M_A M_B} \frac{RT}{D_{AB}} \frac{\rho_B}{\rho} + \frac{\eta \phi^2}{\rho k}} \frac{\partial p_A}{\partial x} . \tag{4.315}$$

This can be written as

$$\frac{\rho_B}{\rho} = \frac{p_B M_B}{pM} = \frac{p - p_A}{p} \frac{M_B}{M}$$

and

$$\frac{\eta}{\rho} = \frac{\eta}{\phi d} = \frac{\nu}{\phi}.$$

Substituting these into Eq. (4.315) after grouping terms,

$$\rho_A v_{Ax} = -\frac{\phi}{1 + \frac{p}{p - p_A}\frac{M_A}{RT}D_{AB}\nu\frac{\phi}{k}} \frac{p}{p - p_A}\frac{M_A}{RT}D_{AB}\frac{\partial p_A}{\partial x} \quad . \tag{4.316}$$

The term

$$\epsilon = \frac{\phi}{1 + \frac{p}{p - p_A}\frac{M_A}{RT}D_{AB}\nu\frac{\phi}{k}} \tag{4.317}$$

is the resistance factor caused by the material. Using Eq. (4.317), the diffusion flow is

$$\rho_A v_{Ax} = -\epsilon\frac{p}{p - p_A}\frac{M_A}{RT}D_{AB}\frac{\partial p_A}{\partial x} \quad . \tag{4.318}$$

The term $p/(p - p_A)$ derives from assumption (4.313) representing the effects of Stefan flow. If $\epsilon = 1$, Eq. (4.318) gives the diffusion flow in a free space.

Equation (4.318) indicates that if $k \longrightarrow \infty$, the diffusion resistance remains under 1, namely, $\epsilon_d = \phi$. This is easy to understand, as ϕ represents that part of the material cross-sectional surface through which the vapor diffuses.

4.3.9 Example of Drying Process Calculation

The problems experienced in drying process calculations can be divided into two categories: the boundary layer factors outside the material and humidity conditions, and the heat transfer problem inside the material. The latter are more difficult to solve mathematically, due mostly to the moving liquid by capillary flow. Capillary flow tends to balance the moisture differences inside the material during the drying process. The mathematical discussion of capillary flow requires consideration of the linear momentum equation for water and requires knowledge of the water pressure, its dependency on moisture content and temperature, and the flow resistance force between water and the material. Due to the complex nature of this, it is not considered here.

We will cover a simple drying model to examine the radiation drier of coated paper. We assume there are no major temperature or humidity variations in the direction of the paper web thickness, and that temperature T and humidity u are constant in the direction of thickness. This assumption requires that the capillary action be ignored, and the pressure gradient of water is zero on the assumption $\partial u/\partial x = \partial T/\partial x = 0$. How is it possible that the humidity distribution remains uniform?

The only approach is to ignore the capillary flow and to assume water vaporization takes place evenly in the thickness of the paper web. With a

radiation drier, this approach is reasonable if the radiation energy is absorbed evenly inside the web. Assuming the boundary layers on both sides of the web are similar, the vapor flow is distributed symmetrically to the center of the web. The model of vaporization and water drift is shown in Fig. 4.38.

To derive formula (4.318) for vapor flow in a porous material, we approximate the pressure gradient in Eq. (4.318) with

$$\frac{\partial p_A}{\partial x} = \frac{p_A(s) - p_A(T,u)}{\Delta x}, \tag{4.319}$$

where $\Delta x = s/4$ and s is the thickness of the paper web (Fig. 4.38). The vapor flow through the boundary layer can be represented as

$$\rho_A v_{Ax} = k_c' \frac{M_A p}{RT} \ln \frac{p - p_A(y)}{p - p_A(s)}, \tag{4.320}$$

where $k_c' = (\alpha/\rho c_p)\mathrm{Le}^{1-n}$ (Eq. (4.300)).

Equation (4.314) follows from Eqs. (4.250), (4.253), (4.256a), and (4.259):

$$\begin{aligned} j_A &= k_c(c_A(s) - c_A(y)) && \text{(Eq. (4.256a))} \\ &= k_c' \frac{p}{p_{BM}}(c_A(s) - c_A(y)) && \text{(Eq. (4.259))} \\ &= k_c' \frac{c}{p_{BM}}(p_A(s) - p_A(y)) && \text{(Eq. (4.250))} \\ &= k_c' \frac{c \ln \frac{p_B(y)}{p_B(s)}}{p_B(y) - p_B(s)}(p_A(s) - p_A(y)) && \text{(Eq. (4.253))} \\ &= k_c' \, c \ln \frac{p - p_A(y)}{p - p_A(s)} && (p = p_A + p_B) \end{aligned}$$

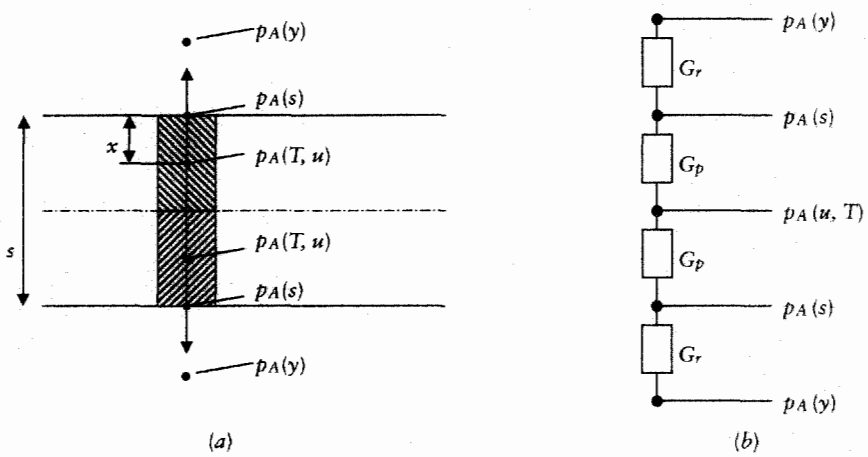

FIGURE 4.38 (*a*) The uniform vaporization of water in paper. (*b*) Resistance web analogy for steam flow; $1/G_p$ = resistance due to the paper, $1/G_r$ = resistance due to the boundary layer.

with reference to Eq. (4.251),

$$\rho_A v_{Ax} = M_A j_A = k_c' \frac{M_A p}{RT} \ln \frac{p - p_A(y)}{p - p_A(s)},$$

or Eq. (4.320).

The logarithmic function in Eq. (4.320) can be written as

$$\ln \frac{p - p_A(y)}{p - p_A(s)} = \ln\left(1 + \frac{p_A(s) - p_A(y)}{p - p_A(s)}\right).$$

When $(p_A(s) - p_A(y))/(p - p_A(s)) < 1$, a logarithmic function to a series ($\ln(1+x) = x - x^2/s + \cdots$) can be developed, and using the first term gives the approximation

$$\ln \frac{p - p_A(y)}{p - p_A(s)} \approx \frac{p_A(s) - p_A(y)}{p - p_A(T, u)}. \tag{4.321}$$

In this approximation $p_A(s)$ in the denominator is replaced by $p_A(T, u)$.

We use the following notations:

$$G_r = k_c' \frac{M_A p}{RT} \frac{1}{p - p_A(T, u)} \tag{4.322}$$

$$G_p = \epsilon \frac{p}{p - p_A(T, u)} \frac{M_A}{RT} D_{AB} \frac{1}{\Delta x}. \tag{4.323}$$

Using approximation (4.319) in Eq. (4.318) and Eq. (4.317) in Eq. (4.320) leads to the steam flow formula

$$\rho_A v_{Ax} = G_p(p_A(T, u) - p_A(s)) = G_r(p_A(s) - p_A(y)).$$

Eliminating $p_A(s)$ gives

$$\rho_A v_{Ax} = G(p_A(T, u) - p_A(y)), \tag{4.324}$$

The total conductance is determined from

$$\frac{1}{G} = \frac{1}{G_r} + \frac{1}{G_p}. \tag{4.325}$$

The total vaporization on both sides of the web is determined by Eq. (4.324) multiplied by 2. If the radiation power absorbed in the web is $\dot{Q}''(\mathrm{W\ m^{-2}})$, the energy balance can be written as

$$\dot{Q}'' = C'' \frac{dT}{dt} + 2G(p_A(T, u) - p_A(y))l(T, u), \tag{4.326}$$

where $l(T, u)$ is the vaporization heat of water and C'' is the heat capacity of the web ($\mathrm{J\ m^{-2} K^{-1}}$). This can be calculated from

$$C'' = m''(c_{p1} + u c_{p2}), \tag{4.327}$$

where m'' is the square mass of the dry substance of the paper web ($\mathrm{kg\ m^{-2}}$), c_{p1} is the specific heat of the dry substance, and c_{p2} is the specific heat of water.

The humidity change due to vaporization is

$$-m''\frac{du}{dt} = 2G(p_A(T,u) - p_A(y)) . \tag{4.328}$$

The negative sign in Eq. (4.328) is due to the fact that $(du/dt) < 0$ represents the net vaporization to the surroundings.

Calculating the temperature rise at each time t with Eq. (4.326) and Eq. (4.328) gives the corresponding change in humidity. As the function G and the pressure $p(T, u)$ are complex, numerical solutions are used.

Example 6

Calculate the humidity change and the temperature rise in a paper web at the time when the web humidity $u = 0.20$ and temperature $\theta = 70$ °C. Assume the heat transfer factor on the web surface is $\alpha = 40$ W m^{-2} K^{-1} and the humidity of the surrounding air is $x = 0.05$ kg H_2O/kg dry air. The radiation power density absorbed by the web surface is 250 kW m^{-2}.

The vaporization heat of water, which depends on the humidity, is accurately determined by

$$l(T,u) = l_o(T) + r(T,u), \tag{4.329}$$

where

$l_o(T)$ is the vaporization heat of free water
$r(T, u)$ is the required auxiliary heat (sorption heat)

The sorption heat for the newsprint is calculated as

$$r = A_6 u^{A_2} \exp(A_4 u) T^2 \left(\frac{T_{cr} - T}{A_7}\right)^{A_3 - 1} , \tag{4.330}$$

where $A_2 = -1.3820$, $A_3 = 7.557$, $A_4 = -3.372$, $A_6 = 8.633 \times 10^{-3}$ kJ kg^{-1} K^{-2}, $A_7 = 696.0$ K, and $T_{cr} = 647.3$ K. Substituting $u = 0.20$ and $T = 343$ K in this equation gives $r = 21.1$ kJ kg^{-1}. Table 4.7 gives $l_o(\theta = 70\ °C) = 2333.3$ kJ kg^{-1}; hence, $l(T, u) = 2354 \times 10^3$ J kg^{-1}.

The partial pressure of the surrounding air $p_A(y)$ is calculated using the humidity $x = 0.05$ kg H_2O/kg dry air:

$$p_A(y) = \frac{x}{0.622 + x} p = \frac{0.05}{0.622 + 0.05} 10^5 = 7440 \text{ Pa}$$

The steam pressure inside the paper web $p_A(T, u)$ calculated in the previous example was $p_A(T, u) = 27.7 \times 10^3$ Pa and the diffusion resistance factor $\epsilon = 0.50$. If the thickness of the paper web $s = 0.09$ mm, the mean diffusion distance inside the paper is $\Delta x = s/4 = 0.0225$ mm.

Substituting the numerical values in Eq. (4.323) to determine the conductance,

$$G_p = 0.5\left(\frac{10^5}{10^5 - 27.7 \times 10^3}\right)\left(\frac{18 \times 10^{-3}}{8.314 \times 343}\right) \times 36.3 \times 3 \times 10^{-6} \frac{1}{0.0225 \times 10^{-3}}$$
$$= 7.04 \times 10^{-6} \text{ kg m}^{-2} \text{ s}^{-1} \text{ Pa}^{-1} .$$

To calculate the conductance of the boundary layer we first calculate the mass transfer factor using Eq. (4.300):

$$k_c' = \frac{\alpha}{\rho c_p} \mathrm{Le}^{1-n}.$$

Assume that $n = 0.4$. Table 4.7 gives ($\theta = 70$ °C):

$$\rho_A = 0.1981 \text{ kg m}^{-3}, \qquad \rho_B = 0.715 \text{ kg m}^{-3}$$
$$D_{AB} = 36.3 \times 10^{-6} \text{m}^2 \text{ s}^{-1}, \qquad \lambda = 0.02418 \text{ W m}^{-1} \text{ K}^{-1}$$
$$\rho c_p = \rho_A c_{pA} + \rho_B c_{pB} = 0.1981 \times 1850 + 0.715 \times 1006 = 1086 \text{ J m}^{-3} \text{ K}^{-1}$$
$$\mathrm{Le} = \frac{D_{AB} \rho c_p}{\lambda} = 1.63$$
$$k_c' = \frac{40}{1086} \times 1.63^{1-0.4} = 4.93 \times 10^{-2} \text{ m s}^{-1}$$

Boundary layer conductance is, from Eq. (4.322),

$$G_r = 4.93 \times 10^{-2} \frac{18 \times 10^3 \times 10^5}{8.314 \times 343} \frac{1}{10^5 - 27.7 \times 10^3}$$
$$= 0.432 \times 10^{-6} \text{ kg m}^{-2} \text{ s}^{-1} \text{ Pa}^{-1}.$$

Total conductance is, from Eq. (4.325),

$$G = \left[\frac{1}{0.432 \times 10^{-6}} + \frac{1}{7.04 \times 10^{-6}} \right]^{-1} = 0.407 \times 10^{-6} \text{ kg m}^{-2} \text{ s}^{-1} \text{ Pa}^{-1}.$$

Vaporization at time $t = 2 \times 0.407 \times 10^{-6}(27.7 \times 10^3 - 7.44 \times 10^3) = 16.49 \times 10^{-3}$ kg m^{-2} s. The humidity change rate is calculated from Eq.(4.328) when the square mass of the dry substance of the paper web is $m'' = 40.5 \times 10^{-3}$ kg m^{-2}.

$$\frac{du}{dt} = -\frac{16.49 \times 10^{-3}}{40.5 \times 10^{-3}} = -0.41 \text{ s}^{-1}.$$

Heat capacity $C'' = 40.5 \times 10^{-3}(1400 + 0.2 \times 4186) = 90.6$ J m^{-2} K^{-1}. The temperature rise, Eq. (4.326), is

$$\frac{dT}{dt} = \frac{1}{90.6}(250 \times 10^3 - 16.49 \times 10^{-3} \times 2354 \times 10^3) = 2330 \text{ K s}^{-1}.$$

The velocity of a coated paper web is 17 m s^{-1} and the width of the IR drier is 0.4 m. Thus the delay time in one drier is $0.4/17 = 0.0235$ s. This yields an indication of the processes inside the drier, using the above calculated values:

$$|\Delta u| \approx 0.41 \times 0.0235 = 0.01$$
$$\Delta T \approx 2330 \times 0.0235 = 55 \text{ K}$$

An accurate indication is achieved by carrying out the calculations in small time steps, such as $\Delta t = 0.004$ s, and then by calculating the vaporization, humidity change, and corresponding temperature rise at each time step. This is the numerical solution of differential equations (4.326) and (4.328). The results of a calculation of this type are shown in Table 4.12.

TABLE 4.12 Calculations for Infrared Drier

Infra power = 250 kW/m²		
Time (s)	**Temperature (°C)**	**Humidity (kg water/ kg dry air)**
0.0040	47.58	0.2317
0.0080	57.32	0.2310
0.0120	66.05	0.2294
0.0160	73.57	0.2265
0.0200	79.59	0.2220
0.0240	83.83	0.2157
0.0280	77.01	0.2091
0.0320	72.21	0.2046
0.0360	68.43	0.2010
0.0400	65.31	0.1981
0.0440	62.64	0.1957
0.0480	60.34	0.1936
0.0520	58.32	0.1918
0.0560	56.53	0.1902
0.0600	54.93	0.1887
0.0640	53.50	0.1875
0.0680	52.22	0.1863
0.0720	51.05	0.1853
0.0760	49.99	0.1844
0.0800	49.03	0.1835
0.0840	48.16	0.1827
0.0880	47.36	0.1821
0.0920	46.63	0.1814
0.0960	45.96	0.1808
0.1000	45.34	0.1803
0.1040	44.78	0.1798
0.1080	44.26	0.1794
0.1120	43.78	0.1789
0.1160	43.33	0.1786
0.1200	42.93	0.1782

Note: Initial web temperature is 37 °C and the initial humidity is 0.23. After the infrared drier ($t \geq 0.024$ s), there is a free draw, where the water vaporizes from the web to the surroundings ($x = 0.03$ kg H_2O/kg dry air), resulting in the cooling down of the web. The heat transfer factor in the drier and after the drier is $\alpha = 40$ W/m² K.

4.3.10 Evaporation from a Multicomponent Liquid System

In many industrial processes, the many components contained in the liquid evaporate simultaneously. Evaporation of individual components is easy to determine. For multicomponent liquid systems, the individual evaporation rates are summed to obtain the total evaporation rate.

Applying mass transfer theory to a component i in the liquid, assuming good mixing and neglecting atmospheric concentrations, the evaporation molar rate of a single component can be expressed as

$$\frac{dn_i}{dt} = \frac{k_{G,i}A}{n_t} p_i^s n_i, \tag{4.331}$$

where

$k_{G,i}$ is the mass transfer coefficient
A is the surface area of the liquid
n_t is the total moles of liquid
p_i^s is the saturation vapor pressure of pure component i

Integrating Eq. (4.331) and knowing that n_i^o is the initial number of moles of component i yields

$$n_i = n_i^o \exp(-K_i p_i^s t), \tag{4.332}$$

where

$$K_i = \frac{k_{G,i}A}{n_t}. \tag{4.333}$$

Equation (4.333) assumes a constant ratio.

The total mass is

$$m_t = \sum_1^N n_i M_i. \tag{4.334}$$

The total evaporation mass flow rate is obtained as

$$-\dot{m}_t = \frac{dm_t}{dt} = \sum_1^N M_i \frac{dn_i}{dt} = \sum_1^N -K_i M_i p_i^s n_i^o \exp(-K_i p_i^s t) \ . \tag{4.335}$$

Defining

$$m_t^o = n_t^o M_{\text{av}} \tag{4.336}$$

$$M_{\text{av}} = \sum_1^N x_i M_i \tag{4.337}$$

$$x_i^o = \frac{n_i^o}{n_t^o}, \tag{4.338}$$

we obtain the following:

$$\frac{dm_t}{dt} = m_t^o \frac{\sum_1^N K_i M_i p_i^s x_i^o \exp(-K_i p_i^s t)}{\sum_1^N x_i^o M_i}, \tag{4.339}$$

where x_i is the mole fraction of component i in the liquid phase, and M is the molecular weight.

The partial pressure of the component i is obtained from

$$p_i = \frac{x_i^o p_i^s \exp(-K_i p_i^s t)}{\sum_1^N x_i^o \exp(-K_i p_i^s t)}. \tag{4.340}$$

For a nonideal liquid solution, multiplying Eq. (4.331) by the activity coefficient γ gives

$$\frac{dn_i}{dt} = \frac{k_{G,i}A}{n_t} p_i^s n_i \gamma_i, \tag{4.341}$$

For an ideal solution the activity coefficient is $\gamma_i = 1$.

$$k_{G,i} = \frac{h_{m,i}}{RT}, \tag{4.342}$$

where $h_{m,i}$ is the mass transfer coefficient in m/s, which is calculated from the heat and mass transfer analogy correlations, R is the universal gas constant, and T is the absolute temperature (K).

4.4 WATER PROPERTIES AND TREATMENT

4.4.1 Introduction

It is essential that the industrial ventilating engineer have a basic understanding of the properties of water and its treatment. This is to ensure an efficiently running and trouble-free plant. Additional to these issues are the problems relating to the discharge of contaminated water to the surrounding environment.

Water treatment over the past 100 years has grown into a complex science. It is of interest to note that in the 1880s a steamship left the port of Liverpool in the UK with instructions that the boiler water was to be treated with a mixture of cow dung and peat. A short time after leaving Liverpool, the ship's boiler exploded and the ship sank. It was not reported whether the explosion was due to the unusual method of water treatment.

4.4.2 Common Water Impurities

The following factors indicate the problems that poor-quality water may cause to the engineering plant and to human health:

- Metal corrosion
- Scale formation on the heat transfer surface
- Dezincification
- Plumbosolvency
- Biological health hazards

Water supplies should never be assumed to be chemically pure. Groundwater from wells and springs contains dissolved impurities. Its properties depend

TABLE 4.13 Common Water Impurities

Constituent	Formula	Problems caused	Methods of treatment
Alkalinity	Bicarbonates (HCO_3) Carbonates (CO_3) Hydroxyl (OH) as $CaCO_3$	Steam systems: foaming and solid carry over Steel embrittlement (HCO_3) and (CO_3) Corrosion	Distillation Demineralization Lime and lime soda Dealkalization (ion exchange) Acid treatment hydrogen zeolite
Ammonia	NH_3	Corrosion of copper & zinc alloys	Cation exchanger (hydrogen zeolite) Chlorinating Deaeration
Carbon dioxide	CO_2	Severe corrosion in condensate lines	Aeration Deaeration Alkalies (neutralization) Filming and neutralization amines
Chloride	Cl	Increases solid contents Produces a corrosive solution	Distillation Demineralization
Color	—	Boiler foaming Presents problems with iron removal Discoloration of manufactured product	Adsorption (activated carbon) Coagulation Filtration Chlorination
Conductance	μS	Due to ionizing solids in solution; an increase in conductivity occurs resulting in corrosive water	Reduce dissolved solids by lime softening or demineralization
Dissolved solids	—	Caused by evaporation, in steam generation resulting in blockage and foaming Frequent blow down Loss of treated water Loss of heat	Lime softening Distillation Cation exchange. (hydrogen zeolite) Demineralization
Fluoride	F	Few major industrial water problems Reduces dental decay	Alum coagulation Magnesium Hydroxide reaction Anion exchange Membrane separation
Free mineral acids	HCl H_2SO_4	Corrosion	Any process using alkalines to neutralize
Hydrogen sulphide	H_2S	Corrosion (rotten egg smell)	Aeration Chlorination Ozone
Iron	Fe(II) (ferrous) Fe(III) (ferric)	Discolored water Deposits formed will foul surfaces	Coagulation and filtration Catalytic filtration Lime softening Aeration

(continues)

TABLE 4.13 *(continued)*

Constituent	Formula	Problems caused	Methods of treatment
Manganese	Mn(II)	See iron	See iron
Nitrate	NO_3	Increased solid content assists in the reduction of metal embrittlement Health problems with infants if used in foods	Distillation Demineralization
Oil	—	Scale Sludge Foaming Fouling of pipe work and heat exchangers	Baffle separators Strainers Coagulation Diatomaceous earth
Oxygen	O_2	Severe metallic corrosion	Addition of corrosion inhibitors, sodium sulfite Automatic air vents, deaeration
pH	$pH = \log \frac{1}{H^+}$	Graded into acidic or alkaline water Scale 0–14: 0 = highly acidic 7 = neutral 14 = highly alkaline	Increased by alkaline addition Decreased by the addition of acid
Silica	$Si\ 0_2$	Scale buildup on surrounding surfaces, reducing flow and heat transfer	Removed by applying hot magnesium salts Demineralization processes
Sulphate	SO_4	Increased solid content Combines with Ca to form calcium sulfate salt	Distillation Demineralization
Suspended solids	—	Clogs pipelines Fouls heat exchanger Surfaces	Settling Filtration
Total solids	—	Sum of dissolved and suspended solids	See dissolved and suspended solids

on the nature of the ground over which it flows or passes through. Surface water from lakes and rivers contains silt, dissolved impurities, and organic matter; its quality varies widely depending on flow rate.

Table 4.13 lists and briefly describes some of the impurities found in typical water supplies. As can be seen, a wide range of problems have been considered, and no one method of treatment is suitable for all cases. The

pharmaceutical industry and silicon chip manufacturers require the greatest purity in the water used.

4.4.2.1 Heavy Metals

Table 4.13 lists the most commonly encountered pollutants in water; however, in many industrial applications various heavy metals are frequently combined in the process discharge.

Some heavy metals are essential to life at low concentrations but are dangerous to animal and plant life in higher concentrations. Generally, it is the free metal ion that is the most toxic; however, with Hg and Sn certain organic forms have a greater toxicity.

The WHO, the CEN, and the Environmental Protection Agency in the United States specify the maximum permissible concentrations of these metals and other pollutants in the environment.

Due to the many variables involved, no attempt is made at this stage to cover the various methods used to remove these pollutants before the water is released into the environment. Table 4.14 lists the common heavy metals in water.

TABLE 4.14 Heavy Metals

Constituent	Chemical formula	Problems caused
Antimony	Sb	Moderately toxic
Arsenic	As	Highly toxic, corrosive, carcinogen
Beryllium	Be	High toxicity, long-term effects
Cadmium	Cd	Highly toxic, carcinogen
Chromium	Cr	Compounds may be highly toxic
Cobalt	Co	Moderate toxic
Copper	Cu	Highly toxic
Lead	Pb	A cumulative poison
Mercury	Hg	Very highly toxic
Molybdenum	Mo	Compounds are highly toxic
Nickel	Ni	Highly toxic, carcinogenic
Selenium	Se	Highly toxic
Silver	Ag	Low toxicity
Tellurium	Te	Highly toxic
Thallium	Tl	Sulfates highly toxic
Tin	Sn	Irritation of skin, eyes, lungs, and stomach
Titanium	Ti	Chlorides are moderately toxic
Uranium	U	Toxic, insoluble in water
Vanadium	Va	Oxides and chlorides have a high toxicity
Zinc	Zn	Moderately toxic, carcinogenic

4.4.3 Cooling Water Systems

Cooling water systems used for process heat rejection can be classified under one of the following headings:

- Open recirculation
- Closed recirculation
- Once-through system

4.4.3.1 Open Recirculation

Open recirculation includes the standard cooling tower, spray pond, or evaporator condenser as shown in Fig. 4.39. An arrangement of this type provides an efficient cooling system. Its main disadvantage is growth of microorganisms such as the *Legionella* species. To protect people from these bugs, the biological water treatment represents a very high cost in the operation of the plant. This arrangement is losing favor with many engineers and is being replaced by the less efficient closed systems.

Typical applications include heat rejection from the refrigeration plant. The highest proportion of cooling takes place by evaporation.

Advantages

1. Can cool water down to 2 °C above the wet bulb temperature

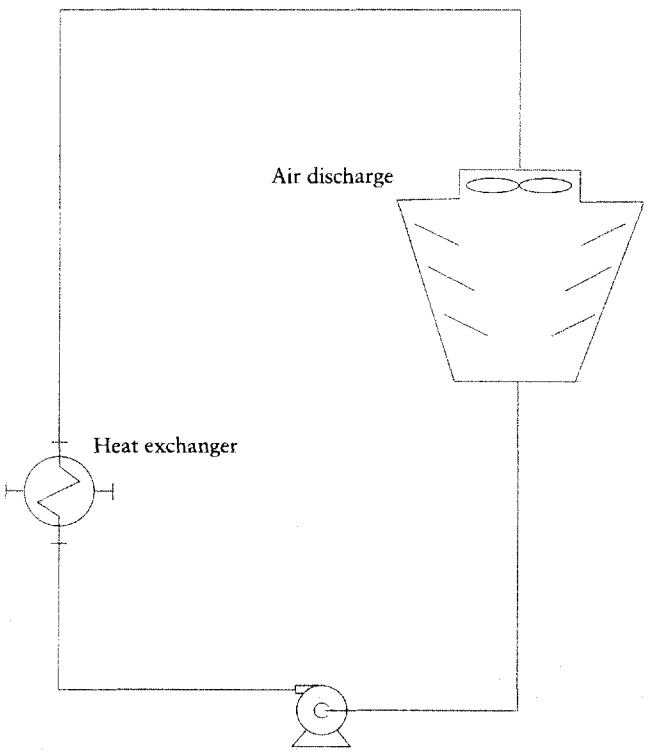

FIGURE 4.39 Cooling water system (open recirculation).

2. Average temperature drop through tower in 10–18 °C range depends on wet bulb temperature

Disadvantages

1. Corrosion due to absorption from the atmosphere of pollutants as the water droplets pass through the tower
2. Fouling of surfaces, resulting in decreased heat transfer efficiency
3. Scale buildup, resulting in a reduction of fluid flow through the heat exchanger and loss of effectiveness
4. Microbiology problems (such as 2 and above 3) together with corrosion of materials and health hazards
5. Decay problems in wooden cooling towers
6. Spray water loss, resulting in costly additional water treatment for the makeup water
7. Spray drift may cause annoyance to people in its path, as well as corrosion of adjacent metals and concrete breakdown; improved design of drift eliminators available (in PVC) for critical control of drift

The temperature difference between the recooled water temperature and the inlet air wet bulb temperature is called the *approach*. The lower the approach, the more complex the tower's design becomes. The normally used minimum approach temperature is 2 °C.

4.4.3.2 Closed Recirculation

The arrangement for closed recirculation is shown in Fig. 4.40. It overcomes many of the problems encountered with the open system. Typical applications include engine cooling and heat rejection from refrigeration plant.

Advantages

1. Compared with the open system, the average cooling water temperature drop is small, only in the 6–8 °C range.
2. Provided no water losses occur due to pipeline leaks, the cost of water treatment is at a minimum.

Disadvantages

1. Corrosion and fouling will occur, though normally considerably less than that experienced in the open system.

4.4.3.3 Once-Through System

This is the simplest of the three systems (see Fig. 4.41). Typical applications include

- Process water
- Potable water
- General service supplies

Advantages

1. Low initial cost
2. Space savings, small footprints

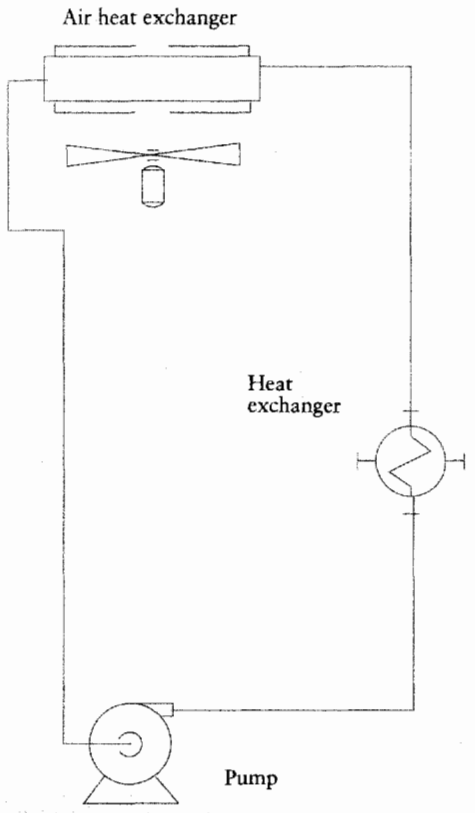

FIGURE 4.40 Cooling water system (closed recirculation).

Disadvantages

1. Low average temperature change, only in the 3–6 °C range
2. Expensive in water consumption, with large volume flow rates
3. Sewer discharge costs
4. Corrosion

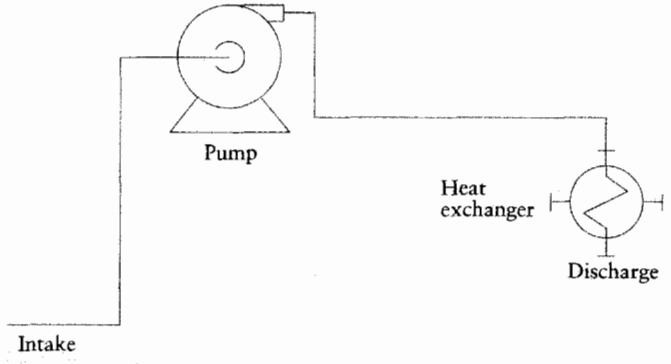

FIGURE 4.41 Cooling water system (once-through system).

5. Fouling and scale problems
6. Microbiological problems

4.4.4 Water Treatment

In most engineering applications the supply water is not suitable for immediate use without treatment. It is essential that the method of water treatment selected be the one most suited to the application. If steam is used as the working medium for a process, it is essential that water treatment be used to prevent the precipitation of substances in the water from fouling pipe work and heat exchangers; otherwise costly plant damage will result.

The method of treatment selected depends on many factors, such as the nature of the salts and the pH of the water, and the assistance of a reputable specialist company is necessary to carry out regular testing and an analysis report.

4.4.4.1 Methods of Feedwater Treatment

The treatment may be internal, which involves the addition of chemicals to the water to make the salts causing scale and sludge less likely to bond to pipe work and heat exchanger surfaces. In the case of boilers and cooling towers, blowdown of the water on a continuous or regular basis is required. Care must be taken in the case of blowdown to ensure that the exiting water temperature does not damage the drains or that the chemicals pollute waterways. The consent of the water authorities is required in order to determine what levels can be discharged into waterways. In certain cases further treatment may be necessary before discharge.

In the case of boilers operating at low pressure, organic materials such as natural and modified tannins, starches, or alginates are added to aid blowdown. For boilers operating at high pressure, synthetic materials such as polyacrylates and polymethacrylates have been developed. The most commonly used chemicals for boiler feedwater treatment are phosphates and hydrazine.

External treatment involves the removal of impurities from the water by various methods before it enters the plant; this is the most effective method of water treatment. This category of treatment involves one or more of the following processes.

Sedimentation

In sedimentation the water to be treated flows slowly through a tank, allowing the suspended material in the water to fall to the base of the tank. The use of coagulating compounds, such as aluminum and ferric sulfate, increases the efficiency.

Oxidation

It is during oxidation that iron and manganese in suspension are removed from the water. Oxidizing agents (chlorine, ozone, hydrogen peroxide, potassium permanganate, etc.) or direct aeration is used; the metals in

solution are converted to insoluble oxides, which are removed by filtration. The use of gaseous chlorine is not recommended if the water contains organics, or else car- cinogenic by-products can be formed (trihalomethanes). Gaseous chlorine also presents health problems in the case of leaks and is corrosive.

Filtration

If the solution is allowed to flow through a granular bed such as sand, the larger particulate matter remains on the surface, while the smaller material is collected in the thickness of the granular bed. Pressurization of the filter accelerates the process. Besides sand, other materials used as filtering media are anthracites, manganese dioxide, and activated carbon.

Softening

The sense of touch allows one to determine if water is hard or soft. For a domestic application in a hard-water area, more soap is required to produce lather than is required in a soft-water area.

The temporary hardness salts can be removed by boiling; these salts may be classified as alkaline or carbonate hardness salts. These salts in solution are calcium carbonate, $CaCO_3$, calcium hydrogen carbonate, $Ca(HCO_3)_2$, and magnesium hydrogen carbonate, $Mg(HCO_3)_2$. Heating $Ca(HCO_3)_2$ produces water, carbon dioxide, and calcium carbonate, and this compound is deposited on heat exchangers.

The salts that cause permanent hardness are calcium sulfate, $CaSO_4$, calcium chloride, $CaCl_2$, magnesium sulfate, $MgSO_4$, and magnesium chloride, $MgCl_2$. These are known as nonalkaline or noncarbonate hardness salts and cannot be removed by boiling; they must be removed by chemical treatment.

The internal process complements the external process by taking care of any contamination that may enter the water from the process.

The following is a brief introduction to the various types of water softening plants encountered.

Lime Soda. If carbon dioxide is in solution in water and calcium hydroxide is added, the resulting precipitation product is $CaCO_3$; this can be removed by sedimentation.

If the water is temporarily hard due to the presence of $Ca(HCO_3)_2$, and calcium hydroxide is added, the resulting products will be a precipitate.

If the water is permanently hard due to $MgSO_4$, and lime is added, the precipitates calcium sulfate, $CaSO_4$, and magnesium hydroxide, $Mg(OH)_4$, result, which are removed by sedimentation.

Permanent hardness can also be due to the presence of $CaSO_4$, in which case the addition of soda (sodium carbonate), Na_2CO_3, produces sodium sulfate, Na_2SO_4, and calcium carbonate, $CaCO_3$; this precipitate once again is removed by sedimentation.

Ion Exchange. When water flows through a resin ion exchange material bed, some of the undesirable ions are adsorbed and replaced with less objectionable ones. The process may be either

- Base exchange
- Dealkalization
- Demineralization

The base exchange process removes both the temporary and permanent hardness salts from the water by allowing the water to flow through resin beads containing sodium zeolite, Na_2Z.

When the permanent hardness salt $CaSO_4$ passes through the bed, calcium zeolite (CaZ) and sodium sulfate (Na_2SO_4) are formed, which are then flushed away.

A temporary hardness salt such as calcium carbonate ($CaCO_3$) passing through a sodium zeolite bed will produce calcium zeolite (CaZ) and sodium carbonate (Na_2CO_3). This solution is flushed away. But the temporary hardness salt calcium hydrogen carbonate, $Ca(HCO_3)_2$, passing through a sodium zeolite bed, will produce calcium zeolite and sodium hydrogen carbonate, $NaHCO_3$. The latter increases the alkalinity of water, causing foaming of the boiler water due to the formation of sodium hydroxide, NaOH. Similar reactions are possible involving magnesium chloride and sodium zeolite.

After a time, depending on the concentration of salts and the flow rate, the remaining sodium zeolite is converted to either calcium or magnesium zeolite. When the zeolite becomes saturated, the resin bed must be regenerated. The regeneration process is achieved by backwashing (flushing) the bed with fresh water to remove some of the remaining solids, followed by passing a solution of salt through the resin bed. This flushing removes the calcium chloride (CaCl) and the sodium zeolite; a final rinse removes any salt remaining, allowing the process to continue.

The dealkalization process removes the temporary hardness in water. This uses an acid resin bed for regeneration—in this case sulfuric acid (H_2SO_4).

To remove the majority of the salts from water, a mixture of resins is used; the process in this case is called demineralization.

Basically, the hardness salts of calcium and magnesium ions are exchanged for sodium ions in the dealkization process; the carbonate and bicarbonate salts, which cause high levels of alkalinity, are replaced with chloride ions. Reverse osmosis can also be used to produce demineralized water.

Precipitation Softening. This process depends on sufficient holdup time within a vessel to allow sedimentation and clarification to occur. A coagulation chemical such as alum or iron salts added to the solution will improve the process efficiency.

Evaporation. The process of evaporation or distillation in the past was carried out in submerged-tube evaporators. These have been superseded by flash-type evaporators, which are more economical to run and reduce scale problems. The process is suitable for brackish water, where the cost of chemical methods is excessive. The resulting distilled water is not palatable and requires aeration to make it potable.

The operating cost is high due mainly to the energy used for the heat source, cooling water, and the necessary chemical treatment. To reduce the running costs, waste process heat or solar collectors are used.

Falling-film vertical evaporators, direct expansion systems, and vacuum freezing techniques may also be used.

Reverse Osmosis. The process of osmosis is used by plants to obtain food and moisture from the soil. The density of the sap in the roots of the plant is greater than that of the soil water surrounding it. The root wall provides a semipermeable membrane, and the difference in suction across it is the osmotic pressure.

In reverse osmosis, the osmotic pressure is increased manually to get the water to flow from a high-density area through a semipermeable membrane to the lower-density weaker solution. The water will pass through the membrane and leave the solids behind. A pressure of about 2.76 MPa will extract 90% or more of the dissolved absorbed solids; further refinement may be achieved through a base exchange process.

Magnetic Water Treatment. This method is used in marine engineering and district heating networks in Russia. The hard water to be treated, either hot or cold, flows first through a filter and then at high velocity through permanent magnets. The magnetic field influences the nature of the crystallization of the hardness salts. This results in numerous nuclei being formed in the solution, creating sludge instead of a hard scale, which is easily removed by blowdown.

Deaeration

The removal of all gases in the water by means of traps or chambers will improve the pumping characteristics and reduce corrosion and noise.

In the case of hot water, the oxygen in the water becomes about twice as corrosive for every 20 °C increase in temperature; hence, removal of the oxygen is of prime importance. Oxygen is extremely corrosive in hot-water systems containing demineralized water

In groundwater, gases such as carbon dioxide, hydrogen sulfide, and radon may be dissolved under pressure. For efficient removal, an intensive degassing process (GDT, or Gas-Degas Technology) has been developed by the GDT Corporation (USA). It consists of groundwater and air (or ozone) being intensively mixed in a venturi injector, followed by optimum residence time in a reactor vessel, and finally the efficient removal of unwanted stripped gases in a centrifugal separator.

Oxygen Scavenging

By removing oxygen completely, corrosion by this gas is eliminated. It can be achieved by the addition of sodium sulfite or hydrazine, which reacts with oxygen. The reaction product will not normally cause any problems.

Scale Control

Chemicals such as disodium or the polyphosphates are used to precipitate scale-forming solids in the water. If alkalinity control is required, caustic soda

or soda ash is used in controlled amounts. For some boiler water, treatment-chelating agents are used to full advantage.

For a high-pressure boiler plant with a high evaporation rate, demineralized feedwater is classified as having an electrical conductivity of less than 0.2 $\mu S\ cm^{-1}$; for less critical plant conditions an electrical conductivity greater than 0.2 $\mu S\ cm^{-1}$ may be acceptable.

The water chemistry relating to power plants operating at high temperatures and pressures is a complex issue. To determine if water is corrosive or scale forming, use is made of the Langelier or Ryznar index. For further information, refer to the VGB guidelines for plants operating at pressures above 68 bar (VGB-450L) and the Scandinavian recommendations (DENA).

Sludge

Either straightforward drainage or blowdown can readily remove sludge from the plant. It is, however, necessary in some cases to ensure that the residual solids are free-flowing; this is achieved by the use of tannin, lignin, seaweed derivatives, and starch organics.

Foam

Water level control and the use of organic antifoam chemicals are essential in steam plants in order to break down the bubbles at the water surface in steam systems, which cause foaming.

Condensate

Condensate formed in steam systems may require treatment to remove the carbon dioxide in suspension or free-flowing in the condensate. Due to the nature of the water source, carbon dioxide and oxygen as dissolved gases are always present to some degree in water supplies, and in some instances hydrogen sulfide (H_2S) and ammonia (NH_3) may be present, producing a weak carbonic acid gas and causing elevated-temperature corrosion of metals. Treatment in this case is achieved by the addition of chemicals, pH control, oxygen removal, etc.

When dealing with a large steam plant, the chemistry and the methods of water treatment required are complex.

The efficiency of water separation varies considerably from boiler to boiler. The purity of the steam supplied to a steam turbine should be checked. On the basis of the results, the maximum allowable salt concentration in the boiler water can be determined. This concentration may be much lower than the values given in the table.

When the heat load even locally exceeds 230 $kW\ m^{-2}$ the target values for drum pressure, 160 bar (except for SiO_2), should be used for all boiler pressures. For feedwater, the recommended values for >67 bar should be used.

1. The maximum *p*-value is independent of feedwater treatment.
2. The gauge pressure when using phosphates to reduce the residual hardness and when using a coordinated phosphate method for pH

control fall in the pressure range of 35–90 bar PO_4 between 10 and 20 mg kg^{-1} and in the range 67–125 bar between 7 and 15 mg^{-1}.

3. γ_{25} = Conductivity of boiler water from a neutralized sample at 25 °C.

Although the table is outside the scope of most industrial ventilating engineering requirements, it does indicate the many problems to be considered in the measurement techniques.

To finish this section, a typical flow diagram has been included (Fig. 4.42).

Biological Factors

It is essential that the engineer not lose sight of the numerous potential problems related to microbiological concentration. These include

- Microbiological fouling in heat exchanger pipelines, cooling towers, etc.
- Microbiological corrosion in pipe work
- The effects of contaminated water on human health

In the case of a closed water system, once the correct water treatment is provided, the incidence of microbiological fouling or corrosion is virtually eliminated, provided that the addition of fresh water is not a frequent occurrence. It is, however, essential to have water tests carried out at regular intervals by a water laboratory.

In the case of an open water system, the problem is compounded due to the addition of microorganisms from the atmosphere. Water temperature control is critical to stop the water from becoming a breeding soup culture for the microorganisms.

The aerosols formed in an open system, if inhaled, can cause various forms of *Legionella.* No one biocide is adequate to control these, as there are some 30 known groups, the most virulent being *Legionella pneumophila.*

It is essential to practice good design of all open systems by adhering to set guidelines. A well-planned and effective maintenance program is of prime importance.

The use of ozone for water treatment is now well established and has the following advantages:

- An efficient biocide
- Low owning and operating costs compared with other methods
- No chemical handling, storage, or discharge problems
- Simple methods of automatic control

Ozone is more effective than chlorine in deactivating poliovirus, *Cryptosporidium parvum, Giardia lamblia,* and other protozoa. It also improves the color, taste, and odor of water dramatically. However, since no residual amount remains, it is always necessary to add a small amount of a more stable disinfectant as well (sodium hypochlorite, chlorine dioxide, etc.).

The disadvantages are

- High or medium initial cost. The energy cost for ozone synthesis is about 12–15 kW h $(kg\ O_3)^{-1}$ consumed (1999), while 10–15 years ago it was in the 25–30 kW h $(kg\ O_3)^{-1}$ range.
- Limitations on water temperature and quality.

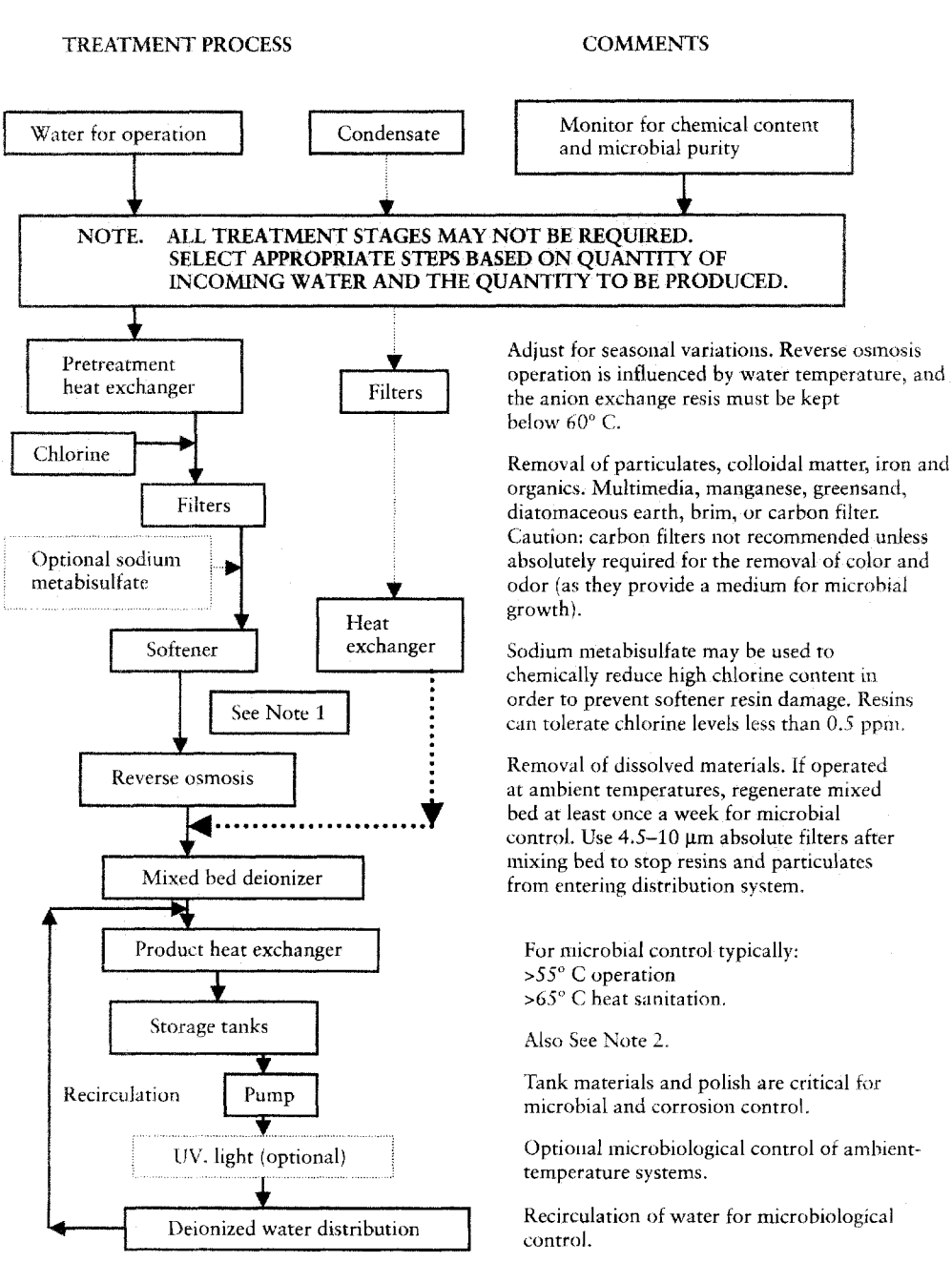

Note 1: Older systems may have cation/anion deionizers in place of softeners/reverse osmosis.
Note 2: Older systems may use chlorination for microbial control.

FIGURE 4.42 Typical flow diagram of water treatment.

References

TM.13, *Minimising the Risk of Legionnaire's Disease* (CIBSE).
Approved Code of Practice on the Prevention or Control of Legionellosis (Health and Safety Commission, UK).
The Control of Legionellosis Including Legionnaires' Disease (Health and Safety Executive, UK).

4.4.4.2 Separation Techniques

Up to now, only the water treatment aspects relating to the efficient running of a plant have been covered. It is necessary to consider the discharge of the water from any cleaning process into the waterways or drainage systems, in order to ensure that statutory regulations are not violated. The following techniques are briefly considered:

- Separation of a liquid from a solid.
- Separation of a solid from a liquid.

The selection of the method used depends on many complex factors, which are not covered in this paper. The basics of each of the two methods are briefly covered. Only a few of these techniques would be used in the water treatment procedure encountered in the industrial ventilation field; however, for the sake of completeness others are also covered.

Separation of a Liquid from a Solid

The removal of the various solid particulates from a gas stream may be achieved by washing either with chemicals or with water. Once this process has been carried out, the problem is to remove the solids from the liquid in order to

- Reuse the liquid
- Collect any valuable particulate matter for recycling
- Ensure that the drainage system is not contaminated

Numerous techniques may be used, each with disadvantages and advantages. The methods used are

- Gravitational force
- Centrifugal force
- Application of a vacuum
- Application of mechanical force
- Action of a solvent
- Displacement
- Vaporization

In considering each of these techniques, the properties and principles on which they depend are related to the liquid only.

The solid in the liquid mixture must be considered as

- Nonvolatile
- Insoluble

- Unaffected by the treatment to which it is subjected
- Capable of being reused with a minimum of treatment
- Not causing any problems when discharged into the drains
- Discharging into drains less than 40 °C with pH in the 6–11 range

Removal by Gravitational Force. This method simply involves a settling chamber in which the fact that the liquid–solid mixture–solid pore interface has little holding power. Thus, given sufficient time, the solids will settle into the base of the chamber due to gravitational forces.

The efficiency of this operation can be improved by the use of finely perforated vee troughs, which will contain the particulate matter and allow the liquid to descend to the base of the container, where it then drains away either for further treatment or for reuse.

Removal by Centrifugal Force. This method is more efficient in extracting the particulate matter from a liquid due to the fact that the forces developed are many times greater than the force of gravity.

The machine used is normally the basket-type centrifuge, which is a rotating perforated drum with a vertical axis. The solids remain in the drum and the liquid passes out through perforated holes. The smaller the holes, the greater the collection efficiency. However, there is the risk of hole clogging, causing a rapid fall in operating efficiency. The fluid viscosity and the particulate size are of prime importance. Plant arrangement in series using different-size perforations tends to overcome the clogging problems.

Vacuum Removal. This approach is used in the paper industry for denaturing the paper, in which a vacuum is applied under the paper stock.

Mechanical Force. Liquid can be readily expelled from a spongelike particulate mass of solid by using various pressing techniques. With this method, mechanical energy is used to force the liquid containing the particulate matter through a porous bed. The particulate matter is held in the pores in the bed. When the pressure drop reaches a certain level, replacement or backwashing takes place. This process may be either intermittent or continuous.

Solvent Action. Materials that tend to respond well to extraction by pressing will be more effective in solids removal when solvents are used. The complication is that it becomes necessary to separate not only the solids and the containing liquid from the finished process, but the solvent as well.

Displacement. This approach, which displaces one liquid from a solid mass by the introduction of another, is seldom used.

Vaporization Methods. The above methods may be unacceptable on certain counts, and if complete removal of the liquid from the solid is required, vaporization methods are used. A nonvolatile solid can be removed from a volatile liquid by the application of heat, a vacuum, or both.

The various techniques can be classified as

- Heat applied at atmospheric pressure
- Heat applied at reduced pressure
- Vapor distillation

The dryers make use of warm air, flue gases, and direct radiant heat to the liquid-particle mixture. This method allows complete extraction of the solid through removal of the liquid by vaporization. Due to the energy input required with this method, it is the most costly.

Separation of a Solid from a Liquid

A solid in a liquid medium may be in either of the conditions:

1. The solid may be dissolved into the liquid medium.
2. It may be insoluble and remain suspended in the liquid.

The liquid is assumed to be saturated if undissolved material is present, with solids both in suspension and in solution in the liquid phase.

The efficiency of separation will obviously affect the purity of the liquid, and it may be necessary to provide a series of separate stages to meet the standard required by the specification.

The most important consideration is the actual condition of the solid in the liquid. Is it in solution, or is it in suspension? Other considerations are

1. The relationship of the solid to the liquid
   (a) Solids in solution in the liquid
      - The solid concentration in the solution
      - Degree of solubility
      - The relationship between temperature and solubility
      - The viscosity of the liquid

   (b) Solid in suspension in the liquid
      - The relative amounts of solids in suspension
      - The size of solid particulate matter
      - The density of the particulate matter
      - The compacting properties of the solid
      - The viscosity of the liquid medium
      - The nature of the solid— spongelike, gritty, etc.
2. The degree of separation required
3. The heat-sensitive properties of the solid or liquid
4. Corrosive nature of solids and liquids
5. The degree of separation required for both the liquid and the solid

6. The value of the recovered solids or liquids
7. The volume of materials to be treated

The following list provides an indication of the various techniques on which the separating methods are based.

- Relative vapor pressure of the solid and liquid
- The phase relationship between the solid and liquid
- The relative solubility of immiscible solvents
- Reduction of solubility
- Chemical precipitation
- Ion exchange
- Electrolytic deposition
- Adsorptive properties

The separation of solids in suspension in liquids can be achieved by either of the following techniques

- Density difference
- The cross-section of the solid particulate matter
- The electrostatic properties of the solid

Next we briefly consider each of the above in turn.

Relative Vapor Pressure of Solid and Liquid. If the dissolved solids in a liquid have a low vapor pressure relative to the liquid in which they are dissolved, provided the solid is not affected by the liquid boiling point, it is an easy matter to vaporize the liquid, leaving a dry residue.

Phase Relationship between the Solid and Liquid. A phase relationship may involve a number of crystalline forms from which materials can be separated. When a solid material is precipitated as a result of the solution becoming supersaturated, crystallization occurs. Crystallization may be achieved by

- Cooling alone
- Concentration
- Concentration followed by cooling
- Simultaneous concentration and cooling

Relative Solubility of Immiscible Solvents. Many solid materials in solution can be removed by transferring them to a second solvent; it is essential that the solvents be mutually insoluble.

This approach will not produce a solid; it can, however, be used to remove a solid from one solution or solvent and transfer it to another, from which it can be readily removed.

Reduction of Solubility. It is possible to remove a solid from a solution by changing the condition of a solvent. One method is the addition of a second solvent miscible with the first, in which the solid in solution is relatively

insoluble. Another method depends on the fact that if the substance can be ionized, its solubility can be suppressed. This is achieved by adding a highly ionized second substance having one ion in common with the original dissolved solid.

Chemical Precipitation. If physical separation techniques do not work, separation may be achieved by chemical conversion to a soluble precipitate.

Ion Exchange. Certain solid substances have the property of exchanging one ion for another if placed in a solution containing the ions. Typical substances with this property are the zeolites and certain synthetic resins.

Electrolytic Deposition. The separation of a metal from a solution can be achieved by electrolysis.

Adsorptive Properties. Substances such as silica gel and activated charcoal can be used to collect (adsorb) certain solids from solution. The adsorber bed may be discarded when depleted or recycled by washing and heating.

Separation of Solids in Suspension in Liquids. This can be achieved using

1. Density difference
2. The difference in cross-section between the solid particulate matter and the liquid molecule
3. The electrostatic properties of the solid

Density Techniques. Many methods are in use, with the selection depending on

- Particulate size
- Settling velocity
- Quantity of solids in suspension

In the case of gravitational settling, the unit design depends on the method of solid removal after settling. The methods in use are

- Removal of solids from the separation unit in which they are contained
- Intermittent or continuous discharge of the solids from the base of the unit
- Continuous discharge over the rim of the settling tank
- Separation by centrifugal force

Gravity filters used in the density removal are subdivided into

- Sand gravity
- Continuous gravity

Vacuum Filters. If, due to the nature of the liquid, the gravity filter becomes unsuitable, a vacuum filter is used to create a substantial pressure difference. Vacuum filters can be divided into the following types:

- Intermittent filters
- Leaf filters
- Continuous (e.g., rotary vacuum) filters
- Vacuum pressure filters, as used in desulfurization plant
- Pressure filters

In the true gravity case, pumps are not used. If, however, the liquid is highly viscous, to achieve efficient operation, pumps are required to force the fluid through the pressure filters. The pump can be considered essentially as a press with a plate-and-frame filter. The plate-and-frame filter consists of a series of frames over which the filter medium is stretched. A centrifugal basket of fine mesh is another method of particulate removal.

Dialysis. If a solution containing colloidal particle is placed on one side of a dialysis membrane, the water on the other side will allow the solution to be reduced in concentration as it passes through the membrane.

Electrostatic Properties of Solids in Suspension. Some solids in suspension will migrate from one pole to another when placed between direct current electrodes. The phenomenon of solids moving toward an electrode is known as cataphoresis.

To close this section on treatment, two more methods that depend on bacteriological action are considered:

- Aerobic treatment
- Anaerobic treatment

Aerobic Treatment. The activated sludge process depends on aerobic biological action. In this case the microorganisms, in searching for food, break down the complex organic substances into simple stable substances. This process results in the removal of soluble and suspended organic matter from wastewater.

The growth of microorganisms in the presence of dissolved oxygen removes the majority of pollutant matter; in turn, protozoa grow and feed on these organisms. The resulting balance is of a living culture in suspended form in the activated sludge floc. This process is ideally suited for the removal of carbonaceous matter and nitrification from wastewater.

The principal elements of the system include an aeration tank in which the wastewater is thoroughly mixed with continuously activated sludge and oxygen. From this part of the process, it passes into a clarifier tank, where the settled sludge is removed from the purified water to be recycled by the return activated sludge pumps.

For this system to work, two exacting requirements must be met. The aeration device must be capable of both transferring oxygen from the atmosphere to the liquid, and distributing this oxygen throughout the wastewater to the

suspended living microorganism. This type of system is suited for low-strength waste, typically on the order of 50–200 mg L^{-1} BOD.

To enhance the purification process and increase the degree of purification, powdered activated carbon (PAC) may be added directly to the aeration tank, or the biologically treated wastewater may be filtered through granulated activated carbon (GAC) for posttreatment.

Pre- or post-treatment with ozone of wastewater may also be applied. Pretreatment with ozone takes place in the presence of biorefractory compounds, as ozone increases the BOD/COD ratio.

Anaerobic Treatment. Typical of this method is the upflow anaerobic sludge blanket. This consists of a corrosion-resistant tank complete with separators. The flow network enters the reactor base without short-circuiting, ensuring the proper formation of the granular sludge. New bacterial cells are formed in the reactor and aggregate into tiny granules, which have good settling characteristics.

Biogas is produced by the bacteria in the form of small bubbles; these float upward through the sludge bed/blanket, providing a good mixing action. When the biogas reaches the top of the reactor, it is collected and used as a fuel.

Design Considerations

In determining the best method of treatment, the following factors have to be considered:

Owning and Operating Costs

- Initial cost
- Maintenance
- Energy costs
- Water treatment
- Corrosion costs
- Odor treatment
- Abrasion problems
- Slurry pumping problems
- The maximum temperature the drains and the water sinks can accept (bearing in mind thermal stresses and corrosion in discharge pipelines, and algae growth and oxygen depletion in the watercourses)

Properties of Liquid Used

- Vapor pressure
- Temperature of decomposition
- Viscosity
- Density

Properties of Solid Being Extracted

- Temperature of decomposition
- Solubility
- State of subdivision
- Surface absorptive properties
- Elasticity

In some cases, fragility related to the dryness of the resultant solid, which will influence the removal technique

Relationship between Liquid and Solid

- Mechanically held liquid
- Liquid absorbed on solid surfaces

Removal Efficiency Required. This depends on design requirements and current legislation.

Requirements for Regeneration

- Of liquid
- Of solid
- Of both liquid and solid

Equipment Availability. In many cases the equipment is not available "off the shelf," and the delivery time may be lengthy; hence, adequate planning is necessary to ensure that the commissioning date can be met with the plant selected.

4.4.4.3 Heat Transfer Fluids

It is prudent at this stage to briefly consider the problems that can be experienced in either refrigeration or heat recovery systems when water treatment is required to prevent freezing. The antifreeze treatment of pure water may be achieved by various means, typical ones being various brines, ethylene glycol, and propylene glycol.

In the treating of water by any of these methods, it must be remembered that due to property changes, they can cause problems on both the heat transfer characteristics and fluid flow characteristics compared with pure water.

Many proprietary trade heat transfer fluids are in common use. Depending on operating temperatures, typical characteristics are

- Density from 600 to 1100 kg m^{-3}
- Specific heat capacity from 1.12 to 2.75 kJ kg^{-1} K
- Thermal conductivity from 0.1 to 0.29 W m^{-1} K.
- Boiling points up to 340 °C at atmospheric pressure
- Freezing points down to –15 °C

TABLE 4.15 Typical Properties of Some Fluids

Temperature (°C)	Solution	Solution by weight	Density (kg m^{-3})	Specific heat (kJ kg^{-1} $°C^{-1}$)	Thermal conductivity W m^{-1} °C	Viscosity (pa s × 10^{-3})	Freezing point (°C)	Boiling point (°C)
−1	Sodium chloride	12	1092.6	3.6	0.485	2.2	−8.5	102.0
	Calcium chloride	12	1109.0	3.47	0.57	2.4	−7.2	101.0
	Methanol water	15	985.3	4.187	0.485	3.2	−10.3	86.0
	Ethylene water	20	977.2	4.35	0.47	5.3	−11.1	87.2
	Ethylene glycol	25	1036.5	3.85	0.52	3.7	−10.7	102.8
	Propylene glycol	30	1033.3	3.93	0.45	8.0	−10.6	102.2
−10	Sodium chloride	21	1166.3	3.35	0.43	4.2	−17.2	102.2
	Calcium chloride	20	1198.3	3.0	0.54	4.8	−17.2	101.1
	Methanol water	22	967.6	4.06	0.45	5.3	−15.5	83.3
	Ethylene water	25	977.2	4.27	0.43	8.3	−15.5	86.1
	Ethylene glycol	35	1057.3	3.60	0.48	6.8	−17.8	103.9
	Propylene glycol	40	1046.0	3.73	0.41	20.0	−4.2	103.3
Water at (0 °C)			999.87	4.2174	0.569	1.792	0	100

- Dynamic viscosity of 0.9×10^{-3} to 1.2×10^{-3} Pa s
- Flash points from 108 to 263 °C

The influences these factors have on fluid flow in the tubes are as follows:

- What may be turbulent flow in the heat exchanger for water will reduce to transitional or laminar flow for the heat transfer fluid, reducing the coefficient of heat transfer to a value 70% or more of that for water.
- Viscosity changes make conventional water pipe sizing tables useless; these must be upgraded by the application of appropriate correction factors.
- Density changes.
- Specific heat capacity changes.
- Thermal conductivity changes.

Table 4.15 gives typical properties of some fluids. For other fluids, contact the manufacturer for exact data. With heat transfer oils, care must be taken that chemical changes such as carbonization do not take place.

This page intentionally left blank

5

PHYSIOLOGICAL AND TOXICOLOGICAL CONSIDERATIONS

LARRY G. BERGLUND

Tohoku University, Japan

JONATHAN W. KAUFMAN

Naval Air Warfare Center, United States

ULF LANDSTRÖM

National Institute for Working Life, Umeå, Sweden

KAI M. SAVOLAINEN

Department of Industrial Hygiene and Toxicology, Finnish Institute of Occupational Health, Helsinki, Finland and Department of Environmental Medicine, National Public Health Institute, Kuopio, Finland

PENTTI KALLIOKOSKI

Department of Environmental Sciences, University of Kuopio, Kuopio, Finland

Industrial Ventilation Design Guidebook

5.1 THERMAL COMFORT

5.1.1 Introduction

Humans seek and want thermal comfort, even at work in industrial settings. Clothing, activities, posture, location, and shelter are chosen, adjusted, altered, and sought consciously and unconsciously to reduce discomforts and enable us to focus more on the other tasks of life. Discomfort can contribute to mistakes, productivity decreases, and industrial accidents.[1–4] Thermal discomfort results from the physiological strain of thermoregulation. The strain can be in the form of altered body temperatures, sweating and excessive skin moisture, muscle tension and stiffness, shivering, and loss of dexterity. A small

amount of discomfort can sometimes enhance concentration and productivity by heightening arousal but too much discomfort is clearly detrimental.

Thus, thermal comfort is clearly desirable and important to the well-being and productivity, and thereby the financial health, of industry. An understanding of the principles of thermal comfort and discomfort can help guide a designer's efforts in creating and operating industrial environments that are both energy-efficient and thermally acceptable to the occupants.

A commonly expressed definition[5] is: "Thermal Comfort is that condition of mind that expresses satisfaction with the thermal environment." The definition implies that the judgment of comfort is a mental process that results from physical, physiological, and psychological factors and processes. Dissatisfaction can lead to complaints and other undesirable side effects.

Manufacturing engineers, operators, and owners, of course, want to minimize complaints. A goal in the design process should be to recognize this objective and work to minimize discomfort from the outset. In general, designs that provide satisfying or acceptable environments will be financially more successful for the designer. That is, individual productivity will not be impaired by the environment, resulting in fewer accidents and lost time, fewer complaints, reduced employee turnover, and lower insurance costs.

Why Is One Comfortable? What Affects Our Comfort?

Both primary factors and lesser secondary factors affect our sense of satisfaction with the thermal environment. The primary factors have significant reproducible effects and directly affect heat transfer and the occupant's thermal state. Secondary factors that may affect one's sense of satisfaction with a space are conditions such as color and ambiance, local climate, age, physical fitness, sound, food, and illness. These secondary factors have smaller to negligible effects on one's thermal state and will not be discussed here, but such information is available.[6]

5.1.2 Primary Factors

Humans and the other warm-blooded animals have developed thermoregulatory systems to carefully control body temperature to levels that enable them to function and survive effectively. In general, thermal comfort occurs when the physiological effort to control body temperature is minimized for the activity. Table 5.1

TABLE 5.1 Thermal Environment and Physiological Responses of Thermoregulation

Thermal environment	Physiological responses
HOT	↑blood flow to skin (vasodilation), heart rate ↑, sweating ↑, skin moisture ↑, body temperatures ↑, metabolism ↑
NEUTRAL	comfort, minimized effort, T_{mb} (mean body temperature) ~ 36.2 °C
COLD	↓blood flow to skin (vasoconstriction), muscle tension and shivering ↑, body temperatures ↓, metabolism ↑

illustrates that as conditions deviate from neutral the body activates mechanisms to stabilize body temperature. These efforts all result in small but noticeable and measurable increases in metabolism and physiological effort.

Body Temperature

To maintain proper body temperatures (T), metabolic energy (M) must be continuously transferred to the environment.

Energy balance:

$$\text{metabolism} - \text{energy losses} - \text{work} = \text{rate of energy storage in body}$$
$$M - L - W = C\,dT/dt$$

where

$$\text{energy losses } (L) = \text{dry heat loss} + \text{evaporative heat loss}$$

If $M - W > L$, then body $T \uparrow$ — feel warmer
If $M - W < L$, then body $T \downarrow$ — feel cooler

The body temperature limits for health in terms of internal or core temperature are fairly limited. The limits are basically related to the function of nervous tissue. Body temperatures around 28 °C or less can result in cardiac fibrillation and arrest. Temperatures of 43 °C and greater can result in heat stroke, brain damage, and death. Often, too high a temperature causes irreversible shape changes to the protein molecules of nervous tissue. That is, cooling overheated tissue to normal temperatures may not restore its original function.

Metabolism

Metabolism is often characterized by a convenient, relative, and dimensionless quantity called the met unit:

$$\text{met} = \text{metabolism/resting metabolism} \tag{5.1}$$

The metabolism of a resting person is then 1 met. Some met levels of various activities are listed in Table 5.2.

Metabolic energy is often normalized in terms of energy per unit area of skin (1 met = 58.2 W/m^2):

$$M/A_D = 58.2 \cdot \text{met watts/m}^2 \tag{5.2}$$

TABLE 5.2 Met Level of Various Activities

Reclining	~0.8 met	Walking 5 km/h	~3 met
Seated and quiet	~1.0 met	Standing and heavy activity (heavy work, garage work)	~3 met
Standing	~1.2 met	Basketball	~5–8 met
Standing and light activity (shopping, lab, light industry)	~1.6 met	Max	~10–12 met
Standing and medium activity (house work, machine work)	~2 met		

or

$$M = A_D \cdot 58.2 \cdot \text{met watts}, \tag{5.3}$$

where A_D is body surface area in m^2. The subscript D refers to the DuBois equation[6] commonly used for calculating the area of the skin:

$$A_D = 0.202 m^{0.425} h^{0.725} \ m^2, \tag{5.4}$$

where m = mass (kg), h = height (m). Surface areas are generally in the range of 1.4 to 2.2 m^2.

In some activities metabolic energy may be converted to useful work (force · distance). At steady state the rate of doing work P = force · distance/time and the thermal losses must balance with metabolism:

$$M = P + L \tag{5.5}$$

and if the rate of work is expressed as a thermal efficiency, $\eta = P/M$, then Eq. (5.5) simplifies to

$$M(1 - \eta) = L \ . \tag{5.6}$$

Example

Determine the met level of a person who bicycles up a 150 m-high hill in 10 minutes. The person weighs 75 kg and is 182 cm tall. The bicycle weighs 10 kg.

work of cycling up the hill = force · distance

$$= (75 + 10) \cdot 9.8 \cdot 150 = 124\ 950 \text{ N m}.$$

The work is accomplished over a period of 10 minutes, so

$$P = 124\ 950/(10 \cdot 60) = 208 \text{ Nm/s} = 208 \text{ watts}.$$

Cycling with the legs is rather efficient and it can be reasonably assumed that the thermal efficiency (η) is about 20%. Thus

$$M = P/\eta \cong 208/0.2 \cong 1040 \text{ W}.$$

This energy, normalized per unit of body surface area (M/A_D) where

$$A_D = 0.202 m^{0.425} h^{0.725} = 0.202 \cdot 75^{0.425} \cdot 1.82^{0.725} = 1.95 \ m^2,$$

is

$$M/A_D = 1040/1.95 = 533.3 \ W/m^2.$$

Expressed in terms of met:

$$M/A_D = 533.3/58.2 = 9.2 \text{ met}.$$

Since this activity is greater than about 7 met, the effort of breathing may make it difficult to talk during the climb.

Physiological Temperature Regulation

For most situations and conditions in daily life, the human can be represented adequately by a simple model that is helpful for understanding human thermal regulation.[7] The model has two thermal compartments (Fig 5.1). The

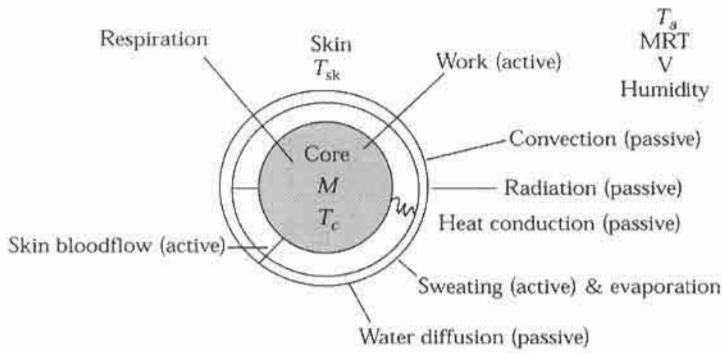

FIGURE 5.1 Simple representation of physiological temperature regulation in man.

compartments are characterized as having relatively uniform temperatures throughout. The bigger compartment (85 to 95% of body weight) represents the body's core and contains all of the muscles and other significant heat- and energy-generating tissue. Blood profusion of the muscles and internal organs distributes the heat fairly well so the core can be represented as having an approximately uniform temperature (T_c). The smaller compartment represents the skin with uniform temperature T_{sk}. The temperature uniformity of this simple lumped parameter model is reasonable for people at sedentary to medium activities (0.7–5 met) in conditions where healthy people feel slightly cool to very hot.

Essentially all the energy produced in the body by the various metabolic activities is generated in the core. The skin functions as a protective and heat transfer surface for the core. As such, the skin, which is about 1.6 mm thick on average, has tissue with very small oxygen needs and heat-producing capabilities. The energy (M) produced by the core includes the extra heat generated by muscles in tensioning and shivering (Table 5.3) under active control for thermoregulation. In humans, shivering thermogenesis potentials are small with a maximum incremental heat increase capability of about 1 met.

The metabolic energy generated by the core (M) is lost by (1) doing work, (2) respiration, (3) passive heat conduction to the skin, and (4) active blood flow to the skin. Any heat not transferred from the core is stored, with a resulting increase in core temperature. Work is energy that leaves the body as in

TABLE 5.3 Active Physiological Controls: Shivering, Sweating and Skin Blood Flow

shivering $= K_{shiv} \cdot (T_{skset} - T_{sk}) \cdot (T_{cset} - T_c)$ W/m^2, $T_{skset} \equiv 33.7°$ C $T_{cset} \equiv 36.8°$ C

skin blood flow $= (BFN + C_{dil} \cdot (T_c - T_{cset}) / (1 + Str \cdot (T_{skset} - T_{sk}))$ liters/(h m^2)
where BFN is normal blood flow to skin for its metabolic needs. It is small ~6.3 L/h/m^2. SKBL↑ as T_c↑ >36.8° C , SKBL↓ as T_{sk}↓ <33.7° C

sweat $= K_{sw} \cdot (T_{mb} - T_{mbset})e^{(T_{sk} - T_{sksct})/10.7}$ g/min/m^2, where $T_{bm} = \alpha T_{sk} + [1 - \alpha]T_c$
and $\alpha \approx 0.1$.

the raising of a weight or other thermodynamic work (force · distance) activities. Respiratory heat loss occurs from bringing ambient air into the core, raising its temperature to near core temperature, humidifying it to near saturation at core temperature, and exhaling it. The resulting heat loss is proportional to breathing rate and to the temperature and humidity differences. The breathing rate or air flow through the lungs is regulated mainly by CO_2 levels in the blood and as a result is proportional to metabolic rate.

The skin receives heat from the core by passive conduction and active skin blood flow (Table 5.3). It transfers this heat to the surroundings by convection, radiation, and evaporative (perspiration and diffusion) mechanisms. All of these mechanisms are unregulated or passive except evaporation from sweating. The sweating process is actively controlled by the human's thermoregulatory center where the rate of sweat secretion is proportional to elevations in core and skin temperature from respective set point temperatures (Table 5.3).

The physiologically active elements in body temperature regulation, summarized in Table 5.3, function and regulate in part on deviations in body temperatures from set points. In humans thermogenesis by shivering is small and inefficient in comparison to other animals. Thus the very precise regulation of body temperature in man is primarily due to only two active mechanisms associated with the skin: blood flow and sweating. Under normal comfort conditions, blood flow to skin is about 6 liters per hour per m^2 of skin. Of this about 1.5 L/(h m^2) is for the relatively constant minimal metabolic needs of the skin. In hot environments and during exercise skin blood flow can be increased by 15 times to about 90 L/(h m^2).[7] When necessary to reduce heat loss in cold environments, the vessels can restrict blood flow to as little as 1 L/(h m^2). With continued heat exposure, the thermoregulatory system increases its sensitivity so that blood flow increases with smaller and smaller changes in body temperature as the body acclimates to the hot environment.

Sweating, the other powerful heat loss mechanism actively regulated by the thermoregulatory center, is most developed in humans. With about 2.6 million sweat glands distributed over the skin and neurally controlled, sweat secretion can vary from 0 to 1 L/(h m^2). The other, lesser, passive evaporative process of the skin is from the diffusion of water. The primary resistance to this flow is the stratum corneum or outermost 15 μm of the skin. The diffusion resistance of the skin is high in comparison to that of clothing and the boundary layer resistance and as a result makes water loss by diffusion fairly stable at about 500 grams/day.

When the energy flows in and out of a compartment do not balance, the energy difference accumulates and the temperature increases or decreases. The changes in core and skin temperature then in turn alter the physiological control signals to restore balance and thermal stability.

5.1.3 Body Control Temperatures

Body temperatures are primarily sensed by temperature sensors in the hypothalamus near the center of the brain. Arterial blood flowing over and near the hypothalamus gives it information about the average thermal condition of

the body. In addition, there is evidence that temperature sensors in the spinal cord and gut also give the hypothalamus core temperature information.[8] The skin has abundant numbers of warm and cold sensors that also communicate to the hypothalamus (Fig. 5.2).

Thermal Sensation

The temperatures monitored in Fig. 5.2 are used by the brain to regulate shivering, blood flow to the skin, and sweating. The sensed temperatures also contribute to our overall feelings of warmth and other thermal sensations. Thermal sensation (TS) can be predicted over a wide range of activities (0.8 to 4 met) from simple deviations in the mean body temperature (T_{mb}) from the mean body temperature when the person feels neither warm or cool but neutral (T_{mbn}) (Fig. 5.2).

The mean body temperature is a weighted average of core and skin temperatures, with core temperature being much more important. That is as it should be as the purpose of the regulation system's operations is to maintain core temperature for the brain and other vital organs. The mean body temperature for a neutral thermal sensation is about 36.2 °C. At temperatures above or below that, one feels progressively warmer or cooler, which further protects the individual by stimulating conscious behavioral actions to reduce physiological strain and restore neutral sensations.

During transients the rate of change of mean body temperature can have a strong effect on thermal sensation.

$$\frac{dT_{mb}}{dt} = 0.9\frac{dT_c}{dt} + 0.1\frac{dT_{sk}}{dt} \tag{5.7}$$

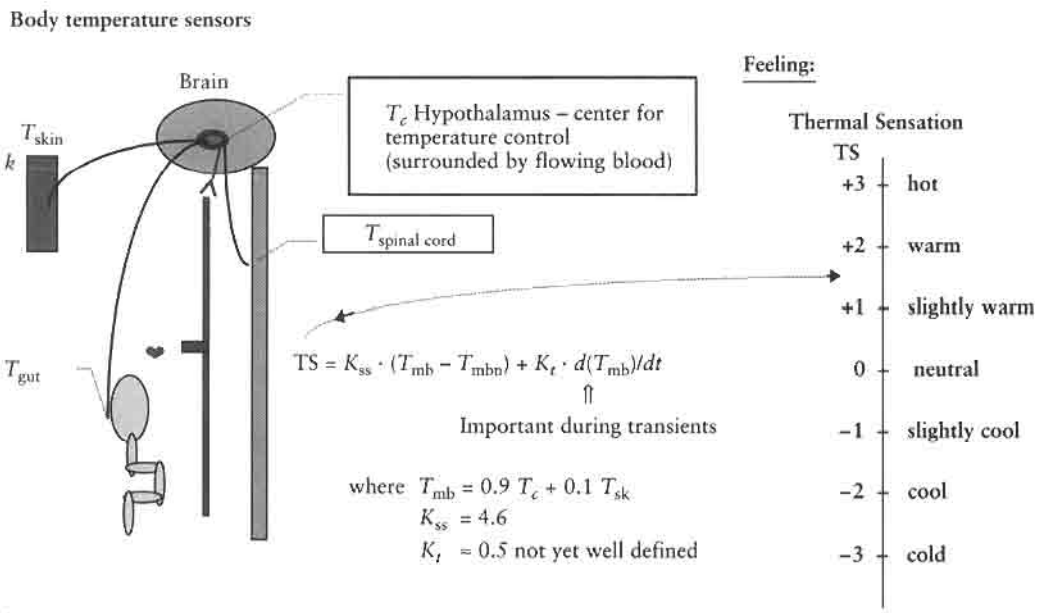

FIGURE 5.2 Temperature sensors for temperature regulation and thermal sensation.

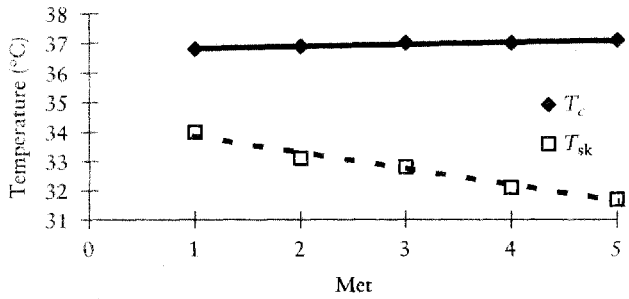

FIGURE 5.3 Schematic of skin and core temperatures for a neutral thermal sensation.

In most transient environmental situations, it is rapid changes in skin temperature that affect our feelings of warmth; rapid changes in core temperature only occur during rapid changes in metabolism and possibly during transient radar or other microwave exposures. Diving into cold water after a hot sauna is pleasant rather than cold because core temperature remains high and dT_{sk} reduces the hot thermal sensation.

In summary, core temperature is much more important than skin temperature in determining how warm we feel. Core temperature is affected by metabolic activity and heat storage. It is relatively isolated from the environment except through whole-body heat balance and resulting heat storage. Feet and hands have little metabolic heat generation themselves and depend on warm blood from the core for their temperature. The feeling of cold feet then means that the whole body heat balance has caused the core to lose temperature and the hypothalamus is restricting heat flow to the feet in order to stabilize the core temperature.

The consequence of the relationships of Table 5.3 and Fig. 5.2 is that for a neutral thermal sensation, at steady state, the core temperature increases while the skin temperature decreases with increased metabolic activity (Fig. 5.3). The increase in metabolism causes sweating which decreases skin temperature.

5.1.4 Clothing

Thermal Insulation

Clothing affects heat and moisture loss. Increasing the thickness or number of layers of clothing increases its insulating capability and reduces body heat loss. Clothing insulation is usually described with the clo unit. Originally, 1 clo was defined as the thermal resistance necessary for comfort while sedentary in a uniform still air environment of 21 °C. In conventional SI nomenclature 1 clo has a thermal resistance of 0.155 K m^2/W. Some ensembles' clo values and associated comfort temperatures are shown in Fig. 5.4.

The clothing insulation necessary for comfort or a neutral thermal sensation (TS = 0) in a thermally uniform 50% RH still-air environment is graphed in Fig. 5.5.[9] The slope of the graph is such that comfort temperature is decreased about 0.6 °C for each 0.1 clo increase in clothing insulation. The

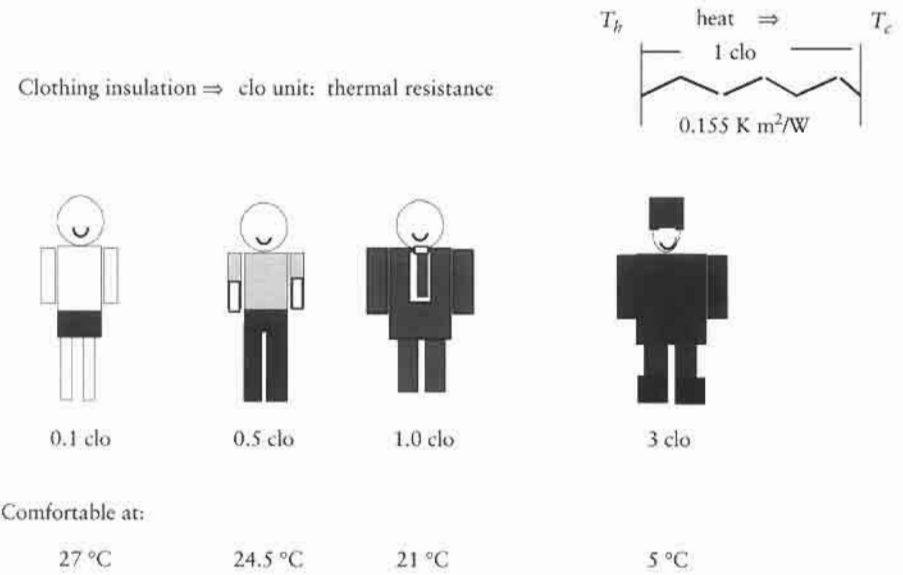

FIGURE 5.4 Some clothing ensembles with associated clo values and comfort temperatures.

graph is for 1 met but the line can be shifted to cooler temperatures for increased metabolism at the rate of −1.4 K/met.

From Fig. 5.5, comfort is possible in still air from 18 to 27 °C by adjusting clothing insulation from 1.5 to 0 clo. This has significant building energy reducing potential with buildings only heated to 18 °C and cooled to 27 °C. However, personal, societal, and institutional preferences, norms, and codes usually limit the possible clo variation to a narrower range. For sedentary-

TABLE 5.4 Clo Values of Some Individual Clothing Items

Item	clo_i	Item	clo_i
Trousers (thin)	0.15	Sweater (thin)	0.25
Trousers (thick)	0.24	Sweater (thick)	0.36
Sweat pants	0.28	Jacket (thin)	0.4
Overalls	0.30	Jacket (thick)	0.7
Coveralls	0.49	Sleeveless vest (thin)	0.13
Walking shorts	0.08	Sleeveless vest (thick)	0.22
Short-sleeved knit sport shirt	0.17	Sandals	0.02
Short-sleeved dress shirt	0.19	Shoes	0.03
Long-sleeved dress shirt	0.25	Boots	0.1
Long sleeved flannel shirt	0.34	Ankle-length athletic socks	0.02
Long-sleeved sweatshirt	0.34	Calf-length socks	0.03
T-shirt	0.08	Long underwear (top)	0.2
Underwear	0.05	Long underwear (bottom)	0.15

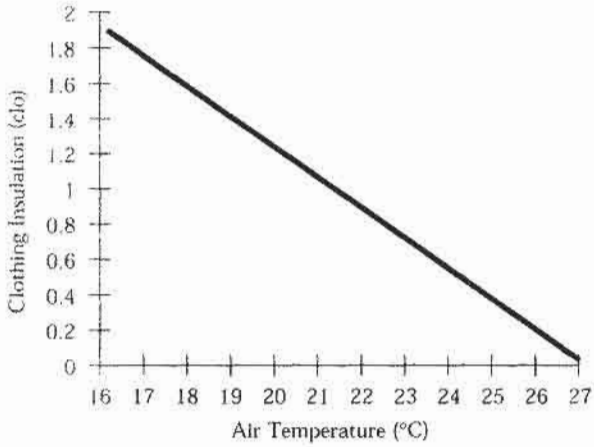

FIGURE 5.5 Clothing insulation necessary for neutral thermal sensation of sedentary persons (1 met) in a thermally uniform still-air environment with 50% relative humidity.[9] For higher activity levels the temperature at a clo level can be reduced about 1.4 °C per met increase.[10]

long-term comfort and because the hands are usually uncovered, the minimum practical temperature is about 20 °C.[11]

Clo values are usually measured on heated manikins in specialized laboratories. The skin temperature of the manikin is controlled to about 33 °C and the power input is measured (Fig. 5.6). Clo can also be similarly measured on humans with instruments to measure T_{sk}, metabolism, and rate of weight loss.

A very useful way to estimate clo is by summing the clo values of the individual items worn:

$$\text{clothing insulation (clo)} = \sum \text{clo}_i. \tag{5.8}$$

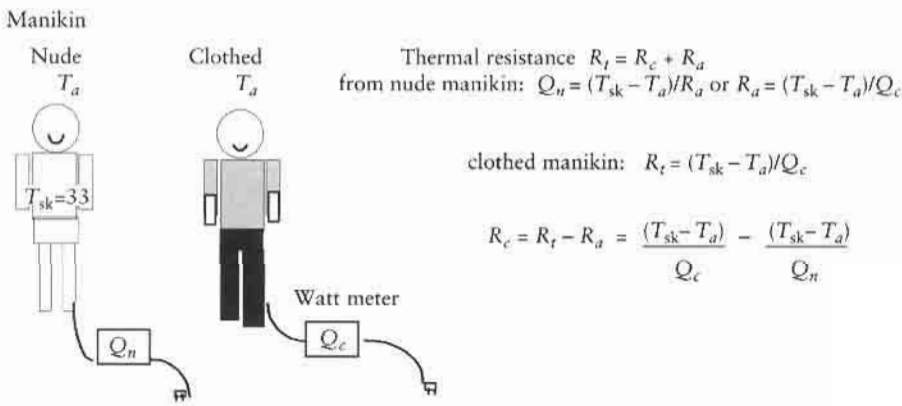

FIGURE 5.6 Clo value measured on heated manikins in a controlled environment.

Some clothing item clo values are listed in Table 5.4.[9] For example, the clo value of a person wearing a thin shirt, thin trousers, underwear, shoes, and socks estimated by this method would be: $0.17 + 0.25 + 0.05 + 0.05 = 0.52$ clo. If the person were to add a T-shirt under the shirt, the clothing insulation would be expected to increase to 0.6 clo.

Effect of Chairs on Clothing Insulation

When a person is sitting, the chair generally has the effect of increasing clothing insulation (ΔI_{cl}) by up to 0.15 clo depending on the contact area (CSAC) between the chair and body. Specifically,

$$\Delta I_{cl} = 7.48 \cdot 10^{5} \cdot \text{CSAC} - 0.1\text{clo}, \tag{5.9}$$

where CSAC is the chair surface area contact in cm^2 or the surface area of the chair in contact with the human.[6,12]

For example, a desk chair with a body contact area of 2700 cm^2 has a ΔI_{cl} of 0.1 clo. This amount should be added to the insulation of the standing clothing ensemble to obtain the insulation of the ensemble when a person is sitting in the desk chair,

$$\text{clo}_{\text{sitting}} = \text{clo}_{\text{standing}} + \Delta I_{cl}. \tag{5.10}$$

Effect of Walking on Clothing Insulation

Body motion generally increases the ventilation of garments and thereby carries away heat and decreases the clothing ensemble's effective insulation. The increased airflow between the garment and the skin is due to a combination of increased air speed and the pumping action of the garment as it flexes during movement. As a result, walking decreases clo. The change in clothing insulation (ΔI_{clw}) can be estimated from the standing intrinsic insulation of the ensemble ($\text{clo}_{\text{standing}}$) and the walking speed (S) in steps per minute:[6,13]

$$\Delta I_{clw} = 0.504 \cdot I_{cl} + 0.0281 \cdot 10^{-3} \cdot S - 0.24 \text{ clo} \tag{5.11}$$

Thus the insulation of the walking person is found by subtracting the walking effect from the insulation of the standing clothing ensemble,

$$\text{clo}_{\text{walking}} = \text{clo}_{\text{standing}} - \Delta I_{clw}. \tag{5.12}$$

For example, the clothing insulation of a person wearing a winter business suit with a standing intrinsic insulation of 1 clo would decrease by 0.52 clo when the person walks at 90 steps per minute (about 3.7 km/h). Thus the ensemble's intrinsic insulation when walking would be 0.48 clo. More complete clothing tables and figures are available in the literature, for example Chapter 8 of the *ASHRAE Handbook of Fundamentals*.[6]

5.1.5 Comfort Zones

In general, when a person is thermally comfortable, the person's thermal sensation for the whole body is at or near neutral as depicted in Fig. 5.7*a*. As we have seen, the thermal conditions necessary for comfort are affected by clothing insulation. Figure 5.7*b* shows the range of temperatures and humidities

that are considered comfortable by ASHRAE Standard 55-94 for the typical summer and winter clothing levels of Fig. 5.7*a*.

In Fig. 5.7*b*, the comfort zone at 50% RH for the 0.9 clo winter clothing is from 20 °C to 23.5 °C and for the 0.5 clo summer clothing is from 22.5 °C to 26 °C. The temperature boundaries on the right and left sides of the comfort zones have constant ASHRAE Effective Temperature (ET*) levels. An ET* line is the locus of conditions that are calculated to have the same heat loss from the skin, skin temperature, and skin moisture levels. Since the physiology of the skin is the same for a constant ET* line, the thermal sensation and comfort judgments are also generally constant along the line. The temperature value of this line is the temperature where the relative humidity is 50%. Along an ET* line the environment feels the same as it feels for air at temperature T at 50% RH. The ET* lines are not vertical but are affected by humidity and the human's physiological responses to the environment. Thus on the warm side of a comfort zone the humidity has more of an effect than on the cool side of the zone. But the differences in the slopes are not large and both

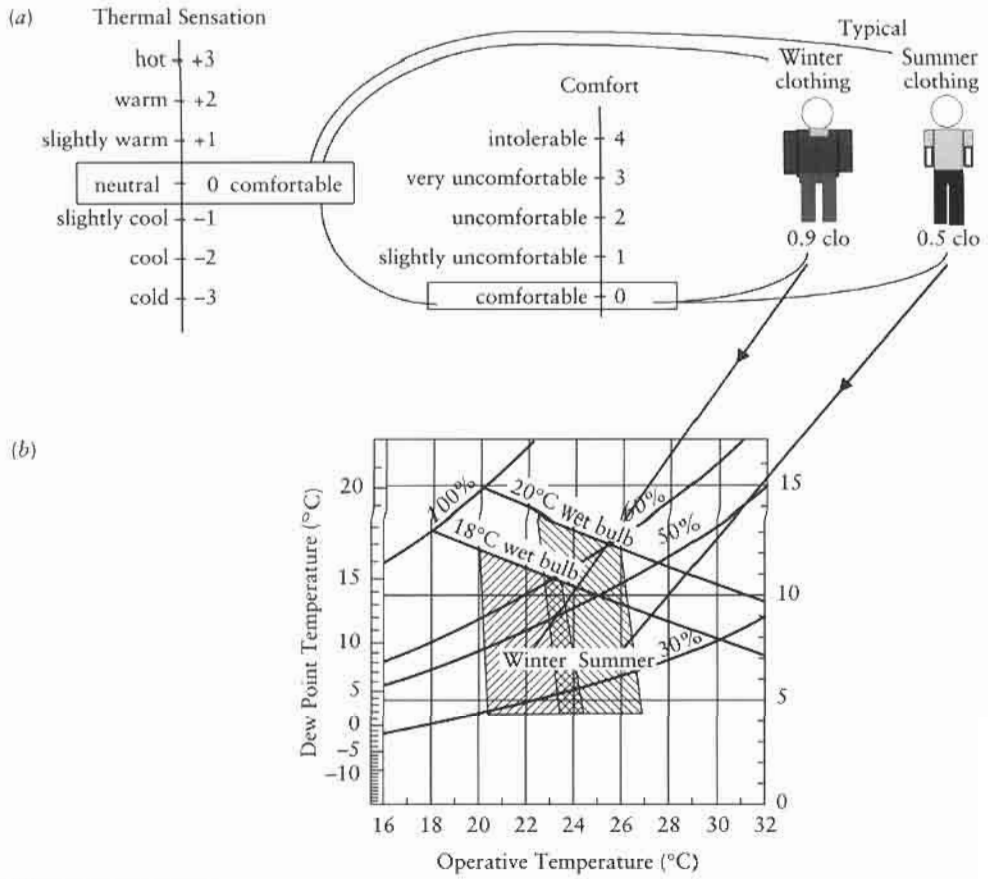

FIGURE 5.7 (*a*) Comfort and thermal sensations of a comfort zone. (*b*) Conditions for comfort on pyschometric chart for sedentary persons (≤ 1.2 met).[14]

indicate that temperature has a much stronger effect than humidity on the human thermal response. That is, the ET* lines show that for the same thermal sensation at a higher humidity the temperature must be lower. On average, for an 11 °C increase in dew point the temperature would need to be 1 °C lower to have the same thermal sensation. In terms of human response the boundaries are not hard and sharp as indicated in Fig. 5.7*b* but instead are more soft and fuzzy in nature.

Optimum comfort would be in the center of each zone. Moving away from the center, some people would be expected to have thermal sensations approaching −0.5 and +0.5 at the cooler and warmer ET* borders. The zones of Fig. 5.7*b* are for sedentary or slightly active ($M \leq 1.2$ met) people. If the activity level is higher than that, then the ET* line borders can be shifted about 1.4 K lower per met of increased activity. Similarly, if the clothing is different than the 0.9 and 0.5 clo vales of Fig. 5.7*a*, the temperature boundaries can be decreased about 0.6 K for each 0.1 clo increase in clothing insulation. Another, similar way to adjust the comfort zone for both different activity levels and clo values is to shift the zone centered on the optimum temperature ($T_{\text{sedentary}}$) at 50% RH as

$$T_{\text{active}} = T_{\text{sedentary}} - 3(1 + \text{clo}) \cdot (\text{met} - 1.2)\ ^{\circ}\text{C} \quad . \tag{5.13}$$

Conditions that are warmer than the applicable still-air comfort zone of Fig. 5.7*b* can often be made comfortable by increasing the air speed. If the conditions are 1 to 6 °C warmer than the still-air comfort zone of Fig. 5.7*b*, the necessary air speed (v) to restore thermal balance and comfort can be estimated from Fig. 5.8, where $T - T_{\text{comf}}$ is the temperature difference between the environment and the still-air comfort temperature. Though the increased air speed will bring the whole-body thermal sensation to the comfort level, air motions above 0.8 m/s or so may cause other kinds of discomfort from

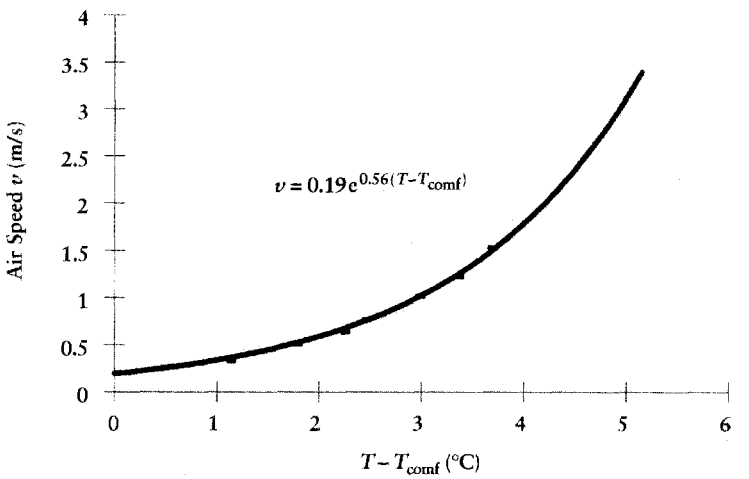

FIGURE 5.8 Air speed necessary at temperature T for the same thermal response as T_{comf} in a still-air environment (≤0.2 m/s).

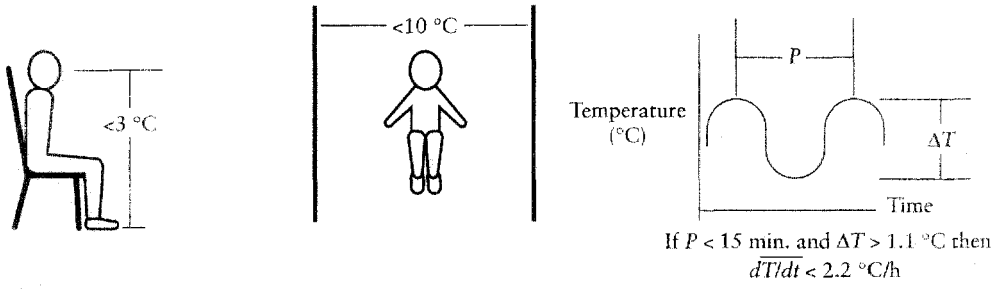

FIGURE 5.9 Nonuniformity limits to avoid discomfort.

moving papers, hair, and other light objects, and the pressure of the air speed itself may affect some people.

5.1.6 Spatial and Temporal Nonuniformity

The thermal parameters for comfort should be relatively uniform both spatially and temporally. Variations in heat flow from the body make the physiological temperature regulation more difficult. Nonuniform thermal conditions can lead to nonuniform skin temperatures. The active elements of the regulatory system may need to make more adjustments and work harder in order to keep thermal skin and body temperatures stable. To avoid discomfort from environmental nonuniformities, the temperature difference between feet and head should be less than about 3 °C (Fig. 5.9) and the mean surface temperature or radiant difference from one side of the body to the other should not be greater then about 10 °C.

Similarly, with cycling temperatures, large fast cycles can cause discomfort. To avoid this, if the time to complete one cycle is less than 15 minutes and the peak-to-peak temperature variation is greater than 1.1 °C, the average rate of temperature change should be less than 2.2 °C/h (Fig. 5.9). Very slow rates of temperature change ($dT/dt < 0.5$ °C/h) are much less difficult to adjust to and the change can go unnoticed until the temperature is beyond the comfort zone temperature.

Local air motion is another thermal nonuniformity that can cause a local cooling of the skin and the feeling of a draft. Draft discomfort from local air motion increases as the air temperature decreases below skin temperature. Fluctuations in the local air motion increase the perception of drafts and should be avoided. The unsteadiness of air motion is often described in terms of its turbulence intensity (Tu):

$$\mathrm{Tu} = \mathrm{SD}_v / \bar{v}, \tag{5.14}$$

where $\bar{v}$ is the average air speed of the draft and SD_v is its standard deviation. In spaces with forced air systems, the turbulence intensity is typically between 0.3 and 0.6.[15] That level of turbulent intensity generally limits maximum air speeds to < 0.2 m/s for occupants in cool environments.[16] However, in warm environments turbulence intensity is desirable as it increases the cooling effectiveness of the air motion.[17]

5.1.7 Thermal Radiation and Operative Temperature

In buildings away from outside perimeter walls, air and surface temperatures are usually approximately equal. The heat losses from a person by radiation (q_r) and convection (q_c) are then flowing to the same temperature level. In such uniform spaces, the radiant and convective losses are about equal and together account for about 80–90% of the total heat loss of a sedentary comfortable individual. In the presence of hot or cold surfaces, as may occur in perimeter or other locations in a building, the average surface temperature of the surroundings (called mean radiant temperature) as seen by the person's body may be substantially different from air temperature. If the mean radiant temperature (MRT) is greater or less than air temperature (T_a) the person will feel warmer or colder than in a thermally uniform space where MRT = T_a.

To simplify the effects of radiation and convection on dry heat transfer, the concept of operative temperature is often used. By definition operative temperature is the temperature of a uniform environment (T_a = MRT) that has the same total dry heat loss (convection + radiation) as the actual environment where $T_a \neq$ MRT.

Dry heat losses (q_{dry}) from the person's surface at temperature T_s can be expressed as

$$q_{\text{dry}} = q_c + q_r = h_c \cdot (T_s - T_a) + h_r \cdot (T_s - \text{MRT}) \quad , \tag{5.15}$$

where the convective (h_c) and linearized radiation (h_r) heat transfer coefficients are

$$h_c = 8.5v^{0.5} \text{W/m}^2\,\text{K with } v \text{ in m/s} \tag{5.16}$$

and

$$h_r = 4e\sigma(A_r/A_D)[273.2 + (T_s + \text{MRT})/2]^3 \ \text{W/m}^2\,\text{K}, \tag{5.17}$$

where

e = emissivity of clothing-body surface ≈ 0.9,
σ = Stefan-Boltzmann constant, 5.67×10^{-8} W/m^2 K
A_r = effective radiation area of body, m^2 $(A_r/A_D) \approx 0.7$

A_r is less than the skin area A_D because some of the skin of fingers, arms, legs, and feet radiates to other skin and is not as effective for radiant heat loss. Equation (5.15) can be rearranged to

$$q_{\text{dry}} = (h_c + h_r) \cdot [T_s + T_o] \tag{5.18}$$

where T_o is the operative temperature,[6] evaluated as $T_o = [h_c \cdot T_a + h_r \cdot T_r]/(h_c + h_r)$. The equation shows that operative temperature is the average of air and mean radiant temperatures weighted by their respective heat transfer coefficients. It is the temperature of a uniform environment that physically and mathematically represents the actual environment. Fortunately, for the low air speeds ($v < 0.25$ m/s) of most indoor environments $h_c \cong h_r$ and operative temperature becomes the simple average of the air and mean radiant temperatures,

$$T_o \cong (T_a + T_r)/2. \tag{5.19}$$

At higher air speeds $h_c > h_r$, convective heat loss becomes greater than radiation and T_o approaches T_a. For such conditions Eq. (5.20) is recommended:[9]

$$T_o = AT_a + (1 - A)\text{MRT}, \tag{5.20}$$

where A depends on air speed (v):

v (m/s)	0–0.2	0.2–0.6	0.6–1.0
A	0.5	0.6	0.7

The above indicates that to maintain a constant level of comfort when MRT decreases, T_a must be increased an equal amount. This is the difficulty of perimeter zones. In many such environments the air and surface temperatures differ and operative temperature is a convenient way to characterize the environment.

How is mean radiant temperature (MRT) determined? One could calculate or measure the surface temperatures of the room and calculate MRT from

$$\text{MRT} = [(F_{p-w} \cdot T_{rw}^4 + F_{p-f} \cdot T_{rf}^4 + F_{p-c} \cdot T_{rc}^4) \quad + + + \quad [F_{p-n} \cdot T_{rn}^4]^{1/4}, \tag{5.21}$$

where T_{rn} is the absolute temperature (K) of the radiating surface n and F_{p-n} is the angle factor from the person to surface n,[6,18] and F_{p-n} is the fraction of radiation leaving p that strikes n.

If the surface temperatures are not widely different, Eq. (5.21) can be simplified to

$$\text{MRT} = [(F_{p-w} \cdot T_{rw} + F_{p-f} \cdot T_{rf} + F_{p-c} \cdot T_{rc}) \quad + + + \quad F_{p-n} + T_{rn}. \tag{5.22}$$

At a location MRT and T_o are often measured with a sphere or ellipsoid representing the person, as shown in Fig. 5.10. In the diagram the energy balance on the globe at steady state is $q_c = q_r$, or

$$h_c \cdot (T_g - T_a) = h_r \cdot (\text{MRT} - T_g), \tag{5.23}$$

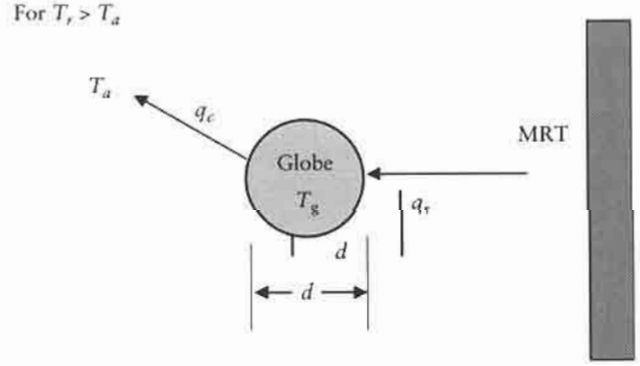

FIGURE 5.10 The determination of MRT.

and after rearranging:

$$\text{MRT} = T_g + [h_c/h_r] \cdot (T_g - T_a) \tag{5.24}$$

Substituting numerical values for h_c and h_r with $d = 15$ cm and v in m/s,

$$\text{MRT} = T_g + 0.247v(T_g - T_a) \ . \tag{5.25}$$

Further, from the definition of operative temperature (T_o),

$$T_o = (h_c \cdot T_a + h_r \cdot \text{MRT})/(h_c + h_r) . \tag{5.26}$$

Substituting Eq. (5.24) into Eq. (5.26) and rearranging,

$$T_o = \frac{T_a + [h_r + h_c]_h \cdot T_g + [h_r/h_c]_h \cdot [h_c + h_r]_g \cdot (T_g - T_a)}{1 + [h_r/h_c]_h} \ , \tag{5.27}$$

where subscripts h and g designate the human and globe. For 15 to 20 cm diameter globes $[h_r/h_c]_g \cong [h_r/h_c]_h$, which after substituting and rearranging Eq. (5.27) simplifies to

$$T_o = T_g . \tag{5.28}$$

Globes can be made of any opaque material. A globe of low mass is helpful to provide a short time constant for transient conditions. Globes are typically gray or black, but color is not important if they do not receive high temperature radiation from the sun or other glowing objects. If significant high-temperature radiation is present, then they should have a color similar to that of the occupant. The comfort zones of Fig. 5.7*b* should be entered with T_o when it is known that $\text{MRT} \neq T_a$ because T_o is the temperature that the environment feels like to the occupant of the space.

Warm Discomfort and Skin Moisture

In warm environments or situations with prolonged activities above about 1.2 met there is sweating. The sweat glands put water on the skin for evaporative cooling. Since the latent heat of evaporation of water is so high very little water is consumed in this cooling process. In the process the skin gets wet. If the conditions are very good for evaporation the skin can remain nearly dry while sweating occurs, as for example in windy desert conditions. In humid still-air conditions a larger surface of water is necessary to evaporate the sweat and the skin becomes wetter. The fraction of the surface of the skin that is covered with water for evaporation is called skin wettedness (w).[19] It is a measure of the physiological strain or effort of evaporative cooling and has long been associated with warm discomfort (Fig. 5.11). It is rare that a person feels comfortable with a skin wettedness above 20 to 25%.

Some of the discomfort of warm environments, the perception of skin moisture, and the interactions of clothing fabrics with the skin may be due to the moisture itself. The skin's outer layer of dead squamous cells of the stratum corneum can readily absorb or lose water. With moisture addition, the cells swell and soften. With drying, they shrink and become hard. In this setting the skin's moisture may be better indicated or characterized by the relative humidity of the skin (RH_{sk}) rather than skin wettedness,[24]

$$\text{RH}_{\text{sk}} = P_m/P_{\text{s,sk}}, \tag{5.29}$$

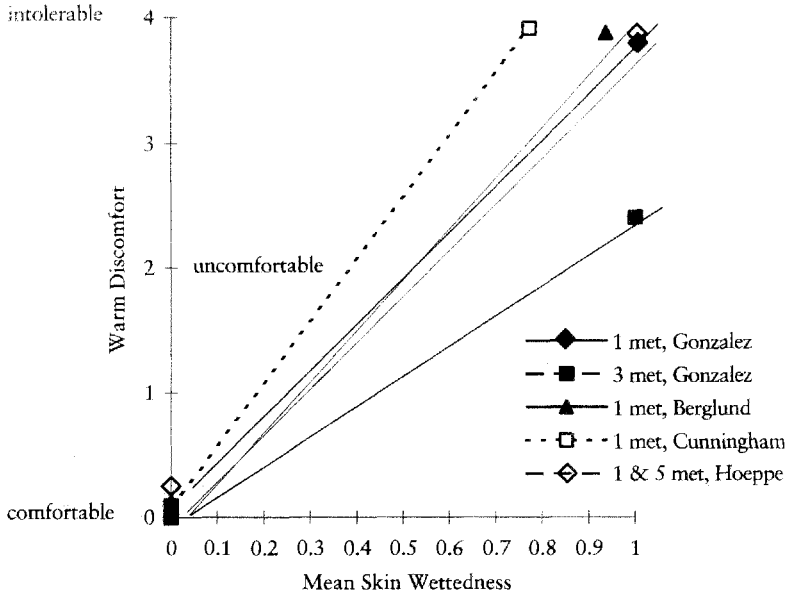

FIGURE 5.11 Warm discomfort related to skin wettedness from various studies.[20]

where P_m is the average vapor pressure of the skin and $P_{s,sk}$ is the saturated vapor pressure of water at skin temperature. Typically, the water content (water/dry skin) of the stratum corneum is about 10% but it can absorb as much as four times its dry weight.

Skin moisture may be detected by mechanoreceptors of the skin and hair follicles or some other neural mechanism that senses the skin's swelling and shrinking. At high levels of skin moisture the swelling is sufficient to close or reduce the lumen of sweat glands and reduce sweating (called hydromeiosis). Hydromeiosis occurs at $RH_{sk} \geq 0.9$.[25] Conversely, under good drying conditions the skin can shrink to the extent that lesions form.

As mentioned previously, the other term for characterizing skin moisture is skin wettedness (w) or the size of the water film as a fraction of total skin area that is necessary to account for the observed evaporative heat loss from the skin (E_{sk}),

$$E_{sk} = w \cdot A_{du} \cdot h_e \cdot (P_{s,sk} - P_a), \tag{5.30}$$

where A_{du} is total skin area, h_e is evaporative heat transfer coefficient, and P_a is the ambient vapor pressure.

Skin wettedness and skin relative humidity are related by

$$RH_{sk} = w + (1 - w)(P_a / P_{s,sk}) . \tag{5.31}$$

From Eq. (5.30) it is clear that RH_{sk} will be greater than w except when $w = 1$. It is also evident that with a constant w, RH_{sk} increases with ambient absolute humidity. Thus, though the ET* temperature boundaries have con-

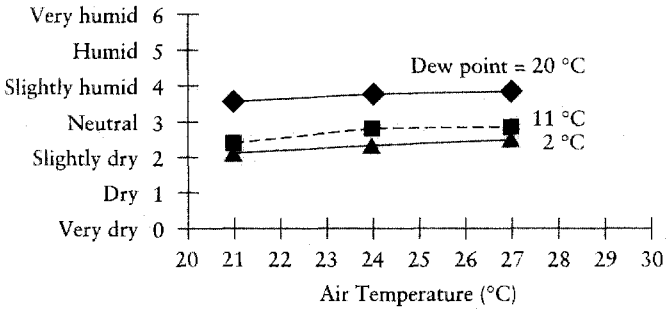

FIGURE 5.12 Perceived ambient humidity by sedentary subjects.

stant skin wettedness levels, the RH_{sk}, swelling, and softening of the skin increase with increasing ambient absolute humidity.

Humans are sensitive to moisture and can reliably describe the humidity of the environment using word scales as demonstrated in Fig. 5.12.[10] The subject's humidity judgments appear to be functions of the air's dew point, a measure of absolute humidity, and are relatively unaffected by the ambient temperature. Further, people are also good at perceiving skin moisture, as illustrated in Fig. 5.13, where perceived skin wettedness is seen to correlate well with measured skin wettedness.

In situations of prolonged sweating, skin wettedness slowly increases with time because of accumulating salt on the skin. The increasing salt occurs because the water in perspiration evaporates while the dissolved materials, principally sodium chloride, remain on the surface. The salt lowers the vapor pressure of the sweat film, decreasing its rate of evaporation per unit area. The area of the film then naturally increases in order that evaporation will equal the rate of sweat secretion. It is thought that part of the relief that bathing brings after a warm day or strenuous activity is that by cleaning the skin, perspiration can then evaporate more efficiently with reduced skin wettedness.

Clothing can be one of the detractors from acceptability in humid environments. Measurements by Gwosdow[26] reveal that the friction between skin and clothing increases abruptly for skin wettedness levels above 25%. Further, fabrics are perceived to be rougher or to have a coarser texture and to be less pleasant with increasing skin moisture. This may be one of the reasons that, in the comfort studies cited earlier, the people have rarely indicated they were comfortable when they had skin wettedness levels near and above 25%.

Low Humidity

Low humidity also affects comfort and health. Comfort complaints about dry nose, throat, eyes, and skin occur in low-humidity conditions, typically when the dew point is less than 0 °C. Low humidity can lead to drying of the skin and mucous surfaces. On respiratory surfaces, drying can concentrate mucus to the extent that ciliary clearance and phagocytic activities are re-

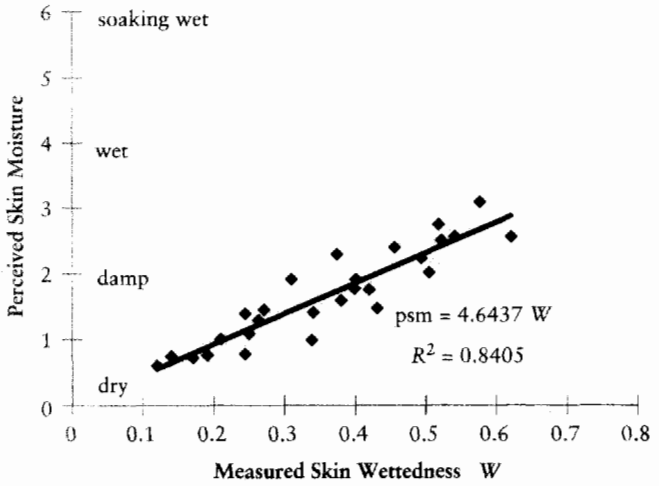

FIGURE 5.13 Perceived skin moisture correlated to measure skin wettedness for activities from 1 to 3 met.

duced, increasing susceptibility to respiratory disease as well as discomfort. Green[27] quantified that respiratory illness and absenteeism increase in winter with decreasing humidity. He found that any increase in humidity from the low winter levels decreased absenteeism. Excessive drying of the skin can lead to lesions, skin roughness, and discomfort and impair the skin's protective functions. Dusty environments can further exacerbate low-humidity dry skin conditions.[28]

Liviana et al.[29] found that drying from low humidity can contribute to eye irritation. Eye discomfort increased with time in low-humidity environments $T_{dp} < 2$ °C.

High Humidity

Comfort is reduced by elevated humidity levels. It is recommended[30] that on the warm side of the comfort zone the relative humidity should not exceed 60% to prevent warm discomfort. On the cool side of the comfort zone, high humidity is less important because there is no sweating to increase skin moisture. For these reasons the upper boundaries of comfort zones in Fig. 5.7*b* are wet bulb temperatures of 18 and 20 °C for the winter and summer comfort zones respectively.

References

1. Langkilde, G., Alexandersen, K., Wyon, D. P., and Fanger, P. O. (1973). Mental performance during slight cool and slight warm discomfort. *Archives Des Sciences Physiologiques* 27, 511–518.
2. Macworth, N. H. (1946). Effects of heat on wireless operators hearing and recording Morse Code messages. *Brit. J. Ind. Med.*, 3:143–158.
3. Vernon, H. M. (1948). An investigation of the factors concerned in the causation of industrial accidents. In *Basic Principles of Ventilating and Heating*. T. Bedford, Lewis & Co., p. 346.

4. Wyon, D. (1978). Human productivity in the environments between 65 and 85 °F (18-30 °C). In *Energy Conservation Strategies in Buildings*. editor, Stolwijk, J. A. J., Yale University Printing Service, p. 192–216.
5. ASHRAE (1966). ASHRAE Standard 55–66: Thermal Environmental Conditions for Human Occupancy. American Society of Heating Refrigeration and Air-Conditioning Engineers, Atlanta.
6. ASHRAE (1997). *Handbook of Fundamentals*, Chapter 8, American Society of Heating, Refrigeration and Air-Conditioning Engineers, Atlanta.
7. Gagge, A. P., Stolwijk, J., and Nishi, Y. (1971). An effective temperature scale based on a simple model of human physiological regulatory response. *ASHRAE Trans*, 77(1), 247–262.
8. Hardy, J. D., Stolwijk, J. A. J., and Gagge, A. P. (1971). In *Comparative Physiology of Thermoregulation*, Chapter 5, Charles C. Thomas, Springfield, IL.
9. ASHRAE (1992). ANSI/ASHRAE Standard 55–1992: Thermal Conditions for Human Occupancy. American Society of Heating, Refrigeration and Air-Conditioning Engineers, Atlanta.
10. Berglund, L. G. and Cain, W. S. (1989). Perceived air quality and the thermal environment. *In The Human Equation: Health and Comfort*. Proceedings of ASHRAE/SOEH Conference IAQ '89. ASHRAE, Atlanta, pp. 93–99.
11. Goldman, R. F. (1978). The role of clothing in achieving acceptability of environmental temperatures between 65 °F and 85 °F (18 °C and 30 °C) In *Energy Conservation Strategies in Buildings*. Stolwijk, J. A. J., Yale University Printing Service, p. 49.
12. McCullough, E. A., Olesen, B. W., and Hong, S. W. (1994). Thermal insulation provided by chairs. *ASHRAE Trans.*, 100(1).
13. McCullough, E. A. and Hong, S. W. (1994). A data base for determining the decrease in clothing insulation due to body motion. *ASHRAE Trans.*, 100(1).
14. ASHRAE (1994). ANSI/ASHRAE Standard 55–1992, Addendum 55a, American Society of Heating, Refrigeration and Air-Conditioning Engineers, Atlanta.
15. Hanzawa, H., Melikov, A. K. and Fanger, P. O. (1987). Air flow characteristics in the occupied zone of ventilated spaces. *ASHRAE Trans.*, 100(2), 937–952.
16. Fanger, P. O., Melikov, A. K., Hanzawa, H., and Ring, J. (1988). Air turbulence and sensation of draught. *Energy and Buildings*, 12, 21-39.
17. Xia, Y., and Zhao, R. (1999). Effects of air turbulence on human thermal sensation in warm isothermal environment. *The Third International Symposium on Heating, Ventilation and Air Conditioning*, 1:147–152.
18. Fanger, P. O. (1972). *Thermal Comfort*, McGraw-Hill, New York.
19. Gagge, A. P. (1937). A new physiological variable associated with sensible and insensible perspiration. *Am. J. of Physiol*, 20(2), 277–287.
20. Berglund, L. G., and Cunningham, D. J. (1986). Parameters of human discomfort in warm environments. *ASHRAE Trans.*, 92(2), 732–746.
21. Gonzalez, R. R., and Berglund, L. G. (1978). Indices of thermoregulatory strain for moderate exercise in the heat. *J. Appl. Physiol. Resp. Environ. Excercise Physiol.* 44(6), pp. 889–899.
22. Cunningham, D. and Berglund, L. G. (1985). Skin wettedness under clothing and its relationship to thermal comfort in men and women. In *CLIMA 2000: Indoor Climate*, 4, VSS Kongres, Copenhagen. pp. 91–96.
23. Hoeppe, P., Oohori, T., Berglund, L., and Gwosdow, A. (1985) Vapor resistance of clothing and its effect on human response during and after exercise. In *CLIMA 2000: Indoor Climate*, 4, VSS Kongres, Copenhagen. pp. 97–102.
24. Mole, R. H. (1948). The relative humidity of the skin. *J. Physiol.*, London, 107:399–411.
25. Kerslake, D. M. (1972). *The Stress of Hot Environments*, University Press, Cambridge.
26. Gwosdow, A. R., Stevens, J. C., Berglund, L., and Stolwijk, J. A. J. (1986). Skin friction and fabric sensations in neutral and warm environments. *Textile Research Journal*, 56, 574–580.
27. Green, G. H. (1982). Positive and negative effects of building humidification. *ASHRAE Trans*, 88(1), 1049–1061.
28. White, I. R., and Rycroft, R. J. G. (1982). Low humidity occupational dermatosis. *Contact Dermat.*, 8, 287-290.
29. Liviana, J. E., Rohles, F. H. and Bullock, O. D. (1988). Humidity, comfort and contact lenses. *ASHRAE Trans*, 94(1), 3–11.
30. Nevins, R., Gonzalez, R. R., Nishi, Y., and Gagge, A. P. (1975). Effect of changes in ambient temperature and level of humidity on comfort and thermal sensations. *ASHRAE Trans.*, 81(2).

5.2 HUMAN RESPIRATORY TRACT PHYSIOLOGY

5.2.1 Introduction

Industrial environments expose individuals to a plethora of airborne chemical compounds in the form of vapors, aerosols, or biphasic mixtures of both. These atmospheric contaminants primarily interface with two body surfaces: the respiratory tract and the skin. Between these two routes of systemic exposure to airborne chemicals (inhalation and transdermal absorption) the respiratory tract has the larger surface area and a much greater percentage of this surface exposed to the ambient environment. Ordinary work clothing generally restricts skin exposures to the arms, neck, and head, and special protective clothing ensembles further limit or totally eliminate skin exposures, but breathing exposes much of the airway to contaminants.

Inhaling potentially noxious airborne mixtures exposes respiratory tissue and the supporting vasculature to disease and injury. In addition, other organs can be injured due to transepithelial transport along the airway to the bloodstream and subsequent bulk transport throughout the body. Consequently, understanding the relationship between industrial ventilation and human health requires knowledge of how the respiratory tract interacts with the surrounding environment. It is the goal of this chapter to lay the groundwork for understanding how the human airway deals with potential airborne threats.

5.2.2 Anatomical Overview

The human respiratory tract serves to deliver oxygen to the bloodstream and remove carbon dioxide. It accomplishes this by utilizing two large air bags (lungs) with extremely large internal surface areas to transport these gases between the pulmonary airstream and capillaries. The lungs are situated inside a semirigid bony structure (rib cage), which is joined together by intercostal muscles and supported from below by a large sheet of muscle tissue (diaphragm). These structures serve to physically protect the lungs and generate the forces required for inspiration and exhalation. Immediately surrounding the lungs are bags (pleura), which transfer force generated by the diaphragm and intercostal muscles to the lungs and are penetrated by numerous blood vessels.

The respiratory tract can be theoretically subdivided into distinct functional regions (Fig. 5.14). Dividing the respiratory tract into conducting and respiratory airways is perhaps the simplest division. Framed in this way, the respiratory tract consists of two airway regions: a series of tubes (nasal and oral cavities, pharynx, larynx, trachea, bronchi, and nonalveolated bronchioles) leading to a terminal region of essentially bag-like structures (respiratory bronchioles, alveoli), where gas is exchanged between the airway lumen and the surrounding capillaries.

A slightly more detailed airway organization suggested by the ICRP Task Group on Lung Dynamics[1] divides the airway into five regions: nasal

and oral cavities, pharynx and larynx, tracheobronchial tree, bronchioles, and alveoli. This construct essentially refines the view of conducting airways into a portal region (extrathoracic airways) and conducting tubes (tracheobronchial tree). Extrathoracic airways comprise all airway structures proximal to the larynx. Figure 5.14*a* shows this to include the nasal passages, nasopharynx, oral cavity, oropharynx, pharynx, and larynx. These structures have the functions of removing gross contaminants from the inspired airstream, humidifying and warming inspired air, and primary recovery of whatever heat and humidity can be retained from expired air. The tracheobronchial tree consists of a straight tube (trachea) terminating in a series of bifurcating tubes, which subsequently terminate at the pulmonary airways. The trachea, bronchi, and nonrespiratory bronchioles have the functions of removing fine particulates from the inspired airstream and completing the conditioning (raising to body temperature and complete saturation) of inspired air. Distal to the terminal bronchioles (the most distal nonrespiratory bronchioles) is the lung parenchyma, where gas exchange occurs in the respiratory bronchioles and alveoli.

5.2.2.1 Extrathoracic Airway Anatomy

The most proximal regions of the extrathoracic airways are the nasal and oral cavities, which act as portals to and from the ambient environment. Figure 5.14*b* shows how, during nasal breathing, inspired air enters at the two nares, passes through the nasal vestibules and turbinates, and exits at the nasopharynx. Total distance along the nasal passageway from the nares to the nasopharynx is approximately 10–14 cm. This narrow conduit (1–3 cm in width) divides into two paths by a septum extending from the nares to the distal edge of the turbinates. Though relatively short and narrow, the nasal passageways have a large surface area ($\approx$160 cm^2 compared with $\approx$69 cm^2 for the trachea) because of the highly convoluted turbinate structure.

Inspired air enters the nasal passages via two nares (nostrils), whose cross-sectional area can be enlarged by circular muscles (dilator naris muscles). Immediately distal to the nares are the nasal vestibules, pyramidal openings lined by squamous epithelium with nasal hairs projecting from the epithelium. These hairs achieve coarse filtration of the inspired airstream. Inspired air passes out of the vestibules via the nasal valves, slit-like openings at the back of the vestibules (each valve having a cross-sectional area of $\approx$30 mm^2), and enters the turbinates.

The turbinate regions are 5–8 cm long and defined by bony projections (superior, middle, and inferior conchae) forming convoluted passages through this region of the nasal cavity. Corresponding openings (superior, middle, and inferior meatus) define three airway passages. Ciliated epithelia and mucus-secreting goblet cells generally line the luminal surfaces of the turbinate region, though olfactory tissues are found in the superior meatus. Figure 5.15 shows how air traveling within the turbinates can easily pass between the different meatus. The tortuous passageways promote deposition of inspired particles as well as the exchange of heat and water

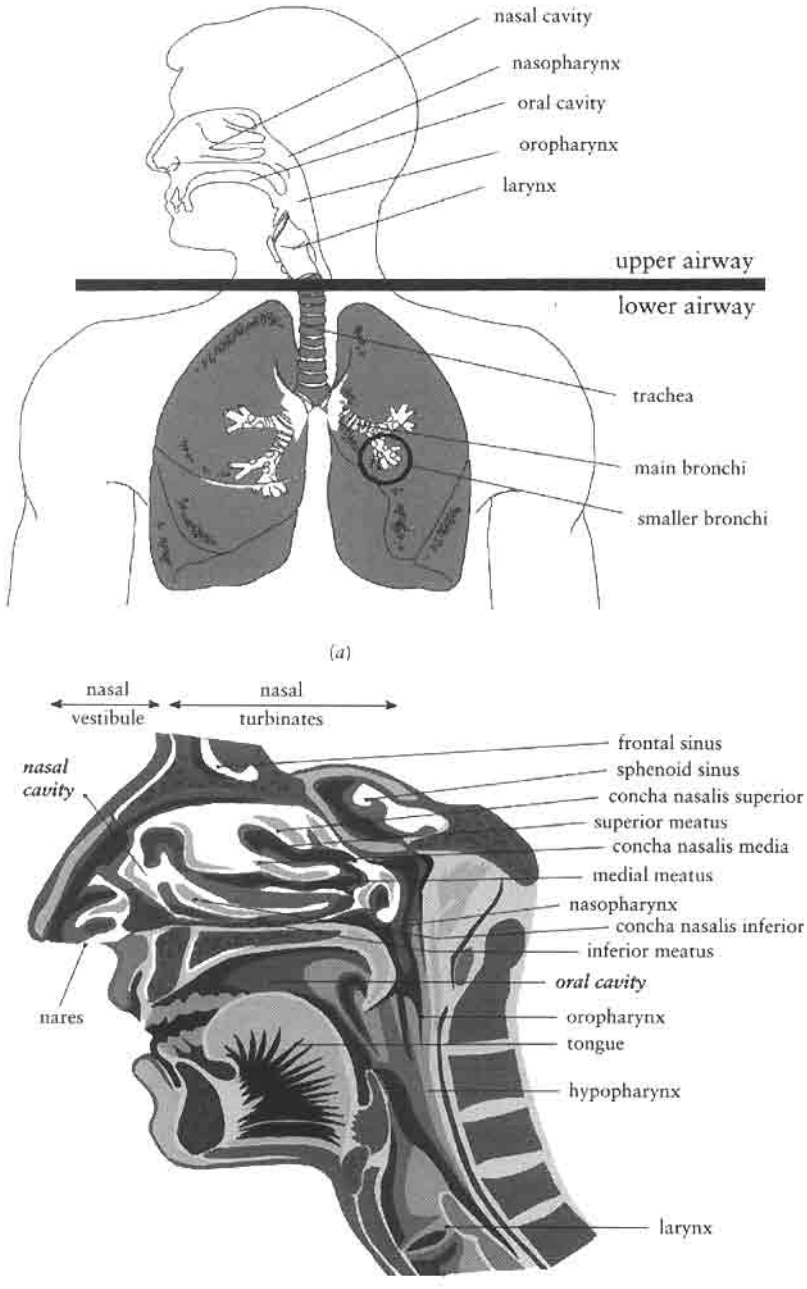

FIGURE 5.14 (a) Anatomical overview of the human respiratory tract. The larynx generally serves as the boundary between the upper (extrathoracic) and lower airways. (b) Anatomy of the upper airway.

vapor between the airway wall and the inspiratory or expiratory airstreams. Meatus cross-sectional areas correlate to airflow, the greatest quantity of air passing through the inferior meatus. Slower airflow within the superior meatus allows for greater residence times along these airway surfaces. Increased residence times enhance olfaction occurring at the olfactory bulbs located along the superior surface of the superior meatus. Airstream mixing caused by eddy currents within the superior meatus further enhances olfaction.

The two (left and right) inspiratory nasal airstreams merge in the distal end of the turbinates before experiencing a 90° bend in the airway upon entering the nasopharynx. The nasopharynx is roughly 5 cm long, has a volume of 12 cm^2, and is lined with squamous epithelium, which appears to protect underlying tissue from gross mechanical injury. Any relatively large particles (>3 μm) successfully navigating the nasal passages will likely impinge upon the nasopharyngeal wall because of inertia. Ciliated columnar epithelium interspersed with mucus-secreting goblet cells appearing distal to the nasopharynx marks the start of the oropharynx.

Ambient air entering the oral cavity during oral breathing confronts a variety of surface structures. Inspired air initially passes between highly vascular lips and across the teeth, which can be viewed as a series of heat transfer fins. The tongue and buccal surfaces (both rough, highly vascular

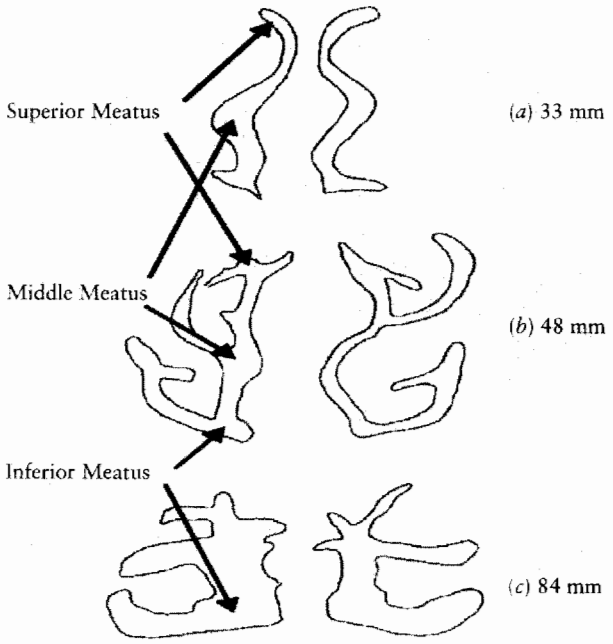

FIGURE 5.15 Cross-section of human nasal turbinates at various positions along the airway. Distances indicated are from the nares. The medial surface in each cross-section represents the nasal septum. (Modified from Guilmette et al.[2])

surfaces) and the hard palate border the cavernous opening beyond the teeth. The soft palate defines the distal limit to the oral cavity, beyond which the airstream bends 90° to enter the oropharynx. Oral cavity dimensions vary greatly depending on tongue position and extension of the buccal surfaces but a simple cylindrical model (8 cm length, 1.8 cm diameter) has been used to characterize the oral cavity.[3] Inspired air passing out of the oral cavity enters the oropharynx.

The pharynx (nasopharynx, oropharynx, and hypopharynx) serves to pass air between the airway portals (nasal and oral cavities) and the thoracic airways (tracheobronchial tree, alveoli). It terminates at the epiglottis, a valve that prevents swallowed food and liquids from entering the lower airways. Beyond the epiglottis lies the larynx, which serves as a conduit for air passing in and out of the lower airways and as a tone-producing structure. Both pharyngeal and laryngeal surfaces are lined with columnar ciliated epithelium and goblet cells, except for the squamous epithelium lining the nasopharynx and a small area on the vocal folds of the larynx.

5.2.2.2 Central and Pulmonary Airway Anatomy

Inspired air passing out of the larynx forms a jet as it enters the trachea, the largest conducting tube in the airway. The most proximal tube in the tracheobronchial tree (generation zero in the Weibel "A" model),[4] the trachea has an approximate diameter of 1.8 cm and extends in adults roughly 12 cm from the distal edge of the larynx to the carina. Columnar ciliated epithelium and goblet cells are the primary cell types lining the tracheal lumen. Negative pressures within the tracheal lumen during strenuous inspiration can produce significant radial pressure gradients that would, if possible, collapse the trachea. Tracheal patency during strenuous breathing is ensured by a series of incomplete cartilaginous rings supported by fibroelastic and smooth muscle tissues extending along the length of the trachea.

The trachea terminates at the carina, the site at which the main bronchi bifurcate. Bronchial tube diameters and generally lengths decrease distally from the carina with successive bifurcations. The right and left main bronchi have diameters of approximately 1.2 cm and lengths of 4.76 cm, decreasing to diameters of approximately 0.13 cm and lengths of 0.46 cm in the smallest bronchi (generation 10). Cartilage occurring in airway walls down to the tenth generation of bifurcations assists bronchial smooth muscle in maintaining bronchial patency during strenuous breathing. Bronchioles (generations 11–18) lack cartilage and rely entirely on smooth muscle for maintaining luminal patency during breathing. Alveolar ducts (generations 19–23) and alveoli (generation 24) lack any cartilage or smooth muscle and maintain patency by a balance between tensile forces generated by gases present within the alveolar lumen and alveolar fluid surface tension. Surfactants present in alveolar fluid prevent surface tension from collapsing the alveoli (atelectasis).

The estimated number of tubes in each airway generation depends on the bifurcation model used in describing the tracheobronchial tree. Though bronchial bifurcations are asymmetric, symmetric models, exemplified by Weibel,[5] or asymmetric models, such as one suggested by Horsfield,[6] can

each serve to represent airway branching. Recent studies have also suggested a fractal pattern to the bifurcations.[7,8] Whatever the overall bifurcation pattern, the general structure can be most easily summarized by the Weibel "A" model,[4] in which successive bronchial generations are more numerous, shorter, and have smaller individual cross-sectional areas than more proximal generations. According to the Weibel "A" model, the number of branches in generation z is

$$N(z) = 2^z \tag{5.32}$$

and the mean diameter of airways in generation z, $d(z)$, is given by

$$d(z) = d_0 2^{-z/3} \tag{5.33}$$

where d_0 = tracheal diameter (Table 5.5). Consequently, overall cross-sectional area increases exponentially as a function of distance from the nares, producing a predicted alveolar surface area of 43–80 m^2. Respiration (exchanging O_2 for CO_2) depends on this large exchange surface to provide sufficient gas exchange capacity during strenuous activity to accommodate demands by active muscles for greater volumes of O_2 and the need to remove excess CO_2.

5.2.2.3 Airway Wall Anatomy

Airway cross-sections have the nominal anatomy shown in Fig. 5.16. Airway surface liquid (ASL), primarily composed of mucus gel and water, surrounds the airway lumen with a thickness thought to vary from 5 to 10 mm. ASL lies on the apical surface of airway epithelial cells (mostly columnar ciliated epithelium). This layer of cells, roughly two to three cells thick in proximal airways and eventually thinning to a single cell thickness in distal airways, rests along a basement membrane on its basal surface. Connective tissue (collagen fibers, basement membranes, elastin, and water) lies between the basement membrane and airway smooth muscle. Edema occurs when the volume of water within the connective tissue increases considerably. Interspersed within the smooth muscle are respiratory supply vessels (capillaries, arteriovenous anastomoses), nerves, and lymphatic vessels.

Certain respiratory diseases (e.g., asthma and emphysema) alter airway dimensions, thereby modifying airflow patterns and adversely affecting gas exchange and particle deposition. Emphysema breaks down alveolar walls, enlarging alveolar sac volume but significantly reducing overall alveolar surface area. Assuming a constant gas exchange flux, reducing alveolar surface area decreases gas exchange and diminishes the body's ability to obtain oxygen from the inspired airstream. In addition, eliminating alveolar walls reduces the number of alveoli and shortens overall path length. A shorter path may allow larger inhaled particles to reach and deposit in the pulmonary airways, potentially leading to adverse clinical consequences. Diseases that reduce bronchial diameter (asthma, chronic bronchitis, and cystic fibrosis) increase airstream velocity in occluded airway regions, increasing heat and water vapor exchange and particle impaction while reducing sedimentation in the affected bronchi. This results in a greater volume of fine inhaled particles [<3.0 μm mean mass aerodynamic diameter (MMAD)] passing to more distal (and potentially

TABLE 5.5 Representative Conducting Airway Dimensions Based on the Weibel "A" Model

				Reynolds number		
				Minute ventilation		
Airway region	Cross-sectional area (cm)	Equivalent diameter (cm)	Airway segment length (cm)	8 L/min	16 L/min	30 L/min
Nasal vestibule	1.3	67	0.9	1515	3029	5679
Nasal cavity	2.4	0.61	1.8	1664	3327	6238
Nasal turbinates	2.3	0.44	1.3	2306	4612	8648
Nasal turbinates	2.6	0.36	4.4	2819	5637	10570
Nasal turbinates	3	1.18	0.6	860	1720	3225
Proximal nasopharynx	3.9	2.03	2	500	1000	1875
Distal nasopharynx	2.9	1.45	3	700	1400	2624
Proximal oropharynx	2.8	1.26	1.7	805	1611	3020
Distal oropharynx	3	1.3	1.3	781	1561	2927
Proximal hypopharynx	2.3	1.5	2.4	676	1353	2537
Distal hypopharynx	1.9	1.3	1.3	781	1561	2927
Larynx	1.8	1.5	1.1	676	1353	2537
Proximal trachea	2.1	1.6	2.7	634	1268	2378
Distal trachea	2.8	1.9	9.3	534	1068	2003
Bronchii gen. 1	3.4	1.47	4.8	345	689	1292
Bronchii gen. 2	3.9	1.11	1.9	227	454	851
Bronchii gen. 3	3.9	0.79	0.8	161	323	605
Bronchii gen. 4	3.9	0.56	1.3	114	229	429
Bronchii gen. 5	4	0.4	1.1	80	159	299
Bronchii gen. 6	4.3	0.29	0.9	54	107	202
Bronchii gen. 7	4.7	0.22	0.8	37	75	140
Bronchii gen. 8	5.4	0.16	0.6	24	47	89
Bronchii gen. 9	6.7	0.13	0.5	15	31	58
Bronchii gen. 10	8	0.1	0.5	10	20	37
Bronchii gen. 11	19.6	0.11	0.4	4.4	8.9	17
Bronchii gen. 12	28.8	0.1	0.3	2.8	5.5	10
Bronchii gen. 13	44.5	0.08	0.3	1.4	2.9	5.4
Bronchii gen. 14	69.4	0.07	0.2	0.8	1.6	3
Bronchii gen. 15	113	0.07	0.2	0.5	1	1.9
Bronchii gen. 16	180	0.06	0.2	0.3	0.5	1
Bronchii gen. 17	300	0.05	0.1	0.1	0.3	0.5

Note that turbulent flow (Reynolds number > 3000 is predicted only in the extrathoracic airways at flow rates < 30 L/min.

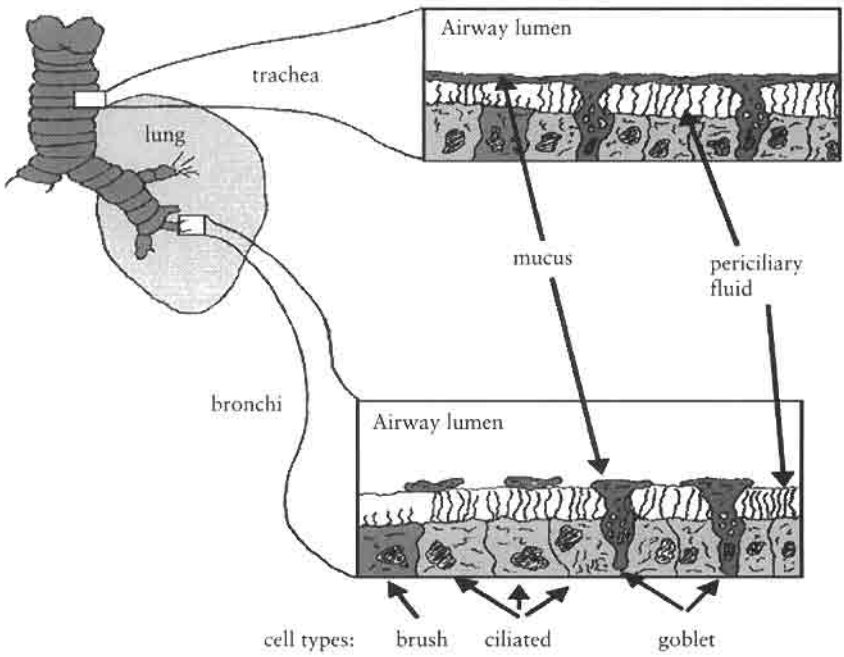

FIGURE 5.16 Depiction of representative airway cross-section at various points (trachea, bronchi, and pulmonary airway) along the respiratory tract showing common cell types. Note how mucus gel is generally presumed to form sheets in the more proximal airways. The pulmonary airway depiction includes both a section of respiratory bronchi and an alveolus.

more vulnerable) regions, permitting more of these fine particulates to settle in distal airways by sedimentation (see Section 5.2.7).

Airway Surface Liquid

ASL lining the airway luminal surface serves to protect airway epithelium against airborne pathogens and toxins, desiccation, and abrupt pH changes. This fluid is secreted along all airway surfaces except portions of the extrathoracic and respiratory airways (respiratory bronchi and alveoli). ASL composition is unclear,[9,10] though it is theorized to consist of a periciliary layer composed mainly of water and various ions approximately 5–7 μm in depth[10] and the epiphase, an overlying gel layer of hydrated mucins in the form of droplets, sheets, or blankets[11–13] (Fig. 5.16). Epithelial cells control periciliary fluid water and ion concentration by chloride secretion and sodium absorption. Solids constitute approximately 5% of periciliary fluid mass, with water comprising the remaining 95%, though disease can raise solids concentration above 10%. Periciliary fluid solids include glycoproteins, proteins, peptides, glycosaminoglycans, immunoglobins, and lipids in addition to materials deposited from the passing airstream. The epiphase is thought to be a hydrogel consisting of various complex glycoproteins, with hydration controlled by a Donnan effect.[14,15] Control of periciliary fluid hydration is a complex interaction of evaporation,[10,16] osmotic pressure differentials regulated by ion transport,[11,17,18]

and hydrostatic pressure.[19] Estimates of daily mucus production range from 7–12 mL/day in healthy individuals to > 100 mL/day in cystic fibrosis patients.

Airway Epithelial Cell Types

Conducting airway passages are generally composed of ciliated pseudostratified cuboidal columnar epithelial cells interspersed with basal, brush, and secretory cells (goblet, serous, Clara). Cilia found on ciliated epithelial cell apical surfaces (along the lumen) provide motive force for propelling mucus gel along the airway. Extrathoracic airway surfaces are lined with ciliated epithelium, except for squamous epithelium covering the nasal vestibule, nasopharynx, oral cavity, oropharynx, and portions of the larynx. Squamous epithelium protects airway surfaces against mechanical impact or shear in areas where relatively large inspired particles usually impact. Also, nasal olfactory surfaces are not lined with ciliated epithelium but covered instead by special sensory cells. These specialized olfactory receptor cells react with inhaled odorant molecules, generating neural signals sent to the olfactory bulbs of the brain that produce a sense of smell. All tracheobronchial surfaces are lined with ciliated epithelium down to the pulmonary airways. Proximal airway epithelium is thickest and progressively flattens and thins toward the lung parenchyma, gradually transitioning into alveolar endothelium.

Secreting cells found along the conducting airways include nonciliated goblet and serous cells. Goblet cells produce glycoproteins that form droplets or sheets of mucus gel floating on periciliary fluid. Serous cell exudates are believed to include periciliary fluid, various proteins and peptides (including lysozyme and lactoferrin), and protease inhibitors. Periciliary fluid also derives from interstitial fluid transudate. Glycosaminoglycans, lipids, serum proteins, and ions found in ASL appear to originate from all surface epithelial cells and submucosal glands (serous and mucous). The quantity of submucosal glands decreases in more distal airways and are absent from pulmonary airways.

Microvilli, approximately 2 μm long, give a "brush-like" appearance as they project from the apical surface of brush cells. These cells contribute to fluid regulation along the luminal surface by absorbing excess periciliary fluid either secreted by neighboring serous cells or transported from distal airways by the mucociliary elevator. Basal cells are progenitors of the other epithelial cells and are the most actively mitotic epithelial cells. Lymphocytes also appear in ASL as either migratory or basal cells.

Pulmonary airways are lined with specialized cells generally not found in the conducting airways. Alveolar epithelium, composed of thin sheet-like cells separated from pulmonary capillaries by only a basement membrane, permits easy exchange of gases between alveolar sacs and blood (Fig. 5.17). Secretory Clara and Type II pneumonocyte cells produce surfactant, lipids, and protease inhibitors within the pulmonary airways. Macrophages are scavenger cells that remove microorganisms and particulates depositing along alveolar surfaces.

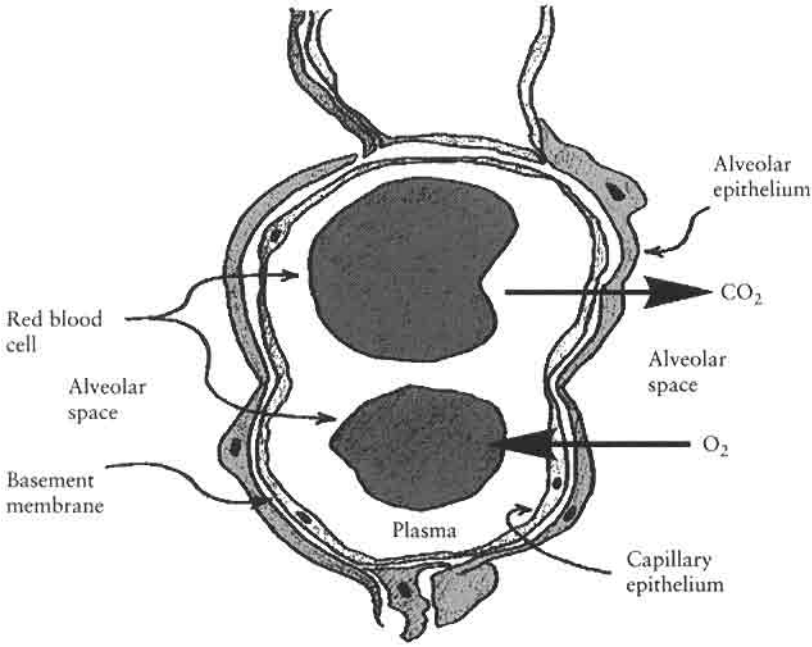

FIGURE 5.17 Gas exchange between alveolar and capillary compartments.

5.2.2.4 Airway Vasculature

Pulmonary gas exchange is intimately connected to cardiovascular function. Deoxygenated blood from the right ventricle of the heart passes through the pulmonary artery to the lungs, exchanges carbon dioxide and oxygen across the alveolar wall, and returns to the left atrium of the heart via the pulmonary veins. The heart propels this oxygenated blood from the left ventricle through the aorta and hence throughout the body via a high-pressure system of thick-walled vessels known as arteries branching out from the aorta. Further branching gradually reduces the cross-section of arteries until, at a diameter of approximately 30 μm, they are termed arterioles. Total vascular surface area increases as arterioles continue to branch and diminish in diameter until they terminate at a capillary bed or connect directly with venuoles in an anastomosis, a dense network of interconnected vessels.

Arteriole wall smooth muscle controls vascular diameter and regulates blood flow by modulating the pressure drop along the length of the vessel. Enlisting groups of arterioles regulates local or regional vascular resistance by modulating capillary flow in response to temperature changes or other stimuli. Active control of arteriole wall smooth muscle tone due to a variety of internal and external stimuli also regulates blood flow through anastomoses and consequently peripheral blood volume and pressure. Anastomoses control peripheral blood flow by allowing a portion of total blood flow to bypass capillary beds.

Intravascular blood pressure drops as a function of arterial and arteriole diameter to such an extent that capillary walls can consist of a single layer of endothelial cells. Capillaries, with diameters of 6–8 μm, transport blood close enough (roughly 20–30 μm) to cells throughout the body to allow gas (O_2 and CO_2), heat, nutrient and waste, and water exchange between blood and cells via diffusion. Interstitial tissue containing collagen fibers, basement membranes, elastin, and water supports capillary endothelial cells and provides additional tensile strength. Capillaries merge to form venules, which in turn merge to form veins. These low-pressure components of the cardiovascular system—capillaries, venules, and veins—transport deoxygenated blood from the capillaries to the right atrium of the heart via the largest vein, the inferior vena cava.

Blood supplying conducting airway tissues derives from large bronchial arteries branching off either the aorta or intercostal arteries. These vessels also supply blood to the visceral pleura, regional nerves and lymph nodes, and vascular walls of the pulmonary arteries and veins. Bronchial artery branches follow the conducting airways and provide blood to the bronchial walls down to the respiratory bronchioles. Smaller arterial branches form anastomoses along the peribronchial surface (Fig. 5.18). Arterioles originating from the peribronchial anastomoses penetrate the bronchial smooth muscle and form relatively straight, thin bronchial capillaries and submucosal anastomoses. Conducting airway luminal cells

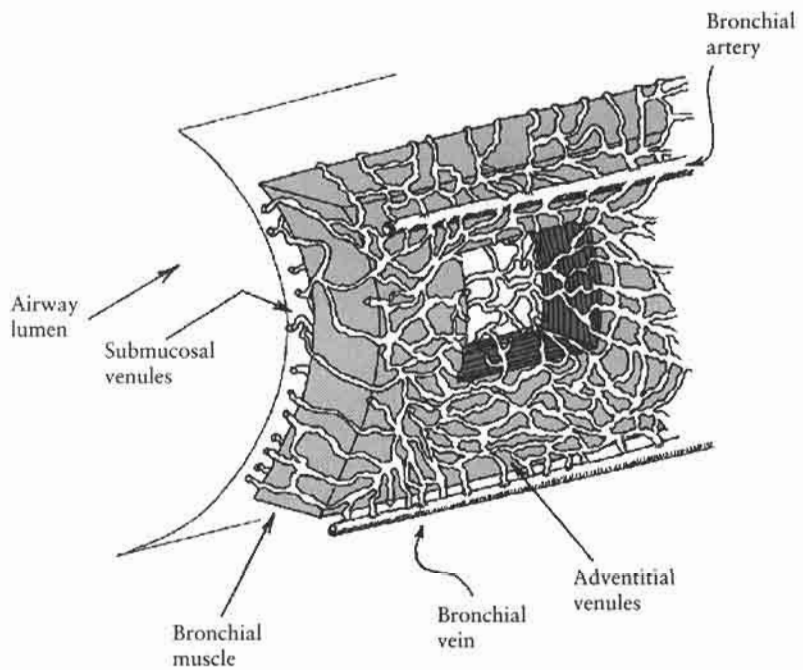

FIGURE 5.18 Vasculature structure along a portion of bronchial muscle. Airway epithelia are not shown in this figure but lie between the submucosal venules and the airway lumen. Modified from Deffebach et al.[20]

(ciliated epithelium, serous, and goblet cells) are supplied with nutrients, oxygen, water, and heat via these submucosal anastomoses.

Respiratory bronchioles and alveoli are supplied with deoxygenated blood from the right ventricle of the heart by the pulmonary arteries. Five lobar arterial branches follow the bronchi, and subsequent bronchopulmonary arterial branches run adjacent to smaller airways to the level of the respiratory bronchioles. Dense coiled capillary networks beyond this point distribute deoxygenated blood to capillaries and return oxygenated blood to the venules arising from the respiratory bronchiolar, alveolar, and alveolar duct capillary beds. Pulmonary capillaries directly attach to lung connective tissue, reducing diffusive resistance to gas exchange.

Vessels linking bronchial arteries directly with pulmonary alveolar microvessels are commonly found in neonates but apparently decrease in frequency with age. There is also evidence of direct communication between bronchial arteries and pulmonary veins. Venous blood originating from extrapulmonary airways (proximal to approximately generation 3 bronchi) drains into the right atrium via the azygos and hemiazygos veins. Intrapulmonary bronchial venous flow, returning blood to the heart from bronchi distal to the third generation, drains into the pulmonary circulation, which subsequently drains into the left atrium either directly or via the pulmonary vein.

Airway surfaces, like skin, are continually exposed to the ambient environment. In contrast to skin submucosal vessels, however, which shed excess heat by vasodilating when heated and conserve heat by vasoconstricting when chilled, it is unclear how the airway vasculature responds to temperature extremes. Inspiring cold air poses two challenges to conducting airway tissues: the risk of tissue injury should inadequate heat reach the airway surface and excessive body heat loss due to increasing the radial temperature gradient. Vasodilation would protect airway tissue but increase heat loss, while vasoconstriction would produce the opposite effect.

Nasal vasculature may offer some insight into this question, though research to date has been equivocal. Nasal turbinate vessels can be classified as either capacitance vessels or resistive vessels. Capacitance vessels appear to vasodilate in response to infection[21] while resistance vessels appear to respond to cold stimuli by vasoconstriction.[22] Buccal vascular structures also respond to thermal stimuli but appear to respond principally to cutaneous stimuli.[23] How pharyngeal and tracheobronchial submucosal vessels react to thermal stimuli is not known, though cold-induced asthma is believed to result from bronchospasms caused by susceptible bronchial smooth muscle responding to exposure to cold dry air.[24,25] This asthmatic response suggests an inadequate vascular response to surface cooling.

5.2.3 Ventilation Patterns

5.2.3.1 Breathing Mechanics

Breathing consists of the cyclic action of the lungs to inspire and expire atmospheric gases. Inspiration occurs when the diaphragm and intercostal muscles contract, generating a negative pressure in the pleura surrounding

the lungs and causing the lungs to expand. Air enters the respiratory tract from the surrounding atmosphere when the inspiratory pressure exceeds airway resistance. Expiration occurs when the diaphragm and intercostal muscles relax, causing elastic recoil from the pleura, which reduces the forces expanding the lungs. When lung viscoelastic forces overcome pleural pressure, the lungs constrict and air is expelled.

Movement of the chest wall in relationship to lung volume can be represented on a pressure-volume diagram (Fig. 5.19). The pressure term refers to pleural pressure, a measure of pressure within the space between the pleural membranes surrounding the lungs. The volume term represents changes in percent vital capacity (%VC), changes in lung volume, or other convenient measures of lung volume. Hysteresis, i.e., the failure of the chest wall and lungs to follow identical pressure-volume paths during inspiratory and expiratory loads, is caused by viscoelastic and plastic properties of the lung and chest wall. Specifically, mechanical differences between lung surfactant properties and alveolar recruitment, on the one hand, and chest wall skeletal muscle and elastic fiber properties, on the other, are believed to account for most of the observed hysteresis. It is worth noting that posture also affects pressure-volume relationships by shifting gravitational forces within the abdomen.

Gases entering the airways first fill the volume of the anatomical dead space (conducting airways) before filling the pulmonary airway. Alveolar ventilation ($\dot{V}_A$) defines the volumetric rate of gas passing through pulmonary airways that participate in O_2 and CO_2 exchange, with O_2 uptake ($\dot{V}_{O_2}$) and CO_2 production ($\dot{V}_{CO_2}$) determined by metabolic demands.

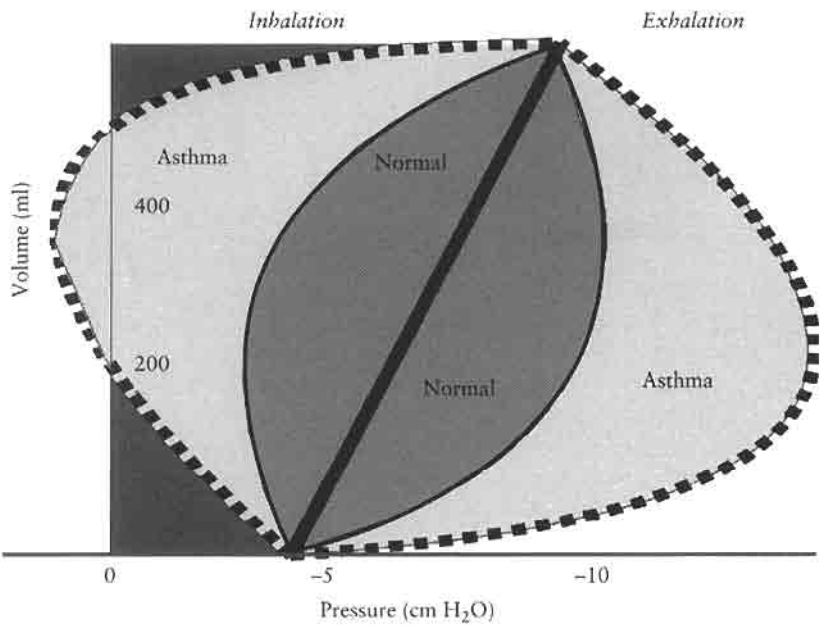

FIGURE 5.19 Relationship of transpleural pressure to volume in normal and asthmatic individuals.

TABLE 5.6 Effect of Dead Space Volume, Tidal Volume, and Breathing Frequency on Alveolar Ventilation at a Fixed Minute Ventilation ($\dot{V}_E$ = 58.0 L/min). Modified from Cherniack.[26]

$\dot{V}_A$(L/min)	V_D (m/L)	V_T (mL)	f (min^{-1})
3.2	150	250	32
4.0	250	500	16
4.8	200	500	16
5.6	150	500	16
6.8	100	1000	8

$\dot{V}_A$, alveolar gas volume; V_D, dead space volume; V_T, tidal volume; f, breathing frequency

Air entering alveolar spaces but not partaking in gas exchange due to poor perfusion of individual alveoli is not part of V_A but adds to the total dead space volume (V_D). This additional dead space leads to the concept of a physiological dead space that includes not only an anatomical component (conducting airways) but also a functional component (poorly perfused or nonperfused alveoli). Diseases affecting either conducting airway geometry or pulmonary perfusion can thus alter V_D. The total volume of air ($\approx$500 mL) inspired (or expired) during each breath is known as the tidal volume, V_T and can be described by

$$V_T = V_D + \frac{\dot{V}_A}{f}, \tag{5.34}$$

where f = breathing frequency (breaths min^{-1}) so that

$$\dot{V}_A = f(V_T - V_D). \tag{5.35}$$

Expired minute ventilation, $\dot{V}_E$, defines the gas volume inspired or expired in 1 minute and is given by

$$\dot{V}_E = V_T f, \tag{5.36}$$

Typical $\dot{V}_E$ for normal quiet breathing is approximately 6–8 L/min. In extreme circumstances, individuals can live for brief periods with minute ventilation rates as low as 1–2 L/min or as high as 300 L/min. Table 5.6 shows the dependence of $\dot{V}_A$ on V_D, V_T, and f for a given $\dot{V}_E$.

Alveolar ventilation supplies O_2 to the bloodstream while alveolar capillary perfusion provides alveolar gas with CO_2. Resting individuals consume approximately 250 mL O_2/min and produce approximately 200 mL CO_2/min because, stoichiometrically, metabolic processes require a greater supply of O_2 than the quantity of CO_2 produced. Defining the respiratory exchange ratio, R, as

$$R = \frac{\dot{V}_{CO_2}}{\dot{V}_{O_2}}, \tag{5.37}$$

then R = 0.8 during normal resting breathing and$\dot{V}_A$ = 4 L/min is required to lower the arterial CO_2 partial pressure to 40 torr and raise arterial O_2 partial

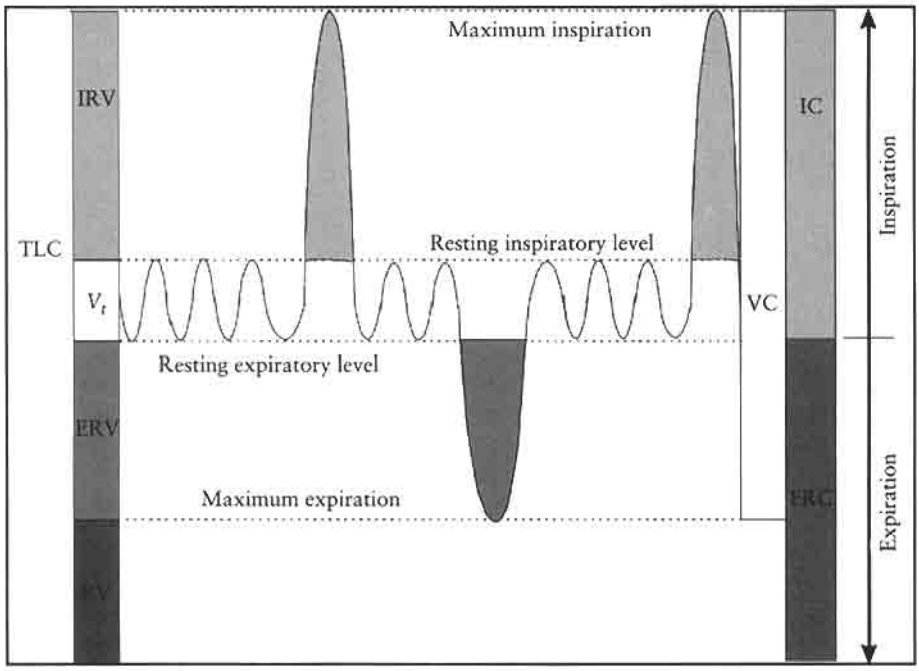

FIGURE 5.20 Graphical representation depicting relationship between airway volume measurements. The curve represents both tidal and forced breathing patterns.

pressure to 100 torr in order to maintain blood hemoglobin saturation levels (97.5%) in the venous end of pulmonary capillaries. A corresponding pulmonary perfusion rate, $\dot{Q}$, equal to 5 L/min of arterial blood is necessary when both ventilation and flow are uniform. The subsequent ventilation-perfusion ratio, $\dot{V}_A/\dot{Q}$, provides a quantitative measure of gas exchange efficiency. $\dot{V}_A/\dot{Q} = 0.8$ in this ideal case but generally ranges from 1.0 at rest to 3.0 or greater during heavy exercise.

Summing V_T, the inspiratory reserve volume (IRV), the expiratory reserve capacity (ERV), and the residual volume (RV) gives the total lung capacity (TLC). IRV is the maximum additional volume one can inspire from end-tidal inspiration. ERV measures the maximum additional volume one can expire from an end-tidal expiration level. RV measures the gas remaining in the respiratory tract after the maximum possible exhalation and reflects the minimum noncollapsible volume (under normal circumstances) within the airway. In contrast, the functional residual capacity (FRC) measures the gas volume remaining in the airway at an end-tidal exhalation. The deepest possible breath (TLC-RV) is defined as the vital capacity (VC). Figure 5.20 graphically depicts the various components of airway volume. Values for TLC, VC, and RV depend on health, body size, gender, and age. Table 5.7 lists predictive equations for healthy individuals. In general, females have 10–25% smaller volumes than men of the same age and size. Age has its greatest effect on RV, which increases by 50% or more from age 20 to age 60.

TABLE 5.7 Predictive Equations for Static Lung Volumes and Dynamic Pulmonary Function[26]

Parameter	Gender	Prediction Equation
Vital capacity	Female	$0.0404H - 0.022A - 2.35 - \frac{147.1}{H} - 0.00828A + 0.5673\log A - \frac{0.5509}{W} + 0.0242$
	Male	$0.0481H - 0.020A - 2.81 - \frac{1.4892}{H} - 0.0069A + 0.5191\log A - \frac{0.6347}{W} + 1.0206$
Residual volume	Female	$0.032H - 0.009A - .390 - \frac{2.1684}{H} - 0.00374A + 0.0185\log A - \frac{9.2457}{W} + 1.2934$
	Male	$0.027H - 0.017A - 3.447 - \frac{2.3637}{H} - 0.00338 + 0.6387\log A - \frac{10.5711}{W} + 0.694$
Total lung capacity	Female	$0.079H - 0.008 - 7.49 - \frac{171.34}{H} - 0.00380A + 0.3481\log A - \frac{3.0601}{W} + 1.3667$
	Male	$0.094H - 0.015A - 9.167 - \frac{173.61}{H} - 0.00561A + 0.5292\log A - \frac{3.5461}{W} + 1.2155$
Forced expired volume, 1 s*	Female	$3.95H - 0.025A - 2.60$
	Male	$4.30H - 0.029A - 2.49$
Forced vital capacity*	Female	$4.43H - 0.026A - 2.89$
	Male	$5.76H - 0.026A - 4.34$
Peak expired flow*	Female	$5.50H - 0.030A - 1.11$
	Male	$6.14H - 0.043A + 0.15$

A = age (years); H = height (cm); W = weight (kg)
*Health Survey for England (1996)
http://www.official-documents.co.uk/document/doh/survey 96/ehch3.htm#3.7

Forced expiration is commonly used to assess pulmonary function in both healthy and impaired individuals. Static measures of lung volumes (TLC, V_T, FRC) fail to detect dynamic changes in pulmonary function that are attributable to disease (e.g., asthmatic airway constriction). Obtaining maximum expiratory flow-volume (MEFV) curves (Fig. 5.21) permits derivation of key parameters in detecting changes in lung function.

Forced vital capacity (FVC) quantifies the maximum air volume expired following a maximal inspiration and is one of the basic measures of analyzing flow changes such as reduced airway patency observed in asthma. To measure FVC, an individual inhales maximally and then exhales as rapidly and completely as possible. FVC primarily reflects the elastic properties of the respiratory tract. The gas volume forcibly expired within a given time interval, FEV_t (where t is typically one second, $FEV_{1.0}$)

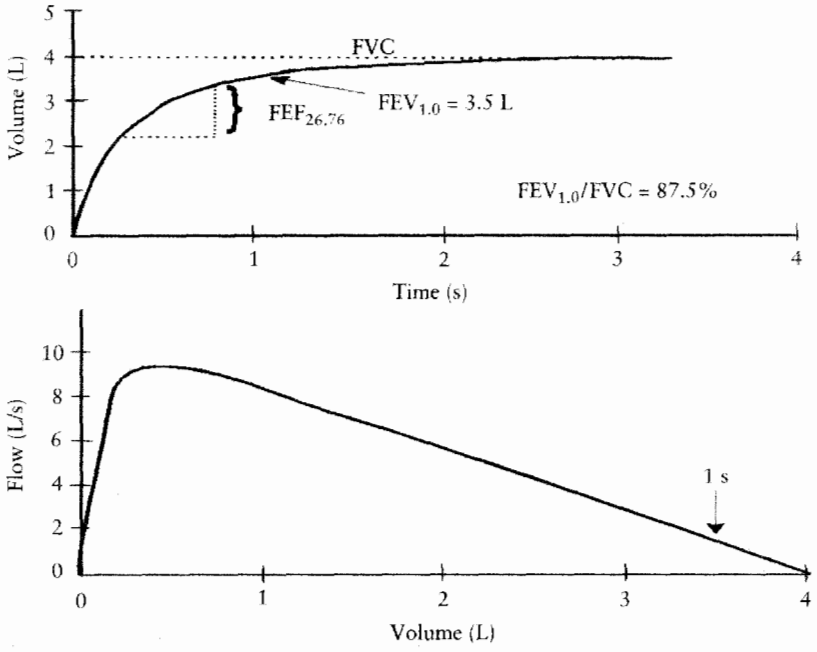

FIGURE 5.21 Representative spirogram (top) and flow–volume curve (bottom) during forced expiration. $FEV_{1.0}$ shown in the spirogram corresponds to the arrow in the flow–volume curve indicating forced expired volume in one second.

is also commonly used for diagnostic purposes and represents expiratory flow resistive properties of the respiratory tract. $FEV_{1.0}$ has the advantage of being relatively independent of effort and sufficiently sensitive to detect airway obstruction even at low flows. Other timed expiratory intervals are either too short ($FEV_{0.5}$) and dependent on effort, or too long ($FEV_{2.0}$) and include low flows occurring at the end of expiration. The $FEV_{1.0}/FVC$ ratio quantifies the percentage of FVC expired in one second and is often used to detect changes in flow resistance (e.g., asthma) or airway restriction (e.g., pulmonary fibrosis, obesity). Another common measure of lung function derived from the MEFV curve is the peak expiratory flow, PEF, which is used as a simple method to predict airway conductance. Unfortunately, PEF is sensitive to effort during testing, depends much more on extrathoracic and tracheal conductance rather than pulmonary conductance, and is insensitive to lesser airway obstruction.

5.2.3.2 Intra-airway Airflow Patterns

Transporting inspired and expired gases through the airway, depositing particulates onto mucosal surfaces, and exchanging heat and water vapor between the airstream and airway surfaces depends on a number of factors, one of the more important being airway flow characteristics. Airway geometry, airstream velocity, and gas density determine the flow regime prevailing in each airway region. Turbulence in fluid flow through a conduit is generally associated with fluid inertial forces greatly exceeding fluid viscous forces

such that Poiseuille flow (parabolic laminar flow) is not established and eddy currents develop. The Reynolds number, Re, quantifies this relationship between inertial and viscous forces and is given by

$$\mathrm{Re} = \frac{\mu D u}{\rho}, \tag{5.38}$$

where μ = fluid viscosity, D = tube diameter, u = mean fluid velocity, and ρ = fluid density. The equivalent diameter, $D_e = 4A/P$, where A = conduit cross-sectional area and P = wetted perimeter, replaces D for noncircular conduits. In circular straight tubes, Re > 2300 typically indicates the presence of turbulence. Convection caused by eddy currents enhances deposition of buoyant airborne particles by bringing more of these particles into contact with the mucosal surface. Airway heat and water vapor exchange is also enhanced by turbulent airflow.

Turbulence in nasal cavity airflow is a consequence of both high airstream velocities, caused by small nasal cross-sectional areas, and very irregular nasal airway geometry, which induces flow distortions. Nasal turbinate Re exceeds 2300 even during normal quiet breathing and nasal cavity airflow is apparently turbulent at most $\dot{V}_E$. Flow in the pharynx, larynx, and trachea is also generally turbulent at most $\dot{V}_E$ despite Re > 2300 only at higher $\dot{V}_E$ (30 L/min and greater). This airstream mixing enhances convective heat and mass transfer in extrathoracic airways and plays a major role in airway defense mechanisms.

Humans preferentially breathe nasally, possibly because of the highly efficient filtration, humidification, and warming performed on the inspiratory airstream, but inspiratory flow passing through the convoluted passageways incurs a substantial pressure drop. Filtration by the oral cavity is much less effective, but the pressure drop is also lower. As a result, humans normally breathe nasally until $\dot{V}_E$ reaches approximately 30 L/min, when oronasal breathing begins. This shift in breathing pattern occurs because, at lower flow rates, the pressure gradient between the atmosphere and pulmonary airways generated by inspiratory negative pressure in the lungs can overcome nasal resistance, but as flow rates increase, the nasal cavity pressure drop increases proportionally with Re. Consequently, oral breathing must supplement nasal breathing above roughly 30 L/min in order to maintain respiratory airflow. Since flow through the oral cavity has a lower pressure drop than flow through the nasal cavity, a greater proportion of airflow during oronasal breathing passes through the oral cavity. It is unclear whether oronasal breathing produces laminar or turbulent airflow in the oral cavity, though Re < 2100 at $\dot{V}_E \leq 30$ L/min.

Pharyngeal turbulence results from the 90° bend at the nasopharynx and irregular surfaces at the oropharynx and larynx. Vocal cords constrict the passageway and cause significant flow distortions and turbulence within the larynx. The passageway abruptly expands from the laryngeal orifice into the trachea. Rapid expansion produces a jet in proximal tracheal airflow and turbulence all along the trachea. Turbulent tracheal airflow occurs because the abrupt expansion causes reverse flow in the boundary layer, causing flow separation in the proximal trachea (Fig. 5.22). Under these conditions, turbulence forms at Re much less than 2300 in an abrupt expansion (often at Re ≈ 300).

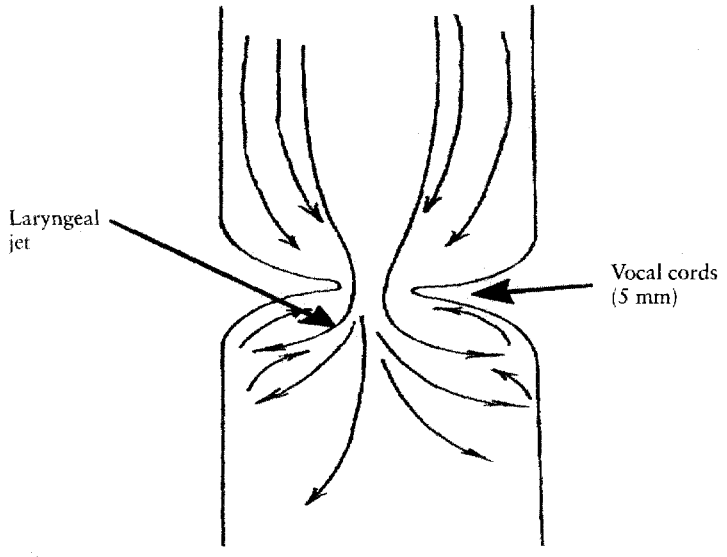

FIGURE 5.22 Schematic depiction of airflow pattern through the larynx. Note how eddies form downstream as air passes through the tracheal jet created by the vocal cords. This effect varies according to vocal chord position.

Studies of airflow through models of bifurcating airways[27,28] show that turbulence generated in the trachea does not sufficiently decay in the largest bronchi to produce laminar flow. Despite Re diminishing to below 1000, flow through at least the fourth generation bronchi is believed to be turbulent at all but the lowest $\dot{V}_E$. Eventually, however, flow disturbances dampen along the bronchial tree and flow becomes laminar. Entrance flow predominates because bronchi are typically only three to four diameters long. In addition, bifurcations modify velocity profiles because of asymmetric shear forces along inner and outer walls possibly caused by flow separation along the outer wall near the bifurcation (Fig. 5.23). Consequently, disturbed laminar flow appears to exist during both inspiration and exhalation in most bronchi.

Mean airstream velocity diminishes as inspiratory flow moves toward the lung parenchyma because of the rapid increase in total cross-sectional area. The largest increases in area occur in the distal bronchioles and pulmonary airways, causing u to approach zero because

$$u = \frac{Q}{A}, \tag{5.39}$$

where Q = volumetric flow rate ($\dot{V}_E$). Although flow is laminar, Poiseuille flow does not occur despite Re < 1.0 because of the complex geometry of these airways. Axial diffusion (also known as Taylor dispersion) accounts for mass transport within distal bronchioles and combines convection and diffusion in an oscillating fluid with a low Re such that

$$\frac{\partial c}{\partial x} = K\left[\frac{\partial^2 c}{\partial y^2} + \frac{\partial^2 c}{\partial z^2}\right], \tag{5.40}$$

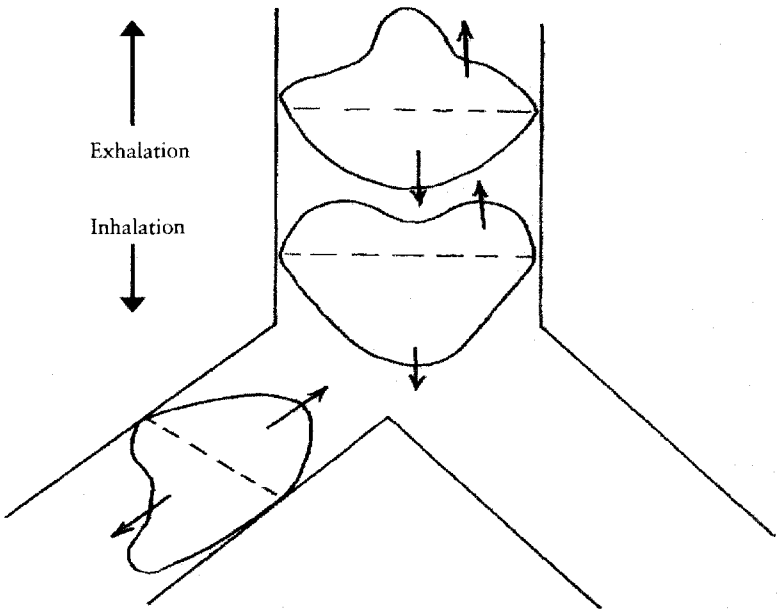

FIGURE 5.23 Airstream velocity profiles through a bronchial bifurcation. Shear forces along the medial bronchial wall cause flow distortions in the daughter tubes during inspiration. Bimodal velocity profiles generated in the parent tube during expiration are also caused by shear along the daughter tube medial walls. Modified from Scherer and Haselton.[28]

where c = solute concentration; x = direction of airflow; y, z = transverse directions to flow; and K = dispersion constant. K depends on the molecular diffusion coefficient, D_{ab}, where Fick's law defines mass transport by molecular diffusion as

$$m = -D_{ab} A \frac{dc}{dx}, \tag{5.41}$$

so that

$$K = f\left(D_{ab}, \frac{1}{U}\right), \tag{5.42}$$

where U = convective velocity. Pulmonary airways rely solely on molecular diffusion for mass transport.

5.2.4 Mucociliary Clearance

Mucus gel floating on airway periciliary fluid becomes contaminated by atmospheric contaminants deposited onto the air-mucus interface during respiration. Deposition generally traps these materials, especially particulates, in the mucus gel and prevents them from being transported further by the airstream. Merely trapping these materials, however, serves little purpose because they would diffuse through the periciliary fluid to enter the epithelia and blood-

stream. Cilia projecting from the apical surface of ciliated columnar epithelial cells, however, continuously propel mucus toward the epiglottis. Given sufficient mucus velocity, trapped contaminants will reach the epiglottis before they can diffuse through the periciliary fluid in sufficient quantity to cause injury or disease. Swallowing passes the contaminated mucus into the esophagus and eliminates the threat to the respiratory tract.

Ciliary Location

Cilia are present along most extrathoracic airway surfaces except for the nasal vestibule, olfactory surfaces, nasopharynx, oropharynx, oral cavity, and portions of the larynx. Extrathoracic airway cilia gradually push mucus distally toward the epiglottis. In nonciliated regions, mucus moves by mechanical force (coughing, sneezing, and swallowing) or by gravity. Cilia line all tracheobronchial surfaces down to the pulmonary airways, propelling mucus proximally toward the epiglottis. Respiratory airway surfaces (respiratory bronchi, alveoli) are devoid of cilia.

Ciliary Structure

Cilia are thin cylindrical hair-like structures with a cross-sectional radius of 0.1 μm projecting from the apical epithelial surface of ciliated columnar cells. Ciliary length is thought to correspond to periciliary fluid depth and range from approximately 7 μm in proximal airways to roughly 5 μm in more distal airways.[29] Each ciliated epithelial cell supports approximately 200 cilia at a density of eight cilia/μm^2. Short microvilli, possibly associated with secretory functions, are interspersed among the cilia.

Nonciliated cells separate fields of ciliated epithelial cells from each other. Synchronized ciliary movement, with a beat frequency in human proximal airways under normal conditions of 8–15 Hz,[30–34] propels mucus along the mucociliary escalator at a rate of up to 25 mm/min.[35,36] Beat frequencies appear to slow to roughly 7 Hz in more distal airways. Cilia move in the same direction and in phase within each field but cilia in adjacent fields move in slightly different directions and are phase shifted. These beat patterns result in metachronal waves that steadily move mucus at higher velocities (≈12–18 mm/min) than would be achievable by summing the motion of individual cilia.

Relationship of Ciliary Motion to Mucus Movement

Mucus gel is propelled toward the epiglottis by a two-phase ciliary beat cycle. Forward mucus movement occurs during the effective or power phase of the cycle, when cilia fully extend and traverse an arc perpendicular to the epithelial surface (Fig. 5.24). Claw-like structures, 25–35 nm long, project from each cilia tip and appear to assist in the mechanical transfer of momentum from cilia to mucus gel. Maximum mucus velocity depends on the extent cilia penetrate the epiphase during the power phase, periciliary and mucus gel viscosity, and cilia density.

During the recovery or preparatory phase, cilia bend over, swing back to start position generally parallel to the epithelial surface, and stiffen in anticipation of the next power phase. Ciliary bending and axial movement

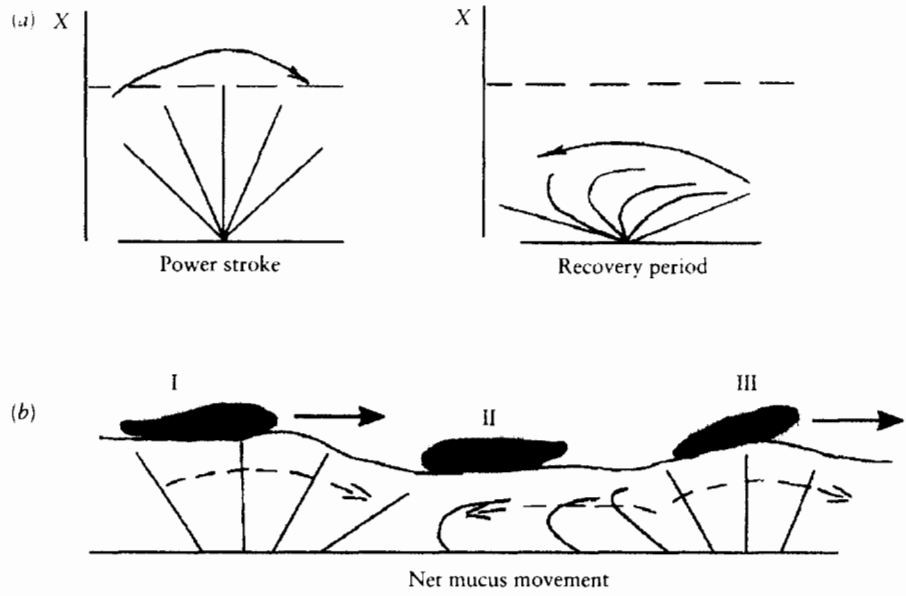

FIGURE 5.24 Components of ciliary movement. (*a*) Power and recovery phases of ciliary movement. Arrows indicate the direction of ciliary travel. (*b*) Net mucociliary transport. Dotted arrows show the direction of cilia while the solid arrows show mucus transport. Note that net gel movement is forward in I and III while no gel movement occurs in II during the cilia recovery phase. Modified from Fulford and Blake.[29]

parallel to the cell surface significantly reduce retrograde momentum exerted on the surrounding fluid during the ciliary recovery phase because periciliary fluid viscosity is much lower than that of mucus gel. In addition, the no-slip condition along the epithelial surface also retards retrograde movement. Mucus viscosity and the presence of surrounding cilia further retard any retrograde mucus movement such that gravity has little effect on tracheobronchial mucociliary transport.

Derangement of metachronal motion impedes mucosal movement and increases the risk of disease or injury. Slowing mucosal velocity increases residence times in the affected airway region, permitting greater diffusion of deposited pathogens and toxins through periciliary fluid and increasing the risk of direct injury to airway epithelium and systemic injury via the bloodstream. Reducing the number, activity, or coordination of adjacent cilia or ciliary fields, hypersecretion of serous fluid or mucus gel, increased periciliary or mucus viscosity, and excessive periciliary fluid evaporation can each adversely affect mucociliary transport. Inspiring dry or cold air or cigarette smoke decreases periciliary fluid depth (altering cilia penetration into mucus gel) and cilia beat frequencies, which slows mucociliary transport. In addition, changes in periciliary fluid pH, ion concentration, or viscosity due to deposited chemicals, microorganisms (e.g., influenza, mycoplasmas), or systemic disease (e.g., asthma, cystic fibrosis) also inhibit ciliary beat frequency.

5.2.5 Airway Heat and Water Vapor Transport

5.2.5.1 Longitudinal and Radial Temperature/Humidity Gradients

Air passing through the respiratory tract must be properly conditioned (warmed and humidified) in order to optimize alveolar O_2 and CO_2 transport and minimize heat and water losses from the body. Respiratory air conditioning, as shown in Fig. 5.25, occurs as the airstream passes over the airway mucosal surfaces and results in both spatial and temporal humidity and temperature changes during each phase of respiration.[37,38] Submucosal blood temperatures (T_{blood}) are thought to be cooler in the extrathoracic airways and gradually warm along the length of the conducting airways until body core temperature (T_{core}, roughly 37 °C) is achieved within the bronchi. This longitudinal temperature gradient exists because ambient air temperatures are generally lower than T_{core}. Inspired air extracts heat and water from airway walls as it passes through the lumen, warming the airstream and cooling the wall. The radial temperature gradient lessens as the ever-warmer airstream moves along the airway, causing gradually less heat extraction from the wall until eventually no heat is exchanged. The process is reversed during expiration. At the onset of inspiration, the walls of the airway are their warmest and approach end-expiratory airstream temperatures throughout most of the respiratory tract.[38,39] Typically, inspired air

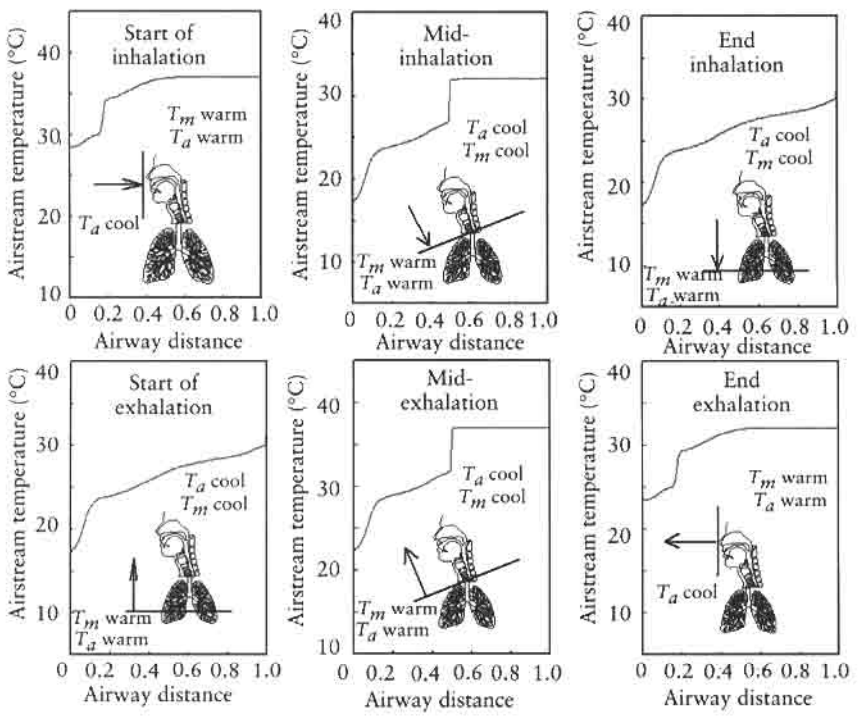

FIGURE 5.25 The relationship between the inspiratory and expiratory airstream front boundary and air, T_a, and wall, T_m, temperatures as a function of nondimensional distance from the nares. Solid lines shown on the airway picture indicate respiratory fronts and arrows depict the direction of airflow. Qualitative temperatures indicate relative temperature gradients across front boundaries. The graph depicts airstream temperatures as a function of nondimensional distance along the airway while breathing normal room air. Nondimensional distance is distance from the nares (x) divided by overall airway length (L).

is cooler than this, creating a radial temperature gradient, such that the air within the airway lumen is cooler than the walls (Fig 5.25). A radial water vapor concentration gradient also exists because air at the air-mucus interface (airway wall) is fully saturated,[40] while inspired air has a lower absolute humidity due to its being at a lower temperature than the airway wall.

Under most circumstances, passage of relatively cool inspiratory air along the airway results in convective and evaporative cooling of the mucosa while warming and humidifying the inspired air.[38,39] Airflow patterns caused by convoluted upper airway morphology augment heat and water vapor transport.[41–44] Radial temperature gradients can persist at least as far as the carina during oral breathing of room air,[45,46] causing heat and water vapor exchange to occur for much of the length of the upper airway. At the end of inhalation, longitudinal temperature and water vapor concentration gradients exist along the airway (Fig. 5.25). Air reaching the most distal airway regions (beyond about the fourteenth bronchial generation) is believed to be fully conditioned (37 °C, 100% humidity) during normal breathing. Exhalation causes warm air originating in the distal airway to pass over airway walls in proximal airway segments, which had been cooled during inspiration and are normally maintained below body core temperature.[47] The resulting temperature gradient causes airstream water vapor to condense and the airstream to lose heat to the airway walls. This acts to minimize net heat and water losses.[48]

Effectiveness of the conditioning process is dependent upon respiratory tract geometry, ambient air temperature (T_{amb}) and humidity (C_{amb}), inspiratory and expiratory flow rates and volumes,[48] mucus temperature (T_m), airway wall blood temperature (T_{blood}), and flow rate in the submucosal capillary bed.[49–52] These variables interact and their effects are interdependent. For example, airway geometry plays a major role in conditioning since the rate of heat exchange between the wall and airstream, $\dot{q}$ is given by

$$\dot{q} = hA_s\Delta T, \tag{5.43}$$

where h = heat transfer coefficient, A_s = airway wall surface area, and ΔT = temperature difference between the airstream and wall.[53] Water vapor exchange is analogous to heat exchange and thus is also a function of A_s.[54] In addition, both mean gas velocity, $\bar{u}$ and residence time, t_w, are dependent on airway geometry since $t_w = f(\bar{u})$, $u = f(A)$, and conduit geometry directly affects the generation of flow disturbances and subsequent development of turbulent flow.

5.2.5.2 Role of Airway Heat and Water Vapor Exchange in Disease and Injury

Exchange of heat and water vapor in the respiratory tract can significantly influence airway patency, alveolar gas transport, and whole body homeostasis, such as seen with cold- or exercise-induced bronchospasms. Maintaining airway patency is important in reducing airway resistance, maximizing inspiratory volume, and minimizing the work of breathing. The mechanism by which heat and water vapor exchange influences airway resistance has been widely debated[55–57] but probably depends on both airway mucosa heat and water losses.[47,58] It has been suggested that alterations in the conditioning of inspired and expired air can lead to increased total airway resistance[39,47,49,55] by causing increased nasal blood flow,[59,60] altering vascular tone and permeability in the

bronchial circulation,[61] and increasing airway smooth muscle tension.[62–65] Under pathological conditions, diminished conditioning may also increase mucus thickness,[17,66] which in extreme cases causes increased airway resistance by reducing airway cross-sectional area and increasing shear stress at the air/mucus interface.[67] In addition to effects on the conducting airways, alveolar O_2 and CO_2 transport could be hampered if air has not been warmed to body temperature (37 °C) and fully humidified by the time it reaches the alveoli.

The importance of respiratory heat and water losses is not confined to the respiratory structures. Inspiration of cold, hot, or dry air poses the potential threats of thermal injury or desiccation to the airway epithelium[46,52,66,68,69] and is a challenge to whole-body thermoregulation. Under certain conditions, such as hyperbaria,[70,71] airway heat losses can account for a considerable percentage of total body heat production (in some cases $> 100\%$).[71] Normally these threats are ameliorated by rapid moderation of inspired air temperature and humidity by exchanging heat and water vapor between the mucus and airstream in the upper airway.[72–74] Recovering much of the heat and water vapor contained in expired air minimizes heat and water losses to the ambient environment[75] and aids in whole-body thermoregulation.

Heat and water vapor transport can also lead to respiratory impairment, infection, and injury through thermal and osmotic stresses occurring at the mucosal epithelium.[66,75] These stresses cause changes in mucus osmolarity, pH, ciliary activity, and cellular transport,[73,76] resulting in altered mucosal thickness[17,66] and impaired airway defenses. Normal breathing allows microorganisms, pollutant gases, and particulate matter to contact the mucus coating (comprised of mucus gel and periciliary fluid) atop the apical surface of respiratory epithelium. A complex system of chemical, immunological, and mechanical defense mechanisms protects the respiratory epithelium and alveoli from potential diseases or injury caused by noxious airstream components.[77] Aside from chemical neutralization of pollutants in the airstream[78,79] and physical defenses such as bronchoconstriction, coughing, and particle impaction caused by airway morphology,[77,80–82] the defense of the airway depends on the physical and chemical properties of airway mucus (e.g., chemical detoxification reactions with proteins[83]) and the ciliary mechanism which moves it toward the epiglottis (mucociliary escalator). Inspiring cold dry air can impede mucociliary transport, reducing mucus velocity and increasing the risk of airway disease or injury.

Airway deposition patterns of inspired hygroscopic particles are also affected by airway heat and water vapor exchange. Inspired particles passing from a relatively dry ambient environment into the fully saturated airway quickly adsorb water from the surrounding airstream. Water vapor adsorption at the particle surface increases hygroscopic particle mass m_p as a function of particle diameter d_g and the water vapor concentration gradient between the bulk fluid, c_∞, and particle surface, c_0, according to

$$\frac{dm_p}{dt} = 2\pi d_g D_w C_w (c_\infty - c_0), \tag{5.44}$$

where D_w = diffusion coefficient of water vapor in air and C_w = slip correction factor = $f(d_g, D_w, T)$.[84] In addition, d_g can be determined from m_p and particle density, ρ,

$$d_g = 2\left[\frac{3m_p}{4\pi\rho(X)}\right]^{1/3}, \tag{5.45}$$

where X = particle composition at time t.[85] Particle growth continues until equilibrium is reached between particle surface and bulk airstream water vapor pressure. Given sufficient growth, extremely fine particles that might otherwise pass entirely through the airway during the breathing cycle deposit along the airway because of the increase in mass. Compromised extrathoracic submucosal blood flow due to injury or disease will change water vapor exchange between the mucosal surface and inspired airstream. This in turn will alter the growth patterns of inspired hygroscopic particles. This process may play a role in lower airway injury caused by inspired toxins (e.g., acid aerosols) or succumbing to diseases normally present in the ambient environment (e.g., pneumonia) that seem to affect weakened individuals.

5.2.6 Endogenous Ammonia Production

Evidence suggests that the highest airway NH_3 concentrations occur in the oral cavity,[78] the only segment of the respiratory system that is normally colonized by bacteria, and that the remainder of the airway, including the nasal passages, have significantly lower levels. Diffusion of NH_3 from the bloodstream into the airway lumen is probably the primary source of NH_3 for the entire airway except the oral cavity.[78] Blood ammonium concentration, $[NH_4^+]_B$, is normally the consequence of protein deamination during dietary protein digestion,[86] though deamination of AMP in muscle tissue during strenuous exercise can significantly increase $[NH_4^+]_B$.[86–88] Ureolysis by gastrointestinal bacteria can also contribute to $[NH_4^+]_B$.[86] It is theorized that airstream NH_3 concentration, $[NH_3]_A$, is in equilibrium with $[NH_4^+]_B$ throughout most of the respiratory tract,[78] though this has not been demonstrated. Airway mucus may impede diffusion of blood ammonia into the airway lumen because of its net negative charge.[83] The effect this Donnan exclusion phenomenon may exert on airway NH_3 diffusion has not been demonstrated, since $[NH_4^+]_B$ has not yet been correlated with $[NH_3]_A$ in humans.

Bacterial catabolism of oral food residue is probably responsible for a higher $[NH_3]_A$ in the oral cavity than in the rest of the respiratory tract.[78] Ammonia, the by-product of oral bacterial protein catabolism and subsequent ureolysis, desorbs from the fluid lining the oral cavity to the airstream.[89,90] Saliva, gingival crevicular fluids, and dental plaque supply urea to oral bacteria[90] and may themselves be sites of bacterial NH_3 production, based on the presence of urease in each of these materials.[89,91] Consequently, oral cavity $[NH_3]_A$ is controlled by factors that influence bacterial protein catabolism and ureolysis. Such factors may include the pH of the surface lining fluid, bacterial nutrient sources (food residue on teeth or on buccal surfaces), saliva production, saliva pH, and the effects of oral surface temperature on bacterial metabolism and wall blood flow. The role of teeth, as structures that facilitate bacterial colonization and food entrapment, in augmenting $[NH_3]_A$ is unknown.

The significance of pH is particularly interesting since pH may either augment or diminish NH_3 production. The possible mechanisms by which pH affects NH_3 production are: (a) inhibition of bacterial metabolism, (b) pH-dependent changes in urea metabolic pathways, (c) pH-dependent bacterial utilization of glucose and urea as energy sources, and (d) increased bacterial uti-

lization of NH_3 in amino acid synthesis. Ureolysis appears to be very sensitive to pH; NH_3 production increases as salivary pH is reduced from 7.0 to 6.0[92] but decreases significantly when pH is lowered to approximately pH 2.5.[93] A salivary pH of 2.5, however, only temporarily depresses NH_3 production[93] since NH_3 diffusing from the bloodstream may neutralize acids responsible for reduced oral cavity pH and slowly increase oral pH. Ureolysis may increase rapidly at some pH threshold, perhaps near pH 5.5,[94] because of the steady supply of salivary urea.[90] Oral pH continues to increase as NH_3 is generated,[94] with peak NH_3 production thought to occur near an oral pH of 6.0.[92] Salivary HCO_3^- may act to buffer increases in oral pH and thus maintain NH_3 production rates.[95] Therefore, an increase in salivary flow will not only increase the availability of urea to oral bacteria but also help maintain oral conditions advantageous for NH_3 production. Theories regarding in vivo regulation of oral NH_3 production are speculative since the bulk of data was obtained from in vitro studies of salivary sediments and dental plaque samples; greater knowledge of in vivo interaction between oral cavity NH_3 production, pH, and saliva is needed.

Fasting combined with poor oral hygiene results in an elevated dental plaque pH ($\sim$7.6),[96] suggestive of active ureolysis. Whether fasting or poor oral hygiene is responsible for the higher pH is unclear. Carbohydrates in the mouth lower dental plaque pH,[96] while glucose, in particular, buffers oral pH[97] thereby inhibiting NH_3 production.[92] The formation of NH_3 appears to be inhibited by glucose for two other reasons: (a) it is preferentially used for bacterial energy production in place of proteins and peptides, and (b) its presence favors acid-producing bacteria that scavenge NH_3.[92] Oral food residues with a high protein content should serve as a rich substrate for oral NH_3 production through bacterial deamination.

5.2.7 Respiratory Defense Mechanisms

Breathing exposes a large body surface area to attack by noxious materials or pathogens present in the ambient atmosphere. A complex series of defense mechanisms, including physical removal, chemical neutralization, and immunological response, protect against biological, chemical, or mechanical injury. Physically removing toxins or pathogens from the airstream by coughing, sneezing, movement along the mucociliary escalator, or phagocytosis in the alveoli reduces exposure concentrations in vulnerable airway regions. Airborne toxins can be neutralized by endogenous NH_3, while deposited materials are diluted, buffered, and neutralized by periciliary fluid and mucus gel. Immunoglobins and enzymes present in periciliary fluid and along alveolar surfaces can eliminate deposited pathogens that have not been physically removed.

5.2.7.1 Vapor Phase Neutralization

In addition to typical atmospheric or metabolic constituents (N_2, O_2, H_2O, and CO_2), breathing transports chemical species in the form of vapors and particulates along the respiratory tract. While O_2 and CO_2 gas exchange occurs solely in the lung parenchyma, air/blood exchange of other species can and does occur throughout the airway. The principal airway absorption sites of gases such as O_3 and SO_2 are largely determined by their water:air partition coefficient (the concentration ratio at equilibrium) and water solubility.[98] Highly water-soluble

chemical species with high water:air partition coefficients are generally absorbed in the extrathoracic airways, while less soluble species pass beyond the extrathoracic airways in relatively high concentrations (see Section 5.3).

Concentration gradients provide the driving force for gaseous chemical species diffusion between the luminal gas mixture and ASL. Factors that alter this gradient, such as local airstream concentration, chemical reactivity, lipid solubility, and ASL metabolism, modulate local absorption or reentrainment into the airstream. Local airstream/ASL concentration gradients drive diffusion into or out of ASL along a given airway length.[99,100] As the inspiratory air passes along the airway and comes into contact with previously unexposed ASL, chemical species follow the concentration gradient and diffuse into ASL. The leading edge of the inspiratory wave becomes increasingly depleted of the diffusing species, increasing proximal ASL concentrations while reducing airstream concentrations downstream. Consequently, ASL absorption decreases in more distal airways. Reentrainment can occur during expiration if concentration gradients are reversed, i.e., tracheobronchial and extrathoracic ASL concentrations exceed those found in gases flowing outward from the lung parenchyma.

The rate at which an absorbed chemical species is removed from the ASL determines whether reentrainment occurs during a breathing cycle.[98] Slow removal rates relative to the breathing cycle allow the concentrations in the ASL to be higher than in the expiratory airstream. Figure 5.26 shows processes that diminish the ASL concentration of absorbed chemical species. Metabolic processes or interactions with ions and other chemically reactive substances found

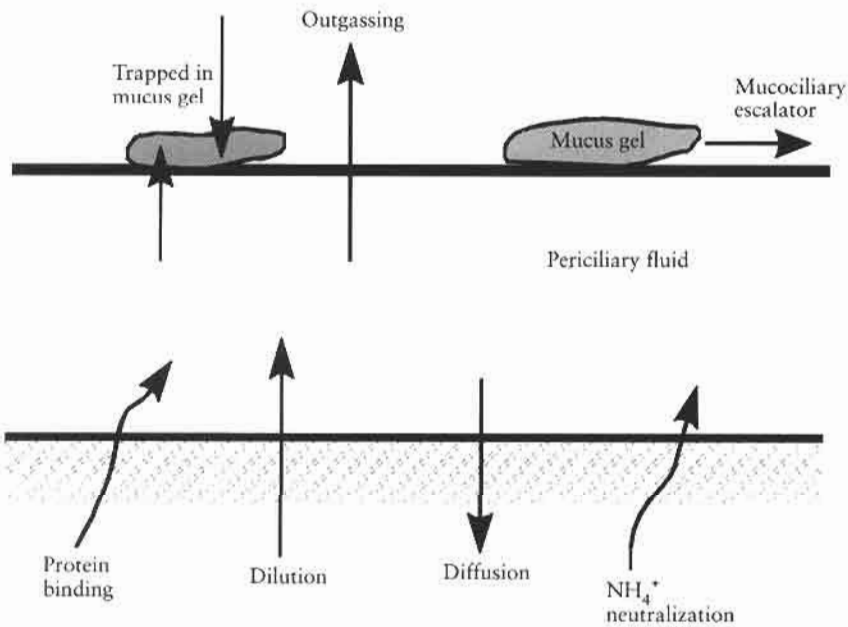

FIGURE 5.26 Various chemical and physical mechanisms which can affect ASL chemical concentration during breathing. Dilution due to transepithelial water exchange depends on the osmotic pressure gradient between periciliary and interstitial fluid.

in ASL can eliminate absorbed chemicals. Diffusion through airway epithelium into the submucosal bloodstream is an alternative removal pathway (Fig. 5.27) that depends on lipid solubility or facilitated transport across cell membranes.

5.2.7.2 Aerosol Defense

Particle Deposition

Particles entrained in the airstream deposit along the airway as a function of size, density, airstream velocity, and breathing frequency. Sizes of roughly spherical or irregularly shaped particles are commonly characterized by relating the settling velocity of the particle to that of an idealized spherical particle.[101] For example, an irregular particle which settles at the same rate as a 5 μm spherical particle has a mean mass aerodynamic diameter (MMAD) of 5 μm. Since spherical particle mass, m_p, is a function of particle diameter, d

$$m_p = \frac{\pi}{6} d^3 \rho, \tag{5.46}$$

where ρ = particle density, MMAD can be viewed as representing the mass and buoyancy of a spherical particle equivalent to the randomly shaped airborne particle.[101] Three basic deposition mechanisms, impaction, sedimentation, and diffusion, act on all entrained particles, but each mechanism predominantly affects specifically sized particles within a given airway region.[101]

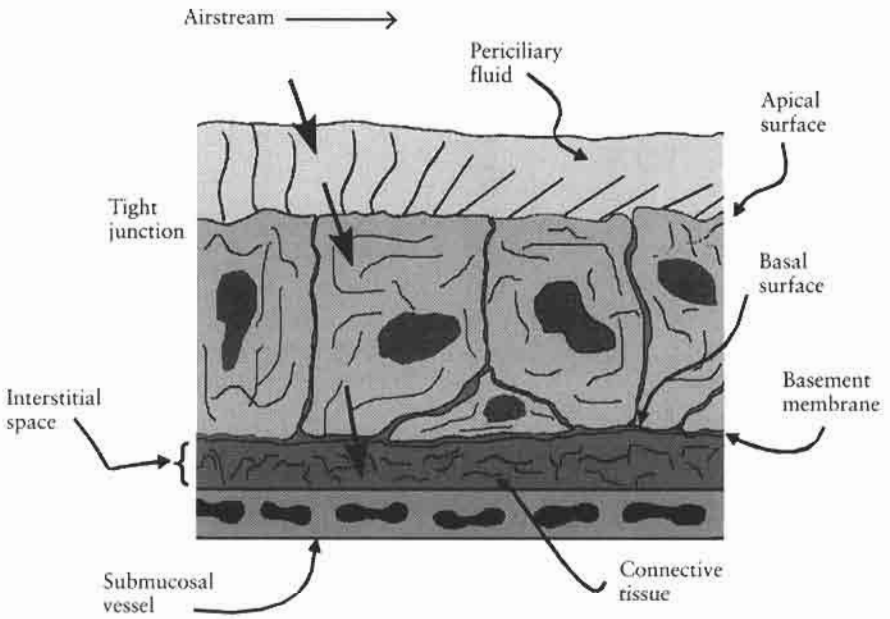

FIGURE 5.27 Diffusional pathway of deposited materials from the airstream to interstitial space. Large arrows depict diffusion across the ASL, apical, and basal call membranes. Na^+ and Cl^- passively diffuse across the cellular apical surface while K^+ diffuses and a Na^+-K^+-$2Cl^-$ co-transporter exchanges these ions across the cellular basal surface. Active transport (Na+-K+ pump) also transports Na^+ out of and K^+ into the cell across the cellular basal surface. Water diffuses across the different cell membrane surfaces depending upon the existing osmotic pressure gradient. Diffusion of water and salts through the paracellular spaces between cells can also occur.

The nasal passages form an efficient filtration mechanism for inspired air, removing larger particulates (>3 μm MMAD) before they can enter the thoracic airways. The very largest inspired particles (roughly 10 μm MMAD and larger) impinge on nasal hairs (vibrissae) and are mechanically removed from the nasal cavity (e.g., by blowing one's nose). Particle inertia generally causes the remaining larger particles to deposit along the nasal cavity surfaces by impaction because of convoluted nasal geometry. A particle impacts an airway wall when the path length to the wall equals the lateral displacement, L, occurring while the particle moves at a velocity u along a streamline altering direction by an angle θ, which is given by

$$L = \frac{u u_t \sin\theta}{g}, \tag{5.47}$$

where terminal velocity, u_t, is the particle velocity at which particle inertia is balanced by drag forces. For $1.0\ \mu\text{m} \leq d \leq 40\ \mu\text{m}$,

$$u_t = \frac{g d^2}{18 \mu_a}(\rho_p - \rho_a), \tag{5.48}$$

where g is the gravitational constant, μ_a is the air viscosity, and ρ_p and ρ_a are the density of the particle and air, respectively. Larger particles that successfully traverse the nasal passages typically impact the nasopharyngeal wall at the 90° turn beyond the distal edge of the nasal cavity.

Finer particles (<3 μm), termed respirable particles, pass beyond the extrathoracic airways and enter the tracheobronchial tree. Impaction plays a significant role near the tracheal jet, but sedimentation predominates as the effects of rapid conduit expansion dampen in the distal trachea and beyond. Sedimentation occurs when gravitational forces exerted on a particle equal drag forces, i.e., when particle velocity falls to u_t. As mean inspiratory airstream velocity gradually declines along the tracheobronchial tree, particle momentum diminishes and 0.5–3 μm MMAD particles settle out of the airflow and onto mucosal surfaces.

Mean airflow velocities approach zero as the inspired airstream enters the lung parenchyma, so particle momentum also approaches zero. Most of the particles reaching the parenchyma, however, are extremely fine ($<0.5\,\mu$m MMAD), and particle buoyancy counteracts gravitational forces. Temperature gradients do not exist between the airstream and airway wall because the inspired airstream has been warmed to body temperature and fully saturated before reaching the parenchyma.[50,51] Consequently, diffusion driven by Brownian motion is the only deposition mechanism remaining for airborne particles. Diffusivity, D_c, can be described under these conditions by

$$D_c = \frac{kT}{3\pi\mu d}, \tag{5.49}$$

where k is the Boltzmann constant, T is the absolute temperature, μ is the air viscosity, and d is the particle diameter. Particle displacement, δ, is a function of residence time, t, and D_c such that

$$\delta = (6 D_c t)^{0.5}. \tag{5.50}$$

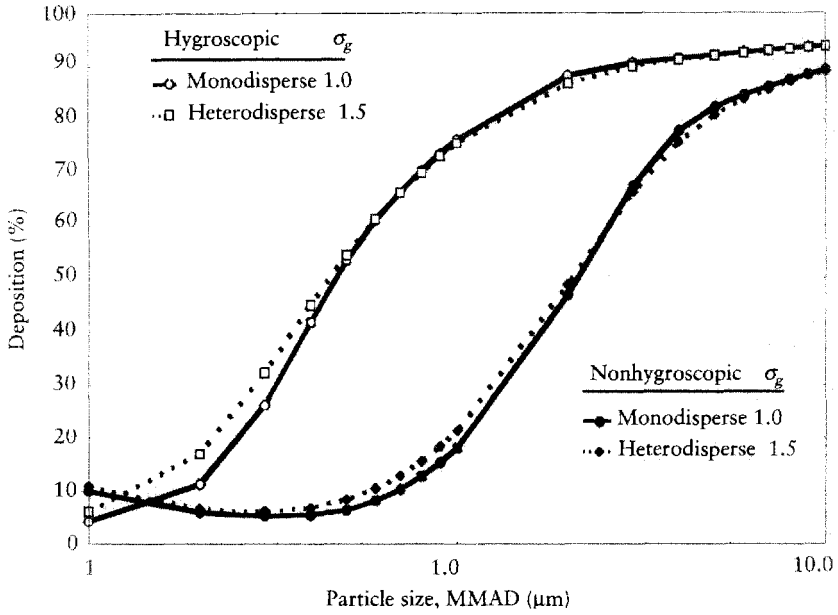

FIGURE 5.28 Estimated overall airway deposition as a function of initial particle size and particle hygroscopicity for particles with mass median aerodynamic diameters (MMAD) between 0.1 and 10 μm.[102] Geometric dispersion, a measure of particle size distribution, principally affects only smaller MMAD.

Consequently, any breathing pattern which increases pulmonary residence times, such as breath-holding, increases fine particle deposition throughout the airway.

Where along the airway inspired particles deposit depends on particle mass, since the deposition mechanism depends on particle MMAD. Passage through the airway has no effect on nonhygroscopic particle mass (e.g., fly ash), and initial MMAD determines the deposition pattern (Fig. 5.28). In contrast, hygroscopic particles (e.g., acid droplets) increase in mass when exposed to humid environments like the respiratory tract. Particle properties (e.g., chemical composition, ionic concentration, and particle surface area) and airstream conditions (e.g., temperature, RH, and $\dot{V}_E$) which affect hygroscopic growth consequently play major roles in determining particle mass and deposition patterns (Fig. 5.29).

Acid Aerosol Neutralization

Sulfuric acid (H_2SO_4) and ammonium bisulfate (NH_4HSO_4) contribute importantly to ambient acid aerosols, particularly in geographic locations where sulfur-rich coal is used for power plant fuel, such as the eastern United States.[103] Studies on animals and human subjects have shown that H_2SO_4 and NH_4HSO_4 alter mucociliary transport in a dose-dependent fashion[104–106] and can adversely affect pulmonary function in humans.[106] While this effect on clearance has generally been attributed to hydrogen ion concentration, $[H^+]$, the work of Schlesinger et al.[107] suggests that, for equivalent inhaled $[H^+]$, H_2SO_4 elicits a greater change than NH_4HSO_4. If this observation is confirmed, it

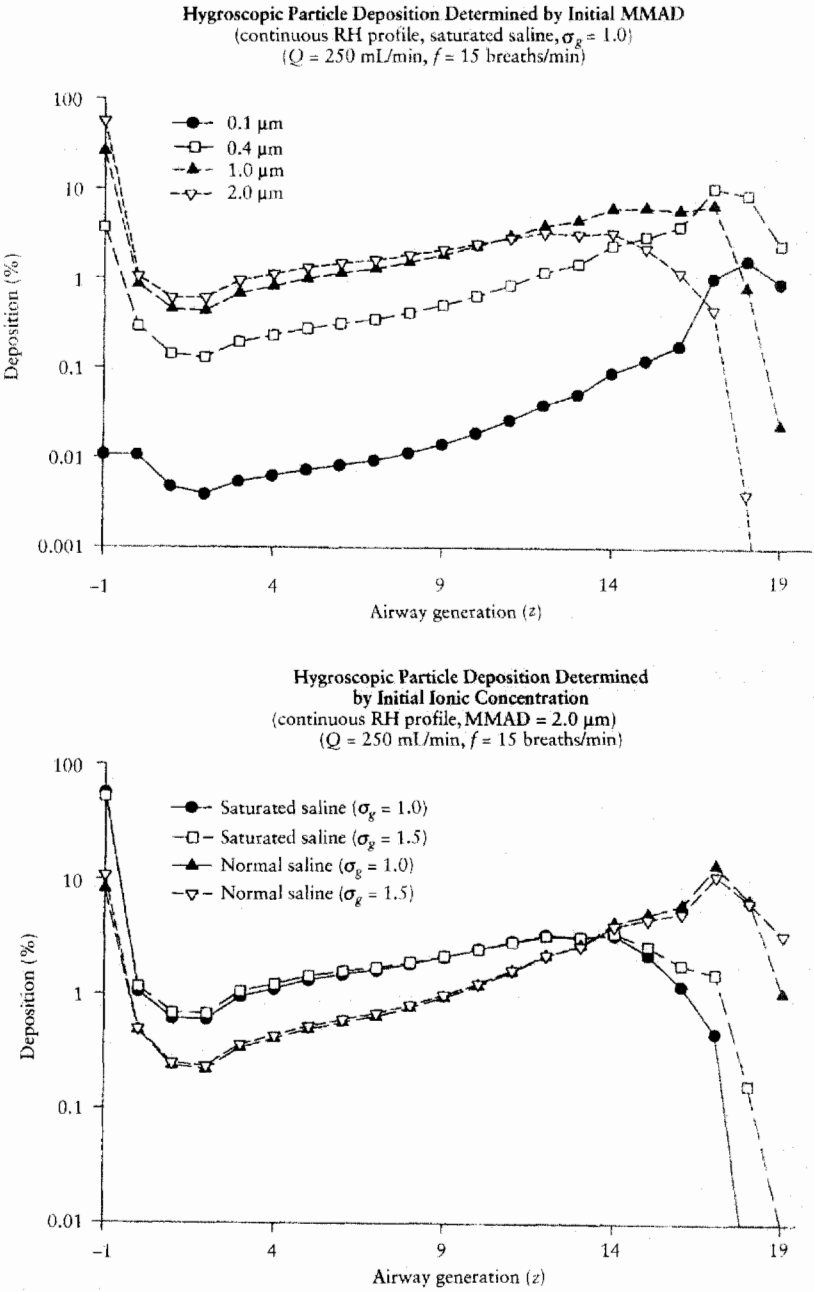

FIGURE 5.29 Predicted effects of initial hygroscopic particle properties (initial diameter, ionic concentration) on the airway deposition profile.[102] Larger initial particles are predicted (left) to deposit in the more proximal airways while fine particles reach pulmonary airways in much greater concentrations. Initially high ionic concentrations (saturated saline) are predicted (right) to deposit primarily in upper airways, probably due to their rapid growth during transit through the upper airway. More moderate growth rates represented by normal saline aerosol result in greater predicted deposition in the pulmonary airways. Airway generation −1represents the upper airway while the trachea is given as generation 0.

would appear that the molecular form of the inhaled acid may play a significant role, perhaps through differences in hygroscopic growth and neutralization rate between H_2SO_4 and NH_4HSO_4 particles.

For a given ambient concentration of acid aerosol, the dose of acid delivered to the respiratory tract is in large measure determined by the pH and particle size of the aerosol. Due to the efficiency of the upper airways (particularly the nasal passages) in filtering coarse (>3 μm) particles, submicrometric acid aerosol particles pose the greatest risk to the lower airways. Ambient acid aerosols are overwhelmingly submicrometric in size distribution at most relative humidities.[108] Submicron acid particles therefore merit special attention in the attempt to understand the action of acid aerosols on airway health, particularly as they comprise a large proportion of acidic environments.[108]

Airstream neutralization of acid aerosols by NH_3 present in the airway lumen reduces the health risk associated with acid particles by reducing the acid concentration prior to particle deposition.[78,109] In addition, the liquid lining of the respiratory tract probably acts as a chemical buffer,[110] further reducing the health hazard posed by inspired acid particles. Principal factors controlling airstream neutralization of acid aerosols, which is considered to be a diffusion-limited process, are particle surface area, $[NH_3]_A$, and particle residence time in the airstream.

Since NH_3 is highly water-soluble and neutralization within the droplet occurs rapidly,[111] the rate-limiting step in acid neutralization is normally NH_3 transport to the air/droplet interface, which is dependent on $[NH_3]_A$ and particle surface area. At high $[NH_3]_A$, the rate of NH_3 uptake across the air/droplet interface is given by

$$\frac{dC_s}{dt} = \frac{3D_g}{r^2}([NH_3]_A - C_s H q_{NS}), \tag{5.51}$$

where C_s is the NH_3 concentration in the acid droplet, D_g, is the airstream NH_3 diffusion coefficient, r is the droplet radius, H is the Henry's law coefficient, and q_{NS} is the activity coefficient of neutral undissociated species in solution in the droplet.[112] Particle size of inhaled liquid aerosols does not remain constant within the airways, however. Water will condense on the surface of particles as they move distally along the airway because of local increases in relative humidity.[85,113,114] The resulting increase in particle radii due to hygroscopic growth will reduce NH_3 concentration according to Eq. (5.49), while the increase in particle size will increase particle deposition.[102,115] However, increasing the particle radius results in greater particle surface area, which should increase NH_3 uptake, thereby opposing the reduction in particle $[NH_3]$.

Elevated inspiratory flow rates reduce airway $[NH_3]$ by diluting the endogenous NH_3. The effect of flow rate on $[NH_3]_A$ should be most apparent in the upper airway due to the large NH_3 concentration difference between ambient air (as the diluent) and the upper airway (containing endogenous NH_3). The diluting effects of ventilation should be less evident in the large central airways and diminish steadily as the inspiratory wavefront moves distally along the airway because air velocity declines as airway volume increases and NH_3 is a highly soluble gas and most likely equilibrates rapidly with blood ammonia. As a result, flow-rate effects on $[NH_3]_A$ should be negligible after approximately the eighth bronchial generation because the rapid increase in airway volume

causes air velocity to decline and the airstream to become more diluted. Since the expiratory wavefront is anticipated to encounter uniform $[NH_3]_A$ throughout the lower conducting airways, increased expiratory flow rates should have no effect on $[NH_3]_A$ until the wavefront reaches the upper airway. With nasal expiration, there may be no longitudinal NH_3 concentration gradient except at the nares, unless NH_3 diffuses from the oral cavity into the oropharynx.

Despite our limited knowledge of $[NH_3]_A$ distribution and control, there are at least two mathematical models[80,112] that attempt to predict the neutralization of inhaled acid aerosols. Cocks and McElroy[112] base their model on acid particle growth by predicting equilibrium particle size as a function of initial particle diameter and relative humidity (RH). Molecular diffusion is a major determinant of particle growth in the Cocks and McElroy[112] model, particularly for submicrometric particles, because their size approaches the mean free path of water vapor. Neutralization of acid particles was determined as a function of time and constant $[NH_3]_A$ at parenchymal conditions. Cocks and McElroy[112] did not account for higher levels of ammonia in the upper airways, which suggests that the bulk of neutralization will occur in the upper airway, at lower RH and temperature than in the parenchyma. The effect of a longitudinal intra-airway $[NH_3]_A$ gradient on neutralization was also not considered.

Larson[80] developed a model of acid aerosol neutralization that accounts for RH and temperature gradients along the airway. The longitudinal gradients used in the model were taken from the model of Martonen and Miller[116], which did not account for airway geometry or ventilation. Two fixed intra-airway $[NH_3]_A$ gradients, reflecting oral and nasal breathing, were modeled and both assumed linear concentration gradients along the airway (with a step change at the oropharynx during nasal breathing). Dilution due to increased flow rate was not modeled, nor is it clear whether the $[NH_3]_A$ gradients changed during exhalation. Neither Cocks and McElroy[112] nor Larson[80] accounted for gas-phase NH_3 transport (except at the particle surface) or the possible effect a reduction in oral wall pH, caused by exposure to acid aerosol, would have on segmental control of $[NH_3]_A$.

Both models predict that two factors would decrease $[H^+]$ in the particle: (1) hygroscopic growth of the particle, which is thought to be capable of reducing particle $[H_2SO_4]$ from 15.3 M to 0.22 M; and (2) particle neutralization due to $[NH_3]_A$, which is potentially more significant but likely to be more variable within an exposed population. Without neutralization, highly acidic submicrometric particles (pH = 0.66) were predicted to be deposited onto distal airway tissues.[80] To refine our understanding of the potential for acid neutralization to mitigate adverse health effects, the assumptions regarding NH_3 concentration appear to be critical for any mathematical description of acid aerosol effects. Cocks and McElroy[112] demonstrated the importance of NH_3 concentration estimates, with complete neutralization of submicron droplets at 500 $\mu g/m^3$ NH_3 but less than 15% neutralization at 50 $\mu g/m^3$ NH_3. Since measured oral NH_3 concentration vary over a wide range, 144–1536 $\mu g/m^3$,[78,93] model predictions would improve if the factors controlling NH_3 production and $[NH_3]_A$ were known.

Mucociliary Escalator

Bacterial and viral inoculants deposited onto airway mucus are normally inactivated by immunoglobins and macrophages[117] while being physically

removed by the mucociliary escalator (mucociliary clearance).[17,77] Deposition and adherence of particulates onto airway mucus also prevents aspirated pollutants,[108,118] viral particles,[77,119] and infected epithelial cells shed from the airway wall[77] from reaching the alveoli.[17,22,119] Airway mucus also plays an important role in buffering and chemically neutralizing inhaled pollutant gases.[120] In addition, mucus serves to protect the airway epithelium against injury caused by rapid fluctuations in airstream temperature, T_a, and humidity, C_a.[66]

Disruption of these defense mechanisms can lead to bacterial colonization or viral infection. Mucus temperature is important in controlling respiratory infections because decreasing T_m below central body core temperature not only impairs ciliary movement,[73,76] but also enhances viral replication,[21] greatly increasing the likelihood of respiratory infection. Drying of airway mucus also increases the possibility of respiratory infection by reducing mucus thickness and impairing mucociliary clearance.[121,122]

References

1. International Commission on Radiological Protection. (1994). *Human Respiratory Tract Model for Radiological Protection* (Vol. Publication 66). Elsevier Science, Tarrytown, NY.
2. Guilmette, R. A., Wicks, J. D., and Wolff, R. K. (1989). Morphometry of human nasal airways in vivo using magnetic resonance imaging. *J. Aerosol Med.* **2**, 365–377.
3. Daviskas, E., Gonda, I., and Anderson, S. D. (1990). Mathematical modeling of heat and water transport in human respiratory tract. *J. Appl. Physiol.* **69**, 362–372.
4. Weibel, E. R. (1989). Lung morphometry and models in respiratory physiology. In *Respiratory Physiology: An Analytical Approach* (H. K. Chang and M. Paiva, Eds.), pp. 1–56. Marcel Dekker, New York.
5. Weibel, E. R. (1963). *Morphology of the Human Lung*. Academic Press, New York.
6. Horsfield, K. (1986). Morphometry of airways. In *The respiratory system: Section 3. Mechanics of Breathing, Part 1vol. III* (P.T. Macklem and J. Mead, Eds.), pp. 75–88. American Physiological Society, Bethesda, Maryland.
7. McNamee, J. E. (1991). Fractal perspectives in pulmonary physiology. *J. Appl. Physiol.* **71**, 1–8.
8. Nelson, T. R., West, B. J., and Goldberger, A. L. (1990). The fractal lung: universal and species-related scaling patterns. *Experientia* **46**, 251–254.
9. Robinson, N. P., Kyle, H., Webber, S. E., and Widdicombe, J. G. (1989). Electrolyte and other chemical concentrations in tracheal airway surface liquid and mucus. *J. Appl. Physiol.* **66**, 2129–2135.
10. Widdicombe, J. G. (1989). Airway mucus. *Eur. Respir. J.* **2**, 107–115.
11. Jeffery, P. K. (1987). The origins of secretions in the lower respiratory tract. *Eur. J. Respir. Dis.* **71**, Suppl 153, 34–42.
12. Pavia, D., Agnew, J. E., Lopez-Vidreiro, M. T., and Clarke, S. W. (1987). General review of tracheobronchial clearance. *Eur. J. Respir. Dis.* **71**: (Suppl. 153), 123–129.
13. Welsh, M. J. (1987). Electrolyte transport by airway epithelium. *Physiol. Rev.* **67**, 1143–1184.
14. Verdugo, P. (1984). Hydration kinetics of exocytosed mucins in cultured secretory cells of the rabbit trachea: a new model. *Mucus and Mucosa* (**Ciba Foundation symposium 109**), 212–225.
15. Verdugo, P., Aitken, M., Langley, L., and Villalon, M. J. (1987). Molecular mechanism of product storage and release in mucin secretion II. The role of extracellular Ca^{++}. *Biorheology* **24**, 625–633.
16. Boucher, R. C., Stutts, M. J., Bromberg, P. A., and Gatzy, J. T. (1981). Regional differences in airway surface liquid composition. *J. Appl. Physiol.* **50**, 613–620.
17. Kaliner, M., Shelhamer, J. H., Borson, B., Nadel, J., Patow, C., and Marom, Z. (1986). Human respiratory mucus. *Am. Rev. Respir. Dis.* **134**, 612–621.
18. Widdicombe, J. G. (1989). Fluid transport across airway epithelia. Mucus and Mucosa 109, 109–120.
19. Taylor, A. E., and Drake, R. E. (1978). Fluid and protein movement across the pulmonary microcirculation. In *Lung Water and Solute Exchange* (N. C. Staub, Ed.), pp. 129–166. Marcel Dekker, New York.

20. Deffebach, M. E., Charan, N. B., Lakshminarayan, S., and Butler, J. (1987). The bronchial circulation: Small, but a vital attribute of the lung. *Am. Rev. Respir. Dis.* **135**, 463–481.
21. Bende, M., Barrow, I., Heptonstall, J., Higgins, P. G., Al-Nakib, W., Tyrrell, D. A. J., and Akerlund, A. (1989). Changes in human nasal mucosa during experimental coronavirus common colds. *Acta Otolaryngol. (Stockh)* 107, 262–269.
22. Olsson, P., and Bende, M. (1985). Influence of environmental temperature on human nasal mucosa. *Ann. Otol. Rhinol. Laryngol.* 94, 153–155.
23. Fouke, J. M., Wolin, A. D., Bowman, H. F., and McFadden, E. R. J. (1990). Effect of facial cooling on mucosal blood flow in the mouth in humans. *Clinical Science* 79, 307–313.
24. Anderson, S. D., Schoeffel, R. E., Follet, R., Perry, C. P., Daviskas, E., and Kendall, M. (1982). Sensitivity to heat and water loss at rest and during exercise in asthmatic patients. *Eur. J. Respir. Dis.* 63, 459–471.
25. McFadden, E. R., Jr. (1983). Respiratory heat and water exchange: physiological and clinical implications. *J. Appl. Physiol.* 54, 331–336.
26. Cherniak, R. M. (1992). *Pulmonary Function Testing* (2nd ed.). Philadelphia: W. B. Sanuders.
27. Dekker, E. (1961). Transition between laminar and turbulent flow in human trachea. *J. Appl. Physiol.* **16**, 1060–1064.
28. Scherer, P. W., and Haselton, F. R. (1979). Convective mixing in tube networks. *AIChE J.* 25, 542–544.
29. Fulford, G. R., and Blake, J. R. (1986). Muco-ciliary transport in the lung. *J. Theor. Biol.* **121**, 381–402.
30. Luk, C. K., and Dulfano, M. J. (1983). Effect of pH, viscosity and ionic-strength changes on ciliary beating frequency of human bronchial explants. *Clin. Sc.* 64, 449–451.
31. Mercke, U., Hakansson, C. H., and Toremalm, N. G. (1974). The influence of temperature on mucociliary activity: Temperature range 20°C–40°C. *Acta Otolaryngol.* 78, 444–450.
32. Munro, N. C., Barker, A., Rutman, A., Taylor, G., Watson, D., McDonald-Gibson, W. J., Towart, R., Taylor, W. A., Wilson, R., and Cole, P. J. (1989). Effect of pyocyanin and 1-hydroxyphenazine on in vivo tracheal mucus velocity. *J. Appl. Physiol.* 67, 316–323.
33. Reimer, A., von Mecklenberg, C., and Toremalm, N. G. (1978). The mucociliary activity of the upper respiratory tract. III. A functional and morphological study on human and animal material with special reference to maxillary sinus diseases. *Acta Otolaryngol.*, 1–20.
34. Seybold, Z. V., Mariassy, A. T., Stroh, D., Kim, C. S., Gazeroglu, H., and Wanner, A. (1990). Mucociliary interaction in vitro: effects of physiological and inflammatory stimuli. *J. Appl. Physiol.* 68, 1421–1426.
35. Giordano, A., Jr., Shih, C. K., Holsclaw, D. S., Jr., Khan, M. A., and Litt, M. (1977). Mucus clearance: In vivo canine tracheal vs. vitro palate studies. *J. Appl. Physiol.* 42, 761–766.
36. Toremalm, N. G. (1985). Aerodynamics and mucociliary function of upper airways. *Eur. J. Respir. Dis.* 66 (Supp. 139), 54–56.
37. Solway, J. (1990). Airway heat and water fluxes and the tracheobronchial circulation. *Eur. Respir. J.* 3 (**Suppl. 12**), 608s–617s.
38. Walker, J. E. C., Wells, R. E., Jr., and Merrill, E. W. (1961). Heat and water exchange in the respiratory tract. *Am. J. of Med.* 30, 259–267.
39. Cole, P. (1954). Respiratory mucosal vascular responses, air conditioning and thermoregulation. *J. Laryngol. Otol.* 68, 613–622.
40. Tsai, C.-L., Saidel, G. M., McFadden, E. R., Jr., and Fouke, J. M. (1990). Radial heat and water transport across the airway wall. *J. Appl. Physiol.* 69, 222-231.
41. Narezhnyy, E. G., and Sudarev, A. V. (1971). Local heat transfer in air flowing in tubes with a turbulence promoter at the inlet. *Heat Transfer* 3, 62–66.
42. Proetz, A. W. (1951). Air currents in the upper respiratory tract and their clinical importance. *Ann. Otol. Rhinol. Laryngol.* 60, 439–467.
43. Sandall, O. C., Hanna, O. T., and Mazet, P. R. (1980). A new theoretical formula for turbulent heat and mass transfer with gases or liquids in tube flow. *Can. J. Chem. Eng.* 58, 443–447.
44. Sparrow, E. M., and Kalejs, J. P. (1977). Local convective transfer coefficients in a channel downstream of a partially constricted inlet. *Int. J. Heat Mass Transfer* 20, 1241–1249.
45. McFadden, E. R., Jr., Denison, D. M., Waller, J. F., Assoufi, B., Peacock, A., and Sopwith, T. (1982). Direct recordings of the temperatures in the tracheobronchial tree in normal man. *J. Clin. Invest.* 69, 700–705.
46. Moritz, A. R., and Weisiger, J. R. (1945). Effects of cold air on the air passages and lungs: an experimental investigation. *Arch. of Inter. Med.* 75, 233–240.

47. Ingenito, E. P., Solway, J., Lafleur, J., Lombardo, A., Drazen, J. M., and Pichurko, B. M. (1988). Dissociation of temperature-gradient and evaporative heat loss during cold gas hyperventilation in cold-induced asthma. *Am. Rev. Respir. Dis.* **138**, 540–546.
48. Solway, J., Pichurko, B. M., Ingenito, E. P., McFadden, E. R., Jr., Fanta, C. H., Ingram, R. H., Jr., and Drazen, J. M. (1985). Breathing pattern affects airway wall temperature during cold air hyperpnea in humans. *Am. Rev. Respir. Dis.* **132**, 853–857.
49. Gilbert, I. A., Fouke, J. M., and McFadden, E. R., Jr. (1988). Intra-airway thermodynamics during exercise and hyperventilation in asthmatics. *J. Appl. Physiol.* **64**, 2167–2174.
50. Hanna, L. M. (1983). *Modeling of heat and water vapor transport in the human respiratory tract.* Ph.D. Dissertation, University of Pennsylvania, Philadelphia.
51. Ingenito, E. P. (1984). *Respiratory fluid mechanics and heat transfer.* Ph.D. dis, MIT, Cambridge, MA.
52. Scherer, P. W., and Hanna, L. M. (1985). Heat and water transport in the human respiratory tract. In *Mathematical Modeling in Medicine and Biology* (A. Shitzer and R. C. Eberhart, Eds.), pp. 287–306. Plenum Press, New York.
53. Welty, J. R., Wicks, C. E., and Wilson, R. E. (1969). *Fundamentals of Momentum, Heat and Mass Transfer.* John Wiley & Sons, New York.
54. Bird, R. B., Stewarr, W. E., and Lightfoot, E. N. (1960). *Transport Phenomena.* John Wiley & Sons, New York.
55. Anderson, S. D., and Schoeffel, R. E. (1982). Respiratory heat and water loss during exercise in patients with asthma: Effect of repeated exercise challenge. *Eur. J. Respir. Dis.* **63**, 472–480.
56. Deal, E. C., McFadden, E. R., Jr., Ingram, R. H., Jr., Strauss, R. H., and Jaeger, J. J. (1979). Role of respiratory heat exchange in production of exercise-induced asthma. *J. Appl. Physiol.* **46**, 467–475.
57. McFadden, E. R., Jr. (1987). Exercise-induced asthma: Assessment of current etiologic concepts. *Chest* **91**, 151s–157s.
58. Chen, W.Y., and Horton, D. J. (1977). Heat and water loss from the airways and exercise-induced asthma. *Respiration* **34**, 305–313.
59. Ohki, M., Hasegawa, M., Kurita, N., and Watanabe, I. (1987). Effects of exercise on nasal resistance and nasal blood flow. *Acta Otolaryngol. (Stockh)* **104**, 328–333.
60. Paulsson, B., Bende, M., and Ohlin, P. (1985). Nasal mucosal blood flow at rest and during exercise. *Acta Otolaryngol. (Stockh.)* **99**, 140–143.
61. Gilbert, I. A., Fouke, J. M., McFadden, E. R., Jr., Lenner, K. A., and Coreno, A. J., Jr. (1990). The effect of repetitive exercise on airway temperatures. *Am. Rev. Respir. Dis.* **142**, 826–831.
62. Black, J. L., Armour, C. L., and Shaw, J. (1984). The effect of alteration in temperature on contractile respsonses in human airways in vitro. *Resp. Physiol.* **57**, 269–277.
63. Bratton, D. L., Tanaka, D. T., and Grunstein, M. M. (1987). Effects of temperature on cholinergic contractility of rabbit airway smooth muscle. *J. Appl. Physiol.* **63**, 1933–1941.
64. Souhrada, M., and Souhrada, J. F. (1981). The direct effect of temperature on airway smooth muscle. *Resp. Physiol.* **44**, 311–323.
65. Souhrada, J. F., Presley, D., and Souhrada, M. (1983). Mechanisms of the temperature effect on airway smooth muscle. *Resp. Physiol.* **53**, 225–237.
66. Barbet, J. P., Chauveau, M., Labbe, S., and Lockhart, A. (1988). Breathing dry air causes acute epithelial damage and inflammation of the guinea pig trachea. *J. Appl. Physiol.* **64**, 1851–1857.
67. Clarke, S. W., Jones, J. G., and Oliver, D. R. (1970). Resistance to two-phase gas-liquid flow in airways. *J. Appl. Physiol.* **29**, 464–471.
68. Proctor, D.F., and Swift, D.L. (1977). Temperature and water vapor adjustment. In *Respiratory Defense Mechanisms, Pt 1* (J. D. Brain, D. F. Proctor, and L. M. Reid, Eds.), pp. 95–124. Marcel Dekker, New York.
69. Widdicombe, J. G. (1977). Defense mechanisms of the respiratory tract and lungs. In *International Review of Physiology: Volume 14. Repiratory Physiology II* (J. G. Widdicombe, Ed.), pp. 291–316. University Park Press, Baltimore.
70. Hoke, B., Jackson, D. L., Alexander, J. M., and Flynn, E. T. (1976). Respiratory heat loss and pulmonary function during cold-gas breathing at high pressure. In *Underwater Physiology VI* (C.J. Lambertsen, Ed.). FASEB, Bethesda, MD.
71. Piantadosi, C. A., Thalmann, E. D., and Spaur, W. H. (1981). Metabolic response to respiratory heat loss—induced core cooling. *J. Appl. Physiol.* **50**, 829–834.
72. Proctor, D. F., Andersen, I., and Lundqvist, G. R. (1977a). human nasal mucosal function at controlled temperatures. *Respiration Physiology* **30**, 109–124.

73. Proctor, D. F., Andersen, I., and Lundqvist, G. R. (1977b). Nasal mucociliary function in humans, Part 1. In *Respiratory Defense Mechanisms* pp. 427–452. Marcel Dekker, New York.
74. Webb, P. (1951). Air temperatures in respiratory tracts of resting subjects in cold. *J. Appl. Physiol.* 4, 378–382.
75. Deffebach, M. E., Salonen, R. O., Webber, S. E., and Widdicombe, J. G. (1989). Cold and hyperosmolar fluids in canine trachea: Vascular and smooth muscle tone and albumin flux. *J. Appl. Physiol.* **66**, 1309–1315.
76. Baetjer, A. M. (1967). Effect of ambient temperature and vapor pressure on cilia-mucus clearance rate. *J. Appl. Physiol.* **23**, 498–504.
77. Reynolds, H. Y. (1988). Normal and defective respiratory host defenses. In *Respiratory Infections: Diagnosis and Management* (J. E. Pennington, Ed.), pp. 1–33. Raven Press, New York.
78. Larson, T. V., Covert, D.S., Frank, R., and Charlson, R.J. (1977). Ammonia in the human airways: neutralization of inspired acid sulfate aerosols. *Science* **197**, 161–163.
79. Larson, T. V., Frank, R., Covert, D.S., Holub, D., and Morgan, M.S. (1982). Measurements of respiratory ammonia and chemical neutralization of inhaled sulfuric acid aerosol in anesthetized dogs. *Am. Rev. Respir. Dis.* **125**, 502–506.
80. Larson, T. V. (1989). The influence of chemical and physical forms of ambient air acids on airway doses. *Environ. Health Perspect.* **79**, 7–13.
81. Martonen, T. B. (1993). Mathematical model for the selective deposition of inhaled pharmaceuticals. *J. Pharmacol. Sci.* **82**, 1191–1199.
82. Persons, D. D., Hess, G. D., Muller, W. J., and Scherer, P. W. (1987). Airway deposition of hygroscopic heterodispersed aerosols: results of a computer model. *J. Appl. Physiol.* **63**, 1195–1204.
83. Lee, S. P., and Nicholls, J. F. (1987). Diffusion of charged ions in mucus gel: effect of net charge. *Biorheology* **24**, 565–569.
84. Ferron, G. A., Haider, B., and Kreyling, W. G. (1988). Inhalation of salt aerosol particles-1. Estimation of the temperature and relative humidity of the air in the human upper airways. *J. Aerosol Sci.* **19**, 343–363.
85. Cocks, A. T., and Fernando, R. P. (1982). The growth of sulphate aerosols in the human airways. *J. Aerosol Sci.* **13**, 9–19.
86. Mutch, B. J. C., and Banister, E. W. (1983). Ammonia metabolism in exercise and fatigue: a review. *Med. Sci. Sports* **15**, 41–50.
87. Broberg, S., and Sahlin, K. (1988). Hyperammoniemia during prolonged exercise: an effect of glycogen depletion? *J. Appl. Physiol.* **65**, 2475–2477.
88. Denis, C., Linossier, M.-T., Dormois, D., Cottier-Perrin, M., Geyssant, A., and Lacour, J.-R. (1989). Effects of endurance training on hyperammonaemia during a 45-min constant exercise intensity. *Eur. J. Appl. Physiol.* **59**, 268–272.
89. Kopstein, J., and Wrong, O. M. (1977). The origin and fate of salivary urea and ammonia in man. *Clin. Sc. and Mol. Med.* **52**, 9–17.
90. MacPherson, L. M. D., and Dawes, C. (1991). Urea concentration in minor mucus gland secretions and the effect of salivary film velocity on urea metabolism by streptococcus vestibularis in an artificial plaque. *J Periodont. Res.* **26**, 395–401.
91. Sissons, C. H., Cutress, T. W., and Pearce, E. I. F. (1985). Kinetics and product stoichiometry of ureolysis by human salivary bacteria and artificial mouth plaques. *Arch. Oral Biol.* **30**, 781–790.
92. Biswas, S. D. (1982). Effect of urea on pH, ammonia, amino acids and lactic acid in the human salivary sediment system incubated with varying levels of glucose. *Arch. Oral Biol.* **27**, 683–691.
93. Norwood, D. M., Wainman, T., Lioy, P. J., and Waldman, J. M. (1992). Breath ammonia depletion and its relevance to acidic aerosol exposure studies. *Arch. of Environ. Health* **47**, 309–313.
94. Sissons, C. H., and Cutress, T. W. (1987). In-vitro urea-dependent pH-changes by human salivary bacteria and dispersed, artificial-mouth, bacterial plaques. *Arch. Oral Biol.* **32**, 181–189.
95. Shellis, R. P., and Dibdin, G. H. (1988). Analysis of the buffering systems in dental plaque. *J. Dent. Res.* **67**, 438–446.
96. Kleinberg, I., and Jenkins, G. N. (1964). The pH of dental plaques in the different areas of the mouth before and after meals and their relationship to the pH and rate of flow of resting saliva. *Arch Oral Biol.* **9**, 493–516.
97. Sissons, C. H., and Cutress, T. W. (1988). pH changes during simultaneous metabolism of urea and carbohydrate by human salivary bacteria in vitro. *Arch. Oral Biol.* **33**, 579–587.

98. Dahl, A. R., Snipes, M. B., and Gerde, P. (1991). Sites for uptake of inhaled vapors in beagle dogs. *Tox. Appl. Pharmacol.* **109**, 263–275.
99. Miller, F. J., Overton, J. H. J., Jaskot, R. H., and Menzel, D. B. (1985). A model of regional uptake of gaseous pollutants in the lung. I. The sensitivity of the uptake of ozone in the human lung to lower respiratory tract secretions and exercise. *Toxicol. Appl. Pharmacol.* 79, 11–27.
100. Gerde, P., and Dahl, A. R. (1991). A model for the uptake of inhaled vapors in the nose of the dog during cyclic breathing. *Tox. Appl. Pharmacol.* **109**, 276–288.
101. Hinds, W. C. (1999). *Aerosol Technology: Properties, Behavior, and Measurement of Airborne Particles* (2nd ed.). John Wiley & Sons, New York.
102. Kaufman, J. W. (1999). The role of upper airway heat and water vapor exchange in hygroscopic aerosol deposition in the human airway. In *Toxicity Assessment Alternatives: Methods, Issues, Opportunities* (H. Salem and S.A. Katz, Eds.), pp. 63–70. Humana Press Inc., Totowa, NJ.
103. Lipfert, F. W., Morris, S. C., and Wyzga, R. E. (1989). Acid aerosols: the next criteria air pollutant? *Environ. Sci. Tech.* **23**, 1316–1322.
104. Folinsbee, L. J. (1989). Human health effects of exposure to airborne acid. *Environmental Health Perspectives* **79**, 195–199.
105. Gearhart, J. M., and Schlesinger, R. B. (1989). Sulfuric acid-induced changes in the physiology and structure of the tracheobronchial airways. *Environ. Health Perspect.* **79**, 127–137.
106. Hanley, Q. S., Koenig, J. Q., Larson, T. V., Anderson, T. L., Belle, G. V., Rebolledo, V., Covert, D. S., and Pierson, W. E. (1992). Response of young asthmatic patients to inhaled sulfuric acid. *Am. Rev. Respir. Dis.* **145**, 326–331.
107. Schlesinger, R. B., Chen, L. C., Finkelstein, I., and Zelikoff, J. T. (1990). Comparative potency of inhaled acidic sulfates: speciation and the role of hydrogen ion. *Environ. Res.* **52**, 210–224.
108. Covert, D. S., and Frank, N. R. (1980). Atmospheric particles: Behavior and functional effects. In *Physiology and Pharmacology of the Airways* (J.A. Nadel, Ed.), pp. 259–295. Marcel Dekker, New York.
109. Utell, M. J. (1985). Effects of inhaled acid aerosols on lung mechanics: an analysis of human exposure studies. *Environmental Health Perspect.* **63**, 39–44.
110. Holma, B. (1989). Effects of inhaled acids on airway mucus and its consequences for health. *Environ. Health Perspect.* **79**, 109–113.
111. Huntzicker, J. J., Cary, R. A., and Ling, C. S. (1980). Neutralization of sulfuric acid aerosols by ammonia. *Environ. Sci. Tech.* **14**, 819–824.
112. Cocks, A. T., and McElroy, W. J. (1984). Modeling studies of the concurrent growth and neutralization of sulfuric acid aerosols under conditions in the human airways. *Environmental Res.* 35, 79–96.
113. Scherer, P. W., Haselton, F. R., Hanna, L. M., and Stone, D. J. (1979). Growth of hygroscopic aerosols in a model of bronchial airways. *J. Appl. Physiol.* **47**, 544–550.
114. Tang, I. N., and Munkelwitz, H. R. (1977). Aerosol growth studies—III: Ammonium bisulfate aerosols in a moist atmosphere. *J. Aerosol Sci.* **8**, 321–330.
115. Scheuch, G., and Stahlhofen, W. (1992). Deposition and dispersion of aerosols in the airways of the human respiratory tract: the effect of particle size. *Exper. Lung Res.* **18**, 343–358.
116. Martonen, T. B., and Miller, F. J. (1984). A dosimetry model for hygroscopic sulfate aerosols in selected temperature and relative humidity patterns. *J. Aerosol Sci.* **15**, 203–208.
117. Farzan, S., and Farzan, D. (1997). *A Concise Handbook of Respiratory Diseases* (4th ed.). Appleton & Lange, Stamford, CT.
118. Schlesinger, R. B. (1989). Factors affecting the response of lung clearance systems to acid aerosols: role of exposure concentration. *Environ. Health Perspect.* **79**, 121–126.
119. Richardson, P. S., and Peatfield, A. C. (1987). The control of airway mucus secretion. *Eur. J. Resp. Dis.* 71, (Suppl 153), 43–51.
120. Holma, B. (1985). Influence of buffer capacity and pH-dependent rheological properties of respiratory mucus on health effects due to acidic pollution. *Sci. Total Environ.* 41, 101–123.
121. Salah, B., Dihn Xuan, A. T., Fouilladieu, J. L., Lockhart, A., and Regnard, J. (1988). Nasal mucociliary transport in healthy subjects is slower when breathing dry air. *Eur. Respir. J.* 1, 852–855.
122. Sleigh, M. A., Blake, J. R., and Liron, N. (1988). The propulsion of mucus by cilia. *Am. Rev. Respir. Dis.* 137, 726–741.

Bibliography

Hickey, A. J., and Martonen, T. B. (1993). Behavior of hygroscopic pharmaceutical aerosols and the influence of hydrophobic additives. *Pharm. Res.* 10, 1–7.

Martonen, T. B., Bell, K. A., Phalen, R. F., Wilson, A. F., and Ho, A. (1982). Growth rate measurements and deposition modelling of hygroscopic aerosols in human tracheobronchial models. *Ann. Occup. Hyg.* 26, 93–108.

Glossary

Airstream: Volume of air traversing a portion of or the entire respiratory tract.

Airway defense mechanisms: Group of physical, physiological, and immunological mechanisms that protect the respiratory tract against disease or injury.

Airway generation: Theoretical representation of bronchi position within the airway based on the number of successive bifurcations leading to a given level. Generally assumes a symmetric series of bronchial bifurcations. Asymmetric models typically use the concept of order, based on branching angle of daughter tubes, to describe relative position within the airway.

Airway lumen: Opening in conducting airway through which air moves during inhalation and exhalation.

Airway surface liquid (ASL): A mixture of periciliary fluid and submucosal gland secretions.

Alveolar duct: Airway distal to respiratory bronchiole leading to individual alveoli and alveolar sacs.

Alveolar gas transport: Exchange of oxygen and carbon dioxide between alveolar gases and the adjacent capillary bloodstream.

Alveolar sac: Group of alveoli originating from an expansion of the alveolar duct surface.

Alveolar ventilation: Volume of air passing through the alveoli and alveolar ducts in one minute.

Anastomoses: Lattice-like network of direct connections between arterioles and venules. They can allow for flow regulation and pressure equalization.

Apical epithelial surface: In the airway, surface interfacing with lumen.

Atelectasis: Collapse of the expanded lung.

Axial diffusion: Mass transfer by diffusion along streamlines that occurs at very low velocities. In the respiratory tract, axial diffusion likely occurs in the pulmonary airways.

Basal epithelial surface: In the airway, surface interfacing with basement membrane.

Basal cells: Stem cells for other airway cell types that do not interface with the airway lumen.

Basement membrane: Layer of dense amorphous material on which cells associated with connective tissue rest (e.g., epithelia). Appear to structurally support cells and may play a role in regulating ion and molecular transport across tissues.

Bifurcation: In the airway, a relatively large bronchi divides into two smaller, more distal branches.

Bloodstream: Volume of blood circulating through the heart, arteries, capillaries, and veins or within a certain anatomical region.

Body core temperature: Hypothetical "average" internal organ temperature, typically referenced to either right atrial or brain temperature. A reference value of 37 °C is generally used under normal environmental conditions.

Breathing frequency: Number of breaths per minute.

Bronchioles: Noncartilaginous, smaller, more distal subdivision of tracheobronchial tree. Walls consist of smooth muscle and elastic fibers.

Buccal: Pertaining to the lateral inner surface of the oral cavity (cheek).

Bulk transport: Transport of relatively large quantities of material by forced convection.

Capacitance vessels: Larger venules and veins forming a large-volume, low-pressure system of blood vessels.

Carbon dioxide production: Rate at which the pulmonary bloodstream transports carbon dioxide, produced by metabolic processes, to the pulmonary airstream.

Cartilaginous: Consisting of cartilage.

Catabolism: Destructive metabolism; breakdown of complex chemical compounds into simpler ones.

Chemical neutralization: Chemical reaction that converts acids or bases to nonreactive salts.

Cilia: Hair-like motile extensions of a cell wall. Airway cells use cilia to propel mucus gel toward the epiglottis.

Ciliary beat frequency: Rate at which cilia travel through both the power and recovery phases of the ciliary beat cycle.

Ciliary beat power phase: Interval during which forward ciliary movement propels mucus gel toward the epiglottis.

Ciliary beat recovery phase: Interval during which cilia bends and returns to initial position before power stroke. Minimal mucus gel retrograde movement is thought to occur.

Clearance: Removal of a substance from the airway.

Concentration gradient: Difference in concentration measured between two points.

Concha: One of three bony projections in the nasal turbinate region.

Conducting airways: Portion of respiratory tract through which air is transported but in which oxygen and carbon dioxide are not exchanged with the bloodstream.

Dead space: The portion of each breath that does not participate in gas exchange. Anatomical dead space is the volume of the conducting airways; physiological dead space also includes the contribution of pulmonary airways that are well-ventilated but poorly perfused.

Dental plaque: Mass of microorganisms attached to a tooth surface.

Deoxygenated blood: Blood containing hemoglobin with oxygen levels below fully saturated.

Diaphragm: Large abdominal muscle that varies pleural pressure resulting in movement of air through the respiratory tract.

Diffusion-limited: A chemical or physical process that depends upon the supply of material via diffusion.

Distal: In the airways, positioned relatively further from the nares.

Donnan equilibrium: Both concentration gradients and charge gradients contribute to the distribution of ions on either side of a membrane. Consequently, if there is a concentration gradient of an impermeable charged solute (e.g., protein) across a semipermeable membrane, then concentrations of permeable ions on either side of the membrane will not be equal.

Dose-dependent: Response to applied stimuli directly proportional to concentration of stimuli.

Edema: Excessive accumulation of fluid in cells, interstitial spaces, or tissues.

Eddy currents: Vortices that characterize turbulent flow.

End-expiratory: Airstream conditions measured when expiration ceases and just prior to initiating inspiration.

Endogenous ammonia: Byproduct of metabolism and bacterial catabolism that diffuses into the airway lumen. Highest concentrations are found in the oral cavity.

Endothelium: Layer of flat cells lining blood vessels.

Entrance flow: Flow within the inlet region of a conduit that has not developed a parabolic velocity profile. Airflows within the respiratory tract are not fully developed (parabolic) because of the relatively short tube lengths and irregular geometry.

Epiglottis: Leaf-shaped cartilage which closes larynx during swallowing.

Epiphase: Airway surface liquid gel layer composed of mucins in the form of droplets, sheets, or blankets.

Epithelium: Cellular layer interfacing with external environment which contains no blood vessels. In the airway, the epithelium lines the airway lumen.

Expiratory reserve volume (ERV): Maximum additional volume one can expire from end-tidal expiration.

Extrapulmonary airways: All airways not involved in gas exchange. These include the extrathoracic airways and the tracheobronchial tree down to the terminal bronchioles.

Extrathoracic airways: The portion of the human conducting airways proximal to and including the larynx. Also called the upper airways.

Fibroelastic: Fibrous material possessing elastic properties. In the airway, fibroelastic tissue throughout the lung contributes to its overall elasticity, generating a positive recoil force at the functional residual capacity, or resting state of the lungs.

Flow distortion: Nonuniform airstream velocity profile due to asymmetric shear, as in inspiratory bronchial airflow distal to a bifurcation.

Flow separation: Formation of turbulent eddies away from boundary as flow streamlines diverge.

Forced expired volume (FEV_t): Gas volume forcibly expired within the time interval t (typically $t = 1.0$ seconds).

Forced vital capacity (FVC): Maximum forced expired volume following a maximum inspiratory effort.

Fully conditioned airstream: Inspired airstream which has been warmed and humidified to approximate alveolar conditions (theoretically 37 °C, 100% relative humidity).

Functional residual capacity (FRC): Gas volume remaining in the airway at end-tidal exhalation.

Gingival crevicular fluid: Liquid found in gingival crevices located around the base of teeth.

Hemoglobin saturation level: The extent to which the oxygen-bearing capacity of hemoglobin in red blood cells is utilized.

Homeostasis: Tendency for an organism to maintain internal physiological stability.

Hydrostatic pressure: Force generated by a fluid at rest, directed perpendicular to a surface.

Hygroscopic: Material that readily adsorbs or absorbs moisture from the atmosphere.

Hyperbaria: Pressures greater than standard atmospheric pressure (760 mm Hg).

Inspiratory reserve volume (IRV): Maximum additional volume one can inspire from end-tidal inspiration.

Intercostal muscles: Muscles connecting the ribs that aid the diaphragm in propelling air through the respiratory tract.

Interstitial: Space found between cells.

Jet: Rapidly expanding flow exiting from a very small orifice.

Lower airways: The portion of the human conducting airways distal to the larynx.

Macrophage: A large ameboid phagocytic cell.

Mean mass aerodynamic diameter (MMAD): Mean diameter of theoretical particles with a 1 g/cm density having the same settling velocity as an actual group of measured particles calculated on the basis of particle mass.

Meatus: An opening or passage;. . . **of the nasal cavity:** air passages between the nasal conchae and the later wall of the nasal septum.

Metachronal wave: Synchronized ciliary movement over a relatively large airway region that is responsible for the transport of objects and materials along the mucociliary escalator.

Microvilli: Minute projections of cell membrane that greatly increase apical surface area.

Minute ventilation: Volume of air expired or inspired during one minute of breathing.

Mucociliary escalator: Mechanism that removes extracellularly-derived materials from the conducting airways by entrapping these materials in mucus that is continuously moved toward the epiglottis by synchronized ciliary movement.

Mucus: Viscous glycoprotein, proteoglycan secretion of goblet cells and mucus glands.

Nares: Orifices leading into the nasal cavity; nostrils.

Nasal cavity: Airway passages between the nares and posterior termination of the nasal septum.

Nasal turbinates: Region within the nasal cavity denoted by convoluted bony projections (conchae).

Nasopharynx: Airway passage between the posterior termination of the nasal septum and lower border of the soft palate.

Nonhygroscopic: Material that resists adsorbing or absorbing atmospheric water vapor.

Noxious: Injurious.

Olfaction: The physiological function of sensing odors.

Oral cavity: Airway passage between the lips and lower border of the soft palate.

Oronasal breathing: Breathing simultaneously through both the nasal and oral cavities.

Oropharynx: Airway passage between the lower border of the soft palate and epiglottis.

Oxygen uptake: Rate of oxygen transfer from air resident in the pulmonary airways to the pulmonary bloodstream. This is driven by the oxygen concentration gradient and depends on metabolic demand.

Parenchyma: The essential or specialized part of an organ; gas exchange portions of the respiratory tract (alveoli, respiratory bronchioles).

Particle growth: Increase in particle size due to hydration.

Partition coefficient: Quantitative expression of the partition equilibrium of a material between two immiscible liquid phases; usually expressed as the ratio of concentrations between the two phases.

Patency: Extent of a conduit (airway, blood vessel) being open or not obstructed.

Pathogen: Disease-producing organism or substance.

Peak expired flow (PEF): Gas volume forcibly expired within the time interval t (typically $t = 1.0$ seconds).

Perfusion: Passage of blood through a blood vessel.

Peribronchial surface: Surface surrounding a bronchus.

Periciliary fluid: Transepithelial secretion along the conducting airways consisting primarily of water.

Phagocytosis: Process describing the engulfment and destruction of extracellularly-derived materials by phagocytic cells, such as macrophages and neutrophils.

Pleura: Folded membrane surrounding the lungs. Space between the visceral and parietal layers (pleural space) is fluid-filled and determines transpulmonary pressure.

Poiseuille flow: Parabolic laminar flow in a straight tube.

Portal: The point at which something enters the body; in the airway, the nares or lips.

Proximal: In the airways, positioned relatively closer to the nares.

Pulmonary: Pertaining to or affecting the lungs.

Pulmonary airways: Portion of respiratory tract (alveoli, respiratory bronchioles) where gas exchange occurs.

Pulmonary perfusion rate: Volumetric flow rate within the pulmonary veins.

Reentrainment: Return of material to an airstream after deposition onto a surface.

Residence time: Time interval during which an identifiable portion of a fluid flow remains within a given volume.

Residual volume (RV): Minimum non-collapsible volume within the airway.

Resistance vessels: Microcirculatory blood vessels (arterioles, pre-capillary sphincters) used to regulate blood flow in a specific tissue.

Respiration: Physiological process of taking in oxygen and expelling oxidative waste products (carbon dioxide, water).

Respiratory air conditioning: Heat and water vapor exchange occurring in proximal airways that warms and humidifies inspired air to approximate alveolar conditions.

Respiratory bronchioles:

Respiratory exchange ration: Ratio of carbon dioxide production to oxygen uptake, a measure of aerobic metabolism.

Reverse flow: Portion of a flow moving in a direction opposite that of the bulk of the flow.

Secretory cells: Cells producing substances (e.g., mucus) with physiochemical properties differing from cellular components.

Smooth muscle: Involuntary muscle tissue found in viscera and blood vessel walls.

Soft palate: Movable fold along the posterior superior portion of the oral cavity dividing the nasopharynx and oropharynx.

Squamous epithelium: Flattened, interlocking, toughened epithelial cells.

Submicrometric particle: Airborne particle with a diameter less than one micrometer.

Submucosa: Layer of tissue beneath the airway epithelium.

Surfactant: Monomolecular layer of material secreted by Type II alveolar cells that lowers alveolar surface tension and stabilizes alveolar volume.

Temperature gradient: Difference in temperature measured between two points.

Thermoregulation: Physiological process attempting to maintain body core temperature at approximately 37 °C.

Tidal volume (V_T): Volume of air inspired or expired with each breath.

Total lung capacity (TLC): Total volume of air that can be contained within the respiratory tract during maximal inspiration.

Toxin: Poisonous material.

Tracheobronchial tree: Series of bifurcating tubes originating at the trachea that conduct air to and from the respiratory airways.

Transepithelial: Passing across a layer of epithelial cells.

Upper airway: The portion of the human conducting airways proximal to and including the larynx.

Ureolysis: Physiological process that breaks down urea and releases ammonia.

Vasculature: Blood supply consisting of arteries, capillaries, and veins.

Vital capacity (VC): Greatest possible inspired volume.

Wetted perimeter: Perimeter of conduit in contact with moving fluid.

Work of breathing: Metabolic cost of breathing.

5.3 TOXICITY AND RISKS INDUCED BY OCCUPATIONAL EXPOSURE TO CHEMICAL COMPOUNDS

5.3.1 Introduction and Background

5.3.1.1 Health Hazards Due to Occupational Exposure

Workers exposed to chemicals often experience discomfort and adverse health effects which may progress to occupational diseases. Even though working conditions have improved markedly during recent decades, in general

the number of individuals suffering occupational diseases has declined rather slowly. In addition, the number of new cases of registered occupational health diseases depends on employment circumstances; there is a natural decline during times of economic recession. This gradual change is due to several factors: the diagnostic criteria have become less stringent, physicians have learned to recognize occupational diseases better, and many occupational diseases develop slowly and thus the present situation reflects, at least to some extent, past exposures. Furthermore, the significance of occupational allergies has increased and allergic reactions can be caused even by low exposure levels.

Toxic chemicals, such as benzene and carbon disulfide, which in the past were common causes of occupational diseases, are nowadays generally well controlled. Most of the current occupational diseases are caused by exposures which are not particularly acutely toxic, but cause allergies. Typical exposures causing allergies are animal and flour dusts. If one considers actual chemicals, then isocyanates have become a major problem, principally via their ability to cause sensitization. Historical exposure to asbestos and other mining dusts still leads to numerous new diseases, many of which are very serious, even fatal. Solvents and pesticides are the groups of chemicals probably causing the largest amount of acute poisoning-type occupational diseases.[1,2]

Traditionally, the greatest risk due to chemicals has been considered to occur via inhalation. Chemicals may also penetrate through the skin. Water-based products are increasingly replacing solvent-based products in many applications, such as painting, printing, and gluing. The water-based products may, however, contain glycol derivatives which penetrate through the skin with ease. Many chemicals also irritate or sensitize the skin. Chromium, nickel, and epoxy resins are examples of common occupational skin allergens.

Ventilation engineers and occupational hygienists must be aware of the risks of chemicals with a high acute toxicity. Chemicals which are odorless (e.g., carbon monoxide), paralyze the sense of smell (e.g., hydrogen sulfide), or cause pulmonary edema as a delayed effect (e.g., nitrogen dioxide and ozone) are especially insidious. Often these gases are produced as unwanted by-products. For example, nitrogen dioxide and ozone may be formed due to oxidation of air during welding. Welding near sources of chlorinated solvents, such as perchloroethylene, may cause pyrolysis and the formation of phosgene.

Occupational exposure limits (OELs) have been set in most industrial countries to prevent excessive exposures. The limits for the most common exposures are based on experimental animal and epidemiological studies. Most novel agents have now generally gone through extensive toxicological testing. For the older chemicals, usually a plethora of epidemiological data is available.

When the incidence of occupational diseases was compared with the frequency of OEL violations in Finland, a rather good correlation was observed. This indicates that these OELs are reasonably well defined. This is also natural because they are based on long-term exposure history of a large number of people. However, the OELs for many chemicals are still only educated guesses, and numerous and often large changes have been made when the OEL lists have been revised. In addition, most chemicals still have no OEL. Only about 2000 chemicals have an OEL in some country.[3]

A particularly strict exposure-control policy is applied for carcinogenic chemicals. The OELs are usually lowered considerably even when a chemical

is only suspected of being a carcinogen. When the evidence becomes stronger, the OELs are usually tightened further. Vinyl chloride provides a good example; its OEL was first lowered to 20 ppm from 500 ppm and then further to 3 ppm in Sweden in 1974-5 when its ability to cause a very rare type of cancer, angiosarcoma of the liver, was detected. The rarity of the disease made it possible to locate the association; on the other hand, the practical impact of this carcinogenic potency also remains rather low. It has been estimated that less than 400 angiosarcoma cases will appear worldwide due to vinyl chloride exposure (in comparison with the number of occupational cancers caused by asbestos which is already about 1000-fold higher).[4,5] Internationally, there is an ongoing vigorous discussion on whether there are possible thresholds for genotoxic carcinogens. In many instances these compounds are considered to have no safe dose. If one assumes that there is some threshold also for genotoxic carcinogens, this would have major consequences for the assessment of risks of carcinogenic compounds.[6–8]

Since the OELs provide the basis for ventilation requirements, an astute designer tries to find out how secure the OELs of the chemicals which will be used in the plant he or she is planning. Some of the chemicals used may totally lack OELs. Therefore, it is advisable to become familiar with the relevant literature, preferably together with a specialist. It is clear that the ventilation engineer needs to be aware of the possible significance of toxicology for industrial ventilation construction.

The epidemiological data have the advantage of being based on human exposures. However, the results of epidemiological studies often remain inconclusive because of various confounding factors and poor exposure assessments. In addition, epidemiological data are available for only a small number of agents. The target level approach, presented in chapter 6 of this book, uses inherently large safety margins in relation to OELs. Unfortunately, it is also applicable only for the most common exposures. Since zero exposure is the best, the ALARA (As Low As Reasonably Achievable) principle, adopted in radiation protection, is, in principle, also a good approach for other exposures.[9,10] However, even then the question, how low is low enough, may remain unanswered. This chapter has been written with the intention of lowering the threshold for a ventilation engineer to seek a toxicological consultation and to provide the fundamental background information needed to utilize the available toxicological literature. Occupational hygienists may also find the text to be a useful compact overview of the essential concepts of toxicology.

5.3.1.2 Epidemiology

Epidemiological studies usually consist of the knowledge obtained from human exposures supplementing data derived from experimental studies. Epidemiological data often provide the ultimate proof of the deleterious effects of a chemical compound on humans, and form an important component of the assessment of the risks of some chemical compounds. In the future, the role of epidemiological data should be confirmatory rather than decisive in the risk assessment of existing and, especially, of new chemicals, since toxicology is becoming more and more a preventive rather than an observational science in protecting the health of workers exposed to chemicals and mixtures of chemicals in occupational environments.

The purpose of epidemiological studies is to try to identify whether there are causal relationships between the occurrence of diseases or other biological effects and exposures to various agents. There are three main types of epidemiological studies: cross-sectional, cohort, and case-control studies. The working population is, on the average, healthier than the general population. Due to this "healthy worker effect," comparisons should be made with another worker group instead of the general population. The reason for the healthy worker effect is the fact that it is difficult for sick or disabled people to stay in employment due to the limitation caused by their diseases. Poor health may also prevent a person from getting a job in the first place.

Cross-sectional Studies

In a cross-sectional study, exposure and effect are studied simultaneously. This approach contains an inherent problem because exposure must precede the effect. However, it can be used to investigate acute effects and also mild chronic effects (which do not force people to leave their jobs) if exposure has remained rather stable for a long time. When the prevalence of the effects studied are compared with the prevalence in other worker groups (controls or references) which correspond otherwise with the study group but are not exposed to the agent investigated, indicative evidence of possible causality may be obtained. For example, cross-sectional studies have been applied successfully to reveal the associations between mild neurotoxic effects and exposure to organic solvents.[11]

Cohort Studies

In a cohort or follow-up study, a group of workers exposed to the same agent is followed for a certain period, which can be either retrospective (starts at some time in the past and continues to the present) or prospective (starts in the present and continues for a certain time into the future). A cohort of controls should be formed with the same selection criteria as used for the study groups, except that they lack the exposure. Thus, exposure to one agent only can be studied whereas several health outcomes can be included. A cohort study is the only possible study method when the exposure studied is rare. The results of the cohort study are expressed as relative risks (risk ratios, RR) for various diseases (see Table 5.8 for results of different types of epidemiological studies on cancers in printing workers and epidemiological terms) (IARC, 1996),

$$\text{Relative Risk (RR)} = \frac{(\text{exposed with disease})/(\text{all exposed})}{(\text{controls with disease})/(\text{all controls})}$$

$$\text{Odds Ratio (OR)} = \frac{(\text{exposed cases})/(\text{non-exposed cases})}{(\text{exposed controls})/(\text{non-exposed controls})}$$

The benefit of a prospective cohort study is the possibility for accurate exposure assessment. However, these are not common, because many occupational diseases (including cancers which are being intensely investigated currently) require long exposure times to develop. It is not practical or ethical to wait for decades before one obtains the result.

The problems often encountered in retrospective cohort studies include poor exposure data and incomplete follow-up of all individuals. The accuracy of health outcome data may also be low.

TABLE 5.8(*a*) Record-linkage Studies among Workers in the Printing Industry (IARC, 1996)

Reference, country	Study subjects	Period of follow-up	Occupation/exposure	Cancer site/ cause of death	No. obs.	RR	95% CI	Comments
Malker and Gemne,[13] Sweden	24 652 men and 6450 women registered at 1960 census as printing workers	1961–73	Printing workers (M)	Lung	190	1.5	[1.3–1.8]	Morbidity
			Blue-collar workers (M) in printing enterprises (newspaper, journal/book printing, others)	Lung	149	1.6	[1.4–1.9]	
			Birth cohort around 1990 (M)	Lung	45	1.9	1.4–2.5	
				Urinary bladder	76	1.3	NG	P > 0.01
				Kidney	48	1.1	NG	P > 0.01
				Skin melanoma	27	1.2	NG	P > 0.01
			Printing workers (F)	Lung	9	1.3	NG	P > 0.01
				Urinary bladder	5	0.8	NG	P > 0.01
				Kidney	7	1.1	NG	P > 0.01
				Skin melanoma	8	1.2	NG	P > 0.01
				Cervix/uterus	162	1.3	[1.1–1.5]	
McLaughlin et al. (1988) Sweden	Male printing workers at 1960 census; 91 melanomas	1961–79	Printing industry	Skin melanoma	91	1.4	[1.1–1.7]	Morbidity
			Newspaper printing industry		39	1.9	[1.1–1.7]	
			Newspaper publishing industry		7	3.1	[1.2–6.4]	
			Typographets in newspaper printing industry		19	2.0	[1.2–3.1]	
			Machine repairers in newspaper printing industry		2	14.5	[1.6–52.3]	
			Journalists/editors in newspaper printing industry		16	2.4	[1.4–3.9]	
			Business/executives in newspaper printing industry		5	9.1	[2.9–21.2]	

(continues)

TABLE 5.8(*a*) Record-linkage Studies among Workers in the Printing Industry (IARC, 1996) *(continued)*

Reference, country	Study subjects	Period of follow-up	Occupation/exposure	Cancer site/ cause of death	No. obs	RR	95% CI	Comments
Aronson and Howe (1994) Canada	242 196 women identified through employment survey	1965–79	Printing and publishing industry	Breast	11	2.2	1.1–3.9	Mortality; other sites not significantly elevated Mortality
Costa et al. (1995) Italy	1981 population census of Turin, Italy, residents; 10 798 deaths among persons employed	1981–89	Printing and publishing industry (M)	Pleura	2	6.0	0.7–22	
				Colon	7	2.1	0.9–4.4	
				Lung	22	1.1	[0.7–1.7]	
				Urinary bladder	2	1.0	[0.1–3.6]	
				Haematopoietic	7	1.6	0.6–3.3	
			Printing and publishing industry (F)	Lung	3	2.6	0.5–7.6	
				Colon	2	2.7	0.3–9.7	
				Ovarian	3	3.2	0.6–9.3	
				Haematopoietic	2	2.0	0.2–7.2	
			Printers (M)	Liver	3	1.7	0.3–5.0	
				Colon	3	1.8	0.4–5.3	
				Multiple myeloma	2	[9.7]	[1.1–33.1]	
				Lung	12	1.2	[0.6–2.1]	
				Urinary bladder	0	–	–	
Costa et al. (1995) Italy	1981 population census of Italian residents; 15 734 deaths among persons employed	1981–82	Printing and publishing industry (M)	Kidney	3	4.8	1.7–13.4	Mortality
				Lung	11	1.1	[0.8–1.4]	
				Urinary bladder	2	2.9	[0.8–11.1]	

Pukkala (1995) Finland	1970 population census 47 178 men, 46 853 women	1971–85	Printing occupations (M)	Colon	16	2.2	1.2–35.	Morbidity
				Lung	50	0.8	0.6–1.1	
			Printing occupations (F)	Colon	10	1.4	0.7–2.5	
				Lung	12	1.8	0.9–3.2	
			Printers (F)	Breast	74	1.4	1.1–1.8	
				Ovarian	30	2.2	1.5–3.1	
				Skin melanoma	5	1.1	0.3–2.5	
			Printers (M)	Skin melanoma	7	1.1	0.5–2.4	
				Urinary bladder	9	1.1	0.5–2.0	
				Leukemia	2	0.4	0.1–1.4	
				Lung	19	1.1	0.7–1.7	
			Lithographers	Skin basal-cell carcinoma	4	4.4	1.2–11.2	

RR, relative risk estimated by SMR (for mortality) or SIR (for morbidity); M, male; F, female; NG not given.

International Agency for Research on Cancer (1996) "Printing processes and printing inks, carbon black and some nitro compounds". IARC monographs on the evaluation of carcinogenic risks to humans, Vol. 65, pp. 67-70. International Agency for REsearch on Cancer, Lyon, France.

TABLE 5.8(*b*) Case-control Studies of Urinary Bladder Cancer among Workers in the Printing Industry[12]

Reference, country	Type of controls	Exposure	Sex	No. of exposed cases/ controls	Odds ratio	95% CI	Comments
Najem et al.[18] USA	Hospital-based, tobacco-related heart diseases and neoplasms excluded	Printing industry (≥ 1 year)	M + F	7/5	2.7	0.8–9.6	Crude odds ratio
Cartwright[19] United Kingdom	Hospital-based, non-malignant diseases	Printers (exposed to ink-fly from high-speed presses)	M + F	18/NG	3.1	1.4–6.8	Adjusted for type of case (incident or prevalent) and sex
Silverman et al.[20] USA	Population-based	Printing industry (ever) Printers (ever)	M M	50/45 6/2	1.1 3.0	0.7–1.7 0.6–14.8	Crude odds ratio
Schoenberg et al.[21] USA	Population-based	Printing workers (ever) Printing ink (self-reporting)	M M	20/38 42/53	0.9 1.6	0.5–1.5 1.0–2.5	Adjusted for age, smoking, and other employments
Baxter and McDowall[22] United Kingdom	Other cancers All causes of death	Printers (stated on death certificates)	M	21/NG	1.5 1.2	P 0.05 P 0.05	Against other cancers; matched on residence, year of death, age
Brownson et al.[23]	Population-based, other non-smoking-related	Printing machine operators (longest-held job)	M M	7/8 7/6	3.1 2.3	1.1–8.9 0.8–7.2	All controls Prostate cancer excluded
Silverman et al.[25, 26] USA	Population-based	Printer (ever)	M (white) F	37/77 1/10	0.8 0.2	0.5–1.2 <0.1–1.4	Adjusted for smoking; frequency matching for age and geographic area
Kunze et al. [27] France	Hospital-based, non-neoplastic diseases of the lower urinary tract	Printing industry (ever) Printing worker (ever)	M M	11/3 7/3	5.0 3.0	1.3–19.6 0.7–13.8	Crude odds ratio
Cordier et al.[28] France	Hospital-based, neoplastic, respiratory and urological conditions excluded	Printing and publishing industry (ever) Printers	M M	26/28 14/9	0.9 1.5	0.5–1.5 0.6–3.5	Adjusted for age, hospital residence, smoking
Siemiatycki et al.[29], Canada	Population and hospital-based, other cancers, excluding lung and kidney sites	Printing and publishing industry < 10 years ≥ 10 years Photographic products (substantial exposure)	M 	 2/NG 11/NG 4/NG	 0.3 1.9 3.0	 0.1–1.2 0.9–3.9 0.9–10.1	Adjusted for age, family income, smoking, coffee consumption, ethnicity, respondent status

TABLE 5.8(c) Case-Control Studies of Lung Cancer among Workers in the Printing Industry

Reference, country	Type of controls	Exposure	Sex	No. of exposed cases/controls	Odds ratio	95% CI	Comments
Coggon et al.[30] (1984) United Kingdom	Deaths from other causes	Printing inks	M	28/36	1.6	0.9–2.7	Job exposure matrix applied to occupations recorded on death certificates; age <40 years, cases and controls
		Printing inks (high exposure)	M	9/9	2.0	0.8–5.0	
Schoenberg et al.[31] USA	Population-based	Printing workers ≥ 10 years	M	20/11	2.5	1.0–6.1	Adjusted for smoking
			M	7/1	8.4	NG	(p.20.05, crude)
		Printing industry	M	37/31	1.3	0.8–2.3	Adjusted for smoking
Benhamou et al.[32] France	Hospital-based, non-tobacco related diseases	Printers and related workers	M	32/51	1.2	0.7–1.9	Matched for sex, age at diagnosis, hospital, interviewer; adjusted for smoking
Hoar Zahm et al.[33] USA	Selected cancer sites	Printing occupations	M	21/41	1.1	0.6–1.9	Adjusted for age, smoking
				7/[4] (adenocarcinoma)	1.8	0.7–4.2	Occupations unknown for about half of cases and controls
Siemiatycki[34] (1991) (Canada)	Hospital-based, other cancers	Printing and publishing industry	M	35/NG	2.0	[1.2–3.5]	Smoking-adjusted
		Printers	M	26/NG	2.1	[1.1–4.1]	Smoking-adjusted
		Printers (>10 years)	M	13/NG	1.7	[0.7–4.1]	Smoking-adjusted
		Printing process workers	M	15/NG	3.1	[1.1–8.7]	Smoking-adjusted
			M	6/NG (adenocarcinoma)	7.0	[1.8–27.9]	Smoking-adjusted
		Inks (any)	M	37/NG	1.6	[1.0–2.7]	Smoking-adjusted
		Inks (substantial)	M	18/NG	1.5	[0.7–3.1]	Smoking-adjusted

Case-control Studies

In case-control studies, only one disease can be investigated. The cases include all patients with a certain disease observed in a hospital, city, or a larger area in a given period of time. Their exposure histories are compared with those of the controls. Thus, several exposures can be investigated. The exposure data are not very accurate because they are obtained by interview. Especially in cases of serious diseases, patients are often desperate to seek some reason for their disease. Therefore, patients of some other disease are usually employed as controls to avoid this information bias. The selection of controls is a crucial but extremely difficult task. Since factors such as age, sex, smoking, living habits, and place of abode are known to be risk factors for several diseases, the effects of these confounding factors are eliminated by matching. However, overmatching should also be avoided. Odds ratio (see Table 5.8*b*,*c*) is used to express how often the cases have been exposed to various exposures compared to controls. Case-control studies are common because they are inexpensive and relatively easy to perform. If the disease studied is rare, this approach is also the only practical alternative.[12]

5.3.1.3 Classifications of Toxicology

The word toxicology originates from the Greek word toxicon, which means arrow. In ancient times, arrows were dipped into plant poisons to increase their lethality in hunting. Today, toxicology refers to that scientific discipline that explores the deleterious effects of chemicals or of physical or biological factors on living organisms. Toxicology also explores the mechanisms whereby chemicals, or physical or biological factors induce their harmful effects in the organism.

There are several definitions and classifications of toxicology. One classification is based on the target organs which are harmfully affected by chemicals. Hence, there are terms such as neurotoxicology, liver or hepatic toxicology, kidney or renal toxicology, and toxicology of the eye (ocular toxicology). Inhalational toxicology emphasizes the importance of the lungs as the target organ of chemicals. In addition to these descriptive classifications, toxicology can be divided into mechanistic toxicology, conducted mainly in university and governmental research institutions, and descriptive or regulatory toxicology, which is required for classification and labelling of chemicals for registration purposes. Even if mechanistic toxicology is essential for understanding how chemicals and other factors induce their toxic effects, descriptive toxicology is also important in characterizing the properties of a chemical compound. Descriptive toxicology is a prerequisite for regulatory purposes and risk assessment. When the qualitative requirements for risk assessment increase, the importance of mechanistic information on chemicals in risk assessment will also increase.

Toxicology can also be divided into different classes based on the goals it serves. Clinical toxicology explores ways of treating poisoned patients, and also aims to develop quick methods to diagnose poisonings. Forensic toxicology is the science involved in detecting the role of poisons in fatalities. Environmental toxicology assesses the importance of environmental pollution and the effects of exposure through various environmental compartments on human health. Ecotoxicology is interested in the effects of environmental chemicals on

TABLE 5.9 Classifications of Toxicology

Area of toxicology	Scope
Mechanistic	Understanding of cellular and molecular mechanisms
Regulatory	Drafting regulations and legislation
Organ-specific	Defining organ-specific effects and defining chemically induced critical effects
Forensic	Diagnosis and fatalities
Occupational	Delineating occupational hazards and risks and prevention
Environmental	Identification of chemical hazards in the environment, and their effects on humans and wildlife species
Clinical	Diagnosis and treatment of poisoning

animals such as fish, insects, birds, and other wild animals. Industrial or occupational toxicology aims to study the effects of chemicals on workers exposed in an occupational environment (see Table 5.9).

Toxicology often provides the basis for a number of regulations aimed at protecting workers from potentially harmful effects. Today, more than ever before, toxicology has a preventive function that provides information on chemicals that can be used safely. It is difficult to imagine occupational or other safety regulations without a major input from toxicology.

The main role of toxicology in the industrial setting originates from its ability to identify harmful chemicals and other hazards in advance. After toxicological research has identified exposure-effects relationships for different chemicals, occupational exposure limits (OELs) for various industrial chemicals can be established. Subsequently, workers can be protected against excessive exposures by measuring the exposure and ensuring that the OELs are not violated; ventilation engineers and occupational hygienists are the key persons in this field. Careful planning and design can ensure that most workers can be protected, nevertheless the most sensitive individuals may still react to exposure levels that are below the acceptable exposure limits. These relationships also indicate the close relationship between industrial toxicology and industrial hygiene. Without a broad knowledge of the toxicological characteristics of chemicals, industrial hygiene is more or less irrelevant. On the other hand, without industrial hygiene, toxicology would be helpless in protecting the workers against chemical hazards.

5.3.1.4 Industrial Toxicology, Hygiene, and Occupational Medicine

Industrial toxicology, industrial hygiene, and occupational medicine all have a common goal: to protect workers from occupational hazards in the workplace. The goal of toxicological research is to protect the worker by characterizing the biological effects of chemicals and by identifying the hazardous agents, whereas the goal of occupational hygiene is to protect workers by improving the occupational environment. The goal of occupational medicine, in turn, is to protect workers' health by identifying early signs of harmful effects, and to diagnose and treat occupation-related diseases. In

many cases, reduction of exposure will suffice to prevent many occupation-related diseases after the first symptoms, but the exposure may also need to be stopped completely. However, before such radical measures can be taken, the association between the exposure and the disease has to be established, i.e., the occupational nature of the disease needs to be demonstrated. Therefore, occupational medicine relies on toxicological and occupational hygienic knowledge in solving occupational health problems. However, the scope of occupational medicine is much wider than simply examining chemical-induced toxicity, as it covers a wide area of interests such as occupational ergonomics and psychophysiological factors in the occupational setting.[35]

Poisoning Incidents in the Workplace

The hazards of chemicals are commonly detected in the workplace first, because exposure levels there are higher than in the general environment. In addition, the exposed population is well known, which allows early detection of the association between deleterious health effects and the exposure. The toxic effects of some chemicals, such as mercury compounds and soot, have been known already for centuries. Already at the end of the eighteenth century, small boys who were employed to climb up the inside of chimneys to clean them suffered from a cancer of the scrotum due to exposure to soot. This was the first occupational cancer ever identified. In the viscose industry, exposure to carbon disulfide was already known to cause psychoses among exposed workers during the nineteenth century. As late as the 1970s, vinyl chloride was found to induce angiosarcoma of the liver, a tumor that was practically unknown in other instances.[36]

Even in the Nordic countries, exposure to carbon disulfide still caused severe central nervous effects among exposed workers during the late 1960s and early 1970s, and exposure to lead caused several lead poisonings at the same time. Exposure to asbestos remained a major health hazard until the 1970s. The use of asbestos is nowadays strictly controlled and it has been banned in many countries. Nevertheless, it continues to be an important occupational health problem because of the long latency period of asbestos for causing lung cancer and mesothelioma, a time period of 20–40 years. In addition, there are large amounts of asbestos remaining in buildings, and renovation of old buildings will pose a health risk to workers for a long time to come.[37]

Many very hazardous solvents, such as benzene and carbon tetrachloride, were widely used until the 1970s. The situation was very similar for the use of pesticides. Among the toxic pesticides that were still in wide use 20 years ago were chlorophenols, DDT, lindane, and arsenic salts, all of which are classified as human carcinogens as well as being acutely toxic.[4,38] Fortunately, use of these kinds of very toxic chemicals is now limited in the industrialized world. However, because the number of chemicals used in various industries continues to increase, the risks of long-term health hazards due to long-term exposure to low concentrations of chemicals continues to be a problem in the workplace.

Association of Industrial Activity and Poisonings in the General Environment

The harmful effects of industrial emissions are not confined to the workers but extend beyond the plant boundary line. Chemically-induced diseases among workers exposed to industrial chemicals are a warning sign of the risks to which a larger population is also being exposed; usually the chemical hazards are in principle similar in the occupational and general environment. However, occasionally environmental exposures can be qualitatively different from the occupational environment and may also cause deleterious health effects in the general population.[39,40]

Since the general population is much larger than the occupationally exposed worker groups, and also includes very sensitive individuals, some deleterious effects have been detected only in the general population. Urban air pollution is a good example. In the 1930s, an air pollution incident in the valley of the River Maas in Belgium was responsible for the deaths of tens of individuals due to increased concentrations of coal dust and sulfur dioxide in the ambient air. At that time, it was already predicted that this could be a harbinger of future catastrophes in a major city like London, and, indeed, in 1952, a dramatic increase of concentrations in small coal particles and sulfur dioxide took place during weather inversion in the London metropolitan area. In consequence, an excess mortality of more than 4000 individuals occurred during a few days. Similar though less severe smogs (a fog caused by air pollution) took place in the late 1950s. Subsequently the use of coal was prohibited in London and today the air quality in the city is much better than it was 40 years ago. In addition to this classic kind of smog, photochemical smog, consisting of nitrous oxides and ozone and their reaction products with hydrocarbons, is encountered in warm and sunny areas where there is major traffic-related pollution. A model area for such a situation is Los Angeles, California, where the air quality is a continuous concern.[41]

The emphasis on air pollution in different parts of the world has led to marked improvements in air quality. However, there are several metropolitan areas in the world where the air pollution situation is still deteriorating. Examples of such areas are Mexico City, Mexico, New Delhi, India, Cairo, Egypt, and Sao Paulo, Brazil. Most of these badly polluted areas are in developing countries where resources for improving the situation are limited. Thus, these problems are difficult to solve (see Fig. 5.30).[41]

Recently, much emphasis has been put on the harmful effects of small particles, i.e., particulate matter (PM), on human health. A number of standards have been established to characterize the PM fractions in the air and their effects on human health. A widely used PM standard in force in both Europe and the United States is based on the mass concentration of particles with a diameter of 10 μm or less (PM_{10}). However, recently the U.S. Environmental Protection Agency (EPA) proposed a new standard that is based on the aerodynamic diameter of 2.5 μm particles. This new standard emphasizes the significant impact of small particles on human health, especially on the respiratory and cardiovascular systems.[41,42]

It has been known for years that professional bus and truck drivers as well as railroad workers suffer a larger than average risk of lung cancer because of

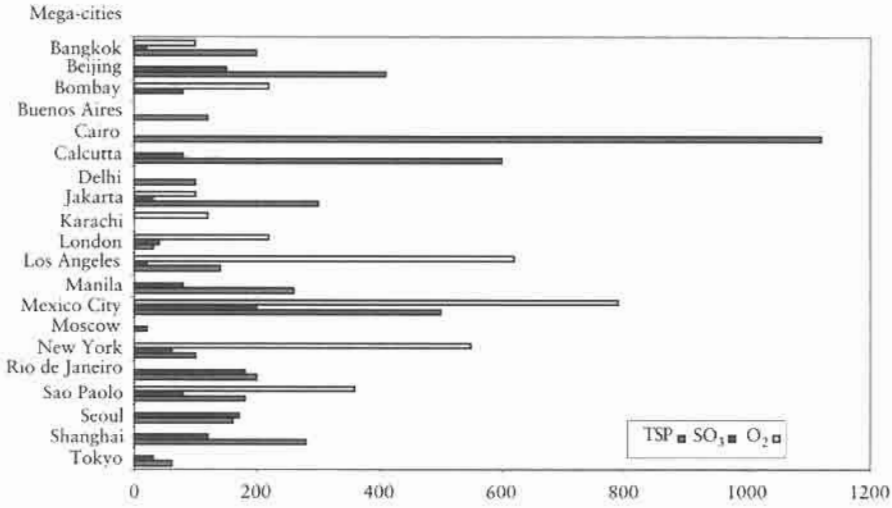

FIGURE 5.30 Comparison of ambient levels of 1 h maximum ozone, annual average of total suspended particulate matter (TSP), and sulfur dioxide in selected cities from around the world to illustrate the variation in these levels from country to country with respect to the United States. [Reproduced from the National Air Quality and Emission Trends Report (1992), with permission.][41]

exposure to gas engine, especially diesel engine, exhausts. These individuals are also at a larger than average risk of sudden death due to myocardial infarction, cardiovascular disease, and pulmonary disease. Several studies from the U.S. and Europe have demonstrated that exposure to inhalable particles, especially those generated by traffic and energy production, cause a one to five percent increased risk of mortality among the general population. At the European level, this would represent 50 000 to 100 000 additional deaths annually.[43,44] It is probable that the previous examples of increased mortality during historical air pollution episodes were largely due to exposure to small particles. Unfortunately, no clear conclusions can yet be made concerning occupational dust exposure in general.

5.3.1.5 Concept of Risks

The term risk has wide implications. It is used to characterize difficulties in predicting changes in the currency markets and to indicate the probability of potential financial losses due to such changes. A surgeon prior to a major operation also needs to evaluate the risks to the patient, not only due to the disease, but also risks associated with the operation itself and the anesthesia. Car drivers seldom consider the risk of a traffic accident when starting a car even though the risk of a fatal car accident is many times greater than the calculated risks associated with exposure to chemicals. Another example, widely discussed in the media, is the comparison of risks from energy production by fossil fuels and nuclear energy. This comparison has proven to be extremely difficult due to a number of philosophical aspects. We can calculate with some degree of certainty the risks involved in the production of energy with

fossil fuels. There are major risks in mining or oil drilling, during the transportation of the fuel, and due to the extensive emissions emanating from the combustion of the fuel. In Europe, annual loss of life due to energy production utilizing fossil fuels, and due to traffic exhaust, is close to 100 000. The verifiable health hazards due to nuclear energy are only a small fraction of the losses due to the use of fossil fuels. However, the potential risk due to a nuclear accident raises alarm in individuals, because the true risk due to nuclear energy cannot be calculated. Even if the accident probability is small, the losses due to even one incident may be catastrophic. This is well illustrated by the accident in Chernobyl in 1986.[45,46]

If one is to estimate the potential hazards of some chemicals prior to their release to the market, the chemicals must be tested for their toxicity in experimental animals. Animals are exposed to high doses of chemicals to avoid the use of large numbers of animals. When the results of animal experiments are applied to humans, several assumptions have to be made, including (1) that animals are a good model to predict human hazards caused by chemicals, and (2) that large doses of chemicals used in studies utilizing small groups of experimental animals cause similar effects to what would be seen in humans though at a lower frequency or with a milder change in functions of target organs. Toxic effects of chemicals may, however, be quite different in rodents than in humans. For example, guinea pigs tolerate the effects of strychnine rather well, in contrast to humans. For organ toxicity (neurotoxicity, liver toxicity, kidney toxicity) endpoints, safety factors can be used for assessing safe levels for humans (see below). Dose-responses are regularly used to delineate the toxicological characteristics of chemical compounds, and to make comparisons of effects between species.[1,47]

In most cases, experimental animal studies are used to define the so-called no-observable-adverse-effect level (NOAEL), i.e., the lowest dose that does not cause an adverse effect in experimental animals. This dose is then divided by a safety factor of 100, ten for interspecies differences between rodents and humans and ten for intraspecies differences between humans, to calculate the dose (mg/kg) which is considered to be safe for humans. This approach contains the assumption that there is a safe dose below which a chemical does not cause harmful effects on humans (for the safety factor of 100, see Fig. 5.31). This assumption of a safe threshold dose is used for most endpoints of deterministic toxicology, i.e., organ toxicology. However, whether in fact there can be any safe dose for carcinogens, especially for genotoxic carcinogens, has been challenged, and the linear extrapolation models widely used in carcinogenic risk assessment do not utilize safety factors. However, this approach has also been recently challenged because throughout biology, one does not find effects without any threshold, and because it neglects biological defence mechanisms present within cells. The thresholds may, however, be so low in some instances that the arguments are purely theoretical. However, they have important implications for risk assessment.[47,49] Furthermore, one can argue that none of the toxicological endpoints, whether deterministic (organ toxicity) or stochastic (cancer) in nature, have a threshold. This may be true conceptually, and it is especially true experimentally because in most cases determination of a true threshold is beyond the limit of detection of the experimental approach.

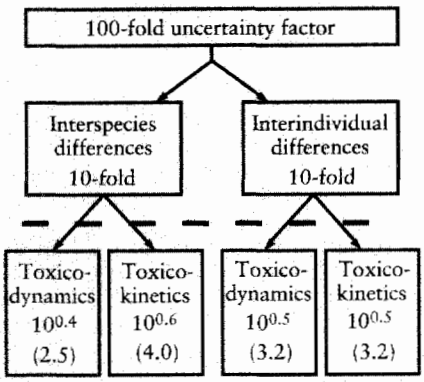

FIGURE 5.31 Subdivision of the 100-fold uncertainty factor showing the relationship between the use of uncertainty factors (above the dashed line) and proposed subdivisions based on toxicokinetics and toxicodynamics. Actual data should be used to replace the default values if available.[48]

Usually risk assessment procedure, discussed in more detail later (see Chapter 6), is divided into four different stages or steps (see Fig. 5.32):[49]

1. Hazard identification through animal experiments, epidemiological studies, or structure activity analyses
2. Hazard characterization, or dose-response characterization, by using experimental animals to reveal target organs and toxic doses, and the shape of the dose-response curve
3. Exposure assessment to reveal the exposure of different groups of people, and to compare their exposure levels to the doses that cause harmful effects in humans as shown in epidemiological studies, or to doses that cause toxic effects in experimental animals
4. Risk assessment, a synthesis of the preceding three steps, which aims to assess both qualitatively and quantitatively the risks induced by a chemical at a given or at different exposure levels. This step utilizes either a safety factor approach or various extrapolation models.

Based on the results of risk assessment, decision makers have to attempt to manage risks, e.g., by determining various exposure limits to protect individuals against deleterious effects of chemical exposures. This kind of procedure is commonly used for determining acceptable daily intake values (ADIs)[49] for contaminants in foods and acceptable operator exposure level (AOELs) for pesticides. Even though the results obtained in experimental animal tests are part of the basic data on which the OELs have been based, the levels result from consideration of many other aspects, especially epidemiological data. In addition, these decisions take into consideration economic and political consequences of the decisions, as well as perception of various risks by the general public. Furthermore, properties such as strong odor or irritation influence the levels of OELs. It needs to be kept in mind that even though risk assessment of exposures

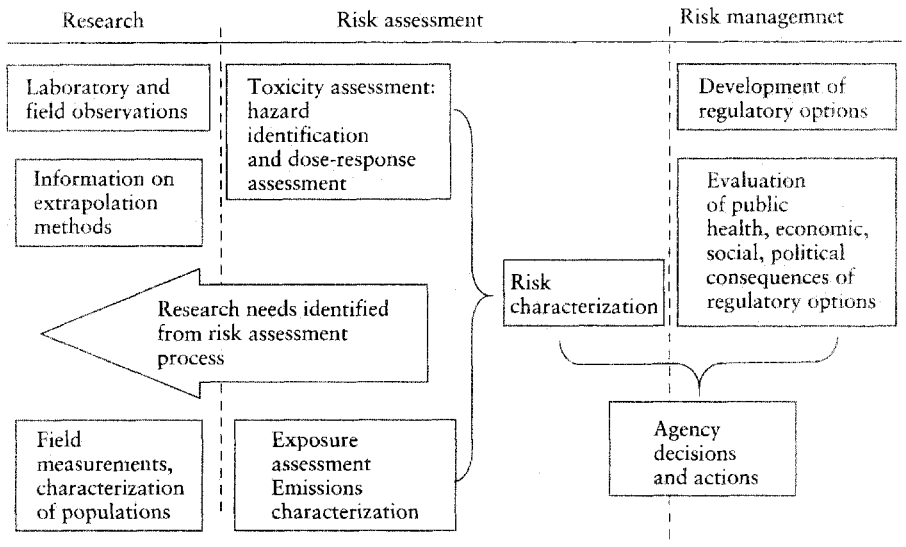

FIGURE 5.32 Elements of risk assessment and risk management.[49](used with permission.)

to single chemicals is still far from complete, much greater difficulties are encountered in assessing the risks of multiple exposures.

5.3.2 Exposure to Chemical Substances

Among the 10 million known chemical compounds, there are some 50 000 which are in common use. Workers are usually exposed to several agents simultaneously (their interactions are considered in section 5.3.4.2). In addition, many impurities in workplace air are inherently complex mixtures, which may consist of hundreds of different compounds. Mineral oils and wood dusts are examples of common complex mixtures.

5.3.2.1 Characterization of Exposures

Indoor and Outdoor Exposure to Pollutants

Occupational and environmental exposure to chemicals can take place both indoors and outdoors. Occupational exposure is caused by the chemicals that are used and produced indoors in industrial plants, whereas nonoccupational (and occupational nonindustrial) indoor exposure is mainly caused by products. Toluene in printing plants and styrene in the reinforced plastic industry are typical examples of the two types of industrial occupational exposures. Products containing styrene polymers may release the styrene monomer into indoor air in the nonindustrial environment for a long time. Formaldehyde is another typical indoor pollutant. The source of formaldehyde is the resins used in the production process. During accidents, occupational and environmental exposures may occur simultaneously. Years ago, dioxin was formed as a by-product of production of phenoxy acid herbicides. An explosion in a factory in

Seveso, Italy, caused wide-spread pollution of the industrial site as well as its surroundings. Serious effects of dioxin were detected both in domestic animals, such as cows and sheep, and in humans, the most serious early effects being a serious skin disease, chloracne, and alterations in the function of the immune system. Follow-up studies have demonstrated that this accident also increased the cancer risk in exposed individuals.[51]

Outdoor inhalation exposure is mainly due to traffic, energy production, heating, and natural factors such as pollen and mineral dusts. These outdoor sources of pollution also affect indoor air quality. The indoor concentration is typically 20–70% of the corresponding outdoor concentration. Occasionally the indoor concentrations of an external pollutant (especially radon) may even exceed the concentrations outdoors.[41]

In densely populated areas, traffic is responsible for massive exhausts of nitrous oxides, soot, polyaromatic hydrocarbons, and carbon monoxide. Traffic emissions also markedly contribute to the formation of ozone in the lower parts of the atmosphere. In large cities, fine particle exposure causes excess mortality which varies between one and five percent in the general population.[43] Contamination of the ground water reservoirs with organic solvents has caused concern in many countries due to the persistent nature of the pollution. A total exposure assessment that takes into consideration all exposures via all routes is a relatively new concept, the significance of which is rapidly increasing.[52,53]

Characteristics of Industrial Processes

The in-plant emissions can be divided into process and manual emissions. In the process industry, the emission sources can usually be enclosed and the workers do not need to stay for long periods close to the emissions. The emissions are minor, and even if they do occur, they are generally released far from the areas where workers have their accommodation. Often, workers can spend most of their time in clean control rooms. In certain process industries, such as the petrochemical industry, the processes are located largely outdoors, and the emissions are mainly fugitive emissions from leaking seals of flanges, valves, and pump shafts. Manual emissions occur in the immediate vicinity of the worker due to the task he or she is performing. Typical examples include welding, painting, gluing, sawing, and grinding. It is natural that the exposure control is much easier for process emissions than for manual ones. Even very toxic substances can be used safely in the process industry whereas even moderately noxious chemicals may cause major problems in manual tasks. Thus, avoidance of those manual tasks with chemicals known to cause adverse health effects is important. If the automation of these tasks becomes very expensive, it may be possible to use subcontractors who specialize in this kind of work and have adequate control arrangements in their production facilities.

The best way to control exposure is to replace dangerous agents with safer ones. Today, highly toxic solvents, such as benzene, bromobenzene, carbon tetrachloride, and chloroform are no longer extensively used. Benzene remains, however, an important chemical in the petrochemical industry, but the processes where it is used are closed.

The use of other highly toxic substances, such as lead and carbon disulfide, which have in the past caused many occupational diseases, is also rare in

manual tasks nowadays. Thus, relatively few possibilities for substitution are left in individual workplaces. One rather common exception does exist; very fine powders can often be replaced with granular or liquid products. All possibilities to replace solvent-based products with water-based alternatives have not yet been utilized. However, one must be aware of the possible novel risks involved with the use of the new products; for example, when acid-cured furniture paints and lacquers, which released formaldehyde, have been replaced with acrylic resins, skin sensitization has become more common among furniture painters.

Since process disturbances do take place, and accidental releases are possible, even from processes closed under normal conditions, the plants where highly toxic or sensitizing substances are in use or may be generated should be provided with continuous monitoring and alarm systems in the critical areas.

5.3.2.2 Exposure Routes

The exposure routes include the lungs, i.e., inhalational exposure, the skin, i.e., dermal exposure, and the mouth, i.e., oral exposure.[52,54] Inhalation is usually considered to be the most important route for occupational exposure. Some chemicals are also absorbed via the skin or damage (irritation or sensitization) to the skin, and thereby amplify their own absorptions. Poor personal hygiene may result in oral exposure from eating or smoking with dirty hands. Toxic effects also often depend on the exposure route. The effects of irritating agents occur at the contact site. On the other hand, many compounds are distributed widely in the body and the target organ may be situated far from the entry site. Compounds may become concentrated in certain organs. The organ with the highest concentration is, however, not necessarily the target organ; for example, lead is accumulated in the bones but its most severe effects appear in the central nervous system. Many lipophilic carcinogens are accumulated in the adipose tissue but the cancer does not usually develop there but rather in the target organs, such as the liver, the kidneys, or the lungs.[5,55–57]

Inhalational Exposure

Gases, vapors, mists, and dusts are mainly absorbed into the body through the lungs. Lipid-soluble vapors, especially those of solvents, and gases reach the alveolar space without any difficulty from where they pass through the respiratory tract, and diffuse readily across alveolar lining to reach the systemic circulation. Passive diffusion is based on a concentration gradient between alveolar air and the blood. The rapidity of the saturation of the blood with gaseous compounds largely depends on the blood and lipid solubility of the gas. Highly blood- and lipid-soluble compounds reach saturation slowly whereas vapors and gases with low blood- and lipid-solubility rapidly become saturated in the blood.[58–60] Also, water-solubility and reactivity greatly affect penetration through the lung. Very water-soluble and reactive compounds tend to dissolve in the mucus in the upper respiratory airways, or react with proteins in the mucus, and only a small portion of the dose of such compounds ever reaches the alveolar region of the lungs. Examples include sulfur dioxide and formaldehyde. Especially, the latter

reaches the alveolar region only at high concentrations because it reacts with proteins in the mucus and in the cells of the epithelial lining of the upper respiratory tract. On the other hand, as a consequence of its reactivity, high concentrations of formaldehyde cause serious lung injury and lung edema upon reaching the alveolar region.[58,59]

Aerosols reach the alveolar space depending on their particle size and physico-chemical characteristics. Small particles that reach the alveolar region (see Sections 2.3.7 and 3.1.1) may reach the circulation through the lymphatic drainage of the alveolar region.

Dermal Exposure

Skin is also important as an occupational exposure route. Lipid-soluble solvents often penetrate the skin, especially as a liquid. Not only solvents, but also many pesticides are, in fact, preferentially absorbed into the body through the skin. The ease of penetration depends on the molecular size of the compound, and the characteristics of the skin, in addition to the lipid solubility and polarity of the compounds. Absorption of chemicals is especially effective in such areas of the skin as the face and scrotum. Even though solid materials do not usually readily penetrate the skin, there are exceptions (e.g., benzo(*a*)pyrene and chlorophenols) to this rule.[37,60,61]

Oral Exposure

In the occupational setting, oral exposure is of minor significance, being mainly due to poor personal hygiene. In addition, gases that dissolve or are otherwise trapped in the upper respiratory tract, usually are swallowed and enter the gastrointestinal tract. Particles that are removed as such or are captured by macrophages by the mucociliary escalator from the respiratory tract are also ultimately swallowed and enter the gastrointestinal tract.

5.3.2.3 Physico-Chemical Determinants of Exposure

Physico-chemical characteristics greatly determine the entry of chemicals into the body, and also their behavior in the body (distribution, biotransformation, and excretion). Therefore, the physico-chemical characteristics of a compound affect its dose and its subsequent effects by determining how quickly and extensively a chemical reaches the target organs. In the following section, some of these important physical-chemical characteristics of chemicals will be discussed.

Water Solubility

The site and the severity of the effect of respiratory irritant gases depend largely on their water solubility. Very water-soluble gases and vapors, such as ammonia, hydrogen chloride, sulfur dioxide, and formaldehyde dissolve in the mucus of the nose and upper airway and cause inflammation. Poorly water-soluble gases, such as nitrogen dioxide and ozone, are able to reach the deep lung area. Inflammation results from damage to cellular membranes of bronchiolar and alveolar cells, and subsequent accumulation of liquid in the lungs (edema). Because the alveoli have no receptors for irritation, the effects are generally noticed only several hours after the exposure when the amount of

liquid accumulating has become so large that it impairs gas exchange. In addition to water-solubility, the reactivity of the gas with airway proteins is important. Thus, sulfur dioxide is removed effectively by the nose while ethanol is partially absorbed. If a soluble gas is adsorbed on fine particles, it can be transported deep to the lungs.[58,59]

The solubility coefficient S is used as a measure of water solubility. It is the ratio between the concentrations in water and air phases at equilibrium. Ethanol, a very soluble gas, has a solubility coefficient of 1 100 at 37 °C while the coefficient for nitrous oxide, a poorly soluble gas, is 0.15.

The Importance of pH and pK_a

Under physiological conditions, pK_a (negative common logarithm of the acid constant) of a compound largely determines its behavior at varying pH. This is important because the dissolution of polar molecules in lipid bilayers is a difficult and slow process, and from a practical toxicokinetic point of view, most polar compounds fail to penetrate biological membranes to any significant extent. Ionization of most weak acids and bases depends on their dissociation constant and pH according to the Henderson-Hasselbach equation:[62]

$$\log[A^-/HA] = \text{pH} - \text{pK}_a \quad \text{(for weak acids)}$$
$$\log[B/BH^+] = \text{pH} - \text{pK}_a \quad \text{(for weak bases)}$$

The proportion of ionized and unionized forms of a chemical compound can be readily calculated according to the above equation. It can be easily seen that pK_a is also a pH value at which 50% of the compound exists in ionized form. The ionization of weak acids increases as the pH increases, whereas the ionization of weak bases increases when the pH decreases. As the proportion of an ionized chemical increases, the diffusion of the chemical through the biological membranes is greatly impaired, and this attenuates toxicokinetic processes. For example, the common drug acetosalicylic acid (aspirin), a weak acid, is readily absorbed from the stomach because most of its dose is in an unionized form at the acidic pH of the stomach.[62,63]

Lipid Solubility

Cell membranes are composed of lipid bilayers which contain large protein molecules and glycoproteins. To be able to penetrate through the cell membrane, a compound has to dissolve in the lipid bilayer, where it diffuses according to the concentration gradient across both sides of the membrane, and after passing through the membrane, dissolve once more in the water phase within the cell. Lipid-soluble compounds can reach high concentrations in lipid-rich organs, such as the adipose tissue, brain, bone marrow, and spleen. Lipid-solubility is often characterized by an octanol/water coefficient which indicates the concentration ratio of the compound between these two phases. For example, xylene, a non-polar lipid-soluble organic solvent, has an octanol/water coefficient of 3200. In addition to polar organic compounds, many inorganic gases have low octanol/water coefficients.[62]

Blood Solubility

Absorption of a gaseous compound from the lungs depends on its blood solubility. For most compounds, blood solubility is similar to water solubility. However, the blood solubility coefficient may become much higher than the water solubility coefficient if the blood proteins have a high affinity for the compound. Carbon monoxide, for which hemoglobin has a high affinity, is a good example (see Section 4.3.3). Blood solubility is decisive for the rapidity of the action of the compound, especially on the central nervous system, but also on other organs. Often lipid-soluble vapors such as diethyl ether or organic solvents such as xylenes also have a high blood solubility.[62,63]

The toxic effect depends both on lipid and blood solubility. This will be illustrated with an example of anesthetic gases. The solubility of dinitrous oxide (N_2O) in blood is very small; therefore, it very quickly saturates in the blood, and its effect on the central nervous system is quick, but because N_2O is not highly lipid soluble, it does not cause deep anesthesia. Halothane and diethyl ether, in contrast, are very lipid soluble, and their solubility in the blood is also high. Thus, their saturation in the blood takes place slowly. For the same reason, the increase of tissue concentration is a slow process. On the other hand, the depression of the central nervous system may become deep, and may even cause death. During the elimination phase, the same processes occur in reverse order. N_2O is rapidly eliminated whereas the elimination of halothane and diethyl ether is slow. In addition, only a small part of halothane and diethyl ether are eliminated via the lungs. They require first biotransformation and then elimination of the metabolites through the kidneys into the urine.[62,63]

Partition Coefficients

Other important determinants of the effects of compounds, especially solvents, are their partition coefficients, e.g., blood-tissue partition coefficients, which determine the distribution of the compound in the body. The air-blood partition coefficient is also important for the absorption of a compound because it determines how quickly the compound can be absorbed from the airspace of the lungs into the circulation. An example of a compound that has a high air-blood partition coefficient is trichloroethane (low blood solubility) whereas most organic solvents (e.g., benzene analogues) have low air-blood partition coefficients (high blood solubility).[62,63]

Vapor Pressure

Vapor pressure is important simply because a compound that is easily vaporized can also readily cause a marked exposure through the lungs. Organic solvents are good examples of volatile compounds, and known to cause marked exposure via the lungs, in addition to exposure via the skin.[64]

Particle Size

The size of inhaled particles varies markedly. The size distribution approximates a log-normal distribution that can be described by the median or the geometric mean, and by the geometric standard deviation. For fibers, both

fiber diameter and length are important determinants of their behavior in the airways. The effect of particle size on the fate of particles is discussed in more detail in sections 3.1 and 5.2.[50]

5.3.2.4 Physiological Determinants of Exposure

Anthropologic features of humans, their physical activities, ventilation capacities, and the state of their circulation all affect exposure to chemical compounds. Some of the physiological determinants of exposure will be dealt with below. Exercise typically increases cardiac output, facilitates circulation, increases the minute volume of ventilation, is associated with vasodilation of the skin circulation, and increases perspiration and secretory activity of the sweat glands. All of these changes tend to facilitate the absorption of chemicals through multiple routes.

Inhalational Exposure

During exercise, both minute ventilation and cardiac output increase dramatically. Whereas minute ventilation averages 7–10 L/min at rest for an average person of about 70 kg, it can increase to 160 L or more/min during intense exercise, and be 25–40 L/min with moderate exercise. This has a considerable direct effect on exposure through the lungs. For example, when young persons were exposed to *m*-xylene at a concentration of 100 ppm, the concentration of *m*-xylene in their venous blood reached a level of 19 μmol/L whereas after a moderate exercise at 100 W, a concentration of 100 μmol/L was reached in their blood. Thus, the exercise caused about a five-fold increase in the concentration of *m*-xylene in the blood compared to values in sedentary subjects even though the ambient air xylene concentration was the same.[65] The increase was approximately equivalent to the change in minute ventilation (which was four to six fold). Increased cardiac output and thereby increased circulation helped in maintaining the concentration gradient between the alveolar space and the blood and thereby facilitated pulmonary absorption of *m*-xylene.[66,67]

Dermal Exposure

Exercise also increases skin circulation and perspiration, which both enhance dermal penetration of compounds into the body. Furthermore, skin lesions, such as wounds and dermatitis, can increase the permeability of the skin to chemicals. Also, exposure of the skin to solvents and removal of skin fat increase dermal penetration of a number of compounds. Compounds penetrate the skin more readily in places where the skin is thin, like the face, hands and scrotum. Increased dermal blood flow due to exercise facilitates the penetration of the skin by chemicals.[65–67]

Considerable protection against dermal exposure can be achieved by using the appropriate protective clothing, such as overalls, rubber gloves, and boots. For example, protective clothing provided 80–95% protection when workers manually handled ethylenebisdithiocarbamate fungicides in agriculture.[52,54,57] It would seem that a similar protection against dermal exposure can be achieved in agriculture and industry in general. Figure 5.33 shows that urinary excretion of ethylenethiourea mainly depends on dermal absorption of the parent compound, maneb (a dithiocarbamate) because a delay can be seen before the start

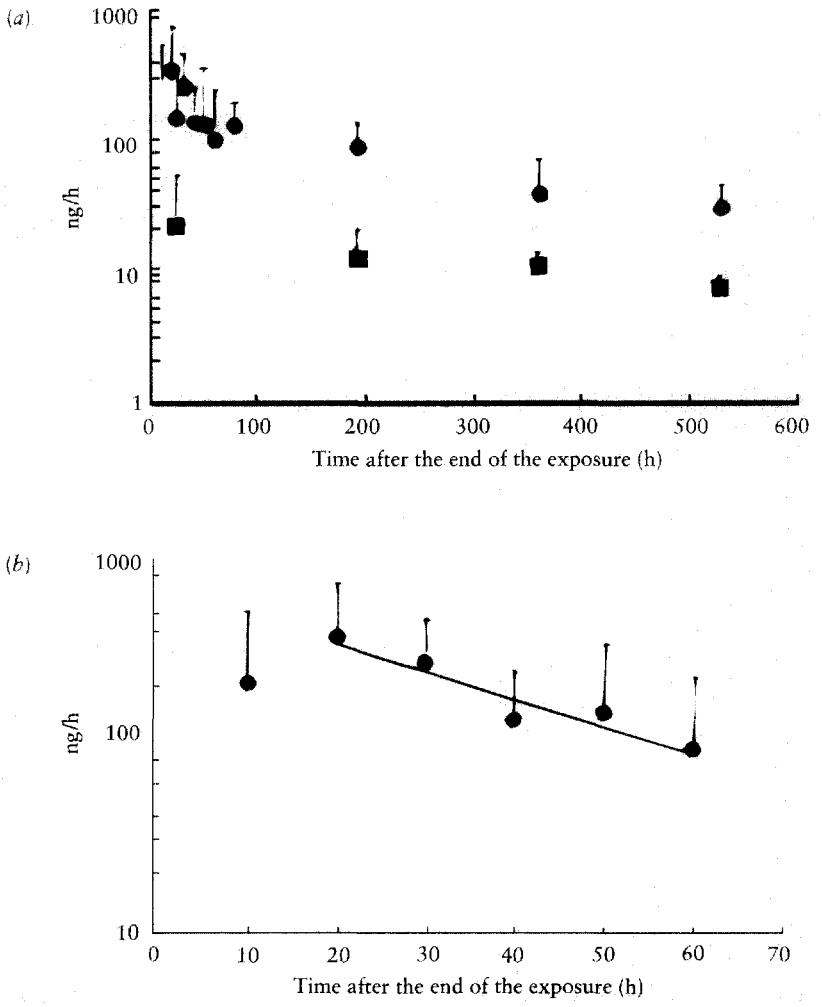

FIGURE 5.33 (a) Excretion rate (means and standard deviations of the means) of ethylenethiourea (ETU) in the urine (ng/h) of potato field applicators (circles) (groups I and II) and pine nursery weeders (squares) (group IV) after exposure to ethylene bisdithiocarbamates during pesticide application (groups I and II) and the weeding of the sprayed vegetation (group IV). The ETU concentrations were at the detection limit in group IV after two weeks of follow-up (two last time points). (b) Excretion rate of ethylenethiourea (ETU) (means and standard deviations of the means) in the urine (ng/h) of potato field applicators (group I) during 60 h after the cessation of exposure to ethylene bisdithiocarbamate fungicides. The first time point at 10 h after the cessation of the application was omitted from the analysis because of possible continuous exposure for a few hours after the application and because of the effect of dermal absorption. The regression equation is $y = -6x + 455$, where y is the excretion rate of ETU (ng/h), x is the time (h), and the correlation coefficient squared (r^2) is 0.86. [With permission from Kurttio, P., and Savolainen, K., (1990). Ethylenethiourea in air and in urine: Implications to exposure to ethylenebisdithiocarbamate fungicides. *Scand. J. Work Environ. Health* **16**, 203–207.]

of urinary elimination of ethylenethiourea (Fig. 5.33*b*). Figure 5.33*a* shows that the urinary elimination of ethylenethiourea has several elimination phases due to the distribution of the compound in different body compartments.

5.3.3 Kinetics of Chemical Compounds

The kinetic properties of chemical compounds include their absorption and distribution in the body, their biotransformation to more soluble forms through metabolic processes in the liver and other metabolic organs, and the excretion of the metabolites in the urine, the bile, the exhaled air, and in the saliva. An important issue in toxicokinetics deals with the formation of reactive toxic intermediates during phase I metabolic reactions (see Section 5.3.3).

5.3.3.1 Absorption

As stated earlier, inhalation is the main route of absorption for occupational exposure to chemicals. Absorption of gaseous substances depends on solubility in blood and tissues (as presented in Sections 2.3.3–2.3.5), blood flow, and pulmonary ventilation. Particle size has an important influence on the absorption of aerosols (see Sections 2.3.7 and 3.1.1).

Absorption via the skin depends on the lipid- and water-solubility of the compound, its polarity, and the molecular size. Dermal absorption is also markedly affected by the size of the exposed skin area.[52,54,65,67]

Chemicals have to pass through either the skin or mucous membranes lining the respiratory airways and gastrointestinal tract to enter the circulation and reach their site of action. This process is called absorption. Different mechanisms of entry into the body also greatly affect the absorption of a compound. Passive diffusion is the most important transfer mechanism. According to Fick's law,[57] diffusion velocity v depends on the diffusion constant (D), the surface area of the membrane (A), concentration difference across the membrane (Δc), and thickness of the membrane (L)

$$v = \frac{DA\Delta c}{L} \tag{5.52}$$

The diffusion constant depends on the lipid solubility, molecular weight, and structure of the substance. Lipid-soluble compounds with a molecular weight less than about 500 diffuse readily through the membranes. Polar compounds are poorly absorbed. However, active transport systems play a major role in the absorption of a number of amino acids, sugars, ions, and other nutrients. The blood-brain barrier, a functional structure that protects the central nervous system (CNS) against foreign substances, prevents the entry of most compounds in to the CNS. In fact, only lipid-soluble compounds, and polar compounds which have an active transport mechanism, can readily enter the CNS. Examples of such polar compounds include amino acids and sugars. Active transport also plays an important role in the testicles, which are protected by a testicular-blood barrier which has a role similar to the blood-brain barrier.[57,68] Figure 5.34*a* shows how mevinphos, a greenhouse organophosphorus insecticide which mainly gains access to the body via the skin, is absorbed. Figure 5.34*b* shows that exposure through lungs was negligible, because there was an excellent correlation between mevinphos on the foliage, the source of the compound, and mevinphos level on the skin.[54]

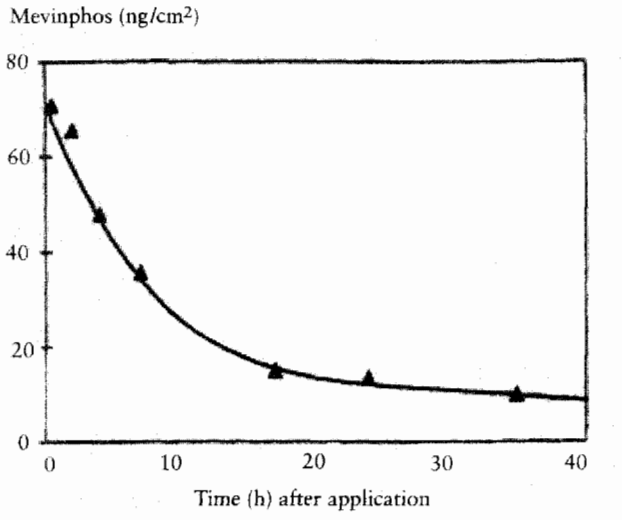

(*a*)

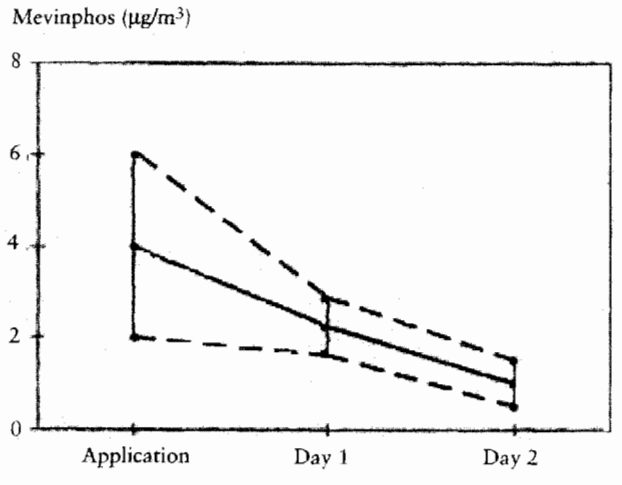

(*b*)

FIGURE 5.34 (a) Correlations ($y = 7.2x \leq 3.5$; $r = 0.97$) between the amount of mevinphos on the foliage and the dermal exposure rate to mevinphos via the hands.[54] (b) Mean (±SD) concentrations of mevinphos in the breathing zone of the workers immediately after application and on the morning of the two first working days after the application.[54] (Used with permission.)

Entry of Particles into the Body

The aerodynamic particle diameter determines the fate of particles in the respiratory system. Coarse particles are deposited in the nose and nasopharynx. Smaller particles that pass the upper airway can be deposited in the bronchial region and lower airway. A size-selective deposition model and sampling of particles has been standardized both in Europe[69] and internationally.[70] The

standard includes size definitions for three mass fractions. The inhalable fraction consists of particles that can enter the upper airway. Its upper size limit is 100 μm (the diameter of human hair is 50–100μm). The thoracic mass fraction consists of particles that can penetrate past the larynx. Its upper size limit is about 30 μm and median cut point 10 μm. The respirable mass fraction consists of particles that can enter the alveolar region. Its upper size limit is about 10 μm and median cut point 4 μm (see Fig. 5.35).

5.3.3.2 Distribution

After absorption, a chemical compound enters the circulation, which transfers it to all parts of the body. After this phase, the most important factor affecting the distribution is the passage of the compound through biological membranes. From the point of view of the distribution of a chemical compound, the organism can be divided into three different compartments: (1) the plasma compartment; (2) the intercellular compartment; and (3) the intracellular compartment. In all these compartments, a chemical compound can be bound to biological macromolecules. The proportion of bound and unbound (free) chemical compound depends on the characteristics of both the chemical and the binding macromolecules.[63,64]

In the plasma, most chemicals are bound to plasma proteins. Albumin is quantitatively the most important binding protein but beta globulin and acidic glycoprotein also bind chemicals. The number of binding sites is limited, and, therefore, high doses of chemicals may cause saturation of protein binding. In most cases, an adverse effect does not require saturation of protein binding sites because free and bound chemical are in equilibrium in the plasma, and the free chemical is available for toxic action in the target tissues. The circulation is extremely important for distribution of chemicals. Heavily perfused organs, i.e., the brain, liver, and kidneys, receive most of the cardiac output, and in these organs the concentration of a chemical increases much more rapidly than in the other organs. Organs whose perfusion is small, e.g., resting muscles and adipose tissue, receive only a small portion of the cardiac output, and therefore concentration of a chemical in these organs increases much more slowly than in the heavily perfused organs.[62–64]

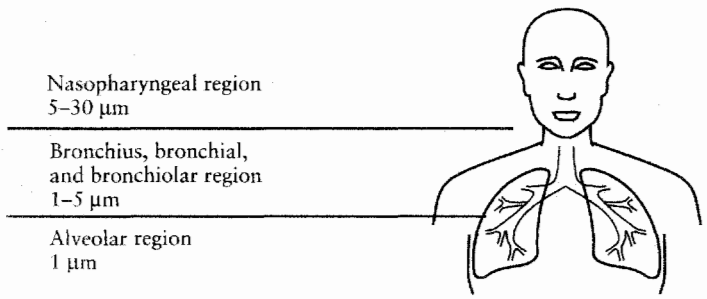

FIGURE 5.35 Regions of pulmonary pathways and size of particles that can reach different regions of the lungs.[4]

Adipose tissue and bones function as storage sites for many substances. Most chemicals have some tissue specificity with regard to their tissue binding. In many cases, this property of a chemical is not important, but, especially for lipid-soluble chemicals, adipose tissue often becomes an important storage depot from which they are slowly released. Both accumulation and release of compounds from the adipose tissue are slow processes, partly because adipose tissue receives only 2% of the cardiac output. The accumulated compound may be released if the size of the fat depot decreases. For example, lipid-soluble insecticides, such as chlordane, may even cause acute intoxication due to dieting, and dieting also causes release of the supertoxic compound dioxin into the circulation. Lipid-soluble compounds can also be released from their depots in the adipose tissue during breast feeding of infants, and this may cause excessive exposure.[63,71] The features of absorption, distribution, and excretion have been depicted in Fig. 5.36.

Another important storage depot for toxic compounds is the skeleton. In particular, cadmium and lead bind and accumulate in the bone tissue from which they are released very slowly. The half-life of elimination of cadmium is several years, the half-life of lead is several months.

Theoretical volume of distribution (V_d) of a chemical is the volume in which the chemical would be distributed if its concentration were equal to a theoretical steady-state plasma concentration (C_0) at time zero. The volume of distribution is thus obtained quite similarly as the steady state concentration of a compound in the workroom air:

$$V_d = \frac{m}{C_0}, \tag{5.53}$$

where m is the mass of a chemical and C_0 is its theoretical plasma concentration at time zero. Even though the compound does not ever reach the theoretical

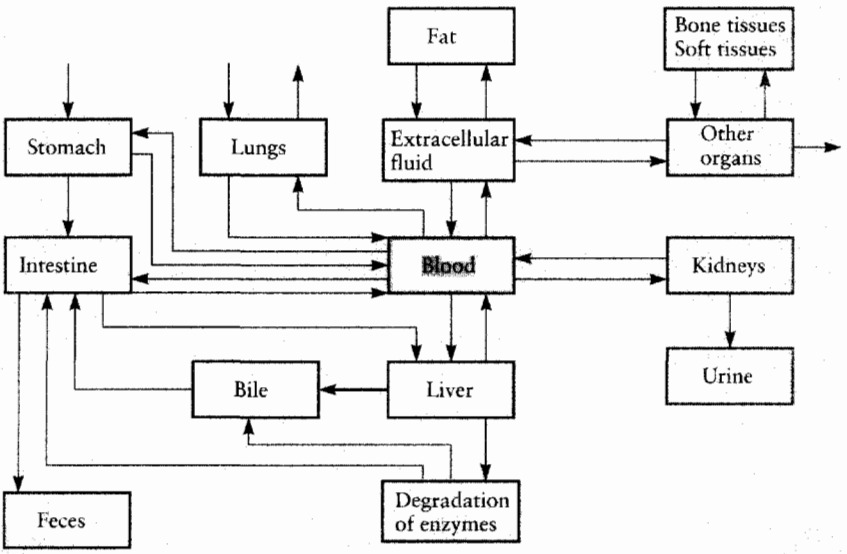

FIGURE 5.36 Schematic representation of absorption, distribution, and excretion of xenobiotics.[2]

volume of distribution in practice, it provides valuable information on the characteristics of the compound, that can be used in a number of pharmaco/toxicokinetic models.[62,68]

Special Considerations

Chemical compounds may also be distributed to the placenta and through the placenta to the fetus and thereby cause exposure of the offspring. Even though the placental wall consists of several layers, it is a biological membrane, and the same principles apply to the placenta as to any other biological membrane, i.e., penetration depends on lipid-solubility and ionization of chemical compounds. However, the concentrations of lipid-soluble compounds increase slowly in the fetus, because it is a separate body compartment, and redistribution with this compartment is a time-consuming process. However, an equilibrium will be reached between the mother and the fetus during long-term exposure. This is the main reason chemical exposure during pregnancy is strictly controlled in most developed countries.

5.3.3.3 Biotransformation

The purpose of metabolism or biotransformation of xenobiotics (foreign compounds) is to transform them into a water-soluble form so that they can be excreted either in the urine or in the bile. These processes are catalyzed by a number of enzymes. Biotransformation reactions are divided into phase I and phase II reactions: in phase I reactions, functional groups, such as the hydroxyl group, are linked to the xenobiotic (Fig. 5.37). This is why phase I reactions are also called functionalization reactions. In phase II, the functional group is conjugated with one of several chemical compounds in the body, e.g., glucuronic acid, glutathione, sulfates, glycine, or methionine. Most xenobiotics undergo both phase I and phase II reactions, but some compounds undergo only one of the phases. It is noteworthy that rarely will all of the absorbed

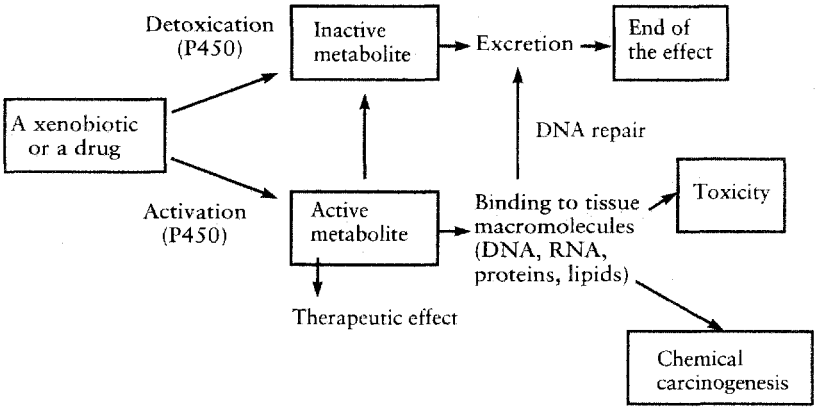

FIGURE 5.37 Janus faces of the biotransformation of xenobiotics. On one hand metabolism leads to inactivation and elimination of xenobiotics, but on the other hand many metabolites are reactive and may cause deleterious effects by binding to DNA, proteins, and other macromolecules.

compound be metabolized; in most cases small amounts of unchanged parent compound can also be found in the urine. This can also be utilized as a specific biological monitoring test. The enzymes responsible for biotransformation of xenobiotics also catalyze the metabolism of endogenous compounds, such as hormones and neurotransmitters. For example, steroid hormones undergo phase I oxidation catalyzed by P450 enzymes and then conjugation reactions of the functional groups catalyzed by glucuronyltransferase or sulfotransferase. The number of possible metabolites of various chemicals is often very large because of the variety of different phase I and phase II enzymes in the cells.[63,72]

The highest activities and amounts (the amount of enzyme protein/g protein in the tissue) of biotransformation enzymes are found in the liver, and this organ plays a key role in the metabolism of endogenous and foreign compounds. However, these enzymes can be found in many other organs, and one can hypothesize that enzymes expressed at the entries to the body, i.e., the skin and the mucosa of the gastrointestinal tract and airways, have developed during evolution to protect the organism against foreign compounds. In fact, the liver and kidneys are also direct or indirect sites of entry of foreign compounds into the body. The liver is an important port of entry because of the portal vein that carries most foreign compounds directly from the intestine to the liver. The kidneys can also be a port for chemical compounds into the body because a number of compounds excreted in the urine may be reabsorbed in the proximal tubules of the kidney. Such compounds include those with an active transport system, many lipid-soluble compounds, and metabolites that have been hydrolyzed in the urine. On the other hand, metabolites of these parent compounds conjugated with biological macromolecules or amino acids are readily excreted in the urine or bile.[68,72]

Biologically active compounds are often inactivated during phase I biotransformation. However, in some instances, biological activity of chemical compounds may be increased, and they can become activated especially by the P450 enzyme (CYP enzymes) system that catalyzes oxidation, hydroxylation, and epoxidation. These reactions may yield electrophilic intermediates that readily react with the nucleophilic groups of biological macromolecules, such as nucleic acids and proteins, with toxic consequences, such as cell death, mutagenesis, malignant transformation of cells, or teratogenesis. For example, activation of carbon tetrachloride, bromobenzene, and acetaminophen (paracetamol) after high doses cause liver necrosis. At lower doses, they may cause genotoxic alterations in the cells and subsequent malignant transformation of the exposed cells. Active metabolites of aflatoxin B1 (a fungal toxin), benzo(a)pyrene (a combustion product), and vinyl chloride (a plastic monomer), induce cancer subsequent to their binding with bases in the DNA. Since all of the compounds that are absorbed in the gastrointestinal tract enter the liver directly through the portal vein, their biotransformation is very effective in the liver because of their extensive contact with metabolically active liver cells, the hepatocytes. The anatomical structure of the liver further promotes effective biotransformation of xenobiotics in this organ (Fig. 5.38). A number of factors affect the metabolizing capacity of the liver. These include the concentration of phase I CYP enzymes, the uptake of the compounds by the liver

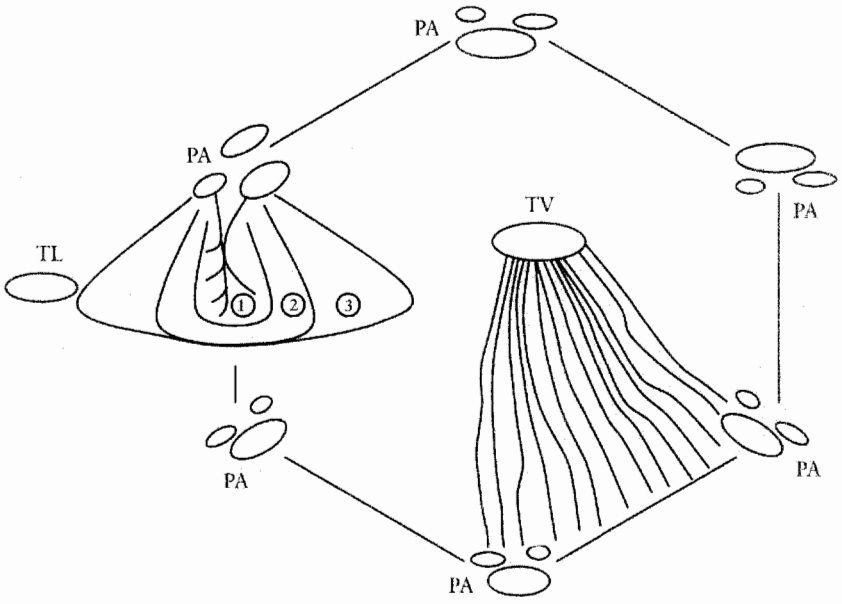

FIGURE 5.38 Pictorial presentation of the microscopic structure of the liver. The picture shows the classical liver lobulus. The functional acinus and its three zones are at the left. The acinal zones are marked by numbering them 1-3. These zones correspond to the direction of blood flow from the portal arteries (PA) to the terminal veins (TV). Zone 1 corresponds to the periportal area in classical liver pathology, zone 2, the interlobular region (midzone), and zone 3, centrelobular region.[74]

cells, blood flow through the liver, and different pathological processes such as collagen formation due to cirrhosis and hepatitis.[55,56]

5.3.3.4 Excretion

Water solubility (polarity) is essential for excretion. Even though lipid-soluble compounds may also be excreted to primary urine, they are usually at least partially reabsorbed. The metabolites formed in the liver and extrahepatic tissues remain free (i.e., not bound to proteins) and are, therefore, readily excreted.

Cadmium is effectively accumulated in the kidneys. When the cadmium concentration exceeds 200 μg/g in the kidney cortex, tubular damage will occur in 10% of the population, and proteins begin to leak into urine (proteinuria). When the concentration of cadmium in the kidney cortex exceeds 300 μg/g, the effect is seen in 50% of the exposed population. Typically, excretion of low-molecular weight proteins, such as beta-microglobulin, is increased, due to dysfunction of proximal tubular cells of the kidney. The existence of albumin or other high-molecular weight proteins in the urine indicates that a glomerular injury has also taken place. The excretion of protein-bound cadmium will also be increased.[62,63,73]

Pulmonary excretion takes place for volatile compounds. Alveolar air is at equilibrium with capillary blood. Thus, pulmonary excretion depends on the vapor pressure of the compound and its blood solubility. If blood solubility is

low, the compound will be rapidly excreted (see Section 2.3.9). The determination of alveolar air concentration can be used as biological exposure test for organic solvents. This test is also widely applied to control for drunken driving. The concentration of a solvent in the blood is obtained by multiplying the alveolar air concentration by the blood solubility coefficient.[62,74]

Lungs also secrete nonvolatile compounds. Lipid-soluble compounds may thus be transported with the alveobronchotracheal mucus to the pharynx, where they are swallowed. They may then be excreted or reabsorbed. Particles are also removed by this mucociliary escalator.

The particle size is the most important factor that contributes to the clearance of particles. For particles deposited in the anterior parts of the nose, wiping and blowing are important mechanisms whereas particles on the other areas of the nose are removed with mucus. The cilia move the mucus toward the glottis where the mucus and the particles are swallowed. In the tracheobronchial area, the mucus covering the tracheobronchial tree is moved upward by the cilia beating under the mucus. This mucociliary escalator transports deposited particles and particle-filled macrophages to the pharynx, where they are also swallowed. Mucociliary clearance is rapid in healthy adults and is complete within one to two days for particles in the lower airways. Infection and inflammation due to irritation or allergic reaction can markedly impair this form of clearance.

Particles deposited in the alveoli are phagocytized by alveolar macrophages and cleared either through the mucociliary escalator or through the lymphatic drainage system. Fibers may be too long to become phagocytized by single macrophages. In such a case, several macrophages can participate in the phagocytosis in a cooperative manner (see Fig. 5.39). Macrophages are able to dissolve synthetic miner fibers to some extent but asbestos (especially amfiboles) fibers remain mostly unaffected. This leads to the production of oxygen radicals and inflammation mediators which induce macrophages to kill themselves. Another macrophage will then phagocytize the asbestos fiber and it too will die. This vicious cycle will continue and it may ultimately lead to lung fibrosis and cancer. Small particles may also directly penetrate the epithelial membrane and enter the blood stream.

5.3.3.5 Movements of Chemical Compounds in the Body

Absorption, distribution, biotransformation, and excretion of chemical compounds have been discussed as separate phenomena. In reality all these processes occur simultaneously, and are integrated processes, i.e., they all affect each other. In order to understand the movements of chemicals in the body, and for the delineation of the duration of action of a chemical in the organism, it is important to be able to quantify these toxicokinetic phases. For this purpose various models are used, of which the most widely utilized are the one-compartment, two-compartment, and various physiologically based pharmacokinetic models. These models resemble models used in ventilation engineering to characterize air exchange.

One-Compartment Model

The simplest toxicokinetic analysis involves measurement of the plasma concentrations of a chemical at several time points after the administration of

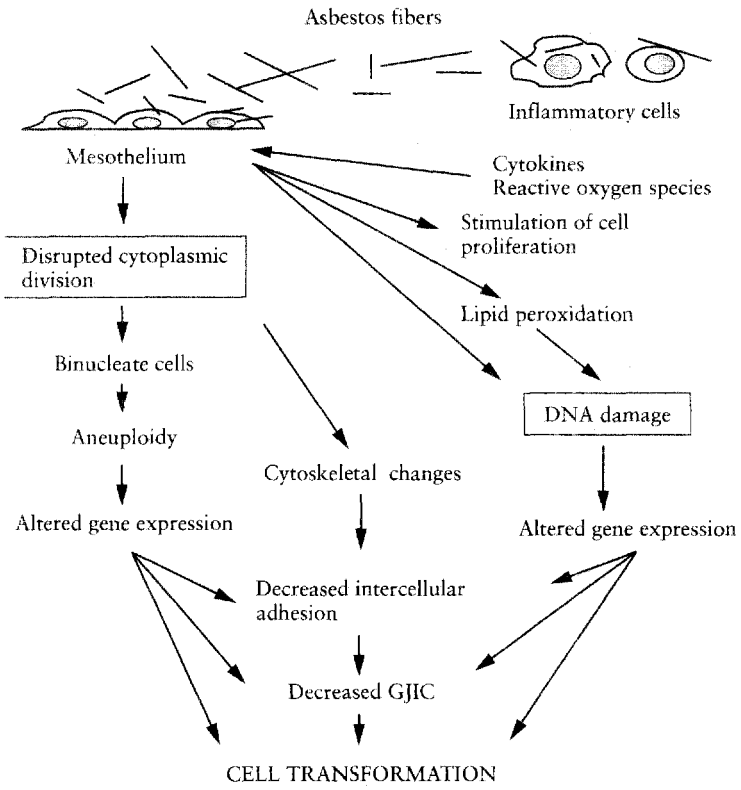

FIGURE 5.39 Possible pathways in fiber carcinogenesis. The figure is based on review articles by 1992 and Kamp et al. 1992, and original publications by Marsh and Mossman 1991,[76] Heintz et al. 1993, Kodama et al. 1993, Kinnula et al. 1994b, as well as the results presented in studies II and V. The connection between disrupted cytoplasmic division, cytoskeletal changes, and decreased intercellular adhesion has not been studied in relation to fibers. The pathway is based on articles dealing with linkage between cadherins, catenins, and cytoskeleton, as well as their role in cell transformation.[78–80] The connection between decreased cell-cell adhesion and decreased GJIC has been reported by Musil et al.[81] and Meyer et al.,[82] and the role of GJIC in cell transformation has been reviewed by Yamasaki.[83] (modified from Pelin).[84]

a single intravenous injection. If the kinetic data obtained yield a straight line when plotted as the logarithm of plasma concentrations versus time, the kinetics of the compound can be described by a one-compartment model, in which the whole body is treated as one single space or compartment. Even though the one-compartment model is an extreme simplification of the organism in the physiological and toxicological sense, the behavior of several chemical compounds can be well described and understood by using this model. Usually, only the kinetics of compounds that are rapidly distributed in the body can be described with the one-compartment model. As described below (Fig. 5.40), the theoretical concentration C_0 can then be calculated.

The rate of elimination of a chemical compound from the body is usually proportional to the amount of the chemical in the body. Elimination processes include biotransformation, exhalation, and excretion in the urine, bile, saliva, and sweat, and even in the hair and nails. The first-order

elimination rate constant k_{el} has units of reciprocal time (e.g., min^{-1} and h^{-1}). For example, if the elimination rate constant is 0.5 h^{-1} the percentage of the dose excreted after one, two, or three hours is the same, regardless of the given dose. In this case, the percentage of the dose excreted is 43%, even though the rate constant is 0.5/h (or 50%/h), because the dose remaining in the body (C) decreases continuously with time. The elimination rate decreases ($k_{el} \cdot C$) when the dose remaining in the body (C) decreases. The first-order elimination rate of the compound is mathematically expressed as an exponential equation $C = C_0 \cdot \exp(-k_{el}t)$ where C is the plasma concentration, k_{el} the first-order elimination rate constant, and t the time of blood sampling. With logarithmic transformation a straight line is obtained:

$$\ln C_t = \ln C_0 - k_{el} \cdot t \tag{5.54}$$

where ln C_0 represents the intercept and $-k_{el}$ represents the slope of the line. Therefore, the first-order elimination rate constants can be determined by utilizing the slope of the ln C versus time plot.

In addition to the elimination rate constant, the half-life ($t_{1/2}$) is another important parameter that characterizes the time-course of chemical compounds in the body. The elimination half-life ($t_{1/2}$) is the time to reduce the concentration of a chemical in plasma to half of its original level. The relationship of half-life to the elimination rate constant is $t_{1/2} = 0.693/k_{el}$ and, therefore, the half-life of a chemical compound can be determined after the determination of k_{el} from the slope of the line. The half-life can also be determined through visual inspection from the log C versus time plot (Fig. 5.40). For compounds that are eliminated through first-order kinetics, the time required for the plasma concentration to be decreased by one half is constant. It is important to understand that the half-life of chemicals that are eliminated by first-order kinetics is independent of dose.[68,85,86]

Two-Compartment Model

If the plotting of the logarithm of the plasma concentration against time does not result in a straight line but rather in a curve, the use of multicompartment models is required. Multicompartment models are required for compounds that distribute to different organs at different rates. Such compounds are usually lipid-soluble and reach equilibrium in lipid-containing organs relatively slowly. This results in multiexponential elimination because chemical compounds are eliminated in a reverse order as compared with their distibution. In the simplest case, this type of curve can be resolved into two exponential terms (a two-compartment model). Concentration can be expressed as $C = Ae^{\alpha} + B^{\beta}$ where A and B are proportionality constants and α and β are rate constants with dimensions of reciprocal time. During the distribution alpha phase, concentrations of the chemical in plasma decrease more rapidly than they do in the postdistribution phase (beta). The length of the distribution phase may vary from minutes to hours to days. Whether the distribution phase becomes apparent depends on the time of the sampling after the cessation of the exposure. Since most chemicals in the occupational environment

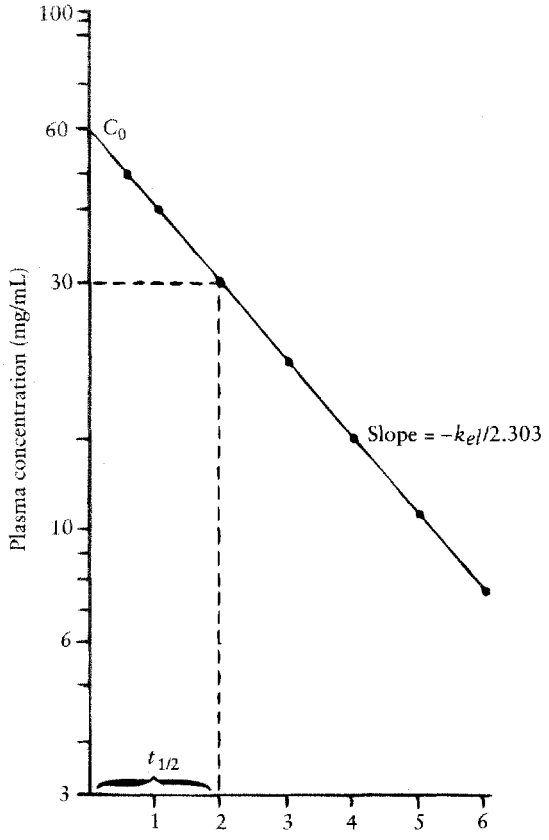

FIGURE 5.40 Schematic representation of the concentration of a chemical in the plasma as a function of time after an intravenous injection if the body acts as a one-compartment system and elimination of the chemical obeys first-order kinetics with a rate constant (k_{el}).[68]

follow two- or other multicompartmental elimination kinetics, the correct timing of blood sampling for biological monitoring is essential.[68,85,86]

In a two-compartment model, β is equivalent to k in the one-compartment model. Therefore, the terminal half-life for the elimination of a chemical compound following two-compartment model elimination can be calculated from the equation $\beta = 0.693/t_{1/2}$.

Saturation of Elimination

Saturation kinetics are also called zero-order kinetics or Michaelis-Menten kinetics. The Michaelis-Menten equation is mainly used to characterize the interactions of enzymes and substrates, but it is also widely applied to characterize the elimination of chemical compounds from the body. The substrate concentration that produces half-maximal velocity of an enzymatic reaction, termed K_m value or Michaelis constant, can be determined experimentally by graphing v_i as a function of substrate concentration, [S].

The Michaelis-Menten equation is written

$$v_i = \frac{v_{max}[S]}{K_m + [S]} \tag{5.55}$$

where v_i is the measured initial velocity of an enzymatic reaction, v_{max} is the maximal velocity of the enzymatic reaction, and K_m is the Michaelis constant. Note that when [S] far exceeds the K_m, the initial velocity, v_i, is close to the maximal velocity, v_{max}.

In zero-order kinetics, a constant amount of a chemical compound is excreted per unit of time. In most cases, this phenomenon is caused by the saturation of a rate-limiting enzyme, and the enzyme commonly functions at its maximal rate, i.e., a constant amount of a chemical compound is metabolized per unit time. A good example is ethyl alcohol; alcohol dehydrogenase becomes saturated at relatively low concentrations. Because of this saturation, ethyl alcohol is eliminated at a constant rate about 7 g/h. However, the reason is not always an enzyme; any

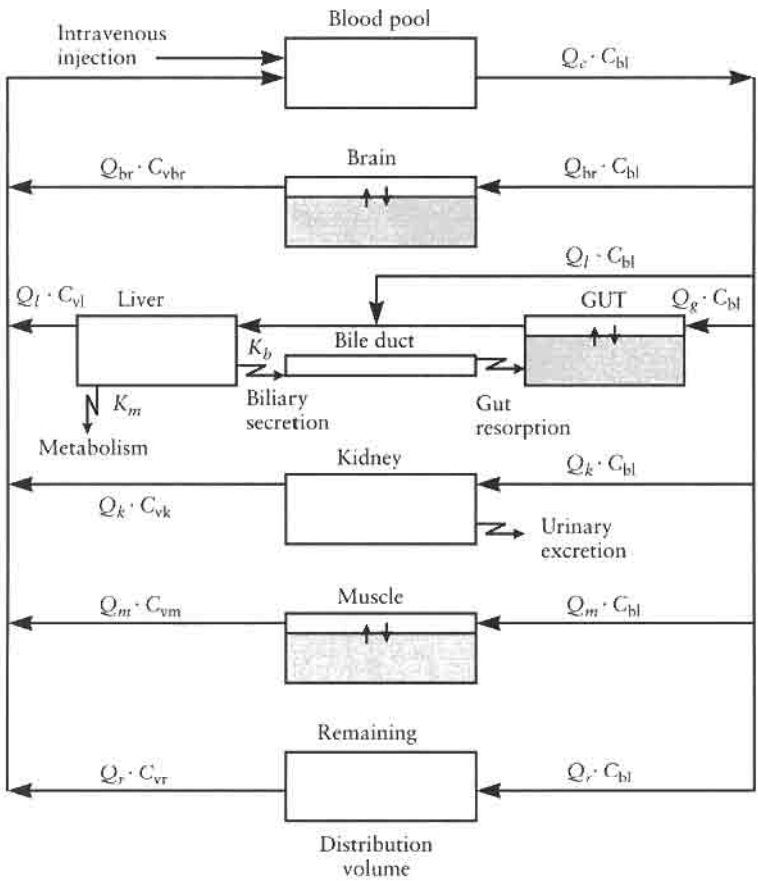

FIGURE 5.41 (a) Physiological model for phenobarbital. (b) Physiological model for the volatile organic chemical benzene.[68] (Used with permission.)

system that may become saturated follows zero-order kinetics. As the concentration of a chemical compound decreases to below the concentration at which the enzyme becomes saturated, it changes to first-order kinetics.

From a practical point of view, saturation of elimination has important consequences. If the metabolism becomes saturated, the duration of the action of the compound is prolonged. In such a case, correct timing for collection of biological monitoring samples also becomes difficult to assess. Furthermore, saturation of metabolism may also have qualitative effects. For example, it has been argued (but not yet proved) that arsenic compounds cause cancer at high doses at which methylation of inorganic arsenic becomes saturated.[68]

Physiologically Based Toxicokinetic Models

Physiologically based toxicokinetic models are nowadays used increasingly for toxicological risk assessment. These models are based on human physiology, and thus take into consideration the actual toxicokinetic processes more accurately than the one- or two-compartment models. In these models, all of the relevant information regarding absorption, distribution, biotransformation, and elimination of a compound is utilized. The principles of physiologically based pharmaco/ toxicokinetic models are depicted in Fig. 5.41*a* and *b*. The

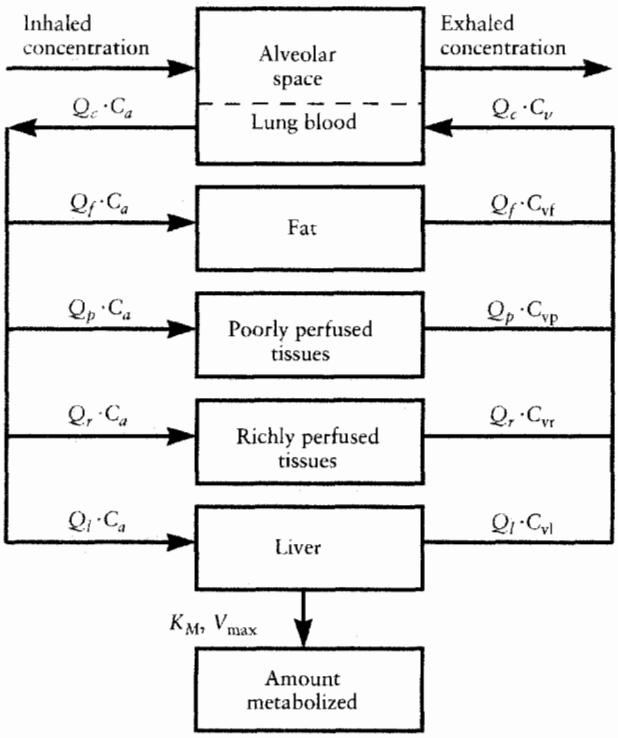

(*b*)

FIGURE 5.41 (*continued*)

main difficulty in using these models is that in most cases not enough information is currently available about the compound under study.[68,85]

5.3.4 Toxic Effects of Chemical Compounds

5.3.4.1 The Nature of Toxic Reactions

A toxic reaction may take place during or soon after exposure, or it may only appear after a latency period. Chronic toxicity requires exposure of several years for a toxic effect to occur in humans. With respect to experimental animals, the animals are usually exposed for most or all of their life time to ascertain the occurrence of chronic toxicity. Acute toxic reactions that occur immediately are easy to associate with the exposure and the exposure-effect relationship can readily be demonstrated. The longer the time interval between exposure and effect, the more difficult it is to delineate the relationship between exposure and effect.

Toxic effects often disappear after the cessation of the exposure, but they can also be permanent. The tissue's ability to regenerate is one of the most important factors that determines the nature of toxic effects. For example, liver tissue has a remarkable capacity to regenerate, and therefore liver injury is often reversible. On the other hand, neuronal cells do not regenerate at all, thus neuronal injury is irreversible. It is true that neuronal cells can compensate for possible losses, but only to a minor degree. In particular, chronic effects tend to be irreversible.[64]

There are some basic differences between toxic and allergic reactions. The most important differences are: (1) an allergic reaction always requires a prior exposure to the compound, and this reaction only occurs in sensitized individuals; and (2) a dose-response relationship is characteristic to a toxic reaction, whereas such a relationship is much less clear for an allergic reaction. Even minute doses can elicit an allergic reaction in a sensitized individual (see Fig. 5.42).[64]

5.3.4.2 Antagonism and Synergism

Industrial workers are almost always exposed to several agents simultaneously. The possible interactions of these multiple exposures are and will remain (because the possible combinations are almost infinite) an area of great uncertainty. The situation is further complicated by the simultaneous presence of many lifestyle factors, especially smoking and the use of alcohol and drugs. Other exposures may enhance the toxic effect of an agent. The increased combined effect may be additive ($1 + 1 = 2$) or synergistic ($1 + 1 > 2$). The neurotoxic effects of most organic solvents are usually considered to be additive; therefore, industrial hygienists use the combined exposure level to assess the conditions. It is obtained by dividing the concentration of each solvent by its OEL and by adding the quotients. If the sum exceeds one, the exposure is considered excessive. There are cases of synergism, where the toxic effects of individual exposures become greatly potentiated. A well known example is the combination of asbestos exposure and smoking. The various constituents may have no mutual interactions. In such a case, the effects of different agents can be considered individually. Since in most cases we are ignorant of these

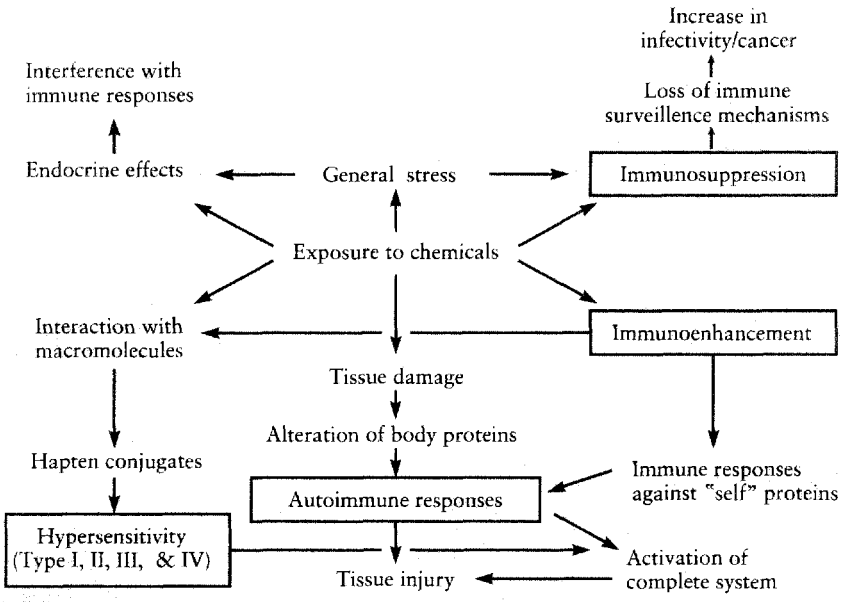

FIGURE 5.42 Responses of the immune system to exposure to some chemicals.[65] (Used with permission.)

potential interactions, the no-interaction assumption is the most common premise. Finally, it is also possible that some constituents reduce the effects of other exposures; however, there are no well-demonstrated examples of this kind of antagonistic action between occupational exposures. [56,57,85–87]

The interactions may be physicochemical without the participation of biological mechanisms; for example, deep lung exposure to highly soluble irritative gases, such as sulfur dioxide, may become enhanced due to adsorption of the gas onto fine particles. Biological interactions may occur at all stages and body sites. For example, toxicity is increased when adverse effects are due to some reactive metabolic intermediate and exposure to another agent stimulates its metabolic activation (enzyme induction).

5.3.4.3 Mechanisms of Toxicity

Paracelsus, a Swiss physician of the sixteenth century, stated that everything is toxic, it is just the dose that matters.[88] This statement still holds true 500 years after Paracelsus developed it to defend the use of toxic compounds such as lead and mercury in the treatment of serious diseases such as syphilis. Chemical compounds cause their toxic effects by inducing changes in cell physiology and biochemistry, and an understanding of cellular biology is a prerequisite if one wishes to understand the nature of toxic reactions.

Toxic reactions occur by several mechanisms: activation of metabolism, production of reactive intermediates and subsequent reactions with cell macromolecules, changing receptor responses, or through abnormal defence reactions. Several compounds cause toxicity by mimicking the organism's own hormones or neurotransmitters, or activating the body's endogenous receptors in some non-physiological way.[89]

Cells are capable of repairing minor damage, but extensive damage leads to cell death. This takes place through either necrosis, which is a chemical-driven chaotic and passive process, or programmed cell death, apoptosis, which is a genetically controlled and energy consuming process. Apoptosis is also a part of normal cell physiology in organogenesis during the development of the embryo before superfluous cells commit a form of cellular suicide by activating their apoptotic programs. However, many chemicals, e.g., several quinone oxidants, and heavy metals may overtly augment apoptosis in adults when it can turn into a pathological process. Thus, cell death is a crucial toxic injury which is affected by the rapidity of the cell injury as well as the target organ. It is noteworthy that the dose of a compound may determine whether cells will proliferate in a tissue or undergo apoptosis or necrosis (see Fig. 5.43 for necrosis and apoptosis).[64,89,91]

Cells in various tissues such as liver, kidney, or gastrointestinal tract, have a remarkable capacity to repair injuries inflicted by chemicals. Furthermore, the ability of most organs to fulfill their functions usually far exceeds requirements that they need to perform. For example, humans can live with one lung, one kidney, and only part of their liver. In this regard, the central nervous system is an exception because neuronal cells do not regenerate. However, even neuronal cells are capable of compensating for an injury. This does not take place through the replacement of dead cells but through the outgrowth of new extensions of existing neurons and through the formation of new synapses, i.e., contacts between neurons that allow chemical neurotransmission between neurons. Even though many toxic effects are due to cell death, toxicity may

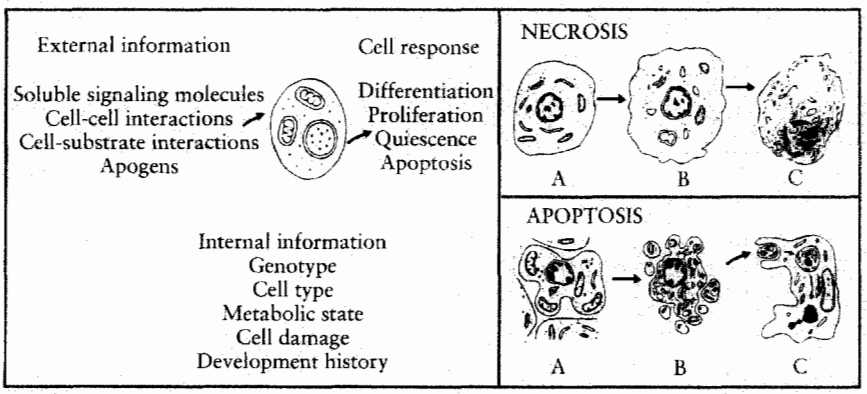

FIGURE 5.43 *Left:* External and internal stimuli triggering various cellular responses including aptosis. *Right:* Comparison of morphologic characteristics of necrosis (*top*) with apoptosis (*bottom*). A normal cell (*top, A*) usually begins the process of necrosis with an initial phase of generalized swelling (*top, B*), which progresses to a dissolution of organelles and rupture of plasma membranes (*top, C*). The earliest phase of apoptosis (*bottom, A*) involves retraction from adjacent cells, loss of specialized surface structures, shrinkage with condensation of cytoplasm, margination of compacted nuclear chromatin, and localized protrusions of the cell surface. Nuclear fragmentation may occur at this time. In the next phase, the protuberances of the cell surfaces separate into multiple membrane-bound bodies (apoptotic bodies) that contain nuclear remnants and intact organelles. The apoptotic bodies are then engulfed and degraded by resident tissue cells (*bottom, C*) or phagocytes. Note that the light microscopic appearances of nuclear rupture and chromatin disintegration (karyorrhexis) may be seen in both late necrosis (*top, C*) and apoptosis (*bottom, B*). Modified from Searle et al.[104]

occur with functional consequences without there being any visible morphological alterations in cells or tissues.[89]

Chemically induced changes in DNA, i.e., mutations and chromosomal damage, are also an important toxicity mechanism. The bases in DNA, like bases in general, are nucleophilic (electron donors) and react with electrophiles (electron acceptors). Strong electrophiles, such as carbonium ions and epoxides, are formed during the metabolism of many known potent carcinogens. Thus, the formation of DNA adducts may cause malignant transformation of cells and lead to initiation of cancer. In the following section, mechanisms whereby chemical compounds induce their toxicity will be discussed.[37,89]

Receptor-mediated Toxicity

Several chemical compounds induce their toxic and other effects through stimulating specific receptors and events occurring after receptor activation, a process called signal transduction. Receptors themselves are protein molecules sitting in the lipid bilayer of the cell membrane. They have the ability to recognize physiological intercellular transmitters such as hormones, neurotransmitters, or growth factors (also called first messengers). Normally a very small amount of a transmitter is sufficient to activate the receptor. Many of the receptors are ion channels and their activation leads to the influx of ions into the cell. There are specific receptor-coupled receptors for sodium, potassium, and calcium. Increased influx of these ions usually leads to increased enzymatic activity, and activation of the cell. Some receptors are intimately associated with enzymes such as tyrosine kinase, adenylate cyclase, or phospholipase C.[92–95]

Some of the cell membrane receptors are coupled to an amplifier, called the G-protein. Activation of a G-protein leads either to activation or inhibition of an effector enzyme on the internal side of the cell membrane (see Fig. 5.44).[92] These effector enzymes are responsible for the generation of second messengers that are essential for cellular signal transduction. Whereas first messengers, described above, are responsible for chemical intercellular communication, second messengers are responsible for transducing the information that has reached the cell surface receptor to all parts of the cell interior. There is also a specific enzyme machinery for inactivating the second messengers to terminate the action that was initiated by the first messenger. Typical effects of a second messenger are elevation of free intracellular calcium associated with cellular activation, activation of specific enzymes such as protein kinase C,[92] or production of a tertiary cellular messenger such as nitric oxide (NO). Nitric oxide is a gaseous cellular messenger that can act as both an intra- and intercellular signal transduction factor. Being lipid-soluble, NO easily diffuses in the cell as well as penetrating through the cell membrane and thereby also reaching other cells.[96,97]

There are even receptors that are known to become activated only due to interaction with a synthetic chemical, and no physiological agonist for such a receptor has been characterized. A model receptor in this class is the so-called Ah receptor complex that becomes activated subsequent to its exposure to 2,3,7,8-tetrachlorodibenzo-*p*-dioxin (TCDD). Activation of the Ah receptor

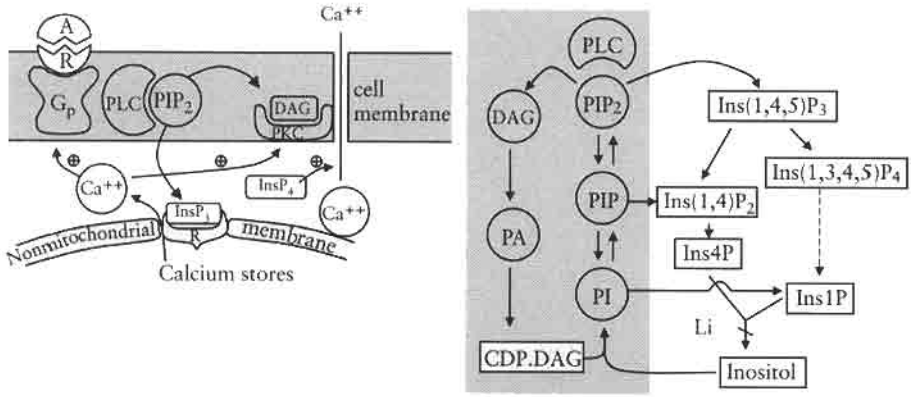

FIGURE 5.44 Acetylcholine (A) binds to a receptor (R) coupled to a G-protein (G_p), and stimulates phospholipase C (PLC). PLC hydrolyzes phosphatidylinositol-(4,5)-bisphosphate (PIP_2) to inositol-(1,4,5)-triphosphate ($Ins(1,4,5)P_3$) and diacylglycerol (DAG). DAG stimulates protein kinase C (PKC), and $Ins(1,4,5)P_3$ binds to its receptor (R) in the intracellular Ca^{2+} store, releases Ca^{2+}, and elevates the levels of free intracellular calcium ($[Ca^{2+}]_i$). Inositol-(1,3,4,5)-tetracisphosphate ($Ins(1,3,4,5)P_4$) is formed from $Ins(1,4,5)P_3$ by phosphorylation, and it, together with $Ins(1,4,5)P_3$ controls influx of Ca^{2+}. PKC and Ca^{2+} cause neuronal stimulation.[92] (Used with permission.)

complex by TCDD leads to increased expression of multiple genes that encode for many proteins such as the enzymes belonging to the phase I CYP P450 family (see Fig. 5.45). This may cause major alterations in the biotransformation of xenobiotics.[89,98–100]

In the CNS, acetylcholine (ACh) is one of the key excitatory neurotransmitters (first messengers). In neuronal cells, it binds preferentially to muscarinic receptors. Stimulation of muscarinic receptors increases levels of neuronal free intracellular calcium leading to neuronal activation. If present in excess, ACh leads to epileptiformic seizures and tonic-clonic convulsions which may be associated with neuronal injury.[92,101,102] Glutamate (Glu) is the most ubiquitous excitatory neurotransmitter in the CNS which binds to several subtypes of glutamatergic receptors. Glutamate is released from nerve endings of glutamatergic neurons subsequent to neuronal stimulation, and also during hypoxia and neuronal injury. Glu also elevates neuronal levels of free intracellular calcium, activates cells, and, when in excess, can cause neuronal injury.[93] Thus, both of these molecules are endogenous neurotransmitters which in excess are harmful to the CNS. Occupational and environmental contaminants such as lead may amplify the effects of Glu, and thereby cause severe neurotoxic risks to exposed individuals.[103,104]

One of the important consequences of neuronal stimulation is increased neuronal aerobic metabolism which produces reactive oxygen species (ROS). ROS can oxidize several biomolecules (carbohydrates, DNA, lipids, and proteins). Thus, even oxygen, which is essential for aerobic life, may be potentially toxic to cells. Addition of one electron to molecular oxygen (O_2) generates a free radical (O_2^-), the superoxide anion. This is converted through activation of an enzyme, superoxide dismutase, to hydrogen peroxide (H_2O_2), which is, in turn, the source of the hydroxyl radical (OH). Usually catalase

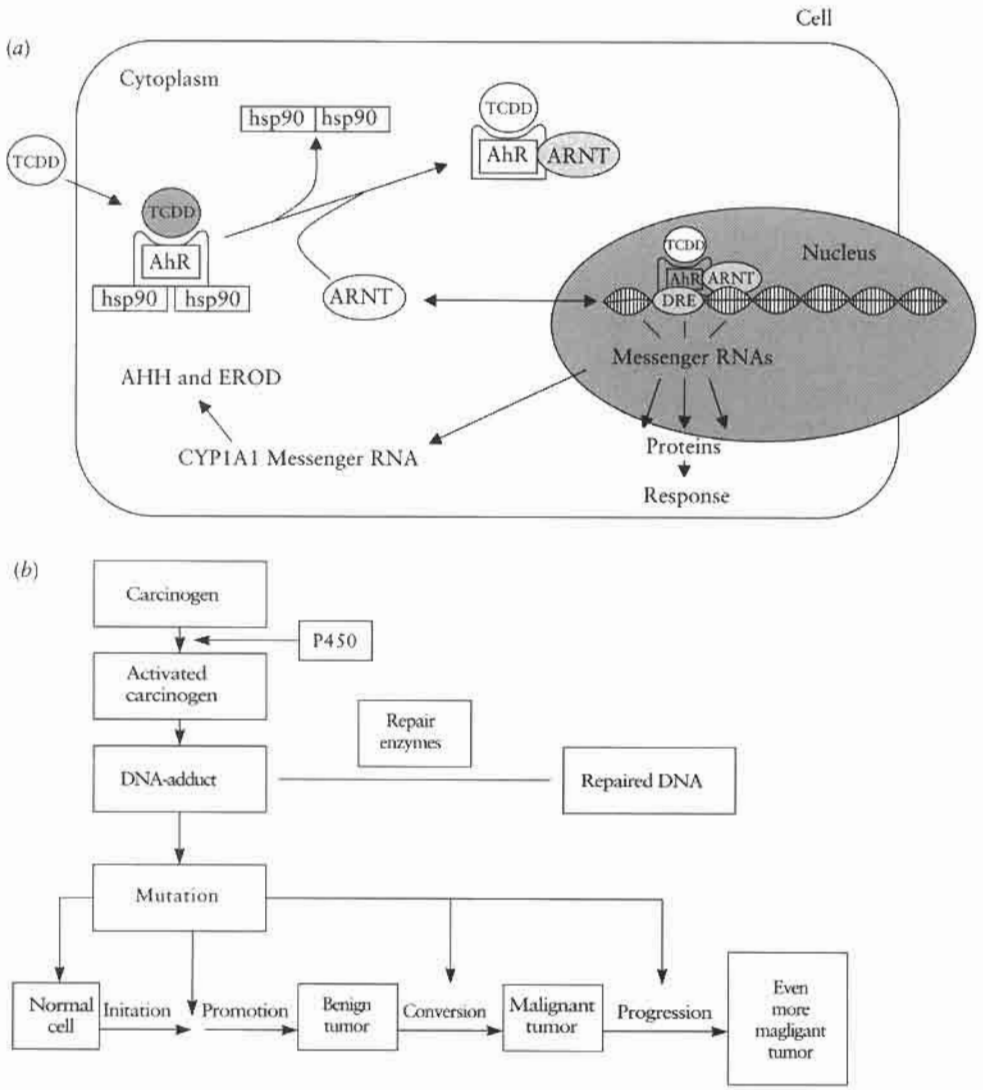

FIGURE 5.45 (*a*) Mechanism of induction of xenobiotic metabolism caused by TCDD and polycyclic aromatic hydrocarbons via the Ah-receptor (AhR). In the cytosol, soluble Ah-receptor is associated with two heat shock proteins (hsp). When TCDD molecule binds to the Ah-receptor, the stress proteins are released, and the TCDD-Ah-receptor complex dimerizes with an Ah-receptor nuclear translocater protein. In the nucleus, this dimer binds to the dioxin response element (DRE) and causes an induction of the synthesis of messenger RNA, subsequent translocation to ribosomes, and formation of proteins, e.g., P450 enzymes. (*b*) Mutations according to our current understanding are an essential part of every stage of chemical carcinogenesis.

further metabolizes hydrogen peroxide to molecular oxygen and water. Oxygen may also be activated to the highly reactive singlet oxygen. It is important to note that the formation of reactive oxygen species is a part of normal cell respiration, i.e., in electron transfer during metabolism of oxygen by the CYP enzyme system. During this process, a part of the ROS formed leaks into the cell.[93,105]

Production of ROS is not only a detrimental process; several cells carry out their functions in the body by generating ROS. For example, neutrophils and macrophages produce ROS upon activation. This is one of their ways of destroying invading microorganisms. However, other exposures, such as mineral fibers, and inorganic and biological particles are also able to activate phagocytes to produce ROS. Excessive ROS production may be harmful to the host cell and surrounding cells.[93,105]

Cells have defense systems to protect themselves against these radical species. The defense systems constitute intracellular thiols, such as glutathione (GSH), a molecule rich in SH groups, and thus capable of scavenging the reactive species through oxidation of the SH groups. This oxidation leads to the formation of disulfide bridges; oxidized GSH (GSSG) is unable to scavenge oxygen radicals. GSH has to be regenerated and this reduction is performed by a specific enzyme, glutathione reductase.[105] Cells also contain water- and lipid soluble molecules that remove ROS. The most important of these molecules are a water-soluble vitamin, vitamin C, that acts in the cytoplasm, and a lipid-soluble vitamin, vitamin E, that functions in the cell membrane. Cellular defense mechanisms against excessive production of ROS also include enzymes that metabolize these reactive species; superoxide dismutase (SOD) metabolizes superoxide anion to hydrogen peroxide, and catalase breaks down hydrogen peroxide to molecular oxygen and water. Oxidative stress results when activation of cells leads to such a high production of ROS that it overwhelms the capacity of the defense mechanisms. The initial phases of stress are associated with depletion of cellular GSH. Then the depletion of defense vitamins C and E occurs. This means that vital biological macromolecules, notably DNA, proteins, carbohydrates, and lipids, can be attacked by the reactive species. This cascade of events may lead to cell death through necrosis or apoptosis.[104–106]

Effects on Excitable Membranes

Maintenance of electrical potential between the cell membrane exterior and interior is a necessity for the proper functioning of excitable neuronal and muscle cells. Chemical compounds can disturb ion fluxes that are essential for the maintenance of the membrane potentials. Fluxes of ions into the cells or out of the cells can be blocked by ion channel blockers (for example, some marine toxins).[107]

Insecticides, such as DDT and lindane, cause their neurotoxic effects by affecting the functions of ion channels in the neuronal cell membrane, thereby altering depolarization of the cell membrane. Organic solvents also modify the normal functioning of excitable neuronal membranes. It was originally assumed that organic solvents non-specifically altered the fluidity of the cell membrane. Current knowledge is that the effects of organic solvents are more specifically directed toward cell membrane proteins such as ion channels, other receptors, and specific enzymes.[107]

Effects on Cellular Energy Metabolism

Several toxic compounds act by inhibiting the oxidation of carbohydrates or by inhibiting the formation of adenosine triphosphate (ATP), a molecule that

is an essential energy source of the cells. Cellular energy metabolism can be prevented by inducing anoxia, for example, by exposure to carbon monoxide.[89] Carbon monoxide reacts with hemoglobin and forms carboxyhemoglobin, which is unable to bind oxygen. Nitrite-induced oxidation of heme iron causes formation of methemoglobin from hemoglobin. An increased amount of methemoglobin also prevents oxidation of cells and tissues because methemoglobin does not bind oxygen. However, the treatment of methemoglobinemia is much easier than the treatment of CO-induced carboxyhemoglobinemia. In fact, induction of slight methemoglobinemia with nitrite can be used as an antidote in cyanide poisonings, because the ferric (trivalent iron) form present in methemoglobin acts as a sink by binding free cyanide.[108]

Cyanide, hydrogen sulfide, and azides prevent cells and tissues from utilizing oxygen by binding to cytochrome oxidase and thereby preventing mitochondrial energy production. The release of hydrogen cyanide may take place if cyanides make contact with acids, and, for example, sewage workers may be exposed to hydrogen sulfide if anaerobic conditions occur. Formation of hydrogen sulfide also takes place in many industries. This gas is insidious because its very unpleasant odor virtually disappears at high concentrations.[109] The inhibition of ATP formation can also take place through other mechanisms. Dinitrophenol (a herbicide) blocks the citric acid cycle by uncoupling it from mitochondrial oxidative metabolism. Fluoro-aceticacid, in turn, blocks the citric acid cycle by inhibiting several key enzymes in the cycle.[99,110,111]

Depletion of ATP in the cells prevents maintenance of the membrane potential, inhibits the functioning of ion pumps, and attenuates cellular signal transduction (e.g., formation of second messengers such as inositol phosphates or cyclic AMP). A marked ATP depletion ultimately impairs the activity of the cell and leads to cell death.

Disturbances in Cellular Calcium Metabolism

As stated above, calcium is an extremely important cellular ion for several cellular functions. The concentration of calcium in human extracellular fluid is about 2.5 mM, while the intracellular concentration is only 100–200 nM depending on the cell type. Thus, there is 10 000–20 000 fold concentration difference between the cell interior and exterior that has to be maintained by cellular pumping mechanisms. This requires a large amount of energy.[93,112,113]

The behavior of calcium in the cells can be considered as a metabolic process. There is uptake, distribution, and excretion of calcium in the cells. The uptake of calcium occurs via activation of calcium channels. The end result is elevation of intracellular calcium levels and subsequent activation.[89,91,114] Because calcium is a powerful cell-activating ion, increased calcium levels in the cell have to be controlled carefully. There are a number of calcium pumps that are responsible for pumping of calcium out of the cells. This again requires a large amount of energy.[115]

Nitric Oxide

Nitric oxide (NO) is a gaseous cellular messenger that transmits information between cells and within cells. In spite of its physiological role, NO is also a reactive species which is capable of reacting with biological molecules, and

therefore in some instances tissue damage may ensue. NO is produced by an enzyme, nitric oxide synthase (NOS) which acts on arginine, transforming it into citrulline and NO. This enzyme has both inducible and constitutive forms. Inducible NOS (iNOS) is expressed in immunological cells, mainly phagocytes such as macrophages and neutrophiles, and in epithelial cells of the airways as well as endothelial cells of the circulatory system.[97,116] Constitutive NOS (cNOS) is expressed in many cells e.g. neuronal cells. It is characteristic of iNOS that NO is produced only subsequent to persistent induction of the enzyme. Upon stimulation, the induction of iNOS (stimulated synthesis of the enzyme protein) may take several hours, but after this time period, the cell can produce large amounts of NO. When airway epithelial cells and circulatory endothelial cells produce NO, they contribute to the control of the tone of the smooth muscle in these systems and thus modify airway resistance and blood pressure.[97] NO production is associated with asthma and airway infections; in both situations, an increased concentration of NO can be measured in the exhaled air.[96]

On the other hand, cNOS is continuously expressed in the cells, and upon stimulation of the cell, the formation of NO begins immediately. However, the amounts of NO produced are minute. The nature of NO in cells expressing cNOS is only to act as a messenger molecule, whereas NO has also other functions in cells expressing iNOS. For example, NO has bacteria and cell killing properties in immunological cells, such as phagocytes.[97,116,117]

Nitric oxide may induce deleterious effects when airway epithelial or immunological cells are exposed to mineral particles (asbestos, quartz). These particles also stimulate cells to produce NO in large quantities, but pulmonary cells are unable to destroy these particles, and a non-physiologically excess production of NO results, perhaps causing tissue damage due to a reaction of NO with cellular macromolecules.[118,119]

Immunological Responses and Sensitization

A number of chemical compounds are potent sensitizers that can lead to serious immunological reactions. Immunotoxicology explores interactions between chemical compounds and the immune system. Chemicals can amplify, attenuate, or otherwise modify immunological reactions subsequent to exposure.[120]

The basic function of the immunological system is to detect and destroy foreign material that may be harmful to the organism. Cells that belong to the immunological system include macrophages, monocytes, granulocytes, and T- and B-lymphocytes. All cells that belong to the immune system have differentiated from the same stem cell. In harmful immunological reactions, the response of an organism to an exposure changes. The environmental factor does not act directly, but alters the reaction of the person exposed. The most important forms of this kind of immunological reactions are (1) immunosuppression; (2) uncontrolled cell growth, e.g., leukemia and lymphoma; (3) disturbances of immunological defense mechanisms against infectious agents and malignant cells; (4) allergies; and (5) autoimmunity. Allergies will be dealt with in more detail later in this chapter.[120]

Necrotic and Apoptotic Cell Death

The main types of cellular injury induced by chemical compounds are necrotic and apoptotic (programmed) cell death. Necrosis implies chaotic ending

of cellular functions, and it always represents an unwanted effect on the cell by a chemical. Apoptosis is a physiological phenomenon that is required during development of the embryo in shaping the developing organs into their final size and form, and it is also functionally important in the development of organs and even body parts (e.g., fingers and toes). Apoptosis is also important in maintaining the integrity and renewal of mucous membranes and the skin. In direct contrast to necrosis which is a passive, non-energy-requiring phenonomenon, apoptosis requires gene expression and synthesis of new proteins, and it is an energy-expensive process.[89,91]

Necrotic cell death is often due to binding of reactive species to biologically important cellular macromolecules, such as proteins, lipids, and DNA. Biotransformation of a number of chemicals such as carbon tetrachloride or styrene leads to formation of epoxides that bind to nucleophilic sites on proteins and DNA. Many of these compounds are also carcinogens. Furthermore, several compounds also cause increased production of ROS. These phenomena may also damage the cell membrane, leading to its leakage and rupture. Necrosis is characterized by cell swelling and leakage of cell constituents into the surroundings of the cell.

In apoptotic cell death, several factors such as growth factors, NO, the tumor suppressor gene p53, and the protein encoded by this gene contribute to the process that leads to cell death. One of the functions of p53 protein is the activation of apoptosis if a cell is transformed to a malignant cell. Apoptosis typically leads to the formation of smaller membrane-encapsulated particles within the cell. Apoptotic cell death begins in the nucleus and proceeds to other parts of the cell. The death process may be quite advanced before it can

TABLE 5.10 Some Important Biochemical Events in Apoptotic Control[91]

1. The detachment of chromatin from the nuclear scaffold, leading to chromatin condensation.
2. Endonuclease-catalyzed hydrolysis of DNA at the internucleosomal linker regions into multimers of 180 base pairs which are visualized by electrophoresis as a "ladder" of nuclear DNA fragments. Access of the endonuclease to DNA is facilitated by depletion of polyamines, and the activity of the enzyme is increased by Ca^{2+} and decreased by ADP-tibosylation. Thus, agents that increase intracellular Ca^{2+} or inhibit poly(ADP-ribose) polymerase can induce apoptosis.[121]
3. Induction of transglutaminase, an enzyme that cross-links proteins through ε-(γ-glutamyl)lysine bonds and presumably contributes to the formation of membrane-bound apoptosis bodies.
4. Protein kinase A activation usually promotes, whereas protein kinase C activation retards, apoptosis.
5. Increased synthesis of transforming growth factor-beta1, which blocks cell division and promotes apoptosis by interacting with its own membrane receptor.[122]
6. Cytotoxic T lymphocytes induce apoptosis of target cells by producing the Fas ligand, a signaling protein that activates Fas, a membrane receptor on potential target cells, including those of the liver, the heart, and the lungs.[123]

Source: Modified from Gregus and Klaassen.[89]

be observed from outside the cell. Ultimately, the cellular particles are phagocytized by the surrounding cells without any inflammatory process. This is one of the characteristic morphological differences between necrotic and apoptotic cell death: whereas inflammation is typical for necrosis, lack of inflammation is the hallmark of apoptosis.[89,91] See Table 5.10 for features of apoptosis. Table 5.11 lists events important for necrosis.

Exposure to chemical compounds such as some heavy metals (e.g., lead) may activate apoptosis in a non-physiological way, leading to organ injury

TABLE 5.11 Agents Causing Sustained Elevation of Cytosolic Ca^{2+} and/or Impaired Synthesis of ATP

A. Agents inducing Ca^{2+} influx into the cytoplasm
   I. Via ligand-gated channels in neurons:
      1. Glutamate receptor agonists ("excitotoxins"): glutamate, kainate, domoate
      2. "Capsaicin receptor" agonists: capsaicin, resiniferatoxin
   II. Via voltage-gated channels: maitotoxin (?) $OH^{\bullet}$
   III. Via "newly formed pores": maitotoxin, amphotericin B, chlordecone, methylmercury alkyltins
   IV. Across disrupted cell membrane:
      1. Detergents: exogenous detergents, lysophospholipids, free fatty acids
      2. Hydrolytic enzymes: phospholipases in snake venoms, endogenous phospholipase A_2
      3. Lipid peroxidants: carbon tetrachloride
      4. Cytoskeletal toxins (by inducing membrane blebbing): cytochalasins, phalloidin
   V. From mitochondria: see D

B. Agents inhibiting Ca^{2+} export from the cytoplasm (inhibitors of Ca^{2+}-ATPase in cell membrane and/or endoplasmic reticulum)
   I. Covalent binders: acetaminophen, bromobenzene, CCl_4, chloroform, DCE
   II. Thiol oxidants: cystamine (mixed disulfide formation), diamide, *t*-BHP, menadione, diquat
   III. Others: vanadate

C. Agents impairing mitochondrial ATP synthesis

D. Agents causing hydrolysis of $NAD(P)^+$ in mitochondria
   I. By increasing $NAD(P)^+$ availability via oxidation of NAD(P)H
      1. Directly: alloxan
      2. Enzymatically: *t*-BHP, NAPBQI, divicine, fatty acid hydroperoxides, menadione, MPP^+
   II. By activation of "NAD-glycohydrolase": phenylarsine oxide, gliotoxin, $NO^{\bullet}$

DCE = 1,1-dichloroethylene; *t*-BHP = *t*-butyl hydroperoxide; MPP^+ = 1-methyl-4-phenylpyridinium; NAPBQI = *N*-acetyl-*p*-benzoquinoneimine.
Source: Modified from Gregus and Klaassen.[89]

and reduced functional capacity of the organ. It is noteworthy that effects of various oxidants, such as quinones, can vary as a function of dose: at low doses they may induce cellular proliferation, at moderate doses apoptosis, and at high doses they induce necrosis. Thus again dose is the ultimate determinant of the effect, even when very basic cellular responses such as death or survival are involved.[124]

Binding to Cellular Macromolecules

Many chemical compounds induce their toxic effect by binding to the active site of an enzyme or to other proteins that are vital for cellular functions. As described above, hydrogen sulfide and cyanide bind to the Fe^{3+} of cytochrome oxidase whereas carbon monoxide binds to the Fe^{2+} of hemoglobin.[89] Consequently, cyanide prevents a cell from utilizing oxygen even if it would be available and carboxyhemoglobin formation during CO exposure inhibits the access of cells to oxygen and thereby terminates oxidative metabolism inside the cells. Lead, mercury, and cadmium bind to SH-groups of proteins and thereby inhibit their functions.[89,125] A classic example of fatal enzyme inhibition is the covalent binding of organophosphate insecticides, such as the activated form of parathion, paraoxon, to the acetycholinesterase enzyme. This leads to accumulation of acetylcholine in the central nervous system, endocrine glands, smooth muscle, and other organs. This, in turn, leads to clinical signs such as breathing difficulties, excessive salivation, tremors, convulsions, and even death.[126,127] The mechanism of this enzyme inhibition is illustrated in Fig. 5.46.

Covalent binding of chemicals to biological macromolecules can also cause toxicity. During biotransformation and metabolic activation, chemical compounds can be changed to free radicals, which have an unpaired

Organophosphate

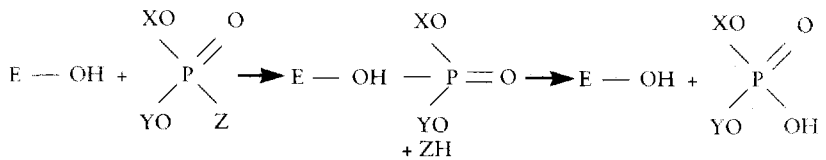

Carbamate

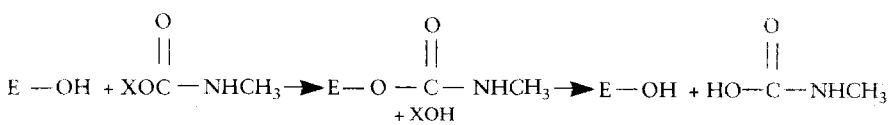

FIGURE 5.46 Interaction of the serine hydroxyl residue in the catalytically active site of acetylcholinesterase enzyme with esters of organophosphates or carbamates. The interaction leads to binding of the chemical with the enzyme, inhibition of the enzyme, inhibition of acetylcholine hydrolysis, and thus accumulation of acetylcholine in the synapses.

electron. These are extremely reactive, and readily react with cellular lipids, causing lipid peroxidation, where polyunsaturated fatty acids are converted to lipid peroxyradicals that are further changed to lipid hydroxy-peroxides. These are then the source for lipid peroxides. This is a typical chain reaction that continues until it is stopped by antioxidants.[128] If there is a shortage of antioxidants in the cell e.g., due to oxidative stress that has depleted GSH, the end result may be cell death. Thus, intracellular thiols, especially glutathione, are extremely important in preventing radical-induced cellular injuries.[128] Figure 5.47 depicts the role of glutathione in the protection of cells against attack by electrophiles, oxidants, and reactive oxygen species.[64]

Nucleic acids in the DNA contain a high number of nucleophilic sites that can be attacked by electrophilic intermediates (metabolites) of chemical compounds. DNA adducts formed may cause alterations in the expression of a critical gene in the cell and thus lead to cell death. For example, modification of p53 tumor suppressor gene may inactivate the functions of the p53 protein and render cells sensitive to malignant transformation. Also, formation of RNA adducts may inhibit key cellular events because RNA is essential for protein synthesis.

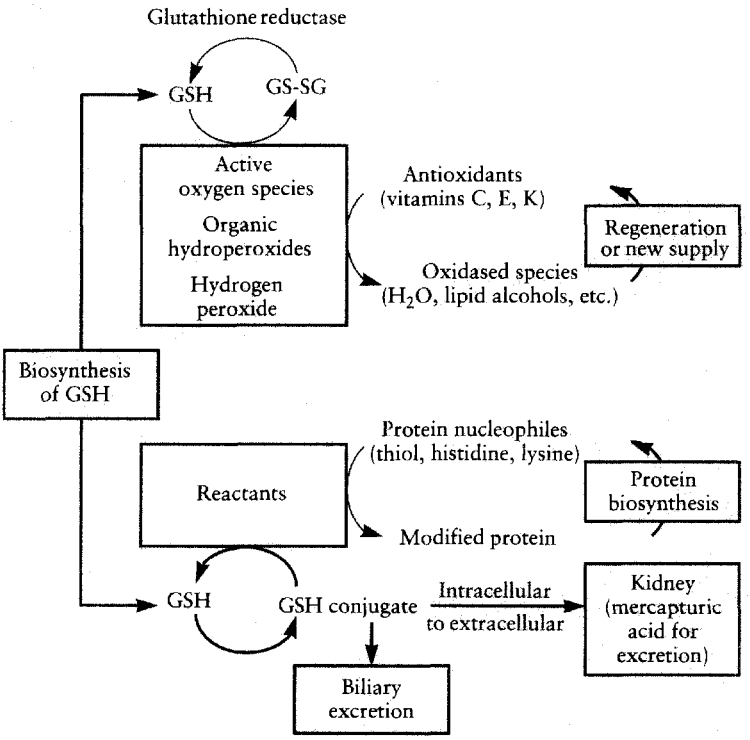

FIGURE 5.47 The role of glutathione and metabolic pathways involved in the protection of tissues against intoxication by electrophiles, oxidants and active oxygen species.[65] (Used with permission.)

Genetic Damage

A genetic injury often leads to the formation of inactive protein or inhibition of synthesis of a certain protein. There are endless possibilities for such interactions between DNA and chemical compounds because each human cell contains about 100 000 genes. Genetic damage leads to an inheritable injury only when it occurs in a germ cell that is involved in fertilization and development of a new organism. Genetic damage in a somatic cell may lead to a deleterious effect in an individual since it can ultimately lead to a toxic end result such as cancer.

Most of the compounds that induce alterations in genetic material, i.e., mutagens, also induce cancer, i.e., they are also carcinogens. For this reason, mutagenicity tests have been widely used to predict carcinogenicity. They are also used for biological monitoring of exposed workers to identify early damage to the genetic material in human cells. It has to be noted, however, that recently mutagenic tests have been heavily criticized for a number of reasons, and a positive result in a single mutagenic test can never be considered as a clear indication of carcinogenicity or even mutagenicity. Instead, a combination of several mutagenicity tests all producing positive results is clearly a cause for concern.[129]

Genetic damage can take place at the level of the chromosome or at the gene level. In addition, chemicals can also induce alterations in the number of chromosomes in the cells. Aneuploidy is an excess or a shortage of a single chromosome. Polyploidia is an excess of a whole set of chromosomes in the cell.

Chromosomal aberrations represent damage to the chromosomal structure that can be detected microscopically. The most frequent chromosomal aberrations are deletion (lack of a chromosome or its part), duplication (part of a chromosome has been duplicated), inversion (parts of a chromosome have changed place within that particular chromosome), and translocation (parts of chromosomes have changed their position between two chromosomes). Many of these chromosomal changes are transferred to sister cells when the cell divides, and become, therefore, stable chromosomal aberrations. Cytostatic drugs and cigarette smoke are examples of chemical exposures known to induce chromosomal aberrations. Chromosomal aberrations themselves do not, however, give any clue of the causative agents for the changes.[129]

Genotoxic compounds can induce a number of different mutations. A gene or a part of a gene can be missing (deletion), additional genetic material may become added to a gene (insertion), a gene may be amplified (amplification), or a genetic change may concern only one nucleotide, a basic structural unit of nucleic acid. The latter change causes deletion of one single amino acid in a protein encoded by the gene, and may lead to inactivation of a protein. The result is a frame-shift mutation if a number of nucleotides (usually one or two) upset the regular arrangement of the three nucleotide-code. This kind of change alters the amino acids throughout the protein because each amino acid has its own code consisting of three nucleotides. A number of chemical compounds bind to DNA, and may cause point mutations. Ionizing radiation-induced DNA damage typically causes deletions. Table 5.12 lists the principal assays used in genetic toxicology.[130]

TABLE 5.12 Principal Assays in Genetic Toxicology

I. Pivotal assays
  A. An assay for gene mutations
    Salmonella/mammalian microsome assay (Ames test)
  B. A mammalian assay for chromosome damage in vivo
    Metaphase analysis or micronucleus assay in rodent bone marrow
II. Other assays offering an extensive database or unique endpoint
  A. Assays for gene mutations
    E. coli WP2 trytophan reversion assay
    TK or HPRT forward mutation assays in cultured mammalian cells
    Drosophila sex-linked recessive lethal assay
  B. Cytogenetic analysis in cultured Chinese hamster or human cells
    Assays for chromosome aberrations and micronuclei
    Assays for aneuploidy
  C. Other indicators of genetic damage
    Assay for mitotic recombinarion in yeast and *Drosophila*
    Assay for unscheduled DNA synthesis in cultured hepatocytes and rodents
  D. Mammalian germ cell assays
    Mouse visible or electrophoretic specific-locus tests
    Assays for skeletal and cataract mutations
    Cytogenetic analysis and heritable translocation assays
    DNA damage and repair in rodent germ cells
    Dominant lethal assay

Source: Modified from Hoffmann.[130]

5.3.4.4 Target Organs

Organs as Targets of Chemical Compounds

Blood acts as the transport system for distribution of absorbed substances throughout the body. The distribution is often uneven. Adverse responses may occur if the concentration exceeds a critical concentration in the target organ. As stated previously, the target organ is not necessarily the same as the organ with the largest accumulation of the substance. Many compounds are stored in the skeleton and fatty tissue but critical effects usually occur in other organs. Lipophilic organic materials are deposited in fatty tissue, whereas some inorganic materials accumulate in the bones due to their resemblance to calcium (e.g., lead) or their ability to bind with calcium (e.g., fluoride).[131,132]

Water-soluble compounds are naturally easily transported in the blood. Non-soluble compounds are usually transported bound to plasma proteins (albumins). This binding is reversible in most cases but may vary remarkably. The degree of protein binding may vary between 50% and 99%. The proportion of the free (unbound) compound in the circulation is the amount of the compound that can reach the tissues and thus the target organs. Very lipid-

soluble compounds are also easily transported in the blood, mainly bound to lipoproteins. They move freely from the circulation to the organs depending on the lipid content of various organs. Thus, at equilibrium, organs such as the brain and other lipid-containing organs have the highest concentration of the agent at equilibrium. Typical examples of very lipid-soluble components are aromatic solvents such as benzene, xylenes, toluene, styrene, and ethylbenzene. Also, chlorinated hydrocarbons such as tri- and tetrachloroethylene belong to this category.[2,68]

The reactivity of a compound greatly affects its distribution and, therefore, the potential target organs. For example, formaldehyde is a very reactive and irritating gas. Because of its reactivity, inhaled formaldehyde binds with mucus and proteins in the nasal and oral cavities and perhaps in the upper respiratory tract, but it does not reach the alveolar region or the systemic circulation through inhalational exposure. For this reason, the most serious health effects of formaldehyde, notably cancer, are only seen in the upper respiratory tract. In fact, a considerable amount of formaldehyde is being formed endogenously in normal metabolism. However, it does not cause any harm under these conditions because it is tightly bound to serum proteins. Thus, harmful reactions of formaldehyde with macromolecules such as DNA only occur in very limited areas in the body. Due to its reactivity, formaldehyde also readily forms protein adducts which in some cases can be used for biomonitoring of formaldehyde exposure.[129]

Toxicity to the Central and Peripheral Nervous Systems

The nervous system consists of two main categories of cells: neurons and glial cells. Neurons are the actual nerve cells, which are responsible for transmitting information. There are fewer nerve cells than glial cells present in the brain. Glial cells play a variety of supportive functions. The brain and spinal cord form the central nervous system (CNS). Most parts of the CNS are isolated from other parts of the body by the blood-brain barrier, which is a functional rather than a morphological entity that consists of tightly connected cell membranes. Some substances, however, pass through the blood-brain barrier due to their lipophilicity. In addition, there are active transport mechanisms for hydrophilic nutrients and minerals which are vital for CNS function. Some toxic compounds can use these mechanisms to cross the barrier. The remaining parts of the nervous system are called the peripheral nervous system (PNS). The PNS can be considered, in fact, as an extension of the CNS.[133–135]

Neurons have three parts: the cell body and dendrites, the axon, and axon terminals. The cell body contains the nucleus and the organelles needed for metabolism, growth, and repair. The dendrites are branched extensions of the cell body membrane. The axon is a long, thin structure which transfers electrical impulses down to the terminals. The axon divides into numerous axon terminals and it is in this specialized region that neurotransmitters are released to transmit information from one neuron to its neighbors. The synapse has been defined as the space between two subsequent interrelated neurons.[107]

The glial cells support the neurons physically. Certain glial cells (oligodendroglial cells) synthesize myelin, a fatty insulation layer wrapped around the axons. Myelin is necessary for the so-called saltatory conduction of electrical

impulses. The myelin layer is not continuous but has breaks called the nodes of Ranvier. Action potentials occur only at those nonprotected nodes where they "jump" (the Latin verb *saltare* means "jump") from one node to the next. The glial cells also have various maintenance functions (e.g., maintaining ionic equilibrium).[136,137]

The nervous system is vulnerable to attack from several directions. Neurons do not divide, and, therefore, death of a neuron always causes a permanent loss of a cell. The brain has a high demand for oxygen. Lack of oxygen (hypoxia) rapidly causes brain damage. This manifests itself both on neurons and oligodendroglial cells. Anoxic brain damage may result from acute carbon monoxide, cyanide, and hydrogen sulfide poisonings. Carbon monoxide may also be formed in situ in the metabolism of dichloromethylene.[107,138]

Organic solvents have acute narcotic effects. Aromatic and chlorinated hydrocarbons seem to be especially effective. As stated, the combined effect of several organic solvents is usually considered to be additive. However, there is some evidence that the combined effect may in fact be synergistic. The symptoms caused by organic solvents, often called prenarcotic symptoms, resemble those caused by the use of alcohol. A decrease in reaction time and impairment in various psychological performances can be observed. Acute neurotoxicity can also be detected as abnormalities in the electroencephalogram (EEG), which records the electrical activity of the brain.[107]

Chronic neurotoxic effects can be divided into four groups. Neuronopathy, where the whole neuron is destroyed, is the most dramatic of these four. In axonopathy, the axon partly degenerates. The damage usually begins from a certain site and progresses towards the terminal. One can imagine it as a break in the axon. Carbon disulfide and n-hexane are examples of chemicals causing this kind of damage. The toxic effect results in reactions with the amino groups in proteins. In the case of n-hexane, the toxic compound (2,5-hexadione) is formed via oxidative metabolism. The reactions cause precipitations of neurofilaments in the axons which hinder its transport capabilities. The sensomotoric neuropathy caused by n-hexane exposure appears in extremities as numbness, weakness, and muscle pain. Myelinopathy slows the velocity of nerve conduction. The damage cannot be easily rectified in the CNS. Demyelination may also occur in the PNS. Lead is the most common agent causing myelinopathy.[107,139]

Eye Toxicity

Vision is vital for human activities, and eyes are very sensitive to a number of toxic insults induced by chemical compounds. The most serious outcome is permanent eye damage which may be so severe as to cause loss of vision. The eye consists of the cornea and conjunctiva, the choroid, the iris, and the ciliary body. It also contains the retina, which is of neural origin, and the optic nerve. The retina contains photoreceptors, a highly specific light-sensitive type of neural tissue. The eye also contains the lens and a small cerebrospinal fluid system, the aqueous humor system, that is important for the maintenance of the steady state of hydration of the lens and thus the transparency of the eye.[140]

The cornea must be transparent to allow normal function of the eye. Therefore even a tiny degree of scar formation, commonly induced by exposure

to acids or alkalies, in the cornea may seriously damage the visual system. Acid and alkali burns of the eye have to be washed immediately for at least 30 min with water.[41]

A special feature of the iris is its autonomic innervation. Sympathetic activation widens the aperture of the iris whereas impulses from the parasympathetic nervous system decrease the aperture size. Therefore adrenergic agonists and anticholinergic compounds both increase the aperture of the iris, i.e., cause mydriasis, and antiadrenergic and cholinergic agonists decrease it, i.e., cause miosis. The iris can thus be considered an excellent mirror reflecting the balance of the autonomic nervous system in the body.[140]

The eye has its own hydraulic system, and disturbances in it may cause serious damage to the eye. The normal eye pressure is 22 mm Hg, but when the pressure increases to 28–30 mm Hg, the optic nerve is squeezed and becomes hypoxic. This increase in the eye pressure may be due to acids or alkali causing inflammation in the anterior chamber of the eye, blocking the outflow of aqueous humor back into the systemic circulation.

The lens is an avascular transparent tissue surrounded by an elastic, collagenous capsule. Disturbances in the normal metabolism of the lens and rupture of the lens alter its optical characteristics, and may cause cataract, i.e., reduced transparency of the lens. For example exposure to a herbicide, 2,4-dichlorophenol, may cause cataract.[99]

The retina is the part of the eye that belongs to the nervous system. Rods and cones are the photoreceptors of the retina that synapse with the cells in the bipolar layer in the retina, and these cells, in turn, make connections with ganglion cells. The metabolism of retina is very active and, therefore, the retina is sensitive to toxic insults. For example, natural retinols that were being used in skin therapies have provoked retinal damage, perhaps by replacing the retinoids of the photoreceptors. Hyperbaric oxygen can also cause serious retinal damage in immature newborn children that have had respiratory difficulties.[107,137]

Methanol intoxication can cause blindness due to damage to ganglion cells in the retina. The blindness results from the accumulation of formaldehyde and formic acid, which are metabolites of methanol. Chemical compounds can also damage the visual cortex, for example, visual damage was observed among the victims of organic mercury intoxication in Japan (the fishermen of Minamata Bay).[107,137]

Pulmonary Toxicity

The lungs are an important port of entry for toxic compounds into the body, and also an important target organ for chemical compounds. Gas exchange is the most important function of the lungs—oxygen enters the circulation through the lungs, and carbon dioxide and other products of metabolism are exhaled. In addition, the lungs are an important metabolizing organ. Lungs possess a number of non-specific defense systems, such as sneezing and coughing, active movement of the cilia of the pulmonary epithelial cells, and secretion of mucus in the airways. In addition, there are a number of specialized phagocytic cells such as neutrophils, eosinophils and macrophages, that destroy foreign particles through phagocytosis, i.e., they

first engulf the particles and then destroy them by bombarding them with proteolytic enzymes. The immunological system is responsible for providing specific responses against specific antigens.[4,41]

Inhaled gaseous compounds are absorbed in all parts of the respiratory system whereas particle size determines how deep into the airways the particles will be transported in the airstream. Shortness of breath is a typical sign of a chemical exposure that has affected the lungs, and it may be evoked through immunological mechanisms (e.g., formaldehyde, ethyleneoxide), or through toxic irritation (formaldehyde, isocyanates, sulfur dioxide, nitrogen dioxide, ozone). Frequently the mechanism depends on the concentration of the compound in the inhaled air. The accident in Bhopal, India, is an example of a poisoning epidemic that caused serious lung injuries. There, an explosion of a large container led to poisoning of thousands of individuals by methylisocyanate, and subsequently to blindness, serious lung injuries, and deaths in the exposed population.[41]

Acute Lung Toxicity Toxic compounds can induce acute deleterious effects in various parts of the airway. Irritating compounds may cause bronchoconstriction within the bronchial tree, edema of its mucous membranes, and increased secretion of mucus. In addition, ciliar activity may decrease in the bronchial and bronchiolar regions, and thereby prevent the clearance of mucus and foreign particles from the airway.[58,59,86]

Bronchoconstriction may take place without any cellular injury. For example, low concentrations of sulfur dioxide induce bronchoconstriction. Asthmatics are especially sensitive; a concentration of sulfur dioxide as low as 0.4 ppm may induce bronchoconstriction.[58,59] Cholinergic activation mediated via the vagal nerve is responsible for this reaction because it can be prevented with anticholinergic compounds.[74] An inflammatory reaction may also cause bronchoconstriction. Inflammatory mediators, such as metabolites of arachidonic acid released from the epithelial cells of the airways, may increase the extent of the bronchoconstriction. Epithelial cells also produce relaxing compounds that antagonize bronchoconstriction, but in inflammation, there is reduced production of these compounds (e.g., prostaglandin E_2). Also, exposure to inorganic particles may induce a dramatic acute inflammation in the lungs, leading to the excretion of a number of bioactive molecules from pulmonary phagocytic cells.

Compounds that induce bronchoconstriction include tobacco smoke, formaldehyde, and diethyl ether. Several other compounds, such as acidic fumes (e.g., sulfuric acid) and gases, such as ozone and nitrogen dioxide, as well as isocyanates, can cause bronchoconstriction. Also, cellular damage in the airways induces bronchoconstriction because of the release of vasoactive compounds. Frequently, different mechanisms work at the same time, provoking bronchoconstriction and increased secretion of mucus, both of which interfere with respiration.[58,59]

The alveolar surface is predominantly covered by alveolar type I cells. These cells are the primary targets of chemical compounds causing alveolar damage. Typically, alveolar type I cells are replaced by alveolar type II cells subsequent to alveolar damage induced by deep lung irritants (e.g., nitrogen dioxide and ozone).[74] On the other hand, when small particles reach the alveolar region, specialized phagocytes, mainly macrophages, phagocytize the particles and are then removed from the lungs by the mucociliary escalator in the trachea, or by the lym-

phatic system. Alternatively they may persist in the lungs.[58,59] When macrophages are phagocytizing the particles, they become activated and secrete large amounts of oxygen radicals. While the radicals may have no effect whatsoever on the particles, they may well damage the surrounding cells and tissues. It has been suggested that the mechanisms by which asbestos particles induce lung cancer and mesothelioma (a fatal cancer type in the pleura) may be associated with excessive production of reactive oxygen species by specialized phagocytes.[37] An important consequence of alveolar level damage is that it may sensitize the lungs to inflammation. Serious air pollution episodes are associated with increased incidence of lung inflammations, especially in the elderly.

Chronic Pulmonary Toxicity Chronic damage to the lungs may be due to several subsequent exposures or due to one large dose that markedly exceeds the capacity of pulmonary defense, clearance, and repair mechanisms. Chronic pulmonary toxicity includes emphysema, chronic bronchitis, asthma, lung fibrosis, and lung cancer. The single most important reason for chronic pulmonary toxicity is tobacco smoke, which induces all types of chronic pulmonary toxicity, with the exception of fibrosis.[141]

In developed countries, where the prevalence of chronic obstructive lung diseases has increased rapidly, the finger of suspicion is often pointed at the air quality, especially that in large cities.[41] In emphysema, the walls separating alveoli from each other disappear, and this reduces the surface area for gas exchange. Chronic bronchitis is characterized by persistent cough and increased mucus secretion. In asthma, the lungs become sensitive to bronchoconstriction induced by environmental agents. In addition, asthma also involves inflammation of the airways.[58,59]

Lung Cancer Lung cancer is one of the most common cancers. In many countries, lung cancer is the most common cancer among the male population, and its incidence among females has shown a dramatic and alarming increase. The incidence of lung cancer has always carried a strong association with smoking in the past, i.e., the latency period of lung cancer is about 20 years after the beginning of the exposure to tobacco smoke. In addition to tobacco smoke, many chemicals can increase the risk of lung cancer. These include asbestos, radon, nickel, chromium and beryllium. Asbestos and radon are considered to be the next most important factors after tobacco smoke causing lung cancer. Both also have a synergistic effect with smoking. The number of asbestos-related diseases has remained high (these include pleural diseases, asbestosis, and cancers), even though the use of asbestos has dramatically decreased and is now totally banned in many countries. This is due to the long latency period of asbestos-induced diseases.[41,58,59] Figure 5.48 provides epidemiological data on the relationship between smoking and lung cancer. See also Fig. 5.39 for the mechanism of asbestos toxicity.[64]

Cardiovascular Toxicity

Several chemical compounds can have an adverse effect on the heart and the vascular system. The effect may first appear as a transient change in the cardiac function. However, prolonged exposure increases the risk of permanent effects. Occasionally, functional effects such as cardiac arrhythmias may even lead to death. Furthermore, in many cases the effects of chemicals

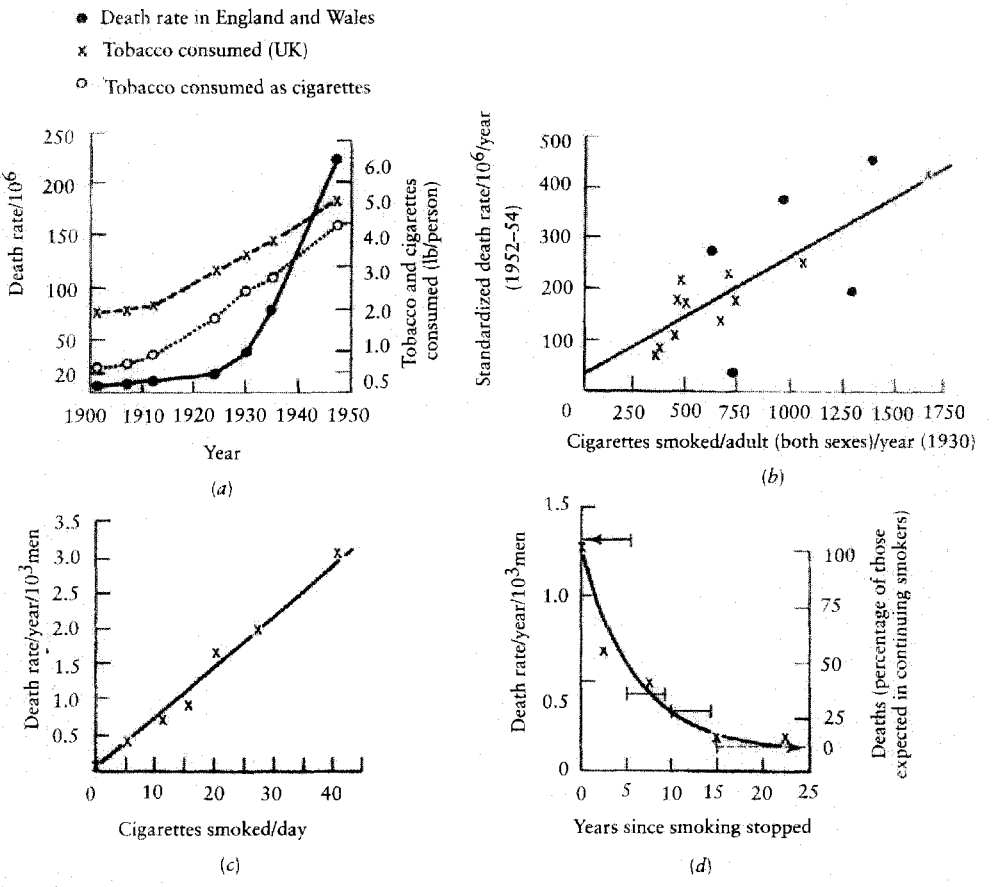

FIGURE 5.48 Epidemiological data defining the relationships between smoking of cigarettes and carcinoma of the lung. (*a*) Death rate from cancer of the lung and the rate of consumption of tobacco in the UK. The rates are based on three-year averages for all years except 1947. (*b*) Relationship between lung cancer mortality and previous cigarette consumption in sixteen countries. From left to right the solid dots below the line (lower incidence) are from Japan and USA and above the line (higher incidence) are from the Netherlands, Austria and England/Wales. (c) Death rate from lung cancer, standardized for age among doctors smoking different daily numbers of cigarettes. (*d*) Death from lung cancer among doctors who had given up smoking cigarettes for different periods (used with permission). |——| indicates data for <5, 5–9, 10–14, and >15 years since stopping smoking.[64,142–144] (Used with permission.)

on the cardiovascular system are secondary; i.e., a compound may affect lipid metabolism and thereby amplify atherosclerotic alterations in the circulatory system.

Mechanisms of Cardiotoxicity Chemical compounds often affect the cardiac conducting system and thereby change cardiac rhythm and force of contraction. These effects are seen as alterations in the heart rate, conduction velocity of impulses within the heart, and contractivity. For example, alterations of pH and changes in ionic balance affect these cardiac functions. In principle, cardiac toxicity can be expressed in three different ways: (1) pharmacological actions become amplified in an nonphysiological way; (2) reactive metabolites of chemical compounds react covalently with vital macromolecules

in myocytes (cardiac muscle cells) causing permanent functional and morphological alterations; and (3) the reaction is mediated through immunological mechanisms. Also, a reactive intermediate of allylamine, acrolein, may cause cardiac damage. When cardiac injury is mediated through immunological mechanisms, the reaction is usually due to the formation of a complex of the chemical compound with some protein, also termed a hapten.[145]

Mean arterial pressure and cardiac output, an expression of the amount of blood that the heart pumps each minute, are the key indicators of the normal functioning of the cardiovascular system. Mean arterial pressure is strictly controlled, but by changing the cardiac output, a person can adapt, e.g., to increased oxygen requirement due to increased workload. Blood flow in vital organs may vary for many reasons, but is usually due to decreased cardiac output. However, there can be very dramatic changes in blood pressure, e.g., blood pressure plummets during an anaphylactic allergic reaction. Also cytotoxic chemicals, such as heavy metals, may decrease the blood pressure.

Compounds Causing Cardiovascular Toxicity Alcohols are the most important compounds causing vascular toxicity. Ethanol depresses cardiac muscle and attenuates its contractivity when the concentration of ethanol in the blood exceeds 0.75 mg/100 mL. Ethanol also causes arrhythmias, and a metabolite of ethanol, acetaldehyde, also depresses the heart. Furthermore, high concentrations of acetaldehyde cause cardiac arrhythmias. The cardiovascular toxicity of methanol is about the same as that of ethanol, whereas alcohols with longer chains are more toxic than ethanol.

Halogenated hydrocarbons depress cardiac contractility, decrease heart rate, and inhibit conductivity in the cardiac conducting system. The cardiac toxicity of these compounds is related to the number of halogen atoms; it increases first as the number of halogen atoms increases, but decreases after achieving the maximum toxicity when four halogen atoms are present. Some of these compounds, e.g., chloroform, carbon tetrachloride, and trichloroethylene, sensitize the heart to catecholamines (adrenaline and noradrenaline) and thus increase the risk of cardiac arrhythmia.

Some metals, such as cadmium, cobalt, and lead, are selectively cardiotoxic. They depress contractivity and slow down conduction in the cardiac system. They may also cause morphological alterations, e.g., cobalt, which was once used to prevent excessive foam formation in beers, caused cardiomyopathy among heavy beer drinkers. Some of the metals also block ion channels in myocytes. Manganese and nickel block calcium channels, whereas barium is a strong inducer of cardiac arrhythmia.

Several chemical compounds may cause inflammation or constriction of the blood vessel wall (vasoconstriction). Ergot alkaloids at high doses cause constriction and thickening of the vessel wall. Allylamine may also induce constriction of coronary arteries, thickening of their smooth muscle walls, and a disease state that corresponds to coronary heart disease. The culprit is a toxic reactive metabolite of allylamine, acrolein, that binds covalently to nucleophilic groups of proteins and nucleic acids in the cardiac myocytes.[145]

Atherosclerosis is a degenerative disease which is characterized by cholesterol-containing thickening of arterial walls. Saturated fatty acids, high levels of cholesterol, elevated blood pressure, and elevated serum lipoprotein are well-known risk

factors for atherosclerosis. Exposure to some chemical compounds, such as carbon disulfide (CS_2) and CO may promote the development of the disease.[36]

Liver Toxicity

The liver is the most important metabolizing organ in the body. It is largely responsible for the biotransformation of chemicals and drugs to water-soluble forms that can be excreted in the urine or bile. The functional unit of the liver is the triangular-shaped acinus, the tip of which is located between the terminal vein and adjacent portal arteries (see Fig. 5.49).[61] Liver damage may cause dramatic changes in the biotransformation of chemicals, and lead to alterations in metabolic pathways. Severe liver damage is characterized by fibrosis and scar formation and the loss of functional capacity of the organ. There are many chemical compounds capable of inducing liver damage.[147,148]

Yellow phosphorus was the first identified liver toxin. It causes accumulation of lipids in the liver. Several liver toxins such as chloroform, carbon tetrachloride, and bromobenzene have since been identified. The forms of acute liver toxicity are accumulation of lipids in the liver, hepatocellular necrosis, intrahepatic cholestasis, and a disease state that resembles viral hepatitis. The types of chronic hepatotoxicity are cirrhosis and liver cancer.

Acute Liver Damage Several compounds (e.g., dimethyl nitrosoamine, carbon tetrachloride, and thioacetamide) cause necrosis of hepatocytes by inhibiting protein synthesis at the translational level, i.e., by inhibiting the addition of new amino acids into the protein chain being synthetized. This is not, however, the only mechanism. Ethionine is a compound which inhibits protein synthesis but does not induce

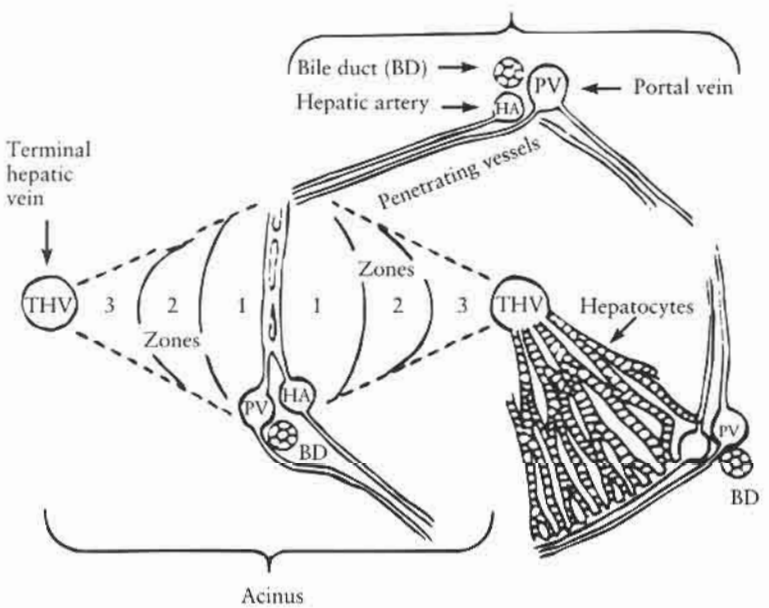

FIGURE 5.49 Schematic of liver operational units: the classic lobule and the acinus.[146] (See also Fig. 5.38.)(Used with permission.)

liver necrosis. Carbon tetrachloride, tetrachloroethylene, and yellow phosphorus induce lipid peroxidation, one common mechanism of liver necrosis. There are, however, a number of compounds (e.g., dimethyl nitrosoamine) that cause liver necrosis without causing lipid peroxidation. Recent findings suggest that neutrophil-mediated cytotoxicity may play a role in some forms of liver toxicity, perhaps due to inflammatory mediators or reactive oxygen species excreted by these inflammatory cells.[147,148]

Accumulation of lipids in the liver (steatosis) is one possible mechanism for liver toxicity. Several compounds causing necrosis of hepatocytes also cause steatosis. There are, however, some doubts that steatosis would be the primary cause of liver injury. Several compounds cause steatosis (e.g., puromycin, cycloheximide) without causing liver injury. Most of the accumulated lipids are triglycerides. In steatosis, the balance between the synthesis and excretion of these lipids has been disturbed (see Table 5.13).[147,148]

TABLE 5.13 Examples of Drugs that Induce Intrahepatic Cholestasis or Liver Damage Resembling That Induced by Viral Hepatitis

Intrahepatic cholestasis	Viral hepatitis–like liver damage
Amitriptyline	Ethacrynic acid
Azathioprine	Halothane
Carbamazepine	Indomethacin
Chlorodiazepoxide	Imipramine
Chlorpromazine	Iproniazid
Chlorthiazide	Carbamazepine
Diazepam	Alphamethyldopa
Erythromycin estholate	Nialamide
Estradiole	Phenylbutazone
Ethacrynic acid	Pyrazinamide
Fluphenazine	Sulphamethoxazole
Haloperidol	Isoniazid
Imipramine	
Mestranole	
17-methylnortestosterone	
Methyltestosterone	
Nitrofurantoin	
Noretandrolone	
Oxacillin	
Oxandrolone	
Penicillamine	
Perphenazine	
Perchloroperazine	
Promazine	
Thioridazine	
Tolbutamide	

Source: Modified from Savolainen and Vähäkangas.[151]

TABLE 5.14 Chemical Compounds that Induce Chronic Liver Damage

Chemical compound	Cirrhosis	Cancer*
Natural Compounds		
Aflatoxin**	x	x
Ethanol**	x	?
Pyrrolizidine alkaloids	?	x
Saffrole	?	x
Synthetic Compounds		
Anabolic androgens**	—	x
Dialkylnitroamines	?	x
Organochlorine pesticides	?	x
Polychlorinated hydrocarbons	?	x
Carbon tetrachloride	x	x
Chloroform	?	x
Vinyl chloride**	?	x
Dimethylaminobenzene	?	x
Acetylaminofluorene	?	x
Thioacetamide	?	x
Urethane	?	x
Ethiomine	?	x
Dimethylbenzanthrazene	?	x
Galactosamine	?	x

* In experimental animals
** Is also a human carcinogen
? Unknown
— Does not cause any effect
Source: Modified from Savolainen and Vähäkangas.[151]

Chronic Liver Damage Cirrhosis is one the main forms of chronic liver damage. Formation of a collagen network that destroys the typical liver structure is characteristic of cirrhosis. In cirrhosis, the blood circulation to the liver is severely disturbed because of altered liver morphology. The underlying mechanism of this disruption is most likely necrosis of individual hepatocytes leading to scar formation. The same compounds that induce liver cancer also induce liver cirrhosis. In humans, the most important compound causing liver cirrhosis is ethyl alcohol.[149,150] Table 5.14 lists chemical compounds that can induce acute liver damage.

Liver cancer can also be a consequence of exposure to hepatotoxic chemicals. Natural hepatocarcinogens include fungal aflatoxins. Synthetic hepatocarcinogens include nitrosoamines, certain chlorinated hydrocarbons, polychlorinated biphenyls (PCBs), chloroform, carbon tetrachloride, dimethylbenzanthracene, and vinyl chloride.[150] Table 5.15 lists the chemical compounds that induce liver cancer or cirrhosis in experimental animals or

TABLE 5.15 Chemical Compounds that Induce Acute Liver Damage

Chemical compound	Necrosis	Steatosis
Natural Compounds		
Aflatoxin**	x	x
Ethanol**	—	x
Pyrrolizidine alkaloids	x	x
Saffrole	?	?
Synthetic Compounds		
Anabolic androgens**	—	—
Dialkylnitroamines	x	x
Organochlorine pesticides	?	?
Polychlorinated hydrocarbons	?	?
Carbon tetrachloride	x	x
Chloroform	x	x
Vinyl chloride**	?	?
Dimethylaminobenzene	x	x
Acetylaminofluorene	?	?
Thioacetamide	x	—
Urethane	x	—
Ethiomine	—	x
Dimethylbenzanthrazene	?	?
Galactosamine	x	x

* In experimental animals
** Is also a human carcinogen
? Unknown
— Does not cause any effect
Source: Modified from Savolainen and Vähäkangas.[151]

humans. Humans are exposed to aflatoxins in hot and humid regions in Africa and Asia where peanuts and grain have to be stored in inappropriate conditions which favor the growth of fungi. In these regions, hepatitis is also common, and these two factors may, in fact, act synergistically to promote the formation of liver cancer.[5,150] Historically, workers involved in the production of polyvinylchloride (PVC) polymers (plastics, elastomers) were exposed to high concentrations of vinyl chloride. In these workers, the incidence of liver angiosarcoma increased dramatically, and the incidence of brain tumors has also been reported to be higher than the incidence in control workers.[36] Ethyl alcohol can increase the risk of liver carcinoma. It is not primarily considered a very potent liver carcinogen, but nonetheless is important because the doses of ethyl alcohol to which humans are exposed are so high.

Kidney Toxicity

The integrity of mammalian kidneys is vital to body homeostasis, because the kidneys play the principal role in the excretion of metabolic wastes and the regulation of extracellular fluid volume, electrolyte balance, and acid-base

balance. In addition, the kidney is responsible for the synthesis of a number of hormones that regulate several systemic metabolic events. These hormones include 1,25-dihydroxyvitamin D_3, erythropoietin, renin, and several vasoactive prostanoids and kinins. In addition to these physiologically important functions, the kidneys are also metabolically active organs that contribute to the biotransformation of xenobiotics.

The sensitivity of the kidneys to various toxic insults is due to large blood flow, ability to concentrate compounds to be excreted in the urine, and to metabolically activate xenobiotics. About 25% of cardiac output continuously flows through the kidneys even though the relative weight of the kidneys is only 0.5% of the human body mass. Due to the key role of the kidney in the excretion of metabolic wastes, it inevitably becomes exposed to high concentrations of metabolic endproducts. The primary urine filtrated in the glomeruli is concentrated 100-fold before its excretion. The amount of primary urine formed during a 24-hour period is about 100 L, and is being concentrated down to one liter. Therefore, the concentrations of several toxic compounds in the urine may become very high compared to their corresponding concentrations in the bloodstream. Furthermore, excretory and reabsorptive functions may expose kidney cells to high concentrations of harmful compounds.[148]

Alterations in the ability of the kidneys to excrete or reabsorb compounds from the proximal and distal tubules are immediately reflected in the amount of extracellular fluid in the mammalian organism. For example, reduced excretion in the glomeruli leads to increased volume of extracellular fluid, and this may contribute to cardiac insufficiency, in which the working capacity of the heart is exceeded. The kidneys are active metabolic organs; this ability has toxicological significance when it leads to the formation of toxic reactive metabolites that damage kidney cells.[147,148]

Mechanisms of Kidney Toxicity Alterations in the levels of free intracellular calcium in kidney cells are important in kidney toxicity caused by several chemical compounds since cell calcium participates in cell activation and the formation of reactive oxygen species that contribute to hypoxic cell injury.[89] Kidney injury may also be due to an indirect mechanism: long-term hypotension may be a reason for kidney injuries, e.g., due to reduced oxygen supply. Immunological mechanisms may also play a role in kidney injuries, and for example, metallothionein, a protein synthesized by the liver to complex heavy metals, may accumulate in the kidneys as a protein-metal complex and cause kidney injury. The primary goal of the protein is to protect the mammalian organism against metal toxicity, but excessive accumulation of the metal-metallothionein complex in the kidneys leads to cellular damage and impaired kidney function, e.g., reduced formation of urine. Also accumulation of calcium oxalate, which occurs after exposure to ethylene glycol, the parent compound of the oxalate, may induce kidney injury.[36]

Compounds that Cause Kidney Damage Several drugs and some anesthetic compounds such as methoxyflurane cause kidney damage when present at high doses. Kidney-toxic compounds found in occupational environments include mycotoxins, halogenated hydrocarbons, several metals, and solvents (see Table 5.16).

TABLE 5.16 Nephrotoxic Compounds in Occupational and General Environments

- Mycotoxins
  - Aflatoxin B
  - Ochratoxin A
  - Pyrrolizidine alkaloids
  - Rubratoxin B
- Volatile hydrocarbons
  - Gasoline
- Herbicides and Fungicides
  - Paraquat
  - Diquat
  - Succinimides
  - 2,4,5-trichlorophenoxyacetic acid
- Metals
  - Cadmium
  - Gold
  - Lead
  - Nickel
  - Mercury
  - Chromium
  - Uranium
- Organic solvents
  - Ethylene glycol
  - Diethylene glycol
  - Toluene
- Halogenated aliphatic hydrocarbons
  - Bromobenzene
  - Carbondichloride
  - Chlorofluoroethene
  - Dibromoethane
  - Hexachlorobutadiene
  - Trifluoroethene
  - Bromodichloromethane
  - Chloroform
  - Dibromochloropropane
  - Dichloroethene
  - Pentachlotoethene
  - Trichloroethene
- Other compounds
  - Benzidine
  - *p*-Aminophenol
  - Maleate

Source: Modified from Savolainen and Vähäkangas.[151]

Many metals are potent kidney toxins. These metals cause similar signs and symptoms. At low doses, the symptoms include leakage of sugars and amino acids into the urine due to glomerular damage and polyuria due to lack of concentrating capability of the kidney. Large doses cause cellular necrosis, anuria, increased concentrations of blood-urea-nitrogen, and subsequently the total breakdown of kidney function and ultimately death. In addition to direct cell injury, some metals induce vasoconstriction in the kidney. Metals such as nickel and cadmium strongly induce the synthesis of metal binding proteins in the liver, notably metallothionein.[152]

Halogenated hydrocarbons may cause kidney damage in addition to liver damage. A nephrotoxic dose of carbon tetrachloride increases the relative weight of the kidneys, induces swelling of tubular epithelium in the kidneys, and causes lipid degeneration, tubular casts, and necrosis of the epithelium of the proximal tubulus. Several other halogenated hydrocarbons, e.g., tri-and tetrachloroethylene, also induce this kind of kidney damage.[153]

Reproductive Toxicity

The reproductive system is a very complex, hormonally-controlled entity. The female endocrine system is more complex than that of the male, and toxic effects that are directed toward the female reproductive system are, therefore, more difficult to assess than those targeted at the male system. In addition, the effects of toxic compounds on the reproductive system clearly differ between females who are pregnant and those who are not, because pregnancy changes. female physiology and because the target of the toxic effects may also be the fetus. The effects of chemicals on the fetus will be discussed in the section on teratogenesis (see Section 5.3.4.5). The assessment of reproductive toxicity is further complicated by the fact that the timing of essential events, e.g., the process of organogenesis, is different in different species, and therefore extrapolating results obtained in animal experiments to predict the toxic effects of chemicals on human reproduction is problematic.

It needs to be noted that a toxic effect on the reproductive system may be mediated through alterations in normal functions of the central nervous system, gonads (ovaries, testicles), or on the pharmacokinetics of reproductive hormones.[98,154,155]

Compounds Affecting Reproduction Compounds that can affect reproductive function include several drugs and occupationally important chemicals such as solvents and pesticides as well as a number of environmentally relevant compounds. A group of chemical compounds that has received much attention recently is endocrine disruptors, many of which are halogenated hydrocarbons, e.g., PCBs. These are known to induce feminization in fish and other animal species.[98,156,157] There is intense debate about the significance of these compounds to human health. Tobacco smoke and ethyl alcohol also have major effects on human reproduction, the effects of alcohol being especially important. Table 5.17 lists compounds that may disturb the functions of female and male reproductive functions.

Toxicity to Blood and Blood-Forming Tissues

Blood-forming tissues consist of bone marrow, spleen, lymph nodes and the reticuloendothelial system. These produce the elements of blood and are important for the immunological defense systems.

TABLE 5.17 Examples of Chemical Compounds that Affect the Reproductive System

Females	Males
Environmental chemicals	Environmental chemicals
Aniline	Carbon disulfide
Benzene	Chlordecone
Ethylene oxide	Dibromochloropropane
Glycol ethers	Ethylene dibromide
Formaldehyde	Ethylene oxide
Inorganic and organic lead	Glycol ethers
Carbon disulfide	Hexane
Methyl mercury	Inorganic and organic lead
Pesticides (occupational exposure)	Pesticides (occupational exposure)
Phthalates	Vinyl chloride
Polychlorinated biphenyls	
Styrene	Drugs
Toluene	Steroids
Vinyl chloride	Cell cycle inhibitors
	Central nervous system drugs
Drugs	- Anesthetic gases
Anesthetic gases	- Levodopa
Steroids	- Opioids
Cell cycle inhibitors	- Tricyclic antidepressants
Opioids	Phenacetin
	Phenytoin
Social poisons	Thiazide diuretics
Tobacco smoke	
Alcohol	Social poisons
	Tobacco smoke
Narcotic drugs	Alcohol
Marijuana	Caffeine
Cocaine	Theobromine
Heroin	
	Narcotic drugs
	Marijuana
	Cocaine
	Heroin
	Physical factors
	Temperature
	Lightning
	Hypoxia
	Irradiation

Source: Modified from Savolainen and Vähäkangas.[151]

There are undifferentiated stem cells of the blood elements in the bone marrow that differentiate and mature into erythrocytes, (red blood cells), thrombocytes (platelets), and white blood cells (leukocytes and lymphocytes). The production of erythrocytes is regulated by a hormone, erythropoietin (see the section on kidney toxicity), that is synthetized and excreted by the kidney. An increase in the number of premature erythrocytes is an indication of stimulation of erythropoiesis, i.e., increased production of erythrocytes in anemia due to continuous bleeding.

Toxic Effects on the Blood-Forming Tissues Reduced formation of erythrocytes and other elements of blood is an indication of damage to the bone marrow. Chemical compounds toxic to the bone marrow may cause pancytopenia, in which the levels of all elements of blood are reduced. Ionizing radiation, benzene, lindane, chlordane, arsenic, chloramphenicol, trinitrotoluene, gold salts, and phenylbutazone all induce pancytopenia. If the damage to the bone marrow is so severe that the production of blood elements is totally inhibited, the disease state is termed aplastic anemia. In the occupational environment, high concentrations of benzene can cause aplastic anemia.[158]

Platelets are essential as the first line of defense in clot formation to stop bleeding. Platelets gather quickly around the damaged vessel wall and clump together with fibrin filaments to form a clot that prevents bleeding. Platelets also become activated by exposure to adrenaline, thrombin, and collagen. Drugs and chemicals that disturb normal functioning of the bone marrow also decrease the number of circulating platelets, a state termed thrombocytopenia. Vinyl chloride is an example of a chemical which may cause this kind of disturbance.

Specialized phagocytes (i.e., actively phagocytizing cells of the immune system) include granulocytes (neutrophils, eosinophils, and basophils), monocytes, and macrophages, which often originate from circulating monocytes. Many environmental factors may decrease the number of these cells. Ionizing radiation and several drugs may cause granulocytopenia. Erythrocytes can be degraded if they are exposed to chemical compounds, the end result being hemolytic anemia. Hemolytic anemia reduces the capacity of blood to carry oxygen, and thereby prevents oxygenation of various tissues, especially the central nervous system and the heart, organs that are particularly sensitive due to their large oxygen need. Aniline and nitrobenzene cause hemolytic anemia, and several other nitrocompounds also induce this effect. Phenols and propylene glycol are also capable of inducing hemolytic anemia.[158,159]

Toxicity to the Skin

The skin is the largest organ in the human being. In particular, the surface layer of the outer epidermis, the stratum corneum, usually provides quite good protection against chemical compounds. Nevertheless, the skin is an important entry route for chemical compounds into the body.

Skin has several protective mechanisms in addition to its thick epidermis that prevent many chemical compounds from penetrating it. Eccrine (sweat)

glands, phagocytic cells, skin metabolism, and melanin pigmentation (which protects the skin from ultraviolet irradiation from the sun) belong to the battery of the dermal defense systems. However, skin is exposed to many chemical compounds. Skin diseases account for a considerable percentage of all occupational diseases (20% in Finland). Among exposure-induced skin diseases, inflammations due to both irritation and sensitization are common.

Assessment of skin exposure continues to be relatively difficult because it is difficult to measure or estimate the dose actually absorbed by the skin.

Toxic Reactions of the Skin Irritation is the most common reaction of the skin. Skin irritation is usually a local inflammatory reaction. The most common skin irritants are solvents; dehydrating, oxidizing, or reducing compounds; and cosmetic compounds.[160] Acids and alkalies are common irritants. Irritation reactions can be divided into acute irritation and corrosion. Necrosis of the surface of the skin is typical for corrosion. Acids and alkalies also cause chemical burns. Phenols, organotin compounds, hydrogen fluoride, and yellow phosphorus may cause serious burns.[161] Phenol also causes local anesthesia, in fact it has been used as a local anesthetic in minor ear operations such as puncture of the tympanous membrane in cases of otitis.[36]

The common skin reaction allergic contact dermatitis is evoked subsequent to exposure to a chemical compound via a cell-mediated type IV allergic reaction. Allergic contact dermatitis is also a common skin disease in the occupational environment. The reaction is compound-specific and re-exposure to very small amounts of chemical compounds provoke a severe reaction. Skin allergens often have small molecular size and are frequently haptens that become bound to a protein and in that way induce an immunological reaction. Many chemical compounds can induce allergic contact dermatitis (see Table 5.18).[161] Especially important inducers of allergic contact dermatitis are metals (nickel) and metallic compounds (cobalt, chromium, and nickel salts as well as organic mercurial compounds). Also several cosmetic products, resins, a number of colors, rubber (latex) and leather additives, and pesticides (fungicides such as thiurams and dithiocarbamates) are skin allergens. Compounds that belong to the same group of chemical compounds may cross-sensitize sensitive individuals. Thiurams and dithiocarbamates are good examples of this: if you are sensitive to one compound in this group you are allergic to all members of this group of chemicals.[162,163] Table 5.19 lists common cross-reacting chemicals.[161]

Light and Toxic Reactions In many individuals, exposure to ultraviolet radiation from the sun causes skin reactions such as erythema, thickening of the epidermis, and darkening of existing pigment. Exposure to ultraviolet light also increases the risk of different forms of skin cancers, especially malignant melanoma.[161]

Chemical Acne Many chemical compounds induce skin lesions that are similar to acne. Oils, tar, creosote, and several cosmetic products induce chemical acne. These compounds induce keratinization of the sebaceous glands of the skin, obstruction of the glands, and formation of acne. Chloracne is a specific skin lesion that is induced by chemical compounds that are structurally similar to 2,3,7,8-tetrachloro dibenzo-p-dioxin (TCDD). Chloracne is slow to heal and difficult to

TABLE 5.18 Common Contact Allergens

Source	Common allergens	Source
Topical medications/ Hygiene products	Antibiotics	Therapeutics
	Bacitracin	Benzocaine
	Neomycin	Fluorouracil
	Polymyxin	Idoxuridine
	Aminoglycosides	α-Tocopherol (vitamin E)
	Sulfonamides	Corticosteroids
	Preservatives	Others
	Benzalkonium chloride	Cinnamic aldehyde
	Formaldehyde	Ethylenediamine
	Formaldehyde releasers	Lanolin
	Quaternium 15	*p*-Phenylenediamine
	Imidazolidinyl urea	Propylene glycol
	Diazolidinyl urea	Benzophenones
	DMDM Hydantoin	Fragrances
	Methylchloroisothiazolone	Thioglycolates
Plants and trees	Abietic acid	Pentadecylcatechols
	Balsam of Peru	Sesquiterpene lactone
	Rosin (colophony)	Tuliposide A
Antiseptics	Chloramine	Glutaraldehyde
	Chlorohexidine	Hexachlorophene
	Chloroxylenol	Thimerosal (Merthiolate)
	Dichlorophene	Mercurials
	Dodecylaminoethyl glycine HCl	Triphenylmethane dyes
Rubber products	Diphenylguanidine	Resorcinol monobenzoate
	Hydroguinone	Benzothiazolesulfenamides
	Mercaptobenzothiazole	Dithiocarbamates
	p-Phenylenediamine	Thiurams
Leather	Formaldehyde	Potassium dichromate
	Glutaraldehyde	
Paper products	Abietic acid	Rosin (colophony)
	Formaldehyde	Triphenyl phosphate
	Nigrosine	Dyes
Glues and bonding agents	Bisphenol A	Epoxy resins
	Epichlorohydrin	*p*-(*t*-butyl)formaldehyde resin
	Formaldehyde	Toluene sulfonamide resins
	Acrylic monomers	Urea formaldehyde resins
	Cyanoacrylates	
Metals	Chromium	Mercury
	Cobalt	Nickel

Source: Modified from Rice and Cohen.[161]

TABLE 5.19 Common Cross-Reacting Chemicals

Chemical	Cross-Reactor
Abietic acid	Pine resin (colophony)
Balsam of Peru	Pine resin, cinnamates, benzoates
Bisphenol A	Diethylstilbestrol, hydroquinone monobenzyl ether
Canaga oil	Benzyl salicylate
Chlorocresol	Chloroxylenol
Diazolidinyl urea	Imidazolidinyl urea, formaldehyde
Ethylenediamine di-HCl	Aminophylline, piperazine
Formaldehyde	Arylsulfonamide resin, chloroallyl-hexaminium chloride
Hydroquinone	Resorcinol
Methyl hydroxybenzoate	Parabens, hydroquinone monobenzyl ether
p-Aminobenzoic acid	*p*-Aminosalicylic acid, sulfonamide
Phenylenediamine	Parabens, *p*-aminobenzoic acid
Propyl hydroxybenzoate	Hydroquinone monobenzyl ether
Phenol	Resorcinol, cresols, hydroquinone
Tetramethylthiuram disulfide	Tetraethylthiuram mono- and disulfide

Source: Modified from Rice and Cohen.[161]

treat. Chloracne is characterized by hyperplasia of the epithelial cells of the sebaceous glands associated with inflammatory skin changes typical of acne.[164]

TCDD is the most potent inducer of chloracne. This has been well known since the accident in Seveso, Italy, in 1976 in which large amounts of TCDD were distributed in the environment subsequent to an explosion in a factory that produced a chlorophenoxy herbicide, 2,4,5-T. TCDD is an impurity produced during the production of 2,4,5-T. The most common long-term effect of TCDD exposure was chloracne. Exposed individuals also suffered increased excretion of porphyrins, hyper-pigmentation, central nervous system effects, and liver damage and increased risk of cancer was a long-term consequence of the exposure. In addition to TCDD, polychlorinated biphenyls (PCBs), polychlorinated dibenzofurans, and polychloronaphthalens cause chloracne as well as other effects typical of TCDD.[51,150,165]

Allergies

Allergies are diseases in which immune responses to antigens, compounds which otherwise would be innocuous, cause inflammation. The immune response occurs in two stages. First, the person becomes sensitized to an antigen. He or she will remain asymptomatic until there is a new exposure, which will provoke an inflammatory response. Hypersensitivity is often used as a synonym for allergy. Allergic disease can be classified according to the immunologic mechanism provoking it. Traditionally, a classification into four types is used, as first presented by Gell and Coombs.[166]

Type I allergies are mediated by immunoglobulin E (IgE). Unlike the other immunoglobulins (G,M,A, and D), which are part of the essential defense

mechanisms against foreign proteins, IgE is an antibody type that has virtually only adverse effects. Often allergy is defined to include only type I reactions. The symptoms due to IgE-mediated responses depend on the exposure route. In occupational environments, inhalation is usually the most important route and allergic rhinitis and asthma are common occupational diseases. Atopic dermatitis also belongs to this allergy type. The individual susceptibility for this kind of reaction varies considerably. Those persons who inherently are sensitive are called atopics. The allergens are usually proteins or glycoproteins with molecular weights ranging from 10 to 40 kDa. Common allergen sources include pollen, mites, molds, and animal dander.[120]

Sensitization is a consequence of a complex chain of events which includes presentation of the allergen by antigen-presenting cells (APC) to naive (Th0) lymphocytes, which then differentiate into Th2 lymphocytes. These lymphocytes then release a barrage of cytokines (particularly IL-4) that cause B lymphocytes (B cells) to differentiate into specialized plasma cells which secrete IgE antibodies (cytokines are chemical mediators, small soluble proteins that affect the specific receptors of other cells initiating and maintaining many biological processes). Circulating IgE binds to the receptors on the surfaces of mast cells (located mainly in the mucosal and epithelial tissues).[89,120]

When exposure is repeated, the allergen binds between two adjacent IgE molecules. This causes release of inflammatory mediators (histamine, leukotrienes, chemotactic factors). These act locally and cause smooth muscle contraction, increased vascular permeability, mucous gland secretion, and infiltration of inflammatory cells (neutrophils and eosinophils). However, histamine can also be released by non-IgE-mediated mechanisms (e.g., due to exposure to certain fungi).[162,163]

In addition to the proteins discussed above, a large number of reactive chemicals used in industry can cause asthma and rhinitis. Hypersensitivity pneumonias have also been described. Isocyanates and acid anhydrides are industrial chemicals that cause occupational asthma. Acid anhydrides, such as phthalic anhydride, seem to cause mainly type I reactions, whereas the IgE-mediated mechanism explains only a part of the sensitizations to isocyanates. Several mechanisms have been suggested, but despite intensive research no models have been generally accepted. The situation is even more obscure for other sensitizing chemicals; therefore, the term specific chemical hypersensitivity is often used for chemical allergies. This term should not be confused with multiple chemical sensitivity (MCS) syndrome, which is a controversial term referring to hypersusceptibility to very low levels of environmental chemicals.[120]

Type II reactions include cytotoxic reactions in which the antigen binds to the surface of certain cells (e.g., red blood cells) and B cells then produce IgG antibodies against these cells, which results in cytotoxic injury mediated by complement (a group of blood plasma proteins acting together) activation and an influx of inflammatory cells. For example, some drug allergies are caused by this mechanism. However, this is not an important mechanism in occupational allergies.[120]

In type III or immunocomplex-mediated allergy, IgG antibodies form complexes with antigen. At low exposures, the body is able to remove these complexes, but if there is a severe exposure, immunocomplexes release a variety of proinflammatory cytokines. The involvement of this mechanism is clearest in serum sickness. This mechanism is also considered to be most important in the development of extrinsic allergic alveolitis (hypersensitivity pneumonitis, especially

the acute form) in persons having massive bioaerosol exposure. The symptoms include fever, cough, shortness of breath, and malaise. Prolonged exposure can result in lung fibrosis. The disease is common among farmers who handle moldy hay (the syndrome is also called farmers' lung disease). Trimellitic anhydride is an example of a reactive chemical causing a type III response.[120]

Type IV reactions differ from the previous hypersensitivity reactions in that they are not immunoglobulin-mediated, but mediated by T cells. It is probable that this mechanism is also involved in the pathogenesis of extrinsic alveolar alveolitis, especially in the chronic form. Allergic contact dermatitis is the most common example of this allergy type. Allergic contact dermatitis is caused by substances with low molecular weights (below 500 Da). The small molecule (e.g., Ni and Co), called a haptene, cannot act as an allergen alone, but needs to bind to certain proteins (Ia-antigens) on the surface of Langerhans' cells. This combined hapten and Ia-antigen forms the allergen. Langerhans' cells then transfer the allergen to the small lymphocytes. This is carried by the lymphatic vessel to the lymph node where it initiates the production of activated T cells (Th1 lymphocytes). When these encounter their antigens, cytokines are secreted (e.g., interferon γ; IFNγ). These activate the inflammatory cells leading to visible eczema usually within 1–4 days. T memory cells remain viable for a long time (a year or even longer), after which the sensitivity disappears.[162,163] The mechanisms underlying type I–IV allergic reactions have been depicted in a simplified way in Fig. 5.50.

Over 3000 chemicals have been classified as contact allergens. Among them are some substances (so-called "superallergens") that are so potent that they sensitize most exposed persons possibly on the first contact (e.g., dinitrochlorobenzene).[120] In practice, it would be useful to be able to classify contact allergens according to their potency. In the Nordic countries, a classification system for skin-contact allergens resembling the criteria of IARC for the classification of carcinogenic substances has been proposed, but it is not yet widely accepted. However, allergenicity evaluation has become an important part of toxicity testing with experimental animals. The guinea pig is the most commonly used animal, and the guinea pig maximation test is probably the most sensitive method for detecting the sensitizing potential of a compound.

Many irritative chemicals may cause non-specific hyper-responsitivity of the airways and skin. The number of irritating chemicals is very large, several thousands. The symptoms caused by exposure to irritants may resemble allergic symptoms. In addition, exposure to irritating substances (such as sulfur dioxide or solvent vapors) often triggers the symptoms in individuals with allergic asthma.

5.3.4.5 Chemical Teratogenesis

A teratogen is a chemical compound that induces malformations in the fetus. The term can also be defined to have a wider meaning, that a teratogen is a compound that can permanently damage the fetus during pregnancy. In the latter case, teratogens include compounds that induce morphological and/or functional alterations in the fetus. Brain tissue is especially sensitive to the effects of chemical compounds, because unlike most other organs, which undergo most of their organogenesic development during the first trimester of the pregnancy, the brain continues to develop throughout the entire pregnancy, and even after birth, the brain continues to develop for a number of years.[167]

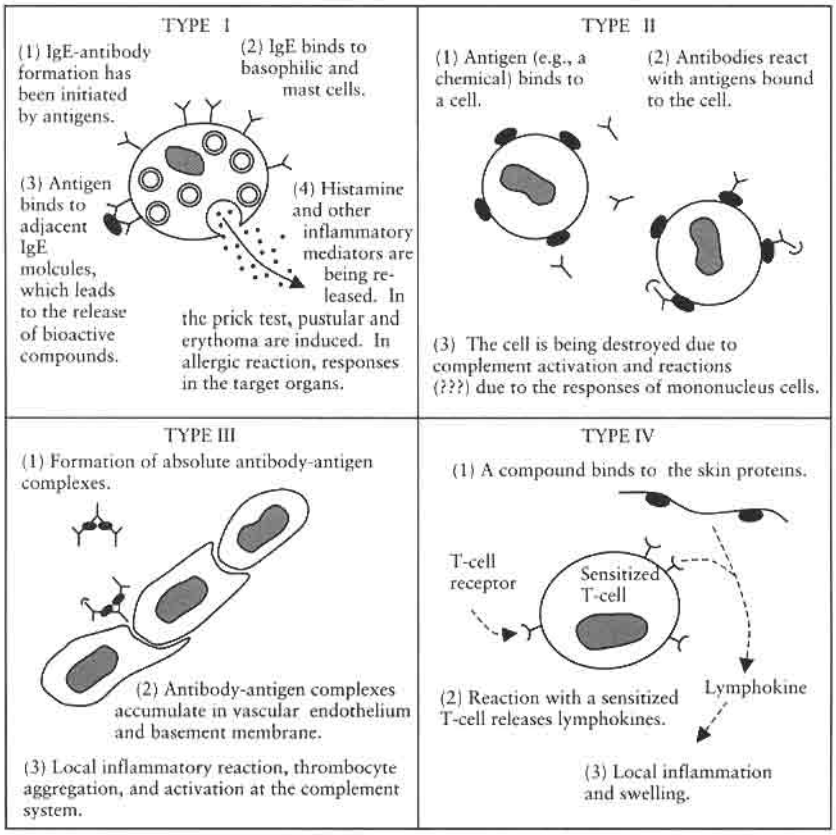

FIGURE 5.50 Four allergic (types I-IV) reaction types based on Coomb's classification. Type I reaction is an immediate allergic reaction. Type II reaction is an antibody-dependent cytotoxic reaction. In a type III reaction, injuries are due to soluble circulating antibody-antigen complexes. Type IV reactions are cell-mediated delayed allergic reactions. In the figure, the characteristics of different allergic reactions have been depicted in more detail.[151]

About three percent of children are born with some degree of morphological malformation. It is claimed that up to 16% of children may be malformed to some degree. However, most of the malformations are barely appreciable and, thus, the incidence of severe malformations is much lower. In about 30% of malformation cases, a genetic reason can be found, and in about 10% of cases, some external factor can be implicated. In most cases, however, the reason for the malformations remains unknown. It should be stressed that it is even extremely difficult to identify chemical compounds that cause functional damage, since regardless of the mechanism of the disturbance in development, the timing when it causes the damage is critical. Compounds with very different mechanisms can cause the same functional deficiency in a child. A chemical compound is rarely suspected as being the cause of a malformation.[167]

Mechanisms of Chemical Teratogenesis

The effects of a teratogen on a fetus depend on the timing of the exposure, i.e., at which stage of organogenesis the exposure takes place. Exposure to a teratogen before implantation usually leads to death and abortion of the fetus. How-

ever, experimental animal data provide evidence that exposure even at this stage may lead to birth of a malformed pup. Organogenesis is the period between the 21st and 56th days of pregnancy in humans, when most organs are undergoing rapid development. This time is the most sensitive period for a teratogen to exert its effects. For example, the closure of the palate in humans takes place between 56th and 58th day of pregnancy. This is the time when the risk of cleft palate is the greatest for the fetus if exposure to a teratogen occurs. After the end of organogenesis, morphological malformations are unlikely, but biochemical and functional alterations are still possible.[168]

Several chemical carcinogens are also chemical teratogens. In these cases, both carcinogens and teratogens may have an ultimate common mechanism, DNA damage. In this context, both chemical carcinogens and teratogens require metabolic activation to be able to react with the nucleic acids in DNA. Like chemical carcinogenesis, chemical teratogenesis constitutes a cascade of complex events, and is rarely induced by a single factor. This is exemplified by the fact that, depending on the dose and timing of exposure, a chemical teratogen may cause death of the fetus, induce a malformation, or result in growth retardation of the fetus. If the dose is large, the fetus dies. If the dose is lower than the lethal dose and exposure takes place during an early phase of a critical period, compensatory hyperplasia may replace the dead cells in the damaged organ, resulting in growth retardation in a morphologically normal fetus. However, even a small dose of a teratogen may lead to specific malformations when the exposure takes place during a critical period of organogenesis of a given organ. In addition to chemical compounds, ionizing radiation may also cause DNA damage potentially leading to teratogenesis.[169]

In addition to direct effects of chemical compounds on the fetus, metabolic disturbances in the mother, such as diabetes or hyperthermia, or deficiencies of calories or specific nutrients such as vitamin A, zinc, and folic acid may lead to teratogenesis. Compounds that inhibit placental functions may also induce malformations, e.g., by inhibiting placental circulation. For example, hydroxyurea disrupts the placental circulation and induces malformations. In addition, it also induces DNA damage.[170–173]

Chemical Teratogens

More than 900 teratogens have been identified in experimental animals. However, only about 30 human teratogens have been identified. Human teratogens have been listed in Table 5.20. In this section, some of the best-known teratogenic compounds are briefly described.[167]

Thalidomide was introduced in 1956 as a sedative which also prevented nausea and vomiting. Since the compound was effective and did not induce addiction, and because its acute side-effects were minor, it became popular to prevent the nausea associated with early pregnancy. Within a few years after its introduction, there was an outbreak of an epidemic of very rare malformations of the extremities, hands, and legs. Typical malformations due to thalidomide were lack of extremities (anamely), a shortening of long bones of the extremities (phocomelia or seal-like limbs), and malformations of the heart, eyes, intestine, external ears, and kidney. The sale of thalidomide was prohibited in 1961, and within a year no more children were born with its tragic trademark deformities.[174] Had the malformations induced by thalidomide been less spectacular and

TABLE 5.20 Human Developmental Toxicants

- Radiation
  - Therapeutic
  - Radioiodine
  - Atomic fallout
- Infections
  - Rubella virus
  - Cytomegalovirus
  - Herpes virus hominis
  - Toxoplasmosis
  - Venezuelan equine encephalitis virus
  - Syphilis
  - Parvovirus B-19
- Maternal metabolic imbalances
  - Alcoholism
  - Cretinism
  - Diabetes
  - Folic acid deficiency
  - Hyperthermia
  - Phenylketonuria
  - Rheumatic disease
  - Virilizing tumors
- Drugs and chemicals
  - Androgenic chemicals
  - Angiotensin-converting enzyme inhibitors
    - Captopril, enalapril
  - Antibiotics
    - Tetracyline
  - Anticancer drugs
    - Aminopterin, methylaminopterine, cyclophosphamide, busulfan
  - Anticonvulsants
    - Phenytoin, trimethadione, valproic acid
  - Antithyroid drugs
    - Methimazole
  - Chelators
    - Penicillamine
  - Chlorohiphenyls
  - Cigarette smoke
  - Cocaine
  - Coumarin anticoagulants
    - Warfarin
  - Diethylstilbesterol
  - Ethanol
  - Ethylene oxide
  - Iodides
  - Lithium
  - Metals
    - Mercury (organic)
    - Lead
  - Retinoids
    - 13-*cis*-retinoic acid
    - Etretinate
  - Thalidomide

Source: Modified from Rogers and Kavlock.[167]

rare (e.g., if it had induced cleft palate), it would have taken much longer to identify the causal relationship between the use of thalidomide and the malformations. In the case of thalidomide, the causal relationship was clear; about 84% of mothers whose children had limb malformations had taken thalidomide. It is estimated that thalidomide damaged about 7000–10 000 children, mainly in Western European countries.

Another well-known chemical teratogen is methyl mercury. Environmental health disasters in Japan, in Minamata Bay and Nigeta in the 1950s, and in Iraq in 1971, have provided detailed information of the effects of methyl mercury on fetuses.[175] Exposure to methyl mercury during pregnancy affected mainly the central nervous system of the children, and these changes were permanent. The most important sign was progressive retardation of psychomotor development of a child that seemed to be normal at birth. In addition, the exposure may also have caused blindness, deafness, and convulsions which appeared as the child grew (see Fig. 5.51). Methyl mercury seriously disturbs the normal organization of various brain structures during organogenesis. It binds to SH groups of proteins and also disturbs DNA and RNA synthesis. It used to be thought that the mother could somehow protect the growing fetus from chemical insults. Methyl mercury is a compound which reveals the fallacy of the claim that doses of methyl mercury which do not damage the mother cannot be teratogenic to the fetus. Furthermore, male fetuses seem to be more sensitive than female fetuses to the effects of this compound.[176]

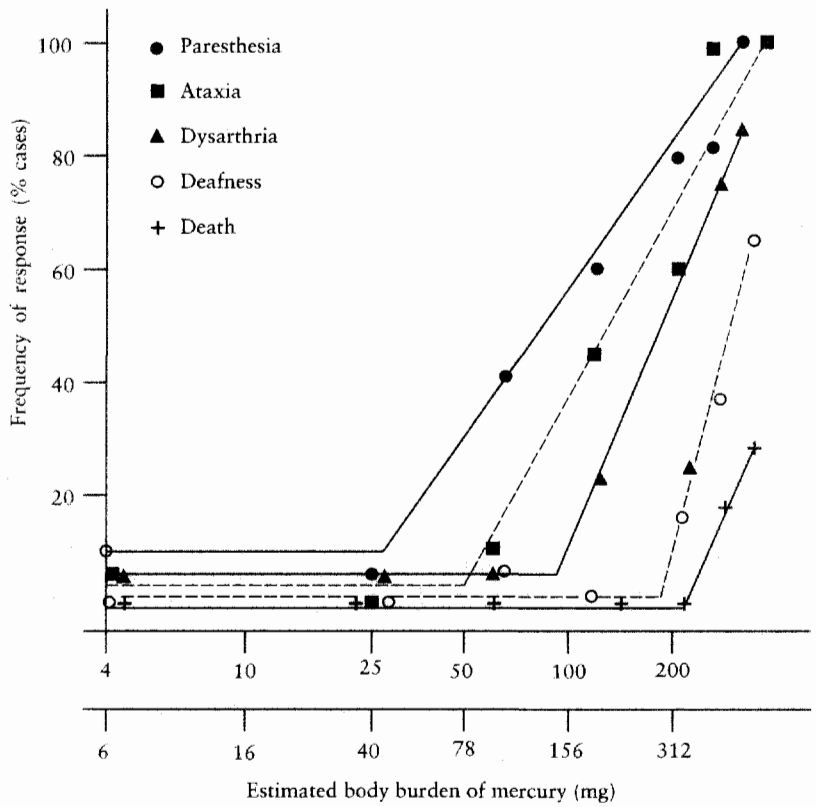

FIGURE 5.51 Dose-response relationships for methyl mercury.[176] (Used with permission.)

Fetal alcohol syndrome (FAS) was only defined in 1973, even though harmful effects of ethyl alcohol on the fetus have been known for a long time. During the past 25 years, the estimates of the dose required to damage the fetus have decreased, and today the consumption of ethyl alcohol during pregnancy is not recommended at all. The incidence of FAS has been found in different epidemiological studies to be about 2–7 cases/1000 live births.[177]

FAS is normally characterized by growth retardation, anomalies of the head and face, and psychomotor dysfunctions. Excessive consumption of ethyl alcohol may lead to malformations of the heart, extremities, and kidneys. Since consumption of ethyl alcohol is socially acceptable and prevalent even in pregnant women, the risks associated with the use of ethyl alcohol are remarkable. However, it should be kept in mind that there are several chemical compounds in the occupational environment that may also cause malformations even at low doses. The occupationally-important known human teratogens include methyl mercury, ethyl alcohol, PCB compounds, tobacco smoke, lead, TCDD, 2,4,5-T, carbon monoxide, nitrogen dioxide, gasoline, and fluoride.[167]

5.3.4.6 Carcinogens and Mutagens

A mutagen is a chemical that can induce alterations in the DNA. Mutations occurring in germ cells are inheritable and may lead to genetic diseases. If mutations take place in somatic cells, carcinogenesis may be initiated.

The International Agency for Research on Cancer (IARC) classifies carcinogens into five groups: human carcinogens (Category I), probable human carcinogens (Category 2A), possible human carcinogens (Category 2B), not classified (Category 3), and compounds with no evidence of carcinogenicity for humans (Category 4). Before an agent can be classified as a human carcinogen, there must be sufficient epidemiological evidence for a causal association between exposure to this agent and cancer. Probable human carcinogens include agents for which the epidemiological evidence is more limited and/or animal test carcinogenicity evidence is available. A compound is classified as possible human carcinogen when there is limited evidence of animal carcinogenicity. If the animal evidence is inadequate, the agent belongs to the not classified category. The final category includes agents with no evidence of carcinogenicity as determined by adequate animal testing or epidemiological studies. By the year 1993, IARC had classified the carcinogenicity of 763 chemical compounds, groups of chemical compounds, and mixtures of chemical compounds. Of these, 58 were placed in Category 2A, and 205 compounds were placed in Category 2B. The number of chemical compounds belonging to Category 3 was 405, and only one compound was classified as Category 4. These figures reveal some of the difficulties associated with the assessment of the carcinogenicity of chemical compounds: (1) usually only a limited number of studies on the carcinogenicity of chemicals are available; (2) human carcinogenicity is difficult to demonstrate; and (3) experimental or epidemiological evidence of the lack of carcinogenicity is practically impossible to obtain. This is the reason for not having a "not carcinogenic in humans" category in the IARC classification.[150] Some of the difficulties in assessing the carcinogenicity of chemical compounds are discussed below.[178] Table 5.21 lists categories of human carcinogens according to IARC.

TABLE 5.21 Classification of Carcinogenicity of Chemicals According to the International Agency on Research on Cancer

Class	Explanation
1. Carcinogenic to humans	Enough epidemiological evidence on carcinogenicity in humans
2A. Probably carcinogenic to humans	Limited evidence on carcinogenicity in humans and sufficient evidence on carcinogenicity in experimental animals and other relevant evidence
2B. Possibly carcinogenic to humans	Limited evidence on carcinogenicity in humans, and other relevant evidence missing; occasionally a compound with insufficient human evidence but limited evidence on carcinogenicity in experimental animals
3. Not classifiable	Not enough scientifically relevant data available for classification
4. Probably not carcinogenic in humans	Evidence both in humans and experimental animals indicates a lack of carcinogenicity

Source: Modified from Vähäkangas and Savolainen.[179]

Since animals are biological systems which differ from humans in many ways, epidemiological evidence on the carcinogenicity of chemicals is naturally much stronger than that derived from experimental animal studies. However, it is often difficult to obtain conclusive evidence due to several problems which are characteristic of epidemiological studies (see Section 5.3 IPR, pages 3–5). It should also be noted that agents causing very rare types of cancer are much easier to detect than those causing more common cancers. Angiosarcoma of the liver and adenocarcinoma of the nose are rare cancers (annual incidences about one per million in the general population); therefore, the human carcinogenicity of vinyl chloride (angiosarcoma) and wood dust (adenocarcinoma of nasal cavity) was identified on the basis of a few cases, whereas increased risk of lung cancer (annual incidence about 400–500 per million) is much more difficult to demonstrate. However, when the evidence derived from experimental animal studies on the carcinogenicity of a given chemical is utilized in assessing human risks of chemical carcinogenesis, several new difficulties are encountered.[178,180–182]

The biotransformation of a given chemical compound in experimental animals and in humans may differ. Furthermore, high doses of chemical compounds are used in studies with experimental animals, and this may cause alterations in biotransformation of the tested chemicals that do not occur at the lower doses relevant to the human exposure situation. For example, a metabolic pathway dominating at low doses may become saturated, and a salvage metabolic pathway, e.g., one that produces reactive intermediates of the compound, may become involved in the biotransformation of the chemical. Since this intermediate could never be produced at the exposure levels encountered in humans, the overall result

of such a carcinogenicity trial is irrelevant. It has also been argued that high doses of chemicals used in animal carcinogenicity bioassays induce mitogenesis (increased rate of cell division), and thus carcinogenesis, and are therefore not specific to the compound itself.[182,183]

Mechanisms of Chemical Carcinogenesis

Carcinogens can be divided into two broad classes based on their mechanism of chemical carcinogenicity: genotoxic and epigenetic carcinogens. Genotoxic carcinogens initiate the process of chemical carcinogenesis by acting as mutagens. All other carcinogens belong to the group epigenetic carcinogens, which includes foreign compound carcinogens, carcinogens acting through a hormonal mechanism, carcinogens that amplify the carcinogenic effects of true carcinogens when they are given after the true carcinogen, and cocarcinogens that stimulate chemical carcinogenesis when delivered in conjunction with a true carcinogen. Chemical carcinogenesis is a very complex cascade of events, this being typical of all forms of carcinogenesis, such that the alterations leading to cancer take place in a stepwise and usually subtle fashion. In fact, it is difficult if not impossible to find the point at which one step is over and the next one begins.[178,180]

Experimental animal studies have played a key role in the understanding of the mechanisms of chemical carcinogenesis. The duration of development of a cancer in humans may be several decades, and the development probably includes several steps. Furthermore, individual susceptibility is also important for the disease. Therefore, it has been extremely difficult to make the required observations in exposed individuals.

Most genotoxic carcinogens require metabolic activation. The most important group of enzymes that participates in these processes are the P-450 enzymes, of which CYP1A1 is involved in the activation of polycyclic aromatic hydrocarbons, CYP2 in the activation of aromatic amines, and CYP3A in the activation of aflatoxins.[131] An activated compound binds to several macromolecules within cells, and an important event in chemical carcinogenesis is binding to the genetic material, i.e., the formation of carcinogen-DNA adducts which lead to alterations in the genes. Typically, activated compounds favor guanine as the base to which they bind. In addition to the balance between the activity of enzymes that activate chemicals and the activity of enzymes that repair the chemical-induced damage to DNA, the stability of the adducts and the amount of the adducts in the cells are important factors in the initial stages of chemical carcinogenesis induced by genotoxic carcinogens.[184–186]

If enzymes responsible for DNA repair are unable to remove the DNA adduct, or if an error takes place in the repair, then the error in the genetic code remains when the cell divides. Thus, cellular proliferation is also required, in addition to a mutation, for there to be a permanent effect of a chemical compound. Accumulation of genetic errors, i.e., mutations, has been suspected to be an important factor in chemical carcinogenesis.[183,185]

Recently a number of genes that are important in chemical carcinogenesis have been identified. These include oncogenes (genes that promote carcinogenesis) and tumor suppressor genes (genes that prevent carcinogenesis). A mutation of a proto-oncogene may be required for the transformation of a

proto-oncogene to an oncogene, which then amplifies the carcinogenic process. On the other hand, mutations that inactivate tumor suppressor genes also greatly amplify carcinogenesis induced by exposure to chemical compounds.[187,188] In fact, inactivating mutations in tumor suppressor genes may be vital for the initiation and progression of the carcinogenic process. For example, mutations of ras-, raf-, jun-, fur-, and myc-oncogenes are known to be crucial in the development of lung cancer.[189] Table 5.22 lists important oncogenes and tumor suppressor genes that may be involved in human carcinogenesis.

A few tumor suppressor genes have also been identified. The most important of these are the p53 tumor suppressor gene and the retinoblastoma gene.[190] When functioning normally, the p53 tumor suppressor gene will stop cell division after DNA damage to give the cell time to repair the damage. Inactivating mutations in the p53 tumor suppressor gene may, therefore, amplify carcinogenesis by preventing the cell from repairing damage to its genetic material. In fact, mutations of p53 tumor suppressor gene are the most usual genetic changes in human cancers, and it seems that some chemical carcinogens

TABLE 5.22 Important Oncogenes and Tumor Suppressor Genes in Human Cancers

	Tissues associated with the cancer
Oncogene	
ras	Lung, colon, pancreas
raf	Lung
jun	Lung
erb-B2(neu)	Breast, lung
fur	Lung
myb	Lung
myc	Bone marrow (acute leukemia)
	Lymphatic tissue (Burkitt lymphoma), lung
	Nervous tissue (neuroblastoma)
abl	Bone marrow
Tumor suppressor gene	
Rb	Retina (retinoblastoma), lung
p53	Lung, urinary bladder, intestine, breast
WT-1	Kidney (Wilms' tumor)
APC	Colon
DCC	Colon
BRCA	Breast
HNPCC	Colon

Source: Modified from Vähäkangas and Savolainen.[179]

induce typical and very specific mutations in the p53 tumor suppressor gene. One example is the aflatoxin-induced mutation in codon 249 in the p53 gene.[191] In contrast, benzo(a)pyrene, present in tobacco smoke, does not bind to this codon, but does bind to other areas of the gene, so-called hot spots. Exposure to UV light also seems to induce typical and specific mutations in thep53 gene. In addition, there are other typical mutations of the p53 gene that seem to be associated with cancer that are induced by environmental or occupational chemical carcinogens.[190]

Transplacental Carcinogenesis

Transplacental carcinogenesis indicates that exposure of the mother during pregnancy may induce cancer in the child as it grows. In animals, more than 50 transplacental carcinogens have been found, but in humans only one such compound has been identified, diethylstilbesterol, a synthetic estrogen that was used to prevent spontaneous abortions. However, there is data to suggest that several chemical compounds that are important in the occupational environment may also mediate their effect transplacentally. Such compounds include polycyclic aromatic hydrocarbons, nitrosoamines, hydrazines, and isoniazide. Thus, exposure to these compounds should be strictly controlled due to the potential hazard they pose to the developing fetus.[5]

5.3.5 Exposure Assessment

Workers' exposure levels can be estimated either by occupational hygiene sampling or by biological monitoring. Since inhalation is usually the most important exposure route, occupational hygiene surveys generally include the measurements of airborne concentrations of many impurities in workroom air. However, dermal exposure is also important for many substances. It can be assessed by analyzing hand-wash and patch samples. In biological monitoring, the concentration of a substance or its metabolite is determined from biological samples. Urine, blood, and exhaled air are the most common biological samples. Furthermore, molecular dosimetry, or target-dose monitoring, usually based on the analysis of DNA or protein adducts in lymphocytes or hemoglobin adducts in erythrocytes in exposed individuals, has become popular and holds great promise in the assessment of the association between exposure and the effects of carcinogens.

5.3.5.1 Determination of Airborne Concentrations

Major time variation is typical for occupational inhalation exposure. It is not unusual if a worker's daily average exposure levels varies by a factor of ten within a single week. The concentration distribution is usually close to lognormal (the logarithms of concentrations are distributed normally). In fact, the distribution may be slightly skewed so that its right side is less steep than its left. The concentration distributions can be characterized by their geometric mean (m_g) and geometric standard deviation (s_g). However, the geometric mean should never be used to describe exposure because the exposure dose depends on the arithmetic mean. The geometric standard deviation is typically 1.5–2.5. In industries with continuous processes, s_g

may be lower (1.1–1.5), whereas s_g may exceed 2.5 in some manual occupations. The lognormal distribution becomes a straight line on logarithmic probability paper. The concentration corresponding to the probability of 50% is m_g (also the median) and s_g is obtained from the ratio $c_{50}/c_{15.9}$ or $(c_{84.1}/c_{50})$ as shown in Fig. 5.52.[192]

A European standard (EN 689/95) has been set for occupational exposure assessment. However, this is primarily intended to be used to guarantee that the concentrations of air impurities are in compliance with OELs. According to the standard, exposures exceeding 10% of OEL level should be followed with repeated measurements, the interval of which depends on the concentration observed. The interval decreases as the concentration approaches the OEL.[193] The standard also includes the concept that workers should be divided into homogeneous exposure groups (HEGs). These consist of workers who have similar jobs and are exposed to the same agents. This is practical because it would be unnecessarily laborious to investigate every worker. On the other hand, the prerequisite of the standard that the exposure levels of the members of a HEG remain within the range 0.5–2 times the mean exposure level is impractically tight. In addition, airborne concentrations usually fluctuate greatly with time. The within- and between-worker components of exposure variability can be calculated by using the random-effects analysis of variance.[194] However, this would require extensive sampling. Even though repeated random personal sampling is, in principle, the most accurate method for exposure assessment, it has the serious limitation that it does not provide information on the reasons for the exposure. Without this basic knowledge, it may be difficult to institute effective remedial measures.[52]

It is appropriate to consider the differences between manual tasks and process industries (see Section 5.3.2.1) while assessing the exposure, and to perform air sampling so that it also can support planning of engineering control. Because of steep concentration gradients, breathing zone sampling must be performed when investigating manual tasks. A worker often performs several tasks, and the exposure may be very different during different tasks. Therefore, all major tasks done by the worker should be studied under various conditions. If the position of the local exhaust is not fixed, its influence should also be examined. The time-weighted average (TWA) concentration is obtained using the lengths of various tasks as the weights. It is common practice to determine the TWA of a working day (shift). Since the health effects usually depend on long-term average exposure level, this should also be estimated. Past exposures are often very difficult to assess because working conditions and methods may have been changed. However, the present (e.g., annual) average exposure level can be estimated by asking the worker how much time he/she spends on average (e.g., during the past year) for various tasks and use these as weights. For example, if we want to assess a construction painter's exposure to organic solvents, we must first list all tasks in which solvent-based paints are used. The exposure during painting depends mainly on the size of the surface painted (or on paint consumption rate), the room volume, and the ventilation. Since

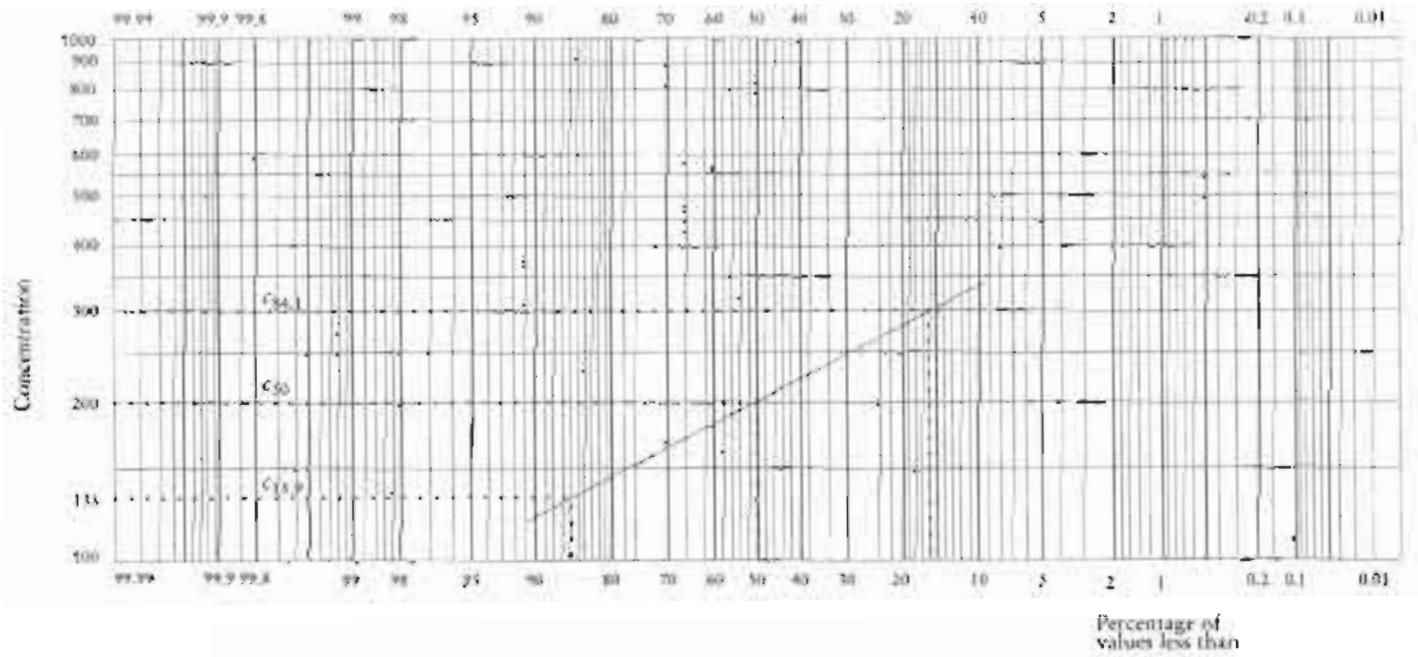

FIGURE 5.52 The determination of the geometric mean concentration and geometric standard deviation. In the sample: m_g c_{50} 200 ppm; s_g $c_{50}/c_{15.9}$ 200 ppm/133 ppm 1.5 = $c_{84.1}/c_{50}$ = 300 ppm/200 ppm.[92]

local exhausts cannot be used generally, the ventilation may depend on the possibility of keeping the doors and windows open. Breathing zone samples are collected during painting of doors, window frames, floors, walls, etc. in rooms of different size (e.g., small, medium, and large), both with doors and windows open and with them closed. The time use distribution can be obtained with a questionnaire.

In process industries, the areal distribution of airborne pollutant concentrations becomes important. Thus, workers' exposure levels depend on their movement patterns during the working day. Ideally, the processes are closed, but, in practice, in-plant emissions occur from openings needed for material flows and sampling. Sometimes, in-plant emissions are intentionally allowed to be discharged into workroom air in areas where workers do not spend any time. In addition, fugitive emissions commonly take place due to leaking seals in flanges, valves, pumps, and fans. For continuous processes, the time variation of airborne concentration often depends predominantly on relatively few process parameters, such as production rate, temperature, and pressure. These are also important for batch processes, but there are usually certain process phases during which the emissions are heaviest. Batch processes generally also include several manual tasks, such as emptying sacks and barrels.

Since the concentration gradients are not very steep at the actual working areas, it is more convenient to use stationary monitoring instead of personal sampling, and ask how much time, on average, each worker spends in various areas. Direct reading instruments provided with a multi-point sampling system are especially useful because they permit long-term concentration follow-up without excessive costs. Even though accurate information on time use cannot be obtained with questionnaires or interviews, and the coverage of stationary sampling points remains incomplete, the error due to these inadequacies is, nevertheless, usually much smaller than that caused by too brief a sampling time in personal monitoring. In addition, relationships between process parameters and airborne concentrations may be identified. This allows the assessment of long-term exposure because long-term statistics of the important process parameters are usually available. In industries using batch processes, the concentration variation during various process phases should also taken into consideration. Figure 5.53 shows the linear relationship between airborne toluene concentration and toluene concentration observed at stationary sampling sites in a printing plant. The annual average concentration is now obtained for each monitoring site simply from the point on the line corresponding to the average use of toluene during the year.[195]

5.3.5.2 Biological Monitoring

While occupational hygiene measurements always measure only the concentrations of chemical compounds present in the occupational environment, i.e., the potential dose, the analysis of biological specimens predominantly reflects the body burden. Furthermore, biological monitoring is always limited to assessment of individual exposure. Personal occupational hygiene sampling takes into consideration only some of the individual factors, e.g., working

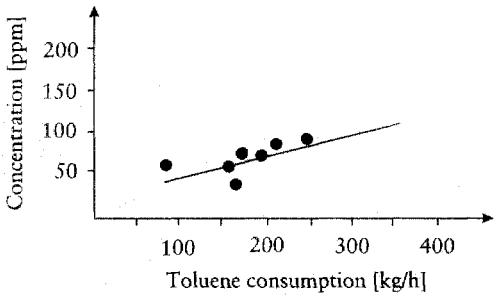

FIGURE 5.53 Relationship between the concentration of toluene in front of a gravure press and the consumption of toluene.[195]

habits and height, which can affect exposure. In biological monitoring, factors such as physical activity, i.e., cardiac output and minute volume of ventilation, metabolism, and the mass of depot tissues (e.g., adipose tissue) may also be considered.[66,67] Figure 5.54 depicts the difference between occupational hygiene and biological monitoring.

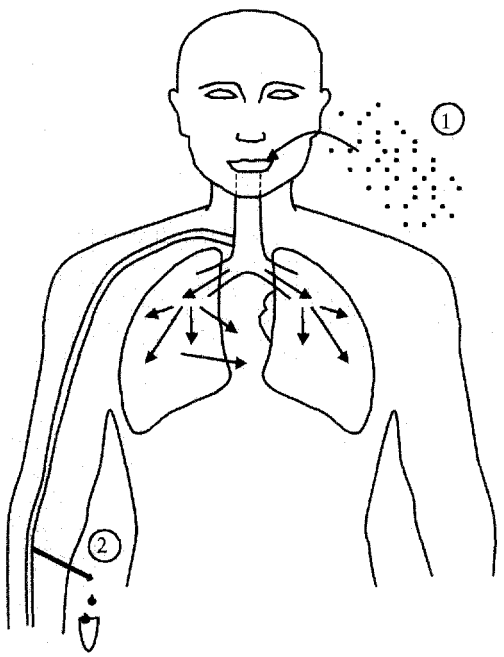

FIGURE 5.54 The idea of biomonitoring compared to the concept of occupational/ environmental hygienic monitoring. Hygienic monitoring (1) means measurement of concentration of a compound or a factor (e.g., fungal spores) outside the organism, e.g., air monitoring. Biomonitoring (2) means measurement of a compound or its metabolites within the organism, for example in the blood, urine, or exhaled air; measurement of binding products in the blood or urine or assessment of an existing effect such as chromosomal or DNA damage in white blood cells.[151]

Biological monitoring provides integrated information on exposure via all routes, including dermal and oral routes.[52] It also includes exposure that takes place outside the workplace. These are benefits in individual risk assessment; on the other hand, they can also be considered disadvantages in occupational health because its aim is to provide safe working conditions for everybody, irrespective of individual characteristics. Biological monitoring can also be used to ascertain effectiveness of personal protective equipment. It also has inherent benefits for substances with long half-lives. The accumulation of substances with very long biological half-lives, such as cadmium, is suitable for biological monitoring because a single sample can provide valuable information provided that a steady-state situation in the body has been reached. In addition, the variation of exposure with time will be attenuated for biological indicators with long half-lives. Therefore, fewer biological monitoring samples are needed for long-term exposure assessment than with conventional occupational hygiene monitoring. However, even this advantage is occasionally negated by the large individual variability typical of biological indicators.

Biological monitoring has several other limitations, in addition to those presented above. Biological monitoring is not suitable for agents which do not need to enter blood, such as irritating gases and many dusts. Neither is it very useful for substances with high acute toxicity (in fact occupational hygiene surveys are not very practical in such cases, but the working area should be provided with some kind of continuous monitoring equipped with an automatic alarm system). Another limitation is the small number of compounds for which there are biological exposure limits or indices (BEI) compared to those for occupational exposure limits (only ca. 10%). However, it should be noted that biological monitoring of exposure to a certain agent is often useful even if no BEI has been established for it. Biological monitoring is especially beneficial for substances with significant skin penetration. Urine sampling may well represent the most convenient means for exposure trend analysis.[196] Blood sampling may be slightly more difficult due to the analytical procedures and unpleasantness of blood sampling. The main limitation is, however, that biological monitoring as such does not provide any information on the causes of exposure. New technologies have become available in which cell samples can be collected, e.g., from the oral cavity, and possible protein or DNA adducts (reaction products between a reactive compound and proteins or DNA) can be quantitated, e.g., with high-pressure-liquid-chromatography. Examples of such compounds are formaldehyde and isocyanates.

5.3.5.3 Biomarkers

Extensive research is currently underway to use biological markers (biomarkers) in exposure and risk assessment. Biomarkers include the reaction products of chemicals or their metabolic products with biological macromolecules, especially with DNA. They also involve indicators of effect, such as chromosomal damage, and indicators of individual genetic susceptibility.

Formation of DNA adducts has been demonstrated for many carcinogens. DNA bases are nucleophilic and react with electrophilic compounds. Guanine seems to be especially reactive. Several studies have described how adduct formation can increase with exposure. However, the individual variability is larger than with conventional biological monitoring. Very high interindividual variation has been

observed with compounds that require metabolic activation (e.g., polycyclic aromatic compounds). Even though the formation of the adducts is an expression of an interaction of a carcinogen with DNA, the significance of these adducts in chemical carcinogenesis is not yet known. DNA repair and cell proliferation mechanisms remove damage caused by adducts. Peripheral white blood cells are often used in DNA adduct studies; T cells are especially popular because they are long-lived (half-life is about three years) and therefore they do not solely reflect current exposure. Peripheral white blood cells have also been frequently used for studies of chromosomal changes. Individuals who have high enzyme activity for formation of reactive metabolites and/or abnormally low metabolic activity of detoxifying enzymes are probably especially susceptible to toxicity.[197–199] The use of biomarkers in biomonitoring is likely to provide a valuable tool for this purpose in the future. This technology can also be used for molecular dosimetry, or target dose monitoring, in exposed individuals. The goal is to assess the dose at a critical organ or site, such as DNA or a protein.[187,198,200] Figure 5.55 depicts some essential features and prerequisites of biomonitoring.[64] Table 5.23 indicates the main purposes of biological monitoring of exposure to chemical compounds in the workplace.

5.3.6 Toxicity, Risks, and Risk Assessment

Earlier in this chapter, a short introduction to risk assessment and the concept of risk was given (see section 5.3.1.5). In this context, the same issues will not be repeated. However, the risk assessment concepts and methodologies will be discussed in more depth after the reader has received more insight into the role of toxicology in risk assessment, and after many of the principles of risk assessment, such as dose-effect and dose-response relationship, have been clarified. It is still worth emphasizing that the concept of risk is utilized to indicate hazards in the traffic, sports, health care, and even in the monetary markets, not to mention in relation to alternatives of energy production, e.g., nuclear power and its utilization. Toxicology has taken advantage of the concept of risk because it so neatly crystallizes the key issues of toxicology, prevention of chemical and other health hazards, and guaranteeing safety to humans.[49,129,180]

The term risk implies the probability that a certain deleterious health effect will take place under defined circumstances. Likewise, the term security implies the probability that no such deleterious incident will take place under defined circumstances. This kind of definition of risk or security has its foundation in an experimental setting. However, humans or wild animals do not live under defined conditions, but rather face a variety of challenges each day. Therefore, reliable risk assessment is an extremely difficult and tedious undertaking. One of the most challenging issues of toxicology has been assessment of carcinogenic risks induced by chemicals. In the first phase, we shall assess, on the basis of weight of evidence, whether a chemical is a carcinogen or not. This estimation is followed by another, even more demanding task with the goal of estimating the magnitude of the risk of humans exposed to a given chemical in an occupational setting or in their general environment. The outcome of such an assessment should be an estimate of the actual number of additional cases of cancer among exposed persons. This risk assessment utilizes data from experimental animal studies, epidemiological human studies, and all available information on human exposure under different occupational and other living conditions.[49]

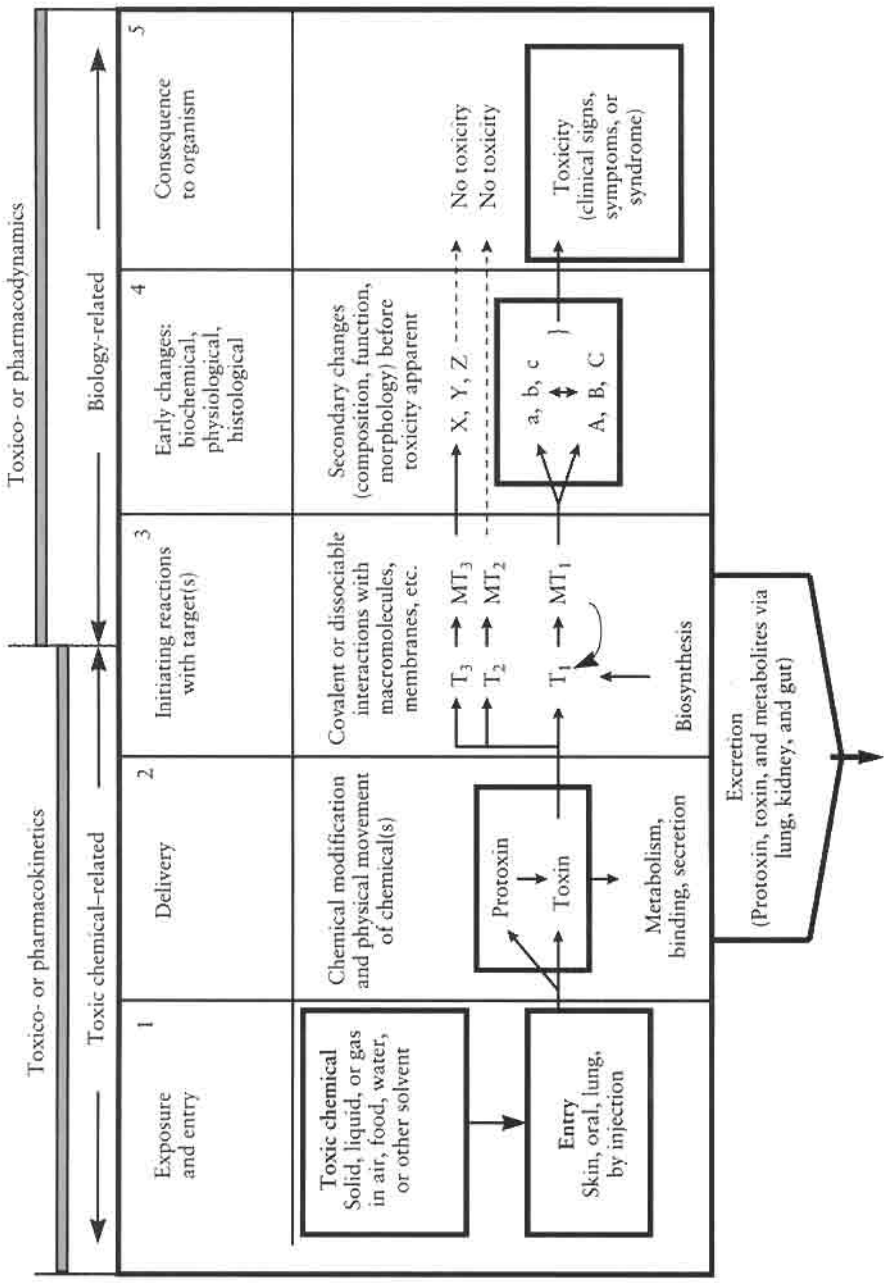

FIGURE 5.55 Scheme for developing toxicity due to chemicals. The stages covered by the terms toxico- or pharmacokinetics and toxico- and pharmacodynamics are marked on the figure.[64]

5.3.6.1 Phases of Risk Assessment

Risk assessment has usually been divided into four different and well-defined phases to ensure that all important issues will be given a fair consideration. The phases of systematic risk assessment include:

1. Hazard identification

TABLE 5.23 Biomonitoring Serves Three Different Purposes of Identifying and Using

1. Biomarkers for susceptibility of an individual within a population of one species to exposure to an intoxicant—genetically determined susceptibility.
2. Biomarkers for internal dose of the intoxicant—dose monitoring.
3. Biomarkers for early biological changes following exposure— effect monitoring.

Source: Modified from Aldridge.[64]

2. Hazard characterization and delineation of dose-effect or dose-response relationships
3. Assessment of exposure
4. Risk characterization

Risk characterization should preferentially include qualitative and, if possible, also quantitative risk assessment based on steps 1–3.

Hazard identification, step one, means identification of new chemicals or other factors that may cause harmful health effects. Previously, novel hazards were usually observed in case studies or after accidents or other excessive exposures, usually in occupational environments. Today, thorough toxicity studies are required on all pesticides, food additives, and drugs. New chemicals also have to be studied for their potential toxic effects. Thus, earlier hazards were in most cases identified after they had caused harmful effects in humans. Today, most chemical products have been evaluated for their toxicity with experimental animals. Therefore, hazard identification has become a preventive procedure based on safety studies conducted before a chemical compound or product reaches the market, and before individuals are exposed to it.[49]

Hazard characterization, step two, usually utilizes data from toxicity studies with experimental animals. In step one, compounds that have to be studied for their toxicity were briefly described. Health authorities in different countries have issued strict guidelines and regulations on the studies that have to be carried out to evaluate the toxicity of pesticides, food additives, and drugs. Furthermore, the European Union and the OECD have issued regulations that are followed in these countries. For example, in the United States, the U.S. Environmental Protection Agency and Food and Drug Administration carefully control the safety of drugs, food additives, pesticides, and other chemicals. The technical quality of the studies has been regulated in detail by good laboratory practice (GLP) guidelines. In Table 5.24, the toxicity/safety studies utilizing experimental animals or other test systems required for the registration of drugs, pesticides, and food additives have been listed.[49]

Exposure assessment, step three, allows a risk assessor to estimate the significance of the effects induced by high doses of a chemical in experimental animals in a human situation. Exposure assessment is, in fact, a prerequisite for quantitative risk assessment because it allows a comparison between effects induced by high dose with those induced by low doses, and also allows

TABLE 5.24 Toxicity Studies for Safety Evaluation of Drugs, Pesticides, Food Additives, and Other Chemicals Utilizing Experimental Animals and Other Systems Required by Health Authorities

Name of study	Animal species	Duration of study	Reason for study
Biotransformation	Rats/mice	One day to weeks	Metabolism
Kinetic studies	Rats/mice	One day to weeks	Absorption, distribution, and elimination
Acute toxicity	Rats/mice	2 weeks	Acute effects
Subacute toxicity	Rats/mice	2–3 weeks	Delayed effects, target organs
Subchronic study	Rats/mice/dogs/rabbits	6 months	Target organs, delayed effects
Chronic studies	Rats/mice	18–24 months	Chronic effects of low exposures
Carcinogenicity	Rats/mice	18–24 months	Carcinogenic potential
Teratogenicity	Rats/rabbits	3–4 weeks	Teratogenic potential
Reproductive toxicity	Rats/mice/rabbits	Several months	Potential to affect reproduction
Irritation	Rats/rabbits	Few days	Irritation index
Sensitization	Guinea pigs/rats	Few weeks	Potential to sensitize
Mutagenicity, genotoxicity	Rats, mice, bacterial strains, yeasts	Few days	Potential to cause mutations, chromosomal damage, and other genotoxic effects

one to compare a dose that causes a toxic effect in an experimental animal with the human dose in an occupational setting or general environment. This is vital because, in most cases, assessment of toxicity, e.g., hazards of new chemicals, is based purely on experimental animal studies. Assessment of exposure in the occupational environment relates the human situation to the toxicity data derived from experimental animal studies.

In risk characterization, step four, the human exposure situation is compared to the toxicity data from animal studies, and often a safety-margin approach is utilized. The safety margin is based on a knowledge of uncertainties and individual variation in sensitivity of animals and humans to the effects of chemical compounds. Usually one assumes that humans are more sensitive than experimental animals to the effects of chemicals. For this reason, a safety margin is often used. This margin contains two factors, differences in biotransformation within a species (human), usually 10, and differences in the sensitivity between species (e.g., rat vs. human), usually also 10. The safety factor which takes into consideration interindividual differences within the human population predominately indicates differences in biotransformation, but sensitivity to effects of chemicals is also taken into consideration (e.g., safety factor of 4 for biotransformation and 2.5 for sensitivity; $4 \times 2.5 = 10$). For example, if the lowest dose that does not cause any toxicity to rodents, rats, or mice, i.e., the no-observable-adverse-effect level (NOAEL) is 100 mg/kg, this dose is divided by the safety factor of 100. The safe dose level for humans would be then 1 mg/kg. Occasionally, a NOAEL is not found, and one has to use the lowest-observable-adverse-effect level (LOAEL) in safety assessment. In this situation, often an additional un-

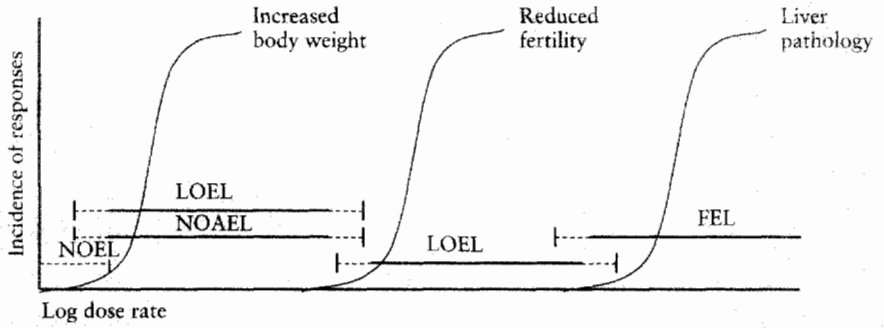

FIGURE 5.56 The "threshold region" for chronic dose-response curves.[49] [Reprinted with permission from Tardiff, R.G., and Rodricks, J.V. (1987). (Eds.), *Toxic Substances and Human Risks: Principles of Data Interpretation*. New York: Plenum Press.]

certainly factor is added, and then the dose is divided by a factor of 1000. A similar approach is also used when one deals with an exceptionally serious toxicological end point, such as epigenetic carcinogenesis or malformations, which has a threshold dose. This kind of approach is utilized when one deals with deterministic toxicological effects, e.g., target organ toxicity (neurotoxicity, kidney toxicity). This approach also requires the assumption of a threshold for the effect, i.e., that there is a safe dose below which no harmful effects occur. Typically, this approach assumes that a chemical compound expresses a typical sigmoidal dose-effect curve in its toxic effects (see Fig. 5.56).[49]

When one has to assess risks of compounds with carcinogenic or allergic properties, risk assessment becomes much more difficult. This applies especially to genotoxic carcinogens, which have been assumed not to have a safe level; the only safe level would be zero. In this circumstance, linear extrapolation (straight line from LOAEL to zero) or various mathematical models that assume the absence of a safe dose have been utilized in human risk assessment. In these instances, the acceptable risk level has been set to 1/1000000. It has to be kept in mind that linear extrapolation or mathematical models are being used because the true mechanisms of chemical carcinogenesis are not known. Therefore, risk regulators, when carrying out risk assessment, are conservative in their risk assessment to guarantee safety of exposed populations. This does not mean, however, that the approach is correct.[49,180,201,202] Figure 5.57 indicates the differences in risk estimates that can be obtained from the same set of data utilizing different mathematical models.[49]

Recently it has been argued that genotoxic carcinogens may also have a threshold in their carcinogenic effect. If this assumption were to be accepted by the regulators, it would have a tremendous impact on risk assessment throughout the world. It would mean that safety factors would also be used when determining safe dose levels for genotoxic carcinogens, and this would affect most of the regulatory limits set for chemicals.

5.3.6.2 The Significance of Health Risks Caused by Chemical Compounds

Assessing health risks induced by exposure to chemical compounds is different in different societies. Typically, in industrialized societies, traffic exhausts, ex-

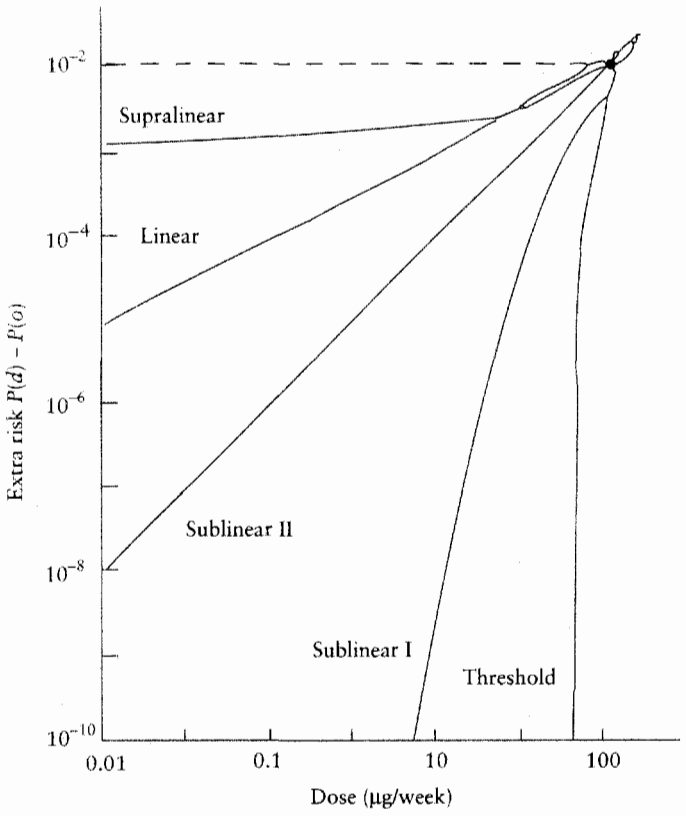

FIGURE 5.57 Results of alternative extrapolation models for the same experimental data.[49] (Reprinted with permission from *Risk Assessment in the Federal Government*. Copyright 1983 by the National Academy of Sciences. Courtesy of the National Academy Press, Washington, DC.)

hausts of power plants, and indoor and outdoor emissions of the chemical industry are the greatest concerns. In the occupational environment, one deals with relatively high exposure levels, whereas among the general public, one deals with very low exposure concentrations but large exposed populations, which complicates the assessment of the additional risks caused by the exposure. Also, the magnitude of risks may vary widely. The excess risks of the general population due to air pollution (nitric and sulfur dioxide, ozone, small particles) in Europe and the United States are between one and five percent in terms of excess mortality. In Europe this corresponds, however, to between 50 000 and 100 000 extra deaths. In occupational environments, the exposure levels may be several fold as compared to environmental risks, perhaps even orders of magnitude higher, but usually the exposure levels are relatively low when compared with the situation 20 or 30 years ago. Also, in occupational environments, the exposed populations can be clearly defined, and appropriate measures can be undertaken to avoid excessive exposure. In industrialized countries, the exposures are nowadays much better regulated than before. This does not imply that toxicity and risk assessment are any less important for guaranteeing chemical safety for workers

and the general population. It simply means that the nature of exposures and their consequences have changed; rather than causing acute poisonings, exposures in these societies cause long-term effects such as allergies, cancers, and other chronic diseases such as cardiovascular diseases and asthma. The risk assessment of long-term effects of chemical exposures is much more demanding than assessing the risks of deterministic effects due to high exposures.[49,180,201–204]

In developing countries, exposure to chemicals, e.g., pesticides, is responsible for millions of acute poisoning cases and hundreds of thousands of fatalities every year.[203] This is due to the low standard of living, poor education, failure to appreciate the significance of hygienic measures and the effects of the compounds, and general attitudes. Furthermore, most developing countries are situated in subtropical or tropical areas where the use of a number of chemicals, such as pesticides, is a necessity. Thus, inadequate safety measures, regulations, and education easily lead to careless use of highly toxic compounds. Much can be done to alleviate this situation, e.g., experts can visit to highlight problems in these countries, but ultimately the situation can only be improved by measures in each country. These measures will include improved education and increased awareness of the toxicity of the compounds and appropriate safety measures.

A good example is the accident that took place in Bhopal, India, in 1984. An explosion in a pesticide plant producing carbaryl, a highly toxic insecticide, caused a release of the raw material of the pesticide, methyl isocyanate, into the environment. In all, 10–25 tons of this highly toxic and reactive compound were released into the densely populated area surrounding the plant. The LC_{50} value (concentration that kills 50% of the exposed experimental animals) of the gas is 10–30 ppm. In the Bhopal region, the exposure resulted in 5000 deaths and 100 000 less severe poisonings, with 5000 persons suffering permanent damage to their respiratory systems.[41]

5.3.6.3 Perception of Risks by Experts and the General Population

Communication of risks to the general public is extremely important for policy-making in consideration of toxic substances. Policy makers should be able to educate the public concerning the differences between different chemical hazards, and that the magnitude of the exposure and thus the dose is essential for assessing the magnitude of the risk. The existence of a chemical hazard does not imply as such a risk to human populations. However, risk communication is usually a difficult task because the concept of risk is so difficult to understand, and, especially in a crisis, failure in risk communication is the rule rather than the exception. Several investigators have extensively studied risk perception and risk communication between lay people and experts. They have found marked differences in the perception of risks between these groups. Especially among the lay people, the familiarity of the risk (e.g., occupational exposure vs. smoking), the magnitude of the outcome of the risk (release of a chemical in the workplace vs. car accident), and the severity of the outcome of an event (release of minute amounts of radon within a nuclear plant vs. fire) all have a major impact on the perception of risks (see Fig. 5.58).[49] Alcohol consumption is a good example. Consumption of ethyl alcohol is one of the most important health hazards in in-

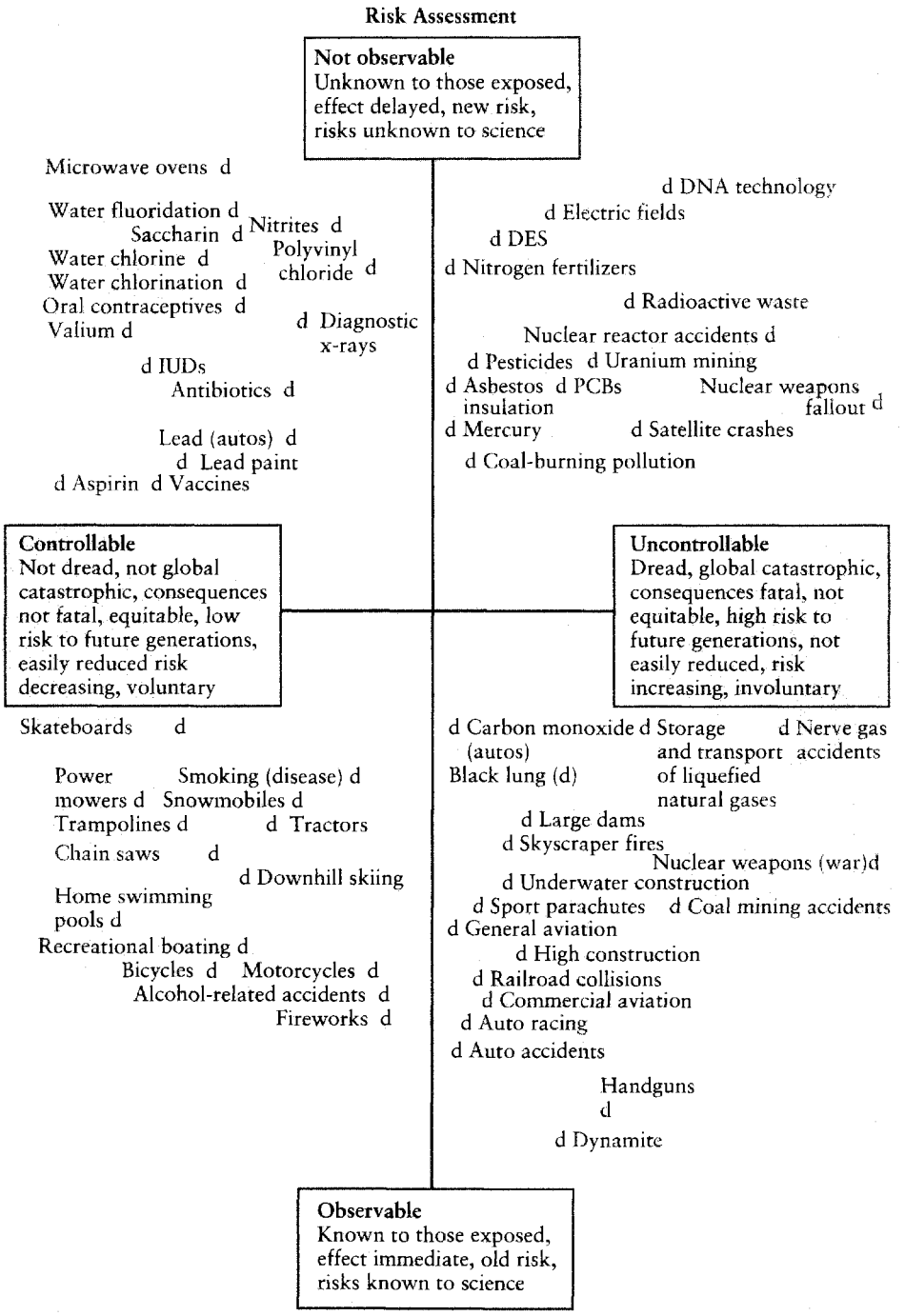

FIGURE 5.58 Risk space has axes that correspond roughly to a hazard's "dreadfulness" (d) and the degree to which it is understood.[49]

dustrialized countries, whereas food additives or pesticide residues are not causes of concern. Nonetheless alcohol use is considered a minor risk compared to the nonsignificant effect of food additives or pesticide residues. Similarly with occupational health risks, exposure to chemicals in industrialized countries is in most cases a minute hazard when compared to lifestyle factors. This does not mean, however, that one should not always strive to prevent industrial exposures and accidents at all times. Perception of risks is important because it ultimately determines how effectively the knowledge produced by toxicological research can be utilized in the protection of human health in the occupational setting and the general environment.

5.3.6.4 Special Considerations

After the use of a chemical becomes widespread, new deleterious effects on human health may be observed. In such situations, the occupational limit values will have to be modified. Usually the OELS tend to decrease when more information on the toxicity of a chemical is obtained.[52] Knowledge of the specific features of various chemicals is thus extremely important for planning ventilation of industrial premises. It is important to be especially aware of those chemicals that may cause long-term effects without causing any acute effects. There are also compounds such as isocyanates that are extremely irritating at concentrations as low as 0.5 ppm. However, some workers may become sensitized to isothiocyanates at a concentration of 10 ppb, and therefore this has to be taken into consideration when planning the industrial ventilation. Thus, one has to plan against compounds that can cause serious health effects at concentrations at which their presence cannot be observed by the human senses, i.e., irritation or odor.

Ultimately, the final stage of risk assessment, risk characterization, aims at achieving a synthesis from data gathered in steps 1–3. The goal of such a synthesis is, in addition to qualitative risk assessment, quantitative risk assessment. This implies that the outcome of the process should be numerical, e.g., a number or other estimate which indicates how many extra cases of a deleterious health outcome are produced due to exposure to a given exposure level in a given population.[49] Decisionmakers demand that toxicologists be able to come up with a reliable estimate of the relative importance in terms of severity of the health outcome or the number of new cases of disease. This would then allow them to prioritize the health hazards, and also carry out the kinds of expense/benefit analysis usually utilized in these situations. It would then be easier to make decisions on which chemical problems to tackle first, and at which concentration level the occupational limit value of a given chemical should be set. These measures are important for the preventive measures to be undertaken.

An important issue in the toxicity of chemicals and in assessing their risks is the *inherent toxicity* of a chemical. This implies the potency, i.e., the magnitude of the dose, at which the chemical can induce a toxic effect, whether cancer, liver damage, or nervous dysfunction. One example of a characteristic of a chemical is its reactivity, which may markedly affect its potential to cause allergic reactions or cancer or to induce irritation of the respiratory tract. Thus, detailed information on the characteristics of a compound is of major significance in understanding the mechanisms of the effects that it can induce in humans and in other living organisms and in understanding the effects themselves.[87]

5.3.6.5 Important Chemical Carcinogens

Polycyclic aromatic hydrocarbons have been classified as human carcinogens because they induce cancers in experimental animals and because smoking and exposure to mixtures of chemicals containing polycyclic aromatic hydrocarbons in the workplace increase the risk of lung cancer in exposed individuals. In experimental animals, benzo(a)pyrene induces cancer in different organs depending on the route of administration.[204] Furthermore, exposure to polycyclic aromatic hydrocarbons commonly occurs in occupations related to traffic (use of diesel engines in transportation and railways).

Tobacco smoke induces a myriad of deleterious health effects in exposed individuals. Carbon monoxide decreases oxygenation of tissues by erythrocytes, nicotine causes vasoconstriction and disturbs circulation especially in the periphery, e.g., in the placenta, and tar contains a number of carcinogenic compounds. In addition, tobacco smoke irritates the mucous membranes in the respiratory airways and eyes, depresses cilia in the bronchi, and also has immunosuppressive effects. These effects may also contribute to the increased risk of lung cancer due to smoking. Furthermore, all forms of smoking increase the risk of lung cancer. The association between smoking and lung cancer is no longer open to debate; there is a dose-effect relationship between the number of cigarettes smoked per day and the magnitude of the risk, and an association between the duration of smoking and the lung cancer risk. Also, an increased risk of bladder cancer and kidney-pelvis cancer is associated with smoking. These observations are not surprising because tobacco smoke contains many known carcinogens, such as benzo(a)pyrene, at relatively high concentrations.[204]

Asbestos fibers and arsenic compounds are also clear-cut human carcinogens.[205,206] Today, substitutes of asbestos or insulation materials, notably man-made vitreous fibres containing ceramic, glasswool, lockwool, and slogwool fibres are suspected human carcinogens,[222] but further information is required before one can come to a final carcinogenic classification. Other potentially important human carcinogens include reactive agents such as formaldehyde and isocyanates.

IARC has also classified ethyl alcohol as a human carcinogen. The use of ethyl alcohol is associated with increased risk of cancers of the oral cavity, pharynx, larynx, esophagus, and liver. Ethanol is usually considered to be a cocarcinogen which amplifies the effects of other carcinogens. For example, the carcinogenic effects of tobacco smoke are amplified by ethyl alcohol. In addition, ethyl alcohol is also genotoxic, and causes chromosomal aberrations, sister chromatid exchanges, and point mutations in test systems where ethyl alcohol can be metabolized. Thus, it seems likely that acetaldehyde, the primary metabolite of ethyl alcohol, is the compound responsible for mutagenicity of ethyl alcohol.[207]

5.3.6.6 Future Perspectives

In the future, the preventive role of toxicology will be emphasized. It will be increasingly important to develop early indicators to monitor long-term subtle exposures that predict deleterious effects that are known to have a causal relationship with occupational exposures. In addition to collection of blood and urine samples, also collection of cells from points of

entry into the body, e.g., by nasal or bronchoalveolar lavage, will provide possibilities to explore functional chemical-induced changes at the cellular and molecular level. Routine measurements of alterations of gene expression in cells so collected may provide valuable information on causality between inhalation exposures and effects in target cells in the nasal cavity or lungs. In many instances, cells collected with nasal or broncho-alveolar lavage (BAL) methods may be used to demonstrate a causal relationship between inhalational exposure and an effect in the airways. This would then allow protection of exposed workers by assessing the exposure through occupational hygienic measurements.

References

1. Klaassen, C. D., Ed. (1996). *Casarett and Doull's Toxicology: The Basic Science of Poisons.* McGraw-Hill, New York.
2. International Agency for Research on Cancer (1995). *Dry cleaning, some chlorinated solvents and other industrial chemicals.* IARC Monographs on the Evaluation of Carcinogenic Risks to Humans, vol. 63. International Agency for Research on Cancer, Lyon, France.
3. International Labor Office, 1991. Occupational exposure limits for airborne toxic substances. Occupational Safety and Health Series, No. 37. International Labour Office, Geneva.
4. Borm, P. J. A., and Henderson, P. T. (1996). Occupational toxicology. In *Toxicology: Principles and Applications* (R. J. M. Niesink, J. de Vries, J. and M.A. Hollinger, Eds.), pp. 1141–1180. CRC Press, Boca Raton, FL.
5. Pitot, H. C. III, and Dragan, Y. P. (1996). Chemical carcinogenesis. In *Casarett and Doull's Toxicology: The Basic Science of Poisons* (C. D. Klaassen, Ed.), pp. 201–267. McGraw-Hill, New York.
6. Olden, K., and Klein, J.-L. (1995). Environmental health science research and human risk assessment. *Mol. Carcinogen.* **14**, 2–9.
7. Abernathy, C. O., Chappel, W. R., Meek, M. E., Gibb, H., and Guo, H.-R. (1996). Is ingested inorganic arsenic a "rhreshold" carcinogen? *Fundam. Appl. Toxicol.* **29**, 168–175.
8. Crump, K. S. (1996). The linearized multistage model and the future of quantitative risk assessment. *Human Exper. Toxicol.* **15**, 787-798.
9. ICRP, (1966). Reommendation of the International Committee on Radiological Protection. Publication 9. Pergamon Press.
10. NCRP (1994). Permissible does from external sources of Ionizing Radition. National Committee on Radition Protection and Measurement, Bethesda, Maryland.
11. Grandjean, P., White, R. F., and Weihe, P. (1996). Neurobehavioral epidemiology: Application in risk assessment. *Environ. Health Perspect.* **104**(2), 397–400.
12. International Agency for Research on Cancer (1996). *Printing processes and printing inks, carbon black and some nitro compounds.* IARC Monographs on the Evaluation of Carcinogenic Risks to Humans, vol. 65, pp. 94–98. International Agency for Research on Cancer, Lyon, France.
13. Malker, H. S. R. and Gemne, G. (1987). A register-epidemiology study on cancer among Swedish printing industry workers. *Arch. Environ. Health* **42**, 73–82.
14. McLaughlin, J. K., Malker, H. S. R., Blot, W. J., Ericsson, J. L. E., Gemne, G., and Fraumeni, J. F., Jr. (1988). Malignant melanoma in the printing industry. *Am. J. Ind. Med.* **13**, 301–304.
15. Aronson, K. J., and Howe, G. R. (1994). Utility of a surveillance system to detect associations between work and cancer among women in Canada, 1965-1991. *J. Occup. Med.* **36**, 1174-1179.
16. Costa, G., Faggiano, F., and Lagorio, S. (Eds.) (1995). *Mortality by Occupation in Italy in the 1980's.* Instituto Superiore per la Prevenzione e la Sicurezza del Lavoro, Rome (in Italian).
17. Pukkala, E. (1995). *Cancer risk by social class and occupation. A survey of 109 000 cancer cases among Finns of working age. Contributions to Epidemiology and Biostatistics,* vol. 7, Karger, Basel.
18. Najem, G. R., Louria, D. B., Seebode, J. J., Thind, I. S., Prusakowski, J. M., Ambrose, R. B. and Fernicola, A. R. (1982). Life time occupation, smoking, caffeine, saccharine, hair dyes and bladder carcinogenesis. *Int. J. Epidemiol.* **11**, 212–217.
19. Cartwright, R. (1982). Occupational bladder cancer and cigarette smoking in West Yorkshire. *Scand. J. Work Environ. Health* 8 (Suppl. 1), 79–82.

20. Silverman, D. T., Hoover, R. N., Albert, S. and Graff, K. M. (1983). Occupation and cancer of the lower urinary tract in Detroit. *J. Natl. Cancer Inst.* 70, 237–245.
21. Schoenberg, J. B., Stemhagen, A., Mogielnicki, A. P., Altman, R., Abe, T. and Mason, T. J. (1984). Case-control study of bladder cancer in New Jersey: I. Occupational exposures in white males. *J. Natl. Cancer Inst.* 72, 973–981.
22. Baxter, P. J. and McDowall, M. E. (1986). Occupation and cancer in London an investigation into nasal and bladder cancer using the Cancer Atlas. *Br. J. Ind. Med.* 43, 44–49.
23. Brownson, R. C., Chang, J. C., and Davis, J. R. (1987). Occupation, smoking, and alcohol in the epidemiology of bladder cancer. *Am. J. Public Health* 77, 1298–1300.
24. González, C., López-Abente, G., Errezola, M., Escolar, A., Riboli, E., Izarzugaza, I., and Nebot, M. (1989). Occupation and bladder cancer in Spain: a multi-centre case-control study. *Int. J. Epidemiol.* 18, 569–577.
25. Silverman, D. T., Levin, L. I., Hoover, R. N., and Hartge, P. (1989). Occupational risk factors of bladder cancer in the United States: I. White men. *J. Natl. Cancer Inst.* 81, 1472–1480.
26. Silverman, D. T., Levin, L. I., and Hoover, R. N. (1990). Occupational risk factors of bladder cancer among white women in the United States. *Am. J. Epidemiol.* 132, 453–461.
27. Kunze, E., Chang-Claude, J., and Frentzel-Beyme, R. (1992). Life style and occupational risk factors for bladder cancer in Germany. *Cancer* 69, 1776–1790.
28. Cordier, S., Clavel, J., Limasset, J. C., Boccon-Gibod, L., Le Moual, N., Mandereau, L., and Hemon, D. (1993). Occupational risks of bladder cancer in France: A multicentre case-control study. *Int. J. Epidemiol.* 22, 403–411.
29. Siemiatycki, J., Dewar, R., Nadon, L., and Gerin, M. (1994). Occupational risk factors for bladder cancer: Results from a case-control study in Montreal, Quebec, Canada. *Am. J. Epidemiol.* 140, 1061–1080.
30. Coggon, D., Pannett, B., and Acheson, E. D. (1984). Use of job-exposure matrix in an occupational analysis of lung and bladder cancers on the basis of death certificates. *J. Natl. Cancer Inst.* 72, 61–65.
31. Schoenberg, J. B., Stemhagen, A., Mason, T. J., Patterson, J., Bill, J., and Altman, R. (1987). Occupation and lung cancer risk among New Jersey white males. *J. Natl. Cancer Inst.* 79, 3–21.
32. Benhamou, S., Benhamou, E., and Flamant, R. (1988). Occupational risk factors for lung cancer in a French case-control study. *Br. J. Ind. Med.* 45, 231–233.
33. Hoar Zahm, S., Brownson, R. C., Chang, J. C., and Davis, J. R. (1989). Study of lung cancer histologic types, occupation, and smoking in Missouri. *Am. J. Ind. Med.* 15, 565–578.
34. Siemiatycki, J. (Ed.) (1991). *Risk Factors for Cancer in the Workplace*, CRC Press, Boca Raton, FL.
35. ILO (1983). *Encyclopedia of Occupational Health and Safety* (L. Parmeggiani, Ed.), vols. 1 and 2, International Labour Office, Geneva.
36. Snyder, R., and Andrews, L. S. (1996). In *Casarett and Doull's Toxicology: The Basic Science of Poisons* (C. D. Klaassen, Ed.), pp. 737–771. McGraw-Hill, New York.
37. Kane, A. B., Boffetta, P., Saracci, R., and Wilbourn, J. D. (Eds.) (1996). *Mechanisms of Fibre Carcinogenesis*. IARC Scientific Publications No. 140. International Agency for Research on Cancer, Lyon, France.
38. Peters, G. R., McCurdy, R. F., Hindmarsh, J. T. (1996). Environmental aspects of arsenic toxicity. *Crit. Rev. Clin. Lab. Sci.* 33, 457–493.
39. Morris, R. D. (1995). Drinking water and cancer. *Environ. Health Perspect.* 103, 225–231.
40. Schwarz, R. A. (1997). Arsenic and the skin. *Int. J. Dermatol.* 36, 241–250.
41. Costa, D. L., and Amdur, M. O. (1996). Air pollution. In *Casarett and Doull's Toxicology: The Basic Science of Poisons* (C. D. Klaassen, Ed.), pp. 857–882. McGraw-Hill, New York.
42. Vedal S. (1997). Ambient particles and health: lines that divide. *J. Air and Waste Manage. Assoc.* 47, 551–581.
43. Dockery, D. W., Pope, C. A. III, Xu, X., Spengler, J., Ware, J. H, Fay, M. E., Ferris B. G. Jr., and Speizer, F. E. (1993). An association between air pollution and mortality in six U.S. cities. *N. Engl. J. Med.* 329(24), 1753–1759.
44. Katsouyanni, K., Touloumi, G., Spix, C., Schwartz, J., Balducci, F., Medina, S., Rossi, G., Wojtyniak, B., Sunyer, J., Bacharova, L., Schouten, J. P., Ponka, A., and Anderson, H. R. (1997). Short term effects of ambient sulphur dioxide and particulate matter on mortality in 12 European cities: Results from time series data from the APHEA project. *Brit. Med. J.* 314, 1658–1663.
45. Jantunen, M., Reponen, A., Kauranen, P., and Vartiainen, M. (1991). Chernobyl fallout in southern and central Finland. *Health Physics* 60: 427–434.

46. Harley, N. H. (1996). Toxic effects of radiation and radioactive materials. In *Casarett and Doull's Toxicology: The Basic Science of Poisons* (C. D. Klaassen, Ed.), pp. 773–800. McGraw-Hill, New York.
47. Ashby, J., Odum, J., Tinwell, H., and Lefevre, P. A. (1997). Assessing the risks of adverse endocrine-mediated effects: Where to from here? *Reg. Toxicol. Pharmacol.* 26, 80–93.
48. WHO (1994). Environmental Health Criteria, 170. Assessing human health risks of chemicals: derivation of guidance values for health-based exposure limits. World Health Organization, Geneva.
49. Faustman, E. M., and Omenn, G. S. (1996). Risk assessment. In *Casarett and Doull's Toxicology: The Basic Science of Poisons* (C. D. Klaassen, Ed.), pp. 75–88. McGraw-Hill, New York.
50. Jantunen, M. (1999). Risks, estimation, management and perception. In *The Urban Atmosphere and Its Effects* (P. Brimblecombe and B. Maynard, Eds.). Imperial College Press (in press).
51. Fingerhut, M. A., Halperin, W. E., Marlow, D. A., et al. (1991). Cancer mortality in workers exposed to 2,3,7,8-tetrachlorodibenzo-*p*-dioxin. *N. Engl. J. Med.* 324, 212–218.
52. Savolainen, K., and Kangas, J. (1995). Strategies for biological monitoring of workers exposed to pesticides. In *Bioindicators of Environmental Health, Ecovision World Monograph Series* (M. Munawar, O. Hänninen, S. Roy, N. Munawar, L. Kärenlampi, and D. Brown, Eds.), pp. 165–178. SPB Academic Publishing, Amsterdam.
53. de Raat, W. K., Stevenson, H., Hakkert, B. C., Hemmen van, J. J. (1997). Toxicological risk assessment of worker exposure to pesticides: Some general principles. *Reg. Toxicol. Pharmacol.* 25(3), 204–210.
54. Kangas, J., Laitinen, S., Jauhiainen, A., and Savolainen, K. (1993). Exposure of sprayers and plant handlers to mevinphos in Finnish greenhouses. *Am. Ind. Hyg. Assoc. J.* 54, 150–157.
55. Van Cauteren, H., de Kok, T. M. C. M., and van Schooten, F.-J. (1996). Introduction to carcinogenesis. In *Toxicology: Principles and Applications* (R. J. M. Niesink, J. de Vries, J. and M. A. Hollinger, Eds.), pp. 346–383. CRC Press, Boca Raton, Florida.
56. Van Cauteren, H., de Kok, T. M. C. M., and van Schooten, F.-J. (1996). Cancer risk evaluation. In *Toxicology: Principles and Applications* (R. J. M. Niesink, J. de Vries, J. and M. A. Hollinger, Eds.), pp. 385–412. CRC Press, Boca Raton, FL.
57. Niesink, R. J. M. (1996). Dermatotoxicology: Toxicological pathology and methodological aspects. In *Toxicology: Principles and Applications* (R. J. M. Niesink, J. de Vries, J. and M. A. Hollinger, Eds.), pp. 502–529. CRC Press, Boca Raton, FL.
58. Feron, V. J., Beems, R. B., Reuzel, P. G. J., and Zwart, A. (1996). Respiratory toxicology; pathophysiology, toxicological pathology and mechanisms of toxicity. In *Toxicology: Principles and Applications* (R. J. M. Niesink, J. de Vries, J. and M. A. Hollinger, Eds.), pp. 531–574. CRC Press, Boca Raton, FL.
59. Feron, V. J., Beems, R. B., Reuzel, P. G. J., and Zwart, A. (1996). Inhalatory exposure and methodological aspects. In *Toxicology: Principles and Applications* (R. J. M. Niesink, J. de Vries, J. and M. A. Hollinger, Eds.), pp. 575–604. CRC Press, Boca Raton, FL.
60. Klemmer, H. W., Wong, L., Sato, M. M., Reichert, E. L., Korsak, R. J., and Rashad, M. N. (1980). Clinical findings in workers exposed to pentachlorophenol. *Arch. Environ. Contam. Toxicol.* 9, 715–725.
61. Pekari, K., Järvisalo, J., and Aitio, A. (1985). Kinetics of urinary excretion of 2,4,6-tri-, 2,3,4,6-tetra- and pentachlorophenol in workers exposed in lumber treatment. Abstract. In *Proceedings of the 26th Congress of the European Society of Toxicology*, p. 183. University of Kuopio, Kuopio, Finland.
62. Niesink, R. J. M. (1996). Absorption, distribution and elimination of xenobiotics. In *Toxicology: Principles and Applications* (R. J. M. Niesink, J. de Vries, J. and M. A. Hollinger, Eds.), pp. 92–135. CRC Press, Boca Raton, FL.
63. Rozman, K. K., and Klaassen, C. D. (1996). Absorption, distribution, and excretion of toxicants. In *Casarett and Doull's Toxicology: The Basic Science of Poisons* (C. D. Klaassen, Ed.), pp. 91–112. McGraw-Hill, New York.
64. Aldridge, W. N. (Ed.) (1996). *Mechanisms and Concepts in Toxicology*. Taylor and Francis Ltd, London.
65. Riihimäki, V., Pfäffli, P., Savolainen, K., and Pekari, K. (1979). Kinetics of *m*-xylene in man. *Scand. J. Work Environ. Health* 5, 217–231.
66. Riihimäki, V. (1979). Kinetics of *m*-xylene in man. *Scand. J. Work Environ. Health* 5, 232–248.
67. Riihimäki, V. (1979). Percutaneous absorption of *m*-xylene from a mixture of *m*-xylene and isobutyl alcohol in man. *Scand. J. Work Environ. Health* 5, 143–150.

68. Medinsky, M. A., and Klaassen, C. D. (1996). Toxicokinetics. In *Casarett and Doull's Toxicology: The Basic Science of Poisons* (C. D. Klaassen, Ed.), pp. 187–198. McGraw-Hill, New York.
69. CEN (1993). *Workplace Atmospheres—Size Fraction Definitions for Measurements of Airborne Particles*. EN 481.
70. ISO (1992) *Air Quality—Particle Size Fraction Definitions for Health-Related Sampling*. ISO/CD 7708 International Standardization Organization, Geneva.
71. Vartiainen, T., Saarikoski, S., Jaakkola, J., and Tuomisto, J. (1997). PCDD, PCDF, and PCB concentrations in human milk from two areas in Finland. *Chemosphere* **34**(12), 2571–2583.
72. Blaauboer, B. J. (1996). Biotransformation: Detoxication and bioactivation. In *Toxicology: Principles and Applications* (R. J. M. Niesink, J. de Vries, J. and M. A. Hollinger, Eds.), pp. 40–65. CRC Press, Boca Raton, FL.
73. Nagelkerke, J. F. (1996). Nephrotoxicology: Toxicological pathology and biochemical toxicology. In *Toxicology: Principles and Applications* (R. J. M. Niesink, J. de Vries, J. and M. A. Hollinger, Eds.), pp. 724–755. CRC Press, Boca Raton, FL.
74. Witschi, H. R., and Last, J. A. (1996). Toxic responses of the respiratory system. In *Casarett and Doull's Toxicology: The Basic Science of Poisons* (C. D. Klaassen, Ed.), pp. 443–462. McGraw-Hill, New York.
75. Kamp, D. W., Graceffa, P., Pryor, W. A., and Weitzma, S. A. (1992). The role of free radicals in asbestos-induced diseases. *Free Radic. Biol. Med.* **12**(4), 293–315.
76. Marsh, J. P., and Mossman, B. T. (1991) Role of asbestos and active oxygen species in activation and expression of ornirhine decarboxylase in hamster tracheal epithelial cells. *Cancer Res.* **51**(1), 167–173.
77. Heintz, N. H., Janssen, Y. M., and Mossman, B. T. (1993). Persistant induction of c-fos and c-jun expression by asbestos. *Proc. Natl. Acad. Sci. USA* **90**(8), 3299–3303.
78. Kemler, R. (1993). From cadherins to catenins: Cytoplasmic protein interactions and reglation of cell adhesion. *Trends Genet.* **9**(9), 317–321.
79. Hamaguchi, M., Matsuyoshi, N., Ohnishi, Y., Gotoh, B., Takeichi, M., and Nagai, Y. (1993). p60v-src casues tyrosine posphorylation and inactivation of the N-cadherin-catenin cell adhesion system. *EMBO J.* **12**(1), 307–314.
80. Su, L. K., Vogelstein, B., and Kinzler, K. W. (1993). Association of the APC tumor supressor protein with catenins. *Science*. **262**(5140), 1734–1737
81. Musil, L. S., Cunningham, B. A., Edelman, G. M. and Goodenough, D. A. (1990). Differential phosphorylation of the gap junction protein connexin43 in junctional communication-competent and -deficient cell lines. *J. Cell Biol.* **111**(5, pt. 1), 2077–2088.
82. Meyer, M., Schreck, R., and Baeuerle, P. A. (1993). H_2O_2 and antioxidents have opposite effects on activation of NF-kappa B and AP-1 in intact cells: AP-1 as secondary antioxidant-responsive factor. *EMBO J.* **12**(5), 2005–2015.
83. Yamasaki, H., Krutovskikh, V., Mesnil, M., Columbano, A., Tsuda, H., and Ito, N. (1993). Gap junctional intercellular communication and cell proliferation during rat liver carcinogenesis. Academic diss., University of Helsinki.
84. Pelin, K. (1994). Asbestos-related malignant mesothelioma: Tumor cel characteristics and mechanisms in fibre carcinogenesis. Academic diss., University of Helsinki.
85. de Vries, J. (1996). Toxicokinetics: quantitative aspects. In *Toxicology: Principles and Applications* (R. J. M. Niesink, J. de Vries, J. and M. A. Hollinger, Eds.), pp. 136–183. CRC Press, Boca Raton, FL.
86. de Vries, J. (1996). Cytotoxicity: molecular mechanisms of cell death. In *Toxicology: Principles and Applications* (R. J. M. Niesink, J. de Vries, J. and M. A. Hollinger, Eds.), pp. 288–313. CRC Press, Boca Raton, FL.
87. Eaton, D. L., and Klaassen, C. D. (1996). Principles of toxicology. In *Casarett and Doull's Toxicology: The Basic Science of Poisons* (C. D. Klaassen, Ed.), pp. 13–33. McGraw-Hill, New York.
88. Deichmann, W. B., Henschler, D., Holmstedt, B., and Keil, G. (1986). What is there that is not poison? A study of the third defense by Paracelsus. *Arch. Toxicol.* **58**, 207–213.
89. Gregus, Z., and Klaassen, C. D. (1996). Mechanisms of toxicity. In *Casarett and Doull's Toxicology: The Basic Science of Poisons* (C. D. Klaassen, Ed.), pp. 35–74. McGraw-Hill, New York.
90. Searle, J., Kerr, J. F., and Bishop, C. J., (1982). Necrosis and apoptosis: Distinct modes of cell death with fundamentally different significance. *Pathol. Annu.*, 17(pt. 2), 229–259.

91. Corcoran, G. B., Fix, L., Jones, D. P., Moslen, M. T., Nicotera, P., Oberhammer, F. A., and Buttyan, R. (1994). Contemporary issues in toxicology. Apoptosis: molecular control point in toxicity. *Toxicol. Appl. Pharmacol.* **128**, 169–181.
92. Savolainen, K., Hirvonen, M.-R., and Naarala, J. (1994). Phosphoinositide second messengers in cholinergic excitotoxicity. *Neuro toxicology* **15**(3), 493–502.
93. Coyle, J. T., and Puttfarcken, P. (1993). Oxidative stress, glutamate, and neurodegenerative disorders. *Science* **262**, 689–694.
94. Felder, C. C. (1995). Muscarinic acetylcholine receptors: Signal transduction through multiple effectors. *FASEB J.* **9**, 619–625.
95. Gustafsson, J.-Å., Kuiper, G., Enmark, E., Treuter, E., and Rafter, J. (1998). Receptor-mediated toxicity. In *Diversification in Toxicology—Man and Environment* (J. P. Seiler, J. L. Autrup, and H. Autrup, Eds.), pp. 21–28. Proceedings of the 1997 EUROTOX Congress, June 25-28, 1997. Århus, Denmark.
96. Barnes, P. J., and Belvisi, M. G. (1993). Nitric oxide and lung disease. *Thorax* **48**, 1034–1043.
97. Moncada, S., and Higgs, A. (1993). The L-arginine-nitric oxide pathway. *N. Engl. J. Med.* **329**, 2002–2012.
98. Capen, C. C. (1996). Toxic responses of the endocrine system. In *Casarett and Doull's Toxicology: The Basic Science of Poisons* (C. D. Klaassen, Ed.), pp. 617–640. McGraw-Hill, New York.
99. Ecobichon, D. J. (1996). Toxic effects of pesticides. In *Casarett and Doull's Toxicology: The Basic Science of Poisons* (C. D. Klaassen, Ed.), pp. 643–689. McGraw-Hill, New York.
100. Tilson, H. A., and Kodavanti, P. R. S. (1998). The neurotoxicity of polychlorinated biphenyls. *Neuro toxicology* **19**(4–5), 517–526.
101. Pazdernik, T. L., Cross, R. S., Giesler, M., and Samson, F. E. (1985). Changes in local cerebral glucose utilization induced by convulsants. *Neuroscience* **14**(3), 823–835.
102. Hirvonen, M. R., Paljärvi, L., and Savolainen, K. M. (1993). Sustained effects of pilocarpine-induced convulsions on brain inositol and inositol monophosphate levels, and brain morphology in young and old male rats. *Toxicol. Appl. Pharmacol.* **122**, 290–299.
103. Naarala, J., Loikkanen, J. J., Ruotsalainen, M. H., and Savolainen, K. M. (1995). Lead amplifies glutamate-induced oxidative stress. *Free Rad. Biol. Med.* 19, 689–693.
104. Loikkanen, J., Naarala, J., and Savolainen, K. M. (1998). Modification of glutamate-induced oxidative stress by lead: The role of extracellular calcium. *Free Rad. Biol. Med.*, **24**, 377–384.
105. Halliwell, B. (1992). Reactive oxygen species and the central nervous system. *J. Neurochem.* 59, 1609–1623.
106. Savolainen, K. M., Loikkanen, J., Eerikäinen, S., and Naarala, J. (1998). Interactions of excitatory neurotransmitters and xenobiotics in excitotoxicity and oxidative stress: Glutamate and lead. *Toxicol. Lett.* **102–103**, 363–367.
107. Anthony, D. C., Montine, T. J., and Graham, D. G. (1996). Toxic responses of the nervous system. In *Casarett and Doull's Toxicology: The Basic Science of Poisons* (C. D. Klaassen, Ed.), pp. 463–486. McGraw-Hill, New York.
108. Snodgrass, W. R. (1996). Clinical toxicology. In *Casarett and Doull's Toxicology: The Basic Science of Poisons* (C. D. Klaassen, Ed.), pp. 969–986. McGraw-Hill, New York.
109. Laywerys, R. R. (1972). *Precis de toxicologie industrielle et des intoxications professionelles.* Ed. J. Duculot, Gembloux.
110. Clarkson, T. (1991). Methylmercury. *Fundam. Appl. Toxicol.* **16**(1), 20–21.
111. Stevens, J. T., and Sumner, D. D. (1991). Herbicides. In *Handbook of Persticide Toxicology, Classes of Pesticides* (W. J. Hayes, and E. R. Laws, Eds.), vol. 3, pp. 1317–1391. Academic Press, San Diego.
112. Tsien, R. W., and Malinow, R. (1991). Changes in presynaptic function during long term potentiation. Ann. N Y Acad. Sci. **635**(1992), 208–220.
113. Stendahl, O., Krause, K.-H., Krischer, J., Jerström, P., Theler, J.-M., Clark, R. A., Carpertier, J.-L., and Lew, D. P. (1994). Redistribution of intracellular Ca^{2+} stores during phagocytosis in human neutrophils. *Science* **265**, 1439–1441.
114. Orrenius, S., McCabe, M. J., and Nicotera, P. (1992). Ca^{2+}-dependent mechanisms of cytotoxicity and programmed cell death. *Toxicol. Lett.* **64/64**, 357–364.
115. Nieminen, A.-L., Gores, G. J., Wray, B. E., Tanaka, Y., Herman, B., and Lemasters, J. J. (1988). Calcium dependence of bleb formation and cell death in hepatocytes. *Cell Calcium* **9**, 237–246.
116. Dörger, M., Jesch, N. K., Rieder, G., Hirvonen, M.-R., Savolainen, K., Krombach, F., and Messmer, K. (1997). Species differences in NO formation by rat and hamster alveolar macrophages in vitro. *Am. J. Respir. Cell Mol. Biol.* **16**, 413–420.

117. Clancy, R. M., and Abramson, S. B. (1993). Nitric oxide: A novel mediator of inflammation. *Proc. Soc. Exp. Biol. Med.* **210**, 93–101.
118. Hibbs, J. B., Taintor, R. R., Vavrin, Z., and Rachlin, E. M. (1988). Nitric oxide: A cytotoxic activated macrophage effector molecule. *Biochem. Biophys. Res. Commun.* **157**, 87–94.
119. Laskin, J. D., Heck, D. E., and Laskin, D. L. (1994.) Multifunctional role of nitric oxide in inflammation. *TEM* **5**, 377–382.
120. Burns, L. A., Meade, B. J., and Munson, A. E. (1996). Toxic responses of the immune system. In *Casarett and Doull's Toxicology: The Basic Science of Poisons* (C. D. Klaassen, Ed.), pp. 355–402. McGraw-Hill, New York.
121. Corcoran, G. B., and Ray, S. D. (1992). The role of the nucleus and other compartments in toxic cell death produced by alkylating hepatotoxicants. *Toxicol. Appl. Pharmacol.* **113**(2), 167–183.
122. Bursch, W. Oberhammer, F., and Schulte-Hermann, R. (1992). Cell death by apoptosis and its protective role against disease. *Trends Pharmacol. Sci.* **13**(6), 245–251.
123. Nagata, S., and Goldstein, P., (1995). The Fas death factor. *Science* **267**(5203), 1449–1456.
124. Dybukt, J. M., Ankarcrona, M., Burkitt, M., Sjöholm, Å., Ström, K., Orrenius, S., and Nicotera, P. (1994). Different prooxidant levels stimulate growth, trigger apoptosis, or produce necrosis of insulin-secreting RINm5F cells. *J. Biol. Chem.* **269**, 30553–30560.
125. Dekant, W., and Vamvakas, S. (1996). Biotransformation and membrane transport in nephrotoxicity. *Crit. Rev. Toxicol.* **26**(3): 309–334.
126. Solberg, Y., and Belkin, M. (1997). The role of excitotoxicity in organophosphorous nerve agents central poisoning. *Trends. Pharmacol. Sci.* **18**(6), 183–185.
127. Brown, M. A., and Brix, K. A. (1998). Review of health consequences from high-, intermediate- and low-level exposure to organophosphorus nerve agents. *J. Appl. Toxicol.* **18**, 393–408.
128. Halliwell, B. (1997). Antioxidants: The basics—what they are and how to evaluate them. *Adv. Pharmacol.* **38**, 3–20.
129. van Delft J. H. M., Baan, R. A., and Roza, L. (1998). Biological effect markers for exposure to carcinogenic compound and their relevance for risk assessment. *Crit. Rev. Toxicol.* **28**(5), 477–510.
130. Hoffmann, G. R. (1996). Genetic toxicology. In *Casarett and Doull's Toxicology: The Basic Science of Poisons* (C. D. Klaassen, Ed.), p. 281. McGraw-Hill, New York.
131. Parkinson, A. (1996). Biotransformation of xenobiotics. In *Casarett and Doull's Toxicology: The Basic Science of Poisons* (C. D. Klaassen, Ed.), pp. 113–186. McGraw-Hill, New York.
132. Kraeling, M. E. K., Reddy, K., and Bronaugh, R. L. (1998). Percutaneous absorption of trinitrobenzene: animal models for human skin. *J. Appl. Toxicol.* **18**, 387–392.
133. Cavanagh, J. B. (1985). Mechanism of organic solvent toxicity: Morphological changes. WHO Environmental Health Series 5, 110–135.
134. Mikkelsen, S., Jorgensen, M., Browne, E., and Gyldensten, C. (1988). Mixed solvent exposure and organic brain damage: A study of painters. *Acta Neurol. Scand.* **78**, 1–143.
135. Atterwill, C. K. (1989). Brain reaggregate cultures in neurotoxicological investigations: Adaptational and neurodegenerative processes following lesions. *Mol. Toxicol.* **1**, 489–502.
136. Spencer, P. S., and Schaumburg, H. H. (1985). Organic solvent neurotoxicity: Facts and research needs. *Scand. J. Environ. Health* **11**, 53–60.
137. Bast, A. (1996). Anatomy and toxicological pathology of the nervous system. In *Toxicology: Principles and Applications* (R. J. M. Niesink, J. de Vries, J. and M. A. Hollinger, Eds.), pp. 974–1001. CRC Press, Boca Raton, FL.
138. Ruff, R. L., Petito, C. K., and Acheson, L. S. (1981). Neuropathy associated with chronic low level exposure to *n*-hexane. *Clin. Toxicol.* **18**, 515–519.
139. Bernsen, H. J. J. A., Verhagen, V. I. M., De Bijl, M. A. O., and Heerschap, A. (1992). Magnetic resonance studies on brain dysfunction induced by organic solvents. *Acta Neurol. Belg.* **92**, 207–214.
140. Potts, A. M. (1996). Toxic responses of the eye. In *Casarett and Doull's Toxicology: The Basic Science of Poisons* (C.D. Klaassen, Ed.), pp. 583–615. McGraw-Hill, New York.
141. Doll, R., Peto, T., Wheatley, K., Gray, R., and Sutherland, I. (1994). Mortality in relation to smoking: 40 years' observations on male British doctors. *Brit. Med. J.* **309**, 901–911.
142. Doll, R., and Hill, A. B. (1950). Smoking and carcinoma of the lung: Preliminary report. *BMJ* ii, 739–748
143. Doll, R., and Hill, A. B. (1964). Mortality in relation to smoking: Ten years' observation of british doctors. *BMJ* ii, 1399–1414, 1460–1467.

144. Doll, R., and Peto, R., (1976). Mortality in relation to smoking: 20 years' observations of British doctors. *BMJ* ii, 1525–1536.
145. Verheyen, A. (1996). Cardiovascular toxicology: Toxicological pathology and methodological aspects. In *Toxicology: Principles and Applications* (R. J. M. Niesink, J. de Vries, J. and M. A. Hollinger, Eds.), pp. 788–815. CRC Press, Boca Raton, FL.
146. Moslen, M. T. (1996). Toxic responses of the liver. In *Casarett and Doull's Toxicology: The Basic Science of Poisons* (C. D. Klaassen, Ed.), pp. 403–416. McGraw-Hill, New York.
147. Vandenberghe, J. (1996). Hepatotoxicology: Structure, function and toxicological pathology. In *Toxicology: Principles and Applications* (R. J. M. Niesink, J. de Vries, J. and M. A. Hollinger, Eds.), pp. 668–700. CRC Press, Boca Raton, FL.
148. Vandenberghe, J. (1996). Hepatotoxicology: Mechanisms of liver toxicity and methodological aspects. In *Toxicology: Principles and Applications* (R. J. M. Niesink, J. de Vries, J. and M. A. Hollinger, Eds.), pp. 702–723. CRC Press, Boca Raton, FL.
149. Sotaniemi, E. A., Ahlqvist, R. O., Pelkonen, R. O. et al. (1977). Histologic changes in the liver and indices of drug metabolism in alcoholics. *Eur. J. Clin. Pharmacol.* **11**, 295–303.
150. International Agency for Research on Cancer (1987). Overall Evaluations of Carcinogenicity: An Updating of IARC Monographs Volumes 1 to 42. IARC Monographs on Evaluation of the Carcinogenic Risks of Chemicals to Humans, Suppl. 7. International Agency for Research on Cancer, Lyon, France.
151. Savolainen, K., and Vähäkangas, K. (1998). Toksikologian perusteet. Elintoksikologia. In *Lääketieteellinen Farmakologia ja Toksikologia* (O. Pelkonen and H. Ruskoaho, Eds.). Duodecim, Helsinki.
152. Klaassen, C. D., Watkins, J. B. (1984). Mechanisms of bile formation, hepatic uptake, and biliary excretion. *Pharmacol. Rev.* **36**, 1–67.
153. Recknagel, R. O. (1967). Carbon tetrachloride hepatotoxicity. *Pharmacol. Rev.* **19**, 145–208.
154. Thomas, J. A. (1996). Toxic responses of the reproductive system. In *Casarett and Doull's Toxicology: The Basic Science of Poisons* (C. D. Klaassen, Ed.), pp. 547–581. McGraw-Hill, New York.
155. van Leeuwen, F. X. R., Krajnc-Franken, M. A. M., and Loeber, J. G. (1996). Endocrinotoxicology: Methodological aspects. In *Toxicology: Principles and Applications* (R. J. M. Niesink, J. de Vries, J. and M. A. Hollinger, Eds.), pp. 890–926. CRC Press, Boca Raton, FL.
156. Perez, P., Pulgar, R., Olea-Serrano, F., Villabos, M., Rivas, A., Metzler, M., Pedraza, V., and Olea, N. (1998). The estrogenicity of bisphenol A-related diphenylalkanes with various substituents at the central carbon and the hydroxy groups. *Environ. Health Perspect.* **106**(3), 167–174.
157. Reiter, L. W., DeRosa, C., Kavlock, R. J., Lucier, G., Mac, J. M., Melillo, J., Melnick, R. L., Sinks, T., and Walton, B. T. (1998). The U.S. federal framework for research on endocrine disruptors and an analysis of research programs supported during fiscal year 1996. *Environ. Health Perspect.* **106**(3), 105–113.
158. Smith, R. P. (1996). Toxic responses of the blood. In *Casarett and Doull's Toxicology: The Basic Science of Poisons* (C. D. Klaassen, Ed.), pp. 335–354. McGraw-Hill, New York.
159. Marx, J. J. M. (1996). Immunotoxicology: Determination of immunotoxic effects and immunotoxicity mechanisms. In *Toxicology: Principles and Applications* (R. J. M. Niesink, J. de Vries, J. and M. A. Hollinger, Eds.), pp. 816–839. CRC Press, Boca Raton, FL.
160. Leino, T., Tammilehto, L., Hytönen, M., Sala, E., Paakkulainen, H., Kanerva, L. (1998). Occupational skin and respiratory diseases among hairdressers. *Scand. J. Work Environ. Health* **24**(5), 398–406.
161. Rice, R. H., and Cohen, D. E. (1996). Toxic responses of the skin. In *Casarett and Doull's Toxicology: The Basic Science of Poisons* (C. D. Klaassen, Ed.), pp. 529–546. McGraw-Hill, New York.
162. Vos, J. G., and van Loveren, H. (1996). Immunotoxicology: Determination of immunotoxic effects and immunotoxicity mechanisms. In *Toxicology: Principles and Applications* (R. J. M. Niesink, J. de Vries, J. and M. A. Hollinger, Eds.), pp. 841–868. CRC Press, Boca Raton, FL.
163. Vos, J. G., and van Loveren, H. (1996). Immunotoxicology: Examples of immunotoxic substances. In *Toxicology: Principles and Applications* (R. J. M. Niesink, J. de Vries, J. and M. A. Hollinger, Eds.), pp. 870–889. CRC Press, Boca Raton, FL.
164. Moses, M., and Prioleau, P. G. (1985). Cutaneous histologic findings in chemical workers with and without chloracne with past exposure to 2,3,7,8-tetrachlorodibenzo-*p*-dioxin. *J. Am. Acad. Dermatol.* **12**, 497–506.

165. Hardell, L., Eriksson, M., Degerman A. (1994). Exposure to phenoxyacetic acids, chlorophenols, or organic solvents in relation to histopathology, stage, and anatomical localization of non-Hodgkin's lymphoma. *Cancer Res.* **54**, 2386–2389.
166. Coombs, R. R. A., and Gell, P. G. H. (1975). Classification of allergic reactions responsible for clinical hypersensitivity and disease. In *Clinical Aspects of Immunology* (P. G. H. Gell, R. R. A. Coombs, and P. J. Lachmann, Eds.), p. 761. Oxford University Press, Oxford.
167. Rogers, J. M., and Kavlock, R. J. (1996). Developmental toxicology. In *Casarett and Doull's Toxicology: The Basic Science of Poisons* (C. D. Klaassen, Ed.), pp. 301–331. McGraw-Hill, New York.
168. Shepard, T. H. (1992). *Catalog of Teratogenic Agents* (7th ed.) Johns Hopkins University Press, Baltimore.
169. Teratology Society (1994). FDA classification system of drugs for teratogenic risk. *Teratology* **49**, 446–447.
170. Wilson, J. G. (1973). *Environment and Birth Defects*. Academic Press, Baltimore.
171. MacDonald, H., and Tobin, J. O. H. (1978). Congenital cytomegalovirus infection: A collaborative study on epidemiological, clinical and laboratory findings. *Dev. Med. Child Neurol.* 20, 271–282.
172. Edwards, M. J. (1986). Hyperthermia as a teratogen: A review of experimental studies and their clinical significance. *Teratog. Carcinog. Mutag.* **6**, 563–582.
173. Keen, C. L., Bendich, A., Willhite, C. C. (Eds.) (1993). Maternal nutrition and pregnancy outcome. *Ann. NY Acad. Sci.* **678**, 1–372.
174. Taussig, H. B. (1962). A study of the German outbreak of phocomelia: The thalidomide syndrome. *JAMA* **180**, 1106.
175. Bakir, R., Damluji, S. F., Amin-Zaki, L., et al. (1973). Methyl mercury poisoning in Iraq. *Science* **181**, 230–241.
176. Goyer, R.A. (1996). Toxic effects of metals. In *Casarett and Doull's Toxicology: The Basic Science of Poisons* (C. D. Klaassen, Ed.), pp. 691–736. McGraw-Hill, New York.
177. Pratt, O. E. (1982). Alcohol and the developing fetus. *Br. Med. Bull.* **38**, 48–53.
178. Ames, B. N., Magaw, R., Gold, L. S. (1987). Ranking possible carcinogenic hazards. *Science* **236**, 271–280.
179. Vähäkangas, K., and Savolainen, K. (1998). Toksikologian perusteet. Periaatteet ja yleistoksikologia. In *Lääketieteellinen Farmakologia ja Toksikologia* (Pelkonen, O., and Ruskoaho, H., Eds.) Duodecim, Helsinki.
180. Purchase, I. F. H. (1994). Current knowledge of mechanisms of carcinogenicity: Genotoxins versus non-genotoxins. *Hum. Exp. Toxicol.* 13, 17–28.
181. Slovic, P., Malmfors, T., Mertz, C. K., Neil, N., and Purchase, I. F. (1997). Evaluating chemical risks: Results of a survey of the British Toxicology Society. *Hum. Exp. Toxicol.* **16**(6), 289–304.
182. Savolainen, K. M. (1997). The use of maximum tolerated dose in rodent carcinogenicity bioassays and its relevance to human risk assessment. *Hum. Exp. Toxicol.* **16**, 190–192.
183. Ames, B. N., and Gold, L. S. (1990). Too many rodent carcinogens: Mitogenesis increases mutagenesis. *Science* **249**, 970–971.
184. Beach, A. C., and Gupta, R. C. (1992). Human biomonitoring and the ^{32}P-postlabelling assay. *Carcinogenesis* **13**, 1053–1074.
185. dell'Omo, M., Muzi, G., Bernard, A., Filiberto, S., Lauwerys, R. R., and Abbritti, G. (1997). Long-term pulmonary and systemic toxicity following intravenous mercury injection. *Arch. Toxicol.* 72(1), 59–62.
186. Hemminki, K., Soederling, J., Ericson, P., Norbeck, H. E., and Segerbaeck, D. (1994). DNA adducts among personnel servicing and loading diesel vehicles. *Carcinogenesis* **15**, 767–769.
187. Hsu, I. C., Metcalf, R. A., Sun, T., Welsh, J. A., Wang, N. J., and Harris, C. C. (1991). Mutational hotspot in the p53 gene in human hepatocellular carcinomas. *Nature* **350**, 427–428.
188. Mass, M. J., Abu-Shakra, A., Roop, B. C., Nelson, G., Galati, A. J., Stoner, G. D., Nesnow, S., and Ross, J. A. (1996). Benzo[*b*]fluoranthene: tumorgenicity in strain A/J mouse lungs, DNA adducts and mutations in the Ki-ras oncogene. *Carcinogenesis* 17, 1701–1704.
189. Perera, F. P., Hemminki, K., Gryzbowska, E., Motykiewicz, G., Michalska, J., Santella, R. M., Young, T. L., Dickey, C., Brandt-Rauf, P., DeVivo, I., Blaner, W., Tsai, W.-Y., and Chorazy, M. (1992). Molecular and genetic damage in humans from environmental pollution in Poland. *Nature* **360**, 256–258.

190. Suzuki, H., Takahashi, T., Kuroishi, T., Suyama, M., Ariyoshi, Y., Takahashi, T., and Ueda, R. (1992). p53 mutations in non-small cell lung cancer in Japan: Association between mutations and smoking. *Cancer Res.* **52**, 734–736.
191. Soini, Y., Welsh, J. A., Ishak, K. G., and Bennet, W. P. (1995). p53 mutations in primary hepatic angiosarcomas not associated with vinyl chloride exposure. *Carcinogenesis* **16**, 2879–2881.
192. Kalliokoski, P., Pfäffli, P., Riihimäki, V., Starck, J., Vaaranen, V., and Helminen, P. (1992). *Occupational Hygiene—Working Conditions and Their Improvement*, p. 165. The Finnish Institute of Occupational Hygiene, Helsinki (in Finnish).
193. CEN (1992). Workplace atmospheres — Guidance for the assessment of exposure by inhalation to chemical agents for comparison with limit values and measurement strategy. EN 689.
194. Boleij, J. S. M, Buringh, E., Heederik, D., and Kromhout, H. (1995). *Occupational Hygiene of Chemical and Biological Agents*, pp. 106–109. Elsevier, Amsterdam.
195. Kalliokoski, P. (1990). Estimating long-term exposure levels in process-type industries using production rates. *Am. Ind. Hyg. Assoc. J.* **51**, 310–312.
196. AIHA and ACGIH (1998). No value BEIs issues and implications of biomonitoring without limits. Roundtable 214, American Industrial Hygiene Conference and Exposition, May 9-15, 1998, Atlanta, Georgia.
197. Harris, C. C. (1989). Interindividual variation among humans in carcinogen metabolism, DNA adduct formation and DNA repair. *Carcinogenesis* **10**, 1563–1566.
198. van Delft, J. H. M., Steenwinkel, M.-J. S. T., van Asten, S., and Baan, R. A. (1997). Monitoring of occupational exposure to polycyclic aromatic hydrocarbons in a carbon-electrode manufacturing plant. *Ann. Occup. Hyg.* **42**, 105–114.
199. dell'Omo, M., and Lauwerys, R. R. (1993). Adducts to macromolecules in the biological monitoring of workers exposed to polycyclic aromatic hydrocarbons. *Crit. Rev. Toxicol.* **23**, 111–126.
200. Timbrell, J. A. (1998). Biomarkers in toxicology. *Toxicology* **129**, 1–12.
201. Hard, G. C. (1998). Recent developments in the investigation of thyroid regulation and thyroid carcinogenesis. *Environ. Health Perspect.* **106**(8), 427–436.
202. Hurley, P. M., Hill, R. N., and Whiting, R. J. (1998). Mode of carcinogenic action of pesticides inducing thyroid follicular cell tumors in rodents. *Environ. Health Perspect.* **106**(8), 437–445.
203. Hill, R. N., Crisp, T. M., Hurley, P. M., Rosenthal, S. L., and Singh, D. V. (1998). Risk assessment of thyroid follicular cell tumors. *Environ. Health Perspect.* **106**(8), 447–457.
204. International Agency for Research on Cancer (1989). *Diesel and Gasoline Engine Exhausts and Some Nitroarenes.* IARC Monographs on the Evaluation of Carcinogenic Risks to Humans, vol. 46. International Agency for Research on Cancer, Lyon, France.
205. Pelin, K., Hirvonen, A., Taavitsainen, M., and Linnainmaa, K. (1995). Cytogenetic response to asbestos fibers in cultured human primary mesothelial cells from 10 different donors. *Mutat. Res.* **334**, 225–233.
206. Pelin, K., Kivipensas, P., and Linnainmaa, K. (1995). Effects of asbestos and man-made vitreous fibers on cell division in cultured human mesothelial cells in comparison to rodent cells. *Environ. Mol. Mutag.* **25**, 118–125. International Agency for Research on Cancer (1988). *Man-made Mineral Fibres and Radon.* IARC Monographs on the Evaluation of Carcinogenic Risks to Humans, vol. 43. International Agency for Research on Cancer, Lyon, France.
207. International Agency for Research on Cancer (1988). *Alcohol Drinking.* IARC Monographs on the Evaluation of Carcinogenic Risks to Humans, vol. 44. International Agency for Research on Cancer, Lyon, France.

Bibliography

Corcoran, G. B., Fix, L., Jones, D. P., Moslen, M. T., Nicotera, P., Oberhammer, F. A., and Buttyan, R. (1994). Contemporary issues in toxicology. Apoptosis: molecular control point in toxicity. *Toxicol. Appl. Pharmacol.* **128**, 169–181.

Grynkiewicz, G., Poenie, M., and Tsien, R. Y. (1985). A new generation of Ca^{2+} indicators with greatly improved fluorescence properties. *J. Biol. Chem.* **260**, 3440–3450.

Hirvonen M.-R., Nevalainen, A., N, Mönkkönen, J., and Savolainen, K. (1997). Streptomyces spores from mouldy houses induce nitric acid, TNFα and IL-6 secretion from RAW264.7 macrophage cell line without causing subsequent cell death. *Environ. Toxicol. Pharmacol.* 4, 57–63.

Kurttio, P., and Savolainen, K. (1990). Ethylenethiourea in air and in urine: Implications to exposure to ethylenebisdithiocarbamate fungicides. *Scand. J. Work Environ. Health* **16**, 203–207.

5.4 VENTILATION NOISE—CHARACTERISTICS, EFFECTS, AND SUGGESTED COUNTER-MEASURES

5.4.1 Occurrence

Ventilation is encountered today in practically all types of indoor environments, e.g., in dwellings, leisure facilities, service facilities, schools, hospitals, factories, machine rooms, workshops, stores, offices, vehicles, meeting rooms, teaching areas, restrooms, and control rooms. The problem affects a very large number of people, both at work and during their leisure time. Complaints about ventilation noise have increased in recent years, at the same time as very limited efforts have been made to deal with the problem. The recommendations applicable to ventilation noise usually indicate a maximum acceptable level of 35–40 dB(A). The highest recommended levels are exceeded, however, in many environments.

A schematic view of a typical central station ventilation system, including a fan, ducts, and diffusers, is given in Fig. 5.59.

5.4.2 Ventilation Noise as an Environmental Problem

Noise generated from ventilation systems can constitute a big problem, particularly in environments where other ambient noise is low. For this reason, ventilation noise has attracted particular attention in environments such as offices, schools, and public areas. The effects which occur there are due primarily to ventilation noise levels that are below the level at which there is a risk of hearing damage. The most common effects are a feeling of annoyance and disturbance of work due to fatigue or disturbed concentration. Ventilation noise also occurs, of course, in other environments with special demands on air quality and air change. In some environments, such as workshops, warehouses, machine rooms, garages, etc., the great need for air changing may lead to relatively high ventilation noise levels. The noise from large fans may in

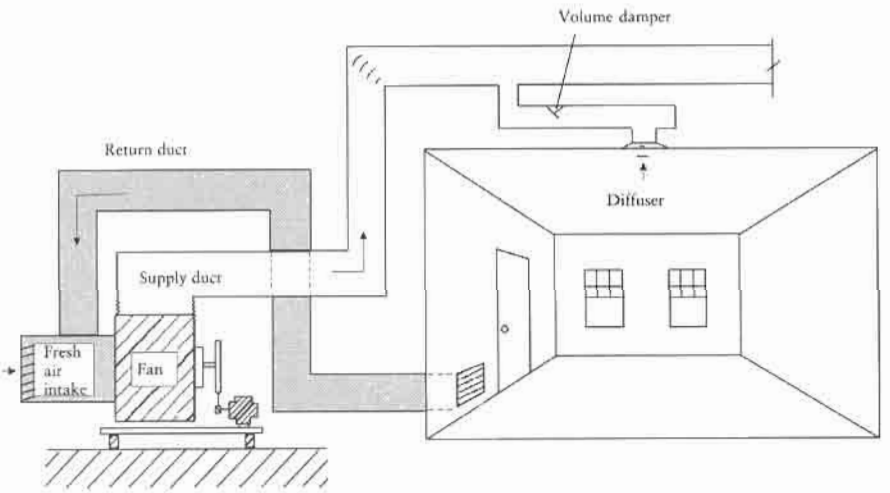

FIGURE 5.59 Schematic view of a typical central station ventilation system, including a fan, ducts, and diffusers.[1]

such cases sometimes reach levels around the threshold for hearing damage. A risk for hearing damage appears in cases of repeated daily exposure above 70 dB(A). Another problem which may arise at high levels of ventilation noise is masking of speech or of other sound signals. In most cases, the sound from ventilation noise is dominated by low-frequency components, which means that the speech-masking effect is not always pronounced. The biggest speech-masking effect occurs if the background noise coincides with the speech frequency range, 500–4000 Hz.

Ventilation noise and the annoyance effects which may result have been a recurring question in recent years for researchers, occupational health services, and various authorities. In spite of this, there are still major shortcomings in our knowledge about the links between human effects and exposure to ventilation noise. Current regulations and recommendations are thus based on uncertain principles in certain respects.

Today there is a pronounced need to take more effective measures against this type of noise. The problem is complicated, however, by the fact that these measures in many instances are unilaterally targeted at achieving a lowering of the dB(A) level, which in many cases has resulted in only a marginal restriction of the inconvenience, or even none at all.

5.4.3 Physical Characteristics

Ventilation noise originates primarily from fans and the air turbulence generated inside ducts and around supply air and exhaust air terminal devices. The appearance of the noise is, of course, affected by factors such as the speed of rotation and the power of the fan, and by how the fan is stabilized or in other ways acoustically insulated. The noise level and the frequency characteristics are also largely determined by the velocity of the air inside ducts and around terminal devices, where factors such as the dimensions and appearance of the ducts and terminal devices may play a decisive role in the appearance of the noise.

The description of the physical characteristics of ventilation noise is based on more reliable knowledge than the description of the human effect. Misconceptions about the levels and frequency characteristics of ventilation noise are still common. This in turn has sometimes led to wrong suggestions about the measures that should be taken in order to eliminate the effects of a ventilation noise exposure.

The links between levels of exposure and inconvenience caused by ventilation noise are described in an investigation carried out on office workers.[2] Technical measurements and analyses of the ventilation noise at 155 typical office workplaces were in this study combined with assessments by the office workers of the level of disturbance that they experienced, the effect on working performance, fatigue, stress-related pain, and headaches. The average noise level was about 40 dB(A) at two of the workplaces, while it was about 35 dB(A) at two others. It emerged from the narrow-band analyses that the sound pressure levels of the infrasound were not in any event of an order that this type of sound frequencies (below 20 Hz) could contribute to any disturbance effects. Any steps taken to counter the sound frequencies of the ventilation noise under 50 Hz, i.e., the point of intersection between the threshold curve of auditory perception and the spectral level distribution curve of

the ventilation noise, would thus be ineffective in these cases. This conclusion is based on the fact that the sound pressure levels of the ventilation noise frequency under 50 Hz were significantly below the threshold curve of auditory perception, and as such were not audible. This situation is considered to be representative of today's ventilation noise in offices. The same results were obtained in a study by Pääkkönen.[3] It must be pointed out, however, that levels above the perception threshold in the infrasound range can, of course, be generated from heavy-duty ventilation systems, for example in factories, stores, and department stores.

It should also be pointed out that the levels from ventilation noise in, for example, workshop premises are often lower than those emanating from other sources, for example machines of various kinds. It is not uncommon for the ventilation noise from industrial premises to cause more disturbance in adjacent offices than in the industrial premises themselves. The fact that ventilation noise propagates in this manner is due to its pronounced low-frequency character. The more low-frequency components in the noise, the greater the propagation. Sound radiation from industrial premises, via duct openings in facades and roofs, may in this manner also cause disturbances in nearby residential accommodations.

5.4.4 Noise Generation

The fan is usually the main source of noise generation in a ventilation system. Rotating fans always constitute a source of noise generation. However, aerodynamically designed fan blades may reduce the noise generated. Another important source of noise is the bearings of various kinds inside the fan motor. Defective bearings add directly to the ventilation noise. Another common reason for high noise levels may be the imbalances which easily arise in a fan system or ductwork. Imbalances give rise to vibration and hence to noise generation. The noise generated by a fan may also be due to poor impact sound insulation in the fan mountings and duct connections. Noise from drive motors for the fan may cause strong radiation from a fan room, especially if it has poor sound insulation.

The noise from the fan is propagated in the duct to the openings inwards or outwards in the premises. The ventilation noise often propagates into the surrounding area from the supply air and exhaust air terminal units in the rooms. The ducts in themselves may also be important sources of noise, particularly if they are poorly insulated or otherwise designed in such a way that noise generation may occur.

Noise generation in the ducts may occur as a result of unfortunately positioned bends, inappropriate geometry, or imbalances. Supply and exhaust air terminal devices may themselves create noise if the air velocity is high or the devices are designed in such a way as to cause air turbulence. The higher the air velocity, the greater the risk of noise-generating turbulence occurring in the ducts.

5.4.5 Effects on Humans

5.4.5.1 Influence on Disturbance and Working Performance

The office workers involved in the study mentioned above[2] rated the ventilation noise as "somewhat disturbing" to "quite disturbing" at the two workplaces where the level of exposure was about 40 dB(A). At the two workplaces

where the mean level was 5 dB lower, the mean rating lay between "not at all disturbing" and "somewhat disturbing." The difference in level resulted in a clearly perceivable lowering of the average disturbance and inconvenience levels. The fact that a 5-dB reduction in the ventilation noise level can result in such a pronounced reduction of the perceived inconvenience can be explained by the circumstance that a change in level in the low-frequency range has a significantly greater effect on the loudness than would be the case in a high-frequency sound range. Measures to achieve a reduction in ventilation noise of the order of 5 dB can thus result in measurable gains in the form of lower inconvenience reactions.

The range of answers to the question, "How does ventilation noise affect your ability to perform your tasks?" reveals that about one in every five office workers on average felt that ventilation noise made their work more difficult. A significantly greater number assessed the higher level at 40 dB(A) as an aggravating factor in the performance of their tasks at the office. About 20% considered that the higher level made their work "somewhat" or "much" more difficult. About 10% made a similar assessment at the noise level of 35 dB(A).

5.4.5.2 Influence Due to Spectral Distribution

Systematic studies have been carried out for the purpose of studying how low-frequency tones, broad-band components, and/or time fluctuations in ventilation noise interfere with disturbance reactions.[4] In one of these studies, the respondents were exposed to ventilation noise that is representative of the noise encountered in office premises. The respondents were asked to use a rotating potentiometer to "set" the "most acceptable noise level" and the "least acceptable noise level" for each noise, taking account of comfort, disturbance, and performance, while performing their work at the same time. The noise level was maintained at a constant level of 40 dB(A).

When setting the most acceptable ventilation noise level consisting of a single tone, all the respondents selected a lower tone frequency for both settings than when they set the least acceptable level. The average frequencies set for the most acceptable and the least acceptable noise levels were 58 and 380 Hz respectively. The disturbance experienced and the discomfort experienced were significantly higher, and the performance was significantly lower, during exposure to the least acceptable noise. A higher level of exertion was also experienced when exposed to the most acceptable noise.

The results clearly indicated that the ventilation noise was perceived as most acceptable when the tone was situated in the lower part of the frequency range. The experience of disturbance and the associated effects occur at exposure levels above the auditory perception threshold. Above this level, the risk of these effects increases as the perceived loudness increases, provided that the other conditions remain constant. Since the loudness can be predicted relatively accurately by means of technical measurements, any differences in the degree of disturbance can also be predicted by reference to these measurements, provided that they are dependent on differences in the loudness.

At the same dB(A) level, the noise with the stronger low-frequency feature was thus experienced as being significantly less disturbing than the more high-frequency noise. This result suggests that the A-weighting overestimates the contribution made by low-frequency tones to the disturbance experienced. This could be taken to mean that the general applicability of the dB(A) level is extremely limited at times when the goal is to carry out evaluations of the anticipated disturbance effects of ventilation noise containing tones.

An investigation designed as a tone experiment was also carried out on a broad-band ventilation noise. The average mid-range frequency for the broad band indicated by each respondent when the most acceptable and least acceptable noise levels were set reflects the situation applicable to tone exposures. The average set mid-range frequencies for the broad-band components were 129 and 456 Hz, respectively. The most acceptable noise level had a lower frequency than the least acceptable noise level for all the respondents. The estimate of the mean values in all the inconvenience variables was significantly higher for the least acceptable noise level than for the most acceptable noise level in all variables.

The results revealed by these investigations on the whole indicated that the measures taken to counter ventilation noise in order to reduce the effects on disturbance, performance, and exertion should be directed at higher frequency components within the low-frequency range. A greater general lowering of the dB(A) level based on measures to counter the low-frequency parts of the ventilation noise may involve a smaller limitation of the inconvenience effects than a smaller comprehensive lowering of the dB(A) level based on a measure to counter the higher frequencies of the ventilation noise.

5.4.5.3 Influence Due to Exposure Period

The influence of the period of exposure on the disturbance experienced due to ventilation noise has been studied both in authentic exposure situations in offices and in laboratory experiments. The link between the estimated disturbance experienced due to ventilation noise and the period of exposure, i.e., the time during which the office personnel stated that they could hear the ventilation, was tested on quite a large group of respondents.[2] The whole test group was divided into two groups, based on estimated values above or below 50 mm on a 100 mm estimation scale. The group with a lower average disturbance experience exhibited significantly lower experience periods (231 min) than the group with a higher average disturbance experience (390 min). The link between the estimated disturbance experience and the time for which the ventilation noise could be heard points to a positive linear correlation, according to which the disturbance experience increases in line with the increase in the period for which it is experienced. This can be interpreted as indicating that exposed persons become habituated to or adapt to the low-frequency ventilation noise only to a very small extent, or not at all. It is felt that similar conclusions can be drawn from a recent, more systematic field study into the significance of the period of exposure prior to

the experience of disturbance.[5] The phenomenon of habituation and adaptation is believed to be consistently stronger for high-frequency noises than for low-frequency noises.

Laboratory experiments strengthen the picture and the conclusions formed from the field studies. Both the estimated disturbance experience and the degree of exertion exhibit gradually higher values over time during a studied exposure period of 60 minutes.[6] The investigation included exposure to ventilation noises with different characteristics at levels ranging from 35–40 dB(A). The requirement to correlate the disturbance experience to the period for which a ventilation noise was experienced gave rise to the idea of possibly masking the experience of an unfavorable ventilation noise. Pure-tone (100 Hz), broad-band, and masked ventilation noise were compared in a laboratory experiment with regard to the effects on performance, alertness, and experience of disturbance.[7] When a masking "pink noise" was added to the pure-tone ventilation noise, there was a tendency for performance to improve and for alertness to increase, although at the same time people were more disturbed by the noise. All the effects were weak, however, and in most cases they were not statistically confirmed. The opportunities for improving the acoustic climate in an environment with ventilation noise via masking effects are thus regarded as limited. Efforts should rather be targeted at a more general reduction of the level of those parts of the ventilation noise that contribute to the overall experience of loudness.

5.4.5.4 Influence Due to Time Fluctuations

Laboratory studies have demonstrated clearly that the experience of disturbance, the degree of exertion, and the performance are consistently affected more negatively when exposed to intermittent noises than when exposed to continuous noises at the same equivalent level.[8] Studies into ventilation noise in authentic environments are still very limited, however. Systematic evaluations of the links between inconvenience symptoms and fluctuations have, as expected, indicated an increased risk of symptoms with an increased breadth of fluctuation in the level.[8] The effect of an increased breadth of fluctuation in the level was also higher at higher dB(A) levels. Fluctuations in level in the vicinity of the threshold of auditory perception were correlated to lower disturbance reactions. More rapid fluctuations (2 Hz) were also experienced as more disturbing than slower fluctuations (0.5 and 1 Hz).[8] Comparisons also indicate that fluctuating tones and fluctuating higher noise frequencies are experienced as more disturbing than corresponding broad-band noise and lower noise frequencies.[8] The situation relating to the effect of fluctuations on inconvenience reactions thus reflects, as anticipated, an increased risk of influence with greater psycho-physical potential for experiencing a ventilation noise. There are strong indications that the particularly disturbing effects of ventilation noise can be explained in many cases by the pronounced fluctuations which often characterize experiences of this type of noise. Fluctuations in ventilation noise can be the reason for marked increases in the experiences of inconvenience. The importance of countering the fluctuating characteristics of the ventilation noise in various ways should be emphasized.

5.4.5.5 Effects on Hearing

The most usual effect of exposure to ventilation noise, as previously mentioned, consists of annoyance and disturbance of various kinds. Such effects may occur as a result of the relatively low levels of exposure occurring in offices, schools, etc. In industrial environments, workshops, warehouses, etc., however, the levels from a fan system may sometimes even reach the level of risk of hearing damage or of speech-masking. The risk of hearing damage and the speech-masking effect arise at levels around 70 dB(A). Pronounced or well-defined health effects expressed as a function of long time or repeated exposure to ventilation noise have not been demonstrated. However, the possibility that repeated exposure to ventilation noise may cause increased stress and in this way may have an effect on health cannot be ruled out. An increased risk of stress-related complaints may occur, not least because human ability to acclimatize to low-frequency noise seems very limited.[5]

5.4.6 Measures

The significant differences in disturbance, when evaluated with regard to the average noise levels, shows that the noise level is a decisive factor with regard to disturbance. Measures to limit the disturbance reaction due to ventilation noise should, therefore, naturally be directed in the first instance at lowering the noise level.

The extent to which a ventilation noise is perceived as disturbing depends not only on its dB(A) level, but also on the spectral distribution and the presence of tones or intermittent components in the noise. From an experiment carried out on respondents exposed to ventilation noises with different characteristics in a simulated office room, it emerged that the highest acceptable level was about 7 dB higher for ventilation noise with a superimposed tone at 30 Hz than for other types of noise.[8] In another experiment, it was found that the tolerance level was much higher for a tone than for a noise at 100 Hz, whereas the opposite tendency applied at 1000 Hz.[8]

Earlier experiments indicate clearly that a lowered sound pressure level can be an effective measure to reduce the inconvenience reactions due to a ventilation noise, provided that it is targeted at the most critical frequency range from the point of view of influence or that the measure results in a general lowering over the entire spectral range of the ventilation noise.

5.4.6.1 Elimination of Different Ventilation Noise Sources

Efforts to reduce the noise from a ventilation system may be concentrated on measures concerning the fan, the fan room, the fan ducts, and the supply and exhaust air terminals.[1,9]

5.4.6.2 The Fan

Fans with poorly designed or excessively simple straight blades should be replaced with quality fans with lower noise generation. As the accumulation of dirt on impellers often causes imbalance, leading to vibration and

unnecessary noise, these should be cleaned regularly. Imbalance, whether due to dirt or to other causes, should be corrected by adjustment. Defective bearings should be adjusted or replaced. Struts and sharp edges in front of an impeller should be avoided. Impact noise insulation should be introduced between fan room and floor structure and between fan room and connecting ducts. The fan unit should be enclosed, with satisfactory airborne sound insulation as the objective.

5.4.6.3 The Fan Room

The roof and walls of the fan room should be lined internally with absorbent materials in order to reduce the sound level in the fan room. The wall insulation should be sufficient to reduce the transmission of sound to adjoining silent premises.

5.4.6.4 The Fan Ducts

Straight, internally smooth ducts should be avoided as these give very little noise reduction. Fan noise can pass virtually unobstructed. Silencers should be installed inside the ducts by covering the walls with absorbent material. In this way noise in the higher-frequency range may be reduced. The low-frequency components of the fan noise are more difficult to attenuate. Very thick absorbent linings are needed to reduce such noise. Altering the area of the duct produces a damping of the noise because parts of the sound are reflected back into the duct. This kind of damping, which may also be achieved at the openings of a ventilation duct, is most effective for low-frequency noise. By inserting internally smooth bends in the duct, damping of the noise may be obtained. The larger the duct widths, the better the damping for low frequencies. Narrow ducts dampen very little. Sound-absorbent bends may produce very sharp reductions in noise level. High frequencies are dampened most easily with duct bends. To obtain damping in the low-frequency range with bends, wide ducts are required. Larger spaces with absorbent walls, "absorption chambers," built into the ductwork, also give effective damping in the lower frequency ranges. The ventilation duct often consists of large noise-generating surfaces which may need to be insulated or enclosed. Counter noise may be an alternative method of reducing the noise level in a ventilation duct. However, this method is relatively costly compared with other technical solutions.

5.4.6.5 The Supply and Exhaust Air Terminals

There is usually a certain damping of the fan noise at the opening of the duct. The damping is greatest if the opening consists of a pipe projecting clear of the wall. The noise radiation is also lowest if it is on the level of the roof or the wall in a corner of the room. Excessive air velocities in the opening may also cause noise in the terminal device, as may inappropriately shaped devices with sharp edges, etc. Supply and exhaust air terminal devices may be fitted with silencers or absorbents.

5.4.7 Exposure Limits

The link between the experience of disturbance and the dB(A) level, which has been analyzed in various studies, indicates that 40 dB(A) would be equivalent to a degree of disturbance immediately below "somewhat disturbing." This result indicates that the ventilation noise in offices should lie beneath this level. When assessing noise, however, it is necessary to take into account the fact that the reaction to disturbance is influenced by many noise characteristics other than the noise level, and also by working environment factors other than the noise environment. The tolerance to noise is also reduced when working on particularly challenging tasks.[8] Under conditions of exposure and working situations of this kind, the noise level should not exceed 35 dB(A). Concerning the dB(A) weighting of the ventilation noise, it should be pointed out that this alternative can exhibit a very poor correlation to the experience of disturbance by the noise in question.[8] Previous analyses indicate, however, that the correlation of the A-weighting procedure is no poorer than that of other weightings, for example dB(B), dB(C), or dB(D).[8] The most reliable conclusions with respect to the negative influence of ventilation noise on exposure are obtained from an analysis of the actual symptoms of inconvenience.

References

1. Kingsbury, H. F. (1991). In *Handbook of Noise Control*, C. M. Harris (Ed.). McGraw-Hill, New York.
2. Landström, U., Kjellberg, A., and Söderberg, L. (1991). Spectral character, exposure levels and adverse effects of ventilation noise in offices. *J. Low Frequency Noise and Vibration* 10(3).
3. Pääkkönen, R. (1988). Low frequency noise and complaints about indoor climate. Proceedings of Nordic Acoustical Meeting, 15–17 June, Tampere.
4. Landström, U., Söderberg, L., Nordström, B., and Kjellberg, A. (1994). Measures against ventilation noise—Which tone frequencies are least and most annoying. *J. Low Frequency Noise and Vibration* 13(3).
5. Landström, U., Holmberg, K., Kjellberg, A., Söderberg, L., and Tesarz, M. (1996). Exposure time and its influence on noise annoyance at work. *J. Low Frequency Noise and Vibration* 14(4).
6. Holmberg, K., Landström, U., and Kjellberg, A. (1993). Effects of ventilation noise due to frequency characteristics and sound level. *J. Low Frequency Noise and Vibration* 12(4).
7. Landström, U., Kjellberg, L., Söderberg, L., and Nordström, B. (1991). The effects of broadband, tonal and masked ventilation noise on performance, wakefulness and annoyance. *J. Low Frequency Noise and Vibration* 10(4).
8. Landström, U. (1995). Exposure parameters involved in low frequency noise annoyance. Proceeding "Assessing and Controlling Community Noise with Low Frequency Components," Copenhagen, December.
9. Sharland, I. (1972). *Woods Practical Guide to Noise Control*. Woods of Colchester, Ltd.

This page intentionally left blank

6 TARGET LEVELS

BJARNE W. OLESEN
Wirsbo-Velta GmbH

DOMINGO L. MORENO-BELTRÁN
Escuela Tecnica Superior de Ingenieros Industriales, Universidad Politecnica de Madrid, Spain

MARIO GRAU-RIOS
Instituto Nacional de Higiene y Seguridad en el Trabajo, Madrid, Spain

ESKO TÄHTI
Finnish Development Centre for Building Services LTD, Helsinki, Finland

RAIMO NIEMELÄ
Finnish Institute of Occupational Health, Vantaa, Finland

LARS OLANDER
Building Services Engineering KTH, Royal Institute of Technology, Stockholm, Sweden

KIM HAGSTRÖM
Faculty of Mechanical Engineering, Helsinki University of Technology, Espoo, Finland

Industrial Ventilation Design Guidebook

6.1 DEFINITIONS AND CONNECTION TO DESIGN METHODOLOGY

6.1.1 Introduction

In process technology and in the manufacture of equipment and systems, the starting point of design includes very precise targets. For example, in car manufacture target levels for main characteristics of the car (e.g., acceleration, maximum speed, and gasoline consumption) are already set in the drawing table. In this case the target values of engineering are also the characteristics to be validated when the product is ready.

Target levels (TLs) refer to the expected values of the system that are determined at the early stages of the design process. Fulfillment of the target levels should be validated or measured by the individuals or organizations responsible at the end of the construction process. Target levels are needed as a standard against which system solutions are compared. During the comparison it may be found that target values cannot be met by any solution or they can lead to very expensive solutions. In such cases the target levels have to be

reconsidered. The target level assessment is a feedback process, as explained in Chapter 3.

Target levels can be utilized at many levels and areas of technology. Some examples from industrial air technology follow:

- Energy efficiency given as a percentage
- Energy usage per cubic meter or square meter of a building, such as for the heat consumption in buildings
- Energy usage per produced unit of final product(s), for example, energy use for each produced ton of stainless steel
- Indoor air quality
- Reliability, for example, how many breaks are accepted per day
- Emission rate
- Capture efficiency of the local exhaust
- Investment cost and maintenance cost
- Expected lifetime of a plant and its components
- Ecological issues

Because the goal of industrial air technology, as defined in Chapter 1, is to control indoor environmental conditions and emissions, special attention must be paid to the indoor conditions and contaminant content of the exhaust air. The need to define target levels for indoor conditions and exhaust air blown outdoors originates from legal requirements, human health requirements, production processes and equipment, and is also related to the type of premises and construction. Target levels should be defined for ventilation systems as well as many other items in the construction process. Target levels should always be dealt simultaneously with design methodology. A decision tree for the target level steps and design methodology is provided in Chapter 3.

6.1.2 Use of Target Levels

It is the responsibility of the end user and the contractor to determine target levels. It is essential that the target levels be specified in such a way that they can be unambiguously measured. It is also important that the responsibilities of each stakeholder be clearly defined, particularly in case something goes wrong. This includes financial responsibilities. In addition to the designer and end user, other stakeholders are involved in the construction of a plant or building. In the simplest case, the overall contractor takes care of the design and construction of the plant or system, and then the end user buys it. In this case only two stakeholders are involved. In more complicated cases, the number of stakeholders may total 10. For instance, the supplier side may be represented by the consulting engineer, manufacturer, ventilation contractor, and building contractor, and the end user side by the real estate company, plant owner, plant engineers, and other occupants.

The use of clearly defined target levels has become more and more important in industrial ventilation. The targets must be realistic and verifiable

by measurements. Different kinds of target levels can be set—for example, for indoor air quality, temperature, energy usage, and various efficiencies. In specific areas of process ventilation, the determination of target levels has been a common procedure for a long time. For example, in paper machine hall ventilation, the contractor guarantees the use of energy per produced kilogram of paper or fresh steam used (see the example at the end of this section).

The use of target levels is spreading to other branches of industrial ventilation, and one big problem associated with the verification of system performance has occurred. In the absence of clearly defined target values, administrative regulations have been used as targets. However, administrative regulations, such as occupational exposure limits, are seldom rigorous. In most cases the fulfillment of these figures guarantees only satisfactory performance of the system. On the other hand, the use of administrative regulations as targets has obviously led to the prominence of equipment-based thinking because of the lack of other, exact figures. Typically, in equipment-based thinking the focus is placed on such parameters as fan power, performance of filters, and efficiency of heat exchangers instead of the target value for the entire system.

Exposure to air contaminants in work rooms is regulated by the occupational exposure limits (OELs) (see Sections 5.2 and 6.2). From the point of view of design and construction, these limits cannot be regarded as proper generic targets for various reasons. In addition to physiological and toxicological factors, the process of setting occupational exposure limits involves expert judgments nearly always resulting in compromises in numerical values. Furthermore, the national occupational exposure limits may differ from country to country due to differences in national priorities, technological development, and revising periods. Full harmonization among all industrial countries cannot be expected in the near future. In addition, the legal status of the OELs may vary from binding regulations for some substances to simple recommendations for others.

In the ideal case the target level procedure for industrial ventilation can be compared with materials selection. Somebody who wants steel AISI 316, for instance, just selects and buys it by specifying this standard. The person will obtain steel with the desired properties, because the steel is made according to the producer's quality requirements and the producer guarantees its quality.

A similar procedure must be followed in industrial ventilation in the future. If the end user wants target class 1, the manufacturer must produce it. If the producer fails to deliver target class 1, the end user can ask the producer to make changes in the system such that the target can be achieved. In the worst case the producer will have to change the whole system. Specifying the different targets is just like selecting materials. The end user selects the IAQ, thermal conditions, energy efficiencies, and other efficiencies. Fulfilling all requirements in industrial ventilation is, of course, more difficult than in materials production, because industrial ventilation is affected by many different items that may be outside the hands of the contractor. In any case, all relevant items should be attached to the contract.

In most cases the main steps in defining target levels relating to industrial ventilation are as follows.

Step1: Musts

Ascertain the requirements of laws, regulations, and standards related to legislation, processes, and equipment, and compare them with customer needs. Of course, before this step, needs of the end user—for example, economical boundary conditions—are identified. At this stage the tentative target levels have also been selected.

Step 2: Needs

Ascertain nonbinding standards, human comfort standards, guidelines, codes of practice, and custom needs.

Step 3: Target Levels

Define the target levels based on musts and needs.

Step 4: Design Conditions

Suggest and confirm with customer the outdoor or process conditions within which the target levels must be met (e.g., absolute maximum temperature versus 95 percentile temperature).

Step 5: Reliability

Find out the customer reliability requirements of the process. Define and obtain the customer's acceptance of the needs for ventilation system reliability (e.g., what is the allowed break-off time).

6.1.3 Combination of Target Levels and Design Methodology

The combination of target levels and design methodology is of vital importance. One of the main items in the INVENT program in Finland over the years 1991–1996 was the development and utilization of these concepts in the ventilation of industrial premises.[1] Together, these two concepts form the basis for industrial ventilation systems.

The target level concept was introduced and developed by the Association of Finnish Manufacturers of Air Handling Equipment (AFMAHE) in 1985.[2,3] Indoor climate target levels have been utilized in the ventilation of public buildings, apartments, and offices for years.[4–6] The Finnish Institute of Occupational Health began to develop the concept for industrial ventilation in 1991.[7,8] The target level procedure for industrial air quality is described in more detail in Section 6.4.

In the design methodology, the whole life cycle of the process must be considered. The life cycle of the process can be divided into four parts: design, construction, operation, and end of the process. Each consists of different tasks. The design methodology process can be described as follows:

Given Data

- Collect and identify data that do not change during the design process, such as outdoor conditions.

Process Description

- Understand the industrial process and identify subprocesses.
- Identify possible emission sources, occupational areas, effects of environmental parameters on production, needs for enclosure, and ventilation equipment.
- Divide the process in parts such that their inputs and outputs to the environment can be defined.

Building Layout and Structures

- Collect data on building layout, openings, and their properties as basic values for load calculations.
- Complete zoning of the building based on division of the process and building layout.
- Make space reservations and add structures needed for ventilation equipment.

Target Level Assessment

- Define target levels for indoor zones and outdoor conditions.
- Specify design conditions for which the target levels are to be met.
- Define target levels for ventilation system, such as reliability, energy consumption, investment, and life cycle costs, etc.

Source Description

- Determine characteristics of the sources and methods for calculation of local loads.

Calculation of Local Loads

- Calculate loads from individual sources to the environment.

Calculation of Total Building Loads

- Calculate total loads (heat, humidity, contaminants) from different subprocesses and the environment to ventilated enclosures.
- Take into account the fact that loads are usually time dependent.

Selection of System

- Select an applicable system on the basis of the target levels.
- Compare acceptable systems to choose the most desirable one.

Detailed Design

- Provide detailed layout and dimensioning.
- Design adjustment and control system.
- Consider special issues, such as thermal insulation, condensation risk, fire protection, and sound and vibration damping.

These are the main steps of design methodology. In some cases all the steps are not needed, but in most cases it is important to take all of them into consideration. In addition to the construction and the use of the system,

attention should also be paid to its demolition. It is worth noting that the feedback is always a typical feature of the design methodology.

Using the procedure described above, the target levels can be determined. Relevant calculation methods and expertise are needed in all the phases. Although the calculation of target levels takes place in different ways for particular cases, the basic procedure remains the same. The target level calculation also varies for different outside temperatures and different process parameters.

6.1.4.1 Example from Paper Industry

Industrial ventilation in a paper mill is always combined with the process itself. Process ventilation together with machine hall ventilation has an impact on the energy efficiency of the whole process. Contractors assign target levels to environmental conditions in a machine hall for parameters such as air quality, air temperature, air humidity, and draftiness. Another target level parameter may be the number of stops over a certain period of time. Table 6.1 gives the target levels for thermal factors combined with the design methodology of one paper mill ventilation case.

The setting of indoor air quality targets is much more complicated and individualized. This is due to the fact that the chemical process in paper making differs from paper type to paper type. Also, the amount of particles is highly dependent on the speed of the machine, the percentage of recycled mass, and the percentage of "stone" in the paper.

The target level for particles in the air of a paper printing machine hall is 0.5 mg/m^3, but in some cases the level can be as low as one-tenth of this number. Tissue paper mills are very complicated in this respect. Depending on the process and other factors, the particle level can be as high as 10 mg/m^3, but levels as low as 1 mg/m^3 can be found. The targets are selected between those figures depending on the type of paper mill.

The target level assessment process for paper machine halls is the result of long historical development. The performances of installed paper machine hall ventilation systems are measured very often and the results are compared with input data used as the basis for design. As a result of these comparisons corrections are made to the design process as necessary.

TABLE 6.1 Example of Target Values for a Paper Machine Hall Ventilation

Location	Air temperature	Air velocity
Machine room		
•Winter	+20 °C	<0.5 m/s
•Summer	< outside temp + 5 °C	0.5 m/s
Basement	< +15 °C	
•Winter	< outside temp + 10 °C	
•Summer		

*No visible condensation on the ceiling or absolute water content < outdoor water content + 20 g/kg.

References

1. K. Hagström, K. Pöntinen, J. Railio, and E. Tähti. *Design methodology of industrial air technology.* INVENT report 55, 1996.
2. J. Railio. Advanced energy-efficient ventilation. In *Proceedings of 6th AIVC Conference, Netherlands, 16–19 Sept. 1985.* Air Infiltration and Ventilation Centre.
3. V. Matilainen and J. Railio. Indoor air classification. In *Proceedings of Healthy Buildings '88,* vol. 3, pp. 633–638. Swedish Council for Building Research, D21, Stockholm 1988.
4. P.O. Fanger. New principles for a future ventilation standard. In *Proceedings of the 5th International Conference on Indoor Air Quality and Climate: Indoor Air '90,* vol. 5, pp. 353–363, 1990.
5. Scanvac. *Classified indoor climate system: Guidelines and specifications.* Swedish Indoor Climate Institute, Stockholm, 1991.
6. O. Seppänen, R. Ruotsalainen, A. Hausen, et al. The classification of indoor climate, construction and finishing materials. *In Proceedings of Healthy Buildings '95,* vol. 3, pp. 1667–1673, 1995.
7. R. Niemelä, A. Tossavainen, V. Riihimäki, and P. Kalliokoski. An extension of indoor air quality classification. In *Proceedings of the 6th International Conference on Indoor Air Quality and Climate,* vol. 3, pp. 483–487. Indoor Air '93, Helsinki, 1993.
8. R. Niemelä, A. Tossavainen, V. Riihimäki, P. Kalliokoski, and T. Mannelin, Target levels of indoor air quality in industrial buildings. *In Proceedings of the 4th International Symposium on Ventilation for Contaminant Control,* vol. 18, pp. 71–76, 1994.

6.2 OCCUPATIONAL EXPOSURE LIMIT VALUES

6.2.1 Introduction

The harmful effects of an environment in which certain chemical agents are present in the air inhaled by employees have been known for a long time. A person may be exposed to many potentially harmful chemical, physical, and biological agents during his or her working life and, depending on the magnitude of the dose, the result can be disease and even death.

In this chapter we will consider only exposure to chemical agents in the air. We will not address other risks that do not influence the dose received by a worker.

These chemical agents can be any chemical element or compound, on its own or mixed, as it occurs in the natural state or as produced by any work activity, whether or not produced intentionally, and whether or not it is placed on the market. According to EINECS (European Inventory of Existing Commercial Substances) and the ELINCS (European List of Notified Chemical Substances), the number of such substances, not counting their mixtures or preparations, is well over 150 000. To these single agents we must add mixtures and solutions composed of two or more substances, intermediate substances formed during chemical reactions, and by-products formed during chemical reactions that remain at the end of the reaction or process. Fortunately, only a few hundred of these chemical substances are used regularly on a commercial basis.

Thus, it can be said that in practically all activities there are risks to health related to the presence of chemical agents. To evaluate their severity we should consider whether the exposure occurs continuously or at irregular intervals, the possible entry routes to the body, the concentration changes with time and place, as well as the aggregation state of the contaminant in liquid, dust, mist, fume, or vapor form.

The mechanisms behind the different types of risks are also quite varied, because manufacturers may apply different conditions and agents, and each manufacturing stage may involve different job functions and therefore different exposure conditions. Distance to emission sources and physical parameters such as rate of release, air currents, and meteorological variations have a profound influence. The variability of exposure conditions is made even greater by work patterns, individual practices, and simultaneous exposure to several substances acting together.

Thus, there is a clear need to establish the relationship between the health effects of hazardous chemical agents in the environment and the level of occupational exposure to the body by means of an occupational exposure limit, in which a reference figure for the concentration of a chemical agent is set. In fact, occupational exposure limits (OELs) have been a feature of the industrialized world since the early 1950s. They were introduced, primarily in the United States, at a time when measures to prevent occupational diseases were considered more beneficial than compensating victims, and in this sense OELs have played an important part in the control of occupational illnesses.

The idea behind OELs is to identify the highest level of exposure concentration and the corresponding reference time period for which we can be confident that there will be no adverse effects on health. However, the concentrations and lengths of exposure at which the presence of airborne chemical agents could damage health have not been clear for many years, and even today there are many questions to be answered.

Generally, OELs are set in reference to the airborne route such that exposure, even when repeated on a regular basis during the working schedule throughout the working life of a *normal* worker, will not lead to adverse effects on the health of exposed persons or their progeny for any time—short term, long term, or beyond the end of the working life—as far as can be predicted from the state of knowledge.

One problem may arise in defining who is a *normal* worker. This means taking account of the variability in biological response together with the uncertain environmental data. A small percentage of workers may experience discomfort from some substances at concentrations at or below the OEL. Moreover, some may be affected more seriously by the aggravation of preexisting conditions or the development of an occupational illness. Therefore, OELs should not apply to special-risk workers, those who are hypersusceptible or otherwise unusually responsive to industrial chemicals because of genetic factors, age, personal habits, medication, or previous exposure.

Usually, OELs are stated as the eight-hour time-weighted average concentration of exposure to a substance in gaseous, vaporous, or suspended form in the air at the workplace. Later on we will give a more precise formula.

With all this in mind, OELs should be regarded as an important part of the overall approach to ensuring the protection of health in the workplace, providing a criteria by which decisions can be made as to whether the airborne concentration of a given substance is sufficiently low to avoid adverse health effects.

In essence, OELs may be used for a number of purposes, for which the principal objective is to provide standards or criteria against which the results

of environmental monitoring in existing workplaces may be compared to ensure that, as far as the current state of knowledge permits, control is adequate to protect health. They may also be used for design purposes, to ensure that new plants and process are engineered in such a way that exposures can be controlled at levels that will not damage health. They should not be used as a basis for assessing the acceptability of nonoccupational exposure, for comparing the toxicity of one substance with that of another, in the evaluation or control of community air pollution nuisances, or as proof or disproof of an existing disease or physical condition.

6.2.2 Setting OELs

The next topic to address is the process of setting OELs. The rationale for setting OELs has no basis in absolute information, and the procedure to be followed may differ from country to country and from substance to substance. Scientific criteria for health protection should be used in combination with considerations of their technical and economic feasibility in a dynamic process in which the development of scientific knowledge underlies rapid changes entailing the need to periodically review the data.

In general, it requires a multidisciplinary approach that takes data on toxicological and other relevant properties of chemicals developed in the fields of industrial hygiene, chemistry, toxicology, epidemiology, engineering, occupational medicine, etc., so that interrelated data from all sources combines to give the most rational input upon which to base OELs, even though adequate documentation is not available for the majority of chemical agents.

Scientific information for the process of establishing OELs may come from human or animal data obtained using different methods, from studies of acute, subacute, and chronic toxicity through various routes of entry. Human data, which is usually the best source, is not easily available, and frequently it is incomplete or inadequate due to poor characterization of exposure and clear dose-response relationships. Human data falls into one of the following categories:

- Epidemiological and clinical studies of workers and other long-term case-control studies
- Experimental studies with volunteers, especially for situations involving the acute effects of an identified adverse agent
- Literature from industrial experience, especially individual case reports showing relationship between exposure to a chemical agent and specific adverse effects

Data coming from laboratory studies with animals offer good characterization of exposure, adequate use of controls, extensive pathological investigations, and the potential to give clear indications of dose-response relationships. However, extrapolating this data to human exposure is not straightforward and may lead to mistakes. Therefore, studies of this type should be used primarily to complement other studies, in order to check certain aspects or to guide the study.

The crucial objective is to identify what effects can be produced by exposure to chemical agents and to select which effects should be considered

adverse to health or well-being in order to quantitatively define exposure levels. The problem arises from the definition of adverse effects to workers' health. That definition should have a broad scope, including, when possible, effects on the offspring of workers and concepts such as nuisance, irritant, and systemic health effects. In this sense, some scientists define the following categories of effects due to increasing exposure to chemical agents:

- No effects observed
- Compensatory effects or early effects of dubious significance, without adverse health consequences
- Early health impairment with clear adverse effects
- Overt disease with severe consequences

In this scheme, OELs should be a dose somewhere between compensatory effects, in which the organism is able to detoxify, metabolize, or excrete the substance, and early impairment. Although there may be profound differences of opinion as to what constitutes this dose, this approach leads to the conclusion that available scientific data permits identification of a clear threshold dose below which exposure to the substance in question is not expected to lead to adverse effects.

However, for some type of adverse effects, such as genotoxicity, carcinogenicity, and respiratory sensitization, it may not be possible from present knowledge to define this threshold of activity, so we may conclude that any level of exposure might carry some finite risk. In this case, OELs should be established at levels sufficiently low to avoid risks; these are called pragmatic OELs.

Another difficulty comes from the consideration of the route of entry of the contaminant, as chemicals can enter the body by various routes and the human body responds to the action of a toxic agent primarily on the basis of the rate and route of exposure. Without any doubt, the most important route of exposure at the workplace is inhalation, and this should be the route used to set OELs. However, if there is a threat of significant exposure by other routes, such as cutaneously (including mucous membranes and the eyes), either by contact with vapors or by direct skin contact with the substance, additional recommendations may be necessary.

6.2.3 Types of OELs

In principle, OELs are based on the measurement of chemical agent concentrations in working air, but in a few cases it is possible to define *biological exposure indices* (BEIs), which are based on measurements on certain biological media. The biological limit value is the limit of the concentration in the appropriate biological medium of the relevant agent or its metabolite, or an indicator of effect. However, considering that BEIs are used as a complement to environmental OELs, and considering also that they do not have much application to industrial ventilation, we will not devote attention to them.

With this in mind, it is possible to define two types of OELs:

- Time-weighted average exposure limit with a specific reference period
- Instantaneous exposure limit

The time-weighted average exposure limit might refer to *long* (TWA = *time-weighted average*) or *short* (STEL = *short-term exposure limit*) periods of time. These OELs always refer to the concentration of a chemical agent in gaseous, vaporous, or suspended form in the air within the breathing zone of a worker.

It is normal to establish OELs for long periods (TWAs) in relation to a reference period of 8 hours, which is a typical working-day schedule. Values above the OEL are allowed provided these are compensated by equivalent excursions below the TWA during the working day. OELs are also normally set on the basis of a nominal 40-hour work week, with a maximum of 240 working days in a year and for a working lifetime that might reach 45 years. The long reference period could be a different one, such as a month, a year, and so on. In general, an 8-hour OEL is recommended as the most satisfactory and practical way of monitoring airborne agents for the purpose of preventing adverse health effects, although, in any case, OELs do not constitute an absolute dividing line between harmless and harmful concentrations.

In addition, it may be necessary to limit permissible upward excursions from the TWA. In practice, concentrations of chemical agents in workplace air fluctuate frequently and to a considerable extent. The amount by which the OEL-TWA may be exceeded for short periods without impairment of health depends upon several factors, such as the nature of the substance, the frequency with which high concentrations occur, and the duration of such periods.

According to the ACGIH (American Conference of Governmental Industrial Hygienists, USA), variations in worker exposure levels may exceed three times the OEL-TWA for no more than a total of 30 minutes during a workday, and under no circumstances should they exceed five times the TWA.

However, there are substances for which an 8-hour OEL-TWA alone provides insufficient protection. In such cases the OEL-STEL is used in relation to a 15-minute period, unless otherwise specified, in order to prevent adverse health effects, immediate or delayed, due to peaks in exposure that cannot be controlled by the application of an 8-hour OEL-TWA. The OEL-STEL indicates a limit value above which exposure should not occur, and it is needed when there are recognized acute effects from a substance whose toxic effects are primarily of a chronic nature.

For ACGIH, exposures above the OEL-TWA up to the OEL-STEL should not be longer than 15 minutes and should not occur more than four times per day. Also, there should be at least 60 minutes between successive exposures in this range.

In any case, the OEL-STEL is not a separate, independent exposure limit; rather, it supplements the OEL-TWA and is intended to be used in normal work situations, not for emergencies. However, the OEL-STEL needs to be complemented by other precautions for substances that may be lethal at very high concentrations and for substances whose toxic or irritant effects are pronounced upon exposure to high concentrations for very short periods.

Another type of time-weighted average exposure limit is the *decision level* (DL), which is expressed as a fraction of the OEL. In general, it is based on judgment, and it is greater than a dose of 50% and usually corresponds to one-fourth of the dose. For special substances, such as carcinogens, it should

be one-tenth. Unlike the OSHA (Occupational Safety and Health Administration, USA) *action level*, the European DL is primarily used for monitoring decisions implying the need to adopt certain types of preventive measures.

Instantaneous OELs represent concentrations that should not be exceeded during any part of the working exposure; that is, they represent the maximum permissible concentration of a chemical compound (or element) present in the air within a working area that, according to current knowledge, generally does not impair the health of the employee or cause undue annoyance. These OELs are also called *ceiling values* and are used for agents that present acute effects such as irritants or for other type of substances that present chronic and acute effects simultaneously and therefore may be used with appropriate medical surveillance. This OEL uses no specific time reference period, but for some situations instantaneous monitoring is not feasible, requiring the use of a 15-minute sampling period.

For some substances, in order to consider all absorption pathways—including dermal, which may lead to skin penetration and consequently increase the total body burden—a *skin notation* must be assigned to an OEL. Although it is recognized that for many substances with a skin notation, quantitative data on dermal penetration may not be available, for other chemical agents uptake through the skin may be on the order of 10% or more of the uptake from respiratory exposure at the 8-hour OEL, especially in operations involving high airborne concentrations where significant areas of the skin are exposed for a long period of time. In general, a substance with a skin notation requires additional risk management measures to ensure the best possible level of protection and to control total systemic exposure at the workplace.

The OELs are expressed in terms of concentration, such as ppm (volume/volume) or mg/m^3. For gases and vapors it is stated in terms independent of temperature and air pressure variables, in mL/m^3, or parts per million by volume in air, and in terms dependent on those variables in milligrams of substance per cubic meter of air at a temperature of 20 °C and a pressure of 101.3 kPa.

The limit value for suspended matter is given in mg/m^3 or multiples thereof for actual environmental conditions (temperature and pressure) at the workplace. The limit values for fibers are given in fibers/m^3 or fibers/cm^3 for actual operating conditions of temperature and pressure. It is possible to convert one expression to the other using the formula

$$\text{TWA } (mg/m^3) = (\text{TWA (ppm)} \times MW)/24.04,$$

where MW is the molecular weight of the substance and 24.04 is the molar volume in liters under these conditions.

Correct and appropriate use of OELs in practice requires considerable knowledge and experience, particularly in cases where there is exposure to mixtures rather than to one substance in isolation, where it is not practical to evaluate the effects of all possible conditions of exposure, or where the working patterns are nonstandard.

Established OELs such as OSHA PELs and ACGIH TLVs, cover only a small fraction of the substances that are found in the workplace, and even for those chemicals discrepancies are commonly encountered among the different lists. For this reason, the European Union (EU) is trying an approach in which

the OELs represent levels of exposure that are perceived to be realistic and attainable at the time they are established. Political and socioeconomic aspects are combined with scientific considerations in order to avoid the imposition of administrative, financial, and legal constraints that would hold back the development of enterprises while maintaining the aim of ensuring the health of workers.

Toward this goal the EU defines two types of OELs:

- Binding limit value
- Indicative limit value

Binding occupational exposure limit values reflect feasibility factors related to social acceptability. When the results of environmental monitoring have to be compared with OELs, factors that influence exposure and that entail preventive policies are considered. For these values member states shall establish a corresponding national binding occupational exposure limit value based on but not exceeding the community limit value. That is, a binding limit means a minimum requirement.

An *indicative limit value* is a more common type of limit that reflects expert evaluation based on scientific data where it is possible to identify the highest level of exposure along with the corresponding reference time period for which one can have confidence that there will be no adverse effects on health. For any chemical agent for which an indicative occupational exposure limit value is established at the community level, member states shall establish a national occupational exposure limit value, taking into account the community limit value and determining its nature in accordance with national legislation and practice.

This approach may provide an opportunity for consolidating and simplifying old legislation on chemicals and for bringing OEL setting up to date with respect to social aspects, balancing the participation of all interested parties (the scientific community, industry, unions, and governments) and therefore advancing the establishment process much more rapidly.

6.2.4 Assessment of Exposure to Chemical Agents

It is appropriate here to give a few ideas on the assessment of workplace exposure to chemical agents, although specialized literature in this field should be consulted for details.

Determination and assessment of the risks of hazardous chemical agents requires knowledge of, among other things, the nature of the agents, the type and duration of the exposure, the gravity of risk, and the criteria chosen for the OEL. The purpose is to make quantitative measurements of the work environment in order to compare the exposure with the limit value by means of an independent scientific assessment using the best available scientific methodology.

However, assessing occupational exposure to airborne contaminants in a representative way is not an easy task and requires a good deal of professional judgment and reliance on a good methodology. There are many issues to be resolved, such as

- Patterns of contaminant generation that change with time
- Interaction among several release points
- Worker variability in relation to location and time

This implies, for example, that measurements taken over a given period of time may give insufficient data to integrate workplace factors in the series of activities in the period under consideration in such a way as to permit assessment of the likely maximum risk to which the individual workers are exposed.

The occupational exposure assessment (OEA) should take into account the future working conditions for the employee, which implies some degree of uncertainty, especially if the exposure is close to the limit value. Therefore, the initial assessment of exposure may require periodic measurements to check for any change in exposure conditions that may increase the risk to workers—for example, if there has been a significant change in working conditions caused by the introduction of a new industrial process or technology or new chemical agents, which could make the risk assessment out of date. In the case of a new risk-involving activity, work could commence only after an assessment of the risk of such activity has been made and any identified preventive measures have been implemented.

6.2.4.1 Procedure for Evaluation of Exposure

The standardized procedure for evaluation of exposure to chemical agents is done in three steps:

- Identification of potential exposure
- Determination of workplace factors
- Assessment of exposure

The first step is to identify the substances present at the workplace. As a starting point, knowledge of the process is needed in order to formulate a list of all chemical agents used in the establishment. The list should include not only primary products but also intermediate and final products, as well as reaction products and by-products. For the chemical agents in the list, it is necessary to know their chemical properties, especially hazardous ones; their OEL values, including biological limit values; and, where these are not available, other technical criteria that can be used to evaluate the risk. It is also helpful to include any information on the safety and health risks of those substances provided by the supplier or other readily available sources. This information on dangerous substances and preparations, in the form of safety data sheets, is intended primarily for industrial users, to enable them to take the measures necessary to ensure the safety and health of workers.

The next step is the determination of workplace factors that have to be considered in estimating the potential for exposure to chemical agents. This includes all points related to work processes and procedures which may be relevant to exposure, such as

- Operations, technical installations, and processes
- Emission sources
- Job functions and activities of each worker
- Work patterns and techniques
- Process layout and workplace configuration

- Engineering prevention measures taken or to be taken
- Workloads and exposure times

The identification of chemical agents and the data on workplace factors leads to the assessment of exposure, which can be done in three different stages that depend on the risk level for the worker and the type and amount of data required:

- An initial appraisal
- A basic survey
- A detailed survey

The assessment of exposure brings together all the data and compares the results of this integration with the chosen OEL. It begins with an initial appraisal and continues with a basic survey and then a detailed one until it is confirmed either that exposure exceeds the limit value or that it is sufficiently below that limit.

The initial appraisal allows consideration of the likelihood of exposure due to the presence of chemical agents. When the conclusions of the initial appraisal show a possible risk exposure for the worker, more data are gathered taking special account of tasks with high exposures. If necessary, workplace measurements are taken if the input data are not sufficient to enable valid comparison with the limit values.

Finally, for situations in which it is not clear that exposure is and will continue to be below the limit values, a detailed survey with a measurement strategy is required. The methods used are based mostly on instruments for sampling the environment in order to obtain reliable measurements of workplace air concentrations. In general, the measurement strategy must consider the most efficient use of resources for the purpose of obtaining quantitative data on exposures by having a clear idea of what the data will be used for or whether it meets the specified need. For example, if the data pertain to peak exposures, these peaks have to be assessed according to the STEL requirements, if any.

For this reason, in order to save time and money, it may be convenient to subdivide the exposed workers into more or less homogeneous groups with respect to exposure—that it is to say, based on similar work patterns—and take direct measurements of air samples within the breathing zone of a worker in the area or areas in which the work activities are carried out during a reference period. However, the use of homogeneous groups should be reconsidered if any individual exposure differs greatly from the average value of the group, which may occur if workers do not perform repetitive tasks.

The measurement procedure must have been tested previously under realistic conditions and should give representative results of worker exposure. Thus, it should not be influenced by unusual work schedules, where tasks may not be well defined or planned. The procedure should include

- The chemical agents
- The sampling procedure
- The analytical procedure
- The sampling location
- The duration of sampling
- The timing and the interval between measurements

- The calculations that yield the occupational exposure concentration from the individual analytical values
- The jobs to be monitored

The measuring procedure used must be appropriate to the chemical agent to be measured, its limit value, and the workplace atmosphere so that the results show the concentration of the agent in the same terms as the limit value. Also, the limits of detection, sensitivity, and precision of the measuring procedure must be appropriate to the limit value.

The sampling period and interval of sampling are related to concentration patterns and to the method of analysis used.

For the sampling location, fixed-point measurement may be used if the results make it possible to assess exposure of the worker at the workplace. In general, however, personal sampling devices are preferred, which give more representative results of worker exposure.

Recently in the surveillance of exposed workers, it has proved useful to carry out analysis of the harmful compound or its metabolites using biological material or a change of biochemical parameters caused by the harmful chemical or its metabolites.

The coordination of ambient chemical agents and biochemical analyses of exposed workers and medical data is intended to confirm the validity of risk assessment.

6.2.4.2 Calculation of the Occupational Exposure Concentration

Calculation of the occupational exposure concentration (OEC) depends on the type of OEL. For example, when the limit value has been set as an eight-hour time-weighted average, the cumulative exposure for an eight-hour work shift should be computed as follows:

$$\mathrm{DE} = \sum c_i t_i / \sum t_i = (c_1 t_1 + c_2 t_2 + \cdots + c_n t_n)/8,$$

where

DE is the equivalent exposure for the working shift, or daily exposure
c_i is the concentration during any period of time t where the concentration remains constant
t_i is the duration in hours of the exposure at the concentration c_i

When the limit value is a STEL type, usually based on a 15-minute period, the exposure concentration is

$$\mathrm{SE} = \left(\sum c_i t_i \right) / 15,$$

where c_i is the measured concentration from direct-reading instruments or from air samples during a 15-minute period.

Finally, for some substances it may be convenient to define a weekly exposure WE:

$$\mathrm{WE} = \left(\sum (\mathrm{DE})_i \right) / 5,$$

where $(\mathrm{DE})_i$ represents the daily exposure corresponding to successive days of the working week.

The daily or weekly exposure should not exceed the eight-hour time-weighted average OEL for the chemical agent involved, and exposure peaks that may occur during the shift must fulfill the STEL; that is, any measured short exposure, SE, during the whole working shift must be lower than the STEL for that agent, if any.

If workers are exposed simultaneously or successively to more than one chemical agent, the risk shall be assessed on the basis of the risk presented by all such chemical agents in combination. Usually, additive effects are assumed for the mixture of chemical agents, so the cumulative exposure is calculated as follows:

$$E(m) = \sum (\mathrm{DE/TWA})_i$$
$$= (\mathrm{DE/TWA})_1 + (\mathrm{DE/TWA})_2 + \cdots + (\mathrm{DE/TWA})_n,$$

where

$E(m)$ is the equivalent exposure index for the mixture
DE is the daily exposure for a particular substance
TWA is the OEL for that chemical agent

To comply with the OEL, the value of the cumulative exposure index shall not exceed unity.

6.2.4.3 Conclusions of the Occupational Exposure Assessment

Comparison of the results of the occupational exposure concentration with the OEL leads to three different possibilities.

When the exposure is well below the limit values and it is possible to be confident that on a long-term basis the probability of exceeding the limit value is very low, the risk assessment may conclude that the nature and extent of the risks related to those chemical agents make a further detailed risk assessment unnecessary unless work conditions are modified in a significant way. In these cases, however, it must be regularly checked whether the assessment leading to that conclusion is still applicable.

If the assessment shows that the exposure approaches the limit values, so that the OEL is met but there is a probability of exceeding the limit values, subsequent measurements at appropriate intervals must be taken to ensure that the assessment situation continues to prevail. The frequency of these measurements will depend on the previous results, so that the nearer the concentration recorded comes to the limit value, the more frequently measurements must be taken under normal working conditions. However, if the values are borderline, the decision of whether exposures are below the limit values within the OEA is not clear, and a more comprehensive sampling exercise may be required using, for example, worst-case measurements. This becomes more important the fewer the measurements that have been taken, so in case of doubt the evaluation results should be verified through additional selective measurements.

When the results of the assessment reveal a risk to the safety and health of workers, with exposure values clearly above the OEL for the chemical agent, or if the probability of exceeding the limit value is high, specific protection, preventive, and monitoring measures must be applied as soon as possible to remedy the situation. The reasons for the limit value being exceeded must be

identified to allow elimination of the hazardous agents through process design, engineering control, or other administrative practices to keep exposures within acceptable limits. A new assessment should be made to check the new situation, and periodic measurements should be done to check that control measures remain effective.

In any case, the risk assessment must be documented in a suitable report, including the existing working conditions and the reasons for the chosen procedures. It should contain, at least, the following data:

- The names of the chemical agents considered
- The description of the workplace factors
- The description of the working conditions during the measurements
- The measuring procedure
- The time schedule
- The results of occupational exposure concentrations
- All events or factors liable to influence the results
- Results of the comparison with the OEL

Retention of this data is essential for future work in order to compare and analyze successive sets of assessment exposures.

Bibliography

American Conference of Governmental Industrial Hygienists. *Threshold limit values for chemical substances and physical agents and biological exposure indices.* ACGIH, Cincinnati, OH, 1999.

The Council of the European Union. Council Directive 98/24/EC of 7, April 1998 *on the protection of the health and safety of workers from the risks related to chemical agents at work.* Official Journal No. L131, May 1998.

European Committee for Standardization. EN 689:1. *Workplace atmospheres: Guidance for the assessment of exposure to chemical agents for comparison with limit values and measurement strategy,* 1995.

6.3 TARGET VALUES FOR THERMAL FACTORS: AN OVERVIEW OF INTERNATIONAL STANDARDS

6.3.1 Introduction

The main purpose for the heating and air conditioning of work spaces is to provide an environment that is acceptable and does not impair the health and performance of the occupants. During production processes and in the external environment it may be necessary to work in unacceptable conditions for a limited time period. However, it must be ensured that these conditions do not impair the health of the employees. Light, noise, air quality, and the thermal environment are all factors that influence the acceptability of conditions for and performance of the occupants. This section will only deal with the thermal environment. Several standards dealing with methods for the evaluation of the thermal environment have been published by international standard organizations such as ISO and CEN.

This section deals with the ISO standards, which have been or are being prepared by ISO/TC159/SC5/WG1 and CEN/TC122/WG11. An overview of the standards issued and the documents under preparation is given in Table 6.2. CEN Technical Report CR 1752 will also be used in this section.[1] Several of these standards may be used as the basis for the design and evaluation of buildings, HVAC (heating, ventilation, and air conditioning) systems, and protective equipment (clothing) and the optimization of work/rest schedules.

The basic philosophy has been to standardize evaluation methods, with recommended limit values for the different parameters or indices listed in informative annexes. These or other values may then be adapted in national rules for the thermal environment.

6.3.2 The Thermal Environment

Existing methods for evaluation of the general thermal state of the body, both in comfort and under heat or cold stress, are based on an analysis of the heat balance for the human body:

$$S = M - W - C - R - E_{sk} - C_{res} - E_{res} - K \quad , \tag{6.1}$$

where

S = heat storage in body
M = metabolic heat production
W = external work
C = heat loss by convection
R = heat loss by radiation
E_{sk} = evaporative heat loss from skin
C_{res} = convective heat loss from respiration
E_{res} = evaporative heat loss from respiration
K = heat loss by conduction

The factors influencing this heat balance are activity level (metabolic rate, met or W/m^2), thermal resistance of clothing I_{cl}, (clo or m^2 °C/W), evaporative resistance of clothing $R_{e,cl}$ (m^2 Pa/W), air temperature t_a (°C), mean radiant temperature $\bar{t}_r$ (°C), air speed v_a (m/s), and partial water vapor pressure p_a (Pa). These parameters must be combined so that the thermal storage is 0, or else the working time has to be limited to avoid too much strain on the body. For comfort, the mean skin temperature also has to be within certain limits and the evaporative heat loss must be low. In existing standards, guidelines, or handbooks, different methods are used to evaluate the general thermal state of the body in moderate environments, cold environments, and hot environments; however, all are based on the above heat balance and the listed factors.

Aside from the general thermal state of the body, a person may find the thermal environment unacceptable or intolerable if local influences on the body from asymmetric radiation, air velocities, vertical air temperature differences, or contact with hot or cold surfaces (floors, machinery, tools, etc.) are experienced.

TABLE 6.2 Developments of International Standards for the Ergonomics of the Thermal Environment

Standard	Aims of the standard	Title of the document
ISO EN 11399	General presentation of the set of standards in terms of principles and application	Ergonomics of the thermal environment: Principles and application of international standards
ISO 13731	Standardization of quantities, symbols, and units used in the standards	Ergonomics of the thermal environment: Vocabulary and symbols
ISO 7933 (EN 12515)	Thermal stress evaluation in hot environments. Analytical method	Hot environments: Analytical determination and interpretation of thermal stress using calculation of required sweat
ISO EN 7243	Diagnostic method for hot environments	Hot environments: Estimation of the heat stress on working man, based on the WBGT index (wet bulb globe temperature)
ISO EN 7730	Comfort evaluation in moderate environments	Moderate thermal environments: Determination of the PMV and PPD index and specification of the conditions for thermal comfort
ISO TR ENV 11079	Thermal stress evaluation in cold environments	Evaluation of cold environments: Determination of required clothing insulation, I_{req}
ISO EN 8996 (EN 28996)	Data collection standards for metabolic rate	Ergonomics: Determination of metabolic heat production
ISO EN 7726	Requirements for measuring instruments	Thermal environments: Instruments for measuring physical quantities
ISO EN 9920	Clothing insulation	Estimation of the thermal insulation and evaporative resistance of clothing ensemble
ISO EN 9886	Evaluation of thermal strain using physiological measures	Evaluation of thermal strain by physiological measurements
ISO EN 10551	Subjective assessment of the thermal environment	Assessment of the influence of the thermal environment using subjective judgment scales
ISO DIS 12894	Selection of an appropriate system of medical supervision for different types of thermal exposure	Ergonomics of the thermal environment: Medical supervision of individuals exposed to hot or cold environments
ISO DIS 13732	Contact with hot, moderate, and cold surfaces	Ergonomics of the thermal environment: Methods for assessment of human responses to contact with surfaces
NP 14505	Vehicle environments	Evaluation of the thermal environments in vehicles
ISO DIS 14415	People with special requirements	Ergonomics of the thermal environment: The application of international standards for people with special requirements
ISO CD 15265	Assessment of risk in moderate, hot and cold environments	Risk assessment
NP 15743	Work practice in cold environments	

6.3.3 Moderate Thermal Environments

The main standards for comfortable thermal environment are ISO EN 7730 and ASHRAE 55-92.[2] The research that forms the basis for these two standards is mainly performed under environmental conditions similar to those for commercial and residential buildings, with activity levels of 1 to 2 met, normal indoor clothing (0.5 to 1.0 clo), and a limited range of environmental parameters.

6.3.3.1 General Thermal Comfort

ISO EN 7730 standardizes the PMV-PPD index as the method for evaluation of moderate thermal environments. To quantify the degree of comfort, the PMV (predicted mean vote) index gives a value on a 7-point thermal sensation scale: +3 hot, +2 warm, +1 slightly warm, 0 neutral, −1 slightly cool, −2 cool, −3 cold. An equation in the standard calculates the PMV index based on the six factors (clothing, activity, air and mean radiant temperatures, air speed, and humidity).

The PMV index can be determined when the activity (metabolic rate) and the clothing (thermal resistance) are estimated and the following environmental parameters are measured: air temperature, mean radiant temperature, relative air velocity, and partial water vapor pressure (see ISO EN 7726).

The PMV index is derived for steady-state conditions but can be applied with good approximation with minor fluctuations of one or more of the variables, provided that time-weighted averages of the variables during the previous 1 h period are applied. Because the PMV index assumes that all evaporation from the skin is transported through the clothing to the environment, this method is not applicable to hot environments. It can be used for a range of PMV index of −2 to +2, i.e., thermal environments where sweating is minimal.

Use of the PMV index is only recommended when the six main parameters are within the following intervals:

M = 46–232 W/m^2 (0.8 to 4 met)
I_{clo} = 0–0.310 m^2 °C/W (0 to 2 clo)
t_a = 10–30 °C
$\bar{t}_r$ = 10–40 °C
v_a = 0–1 m/s
p_a = 0–2700 Pa

The metabolic rate can be estimated by ISO EN 9886, and the thermal resistance of clothing can be estimated by ISO EN 9920, taking into account the type of work and the time of year. For varying metabolic rates, it is recommended to estimate a time-weighted average during the previous 1 h period. For sedentary people, the insulation of a chair must also be taken into account.

The PMV index can be used to check whether a given thermal environment complies with specified comfort criteria and to establish requirements for different levels of acceptability. By setting PMV = 0, an equation is established that predicts combinations of activity, clothing, and environmental parameters that will provide a thermally neutral sensation. Figure 6.1 shows the optimal operative temperature as a function of activity and clothing for different levels of acceptability.

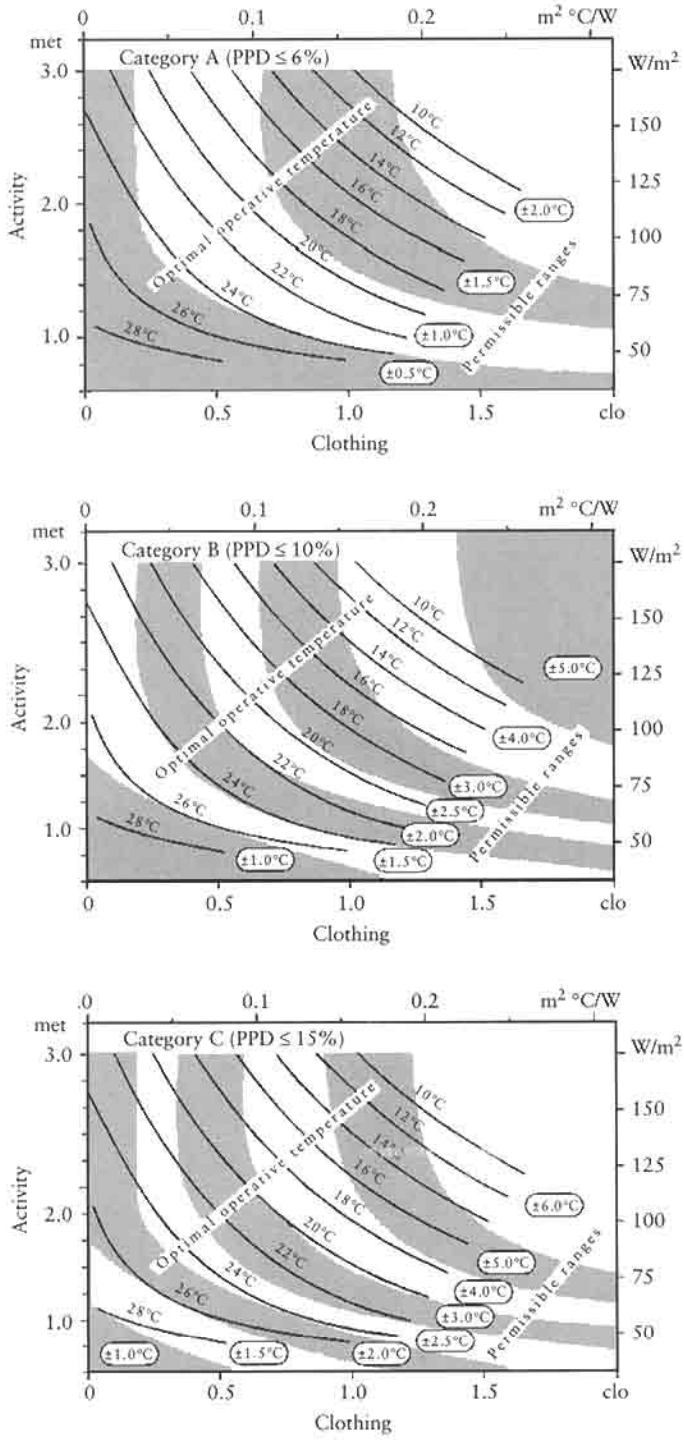

FIGURE 6.1 The optimal operative temperature as a function of clothing and activity for the three categories of thermal environment. The three diagrams also show the range around the optimal temperature for each of the three categories. The air velocity in the space is assumed to be < 0.1 m/s. The relative air velocity, v_a, caused by body movement is estimated to be zero for a metabolic rate M less than 1 met and $v_a = 0.3(M - 1)$ for $M > 1$ met. The diagrams are determined for a relative humidity of 50%, but the humidity has only a slight influence on the optimal and permissible temperature ranges.

The PMV index predicts the mean value of the thermal preferences of a large group of people exposed to the same environment. But individual votes are scattered around this mean value, and it is useful to predict the number of people likely to feel uncomfortably warm or cool. The PPD (predicted percentage of dissatisfied) index establishes a quantitative prediction of the number of thermally dissatisfied people. The PPD predicts the percentage of a large group of people likely to feel too warm or cool, i.e., voting hot (+3), warm (+2), cool (−2), or cold (−3) on the 7-point thermal sensation scale.

Once the PMV value has been determined, the PPD can be found from Fig. 6.2 or from the equation

$$\mathrm{PPD} = 100 - 95e^{(-0.03353\mathrm{PMV}^4 - 0.2179\mathrm{PMV}^2)}. \tag{6.2}$$

6.3.3.2 Local Thermal Discomfort

Aside from the general thermal state of the body, a person may find the thermal environment unacceptable if local influences on the body from asymmetric temperature radiation, draft, vertical air temperature differences, or contact with hot or cold surfaces (floors, machinery, tools, etc.) are experienced. The data for local thermal discomfort is mainly based on studies of people under low activity levels (1.2 met). For higher activities it can be expected that people are less sensitive to local thermal discomfort. The relations between dissatisfaction and local discomfort parameters are found in CR 1752.

Draft: Local Air Velocities

One of the most critical factors is draft. Many people at low activity levels (seated/standing) are very sensitive to air velocities, and therefore draft is a very common cause for occupant complaints in ventilated and air-conditioned spaces. Fluctuations of the air velocity have a significant influence on a person's sensation of draft. The fluctuations may be ex-

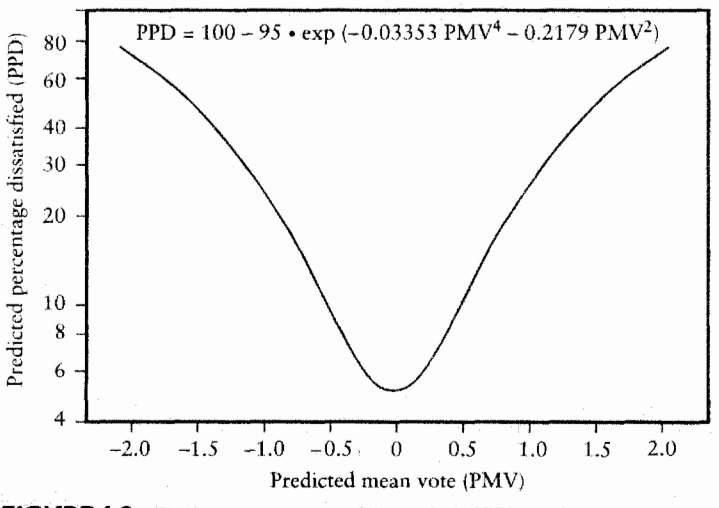

FIGURE 6.2 Predicted percentage of dissatisfied (PPD) as a function of predicted mean vote (PMV).

pressed either by the standard deviation of the air velocity or by the turbulence intensity Tu, which is equal to standard deviation divided by the mean air velocity, v_a. The percentage of people feeling draft (draft rating, DR) may be estimated from the equation

$$DR = (34 - t_a)(v_a - 0.05)^{0.62}(3.14 + 0.37 \cdot SDv_a) \quad (6.3)$$

where

v_a = mean air velocity (3 min), m s^{-1}
SDv_a = standard deviation of air velocity (3 min), m s^{-1}
t_a = air temperature, °C

For $v_a < 0.05$ m s^{-1}, use $v_a = 0.05$ m s^{-1}. For DR > 100%, use DR = 100%.

The model applies to people at light, mainly sedentary activity with a thermal sensation for the whole body close to neutral. The sensation of draft is lower at activities higher than sedentary and for people feeling warmer than neutral.

For people at higher activity levels or at ambient temperatures above the comfort range, an increased air velocity may improve the general thermal comfort. This influence is taken into account by using the PMV equation. Also, high local velocities (spot cooling) may decrease discomfort from high activity or high ambient temperatures.

Vertical Air Temperature Difference

A high vertical air temperature difference between one's head and ankles may cause discomfort. Figure 6.3 shows the percentage of dissatisfied as a function of the vertical air temperature difference between head and ankles (1.1 and 0.1 m above the floor, respectively). The figure applies when the temperature increases with height. People are less sensitive to decreasing temperature.

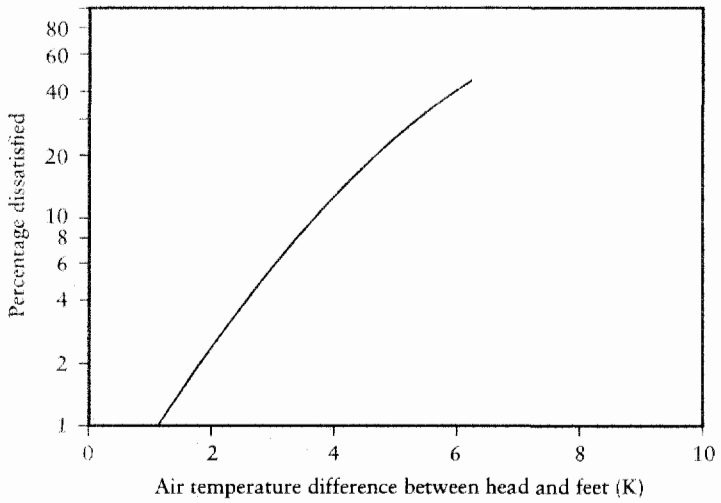

FIGURE 6.3 Local discomfort caused by vertical air temperature difference (applies when the temperature increases with height).

Warm and Cool Floors

If the floor is too warm or too cool, occupants may feel uncomfortable due to warm or cool feet. For people wearing light indoor shoes, it is the temperature of the floor rather than the material of the floor covering that is important to comfort. Figure 6.4 shows the percentage of dissatisfied for seated or standing people as a function of floor temperature.

Radiant Temperature Asymmetry

Radiant asymmetry may also cause discomfort. People are most sensitive to radiant asymmetry caused by warm ceilings or cool walls (windows). Figure 6.5 shows the percentage of dissatisfied as a function of radiant temperature asymmetry caused by a warm ceiling, a cool wall, a cool ceiling, or a warm wall. These data apply for sedentary people and low ceiling height. A study involving a high ceiling (9 m) and asymmetry from ceiling-mounted gas-fired infrared heaters showed a higher acceptable temperature asymmetry.[3] For seated and standing people, a temperature asymmetry of 10–14 K resulted in less than 5% dissatisfied.

6.3.3.3 Target Values for Acceptable Thermal Environments for Comfort

Thermal comfort is defined as the condition of mind that expresses satisfaction with the thermal environment. Dissatisfaction may be caused by thermal discomfort of the body as a whole as expressed with the PMV and PPD indices, or it may be caused by unwanted cooling (or heating) of a particular part of the body. Due to individual differences, it is impossible to specify a thermal environment that will satisfy everybody. There will always be a percentage of dissatisfied occupants, but it is possible to specify an environment predicted to be acceptable by a certain percentage of the occupants.

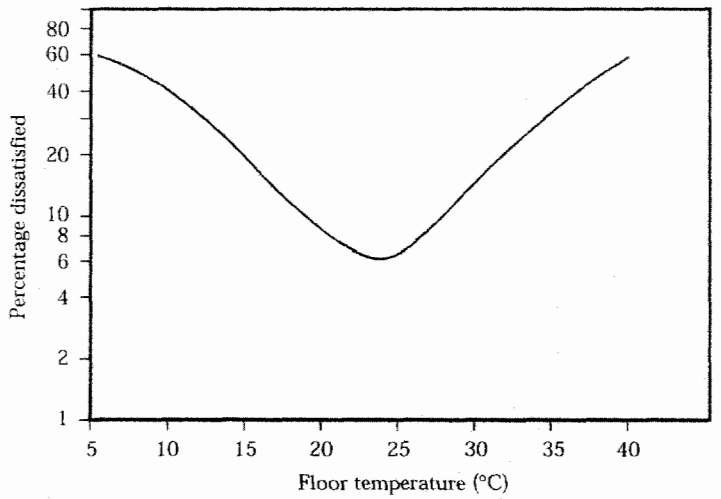

FIGURE 6.4 Local thermal discomfort caused by warm or cold floors.

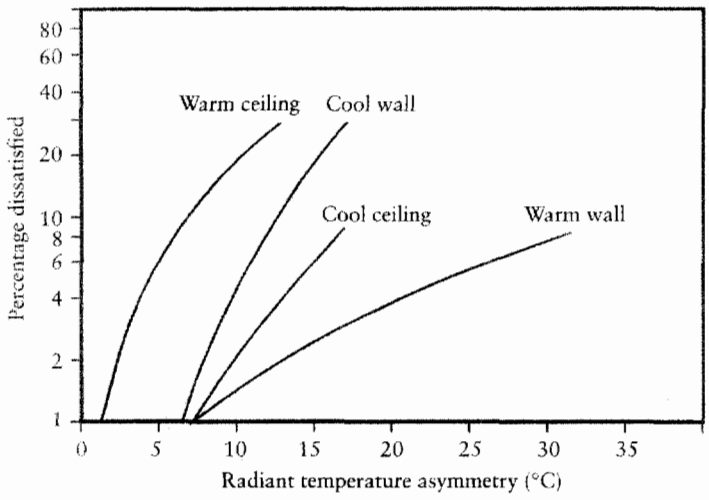

FIGURE 6.5 Local thermal discomfort caused by radiant temperature asymmetry.

Due to local or national priorities, technical developments, and climatic regions, in some cases a higher thermal quality (fewer dissatisfied) or a lower quality (more dissatisfied) may be sufficient. In both cases the PMV and PPD indices, the model of draft, and the relation between local thermal discomfort parameters and the expected percentage of dissatisfied people may be used to determine different ranges of parameters for the evaluation and design of the thermal environment.

While some existing standards specify only one level of comfort (e.g., ISO EN 7730, ASHRAE 55-92), a CEN report (CR 1752) recommend three categories, as shown in Table 6.3. Each category prescribes a maximum percentage of dissatisfied for the body as a whole (PPD) and for each of the four types of local discomfort. Some requirements are hard to meet in practice while others are quite easily met. The different percentages express a balance between the aim of providing few dissatisfied and what is practically obtainable using existing technology.

The three categories in Table 6.3 apply to spaces where persons are exposed to the same thermal environment. It is advantageous if some kind of individual control over the thermal environment can be established for each person in a space. Individual control of the local air temperature, mean radiant temperature, or air velocity may contribute to reducing the rather large differences between individual requirements and therefore provide fewer dissatisfied.

Modification of the clothing may also contribute to balancing individual differences. The effect of adding (or removing) different garments on the optimal operative temperature is given in Table 6.15.

Operative Temperature Range

For a given space there is an optimal operative temperature corresponding to PMV = 0, depending on the activity and the clothing of the occupants. Figure 6.1 shows the optimal operative temperature and the permissible temperature

TABLE 6.3 Three Categories of Thermal Discomfort

	Thermal state of the body as a whole		Local discomfort			
Category	Predicted percentage of dissatisfied (PPD)	Predicted mean vote (PMV)	Percentage of dissatisfied due to draft (DR)	Percentage of dissatisfied due to vertical air temperature difference	Percentage of dissatisfied due to warm or cool floor	Percentage of dissatisfied due to radiant asymmetry
A	<6	$-0.2 < PMV < +0.2$	<15	<3	<10	<5
B	<10	$-0.5 < PMV < +0.5$	<20	<5	<10	<5
C	<15	$-0.7 < PMV < +0.7$	<25	<10	<15	<10

range as a function of clothing and activity for each of the three categories. The optimal operative temperature is the same for the three categories, while the permissible range around the optimum operative temperature varies.

The operative temperature at all locations within the occupied zone of a space should at all times be within the permissible range. This means that the permissible range should cover both spatial and temporary variations, including fluctuations caused by the control system.

Figure 6.1 applies for a relative humidity of 50%; however, in moderate environments the air humidity has only a modest impact on the thermal sensation. Typically, a 10% increase in relative humidity is experienced as equally warm as a 0.3 °C increase in operative temperature.

The numbers of dissatisfied persons in Table 6.3 are not additive. Some of the people experiencing general thermal comfort (PMV-PPD) may be the same as the people experiencing local thermal discomfort. In practice, a higher or lower number of dissatisfied persons may be found using subjective questionnaires in field investigations (ISO 10551).

Local Thermal Discomfort

Figure 6.6 and Tables 6.4–6.6 give ranges for local thermal discomfort parameters for the three categories listed in Table 6.3. The acceptable mean air velocity is a function of local air temperature and turbulence intensity. The turbulence intensity may vary between 30% and 60% in spaces with mixed flow air distribution. In spaces with displacement ventilation or without mechanical ventilation, the turbulence intensity may be lower.

6.3.4 Hot Environments

The ISO philosophy for the assessment of hot environments is to use a simple, "fast" method of monitoring the environment, based on the wet bulb globe temperature (WBGT) index (ISO 7243). If the WBGT value exceeds the provided "reference" value, or if a more detailed analysis is required, then ISO 7933 provides an analytical method of assessment.

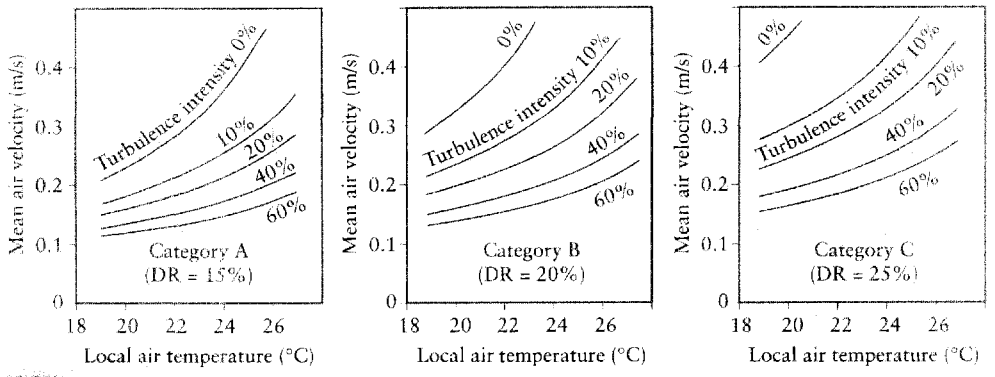

FIGURE 6.6 Acceptable mean air velocity as a function of local air temperature and turbulence intensity for the three categories of thermal environment.

TABLE 6.4 Vertical Air Temperature Difference between Head and Ankles (1.1 and 0.1 m, Respectively, above the Floor) for the Three categories of Thermal Environment

Category	Vertical air temperature difference (°C)
A	<2
B	<3
C	<4

TABLE 6.5 Range of Floor Temperature for Three Categories of Thermal Environment

Category	Range of surface temperature of the floor (°C)
A	19–29
B	19–29
C	17–31

TABLE 6.6 Radiant Temperature Asymmetry for the Three Categories of Thermal Environment

	Radiant temperature asymmetry (°C)			
Category	Warm ceiling	Cool wall	Cool ceiling	Warm wall
A	<5	<10	<14	<23
B	<5	<10	<14	<23
C	<7	<13	<18	<35

The WBGT heat stress index is calculated inside buildings and outside buildings without solar load as

$$\text{WBGT} = 0.7t_{\text{nw}} + 0.3t_g \tag{6.4}$$

and outside buildings with solar load as

$$\text{WBGT} = 0.7t_{\text{nw}} + 0.2t_g + 0.1t_a, \tag{6.5}$$

where

t_{nw} is the natural wet bulb temperature, °C
t_g is the temperature at the center of a 150 mm–diameter black globe thermometer, °C
t_a is the air temperature, °C

The WBGT value for the hot environment is compared against a WGBT reference value, which is included in an informative annex (Table 6.7). The reference values have been established allowing for a maximum rectal temperature of 38 °C for the persons concerned. This corresponds to levels to which almost all individuals can be ordinarily exposed without any harmful effect, provided there are no preexisting pathological conditions.

TABLE 6.7 Reference Values for WBGT (ISO 7243)

	Metabolic rate, *M*		Reference value of WBGT			
Metabolic rate class	Related to a unit skin surface area (W m^{-2})	Total (for a mean skin surface area of 1.8 m^2) (W)	Person acclimatized to heat (°C)		Person not acclimatized to heat (°C)	
0 (resting)	$M < 65$	$M < 117$	33		32	
1	$65 < M < 130$	$117 < M < 234$	30		29	
2	$130 < M < 200$	$234 < M < 360$	28		26	
3	$200 < M < 260$	$360 < M < 468$	No sensible air movement	Sensible air movement	No sensible air movement	Sensible air movement
			25	26		23
4	$M > 260$	$M > 468$	23	25		20

Note: The values given have been established for a maximum rectal temperature of 38°C for the person concerned.

If the WBGT of the hot environment exceeds the WBGT reference value, then the heat stress at the workplace needs to be reduced or a more detailed analysis made (i.e., using ISO 7933). The standard also includes a method to plan a work/rest schedule that will provide a tolerable environment.

The value used in ISO 7933, required sweat rate, SW_{req}, is based on the heat balance equation (6.1). Assuming the heat storage is equal to 0, the necessary evaporation from the skin, E_{req}, to ensure a heat balance is calculated as follows:

$$E_{req} = M - W - C - R - E_{res} - C_{res}. \tag{6.6}$$

The maximum evaporation, E_{max}, that can be absorbed by the environment is estimated from the equation

$$E_{max} = (p_{sk_s} - p_a)/R_{e_T}, \tag{6.7}$$

where

p_{sk_s} = saturated water vapor pressure at the skin
p_a = water vapor pressure in the environment
R_{e_T} = total evaporative resistance of clothing and boundary layer

Based on the required evaporation and the maximum evaporation it is then possible to estimate the following factors:

- Required skin wettedness,

$$w_{req} = E_{req}/E_{max} \tag{6.8}$$

- Sweating efficiency,

$$r = 1 - 0.5e^{-6.6(1-w_{req})} \tag{6.9}$$

- Required sweat rate,

$$SW_{req} = E_{req}/r \tag{6.10}$$

These parameters are used to evaluate how stressful a given hot working environment is. Depending on the physiological limitations for factors such as sweat rate, total sweat loss, heat storage, and skin wettedness, which are listed in Table 6.8, it is possible to evaluate whether a given environment is acceptable for continuous work. The method also allows calculation of an acceptable working time. Detailed equations for the calculations can be found in the standard (ISO 7933). The relation between the operative temperature and SW_{req} for different combinations of activity and clothing is shown in Table 6.9.

A computer program is provided for ease of calculation and efficient use of the standard. This rational method of assessing hot environments allows identification of the relative importance of different components of the thermal environment, and hence can be used in environmental design. The WBGT index is an empirical index, and it cannot be used to analyze the influence of the individual parameters. The required sweat rate (SW_{req}) has this capability, but lack of data may make it difficult to estimate the benefits of protective clothing.

6.3.5 Cold Environments

Many industrial workplaces are located in cold environments, such as cold storage, meat packing areas, and outdoor sites. In cold environments, clothing is the

TABLE 6.8 Reference Values for the Different Criteria of Thermal Stress and Strain

	Non-acclimatized subjects		Acclimatized subjects	
Criteria	**Warning**	**Danger**	**Warning**	**Danger**
Maximum skin wettedness, w_{max}	0.85	0.85	1.0	1.0
Maximum sweat rate				
Rest: $M < 65$ W/m				
Sw_{max}, W/m^2	100	150	200	300
g/h	260	390	520	780
Work: $M > 65$ W/m^2				
Sw_{max}, W/m^2	200	250	300	400
g/h	520	650	780	1040
Maximum heat storage,				
Q_{max} W h/m^2	50	60	50	60
Maximum water loss,				
D_{max}, W h/m^2	1000	1250	1500	2000
g	2600	3250	3900	5200

most important factor in obtaining an acceptable thermal environment. Based on the heat balance equation (6.1), an analytical method has been proposed by CEN and ISO: required clothing insulation, I_{req} (ISO/TR ENV 11079). The method calculates the insulation of the clothing necessary to keep a heat balance

TABLE 6.9 Required Sweat Rate Index SW_{req} W/m^2, and Wettedness (w_{req}) as a Function of Clothing, Temperature, Air Speed, and Humidity at an Activity Level *M* Equal to 70 W/m^2

Clothing I_{cl}, clo	Relative humidity, %	Operative temperature t_o, °C	Air velocity v_a, m/s				
			<0.1	0.2	0.5	1.0	2.0
0.50	20	25	10(.03)	8(.02)	2(.01)		
		30	37(.13)	36(.12)	33(.09)	29(.06)	24(.04)
		35	65(.24)	64(.22)	64(.18)	63(.14)	62(.11)
		40	93(.37)	94(.34)	95(.29)	98(.24)	101(.20)
		50	169(.78)	165(.72)	165(.62)	171(.52)	182(.45)
	50	60	*(1.00)	(1.00)	*(1.00)	*(1.00)	*(1.00)
		25	10(.04)	8(.03)	2(.01)	29(.08)	24(.05)
		30	37(.17)	35(.15)	33(.12)	63(.22)	62(.17)
		35	65(.37)	65(.34)	64(.28)	99(.47)	102(.39
		40	102(.74)	99(.69)	98(.57)	29(.12)	24(.08)
	80	30	37(.26)	36(.23)	33(.18)	64(.48)	63(.38)
		35	76(.82)	71(.75)	66(.61)		

in a given cold environment given the activity level, air and mean radiant temperatures, air velocity, and humidity according to the following equations:

$$I_{req} = \frac{t_{sk} - t_{cl}}{M - W - E_{sk} - C_{res} - E_{res}} \tag{6.11}$$

$$M - W - E_{sk} - C_{res} - E_{res} = C + R \tag{6.12}$$

The relationship between activity level, operative temperature, and I_{req} may be calculated with this new method; however, it has not been widely used, and little experience is available. Therefore, the method has been proposed in the form of a technical report, which in the future may be published as an ISO standard.

The index value may be used to select a clothing ensemble that will provide the required insulation. The clothing insulation can, as shown in Table 6.10, be predicted either as a minimum, where some strain may be imposed on the people, or as a neutral value, where people are expected to feel neutral. It is important when selecting the actual clothing (ISO 9920) to allow for individual adjustment of the insulation. Also, the clothing insulation values listed in ISO 9920 are valid for people engaged in standing and sedentary work. For people at higher activity levels, the clothing values from the tables in ISO 9920 should be reduced by approximately 20% owing to body movements (pumping effect).

If it is not possible to use a clothing ensemble with enough insulation, the method includes a procedure for calculation of a recommended exposure time. The basis for the calculations are the physiological requirements listed in Table 6.10.

For outdoor work there may be a risk of frostbite in the wintertime. The report uses the wind chill temperature, WCI, calculated as

$$t_{ch} = \frac{33 - \text{WCI}}{25.5} \ ^\circ\text{C} \tag{6.13}$$

$$\text{WCI} = 1.16(10.45 + 10\sqrt{v_a} - v_a)(33 - t_a) \ (\text{W/m}^2) \ , \tag{6.14}$$

where t_a = outside air temperature (°C), WCI = wind chill index (W/m^{-2}), and v_a = relative air velocity (m s^{-1}). Table 6.11 shows the values depending on the outside temperature and wind velocity, and Table 6.12 shows the expected effect.

TABLE 6.10 Proposed Physiological Criteria for Determination of I_{req}, DLE, and Local Cooling (ISO 7R 11079)

Type of cooling	Parameter	Minimal I_{req} (high strain)	Neutral I_{req} (low strain)
General	I_{req}	30	35.7–0.028 5M
	t_{sk} (°C)	0.06	0.0001M
	w (n.d.)		
	DLE		
	Q_{hm} (W h m^{-2})	–40	–40
Local	Hand temperature (°C)	15	24
	WCI (W h m^{-2})	1600	—
	Respiratory tract and eye temp. (°C)	$t_a < -40$	—

TABLE 6.11 Cooling Power of Wind on Exposed Flesh Expressed as a Chilling Temperature, t_{ch}, under Almost Calm Conditions

Wind speed ($m\ s^{-1}$)	Actual thermometer reading										
	0	−5	−10	−15	−20	−25	−30	−35	−40	−45	−50
1.8	0	−5	−10	−15	−20	−25	−30	−35	−40	−45	−50
2	−1	−6	−11	−16	−21	−27	−32	−37	−42	−47	−52
3	−4	−10	−15	−21	−27	−32	−38	−44	−49	−55	−60
5	−9	−15	−21	−28	−34	−40	−47	−53	−59	−66	−72
8	−13	−20	−27	−34	−41	−48	−55	−62	−69	−76	−83
11	−16	−23	−31	−38	−46	−53	−60	−68	−75	−83	−90
15	−18	−26	−34	−42	−49	−57	−65	−73	−80	−88	−96
20	−20	−28	−36	−44	−52	−60	−68	−76	−84	−92	−100

6.3.6 Supporting Standards

The application of the above standards requires measurement or estimation of a number of parameters. The supporting and complementary standards described below provide information that is required for the application of standards for assessing thermal environments. They can also be used independently in ergonomics and other investigations.

6.3.6.1 Metabolic Rate

All assessments of thermal environments require an estimate of the metabolic heat production of the occupants. ISO EN 8996 presents three types of methods. The first is by use of tables, where estimates are provided based on a description of the activity. These range from a general description (light,

TABLE 6.12 Wind Chill Index, WCI, Chilling Temperature, t_{ch}, and Effect on Exposed Flesh

WCI ($W\ m^{-2}$)	t_{ch} (°C)	Effect
1200	−14	Very cold
1400	−22	Bitterly cold
1600	−30	Exposed flesh freezes within 1 h
1800	−38	
2000	−45	Exposed flesh freezes within 1 min
2200	−53	
2400	−61	Exposed flesh freezes within 30 s
3600	−69	

heavy, etc.) to methods of summing components of tasks (e.g., basal metabolic rate + posture component + movement component). An example of activity levels is given in Table 6.13.

The second method is by use of the heart rate. The total heart rate is regarded as a sum of several components and, in general, is linearly related to the metabolic heat production for heart rates above 120 beats per minute. Heat stress will, however, also increase the heat rate. The third method is to calculate the metabolic heat production from measures of oxygen consumption, and carbon dioxide production during activity and recovery.

6.3.6.2 Clothing

ISO EN 9920 provides a large database of thermal insulation values, which have been measured on a standing thermal manikin. One set of tables gives the insulation values for a large number of ensembles (Table 6.14). Another set of tables gives insulation values for individual garments (Table 6.15), on the basis of which the insulation for a whole ensemble can be estimated.

The insulation of an ensemble, I_{cl}, may be estimated as the sum of the individual garment insulation values: $I_{cl} = \sum I_{clu}$. The data on evaporative resistance are not so extensive. A few data are given in the standard, and a method to calculate the evaporative resistance based on the thermal insulation is also given. In the present standard no values are listed for the insulation of chairs, which may add 0.1–0.4 clo. Especially for the assessment of the level of heat stress, data on the evaporative resistance of clothing ensembles are important.

6.3.6.3 Instruments and Measurements

ISO 7726 provides a description of the parameters that should be measured (air temperature, mean radiant temperature, plane radiant temperature, air velocity, and humidity) together with methods of measurement

TABLE 6.13 Metabolic Rates

Activity	($W\ m^{-2}$)	met
Reclining	46	0.8
Seated, relaxed	58	1.0
Sedentary activity (office, dwelling, school, laboratory)	70	1.2
Standing light activity (shopping, laboratory, light industry)	93	1.6
Standing, medium activity (shop assistant, domestic work, machine work)	116	2.0
Walking on the level		
2 km h^{-1}	110	1.9
3 km h^{-1}	140	2.4
4 km h^{-1}	165	2.8
5 km h^{-1}	200	3.4

TABLE 6.14 Thermal Insulation for Typical Clothing Ensembles

	I_{cl}			I_{cl}	
Work clothing	**clo**	**m^2 K /W**	**Daily wear clothing**	**clo**	**m^2 K /W**
Underpants, boiler suit, socks, shoes	0.70	0.110	Panties, T-shirt, shorts, light socks, sandals	0.30	0.050
Underpants, shirt, boilersuit, socks, shoes	0.80	0.125	Underwear, shirt with short sleeves and legs, light trousers, light socks, shoes	0.50	0.080
Underpants, shirt, trousers, smock, socks, shoes	0.90	0.140	Panties, petticoat, dress, stockings, shoes	0.70	0.105
Underwear with short sleeves and legs, shirt, trousers, jacket, socks, shoes	1.00	0.155	Underwear, shirt, trousers, socks, shoes	0.70	0.110
Underwear with long sleeves and legs, thermo-jacket, socks, shoes	1.20	1.85	Panties, T- shirt, trousers, jacket, socks, shoes	1.00	0.155
Underwear with short sleeves and legs, shirt, trousers, jacket, heavy quilted outer-jacket and overalls, socks, shoes, cap, gloves	1.40	0.220	Panties, blouse, long shirt, jacket, stockings, shoes	1.10	0.170
Underwear with short sleeves and legs, shirt, trousers, jacket, heavy quilted outer-jacket and overalls, socks, shoes	2.00	0.310	Underwear with long sleeves and legs, shirt, trousers, V-neck sweater, jacket, socks, shoes	1.30	0.200
Underwear with long sleeves and legs, thermo-jacket and trousers, heavy quilted outerjacket and overalls, socks, shoes, cap, gloves	2.55	0.395	Underwear with short sleeves and legs, shirt, trousers, vest, jacket, coat, socks, shoes	1.50	0.230

TABLE 6.15 Thermal Insulation for Individual Garments

Garment description	Thermal insulation (clo)
Underwear	
Panties	0.03
Underpants with long legs	0.10
T-shirt	0.09
Shirts, blouses	
Short sleeves	0.15
Normal, long sleeves	0.25
Trousers	
Shorts	0.06
Normal	0.25
Dresses, skirts	
Light skirts (summer)	0.15
Heavy skirts (winter)	0.25
Winter dress, long sleeves	0.40
Sweaters	
Thin	0.20
Thick	0.35
Jackets	0.90
Light, summer jacket	0.35
Jacket	0.40
High-insulative, fiberpelt	
Boiler suit	0.90
Trousers	0.35
Jacket	0.40
Outdoor clothing	
Coat	0.60
Parka	0.70
Sundries	
Socks	0.02
Thick, long socks	0.10
Shoes (thick-soled)	0.04
Boots	0.10

and specifications for the instruments (accuracy, response time, measuring range). Table 6.16 gives the accuracy required in the standard.

6.3.7 Measurements on Individuals

The methods listed above to evaluate the thermal environment assume an average person. As individuals can react very differently, both regarding acceptance of a given environment and regarding the strain that a given environment imposes, it may under certain circumstances be beneficial to incorporate individual physiological and subjective measurements. Also, there may be a need for evaluation of an individual's capability for performing a certain job under severe conditions in the field or in an ergonomics laboratory investigation.

6.3.7.1 Physiological Measurements

ISO EN 9886 presents the principles, methods, and interpretation of measurements of relevant human physiological responses to hot, moderate, and cold environments. The standard can be used independently or to complement other standards. Four physiological measures are considered: body core temperature, skin temperature, heart rate, and body mass loss. Comments are also provided on the technical requirements, relevance, convenience, annoyance to the subject, and cost of each of the physiological measurements. The use of ISO 9886 is mainly for extreme cases, where individuals are exposed to severe environments, or in laboratory investigations into the influence of the thermal environment on humans.

6.3.7.2 Subjective Measurements

Subject scales are useful in the measurement of subjective responses of persons exposed to thermal environments. They are particularly useful in moderate environments and can be used independently or to complement the use of the objective methods (e.g., thermal indices) that were described previously. ISO EN 10551 presents the principles and methodology behind the construction and use of subjective scales and provides examples of scales that can be used to assess thermal environments.

The medical screening standard, ISO DIS 12894, provides advice to those concerned with the safety of human exposures to hot or cold thermal environments, about health screening and surveillance that may be appropriate prior to and during such exposures. This guidance is applicable to both occupational and laboratory exposures to extreme environments. In either case an assessment should be made of the expected thermal stress on the individual, but the detailed arrangements for medical supervision may differ between the two situations. Control of occupational exposures must also satisfy national health and safety legislation. The laboratory or climatic chamber studies for which this standard is relevant include those in which people may be exposed to high or low ambient conditions or local heating or cooling.

TABLE 6.16 Characteristics of Measuring Instruments

		Class C (comfort)			Class S (thermal stress)			
Quantity	Symbol	Measuring range	Accuracy	Response time (90%)	Measuring range	Accuracy	Response time (90%)	Comments
Air temperature	t_a	10 to 40 °C	Required: ±0.5 °C Desirable: ±0.2 °C These levels shall be guaranteed at least for a deviation $\lvert t_r - t_a \rvert$ equal to 10 °C	The shortest possible. Value to be specified as characteristic of the measuring instrument	− 40 to + 120 °C	Required: − 40 to 0 °C: $\pm (0.5 + 0.01 \lvert t_a \rvert)$ °C > 0 to 50 °C: ± 0.5 °C > 50 to 120 °C: $\pm [0.5 + 0.04(t_a - 50)]$ °C Desirable: $\frac{\text{required accuracy}}{2}$ These levels shall be guaranteed at least for a deviation $\lvert t_r - t_a \rvert$ equal to 20 °C	The shortest possible. Value to be specified as characteristic of the measuring instrument	The air temperature sensor shall be effectively protected from any effects of thermal radiation coming from hot or cold walls. An indication of the mean value over a period of 1 min is also desirable.
Mean radiant temperature	$\bar{t}_r$	10 to 40 °C	Required: ±2 °C Desirable: ±0.2 °C These levels are difficult or even impossible to achieve in certain cases with the equipment normally available. When they cannot be achieved, indicate the actual measuring precision	The shortest possible. Value to be specified as characteristic of the measuring instrument	− 40 °C to + 150 °C	Required: − 40 to 0 °C: $\pm (5 + 0.02 \lvert t_a \rvert)$ °C > 0 to 50 °C: ± 5 °C > 50 to 120 °C: $\pm [5 + 0.08(t_a - 50)]$ °C Desirable: − 40 to 0 °C: $\pm (0.5 + 0.01 \lvert t_a \rvert)$ °C > 0 to 50 °C: ± 0.5 °C > 50 to 120 °C: $\pm [0.5 + 0.04(t_a - 50)]$ °C	The shorrest possible. Value to be specified as characteristic of the measuring instrument	When the measurement is carried out with a black sphere, rhe inaccuracy relation to the mean radiant remperature can be as high as ± 5 °C for class C and ± 20 °C for class S according to the environment and the inaccuracy for v_a, t_a and t_g
Plane radiant temperature	t_{pr}	0 to 50 °C	Required: ±0.5 °C Desirable: ±0.2 °C These levels shall be guaranteed at least for a deviation $\lvert t_{pr} - t_a \rvert < 10$ °C	The shortest possible. Value to be specified as characteristic of the measuring instrument	0 to 200 °C	Required: − 60 to 0 °C: $\pm (1 + 0.01 \lvert t_{pa} \rvert)$ °C > 0 to 50 °C: ± 1 °C > 50 to 200°C: $\pm [1 + 0.04(t_{pa} - 50)]$ °C Desirable: $\frac{\text{required accuracy}}{2}$ These levels shall be guaranteed at least for a deviation $\lvert t_{pr} - t_a \rvert < 20$ °C	The shortest possible. Value to be specified as characteristic of the measuring instrument.	

(continues)

TABLE 6.16 *(continued)*

		Class C (comfort)			Class S (thermal stress)			
Quantity	**Symbol**	**Measuring range**	**Accuracy**	**Response time (90%)**	**Measuring range**	**Accuracy**	**Response time (90%)**	**Comments**
Air velocity	v_a	0,05 to 1 m/s	Required: $\pm(0.05 + 0.05v_a)$ m/s Desirable: $\pm(0.02 + 0.07v_a)$ m/s These levels shall be guaranteed whatever the direction of flow within a solid angle $\omega = 3\pi$sr	Required: 0.5 s Desirable: 0.2 s	0.2 to 20 m/s	Required: $\pm(0.1 + 0.05\ v_a)$ m/s Desirable: $\pm(0.05 + 0.05\ v_a)$ m/s These levels shall be guaranteed whatever the direction of flow within a solid angle $\omega = 3\pi$sr	The shortest possible. Value to be specified as characteristic of the measuring instrument.	Except in the case of a unidirectional air current, the air velocity sensor shall measure the velocity whatever the direction of the air. An indication of the mean value and standard deviation for a period of 3 min is also desirable.
Absolute humidity expressed as partial pressure of water vapor	p_a	0.5 to 3.0 kPa	$\pm$0.15 kPa This level shall be guaranteed even for air and wall temperatures equal to or greater than 30 °C and for a difference $\lvert t_r - t_a \rvert$ of at least 10 °C	The shortest possible. Value to be specified as characteristic of the measuring instrument	0.5 to 6.0 kPa	$\pm$0.15 kPa This level shall be guaranteed even for air and wall temperatures equal to or greater than 30 °C and for a difference $\lvert t_r - t_a \rvert$ of at least 20 °C.	The shortest possible. Value to be specified as characteristic of the measuring instrument.	
Surface temperature	t_s	0–50 °C	Required: $\pm$1 °C Desirable: $\pm$0.5 °C	The shortest possible. Value to be specified as characteristic of the measuring instrument	– 40 to + 120 °C	Required: < –10 °C: $\pm[1 + 0.05(t_s - 10)]$°C – 10 to 50 °C: $\pm$1°C > 50 °C: $\pm[1 + 0.05(t_s - 50)]$°C Desirable: $\frac{\text{required accuracy}}{2}$	The shortest possible. Value to be specified as characteristic of the measuring instrument.	

6.3.8 Other and Future Standards

To help the user, an overview standard (ISO 11399) is being issued. This summarizes the different standards and guides the user to which method and standard are applicable for the given situation. In addition, a standard has been prepared that lists all definitions, symbols, and units (ISO 13731). Ongoing work is dealing with standards for contact with hot, cold, and comfortable surfaces, application of the standards in vehicles, and precautions to take when assessing thermal environments for the disabled, aged, or other groups with special needs.

6.3.9 Conclusion

The series of standards presented in this paper provides a useful package for assessment and design of HVAC systems and protective equipment to be used in moderate, cold, and hot environments. The standards may be used to estimate the optimal combination of environmental thermal factors that will provide comfortable or tolerable healthy working conditions. The standards may also be used to establish optimal work/rest schedules for environments where the working time must be limited owing to strain on the human body. Several of these standards are being adopted as national standards in several countries.

Some of the methods used in the standards are based on many years of research and validation, while others are relatively new and not validated to the same degree. It is therefore important to realize that a standard is not an everlasting document, but must be revised on a regular basis. These revisions take place at least every fifth year, and experience with use and new knowledge are incorporated into the review process.

6.3.10 Examples

Table 6.17 shows recommended operative temperatures and maximum mean air velocities for different types of spaces. The table is based on ISO EN 7730 and CR 1752.

Table 6.18 shows the effect of adding or removing garments on the preferred operative temperature. By individual adaption of clothing it is possible to compensate for individual differences in preferred temperature or for differences in activity level. The table is based on ISO EN 7730 and ISO EN 9920.

References

1. CR 1752. *Ventilation for buildings: Design criteria for the indoor environment.* CEN, Brussels, 1998.
2. ASHRAE Standard 55-92. *Thermal environment conditions for human occupancy.* ASHRAE, New York, 1992.
3. G. Langkilde, L. Gunnarsen, and N. Mortensen. Comfort limits during infrared radiant heating of industrial spaces. *CLIMA 2000*, Copenhagen, 1985.

TABLE 6.17 Examples of Recommended Operative Temperature and Air Velocity Based on ISO EN 7730 and CR 1752

Type of building/space	Clothing season (summer) (clo)	Clothing season (winter) (clo)	Activity (met)	Category	Operative temperature Cooling season (summer) (°C)	Operative temperature Heating season (winter) (°C)	Mean air velocity cooling heating Cooling season (summer) (m/s)	Mean air velocity cooling heating Heating season (winter) (m/s)
Single office (cellular office)	0.5	1.0	1.2	A	24.5 ± 0.5	22.0 ± 1.0	0.18	0.15
				B	24.5 ± 1.5	22.0 ± 2.0	0.22	0.18
				C	24.5 ± 2.5	22.0 ± 3.0	0.25	0.21
Landscaped office	0.5	1.0	1.2	A	24.5 ± 0.5	22.0 ± 1.0	0.18	0.15
				B	24.5 ± 1.5	22.0 ± 2.0	0.22	0.18
				C	24.5 ± 2.5	22.0 ± 3.0	0.25	0.21
Conference room	0.5	1.0	1.2	A	24.5 ± 0.5	22.0 ± 1.0	0.18	0.15
				B	24.5 ± 1.5	22.0 ± 2.0	0.22	0.18
				C	25.5 ± 2.5	22.0 ± 3.0	0.25	0.21
Auditorium	0.5	1.0	1.2	A	24.5 ± 0.5	22.0 ± 1.0	0.18	0.15
				B	24.5 ±1.5	22.0 ± 2.0	0.22	0.18
				C	24.5 ± 2.5	22.0 ± 3.0	0.25	0.21
Cafeteria/ restaurant	0.5	1.0	1.4	A	23.5 ± 1.0	20.0 ± 1.0	0.16	0.13
				B	23.5 ± 2.0	20.0 ± 2.5	0.20	0.16
				C	23.5 ± 2.5	20.0 ± 3.5	0.24	0.19
Classroom	0.5	1.0	1.2	A	24.5 ± 0.5	22.0 ± 1.0	0.18	0.15
				B	24.5 ± 1.5	22.0 ± 2.0	0.22	0.18
				C	24.5 ± 2.5	22.0 ± 3.0	0.25	0.21
Kindergarten	0.5	1.0	1.4	A	23.5 ± 1.0	20.0 ± 1.0	0.16	0.13
				B	23.5 ± 2.0	20.0 ± 2.5	0.2	0.16
				C	23.5 ± 2.5	20.0 ± 3.5	0.24	0.19
Department store	0.5	1.0	1.6	A	23.0 ± 1.0	19.0 ± 1.5	0.16	0.13
				B	23.0 ± 2.0	19.0 ± 3.0	0.20	0.15
				C	23.0 ± 3.0	19.0 ± 4.0	0.23	0.18

TABLE 6.18 Examples of the Relation between a Change in Garments and the Acceptable Change in Operative Temperature

Garment description	Thermal insulation (clo)	Change of operative temperature (K)
Panties	0.03	0.2
Underpants with long legs	0.10	0.6
T-shirt	0.09	0.6
Short sleeve shirt	0.15	0.9
Light shirt, long sleeves	0.20	1.3
Normal shirt, long sleeves	0.25	1.6
Shorts	0.06	0.4
Light-weight trousers	0.20	1.3
Normal trousers	0.25	1.6
Light skirts (summer)	0.15	0.9
Heavy skirt (winter)	0.25	1.6
Sleeveless vest	0.12	0.8
Thin sweater	0.20	1.3
Light summer jacket	0.25	1.6
Normal jacket	0.35	2.2
Coat	0.60	3.7
Down jacket	0.55	3.4
Parka	0.70	4.3

6.4 TARGET LEVELS FOR INDUSTRIAL AIR QUALITY

6.4.1 Introduction

The need for exact target values relating to processes and products is self-evident in the design phase of process technology, equipment manufacture, and many other areas of engineering. Industrial ventilation is defined as "airflow technologies" to control the workplace indoor environment and emissions." It is therefore logical that the goals of industrial ventilation are unambiguously quantified. In the past the design goals of industrial ventilation have been expressed in many terms, such as airflow rates, filter classes, control velocity of a local exhaust hood, and surface temperature of a radiator. Although these are indispensable quantities in the design and realization processes, they account only indirectly for the environment within the premises. Therefore, the goal of industrial air quality should be defined using target values of the relevant contaminants occurring in the room.

The need for the implementation of target levels for air quality in industrial work rooms stems from different concerns. In addition to technological factors, the systematic design methodology, life cycle assessment, advances in air distribution methods, and increased integration with the process and

building automation have to be considered. The recent changes in the standards of working conditions that favor the target level process also must not be forgotten.

Occupational exposure limits (OELs) have been used for decades as exposure criteria for air contaminants (see Sections 5.3 and 6.2). OELs are quantitative health standards expressed as a maximum mean concentration of dangerous air contaminants over a given reference period. Although OELs are required for the establishment of health-based standards, the limits entail a great deal of uncertainty. They indicate the minimum level of air quality corresponding to the present understanding of what is an acceptable risk, but they do not serve as a criterion for planning a comfortable environment and control technologies for the whole life cycle of the system, say over a period of 20 years.

Although high exposures to air contaminants still occur in a number of industries, the general trend is that the current levels of most commonly used chemicals are decreasing and are clearly lower than the corresponding OELs. This means that more people are working in cleaner environments than previously. In the 1990s a discussion began by industrial hygienists and associated work environment specialists on the role of the OELs and the system for setting the limits.[1] There is the opinion that the OELs have less impact on the improvement of occupational environment than in previous decades, and that they focus on compliance testing instead of control. It is also worth noting that compliance with the occupational exposure limits does not guarantee 100% protection for all individuals.

Nowadays many companies have adopted a policy of continuous improvement of working conditions. Therefore, it is desirable to create target levels for those who want to pursue more efficient control by applying the best available control technologies. There are also endeavors to create optimal working conditions in order to improve the performance and the innovativeness of a staff, and hence enhance productivity. A series of laboratory and case studies show that employee productivity is higher when the work environment is appropriate for the tasks being done.[2] Such efforts are typical in the advanced sector of industry. One can say that there is a transition from "blue-collar to white-collar work."

Today occupants, building owners, and other end users of ventilation systems are more interested in the level of air quality and thermal climate than in the techniques by which that level is achieved. This is supported by the fact that industrial ventilation systems in modern premises are more complicated and tightly integrated with the process and building automation. It is therefore difficult for end users or nonprofessionals to evaluate whether a ventilation system is functioning correctly.

The aim of this section is to consider the scientific and technological grounds for assessing target levels of contaminants that frequently occur in the occupational environment as well as use of the target levels. The target level (TL) of a contaminant is defined as the predetermined concentration of a dominant contaminant to be achieved by air technology or other control methods. A target level can be considered for an entire room volume or a zone, such as an occupied zone or a limited part of the occupied zone.

Unlike OELs, the proposed target levels for air contaminants are voluntary guidelines.

6.4.2 Grounds for Assessing TLs for Industrial Air Quality

In order to assess the target concentrations of air contaminants both human risk-based and technology-based approaches can be used (Fig. 6.7). The various approaches are dealt with in more detail elsewhere.[3,4]

The procedure of assessing health-based occupational exposure limits for chemical substances includes determination of no-observed-adverse-effect level (NOAEL) for the critical toxic effect and application of an appropriate safety factor based on expert judgment (see Section 5.3). In principle, the same procedure could be used for assessing the TLs. However, the quantitative risk assessment procedure entails notable uncertainties at low-dose regions—say, below one-tenth of the current OELs. In addition, exposure limits are revised at certain intervals in the light of new research information and actual policy objectives. In most cases, the limits have been reduced over the years. In theory, one possibility for assessing a target level for desired air quality could be the determination of an exposure that cannot be distinguished from the biological monitoring values of the nonoccupational population. However, adequate data for this purpose exist only for a few substances in advanced industrialized countries, and for that reason a technology-based approach for target level assessment is considered in this paper. Similar control strategies, based on performance standards and risk assessment, have been proposed for some industries—for example, the pharmaceutical industry and technology transition in the defense sector.[5,6]

In the technological approach, qualitative and quantitative information on emissions released by various production and work processes, as well as data on control technology performance, are required in order to specify the air quality target levels that are technically and economically feasible. The approach is based on information on current concentration levels that are achieved by different control technologies, ranging from standard practices to the most advanced technology options (Fig. 6.7).

Existing contaminant exposure data banks can be utilized to survey the standard practices.[7,8] For example, the register of occupational hygiene measurements at the Finnish Institute of Occupational Health, containing information on more than 150 000 determinations of airborne pollutants, has been used. In most cases the measurements have been requested due to concern over working conditions. Consequently, the data in the registry likely reflect worst-case circumstances, in which the exposure levels have been high due to heavy emission rates or inefficient control. Based on the data in the register, cumulative frequency distributions of contaminant concentrations were created. As an example, the cumulative frequency distribution of concentrations of xylenes is shown in (Fig. 6.8). The median concentration levels and the lower and upper tails can be seen from the cumulative distribution curves. Usually attention has been focused on higher concentrations in order to prioritize the required control actions. However, from a design point of view, low values are of particular interest, as they reflect conditions in the work rooms with efficient engineering controls.

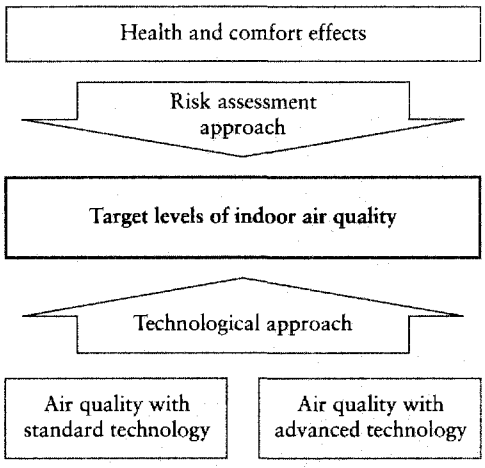

FIGURE 6.7 Approaches for the assessment of target level air quality.

In recent years, benchmarking has proved to be a very successful tool in total quality management (TQM).[9] Basically, benchmarking is a target-setting and comparison process in which the current standard performance is compared with the best possible performance. A typical feature of the benchmarking process is periodic upgrading of the targets. Applying the benchmark philosophy to air quality control means that the air quality level produced by the best available technology (BAT) must be defined. In this section, the benchmark air quality is obtained by determining the contaminant concentrations in plants with advanced production and control technology. For selection of the benchmark plants, the following criteria were set:

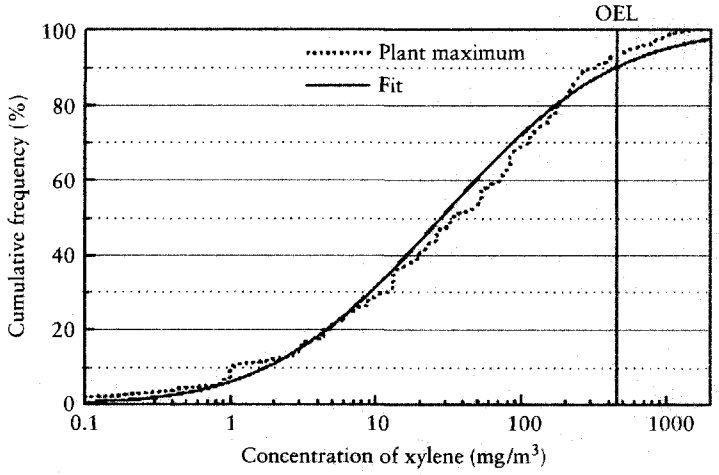

FIGURE 6.8 Plant maximum concentrations of xylene (number of plants = 139, number of measurements = 865).

- Effective elimination of emission sources through the selection of the best process technology or effective control of emissions from sources that cannot be avoided
- Balanced mechanical supply and exhaust ventilation equipped with an advanced air distribution strategy to accurately control the flow patterns in a work space
- Air-handling units equipped with heat recovery and sophisticated control of the key parameters of HVAC systems, such as temperature, airflow rate, and pressure difference
- New or renovated premises

As an example, the measurement data on inorganic total dust collected in conventional factories and benchmark factories is shown in Fig. 6.9.

It is practical to present target concentrations in terms of concentration bands representing different categories of air quality (Fig. 6.10). The first category, representing the cleanest air, reflects the special requirements of certain processes (the electronics industry, biotechnology, etc.). The second category represents good occupational levels achieved by using BAT controls. For most contaminants the upper concentration limit of this category is less than one-tenth of the OEL for the corresponding compound, implying that the employer need not carry out repeated air monitoring according to the European standard.[10] The next two categories for occupied spaces with notable contaminant sources cover the concentration range up to the OEL for a particular

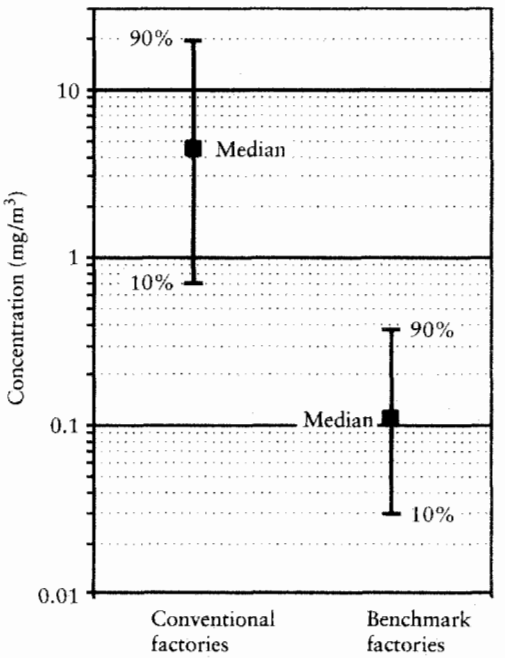

FIGURE 6.9 Concentrations of inorganic total dust in the breathing zone in conventional and benchmark factories.

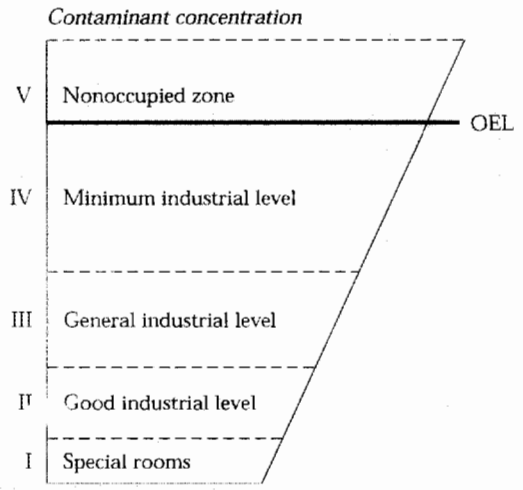

FIGURE 6.10 Target level categories of air quality.

contaminant. In the following four quality categories, numerical values of target levels are given. It may be useful to set a fifth category, for nonoccupied zones or spaces—for instance, the upper part of a room. The occupied zone is defined in terms of certain distances from the floor and walls by a European standard.[11]

6.4.3 Target Levels for Common Contaminants

The target level procedure was applied to 16 common air contaminants (Table 6.19). These are common contaminants in the industrial environment, and in many cases are the most critical compounds from the viewpoint of need for control measures. The prevailing concentration data as well as the benchmark levels were taken from Nordic databases, mainly the Finnish sources, and described elsewhere.[12,13] In addition, a general model for assessing target values for other contaminants is presented in the table.

The target levels for 16 common contaminants were grouped into four categories in terms of concentration bands. The numerical values of the target level categories II and III were obtained by using information on current concentrations in standard practice and benchmark plants. As an example, information on inorganic total dust is shown in (Fig. 6.9). The register of the occupational hygiene measurements revealed that the ratio of the current concentration levels to OELs depends greatly on the particular contaminant. Therefore, target levels are not given as the same fraction of the OEL. Excluding ozone and formaldehyde, the upper limit of "good industrial level" (category II) varies from 1% to 9% of the corresponding OEL in Finland. The upper limit of cat-

TABLE 6.19 A Classification Scheme of Target Levels for Common Air Contaminants in Industrial Settings

Contaminant	Target level category			
	I. Special rooms	II. Good industrial level	III. General industrial level	IV. Minimum[c] industrial level
Inorganic dust (mg/m^3)	<0.01[a]	<0.5	0.5–2.5	2.5–10
Cr(III) compounds ($\mu g/m^3$)		<10	10–100	100–500
Cr(VI) compounds ($\mu g/m^3$)		<2	2–10	10–50
Nickel compounds ($\mu g/m^3$)		<5	5–20	20–100
Oil mist (mg/m^3)		<0.2	0.2–1	1–5
Formaldehyde (mg/m^3)	0.02[b]	<0.1	0.1–0.2	0.2–0.37
Nitrogen dioxide (mg/m^3)	<0.1[a]	<0.2	0.2–1.4	1.4–5.7
Carbon monoxide (mg/m^3)		<3	3–12	12–35
Ozone ($\mu g/m^3$)	10[a]	<50	50–75	75–100
Acetone (mg/m^3)		<12	12–120	120–1200
Butanol (mg/m^3)		<2	2–20	20–150
Aliphatic mineral spirits (mg/m^3)		<10	10–100	100–1200
Isopropanol (mg/m^3)		<5	5–50	50–500
Toluene (mg/m^3)		<5	5–40	40–190
Xylenes (mg/m^3)		<5	5–40	40–440
Styrene (mg/m^3)		<1	1–20	20–86
General model for other contaminants		<0.1 × OEL	0.1 × OEL to 0.25 × OEL	<OEL

[a]As an example of special rooms, air quality requirements in electronics work rooms according to standard IEC 721-3-3 were used.

[b]A preliminary proposal, based on the fact that 5% of the current concentrations of formaldehyde are equal to or below this level.

[c]The upper limit is the current OEL in Finland.

egory "general industrial level" (category III) also varies from substance to substance. Again apart from ozone and formaldehyde, the limit is 10–34% of the corresponding OEL. Ozone is an exceptional

compound because outdoor concentrations of ozone may be higher than indoor concentrations. Formaldehyde, which is one of the most common compounds in the manufactured environment, is also a critical contaminant, as the guideline value for residential air is relatively close to the corresponding OEL. It is worth emphasizing, however, that this scheme is still subject to further development.

6.4.4 Use of TLs

The previous procedure can be used for assessing target levels for a variety of substances in work rooms with notable contaminant emissions. A different set of target levels has already been proposed for nonoccupied environments.[14,15]

In the design phase, "good industrial levels" should be set as the starting point, with design then proceeding according to the method described in Chapter 3. A target level should be set for dominant and critical contaminants in the space. For instance, for the welding of stainless steel, a target level should be set for hexavalent chromium, which is of concern as a health risk. If the "good industrial level" cannot be achieved—for example, due to the high emission of welding fumes—a higher target level can be considered.

Implementation of the target level procedure has clear benefits in both the short and long terms. The procedure is particularly useful in cases where the occupational exposure limit is later reduced. The reduction of exposure limits occurs from time to time in the light of new research information. For instance, for the occupational exposure limit of formaldehyde, the TLV given by ACGIH was reduced from 1.2 mg m^{-3} to 0.37 mg m^{-3} in 1992.[15] The corresponding change took place in Finland in 1998. If the target level of formaldehyde was set just below 1.2 mg m^{-3}, the performance of the whole ventilation system and other control systems would have been insufficient after the decrease of the TLV. Investments in a more efficient control technology are of benefit. If the original system was designed to comply with "good industrial level" (i.e. 0.1 mg m^{-3}) or "general industrial level" (i.e., 0.2 mg m^{-3}), no improvements would be needed regardless of the OEL reduction.

The setting of quantitative goals for indoor air quality also supports an organization's quality policy in the area of safety and health. Furthermore, the introduction of the target level concept for indoor quality will enhance the development of more advanced and efficient control technologies on a voluntary basis. One can assume that the diffusion of technology will make the present-day benchmark air quality common practice in, say, 10 to 20 years.

Therefore, if the desired indoor air quality goals are clearly defined, they will benefit the designers, health and safety professionals, manufacturers of control technology equipment, end users, and other experts who are responsible for maintaining a safe and healthy indoor climate. In conclusion, introduction of the target level process for industrial air quality will benefit both the health sector and the production sector.

References

1. J. Vincent. *Am. Ind. Hyg. Assoc. J.*, October 1998.
2. W. J. Fisk and A.H. Rosenfeld. *Indoor Air 7*, 158, 1997.
3. R. Niemelä, P. Kalliokoski, J. Rantanen, A. Tossavainen, V. Riihimäki, and J Räisänen. In *Ventilation '97: Global development in industrial ventilation. Proceedings of the 5th International Symposium on Ventilation for Contaminant Control*, ed. by H. Goodfellow and E. Tahti, 133–140, 1997.
4. R. Niemelä, J. Rantanen, and M. Kiilunen. *Risk Anal. 18*, 679, 1998.
5. B.D. Nauman, E.V. Sargent, B.S. Starkman, W.J. Fraser, G.T. Becker, and G.D. Kirk. "Performance-based exposure control limits for pharmaceutical active ingredients." *Am. Ind. Hyg. Assoc. J. 57*, 33–42, 1996.
6. H.G. Claycamp. "Industrial health risk assessment: Industrial hygiene for technology transition." *Am. Ind. Hyg. Assoc. J.* 57, 423–434, 1996.
7. P. Swuste and A. Hale. *Appl. Occup. Environ. Hyg. 9*, 57–61, 1994.
8. M.R. Gomes and G. Rowls. *Appl. Occup. Environ. Hyg. 10*, 238–243, 1995.
9. G.H. Watson. *Strategic benchmarking*. John Wiley & Sons, New York, 1992.
10. European Committee for Standardization. EN 689. Workplace atmospheres: Guidance for the assessment of exposure to chemical agents for comparison with limit values and measurement strategy, 1995.
11. European Committee for Standardization. EN TC 156.
12. R. Niemelä, E. Priha, and P. Heikkilä, "Trends of formaldehyde exposure in industries." *Occup. Hyg. Risk Manag. Occup. Haz. 4*, 31–46, 1997.
13. O. Seppänen, R. Ruotsalainen, A. Hausen, et al. In *Proceedings of Healthy Buildings '95*, vol. 3, 1667–1673, 1995.
14. Scanvac. *Classified indoor climate system: Guidelines and specifications*. Swedish Indoor Climate Institute, Stockholm, 1991.
15. ACGIH. *Threshold limit values for chemical substances and physical agents and biological exposure indices*. Cincinnati, 1992.

6.5 REQUIREMENTS DUE TO BUILDING CONSTRUCTION, EQUIPMENT, PROCESSES, AND TYPE OF PRODUCTION PREMISES

6.5.1 Introduction

Nonindustrial buildings are made as shelters for people and to create a proper indoor environment for the occupants. By contrast, industrial buildings are made around a process, and consequently nearly all decisions are based on the process needs. Due to these fundamental differences, the main targets in industrial buildings generally differ from those of nonindustrial buildings. Of course, the process also consists of human beings in many industries, and therefore ventilation is designed and constructed based on the needs of the people working inside the building. The requirements on target levels due to type of premises can be divided in two parts: the effect of the different parameters and their target levels on the building, and the building's effect on the different parameters and their target levels.

Requirements on parameters that may influence the building and its performance and target levels to be determined for occupational zones and nonoccupational zones are the following: temperature, humidity, air velocity, contaminant concentration (particles, gases), odors, biocontamination (in air and on surfaces), fire/explosion risk, noise, vibrations, radiation (IR, UV, radioactive, etc.), sunshine, loading on floors, and pressure differences (inside-outside and between rooms).

Requirements on building parameters that may influence the performance of the ventilation system and target levels to be determined are the following: emissions from surfaces; heat transfer coefficients; diffusion and leakage through walls, floors, ceilings, and windows; thermal needs; pressure differences; layout; stack height; natural ventilation—orientation, place, wind directions, height, surrounding environment—floors, walls, ceilings, windows, doors, gates; floor and ceiling heating systems; sunshielding load; spreading around and close to the building; process conditions; and interference of one parameter with another.

The process itself often sets requirements on the ventilation parameters, and it also affects the ventilation—for example, by secondary flows coming from moving wires or trucks. A very special case is clean rooms, where the high purity requirements set strict target conditions for ventilation.

Equipment inside the building also often influences the ventilation parameters. For example, some electrical equipment needs especially precise indoor conditions. The requirements of these parameters can be one decade stricter than the target levels for people working inside the building.

In industrial premises it is also important that the target level values are guaranteed and that the ventilation system operation can be secured so that the process is not violated because of the ventilation. There are many examples where important fans have failed or important components have corroded, causing extensive losses for the company. In many cases the whole production plant has stopped.

A summary of essential items to be taken into account in determining the target levels is presented in Table 6.20. The table shows that the process is the main determining factor for industrial ventilation.

TABLE 6.20 Relationship of the Items in Assessing Target Levels

	Building	Ventilation	Process	Humans	Equipment	Outdoor environment
Building	—	—	Tightness	—	—	—
Ventilation	Corrosion Materials Pressure difference	—	Corrosion Thermal conditions Materials Openings Tightness	Comfort IAQ	Corrosion Materials	Emissions Immissions
Process	Corrosion Materials Life cycle Heavy loads Layout Air tightness Orientation Openings	IAQ Corrosion Materials Life cycle Layout Air tightness Air distribution Heating & cooling	—	Comfort IAQ	Corrosion Materials	Emission Immissions
Humans	Layout Openings	Heating & cooling Thermal targets Air distribution IAQ targets	—	—	—	—
Equipment	Heavy loads Materials	Thermal conditions IAQ Heating & cooling	—	—	—	Emissions Immissions
Outdoor environment	Materials Insulation Heating & cooling	Heating & cooling Air distribution	Emissions Immissions	—	Layout	—

6.5.2 Ventilation Parameters that Influence the Building Construction and Process Design

Many parameters and variables in a ventilation system may influence the requirements on the building (and sometimes also the equipment inside the building) and the process. This makes it necessary to take into account the decided target levels when designing the building and sometimes also when choosing the process. It is impossible to assign detailed numbers to effects, so only a description of different parameters and their importance will be given here.

The main target levels inside a building are normally set for temperature, humidity, air velocity, airflow rate (and air distribution), and contaminant concentration.[1,2]

The temperature limits inside a building are mostly within the variations of the temperature outside, and the heat resistance requirements on the building materials inside are the same as the requirements on materials used outside. There could be some additional requirements on outside materials depending on rain, snow, wind, sunshine, etc. When the temperatures inside, whether higher or lower than outside, will be used because of the process, the building materials must be chosen with these requirements taken into account, especially when heat radiation is a factor. This should not be confused with demands on temperature and humidity insulation.

To maintain the target level for temperature, a specific amount of insulation may be needed, since too little insulation makes it impossible to keep the temperature levels. For each building it is necessary to make a detailed cost-benefit calculation of insulation and heating/cooling costs. The same discussion is applicable to temperature variation requirements, both for the rate of change and the period lengths (see Chapter 16).

The requirements on the building materials for resistance against humidity and moisture are connected to the requirements for temperature, since the vapor pressure could have large variations in a small temperature range. Moreover, if there is a risk of condensation (e.g., when the process generates water vapor), it is necessary to have surfaces that do not adsorb moisture. There is also the possibility of rust with high humidity. Normally, a relative humidity below 40–50% is assumed sufficient to prevent rust. If there are some contaminants present, this value can change.[3] There is also some evidence that higher humidity provides greater exposure to contaminants.[4] High humidity may promote the growth of some biocontaminants, such as molds, but generally humidity levels below 70% prevent the formation of mold. On the other hand, there are a few types of biocontaminants (bacteria) that grow better in low humidity. Depending on the process and likely biocontaminants, it is necessary to choose both the humidity level and the quality of surface material. This is especially important for those processes where changes in temperature and humidity level are frequent.

The requirements on building materials due to air velocities inside the building are generally negligible. However, sometimes the allowed contaminant concentrations can be of such magnitude that moving air may affect surfaces. In such cases it is necessary to use materials with sustainable surfaces. Normally this demand is valid only for the transport of dust-laden air in

ducts. For the process the air velocity may have a major influence, both on the possibilities of using local ventilation (see Chapter 10) and on many processes in which a high air velocity disturbs the process and changes the result (product). Examples are weaving, pharmaceutical manufacture, and steel casting.

The airflow rate does not interfere with the building or the building materials, and usually not with the process. The air distribution may vary a lot, however, if the building and process layout and sometimes the building materials are not chosen with great care. Lamps, ladders, window shutters, cabins, process equipment, etc. are often placed where the ventilation designer did not expect any obstructions. Thus continuous cooperation between the different designers is necessary to prevent mistakes and to facilitate common solutions to this type of problem (see Chapter 8).

Normally there is some connection between the airflow rate and noise and vibration generation. This could modify the building construction either to prevent spreading or to diminish the levels of noise and vibrations from the air-handling units. This naturally includes all parts of these units, i.e., fans, pumps, and valves (see Chapters 5 and 9). The demands on noise insulation also include the noise and vibrations from the process equipment, which often has a higher level of noise and vibration than the ventilation system.

Contaminants nearly always need some air humidity to cause damage to the building and building materials. This is mainly an environmental problem. Since the outside air is often used inside without being cleaned of gases and some outside air can enter through other ways than the ventilation system, this may be important for the materials used inside. The contaminants that do most damage are liquid acids and particles consisting of acid compounds. If these types of contaminants are generated in a process inside the building, all materials must be chosen very carefully for both the building and the process.[3,5] For particles the primary effect on materials is surface dirtying. In many cases this can be prevented by proper cleaning procedures. The damage on internal surfaces by air pollution is usually of little significance, and the cost for material of a higher grade must be compared with the building's lifetime and the cost for cleaning.[6]

One other important factor that determines the building construction is the mechanical load on the building by the process equipment and by different parts of the ventilation system. These can either be surface loads or concentrated loads. For example, it is necessary to design for a high load on a roof when fans and other air treatment units are to be placed there. Since cranes are often fastened to walls or roofs, the loads on these parts must be carefully analyzed. For all placings of ventilation systems there are demands on availability, accident prevention, and emergency exits that may change the building construction and process design. There should be no problems with necessary space for ducts and other equipment inside or outside buildings with industrial ventilation. Sometimes, however, it may be necessary to make sure all ventilation equipment gets enough space on the floor or the roof. This naturally includes proper space for spare parts and maintenance.

Sometimes the mechanical load can be in the form of air pressure on the surfaces. If the ventilation system has a pressure difference to the outside or between rooms, the building must withstand the pressure differences. It must

also have a structural tightness that permits the ventilation system to maintain these differences.[7] The sensitivity of the process to air pressures and air pressure changes must also be checked.

In addition to the building parameters, there are often some requirements from suppliers of processes and equipment to make sure their parts function properly. This may mean that the requirements for the equipment decide the target levels (e.g., in pharmaceutical and electronics industries). In other cases there are restrictions on deviations from the target levels (e.g., on temperature for machine control system or on humidity and vibration for optical measurement systems).[7]

When there are requirements from the manufacturers of equipment regarding the environment and building, it is necessary to check these values—first, to decide if the limits given by the manufacturer are appropriate, and second, to make a comparison with the target levels. If the target levels are more stringent than the demands for the equipment, there will be no problem. If one or more of the demands is more stringent than the corresponding target level, it is necessary to change the target levels or in some cases to reevaluate the requirements.

Whatever the case, the levels necessary for the processes and the machines and their influence on the target levels must be quantified, and the designer of the ventilation system must take appropriate action.

A summary of the different influences on the building and the process is given in Table 6.21. "Large" means that the (ventilation) parameter usually has a large influence on the construction variables. "Variable" indicates that the parameter's influence usually varies depending on other ventilation parameters or construction variables. "Small" means that the parameter's influence usually has little influence. The numbers describe the required target levels according to Section 6.4. For example, if the target level is II (good industrial level), the temperature limits could have a large influence on the building's construction and choice of material. On the other hand, the target levels III to V usually have a limited influence on how the building is constructed and materials chosen.

TABLE 6.21 Simplified Table Showing How Parameters, Mainly of the Ventilation System, Influence the Building and Process

Ventilation parameter	Large	Variable	Small
Temperature limits	I, II		III–V
Humidity levels	I, II	III, IV	V
Air velocities	I		II–V
Airflow rate	I	II–IV	V
Contaminant concentration	I, II	III	IV, V
Mechanical load (including pressure differences)	I, II	II, III	IV, V
Equipment demands	I	II–V	

Numbers refer to the target level classes presented in Fig. 6.10.

The distribution given in the table should be used only as a guide, not for designing. There are many cases where low demands on target level for some ventilation parameter have a great influence on the building system.

6.5.3 Building and Process Parameters that Influence the Ventilation System

The building parameters generally do not influence the target levels and the ventilation system in industrial ventilation. The process influences the ventilation system in many different ways, and these are described in the respective chapters (Chapters 5, 7, 8, 10, 13, and 14). However, many buildings exist where the building parts, and also the equipment used, may influence the ventilation system and therefore also the target levels.[8] Naturally, the number of floors and the building height influence the ventilation design. This should not change the target levels. Emissions from surfaces and the tightness of walls, roof, and floor can also be of importance. Other parameters are also involved. For example, the size of the windows influence the temperature inside; and light walls and floors diffuse vibrations from machinery and fans and do not store any heat, but thick walls store heat. This changes the temperature variation and makes control of the temperature more complex. Doors that do not close make temperature and airflow control difficult, surface materials can adsorb contaminants and act as secondary emission sources, and so on.[9]

Normally there are no exceptional demands on buildings. For target levels II (good industrial level) and III (general industrial level), there is a great possibility that the building's performance influences the ability to maintain the specified levels. For levels IV (minimum industrial level) and V (nonoccupied zone), the influence from the building on the maintenance of these levels is normally negligible. Target level I (special rooms) always demands careful design, taking into account all possible mechanisms that may influence the environment.

The building parameters have varying importance depending on whether they affect the occupied zone or the nonoccupied zone, just as the process has different influences on these zones. For the nonoccupied zone it is of little significance if a high contaminant concentration is achieved, since no person will be in that zone. However, there could be some limits depending on the equipment or control systems situated in this zone. Since the size and location of the occupied zone can change during the building's use, it is necessary to be very cautious. To treat the whole volume as an occupied zone is a conservative and safe measure.

There are many different types of equipment that are not directly connected to the process. One example is elevators, which can influence the ventilation system both when moving and when standing. In addition to the need for ventilation of the elevator, elevator shaft, and machine room, the moving elevator can induce airflows that change the air distribution and airflows in different parts of the building.

The influence of the building on the ventilation system, and indirectly on the target levels, can take many forms. There are, e.g., emissions from the materials that demand increased airflow rates and also door and window open-

ings that influence the airflow distribution. These influences can sometimes differ between operating and nonoperating times.

The emissions of gases and vapors (and particles) from surfaces (both building materials and equipment) are easy to define in theory but can be very difficult to quantify in practice. There are many contaminants that can be generated, which makes it necessary to define the levels for a few, which are to be chosen from data from suppliers or from contaminants known to be generated by used materials.[10]

Adsorption by surfaces is normally of little significance, except when the adsorbed material can change the performance of the surface (e.g., its strength through corrosion) or when the adsorbed contaminants can be reemitted to generate new contaminants.

Leakage through walls, floors, and ceilings must be taken into account for contaminants (gases, vapors, particles, moisture, etc.) and leakage between building parts for air (with contaminants). Leakage from the ground of water vapor or radioactive gases is better prevented by construction measures than by ventilation measures. It is possible to use ventilation to diminish the influence of these parameters, but that could be unnecessarily expensive. Infiltration of radon depends on the pressure difference between the inside and outside, and by avoiding unnecessary high pressure differences it is possible to keep radon infiltration low.

Incoming radiation from the sun is dependent on the size, type, placement, and shading of windows (and placement of the building), and the subsequent heating or cooling of surfaces can change the air distribution in the room.

In general, it is mandatory to have some kind of partition between different parts of a building because of fire risks and regulations. These partitions can easily change both the airflow rate and the air distribution if proper preventive measures are not taken.

The influence of the sewage and the waste-handling systems on air quality must be taken into account, since both odorous and toxic gases may be emitted from these systems to the ventilation system.

Placement of the building in relation to wind directions and surrounding activities, such as other industrial plants and their exhausts and neighboring roads, can be important for the performance of the ventilation system and thus also for the possibility of keeping to the target levels. Trees and bushes generate bioaerosols that may enter the ventilation system.[11]

The location of the ventilation system's different parts can also have some consequences. For example, one common fault is the placing of the air intake in the wake of the building or downstream from the air outlets. The locations of air intakes should be decided by the ventilation designer in connection with the building designer, but there are other parameters beside the outlet air that may change the quality of the incoming air. Lorry quays and transport openings in the building can be difficult to move and may require another place for the air intake. (They may also change the air distribution, depending on wind directions and velocities.) The placement of the air intake is more important if natural ventilation is used in some part of the building.

The energy distribution system used for the building could influence the possibilities of maintaining the target levels. This is due to the influence on the ventilation system or because the energy system requires some separate target levels, e.g., for tightness between some rooms in the building or for emission rates of contaminants to the building's interior or surroundings. The choice of heating/cooling distribution through the floor or ceiling affects the air distribution and normally also the temperature distribution in the building. The contaminant distribution can also be changed.

The different target levels can interfere with each other depending on the process, climate, and building. For example, the target level for some contaminant's concentration could demand a flow rate such that it is nearly impossible to keep to the target levels for air velocities. In such cases it is necessary to first look for another solution for the ventilation system (including local ventilation) and then to evaluate the different target levels against each other. This could result in changes of one or more of the target levels. If this situation occurs, the whole system (process, building, protection, etc.) must be carefully reviewed to find an appropriate solution to accomplish the main task, which normally is to manufacture a product.

Building parameters influencing the ventilation system are reviewed in Table 6.22. "Large" means that the building parameter usually has large influence on the ventilation system's performance. "Variable" means that the building parameter's influence usually varies depending on other building or ventilation variables. "Small" indicates that the building parameter usually has little influence on the ventilation system's performance. The numbers refer to the required target levels presented in Section 6.4. For instance, if the target level is II (good industrial level), the tightness of the building has a large influence on the ventilation system's performance. On the other hand, with target levels III (general industrial level) to V (nonoccupied zone) the influence of tightness on the ventilation system's performance is usually limited.

TABLE 6.22 Simplified Table of Building Parameters that Influence the Ventilation System

Building parameter	Large	Variable	Small
Wall, ceiling materials	I, II	III	IV, V
Tightness	I, II		III–V
Windows	I, II	III	IV, V
Fire and waste systems	I	II, III	IV, V
Building orientation	I	II	III–V
Openings (doors, air intakes, etc.)	I–III		IV, V
Energy system	I, II	III	IV, V

Numbers refer to the target level classes presented in Fig. 6.10.

The distribution given in the table should, as for Table 6.21, be used only as a guide, not for designing. There are many cases where one parameter of the building system can have a large influence on the performance of the ventilation system, even when there are low demands on the target levels.

6.5.4 Summary

It is very difficult to impose target levels on building parameters or to determine the magnitude of these parameters' influence on the possibilities of maintaining the different primary target levels. It is recommended that suppliers of equipment state their requirements in terms of specific values for the appropriate parameters, e.g., contaminant concentration, humidity, temperature, and vibrations. It is also recommended that the design of the ventilation systems and the building be done in close cooperation. There are many details in a building's construction that could influence the performance of the ventilation system and thus also the target levels.

References

1. R. Niemelä, A. Tossavainen, V. Riihimäki, P. Kalliokoski, and T. Mannelin. Target levels of indoor air quality in industrial buildings. In A. Jansson and L. Olander, eds. *Ventilation '94: Proceedings of the 4th International Symposium on Ventilation for Contaminant Control*, pp. 71–76, 1994.
2. G. Allhammar. *Checklista för projektering av industriventilation*. R142:1983. Byggforskningsrådet (Swedish Council for Building Research), 1983.
3. P.J. Tunturi and J. Railio. Expert system for selection of materials and coatings in ventilation systems in pulp and paper industry. In A. Jansson and L. Olander, eds. *Ventilation '94: Proceedings of the 4th International Symposium on Ventilation for Contaminant Control*, pp. 149–152, 1994.
4. N.O. Breum. Air humidity for control of exposure to dust and formaldehyde at a garment sewing plant. In A. Jansson and L. Olander, eds. *Ventilation '94: Proceedings of the 4th International Symposium on Ventilation for Contaminant Control*, pp. 301–306, 1994.
5. J.E. Yocom and A.R. Stankunas. Pollutant effects on materials. In S. Calvert and H.M. Englund, eds. *Handbook of air pollution technology*, pp. 25–41. John Wiley & Sons, New York, 1984.
6. National Research Council, Committee on Medical and Biological Effects of Environmental Pollutants, Subcommittee on Airborne Particles. *Airborne particles*. University Park Press, Baltimore, 1979.
7. G.J. Farquharson. Building and facility design for clean and sterile pharmaceutical product manufacture. In J.H. Vincent, ed. *Ventilation '88: Proceedings of the Second International Symposium on Ventilation for Contaminant Control*, pp. 231–236. Pergamon Press, Oxford, 1989.
8. J.R. Rosenzweig-Witherspoon and G.D. Landrus. A total building performance approach to indoor environment concerns. In J.H. Vincent, ed. *Ventilation '88: Proceedings of the Second International Symposium on Ventilation for Contaminant Control*, pp. 535–542. Pergamon Press, Oxford, 1989.
9. SCANVAC. *Classified indoor climate systems: Guidelines and specifications*. Swedish Indoor Climate Institute, 1991.
10. J.B. White, J.C. Reaves, P.C. Reist, and L.S. Mann. A data base on the sources of indoor air pollution emissions. In *Engineering solutions to indoor air pollution: Proceedings of the ASHRAE Conference IAQ 88*, pp. 34–48. ASHRAE, Atlanta, 1988.
11. P.R. Morey. Microorganisms in buildings and HVAC systems: A summary of 21 environmental studies. In *Engineering solutions to indoor air pollution: Proceedings of the ASHRAE Conference IAQ 88*, pp. 10–24. ASHRAE, Atlanta, 1988.

This page intentionally left blank

7

PRINCIPLES OF AIR AND CONTAMINANT MOVEMENT INSIDE AND AROUND BUILDINGS

ALEXANDER ZHIVOV

University of Illinois at Urbana-Champaign, U.S.A.

HÅKON SKISTAD

SINTEF Energy Research, Refrigeration, and Air Conditioning, Norway

ELISABETH MUNDT

KTH, Royal Institute of Technology, Sweden

VLADIMIR POSOKHIN

Kazan State Architectural–Construction Academy, Russia

MIKE RATCLIFF

Rowan Williams Davies & Irwin Inc., Canada

EUGENE SHILKROT

TsNIIPromzdanii, Thermec, Russia

ANDREY STRONGIN

TsNIIPromzdanii, Thermec, Russia

Industrial Ventilation Design Guidebook

7.1 INTRODUCTION

Proper selection and sizing of ventilation systems require knowledge of emissions from internal contaminant and heat sources and an understanding of the mechanisms and characteristics of air and contaminant movement.

Major factors affecting air and contaminant movement inside ventilated space are summarized in Section 7.3 and can be classified as

- Sources of heat and contaminants (Section 7.2);
- Air currents produced by process equipment and moving people (Section 7.3);
- Forced convection or supply air jets introduced into the room by mechanical or natural ventilation systems, or their combination (Section 7.4);
- Free convection flows along heated and cooled vertical surfaces and above heat sources, covered in Section 7.5;
- Airflow created in the vicinity of local and general exhausts (Section 7.6);
- Airflow through intended and unintended openings and cracks in the building envelope (Section 7.8.2), and aerodynamic means of the large opening protection, described in Section 7.7;
- Airflow around the building under the influence of natural winds (Section 7.8.1); and
- Airflow between different building zones caused by pressure and temperature differences, or turbulent exchange, addressed in Section 7.8.5.

In some cases, the ventilation process in the room can be simplified and mechanisms of air and contaminant movement under the influence of each of the above factors can be described using simplified theoretical principles of fluid mechanics, empirical data, and observations from numerous research studies. In general, the ventilation process in a room is complex and different factors have a joint effect on airflow patterns and characteristics, in continued spaces and in industrial buildings particularly.

Though there are no ready recipes available, this chapter provides some guidance on

- How to select predominant factors affecting air and contaminant movement in ventilated spaces,
- How to account for their joint effects, and
- How to predict the airflow characteristics with an accuracy acceptable in ventilation design.

7.2 CONTAMINANT SOURCES

7.2.1 Classification

Knowledge of the process or operation and contaminant sources is essential before ventilation systems can be selected and designed. Contaminant sources affecting the working environment may be external, associated with the elements of HVAC systems, or internal.

External Sources

Outdoor air is generally less polluted than the system return air. However, problems with reentry of previously exhausted air occur as a result of improperly located exhaust and intake vents or periodic changes in wind conditions. Other outdoor contamination problems include contaminants from other industrial sources, power plants, motor vehicle exhaust, and dust, asphalt vapors, and solvents from construction or renovation. Also, heat gains and losses through the building envelope due to heat conduction through exterior walls, floor, and roof, and due to solar radiation and infiltration, can be attributed to effects from external sources.

HVAC System

The HVAC system also acts as a pollutant source when it is not maintained properly. Microorganisms breed in various environments present within components (e.g., cooling coils, ducts) of the system and may be distributed throughout the building. Improper maintenance of filters leads to loss of efficiency and re-emission of contaminants.

Internal Sources

This section discusses primarily internal sources of contaminants and other occupational hazards related to the process or the building envelope.

Among the major potential hazards affecting working environment are chemical (airborne contaminants), biological, and physical hazards. Air contaminants are commonly classified as either particulate contaminants or gas and vapor contaminants.[1] Common particulate contaminants include dusts, fumes, mists, aerosols, and fibers.

Dusts are solid particles generated by such processes as handling, crushing, and grinding.

Fumes are formed when material from a volatilized solid condenses in cool air (e.g., welding fumes).

Fibers are solid particles whose length is several times their diameter, such as asbestos.

Gases are formless fluids that expand to occupy the space enclosure in which they are confined. They are atomic, diatomic, or molecular in nature, as opposed to droplets or particles, which are made up of millions of atoms or molecules.

Vapors are the volatile form of substances that are normally in a solid or liquid state at room temperature and pressure. Through evaporation, liquids change into vapors and mix with the surrounding atmosphere.

Mist is a liquid suspended in air. Mists are generated by liquids condensing from a vapor back to a liquid or by a liquid being dispersed by splashing or atomizing.

Aerosols are also a form of a mist characterized by highly respirable, minute liquid particles. They can be formed by atomizing, spraying, or mixing, or by violent chemical reactions, evolution of gas from a liquid, or escape of a dissolved gas when pressure is released.

Fogs are fine airborne droplets usually formed by condensation of vapor. Many droplets in fogs are microscopic and submicroscopic and serve as a transition stage between mists and vapors.

Smog commonly refers to air pollution; it implies an air mixture of smoke particles, mists, and fog droplets of such concentration and composition as to impair visibility, in addition to being irritating or harmful. Smog is often associated with temperature inversions in the atmosphere that prevent normal dispersion of contaminants.

Biological hazards include bacteria, viruses, fungi, and other living organisms that can cause acute and chronic infections by entering the body either directly or through breaks in the skin. Physical hazards include thermal para-meters (temperature, relative humidity, and velocity) beyond the comfort range, excessive levels of ionizing and nonionizing electromagnetic radiation, noise, vibration, and illumination.

Airborne contaminant movement in the building depends upon the type of heat and contaminant sources, which can be classified as (1) buoyant (e.g., heat) sources, (2) nonbuoyant (diffusion) sources, and (3) dynamic sources.[2] With the first type of sources, contaminants move in the space primarily due to the heat energy as buoyant plumes over the heated surfaces. The second type of sources is characterized by contaminant diffusion in the room in all directions due to the concentration gradient in all directions (e.g., in the case of emission from painted surfaces). The emission rate in this case is significantly affected by the intensity of the ambient air turbulence and air velocity. The third type of sources is characterized by contaminant movement in the space with an air jet (e.g., linear jet over the tank with a push-pull ventilation), or particle flow (e.g., from a grinding wheel). In some cases, the above factors influencing contaminant distribution in the room are combined.

The effect of buoyancy in gases released into the air can be related either to the difference in the molecular weights or to the difference in temperature. To characterize the buoyancy for gases with a molecular density significantly different from the density of air, Elterman proposed a parameter P, with units of g/(m^3 K):[3]

$$P = C\frac{1 - 29/M_g}{\Delta\theta}, \tag{7.1}$$

where C = gas concentration in the air, g/m^3; M_g = relative molecular density of the gas; $\Delta\theta = \theta - \theta_o$ = air temperature difference between the reference point and the air supply, °C.

According to Elterman, when $P < 5 \times 10^{-3}$ g/(m^3 K), the distribution of gas concentrations along the room height is similar to the temperature distribution, and thus the contaminant removal efficiency and heat removal coefficients will have the same values. When $5 \times 10^{-3} < P < 0.1$, gas concentration in the air of the upper zone is higher than that in the occupied zone, and the gas removal efficiency is higher than the heat removal efficiency. When $P \approx 0.4$, the gas concentration distribution is uniform along the room height. Only when $P > 0.4$ g/(m^3 K) is the concentration of the gas, which is heavier than air, higher in the occupied zone than in the upper zone.

7.2.2 Nonbuoyant Contaminant Sources

Gases, vapors, and small dust particulates are distributed in the space by airflows produced by supply jets, convective flows, or air currents entering the building through the building apertures and cracks. Also, gases and vapors are distributed due to turbulent and molecular diffusion. Distribution of contaminants with airflows is significantly faster (hundreds of times) than distribution due to molecular diffusion.

Theories of hood performance with nonbuoyant pollution sources are based on the equation of turbulent diffusion. The following equation allows the engineer to determine the contaminant concentration decay in the uniform airflow upstream from the contaminant source:

$$C_x = C_o e^{-\frac{V}{D}X}, \tag{7.2}$$

where

X = distance from the source, m
C_o = contaminant concentration at the source, mg/m^3
C_x = contaminant concentration at the distance X from the source, mg/m^3
v = air velocity in the flow, m/s
D = coefficient of the turbulent diffusion, m^2/s

The value of the coefficient of turbulent diffusion, D, depends upon the air change rate in the ventilated space and the method of air supply. Studies by Posokhin[2] show that approximate D values for locations outside supply air jets is equal to 0.025 m^2/s. Air disturbance caused by operator or robot movement results in an increase in the D value of at least two times. Studies by Zhivov et al.[4] showed that the D value is affected by the velocity and direction of cross-drafts against the hood face, and the presence of an operator; e.g., for a cross-draft directed along the hood face with velocity $v = 0.5$ m/s with $D = 0.15$ m^2/s (with the presence of an operator), an increase to $v = 1.0$ m/s results in $D = 0.3$ m^2/s.

Contaminant Emission by a Process

The quantity of contaminant (fume, oil mist, VOC, gas, or particulates), G, kg/h, generated in the space can be calculated using one of the following equations:

$$G = R_1 \times T_{\text{process}}, \tag{7.3}$$

where R_1 is a fume, oil mist, VOC, gas, or particulate generation rate, kg/min, and T_{process} is an average contaminant release time per hour (e.g., arc time for the welding process), min/h; or

$$G = R_2 \times U, \tag{7.4}$$

where R_2 is a contaminant generation rate per production unit, kg/(production unit), and U is an average production unit output (e.g., units/h) for the given process.

For a welding process, for example, total welding fume generation rate R_1 is a fume (gas, particulate) generation rate, kg/min; T_{arc} is an average arc time for the welding process used, min/h; R_2 is a fume generation rate, kg, per kg of electrodes used; and U is average electrode usage, kg/h, in the given welding process. R_1 and R_2, percentages of the critical components in the fume for the typical welding processes, and an average arc time for the typical welding processes are listed in AWS.[5]

Gas and Vapor Emission through Looseness in Process Equipment and Pipelines

When the pressure inside the equipment/pipeline is greater than the room pressure, this emission can be calculated using the equation suggested by Repin:[6]

$$G = kCV\sqrt{\frac{m}{T}}, \tag{7.5}$$

where k is a reserve coefficient that varies from 1 to 2 depending upon the state of the equipment, C is a coefficient that depends upon the gas pressure inside the equipment (see Table 7.1), V is the internal volume of the equipment/pipeline with an excessive gas pressure (m^3), m = molecular weight of gas/vapor, and T = gas/vapor temperature inside the equipment (°C).

Gas and Vapor Emission Processes from an Open Liquid Face

Emission from an open liquid face (e.g., open tanks, liquid spills on the floor surface) can be evaluated using equations based on criteria relations and empirical data. Assuming that the heat and mass transfer processes can be described using similar differential equations, the criteria equation describing the evaporation process will be similar to one describing the heat transfer:[3]

$$\text{Nu} = C(\text{Gr} \cdot \text{PR})^n, \tag{7.6}$$

where Nu, Gr, and Pr are the Nusselt, Grashof, and Prandtl numbers for evaporation processes:

$$\text{Nu} = \frac{g_0 d}{D}, \qquad \text{Pr} = \frac{\nu}{D}, \qquad \text{Gr} = \frac{gd^3(\rho_0 - \rho_1)}{\nu^2 \rho_1},$$

TABLE 7.1 Coefficient C

Gas pressure, atmospheres	< 2	2	7	17	41	161	401	1001
C	0.121	0.166	0.182	0.189	0.152	0.289	0.297	0.370

where

g_0 = mass rate of liquid evaporation (liquid mass evaporated from unit of surface area in a unit of time, and related to the unit of vapor concentration at the surface and in the ambient air), m/s
d = characteristic dimension, m
D = molecular diffusion coefficient, m^2/s
ν = kinematic viscosity coefficient, m^2/s
ρ_0 = ambient air density, kg/m^3
ρ_1 = air density near the liquid surface at the surface temperature, kg/m^3

Film Regime In the film regime, there is a thick film of undisturbed air formed adjacent to the liquid surface (e.g., evaporation from the surface of small mercury droplets). In Eq. (7.6), $Gr \times Pr < 1$, $n = 0$, and Nu is constant.

The mass flow rate, G, g/s, from the surface can be evaluated using

$$G = 2Dd(C_1 - C_0), \tag{7.7}$$

where C_1 and C_0 are vapor concentration, g/m^3, in the air adjacent to the liquid surface and in the ambient air.

Laminar Regime In the laminar regime, $2 \times 10^2 < Gr \times Pr < 2.3 \times 10^8$, and $n = 1/4$. The mass flow rate, G, g/s, from the surface can be evaluated using

$$G = FAd^{-1/4}D^{1/2}(C_1 - C_0)^{5/4}|(M_{air}/M_l - 1)|^{1/4}, \tag{7.8}$$

where M_{air} = relative molecular weight of air, M_l = relative molecular weight of vapor evaporated from the liquid surface, and A = surface area, m^2.

For a horizontal surface, $F = 0.334$ when $M_{air} > M_l$, and $F = 0.184$ when $M_{air} < M_l$. For a wet vertical surface, $F = 0.224$.

Turbulent Regime In the turbulent regime, $Gr \times Pr > 2.3 \times 10^8$, and $n = 1/3$. This regime may occur only when the area of evaporating liquid is very large (tens of square meters).

The mass flow rate, G, g/s, from the surface can be evaluated using

$$G = FAD^{1/3}(C_1 - C_0)^{4/3}|(M_{air}/M_l - 1)|^{1/3}. \tag{7.9}$$

For a horizontal surface, $F = 150$ when $M_{air} > M_l$, and $F = 75$ when $M_{air} < M_l$. For a wet vertical surface, $F = 113$.

7.2.3 Emission from Heat Sources

Heating and cooling load calculation for HVAC system design is based on the heat balance principle. For the given building, room, or independent building zone, heat balance components should be established and analyzed. The major heat sources and sinks in industrial buildings are:

- Heat losses and gains by heat conduction through the building envelope
- Heat gains by solar radiation
- Heat losses and gains with infiltration and exfiltration through cracks in the building envelope
- Heat gains from people activity
- Heat gains from lighting
- Heat gains from process equipment powered by electric motors
- Heat gains from processes with conversion of mechanical energy into heat
- Heat gains and losses for heating or cooling raw materials and parts brought into or taken out of the building, melted metal solidification, vapor condensation, or liquid evaporation
- Heat losses with vehicles entering the building, etc.

The total heat gains and losses, ΔW, which should be compensated by the HVAC system, can be determined by

$$\Delta W = \sum_{1}^{n} W_{\text{gains},} - \sum_{1}^{m} W_{\text{losses},} . \tag{7.10}$$

Heat gains and losses can be only sensible or sensible and latent. Sensible heat gains result from conduction, convection, and/or radiation. Latent heat gains occur when moisture is added to the space (e.g., from evaporation).

Sensible Heat Sources

The total heat load is introduced by each source by convection and radiation:[7]

$$W_0 = W_{\text{conv}} + W_{\text{rad}} = \psi W_0 + (1-\psi) W_0. \tag{7.11}$$

The total radiant component of the heat load introduced by each source into the space can be divided between the upper and the lower (occupied) zones of this space:[7]

$$W_{\text{rad}} = W_{\text{rad low}} + W_{\text{rad up}} = \varphi(1-\psi) W_0 + (1-\varphi)(1-\psi) W_0 . \tag{7.12}$$

The total convective component of the heat load introduced by each source is

$$W_{\text{conv}} = W_{\text{conv low}} + W_{\text{conv up}} = \beta\psi W_0 + (1-\beta)\psi W_0 , \tag{7.13}$$

where ψ, φ, and β are nondimensional coefficients reflecting the portion of the convective component of the total heat load released into the space for each heat source, the portion of the radiant component of the total radiant heat load in the low zone, and the portion of the convective component of the total convective heat load in the low zone, respectively.

Coefficients ψ, φ, and β vary within a range from 0 to 1. The coefficient ψ value depends on the heated surface temperature and emittance, and can be estimated from Table 7.2.

TABLE 7.2 Coefficient ψ

	Surface temperature, θ_{surf}, °C										
ϵ	40	50	60	100	150	200	300	500	800	1000	1200
0.8	0.42	0.44	0.45	0.48	0.45	0.4	0.32	0.2	0.1	0.1	0
0.5	0.52	0.55	0.58	0.59	0.56	0.51	0.42	0.29	0.14	0.1	0.1
0.2	0.73	0.76	0.77	0.78	0.76	0.73	0.65	0.59	0.3	0.2	0.14

The coefficient φ value depends on the source location in the ventilated room (e.g., in the center, close to the wall, etc.) and the source dimensions relative to the room size. Coefficient φ values for small sources ($<1/10$ of the room size) can be estimated using Tables 7.3. and 7.4.

Coefficients ψ and φ for some typical heat sources are as follows:

For a sitting or standing person $\psi = 0.57$, $\varphi = 0.63$
For machining equipment $\psi = 0.5$, $\varphi = 0.6$

The β coefficient value depends upon the supply air method (e.g., $\beta = 0$ with displacement and natural ventilation, $\beta = 1$ with convective plume dissipating within the occupied zone due to interaction with supply jets, airflows created by moving objects, etc.).

Heat Gain from Process Equipment

Heat load from hot process equipment with a relatively simple configuration (e.g., tanks with hot water, solution, or oil) can be calculated using the following equation:

$$W_{eq} = \alpha_{conv} A_{conv} (\theta_{surf} - \theta_0) + \alpha_{rad} A_{rad} (\theta_{surf} - \theta_0), \tag{7.14}$$

where θ_{surf} = surface temperature, °C; θ_0 = room air temperature, °C; A_{conv} = convective heat exchange surface area, m^2; and A_{rad} = radiant heat exchange surface area, m^2. In general, $A_{rad} \leq A_{conv}$ (i.e., the ratio $K_A = A_{rad}/A_{conv} \leq 1$). The convective and radiant heat flux, α_{conv} and α_{rad}, W/(m^2 °C), are

$$\begin{aligned} \alpha_{conv} &= K\sqrt[3]{\theta_{surf} - \theta_0} \\ \alpha_{rad} &= \epsilon_0 C_0 b, \end{aligned} \tag{7.15}$$

$$W_{eq} = \epsilon_0 C_0 b + K\sqrt[3]{\theta_{surf} - \theta_0}(\theta_{surf} - \theta_0)A, \tag{7.16}$$

TABLE 7.3 Coefficient $\varphi_{horizontal}$

	B/H			
Source location in the room	1	2	3	4
Along the room axis	0.3	0.12	0.04	0
Between the axis and the wall	0.38	0.17	0.11	0.07
Close to the wall	0.51	0.3	0.23	0.16

TABLE 7.4 Coefficient $\varphi_{vertical}$

	B/H			
Source location in the room	**1**	**2**	**3**	**4**
Source along the room axis	0.8	0.7	0.65	0.6
Between the axis and the wall	0.8	0.72	0.67	0.63
Close to the wall	0.85	0.75	0.7	0.68

TABLE 7.5 Values of *K* and *b* Coefficients[8]

θ_{surf}, °C	*b*	*K*
20	1.01	1.67
80	1.36	1.6
180	2.3	1.53
280	3.3	1.47
380	4.87	1.41
480	6.92	1.36
580	9.43	1.33
980	25.5	1.19

where $C_0\epsilon_0$ = surface emittance, W/m^2 °C, and K and b are coefficients depending on the surface temperature (see Table 7.5).

For horizontal surfaces facing upward, coefficient K should be increased by 30%, and for horizontal surfaces facing downward, it should be decreased by 30%, compared with the data from Table 7.5.[8]

The total unit heat gain from the process equipment, W_{eq}, can be evaluated using the graph in Fig. 7.1.

Heat Gain from Lighting

This can be calculated from

$$W_{light} = K_u K_{sa} W_0, \tag{7.17}$$

where K_u = lighting use factor (applied to lighting when use is known to be intermittent), K_{sa} = special allowance factor, and W_0 = total light wattage. The special allowance factor is for fluorescent fixtures and fixtures that are either ventilated or installed so that only part of their heat contributes to a space heat load.[1]

Heat Gain from Equipment Operated by Electric Motors

Heat gain related to electric motors is calculated as[1]

$$W_{eq} = \left(\frac{P}{E_M}\right) F_{UM} F_{LM}, \tag{7.18}$$

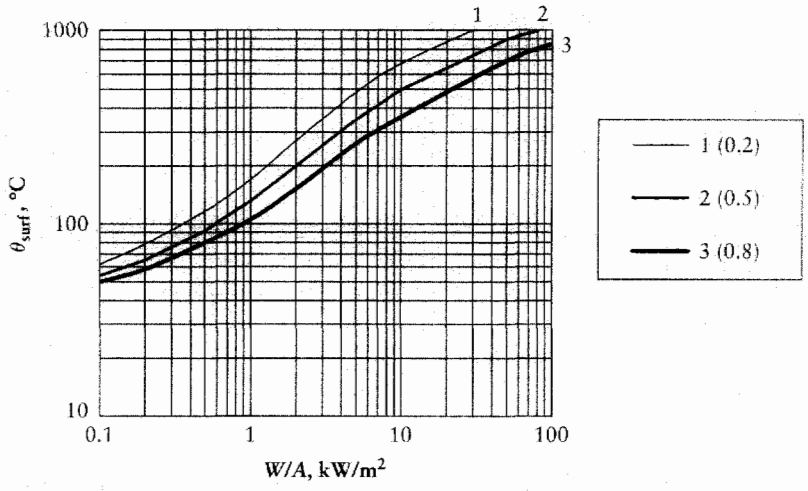

FIGURE 7.1 Relationship between the heat source surface temperature, θ_{surf}, heat flux, W/A_{surf}, and the heat source emittance ϵ/K_A: 1—$K_A = 0.2$; 2—$K_A = 0.5$; 3—$K_A = 0.8$.

where P = motor power rating, W; E_M = motor efficiency, expressed as a decimal fraction < 1.0; F_{UM} = motor use factor, 1.0 or a decimal fraction < 1.0; F_{LM} = motor load factor, 1.0 or a decimal fraction < 1.0.

Heat Loss/Gain for Heating or Cooling Materials and Parts Brought into or Taken out of the Space

This heat loss/gain is calculated as

$$W_{mat} = c(\theta_1 - \theta_0)GB, \tag{7.19}$$

where c = specific heat, W/(m³ °C); t_1 = material initial temperature, °C; G = material mass, kg; B = share of heat load lost/gained during the time period ΔZ from the time the material was brought in (see Fig. 7.2), $B = f(\text{Fo})$; $\text{Fo} = \Delta Z/cGR$, where

$$R = \frac{G}{\rho\lambda A^2} + \frac{1}{\alpha_0 A}, \tag{7.20}$$

λ = heat conductivity coefficient, W/(m °C) (increased by 25% for loose materials), and α_0 = total heat flux coefficient, W/(m² °C).

Heat Load from Molten Metal Cooling

This can be calculated as

$$W_{\text{molten mat}} = [c_l(\theta_1 - \theta_s) + c_s(\theta_s - \theta_0)]G, \tag{7.21}$$

where c_l = specific heat of the material in the liquid phase, W/(m³ °C); c_s = specific heat of the material in the solid phase, W/(m³ °C); and θ_s = temperature of solidification, °C.

7.2.4 Sources of Dust

Many industries, such as chemical, printing, metallurgy, fine ceramics, and welding operations, have processes generating dust. Crushing, blasting, material transporting and processing, finishing, and other opera-

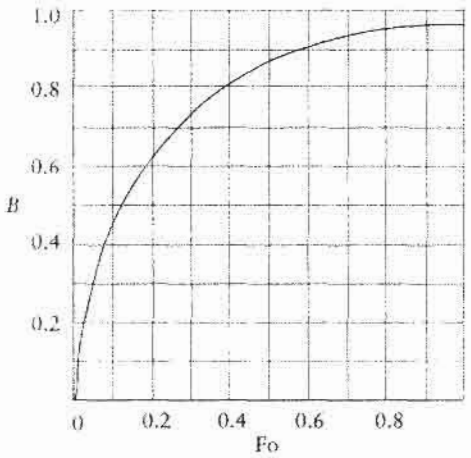

FIGURE 7.2 Influence of Fo criteria on coefficient B.[8]

tions result in dust release into the building space. Other particle sources may include construction and renovation, deteriorated insulation, cleaning, etc. The dust resulting from each of these processes differs in its chemical and physical characteristics. Particle size, shape, density, and release method influence the distribution of dusts inside the space, and the methods of particle control and air cleaning technology used. Dusts in the work environment vary in particle size from 0.1 μm to 25 μm (Fig. 7.3). Respirable particle sizes vary from less than 1 μm to 10 μm. Large particles with a size of tens of microns deposit on surfaces, while smaller particles remain suspended in the air and migrate in the space with airflows.

Grinding, polishing, and other finishing operations produce particles imparted with some momentum and thus are considered to be dynamic sources. A particle ejected into still air with an initial velocity will travel some distance (stopping distance) before decelerating to rest due to drag forces. The data from Hinds show the difficulty in throwing even fairly large

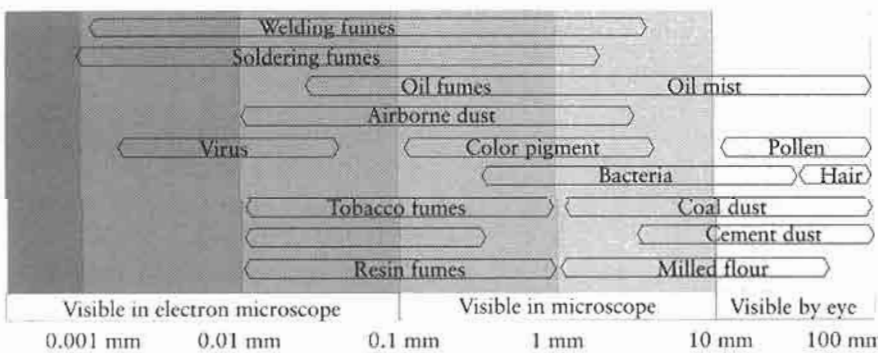

FIGURE 7.3 Range of particle sizes for typical dusts.

particles an appreciable distance in still air.[9] When the receiving hood is designed, any particles that are in the inhalable range should be considered immovable.[10]

Granular and other bulk materials processing and conveying, bag emptying and disposal, and similar operations air into the process enclosure. Induced air picks up dust. If the system component, such as a bin, is tight, the induced air will reverse its path and carry the entrained dust back through the upstream opening, as shown in Fig. 7.4.[10]

Resistance and arc welding operations, and plasma and laser cutting produce fumes by expulsion or evaporation of the base material, coating, and electrode wear. Larger particles deposit on the surrounding surfaces, while smaller particles move upward with convective flows. Specific contaminants associated with different welding and cutting operations are listed in AWS.[5]

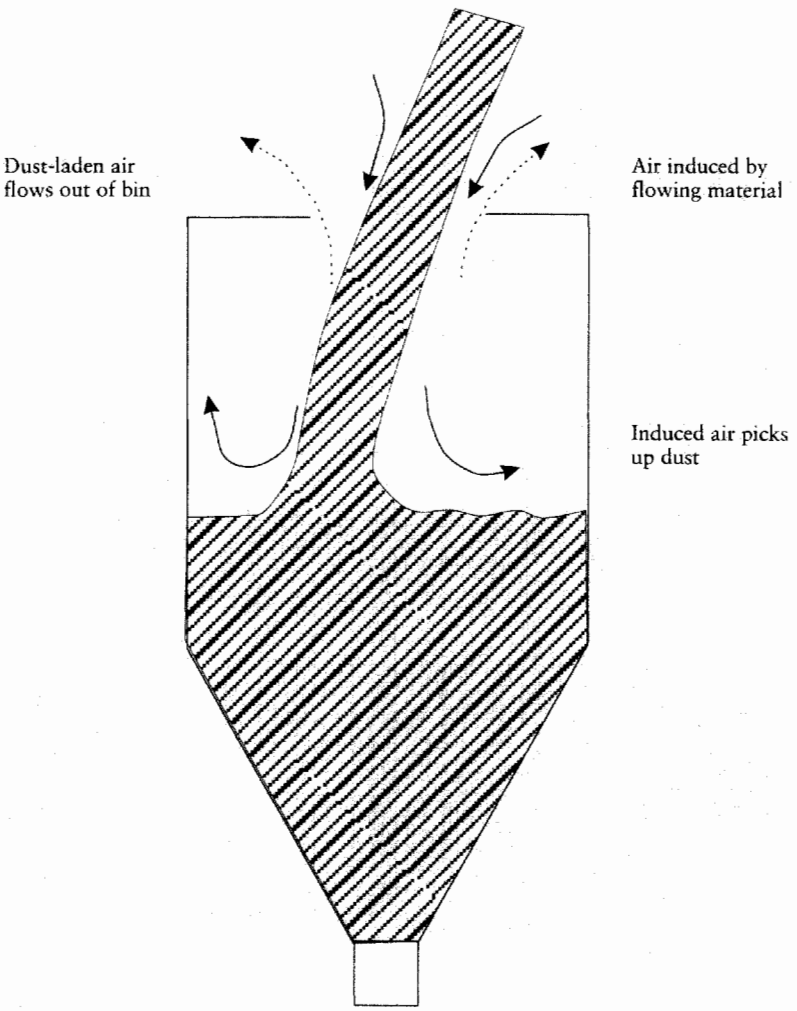

FIGURE 7.4 Air induction into a bin from flowing granular materials.

7.2.5 Sources of Moisture Emission

Moisture control in industrial buildings is necessary to avoid problems related to

- Human comfort, health, and productivity
- Process requirements (e.g., in pharmaceutical and semiconductor manufacturing, painting processes, plastic injection molding, and breweries)
- Building durability, by preventing decay of wood-based materials, corrosion of metals, and spalling of masonry and concrete caused by freeze-thaw cycles
- Degradation of the thermal resistance of building materials

Principal sources of moisture in the building include

- Evaporation from wet surfaces and open tanks
- Steam leakage from process equipment or pipelines
- Evaporation from people breathing and from perspiration
- Permeation through floors, walls, and ceiling
- Desorption from moist products
- Generation from combustion, i.e., open flame in the space
- Air infiltration through leaks, holes, and door openings
- Untreated outside air supplied by the mechanical or natural ventilation system

Moisture Diffusion through the Building Envelope

The permeation moisture load through building materials can be calculated using

$$M = pA\ \Delta\text{VP}, \tag{7.22}$$

where p = permeance factor, g/(h m^2 kPa), A = surface area, m^2; ΔVP = difference in vapor pressure across the material, kPa.

Evaporation from Wet Surfaces and Open Tanks

The amount of water evaporated from wet surfaces (i.e., process equipment, floors) or water tanks, M, kg/h, is proportional to the difference in vapor pressure between the surface and air, the surface temperature, and the air velocity across the water surface:[11]

$$M = 7.4(a + 0.017V)(P_2 - P_1)101.3\frac{A}{P_b}, \tag{7.23}$$

where M = evaporation load, kg/h; V = air velocity across the surface, m/s; P_2 = water vapor pressure in the air above the surface, kPa; P_1 = vapor pressure of air saturated at the water temperature, kPa; A = total surface area wetted or of the water face, m^2; P_b = barometric pressure, kPa; and a = coefficient reflecting the influence of air movement. For air temperature between 15 °C and 30 °C, a can be evaluated as shown in Table 7.6.

If the water temperature is held constant and the water is still, Table 7.7 can be used to evaluate the temperature of the water surface (at room air temperature 20 °C and RH = 70%). When the water is stirred, the surface temperature can be assumed to be equal to the mean water temperature.

TABLE 7.6 Determination of *a* for Various Water Temperatures

Water temperature, °C	30	40	50	60	70	80	90	100
a	0.022	0.03	0.03	0.04	0.041	0.05	0.051	0.06

TABLE 7.7 Water Surface Temperature Evaluation

Water temperature, °C	20	30	40	50	60	70	80	90	100
Water surface temperature, °C	18	28	37	45	51	58	69	82	97

Evaporation load from wet surfaces or floors can be evaluated using the following equation:[11]

$$M \approx (6 \sim 6.5)(\theta_0 - \theta_w)A, \tag{7.24}$$

where θ_0 = dry-bulb room air temperature, °C; θ_w = wet-bulb room air temperature, °C.

Moisture from Air Leaks through Cracks and Apertures

Moisture load from infiltrating air can be evaluated as

$$M = G_{\text{inf}}(m_{\text{out}} - m_0), \tag{7.25}$$

where G_{inf} = infiltrating air flow rate, kg/h; m_{out} and m_0 = moisture content in outside and inside air, gr/kg.

Moisture from Personnel

The moisture release rate from people's respiration and perspiration can be calculated as follows:[12]

$$M = (P_A \times F_A) + (P_B \times F_B) + (P_C \times F_C) + (P_D \times F_D), \tag{7.26}$$

where (P_A, F_A), (P_B, F_B), (P_C, F_C) and (P_D, F_D) = evaporation rate and number of people seated (A), standing (B), with light activity (C), and with moderate activity (D) (see Fig. 7.5).

Moisture from Combustion

The amount of water vapor resulting from combustion varies with composition of the burned gas. When the value is unknown, one can estimate that each cubic meter of gas burned produces 42 grams (650 grains) of water vapor.

7.2.6 Explosive Gases, Vapors, and Dust Mixtures

Some gases, vapors, and dust mixtures with air or oxygen may produce explosions. For explosion to occur, a flammable gas or combustible material

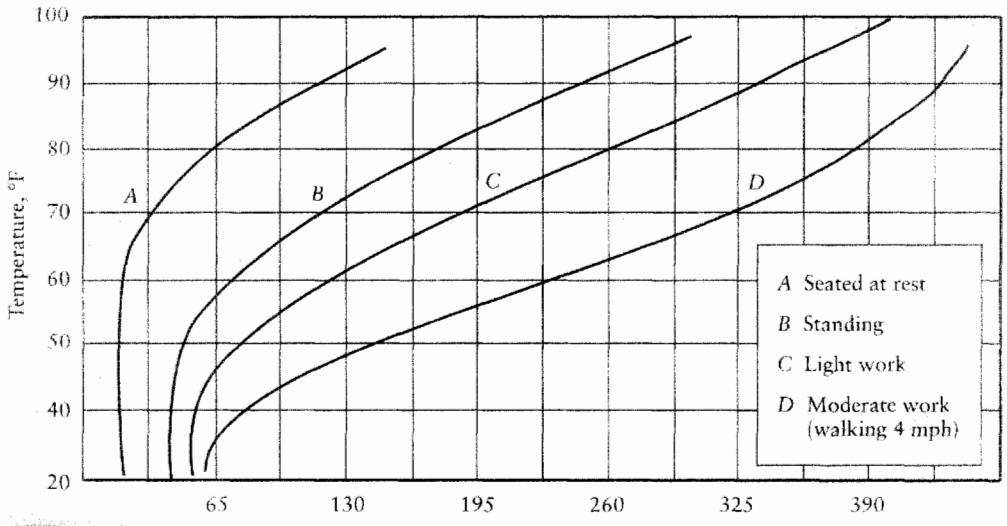

FIGURE 7.5 Moisture evaporation, gr/h, per average man.

mixture with air or oxygen must be in proportion within the explosive ("flammable") limits, and an ignition source must be present and have sufficient energy to ignite the explosive mixture. Ignition can be caused either by electrical arc, spark, or by a hot surface. The surface temperature that can cause ignition varies for different gas mixtures. Ignition of carbon disulfide and ethyl nitrite, for example, requires a surface temperature of only 85 °C.

Flammable gases and vapors include acetylene, hydrogen, butadiene, ethylene oxide, propylene oxide, acrolein, ethyl ether, ethylene, acetone, ammonia, benzene, butane, cyclopropane, ethanol, gasoline, hexane, methanol, methane, natural gas, naphtha, and propane.

Combustible dusts include metal dust (e.g., aluminum, magnesium, and their commercial alloys), carbonaceous dust (e.g., carbon black, charcoal, and coal), flour, grain, wood, plastics, and chemicals.

Flammable gases and vapors or combustible dust may be present in quantities sufficient to produce explosive or ignitable mixtures due to[13]

- Leakage from maintenance operations, breakdown of equipment, or faulty operation of equipment
- Escape in the event of an accidental rupture or breakdown of equipment, or in abnormal equipment operation

Among common areas where explosion can occur are coal mines, petrochemical plants, chemical plants, paint shops, grain handling industry, etc. Explosive limits for gases and vapors are expressed as percentages (%), and may be defined as minimum and maximum concentrations of a flammable gas or vapor between which ignition occur.[14] Concentrations below the lower explosive limit (LEL) are too lean to burn, while those above the upper explosive limit (UEL) are too rich. Table 7.8 lists explosive limits for some common gases.

TABLE 7.8 Explosive Limits of Some Gases in Air and Oxygen Mixtures[14]

Gas	Explosive limits in air	Explosive limits in oxygen
Ammonia	15.50–27.00	13.50–79.00
Carbon monoxide	12.50–4.20	15.50–93.90
Hydrogen	4.00–74.20	4.65–93.90
Methane	5.00–15.00	5.40–59.20
Diethyl ether	1.85–36.50	2.10–82.00
Propylene	2.00–11.10	2.10–52.80

Upper and lower explosive limits EL_{mix} for mixtures of several gases can be calculated using the Le Chatelier equation[15]

$$EL_{mix} = \frac{100}{\frac{P_1}{EL_1} + \frac{P_2}{EL_2} + \frac{P_3}{EL_3} + \cdots}, \tag{7.27}$$

where P_i = proportion of gas i in the gas mixture; EL_i = explosive limit for gas i.

Dust particles have a lower explosive limit expressed in mg/m^3 and almost no upper limit. Examples of LEL for dusts are polystyrene, 0.02 mg/m^3; corn starch, 0.04 mg/m^3; and coal, 0.055 mg/m^3.

A liquid not considered flammable may still have an explosive potential. An example is dichloromethane or methylene chloride, often used in paint strippers, which evaporates very quickly. It is not flammable, but its vapors may be explosive (explosive limits 12% to 22%).

References

1. ASHRAE. 1997. *ASHRAE Handbook of Fundamentals.* American Society of Heating, Refrigeration, and Air Conditioning Engineers, Atlanta.
2. Posokhin, V. N. 1984. *Design of Local Ventilation Systems for Process Equipment with Heat and Gas Release* (in Russian). Mashinostroyeniye, Moscow.
3. Elterman, V. M. 1980. *Ventilation of Chemical Plants.* KHIMIA, Moscow.
4. Zhivov, A. M., L. L. Christianson, and G. L. Riskowski. 1997. *Influence of Space Air Movement on Hood Performance.* ASHRAE Research Project RP-744. American Society of Heating, Refrigeration, and Air Conditioning Engineers, Atlanta.
5. AWS. 2001. *Ventilation Guide.* F3.2. American Welding Society.
6. Repin, N. N. 1938. Method of ventilation design for chemical industry. *Heating and Ventilating*, nos. 4–5.
7. Shilkrot, E. O. 1993. Determination of design loads on room heating and ventilation systems using the method of zone-by-zone balances. *ASHRAE Transactions*, vol. 99, no. 1.
8. Bogoslovski, V. N. 1976. *Heating and Ventilation. Part 2: Ventilation* (in Russian). Stroizdat, Moscow.
9. Hinds, W. 1982. *Aerosol Technology: Properties, Behavior, and Measurement of Airborne Particles.* John Wiley & Sons, New York.
10. Burgess, W. A., M. J. Ellenbecker, and R. D. Treitman. 1989. *Ventilation for Control of the Work Environment.* John Wiley & Sons, New York.
11. Stroizdat. 1992. *Designer's Guidebook: Ventilation and Air-Conditioning.* Stroizdat, Moscow.
12. Munters. 1990. *The Dehumidification Handbook.* 2nd ed. Munters Cargocaire.
13. NFPA. 1999. *National Electrical Code Handbook*, Articles 500–504.
14. LeBreton, E. 1996. Confined space. *TDG Dangerous Goods Newsletter*, vol. 16, no. 1, Spring.
15. Baturin, V. V. 1990. *Fundamentals of Industrial Ventilation.* PROFIZDAT, Moscow.

7.3 AIRFLOW

7.3.1 Factors Influencing Room Airflow

Air and contaminant movement and turbulent intensity in the ventilated space are affected by different external and internal forces, such as

- Supply air jets forced into the room by mechanical systems
- Free convection currents generated by air heating or cooling by surfaces (process equipment, external walls)
- Airflow in the vicinity of local exhausts (hoods) or general exhaust (due to negative pressure in the duct produced by mechanical systems)
- Airflow forced through intended and unintended openings in the building envelope, which depends on the pressure difference across the opening resulting from wind pressure on the building envelope, temperature difference between the indoor and outdoor air, and an imbalance in the mechanical exhaust ventilation system performance versus the mechanical air supply (positive or negative pressure building)
- Air currents produced by process equipment or moving people (e.g., high-speed rotating machines such as pulverizers, high-speed belt material transfer systems, falling granular materials, and escaping compressed air from pneumatic tools)

The airflow pattern and the scale of air currents in the room depend upon the types of sources and the energy introduced by each source, as well as the configuration and dimensions of the room. The energy of the predominant turbulent flow created by each source transfers into transverse turbulent pulsations, which convert large eddies into smaller eddies. This energy is finally converted into heat. Kinetic energy of air leaving the room through exhaust openings can be neglected. Typically, exhaust openings are protected by a grill, which does not let through large or medium-size energy-containing eddies.

The energy of large and medium-size eddies can be characterized by the turbulent diffusion coefficient, A, m^2/s. This parameter is similar to the parameter used by Richardson to describe turbulent diffusion of clouds in the atmosphere.[1] Turbulent diffusion affects heat and mass transfer between different zones in the room, and thus affects temperature and contaminant distribution in the room (e.g., temperature and contaminant stratification along the room height—see Chapter 8). Also, the turbulent diffusion coefficient is used in local exhaust design (Section 7.6).

Studies by Elterman show that turbulent diffusion coefficients in ventilated rooms outside jets and plumes can be described using the relationship[2]

$$A = C\epsilon^{1/3} l^{4/3}, \tag{7.28}$$

where C can be evaluated from the equation

$$C = 0.25 \pm \Delta, \tag{7.29}$$

where Δ = confidence interval, which depends upon the required confidence probability, as shown in Table 7.9. In most cases, the average value $C = 0.25$ can be used in Eq. (7.28).

TABLE 7.9 Coefficient C

Confidence probability	80%	85%	90%	95%	97%
Confidence interval, Δ	0.051	0.063	0.078	0.10	0.114
C Maximum	0.301	0.313	0.328	0.35	0.364
Minimum	0.199	0.187	0.172	0.15	0.136
Average	0.25	0.25	0.25	0.25	0.25

Characteristic length, l in Eq. (7.28), depends on the application; e.g., for local exhaust design l equals the characteristic hood dimension, and for room air distribution design with a temperature or contaminant stratification, l equals the room height.

Another important parameter used in Eq. (7.28) is ϵ, which is the kinetic energy, E_{room}, kg m²/s, dissipated in the mass of air, M, kg, in time τ, s:

$$\epsilon = \frac{E_{room}}{M\tau} = \frac{\text{kg m}^2/\text{s}}{\text{kg s}} = \frac{\text{m}^2}{\text{s}} \tag{7.30}$$

The total kinetic energy introduced by different sources can be calculated by summation of all sources,

$$E_{room} = \sum E_{jet} + \sum E_{conv} + \sum E_{m.o.} \tag{7.31}$$

Contributing energies can be calculated using the following equations:[2]

- Kinetic energy introduced by supply air jet:

$$E_{jet} = \frac{1}{2}\rho_0 Q_0 V_0^2 \tag{7.32}$$

- Kinetic energy generated by convective heat source (W_{conv}):

$$E_{conv} = \frac{g W_{conv} H}{1.8 C_p T_0} \tag{7.33}$$

  where W_{conv} is a convective component of the heat source, H_r is the room height above the heat source, and C_p and T_0 are the specific heat and absolute temperature of the room air, respectively.
- Kinetic energy from the moving objects, calculated from the body's drag coefficient k, area A, velocity V, percent movement t, and the room air density ρ:

$$E_{m.o.} = \frac{1}{2} k A V^2 \rho_0 t \tag{7.34}$$

7.3.2 Airflow in Rooms Dominated by Supply Jets

In rooms where energy is introduced primarily by supply air jets, air distribution methods are referred to as mixing type. With a perfect mixing-type air distribution, airflow pattern and air velocity at any point in the room are

governed by supply jet momentum. In this case, if the air supply and air exhaust openings are located close to each other, a large proportion of supply air is extracted from the room without passing the occupied zone. Such a situation, called short-circuiting, results from poor design and leads to undesirable airflow patterns.

Current mixing-type air distribution methods typically consider ventilation of the occupied zone with jets intercepting its upper boundary (e.g., Fig. 7.6*a*, *c*). Also, the occupied zone can be ventilated by the reverse flow produced as the supply jet degrades above the occupied zone level (Fig. 7.6*b*). Mixing-type air distribution methods include air supply with jets projected vertically downward, inclined jets, jets directed vertically upward, and horizontal jets along room surfaces.

In the latter case, the jet reaches the opposite wall/ceiling and follows room surfaces until it reaches the occupied zone (Fig. 7.7*a*). If the combination of room sizes (height, length, and width) allows such an airflow pattern, this room is considered to be "short."[5] The room where an air jet dissolves before it reaches the opposite wall is considered to be "long." In such rooms, the occupied zone is ventilated by "reverse" flow, and secondary and tertiary vortexes (Figure 7.7*b*, *c*).Buoyant forces, e.g., when supply air is heated, can significantly affect the airflow pattern created by supply jets (Fig. 7.6). Applying proper design principles prevents warm air from rising to the upper zone of the room without heating the occupied zone. More detailed discussion of airflow created in confined spaces with mixing-type air supply can be found in Section 7.4.5.

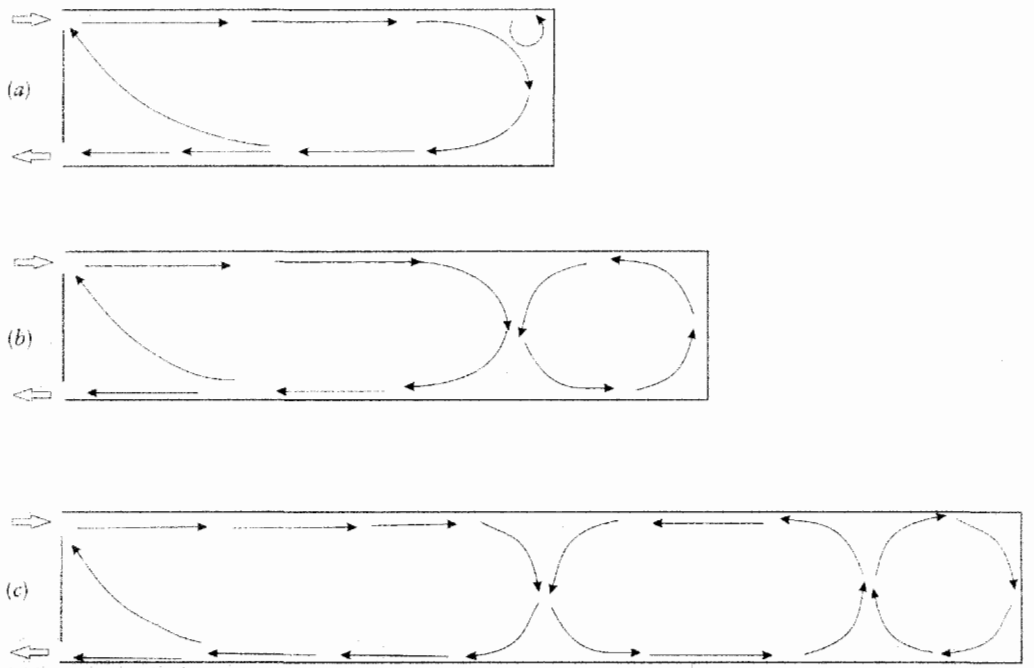

FIGURE 7.6 Flow patterns in rooms with horizontal air supply along the ceiling surface: (*a*) primary airflow in a short room; (*b*) primary airflow; (*c*) secondary and tertiary eddies in long rooms.[3]

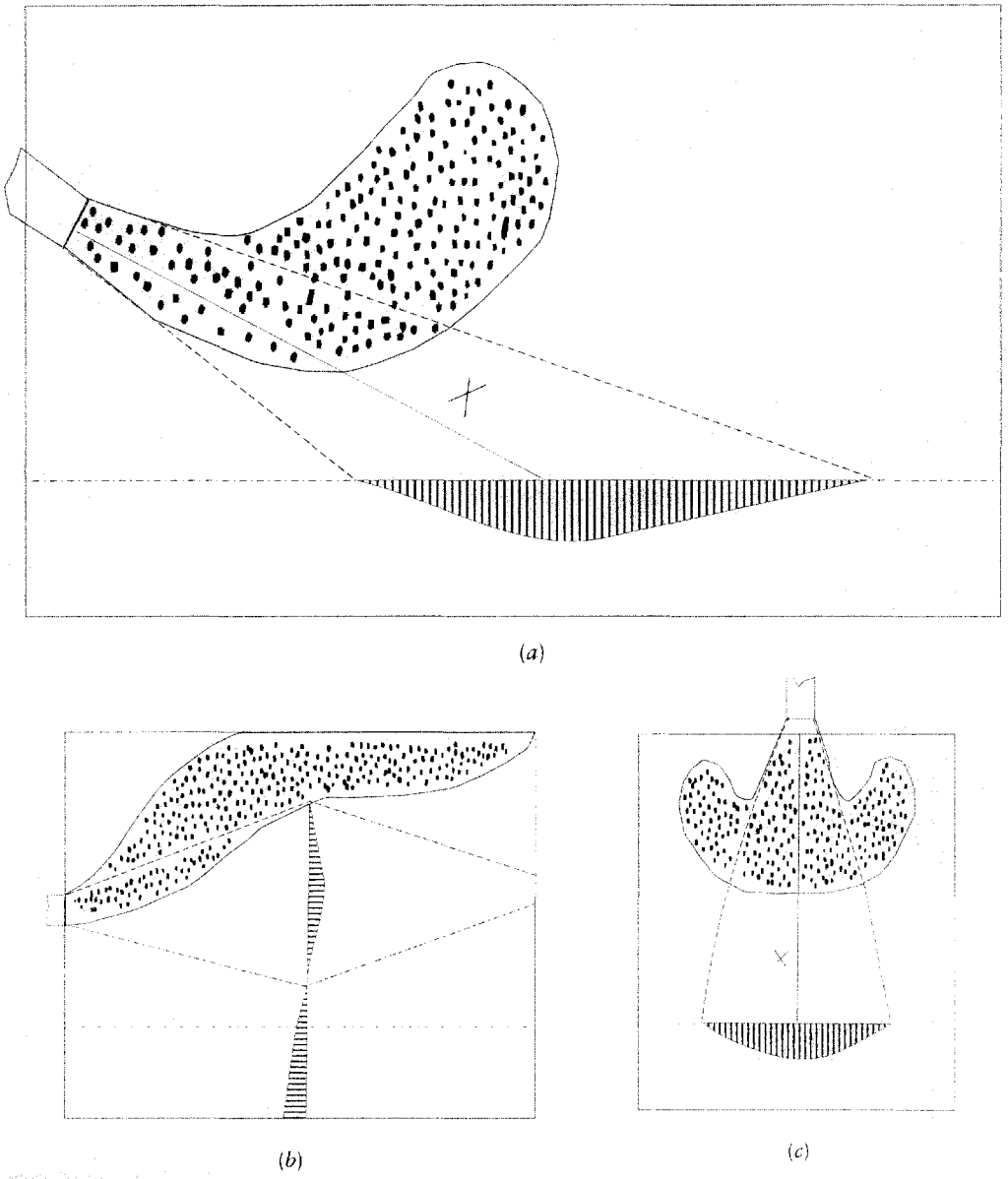

FIGURE 7.7 Schematics of air supply: (*a*) with inclined jets toward the occupied zone; (*b*) with horizontal jets and occupied zone ventilated by reverse flow; (*c*) with vertical jets. Shaded areas show the effect of buoyant forces on airflow pattern when supply air is excessively heated over the room air.[4]

7.3.3 Airflow Dominated by Thermal Plumes

In rooms where air and contaminant movement is dominated by thermal energy of heat sources (e.g., in rooms with natural or displacement ventilation), temperature and contaminant stratification along the room height is created. Air supply and exhaust in such rooms are designed not to disturb the natural pattern of air movement created by heat sources: cooled air enters the room in

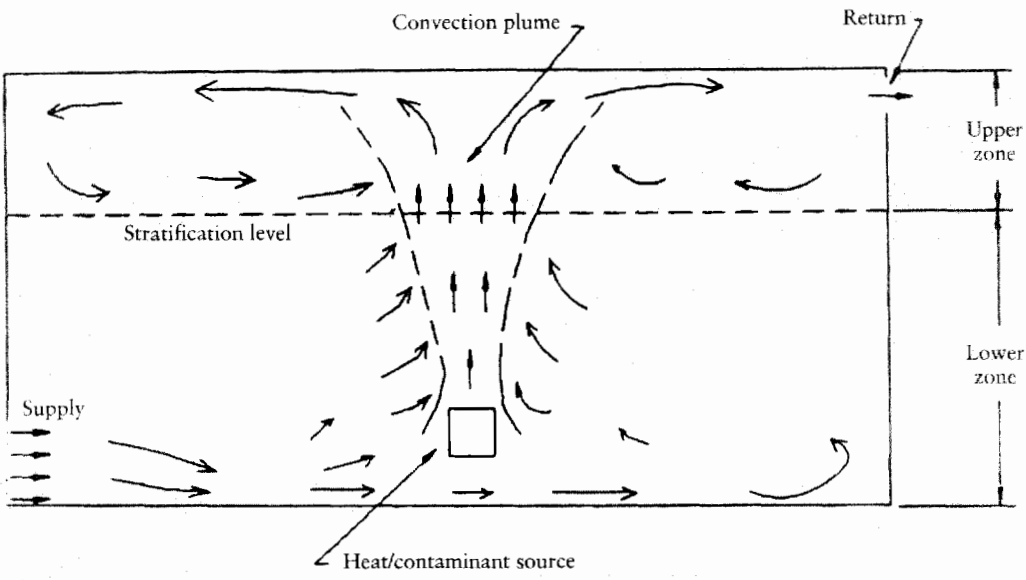

FIGURE 7.8 Schematic of airflow in rooms with a displacement ventilation.[6]

the lower zone close to the floor level and is exhausted from the upper zone. Under the influence of buoyancy, cold air spreads along the floor and floods the lower zone of the room. The air close to the heat source is heated and rises upward as a convective airstream (Fig. 7.8). In the upper zone this stream spreads along the ceiling. The lower part of the convective stream induces the colder air of the lower zone of the room, and the upper part of the convective airstream induces the heated air of the upper zone of the room. The height of the lower zone depends on the air volume discharged into the occupied zone and on the amounts of convective heat discharged by the sources (Fig. 7.9). In the presence of the temperature gradient, the convective plume may reach the height where the temperature difference in the plume and in the ambient air at the corresponding height disappears. This can happen with convective plumes above weak heat sources (e.g., above cigarette, point welding, person's body) in the presence of stronger heat sources (Fig. 7.10).

Temperature and contaminant gradients along the room height and separation stability between the upper and lower zones are influenced by turbulent exchange between these zones. The heat flux density due to turbulent exchange can be determined as[7]

$$q_{\text{turb}} = A_{\text{turb}} C_p g \rho \frac{\delta\theta}{\delta z}, \tag{7.35}$$

where $\delta\theta/\delta z$ is the air temperature gradient in the separation zone. To calculate the turbulent exchange coefficient, A_{turb}, for the separation zone, Shilkrot[7] used the V. H. Munk and E. R. Anderson relationship,[9] which is in good agreement with empirical data:

$$A_{\text{turb}} = A_{\text{ex}}(1 + 3.3\text{Ri})^{-3/2} \tag{7.36}$$

The exchange coefficient, A_{ex}, has been evaluated experimentally.

(*a*)

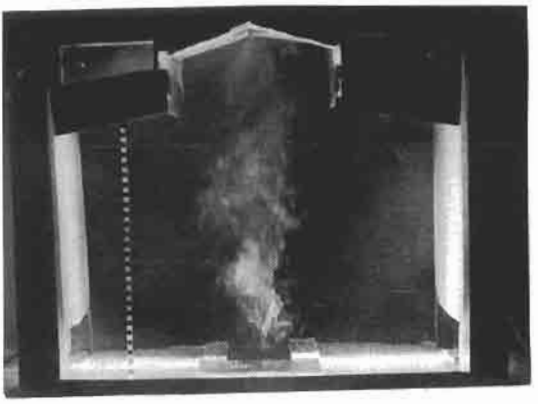

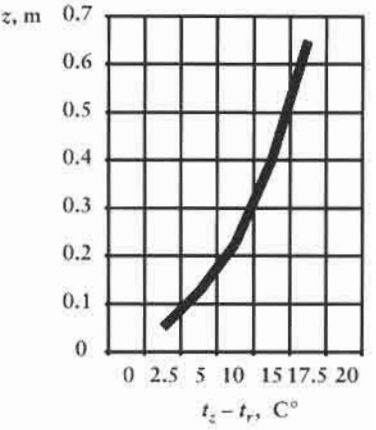

(*b*)

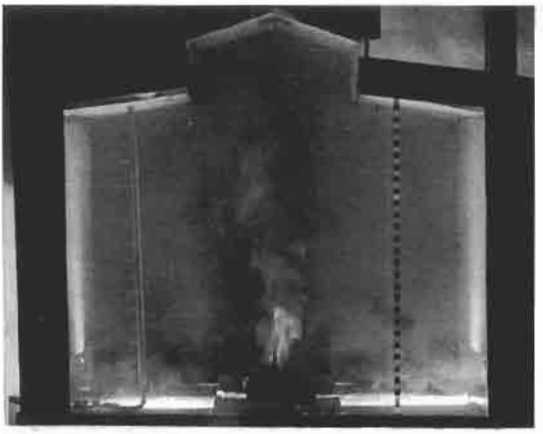

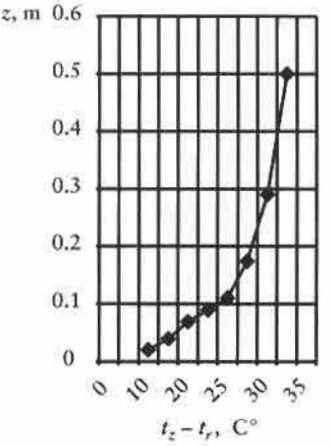

(*c*)

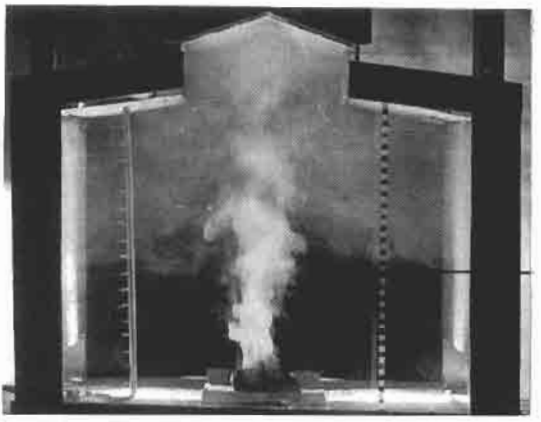

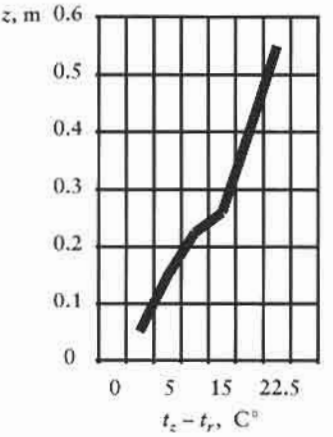

FIGURE 7.9 Influence of exhausted airflow on airflow pattern in the naturally ventilated room: (*a*) airflow in the convective plume smaller than exhausted airflow; (*b*) airflow in the convective pluime equal to the exhausted airflow; (*c*) airflow in the thermal plume at the stratification level equal to the exhausted airflow.[8] (t_z = air temperature along the room height, t_r = average room temperature)

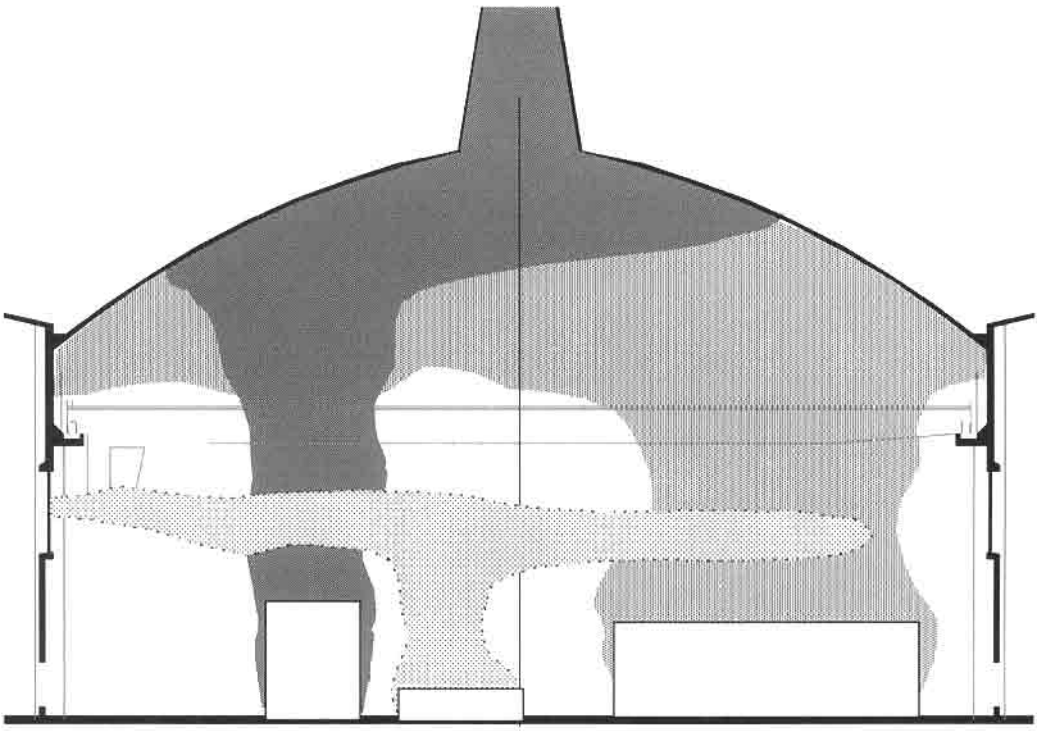

FIGURE 7.10 Stratification in rooms with several heat sources of different strength.[9]

To characterize the airflow in the stratified space, Elterman[2] proposed K, which is a ratio of kinetic energy dissipating in the ventilated space to the energy used to suppress the buoyancy forces:

$$K = \frac{V^3 C_p \rho L B H}{\beta g W_{\text{conv}} l} \tag{7.37}$$

The criteria K is similar to the Archimedes number introduced in 1930 by Baturin and Shepelev[7] to characterize air jets influenced by buoyancy, or to the Richardson criteria used in meteorology to characterize the ratio of the turbulence suppression by the buoyancy forces over the turbulence generation by the Reynolds tension.[10,11] In the case of displacement ventilation, the Richardson criteria can be defined by the relationship[12]

$$\text{Ri} = \frac{g}{T}\frac{\delta\theta/\delta z}{(\delta v/\delta z)^2} \approx \frac{g}{T_0}\frac{\Delta\theta/\Delta z}{(\Delta v/\Delta z)^2} \tag{7.38}$$

where $\delta v/\delta z$ is the room's velocity gradient in the separation zone.

Analysis conducted by Shilkrot[7] for the parameter ranges

- Convective component of heat sources up to 11.6×10^3 kW
- Heights of the temperature separation level up to 15 m
- Room air exchange rates up to 50 h^{-1},
- Room heat intensity up to 116 W/m^2
- Velocity of air supply up to 2 m/s
- Richardson number below 5

showed that the heat flux density value due to the turbulent exchange between the upper and lower zones does not exceed 10% of the total heat released into the occupied zone, and thus can be neglected.

Energy generated by physical activity in the room (i.e., movement of people, transport, conveyor, operation of machines) increases turbulent exchange between the upper and the lower zones and may even disrupt temperature and contaminant stratification along the room height.

7.3.4 Unidirectional Flow

To create unidirectional low-turbulence flow, air is supplied with a low velocity; supply diffusers and exhaust openings have large surfaces (e.g., filter mats). Airflow can be either vertical (air supplied from the ceiling and exhausted through the floor or vice versa (Fig. 7.11*a*)), or horizontal (air supplied through

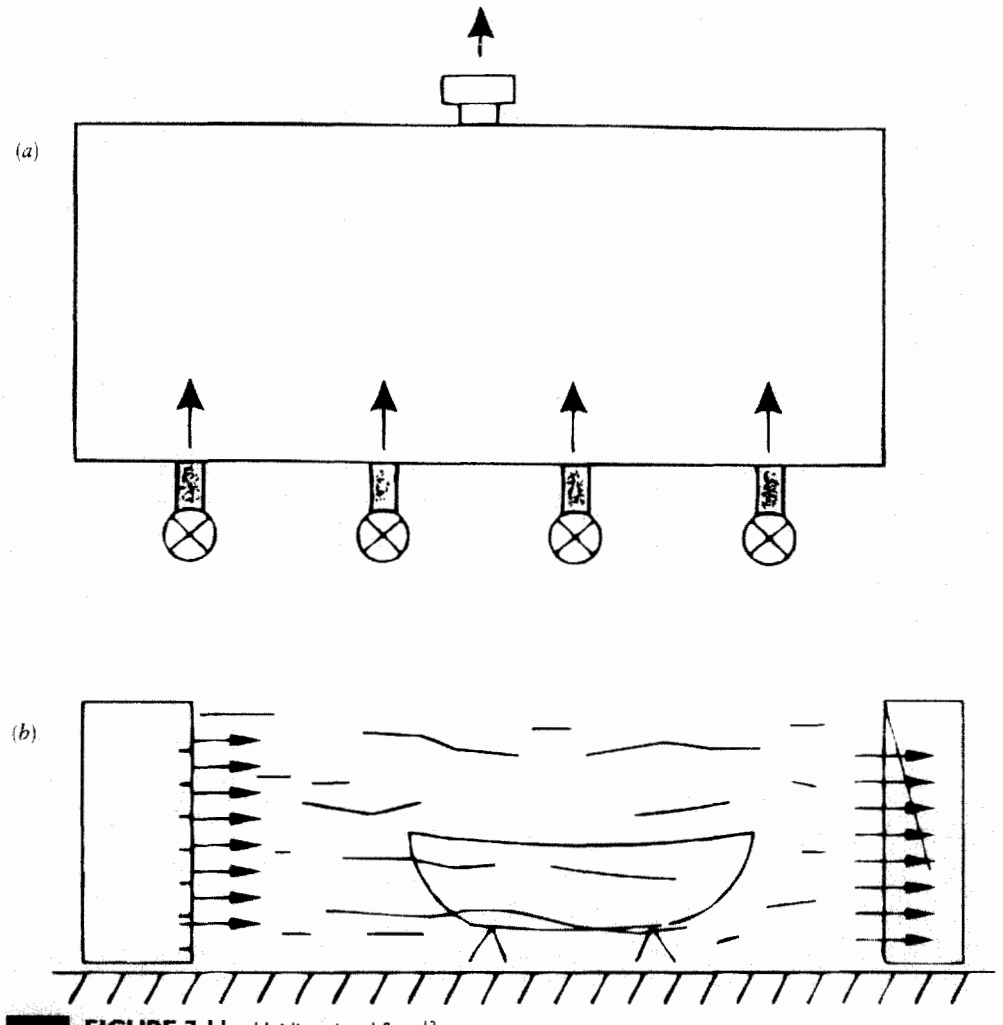

FIGURE 7.11 Unidirectional flow.[13]

one wall and exhausted through returns located on the opposite wall (Fig. 7.11*b*)). The outlets are uniformly distributed over the ceiling, floor, or wall to provide a low-turbulence plug-type flow across the entire room. This type of system is mainly used for ventilating clean rooms, in which the main objective is to remove contaminant particles within the room, or in halls with high heat and/or contaminant loads and a high air change rate.

One of the unidirectional flow system modifications is air supply through diffusers located above the occupied zone. The supply air temperature is lower than the desired room air temperature in the occupied zone, and air velocity is lower compared to a mixing-type air supply, but higher than for a thermal displacement ventilation. Polluted air of the occupied zone is suppressed by an overlying air cushion that displaces the contaminated air toward floor-level exhausts (Fig. 7.12).

7.3.5 Spiral Vortex Flow

Spiral vortex air distribution can be used to localize air contaminants in certain room areas and to evacuate the polluted air from those areas. A spiral vortex in a space can be formed by supplying air through the vertical supply ducts located along a closed contour (preferably along the walls), thus generating a vertical vortex. An exhaust outlet can be located in the ceiling near the center of the rotational flow. Such a combination of air supply and exhaust-systems allows a means for concentrating contaminants in the vortex core and transporting them to the exhaust outlet along the core axis (Fig. 7.13). Low pressure in the vortex core allows for the collection of contaminants and for preventing their diffusion to the clean space.[15,16]

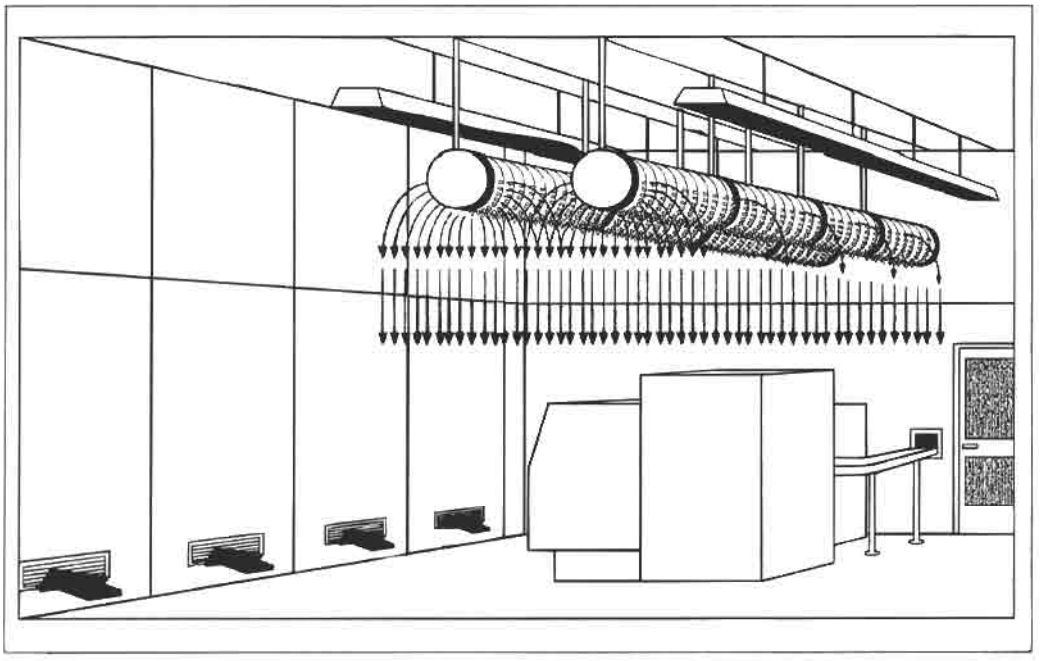

FIGURE 7.12 Unidirectional flow system with air supply through diffusers located above the occupied zone.[14]

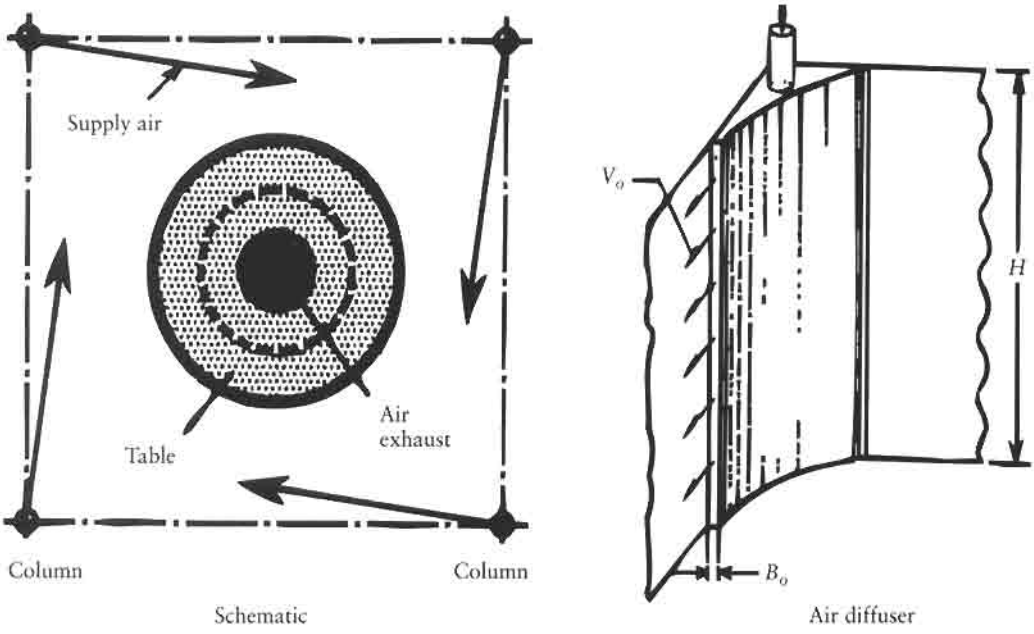

FIGURE 7.13 Spiral vortex flow.[15,16]

7.3.6 Airflow Created by Exhaust Performance

The effect of exhaust performance on room air movement is limited compared to the effect produced by air jets. The distance from the opening to the point where air velocity drops to 10% of the initial velocity value (Fig. 7.14) is approximately equal to one characteristic size of the exhaust opening (D for the round duct) and 60 characteristic sizes for the supply outlet ($60D$ for the round nozzle).

Local exhausts are designed to capture air pollutants and heat at the source, and thus their location and the exhausted airflow rate should ensure sufficient capture velocity.

General exhausts typically do not prevent contaminants and heat from mixing with the room air, and thus, theoretically, it does not matter where the exhaust openings are located (Fig. 7.15).

In practice, the air seldom mixes as completely as in theory. The pollutants spread with the room air, but there may be areas where the concentration is higher than the average for the room. This has to be taken into account in determining the location of the exhaust opening.

In rooms with ventilation systems creating temperature and/or contaminant distribution (see Section 7.5.4), one might consider placing an exhaust opening at, or close to, the equilibrium height for the main contaminant (Fig. 7.16). In addition, there should be a general exhaust either at ceiling level or at floor level, depending on the buoyancy of the contaminants. When it is not certain if the contaminants have negative or positive buoyancy, one should place exhaust openings both under the ceiling and at floor level (Fig. 7.17). More about general exhaust location selection is covered in Section 8.10.

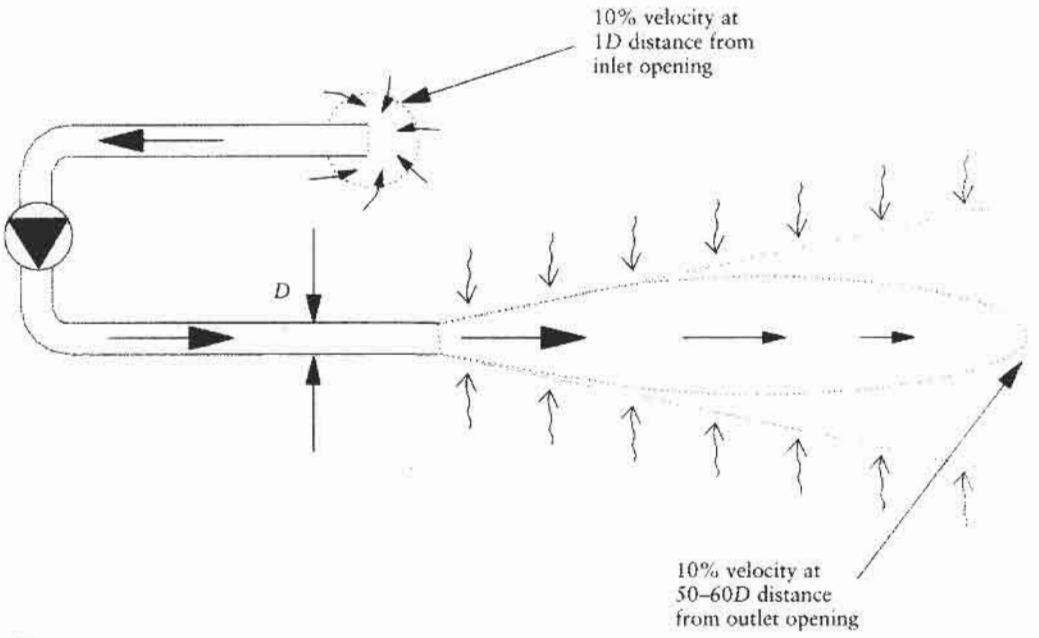

FIGURE 7.14 A jet reaches a long way in one direction, but the capture length of a sink is very limited.

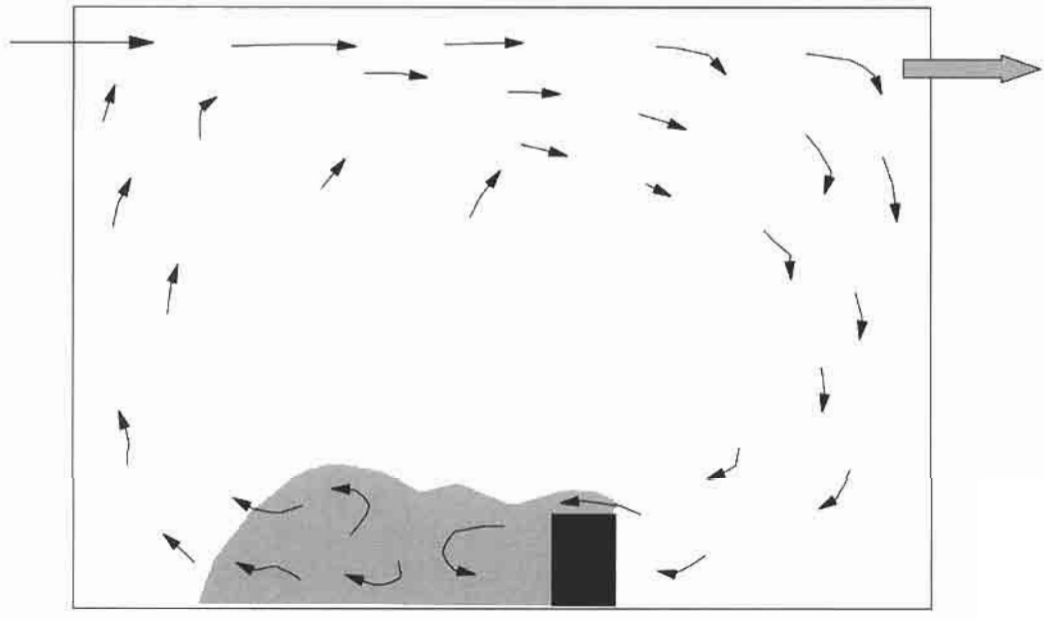

FIGURE 7.15 Exhaust from a room with perfect mixing. The location of exhaust openings is not important.

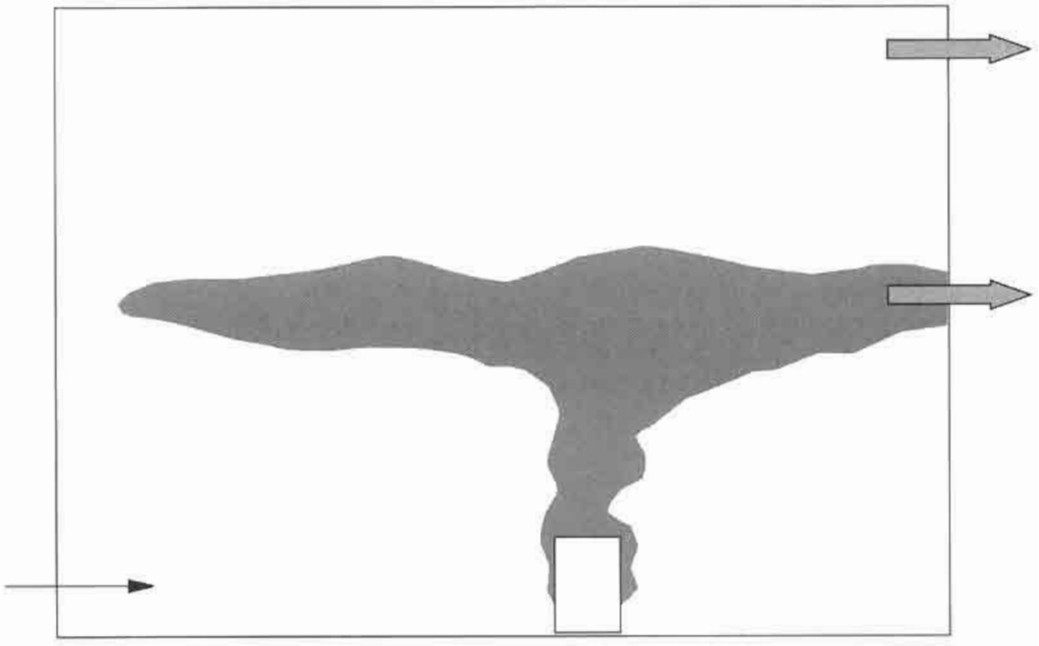

FIGURE 7.16 Thermal stratification should be taken into account in locating the exhaust openings.

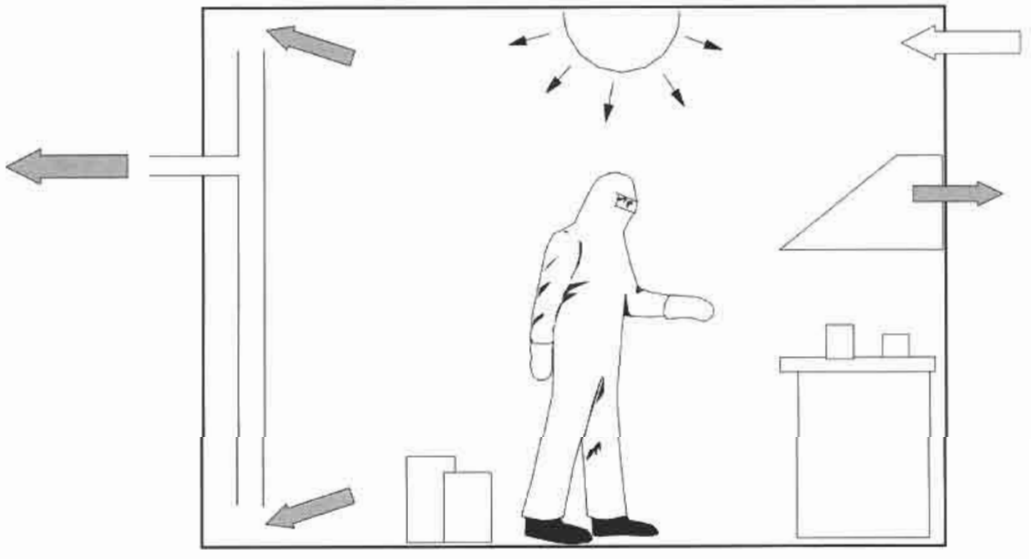

FIGURE 7.17 When contaminants can be both negatively and positively buoyant, exhausts should be located both high and low.

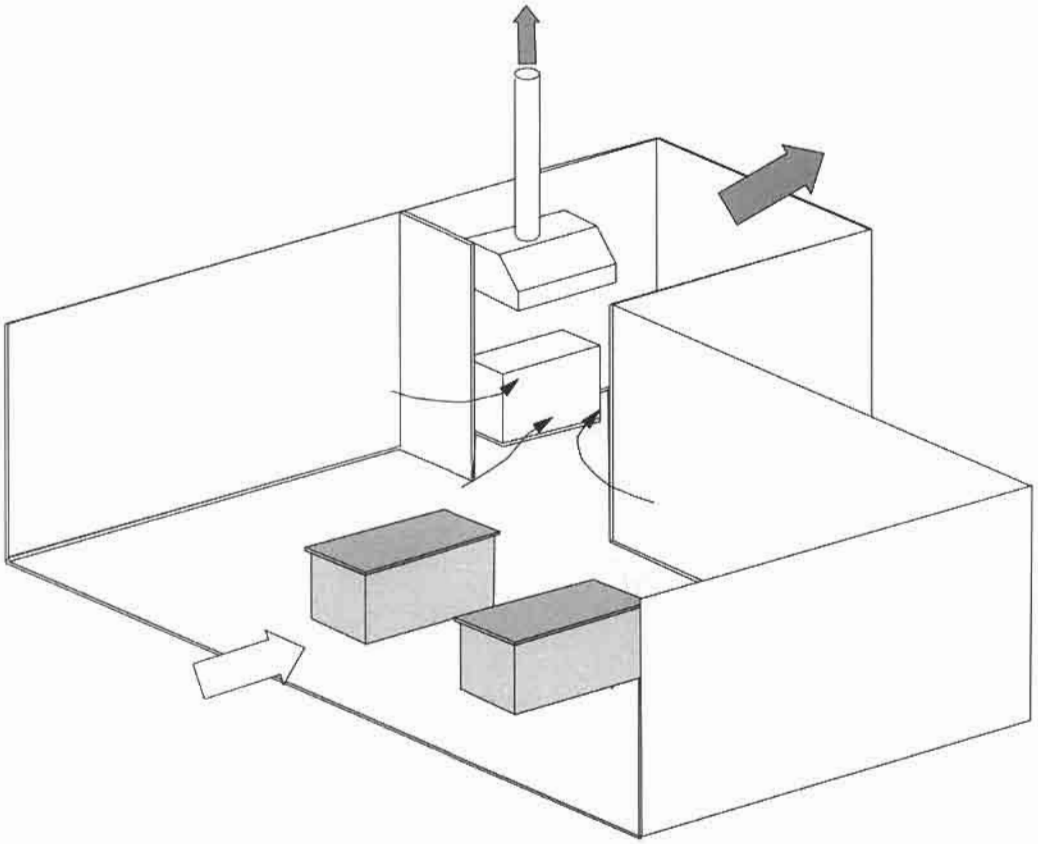

FIGURE 7.18 General exhaust placed to give a displacement flow through a passage.

When special contaminating processes are located in a semi-enclosed part of a room as in Fig. 7.18, the exhausts should be located so that a displacement flow is created through the passage into the semi-enclosure. With this arrangement there may be no need for a door, which may be very practical.

References

1. Richardson, L. F. 1926. *Proceedings of the Royal Society.* Ser. A.V., vol. 26.
2. Elterman, V. M. 1980. *Ventilation of Chemical Plants.* KHIMIA, Moscow.
3. Müller, H. J. 1977. Einfluß der geometrischen verhältnisse auf die raumunsströmung bei der strahllüftung. *Luft-und Kältetechnik*, no. 6.
4. Grimitlyn, M. I. 1982. *Air Distribution in Rooms.* Stroizdat, Moscow.
5. Etheridge, D., and M. Sandberg. 1996. *Building Ventilation: Theory and Measurements.* John Wiley & Sons, New York.
6. ASHRAE. 1997. *Handbook of Fundamentals*, Chapter 31. American Society of Heating, Refrigeration, and Air-Conditioning Engineers, Atlanta.
7. Shilkrot, E. O. 1993. Determination of design loads on room heating and ventilation systems using the method of zone-by-zone balances. *ASHRAE Transactions*, vol. 99, no. 1.
8. Shilkrot, E. O. 1977. Natural ventilation of single-story industrial buildings with significant heat loads. Ph.D. Thesis, MISI, Moscow.
9. Skistad, Håkon. 1999. Private communications.

10. Merrit, G., and G. Redinger. 1973. Measurements of heat and impulse transfer coefficient in turbulent stratified flow. *Journal of Rocket Technology and Astronautics*, no. 11.
11. Munk, W. H., and E. R. Anderson. 1948. Notes on the theory of the thermocline. *Journal of Marine Research*, vol. 1.
12. Shilkrot, E. O., and A. M. Zhivov. 1992. Room ventilation with designed temperature stratification. In *Roomvent '92: Proceedings of the Third International Conference on Air Distribution in Rooms*, vol. 1. Aalborg, Denmark.
13. ABB. 1993. *Technical Information*. SEFIC/E 2761 Reg. 8.
14. AIR-IX. 1987. *Teollisuusilmanvaihdon suunnittelu: Kauppaja teollissusministerio*. Helsinki.
15. Kuz'mina, L. V., A. M. Kruglikova, and A. S. Gus'kov. 1986. Contaminant distribution in industrial hall with spiral vortex ventilation. In *Occupational Safety in Industry: Transactions of the All-Union Research Institutes for Labor Protection*. Profizdat, Moscow.
16. Nagasawa, Y., M. Nitadori, and S. Matsui. 1990. Characteristics of spiral vortex flow and its application to control indoor air quality. In *Roomvent '90: Proceedings of the International Conference on Air Distribution in Ventilated Rooms*. Oslo, Norway.

Bibliography

Alden, J. L., and J. M. Kane. 1982. *Design of Industrial Ventilation Systems*. 5th ed. Industrial Press, New York.
LVIS. 1996. *Ilmastointi*. LVIS-2000. Painopaikka, Kausalan Kirjapaino Oy.
Seliverstov, A. N. 1934. *Ventilation of Chemical Industry Plants: ONTI* (in Russian). Gosstriizdat, Moscow.

7.4 AIR JETS

7.4.1 Introduction

Air supplied into the room through the various types of outlets (grills, ceiling-mounted air diffusers, perforated panels, etc.) is distributed by turbulent air jets. In mixing-type air distribution systems, these air jets are the primary factor affecting room air motion. Numerous theoretical and experimental studies that developed a solid base for turbulent air jets theory were conducted concurrently in different countries (Germany, Sweden, Russia, the UK, and the United States) from the 1930s through the 1980s. Theory of air jets and air distribution design principles are discussed in this section.

7.4.2 Classification

If there is no influence of the walls, ceiling, or obstructions on the air jet, it can be considered a free jet. If the air jet is attached to a surface, it is called an *attached air jet*.

Characteristics of the air jet in the room might be influenced by reverse flows, created by the jet entraining the ambient air. This air jet is called a *confined jet*. If the temperature of the supplied air is equal to the temperature of the ambient room air, the jet is an *isothermal jet*. A jet with an initial temperature different from the temperature of the ambient air is called a *nonisothermal jet*. The air temperature differential between supplied and ambient room air generates buoyancy forces in the jet, affecting the trajectory of the jet, the location at which the jet attaches and separates from the ceiling/floor, and the throw of the jet. The significance of these effects depends on the relative strength of the thermal buoyancy and inertial forces (characterized by the Archimedes number).

Air jets can be classified according to the diffuser type as follows (Fig. 7.19):[1]

1. *Compact* air jets are formed by cylindrical tubes, nozzles, and square or rectangular openings with a small aspect ratio that are unshaded or shaded by perforated plates, grills, etc. Compact air jets are three-dimensional and axisymmetric at least at some distance from the diffuser opening. The maximum velocity in the cross-section of the compact jet is on the axis.

2. *Linear* air jets are formed by slots or rectangular openings with a large aspect ratio. The jet flows are approximately two-dimensional. Air velocities are symmetric in the plane at which air velocities in the cross-section are maximum. At some distance from the diffuser, linear air jets tend to transform into compact jets.

3. *Radial* air jets are formed by ceiling cylindrical air diffusers with flat disks or multidiffusers that direct the air horizontally in all directions.

4. *Conical* air jets are formed by cone-type or regulated multidiffusers in ceiling air distribution devices, and have an axis of symmetry. The vectors of

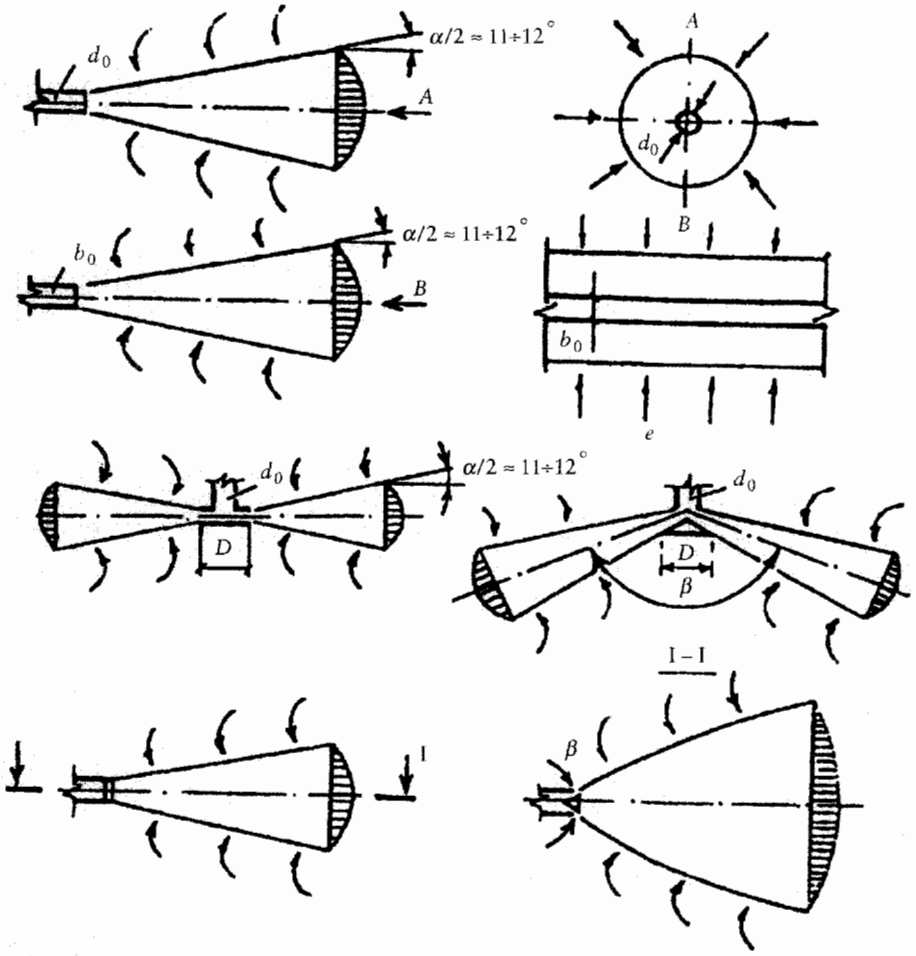

FIGURE 7.19 Types of diffuser jets: (*a*) compact; (*b*) linear; (*c*) radial; (*d*) incomplete radial; (e) conical.[1]

air velocities are parallel to the conical surface (with an angle at the top of the cone equal to 120°). Maximum velocities in cross-sections perpendicular to the axis occur at the conical surface.

5. *Incomplete radial jets* are supplied through outlets with grills having diverging vanes, and have a coerced angle of expansion. At some distance this kind of jet tends to transform into a compact one.

6. Swirling jets are supplied to the room through air diffusers with vortex-forming devices creating rotation motion, and have tangential as well as radial velocity vectors. Depending upon the type of air diffuser, swirling jets can be compact, conical, or radial.

7.4.3 Isothermal Free Jet

7.4.3.1 Zones in a Jet

For different types of free jets and air diffusers there are similarities in the resulting flows. Four major zones are recognized along a free jet. These zones, as described by Tuve,[2] may be roughly defined in terms of the maximum or center core velocity that exists at the jet cross-section being considered (see Fig. 7.20*a*).

Zone 1 is a short zone, extending about two to six diffuser diameters (for compact and radial jets) or slot widths (for linear jets) from the diffuser face. In this zone, the centerline velocity of the jet remains nearly equal to the original supply velocity throughout its length.

Zone 2 is a transition zone, and its length depends upon the diffuser type. For a compact jet the transition zone typically extends to eight or ten diameters from the outlet. Within this zone, the maximum velocity may vary inversely with the square root of the distance from the outlet. Some researchers 3–5 suggest use of a simplified scheme of the jet (Fig. 7.20*b*) with a transition cross-section for practical purposes.

Zone 3 is the zone of fully established turbulent flow. It has major engineering importance, since it is usually in this zone that the jet enters the occupied region. The length of this zone depends on the air jet shape, the type and size of supply air diffuser, the initial velocity of the air jet, and the turbulence characteristics of the ambient air.

Zone 4 is a terminal zone in which the residual velocity decays quickly into large-scale turbulence. Within a few diameters, the maximum velocity subsides to below 0.25 m/s. Though this zone has been studied by several researchers,[6,7] its characteristics are still not well understood.

In some practical applications of air supply (e.g., multiple-jet ceiling diffusers, an annular jet collapsing into a compact jet, jets from rectangular outlets becoming round or elliptical, or multiple streams merging when air is supplied through perforated panels), measurements and accurate jet description in Zone 1 and Zone 2 may be difficult.

7.4.3.2 Velocity Distribution in Jet Cross-Section within Zone 3

Velocity distribution profiles in Zone 3 of the jet were found to be similar.[8–10] They can be computed by applying momentum-transfer theory (Prandtl-Tollmein) and vorticity-transfer theory (Taylor-Goldstein). Modification of these theories with different assumptions has resulted in several equa-

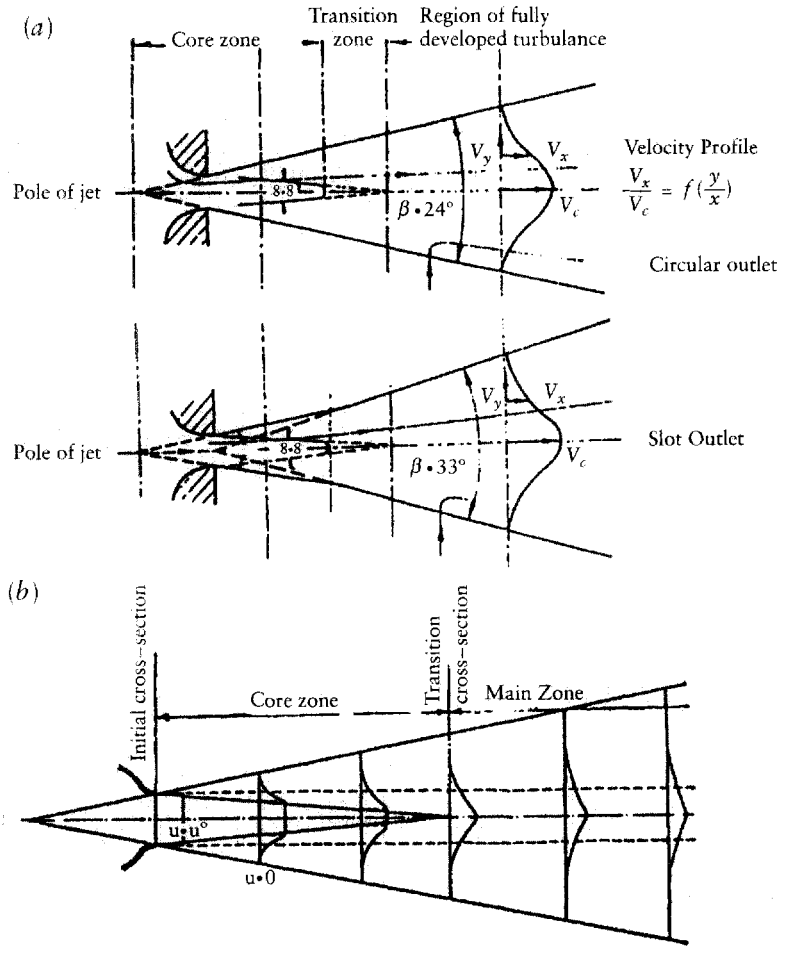

FIGURE 7.20 Turbulent jet: (*a*) schematic with four zones; (*b*) simplified jet schematic.

tions for jet velocity profiles. These equation are presented in Table 7.10 and can be divided into two groups:

- Profiles with finite boundaries[11,12] with a velocity of zero at the specified distance from the jet axis
- Profiles with indefinite boundaries[13,14] with air velocity decreasing with distance from the axis asymptotically approaching zero

TABLE 7.10 Equations for Velocity Profiles in a Free Jet.

	v_i/v_x	
Author	**Round jet**	**Linear jet**
Schlichting[12]	$(1-(r/\delta)^{3/2})^2$	$(1-(y/\delta)^{3/2})^2$
Reichardt[13]	$e^{-(r/\delta)^2}$	$e^{-(r/\delta)^2}$

In the equations listed in Table 7.10, $r(y)$ is the distance from the point of interest to the jet axis, and δ is the distance to the jet boundary, which can be obtained from equations summarized in Table 7.11.

It has been demonstrated by Ruden,[16] Albertson et al.,[10] Taylor et al.,[17] Keagy and Weller,[18] Pai,[19] Becher,[20] Förthmann,[9] Nottage et al.,[21] Shepelev,[4] Grimitlyn,[1] and other researchers that the Gauss error-function profile by Reichardt is in agreement with data from studies of both nozzle jets and manufactured air diffusers supplying similar jets. This profile is utilized mostly by researchers using the analytical (semi-empirical) approach in air jet studies. Table 7.12 lists some modifications of the Gauss error-function velocity profile equations used for practical applications.

The Schlichting finite-boundaries profile is another one that is frequently used.[23] Utilization of this profile is specifically fruitful for describing velocity distribution in complex flows, e.g., a jet in a cross-flow[24] and jet interaction under the right angle.[25] In such cases, distance from the jet axis, r_i, to the point with an air velocity V_i is replaced by the parameter $r_i = (S_i/\pi)^{1/2}$, where S_i is the area within a contour with a constant velocity V_i.

7.4.3.3 Centerline Velocity in Zone 3

Compact Jet

Centerline velocity in Zone 3 of the supply jet can be calculated from the equations based on the principle of momentum conservation along the jet:[26,27]

$$M_0 = 2\pi\rho \int_0^{y^*} V^2 y \, dy \tag{7.39}$$

TABLE 7.11 Equations for Jet Boundaries

	δ		
Author	**Round**	**Linear**	**Radial**
Tollmein[11]	$0.151x$	$0.272x$	—
Reichardt[13]	$0.085x$	—	—
Heskestad[15]	—	—	$0.288x$
Tuve[2]	—	—	$0.185x$

TABLE 7.12 Practical Modifications of the Gauss Error-Function Velocity Profile Equations

	v/v_x		
Author	**Round jet**	**Linear jet**	**Radial jet**
Tuve[2]	$e^{-0.7(y/y_{0.5v})^2}$	$e^{-0.7(y/y_{0.5v})^2}$	$e^{-0.7(y/y_{0.5v})^2}$
Grimitlyn[22]	$y_{0.5v} = x \tan \alpha_{0.5v}$	$y_{0.5v} = x \tan \alpha_{0.5v}$	$y_{0.5v} = x \tan \alpha_{0.5v}$
Shepelev[4]	$e^{-\frac{1}{2}\left(\frac{y}{0.082x}\right)^2}$	$e^{-\frac{1}{2}\left(\frac{y}{0.1x}\right)^2}$	$e^{-\frac{1}{2}\left(\frac{y}{0.1x}\right)^2}$

where $M_0 = \rho v_0^2 A_0$ = initial jet momentum and y^* = distance from the axis to the jet boundary.

Application of the Gauss error-function equation for velocity profile in the form proposed by Shepelev (Table 7.12) in Eq. (7.39) results in the following formula for the centerline velocity in Zone 3 of the compact jet:

$$v_x = \frac{1}{\sqrt{\pi} c} \sqrt{\frac{M_0}{\rho_\infty}} \frac{1}{x}. \tag{7.40}$$

Equation (7.40) can be also presented as

$$v_x = \frac{\theta\varphi}{\sqrt{\pi}} c \frac{V_0 \sqrt{A_0}}{x}, \tag{7.41}$$

where

$$\theta = \sqrt{\rho_0 / \rho_\infty} = \sqrt{T_\infty / T_0} \tag{7.42}$$

and

$$\frac{A}{A_0}\varphi = \left[\int_0^1 \left(\frac{V}{V_0} \right)^2 d\left(\frac{A}{A_0}\varphi \right) \right]^{1/2} \tag{7.43}$$

are the coefficients of the velocity distribution at the diffuser outlet.

When outlet velocity distribution is uniform, $\phi = 1$, and v_0 = average air velocity at the diffuser outlet ($v_0 = q_0/A_0$). The complex of coefficients $\Theta\varphi/\sqrt{\pi}c$ reflecting the conditions of the air supply has a constant value for a given situation and is called the dynamic characteristic of the diffuser jet.[4] Dynamic characteristic describes the intensity of velocity decay along the air jet axis:

$$K_1 = \frac{\Theta\varphi}{\sqrt{\pi} c}. \tag{7.44}$$

The above approach for the centerline velocity computation was utilized by different researchers using other velocity profiles and resulted in

$$v_x = K_1 v_0 \frac{\sqrt{A_0}}{x}. \tag{7.45}$$

Theoretical values of characteristic K_1 depend upon the type of velocity profile equation and supply conditions assumed. According to Shepelev, $K_1 = 6.88$; another estimate is $K_1 = 6.7$.[28] The Schlichting profile results in $K_1 = 7.4$, and with the Tollmein profile $K_1 = 7.76$.[29] According to experimental studies reported by Tuve,[2] the range of K_1 characteristic for compact jets discharged from round outlets varies between 5.7 and 7 depending upon supply air velocity and type of outlet. Analysis of experimental data from different researchers by Rodi[30] indicates that K_1 is close to 7.

Some researchers (e.g., Abramovich,[26] Baturin,[31] Rajaratnam,[32] and Nielsen and Moller[33]) consider x to be the distance from a point located at some distance x_0 upstream from the diffuser face. Equations for the jet boundaries and velocity profile used in the centerline velocity derivation assume that the jet is supplied from the point source. Addition of the distance x_0 to the distance from the outlet corrects for the influence of the outlet size on the jet geometry. For practical reasons some researchers neglect x_0.

Linear Jet

The equations for centerline velocities in a linear diffuser jet can be derived using the same principles as in the case of a compact jet. For a linear jet:

$$v_x = K_1 v_0 \sqrt{\frac{H_0}{x}}, \tag{7.46}$$

where H_0 = height of the slot.

Similar to the case with compact air jet supply, theoretical values of characteristic K_1 depend upon the type of velocity profile equation and supply conditions. According to Shepelev, $K_1 = 2.62$. The Görtler profile results in $K_1 = 2.43$ and the Tollmein profile in $K_1 = 2.51$.[29] Becher[34] reported the K_1 characteristic for a linear jet to be equal to 2.55. Experimental results by Heskestad,[35] Miller and Comings,[36] van der Hegge Zijnen,[37,38] Gutmark and Wygnanski,[39] and Kotsovinos and List[40] appear to satisfy $K_1 = 2.43$.

Radial Jet

The application of the principle of momentum conservation to the radial jet by Koestel[41] resulted in the following equation for the centerline velocity (Fig. 7.21):

$$\frac{v_R}{v_0} = \frac{\sqrt{K(H_0/R_0)\cos\theta[K(H_0/R_0)\cos\theta + 1]}}{\sqrt{\frac{R(R - R_0)}{R_0}}}. \tag{7.47}$$

The value of the numerator of the right-hand side of Eq. (7.47) depends on the geometric configuration of the outlet (R_0, H_0, $\cos\theta$). The denominator represents the dimensionless distance from the outlet. For a given diffuser or a plaque Eq. (7.47) becomes

$$\frac{v_R}{v_0} = \frac{CR_0}{\sqrt{R(R - R_0)}}. \tag{7.48}$$

Experimental C values for a radial slot and a radial nozzle tested by Koestel are 1.13 and 1.19, respectively. Eq. (7.48) is similar to Eq. (7.45) if the distance from the outlet is large enough so that $(R - R_0)$ is approximately equal to R. The theoretical value of the characteristic K_1 in Eq. (7.45) applied to a radial jet is equal to 1.05, according to Shepelev.[42]

Similar derivations by Regenscheit[43] resulted in the following equation for the radial jet centerline velocity:

$$\frac{v_R}{v_0} = \frac{R_0}{R} \frac{A_F}{\sqrt{1 + R_0/R}}, \tag{7.49}$$

where

$$\alpha_F = \frac{h_0}{R_0 m} \tag{7.50}$$

and

$$A_F = \alpha_F \sqrt{1 + 1/\alpha_F}. \tag{7.51}$$

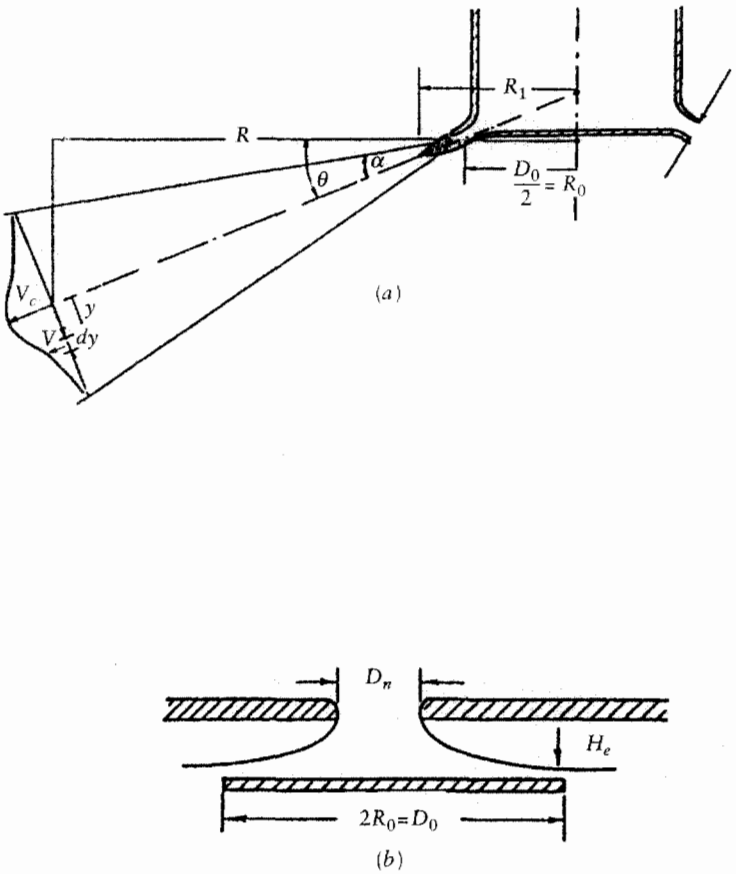

FIGURE 7.21 Schematic of a radial jet: (*a*) general case $\theta \geq 0$ (*b*) air supplied through a diffuser with a plaque: $\theta = 0$.[41]

Referring to the data from Baturin,[44] Regenscheit evaluated α_F to be 0.377. At a significant distance from the supply outlet ($R_0/R \longrightarrow 0$), Eq. (7.49) can be transformed into Eq. (7.45).

Equations (7.45) and (7.46) show that air velocity along compact, linear, and radial jets is proportional to the value of K_1. This parameter depends upon

1. Jet type
2. Diffuser type
3. Initial air velocity[45] or Reynolds number[46–48]

7.4.3.4 Universal Equations for Velocity Computation along Jets Supplied from Outlets with Finite Dimensions

A fruitful approach for velocity computation in the first three zones of jets supplied from outlets with finite size was developed based on the hypothesis that momentum diffuses with distance from the source in the same manner as heat energy.[49,50] This approach, developed by Elrod,[51] Shepelev and Gelman,[52] and Regenscheit,[53] utilizes the method of superposition of jet momentum from the multiple-jet system. These jets originate from the points with supply air veloc-

ity equal to the average air velocity at the outlet. This approach utilizes the following principles:

1. Momentum conservation along the jet
2. Air velocity in each jet cross-section, described using the Reichardt Gauss error-function profile
3. Constant angle of divergence along the jet

This method was applied by Shepelev and Gelman[52] to air supply through a rectangular outlet with dimensions $2L \times 2B$ (Fig. 7.22), resulting in the following equation for air velocities in the jet cross-section located at the distance x from the outlet:

$$v_{x,y,z} = \frac{v_0}{2}\sqrt{\left(\operatorname{erf}\frac{L-y}{cx} + \operatorname{erf}\frac{L+y}{cx}\right)\left(\operatorname{erf}\frac{B-z}{cx} + \operatorname{erf}\frac{B+z}{cx}\right)}. \tag{7.52}$$

From Eq. (7.52) the centerline velocity can be calculated by substituting $y = 0$ and $z = 0$:

$$v_x = v_0\sqrt{\operatorname{erf}\frac{L}{cx}\operatorname{erf}\frac{B}{cx}}. \tag{7.53}$$

Equations (7.52) and (7.53) describe air velocity in cross-sections of the jet located in Zone 1 through Zone 3. The shape of the outlet can be from square ($2B \times 2B$) to infinite slot with a width $2B$ ($L = \infty$). In the case of a linear jet supplied through the slot, Eqs. (7.52) and (7.53) become

$$v_{x,y,z} = \frac{v_0}{\sqrt{2}}\sqrt{\operatorname{erf}\frac{B-z}{cx} + \operatorname{erf}\frac{B+z}{cx}} \tag{7.54}$$

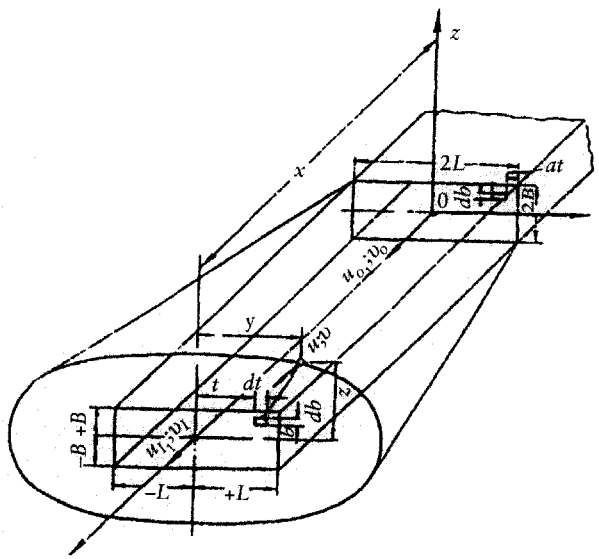

FIGURE 7.22 Schematic of a jet supplied through a rectangular outlet.[52]

and

$$v_x = v_0 \sqrt{\text{erf}\frac{B}{cx}}. \tag{7.55}$$

The solution for a circular jet as presented by Elrod[51] and Regenscheit[53] cannot be evaluated in closed form. The exact solution can be determined only for the centerline velocity:

$$\frac{v_x}{v_0} = 1 - \exp\left(\frac{-D^2}{4c^2x^2}\right). \tag{7.56}$$

7.4.3.5 Jet Throw

Diffuser jet throw, L, is a parameter commonly used in air diffuser sizing defined as the distance from the diffuser face to the jet cross-section where the centerline velocity equals a terminal velocity v_x (v_x is often assumed to be 0.25 m/s). Therefore, the throw (L) can be determined by velocity decay equations with v_x equal to the terminal velocity:

$$L = K_1 \sqrt{A_0} \frac{v_0}{v_x}. \tag{7.57}$$

7.4.3.6 Entrainment Ratio

Entrainment ratio is another jet characteristic commonly used in air distribution design practice. Specifically, it is used in analytical multizone models (see Chapter 8) when one needs to evaluate the total airflow rate transported by the jet to some distance from a diffuser face. Airflow rate in the jet, Q_x, can be derived by integrating the air velocity profile within the jet boundaries:

$$Q_x = 2\pi \int_0^{y^*} Vy \, dy. \tag{7.58}$$

Equations for airflow rate computation in compact, linear, and radial jets are presented in Table 7.13.

For a given area of diffuser opening A_0, the entrainment ratio is proportional to the distance x (for compact, radial, and conical diffuser jets)

TABLE 7.13 Airflow Rate through a Jet Cross-sectional Area

	Q_x/Q_0		
Author	**Compact jet**	**Linear jet (per 1 m slot length)**	**Radial jet**
Baturin[58]	$0.275 \frac{x-x_0}{\sqrt{A_0}}$	$0.530 \sqrt{\frac{x-x_0}{H_0}}$	$0.530 \sqrt{(1-R/R_0)\frac{R-R_0}{H_0}}$
Regenscheit[43]	$1.77m \frac{x}{\sqrt{A_0}}$	$\sqrt{m} \sqrt{\frac{x}{H_0}}$	$1.96 \frac{R\sqrt{1-R_0/R}}{R_0}$
Shepelev[4]	$0.29 \frac{x}{\sqrt{A_0}}$	$0.43 \sqrt{\frac{x}{H_0}}$	$0.069 \frac{R}{\sqrt{R_0 H_0}}$
Grimitlyn[1]	$\frac{2}{K_1} \frac{x}{\sqrt{A_0}}$	$\frac{\sqrt{2}}{K_1} \sqrt{\frac{x}{H_0}}$	$\frac{\sqrt{2}}{K_1} \frac{x}{\sqrt{A_0}}$

or proportional to the square root of the distance x (for linear jets). For the same type of jet, the entrainment ratio is less with a large K_1 than with a small K_1. Radial and conical diffuser jets have a smaller entrainment ratio than compact or incomplete radial jets with the same K_1 value. Linear diffuser jets have a smaller entrainment ratio than radial and conical jets.

7.4.4 Nonisothermal Free Jets

7.4.4.1 Criteria for Nonisothermal Jets

Buoyant flows can be classified as[55]

- Buoyant jets when the buoyant force acts in the direction of the jet supply velocity at the origin, i.e., upward-projected heated air jet or downward-projected cooled air jet
- Negative buoyant jets when the buoyant force acts in the opposite direction, i.e., downward-projected heated air jet or upward-projected cooled air jet
- Nonbuoyant jets when the effect of buoyancy is negligible
- Plume when the buoyant force completely dominates the flow, as for flow generated with a heat source

In the general case, a buoyant jet has an initial momentum. In the region close to discharge, momentum forces dominate the flow, so it behaves like a nonbuoyant jet. There is an intermediate region where the influence of the initial momentum forces becomes smaller and smaller. In the final region, the buoyancy forces completely dominate the flow and it behaves like a plume. When the jet is supplied at an angle to the vertical direction, it is turned upward by the buoyancy forces and behaves virtually like a vertical buoyant jet in a far field. A negative buoyant jet continuously loses momentum due the opposite direction of buoyancy forces to the supply air momentum and eventually turns downward.

Between the nonbuoyant jet region and the plume region lies an intermediate region in which the flow changes from the former to the latter.[55] The axial location of the beginning of this intermediate region depends primarily on the exit Froude number:

$$F = \frac{V_0^2}{gD_0}\frac{T_\infty}{(T_0 - T_\infty)}. \tag{7.59}$$

The beginning of the transition zone in the linear jet is at approximately

$$\frac{x_{\text{beg}}}{H_0} = 0.5F^{2/3}\left(\frac{T_\infty}{T_0}\right)^{-1/3}. \tag{7.60}$$

Using the relation between the Froude number and the Archimedes number, $\text{Ar}_0 = 1/F$, the length of the linear jet zone, x, where the buoyancy forces are negligibly small can be calculated as follows:

$$\frac{x}{H_0} = \frac{0.5}{\text{Ar}_0^{2/3}}\left(\frac{T_\infty}{T_0}\right)^{-1/3}. \tag{7.61}$$

To characterize the relationship between the buoyancy forces and momentum flux in different cross-sections of a nonisothermal jet at some distance x, Grimitlyn[56] proposed a local Archimedes number:

$$\mathrm{Ar}_x = \frac{g x \Delta\theta_x}{V_x^2 T_\infty} \tag{7.62}$$

where g is acceleration due to buoyancy. Equations for the local Archimedes number can be derived by substituting the expressions for axial velocity V_x and temperature differential $\Delta\theta_x$ into Eq. (7.62):

- For compact and radial jets

$$\mathrm{Ar}_x = \frac{K_2}{K_1^2}(\mathrm{Ar}_0)\left(\frac{x}{\sqrt{A_0}}\right)^2 \tag{7.63}$$

- For linear jets

$$\mathrm{Ar}_x = \frac{K_2}{K_1^2}(\mathrm{Ar}_0)\left(\frac{x}{H_0}\right)^{3/2}, \tag{7.64}$$

where the Archimedes number at the outlet is

$$\mathrm{Ar}_0 = \frac{g\sqrt{A_0}}{V_0^2}\frac{\Delta\theta_0}{T_r}, \tag{7.65}$$

characterizing the ratio of buoyancy and inertial forces at the jet discharge from the outlet.

When calculating Ar_0 for a linear jet, $\sqrt{A_0}$ is replaced by the width of the slot H_0.

Introduction of the local Archimedes criterion helped to clarify nonisothermal jet design procedure. Grimitlyn suggested critical local Archimedes number values, $\mathrm{Ar}_x^{\mathrm{crit}}$, below which a jet can be considered unaffected by buoyancy forces (moderate nonisothermal jet): $\mathrm{Ar}_x \leq 0.1$ for a compact jet, $\mathrm{Ar}_x \leq 0.15$ for a linear jet.

A similar limitation for a linear jet from Eq. (7.64) at $K_1 = 2.5$, $K_2 = 2.0$, $T_0 = 293°\mathrm{C}$, and $T_\infty = 313°\mathrm{C}$ is $\mathrm{Ar}_x < 0.14$.

7.4.4.2 Temperature Profile Distribution in a Jet

Along with a constant velocity zone (Zone 1), there is a constant temperature zone in a jet. Heat diffusion in a jet is more intense than momentum diffusion; therefore the core of constant temperatures fades away faster than that of constant velocities and the temperature profile is flatter than the velocity profile. Thus the length of the zone with constant temperature (Fig. 7.23) is shorter than the length of the constant velocity zone (Zone 1).[5,57,58]

From Tolmin's theory and experimental data (e.g., Reichardt[59]) the relationship between velocity profile and temperature profile in the jet cross-section can be expressed using an overall turbulent Prandtl number $\mathrm{Pr} = \nu_t/\alpha_t$, where ν_t is a turbulent momentum exchange coefficient and α_t is a turbulent heat exchange coefficient:

$$\frac{v}{v_x} = \left(\frac{\theta - \theta_\infty}{\theta_x - \theta_\infty}\right)^{1/\mathrm{Pr}} \tag{7.66}$$

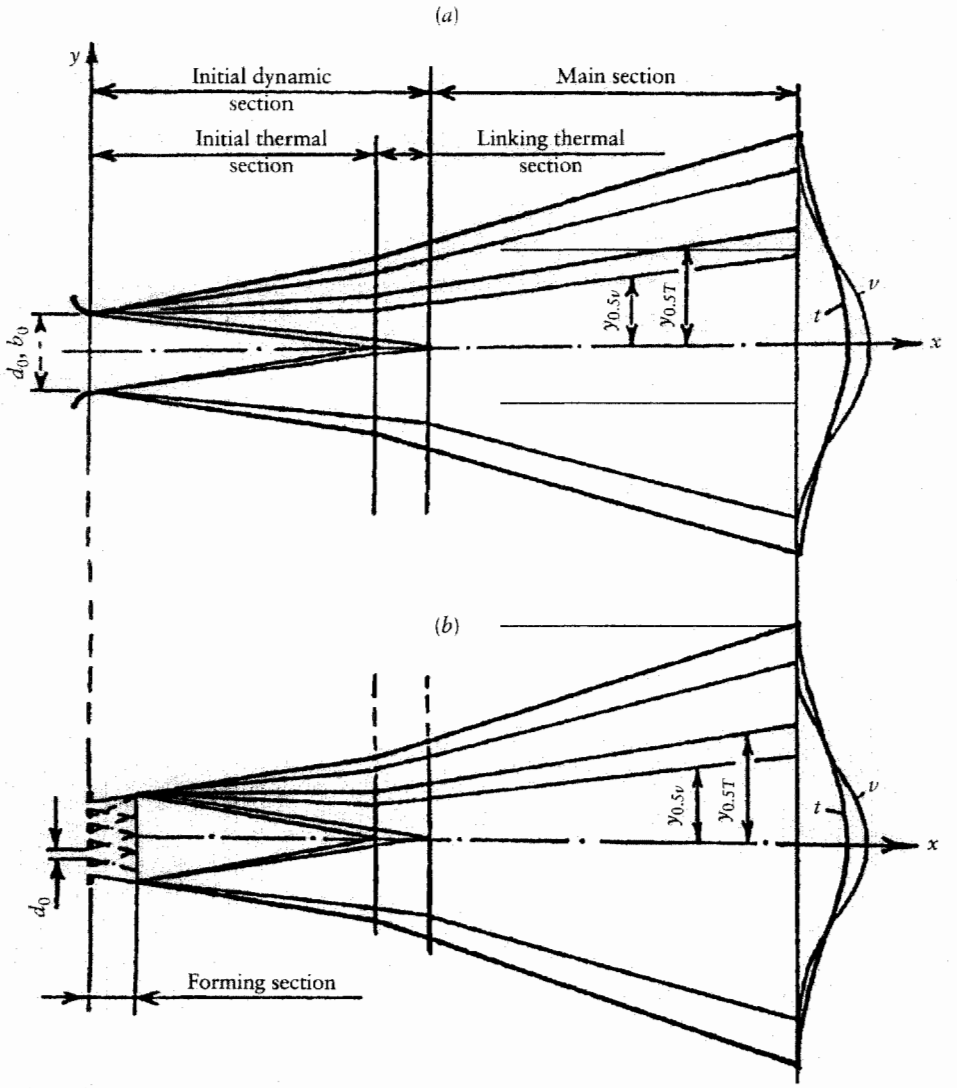

FIGURE 7.23 Schematic of a jet: (*a*) from an open outlet (*b*) from a louvered (perforated) outlet. [56]

where θ is the air temperature at the point of consideration, and θ_x is the maximum air temperature in the cross-section of the jet.

A Prandtl number of 0.7 has been suggested for nonisothermal jets by Nottage,[60] Forstall and Shapiro,[61] Corrsin and Uberoi,[62] and Grimitlyn.[63] Abramovich[3] suggested a Prandtl number for a compact jet of 0.75, and for a linear jet, 0.5.

According to Abramovich,[57] Regenscheit,[64] and Shepelev,[4] the relation between the velocity distribution and the temperature distribution in the cross-section of nonisothermal compact, linear, or radial jets within Zone 3 can be expressed as

$$\frac{\Delta_\theta}{\Delta_{\theta x}} = (\theta - \theta_\infty)/(\theta_x - \theta_\infty) = \sqrt{\frac{v}{v_x}}, \tag{7.67}$$

and thus the Prandtl number is equal to 0.5. Table 7.14 lists some temperature profile equations as they are used for practical applications.

7.4.4.3 Centerline Temperature Differential in a Horizontally Supplied Jet

Compact Jet

The centerline temperature differential within the zone of fully established turbulent flow (Zone 3) of a nonisothermal jet can be derived using equations of momentum (Eq. (7.39)) and excessive heat conservation along the jet:[3,4,58]

$$W_0 = 2\pi C_p \rho_\infty \int_0^{y^*} V(\theta - \theta_\infty) y \, dy, \tag{7.68}$$

where $W_0 = c_p \rho_\infty v_0 (\theta_0 - \theta_\infty) A_0$ = excessive heat in supplied air, and C_p = specific heat of air.

The equation for the centerline temperature differential in Zone 3 of the compact jet derived[4] from Eq. (7.61) using the Gauss error-function temperature profile (Table 7.14) is

$$\Delta\theta_x = \frac{1+\sigma}{2\sqrt{\pi}c} \frac{W_0}{C_p \rho_\infty} \frac{1}{\sqrt{M_0/\rho_\infty}} \frac{1}{x}. \tag{7.69}$$

Equation (7.69) also can be presented as follows:

$$\Delta\theta_x = \frac{(1+\sigma)\theta}{2\sqrt{\pi}c\varphi} \frac{\Delta\theta_0 \sqrt{A_0}}{x}, \tag{7.70}$$

where

$$\Delta\theta_x = T_0 - T_\infty = \frac{W_0}{C_p \rho_0 Q_0}. \tag{7.71}$$

The complex of coefficients having constant value $(1+\sigma)\theta / 2\sqrt{\pi}\, c\phi$ is called[4] the thermal characteristic of the diffuser jet, K_2, and characterizes the temperature decay along the air jet. Assuming perfect mixing in the room (i.e., $\theta_{oz} \approx \theta_\infty$), θ_∞ can be substituted for θ_{oz}, and Eq. (7.70) can be presented as follows:

$$\frac{\theta_x - \theta_{oz}}{\theta_0 - \theta_{oz}} = K_2 \frac{\sqrt{A_0}}{x}. \tag{7.72}$$

As in the case of equations for the velocity decay computation, in the equations for the temperature decay computation, some researchers consider x to be a distance starting from some virtual source located at some distance x_0 from the diffuser face; others for practical reasons neglect x_0.

As in the case of the K_1 characteristic, theoretical values of characteristic K_2 depend upon supply conditions. According to Shepelev,[4] in the case of air supply through a nozzle with a uniform outlet velocity profile, $K_2 \times K_1 = (1 + \mathrm{Pr})/(2\pi 0.082^2)$. Thus, when $K_1 = 6.88$ and $\mathrm{Pr} = 0.7$, $K_2 = 5.85$. Grimitlyn[1] suggests the following relation between K_2 and K_1 coefficients:

$$K_2 = \sqrt{\frac{1+\mathrm{Pr}}{2}} K_1. \tag{7.73}$$

According to Helander's unpublished data (Progress Report, Downward Projection of Heated Air, January 6, 1951, referenced by Koestel[58]), $K_2 = 6$.

TABLE 7.14 Temperature Profile Equations

	$\frac{\theta - \theta_\infty}{\theta_x - \theta_\infty}$		
Author	**Round jet**	**Linear jet**	**Radial jet**
Shepelev[4]	$e^{-\frac{1}{4}\left(\frac{y}{0.082x}\right)^2}$	$e^{-\frac{1}{4}\left(\frac{y}{0.1x}\right)^2}$	$e^{-\frac{1}{4}\left(\frac{y}{0.1x}\right)^2}$
Grimitlyn[1]	$e^{-0.7\,(y/y_{0.5t})^2}$ $y_{0.5t} = x \tan \alpha_{0.5t} = x\frac{tg\ \alpha_{0.5v}}{\sqrt{\mathrm{Pr}}}$	$e^{-0.7\,(y/y_{0.5t})^2}$ $y_{0.5t} = x \tan \alpha_{0.5t} = x\frac{tg\ \alpha_{0.5v}}{\sqrt{\mathrm{Pr}}}$	$e^{-0.7\,(y/y_{0.5t})^2}$ $y_{0.5t} = x \tan \alpha_{0.5t} = x\frac{tg\ \alpha_{0.5v}}{\sqrt{\mathrm{Pr}}}$
Abramovich[23]	$(1 - r/\delta^{3/2})^{1.4}$	$(1 - y/\delta^{3/2})$	—

Linear Jet

Derivation of the equation for the centerline temperature differential in a linear jet is based on the same principles that are used in the case of a compact jet. For the linear diffuser jet, centerline temperature differential can be computed from the following equation:

$$\frac{\theta_x - \theta_{oz}}{\theta_0 - \theta_{oz}} = K_2 \sqrt{\frac{H_0}{x}}. \tag{7.74}$$

The centerline temperature differential in Zone 3 of the diffuser jet is proportional to the value of the K_2 coefficient, which, along with the K_1 coefficient, depends upon jet and diffuser types and supply conditions. The theoretical value of the K_2 coefficient, according to Shepelev,[4] is 2.49. Experimental data reported by Grimitlyn[1] show K_2 to be 2.0.

Radial Jet

Equations for the centerline temperature differential in radial and in conical jets (Fig. 7.21) is derived in the same way as for compact and linear jets[4] and is similar to Eq. (7.70):

$$\frac{\theta_x - \theta_\infty}{\theta_0 - \theta_\infty} = \sqrt{\frac{1 + \Pr}{4\sqrt{\pi} c \sin\alpha}} \frac{\theta}{\varphi} \frac{1}{\sqrt{\beta}} \sqrt{\frac{A_0}{x}} \tag{7.75}$$

The complex of parameters

$$\sqrt{\frac{1 + \Pr}{4\sqrt{\pi} c \sin\alpha}} \frac{\theta}{\varphi} \frac{1}{\sqrt{\beta}} \tag{7.76}$$

is a thermal characteristic, K_2. In the case of a radial jet $\beta = 2\pi$ and $\alpha = 90°$. Assuming $\theta = 1$, $\varphi = 1$, $c = 0.082$, and $\Pr = 0.5$, $K_2 = 1$. For conical jet with $\alpha = 60°$ ($\beta = 2\pi$, $\theta = 1$, $\varphi = 1$, $c = 0.082$, and $\Pr = 0.5$), $K_2 = 1.07$. Table 7.15 lists some equations used for centerline temperature differential computation in horizontal jets.

According to Shepelev,[42] the theoretical values of the K_2/K_1 ratio for air supply through nozzles with uniform velocity distribution at the outlet cross-section is 0.9 for compact jets and 0.95 for radial, conical, and linear jets. Practically, for different types of air diffusers, this ratio can vary from 0.7 to 3.0.

7.4.4.4 Universal Equations for Temperature Difference Computation along Jets Supplied from Outlets with Finite Dimensions

Shepelev and Gelman[52] and Regenscheit[53] computed air temperature along the first three zones of jets supplied from outlets with finite size using the method of superposition of the multiple-jet system. These jets originate from the points with supply air velocity equal to the average air velocity at the outlet.

Along with principles described in Section 7.4.3, this approach utilizes the following equations describing temperature distribution in a compact jet and a heat flux at a given point (x, y, z):

$$\frac{\theta - \theta_\infty}{\theta_0 - \theta_\infty} = \frac{1 + \Pr}{2 \times 0.082\sqrt{\pi}} \frac{\sqrt{A_0}}{x} e^{-\frac{\Pr}{2}\left(\frac{r}{0.082x}\right)^2} \tag{7.77}$$

$$\frac{\nu(\theta - \theta_\infty)}{\nu_0(\theta_0 - \theta_\infty)} = \frac{1 + \Pr}{2\pi 0.082^2} \frac{A_0}{x^2} e^{-\frac{1 + \Pr}{2}\left(\frac{r}{0.082x}\right)^2}. \tag{7.78}$$

TABLE 7.15 Centerline Temperature Differential in Horizontal Jets

	$\frac{\theta - \theta_\infty}{\theta_x - \theta_\infty}$		
Author	**Round jet**	**Linear jet**	**Radial jet**
Shepelev[4] Grimitlyn[22]	$K_2\frac{\sqrt{A_0}}{x}$	$K_2\frac{\sqrt{H_0}}{x}$	$K_2\frac{1}{\sqrt{\beta \sin \alpha}}\frac{\sqrt{A_0}}{x}$ $K_2\frac{\sqrt{A_0}}{x}$
Abramovich[57]	$\frac{0.7}{\frac{ax}{R_0}+0.29}$ $a = 0.66\text{–}0.76$	$\frac{1.04}{\sqrt{\frac{ax}{B_0}}+0.41}$ $a = 0.09\text{–}0.12$	—
Koestel[58]	$5.35\frac{D}{x}$	—	—
Baturin[54]	$\frac{9.24R_0}{x-x_0}\sqrt{\frac{\theta_\infty}{\theta_0}}$	$3.27\sqrt{\frac{B_0}{x}\sqrt{\frac{\theta_\infty}{\theta_0}}}$	$3.27\sqrt{\frac{R_0}{(x-x_0)\left(1+\frac{x}{x_c}\right)}\sqrt{\frac{\theta_\infty}{\theta_0}}}$

The heat flux through the finite element dA of the jet cross-section at the distance x from the outlet can be calculated as

$$\frac{d[v(\theta-\theta_\infty)]}{v_0(\theta_0-\theta_\infty)} = \frac{1+\mathrm{Pr}}{2\pi 0.082^2}\frac{dA_0}{x^2}e^{-\frac{1+\mathrm{Pr}}{2}\left(\frac{r}{0.082x}\right)^2}. \tag{7.79}$$

The double integral of Eq. (7.79) across the outlet area $2A \times 2B$ results in the following equation for a heat flux through a given point of a jet supplied through a rectangular outlet:

$$\frac{v_{xyz}(\theta_{xyz}-\theta_\infty)}{v_0(\theta_0-\theta_\infty)} = \frac{1}{4}\left(\mathrm{erf}\sqrt{\frac{1+\mathrm{Pr}}{2}}\frac{y+A}{0.082x} - \mathrm{erf}\sqrt{\frac{1+\mathrm{Pr}}{2}}\frac{y-A}{0.082x}\right)$$
$$\times\left(\mathrm{erf}\sqrt{\frac{1+\mathrm{Pr}}{2}}\frac{z+B}{0.082x} - \mathrm{erf}\sqrt{\frac{1+\mathrm{Pr}}{2}}\frac{z-B}{0.082x}\right). \tag{7.80}$$

Joint solution of Eqs. (7.68) and (7.80) results in the following equation for the temperature differential along the jet axis:

$$\frac{\theta_{xyz}-\theta_\infty}{\theta_0-\theta_\infty} = \frac{\mathrm{erf}\sqrt{\frac{1+\mathrm{Pr}}{2}}\frac{A}{0.082x}\,\mathrm{erf}\sqrt{\frac{1+\mathrm{Pr}}{2}}\frac{B}{0.082x}}{\sqrt{\mathrm{erf}\frac{A}{0.082x}\,\mathrm{erf}\frac{B}{0.082x}}}. \tag{7.81}$$

In the case when air is supplied through a slot with a width $2B$ ($A = \infty$), Eq. (7.81) can be converted into

$$\frac{\theta_{xyz}-\theta_\infty}{\theta_0-\theta_\infty} = \frac{\mathrm{erf}\sqrt{\frac{1+\mathrm{Pr}}{2}}\frac{B}{0.082x}}{\sqrt{\mathrm{erf}\frac{B}{0.082x}}}. \tag{7.82}$$

Velocities and Temperatures in Vertical Nonisothermal Jets

Studies by Helander et al.,[65–68] Knaak,[69] Koestel,[58] Shepelev,[4] Regenscheit,[70] and Grimitlyn[5] resulted in equations for downward and upward projected diffuser jets.

For the circular jet, Regenscheit[70] obtained empirical equations for the maximum velocity in the downward and upward vertical jets of heated and cooled air. For a compact (round) jet,

$$\frac{v_x}{v_0} = \frac{m\sqrt{A_0}}{x} \pm \sqrt{\frac{\mathrm{Ar}_0}{m}\left[1 + \ln\frac{2x}{m\sqrt{A_0}}\right]}, \tag{7.83}$$

where m = parameter characterizing the diffuser jet (m from 0.1 to 0.3). For a linear jet,

$$\frac{v_x}{v_0} = \sqrt{\frac{H_0}{x}} \pm \sqrt{\frac{\mathrm{Ar}_0}{0.2}\left(2.83\sqrt{\frac{x}{H_0}} - 1\right)}. \tag{7.84}$$

Based on theoretical analyses, Koestel,[58] Shepelev,[4] and Grimitlyn[5] developed equations for velocities and temperatures in vertical heated and chilled air jets. The assumptions used by these authors are similar, and the method used is described in Koestel.[58] The assumptions used in the analysis can be summarized as follows:

1. The jet of warmed or cooled air is projected into an unbounded atmosphere of still air of uniform temperature.
2. The only force opposing the downward flow of the heated air or upward flow of the cooled air is a buoyancy force. In their analysis, Helander and Jakowatz[65] also suggested accounting for inertial forces due to the entrainment of room air. However, this suggestion is not in an agreement with a principle of momentum conservation used in most of the existing models for isothermal jets.
3. The air entrained by the jet has room air temperature.
4. A velocity profile and a temperature difference profile have shapes that can be approximated by an error-function type curve.

For practical use the influence of buoyancy forces on temperature and velocity decay in vertical nonisothermal jets, as proposed by Grimitlyn,[56] can be accounted for by the coefficient K_n of nonisothermality. For compact jets,

$$\frac{v_x}{v_0} = K_1\frac{\sqrt{A_0}}{x}K_n \tag{7.85}$$

$$\frac{\theta_x - \theta_{oz}}{\theta_0 - \theta_{oz}} = K_2\frac{\sqrt{A_0}}{x}\frac{1}{K_n}, \tag{7.86}$$

where K_n for a compact jet can be computed as

$$K_n = \sqrt[3]{1 \pm 2.5\frac{K_2}{K_1^2}\mathrm{Ar}_0\left(\frac{x}{\sqrt{A_0}}\right)^2}. \tag{7.87}$$

For linear jets,

$$\frac{v_x}{v_0} = K_1\sqrt{\frac{H_0}{x}}K_n, \tag{7.88}$$

$$\frac{\theta_x - \theta_{oz}}{\theta_0 - \theta_{oz}} = K_2 \sqrt[3]{\frac{H_0}{x}} \frac{1}{K_n}, \tag{7.89}$$

where

$$K_n = \sqrt[3]{1 \pm 1.8 \frac{K_2}{K_1^2} \mathrm{Ar}_0 \left(\frac{x}{H_0}\right)^{1.5}}. \tag{7.90}$$

By applying the Ar_x criterion, Eqs. (7.87) and (7.90) can be transformed into

$$K_n = \sqrt[3]{1 \pm a\mathrm{Ar}_x}, \tag{7.91}$$

where $a = 2.5$ for axially symmetric and incomplete radial jets and $a = 1.8$ for linear jets. The plus sign in Eq. (7.91) corresponds to the situation when the directions of buoyancy and inertia forces coincide, whereas the minus sign corresponds to their counteraction. This equation can be used for vertical nonisothermal jets at $\mathrm{Ar}_x \leq 0.25$.

Nonisothermal Jet Throw

The throw of downward-projected heated jets or upward-projected chilled jets can be derived from Eqs. (7.85) and (7.88) for K_n equal to some value, e.g., 0.1. Helander and Jakowatz,[65] in their work on heated jets projected downward, have called attention to some of the differences between the actual conditions and those assumed for analysis. One of these is the radial escape of warm air in the terminal zone of a hot stream projected downward. This escaping warm air then rises and causes a change in ambient conditions for the upper part of the jet. The terminal zone and the edges of the jet are zones of marked instability, with definite surges and fluctuations, so that the jet envelope is very difficult to define or to determine experimentally. In the closure to the paper presented by Knaak,[69] Dr. Helander suggested that from the point of view of practical application, the distance to the beginning of the unstable, terminal zone of the jet is about 80% of the jet throw.

The data from Baturin and Shepelev,[71] Helander et al.,[66] Regenscheit,[64] Turner,[72] Shepelev,[4] Seban et al.,[73] Sato et al.,[74] Grimitlyn,[56] Mizuchina,[75] and Weidemann and Hanel[76] show that maximum downward/upward travel of heated/cooled compact jets can be evaluated using the equation

$$\frac{z_{\max}}{\sqrt{A_0}} = \frac{a}{\sqrt{\mathrm{Ar}_0}}, \tag{7.92}$$

where the coefficient a varies between 1.59 and 2.57 with a mean value of $a = 1.8 \pm 0.3$.

Considering that most of the data were obtained using round nozzles with jet characteristics close to ideal discharge conditions ($K_1 = 6.88$, $K_2 = 5.85$), Eq. (7.92) can be presented as[56]

$$\frac{z_{\max}}{D} = \frac{0.63 K_1}{\sqrt{K_2 \mathrm{Ar}_0}}. \tag{7.93}$$

The throw of downward-projected heated linear jets or upward-projected chilled air jets can be calculated as[56]

$$\frac{z_{\max}}{D} = \frac{0.67 K_1^{4/3}}{(K_2 \mathrm{Ar}_0)^{2/3}}. \tag{7.94}$$

Trajectory of Horizontal and Inclined Jets

Buoyancy forces influence the trajectory of horizontally projected air jets or air jets supplied at some angle to the horizontal plane (Fig. 7.24). Most nonisothermal air jet studies were devoted to horizontally projected compact air jets. Based on the analytical studies,[3,42,77–80] the trajectory axis of inclined jets can be described by a polynomial function

$$\frac{z}{\sqrt{A_0}} = \Psi \frac{K_2}{K_1^2} \mathrm{Ar}_0 \left(\frac{x}{\sqrt{A_0}} \right)^3. \tag{7.95}$$

Similar equations were suggested by experimental studies.[81–83] Some authors determine the trajectory axis from equations of another kind—parabola, for example.[84,85]

In some studies on inclined air jets, the equation for the trajectory differs from Eq. (7.95) by the additional term as follows:

$$\frac{z}{\sqrt{A_0}} = \frac{x}{\sqrt{A_0}} tg\alpha_0 \pm \Psi \frac{K_2}{K_1^2} \mathrm{Ar}_0 \left(\frac{x}{\sqrt{A_0}} \right)^3. \tag{7.96}$$

Taliev[86] and Schneider[87] derived the equations for the trajectories by numerical methods. Experimental data for the trajectory of the inclined jet ($\alpha_0 \neq 0$) were obtained only by Fleishbacker and Schneider.[80]

As was shown by Zhivov,[88] the main difference in most of the equations for the jet trajectory is the value of the coefficient ψ. The differences in experimental data obtained by different authors are mainly due to the difficulties in the measurements of nonisothermal air jets supplied with low initial velocities (2–10 m/s). There is also a different understanding of the term "air jet trajectory." Some authors mean the points with maximum velocity values, while others mean the centers of gravity of the cross-sections of the jet.

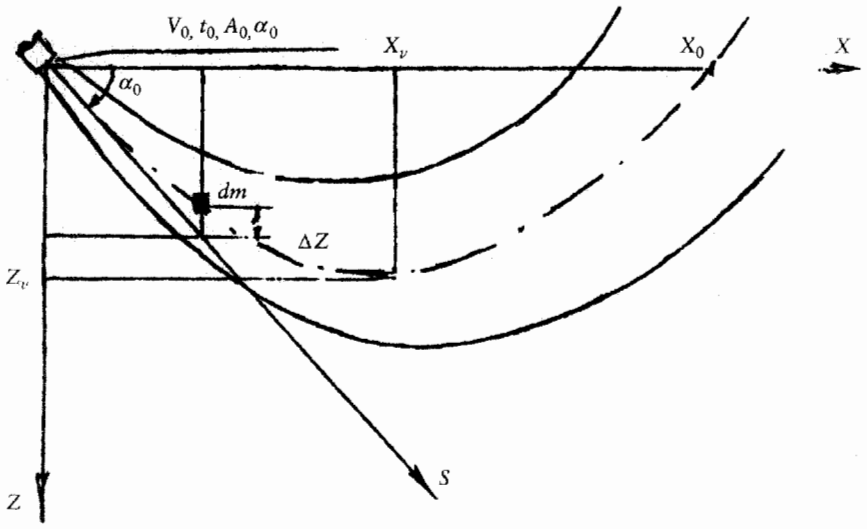

FIGURE 7.24 Schematic of an inclined jet.

The analytical method of jet trajectory study developed by Shepelev[4] allows the derivation of several other useful features and is worth describing. On the schematic of a nonisothermal jet supplied at some angle α_0 to the horizon (Fig. 7.25), S is the jet's axis, X is the horizontal axis, and Z is the vertical axis. The ordinate of the trajectory of this jet can be described as $z = xtg\alpha + \Delta z$, where Δz is the jet's rise due to buoyancy forces. To evaluate Δz, the elementary volume dW with a mass equal to $dm = \rho_s dV$ on the jet's trajectory was considered. The buoyancy force influencing this volume can be described as $dP = g(\rho_\infty - \rho_s)$. Vertical acceleration of the volume under the consideration is $j = dP/dm = g(\rho_\infty - \rho_s)/\rho_s \approx g(T_s - T_\infty)/T_s$. Vertical acceleration can be presented with the help of the vertical velocity component $j = dV_z/d\tau$, where the time interval $d\tau$ can be described as dS/V_s. Based on these equations, the vertical component of air velocity can be presented as

$$v_z = \frac{g}{T_\infty}\int_0^s \frac{T_s - T_\infty}{v_s} dS. \qquad (7.97)$$

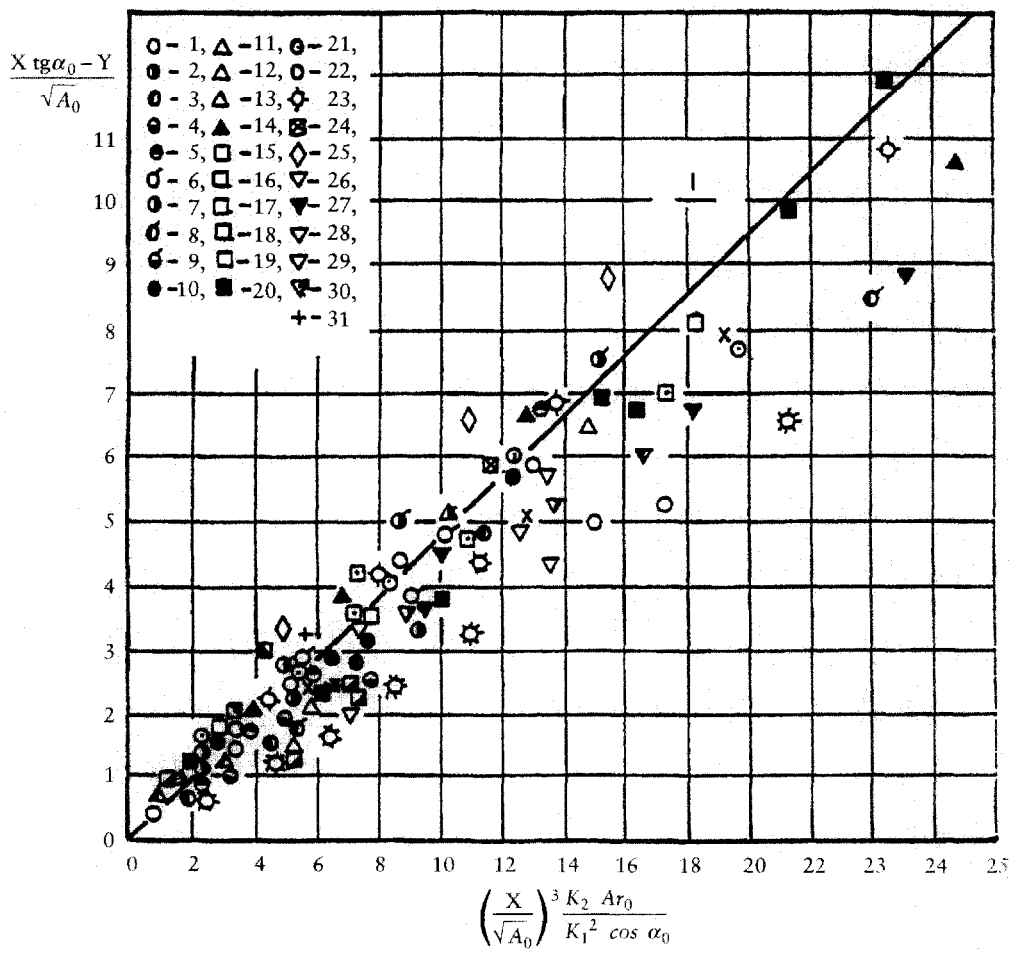

FIGURE 7.25 Experimental evaluation of the coefficient ψ. Reproduced from Zhivov.[88]

The ratio of local temperature difference and velocity on the jet's axis in Eq. (7.97) can be substituted by

$$\frac{T_s - T_\infty}{v_s} = \frac{K_2}{K_1}\frac{g}{T_\infty}\frac{T_0 - T_\infty}{v_0}, \tag{7.98}$$

resulting in

$$v_z = \frac{K_2}{K_1}\frac{g}{T_\infty}\frac{T_0 - T_\infty}{v_0}S. \tag{7.99}$$

Considering that $v_z = dz/d\tau$, $v_z/v_s = dz/dS$ and $v_s = K_1 v_0\sqrt{A_0}/S$, the equation for calculating Δz can be rewritten as

$$\Delta z = \frac{K_2}{K_1}\frac{g}{T_\infty}\frac{T_0 - T_\infty}{v_0}\int_0^s \frac{S\,dS}{v_S} \tag{7.100}$$

or

$$\Delta z = \frac{K_2 g(T_0 - T_\infty)}{3K_1^2 T_\infty v_0^2\sqrt{A_0}}S^3. \tag{7.101}$$

Substituting $x\cos\alpha_0$ for S, and Ar_0 for the complex of parameters, the resulting equation for the trajectory is

$$z = x\,tg\alpha_0 \pm \frac{1}{3}\frac{K_2}{K_1^2}\mathrm{Ar}_0\left(\frac{x}{\cos\alpha_0}\right)^3. \tag{7.102}$$

When a chilled air jet is supplied at the angle α_0 upward, it will cross the level of the supply outlet at the distance x_0. This distance can be calculated by substituting $z = 0$ in Eq. (7.102):

$$x_0 = \frac{\sqrt{3}K_1\cos\alpha_0\sqrt{\sin\alpha_0}}{\sqrt{K_2\mathrm{Ar}_0}}. \tag{7.103}$$

The abscissa and ordinate of the jet vortex in the case of upward inclined cold air jet supply or downward inclined warm air supply were derived from Eq. (7.103):

$$x_v = \frac{K_1\cos\alpha_0\sqrt{\sin\alpha_0}}{\sqrt{K_2\mathrm{Ar}_0}} \tag{7.104}$$

$$z_v = \frac{2}{3}\frac{K_1(\sin\alpha_0)^{3/2}}{\sqrt{K_2\mathrm{Ar}_0}}. \tag{7.105}$$

The ratio x_v to z_v depends only on $tg\alpha_0$: $z_v/x_v = 2/3\ tg\alpha_0$, and the ratio of x_v/x_0 has a constant value equal to 0.578. To clarify the trajectory equation of inclined jets for the cases of air supply through different types of nozzles and grills, a series of experiments were conducted.[88] The trajectory coordinates were defined as the points where the mean values of the temperatures and velocities reached their maximum in the vertical cross-sections of the jet. It is important to mention that, in such experiments, one meets with a number of problems, such as deformation of temperature and velocity profiles and fluctuation of the air jet trajectory, which reduce the accuracy in the results. The mean value of the coefficient Ψ obtained from experimental data (Fig. 7.25) is 0.47 ± 0.06. Thus the trajectory of the nonisothermal jet supplied through different types of outlets can be calculated from

$$\frac{z}{\sqrt{A_0}} = \frac{x}{\sqrt{A_0}}tg\alpha_0 \pm 0.47\frac{K_2}{K_1^2}\mathrm{Ar}_0\left(\frac{x}{\sqrt{A_0}}\right)^3. \tag{7.106}$$

The accuracy of this value is sufficient (Fig. 7.26) to be used in designing the trajectory of inclined ventilation jets at an angle $\alpha_0 \leq \pm 45°$. Using the experimental value of the coefficient, the equation for the vortex abscissa x_v can be presented as follows:

$$x_v = \frac{\cos\alpha_0 \sqrt{|\sin\alpha_0|}\sqrt{A_0}}{\sqrt{3 \times 0.47(K_1/K_2^2)\mathrm{Ar}_0}}. \tag{7.107}$$

However, this clarification does not affect the ordinate-to-abscissa ratio, which remains equal to 0.578.

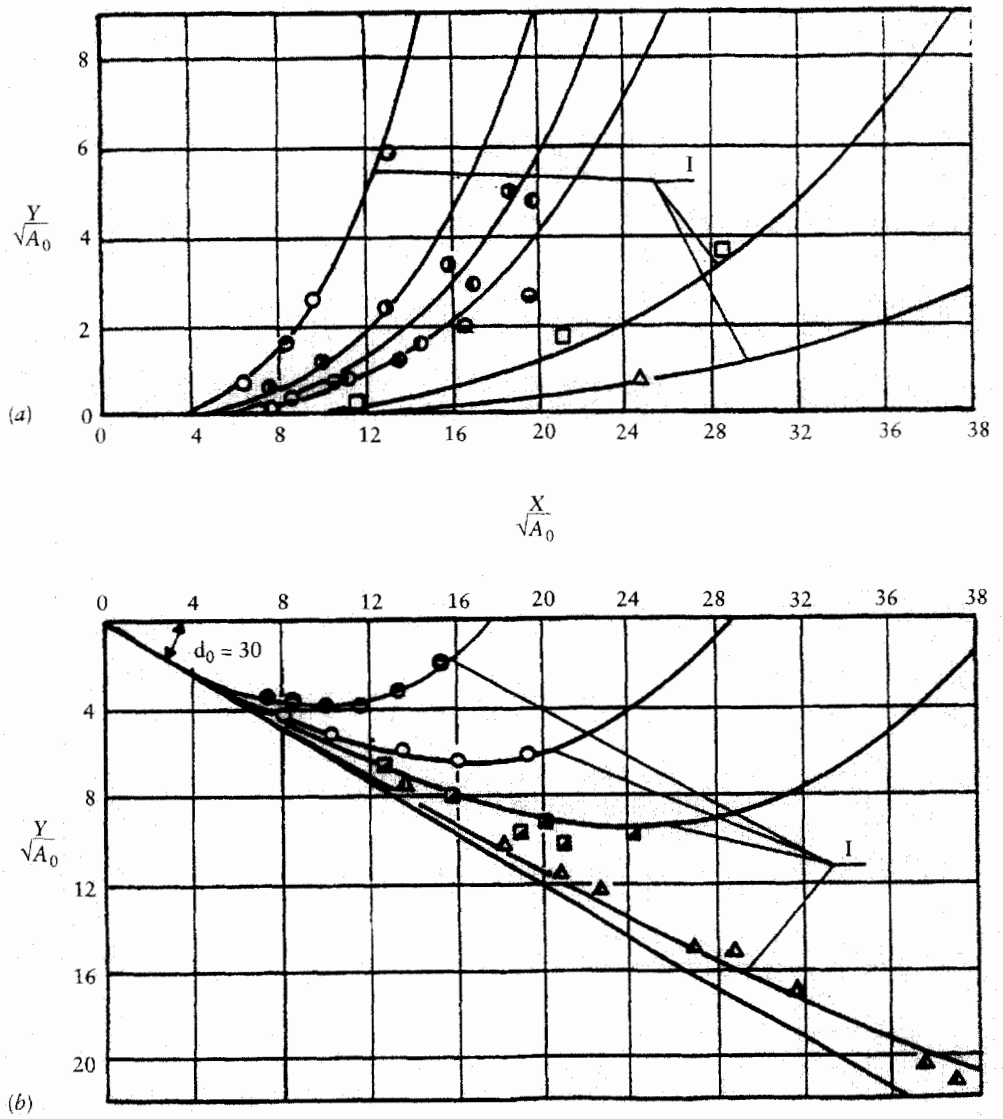

FIGURE 7.26 Trajectory of a nonisothermal jet supplied at an angle: (*a*) – $\alpha_0 = 30°$; 1 – equation (7.106). Reproduced from Zhivov.[88]

For the nonisothermal linear air jet, the trajectory equation is derived by Shepelev[4] is

$$\frac{z}{H_0} = \frac{x}{H_0} tg\alpha_0 \pm 0.4 \frac{K_2}{K_1^2} \mathrm{Ar}_0 \left(\frac{x}{H_0}\right)^{5/2}. \tag{7.108}$$

7.4.4.5 Jet Attachment

Jets discharging close to the plane of the ceiling or wall are common in ventilation practice. The presence of an adjacent surface restricts air entrainment from the side of this surface. This results in a pressure difference across the jet, which therefore curves toward the surface. The curvature of the jet increases until it attaches to the surface. This phenomenon is usually referred to as a Coanda effect. The attached jet or, as it is commonly called, wall jet, can result from air supply through an outlet with one edge coincident with the plane of the wall or ceiling (Fig. 7.27). Jets supplied at some distance from the surface or at some angle to the surface can also become attached (Fig. 7.28)

The results of studies by Kerka of jets supplied through rectangular outlets[2] with and without an adjacent surface indicate an increase of 1.27 to 1.45 times in the velocity decay coefficient for wall jets compared with free jets from the same outlets. The angle of divergence of the wall jet in the direction perpendicular to the wall was slightly less than one-half of a free jet, while the angle of spread of the jet along the wall was greater than the divergence of a free jet.

The results of experimental studies of compact wall jets by Mitkalinny,[91] Abdushev, Baharev, and Fedorov; on linear wall jets by Kerka and Sakipov; and on radial wall jets by Gelman are summarized by Grimitlyn[1] and presented in

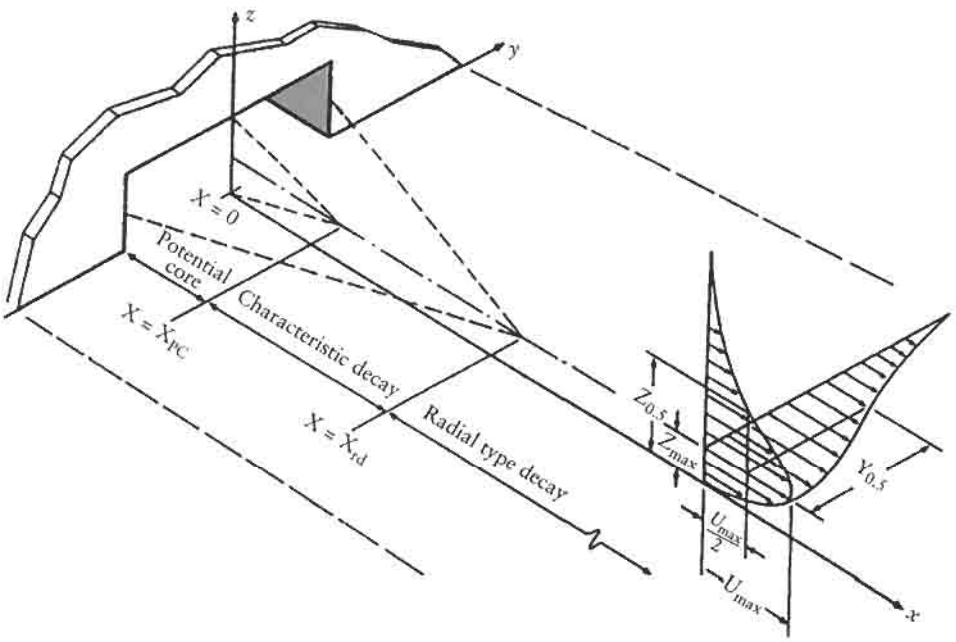

FIGURE 7.27 Three-dimensional wall jet. Reproduced from Etheridge and Sandberg.[81]

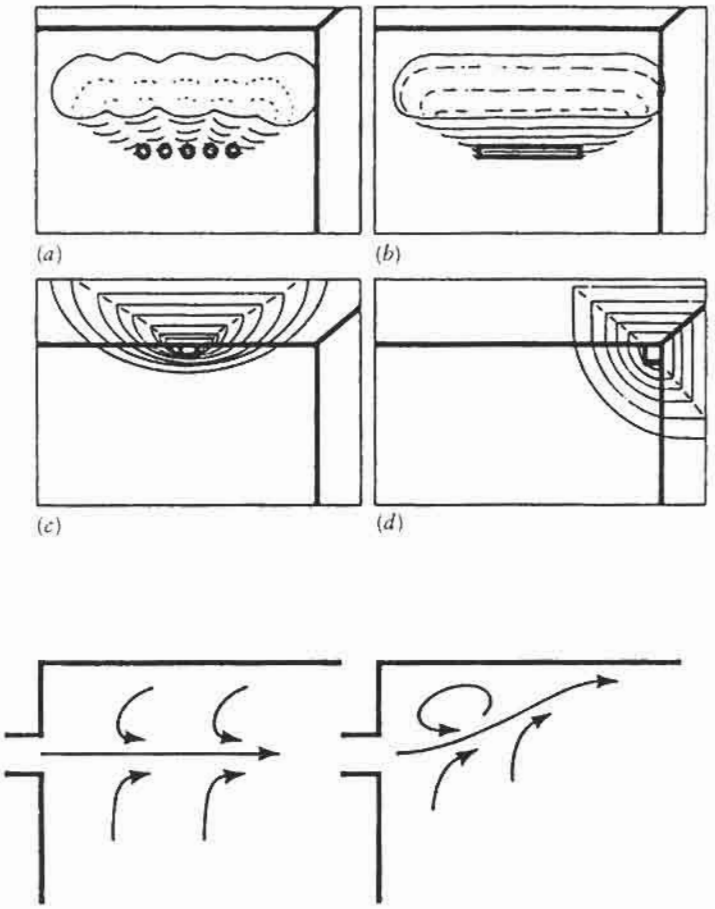

FIGURE 7.28 Jet attachment with air supply through outlets located at some distance from the surface: (*a*) multiple jets; (*b*) long slot jet; (*c*) rectangular jet; (*d*) rectangular corner jet; (e) general schematic. Reproduced from Nielsen[90].

Fig. 7.29. These data indicate that the parameter $K^{wall} = K_1{}^{wall}/K_1$ reflecting the influence of the wall on the velocity decay along the jet increases from 1 to 1.4 with distance from the outlet. For a compact jet $K^{wall} = 1$ when $x < 5d_0$; for a linear jet K^{wall} reaches its maximum value of 1.4 only at $x < 20b_0$, where b_0 is an outlet width.

Studies of wall jets[54,55] show that they have two layers: a turbulent boundary layer close to the wall and an outer shear layer. The thickness of the boundary wall layer can be neglected for practical purpose. Accordingly, to compute the maximum velocity in the wall jet, researchers[42,64,89] apply the method of images by treating the wall jet as one-half of a free jet. Application of this method gives a relationship between the characteristics of a wall jet and a free jet, which results in a correction factor equal to $\sqrt{2}$. This approach has some inaccuracy even with linear and radial jets. in a For a three-dimensional wall jet, the procedure is even more approximate. Discussion by Etheridge and Sandberg[89] of some previous studies of attached jets indicates some loss of momentum in an attached jet due to the friction against the surface. The authors compiled information from previous stud-

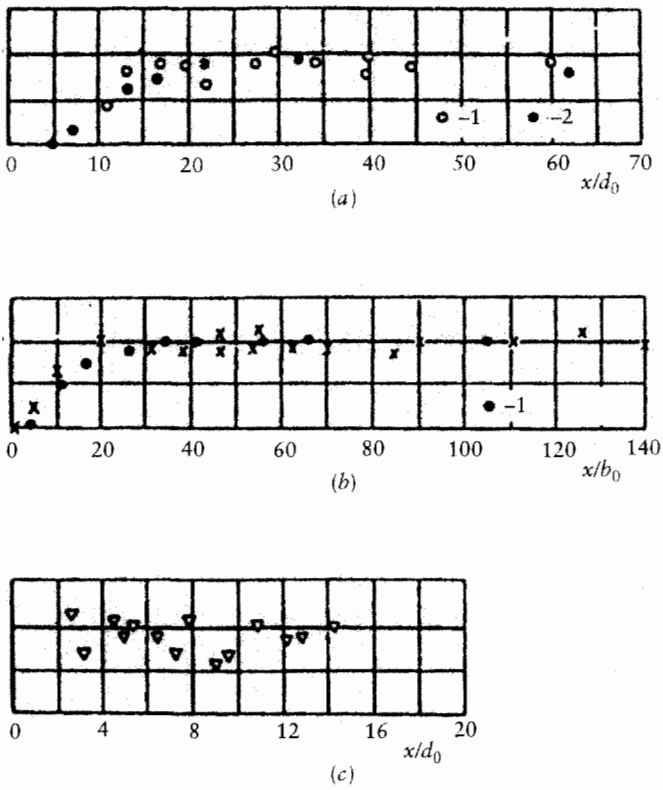

FIGURE 7.29 Correction parameter K_{wall} reflecting the influence of the wall: (*a*) compact jets (experimental data from V. Mitkalinny, A. Abdushev, V. Baharev and L. Fedorov); (*b*) linear jets (experimental data from W. Kerka and Z. Sakipov); (*c*) radial jets (experimental data from N. Gelman). Reproduced from Grimitlyn.[56]

ies, which is summarized in Table 7.16. According to the equations presented in Table 7.16, the maximum velocity in a wall jet is inversely proportional to the distance from the outlet in a different power compared to a free jet.

It is not uncommon to supply air into the room with jets attached both to the ceiling and to the wall surfaces.[1,90] Air jets can be parallel to both surfaces or be directed at some angle to one or both surfaces (Fig. 7.28). Studies of compact wall jets supplied parallel to both surfaces reported by Grimitlyn[1] show that the correction factor value is in the range from 1.6 to 1.7, which means that restriction of entrainment from two sides reduces velocity decay by 20% to 30% compared to the case of a wall jet.

When a jet is supplied at some distance from the surface, the attachment occurs when the distance between the outlet and the surface is below a critical distance; otherwise the jet will propagate as a free jet.[97] If the jet attaches to the surface, the flow downstream of the attached point is similar to that of a wall jet. For a compact isothermal jet, the critical distance for jet attachment to the surface is $L_{crit} = 6A_0^{1/2}$.[98] For $L_{crit} < 6A_0^{1/2}$ the velocity decay coefficient K_1

TABLE 7.16 Maximum Velocity Decay in Wall Jets

Type of jet		Decay of the maximum velocity	Reference
Linear wall jet		$\sim x^{-0.555}$	Schwarz and Cosart[92]
		$\sim x^{-0.375}$	Regenscheit[64]
Radial wall jet		$\sim x^{-1.12}$	Bakke[93]
		$\sim x^{-1.15}$	Waschke[94]
Rectangular wall jet	$H_0/L = 0.025$	$\sim x^{-1.15}$	Sforza and Herbst[95]
	$H_0/L = 0.05$	$\sim x^{-1.09}$	
	$H_0/L = 0.01$	$\sim x^{-1.15}$	
	$H_0/L = 1.0$	$\sim x^{-1.14}$	
Compact wall jet		$\sim x^{-1}$	Nielsen[96]

becomes greater than it would be in the case of free jet, and should be corrected using correction factor F (see Fig. 7.30) to compensate for surface proximity.

The length of the recirculation zone, x_a, for a linear jet (the distance to the point of jet attachment to the surface) was studied by Sawyer,[99] Miller and Comings,[36] and Bourque and Newman.[100] The results of these studies, summarized in Awbi,[97] show that the length of the recirculation zone (Fig. 7.31) is proportional to the distance from the outlet to the surface and can be described as

$$x_a/H_0 = 0.73(D/H_0) - 2.3, \tag{7.109}$$

where H_0 is the width of the outlet.

Sandberg et al.[101] conducted similar tests with a heated linear jet so that the buoyancy forces opposed the forces due to the lower pressure in the circulation zone (bubble). Based on the results of these tests, it was concluded that

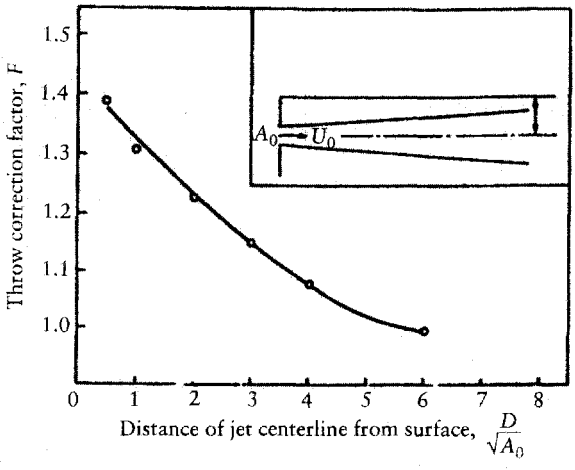

FIGURE 7.30 Correction factor F for surface proximity. Reproduced from Farquharson.[98]

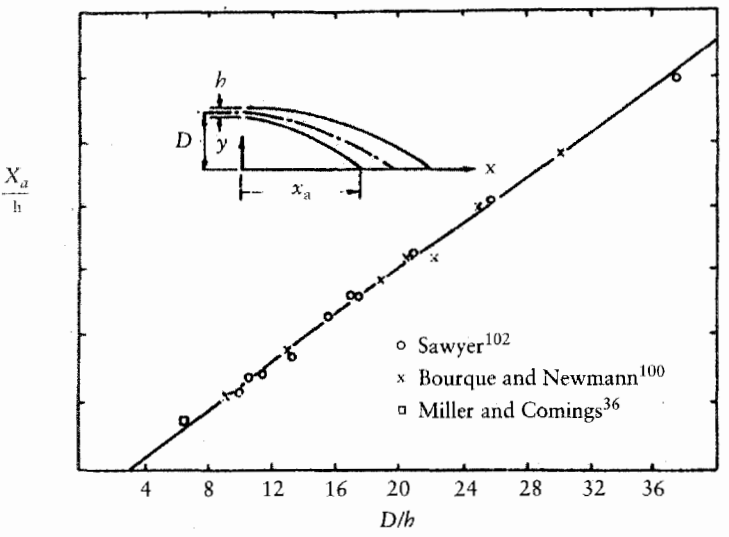

FIGURE 7.31 Effect of supply distance from surface on the attachment distance for a linear jet. Reproduced from Awbi.[97]

heating the jet does not change the location of the attachment point. For $5 < D/H_0 < 13$ the length of the circulation zone followed the relation

$$x_a/H_0 = 1.175(D/H_0) + 6.25\,. \tag{7.110}$$

Calculation of x_a/H_0 using Eqs. (7.109) and (7.110) results in significantly different results. For $D/H_0 = 8$, $x_a/H_0 = 3.54$ according to Eq. (7.109), and $x_a/H_0 = 15.65$ according to Eq. (7.110).

The length of the circulation zone (bubble), L_b, created when the linear jet is supplied at an angle α to the surface was studied experimentally by Bourque and Newman[100] and theoretically by Sawyer.[99] The effect of the angle between the jet axis at the outlet and the surface on the length of the circulation bubble is shown in Fig. 7.32, reproduced from Awbi.[97] The data presented in Fig. 7.32 show that at sufficiently high Reynolds number the length of the circulation zone is independent of the Reynolds number.

Linear jet attachment to a plane not parallel to the supply direction was studied by Katz.[103] The critical angle, θ_c, of the plane to the jet supply direction, as indicated in Fig. 7.33, was found to be dependent on the supply velocity (Reynolds number). It also depends on the distance of the plane edge from the supply outlet (see Fig. 7.34).

Baturin[54] studied air jets supplied from rectangular nozzles at some angle to the plane with an edge of the nozzle coincident with the plane. The results of his studies indicate that the critical value of the angle of the jet supply direction to the plane is 45°. It was also shown that the jet supplied through a rectangular outlet with a nozzle located at some distance from the plane does not attach to the surface.

7.4.4.6 Jet Separation

When the temperature of an air jet attached to the ceiling is lower than the temperature of the ambient air, the jet will remain attached to the ceiling until the downward buoyant force becomes greater than the upward static pressure (Coanda force). At this point, the jet separates from the ceiling and

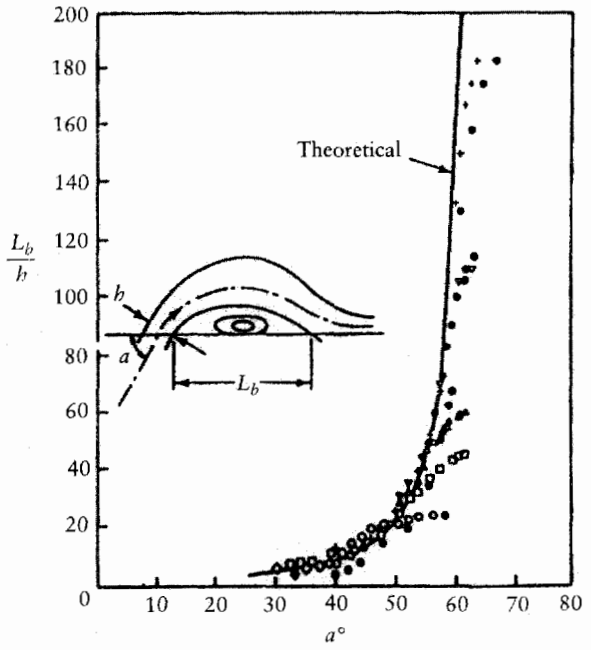

FIGURE 7.32 Effect of supply jet angle on recirculation bubble length. Experimental data and theoretical curve from Sawyer.[42] Reproduced from Awbi.[97]

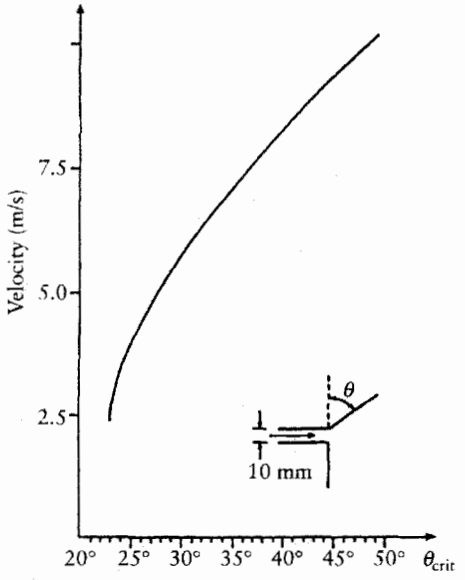

FIGURE 7.33 Critical angle. Wall is located close to supply outlet. Reproduced from Katz.[103]

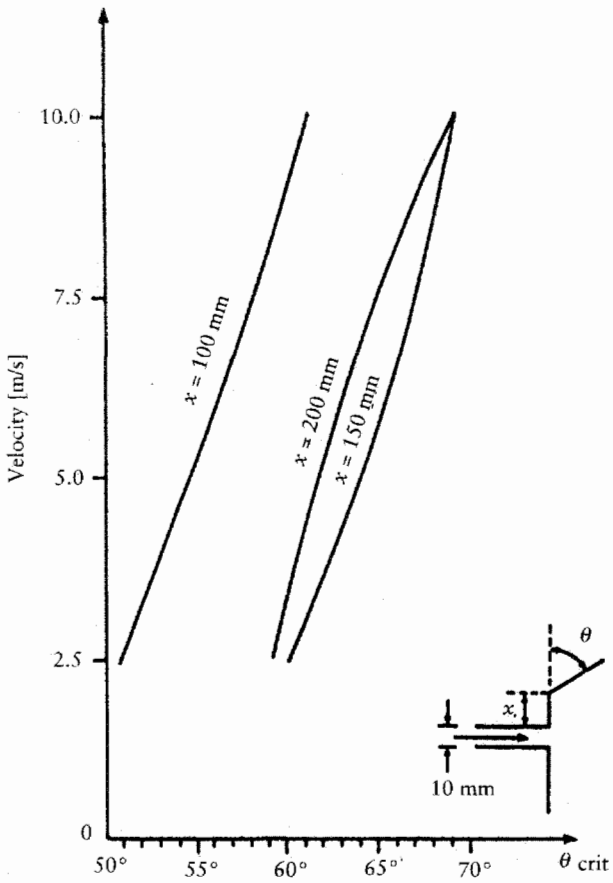

FIGURE 7.34 Critical angle. Wall is located at different distances from the air supply outlet. Reproduced from Katz.[103]

begins a downward-curving trajectory.[104] Studies of nonisothermal jets conducted by Grimitlyn,[5] Schwenke,[105] Nielsen and Moller,[106] Miller,[104] Anderson et al.,[107] and Kirkpatrick et al.[108] showed that the distance to the point of the jet's separation can be computed using the following equation:

$$x_{sep} = \frac{a}{(\mathrm{Ar}_0)^b}. \tag{7.111}$$

For linear diffuser jets[109] $a = 2.5H_0$ and $b = 2/3$. For compact diffuser jets $a = 1.6A_0^{0.5}$ and $b = 0.5$.[107,108] According to theoretical analysis and experimental data collected by Grimitlyn,[5] the separation distance of jets could be expressed by equations similar to Eq. (7.111) considering diffuser characteristics K_1 and K_2. For compact and incomplete radial jets,

$$x_s = \frac{0.55K_1\sqrt{A_0}}{\sqrt{K_2\mathrm{Ar}_0}}. \tag{7.112}$$

For linear jets,

$$x_s = \frac{0.4K_1^{3/4}H_0}{(K_2\mathrm{Ar}_0)^{2/3}}. \tag{7.113}$$

For radial jets,

$$x_s = \frac{0.45K_1\sqrt{A_0}}{\sqrt{K_2 \mathrm{Ar}_0}}. \tag{7.114}$$

7.4.5 Jets in Confined Spaces

7.4.5.1 General Description of Confined Flow

Current mixing-type air distribution methods typically consider occupied zone ventilation with jets intercepting its upper boundary. These methods include air supply with vertical jets through ceiling-mounted air diffusers and air supply with inclined jets. They also include air supply with vertical upward-directed jets or horizontal jets along room surfaces. In the latter case, the jet reaches the opposite wall/ceiling and follows room surfaces until it reaches the occupied zone (Fig. 7.35). If the combination of room sizes (height, length, and width) allows such an airflow pattern, this room is considered to be "short."[89] The room in which air jets dissolve before reaching the opposite wall is considered to be "long." In such rooms, the occupied zone is ventilated by "reverse" flow. Initially, studies of jets in confined spaces were carried out for mining, chemical, and mechanical engineering applications.[3,32,84] In the current chapter three methods of air supply in confined spaces are discussed:

- Horizontal jet supply
- Inclined jet supply
- Horizontal jet supply with directing jets
- Vertical jets

7.4.5.2 Experimental Studies of Isothermal Horizontal Jets in Confined Spaces: Airflow Pattern, Throw, Velocities

The first experimental data on confined air jets used for ventilation date back to 1939, when Baturin and Hanzhonkov studied air supply method with

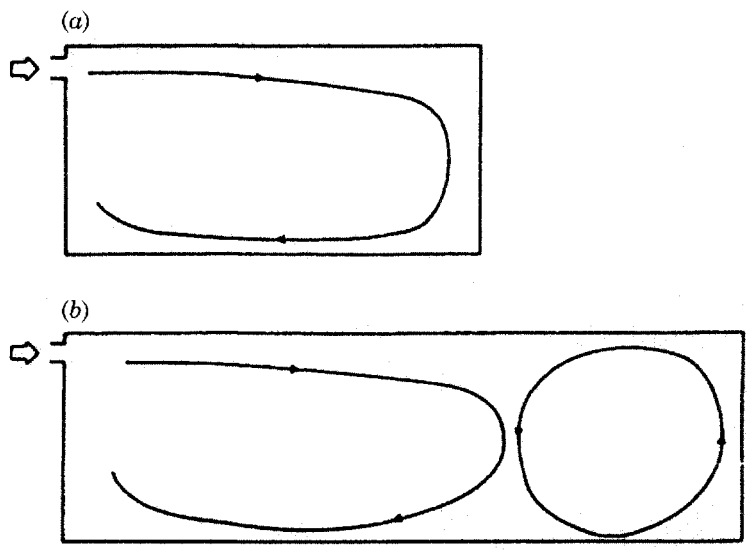

FIGURE 7.35 Jet flow in a room: (*a*) "short" room; (*b*) "long" room. Reproduced from Etheridge and Sandberg.[90]

the occupied zone ventilation by "reverse" flow. Later, this method was called concentrated air jet supply. Baturin and Hanzhonkov concluded that the airflow pattern in the ventilated space depends on the location of air supply outlets and practically does not depend upon location of air exhausts.[110]

Studies by Nelson and Stewart,[111] Bromley,[112] and Gunes[113] provide experimental data on air velocities and temperature distribution for this method of air supply at different room configurations, locations of air supply outlets, and velocities and temperatures of air supply.

The effect of the room length and position and shape of the air supply outlets was studied by Linke.[114,115] These studies show that there is a maximum room length that can be effectively ventilated by the supply air jet (Fig. 7.36*a*). For the

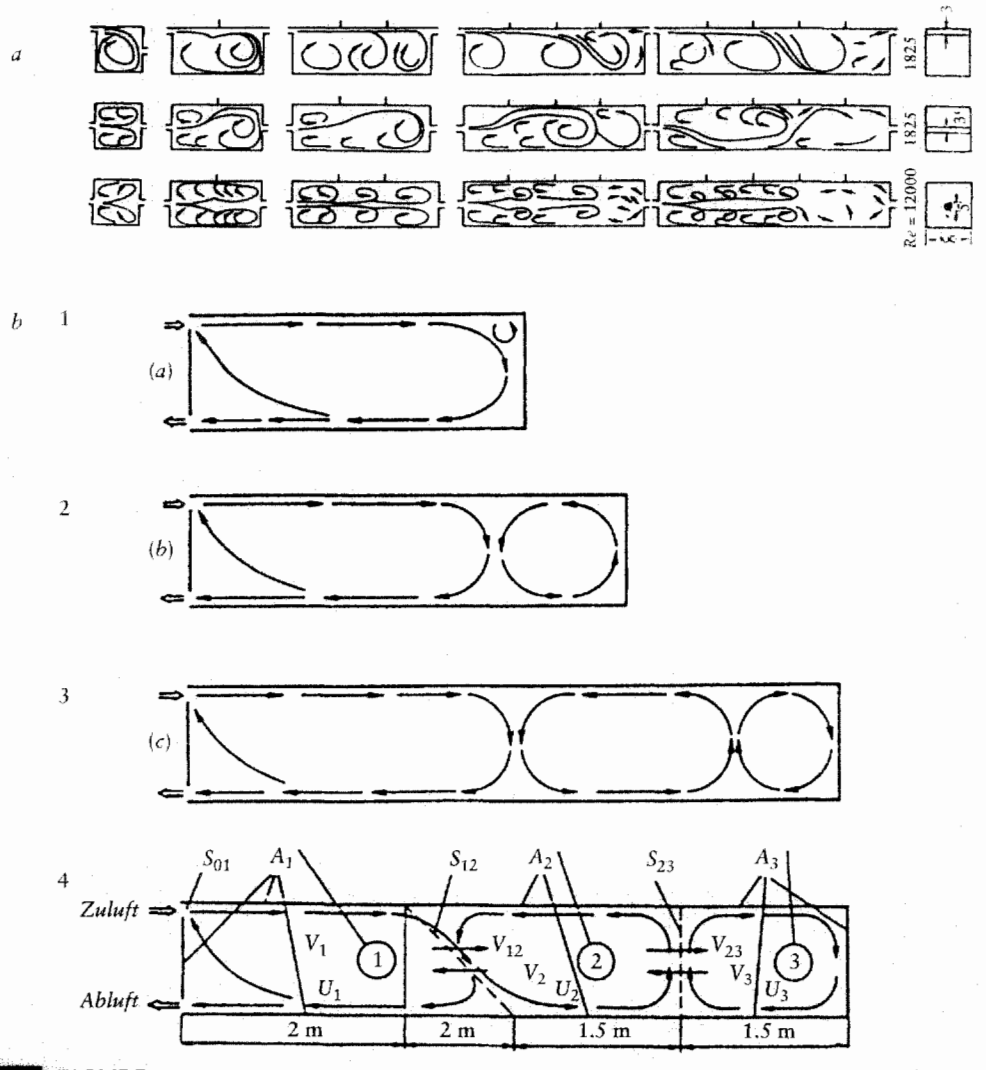

FIGURE 7.36 Flow patterns in rooms of different lengths with various types of air supply and exhaust: (*a*) reproduced from Linke[118], (*b*) reproduced from Müller.[119] 1—$L_r/H_r = 3$; 2—$L_r/H_r = 4$; 3—$L_r/H_r = 6$; 4—schematic of primary, secondary and tertiary vortexes in the room with $L_r/H_r = 6$.

linear (2-D) air jet attached to the ceiling supplied at the Reynolds number in the range from 1825 through 12 000, the maximum room length does not exceed three times the room width. The rest of the room downstream is poorly ventilated. When the air supply slot is symmetrical (located at $1/2H$), the effectively ventilated room length increases to four room widths. Air supply through a round nozzle with a nonattached jet allows the effectively ventilated room length to increase up to five transversal cross-section sizes, $(B \times H)^{1/2}$, of the room.

The airflow pattern in rooms ventilated by linear attached jets with L/H ratio greater than that for effectively ventilated rooms was studied by Schwenke[105] and Müller.[116] The results of their air velocity measurements and visualization studies indicate that there are secondary vortexes formed downstream in the room and in the room corners. The number of downstream vortexes and their size depend upon the room length (Fig. 7.36*b*). Mass transfer between the primary vortex and the secondary vortex depends upon the difference in characteristic air velocities in the corresponding flows U_1 and U_2 and can be described using the Stanton number, St:[116].

$$\mathrm{St} = \frac{U_1 + U_2}{U_1 - U_2} \frac{1}{4\sigma\sqrt{\pi}}, \tag{7.115}$$

where

$$\sigma = \frac{1}{2\sqrt{\chi c \dfrac{U_1 - U_2}{U_1 + U_2}}}, \tag{7.116}$$

where χ and c are empirical coefficients. For the jet spreading along the wall ($U_2 = 0$), the Stanton number is equal to 0.01. This approach was used to predict mass transfer between the primary and secondary vortexes and the characteristic air velocities in the secondary vortexes. These predictions were compared with experimental data. Though experimental data deviate from predicted air velocities, the proposed model provides some understanding of the mechanism of mass transfer between different room zones. Average rotation velocity and mass transfer decreases from the primary vortexes to the secondary and the subsequent vortexes.

The influence of room transverse cross-section configuration on airflow patterns created by air jets supplied through round nozzles in proximity to the ceiling was studied by Baharev and Troyanovsky[117] and Nielsen[90] (see Fig. 7.37). Based on experimental data, they concluded that when the room width B is less than $3.5H$, the jet attaches to the ceiling and spreads, filling the whole width of the room in the manner of a linear jet. The reverse flow develops under the jet. When $B > 4H$, the reverse flow also develops along the jet sides. Baharev and Troyanovsky[117] indicated that air temperature and velocity distribution in the occupied zone is more uniform when the jet develops in the upper zone and the occupied zone is ventilated by the reverse flow. Thus, they proposed limiting room width to $3–3.5H_r$

Detailed experimental data were obtained by Sadovskaya[118,119] on a physical model in isothermal conditions. She has found that the confined air jet has two critical cross-sections (Fig. 7.38). In the first cross-section, where the ratio of jet cross-sectional area to the area of ventilated space equals 0.24, the jet

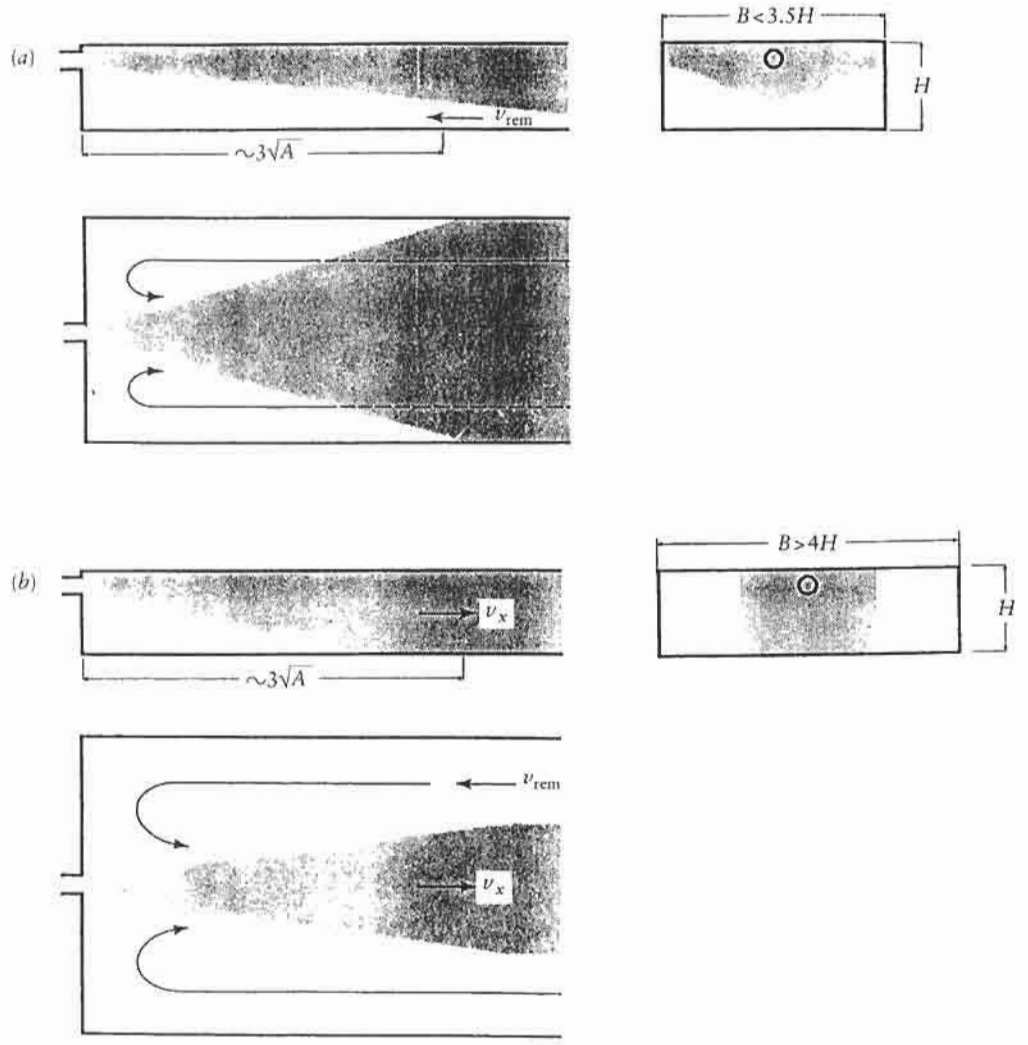

FIGURE 7.37 Influence of room configuration on airflow pattern: (*a*) $B/H < 3.5$; (*b*) $B/H > 4$. Reproduced from Nielsen.[91]

develops as a free jet. Between the first and second critical cross-sections, where the jet occupies 40% of the room cross-sectional area, is the zone of confined jet. Beyond the second critical cross-section is the zone of jet degradation. Sadovskaya has found that the lengths of all three zones depend upon the coefficient of turbulent structure a of the jet at the air supply and determined empirical equations for the length of each zone and air velocities in the air jet and in the reverse flow:

$$x_1 = \frac{0.1\sqrt{BH}}{a} \tag{7.117}$$

$$x_2 = [0.21(BH^{1/2})]/a. \tag{7.118}$$

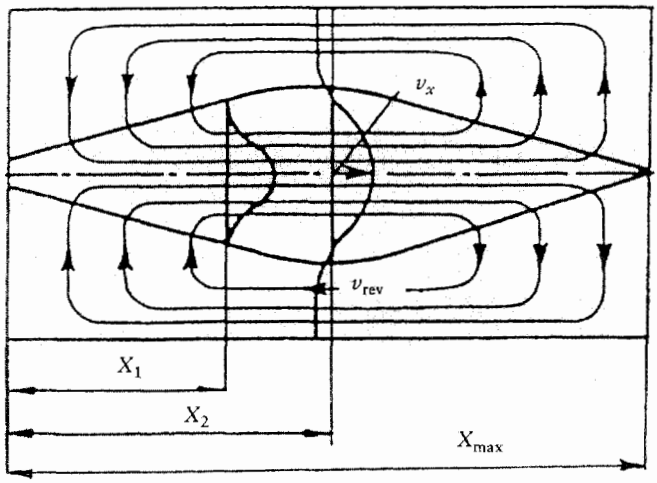

FIGURE 7.38 Schematic of air jet in confined space proposed by N. N. Sadovskaya. Reproduced from Grimitlyn.[5]

In these studies, nozzles with $a = 0.07$ were used. For the values of parameter $(BH/A_0)^{1/2}$ used in the studies, from 2.44 through 71.5, maximum jet throw is in the range

$$x_{max} = (\text{from } 4.07 \text{ through } 5.1)\sqrt{BH}.$$

Based on experimental data from Sadovskaya[118,119] and Rozenberg[120] as well their own experimental results, Baharev and Troyanovsky[117] derived empirical equations to design air distribution with horizontally supplied confined jets.

Studies conducted by Grimitlyn[56] led to generalized Eqs. (7.117) and (7.118) for air diffusers with different velocity decay characteristics K_1:

$$x_1 = 0.22K_1\sqrt{BH}$$

$$x_2 = 0.31K_1\sqrt{BH}$$

$$x_{max} = 0.62K_1\sqrt{BH}$$

for compact jets, and

$$x_1 = 0.1K_1^2H_r$$

$$x_2 = 0.15K_1^2H_r$$

$$x_{max} = 0.3K_1^2\sqrt{BH}$$

for linear jets.

To avoid high velocities in the occupied zone due to direct effect from the supply air jet, and to increase the length of the effectively ventilated zone for a single jet in rooms with height H_r from 4 m to 10 m, Baharev and Troyanovsky[117] proposed supplying air from the height $h_0 = 0.6$–$0.7H_r$.

Effect of Jet Proximity to the Ceiling

Studies by Sawyer,[102] Bourque and Newman,[100] and Regenscheit[121] showed (Fig. 7.39) that a two-dimensional jet supplied from a slot with a

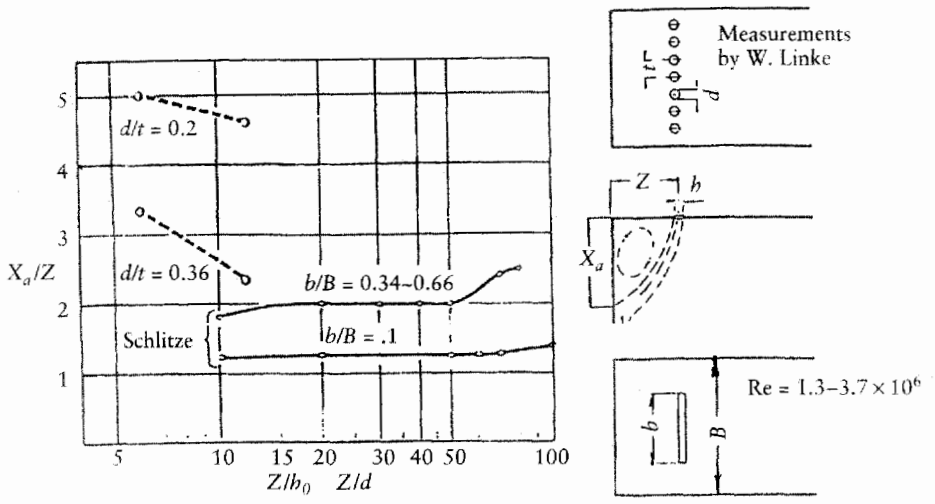

FIGURE 7.39 Reattachment length x_a vs. the distance z from the ceiling surface to the supply outlet. Reproduced from Regenscheit.[121]

width h_0 at the distance z from the ceiling surface will become attached to this surface at the distance x_a given by

$$\frac{x_a}{h_0} = 0.2 + 2.7\left(\frac{z}{h_0}\right)^{0.8} . \tag{7.119}$$

Research reported by Jackman[122] showed that the effect of proximity of air supply to the ceiling is also important when air is supplied with compact jets. The nonuniform entrainment from either side of the jet resulted in a force deflecting the jet toward the ceiling. The attraction of the jet toward the surface is greater the closer the air supply is to the ceiling and the higher its aspect ratio (grill width over grill height).

Effect of Ceiling Beams or Obstructions in the Jet Zone

Ceiling beams will not affect jet attachment to the ceiling if they are located further than $1.6x_a$ from the air supply outlet.[123] If a beam is located closer than $1.6x_a$, the impingement of the jet on this beam will change the jet direction.

The effect of ceiling beams and light fittings on ventilation jets was also studied by Holmes and Sachariewicz.[124] Their studies were limited to the two-dimensional case: air supply through linear slot and a two-dimensional barrier (Fig. 7.40). The results of these studies show that the ceiling jet can take one of three courses when it encounters an obstruction:

1. Separate from the surface and take up a flow angle approximately equal to the angle between the upstream face of the obstruction and the surface;
2. Separate from the surface and reattach some distance downstream from the barrier; or
3. Almost ignore the existence of the barrier.

The jet will separate from the surface if the axial distance between the slot and the obstruction, x_d, is less than a specified critical distance x_c (Fig. 7.41). The

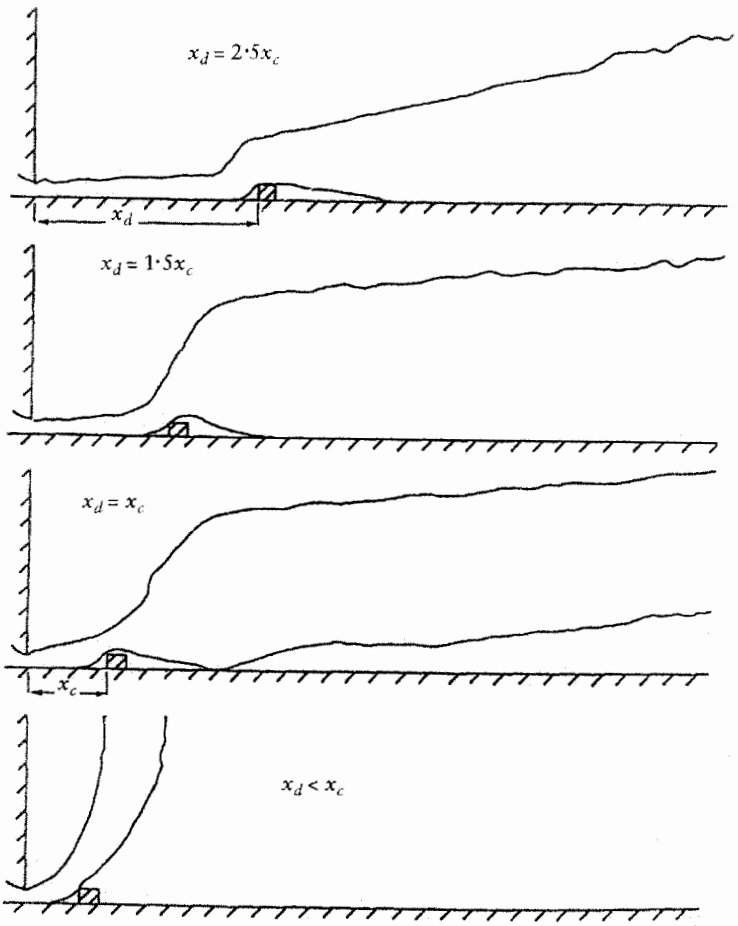

FIGURE 7.40 Beam influence on the airflow pattern along the ceiling. Reproduced from Holmes and Sachariewitz.[124]

values of x_c given in Fig. 7.41 are only for an obstruction of transverse dimension w equal to or less than the slot span s.

In the second course, the flow downstream of the barrier can be adequately represented by a determination of both the maximum separation of the line of maximum velocity from the surface (Fig. 7.42) and the velocity decay after the barrier

$$\frac{v_{\max}}{v_0} = 2.2\left(1 - 0.785\frac{w}{s}\right)^{1/2}\left(\frac{b_0}{x - x_d}\right)^{1/2}, \tag{7.120}$$

where x_d is the distance from obstruction to the slot, $0.5 < w/s < 1$.

Obstruction does not affect the jet if the obstruction is further than about eight critical distances (x_c) from the slot. In this case the velocity decay of the jet may be obtained from

$$\frac{v_m}{v_0} = 2.2\left(\frac{b_0}{x - x_0}\right)^{1/2}, \tag{7.121}$$

where b_0 is an effective slot width and x_0 is the virtual origin of the jet.

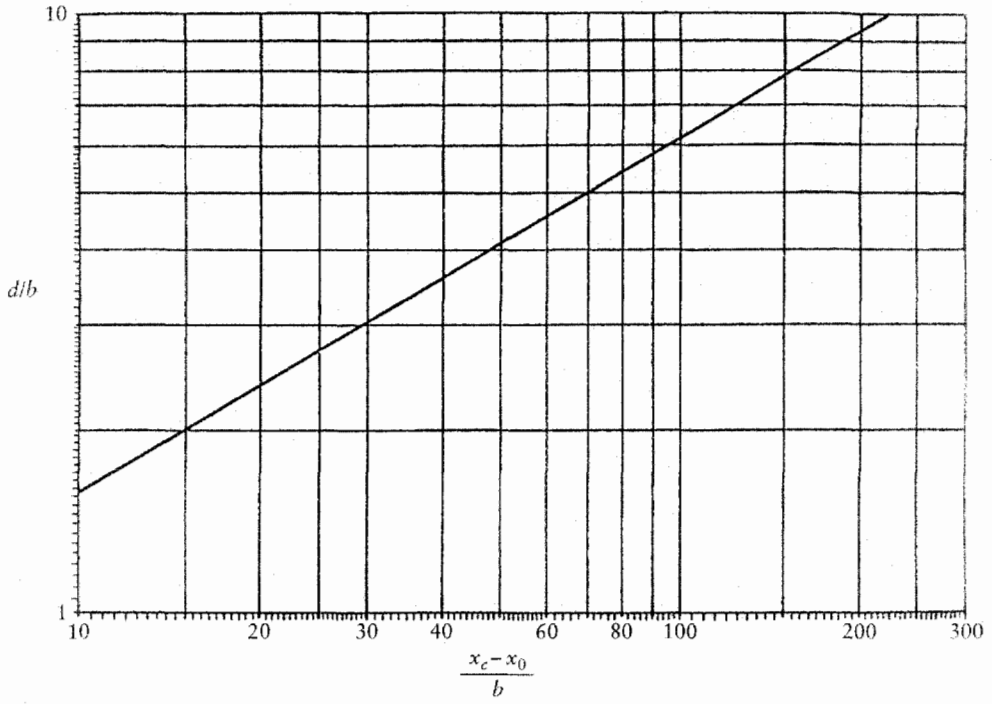

FIGURE 7.41 Critical distance x_c from the slot to the beam: b = width of two dimensional slot, d = beam height, x_0 = jet core zone length. Reproduced from Holmes and Sachariewicz.[128]

Although the tests were conducted only for two-dimensional cases, the authors suggest that their results can be extended to three-dimensional cases as follows:

- If the obstruction span is less than half the slot span, the effect of obstructions can be ignored provided $x_d > x_c$.
- The value of x_c for a short barrier will be less than for a long one and it will be safe to use the values obtained in the studies.
- The velocity decay downstream of a short barrier may be represented by

$$\frac{v_m}{v_0} = 2.2\left(1 - 0.785\frac{w}{s}\right)^{1/2}\left(\frac{b_0}{x - x_d}\right)^{1/2}, \tag{7.122}$$

  where $0.5 < s/w < 1$.
- If the barrier is longer than the slot, the flow will be deflected at right angles to the normal jet trajectory, causing a possible thinning of the jet at the barrier and increasing the critical barrier distance. It is not possible to estimate accurately the extent of such an increase from the studies of two-dimensional situations. The authors consider that such an increase will not exceed 100%.

Graphical interpretation of the factors influencing the critical distance x_c from air supply to the linear obstacle with a height d_c for air supply through a slot diffuser with height h_0 and for air supply through a round nozzle with outlet diameter d_0[125] are presented in Fig. 7.43. Nonisothermal flow has an influence on

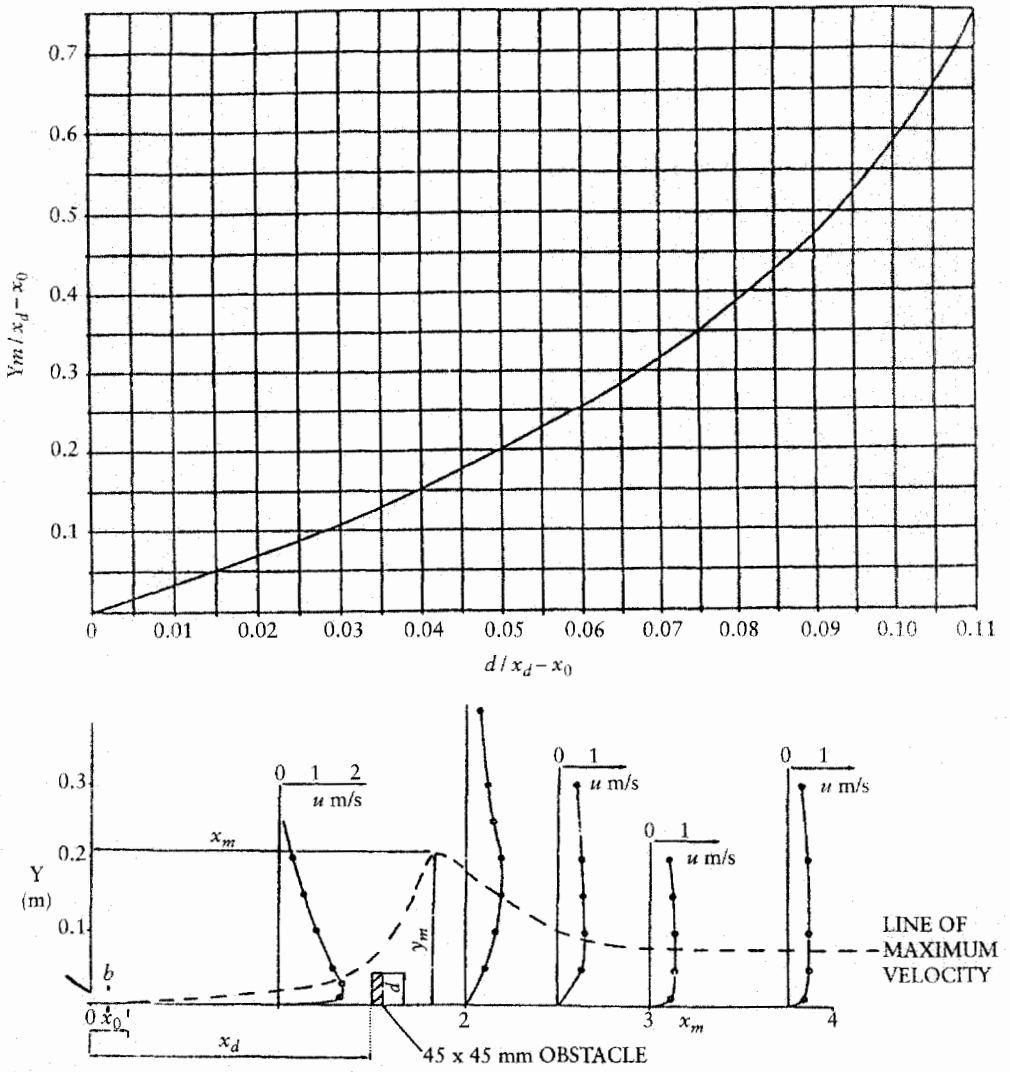

FIGURE 7.42 Maximum jet separation y_m from ceiling: b = width of two-dimensional slot, b = beam height, x_0 = jet core zone length. Reproduced from Holmes and Sachariewicz.[128]

the critical distance, and Archimedes number, Ar, is an important parameter together with the geometrical relations.[125] Ventilation with cooled air increases the effect of obstacles, and warm air supply decreases this effect.[126,127]

Air can be supplied in rooms by one or several jets. Air supply openings can be located along one wall—parallel air jet supply (Fig. 7.44*a*)—and/or on opposite walls—contrary-directed jets supply (Fig. 7.44*b*). In special cases air can be supplied in a fan-type manner (Fig. 7.44*c*).

Air circulation with a parallel jet supply is illustrated in Fig. 7.45. Jets are located at distance t from each other, and each jet forms return flow similar to that induced by a single jet in the room with a width $B = t$. Thus, in the case of N parallel jets, the room should be considered divided into several zones with a width $B = B_r/N$, separated from each other by airtight walls.

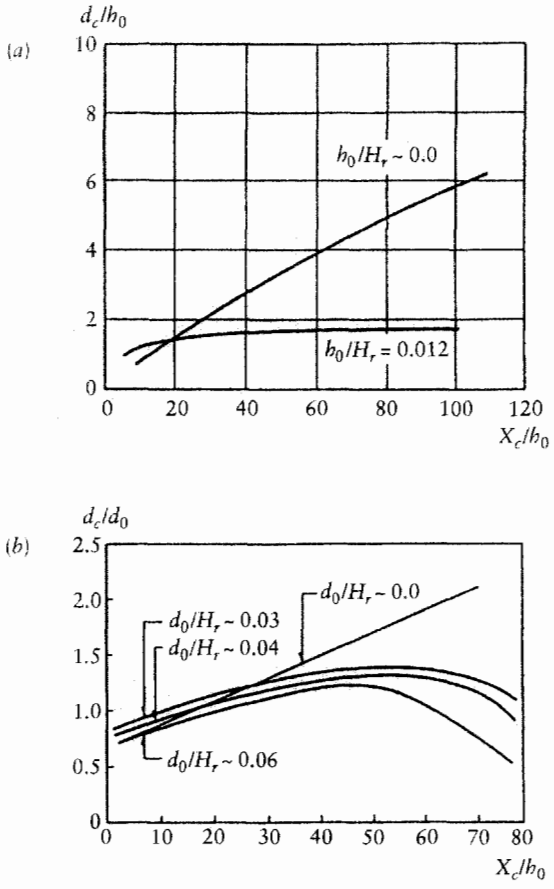

FIGURE 7.43 Critical height of an obstacle d_c vs. distance from supply slot with a height h_0 (*a*) and supply nozzle with diameter d_0 (*b*) Reproduced from Nielsen.[129]

7.4.5.3 Analytical Studies

Abramovich[3] was the first to study axisymmetric confined jets analytically. He suggested the method based on utilizing the equations of continuity and momentum conservation. He also assumed that the width of the layer of a jet mixing with a counterflow equals the width of a free jet with a velocity distribution according to Schlichting's formula:

$$\frac{v - v_{rev}}{v_x - v_{rev}} = \left[1 - \left(\frac{y}{b}\right)^{3/2}\right]^2 \tag{7.123}$$

where $b = 0.22x$ –half of the free jet width.

Analytical methods suggested by Shepelev and Tarnopolsky,[128] Grimitlyn and Pozin,[129] and Sychev and Volov[130] differ from the one described above only in the way the authors described velocity distribution in the mixing layer:

- Shepelev and Tarnopolsky:

$$\frac{v - v_{rev}}{v_x} = e^{-\frac{1}{2}\left(\frac{y}{cx}\right)^2} \tag{7.124}$$

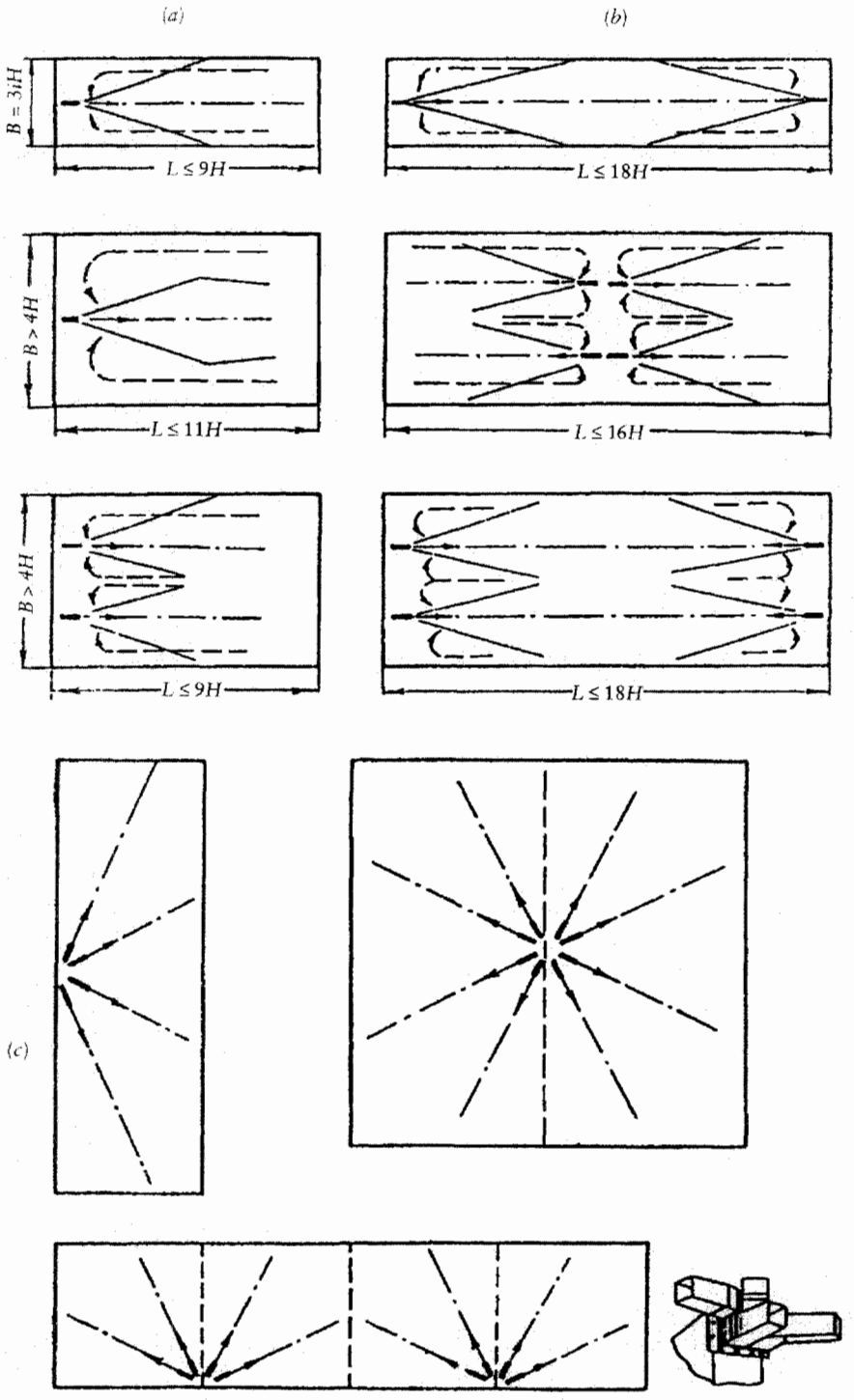

FIGURE 7.44 Schemes of room ventilation with parallel jet supplied from the same wall (*a*), from opposite walls (*b*), and in a fan-type manner (*c*). Reproduced from Baharev and Troyanovsky.[117]

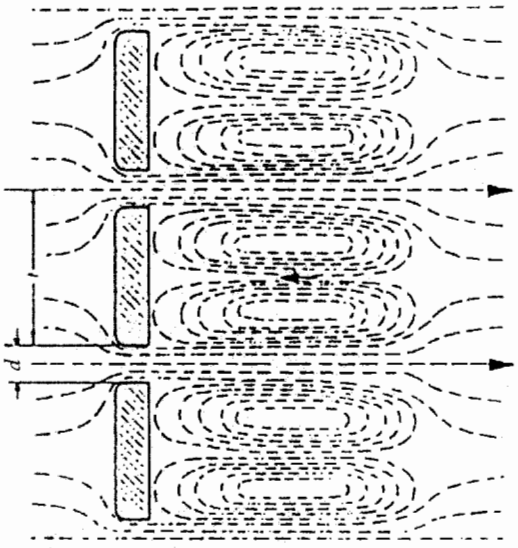

FIGURE 7.45 Room ventilation by parallel jets. Reproduced from Regenscheit. (1975)

- Grimitlyn and Pozin:

$$\frac{v - v_{rev}}{v_x} = e^{-0.7\left(\frac{K_1 y}{0.66x}\right)^2} \tag{7.125}$$

- Sychev and Volov:

$$\frac{v - v_{rev}}{v_x - v_{rev}} = 1 - 6\left(\frac{y}{b}\right)^2 + 8\left(\frac{y}{b}\right)^3 - 3\left(\frac{y}{b}\right)^4 \tag{7.126}$$

It is assumed in the above-mentioned methods that the influence of confined space on the supplied jet can be described by the reduction of the axial component and the value v_{rev}, as for jet development in the counterflow. The value of v_{rev} is assumed to be the same throughout each cross-section but variable along the jet length. The value of v_{rev} can be found from the continuity equation, which in the case of jet distribution in a space of cylindrical shape can be presented as

$$2\int_0^{r^*} v r \, dr + v_{rev}(R^2 - r_*^2) = 0 \tag{7.127}$$

for air supply and air exhaust located in the same wall and for air supply and air exhaust located in opposite walls.

According to Shepelev and Tarnopolsky[128] air velocity on the axis of the jet at the distance x from the outlet for air supply and exhaust located on the same wall can be calculated from

$$v_{xc} = v_x \left[1 - \frac{r_0}{R} \frac{1 - \exp\left[-\frac{1}{2}\left(\frac{R}{cx}\right)^2\right]}{\frac{1}{2}\left(\frac{R}{cx}\right)^2 K_1 \sqrt{\pi} \frac{r_0}{R}} \right], \tag{7.128}$$

and the maximum (in the cross-section) velocity in the reverse flow can be calculated from

$$v_{rev} = v_0 \left(K_1 \frac{\pi r_0^2}{x} \exp\left[-\frac{1}{2}\left(\frac{R}{cx}\right)^2 \right] \left(-\frac{r_0}{R} \frac{1 - \exp\left[-\frac{1}{2}\left(\frac{R}{cx}\right)^2 \right]}{\frac{1}{2}\frac{R}{cx}} \right) \right). \tag{7.129}$$

Velocity in the reverse flow reaches its maximum value at $x^* = 4.88R$ equal to

$$v_{rev}^{max} = 0.656 \sqrt{\frac{M_0}{\rho \pi R^2}}. \tag{7.130}$$

The equations presented above can be applied to spaces of rectangular shape by replacing πR^2 by BH.

A similar approach was used by Zhivov[131,132] in his studies of systems of coaxial jets in confined space. The distance x from the air diffuser to the cross-section with a maximum velocity in the reverse flow for the case without coaxial jets was found to be $1.9(BH)^{0.5}$ at $K_1 = 6.2$, and $1.4(BH)^{0.5}$ at $K_1 = 4.5$. For a nonisothermal jet, it was also found[132] that the reverse flow and confining surfaces increase the upper limit of the cold or heated supply air temperature Δt_0, which ensures a horizontal jet projection.

The results of different analytical and experimental studies of the confined horizontal jet described above are presented in Table 7.17. The main reason for the differences in the analytical results is different approximations of reverse flow velocity profiles.

The influence of the reverse flow on the centerline velocities v_{xc} was proposed[1] to be expressed by the coefficient K_c,

$$v_{xc} = v_x K_c,$$

which, as was shown above, can be derived analytically. The value of K_c depends on the ratio of the cross-section area of the free jet and the corresponding cross-section of the room. The graphs for evaluating K_c for compact, radial, and linear air jets are presented in Fig. 7.46.

7.4.5.4 Experimental Studies of Horizontal Heated and Cooled Air Supply in Confined Spaces

Gobza[134,135] studied air supply with concentrated jets on physical models and in the field and concluded that temperature stratification along the room height may occur if improper supply air temperature difference and air exchange rate are selected. Among the field cases reported by Gobza are industrial halls as long as 150 m (at width equal to 50 m and height 12–15 m).

The effect of supply air temperature on jet behavior in confined spaces was studied by Müllejans.[48] Studies of cooled air jets were conducted in rooms with a size from 1.0 m × 1.0 m × 1.6 m to 2.27 m × 3.33 m × 5.31 m with an air supply through the slot ($b = B_r$) or rectangular opening ($b \ll B_r$). Numerous smoke photographs were taken reflecting supply situa-

TABLE 7.17 Results of Experimental and Analytical Studies of the Compact Confined Jet

Reference	Throw	Throw definition	Zone 1 + Zone 2	Maximum velocity in the reverse flow
Baharev and Troyanovsky[117]	$(4.7-5.4)\sqrt{BH}$	$(v_{rev} = 0.05\text{–}0.01 v_0)\cdot \sqrt{A_0/BH}$	$2.0\sqrt{BH}$	$0.78 v_0\sqrt{(A_0/BH)}$
Abramovich[3]	$3.5\sqrt{BH}$	$v_x = 0.05\text{–}0.01 v_0$	$2.4\sqrt{BH}$	$0.88 v_0\sqrt{(A_0/BH)}$
Shepelev and Tarnopolsky[128]	$5\sqrt{BH}$	$v_{rev} = 0.07 v_0\sqrt{A_0/BH}$	$2.75\sqrt{BH}$	$0.66 v_0\sqrt{(A_0/BH)}$
Grimitlyn and Pozin[129]	$0.7K_1\sqrt{BH}$	—	$0.31\ K_1\sqrt{BH}$	$0.78 v_0\sqrt{(A_0/BH)}$
Gnatyuk et al.[133]	$4.3\sqrt{BH} - 3.3\sqrt{A_0/BH}$	$v_x = (0.07 - 0.01)v_0$	—	—
Sychev and Volov[130]	$5.5\sqrt{BH}$	$v_x = 0$	$3.2\sqrt{BH}$	$0.7 v_0\sqrt{(A_0/BH)}$
Schwenke[105]	$5.0\sqrt{BH}$ – compact jet $3H$ – linear nonattached jet	$v_{x\ ave} = 0.2$ m/s or $v_{x\ max} = 0.5$ m/s	—	—
Nielsen[90,96]	$5.0\sqrt{BH}$ – compact jet $4H$ – linear attached jet	—	$3\sqrt{BH}$	$0.95 v_0\sqrt{(A_0/BH)}$ round attached jet
Zhivov[131,132]	$3.9\sqrt{BH}$, $K_1 = 6.2$ $3.4\sqrt{BH}$, $K_1 = 4.5$	Cross-section velocities are uniform with an unstable direction	$1.9\sqrt{BH}$, $K_1 = 6.2$ $1.4\sqrt{BH}$, $K_1 = 4.5$	$0.73 v_0\sqrt{(A_0/BH)}$

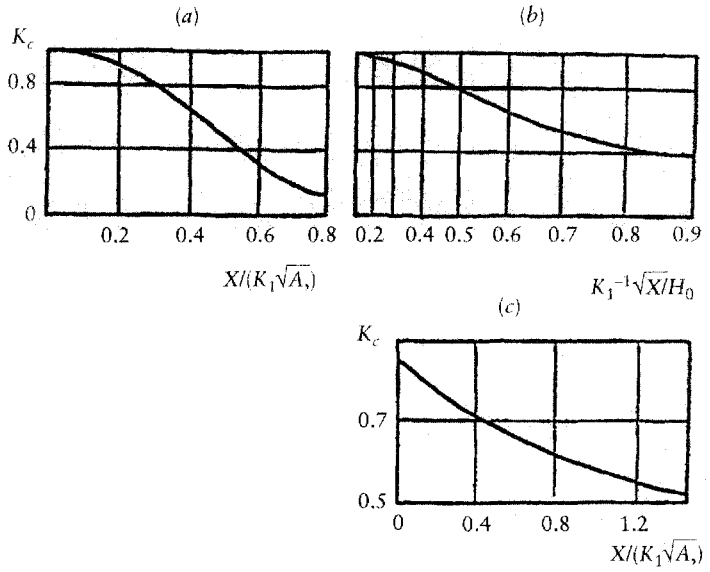

FIGURE 7.46 Coefficient of confinement: (*a*) compact jet, $A_r = B \times H$; (*b*) linear jet; (*c*) radial jet, $A_r = B \times L$. Reproduced from Grimitlyn and Pozin.[137]

tions with different Re and Ar numbers. Archimedes number was defined by Müllejans as

$$\mathrm{Ar} = \frac{gD_h(\theta_w - \theta_0)}{v^2(T_w + T_0)/2}, \tag{7.131}$$

where $v = Q_0/(B_rH_r)$ [m/s], $\theta_w\,(T_w)$, $\theta_0(T_0)$ = wall and supply air temperatures [°C, K], g = acceleration due to gravity, and D_h is the hydraulic diameter,

$$D_h = \frac{4B_rH_r}{2(B_r + H_r)}. \tag{7.132}$$

Müllejans has reported that with air supply through rectangular openings the jet behaves more or less as an isothermal flow when $\mathrm{Ar} < 10^4$.

To establish a criterion for any size room and outlet, the Ar number was adjusted using a geometrical factor. The modified Ar* was defined as

$$\mathrm{Ar}^* = \mathrm{Ar}\frac{b_0h_0}{D_h^2}. \tag{7.133}$$

With a common value of $b_0h_0/D_h^2 = 1/250$, the airflow pattern will be similar to isothermal with a modified Ar* number limited to 40.

In the case of a room ventilated by a linear jet, this jet deflects toward the ceiling immediately after entering the room. Maximum Ar values depend upon the L/H ratio and are shown in Table 7.18.

Experimental studies conducted by Grimitlyn[56] on heated and chilled confined jets showed that the airflow pattern remains the same as for isothermal

TABLE 7.18 Ar Values

L/H	4.7	3.0	2.0	1.0
Ar_{max}	2000	3000	10 000	11 000

air supply when $Ar_x < 0.2$ at $x = 0.22K_1(BH)^{0.5}$, in rooms with H/B ratio from 0.3 to 1.0, where

$$Ar_x = \frac{K_2 g\sqrt{A_0}\Delta\theta_0}{K_1^2 v_0^2 T_{oz}}\left(\frac{x}{\sqrt{A_0}}\right)^2. \tag{7.134}$$

The above limitation on the local Archimedes number results in the following equation for maximum temperature difference of supplied air:

$$\Delta\theta_0 = 122\frac{v_0^2\sqrt{A_0}}{K_2 BH}. \tag{7.135}$$

Similar studies were conducted by Troyanovsky,[136] who concluded that to maintain the airflow pattern in rooms with heated or cooled air supply as in isothermal conditions, it is necessary that the rise of horizontally supplied jet does not exceed $\Delta y = 0.1BH$ at the distance from the outlet $x = 0.15K_1(BH)^{0.5}$. From this assumption the following equation for the maximum air temperature difference was derived:

$$\Delta\theta_0 = 1300\frac{v_0^2\sqrt{A_0}}{K_1 K_2 BH}. \tag{7.136}$$

Comparing Eq. (7.135) to Eq. (7.136), one can see that the value of the maximum temperature difference computed using Eq. (7.136) is higher than that determined using Eq. (7.135). Results of experimental studies on physical models[1] indicate that when $H/B > 1$, the limitation on supply air temperature difference should be even more restrictive.

7.4.5.5 The Effect of Confinement on Inclined Air Jets

The investigations of horizontal and inclined air jet trajectory, velocity, and temperature decay under buoyancy discussed in the previous section were conducted with free (nonconfined) jets. Only limited research data is available describing the behavior of inclined jets in confined spaces. Studies by Regenscheit[70] of horizontal cooled air supply from linear and rectangular openings can be related to this topic. Graphs in Fig. 7.47 show how the relative distance x_0/L from the supply opening to the point of jet impingement with the floor surface is influenced by the modified Archimedes number Ar:

$$Ar = \frac{g\Delta T_0 4(BH)^3}{T_{oz}Q_0^2 2(B+H)}. \tag{7.137}$$

Other experimental and analytical studies of nonisothermal inclined jets in confined spaces were carried out by Zhivov.[88] Experimental studies were conducted on the physical models. The ratio of the model dimensions $L \times B \times H$ was changed so that the value H/B was from 0.3 to 3.0 and $L/(B \times H) = 2.4$–4.9.

Visualization of airflow in the room with smoke and silk threads was used to describe airflow patterns in rooms with inclined jet supply. Airflow created

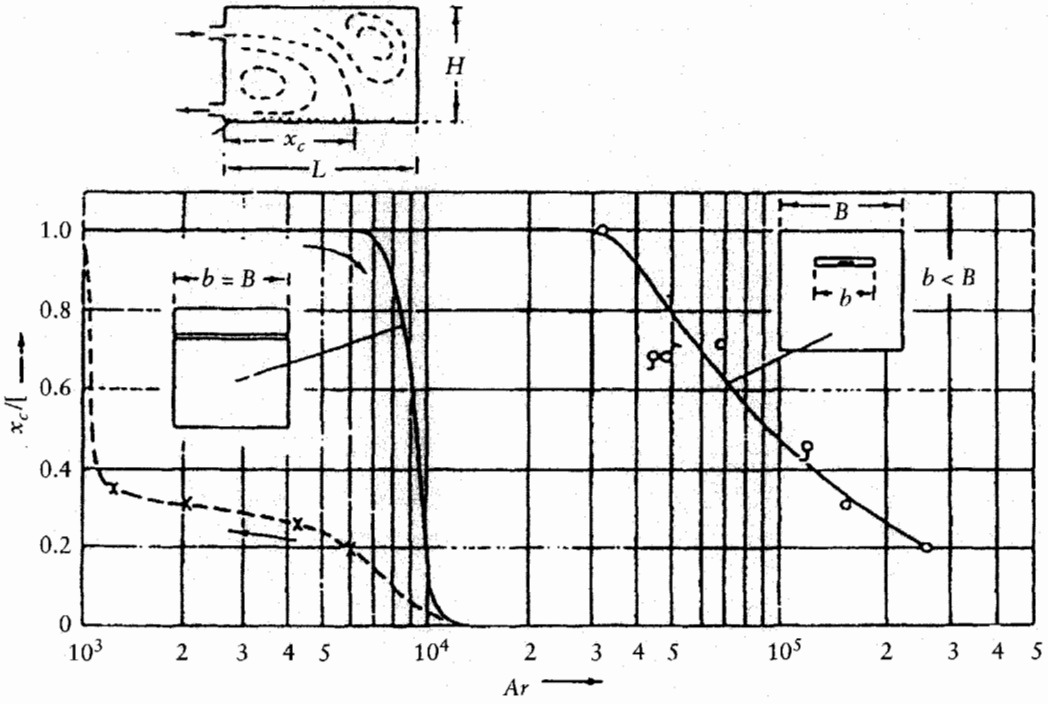

FIGURE 7.47 Nonisothermal jet trajectory in a room. Reproduced from Regescheit. [70]

by inclined jets impinging on the floor surface can be divided conditionally into three zones (Fig. 7.48): (1) free or confined jet, (2) impingement zone, and (3) flow along the floor. The width of the jet depends upon the supply characteristics, which can be primarily described by the velocity decay characteristic K_1. Some air diffusers (e.g., ventilation grills) can create jets with coerced angle of deflection only in one direction.

The first zone of the jet can be described using equations for velocity and temperature decay as well as jet trajectory with a coefficient K_c accounting for jet confinement. The impingement zone can be characterized by a significant change in the static pressure and great curvature of the air current lines. After the impingement, the radial flow is formed as if it is supplied from the side surface of the truncated cylinder with a uniform initial velocity of U_m^*. In the basement of the cylinder, there is a particular line that crosses the quasi source of the radial flow. Equations provided in the paper can be used to evaluate velocities along the branches with maximum airflow, minimum airflow, and along the particular line.

When the width of the jet (calculated for free conditions) is less than the width of the room, airflow after jet impingement on a floor is similar to that in nonconfined conditions. When the horizontally directed flow (along the particular line) reaches the wall, it is divided into two branches: one following the direction of the branch with a maximum airflow and another flowing in the opposite direction.

When the air directed backward reaches the back wall of the room, it flows upward to be induced by the jet within its first zone (Fig. 7.49).

The circulation zone is created above the branch with maximum airflow spreading along the floor. The reverse flow is also induced by the inclined jet within its first zone.

If the width of the jet (calculated for free conditions) at the point of its intercept with the occupied zone exceeds the room width, side walls transform the jet as if it was formed by the linear jet impingement on a floor.

In design of air distribution with inclined cooled air jets, the following parameters should be considered: air velocity and temperature at the point of jet

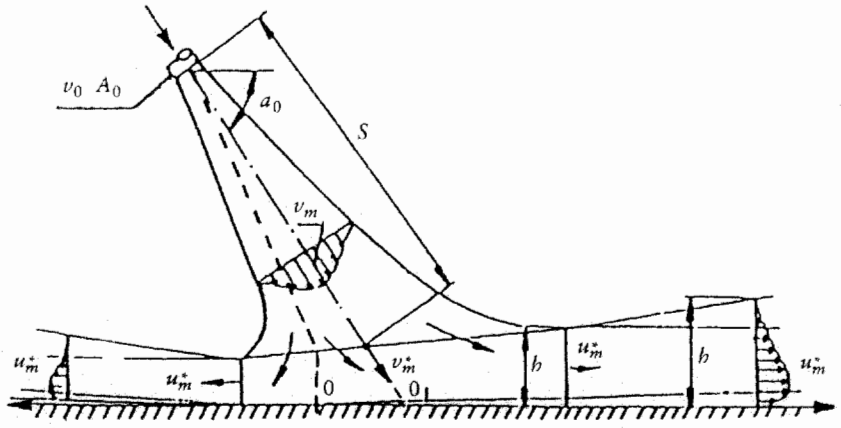

FIGURE 7.48 Schematic of inclined jet impingement with a floor surface. Reproduced from Zhivov.[88]

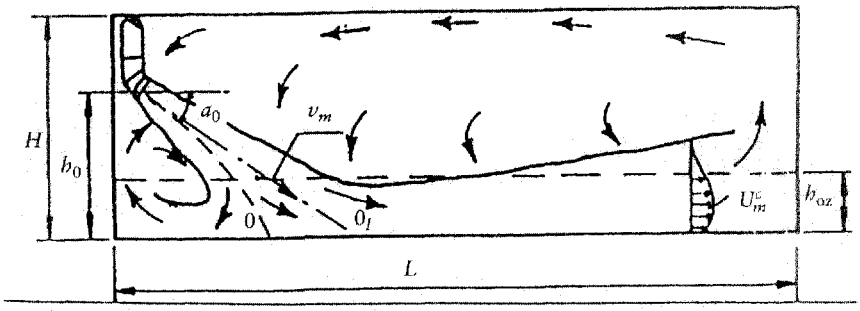

FIGURE 7.49 Airflow in a room with an inclined jet supply. Reproduced from Zhivov.[88]

intercept with the occupied zone—for practical purposes this cross-section can be considered the border between the first and the second zone of the impinging jet; and velocities along jet branches—maximum airflow branch, minimum airflow branch, and the branch along the particular line.

The latter information is important in evaluating the size of the occupied zone that can be effectively ventilated by inclined jets. It was proposed[88] that the occupied zone of rooms is well ventilated by inclined jets (particularly in industrial rooms with contaminant release) if air velocity in the occupied zone exceeds 0.1 m/s.

The influence of confinement on air velocity u_m in the flow along the floor can be accounted for with the coefficient K_c:

$$u_m^c = K_c u_m . \tag{7.138}$$

The value of this coefficient depends on the relative height of the flow along the floor h_f / H_r (calculated in the free conditions), where

$$K_c = 1 \quad \text{when } h_f \leq 1.1, \quad K_c = 1.79 - 0.72\, h_f / H_r \quad \text{when } h_f > 1.1. \tag{7.139}$$

7.4.5.6 Air Supply with Vertical Jets

Air supplied in confined space by downward vertical jets creates a similar flow pattern as in the case of air supply by horizontal nonattached jets. With vertical air supply, the occupied zone is ventilated directly by air jets. Grimitlyn[137] suggests that the area of occupied zone ventilated by one jet be sized based on the jet's cross-sectional area at the point it enters the occupied zone. The jet cross-sectional area and configuration depend upon the height of the air supply, the type of air jet, and diffuser characteristics (K_1 and K_2).

7.4.6 Jet Interaction

Diffuser jet interaction is a common case when air is supplied into ventilated rooms through multiple air diffusers (e.g., sidewall-mounted grills or ceiling-mounted air diffusers) or using speciality air distribution systems. Interacting jets can be supplied

- Parallel to each other
- In the opposite direction toward each other (e.g., from the outlets located on the opposite walls)
- Coaxially
- At an angle to each other

Studies of some common cases of jet interaction are discussed in this section.

7.4.6.1 Interaction of Parallel Jets

Interaction of parallel air jets is the most common case. It was thoroughly studied by Baturin,[138] Koestel and Austin,[139] Grimitlyn,[56,140] Bashus and Kocheva,[141] Posokhin,[142] Nosovitsky,[143] Kuzmina,[144] Vasilyeva,[145] and Shepelev.[42] Researchers developed equations describing velocities and temperatures in two or more interacting jets assuming that momentum and heat content of the flow through the elementary area in the cross-section of the resulting jet is equal to the sum of momentums and heat contents through the same area of the separate interacting jets. It was also assumed that separate jets do not influence each other. Derivation of velocities based on these assumptions described by Shepelev[42] is presented below.

Air velocity v_{Σ} at any point (X,Y,Z) of the flow created by interaction of two parallel jets supplied from outlets located at a distance $2a$ from each other (Fig. 7.50) can be described by

$$v_{\Sigma}^2 = v_1^2 + v_2^2, \tag{7.140}$$

where

$$v_1 = \frac{K_1 v_0 \sqrt{A_0}}{X} e^{-\frac{1}{2}\frac{(Y-a)^2+Z^2}{(cX)^2}} \tag{7.141}$$

$$v_2 = \frac{K_1 v_0 \sqrt{A_0}}{X} e^{-\frac{1}{2}\frac{(Y+a)^2+Z^2}{(cX)^2}}. \tag{7.142}$$

Air velocity in the resulting flow in the plane of the interacting jets' axis ($Z = 0$) derived from Eqs. (7.140)–(7.142) is

$$v_{\Sigma} = \frac{K_1 v_0 \sqrt{A_0}}{X}\left[e^{-\left(\frac{Y-a}{cX}\right)^2} + e^{-\left(\frac{Y+a}{cX}\right)^2}\right]^{\frac{1}{2}}. \tag{7.143}$$

Air velocity on the axis of one of interacting jets ($Y = a$ or $Y = -a$) is

$$v_{x1} = \frac{K_1 v_0 \sqrt{A_0}}{X}\left[1 + e^{-\left(\frac{2a}{cX}\right)^2}\right]^{\frac{1}{2}} \tag{7.144}$$

If $\lambda = (v_{x1} - v_x)/v_x$ is the relative increase of axial air velocity in one of the interacting jets due to the influence of the other, then the length of the jet X^*

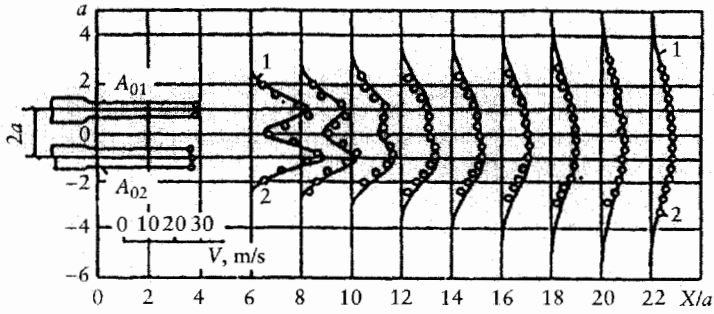

FIGURE 7.50 Interaction of two parallel compact jets.

within which the influence of the interacting jet would be less than, e.g., 10% ($\lambda = 0.1$) can be obtained from

$$X^* = \frac{2a}{c}\frac{1}{\sqrt{-\ln\lambda(2-\lambda)}} \approx \frac{24.4a}{\sqrt{-\lambda(2-\lambda)}} = 26.4a, \tag{7.145}$$

which means that the axial velocity of the interacting jet is influenced by another jet only beginning with X^* exceeding 13.2 times the distance between the outlets.

Velocity along the axis of symmetry between the interacting jets can be calculated assuming $Y = 0$ in Eq. (7.143):

$$v_{\Sigma x} = \frac{K_1 v_0 \sqrt{2A_0}}{X} e^{-\left(\frac{a}{cX}\right)^2}. \tag{7.146}$$

Air velocity along the jet supplied from the outlet with opening area equal to $2A_0$ is

$$v_x = \frac{K_1 v_0 \sqrt{2A_0}}{X}. \tag{7.147}$$

If $\lambda = (v_x - v_{x1})/v_x$ is the relative difference between the axial air velocity in the jet with double opening area and the air velocity along the axis of symmetry of the interacting jets, then the length of the jet X^{**} within which this ratio would be less than, e.g., 10% ($\lambda = 0.1$) can be obtained from

$$X^{**} = \frac{a}{\sqrt{2}c}\frac{1}{\sqrt{-\ln(1-\lambda)}} \approx \frac{8.62}{\sqrt{-\ln(1-\lambda)}} = 26.5a. \tag{7.148}$$

This approach can be used for interacting jets supplied from outlets with different area of discharge with different initial air velocities. In this case the equation for air velocity in the flow of interacting jets will be

$$v_\Sigma = \frac{K_1}{X}\left[v_{01}^2 A_{01} e^{-\left(\frac{Y-a}{cX}\right)^2} + v_{02}A_{02} e^{-\left(\frac{Y+a}{cX}\right)^2}\right]. \tag{7.149}$$

Comparison of the calculations using Eq. (7.143) with experimental data collected by Vasilyeva[145] at $v_{01} = 38.1$ m/s, $v_{02} = 36.6$ m/s, $D_{01} = 0.03$ m, $D_{02} = 0.04$ m, $a = 0.05$ m is presented in Fig. 7.50 from Shepelev.[42]

Jet interaction should not be taken into account when the jets are closely adjacent to each other, are propagated in confined conditions, and entrainment of the ambient air is restricted. This may be the case for concentrated air supply when air diffusers are uniformly positioned across the wall and the jets are replenished by the reverse flow, which decreases the jet velocity. This effect should be taken into consideration using the confinement coefficient K_c discussed in Section 7.4.5. For the same reason, jet interaction should not be taken into consideration when air is supplied through the ceiling-mounted air diffusers and they are uniformly distributed across the ceiling.[56]

For the most common practical situation, when air is supplied by parallel jets from several diffusers placed in one plane and having the same outlet area A_0 and discharge velocity v_0, the resulting velocity on the axis of the coalesced flow v_Σ can be found:[56]

- For compact and incomplete radial jets from

$$\frac{v_\Sigma}{v_0} = K_1 \frac{\sqrt{A_0}}{X} K_{\text{int}} \tag{7.150}$$

- For linear jets from

$$\frac{v_\Sigma}{v_0} = K_1 \sqrt{\frac{H_0}{X}} K_{\text{int}}. \tag{7.151}$$

The above relations can also be used as a first approximation to find the temperature drop in interacting jets by substituting $\Delta\theta_\Sigma$, $\Delta\theta_0$ and ΔK_2 for v_Σ, v_0, and K_2, respectively. The values of interaction coefficient K_{int} for even and odd numbers of outlets are given in Fig. 7.51, reproduced from Grimitlyn.[56]

7.4.6.2 Interaction of Jets Supplied from Opposite Directions

For practical applications related to space ventilation and air-conditioning, interaction of similar jets with equal size and initial momentum supplied from the opposite walls (Fig. 7.52) were studied by Roeder,[146] Conrad,[147] Urbach,[148] Regenscheit,[149] and Smirnova.[1]

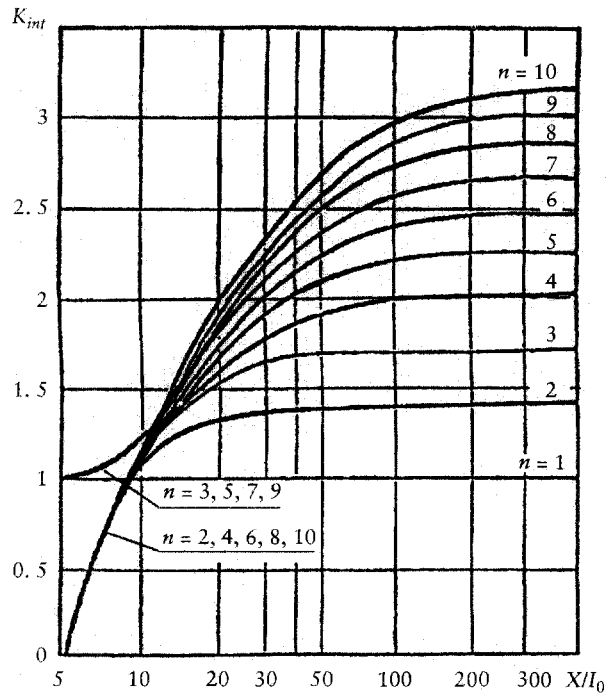

FIGURE 7.51 Coefficient K_{int} of interaction for the jets discharging from the opening located in a single row. Reproduced from Grimitlyn.[56]

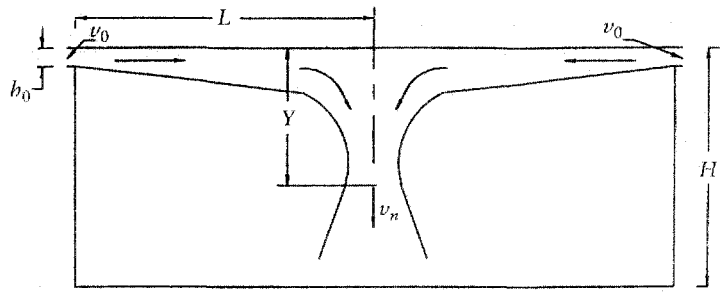

FIGURE 7.52 Interaction of two jets supplied from the opposite walls.

Conrad[147] compared impingement of two opposite linear jets attached to the ceiling with a linear jet changing its direction after impingement with a wall. For the attached jet, maximum air velocity along the jet can be described by

$$\frac{v_m}{v_0} = \left(\frac{h_0}{mX}\right)^{0.375}, \tag{7.152}$$

where m is a supply outlet characteristic that can range from 0.1 to 0.4,[58] and X is the distance from the slot to the point of interest. After changing the jet direction, the velocity in the vertical jet can be obtained from

$$\frac{v_m}{v_0} = K\left(\frac{h_0}{mL}\right)^{0.375}\left(\frac{L}{L-Y}\right)^q, \tag{7.153}$$

where Y = vertical distance from the ceiling to the point of interest, L = length of jet travel along the ceiling; $K = 1$, $q = 0.2$ when the jet travels vertically along the wall; $K = 0.65$, $q = 1$ in the case of two-jet interaction. In discussion of the data obtained by Conrad and Roeder, Regenscheit[149] suggested that the values of K and q also depend upon the relative distances L/h_0 and Y/h_0 and the characteristic m. Based on the data by Urbach,[148] Regenscheit concluded that K and q parameters also depend upon ratios L/H and h_0/H. Research data also show that air velocities in the combined vertical jet are lower than in the jet after its interaction with a wall.

The above data as well as studies of compact and radial jet interaction conducted by Smirnova, Avdeeva, and Gunes were summarized by Grimitlyn.[1] Grimitlyn suggested that the air velocity in the jet resulting from impingement of two similar opposite jets is

$$v_\Sigma = K_{\text{int}}^{\text{op}} v_x \tag{7.154}$$

where $K_{\text{int}}^{\text{op}}$ can be evaluated from the graph in Fig. 7.53. The graph shows that smaller relative distance between jet supply outlets and the point of jet interaction, a/b_0 (for linear jets) or $a/\sqrt{A_0}$ (for radial and compact jets), results in smaller air velocities in the combined jet.

7.4.6.3. Interaction of Coaxial Jets

During the last two decades, a new generation of HVAC systems with concentrated air supply assisted by directing jets was introduced in several European countries.[150,151] In one common modification, the main streams of ventilating air (heated or chilled) are supplied through a small number of air openings (grills) at low initial velocities and distributed within the space by horizontal (coaxial with main streams)

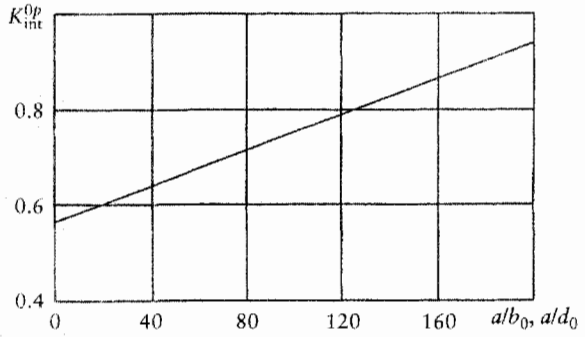

FIGURE 7.53 Coefficient K_{int} of opposite jets interaction. Reproduced from Grimitlyn.[1]

and vertical (supplied perpendicular to the main streams), or only horizontal, directing jets (Fig. 7.54). These jets are discharged at high velocities from nozzles having small outlet diameters. The air is delivered to these nozzles from a separate air handling unit. The same principle is utilized by the "air piston system,"[151] in which horizontal directing jets are created by axial or radial fans located along the main streams. Analytical and experimental studies on the interaction of main streams of supplied air and horizontal directing jets in laboratories and in the field conducted by Zhivov[25,132,152] laid the ground for the design method of such systems.

Interaction of the Free Isothermal Main Stream and Horizontal Directing Jets

The characteristic feature of the main stream and horizontal directing jet interaction is that the directing jets are supplied through nozzles located at some distance from each other and from the outlet supplying the main stream (Fig. 7.55).

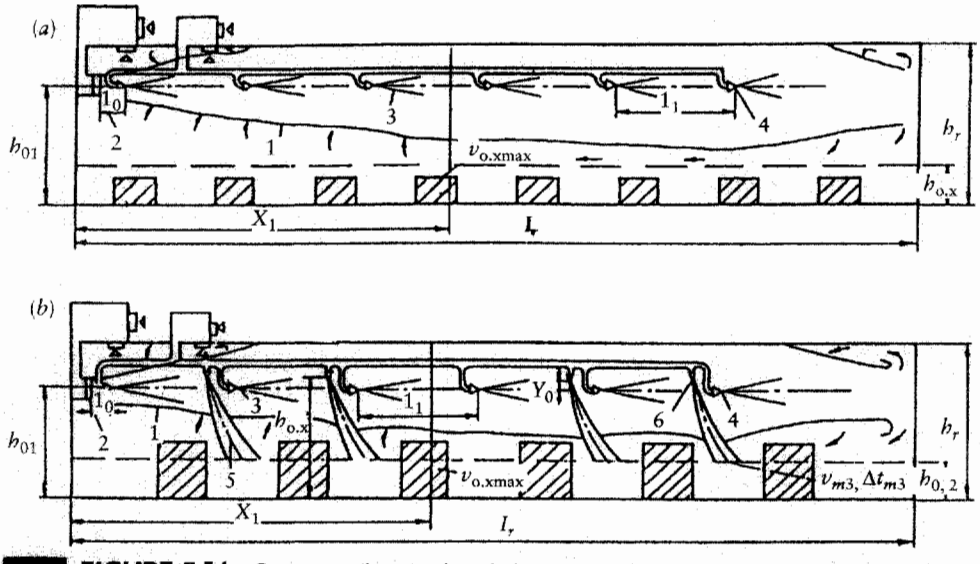

FIGURE 7.54 Concentrated air supply with directing jets: (*a*) with horizontal directing jets; (*b*) with vertical directing jets; 1—main stream; 2—main stream air diffuser; 3—horizontal directing jet; 4—horizontal directing jet nozzle; 5—vertical directing jet; 6—vertical directing jet nozzle. Reproduced from Zhivov,[131].

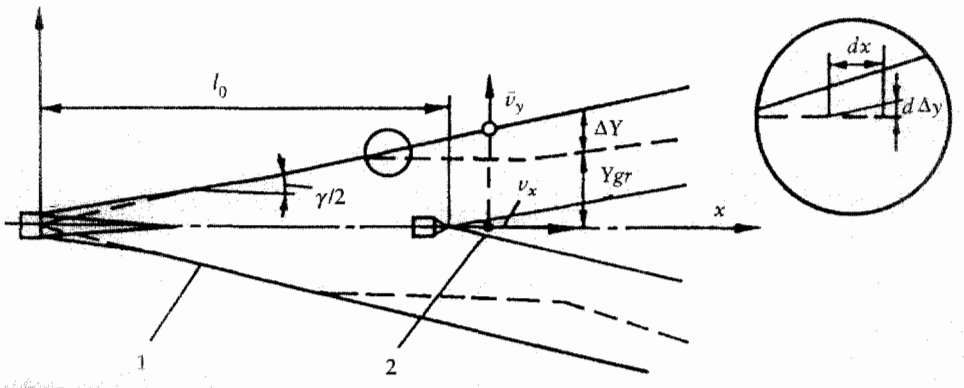

FIGURE 7.55 Schematic of free isothermal main stream and horizontal directing jet interaction: 1—main stream (D_{01}, V_{01}, I_{01}, d_{01}, K_{11}); 2—directing jet (D_{02}, V_{02}, I_{02}, d_{02}, K_{12}). Reproduced from Zhivov,[131]

Experimental studies with propane, as a tracer gas, introduced into the main stream showed that directing jets make the main stream narrower. Velocity profiles $v_{i\Sigma}$ in cross-sections of the resulting stream (created by the main stream and directing jets) can be described by the formula derived, assuming the resulting stream momentum is equal to the sum of interacting jet initial momentums. For maximum velocity in the resulting airflow in the cross-section of the $(N-1)$ nozzle, this equation is

$$v_{m\Sigma} = v_{02}\frac{d_{02}}{l_i}\sqrt{\frac{I_{01}}{I_{02}}\left(\frac{K_{11}}{K_{12}}\right)^2 + \sum_{k=1}^{N-1}\frac{1}{k^2}}, \tag{7.155}$$

where K_{11} and K_{12} are coefficients of velocity decay in the main stream and directing jets, respectively, v_{02} is the horizontal directing jet supply air velocity, I_{01} and I_{02} are main stream and horizontal directing jet momentum, respectively, and d_{02} is the horizontal directing jet nozzle diameter.

To derive the equation for the jet boundary resulting from the interaction of coaxial main flow and a directing jet supplied at the distance l_0 from the main outlet, this interaction was presented[152] as the interaction of the main jet with a sink distributed along its axis (Fig. 7.55). Considering the influence of the directing jet on the main flow boundary as ΔY, the half width of the resulting flow can be presented as

$$Y_b = \Lambda X - \Delta Y, \tag{7.156}$$

where

$$\Delta Y = \int_x^0 \frac{d(\Delta Y)}{dX}dX. \tag{7.157}$$

Λ is the coefficient characterizing the angle γ of the main flow divergence (Fig. 7.55) without the directing jets' influence. The following relationship was derived for the resulting flow boundary:

$$Y_b = \Lambda X - \frac{\theta}{K_{12}^2}\frac{I_{02}}{I_{01}}l_0\Phi(\bar{X}) \tag{7.158}$$

$$\Phi(\bar{X}) = \int_0^X \left(1 + \frac{1}{\sqrt{1 + K_{11}^2\left(\frac{\bar{X}}{\bar{X}-1}\right)^2}}\right)^2 d\bar{X}, \tag{7.159}$$

where θ is an experimental coefficient and $\bar{X} = X/l_0$.

In the case of several directing jets interacting with a main stream, the above approach was used assuming that each following directing jet interacts with the resulting flow created by the main flow and the previous directing jets. The equation for the resulting flow boundary differs from Eq. (7.158) only by the expression for the $\Phi(X)$ function.

Interaction of the Confined Isothermal Main Stream with Horizontal Directing Jets

The experimental studies[152] show that the resulting jet length in the confined space can be divided into three zones (Fig. 7.56). In the first zone, there is an expansion of the resulting jet boundaries. The length of this zone (X_I) depends upon the relative momentum (I_{02}/I_{01}) value and the relative distance ($l_i/\sqrt{A_r}$) between the directing nozzles, where A_r is the room vertical cross-section area ($b_r \times h_r$). The distance (X_I) increases when the relative momentum (I_{02}/I_{01}) increases and the relative distance ($l_i/\sqrt{A_r}$) decreases. In the second zone, the resulting jet width stays relatively constant. It expands up to the last nozzle, and its length is equal to ($X_{II} - X_I$) and depends on the number of directing nozzles and the distance between them.

In the third zone, there is a significant decrease in resulting jet width. The cross-section in which the jet flow degrades is considered the end of the third zone. The length of the third zone ($X_{III} - X_{II}$) is practically equal to the length of the jet's degradation zone in the confined space without directing jets, which is $2\sqrt{A_r}$. Within the studied range of parameters, the resulting jet throw (X_{III}) reached $10\sqrt{A_r}$.

Beyond the third jet zone, there is a stagnant zone in which the velocity values are relatively uniform and have an unstable direction. There is reverse flow in zones I through III which is located between the jet boundaries and the cylinder walls. The maximum value of the velocity in the reverse flow is in the cross-section at the end of zone I at the distance X_I. The following equation was derived to calculate the length of the first zone X_I:

$$X_I = \frac{0.755}{\Lambda} Y_b + \frac{\theta}{\Lambda K_{11}^2} \frac{I_{02}}{I_{01}} l_i \Phi(\bar{X}). \tag{7.160}$$

The average experimental value of the coefficient θ is 1.7 with a standard deviation (σ_θ) of 0.05. Equation (7.160) allows one to calculate the momentum ratio (I_{02}/I_{01}) required to extend the length of zone I to the value equal to X_I, given that the distance between the directing nozzles is equal to l_i. The graph presented in Fig. 7.56 is plotted according to Eq. (7.160) for K_{11} and K_{12} equal to 6.2. The maximum value of reverse flow velocity (v_{rev}) was found to be in the cross-section at X equal to X_I:

$$v_r^{\max} = 0.73 v_{01} \sqrt{\frac{A_{01}}{A_r}\left(1 + \frac{SI_{02}}{I_{01}}\right)}, \tag{7.161}$$

where A_0 is the main stream supply air diffuser area, and S is the number of horizontal directing jets in zone 1.

Interaction of a Nonisothermal Main Stream with Horizontal Directing Jets

Studies of nonisothermal main stream and horizontal directing jet interaction were conducted to evaluate the maximum heat load that can be effectively supplied by such HVAC systems. To summarize experimental data both in free and confined conditions, it was suggested that the above limiting condition is achieved when the current Archimedes number Ar_x (ratio of the buoyancy forces over inertia forces along the resulting jet axis) does not exceed some value μ:

$$\mathrm{Ar}_x = \frac{gX}{v_{x\Sigma}^2}\frac{2\theta_m - \theta_r}{273 + \theta_r} \le \mu. \tag{7.162}$$

For the interaction of the main stream with N directing nozzles, the resulting expression for Ar_x can be presented as:

$$\mathrm{Ar}_x = \frac{K_{21}}{K_{11}^2}\mathrm{Ar}_0\left(\frac{X}{d_{01}}\right)^2\frac{1}{f}, \tag{7.163}$$

where

$$f = \frac{1}{N^2} + \frac{I_{02}}{I_{01}}\left(\frac{K_{12}}{K_{11}}\right)\left(\frac{X}{l_i}\right)^2\sum_{i=1}^{N}\frac{1}{i^2}. \tag{7.164}$$

The current Archimedes number for the resulting jet grows along the jet as it does in any nonisothermal jet. However, the consequent momentum additions by directing jets increases the inertial forces in the resulting jet and thus at a certain cross-section the current Archimedes number falls. The number of directing jets after which Ar_x reaches the peak can be calculated using

$$N^* = \frac{1}{\sqrt{\frac{I_{02}}{I_{01}}\left(\frac{K_{12}}{K_{11}}\right)^2\left(1.202\sum_{i=1}^{N^*}\frac{1}{i^3}\right)}}. \tag{7.165}$$

From the experimental data for the free resulting jet, the μ value in Eq. (7.162) is equal to 0.075. Tests in field showed that the influence of the re-

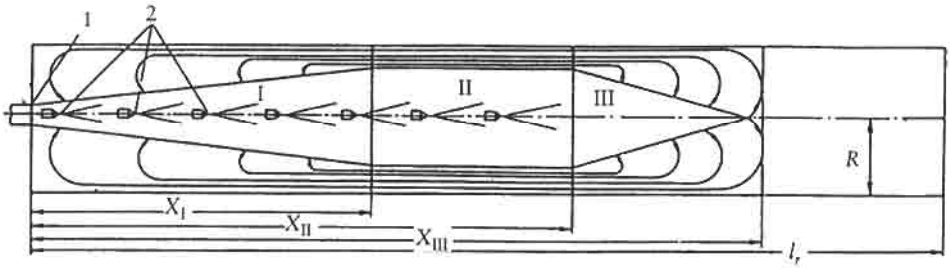

FIGURE 7.56 Schematic of confined main and horizontal directing jets interaction: 1—main flow; 2—directing jet. Reproduced from Zhivov.[132]

verse flow and confining surfaces increases the value of μ to 0.2. Based on Eq. (7.162) and experimental μ values, the maximum initial air temperature supplied by the main stream is limited by

$$\theta_0 - \theta_r \leq a \frac{K_{f1}^2}{K_{21}} \frac{v_{01}^2 d_{01}}{l_i^2} f, \tag{7.166}$$

where a is a coefficient equal to 2.65 for a free jet and 7.07 for a confined jet.

7.4.6.4 Interaction of Jets Supplied at an Angle to Each Other

There are only a few studies of air jets supplied at some angle α ($0° < \alpha < 90°$) to each other. To predict characteristics (trajectory, velocity decay, etc.) of the flow resulting from interaction of two jets supplied at some angle toward each other, Hudenko[153] proposed to sum momentums of interacting jets as in the case with parallel jets. He has estimated that the error of prediction will be smaller at a smaller

- Interaction angle
- Distance between the supply nozzles
- Difference in the nozzle sizes
- Supply air velocity values

Meshalin[154] conducted experimental studies of two equal jets supplied at angles of 15°, 30°, and 45° to each other. Based on the results of his studies, the author concluded that

- The turbulent mass transfer in the flow resulting from the interaction of the two jets is more extensive than in a single jet under the same supply conditions.
- The intensity of mass transfer in the flow in the plane of the interacting jets' axis is lower than in the plane of symmetry.
- The intensity of mass transfer in the resulting flow increases with the angle of interaction.

Numerous studies of jets supplied into a uniform or nonuniform cross-flow were conducted in application to such areas as air pollution control, burning processes, etc. Detailed discussion of these studies is beyond the current review. However, some results of these studies will be mentioned as needed in the following section.

Interaction of a Free Isothermal Main Stream with Directing Jets Supplied at a Right Angle to the Main Stream

As in the case of the interaction of coaxial directing jets, the interaction of main streams with directing jets supplied at a right angle was studied[25,131] to develop a design method for air distribution with horizontal and vertical directing jets.

The discussion of the interaction of air jets supplied at some angle to each other shows that application of the method of superposition of the interacting jets' momentums and surplus heat to predict velocity and temperatures in the combined flow results in inaccuracy when two unequal jets are supplied at a right angle. A different approach was undertaken in the studies of interaction of the main stream with vertical directing jets.[25,131]

Visualization studies of the resulting flow showed that the directing jet changes its initial direction due to its interaction with a main stream. The interaction results in two separate flows; the first is a continuation of the main stream and the second is a continuation of the directing jet. The specific feature of this interaction is that vertical directing nozzles are located within a main stream (Fig. 7.57). The median diameter of the directing jet is significantly (several times) smaller than the main stream diameter within a zone of their interaction. Thus, the interaction of the main stream and the vertical directing jet can be seen as an interaction of the axisymmetric (directing) jet with an infinite cross-draft with a nonuniform velocity profile.

An analytical solution of the interaction in the case of isothermal main and directing jets, assume that the main stream (Fig. 7.57), supplied with initial velocity (v_{01}) through a nozzle that has internal diameter (d_{01}), is developing within a zone ($-l_0$, 0) as a free jet. The momentum (I_1) of the jet within the zone ($-l_0 + l_c$, 0) remains equal to the initial momentum (I_{01}), and the velocity distribution in the cross-section of interaction in the plane XY remains the same within the zone (0, X_A). The axisymmetric main stream within the zone (0, X_A) is substituted by the linear flow with velocity profile that can be described by the formula

$$v_{i1} = v_{m1} e^{-\frac{1}{2}\left(\frac{Y - Y_0}{c l_0}\right)^2}, \quad X \in [0, X_A], \quad c = 0.082 \tag{7.167}$$

The directing jet is supplied at a right angle to the main stream axis with an initial velocity of v_{03} from the nozzle with an inner diameter (d_{03}) located at the distance (l_0) from the plane of main stream supply and at the distance Y_0 from its geometrical axis. The momentum vector component along the Y axis remains constant and equal to the initial momentum (Fig. 7.57):

$$I_3 \cos\beta = I_{03}, \tag{7.168}$$

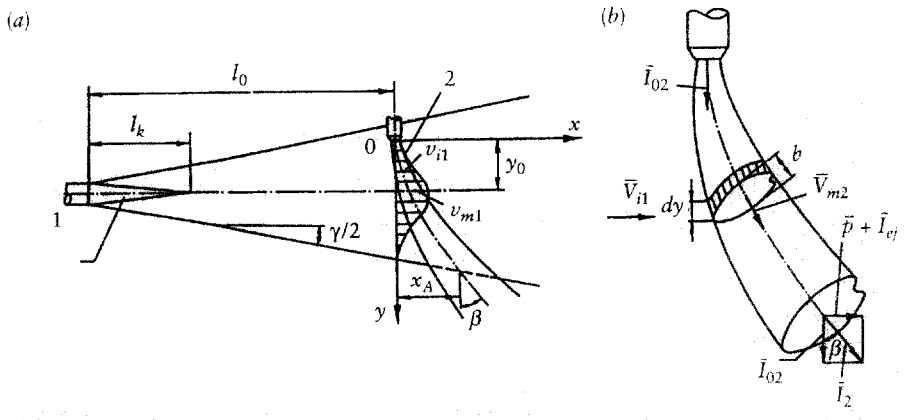

FIGURE 7.57 Schematic of free isothermal main stream and vertical directing jet interaction: 1—main stream (D_{01}, V_{01}, l_{01}, d_{01}, K_{11}); 2—directing jet (D_{03}, V_{03}, l_{03}, d_{03}, K_{13}). Reproduced from Zhivov. [13]

where β is the angle between the Y axis and the tangent to the directing jet trajectory

$$I_{03} = \rho_{03} v_{03}^2 \frac{\pi d_{03}^2}{4}. \tag{7.169}$$

The aerodynamic force (P) of the main stream and the momentum of the injected air (I_{inj}) change the X component of the directing jet. The X component of the directing jet can be calculated from

$$I_3 \sin\beta = P + I_{inj}. \tag{7.170}$$

Experimental studies have shown that velocity distribution in the cross-section of the directing jet can be described by the same equation as those in the axisymmetric jet in a cross-draft,

$$\frac{V_{i3}}{V_{03}} \cos(\bar{v}_{i3}, \bar{n}) = \left[1 - \left(\frac{r_i}{R_b}\right)^{1.5}\right]^2, \tag{7.171}$$

where $r_i = \sqrt{S_i/\pi}$, $R_b = b/2$, and S_i is a cross-sectional area limited by the constant velocity line. The joint solution of Eqs. (7.168), (7.170), and (7.171) results in the following expression for the maximum velocity along the directing jet:

$$\frac{V_{m3}}{V_{03}} = \chi_v \frac{d_{03}}{Y}, \tag{7.172}$$

where

$$\chi_v = \frac{m_2}{1 + \frac{a}{q^k}} \frac{1}{\sqrt{\cos\beta}}. \tag{7.173}$$

When $\beta < 25°$, $\sqrt{\cos\beta} \approx 1$.

The differential equation for the directing jet trajectory was obtained by the joint solution of Eqs. (7.168) and (7.170) assuming $\sqrt{\cos\beta} = 1$:

$$tg\beta = \frac{dX}{dY} = \frac{P + I_{inj}}{I_{03}} = \frac{c^2 k_0}{3} \frac{m_1}{\chi_v} I_0 \frac{1}{I_{03}} A, \tag{7.174}$$

where

$$A = e^{-\left(\frac{Y_0}{cl_0}\right)^2} - e^{-\left(\frac{Y - Y_0}{cl_0}\right)^2} + \frac{\sqrt{\pi} Y_0}{cl_0}\left[\operatorname{erf}\left(\frac{Y - Y_0}{cl_0}\right) + \operatorname{erf}\left(\frac{Y}{cl_0}\right)\right] \tag{7.175}$$

The equation for the directing jet trajectory was obtained by the integration of Eq. (7.174) at $X = 0$, $Y = 0$:

$$X = \frac{ck_0}{3} \frac{m_1^2}{\chi_v} \frac{I_{01}}{I_{03}} B, \tag{7.176}$$

where

$$B = (Y - Y_0)\left[e^{-\left(\frac{Y_0}{cl_0}\right)^2} + \frac{\sqrt{\pi} Y_0}{cl_0}\left(\frac{Y_0}{cl_0}\right)\right] - \frac{cl_0\sqrt{\pi}}{2}\left[\operatorname{erf}\left(\frac{Y - Y_0}{cl_0}\right) + \operatorname{erf}\left(\frac{Y_0}{cl_0}\right)\right]$$
$$+ Y_0\left[e^{-\left(\frac{Y - Y_0}{cl_0}\right)^2} + \frac{\sqrt{\pi}(Y - Y_0)}{cl_0} \operatorname{erf}\left(\frac{Y - Y_0}{cl_0}\right)\right]. \tag{7.177}$$

Based on Eqs. (7.175) and (7.177) one can conclude that beyond the boundary of the main stream the directing jet has a straight trajectory.

Visualization studies of the directing jet showed that after interacting with a main stream the directing jet has a straight trajectory when β is less than 50°. At a greater value of β ($tg\beta > 1.2$) the directing jet trajectory is significantly curved.

In the case of a nonisothermal directing jet, the above assumptions are true, except that the momentum vector component along the Y axis changes due to the buoyancy force:

$$dI_{y3} = \pm dG \tag{7.178}$$

The amount of heat W_3 along the directing jets remains constant.

Experimental studies have shown[131] that the temperature distribution in the cross-section of the directing jets can be described as follows:

$$\frac{\theta_{i3} - \theta_r}{\theta_{o3} - \theta_r} = 1 - \left(\frac{r_i}{R_b}\right)^{1.5} \tag{7.179}$$

Based on the above assumptions, the following equations were derived to calculate the velocity and temperature decay along the nonisothermal directing jet:

$$\frac{V_{m3}}{V_{03}} = \chi_r \frac{d_{03}}{Y} \sqrt{1 \pm 1.8 \mathrm{Ar}_y \sqrt{\cos\beta} \sqrt{\frac{\rho_{03}}{\rho_r}}} \tag{7.180}$$

$$\frac{\theta_{m3} - \theta_r}{\theta_{o3} - \theta_r} = \chi_t \frac{\sqrt{\cos\beta} \sqrt{\frac{\rho_{03}}{\rho_r}}}{\sqrt{1 \pm 1.8 \mathrm{Ar}_y \sqrt{\cos\beta} \sqrt{\frac{\rho_{03}}{\rho_r}}}} \frac{d_{03}}{Y} \tag{7.181}$$

where

$$\mathrm{Ar}_y = \frac{1}{\chi_v} \frac{g d_{03}}{v_{03}^2} \frac{\theta_{03} - \theta_r}{273 + \theta_r} \left(\frac{Y}{d_{03}}\right)^2 \tag{7.182}$$

and

$$\chi_t = \frac{n_3}{1 + \frac{a}{q^k}}. \tag{7.183}$$

In the case when there is no main stream ($v_{01} = 0$, $q = \infty$, and $\beta = 0$), Eqs. (7.180) to (7.183) reduce to those for free jets.

Joint solution of Eqs. (7.170) and (7.178) allows one to calculate the maximum amount of heat supplied by a directing jet with the assumption that the jet reaches the occupied zone ($v_{m3} > 0.1$ m/s) and $(tg\beta_n - tg\beta)/tg\beta$ is less than 0.2 at the point where it enters the occupied zone. The maximum initial temperature difference of the air supplied by vertical directing jet is

$$(\theta_{03} - \theta_r)^{\max} = 32 \frac{v_{03}^2 d_{03}}{(h_{03} - h_{o,z})^2} \frac{1}{1 + 23.7 \sqrt{\frac{d_{01}}{l_0}}} \tag{7.184}$$

Based on the experimental results, the following values of coefficients were found: $a = 9.5$, $k = 0.25$, $k_0 = 3.3$ at $0° < \beta < 25°$ and $k_0 = 2.4$ at $25° < \beta < 50°$.

References

1. Grimitlyn, M. I. 1994. *Air Distribution in Rooms.* St. Petersburg.
2. Tuve, G. L. 1953. Air velocities in ventilating jets. *Heating, Piping and Air Conditioning*, January, pp. 181–191.
3. Abramovich, G. N. 1960. *Theory of Turbulent Jets.* Fizmatgiz, Moscow.
4. Shepelev I. A. 1961. Supply ventilation jets and air fountains. In *Proceedings of the Academy of Construction and Architecture of the USSR*, no. 4.
5. Grimitlyn, M. 1970. Zurluftverteilung in raumen. *Luft und Kältetechnik*, no. 5, pp. 246–256.
6. Madison, R., and W. R. Elliot. 1946. Throw of air from slots and jets. *Heating, Piping and Air Conditioning*, November, pp. 108–109.
7. Weinhold, K., R. Dannecker, and U. Schwiegk. 1969. Über auslegungsverfahren von lüftungsdecken. *Luft und Kältetechnik*, no. 2, pp. 78–84.
8. Trüpel, T. 1915. Uber die einwirkung eines luftstrahles auf die umgebende luft. *Z. fur das Gesammte Turrbinenwesen*, nos. 5–6.
9. Förthmann, E. 1934. Über turbulente strahleasbreitung. *Ing. Archiv.*, vol. V, no. 1, pp. 42–54.
10. Albertson, M. L., Y. B. Dai, R. A. Jensen, and H. Rouse. 1948. Diffusion of submerged jets. In *Proceedings of the ASCE*, vol. 74, p. 1751.
11. Tollmien, W. 1926. Sonderabdruck aus zeitschrift für angewandte. *Mathematik und Mechanik*, vol. 6, pp. 468–478.
12. Schlichting, H. 1930. Ueber das ebene windschaftenproblem. *Ing. Arch.*, no. 5.
13. Reichardt, H. 1942. Gesetzmäßigkeiten der freien turbulentz. *VDI*, Forschungsheft 414.
14. Görtler, H. 1942. Berechnung von aufgaben der freien turbulentz auf grund eines neunen näherungsansatzes. *Z. Angewandte Math. Mech.*, vol. 22, no. 3, pp. 245–254.
15. Heskestad, G. 1966. Hot-wire measurements in a radial turbulent jet. *Transactions ASME: Journal of Applied Mechanics*, no. 33, pp. 417–424.
16. Ruden, P. 1933. Turbulente ausbreitungsvorgänge im freistrahl. *Naturwissenschaften*, bd. 21, nos. 21–23.
17. Taylor, J. F., H. L. Grimmett, and E. W. Comings. 1951. *Chemical Engineering Progress*, no. 4, pp. 175–180.
18. Keagy, W. R., and A. E. Weller. 1949. *Proceedings of the Heat Transfer and Fluid Mechanics Institute*, ASME, pp.89–98.
19. Pai, S. I. 1949. Two dimensional jet mixing of a compressible fluid. *Journal of Aeronautical Sciences*, August, pp. 463–469.
20. Becher, P. 1949. Calculation of jets and inlets in ventilation. Ph.D. thesis. Technical University of Denmark, Copenhagen.
21. Nottage, H. B., J. G. Slaby, and W. P. Gojza. 1952. ASHVE Research Report No. 1459: Exploration of a chilled jet. *ASHVE Transactions*, vol. 58, p. 357.
22. Grimitlyn, M. I. 1973. Principles of air distribution in ventilated spaces. D.Sc. thesis. VVISKU, Leningrad.
23. Abramovich, G. N. 1984. *Theory of Turbulent Jets.* Fizmatgiz, Moscow.
24. Gendrikson, V. A., and Y. V. Ivanov. 1973. Some regularities of axisymmetric jets supplied at an angle to the cross-draft. In *Proceedings of the Tashkent Polytechnical Institute*, vol. 101, pp. 184–198.
25. Zhivov, A. M. 1982. Investigation of the interaction of axially symmetric turbulent jets supplied under straight angles to each other. In *Turbulent Jet Flows: Theses of Reports of the Fourth All Union Scientific Conference on Theoretical and Applied Aspects of Turbulent Flows*, part II. Estonian Academy of Sciences, Tallinn.
26. Abramovich, G. N. 1948. *Turbulent Free Jets of Liquids and Gases.* Gosenergoizdat, Moscow.
27. Loitzansky, L. G. 1973. *Mechanics of Fluid and Gas.* Nauka, Moscow.
28. Rydberg, J., and P. Norback. 1949. ASHVE Research Report No. 1362: Air distribution and draft. *ASHVE Transactions*, vol. 55.

29. Kraemer, K. 1971. Die potentialströmung in der umgebung von freistrahlen. *Zeitschrift für Flugwissenschaften*, vol. 19, no. 3, pp. 93–104.
30. Rodi, W. 1982. *Turbulent Buoyant Jets and Plumes*. Pergamon Press, New York.
31. Baturin, V. V. 1972. *Fundamentals of Industrial Ventilation*. 3rd English ed. Pergamon Press, New York.
32. Rajaratnam, N. 1976. *Turbulent Jets*. Elsvier, Amsterdam.
33. Nielsen, P. V., and Åke T. A. Moller. 1988. Measurements on buoyant jet flows from a ceiling-mounted slot diffuser. In *The 3rd Seminar on Applications of Fluid Mechanics in Environmental Protection-88*. Selesian Technical University, Gliwice, Poland.
34. Becher, P. 1950. Luftstrahlen aus ventilationsöffnungen. *Gesundheits-Inginieur*, vol. 71, p. 139.
35. Heskestad, G. 1965. Hot-wire measurements in a plane turbulent jet. *Transactions ASME: Journal of Applied Mechanics*.
36. Miller, D. R., and E. W. Comings. 1960. Force momentum fields in a dual-jet flow. *Journal of Fluid Mechanics*, vol. 7, no. 2, p. 237.
37. van der Hegge Zijnen, B. G. 1958. Measurement of the velocity distribution in a plane turbulent jet of air. *Applied Sci. Res.*, A7, pp. 256–276.
38. van der Hegge Zijnen, B. G. 1958. Measurement of the distribution of heat and matter in a plane turbulent jet of air. *Applied Sci. Res.*, A7, pp. 277–292.
39. Gutmark, E., and I. Wygnanski. 1976. The planar turbulent jet. *Journal of Fluid Mech.*, vol. 73, p. 3.
40. Kotsovinos, N. E., and E. L. List. 1977. Plane turbulent buoyant jets. Part 1: Integral properties. *Journal of Fluid Mechanics*, vol. 81, pt. 1.
41. Koestel, A. 1957. Jet velocities from radial flow outlets. *ASHVE Transactions*, vol. 63, p. 505–526.
42. Shepelev, I. 1978. *Aerodynamics of Air Flows in Rooms*. Stroyizdat, Moscow.
43. Regenscheit, B. 1971. Die berechnung von radial strömenden frei- und wandstrahlen, sowie von rechteckstrahlen. H. Krantz-Luttechnik. Aahen-Richterich. *Gesundheits-Ingenieur*, no. 7, pp. 193–201.
44. Baturin, V. V. 1959. *Lüftungsanglagen für Industrielbaten*. Auft, Berlin.
45. ASHRAE. 1997. *Handbook of Fundamentals*, Chapter 31. Amercian Society of Heating, Regrigeration and Air-Conditioning Engineers, Atlanta.
46. Vulis, L. A., V. G. Zhivov, and L. P. Yarin. 1969. Transition zone in a free jet. *Inz.-Phyz. Zhurnal*, vol. XVII, no. 2.
47. Hanel, B., and E. Rechter. 1979. Das verhalten von freistrahlen in verschiedenen Reynolds-Zahlbereichen. *Luft und Kältetechnik*, bd. 15, no. 1, pp. 12–14.
48. Müllejans, H. 1966. *Über die Ähnlichkeit der nicht-isothermen Strömung und den Wandurbergang in Räumen mit Strahlüftung*. Forschungsber des Landes NRW, no. 1656. Westdeutscher Verlag, Köln. (The similarity between non-isothermal flow and heat transfer in mechanically ventilated rooms. BSRIA Translation 202, Bracknell, UK.)
49. Carslaw and Jaeger. 1947. *Conduction of Heat in Solids*. Oxford University Press, New York.
50. Vulis, L. A. 1960. Regarding free turbulent jets computation applying the heat conductivity method. In *Proceedings of Acad. Sci. Kaz. SSR*, Ser. Energy, vol. 2, no. 18.
51. Elrod, H. G. 1954. Computation charts and theory for rectangular and circular jets. *ASHVE Journal: Heating, Piping and Air Conditioning*, March, pp. 149–155.
52. Shepelev, I. A., and N. A. Gelman. 1966. Universal equations for velocity and temperature computation along the ventilation jets, supplied from rectangular outlets (in Russian). *Water-Supply and Sanitary Technique*, no. 7.
53. Regenscheit, B. 1981. *Isotherme Luftstrahlen: Klima+Kälteingenieur*. Verlag C.F. Müller, Karlsruhe.
54. Baturin, V. V. 1965. *Fundamentals of Industrial Ventilation* (in Russian). VtsSPS: Profizdat, Moscow.
55. Chen, C. J., and W. Rodi. *Vertical Turbulent Buoyant Jets: A Review of Experimental Data*. Pergamon Press, New York.
56. Grimitlyn, M. I. 1982. *Air Distribution in Rooms*. Stroiizdat, Moscow.
57. Abramovich, G. N. 1940. Turbulent free jets of liquids and gases. In *Proceedings of TsAGI*, no. 512.
58. Koestel, A. 1954. Computing temperatures and velocities in vertical jets of hot or cold air. *ASHVE Transactions*, vol. 60, pp. 385–410.
59. Reichardt, H. 1944. Impuls und warmeaustausch in freien turbulenz. *ZAMM*, bd. 24, no. 5, 6.
60. Nottage, H. B. 1951. Ventilation jets in room air distribution. Ph.D. thesis. Case Insritute of Technology.
61. Forstall, W., and A. H. Shapiro. 1950. Momentum and mass ttansfer in coaxial gas jets. *Journal of Applied Mechanics*, vol. 17, no. 4.

62. Corrsin, S., and M. S. Uberoi. 1950. *Further Experiments on the Flow and Heat Transfer in a Heated Turbulent Jet.* NACA Report no. 998.
63. Grimitlyn, M. I. 1965. Fundamentals of isothermal and non-isothermal jets. *Theory and design of ventilation jets.* VNIIOT, Leningrad, pp. 27–56.
64. Regenscheit, B. 1959. Die Luftbewegung in klimatisierten räumen (Movement of air in air-conditioned rooms). *Kältetechnik*, heft 1, pp. 3–11.
65. Helander, L., and C. V. Jakowatz. 1948. ASHVE Research Report No. 1327: Downward projection of heated air. *ASHVE Transactions*, vol. 59, p. 71.
66. Helander, L., S. M. Yen, and R. E. Crank. 1953. ASHVE Research Report No. 1475: Maximum downward travel of heated jets from standard long radius ASME nozzles. *ASHVE Transactions*, vol. 59, pp. 241–259.
67. Helander, L., S. M. Yen, and L. B. Knee. 1954. ASHVE Research Report No. 1511: Characteristics of downward jets of heated air from a vertical delivery discharge unit heater. *ASHVE Transactions*, vol. 60, p. 359.
68. Helander, L., S. M. Yen, and W. Tripp. 1957. ASHRAE Research Report No. 1601: Outlet characteristics that affect the down throw of heated air jets. *ASHVE Transactions*, vol. 63, p. 255.
69. Knaak, R. 1957. ASHVE Research Report No. 1619: Velocities and temperatures on axis of downward heated jet from 4-inch long-radius ASME nozzle. *ASHVE Transactions*, vol. 63, pp. 527–538.
70. Regenscheit, B. 1970. Die Archmedes-zhal-kenzah zur beurteilung von raumstromungen. *Gesundheits Ingenieur*, vol. 91, no. 6.
71. Baturin, V. V., and I. A. Shepelev. 1935. Publication in *Heating and Ventilation*, no. 5, Moscow.
72. Turner, J. S. 1973. *Buoyancy Effects in Fluids.* Cambridge University Press, Cambridge.
73. Seban, R. A., M. M. Behnia, and K. E. Abrea. 1978. Temperatures in a heated air jet discharged downward. *International Journal of Heat and Mass Transfer*, vol. 21, pp. 1453–1458.
74. Sato, K., H. Osuka, and J. Inone. 1981. Maximum penetration distance of a vertical buoyant jet. *Int. Chem. Engin.*, vol. 21, no. 3, pp. 435–442.
75. Mizuchina, T. 1982. An experimental study of vertical turbulent jet with negative buoyancy. *Wärme- u. Stoffübertragung*, vol. 16, no. 1.
76. Weidemann, B., and B. Hanel. 1988. Untersuchengen zum verhalten des vertical von oben nach unten ausströmenden runden warmen freistrahls. *Luft und Kältetechnik*, no. 3, pp. 119–124.
77. Nosovitsky, A., and V. Posokhin. 1966. Inclined fountains of heated and chilled air, created by nonisothermal jets supply. In *Heat, Gas Supply and Ventilation.* Budivelnik, Kiev.
78. Omelchuk, V. 1966. Laws of nonisothermal jet development, banded by buoyancy forces. *Water Supply and Sanitary Technique*, no. 2.
79. Filney, M., and A. Nosovitsky. 1967. Air supply by free compact jets. *Proceedings of High School Construction and Architecture*, no. 2.
80. Fleischbacker, G., and W. Schneider. 1975. Experimentelle und theoretische untersuchungen über den einfluß der schwerkraft auf anisoterme, turbulente freistrahlen. *Abhandl. Aus dem Aerodynamischen Institute*, H. 22.
81. Stein, M. 1953. Studies on air jets. *Journal of the Institute of Heating and Ventilating Engineers*, vol. 21.
82. Koestel, A. 1955. Paths of horizontally projected heated and chilled air jets. *Heating, Piping and Air Conditioning*, July, pp. 221–226.
83. Grimitlyn, M. I. 1969. *Modeling and Designing of Air Distribution Devices: Filtration of Industrial Exhausts and Problems of Air Distribution.* Institut Ohranu Truda VtsSPS, Leningrad.
84. Lyakhovsky, D., and S. Syrkin. 1939. Aerodynamics of the torch flowing out into the medium of another density. *Journal of Technical Physics*, vol. 9, no. 9.
85. Frean, D. H., and N. S. Billington. 1955. The ventilating air jets. *Journal of the Institution of Heating and Ventilating Engineers*, December.
86. Taliev, V. 1969. Laws of free non-isothermal axially symmetric jet development. *Water Supply and Sanitary Technique*, no. 1.
87. Schneider, W. 1975. Uber den einfluß der schwerkraft auf anisotherme turbulente freistrahlen.—Abhandl. aus dem Aerodynamischen Institute der Rhein-Westf. Techn. Hochschule Aahen. H. 22.
88. Zhivov, A. M. 1993. Theory and practice of air distribution with inclined jets. *ASHRAE Transactions*, vol. 99, no. 1.
89. Etheridge, D., and M. Sandberg. 1996. *Building Ventilation: Theory and Measurements.* John Wiley & Sons, New York.
90. Nielsen, P. V. 1981. *Luftstrømning i Ventilerede Arbejdslokaler* (Ventilation of Working Areas). SBI-Rapport 128. Statens Byggefoskningsinstitut.

91. Mitkalinny, V. 1961. *Gas Jet Flow in Ovens.* Metallurgisdat, Moscow.
92. Schwarz, W. H., and W. P. Cosart. 1960. The two-dimensional turbulent wall jet. *Journal of Fluid Mechanics*, vol. 10, pp. 481–495.
93. Bakke, P. 1957. An experimental investigation of a wall jet. *Journal of Fluid Mechanics*, vol. 2, pp. 467–472.
94. Waschke, G. 1974. Über die Lüftung mittels isothermer turbulente radialer Deckenstrahlen. Dissertation. RWTH, Aachen, Germany.
95. Sforza, P. M., and G. Herbst. 1970. A study of three dimensional incompressible turbulent wall jets. *AIAA Journal*, vol. 8, pp. 276–293.
96. Nielsen, P.V., L. Evenson, P. Grabau, and J.H. Thulesen-Dahl. 1987. Air distribution in rooms with ceiling-mounted obstacles and three-dimensional isothermal flow. RoomVent '87. *Proceedings of the International Conference on Air Distribution in Ventilated Spaces*, Stockholm.
97. Awbi, H. B. 1991. *Ventilation of Buildings.* Chapman and Hall, London.
98. Farquharson, I. M. C. 1952. The ventilating air jet. *JIHVE*, vol. 19, pp. 449–469.
99. Sawyer, R. A. 1963. Two-dimensional reattaching jet flows including the effects of curvature on entrainment. *Journal of Fluid Mechanics*, vol. 17, pp. 481–498.
100. Bourque, C., and B. G. Newman. 1960. Reattachment of a two-dimensional incompressible jet to an adjacent flat plate. *Aeromechanical Quarterly*, vol. XI, August, pp. 201–232.
101. Sandberg, M., B. Wirén, and L. Claesson. 1992. Attachment of a cold plane jet to the ceiling—length of recirculation region and separation distance. In *Roomvent '92*, vol. 1, Aalborg, Denmark.
102. Sawyer, R. A. 1960. The flow due to a two-dimensional jet issuing parallel to a flat plate. *Journal of Fluid Mechanics*, no. 9, part 4, pp. 543–561.
103. Katz, P. 1973. Der Coanda-effect. *Gesundheits-Ingenieur*, no. 6, pp. 169–192.
104. Miller, P. L., Jr. 1991. Diffuser selection for cold air distribution. *ASHRAE Journal*, vol. 33. September, pp. 32–36.
105. Schwenke, H. 1976. Zur luftstromung in räumen mit wurfluftung. *Luft und Kältetechnik*, no. 1, pp. 11–14.
106. Nielsen, P. V., and Åke T. A. Moller. 1987. Measurement on buoyant wall jet flows in air-conditioned rooms. In *Roomvent '87*. Stockholm.
107. Anderson, R., V. Hassani, A. Kirkpatrick, K. Knappmiller, and D. Hittle. 1991. Experimental and computational visualization of cold air ceiling jets. *ASHRAE Journal*, vol. 33, no. 5.
108. Kirkpatrick, A., T. Malmstrom, K. Knappmiller, D. Hittle, P. Miller, V. Hassani, and R. Anderson. 1991. Use of low temperature air for cooling of buildings. In *Proceedings of the 1991 Building Simulation Conference.*
109. Rodahl, E. 1977. The point of separation for cold jets flowing along the ceiling. In *CLIMA 2000.* Belgrade, Yugoslavia.
110. Baturin, V. V., and V. I. Hanzhonkov. 1939. Air circulation in rooms depending on the location of supply and exhaust openings. *Heating and Ventilating*, Nos. 4–5.
111. Nelson, D. W., and D. J. Stewart. 1938. ASHVE Research Report No. 1076: Air distribution from side wall outlets. *ASHVE Transactions*, vol. 44, no. 77.
112. Bromley, M. F. 1946. Experimental studies of flows distribution. D.Sc. thesis. MISI.
113. Gunes, I. L. 1948. Ventilation of rooms with surplus heat and concentrated air supply. Ph.D. thesis. LISI, Leningrad.
114. Linke, W. 1957. Strömungsvorgänge in zwangsbelüfteten räumen. *VDI-Berichte*, bd. 21, pp. 29–39.
115. Linke, W. 1966. Eigenschaften der strahlüftung (Aspects of jet ventilation). *Kältetechnik Klimatechnik*, vol. 18, no. 3 (BSRAE Translation 103).
116. Müller, H. J. 1977. Einfluß der geometrischen verhältnisse auf die raumunsträmung bei der strahllüftung. *Luft- und Kältetechnik*, no. 6.
117. Baharev, V. A., and V. N. Troyanovsky. 1958. *The Basis of Heating and Ventilating Systems with the Concentrated Air Supply Design and Calculation.* Profizdat, Moscow.
118. Sadovskaya, N. N. 1950. Studies of air circulation in the spaces with heating and ventilating by concentrated air jet supply. Ph.D. thesis. VNIIOT VtsSPS, Leningrad.
119. Sadovskaya, N. N. 1955. Air circulation in spaces with concentrated air jet supply. In *Proceedings of the Conference: Concentrated Air Supply*, issue 4. LIOT, Leningrad.
120. Rozenberg, V. N. 1949. In Lyakhovsky, D. N. *Aerodynamics of the Jet and Torch Processes.* TsKTI, Book 12: Heat Transfer and Aerodynamics. MASHGIZ.
121. Regenscheit, B. 1962. *Das Wierderlengen eines ebenen Strahles an eine Wand.* Hausbericht H. Krantz Lufttechnik. E. Bericht 2376.

122. Jackman, P. J. 1970. *Air Movement in Rooms with Side-Wall Mounted Grilles.* BSRIA Laboratory Report No. 81. Bracknell, UK.
123. Regenscheit, B. 1975. Strahlgesetze und raumströmung. *Klima-Kälte-technik*, vol. 6, pp. 147–150.
124. Holmes, M. J., and E. Sachariewicz. 1973. *The Effect of Ceiling Beams and Light Fittings on Ventilating Jets.* Heating and Ventilating Research Association Laboratory Report No. 79. Bracknell, UK.
125. Nielsen, P. V. 1995. Lecture notes on mixing ventilation. University of Aalborg, Department of Building Technology, Denmark.
126. Söllner, G., and K. Klinkenberg. 1972. Leuchen als störkörper im luftstrom. *HLH*, vol. 23, no. 4.
127. Nielsen, P. V. 1980. The influence of ceiling-mounted obstacles on the airflow pattern in air-conditioned rooms at different heat loads. *Building Service Engineering Research and Technology*, vol. 1, no. 4.
128. Shepelev, I. A., and M. D. Tarnopolsky. 1965. Turbulent air jet spreading in the confined space. In *Heat-, Gas Supply and Ventilation: Proceedings of the Conference.* Budivelnik, Kiev.
129. Grimitlyn, M. I., and G. M. Pozin. 1973. Determination of parameters of the jet developing in a confined space and following a blocked or through-motion pattern. In *Proceedings of VTsNIIOT VTsSPS 91.* Profizdat, Moscow.
130. Sychev, A.T., and G.Y. Volov. 1981. Method of confined jets calculation. In *Proceedings of Acad. Sci. BSSR.* Ser. Phys.-Energ. Sci., no.1.
131. Zhivov, A. M. 1983. Concentrated air distribution with directing jets. Ph.D. thesis. All-Union Research Institute for Labor Protection, St. Petersburg, Russia.
132. Zhivov, A. M. 1994. Air supply with directing jets. In *Ventilation '94: Proceedings of the Fourth International Symposium on Ventilation for Contaminant Control.* Stockholm, Sweden.
133. Gnatyuk, V. V., T. A. Gnatyuk, and L. P. Yarin. 1977. Studies of the axis-symmetric blocked flow structure. In *Proceedings of the USSR Acad. Sci., Mechanics of Liquids and Gases*, no. 2, pp. 16–23. Nauka, Moscow.
134. Gobza, R. N. 1947. *Warm Air Heating with Concentrated Air Jet Supply.* Ser. 436, KTIS. Stroizdat, Moscow.
135. Gobza, R. N. 1965. The results of heating systems with concentrated air supply field studies: Transactions of the scientific session of the institute, June 21–26, 1954. *Concentrated Air Supply into Rooms*, issue 4, pp. 83–106. Liot, Leningrad.
136. Troyanovsky, V. N. 1969. *Studies of the Allowable Initial Air Temperature Difference of the Ambient Air and Air Supplied by the Ventilation System with Concentrated Jets.* Research Report T-5-69. KazIOT, Kazan.
137. Grimitlyn, M. I., and G. M. Pozin. 1993. Fundamentals of Optimizing Air Distribution in Ventilated Spaces. *ASHRAE Transactions*. vol. 99, no. 1.
138. Baturin, V. V. 1951. *Fundamentals of Industrial Ventilation* (in Russian). VTsPS: Profizdat, Moscow.
139. Koestel, A., and J. B. Austin, Jr. 1956. Air velocities in two parallel ventilating jets. *ASHVE Transactions*, vol. 62, pp. 425–436.
140. Grimitlyn, M. I. 1960. *Air Distribution through Perforated Ducts.* Leningrad.
141. Bashus, V., and V. Kochova. 1963. Vzajemne pusobeni volnich proudu. *Zdravonti Technika a Vzduchotechnika*, no. 4, pp. 150–168.
142. Posokhin, V. 1966. Interaction of supply air jets. *Water Supply and Sanitary Technique*, no. 7.
143. Nosovitsky, A. 1968. Single jet and system of multiple jets development between the walls. In *Proceedings of High School (Isvestia VUZOV) Construction and Architecture*, no. 5.
144. Kuzmina, L. V. 1968. *On the Interaction of Parallel Supply Jets: Collected Papers of the Occupational Safety Institutes under the VTsPS.* Profizdat, Moscow.
145. Vasilyeva, L. V. 1969. Studies on parallel air streams interaction. Ph.D. thesis. NIIST, Moscow.
146. Roeder, H. 1967. Das Verhalten ebener Luftstrahlen, die an einer Wand abgelenkt werden. *Hausbericht H. Krantz Lufttechnik, E.* Nr. 2736.
147. Conrad, O. 1972. Untersuchung über das verhalten gegeneinander strömender wandstrahlen. *Gesundheits-Ingenieur*, Heft 10, pp. 303–308.
148. Urbach, D. 1971. Modelluntersuchungen zur Strahllüftung. Dissertation. RWTH. Aachen.
149. Regenscheit, B. 1974. Der Einfluß von raumwänden auf die strahlgesetze der lufttechnik (The influence of the room enclosing walls on the laws of jets in ventilation technology). *Ki*, no. 1, pp. 9–16.
150. Fläkt. 1977. Svenska fläktfabriken AB. *Dirivent — Air Treatment System for Large Premises.* E1472A.
151. Wasiluk V., M. Jaskolski, and J. Olezsko. 1980. Model testing a large-plane exhaust of inflowing air as a possible solution for ductless ventilation system "air piston." In *Clima 2000: 7th International Congress of Heating and Air Conditioning.* Budapest.

152. Zhivov, A. M. 1985. The interaction of axially symmetric coaxial jets in free and confined conditions. In *Turbulent Jet Flows: Theses of Reports of Fifth All Union Scientific Conference on Theoretical and Applied Aspects of Turbulent Flows*, part I, pp. 27–32. Estonian Academy of Sciences, Tallinn.
153. Hudenko, B. G. 1966. About the calculation of turbulent jet mixing based on the principle of superimposing. In *Studies of Heat and Mass Exchange in Production Processes and Equipment*, Science and Technology, Minsk.
154. Meshalin, V. S. 1974. About turbulent stress in impinging jets. In *Mechanics of Gases and Fluids*. Moscow.

Bibliography

AICVF. 1991. Aeraulique. In *Principles de l'Aeraulique Appliaues au Genie Climatique. Collection des Guides de l'AICVF.*
Andersen, K. T. 1996. *Beregning af Luftstråler og returstrømme i rum* (Calculation of air jets and reverse flows in rooms). SBI-Report 248. Statens Byggeforskningsinstitut.
Andersen, K. T. 1995. Vurdering af luftstrømningsmodeller for glasbygninger (Evaluation of air flow models in glass buildings). SBI-Report 247. Statens Byggeforskningsinstitut.
Angel L. K., and B. M. Rudman. 1974. *Ventilation of Non-ferrous Metallurgy Plants*. Moscow: Metallurgy.
Bach, H. 1973. Ähnlichkeitskriterien bei raumströmungen (Analogy criteria with space flow). *Ki.*, vol. 9, no. 6, pp. 37–42.
Becher, P. 1966. Lüftverteilung in gelüfteten räumen. *Heizung, Lüftung-Haustechnik*, vol. 17, no. 10, pp. 379–384.
Beck, E. 1992. Luftführung in Industrieräumen. *TGA-Magazin*, vol. 6, pp. 36–42.
Beltaos, S. 1976. Oblique impingement of circular turbulent jets. *Journal of Hydraulic Research*, vol. 14, no. 1, pp. 17–36.
Beyersdorfer, S. 1986. Proportionalität der geschwindigkeitsfelder in strömungssystemen mit unrerschiedlichen werten der ähnlichkeitskennzahlen. *Luft- und Kältetechnik*, no. 2, pp. 94–95.
Brunig, M. 1984. Bei prallstromung senkrecht gegen eine wand auftretende umfeldströmung. *HLH* vol. 35, no. 10, October, pp. 503–504.
Chow, W. K., and W. Y. Fung. 1997. Experimental studies on the airflow characreristics of spaces with mechanical ventilation. *ASHRAE Transactions*, p. 1.
Chen Q., A. Moser, and A. Huber. 1990. Prediction of buoyant, turbulent flow by a low Reynolds-number k-ε model. *ASHRAE Transactions*, vol. 96, no. 1, p. 15.
Christianson, L. L. 1989. *Building Systems: Room Air and Air Contaminant Distribution*. ASHRAE, Atlanta.
CIBSE. 1988. *CIBSE Guide: Installation and Equipment Data*, vol. B. Chartered Institution of Building Services Engineers, London.
Coli, G. 1974. Distribuzione dell'aria con diffusori a lancio orizzontale. *Condizionamento dell'Aria*, no. 7.
Corrsin, S. 1943. *Investigation of Flow in an Axially Symmetric Heated Jet of Air.* NACA Wartime Report W-94.
Croom, D. J., and B. M. Roberts. 1981. *Air Conditioning and Ventilation of Buildings*. 2nd ed., vol. 1. Pergamon Press, New York.
Curilev, E. S., and M. Z. Pechatnikov. 1966. Laws of jet distribution in heavily obstructed spaces. In *Proceedings of the Conference "Heat Supply and Ventilation."* Budivelnik, Kiev, pp. 137–141.
Davis, J.A. 1977. The unidirectional flow ventilation systems. *Heating, Piping and Air Conditioning*, March, pp. 63–67.
Delicieeux, P., H. Bouia, and D. Blay. 1992. Simplified modelling of air movements in a room and its first validation with experiments. In *Roomvent '92: Proceedings of the Third International Conference on Air Distribution in Rooms*, vol. 1. Aalborg, Denmark, pp. 383–397.
Designer's Guide. 1992. *Ventilation and Air-Conditioning*. Stroizdat, Moscow.
Didenko, V. G. 1972*a*. Studies of the process equipment location density on the ventilation effectiveness at different methods of air supply. *Transactions on Sanitary Technique*, Nizhne-Vozhskoye, Volgograd, issue IV, pp. 115–117.

Didenko, V. G. 1972*b*. Studies of the process equipment sizes on the ventilation effectiveness at different methods of air supply. *Transactions on Sanitary Technique*, Nizhne-Vozhskoye, Volgograd, issue IV, pp. 124–126.

Drkal, F. 1990. Belüftung durch stabilisierte lutströmung, kombiniert mit strahlungsbänderheizung. *HR*, vol. 9.

Ebrahimi, I. 1968. Turbulentz in isothemen freistrahlen. *Forsch. Ing.-Wes.*, vol. 34, no. 6, pp. 177–182.

Elbanna, H., S. Gahin, and M. I. I. Rashed. 1983. Investigation of two-plane parallel jets. *AIAA Journal*, vol. 21, no.7, pp. 986–991.

Elleson, J. S., and A. T. Kirkpatrick. 1997. Overview of the ASHRAE Cold Air Distribution System Design Guide. *ASHRAE Transactions*, vol. 107, p. 1.

Finkelstein, W., K. Fitzner, and W. Moog, 1973. Messungen von raumluftgeschwindigkeiten in der klimatechnik. *Heizung-Luftung-Haustechnik*, vol. 24, no. 2, February.

Fissore, A. A., and G. .A. Liebeck. 1991. A simple empirical model for predicting velocity distributions and comfort in a large slot ventilated space. *ASHRAE Transactions*, vol. 97, no. 2.

Franchuk, A. U. 1949. *Method of Temperature Calculation at Different Room Heights—Studies on Building Physics* (in Russian). Gosstroizdat, Moscow/Leningrad.

Frings, P., and J. Pfeifer. 1981. Einfluß der raumbegrenzungsflächen auf die geschwindigkeitsbnahme im luftstrahl. *HLH*, vol. 32, no. 2, pp. 49–61.

Fry, D. J., and E. E. Adams. 1983. Confined radial buoyant jet. *Journal of Hydraulic Engineering*, vol. 109, no. 9, September.

Gartenmann, F. C. 1959. Versuche uber die strahlausbreitung an lüftungsdecken. *Aerodynamnische Versuchsanstalt*, 59/A/12.

Gendrikson, V. A. 1968. Mixing processes in the axisymmetric jet supplied in cross draft. In *Proceedings of the Acad. Sci. Estonian SSR.*, Tallinn.

Ginevskii, A. S. 1969. Theory of turbulent jets and wakes. *Mashinostroyeniye*, Moscow.

Greenlaw, A. L., and T. S. Hart. 1938. Air paths from grilles. *Heating, Piping and Air Conditioning*, July, pp. 452–455.

Grimitlyn M. I., G. A. Smirnova, V. I. Filatov, E. M. Elterman, L. E. Elterman, and L. M. Brailovsky. 1983. *Ventilating and Heating of Plastic Processing Shops*. Chemia, Leningrad.

Grimitlyn, M. I., and A. M. Zhivov. 1983. Improvement of air-conditioning systems effectiveness in the operation halls of the automatic telephone exchange stations. In *Proceedings of the Conference: Improvements in the Ventilation and Air-Conditioning Systems Effectiveness*. LDNTP, Leningrad.

Gunes, I. L. 1970. Concentrated air supply in industrial spaces. In *Transactions of VNIIGS: Design and Installation of Sanitary-Technique Systems*, vol. 28, pp. 3–15. VNIIGS, Leningrad.

Gunes, I. L., and I. L. Leshinskaya. 1977. Evaluation of the required air change rate with air supply through ceiling mounted air diffusers. In *The Issues of Sanitary-Technique Systems Design and Installation*. VNIIGS, Leningrad.

Gunes, I. L., and I. L. Leshinskaya. 1974. Selection and design of air diffusers for combined heating and ventilating systems. In *Transactions of VNIIGS: Design and Installation of Sanitary-Technique Systems*, vol. 38, pp. 13–31. VNIIGS, Leningrad.

Hanel, B. 1994. *Raumluftströmung*. C. F. Müller Verlag. GmbH, Heidelberg.

Harris, P. R. 1967. The densimetric flows caused by the discharge of heated two-dimensional jets beneath a free surface. Ph.D. thesis. University of Bristol, Department of Civil Eng.

Hassani, V., T.-G. Malmstrom, and A. T. Kirkpatrick. 1993. Indoor thermal environment of cold air distribution systems. *ASHRAE Transactions*, vol. 99, no. 1, pp. 1359–1365.

Hauesmann, K. 1966. Eigenschaften turbulenter strahlenbündel. *Chemie-Ing.-Techn*, vol. 38, no. 3, pp. 293–297.

Heins, T. 1996. Brandsimulation mit mehrraum-zonenmodellen. *TAB*, vol. 94, no. 4, pp. 75–81.

Heselberg, P., S. Murakami, and C.-A. Roulet. 1996. Annex 26: Air flow patterns in large enclosures. In *Ventilation of Large Spaces in Buildings. Part 3: Analysis and Prediction Techniques*. IEA.

Holmes, M. J., and C. Caygill. 1973. *Air Movement in Rooms with Low Supply Air Flow Rates*. Heating and Ventilating Research Association Laboratory Report No. 83. Bracknell, UK.

Hosni, M. H., A-El Hassan, B. Mohamed, and P. L. Miller. 1996. Airflow characteristics of jet expansion for non-isothermal flow conditions. *ASHRAE Transactions*, vol. 102, no. 2.

Howarth A. T. 1980. Temperature distribution and air movement in rooms heated with a convective heat source. Ph.D. thesis. University of Manchester.

Hwang, C. L., F. A. Tillman, and M. J. Lin. 1984. Optimal design of an air jet for spot cooling. *ASHRAE Transactions*, vol. 90, no. 1B, pp. 476–498.

Jackman, P. J. 1973. *Air Movement in Rooms with Sill-Mounted Diffusers*. BSRIA Laboratory Report No. 81. Bracknell, UK.

Jackman, P. J. 1971. *Air Movement in Rooms with Sill-Mounted Grilles—A Design Procedure*. BSRIA Laboratory Report No. 71. Bracknell, UK.

Jendroßek, J. U. 1992. Kanalloses luftführungssystem. *TAB*, vol. 690, no.1, pp. 45–49.

Karimipanah, T. 1996. Behavior of jets in ventilated enclosures. In *Roomvent '96: Proceedings of the 5th International Conference on Air Distribution in Rooms*, vol. 1, July. Yokohama, Japan.

Karimipanah, T. 1996. Turbulent jets in confined spaces. Ph.D. thesis. Royal Institute of Technology, Center for Built Environment, Gävle, Sweden.

Koestel, A. 1955. Paths of horizontally projected heated and chilled air jets. *ASHVE Transactions*, vol. 61, pp. 213–232.

Koestel, A., P. Hermann, and G. L. Tuve. 1950. ASHVE Research Report No. 1404: Comparative study of ventilating jets from various types of outlets. *ASHVE Transactions*, vol. 56, p. 459.

Koestel, A., P. Hermann, and G. L. Tuve. 1949. Air streams from perforated panels. *Heating, Piping and Air Conditioning*, July, pp. 107–113.

Koestel, A., and G. L. Tuve. 1955. Performance and evaluation of room air distribution systems. *ASHVE Transactions*, vol. 61, pp. 533–550.

Koestel, A., and C.-Y. Young. 1951. The control of air streams from a long slot. *Heating, Piping and Air Conditioning*, July, pp. 111–115.

Kotsovinos, N. E. 1977. A study of the entrainment and turbulence in a plane buoyant jet. *Journal of Fluid Mechanics*, vol. 81, pt. 1, pp. 25–62.

Kristensson, J. A., and O. A. Lindqvist. 1993. Displacement ventilation systems in industrial buildings. *ASHRAE Transactions*, vol. 99, no. 1.

Landau, L. D., and E. M. Lifshits. 1953. *Mechanics of Continuous Medium*. GOSIZDAT, Moscow.

Landis F., and A. H. Shapiro. 1951. *The Turbulent Mixing of Coaxial Gas Jets*. Heat Transfer and Fluid Mechanics Institute, Preprints and Papers. Stanford University Press, California.

Laret, L. 1980. Contribution au développement de modéles mathématiques du comportement thermique transitoire de structures d'habitation. Ph.D. thesis. University of Liège.

Li, Z. H. 1994. Fundamental studies on ventilation for improving thermal comfort and IAQ. Ph.D. thesis. University of Illinois.

Li Z., L. L. Christianson, J. S. Zhang, and A. Zhivov. 1994. Cold air jets systems effects on the occupied regions. In *Roomvent '94: Proceedings of the Fourth International Conference on Air Distribution in Rooms*,. vol. 2. Krakow, Poland.

Li, Z. H., J. S. Zhang, A. M. Zhivov, and L. L.Christianson. 1993. Characteristics of diffuser air jets and airflow in the occupied region of mechanically ventilated rooms—a literature review. *ASHRAE Transactions*, vol. 99, no. 1.

Lin, Y. F., and M. J. Sheu. 1991. Interaction of parallel turbulent plane jets. *AIAA Journal*, vol. 29, no. 9, pp. 1372–1373.

Maksimov, G. A., and V. V. Der'ugin. 1972. *Air Movement in Heated and Ventilated Spaces*. LISI, Leningrad.

Malmström, T.-G. 1996. Archimedes number and jet similarity. In *Roomvent '96: Proceedings of the 5th International Conference on Air Distribution in Rooms*, vol. 1, July. Yokohama, Japan.

Malmström, T.-G., and V. Hassani. 1992. Use of constant momentum for supply of cold air. In *Roomvent '92: Proceedings of the 3rd International Conference on Air Distribution in Rooms*, vol. 3. Aalborg, Denmark.

Masuch, J. 1992. The influence of air outlet directions on the stability of air flow patterns in large halls. In *Roomvent '92: Proceedings of the 3rd International Conference on Air Distribution in Rooms*, vol. 1, pp. 539–552. Aalborg, Denmark.

McRee, D. I., and H. L. Moses. 1967. The effect of aspect ratio and offset on nozzle flow and jet reattachment. In *Advances in Fluidics: The 1967 Fluidics Symposium*. ASME.

Merrit, G., and G. Redinger, 1973. Measurements of heat and impulse transfer coefficient in turbulent stratified flow. *Journal of Rocket Technology and Astronautics*, no. 1.1.

Miller, P. L. 1971. *Room Air Distribution Performance of Four Selected Outlets*. ASHRAE Research Report No. 2210 RP–88. Washington, D.C.

Miller, P. L. 1969. ASHRAE Research Report RP–55 No. 2100: Room air distribution with air distributing ceiling—Part 1. *ASHRAE Transactions*, vol. 75, pp. 118–131.

Moog, W. 1978. Ähnlichkeitstheoretische überlegungen bei raumstromüngen. (Theoretical considerations of similarity for airflow within the open space). *KI* 11/1978, Teil 4.3, pp. 267–270.

Müller, H. J. 1975. Beitrag zum thema der luftführung in tierproduktions-anlagen. *Luft und Kältetechnik*, no. 2.

Nielsen, P. V. 1994. Air distribution in rooms—Research and design methods. In *Roomvent '94: Proceedings of the Fourth International Conference on Air Distribution in Rooms*, vol. 1. Krakow, Poland.

Nielsen, P. V. 1992. Velocity distribution in the flow from a wall-mounted diffuser in rooms with displacement ventilation. In *Roomvent '92: Proceedings of the Third International Conference on Air Distribution in Rooms*, vol. 3. Aalborg, Denmark.

Oosthuizen, P. H. 1983. *An Experimental Study of Low Reynolds Number Circular Jet Flow.* ASME Preprint 83-FE-36.

OSHA. 1989. Air Contaminants: Permissible Exposure Limits. Title 29 Code of Federal Regulations, Part 1910.1000. U.S. Department of Labor. OSHA 3112.

Padmanabham, G., and B. H. L. Gowda. 1991. Mean and turbulence characteristics of a class of three-dimensional wall jets. Part 2: Turbulence characteristics. *Journal of Fluid Engineering*, vol. 113, December, pp. 629–634.

Pechatnikov, M. Z. 1967. Principles of jet flows in cold rooms. Ph.D. thesis. LTIHP, Leningrad.

Poz, M. Y. 1994. Experimental investigation of planar turbulent jet in enclosures. *ASHRAE Transactions*, vol. 100, no. 1, pp. 1182–1194.

Poz, M. Y. 1993. Theoretical investigation and practical applications of non-isothermic jets for the purpose of ventilating rooms. *ASHRAE Transactions*, vol. 99, no. 1, pp. 950–959.

Prandtl, L. 1942. Bemerkungen zur theorie der freien turbulenz. *Z. für Angewandte Math., Mech.*, vol. 22, no. 5, pp. 241–243.

Priest, J. B. 1996. Ph.D. thesis. University of Illinois.

Rakoczy, T. 1977. Dimensionierung von düsen als luftdurchlässe für raumlufttechnische anlagen. *HLH*, vol. 28, May, pp. 173–175.

Regenscheit, B. 1976. Einfluß der Reynoldszahl auf die geschwindigkeitsabnahme turbulenter freistrahlen. *HLH*, vol. 27, no. 4, pp. 122–126.

Regenscheit, B. 1964. Modellversuche zur erforschung der raumströmung in belüfteten räumen. *Staub*, no. 1, January, pp. 14–20.

Regenscheit, B. *Strahlen in Begrenzten Räumen.* From the B. Regenscheit archive at Essen University. Courtesy of Prof. Fritz Steimle.

Rietschil, H. 1930. *Leitfaden der Hier—und Luftungstechnik.* Neunte Auflage.

Rouse, H., C. S. Yih, and H. W. Humphreys. 1952. Gravitational convection from a boundary source. *Tellus*, vol. 4, pp. 201–210.

Rubel, A. 1980. Computations of jet impingement on a flat surface. *AIAA Journal*, vol. 18, no. 2, pp. 168–175.

Rydberg, J. 1962. Luftinblåsning genom perforerade tak. *VVS*, no. 6.

Rydberg, J. 1962. Maximala ventilationsluftmängder för olika insblåsninganodningar. *VVS*, no. 12.

Sato, H., and F. Sakao. 1964. An experimental investigation of the instability of two-dimensional jet at low Reynolds number. *J. Fluid Mech.*, vol. 20, no. 2, pp.337–352.

Schädlich, S. 1993. Der einfluss verschiedener luftdurchlassgeometrien auf das freistrahlverhalten. D.-Ing. thesis. *Deutscher Kälte- und Klimatechnischer Vereins*, no. 43.

Schlanzke, G. 1975. Die turbulente vermischung in freistrahlen unter berücksichtigung von dichteunterschieden. *Luft und Kältetechnik*, no. 2, pp. 71–75.

Schlichting, H. 1969. Boundary layer theory. In *Handbook of Fluid Dynamics.* New York.

Schlünder, U. 1971. Über die ausbreitung turbulenter freistrahlen. *Z. Flugwiss*, vol. 19, no. 3, pp. 108–113.

Schobesberger, R. 1985. Gezielte zuluftverteilung in industriehallen mit dem hoval-dralluftverteiler (Directed supply air distribution in large manufacturing shops with the HOVAL-screw-type air diffusers). *Klima-Kälte-Heizung.* 1/1985, Teil 6, 1408.

Schramek, E. R. *Tachenbuch für Heizung und Klimatechnik. Recnagel-Sprenger-Hönmann.* R. Olenbourg, Verlag München Wien.

Schultz-Hausmann, F. K. 1985. Wechselwirkung ebener freistrahlen mit der umgebung. VDI-Verlag GmbH, Düsseldorf.

Schwarz, W. 1995. Auslegung von düsenstrahlbündeln. *Ki Luft und Kältetechnik*, no. 11., pp. 518–521.

Schwenke, H. 1975. Uber das verhalten ebener horizontaler zuluftstrahlen im begrenzten raum. *Luft und Kältetechnik*, no. 4.

Sefker, T. 1989. Verallgemeinerte darstellung des verhaltens isothermer freistrahlen. D.-Ing. thesis. Deutscher Kälte- und Klimatechnischer Vereins, no. 27.

Seliverstov, A. N. 1934. *Ventilation of Chemical Industry Plants* (in Russian). ONTI. Gosstrizdat, Moscow.

Seliverstov, A. N. 1932. *Room Ventilation in Plants and Factories* (in Russian). ONTI. Gosstrizdat, Moscow.

Sigalla, A. 1958. Experimental data on turbulent wall jets: A correlation of existing data. *Aircraft Engineering*, May, pp. 131–134.

Skåret, E. 1993. Advanced design of ventilation systems: Ventilation models. Lecture Series, Von Karman Institute for Fluid Dynamics.

Skåret E. 1986. Industrial ventilation—Model tests and general development in Norway and Scandinavia. In *Proceedings of Ventilation '85 Conference*. Elsevier Science Publishers BV, Amsterdam.

Skistad, H. 1995. Industriventilasjon: Innblasning og avsug, hefte 1. Scarland Press AS.

Stark, S. V. 1950. Submerged turbulent flows mixing. Ph.D. thesis. Moscow Institute of Steel and Alloys (MISiS).

Stoecker, W. F. 1968. *Principles for Air Conditionmg Practice*. Industrial Press, New York.

Ströder, R. 1991. RLT-Analagen für fertigunshallen. *TAB*, vol. 2, pp. 125–130.

Takemasa, Y., S.Togari, and Y. Arai. 1996. Application of an unsteady-state model for predicting vertical temperature distribution to an existing atrium. *ASHRAE Transactions*, vol. 102, no. 1.

Taliev, V. N. 1979. *Aerodynamics of Ventilation*. Stroyizdat, Moscow.

Tarnopolsky, M. D. 1994. Approved calculation of air distribution in an auditorium. *ASHRAE Transactions*, vol. 100, no. 1, pp. 1195–1209.

Tarnopolsky, M. D. 1966. Concentrated air supply design in ventilated rooms. *Water Supply and Sanitary Technique*, no. 6.

Tavakkol, S., M. H. Hosni, P. L. Miller, and H. E. Straub. 1994. A study of isothermal throw of air jets with various room sizes and outlet configurations. *ASHRAE Transactions*, vol. 100, no. 1, pp. 1679–1686.

Timofeeva, O. N., and G. S. Veksler. 1972. Experimental results of concentrated air supply in large rooms. In *Transactions of the Institutes for Labor Protection of the VTsSPS*, vol. 76. Profizdat, Moscow.

Trapani, R. D. 1967. An experimental study of bounded and confined turbulent jets. In *Advances in Fluidics: The 1967 Fluidics Symposium*, pp. 1–13. ASME, New York.

Trogisch, A. 1990. Zur gestaltung und dimensionierung von lüftungstechnischen systemen in industriehallen (Designing ventilation systems for industrial halls). *Ki Klima-Kälte-Heizung*, no. 2, pp. 73–76.

TsNIIPromzdanii. 1984. *Recommendations on Heating and Ventilating Systems Design with Directing Nozzles*. Central Research Institute for Industrial Buildings, Moscow.

TsNIIPZ. 1985. *Develop Recommendations on Design of VAV Heating and Ventilation Systems with Inclined Jet Air Supply*. Final Report No. 02880089962. Central Research Institute for Industrial Buildings (TsNIIPZ), Moscow.

Tuve, G. L., and G. B. Priester. 1944. ASHVE Research Report No. 1248: Control of air streams in large spaces. *ASHVE Transactions*, pp. 153–172.

Uspenskaya, L. B., L. S. Klyatchko, and Z. I. Rashkovsky. 1975. Ventilation of textile shops of the synthetic fiber production plants. In *The Issues of Sanitary Technique Systems Design and Installation*. VNIIGS, Leningrad.

Uspenskaya, L. B., and S. M. Slavina. 1970. Experimental studies of temperature distribution in modular industrial spaces with a non-uniform heat source. In *The Issues of Sanitary Technique Systems Design and Installation*. VNIIGS, Leningrad.

Vialle, P., D. Blay, and B. Lionner. 1996. Decay laws in the case of 3D vertical free jets with positive buoyancy. In *Roomvent '96: Proceedings of the 5th International Conference on Air Distribution in Rooms*, vol. 1, July. Yokohama, Japan.

VNIIOT. 1970. In Grimitlyn, M. I. 1973. *Principles of air distribution in ventilated rooms*. D.Sc. thesis. VVISKU, Leningrad.

Weidemann, B., B. Hanel, and G. Hopper. 1985. Experimentelle unter-suchungen des temperaturfeldes nichtisotherme, horizontal ausstromender, runder fleistrahlen. *Luft und Kältetechnik*. no. 4.

Weidemann, B., G. Makara, and A. Trogisch. 1983. Zur problematik der lüftung von industriehallen. *Luft und Kältetechnik*, no. 3, pp. 123–128.

Wille, R. 1963. Beiträge zur phänomenologie der freistrahlen. *Z. Flugwiss*, vol. 11, no.6, pp. 222–233.

Wygnanski, I. 1964. The flow induced by two-dimensional and axisymmetric turbulent jets issuing normally from an infinite plane surface. *Aeronautical Quarterly*, November, pp. 373–380.

Yakovlevskii, O. V., and A. N. Sekundov. 1964. Fluid flows generated by turbulent jets, In *Proceedings of the Academy of Science of the USSR: Mechanics and Machine-Building*. Nauka.

Zhang, G., J. S. Strom, and S. Morsing. 1996. Jet drop models for control of cold air trajectories in ventilated buildings. In *Roomvent '96: Proceedings of the 5th International Conference on Air Distribution in Rooms*, vol. 1, July. Yokohama, Japan.

Zhivov, A. M. 1992. Selection of general ventilation method for industrial spaces. Presented at 1992 annual ASHRAE meeting ("Supply air systems for industrial facilities" seminar).

Zhivov, A., J.B. Priest, and L.L. Christianson. 1996. Air distribution design for realistic rooms. In *Roomvent '96: Proceedings of the 5th International Conference on Air Distribution in Rooms*, vol. 1, July. Yokohama, Japan.

Zhivov, A. M. 1994. Air supply with directing jets. In *Ventilation '94: Proceedings of the Fourth International Symposium on Ventilation for Contaminant Control*. Stockholm, Sweden.

Zhivov, A. M. 1993. Theory and Practice of air distribution with inclined jets. ASHRAE *Transactions*, vol. 9, no. 1. Stockholm, Sweden.

Zhivov, A. M. and G. M. Pozin, 1989. Improvement of the design for air distribution by inclined jets. In Theses of Reports at the Eighth Conference on Ventilation and Air Conditioning, pp. 182–191. Gdansk, Poland.ASHRAE *Transactions*, vol. 9, no. 1. Stockholm, Sweden.

Zhivov, A. M. and Kelina, E. L. 1989. Evaluation of air exchange rate with air supply with inclined jets. In Occupational Safety Technique and Industrial Sanitary: Collected Papers of the Occupational Safety Institutes under AUCCTU, Mosciow. Profizdat, pp. 33–38.

Zhivov, A. M. 1985. The interaction of axially symmetric coaxial jets in free and confined conditions. In *Turbulent Jet Flows. Theses of Reports of Fifth All Union Scientific Conference on Theoretical and Applied Aspects of Turbulent Flows*, part 1, Estonian Academy of Sciences. Tallinn. pp. 27–32.

Zhivov, A. M. 1983. Concentrated air distributed with directing jets. Ph.D. thesis. All-Union Research Institute for Labor Protection, St. Petersberg, Russia.

Zhivov, A. M. 1982. Investigationof the interaction of Axially symmetric turbulent jets supplied under straight angles to each other. In *Turbulent Jet Flows. Theses of Reports of Fourth All Union Scientific Conference on Theoretical and Applied Aspects of Turbulent Flows*. Part II. Estonian Academy of Sciences, Tallinn.

7.5 PLUMES

7.5.1 Natural Convection Flows

When an object is warmer than the surrounding air, the air is heated, and the warm air moves upward due to buoyancy. The air current created in this way is called a natural convection flow or plume. Also, if the object is colder than the surroundings, the descending cool air current is called a natural convection flow or plume. Generally, heat transfer involving motion of air or some other fluid caused by a difference in density is called natural or free convection. As a result of free convection, a flow of air or other fluid is produced in the form of a boundary layer moving along a surface or as a thermal plume above a surface. In a building, natural convection flows can be formed along the cold or warm vertical surfaces of the external walls and windows, along vertical hot surfaces of process equipment, etc., as shown in Fig. 7.58. Convection flows or thermal plumes are created above people, lights, hot horizontal surfaces of process equipment, and other objects with a surface temperature greater than the room air temperature (Fig. 7.59).

As can be seen from Figs. 7.58 and 7.59, the amount of air in the convection flows increases with height, due to entrainment of the surrounding air. The amount of air transported in a natural convection flow depends on the temperature and the geometry of the surface or source and the temperature of the surrounding air. Because the driving force in convection flows

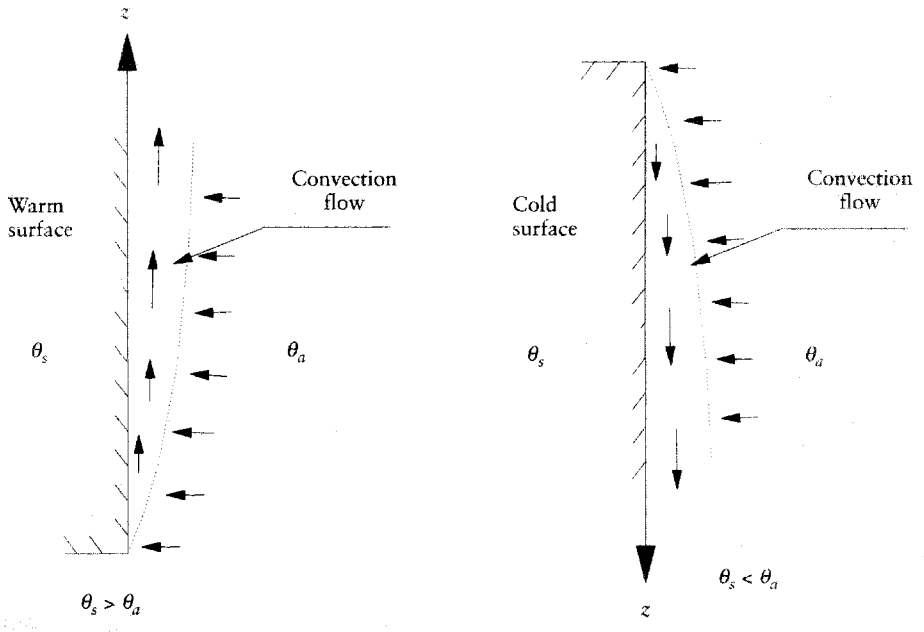

FIGURE 7.58 Convection flows along vertical surfaces.

is the buoyancy force caused by the density difference (i.e., the temperature difference), a temperature gradient in the room influences the plume rise height. Information on thermal plume characteristics is essential for designing ventilation systems with displacement air supply and for dimensioning overhead hoods above heat sources. Empirical, analytical, and computational fluid dynamics are the commonly used approaches to evaluate air temperatures, velocities, and airflow rates in thermal plumes above different heat sources and in convection flows at vertical surfaces.

This section treats

- Natural convection flows in nonconfined and nonstratified environments (Section 7.5.2)
- Plume interaction (Section 7.5.3)
- The influence of a confined space on convection flows (Section 7.5.4)
- The influence of a temperature stratification (Section 7.5.5)

7.5.2 Nonconfined and Nonstratified Environments

7.5.2.1 Plumes from Point and Line Sources

Thermal plumes above point (Fig. 7.60) and line (Fig. 7.61) sources have been studied for many years. Among the earliest publications are those from Zeldovich[1] and Schmidt.[2] Analytical equations to calculate velocities, temperatures, and airflow rates in thermal plumes over point and line heat sources with given heat loads were derived based on the momentum and energy conservation equations, assuming Gaussian velocity and excessive temperature distribution in

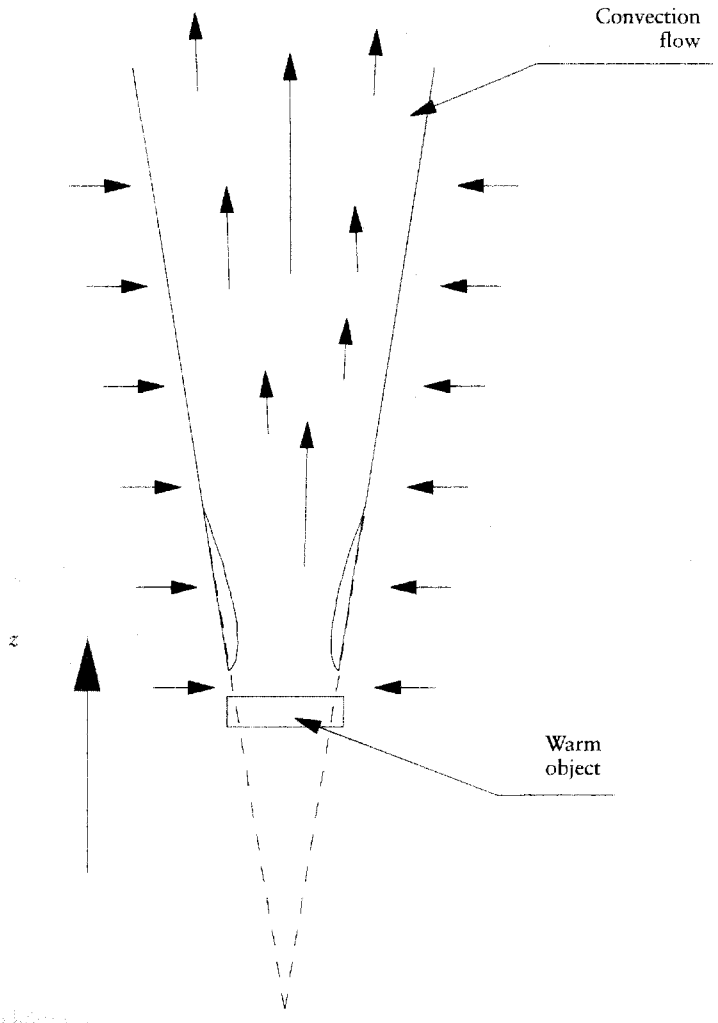

FIGURE 7.59 Thermal plume above a horizontal surface.

thermal plume cross-sections.[3] These equations correspond to those determined experimentally by other researchers[4,5] and are listed in Table 7.19. The equations in Table 7.19 were derived with the assumption that the heat source size was very small and did not account for the actual source dimensions.

The coefficients in the equations differ slightly in different references, depending on the entrainment coefficients used. The convective heat flux Φ, in W or W/m from the heat source, can be estimated from the energy consumption of the heat source Φ_{tot} by

$$\Phi = k\Phi_{tot} \tag{7.185}$$

The value of the coefficient k is 0.7–0.9 for pipes and ducts, 0.4–0.6 for smaller components, and 0.3–0.5 for larger machines and components.[6]

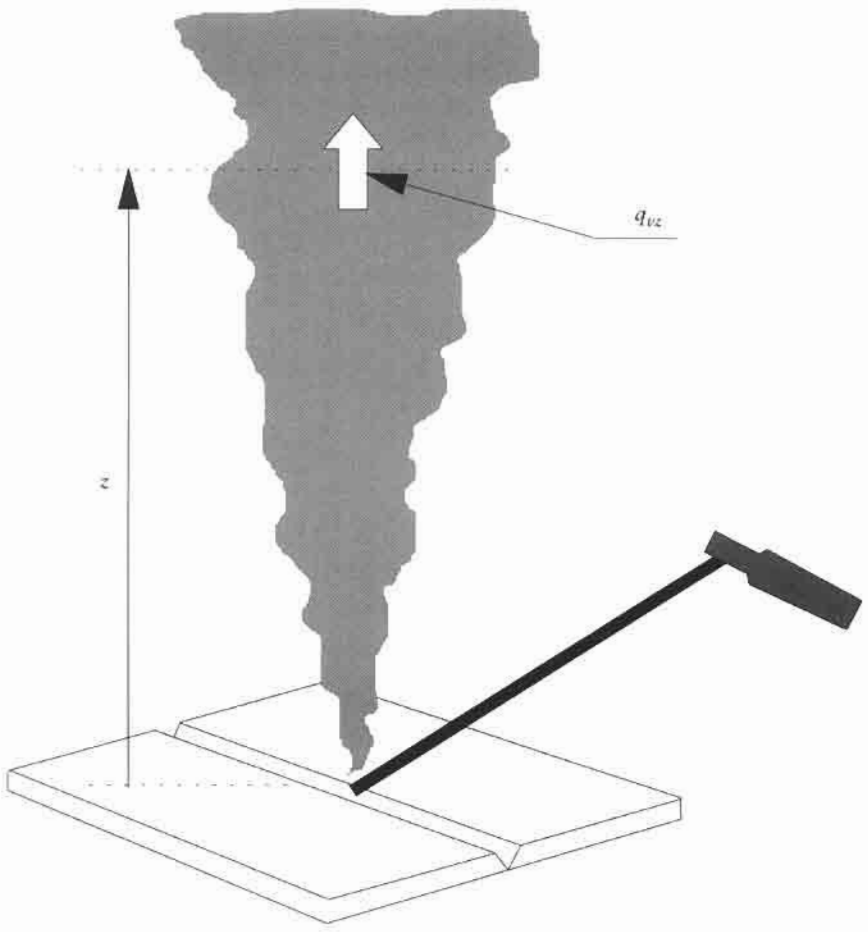

FIGURE 7.60 Plume from a point source.

Example 7.5.1

A point source has a convective heat output of 100 W (see Fig. 7.62). Determine the airflow rate 1 m above the source.

Solution Table 7.19 gives the equation to be used:

$$q_{v,z} = 0.005\Phi^{1/3}z^{5/3}. \tag{7.186}$$

This gives

$$q_{v,z} = 0.005 \cdot 100^{1/3} \cdot 1^{5/3} = 0.023 \text{ m}^3/\text{s}.$$

7.5.2.2 Convection Flow along Vertical Surfaces

Convection flow along vertical surfaces (Fig. 7.63) is also of major interest in industrial ventilation, where large production units with a vertical extension are often present. When the vertical extension of the surface is small, the convection flow is mainly laminar, but at larger extensions the flow is tur-

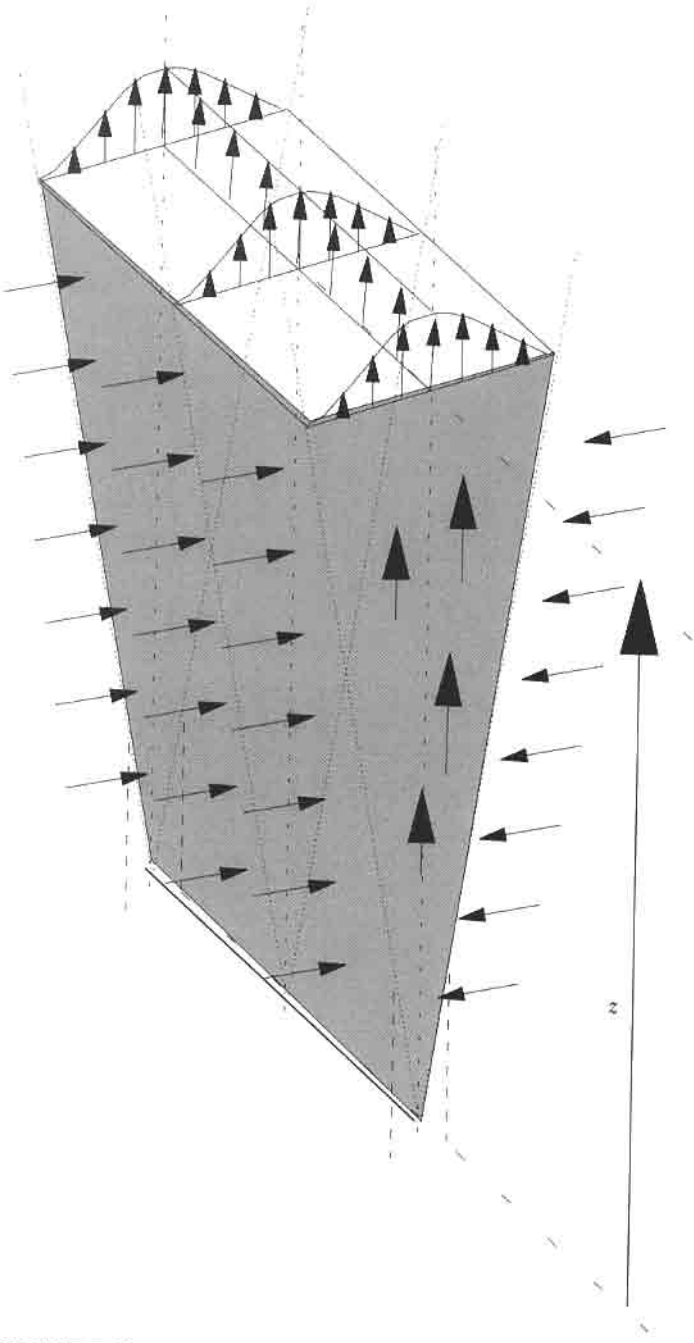

FIGURE 7.61 Plume from a line source.

TABLE 7.19 Characteristics of Thermal Plumes above Point and Line Sources

Parameter	Point source	Line source
Centerline velocity (m/s)	$v_z = 0.128\Phi^{1/3}z^{-1/3}$	$v_z = 0.067\Phi^{1/3}$
Centerline excess temperature (°C)	$\Delta\theta = 0.329\Phi^{2/3}z^{-5/3}$	$\Delta\theta = 0.094\Phi^{2/3}z^{-1}$
Airflow rate (m³/s m)	$q_{v,z} = 0.005\Phi^{1/3}z^{5/3}$	$q_{v,z} = 0.013\Phi^{1/3}z$

Φ = convective heat output (W/m)

z = height above source (m)

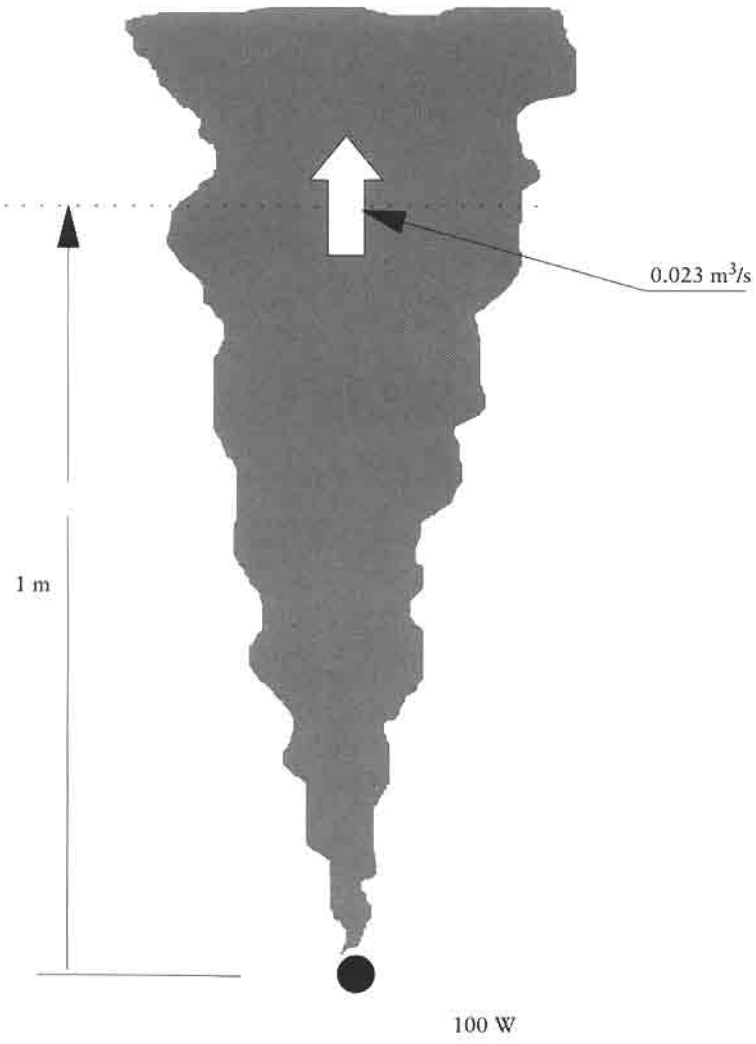

FIGURE 7.62 The plume of Example 7.5.1

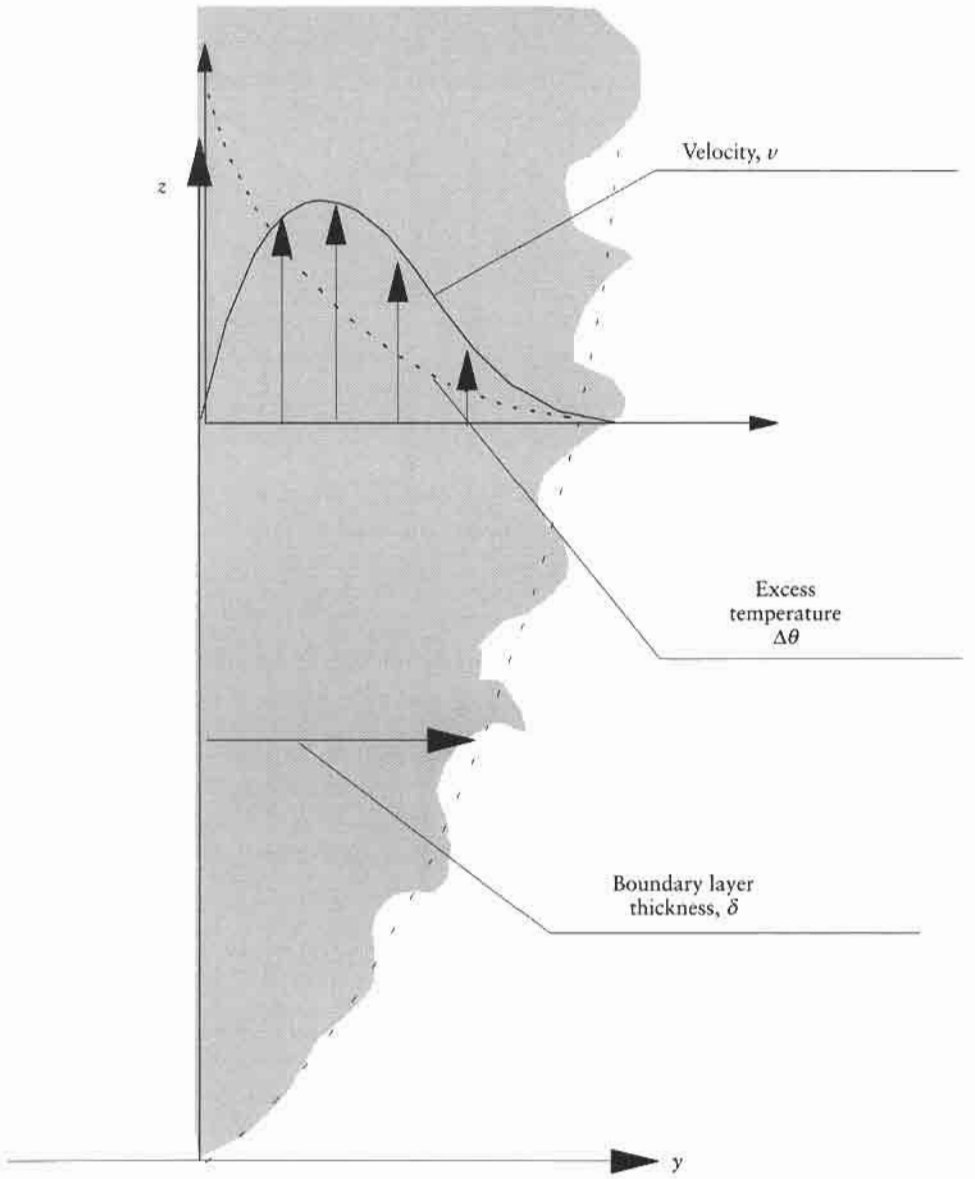

FIGURE 7.63 Convection flow along a vertical surface.

bulent. The basic equations for a surface with a constant temperature are given in Table 7.20.[7,8] The temperature difference between the surface and the surrounding air is $\Delta\theta$, and z is the height from the bottom of the surface. The flow changes from laminar to turbulent at

$$\mathrm{Gr} \cdot \mathrm{Pr} = 7 \times 10^8 \tag{7.187}$$

which for air at moderate temperature differences means around $z = 1$ m, and for air at higher temperatures around $z = 0.5$ m.

TABLE 7.20 Characteristics of Convection Flows along Vertical Surfaces

Parameter	Laminar region	Turbulent region
Maximum velocity (m/s)	$v_z = 0.1(\Delta\theta z)^{1/2}$	
Thickness of boundary layer (m)	$\delta_z = 0.05(z/\Delta\theta)^{1/4}$	$\delta_z = 0.11 z^{0.7}\Delta\theta^{-0.1}$
Airflow rate	$q_{v,z} = 0.00287\Delta\theta^{1/4} z^{3/4}$ (m³/s)	$q_{v,z} = 0.00275\Delta\theta^{0.4} z^{1.2}$ (m³/sm)

Example 7.5.2

Calculate the airflow rate along an external wall with a surface temperature 3°C above room temperature, at a height of 4 meters above the lower edge of the surface.

Table 7.20 gives the equation to be used:

$$q_{v,z} = 0.00275\Delta\theta^{0.4} z^2 \tag{7.188}$$

which gives

$$q_{v,z} = 0.00275 \cdot 3^{0.4} \cdot 4^{1.2} = 0.0225 \text{ m}^3/\text{sm}$$

7.5.2.3 Convection Flow from Horizontal Surfaces

Convection flows from horizontal surfaces are very difficult to determine in the same basic way as for point, line, or vertical sources. The reason is that the flows behave in a very unstable way and leave the flat surface from different positions at different times, partly depending on the total air movement in

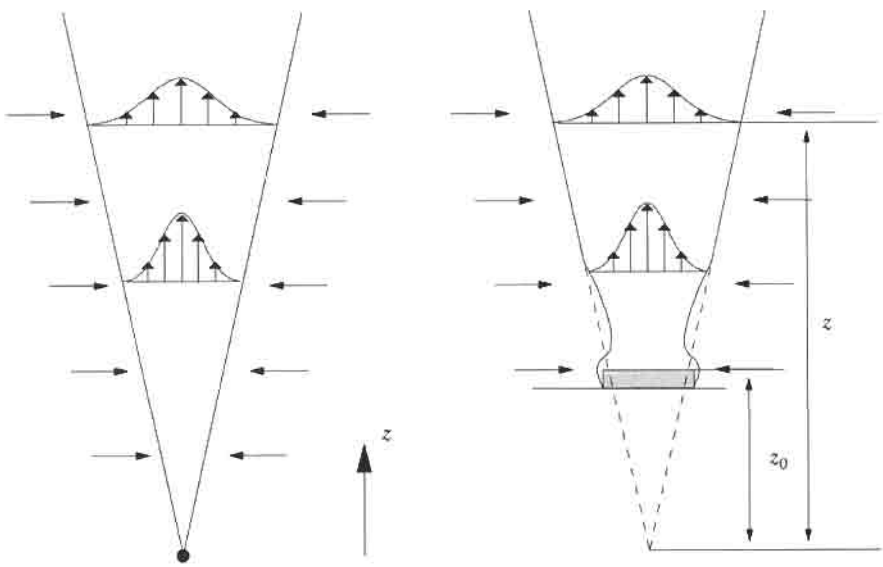

(*a*) Point source (*b*) Extended source

FIGURE 7.64 Illustration of the position of the virtual source.

the room. These surfaces are mostly treated as plumes from extended surfaces; see below.

7.5.2.4 Plumes from Extended Sources

In reality, heat sources are seldom a point, a line, or a plane vertical surface. The most common approach to account for the real source dimensions is to use a virtual source from which the airflow rates are calculated;[9–12] see Fig. 7.64. The virtual origin is located along the plume axis at a distance z_0 on the other side of the real source surface. The adjustment of the point source model to the realistic sources using the virtual source method gives a reasonable estimate of the airflow rate in thermal plumes. The weakness of this method is in estimating the location of the virtual point source.

The method of determining a maximum case and a minimum case provides a tool for such estimation; see Fig. 7.65.[12] In the maximum case, the real source is replaced by a virtual point source such that the border of the plume above the point source passes through the top edge of the real source (e.g., cylinder).

The minimum case is when the diameter of vena contracta of the plume is about 80% of the upper surface diameter and is located approximately one-third of a diameter above the source. The spreading angle of the plume is set to 25°. For low-temperature sources, Skistad[12] recommends the maximum case, whereas the minimum case best fits the measurements for larger, high-temperature sources.

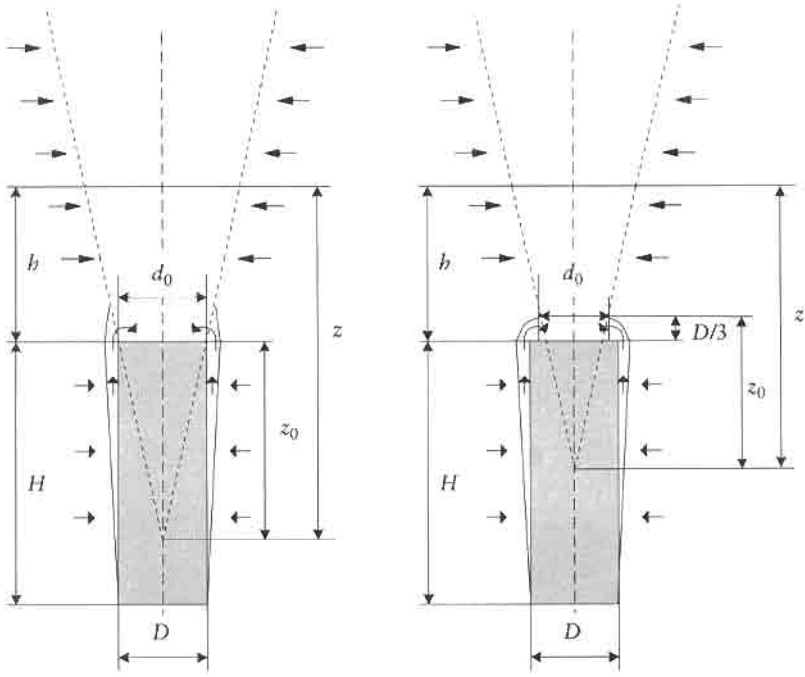

(*a*) Maximum case (*b*) Minimum case

FIGURE 7.65 Convection flow above a vertical cylinder.

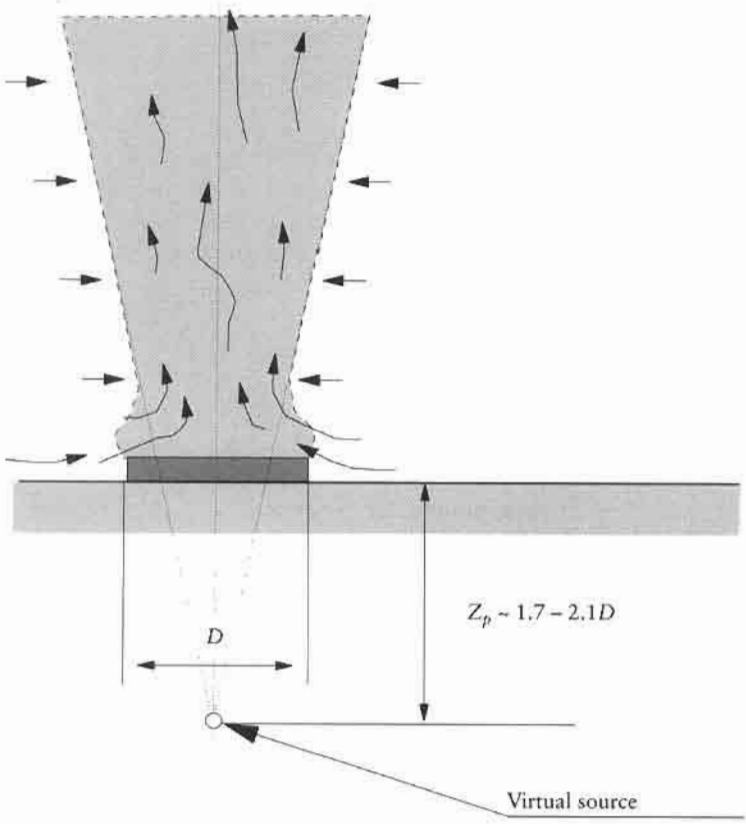

FIGURE 7.66 Virtual source according to Morton.

For a flat heat source Morton et al.[13] suggested that the position of the virtual source be located at $z_0 = 1.7 - 2.1 \times D$ below the real source (Fig. 7.66). This corresponds well with the maximum and minimum method described above, which gives $z_0 = 1.47 - 2.25 \times D$ below a flat plate.

Mundt[3] calculates the thickness of the boundary layer (see Table 7.20) at the top of a vertical extended heat source and adds this to the source radii, and then calculates the position of the virtual source as $z_0 = 2.1(D + 2\delta)$ before using the point source equation.

According to Bach et al.[14] the volume flow from the vertical surfaces should be added to the volume flow calculated by the equations for point or line sources.

Example 7.5.3

Calculate the convection flow rate, q_v at a height $z_{floor} = 2$ m above the floor in the plume above a hot cylinder with a diameter of $D = 0.66$ m and a height of $H = 0.66$ m. The convective heat flux is $\Phi = 5$ kW.

(a) **The Maximum Case (Fig. 7.67)** In the maximum case we get

$$z_0 = D/(2\tan 12.5°) = 2.25D = 1.49 \text{ m},$$

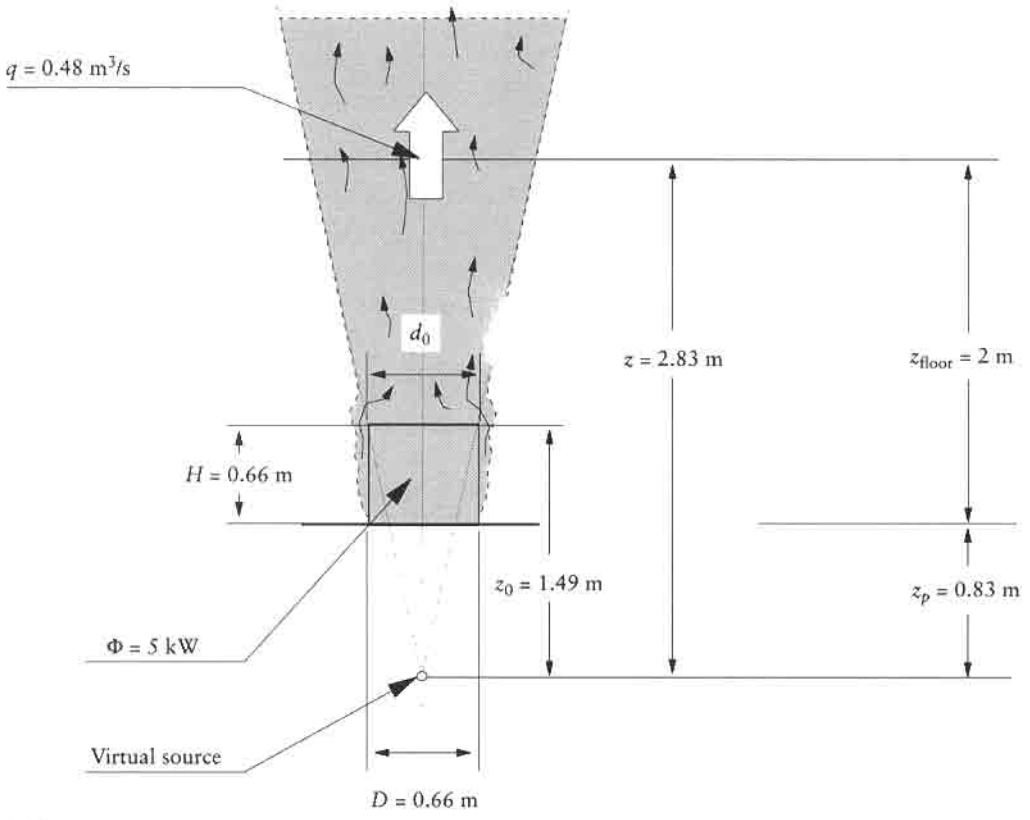

FIGURE 7.67 Plume above a cylinder, maximum case.

which means that the virtual source is located below the floor:

$$z_p = H - z_0 = 0.66\ \text{m} - 1.49\ \text{m} = -0.83\ \text{m}.$$

The vertical distance to be used in the plume formula is

$$z = z_{\text{floor}} - z_p = 2.0\ \text{m} - (-0.83\ \text{m}) = 2.83\ \text{m},$$

and from Table 7.19, we find the formula for the volume flow above a point source:

$$q_v = 0.005\Phi^{1/3}z^{5/3}, \tag{7.189}$$

which gives

$$q_v = 0.005 \cdot 5000^{1/3} \cdot 2.83^{5/3} = 0.48\ \text{m}^3/\text{s}$$

(b) The Minimum Case (Fig. 7.68) In the minimum case we get

$$z_0 = 0.8D/(2\tan 12.5°) = 1.804D = 1.19\ \text{m}.$$

The virtual source is located slightly below the floor:

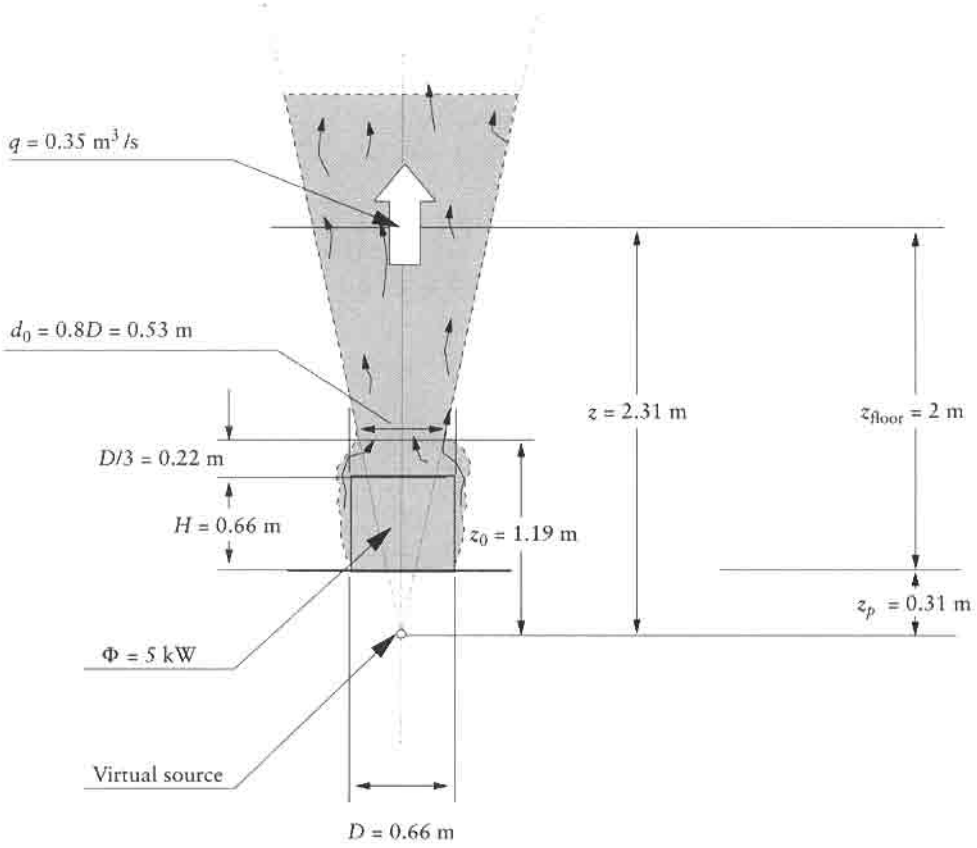

FIGURE 7.68 Plume above a cylinder, minimum case.

$$z_p = (D/3) + H - z_0 = 0.22\ m + 0.66\ m - 1.19\ m = -0.31\ m.$$

The vertical distance to be used in the plume formula is

$$z = z_{floor} - z_p = 2.00\ m - (-0.31\ m) = 2.31\ m,$$

which gives the volume flow rate from Eq. (7.189):

$$q_v = 0.005 \cdot 5000^{1/3} \cdot 2.31^{5/3} = 0.35\ m^3/s$$

Conclusion According to the maximum and minimum method, the convection flow rate through a level 2 m above the floor is between 0.35 m³/s and 0.48 m³/s.

7.5.3 Plume Interaction

When a heat source is located close to a wall, the plume may attach to the wall; see Fig. 7.69. In this case the entrainment will be reduced compared to the entrainment in a free plume, and the attached plume can be regarded as half the plume from the source, with its mirror image on the other side of the wall; see Fig. 7.70.

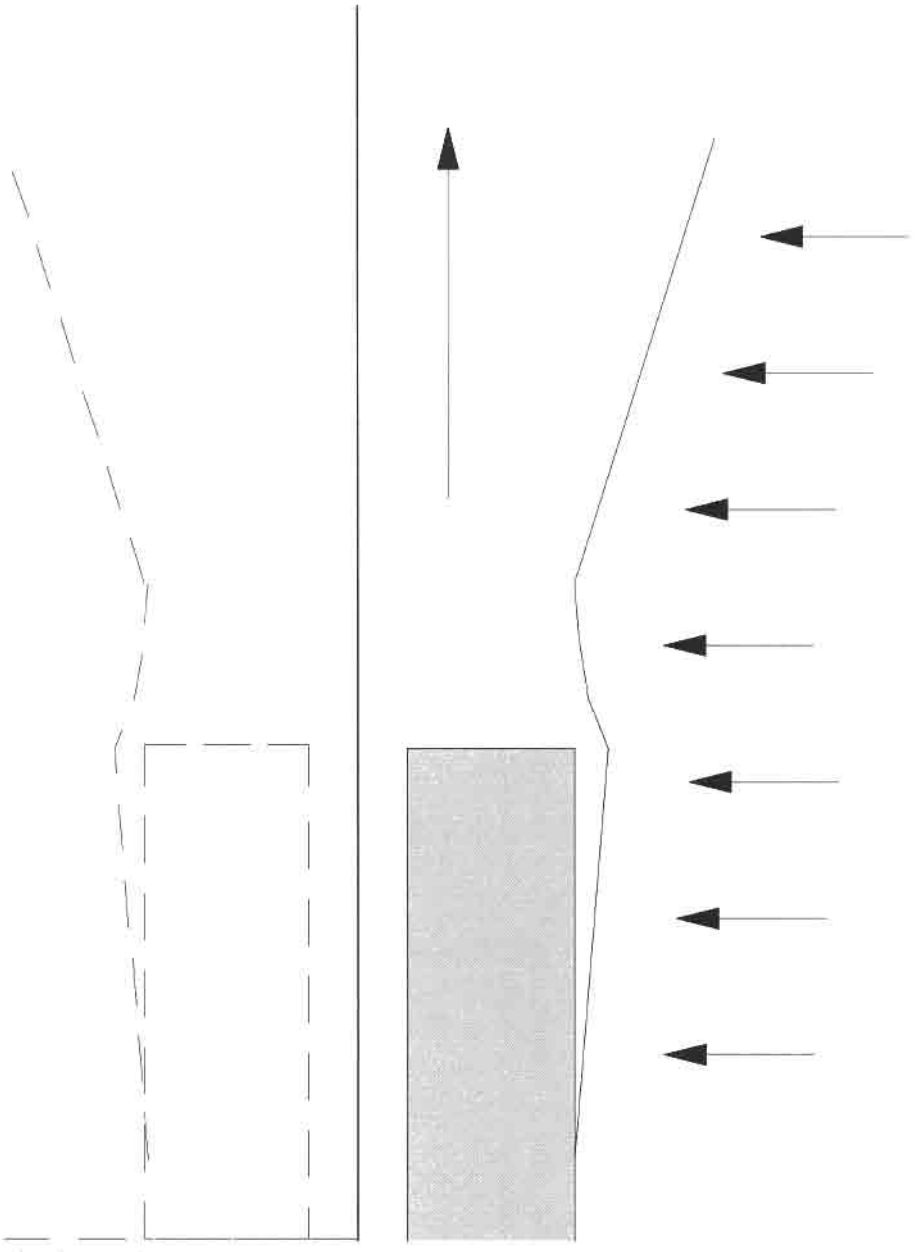

FIGURE 7.69 Thermal plume attached to a wall.

The airflow rate from a heat source can then be calculated as half of the flow from a source with a heat emission of 2Φ:[6]

$$q_v = 1/2 \cdot 0.0052\Phi^{1/3}z^{5/3} = 0.0032\Phi^{1/3}z^{5/3}. \tag{7.190}$$

If the heat source is located in a corner, the airflow rate is equal to 25% of the airflow from a heat source with a heat emission of 4Φ:[15]

$$q_v = 1/4 \cdot 0.005(4\Phi)^{1/3}z^{5/3} = 0.002\Phi^{1/3}z^{5/3}. \tag{7.191}$$

This follows from the same reasoning as above. See Fig. 7.71.

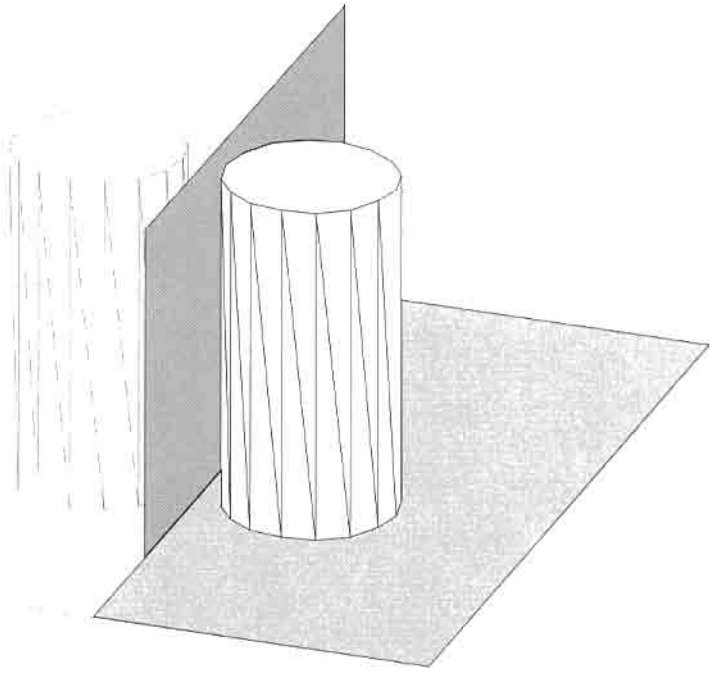

FIGURE 7.70 Convection source close to a wall.

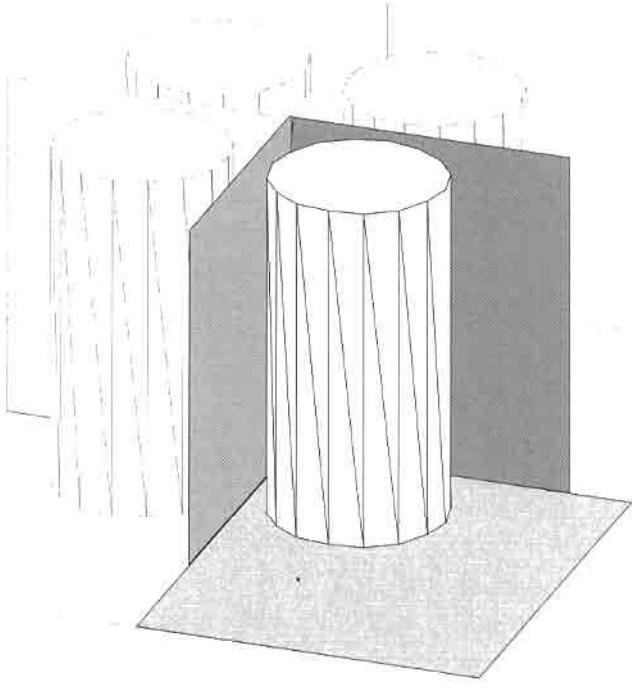

FIGURE 7.71 Convection source in a corner.

When several heat sources are located close to each other, the plumes may merge into a single plume; see Fig. 7.72. In this case, the source should be regarded as one single source, with the heat emission equal to the sum of the heat emission from each of the sources:

$$q_v = 0.005(\Sigma\Phi)^{1/3} z^{5/3} \tag{7.192}$$

where $\Sigma\Phi$ = the sum of the individual heat emissions (W), and z = the height above the virtual source (m). The total flow from N identical sources is then given by[16]

$$q_{v,N} = q_{v,1} N^{1/3} \tag{7.193}$$

where $q_{v,1}$ is the volume flow in the plume from one of the sources.

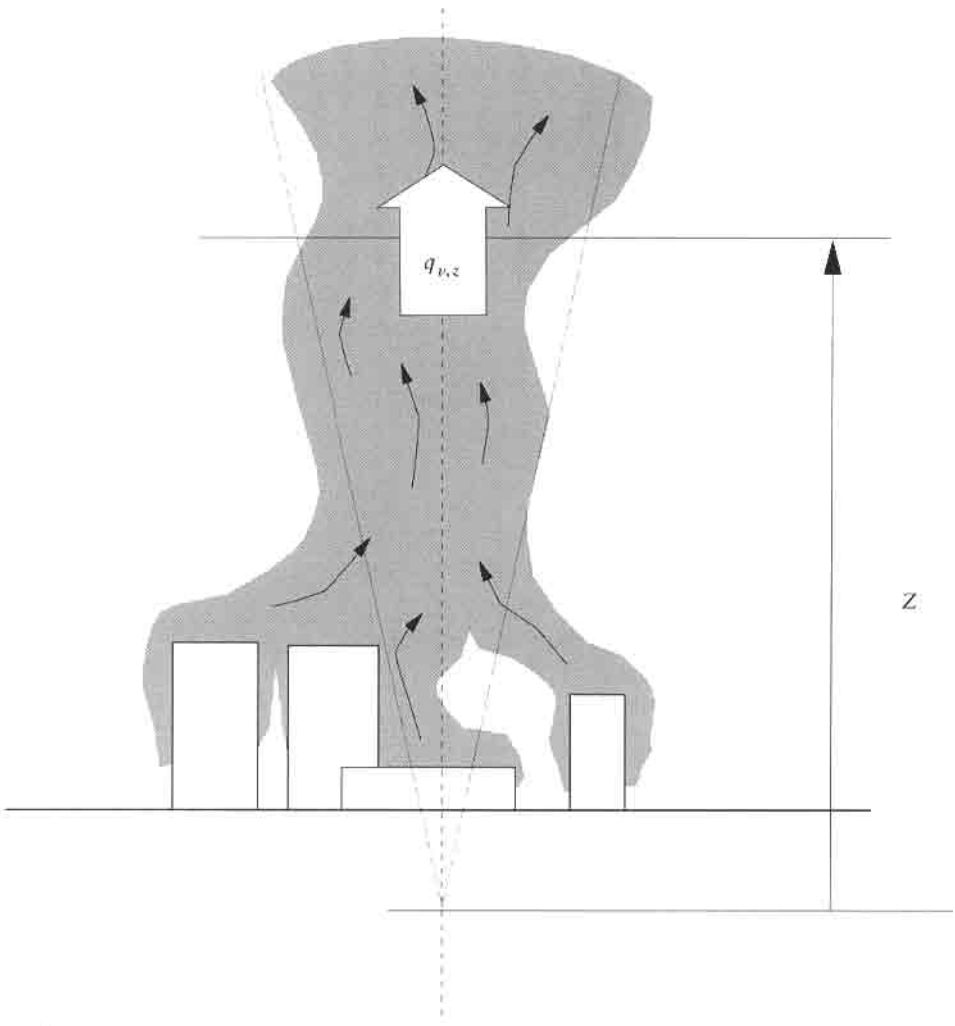

FIGURE 7.72 Interaction between several plumes.

7.5.4 Plumes in Confined Spaces

Figure 7.73 shows a plume in an open environment. The hot air from the source entrains ambient air into the convection current (the plume), thus making the air volume flow increase with height.

Imagine that we enclose the plume, as shown in Fig. 7.74. The plume still entrains air from the surroundings, but the available fresh air is limited. This means that fresh air will surround the plume only up to a certain level. Above this level, the entrained air has to be recirculated from the plume itself. This leads to a two-zone flow model, with a layer of fresh air at the bottom, and warmer air from the plume at the top. The interface between the two layers is located at the height at which the entrained air in the plume equals the supplied air. This can be found from the volume-flow formulae of Section 7.5.2.

Example 7.5.4 Confined Plume

We now put the hot cylinder of Example 7.5.3 inside a room. The convective heat output is still $\Phi = 5$ kW. The air is supplied at the floor, as shown in

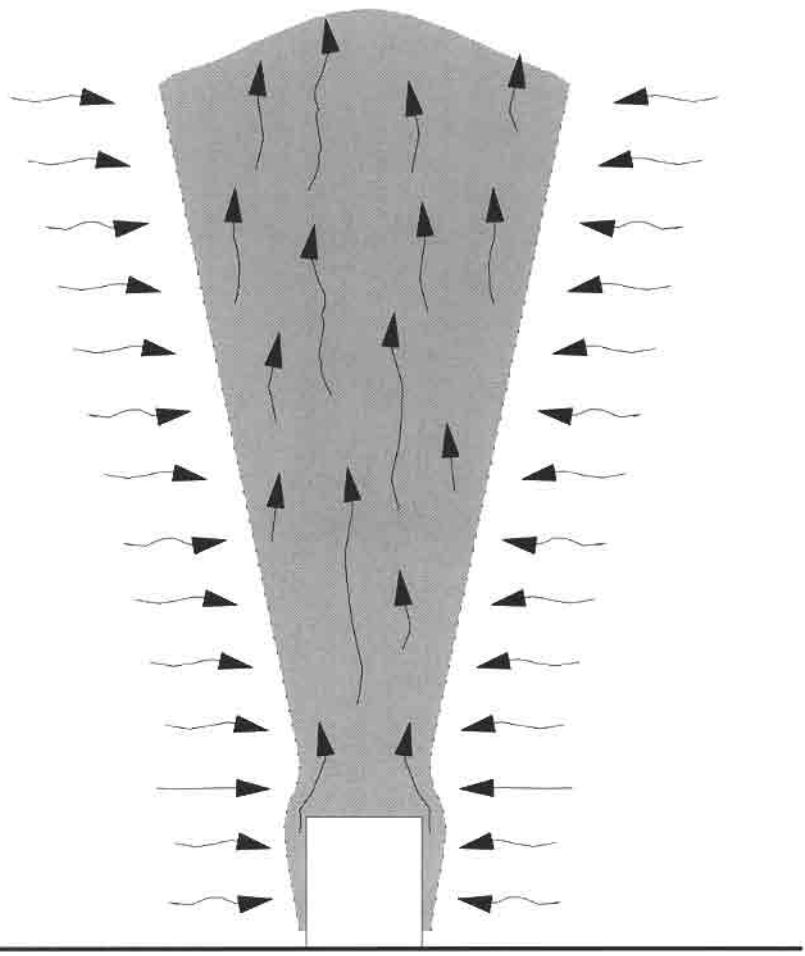

FIGURE 7.73 Plume in an open environment.

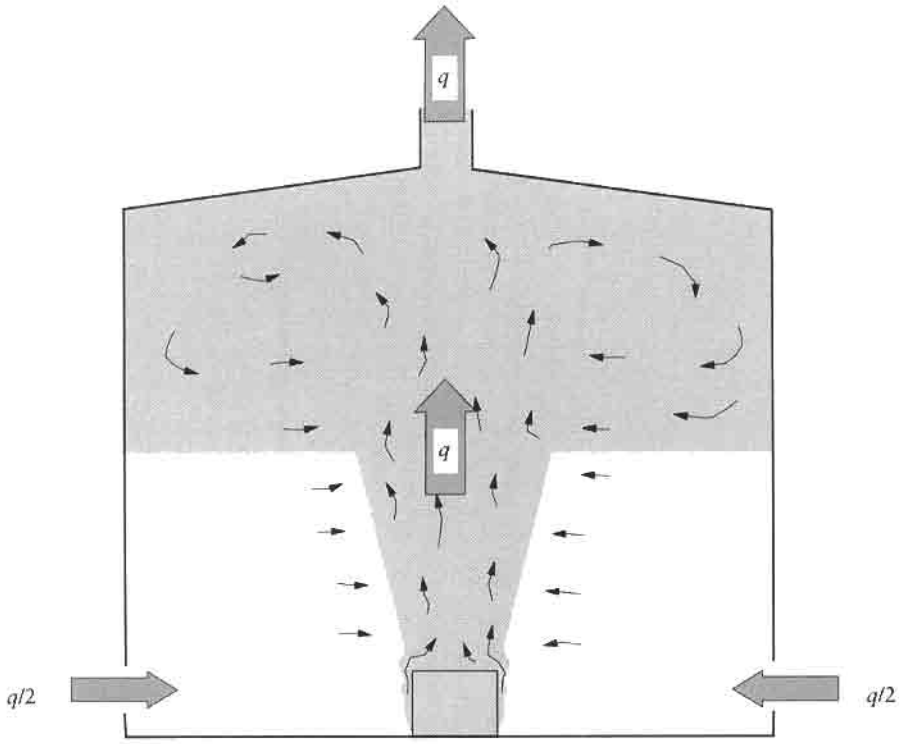

FIGURE 7.74 Plume in an enclosure.

Fig. 7.75, at a rate of $q_v = 1$ m³/s at 10 °C, corresponding to an air mass flow of 1.25 kg/s. The same air mass flow is allowed to escape through the opening in the ceiling. This corresponds to a temperature increase of $\Delta\theta = 4$ °C. At what height will the interface between the fresh bottom layer and the upper recirculation layer stabilize?

From Table 7.19 we find the air volume flow (q_v) in the plume as a function of the height above the floor (z):

$$q_v = 0.005\Phi^{1/3}z^{5/3} \tag{7.194}$$

We can rearrange the equation so that we find the height for a given air volume flow in the plume:

$$z = \left(\frac{q_v}{0.005}\right)^{3/5}\frac{1}{\Phi^{1/5}},$$

which yields the height of the interface:

$$z = (1/0.005)^{3/5} \cdot (5000)^{-1/5} = 4.37 \text{ m}.$$

See Fig. 7.75.

7.5.5 Plumes in Rooms with Temperature Stratification

The idealized case of Fig. 7.75 assumes that the room air temperature is constant in the lower, fresh air layer. In reality, the temperature increases with height in both the lower and upper layers. Figure 7.76 shows a typical vertical

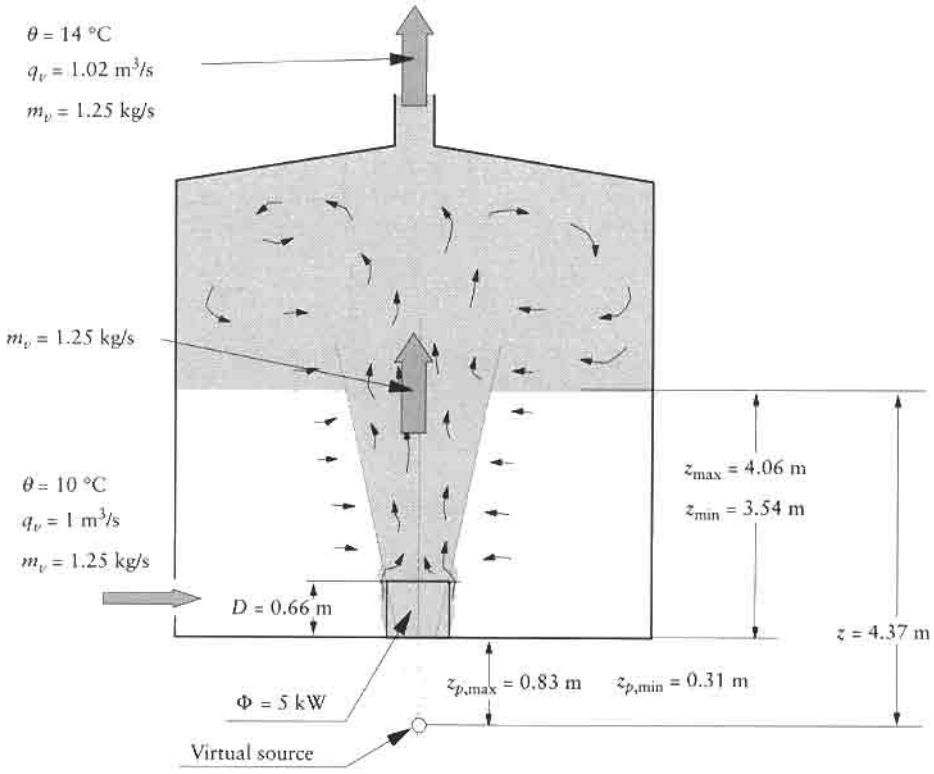

FIGURE 7.75 Calculated results of Example 7.5.4.

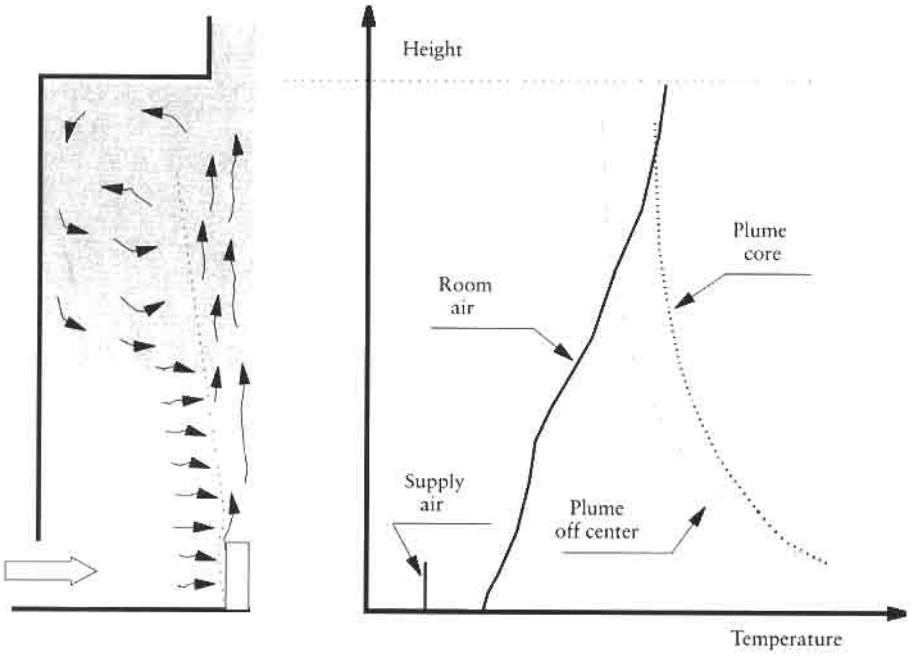

FIGURE 7.76 Vertical temperature distribution in the room of Fig. 7.74.

temperature distribution in a room enclosing a convection current. The air enters the room at low temperature, and is mixed slightly with the room air and heated by convection from the floor, thus making the air temperature at floor level higher than the supply temperature. The air temperature increases from the floor level up to the ceiling, more or less linearly, because the hottest air (in the core of the plume) rises to the ceiling due to its buoyancy, while the outer, cooler parts of the plume layer according to their temperature.

Plumes are influenced by the temperature stratification. The driving force of the plume is the temperature difference between the plume and the surroundings. When this difference diminishes, the plumes will disintegrate and spread horizontally in the room; see Fig. 7.77.

Batchelor[17] noticed the influence of a temperature gradient in the surroundings, and Morton et al.[13] gave a method for calculating the maximum plume rise from a point source in surroundings with a temperature gradient. The volume flow rate in plumes in a room with a temperature stratification is slightly decreased compared to the volume flow rates calculated with the equations presented for nonstratified media.[12] Jin[18] studied the maximum plume rise height for plumes above welding arcs.

In the presence of the temperature gradient, the convective plume reaches its terminal height (z_t), where the temperature difference between the plume and the ambient air disappears. Also, there is another point in the plume at which the air velocity equals zero. This is referred to as the maximum height of the plume (z_{max}). The plume spreads horizontally between these two heights.

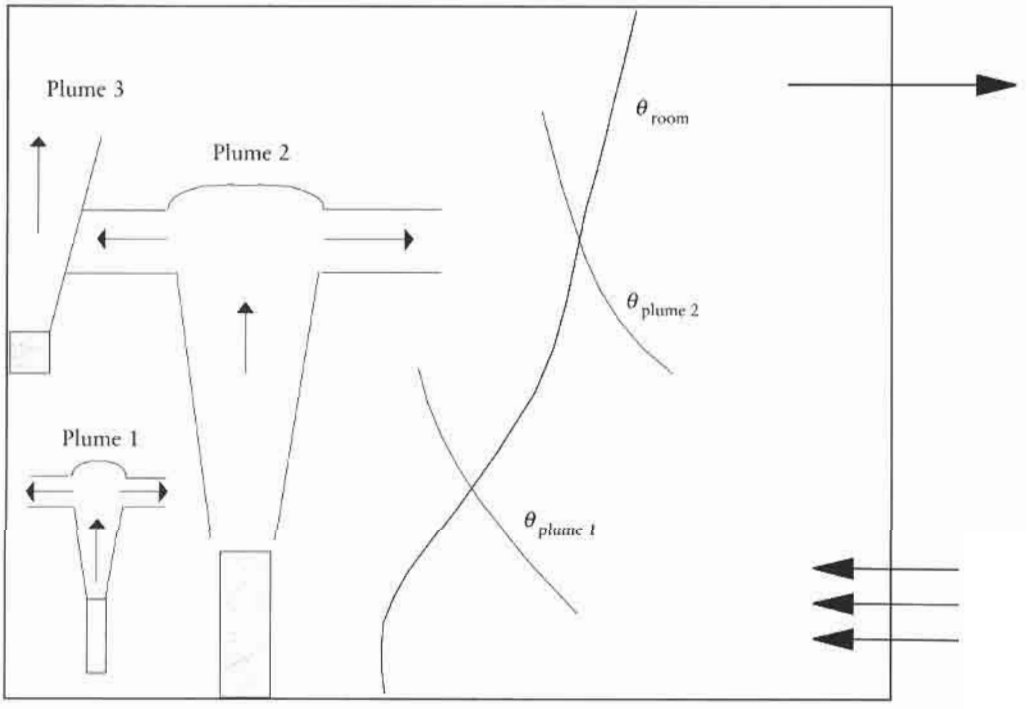

FIGURE 7.77 Schematic illustration of the airflow pattern in a room ventilated by displacement.

7.5.5.1 Point Source

For a point source, Mundt[3] gives the following plume rise formulae:

Maximum height:

$$z_{\max} = 0.98\Phi^{1/4}\left(\frac{d\theta}{dz}\right)^{-3/8} \tag{7.195}$$

Equilibrium height:

$$z_t = 0.74\Phi^{1/4}\left(\frac{d\theta}{dz}\right)^{-3/8} \tag{7.196}$$

where

$d\theta/dz$ = vertical temperature gradient in the room air (°C/m)
Φ = convective heat from the source (W)
$z_{\max}$ = maximum plume rise height (m)
z_t = equilibrium height of the plume (m)

Volume flow rate: The volume flow rate through a given height above the virtual point source in the plume can be found by the following calculation procedure, according to Mundt:[3]

1. Calculate the location of the virtual source and the corresponding z.
2. For the height z above the virtual source, calculate z_1 according to the formula

$$z_1 = 2.86z\left(\frac{d\theta}{dz}\right)^{3/8}\Phi^{-1/4} \tag{7.197}$$

   If $2.125 < z_1 < 2.8$, the density difference disappears and the calculations become uncertain; if $z_1 \geq 2.8$, the plume has reached its maximum height below the actual level.
3. Calculate

$$m_1 = 0.004 + 0.039z_1 + 0.380z_1^2 - 0.062 \cdot z_1^3 \tag{7.198}$$

4. The volume flow rate in the plume through the height z can be found by

$$q_v = 0.00238\Phi^{3/4}\left(\frac{d\theta}{dz}\right)^{-5/8}m_1\,, \tag{7.199}$$

   where q_v is the volume flow rate in m^3/s.

7.5.5.2 Line Source

For a line source, Mundt[3] gives the following plume rise formulae:

Maximum height:

$$z_{\max} = 0.51\Phi^{1/3}\left(\frac{d\theta}{dz}\right)^{-1/2} \tag{7.200}$$

Equilibrium height:

$$z_t = 0.35\Phi^{1/3}\left(\frac{d\theta}{dz}\right)^{-1/2} \tag{7.201}$$

Volume flow rate:

1. Calculate the location of the virtual source and the height z above the virtual source.

2. For the height z above the virtual source, calculate z_1:

$$z_1 = 5.78z(d\theta/dz)^{1/2}\Phi^{-1/3} \tag{7.202}$$

If $2.0 < z_1 < 2.95$, the density difference disappears and the calculations become uncertain; if $z_1 \geq 2.95$, the plume has reached its maximum height below the actual level.

3. Calculate

$$\sqrt{a} = 0.004 + 0.477z_1 + 0.029z_1^2 - 0.018z_1^3 \tag{7.203}$$

4. The volume flow rate is given by

$$q_{v,1} = 0.00482\Phi^{2/3}(d\theta/dz)^{-1/2}\sqrt{a} \tag{7.204}$$

where

$q_{v,1}$ is the volume flow rate in $m^3/s\ m$.

Example 7.5.5 Point Source in a Room with Thermal Stratification

We now put the cylinder of Example 7.5.4 inside a room with a vertical temperature gradient of 1.5 °C/m (see Fig. 7.78). In this case we assume that there are other heat sources in the room. We want to investigate how this temperature stratification influences the volume flow in the plume above the cylinder, and at what height the plume stops.

Following the formulae and calculation procedure of Section 7.5.5.1, we get

a. *Location of the virtual source:* We use the location calculated for the maximum case in Example 7.5.4, i.e.,

$$z_p = -0.83\ m.$$

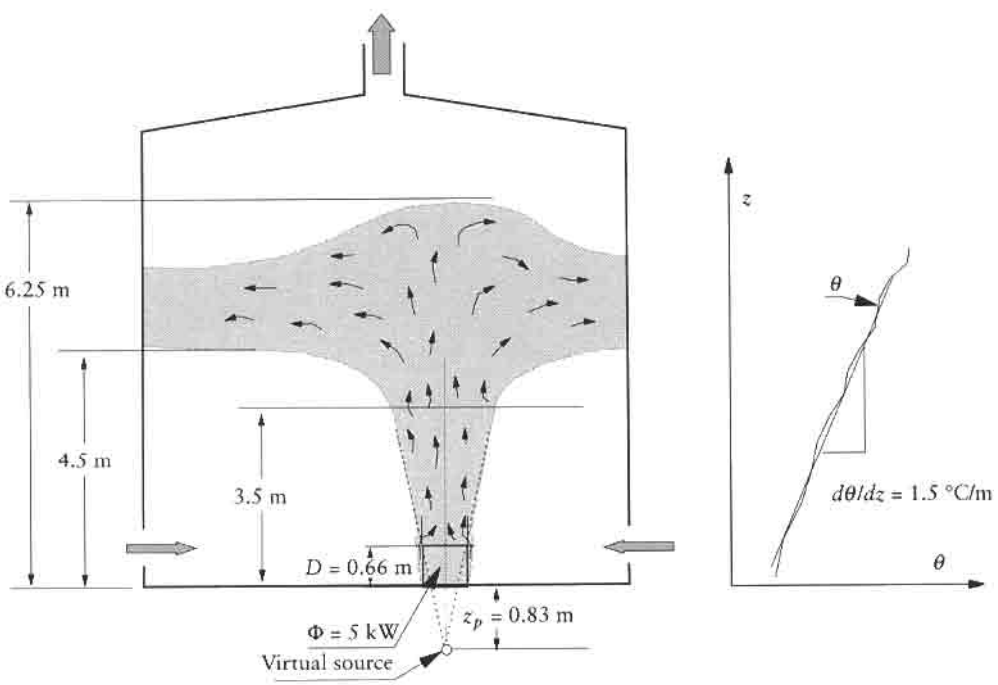

FIGURE 7.78 The cylinder of Example 7.5.4 in a room with thermal stratification.

b. Maximum plume rise: The maximum height above the virtual source is found from Eq. (7.195):

$$z_{max} = 0.98 \cdot 5000^{1/4} \cdot 1.5^{-3/8} = 7.08 \text{ m},$$

i.e., the maximum height is 7.08 m above the virtual source, which is

$$7.08\text{m} - 0.83\text{m} = 6.25 \text{ m above the floor}$$

Equilibrium height (Eq. 7.196):

$$z_t = 0.74 \cdot 5000^{1/4} \cdot 1.5^{-3/8} = 5.34 \text{ m},$$

i.e., the equilibrium or terminal height is 5.34 m above the virtual source, which is

$$5.34 - 0.83 = 4.51 \text{ m above the floor.}$$

c. Volume flow rate in the plume: To find the air volume flow rate through a level $z_{floor} = 3.5$ m, we must first calculate z and then z_1 at this level with Eq. (7.197):

$$z_1 = 2.86 \cdot (3.5 + 0.83) \cdot 1.5^{3/8} \quad 5000^{-1/4} = 1.715$$

With z_1 we can calculate m_1 according to Eq. (7.198):

$$m_1 = 0.004 + 0.039 z_1 + 0.380 z_1^2 - 0.062 z_1^3 = 0.875 \ ,$$

which gives the convection airflow rate from Eq. (7.199):

$$q_v = 0.00238 \cdot (5000^{3/4}) \cdot 1.5^{-5/8} \cdot 0.875 = 0.96 \text{ m}^3/\text{s}.$$

The volume flow calculated 3.5 m above the floor is slightly lower than that calculated for an isothermal atmosphere. The deviation between the volume flows calculated for isothermal room air and stratified room air can be seen from Fig. 7.79.

Example 7.5.6 Comparison with Numerical Modeling

Calculate maximum air velocity, airflow rate, and excessive temperature (relative to the ambient air temperature equal to 20 °C) in thermal plume above the heated cube (0.66 m × 0.66 m × 0.66 m) with convective heat production $W_{conv} = 225$ W, at heights of 2.0 m and 4.0 m above the floor level. Neglect temperature gradient along the room height. Compare the results with predictions made for the same case using CFD code[19] (Fig. 7.80).

To calculate the thermal plume, the cube can be presented as a cylinder with a diameter equivalent to the hydraulic diameter of the top of the cube:

$$D = \frac{4 \times 0.66 \times 0.66}{4 \times 0.66} = 0.66 \text{ m}.$$

In the minimum case,

$$z_o = 0.8D/(2 \tan 12.5°) = 1.19 \text{ m}.$$

The virtual source is located below the floor level:

$$z_p = D/3 + H - z_o = 0.66/3 + 0.66 - 1.19 = -0.31 \text{ m} \ .$$

Thus the vertical distances to be used in the plume characteristics calculation are correspondingly equal to 2.31 m and 4.31 m.

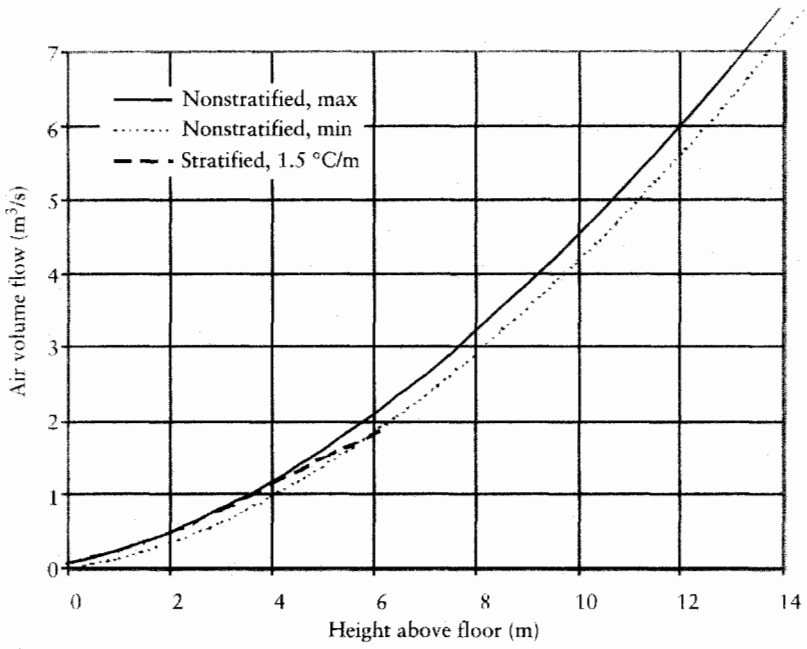

FIGURE 7.79 Airflow rate in the plume above the cylinder of Example 7.5.5.

The maximum velocity in the thermal plume, from Table 7.19, is

$$v_{z,\,2\,\mathrm{m}} = 0.128 \cdot 225^{1/3} \cdot 2.31^{-1/3} = 0.59 \text{ m/s}$$

and

$$v_{z,\,4\,\mathrm{m}} = 0.128 \cdot 225^{1/3} \cdot 4.31^{-1/3} = 0.48 \text{ m/s}\,.$$

The corresponding values of maximum velocities in the plume at heights 2.0 m and 4.0 m above the floor level, from the table in Fig. 7.80, are 0.54 m/s and 0.42 m/s.

The maximum excessive temperature in the thermal plume, from Table 7.19, is

$$\Delta\theta = 0.329 \cdot 225^{2/3} \cdot 2.31^{-5/3} = 3.0 \text{ °C}$$

and

$$\Delta\theta = 0.329 \cdot 225^{2/3} \cdot 4.31^{-5/3} = 1.06 \text{ °C}\,.$$

The corresponding values of maximum excessive temperatures in the plume at heights 2.0 m and 4.0 m above the floor level, from the table in Fig. 7.80, are 3.6 °C and 1.06 °C.

The maximum airflow in the thermal plume, from Table 7.19, is

$$q_{v,z} = 0.005 \cdot 225^{1/3} \cdot 2.31^{5/3} = 0.123 \text{ m}^3\text{s}$$

and

$$q_{v,z} = 0.005 \cdot 225^{1/3} \cdot 4.31^{5/3} = 0.347 \text{ m}^3\text{s}\,.$$

The corresponding values of airflow rates in the plume at heights 2.0 m and 4.0 m above the floor level, from the table in Fig. 7.80, are 0.18 m³/s and 0.35 m³/s.

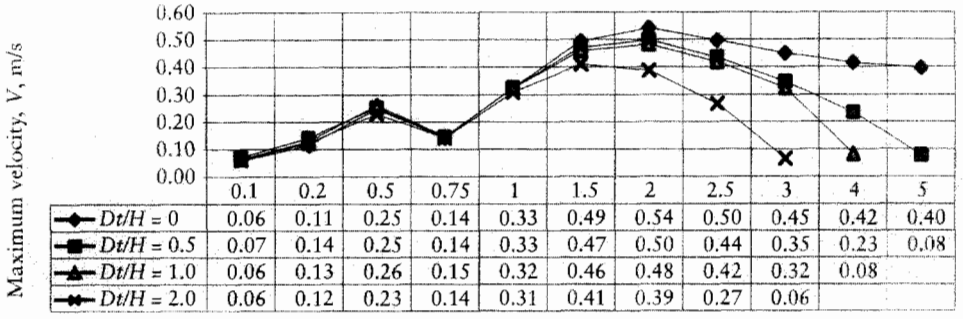

	0.1	0.2	0.5	0.75	1	1.5	2	2.5	3	4	5
Dt/H = 0	0.06	0.11	0.25	0.14	0.33	0.49	0.54	0.50	0.45	0.42	0.40
Dt/H = 0.5	0.07	0.14	0.25	0.14	0.33	0.47	0.50	0.44	0.35	0.23	0.08
Dt/H = 1.0	0.06	0.13	0.26	0.15	0.32	0.46	0.48	0.42	0.32	0.08	
Dt/H = 2.0	0.06	0.12	0.23	0.14	0.31	0.41	0.39	0.27	0.06		

Height above the floor level, m

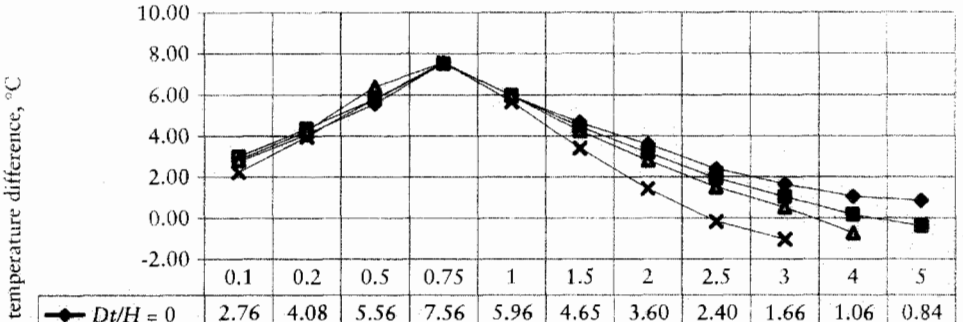

	0.1	0.2	0.5	0.75	1	1.5	2	2.5	3	4	5
Dt/H = 0	2.76	4.08	5.56	7.56	5.96	4.65	3.60	2.40	1.66	1.06	0.84
Dt/H = 0.5	3.00	4.36	5.79	7.51	5.98	4.46	3.19	1.94	1.04	0.16	−0.40
Dt/H = 1.0	2.83	4.25	6.38	7.57	5.96	4.24	2.81	1.50	0.52	−0.74	
Dt/H = 2.0	2.24	3.97	5.80	7.57	5.66	3.39	1.42	−0.17	−1.05		

Height above the floor level, m

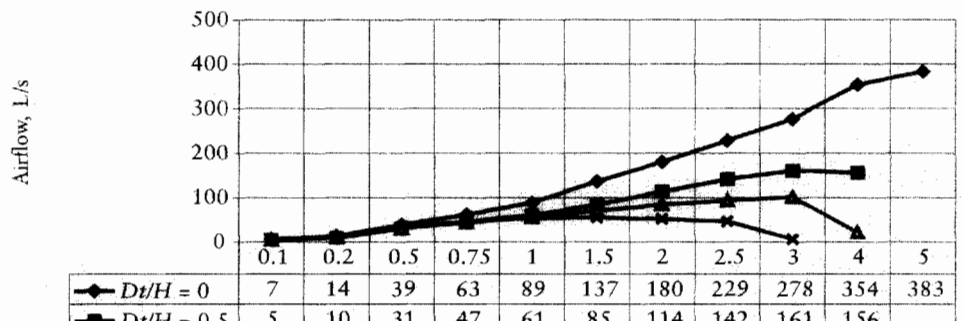

	0.1	0.2	0.5	0.75	1	1.5	2	2.5	3	4	5
Dt/H = 0	7	14	39	63	89	137	180	229	278	354	383
Dt/H = 0.5	5	10	31	47	61	85	114	142	161	156	
Dt/H = 1.0	5	10	31	45	57	71	85	94	102	22	
Dt/H = 2.0	6	11	35	46	54	55	52	47	7		

Height above the floor level, m

FIGURE 7.80 CDF-predicted values of maximum velocity *V*, temperature differential, θ_{max} (°C), and airflow, *q* (L/s), in the horizontal cross-section of the buoyant plume above the heated cube (0.66 m × 0.66 m × 0.66 m, 225 W).[19]

There is a very good correspondence between the analytical and numerical results for temperature and velocity. The airflow rates differ, however, with a factor of 1.46 at a height of 2 m, whereas the correspondence at 4 m is very good.

References

1. Zeldovich, Y. B. 1937. Fundamental principles for free convective plumes. *Journal of Experimental and Technical Physics*, vol. 7, no. 12.
2. Schmidt, W. 1941. *Turbulente Ausbreitung eines Stromes erhitzer Luft ZAMM*, bd. 21.
3. Mundt, E. 1996. The performance of displacement ventilation systems: Experimental and theoretical studies. Ph.D. thesis. Bulletin No. 38, Building Services Engineering, KTH, Stockholm.
4. Mierzwinski, S. 1981. Air motion and temperature distribution above a human body as a result of natural convection. A4-serien no. 45, Inst. för Uppv.- o Vent. teknik, KTH, Stockholm.
5. Popiolek, Z. 1981. Problems of testing and mathematical modeling of plumes above human body and other extensive heat sources. A4-serien no. 54, Inst. för Uppv.- o Vent. teknik, KTH, Stockholm.
6. Nielsen, P. V. 1993. *Displacement Ventilation: Theory and Design.* Aalborg University, Denmark.
7. Jaluria, Y. 1980. *Natural Convection, Heat and Mass Transfer.* Pergamon Press, New York.
8. Etheridge, D., and M. Sandberg. 1996. *Building Ventilation: Theory and Measurement.* Wiley, New York.
9. Elterman, V. M. 1980. *Ventilation of Chemical Plants.* Khimia, Moscow.
10. Holman, J.P. 1989. *Heat Transfer.* McGraw-Hill, New York.
11. Mundt, E. 1992. Convection flows in rooms with temperature gradients: Theory and measurements. In *Roomvent '92: Proceedings of the Third International Conference on Air Distribution in Rooms*, vol. 3. Aalborg, Denmark.
12. Skistad, H. 1994. *Displacement Ventilation.* Research Studies Press, John Wiley & Sons, Ltd., West Sussex, UK.
13. Morton, B. R., G. Taylor, and J.S. Turner. 1956. Turbulent gravitational convection from maintained and instantaneous sources. *Proc. Royal Soc.*, vol. 234A, p. 1.
14. Bach, H., et al. 1993. Gezielte belüftung der arbeitsbereiche in produktionshallen zum abbau der schadstoffbelstung. *Forschungsbericht* HLK-1-92.
15. Kofoed, P. 1991. Thermal plumes in ventilated rooms. Ph.D. thesis. University of Aalborg, Denmark.
16. Nielsen, P. V. 1993. Air distribution in rooms: Room air movement and ventilation effectiveness. In *International Symposium on Room Convection and Ventilation Effectiveness.* ISRACVE and ASHRAE, Tokyo.
17. Batchelor, G. K. 1954. Heat convection and buoyancy effects in fluids. *Quart. J. Roy. Met. Soc.*, vol. 80, pp. 339–358.
18. Jin, Y. 1993. Particle transport in turbulent buoyant plumes rising in a stably stratified environment. Ph.D. thesis. Department of Building Services Engineering, KTH, Stockholm.
19. Aksenov, A.A., A.V. Gudzovski, E.O. Shilkrot, and A.M. Zhivov. 1998. Thermal plumes above heat sources in rooms with a temperature stratification. In *Roomvent '98.*

Bibliography

Zhivov A. M., E.O. Shilkrot, P. V. Nielsen, and G. L. Riskowski. 1997. Displacement ventilation design. In *Ventilation '97: Proceedings of the 5th International Symposium on Ventilation for Contaminant Control*, vol. 1, pp. 427–438. Ottawa, Canada.

Zhivov A. M., G. L. Riskowski, T. W. Ruprecht, L. L. Christianson, P. V. Nielsen, E. O. Shilkrot, and A. A. Rymkevich. 1997. *Design Guide for Displacement Ventilation.* Research Project for Philip Morris Management Corporation. IAT, Savoy, IL.

7.6 AIRFLOW NEAR EXHAUSTS

7.6.1 Introduction

The pollutant-capturing efficiency of local ventilation systems depends on hood design, the hood's positioning near the source of contamination, and the

exhaust air flow. The type and the size of the hood depends on the type and geometry of the pollution source and its characteristics (see Chapter 10 for details). Contaminant movement in the source vicinity is specific to the source type. Pollution sources can be classified (see Section 7.2) as

- A nonbuoyant (diffusion) source
- A buoyant (heat) source
- A dynamic source

The first type of source is characterized by contaminant diffusion in the room in all directions due to the concentration gradient in all directions (e.g., emission from a painted surface). The emission rate in this case is significantly affected by the intensity of the ambient air turbulence and air velocity. With the second type of source, contaminants move in the space primarily due to heat energy as buoyant plumes over the heated surfaces. The third type of source is characterized by contaminant movement in a space with an air jet (e.g., a linear jet over the tank with push-pull ventilation) or particle flow from a grinding wheel. In some cases these factors influencing contaminant distribution are combined.

The geometry of the contaminant source can be *compact* or *linear*. The source geometry affects the hood geometry: round, rectangular, or slot.

Hoods are either *enclosing* or *nonenclosing*. Enclosing hoods provide better and more economical contaminant control because their exhaust rates and the effects of room air currents are minimal compared with nonenclosing hoods. For more detail regarding nonenclosing hoods, see Chapter 10.

For nonenclosing hoods, the airflow rate that allows contaminant capture is called a *target airflow*.[1] The target airflow rate q_0^* is proportional to some characteristic flow rate Q_0 that depends on the type of contaminant source:

$$q_0^* = k_q, \tag{7.205}$$

where

K is a dimensionless coefficient depending on the hood design
q is the characteristic airflow rate depending on the contaminant source

For a nonenclosing hood with a nonbuoyant contaminant source, the characteristic airflow can be calculated using the following equation:

$$q = V_0 \cdot A_0, \tag{7.206}$$

where

v_0 = average air velocity in the hood opening that ensures capture velocity at the point of contaminant release, m/s
A_0 = hood opening area, m^2

For a buoyant source q can be equal to the airflow in the convective plume at the hood suction cross-section. For a dynamic source q can be equal to the airflow rate in the jet.

An exhaust airflow rate lower than q_0^* results in reduced contaminant-capturing effectiveness. An exhaust airflow rate greater than q_0^* results in excessive capturing effectiveness (Fig. 7.81).

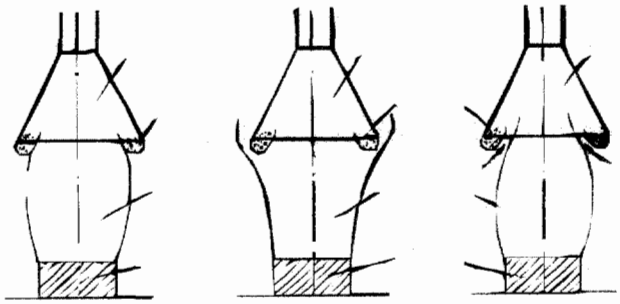

(*a*) (*b*) (*c*)

FIGURE 7.81 Hood performance for different exhaust airflow rates. (*a*) Target airflow rate $q = q^*$. (*b*) Target airflow rate $q < q^*$. (*c*) Target airflow rate $q > q^*$.

7.6.2 Capture Velocity

The capture velocity is the air velocity at the point of contaminant generation upstream of a hood. The contaminant enters the moving airstream at the point of generation and is conducted along with the air into the hood. The concept of capture velocity is primarily used by designers to select a volumetric flow rate for withdrawing air through a hood in the case of a nonbuoyant contaminant source. Ranges of capture velocities for several industrial operations are listed in Table 7.21.[2] The values for capture velocities are based on successful experience under ideal conditions. For the given hood, if design velocities anywhere upstream of the hood are known [$v = f(q_0, x, y, z)$], the capture velocity is set equal to v_c at the point (x, y, z) where contaminants are to be captured and q_0 is found. To ensure that contaminants enter an inlet, the transport equations between the source and the hood have to be solved.

Airflow near the hood can be influenced by drafts created directly by the supply air jets (spot-cooling jets) or by turbulence of the ambient air caused by the jets, upward/downward convective flows, moving people, and drafts from doors and windows.

Process equipment may be responsible for other sources of air movement in the room. For example, high-speed rotating machines such as pulverizers, high-speed belt material transfer systems, falling granular materials, and compressed air escaping from pneumatic tools all produce air currents.

These factors can significantly reduce the capturing efficiency of local exhausts and should be accounted for by the correction coefficient on room air movement, $K_r > 1$, in Eqs. (7.205) and (7.206). For example, Eq. (7.206) is replaced with

$$q_o^* = k_r k q_o . \tag{7.207}$$

7.6.3 Air Movement Near Sinks

7.6.3.1 Theoretical Considerations

Airflow near the hood can be described using the incompressible, irrotational flow (i.e., potential flow) model. The potential flow theory is based on

TABLE 7.21 Ranges of Capture (Control) Velocity

Conditions	Examples	Capture velocity, m/s
Released with essentially no velocity into still air	Evaporation from tanks, degreasing, plating	0.25 to 0.5
Release at low velocity into moderately still air	Container filling, low-speed conveyor transfers, welding	0.5 to 1.0
Active generation into zone of rapid air motion	Barrel filling, chute loading of conveyors, crushing, cool shakeout	1.0 to 2.5
Release at high velocity into zone of very rapid air motion	Grinding, abrasive blasting, rumbling, hot shakeout	2.5 to 10

Note: In each category above, a range of capture velocities is shown. The proper choice of value depends on several factors:

Lower end of range:	*Upper end of range:*
•Room air currents favorable to capture	•Distributing room air currents
•Contaminants of low toxicity or of nuisance value only	•Contaminants of high toxicity
•Intermittent, low production	•High production, heavy use
•Large hood; large air mass in motion	•Small hood; local control only

several assumptions.[3] For instance, the fluid is assumed frictionless. Another assumption is that the flow is steady. That means there are no changes in velocity at a given point with respect to time.

The total pressure p_{tot} in the area upstream of the hood remains constant and can be described with the following equation:

$$p_{tot} = p_{st} + p_d = \text{constant} \tag{7.208}$$

where

p_{st} is the static pressure, Pa, at any point of the flow
$p_d = \rho v^2/2$ is the dynamic pressure, Pa, at any point of the flow
ρ = air density, kg/m^3
v = air velocity, m/s
g = gravitational acceleration, 9.8 m/s^2

At some distance from the hood, the total pressure in the airflow p_{tot} is equal to the ambient air pressure, e.g., $p_{tot} = 0$. Thus,

$$p_d = \frac{\rho v^2}{2} = -P_{st} \tag{7.209}$$

The above discussion does not apply to the wakes, with a vortex air movement (Fig. 7.82).

Numerical simulation of hood performance is complex, and results depend on hood design, flow restriction by surrounding surfaces, source strength, and other boundary conditions. Thus, most currently used methods of hood design are based on experimental studies and analytical models. According to these models, the exhaust airflow rate is calculated based on the desired capture velocity at a particular location in front of the hood. It is easier

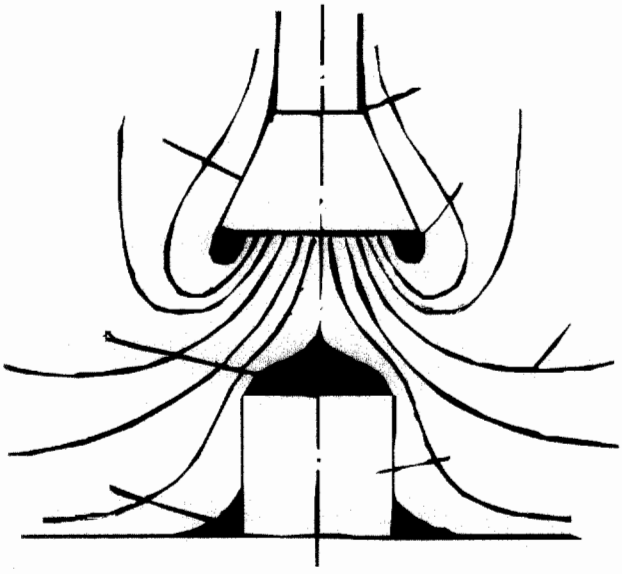

FIGURE 7.82 Airflow in the hood vicinity.

to understand the design process for the sink with vanishingly small dimensions—a point or a linear source of suction.

7.6.3.2 Air Movement Near a Point Sink

The point sink can approximate airflow near a hood with round or square/rectangular shape. The point sink will draw air equally from all directions (Fig. 7.83). The radial velocity v_r (m/s) at a distance r (m) from the sink can be calculated as a volume rate of exhaust airflow q (m^3/s) divided by the surface area of an imaginary sphere of radius r:

$$v_r = \frac{q}{4\pi r^2}. \tag{7.210}$$

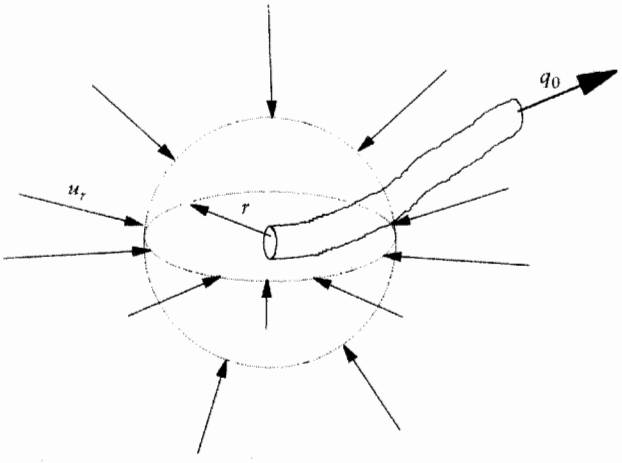

FIGURE 7.83 Airflows toward the point sink.

TABLE 7.22 Values of α (rad) for Some Typical Point Sink Locations

Type of airflow restriction	α, rad
Unrestricted airflow	4π
Sink within the infinite surface	2π
Sink in the vertex of the dihedral angle with the right angle (90°)of deflection	p
Sink in the vertex of the trihedral angle with the right angle (90°)of deflection in all directions	$\pi/2$
Sink in the vertex of the dihedral angle with the angle ϕ, rad, of deflection	2ϕ
Sink in the vertex of the cone with an angle of deflection ϕ, rad	$2\pi(1 - \cos \phi/2)$

Restriction of the airflow by surfaces decreases the area through which the air flows toward the sink, which results in increased radial velocity. For cases with a restricted airflow created by the sink, Eq. (7.210) can be modified to

$$v_r = \frac{q}{\alpha r^2} \tag{7.211}$$

where α is in radians. Values for some typical airflow restrictions are listed in Table 7.22.

Equations for the inflow velocity (v_r) and the corresponding capture distance (r_c) are listed in Table 7.23 for the most common point sink locations.

7.6.3.3 Air Movement Near a Linear Sink

A linear sink will create a two-dimensional airflow. The radial velocity v_r (m/s) at a distance r (m) from the sink is calculated as a volume rate of q(m^3/s) per meter of linear sink length divided by the surface area of an imaginary cylinder of radius r:

$$v_r = \frac{q}{2\pi r} \tag{7.212}$$

The effect of restricting surfaces on the flow created by the linear sink will be similar to that described for the point source. The equations for the inflow velocity (v_r) and the corresponding capture distance (r_c) for some typical situations are listed in Table 7.24.

7.6.3.4 Air Movement Near Sinks with Finite Dimensions

Realistic exhausts used to capture contaminants are complex, varying in their geometry and size. In many cases, the airflow rate ensuring a desired capture velocity at a particular location can be obtained only from empirical studies. Air velocities in front of the hood suction opening depend on the exhaust airflow rate, the geometry of the hood, and the surfaces comprising the suction zone. Studies have established the principle of similarity of velocity contours (expressed as a percentage of the hood face velocity) for zones with similar geometry.[4]

TABLE 7.23 Inflow Velocity and Capture Distance for Some Common Locations of a Point Sink

Schematic of airflow restriction	Inflow velocity, v_r	Capture distance, r_c
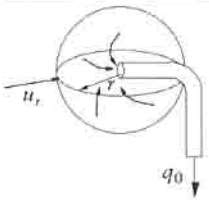 Unrestricted airflow	$v_r = \frac{q}{4\pi r^2}$ (1)	$r_c = \sqrt{\frac{q}{4\pi v_c}}$ (2)
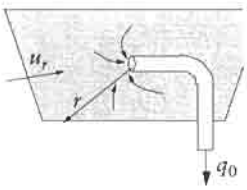 Sink within the infinite surface	$v_r = \frac{q}{2\pi r^2}$ (3)	$r_c = \sqrt{\frac{q}{2\pi v_c}}$ (4)
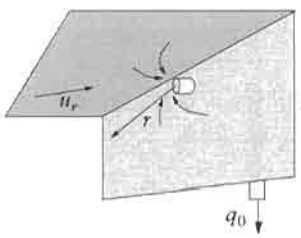 Sink in the vertex of the dihedral angle with the right angle (90°) of deflection	$v_r = \frac{q}{\pi r^2}$ (5)	$r_c = \sqrt{\frac{q}{\pi v_c}}$ (6)
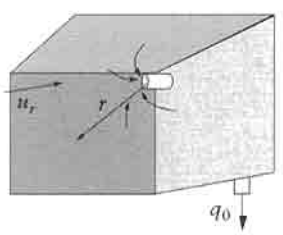 Sink in the vertex of the trihedral angle with the right angle (90°) of deflection in all directions	$v_r = \frac{2q}{\pi r^2}$ (7)	$r_c = \sqrt{\frac{2q}{\pi v_c}}$ (8)

Ill. courtesy H. Skistad

To describe an airflow in the vicinity of some realistic, finite-dimensional hoods, theoretical considerations that are valid for hypothetical point or linear sinks can be applied.

Typically, the velocity distribution in the hood face area is not uniform. Wakes formed close to the hood sides, or vena contracta, reduce the "effec-

TABLE 7.24 Inflow Velocity and Capture Distance for Some Common Locations of a Linear Sink

Schematic of airflow restriction	Inflow velocity, v_r	Capture distance, r_c
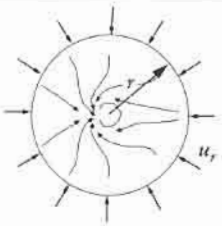 Unrestricted flow	$v_r = \frac{q}{2\pi r L}$ (1)	$r_c = \frac{q}{2\pi v_c L}$ (2)
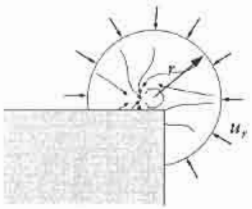 Sink at the vertex of the dihedral angle with the right angle of deflection (270°)	$v_r = \frac{2q}{3\pi r L}$ (3)	$r_c = \frac{2q}{3\pi v_c L}$ (4)
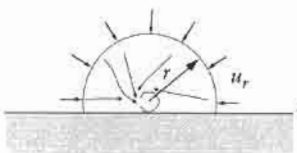 Sink within the infinite surface	$v_r = \frac{q}{\pi r L}$ (5)	$r_c = \frac{q}{\pi v_c L}$ (6)
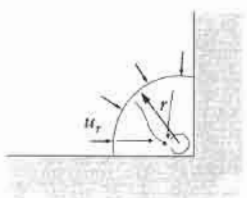 Sink at the vertex of the dihedral angle with the right angle of deflection (90°)	$v_r = \frac{2q}{\pi r L}$ (7)	$r_c = \frac{2q}{\pi v_c L}$ (8)

Ill. courtesy H. Skistad

tive suction area" of the hood. Figure 7.82 shows the wakes in the suction area of an unrestricted rectangular duct. The suction occurs only in the central part of the duct, which constitutes approximately 75% of the duct width.[5] Within the "effective suction width" airflow velocities are relatively uniform, with a maximum air velocity v_m in the center equal to $1.29v_0$,

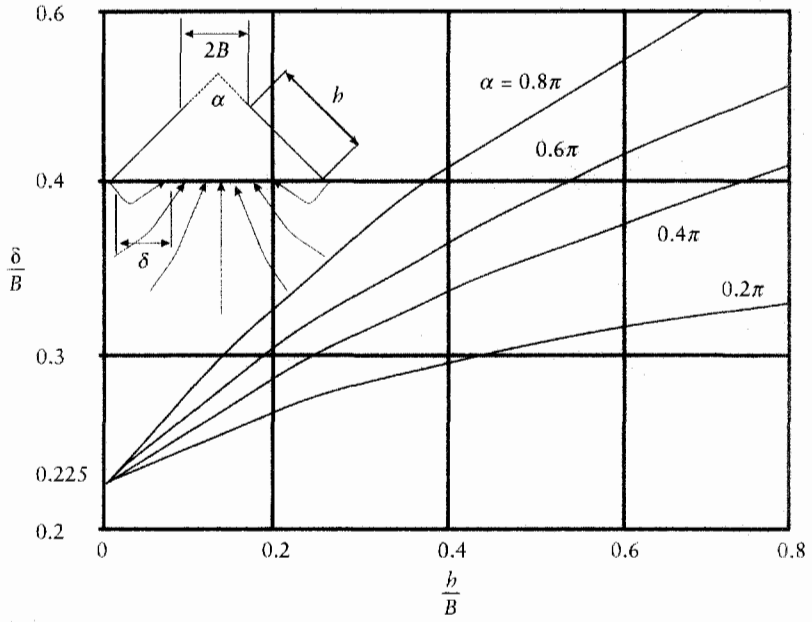

FIGURE 7.84 Influence of hood configuration on hood entrance wake size, δ.

where v_0 is the average velocity calculated based on the total duct width. The velocity distribution in the suction area of an unrestricted round duct is similar, with an "effective suction diameter" $D_e = 0.81D$ and a maximum velocity $V_m \approx 1.1v_0$.

The size of these wakes and the velocity uniformity level depend on the hood design and the airflow pattern in close proximity to the hood face.

Figure 7.84 shows the approximate relation between the wake size and the angle of cone deflection for the typical hood.[5] Wake size increases ("effective suction area" decreases) with an increase in the angle of the hood deflection. Thus, it can be recommended that the value for hood deflection angle not exceed $\pi/4$.

Extensive review of equations for centerline velocities in flows in the vicinity of realistic hoods resulting from experimental and theoretical studies was performed by Braconnier.[6] This review shows certain inconsistencies in equations available from the technical literature due to effects of parameters related to opening (shape, length-to-width ratio, presence of a flange) and the opening location (in an open space or limited by surfaces). The summary of equations from this review complemented by information from Posokhin[5] is presented in Tables 7.25 and 7.26.

Comparison of the relative velocity change in the airflow created by a hood with a finite face area and by a point source is graphically illustrated in Fig. 7.85. At a distance greater than $X/R = 1$, the velocities induced by a realistic hood and by a point source are practically equal. This means that in some cases airflow in front of realistic hoods can be described using the simplified point source equations.

TABLE 7.25 Inflow Velocity for Some Other Common Locations of a Linear Sink

Schematic of airflow restriction	Inflow velocity, v
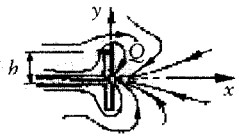 Sink with flanges	$$V_{0X} = -\frac{Q}{2\pi}\frac{X}{X^2 + h^2 - h\sqrt{X^2 + h^2}}$$
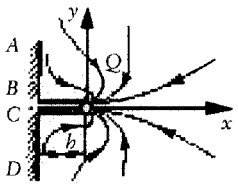 Sink set forth from the infinite surface	$$v_{AB} = -v_{CD} = -\frac{Q}{\pi}\frac{Y}{Y^2 + h^2}$$ $$v_{0X} = -\frac{Q}{\pi}\frac{X - h}{X^2 + 2Xh}$$
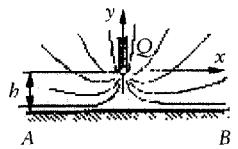 Sink facing the infinite surface	$$v_{AB} = -\frac{Q}{\pi}\frac{X}{X^2 + h^2}$$ $$v_{0C} = -\frac{Q}{\pi}\frac{(h + Y)}{Y(2h + Y)}, \quad Y < 0$$
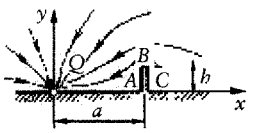 Sink within the infinite surface with an airflow obstruction from one side	$$v_{OA} = \frac{Q}{\pi}\frac{X - a}{\sqrt{(a^2 + h^2)[(X - a)^2 + h^2]} - (X - a)^2 - h^2}$$ $$v_{CD} = -\frac{Q}{\pi}\frac{a - X}{\sqrt{(a^2 + h^2)(X - a)^2 + h^2} - (z - X^2) + h^2}$$
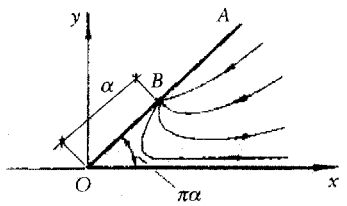 Sink on one of the surfaces of the dihedral angle απ (rad)	$$v_{0X} = -\frac{Q}{\alpha\pi}\frac{x^{\left(\frac{1-\alpha}{\alpha}\right)}}{x^{1/\alpha} + a^{1/\alpha}}$$ $$v_{OA} = -\frac{Q}{\alpha\pi}\frac{\left(\frac{x}{\cos\pi\alpha}\right)^{\left(\frac{1-\alpha}{\alpha}\right)}}{\left(\frac{x}{\cos\pi\alpha}\right)^{1/\alpha}} - a^{1/\alpha}$$

(continues)

TABLE 7.25 *(continued)*

Schematic of airflow restriction	Inflow velocity, v
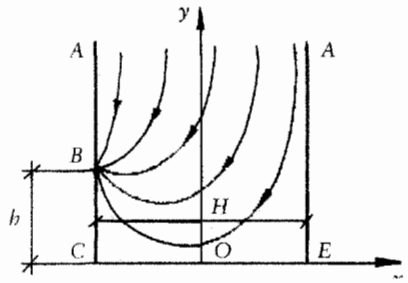 Linear exhaust from confined space (a)	$v_{AC} = \frac{Q}{H}\frac{\sin h(\pi \bar{Y})}{\cos h(\pi h) - \cos h(\pi \bar{Y})}, \quad \bar{h} = \frac{h}{H}$
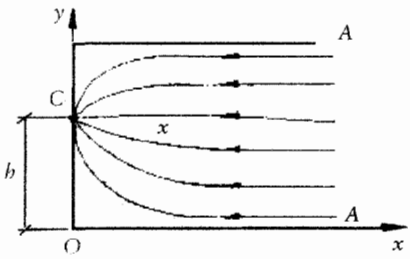 Linear exhaust from confined space (b)	$v_{OA} = -\frac{Q}{2H}\frac{\sin h(\pi \bar{X})}{\cosh^2\left(\frac{\pi}{2}\bar{X}\right) - \cos^2\left(\frac{\pi}{2}\bar{h}\right)}$ $v_{BA} = -\frac{Q}{2H}\frac{\sin h(\pi \bar{X})}{\sinh^2\left(\frac{\pi}{2}\bar{X}\right) + \cos^2\left(\frac{\pi}{2}\bar{h}\right)}$ $v_{OB} = -\frac{Q}{2H}\frac{\sin(\pi \bar{Y})}{\cos^2\left(\frac{\pi}{2}\bar{Y}\right) - \cos^2\left(\frac{\pi}{2}\bar{h}\right)}$

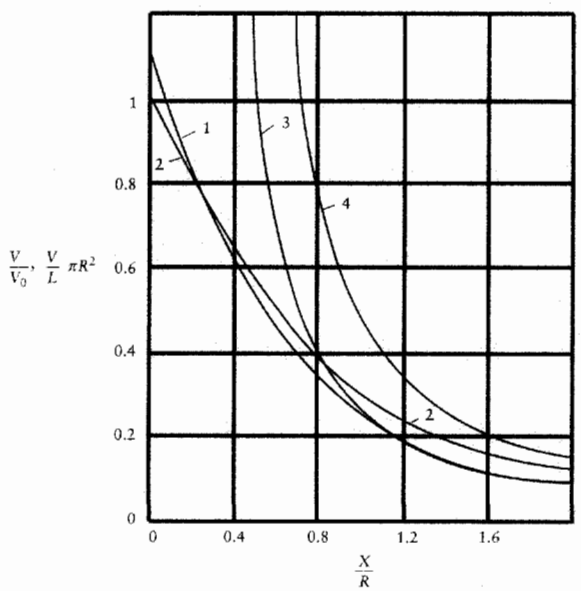

FIGURE 7.85 Centerline velocity, V, and decay in the flow created by exhausts with finite dimensions and point sinks. *1*, round free-standing pipe; *2*, round opening in a infinite surface; *3*, unrestricted point sink, $V = q/\pi r^2$; *4* point sink in an infinite surface, $V = 2q/\pi r^2$.

TABLE 7.26 Centerline Air Velocities Induced by Sinks with Finite Dimensions

Hood type	Schematic	Equation	Applicable range	Reference
Round free-standing hood, unflanged	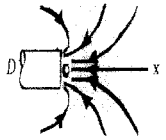	$\frac{v_X}{v_0} = (1 + 10x^2/A)^{-1}$	$x \le 1.7\sqrt{A}$ $\alpha \le 30°$	Dalla Valle[4]
Round free-standing hood, flanged	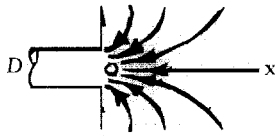	$\frac{v_X}{v_0} = 1.1(0.07)^{-x/D}$ $\frac{v_X}{v_0} = 1(x/D)^{-1.5}$	$0 \le \frac{x}{D} \le 0.5, C \ge D$ $0.5 \le \frac{x}{D} \le 1.5, C \ge D$	Garrison (1977)[7]
Rectangular free-standing hood, unflanged	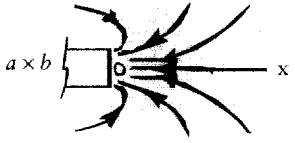	$\frac{v_X}{v_0} = (0.93 + 8.58\alpha_F^2)^{-1}$ $\alpha_F = (x/\sqrt{A})(a/b)^{\beta F}$ $\beta_F = 0.2(x/\sqrt{A})^{-1.3}$	$1 \le \frac{a}{b} \le 16$ $0.05 \le \frac{x}{\sqrt{A}} \le 3$ $a \le 30°$	Fletcher (1977)[8]
Rectangular free-standing hood, flanged	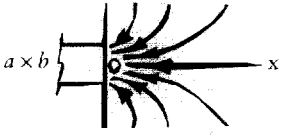	$\left[\frac{v_X}{v_0} = 1 - \frac{2}{\pi}\text{atan}\left(\frac{2x\sqrt{x^2 + a^2 + b^2}}{ab}\right)\right]$	$1 \le \frac{a}{b} \le 16$ $0.05 \le \frac{x}{\sqrt{A}} \le 3$ $\frac{C}{\sqrt{A}} \ge 1$	Tyaglo and Shepelev (1970)[9]
Slot in the pipe wall	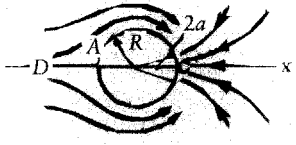	$\frac{v_{ez}}{v_p} = \frac{v_{AD}}{v_0} = \frac{2R}{R\pi}\text{atan}\left[\frac{x + R}{x - R}\tan\left(\frac{\alpha}{2}\right)\right]$	$\lvert x\rvert \ge R$	Posokhin[5]

References

1. Posokhin, V. N., and A. M. Zhivov. 1997. Principles of local exhaust design. In *Proceedings of the 5th International Symposium on Ventilation for Contaminant Control*, vol. 1. Canadian Environment Industry Association, Ottawa.
2. Alden, J. L., and J. M. Kane. 1982. *Design of Industrial Ventilation Systems*. 5th ed. Industrial Press, New York.
3. Stoecker, W. 1968. *Principles for Air Conditioning Practice*. Industrial Press, New York.
4. DallaValle, J. M. 1952. *Exhaust Hoods*, 2nd ed. Industrial Press, New York.
5. Posokhin, V. N. 1984. *Design of Local Ventilation Systems for the Process Equipment with Heat and Gas Release* (in Russian). Mashinostroyeniye, Moscow.
6. Braconnier, R. 1988. Bibliographic review of velocity field in the vicinity of local exhaust hood openings. *American Industrial Hygienists Association Journal*, vol. 49 no. 4, 185–198.
7. Garrison, R. P. 1977. Nozzle performance and design for high velocity/low volume exhaust ventilation. Ph.D. thesis. University of Michigan. Ann Arbor, MI.
8. Fletcher, B. 1977. Center line velocity characteristics of rectangular unflanged hoods and slots undersuction. *Ann. Occup. Hyg.* 20:141–46.
9. Tyaglo, I. G. and I. A. Shepelev. 1970. Air flow near exhaust opening. Vodosnabzheniye I Sanitarnaya Tekhnika #5, pp. 24–25.

Bibliography

ACGIH. 1998. *Industrial Ventilation: A Manual of Recommended Practice*. 23rd ed. Committee on Industrial Ventilation, American Conference of Governmental Industrial Hygienists, Cincinnati.

Burgess, W. A., M. J. Ellenbecker, and R. D. Treitman. 1989. *Ventilation for Control of the Work Environment*. John Wiley & Sons, New York.

Designer's Guide. 1992. *Ventilation and Air Conditioning* (in Russian). 4th ed., part 3(1). Stroizdat, Moscow.

Elterman, V. M. 1980. *Ventilation of Chemical Plants* (in Russian). Khimia, Moscow.

7.7 AIR CURTAINS

7.7.1 Introduction

Air curtains are local ventilation devices that are used in industrial buildings to reduce leakage of airflow through apertures in building enclosures and process equipment. Their operation is based on the damping effect of air jets that are supplied into the area of the open aperture. The advantages of air curtains include

- Improvement of working conditions near open apertures
- Reduction of heat (cold) consumption and electrical energy for heating (cooling) of buildings and process equipment
- Reduction of heat loss in the building by using overheated air from an upper zone of the room
- Reduced loss of usable working area near gates due to the ingress of outdoor air into the building

Traditional air curtains, which utilize only indoor air heated in the curtain heaters, are not always economical (due to considerable thermal energy consumption). Reduction of heat consumption is achieved by curtains that utilize unheated indoor or outdoor air, and also combined air curtains, which heat 3only part of the supplied air. Air curtains that use unheated air conserve 30–70% of thermal energy.

7.7.2 Types of Air Curtains and Their Application

According to the application and aerodynamic pattern, the following types of air curtains have been designed:

- Air curtains with heated indoor air
- Air curtains with unheated indoor air
- Combined air curtains with indoor air
- Air curtains with unheated outdoor air
- Air curtains for cooled rooms
- Air curtains for gates with long passages
- Air curtains for process equipment

The first four air curtain types are installed in outer apertures of gates in heated rooms and also in unheated rooms where a standard temperature should be maintained in the working zone. They are designed to prevent the ingress of outdoor air during the cold season of the year. Air curtains for cooled rooms are designed to prevent the ingress of warm outdoor air. If the heating program for the room is to be replaced by the cooling program during the year, it is advisable to equip the gate with both an air curtain that prevents ingress of cold and one that prevents ingress of heat.

Air curtains for process equipment are designed to prevent toxic constituents from entering the room through apertures of the equipment.

7.7.2.1 Air Curtains with Heated Indoor Air

The traditional design pattern (to be described in Section 7.7.5) is recommended for air curtains with heated indoor air. The air curtain may be double-sided with horizontal supply (Fig. 7.86*a*), or it may be single-sided (Fig. 7.86*b*) with horizontal or vertical supply. In all cases, the air curtain is a flat jet discharged at an angle toward the pressure side of the opening.

Air curtains with heated indoor air are used for relatively small gates (up to 3.6 × 3.6) in genial climate and in buildings without skylights, and also in case constructions prevent the installation of combined air curtains (e.g., not enough space at the gate). Air curtains with heated indoor air guarantee the necessary temperature of the air mixture entering through the gate, but they also consume a relatively large amount of thermal energy.

7.7.2.2 Air Curtains with Unheated Indoor Air

Air curtains with unheated indoor air have a similar air supply arrangement. Only the design of the air intake duct might differ; it may be extended to take in warm air, for example, from the upper overheated zone of the room. Air curtains with unheated indoor air are recommended in case the standard temperature of the air coming in through the aperture of the open gate can be maintained without heating the air in the curtain, as in the following cases:

- Rooms with an overheated upper zone of over 2 ×C (if it is possible to use the air from the upper overheated zone of the room)
- Rooms with excess heat (if it is technically possible and reasonable to utilize it)

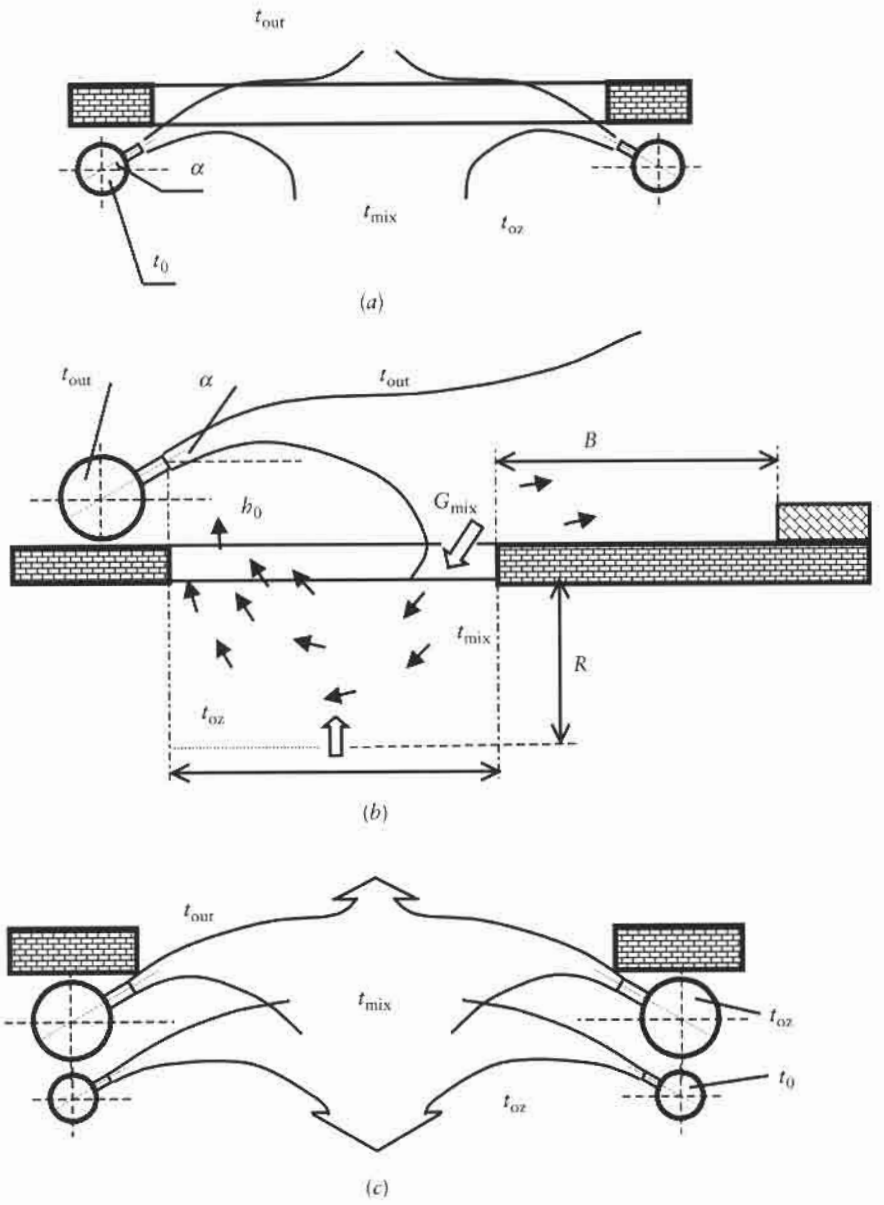

FIGURE 7.86 Schematic of shutter-type air curtains. (*a*) Heated or unheated air supply. (*b*) Outdoor air supply. (*c*) Combined air curtain.

- Rooms with a low standard air temperature in the working zone near the gates (8 °C and below)

Air curtains with unheated indoor air are more restricted in application than air curtains with heated indoor air, but they do not require the installation of air heaters in the curtain devices.

Air curtains with unheated outdoor air are recommended with a one-sided lateral supply of outdoor air in the form of a flat jet at an angle to the plane surface of the gate aperture toward the outdoor air (Fig. 7.86*b*). In

this case the outer surface of the enclosure should not have any obstructions on the opposite side that might prevent the jet from flowing along the surface of the gate. This free length should be no less than the approximate width of the gate.

Air curtains with unheated outdoor air find application in unheated rooms and also in case there are no strict hygiene requirements for the microclimate in the gate zone (no working places near to the gate, e.g.). Air curtains with unheated outdoor air should not be used in double-wing gates, in humid rooms, and in cases of transport with an open driver's cab through the gate.

Air curtains with unheated outdoor air do not provide for the necessary microclimate in the immediate vicinity of the gate, but since no thermal energy is used, they reduce heat losses from the room.

7.7.2.3 Combined Air Curtains with Indoor Air

Combined air curtains with indoor air are recommended with a double-sided supply of heated and unheated air fed to the room in the form of plane jets at an angle of 15° to one another (Fig. 7.86*c*).

7.7.2.4 Air Curtains with Unheated Outdoor Air

Delivery ducts for unheated (outdoor) air are located in the room right against the gate. Delivery ducts for air heated in the air curtain device (indoor) are installed inside the room behind the outdoor delivery ducts, with a clearance for exhaust air between the outdoor and indoor delivery ducts of the air curtain.

Recommended applications of combined air curtains with indoor air include

- Severe climate areas
- Gates of 3.6 m × 3.6 m or larger
- Locations with several gates (three or more)

Combined air curtains with indoor air cut down expenses due to rational utilization of energy by the heated jets. Thermal energy savings are 25–60% depending on the dimensions of the gate and climatic region, and the reduction in expenditures is 30–70%.

7.7.2.5 Air Curtains for Cooled Rooms

Air curtains for cooled rooms are recommended with a one-sided supply of outdoor air from above in the form of a flat jet at an angle to the plane surface of the gate toward the cold indoor air (Fig. 7.87).

Air curtains for cooled rooms are used in all types of rooms with artificial cooling of air: vegetable stores, cold rooms, freezers, air-conditioned plants and storehouses, etc. Installation of air curtains for cooled rooms considerably reduces cold losses through the open gate and also reduces undesirable variations in temperature in the gate zone inside and outside the cooled room.

7.7.2.6 Air Curtains for Gates with Long Passages

Air curtains for gates with long passages use a pattern of air supply "curtains in a channel" (Fig. 7.88). The operating principle is based on the complete conversion of the jet impulse to counterpressure that prevents outdoor air from bursting into the room.

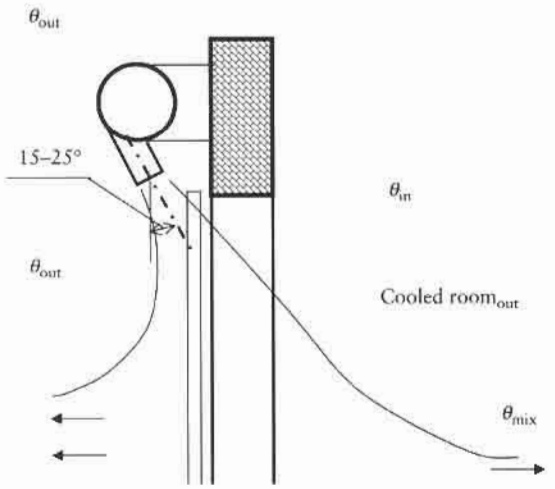

FIGURE 7.87 Schematic of air curtains for cooled rooms.

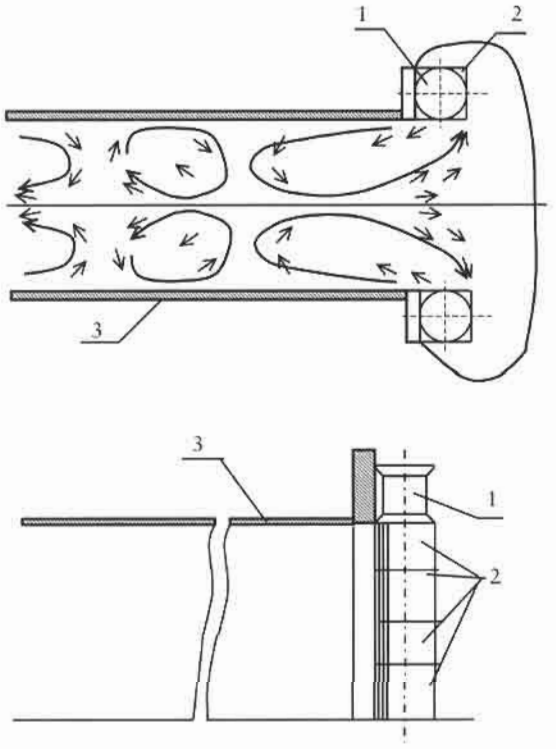

FIGURE 7.88 Air curtain for a medium-size gate with a lobby: *1*, fan; *2*, distribution duct; *3*, lobby.

The air is fed against the bursting airflow or at a minor angle. The jet of the curtain developing in the channel is dampened, and from the end of the channel it turns to the opposite direction. This creates a closed circulation proof against outside effects.

The length of the passage should be chosen so that it prevents the air from being released outside. To reduce the length of the passage, the air is normally supplied in the form of incomplete spray jets with nozzles of special design. Another alternative is to feed outdoor air into the passage (Fig. 7.89).

7.7.2.7 Air Curtains for Process Equipment

Air curtains for process equipment are designed to prevent the ingress of toxic constituents (gases, aerosols, heat flows) into the room through open apertures of the process equipment. They also support necessary parameters of technological processes in the plant. Processes running in the technological equipment are classified as isothermal (e.g., spray-painting chambers) and nonisothermal (e.g., heat dryers). In isothermal processes one uses damper-type air curtains for process equipment in combination with an exhaust system (Fig. 7.90). In nonisothermal processes one uses a circulation system based on the "curtains in a channel" operating principle (Fig. 7.91).

7.7.3 Principle of Calculation

There are currently two approaches to the design of damper-type air heat curtains: cinematic and dynamic.

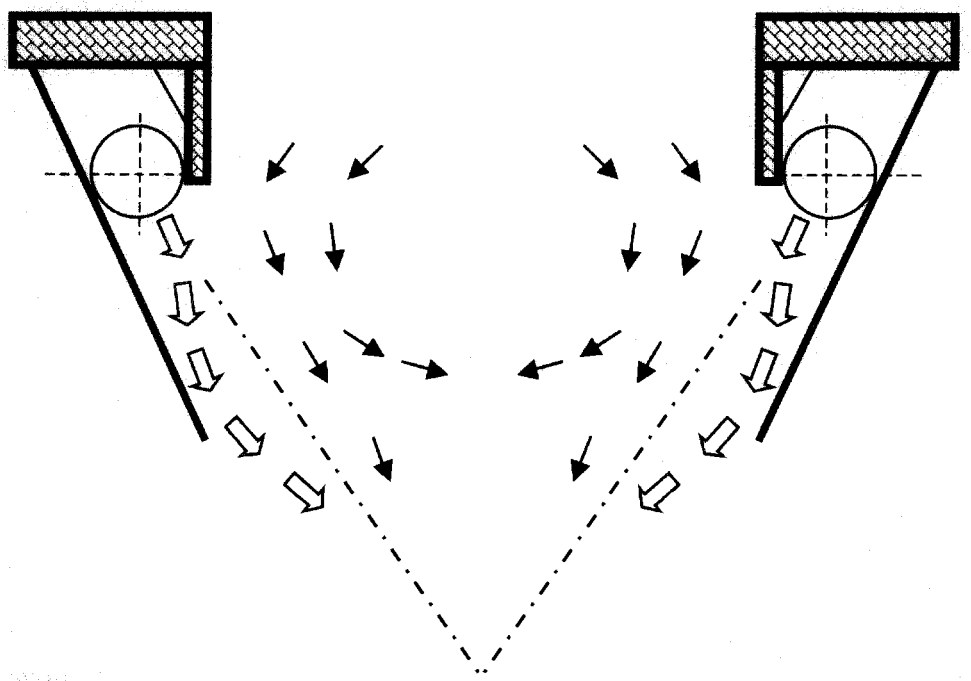

FIGURE 7.89 Air curtain with a lobby and outside air supply.

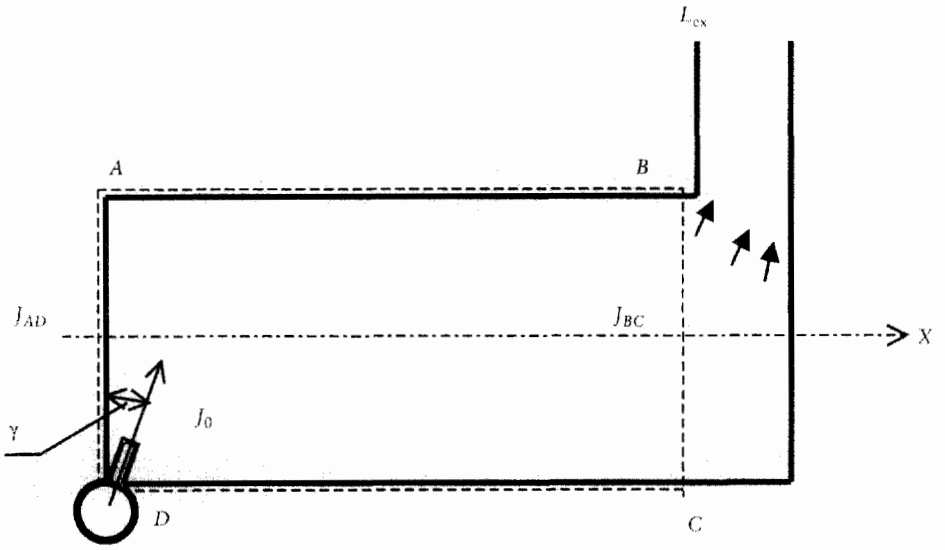

FIGURE 7.90 Schematic of air curtains for process equipment: isothermal processes.

In the cinematic method the airflow in the aperture is understood to be the result of interaction of the air curtain jet and the incident flow. Some of the cinematic methods that were developed[1–6] did not apply the laws of conservation of the impulse and mechanical energy. These methods did not correspond satisfactorily to test results and were not developed further. In these cases the determination of the jet trajectory does not take into account the effect of the enclosures and the interaction of the jets, and the division of airflows between the room and the outer atmosphere is performed with an arbitrary geometrical construction. The above-mentioned facts lead to divergence of design results and existing test results as to both the release speed and the initial temperature of the air curtain.[7,8]

The dynamic method sees airflow as a result of the effect of differential pressure on the jet in the gate aperture. Dynamic methods do consider the law of conservation of the impulse in the isolated circuit. According to the type of isolation of the circuit, dynamic methods are divided into methods that determine the trajectory of the jet[9–14] and methods that determine the integral flow rate of air through the aperture.[7, 8, 15, 16] This method, due to consideration of the aperture and surrounding enclosures in the design circuit and application of the law of conservation of mechanical energy, achieved for the design of the air release speed a dependence that corresponds well to test results.[7, 8] Figures 7.90–7.92 illustrate examples of isolated circuit design.

In the following we apply the dynamic method of air curtain design (see Fig. 7.92). The basic dependency is illustrated for a one-sided air curtain that is supplied at angle a and developed on the plane surface XOY. Since the jet of the air curtain is bent by the effect of differential pressure from outside (P_{out}) and inside (P_{in}) the building, the jet of the air curtain flows to the opposite side of the aperture and splits into two parts. After the division, one part of the jet flows along the outer surface of the enclosure and the other one enters the room at an angle β to the plane surface of the aperture. We isolate the

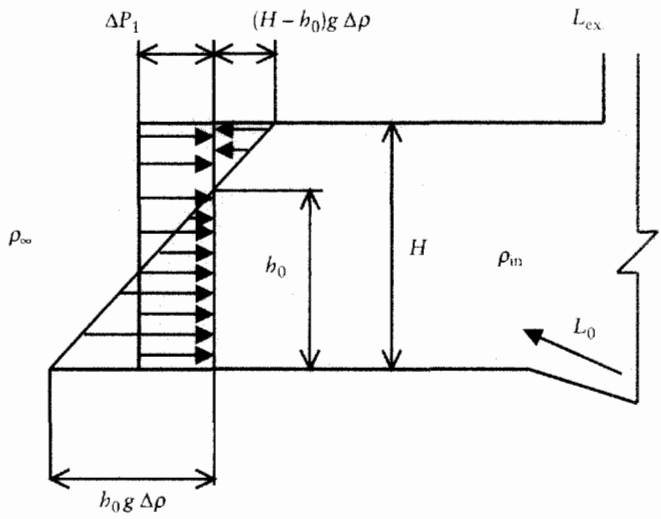

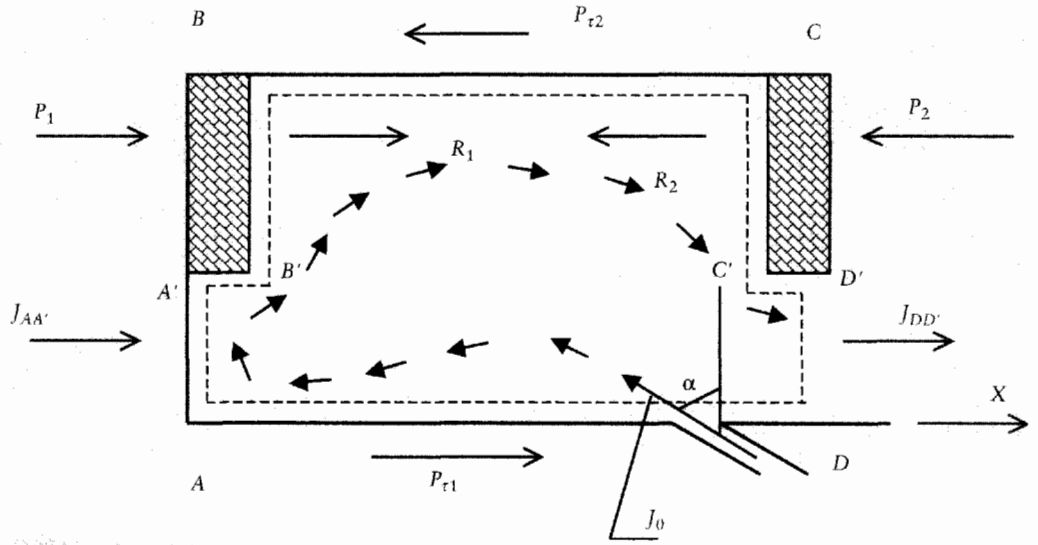

FIGURE 7.91 Schematic of air curtains for process equipment: nonisothermal processes.

circuit *ABVGDKMN*. Surfaces *AB*, *AN*, and *BV* are led at a distance from the gate where the speed of air flowing to the jet is near zero and the quantity of air impulse coming in through the surface *NABV* may be disregarded.

The equation of momentum of the isolated circuit in projection at the Y-axis is

$$J_0 \sin\alpha + J_b \sin\beta = \Delta P A_0 + (P_{in} - N_y)(A_{AB} - A_0), \qquad (7.213)$$

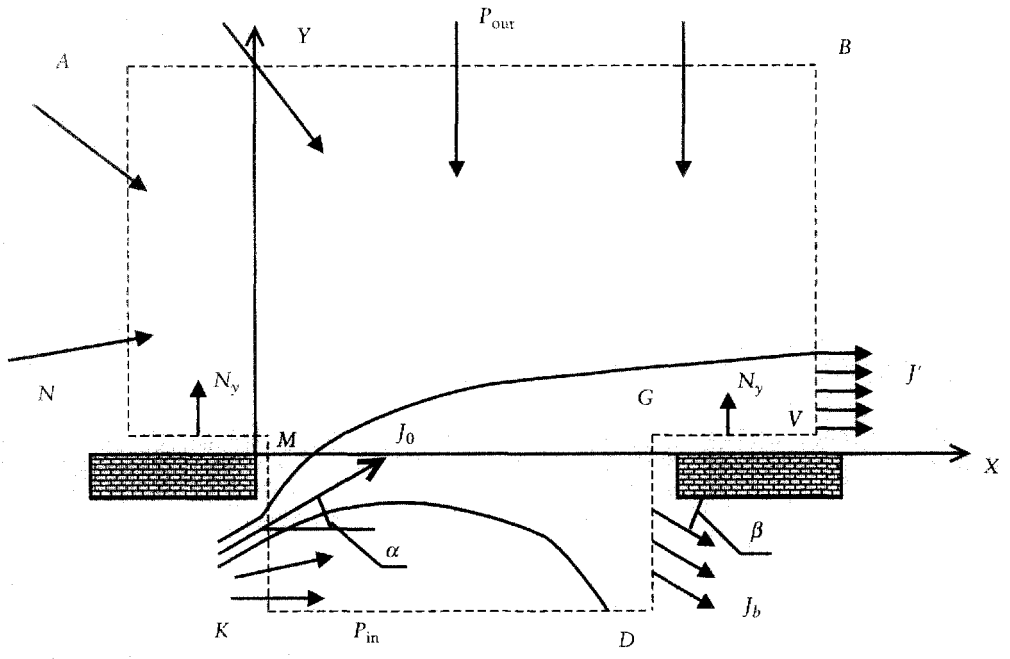

FIGURE 7.92 Theoretical model of air curtains.

where

$$\Delta P = P_{out} - P_{in}(\text{Pa}) \tag{7.214}$$

J_0, J_b are impulses of airflows supplied by the air curtain that flow into and out of the room (N)

A_{AB}, A_0 are the areas of the surface AB and the gate aperture (m^2)

N_y is the average value of reactive pressure in the scope of plane surfaces VG and MN (Pa)

We derive the concept of the dynamic efficiency of the air curtain, E, which is equivalent to the ratio between aerostatic pressure forces affecting the gate aperture and the doubled initial impulse of the air curtain jets:

$$E = \Delta P A_0 / 2J_0 . \tag{7.215}$$

The factor E shows the efficiency of utilization of the initial impulse of the curtain jets. Using this form to represent factor E allows us to estimate the efficiency of the curtain in fractions of the unit.

The dependence for factor E results from the joint solution of the Eqs. (7.213) and (7.215) as follows:

$$E = 0.5(\sin\alpha + R_y) . \tag{7.216}$$

The quantity R_y is a function of geometrical parameters and is determined experimentally. Similar dependencies for the factor E have been obtained for all patterns of the air curtains introduced above.

The initial speed of the air supplied by the air curtain is determined according to the following universal dependence, which results from the joint solution of Eqs. (7.213)–(7.216):

$$v_0 = (\Delta P A_0 / 2\beta_0 \rho A_S E)^{1/2} \text{ [m/s]}, \tag{7.217}$$

where

β_0 = the Boussinesq factor (1.05–1.1)
ρ = density of air supplied by the air curtain [kg/m^3]
A_S = total area of the outlet apertures of the air curtain [m^2]

The value of the ratio $f = A_0 / A_S$ is recommended to be taken based on the following technical and economical considerations:

- For air curtains with heated indoor air, unheated indoor air, or combined air curtains with indoor air: f = 10–20
- For air curtains with unheated outdoor air, air curtains for cooled rooms, air curtains with long passages, or air curtains for process equipment: f = 20–40

The average values of factor E in the recommended range of f are shown in Table 7.27.

The mass flow of air supplied by the air curtain is

$$G_0 = \rho_0 v_0 A_S \text{ [kg/s]}. \tag{7.218}$$

The purpose of the thermal design of the air curtain is to find the dependence between the average initial temperature of the jets supplied by the air curtain and the average temperature of the part of damping airflow coming in through the gate aperture. The temperature distribution of the air curtain jet significantly differs from the temperature distribution of the free jet as a result of the different temperatures of the air masses joined to the air curtain jet (Figs. 7.93 and 7.94).

TABLE 7.27 Factor of Dynamic Efficiency, *E*

	Type of air curtain		
sin α	With heated indoor air, with unheated indoor air, or combined curtains with indoor air	With unheated outdoor air or for cooled rooms	For gates with a long passage
0.1	0.1	0.15	—
0.2	0.15	0.2	—
0.3	0.2	0.25	—
0.4	0.25	0.3	—
0.5	0.3	0.4	—
0.6	0.35	—	—
0.9 – 1.0	—	—	–1.0

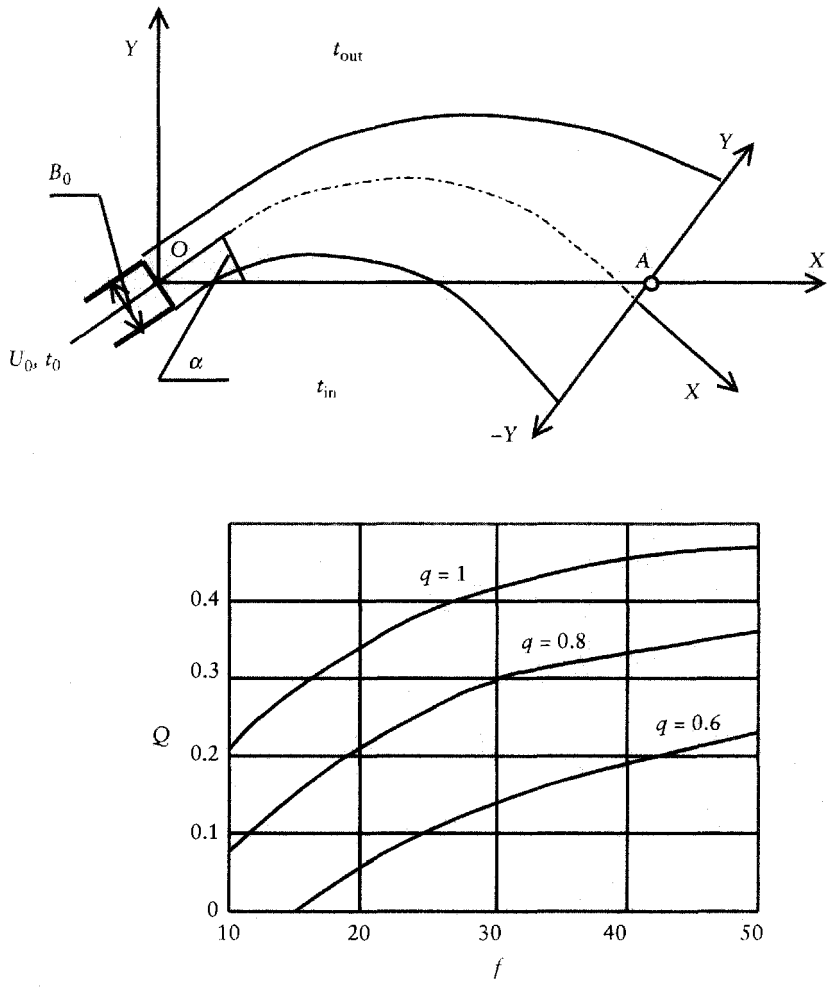

FIGURE 7.93 Heat losses of air curtains.

The distribution of excess temperature of the curtain air (in relation to the outdoor air temperature, t_{out}) is found from the conservation of the heat content of the jet as follows:

$$\Phi = \Delta\theta_{o1} N \cosh^{-1} Y/CX + 0.5\Delta\theta_B(1 - (\tanh Y)/CX)(1 - N \cosh^{-1} Y/CX), \tag{7.219}$$

where

$N = (4/\pi\sqrt{3}Cx)\sqrt{T_\infty}/\sqrt{T_0} \cdot (1/\varphi)$
$\Delta\theta_{o1} = \theta_0 - \theta_{out}$
$\Delta\theta_B = \theta_{in} - \theta_{out}$
C is an experimental constant ($C \approx 0.1$)
$x = X/b_o$
b_o = width of the air outlet slot

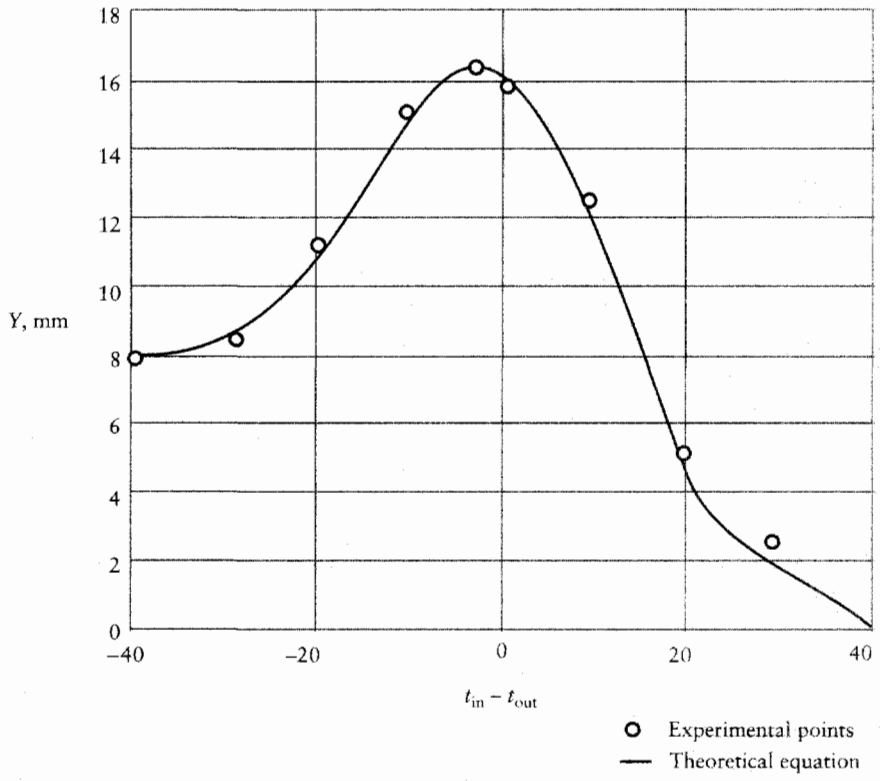

FIGURE 7.94 Air temperature distribution in air curtain jet.

$\sqrt{T_\infty}/\sqrt{T_0}$ = correction factor for the nonisothermal jet
T_∞ = average temperature of the environment (K)
$\varphi = \sqrt[4]{\zeta}$ = correction factor for the jet impulse
ζ = factor of the local resistance of the air outlet nozzle

The formula for the determination of the necessary initial temperature of the air curtain jet results from the integration of the equation for the heat content of the jet in the section X_A corresponding to the inlet of the jet into the room in the scope $(-\infty\ -Y_A)$. The ordinate of point A is obtained from the law of conservation of the mass in the section X_A:

$$Y_A = CX\operatorname{arc\,tanh} D,$$

where

$$D = [2 - (p_{mix}q/p_0)](1/\varphi)(1/\sqrt{T_\infty}/\sqrt{T_0})/(p_{mix}q/p_0)(\sqrt{3}Cx) \qquad (7.220)$$

$q = G_0/G_g$ is the relative mass flow of air through the curtain
G_g is the mass flow of air through the aperture

Simplified formulas are applied in engineering design. For example, in the case of an air curtain with heated indoor air the necessary temperature of the supplied air may be calculated according to the following formula:

$$\theta_0 = \theta_{out} + m_1(\theta_{mix} - \theta_{out}) + m_2(\theta_{in} - \theta_{out}), \qquad (7.221)$$

TABLE 7.28 Values of the Factors m_1 and m_2

f	m_1	m_2
10	2	−0.6
15	2.5	−1
20	2.9	−1.3
30	3.5	−1.8
40	4.1	−2.2

where

θ_{out}, θ_{in} are design temperatures of the outdoor air and room air, respectively (°C)
θ_{mix} is the temperature of the air mixture coming through the aperture of the gate
m_1 and m_2 are factors with average values as shown in Table 7.28 for total damping of the aperture ($q = 1$)

The temperature of air supplied by the air curtain should not exceed 70 °C in case the technological process does not require any other temperature. The thermal capacity of the air curtain is determined according to the equation

$$P = c_p G_0(\theta_0 - \theta_H) \quad [\text{W}], \tag{7.222}$$

where

c_p is the heat capacity of air, 1004 J/kg °C
θ_H is the discharge temperature of the air curtain

Parameters for combined air curtains are determined by optimized calculations based on minimal expenses. Usually the share of heated air in a combined air curtain is 20–40% of the total flow and its temperature is 60–70 °C.

7.7.4 Operation of the Air Curtain

The automation of an air curtain should provide for the following:

- Starting of the fan when the serviced aperture is opened and when the air temperature near the closed aperture deviates from a set value
- Stopping of the fan after the serviced aperture is closed and restoration of the air temperature near the closed aperture to a set value
- Controlling supply air flow in proportion to the square root of the change of the aerostatic pressure difference across the aperture: $q_{m,0} \sim \Delta P^{0.5}$
- Controlling the supply air temperature (in the case of air curtains with heated air) in proportion to the change in temperature of the outdoor air

7.7.5 Design of an Air Curtain Device

7.7.5.1 The Task

An air curtain is to be used in the doorway of an industrial building to prevent the penetration of cold air into the building. The task is to dimension this air curtain device for the following climatic conditions:

Case 1:

- Outdoor air temperature $\theta_{out} = -12$ °C
- Wind velocity $v_w = 0$ m/s

Case 2:

- Outdoor air temperature $\theta_{out} = -5$ °C
- Wind velocity $v_w = 5$ m/s

The wind velocities are local values at the height of the doorway, so no additional wind sheltering coefficients or height corrections are necessary. A solution is sought for which both situations above can be handled with the same air curtain device by just changing the fan speed and the heating power of the air curtain.

7.7.5.2 Data

The building (see Fig. 7.95) is 12 m high and has three large openings. The doorway for which the air curtain is designed is on the ground level, has dimensions 4 m (height) × 6 m (width), and is intended primarily for vehicular traffic.

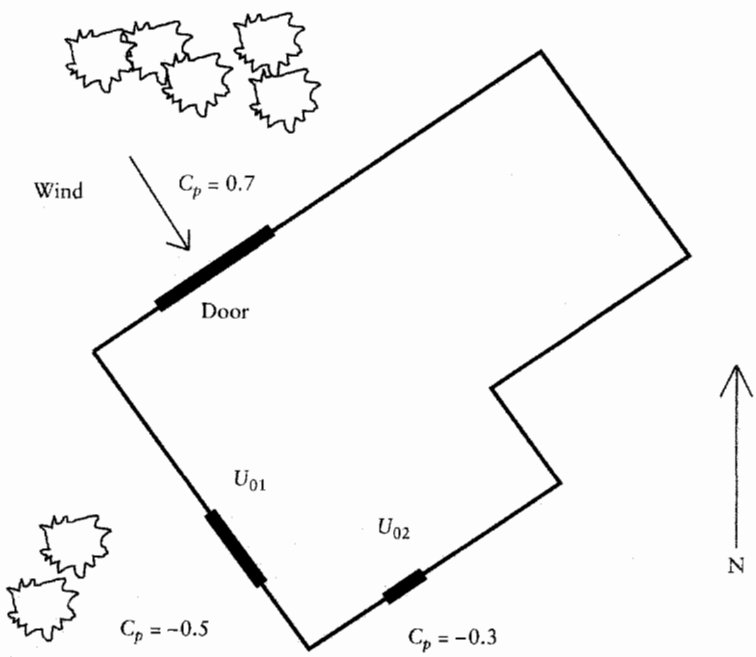

FIGURE 7.95 The object building.

TABLE 7.29 Characteristics of the Building Apertures in the Example

		Gate	Opening 1	Opening 2
Width	L[m]	6	4	2
Height	H[m]	4	2	1
Area	A[m^2]	24	8	2
Center height above ground	h_g [m]	2	9	5.5
Pressure coefficient	c_p [–]	0.7	–0.5	–0.3
Discharge coefficient	μ [–]	0.25	0.8	0.8

There are two large openings in the upper part of the building: U_{01}, which is 4 m wide × 2 m high, and U_{02}, which is 2 m wide × 1 m high. The lower-level of 5 m. Otherwise the building envelope is assumed to be airtight. This information is summarized in Table 7.29.

The indoor air temperature and humidity are assumed to be uniform:

- Temperature: $\theta_{in} = 20$ °C
- Humidity: $\phi = 60\%$

The general ventilation airflows are in balance.

The unbalanced local exhausts take their makeup air through the building openings:

$$q_{v,m} = 4 \text{ m}^3/\text{s}, \qquad q_{m,m} = 4.8 \text{ kg/s}.$$

7.7.5.3 Pressure Distribution in the Building

Calculation is made in accordance with Section 7.8.2, *Infiltration and Exfiltration*.

Mass balance of the airflows through the building envelope:

$$q_{m,g} + q_{m,1} + q_{m,2} + q_{m,m} = 0, \tag{7.223}$$

where

Flow through opening i: $$q_{m,i} = \mu_i A_i \left[2\Delta p_i\right]^{1/2} \text{ [kg/s]} \tag{7.224}$$

Pressure difference across opening i: $$\Delta p_i = p_{i,\text{out}} - p_{i,\text{in}} \tag{7.225}$$

Pressure inside building: $$p_{i,\text{in}} = p_x = \text{const} \tag{7.226}$$

Air densities:

Outdoor air density: $\rho_{\text{out},1} = 1.35$ kg/m^3
Indoor air density: $\rho_{\text{in}} = 1.2$ kg/m^3

Reference level 0 is located in the center of the gate opening, i.e., 2 m above ground level.

Case 1: Temperature –12 °C, Calm Conditions

Design Pressures

$$\Delta p_{1,\text{out}} = 0$$

$$\begin{aligned}\Delta p_{2,\text{out}} &= 0 + (h_1 - h_2)g(\rho_{\text{out},1} - \rho_{\text{in},1}) \\ &= (9\text{ m} - 5.5\text{ m}) \cdot 9.81\text{ m/s}^2(1.35\text{ kg/m}^3 - 1.2\text{kg/m}^3) \\ &= 5.15\text{ Pa}\end{aligned}$$

$$\begin{aligned}\Delta p_{g,\text{out}} &= 0 + (h_1 - h_g)g(\rho_{\text{out},1} - \rho_{\text{in},1}) \\ &= (9\text{ m} - 2\text{ m}) \cdot 9.81\text{ m/s}^2(1.35\text{kg/m}^3 - 1.2\text{kg/m}^3) \\ &= 10.3\text{ Pa}\end{aligned}$$

The design airflows are found from Eq. (7.224):

$$\begin{aligned}q_{m,g} &= 0.25 \cdot 24\text{ m}^2[2(10.3\text{ Pa} - p_x) \cdot 1.35\text{ kg/m}^3]^{1/2} \\ &= 9.86(10.3\text{ Pa} - p_x)^{1/2}[\text{kg/s}]\end{aligned}$$

$$q_{m,1} = 0.8 \cdot 8[2(p_x - 0.675) \cdot 1.2\text{ kg/m}^3]^{1/2} = 9.91(p_x - 5.15)^{1/2}[\text{kg/s}]$$

$$q_{m,2} = 0.8 \cdot 2[2(p_x - 0.0) \cdot 1.2\text{ kg/m}^3]^{1/2} = 2.48(p_x)^{1/2}$$

$$q_{m,\text{m}} = 4.8\text{ kg/s}$$

The mass balance equation (7.223) now gives

$$9.86(10.3 - p_x)^{1/2} = 9.91(p_x - 5.15)^{1/2} + 2.48(p_x)^{1/2} + 4.8 \quad p_x \approx 6.05\text{ Pa}\,.$$

The design differential pressure is

$$\Delta p_{g,1} = 10.3\text{ Pa} - 6.05\text{ Pa} = 4.25\text{ Pa}\,.$$

Case 2: Temperature –5 °C, Wind 5 m/s

Design pressures

$$\Delta p_{1,\text{out}} = 0$$

$$\begin{aligned}\Delta p_{2,\text{out}} &= 0 + (h_1 - h_2)g(\rho_{\text{out},1} - \rho_{\text{in},1}) + (c_{p,2} - c_{p,1})p_w \\ &= (9 - 5.5) \cdot 9.81 \cdot (1.32 - 1.2) + [-0.3 - (-0.5)] \cdot 16.5 \\ &= 7.42\text{ Pa}\end{aligned}$$

$$\begin{aligned}\Delta p_{g,\text{out}} &= 0 + (h_1 - h_g)g(\rho_{\text{out},1} - \rho_{\text{in},1}) + (c_{p,g} - c_{p,1})p_w \\ &= (9 - 2) \cdot 9.81 \cdot (1.32 - 1.2) + [0.7 - (-0.5)] \cdot 16.5 \\ &= 28.04\text{ Pa}\end{aligned}$$

The mass balance equation (7.223) is

$$9.86(28.04 - p_x)^{1/2} = 9.91(p_x - 7.42)^{1/2} + 2.48(p_x)^{1/2} + 4.8$$

$$p_x \approx 13.2\text{ Pa}.$$

The design differential pressure is

$$\Delta p_g = 28.04\text{ Pa} - 13.2\text{ Pa} = 14.84\text{ Pa}\,.$$

7.7.5.4 Calculation of the Parameters of the Air Curtain

We choose the ratio between the gate area and the discharge opening area,

$$f = A_0/A_s = 20,$$

which implies an air curtain discharge aperture of

$$A_s = 1.2 \text{ m}^2.$$

The aperture height equals the height of the gate, 4 meters, which yields the width of the air outlet slot:

$$b_s = A_s/4 \text{ m} = 0.2 \text{ m}.$$

The discharge angle of the air curtain jet is

$$\alpha = 30°(\text{i.e., } \sin\alpha = 0.5).$$

The efficiency factor E, according to Table 7.27 is

$$E = 0.3.$$

Based on the given value f the values of the factors m_1 and m_2 are determined from Table 7.28:

$$m_1 = 2.9$$
$$m_2 = -1.3.$$

To determine the supply temperature of the curtain, θ_0, and the thermal capacity P, we use

$$\theta_{\text{mix}} = \theta_{\text{in}} = \theta_H.$$

The parameters of the air curtain can now be determined.

The initial discharge velocity is calculated according to formula (7.217):

Version a

$$v_0 = [(4.25 \cdot 20)/(2 \cdot 1.05 \cdot 1.2 \cdot 0.3)]0.5 = 10.6 \text{ m/s}$$

Version b

$$v_0 = [(14.84 \cdot 20)/(2 \cdot 1.05 \cdot 1.2 \cdot 0.3)]0.5 = 19.8 \text{ m/s}$$

The mass flow of the air supplied by the air curtain is determined according to formula (7.218):

Version a

$$q_{m,0} = 1.2 \cdot 10.6 \cdot 1.2 = 15.26 \text{ kg/s}$$

Version b

$$q_{m,0} = 1.2 \cdot 19.8 \cdot 1.2 = 28.51 \text{ kg/s}$$

The discharge temperature of the air curtain is determined from formula (7.221):

Version a

$$\theta_0 = -12 + 2.9(20 + 12) - 1.3(20 + 12) = 39.2 \text{ °C}$$

Version b

$$\theta = -5 + 2.9(20 + 5) - 1.3(20 + 5) = 35 \text{ °C}$$

The heat capacity of the air curtain is determined according to formula (7.222):

Version a

$$P = 1.01 \cdot 10^3 \cdot 15.26(39.2 - 20) = 295.9 \cdot 10^3 \text{ W}$$

Version b

$$P = 1.01 \cdot 10^3 \cdot 28.51(35 - 20) = 431.9 \cdot 10^3 \text{ W}$$

Thus, version b is more unfavorable, as the differential pressures ΔP are the greatest. The selection of air curtain equipment is made for version b.

The fan of the air curtain is to be provided with a device regulating the supply airflow, for example, by frequency transformer, multispeed motor, etc. The supply airflow is to change according to the dependence $q_{v,0} \sim \Delta p^{0.5}$, which enables, in particular, provision of the necessary efficiency for version a.

As the temperature of the supplied air increases in case of decreasing outdoor temperature, the heater of the air curtain selected for version b is to be tested according to the calculation designed for the lowest outdoor temperature (version a). The heater is to be provided with devices for automatic regulation of the temperature of the supplied air according to the dependence $\theta_0 \sim \theta_{out}$.

References

1. Shepelyev, I. A. 1950. *Osnovy rascheta vozdushnyh zaves, pritochnyh struj i poristyh filtrov.* Strojizdat, Moscow.
2. Stefanov, E. V, and A. B. Fedorov. 1984. Raschet vozdushno-teplovyh zaves s vertikalnoj podatshei vozdukha. *Vodosnabzhenie i sanitarnaya tekhnika*, no. 7, pp. 23–34.
3. Stolyar, V. A. 1966. Tsirkulyatsionnye vozdushnye zavesy. *Stroitelstvo i arkhitektura. Ser. Izvestiya VUZov*, no. 12, pp. 80–86. NISI, Novosibirsk.
4. Köhler, K., and G. Gruhn. 1962. Theoretische untersuchungen zur berechnung und wirtschaftlichen auslegung von luftschleieranlagen. *Energietechnik*, vol. 12, h. 5, pp. 205–215.
5. Charles, L., and P. Herndon. 1966. Closed open door. *Heating, Piping and Air Conditioning*, vol. 5, pp. 105–108.
6. Energy enters the curtain equation. 1987. *Heating and Air Conditioning Journal*, no. 654, pp. 2–33.
7. Elterman, V. M. 1966. *Vozdushnye Zavesy.* Mashinostroenie, Moscow.
8. Strongin, A. S., and M. V. Nikulin. 1991. Novyi podhod raschetu vozdushno-teplovyh zaves. *Stroitelstvo i arhitektura: Ser. Izvestiya VUZov*, no. 1, pp. 84–87.
9. Butakov, S. E. 1949. *Aerodinamika Sistem Promyshlennoi Ventilyatsii*, Profizdat, Moscow. pp. 162–172.
10. Mott, L. F. 1962. Design for protection by air curtain. *Heating and Air Conditioning Journal*, no. 2, pp. 164–166.
11. Titov, V. P. 1980. Osobennosti struj vozdushnyh zaves. *Teplovoi rezhim sistem otopleniya, ventilyatsii, konditsionirovanya vozduha i teplogazosnabzheniya: Cb. trudov*, pp. 3–15. MISI, Moscow.
12. Danielson, P. O. 1972. Luftridder och luftportar. *Tidskrift for Varme, Ventilation, Sanitet*, vol. 43, no. 7, pp. 21–26.
13. Fekete, K. 1967. Luftschleiertüren. *Gesundheits-Ingenieur*, vol. 88, h. 4, pp. 122–124.
14. Lajos, T. and L. Preszler. 1975. Untersuchung von torschleieranlagen. *Heizung, Lüftung, Haustechnik*, vol. 26, h. 5, pp. 171–176; h. 6, pp. 226–235.
15. Nikulin, M. V., K. V. Savin, and A. S. Strongin. 1991. Eksperimentalnye issledovaniya teploobmena struj vozdushnyh zaves. *Gidrodinamika Otopitelno-Ventilyatsionnyh Ustroistv: Mezhvuzovskij sb*, KISI, Kazan. pp. 14–21.
16. Strongin, A. S. 1993. Aerodynamic protection of hangars against cold ingress through apertures. *Building Services Engineering Research and Technology, CIBSE Ser. A*, vol. 14, no 1, pp. 13–16.

Bibliography

Strongin, A.S., and M. V. Nikulin. 1994. Reduction of the energy consumption in air curtains. In *Proceedings of the Cold Climate HVAC '94 Conference*. Rovaniemi.

7.8 AIR MOVEMENT AROUND BUILDINGS AND THROUGH A BUILDING ENVELOPE

7.8.1 Airflow around Buildings

Airflow around buildings consists of natural winds that travel around and possibly through buildings. Airflow around buildings has two influences on industrial ventilation:

1. Wind pressures exerted on the exterior building surfaces, which can influence air movement indoors
2. The outdoor movement of air contaminants, which can degrade indoor air quality if brought indoors with insufficient dilution.

This section will describe general features of airflow patterns and then present information on the dimensions and locations of recirculating (stagnant) zones around the building envelope, which determine wind pressures and contaminant dilution. This knowledge allows one to select the locations of stacks and air intakes and to calculate infiltration and natural ventilation rates.

7.8.1.1 General Features of Airflow around Buildings

Buildings are immersed in an atmospheric boundary layer in which the wind is influenced by friction with the earth's surface. In this layer, wind speed tends to gradually increase with height and turbulence levels decrease with height, as described in many texts.[1] Surrounding buildings, terrain, and vegetation strongly influence wind and turbulence at a building site. The wind and turbulence levels are also influenced by thermal stratification of the atmosphere, such as ground-level inversion layers. The major parameters of the wind at a building site depend on the Reynolds (Re), Karman (Ka), and Richardson (Ri) dimensionless characteristics:

$$\mathrm{Re} = VI/\nu \quad \mathrm{Ka} = \sqrt{(V')^2}/V \quad \mathrm{Ri} = g1/\rho \ (\partial\rho/\partial Z)/(\partial V/\partial Z)^2, \quad (7.227)$$

where l = building characteristic dimension (height or width), ν = kinematic viscosity, V' = velocity fluctuation, V = mean velocity, ρ = air density, $\partial\rho/\partial Z$ = vertical density gradient, and $\partial V/\partial Z$ = vertical velocity gradient.

Winds traveling past a building will be greatly modified compared with winds in the absence of the building. Hosker reviews the information on flow around both isolated structures and building clusters.[2] Snyder and Lawson present detailed trajectories around isolated buildings obtained with detailed flow measurements.[3]

Figure 7.96 illustrates typical flow patterns for wind directly approaching a building face. Airflow in the undisturbed zone has a speed profile dependent on the terrain roughness and the level of atmospheric stratification. Obviously, most wind will be deflected around and over the building. Wind

traveling toward the upwind face of the building will tend to stagnate, creating relatively high static pressures at the upwind face.

As the wind travels past a building corner or over a roof, it will be unable to negotiate the sharp turn and will separate from the building side and roof surfaces. The flow separation creates strong speed variations (shear), reversed flow directions (upwind vortex), negative (suction) pressures on building surfaces, and added turbulence. Another separation zone, the building or cavity wake, is created immediately downstream of the building as the wind encounters the downwind building corners and roof edge. Negative pressures are also seen on the downwind side of the building within the cavity wake. As the wind travels farther downstream, the shear and turbulence gradually diminish and settle to the condition that would apply without the building in place.

The flow pattern depends on the building's relative dimensions: long buildings (along wind length, $L > 2.5H$) versus short buildings ($L < 2.5H$).

The flow pattern shown in Fig. 7.96 illustrates the case of a short building ($L < 2.5H$) with a W/H ratio greater than 10. Near the upwind wall, a stagnation (recirculating) zone is formed. The direction of airflow in the area close to the surface is opposite the main wind direction. The flow separates at the sharp edge of the building to generate a recirculating flow zone. The boundaries of this zone can be described by the equation

$$\int_0^{Z_b} V dz = 0, \tag{7.228}$$

where V = velocity at the point (x, z); and Z_b = height of the recirculating zone boundary at the distance X.

Wilson indicates that for a flat-roofed building, the recirculation region maximum height H_c at location X_c, and the reattachment length L_r shown in Fig. 7.96 can be evaluated using the following equations:[4]

$$H_c = 0.22R \tag{7.229}$$

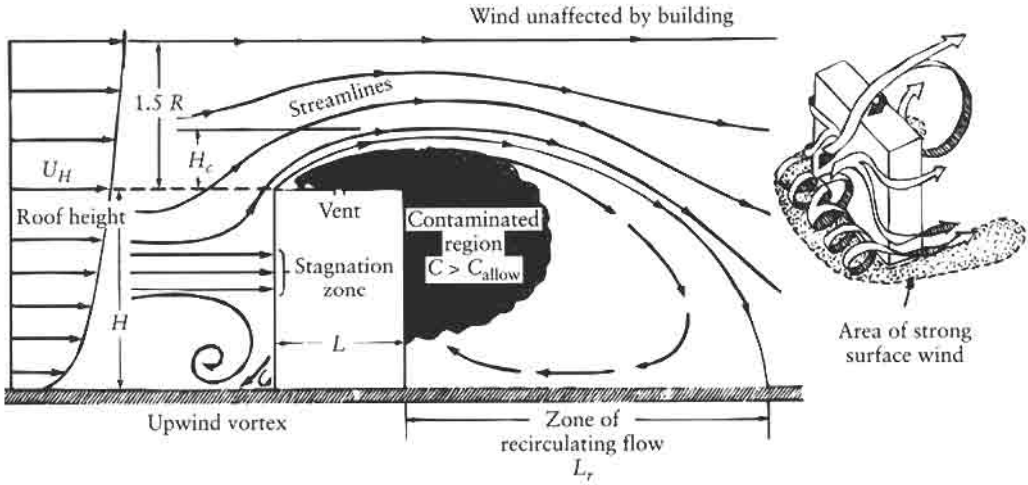

FIGURE 7.96 Flow pattern around a rectangular building. (Reproduced from ASHRAE 1999.)

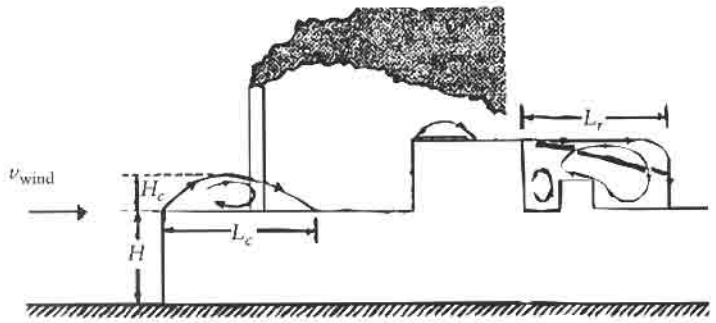

FIGURE 7.97 Flow pattern around a long rectangular building ($L > 2.5H$). (Reproduced from Wilson 1982.)

$$X_C = 0.5R \tag{7.230}$$

$$L_r = 1.0R, \tag{7.231}$$

where

$$R = B_s^{0.67} B_L^{0.33}, \tag{7.232}$$

where B_s = min [H, W], B_L = max [H, W], and H and W = upwind building face height and width, respectively.

If the building has significant length L in the windward direction (Fig. 7.97), the flow will reattach to the building and may generate two distinct recirculating zones—on the building and in its wake. In the case of a long building ($L > 2.5H$), the recirculation zone created by separation of the flow at the front edge of the roof extends to some distance, L_c, smaller than the length of the building ($L_c \sim 0.9R$). Beyond this zone, at a distance of approximately $10H$ to $12H$, the flow streamlines along the roof surface become similar to those absent the effect of the building.

For $W/H < 10$, the length of this recirculating zone is reduced. The values of L_r and H_c can be calculated using the reduction coefficient C_r from Table 7.30.

Winds approaching a rectangular building at an angle will have different flow patterns than winds directly approaching a building face. Figure 7.98 illustrates the case for approach from a 45° angle. On the roof a pair of horizontal, counterrotating vortices emanate from the upwind roof corner. The negative (suction) surface pressures near the upwind corner can be intense, several times the magnitude of the dynamic pressure of the approaching wind.

TABLE 7.30 Values of Coefficient C_r

W/H	1	2	3	4	5	6	7	8	9	10
C_r	0.32	0.45	0.55	0.64	0.71	0.78	0.84	0.90	0.95	1.0

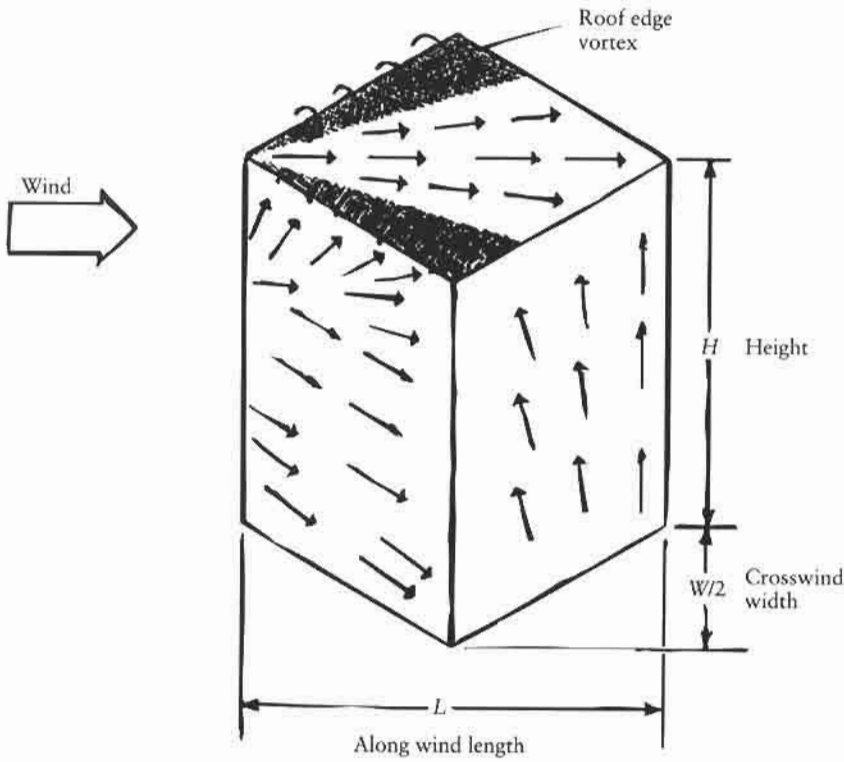

FIGURE 7.98 Flow pattern around a rectangular building with the wind approaching the building at 45°. (Reproduced from ASHRAE 1999.)

The airflow in the center of the roof tends to be downward. The downward motions in the downstream cavity wake are also more intense for winds approaching from an angle.[3]

The above discussion is applicable only to the isolated building. Hosker reviews the effect of nearby buildings on the flow around the building of interest.[2,5]

7.8.1.2 Building Surface Wind Pressures

One of the effects of airflow or wind around buildings is the exertion of wind pressure forces on the surface of the building, which contributes to natural ventilation of the building and infiltration of outside air into the building. As discussed above, pressures tend to be positive (into the building) on upwind surfaces and negative (suction) on lateral, downwind, and roof surfaces.

Pressure at a given location on the building surface is usually expressed as a pressure coefficient times a reference wind pressure at the building height without the building in place:

$$P = C_p \rho v_m^2 / 2, \tag{7.233}$$

where C_p is the pressure coefficient, ρ is the air density, and v_m is the general wind speed at the building height.

Estimation of building pressure comprises two steps:

1. Determination of the reference wind speed for the building site, v_m
2. Determination of the pressure coefficient, C_p, for the particular location on the building

Wind Speed

Wind has a highly turbulent and gusting character. In addition, a time-mean speed varies with the height from the ground and the roughness of the terrain over which the wind passes. The time-mean wind speed profile can be determined using the following expression:

$$v_m / v_{\text{met}} = cH^a, \tag{7.234}$$

where

v_m = mean wind speed at height H above the ground, m/s
v_{met} = mean wind speed measured at a weather station, normally at a height of 10 m above the ground, m/s
c = parameter relating wind speed to nature of the terrain (see Table 7.31)
a = exponent relating wind speed to height above ground

To evaluate the wind speed at height H it is necessary to know the value of v_r for the required location. This may be obtained either from a local weather station or from wind contour maps of the country. Normally, v_r represents the hourly mean wind speed that is exceeded 50% of the time at a particular site.

Other equations describing the wind profile are available from ASHRAE[7] and from Sherman and Grimsrud.[8]

Surface Pressure Coefficient

The second part of computing building pressures involves the pressure coefficient for a particular spot on the building. The surface pressure coefficient, C_p, indicates the share of the wind kinetic energy that is transferred to the static pressure:

$$C_p = 2P/(\rho v^{m2}). \tag{7.235}$$

The value of coefficient C_p at the point on the building surface changes within a range of $-2 < C_p \leq 1$ and is determined by

1. The building geometry
2. The wind velocity (i.e., speed and direction) relative to the building
3. The location of the building relative to other buildings and the topography and roughness of the terrain in the wind direction
4. The location of a point on the building envelope

TABLE 7.31 Terrain factors for Eq. (7.234)

Terrain	c	a
Open flat country	0.68	0.17
Country with scattered wind breaks	0.52	0.20
Urban	0.35	0.25
City	0.21	0.33

The surface pressure coefficient is normally derived from pressure measurements in wind tunnels using reduced-scale models of buildings or building components, or from pressure measurements in the actual buildings. In general, the C_p values depend upon the Re, Ka, and Ri numbers. However, experimental tests are typically conducted at high values of Re (Re $\geq$ 1000), in isothermal conditions (Ri = 0), and considering self-similarity against the Ka number (Ka = idem). Most test conditions allow only geometrical scaling.

For a building with sharp corners, C_p is almost independent of the wind speed (i.e., Reynolds number) because the flow separation points normally occur at the sharp edges. This may not be the case for round buildings, where the position of the separation point can be affected by the wind speed. For the most common case of the building with a rectangular shape, C_p values are normally between 0.6 and 0.8 for the upwind wall, and for the leeward wall $0.6 < C_p < -0.4$. Figure 7.99 and Table 7.32 show an example of the distribution of surface pressure coefficient values on the typical industrial building envelope.

Values of C_p for simple building geometries may be obtained from the British Standards Institution[6,9] or from Liddament.[10] The following relationship between wind incident angle α, building side ratio, and average surface pressure coefficient is based on the database developed by Swami and Chandra:[11]

$$NC_p = \ln[1.248 - 0.703\sin(\alpha/2) - 1.175\sin^2(\alpha) + 0.131\sin^3(2\alpha G) + 0.769\cos(\alpha/2) + 0.07G^2\sin^2(\alpha/2) + 0.717\cos^2(\alpha/2)], \quad (7.236)$$

where

NC_p = normalized C_p
α = angle in degrees between wind direction and outward normal of wall under consideration
G = natural log of ratio of width of wall under consideration to width of adjacent wall

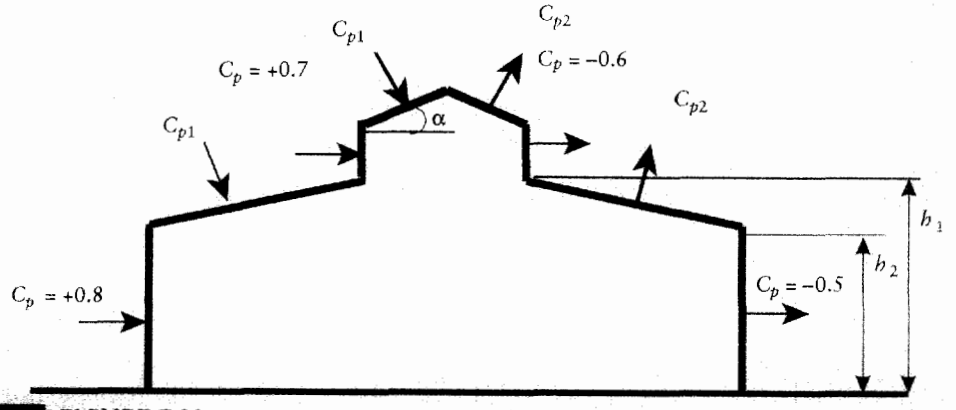

FIGURE 7.99 Example of surface pressure coefficient values for a typical industrial building envelope.

TABLE 7.32 Approximate Surface Pressure Coefficient Values for a Building with a Rooftop Vent

		C_{p1} and C_{p2}			
		h_1/L			
Coefficient	α	**0**	**0.5**	**1.0**	**≥ 2**
C_{p1}	0	0	−0.6	−0.7	−0.8
	20	+0.2	−0.4	−0.7	−0.8
	40	+0.4	+ 0.3	−0.2	−0.4
	60	+0.8	+ 0.8	+ 0.8	+ 0.8
C_{p2}	≤ 60	−0.4	−0.4	−0.5	−0.8

		C_{p3}		
		h_1/L		
Coefficient	W/L	**≤ 0.5**	**1.0**	**≥ 2**
C_{p3}	≤ 1	−0.4	−0.5	−0.6
	≥ 2	−0.5	−0.6	−0.6

A detailed method of determining pressure coefficients is to perform experiments with a wind tunnel facility. Cochran and Cermak compared wind tunnel pressure coefficient measurements with field measures on a test building and found excellent results, with the exception of small areas beneath the vortices near the upwind roof corner for winds approaching at 45°.[12] For infiltration and natural ventilation designs, wind tunnel results should be sufficiently accurate.

Another detailed method of determining pressures is computational fluid dynamics (CFD), which uses a numerical solution of simplified equations of motion over a dense grid of points around the building. Murakami et al.[13] and Zhoy and Stathopoulos[14] found less agreement with computational fluid dynamics methods using the k-ϵ turbulence model typically used in current commercial codes. More advanced turbulence models such as large eddy simulation were more successful but much more costly.[13]

For simplified buildings or in cases where detailed modeling is not practical, simplified tables of coefficients are presented by Liddament for low-rise buildings with two building shapes, for open and sheltered buildings, and for various walls and approach wind angles.[15] ASHRAE also summarizes results from other studies.[7]

7.8.1.3 Contaminant Transport around Buildings

Transport of outdoor contaminants is controlled by both the mean motion of winds and dispersal by turbulence. Since airflow around buildings has

distorted wind trajectories and enhanced turbulence compared with the airflow without buildings, contaminant transport requires special consideration in the presence of buildings.

Contaminants can either be generated by sources within the building or be emitted from exhaust stacks or nearby locations. The goal is to maintain indoor air quality by minimizing the entry of outdoor contaminants into the interior of the building through careful design and location of exhausts, intakes, and building openings. Since most industrial exhausts and air-handling systems are located on the roof, the airflow on the roof is of great interest. As discussed earlier, when wind directly approaches a building side, a separation zone is created on the roof near the upwind edge. This zone will have high turbulence intensities and greatly distorted streamlines. In fact, flow reversal occurs, in which the airflow is in the opposite direction to the approaching wind. Any building exhaust emitted into this zone is quickly dispersed and spread over the roof surface, creating large rooftop contaminant concentrations. It is especially important to avoid placing low-momentum exhausts and air intakes within the same recirculating zone on the roof or side of the building.

Furthermore, winds at an angle to the building side will have downward air motions above the roof and downwind of the building, which also will increase rooftop concentrations.

Therefore, to avoid separation and high-turbulence zones on the roof, contaminant exhaust systems should be designed to extend as high above the roof as practically possible. Two ways to achieve high exhaust trajectories are with the use of taller stacks and greater exhaust vertical momentum, which increases the throw or rise of the exhaust. Tall stacks are an obvious solution but have aesthetic problems, even in an industrial setting. Achieving greater vertical momentum can be gained in several ways:

- Avoiding raincaps over exhausts, which eliminate vertical momentum
- Increasing exit velocity by narrowing the exhaust opening
- Manifolding separate exhausts into fewer stacks
- Placing exhausts *very* close together so that the exhaust plumes can merge (which can help exhausts that cannot be manifolded)

In the design of an industrial facility, a detailed analysis of contaminant transport can be beneficial in specifying exhaust designs and intake locations. As with building pressures discussed above, analysis techniques range from simplified models to experimental methods and sophisticated computational methods. The greater the building geometry complexity, the less useful are the simplified models.

One simplified method for determining stack height is a geometric method described in ASHRAE.[7] The geometric method assumes an exhaust plume shape with a lower boundary having a 1:5 slope relative to the horizontal. The stack and plume are raised until the lower plume boundary is above rooftop penthouses, separation zones, and zones of high turbulence. ASHRAE provides equations for the sizes and locations of the separation and turbulence zones.[7] A stack height reduction credit is provided to account for the vertical exhaust momentum.

Another method is a series of exhaust dilution equations based on Wilson and Lamb[16] and a series of earlier papers summarized in ASHRAE.[7] This method is based on wind tunnel tests on simplified buildings and is intended to provide conservative (low dilution) results. Wilson and Lamb compared the model to actual field data collected at a university campus and found that the model did indeed predict dilutions similar to measured worst-case dilutions suitable for a screening model. However, many cases resulted in conservative underpredictions of dilutions.[16]

An alternative simple model for contaminant dilution of rooftop exhaust stacks is presented in Halitsky.[17] This model combines a jet region specification for the upward exhaust movement with a more traditional Gaussian plume region controlled by atmospheric and building-generated turbulent dilution.

For computing dilutions in the downstream cavity wake (intakes or building openings on the side of a building) due to contaminants from a rooftop stack, another model is presented by Schulman and Scire[18] and is incorporated in a U.S. EPA screening model.[19] More sophisticated analysis may be achieved with wind tunnel models. Saathoff et al. compared wind tunnel dilution predictions with measurements on an actual building and found agreement within a factor of 2, a reasonable limit for dilutions, which can vary over many orders of magnitude.[20] Higson et al. found greater differences between wind tunnel measurements and a miniature building in field conditions, corresponding to a factor of 4 or more.[21]

Computational fluid dynamics (CFD) is becoming more popular, as discussed above for building pressures. However, a recent paper found difficulties in the practical use of current commercial codes due to the wide range of user inputs and decisions.[22] Other papers are exploring alternatives to the standard k- ϵ model typically used in commercial codes today.[23,24]

7.8.2 Infiltration and Exfiltration

Most building envelopes have purposely provided openings (i.e., doors, windows, vents, flues, chimneys, and other ducts) and unintentional openings (i.e., cracks, mortar joints, and gaps around closed windows and doors). Air leakage through unintentional openings in the building envelope result in exchange between outside and indoor air. Uncontrolled outside airflow through cracks and other unintentional openings is called infiltration; the uncontrolled indoor airflow through unintentional openings is called exfiltration. Air leakage through the building envelope is a measure of the air tightness of the building envelope. Air leakage through the building envelope has a positive effect by allowing for natural (free) building ventilation. On the other hand, infiltration increases heat losses (in winter) and gains (in summer) through the building envelope, and also may result in reduced control over contaminant movement within the building.

In general, the air leakage rate through a building envelope is dependent on

- The sizes and distribution of leakage paths
- The flow characteristics of the leakage paths
- The pressure difference across the leakage paths

The flows through the openings in a building are not independent but are based on the mass balance across the whole building envelope. The flow rate through an opening depends upon the pressure difference across it. Normally, the pressure difference occurs due to the wind effect and a temperature difference between the indoor and outdoor air. Also, an imbalance in the mechanical exhaust ventilation system performance over the mechanical air supply (positive or negative pressure building) might be a factor influencing infiltration and exfiltration.

A typical envelope opening has a complicated shape and is often subject to unsteady flow conditions at its inlet and outlet.[25] There are no simple analytical solutions for the flow through such openings. The most-used equation representing flow characteristics is the so-called power law:

$$Q = C_d A(\Delta P/\rho)^{\beta}, \tag{7.237}$$

where Q is the airflow through the opening, $C_d A$ is the effective leakage area, and β is a coefficient.

Experimental evidence regarding the power law is somewhat contradictory. A constant value of $\beta = 0.5$ is considered to give a good fit to experimental data by many authors.[25] According to Awbi, β depends on the flow regime and has a value of 0.5 for fully turbulent flow and 1.0 for laminar flow.[26] In practice the value of β tends to be between 0.6 and 0.7.

Limited information is available on values of C_d for industrial buildings. The effective leakage area, $C_d A$, can be determined by means of a building pressurization or depressurization test.[27, 28] A range of values of C_d for cracks formed around closed windows are given in Table 7.33. These should be used with a value of $\beta = 0.67$.

For practical situations Etheridge et al. suggest representing the typical unintentional opening by a long, narrow straight pipe or duct and describing the flow characteristics by a quadratic relation between Q and ΔP:[25]

$$\Delta P = aQ^2 + bQ, \tag{7.238}$$

where a and b are constants. The first term on the right-hand side represents turbulent flow and the second represents laminar flow. The values of a and b can be obtained from experimental tests on the openings, and some values can be found in Baker et al.[29]

TABLE 7.33 Values of C_d for Windows[6]

	Value of $C_d \times 10^{-5}$	
Window type	**Average**	**Range**
Sliding	8	2–30
Pivoted	21	6–80
Pivoted (weather-stripped)	8	0.5–20

For extremely narrow openings (cracks) with deep flow paths (such as mortar joints and tight-fitting components) the flow is laminar and the flow rate, Q (m^3/s), can be described by the Couette flow equation:[26]

$$Q = [(bh^3)/(12\mu L)]\Delta P, \tag{7.239}$$

where

b = length of crack, m
h = height of crack, m
L = depth of crack in flow direction, m
μ = absolute viscosity of air, Pa s

7.8.2.1 Pressure Difference Due to Stack Effect

The pressure difference across the crack can result from the difference in temperature (air density) between the air inside and outside the building. Static pressure in the vertical column of air varies with height and can be described by the following equation:

$$dp = g\rho\, dh, \tag{7.240}$$

where

g = gravitational acceleration, m/s^2
ρ = density of air, kg/m^3

Thus, static pressure, p_h, at height h can be calculated as

$$p_h = p_o - g\int_0^h \rho\, dh, \tag{7.241}$$

where p_o = static pressure at the reference height in undisturbed flow outdoors, Pa. Assuming that the air density does not change along the building height, Eq. (7.241) can be simplified to

$$p_h = p_o - g\rho h. \tag{7.242}$$

When the air temperature inside the building is greater than the outside air temperature, air infiltrates through the lower openings in the envelope (the pressure difference between the outside air and inside air is positive) and exfiltrates through the upper opening (pressure difference is negative). The height of the neutral plane where the pressure difference across the crack due to stack effect equals 0 depends upon the crack's size, location, and characteristics.

The stack pressure can be expressed relative to the lowest opening height,[26, 30] relative to the static pressure at the floor level,[31] or relative to the point with the minimum static pressure.[32]

7.8.2.2 Wind Pressure

Static pressure over the building surfaces produced by the action of wind is generally positive on the windward side and negative on the leeward side. Pressures on the other sides of a building are negative or positive, depending on wind angle and building shape. The pressure difference across the crack produced by the action of wind can be calculated using Bernoulli's equation:[7]

$$\Delta P = P_o + C_p\rho V^2/2 - P_i, \tag{7.243}$$

where

- $\Delta P = P - P_r$ = pressure difference across the crack (between outdoors and indoors) at the height of the crack, Pa
- P_o = static pressure at the reference height in undisturbed flow outdoors, Pa
- P_i = interior pressure, Pa
- C_p = surface pressure coefficient
- V = wind speed at the datum level (usually the height of the building), m/s
- ρ = air density, kg/m^3

Principles of wind speed and surface pressure coefficient evaluation were covered earlier.

7.8.2.3 Effect of Ventilation System Performance

General and local supply and exhaust ventilation systems can create negative, positive, or neutral pressure in the building. Static pressure created by a mechanical ventilation system inside the building does not change with height. The pressure difference across the crack due to the mechanical system's performance does not change with height and depends on the fan's performance curves and the crack's characteristics. The pressure across cracks due to unbalanced ventilation system performance depends on the difference in supply and exhaust airflow rates, ΔQ_{mech}, and the effective leakage area, C_dA.

7.8.2.4 Combined Effect of Gravity Forces, Wind, and Mechanical Ventilation

The airflow rate infiltrating and exfiltrating through each air leakage pass, Q_i, due to the combined effect of wind, stack, and mechanical ventilation system performance can be calculated from the mass balance equation

$$\sum Q_i + \Delta Q_{mech} = 0. \tag{7.244}$$

The airflow rate Q_i for each air leakage path is expressed with Eqs. (7.237), (7.242), and (7.243) using the information on effective leakage area, C_dA, and a pressure difference across the path. The total pressure acting on an opening from the outside is the sum of the pressure due to wind, gravity forces, and mechanical ventilation performance, and the static pressure inside the building results from Eq. (7.244).

The graphs in Fig. 7.100*a* show the pressure distribution along the building height due to gravity forces using the method suggested by Titov.[32] The reference point with a pressure equal to 0 is located in the upper point outside the building. The graph shape is not affected by the number of openings and their locations. The same approach can be applied to the case with temperature stratification along the room height. The graph in Fig. 7.100*b* illustrates the case for the two-zone model, and the graph in Fig. 7.100*c* illustrates a temperature gradient.

The graphs in Fig. 7.101*a* show the pressure distribution along the building height due to the wind effect (wind velocity does not change along the height). The reference point with a pressure equal to 0 is located at the point with minimum surface pressure coefficient, C_p. The graph reflecting the influence of the nonuniform velocity distribution along the height is presented in Fig. 7.101*b*.

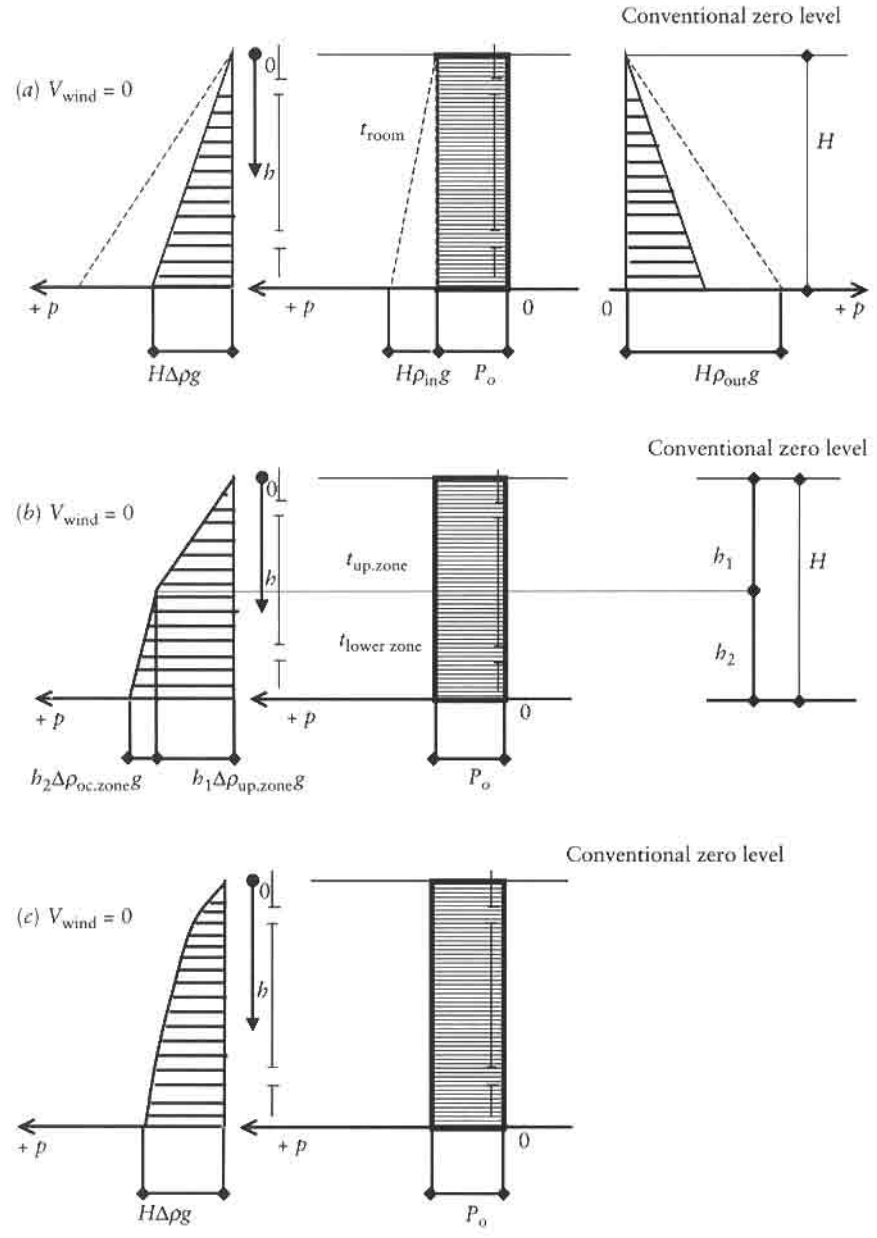

FIGURE 7.100 Pressure change along the building height due to gravity forces: (*a*) even temperature in the room volume; (*b*) room height divided into two zones, upper and lower (two-zone model); (*c*) temperature gradient along the room height.

The combined effect of gravity forces, wind, and mechanical ventilation on the pressure across the opening is illustrated in Fig. 7.102.

When the opening in the building envelope is horizontal or is vertical with a relatively small length, the change in pressure difference along this opening can be neglected. For long vertical openings the change in pressure along the

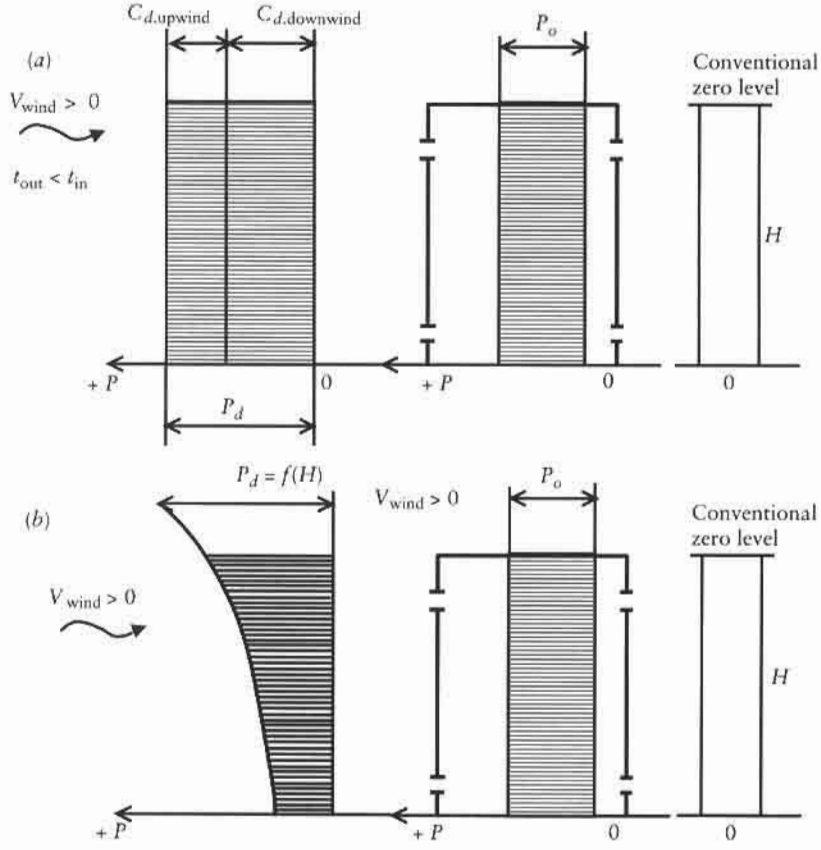

FIGURE 7.101 Pressure distribution due to wind effect: (*a*) uniform wind velocity profile; (*b*) non-uniform wind velocity profile.

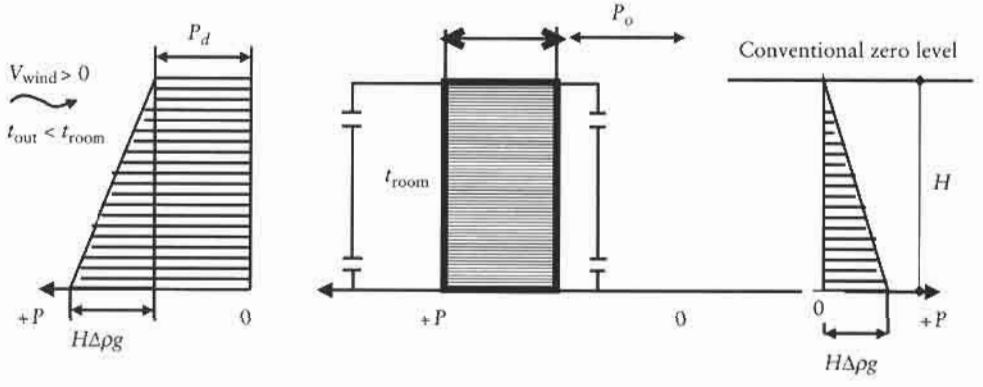

FIGURE 7.102 Pressure change along the building height due to the combined effect of wind and gravity forces, for the case of even temperature in the room volume.

height should be considered, because the lower part of the opening can provide infiltration and the upper part exfiltration

7.8.2.5 Calculation Methods

The principles discussed in this section enable the calculation of air infiltration/exfiltration, provided that the following quantities are known or can be evaluated:[26]

- Wind speed and direction
- Internal and external air temperature
- Position and flow characteristics of all openings
- Pressure coefficients over the building envelope for the wind directions under consideration
- Supply and exhaust ventilation airflow rates

In practice it is difficult, if not impossible, to determine all these quantities accurately, and the following simplified calculation methods based principally on equations discussed in this section are used:

- Empirical methods[6,7]
- Simplified theoretical methods[8,30, 31, 33]
- Network models, primarily for multizone buildings[10,34]

7.8.3 Airflow through Large Openings and Gates

When the building envelope has high openings (e.g., gates or large glazing), the pressure difference across such openings changes with height. In some situations, airflow through a part of the opening enters the building and the airflow through the rest of this opening exits the building. In certain cases this can be neglected, and the pressure difference across the whole opening is assumed to be equal to the one at the center of this opening. However, for openings such as high gates, such simplification results in significant error.

The pressure change outside the building envelope with such an opening is illustrated in Fig. 7.103. The outside air static pressure, P_{out}, is greater than

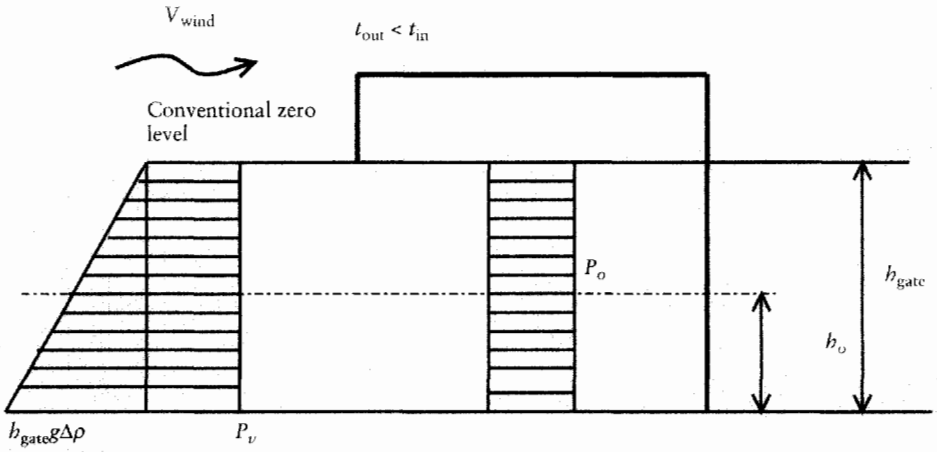

FIGURE 7.103 Pressure distribution inside and outside a building with a single large opening.

the inside air static pressure, P_o, at the lower part of the opening, $h > h_o$, and is lower at its upper part, $h < h_o$. Thus, air is infiltrating through the lower part of the opening and exfiltrating through its upper part.

The airflow rate through an opening area with a height of dh can be calculated as

$$dG = C_d(2\rho_h)^{1/2}(P_{out} - P_o)^{1/2}dh. \tag{7.245}$$

The infiltrating and exfiltrating airflow rates can be calculated using the following equations:

$$G_{inf} = \int_H^h dG \tag{7.246}$$

$$G_{exf} = \int_h^0 dG. \tag{7.247}$$

Let's consider airflow through the gate under the influence of buoyancy forces and wind (Fig. 7.103). The gate has width b and height h_g and is located on the upwind face of the building. The gate pressure loss characteristic does not change with height. Also, assume there are no apertures or cracks in the building envelope, other than the gate.

The mass balance equation for the airflow through the gate can be described as

$$G_{exf} + G_{inf} = 0\,. \tag{7.248}$$

At the height h_o of the boundary between the infiltrating and exfiltrating flows, air pressure across the gate, $P_{out} - P_o$, equals 0, and thus

$$P_o = \Delta\rho g h_o + C_{gate}\frac{\rho v^2}{2}\,. \tag{7.249}$$

Assuming $(\rho_{out}/\rho_o)^{1/3} \approx 1$, the equation allowing calculation of the pressure inside the building can be presented as

$$P_o = \frac{h_o}{2}\Delta\rho g + C_{gate}\frac{\rho v^2}{2}. \tag{7.250}$$

A properly designed air curtain protects the building from outside airflow through the gate. Only air entrained by the air curtain enters the building through the gate.

Total gate protection occurs when the air flow rate exiting the building through the gate, G_{ex} equals the air flow rate, G_o, supplied through the air curtain slot:

$$G_{ex} = G_o \tag{7.251}$$

When the gate is totally protected, there are no other openings in the building envelope and there is a balance between supply and exhaust ventilation systems, $h_o = h_{gate}$ (Fig. 7.104). In this case the pressure difference across the gate is influenced only by the buoyancy forces, and the airflow through the gate can be evaluated using the following equation:

$$G_{ex} = C_d A_o[h_{gate} g(\rho_{out} - \rho_o)\rho_{out}]^{1/2}\,, \tag{7.252}$$

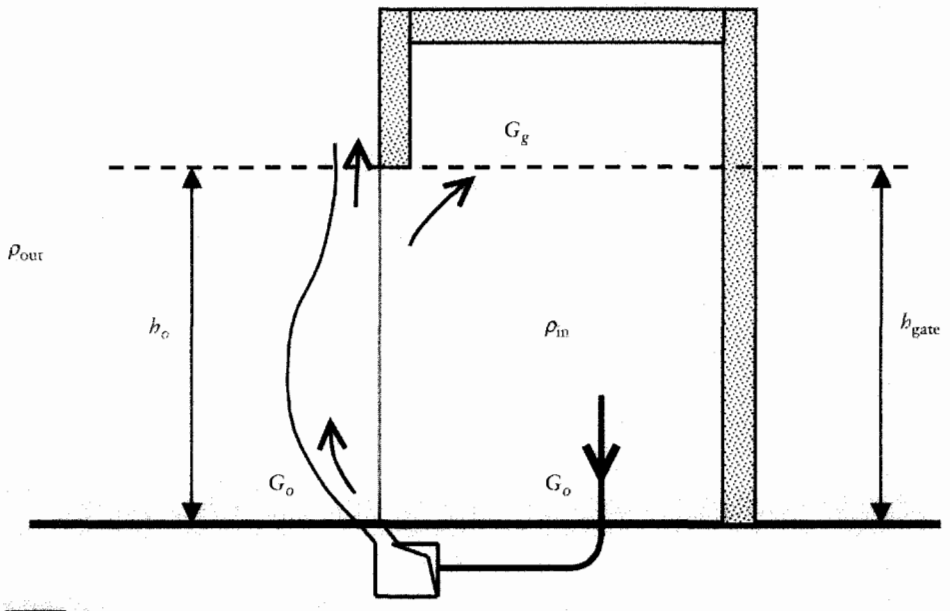

FIGURE 7.104 Schematics of airflow through the gate with an air curtain, for a building having no other openings.

where: C_d is the pressure loss coefficient for the gate; C_d typically has a value between 0.2 and 0.3 (it can be assumed equal to 0.25). For more information about gate protection with air curtains, see Section 7.7.

7.8.4 Controlled Airflow through an Envelope: Principles of Natural Ventilation

Natural ventilation is the controlled flow of air through doors, windows, vents, and other purposely provided openings caused by stack effect and wind pressure. Natural ventilation is used in spaces with a significant heat release, when process and hygienic requirements for indoor air quality allow outdoor air supply without filtration and treatment. Natural ventilation cannot be used when incoming outdoor air causes mist or condensation. Natural ventilation allows significant air change rates (20 to 50 ach) for heat removal with minimal operation costs.

Though airflow through the building with natural ventilation is caused by both wind effect and buoyancy forces, design principles typically do not include a wind pressure component. Wind speed and direction can change over wide ranges and thus wind does not provide a stable force to move air through the building. Thus, the wind effect is frequently considered as a reserve. In general, maximum air change in the building is required in the summer, with a maximum heat load and a minimal temperature difference between outdoor and indoor air. With a change in the heat load, natural ventilation allows for self-adjusting airflow through the building.

Airflow through an opening used for natural building ventilation is approximately turbulent. In this case the flow rate, Q (m^3/s), can be calculated from an equation similar to Eq.(7.237):

$$Q = C_d A(\Delta p/\rho)^{0.5}, \tag{7.253}$$

where

C_d = pressure loss coefficient of opening
A = area of the opening, m^2
Δp = pressure difference across the opening, Pa
ρ = air density, kg/m^3

Air outlets are designed such that their pressure characteristics are negative, which improves their performance in the presence of wind. Different types of ridge vents and roof ventilators have been designed; their sizes and pressure loss coefficients are available from the manufacturers. Examples of some air inlets and their pressure loss coefficients are listed in Table 7.34. All inlets and outlets for natural ventilation must be supplied with controls for easy opening and closing. Ventilated interior halls can obtain outside air through ridge vents in adjacent "cold" halls.

In summer, air inlets for natural ventilation are located in exterior walls; the lower level of the openings is 0.3 to 1.8 m above the floor. Air inlets can be arranged in one, two, or more rows in the longitudinal exterior walls. Windows, doorways, and other types of openings in the exterior walls, or apertures in floors over basements (with air transportation along special channels) also can be used as air inlets. During periods of the year other than summer, air inlets must located higher than 4 m. These inlets must be supplied with baffles to direct air at an upward angle. Air is evacuated from naturally ventilated spaces through wind-protected continuous ridge vents, skylights, or round roof ventilators.

TABLE 7.34 Pressure Loss Coefficients for Inlets[35]

			Pressure loss coefficient				
			Baffle angle, α				
Schematic	Baffle type	h/b	15°	30°	45°	60°	90°
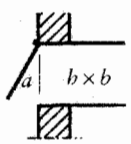	Single, top-hinged	0	30.8	9.2	5.2	3.5	2.6
		0.5	20.6	6.9	4.0	3.2	2.6
		1	16.0	5.7	3.7	3.1	2.6
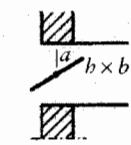	Single, center-hinged	0	59.0	13.6	6.6	3.2	2.7
		1.0	45.3	11.1	5.2	3.2	2.4
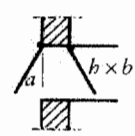	Double, top-hinged	0.5	30.8	9.8	5.2	3.5	2.4
		1.0	14.8	4.9	3.8	3.0	2.4

Natural ventilation design allows one to size the inlets, A_{inl}, and outlets, A_{out}, based on their pressure loss characteristics, C_p, and on the airflow rate, G_o, required to maintain the occupied zone within desired limits. The reverse design procedure is commonly used to evaluate the airflow rate through the building given the sizes, characteristics, and locations of inlets and outlets and the heat load and characteristics of heat sources.

The use of a natural ventilation system assumes temperature stratification throughout the room height. Air close to heat sources is heated and rises as a thermal plume (Fig. 7.105). Part of this heated air is evacuated through air outlets in the upper zone, and part of it remains in the upper zone, in the so-called heat cushion. The separation level between the upper and lower zones is defined in terms of the equality of G_{conv} and G_o, which are the airflow rate in thermal plumes above heat sources and the airflow supplied to the occupied zone, respectively. It is assumed that the air temperature in the lower zone is equal to that in the occupied zone, t_{oz}, and that the air temperature in the upper zone is equal to that of the evacuated air, t_{exh}.

The air exchange rate, G_o, required for temperature control in the occupied zone can be calculated from the room heat balance equation:

$$G_o = W\,[C_p K_\theta(\theta_{uz} - \theta_{oz})]\,, \tag{7.254}$$

where

G_o = air exchange rate, kg/s
W = total surplus heat released in the space, kW
C_p = specific heat of air, kJ/(kg K)

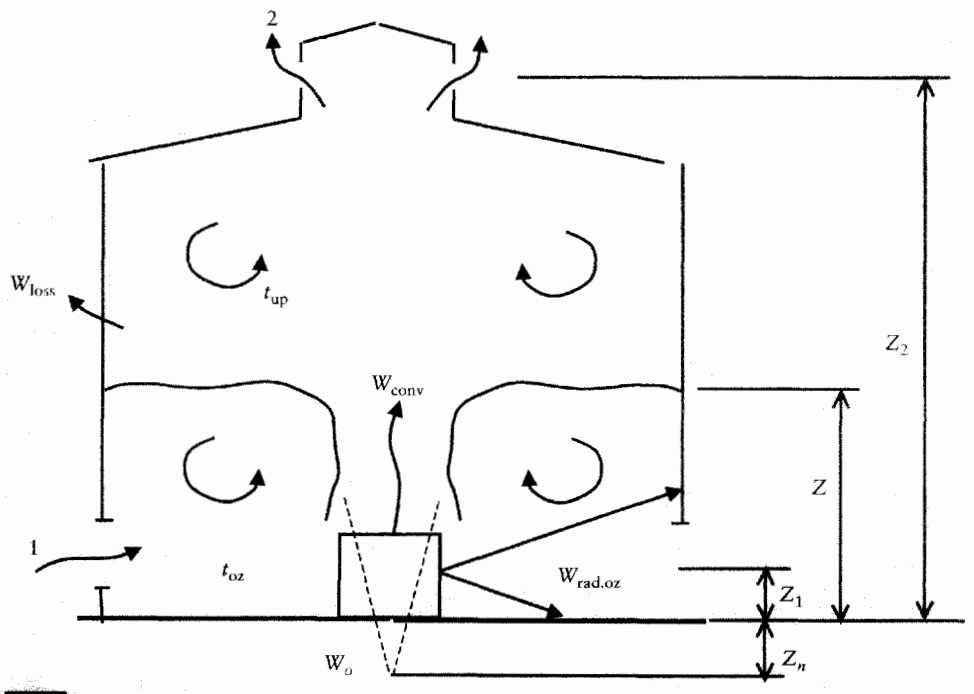

FIGURE 7.105 Schematics of naturally ventilated space: *1*, air inlet; 2, exhaust vents.

K_θ = coefficient of heat removal efficiency, calculated from the air temperatures of the occupied zone, θ_{oz}, the air removed from the upper zone, θ_{exh}, and the outdoor air, θ_o:

$$K_\theta = (\theta_{exh} - \theta_o)/(\theta_{oz} - \theta_o),$$

Coefficient K_θ can be evaluated through measurements in field or on a scaled model. Also, it is possible to predict the K_θ value using the method of zone-by-zone heat balances.[36] According to this method,

$$K_\theta = 1/\{[\varphi(1-\psi) - \lambda]/2\{[\varphi(1-\psi) - \lambda]^2/4 + \lambda\}^{1/2}\}, \quad (7.255)$$

where

$$\psi = \sum (W_o \times \psi)_i / \sum W_o \quad (7.256)$$

$$\varphi = \sum [(W_o \times (1-\psi)\varphi)_i] / \sum [W_o(1-\psi)] \quad (7.257)$$

$$\lambda = \alpha_{rad} A_{oz}(\theta_{oz} - \theta_{out}) / \sum W_o \quad (7.258)$$

where θ_{oz} = occupied zone air temperature, °C; θ_{out} = outside air temperature, °C; A_{oz} = occupied zone area, m^2. A graphical interpretation of Eq. (7.255) is presented in Fig. 7.106.

Typically inlet and outlet locations and heights can be obtained prior to ventilation system design from construction drawings. The static pressure difference across inlets and outlets can be calculated based on the height of the location (Fig. 7.104) and the air density at the respective height:

$$\Delta p = g(Z - Z_1)(p_o - p_{oz}) - g(Z_2 - Z)(p_o - p_{exh}), \quad (7.259)$$

where Z_1 and Z_2 = heights of inlet and outlet centers, m; and Z = separation zone height (typically between $0.4H$ and $0.7H$), with H = ventilated space height, m. For a more detailed calculation of K_t and Z, see Chapter 8 and Stroiizdat.[35]

The temperature of exhausted air can be derived from Eq. (7.246):

$$\theta_{exh} = \theta_o + W/(C_p G_o). \quad (7.260)$$

Based on the static pressure across the inlets, $\Delta p_{inl} = \beta\, \Delta p$, one can calculate the required inlet area, A_{inl}:

$$A_{inl} = G_o/(2\rho_o\, \Delta p_{inl}/C_{p\,inl})^{1/2}. \quad (7.261)$$

Typically, the share of the static pressure across the inlets, β, is selected to be between 0.1 and 0.4. This allows one to keep a low velocity of airflow through inlets so as not to disturb thermal plumes above heat sources.

The residual static pressure available for outlets, Δp_{exh}, and the required outlet area, A_{out}, can be calculated as

$$\Delta p_{exh} = \Delta p - \Delta p_{inl} \quad (7.262)$$

$$A_{exh} = G_{exh}/(2\rho_{exh}\, \Delta p_{exh}/C_{p\,exh})^{1/2}. \quad (7.263)$$

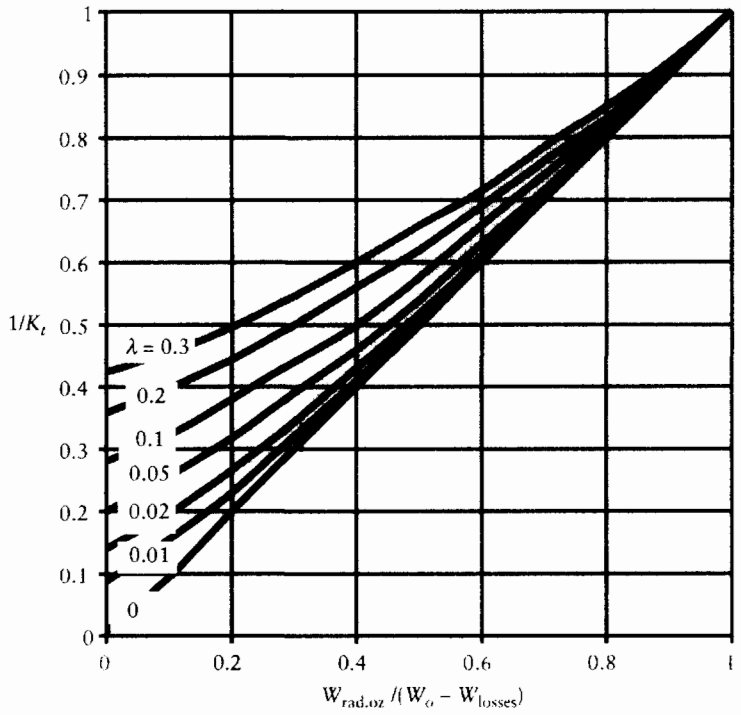

FIGURE 7.106 Supporting graph for the K_t calculation (Eq. 7.255). $\lambda = \alpha_{rad} A_{oz} \Delta t_{o.z} / (W_o - W_{losses})$; $0 \le \lambda \le 1$.

In the case where the area of inlets and outlets is given prior to ventilation design, the static pressure across them can be calculated using the following equations:

$$\Delta p_{exh} = (C_{p\,exh}/2\rho_{exh})(G_o/A_{exh})^2 \tag{7.264}$$

$$\Delta p_{inl} = \Delta p - \Delta p_{exh}\,. \tag{7.265}$$

7.8.5 Air and Contaminant Movement between Building Zones

To evaluate air and contaminant movement within the building, the following classification of building zones is used:

- Building areas separated by physical walls (e.g., halls, rooms, booths) located on the same level. The wall has either intentional apertures or leaks (Fig. 7.107*a*).
- Building areas separated by physical walls located on different levels (floors). Air movement between these zones may occur (e.g., through stairways or ducts) (Fig. 7.107*b*).
- Building areas separated by air jets located on the same level (e.g., jet-assisted hoods, air curtains) (Fig. 7.107*c*).
- Building areas within the same room (with no physical partitions) having different requirements for air cleanliness ("clean" and "dirty" areas) located on the same level (Fig. 7.107*d*).

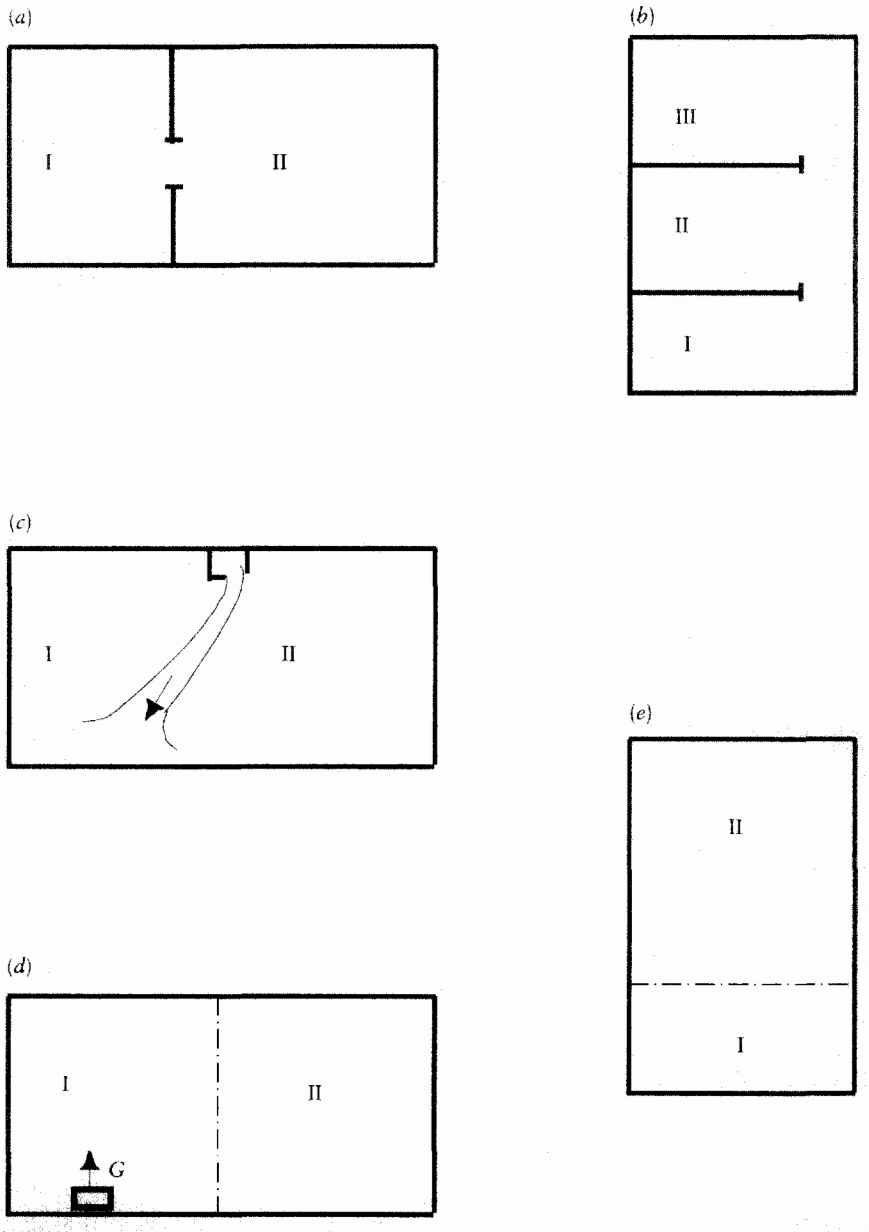

FIGURE 7.107 Zones within a building: (*a*) located on the same level and separated by physical walls with apertures; (*b*) located on different levels and separated by physical walls with apertures; (*c*) located on the same level and separated by air jets; (*d*) located on the same level with no physical separation; (*e*) located in the same room on different levels without physical separation.

- Zones located within the same room on different levels. These zones have different air temperatures and/or contaminant concentrations (Fig. 7.107*e*).

Air and contaminant movement between different zones may be caused by one or several of the following mechanisms:

- Static pressure difference between two zones resulting from the unbalanced air supply and exhaust in each zone. Air and contaminants move from the zone with higher static pressure to the zone with lower static pressure (Fig. 7.108*a*).
- Static pressure difference between two zones resulting from the wind effect on the building envelope (Fig. 7.108*b*).
- Buoyancy forces creating vertical air movement along the passage between two rooms located on different levels, or thermal plumes creating temperature and contaminant differences between two zones located on different levels of the same room (Fig. 7.108*c*).
- Turbulent exchange between air in different zones due to energy introduced by supply air jets, convective currents, or moving objects. In this case the resulting mass transferred between the zones equals 0 (Fig. 7.108*d*).

To control air and contaminant movement between zones, different construction, process-related, and ventilation techniques are used. "Clean" and "dirty" areas can be separated using solid walls, curtains, or partitions (Fig. 7.109*a*). Ventilation techniques used to separate zones include

- Pressure management in different zones (Fig. 7.109*b*)
- Air oasis with specially organized local air supply and exhaust (Fig. 7.109*c*)
- Natural or displacement ventilation systems creating temperature stratification (Fig. 7.109*d*)
- Air curtains and jet-assisted hoods separating "dirty" zones from "clean" zones (Fig. 7.109*e*)

Combined construction, process-related, and ventilation measures include "air locks" between two zones (Fig. 7.109*f*) and process equipment enclosures with air exhaust from the enclosures (Fig. 7.109*g*).

For pressure management between two zones, refer to the information provided in Section 7.8.2. It is important to mention, that the airflow created by pressure difference between the "clean" and "dirty" zones does not completely prevent contaminant movement from the dirty to the clean zone. Let's consider an example of a two-bay building with an air supply into the high "clean" bay and an air exhaust from the low "dirty" bay (Fig. 7.110*a*). The high bay has a higher air temperature than the low bay. The stack effect created between the two bays creates contaminant movement from the dirty zone to the clean zone through leaks and other openings in the walls separating these zones. In order to prevent contaminant movement between the clean and dirty zones, these zones can be separated by an air lock (Fig. 7.110*b*).

Another factor influencing contaminant and heat transfer from dirty to clean zones against the stable airflow is a turbulent exchange between these zones. This process should be considered in the design of displacement or natural ventilation systems and evaluation of the emission rate of contaminants from the encapsulated process equipment (Fig. 7.111*a*).

The mechanism of turbulent heat exchange between the upper and lower zones in the case of ventilation system design with temperature stratification is described in Section 7.3.

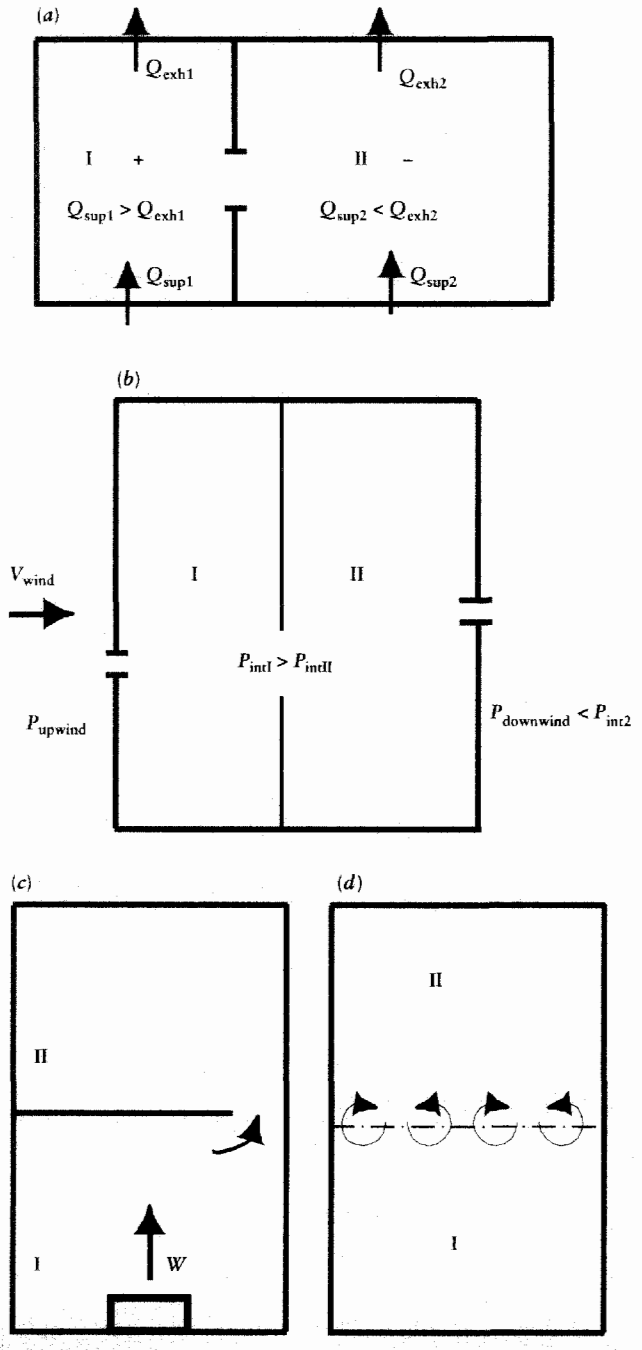

FIGURE 7.108 Mechanisms of contaminant movement between zones: (*a*) difference in static pressure resulting from unbalanced air supply and return; (*b*) difference in static pressure resulting from wind effect; (*c*) buoyancy forces create vertical air movement along the passage between zones located on different levels; (*d*) turbulent exchange between air in different zones due to energy introduced by supply air jets, moving objects, etc.

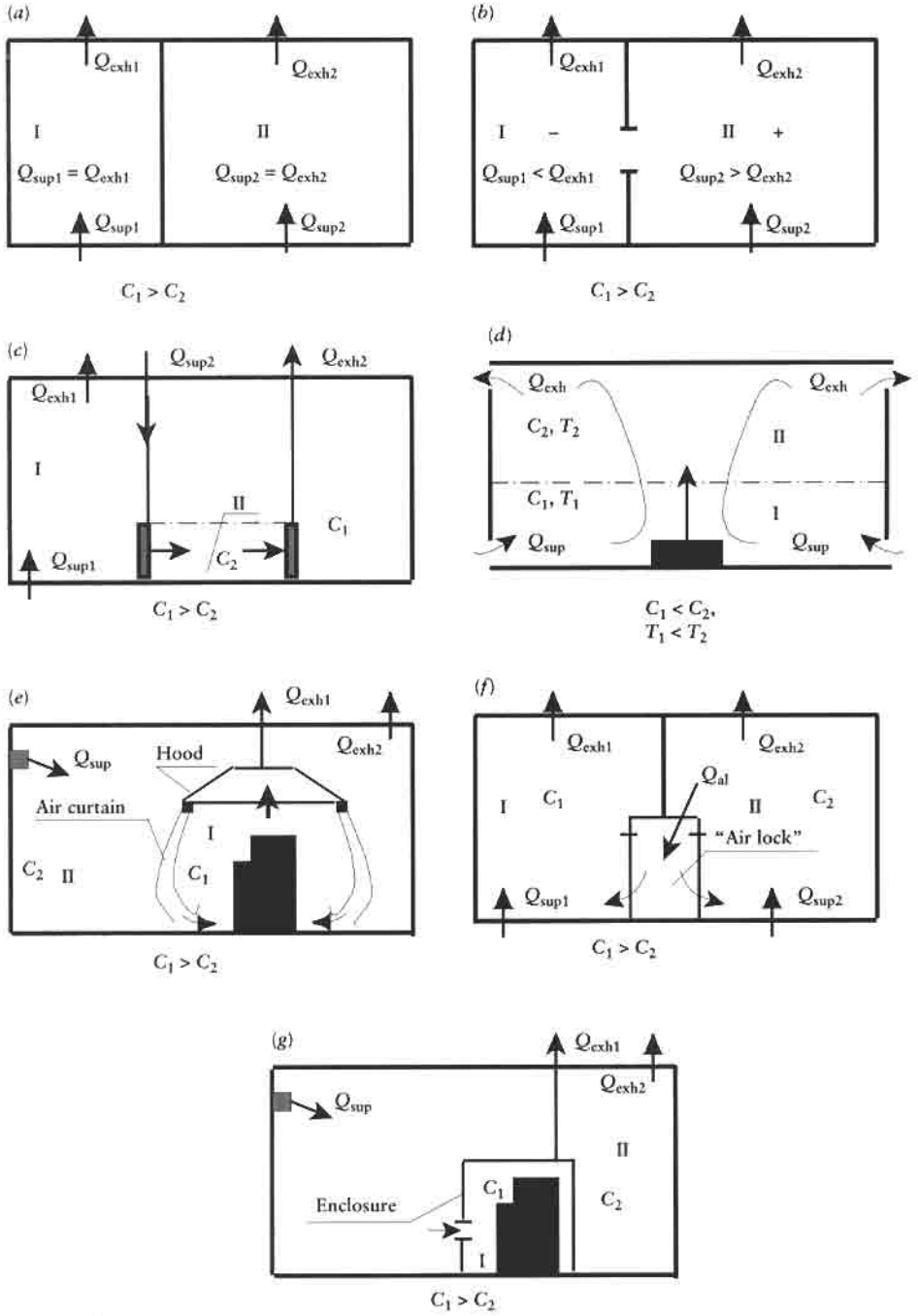

FIGURE 7.109 Construction, process-related, and ventilation techniques used to separate building zones: (*a*) solid wall; (*b*) unbalanced supply and return airflow rates; (*c*) specially arranged local supply and return, creating an "air oasis" with cleaner and cooler air in the desired zone of the building; (*d*) temperature and contaminant stratification along the room height using a natural or displacement ventilation system; (*e*) air curtain supplied around the perimeter of the canopy hood, which separates the contaminated process zone; (*f*) an "air lock" located between two zones; (*g*) enclosing process equipment and extracting air from the enclosure.

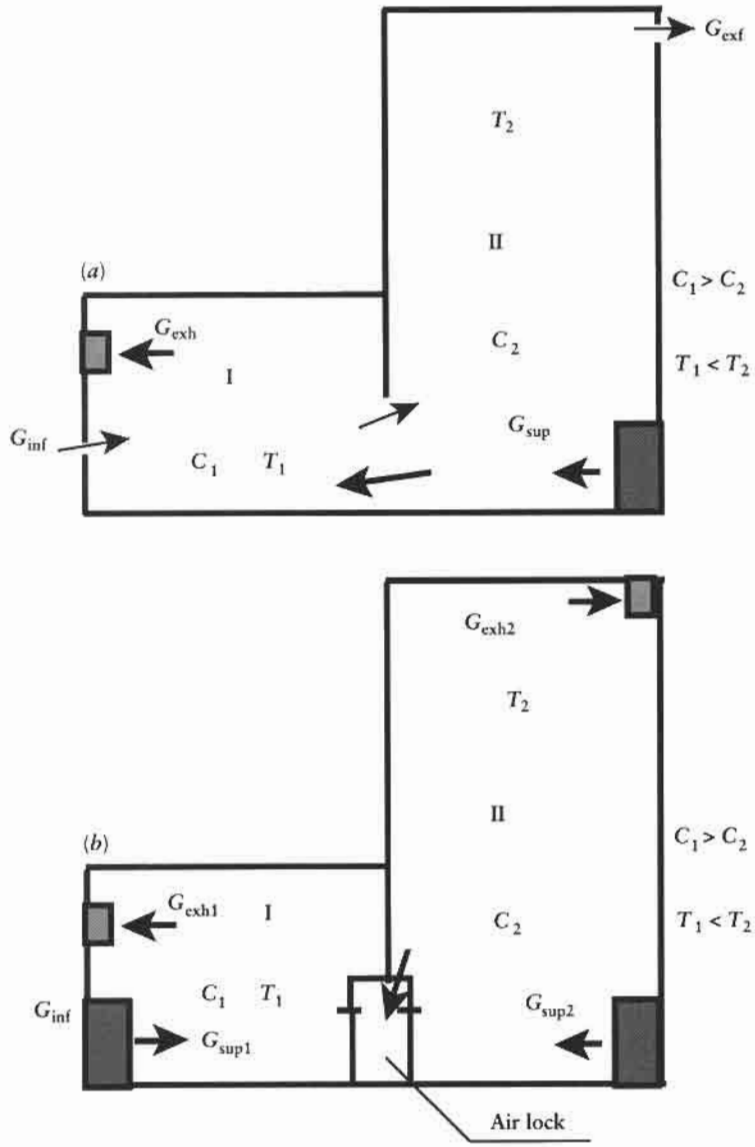

FIGURE 7.110 (*a*) Contaminant movement between two building zones with different ceiling heights due to the combined effect of unbalanced mechanical systems and the "stack" effect. (*b*) Prevention of contaminant movement between two zones using an "air lock."

The effect of turbulent exchange between the contaminated air in the process equipment enclosure and the room air (Fig. 7.111*b*) is described by Elterman. According to Elterman, the air velocity V_{exh} in the process equipment enclosure opening assuring contaminant concentration C_l at the distance l from the opening can be calculated from

$$V_{exh} = \frac{A}{l} \ln \frac{C_o - C_\infty}{C_l - C_\infty}, \tag{7.266}$$

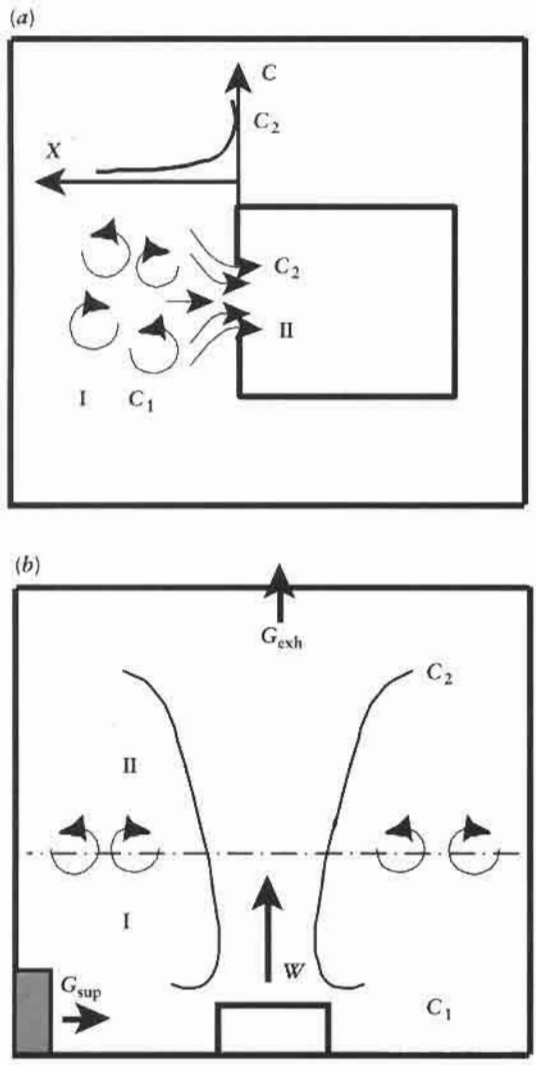

FIGURE 7.111 Contaminant and heat transfer due to turbulent exchange between building zones: (*a*) contaminant movement against the airflow near the vicinity of local exhaust; (*b*) heat and contaminant transfer between the lower and upper zones of the building with displacement ventilation.

where C_o = contaminant concentration under the enclosure, C_∞ = contaminant concentration in the room at the distant point, C_l = contaminant concentration at the point located distance L from the enclosure opening, and A = turbulent exchange coefficient.

Among the most important factors affecting the coefficient A value (see Section 7.3.) are the characteristic enclosure opening size and the air turbulence level under the enclosure. To decrease turbulent exchange with the room air, one can decrease the characteristic opening size (e.g., by inserting a flow equalizer) or install a spigot into the enclosure opening.

References

1. Simiu, E., and R. H. Scanlan. 1986. *Wind Effects on Structures.* 2nd ed. Wiley-Interscience, New York.
2. Hosker, R. P. 1985. Flow around isolated structures and building clusters: A review. *ASHRAE Transactions*, vol. 91, no. 26, pp. 1671–1692.
3. Snyder, W. H., and R. E. Lawson. 1994. Wind tunnel measurements of flow fields in the vicinity of buildings. In *8th Joint Conference on Applications of Air Pollution Meteorology.* American Meteorological Society and the Air and Waste Management Association.
4. Wilson, D. J. 1976. Combination of air intakes from roof exhaust vents. *ASHRAE Transactions*, vol. 82, pp. 1024–1038.
5. Hosker, R. P. 1984. Flow and diffusion near obstacles. *In* D. Randerson (ed.), *Atmospheric Science and Power Production.* DOE/TIC-27601 (DE84005177). U.S. Department of Energy, Washington, D.C.
6. B.S. 5925. 1980. *Code of Practice for Design of Buildings: Ventilation Principles and Designing for Natural Ventilation.* British Standards Institution, London.
7. ASHRAE. 1997. Airflow around buildings. In *Handbook: Fundamentals*, Chapter 15. American Society of Heating, Refrigeration, and Air Conditioning Engineers, Atlanta.
8. Sherman, M. H. and D. T. Grimsrud. 1980. Infiltration pressurization correlation: Simplified physical modeling. *ASHRAE Transactions*, vol. 86, no. 2.
9. BS Code of Practice CP3. 1972. Chapter V: Loading, part 2: Wind loads. British Standards Institution, London.
10. Liddament, M. W. 1986. *Air Infiltration Calculation Techniques: An Application Guide.* Air Infiltration and Ventilation Center, Coventry, UK.
11. Swami, M. V., and S. Chandra. 1988. Correlations for pressure distribution on buildings and calculation of natural-ventilation airflow. *ASHRAE Transactions*, vol. 94, no. 1, pp. 243–266.
12. Cochran, L. S., and J. E. Cermak. 1992. Full- and model-scale cladding pressures on the Texas Tech University experimental building. *J. Wind Engineering and Industrial Aerodynamics*, vols. 41–44, pp. 1589–1600.
13. Murakami, S., A. Mochida, R. Ooka, S. Kato, and S. Iizuka. 1996. Numerical prediction of flow around a building with various turbulence models: Comparison of k-ϵ, EVM, ASM, DSM, and LES with wind tunnel tests. *ASHRAE Transactions*, vol. 102, no. 1.
14. Zhoy Y., and T. Staphopoulos. 1996. Application of two-layer methods for the evaluation of wind effects on a cubic building. *ASHRAE Transactions*, vol. 102, no. 1.
15. Liddament, M. W. 1996. *A Guide to Energy Efficient Ventilation.* Air Infiltration and Ventilation Center, Coventry, UK.
16. Wilson, D. J., and B. K. Lamb. 1994. Dispersion of exhaust gases from roof-level stacks and vents on a laboratory building. *Atmospheric Environment*, vol. 28, pp. 3099–3111.
17. Halitsky, J. 1989. A jet plume model for short stacks. *J. Air Pollution Control Association*, vol. 39, pp. 856–858.
18. Schulman, L. L., and J.S. Scire. 1993. Building downwash screening model for the downwind recirculation cavity. *J. Air and Waste Management Association*, vol. 43, p. 1122.
19. EPA. 1995. *SCREEN3 Model User's Guide.* U.S. Environmental Protection Agency, Washington, D.C.
20. Saathoff, P., H. Wu, and T. Stathopoulos. 1996. Dilution of exhaust from rooftop stacks: Comparison of wind tunnel data with full-scale measurements. In *9th Joint Conference on Applications of Air Pollution Meteorology.* American Meteorological Society and the Air and Waste Management Association.
21. Higson, R. L., R. F. Griffiths, C. D. Jones, and D. J. Hall. 1994. Concentration measurements around an isolated building: A comparison between wind tunnel and field data. *Atmospheric Environment*, vol. 28, no. 11, pp. 1827–1836.
22. Cowen, I. R., I. P. Castro, and A. G. Robins. 1997. Numerical considerations for simulations of flow and dispersion around buildings. In *2nd Conference on Computational Wind Engineering*, Colorado.
23. Delaunay, D., D. Lakehal, C. Barre, and C. Sacre. 1997. Numerical and wind tunnel simulations of gas dispersion around a rectangular building. *J. Wind Engineering and Industrial Aerodynamics*, vols. 67–68, pp. 721–732.

24. Tsuchiya, M., S. Murakami, A. Nochida, K. Kondo, and Y. Ishida. 1997. Development of a new k-ϵ model for flow and pressure fields around bluff body. *J. Wind Engineering and Industrial Aerodynamics*, vols. 67–68, pp. 169–182.
25. Etheridge, D., and Sandberg, M. 1996. *Building Ventilation: Theory and Measurement*. John Wiley & Sons, Chichester, England.
26. Awbi, H. B. 1991. *Ventilation of Buildings*. Chapman & Hall, London.
27. ASTM E783-84. 1984. *Standard Method for Field Measurement of Air Leakage through Installed Exterior Windows and Doors*. American Society for Testing and Materials, Philadelphia.
28. ASTM E779-87. 1987 *Standard Method for Determining Air Leakage Rate by Fan Pressurization*. American Society for Testing and Materials, Philadelphia.
29. Baker, P. H., S. Sharpies, and I. C. Ward. 1987. Air flow through cracks. *Build. Environ.*, vol. 22, pp. 293–304.
30. Kamenev, P. N. 1964. *Heating and Ventilation, Part 2* (in Russian). Stroizdat, Moscow.
31. Baturin, V. V. 1972. *Fundamentals of Industrial Ventilation*, 3rd Engl. ed. Pergamon Press, New York.
32. Titov, V. P. 1976. *Heating and Ventilation, Part 2*. (in Russian). Stroizdat, Moscow.
33. Warren etal. 1980.
34. Liddament, M., and C. Alien, 1983. *The Validation and Comparison of Mathematical Models of Air Infiltration*. Tech. Note AIC 11. Air Infiltration and Ventilation Center, Coventry, UK.
35. Stroizdat. 1992. *Designer's Guidebook: Ventilation and Air-Conditioning*. Stroizdat, Moscow.
36. Shilkrot, E.O. 1993. Determination of design loads on room heating and ventilation systems using the method of zone-by-zone balances. *ASHRAE Transactions*, vol. 99, no. 1.
37. Elterman, V. M. 1980. *Ventilation of Chemical Plants*. Khimia. Moscow.

Bibliography

Baturin, V. V. and V. M. Elterman. 1963. *Aeration of Industrial Buildings* (in Russian). 2nd ed. Moscow.

Charlesworth, P. S. 1988. *Air Exchange Rate and Airtightness Measurement Techniques: An Applications Guide*. Air Infiltration and Ventilation Center, Coventry, UK.

ESDU Data Item 82026. 1982. *Strong Winds in the Atmospheric Boundary Layer —Part 1: Mean Hourly Wind Speeds*. Engineering Sciences Data Unit International, London.

Etheridge, D. W. 1977. Crack flow equations and scale effect. *Build. Environ.* vol. 12.

de Gids, W. F. 1978. Calculation method for the natural ventilation of buildings. *Verwarming Vent*, no. 7, pp. 552–564.

Liddament, M. W. 1987. Power law rules—OK! *Air Infiltration Rev.*, vol. 8, no. 2, pp. 4–6.

Retter, E. I. 1984. *Aerodynamnics of Buildings*. Stroizdat, Moscow.

Thorogood, R. P. 1979. *Resistance to Air Flow through External Walls*. BRE IP 14/79. Building Research Establishment, UK.

Thomas, D. A., and J. B. Dick. 1953. Air infiltration through gaps around windows. *JIHVE*, vol. 21, pp. 85–97.

This page intentionally left blank

8

ROOM AIR CONDITIONING

PER OLAF TJELFLAAT

Department of Refrigeration and Air Conditioning, NTNU, Norweigen University for Science and Technology, Trondheim, Norway

LARS OLANDER

Building Services Engineering KTH, Royal Institute of Technology, Stockholm, Sweden

ESA SANDBERG

Satakunta Polytechnic, Pori, Finland

HANNU KOSKELA

Turku Regional Institute of Occupational Health, Turku, Finland

KIM HAGSTRÖM

Faculty of Mechanical Engineering, Helsinki University of Technology, Espoo, Finland

ALEXANDER ZHIVOV

University of Illinois at Urbana-Champaign, USA

TIMO HAUTALAMPI

Finnish Institute of Occupational Health, Turku, Finland

HÅKON SKISTAD

SINTEF Energy Research, Refrigeration, and Air Conditioning, Norway

RALF WIKSTEN

Laboratory of Applied Thermodynamics, Helsinki University of Technology, Espoo, Finland

MAMDOUH EL HAJ ASSAD

Laboratory of Applied Thermodynamics, Helsinki University of Technology, Espoo, Finland

Industrial Ventilation Design Guidebook

8.1 INTRODUCTION

An industrial hall is an indoor space that is enclosed by walls, ceiling, and floor. Such an enclosure is normally perforated by openings for supply and extract of ventilation air, pipes for industrial processes, and operable hatches, windows, and doors for regular or occasional use.

Air conditioning design for an industrial space must be focused on providing a safe and comfortable environment with a low health risk for workers. The main goal for indoor climate design for an industrial hall is that the selected solution be effective for workers with respect to air quality and thermal comfort. Thus, prescribed design criteria must be met. Secondly, the climatization design should be as energy efficient as possible, which normally involves the minimization of outdoor airflow rate use through application of source control, local ventilation, and efficient space ventilation.

In Chapter 2, *Terminology*, the terminology of zones, systems, and basic strategies for room air conditioning are explained.

The scope of this chapter is to show how to select a strategy and to make calculations to provide efficient room air conditioning for an industrial enclosure. Design examples for simplified scenarios include different ways to condition industrial halls.

Upon starting design for a large enclosure, expected use should be described by informing and questioning the building owner and future users in order to locate zones of occupancy, the related activity level and clothing, and how that is expected to vary over a year. This is also the time to discuss and decide on adequate criteria for acceptable indoor air quality and thermal comfort. National health and building codes and recommendations and international standards apply.

Assumed heat and contaminant emissions inside the room should be estimated. Also, contaminants being admitted into the room by airflow and heat admitted by conduction and radiation through the room envelope should be assessed.

In the good tradition of industrial ventilation design, the possibilities of reducing or eliminating emission sources and using local extracts to avoid spreading to the rest of the room should be addressed.

The prevention of unnecessary heat loss or gain, causing poor thermal comfort due to large glazing areas and infiltration, should also be considered.

The use of local climatization should be considered one way of reducing the requirement for heating, cooling, or ventilating the entire enclosure volume.

8.2 BASIS FOR AIR CONDITIONING DESIGN

Upon starting design for an industrial enclosure, expected use should be described by informing and questioning the building owner and future users.

A scenario of the planned industrial enclosure should be sketched. The scenario should describe:

- The different steps of the flow and batch processes of the industrial production.
- Space demands for machinery, tools, working, and stocking areas for raw materials and products.
- Demand for worker involvement in each part of the industrial process.
- Emission of heat and contaminants from each part of the industrial process.
- Environmental requirements for each part of the industrial process.

The factory scenario must be updated with new information as the design process evolves.

8.2.1 Industrial Process Description

8.2.1.1 Stages of the Industrial Production Process

The different steps of the flow and batch processes of the industrial production must be roughly described early in the design process. A more detailed description may be needed in regions where heat and contaminants are released. Production design engineers are likely to provide the information needed.

8.2.1.2 Space Demands for the Production Process

Space demands for machinery, tools, work areas, and for stocking raw materials and products must be outlined. The logistics for the production line are often the basis for this consideration.

8.2.2 Requirements for Indoor Environment

8.2.2.1 Air Conditioning Demands for Human Occupancy

Requirements for indoor environment quality must be discussed and decided before the air conditioning design is performed. Criteria for acceptable indoor air quality and thermal comfort must be set.

Health hazard due to exposure to contaminants by inhalation is the most important issue. International or national health and building regulations or codes and recommendations are used as basis for the discussion of what requirements should be used for design. In regulations, worker exposure limits for airborne gases are normally expressed as

Time-weighted average concentration, TWA, based on a 40-hour work week,

Short-term exposure limit, STEL, which can be exceeded for periods of up to 15 minutes, and

Threshold limit value, TLV, a concentration level not to be exceeded any time.

Combinations of different substances in the air might be more harmful than the added effect of the two substances.

Most industrial companies would like to set air quality requirements regarding health hazard at a lower concentration level compared to values found in regulations. For example, when a TWA concentration is given as x kg per m^3 of air for a certain contaminant, the required concentration level for design of general ventilation in an industrial enclosure could be chosen as one-third of that value. This value can be considered the target value for the first design.

Target values must be rough for early design and must be refined for later stages in the design process. The main reasons for this are that details often are scarce and that calculation methods are rough at early design. One example of selection of target values is shown in Table 8.1. Some target values are not possible to consider at early design but should nevertheless be satisfied when production has commenced. General advice should be used during the design procedure to avoid such exposure problems at the future work condition.

The company must decide the air quality target values for breathing zones in the work environment after discussion with industrial hygienists and ventilation engineers.

Design criteria with respect to health-hazardous gases could alternatively be given as an accepted daily exposure of contaminant (for each hazardous substance, or a combination of substances).

Hazards from explosions, spills, and extreme working conditions should be considered according to national regulations.

Target values for thermal conditions at different design stages must also be considered. One example, for a scenario similar to regular office work, is shown in Table 8.2. The activity level and clothing insulation of the workers must always be taken into consideration when target values are chosen. Different target values other than the ones used in this table could be required, for example, for very cold and very hot and humid environments.

TABLE 8.1 Example of Target Values for Air Quality at Different Stages of Design

Air quality for breathing zone	First design	Main design	Evaluation
Odor from production processes, materials, and humans[1]			
Humans	Use at least $Q = 0.7$ L/(s p)N + 1.0 L/(s m^2)A_f), where N is the number of persons and A_f is the floor area	CO_2 level < 650 ppm over outdoor level	
Processes and materials	Avoid release of unpleasant odor from processes and materials	Use local extract	Tracer gas experiment with mathematical or physical model to check efficiency
Humidity	Avoid condensation on surfaces	20% < RH < 60%	
Particles	Avoid release of particles	Use local extract	< 20 μg/m^3 for $PM_{2.5}$[2] < 40 μg/m^3 (d < 0.05 μm) < 90 μg/m^3 (all diameters)
Health-hazardous gases			
Radon	Check ground on construction site		< 200 Bq/m^3
TVOC	Avoid moisture and release of fuels and similar contaminants		< 400 μg/m^3
Other substances	Use environment-friendly substances Use one-third of regulation TWA	Concentration in breathing zones lower than chosen target value	Regulation concentration limits given by local authority

[1]European Committee for Standardization. CEN/TC 156/WG6 Ventilation for Buildings: Design Criteria for Indoor Environment. Draft, European Prestandard prENV 1752, June 1996.

[2]$PM_{2.5}$ is the concentration of the fraction of particles where at least 50% (by weight) have an aerodynamic diameter less than 2.5 μm.

The definition of the breathing zone and of the zone of occupancy must be revised at each stage in the design process to make the climatization design effective and efficient.

Accepted acoustical conditions should be considered according to national regulations.

8.2.2.2 Conditioning Demands Other Than for Human Occupants

Industrial processes often require environmental conditions within certain limits.

Air quality requirements may be set as content of particles and as content of chemical substances. Other requirements for temperature, humidity, and air speed could be set. One example is the spray painting process, which is very dependent on a minimum relative humidity (RH) level to

TABLE 8.2 Example of Target Values of Thermal Conditions at Different Stages of Design

Thermal conditions for zone of occupancy	First design	Main design	Evaluation
General comfort			
		Relative air humidity RH < 70%	RH < 70%
Winter (1.1 m above floor)	Air temperature 21°C	Operative temperature 22.0–2.0 °C Air speed < 0.16 m/s	PPD[1] < 10% (−0.5 < PMV < 0.5)
Summer (1.1 m above floor)	Air temperature 25 °C	Operative temperature 24.5 ± 1.5 °C Air speed < 0.22 m/s	PPD < 10%
Local discomfort			
Draft			
Winter (ankles 0.1 m)		Air speed < 0.16 m/s	PPD < 20%
Summer (neck 1.8 m)		Air speed < 0.20 m/s	PPD < 20%
Vertical temperature gradient		<3°C (0.1–1.1 m above floor)	PPD < 5%
Radiant asymmetry		< 10 °C for cold wall < 23°C for warm wall < 14 °C for cold ceiling < 5 °C for warm ceiling	PPD < 5% with respect to cold wall, warm wall, cold ceiling, and warm ceiling
Hot or cold floors		19–26 ° C at surface	PPD < 10%

[1]PPD—percentage of people dissatisfied.

obtain a high-quality result. Refer to Chapter 2 and Chapter 6 for further information.

8.2.3 Architectural Design for an Industrial Enclosure

Once the information on the industrial processes and space requirements, the indoor climate requirements for workers, machinery, and products, and a lot for the factory have been obtained, then the architectural design of the industrial enclosure can be accomplished. A complete factory or industrial building may consist of several enclosures where industrial processes are run. One heating and ventilation plant may service several enclosures, or there may be a separate system for each enclosure.

The architectural design of an industrial enclosure must primarily satisfy the requirements for space and functions to accomplish the industrial process. Secondly, the architectural design should support the goals for good indoor environment and low energy consumption. Good indoor environment and low energy consumption can, for example, be supported by use of windows for day lighting and avoiding problems with down-draft and direct solar radiation.

Development in industrial processes and in work environment during the lifetime of an industrial hall should be predicted and planned for during the architectural design.

Utilization of natural ventilation for air conditioning will normally interact with the architectural design, and it should be considered early in the design process.

8.2.4 Worker Involvement in the Production Process

Demand for worker involvement in every part of the industrial process must be outlined. Then zones of occupancy, the related activity level and clothing, and how that is expected to vary over a typical day and year should be described.

Daily work procedure characterization for each worker must be outlined early in the design process.

At a later stage in the design process, when more detailed information is available, the following parameters should be described as a function of time for each worker: breathing zone position, activity level, and clothing value.

One example of how such information can be presented is shown in Table 8.3. Breathing zone location and activity level for one specific worker during a typical workday are listed.

The actual industrial hall has the form of a box of length, width, and height 48.0, 20.0, and 4.4 m, respectively. The origin of the coordinate system is located in the lower northwest corner of the room. The importance of mapping the breathing zone location can be realized when there is a coincidence of a high contaminant level and a high activity level combined with a long period of occupancy. As the body increases its pulmonary rate to absorb more oxygen, an airborne contaminant is likely to be absorbed to a higher degree in the body.

8.2.5 Load Calculation

8.2.5.1 Heat and Contaminant Emission

An estimate of heat and contaminant emission to the room air is needed early in the design process. Table 8.4 presents typical parameters of interest.

At a later stage in design the position and characteristics of releases are needed such as

Heat, described as power, as temperature on the described surface, or as advection of heat along with substance flowing out of the production process.

Momentum and density of flow released from openings and from processes.

Moisture, as emission of water and vapor from the process.

Contaminant emission, such as mass flow of different substances flowing out of the process.

TABLE 8.3 Example of Worker Behavior During a Typical Workday

Time period (h)	Accumulated time (h)	Work description	Breathing zone position			Activity description	Activity level (met)	Pulm[1] v. rate (kg/h)
			X (m)	*Y* (m)	*Z* (m)			
0.5	0.5	Adjusting machinery	27.7	18.6	1.65	Light work	2.0	1.46
0.5	1.0	Tube-forming quality check	22.9	19.4	1.65	Standing	1.2	0.88
0.5	1.5	Tube-forming quality check	22.9	19.4	1.65	Standing	1.2	0.88
0.5	2.0	Resting outside production hall	—	—	—	Seated	1.0	0.73
0.25	2.25	Checking paint station	17.4	18.6	1.65	Standing	1.2	0.88
0.25	2.5	Checking paint station	17.4	18.6	1.65	Standing	1.2	0.88
0.5	3.0	Checking paint station	17.4	18.6	1.65	Standing	1.2	0.88
0.5	3.5	Checking paint station	17.4	18.6	1.65	Standing	1.2	0.88
0.5	4.0	Checking paint station	17.4	18.6	1.65	Standing	1.2	0.88
0.5	4.5	Checking paint station	17.4	18.6	1.65	Standing	1.2	0.88
0.5	5.0	Checking paint station	17.4	18.6	1.65	Standing	1.2	0.88
0.5	5.5	Furnace adjustment	20.5	18.9	1.65	Light work	2.0	1.46
0.5	6.0	Furnace adjustment	20.5	18.9	1.65	Light work	2.0	1.46
0.5	6.5	Resting outside production hall	—	—	—	Seated	1.0	0.73
0.5	7.0	Resting outside production hall	—	—	—	Seated	1.0	0.73
0.5	7.5	Checking paint station	24.8	19.4	1.65	Standing	1.2	0.88
0.5	8.0	Checking paint station	24.8	19.4	1.65	Standing	1.2	0.88

[1]Pulmonary ventilation can be found from $Q_V = 0.0070M$ (kg/h). $M = 104.4$ W for an adult person at 1 met.

TABLE 8.4 Heat and Contaminant Release to the Air in an Industrial Hall

Source	Position X, Y, Z (m)	Power (W)	Contaminant (kg/s)	Comment
Furnace 1	21, 18, 1.4	30.0×10^3	—	Continuous / 70% in local extract
Furnace 2	23, 18, 1.4	10.0×10^3	—	Continuous / 60% in local extract
Furnace 3	26, 18, 1.4	17.5×10^3	—	Continuous / 80% in local extract
Painting station	17, 19, 1.4	—	Paint aerosol 4×10^{-6}	Substance / TLV = x mg/m^3
Press station	28, 18, 1.5	—	Oil vapor 1×10^{-6}	Substance / TLV = y mg/m^3

Detailed list of the actual contaminant, including properties, health effects, and odor.

It is also useful to make a steady-state balance with respect to airflow, heat flow, and mass flow of substances into and out of the enclosure. See Chapter 7 for details with respect to calculation of heat and contaminant emission.

Assume the use of mechanical ventilation with full mixing ventilation in the room, and calculate a rough estimate of ventilation airflow found by assuming dilution of contaminants released to the room air to one-third of the TLV level given for the substance in question.

8.2.5.2 Room Envelope Characterization

In order to analyze the conditions for air conditioning, the following information must be specified for the industrial enclosure:

Geometric dimensions.
Position and direction, U-value, solar factor, and thermal mass of the different construction elements.
Position of openings for possible infiltration or exfiltration.
Outline of expected opening of doors, windows, and hatches.

8.2.6 Characterization of Room Airflow and Thermal Conditions Based on Industrial Production Process and Envelope

8.2.6.1 Design Winter Conditions

Use the winter design temperature at the site along with the required indoor temperature level.
Estimate the heating power needed to keep that indoor temperature at steady-state conditions. Assume the use of mechanical ventilation with full mixing ventilation in the room; i.e., use the rough estimate of ventilation airflow given in Section 8.2.

8.2.6.2 Design Summer Conditions

Check summer design temperature and humidity outdoors.
Estimate maximum temperature increase in the room, taking into consideration the actual heat release from people and machinery, shading for solar radiation, assuming no thermal mass, and using a typical airflow for ventilation.

8.2.7 Analyses and Actions to Be Considered Prior to Performing Room Air Conditioning Design

The following questions should be considered:

Is replacement of contaminating substances possible?
Is containment of production processes possible, to avoid contaminants and heat being released to the room air?
Is automation of production processes possible, to avoid workers being exposed?
Is use of local extracts possible, to avoid contaminants and heat being released to the room air, and how efficient are extracts?
Is use of personal protection gear for workers possible?
Is use of local fresh-air supply at working stations possible?
Is use of local thermal conditioning possible?
Can changed working procedures reduce exposure to contaminants?
Can clothing be adjusted to correct thermal dissatisfaction problems?
Can activity level be adjusted by changing working routines?
In midsummer, when overheating is a problem, can an afternoon shift be changed into a night shift?

8.3 AIR RECIRCULATION

8.3.1 Introduction

One way to reduce the use of outside air—which needs heating, cooling, humidifying, dehumidifying, or cleaning—is to recirculate the air. Other ways to save energy for a ventilation system should preferably be used, such as the use of a heat exchanger, equipment that uses less energy, use of less air, etc. The main difference between other energy-saving processes and air recirculation is its influence on the contaminant concentration. This is a valid point for both industrial premises and offices and living rooms. Recirculation always includes some cleaning of the air. If the air is not cleaned, the process is seen as transferring instead of recirculating the air.

Through the years many reports have been published on air recirculation. Mostly they have treated the problems in offices,[1] living rooms,[2–6] and schools.[7] There have been many reports on air recirculation, which have concentrated on the use of some specific air cleaning system or on possible health risks.[8,9]

From the literature it is evident that air recirculation has been used and is used for many different types of ventilated areas. For this reason there have been some large investigations into the advantages and disadvantages of using air re-

other difference with central systems is that their performance is heavily influenced by the exhaust hood. If all contaminants generated at a process are captured by the exhaust hood, the performance is similar to a central system, but since this is a very rare phenomenon, the resulting concentration in the room is influenced by the capture efficiency (see Chapter 10).

The following equations separately outline calculating contaminant concentration inside a room with central and local recirculation. The assumptions for the room are that it has one main ventilation system with supply and exhaust air and that the contaminant concentration is the same in the whole volume (except very close to the contaminant source or in the ducts, etc.). The contaminant source is steady and continuous. The model for local ventilation assumes also one main ventilation system to which is added one local exhaust hood connected to a local ventilation system (see Chapter 10) from which all the air is recirculated. In the central system the number of inlets and outlets could vary. The flow rates are continuous and steady.

Different models have been published using two or more zones,[10,28-29] or where a mixing constant is used.[30] Models also exist for multiple ventilation systems in a room or a building,[9] for varying source rates,[13,31-32] and where local and central recirculation take place at the same time.[13,29,31]

The most important part of a recirculating system is the cleaning device. Different types of air cleaning devices are described in Chapters 9 and 13. The cleaner must be suited for the contaminant to be collected and its concentration. This sounds obvious, but is very often forgotten. Cleaners for aerosols (dusts) have efficiencies depending on particle size; for gases, efficiency varies with concentration and type of gas. The efficiency also varies with time, both for particle and gas cleaning systems. For mixtures of gases (vapors) and particles, such as oil mist, it is usually not enough to separate the particles (drops) from the air; the gases must also be collected.

Please note that filtering in dust collectors, vacuum cleaners, etc. does not usually collect the smallest particles. A good rule is not to recirculate such air.

The most common equipment for cleaning recirculated air from particles is fabric filters, mechanical collectors, electrostatic precipitators, and cleaners and wet collectors.[33] For cleaning of recirculated air from gases, absorbers and adsorbers such as activated carbon, sometimes with impregnation for specific gases, and impregnated alumina are most common. The performance of different air cleaning equipment is described in many textbooks and handbooks.[34]

The models described in the following use only one parameter for the cleaning efficiency, which is thus a simplification that must be kept in mind when using these models. This works quite well as long as the efficiency value is the smallest one—e.g., the efficiency for the most penetrating particle size or the efficiency for the most penetrating gas concentration.

8.3.3 Central Recirculation System

Typically, when central recirculation is used the contaminant in the supply air is the main source. This is not the case for industrial use, where the main source is in the ventilated room. This usually results in the concentration being somewhat higher when using recirculation than when not using it. Figure 8.1 outlines the ventilation system, the contaminant source, and the cleaning system.

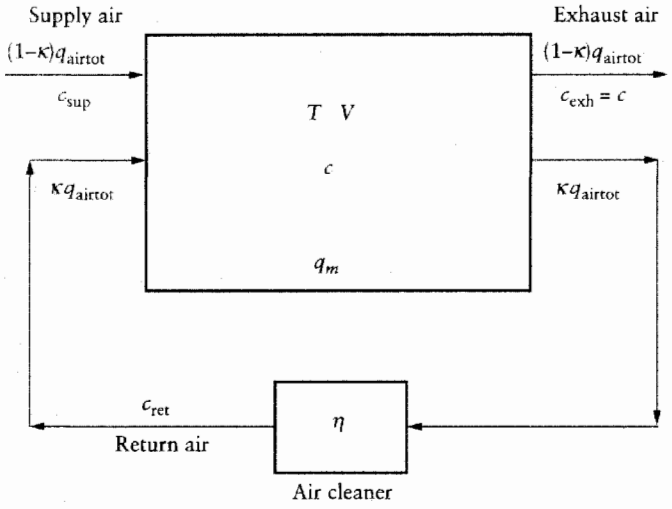

FIGURE 8.1 Model of a central recirculating system used for calculating the connection between contaminant concentrations, airflow rates, contaminant source strength, q_m, and air cleaner efficiency, η. c_{sup} is the concentration in the supply (outside) air, c is the concentration in the room, c_{ret} is the concentration in the returned air, q_{airtot} is the total flow rate through the room, κ is the ratio between recirculated airflow rate and total air flow rate, T is the time constant for the room, and V is the room volume.

In the figure the two flows (supply—exhaust and recirculated) are separated for clarity. Normally they are merged on both the supply and exhaust side.

The following differential equation (or something similar), derived from a mass balance for the room, is solved to find the correlation between flow rates, source rate, contaminant concentrations, cleaning efficiency, and time.

$$(1-\kappa_c)q_{airtot}c_s + \kappa_c q_{airtot}c(1-\eta) + q_m = q_{airtot}c + V\frac{dc}{dt} \quad , \qquad (8.1)$$

where the recirculation ratio, κ_c, is defined as

$$\kappa_c = \frac{q_{airret}}{q_{airtot}}$$

and

κ_c is always less than 1
q_{airret} is the return airflow rate, m^3s^{-1}
q_{airtot} is the total flow rate through the room, m^3s^{-1}
c_s is the concentration in the supply air, mg m^{-3}
c is the concentration in the room, mg m^{-3}
η is the efficiency of the cleaner (0–1)
q_m is the source rate, mg s^{-1}
V is the volume of the room, m^3
t is time, s

It is possible to have a separate recirculating system in addition to the general ventilation system; then there is no restriction on the flow rate. This case is the same as a recirculating local exhaust system (see below)

By assuming the supply air concentration to be zero, since usually there are quite different contaminants in the outside air and from the source, and that the initial concentration also is zero, the time-dependent solution is the following,

$$c = \frac{q_m}{q_{\text{airtot}}} \times \frac{1}{(1 - \kappa_c + \kappa_c \eta)} (1 - e^{-(1 - \kappa_c + \kappa_c \eta)t/T}) \quad . \tag{8.2}$$

where T is the time constant for the room, s, equal to V/q_{airtot}.

By assuming a steady state and since the sum of the supply and return flow rates is equal to the total flow rate through the room, it is possible to manipulate this equation to get the following, where q_{airsup} is the supply airflow rate, $m^3\ s^{-1}$:

$$c = \frac{q_m}{q_{\text{airsup}} + q_{\text{airret}} \eta} . \tag{8.3}$$

This equation shows clearly the influence of the recirculated air. With a source rate of q_m and a general ventilation flow rate of q_{airsup} the concentration is q_m/q_{airsup}. The addition of recirculated air corresponds to an increase of the supply flow rate by the amount q_{airret} times η and decreases the concentration. On the other hand, if a part of the original supply air without recirculation (that is, the total flow rate before recirculation is equal to $q_{\text{airsup}} + q_{\text{airret}}$) is recirculated, the concentration will increase.

Another solution to the differential equation for steady state is the following, where the concentration in the supply air, c_{airsup}, is included:

$$c = \frac{q_{\text{m}}}{q_{\text{airtot}}} \frac{1}{(1 - \kappa_c + \kappa_c \eta)} \times \frac{c_{\text{airsup}}(1 - \kappa_c)}{(1 - \kappa_c + \kappa_c \eta)} \tag{8.4}$$

This equation is the same as the solution for the steady state without contaminant in the supply air, but with an added multiplication term (the third part on the right) that shows the influence of the recirculation.

Another equation that includes the initial concentration and the concentration in the supply air and the mixing factor has been published:[32]

$$c = c_0 e^{-f(q_{\text{airsup}} + \eta q_{\text{airret}})t/V} + \frac{f c_{\text{sup}} q_{\text{airsup}} + q_m}{f(q_{\text{airsup}} + \eta q_{\text{airret}})} \times (1 - e^{-f(q_{\text{airsup}} + \eta q_{\text{airret}})t/V}) \tag{8.5}$$

where c_0 is the initial concentration at time zero, mg m^{-3}, and f is the mixing factor, here defined as the portion of the supply airflow that is completely mixed with room air.

This equation can also be used for steady-state conditions, when the exponential terms are taken away and for complete mixing when f is set to 1.

8.3.4 Local Recirculation

Local recirculation systems differ from central systems in that all exhausted air is passed back to the room after cleaning and that the flow rate could be larger than the flow rate through the room.

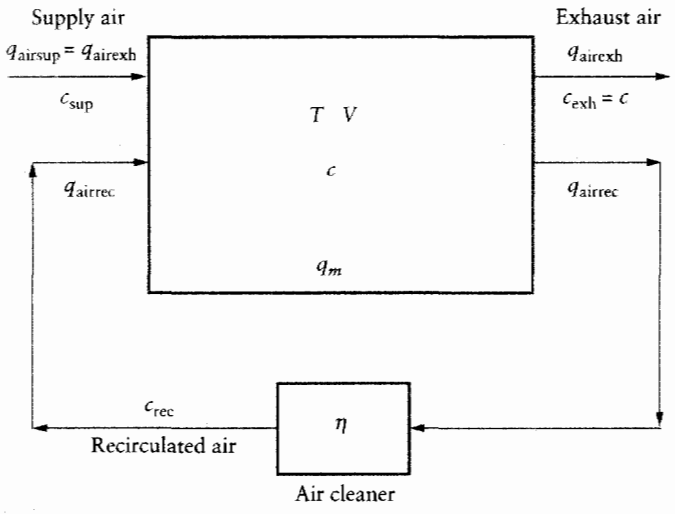

FIGURE 8.2 Model of a local recirculating system (room air cleaner) used for calculating the connections between contaminant concentrations, airflow rates, contaminant source strength, q_m, and air cleaner efficiency, η. c_{sup} is the concentration in the supply (outside) air; c (equal to c_{exh}) is the concentration in the room; c_{rec} is the concentration in the returned air; q_{airtot} is the total flow rate through the room; κ is the ratio between the recirculated airflow rate, q_{airrec}, and total airflow rate; q_{airexh} is the flow rate from the general ventilation system; T is the time constant for the room; and V is the room volume.

One of the most common systems for cleaning air in homes, offices, schools, etc. is the room air cleaner. Figure 8.2 outlines a model of a local recirculating system. Usually these units are situated inside the room if they are small and movable (see Chapter 10). For the model it does not matter if the unit is placed inside or outside the room with the contaminant source, as long as the exhaust and return air openings are inside.

The room air cleaner consists of a fan and some kind of air cleaner for particles or gases or both, usually mounted together as one unit. This is a local recirculating system and the equation for the contaminant concentration in the room, derived with the same assumptions and in the same way as for central systems, is the following:

$$c = \frac{q_m}{q_{airexh}} \times \frac{1}{(1 + \kappa_1 \eta)} \times (1 - e^{-(1 + \kappa_1 \eta)t/T}) \quad , \tag{8.6}$$

where

c is the concentration in the room, mg m^{-3}
q_m is the source rate, mg s^{-1}
q_{airexh} is the exhaust flow rate from the room, m^3 s^{-1}
κ_1 is the local recirculation ratio equal to q_{airrec}/q_{airexh}
q_{airrec} is the flow rate through the unit (cleaner), m^3 s^{-1}
η is the efficiency of the cleaner (0–1)
T is the time constant for the room equal to V/q_{exh}, s

V is the volume of the room, m^3
t is time, s

By manipulating this equation for the steady state, in the same way as for central systems, the following could be achieved:

$$c = \frac{q_m}{q_{airexh} + q_{airrec}\eta}, \tag{8.7}$$

which is similar to the equation for central systems. This relation is often expressed as

$$c = \frac{q_m}{q_{airexh} + q_{airequ}}, \tag{8.8}$$

where q_{airequ} is the so-called equivalent flow rate for the cleaner, because the product of flow rate and cleaning efficiency has the unit of flow rate. In words this could be expressed as follows: The influence of a room air cleaner on the contaminant concentration is the same as if a flow rate of clean air (outside air) equal to q_{airequ} were added to the ventilation flow rate in the room.

From this equation it is clear that if either flow rate or cleaner efficiency for the recirculation system is zero, there will be no change in contaminant concentration. Also, a low flow rate can only be compensated to a small degree by a higher cleaning efficiency, but a low cleaning efficiency can be compensated to some degree by increasing the flow rate.

This equation makes it quite easy to calculate necessary flow rate and cleaning efficiency for a local recirculation system (room air cleaner).

Local ventilation in industry usually differs from the description above in that it is connected to a local exhaust hood (Chapter 10), which has a capture efficiency less than 100%. The capture efficiency is defined as the amount of contaminants captured by the exhaust hood per time divided by the amount of contaminants generated per each time (see Section 10.5). Figure 8.3 outlines a model for a recirculation system with a specific exhaust hood. Here, the whole system could be situated inside the workroom as one unit or made up of separate units connected with tubes, with some parts outside the workroom. For the calculation model it makes no difference as long as the exhaust hood and the return air supply are inside the room.

The solution to the differential equation at steady state in this case is

$$c = \frac{q_m}{q_{airexh}} \times \frac{(1 - \alpha\eta)}{(1 + \kappa_1\eta)}, \tag{8.9}$$

where α is the capture efficiency for the local exhaust hood (0–1). To get the time-dependent solution, the right-hand side is multiplied with the same term (the parentheses including the exponential term) as for the system without an exhaust hood.

This latter equation can also be used for systems without a local exhaust hood by setting the capture efficiency to zero. It could also be used to show the result of recirculation from, e.g., a laboratory fume hood with immediate recirculation. In such a hood all contaminants are generated within the hood and usually also all generated contaminants are captured, so the capture efficiency is 1. The equation demonstrates that if the

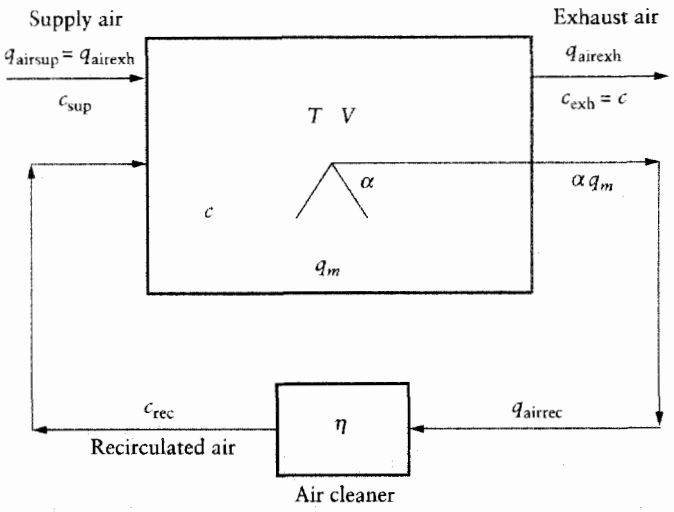

FIGURE 8.3 Model of a local recirculating system with a local exhaust hood, used for calculating the connection between contaminant concentrations, airflow rates, contaminant source strength, q_m, air cleaner efficiency, η and hood capture efficiency, α. c_{sup} is the concentration in the supply (outside) air; c (equal to c_{exh}) is the concentration in the room; c_{rec} is the concentration in the returned air; q_{airsup} is the supply flow rate to the room equal to the exhaust flow rate, q_{airexh}; the recirculated flow rate (through the cleaner) is $q_{air-rec}$; T is the time constant for the room; and V is the room volume.

cleaning efficiency is zero, there is no change in concentration, and the unit only works as a mixing unit.

8.3.5 Conclusion

To design an air recirculation system it is necessary to know the performances of fans, air cleaners, and exhaust hoods included in the current system. The equations described here include the source generation rate and the total airflow rate through the room, which could be difficult to measure. The ratio between source rate and flow rate has the unit of concentration and should in fact be equal to the concentration without recirculation. The equations could thus be transformed to include the contaminant concentration without recirculation instead of this ratio. In this way a direct comparison between concentration without and with recirculation is possible. By using the described equations it is then possible to design an air recirculation system to result in the demanded concentration in a workroom.

References

1. D. W. Vanosdell and L. E. Sparks, *ASHRAE Journal*, 1995, 37, 34.
2. J. J. K. Jaakkola, O. S. Miettinen, K. Komulainen, P. Tuomaala, and O. Seppänen, *Indoor Air '90*, 1990, 1, 281.
3. R. T. Liu and M. A. Huza, *ASHRAE Journal*, 1995, 37, 18.
4. M. Meckler and J. E. Janssen, in *Engineering Solutions to Indoor Air Problems: Proceedings of the ASHRAE Conference IAQ 88*, 130–147, Atlanta, GA: ASHRAE, 1988.

5. C. O. Muller and W. G. England, *ASHRAE Journal*, 1995, 37, 24.
6. T.G. Malmström, *Healthy Buildings*, 1988, 87.
7. A. E. Wheeler, *ASHRAE Journal*, 1992, 26.
8. J. Sundell, *Indoor Air*, 1994, supplement no. 2/94, 1.
9. R. D. Rivers, *ASHRAE Transactions*, 1982, 929.
10. W. J. Astleford, In NIOSH, *Recirculation of Exhaust Air*, Washington, D.C.: U.S. Department of Health, Education and Welfare, NIOSH, 1976, DHEW (NIOSH) Publication No. 76-186.
11. NIOSH, *Recirculation of Exhaust Air: Proceedings of a Seminar, October 1975*, Washington, D.C.: U.S. Department of Health, Education and Welfare, NIOSH, 1976, DHEW (NIOSH) Publication No. 76-186.
12. NIOSH, *The Recirculation of Industrial Exhaust Air: Symposium Proceedings*, Washington, D.C.: U.S. Department of Health, Education and Welfare, NIOSH, 1978, DHEW (NIOSH) Publication No. 78-141.
13. L. J. Partridge, P. R. Nayak, R. S. Stricoff, and J. H. Hagopian, *A Recommended Approach to Recirculation of Exhaust Air*, Washington, D.C.: U.S. Department of Health, Education and Welfare, NIOSH, 1978, DHEW (NIOSH) Publication No. 78-124.
14. J. H. Hagopian, *Validation of a Recommended Approach to Recirculation of Industrial Exhaust Air*, vol. I, Washington, D.C.: U.S. Department of Health, Education and Welfare, NIOSH, 1979, DHEW (NIOSH) Publication No. 79-143A.
15. L. F. Bullock, *Validation of a Recommended Approach to Recirculation of Industrial Exhaust Air*, vol. II, Washington, D.C.: U.S. Department of Health, Education and Welfare, NIOSH, 1979, DHEW (NIOSH) Publication No. 79-143B.
16. M. L. Holcolm and R.C. Scholz, *Evaluation of Air Cleaning and Monitoring Equipment Used in Recirculation Systems*, Washington, D.C.: U.S. Department of Health and Human Services, NIOSH, 1981, DHHS (NIOSH) Publication No. 81-113.
17. R. T. Hughes and A. A. Amendola, *Plant Engineering*, 1982.
18. S. Opiolka, W. Molter, R. Goldschmidt, E. Erich, and G. Schöppe, *Gefahrstoffe Reinhaltung der Luft*, 1998, 58, 291.
19. D. S. Abrams, P. C. Reist, and J. M. Dement, *American Industrial Hygiene Association Journal*, 1986, 47, 22.
20. D. Cucu and H. J. Lippold, *Journal of Electrostatics*, 1985, 17, 109.
21. C. P. Fotos, *Aviation Week & Space Technology*, 1991, 79.
22. A. E. Hall, J.P. Saindon, L. D. Nel, and S. G. Hardcastle, *CIM Bulletin*, 1988, 81, 63.
23. J. R. Luciano, *ASHRAE Journal*, 1983, 38.
24. S. Miller-Leiden, C. Lobascio, W. W. Nazaroff, and J. M. Macher, *Journal of the Air & Waste Management Association*, 1996, 46, 869.
25. G. E. Myers and C. A. Hunckler, *Applied Industrial Hygiene*, 1987, 2, 71.
26. J. R. Swartout, *Plant Engineering*, 1980, 151.
27. J. P. Smith, *Applied Industrial Hygiene*, 1987, 2, 74.
28. L. C. Rodgers, *ASHRAE Transactions*, 1980, 86 part 2, 92.
29. E. Skåret, *Ventilation '85*, 1985, 827.
30. American Conference of Governmental Industrial Hygienists, *Industrial Ventilation, A Manual of Recommended Practice*, metric version, 23rd Ed. Cincinnati, OH: ACGIH, 1998.
31. O. Strindehag, *Heizung, Lüftung, Klimatechnik*, 1979, 30 no. 5, 178–182.
32. Y. Ishizu, *Environmental Science & Technology*, 1980, 14, 1254.
33. J. T. Talty, *Journal of the Air Pollution Control Association*, 1978, 28, 633.
34. S. Calvert and H. M. Englund, eds., *Handbook of Air Pollution Technology*, New York: John Wiley & Sons, 1984.

8.4 TWO-ZONE MODEL DESCRIPTION

8.4.1 Zonal Models

Zonal models are often used in analytical calculation of temperature, concentration, or humidity conditions in ventilated spaces. The space is divided in two or several zones, which typically have different target levels as described in Section 2.1.[1–3] These typical zones can also be divided into additional subzones.

The zoning of the space is based on the assumption of constant temperature, concentration, and humidity in each separate zone.[4,5] The boundaries between the zones can be vertical or horizontal. The balances for air mass flow, contaminant mass flow, water vapor mass flow, and heat flow are determined between zones and between zone and outer boundaries.

Zonal models can be applied for each room air conditioning strategy (see Section 8.6), but they are mostly used in stratification and zoning strategies with different air distribution methods (see Section 8.7).

8.4.2 Two-Zone Model

Two-zone models are especially useful for stratification and zoning strategies because of the typical vertical accumulation of heat, contaminants, or water vapor within these strategies. The level of the boundary between the lower and the upper zone is usually determined on the level of the highest temperature or/and concentration gradient.

In the stratification strategy with a replacing air distribution in the lower zone, the height of the boundary layer between the lower and upper zones can be determined with the criteria of the contaminant interfacial level.[4] This level, where the air mass flow in the plumes is equal to the air mass flow of the supply air, is presented in Fig. 8.4. In this ideal case the wall and air temperatures are equal on the interfacial level. In practical cases they are not usually equal and the buoyancy flows on the walls will raise the level and decrease the gradient.

In the zoning strategy the height of the boundary between lower and upper zones should be determined with the criteria of the air distribution method and devices. The lower zone should be defined high enough to get nearly all the induction air of the supply air devices from the controlled zone, as shown in Fig. 8.5.

8.4.3 Two-Zone Model Calculation

The calculation of the two-zone model is based on the balance equations for air mass flow, contaminant mass flow, water vapor mass flow, and heat flow of both zones.

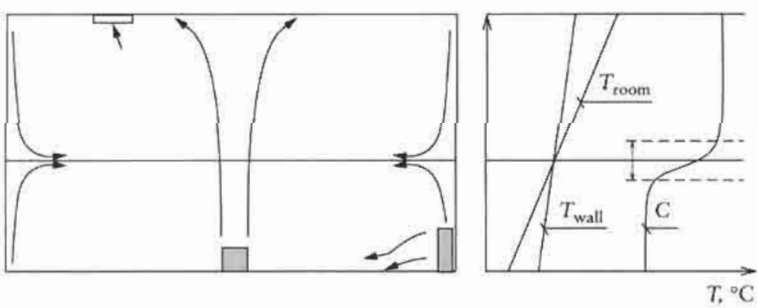

FIGURE 8.4 The height of the contaminant interfacial level in the stratification strategy.

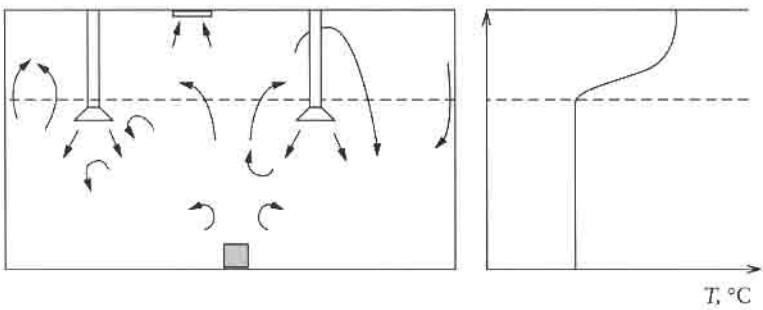

FIGURE 8.5 The height of the lower zone boundary in the zoning strategy.

The air, contaminant, and water vapor mass flow elements in outer boundaries and between the zones are created by

1. Supply air
2. Extract air
3. Heat and contaminant sources
4. Local ventilation
5. Plumes of the buoyancy sources through the zone boundary
6. Possible return air from the upper zone into the lower zone
7. Flows along wall surfaces due to temperature differences
8. Infiltration and exfiltration
9. Mixing between zones due to turbulence and disturbances

The heat flow elements are created by

1. Radiation from heat sources
2. Radiation between room surfaces
3. Heat transport through surface boundary layers

A general steady-state balance calculation of a two-zone model is presented in Figs. 8.6–8.7 and Eqs. (8.10)–(8.17).

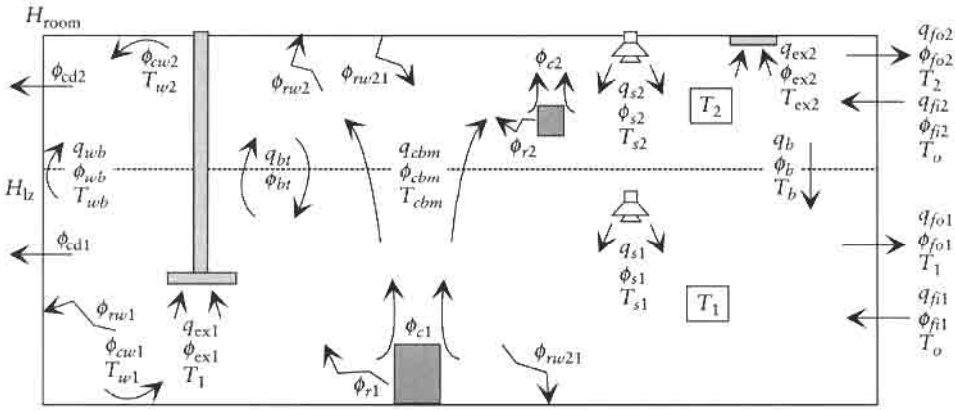

FIGURE 8.6 A general two-zone air mass and heat flow model.

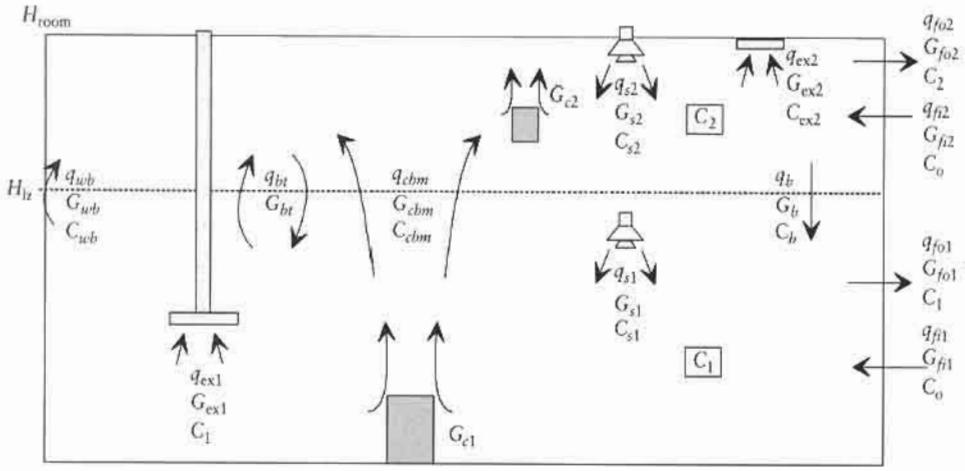

FIGURE 8.7 A general two-zone air and contaminant mass flow model.

Nomenclature for Figs. 8.6–8.7 and Eqs. (8.10)–(8.17)

C = concentration [mg/m^3]
H = height [m]
G = contaminant flow rate [mg/s]
q = airflow rate [dm^3/s]
Q = heat flow rate [W]
T = temperature [K]

Subscripts

1 = upper zone
2 = lower zone
b = boundary, through the boundary
c = convection
cd = conduction
ex = exhaust, extract
f = filtration
i = in
m = mixing, mixed
o = out, outside
r = radiation
s = supply
t = turbulent mixing
w = wall

The model equations are determined by writing the balance equations based on the conservation of mass and energy. The balance equations have the following basic form:

$$\sum \text{flow in} + \sum \text{flow sources} - \sum \text{flow out} = 0$$

Air mass flow balance for the lower zone:

$$\rho_{s1}q_{s1} - \sum\rho_{ex1}q_{ex1} + \rho_b q_b - \sum\rho_{wb}q_{wb} - p_1 q_{fo1} + \rho_o q_{fi1} - \sum\rho_{cbm}q_{cbm} = 0. \tag{8.10}$$

Air mass flow balance for the upper zone:

$$\rho_{s2}q_{s2} - \sum\rho_{ex2}q_{ex2} - \rho_b q_b + \sum\rho_{wb}q_{wb} - p_2 q_{fo2} + \rho_o q_{fi2} + \sum\rho_{cbm}q_{cbm} = 0. \tag{8.11}$$

Heat flow balance for the lower zone air:

$$\Phi_{s1} - \sum\Phi_{ex1} + \Phi_b - \sum\Phi_{wb} - \Phi_{fo1} + \Phi_{fi1} - \sum\Phi_{cbm} + \sum\Phi_{c1} + \sum\Phi_{cw1} + \Phi_{bt} = 0. \tag{8.12}$$

Heat flow balance for the upper zone air:

$$\Phi_{s2} - \sum\Phi_{ex2} - \Phi_b + \sum\Phi_{wb} - \Phi_{fo2} + \Phi_{fi2} + \sum\Phi_{cbm} + \sum\Phi_{c2} + \sum\Phi_{cw2} - \Phi_{bt} = 0. \tag{8.13}$$

Heat flow balance for the lower zone walls:

$$-\sum\Phi_{cw1} + \sum\Phi_{rw1} + \sum\Phi_{rw21} - \sum\Phi_{cd1} = 0 \quad . \tag{8.14}$$

Heat flow balance for the upper zone walls:

$$-\sum\Phi_{cw2} + \sum\Phi_{rw2} - \sum\Phi_{rw21} - \sum\Phi_{cd2} = 0 \quad . \tag{8.15}$$

Contaminant mass flow balance for the lower zone:

$$G_{s1} - \sum G_{ex1} + G_b - \sum G_{wb} - G_{fo1} + G_{fi1} - G_{cbm} + \sum G_{c1} + G_{bt} = 0. \tag{8.16}$$

Contaminant mass flow balance for the upper zone:

$$G_{s2} - \sum G_{ex2} - G_b + \sum G_{wb} - G_{fo2} + G_{fi2} + \sum G_{cbm} + \sum G_{c2} - G_{bt} = 0. \tag{8.17}$$

The balance equations for water vapor flows are similar to balance equations for contaminant flows, but in addition possible condensation and evaporation must be calculated. Also they must be considered in heat flow equations.

The air and wall temperatures and the concentrations in both zones are solved by iteration toward a steady-state situation or by simulating the time-dependent development. In the time-dependent calculation the heat capacity of the walls should be included.

In wall heat balance Eqs. (8.14) and (8.15), the radiation heat flows $\sum\Phi_{rw1}$ and $\sum\Phi_{rw2}$ from the heat sources and $\sum\Phi_{rw21}$ from upper zone wall surfaces to lower zone wall surfaces are assumed to increase the temperature of the walls. In practical cases it is quite complicated to determine how much of the radiation flow rate will be distributed to outer walls and to other surfaces.

Vertical buoyant flows on the wall boundaries $\sum q_{wb}$, $\sum\Phi_{wb}$, and $\sum G_{wb}$ are the sum of several upward and downward flows through the zone boundary, which can be calculated using plume and jet theories.

The convection flows from the heat sources $\sum \Phi_{c1}$ and $\sum \Phi_{c2}$ as well as contaminant flows from contaminant sources are flows loading the room. In the sources additional heat and pollutant flows may be generated, which are exhausted directly out by local ventilation and are not included in the balance calculation.

The pollutant sources $\sum G_{c1}$ and $\sum G_{c2}$ may be without any buoyancy forces or they may be sinks, in other words negative sources or filters.

The flow rate of the plume through the zone boundary depends on the plume strength and vertical temperature gradient.[6] In the case of a zoning strategy, the plume flow rate may also depend on the air distribution method and device because of the interaction between the plume and the supply air.[2]

The turbulent mixing between the zones depends on the air distribution method and device.[7,8]

8.4.4 Two-Zone Model Solutions

Specified solutions of the general two-zone model have been presented previously.[1,6,7,9–11]

Skåret[11] presents a general air and contaminant mass flow model for a space where the air volume, ventilation, filtration, and contaminant emission have been divided for both the zones and the turbulent mixing (diffusion) between the zones is included. A time-dependent behavior of the concentration in the zones with constant pollutant flow rate is presented.

Bach et al.,[1] Pozin,[9] and Shilkrot and Zhivov[10,11] present two-zone models for mixing, zoning, and stratification strategies with different air distribution methods.

Mundt[6] presents a two-zone model for the calculation of temperature gradient within a stratification strategy.

Sandberg et al.[8] present a two-zone model for a zoning strategy and active displacement air distribution method.

Sections 8.7.3 and 8.7.4 give examples of the calculation of two-zone air flow and contaminant flow models applied to stratification and zoning strategies.

References

1. H. Bach, W. Dittes, K. Madjidi, R. Becher, B. Biegert, et al., *Zonal Ventilation of Working Area in Production Halls to Reduce the Load of Contamination*, Research Report 01HK216 Verein der Förderer der Forschung im Bereich Heizung-Luftung-Klimatechnik, Stuttgart e.V., 1992.
2. W. Dittes, New concepts for air flow patterns in industrial halls—Calculation of the ventilation efficiency, in *Ventilation '94: Proceedings of the 4th International Symposium on Ventilation for Contaminant Control*, vol. 1. Stockholm, Sweden, 1994.
3. K. Hagström, K. Siren, and A. Zhivov, *Calculation Methods for Air Supply Design in Industrial Facilities—Literature Review*, Espoo: Helsinki University of Technology, 1999, Report B60.
4. D. Ethridge and M. Sandberg, *Building Ventilation: Theory and Measurement*, Chichester: John Wiley & Sons, 1996.
5. P. Cooper and P. F. Linden, Natural ventilation of an enclosure containing two buoyancy sources, *Journal of Fluid Mechanics*, 1996, *311*, 153–176.
6. E. Mundt, *The Performance of Displacement Ventilation Systems: Experimental and Theoretical Studies*, Stockholm, Sweden: Royal Institute of Technology, 1996

7. E. Shilkrot and A. Zhivov, Zonal model for displacement ventilation design, in *Roomvent* '96 vol. 2. Yokohama, Japan, 1996.
8. E. Sandberg, H. Koskela, and T. Hautalampi, Convective flows and vertical temperature gradient with the active displacement air distribution, in *Roomvent* '98, Stockholm, Sweden, 1998.
9. G. M. Pozin, Mathematical modelling of heat and air processes in mechanically ventilated spaces, in *Roomvent* '92, vol. 1, Aalborg, Denmark, 1992.
10. E. Shilkrot and A. Zhivov, Room ventilation with designed vertical air temperature stratification, in *Roomvent* '92, vol. 1. Aalborg, Denmark, 1992.
11. E. Skåret, *Advanced Design of Ventilation System*, Ventilation Models Lecture Series, Brussels: Von Karman Institute for Fluid Dynamics, 1993.

8.5 EFFECTIVE AND EFFICIENT VENTILATION

8.5.1 Ventilation Efficiency Indices

Effective air distribution in ventilated rooms and proper quantity of conditioned air are essential for creating comfortable conditions, removing contaminants, and reducing initial and operating costs of air conditioning and ventilation systems. The degree to which a ventilation system fulfills ventilation requirements is described in the literature in terms of "ventilation effectiveness," "ventilation efficiency," "ventilation performance," etc. Liddament in his review of technical information related to ventilation effectiveness stated that "the subject of ventilation effectiveness is made unnecessarily complex by the lack of uniformity in terminology. Frequently, terms are interchanged or different terms are used to describe the same concepts."[1]

Ventilation efficiency has traditionally been defined as the ratio between contaminant concentration in the occupied spaces and the concentration in the exhaust air.[2] Sandberg and Skåret differentiate between the terms "air change efficiency" and "contaminant removal effectiveness." Air change efficiency is "a measure of how effectively the air present in a room is replaced by fresh air from the ventilation system," whereas "contaminant removal effectiveness" is "a measure of how quickly an air-borne contaminant is removed from the room." A third similar criterion that is used is "contaminant removal efficiency."[3]

In the current review, the term "effectiveness" of air distribution will be used to describe the ratio of the occupied zone area (where thermal comfort and contaminant concentration are within ranges required by standards and codes) to the total occupied zone area. This hygienic criterion allows one to judge how well the HVAC system fulfills its main task—creating thermal comfort conditions and controlling contaminants in the occupied zone.

Industrial halls are typically large enclosures—indoor spaces that typically comprise one or more zones of occupancy. A large height combined with heat sources often results in room airflow patterns controlled by buoyancy flows.

A characteristic of many industrial halls is that zones of occupancy take up only a small portion of the room volume and height. In addition, the flows are normally buoyancy dominated. This results in a vertical temperature stratification that can be utilized for room air conditioning design in order to achieve effective climatization along with low energy consumption.

A process is found effective when "it produces a desired effect"; e.g., ventilation in a room is effective when it produces sufficiently good air

quality in the breathing zone. However, that air quality may be achieved without the ventilation being efficient. A ventilation process is considered efficient only when it is "effective with little waste of effort,"[4] i.e., being cost-effective.

Being cost-effective is normally equivalent to achieving a ventilation design where the indoor climate meets required specifications (target values), applying a low rate of supply air, along with avoidance of heating or cooling. That way, climatization would be effective as well as efficient.

A review of ventilation efficiency indices is given below. Complete mixing ventilation is the comparative basis for all efficiencies, with the value 1.0. That may be useful, as complete mixing ventilation often is assumed in early design phases.

Which ventilation efficiency index should be chosen for assessment depends on the actual scenario in the enclosure.

The contaminant removal effectiveness can be used when emission data for contaminant sources are available.

Air exchange efficiency indices can be used for cases where no or little information on sources is available, whereas ventilation efficiency, which concerns workers, can be used where very detailed information is available on sources and activities.

8.5.2 Contaminant Removal Effectiveness

As mentioned above, the traditional definition of ventilation efficiency or, in approved terms, "contaminant removal effectiveness," is the ratio between contaminant concentration in the exhaust air and the concentration at a point in the occupied space, i.e.,

$$\epsilon_p^c = C_e / C_p, \tag{8.18}$$

where

ϵ_p^c is contaminant removal effectiveness in the zone of occupancy
C_e is contaminant concentration in the exhaust air
C_p is contaminant concentration at a point in the zone of occupancy

In other words, this contaminant removal effectiveness is a measure of how much cleaner the air is in the occupied spaces than in the exhaust. See Fig. 8.8.

When detailed information on heat and contaminant sources is available, assessment of design is improved by evaluating the effectiveness of contaminant removal achieved by space ventilation. The set of contaminant removal effectiveness indices in Table 8.5 is given in accordance with contemporary use of indices.

The basis of comparison is still the complete mixing scenario, where the concentration of the contaminant in question is homogeneous throughout the room, and equal to the value in the exhaust C_e. All concentrations are net values, i.e., rated above values at the supply opening. It can be shown that

$$\epsilon^c = C_e / \langle C \rangle = \tau_n^a / \bar{\tau}_e^c \tag{8.19}$$

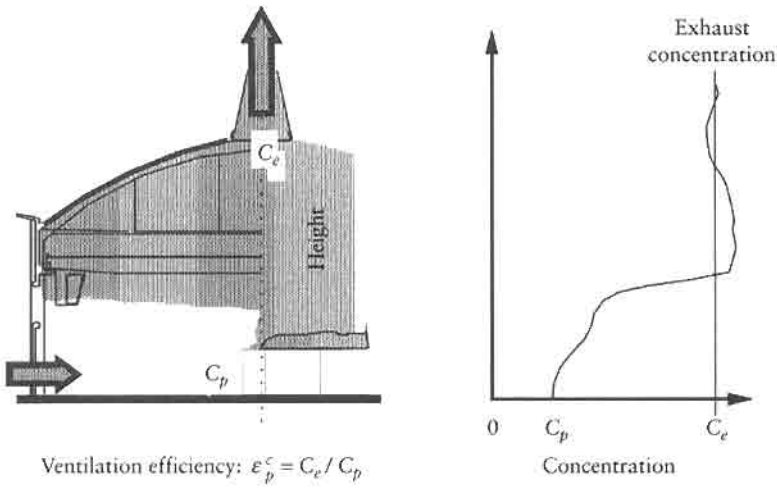

FIGURE 8.8 The original definition of "ventilation efficiency."

for steady-state conditions.[5] $\tau_n^a = V_r/Q$ is the nominal time constant of the ventilation airflow, where V_r is the volume of the room, Q is the airflow rate, and $\bar{\tau}_e^c$ is the mean age of the contaminant in the exhaust.

Application of contaminant removal effectiveness indices is relatively simple for scenarios with one or a few dominant contaminants being released. That is often the case in industrial malls. Where there are many polluting substances to consider, the contaminant removal efficiency should ideally be evaluated for each one. Consequently, applications for regular indoor climate—for example, in a restaurant—are limited, except when addressing specific pollutants like smoking and cooking fumes.

8.5.3 Contaminant Removal Efficiency

The contaminant removal efficiency can be derived from the contaminant removal effectiveness as follows:

$$\eta^c = \left(\frac{\epsilon^c}{1 + \epsilon^c} \right), \tag{8.20}$$

where η^c is contaminant removal efficiency and ϵ^c is contaminant removal effectiveness.

TABLE 8.5 Contaminant Removal Effectiveness Indices

$\epsilon_p^c = C_e/C_p$	Point in room
$\epsilon_b^c = C_e/\langle C \rangle_b$	Breathing zone
$\epsilon_o^c = C_e/\langle C \rangle_o$	Zone of occupancy
$\epsilon^c = C_e/\langle C \rangle$	Complete room

8.5.4 Air Exchange Efficiency

Application of the "age of air" concept can be justified by the fact that the content of contaminants found in the exhaust air normally rises from the value found in supply air entering the room. On its voyage through the room, the air is likely to pick up more contaminants the longer it stays in the room. This is a very simple assumption. It can be argued, however, that using the age of air concept is the best way to evaluate ventilation design for scenarios where little or no information is available on use of the room and locations and emission rates for heat and contaminant sources.

In order to have effective exchange of air in important locations in a room, the age of the air in those locations should be low. The basis for comparison is the complete mixing scenario. That scenario gives the same age for any air volume selected in the room, identical to the nominal time constant for the ventilation airflow, τ_n^a. A steady-state scenario is assumed. See Sutcliffe for an overview of definitions related to age of air.[6] The various air exchange efficiency indices are presented in Table 8.6.

The average age of air for all air molecules in the complete room can be found by performing a step-up tracer gas experiment, and by measuring tracer gas concentration C_e in the exhaust opening. The same procedure can be used for CFD simulations. The definition for average age of air in the room is

$$\langle \bar{\tau} \rangle = \frac{1}{\tau_n^a} \int_0^\infty \left(1 - \frac{C_e(t)}{C_e(\infty)} \right) t \, dt , \tag{8.21}$$

where

$$\tau_n^a = \int_0^\infty \left(1 - \frac{C_e(t)}{C_e(\infty)} \right) dt . \tag{8.22}$$

For ideal displacement ventilation, ϵ_a. Values for the other indices depend on the location of the zone in question.

8.5.5 Air Distribution Performance Index

Among the commonly used criteria is the air distribution performance index (ADPI),[7] defined as the percentage of locations where a combination of air temperature and air velocity meets comfort requirements. This criterion is based on experimental results of air diffuser performance for specifically tested room configurations. Data on the ADPI are available only for sedentary activity.

TABLE 8.6 Air Exchange Efficiency Indices

$\epsilon_p^a = \tau_n^a / \bar{\tau}_p$	Point in room
$\epsilon^a = \tau_n^a / (2\langle \bar{\tau} \rangle)$	Complete room

References

1. M. W. Liddament. *A Review of Building Air Flow Simulation*, Technical Note AIVC 33, Warwick, UK: Air Infiltration and Ventilation Center, March 1991.
2. V. V. Baturin. *Fundamentals of Industrial Ventilation*, 3rd English ed., New York: Pergamon Press, 1972.
3. M. Sandberg, and E. Skåret, E. *Air Change and Ventilation Efficiency—New Aids for Designers*, Swedish Institute for Building Research, 1985.
4. 6.7.ASHRAE, *ASHRAE Handbook: Fundamentals*, Atlanta, GA: ASHRAE, 1997.

8.6 ROOM AIR CONDITIONING STRATEGIES

8.6.1 Introduction

Traditionally the room air conditioning classification has been based on room air distribution methods. The most used division has been the division into mixing and displacement. ASHRAE classifies air distribution (diffusion) methods into mixing systems, displacement ventilation, unidirectional airflow ventilation, and localized ventilation methods.[1] Tapola et al. made a division between mixing and displacement and additionally divided displacement into submethods: thermal displacement, piston displacement, and mixing displacement.[2] Etheridge and Sandberg suggested that air distribution methods be classified as jet controlled or thermally controlled, which raises the important question of how well the room airflow patterns are controlled by the air distribution method.[3]

The direct application of air distribution methods to describe the strategies has led to the wild usage of different terms with unclear definitions. Additionally, in some cases the same term has been used to describe both the air distribution method and air supply devices or in some cases even the whole air conditioning system. Using a wrong term can also lead to a complete misunderstanding of the physical phenomenon in the room. For example, the term "displacement" is currently used for the room air distribution method in which room airflows are primarily driven by the buoyancy of the thermal sources inside the room and not by the supply air that is introduced to replace (substitute) the air removed by the sources in order to prevent the return flow back to the occupied zone. In this case, the term "replace" (substitute) gives a correct picture of the phenomenon, whereas "displace" may mislead the user to believe that the flow field is created primarily by the air distribution method. The results of this inconsistency can also be seen in the presentations of experts in scientific conferences, but much more confusion is caused in the everyday construction business, where the customer often doesn't have any expertise in our technological field.

German guidelines base the division on the resulting airflow pattern within the room rather than distribution methods.[4] They suggest that airflow patterns be divided into four categories: hall-filling mixed flow; zonewise mixed flow; low-momentum, low-turbulence flow for the air supply in the work region; and zonewise displacement ventilation.

This chapter describes a strategy approach for room air conditioning based on the classification and terminology presented by Hagström et al.[5] The basis

of the classification is different aims or ideas of the temperature, gas, particle or humidity distributions, and airflow patterns that can be created within the room. The distributions are often described by using contaminant removal and temperature effectiveness coefficients, which are defined in Section 8.5.

The aim of this classification is not to value one strategy over another. They all have their advantages and disadvantages and it is up to the designer to select the most desirable strategy for each case. In practice a certain type of room air conditioning strategy can be applied by using different kinds of air distribution installations and air supply devices. How well the real situation will fulfill the aim of the ideal strategy depends not only on the physical installation itself, but also on the operating parameters as well as the characteristics of other internal sources that influence the supply airflow patterns and the room airflows, such as heat and contaminant sources, cold drafts, and room heating and cooling methods. It is therefore important to separate ideal strategies from practical room air conditioning solutions.

A clear classification of the ideal strategies will help the evaluation of the present room air distribution methods in different operating conditions. It also creates a solid base for the development and promotion of new innovations in the field.

8.6.2 Classification for Room Air Conditioning Strategies

As the focus of the proposed classification differs from the present practice, it is necessary to explain the terminology used. The aim of room air conditioning is to maintain desired conditions, target levels, in the room during different operating conditions in the most economical way (energy, cost efficiency). Depending on the design criteria, the designer may choose different strategies in order to achieve specified targets. The room air conditioning design and evaluation process is illustrated in Fig. 8.9.

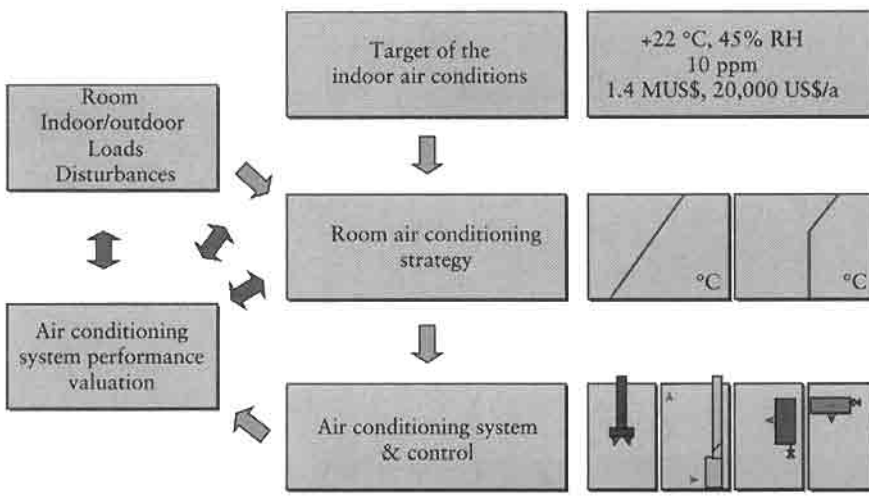

FIGURE 8.9 The room air conditioning design and evaluation process.

TABLE 8.7 Examples of Room Air Distributions, Exhausts, and Heating and Cooling Methods

Air distribution methods	Exhaust methods	Heating methods	Cooling methods
Vertical supply	Local	Convective Air heating Fan coils	Supply air cooling
Concentrated air jets	General	Radiative Infrared	Convective Active, e.g., fan coils Passive, e.g., ceiling baffles
Low-impulse air supply Inclined jets	Mixed	Mixed Local/general	Radiative

The room air conditioning strategy is a fundamental scheme that describes the targeted temperature, humidity, and contaminant distributions as well as airflow patterns within the air-conditioned room. The room air conditioning system consists of different methods and their controls that together create the system performance. The system performance is evaluated by comparing the reached conditions to the chosen strategy. Both the methods (room air distribution, exhaust, room heating and cooling, etc.) and processes and disturbances inside the room influence the resulting conditions. Different room air distributions, exhausts, and heating and cooling methods are listed in Table 8.7. As an example of the terminology we can use a system consisting of low-impulse air devices supplying directly into the occupied zone (often called displacement ventilation) and cooled ceiling methods. At the *Roomvent '98* conference three separate papers were presented, which proved that the system behaves almost as a complete mixing strategy instead of replacement.[6–8]

The following presentation discusses the room air distribution method as a principal parameter to apply to a certain room air conditioning strategy and heating and cooling as assisting methods. However, it must be noted that in some cases a strategy can be fulfilled without any mechanical air distribution installations using buoyancy forces. The classification of ideal room air conditioning strategies is summarized in Table 8.8 and explained more in detail in the text. Though the main emphasis of this presentation is on general room air conditioning, the same ideas behind different strategies can be used for local ventilation. Additionally, as ideal, the classification is not affected by whether the flow direction is horizontal or vertical (upward or downward).

8.6.3 Piston Strategy

8.6.3.1 Description

The highest effectiveness can be achieved with the piston strategy. The contaminant concentration, temperature or humidity, and the local effectiveness are functions of the location and the power of the sources in relation to the supply and exhaust openings. With a homogeneous distribution

TABLE 8.8 Ideal Room Air Conditioning Strategies

	Strategy			
	Piston	**Stratification**	**Zoning**	**Mixing**
Description	To create unidirectional airflow field over the room area by supply air	To support flow field created by density differences by replacing the airflow out from the room area with supply air	To control air conditions within selected zone in the room by the supply air and allow stratification of heat and contaminants in the other room areas	To provide uniform conditions throughout the ventilated space
Heat, humidity, and contaminant distribution*	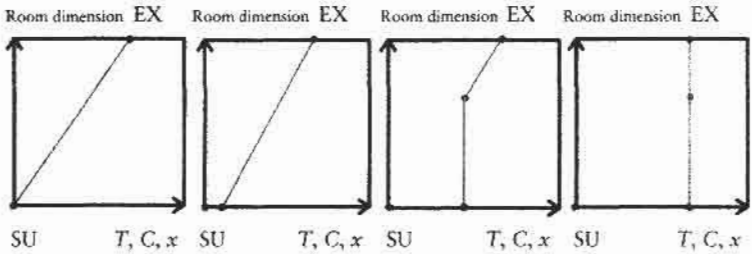			
Main characteristics	Room airflow patterns controlled by low-momentum unidirectional supply airflow, strong enough to overcome disturbances	Room airflow patterns controlled mainly by buoyancy; supply air distribution with low momentum	Room airflow patterns controlled partly by supply and partly by buoyancy	Room airflow patterns controlled typically by high-momentum supply airflow
Ideal efficiency	$\varepsilon_t = (t_{ex}-t_0)/(t_{oz}-t_0)$ $\varepsilon_c = (C_{exh}-C_0)/(C_{oz}-C_0)$ 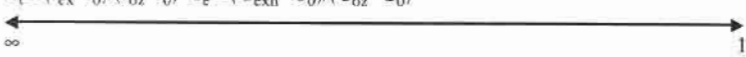			
Typical application (example of a general room air distribution method)	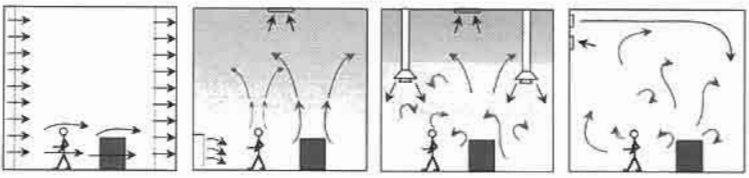			

*x-axis: °C, mg/m³, g/kg; y-axis: room dim. (e.g., height); SU = supply, EX = exhaust

of sources, the contaminant concentration and temperature change linearly between supply and exhaust openings located at opposite ends of the room. With local sources, the concentration upstream of the sources is very low.

8.6.3.2 Advantages and Disadvantages

Advantages include: the whole flow pattern can be controlled, areas upstream of sources can be kept clean, and high contaminant removal and tem-

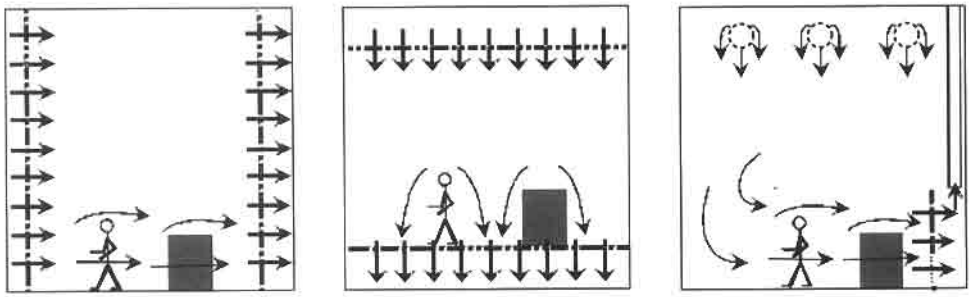

(*a*) Horizontal piston (*b*) Vertical piston (*c*) Partial piston

FIGURE 8.10 Examples of air distribution and exhaust methods for the piston strategy.

perature effectiveness. Disadvantages include the need for high supply airflow rates and large supply areas.

8.6.3.3 Design Criteria

The design criterion of the piston strategy is to overcome all the air currents opposite to the directional airflow created within the room.

8.6.3.4 Application

Piston air conditioning is an expensive strategy due to the high airflow rate that is needed to create a desired airflow pattern inside the room. Thus it is usually used only in applications where it is required, like in the semiconductor industry, where up to about 400 air changes per hour are used. Another example of its application is horizontal piston flow in reinforced plastic plants.[9] Schemes of different ways to apply the piston air conditioning strategy are shown in Fig. 8.10.

8.6.4 Stratification Strategy

8.6.4.1 Description

A similar temperature and contaminant distribution throughout the room is reached with stratification as with a piston. The driving forces of the two strategies are, however, completely different and the distribution of parameters is in practice different. Typical schemes for the vertical distribution of temperature and contaminants are presented in Fig. 8.11.[10] While in the piston strategy the uniform flow pattern is created by the supply air, in stratification it is caused only by the density differences inside the room, i.e., the room airflows are controlled by the buoyancy forces. As a result, the contaminant removal and temperature effectiveness are more modest than with the piston air conditioning strategy.

8.6.4.2 Advantages and Disadvantages

Advantages include: low concentration in the ventilated zone can be achieved and relatively high contaminant removal and temperature effectiveness. However, the stratification strategy is sensitive to disturbances and stagnant areas with high

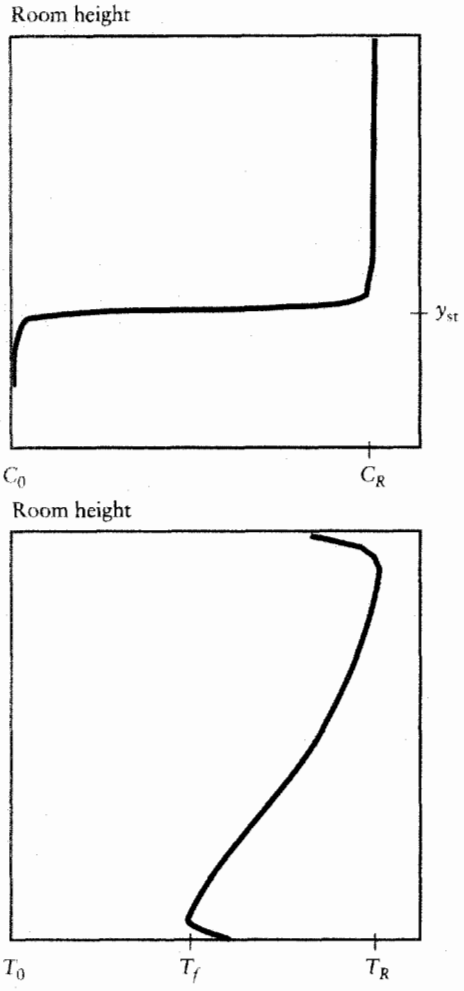

FIGURE 8.11 Vertical temperature and contaminant distribution within the stratification strategy, typical schemes.[3] T_0 is supply air temperature, T_f is the temperature at the floor level, T_R is room temperature, C_0 and C_R are contaminant concentrations in supply and room air above the stratification height, and y_{st} is the stratification height.

local concentrations are possible. It also only functions properly when conditions are favorable.

8.6.4.3 Design Criteria

In the stratification strategy the supply air is used to substitute the outgoing air from the ventilated (in most cases occupied) zone, thus preventing circulation patterns between the zones. The supply air has to be distributed in such a way that the buoyancy flows are not disturbed. Exhaust air openings are to be located "downstream" in order to avoid reverse currents within the room. The location of the contaminant sources and the heat sources causing density differences must be the same in order to carry out the contaminants with equal or higher density than air.

8.6.4.4 Application

Stratification is a desirable strategy to provide efficient room air conditioning with much less effort than using the piston strategy. Its main application in room air conditioning is the thermal replacement method. However, it can also be applied for contaminants without any thermal buoyancy sources that have different density from the room air. Examples of different air distribution methods to create thermal replacement are presented in Fig. 8.12.

However, because of its physical nature—ventilating air having very little authority over the room airflow—the stratification strategy is very dependent on the stability of the density differences and the airflow balances and thus very sensitive to disturbances within the room. Also, the selection of the room cooling and heating method can either aid or prevent the creation of the stratification strategy as described earlier in the chapter.

8.6.5 Zoning Strategy

8.6.5.1 Description

The idea of the zoning air conditioning strategy is to have control over the certain area or volume of the room, while the rest of the room is left with less

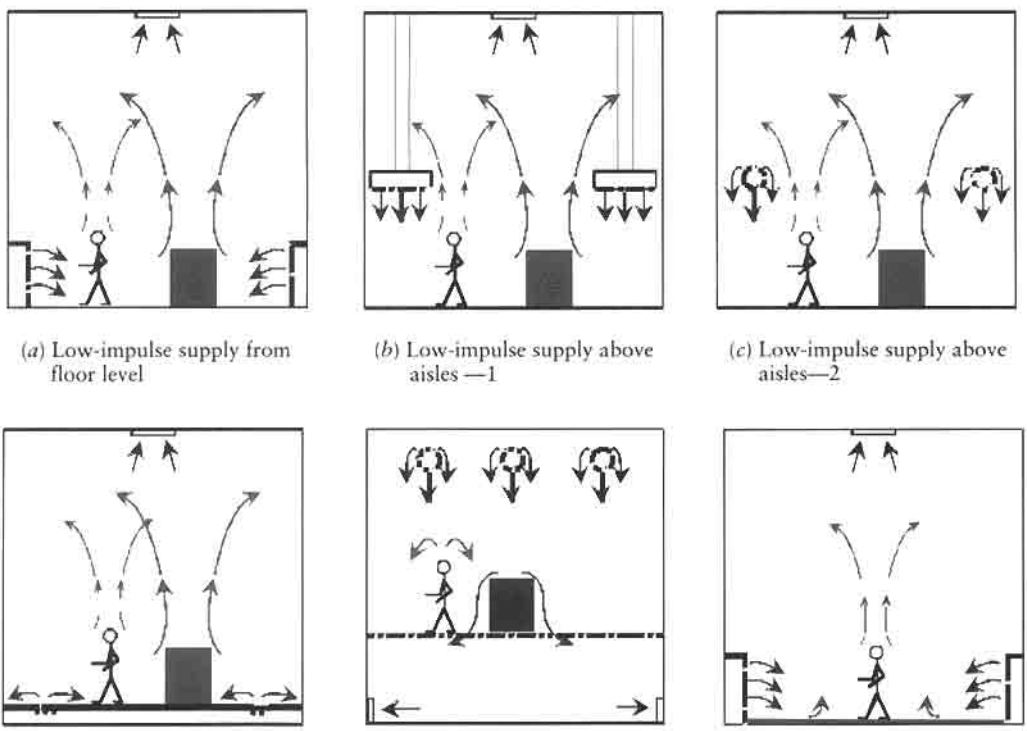

(*a*) Low-impulse supply from floor level

(*b*) Low-impulse supply above aisles —1

(*c*) Low-impulse supply above aisles—2

(*d*) Spare floor supply

(*e*) Negative buoyancy

(*f*) Floor heating

FIGURE 8.12 Examples of air distribution and exhaust methods for the stratification strategy.

attention. In most cases the accumulation of heat, concentration, or humidity outside the controlled zone is desired and utilized. The room airflows are controlled both by the supply air jets and the buoyancy sources. The ventilation effectiveness (temperature, contaminant removal, humidity) using the zoning air conditioning strategy is expected to settle between the values of mixing and stratification strategies. However, the effectiveness is strongly dependent on the methods used and the operating conditions. Concentration and temperature are more homogeneously distributed in the controlled zone than with the stratification strategy.

Zoning can be either vertical or horizontal. Typically vertical zoning is applied in high rooms, when the supply air is distributed close to the occupied zone near floor level and the exhaust air openings are located close to the ceiling. Horizontal zoning can be applied, for example, using air or portable/partial (plastic, etc.) curtains in order to divide room space into different blocks. Within these blocks it is possible to further apply different strategies in the vertical direction semi-independently.[11]

8.6.5.2 Advantages and Disadvantages

The zoning method offers better contaminant removal and thermal effectiveness than with mixing, limited control of the flow patterns in the ventilated zone, and the ability to avoid stagnant areas with high local concentrations in the ventilated zone. However, partial mixing of contaminants in the ventilated zone decreases its effectiveness.

8.6.5.3 Design Criteria

Each method has its own design criteria, but common to most of the methods is that air supply is located close to or inside the controlled zone and the exhaust openings are located inside the uncontrolled zone. The location and power of the buoyancy sources in relation to the supply air jets have a remarkable influence on the accumulations of heat, contaminants, and humidity within the room.

8.6.5.4 Application

A large variety of methods can be used for zoning, such as inclined jets, horizontal cooled jets, vertical jets, floor jets, nozzle ducts, and vortex. Examples of different methods are illustrated in Fig. 8.13.

8.6.6 Mixing Strategy

8.6.6.1 Description

The aim of the mixing air conditioning strategy is to provide uniform conditions throughout the air-conditioned room.

The contaminant removal and temperature effectiveness in the mixing strategy are equal to 1. In practical installations incomplete mixing in the room and unfavorable temperature gradient and location of the exhaust openings in relation to air supply may, however, cause short-circuiting of the supply air into the exhaust openings and the efficiency may remain below 1.

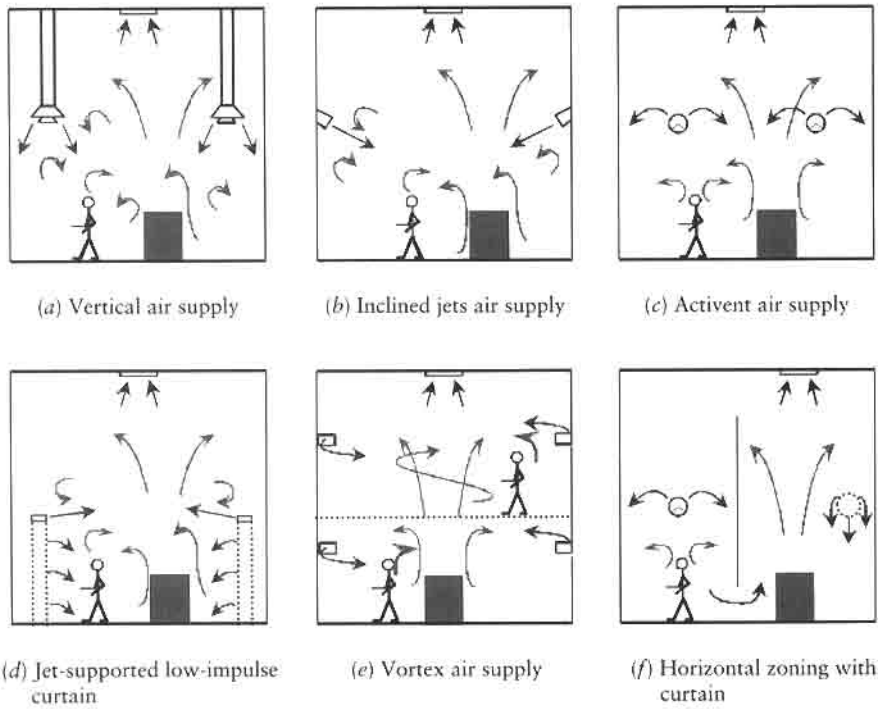

(*a*) Vertical air supply (*b*) Inclined jets air supply (*c*) Activent air supply

(*d*) Jet-supported low-impulse curtain (*e*) Vortex air supply (*f*) Horizontal zoning with curtain

FIGURE 8.13 Examples of air distribution and exhaust methods for the zoning strategy.

8.6.6.2 Advantages and Disadvantages

Using the mixing strategy, stagnant areas with high local concentrations and unfavorable thermal gradients can be avoided during the heating period. At the same time, it has low contaminant removal and temperature effectiveness and its high air velocity may cause drafts.

8.6.6.3 Design Criteria

Air jets are used to create enough air movement inside the room to circulate and mix the whole room air. This strategy is often called dilution ventilation as the contaminants created inside the room are mixed into the whole room volume thus reducing the local peak concentrations.

8.6.6.4 Application

The room airflows are controlled mainly by the supply or/and circulation air jets using, for example, concentrated jets, ceiling air supply, or high-impulse nozzle systems. Examples of different methods are illustrated in Fig. 8.14.

However, the use of other room air distribution methods together with certain exhaust, heating, and cooling methods will also lead (intentionally or unintentionally) to the application of the mixing air conditioning strategy. Some examples are shown in Fig. 8.15.

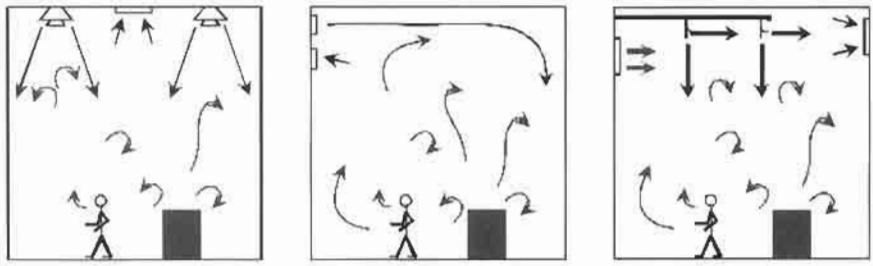

(*a*) Ceiling air supply (*b*) Concentrated air supply (*c*) Air supply with directing jets

FIGURE 8.14 Examples of air distribution and exhaust methods for the mixing strategy.

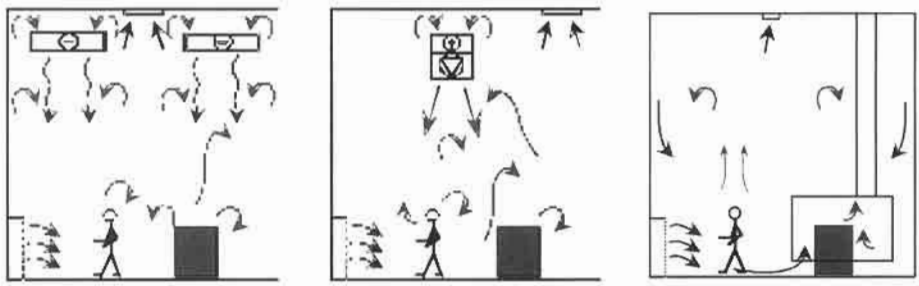

(*a*) Replacing air distribution: cooled ceiling (*b*) Replacing air distribution: recirculating fan heaters (*c*) Replacing air distribution: governing local exhaust

FIGURE 8.15 Examples of systems resulting in the mixing strategy despite the selected air distribution method.

8.6.7 Application of the Strategy in System Selection

The application of the strategies in system selection can be illustrated by using a simple example. Let us think about an industrial hall with some internal heat sources but without any remarkable internal movement that would disturb the stratification.

During summer, Fig. 8.16*a*, there is a need for cooling in the occupied zone (area up to 2 m from the floor level); thus it is desirable to apply the stratification strategy with vertical temperature and contaminant stratification in the hall in order to save cooling energy costs. This can be done, for example, by using a low-impulse air supply with the devices at the floor level.

During winter additional heating is needed in the occupied zone due to the heat losses. The selection of the heating method depends on the selected air conditioning strategy for the heating season. In order to save heating energy costs the exhaust air temperature should not exceed the temperature in the occupied zone. Thus, the desired strategy would be the mixing strategy. An appropriate heating method for that purpose would be, for example, an air and recirculation method with fan heaters located close to the ceiling; see Fig. 8.16*b*.

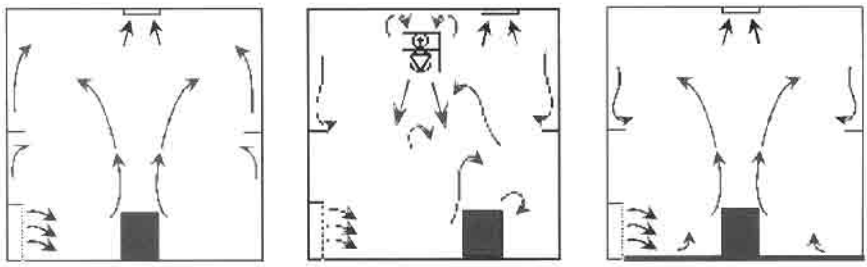

(*a*) Summer:
Stratification methods
* Low-impulse air supply

(*b*) Winter:
Mixing methods
* Low-impulse air supply
* Recirculating fan heaters

(*c*) Winter:
Stratification methods
* Low-impulse air supply
* Floor heating

FIGURE 8.16 Application of the strategy in system selection examples.

If the main reason for the stratification strategy is contaminant control in the occupied zone, the same strategy should be applied in winter conditions, too. Thus, the selected heating method has to fulfill two requirements: to support the creation of the vertical stratification and not to create disturbing airflows into the hall. In this case one option would be the floor heating method; see Fig. 8.16*c*. Additionally, one should consider the prevention of boundary layer flows along the outer walls using, for example, passive methods.[12]

To conclude the example: A different air conditioning strategy can and sometimes should be selected for different seasons or operating conditions. The strategy can be changed by using combinations of available methods.

8.6.8 Summary

The room air conditioning strategy should be used as a target for design and construction of the room air conditioning system. Often it would be desirable to apply several strategies during different operating conditions (e.g., summer–winter). The selection of the system and the set of methods (room air distribution, exhaust, heating, cooling) should be made in such a way that the different strategies can be applied most efficiently.

The clarification of the room air conditioning strategies and their separation from the practical methods at present creates space for creativity and new innovations and their evaluation.

Naming a practical room air distribution method according to a certain strategy may lead to misunderstanding of its performance in varying operating conditions. Though naming probably can't be avoided in business, an understanding of the basic strategies helps customers evaluate offered practical air distribution methods and system solutions.

References

1. ASHRAE, Space air diffusion, *Fundamentals Handbook*, Chapter 31, Atlanta, GA: ASHRAE, 1979.
2. M. Tapola, J. Uimonen, S. Heinänen, and B. Hagner, *Design of Industrial Ventilation* (in Finnish), Ministry of Commerce and Industry in Finland, D:145, 1987.

3. D. Etheridge, and M. Sandberg, *Building Ventilation: Theory and Measurement*, Chichester: John Wiley & Sons,1996.
4. VDI 2262, *Guideline: Workplace Air Reduction of Exposure to Air Pollutants*, Ventilation Technical Measures, Germany: 1994.
5. K. Hagström, E. Sandberg, H. Koskela, and T. Hautalampi, Classification for the room air conditioning strategies. *Building and Environment*, 2000, 35, 699–707.
6. F. Alamdari, Displacement ventilation and cooled ceilings, in *Proceedings of Spacevent '98*, Stockholm: 1998.
7. H. Brohus, Influence of the cooled ceiling on indoor air quality in a displacement ventilated space examined by means of computational fluid dynamics, in *Proceedings of Spacevent '98*, Stockholm: 1998.
8. H. Tan, T. Murata, K. Aoki, and T. Kurabuchi, Cooled ceilings/displacement ventilation hybrid air conditioning system—Design criteria, in *Proceedings of Spacevent '98*, Stockholm: 1998.
9. A. Säämänen, I.M. Andersson, R. Niemelä, and G. Rosen, Assessment of horizontal displacement flow with tracer gas pulse technique in reinforced plastic plants, *Building and Environment*, 1995, 30, 135–141.
10. P. V. Nielsen, Vertical temperature distribution in a space with displacement ventilation, In *IEA Annex26: Energy Efficient Ventilation of Large Enclosures*, Rome: 1995.
11. H. Skistad, Utilizing selective withdrawal in the ventilation of large spaces: "Select-Vent," in *Proceedings of Spacevent '98*, Stockholm: 1998.
12. C. Topp, and P. Heiselberg, Obstacles—an energy-efficient method to reduce downdraught from glazed surfaces, in *Proceedings of the Fifth International Conference on Air Distribution in Spaces, Spacevent '96:* Yokohama, Japan: 1996.

8.7 AIR DISTRIBUTION METHODS AND DIMENSIONING

8.7.1 Selection of Air Supply Method

The choice of room airflow pattern and air supply method is subject to study in each separate case. Table 8.9 presents, however, some guidelines for air distribution methods most commonly applied for various cases.

8.7.2 Mixing Air Distribution

In this chapter we deal with air distribution in a room, where

L = room length
B = room width
H_r = room height

See Fig. 8.17.

8.7.2.1 Penetration of Horizontal Air Jets

Room Length

If the room is to be ventilated by one single air jet, and the jet shall penetrate across the entire room length, the room length should not exceed[1]

$$L \leq 0.62 K_1 \sqrt{BH_r}, \tag{8.22}$$

where

A_0 is the effective discharge area of the jet (m^2)
B = room width (m)

TABLE 8.9 Guidelines for Selection of Air Distribution Method

Pollutant load	Room height	Heat load	Human activity level	Common air supply methods	Type of process
Insignificant		Small	Light	Mixing, horizontal air jets below ceiling	Mechanical assembly
Moderate, dust and fumes	>5 m		Moderate	Displacement, low-velocity air supply at floor level	Welding shop
Moderate, solvent vapors	<5 m		Light	Low-velocity supply from above, local exhausts	Paint shop
High, solvent vapors			Light	Piston flow, vertical from above	Paint booth
Heavy	>10 m	High	Heavy	Displacement, low-velocity air supply at floor level	Foundry, melting works

H_r = room height (m)
K_1 = the decay coefficient of the jet
L = room length (m)
u_{max} = maximum velocity in jet cross-section (m/s)
u_0 = discharge velocity of the jet

The constant K_1 is the decay coefficient used in the formula

$$\frac{u_{max}}{u_0} = K_1 \frac{\sqrt{A_0}}{x}. \tag{8.23}$$

K_1 depends on the type of jet, and varies between 2 and 7. Some K_1 values are given in Table 8.10. See also Section 7.4, *Air Jets*. If the room is longer, one has to take long-room considerations into account. See Section 8.7.2.2.

Room Width

The width of the room, B, should be less than or equal to $3H$ in order to be properly ventilated by one jet. Wider rooms require several jets beside each other, as indicated in Fig. 8.18.

8.7.2.2 Reverse Flow

Short Rooms

When a jet is confined in a short room, the jet will be deflected by the opposite wall, and the flow pattern will be as indicated in Fig. 8.19. Outside the

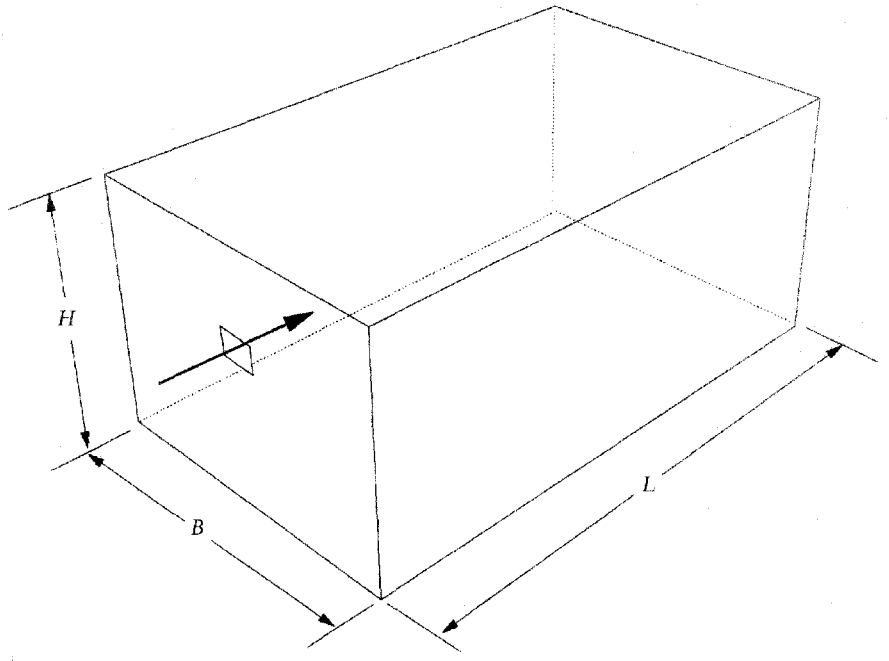

FIGURE 8.17 Room dimensions definition.

jet will be a recirculation zone which consists of the air that is entrained into the jet and the air that is exhausted through the outlet. The amount of entrained air is far greater than the exhaust air. The maximum airflow rate in the reverse flow in Fig. 8.19 equals the airflow rate in the jet.

The velocity distribution in the reverse flow is assumed to be uniform in the case of isothermal conditions. In most practical cases, however, there is a

TABLE 8.10 Decay Coefficients K_1^2

Type of discharge opening	u_0 = 2–5 m/s	u_0 = 8–40 m/s
Single, circular or square	5.7	7.0
Rectangular opening		
$b/h = 25$	5.3	6.5
$b/h = 40$	4.9	6
Grid, opening > 40%	4.7	5.7
Perforated panel, opening 3–5%	3.0	3.7
Perforated panel, opening 10–20%	4.0	4.9
Louvres with diverging vanes		
div. angle 40°	2.9	3.5
div. angle 60°	2.1	2.5
div. angle 90°	1.7	2.0

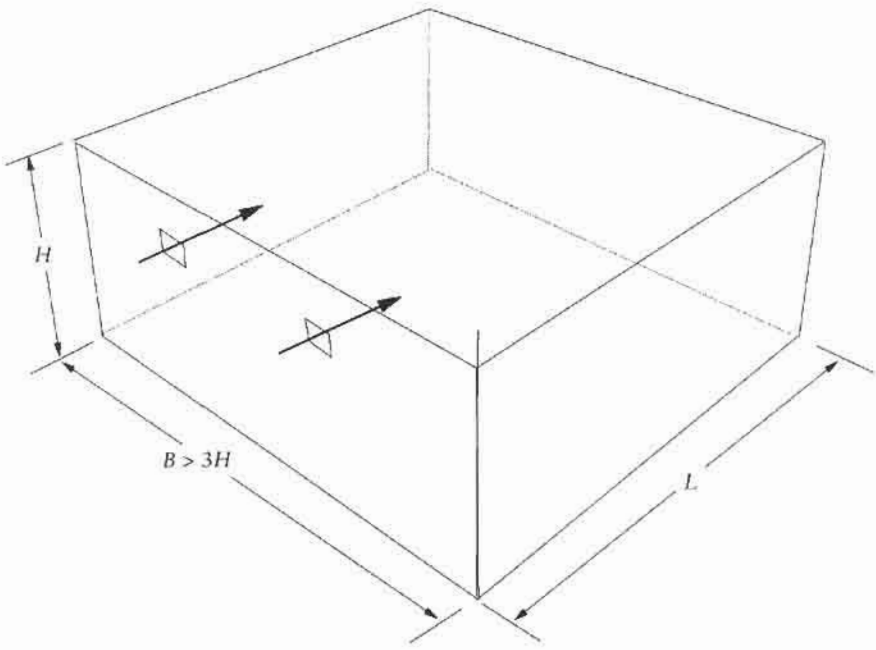

FIGURE 8.18 Wide room.

heat surplus in the room, and the supply air is colder than the room air. In this case the velocity will be higher at floor level, as indicated in Fig. 8.19.

Long Rooms

If the room is longer than the length stated in Eq. (8.22), the air jet reaches a point where it decelerates more than in free air, and the reverse flow becomes more dominant. See Fig. 8.20. We define a critical length, $x_{crit.}$ as the

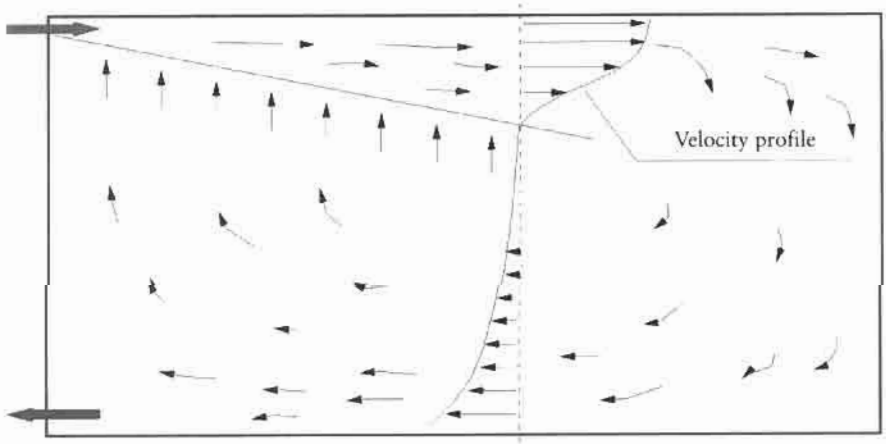

FIGURE 8.19 Reverse flow in a short room.

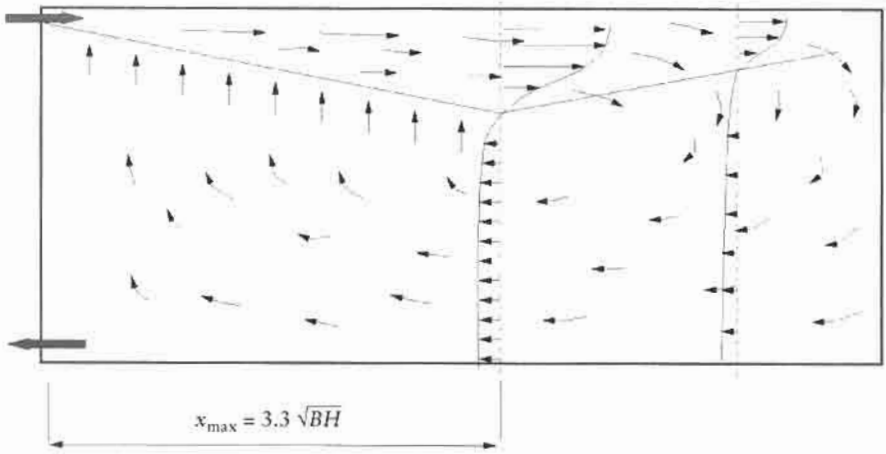

FIGURE 8.20 Maximum penetrating distance for an air jet.

length where the jet starts getting narrower instead of continuing to widen. This critical length is less than the maximum room length defined in Eq. (8.22). Stensaas gives the following estimate for the critical length:[2]

$$x_{max} \approx 3.3\sqrt{BH}. \tag{8.24}$$

Equation (8.24) is about 75–90% of the maximum room length for a compound free jet (decay coefficient of 7.0–5.3 in a decay coefficient equation (8.23).

If the room is longer there will be rotating cells as indicated in Fig. 8.21 in isothermal conditions.

If the room has a certain amount of heat surplus, this will lead to thermal stratification. The thermal stratification will attenuate the rotation, and eventually lead to a flow pattern as shown in Fig. 8.22.

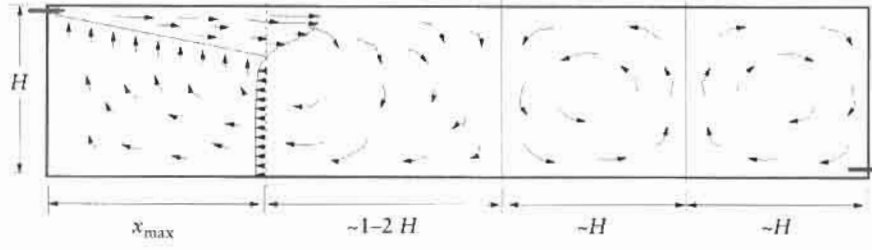

FIGURE 8.21 Multiple rotating cells in a long room: Isothermal conditions.

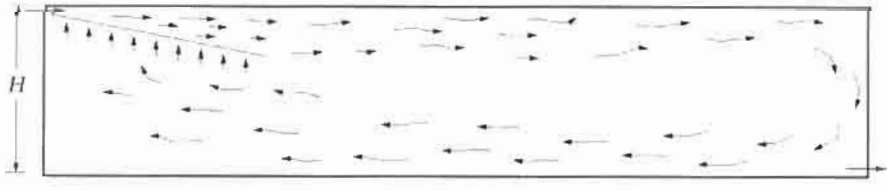

FIGURE 8.22 Long room with thermal stratification.

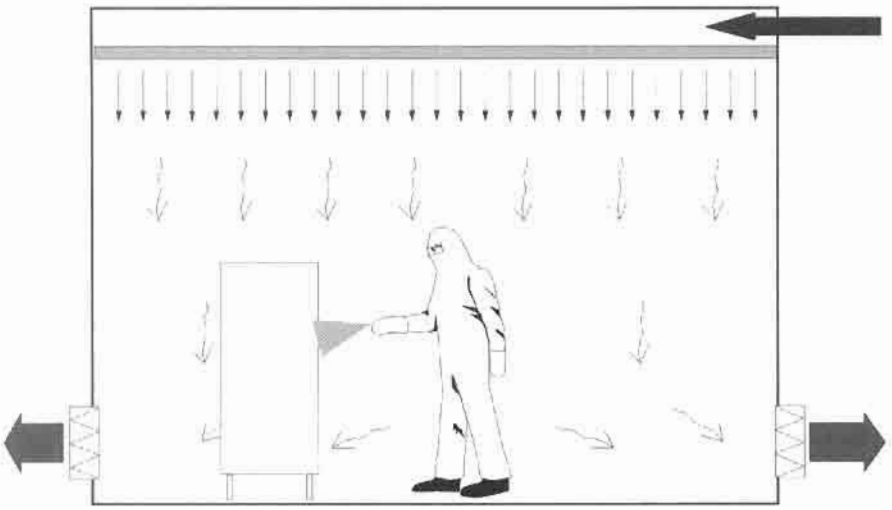

FIGURE 8.23 Piston airflow from a filter mat ceiling in a spray painting booth.

8.7.3 Piston Flow

Piston flow is utilized in several cases where heavily contaminated air needs to be removed, for instance in a spray painting booth (Fig. 8.23).

When there is a very high demand on the cleanness of the air, like in the pharmaceutical industry, piston flow from the ceiling is utilized (Fig. 8.24).

8.7.3.1 Filter Mat Ceilings

In practice, piston flow is not very easy to establish. A common way, utilized in cleanrooms and paint booths, is to have a filter mat placed all across

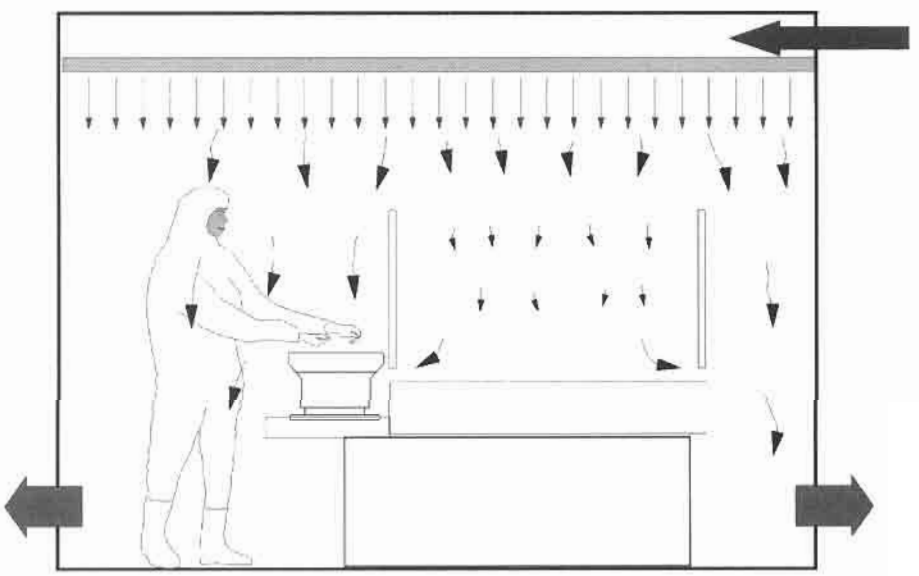

FIGURE 8.24 Piston flow in the pharmaceutical industry.

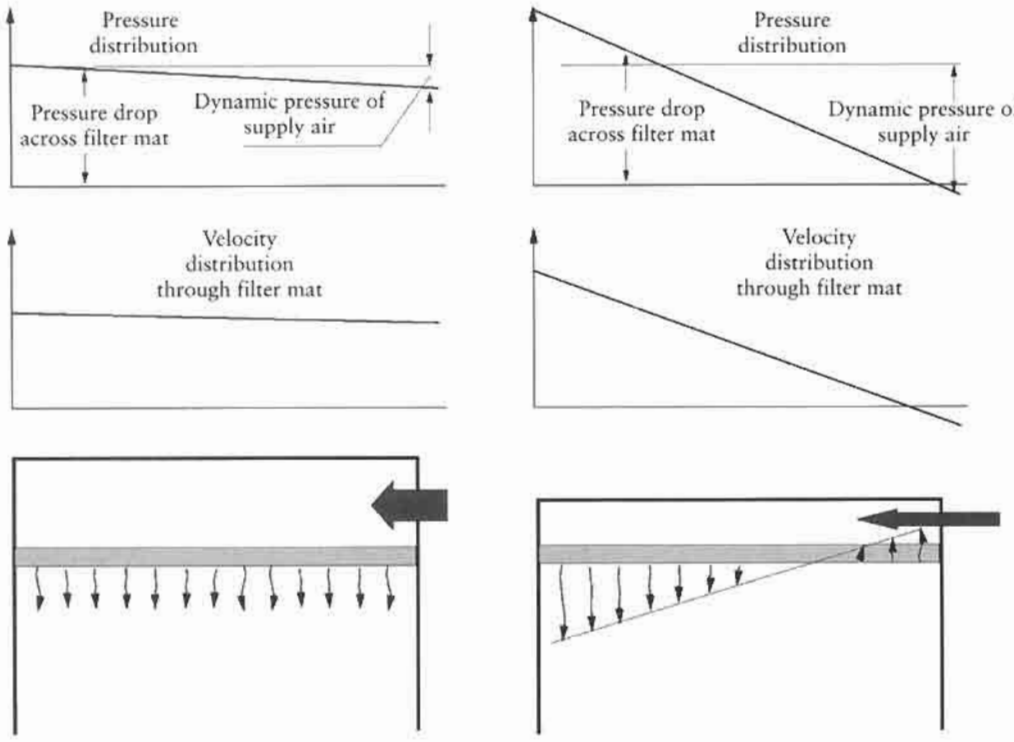

FIGURE 8.25 Velocity distribution along a filter mat.

the ceiling. This gives a good result as long as there is an even pressure distribution above the filter mat. If the supply air jet velocity is high and the pressure difference across the filter mat is low, we may get an uneven velocity distribution along the filter mat, as shown in Fig. 8.25.

When designing air supply through a filter ceiling, one should ensure that the dynamic pressure in the supply air does not affect the static pressure distribution above the filter ceiling too much.

8.7.3.2 Perforated Sheet Ceilings

In rough environments a filter mat may not be desirable, due to wear or dust in the supply air. In those cases, perforated sheets are used as a means of creating a piston flow.

Perforated sheets are, however, much more vulnerable to uneven pressure distributions and tilted inflow of air, as illustrated in Fig. 8.26. The supply air entering horizontally above the perforated sheet partly maintains its horizontal velocity component when being discharged through the holes in the perforated sheet. Thus, it leaves the perforated sheet at an angle less than 90°. The suction between the small outflowing jets also makes the airflow stick to the perforated sheet and flow along the sheet instead of perpendicular to it.

8.7.3.3 Thermal Instabilities in Piston Flows

When designing ventilation systems with piston flow, one should also be aware of the effects of thermal instabilities. Figure 8.27 shows a room with air

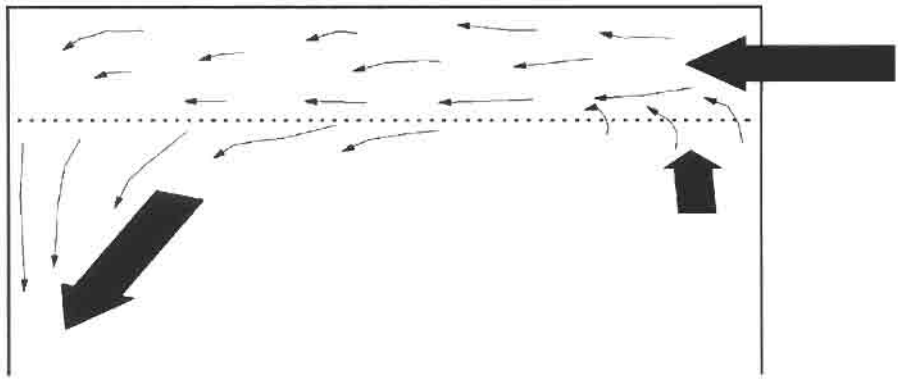

FIGURE 8.26 The outflow from perforated sheets is vulnerable to tilted inflow and to uneven pressure distribution.

supply through a filter ceiling that gives an evenly distributed airflow through the filter mat. However, the supply airflow, being colder than the room air, becomes unstable and turns away from the ascending convection current above the heat source.

Even if there is no concentrated heat source in the room, a flow where colder air is supplied above warmer air always becomes unstable, and tends to turn the flow so that the warmer air goes up and the colder air goes down.

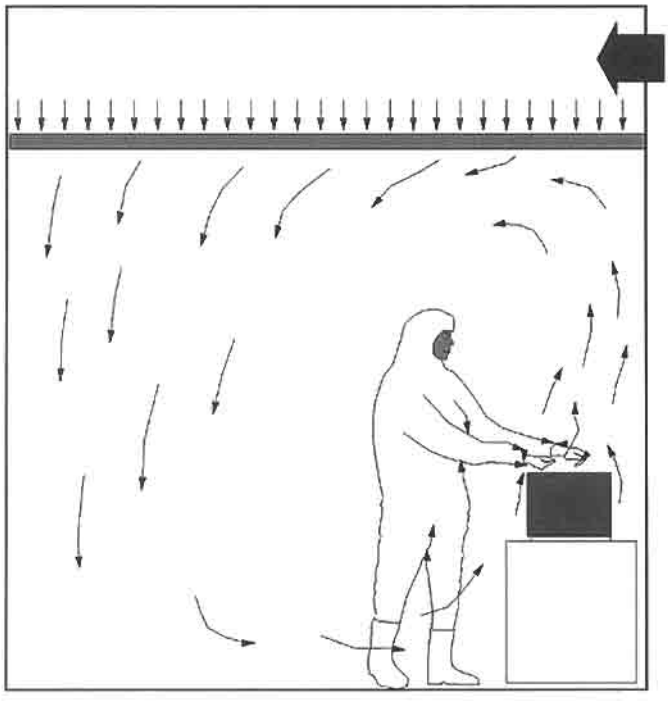

FIGURE 8.27 A cold piston flow from above is unstable, and will make the room air turn upside down.

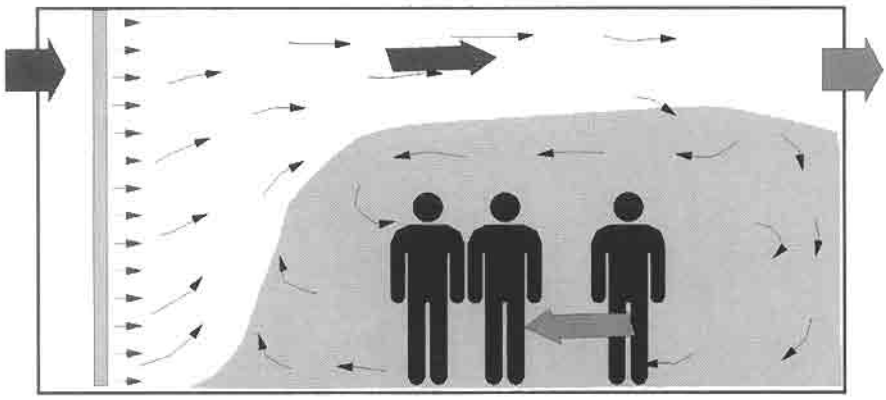

Warm air supply

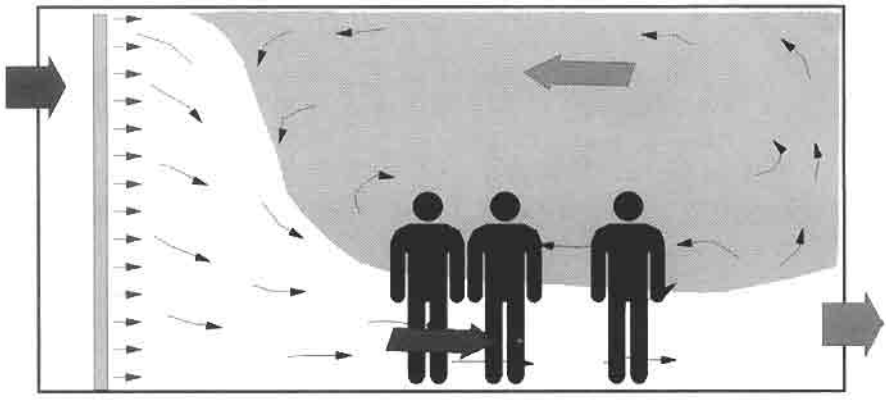

Cold air supply

FIGURE 8.28 Horizontal piston airflows are possible only in isothermal conditions.

If air is supplied horizontally through a wall, the supply air has to have exactly the same temperature as the room air. A temperature difference of 1 °C or more will create flow patterns like those shown in Fig. 8.28.

8.7.4 Displacement Flow

Displacement ventilation means that the supply air pushes the older air away without mixing with it. There are several ways of creating displacement flow. When there are no or negligible temperature differences in the room, displacement may be created as piston flow. In industrial ventilation, temperature differences are commonly present. These cases refer to displacement ventilation as a system where colder fresh air supplants warmer old air, or warmer air replaces the colder air using buoyancy as the main driving force of the process.

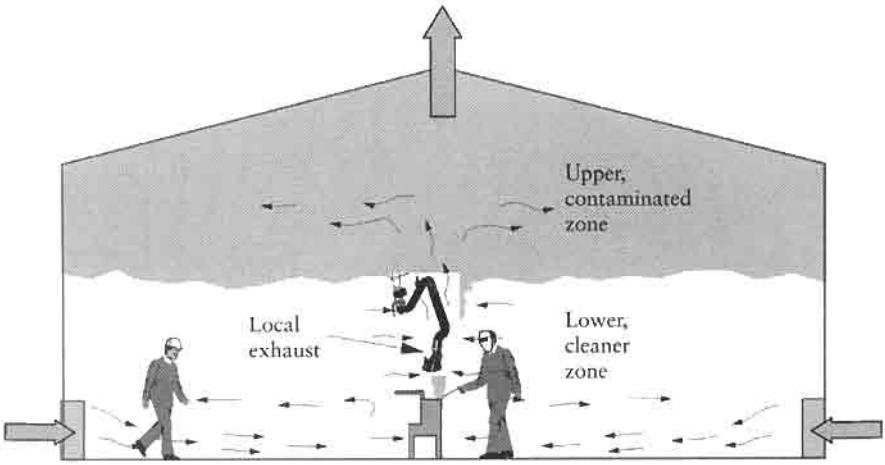

FIGURE 8.29 Displacement ventilation in a welding shop.

8.7.4.1 Warm Contaminants

A simple example of displacement ventilation is shown in Fig. 8.29.

Note that the supply air should be at least 1–2 °C colder than the air in the lower part of the room in order to make the supply air layer at floor level. Thus, the ventilation air cannot be used for heating the room.

The dimensioning of displacement ventilation is shown in the example in Section 7.5.4. That given above is an example of displacement ventilation with weak thermal stratification. Even though the stratification is weak, the contamination in the lower, cleaner zone is normally on the order of one-third of the contamination in the upper zone.

Figure 8.30 shows an example of displacement ventilation in a silicon carbide furnace room. The thermal stratification is very strong, as indicated in the graph on the right-hand side of the figure.

8.7.4.2 Cold Contaminants

An example of displacement ventilation with cold contaminants is shown in Fig. 8.31. The contaminants, i.e., the fumes from the sewer, are colder than the room air, and thus tend to stay low due to the negative buoyancy.

A good arrangement in this case is to locate the air supply below the ceiling. The supply air should not be colder than the room air, in order to layer below the ceiling. The fresh air will fill the room from above.

In this case, heating is possible by means of the supply air.

8.7.5 Zonal Air Distribution

8.7.5.1 Design Requirements for Achieving the Zoning Strategy

The aim of the zoning strategy is to have control of temperature, concentration, or humidity over a certain volume of the room, while the rest of the room is left with less attention. In most cases the accumulation of heat,

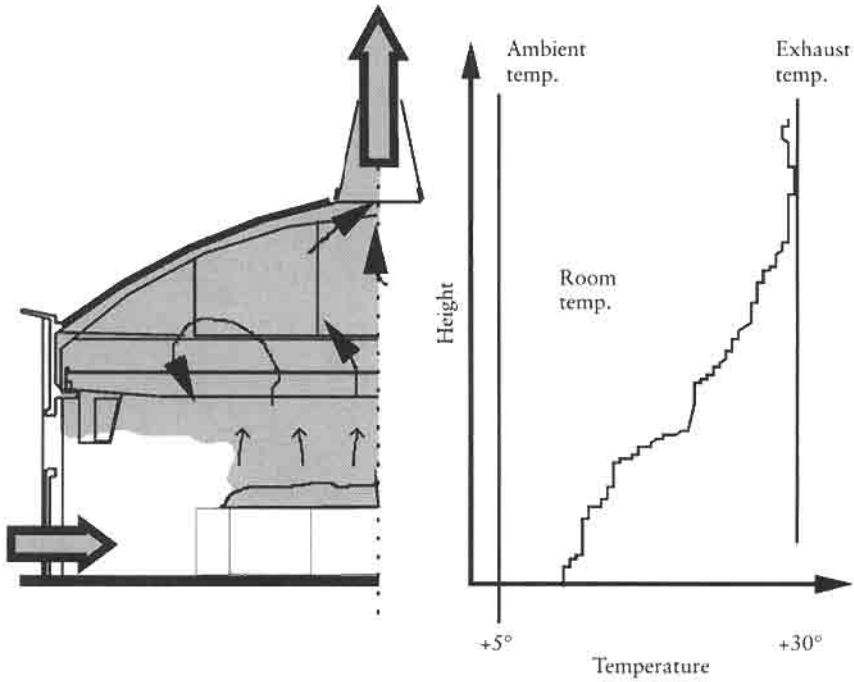

FIGURE 8.30 Displacement ventilation in a silicon carbide furnace room.

contaminants, or humidity outside the controlled zone is desired. The room airflows are controlled partly by the supply air jets, as in the mixing strategy, and partly by the buoyancy sources, as in the stratification strategy. Depending on the air distribution method and dimensioning of the supply air devices, unnecessary mixing is avoided in order to achieve the highest heat and contaminant removal effectiveness possible.

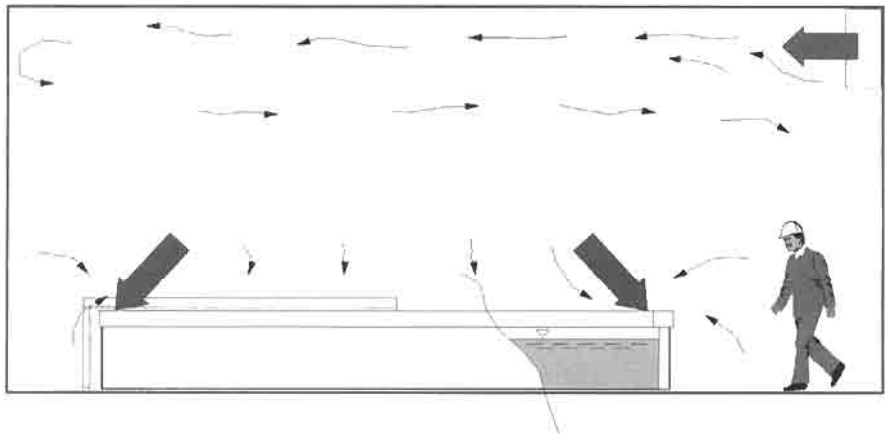

FIGURE 8.31 Sewer treatment plant. The fumes from the sewer are cold, and can be exhausted at the rim of the treatment basin.

The key flow elements in the zoning strategy are the supply air jets, plumes of the buoyancy sources, buoyant airflows along the surfaces, and turbulent mixing between the controlled and the uncontrolled zones, as in Fig. 8.32. These flow elements have significant influence on the effectiveness of the system.

There are four principal ideas in achieving uniform conditions in the controlled zone and a high heat and contaminant removal effectiveness:

1. Supply air is evenly distributed into the controlled zone. The momentum of the jets is high enough to ensure the uniform conditions but also low enough to avoid mixing in the whole room—i.e., the turbulent mixing between the zones is low. This means that usually the number of inlet devices is high.
2. The momentum flux of the plumes is high enough to penetrate the supply airflow patterns. The penetration depends on the location of the plumes in relation to the supply airflow patterns.
3. The plume airflow rate in relation to the extract airflow rate from the uncontrolled zone is low enough to avoid undesired return flow from the uncontrolled zone to the controlled zone.
4. Disturbance flows on the zone boundary should be avoided because of the undesired return flow from the uncontrolled zone to the controlled zone.

The accumulation of heat, contaminants, and humidity is usually vertical in the room, but horizontal zoning is also possible. The same principal ideas should be followed in those cases.

8.7.5.2 Two-Zone Model for Zoning Strategy

When the zoning strategy is applied, the two-zone model is a useful and simple tool for the determination of the thermal, contaminant, and humidity accumulations. Principles of two-zone modeling are presented in Section 8.4.

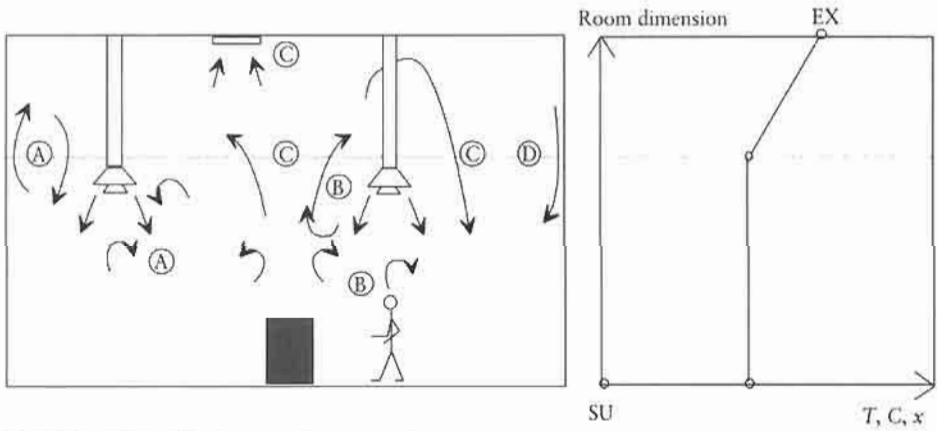

FIGURE 8.32 The key flow elements in the zoning strategy.

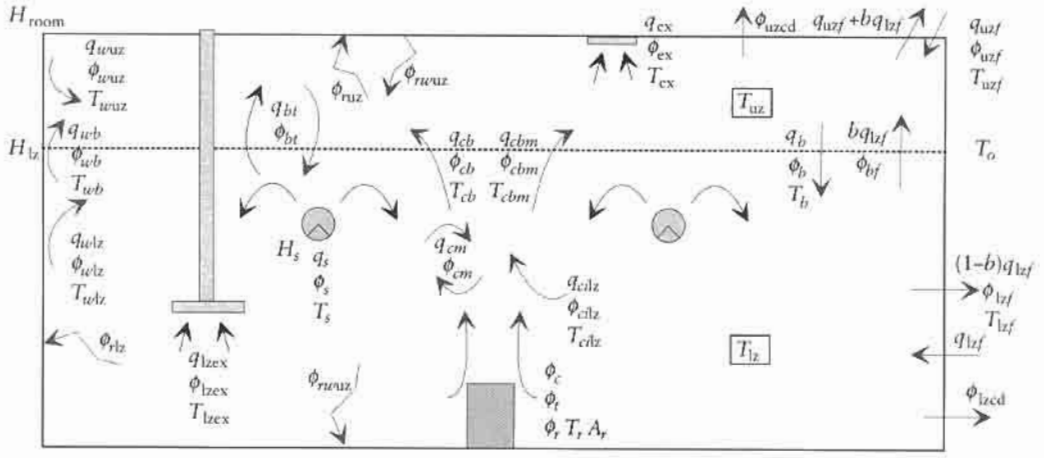

FIGURE 8.33 Two-zone temperature model of the zoning strategy.

Relatively uniform conditions in the controlled zone are characteristic for the zoning strategy. By assuming uniform conditions also in the uncontrolled zone, the following two-zone model can be developed. The controlled zone boundary should be defined high enough to get nearly all the induction air of the supply air devices from the controlled zone. This depends on the air distribution method used and the dimensioning of the devices.

Figures 8.33 and 8.34 describe a two-zone model application of the zoning strategy where all the main variable parameters are presented. Figure 8.33 (temperature model) describes the accumulation of heat and Fig. 8.34 (concentration model) the accumulation of contaminants. After solving for the temperatures, heat flows, and airflows, contaminant concentrations can be calculated. The models are here determined for stationary loads, airflow rates, and indoor/outdoor conditions, but they can be developed also for dynamic simulations.

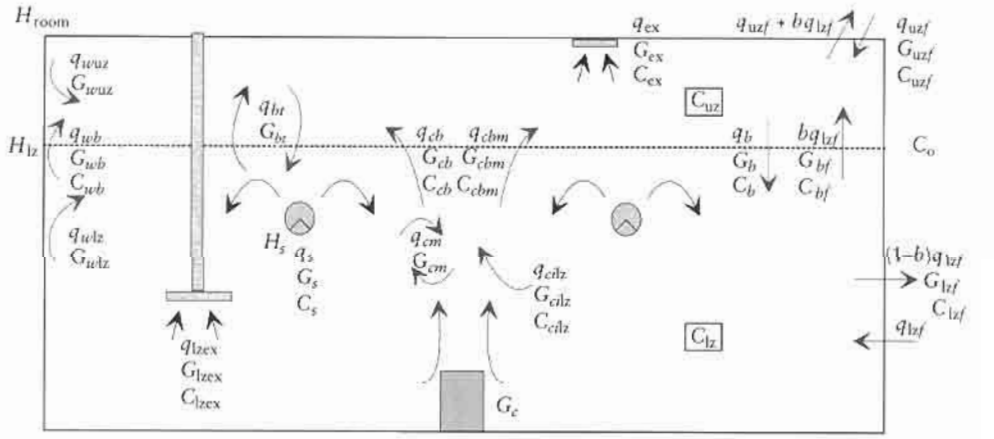

FIGURE 8.34 Two-zone concentration model of the zoning strategy.

The temperature model is based on the air mass flow rate and heat flow rate balances in the lower (controlled) zone (lz) and the upper (uncontrolled) zone (uz).

The plume airflows (q_c) are determined as described in Section 7.5. The turbulent mixing (q_{bt}) between zones and the penetration of the plume airflows (q_{cbm}) through the supply airflow patterns must be determined specially for the air distribution method and devices used as well as the locations of plumes and supply air devices.

The radiation heat transfer (ϕ_r) from the heat loads such as machines, lamps, persons, and sun has to be determined separately for the lower zone (ϕ_{rlz}) and upper zone (ϕ_{ruz}). The radiation between zone wall surfaces (ϕ_{rwuz}) has to be determined as well.

Local exhaust airflows from the hoods in the lower zone (q_{lzex}) reduce the heat removal effectiveness, because the return airflow rate (q_b) from the upper zone to the lower zone is increased.

The infiltration airflow into the lower zone (q_{flz}) is assumed to be higher than the exfiltration. The difference (bq_{flz}) describes the airflow rate into the upper zone caused by filtration.

The wall surface temperatures (T_{wuz}) and (T_{wlz}) are calculated separately for each wall and window surface by means of heat transfer through the wall: $T_{wuz} = T_{uz} - (U_{uz}/h_{uz})(T_{uz} - T_o)$ and $T_{wlz} = T_{lz} - (U_{lz}/h_{lz})(T_{lz} - T_o)$, where h is the heat transfer coefficient on the surface and U is the overall heat transfer coefficient. The airflows along the wall surfaces through the zone boundary (q_{wb}) are calculated separately for each wall and window surface.

The concentration model is based on the air mass flow rate and contaminant flow rate balances in the lower (controlled) zone (lz) and the upper (uncontrolled) zone (uz).

The airflows on the wall surfaces and the air filtration through the walls significantly influence contaminant accumulation, and therefore it is essential to carry out the calculation also for the cold season.

Nomenclature for the figures

A = area [m^2]
b = coefficient
C = concentration [mg m^{-3}]
H = height [m]
G = contaminant flow rate [mg s^{-1}]
q = airflow rate [dm^3 s^{-1}]
ϕ = heat flow rate [W]
T = temperature [K, °C]

Subscripts

a = air
b = boundary, through the boundary
c = convection
cd = conduction
ex = exhaust, extract

f = filtration
lz = lower zone
m = mixing, mixed
o = outside
r = radiation
s = supply
t = turbulent mixing, total
uz = upper zone
w = wall

8.7.5.3 Characteristics of the Zoning Strategy

The air distribution method and dimensioning of the air supply devices are important factors in determining the accumulation of heat and contaminants. Examples of this are presented in Section 8.4. After the behavior of the air distribution method and devices are known, the characteristic effects of the other airflow elements can be calculated.

The simplified examples in Figs. 8.35–8.39 are calculated for the case of an industrial hall with length 40 m, width 25 m, and height 8 m. The zone level is determined at the height of 4 m. The dimensions of the heat (50% convection) and contaminant sources located at floor level are 1 m, 1 m, and 1 m. The heat load of the lights located in the upper zone at the level of 6 m is 15 W m^{-2}. For the walls the U-value is 0.5 W m^{-2} K^{-1}. The turbulent mixing between the zones is estimated as $q_{bt} = 0.5q_s$ or $q_{bt} = 1.0q_s$. The penetration of the plumes through the zone boundary is estimated to be 100%, i.e., $\sum q_{cbm} = \sum q_c$. Contaminant concentration outside is $C_o = 0$. Other values are listed in the tables of the figures.

The effect of the plume airflow rate and the turbulent mixing airflow rate through the zone boundary is presented in Fig. 8.35. The heat removal effectiveness ϵ_T and contaminant removal effectiveness ϵ_C are presented as functions of the relative airflow rate.

The effect of the supply airflow rate and the heat load is presented in Fig. 8.36. The heat removal effectiveness ϵ_T and contaminant removal effectiveness

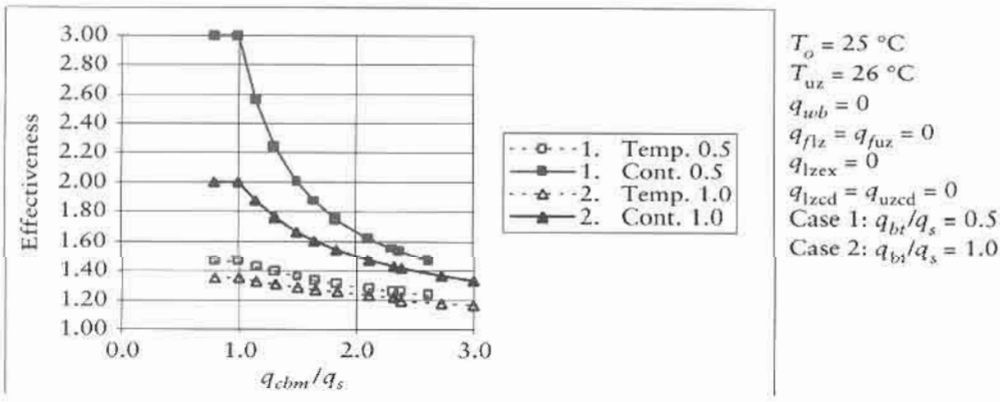

FIGURE 8.35 Effectiveness ϵ_T (temp.) and ϵ_C (cont.) as functions of the ratio q_{cbm}/q_s with the ratio q_{bt}/q_s as a parameter.

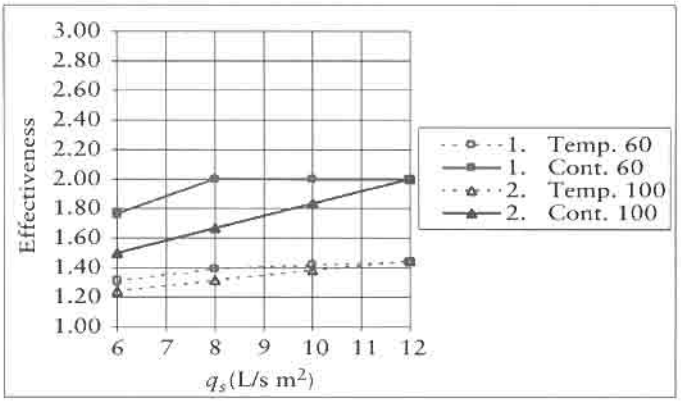

FIGURE 8.36 Effectiveness ϵ_T (temp.) and ϵ_C (cont.) as functions of the supply airflow rate q_s (L s^{-1}m^{-2}) with the total heat load ϕ_t (W m^{-2}) as a parameter.

ϵ_C are presented as functions of the supply airflow rate. The power of one heat source is 500 W.

The effect of the local exhaust airflow rate in the lower zone is presented in Fig. 8.37. The heat removal effectiveness ϵ_T and contaminant removal effectiveness ϵ_C (determined by extract air) are presented as functions of the local exhaust airflow rate. The total heat load is 60 W m^{-2} and the power of one heat source is 500 W. The supply airflow rate is 8 L s^{-1} m^{-2}.

The effect of the downward airflow along the wall surfaces is presented in Fig. 8.38. The heat removal effectiveness ϵ_T and contaminant removal effectiveness ϵ_C are presented as functions of the outdoor temperature T_o. The total heat load is 60 W m^{-2} and the power of one heat source is 500 W. The supply airflow rate is 8 L s^{-1} m^{-2}. In winter seasons heat losses through the walls and the airflow along the walls increase the relative temperature difference and decrease the concentration difference.

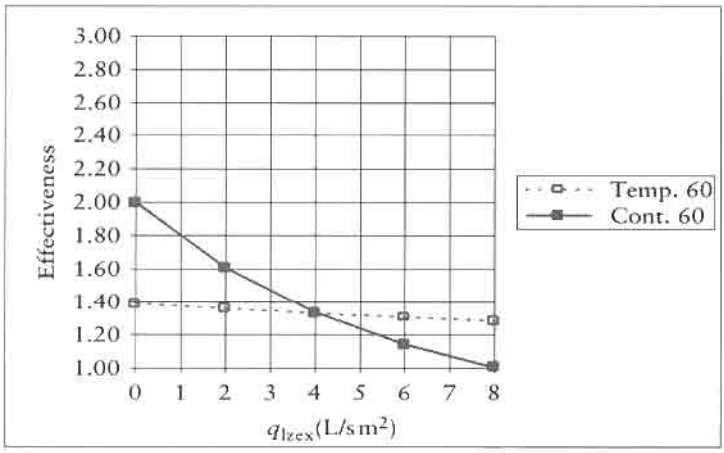

FIGURE 8.37 Effectiveness ϵ_T (temp.) and ϵ_C (cont.) as functions of the local exhaust airflow rate from the lower zone.

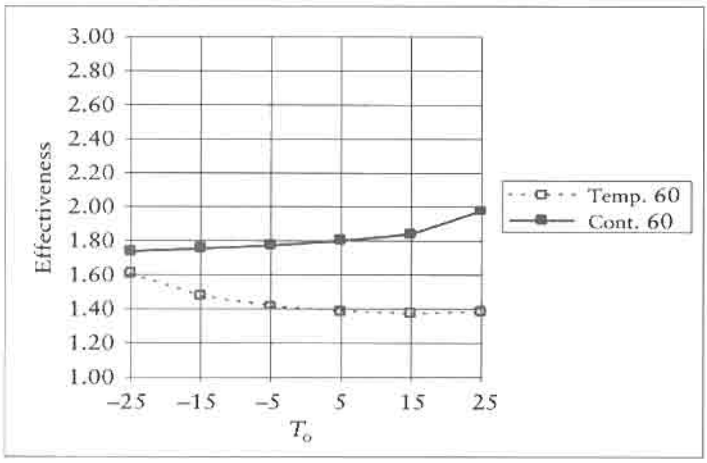

FIGURE 8.38 Effectiveness ϵ_T (temp.) and ϵ_C (cont.) as functions of the outdoor temperature T_o.

The effect of the disturbance of the supply airflow on the plumes is presented in Fig. 8.39. The heat removal effectiveness ϵ_T and contaminant removal effectiveness ϵ_C are presented as functions of the penetration factor Ψ of the plume, which is the ratio of penetrated plume airflow rate to the whole plume airflow rate. The total heat load is 60 W m^{-2} and the power of one heat source is 500 W. The supply airflow rate is 8 L s^{-1} m^{-2}.

These case examples illustrate the dependence of the stratification of temperature and contaminants on several parameters, which in some cases increase and in other cases decrease the effectiveness. All the parameters should be included in calculations when designing the system combination of the room air conditioning methods.

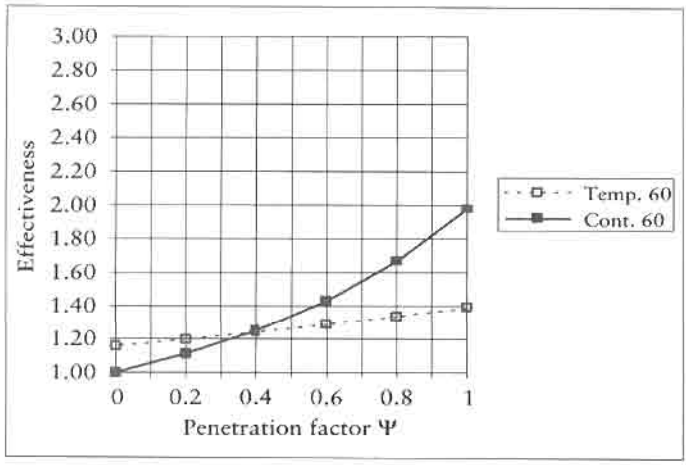

FIGURE 8.39 Effectiveness ϵ_T (temp.) and ϵ_C (cont.) as functions of the penetration factor of the plume airflow rate.

Measured results of effectiveness and turbulent mixing are presented in literature by Bach (several air distribution methods)[3] and Hagström et al. (mixing air distribution methods in zoning strategy).[4,5] A typical example of an air distribution method and device in the zoning strategy is the so-called active displacement method, which is based on a nozzle duct device.[6]

References

1. M. I. Grimitlyn, *Air Distribution in Rooms*, St. Petersburg: Publishing House of Pedagogical University, 1994.
2. L. Stensaas, *Ventilasjonsteknikk 1, Grunnlaget og systemer*, Oslo: Skarland Press AS, 1999.
3. H. Bach, W. Dittes, K. Madjidi, R. Becher, and B. Biegert, *Zonal Ventilation of Working Area in Production Halls to Reduce the Load of Contamination*, Research Report 01HK216 Verein der Förderer der Forschung im Bereich Heizung-Luftung-Klimatechnik, Stuttgart e.V., 1992.
4. K. Hagström, K. Siren, and A. Zhivov, *Calculation Methods for Air Supply Design in Industrial Facilities—Literature Review*, Espoo: Helsinki University of Technology, Report B60, 1999.
5. K. Hagström, A. Zhivov, K. Sirén, and L. L. Christianson, The influence of heat and contaminant source non-uniformity on the performance of three different room air distribution methods. *ASHRAE Transactions*, 1999, 2, 105.
6. E. Sandberg, H. Koskela, and T. Hautalampi, Convective flows and vertical temperature gradient with the active displacement air distribution, in *Roomvent* '98, Stockholm, Sweden, 1998.

Bibliography

Kim Hagström and Alexander Zhivov. Design algorithm for room air distribution design using jet theory and experimental data on temperature and velocity distribution uniformity. Draft, Espoo 14.09, 1998.

8.8 LOCATION OF GENERAL EXHAUST

8.8.1 Exhausts in Nonstratified Room Air

In a room with perfect mixing of the air, it theoretically does not matter where the exhaust opening is located (Fig. 8.40). In practice, air seldom mixes as completely as in theory. One reason for this is temperature differences or density differences. The contaminants are often warmer than the room air, and in some cases the density of the contaminant itself differs from the air density. These topics are treated in the later paragraphs. This paragraph will focus on isothermal, non-buoyant cases.

In long rooms, i.e., where the room is slightly longer than the penetrating distance of the supply jet, the best location of the exhaust is opposite to the air supply opening. See Fig. 8.41.

In very long rooms, the exhaust should be located at the opposite end of the room. Otherwise, the air exchange in the far end of the room may be small, resulting in an accumulation of contaminants in that part of the room. See Fig. 8.42.

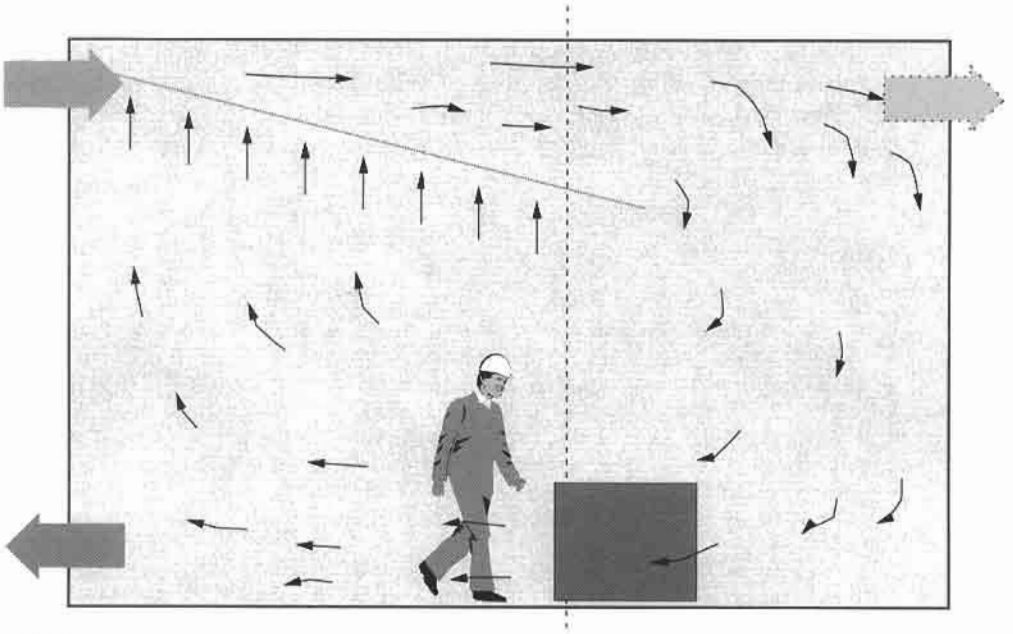

FIGURE 8.40 Exhaust from a room with perfect mixing. The location of the exhaust opening is not important.

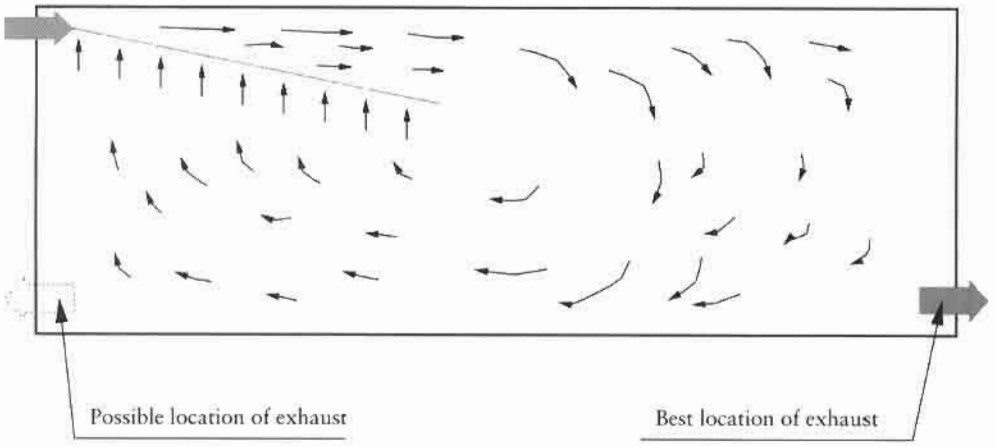

8.8.2 Exhaust of Buoyant Contaminants

8.8.2.1 Exhaust of Warm Fumes

The general rule is that when contaminants are warm, the exhaust should be located as high as possible in the room. Obviously, this applies in the case of displacement ventilation, as shown in Fig 8.43.

In mixing ventilation, the exhaust should be located below the ceiling when the contaminants are buoyant, as illustrated in Fig. 8.44.

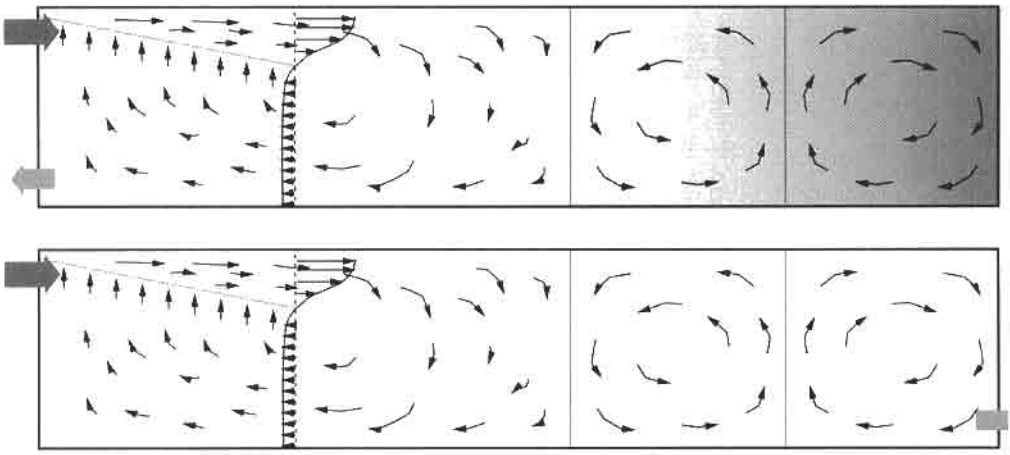

FIGURE 8.42 In very long rooms, the exhaust should be placed opposite to the supply opening.

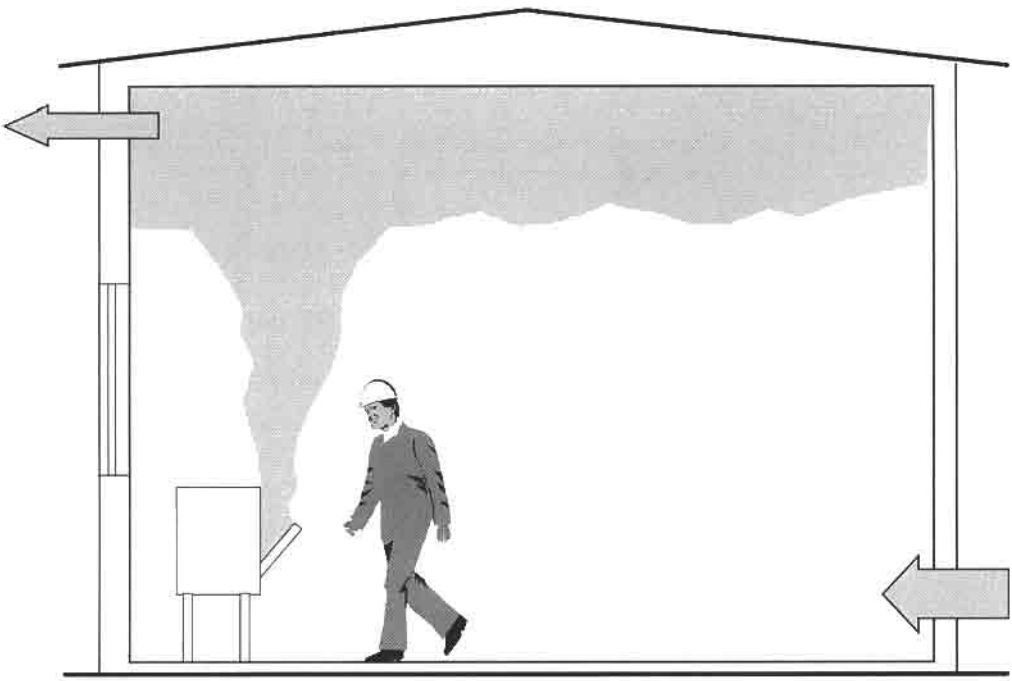

FIGURE 8.43 Warm contaminants should be exhausted below the ceiling, and preferably close to the source.

8.8.2.2 Exhaust of Cold Fumes

Heavy fumes or gases (i.e., negatively buoyant contaminants) should be exhausted at floor level. This applies to displacement ventilation as well as to mixing ventilation (Fig. 8.45).

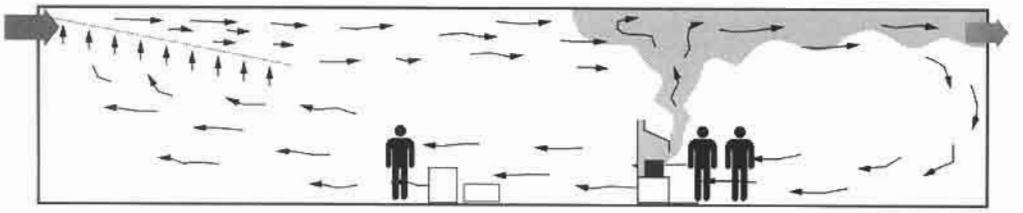

FIGURE 8.44 Buoyant contaminants should be extracted below the ceiling (also in mixing ventilation).

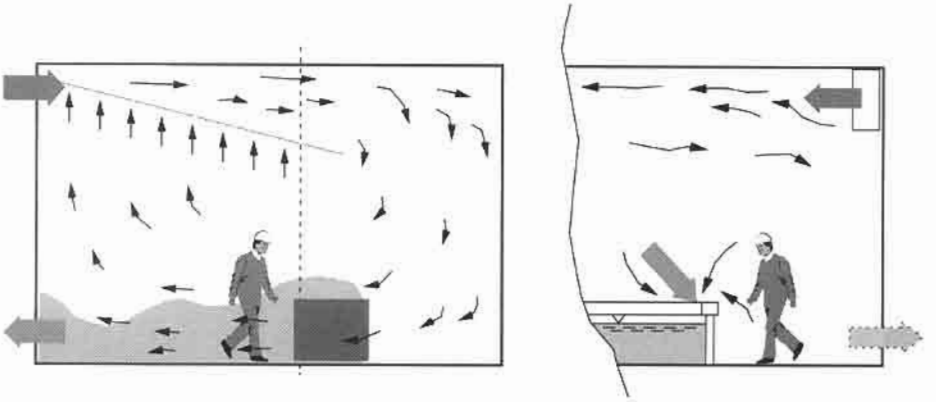

FIGURE 8.45 When the contaminants are heavier than the room air, the exhaust should be at floor level, for displacement ventilation as well as for mixing ventilation.

8.8.2.3 Exhaust of Fumes with Unpredictable Buoyancy

In several cases it is not certain if the contaminants are negatively or positively buoyant. In such cases one should place exhaust openings both below the ceiling and at floor level (Fig. 8.46).

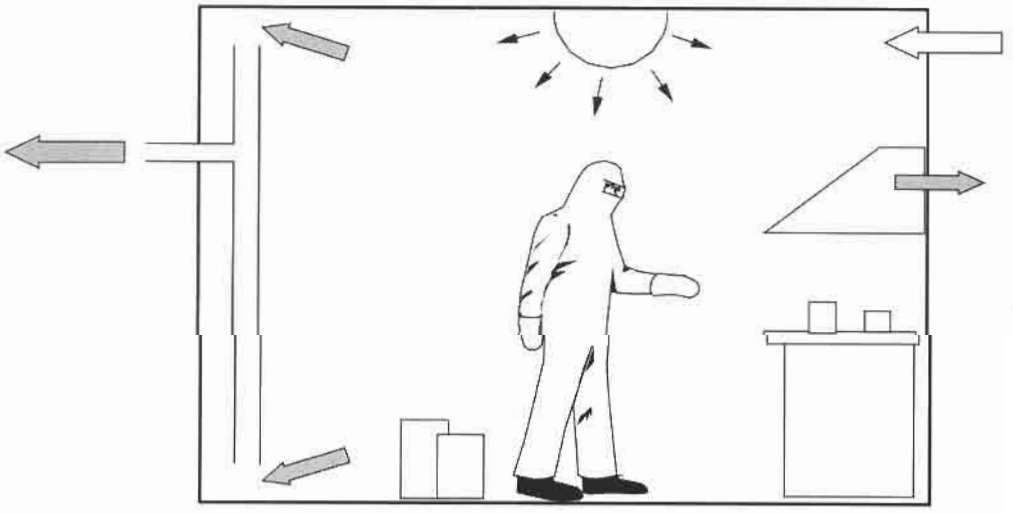

FIGURE 8.46 When contaminants can be both negatively and positively buoyant, exhausts should be located both high and low.

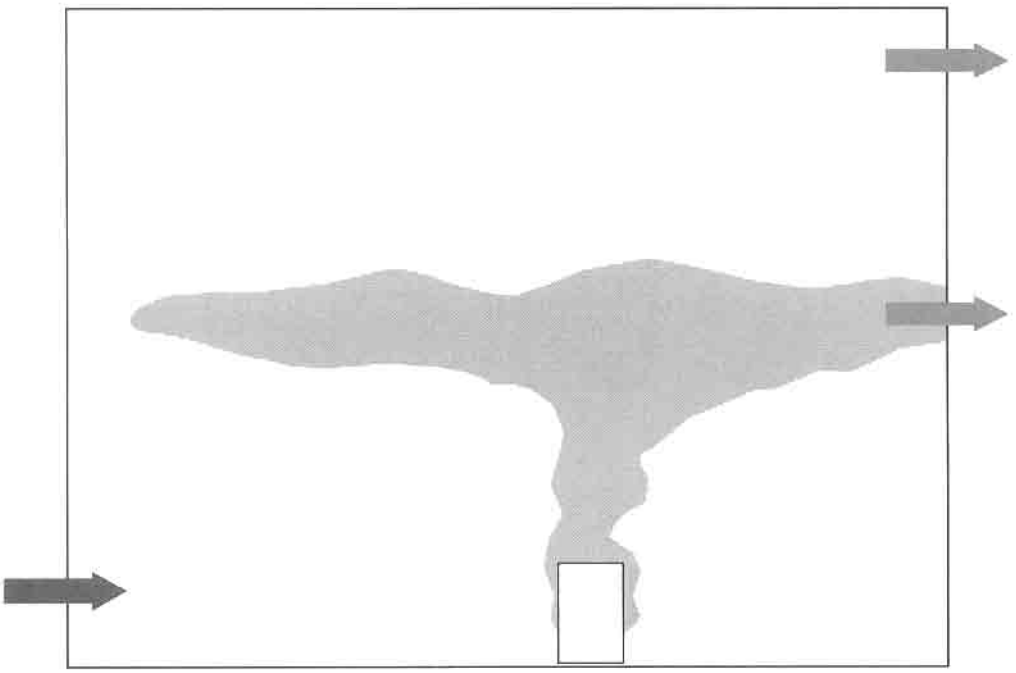

FIGURE 8.47 Thermal stratification should be taken into account when locating the exhaust openings.

8.8.3 Exhausts in Stratified Room Air

Thermal stratification in the room air greatly influences the spreading and dispersion of contaminants (Fig. 8.47). See Section 7.5.4, *Plumes in Confined Spaces*. In such cases, an exhaust opening might be placed at, or close to, the equilibrium height for the main contaminant. In addition, there should be a general exhaust either at ceiling level or at floor level, depending on the buoyancy of the contaminants. A temporary wall (can be canvas) can separate different zones, so that a polluted zone is separated from a clean zone (e.g., the welding zone separated from the mechanical assembly zone, Fig. 8.48).

8.8.4 Location of General Exhaust to Create Displacement Flow

When special contaminating processes are located in a semi-enclosed part of a room like in Fig. 8.49, the exhausts should be located so that a displacement flow is created through the passage into the semi-enclosure.

With this arrangement there may be no need for a door, which may be very practical.

Bibliography

J. L. Alden, and J. M. Kane, *Design of Industrial Ventilation Systems*, 5th ed., New York: Industrial Press, 1982.

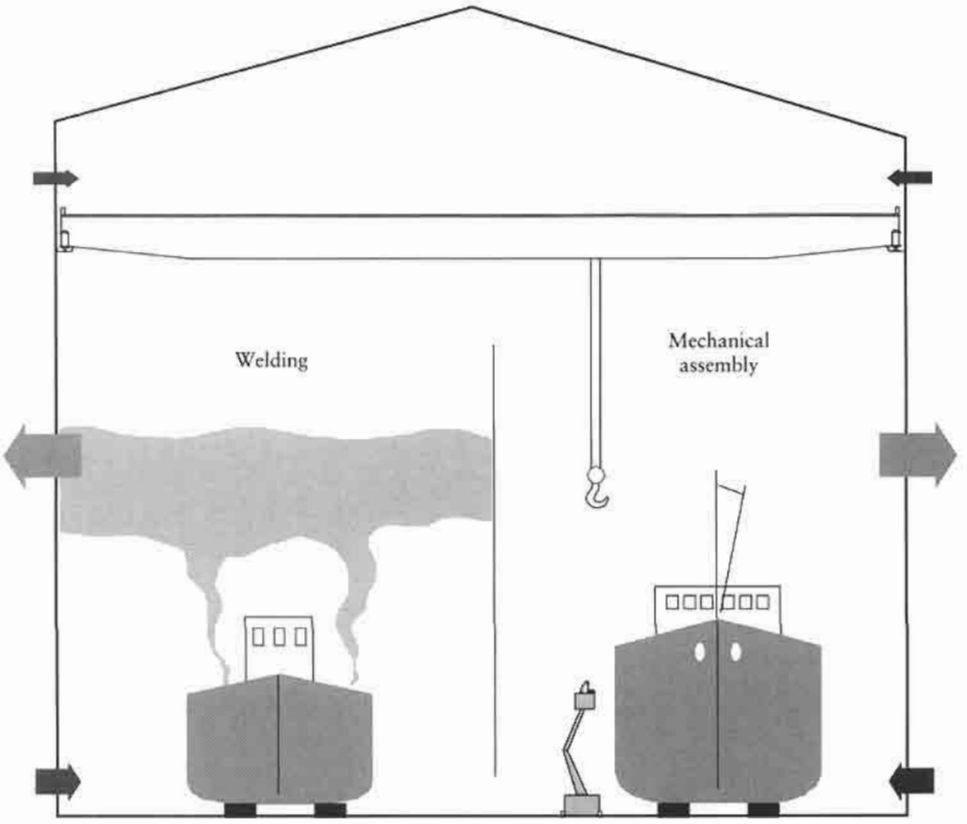

FIGURE 8.48 In stratified air, we can create separate zones in a large enclosure, using the thermal lid as a roof above the zones.

8.9 HEATING OF INDUSTRIAL PREMISES

8.9.1 General

Industrial buildings can generally be divided into three classes with regard to their heating:

1. Buildings that are thermally insulated and airtight. These buildings can be heated with a heating system.
2. Buildings without thermal insulation and/or measures against wind flowing through the outer walls. It is too expensive to heat these buildings totally; local heating or radiant heating at the working places represents a possible solution. An example of buildings of this kind is a warehouse.
3. Buildings where the waste heat from processes is so high that no further heating is needed. This is the case for instance in foundries.

8.9.2 The Heating Power Demand

In the stationary state the heat demand ϕ for an industrial building is

$$\phi = G_b(T_i - T_o) + c_{pa}\rho_a q_{Va}(T_i - T_o) = (G_b + c_{pa}\rho_a q_{Va})(T_i - T_o) \quad . \quad (8.25)$$

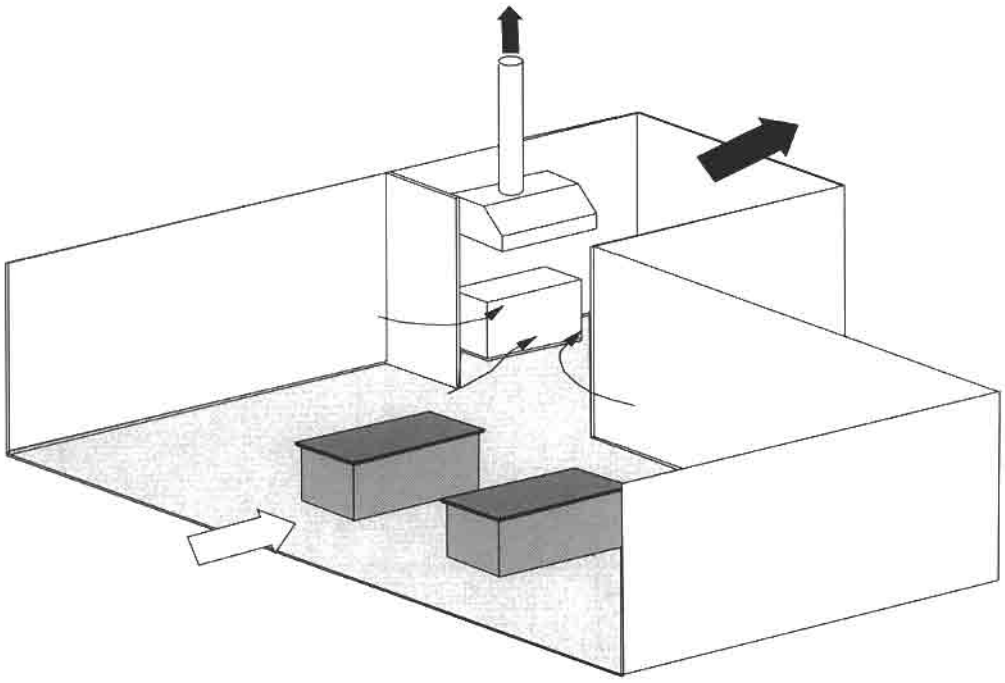

FIGURE 8.49 General exhaust placed to give a displacement flow through a passage.

where G_b is the conductance of the building describing the totality of conduction through outer walls, roof, and floor. It can be considered constant for each specific building. T_i is the temperature inside the building and T_o the temperature outside the building. c_{pa} is the specific heat of air, ρ_a the density of air, and q_{Va} the volume flow of outside air into the building.

from Eq. (8.25) we also get

$$\frac{\phi}{T_i - T_o} = G_b + c_{pa}\rho_a q_{Va} = m \,. \tag{8.26}$$

If the volume flow q_{Va} is practically the same at every outdoor temperature, the quantity in Eq. (8.26) will also be a constant and specific for each individual building. If the quantity in Eq. (8.26) is constant, we also get from Eq. (8.25), if the inner temperature T_i is held constant,

$$\frac{d\phi}{dT_o} = -G_b - c_{pa}\rho_a q_{va} = -m \quad . \tag{8.27}$$

Plotting the heat demand ϕ against T_o should produce a straight line with a negative slope coefficient.

If we look at a measured heat demand (Fig. 8.50) for an industrial building, we see that this is essentially the case. Deviations from the straight line are due to the following three factors:

1. The stationary state is not in reality reached,
2. The inside temperature T_i is not constant, or
3. The volume flow q_{Va} is not constant.

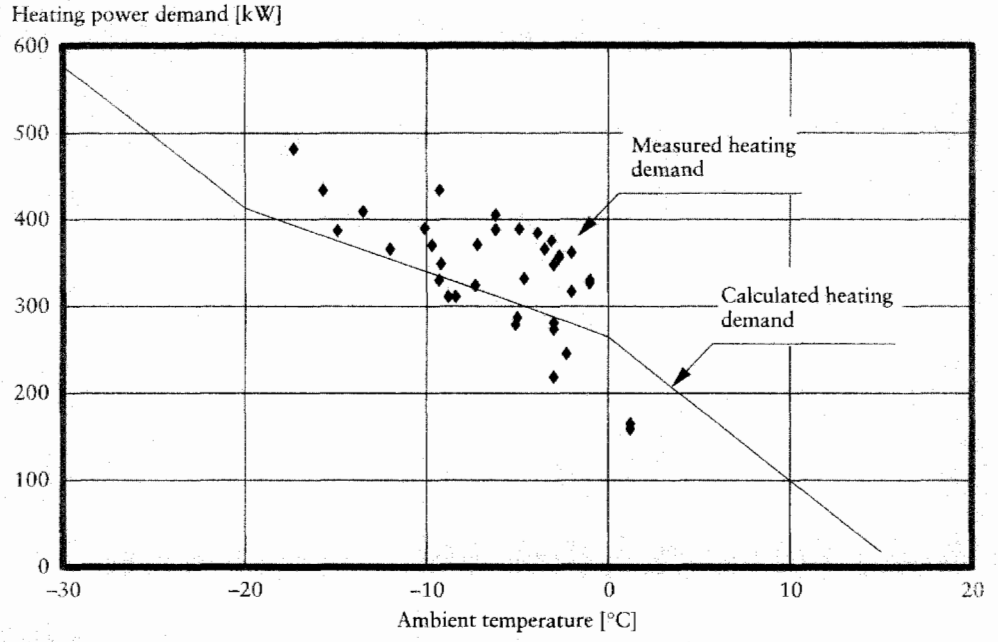

FIGURE 8.50 Heating demand versus ambient temperature for an industrial building. Calculated and measured values compared.

8.9.3 The Heating Energy Demand

The demand of heating energy for an industrial building can be calculated from Eq. (8.25) as

$$Q = \int_{t_1}^{t_2} \phi dt = \int_{t_1}^{t_2} m(T_i - T_o(t))dt\,. \tag{8.28}$$

Here t is the time and $t_1 - t_2$ the time period under consideration (month, year, etc.). The outdoor temperature T_o now depends on time and the indoor temperature is assumed constant.

The quantity m can be considered constant on condition that the flow of outside air q_{Va} is constant within the considered period. Quite often the ventilation is reduced at night and m is then not constant.

If m can be considered constant or if we use an average value of m over the time range $t_1 - t_2$, then we get from Eq. (8.28)

$$Q = m\int_{t_1}^{t_2} (T_i - T_o(t))dt\,. \tag{8.29}$$

The quantity $\int_{t_1}^{t_2}(T_i - T_o(t))dt$ is named the "degree day" and is normally calculated for each month but also on a yearly basis. It depends on the climate where the industrial building is situated. This means that different geographic positions have different degree days. From the definition we also see that the degree day depends on the assumed indoor air temperature, which is assumed constant.

Example

How much energy in January is needed for an industrial building if the heat demand is 50 kW at outside temperature –26 °C and indoor temperature 18 °C? The average outdoor temperature in January at that place is – 4.7 °C.

Solution From Eq. (8.26) we get

$$m = \frac{50\text{kW}}{18°\text{C} - (-26°\text{C})} = 1140\ \text{W}\ °\text{C}^{-1} \quad .$$

The average temperature difference between the indoor air and ambient air is

$$\Delta\theta_{\text{mean}} = 18\ °\text{C} - (-4.7\ °\text{C}) = 22.7\ °\text{C}.$$

That means that the average heating power demand becomes

$$\varphi_{\text{mean}} = m\ \Delta\theta_{\text{mean}} = 1140\ \text{W/°C} \cdot 22.7\ °\text{C} = 25.878\ \text{W}.$$

If the room is heated the whole day and night, i.e., $\dot{m}t$ = 31 days = 744 hours, the heating energy demand becomes

$$Q = \varphi_{\text{mean}}\ \dot{m}t = 25.9\ \text{kW} \cdot 744\ \text{h} = 19.270\ \text{kWh}.$$

8.9.4 Radiant Heating

8.9.4.1 Radiant Temperature

The idea of radiant heating in an industrial hall is to install local heating panels with a high surface temperature. Because of the high temperature, the proportion of thermal radiation in the heating power from the panel will increase drastically. But we must remember that the heating panels will also radiate directly on outer surfaces of the buildings, thus raising their surface temperature and increasing the heat flow through the walls.

The heating panels can be heated with electricity, burning gas flames, or hot water.

The temperature that a thermometer with an almost black bulb indicates when it is placed near the heating panel (Fig. 8.51) is practically the same temperature that a human being will feel in the neighborhood of the panel.

The heat balance for the bulb in Fig. 8.51 is

$$F\sigma\epsilon(T_s^4 - T_b^4) = h_c(T_b - T_a) + (1 - F)\sigma\epsilon(T_b^4 - T_w^4) \quad . \tag{8.30}$$

T_s is the surface temperature of the panel, T_b the thermometer bulb temperature, T_a the air temperature, and T_w the temperature of the walls of the building. F is the view factor from the bulb to the heating panel, ϵ is the emissivity of the thermometer bulb at temperature T_b, σ is the Stefan-Boltzmann constant (5.67×10^{-8} W m^{-2} K^{-4}), and h_c is the convective heat transfer coefficient from bulb to air.

The unknown temperature T_b can be calculated from Eq. (8.30) when the other temperatures T_s, T_a, and T_w are known and also F, h_c, and ϵ. The temperature of the wall and air is practically the same, so we can set $T_a = T_w$. We also use for the heat transfer coefficient h_c = 4 W m^{-2} K^{-1}.

The emissivity ϵ of the bulb is quite insensitive to the material of the bulb, as long as it is not a polished bright metal. Because the bulb radiates long-wave heat radiation, we can use the value ϵ = 0.95.

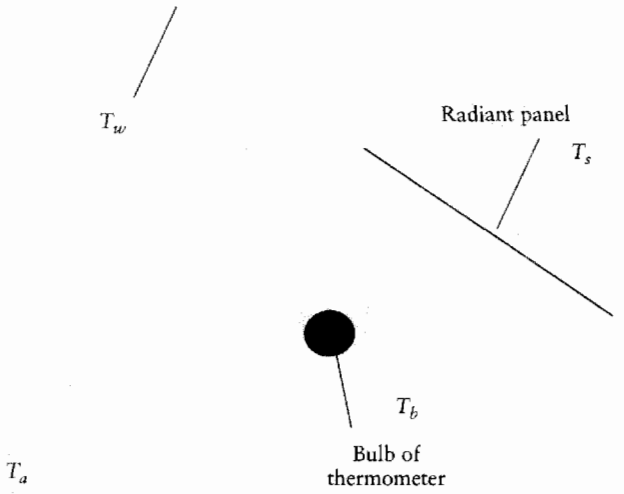

FIGURE 8.51 Heat balance for a black bulb in front of a radiant panel.

The view factor F can be calculated with the aid of Fig. 8.52. With the notations in Fig. 8.52, the view factor for a position for the bulb like that in Fig. 8.52 is

$$F = \frac{1}{4\pi}\arcsin\frac{BC}{\sqrt{1 + B^2 + C^2 + B^2C^2}} . \tag{8.31}$$

If the thermometer is situated symmetrically relative to the heating panel, then the view factor will be four times higher than calculated from Eq. (8.31).

Example

Figure 8.53 gives measured values of the "radiant temperature," which means $T_b - T_a$, caused by an electrical heating panel. The "effective surface" temperature of the panel can be estimated from the curves, then used to calculate the temperature of a thermometer bulb at a few other places. These results can be compared to measured results.

Solution The first step is choosing a reference point. At the point 1 m right below the panel, the radiant temperature is 29 °C, and if we assume that the temperature of air is 20 °C, then $T_b = 49$ °C.

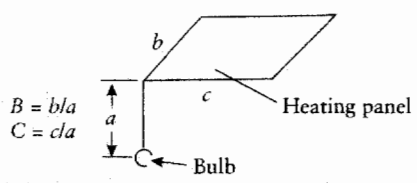

FIGURE 8.52 View factor from thermometer bulb to heating panel.

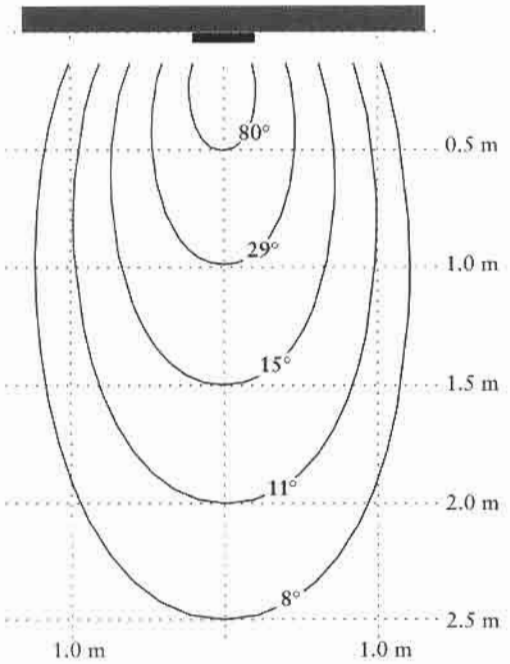

FIGURE 8.53 Measured values of radiant temperature near an electrical heating panel. Length of panel: 1.53 m; width: 0.28 m.

The view factor at that point is

$$F = 4\frac{1}{4\pi}\arcsin\frac{0.14\times 0.765}{\sqrt{1+0.14^2+0.765^2+0.14^2\times 0.765^2}} = 0.02685\ .$$

Inserting this value into Eq. (8.30) and also $T_a = T_w = 20\ °C = 293\ K$, we get (by iteration) the temperature $T_s = 740\ K = 467\ °C$. We can use this value for calculating the radiant temperature at other locations. For each location a new view factor has to be calculated. The results are shown in Fig. 8.54.

We see that the agreement between measured and calculated temperatures is fairly good. Only in the right corner near the heating panel is there a big difference between the measured and calculated temperature. However, the measured results cannot be reliable here either, because it is not possible that the radiant temperature is 80° just near a surface of 467 °C.

8.9.4.2 Radiant Heating Panels Heated by Water

Radiant heating can be realized also by heating the panels by water. The principal construction of such a device is shown in Fig. 8.55.

The temperature of the water in the heating panel is limited by the boiling of the water. The boiling temperature of water increases with increasing pressure. If the pressure of the water is about normal atmospheric pressure, then the temperature of the water can be 90–95 °C. If we want to raise the temperature of water to 120 °C, the absolute pressure of water must be above 2 bar.

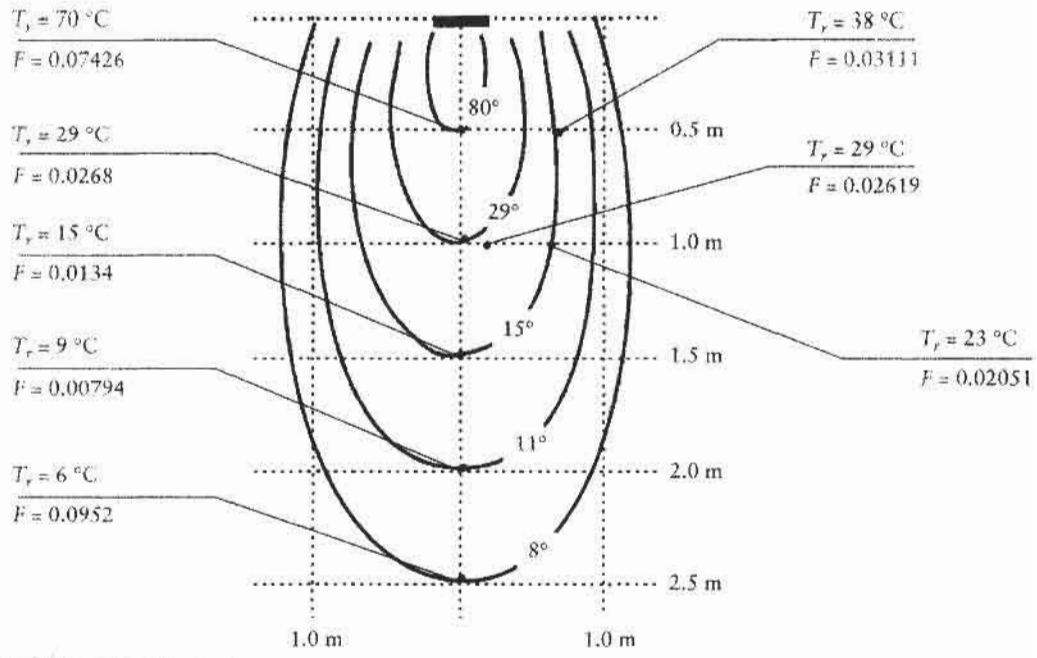

FIGURE 8.54 Measured and calculated radiant temperature at different locations.

The heat balance of a water heated panel is (Fig. 8.56)

$$\phi = \epsilon\sigma A(T_s^4 - T_{sur}^4) + hA(T_s - T_a) + \phi_l \quad , \tag{8.32}$$

where ϕ is the total heat delivered to the panel by the flowing hot water, which is cooled, and ϕ_l is the heat loss through the insulation upward. T_s is the surface temperature of the panel, and we can put

$$T_s = \frac{1}{2}(T_{wi} + T_{wo}) \quad , \tag{8.33}$$

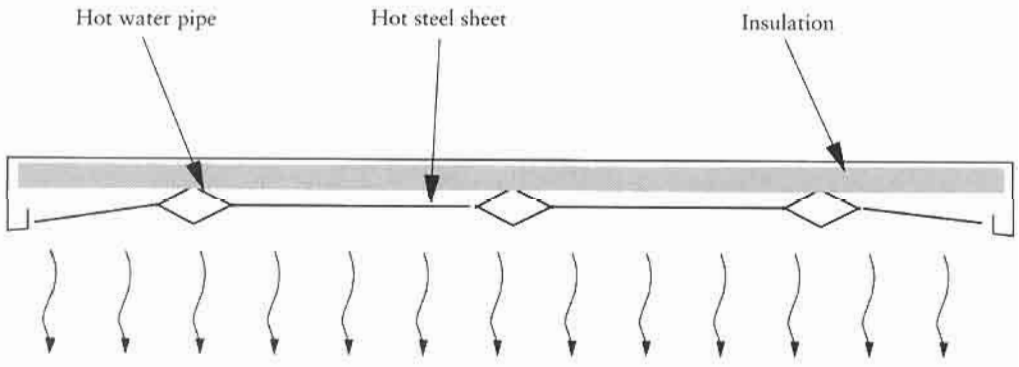

FIGURE 8.55 Radiant heating device using heated panels in water.

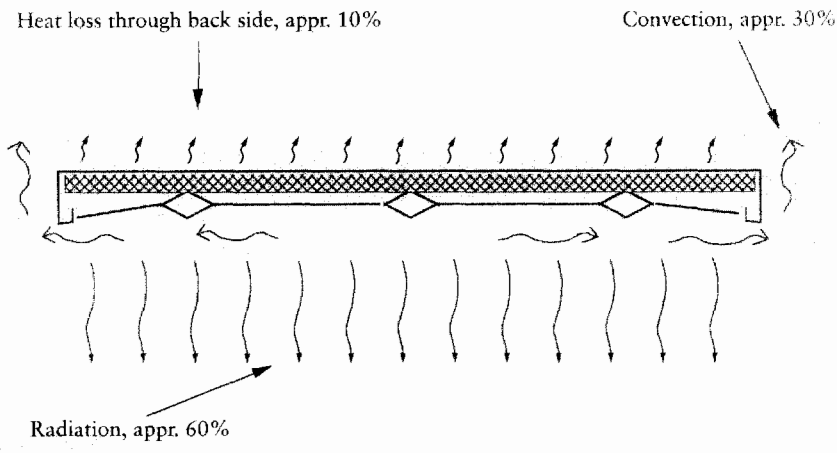

FIGURE 8.56 Heat balance of a heated panel.[2]

where

T_{wi} = inlet temperature of the water to the panel and T_{wo} is the outlet temperature.

T_{sur} = temperature of the walls and roofs of the industrial hall; T_a is the temperature of air in the hall, and we can put $T_{sur} = T_a$.

A = area of the heating panel and h is the convective heat transfer coefficient.

ϵ = emissivity of the surface and, in the considered temperature range, we can put $\epsilon = 0.95$.

ϕ_l can be estimated if we know the type and thickness of the thermal insulation of the panel. One estimation is that ϕ_l is 9–10% of the total heat to the panel.

The convective heat transfer for the panel is free convection from a heated surface faced down. It can be calculated from Incropera and DeWitt:[1]

$$h = 0.27\frac{k}{L_{ef}}\left[\frac{g(T_s - T_a)L_{ef}^3}{\frac{1}{2}(T_s + T_a)\nu\alpha}\right]^{1/4}, \tag{8.34}$$

where

g = gravitational acceleration, 9.81 m s^{-2}

k = thermal conductivity of air

ν = kinematic viscosity of air

α = thermal diffusivity of air

Numerical values for these quantities for a few temperatures are

Temperature (K)	k, W m^{-1} K^{-1}	ν, m^2 s^{-1}	α, m^2 s^{-1}
293	0.0257	15.3×10^{-6}	21.6×10^{-6}
313	0.0273	17.2×10^{-6}	24.4×10^{-6}
333	0.0287	19.2×10^{-6}	27.4×10^{-6}
353	0.0302	21.2×10^{-6}	30.4×10^{-6}

When calculating h from Eq. (8.34), the values for k, ν, and α should be taken at temperature $\frac{1}{2}(T_s + T_a)$.

The length L in Eq. (8.34) is defined as

$$L_{\text{ef}} = \frac{A}{P}, \tag{8.35}$$

where P is the perimeter of the surface area of the heating panel. In case the length of the panel is much bigger than the width, then Eq. (8.35) becomes

$$L_{\text{ef}} = \frac{W}{2}. \tag{8.36}$$

Equation (8.36) can be written as heat per unit length of the heating panel:

$$\phi/L = \epsilon\sigma W T_s^4 - T_{\text{sur}}^4 + h W T_s - T_a + \phi_l/L \ . \tag{8.37}$$

Example

The heat effect per unit length by radiation and convection from a water-heated panel can be calculated theoretically. For example, consider panels of width 0.6 m, 0.9 m, and 1.2 m. Room temperature is 3 °C and surface temperature 30 °C, 50 °C, and 70 °C of the panel. Let us compare the results with calculations for room temperature 15 °C and surface temperature 40 °C, 60 °C, and 80 °C of the panel.

Solution One of the most critical and important quantities to calculate in Eq. (8.32) is the convective heat transfer coefficient. It depends on the temperature conditions and also on the width of the panel. Tables 8.11 and 8.12 collect the calculated heat transfer coefficients in different conditions.

We see from the results that in these situations there is no temperature dependence of the heat transfer coefficient. However, the heat transfer coefficient is lower the larger the width of the panel is. It is quite natural that a narrow panel has a higher heat transfer coefficient because it is easier for the air to rise upwards when the panel is narrow. Using the heat transfer coefficients mentioned above, the heat effect delivered by the heating panels downward is

$$\phi/L = \epsilon\sigma W(T_s^4 - T_{\text{sur}}^4) + h W(T_s - T_a) \ .$$

TABLE 8.11 Heat Transfer Coefficients for $\Delta T_a = 5$ °C

	Heat transfer coefficient, h (W m^{-2} K^{-1})		
Surface temperature T_s for $T_a = 5$ °C	**$W = 0.6$ m**	**$W = 0.9$ m**	**$W = 1.2$ m**
30 °C	2.1	1.9	1.8
50 °C	2.4	2.2	2.0
70 °C	2.6	2.4	2.2

TABLE 8.12 Heat Transfer Coefficients for $\Delta T_a = 15$ °C

	Heat transfer coefficient, h (W m^{-2} K^{-1})		
Surface temperature T_s for $T_a = 15$ °C	$W = 0.6$ m	$W = 0.9$ m	$W = 1.2$ m
40 °C	2.1	1.9	1.8
60 °C	2.4	2.2	2.0
80 °C	2.6	2.4	2.2

Tables 8.13 and 8.14 collect the results and compare them to results given by a manufacturer.

We see that there is a big difference between the calculations and the results given by the manufacturer. The manufacturer's results are about 45–50% higher. The reason for the differences is not clear. One difficulty is that we do not know in the manufacturer's case how much heat is flowing through the insulation upward. We have assumed that this flow is 9% of the total heat effect of the heating panel.

TABLE 8.13 Heat Transfer from Panels. Calculated Values and Manufacturer's Data

	Heat effect per unit length (W m^{-1})					
	$W = 0.6$ m		$W = 0.9$ m		$W = 1.2$ m	
Surface temp T_s for $T_a = 5$ °C	Calc.	Manuf.	Calc.	Manuf.	Calc.	Manuf.
30 °C	110	150	160	230	212	310
50 °C	220	320	330	480	430	650
70 °C	360	520	520	770	680	1040

TABLE 8.14 Heat Transfer from Panels. Calculated Values and Manufacturer's Data

	Heat effect per unit length (W m^{-1})					
	$W = 0.6$ m		$W = 0.9$ m		$W = 1.2$ m	
Surface temp T_s for $T_a = 15$ °C	Calc.	Manuf.	Calc.	Manuf.	Calc.	Manuf.
40 °C	120	150	170	230	230	310
60 °C	240	320	350	480	460	650
80 °C	380	520	560	770	730	1040

8.9.5 Hot Air Blowers

A common heating method in industry is using blowers that blow heated air into the room. See Fig. 8.57. An advantage is that the installation costs are low. A possible disadvantage is that it mixes the air in the room, which may not be desirable in combination with displacement ventilation.

When locating hot air blowers, we need to know the penetration depth for the hot air that is being discharged from the blowers. For a given discharge angle the penetration depth, z, can be expressed as

$$z = k_z l, \tag{8.38}$$

where

z = penetration depth for the centerline of the hot air jet (m)
k_z = penetration factor, see Fig. 8.58
l = characteristic length for the discharge opening, normally the square root of the discharge area (m)

The Archimedes number is defined as

$$\mathrm{Ar} = \Delta T g l / T u_0^2, \tag{8.39}$$

where

g = acceleration of gravity (9.81 m/s²)
ΔT = temperature difference between the discharged warm air and the room air (K)
T = absolute temperature in the discharged air (K)
u_0 = discharge velocity of the warm air (m/s)

To find the penetration depth,

1. Find the Archimedes number from Eq. (8.39).
2. Read the constant k_z from Fig. 8.58.
3. Calculate the penetration depth for the centerline of the jet from Eq. (8.38).

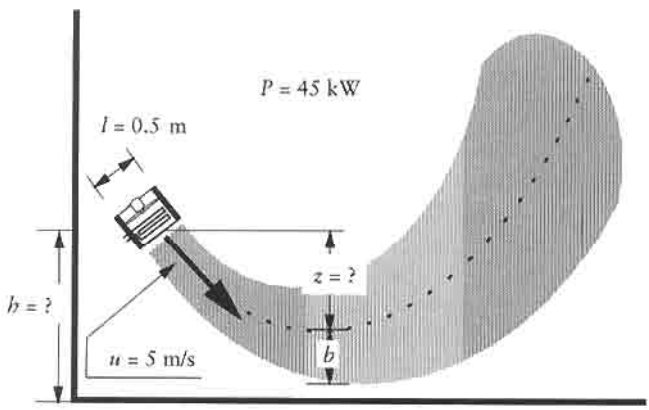

FIGURE 8.57 Hot air blower mounted at the wall.

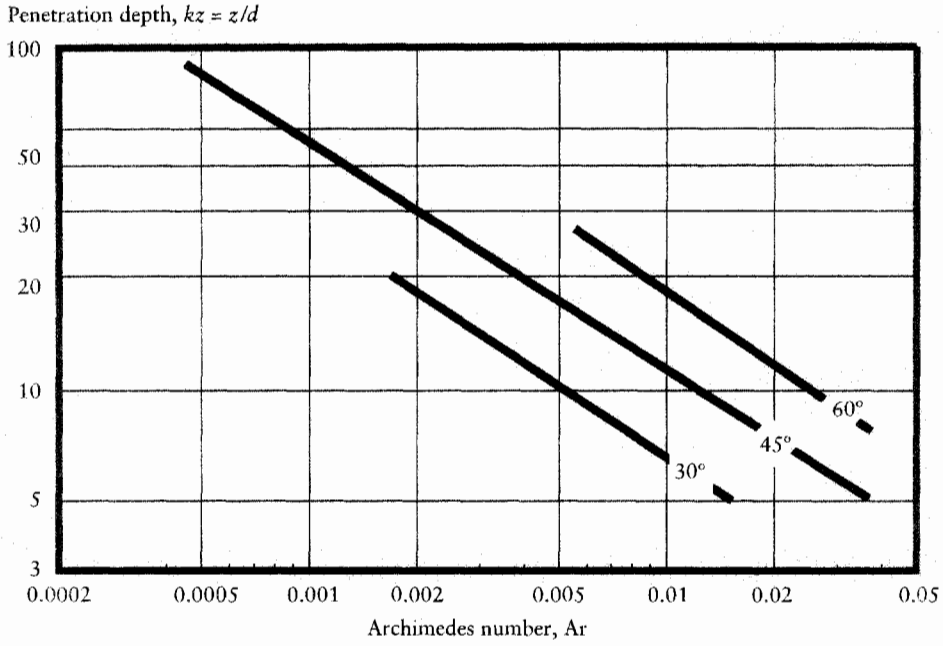

FIGURE 8.58 Penetration depth versus Archimedes number and discharge angle.

Example

A room is heated by hot air blowers. The indoor temperature is +10 °C. Each blower has the following data:

Discharge opening dimensions: $w = h = l = 0.5$ m
Discharge velocity: $u_0 = 5$ m/s
Heater power: $Q = 5$ kW

The blowers are mounted at the walls, and tilted 45° downward. At what height should the blower be mounted so that the air jet reaches the floor? See Fig. 8.57.

Solution First, we find the discharge airflow rate from the blower:

$$q_v = Au_0 = 0.5\text{m} \times 0.5\text{m} \times 5\text{m/s} = 1.25(\text{m}^3/\text{s}) \quad .$$

The temperature increase in the blower is

$$\Delta T = Q/q_v \rho c_p$$
$$= 45\ \text{kW}/1.25\ \text{m}^3/\text{s} \times 1.15(\text{kg/m}^3 \times 1(\text{kW s/kg K})) = 30\ \text{K}.$$

The Archimedes number for the jet at the discharge point, Eq. (8.39), is

$$\text{Ar}_0 = 30\ \text{K} \times 9.81\ \text{m/s}^2 \times 0.5(\text{m}/(313\ \text{K} \times (5\ \text{m/s})^2)) = 0.0196.$$

From Fig. 8.58 we find

$$k_z = z/l = 6$$

for a discharge angle of 45°. Thus, the penetration depth for the centerline of the jet becomes

$$h = z_{max} = 6 \times 0.5 \text{ m} = 3 \text{ m}.$$

The radius of the jet at the lowest point is approximately 1.2 m (calculated from a jet widening angle of 25° and a jet length of 4.2 m from the blower). See Section 7.4.

This means that the hot air blower should not be placed more than 4.2 m above the floor.

8.9.6 Air Jets

An alternative to hot air blowers is air jets that mix the hot air into the occupational zones. See Fig. 8.59.

To avoid generating warmer air layers below the ceiling, air nozzles are utilized to mix the warmer air down into the occupied spaces. This system is well suited for applications where it is important to keep an even temperature throughout the room. It is not suited for rooms with heavy contaminant loads, where zoning is preferable.

8.9.7 Floor Heating

8.9.7.1 General

Floor heating in industrial premises usually means hot-water pipes placed inside the concrete floor. (Electric coils or electric sheets are also used in non-industrial premises; this is, however, not treated here.) Figure 8.60 shows a typical installation of heatpipes inside the floor. Note that the pipes are placed relatively deep down inside the concrete to help even out the surface temperature.

Floor heating has several advantages:

The heat is supplied at the floor, where it normally is most needed.
Putting heating coils or heating pipes into a concrete floor makes a heat reservoir that helps even out temperature fluctuations.
When using hot-water pipes in the floor, the water temperature is usually low (30 °C – 40 °C), so the system is well suited for low-temperature heating.
The system is noiseless and draft-free.

8.9.7.2 Surface Temperature and Heat Emission

One limitation in the use of floor heating is the surface temperature of the floor. Most people will find a floor surface temperature of more than 25 °C uncomfortable.

Heat is transmitted from the floor to the room by radiation and convection. For practical purposes, we can put the heat transfer coefficient to 8 W/m² °C. Based on this assumption, we can make the diagram in Fig. 8.61.

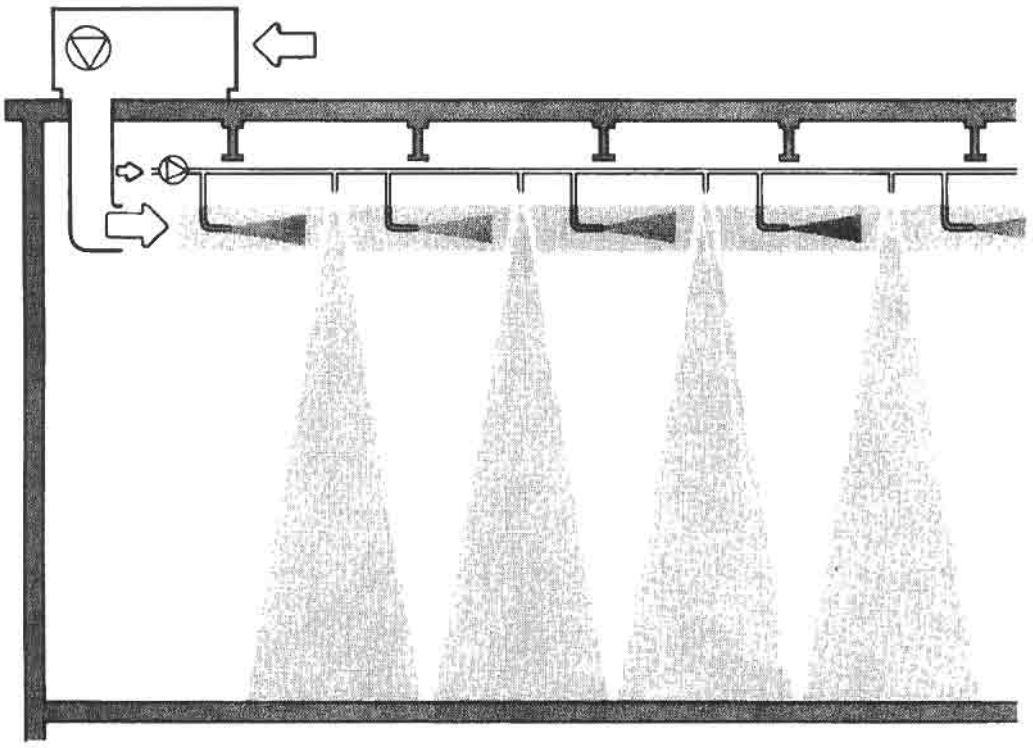

FIGURE 8.59 Mixing jet ventilation. Many nozzles blow the air horizontally and vertically.

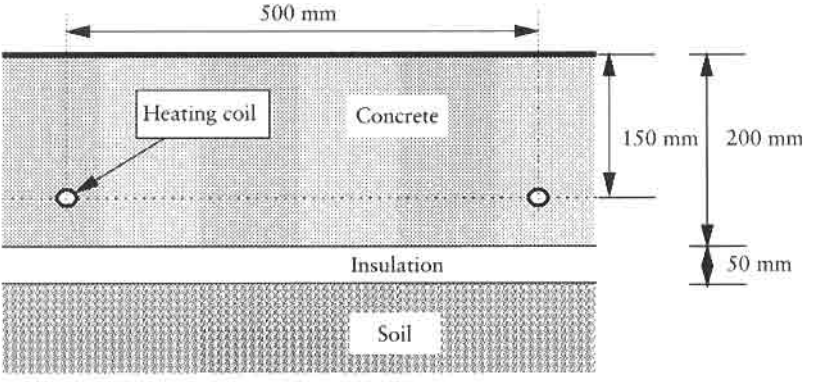

FIGURE 8.60 Arrangement and typical dimensions of hot-water pipes in a concrete floor.

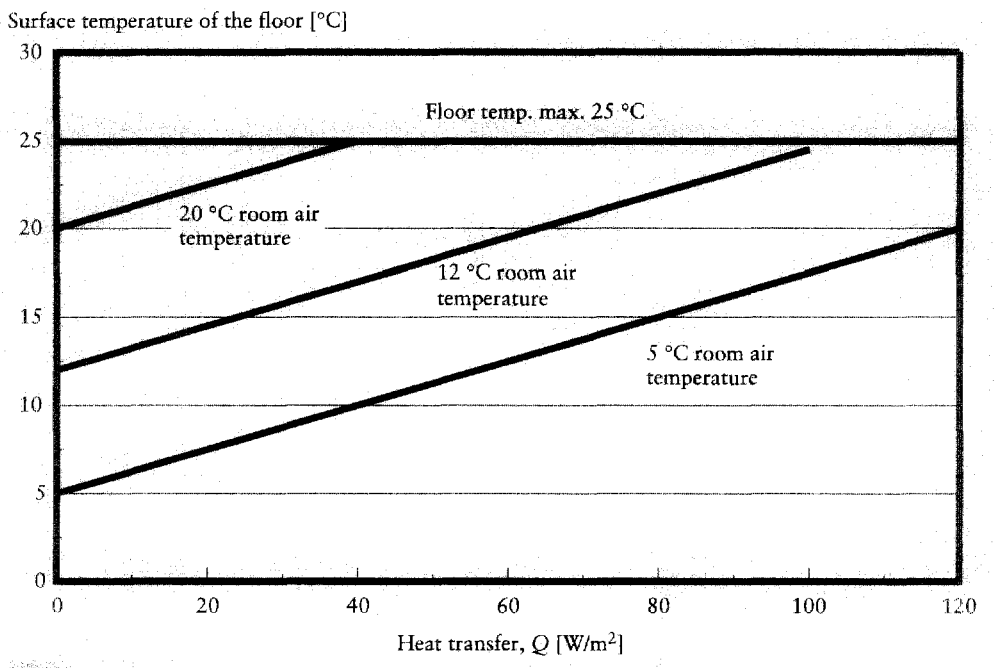

FIGURE 8.61 Heat transfer from a heated floor versus room and floor temperatures.

References

1. F. P. Incropera, and D. P. De Witt, *Fundamentals of Heat and Mass Transfer*, New York: John Wiley & Sons, 1990.
2. H. Skistad, *Industrial Ventilation. Booklet 3: Heating of Industrial Halls*, 1995.

Bibliography

M. Jakob, *Heat Transfer*, vol. II, New York: John Wiley & Sons, 1957.

9 AIR-HANDLING PROCESSES

ERIC F. CURD

John Moores University, Liverpool, United Kingdom

JORMA RAILIO

Association of Finnish Manufacturers of Air Handling Equipment, AFMAHE, Helsinki, Finland

JAN GUSTAVSSON

Camfil Ab, Sweden

JAAP HOGELING

ISSO, Netherlands

MAMDOUH EL HAJ ASSAD

Helsinki University of Technology, Laboratory of Applied Thermodynamics, Finland

JAN EMILSEN

Johnson Controls Norden AS, Norway

SANTE MAZZACANE

Universita di Ferrara, Department of Architecture, Italy

RALF WIKSTEN

Laboratory of Applied Thermodynamics, Helsinki University of Technology, Espoo, Finland

Industrial Ventilation Design Guidebook

9.1 INTRODUCTION

9.1.1 Scope and Purpose

The purpose of this chapter is to present the basic features of air-handling processes and equipment. The aim is to provide a link between the basic theories of air-handling processes, presented in Chapter 4, and the actual equipment covered in the *Systems and Equipment* book.

This chapter deals with the basic air-handling processes: filtration of particles and gaseous substances from the supply and recirculated air, air heating and cooling, heat-recovery processes, and humidification and dehumidification. It also describes fans and ductwork.

This chapter covers the basic issues behind energy-efficient design of air-handling systems and equipment. It deals with equipment space requirements, associated components, and the pressure losses of various components. Good design practices, including system balancing and efficient running, are also addressed.

This chapter deals with the essential factors in the selection of systems and equipment during the design stage: principles of controls, noise-reduction systems, and problems such as erosion, corrosion, maintenance and equipment cleaning, etc.

Safety issues are not covered here. These are dealt with in *Systems and Equipment* book, and some fundamental issues will be taken up in the second edition of the *Fundamentals* book. The following aspects should be taken into account in system design: fan safety; AHU fire protection issues; safety measures in mines, tunnels, underground car parks, etc.; transportation of chemical and explosives.

The basic topic of this chapter is theoretical aspects of air handling units, ductwork design, and the optimization of building energy systems.

9.1.2 Linking with Other Chapters

Chapter 4 covers the physical fundamentals of the air-handling processes, for example, how to construct the Mollier diagram. This chapter describes the basic processes, for example, how to apply the Mollier diagram as a basic tool in

heat-exchanger design. *The Systems and Equipment* volume describes the actual equipment and the associated technical characteristics: heat exchangers and heat-recovery sections in air-handling units, considering the detailed descriptions of various functions, control strategies, etc. This chapter also relates to the basic information presented in

- Chapter 7, basic process design criteria
- Chapter 8, room processes and aspects, air distribution, safety issues
- Chapter 10, local ventilation

Requirements for special items are presented in

- Chapter 11, building system modeling, energy calculations
- Chapter 12, measurements of physical parameters and ventilation processes

Sections 9.2 to 9.8 describe processes and equipment mainly for general industrial ventilation but also for local ventilation.

9.1.3 Aims of an Air-Handling System, Including the Unit and Ductwork

The main objectives are

- Contaminant removal from the indoor space and associated processes
- Supply of safe cleaned and/or treated air for the occupied spaces
- Control of thermal and pressure conditions in treated spaces in a safe, reliable, and energy-efficient manner

Aims of ductwork design are

- Transport of air to and from treated (conditioned) spaces
- Distribution and control of airflows to and from the treated spaces with optimum life-cycle costs.

The air-handling processes should be arranged to take into account the thermal, aerodynamic, and acoustic factors; air quality; moisture control; and cleanliness and other hygiene aspects.

These issues relate certain requirements of the layout of the air-handling system and individual units, including the question of whether to select centralized or decentralized systems, and the number of units required in the building.

9.2 AIR FILTERS

The need to separate impurities from air or other gases has increased as regards both the degree of separation and the necessity to separate both gases and finer particles. Correct dimensioning of filters is a prerequisite for the functioning of ventilation systems, for sensitive production, for protecting humans and the environment, and for improving indoor air quality.

9.2.1 Why Air Filters?

A filter is a component of a system which, in conjunction with other components, can contribute toward a better indoor environment.

9.2.1.1 Ventilation System Protection

Several major studies of indoor-air quality problems[1] have shown that filters would have been able to prevent blocked ducts, fans, and heat exchangers. Other major IAQ problems such as impurities from outside and microorganisms in the system need not arise given the correct choice of filter.

A precondition for maintaining function for a good number of years is that the system should be effectively protected, both on inlet and outlet exhaust systems. *Impurities must be stopped at the inlet and not be allowed to get into the system.* An F7 (EU7) filter is the most economic filter as regards operating costs and cleaning as well as management of the plant.

9.2.1.2 Hygiene Requirement

Every day we breathe about 20–30 kg of air and take in 1 kg of solid and 3 kg of liquid food. We should therefore make the same requirement of the air as we do of food and drink.

9.2.2 Atmospheric Air and Dust

Air is made up of a mixture of different gases and material from natural processes such as wind erosion, evaporation from the sea, earthquakes, and from human activity in the form of combustion products from processes and vehicles.

9.2.2.1 Size of Particles

The size of particles is often indicated in μm (microns). 1 $\mu m = 10^{-6}$ m. Particles in the atmosphere vary, from particles less than 0.01 μm up to leaves and insects.

Studies of atmospheric particles show that their distribution is often bimodal; i.e., the particles are made up of two separate fractions, one with fine and one with coarse particles (Fig. 9.1). The coarse particles, from about 2.5 μm upward, are made up of natural dust from the effect of wind, erosion, plants, volcanoes, etc. The finer fraction is made up of particles smaller than 2.5 μm and consists primarily of particles from human activity, combustion, traffic, and processes.

Hygiene requirements for particle concentrations in the air have been based on concentrations of particles smaller than 10 μm (particulate mass, PM_{10}). Studies have shown a direct connection between the death rate and finer particles, and official requirements are under review, in both Europe and the United States, to be based on the concentration of particles smaller than 2.5 μm ($PM_{2.5}$).

To effectively eliminate these small particles and fulfill official requirements, finer filters are needed, and the requirement for filtering of outdoor air, recycled air, or exhausted air is increasing. With an F7 (EU7) filter, good separation of small particles is achieved.

9.2.2.2 Number of Particles

The number of particles varies considerably with time and place (Table 9.1). To reduce the number of particles in the urban environment to the same number as in the countryside, a filter with 99.9% separation is required. An

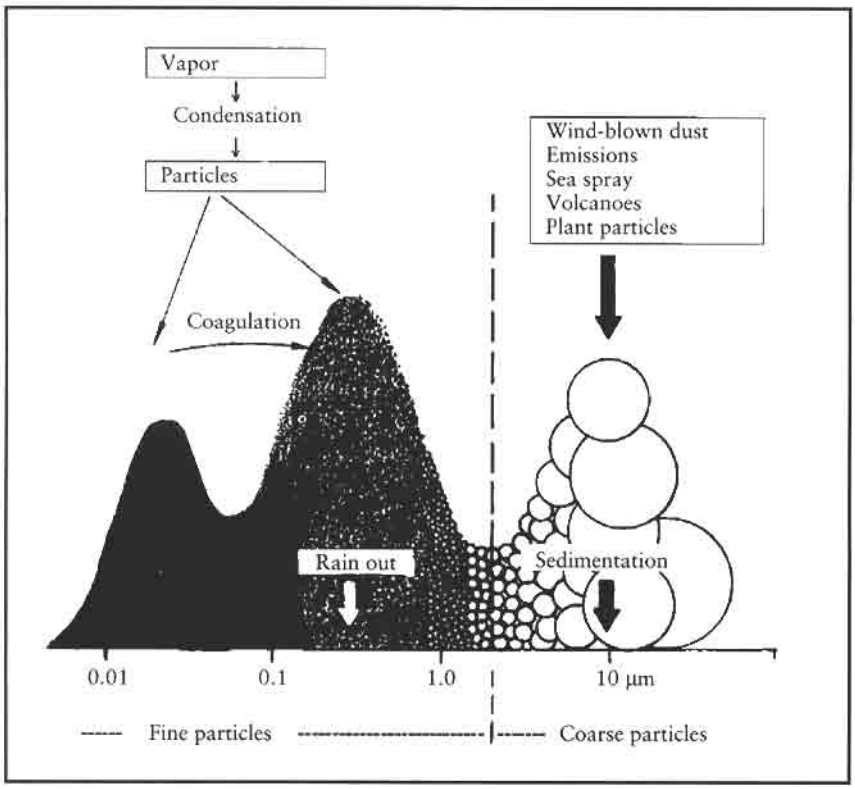

FIGURE 9.1 Size distribution of atmospheric dust.

urban environment or polluted environment thus requires an increasingly better filter quality.

9.2.2.3 Other Aspects

Allergy

The problem of allergies has increased during the last few years. The tendency to develop allergies and asthma is not well understood, but a number of pollutants can trigger the reaction, for instance, airborne allergens such as pollen,

TABLE 9.1 Number of Particles at Different Locations

Place (examples)	Particles/m^3
Clean room	10^3
Arctic	10^7
Countryside	10^9
City	10^{11}
Tobacco smoke	10^{14}

spores, living or dead bacteria, dust, diesel fume, cigarette smoke, etc. Tests have shown that an F7 (EU7) filter can effectively reduce allergens in the air.[2]

Carcinogenic Potential of Pollutants

It is known that the urban traffic environment is carcinogenic due to automotive gases and polyaromatic hydrocarbons. An F8 (EU8) filter reduces their effect by 80%.[2]

Odors/Gases

A large number of odors are borne by particles, but for effective separation, chemical filters are very often required, which can be justified in an urban environment.

9.2.3 Filters and Test Methods

9.2.3.1 Test Methods

EUROVENT has always led the field in measuring and characterizing air filters. Since 1979 EUROVENT 4/5 has set the standard in Europe and provided the basis for European Standard EN 779:1993, Specifications for Particulate Air Filters for General Ventilation.

EN 779:1993 in principle contains two different test methods. The filter is tested both with untreated outdoor air and with the addition of synthetic dust. In the first case, the filter's dust spot efficiency is determined, i.e., its capacity to clean normal outdoor air. In the second case, the filter's arrestance is measured, i.e., its capacity to separate synthetic dust. The average value for dust spot efficiency or arrestance during the course of the test is used for classification of the filter.

Modern measuring techniques, an increased requirement for the indoor environment, and the efficiency of filters in separating particles led to EUROVENT 4/9:1992 "Method of Testing Air Filters Used In General Ventilation for the Determination of Fractional Efficiency." This method also provides the basis for the next revision or upgrade of European Standard EN 779:1999.

In EUROVENT 4/9 the dust spot efficiency has been replaced by measurement of the degree of separation of particles within the 0.2–3 μm range, with a particle size of 0.4 μm used for classification of the filter.

The increased need to control the indoor environment and filter efficiency in the actual environment has led to EUROVENT 4/10:1996, "Recommendations for In Situ Fractional Determination of General Ventilating Filters."

9.2.3.2. Classification of Coarse and Fine Filters

Depending on the test method and test result, particle filters are classified as coarse, fine, HEPA, and ULPA filters (Table 9.2). Electrofilters are usually included in the fine filter group. Chemical filters are used for gases.

Classification is based on laboratory tests with synthetic dust and does not provide a basis for calculation of the life of air filters or assessment of the filter's performance in actual application. Moreover, the dust-holding capacity and average efficiency for each classification vary with final pressure loss and

TABLE 9.2 Filter Classifications

Eurovent 4/9 class	EN 779 class	Average (A_m) arrestance, % synthetic dust	Final pressure drop Pa
Coarse filter	**Coarse filter**		
EU1	G1	$A_m < 65$	250
EU2	G2	$65 \leq A_m < 80$	250
EU3	G3	$80 \leq A_m < 90$	250
EU4	G4	$90 \leq A_m$	250
Fine filter, 0.4 μm efficiency	**Fine filter, dust spot efficiency**	**Average (E_m) efficiency, %**	
EU5	F5	$40 \leq E_m < 60$	450
EU6	F6	$60 \leq E_m < 80$	450
EU7	F7	$80 \leq E_m < 90$	450
EU8	F8	$90 \leq E_m < 95$	450
EU9	F9	$95 \leq E_m$	

airflow. In filters with electrostatically charged material, the charge is neutralized by the collected dust, resulting in poorer separation.[3,4] The influence of electrostatic effect is determined in Nordtest Method VVS 117.[5]

To save energy, the filter is dimensioned in normal ventilation plants, often with a lower final pressure loss than indicated by the classification, and the filter does not achieve the intended filter classification. For reasons of hygiene, the filter is replaced after a certain period of time, rather than a specific final pressure loss.

Coarse Filters

The basic filter material is produced from glass fiber or synthetic plastic fibers (polyester, acrylic, polyamide). Separation is mainly of particles 5 μm and larger.

Fine Filters

To be classified as an F-filter, EN 779 requires that the dust spot efficiency for new filters be greater than 20%, whereas Eurovent 4/5 has no such requirement.

Fine filters are made chiefly from glass fibers with an average diameter of 0.5 μm to 5 μm or of plastic fibers, often in combination with an electrostatic charge.

A new fine filter in the lower fine-filter range, F5 (EU5), separates about 20% of all particles in the air, whereas a better fine filter, F8 (EU8), can take 80% to 90%.

9.2.3.3 HEPA Filters

To meet today's high requirements within the military, nuclear power industry, hospitals, etc., but especially in the electronics industry, new test methods for

HEPA and ULPA filters have been developed. In the CEN EN 1822:1998 test method, the filter's efficiency is determined for the "most penetrating particle size" (MPPS). Depending on the filter's total level of separation and leakage, the filter is classified as H10, H11, . . . , H14 and U15, U16, or U17. HEPA filters are commonly used for inlet air in the pharmaceutical, optical, and food industries.

9.2.3.4 Chemical Filters

Chemical filters are used to collect gases; these are mainly adsorption filters based on activated carbon. By the addition of chemical substances, ("impregnation"), gases which are difficult to adsorb are adsorbed and retained by means of a chemical reaction.

9.2.4 Filters in Operation

9.2.4.1 Separation

It is important to be aware of the filter's properties in different environments. Figure 9.2 shows how, in the case of new filters, separation varies with particle size and filter class. The filter class is based on the average efficiency, and a new filter normally has much lower initial efficiency. In the case of electrostatically charged filters, separation may be significantly higher for new filters. The figure should be seen as an indication of *minimum separation during actual operation.*

As the filter accumulates dust, the pressure loss increases, and the dust removed improves the normal separation. Another effect can be seen with electrostatically charged filter material. During operation, the impurities neutralize the material, and the filter's capacity to separate is reduced. Figure 9.3[4] shows exam-

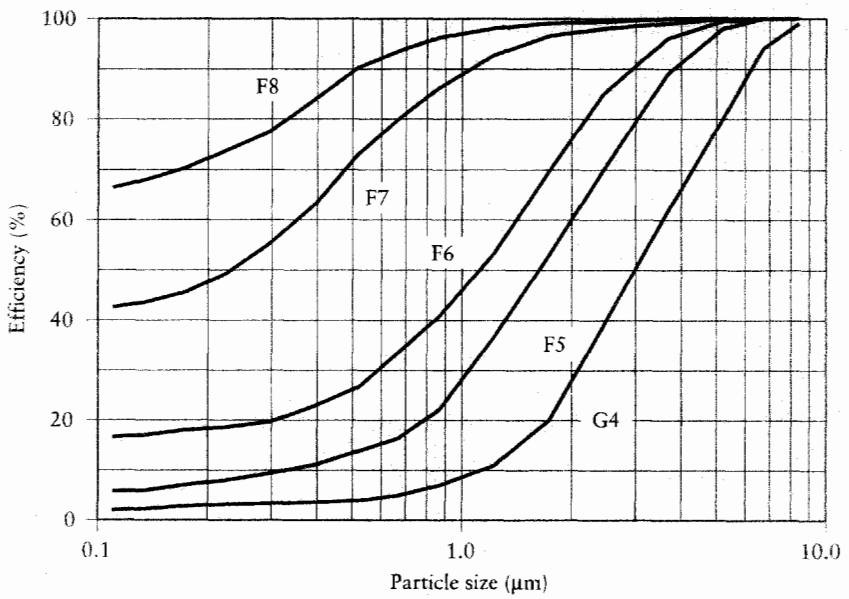

FIGURE 9.2 Efficiency of air filters vs. particle size. The figures should be the minimum efficiencies in an installation.

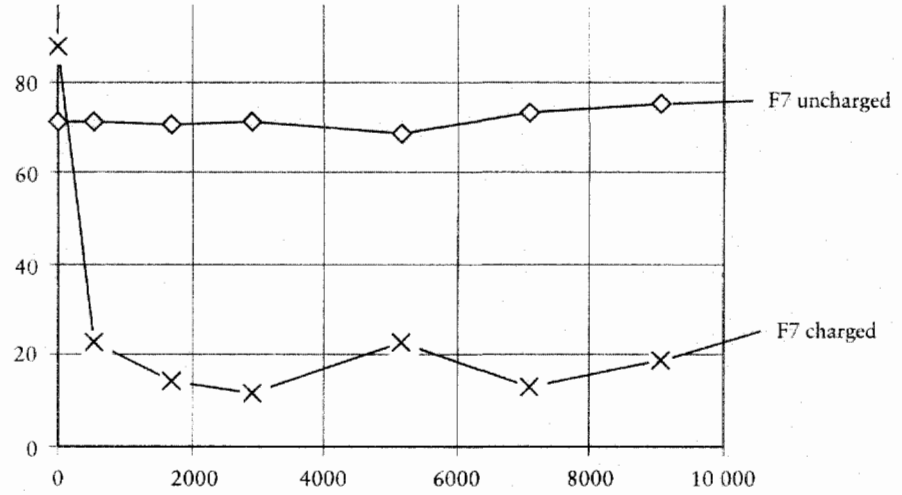

FIGURE 9.3 Example of efficiency changes in an installation with two F7 air filters.

ples of filters shown by laboratory tests to be in accordance with Class F7 (EU7). The efficiency drops dramatically from more than 80% to less than 20% after a few weeks' operation in the case of the filter based on electrostatic charge. The effect varies much with fiber size and charge.

9.2.4.2 Average Pressure Loss

The average pressure loss during operation is dependent on the characteristics of the plant and is often taken to be the average value of initial pressure loss and final pressure loss of the filter. With the lower energy requirement, more and more systems are being dimensioned for constant flow, and average pressure loss is the integrated value. Significant savings can thus be made using filters with a low pressure loss and small increase in pressure during the period of operation.

9.2.4.3 Energy Consumption

A filter's energy consumption, E, based on average pressure loss, can be calculated as

$$E = \frac{q\Delta pt}{\eta 1000}(\text{kW h}),$$

where

q is airflow (m^3/s)
Δp is average pressure loss (Pa)
t is operation time (hours)
η is efficiency of fan

Over one year (8760 hours), a 1 m^3/s filter with an average pressure loss of 100 Pa requires 1250 kW h if the fan's efficiency is set at 70%. The energy cost is generally greater than the filter cost, and pressure loss reduction be-

comes increasingly significant for energy reductions. Lower pressure loss by 10 Pa means 125 kW h less energy in the example above.

9.2.4.4 Lifetime

The lifetime of a filter is dependent on the concentration of dust, type of dust, airflow, and, of course, the selected final pressure loss. Filter material and filter construction are often a compromise or combination of filter effects and installation space. Low speed or large filter surface promotes efficiency, low pressure loss, but above all a longer lifetime.

9.2.4.5 Filter Replacement

Airflow changes in the plant have been the main criterion for changing filters, i.e., when pressure loss increases to the extent that the fan cannot maintain a specific minimum airflow. Reduction of maximum effect, energy consumption or economic evaluation, i.e., when the energy cost and filter cost reach a minimum, are becoming increasingly significant.

Considerations of hygiene are being applied more and more to filter replacement. Studies[6] have shown that with RH (relative humidity) higher than 75% there is a risk of microbial growth in the filter and in the ventilation system. As it is in many cases difficult to avoid a high relative humidity in the air intake, filtering should take place in two steps. The first filter can often be exposed to high humidity or to rain and snow. Organic impurities also become caught in the filters and could be released later. Particles and endotoxins from microorganisms can become loose in low-quality filters.

The first filtration step should thus be carried out using a filter of at least F7 (EU7) quality, which should be changed after a maximum period of one year's continuous operation. The second filter of at least F7 (EU7) quality is not exposed to high RH, effectively stops microorganisms and particles, and can remain in place for about two years, provided the final pressure loss is not reached within this period.

9.2.5 Life-Cycle Issues

9.2.5.1 Environment: Life-Cycle Analysis (LCA)

Global environmental questions have increased in significance during the last few years. A life-cycle analysis (LCA) analyzes the environmental effect with reference to ecological effects, health effects, and consumption of resources.

Life-cycle analysis of a filter shows that operation often corresponds to 70% to 80% of the filter's total environmental load and is absolutely decisive as regards environmental effect.[7] Raw material, refining, manufacturing, and transports correspond to about 20% to 30%, while the used filter contributes at most 1%. Filters of plastic or other inflammable material can render 10 kWh to 30 kWh energy when burned, which correspondingly reduces the total environmental load from 0.5% to 1%. On the other hand, if the pressure loss in the filter is reduced by 10 Pa, the environmental load is reduced by 125 kW h per year, or approximately 5% decrease in total environmental load. Filters in industrial applications can have quite different figures.

TABLE 9.3 Example of Life-Cycle Cost Distribution of an Air Filter

Type of cost	Relative cost (%)
Investment	4.5
LCC_{energy}	80.8
$LCC_{maintenance}$	14.2
$LCC_{environment/dumping}$	0.5
LCC_{total}	100

9.2.5.2 Life-Cycle Cost (LCC)

Life-cycle analysis (LCA) does not account for economic aspects, and such analysis should therefore be considered together with a life-cycle cost analysis (LCC),[8] which takes into account the costs of investment, energy, maintenance, and dumping the final waste product throughout the lifetime of a plant.

Future costs of replacement filters and energy are calculated according to the current value method. The final result for a 1 m^3/s filter with average pressure loss of 200 Pa may be as shown in Table 9.3, if the calculation is based on a 10-year period.

The table shows that energy costs account for 80% of the total cost during the plant's period of operation. The actual costs of the filter, investment, and maintenance correspond to about 20%, while the costs of dumping amount to only 0.5%. The calculation is based on filtering outdoor air, and filters in industrial applications can have quite different figures.

LCC analyses provide an excellent tool for minimizing the filter costs of a plant. As in the case of LCA, the operation and low pressure loss are absolutely decisive as regards the costs of the filter function.

9.2.6 Summary

The following points should be borne in mind when planning filter installations.

- Great care is required regarding the positioning and design of the air intake to avoid drawing in local impurities and rain or snow.
- The risk of microbial growth is low, but to minimize the risk, the plant should be designed so that relative humidity is always below 75% in all parts of the system.
- For reasons of hygiene, the inlet air should be filtered in two steps.[9] The first filter in the air intake must be at least F5 (EU5) quality but preferably F7 (EU7). The second filter step should be effected by a filter of at least F7 (EU7) but preferably F9 (EU9) quality. If there is only one filter step, the minimum requirement is for F7 (EU7) quality.
- As regards recirculated air, at least F5 (EU5) quality must be used to cope with contamination of components in the system, but the minimum requirement is for F7 (EU7) if the environment in the room is to be improved.

- The exhaust air system must be protected from contamination by a filter of at least F5 (EU5) quality.
- Filters must not be installed directly after the fan outlet or across places where there is a big change in area or flow.
- The final pressure drop is dimensioned and selected with regard to permitted variations in flow, the filter's life-cycle costs, and life-cycle analysis.
- Dust-holding capacity and test results from laboratory trials differ from performances in actual use.
- The efficiency must not deteriorate or fall below specific minimum values.
- The tightness and condition of the filter are checked regularly by visual inspection of the plant.
- Filter and aggregate must be clearly marked with the type and designation of the filter, date of installation, etc.
- In the case of more stringent requirements, in situ checks of the filter are carried out according to Eurovent 4/10.
- Filters must be replaced when the pressure loss reaches the dimensioned final pressure loss or when the following hygiene interval is reached, if this is earlier:
  - The first step should be replaced after a maximum operating period of 8700 hours.
  - The second step and filters in exhaust or recycled air systems should be changed after a maximum of two years' continuous operation.
- For reasons of hygiene, the filter should be replaced after the pollen and spore season in the autumn. In the case of high demand, filters can also be changed in the spring after the heating season to eliminate odorous combustion products.
- Filters should be replaced carefully, using protective equipment so that the impurities trapped do not escape.
- It is a good idea to incinerate filters in well-filtered furnaces in order to burn trapped impurities, reduce quantities of waste, and recover some energy. The filters from normal ventilation systems could also be dumped at a landfill.

References

1. Ellringer, P. J., and Whitcomb, L. *Advancing Filtration Solutions*, Indoor Air Quality Studies in the State of Minnesota, no. 263, 1997.
2. Gustavsson, J. Cabin air filters: Performances and requirements. SAE Conference, Detroit, February 1996.
3. Lehtimäki, M. *Performance of Ventilation Filters: Pilot Field Tests, Material Test and Full Scale Field Test*. Tampere, Finland, December 18, 1997.
4. SINTEF. *Lifetime Tests of Air Filters in Real Applications*. STF A95027. Sintef, March 1995.
5. Nordtest. *Electret Filters: Determination of the Electrostatic Enhancement Factor of Filter Media*. Method NT VVS 117. December 1997.
6. Möritz, M. Verhalten von mikroorganismen auf luftfiltern (in German). Universität Berlin, 1996.
7. Camfil Environmental Seminarium, Stockholm. 1998.
8. EUROVENT/CECOMAF Recommendation. *Life Cycle Cost of Air Filters*. 1999.
9. VDI 6022. *Hygienic Aspects for the Planning, Design, Operation, and Maintenance of Air-conditioned Systems*. March 1997.

9.3 HEAT EXCHANGERS AND HEAT-RECOVERY UNITS

9.3.1 General Theory of Heat Exchangers

9.3.1.1 Introduction

A heat exchanger is a device that transfers heat from one medium to another; the medium may be a solid, liquid, or gas. Some of the most complex engineering design problems relate to heat exchangers.

Heat exchangers are divided into the following types.

1. Recuperator: A wall separating the flowing fluids is the most commonly encountered problem.
2. Regenerator: The hot and cold fluids pass alternately through a space containing solid areas/particles, which provide alternately a heat sink and a heat source. An example of the rotating-type matrix is a cooling tower.

The direction of flow is important, as it has a pronounced effect on the efficiency of a heat exchanger. The flows may be in the same direction (parallel flow, cocurrent), in the opposite direction (counterflow), or at right angles to each other (cross-flow). The flow may be either single-pass or multipass; the latter method reduces the length of the pass.

A schematic diagram of a parallel-flow (cocurrent) heat exchanger is shown in Fig. 9.4.

$$\text{Hot fluid: } T_{hi} > T_{ho}$$

$$\text{Cold fluid: } T_{ci} < T_{co}$$

The hot and cold fluids are denoted by the subscripts h and c and the fluid inlet and outlet by i and o, respectively.

In the case of Fig. 9.4, $T_{hi} = T_{h1}$. The *relative temperature differences* are defined by

$$\delta T_h = \frac{T_{hi} - T_{ho}}{T_{hi} - T_{ci}}, \tag{9.1}$$

$$\delta T_c = \frac{T_{co} - T_{ci}}{T_{hi} - T_{ci}}. \tag{9.2}$$

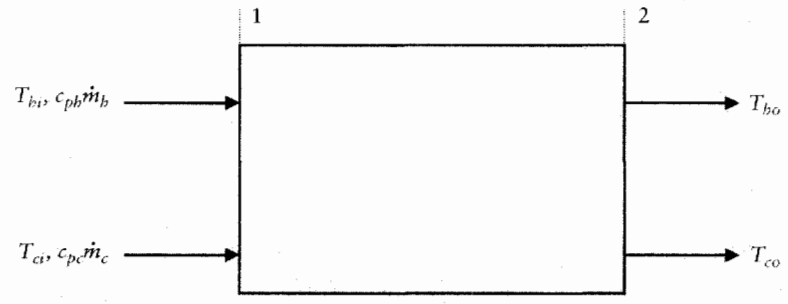

FIGURE 9.4 Heat exchanger with flow notations.

The relative temperature differences can be calculated by dividing the temperature difference of the hot or cold side by the maximum temperature difference, $T_{hi} - T_{ci}$, that occurs in the heat exchanger.

There are two relative temperature changes for a heat exchanger. The greatest of them is the *heat exchanger effectiveness*, ϵ:

$$\epsilon = \max\{\delta T_c, \delta T_h\} \tag{9.3}$$

The maximum temperature difference that takes place in a heat exchanger is $T_{hi} - T_{ci}$. A higher temperature difference cannot occur due to the second law of thermodynamics. The maximum theoretical heat transfer rate in a heat exchanger is

$$\phi_{\max} = \dot{C}_2(T_{hi} - T_{ci}) \quad \text{or} \quad \phi_{\max} = \dot{C}_1(T_{hi} - T_{ci}),$$

where

$$\dot{C} = q_m c_p \tag{9.4}$$

is the *heat capacity rate*, q_m is the mass flow through the heat exchanger, and c_p is the specific heat capacity.

Assuming that the maximum possible temperature difference is on the fluid side with the higher heat capacity rate, then

$$\phi_{\max} = \dot{C}_2(T_{hi} - T_{ci}) \ .$$

The heat exchanger balance is

$$\dot{C}_2(T_{hi} - T_{ci}) = \dot{C}_1 \ \Delta T_1 \ ,$$

where ΔT_1 is the temperature difference of the smallest heat capacity rate fluid in the heat exchanger. Then

$$\Delta T_1 = \frac{\dot{C}_2}{\dot{C}_1}(T_{hi} - T_{ci}) > T_{hi} - T_{ci} \ .$$

This equation, which gives a higher temperature difference than $T_{hi} - T_{ci}$, cannot occur. Then

$$\phi_{\max} = \dot{C}_1(T_{hi} - T_{ci}) \ ,$$

where $\dot{C}_1$ is the smaller heat capacity rate. The actual power is

$$\phi = \dot{C}_1 \Delta T_1 = \dot{C}_2 \Delta T_2 \ ,$$

from which

$$\frac{\phi}{\phi_{\max}} = \frac{\dot{C}_1 \Delta T_1}{\dot{C}_1(T_{hi} - T_{ci})} = \frac{\Delta T_1}{(T_{hi} - T_{ci})} = \frac{\dot{C}_2 \Delta T_2}{\dot{C}_1(T_{hi} - T_{ci})} > \frac{\Delta T_2}{T_{hi} - T_{ci}} .$$

From this it follows that

$$\epsilon = \frac{\phi}{\phi_{\max}} = \frac{\text{temperature difference of smaller heat capacity fluid}}{\text{initial temperature difference}} . \tag{9.5}$$

The heat exchanger effectiveness shows how close the heat exchanger is operating to the maximum heat transfer performance. Equation (9.5) is valid for any type of heat exchanger.

9.3.1.2 Counterflow Heat Exchanger and the Heat Exchanger Effectiveness

In a counterflow or countercurrent heat exchanger, hot and cold fluids enter the exchanger from opposite sides. The counterflow heat exchanger in Fig. 9.5 serves as a reference for all other heat exchanger configurations. A detailed analysis of this type of heat exchanger is therefore necessary.

The heat is transferred by convection and conduction from the hot to the colder fluid through an infinitesimal surface area dA. The temperature of the hot fluid reduces by an amount dT_h, and the temperature of the cold fluid increases by an amount dT_c.

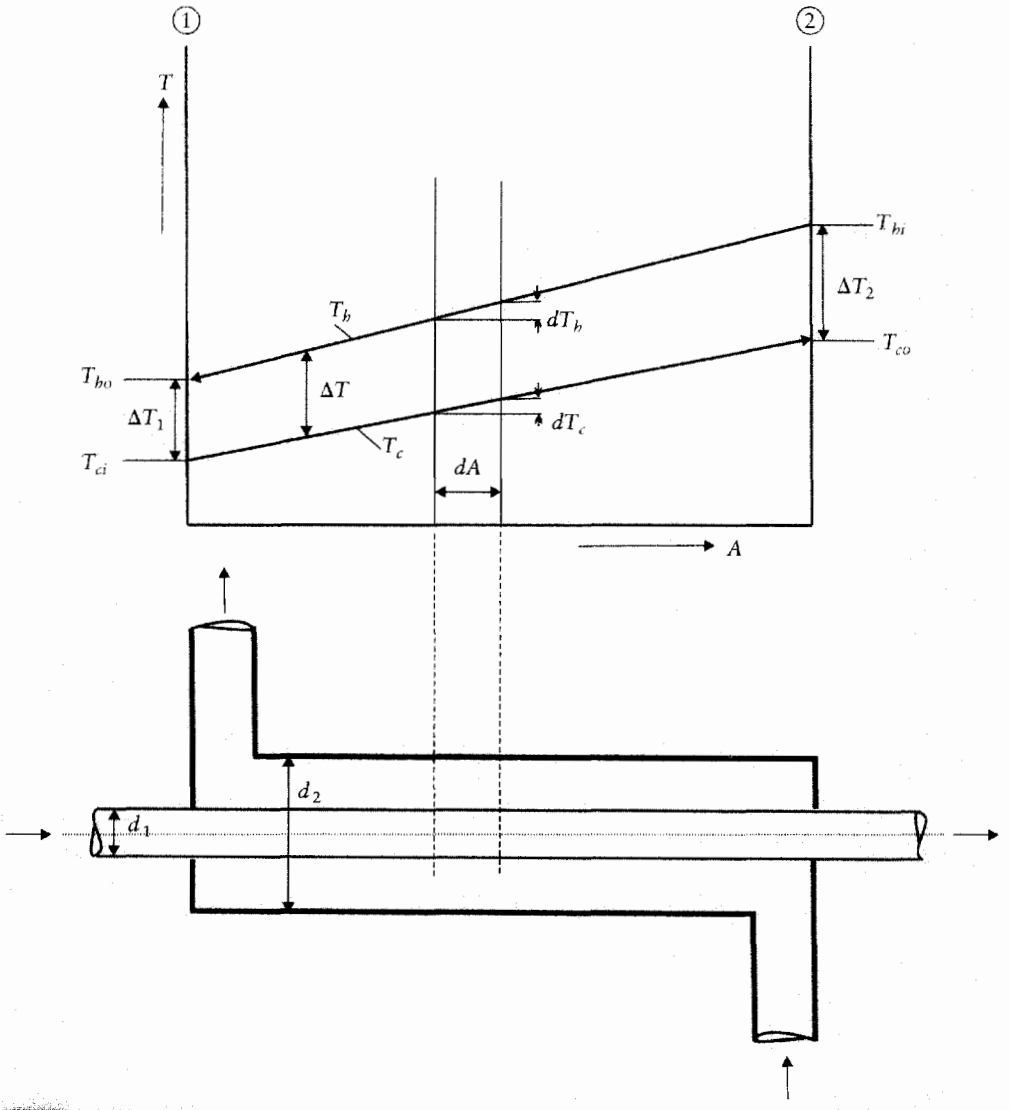

FIGURE 9.5 Counterflow heat exchanger.

The heat balance gives

$$G'' \, dA(T_h - T_c) = \dot{C}_h \, dT_h = \dot{C}_c \, dT_c \,, \tag{9.6}$$

where G'' is the conductance per unit of surface area of the separating wall, which for a plane wall can be written as

$$\frac{1}{G''} = \frac{1}{\alpha_c} + \frac{1}{\alpha_h} + \frac{\delta}{\lambda} \,, \tag{9.7}$$

where α_c and α_h are the cold- and hot-side convective heat transfer coefficients, respectively, δ is the wall thickness, and λ is the wall thermal conductivity.

For a thick circular tube, the conductance per unit tube length is

$$\frac{1}{G'} = \frac{1}{\pi d_o \alpha_o} + \frac{1}{\pi d_i \alpha_i} + \frac{\ln(d_o/d_i)}{2\pi\lambda} \,, \tag{9.8}$$

where α_o is the outer convective heat transfer coefficient, α_i is the inner convective heat transfer coefficient, d_i is the inner tube diameter, and d_o is the outer tube diameter.

Equation (9.6) gives

$$dT_h - dT_c = d(T_h - T_c) = \left(\frac{1}{\dot{C}_h} - \frac{1}{\dot{C}_c}\right) G'' \, dA(T_h - T_c). \tag{9.9}$$

Equation (9.9), after integrating,

$$\int_1^2 \frac{d(T_h - T_c)}{T_h - T_c} = \left(\frac{1}{\dot{C}_h} - \frac{1}{\dot{C}_c}\right) G'' \int_0^A dA, \tag{9.10}$$

gives

$$\ln \frac{\Delta T_2}{\Delta T_1} = \left(\frac{1}{\dot{C}_h} - \frac{1}{\dot{C}_c}\right) G'' \, A = G\left(\frac{1}{\dot{C}_h} - \frac{1}{\dot{C}_c}\right) \tag{9.11}$$

or

$$\frac{\Delta T_2}{\Delta T_1} = \exp \, G''\left(\frac{1}{\dot{C}_h} - \frac{1}{\dot{C}_c}\right). \tag{9.12}$$

Using Fig. 9.5 and Eq. (9.12) gives

$$\frac{T_{hi} - T_{ci} + T_{ci} - T_{co}}{T_{hi} - T_{ci} + T_{ho} - T_{hi}} = \exp\left(G\left(\frac{1}{\dot{C}_h} - \frac{1}{\dot{C}_c}\right)\right). \tag{9.13}$$

For the case of $\dot{C}_h < \dot{C}_c$, the heat exchanger effectiveness is

$$\epsilon = \frac{T_{hi} - T_{ho}}{T_{hi} - T_{ci}}, \tag{9.14}$$

and the heat balance is

$$\dot{C}_h(T_{hi} - T_{ho}) = \dot{C}_c(T_{co} - T_{ci}). \tag{9.15}$$

This then is written as

$$T_{co} - T_{ci} = \frac{\dot{C}_h}{\dot{C}_c}(T_{hi} - T_{ho}) = R(T_{hi} - T_{ho}), \tag{9.16}$$

where $R = \dot{C}_h/\dot{C}_c < 1$.

Using Eqs. (9.13) and (9.16),

$$\frac{1-R\epsilon}{1-\epsilon} = \exp\left(\frac{G}{\dot{C}_h}(1-R)\right) \tag{9.17}$$

from which

$$\frac{1-\epsilon}{1-R\epsilon} = \exp(-z(1-R)), \tag{9.18}$$

where $z = G/\dot{C}_c$ is the dimensionless conductance.

Taking the case $\dot{C}_c < \dot{C}_h$, it can then be shown that we also get

$$\epsilon = \frac{1-\exp(-z(1-R))}{1-R\exp(-z(1-R))}, \tag{9.19}$$

which is the same as Eq. (9.18).

This heat exchanger effectiveness is one of the important parameters that describes the performance of a counterflow heat exchanger.

In Eq. (9.19) $R = \dot{C}_{\min}/\dot{C}_{\max} < 1$ is between the minimum and maximum heat capacity rates. $z = G/\dot{C}_{\min}$ is the heat conductance divided by the minimum heat capacity rate. In heat transfer literature, it is also denoted by z = NTU (number of heat transfer units).

Solving Eq. (9.19) for the dimensionless conductance z gives

$$z = \frac{1}{1-R}\ln\left(\frac{1-R\epsilon}{1-\epsilon}\right). \tag{9.20}$$

If the cold and hot fluids heat capacity rates are equal, then $R = 1$. Equation (9.22) gives an indefinite value, and this equation cannot be used directly.

Using l'Hopital's rule as $R \longrightarrow 1$ gives

$$\begin{aligned}\lim\epsilon &= \frac{\lim\frac{d}{dR}(1-\exp(-z(1-R)))}{\lim\frac{d}{dR}(1-R\exp(-z(1-R)))} \\ &= \frac{\lim(-z\exp(-z(1-R)))}{\lim(-Rz\exp(-z(1-R))-\exp(-z(1-R)))} = \frac{z}{1+z},\end{aligned} \tag{9.21}$$

from which

$$z = \frac{\epsilon}{1-\epsilon}. \tag{9.22}$$

In Fig. 9.6 the temperature profiles in a counterflow heat exchanger are shown when $\dot{C}_h > \dot{C}_c$.

9.3.1.3 Logarithmic Mean Temperature Difference

The rate of temperature drop of a fluid as it flows along the length of a heat exchanger is not constant. In order to take account of this nonlinear relationship, the logarithmic mean temperature difference (LMTD) is used. If the inlet and outlet temperatures do not differ widely, an arithmetic mean can be used, because the relationship is considered to be linear.

In order to calculate the heat transfer from the hot to the cold fluid, the heat exchanger conductance and the temperature of the fluids at both sides of

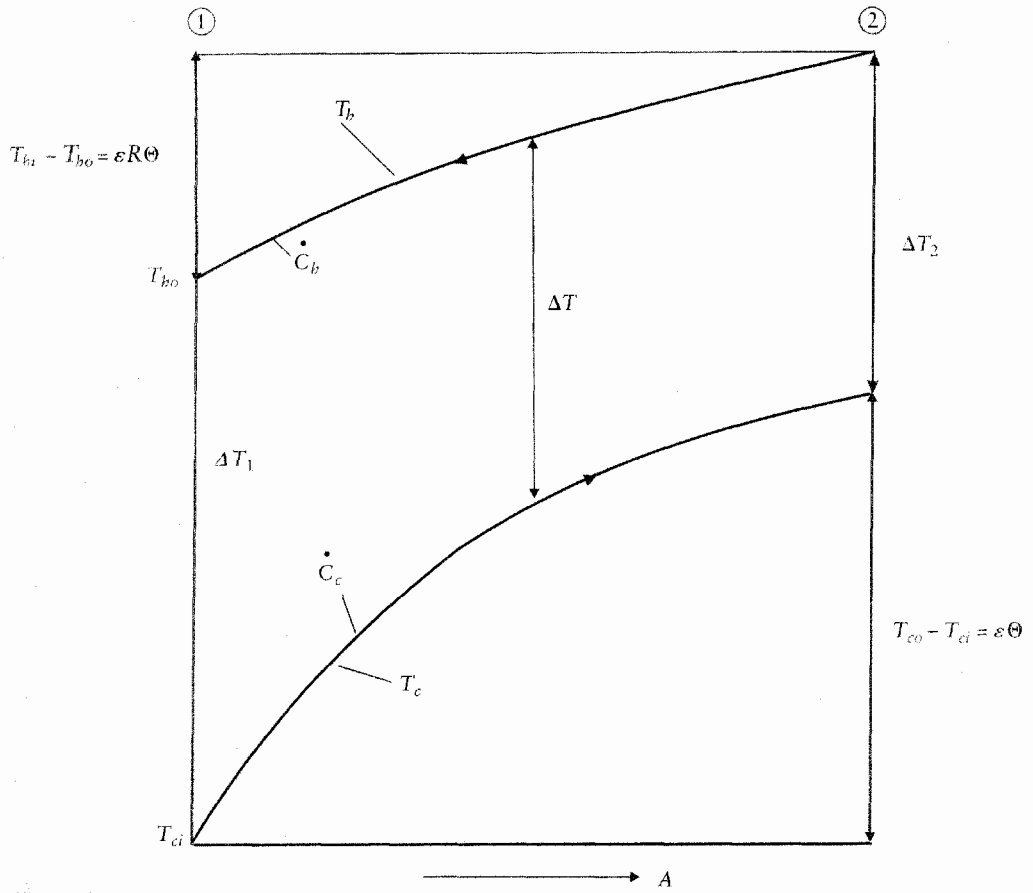

FIGURE 9.6 Counterflow heat exchanger temperature profiles when $\dot{C}_h > \dot{C}_c$. $\theta = T_{hi} - T_{ci}$.

the heat exchanger must be known. The mass flow measurement is often difficult to determine; however, the temperatures are easily measured.

A temperature difference is defined that satisfies the following equation:

$$\phi = G\Delta\overline{T}, \tag{9.23}$$

where ϕ is the heat transfer rate in the heat exchanger and G the conductance. For counterflow Eq. (9.12) gives

$$\ln\frac{\Delta T_2}{\Delta T_1} = G\left(\frac{1}{\dot{C}_h} - \frac{1}{\dot{C}_c}\right) = \frac{\phi}{\Delta\overline{T}}\left(\frac{1}{\dot{C}_h} - \frac{1}{\dot{C}_c}\right). \tag{9.24}$$

On the other hand, Eq. (9.15) gives

$$\phi = \dot{C}_h(T_{hi} - T_{ho}) = \dot{C}_c(T_{co} - T_{ci}) \ , \tag{9.25}$$

giving

$$\begin{aligned}\ln\frac{\Delta T_2}{\Delta T_1} &= \frac{1}{\Delta\overline{T}}(T_{hi} - T_{ho} - (T_{co} - T_{ci})) \\ &= \frac{1}{\Delta\overline{T}}(T_{hi} - T_{co} - (T_{ho} - T_{ci})) = \frac{1}{\Delta\overline{T}}(\Delta T_2 - \Delta T_1).\end{aligned} \tag{9.26}$$

Equation (9.26) gives the temperature difference defined in Eq. (9.23) as

$$\Delta\overline{T} = \frac{\Delta T_2 - \Delta T_1}{\ln\dfrac{\Delta T_2}{\Delta T_1}} = \Delta T_{\ln}. \tag{9.27}$$

From Fig. 9.6 for a countercurrent heat exchanger,

$$\Delta T_1 = T_{ho} - T_{ci}$$

and

$$\Delta T_2 = T_{hi} - T_{co}.$$

For a countercurrent heat exchanger, the logarithmic temperature difference is then

$$\Delta T_{\ln} = \frac{(T_{hi} - T_{co}) - (T_{ho} - T_{ci})}{\ln\dfrac{T_{hi} - T_{co}}{T_{ho} - T_{ci}}}. \tag{9.28}$$

This is the *logarithmic temperature difference* for the counterflow heat exchanger.

The logarithmic mean temperature difference is defined when $\Delta T_2 \neq \Delta T_1$.

Consider the case where $\Delta T_2 = \Delta T_1$. The logarithmic temperature difference is obtained by applying l'Hopital's rule as $\Delta T_2 \longrightarrow \Delta T_1$, giving

$$\lim \Delta T_{\ln} = \lim \frac{\Delta T_2 - \Delta T_1}{\ln\dfrac{\Delta T_2}{\Delta T_1}} = \frac{\lim \dfrac{d}{d\Delta T_2}(\Delta T_2 - \Delta T_1)}{\dfrac{d}{d\Delta T_1}\left(\ln\dfrac{\Delta T_2}{\Delta T_1}\right)} = \Delta T_2. \tag{9.29}$$

The logarithmic mean temperature difference is the same as the temperature difference at the entrance and exit of the heat exchanger, i.e., $\Delta T_1 = \Delta T_2 = \Delta T_{\ln}$

For a counterflow heat exchanger, when $\Delta T_2 = \Delta T_1$,

$$T_{hi} - T_{co} = T_{ho} - T_{ci} \tag{9.30}$$

or

$$T_{hi} - T_{co} = T_{co} - T_{ci}. \tag{9.31}$$

Then from Eq. (9.15), $\dot{C}_h = \dot{C}_c$ when $\Delta T_1 = \Delta T_2 = \Delta T_{\ln}$.

Example 1

A brine solution enters a counterflow heat exchanger at $T_{li} = 31.7$ °C, and air enters at $T_{ai} = 24.4$ °C. The measured outlet temperatures of the brine solution and air are $T_{lo} = 27.2$ °C and $T_{ao} = 30$ °C, respectively.

The mass flow rate of the hot fluid is $q_{ml} = 0.382$ kg s^{-1} and of the cold fluid, $q_{ma} = 0.9$ kg s^{-1}. The specific heat capacity for brine is $c_{pl} = 3.12$ kJ kg^{-1} K^{-1} and for air, $c_{pa} = 1.007$ kJ kg^{-1} K^{-1}.

a. Calculate the total conductance of the heat exchanger.
b. If the liquid mass flow rate is reduced to $q_{ml} = 0.3$ kg s^{-1}, calculate the new outlet temperatures of the brine and air.

Solution

a. The total heat conductance can be calculated from Eqs. (9.23) and (9.28) as $T_{hi} = T_{li}$, $T_{ho} = T_{lo}$, $T_{ci} = T_{ai}$, and $T_{co} = T_{ao}$.

$$G_{\text{tot}} = \frac{\phi}{(T_{li} - T_{ao}) - (T_{lo} - T_{ai})} \ln \frac{T_{li} - T_{ao}}{T_{lo} - T_{ai}},$$

where $\phi = q_{ma} c_{pa} (T_{ao} - T_{ai}) = 5.1$ kW is the heat flow to the air, which gives $G_{\text{tot}} = 2310$ W K^{-1}, $\phi = q_{ml} c_{pl} (T_{li} - T_{lo}) = 5.36$ kW is the heat flow from the liquid, which gives $G_{\text{tot}} = 2430$ W K^{-1}. The difference is due to errors in flow and temperature measurements. The difference between the heat flow in the two cases, 5%, is satisfactory. Then an average estimation can be obtained as $G_{\text{tot}} = 2370$ W K^{-1}.

b. The heat capacity rates of liquid and air are calculated by, respectively,

$$\dot{C}_l = q_{ml} c_{pl} = 0.3 \times 3120 = 936 \text{ W K}^{-1}$$

and

$$\dot{C}_a = q_{ma} c_{pa} = 0.9 \times 1007 = 906 \text{ W K}^{-1}.$$

Therefore,

$$\dot{C}_a < \dot{C}_l.$$

The maximum heat transfer in the heat exchanger is

$$\phi_{\max} = \dot{C}_{\min} (T_{li} - T_{ai}) = 906 \times (31.7 - 24.4) = 6.61 \text{ kW}.$$

The total heat conductance is considered constant and not influenced by the mass flow rate of liquid.

Then the number of heat transfer units is

$$z = \frac{G_{\text{tot}}}{\dot{C}_{\min}} = \frac{2370}{906} = 2.62.$$

Calculating the heat capacity rates ratio gives

$$R = \frac{\dot{C}_{\min}}{\dot{C}_{\max}} = \frac{906}{936} = 0.968.$$

From Eq. (9.19),

$$\epsilon = \frac{1 - \exp(-z(1-R))}{1 - R \exp(-z(1-R))} = \frac{1 - \exp(-2.62(1 - 0.968))}{1 - 0.968 \exp(-2.62(1 - 0.968))} = 0.73.$$

The actual heat transfer is calculated from

$$\phi = \epsilon \phi_{\max} = 0.73 \times 6.61 = 4.84 \text{ kW}.$$

The exit temperature of the liquid is calculated from

$$\phi = \dot{C}_l (T_{li} - T_{lo}),$$

which gives

$$T_{lo} = T_{li} - \frac{\phi}{\dot{C}_l} = 31.7 - \frac{4840}{936} = 26.5 \text{ °C}.$$

Similarly, the exit temperature of air is calculated from

$$\phi = \dot{C}_a (T_{ao} - T_{ai}),$$

which gives

$$T_{ao} = T_{ai} + \frac{\phi}{\dot{C}_a} = 24.4 + \frac{4840}{906} = 29.7\ ^\circ\mathrm{C}.$$

A reduction in liquid flow reduces the outlet temperature of the liquid and air.

9.3.2 Plate Fin-and-Tube Heat Exchangers

9.3.2.1 Introduction

A common type of heat exchanger used in industrial ventilation is the plate fin-and-tube heat exchanger (Fig. 9.7). Liquid or gas flows in the tubes, with a gas or a liquid circulating outside the tubes between the plates.

The plates can be straight or wavy. Wavy plates, due to their greater surface area, enhance the heat transfer between air and the plates but are unsuitable in dusty environments.

9.3.2.2 Annular Fins

The complete study of *annular fins* is essential in order to calculate the amount of conduction in the plate fin. A schematic diagram of annular fins is given in Fig. 9.8.

The temperature distribution within the annular fin is given by the differential equation

$$\frac{d^2T}{dr^2} + \frac{1}{r}\frac{dT}{dr} - \frac{2h}{\lambda t}(T - T_\infty) = 0. \tag{9.32}$$

In Eq. (9.32), h is the heat transfer coefficient between the air and the surface of the annular fin, λ is the thermal conductivity of the fin, and T_∞ is the temperature

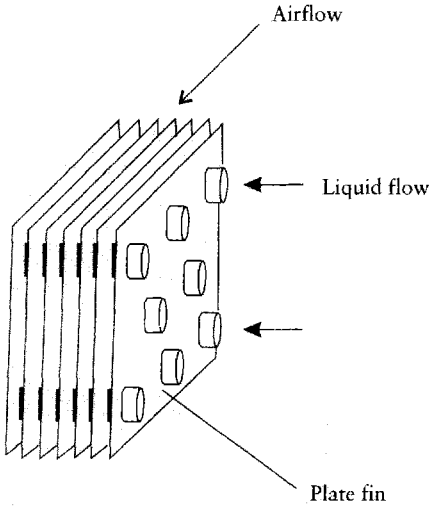

FIGURE 9.7 Plate fin-and-tube heat exchanger.

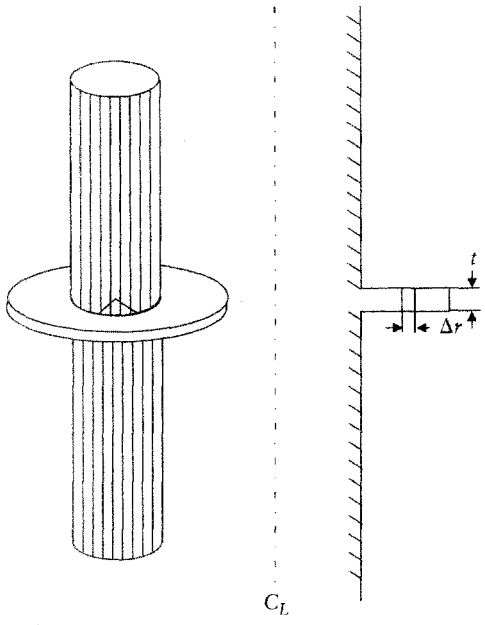

FIGURE 9.8 Annular fin.

of air far away from the fin. The differential equation (9.32) together with the boundary conditions is difficult to solve and is not considered in this chapter.

Normally, heat exchanger tubes are arranged in a staggered manner. The continuous plate is considered as being built up of regular hexagons, with a hole in the center for the pipes. This arrangement is shown in Fig. 9.9.

If hexagons are replaced with an annular area of the same size, the outer radius of the annular area will be

$$r_o = \sqrt{\frac{\sqrt{3}}{2\pi}}\, l = 0.525 l, \tag{9.33}$$

where l is the distance between the pipe centerlines in the heat exchanger. The inner hole diameter in the annular area is the same as the pipe's outer diameter.

9.3.2.3 Fin Efficiency

The fin heat transfer is determined by using fin efficiency. The fin efficiency is calculated using a theoretical approach where the whole fin is considered to be at the same temperature as the fin base. The required parameters necessary to determine the fin efficiency are shown in Fig. 9.10.

The heat transfer through the fin is

$$\phi_{\text{theor}} = hA_s(T_b - T_\infty) = hA_s\theta_t\,, \tag{9.34}$$

where A_s is the surface area of the fin.

The fin efficiency is defined by the division of the actual by the theoretical heat transfer, i.e.,

$$\eta = \frac{\phi_{\text{actual}}}{\phi_{\text{theor}}} = \frac{G\theta_t}{hA_s\theta_t} = \frac{G}{hA_s}. \tag{9.35}$$

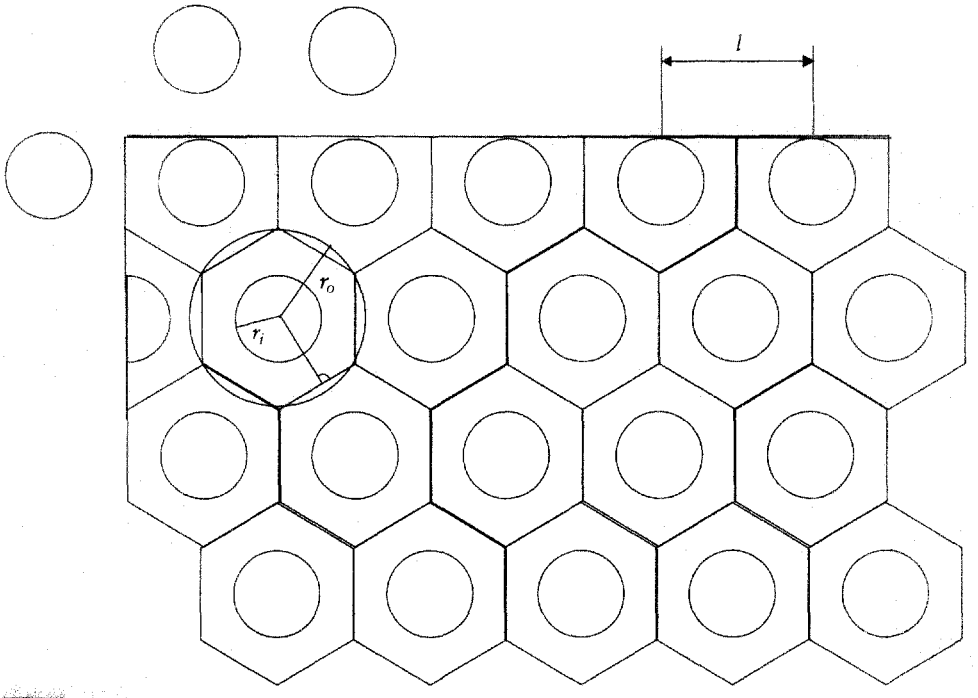

FIGURE 9.9 A continuous plate built up by hexagons.

The actual heat flow through the fin is

$$\phi_{\text{actual}} = G\theta_t = h\eta A_s \theta_t . \tag{9.36}$$

The actual heat flow is calculated by multiplying the fin outer surface area by the fin efficiency. The outer surface area is easy to determine; hence, if the fin efficiency is known, the heat transfer from the fin is easily calculated.

The efficiency depends on the fin geometrical configuration, the fin thermal conductivity, and the heat transfer coefficient at the fin surface.
The use of Eq. (9.36) to determine the heat transfer of annular fins is a practical approach. The fin efficiency curve is constructed by solving Eq. (9.34) for

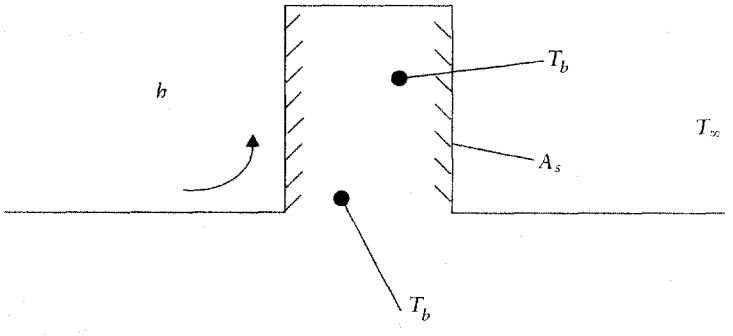

FIGURE 9.10 The comparison for the definition of fin efficiency.

adiabatic boundary condition of the outer surface. Figure 9.11 shows the fin efficiency of an annular fin. (The curves G/G_∞ in the figure are not required in this analysis.)

9.3.2.4 The Convective Heat Transfer Coefficient between the Plate and Flowing Air

To use Fig. 9.11, a means of calculating the heat transfer coefficient between the plate and the flowing air is required. Consider a straight plate. The heat transfer coefficient is calculated using Fig. 9.12.

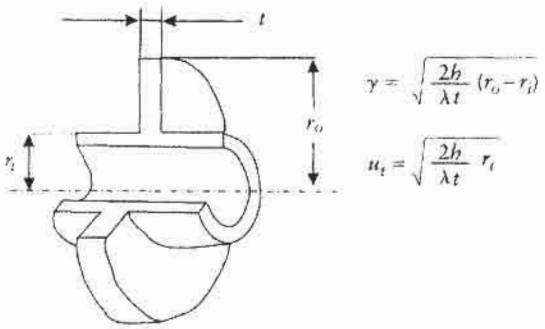

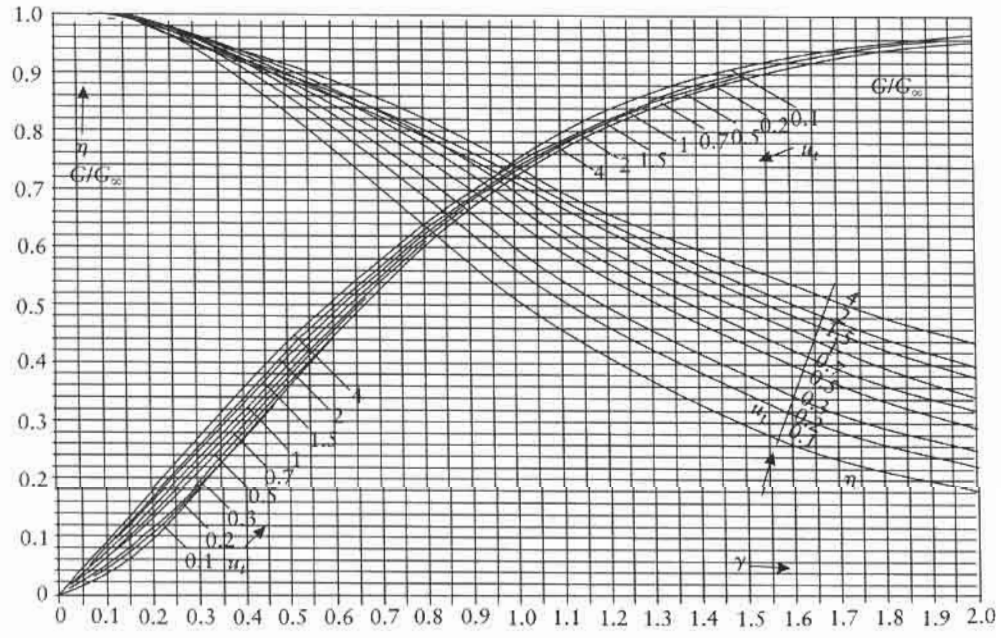

FIGURE 9.11 Fin efficiency of annular fins.

Surface	Fins/cm	Surface	Fins/cm
1	1.15	5	3.61
2	1.74	6	4.60
3	2.62	7	5.71
4	3.02	8	8.11

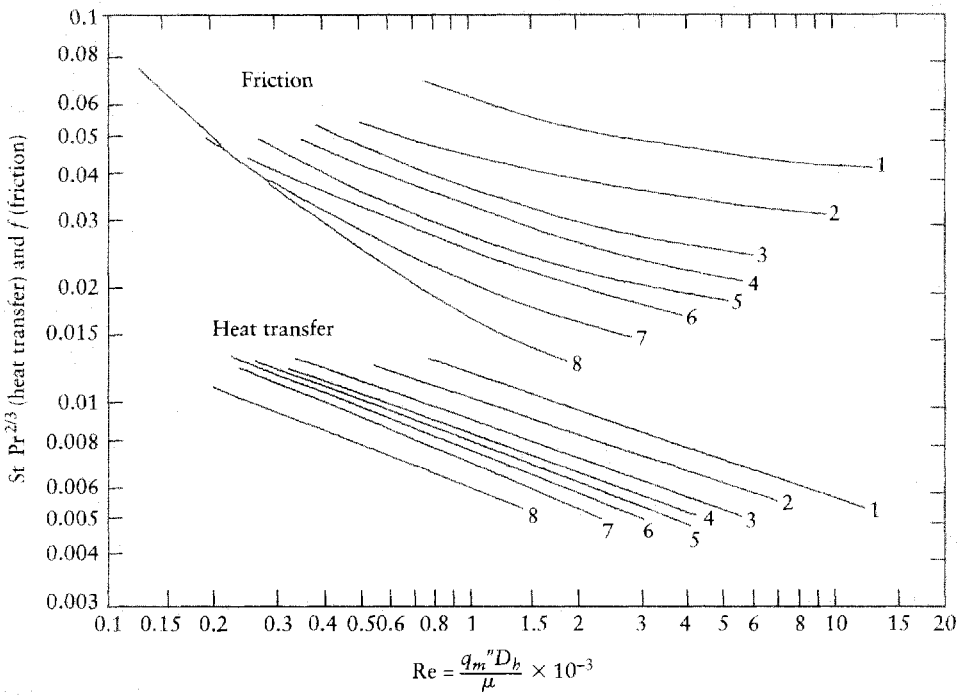

FIGURE 9.12 Diagram for determining the heat transfer coefficient for a straight fin plate.

The abscissa in Fig. 9.12 is

$$\mathrm{Re} = \frac{q_m'' \cdot D_h}{\mu} \cdot 10^{-3}. \tag{9.37}$$

Here

$$q_m'' = \frac{q_m}{A_{\min}}. \tag{9.38}$$

q_m is the mass flow of air through the heat exchanger, and $A_{\min}$ is the total area between the fins perpendicular to the airflow.

D_h is the hydraulic diameter of one cross-section between the plates, calculated from

$$D_h = 2\frac{A_{\min}}{H \cdot N_{pg}}. \tag{9.39}$$

H is the height of the plates in the heat exchanger (assuming the plates are in a vertical position, which is normal), and N_{pg} is the number of gaps between the plates. μ in Eq. (9.37) is the dynamic viscosity of the gas.

The ordinate in Fig. 9.12 is St $Pr^{2/3}$, where Pr is the Prandtl number of air and is defined as

$$\mathrm{Pr} = \frac{c_p \mu}{\lambda}. \tag{9.40}$$

For air at 20–40 °C, the Prandtl number is Pr = 0.71.

St is the Stanton number, defined as

$$\mathrm{St} = \frac{h}{q''_m \cdot c_p}. \tag{9.41}$$

Use Fig. 9.12 to calculate the Reynolds number, Re. Then by reading from one of the curves 1 . . . 8, depending on how many fins there are per centimeter, the value of St $Pr^{2/3}$ can be obtained.

The convective heat transfer coefficient is then

$$h = c_p q''_m \mathrm{St} = c_p q''_m \frac{\mathrm{St} \cdot \mathrm{Pr}^{2/3}}{\mathrm{Pr}^{2/3}}. \tag{9.42}$$

Next consider the wavy plate with herringbone waves. This arrangement with the relevant geometrical parameters is shown in Fig. 9.13.

The heat transfer coefficient for a herringbone plate is calculated from[3]

$$h = \lambda \, \mathrm{Re}_D \, \mathrm{Pr}^{1/3} j/D. \tag{9.43}$$

In Eq. (9.43) we have

$$\mathrm{Re}_D = \frac{q_m \cdot D}{A_c \cdot \mu}, \tag{9.44}$$

where D is the tube outer diameter including the collar of the fin plate, and A_c is the flow area in the heat exchanger where maximum velocity occurs. For a symmetric, staggered configuration, the maximum velocity occurs between the pipes situated vertically on each other.

The factor j is calculated from

$$j = 0.394 \, \mathrm{Re}^{-0.357} \left(\frac{P_t}{P_l}\right)^{-0.272} \left(\frac{s}{D}\right)^{-0.205} \left(\frac{x_f}{p_d}\right)^{-0.558} \left(\frac{p_d}{s}\right)^{-0.133}. \tag{9.45}$$

The relevant geometrical parameters for Eq. (9.45) are given in Fig. 9.13.

Example 2

The data of a heat exchanger is given as follows:

- Copper pipes have outer diameter of 12 mm.
- Symmetric, staggered pipe configuration; distance between the pipe centerlines is 32 mm.
- Aluminum plates ASTM 1110 of thermal conductivity 200 W m^{-1} K^{-1}.
- Plate thickness is 0.3 mm; distance between plates is 3 mm.
- Number of plates is 200.
- Height of plate is 600 mm; depth in flow direction is 290 mm.
- Number of pipe rows is 10, 18 pipes in one vertical row.

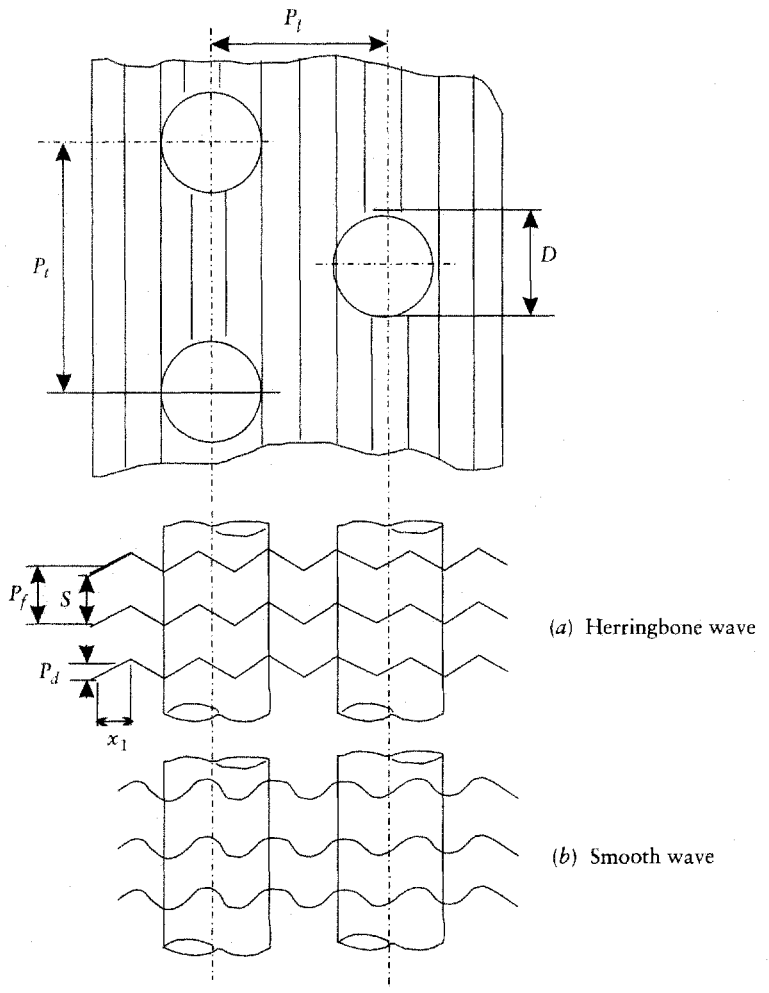

FIGURE 9.13 Wavy fin configuration.

The mass flow of air through the heat exchanger is 0.9 kg s^{-1}. Calculate

a. the fin efficiency,
b. the heat conductance or reciprocal of heat resistance on the air side if the plates are straight, and
c. the air-side conductance if the plates have herringbone waves with $x_f = 4.3$ mm and $p_d = 1$ mm.

The physical properties of air can be determined at 20 °C.

Solution

a. We calculate first the total heat transfer surface of the air side. The distance between the plates is $s = 3$ mm, plate thickness is $t = 0.3$ mm, and outer diameter of the pipe is $d_o = 12$ mm. The height of plates is $H = 600$ mm, and depth of the plates is $L = 290$ mm. The number of gaps between the plates is $N_{pg} = 199$, and the number of plates is $N_{pl} = 200$. The total number of pipes is $N_p = 10 \cdot 18 = 180$.

The outer surface area of the pipes between the fins is

$$A_{pg} = N_{pg}\pi(d_o + 2t)sN_p = N_{pg}\pi DsN_p$$
$$= 199 \cdot \pi \cdot 0.0126 \cdot 0.003 \cdot 180 = 4.3 \text{ m}^2 .$$

The area of the plate fins is

$$A_{pl} = 2 \cdot N_{pl} \cdot \left(H \cdot L - N_p \cdot \frac{\pi D^2}{4} \right)$$
$$= 2 \cdot 200 \left(0.6 \cdot 0.29 - 180 \cdot \frac{\pi \cdot 0.0126^2}{4} \right) = 60.6 \text{ m}^2 .$$

As can be seen, the outer surface area of the pipes between the fins contributes in a small heat transfer area, as expected.

The surface area $A_{\min}$ is

$$A_{\min} = N_{pg} \cdot s \cdot H = 199 \cdot 0.003 \cdot 0.6 = 0.358 \text{ m}^2 .$$

At 20 °C, the physical properties of air are $\mu = 181.1 \cdot 10^{-7}$ N s m^{-2}, $c_p = 1.007$ kJ kg^{-1} K^{-1}, $\lambda = 0.0257$ W m^{-1} K^{-1}, and Pr = 0.709.

For $q_m = 0.9$ kg s^{-1}, Eq. (9.38) gives

$$q''_m = \frac{q_m}{A_{\min}} = \frac{0.9}{0.358} = 2.51 \text{ kg m}^{-2} \text{ s}^{-1} .$$

From Eq. (9.39) we get

$$D_h = 2\frac{0.358}{0.6 \cdot 199} = 0.006 \text{ m} .$$

Equation (9.37) gives

$$\text{Re} = \frac{2.51 \cdot 0.006}{181.1 \cdot 10^{-7}} = 832 .$$

The plates at 1 cm distance are 10/3.3 = 3.03. Using Fig. 9.12 we can read St · Pr$^{2/3}$ = 0.0085.

From this we obtain

$$h = 1007 \cdot 2.51 \cdot \frac{0.0085}{0.709^{2/3}} = 27.0 \text{ W m}^{-2} \text{ K}^{-1} .$$

For $l = 32$ mm, we obtain from Eq. (9.33)

$$r_o = 0.525 \cdot 32 \text{ mm} = 16.8 \text{ mm},$$

$$r_i = \frac{D}{2} = \frac{(12 + 2 \cdot 0.3)}{2} = 6.3 \text{ mm},$$

and

$$r_o - r_i = 16.8 - 6.3 = 10.5 \text{ mm} = 0.0105 \text{ m}.$$

The thermal conductivity of aluminum is $\lambda = 200$ W m^{-1} K^{-1}; thus we obtain

$$\gamma = (r_o - r_i)\sqrt{2h/\lambda t} = 0.0105 \cdot \sqrt{\frac{2 \cdot 27}{220 \cdot 0.0003}} = 0.30$$

and

$$u_t = \sqrt{2h/\lambda t} \cdot r_i = \sqrt{\frac{2 \cdot 27}{220 \cdot 0.0003}} \cdot 0.0063 = 0.180 .$$

Using the above two parameters, the fin efficiency is obtained from Fig. 9.11 as $\eta = 0.95$.

b. Applying Eq. (9.36), we obtain the heat conductance on the air side as

$$G_a = h(\eta A_{pl} + A_{pg}) = 27.0(0.95 \cdot 60.6 + 4.3) = 1638 \text{ W K}^{-1} .$$

c. Because $P_t = l = 32$ mm and the pipe arrangement is staggered and symmetric, we have

$$P_l = \sin 60° \cdot P_t = \sin 60° \cdot 32 = 27.7 \text{ mm} .$$

A_c in Eq. (9.44) is $A_c = 199 \cdot 17(32 - 2 \cdot 6.3) \cdot 3 = 0.197 \text{ m}^2$.

Then in Eq. (9.44)

$$\text{Re}_D = \frac{0.9 \cdot 0.0126}{0.197 \cdot 181.1 \cdot 10^{-7}} = 3180$$

and in Eq. (9.45)

$$j = 0.394 \cdot 3180^{-0.357}\left(\frac{32}{27.7}\right)^{-0.272}\left(\frac{3}{12.6}\right)^{-0.205}\left(\frac{4.3}{1}\right)^{-0.558}\left(\frac{1}{3}\right)^{-0.133} = 0.014.$$

Finally, from Eq. (9.43) we get

$$h = 0.0257 \cdot 3180 \cdot 0.709^{1/3} \cdot 0.0147/0.0126 = 85 \text{ Wm}^{-2}\text{K}^{-1} .$$

We see that the wavy profile of the fin plate increases the heat transfer coefficient greatly.

We now have

$$\gamma = 0.0105 \cdot \sqrt{\frac{2 \cdot 85}{220 \cdot 0.0003}} = 0.53$$

and

$$u_t = \sqrt{\frac{2 \cdot 85}{220 \cdot 0.0003}} \cdot 0.0063 = 0.32 .$$

From Fig. 9.11, we then get $\eta = 0.86$ and finally

$$G_a = 85(0.86 \cdot 60.6 + 4.3) = 4795 \text{ W K}^{-1} .$$

9.3.2.5 Liquid-Side Conductance and Total Conductance of Heat Exchanger

The liquid-side conductance is calculated from

$$G_l = 0.023 \text{ Re}_{D_l}^{4/5} \cdot \text{Pr}_l^{0.3} \cdot \lambda_l \cdot \pi \cdot L, \tag{9.46}$$

where λ_l is the thermal conductivity of the liquid, Pr_l the Prandtl number for the liquid, and L the total length of the pipes in the heat exchanger.

For Re_{D_l} we have

$$\text{Re}_{D_l} = \frac{4q_l}{\pi D_l \mu_l} = \frac{\rho_l w_l D_l}{\mu_l} . \tag{9.47}$$

D_l is the inner diameter of the pipes.

For the total conductance G_{tot} of the heat exchanger, we have

$$\frac{1}{G_{tot}} = \frac{1}{G_f} + \frac{1}{G_c} + \frac{1}{G_a} . \tag{9.48}$$

Here $1/G_c$ is the *heat exchanger contact resistance*. The reason for the contact resistance is that there exists a resistance to heat flow between the outer surface of the pipe and the collar of the plate fins. Normally, the fins are attached to the pipes by mechanical expansion of the tubes out into the plate-fin collars. Because of this manufacturing method, the contact will not be ideal. Small gaps between the pipe surface and the collar of the fins will occur.

It is very difficult to estimate the magnitude of the contact conductance G_c. Normally the total conductance of the heat exchanger is determined, and G_c is calculated from Eq. (9.48). Only in the case that the plate fins are welded to the pipes with a metallurgical contact is the contact conductance infinite, leading to zero contact resistance, that is $1/G_c = 0$.

References

1. Ryti, H. Ripateoria. *Tekniikan kasikirja*, osa 5, pp. 2–13, Jyväskylä: Gummerus, 1965.
2. Webb, R. L. Air-side heat exchanger in finned tube heat exchangers. *Heat Transfer Engineering* 1 (1980) 3, pp. 33–49.
3. Kim, N.-H, Yun, J.-H., and Webb, R. L. Heat transfer and friction correlations for wavy plate fin-and-tube heat exchangers. *Journal of Heat Transfer* 119 (1997) August, pp. 560–567.

9.4 AIR-HANDLING PROCESSES

9.4.1 Air-Heating Equipment

9.4.1.1 Introduction

Many different methods of heating the air for industrial ventilation purposes are possible.

In all warm-air design applications, consideration must be given to the effects of stratification in tall buildings. Stratification increases the roof and high-wall fabric losses and the air change rate by the stack effect, and hence the ventilation loss. These effects may increase the heat loss by 25% over that of a radiant heating system.

In many cases, warm-air heating is the cheapest heating system to install from the initial-cost point of view; the running costs, however, will be higher than for a radiant heating system to provide the same conditions.

The ventilation system can be used to full advantage during the summer months with the heater off to provide outside air and assist in removing the heat gains.

9.4.1.2 Selection

The air may have to be heated for one or more of the following reasons:

- Fabric heating
- Heating makeup air to take care of the ventilation loss

- Comfort heating
- Heating to reduce the incidence of condensation
- Heating to protect goods from damage in store

The selection of equipment to meet the above needs depends on many factors; options include these:

- Direct air warming is achieved by means of air-heater batteries.
- Indirect warming of the air is achieved by the use of radiant heaters.

The heating media used can be classified as

a. Low-temperature hot water (up to 100 °C)
b. Medium-temperature hot water (100 to 120 °C)
c. High-temperature hot water (over 120 °C)
d. Steam
e. Electricity
f. Heat recovery from process hot gases
g. Direct gas fired
h. Heat transfer fluids
i. Direct oil fired
j. Solid fuel firing

Note: Items a, b, and c above are also classed as low-pressure, medium-pressure or high-pressure hot water.

9.4.1.3 Air-Heating Coils

These are used in conjunction with a ventilation or air-conditioning system and may be included in one of the following methods of ventilation.

- Natural ventilation.
- Mechanical extract–induced input.
- Mechanical input–forced extract. This arrangement is known as a plenum system.
- Mechanical inlet–mechanical extract.

In order for coils included in any of the above systems to operate efficiently, they must be designed to have a uniform air velocity across the whole of the heater's face area. This is of prime importance, and the manufacturer's specifications regarding the maximum and minimum air velocities must be met.

From the energy and noise point of view, care must be taken to prevent undue airflow resistance. This is achieved by not normally having more than five tube rows.

Typical face-area air velocity across extended-surface finned coils is normally less than 3.5 m s^{-1}. However, in the case of a plain heater, a velocity of 4 m s^{-1} can be used. In certain instances it is possible to use higher velocities; in all cases, however, the design requirements of the manufacturer should always be met.

In a dusty industrial environment, finned heaters are more liable than plain tube heaters to become blocked or coated with dust. If this dust is greasy, it will bake on the high-temperature surfaces, reducing the rate of heat transfer and in-

creasing the pressure drop across the coils. Special attention must be paid to the provision of easy access to areas for cleaning and maintenance of the coils; the cleaning is readily achieved by using compressed air or steam.

Air heaters in industrial environments require corrosion-protective finishes that are capable of protecting the coil and case from damage by condensation, acid vapors, or aggressive chemicals, in the air or the primary medium. If air washers are used with coils placed after them, copper or other noncorroding metal tubes should be used.

Full consideration of the thermal expansion of the tubes is necessary, with adequate provision for expansion and contraction. It is a wise policy to fit thermometer wells in the pipes near the inlets and outlets of all air-heating batteries, as these provide a useful means of checking the coil performance.

9.4.1.4 Heat Requirements

To determine the heat requirements of makeup air, the following equations can be used.

$$\text{Fabric loss } \Phi_f = \sum(AU)(\theta_{ei} - \theta_{ao}) \tag{9.49}$$

$$\text{Ventilation loss } \Phi_v = 0.33NV(\theta_{ai} - \theta_{ao}) \tag{9.50}$$

Equation (9.50) is a simplified equation that can be used at normal conditions. For practical purposes,

c (specific heat capacity of air) = 1.01 kJ kg^{-1}°C.

ρ air density = 1.2 kg m^{-3}

$$0.33 = \frac{(1.01)(1.2)}{3600}$$

(The number of seconds in one hour is 3600.)

where

Φ_f = fabric loss through all elements (kW)
Φ_v = ventilation loss (kW)
A = surface area of elements (m^2)
U = overall thermal transmittance (W m^{-2} °C)
θ_{ei} = environmental temperature (°C)
θ_{ao} = outdoor air temperature (°C)
θ_{ai} = indoor air temperature (°C)
N = number of air changes per hour
V = volume of room (m^3)

The sum of the two losses, Φ_f and Φ_v, will give Φ_p. This is the plant load. It must be remembered that the plant load is not necessarily the sum of fabric and ventilation loss, as ductwork losses in adjacent areas have to be considered.

For more exact work, the temperature ratios of F_1 and F_2 related to the mode of heating can be used. These relate to 100% convective, such as forced warm air to a high-temperature radiant system, which gives 90% radiant and 10% convective.

These factors compensate for the relationship between the inside air and mean surface temperature and provide similar comfort conditions at

the center of the space, regardless of the mode of heating employed. These ratios are

$$F_1 = \frac{\theta_{ei} - \theta_{ao}}{\theta_c - \theta_{ao}} \tag{9.51}$$

and

$$F_2 = \frac{\theta_{ai} - \theta_{ao}}{\theta_c - \theta_{ao}} . \tag{9.52}$$

The CIBSE Guide Book A.9 has seven tables which cover these ratios for different heating modes.

A space isolated from external building surfaces will have its heat gains from internal sources, such as process, lighting, occupants, etc. And as such, these may be considered as being net sensible and latent heat gains throughout the year requiring cooling.

To form a heat balance for the flows, Net sensible heat flow from the space = Sensible heat absorbed by the ventilating air.

Hence, Sensible heat = Air-mass flow rate (q_m, kg s^{-1}) × Specific heat capacity of humid air at constant volume (c_v), which is 1.012 kJ kg^{-1} K^{-1}.

It is normal in duct design to use volume flow rate rather than the mass flow rate, giving

$$q_v\,(\mathrm{m^3\,s^{-1}}) = q_m\,(\mathrm{kg\,s^{-1}}) \times \rho\ (\text{density, kg m}^{-3}). \tag{9.53}$$

The density of air at 20 °C and 101.325 kPa can be taken as ρ = 1.205 kg m^{-3}.

Supply air to a space can be at any temperature θ_s.

The general gas laws show that air density is inversely proportional to its absolute temperature, hence,

$$pV = mRT$$

where

p = the absolute pressure of the air (Pa)
V = volume of air (m^3)
m = mass of air (kg)
R = gas constant (287.1 J kg^{-1} K^{-1})
T = absolute temperature of the air (K)

and

$$\rho = \frac{m\,(\mathrm{kg})}{V\,(\mathrm{m^3})} = \frac{p\,(\mathrm{Pa})}{RT},$$

assuming that the values of the gas constant, the moisture content, and pressure remain constant in the heating or cooling process.

$$\rho_1 = \frac{1}{T}$$

Let standard air density be ρ_1 and supply air density be ρ_2.

$$\rho_1 = \frac{1}{T_1} \quad \text{and} \quad \rho_2 = \frac{1}{T_2}$$

Dividing and inverting gives

$$\frac{\rho_2}{\rho_1} = \frac{T_1}{T_2}$$

and

$$\rho_2 = \rho_1 \frac{T_1}{T_2}.$$

In practice, the air density has to be corrected for the specific supply temperature by

$$\rho_2 = 1.1906 \times \frac{273 + 20}{273 + \theta_s} \text{ kg m}^{-3}.$$

Substituting into the heat balance equation,

$$\text{Sensible heat } (\Phi_{SH}, \text{kW}) = q_v (\text{m}^3 \text{s}^{-1}) \times \rho_2 (\text{kg m}^{-3}) \times c (\text{kJ kg}^{-1} \text{K}^{-1} \times (\theta_r + \theta_s) \text{K}$$

$$= q_v \times 1.1906 \times \frac{273 + 20}{273 + \theta_s} (1.0048)(\theta_r - \theta_s). \quad (9.54)$$

Hence,

$$q_v \times 351 \times \frac{\theta_r - \theta_s}{273 + \theta_s}, \quad (9.55)$$

or, expressed in terms of volume flow,

$$q_v = \frac{\text{kW}(273 + \theta_s)}{351(\theta_r - \theta_s)}. \quad (9.56)$$

If the space temperature is above its design value, cooling is required. If the space temperature is below the design value, the supply air must be heated. Hence,

$$q_v = \frac{\Phi_{SH}(\text{kW})(273 + \theta_s)}{351(\theta_s - \theta_r)} \text{ m}^3\text{s}^{-1} \quad (9.57)$$

or

$$\Phi_{SH}(\text{kW}) = \frac{q_v(351)(\theta_s - \theta_r)}{(273 + \theta_s)}. \quad (9.58)$$

The rates of extract involved in industrial ventilation are by nature of a high volume. It is of interest to consider the energy required to heat one cubic meter of air from, say, an outdoor temperature of –5 °C to be discharged into the space at 20 °C.

The basic equation is

$$\Phi_{SH}(\text{kW}) = \frac{q_v(351)(\theta_s - \theta_r)}{(273 + \theta_s)}$$

$$= \frac{1.0(351)(25)}{(273 + 20)} = 29.94 \text{ kW, say } 30 \text{ kW}.$$

The above answer gives the heat requirement for the air alone, and normally the fabric losses would be added to this figure.

It will be appreciated that if 30 kW is required for such a small air quantity, it is important to reduce the airflow rate to a value as low as possible in order to save energy.

This reduction in energy use can be achieved without affecting the required pollution levels in the environment by the improved collection methods that are covered in these guides.

9.4.1.5 Low-Temperature Hot-Water Heating Coils

These are used in comfort heating systems and usually have no more than one or two rows of tubes. Various circuit arrangements are possible, depending on the pumping and control methods used.

As well as ensuring that the required design heating capacity is met, the following factors must also be considered.

- The maximum output efficiency must be met with the minimum of air pressure drop.
- The water pressure drop through the coil is as low as economically possible.

The design resistance of hot-water flow through a coil normally never exceeds 4 kPa in accelerated low-pressure hot-water heating installations.

In the case of high-pressure hot-water installations, the resistance to the water flow is determined by other factors, such as the balancing of circuits.

The heaters are fed from hot-water flow and return mains, and to ensure uniform distribution of the heating medium, adequate connections to each row or bank of tubes or sections are necessary. To reduce air-locking problems, venting of the heater flow connections should be arranged. Parallel and counterflow are common arrangements with water coils. Counterflow is preferred, as this gives the highest possible mean temperature difference.

9.4.1.6 Steam-Heated Coils

For a steam coil to operate efficiently, it must have all the latent heat in the steam. This is achieved by the use of a steam trap. The correct trap type must be selected for the particular application in order to prevent waterlogging. All condensate, air, or other noncondensable must be removed from the system without delay; otherwise,

- the rated coil output will fall, and
- corrosion will result, causing premature coil fracture.

The best performance is achieved if the steam is uniformly distributed to the individual tubes. Properly designed and selected steam-distribution tube coils distribute the steam throughout the entire length of all primary tubes. Problems may result with air heaters operating under light load, and these may be overcome by greater sectionalization of the controls. When the entering air temperature is below freezing, the steam supply to the coil should not be modulated. Coils are located in series in the airstream, with each coil sized to be on or completely off in a specific sequence; this depends on the entering air temperature. Low temperatures produce the risk of a coil freeze-up. The use of bypass dampers could be considered, but care should be taken to ensure that cold airstreams do not impinge on the coil through the gaps in the partially closed dampers. Full provision is necessary to accommodate expansion and contraction of the coils.

Provision is necessary for adequate venting of the steam space. Heaters should have pressure gauges fitted at the steam inlet. In order to achieve effi-

cient heat transfer, dry steam must be supplied to the battery; superheated steam is not suitable due to the time necessary for it to lose its latent heat to produce condensate.

9.4.1.7 Electric Air Heaters

These have the advantage that they are low-cost units to install; the running costs, however, depending on the source of electricity, are generally higher than other energy sources.

The air velocity through a heater battery should be to the manufacturer's rated output within its range of safe temperatures. In large units the electrical load is balanced across the three phases of the electrical supply.

The heaters are normally divided into a number of sections in order to provide step control of the unit. Each section of heater elements may consist of two or more rows, each having its individual busbar connections and adequate provision for it to be withdrawn for repair or cleaning, with the other elements remaining in operation. Care has to be taken with electrical isolation of each section before withdrawing them from the casing. The heaters should be electrically interlocked with the fan motors, allowing the electric heater to be switched off when the fan stops or when the air velocity is reduced to a level below that for which the heater has been designed. The risk of fire under abnormal operating conditions must be counteracted by the use of a suitably positioned, temperature-sensitive cutoff trip of the manual reset type.

9.4.1.8 Direct-Fired Air Heaters

These may be

- Gas fired
- Oil fired
- Solid fuel fired

Regardless of the fuel used, the following are the requirements of the flue.

Flues must be of the correct cross-sectional area in order to remove the products of combustion in a safe and efficient manner. The flue terminal should be fitted with a bird guard.

Care has to be taken to ensure that downdrafts do not cause the combustion products to be liberated in the occupied space. To achieve this, it is essential that the stack is of such a height that wind deflecting off adjacent structures does not influence the free passage of the products of combustion.

The appliances must be positioned in a space that has adequately sized combustion air inlet louvers that will not clog with debris and reduce the combustion air supply.

In small installations flueless appliances may be used; the use of these is to be discouraged due to the problems of toxic gases and condensate from the flue gas building up in the space.

9.4.1.9 Gas-Fired Heaters

Only standard, approved appliances should be used. These may operate on

- an atmospheric burner or
- a forced jet burner.

In large industrial installations, the latter is the most common arrangement. The burner has a profile plate that controls the rate of combustion air. The warm air delivery fan may be either centrifugal or axial.

In Europe, the gas safety controls must meet the requirements of CEN standards, including flame failure devices, solenoid control valve, pilot controls, ignition and governor. Overheat-type thermostats and either a pressure switch or an airflow-proving device are fitted to ensure that the burner will cut off in the event of no air flowing through the heater, such as occurs with fan failure.

Thermostatic control of the gas supply to the heater is required so that the air-off temperature can be controlled. This is achieved by a two-stage control that opens a valve partly on low rate and fully on high rate.

The flued appliance is designed to provide maximum heat transfer. The efficiency can be increased by the use of a condensing unit.

The filter banks incorporated require adequate access for cleaning and replacing.

The heat exchanger is normally of the welded type using aluminized steel, stainless steel, or similar materials. It should create the minimum of resistance to the air movement, which has to be turbulent in order to give an efficient transfer of heat.

Depending on the burner system employed, some form of a flue system is required to remove the products of combustion from the appliance to the atmosphere.

In the case of atmospheric type burners, a draft diverter is required on the appliance (in addition to the flue outlet).

The positioning of flue terminations must be selected with care and may be subject to statutory or other regulations.

The flueless appliance has gas supplied to the burner head, and air passes outside the baffles at a designed velocity.

The air paths within these baffles are arranged to provide the correct amount of combustion air. Turndown ratios of up to 35 to 1 are obtainable, providing the correct gas flow for air temperature control.

The control system must satisfy a set sequence, as is required by CEN or other standards. An air switch provides airflow to the unit. A 30-second purge of the unit takes place by the fan; after this period, the ignition spark and pilot gas valve are operated.

On proving the pilot ignition, the main gas valve opens and the burner ignites. Once alight, the main burner will modulate to the temperature set by the room thermostat.

If, during the ignition sequence or the running sequence, flame failure occurs, a lockout will result, which will require manual resetting.

9.4.1.10 Oil-Fired Heaters

Burners of the vaporizing type are used only on low-output equipment. The most common type encountered is the pressure-jet burner.

All burners should meet the requirements of CEN or other national standards. The units must be complete with safety devices for ignition failure and main flame failure.

For safe operation, the heater should have an overheat thermostat and either a pressure switch or airflow-proving device. This control device ensures that the burner will isolate in the event of restricted or no airflow through the heater.

The removal of the combustion products to the external atmosphere takes place through the flue, which may be

- a direct flue connection type,
- a direct flue with a stabilizer (the stabilizer must be compatible with the unit), or
- a fan-assisted or balanced flue.

The oil supply to the heater is thermostat controlled by the air-off temperature.

9.4.1.11 Solid-Fuel-Fired Heaters

Furnace-type air heaters are manufactured from cast iron or steel, and cased in brickwork or steel. The cast-iron heaters are sectional, cemented and bolted together. The steel type are welded or riveted. It is essential that the joints are airtight, so that the cold air can pass over the heated surfaces of the furnace and flues without contamination by the flue gases.

To reduce the possibility of combustion products being drawn into the air if the heat exchanger burns through, the air is blown and not induced through the heater.

Adequate draft is necessary, not only for efficient combustion, but also to reduce the risk of soot being deposited on the heating surfaces. Provision must be made for a cleaning door in the flue and for the tubes.

With a fan-furnace heating system, once the temperature is reached, the fan is controlled to start automatically. Should fan failure occur, provision should be made to damp down the furnace automatically to avoid overheating's causing tube damage.

9.4.1.12 Air-Heating-Coil Selection Factors

When selecting air-heater batteries, the following factors common to all types must be considered.

a. Air volume to be handled (and conditions at which it is measured)
b. Entering air conditions (EAT) (dry-bulb temperature, air density), air quality (possibility of dirt, corrosive, or hazardous atmospheres); whether the coils are suitable to operate in temperatures below freezing
c. Required leaving-air dry-bulb temperature (LAT)
d. The heating medium being used, considering

- Water and steam entering temperatures
- Operating pressure
- Permissible temperature drop of the heating medium

- Electricity supply, voltage, and phase and whether a standby supply is required
- Maximum element operating temperature

e. Allowable air-side velocity
f. Allowable air-side resistance (as it affects fan power)
g. Heating medium connections, size and type, location, circuiting arrangement

h. Provision for air release and drainage
i. Provision for cleaning tubes
j. Electricity: type and location, circuit arrangement; terminal box specification
k. Air-side connections (flanges for duct mounting, etc.)
l. Construction: materials for heaters, coils, and extended surface; number of rows and arrangements; type of extended surface and spacing
m. Division of coil to suit control, manufacturing, or installing arrangement, i.e., number of sections and rows
n. Air pressure at point of installation (and air leakage through coil casting), particularly when located at fan discharge on a high-pressure system
o. Economy of coil selection as related to the system, such as flow rates, temperature rise, pressure drops, and fan and pump power

If a preheater coil is provided and positioned before the air filter, the heater should be either a plain tube or have wide spread fins for easy cleaning

9.4.1.13 Selection of Direct-Fired Air Heaters

Flued Heaters

This method of heating is the recommended one, and the following factors should be considered.

a. Air volume to be handled (q_v), $m^3 s^{-1}$
b. Entering-air conditions (θ_{ao}) (EAT)
c. Leaving-air condition (θ_{lat}) (LAT)
d. Will leaving-air temperature cause discomfort or other problems?
e. Allowable air-side resistance
f. Is the unit provided with all the necessary safety controls?
g. Is the flue outlet suitable for easy discharge of the products of combustion into the atmosphere?
h. Are the ductwork connection flanges provided?
i. Is an access door provided for inspection of the pilot and cleaning the main burner?
j. Are sight glasses or observation ports provided for inspection of pilot and main burner flames?
k. Is a suitable temperature control provided?
l. Does the fan within the unit have sufficient pressure to overcome the system ductwork resistance?
m. Will moisture from the combustion products adversely affect the space humidity requirements?
n. The concentrations of combustion products liberated into the occupied space must be well below the accepted tolerance levels. This is the factor that limits the use of flueless heaters for makeup air supply.

9.4.2 Humidification and Dehumidification

9.4.2.1 Introduction

Humidification and dehumidification (drying) of air are required in many commercial and industrial applications for the following reasons:

- The control of air moisture content within the occupied space to ensure the well-being of human, animal, or plant life
- The control of air moisture content within a space for process control or to protect products in store

Table 9.4 indicates some of the factors that have to be considered when dealing with the moisture content in air. In the case of inert gases used in various industrial processes, other factors have to be considered.

The process of air humidification is achieved by means of a device called a humidifier.

9.4.2.2 Humidifier Types

Many different types of humidifiers are in common use; the humidification process is simply achieved by adding moisture into the air to be conditioned.

TABLE 9.4 Influence of Moisture Content in Air

Factors	High humidity	Low humidity
Ill health and associated allergies	Encourages the growth of spores and fungi.	Lowers the body's resistance to infection and respiratory disease.
Electrostatic shocks	Eliminated at high moisture content.	Increased at low moisture content, causing discomfort to occupants and damage to electronic components. High explosion risk.
Eye conditions	Possible bacteria buildup and health effects.	A high rate of evaporation of the eyeball oil film results in dry, itchy eyes with an increase in eye damage in dusty environments.
Respiratory tract (nose and throat) problems	Increase in bacterial infection.	Resistance to throat, nose, and lung infection is increased, due to the breakdown of the protective mechanisms in the body.
Thermal stress	Reduction in evaporative body cooling. In hot industries, this results in body overheating.	Increase in body cooling with an increase in air movement.
Skin effects	Bacteria growth in skinfolds. Clothing type has to be considered.	As moisture is required to keep the skin supple, low humidity causes cracking of the skin, increasing the risk of chemicals and bacteria entering the body
Materials	Rusting of steel, breakdown of timber and fabrics. Damage of stored goods by insects and mold growth.	Rapid drying out of paper, timber, and fabrics. This is an important factor for storing antiques.
Pollution		The dust concentration is higher in a dry atmosphere, causing health and discomfort problems. Odors, irritant gases, and vapors are more noticeable at low humidiry.
Vegetation effects	Various diseases, depending on produce.	Various diseases, depending on produce.

The selection of a particular method depends on the size of the installation, availability of water or steam, the degree of control required, and the methods used for conditioning and distributing the air.

Humidification is achieved by one of the following methods:

1. By producing a fine mist or spray
2. By evaporation from a pad of absorbent material within the airstream
3. By vaporizing water
4. By steam injection

Figure 9.14 shows the processes of humidification and dehumidification in a skeleton psychrometric chart, while Table 9.5 explains the cycle.

Note: The actual final air conditions given in Fig. 9.14 and Table 9.5 must always be related to the slope of the line, as in some cases the specified conditions may not be met.

Humidifiers Complete with Water Storage

In this type of humidifier, the water required for the humidification process is stored within the unit and is normally fed automatically from the water mains. However, smaller portable units do not have this automatic facility and have to be manually filled with water as required.

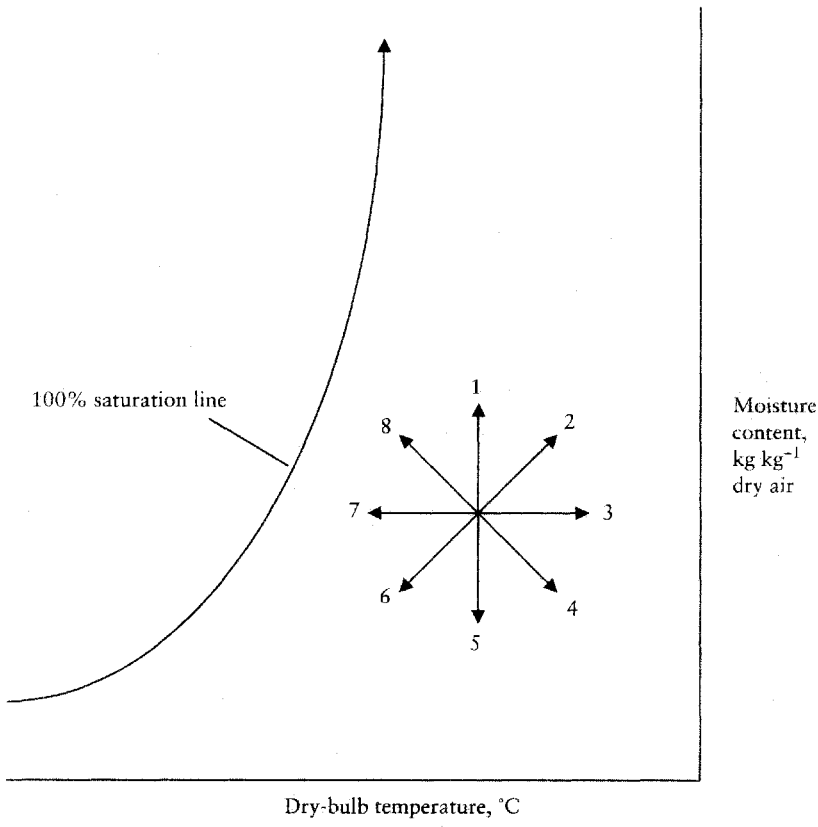

FIGURE 9.14 Humidification and dehumidification processes.

TABLE 9.5 Humidification and Dehumidification Processes

State line: Center point to	Process	Final air conditions	Equipment used
1	Humidification only	Increase in moisture content, specific volume, dry and wet bulb temperature, specific enthalpy, and % saturation	Air washer with heated water
2	Heating and humidification	Increase in moisture content, specific volume, dry- and wet-bulb temperature, and specific enthalpy: decreased % saturation	Steam humidifier or recirculated hot-water spray
3	Sensible heating only	Constant moisture content; increase in specific volume, dry- and wet-bulb temperature, and specific enthalpy; decreased % saturation	Steam, hot-water coils, or electric heating
4	Dehumidification and heating	Decreased moisture content; increase in specific volume and dry- and wet-bulb temperature; decreased specific enthalpy and % saturation	Chemical dehumidification
5	Dehumidification only	Decreased moisture content and specific volume; constant dry-bulb temperature; decreased wet-bulb temperature, specific enthalpy, and % saturation	Not practical
6	Cooling and dehumidifying	Decreased moisture content and specific volume, dry- and wet-bulb temperature, specific enthalpy, and % saturation	Chilled-water washer
7	Sensible cooling only	Constant moisture content; decreased specific volume, dry- and wet-bulb temperature, and specific enthalpy; increased % saturation. When point 7 reaches the 100% saturation line, the air is saturated; further cooling will result in moisture being removed from the air.	Cooling coil and washer at dew point
8	Evaporative cooling only	Increased moisture content and specific volume; decreased dry- and wet-bulb temperature; increased specific enthalpy and % saturation	Washer

To prevent contamination of the water mains by back-siphonage, the water inlet to the appliance should incorporate either

- an air gap,
- an approved type of pipe interrupter, or
- a combined check and antivacuum valve.

The national and local water bylaws and codes should be consulted to ensure that the device fitted is of an approved type.

Spray-Type Humidifier

Water is pumped from a storage tank located at the base of the unit to one or more spray nozzles that inject a fine water spray into the airstream. In large units, the air movement through the ductwork system ensures efficient mixing of the moisture and the air. Units used in small enclosures or rooms use a fan with the pump on the same shaft.

Pan-Type Humidifier

In this type, an absorbent material is partially immersed in a water pan store at the base of the unit. The evaporation of the water into the airstream takes place from the wetted surface of the absorbent material.

Mechanical Pan

In this case, an absorbent material is fixed to a drum or disk. Part of this drum is immersed in the water. When the drum is rotated in the water pan, it absorbs moisture, which is then transferred into the airstream by evaporation.

Steam-Generating Pan

This type consists of an enclosed water tank, which is connected to the main air duct.

High-temperature water coils or direct-fired gas or electrical elements heat the water in the tank. The tank water vaporizes, and the moisture is entrained into the airstream as it passes over the tank.

Humidifiers without Water Storage

Water need not be stored within the unit; this is often the case where the equipment used for humidification forms part of a central station plant or where a suitable source of steam is available.

Spinning-Disk Humidifier

In this case, a controlled quantity of water is discharged against a rapidly rotating disk where centrifugal force spins the droplets radially against circumferentially placed baffles, producing a fine water mist which is discharged into the airstream.

Steam Jet

Steam generated from an external source positioned close to the unit is injected into the airstream. It is essential that the steam supply is uncontaminated and odorless. In order to stop scale buildup, it is essential that some means of water treatment be provided.

Ultrasonic Atomization

Full use can be made of ultrasonic frequencies in producing a fine, atomized jet, which is liberated into the airstream.

Air Washer

A device called an air washer is also used for humidification and dehumidification. It consists of a chamber incorporating a water spray system, a collection tank, and an eliminator section. The eliminator plates are necessary to reduce the incidence of water droplets that are carried out of the plant into the duct run.

The air, in passing through the chamber at velocities in the range 1.5 to 3.5 m s^{-1}, comes into intimate contact with the water, and depending on the conditions required, mass transfer of moisture into the airstream occurs. This transfer produces either addition or removal of moisture; hot or chilled water is used in this process.

The spray bank consists of a series of standpipes with nozzles connected to a horizontal header. The nozzles are arranged to ensure that the spray gives good coverage of the spray chamber without causing any interference with the adjacent nozzles. The pressure through these nozzles is normally between 140 kPa and 280 kPa.

The spray water requirements vary from 0.3 L s^{-1} for a single bank to 0.8 L s^{-1} per 0.5 m^3.

Depending on spray pressure and the strainer, pipeline, and valve resistance, the pumping head is normally in the 16 to 24 m range.

By having more than one spray bank discharging into the direction of airflow, the mixing efficiency is improved. The nozzles provide water atomization by means of forcing the water under pressure through a small orifice, producing a wide-angle rotating spray.

In the past, air washers were used for air cleaning; today, however, more efficient methods are available for the cleaning process.

The continuous recirculation and spraying results in dirty water building up in the sump. In order to reduce the incidence of infection to occupants and fouling of the nozzle, water treatment with biocides and softening of the water supply are required. The sump is complete with strainers in a position which allows easy access for cleaning. See Fig. 9.15.

Another type of air washer is the capillary air washer; see Fig. 9.16. It consists of many thousands of small glass or plastic filaments (cells) providing a large, wetted surface area. These are placed to allow a parallel path of air through them. The surface of each of these strands is covered with the water that is discharged from sprays.

9.4.2.3 Selection Factors

Humidification can be achieved by placing separate humidifiers directly in the conditioned space. In order to maintain the design conditions, however, humidity control should be incorporated into the system. When positioning humidifiers, care has to be taken to ensure that the leaving moisture does not impinge on adjacent surfaces, forming lime or algae deposits.

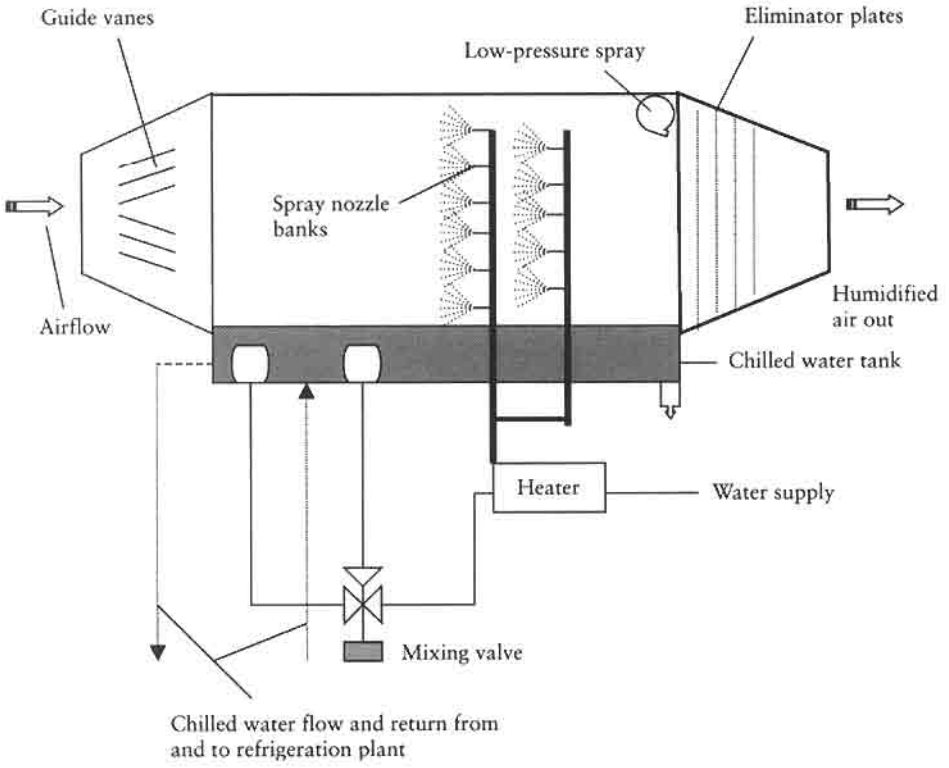

FIGURE 9.15 Air washer.

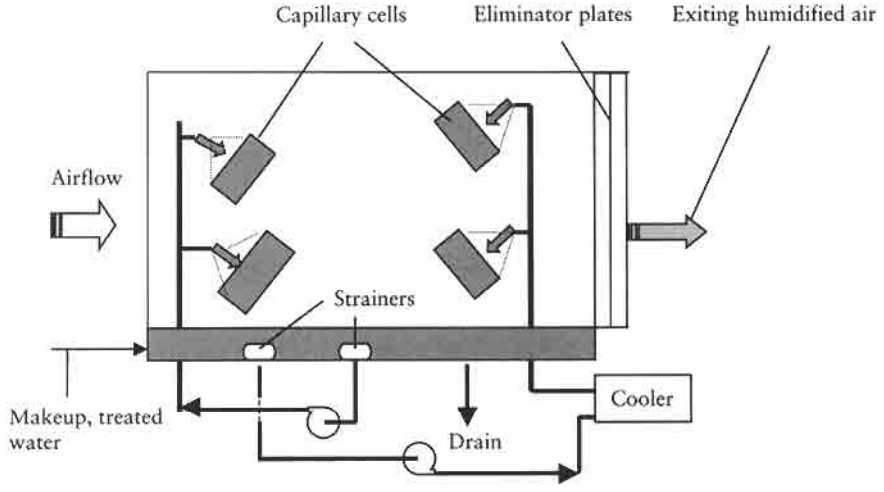

FIGURE 9.16 Capillary air washer.

Regardless of the type of unit used, full consideration should be given to provide a suitable method of water treatment on the following counts:

- To prevent solids from being carried over into the airstream
- To stop deposits from fouling the unit and the associated heat exchanger
- To stop a fine dust of the salts from being discharged into the conditioned space. This is particularly important in the case of spinning-disk or spray-type humidifiers.

For all humidifiers, full consideration should be given to the possibility of the growth of fungi, algae, bacteria, and in particular *Legionella pneumophila,* the microbiological contamination that causes humidifier fever, etc.

Dehumidification

The reverse of the humidification process is that of dehumidification. In this process the water content of air, gases, or fluids is reduced.

In many industrial applications, the moisture extraction takes place at atmospheric pressure; however, certain applications may require a reduction in the atmospheric pressure in order to achieve the maximum efficiency.

The process may be required for the following reasons:

1. Reducing the moisture content of a gas to aid the manufacturing and handling of hygroscopic materials
2. For comfort or process air conditioning in combination with cooling to reduce the latent load
3. Providing protective atmospheres to reduce the oxidization of metals
4. Controlling set humidity conditions in warehouses

Dehumidification can be achieved by one or more the following methods:

1. Compression
2. Refrigeration
3. Liquid sorption
4. Solid sorption
5. A combination of the above

Figure 9.14 and Table 9.5 cover the dehumidification processes.

Compression

If a gas is compressed, its absolute moisture content is reduced, generally resulting in a saturated gas at the elevated pressure. Due to the high cost of providing compression, it is used on its own only in limited applications. It is, however, used as the first stage with one of the other three methods. If a high-pressure gas is allowed to expand, the increase in volume and reduction in pressure result in a lower dew point.

Refrigeration

By allowing moisture-laden, relatively warm gas to come into intimate contact with a cold surface which is below the dew point of the gas, moisture is condensed from the gas.

The term *refrigeration* refers to the gas coming into contact with evaporator coils on a dx vapor-compression cycle, coils on an absorption cycle, vortex

tube, thermoelectric cycle, chilled water coils, or even water mains passing through coils.

The required refrigeration capacity is $\phi r = q_m(h_1 - h_2)$ kW.

Chemical Dehumidification

Certain chemicals (sorbents) have the ability to absorb moisture from a gas; they may be either solid or liquid. Performance of a chemical dehumidification device depends on the sorbent used. The sorbent must be able to attract and remove the sorbate, such as water, from the gas stream. Sorbents absorb water on the surface of the material by adsorption or by chemically combining with water (absorption). If the unit is regenerative, the process is reversible, allowing water to be removed. This is achieved by a sorbent such as silica gel, alumina gel, activated alumina, lithium chloride salt, lithium chloride solution, glycol solution, or molecular sieves. In the case of nonregenerative equipment, hygroscopic salts such as calcium chloride, urea, or sodium chloride are used.

An absorbent material is one which changes either chemically, physically, or both during the sorption process. Certain chemicals, in absorbing moisture during this process, will dissolve into the water from the initial crystalline structure. Further added water results in a phase change from solid to liquid. An adsorbent is another material in which there are no chemical, phase, or physical changes during the sorption process.

Liquid Sorption. If a moist gas is passed through sprays of a liquid sorbent, such as lithium chloride or an ethylene glycol solution, moisture is removed from the air at a rate depending on the vapor pressure difference. This is a function of the absorbent concentration and is maintained at the required level by a regeneration cycle. The regeneration process is continuous and is achieved by allowing a percentage of the chemical into the exhaust-heated air.

If the vapor pressure of the sorbent in its active state is below that of the gas being dehumidified, moisture is absorbed from the gas stream. As the process continues, the sorbent becomes diluted due to the moisture increase. See Fig. 9.17.

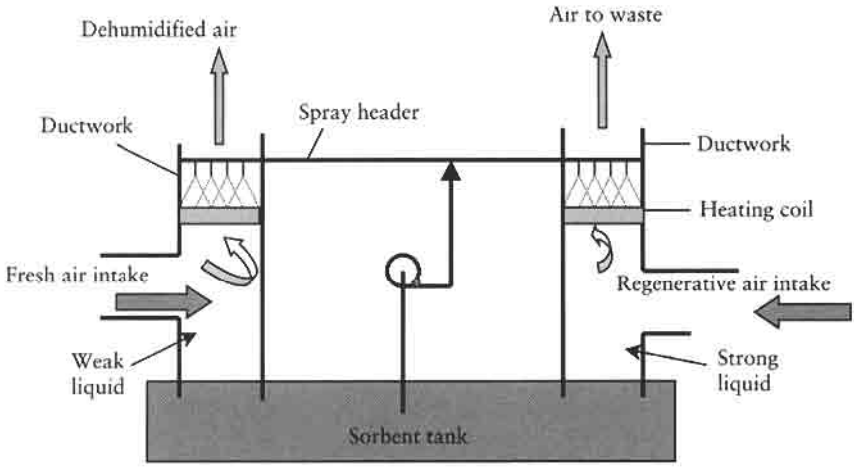

FIGURE 9.17 Liquid sorption.

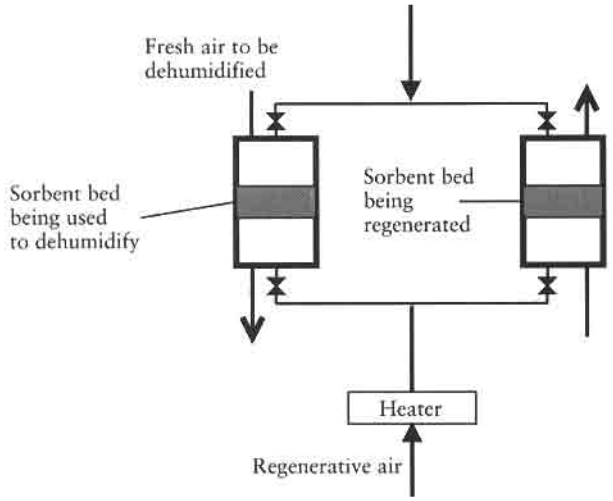

FIGURE 9.18 Solid sorption.

Solid Sorption. A material such as silica gel or activated aluminium through which the moisture-laden gas is passed achieves solid sorption; see Fig. 9.18. The mass transfer that takes place depends on the relative conditions of the chemical and the air conditions. As the material becomes saturated, heating the bed and applying a vacuum to it will reverse the process. Once sufficient water is removed from the material, it can be reused.

The intermittent operation used in the above method is time-consuming; the undesirable effects are overcome by the use of a continuous regeneration process, as shown in Fig. 9.19.

9.4.2.4 Summary

The selection of humidifiers or dehumidifiers must not be taken lightly, as many design factors have to be considered to ensure economic owning and operating costs.

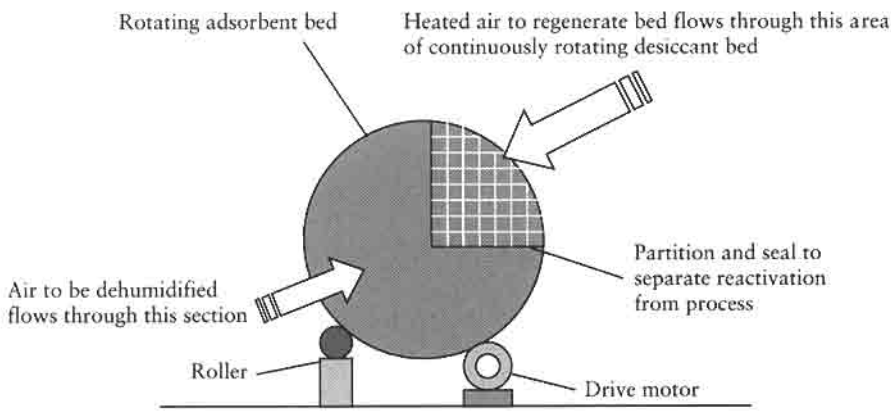

FIGURE 9.19 Automatic rotary regeneration.

9.4.3 Air Distribution

9.4.3.1 Introduction

The aim of this section is to provide a basic introduction to the methods by which air may enter a space and be distributed and to consider the governing equation for the determination of the air quantity and temperature. The governing equation relating to airflow patterns in a space is not covered in this section, as it is discussed elsewhere in the guides.

Ventilation

Ventilation is required in buildings for many different reasons. In this section, the emphasis is on industrial environment; however, the general method of approach is common to all systems for the following reasons:

- To provide adequate oxygen to support life
- To remove all odors by dilution
- To reduce the bacteria count by providing fresh air to the space
- To reduce any toxic gases, vapors, and dusts
- To remove explosive gases and dusts
- To ensure that adequate combustion air is provided to any combustion process
- To lower the moisture content in the air, thus reducing the risk of condensation and mold growth
- To add to or remove heat from the space

All the above must be carried out in the most efficient manner.

The air that enters a space has to be distributed in a manner suitable for the particular application. Regardless of the method selected, the air entering the space must achieve one or more of the above requirements in the following ways:

- Efficient distribution with no stagnation of the air
- Air velocities that will not cause thermal discomfort or disturb papers or manufactured goods such as light powders and fibers
- Low noise transmission level
- Low owning and operating costs
- Capable of maintaining the internal design conditions, regardless of the external environmental conditions

The above factors can be grouped under the following headings:

- Health ventilation
- Safety ventilation
- Comfort ventilation
- Structural heating or cooling

The distribution and the associated extract of air from a space may be

- From high level (the roof or ceiling)
- From the walls, at any level
- From the floor
- From benches

Ventilation of a space can be achieved by the following methods:

- Natural ventilation
- Mechanical extract–induced inlet
- Mechanical input–forced extract
- Mechanical inlet–mechanical extract

The following sections consider each of these methods.

9.4.3.2 Ventilation Methods

Natural Ventilation

This is the usual method of ventilation in domestic dwellings and many small office buildings and workshops. New standards, however, require buildings to have set ventilation rates, which require mechanical ventilation systems. However, as covered later, use is made of natural ventilation to control the air-change rate, regardless of the external conditions. This approach is not practical for industrial applications.

The term *natural ventilation* relates to the airflow in a building that is caused by three natural factors:

1. Temperature differences (thermal density) between the inside and the outside of the building
2. Wind forces around the building
3. A combination of (1) and (2)

Natural ventilation has the advantage that no power supply is required; hence there are no fans and maintenance costs. It has the disadvantage that during the summer months, the temperature difference between the inside and outside is small, and with low wind forces, poor ventilation will result when it is most required. During the winter months, however, the temperature difference between indoors and outdoors is high, with corresponding strong wind forces, resulting in high ventilation and heat-loss rates.

It is not possible to design a system according to a given natural ventilation rate, as this will vary with weather conditions. The cold outdoor air has a greater density for a given volume than the warmer indoor air; it enters through low-level openings, displacing the warmer indoor air and creating air changes. The displaced warmer air escapes through high-level openings (see Fig. 9.20). Ventilation caused by this method is commonly called the *stack effect*.

The greater the distance between the low-level inlets and the high-level outlets, the greater the resulting air change rate will be. The resulting airflow patterns in this arrangement will not ensure satisfactory air distribution in many industrial environments.

The science of building aerodynamics considers the influence of wind forces over buildings and the associated mechanics of fluids; these are complex in nature and are not considered here. It is sufficient to briefly consider Fig. 9.21, which shows how wind passing over a building produces a positive pressure on one side and a negative pressure on the other side. It is this pressure difference that produces airflow through openings. The combined wind and stack effects vary with the seasons.

Figure 9.21 considers the air movement in elevation; the aerodynamic flow in plan is shown in Fig. 9.22. It can be appreciated that adjacent

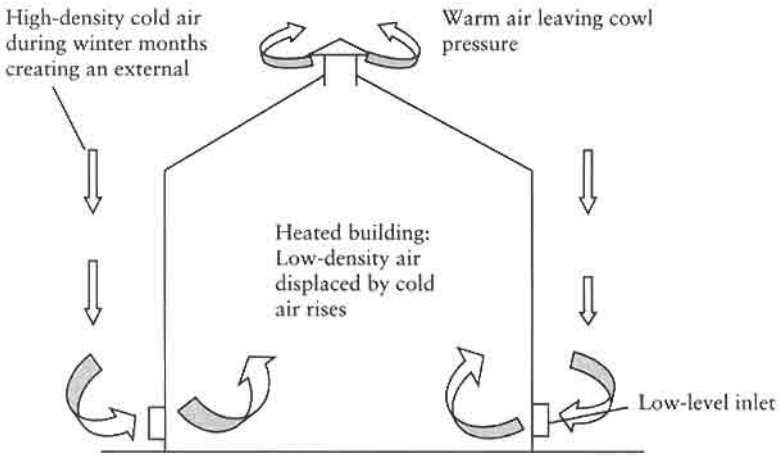

FIGURE 9.20 Stack effect.

structures to the simple block considered result in more complex flow patterns that flow over roof ridges and the geometric shape of the building in relation to the prevailing wind direction. Care has to be taken in the positioning of input or extract fans in relation to the wind direction, as it may have an effect on the fan performance.

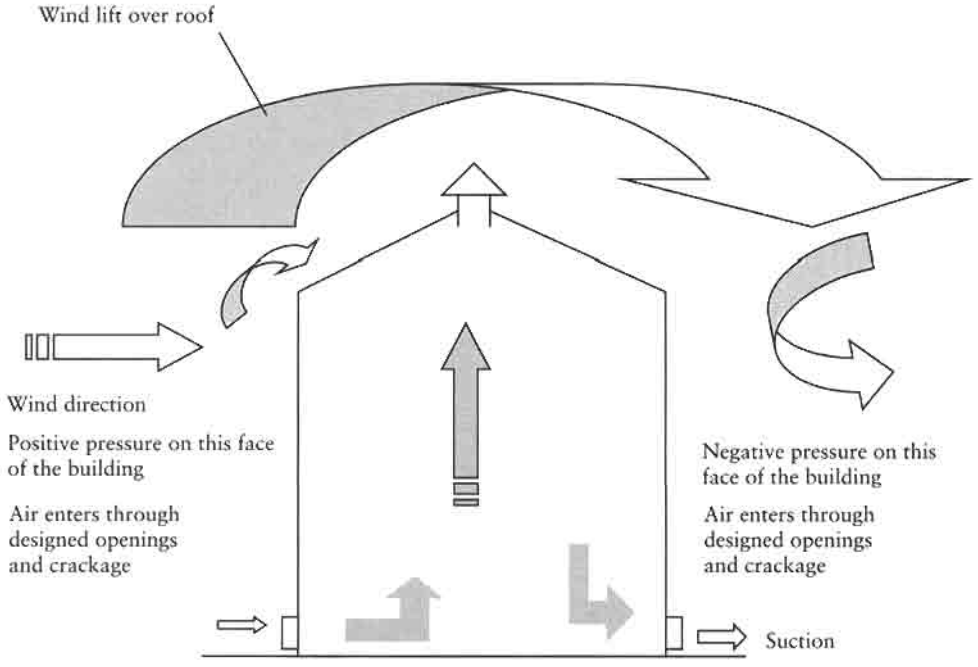

FIGURE 9.21 Wind forces around a building in elevation.

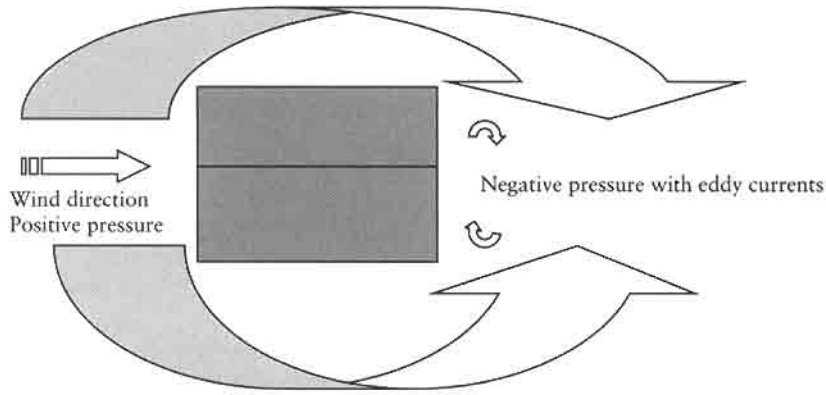

FIGURE 9.22 Wind forces around buildings in plan.

Mechanical Extract–Induced Input

This method of ventilation uses extractor fans. A fan will create a negative pressure within the space. With this method, a set flow rate can be achieved, as the fan will overcome the stack and wind effects; hence, the system is not at the mercy of the weather. This system causes the inside of the building to be held at a negative pressure, so air will be drawn in from outside or from surrounding spaces that are at a high pressure.

A space may need to be held at negative pressure, as in lavatories, kitchens, and process areas for example. In such cases, air will flow into the negative-pressure zone; hence, odors or toxic gases will not escape to other areas. The fan, with its running and maintenance costs, makes this system more expensive than the natural method.

Figure 9.23 shows a typical arrangement of this method of ventilation. The resulting airflow patterns in this arrangement will not ensure satisfactory air distribution in many industrial environments.

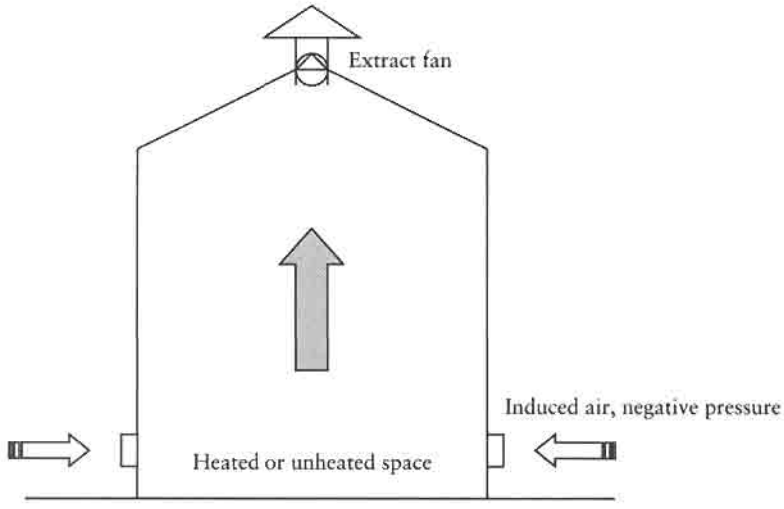

FIGURE 9.23 Mechanical extract–induced input ventilation.

Mechanical Input–Forced Extract

If heating is provided, this is known as a *plenum system*. This is a ducted system, which may provide air to a space in one or more of the following conditions:

- Untreated (no filter)
- Tempered by means of a heater battery (heated to near room conditions)
- Warm, at a temperature high enough to take care of the fabric and ventilation losses from the building

With the air being forced into the space, the pressure is positive; hence, all leakages are outward.

More sophisticated applications of a pressurized system combined with a suitable extractor are found in hospital operating theaters. The positive pressure produced by sterile air entering the room ensures that all leakages are outward. This outward leakage ensures that contaminated air at a lower pressure in the surrounding rooms will not enter the space.

Figure 9.24 shows a typical plenum system of mechanical input and forced extract. The outlets in Fig. 9.24 may be subdivided into two categories:

1. Diffused air distribution
2. Tangential air distribution

In the case of diffused air, the associated characteristics are these:

- The jet has a high degree of entrainment.
- There are no circular air patterns in the occupied zone.
- Air movement is ideal in the working zone, both for thermal comfort and pollution control.
- Temperature gradients (stratification) are at a minimum.

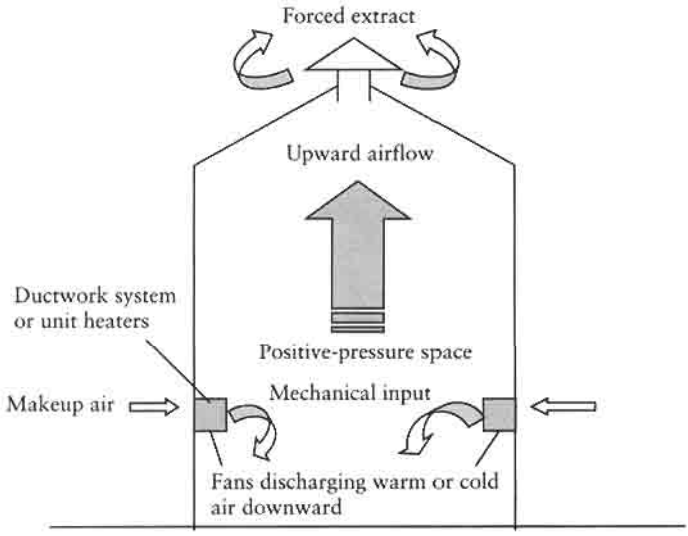

FIGURE 9.24 Plenum system.

The above are achieved by the use of

- Linear air outlets with highly inductive jets discharging directly downward or alternate jets discharging in opposite directions
- Twist outlets with adjustable twist vanes
- Specially designed air outlets
- Whirl outlets, either radial or linear, that have geometrically designed aperture chambers

The tangential method of air distribution has the following features:

- The room airflow patterns are circular.
- Stagnant pockets form between the circular room air patterns.
- The jets come into contact with surrounding surfaces.

In the application of this method of distribution, full use is made of the Coanda effect (wall jet), in which the jet adheres to a surface due to the fact that no entrainment can occur from a solid surface.

The outlets may be square, rectangular, or circular without any air twist being produced.

All outlets must be positioned at such a height that they do not create drafts in occupied zones.

Mechanical Input–Mechanical Extract

In this method of ventilation, powered extract and input systems are provided. The ratio of the supply to extract will control the pressure produced within the space.

If the input fans are handling the same amount of air as the extract fans, a neutral condition will result, with the disadvantages of the natural system.

Figure 9.25 shows a typical layout of this type of system. From the foregoing statements, the advantages of such a system are obvious.

This section has considered methods of ventilation. These should not be considered the same as methods of air distribution, which are now covered.

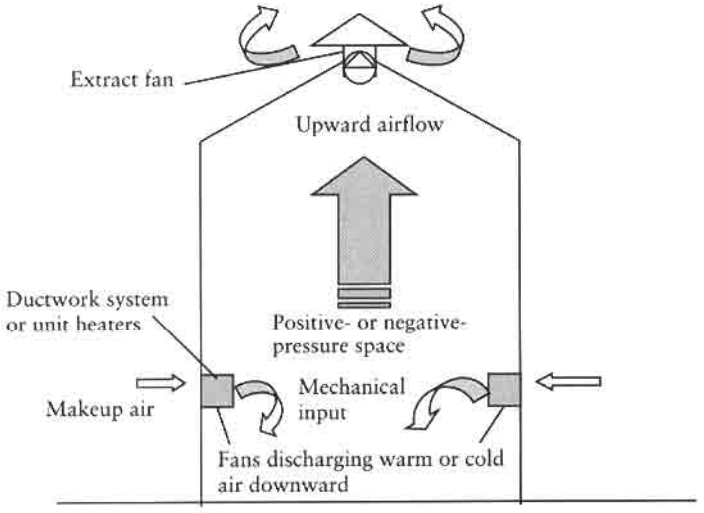

FIGURE 9.25 Mechanical input–mechanical extract.

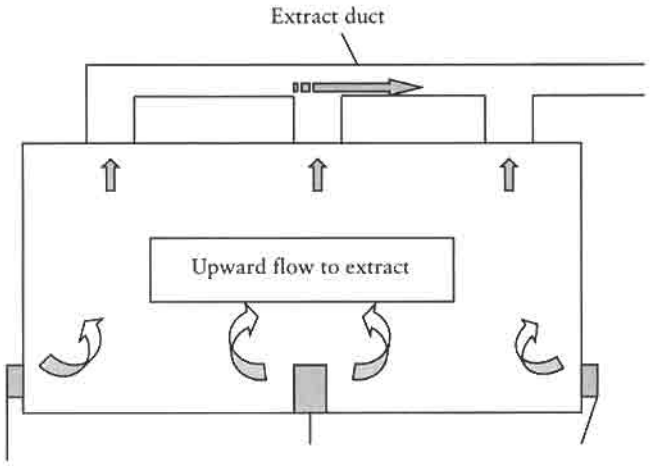

FIGURE 9.26 Upward ventilation, large hall.

9.4.3.3 Methods of Air Distribution

When air is supplied to a space by means of a fan forcing it along the ductwork, it has to be distributed into the space without causing drafts, noise, or poor air distribution, which would result in stagnant conditions in the space. Many variations of the following air-distribution methods are possible.

Upward Ventilation (Displacement)

This arrangement is suited for warm air, as on leaving the grill, hot air will rise. If this air is too hot, it will rise rapidly, and the jet will not reach the middle of the room. Therefore, the leaving velocity and the temperature from the grill are critical.

If the velocity is too high, the occupants will experience drafts, while if it is too low, the occupants in the middle of the room may not receive adequate fresh air. Hence, the arrangement shown in Fig. 9.26 is not suitable for wide spaces. This problem is overcome by using the layout shown in Fig. 9.27.

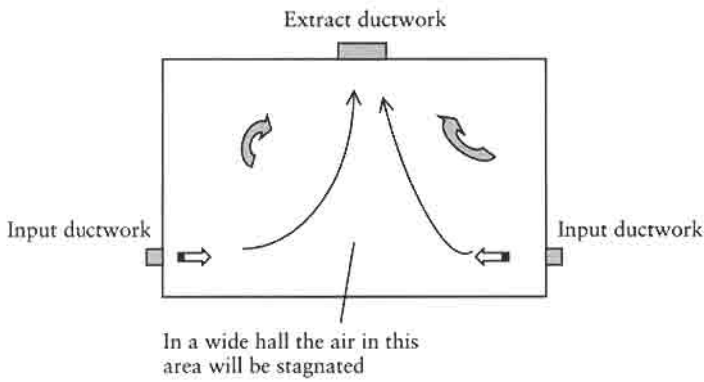

FIGURE 9.27 Upward ventilation, narrow room.

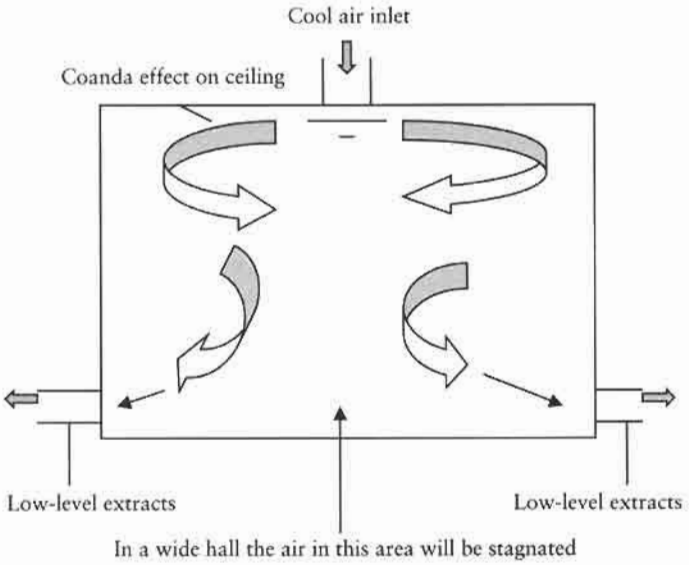

FIGURE 9.28 Downward system.

Downward Systems

Air-conditioning systems make use of this method, as the cooler, dense air supplied from high level will drop to low level, picking up the space heat gains before extraction at low level.

It is essential that the entering air is no more than, say, 9 °C cooler than the room air, for if it is, the cold air will drop, causing complaints from the occupants. In the case of air cooling of hot environments, the temperature difference can be greater.

Full use is made of ceiling diffusers, which ensure that the cold air spreads out over a wide area before dropping. Perforated ceilings may be used, with the ceiling void being the plenum chamber. A typical downward system is shown in Fig. 9.28.

The arrangement shown in Fig. 9.28 is used in industrial halls or auditoriums. Clean rooms have complex systems using laminar flow to ensure that the room is fully ventilated.

Figure 9.29 shows a typical arrangement of a laminar-flow clean room. The flow may be vertical through a perforated ceiling and floor.

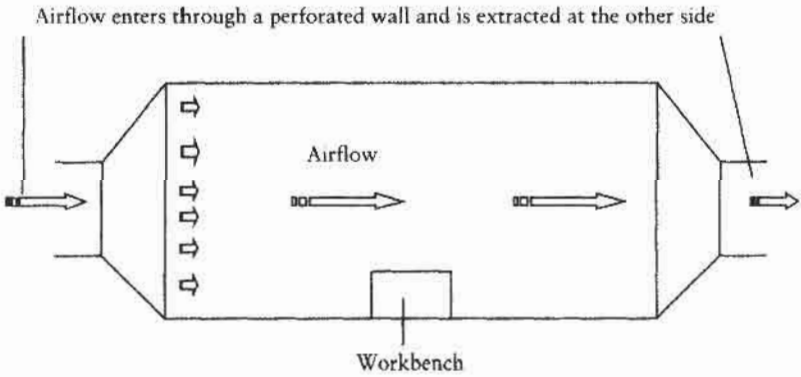

FIGURE 9.29 Laminar-flow room.

Full use can be made in the industrial environment of long jet throws, which entrain room air.

It is essential that the velocity envelope in the occupied zone be in the range of 0.2–0.25 m s^{-1} to avoid drafts. However, in hot industrial environments, these velocities are frequently exceeded in order to provide adequate body cooling.

Mixed Upward–Downward System

The working of this system is shown in Fig. 9.30, from which it will be seen that good air mixing takes place. Care has to be taken to ensure that the high-level inlets and extract are positioned so that short circulating of the air does not occur.

The low-level extract is normally about 25% of the total extract; the actual value is selected to suit the design conditions.

9.4.3.4 Air-Handling Equations

Air Mixing

As the outside air conditions vary from hour to hour, day to day, and month to month, to economize on the heating and cooling loads, the recirculated and fresh airstreams are mixed in varying proportions. If the air contains toxic or inflammable gases, vapors, or dusts, no direct mixing occurs, and a heat-recovery device is used.

In order to appreciate the mixing arrangement, consider the layout shown in Fig. 9.31.

In this instance the following abbreviations are used:

q_m = mass flow rate of the gas
m_w = mass of water vapor present

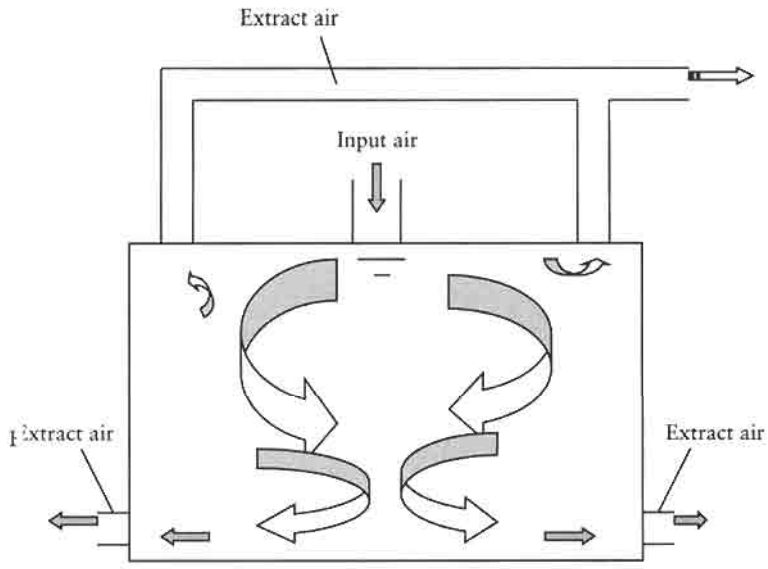

FIGURE 9.30 Mixed upward-downward system.

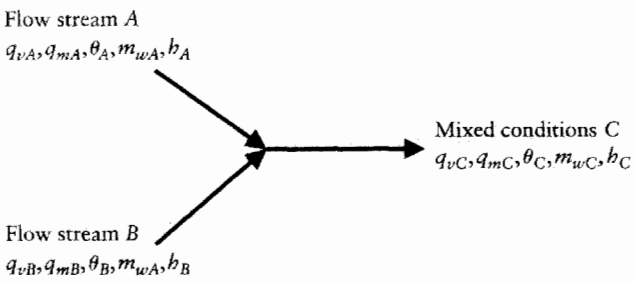

FIGURE 9.31 Mixing arrangement.

h = specific enthalpy of the gas
θ = dry-bulb temperature

Consider any two gas streams A and B which, when combined, produce a mixed condition C.

For Mass Flow

Assuming no flow losses occur, the total mass of a gas introduced into and out of the system must be constant. Hence,

$$q_{mA} + q_{mB} = q_{mC}.$$

For Moisture Content

Similarly, the total quantity of moisture in the system will be the same before and after mixing. However, the amount of moisture per unit mass of the gas will change: hence, in this case the equation must include mass.

$$q_{mA} \times m_{wA} + q_{mB} \times m_{wB} = q_{mC} m_{wC}$$

For Enthalpy

Provided that no gain or loss of heat takes place during the mixing process, the total heat in the two airstreams before mixing must equal that of the combined airstream after mixing.

$$q_{mA} \times h_A + q_{mB} \times h_B = q_{mC} \times h_c$$

For Temperature

When the dry-bulb temperature of a gas is altered, a positive or negative sensible-heat transfer takes place, in terms of both the dry bulb and its associated moisture content.

Because the specific heat capacity of the water vapor is different from that of the dry air, the true dry-bulb mixed-stream air temperature can be determined only by means of a heat balance.

Heat gained or lost by stream A = Heat gained or lost by stream B

$$\begin{bmatrix}\text{Heat gained or lost in stream } A + \\ \text{Heat lost or gained by associated moisture}\end{bmatrix} = \begin{bmatrix}\text{Heat lost or gained in stream } B + \\ \text{Heat lost or gained by associated moisture}\end{bmatrix}$$

$$\begin{bmatrix} q_{mA} \times c_{pg}(\theta_A - \theta_C) + \\ q_{mA} \times m_{wA} \times c_{pW}(\theta_A - \theta_C) \end{bmatrix} = \begin{bmatrix} q_{mB} \times c_{pg}(\theta_C - \theta_B) + \\ q_{mA} \times m_{wB} \times c_{pW}(\theta_C - \theta_B) \end{bmatrix}$$

$$q_{VA}(\theta_A - \theta_C)(c_{pg} + c_{pw}m_{wA}) = q_{VB}(\theta_C - \theta_B)(c_{pg} + c_{pw}m_{wB})$$

Total Room Air Movement

It is essential to ensure that the air distribution in a space provides satisfactory air movement for the occupants' thermal comfort.

When a jet is released into a free space, it induces into its body the room air. The air leaving the grille is the primary air, while that entrained from the room into the body of the jet is the secondary air. The degree of entrainment that takes place is related to the velocity of the leaving jet. The combined airstream is known as the total air.

The induction is expressed by the momentum equation as

$$q_{mP}v_P + q_{ms}v_s = (q_{VP} + q_{VS})_{VT},$$

where

q_m = mass flow rate of the primary air (kg s^{-1})
v_p = entering velocity of the primary air (m s^{-1})
q_{ms} = mass flow rate of the secondary air (kg s^{-1})
v_s = velocity of the secondary air (m s^{-1})
q_{VP} = volume flow of the primary air (m^3 s^{-1})
q_{Vs} = volume flow of the total air (m^3 s^{-1})
v_T = velocity of the total air

The induction ratio (R) is the ratio of the total air to the primary air.

$$R = \frac{\text{Total air}}{\text{Primary air}} = \frac{\text{Primary air + Secondary air}}{\text{Primary air}}$$

Since the throw of a jet is a function of the velocity, and since the rate of velocity decrease is dependent on the rate of induction that occurs, the quantity of air induced into the discharge from an outlet is a direct function of the perimeter of the cross section of the primary airstream.

In the case of two outlets, each of the same area, the outlet having the largest perimeter will induce the greatest amount of secondary air; hence, the throw will only be short. For a given air quantity and pressure discharged into a space, the minimum induction and a single outlet of circular cross section obtains the maximum throw, while the greatest induction and shortest throw occurs with a single, long, narrow slot.

The spread of a jet is the angle of divergence of the airstream after it leaves the outlet. The outlet design may be for horizontal or vertical spread or both.

Example

The following example provides some indication of the effects of induction.

Primary and secondary air are mixed respectively at the rates of 0.5 m^3 s^{-1}, the primary air velocity at outlet being 5.0 m s^{-1}, with the secondary air velocity assumed to be zero.

Determine the velocity and the area of the total airstream when complete mixing of the primary and secondary airstreams has taken place.

Solution The area of the primary airstream before induction is

$$\frac{q_{V1}}{v_1} = \frac{0.5}{5.0} = 0.1 \text{ m}^2.$$

Substituting in the momentum equation,

$$(0.5 \times 5) + (0.5 \times 0) = (0.5 + 0.5)v_3.$$

Hence $v_3 = 2.5 \text{ m s}^{-1}$.

The area of the total airstream is

$$\frac{q_{m1} + q_{m2}}{v_3} = \frac{0.5 + 0.5}{2.5} = 0.4 \text{ m}^2.$$

In basic ventilation design, if a given air change is required, it is a simple matter to determine the capacity of the fan required from

$$q_v = \frac{\text{Volume of space}(\text{m}^3) \times \text{Number of air changes per hour}}{3600}.$$

Depending on the application, the air-change rate may range from 0.5 to 100 air changes per hour. It must be remembered, however, that adequate provision must be made for the makeup air to enter the space without creating discomfort or other problems.

In the case of sensible and latent heat, the cooling procedure becomes a little more complicated.

In the case of summer cooling, the heat balance is

Heat gain to space

= Heat absorbed by chilled air flowing through the room,

or

Sensible heat gain (kW) = Air mass flow × Gain in specific enthalpy,

or

$$\phi_s \text{ (kW)} = q_m \text{ (kgs}^{-1}) \times (h_r - h_s) \text{ (kJ kg}^{-1}).$$

The sensible heat gain is determined by taking into account all the heat gains in a space, such as solar, fabric, infiltration, machines, processes, occupancy, lighting, etc.

The specific enthalpy (h_s) of the room-air design condition is obtained from tables of the property of air or the psychrometric chart.

For deciding to what dry-bulb temperature (θ_s) the incoming supply air has to be cooled, the following approach is applied.

Sensible heat ϕ_s (kW) = Air mass flow rate q_m (kg s^{-1})

× Specific heat capacity (kJ kg^{-1} K^{-1}) × Air temperature rise

$$\Phi_s(\text{kW}) = q_m \times c_p \times (\theta_r - \theta_s)$$

$$q_m = q_v \times \rho$$

$$\Phi_s(\text{kW};SH) = q_v \times \rho \times c_p \times (\theta_r - \theta_s)$$

As the air density depends on both the temperature and moisture content of the air, it is necessary to apply the general gas equation:

$$p_a V = mRT$$

where

p_a is the absolute pressure of the gas (Pa)
V is the gas volume (m^3)
m is the mass of gas (kg)
R is the gas constant (287.1 J kg^{-1} K^{-1})
T is the absolute temperature of the gas (K)

$$\rho = \frac{m}{V} = \frac{p}{RT},$$

assuming that the pressure and moisture content are constant in the flow along the air supply duct.

$$\rho_1 \approx \frac{1}{T}$$

If the standard air density is ρ_1 and the supply air density is ρ_2, then.

$$\rho_1 \approx \frac{1}{T_1}$$

and

$$\rho_2 \approx \frac{1}{T_2}.$$

The above gives

$$\frac{\rho_2}{\rho_1} = \frac{T_1}{T_2}$$

and

$$\rho_2 = \rho_1 \frac{T_1}{T_2}.$$

Correcting the air density for other air supply temperatures,

$$\rho_2 = 1.1906 \times \frac{273 + 20}{273 + \theta_s} \text{kg m}^3$$

where 1.1906 is the density of air at 20 °C and 50% saturated (specific volume 0.8399 m^3 kg^{-1}).

Substituting this into the heat balance equation for sensible heat only gives

$$\Phi_s(\text{kW}) = q_v \times \rho_2 \times c_p \times (\theta_r - \theta_s)$$

$$\Phi_s(\text{kW}) = q_v \times 1.1906 \times \frac{273 + 20}{273 + \theta_s} \times 1.0048 \times 1.0048 \times (\theta_r - \theta_s)$$

$$q_v \times 351 \times \frac{\theta_r - \theta_s}{273 + \theta_s},$$

where 1.0048 is the specific heat capacity of air (kJ kg^{-1} K^{-1}).

On rearranging to obtain q_v,

$$q_v = \frac{\Phi_s(\text{kW}) \times (273 + \theta)}{351(\theta_r - \theta_s)}.$$

Example

The sensible gain in an industrial complex is 1000 kW, and the space temperature has to be controlled at 20 °C.

If the supply air leaves the cooling plant at 11 °C and gains 1 °C in the ductwork before entering the space, determine the air supply volume that is required.

Solution

$\Phi_s = 1000$ kW; $\theta_r = 20$ °C; $\theta_s = 11 + 1$ °C gain $= 12$ °C

so $\Delta\theta = 20 - 12 = 8$ °C.

Hence,

$$q_v = \frac{1000\,\text{kW} \times (273 + 12)}{351 \times (20 - 12)} = 101.5\ \text{m}^3\ \text{s}^{-1}.$$

Answer: 101.5 m^3 s^{-1}.

Question

A workshop is 30 m × 15 m × 4 m and has to be maintained at 20 °C with six air changes per hour with a supply air temperature of 14 °C.

Determine the maximum cooling load that can be met.

Solution

$$q_v = \frac{N \text{ air changes per hour} \times \text{Volume}}{3600}$$

$$\frac{6 \times 30 \times 15 \times 4}{3600} = 3.0\ \text{m}\ \text{s}^{-1}$$

$$\Phi_s = \frac{q_v \times 351(\theta_r + \theta_s)}{273 + \theta_s}$$

Substituting known values,

$$\frac{3.0 \times 351(20 - 14)}{273 + 14} = 22\ \text{kW}.$$

Answer: 22 kW.

In order to determine the summer supply air temperature for a given volume of air necessary to remove a given sensible heat gain, the following equation is used.

$$q_v = \frac{\Phi_s(\text{kW}) \times (273 + \theta_s)}{351(\theta_r - \theta_s)}$$

$$q_v \times 351(\theta_r - \theta_s) = \Phi_s(273 + \theta_s)$$

$$q_v \times 351\theta_r - \Phi_s \times 351\theta_s = \Phi_s \times 273 + \Phi_s \times \theta_s$$

$$q_v \times 351\theta_r - \Phi_s \times 273 = q_v \times 351\theta_s + \Phi_s \times \theta_s$$

$$q_v \times 351\theta_r - \Phi_s \times 273 = \theta_s(q_v \times 351 + \Phi_s)$$

Hence,

$$\theta_s = \frac{q_v \times 351\theta_r - \Phi_s \times 273}{q_v \times 351 + \Phi_s}.$$

Example

A process plant occupies a space of 30 m × 20 m × 4 m. The area has to be maintained at 21 °C with 10 air changes per hour of chilled air. The

refrigeration plant is capable of 35 kW of sensible cooling. Determine the required supply air temperature.

Solution

$$q_v = \frac{30 \times 20 \times 4 \times 10}{3600} = 6.66 \text{ m}^3 \text{ s}^{-1}$$

$$\theta_s = \frac{q_v \times 351\theta_r - \Phi_s \times 273}{q_v \times 351 + \Phi_s},$$

substituting the known values.

$$\theta_s = \frac{6.66_v \times 351 \times 21 - 35 \times 273}{6.66 \times 351 + 35} = 16.6 \text{ °C}$$

Answer: 16.6 °C.

The above examples have dealt with cooling. In the case of heating applications, the supply air temperature must be greater than the room air, hence $\theta_s > \theta_r$.

Example

A workshop has a fabric and ventilation sensible heat loss of 30 kW, and the process requires that the room be maintained at 22 °C dry bulb. Determine the supply air volume required at 34 °C in order to maintain the space at design conditions.

Solution

$$q_v = \frac{\Phi_s \times (273 + \theta_s)}{351(\theta_s - \theta_r)}$$

$$q_v = \frac{30 \times (273 + 34)}{351(34 - 22)}$$

$$= 2.187 \text{ m}^3 \text{ s}^{-1}$$

Answer: 2.187 m^3 s^{-1}

Example

A plenum system provides two air changes per hour of makeup air at 33 °C to a process area of 20 m × 15 m × 3.5 m in order to maintain the space temperature at 21 °C.

Determine the maximum heat loss the above parameters are capable of meeting.

Solution

$$q_v = \frac{2 \times 20 \times 15 \times 3.5}{3600} = 0.583 \text{ m}^3 \text{ s}^{-1}$$

$$q_v = \frac{\Phi_s \times (273 + \theta_s)}{351(\theta_s - \theta_r)}$$

$$\Phi_s = \frac{q_v \times 351(\theta_s - \theta_r)}{273 + \theta_s}$$

$$= \frac{0.583 \times 351 \times (33 - 21)}{273 + 33}$$

Answer: 8.02 kW.

The supply air temperature in the case of a heating system is determined from

$$\theta_s = \frac{351 \times q_v \theta_r + 273 \times \varphi_s}{351 q_v - \theta_s}.$$

Question

Determine the air temperature that is necessary to maintain a volume of 1200 m^3 with six air changes per hour at 20 °C, if the total heat loss is 45 kW.

Solution

$$\frac{1200 \times 6}{3600} = 2.0 \text{ m}^3 \text{ s}^{-1}$$

$$\theta_s = \frac{351 \times 2 \times 20 + 273 \times 45}{351 \times 2 - 45} = 40.07 \text{ °C}$$

Answer: 40.07 kW.

When calculating for heater and cooler batteries, it is the mass flow rate q_m that is required, not the volume flow rate q_V as used above. This is determined by using the appropriate specific volume or density of the air at the actual design temperature and moisture content.

Moisture Content

The water vapor present in the air exists at its own partial pressure. The molecular mass of water vapor is 18.015 kg $kmol^{-1}$. This is less than dry air, which is 29 kg $kmol^{-1}$.

From the above it will be appreciated that the greater the concentration in the air, the less the mixture weighs.

As the moisture content in a dry air mixture increases, the specific volume increases and the density reduces. The specific volume is ν (m^3 kg^{-1}), and the density is ρ (kg m^{-3}).

The relationship between the two parameters is simply $\rho = 1/\nu$.

The base for air density is taken as 101.325 kPa at 0 °C.

Using the general gas law, the standard density is

$$p_a \nu = mRT,$$

hence density

$$\rho = m/\nu = p_a/RT.$$

Taking the vapor pressure of the air supply from hygrometric tables, the value of specific density can be found.

$$\nu = \frac{287.1 \times (273 + \theta_s)}{101.325 - p_s} \text{ m}^3 \text{ kg}^{-1}$$

Example

Air is supplied to a space at the rate of 2.0 m^3 s^{-1} at 12 °C and 70% saturated, at which condition the vapor pressure is 0.9852 kPa. Determine the density and the mass flow rate.

Solution

$$v = \frac{287.1 \times (273 + 12)}{101325 - 0.9852 \times 1000} \text{ m}^3 \text{ kg}^{-1} = 0.8154 \text{ m}^3 \text{ kg}^{-1}$$

The mass flow is then

$$q_m = \frac{q_v}{v} = \frac{2.0}{0.8154} = 2.452 \text{ kg s}^{-1}.$$

Answer: 2.452 kg s^{-1}.

9.5 FANS

9.5.1 General

The fan is the heart of a ventilation system. The industrial engineer requires a comprehensive working knowledge of the subject of fan engineering for the following reasons:

1. The designer must fully appreciate the correct fan selection, by ensuring that its duty meets the requirements of the task for which it is intended.
2. In many cases an existing fan system has to be adapted or modified to meet new demand requirements.
3. The owning and operating costs must be fully considered.

A fan is a rotodynamic device and is the driving part of all mechanical ventilating systems. The energy of rotation applied to the fan shaft is converted into a pressure difference, causing the air, gas, or particulate matter to flow through the ductwork or discharge into a free space.

To be classed as a fan, the work per unit mass on the gas must be less than 25 kJ kg^{-1}; above this value it is called a turbo compressor.

Hence, the fan pressure must not exceed the standard air density of 1.2 kg m^{-3} × 25 kJ kg^{-1}, giving 30 kPa, with the pressure ratio not exceeding 1.30, taking the atmospheric pressure as 100 kPa.

ISO gives the classifications for fans shown in Table 9.6.

TABLE 9.6 Category According to Work per Unit Mass

Description	Code	Work per unit mass, kJ kg^{-1}	Maximum fan pressure, kPa	Class
Low pressure	LB	0 to 0.6	0 to 0.7	0
		0.6 to 0.833	0.7 to 1.0	1
		0.833 to 1.333	1.0 to 1.6	2
		1.333 to 1.667	1.6 to 2.0	3
Medium pressure	MP	1.667 to 3.00	3.0 to 3.6	4
		3.0 to 5.25	3.6 to 6.3	5
		5.25 to 8.33	6.3 to 10	6
High pressure	HA	8.33 to 13.33	10.0 to 16.0	7
		13.33 to 18.67	16.0 to 22.4	8
		18.67 to 25.00	22.4 to 30	9
Turbo compressor	—	25+	30+	—

9.5.1.1 Fan Types

Fans can be divided into four general categories: propeller, axial, centrifugal, and special purpose. These are defined according to the direction of gas flow.

Propeller

This type consists of a propeller or disk-type wheel within a mounting-ring panel or cage. The wheel or housing is constructed from either sheet metal, cast aluminium, plastic, or plastic-coated material. It may be a direct drive with the wheel on the motor shaft or belt driven.

Advantages and Typical Uses

- Wide range of volumes
- A minimum operating cost per $m^3\ s^{-1}$
- Minimum space and weight per $m^3\ s^{-1}$
- Blast or man cooling for hot processes
- Dilution ventilation for toxic and odor removal

Disadvantages/Limitations

- Limited to resistances of 250 kPa
- Sound-level problems with high speeds
- Not suited for corrosive or abrasive applications, bearings to be protected
- Direct-drive fans should not be used in area in which explosive or flammable gases or vapors are handled by the fan
- Operating temperature limitations

Axial Fan

A tube axial fan (see Fig. 9.32) is essentially a propeller fan located in a short cylinder housing, the gas flowing in an axial direction. A vane axial fan incorporates specially designed vanes, which are positioned either upstream or downstream of the fan.

The axial fan consists of an impeller fitted with airfoil blades mounted on a rotating hub. The hub is positioned in a cylindrical casing in line with the gas flow direction. If safe gases are being handled, the motor is located in the airflow. If, however, explosive, abrasive, flammable, or corrosive gases are conveyed, a bifurcated fan is used, with the motor positioned outside the gas stream. A motor located outside the casing allows the fan to be belt driven, providing easy speed changes if necessary. Due to advances in motor electronic speed control, the use of belts for speed control is on the decline.

An airfoil fan may have an efficiency as high as 80%. It has the advantages of being compact and able to fit in line with the ductwork. Its disadvantage is that it may not be capable of developing the high pressures required for many industrial ventilation applications.

The purpose of the blades is to reduce the degree of flow spiraling and to convert some of the velocity component into useful static pressure.

Vane axial fans develop a greater static pressure than tube axial fans. They are constructed from a variety of materials, depending on the application. They may use either a direct drive or a belt drive. More expensive models

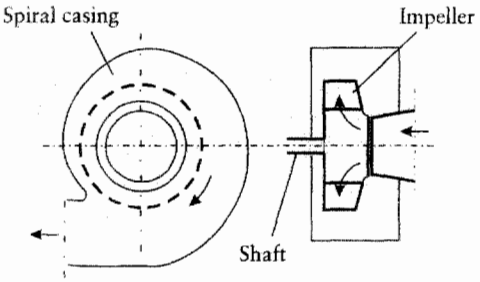

Centrifugal fan

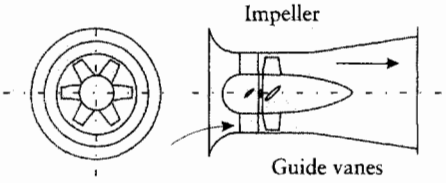

Axial fan

FIGURE 9.32 Centrifugal and axial fans.[1]

are fitted with adjustable pitch blades, allowing a direct-driven fan to cover the same capacities as belt-driven fans of the same diameter.

Advantages and Typical Uses

- Operates from low- to high-volume flow rates.
- The actual pressure range of some vane axials is similar to high-efficiency backward-curved centrifugal fans. By fitting the fans in series, the operating pressure can be increased.
- Compact, low-space environment and low weight per unit volume handled make it second only to the propeller fan.
- Applications include comfort, dilution, man cooling, paint-spray-booth extract, etc.

Disadvantages/Limitations

- Inherently higher sound levels than most efficient centrifugal fans for the same duty
- Unsuitable in abrasive or corrosive atmospheres
- Problems in protecting bearings
- Unsuitable for flammable and explosive gases and vapors unless a bifurcated fan is used
- Fan curve problems with damper closing

Centrifugal Fan

This is the most common type of fan encountered in industrial ventilation systems. These fans are similar to a water wheel, with blades mounted on

back plates. The impeller is positioned in a volute or scroll casing. The air enters with the line of the driving shaft through the eye and discharges at 90° to the entering air.

The centrifugal fan may have one of four impeller designs.

1. Airfoil
2. Backward inclined–backward curved
3. Radial (paddle)
4. Forward curved

Airfoil, Backward Curved

These low-cost fans are of simple construction and have static efficiencies up to 80%.

This fan design is capable of the highest efficiency with the lowest sound level of all the centrifugal fans for a given duty, particularly those with airfoil-shaped double blades.

They are normally fitted with 10–12 blades, the blade tips inclined away from the angle of rotation. They have the advantage of being very efficient, with fan static efficiencies in excess of 80% for airfoil blades. This type of fan has a nonoverloading characteristic curve.

Advantages and Typical Use

- Handles moderate to high airflow rates
- Static pressure up to the 7.5 kPa range
- Highest efficiency of any fan type
- Lowest noise level of any fan type for a given duty
- Self-limiting power characteristics, nonoverloading characteristic
- Variable air volume systems

Disadvantages/Limitations

- For equal pressure and volume, axial fans' weight and size are greater for the backward-curved fan
- Unsuitable for high dust loading, due to particulate buildup on the impeller causing imbalance and vibration
- Wheels are difficult to clean and paint

Radial Blade, Straight Paddle Blade

This fan group, sometimes referred to as industrial exhaust fans', is characterized by its simple, rugged construction.

They may or may not have flat, radial blades. The wheel configuration may be from simple paddle blades to the semi-open and enclosed types. They may be belt or direct driven.

Advantages and Typical Use

- Ease of maintenance and cleaning
- Ease of repair due to simple construction
- Can handle any type of gas or dust
- Used for pneumatic conveying

- Suitable for high-temperature operation
- Suitable for corrosive and abrasive material if correctly designed

Disadvantages/Limitations

- Lowest efficiency of all centrifugal fans.
- Highest sound level of all centrifugal fans for a given duty.
- Shaft power increases as the fan approaches the maximum volume.

Forward-Curved Blade, Centrifugal

These are made up of a large number of wide, shallow blades with a very large inlet area relative to the wheel diameter. For equal duty the speeds are lower than other centrifugal fans. They are sometimes called multivane; the operating efficiencies are in the 65–75% range. They consist of a large number of relatively small blades mounted on the impeller. The blade tips are inclined toward the direction of rotation. The actual flow rate can be 2.5 times as high as the same size backward-curved fan.

Advantages and Typical Uses

- Ideal for any volume at low to medium static pressures.
- Due to low speeds they are quiet in operation.
- The space and weight requirements are about the same as backward-inclined blade fans.

Disadvantages/Limitations

- Lower efficiency than backward-curved fan.
- Greater space requirement for a given duty than an axial flow fan.
- Unsuitable for high dust loading.
- Shaft power increases as fan approaches maximum volume, unlike the backward-curved fan, where it decreases.

The types of fans are given in Fig. 9.32.

As the gas density handled by a fan is relatively constant, the pressure increase is small, and the pressure ratio is less than 1.1.

9.5.2 Centrifugal Fan

In this type of fan, the gas flows initially in an axial direction toward the impeller. After this, in a part of the impeller blade, the gas flow becomes radial.

To force the air to flow through the impeller blades of a centrifugal fan, a tangential force is needed. According to the momentum law this force is

$$F_t = \frac{d}{dt}(mc_{2t} + mc_{1t}) = q_m(c_{2t} - c_{1t}). \tag{9.59}$$

Here c_{1t} is the tangential component of the air velocity at the inlet to the impeller blades, and c_{2t} is the same at the exit. q_m is the mass flow of air through the impeller.

Mechanical power is generally equal to force times velocity, so we get from Eq. (9.59)

$$P_u = q_m(u_2 c_{2t} - u_1 c_{1t}) \,. \tag{9.60}$$

u_1 is the velocity of impeller at the inlet to the blades, and u_2 is the velocity of impeller at the outer edge.

Generally the velocity u can be calculated from

$$u = \pi D n \tag{9.61}$$

where D is the diameter at the point in consideration and n is the speed of revolution of the impeller.

Consider the thermodynamic process in the fan (Fig. 9.33). As the fan is a stationary flow system, consideration is directed to the total enthalpy change. As the suction openings are often at the same, or almost the same level, the potential energy change can be neglected.

Two cases are studied:

- Adiabatic reversible (isentropic) process
- Adiabatic irreversible process in which entropy is generated

In both cases the mass flow, mechanical work, and density are constant. The flow is denoted by subscripts 1 before the fan and 2 after the fan. If there is no entropy generation, subscript 2 is replaced by subscript 2s.

The mass conservation equation gives

$$q_m = \rho c_1 A_1 = \rho c_2 A_2 = \rho c_{2s} A_2, \tag{9.62}$$

where

A_1 is the cross-sectional area of the fan entrance and
A_2 is the cross-sectional area of the fan exit.

Considering the air density to be constant yields $c_2 = c_{2s}$, and using

$$T ds = dh - v dp \,, \tag{9.63}$$

the total enthalpy difference for the isentropic case can be written as

$$\begin{aligned} \Delta h_{\text{tot},s} &= h_{2s} - h_1 + \tfrac{1}{2}c_2^2 - \tfrac{1}{2}c_1^2 \\ &= v(p_{2s} - p_1) + \tfrac{1}{2}(c_2^2 - c_1^2) \\ &= \frac{1}{\rho}(p_{2s} - p_1) + \tfrac{1}{2}(c_2^2 - c_1^2). \end{aligned} \tag{9.64}$$

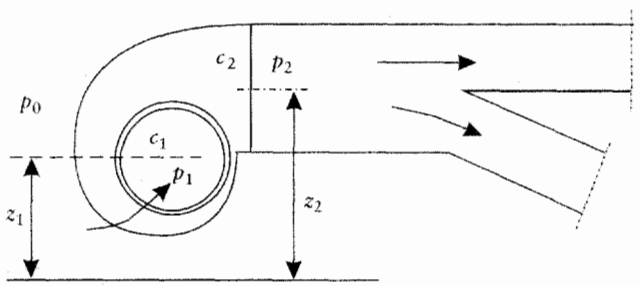

FIGURE 9.33 Fan as a stationary flow system.

In an adiabatic process, an entropy change occurs, giving

$$\int_1^2 T\,ds > 0. \tag{9.65}$$

Thus

$$\begin{aligned}\Delta h_{\text{tot}} &= h_2 - h_1 + \tfrac{1}{2}c_2^2 - \tfrac{1}{2}c_1^2 \\ &= \frac{1}{\rho}(p_2 - p_1) + \int_1^2 T ds + \tfrac{1}{2}(c_2^2 - c_1^2) \\ &= \frac{1}{\rho}(p_2 - p_1) + \int_1^2 T ds + \tfrac{1}{2}(c_2^2 - c_1^2).\end{aligned} \tag{9.66}$$

As the mass flow and power requirements are the same in both cases, $P = q_m\,\Delta h_{\text{tot},s} = q_m\,\Delta h_{\text{tot}}$ or $\Delta h_{\text{tot},s} = \Delta h_{\text{tot}}$.

Comparing Eqs. (9.64) and (9.66) and relating to Eq. (9.65), the following is obtained:

$$p_{2s} > p_2 \tag{9.67}$$

In the isentropic case, the static pressure increases more than for the irreversible case, with the fan operating under the same power input and mass flow.

The total isentropic enthalpy difference can be expressed in terms of the total isentropic pressure difference by

$$\Delta p_{\text{tot},s} = \rho\,\Delta h_{\text{tot},s} = \Delta p_s + \tfrac{1}{2}\rho(c_2^2 - c_1^2)\,. \tag{9.68}$$

Denoting the total pressure by

$$p_{\text{tot}} = p + \tfrac{1}{2}\rho c^2 \tag{9.69}$$

gives the total pressure difference as

$$\Delta p_{\text{tot}} = \Delta p + \tfrac{1}{2}\rho(\Delta c^2)\,. \tag{9.70}$$

In Eq. (9.67), p is the *static pressure*, and $\frac{1}{2}\,\rho c^2$ is the *dynamic pressure*.

Using Eq. (9.65) gives

$$\Delta p_{\text{tot},s} > \Delta p_{\text{tot}} \tag{9.71}$$

for a fan in which the opening suction pressure, mass flow, and power are the same.

Equations (9.60), (9.68), and (9.70) give

$$\text{Isentropic case: } u_2 c_{2u} - u_1 c_{1u} = \frac{1}{\rho}\,\Delta p_{\text{tot},s}\,. \tag{9.72}$$

$$\text{Adiabatic irreversible case: } u_2 c_{2u} - u_1 c_{1u} > \frac{1}{\rho}\,\Delta p_{\text{tot}}\,. \tag{9.73}$$

The isentropic or hydraulic efficiency of the impeller is

$$\eta_s = \frac{\Delta p_{\text{tot}}}{\Delta p_{\text{tot},s}} < 1. \tag{9.74}$$

Using Eqs. (9.60), (9.72), and (9.74) gives

$$P_u = q_m(u_2 c_{2u} - u_1 c_{1u}) = \frac{q_m}{\rho}\frac{\Delta p_{\text{tot}}}{\eta_s} \tag{9.75}$$

where $\eta_s = 1$ if the flow through the impeller is isentropic.

For isentropic or nonisentropic flow, the fan shaft power is greater than the power required for the flow through the impeller.

A proportion of the shaft power is used to overcome the bearing friction. This is allowed by using the mechanical efficiency. Thus, the required axial power is

$$P_a = \frac{P_u}{\eta_m} = \frac{q_v \, \Delta p_{\text{tot}}}{\eta_s \eta_m} = \frac{q_v \, \Delta p_{\text{tot}}}{\eta}, \tag{9.76}$$

where

η is the total efficiency of the fan and

$q_v = \frac{q_m}{\rho}$ is the air volume flow through the fan.

By using the vector equation

$$\begin{aligned} w^2 = \bar{w} \cdot \bar{w} = (\bar{c} - \bar{u}) \cdot (\bar{c} - \bar{u}) &= c^2 + u^2 - 2\bar{u} \cdot \bar{c} \\ &= c^2 + u^2 - 2uc_2 \end{aligned} \tag{9.77}$$

the velocity expression of Eq. (9.73) can be written as

$$\begin{aligned} u_2 c_{2u} - u_1 c_{1u} &= \tfrac{1}{2}(c_2^2 - c_1^2) + \tfrac{1}{2}(u_2^2 - u_1^2) + \tfrac{1}{2}(w_1^2 - w_2^2) \\ &= \frac{1}{\rho}(p_{2s} - p_1) + \tfrac{1}{2}(c_2^2 - c_1^2), \end{aligned} \tag{9.78}$$

from which

$$\Delta p_s = p_{2s} - p_1 = \tfrac{1}{2}\rho(u_2^2 - u_1^2) + \tfrac{1}{2}\rho(w_1^2 - w_2^2). \tag{9.79}$$

The centrifugal force produced increases the impeller static pressure [the first term of the right-hand side of Eq. (9.79)] and reduces the relative velocity w. To increase the static pressure by a change in the relative velocity, the following relationship is necessary:

$$w_1 > w_2.$$

The mass flow through the blade passage is constant; hence, $w_1 > w_2$, and the flow across the surface is greater for the leaving edge than the incoming edge. The cross-sectional area of the passage increases in the direction of flow.

Equation (9.79) shows that the static pressure increases with an increase in the tangential speed and the distance between the incoming and leaving edges of the impeller blade. This will not influence the nature of the flow process in the impeller.

Up to this stage, only the fan characteristics have been considered, without investigating the influence of different impeller blade shapes. Consider the flow at the edge of the impeller blade. Normally, for cost reasons, leading devices are not installed in front of the fan propeller, resulting in radial gas flow into the propeller, with the tangential velocity component $c_{1u} = 0$.

The velocity triangles of the incoming and leaving flow at the blade edges of a centrifugal fan are shown in Fig. 9.34. The flow to the blade is in a radial direction.

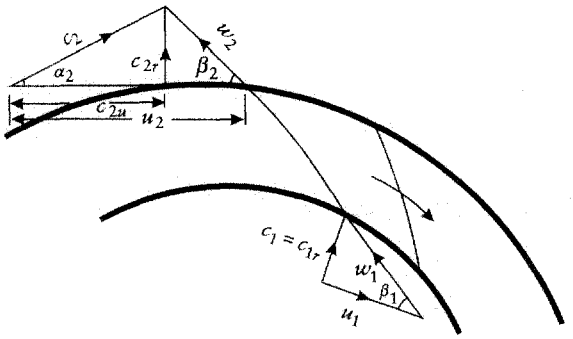

FIGURE 9.34 Velocity triangles at the blade edges of a backward-blade centrifugal fan.[2]

From Fig. 9.34, it can be seen that at the incoming edge of a backward-curved blade, the relative velocity w_1 is in the blade direction when $c_{1u} = 0$.

The blade leaving edge may be

1. Backward curved ($\beta_2 < 90°$), Fig. 9.34
2. Straight ($\beta_2 = 90°$), Fig. 9.35, or
3. Forward curved ($\beta_2 > 90°$), Fig. 9.36.

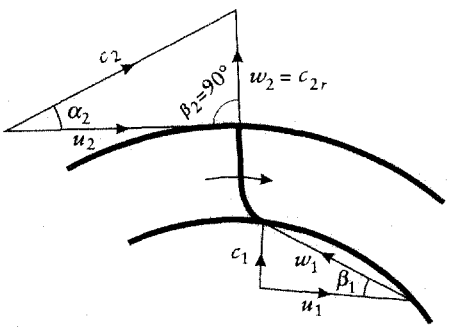

FIGURE 9.35 Straight-blade centrifugal fan impeller. The blade is backward curved at the entrance.[2]

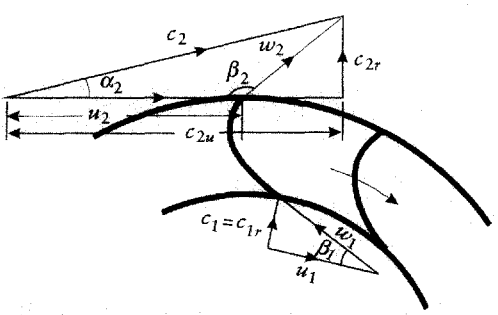

FIGURE 9.36 Centrifugal fan impeller, where the blade is forward curved at the leaving edge and backward curved at incoming edge.[2]

The *reaction ratio* of the fan is defined by

$$r = \frac{\Delta p}{\Delta p_{\text{tot}}}, \tag{9.80}$$

by which the static pressure increase is related to the total pressure increase. The reaction ratio can be determined for different blade shapes for the isentropic case as

$$r_s = \frac{\Delta p_s}{\Delta p_{\text{tot},s}}. \tag{9.81}$$

When $c_{1u} = 0$ and $\eta_s = 1$, Eq. (9.75) gives

$$\Delta p_{\text{tot},s} = \rho u_2 c_{2u}. \tag{9.82}$$

Using Eq. (9.79) gives

$$r_s = \frac{u_2^2 - u_1^2 + w_1^2 - w_2^2}{2u_2 c_{2u}}. \tag{9.83}$$

The radial velocity is approximately constant; thus,

$$c_1 = c_{1r} = c_{2r}. \tag{9.84}$$

At the entrance edge of the blade, the velocity triangle is a right triangle and $c_{1u} = 0$, so Eq. (9.77) gives

$$c_1^2 = w_1^2 - u_1^2 . \tag{9.85}$$

Apply Eq. (9.77) to solve for the reaction ratio in isentropic flow:

$$\begin{aligned} r_s &= \frac{u_2^2 - w_2^2 + c_1^2}{2u_2 c_{2u}} = \frac{2u_2 c_{2u} - c_2^2 + c_{2r}^2}{2u_2 c_{2u}} \\ &= \frac{2u_2 c_{2u} - c_{2u}^2}{2u_2 c_{2u}} = 1 - \frac{1}{2} \cdot \frac{c_{2u}}{u_2}, \end{aligned} \tag{9.86}$$

in which the result $c_2^2 = c_{2r}^2 - c_{2u}^2$ was used.

For backward-curved blade $\beta_2 < 90°$ from Fig. 9.34, it is seen that $c_{2u}/u_2 < 1$. The reaction ratio must be less than 1. In straight-curved blade $\beta_2 = 90°$ of Fig. 9.35, $c_{2u}/u_2 = 1$ and the reaction ratio is $r_s = \frac{1}{2}$. In forward-curved blade $\beta_2 > 90°$ of Fig. 9.36, $c_{2u}/u_2 > 1$ and the reaction ratio is always less than $\frac{1}{2}$.

The reaction ratio of a straight-blade impeller is poor when compared with a backward-curved impeller. The radial (paddle) fan has the advantage that when the air contains much dust, the straight blades remain cleaner than curved blades.

The reaction ratio of forward-curved impeller blades is the lowest. This type is used when a small static pressure increase is sufficient to transport the air. An example of such type is the *drum fan*, with short blades. A large suction opening is required, which allows large volumes of air to be handled. With backward-curved blades, a better reaction ratio is achieved, but with a reduction in total pressure increase. This is because u_2 is only slightly larger than u_1, and for that reason, c_{2u} will be small. By using forward-curved blades, c_{2u} increases, resulting in a larger total pressure differential.

The above discussion assumes that the gas flows parallel to the blades. This is not the case, as the propeller rotation causes the air to rotate between

the blades, against the impeller rotational direction at the same angular velocity. Due to this, the velocity c_{2u} decreases to c'_{2u}; hence,

$$c'_{2u} = c_{2u} - e\omega \tag{9.87}$$

where

ω is the impeller angular velocity
e is the effective radius of the vortex at the outer edge of the impeller (Fig. 9.37)

Figure 9.37 gives

$$\sin \beta_2 \approx \frac{2e}{\pi D_2 / z} \tag{9.88}$$

where

$$e = \frac{\pi D_2 \sin \beta_2}{2z}. \tag{9.89}$$

z is the number of blades.

The fan slip factor is

$$\sigma = \frac{c'_{2u}}{c_{2u}} = \frac{c - \dfrac{\pi D_2 \sin \beta_2}{2z} \cdot \dfrac{2u_2}{D_2}}{c_{2u}} = 1 - \frac{\pi \sin \beta_2}{z} \cdot \frac{u_2}{c_{2u}}, \tag{9.90}$$

in which $\omega = 2u_2/D_2$ is used.

In Eq. (9.90), c_{2u} is the tangential component of the absolute velocity at the exit if the flow is exactly in the blade direction. Since the slip factor is less than 1, the total pressure increase will decrease according to Eq. (9.72) for the same impeller and isentropic flow.

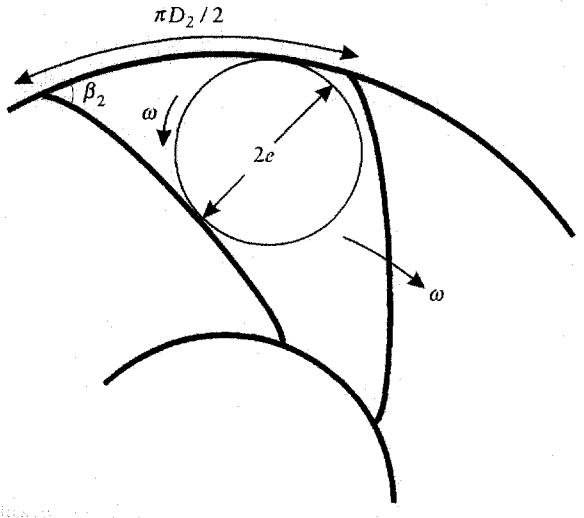

FIGURE 9.37 Secondary flow between the blades of a centrifugal fan.[1]

The reaction ratio is improved, as shown in the following expression:

$$r_s = 1 - \frac{1}{2}\frac{c'_{2u}}{u_2} = 1 - \frac{1}{2}\sigma\frac{c_{2u}}{u_2}. \tag{9.91}$$

The mass flow through the impeller is constant. For constant flow density and volume flow, the volume flow is

$$q_v = \pi D_1 b_1 c_{1r} = \pi D_2 b_2 c_{2r} \tag{9.92}$$

where

b_1 is the blade width at the entrance (Fig. 9.38)
b_2 is the blade width at the exit (Fig. 9.38)
c_{1r} is the absolute radial velocity component at the entrance
c_{2r} is the absolute radial velocity component at the exit

Because $c_{1u} = 0$, we have $c_{1r} = c_1$.

Example 1

The blades of the impeller in a centrifugal fan are backward curved. At the blade entrance $\beta_1 = 22°$, and at the blade exit $\beta_2 = 50°$. The outer and inner diameters of the impeller are $D_2 = 0.8$ m and $D_1 = 0.4$ m, respectively. The width of the blade at the entrance is $b_1 = 22$ cm and at the exit is $b_2 = 12$ cm. The impeller has 15 blades. The impeller rotational speed is $n = 960$ rev min^{-1} $= 16$ s^{-1}. Calculate the volume flow, total pressure increase, static pressure increase, and reaction ratio. Take $c_{1u} = 0$, and air density is 1.22 kg m^{-3}.

Solution. The velocities of the circumferences are

$$u_2 = \pi D_2 n = \pi \cdot 0.8 \cdot 16 = 40.2 \text{ m s}^{-1}$$
$$u_1 = \pi D_1 n = \pi \cdot 0.4 \cdot 16 = 20.1 \text{ m s}^{-1}$$

The velocity triangle at the entrance, taking into consideration that $c_{1u} = 0$, is shown in Fig. 9.39*a*.

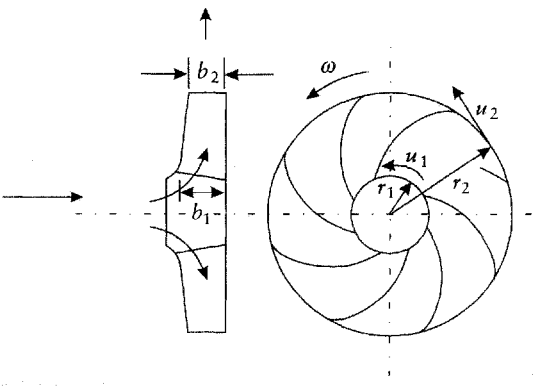

FIGURE 9.38 Dimensions of centrifugal fan impeller.[3]

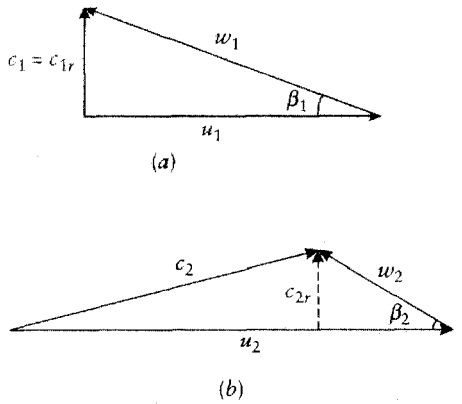

FIGURE 9.39 Velocity triangles.

The triangle gives

$$c_{1r} = c_1 = u_1 \tan \beta_1 = 20.1 \cdot \tan 22° = 8.12 \text{ m s}^{-1}$$
$$w_1^2 = \sqrt{c_1^2 + u_1^2} = \sqrt{8.12^2 + 20.1^2} = 21.68 \text{ m s}^{-1}.$$

Equation (9.92) gives

$$c_{2r} = \frac{D_1 b_1}{D_2 b_2} \cdot c_{1r} = \frac{0.40 \cdot 0.22}{0.8 \cdot 0.12} = 7.44 \text{ m s}^{-1}.$$

Using

$$c_2^2 = c_{2u}^2 + c_{2r}^2$$

gives

$$c_{2u} = \sqrt{c_2^2 - c_{2r}^2} = \sqrt{34.8^2 - 7.44^2} = 34.0 \text{ m s}^{-1}.$$

For $z = 15$, Eq. (9.90) gives

$$\sigma = 1 - \frac{\pi \sin \beta_2}{z} \cdot \frac{u_2}{c_{2u}} = 1 - \frac{\pi \cdot \sin 50°}{15} \cdot \frac{40.2}{34.0} = 0.810,$$

from which $c'_{2u} = \sigma c_{2u} = 27.55$ m s^{-1}, which is the tangential component of the absolute velocity parallel to the circumference velocity component when the blade number is taken into consideration. The flow process is still assumed isentropic. The velocity triangle at the exit is shown in Fig. 9.39*b*.

Using the velocity triangle gives

$$c_2 = \sqrt{c_{2u}^2 + c_{2r}^2} = \sqrt{27.55^2 + 7.44^2} = 28.5 \text{ m s}^{-1}.$$

c_2 and w_2 are now the velocities when the slip factor is $\sigma = 0.81$.

$$w_2 = \sqrt{(u_2 - c'_{2u})^2 + c_{2r}^2} = \sqrt{(40.2 - 27.55)^2 + 7.44^2} = 14.7 \text{ m s}^{-1}$$

Using $c_1 = 8.12$ m s^{-1}, $w_1 = 21.68$ m s^{-1}, and $u_1 = 20.1$ m s^{-1}, the total pressure increase is

$$\begin{aligned}\Delta p_{\text{tot},s} &= \tfrac{1}{2}\rho(c_2^2 - c_1^2 + u_2^2 - u_1^2 + w_1^2 - w_2^2)\\ &= 0.5 \cdot 1.22(28.5^2 - 8.12^2 + 40.2^2 - 20.1^2 + 21.68^2 - 14.7^2)\\ &= 1349 \text{ Pa},\end{aligned}$$

and the static pressure increase is

$$\begin{aligned}\Delta p_s &= \tfrac{1}{2}\rho(u_2^2 - u_1^2 + w_1^2 - w_2^2)\\ &= 0.5 \cdot 1.22(40.2^2 - 20.1^2 + 21.68^2 - 14.7^2) = 894 \text{ Pa}.\end{aligned}$$

The reaction ratio is

$$r_s = \frac{\Delta p_s}{\Delta p_{\text{tot},s}} = \frac{894}{1349} = 0.663\,.$$

For an isentropic process and $c_{1u} = 0$, Eq. (9.75) gives

$$\Delta p_{\text{tot},s} = \rho u_2 c_{2u}. \tag{9.93}$$

Using Fig. 9.33 gives

$$\frac{u_2 - c_{2u}}{c_{2r}} = \cot\beta_2\,, \tag{9.94}$$

from which

$$c_{2u} = u_2 - c_{2r}\cot\beta_2\,. \tag{9.95}$$

Figure 9.35 gives

$$\frac{c_{2u} - u_2}{c_{2r}} = \cot(180° - \beta_2) = -\cot\beta_2\,, \tag{9.96}$$

from which

$$c_{2u} = u_2 - c_{2r}\cot\beta_2\,. \tag{9.97}$$

For all blade shape exits, we can write

$$c_{2u} = u_2 - c_{2r}\cot\beta_2 \qquad \text{when } 0 < \beta_2 < 180°\,. \tag{9.98}$$

Using Eq. (9.92), the total pressure rise is expressed by

$$\Delta p_{\text{tot},s} = \rho u_2\left(u_2 - \frac{q_v \cot\beta_2}{\pi D_2 b_2}\right). \tag{9.99}$$

Equation (9.99) shows the total pressure increase as a function of volume flow for given impeller dimensions and rotational speed at fixed u_2. The blade angle β_2 at the exit is taken as parameter. This function is a linear one. When $\beta_2 > 90°$, $\Delta p_{\text{tot},s}$ increases; for $\beta_2 = 90°$, $\Delta p_{\text{tot},s}$ remains constant; and for $\beta_2 < 90°$, $\Delta p_{\text{tot},s}$ decreases for other parameters given in Eq. (9.97).

The dependency of total pressure increase on volume flow is demonstrated in Fig. 9.40.

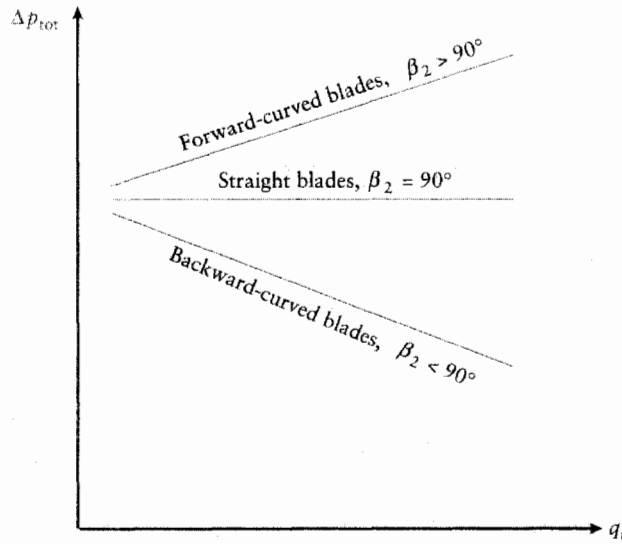

FIGURE 9.40 Total pressure increase versus volume flow for different exit blade angles in isentropic flow. The flow follows the blade shape exactly.

Figure 9.40 is valid only for a single rotational speed. In addition, it is assumed that in the velocity triangle at the leaving edge of the impeller, the velocity component w_2 has the same direction as the angle β_2. The volume flow q_v changes when c_{2r} changes, which means, in the case of constant u_2 and constant direction of w_2, that the absolute velocity c_2 changes. When c_{2r} changes, so does c_{1r}, and the direction of w_1 changes because u_1 is constant. This means that in Fig. 9.40 only for one volume flow is the direction of the velocity w_1 the same as the angle β_1 for the impeller blade. For other values of q_v this is not the case. We still think that the flow process between impeller blades is isentropic, but it is likely that in reality the deviation from an isentropic process is larger the more the direction of w_1 deviates from β_1. This will change the curves in Fig. 9.40 so that we get lower increases in the total pressure.

If the flow is isentropic but does not follow the blade shape exactly, then the slip factor is smaller than 1, and this will directly affect what is shown in Fig. 9.40. Denoting $\Delta p'_{tot,s}$ the total pressure rise when the flow does not follow the blade shape and calculating the slip factor from Eq. (9.90) give

$$\begin{aligned}\Delta p_{tot,s} - \Delta p'_{tot,s} &= \rho u_2 c_{2u} - \rho u_2 c'_{2u} \\ &= \rho u_2 c_{2u}(1-\sigma) = \rho u_2 c_{2u} \cdot \frac{\pi \sin\beta_2}{z} \cdot \frac{u_2}{c_{2u}} \\ &= \rho u_2^2 \cdot \frac{\pi \sin\beta_2}{z}.\end{aligned} \tag{9.100}$$

The total pressure decreases by the same quantity regardless of volume flow; the change is smaller for larger blade number z.

After the impeller the flow is flowing into the fan casing. The purpose of the casing is to collect the flow coming from the impeller and take the flow into the fan exit duct. Air flows to the casing everywhere from the exit edge of the impeller. For that reason the casing has a spiral shape (Fig. 9.41).

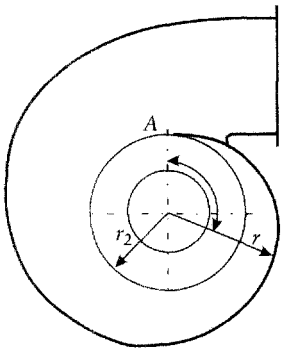

FIGURE 9.41 Centrifugal fan impeller and spiral casing.

If there is no large duct after the fan which needs a large static pressure, then there is no need for spiral casing. The air then leaves steadily from the impeller circumference, and the air is not collected into one point. At the exit side in ventilating systems of buildings, the need for static pressure is small if the leaving air is directly sent to the atmosphere.

Real fan total pressure difference is smaller for the same volume flow than that of an isentropic, theoretical fan. This is a result of the fan losses. These arise from the entropy generation in adiabatic systems. We investigate the losses separately, i.e., entropy generation in the impeller and casing.

At the design point the volume flow is such that the relative velocity is parallel to the blade at the inlet of the impeller. The impeller losses at the design point are

- Friction losses between the flow and blades
- Leakage losses when the gas is transported from pressure side to suction side. Since the phenomenon is equalizing pressure in an adiabatic system, this will increase the entropy in the system.
- Friction in bearings, gasket, and impeller side walls. These losses are taken into consideration by the mechanical efficiency η_m.

The casing losses are due to friction and mixing. The frictional losses and their reasons are the same as those in the impeller channel. The mixing losses develop because the velocity of the impeller exit is not the same at every point as in the spiral casing; it is an average velocity. Mixing of two different flow velocities leads to acceleration and deceleration and pressure difference, whose equalizing increases the entropy.

Outside the design point the direction of the relative velocity is not parallel to the blade, and shock losses are generated.

The theory of losses is very complex. The effect of mixing on the total pressure has been investigated.[4] The calculated results qualitatively match the measured results. Friction in impeller channel and casing decreases the total pressure.

In practice, the fan characteristic curve—i.e., the total pressure difference dependency on the volume flow—is determined experimentally. The measured results are then for the impeller and casing together. Since the losses are greater outside the design point, the fan efficiency is high at the design point.

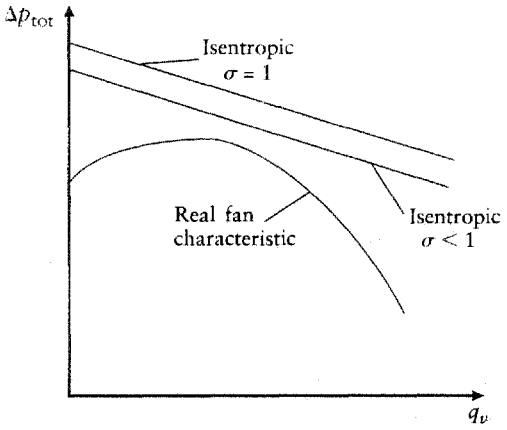

FIGURE 9.42 Typical performance curve of centrifugal fan, $\Delta P_{tot} - q_v$ chart.

Figure 9.42 shows the typical characteristic curve of a centrifugal fan, where the blades are backward curved. The figure also shows the theoretical characteristic curve when the slip factor is 1 and when it is smaller than 1. Characteristic curves for a real fan are closer to the isentropic one at the design point. At this point the efficiency is maximum.

9.5.3 Axial Fans

Figure 9.43 shows the schematic diagram of an axial fan system. The air flows through a nozzle toward the impeller, where static pressure rises. The impeller is attached to a hub. The impeller is also called the propeller. The propeller is followed by a diffuser.

When the aim is to build a cheap fan system and have a small pressure rise, then the nozzle and diffuser are not usually installed in the system.

The performance of an axial fan is based on the external force to drive the propeller, whose blades change the direction of airflow when flowing from the inlet edge to the outlet edge.

Equation (9.59) is valid, but when $u_1 = u_2$, the power needed is

$$P_u = q_m u(c_{2u} - c_{1u}) = q_m u \, \Delta c_u . \tag{9.101}$$

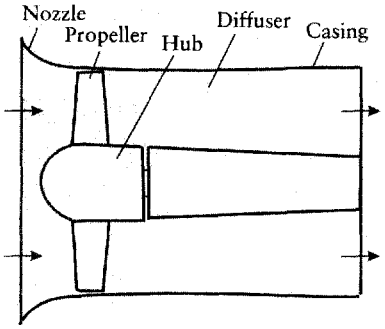

FIGURE 9.43 Schematic diagram of axial fan.[2]

Since P_u is positive, it must be that $c_{2u} > c_{1u}$ when the circumference speed is chosen as the positive direction. Equation (9.101) is valid for every circumference speed between the hub circumference and the outer impeller circumference.

In the following discussion, u is the average circumference speed. The absolute velocity in the shaft direction is denoted by c_a.

The mass flow is constant in the shaft direction, so

$$\rho \cdot \frac{\pi}{4}(D_1^2 - D_2^2)c_{1a} = \rho \cdot \frac{\pi}{4}(D_1^2 - D_2^2)c_{2a} \tag{9.102}$$

where D_1 is the impeller diameter and D_2 is the hub diameter.

Equation (9.102) gives $c_{1a} = c_{2a}$. The axial component does not change, but when $c_{2u} > c_{1u}$, then $c_2 > c_1$. Thus, the axial fan increases the absolute velocity of airflow.

Generally, Eq. (9.80) is valid, but when $u_1 = u_2$, it gives the static pressure increase for an axial fan as

$$\Delta p_s = p_{2s} - p_1 = \frac{1}{2}\rho(w_1^2 - w_2^2) \, . \tag{9.103}$$

Equation (9.79) shows that the rise in circumference velocities at the entrance and exit leads to the static pressure $\frac{1}{2}\rho(u_2^2 - u_1^2)$ increase but not in the axial fan. This results in the axial fan's not having the same pressure rise as that of the centrifugal fan. Axial fans are applicable for large airflows, when the needed pressure increase is relatively small.

The reaction ratio of an axial fan for the isentropic case based on Eqs. (9.75), (9.81), and (9.103) is

$$r_s = \frac{w_1^2 - w_2^2}{2u(c_{u2} - c_{u1})} \, . \tag{9.104}$$

We restrict ourselves to investigate an axial fan, where there is only an impeller. The incoming air has the direction of the axis of the propeller.

The rotating of the impeller increases the absolute velocity of air. In order to increase the static pressure of the gas flow owing to the fan, the velocity relative to the blades should decrease according to Eq. (9.103).

The flow velocity diagrams on both sides of the impeller are shown in Fig. 9.44. The axial direction is the datum for all angles.

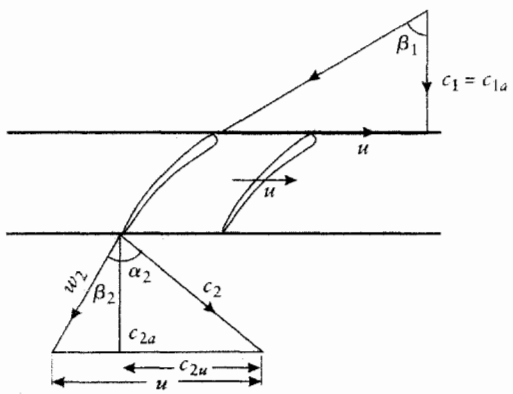

FIGURE 9.44 Velocity triangles of an axial fan impeller.

From the conditions $c_{2a} = c_{1a} = w_{2a} = w_{1a}$ and $w_1 > w_2$, the relative velocity is smaller at the exit than at the inlet. There are two possibilities: the leaving flow direction angle is on the same axis side as that of the coming flow, or the leaving flow direction angle is on a different axis side. Figure 9.44 shows blades where both the relative velocity direction angles β_1 and β_2 are on the same axis side.

The velocity triangle at the entrance gives

$$w_1^2 = u^2 + c_a^2 \tag{9.105}$$

and at the exit gives

$$w_2^2 = (u - c_{2u})^2 + c_a^2 . \tag{9.106}$$

From Eq. (9.103) the isentropic pressure rise is determined by

$$\Delta p_s = \frac{1}{2}\rho(2uc_{2u} - c_{2u}^2) = \rho u^2\left(\frac{c_{2u}}{u} - \frac{1}{2}\frac{c_{2u}^2}{u^2}\right). \tag{9.107}$$

The exit velocity triangle gives

$$\tan\beta_2 = \frac{u - c_{2u}}{c_a}, \tag{9.108}$$

from which

$$\frac{c_{2u}}{u} = 1 - \frac{c_1}{u}\tan\beta_2, \tag{9.109}$$

and from Eq. (9.107)

$$\Delta p_s = \frac{1}{2}\rho u^2\left(1 - \frac{c_a^2}{u^2}\tan^2\beta_2\right). \tag{9.110}$$

Using Eqs. (9.103) and (9.104), the reaction ratio is determined by

$$r_s = \frac{2\,\Delta p}{2\rho u c_{2u}} = \frac{u^2\left(1 - \frac{c_a^2}{u^2}\tan^2\beta_2\right)}{2u^2\left(1 - \frac{c_a}{u}\tan\beta_2\right)} \tag{9.111}$$

$$= \frac{1}{2}\left(1 + \frac{c_a}{u}\tan\beta_2\right) = \frac{1}{2}\left(1 + \frac{\tan\beta_2}{\tan\beta_1}\right).$$

Because $0 < \beta_1 < \pi/2$ and $0 < \beta_2 < \pi/2$, then $\cot\beta_1 > 0$, $\tan\beta_2 > 0$, and $r > \frac{1}{2}$.

From the exit velocity triangle, it can be seen that the gas flow has a tangential velocity component. The gas rotates when it leaves the fan. Normally, the tangential velocity component is of no benefit if a duct is attached to the fan, since it disappears due to friction.

Example 2

The diameter of an axial fan impeller is $D_1 = 0.6$ m, the hub diameter is $D_2 = 0.3$ m, and the rotational speed is $n = 960$ rev min^{-1}. The axial velocity of airflow is $c_{1a} = 5.5$ m s^{-1}, and the blade angle is $\beta_2 = 10°$ (average) at the

blade exit. Calculate the power, isentropic static pressure increase, and reaction ratio. The pressure of the coming air is 1 bar, and the temperature is 45 °C.

Solution. The average diameter is calculated by

$$D = \frac{1}{2}(D_1 + D_2) = \frac{1}{2}(0.6 + 0.3) = 0.45 \text{ m}.$$

The average circumference speed is $u = \pi Dn = 22.6 \text{ m s}^{-1}$. The velocity triangle on the entrance side as shown in Fig. 9.45*a* gives

$$\tan\beta_1 = \frac{u}{c_{1a}} = \frac{u}{c_a} = \frac{22.6}{5.5} = 4.11 \Rightarrow \beta_1 = 76.3°.$$

The velocity triangle at exit has $\beta_2 = 10°$, $w_{2a} = c_{2a} = 5.5 \text{ m s}^{-1}$, which gives

$$\tan\beta_2 = \tan 10° = \frac{w_{2u}}{w_{2a}}$$

$$w_{2u} = w_{2a} \cdot \tan\beta_2 = 5.5 \tan 10° = 0.97 \text{ m s}^{-1}$$

$$c_{2u} = u - w_{2u} = 22.6 - 0.97 = 21.6 \text{ m s}^{-1}.$$

Using ideal gas law, the air density is calculated as

$$\rho = \frac{pM}{RT} = \frac{10^5 \cdot 28.964}{8314.31 \cdot (273 + 45)} = 1.095 \text{ kg m}^{-3}.$$

The flow area is

$$A = \frac{\pi}{4}(D_1^2 - D_2^2) = \frac{\pi}{4}(0.6^2 - 0.3^2) = 0.212 \text{ m}^2.$$

The mass flow through the fan is

$$q_m = \rho c_{1a} A = 1.095 \cdot 5.5 \cdot 0.212 = 1.277 \text{ kg s}^{-1}.$$

Equation (9.101) gives the power as

$$P_u = q_m u(c_{2u} - c_{1u}) = q_m u c_{2u} = 1.277 \cdot 22.6 \cdot 21.6 = 623 \text{ W}.$$

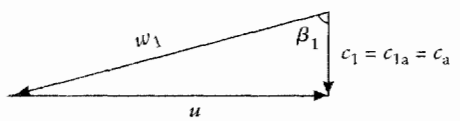

(*a*)

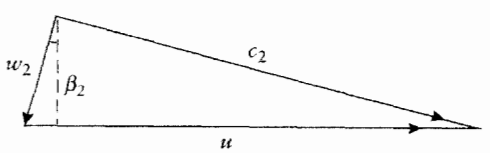

(*b*)

FIGURE 9.45 Velocity triangles.

The isentropic static pressure increase is obtained from Eq. (9.107) as

$$\Delta p_s = \rho u^2 \left(\frac{c_{2u}}{u} - \frac{1}{2} \frac{c_{2u}^2}{u^2} \right) = 1.095 \cdot 22.6^2 \left(\frac{21.6}{22.6} - \frac{1}{2} \cdot \frac{21.6^2}{22.6^2} \right) = 267 \text{ Pa} .$$

Equation (9.111) gives the reaction ratio as

$$r_s = \frac{1}{2} \left(1 + \frac{\tan \beta_2}{\tan \beta_1} \right) = \frac{1}{2} \left(1 + \frac{\tan 10°}{\tan 76.3°} \right) = 0.521 .$$

At the exit the absolute velocity has velocity component c_{2u} on the large circumference parallel to the shaft of Example 3. Component c_{2u} is of no advantage if a duct is connected to the axial fan, since it disappears due to the friction between the walls of the duct and gas flow.

9.5.4 Effect of Speed of Revolution

In the previous sections, the centrifugal and axial fans were investigated for a constant rotational speed.

In this section, the rotational velocity is directly proportional to the rotational velocity n according to the equation $u = \pi D n$. The impeller blade angles remain the same regardless of the rotational velocity of the impeller. Hence, the inlet and exit velocity triangles have the same form. The axial velocity of an axial fan changes directly proportionally to the circumference velocity u. This is also valid for the radial velocity at the outer circumference of a radial impeller fan. These velocities are directly proportional to the fan flow volume; hence,

$$\frac{q_{v2}}{q_{v1}} = \frac{n_2}{n_1}, \tag{9.112}$$

where

n_1 is the rotational velocity of impeller
q_{v1} is the volume flow at rotational velocity n_1
n_2 is another rotational velocity of the impeller
q_{v2} is the volume flow at rotational velocity n_2

As the velocity triangles' shape remains the same,

$$\frac{u_{21}}{u_{22}} = \frac{u_{11}}{u_{12}} = \frac{c_{u21}}{c_{u22}} = \frac{c_{u11}}{c_{u12}} = k. \tag{9.113}$$

In Eq. (9.113), subscript u indicates the velocity to the tangential velocity component, the first subscript 2 indicates impeller exit, the first subscript 1 indicates impeller inlet, the second subscript 2 stands for n_2, and the second subscript 1 stands for n_1. The proportionality constant k is

$$k = \frac{n_1}{n_2}. \tag{9.114}$$

Even though the rotational velocity changes, the flow is still parallel to the blades, and the hydraulic efficiency remains the same regardless of rotational speed.

Using Eqs. (9.75), (9.113) and (9.114) gives

$$\frac{\Delta p_{tot2}}{\Delta p_{tot1}} = \frac{\rho_2}{\rho_1} \cdot \frac{u_{22}c_{u22} - u_{12}c_{u12}}{ku_{22}kc_{u22} - ku_{12}kc_{u12}} = \frac{\rho_2}{\rho_1} \cdot \frac{1}{k^2} = \frac{\rho_2}{\rho_1} \cdot \left(\frac{n_2}{n_1}\right)^2. \tag{9.115}$$

Normally, with fans $\rho_1 = \rho_2$. Then

$$\frac{\Delta p_{tot2}}{\Delta p_{tot1}} = \left(\frac{n_2}{n_1}\right)^2. \tag{9.116}$$

If the rotational velocity change is within reasonable limits and the mechanical efficiency does not change, Eqs. (9.76), (9.112) and (9.115) give the shaft power relation as

$$\frac{P_{a2}}{P_{a1}} = \frac{\rho_2}{\rho_1} \cdot \left(\frac{n_2}{n_1}\right)^3. \tag{9.117}$$

Example 3

The fan is tested at an air pressure of 102.9 kPa, temperature of 10 °C, and a rotational speed of 970 rev min^{-1}. Under these conditions the volume flow is 0.7 m^3 s^{-1}, total pressure difference is 250 kPa, and shaft power is 250 kW. If the operating conditions change to handle an air temperature of 16 °C and pressure of 100 kPa and the efficiency remains unchanged, calculate under the new operating conditions the volume flow, total pressure difference, and shaft power.

Solution

Operating conditions 1: $p_1 = 102.9$ kPa and $T_1 = 10$ °C = 283 K.
Operating conditions 2: $p_2 = 100$ kPa and $T_2 = 16$ °C = 289 K.

Using ideal gas law,

$$\rho_1 = \frac{p_1 M}{RT_1} = \frac{102.9 \cdot 10^3 \cdot 28.964}{8314.31 \cdot 283} = 1.267 \text{ kg m}^{-3}$$

$$\rho_2 = \frac{p_2 M}{RT_2} = \frac{100 \cdot 10^3 \cdot 28.9864}{8314.31 \cdot 283} = 1.205 \text{ kg m}^{-3}.$$

Using $n_1 = 970$ rev min^{-1}, $q_{v1} = 0.73$ m^3 s^{-1}, $\Delta P_{tot1} = 250$ Pa, $P_{a1} = 250$ W, and $n_2 = 500$ rev min^{-1}, Eq. (9.112) gives

$$q_{v2} = \frac{n_2}{n_1} \cdot q_{v1} = \frac{500}{970} \cdot 0.7 = 0.361 \text{ m}^3\text{s}^{-1}.$$

Equation (9.115) gives the total pressure difference as

$$\Delta p_{tot2} = \frac{\rho_2}{\rho_1} \cdot \left(\frac{n_2}{n_1}\right)^2 \Delta p_{tot1} = \frac{1.205}{1.267}\left(\frac{500}{970}\right)^2 \cdot 250 = 63.2 \text{ Pa},$$

and Eq. (9.117) gives the shaft power as

$$P_{a2} = \frac{\rho_2}{\rho_1} \cdot \left(\frac{n_2}{n_1}\right)^3 P_{a1} = \frac{1.205}{1.267}\left(\frac{500}{970}\right)^3 \cdot 250 = 32.6 \text{ W}.$$

Example 4

The total pressure is 500 Pa, and volume flow is 2.4 $m^3 s^{-1}$ for a fan working at standard air conditions (pressure 1 bar and temperature 20 °C). The speed of revolution is 14 rev s^{-1}, and fan efficiency is 60%.

a. Calculate the total pressure, speed of revolution, and power if the volume flow is increased to 3.5 $m^3 s^{-1}$. The fan efficiency is assumed to remain constant.
b. Calculate the total pressure and power at the first volume flow if the temperature is increased to 82 °C and the speed of revolution remains constant.

Solution.

a. Denote $q_{v1} = 2.4$ $m^3 s^{-1}$, $\Delta p_{tot1} = 500$ Pa, $n_1 = 14$ rev s^{-1}, and $q_{v1} = 3.5$ $m^3 s^{-1}$. From Eq. (9.112) we get

$$n_2 = \frac{q_{v2}}{q_{v1}} n_1 = \frac{3.5}{2.4} \cdot 14 = 20 \text{ rev s}^{-1}.$$

From Eq. (9.116) we get

$$\Delta p_{tot2} = \left(\frac{n_2}{n_1}\right)^2 \cdot \Delta p_{tot2} = \left(\frac{20}{14}\right)^2 \cdot 500 = 1020 \text{ Pa}.$$

From Eq. (9.76) we get

$$P_{a2} = \frac{q_{v2} \cdot \Delta p_{tot2}}{\eta} = \frac{3.5 \cdot 1020}{0.6} = 5950 \text{ W}.$$

b. At standard conditions we have $p_1 = 1$ bar and $T_1 = 20$ °C = 293 K. In the new situation we have $p_1 = p_2 = 1$ bar and $T_2 = 82$ °C = 355 K. From ideal gas law we have $\rho_1 = p_1 M / R T_1$ and $\rho_2 = p_2 M / R T_2$ and because $p_1 = p_2$ of we get

$$\frac{\rho_2}{\rho_1} = \frac{T_1}{T_2}.$$

From Eq. (9.115) we then get, for $n_1 = n_2$,

$$\frac{\Delta p_{tot2}}{\Delta p_{tot1}} = \frac{\rho_2}{\rho_1}$$

$$\Delta p_{tot2} = \frac{\rho_2}{\rho_1} \Delta p_{tot1} = \frac{T_1}{T_2} \Delta p_{tot1} = \frac{293}{355} \cdot 500 = 413 \text{ Pa}.$$

From Eq. (9.76) we get

$$P_{a2} = \frac{q_{v1} \cdot \Delta p_{tot2}}{\eta} = \frac{2.4 \cdot 413}{0.6} = 1652 \text{ W}.$$

9.5.5 Fan and Duct Network

In some instances the fan has a free discharge. Typical is the axial fan installed in a wall opening (wall fan). In most cases the fan is connected to a duct run; in this instance the total pressure difference and volume flow are determined from both the fan and duct network characteristics.

Consider the thermodynamic analysis for incompressible gas flow in a duct. Denote the point at the beginning by 1 and at the end by 2. Since there is

$$h_1 + \frac{1}{2}c_1^2 + gz_1 = h_2 + \frac{1}{2}c_2^2 + gz_2 \tag{9.118}$$

where

c is the air velocity
z is the height

Equation (9.63) gives

$$h_2 - h_1 = \int_1^2 T\, ds + \frac{1}{\rho}(p_2 - p_1)\ , \tag{9.119}$$

for which Eq. (9.118) can be written as

$$\begin{aligned} p_1 + \frac{1}{2}\rho c_1^2 + \rho g z_1 &= p_2 + \frac{1}{2}\rho c_2^2 + \rho g z_2 + \rho\int_1^2 T\, ds \\ &= p_2 + \frac{1}{2}\rho c_2^2 + \rho g z_2 + \Delta p. \end{aligned} \tag{9.120}$$

The term $\Delta p = \rho\int_1^2 T\, ds$ is the entropy generation given as pressure loss.

In a straight duct where $z_1 = z_2$ and the cross-sectional area is uniform, then $c_1 = c_2$. This gives $\Delta p = p_1 - p_2 > 0$. Δp is the duct pressure loss, which is a result of entropy generation. Entropy generation is due to the flow friction, which is the reason for pressure loss.

Consider the pressure loss in a duct with straight, uniform cross-sectional area. The pressure loss is caused by friction. When different air sheets move against each other, friction is generated. The velocity and thermodynamic properties of air influence the friction. The duct wall has an overall roughness, which causes vortices to be formed with resulting friction in gas. The velocity has a pronounced effect; in flow with low velocity, the vortices are small. For a straight duct the pressure loss Δp_k can be determined from

$$\frac{\Delta p_k}{L} = \frac{f}{D}\cdot\frac{1}{2}\rho c^2, \tag{9.121}$$

where

L is the duct length
D is the inner diameter
f is the flow friction factor

In velocity and gas property effects, the Reynolds number, Re, is taken into consideration as

$$\mathrm{Re} = \frac{cD}{\nu}, \tag{9.122}$$

where ν is the kinematic viscosity.

The kinematic viscosity is related to density by

$$\mu = \rho\nu \tag{9.123}$$

where μ is the dynamic viscosity.

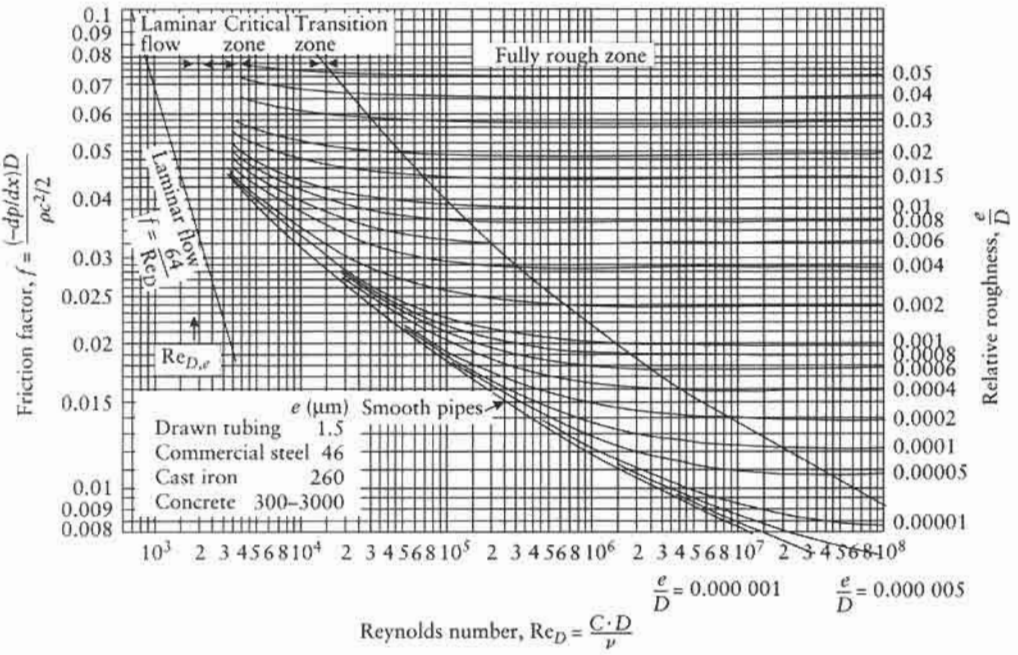

FIGURE 9.46 Friction factor f of duct flow.[5]

The friction factor depends on the Reynolds number and duct wall relative roughness e/D, where e is the average height of the roughness in the duct wall. The friction factor is shown in Fig. 9.46. For a large Reynolds number, the friction factor f is considered constant for rough pipe surfaces. The friction pressure loss is $\Delta p_k \propto c^2$.

For a smooth duct surface,[5] when $\mathrm{Re} > 2000$, the friction factor is

$$f = 0.184\ \mathrm{Re}^{-0.2}. \tag{9.124}$$

Equation (9.121) then shows that $\Delta p_k \propto c^{1.8}$. In practice, $\Delta p_k \propto c^2$ can be used with a high accuracy. For straight, uniform duct cross-sectional area, the static pressure drop in the flow direction is directly proportional to c^2.

The internal friction due to vortices occurs in rapid expansion, diverging, and regulation valves. The entropy generation due to those vortices is taken into consideration in the local resistance. The entropy generation is directly proportional to c^2; thus,

$$\int_1^2 T\,ds = \zeta \frac{1}{2} c^2 \tag{9.125}$$

where ζ is the minor loss coefficient.

$$\Delta p_{kv} = \rho \int_1^2 T\,ds = \zeta \frac{1}{2} \rho c^2. \tag{9.126}$$

The minor loss coefficient depends on the Reynolds number; because this dependency is weak, it is normally ignored. The minor loss coefficients for different resistances are given in textbooks.

Consider next the fan with its connected air duct characteristics when both are operating together. We indicate the fan leaving air by subscript 2 and the suction side by subscript 1.

Using Eq. (9.120) gives

$$p_2 + \frac{1}{2}\rho c_2^2 = p_1 + \frac{1}{2}\rho c_1^2 + \Delta p, \tag{9.127}$$

where $\Delta p = \Delta p_k + \Delta p_{kv}$, the pressure difference in straight ducts, bends, etc. caused by the entropy generation.

Equation (9.127) can be rewritten as

$$\Delta p = p_2 - p_1 + \frac{1}{2}\rho(c_2^2 - c_1^2) = \Delta p_{\text{tot}}, \tag{9.128}$$

which means that the generated pressure loss is large—as much as the fan total pressure difference.

For a special fan situation, a straight air duct of uniform cross-sectional area is used on the leaving side. The outgoing velocity c_3 is the same as the fan leaving velocity c_2. The only minor loss is the outgoing loss $= \frac{1}{2}\rho c_3^2$. Another part of the pressure drop is the frictional pressure drop Δp_k. Equation (9.127) gives

$$\Delta p = \Delta p_k + \frac{1}{2}\rho c_3^2 = \Delta p_k + \frac{1}{2}\rho c_2^2 = \Delta p_{\text{tot}}, \tag{9.129}$$

from which

$$\Delta p_k = \Delta p_{\text{tot}} - \frac{1}{2}\rho c_2^2 = p_2 - p_1 - \frac{1}{2}\rho c_2^2 = p_k. \tag{9.130}$$

The pressure term p_k in Eq. (9.130) is called the obtainable fan pressure.

In steady-state conditions, the mass and volume flow are constant through the fan and duct. If the duct consists of branches of different cross-sectional area A_i, then

$$q_v = c_i A_i \qquad i = 1, \ldots, n \tag{9.131}$$

where n is the number of different cross-sectional areas A_i.

The duct pressure drop can be obtained from Eqs. (9.121) and (9.126) as

$$\Delta p = \sum f_i \frac{L_i}{D_i} \frac{1}{2}\rho c_i^2 + \sum \zeta_j \frac{1}{2}\rho c_j^2 . \tag{9.132}$$

The fan total pressure difference Δp_{tot} also depends on the volume flow. In practice, dependency is determined experimentally, $\Delta p_{\text{tot}} = f(q_v)$. Equations (9.128) and (9.132) give

$$\Delta p_{\text{tot}} = f(q_v) = \sum f_i \frac{L_i}{D_i} \frac{1}{2}\rho c_i^2 + \sum \xi_j \frac{1}{2}\rho c_j^2 . \tag{9.133}$$

The fan volume flow q_v and its corresponding Δp_{tot} can be found when a $\Delta p_{\text{tot}} - q_v$ chart is drawn; the duct parabola and experimental Δp_{tot} both equal $f(q_v)$ (Fig. 9.47). The experimental curve $\Delta p_{\text{tot}} = f(q_v)$ is called the *fan characteristic curve*, and the duct static pressure drop dependency on the duct volume flow is the *characteristic curve*. The characteristic curve intersection point is called *fan operating point*.

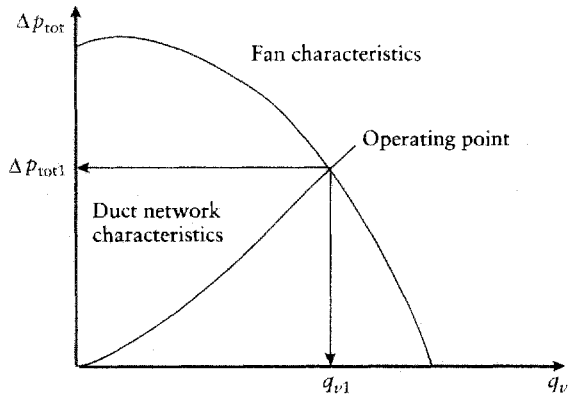

FIGURE 9.47 Fan and duct operating point (Δp_{tot}, q_{v1}).

Example 5

The fan characteristic curve is given by

q_v, L s^{-1}	0	556	1111	1667	2222	2778	3333
Δp_{tot}, Pa	491	535	549	535	491	417	314
P_a, kW	0.40	0.63	0.90	1.20	1.53	1.7	1.75

The duct pressure drop is 589 Pa; airflow is 1944 L s^{-1}. Determine the fan total pressure, volume flow, shaft power, and total efficiency.

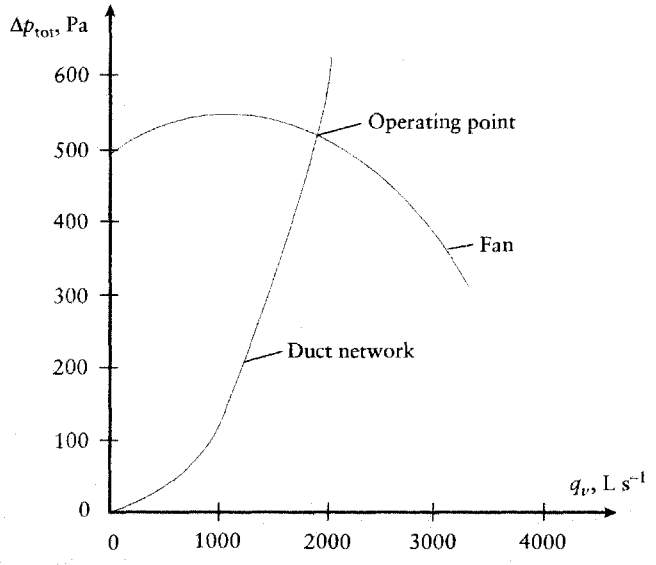

FIGURE 9.48 Fan characteristic curve.

Solution. Draw into the $\Delta p_{tot} - q_v$ diagram the characteristic curve of the fan and the duct-pressure-drop volume flow dependency. The latter is a parabola passing through the origin with the following equation:

$$\Delta p = \frac{589}{1944} \cdot q_v^2 .$$

(Here Δp_{tot} is in Pa and q_v in L s^{-1}.) At the curve's intersection point, $\Delta p = \Delta p_{tot} = 520$ Pa and $q_v = 1900$ L $s^{-1} = 1.9$ m^3 s^{-1}. By interpolation from the above table, the shaft power is 1.34 kW. The total fan efficiency is

$$\eta = \frac{\Delta p_{tot} \cdot q_v}{\text{Pa}} = \frac{520 \cdot 1.9}{1340} = 0.737 = 73.7\% .$$

It may be necessary in a given system to use more than one fan. The fans may be connected either in series or parallel.

9.5.6 Series Fan Connection

In this case the outlet of the first fan is connected to the inlet of the second fan. With this arrangement, the total head developed at a given volume is equal to the sum of the total heads developed by the individual fans. Sometimes more than one fan is used in a duct arrangement. In the series connection (Fig. 9.49), the flow through the fans has the same volume flow, and the leaving flow from the first fan is connected to the suction side of the second fan.

For the series connection, we indicate by 1 and 2 the suction and leaving sides of the first fan, respectively, and by 3 the leaving side of the second fan. The suction side of the second fan is the same as the leaving side of the first

The common total pressure difference is

$$\begin{aligned} \Delta p_{tot} &= p_3 + \tfrac{1}{2}\rho c_3^2 - p_1 - \tfrac{1}{2}\rho c_1^2 = p_3 + \tfrac{1}{2}\rho c_3^2 - p_2 - \tfrac{1}{2}\rho c_2^2 \\ p_2 + \tfrac{1}{2}\rho c_2^2 - p_1 - \tfrac{1}{2}\rho c_1^2 &= \Delta p_{tot1} + \Delta p_{tot2} = f(q_{v1}) + f(q_{v2}), \end{aligned} \tag{9.134}$$

where q_v is the volume flow through both fans and $f(q_v) = \Delta p_{tot1}$ is the total-pressure-difference volume flow dependency of the first fan. The points $(q_v, f_1(q_v))$ are the characteristic curve of the first fan, and the points are the characteristic curve of the second fan.

Equation (9.128) gives

$$\Delta p_{tot} = \Delta p = \Delta p_{tot1}(q_{v1}) + \Delta p_{tot2}(q_{v2}). \tag{9.135}$$

The network and fan combination operating point can be obtained from Eq. (9.134).

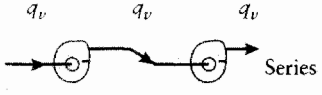

FIGURE 9.49 Series fan connection.

In a $\Delta p - q_v$ chart, the characteristic curve of the ducts is drawn. In the same chart is drawn the characteristic curve of both fans. At each volume flow q_v, the total pressure of each fan is added. In this way, we get a new $\Delta p_{tot} - q_v$ curve. The intersection point of this new curve and the characteristic curve of the ducts is the operating point (Fig. 9.50).

9.5.7 Fan Volume Flow Regulation

If outlet volume flow on the outer side of the attached network of the fan must be adjusted or changed, this will happen by changing the fan characteristic curve or the network impedance. The fan and network then settle in a new operating point, and the volume flow changes.

The impedance of the network can be influenced by

- the change of the minor loss resistance number of a damper.

When the minor loss resistance changes, the impedance of the network and hence the fan and network common operating point also change. The choking regulation with a damper is a bad regulation mode from the point of view of fan energy consumption. The fan is chosen so that in normal conditions the fan is running at the design point. At this point, air absolute velocity, and circumference velocities of the impeller and blade angles are such that the velocity triangles are in the correct form, that is, the flow relative velocity is parallel to the blades, so shock losses are not generated and efficiency is at its highest value.

When choking, neither circumference velocity nor blade angles change. The direction of the flowing gas's absolute velocity toward the impeller does not change, but the magnitude changes. The velocity triangles are now such that the relative speed is not parallel to the blade, and shock losses are generated. This causes a decrease in the efficiency.

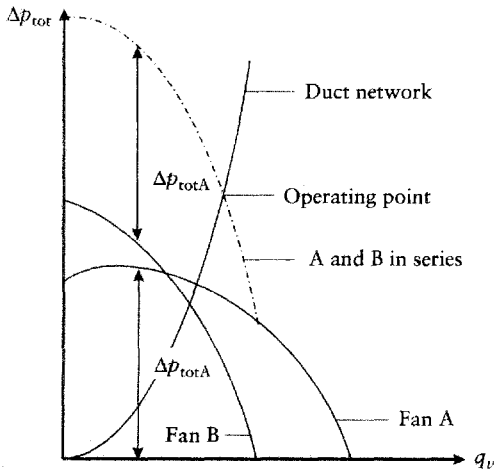

FIGURE 9.50 The determination of the operating point for two fans in series connected a ductwork.

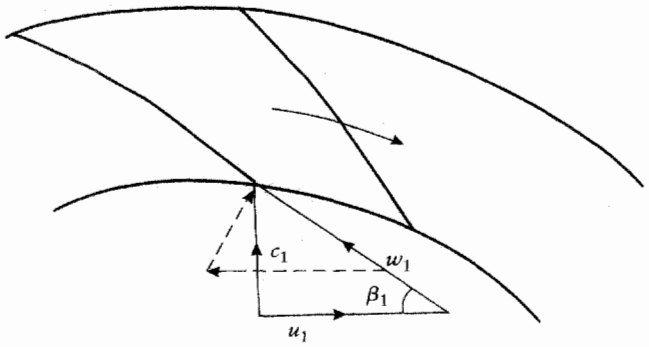

FIGURE 9.51 Leading blades' influence on the inlet velocity triangle of a centrifugal fan. Solid line: velocity triangle without leading blades. Dashed line: velocity triangle with leading blades.

A change in the fan characteristic curve can be made by

- adjustable leading blades (in front of suction opening of centrifugal fans),
- regulation of blade angles of impeller (axial fans), or
- regulation of rotational velocity of impeller.

With adjustable leading blades for a centrifugal fan, the volume flow changes by changing the velocity triangles' form at the impeller inlet. By giving the coming airflow a tangential velocity component, the inlet velocity triangle can be changed in such a way that the absolute velocity radial component changes and the relative velocity remains parallel to the blade. Then the fan efficiency is high. The leading blades change the coming flow's absolute velocity in such a way that the tangential velocity component is in the same parallel direction as the circumference velocity. Leading blades are generally used if the blades are backward curved (Fig. 9.51).

The regulation of axial fan blade angle also influences the inlet and exit velocity triangles in such a way that the axial velocity and thus the volume flow change. When the relative velocity remains parallel to the blade, the efficiency remains high (Fig. 9.52).

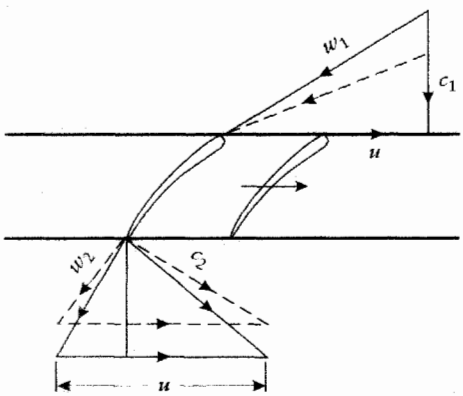

FIGURE 9.52 Influence of axial fan blade angle on volume flow and velocity triangles.

Recently, the regulation of impeller rotational velocity has become a popular regulation mode for volume flow. Electric-motor rotational velocity is regulated by a frequency changer, and its price has dropped lately. Changing the rotational speed also affects the circumference velocity of the impeller. The volume flow can be changed by the same ratio as rotational speed. The form of the velocity triangles and the efficiency remain the same.

Consider the fan characteristic curves for two different rotational velocities n_1 and n_2. Select the operating point for the characteristic curve n_1 as $(\Delta p_{tot1}, q_{v1})$. The corresponding point is $(\Delta p_{tot2}, q_{v2})$ for characteristic curve n_2.

Based on Eqs. (9.112) and (9.116),

$$\frac{q_{v2}}{q_{v1}} = \frac{n_2}{n_1} \quad \text{and} \quad \frac{\Delta p_{tot2}}{\Delta p_{tot1}} = \left(\frac{n_2}{n_1}\right)^2. \tag{9.136}$$

From Eq. (9.136), the characteristic curve of n_2 can be drawn when the characteristic curve of n_1 is known.

Denoting $(\Delta p_{tot}, q_v)$ as the corresponding point of the operating point $(\Delta p_{tot1}, q_{v1})$ and the corresponding rotational velocity $n \neq n$, Eq. (9.136) gives

$$\frac{\Delta p_{tot}}{\Delta p_{tot1}} = \left(\frac{q_{v2}}{q_{v1}}\right)^2 \quad \text{or} \quad \Delta p_{tot} = \frac{\Delta p_{tot1}}{q_{v1}^2} \cdot q_{v2}^2. \tag{9.137}$$

The corresponding points to $(\Delta p_{tot1}, q_{v1})$ compose a parabola, the affinity parabola in the $\Delta p_{tot} - q_v$ chart. The parabola passes through the origin and point $(\Delta p_{tot1}, q_{v1})$.

At the corresponding points of the parabola, the rotational velocity and volume flow change by the same ratio. If the efficiency is high at the point $(\Delta p_{tot1}, q_{v1})$, it is also high at the corresponding point. The fan is connected to a network where there is no static height, so the network $(\Delta p_{tot}, q_v)$ curve is a parabola which passes through the origin. The fan operating point is the intersection point of the characteristic curve and the network $(\Delta p_{tot}, q_v)$ curve. Both parabolas have two common points; the origin and the operating points. If the volume flow is changed, increasing or decreasing the rotational velocity, the new operating point will be on the affinity parabola. If the efficiency is high for the original operating point, then it will also be high for the new one (Fig. 9.53). Hence, rotational speed regulation is a good mode for energy consumption.

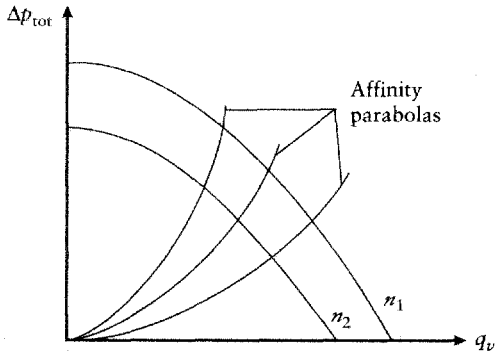

FIGURE 9.53 Fan characteristic curve for two rotational velocities, n_1 and n_2, and three fan affinity parabolas.

Example 6

A fan delivers air to a ventilating system at total pressure difference 500 Pa. The fan is running at 10 rev s^{-1}, and the shaft power needed in these conditions is 7.46 kW. Determine the volume flow, total pressure difference, and shaft power if the fan speed is increased to 12.5 rev s^{-1}.

Solution. Denote $q_{v1} = 1.55\ m^3\ s^{-1}$, $\Delta p_{tot1} = 500$ Pa, $n_1 = 10$ rev s^{-1}, and $P_{a1} = 7.46$ kW. The new fan speed is $n_2 = 12.5$ rev s^{-1}.

The new operating point is on the affinity parabola through $q_{v1} = 1.55\ m^3\ s^{-1}$, and $\Delta p_{tot1} = 500$ Pa. From Eq. (9.136) we have for corresponding points on the affinity parabola

$$q_{v2} = \frac{n_2}{n_1} q_{v1} = \frac{12.5}{10} \cdot 1.55 = 1.937\ m^3\ s^{-1},$$

$$\Delta p_{tot2} = \left(\frac{n_2}{n_1}\right)^2 \Delta p_{tot1} = \left(\frac{12.5}{10}\right)^2 \cdot 500 = 781\ \text{Pa}.$$

Finally,

$$P_{a2} = \frac{\Delta p_{tot2} \cdot q_{v2}}{\eta} = \frac{\Delta p_{tot1}\left(\frac{n_2}{n_1}\right)^2 \cdot \frac{n_2}{n_1} \cdot q_{v1}}{\eta} = \frac{\Delta p_{tot1}\left(\frac{n_2}{n_1}\right)^3 \cdot q_{v1}}{\eta}$$

$$= P_{a1} \cdot \left(\frac{n_2}{n_1}\right)^3 = 7.46 \cdot \left(\frac{12.5}{10}\right)^3 = 14.6\ \text{kW}.$$

References

1. Saarela, M., Puhaltimet. *Tekniikan käsikirja*, osa6p, pp. 123–155, Jyväskylä: K. J. Gummerus, 1960.
2. Yahia, S. M. *Turbines, compressors and fans.* New York: McGraw-Hill, 1990.
3. Douglas, J. F., Gasiorek, J. M., Swaffield, J. A. *Fluid mechanics.* London: Longman, 1985.
4. Iversen, H. W., Rolling, R. E., Carlson, J. J. Volute pressure distribution, radial force on the impeller and volute mixing losses of a radial flow centrifugal pump. *Trans. ASME, Journal of Engineering for Power* 82 (1960), pp. 136–144.
5. Incropera, F. P., De Witt, D. P. *Fundamentals of heat and mass transfer.* New York: Wiley, 1990.

9.6 AUTOMATIC CONTROL OF AIR-HANDLING (HVAC) SYSTEMS

9.6.1 Methods for Automation Control

There are unfortunately no established rules or methods for how an industrial process can be controlled. The methods are usually the necessary and desirable functions and requirements for accuracy, which is necessary for an economical and quality product.

In providing a correctly optimized and accurate control system, all sections of the professional team involved in the project have to work together as a fully cooperating group. This includes persons who have a working knowledge of the process and those who are responsible for the automation and the electrotechnical aspects of the project.

The following control methods are recommended:

- Initially roughly design the systems.
- Survey the functions of the control system.
- Check the system requirements for the required accuracy.
- Select the control system and the user interface.
- Select the process subproduct.
- State the degree of responsibility for delivery and commissioning.

The user interface and the simplicity of usage are important issues. Likewise, stabilized and qualified control for some of the control loops must be as simple as possible.

Also important is the interplay between different sensors, controllers, automation equipment, and objects regulated by the control equipment. The requirements of pumps, fans, batteries, heat exchanger, valves, motors, etc. in standard sizes may greatly differ from the theoretical calculations. Because of this fact, the control equipment, in addition to satisfactory control, must be capable of correcting the differences between the calculated and delivered subproducts.

An automated technical installation is normally no better than the weakest subproduct in the process, system, or installation.

9.6.2 Main Types of Control Equipment and Automation Level

The type of control system and instrumentation to be selected will depend on its location (e.g., the danger of fire, explosion, pollution, moisture, the conditions of temperature and its variations). The control equipment can be classified as

1. Electromechanical and electronic
2. Data-based control (DDC/PLC)
3. Pneumatic control
4. Mixed electronic-pneumatic system

The level of automation depends on the requirements for the technical operation of the attendance system, the need for communication with other processes and data systems, and the requirements for electrical and pneumatic components and cabling methods.

9.6.3 General Technical Requirements

The control and subproducts for the instrumentation are governed by the general technical requirements for the other subproducts in the system. In addition, to fulfill all the general technical requirements, the encapsulation and protection of the environments in which the subproducts are used have to be considered, including danger of explosion, pollution, moisture, temperature, vibration, influence on heating and cooling, etc. See (Table 9.7).

9.6.4 Automation Equipment and Instrumentation

Control and instrumentation can be defined as subproducts for measuring, sending messages, controlling, and regulating. These are installed locally in each system, in the installation as a whole, or in the control technical room.

TABLE 9.7 Important Information and Requirements for Control and Instrumentation

Power supply to buildings	3-phase 400 VAC ±10% 50 Hz
Type of control	Data-based controller (DDC)
Input and output modules	0(2)–10 VDC or 0(4)–20 mA
Climate surroundings	0 to +50 °C and 10 to 90% relative humidity
Electronic norms/requirements	IEC 60364/CENELEC HD384
Level of encapsulation	IP54 (local components)

To ensure flexibility for possible later additions or changes, the instrumentation has to be selected based on standardized subproducts using national or international norms. These standards are mainly based on the measuring areas and signal types. Typical signals for input and output to the data-based controller (DDC and PLC) are

- Measuring and control signals as 0–10 VDC, 0(4)–20 mA, or 0.2–1 bar
- Sensors with receptor of thermal element, platinum or nickel (Pt 100, Pt 1000, Ni 1000)

Other important parts of the instrumentation are

- Local electromagnetic and pneumatic components, damper, and valve actuators
- Fuses, relays, and contactors for control of pumps, fan, light, energy, etc.
- Electrical safety

9.6.5 Process

The term *process* is normally used in connection with the control of a plant in industry; the term, however, also describes the HVAC installation in industry and buildings.

The word *process* is from Latin and defines many different aspects. The automation process relates to the automatic regulation required to control the physical conditions in a system. The term *process* relates to both the optimal conditions within which the operation is maintained and when the operation varies with time or by a predetermined plan.

9.6.6 Controller

Until about 1995 mainly the analog controller was used for controlling an HVAC process. Since then, the digital and data-based controller has taken over (Fig. 9.54). In principle there are no major control technical differences between an analog and similar digital controller. The digital data-based controller has the following advantages:

- Small size, requiring a relatively small installation area
- Accurate reading of the measuring signals
- Keyboard for accurate adjustment of different parameters
- Signals for internal defects and external status and alarms
- A possibility for communication with the computer system

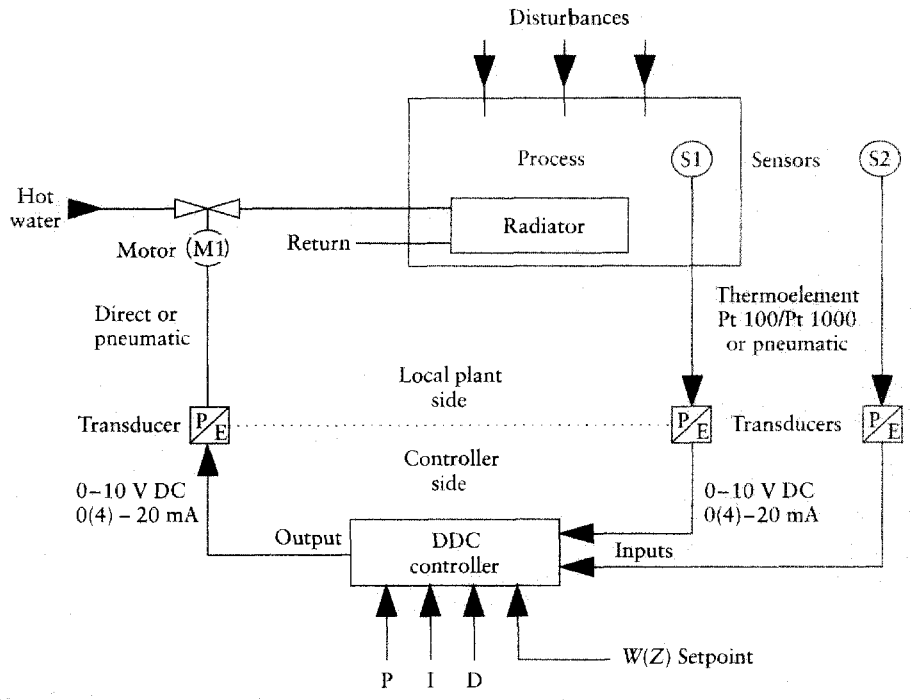

FIGURE 9.54 The controlling loop with sensors, actuators, and controller.

Depending on the control system and components selected, the process variable from the sensors and signals to the actuator control unit is connected either directly or through transducers. Normally, the input and output are adjusted from pneumatic sensors and control units. The signals produced then are transformed into standard electronic values before connecting to the controller's input and output modules.

Data-based controllers are used for controlling energy, lights, cooling, heat, and ventilation in buildings and industrial plants. These are known as DDC controllers. The term *DDC* was used at the beginning of the computer age and includes the original data-based controllers. The term *DDC* derives from American English and is an abbreviation of direct digital control. This term was used to separate the original simple controller PLC (program logic control) from more developed and specialized DDC controllers used for HVAC processes.

The modern DDC controller has only the control function PID. PLC controllers used in process installations may contain more complex regulation functions, for example, the fuzzy or auto-tuning of PID functions. Most DDC controllers are self-sufficient and independent of the controllers or computer programs that are used for system configuration.

They are suited for the technical (HVAC) processes in buildings and include installed and tested computer programs, which cover the most common forms of controlling and regulating in a typical HVAC plant, such as

- Feed-forward (compensating) of air or water temperature from outdoor temperature or for input or extract systems
- Cascade controllers used where the supply and extract air temperatures or return water from heater or cooler batteries requires complete control

- Frost protection of heating coil (where water is used as an energy carrier for heating or cooling)
- Functions for selecting an average of the lowest or highest of different measuring values
- Calculations and mathematical functions
- PLC functions for controlling lights, electrical motors, heating coil, boilers, refrigerating machines, etc.
- Controlling from internal time programs (daily, weekly, or monthly clock with extra program for vacations)
- Optimally starting and stopping for the override of heating, cooling, and ventilation
- Protector for storage of hour rating and measuring values (trend logs)
- Theft-proof admission cards and alarms for water leaks, etc.
- Integrated network for connecting to BAS systems (central operation control)

Analog inputs and outputs in data-based (DDC) controllers are usually standardized and record the signals from sensors or transducers as 0(2)–10 VDC or 0(4)–20 mA. The inputs module can also be standardized for resistances, as Pt 100 DIN, Pt 1000 or Ni 1000 DIN (Pt = platinum, Ni = nickel).

Data-based (DDC) or programmable (PLC) controllers with universal inputs and outputs can be used. It is essential that they are configured before use. In some cases the input may be used only for temperature measurement from special types of thermistors. (Thermistors are constructed from semiconductor materials where the resistance changes reversibly proportional to the temperature, i.e., a negative temperature coefficient.)

9.6.7 The Choice of Controllers

Controllers for decentralized control and regulation are usually positioned locally to the process and connected to the control room.

They attend to and control different technical plants and systems, and they have to deal with all processes required. In data-based plants, controllers usually communicate with one or several local or central computers.

If there are special requirements for communication at all technical data levels, the local controller must still be chosen from the same factory as the other technical operating programs in the central computer or PC. If not, there will be a considerable reduction in the amount of data sent to and from the controller.

In addition to controlling and regulating HVAC plants, DDC controllers have considerable internal memories for the storage of important system data and trend tables. Other important requirements are the interface for using and attending. If the controller is equipped with a graphic dynamic display, service selectors (keyboard) or light diodes for input and output modules, separated operation selectors, and operating or error lights in the electrical distribution may be ignored. The costs for both the new system and future maintenance can be considerably reduced.

The market consists of a considerable assortment of PLC and DDC controllers. Most of the factory types are capable of controlling separate technical plants in a satisfactory manner.

The PLC controller mentioned earlier is used basically for regulating industrial processes or to replace relay controllers (latching) in electrical

processes. Plants with local or central computers are used for operating and controlling energy requirements of HVAC plants. It is impossible to state that the PLC is capable of giving the required results, especially when they are connected in a network and function as self-operating controllers.

Many PLCs can have few and simple data programs, together with a limited internal memory capacity. Due to this fact, it is necessary in many cases to provide extra software and greater memory capacity in the central data station than for more specialized and autonomous DDC controllers. Another reason for selecting the DDC controller is that the skills of the firms who are producing and using DDC controllers are probably better adjusted to the special processes in the HVAC plants which are generally installed in industry and buildings.

9.6.8 Sensors

The receptor that is placed in the process for measuring the physical conditions is called a *sensor*. The receptors, or the sensor elements, may use differ-

measured. Especially important is the accuracy of the measurement, hysteresis, and reaction ability (time constant).

The mechanical shaping of encapsulation and protection is a critical factor when the receptor is placed in an aggressive environment.

Even if the receptor by itself has high accuracy, the sensor may be unable to execute the measurement in a defined place. Quality and total accuracy depend on the combination of receptor, the converter for measured values, and mechanical protection. Mechanical protection can take the form of pockets in water and fluid and also assembly boxes which protect against pollution, humidity, and temperature in the surroundings or against electromagnetic transmissions and noise from power-supplied pipes and cables.

9.6.9 Placing of Sensors in HVAC Systems

Obviously, the sensors have to be installed in a correct and representative place in the process. Determining an optimal installation of sensors for measuring environmental conditions in large halls is not a simple task. Many different factors have to be taken into account. The main place where a certain climate is to be maintained is given priority. Secondly, the influence of infiltration and radiation from surrounding surfaces must be considered.

The influence of airflows from ventilating systems must also be considered. Processes using mediums of different physical qualities when mixed will have separation into different layers. Transmission of energy between molecules in flowing mediums takes place in the direction of the velocity. This strengthens the separation into parallel layers. The level of fluid in containers and tanks is due to stratification of horizontal temperature layers, while airflow after batteries, heat-recovery systems, and humidifiers or dehumidifiers will separate into parallel layers.

Factory-constructed ventilation systems are constructed in a compact manner. Frequently, due to the smaller-space installation, inspection and maintenance of the sensors can be difficult. In ducts, deviations from the real

values of measurements occur due to the sensor or receptor being exposed to moisture or heat or cold radiation from the surroundings. Choosing the incorrect sensor or wrongly positioning it can lead to hunting. The hunting influences the process and makes regulation difficult.

To reduce pollution contamination, sensors or receptors installed in ducts or pipes are placed and installed after the filtration of the air or fluid. Sensors in pipes must be installed primarily in bends and in the direction against dynamic flow. At least two-thirds of the sensor pocket has to be in contact with the fluid. If the pipe diameter is less than the sensor length, the pocket can be installed at an angle less than 90° against the direction of flow to provide the necessary contact area.

Depending on the accuracy required, the pressure difference across components in a flowing gas or fluid is measured by sensors for pressure difference. The quantity of flowing medium can be determined by measuring the flow velocity in pipes or ducts. Sensors for measuring the velocity of gases or liquids are dependent on the nature of the flow if it is laminar. If accurate measurements of the velocity of gas or liquid are required, the sensors have to be installed in straight runs of the pipe or duct. This part of the system should have a straight section longer than five times the diameter of the pipe or the duct. Both velocity and pressure differences can be transformed into respective values by mathematical formulas in the function modules of the DDC controller.

In buildings that are divided into zones with a central heating system, it is common to change the water temperature depending on the outdoor temperature. In this example a function called feed-forward or compensating is used. Figure 9.55 shows how the water temperature changes as a function of the outdoor temperature.

Sensors TS 1-2-4 regulate the batteries for heating and cooling in a sequence to achieve the required temperatures (Fig. 9.56). Regulating valves for heat recovery are controlled by a frequency converter RC1 for the pump motor. When a greater output is required from the heating battery, the pump motor speed increases before the valve MV2 opens. If the extract temperature is lower than the outdoor temperature, the speed of the pump motor increases before valve MV1 opens. To avoid ice formation at low outdoor temperatures, the sensor TS7 operates on a lower limit, depending on the demands of the battery in the exhaust.

Saturated air is difficult to measure accurately; a deviation of 3–5 K must be accepted. In some air conditioning systems, very humid air may condense on surfaces below the dewpoint temperature of the air. Poorly insulated ducts containing humid air can cause serious problems. See Fig. 9.57.

The airflow rate to each room is controlled by a damper operated as a function of the room temperature. Sensors that measure the CO_2 concentration in the room air provide an extra mode of control, in addition to that of air temperature.

The speed of the fans is controlled by sensors PS1 and PS2 and frequency converters RC1 and RC2 (Fig. 9.58). The sensors measure the difference in pressure between duct and atmosphere outside and maintain constant pressure in the ducts.

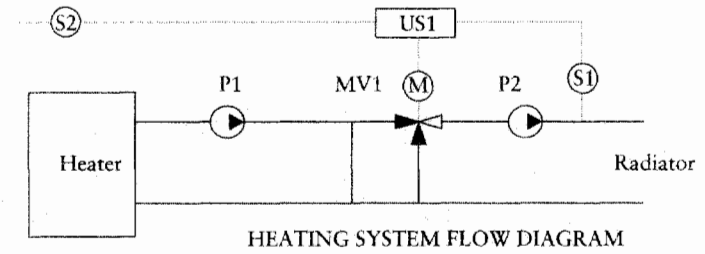

HEATING SYSTEM FLOW DIAGRAM

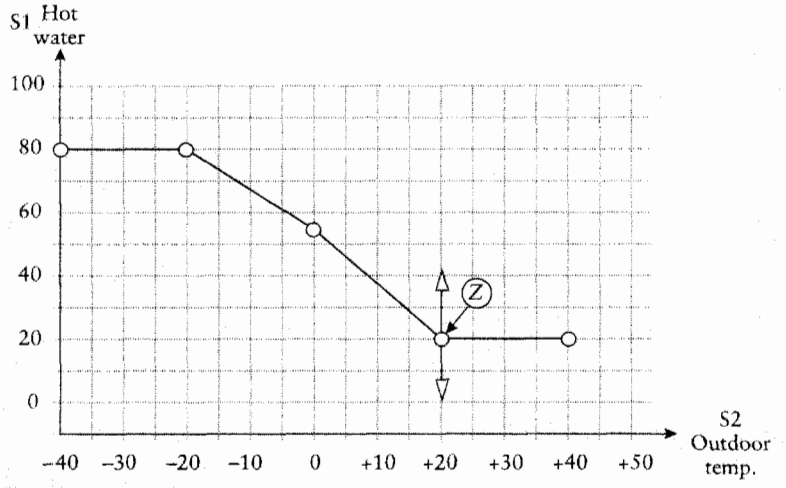

FIGURE 9.55 A central heating system supplying low-pressure hot-water radiators in a building.

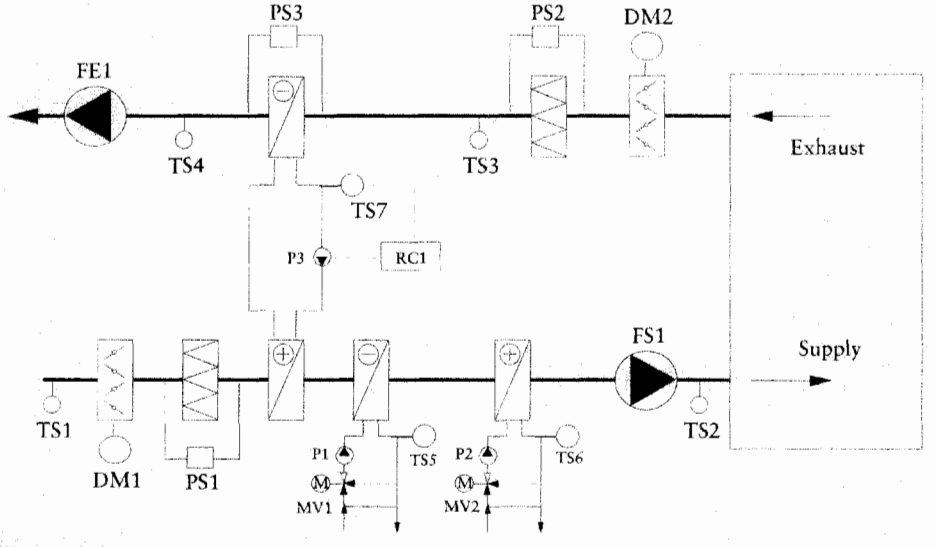

FIGURE 9.56 A ventilation system with provision for heating and cooling batteries.

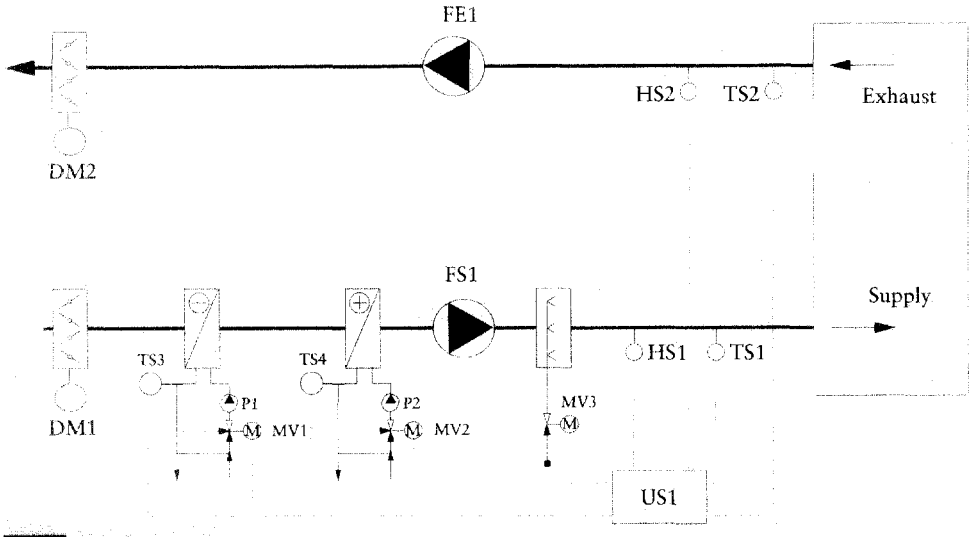

FIGURE 9.57 A ventilation system for controlling the air temperature by humidifying and dehumidifying the air.

9.6.10 Changing Speed by Using Frequency Converters

The speed of an electric motor can be changed by altering the frequency of the electric current. This is because the ratio is the same as 60 or 50 f/p (f = the frequency of the current, p = the number of poles in the stator). Frequency converters are built of electronic components, frequently combined with microprocessors. They provide good motor protection and are superior to the traditional bimetal protection. The characteristic curve for a pump and fan motor is also quadratic, making lower demands to the frequency converters

When the frequency of the electrical current is changed in the frequency converter, the main AC supply is transformed into DC. The DC is then treated

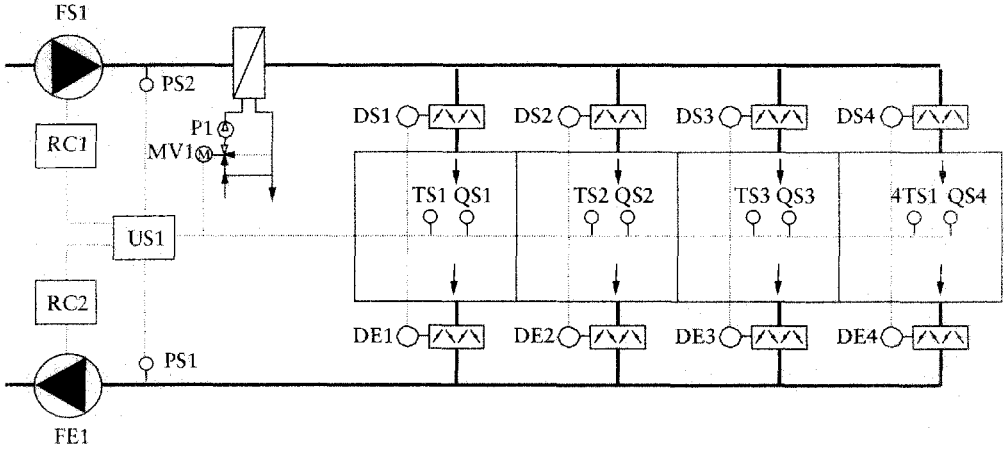

FIGURE 9.58 A variable-air-volume ventilation system (VAV).

in the frequency converter's components, before being transformed back into AC at the required frequency.

Frequency converters constructed for use with three-phase motors less than 4 kW can therefore be delivered with a single-phase supply from the electrical mains. For greater power requirements, it is most common to use a three-phase power supply. Through switches and potentiometers or the programming module of the frequency converter, the important parameters of electrical motors can be adjusted as needed.

The advantage of using frequency converters is that the possibility exists to use a ramp function when starting and stopping the motor (soft start). By using this function, it is possible to avoid starting both fans at full speed with closed dampers; it also reduces stresses on the fan transmission (belts) at the start.

9.6.11 Building the Control Station

When local or central computers are used for controlling the operation of HVAC installations in buildings, they are described as building automation systems. In the control station, operators communicate with control installations, which are connected through the computer plant. Computers for individual use are called personal computers (PCs). The use of PCs for technical and economic tasks in the past few years has increased considerably. The business overflows with PCs, which get greater data power and memory at lower prices.

Building control systems are typically classified as

- Local instrumentation (control system)
- Data-based local controllers
- Control station with computers, mainframe or PC

Because of these solutions, important technical data can be transferred from local instrumentation (control system) through data-based controllers to a control station with computers. The operator may use the many variations that the software data system provides. Technical data operation may be digital off/on messages such as the status of operation and the performance of alarms or analog measurements such as temperature, humidity, pressure, velocity, energy usage, etc.

From the operator's PC in the control station, the operator should be able to perform the following operations:

- Switch on and off electrical lights.
- Control the heating and ventilating systems.
- Switch on and off and control the speed of pump and fan motors.
- Control valves and dampers.
- Detect the condition of and operate filters and dust-cleaning devices.
- Receive and register status and alarm messages.
- Read measured values (temperature, energy, etc.).
- Change set-point for regulation.
- Receive and register energy information, and record the trend log.
- Control and regulate the power consumption.

9.7 AIR DISTRIBUTION SYSTEM, DUCTWORK

9.7.1 Friction Loss Calculation

These are the general principles:

- No internal friction
- Noncompressible gas
- Isothermal
- Stationary
- Bernoulli theorem is applicable

$$p + \frac{\rho v^2}{2} + \rho g h = \text{constant} \tag{9.138}$$

Because the influence of gravitation $\rho g h$ is negligible for horizontal (distribution) systems, this term is ignored in the equations.

Friction losses in ductwork are

$$\Delta p = \frac{\lambda L}{d} + \frac{\rho v^2}{2}, \tag{9.139}$$

in which

λ is friction factor, dimensionless
L is length, m
d is internal diameter, m
ρ is density, kg m^{-3}
v is average air velocity, m s^{-1}

The friction factor λ for laminar flow (Re $\leq$ 2300) is

$$\lambda = \frac{64}{\text{Re}},$$

in which Re is Reynolds number: $\text{Re} = vd/\nu$, in which

v is the average air velocity
ν is kinematic viscosity

For turbulent flow the empirical formula of Colebrook–White applies:

$$\text{Re} > 3500$$

$$\frac{1}{\sqrt{\lambda}} = -2 \log\left(\frac{\epsilon}{3.72D} + \frac{2.51}{\text{Re}\sqrt{\lambda}}\right). \tag{9.140}$$

This expression is difficult to use, as iteration is required. A simplified expression can be used with sufficient accuracy:

$$\frac{1}{\sqrt{\lambda}} = -2 \log\left(\frac{\epsilon}{3.72D} + \frac{5.74}{\text{Re}^{0.901}}\right). \tag{9.141}$$

The formulas are represented in the Moody diagram, which allows a quick solution.

In the transient field where 2300 $<$ Re $<$ 3500, the flow may be laminar or turbulent, and λ is expressed by the following formula:

$$\lambda = \frac{\lambda_{2300}(3500 - \mathrm{Re}) + \lambda_{3500}(\mathrm{Re} - 2300)}{3500 - 2300},$$

in which λ_{2300} and λ_{3500} are the calculated λ values at Re = 2300 and Re = 3500, respectively.

9.7.1.1 The Surface Roughness Factor ϵ

This factor is material dependent. The values in Table 9.8 could be applied. The value for flexible plastic ducts (* in the table) can be estimated by

$$\lambda = \frac{1}{5}\sqrt[10]{(s/d)^6 (S/s)^7} \qquad \text{if } \mathrm{Re} \leq 5 \cdot 10^4, \tag{9.142}$$

in which

d is the internal diameter, m
s is the depth of the winding, m
S is the distance of the windings, m

Hydraulic Diameter

The hydraulic diameter is four times the flow area divided by the duct perimeter.

The formulas given before show the diameter d.

For rectangular and oval ducts, a corrected hydraulic diameter should be used.

$$d_h = 4\frac{A}{P}, \tag{9.143}$$

in which

A is surface area of the duct, m^2
P is perimeter per unit length of the duct, m

TABLE 9.8 The Surface Roughness Factor ϵ

Duct type	Material	ϵ (10^{-3} m)
Seamless ducts	Steel	0.045
	Aluminum	0.045
	Plastics	0.01
Spiral-type ducts	Galvanized steel	0.15
	Stainless steel	0.15
	Aluminum	0.15
Ducts with beams	Galvanized steel	0.07
	Stainless steel	0.07
	Aluminium	0.07
Flexible ducts	Metal	0.5–3
	Plastics	*
Internally insulated ducts	Coated mineral wool	0.25
Masonry ducts	Concrete	2
	Brick	3

Pressure Loss Due to Local Resistance

$$\Delta p = \xi \cdot \frac{\rho v^2}{2} \text{ (Pa)} \tag{9.144}$$

ξ, the local friction resistance factor, depends on the geometrical shape of the ductwork and flow path through the various fittings used in duct systems.

Values for ξ are given in standard handbooks and are based on experimental measurements.

For computer applications, it is useful to have the friction factor in a mathematical expression (empirical).

Theoretical Background of ξ. One example for the case of a round collecting T-piece at 45° is shown in Fig. 9.59.

The impulse balance along the x axis is

$$\rho q_{v1} v_1 \cos \alpha + A_2 p_2 + \rho q_{v2} v_2 = A_3 p_3 + \rho q_{v3} v_3 \tag{9.145}$$

in which

ρ is density, kg m^{-3}
q_v is volume flow rate, m^3 s^{-1}
v is air velocity, m s^{-1}
A is surface area, m^2

Because

$$q_{vi} = q_{v3} - q_{v2}$$
$$A_2 = A_3$$
$$p_1 = P_2,$$
$$p_2 - p_3 = \rho v_3^2 - \rho v_2^2 - \rho v_3 v_1 \cos \alpha + \rho v_2 v_1 \cos \alpha.$$

Bernoulli's law gives

$$p_2 - p_3 = \frac{\rho v_3^2}{2} - \frac{\rho v_2^2}{2} + \Delta p \tag{9.146}$$

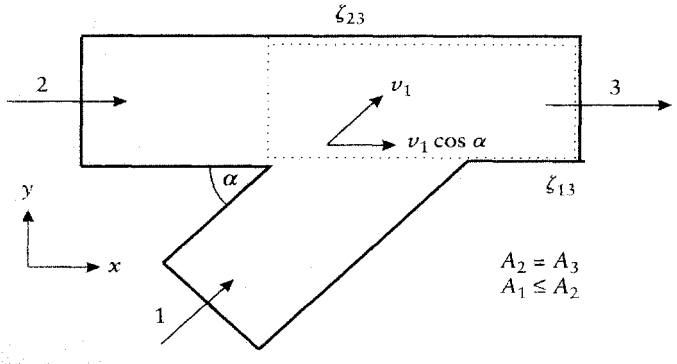

FIGURE 9.59 Round collecting T-piece, 45°.

$$\Delta p = \frac{\rho v_3^2}{2} - \frac{\rho v_2^2}{2} - \rho v_1 v_3 \cos \alpha + \rho v_1 v_2 \cos \alpha \tag{9.147}$$

The friction loss in this branch is expressed as

$$\Delta p = \varsigma_{23} \frac{\rho v_3^2}{2} \tag{9.148}$$

$$\varsigma_{23} = 1 - 2 \cos \alpha \left(\frac{v_1}{v_3}\right) - \left(\frac{v_2}{v_3}\right)^2 + 2 \cos \alpha \frac{v_1 v_2}{v_3 v_3}. \tag{9.149}$$

Using the conservation law, a similar expression can be derived for other connection pieces. The general formula structure is

$$\varsigma = a_0 + a_1 \left(\frac{v_1}{v_3}\right) + a_2 \left(\frac{v_1}{v_3}\right)^2 + a_3 \left(\frac{v_2}{v_3}\right) + a_4 \left(\frac{v_2}{v_3}\right)^2 + a_5 \left(\frac{v_1}{v_3} \frac{v_2}{v_3}\right). \tag{9.150}$$

a_1 through a_5 are regression factors, calculated on the basis of the measured values.

9.7.2 Design Methods

- Constant friction method
- Constant velocity method
- Gradual velocity reduction method
- Pressure recovery method
- Balanced pressure loss method

The design methods are normally a combination of one or more of the above methods.

- Constant friction method. The principle is that the friction losses per meter run of the duct are taken as being constant. Values in the 1 to 5 Pa/m range are typical. The friction losses of connecting elements are expressed as an equivalent length of the straight ductwork runs. This is a simple method. It is ideally suited as a preliminary design method where it is combined with another approach.
- Constant velocity method. This is a simple but not very cost effective approach for systems with a wide range of duct diameters.
- Gradual velocity reduction method. This method is a variation of the constant friction approach, where a maximum velocity is used for the main and branch ducts. This procedure provides a reasonable solution and choice between the velocity, diameter, and resistance. The method is not useful to provide the same static pressure at each outlet.
- Static pressure recovery method. The diameters are selected in such a way that the same static pressure is available before every connection. The duct reduction is selected in such a way that the gain of static pressure is in balance with the friction losses up to the next connection point. This method may result in fewer control devices at connection points or outlets. Low velocities and large diameters at the end of the system may be the result of this design approach.

TABLE 9.9 Recommended Air Velocities to Ensure an Economic Minimum of Noise Production

	Allowable sound pressure level, dB(A), in the room		
Velocity, m s^{-1}, in:	35 dB(A)	40 dB(A)	45 dB(A)
Main duct	6.5	7.5	9.0
Branch	5.5	6.0	7.0
Last branch	3.25	4.0	5.0

- Balanced pressure loss method. This is a method which is used to improve the performance of a preliminary design of a duct system and reduce the number of control dampers.

9.7.2.1 Boundary Conditions

Apart from the energy constraints due to the friction losses, the main reason for limiting the air velocities in ducts is to reduce noise production. Some recommended air velocities are given in Table 9.9.

9.7.3 Thermal Losses by Transmission

9.7.3.1 Circular Ducts

$$\varphi_l = U^*(\theta_{ad} - \theta_a)$$

$$\frac{1}{U^*} = \frac{1}{\pi h_i D_i} + \frac{1}{2\pi\lambda_{is}} \ln \frac{D_i + 2d_{is}}{D_i} + \frac{1}{\pi h_u (D_i + 2d_{is})}, \tag{9.151}$$

in which

φ_l is linear heat flux, $W m^{-1}$
U^* is linear U-value, $W m^{-1} K^{-1}$
θ_{ad} is air temperature in duct, °C
θ_a is surrounding air temperature, °C
h_i is heat transfer coefficient inside, $W m^{-2} K^{-1}$
D_i is internal diameter, m
λ_{is} is heat conduction coefficient of insulation, $W m^{-1} K^{-1}$
d_{is} is insulation thickness, m
h_u is heat transfer coefficient outside, $W m^{-2} K^{-1}$

9.7.3.2 Rectangular Ducts

$$\frac{1}{U_A^*} = \frac{1}{\pi h_i a} + \frac{1}{2\pi\lambda_{is}} \ln\left(\frac{a + d_{is}}{a}\right) + \frac{1}{\pi h_u (a + 2d_{is})}, \tag{9.152}$$

in which a is the internal width of the duct.

This formula is valid for square ducts. For the parallel extension part, one could calculate

$$\frac{1}{U_B^*} = \frac{1}{h_i} + \frac{d_{is}}{\lambda_{is}} + \frac{1}{h_u}. \tag{9.153}$$

The total U^* is calculated as

$$U^* = \frac{2aU_A^* + (b-a)U_B^*/P}{a+b}, \tag{9.154}$$

in which b is the internal height of the duct and $P = 2a + 2b$ is the perimeter length, m.

The energy loss calculation for air temperature losses is

$$\theta_{end} = \theta_a + (\theta_{start} - \theta_a)e^B, \tag{9.155}$$

in which

θ_{end} is air temperature at the end of the duct system, °C
θ_{start} is air temperature at the start of the duct system, °C
θ_a is surrounding air temperature, °C

B is calculated as

$$B = -\frac{U^* L}{q_v \rho c_p}, \tag{9.156}$$

where

U^* is U value of duct, W m^{-1} K^{-1}
L is length of duct, m
q_v is volumetric airflow, m^3 s^{-1}
ρ is density of air in duct, kg m^{-3}
c_p is specific heat of air in duct, J kg^{-1} K^{-1}

9.7.4 Air Leakage from Ductwork

It is of prime importance to keep air and gas leakage from ductwork at a minimum, as it represents increased fan running cost and the waste of treated air. Leakage into extract ductwork reduces the efficiency of the collection system.

9.7.4.1 Leakage Factor

The leakage factor is the rate of air leakage at a given static pressure per m^2 of duct surface area:

$$f_{ref} = \frac{q_{vl}}{A}, \tag{9.157}$$

where

f_{ref} is the leakage factor at a reference pressure Δp_{ref}, m^3 s^{-1} m^{-2}
q_{vl} is the leakage volume flow rate, m^3 s^{-1}
A is the duct surface area, m^2

The leakage factor depends on the pressure Δp_{ref} at which the leakage airflow rate is measured. In this case, it is the arithmetical mean value of the maximum and minimum values of the static pressure difference throughout the ductwork (Pa).

TABLE 9.10 Airtightness Classes as Defined in the EUROVENT Guidelines 2/2 Air Leakage Rate in Sheet Metal Air Distribution Systems

Class A	K_A	0.027×10^{-3} $m^3 s^{-1} m^{-2} Pa^{-0.65}$
Class B	K_B	0.009×10^{-3} $m^3 s^{-1} m^{-2} Pa^{-0.65}$
Class C	K_C	0.003×10^{-3} $m^3 s^{-1} m^{-2} Pa^{-0.65}$

Note that for laboratory duct testing, these values are divided by 2, which gives the upper limits of this quantity for the three different classes.

Leakage Classes

Three classes of airtightness (A, B, and C) are considered.

The classification is based on the following equation:

$$K = \frac{f_{\text{ref}}}{\Delta p_{\text{ref}}^{0.65}}, \tag{9.158}$$

where K is the leakage coefficient per m^2 of duct surface area, $m^3 s^{-1} m^{-2} Pa^{-0.65}$. This quantity provides a measure of the ductwork leakage. This should be independent of the ductwork static pressure test.

Table 9.10 gives the upper limits of this quantity for the three different classes.

Testing

Leakage is determined by means of the fan pressurization method.

The test pressure for class A ductwork should not exceed 1000 Pa or the maximum design static pressure, whichever is smaller.

For class C ductwork, the pressure can be increased to 2000 Pa.

The test pressure should not be less than the design operating (static) pressure.

Table 9.11 gives the upper limits of the leakage volume flow rate for the three ductwork classes at typical test pressures.

High-quality constructed and installed duct systems may perform better than class C. A reduction to 1/3 of the class C values is possible.

TABLE 9.11 Maximum Leakage Factor for the Three Classes and for Typical Test Pressures

Class	Maximum leakage factor ($m^3 s^{-1} m^{-2}$)	Test static pressure difference (Pa)			
		2000 Pa	1000 Pa	400 Pa	200 Pa
A	f_A	—	2.4×10^{-3}	1.32×10^{-3}	0.84×10^{-3}
B	f_B	—	0.8×10^{-3}	0.44×10^{-3}	0.28×10^{-3}
C	f_C	0.42×10^{-3}	0.28×10^{-3}	0.15×10^{-3}	—

TABLE 9.12 Fan Power Increase Due to Ductwork Leakage

Class	Maximum leakage as % of total flow	Increase in fan power
A	6	20%
B	2	6%
C	0.6	2%

9.7.4.2 Fan Power Increase Due to Ductwork Leakage

Leakage may require an increase in the fan power in order to ensure that the required design air distribution to all distribution points is achieved (See Table 9.12).

9.7.4.3 Test Procedure

For circular ducts, at least 10% of the total surface shall be tested, and for rectangular ducts, at least 20% shall be tested. In either case the area to be tested shall normally be at least 10 m^2. Note that there is no specific information regarding the determination of the duct surface area.

If the air leakage rate does not comply with the class requirement, the test shall be extended to include an additional equal percentage of the total surface area.

If the system is still leaking excessively, the total surface area shall be tested.

Bibliography

Eurovent 2/2. Air leakage in sheet metal air distribution systems.

9.8 SOUND REDUCTION IN AIR-HANDLING SYSTEMS

9.8.1 Basic Concepts

The subject of acoustics involving sound transmission is of prime importance in industrial ventilation. Correct system design will ensure that the designer provides a system that will not give rise to complaints regarding noise levels.

Consider the continuous oscillations of a tuning fork. These oscillations generate successive compressions and rarefactions outward through the air. The human ears, when receiving these pressure variations, transfer them to the brain, where they are interpreted as sound. Therefore, the phenomenon of sound is a pressure variation in a fixed point in the air or in another elastic medium, such as water, gas, or solid.

This pressure variation can be considered as the transfer of a pressure wave in space. In the same way, when a stone is thrown into a lake, the ripples generated move radially from the point of entry of the stone. But this observation is only apparent, because a floating buoy will stay in the same horizontal position. It does not move radially in the space; the perturbation, however, moves.

These phenomena can be considered as work processes. In fact, pressure is the force per surface unit, and work is the product of force and displacement of the force. Work is equivalent to energy, and it cannot be created or destroyed.

Therefore, when a noise is to be reduced, the sound energy must be converted into another form of energy, such as kinetic energy of a medium or heat.

This issue must be understood in order to reduce noise problems.

In a fixed point in space, the magnitude of pressure will change according to the nature of the sound source.

A tuning fork gives a pure tone, that is, a pressure variation represented by a sinusoid curve (Fig. 9.60).

The sound speed c, m s^{-1}, is the velocity of propagation of the pressure variations. This depends on the physical properties of the medium and increases with the density of the medium. In air, for example, it is 344 m s^{-1}, while in water, 1410 m s^{-1} and in concrete, 3000 m s^{-1}. The elapsed time between successive compressions is called the period time T.

Frequency is the repetition rate of pressure variations, and it is described by the reciprocal of the period time T:

$$f = \frac{1}{T}\,[\mathrm{Hz}]. \tag{9.159}$$

Its unit is hertz (s^{-1}), corresponding one cycle per second. Pure tone consists of one frequency, but normally all sounds are a mixture of many frequencies. In the audio range, frequency varies normally from 20 Hz to 16000 Hz. The size of the audio range depends on the sensitivity of the listener's ears. When the frequency is below 20 Hz, it is called infrasound, while for frequencies over 16000 Hz, it is called ultrasound.

Wavelength λ is defined as the distance between successive compressions or rarefactions and is

$$\lambda = \frac{c}{f}\,[\mathrm{m}]. \tag{9.160}$$

A sound can be periodic, hence steady, or random (Fig. 9.61).

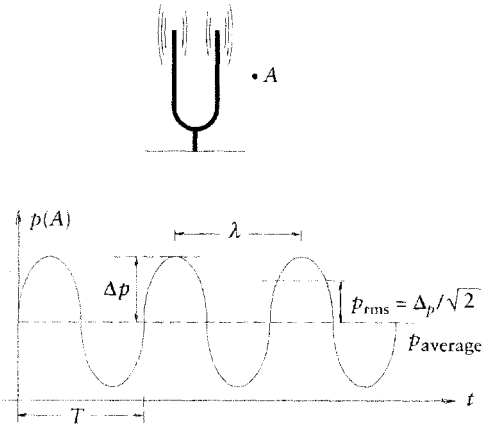

FIGURE 9.60 Sound-waves generation by a tuning fork.

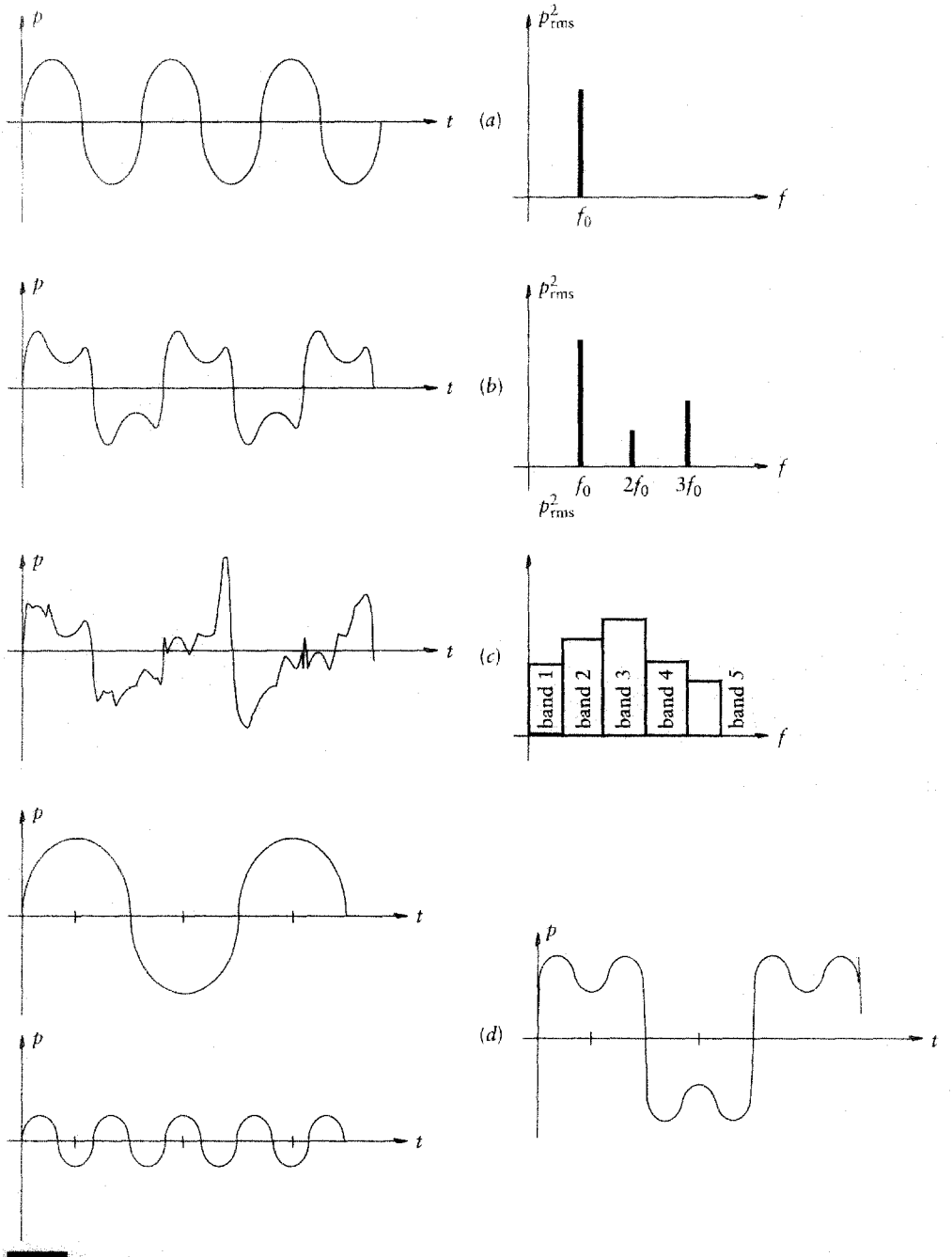

FIGURE 9.61 Different kinds of sounds: (*a*) pure tone, (*b*) periodic sound, (*c*) random noise, (*d*) effects overlapping principle.

A sound is generally not a pure tone, as the latter is only emitted from particular sources. It can be demonstrated that a sound can be divided into different pure tones (superposition method). The waves at different frequencies give the spectrum of the sound, which also describes its energy distribution. In frequency analysis, the spectrum is divided into octave bands. An octave band is defined as the frequency range with its upper boundary twice the frequency of its lower boundary. For every octave band, a central band frequency (f_c) is defined as follows:

$$f_c = \sqrt{f_l \cdot f_u} \tag{9.161}$$

where f_l and f_u are the lower and upper boundary frequencies, respectively. In ventilation technology the normally interesting frequency area is 63–8000 Hz. In this area we have eight octave bands. Sometimes also the frequency band 31.5 Hz is under consideration.

For example, the lowest octave band corresponds to a frequency range between 22 and 45 Hz. Its central value is

$$f_c = \sqrt{22 \cdot 45} = 31.5\,\text{Hz}.$$

In Table 9.13 the standardized octave band series are shown.

Octave bands are divided, on a logarithmic frequency scale, into three equally wide one-third octave bands. This is done often when more exact data of sound spectra are needed. Table 9.14 shows the standardized one-third octave band series.

The sound generation mechanism involves the transmission of acoustic energy in space. Therefore, the power of a sound source is the energy emitted in time units and is measured in W.

TABLE 9.13 Standardized Octave Band Series (ISO 226)

Octave 1			Octave 2			Octave 3		
Lower	Central	Upper	Lower	Central	Upper	Lower	Central	Upper
22	31.5	45	45	63	90	90	125	180
Octave 4			**Octave 5**			**Octave 6**		
Lower	Central	Upper	Lower	Central	Upper	Lower	Central	Upper
180	250	355	355	500	710	710	1000	1400
Octave 7			**Octave 8**			**Octave 9**		
Lower	Central	Upper	Lower	Central	Upper	Lower	Central	Upper
1400	2000	2800	2800	4000	5600	5600	8000	11 200
Octave 10								
Lower	Central	Upper						
11 200	16 000	22 400						

TABLE 9.14 Standardized One-Third Octave Band Series (ISO 226)

First Third of Octave 1			Second Third of Octave 1			Third Third of Octave 1		
Lower	Central	Upper	Lower	Central	Upper	Lower	Central	Upper
22	25	28	28	31.5	35.5	35.5	40	45
First Third of Octave 2			**Second Third of Octave 2**			**Third Third of Octave 2**		
Lower	Central	Upper	Lower	Central	Upper	Lower	Central	Upper
45	50	56	56	63	71	71	80	90
First Third of Octave 3			**Second Third of Octave 3**			**Third Third of Octave 3**		
Lower	Central	Upper	Lower	Central	Upper	Lower	Central	Upper
90	100	112	112	125	140	140	160	180
First Third of Octave 4			**Second Third of Octave 4**			**Third Third of Octave 4**		
Lower	Central	Upper	Lower	Central	Upper	Lower	Central	Upper
180	200	224	224	250	280	280	315	355
First Third of Octave 5			**Second Third of Octave 5**			**Third Third of Octave 5**		
Lower	Central	Upper	Lower	Central	Upper	Lower	Central	Upper
355	400	450	450	500	560	560	630	710
First Third of Octave 6			**Second Third of Octave 6**			**Third Third of Octave 6**		
Lower	Central	Upper	Lower	Central	Upper	Lower	Central	Upper
710	800	900	900	1000	1120	1120	1250	1400
First Third of Octave 7			**Second Third of Octave 7**			**Third Third of Octave 7**		
Lower	Central	Upper	Lower	Central	Upper	Lower	Central	Upper
1400	1600	1800	1800	2000	2240	2240	2500	2800
First Third of Octave 8			**Second Third of Octave 8**			**Third Third of Octave 8**		
Lower	Central	Upper	Lower	Central	Upper	Lower	Central	Upper
2800	3150	3550	3550	4000	4500	4500	5000	5600
First Third of Octave 9			**Second Third of Octave 9**			**Third Third of Octave 9**		
Lower	Central	Upper	Lower	Central	Upper	Lower	Central	Upper
5600	6300	7100	7100	8000	9000	9000	10 000	11 200
First Third of Octave 10			**Second Third of Octave 10**			**Third Third of Octave 10**		
Lower	Central	Upper	Lower	Central	Upper	Lower	Central	Upper
11 200	12 500	14 000	14 000	16 000	18 000	18 000	20 000	22 400

On the basis of a sound wave equation, it is shown that the power of a noise source is equal to

$$\Pi = \frac{p^2}{\rho c} A \,[\mathrm{W}], \tag{9.162}$$

where

A is the orthogonal surface to the waves path (measured in m^2)
ρ is the density of the medium (kg m^{-3})
c is the sound speed in the medium (m s^{-1})
p is the pressure amplitude of the sound (Pa)

If the noise source is a point source and the emission propagation is spherical (Fig. 9.62), then the source power can be written as

$$I = \frac{p^2}{\rho c} 4\pi r^2 . \tag{9.163}$$

Therefore, with constant (steady-state) sound power, p decreases when r increases, not linearly, but quadratically.

Perception of sound by the human ear is not related to sound power but to sound intensity, defined as

$$I = \frac{\Pi}{A} = \frac{p^2}{\rho c}, \tag{9.164}$$

that is, sound power for surface unit $\mathrm{W\,m^{-2}}$. As the listener moves away from the sound-generating source, A increases and intensity decreases.

The lowest intensity audible by human ear is $10^{-12}\ \mathrm{W\,m^{-2}}$, while the maximum value is $1\ \mathrm{W\,m^{-2}}$. Therefore the scale range is very large and inconvenient for technical calculations: it is more convenient to make use of a

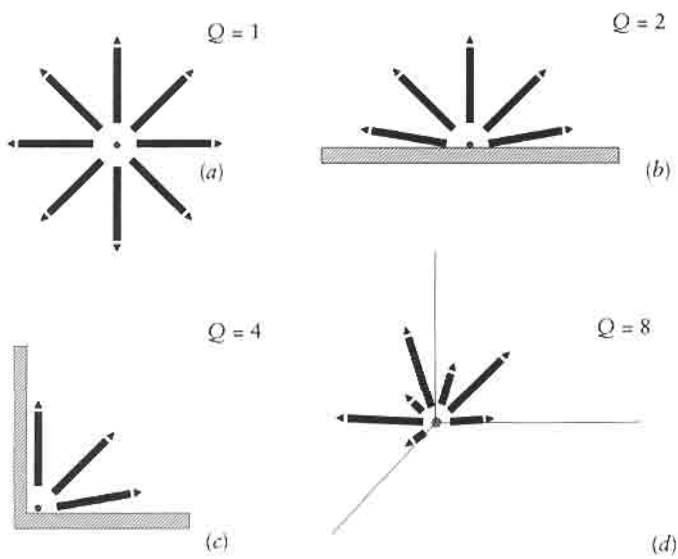

FIGURE 9.62 Different kinds of sound propagation.

logarithmic unit, defined as function of the ratio between the sound intensity and the intensity I_0 of the hearing threshold:

$$L_p = 10 \log\left(\frac{I}{I_0}\right) = 10 \log\left(\frac{p^2}{p_0^2}\right). \tag{9.165}$$

I_0 is fixed equal to 10^{-12} W m^{-2}, and its corresponding pressure is 2×10^{-5} Pa. The new unit is *decibel* (symbol dB) and L_p is called the sound pressure level. In a similar way, we can define sound power level L_W as

$$L_W = 10 \log\left(\frac{\Pi}{\Pi_0}\right) = 10 \log\left(\frac{\Pi}{10^{-12}}\right). \tag{9.166}$$

This unit is also a *decibel*. Note that the decibel is a pure number.

When two sound sources are added, it must be remembered that the decibel is a logarithmic unit. Therefore, they cannot be added arithmetically but must be combined as follows:

Step 1. They must be divided by 10.
Step 2. Then the antilogarithm must be calculated.
Step 3. The obtained values are added.
Step 4. The logarithm is calculated and then multiplied by 10 to obtain the combined value.

In general, when two or more sounds reach the listener at the same time, a composed sound will be received, with pressure level L equal to

$$L = 10 \log[10^{L_1/10} + 10^{L_2/10} + 10^{L_3/10} + \cdots + 10^{L_n/10}] , \tag{9.167}$$

where $L_1, L_2, L_3, \ldots, L_n$ are the pressure levels of each source. This formula can also be applied for the composition of the pressure levels at different frequencies for the same source.

As an alternative to the above Eq. (9.167), it is easier to add to the higher pressure level a term depending on the difference between the considered levels, as shown in Table 9.15.

Example 1

Two noise sources produce 69.2 and 69 dB pressure levels respectively (Table 9.16) at the same space point. The composed sound at said point will have a total pressure level of 72.1 dB, calculated by adding 2.9 dB to 69.2 dB. In a similar way, at 250 hertz, for example, if each of the sources has a pressure level of 60 dB, the total level will be 63 dB (sum of 3 dB and 60 dB).

TABLE 9.15 Coefficients for the Composition of Pressure Levels of Different Sources or of Different Frequencies of the Same Source

Difference in dB between two pressure levels	0	1	2	3	4	5	6	7	8	9	10 or more
Term to add at the higher level	3	2.5	2	2	1.5	1.2	1	1	0.5	0.5	0

TABLE 9.16 Composition of Pressure Levels

Frequency (Hz)	63	125	250	500	1000	2000	4000	8000	Total level
L_1 (dB)	60	62	60	65	60	55	54	48	69.2
L_2 (dB)	60	62	60	60	60	55	60	60	69.0
L total (dB)	63.0	65.0	63.0	66.2	63.0	58.0	61.0	60	72.1

To determine the levels of each frequency for the same source, it is advisable to proceed considering two levels at a time, starting from the lower levels. In this way, for example, by determining the pressure levels of source 1, the total level is 69.2 dB. Thus, the same result can be achieved by applying Eq. (9.138) or the method revealed in Table 9.15.

Example 2

In a work area, a machine has a power level of 50 dB. A second machine in the same room has a power level of 50 dB. Determine the final combined power level.

The total power level will be 53 dB.

In work areas, the noise is usually generated by different sources, such as air-handling units, refrigerating plants, etc. (especially extract and supply air fans).

It is important to quantify the sound pressure levels in dB generated by each source and for each frequency (31.5–8000 Hz) in order to establish which noise will be masked or prevalent. It must be noted that when the pressure levels of two noises differ by more than 10 dB, the resulting level is equal to that of the higher-level source; in other words, the noise at the higher level masks the noise at the lower level, which will not be perceptible to the listener (or the phonometer). In this case it is useless to reduce the latter noise, as the composed noise will remain the same, being influenced by the higher-level noise only.

It is important to remember that the response by a human ear to sound is different from that detected by scientific instruments, as the human ear is more sensitive in the middle frequency range than at the low and high frequencies at the same level.

Therefore, acoustic science has introduced different kinds of weighting curves in order to correlate as accurately as possible the sound level with the level really perceived by a generic listener. In practice, A-weighting correction is used. It consists of a series of coefficients, shown in Table 9.17. These are added to sound levels expressed in dB for each frequency.

The results are expressed in dB(A). The suffix (A) means that the new level has been calculated referring to the A-weighting correction. Phonometers have a special filter called the A-filter, which automatically introduces this correction at measured values, allowing the reading of pressure level in dB(A) directly.

TABLE 9.17 A-Weighting Corrections

Frequency (Hz)	25	31.5	40	50	63	80	100	125	160
A-wt. correction (dB)	-44.7	-39.4	-34.6	-30.2	-26.2	-22.5	-19.1	-16.1	-13.4
Frequency (Hz)	**200**	**250**	**315**	**400**	**500**	**630**	**800**	**1000**	**1250**
A-wt. correction (dB)	-10.9	-8.6	-6.6	-4.8	-3.2	-1.9	-0.8	0	0.6
Frequency (Hz)	**1600**	**2000**	**2500**	**3150**	**4000**	**5000**	**6300**	**8000**	**10000**
A-wt. correction (dB)	1	1.2	1.3	1.2	1	0.5	-0.1	-1.1	-2.5

Example 3

Referring to example 1, the pressure level of the A-weighted combined noise is 68.8 dB(A). Therefore, the acoustic perception of a listener will be 68.8 dB(A), not 72.1 dB (Table 9.18).

9.8.2 Free-Field Noise Transmission

When the noise transmission takes place in a free field (no reflective surfaces), it is possible to calculate the pressure levels at different distances from the source.

For spherical propagation, the following formula can be used:

$$L_p = L_w - 20 \cdot \log r - 11, \tag{9.168}$$

where r is the distance (in m) from the source and L_w is its noise power level. The following formula can be used in the case of hemispherical propagation:

$$= L_w - 809809(20) \cdot \log \, , \tag{9.169}$$

and in general

$$L_p = L_w - 20 \cdot \log r + 10 \cdot \log Q - 11, \tag{9.170}$$

where Q assumes the values indicated in Fig. 9.62, which is a characteristic of the geometry of floor and walls around the source.

TABLE 9.18 A-Weighted Combined Noise

Frequency (Hz)	63	125	250	500	1000	2000	4000	8000	Total level
L total (dB)	63.0	65.0	63.0	66.2	63.0	58.0	61.0	60.0	72.1
A-wt. correction (dB)	-26.2	-16.1	-8.6	-3.2	0.0	1.2	1.0	-1.1	
L total in dB(A)	36.8	48.9	54.4	63.0	63.0	59.2	62.0	58.9	68.8

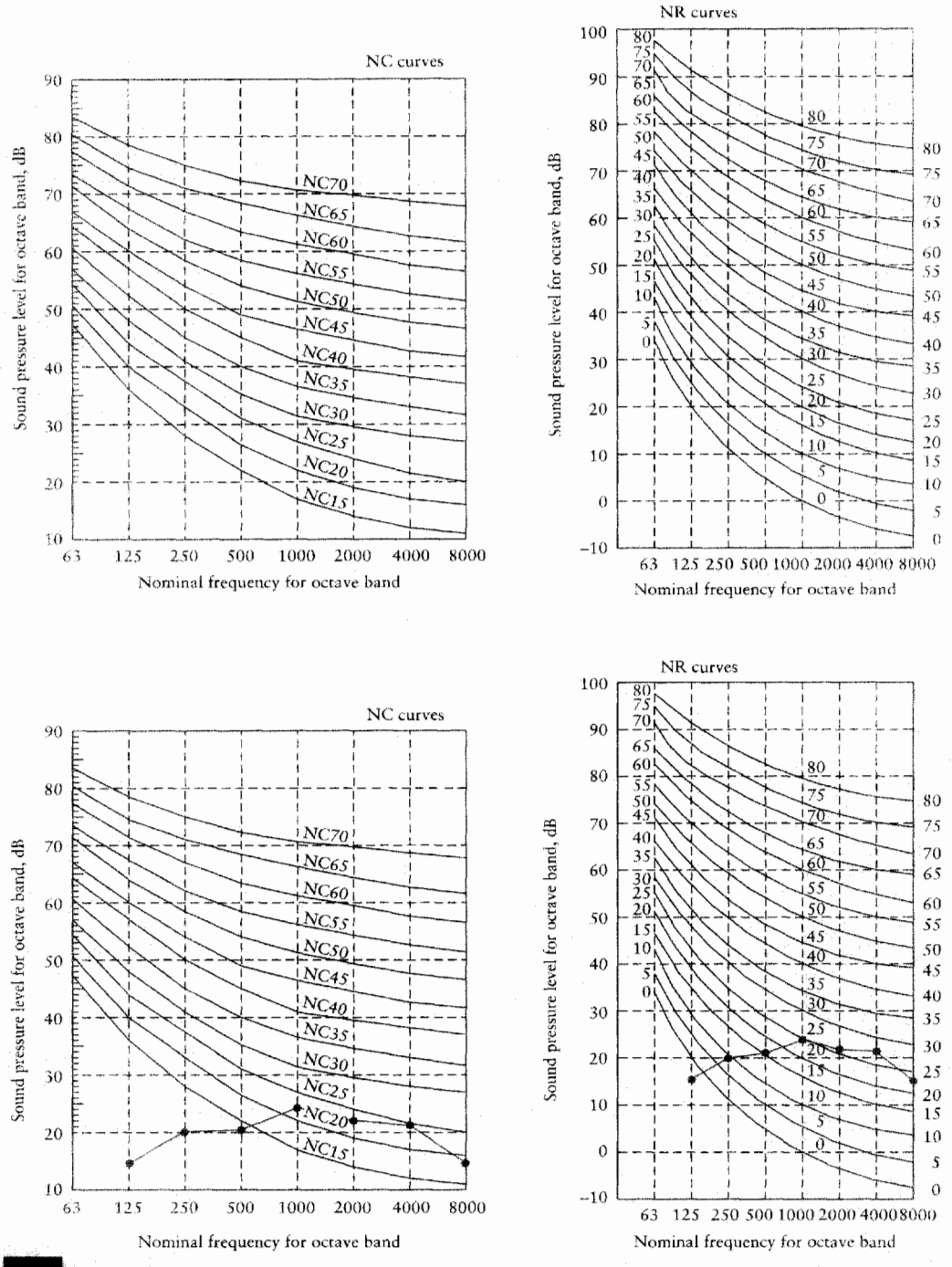

FIGURE 9.63 NC and NR curves and examples of application–The examined noise has an NR index of 28 and an NC index of 25.

9.8.3 Criteria for Acceptable Air-Handling Units and HVAC System Noise Levels

The disturbance caused by a noise depends on its intensity (equivalent pressure level L in dB(A)), its frequency spectrum (that is its energy distribution), and the acoustic characteristics of the medium in which the listener is located.

Concerning the sound pressure level, when a noise generated by an HVAC system or an air-handling unit increases the ambient background noise by 3 dB, the noise increase is just perceptible. On the contrary, an increase of 5 dB or more is clearly perceptible.

As regards the noise spectrum, the different situations can be analyzed approximately with NC (noise criterion) and NR (noise rating) curves (Fig. 9.63). NC and NR curves define the octave band limits of an acceptable background noise: each of them is characterized by a number representing the sound pressure level at 1000 Hz.

The procedure must be carried out in this manner: the noise spectrum is superimposed on NC or NR diagrams, and the highest intercepted NC or NR curve represents the noise. For example, when a noise is represented by an NC 50 curve, it means that its spectrum does not exceed the NC curve, in correspondence of which at 1000 Hz the pressure level is equal to 50 dB(A). If the intercepted point is placed between 250 and 1000 Hz, the noise is classified as neutral; under 250 Hz is called rumbly, while over 1000 Hz is classed as hissy.

A more recent method of analysis uses the RC (room criterion) curves. In this case it must be calculated the arithmetical mean of sound pressure level at 500, 1000, and 2000 Hz. The obtained value identifies the specific RC curve. The noise is classified as rumbly (with excess of energy at low frequencies) if it is under 500 Hz and its sound pressure level exceeds the RC value by 5 or more dB. The noise is classified as hissy (with excess of energy at high frequencies) if it is over 500 Hz and its sound pressure level exceeds the RC value by 3 or more dB.

The acceptability of a noise is fixed from the designer on the basis of specific data for the area depending on state and country laws. In some countries there are regulations requiring that the workers cannot be exposed to a noise exceeding set limits.

Unsteady noise can be evaluated by a phonometer, which measures the sound pressure level for a time period of noise fluctuation and gives the time-weighted average value.

The actual noise levels produced by HVAC systems can vary considerably, and it is not possible to generalize the problems that may be encountered. From a safety point of view, it is advisable to start hearing conservation programs for workers. Permanent hearing damage will result when the noise levels exceed 80 dB(A) for a given time period. Whenever possible, it is desirable to control noise pressure levels to meet the requirements of speech communication; in this case noise should not exceed 65–70 dB(A).

9.9 FUNDAMENTALS OF ENERGY SYSTEM OPTIMIZATION IN INDUSTRIAL BUILDINGS

This section briefly introduces the energy aspects that have to be taken into account in system design. The building-related features are covered in Chapter 11, mainly from the energy-calculation point of view, with less attention paid

to the aspects of optimization of the energy used to run the air distribution systems.

In this section, attention is paid to the energy demand of ventilation and air-conditioning systems as a whole. On the system level, considerable efforts have been made to reduce the heating and cooling demands, and the electrical energy consumption has been regarded as a marginal part. But after the first energy crisis in the mid-1970's, the situation started to change, so rapidly that in many modern air-handling installations, the share of electrical energy can be as high as about 90%. This figure has recently been reported in cold climates, too.

One simple example describes the problem: the efficiency of a heat recovery device can be increased from approximately 50% up to approximately 75% by using a double unit. This will double the pressure drop from, say, 100 Pa to 200 Pa, resulting in the fan energy's increasing respectively.

Measures undertaken to improve the indoor air quality (IAQ) have the same effect by upgrading the filter class, increasing the air change rate, etc. These small improvements have grown both in number and in size, little by little.

Example: A ventilation system (Fig. 9.64) handling 20 m³/s of air needs to heat the supply air from 10 °C to 20 °C. Doubling the number of heat exchangers from one to two increases the heat-recovery efficiency from 50% to 75% and introduces an extra pressure drop of 300 Pa. As we can see from Table 9.19, this is probably a cost-efficient measure.

Therefore, it is essential also in industrial environments to pay serious attention to energy usage of components and systems. This will bring a need to develop standards, guidelines, and other tools for practitioners to achieve the optimum. Some aspects are described in Chapters 15 and 16 relating to Life-Cycle issues. Some criteria to estimate the total energy consumption for the building, and for individual systems, air-handling units, and fans have been developed. These will be described in more detail in the *Systems and Equipment* volume.

Space requirements for air-handling systems are briefly described in the draft European Standard prEN 13779, which, however, is targeted to commercial, public, and office buildings. These requirements also take into account the need for service and maintenance. In industrial applications the

TABLE 9.19 Ventilation System Characteristics (Example)

Air volume flow	q_v	20 m³/s
Air mass flow	q_m	25 kg/s
Extra pressure drop	Δp	300 Pa
Temperature differential	ΔT	10 °C
Extra recovery efficiency	$\Delta \eta$	25%
Extra temperature recovery	ΔT gain	2.5 °C
Extra heat recovery		62.5 kW
Fan power increase		6.0 kW
Net gain		56.5 kW

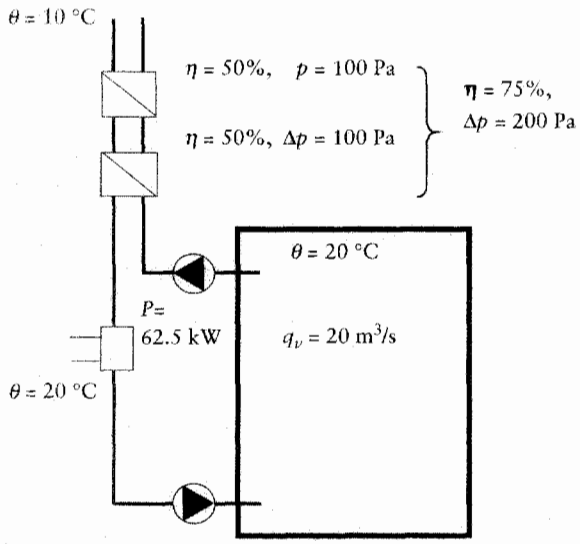

FIGURE 9.64 Ventilation system (example).

same principles apply, but the location of air-handling units, service routes and many other factors have to be considered more from the production-process point of view than for nonindustrial applications.

In ductwork design, attention shall be paid to reduce energy losses using properly designed fittings and proper duct sizing. Balancing also becomes a critical factor in order to ensure that the system operates at its most efficient designed condition. Systems that are designed for easy balancing are good from the energy-consumption point of view, provided that the pressure drops in dampers and terminal devices are within reasonable values. Special attention to equal pressure drops in different duct branches is necessary in design of such ductworks for contaminated air where the use of dampers is not possible. See also Section 9.7 of this chapter.

Demand-controlled ventilation (**DCV**) is one approach to reduce energy consumption due to ventilation, that is gaining popularity in both industrial and nonindustrial applications. It is used in cases where ventilation requirements vary with time, regularly or irregularly. The control is based on a specified level of indoor air quality by means of continuous measurement of the parameters, that are expected to primarily determine the IAQ, such as the concentration of the main contaminant liberated from the production process. The principle is thus similar to the one in some better-known nonindustrial applications, e.g., CO_2 levels in rooms with dense human occupancy (theaters, classrooms, etc.) or nicotine concentration in smoking rooms. See also Section 9.6.

9.9.1 Design Aspects of Energy-Efficient Systems

In the design of air-handling systems, a reasonable energy efficiency can be achieved by relatively simple means, just paying attention to some basic principles.

To give the designer some advice, many recommendations exist in literature. Some general recommendations can be found in prEN 13779 for designing the air distribution system for low energy consumption. These include giving a certain target level for power consumption [the so-called SFP class. SFP means specific fan power, the ratio between the input power of fan motors and the total airflow, in $W/(m^3\ s^{-1})$].

Tables 9.20 and 9.21 present recommendations for maximum pressure drops of components in the supply and extract air systems in order to achieve a certain target level for power consumption in the whole system. In category "Low," this target level is 1500: in "Normal," 2500; and in "High" 4000 $W/(m^3/s)$.

The selection of components to match the target level can be based on the default maximum pressure drop for each component. If a certain component

TABLE 9.20 Recommended Maximum Pressure Drops for Specific Components in Supply Air Systems

	Pressure drop in Pa*		
Component	**Low**	**Normal**	**High**
Ductwork	120	200	300
Heating or cooling coil	40	80	120
Heat-recovery unit	100	150	200
Air filter per section**	100	150	250
Silencer	30	50	80
Terminal device	30	50	100
Air inlet	20	50	70

Note: The values are somewhat different from prEN 13779.

*Values for individual components may be exceeded then the overall target can be achieved by lower pressure drops of other components.

**Final pressure drop before replacement.

TABLE 9.21 Recommended Maximum Pressure Drops for Specific Components in Extract Air Systems

	Pressure drop in Pa*		
Component	**Low**	**Normal**	**High**
Ductwork	120	200	300
Heat-recovery unit	100	200	300
Air filter per section**	100	150	250
Air outlet	20	40	60

Note: The values are somewhat different from prEN 13779.

*Values for individual components may be exceeded then the overall target can be achieved by lower pressure drops of other components.

**Final pressure drop before replacement.

with higher pressure drop is selected (e.g., because of its higher filter class), then the overall target can be achieved by lower pressure drops of other components. For industrial applications, however, the figures in prEN 13779 are not necessarily valid due to the special demands of the production processes, but still their relevant parts can be taken as a design basis. The design process will end up in specific fan power (SFP) categories for each individual air handling unit (SFP_v)—not only as a target value, but as a measurable design value or even as a guarantee value.

These issues are covered in more detail in DGB, Volumes B and C. Here, just a few basic tools have been introduced as guidance toward energy efficient air distribution systems in industry.

Bibliography

prEN 13779. Ventilation for buildings—Performance requirements for ventilation and air conditioning systems. (Draft European Standard.)

9.10 SPECIAL CONSIDERATIONS AND SYSTEM DESIGN ASPECTS

This section addresses special considerations and aspects very briefly. Details will be presented in the Systems and Equipment volume, and more fundamentals, later on, when the basic standards and other background documents are finalized and better known.

9.10.1 Aspects Related to the Quality of Extract or Exhaust Air

In many of these aspects, the Extract Air Classification, summarized in Table 9.22, is a useful tool to assist in system design. Applications of these classifications are described in Annex A of prEN 13779.

Categories for exhaust air (EHA) are also defined in prEN 13779. Normally the EHA category for air to be discharged outdoors is the same as ETA, but if the system includes reliable and monitored cleaning equipment, the category can be one lower. With these provisions, air from industrial processes with very high pollution level, in category ETA 4 can be cleaned to EHA 3 levels.

9.10.1.1 Examples of ETA and EHA Classification Applications

Reuse of Extract Air

The quality of extract air is crucial for its use as recirculated air. The classification described in prEN 13779 is also valid for industrial applications. Air even possibly containing any carcinogenic compound is automatically of category ETA 4 ("very high pollution levels") and must not be used, not even after cleaning, as recirculated air (should be applicable normally only in category ETA 1, and in some cases ETA 2, after cleaning) or transfer air (applicable in categories ETA 1 and ETA 2). This means that reuse of extract air in any industrial application is limited to relatively clean industrial environments) (extract air in category ETA 1 or 2), and even then the quality of air must be continuously controlled and monitored in a reliable way.

TABLE 9.22 Extract Air Categories (ETA)

Pollution level code	Description	Example
	Extract air with low pollution levels	
ETA 1	Air of the same quality as outdoors with respect to humidity. From rooms with pollutant sources from humans and building material.	Offices, storage rooms, public service places. No major pollution sources, including smoking.
	Extract air with moderate pollution levels	
ETA 2	Air from occupied spaces that have impurities in excess of ETA 1.	Smoking lounges, eating areas.
	Extract air with high pollution levels	
ETA 3	Spaces in which moisture, chemical processes, etc. substantially lower air quality.	Toilets, kitchens, garages, tunnels, car parks, solvent areas, laboratories.
	Extract air with very high pollution levels	
ETA 4	Air containing impurities and odors detrimental to health, in concentrations higher than regulations allow.	Industrial processes, laboratories, smoking lounges.

Distances and Locations of Openings

Rough principles are presented in prEN 13779. The general principle is to discharge air with high pollutant levels (category EHA 3 or 4) from openings above the roof level, and upward. Only relatively clean air can be discharged through outer walls. Openings for supply air should be located at the highest practicably possible distance from contamination sources outdoors or from exhaust air.

Pressure Conditions

As a general rule, the system must be designed so that contaminated extract or exhaust air cannot mix with supply air through leakages. This entails requirements for pressure conditions, especially for heat recovery units. For category ETA 1, no limitations are needed: for ETA 2 and 3 using air-to-air

heat exchangers for heat recovery, a positive pressure in the supply air side is required (ETA 2, in average; ETA 3, throughout). When extract air is of category ETA 4, only systems using an intermediate heat transfer medium should be applied. Positive pressure should be avoided in air ducts at least for category ETA 3 and must be avoided altogether for category ETA 4.

9.10.2 Other Questions

More system- and equipment-specific questions will be dealt with in more detail in the *Systems and Equipment* volume. Examples include

System hygiene and cleanliness, and maintenance issues: General requirements presented in ENV 12097 and prEN 13779 apply.

Dampers in air handling units and air distribution systems: Attention has to be paid to reducing the leakages, in accordance with EN 1751. Dampers used in mixing sections of air-handling units must fulfill additional requirements, in accordance with prEN 13053.

Mixing in air-handling units and air distribution systems: Some main principles are presented in Section 9.4. However, air mixing is a complicated process under strong development. Also, the need for major improvements in the equipment has been identified very recently in connection with the standardization work in CEN (prEN 13053).

Air terminals and functional factors affecting the air handling systems: Some basic principles are presented in Chapter 8. However, more attention has to be paid to minimizing the leakages and to sound attenuation.

Materials and corrosion protection: These issues are covered in greater detail in *System and Equipment*. Also, from the hygienic point of view, this issue is growing in importance. Applications with high hygiene requirements are rapidly increasing due to automation of processes.

Flexible ducts (or tubes) and their pressure drops at various flow rates both when extended and when compressed; connection to metal sheet ducts.

Ducts of other materials than metal sheet (plastic, glass fiber wool and aluminium sheet, ceramics, glass, etc.)

Movable or swinging ducts and associated pressure drops in different positions.

Dampers for air ducts handling dust.

Fan selection for air and gases that are dust laden or contain corrosive gases or vapors.

Silencers in air-handling units and air distribution systems.

Bibliography

EN 1751. Ventilation for buildings—Air terminal devices—Aerodynamic testing of dampers and valves.

ENV 12097. Ventilation for buildings—Ductwork—Requirements for ductwork components to facilitate maintenance of ductwork systems.

prEN 13053. Ventilation for buildings—Air handling units—Ratings and performance of components and sections of air handling units.

prEN 13779. Ventilation for buildings—Performance requirements for ventilation and air-conditioning systems. (Draft European Standard.)

10
LOCAL VENTILATION

LARS OLANDER

Building Services Engineering, KTH, Stockholm, Sweden

LORRAINE CONROY

Environmental & Occupational Health Sciences, SPH (M/C 922), University of Illinois at Chicago, Chicago, IL

ILPO KULMALA

VTT Automation, Tampere, Finland

RICHARD P. GARRISON

Department of Environmental Health Sciences, School of Public Health, University of Michigan, Ann Arbor

MICHAEL ELLENBECKER

Department of Work Environment, University of Massachusetts, Lowell

BERNHARD BIEGERT

University of Stuttgart, IKE-LHR, Germany

BERNARD FLETCHER

Health and Safety Laboratory, Broad Lane, Sheffield, UK

HOWARD D. GOODFELLOW

University of Toronto, Department of Chemical Engineering and Applied Chemistry, Toronto, ON, Canada

GUNNAR ROSÉN

National Institute for Working Life, Stockholm, Sweden

BENGT LJUNGQVIST

Building Services Engineering, KTH, Stockholm, Sweden

BERIT REINMÜLLER

Building Services Engineering, KTH, Stockholm, Sweden

ANTONIO DUMAS

Dipartimento di Ingegneria Energetica Nucleare e del Controllo Ambientale, Universitá di Bologna, Italy

MICHAEL ROBINSON

Division of Mathematics, School of Science and Mathematics, Sheffield Hallam University, UK

Industrial Ventilation Design Guidebook

DEREK B. INGHAM

Department of Applied Mathematics, University of Leeds, UK

ALBRECHT LOMMEL

Binzhaldenstrasse 19, Wald, Switzerland (formerly Swiss Federal Laboratories for Materials Testing and Research, EMPA)

KATSUHIKO TSUJI

College of Integrated Arts & Sciences, Osaka Prefecture University, Sakai, Osaka, Japan

IRMA WELLING

Lappeenranta Regional Institute of Occupational Health, Lappeenranta, Finland

XIANYUN WEN

School of the Environment, University of Leeds, UK

10.1 GENERAL

10.1.1 Purpose and Function

Local ventilation is used to diminish or, preferably, to prevent exposure to contaminants (including heat). This includes protection of persons, products, or animals from hazardous and/or nuisance contaminants. This task is not specific for local ventilation and different definitions exist. One is the following:

> Local ventilation systems are used to transport contaminants or heat from the occupancy zone.

A longer definition is

> Local Ventilation uses an airflow rate that is as low as possible, but sufficient to minimize the amount of airborne contaminants entering a specified volume or passing specified point(s). These are usually intended to be at the breathing zone of occupants. This minimization of airflow can be achieved either by capturing (or containing) the airborne contaminant into an exhaust hood before it enters the workspace, by blowing noncontaminated air from a supply inlet through the volume to prevent the contaminant from entering the workspace, or a combination of those. Often an exhaust system is called an extract system. This term is appropriate if the room is seen from the outside, but since in these descriptions the system is seen from inside the room the more adequate name *exhaust system* is used.

Local ventilation is often a very important part of the ventilation system, both in function and in construction, which makes a specific definition difficult. In addition to the above definitions it can be defined as ventilation of a separate volume inside a large room, as opposed to general ventilation, which is for the complete room or building. One problem with this definition is that local ventilation systems could function as localized ventilation in one surrounding and as general ventilation in another surrounding: e.g., a ceiling inlet combined with floor exhaust is a local ventilation system in a

large hall and a general ventilation system in a small room without any other ventilation, although, in this latter case, its main purpose is different from that of a general ventilation system. With these comments as a background, the term *local ventilation* is here used in a very broad sense (See Fig. 1.1 in Chapter 1, where a local ventilation system is outlined).

By using a local ventilation system of good design less air is needed to reach a specific contaminant level than is possible with general ventilation. It can also be said that the purpose of local ventilation is to achieve a more efficient (defined in some way) ventilation in a part of a room or in the whole room. Local ventilation also can be important from a process standpoint, e.g., removal of heat that might damage equipment.

Proper design and construction of a local ventilation system must account for hood flow rate, contaminant generation process and rate, and the generated flow rate of contaminated air. Thus, knowledge about airflow mechanics, process performance, and the contaminant source is essential. The descriptions of different sources are included in Chapter 7 and here only short descriptions are included as necessary to identify different processes and source types.

The demands and design of a local ventilation system (not only local exhausts) should naturally start with the demanded target levels and the toxicity of the air contaminants (see Chapters 5 and 6). For best performance the exhaust should be close to the source and preferably enclose the source, there should be no disturbances of the flow, and at the same time it should have a low flow rate and be able to minimize the concentration of even quite dangerous air contaminants in the working zone.

All processes potentially generate contaminants; i.e., they act as sources. Often the contaminant is spread into and with the air around the process. Control of the contaminants is thus often the same as control of the contaminated air. Other alternatives to control contaminant sources are described in Chapter 3.

The parts of local ventilation systems, situated inside rooms, that influence the flow field are described here. This presumes that the inlet and outlet openings are properly connected to duct systems either directly or through flexible connections (tubes). These ducts and tubes and other parts of importance for the function of these systems are described in other chapters.

Systems worn by a person are not included here. These include personal fresh air supply systems (with pressurized air flasks or connected to a central system by tubes), air belts, air vests, and breathing masks.

10.1.2 Modes

All local ventilation systems can, in principle (and many are in practice), be manufactured for use in one or more of three different modes: fixed, flexible, and mobile.

Fixed systems are those where movement of the hood or other changes to the system, except perhaps opening and closing of lids and doors, is not possible. One example is the hood with a sliding door surrounding a drilling or a milling machine; another is the laboratory fume hood; and another is the canopy hood above or the enclosure around a paper machine.

Flexible systems are those where the suction opening or supply device may be placed at different locations inside a limited area or volume. This is performed by connecting the exhaust (or supply) opening and duct (or tube) to

the fan by flexible connections (ducts with movable elbows or flexible tube). One example is a wall-mounted hood for welding exhaust; another is the exhaust connected to a portable grinding machine; and another is the exhaust for soldering fumes connected to soldering equipment.

Mobile systems are those where the exhaust (supply) opening may be placed almost anywhere inside a workroom. This is performed by placing the whole system (exhaust/supply opening, duct, fan) on wheels or a portable frame. It can also be accomplished by having a separate exhaust part (opening and short tube) which could be connected to a central duct system at many places (in walls, on the floor or from the ceiling). One example of the former is a welding exhaust (with filter) on a small carriage and an example of the latter is a centralized exhaust system for connection to car exhaust pipes. Another example of a mobile system is the sliding connection between an exhaust tube and a fixed duct, which makes it possible to let the exhaust follow the car (or any contaminant generator) around the room.

Mobile exhaust or supply systems also include portable systems—for example, the systems consisting of a fan and a flexible tube used in construction work, either for exhausting or supplying air in work areas without any ventilation system. The work area must have some type of connection, such as windows, to the surroundings.

It is difficult to determine the most common mode for local ventilation and naturally many systems fit into more than one mode.

All the different local ventilation systems can be manufactured in many different materials depending on demands for strength, vibration, abrasion, cleanliness, economy, etc. Most of the time, the material has very little influence on a local ventilation system's performance as long as the original design and flow field is maintained (no holes from abrasion, no clogging, etc.). However, different duct materials could change the friction losses and thus the resulting flow rates.

10.1.3 Classification

For all local ventilation systems the airflow field decides the performance, i.e., how well the contaminant is transported away from the place where it should not be, to a place where it can be transported to an acceptable place (e.g., outside or into the contaminant collector). Thus the disturbance of the intended flow field diminishes the efficiency of the local ventilation system. And all local ventilation systems can be disturbed by tools, machines, and persons, or by anything else that moves air (passing trucks, wind through doors, high temperature gradients, pressure gradients, etc.) or changes in air movements. Naturally, maintenance is as important for local ventilation as for general ventilation.

The necessary containment or transport capability of a local ventilation system depends on the type of contaminant present and its health risks. There could be different demands for gases and particles, for contaminants that have immediate health risks and those that have long-term effects, for contaminants that affect the breathing system and those that affect the skin and eyes, for infectious contaminants, for contaminants that follow the air streamlines closely and those that fall out on floor and work surfaces, etc. (See Chapter 5 for physiological and toxicological considerations.)

There are many possible ways to classify local ventilation systems. When local ventilation is used to describe exhaust hoods only, one classification is hoods that totally surround the contaminant source (enclosing hoods), hoods that partially surround the contaminant source (partially enclosing hoods), and hoods where the contaminant source is outside the hood (exterior hoods). A similar classification is used here for the exhaust hoods. Since local ventilation, as described in this chapter, includes more than exhaust hoods, the following three main categories are used: exhaust hoods, supply inlets, and combinations of exhaust hoods and supply inlets. (See Fig. 10.1.)

The principal classification made here is from the functioning point of view, i.e., how the different flow fields are intended to eliminate the contaminants. When using an exhaust hood the intention is to suck the contaminant into the hood (or prevent it from escaping the hood into the surroundings) by proper design of the flow field and the hood. When using a supply inlet, the intention is to blow the contaminant away (to an exhaust quite close or by spreading the air to an exhaust situated far away) from the volume (breathing zone, etc.) and the air inlet. With a combined system, the intention is to combine the effects of an exhaust outlet and a supply inlet to get a higher efficiency than either of them could achieve separately.

In practice there are many different combinations, such as two exhaust hoods close to each other or two or more air curtains placed around a horizontal (or vertical) source or a hood that is partly an exterior hood and partly an enclosure.

10.1.4 What Is Described

Each of the three categories has many different types of systems. Some common types are described here and for most of the systems the detailed description includes the name and the principle. When and where to apply the different systems and the different forms that may exist are also included. Nearly all systems have some specific issue to be addressed when designing that type of system. Equations and/or parameters are included where available. For some systems, many different equations are available, from which the most accurate or usable have been selected for inclusion. For systems where only one equation exists, it has been described and the limitations identified. If no equations are available, other design parameters and considerations are described.

Many parameters influence the performance of a specific local ventilation system. The main parameters are

- Location of supply and exhaust openings and source(s)
- Location of workers and tools relative to exhaust and source(s)
- Different kind of disturbances
- Changing flow rates

Many of these influences are similar for different types of systems. These parameters' influence is described for each system or for a group of systems depending on feasibility. For some systems, there is no detailed description, which means that there could be differences in the descriptions depending on the actual details of each system.

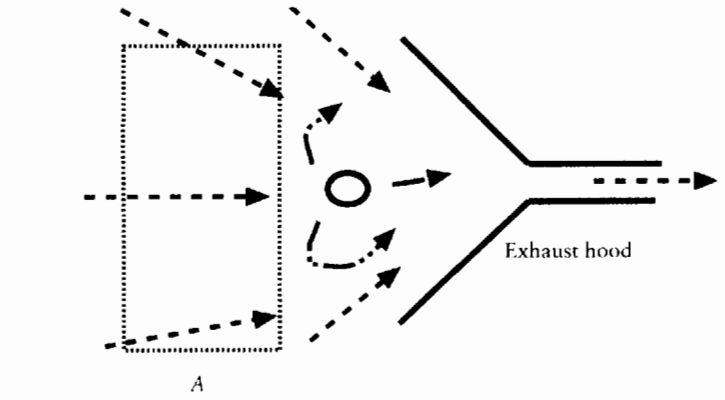

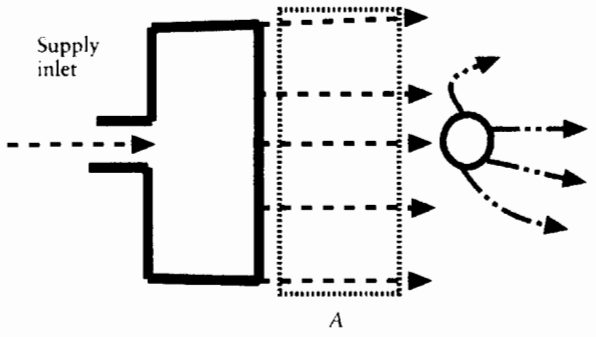

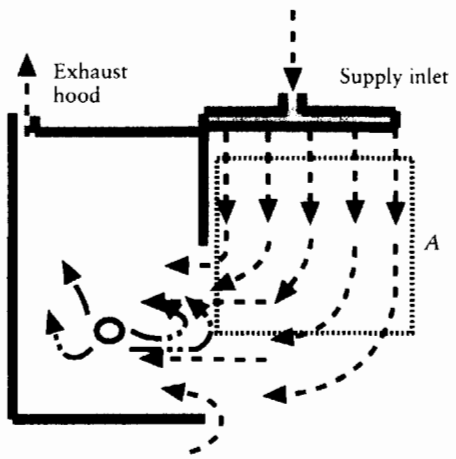

Contaminant source

Air movements

Contaminant movements

A
Protected volume

Walls of exhaust hood/supply inlet

FIGURE 10.1 Principles for the three different ways of protecting a volume by using an exhaust hood (*above*), a supply inlet (*middle*), and a combined exhaust hood and supply inlet (*below*).

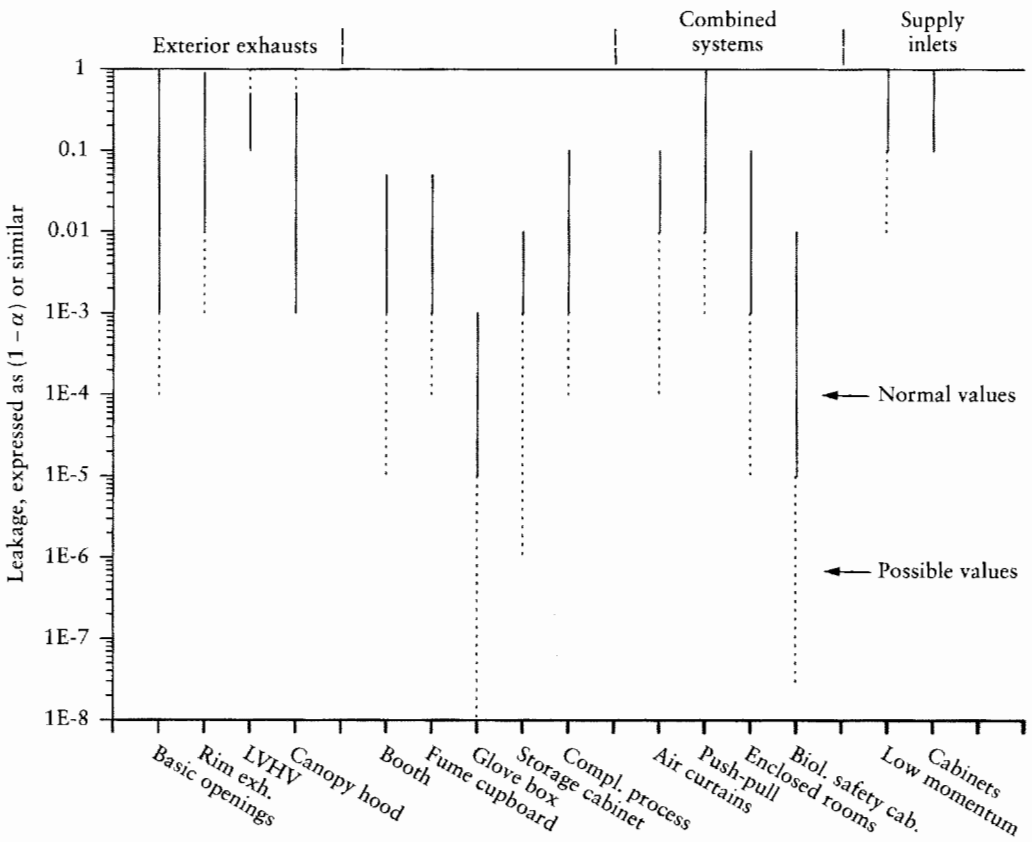

FIGURE 10.2 Approximate leakage of local ventilation systems. The lower the value, the better the system. A value of 1 means no protection. For supply systems, which are not designed to capture contaminants, higher values mean greater protection, and a value of 1 means total protection.

Evaluation procedures for local ventilation are described in Section 10.5. The actual evaluation procedure for a specific system is mostly described in connection with the different parameters that influence the function of the system. Many of the evaluation procedures for general ventilation systems described in Chapter 12 could be used also for local ventilation.

An overview of expected efficiencies for some typical local ventilation systems is shown in Fig. 10.2.

10.2 EXHAUST HOODS

10.2.1 General

10.2.1.1 Use

An exhaust hood requires an adequate supply airflow rate (direct supply or indirect from another room and transported through a transfer opening) inside the room where the exhaust is situated. This means that the supply airflow rate should be approximately equal to the exhaust rate and that the supply devices should be placed in such a way that the incoming air does not

disturb the exhaust flow fields. For some exhaust openings this could be quite easy to arrange; for others it may be difficult. If the disturbance is too great, the efficiency of the exhaust will diminish and it might be necessary to use a different exhaust opening, a different supply opening, a different layout, or a completely new solution (e.g., a combined exhaust and supply). There are usually demands on the cleanliness of the supply air (see Chapters 6 and 8).

Most exhaust hoods are either integrated with the contaminant-generating process equipment or are independent of the process equipment. It is nearly always better to have an integrated hood. The advantages are that the hood is designed to work with that specific tool, process, and contaminant; its airflow rate is less; it is situated at a proper place; it is easier to handle; and it is often less expensive. However, there may be economic or other reasons not to have an integrated hood. A nonspecific exhaust also has advantages: many people know how to handle it (at least in principle); it could be used very near the source (although normally not as close as an integrated hood); it may be useful for different processes at the same workplace; and, if flexible or mobile, it may be less expensive for different uses at the same workplace. However, a nonspecific exhaust usually has lower efficiency than an integrated exhaust with the same flow rate and it may be difficult to get a mobile exhaust to follow the contaminant source.

The more enclosed a process is, the easier it is to keep a low concentration in the workroom. It is usually necessary for the workers or for some equipment to have physical contact with the process, which could make it difficult to use complete enclosures. If it is possible to enclose the contaminant source and the tool, a total enclosure is recommended, especially if the workers only need to access the process during pauses in operation. Total enclosures may also be necessary for processes that generate highly toxic contaminants. Where total enclosures are not practicable, partial enclosures may be used. Exterior hoods are the least effective exhaust hood.

It is strongly recommended to keep the source between the exhaust and the person. When the source is quite close to the person and between the person and the exhaust, the airflow around the person could generate a wake that includes the source or the generated contaminant and thereby the person's exposure could increase (see Fig. 10.3). In these cases, it is better to use a side exhaust, where the person is situated beside the shortest path from source to exhaust.

This phenomenon is more common with large flow rates and large openings, such as use of a laboratory fume hood or a unidirectional horizontal flow field, than with small flow rates and small openings, such as exhaust hoods for welding, soldering, and grinding. Designing the system to place the worker beside the airflow path is generally recommended for all exterior hoods. When using partial enclosures with large openings to the surroundings, a person may also influence the flow field, e.g., by changing the flow into the hood. It is possible to counteract such wakes by using vertically directed supply air around the worker (see Sections 10.3.3 and 10.4.6).

When some natural forces exist, it is essential to utilize, and not to counteract, these forces. Some examples are buoyancy forces from hot sources or contaminant jets from grinding or spray painting (see Fig. 10.4). To completely isolate a volume from its surroundings only using air is impossible. To achieve

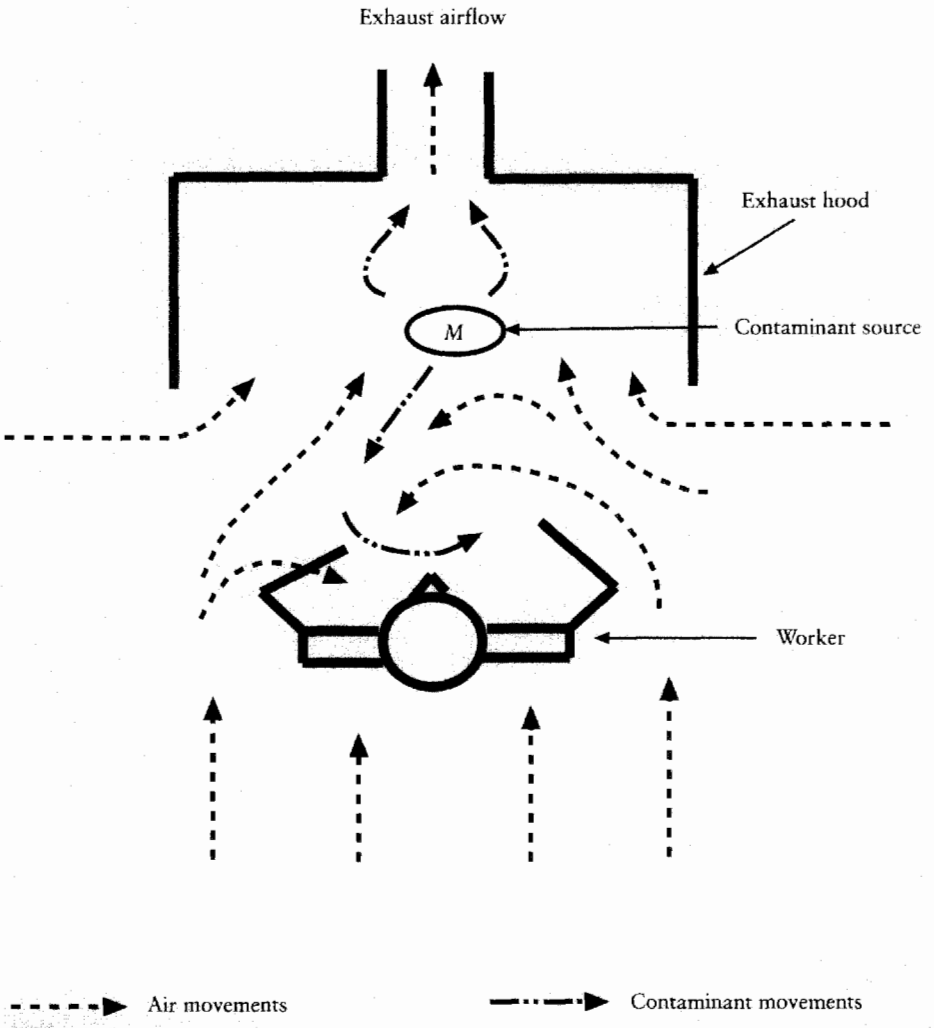

FIGURE 10.3 Possible air and contaminant movements around person in front of opening (or with supply air coming from behind). Seen from above.

this, it is necessary to complement the airflow field with physical barriers. This is easy to understand for exterior hoods, but it is also valid for enclosures.

10.2.1.2 Performance

Many different measures of local ventilation performance exist. These measures can be divided into three main categories: capture velocities, capture efficiencies, and containment efficiencies. Table 10.1 shows the connections between hood types and different efficiency measurements. Section 10.5 describes procedures for measuring each of these performance measures.

Capture velocity is usually defined as the air velocity generated by the exhaust opening necessary to capture a contaminant outside the opening and transport it into the opening. See Fig. 10.5.

The advantage of using capture velocity is that it is possible to calculate the necessary flow rate into the adjacent opening. Its disadvantages are that it

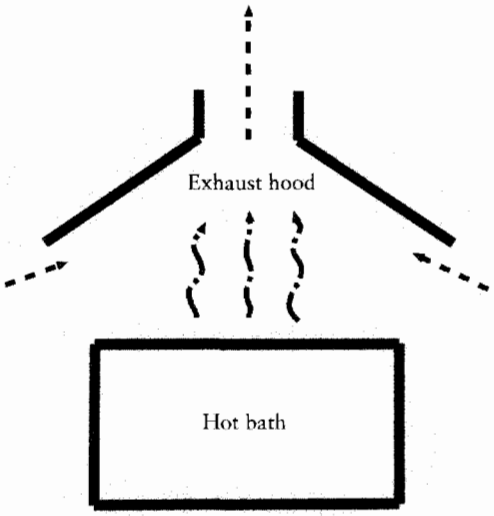

FIGURE 10.4 Example of how a natural force (buoyancy) is used when exhausting generated contaminants.

TABLE 10.1. Relationships between Different Evaluation Procedures and Different Hood Types

Hood types	Exterior hoods	Enclosures
Specific hoods	Basic openings, rim exhausts, LVHV, receptor hoods, special: fit to machines	Booths, laboratory fume hoods, safety cabinets, glove boxes, storage cabinets, built-in processes
Evaluation procedures	Capture efficiency, capture velocity	Containment indices such as protection factor and similar, leakage factor and similar, pressure difference, opening velocity

varies for a specific contaminant, depending on how the contaminant is generated and which type of process is involved, and that it is difficult to measure.

Capture efficiency is the fraction of contaminant generated outside an exhaust that is captured by the exhaust (see Fig. 10.6).

The advantage of using capture efficiency is that it is possible to calculate how much of the contaminant is released into a workspace (if the source rate is known) and thus to judge if the exhaust will reduce workplace exposures to acceptable levels. Its disadvantage is that it is rather difficult to measure and, moreover, it is usually impossible to calculate source generation rate.

Containment efficiencies are often called indices, which are measured and calculated in many different ways. One definition is shown in Fig. 10.7. They are different from the two preceding measures in that they are exclusively used

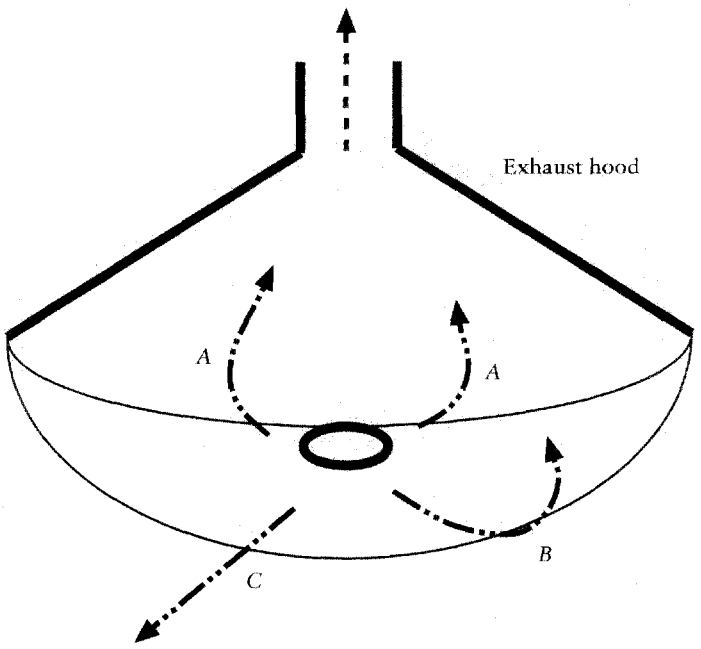

FIGURE 10.5 Illustration of capture velocity.

for enclosures. Their advantages are that they can give a good approximation of the contaminant leakage from a specific work process, that they are not too difficult to measure, and that they make it possible to design a hood for working with a specific hazardous substance. Some of these containment efficiencies could also be defined to measure the efficiency of local supply inlets. The disadvantages are that there are so many different containment indices and that they may give the impression of a measure independent of work, although they are influenced by the process and/or operator.

10.2.2 Exterior Hoods

10.2.2.1 Design Considerations

General

An exterior hood is often a natural choice for an exhaust. It is usually easy to install, less expensive, and does not need any large changes in the outlay of the room or the process. Often it is possible to connect this type of hood to an existing exhaust duct system and when the flow rate is relatively small, the existing supply air system may be maintained without changes.

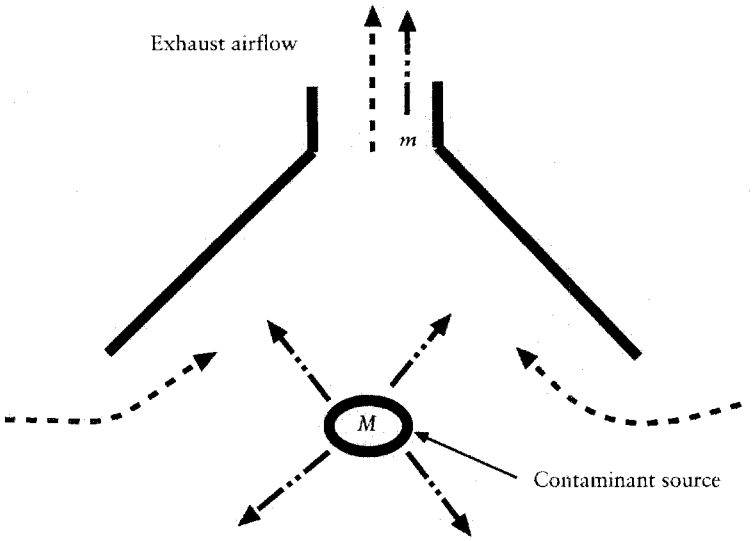

FIGURE 10.6 Definition of capture efficiency, α. M = contaminant source rate, m = contaminant transport (directly) into the exhaust hood, $\alpha = m/M$.

As mentioned before, the efficiency of an exterior hood may be low, which is a disadvantage of this type of system. Before an exterior hood is chosen other alternatives should be investigated regarding efficiency, suitability, and cost.

Exterior hoods are most favorable when one or more of the following conditions are fulfilled:

The exhaust must be very close to the source and it is not possible to surround the source by an enclosure;
The generation has one principal direction and it is necessary to have a distance between the source and the exhaust;
The source is or could be movable; and
The source is temporary in place or time.

The first of these conditions is the most important factor when deciding to use an exterior hood. Exterior hoods are allowed when the demands on the exhaust, and the hazard of the contaminants, are moderate.

The exterior hoods described here are divided into basic openings, rim exhausts, low-volume high-velocity (LVHV) hoods, receptor hoods (canopy hoods), and downdraft ventilation tables. Many varieties of these types of hoods exist. Some of these have been described and investigated more thoroughly than others because they are used more often or they are of more general use and applicability than the more specialized hoods.

The design equations and parameters for the different hoods are quite different, which is the main reason for describing each of these hood types separately.

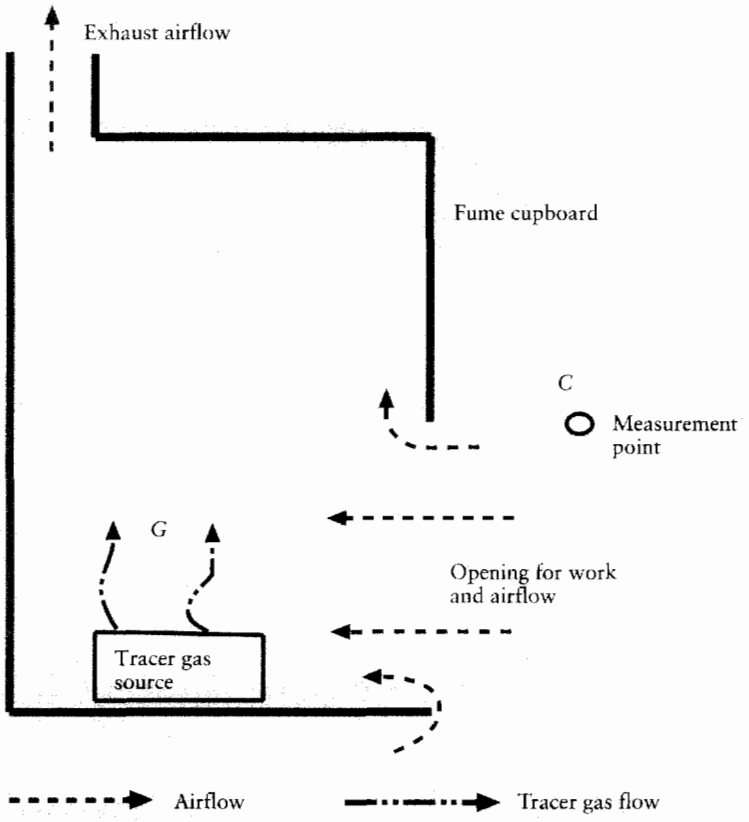

FIGURE 10.7 Definition of protection factor, pF (This is one definition of containment efficiency; see J. Pekkinen et al.[1]) G = gas tracer flow rate, mg min^{-1}, C = concentration in breathing zone, mg m^{-3}, pF = $\log_{10}(G/C)$.

Location of Supply and Exhaust Openings and Sources

The supply air for exterior hoods should be brought into the room without disturbing the exhaust flow. The supply openings are usually placed far away from the exhausts and it is necessary to check that the supply air velocity near the exhaust is much lower than the velocity due to the exhaust. If the supply air velocities are less than one-tenth of the exhaust air velocities at distances less than three exhaust opening diameters from the exhaust, then the influence of the supply on the exhaust should be negligible. This is also true for cross-drafts caused by other activities. For cases with higher supply air velocities or higher cross-draft velocities, supply air velocity or cross-draft velocity must be included in the design of the exhaust, the supply air or cross-draft should be redirected, or the type of exhaust should be changed to one with less sensitivity to supply air or cross-draft velocities.

The exhaust opening should be placed as close as possible to the source. This normally means a distance less than one exhaust opening diameter between source and exhaust opening. If the distance is larger both opening and flow rate must be increased so much that it may be infeasible to use an exterior hood. For sources with one principal generation direction, the distance could be larger with only slightly less efficiency. One example is a canopy hood over a hot bath.

The exhaust could be placed above, below, or beside the source depending on generation direction. If possible, the main exhaust direction (center axis of opening area) should be the same as the main contaminant generation direction. Small changes in location, both sideways and in distance, could result in large changes in the efficiency of exterior hoods. If the exhaust is designed to have the highest efficiency in one specific placing, small moves could decrease the efficiency substantially.

For the supply opening in relation to the source, the same arguments are valid as for the supply in relation to the exhaust. However, it is sometimes possible to use the supply air to increase the transport from the source into the exhaust; these types of systems are described in combined exhaust and supply systems (Section 10.4).

Location of Workers and Tools Relative to Exhaust and Source

The worker and the tool should be outside the exhaust system's distance of influence and the source should be inside this distance, as is shown principally in Fig. 10.8.

This is usually not a problem with small exhausts. With large exhausts (opening area larger than 0.1 m^2), parts of a worker or of tools could easily come between the source and the exhaust. This diminishes the efficiency and could also spread the contaminant in unwanted directions, even if the exhaust velocity is

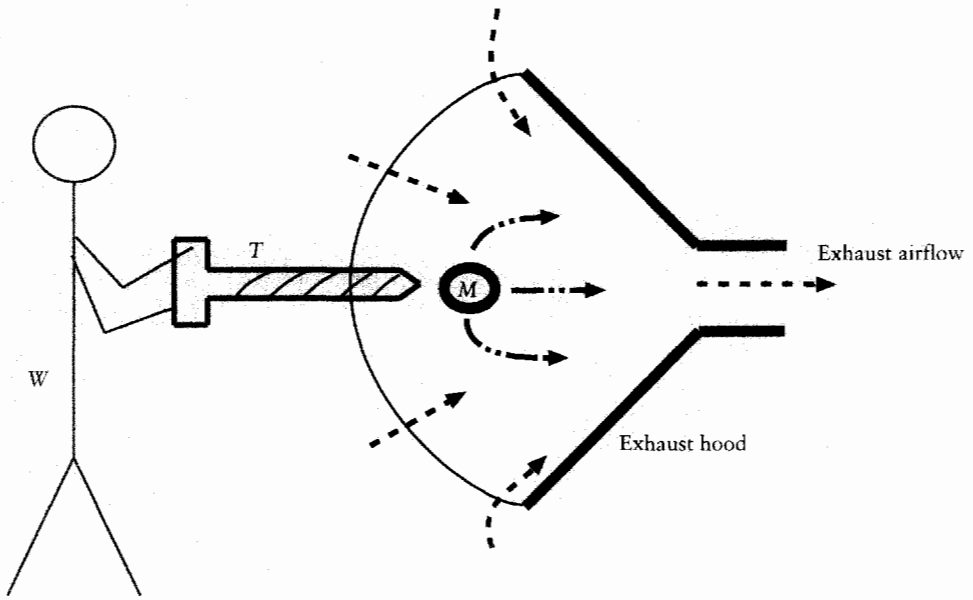

FIGURE 10.8 Schematic ideal placing of worker, tool, and contaminant source when using exterior hoods.

large enough to transport the contaminant into an undisturbed exhaust. With still larger exhausts, a worker too close to the source could be exposed to the contaminant due to vortices created when air flows around the body. See Sections 7.3 and 10.3.4 on airflow around obstacles.

Tools are normally close to the opening. One way to diminish the disturbances from a tool is to shape the opening around that part of the tool where contaminants are generated. Another is to size the opening specifically for the source and place it very close to the source and away from disturbances from the tool.

Disturbances

Since exterior hoods are unshielded, nearly all disturbances can dramatically change the performance of the hood. Changes in direction of contaminant generation could result in contaminant spread outside the exhaust; a variable generation rate could result in intermittent contaminant spread directly to the surroundings when the source volume rate becomes larger than the exhaust flow rate; tools moving around or rotating could either disturb the flow field or redirect the contaminants or both; cross-drafts from moving persons or vehicles, or leakage through door openings or wall cracks could temporarily or permanently disturb the exhaust flow field and result in spreading of the contaminant in the room.[2,3] A moving source demands a moving exhaust or a very large opening to ensure that the hood is as close as possible to the source. An exhaust can be moved virtually, i.e., the openings are not moved, but instead the exhaust flow rate is connected to different openings or parts of one opening (at different locations) depending on where the moving source is at that moment. This is a way of minimizing the exhaust flow rate without diminishing the efficiency. This type of hood puts high demands on the control system for the exhaust. The misplacing of a baffle in the exhaust opening (to diminish the necessary flow rate) could also result in contaminants not being captured.

A laboratory study of surface-treatment tanks by Braconnier et al.[4] showed the effects of cross-drafts and obstructions to airflow on capture efficiency. They found that, without obstructions, capture efficiency decreased with increasing cross-draft velocity but the importance of this effect depended on freeboard height. In their study, cross-draft direction was always perpendicular to the hood face and directed opposite to the hood suction flow. For low cross-draft velocities (less than 0.2 m s^{-1}), efficiency remained close to 1.0 for the three freeboard heights studied. With higher cross-draft velocities, efficiency decreased as freeboard height decreased. For example, when the cross-draft velocity was 0.55 m s^{-1}, efficiency decreased from 0.90 to 0.86 to 0.67 as freeboard height decreased from 0.3 m to 0.15 m to 0.1 m, respectively.

A similar effect was observed for changes in hood flow rate. With a fixed cross-draft velocity, capture efficiency decreased with decreasing hood flow rate. This effect was much more important when freeboard height was small. Their results showed that when hood flow rate was 1.5 $m^3 s^{-1} m^{-2}$, efficiency remained close to 1.0 as long as the cross-draft velocity was less than 0.45 m s^{-1}. The most severe conditions tested were a hood flow rate equal to 0.33 $m^3 s^{-1} m^{-2}$ and cross-draft velocity equal to 1.15 m s^{-1}. Under these conditions, capture efficiency was equal to 0.83 for freeboard height equal to 0.3 m, but decreasing to 0.4 when freeboard height was decreased to 0.1 m.

The effects of obstacles in the flow field were also studied. A bar with dimensions of 0.04 m high $\times$ 0.003 m wide $\times$ 1 m long was used. Capture efficiency was

measured with the obstacle at various heights along the center of the tank (parallel to the exhaust hood). For the experimental conditions studied (hood flow = 0.33 $m^3 s^{-1} m^{-2}$; cross-draft velocity = 0.5 m s^{-1}; freeboard height = 0.3 m), efficiency was reduced from 0.8 when no obstacle was present to 0.28 when the obstacle was removed from the tank to a height of 0.1 m above the rim of the tank. When the obstacle reached a height of 0.4 m, its influence was no longer noticeable. Moving the obstacle upstream of the tank also resulted in effects on hood capture. When the obstacle was placed just above the height of the slot hood, higher capture efficiency resulted. When the obstacle was moved higher in the flow field, efficiency decreased, especially for low hood flow rates. Smoke tests showed the location where the change takes place to be approximately at the height where the flow separates between flow entering the slot hood and flow continuing downstream of the tank. This is similar to the dividing streamline described by Conroy and Ellenbecker[2,5] and Flynn and Ellenbecker[6,7] and to capture envelopes determined experimentally by Fletcher and Johnson.[8]

A field study of vapor degreasing tank emissions and hood capture efficiency was performed by Conroy et al.[9] Solvent emissions to the local ventilation system and to the workspace were measured at 13 sites under operating conditions. In this study, no correlation was found between local ventilation capture efficiency and hood flow rate. The authors found that the ACGIH[10] recommended flow of 0.25 $m^3 s^{-1}$ per m^2 of tank surface was adequate for some conditions and inadequate for others. An increase in flow above design recommendations did not necessarily improve hood performance. It appears that factors in addition to tank surface area need to be considered. Emissions to the workspace were only slightly correlated with local ventilation emissions, suggesting that fugitive emissions are related to factors other than hood flow rate. The authors suggested that these factors are probably more related to work practices. A more detailed analysis[11] of the degreasing activities showed that workplace emissions were positively related to the number of times baskets or parts entered or exited the degreaser and the number of times parts or baskets were removed with visible liquid solvent (carryout). Neither of these activities was correlated with local ventilation emissions.

Iyiegbuniwe[11] also looked at the effects of cross-drafts on hood efficiency. Cross-draft magnitude and direction near the vapor degreaser was measured at eight sites. The author was able to show that as cross-draft velocity parallel to the hood face increased, measured capture efficiency decreased (Fig. 10.9).

Cross-draft velocity was normalized by dividing the measured cross-draft velocity by the capture velocity calculated at the tank centerline. Capture velocity at the tank centerline was calculated using Silverman's[12] centerline velocity (Eq. (10.1)) for unflanged slot hoods. There was considerable scatter in the data, showing that cross-draft velocity alone is not responsible for low capture efficiency.

$$V_c = \frac{Q}{3.7LX}, \tag{10.1}$$

where Q = hood flow rate ($m^3 s^{-1}$ or cfm); V_c = capture velocity (m s^{-1} or fpm); L = tank length (m or ft); and X = 1/2 tank width if two slots are used (m or ft).

Changing Flow Rates

The velocities outside the exhaust opening diminish proportionally to diminishing flow rate. However, the efficiency of the exhaust could diminish more rapidly

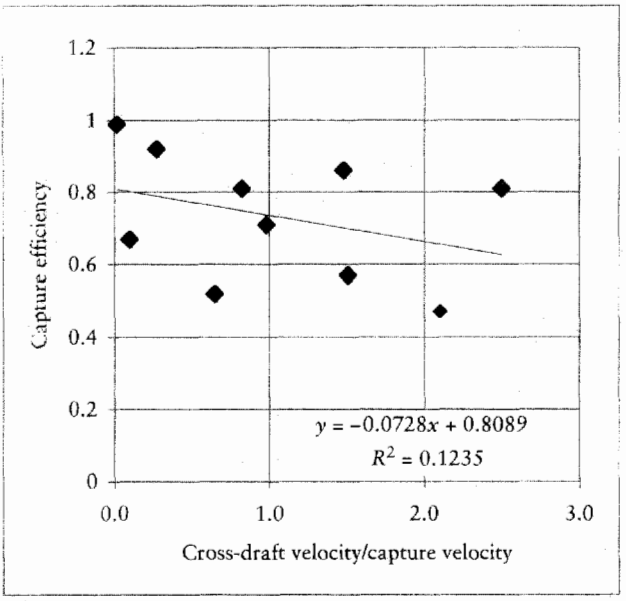

FIGURE 10.9 Hood capture efficiency versus normalized cross-draft velocity.[11]

due to the changed relationship between exhaust air velocity and contaminant velocity. Increased flow rate usually increases efficiency. A large increase could result in drafts that are uncomfortable for the workers. Air velocities that are too high could disturb the process and result in increased material losses.

The supply airflow rate should approximately equal the exhaust flow rate. A minor difference between supply and exhaust flow rates should not disturb the exhaust, since exhaust systems usually are operated with higher pressure differences than supply systems. If the exhaust flow rate is higher than the supply, it could result in lower efficiency due to lower exhaust flow rates and cross-drafts (see *Disturbances*). If the exhaust flow rate is lower than the supply flow rate, there may be fewer problems with exhaust efficiency, but this could result in a supply airflow field different from the designed one and thus result in different kinds of disturbances.

Certain operations require that the workspace be at a lower pressure than surrounding workspaces, e.g., radioisotope laboratories. In these cases, the exhaust flow rate should exceed the supply flow rate, but this excess should be within 10%. The additional resistance resulting from this imbalance should be considered in the design of the exhaust system, specifically in the selection of exhaust fans.

Flow rate changes are sometimes used in the design of local exhaust systems. An example of this is the use of dampers, blastgates, or valves that are interlocked with the machinery of interest. When the tool is on, the damper is opened and air is exhausted from that hood. When the tool is off, the damper is closed and more exhaust air is available to other parts of the system. These kinds of systems diminish the cost for running the system but increase the cost for installation as well as periodic preventive maintenance. The supply system

must be run parallel to the exhaust system, otherwise there will be little to gain by the changing flow rates and the exhaust could be less efficient than desired.

Evaluation Procedures

All exterior hoods should be evaluated regularly. The evaluation procedures can be divided into detailed and simple procedures. Detailed procedures need special instruments and competence, whereas simple procedures may be performed daily. Since simple procedures do not directly measure the performance of the exhaust, it is usually necessary to calibrate them using detailed procedures.

Detailed Evaluation Detailed evaluation is performed by measuring the capture efficiency, either by using the actual contaminant or by using a tracer gas. (In principle, it is possible to use particles as tracers, but gases are usually used as tracers.) The most reliable evaluation is to use the process-generated contaminant, since there are always problems with a tracer, due to the difficulties of feeding the tracer to the source in the same way and in a similar amount as the generated contaminant.[13]

Capture efficiency is the fraction of contaminant generated captured directly by the hood. With the appropriate instruments it is not difficult to measure this efficiency. The total amount of generated contaminant can be found by either shutting off the local exhaust and measuring the concentration in the room or, preferably, by ensuring that all generated contaminant is captured during the concentration measurements in the duct. This can be ensured by putting the exhaust duct very close to or around the source or by making a temporary closed hood around the source. The captured amount is then calculated by comparing the measured concentration in the duct, when the exhaust is working in its normal position, to the measured concentration, when all contaminant is captured.

Capture efficiency can also be measured by first estimating workspace emission rates and local exhaust emissions. The local exhaust emission rate equals the duct concentration (mass/volume) multiplied by the duct flow rate (volume/time). The workspace emission rates can be calculated using appropriate mass balance models and measured ventilation rates and workspace concentrations. Capture efficiency is the ratio of duct emission rate to total emission rate (duct plus workspace).[9,14]

Capture efficiency could be measured in the same way with a tracer gas. The difficulties explained above could make this measurement less reliable even if it usually is easier to measure the concentration of a tracer gas than the concentration of a specified dust or gas mixture.

In theory it should be possible to calculate the capture efficiency without measurements. Some attempts have used computational fluid dynamics (CFD) models, but difficulty modeling air movement and source characteristics have shown that it will be a long time before it will be possible to calculate the capture efficiency in advance.[15]

Simple Evaluation A simple evaluation can be done by checking the airflow rate into the opening, presuming the source characteristics, the placing of the exhaust, and the other parameters (cross-draft, work routines, supply airflow rate, etc.) have not changed since the detailed evaluation was done. It is necessary to do the simple evaluation at the same time as the detailed evaluation. The flow

rate into the exhaust opening can be measured in many different ways: measuring the pressure drop through the opening, using a flow measurement device in the duct, measuring air velocities in the opening plane, etc. Different flow measuring devices are described in, e.g., the ACGIH Industrial Ventilation Manual.[10]

Another simple way to evaluate the exhaust is to use smoke to visualize the air streamlines. It is also possible to see how far the exhaust reaches by observing the smoke generated at different distances. This is best achieved by using the source (if it generates particles or warm gases) and a suitably placed lamp to illuminate the contaminants.

10.2.2.2 Basic Exhaust Openings

General

The basic exhaust opening (BEO) is the simple opening placed at the end of a duct or a tube, which acts as the connection to the suction device (fan). These types of exhausts are commonly used because they can be designed and operated in a way that does not interfere with the process. Most BEOs have quite simple forms—circular, square, rectangular, or nearly any shape—and they can also be tapered with different angles. A rectangular opening is called a slot when it has a large length-to-width ratio (>5). A slot can also consist of many smaller slots or holes in a line. BEOs can be provided with a plane surface covering parts of the opening (baffles). The plane surface could be provided with slots or holes to make a perforated surface. The intention of these surfaces is to improve air distribution over the opening, increase the velocities in the openings, or reduce exhaust flow rate (see *Different Forms and Boundaries Relative to Other Types*). A BEO could, instead of being one opening, consist of many small openings close to each other in the same plane. The opening plane for a BEO is most often straight, but it could be curved to fit the process or the tool.

Most BEOs are situated at the end of a tube, but there are also basic openings situated in walls. BEOs can be used for nearly all kinds of sources, but are usually used for point sources. Use for line or area sources usually demands flexible or movable exhausts, or a slot placed along the line source or along the sides of an area source, or a very large (circular or rectangular) opening placed close to the source. A high flow rate is needed to get efficient exhaust in many cases.

BEOs are used as separate exhausts, as parts of other exhaust systems, or in combined supply and exhaust systems. In these cases there are normally specific design procedures.

Basic exhaust openings are not recommended for use when the distance between source and hood is great, since it is easy for contaminants to spread outside the reach of the exhaust due to the sharp decrease in velocity with increasing distance. It is usually better to use partially closed systems.

Principle

The main principle in designing and operating BEOs is to generate an air velocity at or near the contaminant source or contaminant dispersion direction. This air velocity should be higher than the velocity of the contaminant and any disturbing cross-drafts and should be directed into the exhaust opening. The contaminant is thus transported from the source into the hood. The air velocity outside an opening decreases sharply as distance from the opening increases,

therefore, the exhaust opening should be as close as possible to the source. The exhaust flow rate must be larger than the source's volume generation rate.

Adjacent surfaces can act as barriers to airflow from uncontaminated areas and diminish the necessary flow rate. To prevent suction of air from the uncontaminated region behind the hood, the openings can be provided with flanges, which should be as large as possible. Another variation is to place the source close to surrounding surfaces.[16,17] BEOs can also be integrated into tools, e.g., as part of a frame for automatic welding by spot heating or as small holes in the grinding surface of a portable grinding machine (rotating or oscillating).

BEOs consisting of open tube or duct ends can be connected directly to a source. In principle, these could be called closed systems, since their main function is to exhaust contaminants directly from the source, which is enclosed in the duct. However, they are usually regarded as basic exhausts since they function as such when not connected to the source.

BEOs are also used as exhaust openings in closed volumes or as parts of exhaust systems for different supply systems (Section 10.3). In these cases, it is not the velocity distribution in front of the exhaust opening that is of importance, it is the airflow rate. These applications are described elsewhere (Section 10.4).

Figure 10.10 shows velocity contours outside plain circular openings and outside circular openings with flanges. Figure 10.11 illustrates what happens to the velocity contour outside a plain circular opening when it is placed on a surface. Velocity contours and the streamlines of freestanding circular openings

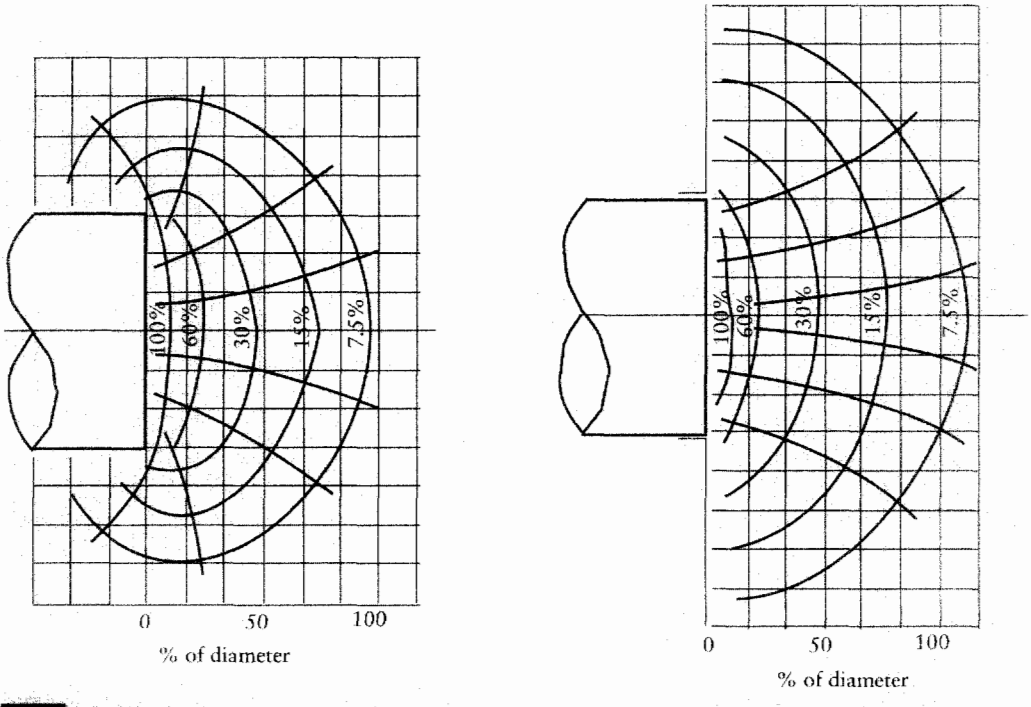

FIGURE 10.10 Velocity field outside circular (*left*) and flanged circular (*right*) opening. Velocities are given on a plane of the diameter and in percentages of opening velocity.[10,18]

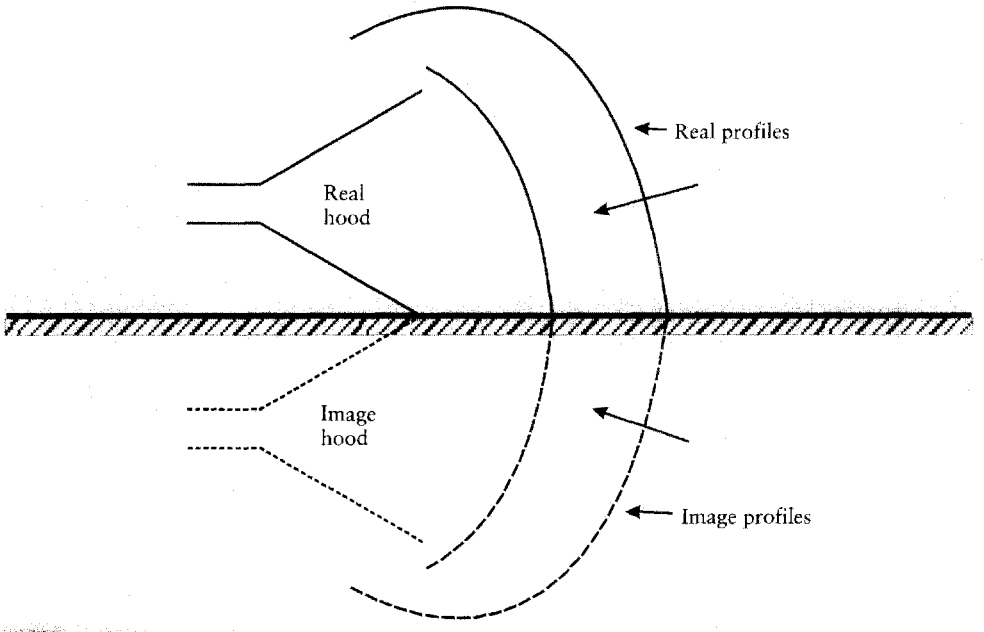

FIGURE 10.11 Influence of adjacent surface on velocity profile for circular opening.[19]

and a circular opening close to a corner are compared in Fig. 10.12. Figure 10.13 shows centerline velocities for circular, flanged openings according to different equations along with some experimental measurements.

Applicability of Sources

BEOs are most often used for point sources or small line or surface sources. See Chapter 7 for descriptions of sources. BEOs are sometimes used for lines or surfaces when the source is moving along the line or on the surface. This naturally demands the exhaust to move with (or be moved with) the source movements (e.g., during painting or seam welding). They have also been used for side suction from baths and tanks[22] and these exhausts are usually called rim exhausts see *Rim Exhausts*. However, for these sources push-pull systems (Section 10.4.3) are often more efficient. Side hoods can also be used, e.g., when molten metal is poured; however, in these cases an enclosed exhaust is more efficient.

BEOs can be used for both warm and cold sources depending on available space. When used for warm sources (e.g., welding fumes or fumes from pouring molten metal) it is much better (usually necessary) to place the exhaust above the source, since the buoyancy force is strong enough to counteract an exhaust flow from below or on the side. See Chapter 7.5 for descriptions of airflow from thermal sources. Sometimes a source could make the contaminants move first upward and when reaching the rim move downward (e.g., during degreasing operations). Usually processes release contaminants in one main direction and the exhaust must be placed in a way that does not try to counteract these natural forces. Whenever possible, the

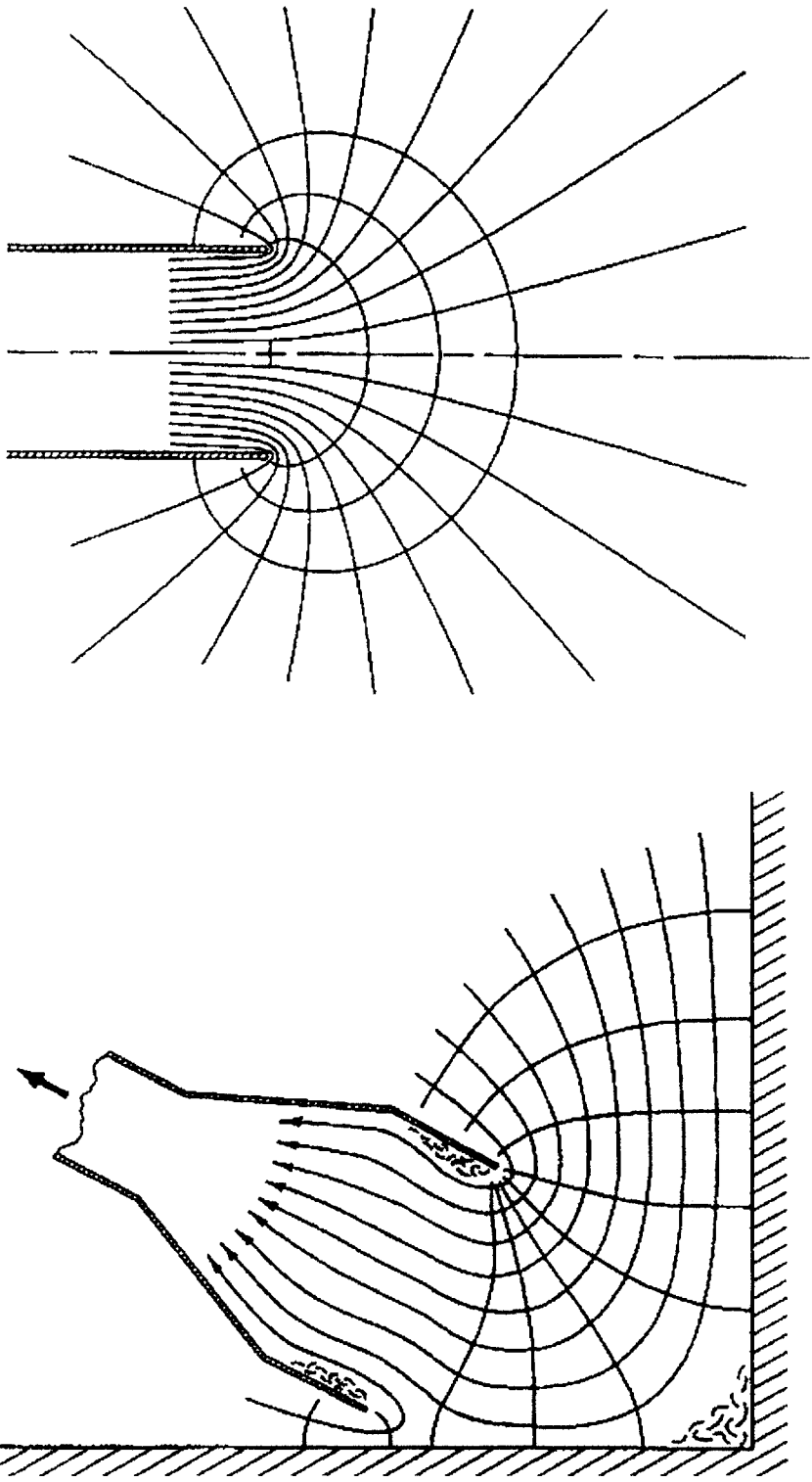

FIGURE 10.12 Comparison of streamlines and velocities outside a circular opening when it is freely suspended and when it is close to an angled wall.[20]

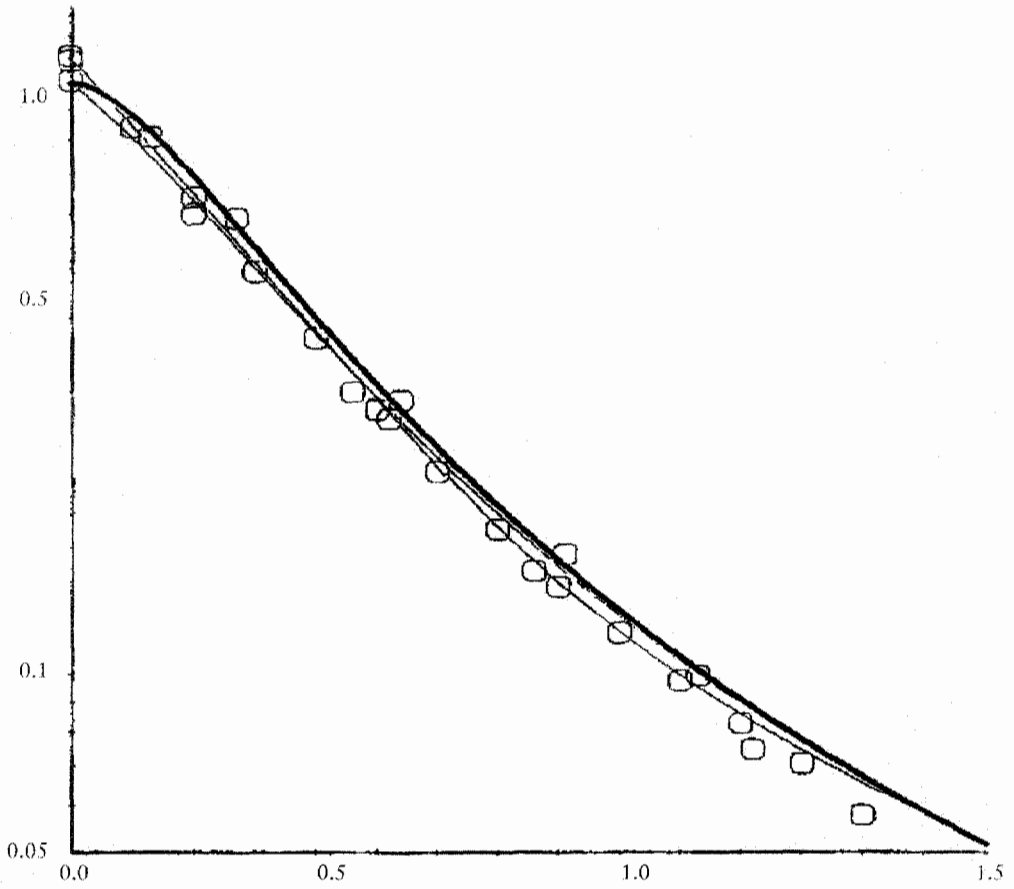

FIGURE 10.13 Velocity changes on centerline outside a flanged circular opening. Vertical axis is nondimensional velocity (real velocity divided by opening velocity) and horizontal axis is nondimensional distance (real distance divided by opening diameter). The lines are drawn according to different formulas and the circles are measured values.[21]

air velocity of the exhaust should have the same direction as that of the contaminant generation (e.g., grinding).

In addition to the advantages of having the exhaust air move in the direction of the generation and the necessity of having a high enough velocity, the exhaust flow rate must be larger than the airflow rate induced by the contaminant generation. This induced flow rate is often many times larger than the flow rate of the generated contaminant (Chapter 7).

For exhausts connected directly to the source, the main problem is to get a tight connection between the exhaust and the source. A common example is exhaust of contaminants from car exhaust pipe when the car is inside a building. In this case, the flow rate must be high enough to transport all generated car exhausts and the connection of the exhaust opening to the tailpipe must be tight enough to prevent car exhaust gases from entering the room air. Other examples are the exhaust around the handle used when pumping gasoline, the exhaust from a lathe machine with a ready-made exhaust connection,[10] and the exhaust from an electric arc furnace.

Different Forms and Boundaries Relative to Other Types

As mentioned above, a basic exhaust can be of nearly any shape with the most common being round, rectangular, or slot openings, with or without flanges. Openings in walls could be said to have the largest flanges. There also are exhausts consisting of multiple holes or perforated plates in a wall or ceiling or floor or table. The latter ones (holes in a floor or table) often have special designs and are treated separately in a later section. The exhaust opening can be tapered to have both a large opening area and a smooth velocity increase inside the opening to the connecting duct, resulting in lower pressure loss. As mentioned above, exterior hoods can be connected directly to a process or to equipment. These have some similarity to industrial vacuum cleaners.

A separate description also exists for low volume high velocity (LVHV) systems. Some of these are similar to BEOs, but they are used in a different way from basic openings. One difference is that BEOs have lower air velocities in the openings than LVHV systems, usually less then 15–20 m s^{-1} and more than 75 m s^{-1}, respectively. Another is that basic openings have opening areas larger than 0.01 m^2, while LVHV openings have areas less than 0.001 m^2. Intermediate systems exist, such as the small circular exhaust opening around a welding rod or the exhaust in the surface of a portable grinding machine.

Specific Issues

The specific problems for BEOs are mostly related to the specific processes at which they are used. One problem that does not, directly, depend on the process is the use of the exhaust system. If an exhaust is not used, naturally it cannot remove contaminants. Although BEOs are less efficient than total or partial booths, their use is still justified. When the location of the BEO is not perfect, higher flow rates are usually required for contaminant control. However, it is better to use this type of hood than to have no local exhaust.

Another issue is the velocity distribution in the opening. Some equations describing the flow field outside a BEO presume that all points in the opening have the same velocity, equal to the flow rate divided by the opening area (*Design Equations*). This is usually a reasonable assumption for design purposes, especially if the opening is provided with baffles to get a smooth velocity distribution. In reality, the velocity distribution in an opening could be quite uneven, which can affect both the velocity distribution outside and the efficiency of the exhaust.

Some other problems include clogging of the opening with exhausted material and an opening shape that is not chosen to fit the process which results in use of higher flow rate than necessary, thus increasing the cost of the process. Other problems are described in *Design Considerations*.

Design Equations and/or Parameters

The first step in designing an exhaust hood is to select the geometry of the hood. As described above, the hood should enclose the process as much as possible. Where enclosures are not possible the hood should be located as close as possible to the source. The next step is to select an appropriate hood flow rate. The most common methods are

A: Calculating contaminant and exhaust velocities at all points in the flow field.

B: Use of capture velocity and centerline velocity.
C: Use of "rules of thumb."

For processes where gases or vapors are generated it is often possible to calculate both the velocity and flow rate of the contaminant. This could be done with different degrees of accuracy by using chemical and physical principles. These are described generally in Perry et al.[22] and Reid et al.[23] Computer programs also exist that calculate source strengths for different kinds of processes and process equipment. By combining these values with the velocity distribution outside an exhaust it is possible to choose the appropriate exhaust airflow rate.

For processes that generate particles (dust, mists, fumes, etc.) there is no general procedure to calculate the contaminant's velocity and flow rate. Data and figures exist for some processes describing the contaminant generation process; however, for dust-generating processes Method B or C is often used.

Method A: Calculating Contaminant and Exhaust Velocities at All Points in the Flow Field Local exhaust hoods are used to remove contaminants at the point of generation before they escape into the workplace air. The efficiency of any local exhaust system is greatly affected by the flow field generated by the exhaust opening. Therefore, accurate modeling of this flow field is essential for reliable predictions. However, solving the airflow field is a formidable task and often must be done numerically.

Potential Flow Airflow fields generated by unobstructed exhaust openings can be satisfactorily described with potential flow models. In these models the flow is idealized by assuming it is inviscid and irrotational, which greatly simplifies the mathematical treatment. This is possible because viscous effects occur appreciably only along solid surfaces and in the region close to the opening. These viscous boundary layers have little influence on the flow field of unobstructed exhaust openings and can therefore be ignored. Moreover, air velocities near exhaust openings in industrial applications are usually so low that the flow can be assumed incompressible.

For an irrotational, incompressible, and frictionless fluid flow there exists a scalar velocity potential ϕ such that the velocity vector V is

$$V = \nabla\phi, \tag{10.2}$$

or for a steady incompressible flow the continuity equation is

$$\nabla \cdot V = 0. \tag{10.3}$$

Substituting the conditions imposed by continuity gives Laplace's equation:

$$\nabla \cdot V = \nabla \cdot \nabla\phi = \nabla^2\phi = 0. \tag{10.4}$$

This equation, taken in conjunction with appropriate boundary conditions, can be solved analytically or numerically to give the ideal flow field.

The Stream Function Stream functions are defined for two-dimensional flow and for three-dimensional axial symmetric flow. The stream function can be used to plot the streamlines of the flow and find the velocity. For two-dimensional flow the velocity components can be calculated in Cartesian coordinates by

$$u = -\frac{\partial \psi}{\partial y}$$
$$v = \frac{\partial \psi}{\partial x}, \tag{10.5}$$

and for axisymmetric flow in spherical coordinates:

$$u_r = \frac{1}{r^2 \sin\theta}\frac{\partial \psi}{\partial r}$$
$$u_\theta = \frac{1}{r \sin\theta}\frac{\partial \psi}{\partial r}, \tag{10.6}$$

where u and v are the velocity vectors in the x and y directions, respectively, ψ is the stream function, r is the distance from the origin, and θ is the polar angle measured from the x-axis.

Two-Dimensional Flow

Line Sink The velocity induced by a line sink is purely radial and is given in cylindrical coordinates by

$$u_r = -\frac{q/L}{k\pi r}, \tag{10.7}$$

where q/L is the exhaust flow rate per unit length, r is the radius of a cylindrical control volume surrounding the sink, and k is a constant which has a value 2 for a line sink withdrawing air from the whole space and 1 for a flanged slot. The negative sign means that flow is toward the sink.

The stream and potential functions are

$$\psi = \frac{q}{2\pi L}\theta \tag{10.8}$$

and

$$\phi = -\frac{q}{k\pi L}\ln r. \tag{10.9}$$

Flanged Slot Slots can be thought of as rectangular hoods with a very large aspect ratio (the ratio of slot length, L, to its width, W). Anastas and Hughes[24] have shown that rectangular exhaust openings behave like slots when the aspect ratio is greater than 100. Usually an aspect ratio greater than 5 is used to define a slot.[25] Slots are an important class of exhaust opening and they are typically used as rim exhaust on large tanks or welding exhaust hoods in high-velocity/low-volume local ventilation systems.

The analytical solution for an infinitely flanged slot can be obtained by assuming that the inlet is composed of elemental point sinks.[26] The velocity field of an infinitely flanged slot can be obtained by assuming the velocity to be uniformly distributed across the opening. The contribution to the velocity potential at point (x, y) due to the elemental line sink of length $d\zeta$ and located at $(0, \zeta)$ is given by

$$d\phi = \frac{q}{\pi L W}\ln r\, d\zeta, \tag{10.10}$$

where W is the width of the slot, L is the length of the slot, and r is the distance between the elemental line sink and point (x, y) which is calculated by Fig. 10.14.

$$r = (x^2 + (y - \zeta)^2)^{1/2} \tag{10.11}$$

The total potential at point (x, y), due to all the elements in the flanged opening, is the sum of all such elements and is given by the integral

$$\phi = -\int_{-W/2}^{W/2} \frac{q}{\pi L W} \ln r d\zeta = -\int_{-W/2}^{W/2} \frac{U_0}{\pi} \ln r d\zeta, \tag{10.12}$$

where U_0 is the mean face velocity. The velocity components can be obtained by using Eq. (10.2):

$$u = \frac{\partial \phi}{\partial x} = -\frac{\partial}{\partial x} \int \frac{U_0}{\pi} \ln r d\zeta = -\int_{-W/2}^{W/2} \frac{U_0}{\pi} \frac{x}{x^2 + (y - \zeta)^2} d\zeta \tag{10.13}$$

and

$$v = \frac{\partial \phi}{\partial y} = -\frac{\partial}{\partial y} \int \frac{U_0}{\pi} \ln r d\zeta = -\int_{-W/2}^{W/2} \frac{U_0}{\pi} \frac{y - \zeta}{x^2 + (y - \zeta)^2} d\zeta \ . \tag{10.14}$$

Integrating Eqs. (10.13) and (10.14) gives the velocity components in the x direction:

$$u(x, y) = -\frac{U_0}{\pi} \left[\arctan\left(\frac{y + W/2}{x} \right) - \arctan\left(\frac{y - W/2}{x} \right) \right], \tag{10.15}$$

and in the y direction:

$$v(x, y) = -\frac{U_0}{2\pi} \ln \left[\frac{\left(y + \frac{W}{2} \right)^2 + x^2}{\left(y - \frac{W}{2} \right)^2 + x^2} \right] . \tag{10.16}$$

The negative sign indicates that the flow is in the negative x and y directions, i.e., toward the hood face. The applicability of this model was verified by Anastas and Hughes[24] and Drkal,[26] who compared theoretical to experimental centerline velocities and found close agreement.

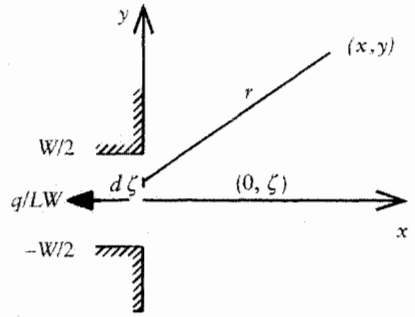

FIGURE 10.14 Coordinate system used in the modeling of a flanged slot.

The velocity contours calculated by this analytical model are shown in Fig. 10.15. The velocities are expressed as parts of the face velocity. In the same figure, velocities produced by the line sink model are also plotted. Near the exhaust opening the line sink model overestimates velocities but further from the opening the agreement is good: the experimental velocities are almost identical to the velocities given by the analytical model at distances $x/W > 2$ from the opening.

The analytical centerline velocities were calculated from

$$\frac{U}{U_0} = \frac{2}{\pi}\arctan\left(\frac{W}{2x}\right), \tag{10.17}$$

which is obtained from Eq. (10.15) by setting $y = 0$. It is interesting to note that when x/W is large, the centerline velocity in Eq. (10.17) can be approximated by the MacLaurin series expansion

$$\frac{U}{U_0} = \frac{W}{x\pi}, \tag{10.18}$$

which is the same as obtained by the simple line sink model.

Plain Slot The analytical solution for the slot in the two-dimensional case can be obtained by conformal transformation:[27]

$$z = e^w + w + 1, \tag{10.19}$$

where $w = \phi + i\psi$ is a complex function of the complex variable $z = x + iy$:

$$x + iy = e^{\phi}e^{i\psi} + \phi + i\psi + 1 = e^{\phi}(\cos\psi + i\sin\psi) + \phi + i\psi + 1. \tag{10.20}$$

Separating the real and imaginary parts gives

$$x = e^{\phi}\cos\psi + \phi + 1 \tag{10.21}$$

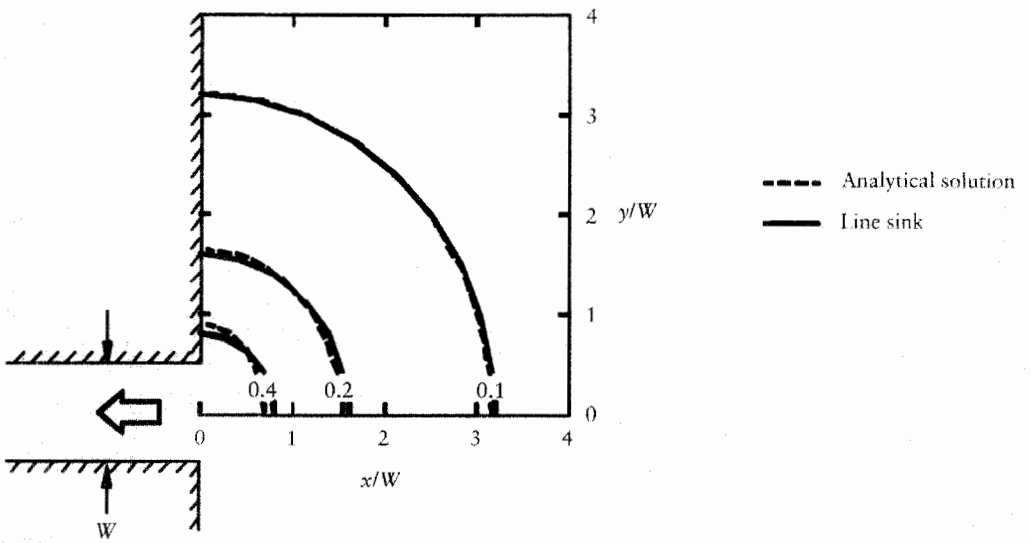

FIGURE 10.15 Analytical and line sink velocity contours for a flanged slot.

and

$$y = e^{\phi}\sin\psi + \psi. \tag{10.22}$$

These equations cannot be used directly, and numerical methods are needed to compute the velocity components. The velocity components can be found by implicit differentiation and using an iterative technique.[24]

Figure 10.16 shows the calculated velocity contours as a fraction of the average velocity in the channel (average face velocity). In addition, velocities obtained from the line sink model are plotted. It can be seen that, compared to the line sink model, the calculated contours are displaced somewhat in the positive x direction, with the greatest relative difference near the exhaust opening and with decreasing relative difference as the dimensionless distance x / W increases.

Three-Dimensional Flow

Point Sink A point sink is defined as a point in space at which the fluid is continuously and uniformly drawn off. The radial velocity into the sink at a distance r from the sink is, in spherical coordinates,

$$u_r = -\frac{q}{k\pi r^2}, \tag{10.23}$$

where q is the flow rate through the sink and k is 2 for a point sink in a plane (infinitely flanged opening) and 4 for an unflanged opening. Since q and r are positive, the negative sign indicates that the fluid flows toward the sink. Due to symmetry, the angular velocity $u_\theta = 0$.

$$\phi = \frac{q}{k\pi}\frac{1}{r} \tag{10.24}$$

$$\psi = -\frac{q}{k\pi}\cos\theta. \tag{10.25}$$

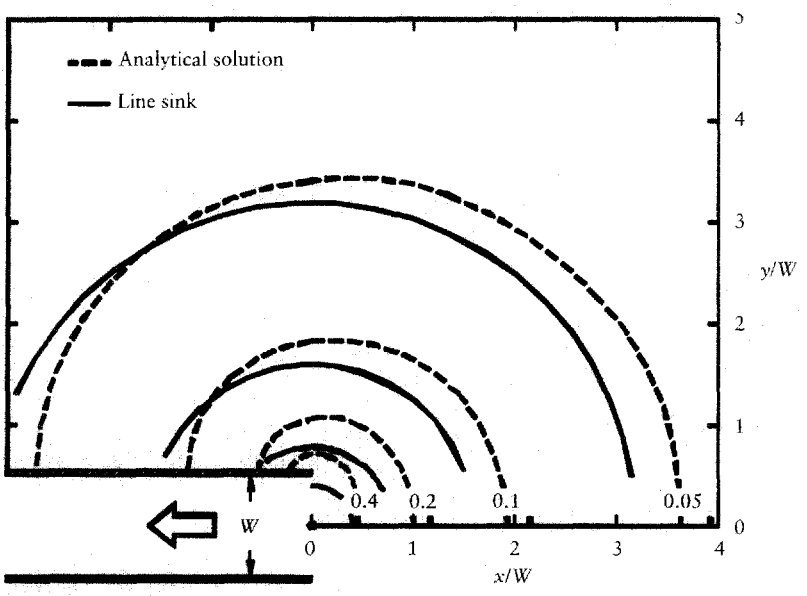

FIGURE 10.16 Velocity contours for the upper half of a plain slot by analytical and line sink solutions.

The potential (Eq. 10.24) and stream (Eq. 10.25) functions for the point sink provide a simple theoretical representation of the velocity variations near real suction openings. Close to the origin the velocity for the point sink approaches infinity and deviates considerably from the actual fluid velocities. However, at distances greater than approximately one diameter from the finite opening, the velocities given by the sink model are reasonable approximations of the true values.

When calculating the velocity potential at a point near an infinitely flanged exhaust opening, the hood face can be assumed to be divided into many area sinks, each of them contributing to the potential at a point in space. The overall velocity potential is then obtained by integrating over the inlet area. The velocity component in the x direction, for example, is then

$$U = \frac{\partial \phi}{\partial x} = \int\int_A \frac{\partial}{\partial x}\left(\frac{q}{2\pi A r}\right) dA, \tag{10.26}$$

where q is the exhaust flow rate, A is the area of the exhaust opening, and r is the distance between a point in space where the velocity is calculated and the elemental area dA at the exhaust opening.

Flanged Rectangular Opening The flow field for an infinitely flanged rectangular opening was first solved in closed form by Tyaglo and Shepelev.[28] In this solution the velocity in the x direction is calculated using the coordinate system shown in Fig. 10.17:

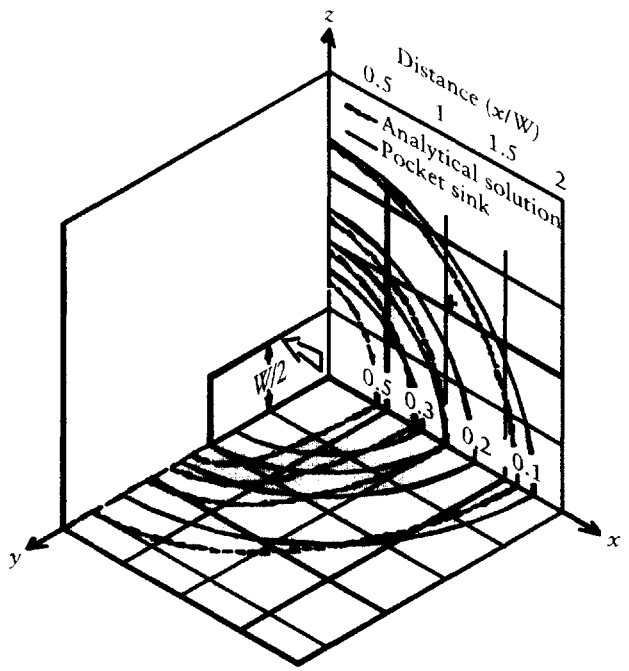

FIGURE 10.17 Velocity contours in symmetry plane for a flanged rectangular opening with an aspect ratio of 2:1 by analytical and point sink methods.

$$u(x, y, z) = -\frac{U_0}{2\pi}\left[\arctan\frac{(y+a)(z+b)}{x\sqrt{(y+a)^2+(z+b)^2+x^2}} - \arctan\frac{(y-a)(z+b)}{x\sqrt{(y-a)^2+(z+b)^2+x^2}} - \arctan\frac{(y+a)(z-b)}{x\sqrt{(y+a)^2+(z-b)^2+x^2}} + \arctan\frac{(y-a)(z-b)}{x\sqrt{(y-a)^2+(z-b)^2+x^2}}\right] \tag{10.27}$$

and in the y direction:

$$v(x, y, z) = -\frac{U_0}{2\pi}\ln\left[\frac{z+b+\sqrt{x^2+(y-a)^2+(z+b)^2}}{z+b+\sqrt{x^2+(y+a)^2+(z+b)^2}} \cdot \frac{z-b+\sqrt{x^2+(y+a)^2+(z-b)^2}}{z-b+\sqrt{x^2+(y-a)^2+(z-b)^2}}\right] \tag{10.28}$$

and in the z direction:

$$w(x, y, z) = -\frac{U_0}{2\pi}\ln\left[\frac{y+a+\sqrt{x^2+(y+a)^2+(z-b)^2}}{y+a+\sqrt{x^2+(y+a)^2+(z+b)^2}} \cdot \frac{y-a+\sqrt{x^2+(y-a)^2+(z+b)^2}}{y-a+\sqrt{x^2+(y-a)^2+(z-b)^2}}\right] \tag{10.29}$$

where $a = L/2$ is the half-length and $b = W/2$ is the half-width of the opening.

Along the hood centerline ($y = 0$ and $z = 0$), the velocity components in the y and z directions disappear and the velocity can be calculated by

$$\frac{U}{U_0} = \frac{2}{\pi}\arctan\frac{LW}{2x\sqrt{4x^2+L^2+W^2}} . \tag{10.30}$$

Flanged Circular Opening The velocity components for an infinitely flanged circular opening with a radius of R are[29]

$$u(r, x) = -\frac{U_0}{2\pi}\int_0^R\int_0^{2\pi}\frac{lx}{(x^2+r^2+l^2+2rl\cos\alpha)^{3/2}}d\alpha dl \tag{10.31}$$

$$v(r, x) = -\frac{U_0}{2\pi}\int_0^R\int_0^{2\pi}\frac{l(r+l\cos\alpha)}{(x^2+r^2+l^2+2rl\cos\alpha)^{3/2}}d\alpha dl . \tag{10.32}$$

The velocities can be calculated by integrating Eq. (10.31) and (10.32) numerically. To perform the calculations, the exhaust opening is divided into several area sinks and their effect on velocity at any point upstream of the exhaust opening is obtained by summing. For the centerline ($r = 0$), Eq. (10.32) yields along the x axis

$$\frac{U}{U_0} = 1 - \frac{\frac{x}{D}}{\sqrt{0.25+\left(\frac{x}{D}\right)^2}} , \tag{10.33}$$

where $D\,(= 2R)$ is the diameter of the opening and x is the distance from the opening (Fig. 10.18).

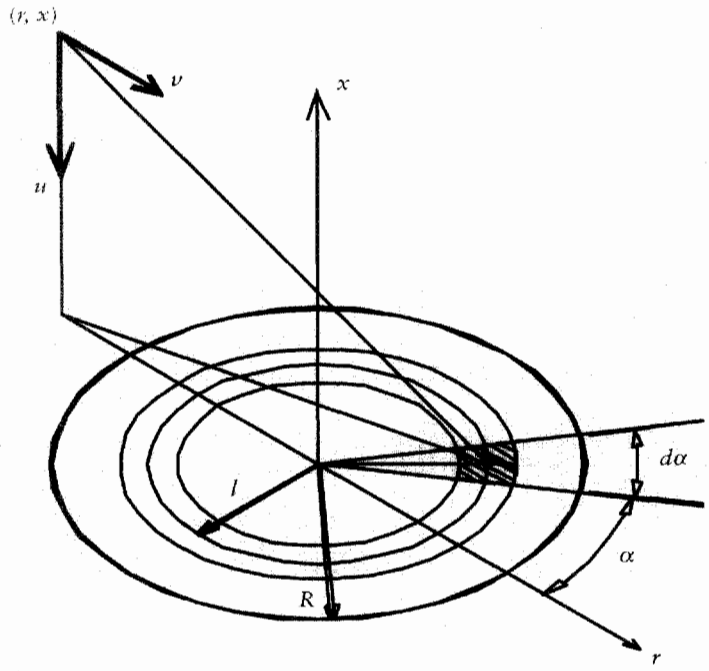

FIGURE 10.18 Geometry for a flanged circular hood.

Flanged Elliptical Opening The potential flow solution for an elliptical aperture in an infinite wall with a constant potential across the hood face is given by Lamb[30] as

$$\Phi = \mp \frac{Q}{4\pi} \int_0^{\lambda} \frac{d\lambda}{[(a^2+\lambda)(b^2+\lambda)\lambda]^{1/2}} \tag{10.34}$$

where λ is the positive root of

$$\frac{x^2}{a^2+\lambda} + \frac{y^2}{b^2+\lambda} + \frac{z^2}{\lambda} = 1. \tag{10.35}$$

Equation (10.34) can be solved to give the velocity components in the x, y, and z directions using the same coordinate system shown in Fig. 10.17:[31]

$$V_x = \frac{dx}{dt} = \frac{\partial \phi}{\partial x} = \frac{Qx(a^2+\lambda)^{3/2}(b^2+\lambda)^{3/2}\lambda^{1/2}}{2\pi E} \tag{10.36}$$

$$V_y = \frac{dy}{dt} = \frac{\partial \phi}{\partial y} = \frac{Qy(a^2+\lambda)^{1/2}(b^2+\lambda)^{3/2}\lambda^{3/2}}{2\pi E} \tag{10.37}$$

$$V_z = \frac{dz}{dt} = \frac{\partial \phi}{\partial z} = \frac{Qz(a^2+\lambda)^{3/2}(b^2+\lambda)^{1/2}\lambda^{3/2}}{2\pi E}, \tag{10.38}$$

where

$$E = x^2\lambda^2(b^2+\lambda)^2 + y^2\lambda^2(a^2+\lambda)^2 + z^2\lambda^2(a^2+\lambda)^2(b^2+\lambda)^2 \tag{10.39}$$

and x is perpendicular to the hood face, y is parallel to the hood length, and z is parallel to the hood width. The hood airflow is q; a is the length of the major axis and b is the length of the minor axis of the modeled ellipse. Laboratory measurements in the x, y plane ($z = 0$) showed Eq. (10.37) to be a good predictor of y velocity. Agreement between measured velocity and velocity predicted by Eq. (10.36) was not as good and the authors provide an empirical correction for Eq. (10.36). The agreement between predicted and measured x velocity changed as a function of location in front of the hood, with better agreement further from the hood face. Assuming constant potential on the hood face results in predicted velocities equal to one-half the average velocity in the center of the hood face and infinite velocities at the edges. Experimental measurements indicate that potential flow underpredicts velocity at the edges of the hood and overpredicts near the center. An empirical factor was determined to force the slope of the predicted versus measured x velocity to be equal to 1. The factor is a function of λ, which in turn is a function of x, y, and z locations. Equation (10.36) is replaced with

$$V_x = \frac{dx}{dt} = \frac{\partial \phi}{\partial x} = \frac{Qx(a^2 + \lambda)^{3/2}(b^2 + \lambda)^{3/2}\lambda^{1/2}}{2\pi E} \cdot \frac{\ln\lambda - 11.8}{-10.7} \quad (10.40)$$

Superposition of Flows Potential flow solutions are also useful to illustrate the effect of cross-drafts on the efficiency of local exhaust hoods. In this way, an idealized uniform velocity field is superpositioned on the flow field of the exhaust opening. This is possible because Laplace's equation is a linear homogeneous differential equation. If a flow field is known to be the sum of two separate flow fields, one can combine the harmonic functions for each to describe the combined flow field. Therefore, if ϕ_1 and ϕ_2 are each solutions to Laplace's equation, $A\phi_1 + B\phi_2$, where A and B are constants, is also a solution. For a two-dimensional or axisymmetric three-dimensional flow, the flow field can also be expressed in terms of the stream function.

Flow Past a Point Sink A simple potential flow model for an unflanged or flanged exhaust hood in a uniform airflow can be obtained by combining the velocity fields of a point sink with a uniform flow. The resulting flow is an axially symmetric flow, where the resulting velocity components are obtained by adding the velocities of a point sink and a uniform flow. The stream function for this axisymmetric flow is, in spherical coordinates,

$$\Psi = \frac{U_s}{2}(s \sin\Theta)^2 - \frac{q}{k\pi}\cos\Theta, \quad (10.41)$$

where s is the distance from the origin and U_S is the velocity of the uniform flow. The model does not take into consideration the location of the unflanged exhaust duct relative to the streaming flow. However, for the flanged opening the only physically meaningful orientation is with the hood axis perpendicular to the flow.

The addition of a uniform flow with the sink flow creates a dividing streamline (Fig. 10.19), so that the contaminants released inside the dividing streamline would be captured while the contaminants released outside would escape. The

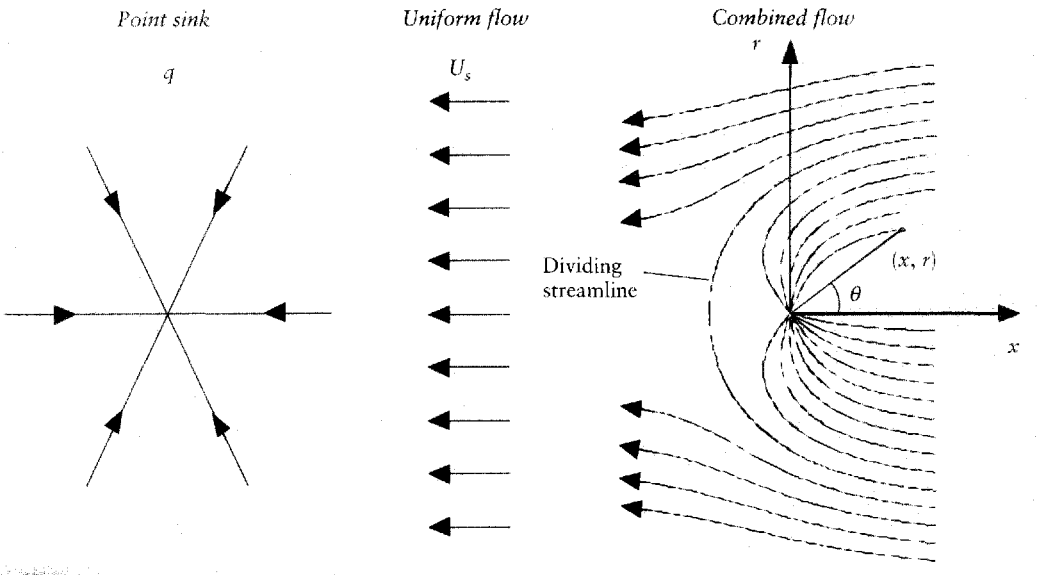

FIGURE 10.19 Combination of a point sink flow field with a uniform flow field.

stream function has value $\Psi = q/(k\pi)$ at the dividing streamline and so its location can be found by expressing Eq. (10.41) in polar coordinates:

$$\frac{q}{k\pi} = \frac{U_s}{2} r^2 - \frac{q}{k\pi} \frac{x}{(x^2 + r^2)^{1/2}} . \tag{10.42}$$

This can be solved for $r(x)$, giving[32]

$$r(x) = \left[\frac{2q}{k\pi U_s} - \frac{x^2}{2} + \frac{xq}{k\pi U_s} \left(\left(\frac{k\pi U_s x}{2q} \right)^2 + \frac{2k\pi U_s}{q} \right)^{1/2} \right]^{1/2} . \tag{10.43}$$

This solution gives unequivocally the effective control range of both unflanged and flanged openings when the exhaust flow rate and velocity of the idealized cross-draft are known. The distance from the hood opening to the dividing streamline for a hood in uniform flow perpendicular to its axis is thus

$$r(0) = \left(\frac{2q}{k\pi U_s} \right)^{1/2} . \tag{10.44}$$

This type of dependence of capture efficiency on the exhaust flow rate and cross-draft velocity has also been seen by Fletcher and Johnson[8] who determined the capture efficiency of a flanged square exhaust hood in a cross flow.

Semi-Theoretical and Empirical Velocity Fields Since the use of formulas to calculate the velocities outside an arbitrary opening could be very tedious, only some examples of these formulae are given. These calculations are best done on computers and there are some dedicated programs to calculate and visualize the flow fields outside exhaust openings. There could sometimes be problems when calculating the velocity field outside an opening close to

one or more surfaces. For example, a BEO placed near a corner with the source either in the corner or on one surface may be easier to calculate by using graphical addition than using computer programs.[19,20]

Circular Flanged Openings[21] This velocity field has a circular symmetry and it suffices to calculate the velocity directed into the opening:

$$v = \frac{\epsilon^2}{1 + \frac{1-\epsilon^2}{2\cdot\epsilon}\cdot \ln\frac{1+\epsilon}{1-\epsilon}}\ , \tag{10.45}$$

where v is the nondimensional velocity, ln is the natural logarithm, and

$$\epsilon = \frac{1}{\sqrt{z^2+(r+0.5)^2}+\sqrt{z^2+(r-0.5)^2}}\ , \tag{10.46}$$

where z is the nondimensional distance (the real distance divided by the opening diameter) along the center axis from the opening plane and r is the nondimensional perpendicular distance from the center axis defined as

$$r = \sqrt{x^2+y^2}\ , \tag{10.47}$$

where x and y are the nondimensional (real distance divided by opening diameter) distances from the center axis along two perpendicular axes parallel to the opening plane.

The equations for calculating the individual velocity components in the x and y directions are given in the source,[21] where suitable forms for computer calculations are also given.

Rectangular Flanged Openings[21,33] The velocity fields for these openings must be calculated for each direction individually. Here v_x and v_y are the nondimensional velocities parallel to the opening plane and v_z is the nondimensional velocity perpendicular to the opening plane directed toward the opening plane:

$$\begin{aligned} v_x = &-\frac{1}{2\pi}\cdot\ln\left(\left[\sqrt{z^2+x_-^2+y_+^2}+y_+\right]\cdot\left[\sqrt{z^2+x_+^2+y_-^2}+y_-\right]\right) \\ &+\frac{1}{2\pi}\cdot\ln\left(\left[\sqrt{z^2+x_+^2+y_+^2}+y_+\right]\cdot\left[\sqrt{z^2+x_-^2+y_-^2}+y_-\right]\right) \end{aligned} \tag{10.48}$$

$$\begin{aligned} v_y = &-\frac{1}{2\pi}\cdot\ln\left(\left[\sqrt{z^2+y_-^2+x_+^2}+x_+\right]\cdot\left[\sqrt{z^2+y_+^2+x_-^2}+x_-\right]\right) \\ &+\frac{1}{2\pi}\cdot\ln\left(\left[\sqrt{z^2+y_+^2+x_+^2}+x_+\right]\cdot\left[\sqrt{z^2+y_-^2+x_-^2}+x_-\right]\right) \end{aligned} \tag{10.49}$$

$$v_z = -\frac{1}{2\pi} \cdot \left[\arctan \frac{x_+ \cdot y_+}{z \cdot \sqrt{z^2 + x_+^2 + y_+^2}} - \arctan \frac{x_- \cdot y_+}{z \cdot \sqrt{z^2 + x_-^2 + y_+^2}} - \arctan \frac{x_+ \cdot y_+}{z \cdot \sqrt{z^2 + x_+^2 + y_-^2}} + \arctan \frac{x_- \cdot y_+}{z \cdot \sqrt{z^2 + x_-^2 + y_-^2}} \right]. \tag{10.50}$$

The nondimensional velocity in the direction toward the opening is

$$v = \sqrt{v_x^2 + v_y^2 + v_z^2}, \tag{10.51}$$

where

$$x_+ = x + 0.5\sqrt{\frac{W}{L}} \qquad x_- = x - 0.5\sqrt{\frac{W}{L}}$$
$$y_+ = y + 0.5\sqrt{\frac{L}{W}} \qquad y_- = y - 0.5\sqrt{\frac{L}{W}} \tag{10.52}$$

and W and L are the extensions of the opening in the x and y directions, respectively, and x, y, and z are the nondimensional distances along the different axes and arctan is the arctangent function. The nondimensional distances are defined as the real distances divided by the square root of the opening area. The opening area is equal to W times L.

Flanged Slot Openings[21,33] The equations given above for rectangular flanged openings can be used or it is possible to use the following equations, except in the region near the slot ends:

$$\frac{V_x}{V_0} = -\frac{1}{2\pi} \cdot \ln \left[\frac{\left(X + \frac{W}{2}\right)^2 + Z^2}{\left(X - \frac{W}{2}\right)^2 + Z^2} \right] \tag{10.53}$$

and

$$\frac{V_z}{V_0} = \frac{1}{\pi} \cdot \left[\arctan\left(\frac{X + \frac{W}{2}}{Z}\right) - \arctan\left(\frac{X - \frac{W}{2}}{Z}\right) \right]. \tag{10.54}$$

Here V_x is the real velocity parallel to the opening plane, V_z is the real velocity perpendicular to the opening plane, and V_0 is the velocity in the opening. Z is the real distance from the opening, perpendicular to the opening plane, X is the distance from the center-plane parallel to the opening plane, W is the slot width, ln is the natural logarithm, and arctan is the arctangent function. Note that the velocity is independent of the slot length as long as the flow rate per unit length is constant.

Unflanged Circular, Rectangular, and Slot Openings For unflanged openings no explicit equations exist for the flow fields. However, it is possible to calculate the velocity field outside a specific BEO using computers. These

calculations are usually done using computational fluid dynamics (CFD).[34,35] Empirical values for an unflanged circular opening are shown in Fig. 10.10. In Figs. 10.20 and 10.21, empirical values for different unflanged rectangular openings (1:1, 1:2, 1:3, 1:10) are shown.

Method B: Use of Centerline Velocity Models with Capture Velocity
Capture velocity is defined as the velocity outside an exhaust necessary to capture the contaminant farthest away from the opening, when it has released its initial energy, and transport it into the opening. Selection of capture velocity depends on the source generation rate, speed, direction, and spread, as well as the effects of disturbances such as cross-drafts. Some problems with this design procedure are: generated contaminants usually do not have one single velocity, and the maximum release velocity is usually not known, nor are the temporal and spatial velocity distributions of the release. Some very approximate recommended capture velocities for different processes are given in Table 10.2.[37] It must be emphasized that these values have been the same since they were first published in the 1940s.[10,16] Few results regarding capture velocity have been published. Most of these studies have shown that capture velocity is not a simple tool to use.[8,38]

Many equations and figures of velocities outside basic exhaust openings have been published. There are some summaries and comparisons of equations.[34,39] These equations are empirical, theoretical, or semi-empirical descriptions, but they have all been thoroughly investigated and tested and they are reliable as long as the prerequisites coincide with the original descriptions.[7] Most equations describe the velocity along the center axis of different opening shapes.

Equations (10.23) and (10.7) have been used as the basis for centerline velocity estimates. Usually these equations are modified empirically depending on the shape of the exhaust. The results are specific equations for circular openings, square openings, rectangular openings with different side relations, slots, etc. Further modifications are made when the hoods are operated with flanges. The modifications for flanges result in lower flow rates for the same capture velocity or higher capture velocities with the same flow rate.

Equations for centerline velocity outside circular, square, rectangular and slot exhausts without and with flanges are presented in Table 10.3. These equations have been chosen to have as large an application as possible. For very detailed calculations it is recommended that the original research references be consulted.[37,39,40]

For exhausts with flanges it is assumed that the flanges have, in principle, infinite width. This is only achieved approximately for an opening in a wall. If the flange width is larger than the square root of the opening area[10,41] the centerline velocities have been found to be practically equal to the velocities for openings with an infinite flange. Velocities in regions other than on the centerline have not been examined in the same way, but velocities not far from the centerline should be influenced approximately in the same amount as on the centerline.

Method C: Rules of Thumb There are many "rules of thumb" for choosing BEOs. Many of these are connected to manufacturers, which

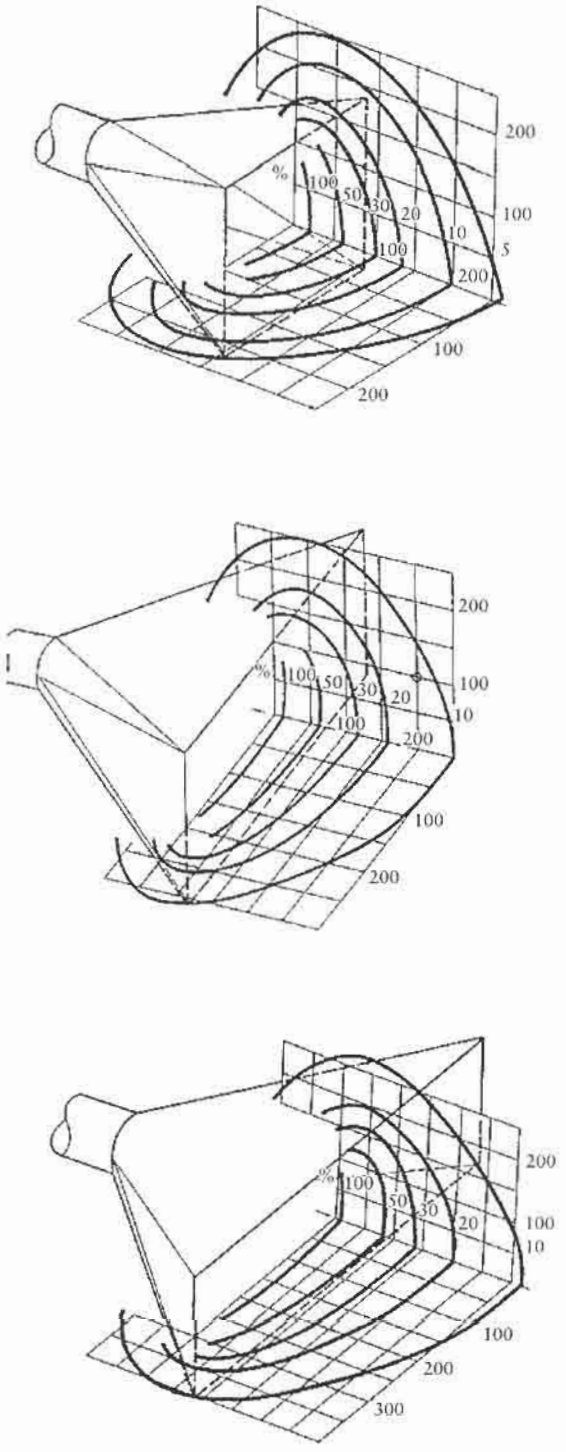

FIGURE 10.20 Velocity contours outside rectangular openings with different relations between the sides. From top to bottom: square, rectangular 1:2, rectangular 1:3. The velocities are in percentages of the opening velocity and for a plane in each side's centerline.[18]

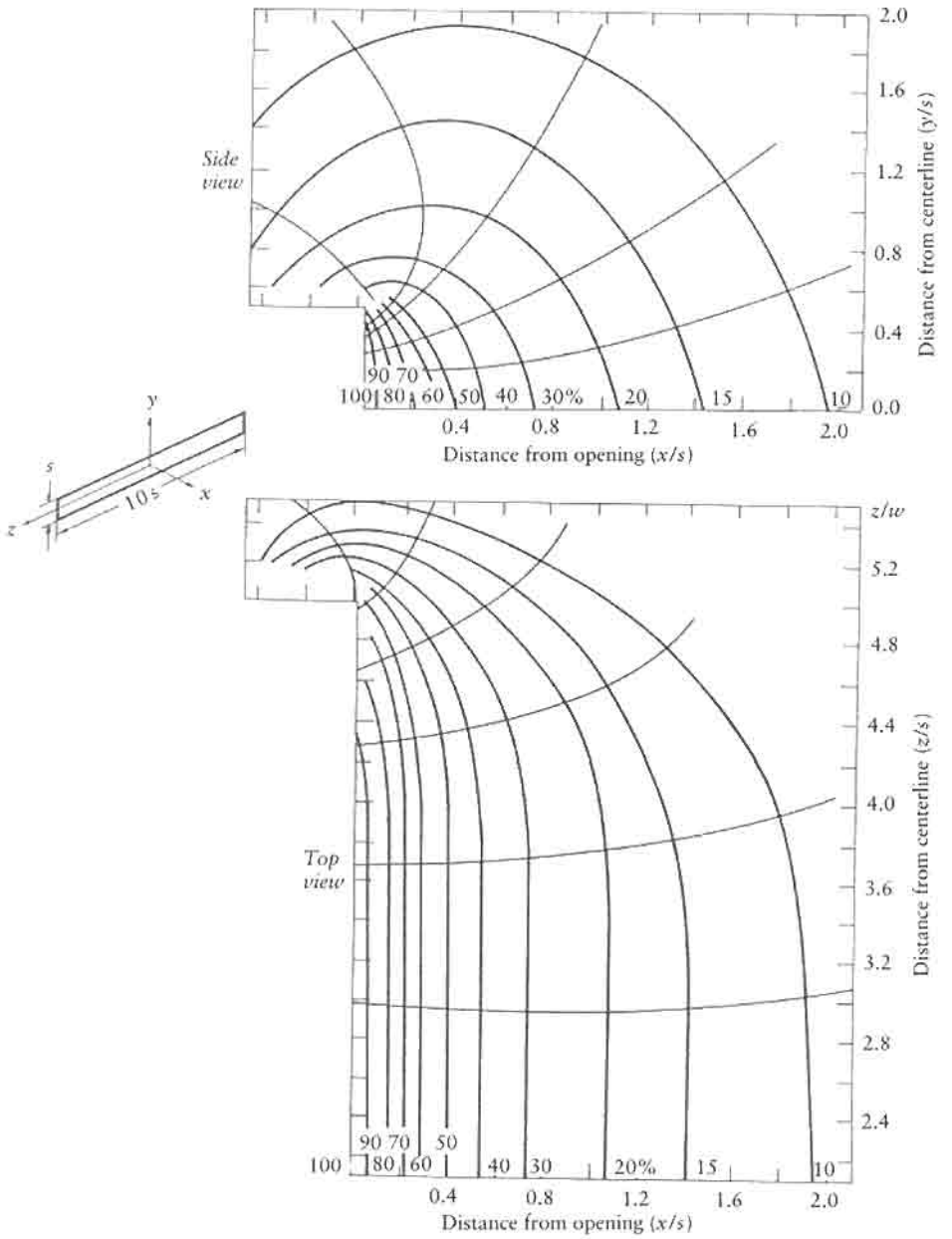

FIGURE 10.21 Velocity contours outside a slot or a rectangular opening with a side ratio of 1:10. The velocities are in percentage of the opening velocity. The top figure shows the velocities along the centerline of the short side. The bottom figure shows the velocities along the centerline of the long side.[36] (Reprinted by permission of John Wiley & Sons, Inc.)

through the years have gathered substantial experience regarding their own products. These rules are usually in the form of recommended airflow rates for specific openings used for specific processes at specified distances and places. The ACGIH[10] also provides design plates for a number of specific processes. Many of these design plates rely on the experience of users and also fall

TABLE 10.2 Capture Velocities for Various Industrial Processes

In each category below a range of capture velocities is shown. The proper choice of values depends on several factors. Lower end of range, 1. Room air currents minimal or favorable to capture, 2. Contaminants of low toxicity or of nuisance value, 3. Intermittent low production, 4. Large hood—large air mass in motion. Upper end of range, 1. Disturbing room air currents, 2. Contaminants of high toxicity, 3. High production or heavy use, 4. Small hood—local control only.

Condition of dispersion of contaminant	Examples	Capture velocities ($m\ s^{-1}$)
Released with practically no velocity into quiet air	Evaporation from tanks, degreasing, etc.	0.25–0.50
Released at low velocity into moderately still air	Spray booths, intermittent container filling, low-speed conveyor transfer, welding, plating, pickling	0.5–1.0
Active generation into zone of rapid air motion	Spray painting in shallow booths, barrel filling, conveyor loading, crushers	1.0–2.5
Released at high initial velocity into zone of very rapid motion	Grinding, abrasive blasting, tumbling	2.5–10

into the "rule of thumb" category. These data include recommended flow rates, expected pressure drops, and geometry specifications. Normally there are no specifications of the efficiency of the exhaust, even when it is possible to make such an evaluation.

The recommendation is to start with Method A, if possible. If this is not possible Method C can be used, but it is recommended that the equations given in Method A, together with approximations of the contaminant's properties, be used to check and/or verify the manufacturer's data. Method B could be used if no other alternative exists. If the design is for a noncommercial or nonstandard exhaust, it is not possible to use Method C and it is strongly recommended to use Method A, even if only approximate values are available.

Pressure Drop

The calculation of the pressure drop for a chosen exhaust depends on the calculation method (Chapter 9). Pressure drop is usually calculated as the product of a hood entry loss factor, F_h, and the dynamic pressure in the connecting duct, p_d. The p_d is expressed as $\rho \cdot v^2/2$, where ρ is the air density and v is the air velocity in the duct. Some common hood entry loss factors are given in Table 10.4.[10,16,36]

The design equations for pressure drops can also be used for evaluation procedures (Section 10.5).

10.2.2.3 Rim Exhausts

General

Rim exhausts are a specific application of slot hoods, which in turn are a type of exterior or capture hood. Rim exhausts are slot hoods placed along the rim or edge of an area source such as an open surface tank or vessel opening. Open surface tanks are widely used in industrial settings for cleaning, stripping,

TABLE 10.3 Centerline Velocity Equations

Hood shape	Centerline velocity	References
Circular, unflanged	$\frac{V}{V_0} = \frac{1}{12.7 \cdot z^2 + 1}$	Burgess et al.,[40] Dittes et al.[37]
Circular, flanged	$\frac{V}{V_0} = \frac{1}{8 \cdot z^2 + 1}$	Burgess et al.,[40] Jansson[34]
V = centerline velocity, V_0 = hood face velocity (Q/A), z = distance from hood face along centerline / opening diameter		
Square, unflanged	$\frac{V}{V_0} = \frac{1}{8.6 \cdot z^2 + 0.93}$	Burgess et al.[40]
Square, flanged	$\frac{V}{V_0} = \frac{1}{6.3 \cdot z^2 + 0.25}$	Burgess et al.[40]
V = centerline velocity, V_0 = hood face velocity (Q/A), z = distance from hood face along centerline / length of one side		
Rectangular, unflanged	$\frac{V}{V_0} = \frac{1}{10\left(\frac{X^2}{(W \cdot L)}\right) + 1}$	Burgess et al.,[40] Braconnier[33]
Rectangular, flanged	$\frac{V}{V_0} = \frac{1}{2\pi\left[0.25 + \left(\frac{X}{W}\right)^{2}\right]^{-0.5} \cdot \left[0.25 + \left(\frac{X}{L}\right)^{2}\right]^{-0.5}}$	Burgess et al.[40]
V = centerline velocity, V_0 = hood face velocity ($Q/(L \cdot W)$), W = hood width, L = hood length, X = distance from hood face along centerline		
Slot, unflanged	$\frac{V}{V_0} = 0.27 \cdot \left(\frac{X}{W}\right)^{-1.0}$	Burgess et al.[40]
Slot, flanged	$\frac{V}{V_0} = 0.36 \cdot \left(\frac{X}{W}\right)^{-1.0}$	Burgess et al.[40]
V = centerline velocity, V_0 = hood face velocity ($Q/(L \cdot W)$), W = hood width, L = hood length, X = distance from hood face along centerline and in the longest plane		

electroplating, and other coatings applications. Rim exhausts are amenable to open surface tanks because they do not generally interfere with the operations of the tank and usually will draw contaminated air away from the breathing zone of workers. This is in contrast to canopy hoods, which may also be used for heated open surface tanks, although these hoods will draw contaminated air through a worker's breathing zone if the worker leans over the tank.

Principle

The rim exhaust is a source of suction that is placed along one or more sides of the area source. Air is drawn across the surface of the source and contaminated air is drawn into the hood. Specific examples of rim exhaust include open-surface tank exhaust such as electroplating, cleaning, degreasing; table exhaust such as mortuary tables; and exhaust used during container filling such as barrel filling.

TABLE 10.4 Entry Loss Factors for Flanged or Unflanged Round, Square, and Rectangular Tapered Openings

Exhaust shape	Hood entry loss factor
Plain duct end	0.93
Flanged duct end	0.49
Bellmouth entry	0.04
Tapered hood, 15°	Round: 0.15; rectangular: 0.25
Tapered hood, 30°	Round: 0.08; rectangular: 0.16
Tapered hood, 60°	Round: 0.08; rectangular: 0.17
Tapered hood, 90°	Round: 0.15; rectangular: 0.25
Tapered hood, 120°	Round: 0.26; rectangular: 0.35

The angle is the major angle on rectangular hoods.[10]

Applicability of Sources

Rim exhausts are suitable for area sources of contaminant. They are limited in the area over which they can draw with adequate velocity. In practice, the slot hood should be within 0.6 m of the far edge of the source. For an open surface tank this means that a slot hood on one long side is necessary for tanks up to 0.6 m in width; hoods on both long sides are necessary for tanks up to 1.2 m in width; and rim exhaust is not practical for tanks wider than 1.2 m. For those situations, push-pull ventilation or enclosure type hoods are recommended.[25]

Different Forms and Boundaries Relative to Other Types

Rim exhausts are slot hoods located on or around the edge of a source such as an open surface tank. Flanges may be added to decrease the airflow from behind the slot (uncontaminated air) and therefore increase the airflow from in front of the slot (contaminated air). The plenum downstream of the slot, if located above the slot, may act as a flange. Flanges may also be added to the sides of the source (tank) away from the slot hood. These flanges also act to increase the flow of contaminated air into the tank. Tank flanges, however, may interfere with process activities by limiting access to the tank.

Design Equations and/or Parameters

Rim exhausts, being one type of slot hood, use the same basic principles as given in the section on basic exhaust openings. The recommendation is to use the equations given in the *Basic Exhaust Openings* section for unflanged or flanged slot hoods or elliptical openings. The most common design method, however, uses Method B, capture velocity. The design procedure involves selecting a capture velocity. The selection depends on the generation rate and toxicity of the contaminant as well as some consideration of disturbances near the local exhaust hood. For the case of open surface tanks, the generation rate and toxicity are usually combined to determine the class of contaminant. The class is then used to select an appropriate capture velocity. The ACGIH[25] gives recommended capture velocities for a number of open-tank processes. Equation (10.55) is applicable:

TABLE 10.5 Values of Hood Flow Rate Coefficient, C[25]

Tank aspect ratio (W/L)	Flanged or baffled	Free-standing or unflanged
0–0.09	1.0	1.5
0.1–0.24	1.25	1.75
0.25–0.49	1.5	2.0
0.49–0.99	1.75[1]	2.25[1]
1.0–2.0	2.0[1]	2.5[1]

[1]A maximum flow rate of 1.27 $m^3 s^{-1} m^{-2}$ tank surface is considered sufficient.

$$Q = CV_cLX, \tag{10.55}$$

where Q = hood flow rate ($m^3 s^{-1}$); C = coefficient, which depends on use of flanging and tank aspect ratio, see Table 10.5 (unitless); V_c = capture velocity ($m s^{-1}$); L = tank length (m); and X = distance the hood must "reach" for contaminant capture, equal to tank width if one slot is used and 1/2 tank width if two slots are used (m).

The rim exhaust is placed on the longer side of the tank and the ratio of the width to length of the tank is the tank aspect ratio. Higher aspect ratios require higher hood flow rates per unit area due to the increased distance that the hood must reach. The highest hood flow rates per unit area would be expected for square hoods. Values of C are given in Table 10.5.[25]

The pressure loss associated with this type of exhaust opening is the sum of two pressure losses. The slot hood is usually thought of as a sharp-edged orifice and the duct entry (from the slot plenum) is a flanged opening. The recommended hood entry loss is given by Eq. (10.56):[25]

$$h_e = 1.78(VP_{slot}) + 0.25(VP_{duct}), \tag{10.56}$$

where h_e = hood entry loss (pressure units); VP_{slot} = velocity pressure in slot (pressure units); and VP_{duct} = velocity pressure in duct (pressure units).

The ACGIH[25] gives design criteria for several specific applications of rim exhaust including vapor degreasing, tables, mortuary tables, and barrel filling. Each of these design plates gives a recommended hood flow rate based on source surface area and has been determined based on some of the design considerations described above as well as practical experience with these types of hoods. As described previously, selecting hood flow rate based solely on source surface area can lead to decreased efficiency in the presence of cross-drafts, worker or process activity, or obstructions in the flow field.

Another design method uses capture efficiency. There are fewer models for capture efficiency available and none that have been validated over a wide range of conditions. Conroy and Ellenbecker[2,5] developed a semi-empirical capture efficiency for flanged slot hoods and point and area sources of contaminant. The point source model uses potential flow theory to describe the flow field in front of a flanged elliptical opening and an empirical factor to describe the turbulent diffusion of contaminant around streamlines.

Potential flow theory is used to predict the velocity components (V_x, V_y, V_z) at any point (x, y, z) in front of an elliptical opening (see Flanged Elliptical Openings). A cross-draft can be added to the velocity components through simple vector addition. The velocity model has been validated in the laboratory.[32] Capture efficiency is calculated from the velocity model for the xy-plane ($z = 0$) with an empirical term to account for turbulent dispersion of contaminant around streamlines. Equation (10.57) is the capture efficiency model:

$$\eta = \frac{\exp\left(\frac{X-\mu}{\omega}\right)}{1+\exp\left(\frac{X-\mu}{\omega}\right)}, \tag{10.57}$$

where η = capture efficiency; X = distance, in the x direction, from the hood face to the point of interest; μ = empirically corrected distance, in the x direction, to the dividing streamline; and ω = empirical parameter to account for the spread of contaminant around streamlines. The dividing streamline is the streamline that just enters the hood.

The spread parameter, ω, is calculated from

$$\omega = -0.15X_c + 0.004 \text{ with } X_c \text{ in meters}. \tag{10.58}$$

The empirically corrected dividing distance, μ, is calculated from

$$\mu = 0.83X_c. \tag{10.59}$$

The theoretical distance to the dividing streamline, X_c, is a function of hood dimensions, hood face velocity, distance parallel to the hood face, and cross-draft velocity, and is calculated from the equations for flanged elliptical openings in Section 10.2.2.2.

Capture efficiency of area sources of contaminant release, such as open-surface tanks, can be calculated by numerically integrating the point predictions over the surface of the source.[2] For open-surface tanks with a liquid level very close to the bottom of the slot hood, the source in front of the hood prevents air from being drawn from below the slot, causing more air to be drawn from in front of the slot. The effect is to increase the distance to the dividing streamline. The velocity field, modified by the presence of the contaminant source, is modeled by an image source of suction below the slot. This modification is necessary for plating, pickling, or cleaning tanks and for tables. With vapor degreasers, the liquid level is much lower than the bottom of the slot and does not interfere with airflow from below the slot. The assumption of an image source of suction is not necessary. This area source model was validated in the laboratory with very good results. An attempt was made to validate this model in the field. Capture efficiency of local ventilation on vapor degreasers was measured at 16 sites. Cross-draft velocities were simultaneously measured at 8 sites. Predicted and measured capture efficiencies did not compare well (Fig. 10.22).[42] As discussed in the *Disturbances* section, there are many possible reasons for the poor agreement. The area capture efficiency model only considers hood flow rate and dimensions, source dimensions, and cross-draft velocities,

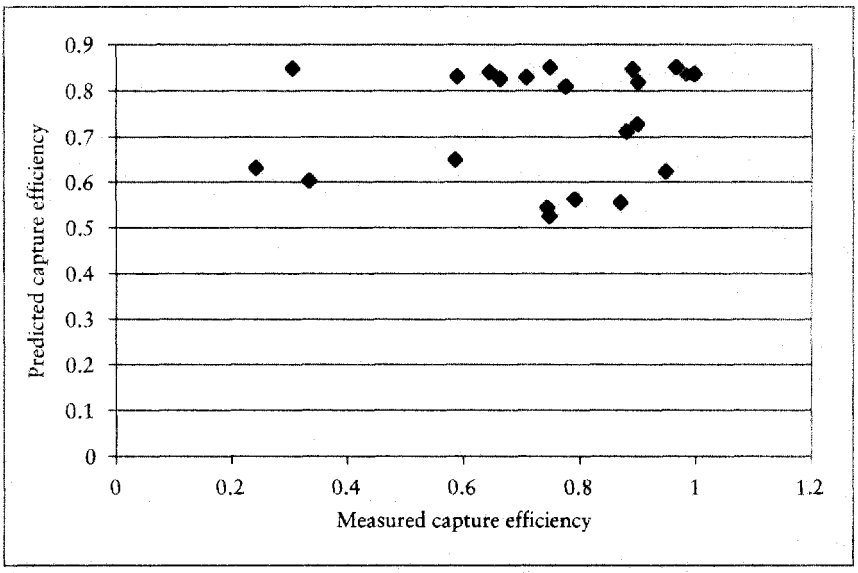

FIGURE 10.22 Predicted versus measured capture efficiency of vapor degreasers under operating conditions.

whereas actual capture efficiency also depends on work practices and activity at the tank.

Computational fluid dynamics methods may allow for more accurate predictions. These models account for turbulence and other parameters such as thermal effects. A description of these methods is included in Chapter 11.

10.2.2.4 Low-Volume/High-Velocity Exhaust Ventilation

General

It can be very difficult to control dust from some industrial operations, especially when particles are released at high velocities. Large particles can travel significant distances before slowing down enough for capture and control by conventional local exhaust ventilation. Fine particles may be caught in the rapidly moving boundary layer of air that develops with rapidly moving surfaces, such as grinding wheels. Fine dust particles can be conveyed within the boundary layer and be dispersed away from the point of generation. These characteristics make it difficult to control personal dust exposures.

This discussion will address needs, applications, performance characteristics, and design considerations for LVHV exhaust ventilation. The applications are primarily for dust control. LVHV systems can be effective for protecting workers from dust exposures and for recovering valuable process materials. The equipment, excepting the nozzles, involves technology that is the same as for large central vacuum cleaning systems.

LVHV nozzles require very careful design. They can be effective in capturing and removing dust from operations that are otherwise difficult to control, e.g., hand-held tools and some fixed-machine grinding and other operations. Installation costs for LVHV systems can be considerably higher than for conventional local exhaust systems. However, operating costs can be lower be-

cause of relatively small exhaust air volume flow rates and resulting lower costs of conditioning replacement air.

LVHV nozzles can create problems that may be sufficiently severe as to prevent their use, usually in the form of ergonomic encumbrances and excessive noise. These problems can be dealt with, to limited extents, and LVHV applications can be effective. It must also be understood that dust control by LVHV systems is ultimately limited. No ventilation control measure can ensure sufficient worker protection down to extraordinarily low acceptable dust levels. Worker protection must always be confirmed by industrial hygiene monitoring and evaluation, and administrative control measures such as respiratory protection may be necessary.

LVHV applications have not developed rapidly. Initial concepts were developed for industrial applications in the 1950s and 1960s. Refinements were made and commercial products have been available from the 1970s until the present time. Unfortunately, there has not been much development of new applications.

Certainly, some workplace operations involving highly toxic and/or valuable materials can be controlled more effectively by LVHV ventilation than by conventional local exhaust ventilation. These situations represent opportunities to improve worker protection, recover valuable materials, and to reduce replacement air requirements. Designers of local exhaust ventilation systems should be mindful of such opportunities and take advantage of LVHV control methods.

Principle

Low-volume/high-velocity (LVHV) local exhaust ventilation is an approach that can be effective in controlling high-velocity dust particles. LVHV ventilation involves careful design and placement of relatively small exhaust inlets, better described as exhaust nozzles. The exhaust nozzles are positioned very close, within 2.5 cm (1.0 inch) of the point(s) of contaminant generation. LVHV nozzles utilize high "face" velocities, typically in the range 50–100 m/s (10 000–20 000 ft min^{-1}, fpm). High inlet velocities and close positioning enable LVHV nozzles to capture much of the dust that is generated, even when released at high velocities.

Applicability of Sources

The most common applications for LVHV ventilation are to control highly toxic and/or highly valuable dusts. These circumstances make it easier to justify the typically high installation costs of LVHV systems. Some of the earliest applications of LVHV ventilation were to control machining operations on radioactive materials and highly toxic metals and alloys, such as those involving beryllium.[43–45] Hand-held high-speed rotating tools can be among the most difficult for achieving effective dust control. A number of specific LVHV applications have been developed for foundry and other dust-generating tools.[25]

If well designed and properly used, LVHV applications have the primary advantage of effective dust control. LVHV systems also require much less replacement airflow than conventional ventilation systems. This can result in significant savings in operating costs to condition the replacement air. These savings can help to offset the typically high installation costs for LVHV systems.

LVHV systems have disadvantages associated with installation costs, e.g., custom-made nozzles, expensive hose and duct, air-cleaning equipment, expensive

air movers, and large electric motors (with high operating costs). Noise levels generated by LVHV nozzles can be hazardous to hearing. And, as for any engineering control, LVHV ventilation may not be sufficiently effective to eliminate potentially hazardous exposures. For example, despite a relatively long history of use with beryllium machining operations, some LVHV systems may not have been sufficiently effective to prevent chronic beryllium disease.[46] The practical limits of LVHV ventilation are not well known. Control of dusts to microgram-per-cubic-meter levels (such as for beryllium) might be achievable by LVHV ventilation for some operations, but possibly not for other operations.

High-Speed Dust Control

Figure 10.23 illustrates a progression of "Before LVHV" and "After LVHV" dust control applications.[47] Figure 10.23*a* shows a simple plain rectangular, wedge-shaped LVHV exhaust nozzle removing dust from a stationary grinding wheel. Figure 10.23*b* shows a prototype LVHV nozzle positioned on a hand-held grinding wheel. Figure 10.23*c* illustrates the effectiveness of a commercially-made LVHV nozzle on a hand-held grinding wheel. LVHV nozzles have been used to control dust from machining on asbestos-containing and structural plastic materials.[40]

Welding Operations Efforts have been made to use the LVHV design approach for controlling welding fumes. Sometimes, this can be an effective method. Sometimes, however, there can be serious problems with the high-velocity exhaust stripping away shielding gases and causing poor quality welds. It is also difficult for exhaust nozzles to survive without damage in industrial welding environments, where even relatively slight damage can cause significant changes in the high-velocity airflow patterns and adversely affect welding. Most successful point-exhaust applications for welding establish capture velocities lower than for LVHV dust control, but still higher than for conventional exhaust hoods.

Other Applications Very small, very low-flow, and relatively high-velocity exhaust inlets, similar to LVHV nozzles, have been used successfully to control fumes from electric soldering irons.[48,49] Some investigations have been made into small, point-control exhaust ventilation for aerosols generated by high-speed dental tools. However, such low-volume point-control ventilation systems have not seen widespread use.

Design Equations and Parameters

Nozzle Performance Characteristics Relatively little has been done to prescribe design guidelines for these applications. Published guidelines consist largely of drawings and limited data originating from LVHV equipment suppliers.[25,40,43,44,47]

Research has been conducted to evaluate the effectiveness of several LVHV nozzle configurations for capturing tracer aerosols for simulated industrial operations.[50] Studies have been conducted to evaluate dust capture for LVHV nozzles on hand-held tools, and have demonstrated over 90% collection efficiencies for operations such as grinding and sanding.[51–53]

Research has also characterized the performance of LVHV nozzles having simple geometric shapes.[54–56] The experimental nozzles included seven profile shape variations for circular nozzles having a diameter (D) of 2.54 cm (1.0 inch)

Before LV/HV

After LV/HV

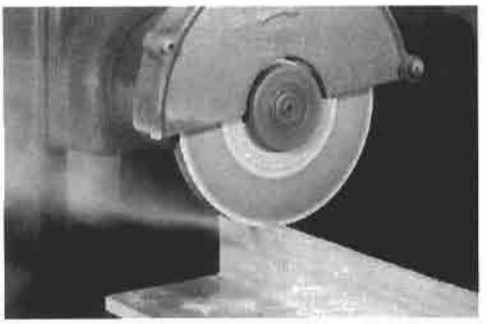

(*a*) Simple rectangular-wedge nozzle near a stationary surface grinder

(*b*) Roughly fabricated nozzle for a hand-held cup-wheel grinder

(*c*) Commercially made nozzle for a hand-held cup-wheel grinder

FIGURE 10.23 Applications of LVHV local exhaust ventilation for dust control.[47]

and eight rectangular nozzles, all having 6.45 cm^2 (1.0 $inch^2$) openings that were tested for plain and flanged profiles. The circular nozzle profile shape variations included plain (with "thick" and "thin" inlet walls), flanged, flared (tapered at 45°), rounded, plain wedge (45°), and rounded wedge (45°). Plain circular nozzles were also tested at different diameters: D = 1.27, 1.91, 2.54, 3.18, and 3.81 cm (0.5; 0.75; 1.0; 1.25, and 1.5 inch). The rectangular nozzles varied in end shape

from square (width-to-length ratio, WLR = 1.0) to rectangular (WLR = 0.5 and 0.25), and narrow slot (WLR = 0.10). These experimental LVHV exhaust nozzles were tested at different volume flow rates (Q), establishing calculated-average nozzle face velocities ($V_0 = Q/A$; A = inlet area) of 50, 75, 100, and 125 m s^{-1} (10 000, 15 000, 20 000, and 25 000 fpm), and at some higher values of V_0.

Centerline Static Pressures Figure 10.24 shows centerline static pressure profiles (SPCL) versus X (cm Hg versus cm; inch Hg versus inch) for several experimental LVHV nozzles. Figure 10.24*a* compares plain, flared, and rounded circular nozzles. The plain nozzle experienced a pronounced vena contracta; the flared and rounded nozzles did not. The effects of a vena contracta can be severe for LVHV nozzles. Figure 10.24*b* shows a progression of SPCL profiles for changing nozzle face velocity, V_0. The vena contracta became more pronounced as V_0 increased, ultimately showing abrupt discontinuities, caused by weak shock waves, when the airflow achieved sonic velocity at the throat of the vena contracta. The achievement of sonic velocity established aerodynamic choking ("critical" flow) in the nozzle flow. Aerodynamic choking has significant effects on nozzle noise, as discussed subsequently.

Nozzle Static Pressure Loss Overall nozzle static pressure loss (SPN) was tested for all of the experimental LVHV nozzles.[55,56] Experimental testing has confirmed what would be expected, that nozzle shape and size variation can cause great differences in overall static pressure loss, especially at high airflow velocities. Figure 10.25*a* compares SPN versus V_0 (cm Hg versus m s^{-1}; inch Hg versus fpm) characteristics for five circular nozzles. The plain wedge had the steepest rising curve, followed by the plain circular nozzle. Both of

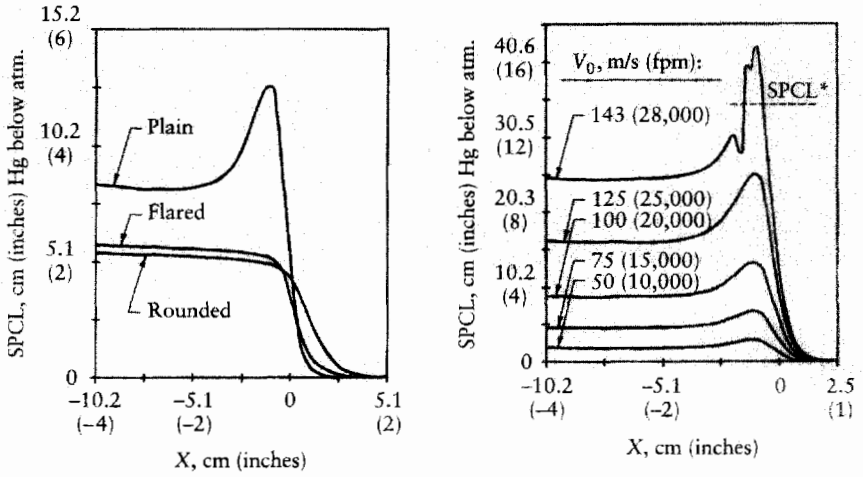

(*a*) Plain, flared, and rounded circular nozzles (D = 2.54 cm, V_0 = 100 m/s)

(*b*) Plain circular nozzle (D = 2.54 cm)

FIGURE 10.24 Centerline static pressure (SPCL) profiles for experimental LVHV exhaust nozzles.[57] The centerline pressure is measured at different distances, X, from the opening plane of the exhaust nozzle. X is positive outside the opening.

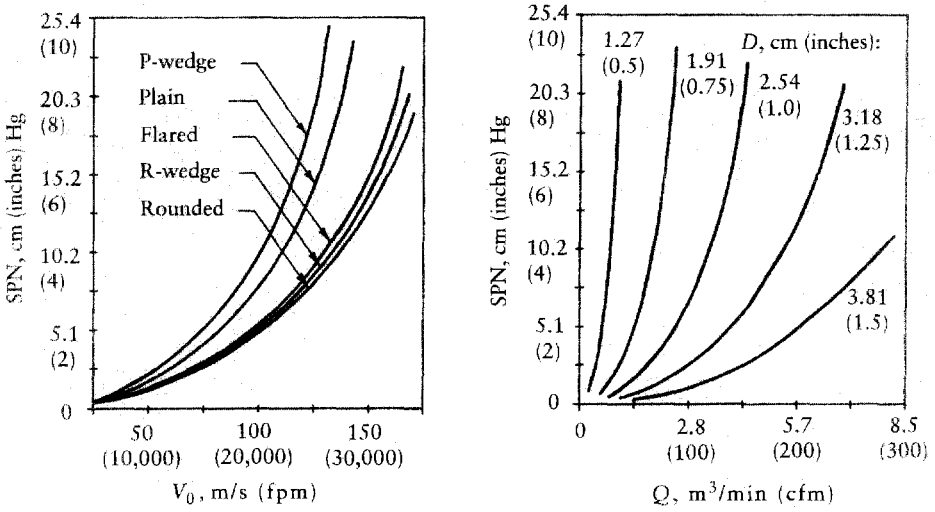

(*a*) Circular nozzle profile shapes (D = 2.54 cm)

(*b*) SPN vs. Q for plain circular nozzles of different diameters

FIGURE 10.25 Nozzle static pressure loss (SPN) characteristics for circular experimental LVHV exhaust nozzles.[55]

these nozzles experienced substantial, irreversible energy losses caused by turbulence in the vena contracta. The flared, rounded, and rounded wedge profiles did not experience pronounced vena contracta effects, and experienced consequently lower values of SPN. Figure 10.25*b* shows SPN versus Q (cm Hg versus $m^3 s^{-1}$; inch Hg versus cfm) for five plain circular nozzles having different diameters; the curves show large differences. Nozzle size has a profound effect on nozzle static pressure loss (SPN). This may prevent the use of very small LVHV nozzles that can experience extremely large static pressure losses.

Noise Characteristics LVHV exhaust nozzles can generate very high noise levels.[55,56] Nozzle noise can present significant hazards to hearing. Options are limited, but actions can be taken to help reduce nozzle noise. Figure 10.26*a* compares nozzle noise profiles, dBA versus V_0 (m s^{-1}, fpm) for plain circular, square, and rectangular (WLR = 0.25) nozzles. The curves are remarkably similar, each showing dramatic increases in noise levels as V_0 approached maximum flow, and each showing significant dBA noise reduction when driven closer to maximum (choked) flow.

Figure 10.26*b* shows noise spectra (dB versus Hz) for a plain circular nozzle at different face velocities, V_0. As V_0 increased, so did the noise levels, especially at frequencies greater than 1000 Hz. This was true at the flow rate causing the maximum noise level, i.e., V_0 = 137 m s^{-1} (27 000 fpm). However, further relatively slight increases in flow rate (increasing V_0) resulted in overall noise levels dropping dramatically (10–15 dB), especially in the highest frequencies (greater than 8000 Hz). These findings confirm that nozzle noise results largely from high-frequency airflow turbulence. The data show that driving an LVHV exhaust nozzle to its maximum flow, i.e., toward aerodynamic choking, can also

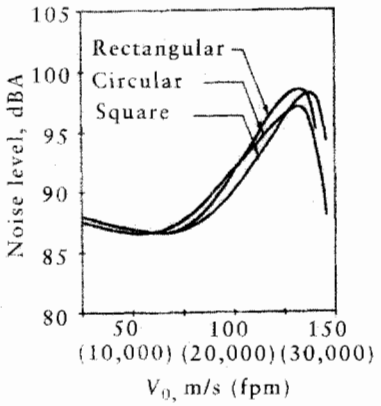

(*a*) Noise profiles for plain circular, square, and rectangular (WLR = 0.25) nozzles (V_0 = 100 m/s)

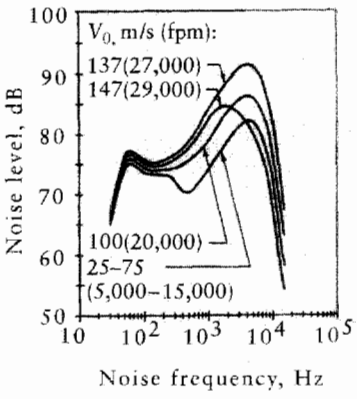

(*b*) Noise spectra for a plain circular nozzle (D = 2.54 cm)

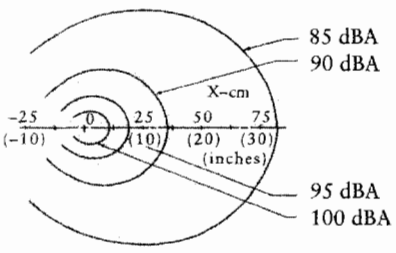

(*c*) Noise potentials for a plain circular nozzle (D = 2.54 cm, V_0 = 100 m/s)

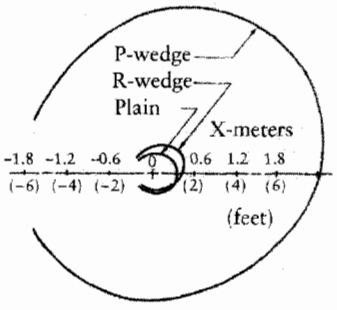

(*d*) 90 dbA noise potentials for plain, plain-wedge, and rounded-wedge circular nozzles (D = 2.54 cm, V_0 = 100 m/s)

FIGURE 10.26 Noise characteristics for experimental LVHV exhaust nozzles.[54, 56]

result in large reductions in nozzle noise levels. Less noise is propagated outside the nozzle because much of the noise is, in effect, "swallowed" by the nozzle.

Noise levels for plain circular nozzles propagated for greater distances as diameter increased for D = 1.27, 1.91, and 2.54 cm (0.5, 0.75, 1.0 inch), but were essentially unchanged for the larger sizes, D = 2.54, 3.18, and 3.81 cm (1.0, 1.25, 1.5 inch). These findings suggest a limiting effect of nozzle size on nozzle noise. This would favor using smaller nozzles to reduce noise, but higher pressure losses will also occur. Increasing nozzle size beyond certain values (e.g., D = 2.5 cm for a plain circular nozzle) may not significantly increase nozzle noise levels.

Figure 10.26 also presents comparisons of nozzle noise potentials, two-dimensional plots of constant noise (dBA) levels in proximity to the experimental LVHV nozzles. Noise potentials for a plain circular nozzle,

Fig. 10.26*c*, demonstrated a progression (85, 90, 95, 100 dBA) of roughly elliptical contours, resembling constant velocity contours. The possible effect of LVHV nozzle noise projecting to great distances is illustrated in Fig. 10.26*d* (note the change in scale to meters (feet) from centimeters (inches)). The plain wedge circular experimental nozzle was extremely loud, establishing a 90 dBA noise potential encompassing an area about 3.8 m × 3.3 m (15 feet × 13 feet)—this area being roughly 50 times that for either the plain or the rounded wedge circular nozzles.

The extreme noise of the plain wedge nozzle resulted from a highly turbulent and obstructive vena contracta forming in the flow, downstream of the short side of the nozzle opening. This example highlights the possibility of entirely unacceptable noise levels from sharp-edged LVHV nozzles, and the significant benefits (noise reduction) that can come from rounding the inlet edges of LVHV nozzles.

Aerodynamic Choking Aerodynamic choking is an important factor to consider in the design of LVHV nozzles. Choking can occur whenever a nozzle is connected to a system capable of generating negative static pressure in the flow low enough (roughly 53% of atmospheric pressure; see Fig. 10.24*b*) to cause "critical" flow through the nozzle. Choking is important because it limits nozzle flow rate and because it can reduce nozzle noise.

When choking occurs in conjunction with a turbulence-caused vena contracta, such as for plain and flanged nozzles, the overall nozzle static pressure losses (SPN) will be quite high. If choking were to occur in conjunction with a carefully designed converging-diverging nozzle wall, then it should be possible to reduce the obstructive turbulent region significantly, thereby reducing static pressure losses and noise levels. Such design could also have the advantage of achieving aerodynamic choking at more predictable flow rates. A converging-diverging type LVHV nozzle probably would require fabrication as a cast metal or as a molded plastic. Despite the potential benefits, nozzle design to facilitate aerodynamic choking has not been developed in LVHV applications.

System Design Considerations

The primary components of LVHV ventilation systems are the exhaust nozzles, flexible hose, fixed duct, air cleaner, and the exhauster and motor. Each of these is discussed below. Figures 10.23, 10.27, and 10.28 illustrate LVHV nozzles. Figures 10.29 and 10.30 illustrate other system components and installations.

LVHV Nozzles Some of the earliest LVHV nozzles were developed for grinding and other high-speed, dust-generating, foundry-type operations. Hand-held tool applications present special opportunities for LVHV applications. Figure 10.25 shows published nozzle designs for cup-shaped, disc, and cone-shaped grinders, a vibratory sander, and a pneumatic chisel.[25] These illustrations are taken from several ACGIH "VS-Prints" and are based on nozzle designs that have been made commercially. The original British and United States patents for designs similar to some of these provide additional details and information.[57–60]

Figure 10.28 shows a complete ACGIH VS-Print for an LVHV nozzle applied to a surface-grinding machine. The figure illustrates an adjustable LVHV nozzle positioned near the point of grinding. Additional details are provided

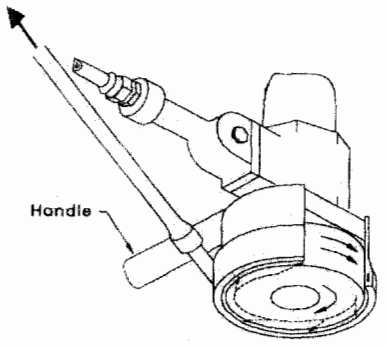

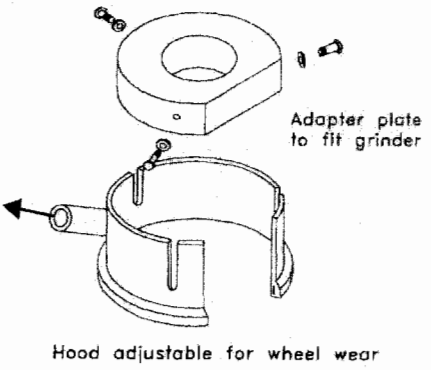

(*a*) Cup-shaped grinder and nozzle design details

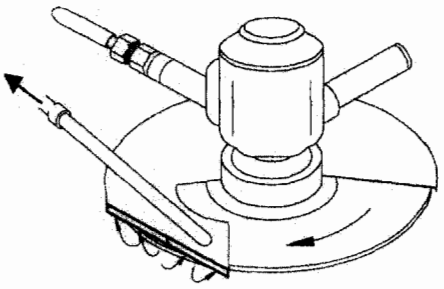

(*b*) Disk grinder

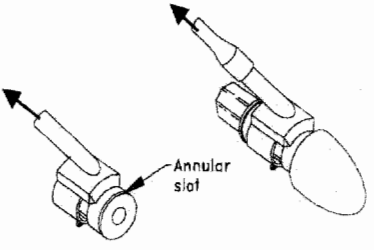

(*c*) Cone-shaped grinder

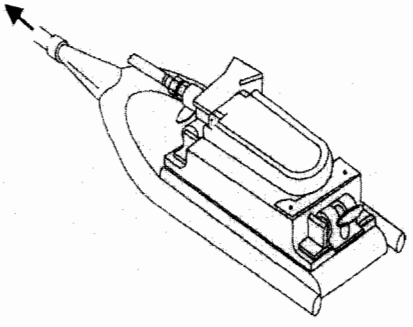

(*d*) Vibratory sander

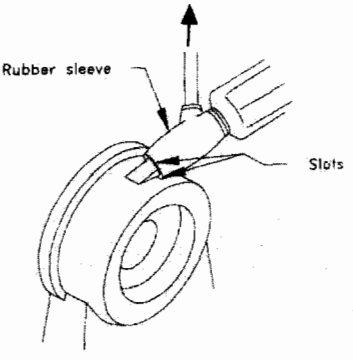

(*e*) Pneumatic chisel

FIGURE 10.27 Examples of LVHV exhaust nozzles for dust control on hand-held tools.[25]

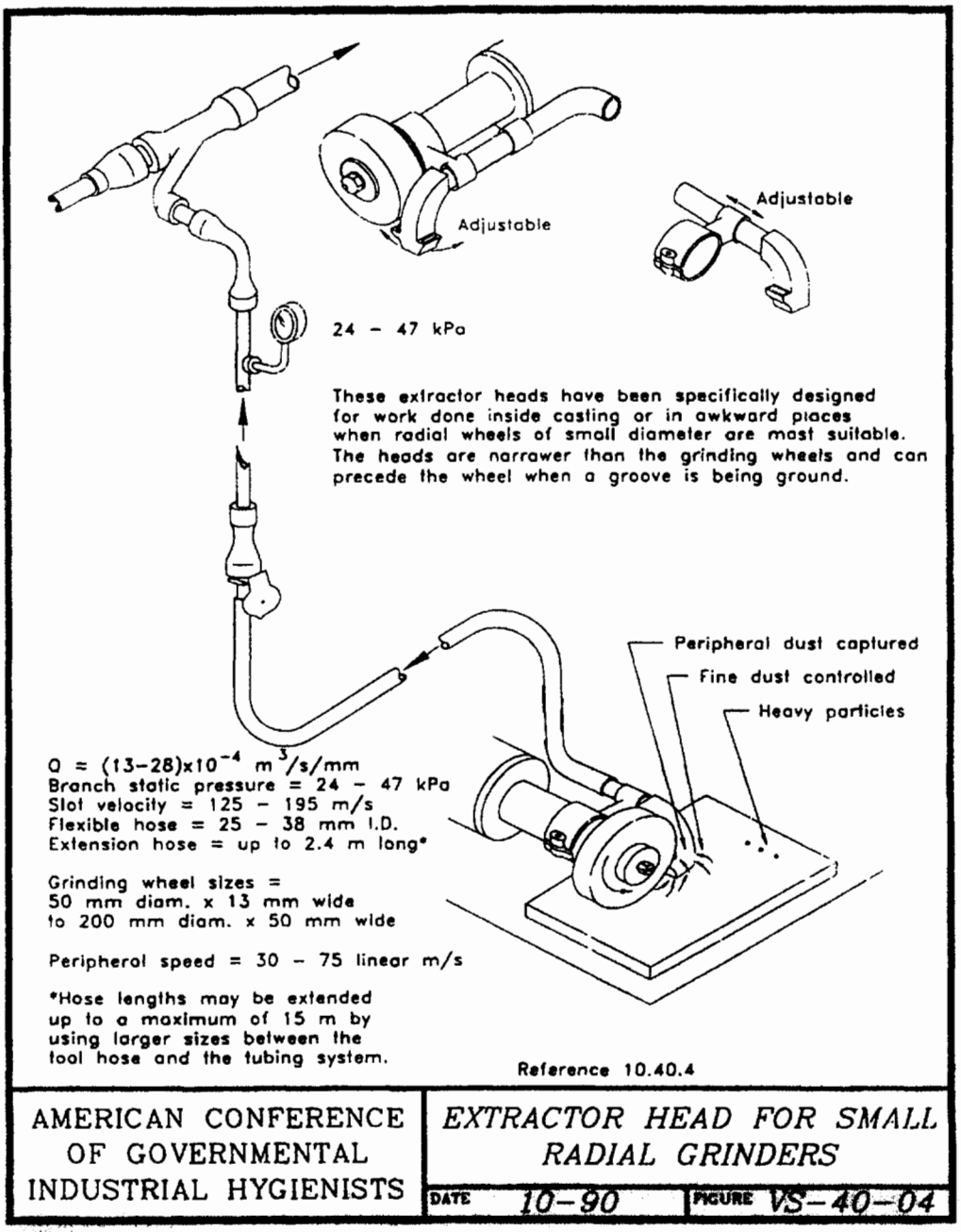

FIGURE 10.28 ACGIH VS-Print for designing an LVHV exhaust nozzle for a stationary surface grinding machine.[25]

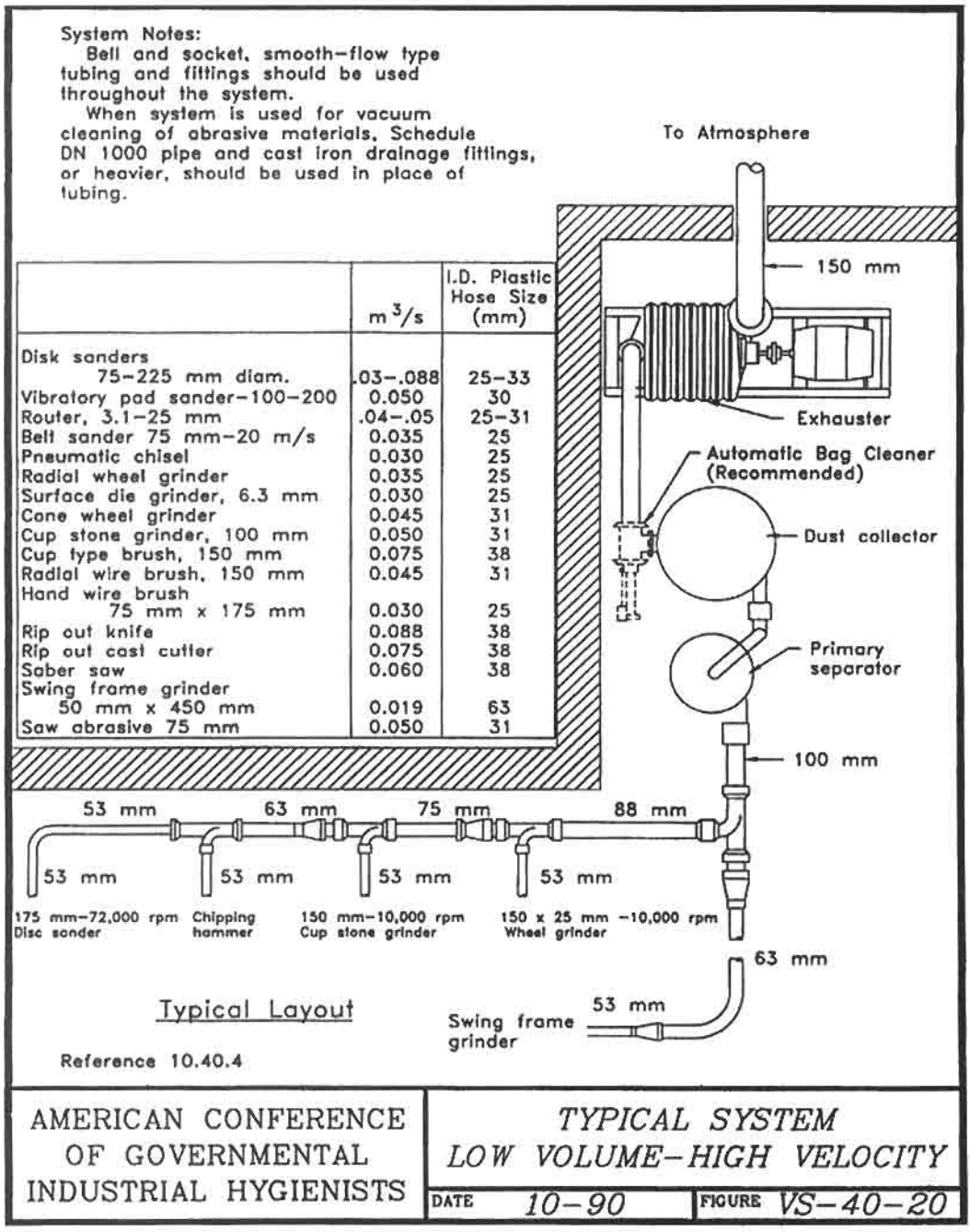

	m^3/s	I.D. Plastic Hose Size (mm)
Disk sanders 75–225 mm diam.	.03–.088	25–33
Vibratory pad sander–100–200	0.050	30
Router, 3.1–25 mm	.04–.05	25–31
Belt sander 75 mm–20 m/s	0.035	25
Pneumatic chisel	0.030	25
Radial wheel grinder	0.035	25
Surface die grinder, 6.3 mm	0.030	25
Cone wheel grinder	0.045	31
Cup stone grinder, 100 mm	0.050	31
Cup type brush, 150 mm	0.075	38
Radial wire brush, 150 mm	0.045	31
Hand wire brush 75 mm x 175 mm	0.030	25
Rip out knife	0.088	38
Rip out cast cutter	0.075	38
Saber saw	0.060	38
Swing frame grinder 50 mm x 450 mm	0.019	63
Saw abrasive 75 mm	0.050	31

FIGURE 10.29 ACGIH VS-Print for designing a multiple-nozzle LVHV exhaust system for dust control in foundry operations.[25]

(*a*) Multiple-stage centrifugal exhauster. Motor connected by coupling or pulleys and belts.

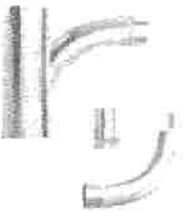

(*b*) Smooth-flow LVHV duct (tubing) components. Slip-fit joints with welded seams.

(*c*) Ground-level installation with a single baghouse air cleaner.

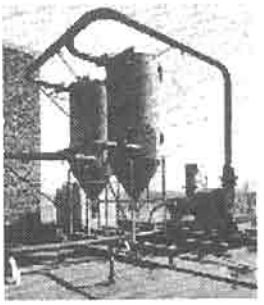

(*d*) Roof installation with dual baghouse air cleaners.

FIGURE 10.30 Illustrations of LVHV exhaust system components and installations.[47]

pertaining to nozzle exhaust flow rates, Q (as a function of wheel diameter), nozzle branch static pressure (–7 to –14 inches Hg), flexible hose inside diameter (1–1.5 inches), and hose length.

Figure 10.29 shows a VS-Print illustrating a complete LVHV system (plan view) for a typical foundry application. This system connects five dust-generating tools, each with its own exhaust nozzle. This figure also includes recommended nozzle volume flow rates and flexible hose inside diameters for several typical foundry-type operations.

Commercial products do exist that integrate shrouded and ventilated grinding wheels and other hand-held tools. It may be possible to find an existing LVHV-type product that will work well for some applications, requiring only to be connected to an appropriate air handling system. However, it is also sometimes necessary to make custom-fabricated LVHV nozzles for some hand-held tools and for essentially all fixed-machine dust-generating tools. The best approach is to consider the following:

Keep the point of suction (nozzle opening) within 2.5 cm (1 inch) from the point of dust release, if possible;
Avoid having any sharp edges at the inlet opening or inside the nozzle;
Consider ergonomics for hand-held tools;
Consider adjustment and movement for stationary machine tools; and
Consider nozzle noise levels and control measures.

Ergonomic problems can cause significant challenges for LVHV applications on hand-held tools. The weights of flexible hoses can greatly alter the balance of tools fitted with LVHV nozzles. Positioning of the tool and nozzle for best dust capture can limit and encumber a tool operator. Noise control options are usually limited to reducing sharp corners and controlling volume flow rate. Some findings suggest that molded plastic nozzles can dampen noise propagation, and thereby generate lower noise levels in comparison to fabricated metal nozzles. Molded nozzles could also incorporate converging-diverging wall surfaces to facilitate aerodynamic choking.

Flexible Hose There are practical limitations on the size (inside diameter) and length of flexible hoses to connect from LVHV nozzles to fixed duct systems. LVHV hose must be smooth and flexible, strong enough not to collapse under low static pressures, and sufficiently durable to withstand industrial environments (e.g., dragging, flexing, impact, temperature variations, abrasive dusts). LVHV hoses are typically made of plastic or rubber materials, but should never be of the corrugated type. Conductive, static-proof hose, or bonding connections may be necessary to reduce accumulation of static charge.

LVHV hose inside diameters are usually recommended to be in the range 2.0–3.5 cm (1–1.5 inches).[25] Hose lengths should be limited to about 2 m (8–10 feet), if possible. If greater lengths are necessary, then the hose inside diameter must be enlarged to reduce friction losses, but not so large as to fail to transport dust to the duct system. It is advisable to obtain accurate hose friction loss data from manufacturers.

Fixed Duct/Tubing The ducts for LVHV systems ordinarily consist of steel tubing designed to minimize turbulent pressure losses and convey airborne dust to an air cleaner. The type of steel-tubing duct that is used in central vacuum cleaning systems is good for LVHV applications. It is designed with long-radius turns and smooth inside joints between the fittings and straight duct sections. The duct fittings have expanded ends to allow a slip-fit with the straight duct and a smooth joint on the inside surface of the duct. The slip-fit components are positioned and welded to create a strong and smooth airflow system.

Materials other than steel are also available, such as galvanized steel, aluminum, or stainless steel. Solid neoprene fittings are available for applications involving highly abrasive dusts.[47] Sometimes, heavy cast iron pipe can be used for highly abrasive applications.[25] Conventional sheet-metal duct cannot be used because it cannot handle the very low static pressures. LVHV and central vacuum cleaning system duct manufacturers should be consulted to provide accurate data for duct friction and turbulence pressure losses. Data available for conventional galvanized duct and fittings may not be sufficiently accurate for LVHV design applications.

Figure 10.29 illustrates duct sizing for a five-nozzle LVHV system. It also illustrates connections to air-cleaning equipment and a multiple-stage centrifugal exhauster. It should be noted that the actual LVHV duct is much smoother than is suggested by the drawings in Figs. 10.28 and 10.29.

Air Cleaner/Dust Collector There are a wide variety of possible types of air-cleaning equipment for LVHV systems. The most common is a fabric dust collector, having a vertical cylindrical baghouse design. This type is common in large central vacuum cleaning systems. Other types of fabric collectors can also be used. For applications involving substantial amounts of large dust particles, it is usually a good idea to have a cyclone-type primary separator upstream of a fabric collector.

Air cleaning (dust collection) can be cost effective for LVHV systems handling valuable dusts. Care must be taken when handling potentially toxic dusts from air cleaners. Regular, routine reconditioning of fabric filters (e.g., by automatic shaking or pneumatic pulsing) is important. This can be accomplished on a set maintenance schedule or as a function of pressure drop across the fabric filter. It is not recommended to recirculate airflow back to the workplace because of the low air volume and potential hazards in the event of filter failures.

Exhauster and Motor Air movers for LVHV systems are not conventional fans. The low static pressures needed to operate LVHV systems can be generated by multiple-stage centrifugal (turbine-type) exhausters. These utilize high-precision rotating blades that can be damaged by dust. Consequently, it is always necessary to have an air cleaner in an LVHV dust control system to protect the fan. The low static pressures also require air volume flow rates to be corrected to standard conditions for exhauster selection.

The exhauster and motor must be mounted on a rigid frame. Installation should include a solid foundation, with vibration isolation of the exhauster and motor frame, and flexible connections between the inlet and outlet ducts and the exhauster. A commercial silencer should be considered to reduce noise levels propagating from the exhauster discharge stack. Electric motors for LVHV systems may need to be quite large in order to drive the exhausters at the necessary speeds and pressures. Motors can be connected by direct-drive couplings or indirectly by pulleys and belts. The operating costs of large motors can be significant, partially offsetting savings from low airflow rates.

Figure 10.30 illustrates a multiple-stage exhauster and smooth-flow duct (pneumatic tubing) components. It also includes pictures of air cleaner–exhauster–motor installations located outside of buildings and connected to LVHV (or central vacuum cleaning) systems inside the buildings.

10.2.2.5 Receptor Hoods

General

Receptor hoods, also called canopy hoods, are designed to capture contaminants given off by heated processes. They take advantage of the thermal updraft caused by such processes; by placing the hood in the path of the updraft, they "receive" the exhaust and capture the contaminants.

Principle

Heated sources can cause strong updrafts that carry contaminants upward. Receptor hoods take advantage of this updraft, as shown in Fig. 10.31. The process shown to the left in Fig. 10.31 is at room temperature, while the process to the right in Fig. 10.31 is operating at elevated temperature. A canopy

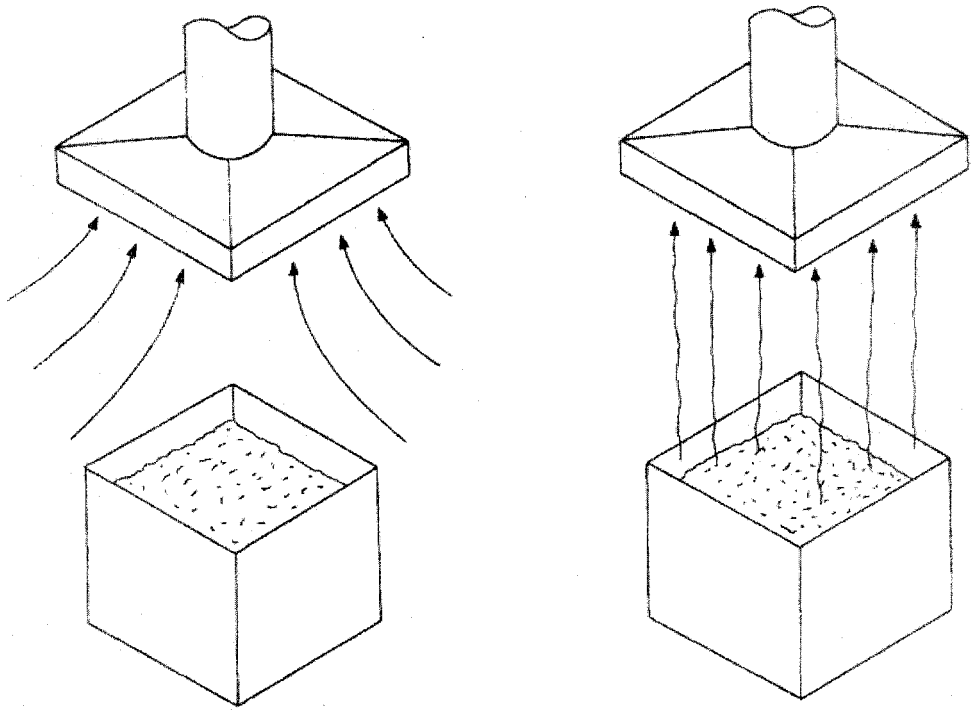

FIGURE 10.31 Canopy hoods over a cold process (*left*) and a hot process (*right*).

hood is shown over each process. The hood to the left is a simple exterior hood (see Section 10.2.2.2); as such, it must create a sufficient capture velocity at the surface of the process to capture the contaminants emitted. The hood to the right, by contrast, utilizes the updraft created by the process to aid in the contaminant capture; here the key design variable is not the capture velocity at the process surface, but the total volume of air set in motion by the updraft. As shown below, canopy hoods work well as receptor hoods on heated processes, but are very poor choices for room-temperature applications.[40]

Applicability of Sources

The key variable in determining the applicability of a receptor hood to a particular source is the temperature of the heated source, and the resulting updraft. The temperature must be high enough to cause an appreciable updraft, or the hood will be ineffective. An estimate must be made of the total amount of buoyant airflow set in motion by the heated source; the airflow through the hood must be greater than this buoyant airflow, in order to ensure complete contaminant capture. This principle is illustrated in Fig. 10.32, which shows the air spill that occurs when a hood's exhaust airflow is less than the thermal updraft airflow.

Different Forms

Hemeon[61] divides receptor hoods into low hoods, located within about 1 m of the heated source, and high hoods, located beyond this distance (Fig. 10.33).

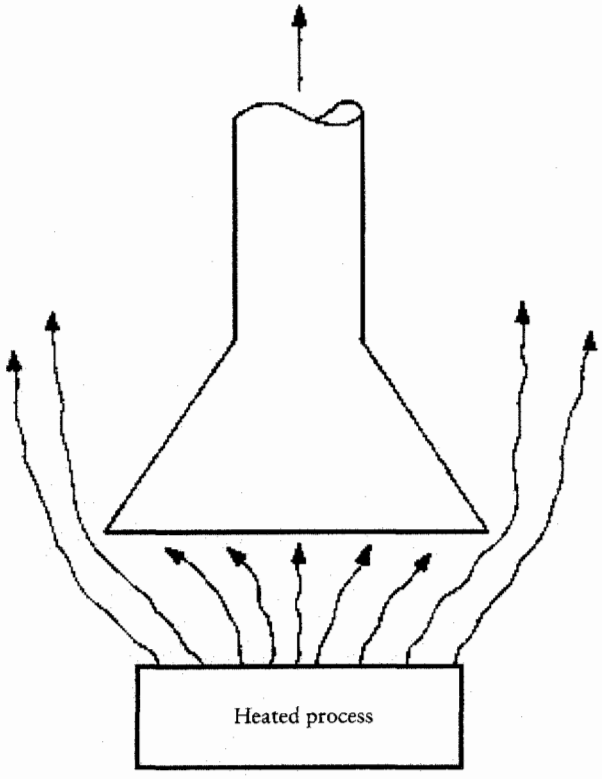

FIGURE 10.32 Canopy hood with an airflow rate less than the thermal updraft airflow from a hot process.

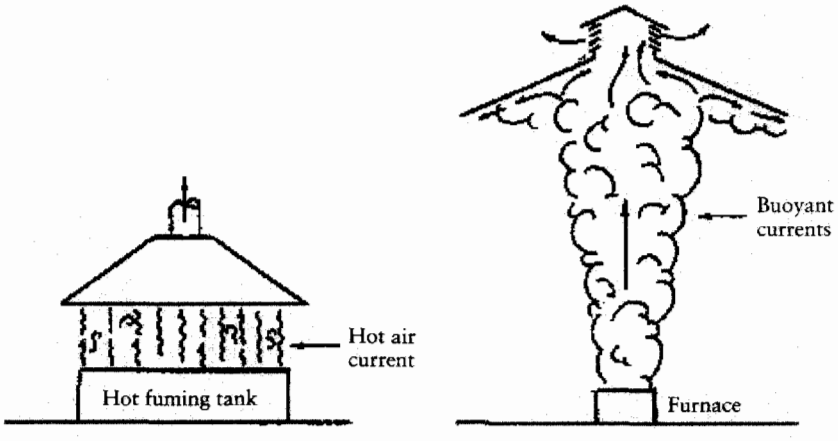

FIGURE 10.33 Canopy hoods according to Hemeon: *left*, low hood, *right*, high hood.

The design of low hoods is much simpler, since the adverse effects of turbulent mixing and cross-drafts are much less important than for high hoods. Low hoods are much more likely to capture a high percentage of the heated air and contaminants than high hoods, so they should be used whenever possible.

Specific Problems

The location of a canopy or receptor hood above a process, in order to take advantage of the thermal updrafts, can be problematic.[40] If the top of the heated source is located below the worker's breathing zone, as is frequently the case for open-surface tanks used in plating, it is very easy for the worker to place his or her head directly into the path of the rising contaminants resulting in very high contaminant exposure even if the hood is 100% efficient at capturing the source emissions. This is illustrated in Fig. 10.34. This represents a serious limitation on the use of receptor hoods; if workers must be positioned over heated sources, it is usually better to forgo the benefits of the thermal updraft and use an alternative design, such as a slot hood (Fig. 10.35).

Design Equations and/or Parameters

Hemeon[61] is the first standard reference book that presents the equations for calculating thermal updrafts. These equations are repeated and expanded in other standard reference books, including Heinsohn,[36] Goodfellow,[16] and the ACGIH Industrial Ventilation Manual.[25] These equations are derived from the more accurate formulas for heat transfer (Nusselt number) at natural convection (where density differences, due to temperature differences, provide the body force required to move the fluid) and both the detailed and the simplified formulas can be found in handbooks on thermodynamics (e.g., Perry[22], and ASHRAE[62]).

High Receptor Hoods The important variable that distinguishes receptor hoods from other exterior hoods is q_{vs}, the upward airflow set in motion by the heated source. Let us first consider the more general (and difficult) case of a high hood. Assume for simplicity that the source and the hood are circular in cross-section. The basic geometry used in this case is shown in Fig. 10.36.

According to Heinsohn:[36]

$$q_{vs} = 0.166 z^{1.67} F^{0.33}, \tag{10.60}$$

where

q_{vs} = buoyant airflow ($m^3 s^{-1}$),
z = virtual source height (m),
F = buoyant flux parameter ($m^4 s^{-3}$)

As shown in Fig. 10.36, the plume expands as it rises. The virtual source height is obtained by extending the actual source downward to the virtual point source:

$$z = h + h', \tag{10.61}$$

where

h = distance between the actual source and the hood (m)
h' = distance between the actual source and the virtual source (m)

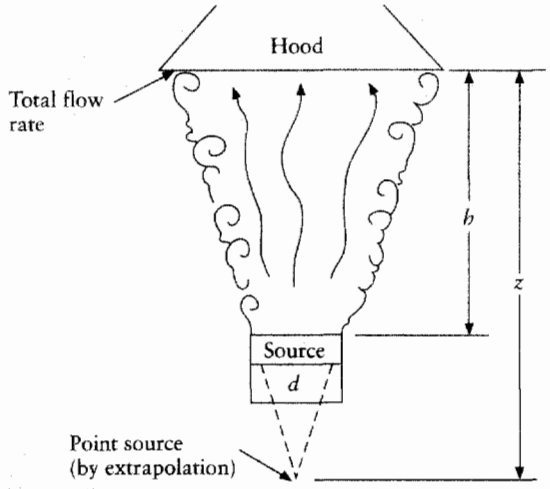

FIGURE 10.34 Basic geometry for calculating necessary flow rate for high canopy hoods.

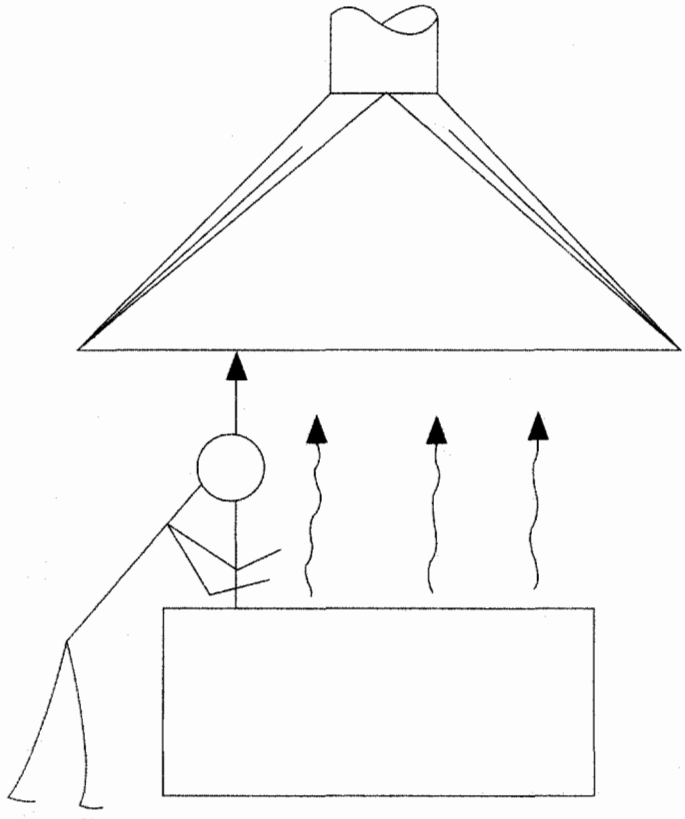

FIGURE 10.35 Inappropriate use of a canopy hood, since worker exposure is not prevented by use of the hood.

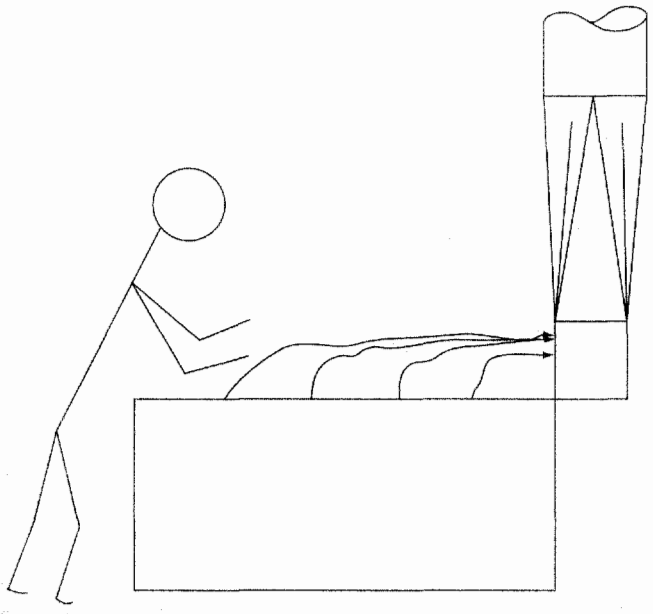

FIGURE 10.36 It is better to use a slot hood when a worker needs to lean over a bath.

Several different equations for h' are given in the references and are shown in Table 10.6.

Given this range of values in the literature, it is probably easiest for the user to go to the original source[61] and assume that $h' = 2d_s$.

The buoyant flux parameter, F, is often very difficult to determine. Theoretically,

$$F = \frac{g\Phi}{c_p T_0 \rho_0}, \tag{10.62}$$

where

g = acceleration due to gravity (9.81 m s^{-2})
ϕ = convective heat transfer from the source to air (W)
c_p = specific heat of air (J kg^{-1} K^{-1})
T_0 = absolute temperature of ambient air (293 K)
ρ_0 = density of ambient air (1.18 kg m^{-3})

The convective heat transfer is given by

$$\Phi = h_c A_s (T_s - T_0), \tag{10.63}$$

where

h_c = convection heat transfer coefficient of the heated surface (W m^{-2} K^{-1})
A_s = heated source surface area (m^2)
T_s = heated source surface temperature (K)

The difficulty in using these equations lies in the determination of h_c for any given heated surface; in general, the value of h_c will not be known since it de-

TABLE 10.6 Equations for Distance between the Actual Source and the Virtual Source, h' (m)

Source	Distance between actual source and virtual source h' (m)
Assuming angle of expansion = 18°	$3.2d_s$
Heinsohn[36]	$1.5d_s$
Hemeon[61]	$2d_s$
Goodfellow[16]	$2.58d_s^{1.138}$
ACGIH[25]	$2d_s^{1.138}$

d_s = diameter of the heated source (m).

pends on the specific geometry of the surface. Hemeon[61] presents equations for calculating h_c for several simple geometries, including horizontal and vertical plates and cylinders; these equations are given in Table 10.7. (The equations given in Section 7.5 could also be used for calculation of plume diameters.)

The solution to the above equations will result in a value for q_{vs}, the airflow set in motion by the heated source. The actual airflow through the hood, q_{vH}, must be larger than q_{vs} to ensure complete contaminant capture. Heinsohn[36] recommends that

$$q_{vH} = 1.21 q_{vs}. \tag{10.64}$$

The diameter of the receptor hood is also a critical design variable. The diameter of the heated plume, d_p, can be determined geometrically if it assumed that the included angle of expansion is 18°. Alternatively, ACGIH[25] and Goodfellow[16] give the following equation for the plume diameter:

$$d_p = 0.5z^{0.88}. \tag{10.65}$$

TABLE 10.7 Heat Loss Coefficients (h_c) by Natural Convection[63]

Shape or disposition of heat surface	Natural convection heat loss coefficient (W m^{-2} K^{-1})
Vertical plates over 0.5 m high	$2.0\ (\Delta t_c)^{0.25}$
Vertical plates less than 0.5 m high (L_v = height in meters)	$1.4\ (\Delta t_c / L_v)^{0.25}$
Horizontal plates facing upward	$2.5\ (\Delta t_c)^{0.25}$
Horizontal plates facing downward	$1.3\ (\Delta t_c)^{0.25}$
Single horizontal cylinders (L_d = diameter in meters)	$1.1\ (\Delta t_c / L_d)^{0.25}$
Vertical cylinders over 0.5 m high (L_d = diameter in meters)	$1.05\ (\Delta t_c / L_d)^{0.25}$

For high hoods, the plume may be deflected by cross-drafts, and the canopy must be larger than d_p to account for this effect. Hemeon[61] gives no specific procedure for calculating the hood diameter, stating only that the hood diameter should be "materially larger" than the plume diameter. Heinsohn[36] recommends that the hood diameter be equal to one-half the effective height (z). ACGIH[25] recommends that

$$d_f = d_p + 0.8h\,, \tag{10.66}$$

where d_f = diameter of hood face (m).

Although the above approach for high receptor hoods is rigorous theoretically, it is difficult to use in practice. ACGIH[25] offers a simpler approach. First, the virtual source height is calculated using Eq. (10.61) where $h' = 2d_s^{1.138}$. Rather than calculating q_{vH}, the velocity of the hot air column at the hood face is calculated using

$$v_f = \frac{0.85A_s^{0.33}(T_s - T_0)^{0.42}}{z^{0.25}}\,, \tag{10.67}$$

where

v_f = upward plume velocity at the face of the hood (m s^{-1})
A_s = area of the heated source (m^2)
z = height of the plume (m)
$T_s - T_0$ = difference between heat source surface temperature and ambient air temperature (K)

The diameter of the hood is then calculated using Eqs. (10.65) and (10.66). An inward velocity, v_r, must be selected for the air flowing into the hood through the parts of the hood without the plume; Hemeon[63] recommends a velocity of 1 m s^{-1}, while Heinsohn[36] suggests 1.5 m s^{-1}.

Finally, the required hood airflow rate is calculated as the sum of the plume airflow and the inward airflow through the rest of the hood:

$$q_{vH} = v_f A_p + v_r(A_f - A_p)\,, \tag{10.68}$$

where

q_{vH} = total airflow through the hood (m^3 s^{-1})
A_p = area of the hot air plume at the hood face (m^2)
A_f = total area of the hood face (m^2)
v_f = 1 or 1.5 (m s^{-1})

This approach is much easier to use than the first, but may give less accurate results since it assumes an average or typical value for the heat transfer coefficient for all heated source geometries.

The same basic procedures as described above can be used if the source and hood are rectangular rather than circular. The two dimensions of the plume and hood must be calculated independently by substituting them for d_s in the equations developed above.

Low Receptor Hoods Low receptor hoods are much easier to design, since entrainment of air into the plume and the effects of turbulent cross-drafts are not significant problems. In this case, the diameter of the plume at the hood face, d_p, is assumed to equal the diameter of the source, d_s. Accord-

ing to ACGIH[25], the diameter (or side length, for a rectangular hood) need only be 0.5 m larger than the source. ACGIH[25] gives the following equation for the airflow into a low circular receptor hood:

$$q_{vH} = 0.045 d_p^{2.33} (T_s - T_0)^{0.42}, \tag{10.69}$$

where

d_p = diameter of plume at hood entrance (m)
$T_s - T_0$ = difference between heat source surface temperature and ambient air temperature (K)
q_{vH} = flow rate into hood ($m^3 s^{-1}$)

If the source and hood are rectangular, the following equation is used:

$$q_{vH} = 0.06 b^{1.33} L (T_s - T_0)^{0.42}, \tag{10.70}$$

where b = the width of the rectangular hood (m), L = the length of the rectangular hood (m), and q_{vH} = flow rate into hood ($m^3 s^{-1}$).

Evaluation

Capture efficiency measurements may be used to evaluate the function of a canopy hood (see Section 10.5). Capture velocity is not a feasible evaluation tool, since a canopy hood does not generate an air velocity close to the source. It is also possible to use exposure measurements for workers outside the plume area. Since most hot processes generate visible contaminants, visual inspection of the flow, especially around hood edges, might provide a qualitative evaluation. Many contaminants could however be invisible when diluted and smoke generators (Section 10.5) may be necessary to find leakages (temporary or permanent) around the hood edges.

10.2.2.6 Downdraft Ventilation Tables

General

For some operations it is advantageous to have the exhaust downward instead of through one of the basic exhaust openings described previously. This is accomplished by suction through the working table, a downdraft table. These exhaust openings are quite like basic exhaust openings with flanges, directed upward. To make the surface function both as an exhaust and as a working table, the opening of the exhaust is covered by a perforated table. To this table could be added vertical and horizontal walls and possibly a ceiling, which makes such an opening more like a partial enclosure than a basic exhaust opening.

Principle

Slots or holes are placed into a horizontal work surface to exhaust air downward in such a way that the surface can also be used as a table. The amount of open area for airflow varies depending on use.

Applicability of Sources

Small versions of downdraft tables (less than approximately 0.5 m^2) are used when small-sized chemical work is to be done on tables instead of in laboratory fume hoods (see Fig. 10.37). This includes work with low-momentum sources (no initial velocity and near room temperature) such as laboratory animal experiments.

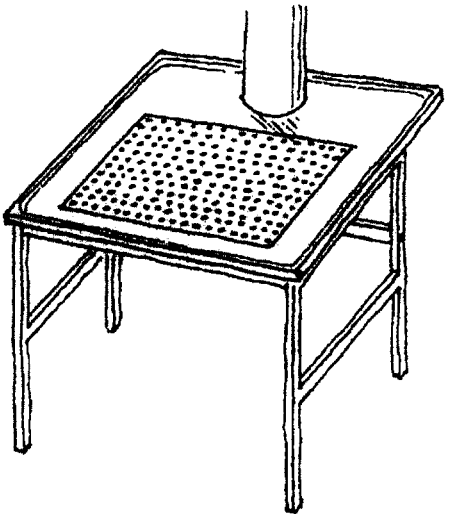

FIGURE 10.37 Downdraft hood for small-scale laboratory work.

Downdraft tables are also used for human dissection tables although rim exhausts (see *Rim Exhausts*) are usually used for this purpose. For manual shoe repair and during application of artificial fingernails, downdraft tables are the only type of exhaust possible.

Larger versions are used for sanding, grinding, polishing, and welding. Since welding generates large amounts of heat together with the contaminants, a downdraft table, although handy, is not suited for this use. There could be problems with grinding, since the contaminants are generated with a high velocity in different directions and a downdraft table is only suited for capturing contaminants with low velocity and a temperature equal to or lower than room temperature. A partial solution to this is to surround the table on three sides with walls (0.2 to 0.5 m high) to deflect the generated contaminants and to diminish the amount of air pulled in from the sides (see Fig. 10.38).

Very large downdraft tables have been used for sources such as electrocutting and welding of large steel sheets.

Different Forms and Boundaries Relative to Other Types

For small-scale laboratory work, the exhaust surface is often made as a separate section added to the side of a table or put into a large hole in a table. These tables usually have a sheet metal surface that is resistant to the chemicals used and is easily cleaned. Many circular holes are cut into the metal surface to allow for airflow. This perforation makes the pressure difference over the table quite high and at the same time gives an even distribution of the airflow over the entire surface. These types of exhaust surfaces could be formed to suit different working conditions, e.g., the surface could be made to fit into a sink or to be placed below and around a balance. Using side walls that are not too high, on three or four sides, transforms the table to a partial enclosure, which increases

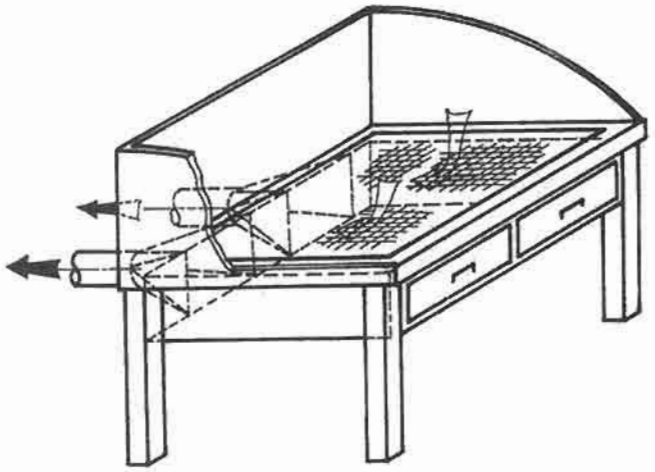

FIGURE 10.38 Downdraft table for grinding, etc. with side walls. This table has two exhaust connections to distribute the flow over the entire surface.

the capture of the contaminants. When a downdraft table is surrounded by three walls and a ceiling its function is more like a booth (see Section 10.2.3.2).

For sanding, grinding, and polishing, both small and large tables exist that use quite large flow rates. These often have built-in fans and filters, which could either return the air to the workroom or blow it to the outside. These tables could be placed into larger working tables but more commonly separate fixed or movable units. They usually do not have a sheet metal surface; instead, the exhaust opening is covered with metal (steel) bars for heavy loads. They could also have a collecting tray beneath the surface and could be surrounded on three sides by vertical shielding walls as mentioned above.

Downdraft tables are available for welding, but the efficiency could be quite low due to low suction velocities and large work pieces.

Similar types of tables are used for electro-cutting of large steel sheets, where it is common to divide the exhaust into segments. The flow rate changes in each segment depending on the location of the cutter. These cutting tables often have an added cooling bath beneath the plate (and the exhaust suction holes). To achieve good capture of the contaminants it is necessary to add an exhaust around the cutter on the upper side.

Many different types of tables exhaust downwards and have a perforated surface covering part of the table, e.g., inside a cabinet. This design is common in biological safety cabinets (see Section 10.4.6.4). Biological safety cabinets use a combination of a supply and an exhaust opening, and therefore are not defined as a downdraft table.

Specific Problems

The downdraft tables used for small-scale chemical work are only recommended for small operations that generate contaminants near the working surface. The items that are used should not cover too large an area of the exhaust. Covering the surface increases the velocity and subsequently also the

reach of the exhaust, but the contaminant generation usually takes place on the covered surface where velocities are too low for adequate capture, resulting in spread of contaminants to the room.

Use of warm processes on a downdraft table should be avoided since the air velocity created by the exhaust is often lower than the velocity due to buoyancy effects. Effective use of a downdraft table for welding requires velocities high enough to counteract the buoyancy, which could result in disturbances of the welding process.

The supply openings in the room must be placed to avoid disturbing the flow into the table. This naturally is easier to accomplish when the table is furnished with side walls.

Also, when using cold processes on a downdraft table, the worker should avoid leaning over the working place or sitting too close to it, since this could disturb the flow into the exhaust and increase the spread of contaminants into the workspace. The same effects as when using fume cupboards could easily be the result (Section 10.2.3.3).

An increase in flow rate could be advantageous since more contaminants could be captured. However, an increased flow could disturb the process and also generate drafts for the worker. A diminished flow rate results in less capture of contaminants.

When a built-in fan and filter is used and the air is recirculated into the workroom, it is necessary to consider the influence of the contaminants on the overall concentration inside the work room. Moreover, it could be difficult to dampen the noise from a built-in fan with a large flow rate. Small tables do not have these problems, since they are connected with ducts to a central fan.

Design Equations and/or Parameters

For small downdraft tables used for chemical work, a flow rate of 0.28 $m^3 s^{-1}$ and m^2 table is used. This gives a mean velocity immediately above the surface of approximately 0.3 m s^{-1}. This is a very low velocity, which can not capture moving contaminants. When these values are used, a maximum use height of 0.15 m is recommended, which should result in a small leakage from the source to the surrounding. This presumes there is at least 0.1 m of uncovered surface between the worker and the source and that the surface is covered to less than 30%. For these tables the pressure difference is between 50 and 100 Pa, depending on the density of holes.[63]

The larger tables (0.8 × 0.5 m to 1.2 × 0.8 m) used for grinding, etc. normally operate with mean velocities of approximately 1 to 1.5 m s^{-1} at the surface. (There are prefabricated tables with face velocity equal to 0.5 m s^{-1}). Mean velocities of 1 to 1.5 m s^{-1} result in flow rates of 3600 and 5400 $m^3 s^{-1}$ and m^2. Some tables use velocities between 2 and 9 m s^{-1}, resulting in flow rates of 7200 and 64 800 $m^3 s^{-1}$ and m^2. These are very high flow rates, which result in noise and high costs. However, at a distance of 0.5 m above the table surface the velocity in the center is 3 m s^{-1}. Tables with these velocities have a good capability to capture most generated particles. The velocity is calculated by using the equations for a square flanged opening 1 m^2 in size and an opening velocity of 9 m s^{-1} (Section 10.2.2).

Recirculation is commonly used for grinding tables due to the large exhaust airflow rates of this design. For these larger tables the free area is much larger than for the small chemical tables, resulting in a much lower pressure difference. In order to maintain an even distribution of airflow over this large surface, it is necessary to use

some type of flow distribution device. The grating bars are usually not enough, and filters placed immediately below the table could have a pressure difference large enough to distribute the flow rate over the entire surface (see Fig. 10.38).

For evaluation the velocity distribution and capture velocity could be used. Since the worker is quite close to the contaminant-generating place, occupational hygiene efficiency is possible (Section 10.5).

10.2.3 Enclosures

10.2.3.1 General

The classification of hoods into exterior hoods and enclosures could sometimes make it difficult to specify a hood. This classification is only an attempt to describe the hoods. Enclosures can be separated into partial and total enclosures: partial enclosures have an opening to the surroundings big enough to use for work, and total enclosures do not. Both have the contaminant source inside a physical volume and for some of these hoods this volume is large enough for some workers to work inside. See Fig. 10.39.

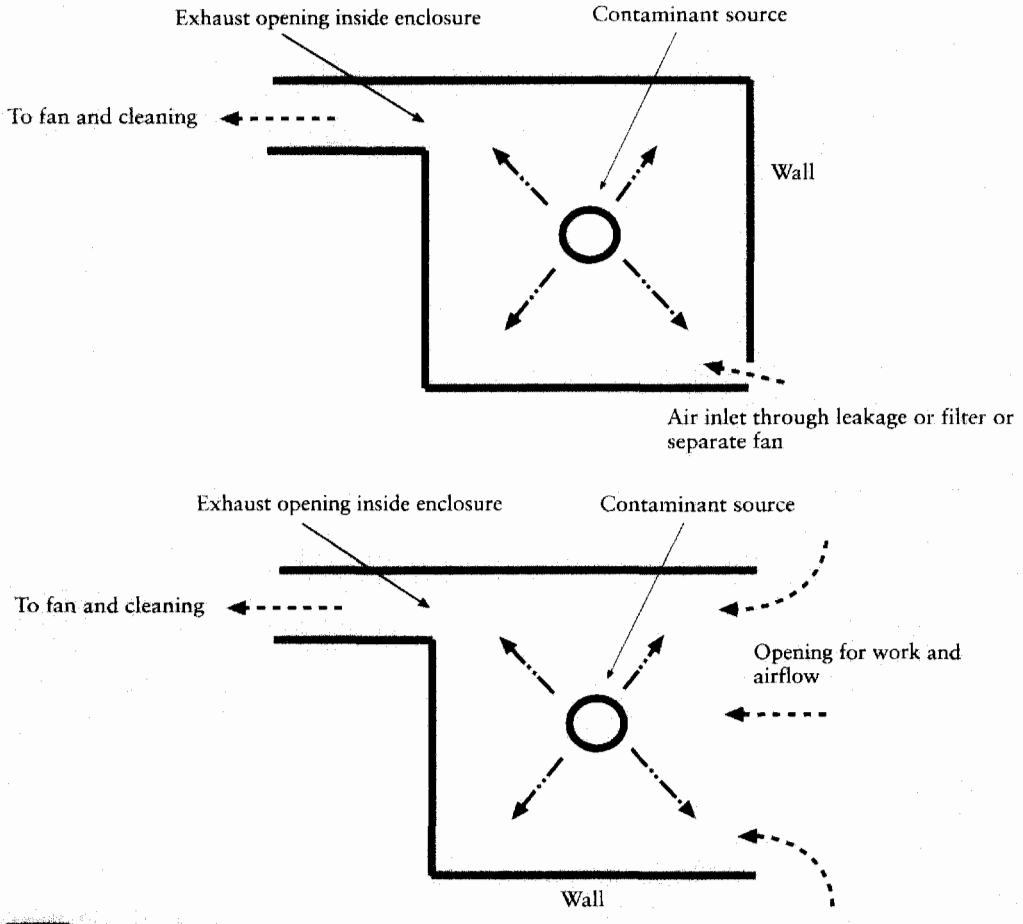

FIGURE 10.39 Principles for total enclosure (*above*) and for partial enclosure (*below*).

Partial enclosures are a compromise between containment and access. Most people misunderstand the function of partial enclosures. It is not possible to completely separate the interior from the surroundings with partial enclosures. Complete separation is only possible with total enclosures. The function of a partial enclosure is as dependent on the flow rate, the flow field, the working procedures, the contaminant generation process, etc. as is the function of exterior hoods. The advantage with a partial enclosure is that the physical walls diminish the possibilities for the contaminants to escape from the hood to the surroundings. Thus these hoods could be used when relatively high demands are put on the contaminant concentration outside the hood.[64] Some of the most commonly used enclosures, such as fume cupboards and booths, are described. Many variations of these exist, e.g., enclosure of the complete process, and some of these are described here.

The total enclosure is the natural choice when very high demands on the containment of generated contaminants exist (e.g., glove boxes). Usually these are not totally closed, since some air must enter the volume before it is exhausted. The connections to the surrounding are either small openings in the walls (cracks) or a designed opening, which could include a filter to ensure clean air inside the enclosure. If the hoods are combined with internal supply airflow inlets they are described in Section 10.4. The main differences between partial enclosures and total enclosures are that the pressure drop for the total enclosure, to get an acceptable flow rate, is much higher than for a partial enclosure, and that the necessary flow rate for adequate contaminant control is usually smaller for the total enclosure than for the partial enclosure.

Access to the interior of the enclosure is much more restricted for a total enclosure than for a partial enclosure. So-called totally closed hoods, where all contact between inside and outside is through air locks or by robot or remote control (see Section 10.4.6.4), these are not only expensive to construct and operate, they also need specialized ventilation systems to function properly.

If the contaminated airflow rate that is to be exhausted, or the internal pressure, varies too much it could be advantageous to use an exhaust connection with a small distance between tube and duct, acting as an opening for additional air when contaminant flow rate is low. This could be in the form of a large exterior hood covering the outlet from the process and leaving only a very small opening gap for external air (thimble). See Fig. 10.40.

There are many different types of these enclosures, such as hoods around transfer points for conveyor belts, hoods connected to electric furnaces, hoods for large storage bins, etc. These hoods are usually designed to use the actual equipment's walls and existing openings as exhaust connections. The contaminant generation rate often varies in these volumes. This makes it necessary to have some kind of volume or flow regulator to prevent leakage. In principle an exhaust flow rate that varies with the generation rate or is large enough for the largest generation rate could be used. There are two other solutions to this problem. One is to make some part of the hood, the wall, or the exhaust connection of flexible material. In this way the volume could vary with the internal pressure, the exhaust flow rate could be kept constant, and leakage could be prevented. The second is to have a large enough volume in the hood to function as a reservoir. This volume stores some of the contaminated air inside

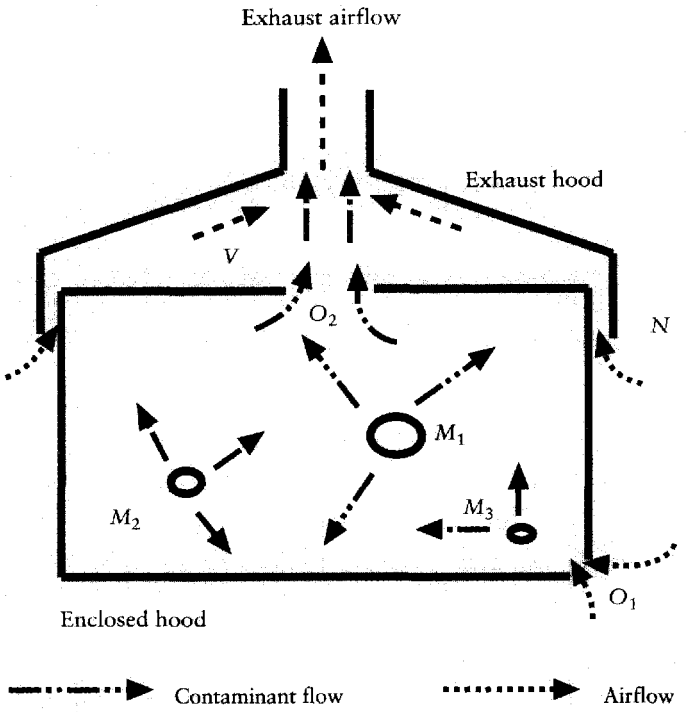

FIGURE 10.40 Connection of exhaust when source rate varies so much that airflow rate is influenced. When the source rate is high, the volume *V* functions as temporary storage. When the source rate is high, the volume *V* functions as temporary storage. When the source rate is low, the exhaust is sucked through *N*. In this way the exhaust airflow rate may be held constant, even if the source rate varies. M_1, M_2, and M_3 are contaminant sources with varying source rates. O_1 is a small opening for air, *N* is one (or more) narrow slit for air bypassing the enclosed hood, *V* is volume where pressure is lower than in the source volume and the pressure loss through *N* is higher than through the opening(s) O_2.

the hood, while the airflow continues to exhaust at a constant rate. When the contaminant generation rate decreases, the stored contaminant is exhausted. However, this construction could lead to high concentrations, or "dead spots," in some sections of the enclosure. This could result in some spreading of the stored contaminant to the surrounding.

The location of the exhaust opening inside the enclosure should be in the main direction of the expected emission direction. The exhaust opening is usually located in the back wall, but many other locations are possible, including the ceiling, side wall, floor, or combinations of these. These other locations are used in practice.

Under normal operating conditions the worker will be situated outside the enclosure. The operator will enter the hood only with his or her hands/arms. During the setting up of equipment it may be necessary to enter the enclosure, but entry should be kept to a minimum and, whenever possible, before the emission of contaminant has commenced.

It has long been recognized that the presence of a worker close to an enclosure, especially a fume cupboard, can have a significant effect on the exhaust hood performance (see Section 10.2.3.3). However, one aspect of

operator interaction that can be modified is operator movements. These create unstable eddies that can have a significant adverse effect on the containment performance of fume cupboards. The effects found for fume cupboards are similar for other partial enclosures. With total enclosures, workers do not normally influence the performance of the hood.

Equipment and supplies should be placed in the enclosure before a contaminant-generating procedure commences. Unnecessary equipment should be removed. High-input heat sources within an enclosure will cause convection currents that can disturb the flow and should be avoided, if possible, or accounted for with correct placement of baffles and/or exhaust connections.

Disturbances to the airflow into and in an enclosure can be caused by

Equipment and the process being carried out in the enclosure,
The presence and movements of the operator,
Movement of other personnel,
Drafts or cross-flows external to the enclosure, and
Fluctuating conditions downstream of the enclosure.

Measures should be adopted to minimize these effects.

Disturbances can be caused by all processes that take place in or that pass through the remaining openings of the enclosure. If the location of the worker is in the opening, between the contaminant source and the surrounding room, recirculation areas in front of the worker can be created that could carry contaminants into the breathing area.

Working locations between the contaminant source and the capture openings dramatically reduce the efficiency of the capture system and should therefore be avoided. If the hood is enclosed on three vertical sides the sensitivity to cross-draft is low.

Enclosures and especially fume cupboards normally remove large quantities of air, need to be replaced via a well-designed makeup air system. The enclosure and the make-up air supply should be regarded as an integral system and the supply must not compromise the performance of the enclosure. As room air currents can have a significant effect on the containment of an enclosure, the problem is to replace the extracted air with a minimum of disturbance to the room air. This may require the use of special diffusers or a perforated ceiling to achieve sufficiently low air velocities. It is usually recommended that the air speed from such devices not exceed 50 to 60% of the face velocity of the enclosure. This would lead to a value much lower than that usually found with conventional ceiling diffusers or grills.

Drafts from windows and doors can have speeds that exceed that through the face of the enclosure. This can be especially so where the makeup air does not balance the amount extracted by the enclosure(s). Doors should be kept closed unless the room has been specifically designed to operate otherwise.

An increase of the capture airflow rate normally results in increased capture efficiency, but the relationship between these quantities is not linear. A case-by-case evaluation is necessary to establish this relationship. In every case an increase of the airflow rate causes an increase of the operating costs. Analogously, a decrease in airflow rate leads to a decrease in capture efficiency and in some cases, a total breakdown of the capture effect (e.g., capture devices working with the vortex principle require minimum airflow rates).

Evaluation can be performed by measuring capture efficiency using real contaminants and applying the real process or by substituting with tracer materials. A simpler, but qualitative, method of evaluation is the visualization of the airflow. If the relationship between capture efficiency and airflow rate is known, a measurement of the airflow rate can be used for frequent evaluation. See Section 10.5.

10.2.3.2 Booths

General

At many workplaces, emissions occur randomly across a certain emission area (e.g., across the area of a workbench or grinding workpiece). In many cases these emissions are difficult to control using exterior exhaust systems because of the undefined emission location and because of work procedure flexibility. Additionally, severe influences (cross-flows) from the surrounding room often reduce the efficiency of single exhaust elements to a minimum. In such cases, booths are the appropriate choice for a local exhaust system.

Booths are partially enclosed workplaces with one or more open face(s) for access by workers. These openings at one or more sides of the enclosure function not only to capture air contaminants directly through their short-distance capture capability but also to cause an airflow in a certain direction (normally away from the worker/work process and into the enclosure). The capture efficiency could be increased by using an existing main flow direction (e.g., thermal flows caused by heat sources) to support the capture process.

Principle

Medium-sized workpieces (workbench size up to 4–5 m square base) often need to be treated during work processes. Depending on the treatment process, different types of emission areas are possible. The actual emission area due to the treatment may be small (e.g., during welding) but time dependent, moving across the whole workpiece, or the emission area could be the whole surface of the workpiece (e.g., during spray painting). In both cases it is nearly impossible to realize an effective capture of the air contaminant while using external capture elements. Either the elements have to be readjusted every moment to ensure proper function or the exhaust airflow has to be increased to unrealistic values in order to increase the grasp of the capture elements.

When using a booth the capture efficiency of one or more basic capture openings (slot, bellmouth inlet, etc.) is enhanced by shielding it against influence from the surrounding airflow (cross-drafts) from at least one side and therefore restricting the flow toward the opening. Since the direct grasp of exhaust openings is very short, the main effect is obtained from the ambient air entering the booth while following the air volume flow deficit, thus generating a general draft into the booth. The aim is to establish a flow across the entire remaining open faces of the booth, uniformly directed into the booth and toward the capture openings.

Generally the capture openings are located in the back wall of the booth but may also be in the ceiling, side wall(s), floor, or a combination of these locations. The location of the exhaust opening depends on the type and direction of the emissions.

If a significant thermal stratification is expected inside the booth, the pressure difference between the inside and the outside of the booth, which increases with height has to be taken into account during the design process. Appropriate design features include efficient capture devices in the ceiling of the booth and an overall dense structure of the booth.

Applicability of Sources

Booths are generally suitable for all sources where the location of the emission can not be restricted to a fixed point (e.g., area sources) or moving point sources (e.g., polishing, grinding, welding, spray painting) and for sources with high momentum-driven emissions (e.g., grinding, spray painting).

Booths are often used for work procedures with momentum-driven emissions. In such cases the capture devices must be placed to take advantage of this momentum. For example, a spray paint booth would have the exhaust location downstream of the painting location, most likely at the back of the booth. The capture devices in the back wall should be suitable to reduce the momentum of the emitted particles in such a way that they are not reflected back into the work area. Floor exhaust should be able to keep the heavier particles down so that they cannot be a source for secondary emissions.

Different Forms and Boundaries Relative to Other Types

Based on the manufacturing process, the existing emission processes, and on workers' demands (e.g., ergonomical aspects), different types of booths are possible. Many of these are commonly used. There can be a division according to the booth type (the shape of the booth), the position of the worker, the type of emission process, and the applied types of capture devices with the corresponding airflow pattern inside the booth.

The essential booth types are

Floor type or cabin: The floors of these booths are at or very near to the facility floor level. They are often very large to accommodate very large workpieces. In some cases, these booths may have flexible or hydraulically movable walls or roof to ensure access to the booth by a crane (see Fig. 10.41).

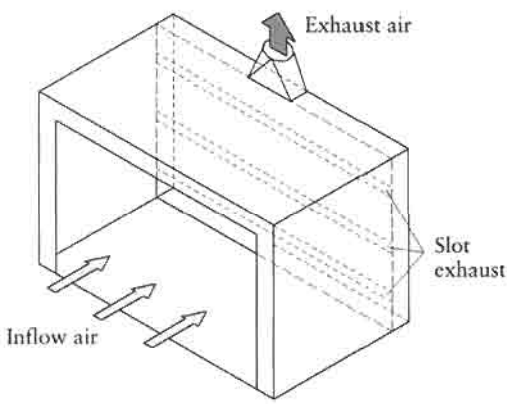

FIGURE 10.41 Scheme of a floor-type booth (cabin).

Workbench type: Booths of this type have at least one open face and thus may be laboratory fume cupboards, safety cabinets, or similar equipment.
Special-purpose type: Booths of this type are specially designed, in shape and function, for a certain production facility and/or process.

The position of the worker could be inside or outside the booth. In some cases, the worker is no longer necessary because of automation. The essential types of emission processes are described in the *Design Equations and/or Parameters* section.

In addition to the location of the capture systems, booths could be assigned to different design categories:

Systems with extraction only: The most common of this type use slot exhaust devices that are more or less uniformly distributed across the exhaust wall of the booth (e.g., the back wall). Some attention has to be paid to maintaining a uniform distribution of the exhaust volume flow across the slit openings. Rows of bellmouth inlets or even vortex hoods are more advantageous because they provide a more uniform flow field.
Combined systems (extraction with additional supply air): It is advantageous to increase the range of the capture system by an additional supply system. The supply air blows the contaminated air toward the capture openings (see Section 10.4.6).

Booths are also available that recirculate the exhaust air, after internal filtering, to the surrounding room or other areas outside the room.

Specific Issues

Problems will arise if the capture principle is not matched to the process or through the process itself (e.g., clogging of floor capture openings, clogging of filters). The structure of the booth could also be used for purposes of noise reduction.

Design Equations and/or Parameters

The size of the booth, accessibility, and other necessary openings have to be designed according to the demands of the manufacturing process.

The design of the exhaust system is first influenced by the type of contaminant emission caused by the process. Contaminant emissions are possible due to

Momentum (e.g., grinding, spraying),
Density differences due to heat (e.g., shaker roast in foundries) or due to high-density vapors,
Pressure differences (e.g., processes with compressed air), or
Diffusion and evaporation (e.g., solvents from painting).

Capture opening(s) locations should be chosen to take advantage of the initial release direction of the contaminant. This leads to locating exhaust openings in the back, floor, ceiling (e.g., for heat-emitting processes), or side walls of the booth. In many cases it is useful to combine exhaust openings in different sides of the booth.

Generally the airflow rate per cross-sectional area of openings or the influx velocity in the opening (equal distribution across the whole area assumed)

is used as a design base. As a first assumption an influx velocity of $v_{in} = 0.1$ to 0.2 m s^{-1} should be used. Based on the total area of all openings A_{tot}, the necessary airflow rate, Q_{ex}, can be calculated as

$$Q_{ex} = A_{tot} \cdot v_{in} \cdot \tag{10.71}$$

At this step in the design procedure, it is necessary to consider the type of contaminant emission that the booth is designed to control. With the above assumption of influx velocity (0.1 to 0.2 m s^{-1}), all emitted material should remain in the booth. With these velocities, it will not be possible to draw in any contaminants that escape the booth. In case of doubt, the influx velocity, v_{in}, should be increased and the necessary hood flow rate should be recalculated.

Additional calculations are necessary if significant heat loads inside the booth cause thermal stratification. A capture system in the ceiling would be advantageous in this case. A check of the pressure in the booth is necessary to avoid spilling of contaminated air near the top of face opening due to the thermal pressure. The height-dependent inflow or spilling velocity due to pressure differences can be calculated as

$$v(z) = \left[2 \cdot \left(\frac{P_1(z) - P_2(z)}{\rho}\right)\right]^{0.5}, \tag{10.72}$$

where $P_1(z)$ and $P_2(z)$ are the linearized functions of the pressure versus height z.

$$P_1(z) = P_{tot,01} - g\left(\rho_{01} \cdot z + b_1 \frac{z^2}{2}\right), \tag{10.73}$$

where $P_{tot,01}$ and ρ_{01} are the values for pressure and density at floor level and b_1 is the linearity factor for the increase or decrease of the density with the height.

It is necessary to check that no outward-directed velocity occurs across the open face of the booth. In such a case, another capture principle must be chosen or the exhaust airflow has to be increased until the needs are fulfilled. The possibility of spilling contaminated air out of the booth could also be reduced by the use of a flexible curtain covering the open face of the booth.

10.2.3.3 Fume Cupboards

General

A fume cupboard is a boxlike, partially enclosed workstation that is used to protect operators and other personnel by limiting the spread of airborne contaminants generated within it. It is ventilated by a mechanically induced inward flow of air through an adjustable working opening or openings (working aperture). This inward airflow is designed to contain the contaminant within the cupboard and to dilute it. The contaminated air is usually ducted away by means of an extract system which should provide for its safe release. Because fume cupboards are partial enclosures, there will be some leakage in the form of transient emissions of contaminant from the opening(s). A fume cupboard should therefore be capable, not only of generally containing the contaminant generated within it, but also of reducing these transient emissions to acceptable levels.

Fume cupboards are frequently referred to as laboratory fume hoods and are a primary method of contaminant control within laboratories.

Principle

Fume cupboards are mostly used for small-scale laboratory work by a single operator either seated or standing outside the cupboard. The opening(s) is furnished with a transparent sash or sashes that shields the operator from the process being carried out within the cupboard. The movement of air around and away from the worker creates a clean-air work zone while at the same time containing the contaminated air within the enclosure. The sash(es) on the working aperture(s), together with the side, back, and top walls, reduce the amount of air needed to produce a sufficiently high inward airflow capable of overcoming the tendency of the contaminant to escape from the cupboard. The sash offers protection against chemical splashes and also shields the source from the effects of cross-drafts. The sides of the cupboard are sometimes transparent, especially if the fume cupboard is to be used for demonstration work. See Fig. 10.42.

A number of design features that are usually associated with good containment by a fume cupboard:

Good entry of the air into the cupboard reduces the size of eddies at the boundaries and can be achieved by using rounded jambs at the side walls, an aerofoil on the sill, and a well designed sash handle.[65]

A back baffle at the rear of the enclosure forms a low-level extract slot in addition to a slot at a high level. The low-level slot helps to make the velocity over the open aperture more uniform as well as producing a flow across the floor of the enclosure which will scavenge any heavy vapors that may not have mixed with the incoming air. The high-level slot removes air and pollutants rising into the upper part of the cupboard.

Applicability of Sources

Fume cupboards are widely used in chemistry laboratories, both in schools and in industry, to control moderately dangerous contaminants generated by small-scale processes. The releases usually have low momentum and ideally the cupboard should be used with the sash in the closed position.

Different Forms and Boundaries Relative to Other Types

Walk-in Fume Cupboards A walk-in fume cupboard is a cupboard in which the working chamber extends to the floor level. Large equipment can be set up in these cupboards before active working commences; it is not intended that they be entered during working. The design is basically the same as that of the bench-mounted cabinet but with either double-hung vertical sashes or horizontal sashes. Horizontal sashes have the advantages of being lighter and easier to move. Walk-in fume cupboards are often fitted with a removable table or shelf as a work surface at normal bench height. This type of cupboard cannot be expected to function well with the front sash fully opened; it would require a large extract volume flow rate and would be susceptible to room air currents and external movements. In practice they should be used with the sash as near to its closed position as possible.

Perchloric Acid Fume Cupboards Use of concentrated perchloric acid gives rise to special hazards and these special fume cupboards should be for perchloric acid use only. Contact of hot perchloric acid with organic materials and certain metals (especially copper) can lead to the formation of perchlorates which,

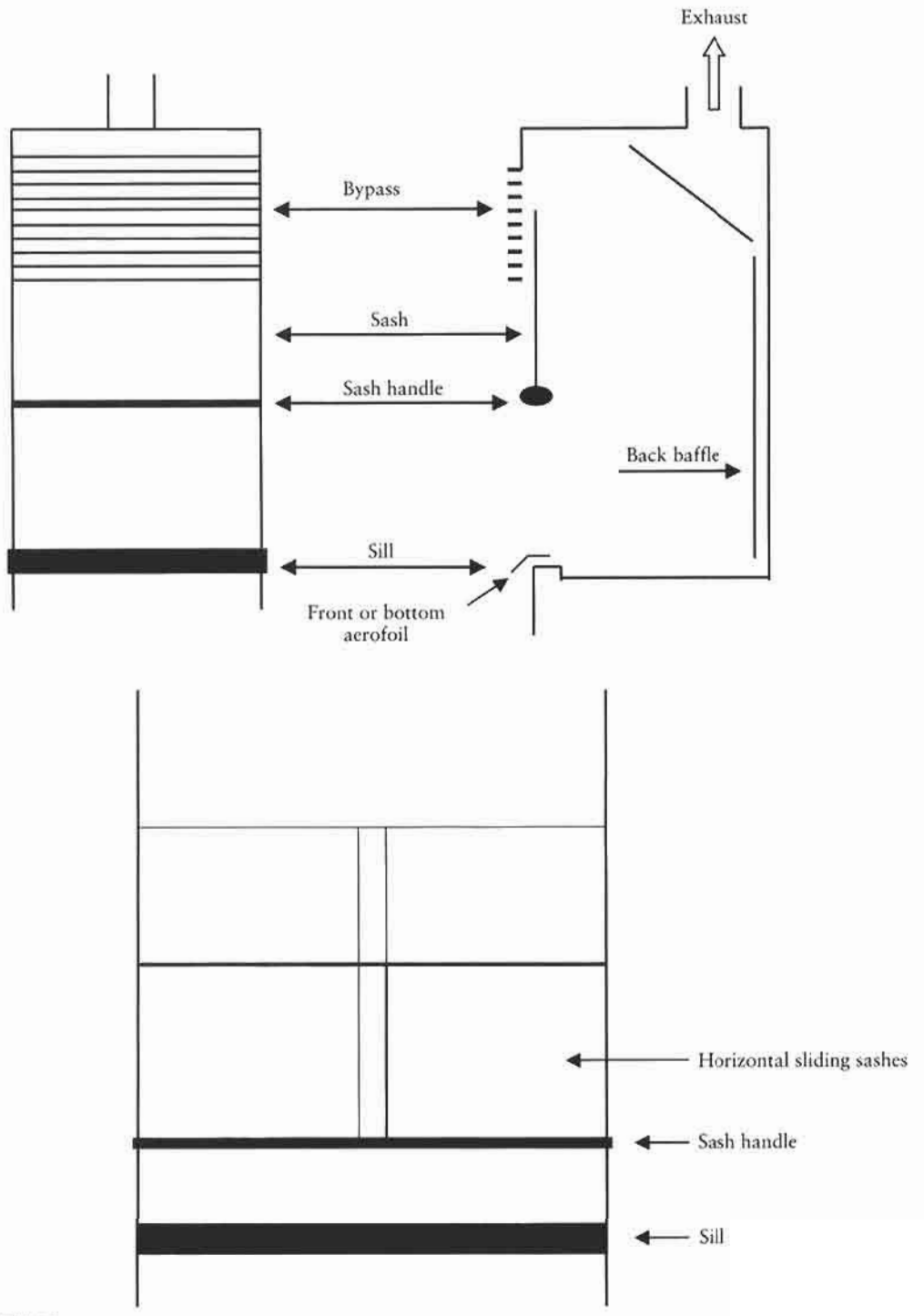

FIGURE 10.42 General nomenclature for a fume cupboard.

in the dry state, can be highly explosive and shock sensitive. In addition, when exposed to perchloric acid certain organic materials, for example wood and cotton, can be very unstable and possibly ignite spontaneously when dry. Perchlorates are water soluble and both this type of fume cupboard and its ductwork system are usually fitted with water wash-down systems. It is particularly important that the area behind the back baffle is thoroughly washed. In consideration of the above comments, the following design features should be incorporated:

1. The materials of construction, from the cupboard to the fan, should be inorganic and resistant to attack by perchloric acid. For the cupboard itself suitable materials include stainless steel of types 316 or 317, solid epoxy resin, and rigid PVC. Stainless steel has been popular for this application as it is easy to form, weld, and polish. It is, however, attacked by the acid, which causes discoloration of the metal surface and the formation of iron(III) perchlorate, which can be explosive. Ductwork, separate from other extract systems, is usually made from stainless steel or plastic materials. Fire regulations may preclude the use of plastic ductwork or require it to be sheathed in an outer casing of metal or GRP. The fan casing and impeller can both be made of plastic.
2. Surfaces should be impervious, smooth, and crevice-free. Joints between walls and the base should be rounded to facilitate cleaning.
3. The whole system should be designed for ease of decontamination. The cupboard will incorporate a wash-down system. Adequate drainage in the cupboard and ductwork is required. Water drained from the system, including that from the fan casing, should be collected and properly disposed of. It should not be possible for water to get onto the work surface.
4. Ignition sources in the cupboard and duct system should be avoided. Plastic fans, electrical sockets external to the cupboard, and explosion-proof light fittings reduce the likelihood of ignitions.

Recirculating Fume Cupboards The recirculating fume cupboard, sometimes called a ductless or filtration fume cupboard, is a type of fume cupboard that recirculates air back to the workspace after it has been filtered. It therefore eliminates the need for an extract and dispersal system. The design and performance of these cupboards has improved greatly since the 1980s, when some early models were found to be inadequate at containing vapors and greatly reduced worker protection.[66] Recirculating fume cupboards have built-in fans that pass the contaminated air through one or more types of filters, e.g., activated carbon, molecular sieves, electret filters, HEPA filters, etc. A pre-filter removes particulate contamination while the main filter, which may be made up of several different types of filter media, removes fine particles, vapors, and gases. The most widely used filters are activated carbon filters, which are used for specific groups of chemicals. The heart of the recirculating fume cupboard is the filtration system and this needs to be selected carefully. It can also be the weakness of this type of cupboard. They are not appropriate for every application. Success and safe use depend on a thorough appraisal of their limitations.

Auxiliary Air Fume Cupboards In this type of fume cupboard, partially treated air is supplied externally to the cupboard directly to or near the face of

the cupboard so as to reduce the demand for fully conditioned air from the workplace, thereby reducing operating costs. The supply air should be distributed uniformly over the height or width of the cupboard and the airflow should be directed into the cupboard at all points over its face. Auxiliary air fume cupboards are dealt with more in Section 10.4.6.

Variable Air Volume Fume Cupboards This type of cupboard incorporates a variable air volume (VAV) controller that regulates the amount of air exhausted from the cupboard such that the face velocity remains essentially constant irrespective of the sash position. A sensor detects either the sash position, the pressure differential between the fume cupboard interior and the room, or the velocity at some point in the cupboard. This information is used to control either the exhaust fan speed or the position of a control damper. The supply air volume flow rate into the laboratory or workspace should also be regulated. It should be remembered that with the sash in the closed position the amount of air to dilute contaminants in both the fume cupboard and the laboratory is reduced and that there could, for example, be difficulty in reducing contaminant levels below the lower explosive level.

Location of Workers and Tools Relative to Exhaust and Source

Under normal operating conditions the worker will be standing or seated outside the fume cupboard and will enter the cupboard only with his or her hands/arms. During the setting up of equipment it may be necessary to enter the fume cupboard, but entry should be kept to a minimum and, whenever possible, should be carried out before any emission of contaminant has commenced.

Disturbances

Disturbances to the airflow into and in a fume cupboard can be caused by

1. Equipment and the process being carried out in the cupboard,
2. The presence and movements of the operator,
3. Movement of other personnel,
4. Fluctuating conditions downstream of the cupboard, and
5. Drafts or crossflows external to the cupboard.

Measures should be adopted to minimize these effects.

Equipment and Processes Equipment and supplies should be placed in the cupboard before a procedure commences. Unnecessary equipment should be removed. High-input heat sources within a cupboard will cause convection currents that can disturb the flow and should be avoided if possible. Work should be carried out well within the cupboard, at least 150 mm from the plane of the sash whenever possible. It should not however be placed closer than 50 mm to the lower extract slot of a back baffle. Large pieces of equipment should if possible be raised 25 to 50 mm above the working surface of the cupboard to improve the flow in the cupboard.

Presence and Movements of the Operator It has long been recognized that the presence of a worker at a fume cupboard can have a significant effect on its performance. Chang and Gonzalez[67] showed that with a person standing in an

airflow, a complex flow pattern is set up in the wake of the body. In the case of a fume cupboard the flow is usually from behind the body so that a region of low pressure develops between the person and the cupboard face. This flow combines with that in the person's thermal boundary layer. Johnson, Fletcher, and Saunders[68] showed that the near-body airflow field could be dominated by these thermal effects, which caused velocities of about 0.2 m s^{-1}. The possibility exists therefore that pollutants could be drawn outward through the aperture of the cupboard and pass into the breathing zone of a person working there. These discharges have been visualized using smoke and are described by several authors.[69,70] It is difficult to do much about the fact that the presence of a person working at a fume cupboard will interfere with the airflow into it. However, one aspect of operator interaction that can be modified is that of operator movement. These movements create unstable eddies that can have a significant adverse effect on the containment performance of fume cupboards.[71] Ljungqvist showed how leakage increased considerably when an operator performed movements as opposed to standing still. Movement of the sash from the closed to the open position causes contaminated air to be released from the cupboard in a pulse lasting for several seconds.[72] Closing the sash has a negligible effect. With systems of working where the closed position is the norm, the sash may need to be opened and closed at frequent intervals, resulting in a relatively high operator exposure.

Movement of Other Personnel A major factor that can influence the containment of a fume cupboard is the movement of personnel in its vicinity. A person walking past a fume cupboard creates eddies in his or her wake with local velocities of the same order as that of the airflow through the face of the cupboard. Measurements of the effects of these eddies on containment of cupboards[72] show that leakage depends on the distance of the moving person from the cupboard. BS7258 recommends that "the distance from the sash to any circulation space should be at least 1000 mm, so as to preserve a zone undisturbed by anyone other than the operator." The size of the leakage will also depend on the speed of the person as well as the air velocity through the face opening. Therefore, although a fume cupboard may perform well under ideal test-room conditions at a low face velocity, movement of personnel close to its face needs to be considered carefully when selecting an operational value for the face velocity.

Conditions Downstream of the Cupboard Variations in conditions downstream of the cupboard may affect the performance of the cupboard. The variations can arise from three causes: atmospheric conditions, multi-extract systems, and VAV controls.

On-site containment measurements[73] made on a fume cupboard on a particularly exposed site showed that very large day-to-day variations in the degree of containment could be attributed to the wind blowing across the stack. A suitable design of stack termination and a high discharge velocity should reduce this problem.

Problems can arise if several cupboards, each with its own fan, are connected to a single common duct and discharge stack. If a fume cupboard was switched off or a fan failed, flow through the cupboard could be reversed causing contaminants to be discharged into the room. The collecting duct should be kept at a lower pressure by its own fan to reduce this risk.

The operation of flow dampers can cause pressure fluctuations in the ductwork system. Measurements by Melin[74] indicate that pressure oscillations in an exhaust system can cause instabilities in the airflow through a fume cupboard sufficient to give rise to outward leakage of contamination, especially when a person stands in front of the cupboard.

Drafts and Cross-Flows Fume cupboards remove large quantities of air, which need to be replaced via a well-designed makeup air system. The fume cupboard and the makeup air supply should be regarded as an integral system and the supply must not compromise the performance of the cupboard. As room air currents can have a significant effect on the containment of a fume cupboard, the problem is to replace the extracted air with a minimum of disturbance to the room air. This may require the use of special diffusers or a perforated ceiling to achieve sufficiently low room-air velocities. It is usually recommended that the air speed from such devices does not exceed 50 to 60% of the fume cupboard face velocity. This would lead to a value much lower than that usually found with conventional ceiling diffusers or grills.

Drafts from windows and doors can have speeds that exceed that through the face of the cupboard, especially where the makeup air does not balance with the amount extracted by the cupboard(s). Doors should be kept closed unless the laboratory has been specifically designed to operate otherwise.

Location of Fume Cupboards

A fume cupboard should be sited to avoid disturbances to the fume cupboard, its operator, and other personnel. It should not interfere with the escape route from the area in the event of an emergency. It should be sited to maximize the working efficiency of the cupboard and the area in which it is installed. Although specified dimensions and layout cannot guarantee performance, the values in Table 10.8[75] are based on experience and are widely used.

A fume cupboard should not be positioned where the only escape route from the area would necessitate passing directly in front of the fume cupboard. Siting with respect to makeup air grills should be considered carefully (see above on drafts and cross-flows) and a minimum separation distance of 1500 mm is recommended.[75]

Changing Flow Rates

Control of contaminant at the face of a fume cupboard depends on the movement of air through the working aperture. The velocity must be sufficiently high to resist the effects of disturbances created by the operator, other personnel, equipment, cross-drafts, etc. It should not be so high, however, as to cause disturbances to equipment in the cupboard or to create eddies in the wake of the operator or from the cupboard itself that will adversely effect containment.

The recommended value of the face velocity has been the subject of much debate and variation over the years. The recommended values have also varied widely with use. For example, CIBSE[76] recommends values as low as 0.2 and 0.25 m s^{-1} for fume cupboards for teaching and research purposes, respectively, and as high as 2.0 m s^{-1} for radioactive work depending on grade. Middleton [77] quotes the optimum range for the face velocity of laboratory fume cupboards to lie between

TABLE 10.8 Recommended Separation Distances for Fume Cupboards

Position	Recommended minimum distance (mm)
Separation from traffic route	1000
Lateral distance from large equipment, pillars, or adjacent wall	300
Distance from opposite wall	2000
Distance from opposite fume cupboard	3000
Distance from opposite bench top used by fume cupboard operator	1500
Distance from door in same wall	1000
Distance from door in wall at right angles	1500

0.5 and 1.2 m s^{-1}. However, ACGIH[25] suggests that face velocities in the range of 0.3 to 0.5 m s^{-1} are suitable. BS7258[75] notes that velocities less than 0.3 m s^{-1} are unlikely to give good containment. A face velocity of 0.3 m s^{-1} is seen by ANSI[78] as being adequate only under near-perfect conditions and not appropriate as a general standard. ANSI sees the value of 0.5 m s^{-1} as adequate and perhaps more than so. The range suggested by ACGIH would therefore seem to be generally acceptable with caution being exercised at the lower end of the range.

Design Equations and/or Parameters

The size of a fume cupboard should be chosen to maximize performance. The height of the work surface above floor level and the overall internal height are determined by the intended usage. Where the required internal height is 2 or more it is worth considering the need for a walk-in cupboard. Widths of cupboards are usually in increments of approximately 300 mm. The choice between vertical and horizontal sashes is to some extent a national preference, e.g., in the UK most sashes are of the vertical type. However, there can be practical reasons for the choice. Some laboratory procedures may require a relatively large vertical reach. To do this with a vertical sash could require several times the airflow rate required using a horizontal sash. The hybrid vertical/horizontal sash could meet most needs. Specification of a face velocity is now regarded as less important than containment but it is worth noting the advice of BS7258[75] that a value less than 0.3 m s^{-1} is unlikely to give good containment. The back baffles should be adjusted to give an even distribution of face velocities; velocities measured at the face should not differ from the mean by more than 15%.

Where a cupboard is fitted with a bypass, it should be designed with an air velocity that is sufficiently high to prevent the escape of contaminants. This is particularly important where the cupboard is likely to be subjected to high heat loads, which could cause strong thermal currents in the upper part of the cupboard. However, the velocity should not be high enough to disturb the flow inside the cupboard and cause loss of containment.

Fume cupboards in themselves generate virtually no noise due to their low air velocities, but they can, and do, amplify noise generated by the exhaust

system. The noise can originate from the ductwork itself, bends, flow controllers, fans, or belt drives. More information on noise generation and amplification in fume cupboard installations is given by Haugen[79].

Evaluation Procedures

Qualitative Testing The use of smoke released around the boundaries and inside a fume cupboard can be a simple and effective way of visualizing the local airflow patterns and gives an indication of the likely containment. It is however a very subjective test. Air movement around and under sash handles can be shown using either titanium tetrachloride applied with a cotton wool swab or a smoke tube. The latter is far more convenient to use and is in the form of a sealed pencil-like glass ampoule. To use, the ends of the tube are broken off. Air is passed through the tube and emerges as a thin plume of dense white smoke. Flow patterns inside the cupboard are better shown by the use of smoke pellets or a smoke generator. The latter has several disadvantages over smoke pellets: it is bulky and heavy, usually requires a power supply, and tends to be fairly uncontrollable in the volume flow rate of the smoke.

The flow should move smoothly into the cupboard and should not re-emerge into the laboratory. It should be remembered that the smoke test is a negative test, i.e., if smoke is seen to emerge from the cupboard, the cupboard does leak; if no smoke is seen to emerge, the cupboard may leak.

More information on flow visualization can be found in Chapter 12.

Quantitative Testing

Face Velocity Measurements Although it is generally accepted that face velocity is not sufficient to specify or describe fume cupboard performance, it is a relatively easily made measurement that is readily understood and widely quoted. Low face velocities make a fume cupboard sensitive to outside disturbances (for example drafts) whereas excessively high velocities can cause eddies in the wakes of operators and under sash handles which can lead to contaminant being drawn out of the cupboard.

There are two main types of instrument in general use for face velocity measurements: vane anemometers and thermo- or heated-element anemometers. The latter type is becoming increasingly popular although the traditional vane anemometer is still widely used. The vane anemometer has a number of disadvantages. It is relatively large and this may physically restrict its use in certain circumstances. The value measured is an average over a large area. The instrument has a slow response to velocity fluctuations and cannot be used to investigate turbulence levels. In addition, the calibration of vane anemometers needs to be checked frequently. With a thermal anemometer the loss of heat from the sensing element is a function of the airstream velocity past it, resulting in a fairly fast response. Commercial instruments usually have two sensing elements to give temperature compensation. This type of instrument will tolerate moderate contamination by dust, can be cleaned (with care), and is in common use in the field.

To make measurements, the working aperture of the cupboard is divided into equal areas by imaginary lines parallel to the sides of the aperture. The air velocity is measured in each of these areas and sometimes its variation with time. If individual velocities are within about ±15% of the mean, there should be little cause for con-

cern.[80] (The accuracy of individual readings is likely to be ±10%.) These measurements can identify problems caused by crossdrafts and badly adjusted back-baffles.

Containment Tests Fume cupboards offer only partial containment. It is therefore logical to seek a test that measures how good the partial containment is. Such information can be useful not only in assessing the safety of a fume cupboard but also in comparing different design features and different manufacturers' cupboards. Although there are several different methods of determining containment, the basic method is the same and involves the release of a tracer inside the cupboard and detection of leakage at a point or points outside of it. The tracer is usually a gas mixture, 10% sulfur hexafluoride (SF_6) in 90% nitrogen. SF_6 is a very dense gas and mixture with nitrogen makes the density of the tracer closer to that of air. The tracer is supplied from a pressurized cylinder via a pressure gauge and flowmeter, at a flow rate between 1 and 8 liters per minute (L min^{-1}), to a gas ejector. The ASHRAE design has been quite widely used in the past. It is used for example in the American ASHRAE 110-1995 and German DIN 12 924 standards. The gas passes through a critical orifice, entrains air through openings in the body of the device, and is ejected through wire-mesh gauze. The tracer is ejected at relatively high speed (over 1 m s^{-1}) into the fume cupboard. In a second type of ejector, the tracer gas passes into the cupboard through a sintered material and emerges into the cupboard at relatively low speeds. Devices of this type are used as silencers when venting air from compressed air systems and have the added advantages of being small, readily available, and cheap. Use of this type of ejector is proposed in a draft CEN Standard on fume cupboards currently under preparation.

Some standards (for example ASHRAE 110-1995,[81] DIN 12 924,[82] and Nordtest[83]) specify the use of a manikin at the face of the fume cupboard during containment while others (for example, BS7258[75]) have an unobstructed entry. Under the ASHRAE protocol the tracer gas leakage is sampled through a collection probe at the breathing zone (nose) of the manikin, whereas the DIN standard specifies sampling over a grid of points outside the cupboard 100 mm from the plane of the sash. The British standard specifies a sampling grid in the plane of the sash. The draft CEN standard will not specify the use of a manikin for this type of containment test and will have sampling grids both in the plane of the sash and at some distance in front of it to allow for a dynamic sash test.

The gas sample taken is analyzed usually by either an infrared or an electron capture gas analyzer. The infrared gas analyzer is the more widely used device and is capable of analyzing a broad spectrum of gases. It is heavy and bulky but portable. Some models have built-in calibrations but on-site calibration will give more accurate results. The gas sample usually passes through a large cell (2 to 5 liters) at a flow rate on the order of 15 L min^{-1} and the response time of the instrument is therefore several seconds. As contaminant is ejected from fume cupboards in bursts lasting a matter of seconds,[63] the output signal of the analyzer is attenuated and does not accurately reflect the true course of events. Electron capture devices will detect any electron capture gas. The instruments are small, portable, can often be battery operated, and have a very small measuring volume. The response time is very short and the output of the instrument gives a close representation of the real-time events. The output signal of early instruments tended to drift with time but this problem seems to have been overcome. Both types of instrument will

measure SF_6 concentrations in the likely range of interest (about 0.01 to 20 ppm). The output of the analyzer can be fed to a chart recorder, datalogger (for downloading into a PC), or directly into a PC for processing.

The effectiveness of the fume cupboard can be expressed in a number of ways. Several of these ways are discussed by Melin[74] and Olander.[13] Nordtest[83] defines an escape safety parameter as

$$E = \frac{C_x}{(C_x + C_{max})} \times 100\%, \tag{10.74}$$

where C_x is the calculated tracer gas in the exhaust air and C_{max} is the maximum recorded tracer gas concentration.

In the ASHRAE standard the fume cupboard performance is summarized by expressions of the following type:

$$\begin{matrix} \text{xx AU yyy} \\ \text{xx AM yyy,} \end{matrix} \tag{10.75}$$

where xx is the tracer gas release rate in L min^{-1}, yyy is the average gas concentration measured in ppm; AM is "as manufactured," usually tested in test room with no equipment in the cupboard; and AU is "as used," installed in a laboratory with equipment as in actual use.

In Section 10.5 other efficiency measurements are described.

10.2.3.4 Gas Storage Cabinets

General

Gas storage cabinets were originally developed for the semiconductor industry in the 1970s. These early storage cabinets consisted of a box that enclosed the tank and connections; they were operated under negative pressure and exhausted to the outside. Gas storage cabinets have become more sophisticated, adding gas detection, fire sprinklers, alarms, and pneumatic controls.[84] Some cabinets have point-of-operation air cleaners such as scrubbers.

Many building and health and safety codes require the use of gas storage cabinets, exhausted enclosures, and/or separately ventilated gas storage rooms for toxic gases. These controls are also recommended for flammable and corrosive gases.

Compressed gases are defined in several ways. In the UK compressed gases are defined as "gases with a gauge pressure exceeding 1.5 kg cm^{-2}" and "liquids with a vapor pressure exceeding 3.0 kg cm^{-2}." The U.S. Department of Transportation defines a compressed gas as "any material or mixture having in the container either an absolute pressure greater than 276 kPa at 21°C or an absolute pressure greater than 717 kPa at 54 °C, or both, or any liquid flammable material having a Reid vapor pressure greater than 276 kPa at 38 °C."[85]

Principle

Gas storage cabinets consist of a box that encloses the tank(s) and all connections. Many include change out capabilities and an access door. The cabinets are exhausted to remove any contaminant that may leak into the cabinet and to maintain the cabinet under negative pressure relative to the

surrounding area. The gas cabinet is designed to control fugitive emissions from the gas cylinder and gas distribution system. In most cases, a violent release of the cylinder contents will not be controlled.

Applicability of Sources

Gas storage cabinets are used to contain compressed gas cylinders containing toxic, flammable, or corrosive gases.

Different Forms and Boundaries Relative to Other Types

Gas storage cabinets are designed to contain one to four gas cylinders. The cylinders are connected to a gas distribution system which is also contained in the cabinet. Very sophisticated systems are available from cabinet manufacturers. These may include automatic or semiautomatic change-over capabilities, fire sprinklers, purging systems, and gas detection systems which may include alarms and automatic shutoff. Point-of-use scrubbers may also be incorporated into the design, depending on the gas being used (see Fig. 10.43).

Specific Issues

In addition to the toxic and/or flammable properties of the gas, the gas cylinder may also pose a hazard due to the potential high-energy release of the contents. For this reason, additional safety considerations are necessary. The cylinders are specifically designed to contain the contents under high pressure. Careful inspection and maintenance is necessary. The fittings used on the cylinder are often specific for the gas of concern and mixing of components among different cylinder types is not recommended and is, in some cases, prohibited. Cylinders need to be restrained to prevent accidental damage to the valve or regulator. During transport the cylinder valve should be covered.

Gas storage cabinet use may be required by local, state, or national codes. These codes vary by location and the designer or user of the cabinet is referred to these codes for further information. One source of building code information in the U.S. is the Uniform Building Code[86] and the Uniform Fire Code.[87]

The Uniform Fire Code requires that pyrophoric, flammable, or highly toxic gases be within ventilated gas cabinets, laboratory fume hoods, or exhausted enclosures.[87]

Gases with a health hazard, flammability, or reactivity ranking of 3 or 4 (toxic or highly toxic) should also be used and dispensed from a ventilated gas cabinet. The cylinder and any fittings subject to leakage should be enclosed by the cabinet.[88]

Toxic gas monitoring including visual and audible alarms and communication with a constantly attended Emergency Control Station may also be necessary in areas that use toxic or highly toxic gases. The monitoring system must also automatically close the shutoff valve on toxic or highly toxic gas supply lines. Smoke detectors are required in rooms or areas where highly toxic compressed gases are stored indoors.[88]

The Uniform Mechanical Code[89] requires that ducts carrying explosive or flammable gases be ducted directly to the outside of the building.

Design Equations and/or Parameters

The average face velocity at all openings into a gas cabinet should be at least 1 m s^{-1} with a minimum velocity at any point of 0.76 m s^{-1}.[89] These

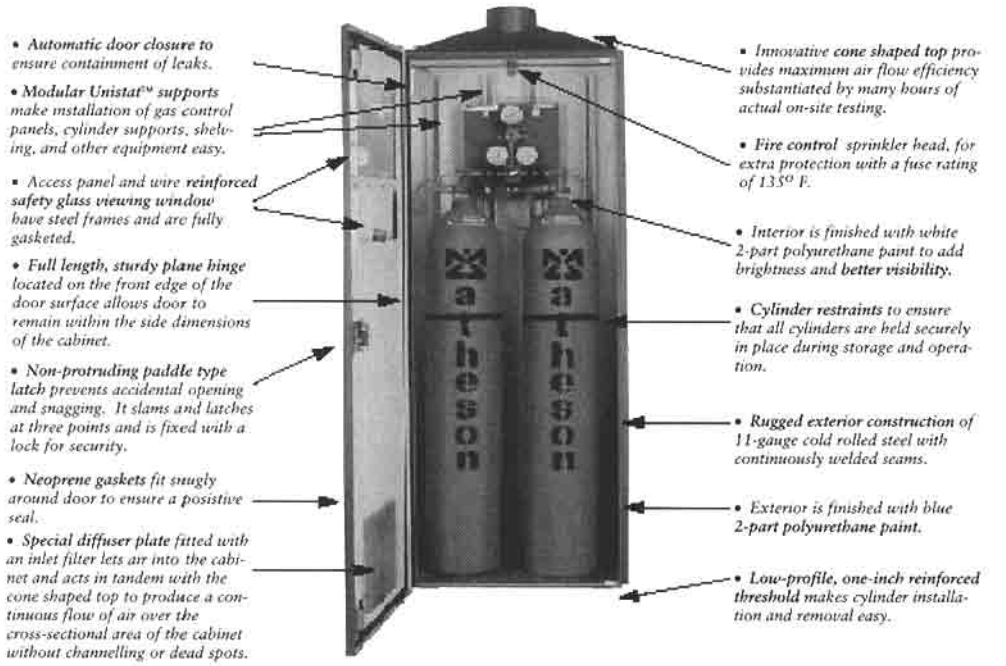

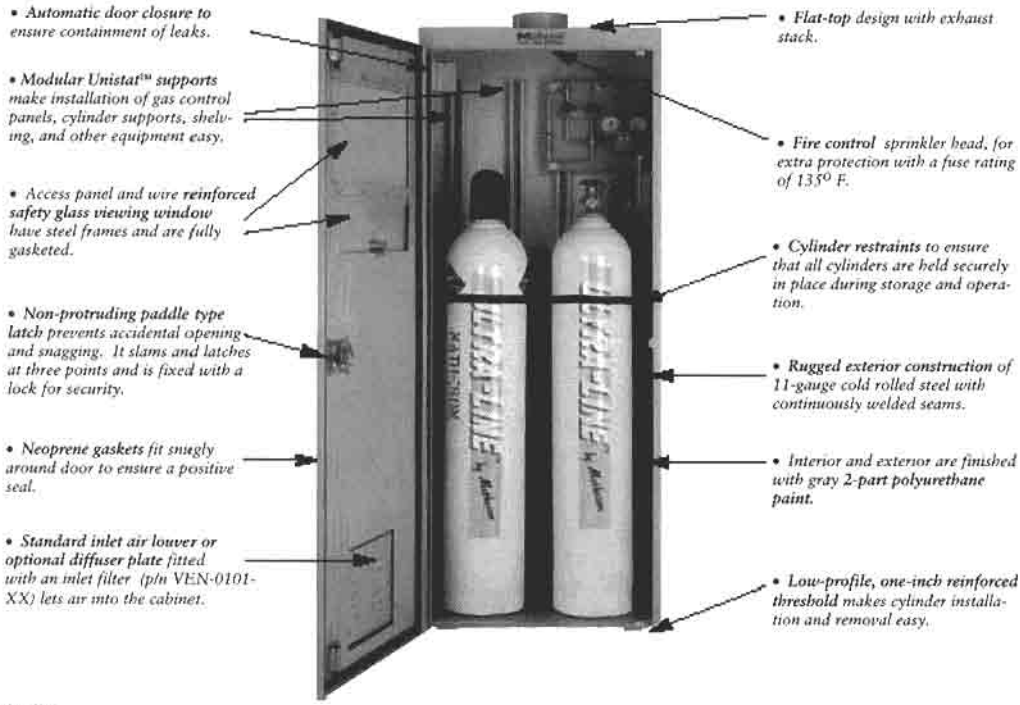

FIGURE 10.43 Typical designs for gas storage cabinets (Matheson Gas Products, used with permission).

velocities must be maintained through the access port at the valve, but also through the door of multiple cylinder cabinets when the door is opened to replace a cylinder. The cabinet may be equipped with a two-position flow operation interlocked with the door which will increase the airflow when the door is opened.[88]

Burgess et al.[40] describe a study of gas storage cabinets. In the study, coefficient of entry (C_e) for various inlet/outlet configurations was measured. A tracer gas study is also described. The tracer gas study involved releasing sulfur hexafluoride (SF_6) at 0.032 L s^{-1} at a critical leak position in the cabinet and measuring SF_6 concentration in the exhaust stream. The tracer gas was turned off when a steady exhaust stream concentration was observed and the time for the concentration to decay to 5% of steady state was measured.

The study found that the slot-type inlet at the bottom of the cabinet door resulted in higher pressure losses (lower C_e) than the diffuser or perforated plate inlet. The exhaust configuration had little effect on C_e or tracer gas clearance time. The study also concluded that an exhaust rate 0.118 m^3 s^{-1} for a two-cylinder cabinet was sufficient as little improvement was seen with an increase to 0.165 m^3 s^{-1}.[40] The slotted inlet took longer to clear a leak than either the perforated plate or diffuser inlet. Measured coefficients of entry for a two-cylinder gas storage cabinet are shown in Table 10.9.

Pyrophoric gases deserve special consideration. Considerable research on storage and use of silane gas has been performed. A summary of some of this research is provided by the Semiconductor Safety Association.[90]

Building codes also require that systems conveying explosive or radioactive materials be prebalanced through duct sizing. Other systems may be designed with balancing devices such as dampers; however, dampers provided to balance airflow must be provided with securely fixed minimum position blocking devices to prevent restricting flow below the required volume or velocity.[88]

10.2.3.5 Enclosures of Complete Process (Buoyant and Nonbuoyant Sources)

Enclosures for Buoyant Sources

Enclosures are used throughout industry to capture emissions from buoyant sources. The following discussion pertains mainly to large enclosures such as those used on metallurgical process vessels. Many of the design equations and procedures developed for buoyant source hoods described by Goodfellow[91,92] apply to large enclosure design. Process vessels successfully using enclosures include electric arc furnaces, top and bottom blown-oxygen steel conversion furnaces, and nonferrous converters.

The use of enclosures for fugitive emission capture on process vessels such as furnaces offers the following advantages:

1. Total capture of emissions is possible (equivalent to total building evacuation). The enclosure offers total containment, unaffected by in-plant drafts.
2. Working conditions outside the enclosure are drastically improved. The bulk of heat, fume, and dust from the process vessels is contained within the enclosure.

TABLE 10.9 Coefficients of Entry for Gas Storage Cabinets[40]

Inlet configuration	Outlet configuration	Coefficient of entry, C_e
Slot	Flat	0.44
	Shallow cone	0.47
	Deep cone	0.47
Diffuser	Flat	0.7
	Shallow cone	0.75
	Deep cone	0.72
Perforated plate	Flat	0.68
	Shallow cone	0.72
	Deep cone	0.72

3. On small and low-production furnaces, the enclosure can be used as both primary and secondary control, thereby reducing the need for other equipment.
4. As a side benefit, on electric arc furnaces the enclosure offers a great potential for noise control.

The main disadvantages of using an enclosure are as follows:

1. The potential for interference with the normal operation and maintenance of a process vessel is high. A major design effort is required to overcome this disadvantage. All aspects of the process vessel operation must be considered. Lines of sight for process vessel and crane operators, access for crane-held ladles and buckets, process vessel movements, and maintenance access must be accommodated by the enclosure design. This is more easily achieved in a new installation.
2. Enclosure design on retrofit cases becomes very difficult and may require a compromise between process vessel operation and fume capture performance.

The design methodology is based on dealing with the following three main aspects:

1. Process and layout,
2. Fume capture, and
3. Mechanical design.

Discussion of design aspects will concentrate on electric arc furnace enclosures, although the design methodology generally applies to most large enclosures.

Process and Layout Requirements The key to a successful enclosure installation is to consider all process and layout requirements during the initial design stage. When planning an enclosure for a metallurgical furnace, the following questions should be asked:

1. Are primary and/or secondary emissions to be controlled by the enclosure?
2. What is the extent of furnace and related equipment movements?

3. How will the enclosure affect the furnace operation process control?
4. Where must enclosure openings be located?

On oxygen steel conversion furnaces, primary fume control is usually achieved by a separate close-capture hood positioned over the vessel mouth. The enclosure is then used for secondary fume control during charging, turndown, tapping, and slagging.

On electric arc furnaces, an enclosure can be used for both primary and secondary fume control. However, for large, high-production furnaces, it is more economical to provide separate direct evacuation control for primary melting emissions. Use of separate gas cooling equipment to handle the high heat content from primary emission off-gas on high-production furnaces is often less expensive than directly quenching with large amounts of dilution air from an enclosure. The amount of air dilution is dictated by fabric filter temperature limitations. Generally, if the enclosure exhaust rate for secondary fume capture is similar to or more than that required for primary control, the enclosure system is designed to handle both emissions.

If primary control by the enclosure is under consideration, the extra wear and tear on electrode holding equipment by the escaping fume must be taken into account. This potential problem is particularly evident on ultra-high-power (UHP) furnaces where the holding equipment would be constantly exposed to high-temperature flame. As a possible solution, the furnace could be equipped with a roof-mounted water-coiled stub stack, which naturally draws fume from the furnace and into the enclosure. This approach would divert the fume and prevent damage to the electrode equipment.

When primary fume capture is performed by the enclosure, furnace off-gas combustion efficiency is lower than experienced by furnace direct evacuation control. The off-gas, rich in carbon monoxide (CO), rises from furnace roof openings and partially burns and cools with enclosure air. Significant levels of CO have resulted in the enclosures and exhaust ducting from this type of combination. These levels are not explosive but present a potential hazard to personnel working in the enclosure or in downstream fume cleaning equipment.

Various furnace movements must be accommodated by the enclosure. Operations such as furnace tilting for tapping and slagging, electrode vertical lift, and direction of furnace roof swing must be coordinated with respect to enclosure shape and the location of the exhaust off-take.

Movement of related equipment must also be considered. Tapping ladle and slag pot positioning may be done by overhead cranes or transfer cars and will dictate the extent of enclosure doors and roof slots. Charge bucket positioning and approach by overhead crane will also determine door and slot requirements. Routine removal of the furnace roof and water-cooled panels by overhead crane may finally dictate the size of openings. Emergency procedures must also be accommodated in the design. For example, a full ladle trapped in the enclosure because of a doorjamb must be removed before the metal solidifies.

The following items affecting furnace operation and process control should be addressed as the enclosure shape is established:

1. Line of sight for crane operators and furnace attendants,
2. Furnace control points and attendant location,

3. Method of charging additives,
4. Furnace ancillary equipment location, and
5. Equipment maintenance access requirements.

Furnace control points and ancillary equipment location must be considered as to whether they are positioned in or out of the enclosure. If the bulk of furnace ancillary equipment is located in the enclosure, layouts must allow for proper servicing. If attendants must work in the enclosure during furnace operation, emission capture design must provide a relatively fume-free work environment. In general, enclosure-opening requirements should be minimized during the layout stage. Bucket charging of an electric arc furnace requires a roof slot for crane access. Sliding doors can be used to cover these openings. After the bucket has entered the enclosure, the side doors are closed but the roof slot doors remain open. An air curtain blowing across the roof slot, as shown in Fig. 10.44, can be used to prevent charging emissions from escaping through the roof slot. Ample clearance is required to fit doors and air curtain equipment on the enclosure roof. A roof slot is also required during tapping if the ladle is held by the crane.

Fume Capture Fume capture is accomplished by a combination of the following enclosure features:

1. Containment and storage of the emission,
2. Air extraction from the enclosure, and
3. Air curtain and exhaust off-take.

If acceptable working conditions must be maintained in the enclosure during furnace operation, attention must be given to internal airflow patterns, i.e., minimization of fume recirculation in the enclosure.

Containment and Storage of the Emission The main function of the physical enclosure is to contain secondary furnace emissions from tapping, slagging, and charging and perhaps primary emissions from melting. These emissions are thermally driven against the enclosure roof and can overcome the in-draft effect of the extraction system if the enclosure is not built tightly. Gaps around roof slot doors can also present a severe leakage problem. When the roof doors are open for crane rope access, an air curtain can be effectively used to contain emissions.

The enclosure is also capable of storing fume surges during bucket charging. With proper design, the top of the enclosure will fill with fume while the lower working level remains clear. The key to producing this effect is to reduce fume recirculation in the enclosure by proper placement of the air curtain with respect to the exhaust off-take.

Tapping, slagging, and melting are prolonged, continuous operations. During these periods, the enclosure should not be used for fume storage. The enclosure exhaust capacity must be greater than the emission plume flow rate to avoid fume buildup in the enclosure during these operations.

Air Extraction from the Enclosure A textbook approach to enclosure design for a hot process would follow a procedure of determining the in-draft veloc-

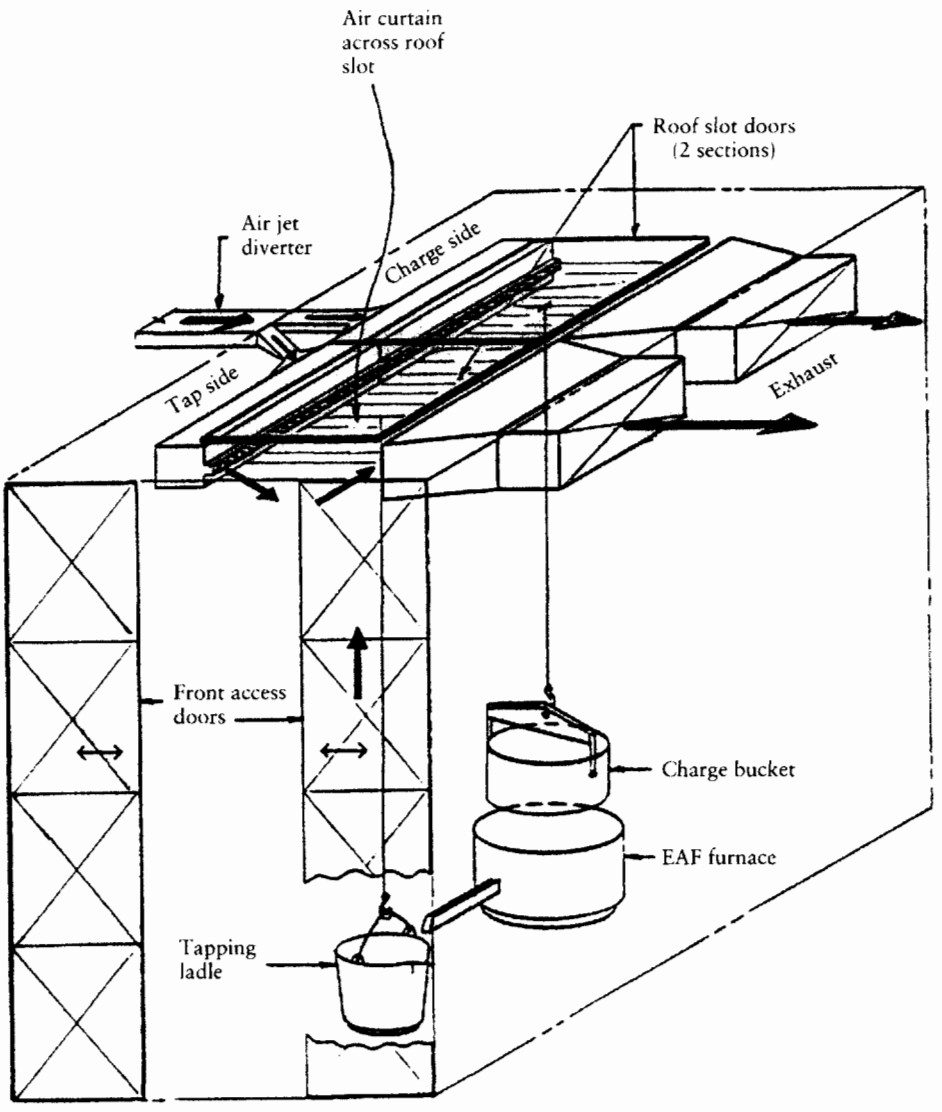

FIGURE 10.44 Air curtain application on an EAF enclosure.

ity required to overcome the stack or "chimney" effect. This calculation could serve as a check, but does not account for plume updrafts in the enclosure.

To determine the air exhaust rate from the enclosure the following steps are recommended.

Step 1: Determine primary emission heat content. This step should be taken early in the design stage to determine if the enclosure will capture both primary and secondary emissions. The heat content of furnace emissions and the temperature limitation on the fume collector are considered for this task. The off-gas heat content is calculated for furnace reactions during melting and refining periods. The maximum heat content should be used for design. Assuming a fabric

filter collector with polyester cloth is used, a 130 °C temperature limit is imposed for continuous operation. The fume volume flow rate after dilution is then determined from the elementary thermodynamic equation:

$$q = \frac{\Phi}{\rho c_p (T_s - T_{amb})}, \tag{10.76}$$

where

q = actual volume flow rate after dilution ($m^3\ s^{-1}$)
Φ = heat release rate from furnace off-gas ($kJ\ s^{-1}$)
ρ = air density at T_s ($kg\ m^{-3}$)
c_p = specific heat of air at T_s ($kJ\ kg^{-1}\ °C^{-1}$)
T_s = specified air temperature after dilution (°C)
T_{amb} = ambient air temperature (°C)

For a high-production furnace the fume volume flow rate after air dilution to 130 °C will be considerably higher than for secondary fume control by enclosure. A separate primary fume capture system would be used for this case.

For the remaining steps, a small, low-production furnace is under consideration with both primary and secondary emissions being captured by the enclosure.

Step 2: Determine secondary emission plume flow rate. The plume flow rate for charging and tapping is predicted by design equations for plume flow rates (compare Section 7.5). The enclosure height is taken as the limit of plume rise. The plume rise from the open furnace before charging should also be calculated. This event is also considered as a prolonged emission.

Step 3: Determine enclosure exhaust rate. The volume flow rate for prolonged emissions during melting, tapping, and periods with the roof swung open sets the minimum exhaust rate required to ensure a relatively fume-free enclosure environment. The fume volume flow rate after dilution (from Step 1) is compared to the highest of the calculated plume flow rates for the prolonged emissions. The greater of these two amounts determines the enclosure exhaust rate. Although the charging plume flow rate can be higher than the tapping plume flow rate, it does not set the enclosure exhaust rate. The enclosure is used to store this approximately 30-second surge for the charging operation.

Air Curtain and Exhaust Off-Take Air curtain design and exhaust off-take location are very important considerations. The air curtain is applied on roof openings that are typically 2 to 3 m wide and used for crane rope access. The opening may extend over the length of the enclosure and should, therefore, be served by two sets of independently operated doors—one for tapping and one for charging. This feature minimizes the pen area when one of the two events occurs.

The optimum position for the exhaust off-take is directly opposite the air curtain discharge. Rising fume with the highest concentration is directed straight into the off-take without excessive recirculation in the enclosure.

The main purpose of the air curtain is to contain the vertical updrafts from charging and tapping emissions. The air curtain slot discharge should therefore be pointed downward (e.g., 15 to 25 degrees from the horizontal) in order to achieve an approximately horizontal resultant flow.

The air curtain design equations are outlined in Chapter 7. The plume data for furnace charging are used in this calculation step. Note that the plume volume flow impinging on the width of the slot should be used rather than the whole plume flow.

During melting, the air curtain should efficiently direct fume towards the exhaust off-take without allowing recirculation within the enclosure. The air curtain design should therefore also consider the fume trajectory when a lower updraft velocity from melting is experienced.

The air curtain supply air can be taken from either inside or outside of the enclosure. However, there is a net flow advantage to taking this air from the outside.

Elevated work area temperatures at operating floor level in the enclosure may be a problem. Limited louver openings or wall-type fans can be used for cooling if operators must normally spend prolonged periods in the enclosure.

Mechanical Design The success of an enclosure installation depends heavily on acceptance by operation and maintenance personnel. Mechanical and structural integrity and reliability must therefore be designed into the enclosure.

The following are a few design details to be considered:

1. After opening locations and proper clearances have been established, the enclosure frame support system should be considered. Major support beams placed at the edge of openings will provide extra strength against the rubbing of crane cables. The overall construction should be light, which allows fast easy repair in the event of collision by crane-held objects. Collision with a robust enclosure would still result in damage and probably be more difficult to repair.
2. Enclosure doors should be designed with generous clearances and be easily operated by simple mechanisms. Wheels, guide rollers, and pneumatic cylinders can be used as part of door mechanisms.
3. Enclosure roof doors that are directly susceptible to fume drafts must be positioned beneath the roof overlapping the opening. Rising fume will then strike, deflect, and disperse within the enclosure, instead of leaking through door clearances. The rest of the roof construction must be tightly sealed.
4. Easy maintenance access must be provided. Removable roof panels for access to furnace subassemblies are desirable. Water-cooled equipment, electrode, and roof movement mechanisms, etc. all require overhead access for proper maintenance.
5. Material selection for the enclosure shell should consider the corrosiveness of the environment. Aluminized sheeting is preferred over zinc-coated material in a steel-production environment.
6. The high sound levels produced by an electric arc furnace can be contained within a furnace enclosure if a proper acoustical design is carried out. Any design should be checked by a competent acoustician. The following points should be considered:

   a. The material of construction of the enclosure should be of sufficient thickness to ensure a heavy-duty and robust design. In most cases structural requirements already ensure this.

b. The cladding should be sufficiently stiffened or damped to preclude resonance at the furnace frequency and its first few harmonics.
c. The inside of the enclosure should be lined with sound-absorbing material (e.g., fiberglass) selected for the frequencies involved and suitably protected from damage.
d. Holes, openings, and air leaks should be minimized, treated, or at least located away from people, where possible.
e. Operating practices should minimize the amount of time operators need to spend inside the enclosure or near an opening while the furnace is operating.

Enclosures for Nonbuoyant Sources

General Design Considerations Design of enclosures for nonbuoyant or inertial sources is completely different from design for buoyant sources. The dust produced by inertial sources arises from the motion of the particulate matter itself, rather than from the thermal head of the air as in the case of buoyant sources. Enclosures are practically the only control technique suitable for large-scale inertial sources such as bulk materials–handling operations. Unlike buoyant sources, dust generated by these operations does not travel in predictable paths, and the range of travel is usually limited. These considerations preclude the use of remote hooding. Local hooding (i.e., a receptor hood) is sometimes used for inertial sources that have a single direction of travel, such as particles projected from a grinding wheel. For large-scale inertial sources, dust generation takes place in all directions and exterior hoods could be used to alter the motion of coarse particulate matter that is projected away from the source.

As with any hood system, design methods are used to obtain required exhaust rates and hood dimensions.[93] The main mechanisms of dust generation are air induction, material splash, air displacement, and air entrainment.

Of these dust-producing mechanisms, air induction and air displacement are important for determining the exhaust rate for enclosures. Air entrainment and material splash are important for determining the size and shape of the enclosure.

A common and important application of exhausted enclosures is to bulk materials transfer points such as at chutes, bins, and dumping sites. Design equations for estimating the required exhaust rate are summarized below. Goodfellow[16] presents further details on design equations. Consideration is also given to sizing the enclosure and positioning the off-take.

The exhaust rate for an enclosure controlling emissions from a falling materials operation should equal the sum of the following quantities:

1. Flow rate of air induced by the falling material,
2. Flow rate equal to the volumetric flow rate of material (i.e., flow rate of displaced air), and
3. Flow rate sufficient to provide a working in-draft velocity through all openings (i.e., control velocity).

Working design equations for each of these flow rates follow. Hemeon[61] developed equations for estimating the volumetric flow rate of induced air based on the power generated by the stream of falling particles (i.e., the work done per unit time by the drag force over the distance

fallen). The recommended equation for estimating the induced airflow rate is the following:[94,95]

$$q_{v_1} = 0.631\left(\frac{q_m h^2 A_s^2}{\rho_s d}\right)^{1/3}, \tag{10.77}$$

where

q_{v_1} = flow rate of induced air ($m^3\ s^{-1}$)
q_m = material flow rate ($kg\ s^{-1}$)
h = drop height (m)
A_s = cross-sectional area of falling stream (m^2)
ρ_s = solids density ($kg\ m^{-3}$)
d = particle mass median diameter (m)
0.631 = empirical constant ($m^{1/3}\ s^{-2/3}$)

The flow rate of displaced air is given by the material flow rate divided by the bulk density

$$q_{v_2} = \frac{q_m}{\rho_s}. \tag{10.78}$$

Lastly, for a recommended control velocity of 0.5–1.0 m s^{-1} through the total area of the openings, A, the flow rate (q_{v_3}) is given by

$$q_{v_3} = Av, \tag{10.79}$$

where v = control velocity (0.5 m s^{-1} for well-protected sources, 1.0 m s^{-1} for vigorous motion operations).

Sizing the enclosure is more important than might first appear. If the enclosure walls are close to the compacting pile of material, material splash effects will cause losses through openings in these walls. Therefore, the use of a larger enclosure allows the velocity of these air streams to decrease before reaching the walls. Since quantitative estimates cannot be made as to the magnitude of the material splash effects, field observations of an existing system and experience are the only guides. Air entrainment becomes a factor when the enclosure has large areas or complete sides that must remain open. Winds or local air currents can then enter and exit the enclosure, thereby removing dust. The flow rate can be calculated in a straightforward manner from the wind velocity, open area, and loss coefficient of the opening. However, the ingress airflow rate is usually found to be quite large so that it may not be practical to attempt to counteract it by enclosure exhaust alone. Positioning the exhaust off-take close to the active zone of dust generation may capture the most concentrated portion of airborne dust before recirculation and mixing with entrained air can occur. This approach reduces the exhaust volume needed for air induction and control velocity.

Selection of the off-take position is important from the standpoint of the amount of material removed. Locating the off-take in the proximity of the material stream or at points of splash will result in greater removal of materials. This positioning may be desirable as a means to control splash effects provided that the off-take velocity is kept low.

Nonexhausted enclosures may be used to contain dust arising from inertial sources and to protect against entrainment by winds. All the difficulties attendant

in the use of exhausted enclosures apply equally to nonexhausted enclosures. Since nonexhausted enclosures do not maintain an inward airflow through openings, tight sealing is the only means for restricting the escape of dust. No design procedures for nonexhausted enclosures can be given, but provisions should be made for removal of settled dust and for access to any equipment inside the enclosure.

The capture efficiency of an existing enclosure installation can be estimated by measuring the portions of captured and spilled dust. The measurement program can be quite involved depending on enclosure size, intermittence of operation, dust settlement in the enclosure, and the extent of air entrainment. The measurement program must be custom designed to best suit the operation.

Gilbert, Hunter, and Ross[96] describe a modeling technique used to improve capture of lime dust from a clamshell unloading operation. The source is typical for bulk materials handling at receiving terminals throughout industry. Large amounts of loose material are handled in the open, thus making control of dust generation and dispersion a constant challenge. In order to design an accurate physical model, it was necessary to identify important variables that were affecting the fugitive emission problem. A detailed account of the variables affecting performance is presented. This makes their paper an excellent reference for demonstrating the design aspects for this type of nonbuoyant source. The paper also has a qualitative description of performance before and after modifications to the hood capture system.

The lime unloading operation simply consists of using a clamshell to unload a barge. The lime is carried by the clamshell into an enclosed hopper and dropped. From this transfer point, conveyors carry the lime to storage silos.

Figure 10.45 illustrates the lime dumping hood. A three-sided enclosure contains the discharge area over the hopper. The top is fitted with a slot for the clamshell trolley. In the original design, the exhaust duct to the dust collection baghouse is located at the enclosure midpoint. A description of the fugitive emissions from this source, as reported by Gilbert, Hunter, and Ross[96] follows:

> During the lime unloading operation when the clamshell is dumped into the hopper inside the enclosure, fugitive emissions of lime dust can sometimes be seen escaping over the front lip of the hopper, escaping at the middle and upper elevation out the front of the enclosure, escaping through the open trolley slot at the top of the enclosure and/or pulled out in the wake of the clamshell. There are many variables that affect the flow patterns inside the hopper and the enclosure to cause these fugitive emissions.
>
> There are several important characteristics of the flow patterns and dust generation that are obvious from watching the field unit in operation. Almost all of the entrained lime dust comes up out of the hopper from below the grizzly starting about 1–2 seconds after the lime starts to fall through the grizzly. The amount of dust, the plume velocity, and the region where it comes up out of the grizzly depend on where the load was dropped, how large a load was dropped, and the elevation of the clamshell above the grizzly. The plume travels upward in the enclosure and sometimes directly out of the front of the enclosure. As the plume rises in the enclosure, it is caught by the wind swirl patterns and carried higher in the enclosure where it can escape through the front or out of the trolley slot at the top of the enclosure. As the plume rises it may move in front of the clamshell, into the clamshell, in back of the clamshell or to the sides of the clamshell, depending on where the drop was made. Because the clamshell is brought out of the enclosure as soon as it is empty, it will generally push or carry out lime dust as it exits from the enclosure. From field observations, it was also obvious that a full clamshell load drop produced more dust in the enclosure than a partially full clamshell. For a severe dust generation drop, it would take 30 to 40 seconds for the enclosure exhaust flow to clear the enclosure of airborne dust.

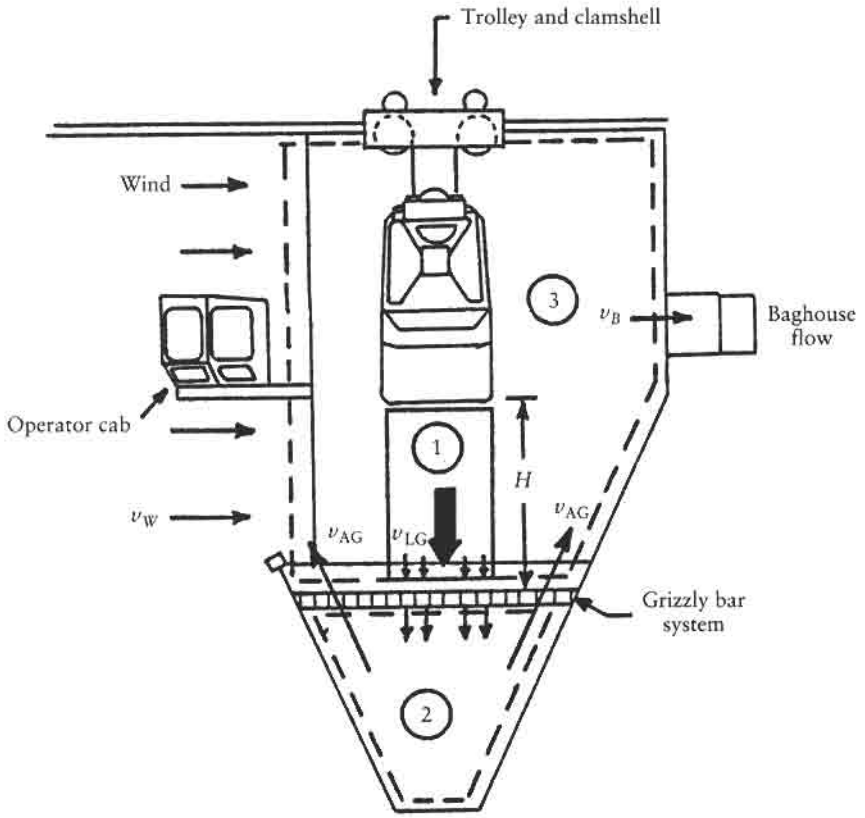

FIGURE 10.45 Capture of lime dust from a clamshell unloading operation (three regions of lime drop flow patterns are modeled).

Cost-effective control of dust problems arising from bulk materials handling requires an initial examination of the overall handling operations. Factors influencing dust generation and dispersion must be understood in order to achieve a proper design.

A number of steps can be taken to minimize dust generation and dispersion. For the clamshell case, an active containment design was pursued to minimize dispersion. Active containment relies upon an inflow of air into some type of enclosure.

A list of important variables affecting dust control during clamshell unloading was established as follows:

1. Baghouse exhaust flow rate
2. Wind direction and velocity
3. Height of lime drop
4. Location of clamshell in enclosure
5. Amount of lime in clamshell
6. Amount of lime in hopper
7. Rate of clamshell opening
8. Dwell time of clamshell in enclosure
9. Rate of clamshell withdrawal

10. Location of enclosure ventilation openings
11. Degree of material dampness
12. Enclosure open-area control velocity

The original design was based on a control velocity recommended by dust control design manuals. The original design of 28 $m^3 s^{-1}$ exhaust flow induced an inward velocity of about 0.5 m s^{-1} through the enclosure entrance and trolley shots. This was not sufficient to overcome plume trajectories aimed outward, or to overcome the effect of moderate wind levels.

A design based on the enclosure open-area control velocity does not consider all the other variables listed as affecting dust control. Calculation procedures to predict many of the other variables would be very complicated if not impossible to perform. Physical modeling of the problem and solution was therefore used as the basic design tool.

A large one-sixth-scale model of the unloader hopper was selected so that flow patterns in the enclosure could be evaluated.[96] Smoke was used to simulate the behavior of the lime dust in the enclosure. The lime drop from the clamshell was simulated by releasing coarse sand, thus modeling the flow patterns caused by the volume displacement and the air entrainment. The effects of local wind speed and direction on the enclosure were also simulated.

Conclusions concerning the causes of the fugitive emissions were developed from extensive model testing. The emissions escaped from the enclosure by direct plume trajectory and wind flow patterns. Lime dropped into the back of the grizzly creates a plume towards the front of the enclosure, whereas a drop near the front produces a plume to the rear. The plume is caused by the rapid displacement of air and dust from the hopper.

Conclusions concerning the elimination of fugitive dust escape were also developed from model testing. The baghouse capacity of 28 $m^3 s^{-1}$ is sufficient to capture most of the emission by implementing the following considerations:

Capture of dust is improved by repositioning the exhaust duct at a lower elevation closer to the grizzly, thus reducing the influence of wind.
By dropping lime in front of the hopper the dust plume is directed to the back, where a baffled off-take effectively captures the lime dust.
A downward flowing exhaust through the grizzly and into the hopper directly counteracts the plume velocity.
Slow opening of the loaded clamshell at as low an elevation as possible minimizes the emission.

The final recommended configuration for improving dust capture is shown in Fig. 10.46. The design change was rather simple and the model test showed a significant reduction in visible fugitive emissions.

This design review example has illustrated the following points:

Dust emissions result from the creation of local airflow caused by wind and from air displacement and entrainment resulting from material movement.
Capture system performance on a nonbuoyant source is influenced by enclosure (hood) design and location of the exhaust point.
Analytical design techniques, which predict the magnitude of local airflow and provide a basis for sizing exhaust systems, are not immediately available for

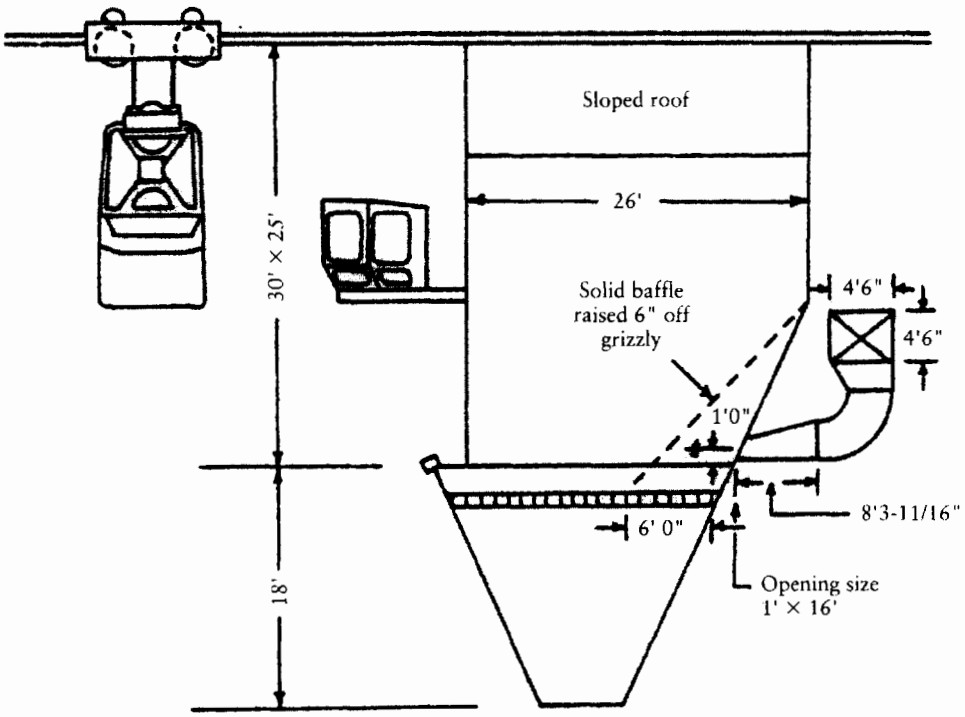

FIGURE 10.46 Capture of lime dust from a clamshell unloading operation. Geometry of final configuration where baghouse flow is drawn from the back of the hopper under a single baffle, which is raised off of the grizzly.

every situation. The designer is, therefore, often forced to use a rule-of-thumb approach or the modeling approach to size a capture system.

The modifications shown in Fig. 10.46 were installed in the field unit. Reports from field unit operators and observers indicated that the significant improvement shown by the model tests was also exhibited in the field.[96]

Partially Enclosed Systems It is common that in different kinds of continuous production lines, only some part of the process is emitting air contaminants. It may not be necessary to enclose the whole production line but rather the part of it where the emission takes place. Examples are different types of surface coating lines and printing lines where organic solvents are emitted from the paint or the printing ink, or in the woodworking industry where slabs of wood are transported and processed in different machines in a production line. These types of production lines are often designed as a long conveyor belt passing the different processing machines. The normal solution is then to enclose the machine as effectively as possible and to connect it to the general exhaust system of the factory. It is not possible to totally encapsulate the machine that is emitting the contaminant since there must be openings for the transportation of material into and out of the enclosure. The inlet opening is normally easier to control than the outlet. One reason is that, many times, it is possible to cover the main area of the opening with some soft material such as brushes or rubber strips that keep the opening almost

closed but allow the material to pass. Another reason is that the conveyor belt causes a slight airflow in the direction it is moving. It is more complicated to control the outlet opening. If the enclosed machine, for example, is applying paint to the material, it is not possible to use brushes or anything else that come in contact with the wet paint. The area of the opening on the outlet side must be larger than on the inlet side. The conveyor belt movement also causes air to be pulled out of the enclosure, bringing the contaminant with it. In this example, as always when paint or ink with organic solvents is applied, the treated material may be a source of contaminant emissions. The enclosure must therefore be extended, covering the conveyor belt until the emission is acceptable or to the next step of the process, e.g., a drying oven. The dimensions of the machine and the need to have access to different parts of it influence the dimensions of the enclosure. The airflow rate needed to achieve a high capture efficiency is normally low.

10.2.3.6 Glove Boxes

General

One way to minimize or eliminate exposure to contaminants is to have a completely closed box with a glass or plastic panel to look through and gloves mounted in one or more walls. This type of local exhaust hood makes it possible to have a completely shielded workplace available nearly anywhere.

Principle

Glove boxes are connected to an exhaust. The form of the box could be similar to any other partially closed hood. Instead of the opening through which the work is performed in a partially closed hood, the box has a wall with two holes attached to a pair of arm-length gloves. This enclosed volume normally does not have any specific opening for entrance of air from the surroundings. The air normally enters through existing cracks. If there is a specific opening to the surroundings a nonreturn valve is placed there to prevent flow from inside the box to the general work area. This valve could be very simple, e.g., a plastic sheet hanging on the inside covering the openings. The opening could also be covered with a filter to prevent contaminants from leaking to the outside, if air somehow should flow backwards. Glove boxes are ready-made from sheet metal or plastic. Work is performed by putting the hands into the fixed gloves and manipulating the tools or materials inside the box by hand. See Fig. 10.47.

Applicability of Sources

Glove boxes are commonly used for small abrasive blasting activities and to control exposure to highly toxic and radioactive materials. Glove boxes used for abrasive blasting are quite similar to the abrasive blasting room (Section 10.4.7.2) but are much smaller and usually do not have mechanical air supply into the box. The same type of system, but with much greater tightness, is used for radioactive and highly toxic biological or chemical materials. For these applications an air supply that flows directly into the box is often used or needed.

Different Forms and Boundaries Relative to Other Types

The transparent surface and the gloves could all be situated in the same wall. Quite often the transparent surface is in one wall and the gloves are on

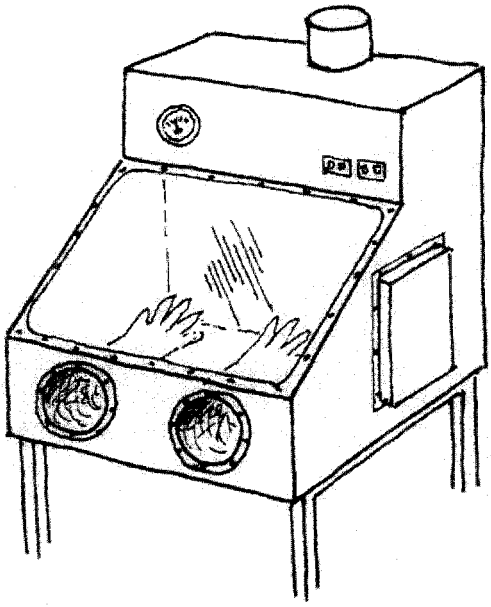

FIGURE 10.47 Example of a glove box for chemical work.

each of the adjoining sidewalls. This could be advantageous when working with both hands in the box. Strippable plastic liners on the interior of the box and filters or other air cleaners at the exhaust connection are often used to facilitate decontamination. For microbiological work, glove boxes are called Class 3 microbiological safety cabinets[97] or Class III Biosafety Cabinets.[98] These have HEPA-filtered inlet air and HEPA-filtered exhaust and are normally a recirculation unit (Section 10.4.6.4). They could be connected to an exhaust duct instead of recirculation. To protect the process or the product, e.g., in the electronics industry, the same construction could be used but with a higher pressure inside than outside the box. These positive-pressure boxes are for product or process protection and do not offer worker protection.

Specific Problems

In order to remove the generated contaminants associated with abrasive blasting and to ensure visibility into the box, a high exhaust airflow rate is necessary. High flow rates may also be necessary to maintain a large pressure difference to prevent leaks of highly toxic and radioactive materials.

The size of the box is usually small, since the whole interior of the box must be reached with the hands in the gloves. Larger boxes could be supplied with more pairs of gloves, and different gloves could be used for different areas inside the box.

Glove box failures are most likely to occur at the glove connection. Normal flexing of the glove material, as well as contact with abrasive, corrosive, or radioactive materials, reduces the integrity of the glove material. Caps on the glove ports are recommended when the gloves are not in use. Periodic inspection and glove replacement are recommended.

For abrasive blasting it is common to have a horizontal grill inside the box for collecting the abrasive material which functions as the stand for the material to be treated. Abrasive blasting generates large amounts of dust with large particles, which should be exhausted as fast as possible. In these boxes, the exhaust connection is above the working area (grill).

Sometimes gases or vapors are used or generated inside the box. Gloves could be permeable for some gases, which may be dangerous to the skin. Selection of glove material must consider the type of contaminant. In cases where suitable glove material is not available, it may be necessary to use a completely closed volume with remote controlled manipulators instead of gloves.

When openings for air supply are used, they should be small, but not too small, since this could generate high, disturbing velocities of incoming air.

To get equipment and the material to be treated into and out of the box it is necessary to have some kind of door. This door should be made in such way that it tightens when negative pressure is applied inside the box. Instead of one door, an airlock volume with one door to the box interior and one door to the exterior can be used.

When these boxes are used to control highly toxic and radioactive materials, provision for emergency power is necessary to ensure continuous exhaust ventilation. In some locations, seismic safety considerations may also be necessary.[99]

Depending on use, the tightness and containment of the box can be tested with a tracer gas or with generated contaminants. Since the pressure inside the box is lower than the pressure outside it could be easier to check the tightness without the exhaust airflow. Measurements similar to those for fume cupboards can be used.

Design Equations and/or Parameters

When glove boxes are used for abrasive blasting, their design must take into account that the ejector of the abrasive material is driven by compressed air. This influences the chosen flow rate, which should be large enough to generate an air velocity of at least 3 m s^{-1} in the openings.[100] The necessary exhaust airflow rate recommended by INRS is then

$$Q = Sv + Q_p, \tag{10.80}$$

where Q is the total exhaust flow rate, $m^3\ s^{-1}$, S the total area of openings to the surroundings, m^2, v the necessary air velocity in the openings, 3 m s^{-1}, and Q_p the airflow rate blown into the box as pressurized air and expanded to atmospheric pressure, $m^3\ s^{-1}$.

The ACGIH[25] recommends 20 air changes per minute for a glove box for abrasive blasting. With a volume of 1 m^3 this is equal to 0.33 $m^3\ s^{-1}$. They also recommend an inward air velocity at all openings of at least 2.5 m s^{-1}.

Several recommendations exist for glove boxes used for highly toxic and radioactive materials. The ACGIH[25] recommends a minimum flow rate equal to 0.25 $m^3\ s^{-1}$ per m^2 of open door area. The box should also operate with a pressure of at least 62 Pa below atmospheric pressure. A minimum duct velocity of 10 to 20 m s^{-1} is also recommended. Lawrence Livermore National Laboratory[99] recommends a minimum velocity through openings of at least 0.5 m s^{-1} and negative pressure relative to the surroundings. In this case, the openings include both operational openings, such as doors and filters, and noncatastrophic accidental

openings, such as glove failure or tear-off of bagout covers. No specific pressure requirements are given. LLNL requires a detailed safety analysis to determine necessary ventilation system requirements and airflow if a large catastrophic failure, such as loss of a window, is credible.[99] Filtration is usually necessary when toxic or radioactive particles are used or may be generated. The filter resistance needs to be considered when sizing the ventilation system.

References

1. J. Pekkinen, J. Eloranta, M. Hyvärinen, J. Muttilainen, and E. Kähkönen. In *Ventilation '94: Proceedings of the 4th International Symposium on Ventilation for Contaminant Control, Stockholm, Sept. 5–9 1994* (eds. A. Jansson and L. Olander). (*Arbete och Hälsa* no. 18), Sweden: National Institute for Working Life, 1994, pp. 276–280.
2. L. M. Conroy and M. J. Ellenbecker. In *Ventilation '88: Proceedings of the 2nd International Symposium on Ventilation for Contaminant Control, 20–23 September 1988, London, England UK* (ed. J. H. Vincent). Oxford, England: Pergamon Press, 1989, 41–46.
3. N. A. Esmen, T. A. Grauel, D. A. Weyel, and A. G. Ilori. In *Ventilation '91: Proceedings of the 3rd International Symposium on Ventilation for Contaminant Control, September 16–20, 1991, Cincinnati, Ohio, USA* (eds. R. T. Hughes, H. D. Goodfellow, and G. S. Rajhans). Cincinnati, OH: American Conference of Governmental Industrial Hygienists, 1993, pp. 321–327.
4. R. Braconnier, R. Regnier, and F. Bonthoux. In *Ventilation '91: 3rd International Symposium on Ventilation for Contaminant Control, September 16–20, 1991, Cincinnati, Ohio, USA.* (eds. R. T. Hughes, H. D. Goodfellow, and G. S. Rajhans). Cincinnati, OH: American Conference of Governmental Industrial Hygienists, 1993, pp. 95–105.
5. L. M. Conroy and M. J. Ellenbecker. *Applied Industrial Hygiene*, vol. 4, no. 6, 1989,135–142.
6. M. R. Flynn and M. J. Ellenbecker. *American Industrial Hygiene Association Journal*, vol. 46, 1985, 318–322.
7. M. R. Flynn and M. J. Ellenbecker. *American Industrial Hygiene Association Journal*, vol. 48, no. 4, 1987, 380–389.
8. B. Fletcher and A. E. Johnson. In *Ventilation '85: Proceedings of the 1st International Symposium on Ventilation for Contaminant Control, October 1–3, 1985, Canada* (ed. H. D. Goodfellow) New York: Elsevier, 1986, pp. 369–390.
9. L. M. Conroy, R. S. Prodans, M. Lachman, X. Yu, R. A. Wadden, J. E. Franke, and P. A. Scheff. *Journal of Environmental Engineering*, vol. 121, no. 10, 1995, 736–741.
10. American Conference of Governmental Industrial Hygienists. *Industrial Ventilation: A Manual of Recommended Practice.* 22nd ed. Cincinnati, OH: ACGIH, 1995.
11. E. A. Iyiegbuniwe. Site-specific emission factors for sixteen degreasers. Doctoral dissertation, University of Illinois at Chicago, 1997.
12. L. Silverman. *Journal of Industrial Hygiene and Toxicology*, vol. 24, no. 9, 1942, 267–276.
13. L. Olander. Efficiency of Local Exhausts—A Review. *Undersökningsrapport* (Investigation report), 1994, 32, Arbetsmiljöinstitutet (NIWL).
14. R. A. Wadden, P. A. Scheff, and J. E. Franke. *American Industrial Hygiene Association Journal*, vol. 50, 1989, 496–500.
15. I. Kulmala. *Annals of Occupational Hygiene*, vol. 39, no. 1, 1995, 21–33.
16. H. D. Goodfellow. *Advanced Design of Ventilation Systems for Contaminant Control.* Chem. Eng. Monograph 23. Amsterdam: Elsevier, 1985.
17. R. P. Garrison and M. Erig. *Applied Industrial Hygiene*, vol. 3, no. 6, 1988, 182–188.
18. J. M. Dallavalle. *Exhaust Hoods.* New York: Industrial Press, 1945.
19. B. Fletcher and A. E. Johnson. *Annals of Occupational Hygiene*, vol. 25, no. 4, 1982, 365–372.
20. R. P. Garrison. *American Industrial Hygiene Association Journal*, vol. 44, no. 12, 1983, 941–947.
21. A. Jansson. *Staub—Reinhaltung der Luft*, vol. 49, 1989, 11–16.
22. R. H. Perry, D. W. Green, and J. O. Maloney. *Perry's Chemical Engineers' Handbook.* 7th ed. New York: McGraw-Hill, 1997, Chapter 5.
23. R. C. Reid, J. M. Prausnitz, and B. F. Poling. *The Properties of Gases and Liquids.* New York: McGraw-Hill, 1987.

24. M. Y. Anastas and R. T. Hughes. *American Industrial Hygiene Association Journal*, vol. 50, 1989, 526–534.
25. American Conference of Governmental Industrial Hygienists. *Industrial Ventilation: A Manual of Recommended Practice, Metric Version.* 23rd ed. Cincinnati, OH: ACGIH, 1998.
26. F. Drkal. *Z. Heiz. Lüft. Klim. Haus.*, vol. 22, 1971, 167–172.
27. V. L. Streeter. *Fluid Dynamics.* New York: McGraw-Hill, 1948.
28. I. G. Tyaglo and I. A. Shepelev. *Vodosnab. Sanit. Tekh.*, vol. 5, 1970, 24–25.
29. F. Drkal. *Z. Heiz. Lüft. Klim. Haus.*, vol. 21, 1970, 271–273.
30. H. Lamb. *Hydrodynamics.* 6th ed. New York: Dover Publications, 1945, pp. 148–152.
31. L. M. Conroy, M. J. Ellenbecker, and M. R. Flynn. *American Industrial Hygiene Association Journal*, vol. 49, no. 5, 1988, 226–234.
32. I. Kulmala. *Advanced Design of Local Ventilation Systems.* VTT Publications 307. Technical Research Centre of Finland, 1997.
33. R. Braconnier. *Cahiers de Notes Documentaires*, no. 124, 1986, 3e trimestre (in French).
34. A. Jansson. Local exhaust ventilation and aerosol behaviour in industrial workplace air. *Arbete och Hälsa*, no. 43, 1990.
35. I. Kulmala. *Annals of Occupational Hygiene*, vol. 37, no. 5, 1993, 451–467.
36. R. J. Heinsohn. *Industrial Ventilation: Engineering Principles.* New York: John Wiley & Sons, 1991.
37. W. Dittes, D. Goettling, and H. Wolf. *Arbeitsplatzluftreinhaltung* (Clean Air at the Workplace). Dortmund: Bundesanstalt für Arbeitsschutz, 1985.
38. T. Masood. In *Ventilation '85: Proceedings of the 1st International Symposium on Ventilation for Contaminant Control, October 1–3, 1985, Canada* (ed. H. D. Goodfellow). New York: Elsevier, 1986, pp. 703–720.
39. R. Braconnier. *American Industrial Hygiene Association Journal*, vol. 49, no. 4, 1988, 185–198.
40. W. A. Burgess, M. J. Ellenbecker, and R. D. Treitman. *Ventilation for Control of the Work Environment.* New York: John Wiley & Sons, 1989.
41. B. Fletcher. *Annals of Occupational Hygiene*, vol. 21, 1978, 265–269.
42. L. M. Conroy. *Field Study of Local Exhaust Hood Performance: Revised Final Report.* National Institute for Occupational Safety and Health (NIOSH) Grant 5 K01 OH00078-03. February 19, 1996.
43. G. F. Cusumano. *High Velocity/Low Volume Dust Control.* Booklet no. 212. New York: Clarkson Industries, 1972.
44. G. F. Cusumano. *Plant Engineering*, 1/10, 3/7, 5/2, 1974.
45. R. I. Chamberlin. *Archives of Industrial Health*, 1959, 19.
46. A. E. Barnard, J. Torma-Krajewski, and S. M. Viel. *American Industrial Hygiene Association Journal*, vol. 58, 1996, 804–808.
47. Hoffman Air Systems. *High Velocity Dust Control and Central Vacuum Cleaning Systems.* Bulletin ASV–623A. New York: Hoffman Air Systems, 1973.
48. H. L. Dalrymple. In *Ventilation '85: Proceedings of the 1st International Symposium on Ventilation for Contaminant Control, October 1–3, 1985, Canada* (ed. H. D. Goodfellow). New York: Elsevier, 1986, pp. 593–601.
49. British Occupational Hygiene Society (BOHS). *Controlling Airborne Contaminants in the Workplace.* Technical Guide No. 7. London: BOHS, 1987.
50. W. A. Burgess and J. Morrow. *American Industrial Hygiene Association Journal*, vol. 37, 1976, 546–549.
51. R. Regnier, R. Braconnier, G. Aubertin, and J. C. Cunin. In *Ventilation '85: Proceedings of the 1st International Symposium on Ventilation for Contaminant Control, October 1–3, 1985, Canada* (ed. H. D. Goodfellow). New York: Elsevier, 1986, 579–591.
52. R. Regnier, R. Braconnier, and G. Aubertin. *Cahiers de notes documentaires*, vol. 131, 1988, 339–354.
53. R. Regnier. *Cahiers de notes documentaires*, vol. 134, 1989, 39–44.
54. R. P. Garrison and D. H. Byers. *American Industrial Hygiene Association Journal*, vol. 41, 1980, 713–720.
55. R. P. Garrison and D. H. Byers. *American Industrial Hygiene Association Journal*, vol. 41, 1980, 803–811.
56. R. P Garrison and D. H. Byers. *American Industrial Hygiene Association Journal*, vol. 41, 1980, 855–863.
57. R. E. Downing and E. B. James. Dust extractors for rotary abrasive tools. British Patent no. 780 761. London: Patent Office, 1957.

58. J. E. Harvey. Dust extractor for flexible disk grinders. U.S. Patent no. 2 954 653. Washington, DC: Patent Office, 1960.
59. F. F. L. Morgan and E. B. James. Dust extractor for chipping chisels. U.S. Patent no. 2 843 929. Washington, DC: Patent Office, 1958.
60. F. F. L. Morgan. Dust extraction systems for surface grinding wheels. U.S. Patent no. 2 819 571. Washington, DC: Patent Office, 1958.
61. W. C. L. Hemeon. *Plant and Process Ventilation*. 2nd ed. New York: Industrial Press, 1963.
62. ASHRAE. *Handbook of Fundamentals*. Atlanta: American Society of Heating, Refrigeration, and Air-conditioning Engineers, 1997.
63. B. Ljungqvist. *Skyddsventilation—En orientering om luftrörelser och föroreningsspridning* (Protective ventilation—An orientation about air movements and contaminant dispersion). Meddelande nr. 20. Stockholm: Dept. Building Services Engineering, Royal Institute of Technology, 1992.
64. J. Koenigsberg. *Heating, Piping and Air Conditioning*, vol. 67, no. 10, 1995, 57–61.
65. C. J. Saunders, A. E. Johnson, and B. Fletcher. In *Ventilation '94: Proceedings of the 4th International Symposium on Ventilation for Contaminant Control, Stockholm, Sept. 5–9, 1994* (eds. A. Jansson and L. Olander). (*Arbete och Hälsa*, no. 18), Sweden: National Institute for Working Life, 1994, pp. 264–269.
66. D. S. Abrams, P. C. Reist, and J. M. Dement. *American Industrial Hygiene Association Journal*, vol. 47, no. 1, 1986, 22–26.
67. S. K. W. Chang and R. R. Gonzalez. *ASHRAE Transactions*, vol. 99, part 1, 1993.
68. A. E. Johnson, B. Fletcher, and C. J. Saunders. *Annals of Occupational Hygiene*, vol. 40, no. 1, 1996, 57–64.
69. R. P. Harvey. In *Proceedings of the Development and Use of Fume Cupboards, Fume Hoods and Ventilated Safety Enclosures in Laboratories: Symposium Organised by the Laboratory of the Government Chemist, London, March 1979*, pp. 32–59.
70. B. Ljungqvist, *ASHRAE Transactions*, vol. 93, pt. 1, 1987, 1304–1317.
71. B. Ljungqvist. *Health and Safety Practitioner*, August 1991, 36–40.
72. A. E. Johnson and B. Fletcher. *Safety Science*, vol. 24, no. 1, 1996, 51–60.
73. B. Fletcher and A. E. Johnson. *In Ventilation '91: Proceedings of the 3rd International Symposium on Ventilation for Contaminant Control, September 16–20, 1991, Cincinnati, Ohio, USA* (eds. R. T. Hughes, H. D. Goodfellow, and G. S. Rajhans). Cincinnati, OH: American Conference of Governmental Industrial Hygienists, 1993, pp. 489–497.
74. J. Melin. *Measurements and Analyses of the Performance of Laboratory Fume Hoods*, Document D40:1997. Göteborg, Sweden: Chalmers University of Technology, 1997.
75. BS7258. *Laboratory Fume Cupboards*. London: BSI, 1994.
76. CIBSE Guide. *Volume B: Installation and Equipment Data. Section B2: Ventilation and Air Conditioning (Requirements)*. London: Chartered Institution of Building Services Engineers, 1986.
77. H. I. Middleton. In *Proceeding of a Symposium on the Development and Use of Fume Cupboards, Fume Hoods and Ventilated Safety Enclosures for Laboratories*. London: Laboratory of the Government Chemist, 22 March 1979.
78. ANSI. *Fundamentals Governing the Design and Operation of Local Exaust Systems*. ANSI Z9.2-1979. American National Standards Institute, New York, 1979.
79. R. Haugen. *American Laboratory*, vol. 28, November, 1991.
80. G. T. Saunders. *Laboratory Fume Hoods: A User's Manual*. New York: John Wiley & Sons, 1993.
81. ASHRAE 110-1995. *Method of Testing Laboratory Fume Hoods*. Atlanta. American Society of Heating, Refrigeration, and Air-conditioning Engineers, 1995.
82. DIN 12 924. *Anforderungen an Anzuge* (Demands on Hoods). Deutsches Institut fur Normungen e V, 1991.
83. Nordtest. *Laboratory Fume Hoods: Performance*. NT VVS 095. Espoo, Finland, 1993.
84. Matheson. Gas containment and distribution systems. Matheson Tri-Gas, Inc., P.O. Box 624, 959 Route 46 East Parsippany, NJ, 215-648-4029, 2000.
85. P. A. Carson and C. J. Mumford. *The Safe Handling of Chemicals in Industry*. Essex, England: Longman Scientific and Technical, 1988.
86. Uniform Building Code. Whittier, CA: International Conference of Building Officials, 1994.
87. Uniform Fire Code. Whitter, CA: International Conference of Building Officials, 1994
88. W. R. Acorn. *Code Compliance for Advanced Technology Facilities: A Comprehensive Guide for Semiconductor and Other Hazardous Operations*. Park Ridge, NJ: Noyes Publications, 1993.
89. Uniform Mechanical Code. Whitter, CA: International Conference of Buildning Officials, 1994

90. Semiconductor Safety Association. *SSA Journal*, vol. 11, Special issue: Silane., Winter 1997.
91. E. R. Kashdan, D. W. Coy, J. J. Spivey, T. Cesta, H. D. Goodfellow, and D. L. Harmon. *Heating, Piping and Air Conditioning*, vol. 58, no. 2, 1986, 47–54.
92. H. D. Goodfellow. *Heating, Piping and Air Conditioning*, vol. 59, no. 2, 1987, 60–66.
93. A. J. Buonicore and W. T. Davis. *Air Pollution Engineering Manual*. New York: Van Nostrand Reinhold, 1992, pp. 173–179.
94. J. N. Morrison. *Transactions of the Society of Mining Engineers*, vol. 250, 1971, 47–53.
95. R. Dennis and D. B. V. Bubenick. *Journal of the Air Pollution Control Association*, vol. 33, no. 12, 1983, 1156–1161.
96. G. B. Gilbert, T. E. Hunter, and D. Ross. In *77th Annual Meeting of the Air Pollution Control Association, San Francisco, Ca., June 24–29, 1984.*
97. R. P. Clarke. *The Performance, Installation, Testing and Limitations of Microbiological Safety Cabinets*. Occupational Hygiene Monograph no. 9. Leeds: Science Reviews, Ltd., 1983.
98. Centers for Disease Control and Prevention and National Institutes of Health. *Primary Containment of Biohazards: Selection, Installation and Use of Biological Safety Cabinets*. Washington, DC: U.S. Department of Health and Human Services, 1995 (available on http://www.niehs.nih.gov/odhsb/biosafe/bsc/bsc.htm)
99. Lawrence Livermore National Laboratory. Work enclosures for toxic and radioactive materials. In *Environmental Safety and Health Manual*. September 1995.
100. INRS. *Cahiers de notes documentaires—hygiène et sécurité du travail*, no. 154, 1994, 5–19.

10.3 SUPPLY INLETS

10.3.1 General

It can sometimes be easier, inside a specific volume, to use supply than to use exhaust air to control contaminants because of the much longer range of influence air from a supply opening has when the openings have the same size and the same airflow rate. For some contaminants and in some processes it may also be necessary to supply additional breathing air to the workers and this air could then also be used to control and transport contaminants. For spot cooling of workers or work pieces it is possible to use point jets originating from specific supply inlets.

10.3.1.1 Choosing

To choose a supply inlet as the local ventilation system is not common because it is difficult to design for the specific spreading of contaminants. This is usually easier with an exhaust hood. However, there are moments when large flow rates or specific flow fields are necessary to transport contaminants or for shielding from contaminants.

When choosing a supply inlet it is always necessary to be very careful, because the influence of the supply air could reach very far. This is most important when using air jets or similar devices to direct the contaminants in an intended direction, since very small changes in direction or momentum could totally destroy the intended flow field and transport the contaminants to, instead of from, the workers.

A supply jet may have several different forms: point jet, swirl jet, line jet, radial jet, etc. The choice depends on available volume and existing demands. A radial jet could be used when it is possible to utilize a wall or a ceiling for distributing the air; a point jet could be used when it is advantageous to have a high air velocity in the volume (room).

Supply inlets are also used when there is no room for an exhaust hood or when the contaminant-generation process has a form such that an exhaust

hood becomes very clumsy. They are also used to enhance the function of exhaust hoods: the most well known are the so-called push-pull systems. However, most of the many exhaust hoods described earlier could be improved by using some kind of directed supply air. It must be remembered that a supply inlet needs much more accurate design than an exhaust hood and that they also need much more maintenance. Supply inlets usually depend on having a defined contaminant concentration in the inlet air; this usually implies clean supply air, but some inlets could use recirculated air with or without cleaning.

For supply inlets in rooms some performance measurements exist, such as air exchange and ventilation efficiencies (see Chapter 8). It is usually not possible to use these for local ventilation supply inlets, and for the moment there are no specific measurements to evaluate the influence of an inlet on contaminants. Some trials with comparison indices, which compare inhaled concentrations (or exposures) with and without a supply inlet, have been done.

10.3.1.2 Combined with Exhausts

Mostly the use of a supply inlet as a local ventilation system presumes that the supply device (with air from outside the room) is located inside a large room, which also has an adequate exhaust airflow rate or has convenient exhaust/transfer openings for the airflow. It is also necessary that the exhaust flow rate is maintained (or pressure difference kept). Otherwise the air supply could change in rate or direction. Instead of using air from a ventilation system, the supply air could be taken from the room (volume) it is situated in. In this case, the room must also have a supply and an exhaust flow rate. It is often necessary to clean the air before it is used in the supply inlet.

A supply inlet could be designed with or without an exhaust. There should naturally be an exhaust opening in the room. If the influence of the exhaust on the supply inlet is low, then it requires no special design, but if the influence of the exhaust is large it must be taken into account. The inlets could be combined with specific exhaust hoods to enhance their efficiency (see Section 10.4). There are many ways to design supply inlets and also to combine different supply inlets; just a few inlets are described in this section.

All supply inlets without a specific exhaust have the same problem, the spreading of contaminants in the room outside the supply air zone. When the inlets are used to create a cleaner zone in a normal workroom this is usually no problem. When a supply inlet is used to blow away some hazardous contaminant it is necessary to combine it with a specific exhaust, or the rest of the room will be contaminated.

10.3.1.3 Pressurization

Some systems normally do not have any specific supply airflow, though they could have some air supply. These are used when a volume (normally a room) is intended to have a lower pressure than the surrounding rooms. This so-called pressurization of zones is used when a high level of safety against spreading of contaminants is needed.[1] A high pressure difference between two rooms causes the air to flow into the room with the lowest pressure if some cracks exist or some connection between the two rooms is opened.

The pressure difference is created by using a large difference between the supply and exhaust flow rates (in either direction). Higher pressure than the surroundings is used to prevent airborne transport into the room and lower pressure to prevent transport from the room. The airflow is then directed from the room with the (initial) higher pressure to the room with the lower pressure, and the transport of contaminants in the other direction is largely prevented. The pressure difference will disappear, for example, when a door is opened between the two zones. When the pressure difference has disappeared, which could happen in fractions of a second, the preventive effect diminishes since, as has been pointed out earlier, it is impossible to have total isolation only by using air.

Closed volumes (confined spaces) exist where supply air is necessary, though not in a specific way. The air could be treated (like in a general ventilation system) to increase its usability or the workers' comfort. The supply air could enter through an inlet device of any form. This could be similar to any normal general ventilation supply device or just an open end of a duct or a tube. The air then exits from the closed volume where possible. This system could be used for temporary work, without high contaminant generation, inside storage tanks, and the supply opening used is usually only the open end of the duct or tube.

There are other small closed volumes where it is necessary to supply a limited flow rate, but where the air sometimes has to be treated carefully through filtering, gas cleaning, heating, cooling, etc. Some examples are the air supply inside a car and airplane and train cabins. These systems are seen mostly as general ventilation systems. Ventilation of control cabins in industry such as crane driver's cabins, with specific demands on heating, cooling, and cleaning, is usually named local ventilation and consists of a supply system only. The air could be treated and distributed through a system in the cabin or from a central system, connected in a way similar to how some mobile local exhaust hoods are connected to a fan (see Section 10.1.2). These cabins have similar functions as cabins used for control purposes, such as traffic toll booths, pay booths, money exchange booths, ticket booths, etc. These have some differences with general ventilation systems regarding choice of opening size of air supply, air velocities, airflow rates, air quality, and temperature. Mostly the demands are similar to demands on general ventilation systems, the difference being that these small volumes have no exhaust system and let the air out of the volume through small openings in the walls. In this way they also to some extent use pressurization of the volume to limit the entrance of contaminants.

When using supply inlets it is more important than for exhaust hoods how the person, working with a process, is placed, relative to the contaminant source and to the inlet. It is nearly always better to keep the person between inlet and source than source between inlet and person. For supply systems it is even more efficient than for exhausts to have the flow passing in front of the person instead of from back to front. The airflow from behind the person could generate a wake, which includes the source or the generated contaminant and thereby increases the person's exposure. This phenomenon is more common with large flow rates and large supply openings than with small flow rates and small inlets. Placing the worker beside the path from the inlet to the source and on to the exhaust is a general rule. It is possible to counteract the wake around a person by using supply air, directed downward around the worker. In this case, the air is normally sucked into an exhaust hood (see Section 10.4).

10.3.2 Air Jets

10.3.2.1 General

Air jets are used for many purposes. Some of these are described in other parts of this chapter, but it is not possible to describe all the possible types and uses. The fundamentals regarding velocity, flow rate, and spreading of round, radial, and plane jets are described in Sections 7.4 and 7.7. When jets are used inside rooms, they do not need to have any corresponding exhaust air. Exhausted air is needed for supply jets in general ventilation, but if the jet's air is taken from the room and blown into the room again, no exhaust is needed. If the air is taken from outside the room, it is necessary to have the same flow rate exhausted from the room.

10.3.2.2 Principle

The main principle is to blow with a velocity higher than that of the surroundings and in this way create a transport of the air in one or more defined directions. The air could be blown to form plane, round, or radial jets. The function of the jet could be to shield a surface, to cover an opening, to cool a person, to transport the air a long distance, or just to change the air velocity inside a closed volume. The air blowing creates a suction effect along the jet and the jet mixes surrounding air into itself and increases the moving flow rate, at the same time decreasing the jet velocity.

Jets used in local ventilation have the same forms and performance as jets in general ventilation, described in Sections 7.4 and 7.7. These sections describe usable equations for flow, velocity, temperature, and concentration distributions. The buoyancy plumes that can result at the end of a jet or from a warm source are described in Section 7.5.

10.3.2.3 Applicability of Sources

The plane jet, mostly blowing vertically, is used to increase the isolation between two volumes, one of which could be the inside of a cabinet, e.g., a laboratory fume cupboard. The plane jet could also transport air along a wall or be used to dry or cool the material in a pulp or paper line.

The round jet is most common in general ventilation and is used in local ventilation for spot cooling, for cleaning surfaces, or to direct air and contaminants in specific direction, e.g., into a large canopy hood or away from a contaminant generation point. The radial jet is not used much in local ventilation.

10.3.2.4 Different Forms and Boundaries Relative to Other Types

Sometimes it is necessary to include the exhaust air when designing an air jet system (see Sections 10.4.2 and 10.4.3). Normally the descriptions assume that the jet is not disturbed by exhaust air, nearby surfaces, or other air movement in the room (see Chapter 7).

10.3.2.5 Specific Issues

Each jet must be designed for a specific function. A jet could easily transport or increase the capturing of contaminants, but could also very easily destroy the intended function of a local ventilation system.

10.3.2.6 Design Equations and/or Parameters

Many different equations describe jets. Some of these are used in Chapter 7. All jets must be placed in such a way that the mixing of surrounding air is not restricted. If it is restricted the jet can behave in an unpredictable manner. For example, a wall close to a plane jet nearly always makes the jet attach to the wall and changes the jet from a free jet to a wall jet.

10.3.2.7 Disturbances

It is quite easy to disturb the flow in a jet either by inserting a small surface at right angles close to the outlet or by using a small air velocity far from the outlet. Usually the latter needs a large flow rate, but a small flow rate with high velocity may also change the direction of the jet, especially as jet velocity decreases.

To change the direction of the jet using another air jet requires that the second jet have a very high velocity near the outlet. To change the direction of a jet far from the outlet using a surface requires a very large surface.

One of the most essential parameters for a jet is the direction. A small deviation in the outlet angle could easily change not only the direction of the jet but also its intended function, be it as a shield or for air transport.

10.3.2.8 Changing Flow Rates

Isothermal jets are not influenced much by small changes in flow rate; the size of the influence can be seen from the different equations. Nonisothermal jets could be changed substantially by small differences in both outlet velocity (flow rate) and/or temperature.

10.3.2.9 Evaluation Procedures

A jet intended for mixing or for a long blowing range could be evaluated by measuring the velocity at different points along and across the jet. It could be necessary to measure the turbulence intensity of the jet, since this changes the transport properties in the jet. This is more important for plane jets intended to function as shields. For evaluating the shielding effect, tracer gas or particles is necessary. In these cases, the measures described in Section 10.5 can be used.

10.3.3 Low-Momentum Supply Systems

Low-momentum air supply systems designed for local ventilation purposes mainly use vertically downward airflow. Some systems with an inlet of low-momentum horizontal airflow for a whole workroom are on the borderline between general and local ventilation and are therefore briefly described here. A more complete description will be found in chapters 7 and 8 dealing with general ventilation.

10.3.3.1 Horizontal Airflow Direction

Horizontal displacement ventilation (see Chapters 7 and 8) is a ventilation principle mainly applied to general ventilation of workrooms. In some instances, a local ventilation problem may be solved by building a separate enclosure or a room around the workstation and arranging for a general ventilation in that enclosure. An example where that principle has been utilized is the control of emissions of and worker exposure to styrene vapors during

lamination of pleasure boats made of glass fiber reinforced polyester plastic.[2] The "room" is then built with one wall using a low-impulse inlet air unit and an exhaust of the same capacity on the opposite wall. The emitted air contaminants (low- or medium-impulse sources) will then be swept away by the predominantly horizontal airflow to the exhaust. With a well-designed system it is possible to reach a very low level of mixing, both horizontally and vertically. If work is also planned and carried out considering the special airflow patterns, a very high degree of reduction of the workers' exposure to the air contaminants may be achieved.

10.3.3.2 Vertically Downward Airflow Direction

General

The aim with air showers is to create locally improved ventilation efficiency. They are characterized by the fact that surrounding air is mixed into the supply air to a very low extent when it reaches the worker and the principle is used with the purpose to create a cleaner or cooler zone without having to consider the heat or contaminant loads in all other areas of the room. Compared to the situation when only general ventilation is used a reduction of workers' exposure to air contaminants from 50% to more than 90% can be achieved by an air shower. Air showers make it possible to reach a chosen target value for local contaminant exposure or climate control with 30 to 70% cost savings compared to mixed ventilation. When this ventilation principle is utilized to reach a defined target level for air contaminant exposure or climate, the investment requirements in general are not higher than compared to the alternative.[3]

Principle Including Sketches/Figures

The basic idea is to create a volume of clean air that includes the breathing zone of one worker by introducing a vertically oriented, low-momentum airflow covering a limited area under the unit with clean air (Fig. 10.48). The airflow can enter with a velocity high enough or slightly chilled to ensure that the introduced, clean air reaches the level where the air contaminant concentration or the temperature is to be controlled. The vertically downward airflow generated by the shower must, therefore, be high enough to counteract the effect of the vertically upward convection airflow around the worker caused by the heat of the body. The area covered by the air shower is often limited to the area in which the worker is mainly moving, normally about 1 m^2, but may be expanded by combining two or more units.

Applicability of Sources

The system may be used to control exposure to air contaminants when the source strength is moderate and has a low-momentum, as is typical in manual handling of processes causing release of gases, vapors, smoke, or dust. Examples are use of glue, paint, printing ink, or other resin-containing products emitting organic solvents and/or gases, soldering, and handling of pulverous raw material as in chemical industries or bakeries. Air showers may also be used to create a high degree of comfort in terms of the freshness of the air or CO_2 in a room with moderately warm sources, e.g., computer workstations.

FIGURE 10.48 The air shower principle creates a zone of clean air around the worker and pushes the contaminant plume away from the breathing zone.

Different Forms and Boundaries Relative to Other Types

A common supply air unit used as an air shower has a flat underside covering an area over the workplace with a typical size approximately 1 m^3 (Fig. 10.49). Another type of unit is shaped as a half sphere, distributing the air over an area much bigger then the cross-section of the unit (Fig. 10.49*b*). Other types of supply air units such as a textile tube may be used for the same purpose.

The same types of units are also used to distribute supply air over larger areas such as a whole factory hall. In those installations, however, the units are mounted higher up. The term "air shower" is therefore reserved in this context for the supplying of fresh air to a workstation with one person.

Air supply units designed for the introduction of air with a high impulse, e.g., an anemostat, are not suitable for air shower systems. Such units may cause a vertical up flow under them and thereby an effect opposite the intention of the air shower.

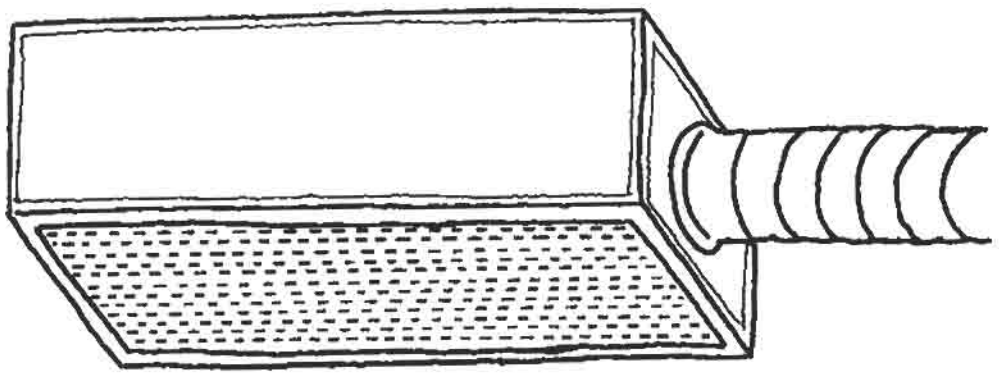

(*a*)

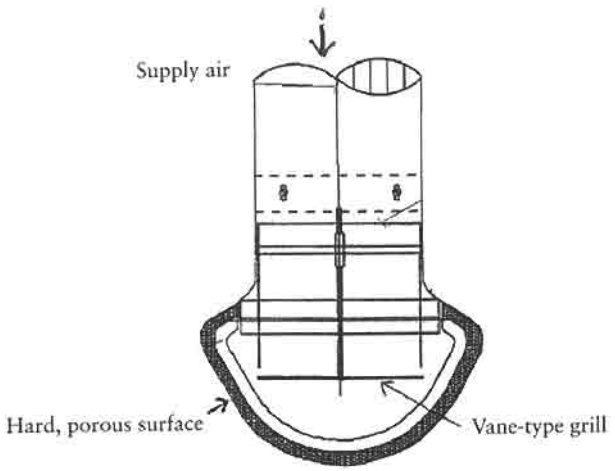

(*b*)

FIGURE 10.49 (*a*) Flat inlet air unit. (*b*) Half sphere inlet air unit.

Specific Issues

The air shower principle is effective but the effect may be drastically reduced if specified design parameters are not followed and maintained. If the system is designed for a supply air temperature of 2 °C below general room temperature, a major divergence from that may drastically reduce the desired effect. A large temperature difference will result in a high acceleration of the supply air and therefore a reduced protected volume, especially when a textile tube is used as the inlet air unit. It is also important to avoid high temperature differences because of the risk that drafts may cause discomfort for workers.

A small temperature difference of the supply air relative to the surrounding air will not result in a protection effect since the density difference will be too low to result in the expected vertical air transport. If the temperature of the supply air is too low problems will result due to drafts on the worker, which will increase the risk that he or she will move from the protected zone if possible.

Design Equations and/or Parameters

The flat supply air unit can be built of, for example, sheet metal as a box with one side perforated. The area of the perforated side must be slightly wider than the area to be protected since the acceleration of the plume (if colder supply air than the surrounding air is used) will cause the cross-section to be reduced. A uniform velocity profile is important to achieve the desired result; divergences may result in negative effects to such a degree that the aim will not be reached. The use of a fabric felt filter downstream of the perforated plate to produce a more uniform velocity profile is therefore recommended.[4]

The unit shaped as a half sphere is a little more complicated but also gives more possibilities to adjust the shape of the protected volume. A factory-made unit[5] was designed according to the following criteria.

To prevent the surrounding air from mixing with the supply air, the air shower should use air-permeable filter material with a harder, load-bearing, nonflammable outer shell and an inner layer of softer material with a high air resistance. This design requires that the supplied air be filtered.

The air shower should have such a shape (plane or hemispherical) as to ensure that the downward airflow from the air shower has a sufficiently wide diameter to counteract the natural tendency of the colder air to form a narrow cylinder of air.

The airflow rate to the unit is determined from the desired vertical air velocity in a cross-section of the airflow. Air velocities between 0.14 and 0.2 m s^{-1} are suggested[4,6,7] when using slightly chilled supply air. This corresponds to an airflow rate of 500 to 720 m^3 h^{-1} per m^2 of supplied area. Systems without cooling have used air velocities between 0.08 and 1.0 m s^{-1} [8,9] or from 290 to 3600 m^3 h^{-1} per m^2 of supplied area. The chilling of the supply air is important to achieve a good result.[3,4,6,7] The temperature is recommended to be 1.5 to 3 °C below the surrounding air ($\Delta\theta$). Figure 10.50 illustrates how a worker's exposure to a gas emitted from a worktable changes when $\Delta\theta$ is changed from 0 to 1.5 °C. A good effect may also be achieved if the supply air velocity is high enough (0.8–1.1 m s^{-1}) or if the air shower is combined with an exhaust unit that forces the airflow in a downward direction.

If the heat generation in the workstation is low, an additional heating may be necessary to compensate for the heat loss induced by chilled supply air

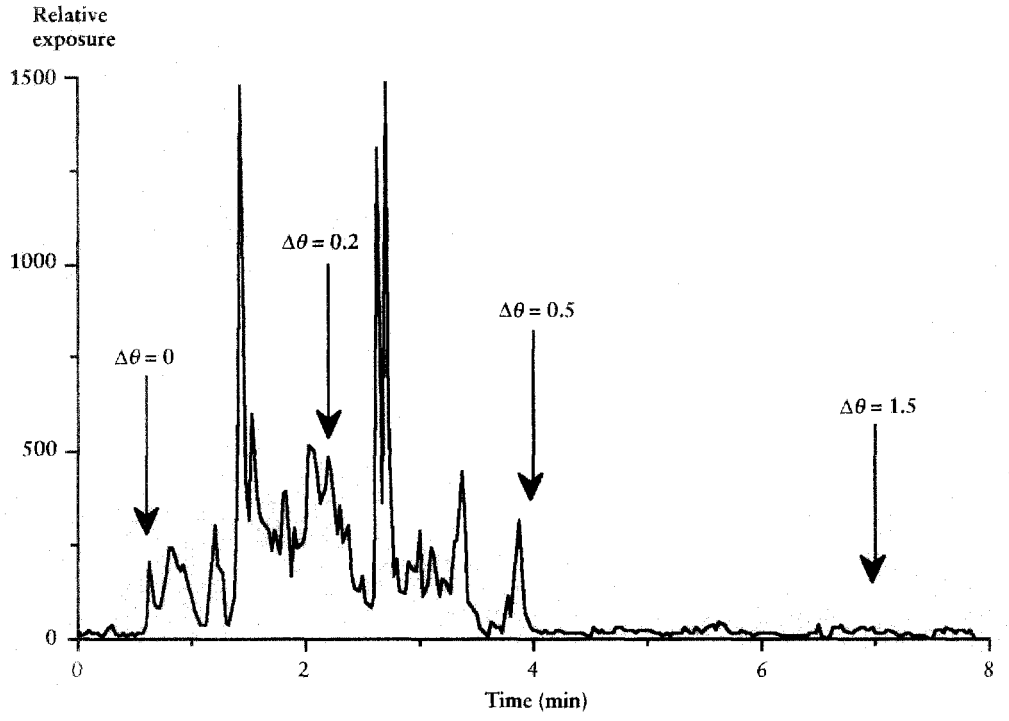

FIGURE 10.50 Worker exposure to tracer gas emitted from worktable as a function of time when the temperature difference between room and inlet air $\Delta\theta$ was gradually changed from 0 to 1.5 °C.

from the air shower. This may be arranged by heating the additional air supply outside the area affected by the air shower[5] or by adding a radiant heating panel close to the worker.[9] It is important to ensure that the worker avoids leaning over the source during work. Raising the source (the worktable) and ensuring good lighting may reduce this risk.

10.3.4 Open Unidirectional Air Flow Benches

10.3.4.1 General

The purpose of open unidirectional airflow benches is to protect products from particulate contaminants by creating a controlled environment. These benches are used, for example, in electronic, biological, pharmaceutical, and food industries. It should be mentioned that within pharmaceutical production, aseptic sterile processes must be carried out in a Class 100 environment (U.S. Federal Standard 209 E, Airborne Particulate Cleanliness Classes in Cleanrooms and Clean Zones). To avoid particle contamination in the bench, horizontal or vertical airflow with high-efficiency particulate air (HEPA)–filtered air is used. The air velocity is normally 0.4–0.5 m s^{-1}. Some examples of typical arrangements of open unidirectional airflow benches are shown in Fig. 10.51.

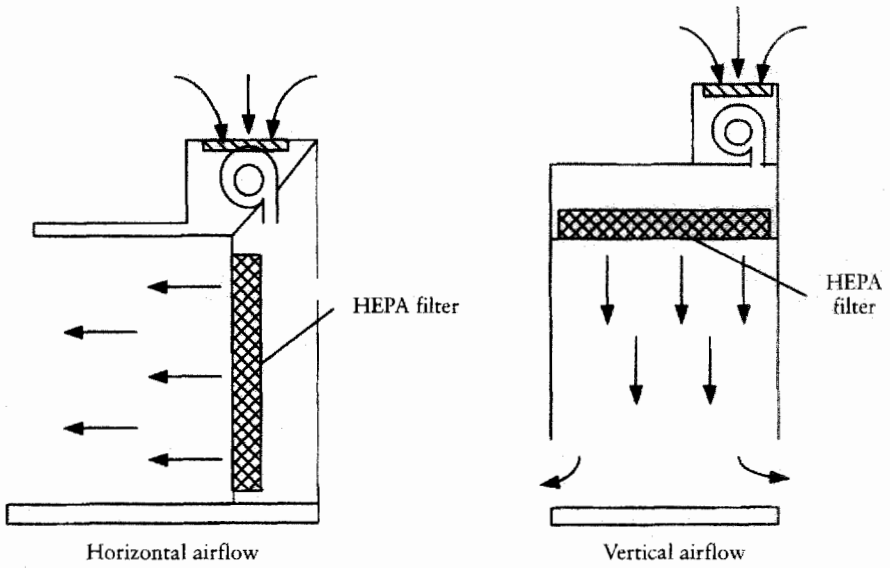

FIGURE 10.51 Examples of typical arrangements of open unidirectional airflow benches.

In order to maintain a high level of air quality, it is necessary to test airflow velocities and HEPA filters for integrity. These tests are described in a variety of standards and recommended practices depending on the use of the airflow bench.

The bench should be supplied with HEPA-filtered unidirectional airflow, having a velocity sufficient to sweep particulate matter away from the working area. Normally a velocity of 0.45 m s^{-1} plus or minus 20% is adequate. It is important to monitor the air velocity at suitable intervals because significant reduction in velocity or uniformity in velocity can increase the risk of contamination.

Integrity testing of HEPA filters should be performed by using an aerosol challenge (dioctylphthalate (DOP) or similar). Initial testing, when the benches are installed, to detect leaks around the sealing gaskets, through the frames, or through the filter media is essential. Thereafter, integrity tests should be performed at suitable intervals. For example, in pharmaceutical production it is common to perform such testing twice a year. When the leakage through the HEPA filter(s) is less than 0.01% of the upstream aerosol challenge level, acceptable conditions are considered to exist.

10.3.4.2 Principle

In order to achieve a high level of product safety it is well known that good work practices in the bench are necessary, and having a clean environment and proper work clothing are of vital importance. Knowledge about the interaction between air movements and the dispersion of contaminants plays an important role. Wake regions and vortex streets can easily be formed behind obstacles.

Dispersion of Airborne Contaminants

Ljungqvist and Reinmüller[11] have described contamination risks in clean environments and have estimated the "critical contamination region" in un-

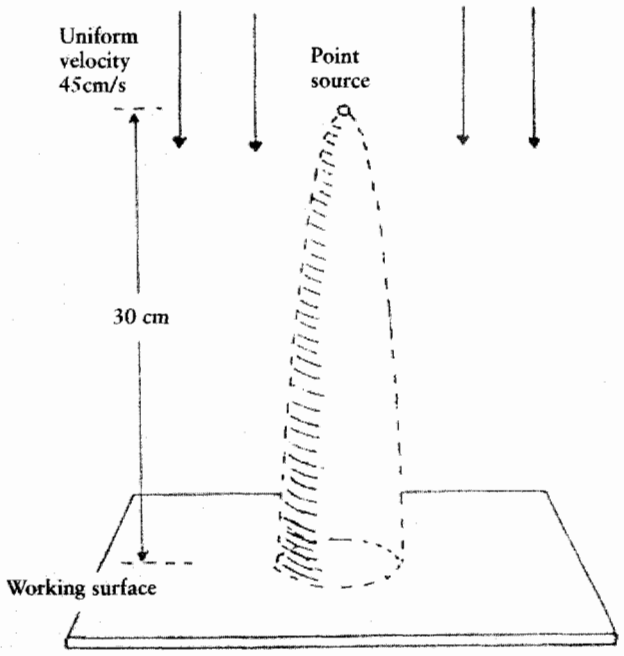

FIGURE 10.52 Critical contamination region in a uniform parallel flow field. Qualitative solution of the diffusion equation in a velocity field with the velocity equal to 0.45 m s^{-1}, diffusion coefficient equal to 2.4 cm^2 s^{-1}, and the distance between the working surface and the contamination source of 30 cm.

disturbed and disturbed parallel flow fields with dispersion from a fixed contamination source. A qualitative solution in an undisturbed parallel flow is given in Fig. 10.52, when the velocity is 0.45 m s^{-1} and the distance between the working surface and the point of source is 30 cm.

In a vortex (rigid-body rotation), Ljungqvist[12] has shown that the mean value of the concentration over the entire region inside the streamline where the point of emission is situated is considerably higher than that of the outside. This allows us to use the concept of contamination accumulation in the context of vortices.

It has also been shown, using visual illustrative methods, that accumulation can occur in the wake of people or objects, provided that the contaminants are emitted in the vortex region. Special consideration must be taken with instabilities and vortices generated by the working person. Vortices can also occur in empty open unidirectional airflow benches.

10.3.4.3 Air Movements

Air Movements in Empty Benches

In vertical unidirectional airflow benches, the area along the vertical wall in front of the operator is usually entirely or partially open. When the other side walls reach down to the working surface in the bench a stagnation flow with stationary vortices is usually created as shown in Fig. 10.53.

To avoid such vortices, the side walls must be designed with openings. At a long bench designed with equally large openings on the longitudinal and opposite wall, the flow can be considered as two-dimensional. If it is further assumed that the flow

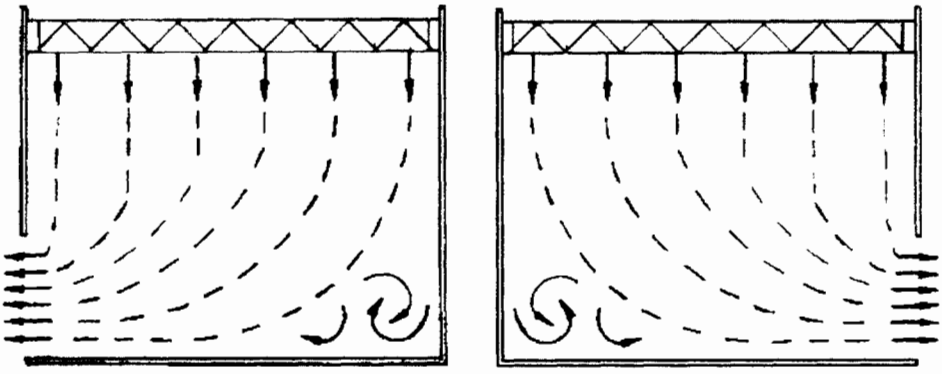

FIGURE 10.53 Vortices in a unidirectional airflow bench with covered side walls.

may be regarded as turbulence free, it is possible to find an exact solution for the Navier-Stokes' equations. The solution was first given in a thesis by Hiemenz.[13]

This plane flow leads to a stagnation point in the middle of the bench on the working surface. Furthermore, it is worth noting that the boundary layer is proportional to the square root of the kinematic viscosity, and that the thickness of the boundary layer does not vary along the working surface. In reality, a stagnation region often arises where the height and appearance can vary as shown in Fig. 10.54.

In the stagnation region shown in Fig. 10.54, contaminants will move in an irregular and often unpredictable manner. This means that production with exposed products in stagnation regions gives rise to contamination risks.

In the unidirectional air flow of an open bench, a vortex street is easily created behind small obstacles. Such an obstacle can be as insignificant as a small lamp or a fixture connecting HEPA filters. Ljungqvist, et al.[14] have, with the help of isothermal smoke, visually depicted the air movements behind such a horizontal 30 mm wide fixture at an air velocity of 0.45 m s^{-1}. The observed flow pattern is schematically shown in Fig. 10.55.

The flow pattern in Fig. 10.55 has a violent turbulent region, characterized by a vortex street and two free vortices rotating in opposite directions

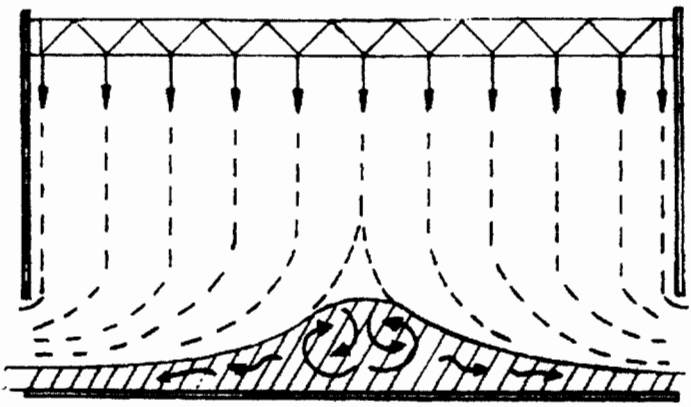

FIGURE 10.54 An example of observed stagnation region in a bench with vertical unidirectional airflow.

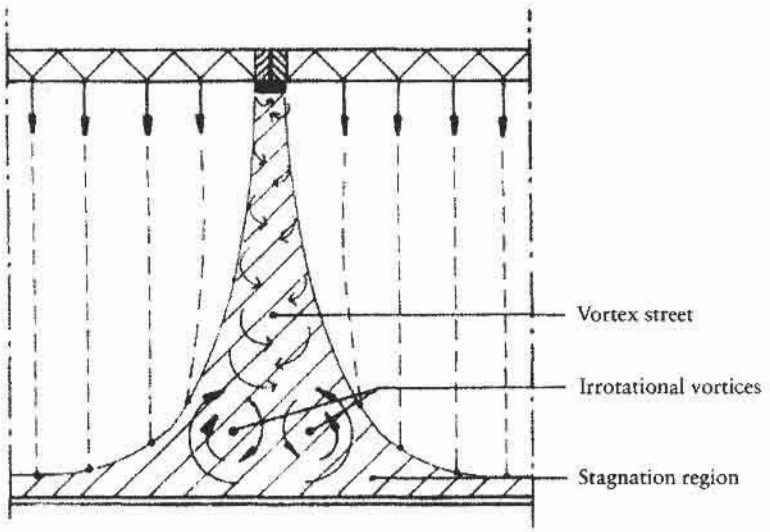

FIGURE 10.55 Observed flow pattern behind an obstacle in a vertical unidirectional air flow bench (long side).

close to the working surface. These observed vortices are known as an irrotational or free vortex and sometimes as a potential vortex. This vortex is characterized by the fact that the velocity varies only with the radius and increases toward the center.

By using a smoke photography technique one of these free vortices (irrotational) in Fig. 10.55 has been visualized (see Fig. 10.56)

FIGURE 10.56 Smoke visualization of a free vortex at the working surface in a vertical uni-directional airflow bench (short side).

Air Movements in Benches with Obstacles

The air movements outside the vortex region in the bench shown in Fig. 10.53 is depicted visually with smoke at an air velocity of 0.45 m s^{-1} in Fig. 10.57.

If a bottle is placed in the bench, a wake is easily created in the region with horizontal flow. This is depicted visually with smoke in Fig. 10.58. If the bottle is situated close to the opening of the unit, ambient air will be entrained into the clean zone in the bench. The length of the reversed region can be estimated to two to three times the diameter of the bottle, and can reach twice this length when the bottle is situated just beside the side wall.

The Reynolds number, which is directly proportional to the air velocity and the size of the obstacle, is a critical quantity. According to photographs presented elsewhere,[15,16] a regular Karman vortex street in the wake of a cylinder is observed only in the range of Reynolds numbers from about 60 to 5000. At lower Reynolds numbers, the wake is laminar, and at higher Reynolds numbers, there is a complete turbulent mixing.

In the case shown in Fig. 10.58, the Reynolds number is approximately 2700. In the situation shown in Fig. 10.55, where the arrangement between two filter modules forms a flow obstacle, the Reynolds number is approximately 900.

FIGURE 10.57 Undisturbed smoke dispersion in the bench shown in Fig. 10.53 at an air velocity of 0.45 m s^{-1}.

FIGURE 10.58 Dispersion of smoke behind a bottle placed in the bench shown in Fig. 10.57.

However, one should be cautious when comparing the Reynolds number from regular Karman vortex streets with the Reynolds number calculated from factual situations in clean benches as the airflow from behind an obstacle is usually not the typically formed Karman vortex street predicted for an indefinitely long circular cylinder. The wake situations during actual conditions often seem to have a three-dimensional structure.

If a hand is placed over the smoke source in Fig. 10.57, a wake region is created in the vertical flow field, as shown in Fig. 10.59.

It is possible that ambient room air can reach the critical region in the bench due to created wakes. Such a wake region is depicted in Fig. 10.60 for a horizontal flow bench with small bottles and an air velocity of 0.45 m s^{-1}.

Essentially, vortices caused by people are of two kinds. Relatively stable and stationary wakes are created by the body. Unstable and nonstationary vortices arise

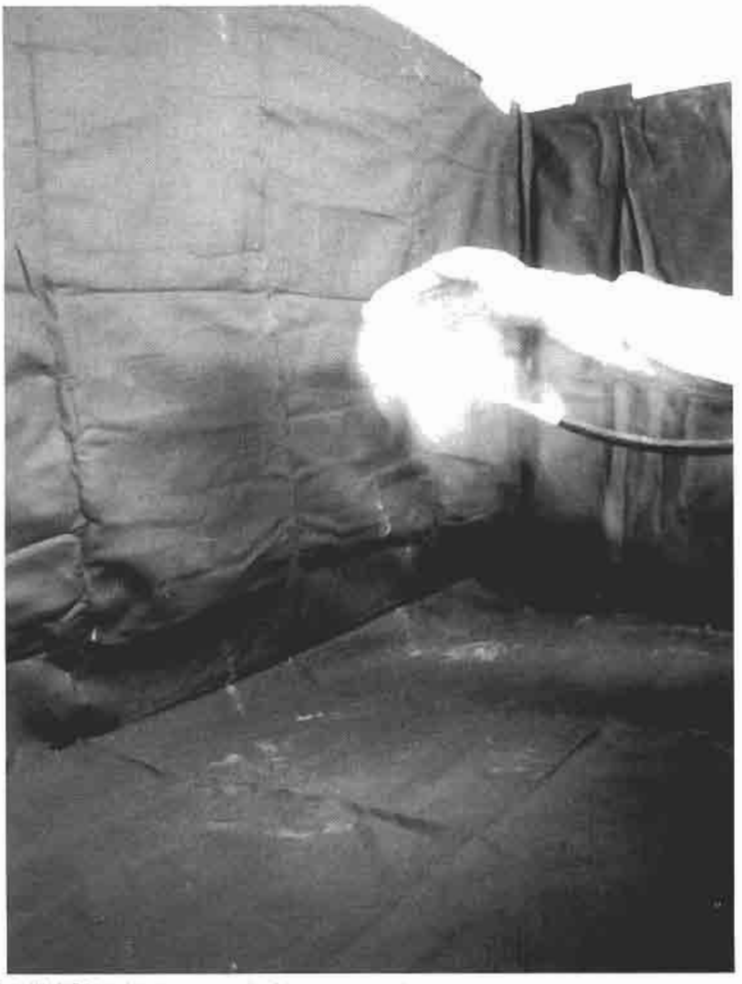

FIGURE 10.59 Dispersion of smoke behind a hand (arm) placed in the bench shown in Fig. 10.57.

FIGURE 10.60 Dispersion of smoke in a horizontal flow bench (wake region behind small bottles).

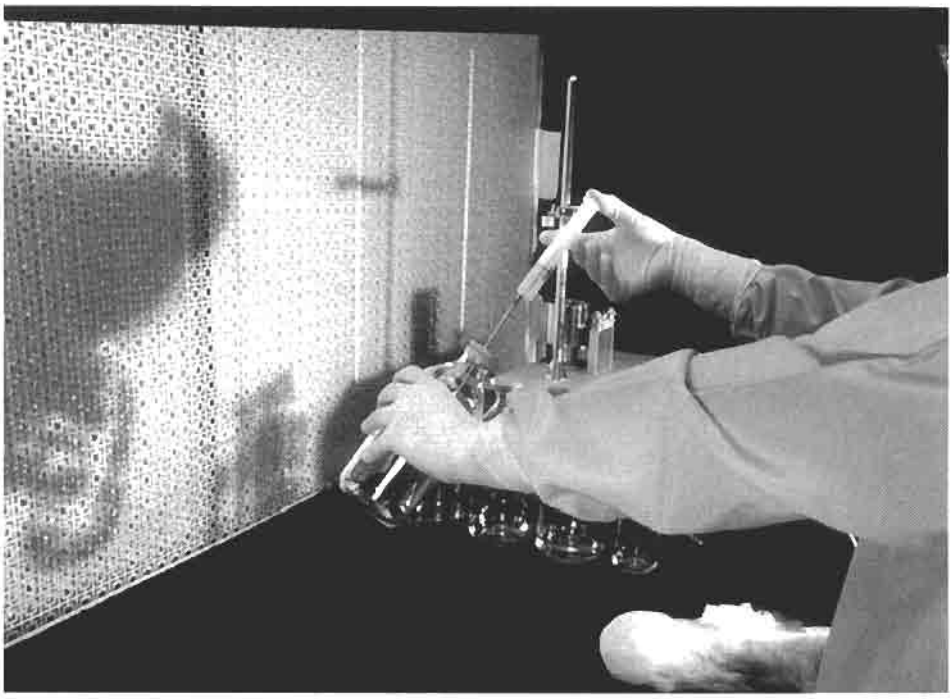

FIGURE 10.61 Dispersion of smoke in a horizontal unidirectional flow bench when operator's hands are in the upper position (undisturbed smoke dispersion).

as a consequence of the movements of the body. In this respect, it is obvious that the movements of the hands and arms play a significant role in creating unstable situations. Work situations in a clean air bench with a horizontal unidirectional airflow are demonstrated by using a smoke technique in Figs. 10.61 and 10.62.

10.3.4.4 Conclusion

When open unidirectional airflow benches are being used in production sensitive to contamination, a thorough function check should always be carried out before the start of production. Studies of air movements with visual illustrative methods give both quick and valuable information.

In order to reduce the influence of unfavorable stagnation regions and vortex structures with their risk for accumulation of contaminants, tests should be carried out to characterize the functioning of the bench. In connection with these tests, induction tests should also be performed. Here smoke (particles) generated outside the bench and the probe of a particle counter placed inside the bench in the critical regions can give valuable information.

Investigations should also be carried out with equipment in place and with test persons performing activities according to a standardized plan of movements.

The above approach, with visualization of air movements and particle challenge tests together with calculation of a risk factor, presents a method, the LR method (Limitation of Risks), to evaluate the risk of human interference in the critical zone of the bench. It also gives valuable information concerning potential weak links. A more thorough description of the LR method is given in Ljungqvist and Reinmüller.[11,17]

FIGURE 10.62 Dispersion of smoke in a horizontal unidirectional flow bench when operator's hands are in motion.

References

1. D. T. Hitchings. *ASHRAE Journal*, February 1994, 36–40.
2. I. M. Anderson, R. Niemelä, G. Rosen, and A. Säämäen. *Applied Occupational Enviornmental Hygiene*, vol. 8, no. 12, 1993.
3. J. A. Kristensson. In *Ventilation '94: Proceedings of the 4th International Symposium on Ventilation for Contaminant Control, Stockholm, Sept. 5–9, 1994* (eds. A. Jansson and L. Olander). (*Arbete och Hälsa*, no. 18). Sweden: National Institute for Working Life, 1994, pp. 477–484.
4. I. Kulmala. *Annals of Occupational Hygiene*, vol. 38, no. 4, 1994, 337–349.
5. J. A. Kristensson and O. A. Lindqvist. In *Proceedings of the 1993 Winter Meeting of ASHRAE, Chicago, January 23–27, 1993*, pp. 992–1008 (ASHRAE Transactions, vol. 99 pt. 1, 1993).
6. A. Säämänen and S. Enbom. In *Ventilation '94: Proceedings of the 4th International Symposium on Ventilation for Contaminant Control, Stockholm*, Sept. 5–9, 1994 (eds. A. Jansson and L. Olander). (*Arbete och Hälsa*, no. 18). Sweden: National Institute for Working Life, 1994, 307–312.
7. I.-M. Andersson, R. Niemelä, G. Rosén, I. Welling, and A. Säämänen. In *Ventilation '91: Proceedings of the 3rd International Symposium on Ventilation for Contaminant Control, September 16–20, 1991, Cincinnati, Ohio, USA* (eds. R. T. Hughes, H. D. Goodfellow, and G. S. Rajhans). Cincinnati, OH: American Conference of Governmental Industrial Hygienists, 1993, pp. 161–166.
8. M. G. Gressel and T. J. Fischbach. *Applied Industrial Hygiene*, vol. 9, 1989, 227–233.
9. L. C. Minor. In *Ventilation '91: Proceedings of the 3rd International Symposium on Ventilation for Contaminant Control, September 16–20, 1991, Cincinnati, Ohio, USA* (eds. R. T. Hughes, H. D. Goodfellow, and G. S. Rajhans). Cincinnati, OH: American Conference of Governmental Industrial Hygienists, 1993, pp. 393–396.
10. I. Welling, J. Auvinen, M. Hyvärinen, I. Kulmala, J. Laurikainen, U. Mooilanen, and A. Niemi. In *Ventilation '94: Proceedings of the 4th International Symposium on Ventilation for Contaminant Control, Stockholm, Sept. 5–9, 1994* (eds. A. Jansson and L. Olander). (*Arbete och Hälsa*, no. 18). Sweden: National Institute for Working Life, 1994, pp. 255–260.
11. B. Ljungqvist and B. Reinmüller. *Clean Room Design: Minimizing Contamination through Proper Design*. Buffalo Grove, IL: Interpharm Press, 1997.
12. B. Ljungqvist. *Some Observations on the Interaction between Air Movements and the Dispersion of Pollution*. Document D8:1979. Stockholm: Swedish Council for Building Research, 1979.

13. K. Hiemenz, Die Grenzschicht an einem in den gleichförmigen flüssigkeitsstrom eingetauchten geraden kreiszylinder (Boundary layer around a cylinder in an even distributed flow). *Dingl. Polytech. J.*, 1911, 326, 321.
14. B. Ljungqvist, R. Nydahl, and B. Reinmüller. *Swiss Contamination Control*, no. 4a, 1990, 36–39.
15. G. K. Batchelor. *An Introduction to Fluid Mechanics*. Cambridge: Cambridge University Press, 1970.
16. H. Schlichting. *Boundary Layer Theory*. 7th ed. New York: McGraw-Hill, 1979.
17. B. Ljungqvist and B. Reinmüller. *PDA Journal of Pharmaceutical Science and Technology*, vol. 49, no. 5, 1995, 239–243.

10.4 COMBINED EXHAUST HOODS AND SUPPLY INLETS

10.4.1 General

These systems can be inside large halls and may have no fixed limits for their influence, except for some parts of the system (inlet device surface, etc.) They can also be situated inside small rooms, where walls, floors, and ceilings are the natural boundaries. The systems usually consist of one exhaust hood and one supply inlet, which interact. There are also special combinations, as two or more inlets and one exhaust hood, or one supply inlet and two or more exhausts. All of these combinations need careful design and an accurate relation between supply and exhaust flow rates and velocities. Some systems also need stable temperature conditions to function properly. All combinations are dependent on having a defined contaminant concentration in the inlet air. This usually implies clean supply air, but some systems may use recirculated air with or without cleaning.

There are many possible combinations of supply and exhaust air. For example, a line jet could be used as a shield in an opening, as a stripping system on surfaces, for blowing contaminants into an exhaust, etc. An enclosure could be designed with a line jet in the opening, with a wall jet inside to increase efficiency, or with a low-momentum jet inside or outside the opening to replace the room air supply. In this section, only some basic combinations are described.

All rooms need both supply and exhaust air. The combined systems described in this section are unique in that they must be chosen and designed simultaneously, since the aim is to get a specific flow field—dependent on the exhaust and the supply simultaneously—inside the specified volume. The flow rates are usually not the same in the supply and the exhaust parts of the system. This means that the same flow difference must exist in the room's ventilation system, if the combined system takes its air from outside the room and disposes of the air to the same place. There is no general rule for how to choose between the systems, except what has been specified for exhaust hoods and supply inlets, respectively. Usually, the choice is made by tradition or the equipment available. This should not prevent the designer from exploring the relative advantages and disadvantages of these systems (which are described for each system) and applying and designing a system that suits his or her demands for a specific process.

Similar to supply inlets, no measurements exist for evaluating the inlets' specific influence on contaminant concentration. The available measurements for the combinations are the same as for exhaust hoods, i.e., capture efficiencies and similar measures. Sometimes the performance of a combined system can be approximated from the performance of the incoming supply inlet and exhaust hood.

Earlier descriptions for exhaust hoods and supply inlets will not be reproduced in this section.

For a combined system it is always important to consider how the person working with a process and the contaminant source are placed in relation to the inlet and outlet. Exactly what their relative positions should be to get the highest efficiency depends on the specific system.

For a push-pull system, the source is usually an open surface tank and the airflow acts as a horizontal curtain above the surface. In this case, the person could be anywhere as long as the system works as intended and the curtain is not broken. The curtain will be broken when parts or material are lifted out of or placed into the bath and the contaminants could be spread either through convection or because the supply air blows against the material or part.

For workbenches or laboratory fume hoods with auxiliary supply it is the working person who could break the shielding curtain, and in that way contaminants are transported from the interior of the exhaust hood to the space where the person is situated.

For unidirectional rooms the placement of inlet, source, and person is as important as when using exhaust hoods. For hospital isolation rooms, it is not only the inlet, outlet, and the person who influences the contaminant concentration; the design of the room and the handling of the room's door are also important.

10.4.2 Air Curtains

10.4.2.1 General

When it is necessary to confine an air volume from the ambient environment and simultaneously have access for operators or machinery, plane air jets offer a possible and simple solution. Air jets (plane and round) are described in Chapter 7. This section describes plane air jets combined with exhaust openings. In principle, they are similar to the air jets described in Chapter 7 and Section 10.3, but the combination with an exhaust opening makes it necessary to consider the influence of the exhaust on the jet. Usually these curtains are used in large doors to shield the interior from the exterior when the door is open. For example, experimental results have shown that from the moment a door is opened, a short time interval, less than 1 minute, is sufficient to get complete development of the airflow through the door.[1] An air curtain allows a reduction of the overall flow through the door. The principles and use of air curtains are described in many textbooks.[2–6] Some basics of air curtains are described here.

10.4.2.2 Principle

When using air curtains the edge effects are neglected and the flow is treated as two-dimensional. The different parts of a two-dimensional jet are sketched in Fig. 10.63.

The theory for plane jets is similar to descriptions of circular jets (see Section 7.4) and many derived equations describe both two-dimensional (plane) and three-dimensional (round) jets. The principle is to generate such high air velocity that a shield against pressure difference, temperature difference, and wind velocity is sustained. However, it is not possible to have complete separation by an air curtain. The main reason for this, is that the jet entrains air

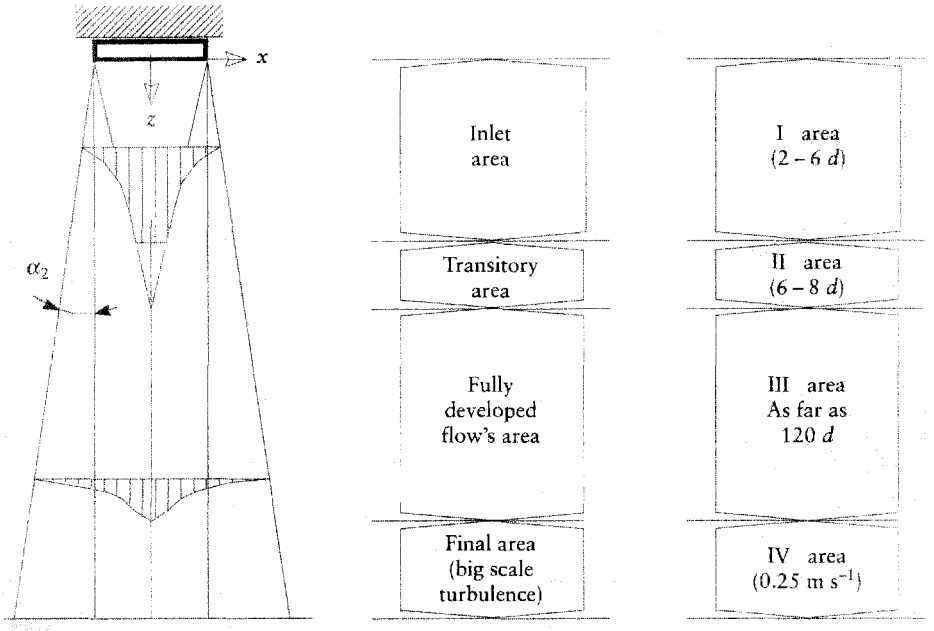

FIGURE 10.63 Plane air jet's outline and development.

(from both sides) along its way and this entrained air is mixed inside the jet and transported together with the original supplied air. Other reasons are the extremely high velocities needed to stop oncoming high wind velocities and the transport of air through the curtain when vehicles or persons pass through the curtain.

10.4.2.3 Applicability of Sources

There are numerous possible applications for air curtains. For example, air curtains may be used to heat a body of linear dimensions (as used to move the fresh snow from the railway exchanges in Canada); to function as a partition between two parts of one volume; to function as a partition between an internal room and an external environment, that have different thermodynamic properties; and to shield an opening in a small working volume (see Section 10.4.6).

10.4.2.4 Different Forms

When used as an air curtain, the flow of the linear jet is blown across a doorway and an exhaust opening pulls the air. The supply air of the air curtain for a door could be either cold or warm, either placed on the inside or the outside, either blowing horizontally or vertically, and either blowing parallel to the opening or at a slight angle to the opening. Usually the curtain has an exhaust opening placed on the other side of the opening. This exhausted air could be circulated back to the supply opening or just transported away. All these alternatives mean that there are innumerable possible configurations for an air curtain. Some of these are shown in the following figures.

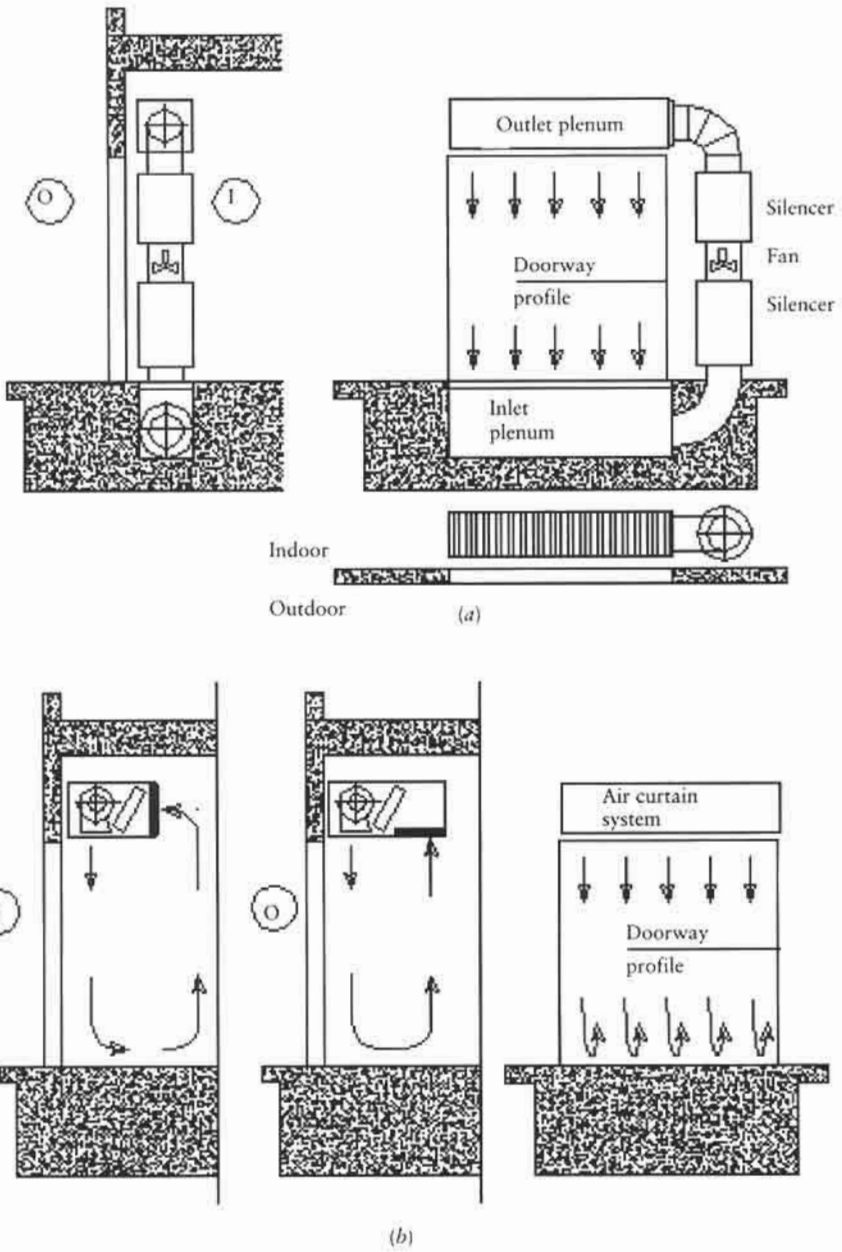

FIGURE 10.64 (a) Jet opening opposite to exhaust grill, (b) Jet opening adjacent to exhaust grill.

A jet blowing vertically downward, with the pull flow downward and upward, is shown in Figs. 10.64*a* and 10.64*b*, respectively.

Air curtains with the jet vertically upward are shown in Fig. 10.65. The configurations differ in the internal or external placement of the air-handling unit.

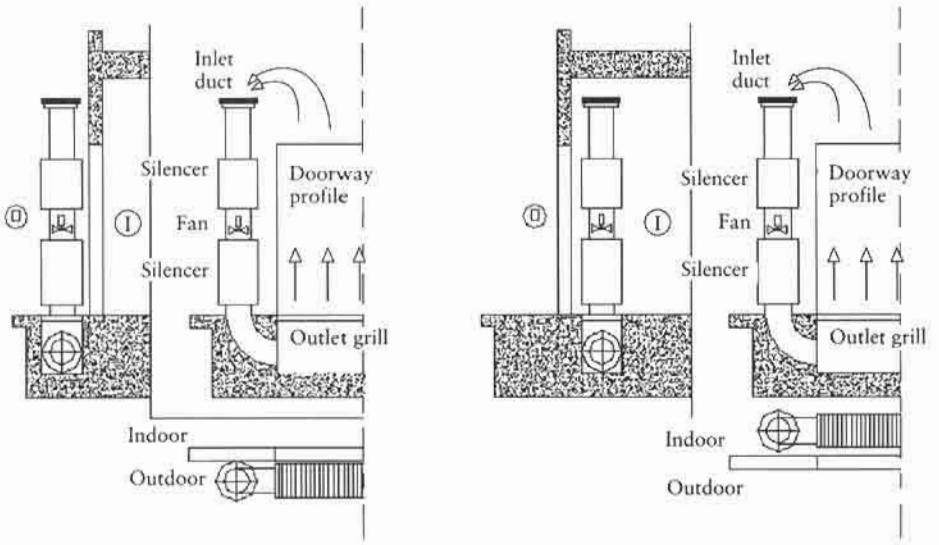

FIGURE 10.65 Three different working configurations of an upward air curtain.

10.4.2.5 Geometrical and Physical Parameters

An isothermal curtain is easily distinguished from the nonisothermal but in practice the mathematical models of a free jet are seldom fully representative of the real jet.

The scheme of an air curtain and some geometrical parameters influencing the behavior of the jet are shown in Fig. 10.66. These parameters are described in Table 10.10.

For the design of an air curtain it is also necessary to take into account the physical parameters of the jet and the surrounding air. A list of these parameters is shown in Table 10.11.

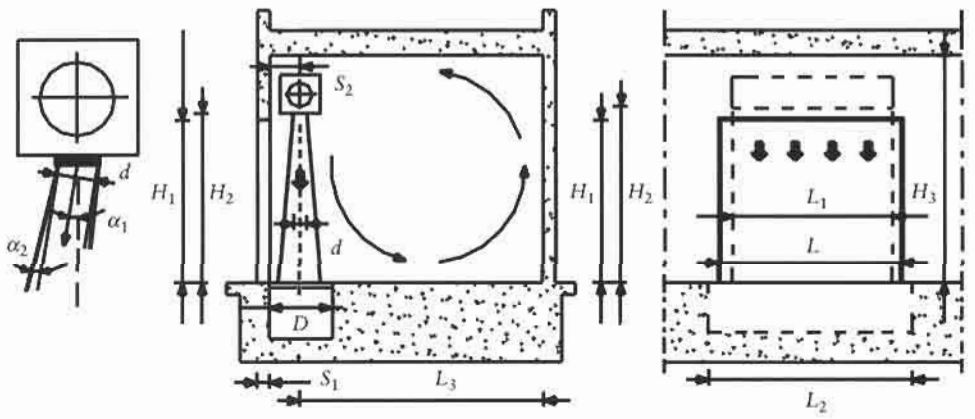

FIGURE 10.66 Characteristic geometrical parameters of air curtains.

TABLE 10.10 Geometrical Parameters Describing an Air Curtain and Influencing Its Performance

L; H_1	Width and height of doorway
d; L_1	Initial width and length of linear jet
s_1	Thickness of the wall that delimits the surface of passage (doorway
s_2	Distance between the axis of the initial section of the linear jet air curtain blade and the surface of the wall that delimits the doorway
D; L_2	Thickness and width of the exhaust opening
α_1	Angle between the axis of the jet and the vertical one
α_2	Angle of divergence of the jet
H_2	Length of longitudal development of the jet
L_3	Distance between the surface of symmetry of the jet and the neighboring wall
H_3	Height of the inside
s_3	Distance between the axis of the opening of the supply device and the axis of the grill

TABLE 10.11 Physical Parameters Influencing an Air Curtain

t	Opening time of doorway
v	Axial velocity of the jet
v_e	Velocity of the air outside normal to the symmetry surface of the linear jet
$T_1 - T_e$	Temperature difference between inside and outside
T_e	Outside temperature
T_g	Initial temperature of the jet
pi	Inside pressure
pe	Outside pressure
ρi	Inside air density
ρe	Outside air density

10.4.2.6 Theoretical Model and Experimental Researches

The influence of the geometrical parameters is not well described in the literature and the design of an air curtain is based on theoretical models of a plane turbulent jet.

One very good description is by Schlichting.[7] Assuming both constant momentum and angle divergence of the jet, the velocity profiles are given by

$$u = \frac{\sqrt{3}}{2}\sqrt{\frac{K\sigma}{z}} \cdot (1 - \tanh^2 \eta) \tag{10.81}$$

and

$$v = \frac{\sqrt{3}}{4}\sqrt{\frac{K}{z\sigma}} \cdot [2\eta(1 - \tanh^2 \eta) - \tanh \eta], \tag{10.82}$$

where

$$\eta = \sigma \cdot \frac{x}{2}, \tag{10.83}$$

where u and v are the air velocities at distance z in the z and x directions, respectively; σ is Reichardt's constant and is equal to 7.67; and x and z are the transverse and longitudinal coordinates of the jet, respectively. K is the kinematic momentum,

$$K = \frac{4}{3} \cdot u_s^2 \cdot \frac{s}{\sigma}, \tag{10.84}$$

where u_s is the centerline velocity at a fixed distance, s, from the outlet opening. The gas density should be included in these calculations, but is canceled out in the calculation of the kinematic momentum.[7] These equations can be used to calculate the mean velocity, velocity distribution across the jet, total flow rate, and entrained flow rate, at a certain distance from the outlet.

Goodfellow[2] has published the following expressions for these relations:

$$\frac{u_{z,c}}{u_0} = 2.5\sqrt{\frac{w}{z}}, \tag{10.85}$$

where $u_{z,c}$ is the centerline velocity at distance z (m) from the opening, m s^{-1}, u_0 is the jet nozzle velocity, m s^{-1}, and w is the nozzle width, m.

The velocity across the jet is

$$\frac{u_z}{u_{z,c}} = e^{-(\alpha x/z)^2}, \tag{10.86}$$

where $u_{z,c}$ is the centerline velocity at distance z (m) from opening, m s^{-1}, u_z is the velocity at distance z (m) from the opening and x (m) from the jet axis, m s^{-1}, and α, a constant, is 6.52.

The mean velocity is given as

$$u_{z,m} = 0.62u_{z,c}, \tag{10.87}$$

where $u_{z,m}$ is the mean velocity across the jet at distance z(m) from the outlet, m s^{-1}, and $u_{z,c}$ is the centerline velocity at distance z (m) from the opening, m s^{-1}.

The entrained air can be calculated as

$$\frac{q_z}{q_0} = 0.62(z/w), \tag{10.88}$$

where q_z is the airflow rate at distance z (m), m^3 s^{-1}, q_0 is the airflow rate at the nozzle, m^3 s^{-1}, and w is the nozzle width, m.

The total amount of air moving at distance z from the nozzle is thus equal to q_z. Of this flow rate, q_0 comes from the nozzle and half of the remaining flow rate comes from either side of the plane jet.

This entrained flow rate is normally many times the original flow rate and it is the total flow rate that the receiving opening must be designed to exhaust. At the same time the entrained air must be available to both sides of the jet,

otherwise the jet will change direction. This is not a problem when there are large volumes on both sides of the curtain, e.g., if the curtain is at an exterior door for a large industrial hall, with separate supply and exhaust ventilation systems. If the curtain is placed at the opening of a small closed volume, e.g., a biological safety cabinet (Section 10.4.6.4), it is necessary to design the supply flow rate inside to include the entrained air in the curtain and the exhaust flow rate inside to include the total flow rate in the jet. Mostly the exhaust is designed still larger to exhaust some more air from the surroundings to increase the separating effect of the curtain.

These relations, which describe the velocity profile sketched in Fig. 10.63, have a similarity property, behind the form of the equations. Guttmark and Wignanski[8] indicate that the similarity profile could be found up to a length of 120 times the outlet opening width.

There are also formulas for calculation of temperature and concentration distribution along and across an air jet. These are based on the similarity profile of the jet.[9]

Another procedure for design of an air curtain is proposed by Tamm[10] based on the Bernoulli equation. Recently Partyka[11] proposed another procedure based on the model of Schlichting previously described.

The theoretical analysis could also be valid for nonisothermal jets assuming that the buoyancy is negligible. Grimitlyn, as reported by Hagström,[12] suggests a local Archimedes number defined as:

$$\mathrm{Ar}_z = \frac{gz(T_z - T_e)}{u_z^2 T_e}, \tag{10.89}$$

where g is 9.81 m s^{-2}, z is the same as above, u_z is the velocity at distance z, T_z is temperature at distance z, and T_e is temperature outside.

He indicates that the buoyancy is negligible for the velocity field for an Archimedes number less than a critical value equal to $\mathrm{Ar}_{z,\mathrm{crit}} = 0.15$.

Experimental laboratory results[13] and results from a full-scale model[1] have shown the relation between the dispersed thermal power inside and the air temperature difference between the two sides of air curtain. The results shown in Fig. 10.67 are for different conditions. There are no other experimental data readily available, so caution is needed when applying these results to the design of an air curtain.

From the experimental results of Azzouz et al.[1] it is possible to obtain an efficiency parameter of an air curtain:

$$\eta = \frac{q_{m,0} - q_{m,1}}{q_{m,0}} = 1 - \frac{q_{m,1}}{q_{m,0}}, \tag{10.90}$$

where η is efficiency, $q_{m,0}$ is the mass flow rate dispersed at the doorway without an air curtain, and $q_{m,1}$ is the mass flow rate dispersed in presence of the air curtain.

Some of the available data are shown in Fig. 10.68 and these indicate that, even if with some uncertainty, η decreases with an increase in the temperature difference—i.e., the higher the temperature difference, the less efficient the curtains are in separating the volumes. The same authors also claim that the efficiency can be as high as 78% with a thermal difference of 5 °C.[1]

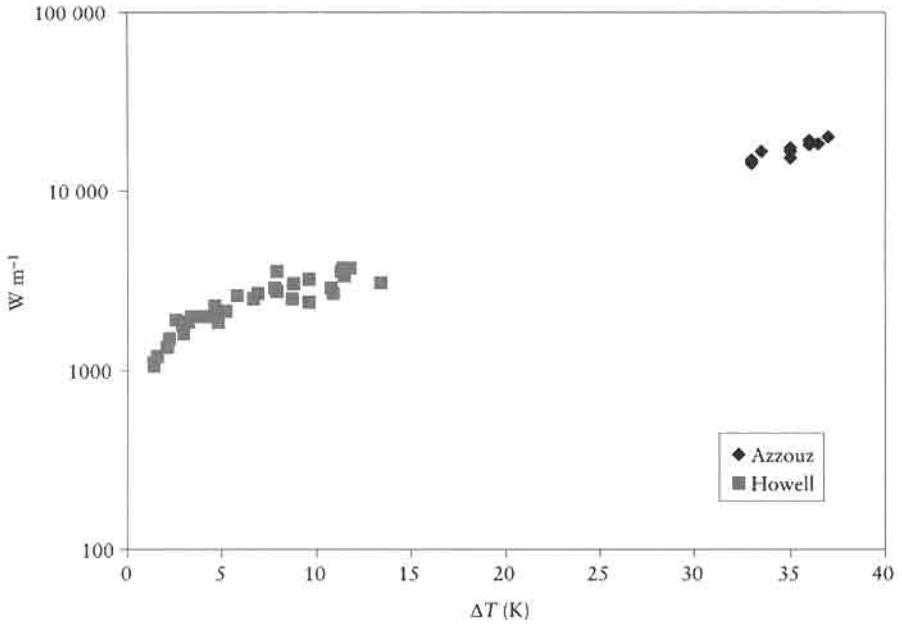

FIGURE 10.67 Thermal power through air curtain versus thermal difference between the air curtain sides.

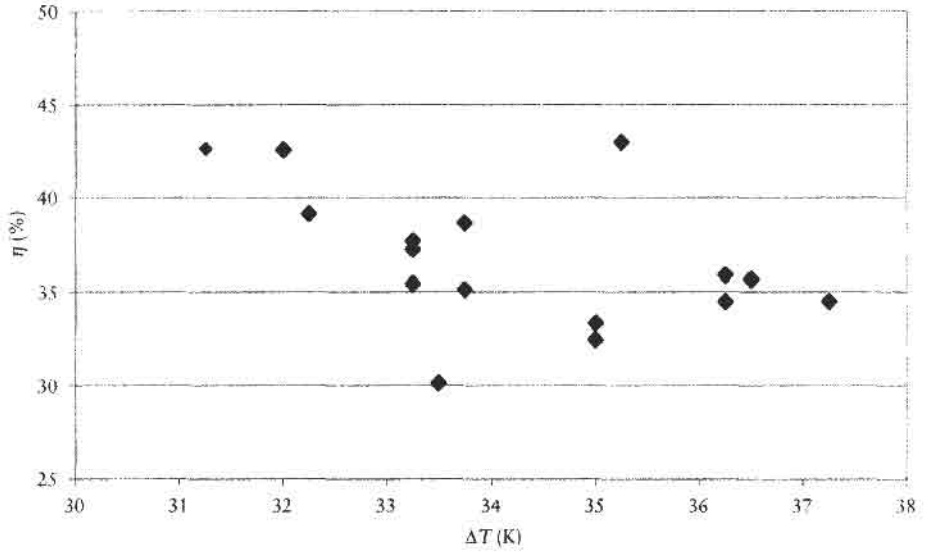

FIGURE 10.68 An air curtain's efficiency versus the difference in temperature between indoors and outdoors.

10.4.2.7 Final Remarks

This short outline suggests that it is difficult to find optimal design parameters for air curtains. CFD may provide a more effective design method for air curtains (see Chapter 13). There are some published articles applying CFD to air jets, but comparison with experimental data is lacking.

10.4.3 Push-Pull Ventilation of Open Surface Tanks

10.4.3.1 General

For large open surface tanks where access for machinery or operators is required above the tank, the options for local ventilation are limited. An overhead canopy would block access, and an exhaust hood placed at the side of the tank is prohibitively expensive for tanks greater than about 0.6 m across.[14] In these cases, push-pull ventilation offers an appropriate mechanism for reducing the overall flow rate required, compared with side exhaust, by up to 50%, while still maintaining clear overhead access.

10.4.3.2 Principle

Push-pull ventilation systems for open surface tanks consist of two components: the push flow is generated by a jet or series of jets that are blown across the surface of the tank towards an exhaust hood along one side of the tank, which pulls and removes the fluid from the jet containing the contaminant. This is shown schematically in Fig. 10.69.

10.4.3.3 Different Forms and Boundaries Relative to Other Types

This section deals mainly with side push-pull ventilation. Center push-pull ventilation is also sometimes used, where two jets of air are blown from a central pipe towards two parallel exhaust hoods at opposite ends of the tank. Much of what we say about side push-pull systems is equally valid to center push-pull.

10.4.3.4 Specific Issues

Background

During the 1980s, the United States' National Institute for Occupational Safety and Health (NIOSH) published a series of papers giving the results of exper-

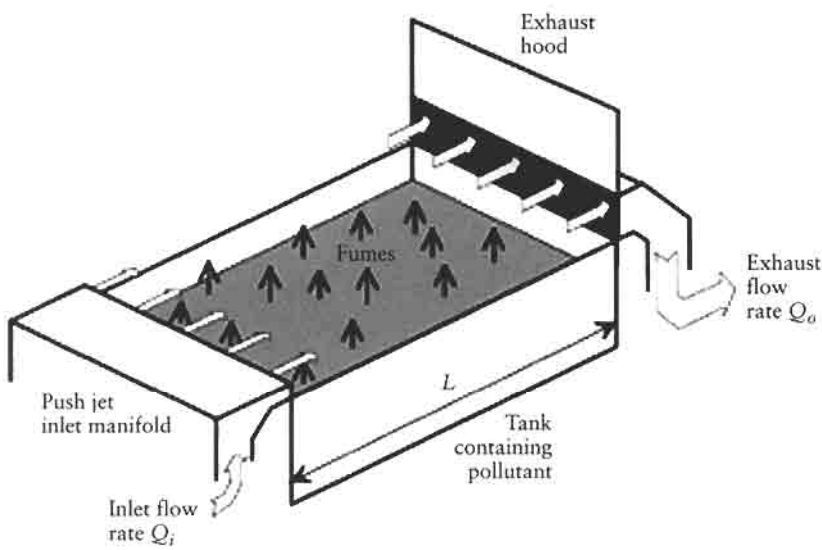

FIGURE 10.69 Schematic diagram of side push-pull system.

imental work on both side and center push-pull systems. Huebener and Hughes[15] examined side push-pull in the laboratory. They used a tank of fixed width, 1.2 m, and variable length, 1.2–1.8 m, with the push-pull system along the shorter sides. The paper suggests minimum inlet and outlet flow rates for different tank sizes and shows velocity profiles for one configuration of the system, and these data are used for comparison with the results to be presented later. Klein[16] published the results of further work by NIOSH, which used the laboratory data of Huebener and Hughes[15] in an industrial situation. He showed that Huebener's data were valid in practical situations, even with significant obstructions in the path of the jet.

A number of workers at Pennsylvania State University examined the push-pull system and found good agreement between their numerical and experimental work. The computational algorithm SIMPLER was used to solve the flow in the two-dimensional push-pull system and it was concluded that for a tank 1.8 m long, the push jet must have an initial velocity of 3.8 m s^{-1}, that the exhaust flow rate per unit width should be 0.495 $m^2 s^{-1}$, and that the ratio of the pull to push flow rates, q_0/q_i, must be between 8.8 and 17.8.

More recently, in the middle 1990s, the UK's Health and Safety Executive (HSE) also reviewed the push-pull system. Hollis and Fletcher[17] offer a comprehensive literature review on push-pull ventilation and note that the main conclusions of previous work on push-pull ventilation of tanks are that the control is primarily supplied by the inlet jet, forming a wall jet along the surface of the tank, and that the main purpose of the exhaust hood is to remove the air and contaminant contained within the push jet.

Flynn et al.[18] applied a finite element based numerical model to solve the problem of a push-pull flow with cross-drafts and demonstrate that the results show good agreement with experimental data. They note, however, that the numerical method is time consuming and therefore computationally expensive.

The ACGIH[14] gives recommendations for the design of a push-pull system, apparently based largely on the work of NIOSH in the 1980s: the nozzle should be between 3.2 mm and 6.4 mm and that the so-called momentum factor of the jet, the product of its velocity and flow rate per unit width, $U_i q_i$, should be between 0.39 and 0.59 $m^3 s^{-2}$. The outlet flow rate may then be calculated using the formula

$$q_0 = 1.2\mathrm{SF}q_i\left(\frac{0.13}{b_i} + 0.41\right)^{0.5}, \tag{10.91}$$

where q_0 is the exhaust flow rate per unit width of tank, L is the tank length, b_i is the jet nozzle height, and SF is some safety factor, recommended to be between 1 and 2.

Flow Patterns Induced by a Push-Pull System

In examining the fluid flow associated with the system, it is advantageous to treat the system as a two-dimensional problem, i.e., to neglect the edge effects. The system can then be represented by Fig. 10.70, where the width is of arbitrary size (usually larger than the length), since all calculations are done per unit width of the tank. Various studies, for example Hollis and Fletcher[17] and Huebener and Hughes,[15] have suggested that it is the flow induced by the jet that is critical to the system, and others, for example Ege and Silverman,[19] have noted that the offset jet deflects towards the tank surface and acts as a

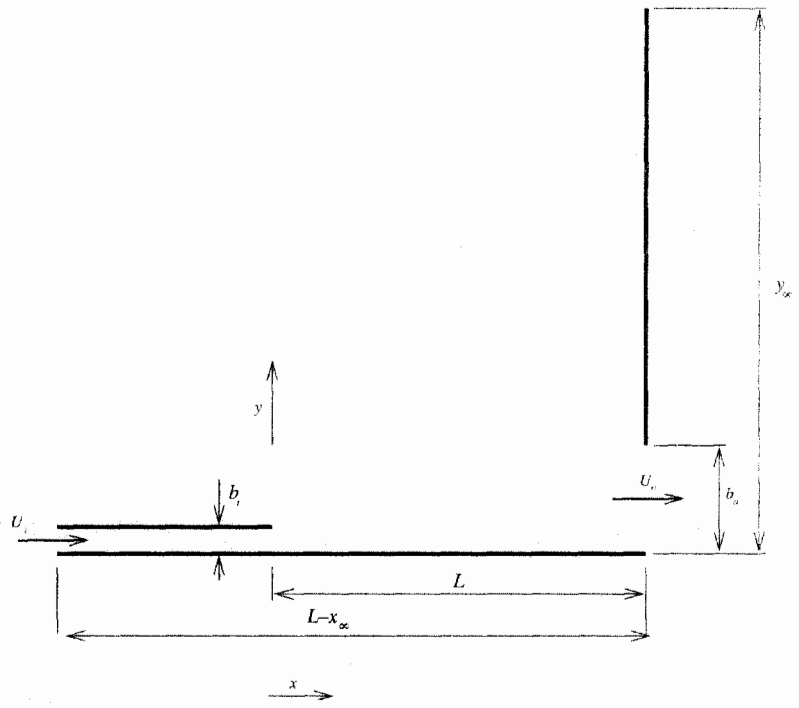

FIGURE 10.70 Simplified model of a wall jet combined with an exhaust flow.

wall jet thereafter. An obvious extension of these findings is to assume first that the flow is dominated by the effect of the push jet, and second that the jet can be treated as a wall jet rather than the offset jet, which it really is. We shall see later that the parameters of the wall jet need to be different from those of the actual offset jet, but that these can be reasonably predicted.

Turbulent wall jets have been extensively studied, and perhaps the most straightforward representation is given by a combination of the work of Verhoff[20] and Launder and Rodi[21] who together show that the fluid flow in a wall jet can be represented by

$$\frac{u}{u_m} = \hat{U}(\eta) \tag{10.92}$$

$$b = \frac{x + \epsilon}{\sigma} \tag{10.93}$$

$$\hat{U}(\eta) = B_1 \eta^d \text{erfc}(B_2 \eta) \tag{10.94}$$

and

$$u_m = \varphi \sqrt{\frac{I_i}{\rho}} x^{-c}, \tag{10.95}$$

where u is the horizontal component of the velocity, b is the jet width, defined to be the perpendicular distance from the surface of the tank to the point where the ve-

locity is half the local maximum, u_m, and the velocity is decreasing with increasing distance; j_i is the initial kinematic momentum of the jet per unit width of tank; ρ is the fluid velocity; x is the horizontal distance from the jet nozzle; and the similarity variable η is given by $\eta = y/b$, where y is the perpendicular distance from the tank surface. The constants, B_1, B_2, σ, φ, ϵ, c and d, take the following values:

$$\begin{array}{lll} B_1 = 1.48 & c = 1/2 & \varphi = 3.98 \\ B_2 = 0.68 & d = 1/7 & \sigma = 13.7 \\ & \epsilon = 10 b_i & \end{array} \tag{10.96}$$

Collectively, for the sake of brevity, we refer to Eqs. (10.92) to (10.96) as the "original Verhoff formulae." A numerical analysis of the wall jet in the push-pull situation suggests that the Verhoff formulae fit the numerical data more closely if the following constants are taken:

$$\begin{array}{lll} B_1 = 1.28 & c = 0.509 & \varphi = 3.86 \\ B_2 = 0.61 & d = 1/13 & \sigma = 9.68 \\ & \epsilon = 0 & \end{array} \tag{10.97}$$

With these values of the constants, we refer to the wall jet formulae as the "modified Verhoff formulae."

The assumptions that the exhaust flow has a negligible effect and that the offset jet can be treated as an equivalent wall jet were tested by Robinson and Ingham[22] and found to be reasonable over the majority of the surface of the tank, except close to the jet nozzle and exhaust hood. Far from the surface of the tank, the exhaust flow has a more noticeable effect.

We have thus introduced two main simplifications: first that the offset jet can be modeled as a simple wall jet, and second that the exhaust flow has a negligible effect. To demonstrate that these assumptions are reasonable, Fig. 10.71 shows the normalized horizontal component of the fluid velocity, $\hat{U}$, as a function of the similarity variable η for numerical results for both the wall jet and offset jet, and the original and modified Verhoff formulae, and the experimental results of Huebener and Hughes.[15] It shows reasonable agreement between all the different methods. A comparison of the other significant variables, such as the width of the jet and the local maximum velocity as a function of distance from the jet nozzle, also show good agreement.

Having established that these assumptions are reasonable, we need to consider the relationship between the parameters of the actual offset jet and the equivalent wall jet that will produce the same (or very similar) flow far downstream of the nozzle. It can be shown that the ratio of the initial kinematic momentum per unit length of nozzle of the wall jet to the offset jet, $j_i/\hat{j}_i$, and the ratio of the two nozzle heights, $b_i/\hat{b}_i$, depend on the ratio $D/\hat{b}_i$, where D is the offset distance between the jet nozzle and the surface of the tank, and $\hat{b}_i$ is the nozzle height of the offset jet. The relationship, which because of the assumptions made in the analysis is not valid at small values of $D/\hat{b}_i$, is shown in Fig. 10.72.

We thus have a means of describing, albeit approximately, the fluid flow induced by the system in terms of the Verhoff formulae and a graphic relationship between the offset jet parameters and the equivalent wall jet parameters. We now wish to be able to calculate the movement of the contaminant in the system

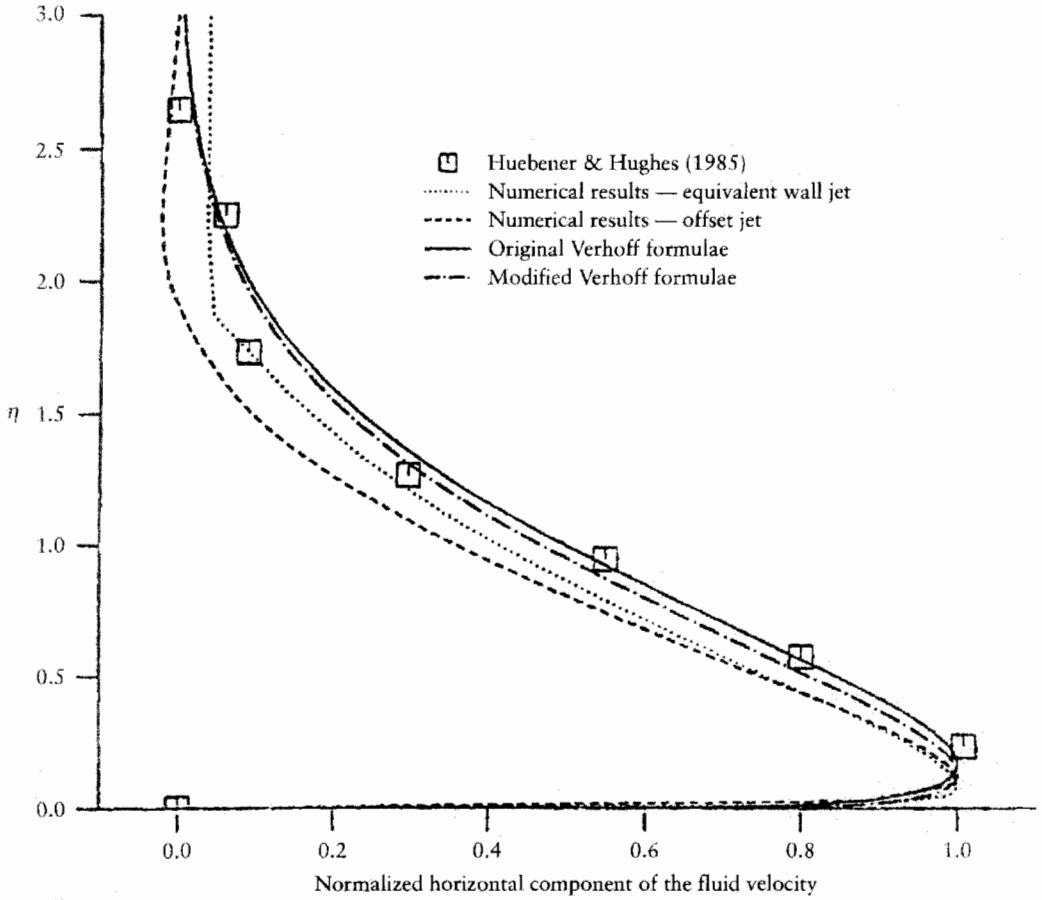

FIGURE 10.71 The ratio of the horizontal component of the fluid velocity to its local maximum u/u_m, as a function of η, at $x = 0.75$ m for the experimental results, the numerical results obtained using the commercial package for the offset and equivalent wall jet models, and the original and modified Verhoff empirical formulae.

and to do this we assume that the diffusion coefficient Γ can be approximated by $\Gamma = \mu_e/\mathrm{Sc}$, where μ_e is the effective turbulent dynamic viscosity and Sc is the Schmidt number, which is usually taken to be 0.7. We have, empirically, a description of the fluid flow, which is a similarity expression. We have determined a self-similar form for the effective turbulent viscosity, namely,

$$\nu_e = -\frac{\phi^* c}{\sigma^2} x^n h(\eta), \tag{10.98}$$

where $\phi^* = \phi\sqrt{j_i/\rho}$ and the function h is given by

$$h = \begin{cases} E\eta^{1-d}\left(1 - \left(\dfrac{\eta}{\eta_0}\right)\right) & 0 \le \eta < (\eta_0 - \epsilon) \\ E(\eta_0 - \epsilon)^{1-d}\left(1 - \left(\dfrac{\eta_0 - \epsilon}{\eta_0}\right)\right) & \eta \ge (\eta_0 - \epsilon) \end{cases} \tag{10.99}$$

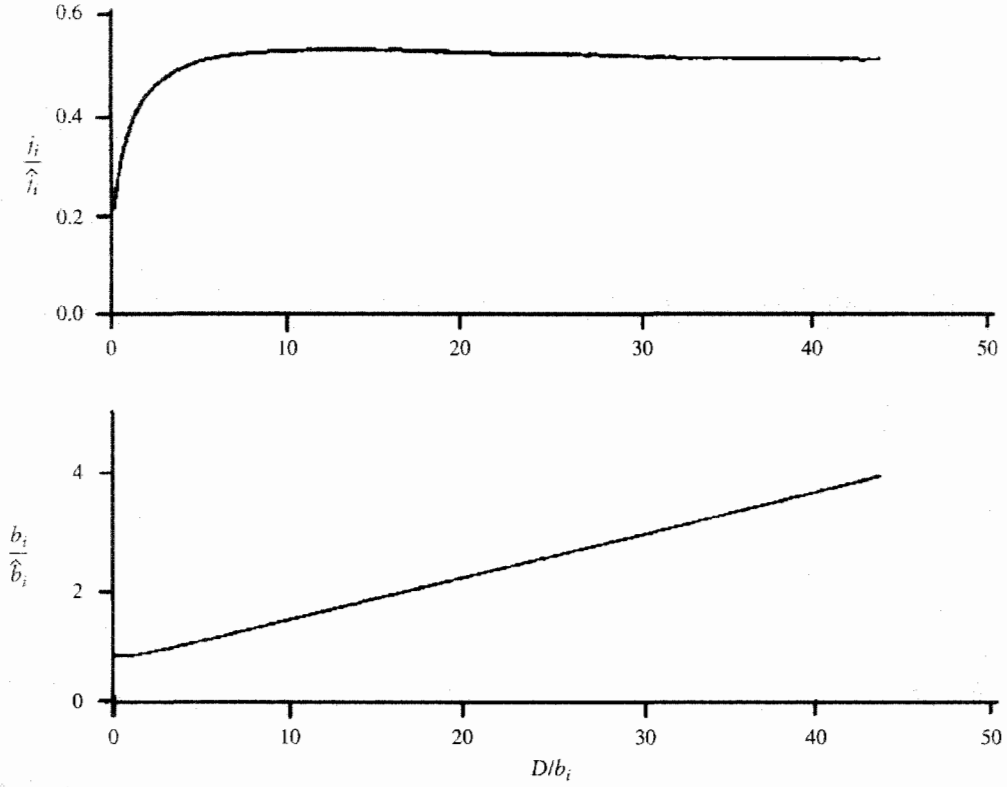

FIGURE 10.72 The variation of the ratios $j_i/\hat{j}_i$ and $b_i/\hat{b}_i$ as a function of $D/\hat{b}_i$.

where E and η_0 are known constants, and ϵ is some small value. As a check that this is a reasonable choice for the effective viscosity, we used this in the boundary-layer approximation to the Navier-Stokes equation to find the velocity profile and compared the result with the empirical formulae. We determined that, except at large η, the predicted flow patterns are graphically indistinguishable from the modified Verhoff formulae, and are a good fit to the numerical results.

Movement of the Contaminant

The full concentration equation for the contaminant may be simplified in the same manner as the Navier-Stokes equations to derive a boundary-layer approximation for the concentration, namely,

$$u\frac{\partial C}{\partial x} + v\frac{\partial C}{\partial y} = \frac{\partial}{\partial y}\left(\frac{\Gamma}{\rho}\frac{\partial C}{\partial y}\right), \tag{10.100}$$

where C is the mass fraction of the contaminant. Writing our formula for the horizontal component of the fluid velocity as $\hat{U} = f'(\eta)$ and using, as described in the previous section, $\Gamma/\rho = -(1/\mathrm{Sc})(\phi^* c/\sigma^2)x^n h(\eta)$, we can reduce Eq. (10.100) to the ordinary differential equation

$$C'' = \frac{1}{h}\left[\frac{1-c}{c}\mathrm{Sc}f - h'\right]C' \tag{10.101}$$

where prime denotes differentiation with respect to η. The natural boundary conditions are to let the concentration be unity on the tank surface and zero far from the tank surface, i.e., $C(0) = 1$ and $C \longrightarrow 0$ as $\eta \longrightarrow \infty$.

The ordinary differential equations for f and C now form a fifth-order system which can be solved using a standard NAG library routine. The results are shown in Fig. 10.73. This figure also shows the numerical results for concentration obtained using a full numerical approach, and there is reasonable agreement between the two.

The results above are for a neutrally buoyant contaminant. In practical situations, the contaminant is often buoyant in air, and so we need to consider the effects of this. To include it, we extend a theory from aerosol science, as given by De Marcus and Thomas,[23] and assume that the governing equation becomes

$$u\frac{\partial C}{\partial x} + (v + v_g)\frac{\partial C}{\partial y} = \frac{\partial}{\partial y}\left(\frac{\Gamma}{\rho}\frac{\partial C}{\partial y}\right). \tag{10.102}$$

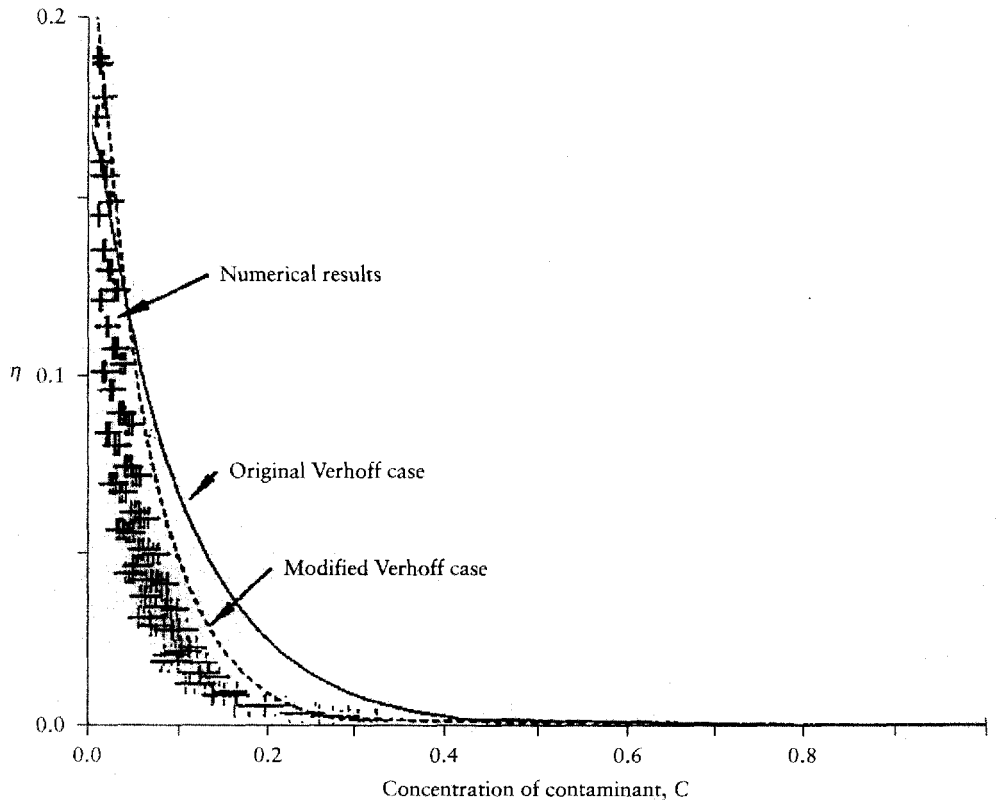

FIGURE 10.73 Concentration of contaminant, C, as a function of η, for the full numerical results and the semi-analytical similarity solution when $h(\eta)$ is given by Eq. (10.99), when $j_i/\rho = 0.54$ m^3 s^{-2}, $b_i = 0.01$ m, $L = 2$m, and SF = 1.5.

In aerosol theory, v_g is the velocity of free fall of a particle, and by extension in the current work v_g is an empirical velocity related to the buoyancy of the contaminant in air. We further assume that the overall fluid flow pattern is unaffected by the minor quantity of the buoyant contaminant.

Now when we substitute $\hat{U} = f'(\eta)$ into our equation, and introduce a change of variable $\xi = \eta^d$ to reflect the need to capture the very rapid changes of variables close to the tank surface, the concentration equation (10.102) becomes

$$h\frac{\partial^2 C}{\partial \xi^2} = 2\Gamma \frac{\partial C}{\partial \eta} - \Lambda \frac{\partial C}{\partial x}, \tag{10.103}$$

where

$$2\Gamma = \frac{\mathrm{Sc}}{cd}\xi^{\frac{1}{d}-1}\left[(1-c)f - \frac{\sigma v_g}{\varphi^*}x^c\right] + \left(\frac{1}{d}-1\right)\xi^{-1}h - h', \tag{10.104}$$

$$\Lambda = \frac{\mathrm{Sc}}{cd}xf', \tag{10.105}$$

and the prime now indicates differentiation with respect to ξ, subject to boundary conditions $C(x, 0) = 1$, $f(x, 0) = f'(x, 0) = 0$ and $C \longrightarrow 0$ as $\xi \longrightarrow \infty$. These equations can be discretized using a semi-implicit Crank-Nicolson method and solved numerically.

We are thus able to find the concentration predicted by this model at any position over the tank surface. Figure 10.74 shows contours of concentration both for the original and modified Verhoff conditions for the operating parameters

$$\begin{array}{lll} L = 4\ \mathrm{m} & b_i = 0.02\ \mathrm{m} & j_i/\rho = 1\ \mathrm{m^3\ s^{-2}} \\ b_0 = 0.1\ \mathrm{m} & v_g = 0.1\ \mathrm{m\ s^{-1}} & \end{array}. \tag{10.106}$$

It is worth commenting here on the more obvious effects of varying the parameters of the system. As we would expect, if we increase the momentum of the initial jet, the movement of the contaminant away from the surface of the tank is restricted. Conversely, if we increase the buoyancy of the contaminant, by increasing v_g, the contaminant moves further from the surface of the tank.

10.4.3.5 Design Equations and/or Parameters

We consider here two possible criteria for deciding on safe operating parameters for the inlet parameters, before turning our attention to the exhaust requirements.

Capture Velocity Criterion

The ACGIH[14] gives guidelines for the minimum capture velocity, V_{cap}, which must be induced to move a contaminant toward an exhaust. The recommended value depends on the industrial process and the local conditions, and Table 10.12 shows the recommendations for typical open-surface-tank processes.

From the ACGIH recommendations, we can say that the system is operating safely if a fluid velocity greater than or equal to the capture velocity is induced across the whole of the tank surface, and the exhaust flow rate is sufficient to capture all the fluid in the jet. Since the maximum velocity at any

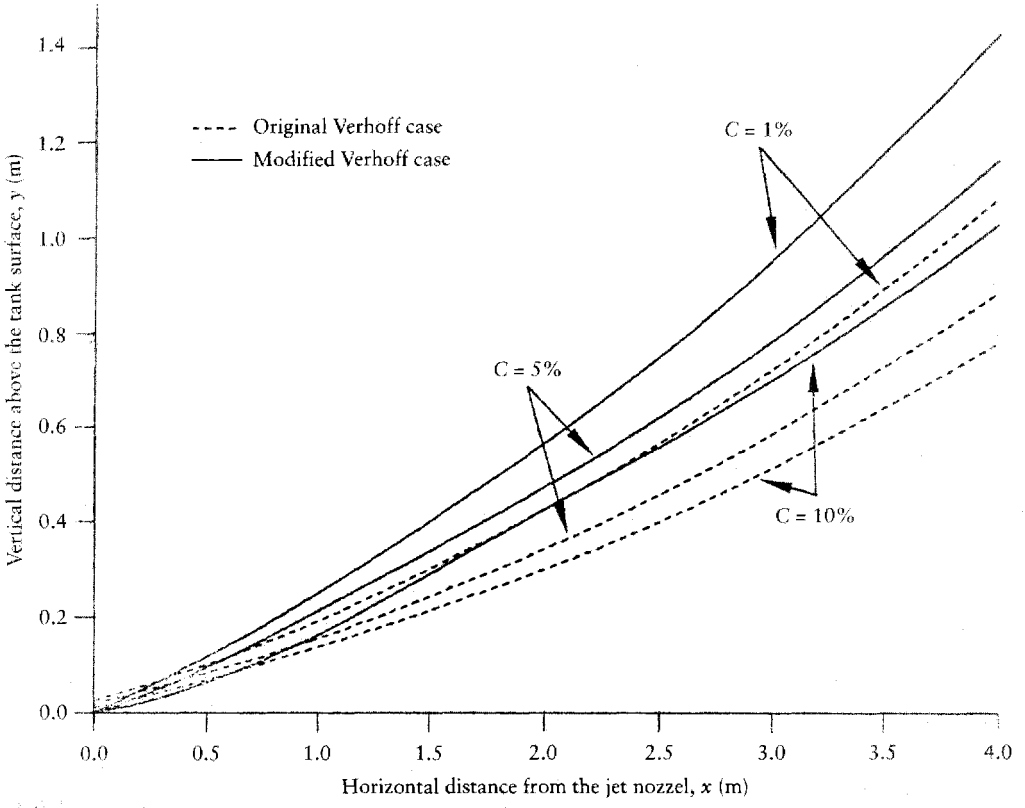

FIGURE 10.74 Contours of concentration derived from the semi-analytical method, in the original and modified Verhoff cases, when the operating parameters are given by Eq. (10.105).

distance from the tank surface is given by $u_m = \phi\sqrt{(j_i/\rho)}x^{-c}$, where c is approximately one-half, we know that the lowest value of u_m will be at $x = L$, and therefore we require $j_i/\rho \geq (V_{cap}/\phi)^2 L^{2c}$. Comparison with those experimental studies that provide enough information to calculate the initial momentum broadly supports this hypothesis; see for example Robinson and

TABLE 10.12 Recommended Capture Velocities for Different Operating Conditions, Based on Table 3.1 (ACGIH[14])

Condition of dispersion of contaminant	Example	Capture velocity (m s^{-1})
Released with practically no velocity into still air	Evaporation from tanks	0.25–0.5
Released at low velocity into moderately still air	Plating, pickling	0.5–1.0

The lower end of the range applies when (a) the room air currents are minimal or favorable to capture, (b) the contaminant is of low toxicity or nuisance value only, (c) the tank is used only intermittently, and (d) there is a large exhaust hood, i.e., there is a large air mass in motion.

The upper end of range applies when (a) the room air currents are significant or unfavorable to capture, (b) the contaminant is of high toxicity, (c) the tank is in heavy use, and (d) there is a small exhaust hood, i.e., small amounts of air are in motion.

Ingham.[24] This gives the required minimum value for the momentum of the equivalent wall jet; we must also recall the relationship shown in Fig. 10.72 to determine the required momentum of the offset jet in the push-pull system.

The biggest drawback to this approach is that the only inclusion of the contaminant buoyancy is in the choice of the appropriate value for V_{cap} and this is necessarily subjective. We therefore consider another alternative criterion.

Critical Contour Criterion

For this safety criterion, we consider the fact that as the velocity decreases with increasing distance from the surface of the tank, it will reach some critical velocity, V_{crit}, at which the induced movement of air will be insufficient to overcome the effects of crossdrafts or the buoyancy velocity v_g. At this point, we must ensure that the concentration is at, or below, some critical allowable concentration, C_{crit}. The values of the critical concentration and velocity will depend on particular circumstances, but it is worth noting that V_{crit} must be at least equal to v_g in order to overcome the effects of buoyancy, and the appropriate value will depend on the crossdrafts, which typically vary between 0.05 m s^{-1} to 0.5 m s^{-1}. For the sake of providing examples, we have chosen V_{crit} to be the maximum of the buoyancy velocity and the typical cross-draft velocity. For the critical concentration we have chosen two values, $C = 0.05$ and $C = 0.10$. The actual value used by a designer would depend on the toxicity of the contaminant in question.

From Fig. 10.72 we can see that the ratio of the momentum of the equivalent wall jet to that of the offset jet is typically about 0.46 and we have taken this value in the sample results presented here.

Figures 10.75 and 10.76 show the initial kinematic momentum required to meet this criterion as a function of the buoyancy velocity and the length of the tank, for different values of the allowable concentration C_{crit} and critical velocity V_{crit}. As we would expect, the required momentum increases both as the length of the tank increases and as the buoyancy of the contaminant increases.

Other Parameters

So far, since we have been treating the flow as being dominated by the jet, we have ignored the effects of the exhaust flow. Of course, the exhaust flow will increase the overall movement of the air, to a small extent far from the exhaust hood but quite significantly close to the hood. We shall discount these positive effects, and consider only the fact that the exhaust hood should remove all the fluid contained within the jet. This can be expressed as

$$q_0 = \mathrm{SF} q_j(L), \tag{10.107}$$

where q_0 is the volume flow per unit width of tank at the exhaust hood; SF is a safety factor greater than unity, the precise value of which is left to the discretion of the designer; and $q_j(L)$ is the flow rate in the jet at $x = L$. This may be calculated by integrating the formula for the fluid velocity (Eq. (10.92)), which yields

$$q_j(L) = \frac{B_1 \phi (L+\epsilon)}{\sigma L^c} \left(\frac{j_j}{\rho}\right)^{1/2} \int_0^\infty \eta^d \mathrm{erfc} B_2 \eta d\eta \tag{10.108}$$

Integrating this equation numerically and substituting the values of the constants from Eqs. (10.99) and (10.100), we obtain the recommended exhaust

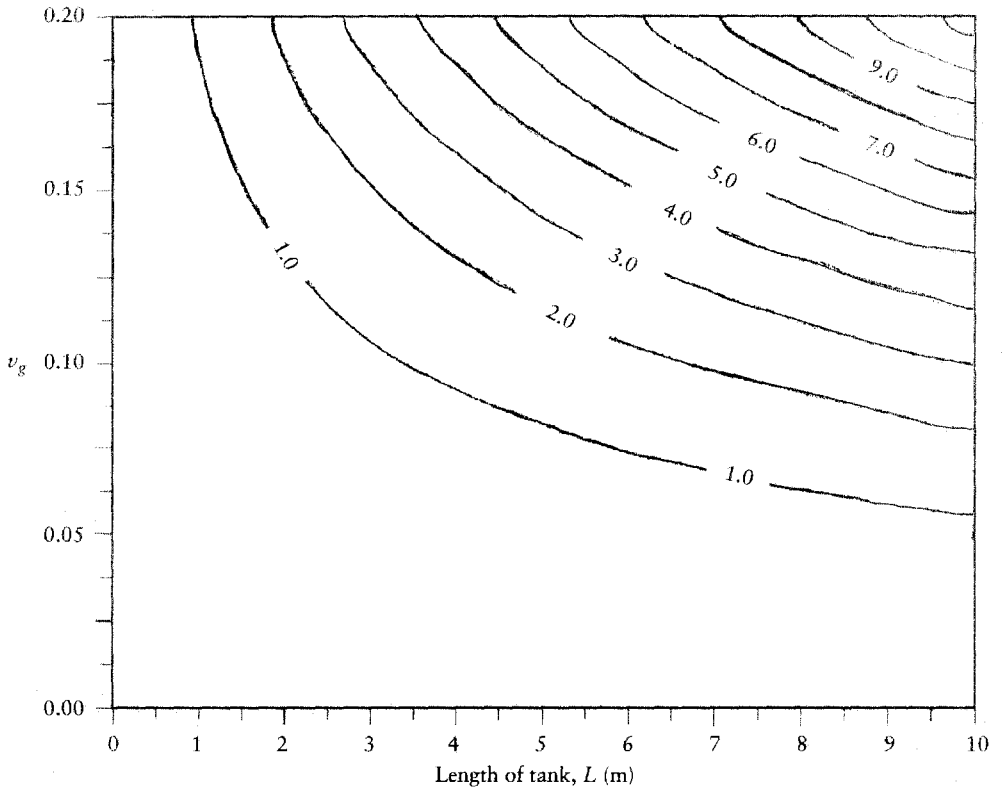

FIGURE 10.75 Required initial kinematic momentum, $\hat{j}_i/\rho$, as a function of the length of the tank, L, and the buoyancy velocity, v_g, when the critical contour criterion is applied with the critical concentration, C_{crit}, equal to 5% and the cross-drafts equal to 0.05 m s^{-1}.

flow rate as a function of the length of the tank, the initial jet momentum, the jet nozzle height, and the safety factor:

$$q_0 = \begin{cases} 0.316\left(\dfrac{L+10b_j}{\sqrt{L}}\right)\sqrt{\dfrac{j_i}{\rho}} & \text{according to the original Verhoff formulae.} \\ 0.443\,L^{0.491}\sqrt{\dfrac{j_i}{\rho}} & \text{according to the modified Verhoff fomulae.} \end{cases} \tag{10.109}$$

Thus the outlet flow rate can be determined once the dimensions of the tank and the inlet jet momentum have been determined.

The above considerations give us a technique for estimating the required jet momentum and outlet flow rates. Other important parameters are the heights of the inlet and outlet apertures. The choice of these parameters will not, in general, have a significant effect on the overall fluid flow pattern and the resulting distribution of the contaminant, and these should be chosen to optimize the performance of the inlet and exhaust pumps.

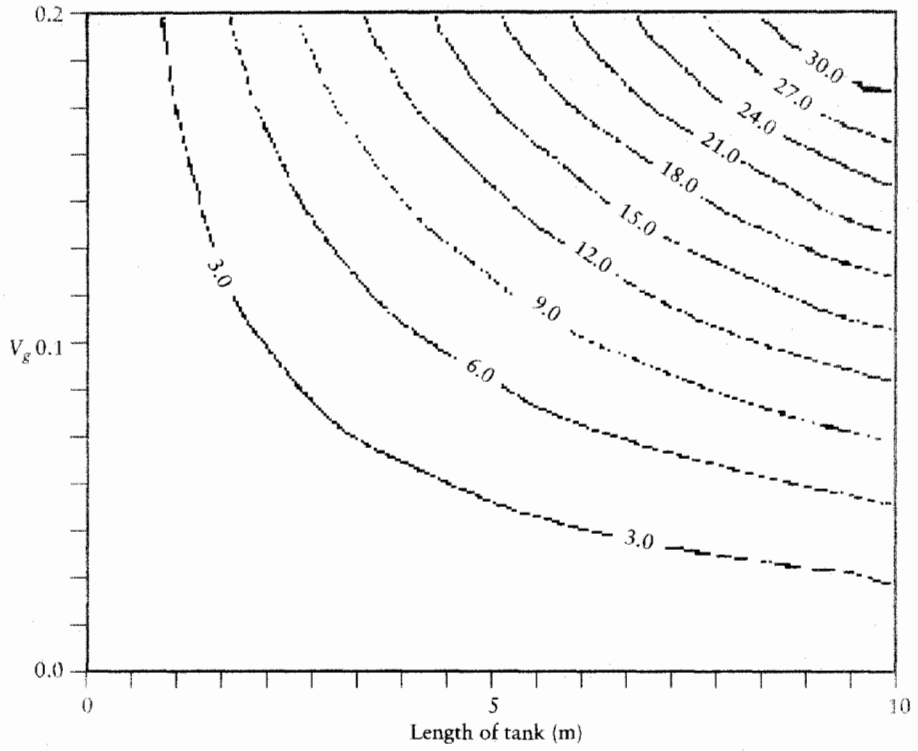

FIGURE 10.76 Required initial kinematic momentum, $\hat{j}_i/\rho$, as a function of the length of the tank, L, and the buoyancy velocity, v_g, when the critical contour criterion is applied with the critical concentration, C_{crit}, equal to 10% and the cross-drafts equal to 0.5 m s^{-1}.

10.4.3.6 Final Remarks

Even with modern CFD commercial software packages, achieving accurate results for a full numerical model for the push-pull system is time consuming because of the very fine grid required close to the jet nozzle and close to the surface of the tank. With the techniques described in this section, it is possible to produce at least first estimates of the required parameters for a given push-pull system. It is then recommended that a designer would conduct full numerical testing of the system at the suggested operating parameters and make final adjustments according to those results. Finally, when the system is installed, it is important to allow for some adjustment of the operating parameters following in situ testing of the ventilation system.

10.4.4 Aaberg Exhaust Hoods

10.4.4.1 General

Simple exhaust hoods have a very short effective range and the hood must be placed very close to the contaminant source to be efficient, which may interfere with technological processes. This lack of direction of the flow may result in the use of excessive exhaust flow rates with large source-to-hood distances and this may result in a large amount of wasted energy.

In order to overcome this limitation in the use of conventional exhaust hoods, Aaberg exhaust hoods (or reinforced exhaust systems) have been developed where the exhaust extracting contaminated air is reinforced by an injected supply jet flow that enhances the exhaust flow considerably in comparison to other outlets. Through a balanced combination of the injection and exhaustion flows, the airflow toward the exhaust opening, in the region where there is the largest concentration of the contaminant, may extend over a far greater distance than is possible by using an exhaust alone.

The two versions of the Aaberg exhaust system, namely an axisymmetrical version and a workbench version, both work on the same principle. In order to illustrate the principle of the Aaberg we describe the axisymmetrical version but the full theoretical, computational, and experimental basis is presented for both systems.

The design of the axisymmetrical Aaberg exhaust hood is very similar to a traditional flanged hood. However, it is fitted with a flange through which air can be ejected radially from a narrow slot (see Fig. 10.77). The dramatic effect of the blowing jet on the hood's overall airflow can be explained as follows: due to the friction developed at the radial jet/air interface an entrainment flow develops which, under the correct conditions, has the property of removing the clean air from in front of the hood (the recycled flow) as well as enhancing and concentrating the exhaust's suction in a zone along the hood's longitudinal axis (the efficient flow). The flow in front of the exhaust opening is now directional and the process is capable of creating a larger fluid flow toward the exhaust opening at greater distances along the axis of the exhaust hood. Further, although replacement air should still be supplied, the Aaberg exhaust works with sig-

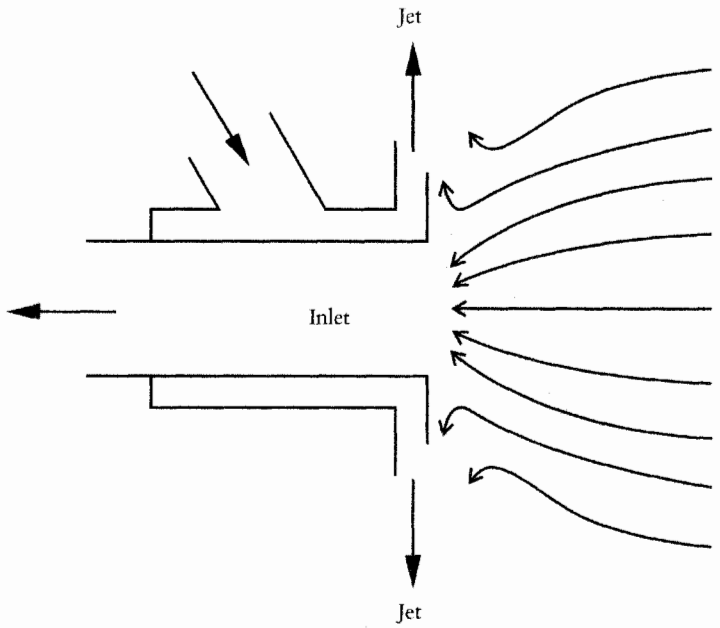

FIGURE 10.77 A schematic representation of the Aaberg principle.

nificantly smaller quantities of air than do traditional exhausts. This, together with a higher concentration of pollutant in the exhaust air, makes the Aaberg process for limiting pollutant emissions more effective than traditional methods. The performance difference between a conventional exhaust hood and the Aaberg system can be seen in Figs. 10.78*a* and 10.78*b*, which show the effects of smoke released at a distance five times the diameter of the exhaust inlet when there is no radial jet, and when there is a jet. When there is no radial jet the pollutant enters the environment and only a few wisps of the contaminant are successfully exhausted. However, when the radial jet is present, virtually all the contaminant is captured.

Figure 10.79*a* shows the typical streamlines for a conventional tube exhaust hood with no radial jet. At large distances from the exhaust opening the flow is approximately radial and behaves very much like a sink flow. The shaded area is

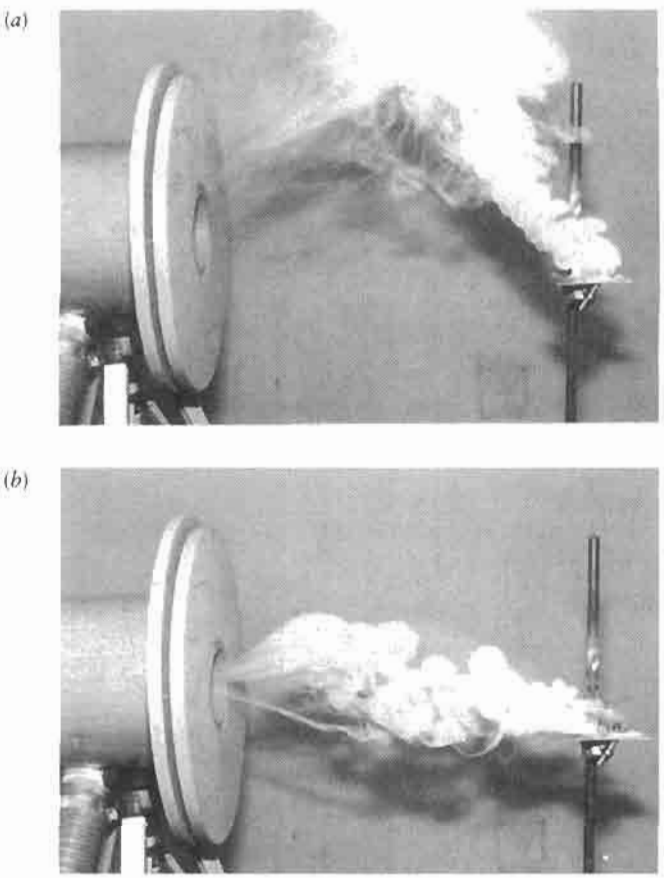

FIGURE 10.78 The capture of tracer gas released at five times the diameter of the exhaust inlet when the radius of the exhaust hood is 0.15 m, the radius of the exhaust hood inlet is 0.037 m, and the width of the exhaust jet is 8.0 mm. (*a*) Suction alone with average inlet velocity of 12.7 m s^{-1}. (*b*) Combined suction and injection with the average inlet and exhaust velocities of 12.8 m s^{-1} and 7.7 m s^{-1}, respectively. (Figures are courtesy of the Health and Safety Executive, Research Division, Sheffield, UK.)

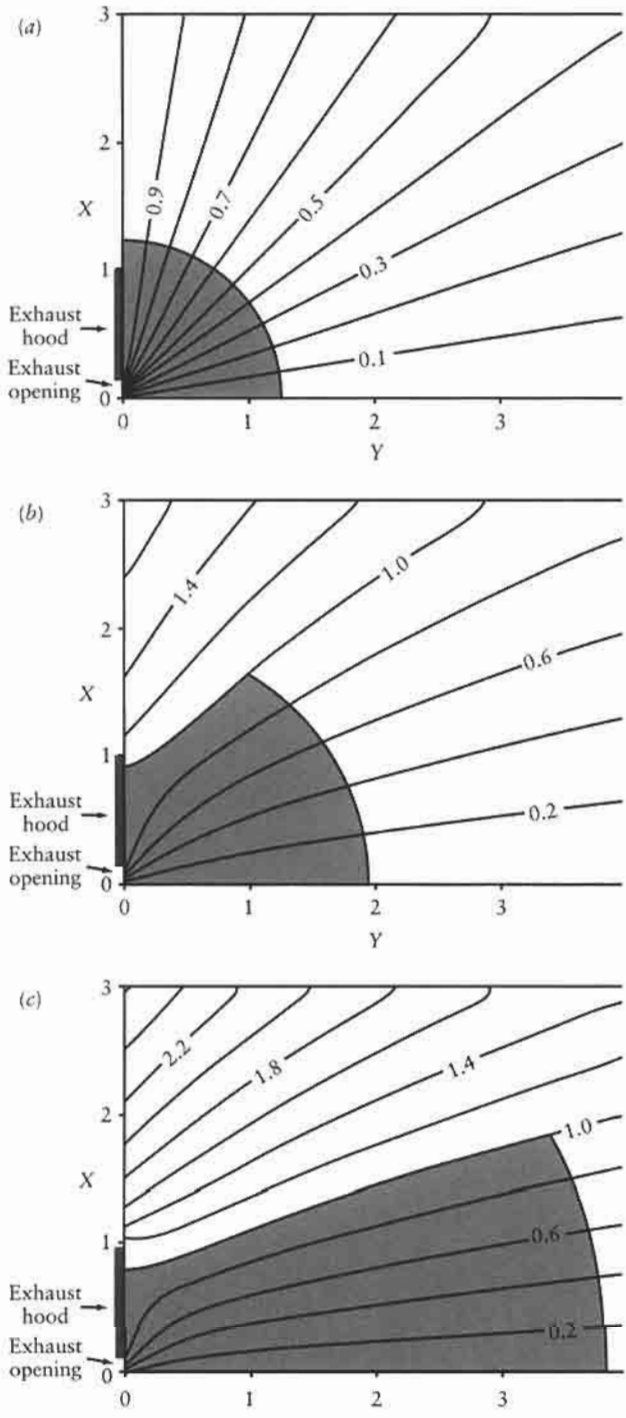

FIGURE 10.79 Typical streamlines for the flow near the exhaust hood when there is (*a*) only suction, (*b*) some exhaust flow, and (*c*) a large exhaust flow. (The flow is symmetrical about $X = 0$.) The shaded area represents the predicted effective capture region.

the region where the fluid speed is greater than the random air speed that is generated in a typical workplace. Thus all the contaminants in the shaded region, the effective capture region, will be exhausted. For the same rate of exhaustion but with the inclusion of the radial jet, i.e., the implementation of the Aaberg principle, Figs. 10.79*b* and 10.79*c* show the streamlines and the effective capture region for increasing values of the momentum of the jet. The streamlines assigned a value of magnitude less than unity all go to the exhaust outlet whereas all the other streamlines form a large recirculating region in the room. Thus the effect of the jet is to concentrate the fluid that flows through the exhaust outlet along the axis of the exhaust hood. Further, the distance from the exhaust hood that the effective capture region extends increases with increasing momentum of the jet. The above discussion clearly explains the reasons for the fluid and contaminant flow observed in Fig. 10.78. It should be noted that in addition to the Aaberg principle being used for a local ventilation system it can be used in the form of a large ventilation unit (see Fig. 10.80). In this case the Aaberg exhaust hood is freely suspended with its axis pointing downward and the contaminant is placed on the floor. This situation has also been investigated by Hunt and Ingham.[25,26]

FIGURE 10.80 A typical Aaberg ventilator unit, which is suspended above the floor while smoke is released on the floor beneath the ventilator.

Finally, the same principle as described above applies to the bench version of the Aaberg principle, which we discuss in detail in the next section.

10.4.4.2 Principle

Bench Aaberg Slot Exhaust

A schematic diagram of the version of the Aaberg slot exhaust (ASE) system is shown in Fig. 10.81. It consists of a horizontal bench to which a vertical flange is attached, housing a rectangular exhaust slot and jet nozzle. Figure 10.82 shows the two-dimensional geometry and the coordinate system of the ASE model.

This situation has also been experimentally investigated by Braconnier et al.,[27] Pedersen,[28,29] Fletcher and Saunders[30] and Hollis.[31] All of these investigations show that as the ratio of the momentum of the exhaust to the inlet flow, increases, the efficiency of the collection of the contaminant increases. Here I is defined as $u_j^2 b / u_i^2 S$ where u_i and u_j are the initial average velocities of the air at the exit of the jet exhaust and the entrance of the slot inlet, respectively, and b and S are the widths of the slot and jet nozzles, respectively. See Fig. 10.81.

The investigators found that the best operating conditions of the Aaberg in disturbed surroundings was when I was approximately 0.6. Further, when the momentum rate, I, becomes too large, then the fluid flow becomes unsteady and highly three-dimensional, with large swirling flows being generated at some distance from the exhaust opening. This flow enhances the level of the turbulence, reducing the capture efficiency by enhancing the diffusion of the contaminant into the induced jet flow.

Axisymmetric Aaberg Exhaust Hood

The Aaberg reinforced exhaust system was first studied in the 1940s,[32] then more extensively in its axisymmetrical form in 1965, but it was not until

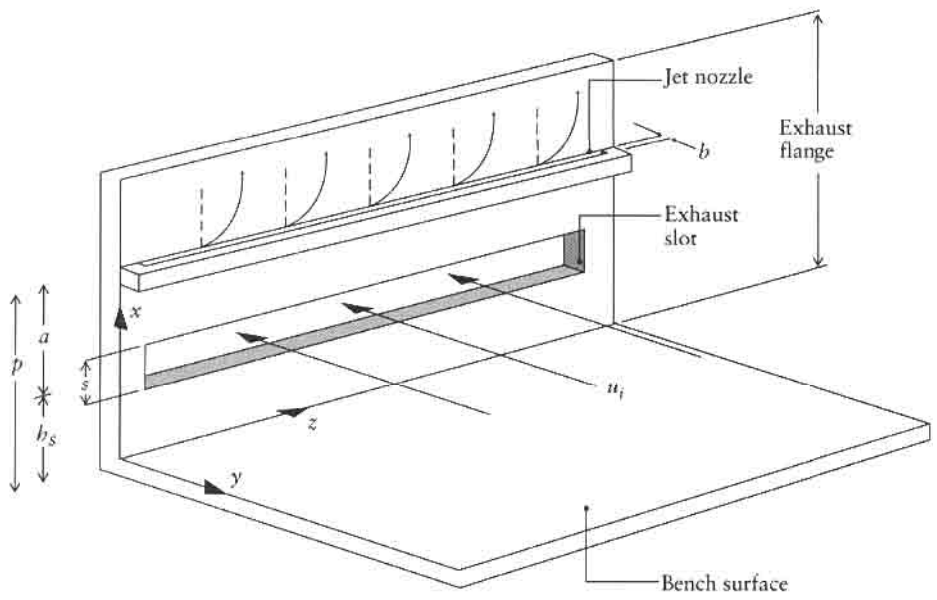

FIGURE 10.81 A schematic diagram of the Aaberg slot exhaust hood.

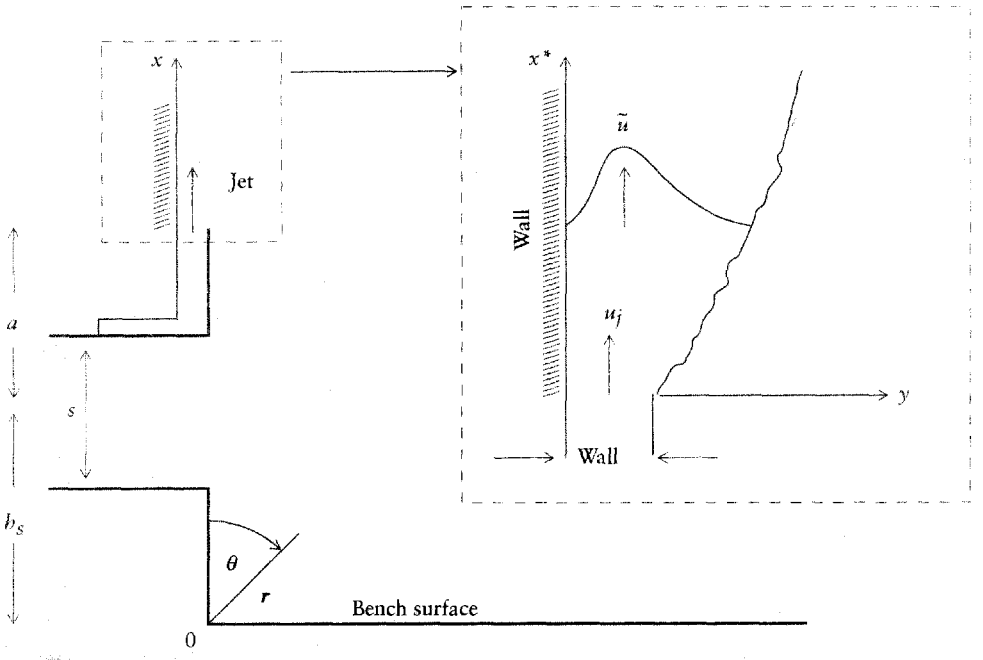

FIGURE 10.82 The geometry and coordinate system of the ASE model.

the 1980s that researchers experimentally attempted to combine the injection and the exhaustion principle; see Hyldgard[33] and Høgsted.[34] Pedersen and Nielsen[35] measured the centerline fluid velocity for three types of Aaberg flows, whereas Fletcher and Saunders used a laser Doppler velocity (LDV) flow analyzer to measure the fluid speeds.

It should be noted that when there is no jet reinforcement of the flow, i.e., the exhaust hood is used in its conventional mode, then in the two-dimensional form of the Aaberg principle the fluid flow velocity due to the exhaust decays approximately inversely proportionally to the distance from the exhaust opening. However, for three-dimensional exhaust hoods the fluid velocity outside the hood decays approximately inversely as the square of the distance from the exhaust hood. Thus in the three-dimensional conventional hood operating conditions the hood has to be placed much closer to the contaminant in order to exhaust the contaminant than is the situation for the two-dimensional hood (see section on *Basic Exhaust Openings*). Thus for ease of operation it is even more vital to develop hoods with a larger range of operation in the three-dimensional situation in comparison with two-dimensional hoods.

10.4.4.3 Applicability of Sources

In general, the Aaberg principle is suitable for all open "processes" which demand an open work area. These processes avoid the use of closed or partially closed systems, for instance a conventional hood with specific walls around the pollution source. In particular, the principle is very suitable for welding (i.e., spraying particle sources) or hot sources of contaminant. Some examples of open

processes where the Aaberg principle may be of use are as follows: removal of pollution by solvents in printing shops and spraying particles and solvents in color spraying units in small car repair and wood spray shops. A good description of the use of an Aaberg hood in a welding shop may be found in Pedersen.[28]

10.4.4.4 Specific Issues

It should be noted that although optimum operating conditions for the Aaberg exhaust system might be accurately found under ideal working conditions, the following points should be considered:

Cross-drafts;
Finite size of the room;
Moving sources of contaminants and moving workers;
Moving particles;
The flow becomes fully three-dimensional, i.e., the flow becomes unstable, when the momentum ratio is too large. This is typically when $I \geq 0.6$;
Noise levels;
Hysteresis/short circuiting (see Pedersen[28]) namely $I \geq 0.1$;
In addition to the momentum ratio I, numerous other geometrical aspect ratios should be investigated.

10.4.4.5 Design Equations and/or Parameters

In the work of Hunt and Ingham[25,26,36] it was found that the experimental predictions, the LDV measurements, the potential flow predictions, and the full turbulent fluid flow calculations all give results that are in extremely good agreement when the Aaberg principle is used both in the axisymmetrical and bench configurations.

Thus it is recommended the simple potential flow model be used to obtain a first estimate for the optimization of the effective capture region in any particular application. Once this has been achieved, the equipment should be built to this specification but with sufficient flexibility to adjust it to obtain the practical optimum effective capture region.

Potential Flow Model for a Bench Slot Exhaust

Outside the jet and away from the boundaries of the workbench the flow will behave as if it is inviscid and hence potential flow is appropriate. Further, in the central region of the workbench we expect the airflow to be approximately two-dimensional, which has been confirmed by the above experimental investigations. In practice it is expected that the worker will be releasing contaminant in this region and hence the assumption of two-dimensional flow appears to be sound. Under these assumptions the nondimensional stream function Ψ satisfies Laplace's equation, i.e.,

$$\frac{\partial^2 \Psi}{\partial X^2} + \frac{\partial^2 \Psi}{\partial X^2} = 0, \tag{10.110}$$

where

$$U = \frac{\partial \Psi}{\partial y} \quad \text{and} \quad V = -\frac{\partial \Psi}{\partial X} \tag{10.111}$$

and U and V are the nondimensional X and Y components of the fluid velocity, respectively, where we have nondimensionalized as follows:

$$X = x/p, \quad Y = y/p, \quad R = r/p, \quad S = s/p,$$
$$H_s = h_s/p, \quad \Psi = \frac{\psi}{m}, \quad U_i = u_i/(m/p) \tag{10.112}$$

where m is the volumetric flow rate of the exhaust and p is the height of the jet nozzle above the bench surface, equal to $a + h_s$.

For a turbulent jet, at the outer edge, we obtain[25]

$$\Psi \longrightarrow A(X-1)^{\lambda}. \tag{10.113}$$

For a free jet,

$$\lambda = \frac{1}{2}, \quad A = \frac{1}{2m}\left(\frac{3bu_0^2 p}{\sigma}\right)^{1/2}. \tag{10.114a}$$

For a wall jet,

$$\lambda = \frac{9}{14}, \quad A = \frac{7.61u_i}{m}(pb)^{1/2}\int_0^{\infty} Y^{1/7}\operatorname{erfc}\left(\frac{10Y}{X-1}\right)dY, \tag{10.114b}$$

σ is an empirical constant which has been taken to be 7.67,[25] and

$$\operatorname{erfc}(z) = 1 - \operatorname{erfc}(z) = 1 - \frac{2}{\sqrt{\pi}}\int_0^z e^{-z^2}dz \ ,$$

where erfc is the well-known error function.

In the case of the free jet, the solution for the Aaberg exhaust system can be found by solving the Laplace equation by the method of separation of variables and assuming that there is no fluid flow through the surface of the workbench. At the edge of the jet, which is assumed to be at $\theta = 0$, the stream function is given by Eq. (10.113). This gives rise to

$$\Psi(R, \theta) = f(R, \theta)$$
$$= A\left\{R^{\lambda}\sin\left(\frac{\lambda\pi}{2}\right)\sin\left[\lambda\left(\frac{\pi}{2}-\theta\right)\right] - \frac{\lambda R^{\lambda-1}}{\sin\left[(\lambda-1)\frac{\pi}{2}\right]}\sin\left[(\lambda-1)\left(\frac{\pi}{2}-\theta\right)\right]\right.$$
$$\left. + \frac{\lambda(\lambda-1)R^{\lambda-2}}{2!\sin\left[(\lambda-2)\frac{\pi}{2}\right]}\sin\left[(\lambda-2)\left(\frac{\pi}{2}-\theta\right)\right]\ldots\right\} + \left(1 - \frac{2\theta}{\pi}\right). \tag{10.115}$$

The exhaust opening is modeled as a finite-sized slot with a uniform velocity distribution. The workbench and the vertical wall below the exhaust slot form a streamline of fluid flow through which the fluid does not cross and, therefore, along this line we have $\Psi = 0$. Between the slot and the jet, the vertical wall is also a streamline and from the dimensionalization given

in Eq. (10.112) we have $\Psi = 1$ on this part of the boundary. Thus we have the following boundary conditions:

$$\left.\begin{aligned} &\Psi(0, Y) = 0 && 0 < Y < \infty \\ &\Psi(X, 0) = \begin{cases} 0 & 0 < X < H \\ (X-H)/S & H < X < H+S, \\ 1 & H+S < X < 1 \\ 1 + A(X-1)^{\lambda} & X > 1 \end{cases} \\ &\Psi(X, Y) = f(R, \theta) && R = R_{\infty} \gg 1 \end{aligned}\right\} \tag{10.116}$$

where R_{∞} is a large value of $(X^2 + Y^2)^{1/2}$ at which the asymptotic solution (Eq. (10.115)) may be considered appropriate. The potential flow resulting from the solution of the Laplace equation (Eq. (10.110)) subject to the boundary conditions (Eq. (10.116)) may be easily solved using boundary integral techniques, e.g., the boundary element method,[37] or the Schwartz-Christoffel transformation technique. However, although these methods give a more elegant mathematical solution of the above problem they are more complex to use than the more straightforward finite-difference approach. In this method the solution domain is divided into a system of rectangular meshes, see Chapter 13 for more details, and an approximate solution may be found at all of the mesh points.

Turbulent Flow Model for a Bench Slot Exhaust

The mathematical model presented in the previous section has been developed under the assumptions that the flow induced by an Aaberg exhaust hood is inviscid and potential and that turbulent effects have been limited to the flow in the jet. However, the typical experimental operating conditions of an Aaberg exhaust hood lead to Reynolds numbers in the order of 10^3 to 10^4. Thus the fluid flow in the jet and in the region surrounding the exhaust inlet are very likely to be turbulent. However, in the region of practical interest, i.e., the region of the flow where there is likely to be large amounts of contaminant, the airflow created by the Aaberg exhaust hood is a convergent flow and therefore in this region we expect a low level of turbulence.

Hunt[38] and Kulmala[39] have solved the full turbulent fluid flow for the Aaberg system using the k-ϵ turbulent model or a variation of it as described in Chapter 13—the solution algorithm SIMPLE, the QUICK scheme, etc. Both commercial software and in-house-developed codes have been employed, and all the investigators have produced very similar findings.

Mathematical Model for an Axisymmetric Aaberg Exhaust Hood

A similar mathematical model to that just described for bench slot exhausts can again be used, but in this case the Laplace equation should be employed in a cylindrical coordinate system (see Fig. 10.83), namely,

$$\frac{\partial^2 \Psi}{\partial R^2} - \frac{\cot\theta}{R^2}\frac{\partial \Psi}{\partial \phi} + \frac{1}{R^2}\frac{\partial^2 \Psi}{\partial \phi^2} = 0 \ , \tag{10.117}$$

where all the quantities are nondimensional as follows:

$$S = \frac{s}{a},\ R = \frac{r}{a},\ X = \frac{x}{a},\ X^* = \frac{x^*}{a},\ Y = \frac{y}{a},\ \Psi = \frac{\psi_r}{a^2 u_j}, \tag{10.118}$$

In the turbulent jet,[38] we have

$$\Psi \longrightarrow GR^{\lambda} \text{ on } \phi = \frac{\pi}{2} \text{ as } R \longrightarrow \infty, \tag{10.119}$$

where

$$\lambda = 1,\ G = \left(\frac{\pi}{2c}\right)^{1/4} K^{1/2},\ K = \left(\frac{u_i s}{u_j a}\right)^2,\ c = 0.693\sigma^2,\ \sigma = 9.31, \tag{10.120}$$

and

$$\Psi = 0 \text{ on } \phi = 0, \text{ for all values of } R. \tag{10.121}$$

Following the procedure discussed previously, we find that at large distances from the Aaberg exhaust hood the stream function is given by

$$\Psi(R, \phi) = g(R, \phi) = \left(\frac{\pi}{2c}\right)^{1/4} K^{1/2}(1 - \cos\phi)\left(R - \frac{1}{2}\right) + \frac{1}{2}\frac{u_i}{u_j} S^2 (1 - \cos\phi) \tag{10.122}$$

Again, as described earlier, we model the exhaust opening as a finite circular opening across which the fluid flows with a constant speed. The axis of the coordinate system is a streamline which we take to be $\Psi = 0$ and on the surface of the flange of the Aaberg exhaust system is also a streamline on which $\Psi = 0$, due to the nondimensionalization given in Eq. (10.112). Further, at the outer edge of the jet, which we assume to be at $\phi = 0$—i.e., it is assumed that the jet is infinitesimally small—the boundary condition (Eq. (10.119)) is appropriate.

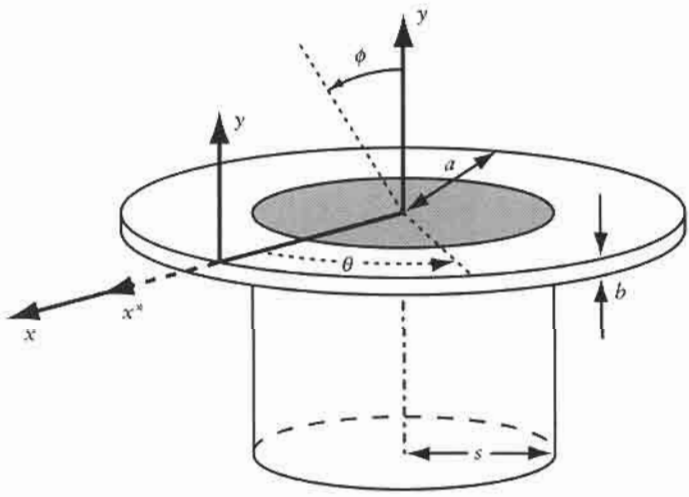

FIGURE 10.83 The geometry and coordinate system used to model the effect of the exhaust inlet size.

Thus the Laplace equation (Eq. (10.117)) has to be solved subject to the following boundary conditions:

$$\left.\begin{aligned} &\Psi(R, 0) = 0 && 0 \le R < R_\infty \\ &\Psi\left(R, \frac{\pi}{2}\right) = \begin{cases} \dfrac{1u_i}{2u_j}R^2 & 0 \le R \le S \\ \dfrac{1u_i}{2u_j}S^2 & R > S \end{cases} \\ &\Psi(R, \phi) = g(R, \theta) && R = R_\infty \end{aligned}\right\} \tag{10.123}$$

where R_∞ is a sufficiently large value of R at which the asymptotic solution (Eq. (10.115)) may be assumed to be appropriate. The solution to this problem may be found using a finite-difference method as described in Chapter 13 or see Hunt and Ingham.[25,26,36]

As with the two-dimensional workbench problem, the numerical solution of this problem can be found by solving the full turbulent fluid flow equations using the methods described in Chapter 13.

10.4.5 Low-Momentum Supply with Exterior Hoods

10.4.5.1 General

Exterior hoods intended to capture contaminants should be placed as close to contaminant sources as possible. In actual practice, however, the hoods can not always be placed close to the source due to circumstances such as working conditions. In such cases, to enhance the exhaust efficiency of exterior hoods, it is useful to use a low-momentum air supply directed toward the exhaust outlet. The supply airflow, which functions to transport contaminants emitted from sources located at a distance from the exhaust outlet, should be relatively low with a uniform velocity but high enough so that it is not disturbed by the surrounding air motions. The advantages of using low-momentum supply with exterior hoods are that (1) a lower supply airflow rate to the workspace is possible, (2) a lower exterior hood exhaust flow rate is possible, and (3) it is possible to supply clean air to the breathing zone of the worker.

10.4.5.2 Principle

Gases, vapors, and fumes usually do not exhibit significant inertial effects. In addition, some fine dusts, 5 to 10 micrometers or less in diameter, will not exhibit significant inertial effects. These contaminants will be transported with the surrounding air motion such as thermal air current, motion of machinery, movement of operators, and/or other room air currents. In such cases, the exterior hood needs to generate an airflow pattern and capture velocity sufficient to control the motion of the contaminants. However, as the airflow pattern created around a suction opening is not effective over a large distance, it is very difficult to control contaminants emitted from a source located at a distance from the exhaust outlet. In such a case, a low-momentum airflow is supplied across the contaminant source and toward the exhaust hood. The

contaminants emitted within the supplied airflow are transported to the exhaust opening and the exterior hood can easily exhaust the contaminated air.

The low-momentum air, which is supplied from a relatively wide supply inlet, functions to transport contaminants to near the exterior hood. In addition, it functions to change the direction of contaminants toward the exterior hood when the direction of contaminated air is initially different from the exhaust direction. The momentum or velocity of the supply air to reach to the exterior hood will be sufficient when the motion of contaminants can be neglected. However, when the contaminated air exhibits significant motion or flows in a direction different from the exterior hood, the supply air velocity should have a sufficient momentum to control the contaminant flow.

The exterior hood could be placed beside, below, or above the contaminant source, and the direction of the supply air could be horizontal, vertical, or diagonal toward the exhaust inlet. The sources should be within the supply airflow, and in some cases, a worker could also be located within the flow. When the worker is within the supply airflow, however, a region of a recirculating airflow, a wake region, can be created downstream. If the breathing zone of the worker and the contaminant source are within this wake region, high exposures may occur. Therefore, the relation between the direction of supply airflow and the position of the worker should always be considered, as the source should never be within the wake region (see Section 10.2.3).

10.4.5.3 Applicability of Sources

Since the low-momentum supply system should enhance the efficiency of an exterior hood by supplying low-momentum airflow to a source, the system can be applied to practically any sources where an exterior hood can be used. In particular, it is effective to apply the system when an exterior hood cannot be placed close to a source or the exhaust direction is different from the initial contaminant release direction.

Many processes generate contaminants in casting plants. Some practical applications of the low-momentum supply system in these plants will be introduced here. Figure 10.84 shows an example of the system applied to the process where molten metal is being poured from a low-frequency furnace to a ladle. The temperature of molten metal is about 1800 K and a highly buoyant plume containing metal fumes is formed above the tapping nozzle and the ladle. To control the plume, a supply inlet is placed horizontally from the center of the ladle by 2.5 m and supply airflow is blown at a uniform velocity of 3.0 $m\,s^{-1}$ toward the ladle. The direction of plume is turned toward the exhaust outlet by the supply airflow, and the flanged exterior hood exhausts the fume-containing plume. The dimensions and operating conditions of the system are indicated in the figure. The velocities of supply and exhaust airflow were determined using CFD simulations.[40,41]

Figure 10.85 shows an example of the system applied to a shaking-out process in a casting plant. In this process, when molding sand around castings is shaken off, high concentrations of dust rise above the shakeout machine in a buoyant plume. To remove the dust, an exterior hood was placed beside the source and a supply inlet was placed on opposite side. Air is blown toward the exhaust outlet to change the direction of the dust toward the exterior hood. The temperature of castings is about 700 K, the

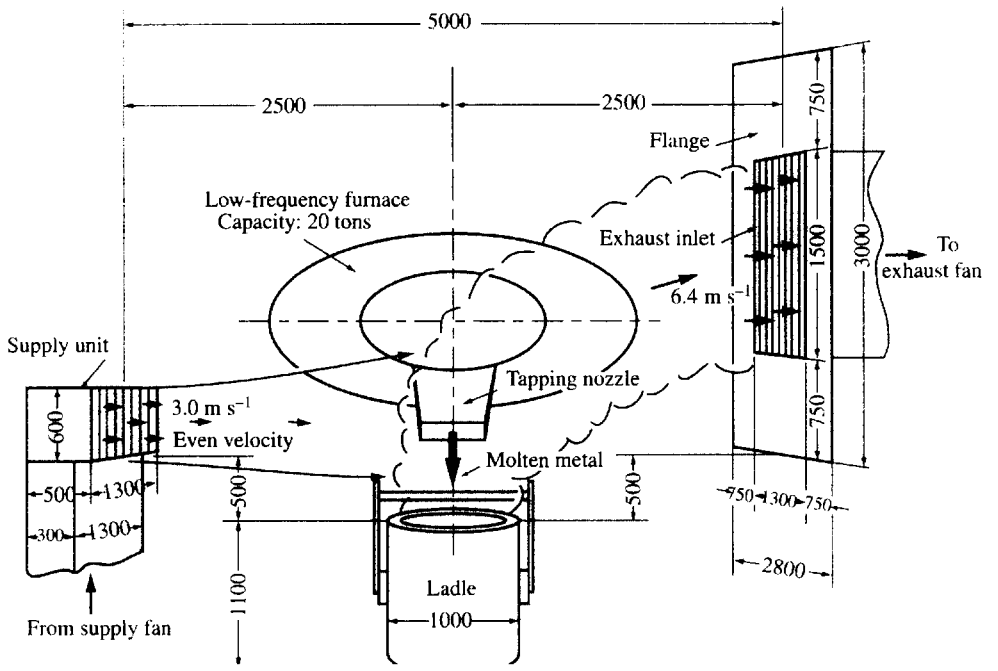

FIGURE 10.84 Practical application to control highly buoyant plume. Supply airflow rate is 2.34 $m^3 s^{-1}$, exhaust flow rate is 12.48 $m^3 s^{-1}$.

velocity of supply air is 1.5 m s^{-1}, and the exhaust velocity at the hood face is 1.5 m s^{-1}. The operating conditions and the dimensions of the system are indicated in the figure. Supply and exhaust flow rates were initially determined using the flow ratio method,[6] but the actual exhaust flow rate was adjusted to an appropriate value after installation.

The final example is shown in Fig. 10.86. Several workers are breaking gates off of castings on the conveyor by hand. Much dust is generated by this operation and the dust rises due to buoyancy. To remove the dust, an exterior hood was placed beside the conveyor and a supply inlet was placed above the workers. The supply airflow is blown toward the breathing zone of the workers and the dust source. In this case, as the workers and the dust source are located within the supply airflow, the airflow functions to supply the workers with clean air and to transport the dust toward the exhaust inlet. The velocity of supply air is relatively low, 1.1 m s^{-1}, and the exhaust velocity at the hood face is 2.75 m s^{-1}. The dimensions of the system are indicated in the figure, and the depth of the device is 6.0 m (compare with Sections 10.3.3 and 10.4.6).

10.4.5.4 Different Forms and Boundaries Relative to Other Types

The inlet opening that supplies the low-momentum airflow should be sufficiently wide to cover the contaminant source and should face toward the inlet of exterior hood. The airflow functions to transport contaminants emitted within the flow to the exterior hood. The exhaust airflow created around the suction opening must exhaust all of the contaminants transported by the supplied airflow. From this point of view, the low-momentum

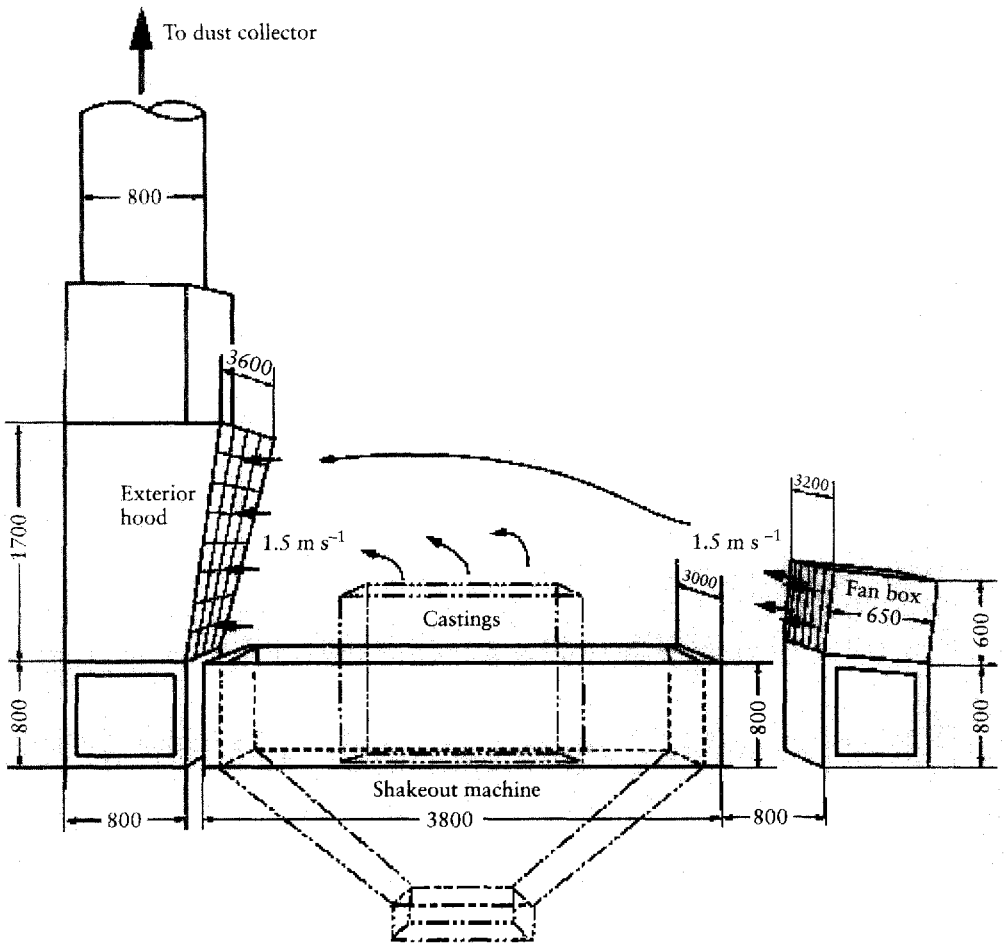

FIGURE 10.85 Practical application to remove dusts from a shaking-out machine. Supply airflow rate is 2.88m^3 s^{-1}, exhaust airflow rate is 9.18 m^3 s^{-1}.

supply with exterior hoods system is similar to the push-pull ventilation system. In the push-pull system described in other sections (10.4.3 and 10.4.6), the main function of the jet is as an injector or as a curtain, whereas in the low-momentum supply system the main function of the supply flow is as a carrier or a transporter of contaminants. The main difference in supply airflow between the push-pull system and the low-momentum supply system is that the supply air is blown at relatively low velocity from relatively wide openings, whereas in the push-pull systems the jet is blown at high velocity from narrow slots.

The low-momentum supply system could also be applied to operations inside booths. If a worker must be inside a booth, to protect the breathing zone, a supply inlet with a relatively wide area is placed above the worker and the low-momentum clean air is blown toward the worker. At the same time, the airflow could transport contaminants to the exhaust outlet.

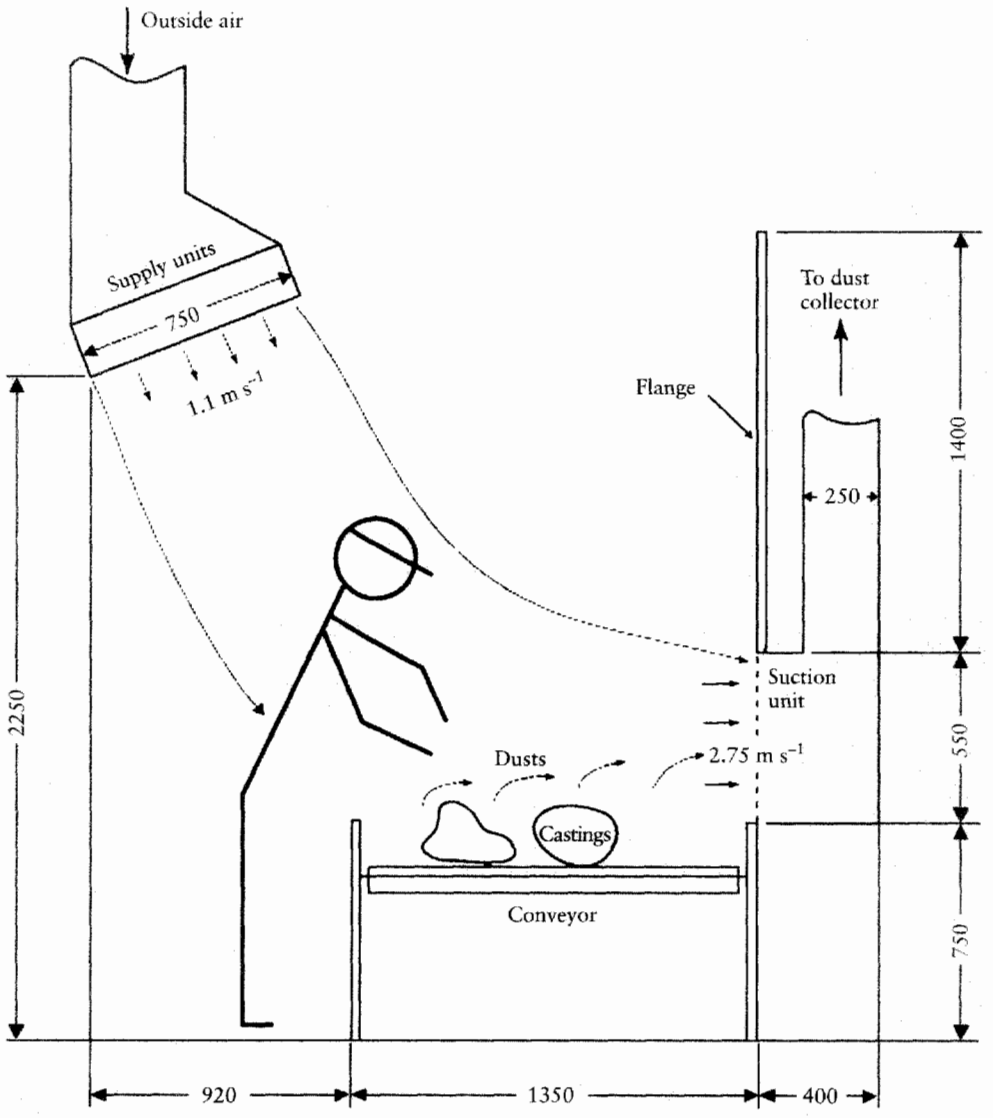

FIGURE 10.86 Practical application to remove dusts generated during handwork. Depth of the system is 6 m, supply airflow rate is 4.95 $m^3 s^{-1}$, and exhaust flow rate is 9.08 $m^3 s^{-1}$.

10.4.5.5 Specific Issues

In the low-momentum supply system, the contaminants are emitted within the low-momentum airflow blown from the supply inlet and they are transported to near the exhaust opening. If the contaminants diffuse into the whole of the supply airflow, the exterior hood must exhaust the whole of the airflow. To diminish the exhaust flow rate, some methods to prevent the contaminants from diffusing into the whole of the airflow are required. One possible method is to supply the air as slowly as possible but with enough velocity to reach the exhaust outlet and to control the surrounding air motion. Another method is to blow supply air with uniform

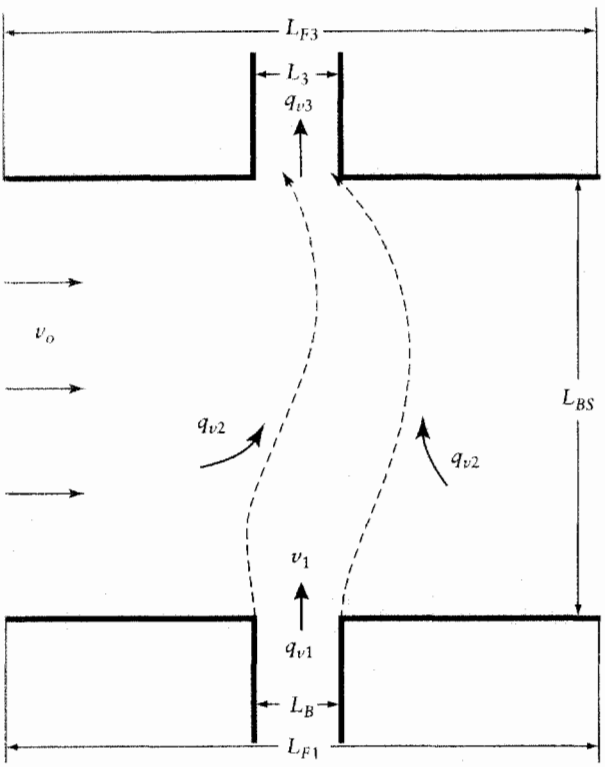

FIGURE 10.87 The fundamental operation and dimensions of the low-momentum supply with exterior hood system.

velocity, but with low turbulence intensity.[42] The exhaust outlet, which is an exterior hood, must exhaust only the contaminated airflow transported from the source; it is not necessary to exhaust the whole of the supply airflow. A flanged exhaust outlet should always be used to enhance the efficiency of the exterior hood.

Workers could be either inside the supply airflow or outside. If a worker is inside the airflow, it is possible that the breathing zone of the worker is within the wake region and he or she may be exposed to the contaminated airflow. To reduce the exposure the worker should always be upstream of the source and should try not to have his or her back to the supply airflow.

10.4.5.6 Design Equations and/or Parameters

An established design method for this type of system is not available. The practical design of the low-momentum supply with exterior hood system described in the previous part of this section used the flow ratio method.[6] However, the actual exhaust flow rate was adjusted visually to the appropriate value in order to exhaust only the contaminants transported by the supply airflow.

The flow ratio method was first suggested for use in designing receptor hoods and then it was suggested for design of push-pull systems. The concept of the method is described as follows.

Figure 10.87 shows the fundamental operation of the push-pull flow. The suction hood should simultaneously exhaust the pushed air (contaminated supply

airflow, q_{v_1}) and the air from the surroundings (q_{v_2}). The total exhaust flow rate (q_{v_3}) is calculated using Eq. (10.122), provided q_{v_1} is less than the exhaust flow rate:

$$\begin{aligned} q_{v_3} &= q_{v_1} + q_{v_2} \\ &= q_{v_1}(1 + q_{v_2}/q_{v_1}) = q_{v_1}(1 + K), \end{aligned} \tag{10.124}$$

where $K = q_{v_2}/q_{v_1}$ is the flow ratio.

Here, one considers the limit value for q_{v_2}/q_{v_1}. It is expressed as

$$(q_{v_2}/q_{v_1})_{\text{limit}} = K_L. \tag{10.125}$$

In designing the push-pull hood, one always applies a safety factor, n, resulting in the exhaust flow rate for design, q_{v_3D}, which is expressed as the following:

$$q_{v_3D} = q_{v_1}(1 + nK_L), \tag{10.126}$$

where K_L is a function of many factors such as the flow and surrounding air motion. It is normally determined from the results of experimental investigations.

The limit value of the flow ratio, K_L, is expressed as the following experimental equation for two-dimensional push-pull flows:

$$\begin{aligned} K_L = 0.55(L_{BS}/L_B)^{1.1}\{0.46((L_{F3}/L_B)^{-1.1} + 0.13)\} \\ \{5.8(v_0/v_1)^{1.4}(L_{BS}/L_B)^{0.25} + 1\}, \end{aligned} \tag{10.127}$$

where v_1 is the velocity of push airflow, v_0 is the velocity of surrounding air motion or contaminant motion, L_{BS} is the distance between push and pull openings, L_B is the width of push opening, and L_{F3} is the length of the flange on the exterior hood.

For practical design, the recommended aspects of the push-pull flow (hood) and the safety factor are as follows:

$$0 < L_{BS}/L_B < 15.0, 2.0 < L_{F3}/L_B < 10.0, 0 < v_0/v_1 < 1.0.$$

For two-dimensional flow $n = 1.1$ and for three-dimensional flow $n = 2.2$.

Applying the flow ratio method to the low-momentum supply system, the required exhaust flow rate is often in excess of practical values. This is because the value of q_{v3} is given as the value at which all the supplied airflow should be exhausted by the exterior hood. In the low-momentum supply system, contaminant sources should usually be between the supply inlet and the exterior hood. The supply airflow is contaminated at the position of the sources and it flows to the exterior hood. Therefore, all of the airflow is not always contaminated. Unfortunately, a design method considering such cases (the diffusion of contaminants within the airflow) has not been established yet, and the appropriate exhaust flow rate has to be adjusted after the system is installed.

10.4.6 Enclosures

10.4.6.1 General

A partial enclosure can be combined with a plane air jet in order to increase the containment of the hood. The jet can be thin or wide, depending on

function and placement, and can be single or multiple. The exhaust hood must be very carefully designed since the exhaust velocity in the opening is usually low and the jet's velocity is usually high.

When using a thin air jet, one common problem is disturbance of the jet when walking or reaching through the jet or passing material through the jet. These activities could deflect the jet and result in a large escape of contaminated air from inside the hood to the worker and the surroundings.

When total isolation of the surroundings is necessary the contaminant source (or the worker) has to be placed in a volume that is physically closed and has both supply and exhaust air. When these systems are situated in small rooms they function as both local and general ventilation. Some smaller systems that normally are of bench size are included in this section.

The systems described illustrate some applications for the use of air jets combined with exhausts. There are many potential combinations of jets and exhausts and most of them have been used at some time. It is not possible to include all potential descriptions here and the ones included were chosen to illustrate the advantages and disadvantages of these systems. More examples are described in the literature (e.g, Hayashi[6] and Goodfellow[2]).

The description of biological safety cabinets is also included in this section. Biological safety cabinets include those with combined supply and exhaust airflow, but also include other designs which are also described.

10.4.6.2 Workbenches

General

A workbench makes use of a local air supply in conjunction with exhaust air to ensure good control of the contaminants generated on a bench process. The local exhaust removes the contaminants, while the local supply air protects the operator and/or the products against airborne contaminants. The local supply air improves the thermal environmental conditions by introducing cool dehumidified air in a hot environment. This ensures that the operator's thermal comfort is maintained in areas of high temperature, where full air conditioning of the entire workspace is not economically feasible.

Principle

Low-velocity supply air enters the space above the operator, providing a clean air zone around an operator working in a contained area. It is arranged so that the contaminated air flows toward the exhaust openings. The low-velocity supply air is usually discharged vertically above the worker, although horizontal flow can be used. A typical example of a workbench is shown in Fig. 10.88.

Applicability of Sources

Workbenches are suitable for area or point sources with low momentum; typical applications are sanding, painting, laminating, soldering, and powder mixing and handling. They are especially useful for industrial operations that, due to operating conditions, cannot be enclosed or isolated. These systems are unsuitable for high-momentum sources such as high convective heat releases or large particles with high release velocities. In such cases, the capture efficiencies

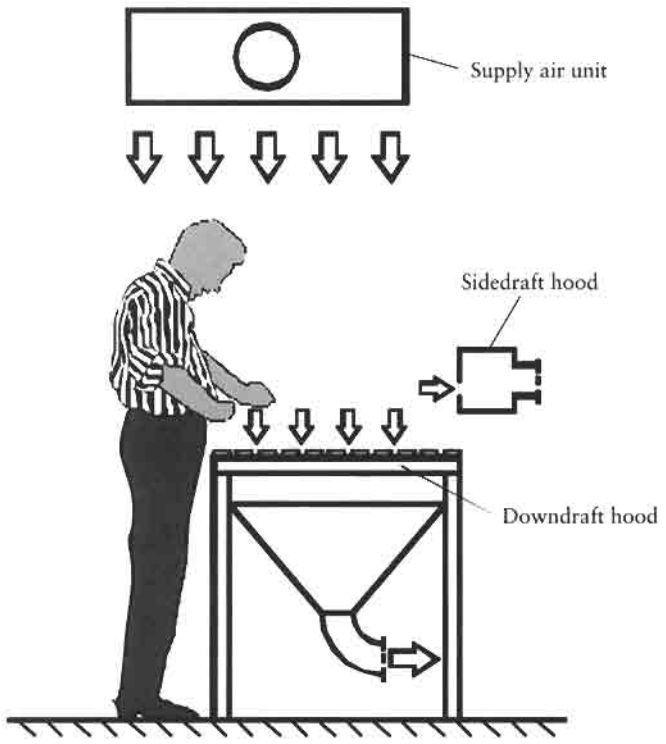

FIGURE 10.88 Example of a workbench with local supply and exhaust ventilation.

of these devices are low. They are also unsuitable for high toxicity materials due to possible contaminant escape into the workplace air.

Different Forms and Boundaries Relative to Other Types

The fitting of limiting boundaries such as walls provides solutions similar to those of laminar airflow (LAF) units or cabinets. An increase in the supply and exhaust supply rates provides a solution similar to ventilated booths (see Section 10.3).

Location of Supply and Exhaust Openings and Sources

The low-velocity supply air is usually delivered above the worker, although horizontal flow may be used. However, use of horizontal supply air must be carefully planned so that it does not spread contaminants toward the operator's breathing zone. Flow from behind the operator should be avoided as it may create recirculating flow regions, resulting in a high operator exposure if the contaminant source is within the wake region (see Section 10.3.4).

The ideal exhaust opening is as close to the pollution source as possible. However, it is important that the exhaust does not interfere with the operation or the process. Typically the exhaust is on the working table opposite the worker, or through a grill or perforated holes on the working table (see Fig. 10.88).

Very good results have been achieved with exhausts located on both sides of the contaminant, with one opening between the operator and the contami-

nant source, and the other opposite the source (Fig. 10.89). The figure shows a typical industrial system in which the measured dust concentrations and standard deviations in the worker's breathing zone are presented with various local ventilation configurations. Without local ventilation, the operator's average dust exposure was 42 mg m^{-3}. With local exhaust only, the exposure was reduced below 1 mg m^{-3}. There was no statistically significant difference between the side draft and downdraft exhausts. The addition of local supply air further reduced the exposure to below 0.5 mg m^{-3}. The best results were achieved when both exhaust inlets were used in combination with supply air. With this combination, the exposure was below 0.2% of the exposure from the dilution ventilation alone. Interestingly, this reduction was obtained without increasing the total airflow rate; hence, a better performance can be achieved for the same energy usage.

Location of Workers Relative to Exhaust Openings and Sources

The standing or sitting worker is normally close to the contaminant source, which is on the working table. The relative location of the exhaust openings should be designed to ensure that contaminants are forced away from the operator's breathing zone.

Disturbances

Any obstructions in the flow field may cause recirculating airflows, which reduce the efficiency of the local ventilation system. The operator's body also causes wakes when bending over the table. This recirculating flow may transport contaminants from the source region to the worker's breathing zone, resulting in potentially high exposures. Ambient disturbances such as airflows due to supply air jets, moving machinery, and drafts from windows and doors may interact with the supply and exhaust openings velocity field and reduce the performance. The worker's physical movements also produce air currents, which may influence the flow field and exposure.

The influence of air disturbances on performance can be minimized by locating the supply air device as close to the operator's breathing zone as practical to improve protection and by using walls or side baffles near the contaminant source.

Specific Issues

High supply air velocities or cool supply air can cause uncomfortable drafts on the worker. Nonuniform supply air velocities with high turbulence intensity may result in decreased capture efficiency, increased contaminant spread, and increased thermal discomfort.

Changing Flow Rates

For a constant exhaust flow rate, an increase in supply airflow provides better operator protection or production protection, but it also increases contaminant spread and risk of draft. Any decrease in supply airflow rate will result in a reduction of the design conditions of the operator or product protection.

With a constant air supply flow rate, an increase in exhaust airflow will result in increased operating costs. Any decrease in exhaust flow rates will result in

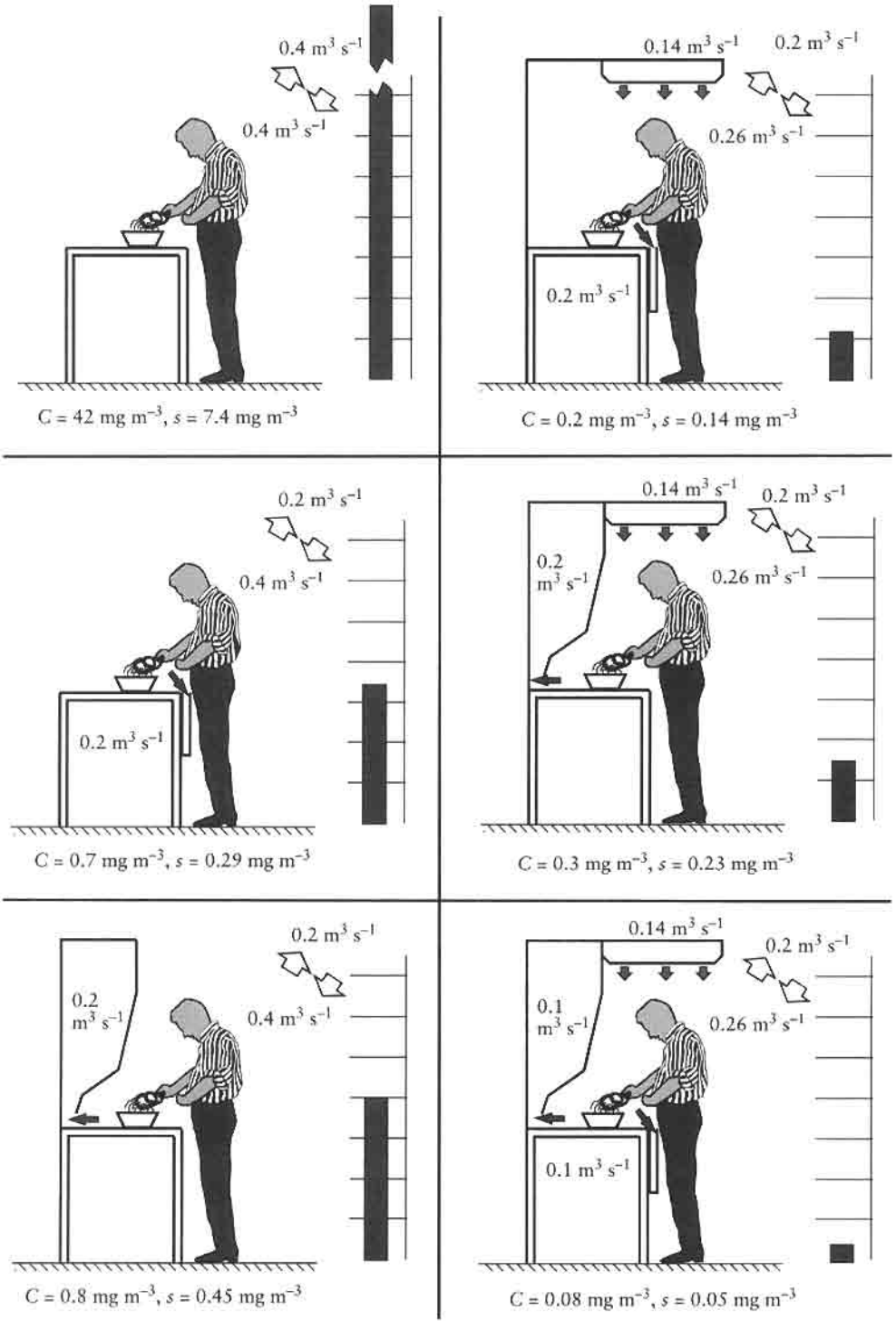

FIGURE 10.89 Measured worker's dust exposure with different ventilation configurations during manual powder handling.[43]

reduced capture efficiency and increased contaminant spread. Reduced exhaust flow rate will cause dust buildup in the ducts due to the reduction in velocity.

Design Equations and/or Parameters

Supply Air When designing workbenches, it is essential that the supply air face area be large enough to cover the contained area. Therefore it is important to have some indication of the operator's range of movements for all intended operations. Moreover, for efficient protection the supply airflow must be adequate to get a stable flow field that will not be affected by ambient disturbances. In industrial applications the suitable mean supply air velocities are typically between 0.2 and 0.45 m s^{-1}. Low velocities should be used when the distance between the supply air unit and the operator is small or for cool supply air. High velocities are applicable at greater distances and in hot environments, with thermal comfort being considered.

The supply air velocity should be uniform to protect against ambient air contaminants. Nonuniform flow results in high velocity gradients and turbulence intensities and rapid supply air mixing with the ambient air. As well as reducing protection efficiency, this will adversely influence thermal comfort. An even velocity distribution can be achieved using distribution manifolds and a filter at the face of the supply air unit.

The flow field created within the protection zone depends mainly on the density difference between supply air and room air (Fig. 10.90). With vertical flow the supply air should be isothermal or cooler than ambient air. If it were warmer, the extension of the controlled flow would be reduced due to buoyancy effects, resulting in the supply air not reaching the operator's breathing zone. As the supply air cannot be used for heating, the operator's thermal comfort should be maintained, preferably with radiant heaters in cold environments. If the supply air temperature is lower than the room air, the denser supply air accelerates down to the operator, and for continuity reasons the supply flow contracts. Excessive temperature differences result in a reduced controlled flow area with thermal discomfort, and should only be used in special cases.

Exhaust Openings The locations of exhaust openings are chosen to suit the particular application, with the hood as close to the generating source as possible. The exhaust opening location depends on the direction of contaminant release and its momentum. For low-momentum sources, exhaust openings should rest on the worktable or appropriate surfaces, thus reducing the amount of air drawn from surrounding clean air regions.

Exhaust airflow rates and exhaust opening locations are designed to ensure air velocities near the contaminant source are in the 0.3–0.5 m s^{-1} range for low-momentum sources. If the exhaust is through a table grille and the source is near the table surface, the exhaust airflow rate is calculated by

$$q_v = A \cdot v, \tag{10.128}$$

where A is the area of the working table and v is the mean air velocity at the opening.

To ensure that contaminants are not spread into the ambient air, the exhaust airflow rate must be higher than the supply flow rate.

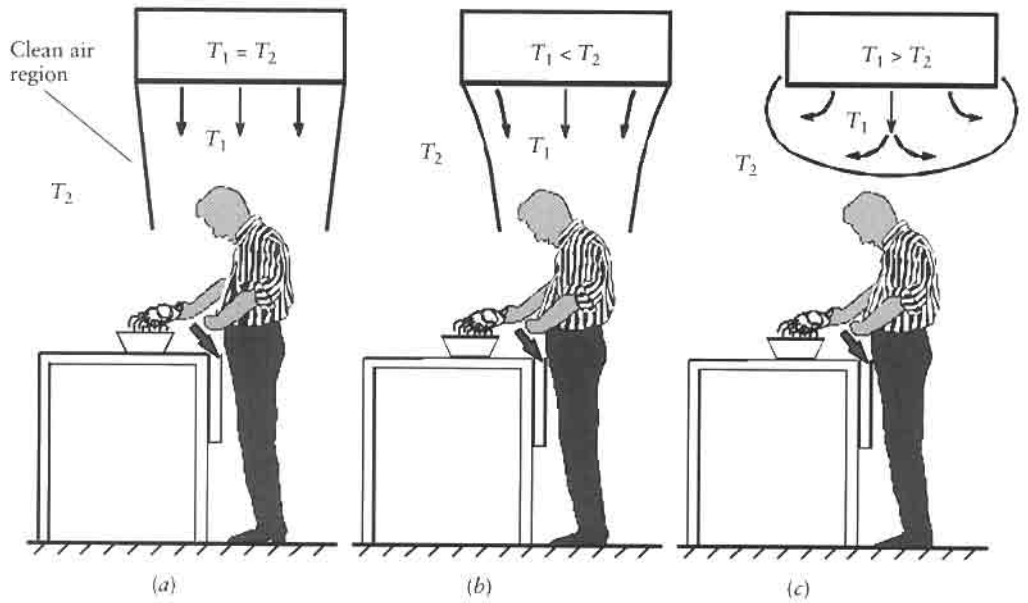

FIGURE 10.90 Supply airflow patterns with (*a*) isothermal supply air, (*b*) cool supply air, and (*c*), warm supply air.

Evaluation Procedures

The ability of the ventilation system to protect the worker efficiently can readily be determined by personal samples. The PIMEX method (see Chapter 12) can be used to determine the worker's exposure during various work phases. The capture efficiency as well as the supply air fraction can be measured using tracer gas techniques. Simple evaluation is carried out visually with smoke tube or pellet tests. Daily system evaluation is recommended using airflow or static pressure measurements at appropriate parts of the system. The air velocities, turbulence intensities, air temperature, mean radiant temperature, and air humidity should also be measured to provide an assessment of thermal comfort.

10.4.6.3 Wall Jet–Enhanced Exhausts

General

To enhance the efficiency of a partial enclosure it is possible to let a plane supply air jet blow inside and/or into the hood along one or more walls or along the table. Other advantages of this system are a reduction in needed supply flow to the room or a reduction in necessary exhaust hood flow for the same level of control. The supply flow (jet) inside the hood usually makes the flow into the hood (through the hood opening) more stable. As for all exhaust hoods with supply air inside, the supply flow rate must be less than the exhaust flow rate and the difference must be large enough to ensure sufficient velocity into the hood.

Principle

A rectangular or a canopy hood is placed close to a wall with the opening facing down. This could be called an open exhaust hood. The hood may have

partial shielding by placing walls on the sides, resulting in a partial enclosure. A wall jet is added to one of these configurations (open or partially enclosed). One possibility is to have a wall jet blow vertically upward along the inner back of the hood (along the inner wall) and then into the exhaust opening (Fig. 10.91). Another possibility is to have the wall jet directed horizontally along the working table (bottom of the open exhaust hood) from the opening toward the inner wall. The jet turns upward at the end of the table, at the inner wall, and then travels into the exhaust outlet (Fig. 10.92). The wall jet can be generated by a fan, from the general supply air system, or from a pressurized air system. The air in the jet could come from either outside or inside the room.

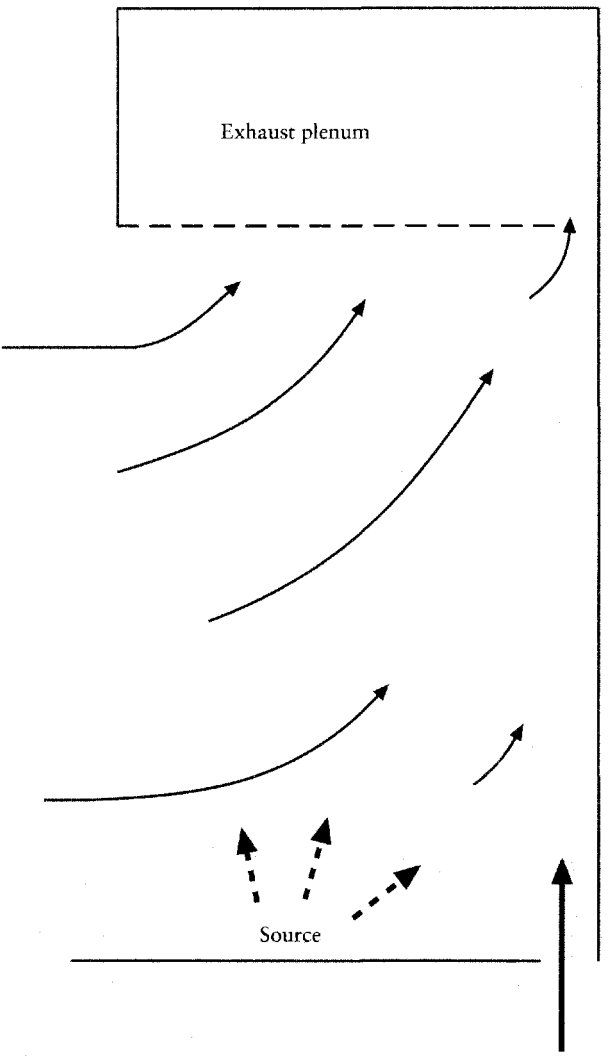

FIGURE 10.91 Vertical jet along inner wall. Dimensional example for kitchen hood. Width is 1.2 m, depth is 0.8 m, height between table and exhaust is 1.15 m, jet inlet width is 3.5 mm, jet flow rate is 28 L s^{-1}, and exhaust flow rate is 278 L s^{-1}.

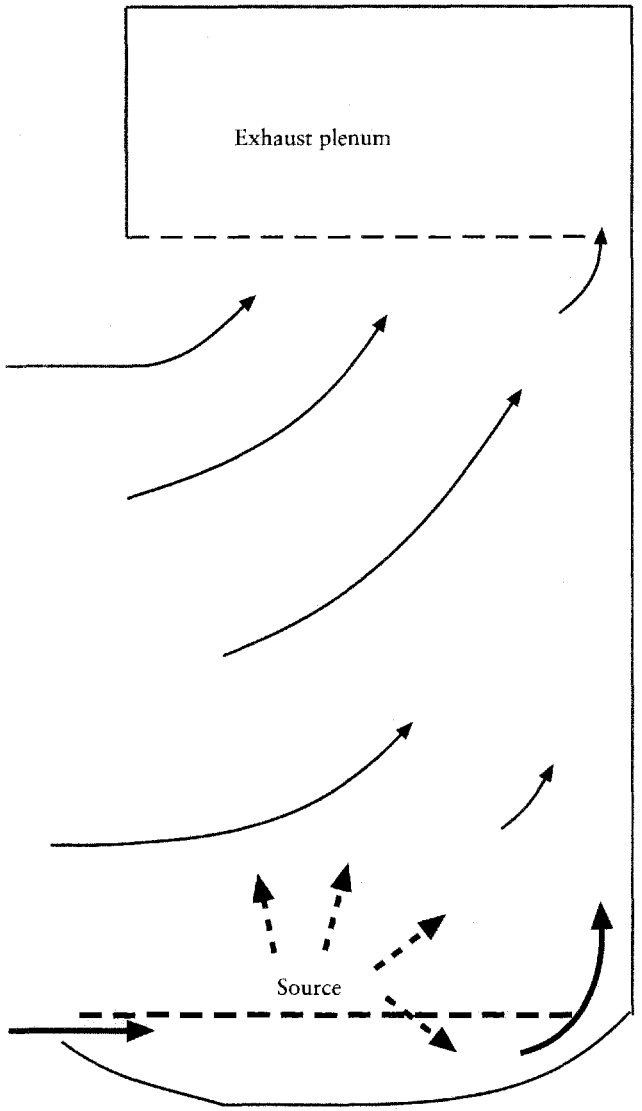

FIGURE 10.92 Horizontal jet along table. Welding table with grid. Exhaust flow rate is 278 L s^{-1} and jet flow rate is 50 L s^{-1}. Dimensions are approximately the same as in Fig. 10.91.

The contaminants are transported into the exhaust opening, from the table, by suction into the supply air (jet) and the movement of the exhausted flow over the table.

Figure 10.91 is shows the principle for a jet along the inner wall. Figure 10.92 shows the principle for a jet along the table, in this case a welding table with grid, where the jet is blown below the grid. Figure 10.93 shows the design of a kitchen hood with the jet along the inner wall, where the grease filter is a part of the connection to the exhaust system. These examples were first described by Lind and Aourell[44] and Petersson and Vikström.[45]

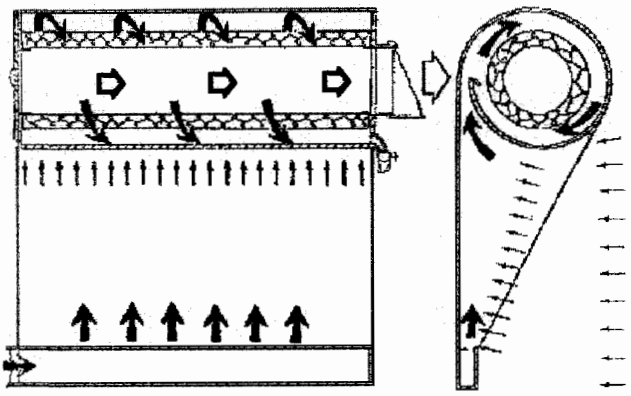

FIGURE 10.93 Design of exhaust with wall jet for a kitchen hood with partly shielded sides and circular grease filter.

Applicability of Sources

These systems can be used for relatively small sources that generate a large amount of contaminants at not too high temperatures and velocities, and where the process is not influenced by cross-drafts.

These systems have been applied to welding tables with open sides, even if the welding processes normally generate too much heat to be appropriate for this kind of local ventilation. In these cases, a plane jet blows along the welding table (from front to back) or an initially plane jet blows from front to back, along the lower part of the welding table (below the grid). These types of systems have also been used for kitchen hoods with open sides. In these cases, the plane jet is blown upward along the back wall. An air jet along the inner back wall of a laboratory fume hood has often been used to increase the flow stability inside the hood.

Different Forms and Boundaries Relative to Other Types

The opening to the exhaust duct is either a horizontal rectangular exhaust opening facing down (with air direction upward) or one or more slots connected to the exhaust duct. These slots should preferably also be placed horizontally, facing down, but could be at some angle to the horizontal plane.

The opening that generates the plane jet could either be a narrow slot or a line of holes placed so close to each other that the jet air forms a continuous plane jet.

The system with a horizontal jet (Fig. 10.92) is similar to the push-pull system used on open surface tanks (Section 10.4.3). One difference is that in this system the jet functions as an injector, whereas in push-pull systems the main function is as a curtain.

If the supply jet is inclined upward, while situated at the front of the table, its function could be similar to an air curtain in an opening. However, the inclination from the horizontal for the jet is usually very slight, since angles above 5 to 10 degrees sharply deteriorate the function of the ventilation system. If the jet is directed vertically, it should be placed along the back wall, blowing upward.

Specific Problems

The connection to the exhaust duct (the exhaust opening) is usually a horizontal surface with suction vertically up, and this connection should be situated above the jet inlet and the source generation point. Sources with heat generation should be on or slightly above the surface and between the jet inlet and the exhaust opening. For a vertical wall jet, the source should be as close as possible to the jet.

The worker must always be outside the hood or in front of the table, that is, the jet should not pass over the worker.

The tools and the contaminant generation should be on or slightly above the working surface. Preferably they should not be directly in the jet, but close to it, when using a horizontal jet. For a vertical jet they should be as far away from the table's front as possible—in other words as close as possible to the vertical jet along the inner back wall, without being in the jet itself. At the same time, they should be as far away as possible from the worker, who naturally is placed behind the jet opening.

The relation between the two flow rates is specific for each hood design. The flow rate into the exhaust duct must be larger than the sum of the jet flow rate and the induced flow rate. The induced flow rate should ideally be of such a size that the flow rate into the hood, passing the operator, keeps the contaminants in the flow into the exhaust.

The jet velocity should fulfill two demands. First, it must be large enough to generate an induced flow rate, which transports the contaminants into the exhaust (for a horizontal jet along the table, it should be large enough to turn upward at the inner wall and continue into the outlet); second, the velocity should not be so large that the jet bounces at the inner wall and returns toward the operator or for a vertical jet that it turns outward along the exhaust opening plane and into the surroundings.

If the hood has side walls the opening to the outside must be large enough to permit work inside the hood and it must also be designed to facilitate flow into the opening and diminish the possibilities for the moving air to transport contaminants to the surroundings.

Pressurized air could be used for the supply jet. Since this normally gives higher initial velocities, the hood becomes more sensitive to changes in the jet flow rate and velocity. Pressurized air systems could also result in more noise problems than a jet resulting from a fan.

The largest disturbances can occur when the supply jet is disturbed or deflected by the process. In this case the jet can blow in unwanted directions, such as to the side or backward into the surroundings. The operator can disturb the horizontal jet by standing too close to the jet inlet and also by preventing the induced flow from passing the contaminant source.

The difference between the supply and exhaust flow rates of the room's general ventilation must be large enough to handle the difference between the hood's supply and exhaust flow rate. If the difference between the room flow rates is too small (the available flow rate into the hood is too small) the hood's containment diminishes and the air inside the hood could be pulled into the room. If the difference is too large, the room supply flow can influence the flow into the hood and possibly inside the hood, which can result in increased

contamination outside the hood. The same condition could occur when the direction of the room supply flow disturbs the flow into and inside the hood.

If the hood's exhaust flow rate is too small (smaller than the sum of the initial jet flow rate and the induced flow rate) the jet will carry some contaminants into the room. The same condition will occur with a jet flow rate or jet velocity that is too large.

An increase in exhaust hood flow rate is not normally a problem, as long as the room supply airflow rate is high enough. If the exhaust hood flow rate diminishes, the same types of problems arise as described above when the initial exhaust flow rate is too low.

An increase in the jet flow rate gives the same result as a supply rate that is initially too high. A decrease in the jet flow rate could result in diminished functioning of the hood, but a small decrease has no deleterious effect.

Design Equations and/or Parameters

The designs that have been published are all empirical. However, it should be possible to use the wall jet equations from Chapter 7 and the equations for velocities outside exhaust openings (Section 10.2.2) to design these types of hoods.

The exhaust flow rate from the hood must always be much larger than the initial flow rate in the jet, since the jet always induces a larger flow rate than the initial jet flow rate. One recommendation is to have the initial jet flow rate approximately equal to 10% of the exhaust flow rate.

The design should start with the necessary air velocity through the hood opening or near the source, from which the induced flow rate can be calculated. This is used, together with operating restrictions on velocities, to calculate the necessary initial jet flow rate and jet opening area, which, together with the distances (height, depth, width), give the jet's velocity and flow rate. These give the necessary minimum exhaust flow rate and the equations in Section 10.2.2 may be used to calculate the size of the exhaust opening. It is possible to start with exhaust opening size and height above the table to calculate the maximum velocity and flow rate of the jet. The same equations presented earlier are used to calculate the velocity gradients outside the exhaust openings. These gradients are used to check that the velocities from the jet are not higher than the velocities from the exhaust, except where the exhaust velocities are too small to capture or transport the contaminants. This usually happens near the contaminant source. Both the velocity and the momentum (or flow rate) into and near the exhaust opening (maintained by the exhaust flow) must be higher than the velocity and momentum generated by the jet at the same place. See Figs. 10.91–10.93 for design examples.

The pressure drop for the exhaust opening, the jet supply opening, and for the hood opening if there are side walls, can be calculated using the normal equations for flow inside ducts and into ducts and openings.

An important design parameter is the jet angle. Normally the jet should be parallel to the table or the inner back wall and can thus be treated as a normal wall jet. If the jet has a small angle upward from the table, the wall jet equations may be unsatisfactory and experiments may be necessary.

The contaminant and heat generation rates must also be assessed in order to determine if the generation rates are too high for the calculated airflow rates or if they influence the passing flow into the exhaust. Generation rates

that are too high could make it necessary to increase the hood's exhaust flow rate or to change to another hood type. It may also be possible to increase the jet flow rate, but since this means increasing velocities at the exhaust, the result must be evaluated before use.

Evaluation

A visual evaluation of ventilation system performance can be performed by injecting smoke into the jet. No quantitative evaluation methods for these systems have been reported, but it should be possible to measure the containment of a hood with side walls (partial enclosure) using one of the containment indices (see Sections 10.2.1 and 10.5). Additional information may be obtained by measuring capture efficiency.

10.4.6.4 Biological Safety Cabinets

General

Biological safety cabinets (BSCs) used in the United States are divided into three classes: I, II, and III. Class II cabinets are further divided into four types: A, B1, B2, and B3.[46] In other countries, other categorization schemes are sometimes used, but usually follow the same general operating conditions. This division is quite unlike the rest of the local ventilation chapter, but since these descriptions are used whenever BSCs are used, it is practical to describe them here.

Class I BSCs are, from the functional view, similar to a fume cupboard (Section 10.2.3). Class II cabinets are used for product and worker protection. Class III cabinets are used for work with very dangerous microbiological or radioactive agents and provide maximum protection to the environment and the worker. The class and type of BSC used is dependent on the demands for worker and product protection.

Principle

A document from the U.S. Centers for Disease Control and Prevention and National Institutes of Health[46] describes, in detail, the different BSC designs and operating parameters. This document is easily available on the Internet and only a short summary will be provided here. For more detail regarding operation, design, use, testing, protection, etc. the reader is referred to the latest edition of the CDC-NIH document.

Class I The Class I BSC provides personnel and environmental protection, but no product protection. It is similar in air movement to a chemical fume cupboard, but has a HEPA filter (see Chapter 9) in the exhaust system to protect the environment (Fig. 10.94). In the Class I BSC, unfiltered room air is drawn across the work surface. Personnel protection is provided by this inward air velocity as long as a minimum velocity of 0.37 m s^{-1} is maintained through the front opening (see the discussion on fume cupboards in Section 10.2.3.3). In many cases Class I BSCs are used specifically to enclose equipment.

The Class I BSC is hard-ducted to the building exhaust system, and the building exhaust fan provides the negative pressure necessary to draw room

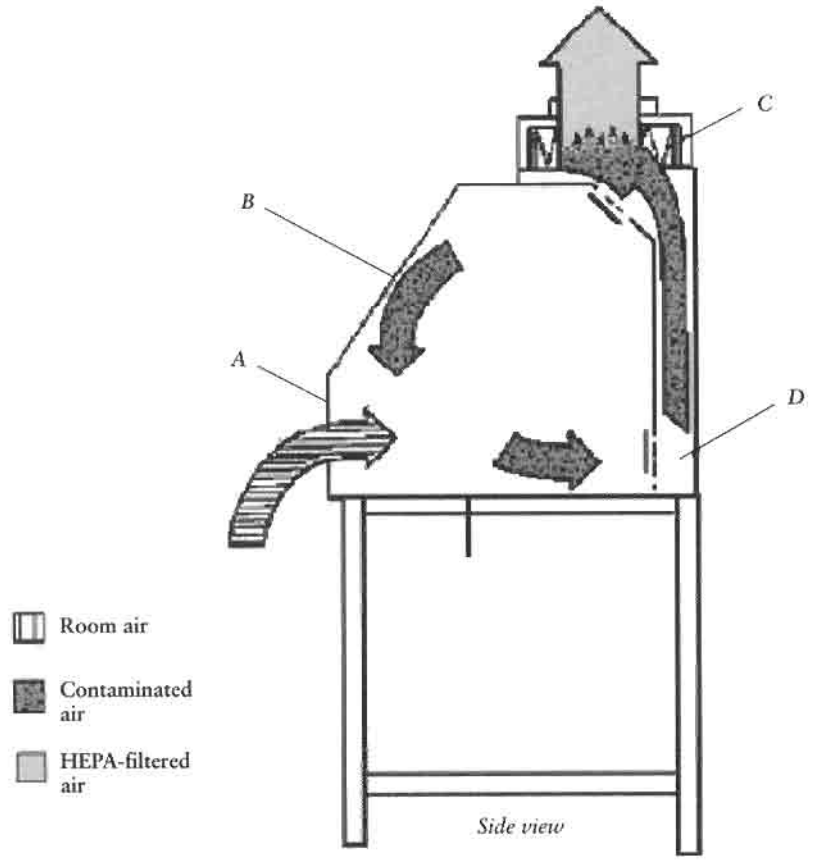

FIGURE 10.94 The Class I BSC (*A*: Front opening. *B*: Sash. *C*: Exhaust HEPA filter. *D*: Exhaust plenum).

air into the cabinet. Cabinet air is drawn through a HEPA filter as it enters the exhaust plenum. A second HEPA filter may be installed at the terminal end of the exhaust.

Some Class I BSCs are equipped with an integral exhaust blower; the cabinet blower must be interlocked with the building exhaust fan. In the event that the building exhaust fan fails, the cabinet exhaust blower must also turn off so that the exhaust ducts are not pressurized. If the ducts are pressurized and the HEPA filter develops a leak, contaminated air could be discharged into other parts of the building or the environment.

Class II The Class II (Types A, B1, B2, and B3)[46] biological safety cabinets provide personnel, environmental, and product protection. Airflow is drawn around the operator, through the hood opening and into the front grill of the cabinet, which provides personnel protection. In addition, the downward flow of HEPA-filtered air provides product protection by minimizing the chance of cross-contamination along the work surface of the cabinet. Because cabinet air has passed through the exhaust HEPA filter, it

is contaminant-free and provides environmental protection. However, when working with hazardous or toxic gases and vapors, only BSCs that are ducted to the outside should be used. All Class II cabinets are designed for work involving microorganisms assigned to all biosafety levels except the highest.

Class IIA In a Class IIA BSC, an internal blower (Fig. 10.95) draws sufficient room air into the front grill to maintain a minimum calculated or measured average velocity of at least 0.37 m s^{-1} at the opening of the cabinet. The supply air flows through a HEPA filter and provides particulate-free air to the work surface. Laminar airflow reduces turbulence in the work zone and minimizes the potential for cross-contamination.

The downward moving air splits as it approaches the work surface; the blower draws part of the air to the front grill and the remainder to the rear grill. Although there are variations among different cabinets, this

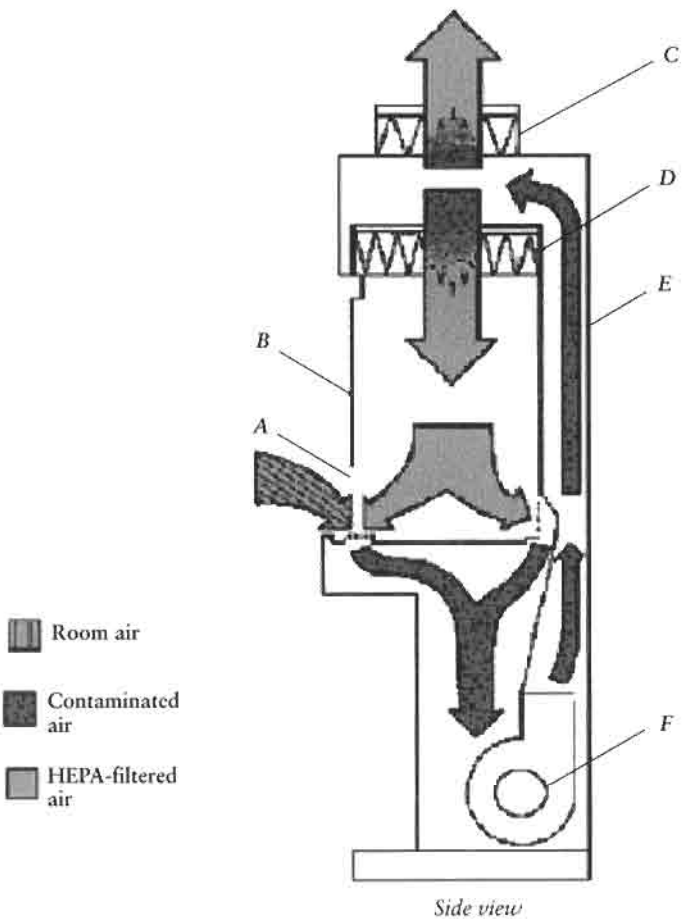

FIGURE 10.95 The Class II A BSC (*A*: Front opening. *B*: Sash. *C*: Exhaust HEPA filter. *D*: Rear plenum. *E*: Supply HEPA filter. *F*: Blower).

split generally occurs about halfway between the front and rear grills, and 5 to 15 centimeters above the work surface.

The air is then discharged through the rear plenum into the space between the supply and exhaust filters located at the top of the cabinet. Due to the relative size of these two filters, approximately 30% of the air passes through the exhaust HEPA filter and 70% recirculates through the supply HEPA filter back into the work zone. Most Class IIA cabinets have dampers to modulate this 30%/70% division of airflow.

An unducted Class IIA BSC should not be used for work involving hazardous or toxic gases and vapors. The buildup of chemical vapors in the cabinet (by recirculated air) and in the laboratory (from exhaust air) could create health and safety hazards.

Class IIB1 In a Class IIB1 cabinet, supply blowers draw room air (plus a portion of the cabinet's recirculated air) through the front grill and then through the supply HEPA filters located immediately below the work surface (Fig. 10.96). This particulate-free air flows upward through a plenum at each side of the cabinet and then downward to the work area through a back-pressure plate. In some cabinets an additional supply HEPA filter removes particulate generated by the blower/motor system.

Room air is drawn through the face opening of the cabinet at a minimum inflow velocity of 0.5 m s^{-1}. As with the Type A cabinet, there is a split in the

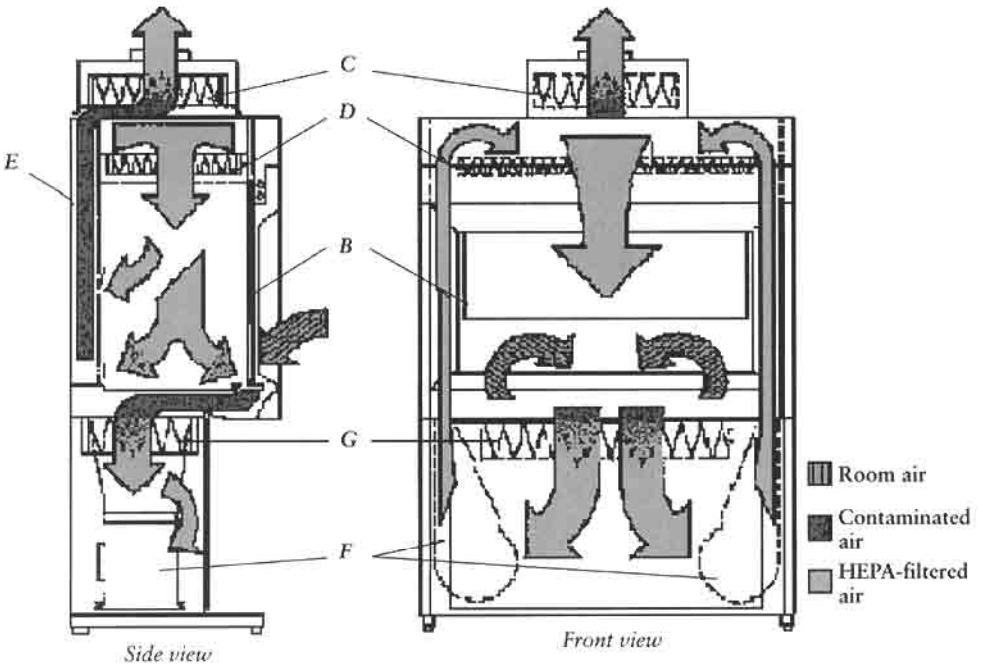

FIGURE 10.96 The Class II B1 BSC, classic design (*A*: Front opening. *B*: Sash. *C*: Exhaust HEPA filter. *D*: Supply HEPA filter. *E*: Negative pressure exhaust plenum. *F*: Blower. *G*: Additional HEPA filter for air supply). *Note*: The cabinet exhaust needs to be connected to the building exhaust.

downflowing air stream just above the work surface. In the Type B cabinet, approximately 70% of the downflow air exits through the rear grill, passes through the exhaust HEPA filter, and is discharged from the building. The remaining 30% of the downflow air is drawn through the front grill. Since the air that flows to the rear grill is discharged into the exhaust system, activities that may generate hazardous chemical vapors or particulate should be conducted toward the rear of the cabinet.

Type B1 cabinets must be hard-ducted, preferably to their own dedicated exhaust system, or to a properly designed laboratory building exhaust. Blowers on laboratory exhaust systems should be located at the terminal end of the duct work. A failure in the building exhaust system may not be apparent to the user, as the supply blowers in the cabinet will continue to operate. A pressure-dependent monitor should be installed to sound an alarm and shut off the BSC supply fan, should failure in exhaust airflow occur. Since this feature is not supplied by all cabinet manufacturers, it is prudent to install a sensor in the exhaust system as necessary. To maintain critical operations, laboratories using Type B1 BSCs should connect the exhaust blower to the emergency power supply.

Class IIB2 The Class IIB2 BSC is a total-exhaust cabinet; no air is recirculated within it (Fig. 10.97). This cabinet provides simultaneous primary biological and chemical containment. The supply blower draws in room air or outside air at the top of the cabinet, passes it through a HEPA filter, and down into the work area of the cabinet. The building or cabinet exhaust system draws air through both the rear and front grills, capturing the supply air plus the additional amount of room air needed to produce a minimum calculated or measured inward face velocity of 0.5 m s^{-1}. All air entering this cabinet passes through a HEPA filter, and perhaps some other air-cleaning device such as a carbon filter, and is exhausted to the outside. Exhausting as much as 0.5 m^3 s^{-1} of conditioned room air makes this cabinet expensive to operate.

Class IIB3 A Class IIB3 BSC (Fig. 10.98) is a ducted Type A cabinet having a minimum inward air velocity of 0.5 m s^{-1}. All positive-pressure contaminated plenums within the cabinet are surrounded by a negative air pressure plenum. Thus, leakage in a contaminated plenum will be into the cabinet and not into the environment.

Class III The Class III biological safety cabinet (Fig. 10.99) was designed for work with microbiological agents demanding the highest biosafety level, and provides maximum protection to the environment and the worker. It is a gas-tight enclosure with a nonopening view window. Access for passage of materials into the cabinet is through a double-door pass-through box that can be decontaminated between uses. Reversing that process allows for safe removal of materials from the cabinet. Both supply and exhaust air are HEPA filtered. Exhaust air must pass through two HEPA filters, or a HEPA filter and an air incinerator, before discharge to the outdoors. Airflow is maintained by a dedicated independent exhaust system

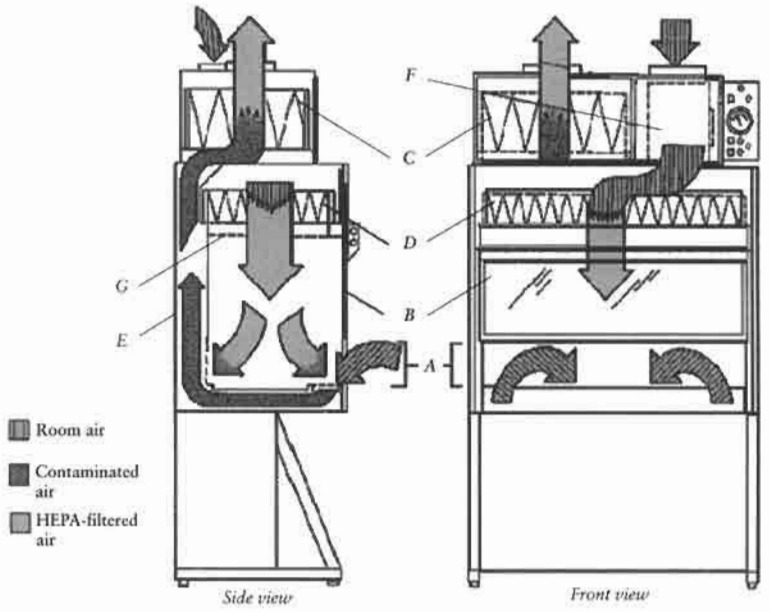

FIGURE 10.97 The Class II B2 BSC (*A*: Front opening. *B*: Sash. *C*: Exhaust HEPA filter. *D*: Supply HEPA filter. *E*: Negative pressure exhaust plenum. *F*: Supply blower. *G*: Filter screen). *Note*: Connection to building exhaust system is required. The carbon filter in the building exhaust is not shown.

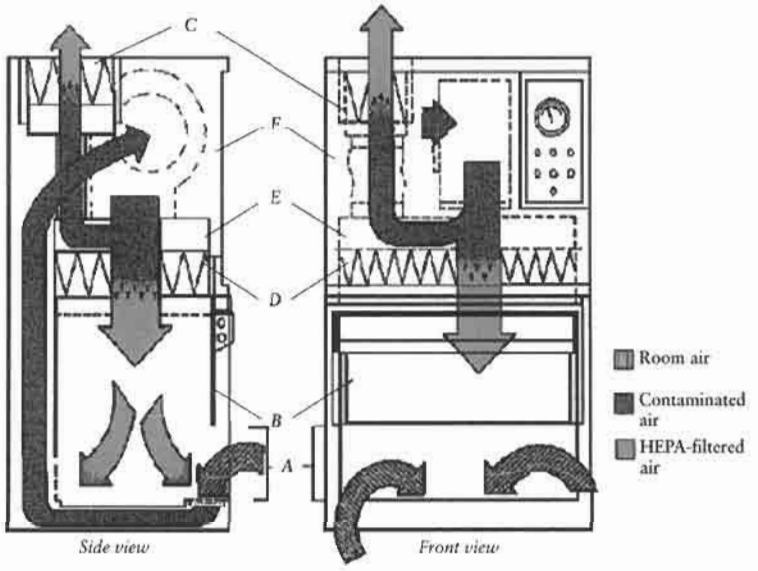

FIGURE 10.98 The tabletop model of a Class II B3 BSC (*A*: Front opening. *B*: Sash. *C*: Exhaust HEPA filter. *D*: Supply HEPA filter. *E*: Positive pressure plenum. *F*: Negative pressure plenum). *Note*: Connection to building exhaust system is required.

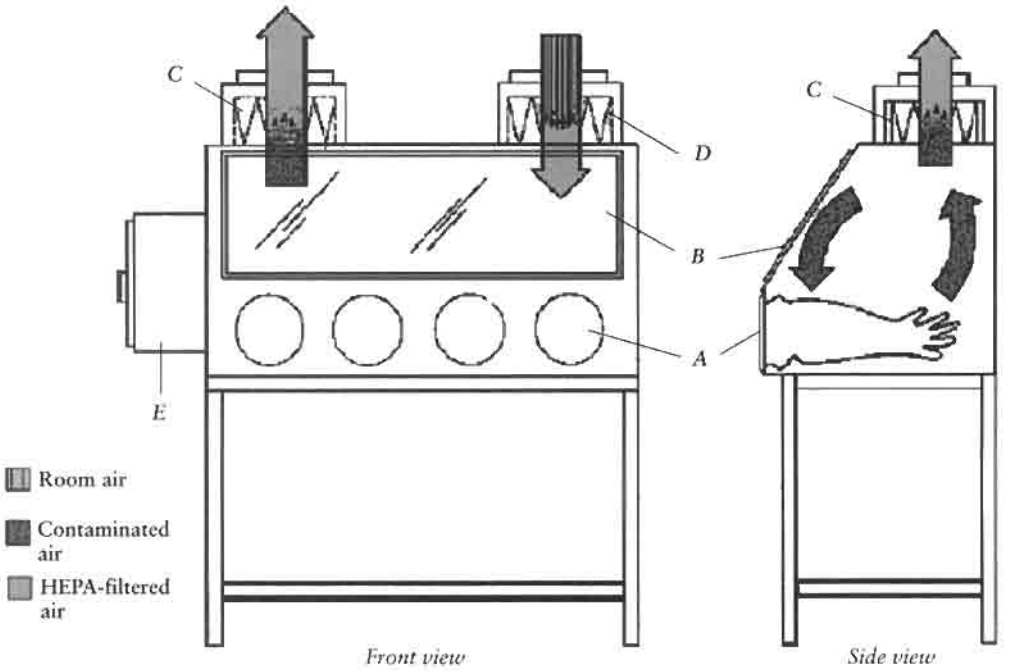

FIGURE 10.99 The Class III BSC (*A*: Glove ports with O-ring for attaching arm-length gloves to cabinet. *B*: Sash. *C*: Exhaust HEPA filter. *D*: Supply HEPA filter. *E*: Double-ended autoclave or pass-through box). *Note*: Connection to building exhaust system is required.

exterior to the cabinet, which keeps the cabinet under negative pressure (usually about 125 Pa).

Long, heavy-duty rubber gloves are attached in a gas-tight manner to ports in the cabinet and allow for manipulation of the materials isolated inside. Although these gloves restrict movement, they prevent the user's direct contact with the hazardous materials. The trade-off is clearly on the side of maximizing personal safety. Depending on the design of the cabinet, the supply HEPA filter provides particulate-free, albeit somewhat turbulent, airflow within the work environment.

Applicability of Sources

BSCs are used for handling microbiological agents and can also be used where other contaminants are handled or generated, such as in the electronics industry. BSCs are primarily designed for particulate contaminants. If toxic or hazardous gases or vapors are used or generated, other air-cleaning systems, in addition to HEPA filters, must be used to achieve a similar protection level. When using BSCs for microbiological work the use of proper procedures and equipment cannot be overemphasized in providing primary personnel and environmental protection (see discussion in Section 10.3.4).

Different Forms and Boundaries Relative to Other Types

A Class I BSC fitted with an added panel covering the opening and fitted with arm-length gloves, becomes, in many ways, similar to a glove box de-

scribed in Section 10.2.3.6. A totally enclosed glove box with added cleaning of inlet and outlet air is a Class III BSC.

Horizontal laminar flow clean air benches are not BSCs (Section 10.3.4). They discharge HEPA-filtered air across the work surface and toward the user. These devices only provide product protection. They can be used for certain clean activities, such as the dust-free assembly of sterile equipment or electronic devices. These benches should never be used when handling potentially infectious materials. The worker can be exposed to materials on the clean bench. Horizontal clean air benches should never be used as a substitute for a biological safety cabinet.

Vertical laminar flow clean benches also are not BSCs. They may be useful, for example, in hospital pharmacies when a clean area is needed. Although these units generally have a sash, the air is usually discharged into the room under the sash, resulting in the same potential problems as the horizontal laminar flow clean benches.

Specific Issues

The CDC-NIH document describes, in detail, the different uses of the different classes and types of BSCs and the type of protection (personnel, product, and environmental) each type provides. The document also provides a detailed comparison of filtration (air cleaning), airflow pattern (into the cabinet from the room or from the supply duct), and necessary performance tests (leak, velocity profile, differential pressure, etc.) for each type of BSC (see also Simons[47]).

BSCs should be designed to operate 24 hours per day, although energy conservation efforts may suggest BSC operation only when needed. The room air balance is of importance in operation of BSCs since room air is removed by ducted BSCs.

Design Equations and/or Parameters

No design parameters for flow rate and pressure loss have been found. The CDC-NIH document specifies the velocity through openings to the surroundings. Class I and IIA BSCs should have a velocity directed into the cabinet larger than 0.37 m s^{-1}. All other Class II BSCs should have a minimum inward face velocity of 0.5 m s^{-1}. Class III BSCs should have no connection to the surrounding work area and should maintain a negative pressure of at least 125 Pa, relative to the surrounding areas.

Most of the BSCs are connected to ducted exhaust systems and have HEPA filters for the supply and the exhaust air. The result is high pressure losses for the BSCs, even if low air flow rates are used. The filters must be handled with care, since much of the protection depends on the proper function of the filter(s).

10.4.6.5 Fume Cupboards with Auxiliary Air

General

Laboratory fume cupboards extract a significant volume of air. The replacement air has to be heated during the cold season and cooled (and

sometimes dehumidified) during the hot season before being supplied to the room. One way to reduce the energy cost associated with fume cupboards is to supply air directly into the fume cupboard. This air, which is treated to a lesser extent than the room supply air, is called auxiliary air. This method of supplying air has some similarities to the distribution of air at workbenches (Section 10.4.6.2) and to the use of air curtains in an opening. In actual practice, these systems are somewhere between the other two systems. Use of one of the other two systems is recommended before using an auxiliary air fume cupboard. The main difference between an auxiliary air fume cupboard and a normal laboratory fume cupboard is the use of both exhaust and supply duct systems. This could result in higher initial costs at the time of construction, but should result in lower energy costs.

Principle

The principle of this system is to connect a supply duct to the fume cupboard and introduce the air along the upper edge of the front opening. The air should be supplied outside of the hood, although there are models with supply on the inside. The air is directed down across the front opening and all the air should flow into the opening. Sometimes air is introduced along the interior side walls of the cupboard and along and over the work surface. Both the air velocity and the flow rate must be low enough to prevent disturbances to the flow into the opening, but high enough to reduce the need for conditioned supply air. The air is commonly distributed through a plenum above the opening when the sash is open and is, by use of a valve, introduced directly into the fume cupboard when the sash is closed. This means that the normal bypass used when the sash is closed is replaced with a duct-connected air supply, which works similarly to the bypass when the sash is closed.

The principle for the auxiliary cupboard is shown in Fig. 10.100. Two other types are shown in Figs. 10.101 and 10.102.[48]

Applicability of Sources

This special type of laboratory fume cupboard is used for the same work as a normal laboratory fume cupboard (Section 10.2.3.3). There is some evidence to suggest that auxiliary air systems are better for walk-in fume cupboards[49] and generally result in better protection than normal fume cupboards.[50] However, several articles have been published which point out the inherent problems with an auxiliary cupboard.[48,51]

Different Forms and Boundaries Relative to Other Types

The main forms of this type of hood are shown in Figs. 10.100–10.102. The difference between this type of hood and workbenches is that for fume cupboards the auxiliary air is only a part of the total exhaust flow rate and the flow is not intended to cover the person standing in front of the exhaust opening. The differences between this type of hood and an air curtain are that the air curtain is thinner, has a higher velocity covering the whole opening, and

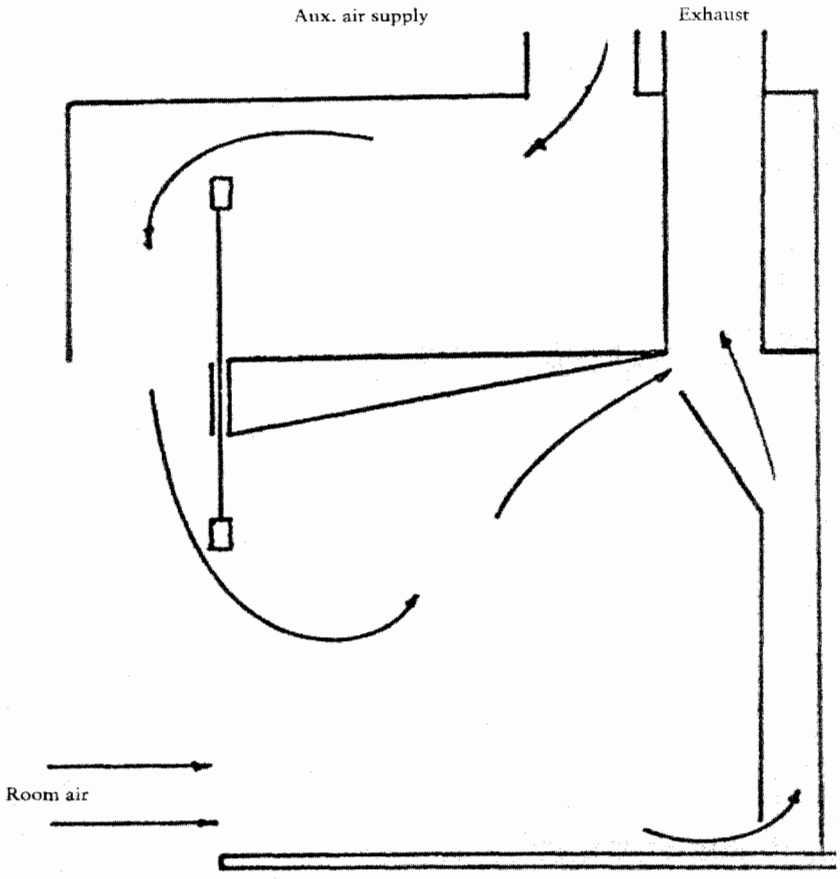

FIGURE 10.100 Principle for auxiliary air supply to a laboratory fume hood.[51]

normally has an exhaust slit in the lower part of the opening to keep the curtain plane over the opening. Auxiliary air fume cupboards look like ordinary laboratory fume cupboards with an added supply air outlet above the opening.

Specific Problems

Auxiliary air cupboards have many problems, most of which have been reported in the literature. A main problem that does not receive much attention is coordination of the flow into the opening controlled by the exhaust with the supply flow directed down immediately above the opening. This includes the complex and simultaneous relationships between velocities, flow rates, flow widths, flow directions, flow stability, turbulence, and temperatures. To this should be added the same problems that exist for normal fume cupboards, such as necessary exhaust flow rate and velocity, flow pattern inside the cupboard, working procedures, and the influence of people on the flow pattern outside and into the opening. The auxiliary air outlet may also be a source of noise.

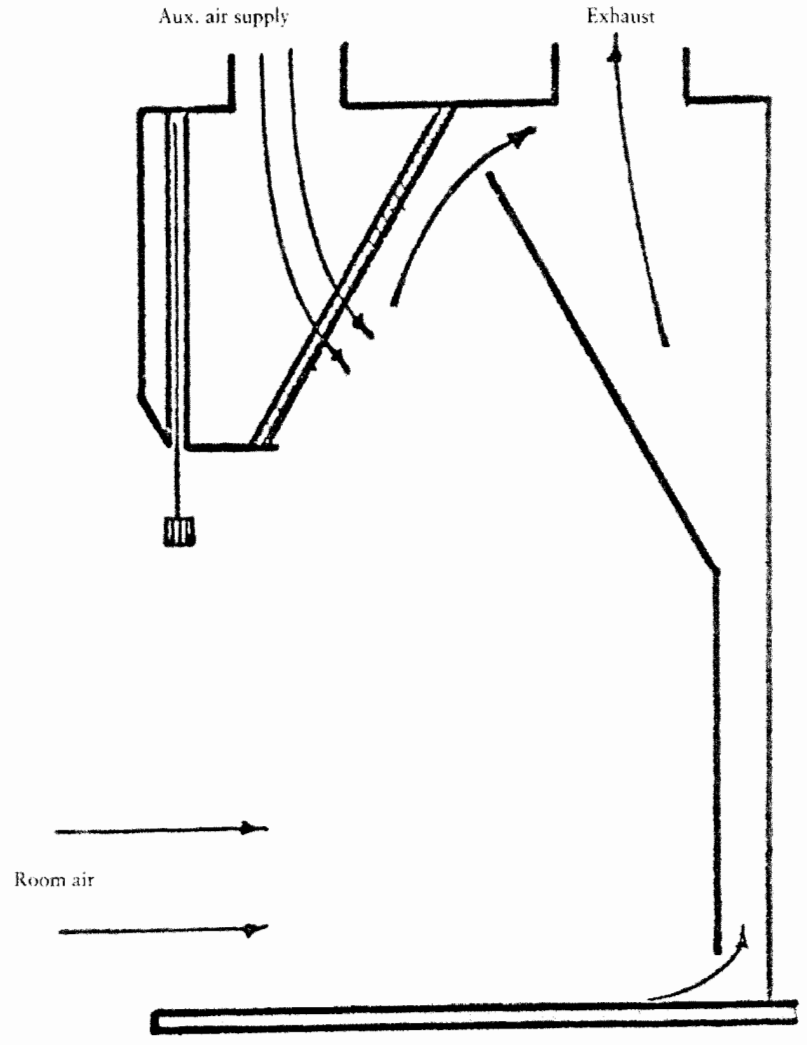

FIGURE 10.101 Auxiliary air supplied directly into the hood volume.[51]

It is quite common to find comments on the problem with different temperatures, different flow rates, and supply flow stability. Most of the other problems seem not to have been investigated.

Comments on the temperature of the auxiliary air are common. Auxiliary cupboards were first introduced to save energy and unconditioned outside air has often been used for the auxiliary supply air. This is usually not acceptable because unconditioned supply air will be too cold during the heating season for a person to work at the hood. It may also be too hot during the cooling season. Today, most auxiliary air systems operate at temperatures close to room temperature.

Even with the use of conditioned auxiliary supply air, these systems have advantages over traditional fume cupboards. It may be possible to lower the

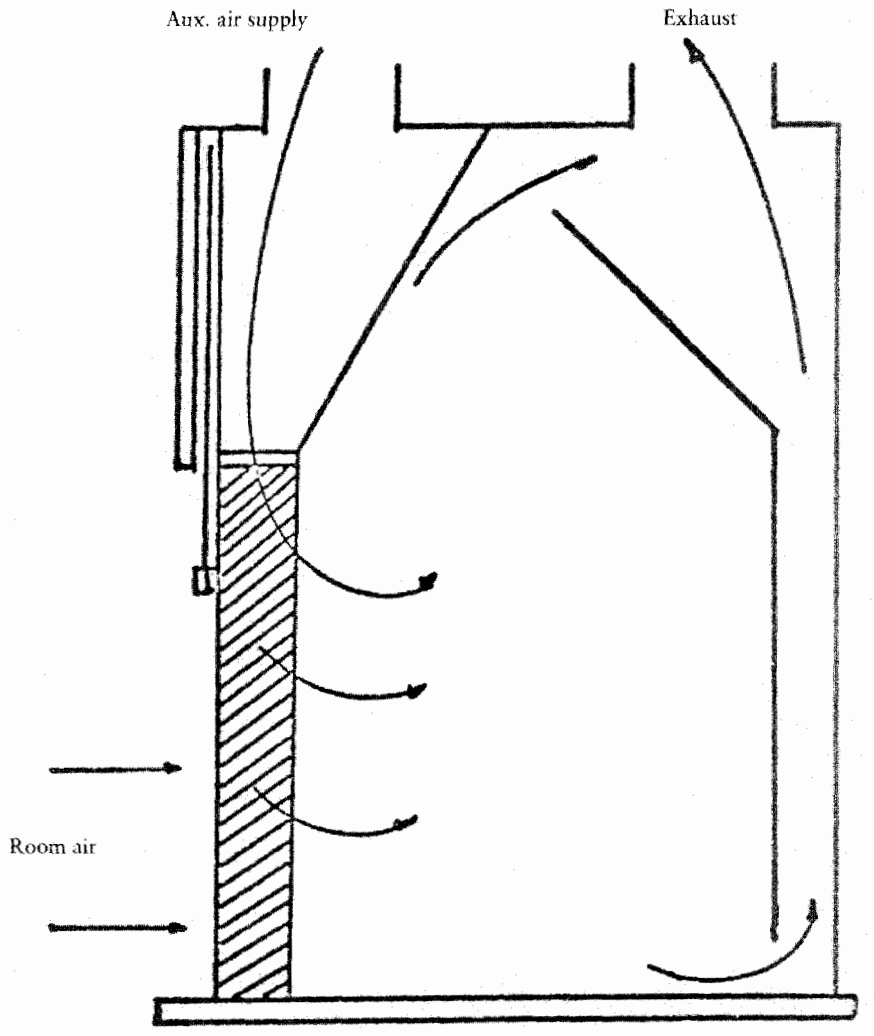

FIGURE 10.102 Auxiliary air supplied along the interior side walls of the hood.[51]

supply airflow rate to the room, to have a constant flow rate to the room, and to achieve better protection of the worker from the contaminants inside the cupboard. To achieve this better protection, it is necessary to have a high air velocity, which could disturb the airflow into the cupboard. This also put demands on design and maintenance.

Design Equations and/or Parameters

There are no specific design equations for this type of hood. Usually the exhaust flow rate is similar to the flow rate for ordinary fume cupboards. The different recommendations for auxiliary cupboards do not generally agree, most likely because all parameters influencing the performance have not been taken into account.

Albern[51] recommends the auxiliary airflow rate be one-third to two-thirds of the exhaust flow rate through the cupboard.

Saunders[49] recommends the auxiliary air have a uniform velocity distribution across the discharge area (±20%). The discharge area must be of a size that the air velocity does not exceed the face velocity of the fume cupboard by more than a factor of 1.2.

Fuller[50] claims that an auxiliary cupboard has better performance than an ordinary cupboard, if properly designed and used. The auxiliary flow rate should be 50% to 75% of the total exhaust flow from the cupboard. Below 50% there is no beneficial effect and above 75% the auxiliary air will aspirate contaminants out of the cupboard. The auxiliary air should enter the hood through the upper one-half to two-thirds of the opening. This should fill the volume between the cupboard operator and the opening and assist in the containment. The auxiliary air should be distributed uniformly across the length of the cupboard for a vertically sliding sash or above only the open sash of a cupboard with a horizontally sliding sash. It should also have a temperature within ±1.5 °C of the room temperature and have a constant flow rate without pulsations.

According to Mitchell[48] the auxiliary flow rate should be between 20% and 40% of the total exhaust flow rate from the cupboard: below 20% results in only small improvements and above 40%, leakage rises quite fast with increasing flow rate.

Based on literature reports and practical experience, the following recommendations are made. The auxiliary air supply should

- Be stable and uniformly distributed air with temperature ±1.5 °C of the room temperature,
- Have an airflow rate between 30% and 50% of the total exhaust air from the cupboard, and
- Be directed vertically or slightly into the opening with a velocity at the upper end of the opening less than the velocity into the opening.

Meeting the final recommendation will dictate the area of the auxiliary air inlet. A common velocity through a fume cupboard opening is 0.5 m s^{-1}. The upper end of the air supply opening is at about the same level as the head of an operator. People are quite sensitive to drafts (too high an air velocity or too low an air temperature or both) on the neck and on the back of the hands. For office work it is recommended that air velocities near a person be less than 0.3 m s^{-1} and preferably less than 0.15 m s^{-1} (see Chapter 5). Laboratory work is often similar to office work, and the design of the auxiliary air supply must be done with great care to prevent conditions that are detrimental to the flow into the cupboard or to the persons working in front of the cupboard.

The advantages and disadvantages of fume cupboards with auxiliary air are probably best summarized by Burgess:[52]

A well-designed auxiliary-air-supplied hood reduces air-conditioning costs and improves hood capture efficiency. The disadvantages of this hood include higher initial cost and maintenance due to the additional replacement air system, the possible introduction of airborne dust into the laboratory, discomfort

to operators during winter conditions unless the air is tempered, disturbance of the exhaust velocity profile at the hood face with poor canopy designs, and the possible hazard that exists in a poorly designed system if the exhaust fan fails and the auxiliary fan continues to operate. Although these objections can be resolved through appropriate system design, they do demonstrate the complexity of the auxiliary-air-supply system. One facility requirement that frequently cannot be met is the overhead space required for the air supply duct and the auxiliary air plenum.

10.4.7 Enclosed Rooms

10.4.7.1 General

There are many different combinations of supply inlets and exhaust enclosures, where the system has been designed as a whole. Two of these enclosures are described in some detail: abrasive blasting rooms with a person working inside the enclosure, and hospital isolation rooms.

Many other combinations exist but will not be described in the following sections. For example, in the electronic and medical industries it is quite common to use so-called unidirectional (UDI) rooms.[53] These utilize the same airflow principles as those used in abrasive blasting rooms (Section 10.4.7) and in cabinets with filtered air (Section 10.3.4), i.e., the air is supplied through one entire wall or the ceiling and is exhausted through the entire opposite wall or the floor.[14] In these cases, it is necessary to design the supply distribution carefully to avoid large turbulent eddies and so that the air velocities created are not uncomfortably high for the workers inside the room.

Most of the combined systems could be designed using information provided in Sections 10.2 and 10.3 and taking into account the mutual influence of the supply and the exhaust system. Many of these local ventilation systems for small enclosures are very similar to general ventilation systems for rooms and could be designed using the methods described in Chapter 8.

It should be noted that the primary purpose of the ventilation systems described for abrasive blasting rooms and hospital isolation rooms is to prevent or minimize exposure to hazardous substances in those persons working outside the blasting or isolation room. The ventilation system may also reduce exposure for workers inside these rooms, but often the reduction is not sufficient to eliminate the need for respiratory protection.

10.4.7.2 Abrasive Blasting Rooms with Person Inside

General

Abrasive blasting normally takes place inside a special room, cabin, or exhaust hood, but if very large equipment must be treated it is usually done without a protective surrounding. When using exhaust hoods and small cabins, where the worker is located outside the hood or cabin, it is possible to work without further protective equipment. Inside an abrasive blasting room, it is always necessary for the worker to wear a protective helmet supplied with breathing air, since the concentrations of the blasting material and other contaminants are very high, irrespective of the ventilation.

The ventilation in an abrasive blasting room has three main functions. The first is to transport the generated dust to the exhaust during the work in such a way that good visibility is achieved. The second is to eliminate, as fast as possible, the dust in the room after the work has ended. The third is to prevent unrestricted dispersal and backwash on the blast operator and the machinery and to keep the dust inside the room, preventing exposure to personnel working outside the room.

The blasting equipment and the air cleaning equipment may be placed outside or inside the room.

Principle

The air is supplied by a ventilation system or from the surrounding area. In both cases, the air is supplied through a diffusing device that covers the larger part of either one wall or the ceiling. The air is exhausted through another wall or the floor. All required openings on abrasive blasting enclosures should be designed with baffling to prevent unrestricted dust leakage. The air flow is intended to be unidirectional and directed from one wall to the opposite wall or from the ceiling to the floor. However, it is not necessary to have unidirectional flow and there are some advantages to good mixing of the air in the room. Good mixing may be achieved, for example, by having the air enter through the ceiling and exit through slots along both longer sides of the floor. Figure 10.103 shows different ways of supplying and exhausting air. Several recommended configurations are shown, as well as two configurations that are not recommended and should be avoided.[54]

The configuration *B1* uses the same flow distribution inside the room as is common in horizontal flow cleanrooms.

Applicability of Sources

The size of the room determines the size of objects that can be treated in the room. The main contaminant source is the blasting equipment and the abrasive material that impacts on the treated surface. The object being blasted can also be a source of hazardous contaminants. For example, removal of paint, which contains lead, cadmium, chromates, or other metals, may result in hazardous concentrations of these contaminants. Removal of fused sand from new castings may result in elevated silica exposure even when non-silica-containing abrasives are used. Except for the size of the room, there are usually no restrictions on the use of these rooms. If the abrasive used is highly dangerous, such as silica sand, the demands on the preventive equipment and the room are higher than when using slag or steel shot. This kind of system may also be used for spray painting small and large objects.

Different Forms and Boundaries Relative to Other Types

These rooms are usually rectangular with doors on one of the short sides for entrance and exit of materials and operators. Room sizes vary from 18 m^3 to more than 300 m^3 and the shapes range from cubic to elongated with rectangular cross-section.

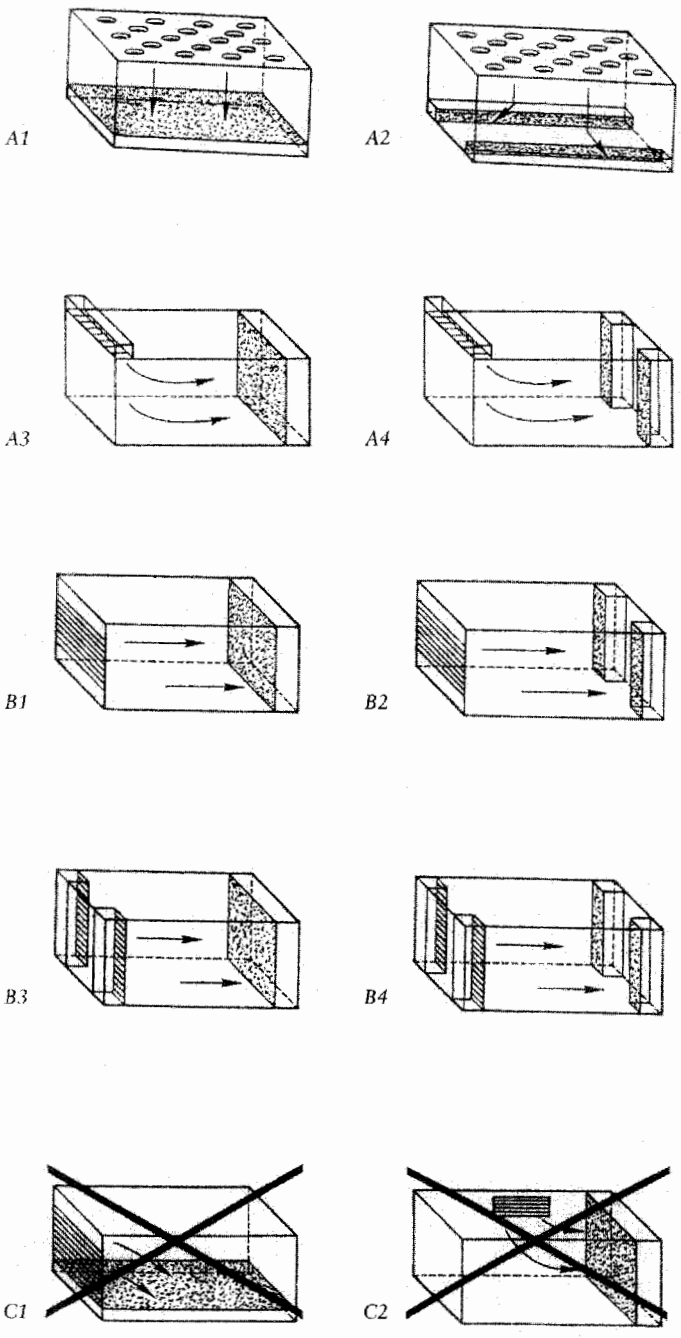

FIGURE 10.103 Different configurations of supply air inlets and exhaust air outlets in an abrasive blasting room. *A1*: Supply in ceiling and exhaust through floor. *A2*: Supply in ceiling and exhaust along floor sides. *A3*: Supply in one end of ceiling and exhaust through one opposite wall. *A4*: Supply in one end of ceiling and exhaust in corners of opposite wall. *B1*: Supply in one wall and exhaust through opposite wall. *B2*: Supply in one wall and exhaust in corners of opposite wall. *B3*: Supply in corners of one wall and exhaust through opposite wall. *B4*: Supply in corners of one wall and exhaust in corners of opposite wall. *C1* and *C2*: Not recommended.[57]

Specific Issues

There are many specific and detailed regulations related to use of blasting equipment, especially when used by an operator inside a room or when using silica sand as an abrasive. These regulations differ from country to country and include specifics on exposure limits for air contaminants (especially for silica dust) and sound levels, airflow rates in the rooms, personal protective equipment, and blast system design and maintenance. One example regarding ventilation is the German regulation that an abrasive blasting room must not be entered without a breathing mask until the room has had 50 air changes of clean air following the cessation of blasting.[55]

Design Equations and/or Parameters

There are very few design recommendations. The following ones are taken from the literature. The NIOSH reference covers nearly all aspects of how to design an abrasive blasting room.[56]

Table 10.13 gives recommended ventilation rates for Germany.[5]

For these rooms, the air should flow horizontally from one end to the other with a velocity greater than 1.3 m s^{-1}. The necessary airflow rate is of course calculated as the volume times the number of air changes per hour.

According to INRS,[54] the supply air velocity should be 2 m s^{-1}. For vertical ventilation (from ceiling to floor), a flow rate minimum of 0.11 m^3 s^{-1} m^{-2} should be used. The cross-sectional area used in the calculation is the room length times its width. When using horizontal ventilation, the flow rate should be greater than 0.28 m^3 s^{-1} m^{-2}. In this case, the cross-sectional area is equal to the room width times its height. These values should be increased by 40% when very dusty operations are performed, when the generated dust is dangerous, or when the room is extremely long (longer than 15 m). According to the reference, these flow rates will result in a contaminant concentration equal to the concentration before work in approximately 100–120 seconds after blasting has stopped.[54]

According to NIOSH,[56] ventilation should be from ceiling to floor or horizontal, but never from floor to ceiling. Vertical (downdraft) ventilation is preferred to prevent leakage through cracks and holes in the room's walls. The recommendation is to use a flow rate of 0.1 m^3 s^{-1} m^{-2} when using non-silica blasting material and 0.4 m^3 s^{-1} m^{-2} if the abrasive contains silica.

TABLE 10.13 Recommended Air Changes for Abrasive Blasting Rooms[5]

Volume (m^3)	Air changes per hour
10	720
10–20	600
20–30	480
30–50	360
50–200	180
More than 200	120

Horizontal ventilation is acceptable if the flow rate is equal to or greater than that recommended for vertically downward ventilation. A minimum entrance velocity for the supply air of 1.2–1.5 m s^{-1} is also recommended. To provide good visibility during blasting, an air change rate of 50 h^{-1} is also recommended, even though the recommended flow rates result in higher air change rates.

10.4.7.3 Hospital Isolation Rooms

General

Infectious patients present a difficult challenge when trying to protect health care workers. These patients must be isolated from the health care workers as well as from the other patients in the hospital. Special isolation rooms are used for this purpose. These rooms are generally used for isolation of infectious tuberculosis (TB) patients, but could be used for patients with other airborne-transmitted diseases. In the United States, there were 22 812 new cases of tuberculosis in 1993, equal to 8.7 per 100 000 population. This represents a 2.8% increase since 1985, following a 6–7% annual decline from 1981–1984.[57,58] Several studies have documented higher than expected tuberculin skin test (TST) conversion rates in hospital personnel.[59–63] The National Institute for Occupational Safety and Health[64] reports that multiple-drug-resistant (MDR) strains of TB have been reported in 40 states and have caused outbreaks in at least 21 hospitals, with 18–35% of exposed workers having documented TST conversions.

A number of these outbreaks gained national attention in the U.S. in the late 1980s and early 1990s. In response to these outbreaks and the identified risk of TB infection in health care workers, the U.S. Centers for Disease Control and Prevention (CDC) issued a series of guidelines for preventing TB transmission in health care facilities.[65,66] These guidelines include the traditional hierarchy of control for occupational hazards which puts primary emphasis on engineering and work practice controls and secondary emphasis on personal protective equipment. The engineering controls used for TB include isolation of the source, in this case an infective patient, and dilution ventilation. Administrative controls include a written infection control program, training of health care workers, and medical surveillance of at-risk workers. For workers who must enter isolation rooms housing infective patients or who are present during cough-inducing procedures, respiratory protection is necessary.

Principle

Specific ventilation recommendations were included in the CDC guidelines. The recommendations for isolation rooms serve two purposes. The first is dilution of contaminant, in this case droplet nuclei in the isolation room. The second is isolation of the space occupied by known or suspected TB patients from adjacent areas. The CDC[65,66] and Conroy, et al.[67] present recommended operating conditions for isolation rooms. These three conditions are presented in the *Different Forms and Boundaries Relative to Other Types* section below.

The principle behind all of the conditions is to use the direction of airflow to prevent contaminated air from traveling out of the isolation room to other areas of the hospital. The direction of the airflow is controlled by creating and maintaining a pressure differential between the space containing the contaminated air and adjacent areas. Additionally, sufficient air must flow through the space to dilute the contaminant concentration to as low as feasible.

Applicability of Sources

The sources for this type of control are infectious hospital or clinic patients, where the infection can be transmitted through the airborne route. The most common application is for control of the spread of tuberculosis, but it could be used for other airborne infections such as varicella or influenza.[68]

Different Forms and Boundaries Relative to Other Types

The different types of infectious isolation rooms are shown in Fig. 10.104. This figure shows three designs which all use an anteroom. It is possible to have isolation without the use of an anteroom, but that is not the preferred method. The three examples shown here are (1) strong negative pressure in room, balanced pressure in anteroom; (2) balanced or positive pressure in room, negative pressure in anteroom; (3) balanced or negative pressure in room, positive pressure in anteroom.

The CDC-recommended ventilation strategy is condition 1, with negative pressure isolation driven by excess exhaust air in the patient room. This is the most effective strategy for protecting workers and other patients. However, the pressurized and depressurized anteroom strategies (conditions 2 and 3) can provide reasonable isolation as well as airflow protection for certain patients who need it (e.g., immunosuppressed patients). The limitations of these latter two strategies (contamination of anteroom, loss of isolation when doors are opened, reduced dilution airflow) must be understood by the hospital workers for their protection. When protection of the patient is an overriding concern, these two strategies are reasonable alternatives.

Specific Issues

Good preventive maintenance programs are needed at the hospitals. Egg-crate-style flow straighteners or other duct obstructions should not be used because they collect lint and block air flow. Exhaust discharge screens and induct fan motors also accumulate lint and reduce airflow. Leaky pre-filters quickly clog high-efficiency particulate air (HEPA) filters with lint and can negate the excess exhaust capacities in the rooms. Airflow and pressure gauges that are not maintained can deceive the hospital and maintenance staff about the performance of the isolation rooms. Windows that are open or ajar have uncontrollable and detrimental effects on room isolation. Maintenance and ward workers who are well informed about the operation and care of the isolation room systems are necessary for effective control.

Door sweeps were effective in controlling isolation of the rooms as long as negative pressurization of the room existed. Although they are a useful supplement to ventilation controls, they can be damaged so that they do not close effectively. Therefore, the preferred way to test these rooms would be with the door sweep retracted so that door gap velocity could be measured.

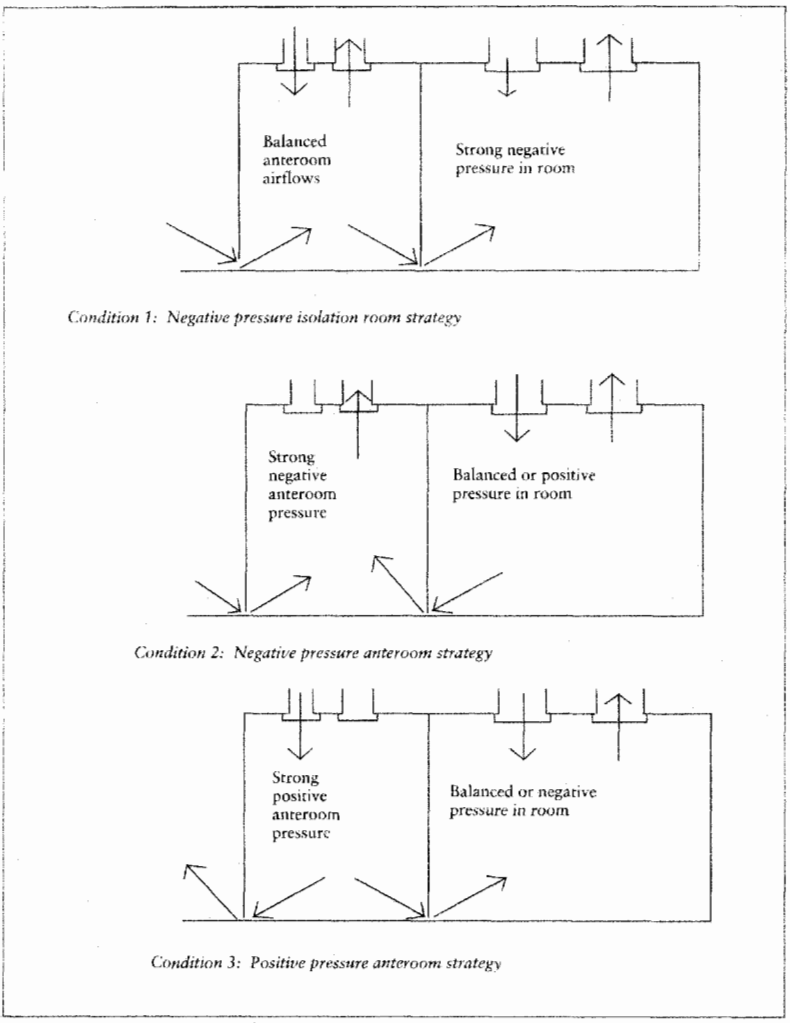

FIGURE 10.104 Isolation strategies using anterooms.

Design Equations and/or Parameters

A dilution ventilation rate of at least 6 air changes per hour (ach) is recommended, with 12 or more ach recommended for new construction or renovation. This may not provide sufficient dilution to allow workers to enter without respiratory protection, but it is considered a feasible dilution rate that will reduce the risk of infection for those workers who must enter the room with respiratory protection. Dilution also reduces the contaminant concentration and therefore the risk when temporary leakage from the room occurs such as when doors are opened or closed.

CDC recommendations for isolation are shown in Table 10.14. Conroy et al.[67] present a modified version of these criteria to take into account different isolation conditions (Table 10.15).

In all cases, it is necessary to supply adequate makeup air while still maintaining appropriate pressure differences. A study of five hospitals in

TABLE 10.14 CDC Isolation Room Criteria [65,66]

Parameter	Criteria
Room excess exhaust	$> 0.024\ m^3\ s^{-1}$
Room door gap velocity	$> 0.5\ m\ s^{-1}$
Room pressure difference	< -0.25 Pa
Room smoke direction	Anteroom or hallway to patient room

Chicago[67] showed that lack of mechanical makeup air resulted in contaminated air reentering the hospital, and therefore these rooms were not isolated from adjacent spaces.

The same study showed that negative pressure rooms with balanced anterooms (condition 1) generally had sufficient negative pressure when there was at least 24 L s^{-1} excess exhaust in the patient room. Rooms using pressurized anterooms (condition 3) provided an excess of supply air to the anteroom, thereby pushing system air into the patient room and into the hall. The advan-

TABLE 10.15 Isolation Room Criteria for Three Different Anteroom Conditions[67]

Condition	Description	Criteria
1	Strong negative pressure in room	Room excess exhaust $> 0.024\ m^3\ s^{-1}$ Room door gap velocity $> 0.5\ m\ s^{-1}$ Room pressure difference < -0.25 Pa Room smoke direction: anteroom to patient room
	Balanced anteroom air flows	Anteroom air flow difference $< 0.024\ m^3\ s^{-1}$ Anteroom door gap velocity $> 0\ m\ s^{-1}$ Anteroom smoke direction: hallway to anteroom
2	Balanced or positive pressure in room	Room excess exhaust from $+0.024\ m^3\ s^{-1}$ to any negative difference Room pressure difference > 0 Pa Room door gap velocity $< 0\ ms^{-1}$ Room smoke direction: patient room to anteroom
	Negative pressure anteroom	Anteroom excess exhaust $> 0.024\ m^3\ s^{-1}$ Anteroom pressure difference < -0.25 Pa Anteroom door gap velocity $> 0.5\ m\ s^{-1}$ Anteroom smoke direction: hallway to anteroom
3	Balanced or negative pressure in room	Room excess exhaust from $-0.024\ m^3\ s^{-1}$ to any positive difference Room pressure difference < -0.25 Pa Room door gap velocity $> 0.5\ ms^{-1}$ Room smoke direction: anteroom to patient room
	Positive pressure anteroom	Anteroom excess exhaust $< -0.024\ m^3\ s^{-1}$ Anteroom pressure difference > 0 Pa Anteroom door gap velocity $< 0\ m\ s^{-1}$ Anteroom smoke direction: anteroom to hallway

tage of this strategy is that it protects the patient from hallway air contaminants. However, most of these rooms failed to provide the recommended dilution airflow rate and necessary excess anteroom supply air. Condition 2, although not observed in this study, uses a strongly depressurized anteroom to induce airflows from both the hallway and the patient room. By design, these rooms fail the CDC guidelines[66] for isolation because of the reversed airflow into the anteroom. However, the rooms provide isolation at the anteroom barrier and protection for the patient from all adjoining spaces. The disadvantage of this strategy is the need to don respiratory protection before entering the anteroom.

10.4.8 Others

10.4.8.1 General

There are many different combinations of supply inlets and exhaust hoods, where these have to be designed together. Some of these are described in some detail. Two examples of using air jets for special purposes are described and the use of wide air curtains is also described.

Many other combinations exist but will not be described here. In small cabins, for storage or work, it is possible to supply and exhaust air in a controlled way to have a defined climate. There are also special sluices, where air is used to rinse the clothes from settled contaminants before a person proceeds to the next, cleaner room. In this case, very high air velocities are used, which could cause discomfort to the person. The residence time for the person usually is less than a couple of minutes and the main objective is to clean the clothes (and sometimes the skin) and therefore the high velocities do not matter.

Glove boxes have been described in Section 10.2.3.6 as systems with only exhaust air. There are glove boxes with both supply and exhaust air openings inside the closed volume (see Section 10.4.6.4) that look and function like the boxes described earlier. The use of supply air directly to the closed volume means that the control of the flow rates must be very accurate. Otherwise the box may be at a higher pressure than the surrounding areas, resulting in leakage of contaminants.

Other examples of combinations include air supply along the center of the ceiling in a room and exhaust along the walls or along the corner between the walls and floor. These are quite similar to abrasive blasting rooms (Section 10.4.7). They have an air supply in the form of a half cylinder, through which the air is evenly distributed over the surface both lengthwise and radially. An alternative is to have the inlets as two or more plane air jets blowing in at some angle downward. The exhaust openings are the same length as the inlet, situated along the room on two sides in the lower part of the walls or in the floor. This combination makes it possible to have quite a large flow rate, at low velocity, through the room.

Combined systems could be designed by using information available in Sections 10.2 and 10.3 and taking into account the mutual influence of the supply and the exhaust system. Some combined systems are described in the literature.[2,3,6]

10.4.8.2 Jets Directed into Hood

One common combination is a jet and an exhaust hood. The jet can be circular or plane and situated around or in front of a (hot) contaminant source. The intention is to direct the contaminant into a basic opening or a receptor hood. Mostly these jets are directed upward into hoods, but may be directed sideways or downward.[6] There is a difference to jets covering openings. When directed into a hood the jet is intended to help the natural flow into the hood and not to act as a shield, even though it sometimes also has this function. Figure 10.105 illustrates two principal ways that air jets could be used to direct contaminants into a hood (see also Section 10.4.5).

Two or more plane jets can be placed above and outside the rim (all sides) of a canopy hood and directed downward. The exhaust flow into the hood makes the down-directed jets turn inward and upward when the jet velocity has slowed down enough to be influenced by the exhaust flow. In many cases, the aim is to diminish the general supply airflow rate into the room and sometimes to use the jets as separators. This method is quite often used on large kitchen hoods to increase their capture efficiency. If the jet is directed toward the front of the fireplace and just reaches the front before turning inward, a high capture efficiency can be achieved.

Another variation is to use a thin air jet around a process or an opening to a process. For welding or soldering on a table, a circular tube with supply holes in the upper side could be used. The circular tube is placed around a fixed welding (soldering) place and blows upward around the welding point into a basic opening hood.

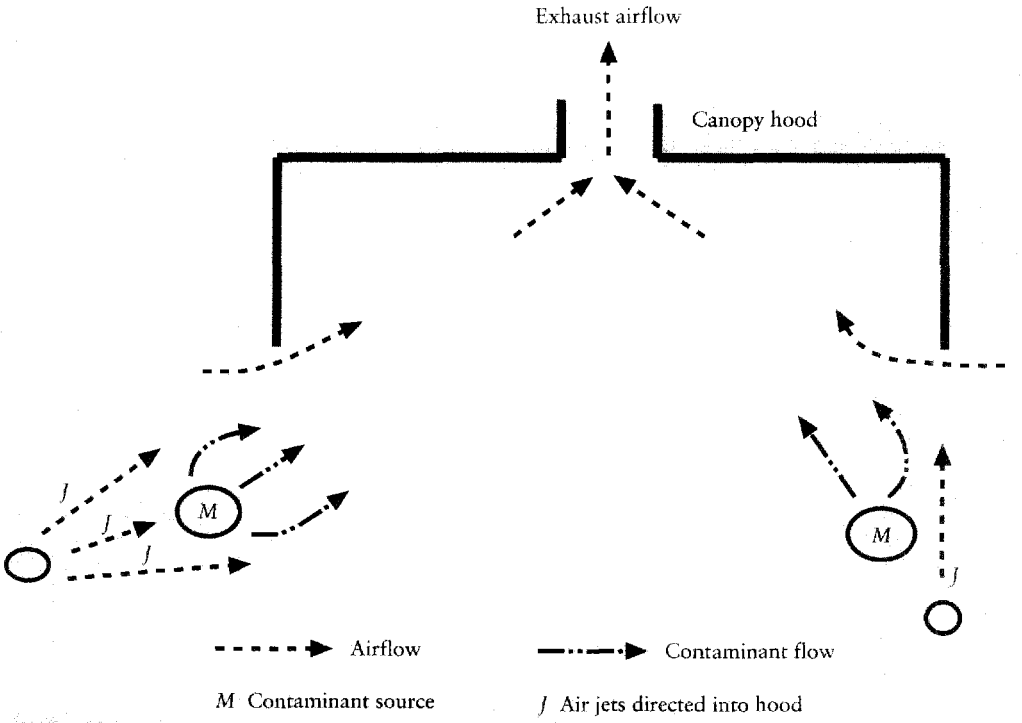

FIGURE 10.105 Two principal ways of using air jets to increase efficiency of a canopy hood.

Such a combination demands careful analysis of distances, air velocities, air directions, and contaminant generation direction and rate. It is necessary to direct the jet into the hood with the correct velocity and flow rate. High velocities or flow rates could result in more spreading of contaminants than without the jet, but the velocity must be large enough to prevent the jet from collapsing into itself due to suction.

For a kitchen hood with a fixed air curtain, good results are possible if the exhaust flow rate is large enough to exhaust the large amounts of contaminants and induced air from the oven. The circular jet around a welding or soldering point is usually too cumbersome to use when working at more than one spot.

10.4.8.3 Vortex Jets

Plane jets could be used to create a closed volume in which a contaminant source could be placed. In some ways, these systems are similar to Aaberg exhaust hoods (Section 10.4.4). The objective is to use plane jets instead of walls around an exhaust opening to create a vortex which enhances the capture efficiency of the exhaust.

Usually a circular exhaust opening is placed in a horizontal surface and directed either downward (airflow upward) or upward (airflow downward). When the exhaust opening is placed in a table and directed upward, it is surrounded by four vertical tubes, which are covered by another horizontal plane. A vertical jet is blown from holes or a slot in each tube. The jets are directed nearly tangential to the circular exhaust and at a certain distance from the opening. This distance depends on the size of the opening and the distance between the two planes. One recommendation is to blow the jet air at 20° from tangential. The four jets blowing at each other create a vortex around the exhaust opening and contain the contaminant inside the vortex.

The exhaust flow rate influences the flow of the jets and some reports recommend a ratio of supply airflow rate to exhaust airflow rate of approximately 0.3. A ratio of 0.2 is unsteady and ratios larger than 0.4 have not been studied. In the cases that have been studied, the exhaust opening was 80 mm in diameter, the distance between the horizontal planes was 750 mm, the tubes were placed in a square with side length equal to 670 mm, and the inward angles of the jets were 10 degrees. This configuration resulted in better capture of hot gases than use of an exhaust system alone.[69]

Figure 10.106 illustrates the vortex jets in combination with a plane exhaust.

10.4.8.4 Wide Air Curtains

Line jets are used as curtains both in bench hoods such as laboratory fume hoods and in large openings such as doors and gates. These jets have to be designed carefully, usually together with an exhaust opening. They must withstand the pressure difference across the opening and their velocities should be of the correct magnitude for the intended purpose. This means that the jet velocity should not be too large, which results in contaminant spreading or high energy consumption. The jet velocity should not be so small that no curtain is achieved. One way to make it easier to enter a department store or pass through an industrial door is to use a wide air curtain instead of a line jet.

From above

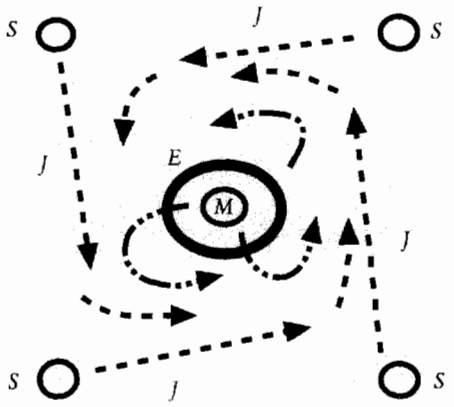

From one side

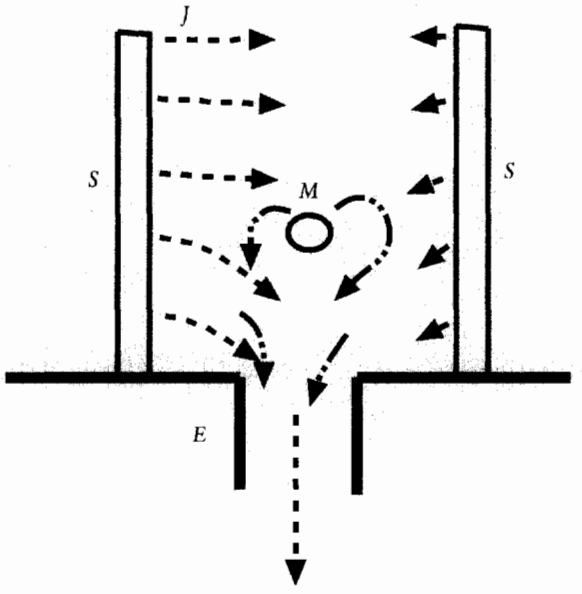

Airflow — Contaminant flow

S Supply tube for air jet — *E* Exhaust opening (in floor)

M Contaminant source — *J* Air jets

FIGURE 10.106 Two principal ways of using air jets to increase efficiency of a canopy hood.

TABLE 10.16 Airflow Rates for Heated Wide Air Curtains (Pressure Difference between Inside and Outside Is 15 Pa)

Door width, m	Airflow rate, $m^3 s^{-1}$	Door height, m	Air velocity in supply opening, $m s^{-1}$
3.0	15	2.2 – 2.5	12
3.5	17.5	2.2 – 2.5	12
4.0	20	2.2 – 2.5	12
4.5	22.5	2.2 – 2.5	12
5.0	25	2.2 – 2.5	12
5.5	27.5	2.2 – 2.5	12
6.0	30	2.2 – 2.5	12

A wide air curtain is usually directed downward from above. The air is blown along the width of the entire door and the jet has a large depth. The exhaust, which could be connected to the inlet (recirculation), is then situated in the floor. The supply air is usually heated, by a heat regenerator, to increase the comfort of people passing through the opening.

The airflow rate should be 4.2 to 5.5 $m^3 s^{-1} m^{-1}$ width of opening, and the exit velocity from the supply side should be 10 to 12 $m s^{-1}$. With an opening height of 6 m, this will result in high-velocity airflow at the head height of passing persons, but this velocity is usually tolerated. The return air opening should be a floor grill with a surface area equal to 1.5 to 2 times the surface area of the supply opening. The recommended size of the floor grill is a depth of 1.5 to 2 m and a width of 3 to 4 m. One recommendation is to operate the system with a supply air temperature that is approximately 5 °C higher than the air temperature of the surrounding spaces.[70]

Another suggestion is to use a supply air temperature equal to 25–30 °C.[5] With an entrance depth of 1.1 m and a pressure difference from outside to inside of 15 Pa (which is equal to a wind velocity of 5 $m s^{-1}$ at a right angle to the door), the values in Table 10.16 are suggested.

These combinations are possible without too detailed design of the combined jet and exhaust, since the wide jet itself will act as a separator between inside and outside and the consequences of an imbalance of supply and exhaust airflow are small. The relative mixing of outside and inside air into the jet is less than for a thin air jet, which also makes it easier to design fan(s) and ducts. The high velocity needed requires a high airflow rate and, with heating, can be expensive to operate.

References

1. H. Azzouz, J. Gosse, and M. Duminil. *Rev. Int. Froid*, vol. 16, no. 1, 1993, 57–66.
2. H. D. Goodfellow. *Advanced Design of Ventilation Systems for Contaminant Control*. Chem. Eng. Monograph 23. Amsterdam: Elsevier, 1985.
3. R. J. Heinsohn. *Industrial Ventilation: Engineering Principles*. New York: John Wiley & Sons, 1991.

4. W. C. L. Hemeon. *Plant and Process Ventilation*. 2nd ed. New York: Industrial Press, 1963.
5. H. Mürmann. *Lufttechnische Anlagen für gewerbliche Betriebe* (Ventilation systems for industrial buildings). 2nd ed. Berlin: Verlagsbuchbehandlung, 1980.
6. T. Hayashi, R. H. Howell, M. Shibata, and K. Tsuji. *Industrial Ventilation and Air Conditioning*. Boca Raton, FL: CRC Press, 1987.
7. H. Schlichting. *Boundary Layer Theory*. 7th ed. New York: McGraw-Hill, 1979.
8. E. Gutmark and I. Wignanski. *Journal of Fluid Mechanics*, vol. 73, 1976, 3–17.
9. C. J. Chen and W. Rodi. *Vertical Turbulent Buoyant Jets: A Review of Experimental Data*. Oxford: Pergamon Press, 1980.
10. W. Tamm. *Kaltetechnik-Klimatisierung*, vol. 18, 1966, 142–144.
11. J. Partyka. *International Journal of Modeling and Simulation*, vol. 15, no. 1, 1995, 14–22.
12. K. Hagström, K. Siren, and A. M. Zhivov. *Calculation Methods for Air Supply Design in Industrial Facilities: Literature Review*. Report B60, Helsinki University of Technology, Espoo: LHVAC, 1999.
13. R. H. Howell, N. Quang Van, and C. E. Smith. *ASHRAE Transactions*, vol. 82, 1976, 191–195.
14. American Conference of Governmental Industrial Hygienists *Industrial Ventilation: A Manual of Recommended Practice*. 22nd Ed. Cincinnati, OH: ACGIH, 1995.
15. D. J. Huebener and R. T. Hughes. *American Industrial Hygiene Association Journal*, vol. 46, 1985, 262–267.
16. M. K. Klein. *American Industrial Hygiene Association Journal*, vol. 48, 1987, 238–246.
17. E. J. Hollis and B. Fletcher. *A Literature Review of Push-Pull Ventilation*. Report IR/I/VE/94/5. Sheffield, UK: Health and Safety Executives, 1994.
18. M. R. Flynn, K. Ahn, and C. T. Miller. *Annals of Occupational Hygiene*. vol. 39, 1995, 573.
19. J. F. Ege and L. Silverman. *Heating and Ventilating*, vol. 10, 1950, 73–78.
20. A. Verhoff. *The Two-Dimensional Turbulent Wall Jet with and without an External Stream*. Report 626. Princeton, NJ: Princeton University, 1963.
21. B. E. Launder and W. Rodi. *Progress in Aerospace Science*, vol. 19, 1981, 81–128.
22. M. Robinson and D. B. Ingham. *Annals of Occupational Hygiene*, vol. 40, 1996, 293–310.
23. W. De Marcus and J. W. Thomas. *U.S. Atomic Commission*, Report ORNL No. 1413. 1952.
24. M. Robinson and D. B. Ingham. *Annals of Occupational Hygiene*, vol. 40, 1996, 693–704.
25. G. R. Hunt and D. B. Ingham. *Math. Eng. Ind.*, vol. 4, no. 3, 1993, 227–247.
26. G. R. Hunt and D. B. Ingham, *Annals of Occupational Hygiene*, vol. 40, no. 2, 1996 171–196.
27. R. Braconnier, D. Thiebaut, G. Aubertin, J. C. Serieys, and J. P Muller. In *Ventilation '85: Proceedings of the 1st International Symposium on Ventilation for Contaminant Control, October 1–3, 1985, Canada* (ed. H. D. Goodfellow). New York: Elsevier, 1986, pp. 743–753.
28. L. G. Pedersen. REEXS—Reinforced exhaust system. Ph.D. thesis, Danish Technological Institute, 1991 (in Danish with English summary).
29. L. G. Pedersen. Private communication. Aarhus: Danish Technological Institute, 1993.
30. B. Fletcher and C. J. Saunders. *Annals of Occupational Hygiene*, vol. 37, 1993, 15–24.
31. E. J. Hollis. *Investigation of an Aaberg Workbench*. HSL Project Report IR/I/VE/95/2. 1995.
32. J. Rydberg and E. Kulmar. *Swedish VVS*, nr. 3, 1947.
33. C. E. Hyldgard. In *Roomvent '87: International Conference on Air Distribution in Ventilated Spaces*. Stockholm, 1987.
34. P. Högstedt. In *Roomvent '87: International Conference on Air Distribution in Ventilated Spaces*. Stockholm, 1987.
35. L. G. Pedersen and P. V. Nielsen. In *Ventilation '91: Proceedings of the 3rd International Symposium on Ventilation for Contaminant Control, September 16–20, 1991, Cincinnati, Ohio, USA* (eds. R. T. Hughes, H. D. Goodfellow, and G. S. Rajhans). Cincinnati, OH: American Conference of Governmental Industrial Hygienists, 1993, pp. 203–208.
36. G. R. Hunt and D. B. Ingham. *Annals of Occupational Hygiene*, vol. 36, 1992, 455–476.
37. D. B. Ingham and M. A. Kelmanson. *Boundary Integral Equation Analysis of Singular, Potential and Biharmonic Problems*. Heidelberg: Springer Verlag, 1994.
38. G. R. Hunt. The fluid mechanics of the Aaberg exhaust hood. Ph.D. thesis, University of Leeds, 1994.
39. I. Kulmala. *Jet Enhanced Exhaust Hood*. Report VALB 317, VTT 1998, FIN-33101. Tampere, Finland, 1998.
40. K. Tsuji, I. Fukuhara, Y. Nakamura, and M. Mizuno. In *Ventilation '97: Proceedings of the 5th International Symposium on Ventilation for Contaminant Control, held in Ottawa,*

Ontario, Canada, September 14–17, 1997 (eds. H. Goodfellow and E. Tähti). Ottawa, Ontario: Canadian Environment Industry Association, 1997, pp. 309–318.
41. K. Tsuji, Y. Nakamura, and M. Mizuno. *Transactions of the Society of Heating, Air-Conditioning and Sanitary Engineers of Japan*, no. 45, 1991, 85–94.
42. H. Komine, K. Tsuji, and Y. Mori. *Advances in the Prevention of Occupational Respiratory Diseases*, New York: Elsevier, 1998, pp. 1120–1126.
43. K. Heinonen, I. Kulmala, and A. Säämänen. *American Industrial Hygiene Association Journal*, vol. 57, 1996, 356–364.
44. L. Lind and I. Aourell. *Utformning av utsugningskåpor i storkök och restauranger* (Design of exhaust hoods for large kitchens and restaurants). ASF-projekt 76/198 and 78/171. Stockholm: Reports K-Konsult, 1978, 1979.
45. N. F. Petersson and P. Vikström. *Punktutsug för svetsarbetsplats* (Local exhaust for a welding workplace). ASF 80/282. Stockholm: Report K-Konsult, 1981.
46. Centers for Disease Control and Prevention and National Institutes of Health. *Primary Containment of Biohazards: Selection, Installation and Use of Biological Safety Cabinets*. Washington, DC: U.S. Department of Health and Human Services, 1995 (available on http://www.niehs.nih.gov/odhsb/biosafe/bsc/bsc.htm).
47. C. G. Simons. *ASHRAE Journal*. August 1991, 31–34.
48. R. N. Mitchell, F. M. Toca, and J. P. Ortiz. *Performance of Auxiliary Air Hoods*. LA-DC-11964. Los Alamos, NM, 1971.
49. G. T. Saunders. *Laboratory Fume Hoods: A User's Manual*. New York: John Wiley & Sons, 1993.
50. F. H. Fuller. *HPAC*, May 1990, 77–80.
51. W. F. Albern, F. Darling and L. R. Farmer. *ASHRAE Journal*, March 1988, 26–30.
52. W. A. Burgess, M. J. Ellenbecker, and R. D. Treitman. *Ventilation for Control of the Work Environment*. New York: John Wiley & Sons, 1989.
53. R. P. Donovan. *Particle Control for Semiconductor Manufacturing*. New York: M. Dekker, 1990.
54. INRS. *Cahiers de notes documentaires—Hygiène et sécurité du travail*, no. 154, 1994, 5–19.
55. W. Pfeiffer. *Staub—Reinhaltung der Luft*, vol. 46, no. 9, 1986, 390–393.
56. J. L. Goodier, E. Boudreau, G. Coletta, and R. Lucas. *Industrial Health and Safety Criteria for Abrasive Blast Cleaning Operations*. HEW Publication no. (NIOSH) 75–122. NIOSH (Arthur D. Little), 1974.
57. Centers for Disease Control and Prevention. Expanded tuberculosis surveillance and tuberculosis morbidity—United States, 1994, *MMWR*, vol. 43, 1994, 361–366.
58. American Thoracic Society. *American Review of Respiratory Disease*, 1992, vol. 146, 1623–1633.
59. A. Catanzaro. *American Review of Respiratory Disease*. vol. 125, 1982, 559–562.
60. S. W. Dooley, M. E. Villarino, M. Lawrence, L. Salinas, S. Amil, J. V. Rullan, W. R. Jarvis, A. B. Bloch, and G. M. Cauthen. *JAMA*, vol. 267, no. 19, 1992, 2632–2634.
61. N. J. Ehrenkranz and J. L. Kicklighter. *Annals of Internal Medicine*, vol. 77, no. 3, 1972, 377–382.
62. C. E. Haley, R. C. McDonald, L. Rossi, W. D. Jones, R. W. Haley, and J. P. Luby. *Epidemiology*, vol. 10, no. 5, 1989, 204–210.
63. Centers for Disease Control. Nosocomial transmission of multidrug-resistant tuberculosis among HIV-infected persons—Florida and New York, 1988–1991, *MMWR*, vol. 40, no. 34, 1991, 585–591.
64. National Institute for Occupational Safety and Health. *Protect Yourself against Tuberculosis: A Respiratory Protection Guide for Health Care Workers*. Washington, DC: U.S. Department of Health and Human Services, 1995.
65. Centers for Disease Control and Prevention. Draft guidelines for preventing the transmission of tuberculosis in health-care facilities, second edition: Notice of comment period, *Federal Register*, vol. 58, no. 195 (October 12, 1993), 52809–52854.
66. Centers for Disease Control and Prevention. Guidelines for preventing the transmission of *Mycobacterium tuberculosis* in health-care facilities, 1994, *MMWR*, vol. 43 (RR-13), 1994, 1-132.
67. L. M. Conroy, J. E. Franke, J. Dimos, J. A. Vittallo, and S. C. Lee. In *Ventilation '97: Proceedings of the 5th International Symposium on Ventilation for Contaminant Control*,

Ottawa, Ontario, Canada, September 14–17, 1997 (eds. H. Goodfellow and E. Tähti). Ottawa, Ontario: Canadian Environment Industry Association, 1997, pp. 497–508.
68. K. E. Gill. *Heating, Piping and Air Conditioning*, February 1994, 45–48, 51–52, 71.
69. S. H. Yarnaguchi, H. Ochi, S. Matsui, and Y. Ishiguro. In *Ventilation '91: Proceedings of the 3rd International Symposium on Ventilation for Contaminant Control, September 16–20, 1991, Cincinnati, Ohio, USA* (eds. R. T. Hughes, H. D. Goodfellow, and G. S. Rajhans). Cincinnati, OH: American Conference of Governmental Industrial Hygienists. 1993, pp. 87–94.
70. P.-O. Danielsson. *Swedish VVS*, no. 7, 1972, pp. 21–26.

10.5 EVALUATION OF LOCAL VENTILATION SYSTEMS

10.5.1 General

Different available measurement instruments and evaluation methods are described in Chapter 12. Some specific methods to evaluate local ventilation systems are described in this section. All local ventilation systems should be evaluated regularly. The evaluation procedures can be divided into detailed and simple, as well as direct and indirect, procedures. The detailed procedures need special instruments and competence, whereas it should be possible to use the simple procedures every day. Since the simple procedures do not measure directly the performance of the exhaust, it is usually necessary to calibrate a simple procedure by using a detailed procedure.[1]

The evaluation methods could be direct, e.g., measuring a containment index, or indirect, e.g., measuring pressure loss or velocity distribution. The direct methods are used to measure the performance of a hood or an inlet during periodic preventive maintenance. Indirect methods are used for verifying or checking on a daily basis (routine checks). How often each method is used depends on the availability of instrumentation and qualified personnel, since direct measurement of a hood's performance can be both expensive and difficult. On the other hand, indirect methods are usually easier to use and can sometimes include inexpensive, continuously monitoring instruments (pressure gauges or velocity indicators).

For some hood types, measurements usually seen as indirect method, are used to measure the hood's performance to determine regulatory compliance. For example, regulations specify minimum and maximum face velocities for laboratory fume hoods and static pressure (negative) inside enclosed hoods. Continuously monitoring instruments can be connected to alarms that sound when the measurement is outside the specified limits.

Capture efficiency is the fraction of generated contaminant that is directly captured by the hood. Measurement of capture efficiency involves measuring concentration of process-generated contaminant or a tracer material. Using process-generated contaminant requires use of instruments suited to each specific contaminant and its conditions (temperature, pressure, concentration, form, etc.). In order to facilitate these measurements, a tracer is often substituted for the process-generated contaminant. The tracer is usually a gas (sulfur hexafluoride, nitrous oxide, helium, or similar), but an aerosol (particles) can also be used (potassium iodide, polystyrene particles, microbiological particles, etc.). The chosen tracer should be as similar to the real contaminant as possible, but at the same time should

be non-toxic, easily and inexpensively measured, and have a low or undetectable background concentration.

Since it is nearly impossible to find an ideal tracer, all measurements made with tracers deviate from measurements made with real contaminants. The efficiency methods, when using real contaminants, are as near to direct measurement of function as is possible. Use of tracers can also give direct measurements, but the conditions of the tracer may differ so much from the real contaminant that these measurements must be seen as indirect.

A simple evaluation can be done by checking the airflow rate into the opening, presuming that the source characteristics, the placement of the exhaust, and other parameters (crossdraft, work routines, supply airflow rate, etc.) have not changed since the detailed evaluation was done. Naturally, it is necessary initially to perform the simple evaluation at the same time that the detailed evaluation is performed. The flow rate into the exhaust opening can be measured in many different ways. These include pressure drop across the opening, flow measurement in the duct downstream of the hood, measuring air velocities in the opening plane, etc. Handbooks and textbooks on ventilation[2,3] and ACGIH Industrial Ventilation Chapter 9[4] have descriptions of different flow-measuring devices.

Since the static pressure loss for a hood is dependent on form and flow rate it can be used alone to monitor the flow rate into the hood. If the flow rate and the pressure loss were measured at the same time as the efficiency, the pressure loss can be used for monitoring hood performance. These methods are also described in the literature mentioned above.

Another simple way to evaluate the exhaust is to use smoke to visualize the air streamlines. It is sometimes possible to see how far an exhaust reaches by observing smoke movement when it is generated at different distances from the hood opening. This is better achieved by using the source (if it generates particles or hot gases) and a suitably placed lamp to look directly at the capture of the contaminants. Some gases can also be visualized, either because of density differences or because of differences in refractive index or light absorption.[5]

In theory it should be possible to calculate the capture efficiency without measurements. There have been some attempts to do that, using CFD, but the problems with air movements and source characteristics have shown that it will be a long time before it is possible to calculate hood capture efficiency in the design stage.

Different methods to measure efficiency are described in Section 10.5.2. Methods to visualize contaminants and airflow are described in Section 10.5.3.

10.5.2 Efficiency Measurements

Performance tests for local ventilation systems are classified in the following three ways: type, commissioning, and in-use tests.

The procedures and requirements for the type and commissioning tests are covered in national and international standards—for example, for laboratory fume cupboards, welding fumes, and kitchen hoods.

Type testing is carried out in special laboratories under controlled conditions using tracer methods. The methods used provide a means of comparing the efficiencies of various local exhausts. Type testing is a method for comparing the efficiencies of various products. It also provides a method for checking the design of airflow rates for general ventilation, and the development of individual products.

The commissioning tests are typically performed before a local ventilation system is put into use; the purpose is to confirm that the design conditions have been achieved. Hence, commissioning tests apply to methods used in type testing, but in a simple and modified way. In-use tests concentrate on the exposure effects of a local ventilation system.

For example, the type test of a laboratory fume hood includes determination of the concentration at various points across the opening of the hood by using various tracer source locations inside the hood. The commissioning test could concentrate on the measurements taken at one point in the opening with one source location.

In-use tests deal with the concentration measurements in the worker's breathing zone for various hood applications. The performance tests presented here are typically in-use tests, where normal work procedures are ongoing.

The initial performance test for all local ventilation systems is a smoke test, which provides easy airflow visualization between the source and the hood. It helps to identify, with little effort, the main features of airflow patterns. Such a test, recorded by a video camera, allows performance comparisons to be made before and after improvements. Real contaminant or tracer gas measurements are necessary in the case of more detailed testing.

For exterior hoods, the measurement of capture velocity provides a quick check of the ideal design conditions. However, it must be remembered that capture velocity is not a direct measure of the ability of an exterior hood to provide personnel protection. Other efficiency measures are required in order to evaluate its performance in practice. The following two efficiency measurements could be useful: capture efficiency and occupational hygiene efficiency. These measures complement each other.

Contaminants captured by an exterior hood can cause exposure if allowed to enter the hood after passing through the operator's breathing zone. The capture efficiency describes the percentage of the generated contaminant that is captured directly by the hood. Occupational hygiene efficiency describes the effect of the use of the hood on the operator's exposure to the contaminant. The occupational hygiene efficiency is performed with the exterior hood working and not working. For example, many wood-processing machines produce large volumes of wood chips and dust and cannot operate without the exhaust hoods in use. With very toxic contaminants, it is essential to work with the hood exhaust operating at all times.

For enclosures, velocity measurements, in the plane of the opening, offer a quick check on the design conditions. However, the opening velocity is not a direct measure of the ability of an enclosure to provide personnel protection. Other measures of efficiency are required and depend on use of the enclosure. In the case of safety cabinets and laboratory hoods, allowance factors for protection and leakage are applied to ensure complete safety when in use.

For exterior hoods and enclosures, the measurement of the breathing zone concentration provides a method of comparing the effects of changes in the supply and exhaust airflow rates.

10.5.2.1 Determination of Capture Velocity

The capture velocity of a hood is defined as the air velocity created by the hood at the point of contaminant generation. The hood must generate a capture velocity sufficient to overcome opposing air currents and transport the contaminant to the hood. For enclosing hoods, capture velocity is the velocity at the hood opening. In this case, the velocity must be sufficient to keep the contaminant in the hood. In practice, hood shape and the influence of cross-drafts on the measured capture velocity have to be considered. All three velocity components should be measured and used to calculate the magnitude and direction of the total velocity. Other methods used, not as good as the previous one, are to measure the velocity with a directional velocity sensor towards the hood or to measure the net velocity by an omnidirectional velocity sensor. In the last method the main airflow direction should be viewed and evaluated by means of a smoke test (see Sections 10.2.1 and 10.2.2.1).

10.5.2.2 Determination of Capture Efficiency

Capture efficiency of the hood (α_c) is defined as the ratio of the directly captured contaminant to the amount of generated contaminant.[6–9] The directly captured contaminant is that part of the emission captured directly into the hood, and does not include that part of the emission captured after dilution into the ambient room air. The room mass balance is determined using the conditions and expressions given in Fig. 10.107 and assuming the room air is well mixed:[10,11]

$$q_{mg} + (q_{vs} + q_{vex})C_o = q_{vs}C_r + q_{vex}C_e \ , \tag{10.129}$$

where

q_{vs} = ventilation flow rate into and out of the space ($m^3\ s^{-1}$)
q_{vex} = rate of extract from the hood and the associated infiltration ($m^3\ s^{-1}$)
q_{mg} = contaminant generated ($mg\ s^{-1}$)
C_r = pollutant concentration in room ($mg\ m^{-3}$)
C_o = pollutant concentration outdoors ($mg\ m^{-3}$)
C_e = pollutant concentration in the extract. ($mg\ m^{-3}$)

The mass balance of the hood is given by

$$q_{mg} + (q_{vex} + q_{vl})C_r = q_{vex}C_e + q_{vl}C_e \ , \tag{10.130}$$

where q_{vl} is the escaped flow rate of the exhaust ($m^3\ s^{-1}$).

By assuming the outdoor concentration is zero, Eq. (10.129) can be expressed as

$$q_{mg} = q_{vex}(C_e - C_r) + (q_{vs} + q_{vex})C_r \ . \tag{10.131}$$

The right-hand side of Eq. (10.131) can be looked at as two parts: $q_{vex}(C_e - C_r)$ is the directly captured part of the emission and $(q_{vs} + q_{vex})C_r$ is the part of the emissions escaping into the room.

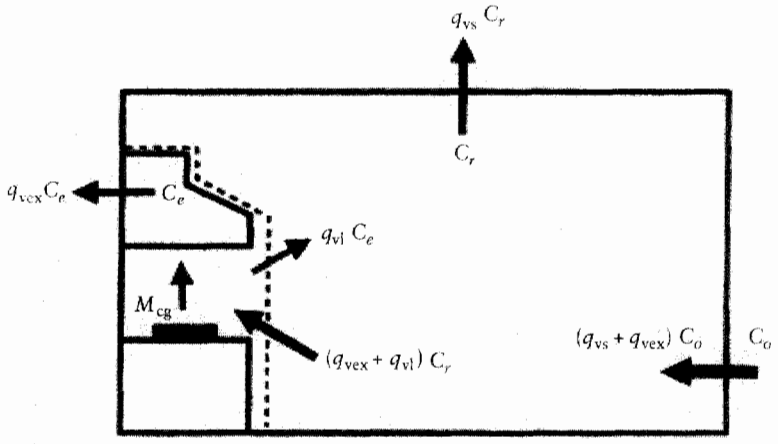

FIGURE 10.107 Room mass balance boundaries for a contaminant source, local exhaust hood, and general ventilation.[11]

q_{vs} = ventilation flow rate into and out of the space, $m^3\ s^{-1}$
q_{vl} = spillage into the space from the hood, $m^3\ s^{-1}$
q_{vex} = rate of extract from the hood and the associated infiltration, $m^3\ s^{-1}$
M_{cg} = contaminant generated, mg s^{-1} (equal to q_{mg} in the equations)
C_r = pollutant concentration in the room, mg m^{-3}
C_o = pollutant concentration outdoors, mg m^{-3}
C_e = pollutant concentration in the extract, mg m^{-3}

Capture efficiency is then defined as

$$\alpha_c = q_{vex}(C_e - C_r)/q_{mg}\ , \tag{10.132}$$

and the emission escaping into the room is given by

$$(1-\alpha_c)q_{mg} = (q_{vs}+q_{vex})C_r\ . \tag{10.133}$$

According to Eq. (10.130), Eq. (10.133) can also be expressed as

$$(1-\alpha_c)q_{mg} = q_{vl}(C_e - C_r)\ . \tag{10.134}$$

Equation (10.133) is more useful than Eq. (10.134), where the escaped airflow q_{vl} is difficult to measure.

At least three factors must be considered when using Eq. (10.132). The first is that the room air is seldom well mixed; the second is that the emission rate is usually unknown; and the third is that measurement of q_{vs} is often very difficult, especially in spaces where a mixture of mechanical and natural ventilation is used. If the room air is poorly mixed, a sampling strategy is needed in order to determine the room air concentration (C_r). There exist different strategies for this, and two are as follows:

The contaminant concentration measurement in the general ventilation exhaust will provide the best average value for room air concentration (C_r).

The room air concentration (C_r) can be determined by measuring the concentration for a grid of points around the room.

The best way to determine the capture efficiency is to use the same contaminants that are encountered in practical applications. The usually unknown emission rate in Eq. (10.132) can be evaluated by the use of different models especially in the case of evaporation, or by weighing the waste material or by measuring the contaminant concentrations and airflow rates in all exhaust ducts in the space and using Eq. (10.131) to calculate q_{mg}.

Sometimes the real contaminant cannot be used for the determination of the capture efficiency, for example, if there is no suitable analysis method available for the real contaminant, or if the analysis method is too expensive. In these cases, tracer gases can be used (see Section 10.2.3.3).

In the case of gaseous contaminants, the tracer gas is selected to simulate as well as possible the properties (density, temperature) and momentum of the real contaminant. It is essential to ensure that the tracers are nontoxic, chemically nonreactive, nonadsorptive on indoor surfaces, and inexpensive. The mixing of the tracer with the actual gaseous contaminant before its release or the release of the tracer with a density near that of the air will improve the validity of the simulation. With tracers, the most difficult task in practice is the relationship of the discharge between the tracer and the real contaminant. Case-by-case techniques to release the tracer are necessary in practice. With tracer gases, the procedure for capture efficiency is described in detail in the European Standard.[12] The tracer gas concentrations are measured in the exhaust duct for two release locations as illustrated in Fig. 10.108.

First, the tracer is released directly into the exhaust duct (Fig. 10.108*a*). Second, the tracer is released with the same flow rate at the contaminant-generation point(s) (Fig. 10.108*b*). The capture efficiency (α_c) is calculated using Eq. (10.132) by taking into account that

$$q_{mg} = q_{vex} C_{ref} \qquad (10.135)$$
$$\alpha_c = (C_e - C_r)/C_{ref},$$

where C_e is the tracer concentration (mg m^{-3}) in the duct, when released at the source release point(s); C_{ref} is the tracer concentration (mg m^{-3}) in the duct, when released directly into the exhaust duct; and C_r is the tracer concentration (mg m^{-3}) in the room, when released at the source release point(s).

The contaminant concentration is measured by a direct reading instrument or by some collecting method (for instance charcoal tubes). Due to the negative pressure in the exhaust duct, powerful sampling pumps are required in order to extract samples from the duct. If the concentration is uniformly distributed in the duct, one measurement point in the duct is sufficient. If the distribution of the concentration in the duct is not uniform, a survey of the concentration distribution and the corresponding duct velocities and cross-sectional areas are required. Various studies[13] have shown that distances ranging from 4 to 50 duct diameters are required, depending on the number of fittings, to ensure complete mixing in the duct.

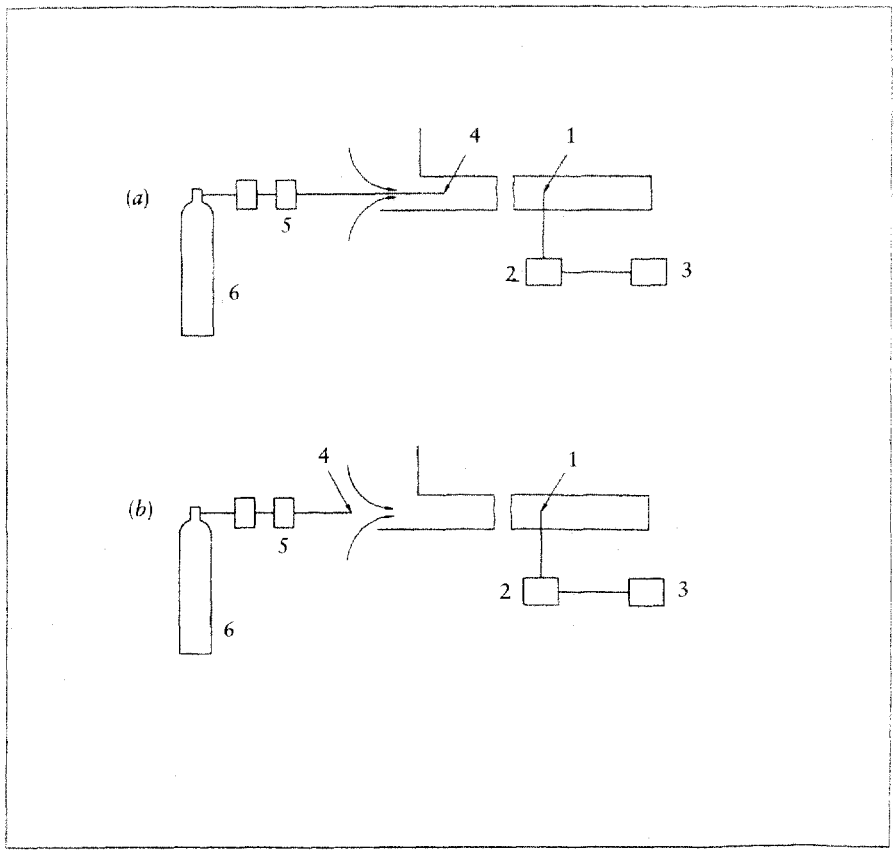

FIGURE 10.108 The procedure to measure the capture efficiency by the tracer gas method. (*a*) The measurement of the reference concentration in the duct, when the tracer is released directly into the duct. (*b*) The measurement of the concentration in the duct, when the tracer is released from the source. *1* = sampling point, *2* = pump, *3* = analyzer, *4* = injection of tracer, *5* = tracer gas flow meter, *6* = tracer gas cylinder.

With particles, the contaminant concentration in the duct is determined by isokinetic sampling with subsequent laboratory analysis use of a calibrated direct reading instrument. If the concentration distribution in the duct is uneven, a complete survey of the concentration distribution with the corresponding duct velocities and cross-sectional area is required. National and ISO standards[14,15] provide information on isokinetic sampling and velocity measurements. In the case of particles, the airborne emission differs from the total emission, for example in the case of granular particulate. The contaminant settling on surfaces depends on particle distribution, airflow rates, direction in the space, electrical properties of the surfaces and the material, and the amount of moisture or grease in the environment.

Test bench methods for machines not too large for test cabins have been developed in order to obtain comparative results. In the case of particles, the tracer gas describes well the behavior of aerodynamic diameter particles less than 5 to 10 μm.[9] For larger particles, correction factors should be used to modify the efficiency results obtained using the tracer gas technique.

10.5.2.3 Determination of Occupational Hygiene Efficiency

The occupational hygiene efficiency (η_h) is defined as the ratio of the contaminant concentrations in the operator's breathing zone (C_{br}) with the exhaust hood operating and not operating:

$$\eta_h = (C_{br}(\text{on}) - C_0)/(C_{br}(\text{off}) - C_o), \tag{10.136}$$

where C_o is the background concentration of the room air contaminant.

This gives a direct measure of the benefits obtained by the hood. In practice, the best way to determine the occupational hygiene efficiency is to measure the actual concentrations in the operator's breathing zone for those two cases. A tracer can also be used with the limitations described above.

10.5.2.4 Determination of the Opening Velocity

The airflow direction is evaluated by a smoke test before commencing velocity measurement at the openings. The velocity is then measured at several points. The airflow direction in each opening should be determined by a smoke test. Rotation of belts and machine parts inside the enclosure generates strong air currents that may escape from the enclosure openings near these moving parts while the other openings may exhibit inward airflow.

10.5.2.5 Determination of Protection Factor (PF)

Different protection factors have been defined.[16] One method is to define it as the ratio of the concentration of a contaminant in the exhaust duct (C_e) to the concentration in the breathing zone (C_{br}) of a person standing in front of the enclosure, for example, a laboratory fume hood:

$$\text{PF} = C_e/C_{br}, \tag{10.137}$$

where C_e and C_{br} are expressed in mg m^{-3}. This approach is useful and easy to measure. By using this method, the determined protection factors may be quite high. For carcinogenic and highly toxic materials, protection factors of 10 000 are common. Protection factors (F) based on the ratio of the breathing zone concentration (C_{br}) to the release rate of the contaminant (q_{mg}) have been used. To obtain convenient numbers for the protection factor, negative logarithms are used:

$$F = -\log(C_{br}/q_{mg}), \tag{10.138}$$

where C_{br} is expressed in mg m^{-3} and q_{mg} is in mg s^{-1}.

Protection factors based on the ratio of the breathing zone concentration to the concentration inside the enclosure have been defined. Without complete mixing of air inside the enclosure, considerable variations in the concentration are expected. The best evaluation for enclosure concentration without complete mixing is the measurement of the concentration in the exhaust duct.

10.5.2.6 Determination of the Efficiency of Local Supply Air

Sometimes local supply air is combined with exterior hoods to protect the worker from escaping contaminants. Measuring the breathing zone concentra-

tion as a percentage of the concentration in the exhaust airflow, with a constant release rate of contaminant or tracer, provides a good method of comparing the effects due to changes in the local supply and exhaust airflow rates.

The dilution effect of the local air supply can be studied by measuring the concentrations in the breathing zone with and without the use of the local supply air.

To determine if the local supply air reaches the breathing zone, a tracer gas is used. The tracer concentrations at various heights below the supply unit are recorded as a percentage of the supply duct tracer concentration. This provides information on the degree of mixing taking place between the supply and ambient air.

10.5.3 Other Methods

10.5.3.1 General

In order to control the movements of contaminants it is useful to be able to see how both the contaminant and the induced airflows move. A number of flow visualization methods have been developed; some are more suitable for laboratory research applications whereas others are quite widely used in industrial situations. We are primarily interested in this latter category. The methods involve releasing a tracer (for example gas, aerosol, or heat) and making visible its path. While in most cases the methods are subjective, their use is invaluable. Ideally the tracer should be nontoxic, nonirritating, inexpensive, and highly visible at low concentrations. The system should be easily portable, self-contained, easy to use, and be controllable.

A review of flow visualization techniques suitable for use in hospital laboratories was carried out several years ago.[17]

Chapter 12 contains more on flow visualization and measurement techniques.

10.5.3.2 Smoke Tubes

Probably the most widely used method for visualizing air movement in the workplace is the smoke tube. They are commercially available and consist of a sealed glass tube that contains a granular medium. Sulfuric acid or titanium tetrachloride is absorbed into the inert granules. To use, the ends of the tube are broken off and air is driven through the tube by means of an aspirator, producing a cloud of white acid fume. A relatively small quantity of smoke is emitted in a fine filament that can be directed to areas of specific interest. Air is often passed through the smoke tube from a small rubber bulb, but a continuous filament of smoke can be generated by using a small positive-pressure pump. The method has several advantages: it is inexpensive, portable, and does not require a power source, and the smoke output is controllable and can be seen without auxiliary lighting. The drawbacks are that the smoke is corrosive and an irritant, although it is generated in small amounts and is not usually a problem. (A battery-powered device, that uses small oil-filled tubes to generate an oil mist has been marketed, but from personal experience its operation is not entirely satisfactory.) Acetic acid smoke tubes are available and

are somewhat less corrosive and irritating; however, they cost approximately twice what titanium tetrachloride tubes cost.

10.5.3.3 Smoke Pellets

Smoke pellets are produced in a range of sizes and are commonly used for the testing of household flues and chimneys. The pellet is ignited and will burn for about 10 seconds producing a dense white smoke. Because this is a combustion process there are obvious restrictions on its use (nonflammable atmospheres, nonflammable surfaces, etc.). In addition the smoke is buoyant because of the heat generated. The smoke can also be an irritant and/or toxic. The production of smoke cannot be controlled, but pellets are inexpensive, easy to use, and readily available, and the smoke is produced in sufficient quantities to make them useful in the evaluation, for example, of fume cupboards and booths.

10.5.3.4 Smoke Generators

These generators vaporize a liquid (oil/mineral oil or glycol and water), which then condenses into a fine aerosol on contact with cooler air. The amount of smoke produced should be controllable by the liquid feed rate and the temperature of the heating chamber, but in practice the output is not easy to control. They will, however, produce a large amount of smoke over a long period. The generators are relatively expensive (several hundred ECUs), are bulky, are not generally portable, and require an electrical connection.

10.5.3.5 Titanium Tetrachloride

This is a clear liquid that vaporizes and, on contact with damp air, combines with water to produce a dense acid mist. Titanium tetrachloride can be painted on to surfaces, such as fume cupboard sills, from which it will evaporate over a period of several seconds showing the airflow patterns close to the surface. (Airflow patterns close to a surface could also be visualized by fastening short filaments of wool or cotton to the surface). Titanium tetrachloride can also be used, when soaked onto a cotton swab, in a similar way to a smoke tube. It is a simple and inexpensive method but the production of smoke, which is toxic and corrosive, is uncontrollable.

10.5.3.6 Fog

Kennedy[17] describes a method using an ultrasonic nebulizer to generate a fog of water droplets which is used in the same way as smoke to visualize airflows. Several types of nebulizers are available but they require an electrical connection and are not hand-held. Food dye can be added to the water to produce colored fog. The nebulizers are expensive (about 1500 ECU) but have negligible operating costs. Although the amount of smoke produced is small, it is nontoxic and nonirritating.

10.5.3.7 Bubbles

Bubble generators are commercially available which will produce small neutrally buoyant soap bubbles for use in the visualization of the general flow patterns in rooms. The bubbles are about 3 or 4 mm in diameter and are filled with a helium/air mixture. In practice, it is difficult to make the bubbles truly

neutrally buoyant and a strong light source is required to view them because of the limited forward scatter of light from the bubbles. They give a good qualitative view of the general flow and are both nonirritating and nontoxic. An investigation by Kerho and Bragg[18] reports on the accuracy of helium bubbles as flow tracers.

10.5.3.8 The Dust or Tyndall Lamp

The above methods use a tracer introduced into a flow to visualize the movement of the air. The dust lamp uses a parallel beam of light to illuminate fine particles normally invisible under diffuse lighting conditions. The fine particles scatter light most intensely in a forward direction (the "Tyndall" effect) and by looking toward the parallel beam at an angle of 5–15 degrees from the centerline, the dust cloud can be seen clearly. The fine particulate cloud will appear as a hazy smoke cloud. Observation of very low-concentration clouds or small leaks may require some suppression of the ambient background light but, although strong sunlight or other sources of bright light should be suppressed, other clouds should be made visible under normal lighting conditions. Dust lamps are commercially available, relatively inexpensive, and, being battery powered, are quite portable. The technique is easy to use and gives good results. Further information on the theory and use of the dust lamp can be found in HSE.[19]

10.5.3.9 Infrared Photography

The movement of gases and vapors is more difficult to visualize than that of particulates. However, most gases and vapors have strong absorption peaks in the infrared band. If a flat screen, heated to some 15 °C or more above ambient temperature, is positioned on one side of a source with an infrared camera and filter on the other side, then the gas cloud will absorb a certain amount of infrared. Although the basic method is simple, special equipment (camera and filters) is required.

10.5.3.10 Schlieren and Shadow Graphs

These methods are based on the visualization of small density differences and gradients due, for example, to temperature or concentration differences. Density differences cause localized changes in the refractive index of the gas. If a parallel beam of light passes the area, the beam will be deflected by the localized changes. If the beam is focused onto a knife edge, the deflections will cause more or less light to fall onto the edge. A camera or viewing screen can be used to observe these changes. The method is basically a research or test room technique. It requires high quality mirrors to produce the parallel beam and setup is time-consuming and delicate. It has been used by Clarke[20] on investigations of outbursts from microbiological safety cabinets.

References

1. V. Hampl and S. Shulman. *American Industrial Hygiene Association Journal*, vol. 46, 1985, 379.
2. W. C. L. Hemeon. *Plant and Process Ventilation*. 2nd ed. New York: Industrial Press, 1963.
3. E. Ower and R. C. Pankhurst. *The Measurement of Air Flow*. 4th ed. Oxford: Pergamon Press, 1966.
4. American Conference of Governmental Industrial Hygienists. *Industrial Ventilation: A Manual of Recommended Practice*. 22nd ed. Cincinnati, OH: ACGIH, 1995.

5. J. N. Woods and J. S. McKarns. *American Industrial Hygiene Association Journal*, vol. 56, 1995, 1208.
6. A. Jansson. Local exhaust ventilation and aerosol behaviour in industrial workplace air. *Arbete och Hälsa*, no. 43, 1990.
7. U. Madsen, N. O. Breum, and P. V. Nielsen. *Building and Environment*, vol. 29, no. 3, 1994, 319–323.
8. U. Madsen, G. Aubertin, N. O. Breum, J. R. Fontaine, and P. V. Nielsen. In *Ventilation '94: Proceedings of the 4th International Symposium on Ventilation for Contaminant Control, Stockholm, Sept. 5–9, 1994* (eds. A. Jansson and L. Olander). (*Arbete och Hälsa*, no. 18). Sweden: *National Institute for Working Life*, 1994, pp. 333–338.
9. U. Madsen, J. R. Fontaine, P. V. Nielsen, G. Aubertin, and N. O. Breum. *American Industrial Hygiene Association Journal*, vol. 57, 1996, 134–141.
10. Y. Li and A. Delsante. *Building and Environment*, vol. 31, 1996, 461–468.
11. Y. Li, A. Delsante, and J. Symons. *Indoor Air*, vol. 7, 1997, 151–157.
12. European Standard EN 1093-4. Safety of machinery—Evaluation of the emission of airborne hazardous substances. Part 4: Capture efficiency of an exhaust system—Tracer method. 1996.
13. V. Hampl, R. Niemela, S. Shulman, and D. Bartley. American Industrial Hygiene Association Journal, vol. 47, 1986, 281–287.
14. ISO 3966. Measurements of fluid flow in closed conduits—Velocity area method using Pitot static tube. 1977, p. 39.
15. ISO 9096. Stationary source emissions—Determination of concentration and mass flow rate of particulate material in gas-carrying ducts: Manual gravimetric method. 1992, p. 30.
16. L. Olander. Efficiency of Local Exhausts—A Review. *Undersökningsrapport* (Investigation report), 1994, 32, Arbetsmiljöinstitutet (NIWL).
17. D. A. Kennedy. *Annals of Occupational Hygiene*, vol. 31, no. 2, 1987, 255–259.
18. M. F. Kerho and M. B. Bragg. *Experiments in Fluids*, vol. 16, 1994, 393–400.
19. HSE. The Dust Lamp—A Simple Tool for Observing the Presence of Airborne Particles. MDHS 82. London: HMSO, 1997.
20. R. P. Clarke. The Performance, Installation, Testing and Limitations of Microbiological Safety Cabinets. Occupational Hygiene Monograph no. 9. Leeds: Science Reviews, Ltd., 1983.

This page intentionally left blank

11 DESIGN WITH MODELING TECHNIQUES

ALFRED MOSER

Insititut für Hochbautechnik, Air & Climate Group, Zurich, Switzerland

ALOIS SCHÄLIN

Air Flow Consulting Alois Schälin, afc, Zurich, Switzerland

LARS DAVIDSON

Chalmers University of Technology, Götenborg, Sweden

VINCENZO CORRADO

Dip. di Energetica del Politecnico di Torino, Facoltà di Architettura, Torino, Italy

VIKTOR DORER

Section 175, EMPA, Dübendorf, Switzerland

MARKUS KOSCHENZ

Section 175, EMPA, Dübendorf, Switzerland

Industrial Ventilation Design Guidebook

11.1 INTRODUCTION

"How does an air curtain respond to a temperature change of, say, 10°?" "How does the air sheet react to an increased pressure difference across it?" Ventilation engineers want answers to such questions, and they want them immediately!

The most popular approach to solve these problems is to use experience and good engineering judgment. A quick experiment may be another solution. A computer simulation is a third option. All those approaches may eventually lead to success. This chapter presents various methods of computer simulation for industrial ventilation design.

Computer simulation involves three stages of simplification:

- Description of the physical situation by mathematical equations
- Transformation of these equations into a form that can be solved by a computer
- Numerical solution of the system of equations

To start the numerical solution, initial and boundary conditions must be specified.

The quality of the computed results is only as good as the quality of the boundary conditions supplied by the user.

Other key issues include the selection of the appropriate model and the abstraction of the physical problem for that model.

Presenting the results graphically completes the simulation. Before a simulation tool is handed to the design engineer, it must be thoroughly validated by computation of cases for which measurements have been performed and by comparison of the calculated results with the measured data. A basic rule:

The computer model is valid only for cases within the parameter range of successful verification.

Example: An airflow model that has been validated at air velocities up to 10 m/s (Mach number below 0.05) cannot be expected to perform reliably at a Mach number of 0.5.

Example: An airflow model that has been validated for temperature differences of 15 K cannot be expected to predict smoke movement accurately in a building that is on fire with temperature differences that are 10 times larger.

The engineer decides when to do a numerical simulation. He or she will consider numerical modeling when one or several of the following apply:

- Measured data for the particular case is unavailable (e.g., during design).
- The structure of the problem involves a large number of interacting zones connected by a complicated network.
- Different physical effects interact (e.g., buoyancy forces acting on an air curtain).
- Boundary conditions and thermophysical properties, etc. are clearly specified (e.g., indoor air quality can be predicted only if the location and strength of the sources are known).
- The influence of parameter variation is to be investigated (e.g., to optimize a local extract system).

Experiment or simulation? A decision may be based on the following considerations, but the final choice rests with the ventilation engineer:

Design or troubleshooting: During design, an on-site experiment with the actual equipment is usually not possible. Numerical prediction may then be easier. However, to investigate comfort complaints, field measurements are quicker, perhaps in combination with simulations.

Availability of facilities and expertise: Are test facilities, instrumentation, and data-acquisition systems available? Are simulation tools, hardware, and specialized staff for numerical simulation available? The decision depends on the answers to these questions.

Scaling laws: If a full-scale test is not possible, reduced-scale experiments are a good alternative. However, certain scaling laws must be observed (see Section 12.4, "*Scale model experiments*"). Correct scaling for isothermal flows is usually possible. However, scaling of buoyant flows in large rooms may be difficult, if not impossible. Then numerical simulation is the better choice.

Ventilation components with small geometric detail: Numerical modeling of diffusers with complex geometry is difficult. Therefore, it is more reliable to measure airflow around such devices at full scale.

Accident simulation: Large-scale accidents normally cannot be staged for experimental purposes. It is impossible to put a building on fire in order to see how smoke spreads. In this case, numerical simulation is the sensible approach.

Parameter variation and optimization: If parameter sensitivity is investigated, simulation is cheaper and quicker than experiments. Trends are usually well predicted by computer models.

Time available: It takes some time to set up a simulation case. After a basic configuration has run successfully, it is easy and quick to do additional computer simulations with different boundary conditions. Experiments, on the other hand, are generally time-consuming.

Cost: If simulation software is in place and trained staff available, computation is considered faster and less expensive than measurement.

Ideally, experiments and simulations should be performed simultaneously, and the results obtained should complement each other. The computer model for a basic configuration can be verified by comparison with experiment and then applied to more complex configurations.

Simple design methods may be found in Chapters 7 and 8 of the *Fundamentals* volume. Methods reported in this chapter are generally powerful and yield detailed information. However, there is a trade-off between simple and complex methods. This is illustrated in Fig. 11.1. More information provided is at the expense of a higher cost and the requirements for more time and skilled staff.

Four methods for industrial air technology design are presented in this chapter: computational fluid dynamics (CFD), thermal building–dynamics simulation, multizone airflow models, and integrated airflow and thermal modeling. In addition to the basic physics of the problem, the methods, purpose, recommended applications, limitations, cost and effort, and examples are provided.

Depending on the purpose of the computer calculations, different tools are selected. The modeling methods described in this chapter and their primary application are listed in Table 11.1.

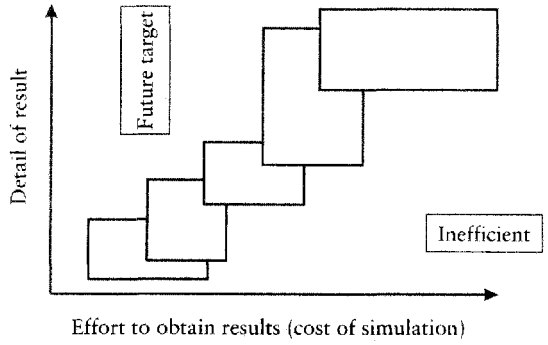

FIGURE 11.1 Trade-off between the complexity of the method and information content of results. Simple methods are at the lower left; complex methods, such as computational fluid dynamics, are near the upper right corner of the graph.

TABLE 11.1 Numerical Methods and Their Purpose

Method	Purpose
Computational fluid dynamics (CFD) (Section 11.2)	Airflow in space, air quality at all points in space, local age of air, entrainment of jets, heating and cooling by airstreams (heat transfer), buoyancy of warm and cold jets, thermal comfort at arbitrary points
Thermal building-dynamics simulation (Section 11.3)	Long-term (e.g., 12 months) thermal response of a building, simulation of thermal storage of building mass and its effect on comfort, energy, and heating and cooling loads. In addition, plant and controls modeling is used to estimate annual energy consumption
Multizone airflow models (Section 11.4)	Air infiltration and exfiltration, air exchange between rooms, mean indoor air quality in a room natural ventilation
Integrated airflow and thermal modeling (Section 11.5)	Air temperature in rooms imposed by building dynamics and ventilation, nighttime cooling, cooling by natural ventilation

In an actual design, thermal modeling (Section 11.3) for different seasons will come first to set temperature boundary conditions. Multizone airflow simulation (Section 11.4) will follow to define ventilation needs in each zone. For large enclosed spaces, for natural ventilation, and for a variety of other special problems, CFD (Section 11.2) and integrated modeling (Section 11.5) are applied.

11.2 COMPUTATIONAL FLUID DYNAMICS IN INDUSTRIAL VENTILATION

11.2.1 Purpose

11.2.1.1 What CFD Is Suited For

Computational fluid dynamics (CFD) is a very promising tool, and its use can be very helpful for analysis and design in industrial ventilation. It is suited for all types of problems where knowledge of a spatial distribution of flow quantities is desired, i.e., where local values at several locations are required.

The flow quantities may include air velocity, temperature, or contaminant concentrations. The term *contaminant* is used here as a general expression for other species at low concentrations carried by the air, such as smoke, CO_2, or toxic gases; even the local age of air can be treated in a similar way.

The availability of local quantities and only a minimal number of physical assumptions are the two key features of CFD. As a result, CFD has the following advantages over other methods such as multizone or flow element methods, which are useful for average values:

- Detailed analysis is possible.
- It is generally applicable for a wide variety of situations and problems.
- Interaction of different flow elements such as jets, plumes, and boundary layers is inherently considered.

- Even flow problems which have not been thought of before can be detected.
- It is very strong, even ideal, in parameter variations of a certain situation.

The last advantage, parameter variations, is in fact common to all the numerical models but is a main advantage over an experimental investigation, as the time effort for changing parameters is very small.

The following example illustrates some of these features. In a clean room with automated transporting and processing facilities, there are two quality classes of air. The space close to the small items under processing and the treating facilities should be exposed only to air of class A quality (very low contaminant level) and the rest of the room air is class B quality (normal standard). Figures 11.2 and 11.3 (see color insert) represent two out of a large number of parameter studies.

Figure 11.2 shows a cross-section through an open oven which is protected by an air curtain of class A air. The oven door must be opened for the loading of the items to be processed in the oven.

The study shows, however, that the air curtain in the original design is bent off the wall due to the presence of the open oven with induced airflow inside the oven. This unexpected flow feature finally leads to a recirculation zone below the oven, and dust particles on the floor can be carried into the oven (class B quality). This effect was then also confirmed by smoke experiments in the real room and the existing ventilation system.

The redesigned airflow system, consisting of a broader air curtain (the broadness needed also for other reasons) and a local exhaust below the oven, ensures class A air quality in the oven when the door is opened for loading (see Fig. 11.3).

11.2.1.2 Application Examples

Quite different flow problems of steady-state and transient nature can be treated. Examples of flow situations that are most important in industrial applications are as follows:

- Impact of air supply or exhaust devices to room airflow
- Thermal plumes originating from machines or high-temperature processes
- Effects of contaminant sources and their distribution in the rooms
- Airflow due to moving parts
- Airflow through openings between rooms or between inside and outside (e.g., natural ventilation or flow through process-related openings to outside)

More recently, the application range seems to be extended with increasing demand to even more complex situations, including additional effects such as

- Influence of solar light through glazings
- Wind influence on large openings to the inside space
- Distribution of heavy gases (i.e., species other than air at high concentrations) in the case of chemical hazards or smoke from fire for occupants' safety reasons (ways of escape)

11.2.1.3 Considering a CFD Study

When a CFD simulation is desired, the following points have to be considered.

What Do I Want to Know Exactly?

It is important to define exactly which results are really required, e.g.:

- Do I need the airflow or turbulence quantities at certain locations, or are toxic concentrations needed?
- Are all the locations of equal importance, or are some more important than others?
- How accurate are results required?

The CFD engineer then has to choose the input values, the resolution of the modeling, and the distribution of the calculation mesh related to the important physics in the flow and to the area and effects of interest.

Effort Needed

It is up to the skill of the CFD engineer to choose the level of simplification of the real situation and the models needed and to judge from experience the accuracy of the results.

A generally valid, simple checklist cannot be given. It is, however, very important to realize that CFD applied to a problem situation is not a simple three step procedure like (1) setting up the problem, (2) letting the computer do the job, and (3) plotting the pictures and getting "yes or no" information ("we build it" or "we don't"). The full truth is more that a CFD application is an iterative procedure (not only within the algorithmic DO loops) between the ventilation designer (and architect) and the CFD engineer. Different levels of simplifications of the real situation will be applied at different stages of the design process, and possibly large numbers of parameter variations of CFD cases have to be carried out in order to reach a conclusion, which in fact can be as simple as "yes" or "no."

How Good Are the Results?

It cannot be stated generally how accurate the predicted results are. Due to the limitations of geometric, physical, and mathematical modeling, not all of the produced numbers (e.g., air velocity vectors) are at a high level of accuracy, and the results are therefore subjected to experienced weighting. In some cases, the values can be as accurate as within 5% of the real values; in other cases, they are not as accurate as could be wished. But results can be still very strong and helpful in a comparative judgment, i.e., if a number of similar cases are compared with observed tendencies.

Costs

A general figure cannot be given either, but usually a case of medium-level complexity with a set of 10 parameter variation needs an effort of two to four man-weeks. In any case, a number of cases have to be calculated (say, 5 or 10, not just 1) to gain knowledge about the sensitivity of the flow to the choice of certain parameters.

Practical Procedure for Carrying out a CFD Study

Usually, in practice, the person who carries out the CFD computation is different from the person who needs the results. It is then very strongly recommended that a strong feedback between the designer who needs the results and the CFD engineer be maintained to prevent disappointments, e.g., results that do not meet the real needs. It is in fact an iterative procedure.

It is furthermore iterative in the sense that one should start from a coarse model, which is then successively refined to the desired or possible depth. Failures in the models or problems of different types tested so far can be detected and treated at an early stage of the design process.

11.2.2 Method

11.2.2.1 Grid

When using any CFD method, we first need to make a grid over the domain. The number of grid nodes in each direction depends on the type of flow, and what accuracy or reliability the user wants for the predictions. The governing equations have been discretized on this grid, and the finer the grid, the more accurate the results. If the user only wants an overall picture of the flow field, a $30 \times 30 \times 30$ grid could be sufficient. The grid should be refined in regions where large gradients are expected. This normally means that the grid should be made finer near walls and in the region of the inlet.

It should also be remembered that the discretization scheme influences the accuracy of the results. In most CFD codes, different discretization schemes can be chosen for the convective terms. Usually, one can choose between first-order schemes (e.g., the first-order upwind scheme or the hybrid scheme) or second-order schemes (e.g., a second-order upwind scheme or some modified QUICK scheme). Second-order schemes are, as the name implies, more accurate than first-order schemes. However, it should also be remembered that the second-order schemes are numerically more unstable than the first-order schemes. Usually, it is a good idea to start the computations using a first-order scheme. Then, when a converged solution has been obtained, the user can continue the calculations with a second-order scheme.

When a coarse grid is used, wall functions are used for imposing boundary conditions near the walls (Section 11.2.3.3). The nondimensional wall distance should be $30 < y^+ < 100$, where $y^+ = u_* y/\nu$. We cannot compute the friction velocity u_* before doing the CFD simulation, because the friction velocity is dependent on the flow. However, we would like to have an estimation of y^+ to be able to locate the first grid node near the wall at $30 < y^+ < 100$. If we can estimate the maximum velocity in the boundary layer, the friction velocity can be estimated as $u_* \simeq 0.04 U_{\max}$. After the computation has been carried out, we can verify that $30 < y^+ < 100$ is satisfied for the grid nodes adjacent to the walls.

If the user wants higher accuracy in the predictions, and if he/she is willing to pay for the increase in accuracy in terms of increased computing cost, more grid nodes should be used. In general, more grid nodes should be located where the flow is complex. For an empty room without furniture or persons, this normally means that more grid nodes should be placed near walls and in

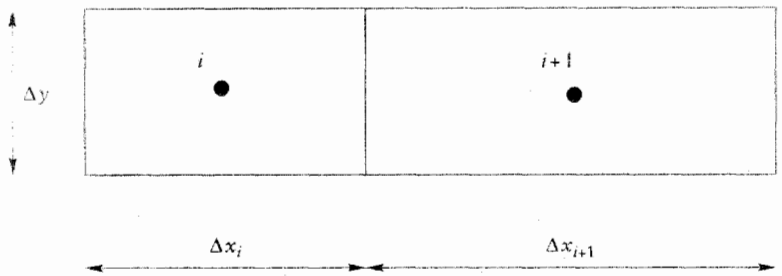

FIGURE 11.4 Aspect ratio and biasing for control volumes. Aspect ratio is defined as $\Delta x_i/\Delta y$ for cell i. Biasing in the x direction is defined as $\Delta x_{i+1}/\Delta x_i$.

the inlet region. If heat transfer at walls is to be predicted, it is usually very important to refine the grid near the walls. When using a fine grid near the walls, low-Reynolds-number (LRN) models should be used (see Section 11.2.3.3). In this case the grid nodes should be located so that $y^+ \simeq 1$ near the wall. As previously explained, we cannot compute the friction velocity u_* in advance, but it can be estimated. After the computation has been carried out, the friction velocity can be computed by using the fact that the velocity in the viscous sublayer is linear (valid for $y^+ < 5$), given by

$$\frac{U_p}{u_*} = \frac{u_* y}{\nu} \quad \Rightarrow \quad u_* = \sqrt{U_p \nu / y}\,.$$

A high aspect ratio (e.g., above 100) usually does not pose any problems (Fig. 11.4). Biasing causes larger problems, both in terms of convergence and accuracy. Preferably, biasing should be smaller than approximately 1.1, that is, the cell size between two adjacent cells in one direction should not increase or decrease by more than 10%.

11.2.2.2 Equations

The incompressible, time-averaged continuity and the Navier-Stokes equations can be written as

$$\frac{\partial \overline{U}_i}{\partial x_i} = 0 \tag{11.1}$$

$$\frac{\partial \overline{U}_i}{\partial t} + \frac{\partial}{\partial x_j}(\overline{U}_j \overline{U}_i) = -\frac{1}{\rho}\frac{\partial \overline{P}}{\partial x_i} + \frac{\partial}{\partial x_j}\left[\nu\left(\frac{\partial \overline{U}_i}{\partial x_j} + \frac{\partial \overline{U}_j}{\partial x_i}\right) - \overline{u_i u_j}\right] + g\beta\delta_{i2}(T - T_{\text{ref}}) \tag{11.2}$$

$$\frac{\partial \overline{T}}{\partial t} + \frac{\partial}{\partial x_j}(\overline{U}_j \overline{T}) = \frac{\partial}{\partial x_j}\left[\frac{\nu}{Pr}\frac{\partial \overline{T}}{\partial x_j} - \overline{u_j t}\right], \tag{11.3}$$

where

$$\begin{aligned} U_i &= \overline{U}_i + u_i' \\ P &= \overline{P} + p' \\ T &= \overline{T} + t' \end{aligned} \tag{11.4}$$

and β is the inverse of the reference temperature in kelvins, so that if T is expressed in °C then $\beta = 1/(273 + T_{\text{ref}})$. The x_2 coordinate increases vertically upwards. Turbulent stresses $\overline{u_i u_j}$ and turbulent heat fluxes $\overline{u_j t}$ appear on the right-hand side of Eqs. (11.2) and (11.3). They act as additional diffusion terms due to correlations between fluctuating velocities and temperature, which are unknown. Transport equations can be derived for $\overline{u_i u_j}$ and $\overline{u_j t}$. The higher-order unknown correlations in the resulting equations are then modeled; this type of model is called a Reynolds stress model.[1]

In ventilation problems, it is often sufficient to use simpler turbulence models, such as eddy-viscosity models. $\overline{u_i u_j}$ and $\overline{u_j t}$ are then replaced by introducing a turbulent viscosity; Eqs. (11.2) and (11.3) can be rewritten as

$$\frac{\partial \bar{U}_i}{\partial t} + \frac{\partial}{\partial x_j}(\bar{U}_j \bar{U}_i) = -\frac{1}{\rho}\frac{\partial \bar{P}}{\partial x_i} + \frac{\partial}{\partial x_j}\left[(\nu + \nu_t)\left(\frac{\partial U_i}{\partial x_j} + \frac{\partial U_j}{\partial x_i}\right)\right] + g\beta\delta_{i2}(T - T_{\text{ref}}) \tag{11.5}$$

$$\frac{\partial \bar{T}}{\partial t} + \frac{\partial}{\partial x_j}(\bar{U}_j \bar{T}) = \frac{\partial}{\partial x_j}\left[\left(\frac{\nu}{Pr} + \frac{\nu}{Pr_t}\right)\frac{\partial \bar{T}}{\partial x_j}\right] . \tag{11.6}$$

Commonly used eddy-viscosity turbulence models are the k-ϵ model and the k-ω model. The eddy viscosities for these models have the form

$$\begin{aligned} \mu_t &= c_\mu \rho \frac{k^2}{\epsilon} \qquad k\text{-}\epsilon \text{ model} \\ \mu_t &= c_\mu \rho \frac{k}{\omega} \qquad k\text{-}\omega \text{ model} . \end{aligned} \tag{11.7}$$

A derivation can be found in the literature.[2–4]

If the flow is isothermal, there is no need to solve for the temperature equation (Eq. (11.6)). In this case the last term in Eq. (11.5) is also dropped. If, however, the thermal comfort is simulated, then the temperature equation must be solved. In ventilation the temperature variations are normally small, which means that it is sufficient to account for density variation only in the gravitation term (the last term in Eq. (11.5)). The gravitation term acts in the vertical direction, and in Eq. (11.5) it is assumed that the x_2 coordinate is directed vertically upward. T_{ref} denotes a reference temperature, which should be constant. It does not influence the predicted results, except that the pressure level is changed. It could, however, affect convergence rate (i.e., increase the number of required iterations required to reach a converged solution), and it should be chosen to a reasonable value, such as the inlet temperature.

The temperature equation is derived from the energy equation, in which the units of each term is joules per unit volume per second, J/(m^3 s) = W/m^3. The temperature equation above has been divided by the specific heat c_p and density ρ (assumed to be constant), and thus the units of each term in Eq. (11.6) is °C/s. If a heat source q is to be added in a cell, it should be divided by c_p (= 1006 J/(kg K) for air).

11.2.3 Required Input

A certain minimal amount of input information is needed to run a CFD case; more information can be provided to achieve higher-quality results. The data required are usually

- Geometric modeling
- Boundary conditions in space and time: thermal, flow (ventilation, mechanical, and natural), sources of contaminants

CFD results can only be as good as

1. Quality of geometric modeling and spatial resolution of computational mesh
2. Models involved in CFD code
3. Knowledge of boundary conditions

This is not as simple as it sounds, as the boundary conditions are very often not well known. The number and distribution of heat sources and ventilation parameters, particularly in naturally ventilated surroundings, are very often not known or even vary. The CFD engineer has to cope with this situation and can do one of the following:

- Choose boundary conditions from his or her knowledge about the given information.
- Perform calculations with parameters varied to check their importance. The CFD results can possibly turn out to be helpful more comparatively (qualitatively) than quantitatively.
- Try to expand the system assumed so far to derive higher-quality boundary-condition values.

The latter is certainly the best if it can be done, which depends on the availability of suited models and resources. Examples of such procedures are

- The problem of unknown amounts of air leakage in the cold season in an industrial hall can be calculated by multizone airflow models during the whole year with local meteorological data.
- A similar approach for unknown temperatures on wall and glass faces can be addressed with the help of thermal building simulation programs.
- The distribution of solar radiation, including surface radiation exchange, can account for solar heat source variations in time and local space.

11.2.3.1 Geometric Modeling

This is the first step, and a very important one, in every CFD study, as it is the basis for the computational mesh. The engineer has to choose the resolution and the details needed for capturing the flow effects desired from the available data. In many cases, the data available are too few; in other cases, the amount of data has to be reduced to a level that can be handled by the resources available.

The following objects usually can be added to the geometric model:

- Bounding shapes of the rooms
  - Inclined bounding faces can cause modeling failures in orthogonal meshes, as the face is modeled as a "stair" instead of a plane face. The wall friction of such a stair is sometimes not accounted for.
- Shapes of inside objects which are obstacles to the airflow (sometimes referred to as "blocked-off" objects), such as machine blocks, partition walls, etc.
  - These objects can contain unused computation nodes, which possibly still occupy memory space, depending on the meshing method used.
  - Within such objects, conductive heat flow can be solved as well. This is sometimes called *conjugate heat transfer* in the literature.
- Shapes of inside objects which are only partly permeable to airflow (sometimes referred to as "porous" objects), such as inlet grills, vents, etc.
- Position of supply and exhaust openings

Note that the codes usually do not support moving objects with either adaptive meshes or a stationary mesh.

11.2.3.2 Physical Boundary Conditions

These conditions govern the flow and are therefore of crucial importance. For each condition (see Table 11.2) the flow value and the scalar values are discussed separately. The table contains volumetric sources, which are not strictly speaking boundary conditions in a mathematical sense. For the CFD engineer they nevertheless define the problem and are therefore included in this table. The problem must also not be overspecified.

Usually the boundary conditions in the following subsections are used.

Inflow

- Used for air supply.
- Flow parameter specified is one of mass flow, velocity, or pressure. Usually mass flow or velocity is taken, as these values are known for air supplies.
- Associated scalar values include temperature, turbulence quantities, contaminant concentrations.

Outlet

- Used for air supply.

Parameters specified are mass flow or velocity. Usually at one outlet, pressure equal to a constant is specified in incompressible flow. If several outlets are present, this pressure boundary condition can only be applied to one outlet, as there are some (unknown) pressure differences between the different outlets. The flow conditions in the rooms are better represented by taking the outlet mass flows when they are known.

TABLE 11.2 Boundary Conditions

Boundary-condition type	Flow value	Scalar value	Special issues in ventilation	App.
Inflow	m, v, or p	T, C_i, turb	Inlet-box method	*
Outflow	m, v, or p	—		
Large opening	p_{total}	T, C_i, turb for inflow	Combination with outside flow	*
Wall	v = 0	T or q	Heat flux or temperature	*
Volumetric sources	—	q, S_c	Simplification	*
Symmetry	—	—	Can be used sometimes for subdivision of large halls	*
Periodicity	—	—		*

m = mass flow, v = velocity components, p = pressure, T = temperature, q = heat flux, C_i = concentration of contaminant species i, S_c = contaminant source, turb = turbulent quantities (depend on the turbulence model used). *Example in appendix.

Large Opening

In such openings, bidirectional flow driven by temperature differences between the two rooms can occur. If a total pressure (static pressure plus dynamic pressure) is specified, this phenomenon can be accounted for. For higher accuracy in the neighborhood of this opening, it is, however, recommended to expand the calculation domain beyond this opening.

Walls

Wall friction slows down the flow.

The temperature boundary condition is in many problems of buoyant flow, e.g., heat sources (machines) or heat sinks (cold glazings), is of great importance.

Walls can also act as sources or sinks of gases or materials.

Moving Walls (Rotating Parts)

Moving walls can be used to represent rapidly moving parts which induce flow in the considered space.

Volume Sources

Heat or contaminant sources can also be assigned to parts of the fluid volume to account for very small real sources or a distribution of a large number of small sources. Care must be taken, however, to make sure that this representation of distributed sources describes correctly the real situation (see the earlier section "Geometric Modeling").

Symmetry or Periodicity

These conditions can be used sometimes for a reduction of the full geometry, but only if the problem is symmetrical or periodic from both the geometric and the physical points of view.

11.2.3.3 Wall Boundary Conditions

Wall Functions

The natural way to treat wall boundaries is to make the grid sufficiently fine that the sharp gradients prevailing near walls are resolved. When computing complex three-dimensional flow, this often requires an excessive amount of computer resources. An alternative is to assume that the flow near the wall behaves like a fully developed turbulent boundary layer and prescribe boundary conditions employing wall functions. Given a maximum number of nodes that we can afford to use in a computation, it is often preferable to use wall functions, which allow us to use a fine grid in other regions far away from the walls where the gradients of the flow variables are large. In this way the CPU time can be reduced substantially. Using wall functions means that the boundary layer near a wall is not resolved, but the first node is located in the log-law region where $30 \leq y^+ \leq 100$ (the upper limit depends on the Reynolds number). The flow between the first node and the wall is supposed to be as in flat-plate boundary layer flow. This assumption is often well satisfied, but in many flow situations it is not true at all. When applying boundary conditions using wall functions, the friction velocity is computed from the log-law, which reads[2–4]

$$\frac{U_P}{u_*} = \frac{1}{\kappa} \ln\left(\frac{E u_* y}{\nu}\right), \tag{11.8}$$

where U_P is the near-wall node velocity tangential to the wall, y is the distance from the wall to the node, κ is the von Karmann constant ($=0.41$), and $E = 9.0$. The friction velocity u_* has to be computed numerically. This is conveniently done by first guessing a value for y^+, then computing a friction velocity (which we denote u_*^{old}). Then the new friction velocity u_* is computed from Eq. (11.8).

$$u_* = \frac{\kappa U_P}{\ln(E u_*^{\text{old}} y/\nu)}.$$

The above equation is solved a few times by iteration, replacing u_*^{old} on the right-hand side in each iteration by the new u_*. Having obtained u_*, the non-dimensional wall distance $y^+ = u_* y/\nu$ can be computed.

For a discussion of wall functions, see refs. 2–4, e.g.

In ventilated rooms buoyant effects are often imported, and wall functions to take this into account are presented in ref. 5.

Low-Reynolds-Number Turbulence Models

In the previous section we discussed wall functions, which are used to reduce the number of cells. However, we must be aware that this is an approximation that, if the flow near the boundary is important, can be rather crude. In many internal flows—where all boundaries are either walls, symmetry planes, inlets, or outlets—the boundary layer may not be that important, as the flow field is often pressure determined. However, when we are predicting heat transfer, it is generally not a good idea to use wall functions, because the convective heat transfer at the walls may be inaccurately predicted. The reason is that convective heat transfer is extremely sensitive to the near-wall flow and temperature field.

When the wall is approached, the viscous effects become more important, and for $y^+ < 5$ the viscous diffusion becomes comparable to the turbulent diffusion. Thus, the standard turbulence models (high-Reynolds-number models) are not correct since fully turbulent conditions have been assumed. The high-Reynolds-number models are modified so that they can be used all the way down to the wall. These modified models are termed low-Reynolds-number (LRN) models. Please note that "high-Reynolds-number" and "low-Reynolds-number" do *not* refer to the global Reynolds number (for example, Re_L, Re_x, Re_D); rather, here we are talking about the local turbulent Reynolds number $\mathrm{Re}_\ell = \mathcal{U}\ell/\nu$ formed by a turbulent velocity fluctuation $\mathcal{U}$ and turbulent length scale ℓ. This Reynolds number varies throughout the computational domain and is proportional to the ratio of the turbulent and physical viscosity ν_t/ν, i.e., $\mathrm{Re}_\ell \propto \nu_t/\nu$. This ratio is of the order of 150 or larger in fully turbulent flow[6] and it goes to zero when a wall is approached.

Examples of LRN k-ϵ and k-ω models can be found in refs. 2 and 9–13. A review can be found in ref. 14.

Time-Scheduled Boundary Conditions

In time-dependent problems, all the above conditions can be time-dependent functions, such as a machine heating cycle or another time-dependent process under study.

Initial Conditions

In stationary problems the initial conditions are in theory not important, but a good guess gives faster convergence. It is even possible that a very bad guess can prevent convergence, if the convergence parameters are chosen a bit aggressively. A very bad guess can also be obtained as an intermediate result of a mistakenly ill-posed problem. A restart from a fresh initial guess is then required.

In time-dependent problems, of course, a good guess (or knowledge) of the initial conditions is much more important.

Data from Thermal Building–Dynamics Programs

In many cases, some boundary conditions are not well known or not known at all. Temperature boundary conditions can be obtained from thermal building–dynamics programs that allow the capture of spatial mean temperatures during a time period as long as a whole year. Some of these programs yield surface temperature values (e.g., TRNSYS), which can be used as temperature boundary conditions at the time of CFD study.

Data from Infiltration and Multizone Airflow Programs

Flow values (mass flows into and out of the CFD domain) can be obtained from infiltration and multizone airflow programs and used as boundary conditions.

Geometry from CAD Database

CAD databases can be helpful, but this depends much on the software set available. Architectural CAD data often contain too many data that have to be simplified and reduced considerably.

11.2.4 CFD Software

When choosing CFD software, there are several aspects that should be taken into account. The most important aspect is probably how complex the configuration is, and what type of grid that complexity requires. Another question is if radiation[15,16] needs to be taken into account; if so, is it sufficient to take radiation between walls, ceiling, and floor into account, or do we need to do ray tracing,[17] including the effects of solid bodies in the room? Does the fluid in the room (for example, moisture) contribute to radiation?[18] A third aspect is the turbulence model. In ventilation problems it is often sufficient to use simple eddy-viscosity models. If heat transfer near surfaces is to be predicted with accuracy, low-Re number models should be used. More complex models, that are better in accurately modeling the physics are Reynolds stress models.[1,19] These models are often considerably more expensive, primarily because they are numerically more unstable. Simplified forms of Reynolds stress models are algebraic Reynolds stress models (ASMs),[20,21] and explicit algebraic Reynolds stress models (EARSMs);[22–24] EARSMs are also often referred to as nonlinear eddy-viscosity models.

Next, the choice of grid type is discussed.

11.2.4.1 Complexity of the Configuration

Depending of the complexity of the computational domain, the user should use CFD software capable of treating different types of grids. There are two different types of grids, structured and unstructured. An unstructured grid (see Fig. 11.5) allows the most complex geometries to be adequately represented. Grids around most types of furniture could be created, as well as grids around persons. An unstructured grid also allows local grid refinement in geometrically complex regions, or in regions where the grid needs to be fine due to strong velocity gradients. The drawback is that the numerical solver usually is less efficient than a solver based on structured grids, which means that more computer time is needed.

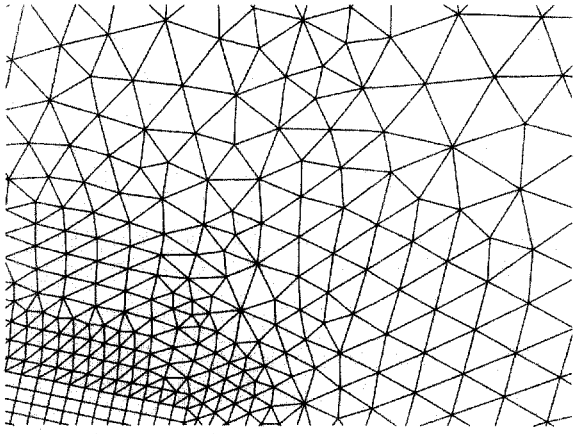

FIGURE 11.5 Example of an unstructured mesh.

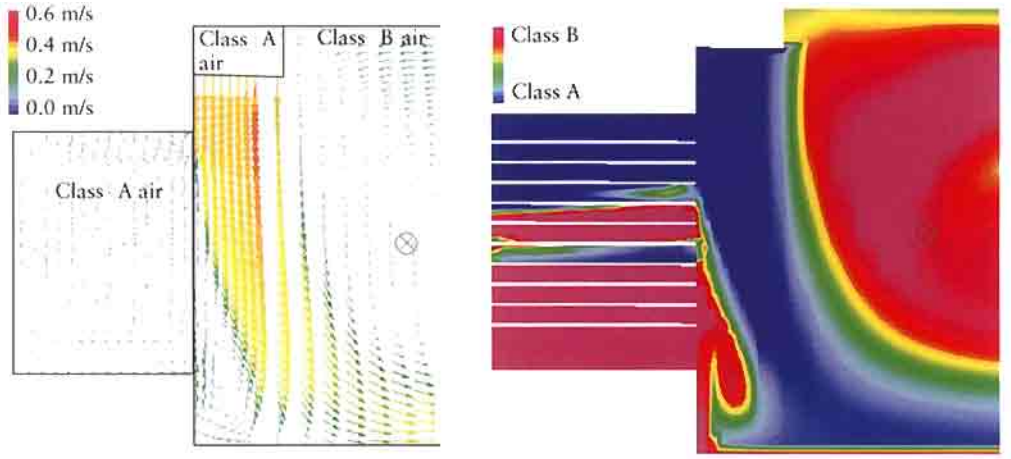

FIGURE 11.2 Cross-section through clean room, with open oven (including shelves) to the left. The air curtain is supposed to protect the inside of the oven when the door is opened to fill in goods. The air curtain, however, was found to be bent outward, and recirculation occurs, which can carry dust into the oven (shown by the class B air to the right).

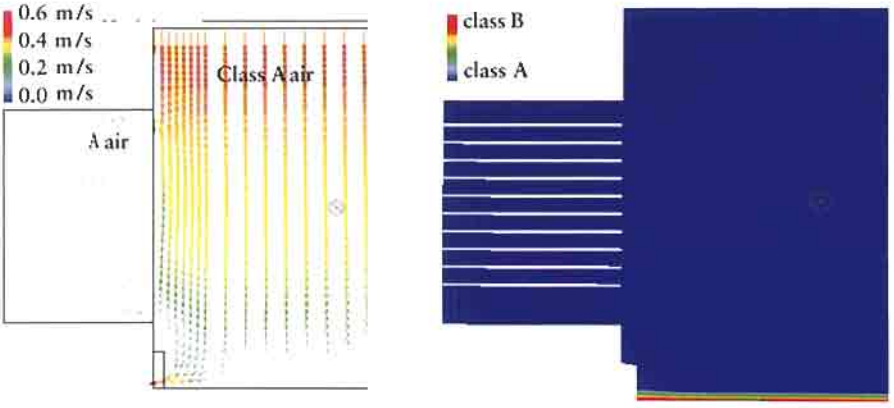

FIGURE 11.3 Improvement of the situation by two steps: (1) an exhaust opening close to the floor below the opening of the oven and (2) a wider air curtain.

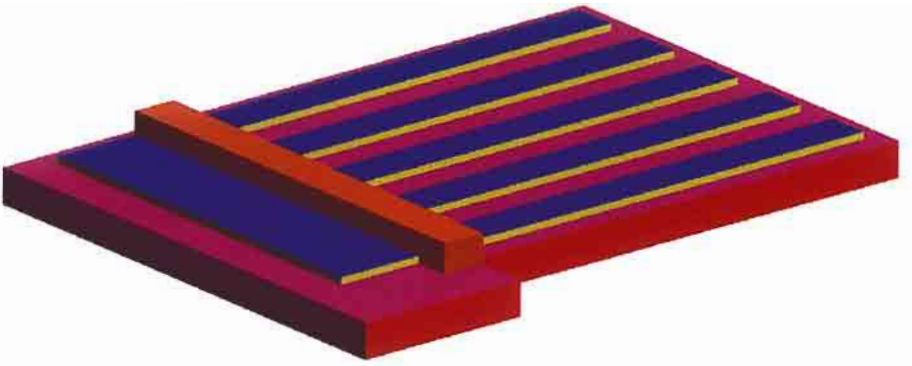

FIGURE 11.17 View of large industrial parcel distribution hall from outside.

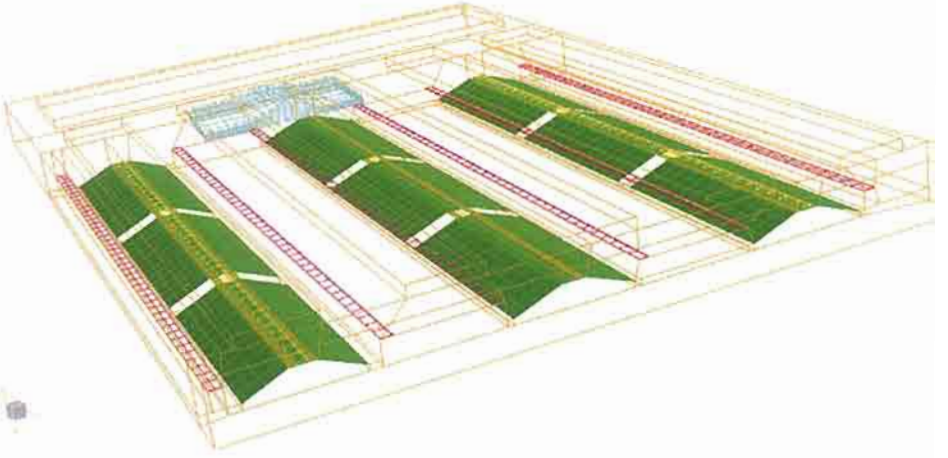

FIGURE 11.18 View of large industrial parcel distribution hall with inside details (CFD model).

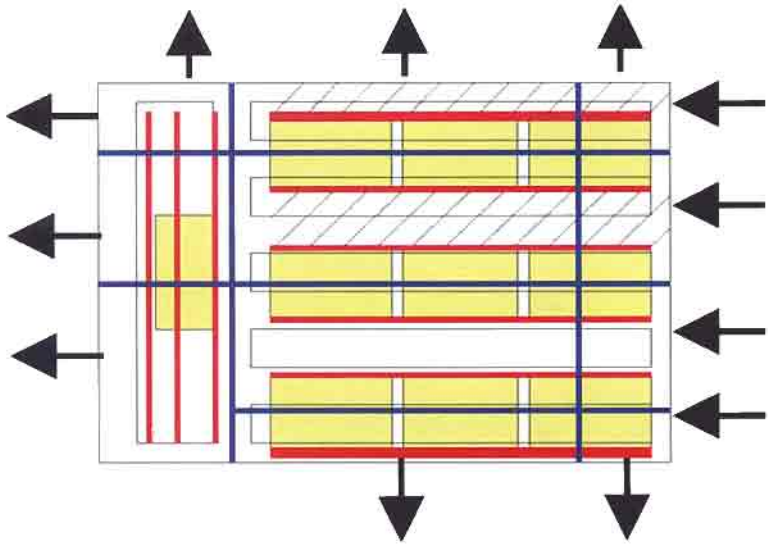

FIGURE 11.19 Zonal division of parcel distribution hall in multizone model.

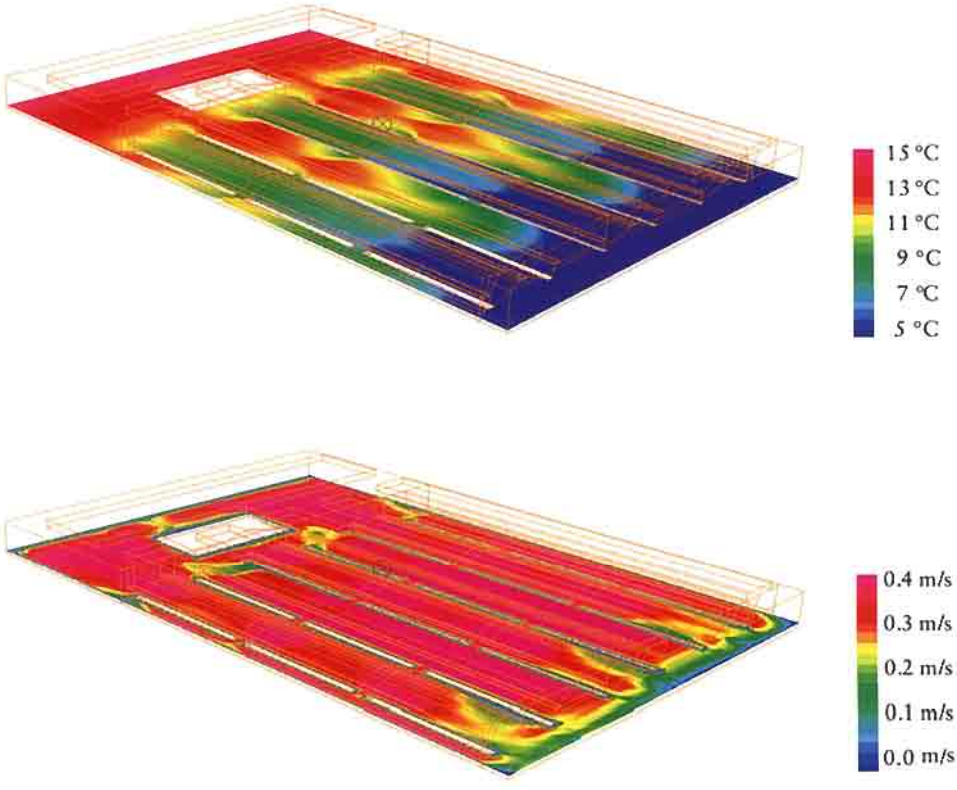

FIGURE 11.20 Resulting air temperatures and velocities in the hall (from CFD model).

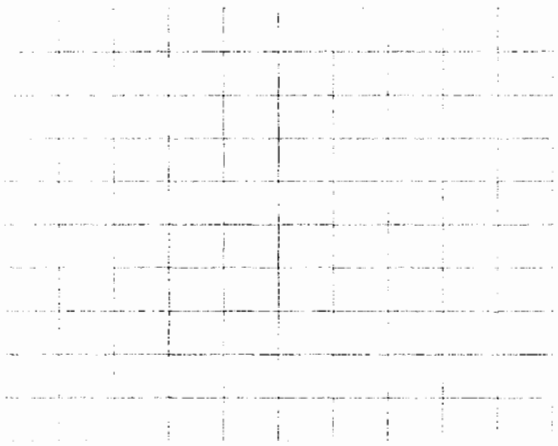

FIGURE 11.6 Example of a Cartesian grid.

For the structured grid, there are at least four subtypes:

1. Cartesian grid (Fig. 11.6).
2. Boundary-fitted (curvilinear) grid (Fig. 11.7).
3. Multiblock, either with Cartesian or boundary-fitted grid; in Fig. 11.8, a two-block Cartesian grid is shown.
4. Multiblock, either with Cartesian or boundary-fitted grid, where the interface of the blocks does not need to be a one-to-one relation; i.e. one cell in one block can meet two cells of the adjacent block (see Fig. 11.9).

When flow in empty rooms is to be computed, a Cartesian grid is sufficient. If the ceiling, floor, or walls of a room are inclined or curved, a boundary-fitted grid should be used. For computing the flow in an apartment or a building with multiple rooms, a multiblock grid should be used. With a grid as

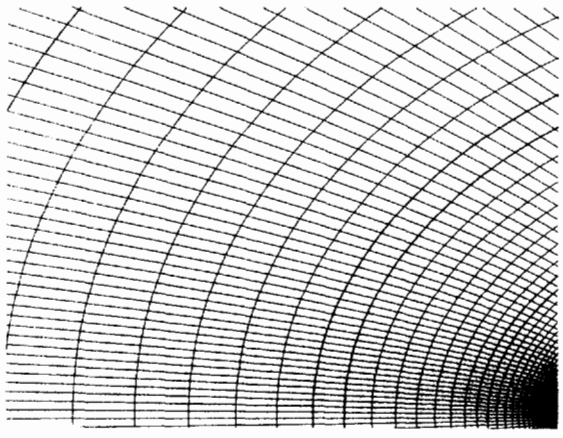

FIGURE 11.7 Example of a curvilinear grid.

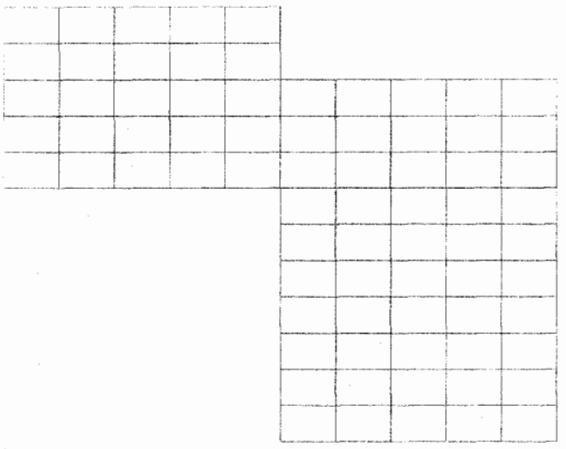

FIGURE 11.8 Example of a multiblock grid.

described in item 4 above, local grid refinement can be used in geometrically complex regions or in regions where large (velocity) gradients prevail.

11.2.5 Case Studies

11.2.5.1 Inlet–Box Method

Often the inlet device (air supply) in a ventilated room is geometrically complicated. To resolve the flow around such a device would require a very fine grid. Instead of trying to resolve the complex flow near the inlet device, one can choose to use the "box method"[25–29] or the "prescribed velocity method."[30,31] Both methods are based on the observation that downstream of the inlet, the flow behaves like a wall jet. Thus it is important that the bound-

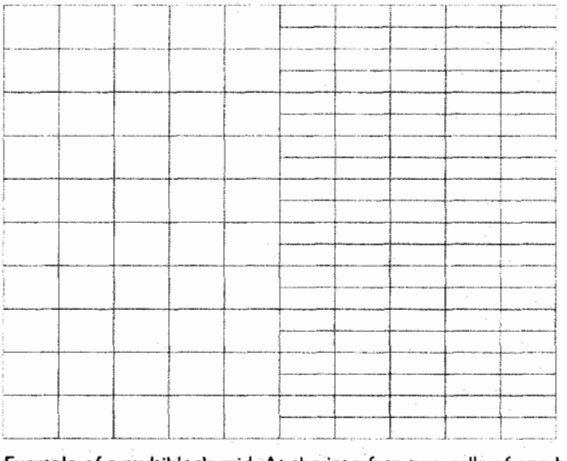

FIGURE 11.9 Example of a multiblock grid. At the interface two cells of one block meet one cell of an adjacent block.

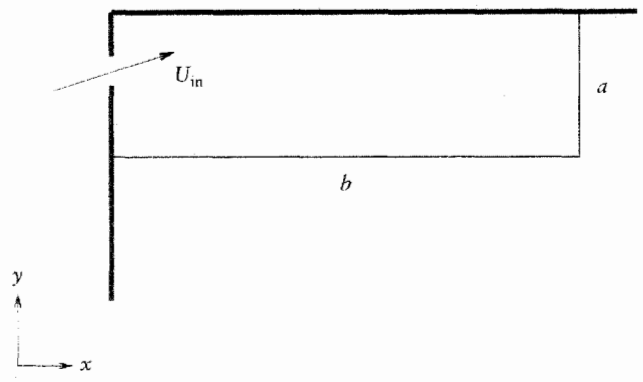

FIGURE 11.10 Inlet region. The flow enters through the inlet with velocity U_{in}.

ary a (see Fig. 11.10) is located sufficiently far downstream that the wall jet is fully developed, but not too far downstream, because the box should be small compared to the room size.

Consider an inlet region as in Fig. 11.10. In the box method all dependent variables are prescribed along surfaces a and b. The variables are not solved for inside the box. Along surface a, the mean flow quantities such as the streamwise velocity component $\overline{U}$ and the temperature are set from wall jet data. The turbulent kinetic energy k is also taken from wall jet data, and together with a prescribed turbulent length scale the dissipation ϵ can be found. Along boundary b zero gradient $\partial\Phi/\partial y$ is prescribed. Special care must be taken to conserve mass and energy in the box. For more details, see ref. 29.

In refs. 32 and 33 a separate computation was carried out for the inlet region (inlet box). The results from this computation were then used for prescribing all variables at all faces of the inlet box when computing the flow in the rest of the room.

The other method is the prescribed velocity (PV) method. In this method only the streamwise velocity component $\overline{U}$ and the temperature profile are prescribed inside the volume ab. The remaining variables ($\overline{V}$, $\overline{W}$, k, and ϵ) are solved for as usual in the whole room, including the ab volume. The temperature level has to be readjusted after each iteration to ensure conservation of energy.

In Fig. 11.11 the predicted $\overline{U}$ velocity is compared with and without use of the PV method.

11.2.5.2 Displacement Ventilation

Because displacement ventilation flow systems have become increasingly popular and are replacing the traditional mixing ventilation systems, it is of great interest to carry out numerical investigation of the flow. In mixing ventilation, fresh air is supplied at high velocity (momentum), inducing an overall recirculation in the room, which gives an efficient mixing. In this way the polluted air is diluted in an efficient way. In displacement

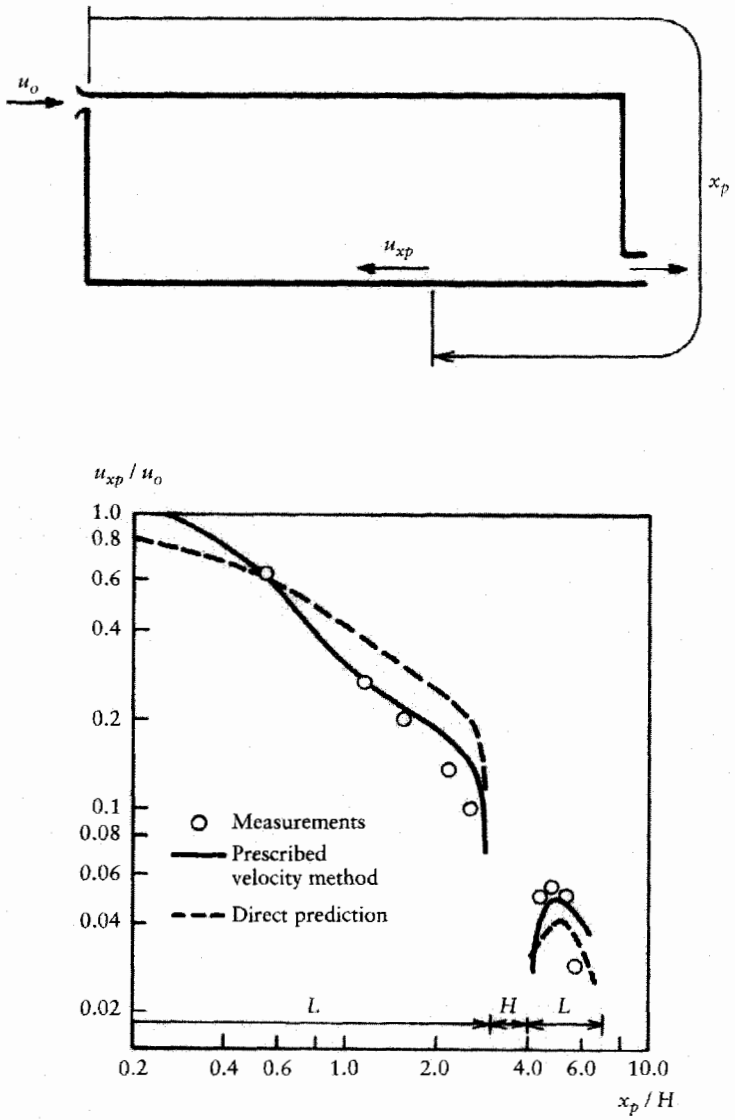

FIGURE 11.11 Comparison of the predicted $\bar{U}$ velocity with and without use of the PV method.[31]

ventilation, however, the object is to keep the fresh and polluted air separated. A schematic diagram of a room ventilated by displacement is shown in Fig. 11.12

In displacement ventilation systems air is supplied to the room at low velocity, with a volume flow rate $\dot{V}_{in}$ near the floor, and is extracted near the ceiling. The temperature of the supplied air is slightly lower than that of the room. Air is heated by the objects in the room, e.g., computer terminals and photocopying machines, and it rises due to buoyancy.

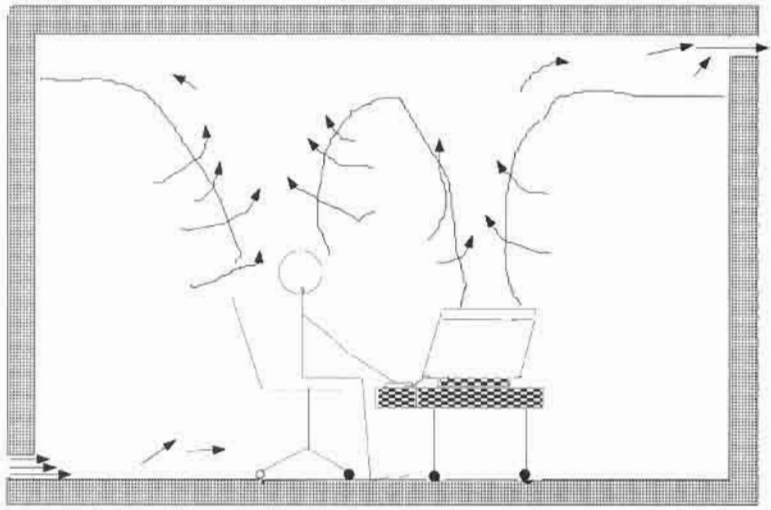

FIGURE 11.12 Ventilation by displacement. (© 1995 Munksgaard International Publishers Ltd., Copenhagen, Denmark.)

When designing a displacement ventilation system, it is important to accurately predict the flow over heat sources. The rising flow above a heat source resembles a plume. The flow in the plume rises up to the ceiling. The volume flow rate in plumes for a given vertical distance from the heat source y is $\dot{V}_{\text{plume}}(y)$, and increases with y due to entrainment. At the ceiling the flow spreads out laterally. Below the ceiling the exit is located through which air is extracted at a rate of $\dot{V}_{\text{in}}$. The remainder of the flow, $\dot{V}_{\text{plume}}(H) - \dot{V}_{\text{in}}$ (H is the height of the room) flows downward. The stratification front y_{front} is located where $\dot{V}_{\text{in}} = \dot{V}_{\text{plume}}$.

One of the first simulations of displacement ventilation was presented in refs. 34 and 35. The predictions were compared with water-model experiments, and hence radiation was not taken into account. In ventilated rooms radiation should be taken into account.[16] In ref. 36 plumes related to displacement ventilation were numerically studied.

In displacement ventilation, there are regions with very low turbulence, and the flow can even be laminar. Hence it is important to use a turbulence model which can handle these regions. The k-ϵ model gives rise to large numerical problems in regions of low turbulence. The reason is that as k goes to zero, the destruction term in the ϵ equation goes to infinity. The ϵ equation is

$$\frac{\partial}{\partial x_j}(\rho \bar{U}_j \epsilon) = \frac{\partial}{\partial x_j}\left[\left(\mu + \frac{\mu_t}{\sigma_\epsilon}\right)\frac{\partial \epsilon}{\partial x_j}\right] + \frac{\epsilon}{k}(c_{\epsilon 1} P_k - c_{\epsilon 2}\rho\epsilon).$$

The destruction term (the last term on the right-hand side) includes ϵ^2/k, and this causes problems as $k \longrightarrow 0$ even if ϵ also goes to zero; they must both go to zero at the correct rate to avoid problems, and this is often not the case.

No such problems appear in the k-ω model. The model was proposed by Wilcox[2,12] and is gaining in popularity; modifications have been presented.[11,13,37] The ω equation is

$$\frac{\partial}{\partial x_j}(\rho \bar{U}_j \omega) = \frac{\partial}{\partial x_j}\left[\left(\mu + \frac{\mu_t}{\sigma_\omega}\right)\frac{\partial \omega}{\partial x_j}\right] + \frac{\omega}{k}(c_{\omega 1} P_k - c_{\omega 2} \rho k \omega).$$

If k goes to zero in region of low turbulence, the turbulent diffusion term simply goes to zero. The other terms remain, giving a nontrivial (i.e., neither zero nor infinity) value of ω. Note that the production term in the ω equation does not include k since

$$\frac{\omega}{k} c_{\omega 1} P_k = \frac{\omega}{k} c_{\omega 1} \mu_t \left(\frac{\partial \bar{U}_i}{\partial x_j} + \frac{\partial \bar{U}_j}{\partial x_i}\right)\frac{\partial \bar{U}_i}{\partial x_j} = c_{\omega 1} c_\mu \left(\frac{\partial \bar{U}_i}{\partial x_j} + \frac{\partial \bar{U}_j}{\partial x_i}\right)\frac{\partial \bar{U}_i}{\partial x_j}.$$

In ref. 38 the k-ω model was used to predict low-Reynolds-number, recirculating flow.

11.2.5.3 Ventilation Parameters

One of the commonly used ventilation parameters is ventilation effectiveness, and it shows how certain regions in the room are influenced by contaminant sources introduced into the room. Three definitions of ventilation effectiveness are often used, namely, the ventilation effectiveness in the occupied zone ϵ_{oc}, the local ventilation index ϵ_P, and the mean ventilation effectiveness $\langle \epsilon \rangle$.[39,40] They are defined as

$$\begin{aligned} \epsilon_{oc} &= \frac{C_{out}}{C_{oc}} \\ \epsilon_P &= \frac{C_{out}}{C_P} \\ \langle \epsilon \rangle &= \frac{C_{out}}{\langle C \rangle}, \end{aligned} \tag{11.9}$$

where C_{oc}, C_P, $\langle C \rangle$ and C_{out} denote the mean concentration in the occupied zone, concentration at a given point P, the mean concentration in the room, and the concentration at the outlet, respectively. To numerically simulate these parameters, the velocity field is first computed. Then a contaminant source is introduced at a cell (or cells) of a region to be studied, and the transport equation for contaminant C is solved. The transport equation for C is

$$\frac{\partial}{\partial x_j}(\rho \bar{U}_j C) = \frac{\partial}{\partial x_j}\left[\left(\mu + \frac{\mu_t}{\sigma_c}\right)\frac{\partial C}{\partial x_j}\right] + S_P, \tag{11.10}$$

where S_P is the contaminant source per unit volume in the chosen cell(s). Note that the magnitude of S_P does not affect the parameters in Eq. (11.9) since Eq. (11.10) is linear. The turbulent Prandtl number is usually set to a constant value $0.7 \leq \sigma_c \leq 0.9$. The boundary conditions for C are: $C = 0$ at inlet(s), zero normal gradient at walls (i.e., $\partial C/\partial n = 0$), and zero streamwise gradient at outlet(s).

The concept of local age and local purging flow rate was introduced in refs. 39 and 41. These parameters were first studied in connection with CFD in refs. 32 and 42. Local age at a point is understood to mean the time that

has elapsed since the particle passing this point entered the room. The definition of local purging flow rate is conceptually more difficult; it is related to how much (volume rate) flow at a point goes directly to the outlet without returning to the point. It turns out that this concept is not possible to determine, either in experiments where the measuring point necessarily has an extent in space (i.e., it is a volume) or in CFD, where finite volumes are used and the concept of a point is not relevant. In refs. 43 and 44, the concept of the local purging flow rate is derived, based on the theory of Markov chain models, for a *region*, and it is termed the *regional purging flow rate*. A number of new ventilation parameters, such as *local purging effectiveness of inlet* A_{sp}, *expected contaminant dispersion index (ECDI)*, and *local specific contaminant-accumulating index*, are presented in refs. 45 and 46.

A review of ventilation parameters can be found in refs. 47–49.

The Local Age and Air Change Efficiency

The transport equation for the local age is[50]

$$\frac{\partial}{\partial x_j}(\rho \bar{U}_j \tau) = \frac{\partial}{\partial x_j}\left[\left(\mu + \frac{\mu_t}{\sigma_\tau}\right)\frac{\partial \tau}{\partial x_j}\right] + \rho \ , \tag{11.11}$$

where σ_τ is the turbulent Prandtl number for τ ($0.7 \leq \sigma_\tau \leq 0.9$). The boundary conditions for τ are: $\tau = 0$ at the inlet, zero normal gradient at walls (i.e., $\partial \tau / \partial n = 0$), and zero streamwise gradient at the outlet. The dimension of τ is time, and the units are seconds.

As an example, the predicted local age for a room with an obstacle is shown in Fig. 11.13.

From the local age, the *air change efficiency* can be defined:

$$\epsilon_a = \frac{\tau_n}{\langle \tau \rangle} \ , \tag{11.12}$$

where τ_n is the nominal time constant, defined as room volume V divided by ventilation flow rate q ($\tau_n = V/q$), and $\langle \tau \rangle$ is the mean age of the air in the room.

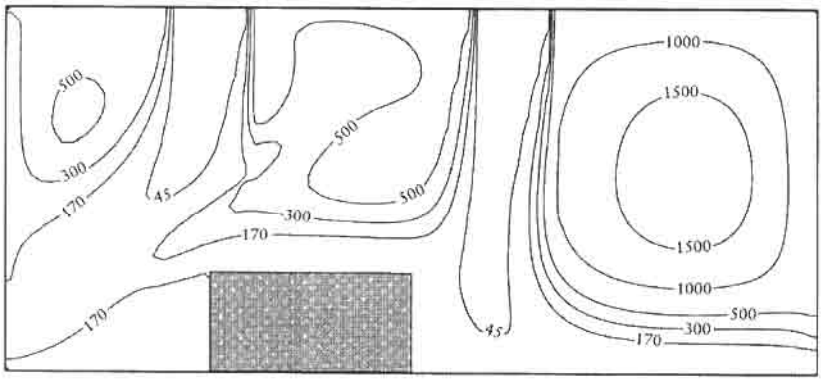

FIGURE 11.13 The local age. There are two inlets at the ceiling and two exits at the sidewalls near the floor. (Reprinted from *Building and Environment*, vol. 32, S.-H. Peng, S. Holmberg, and L. Davidson, "On the Assessment of Ventilation Performance with the Aid of Numerical Simulations," pp. 497–508, ©1997, with permission from Elsevier Science.)

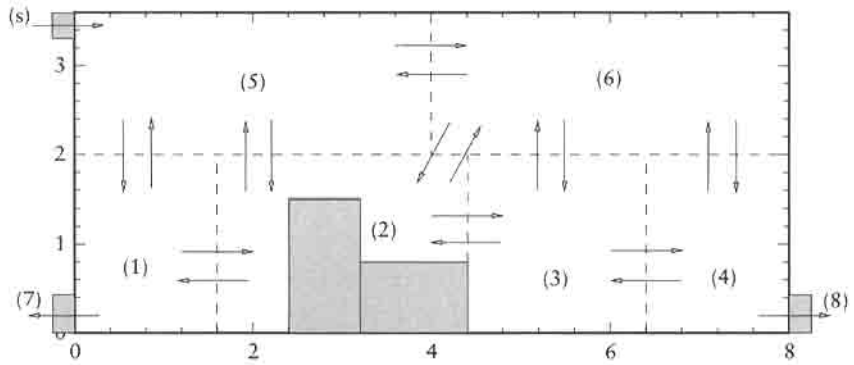

FIGURE 11.14 The purging flow rate. The configuration is divided into six regions. (Reprinted from *Building and Environment*, vol. 32, S.-H. Peng and L. Davidson, "Towards the Determination of Regional Purging Flow Rate," pp. 513–525, ©1997, with permission from Elsevier Science.)

The Regional Local Purging Flow Rate

First the velocity field is computed for the room; the configuration is shown in Fig. 11.14. The regional purging flow rate is computed for regions 1–6.[43] The computed values are tabulated in Table 11.3. As can be expected, U_p is highest in the region near the inlet, and it is low in the region near the workbench. It should be pointed out that U_p is dependent not only on the flow conditions, but also on the size of the region. The fact that U_p is smallest for region 1 is that most of the supplied air is extracted via the other outlet (8).

11.2.5.4 Large Eddy Simulation (LES)

When using LES, the time-dependent three-dimensional momentum and continuity are solved for. A subgrid turbulence model is used to model the turbulent scales that are smaller than the cells. Instead of the traditional time averaging, the equations for using LES are *filtered* in space, and $\bar{u}_i$ is a function of space *and* time.

In refs. 51 and 52 LES of flow in a ventilated room (height H, length L, width W) is presented. The configuration data are

$$L/H = 3,\ W/H = 1,\ h/H = 0.056,\ t/H = 0.16,$$

$$\mathrm{Re} = \frac{u_{\mathrm{in}} h}{\nu} = 5000.$$

TABLE 11.3 The Purging Flow Rate for the Six Regions Defined in Fig. 11.14[43]

Region	U_p (m³/h)
1	281
2	294
3	289
4	372
5	432
6	385

We have used $H = 3$ m, $U_{in} = 0.455$ m/s. The inlet (height h) is located at the left-side wall adjacent to the ceiling, and a wall jet is formed below the ceiling. The exit is located at the right-side wall near the floor (height t).

With LES we get much more information than with traditional time-averaged turbulence models, since we are resolving most of the turbulence. In Fig. 11.15 the computed $\bar{u}$ velocity is shown as a function of time in two cells; one cell is located in the wall jet (Fig. 11.15*a*), and the other cell is in the middle of the room (Fig. 11.15*b*). It is found the instantaneous fluctuations are very large. For example, in the region of the wall jet below the ceiling where the time-averaged velocity $\langle \bar{u} \rangle / U_0$ is typically 0.5, the instantaneous velocity fluctuations are between 0.2 and 0.9. In the middle of the room, which is a low-velocity region, the variation of $\bar{u}$ is much slower, i.e., the frequency is lower.

The probability density function of $\bar{u}$ is shown for four points in Fig. 11.16, two points in the wall jet and two points in the boundary layer close to the floor. For the points in the wall jet (Fig. 11.16*a*) the probability function shows a preferred value of $\bar{u}$ showing that the flow has a well-defined mean velocity and that the velocity is fluctuating around this mean value. Close to the floor near the separation at $x/H = 1$ (Fig. 11.16*b*) it is hard to find any preferred value of $\bar{u}$, which shows that the flow is irregular and unstable with no well-defined mean velocity and large turbulent intensity. From Figs. 11.15 and 11.16 we can see that LES gives us information about the nature of the turbulent fluctuations that can be important for thermal comfort. This type of information is not available from traditional CFD using k-ϵ models.

11.2.5.5 Combination with Outdoor Environment

In many applications there is some sort of airflow interaction between indoors and outdoors through some small openings (small compared with the whole interface area between inside and outside space).

There are two feasible ways of handling this problem: one is to include some of the outdoor space in the CFD computation domain; the other is to calculate the quantities through the interfaces of concern by other methods. Such methods include the use of analytical formulas, e.g., for temperature-difference-driven flow through an opening, or the use of a multizone program. The latter method is illustrated in the following example.[53]

The geometric situation is shown in Fig. 11.17 (see color insert). The figures show a large industrial parcel-distribution hall, where the parcels are collected from the main office and sorted in the rest of the hall for the fine distribution in the region. All the transport is done by trucks which are docked at over 140 doors around the building. When a truck is docked for loading or unloading, some spacings between the open door and the truck remain open. These openings lead to drafts inside the hall, particularly in the neighborhood of this door. As most of the time a large number of trucks are docked around the whole hall, there may be a large net draft through the hall, depending on the wind situation. The building is much exposed to the wind, so in this case obviously the wind-induced draft through all these openings strongly affects the comfort situation for the workers in the hall.

In this case the net draft through the hall was calculated for the whole year using the multizone program COMIS. All the scheduled loading and unloading

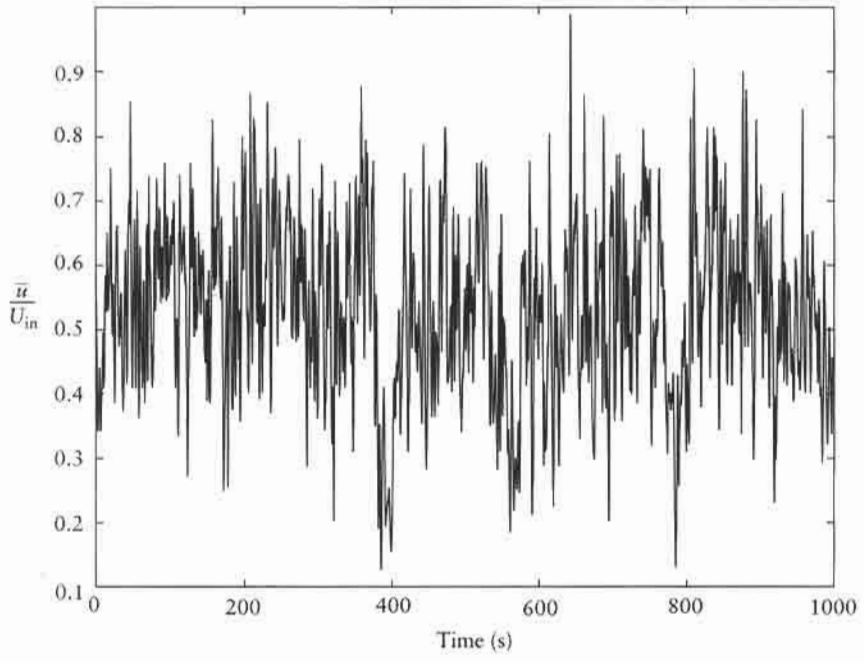

(*a*) $y / H = 0.92$

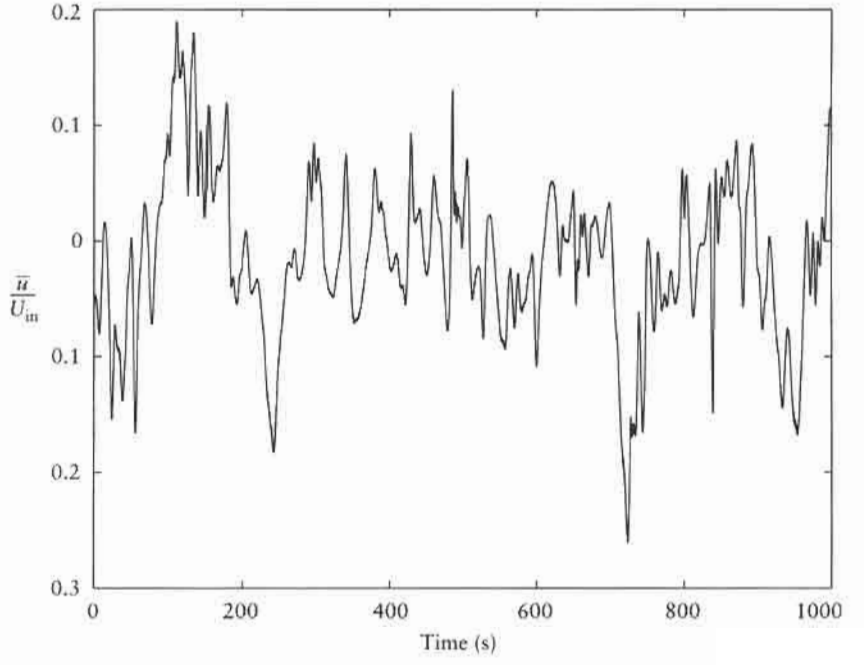

(*b*) $y/H = 0.50$

FIGURE 11.15 Time history of $\bar{u}$ at two chosen cells. $z/H = 0.5$, $x/H = 1$.[51]

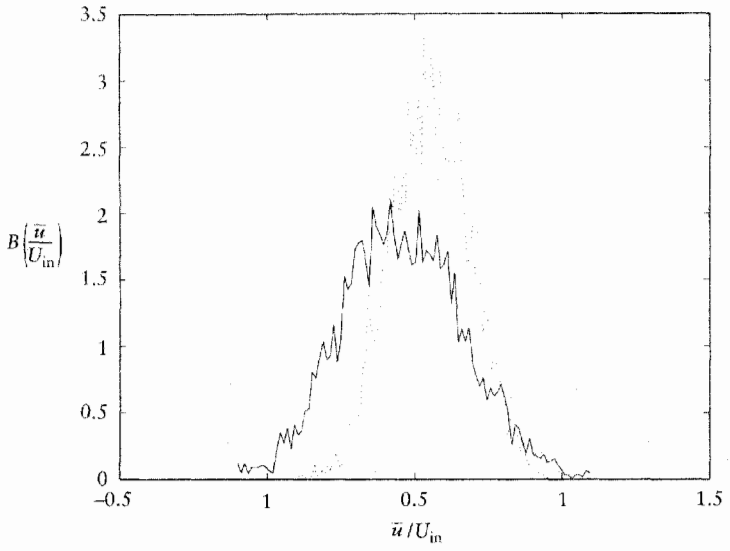

(*a*) $y/H = 0.92$

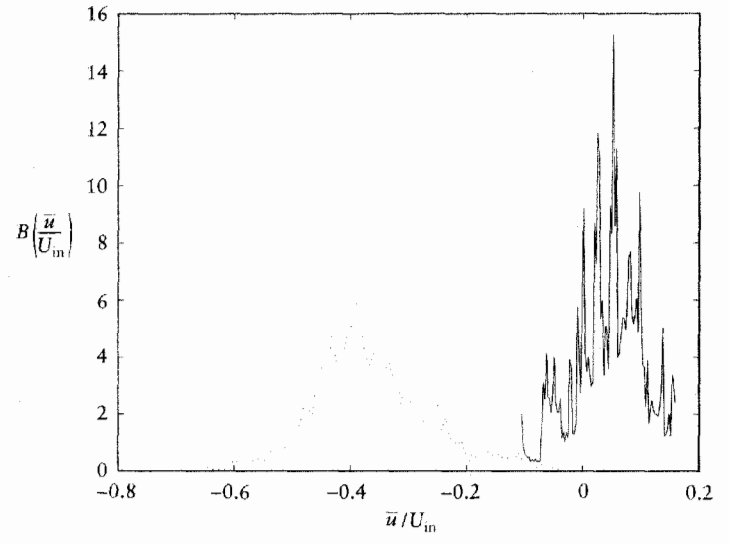

(*b*) $y/H = 0.24$

FIGURE 11.16 Probability density function of $\bar{u}$. Solid line: $x/H = 1.0$; dotted line: $x/H = 2.0$.[52]

processes and the whole wind situation of the design reference year meteorological data for the location of the building have been taken into account (see Fig. 11.18, color insert). For this calculation, the hall has been divided into about 12 zones: 8 at a lower level in the occupants' zone and 4 at a higher level.

An extreme situation (strong wind, low outside temperature, high number of docked trucks with open connections between inside and outside) has been chosen to investigate the influence on the indoor working situation. Figure 11.19 (see color insert) shows the mass flows through the openings on all sides of the building, which have been calculated using the multizone program and are fed as input to the CFD calculation in this case.

Figure 11.20 (see color insert) shows the resulting temperatures in the hall. Along the longer sides and the right of the hall, the lowest air temperatures are found. Air velocities higher than 0.5 m/s are found in this case at many locations inside. Finally, the working comfort was calculated, also taking into account the effect of radiant heating systems above the working area.

11.2.5.6 Simplification of Real Situation

The simplification of the real situation is a very important topic. Simplification is necessary due to limited resources, but the important flow features still should be captured.

No fixed rules can be given; it is up to the experience of the engineer to judge the necessary steps. Good advice, however, is to define a model with only the flow feature of concern, to test several levels of simplification on this model, and to decide from these numerical experiments the level of simplification for the full model under investigation.

The examples in this subsection illustrate some possible problems and solutions.

- Shapes of inside objects which are only partly permeable to airflow (sometimes referred to as porous objects), such as inlet grills, vents, etc.
  - Sometimes a large number of small objects are grouped together and modeled as a large, semiporous object. However, this can give wrong answers in some cases, as the flow through a homogeneously semiporous object is different from the flow around a number of discrete objects.
- Volumetric sources
  - Heat or contaminant sources can also be assigned to parts of the fluid volume to account for very small real sources or a distribution of a large number of small sources. Care must be taken, however, to make sure that this representation of distributed sources correctly describes the real situation.

Example 1: Farm with Animals

Figure 11.21 shows a farm with animals moving around.[54] Due to the symmetry of geometry and ventilation, only half of the scene is modeled and calculated. The pigs are simulated either as discrete objects (Fig. 11.21*a*) or as distributed semiporous objects (Fig. 11.21*b*).

For the first case, Figure 11.22 shows the airflow field above the floor in a plane through the objects. It obviously is very different from the solution obtained with homogeneously distributed semiporous objects, which shows more or less an average velocity all over the plane.

Which model is preferred depends on the final information needed. If the interest is in the magnitude of air velocity that is to be found, the discrete modeling method is certainly better.

Example 2: Textile Machine Hall

Figure 11.23 shows a textile machine hall with a large number of spinning machines. The interest is focused on the distribution of particles generated in the upper part of the machines (large rolls in Fig. 11.11*a*), which should be prevented by the ventilation system from propagating to

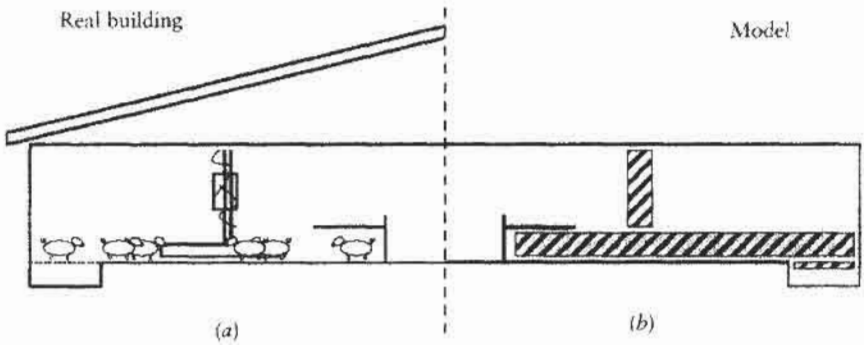

FIGURE 11.21 Groups of objects that are too complex to model (*a*) can be modeled as volumes with certain characteristics (*b*).

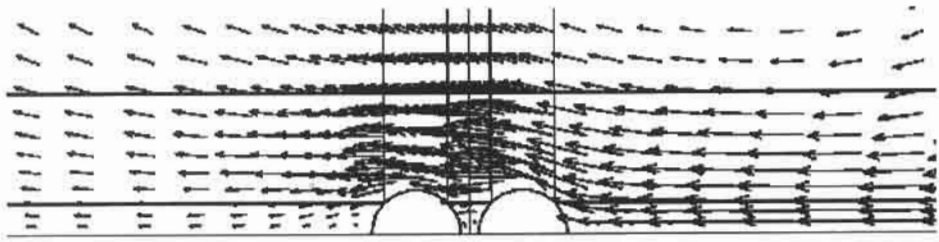

FIGURE 11.22 Calculated airflow field in a plane through discrete objects.

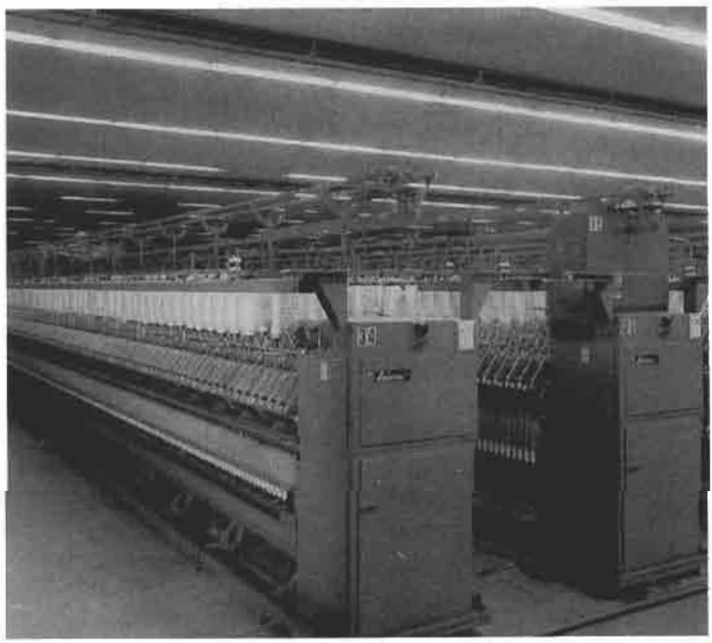

FIGURE 11.23 Textile machine hall with spinning machines.

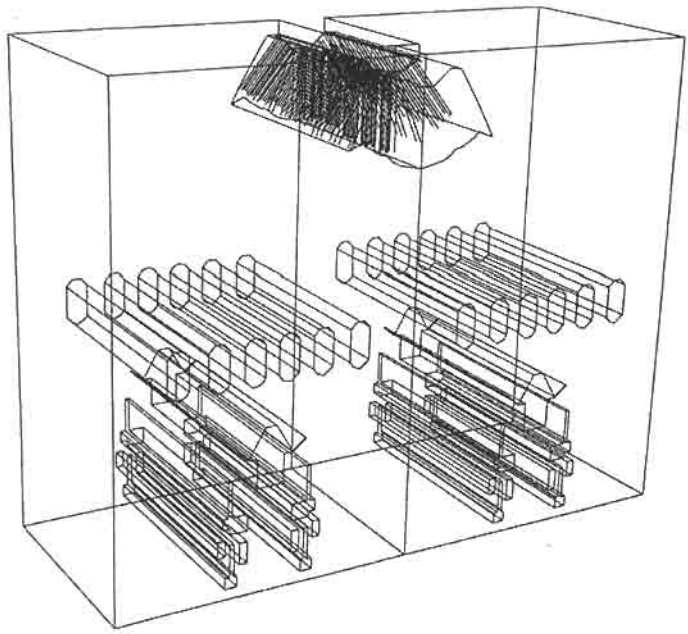

FIGURE 11.24 Model of small part of the hall.

the lower parts of the machines, where the particles would lead to thread damage.

Due to the symmetry of geometry and ventilation, only a small part of the hall is modeled and calculated, i.e., a section about 6 m in width, 2 m in depth, and extending over the full height (Fig. 11.24*b*).

The machines are very complicated, so they are simplified to a level which maintains the main features observed. In this case, the hall already existed, and the ventilation system needed to be improved. In the lower part of the machines are rotating wheels and axes which lead to a net flow across the floor in one direction through all the machines. Such a flow was generated by adding moving walls in the lower part of the machine model (Fig. 11.24), and the size of the velocity was adjusted to fit the measured speed in the real hall. Periodic boundary conditions are attached to the walls to the left and right in Fig. 11.24.

Figure 11.25 shows the flow with the redesigned ventilation system around the machines. In the lower part, the parallel flow along the floor due to the rotating parts is clearly visible. Figure 11.26 illustrates the effectiveness of the ventilation system by tracking massless particles. This method was used here as the particles are considered very small. Particles generated in the upper part of the machines are prevented from reaching the lower parts of the machines.

11.2.5.7 Particle Tracking

Particle tracking can often be very helpful. Sometimes the particle distribution is directly asked for; in other cases, it is an attractive way of illustrating the effectiveness of the ventilation system.

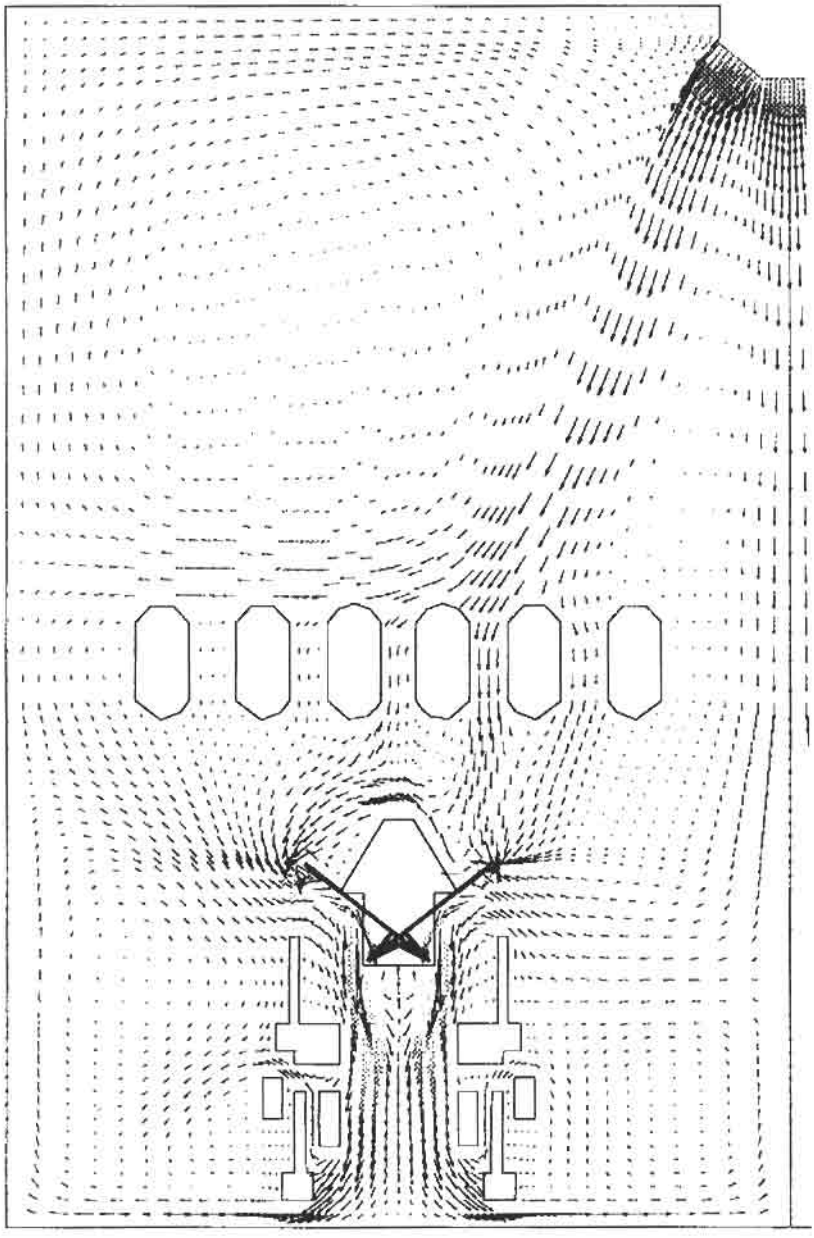

FIGURE 11.25 Airflow in redesigned ventilation system.

For massless particles, only a postprocessing of the result field is needed, where so-called streaklines that follow the given vector field are calculated. If the particles have a certain mass, additional equations have to be solved.

Example 2 in the previous subsection shows the use of massless particles.

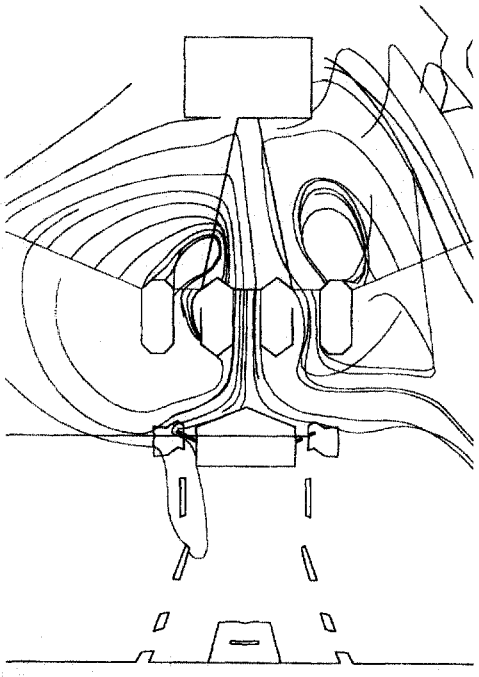

FIGURE 11.26 Streak lines showing path of massless particles.

11.2.6 Conclusions and Recommendations

We conclude by repeating a few general important points.

The application of CFD modeling is a very promising tool, and its use can be very helpful in a large number of applications but also requires some experience of the CFD engineer to produce accurate results.

A number of general methods and methods particularly suited to and needed for ventilation in large industrial rooms are presented in the previous sections. They differ in complexity of effort and accuracy of results and therefore are applied at different stages of the design process.

Usually, quite a number of parameter variations are needed, and different levels of simplification of the real situation have to be applied at different stages of the design process to draw the desired conclusions.

It is greatly recommended that strong feedback between the designer who needs the results and the CFD engineer is maintained to improve the results incrementally and also to produce results that are really needed. It is in fact an iterative design procedure.

References

1. Hanjalić, K. Advanced turbulence enclosure models: A view of current status and future prospects. *Int. J. Heat Fluid Flow*, vol. 15, pp. 178–203, 1994.
2. Wilcox, D. C. *Turbulence modeling for CFD*. La Canada, Calif.: DCW Industries, 1993.

3. Versteegh, H. K., Malalasekera, W. *An introduction to computational fluid dynamics: The finite volume method.* Harlow, England: Longman Scientific & Technical, 1995.
4. Davidson, L. An introduction to turbulence models. Report 97/2, Dept. of Thermo and Fluid Dynamics, Chalmers University of Technology, Gothenburg, 1997.
5. Yuan, X., Moser, A., Suter, P. Wall functions for numerical simulation of turbulent natural convection along vertical plates. *Int. J. Heat Mass Transfer*, vol. 36, pp. 4477–4485, 1993.
6. Launder, B. E. On the computation of convective heat transfer in complex turbulent flow. *Trans. ASME: J. Heat Transfer*, vol. 110, pp. 1112–1128, 1988.
7. Chien, K. Y. Predictions of channel and boundary layer flows with a low-Reynolds-number turbulence model. *AIAA J.*, vol. 20, pp. 33–38, 1982.
8. Lam, C. K. G., Bremhorst, K. A modified form of the k-ϵ model for predicting wall turbulence. *ASME J. Fluids Eng.*, vol. 103, pp. 456–460, 1981.
9. Chen, H. C, Patel, V. C. Near-wall turbulence models for complex flows including separation. *AIAA J.*, vol. 26, pp. 641–648, 1988.
10. Abe, K., Kondoh, T., Nagano, Y. A new turbulence model for predicting fluid flow and heat transfer in separating and reattaching flows: 1. Flow field calculations. *Int. J. Heat Mass Transfer*, vol. 37, pp. 139–151, 1994.
11. Wilcox, D. C. Simulation of transition with a two-equation turbulence model. *AIAA J.*, vol. 32, pp. 247–255, 1994.
12. Wilcox, D. C. Reassessment of the scale-determining equation. *AIAA J.*, vol. 26, no. 11, pp. 1299–1310, 1988.
13. Peng, S. H., Davidson, L., Holmberg, S. A modified low-Reynolds-number k-ω model for recirculating flows. *ASME J. Fluids Eng.*, vol. 119, pp. 867–875, 1997.
14. Patel, V. C., Rodi, W., Scheuerer, G. Turbulence models for near-wall and low Reynolds number flows: A review. *AIAA J.*, vol. 23, pp. 1308–1319, 1985.
15. Jacobsen, T. Airflow and temperature distribution in rooms with displacement ventilation. Ph.D. thesis, Dept. of Building Technology and Structural Engineering, Aalborg University, Aalborg, 1993.
16. Li, Y. Simulation of flow and heat transfer in ventilated rooms. Ph.D. thesis, Dept. of Mechanics, Royal Institure of Technology, Stockholm, 1992.
17. Müller, D., Renz, U. Measurements and predictions of room airflow patterns using different turbulence models. In Mundt, E., Malmström, T. G., eds., *Roomvent '98: 6th Int. Conf. on Air Distributions in Rooms*, vol. 1, pp. 109–116, Stockholm, 1998.
18. Glickman, L. R., Chen, Q. Interaction of radiation absorbed by moisture in air with other forms of heat transfer in an enclosure. In Mundt, E., Malmström, T. G., eds., *Roomvent '98: 6th Int. Conf. on Air Distributions in Rooms*, vol. 2, pp. 111–118, Stockholm, 1998.
19. Chen, Q. Prediction of room air motion by Reynolds-stress models. *Build. Environ.*, vol. 31, pp. 233–244, 1996.
20. Rodi, W. A new algebraic relation for calculating the Reynolds stresses. *ZAMM*, vol. 56, pp. T219–T221, 1976.
21. Kato, S., Marakami, S., Kondo, Y. Numerical simulation of two-dimensional room airflow with and without bouyancy by means of ASM. *ASHRAE Trans.*, vol. 100, pp. 238–255, 1994.
22. Gatski, T. B., Speziale, C. G. On explicit algebraic stress models for complex turbulent flows. *J. Fluid Mech.*, vol. 154, pp. 59–78, 1993.
23. Shih, T. H., Zhu, J., Lumley, J. L. A new Reynolds stress algebraic equation model. *Comput. Methods Appl. Eng.*, vol. 125, pp. 287–302, 1995.
24. Abid, R., Ramsey, C., Gatski, T. Prediction of nonequilibrium turbulent flows with explicit algebraic stress models. *AIAA J.*, vol. 33, pp. 2026–2031, 1995.
25. Nielsen, P. V. Berechnung der luftbewegung in einem zwangsbelüftete raum. *Gesundheits-Ingenieur*, vol. 94, no. 10, 1973.
26. Nielsen, P. V. Flow in air conditioned rooms. Ph.D. thesis, Technical University of Denmark, Copenhagen, 1974.
27. Nielsen, P. V., Restivo, A., Whitelaw, J. H. The velocity characteristics of ventilated rooms. *ASME J. Fluids Eng.*, vol. 100, pp. 291–298, 1978.
28. Nielsen, P. V. Description of supply openings in numerical models for room air distribution. *ASHRAE Trans.*, vol. 98, pp. 963–971, 1992.
29. Nielsen, P. V. The box method—A practical procedure for introduction of an air terminal device in CFD calculation. Report R9744, Dept. of Building Technology and Structural Engineering, Aalborg University, Aalborg, 1997.

30. Nielsen, P. V., Restivo, A., Whitelaw, J. H. The flow properties of rooms with small ventilation openings. *ASME J. Fluids Eng.*, vol. 102, pp. 316–322, 1980.
31. Nielsen, P. V. The prescribed velocity method—A practical procedure for introduction of an air terminal device in CFD calculation. Report R9827, Dept. of Building Technology and Structural Engineering, Aalborg University, Aalborg, 1998.
32. Davidson, L., Olsson, E. Calculation of age and local purging flow rate in rooms. *Bldg. Environ.*, vol. 22, pp. 111–127, 1987.
33. Davidson, L. Turbulence modelling and calculation of ventilation parameters in ventilated rooms. Lic. thesis. Report 86/10, Dept. of Thermo and Fluid Dynamics, Chalmers University of Technology, Gothenburg, 1986.
34. Davidson, L. Numerical simulation of turbulent flow in ventilated rooms. Ph.D. thesis, Dept. of Applied Thermodynamics and Fluid Mechanics, Chalmers University of Technology, Gothenburg, 1989.
35. Davidson, L. Ventilation by displacement in a three-dimensional room: A numerical study. *Build. Environ.*, vol. 24, pp. 363–372, 1989.
36. Shankar, V., Davidson, L., Olsson, E. Numerical investigation of turbulent plumes in both ambient and stratified surroundings, *Indoor Air*, vol. 5, pp. 136–146, 1995.
37. Menter, F. R. Two-equation eddy-viscosity turbulence models for engineering applications. *AIAA J.*, vol. 32, pp. 1598–1605, 1994.
38. Peng, S. H., Davidson, L., Holmberg, S. The two-equation rurbulence k-ω model applied to recirculating ventilation flows. Report 96/13, Dept. of Thermo and Fluid Dynamics, Chalmers University of Technology, Gothenburg, 1996.
39. Sandberg, M., Sjöberg, M. The use of moment for assessing air quality in ventilated rooms. *Build. Environ.*, vol. 18, pp. 181–197, 1983.
40. Nielsen, P. V. Lecture notes on mixing ventilation. Report U9513, Dept. of Building Technology and Structural Engineering, Aalborg University, Aalborg, 1995.
41. Sandberg, M. What is ventilation efficiency? *Build. Environ.*, vol. 16, pp. 123–135, 1981.
42. Davidson, L., Olsson, E. A numerical investigation of the local age and the local purging flow rate in two-dimensional rooms. In *Roomvent '87*, Stockholm, 1987.
43. Peng, S. H., Davidson, L. Towards the determination of regional purging flow rate. *Build. Environ.*, vol. 32, pp. 513–525, 1997.
44. Peng, S. H. Modeling of turbulent flow and heat transfer for building ventilation. Ph.D. thesis, Dept. of Thermo and Fluid Dynamics, Chalmers University of Technology, Gothenburg, 1998.
45. Peng, S. H., Holmberg, S., Davidson, L. On the assessment of ventilation performance with the aid of numerical simulations. *Build. Environ.*, vol. 32, pp. 497–508, 1997.
46. Peng, S. H. New scales for assessing ventilation performance. In Mundt, E., Malmström, T. G., eds. *Roomvent '98: 6th Int. Conf. on Air Distributions in Rooms*, vol. 2, pp. 243–250, Stockholm, 1998.
47. Skåret, E. Ventilation efficiency—A survey of concepts of ventilation effectiveness. Report STF15 A84087, SINTEF, Trondheim, 1984.
48. Sandberg, M. Ventilation effectiveness and purging flow rate—A review. In *Int. Symp. on Room Air Convection and Ventilation Effectiveness*, Tokyo, 1992.
49. Ethridge, D., Sandberg, M. *Building ventilation: Theory and measurement*. Chichester, John Wiley & Sons, 1996.
50. Spalding, D. B. A note on mean residence times in steady flow of arbitrary complexity. *Chem. Eng. Sci.*, vol. 9, pp. 74–78, 1958.
51. Davidson, L. Large eddy simulation: A dynamic one-equation subgrid model for three-dimensional recirculating flow. In *11th Int. Symp. on Turbulent Shear Flow*, vol. 3, pp. 26.1–26.6, Grenoble, 1997.
52. Davidson, L., Nielsen, P. Large eddy simulations of the flow in a three-dimensional ventilated room. In Murakami, S., ed. *Roomvent '96: 5th Int. Conf. on Air Distributions in Rooms*, vol. 2, pp. 161–168, Yokohama, Japan, 1996.
53. Dorer, V., Schälin, A. On the combined application of thermal and CFD modelling in the design of naturally ventilated industrial halls. In *Roomvent 2000*, Reading, UK, 2000.
54. Svidt, K., Zhang, G., Bjerg, B. CFD Simulation of air velocity distribution in occupied livestock buildings. In Mundt, E., Malmstrüm, T. G., eds. *Roomvent '98: 6th Int. Conf. on Air Distribution in Rooms*, Stockholm, 1998.

11.3 THERMAL BUILDING–DYNAMICS SIMULATION

11.3.1 Introduction

Purpose

The main purposes of thermal building–dynamics simulation are

- Energy-demand predictions for heating and cooling
- Energy-performance assessment of a building
- Evaluation of passive cooling options
- Thermal comfort assessments: room air and operative temperatures (but not draft risk evaluations)
- Determination of peak loads and dimensioning of HVAC system components
- Optimization of operation and control of HVAC systems
- Performance assessment of innovative HVAC systems, facades, and glazings
- Daylighting analysis (interaction with solar gains)
- Moisture transport
- Proof of compliance with building regulations or codes expressed in terms of either peak load targets or energy targets

11.3.1.1 Combined and Integral Building Design

Combined thermal and multizone airflow models are needed for problems such as thermal comfort analysis in naturally ventilated buildings, determination of heat-removal capacity by natural ventilation, design and evaluation of passive cooling by nighttime ventilation. This is outlined in more detail in Section 11.5.

For integral building design and performance assessments (thermal comfort, indoor air quality, visual comfort), either integrated building simulation tools must be used or the thermal building simulation must be complemented by airflow and daylighting simulations.

11.3.1.2 Terminology

The structural elements of a building consist of the envelope elements (external walls, floors, ceilings, roof) and internal constructional elements (internal walls). All these opaque (not light transmitting) elements are referred to as *walls* in this section. Translucent elements are referred to as *windows*.

11.3.2 Physical Phenomena

11.3.2.1 Introduction

In this section the basic physical models for the simulation of the dynamic thermal behavior of a building are given. The description starts with the transfer of heat and solar radiation through the building envelope, then summarizes the various ways that this energy is distributed in the room, shows the methods to calculate the instantaneous space sensible load (in other words, the cooling or heating load of the room), and finally deals with the outdoor conditions. In addition, a short overview of the modeling of HVAC components and systems is given.

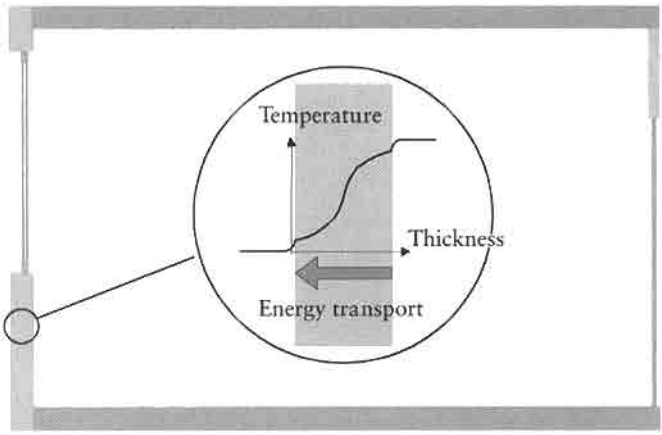

FIGURE 11.27 Heat conduction through an external wall. The temperature distribution over the wall thickness is linear only under steady-state conditions.

11.3.2.2 Heat-Transfer Processes

Heat is transferred by means of three quite different mechanisms:

- Thermal conduction
- Thermal convection
- Thermal radiation

Conduction

Conduction is the heat transfer due to spatial temperature differences (temperature gradient) without any macroscopic material movement. Conduction is important in solids and depends essentially on the material properties (Fig. 11.27).

Convective Heat Transfer

Convection is the heat transfer in the fluid from or to a surface (Fig. 11.28) or within the fluid itself. Convective heat transport from a solid is combined with a conductive heat transfer in the solid itself. We distinguish between free and forced convection. If the fluid flow is generated internally by density differences (buoyancy forces), the heat transfer is termed *free convection.* Typical examples are the cold down-draft along a cold wall or the thermal plume upward along a warm vertical surface. Forced convection takes place when fluid movement is produced by applied pressure differences due to external means such as a pump. A typical example is the flow in a duct or a pipe.

Radiative Heat Transfer

Each body having a temperate above absolute zero radiates energy in the form of electromagnetic waves. The amount of energy emitted is dependent on the temperature and on the emissivity of the material. The wavelength or frequency distribution (the spectrum) of the emitted radiation is dependent on the absolute temperature of the body and on the surface properties.

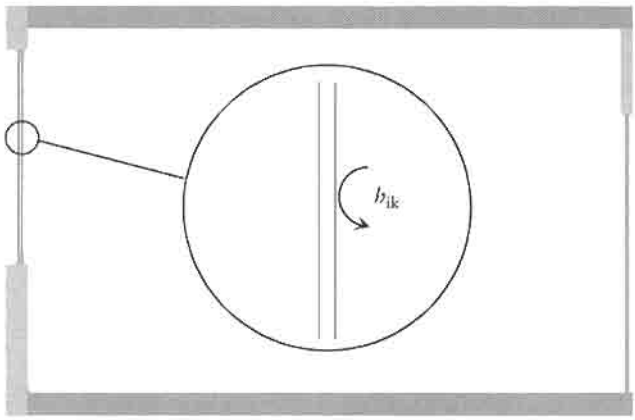

FIGURE 11.28 Convective heat transfer from the glazing surface to the room air.

Long-wave radiation (infrared radiation) is in the range of 0.8–100 μm, short-wave radiation (visible as light) is in the range 0.4–0.8 μm, and solar radiation is in the range 0.3–3.0 μm.

11.3.2.3 Heat-Exchange Processes in the Room

Heat-Balance Equations

The air temperature of a room at any given time is given by a heat-balance equation which includes the heat flux exchanged by convection at each wall element ($A \cdot q_c$), the heat flow exchanged by ventilation (Φ_v), the convective part of heat flow due to internal heat gains (Φ_{ic}), the convective part of heat flow due to the HVAC system (Φ_{hc}), and the variation of energy in the room air($c \cdot M \cdot \partial\theta_a/\partial t$):

$$\sum_{j=1}^{N} (A \cdot q_c) + \Phi_v + \Phi_{ic} + \Phi_{hc} = c \cdot M \cdot \frac{\partial \theta_a}{\partial t}. \tag{11.13}$$

The individual heat fluxes in (Eq. 11.13)—q_c, Φ_v, Φ_{ic},Φ_{hc}—are also time-dependent.

The convection term q_c is given by (h_c, convective heat transfer coefficient; θ_s, inside surface temperature of wall element j; θ_a, room air temperature):

$$q_{c_j} = h_{c_j}(\theta_s - \theta_a). \tag{11.14}$$

The internal surface temperature of each wall element j is given by a heat-balance equation:

$$q_{lr,j} + q_{sr,j} + q_{c,j} + q_{cd,j} + \frac{\Phi_{ir}}{A_j} \cdot \varphi_{ir,j} = 0 \ , \tag{11.15}$$

where q_{lr} is the heat flux by long-wave radiation exchange with other internal surfaces, q_{sr} is the heat flux due to the absorbed short-wave radiation, q_c is the heat flux by convection, q_{cd} is heat flux by conduction, Φ_{ir}/A_j is the heat flux due to the radiative component of the internal heat gains, and $\varphi_{ir,j}$ is the view factor between source and surface j (Figs. 11.29 and 11.30).

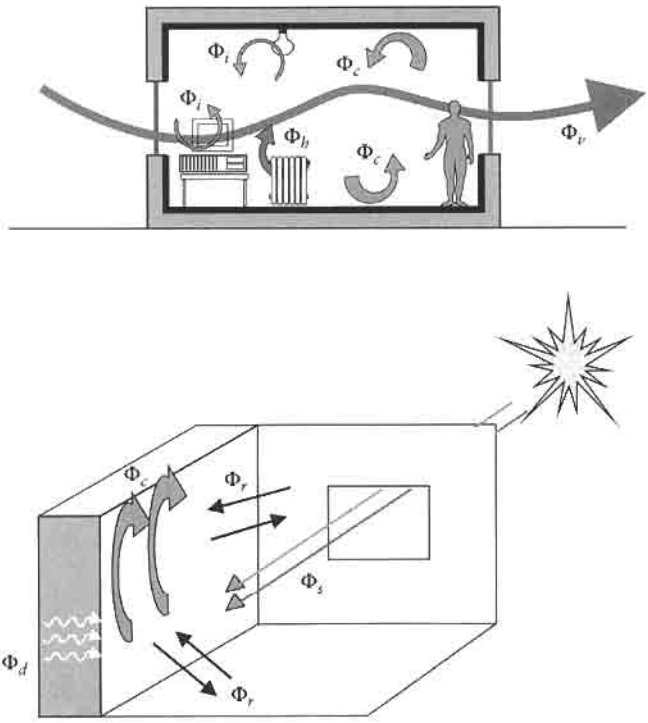

FIGURE 11.30 Heat balance of a wall.

The humidity ratio of a room at any given time is given by a latent heat balance equation including the water vapor flows due to infiltration ($\dot{M}_{w,f}$), to ventilation ($\dot{M}_{w,v}$), to moisture transport through envelope elements ($\dot{M}_{w,d}$), to internal sources ($\dot{M}_{w,i}$), and to the HVAC system ($\dot{M}_{w,h}$), and the variation of moisture content in the zone air mass M ($M\ \partial x_a/\partial t$):

$$\dot{M}_{w,f} + \dot{M}_{w,v} + \dot{M}_{w,d} + \dot{M}_{w,i} + \dot{M}_{w,h} = M \cdot \frac{\partial x_a}{\partial t} \tag{11.16}$$

All heat flux and moisture flux elements in Eqs. (11.13) to (11.16) are also time-dependent.

Solar Radiation Distribution

The heat transferred into a room by solar radiation (short-wave radiation) strongly influences the room climate. Direct and diffuse solar radiation are generally considered separately (Fig. 11.31). Reflections normally are not considered in building simulation codes. According to this assumption, the direct radiation is attributed to the surfaces hit by the beam, while diffuse radiation is distributed to the individual surfaces in the room either according to the area of each surface (area-weighted approach) or according to the geometric situation as seen from the transparent surface (view-factor method, see also long-wave radiation exchange later). At the wall surface, the energy balance is

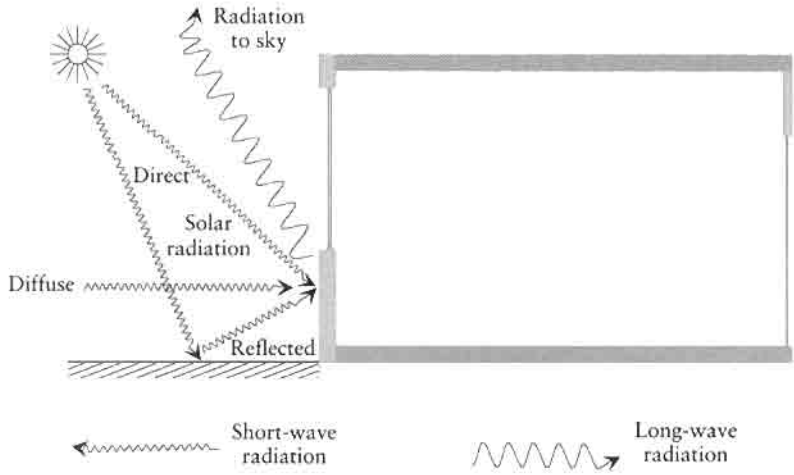

FIGURE 11.31 Radiation fluxes at the building facade: the solar radiation components (direct or beam, diffuse, and reflected radiation from the ground or other buildings) and the components of the radiation back from the building facade (reflected solar and thermal infrared radiation from the building envelope).

established by long-wave radiation exchange to other surfaces, by convection to the room air, and by heat conduction into the wall construction.

Proper consideration of solar radiation exchange between two rooms through a transparent element is important when analyzing atria, sunspaces, or glazed double facades.

Convective Heat Transfer at Surfaces

The kind of convective heat transfer—forced convection or natural (at floor, wall, or ceiling)—must be considered and taken into account by selecting appropriate values for the convective heat transfer coefficient h_c (see Eq. (11.14)). Thus, the heat transfer coefficient implicitly assumes the flow situation at the surface. Normally, coefficients for convective heat transfer are considered as a preset constant parameter (the coefficient may be defined as variable, however, depending on other parameters). Therefore, the selection of appropriate values is crucial. Values for heat transfer coefficients can be found in several references; a comprehensive summary is given in Daskalaki.[1]

Long-Wave Radiation Exchange

All surfaces in a zone exchange long-wave radiation with each other. The net energy transmitted from one surface to another is dependent on the surface temperatures, the surface emissivity, the area, and the orientation of the two surfaces relative to each other. For long-wave radiation, the surface emissivity is assumed to be angle independent. The geometric relation of the two surfaces is described by the view factor. If multireflections are taken into account, the net radiation heat exchange is calculated using exchange factors (e.g., according to Gebhart[2]).

Internal Heat Gains (Casual Gains)

In industrial applications, internal heat gains are very often the most important factor affecting the thermal indoor climate. Typical heat sources are machines, appliances and equipment, and all kind of processes taking place in the room. Artificial lighting and people further contribute to the internal heat load in the room.

In the simulation, the time dependency of the energy release of such sources is defined in so-called schedules. The heat sources transfer energy to the room air by convection and to the surfaces by long-wave radiation. In principle, heat sources can be modeled by two kinds of parameterization:

- Heat source with defined surface temperature and area
- Heat source with predefined total gain and the split between convective and radiative heat release

In the case of a given surface temperature, the amount of energy released is determined by the parameters for the convective and radiative heat exchange. As far as convection is concerned, these are the temperatures of the heat source surface and room air, respectively, and the heat transfer coefficient. The radiative heat exchange is determined by the view factors and the temperatures of the surrounding surfaces.

In the second approach, the energy release is split by a predefined (mostly constant) factor between convection and radiation. The convective part is directly transferred as energy gain to the room air, while the radiative part is distributed to the surrounding walls by the area-weighted method or the view-factor method.

Heat gains from internal loads normally are sensible heat. Nevertheless, many processes release a significant amount of moisture. Also, occupants produce relevant amounts of latent heat, especially at high metabolic rates and at high air temperatures.

Ventilation

When air flows at a certain rate through the space, energy is transported in relation to the difference between supply and extract air temperature. Such airflow can be induced by natural or mechanical ventilation. See Section 11.5 on the interaction between naturally induced airflows and the thermal behavior of the room.

Heat Storage in the Room

Normally, the heat storage capacity of the air in the space can be neglected. Machines, tools, equipment, etc. situated in the room may have a significant influence on the thermal behavior of the room and must be considered in the simulation.

11.3.2.4 Outdoor Conditions

Outdoor Air Temperature

Outdoor air temperature is an important factor regarding the building energy balance. Outdoor air temperature affects the heat transfer through external walls and roofs and the heat transfer by ventilation. Moreover, outdoor air

temperature is a driving force for natural ventilation, as the difference between indoor and outdoor air temperature causes the stack effect.

Outdoor Air Humidity

Outdoor air humidity strongly affects the latent cooling load and energy requirements during summer season. Year-round outdoor air humidity must be considered when studying condensation conditions.

Wind

Wind affects the convective heat transfer on external walls and is a driving force for natural ventilation.

Solar Radiation (Short-Wave Radiation)

The total or global solar radiation has a direct part (beam radiation) and a diffuse part (Fig. 11.31). In the simulation, solar radiation input values must be converted to radiation values for each surface of the building. For nonhorizontal surfaces, the diffuse radiation is composed of (a) the contribution from the diffuse sky and (b) reflections from the ground. The diffuse sky radiation is not uniform. It is composed of three parts, referred to as *isotropic*, *circumsolar*, and *horizontal brightening*. Several diffuse sky models are available. Depending on the model used, discrepancies for the boundary conditions may occur with the same basic set of solar radiation data, thus leading to differences in the simulation results.

The solar radiation absorbed on external building surfaces increases the wall surface temperature, thus leading to a change in the heat conducted through the component. In low-wind conditions, free convective flows drift up the warm external wall surface. This changes the convective heat transfer and leads to increased temperatures of supply air for natural ventilation.

Neither effect normally is accounted for in building simulation programs. Normally, for energy analysis, this is not critical, but it may have a significant effect on natural ventilation of multistory buildings.

Shading

Since insolation often has a very significant effect on the heat balance of a building, shading by buildings or other objects in the surroundings of the building must be taken into account. Also, certain wings or parts of the building itself may shade the part under investigation permanently or over certain time periods. Normally, thermal building–dynamics simulation programs allow for the consideration of such shading.

Long-Wave Radiation

A fictive sky temperature, dependent on ambient temperature, emissivity, and cloudiness, is introduced to account for the long-wave radiative heat exchange between the building envelope and the sky.

11.3.3 Calculation Methods

Simulation is the prediction of a real process by the use of a model. Of the many parameters which influence this process, some must be included in the

model because they are interdependent (e.g., temperatures); others are little affected by other model parameters or by the results of the simulation and thus can be assumed as a preset parameter (e.g., dimensions, material properties, outdoor conditions). Such parameters form the boundary conditions for the model.

This section does not contain any fundamentals or mathematics but tries to describe the basic energy flows and the methods used in thermal building-dynamics simulation codes to model these. Also, the methods are described without stating the underlying algorithms and equations, for which the reader is referred to the literature and references. A short outline of how these models affect the application possibilities and limits is given at the end of this section and also in Section 11.3.7.

11.3.3.1 Outdoor Conditions

In thermal building-dynamics simulation codes, outdoor conditions are mostly input by the so-called weather data file, containing (usually hourly) data for air temperature, wind speed and direction, air humidity, and global and diffuse solar radiation on horizontal surfaces.

Data are provided as measured data or prepared data, representing typical data for a period of several years. Design reference years (DRY) established using methods developed with the framework of the IEA (International Energy Agency) represent characteristic data for a period of 10 years, condensed into a one-year data set. Internal coherence, e.g., between solar irradiation and air temperature, is maintained. For the United States, typical meteorological year (TMY) files are based on measurements in the period 1954 through 1972.

11.3.3.2 Heat Transfer through the Building Envelope

Conduction

Basically, two kinds of heat conduction are distinguished:

- Steady-state conduction
- Unsteady or dynamic conduction

Under steady-state conditions, the temperature distribution in the wall is only spatial and not time dependent. This is the case, e.g., if the boundary conditions on both sides of the wall are kept constant over a longer time period. The time to achieve such a steady-state condition is dependent on the thickness, conductivity, and specific heat of the material. If this time is much shorter than the change in time of the boundary conditions on the wall surface, then this is termed a quasi-steady-state condition. On the contrary, if this time is longer, the temperature distribution and the heat fluxes in the wall are not constant in time, and therefore the dynamic heat transfer must be analyzed (Fig. 11.32).

Calculation Methods for Dynamic Conduction

In reality, heat is conducted in all three spatial dimensions. While specific building simulation codes can model the transient and steady-state two-dimensional temperature distribution in building structures using finite-difference or finite-elements methods, conduction is normally modeled one-

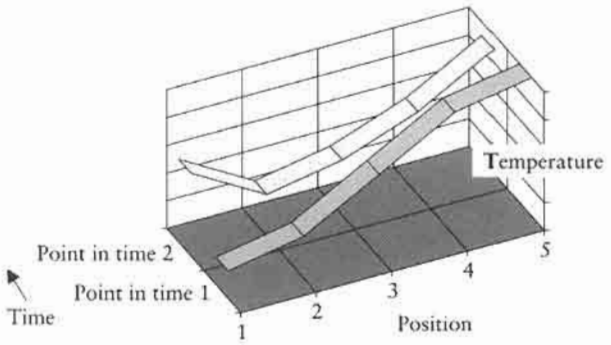

FIGURE 11.32 Temperature distribution in a wall section at two different times.

dimensionally. In-plane conduction is neglected, and cold bridge effects are therefore not considered. However, with the increasing level of building insulation, these effects become more important. They have to be accounted for by setting the material properties and surface areas accordingly.

To describe the dynamic thermal behavior of the envelope and internal structural elements, the following two methods are most often used in thermal building simulation codes:

- Finite differences
- Response factors

In the *finite-difference approach*, the partial differential equation for the conduction of heat in solids is replaced by a set of algebraic equations of temperature differences between discrete points in the slab. Actually, the wall is divided into a number of individual layers, and for each, the energy conservation equation is applied. This leads to a set of linear equations, which are explicitly or implicitly solved. This approach allows the calculation of the time evolution of temperatures in the wall, surface temperatures, and heat fluxes. The temporal and spatial resolution can be selected individually, although the computation time increases linearly for high resolutions. The method easily can be expanded to the two- and three-dimensional cases by dividing the wall into individual elements rather than layers.

The *response-factor approach* is based on a method in which the response factors represent the transfer functions of the wall due to unit impulse excitations. The real excitation is approximated by a superposition of such impulses (mostly of triangular shape), and the real response is determined by the superposition of the impulse responses (see Figs. 11.33 and 11.34).[3]

The response factors are characteristic for the layer buildup of the selected wall and are calculated before (by a preprocessor program) or at the beginning of the simulation. Numerical reasons limit the time step to approximately 10 to 60 min, depending on the thickness and material properties of the wall layers. The method allows the calculation of surface temperatures and heat fluxes but not the determination of the temperature distribution within the wall. Due to the precalculation of these response factors, the computer time for the simulation might be significantly reduced.

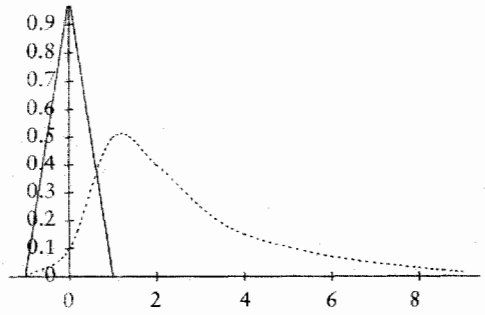

FIGURE 11.33 Typical response function to a unit pulse of the temperature or heat flux boundary.

If energy is supplied to or extracted from a layer within the component, finite-difference models or problem-adapted one-dimensional response-factor- based models have to be used.

Although the method is expandable, it is normally used for the one-dimensional case (wall defined by layers).

Heat Loss to the Ground

The computation time for calculations of energy losses to the ground can be quite significant because of the three-dimensional heat conduction problem. Simplified methods are given in ISO/FDIS 13370: 1998.[4]

Heat Transfer through Windows

Each pane of a window absorbs and reflects a part of the incoming solar radiation in relation to the incident angle and the wavelength band, depending on the properties of the glazing material and coatings if applied (Fig. 11.35). Only a part of the insolation penetrates directly into the room. Energy is also transmitted from one side of the glazing to the other by other means of heat transfer.

For single glazing, the determination of the absorbed and transmitted radiation and of the heat transfer is quite straightforward, but for a window with multipane glazing, the calculation is more complex. Besides conduction in the panes, convection in the gaps as well as multiple reflections between the individual panes must be considered.

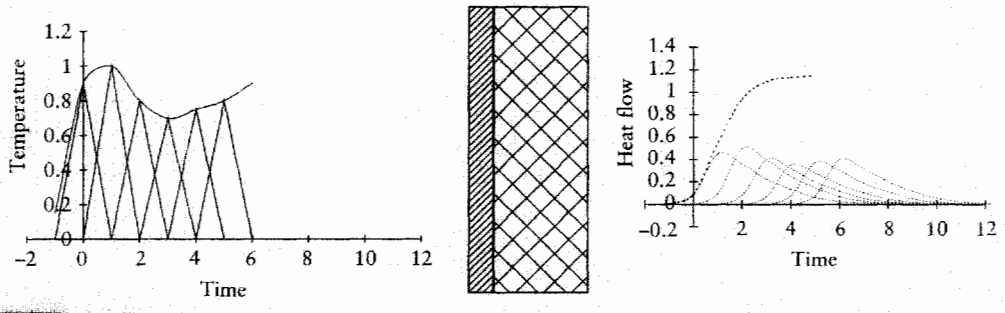

FIGURE 11.34 Determination of the real evolution of the heat flux at the inside wall surface: The temperature condition at the exterior surface is approximated by triangular pulses, and the heat flux response at the interior surface is determined by superposition of the heat flux responses of the individual pulses.

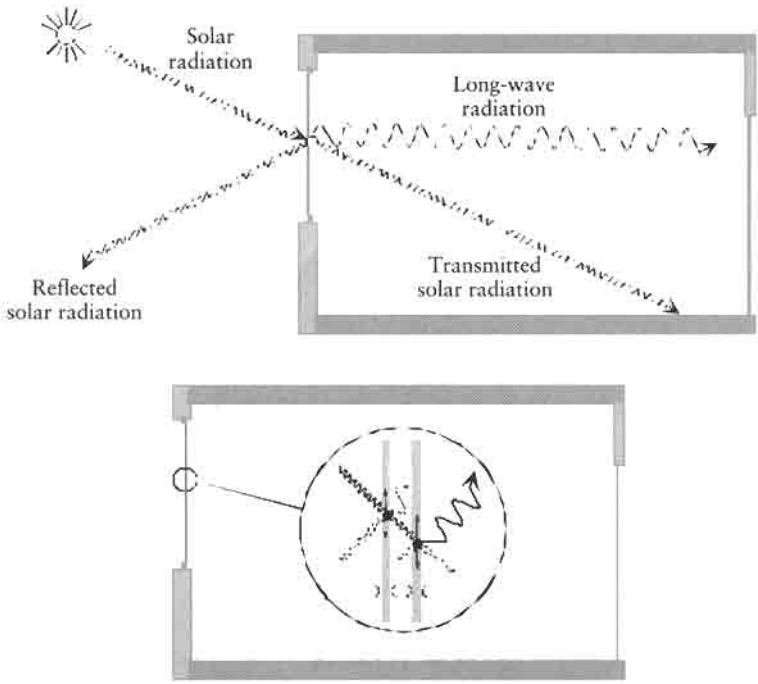

FIGURE 11.35 The solar radiation on a window is partly transmitted directly into the room. Another part of the energy is absorbed in the glazing and released as long-wave radiation. The lower figure shows the individual energy fluxes for a window glazing. The solar radiation is transmitted, reflected, and absorbed in the individual panes of the glazing, from where the energy is released by convection and long-wave radiation both to the room and to the outside.

For the calculation of such glazing in building–dynamics simulation codes, each pane is considered as a layer, exchanging energy with the other panes, with the room, and with the exterior.

For each layer the energy conservation equation is solved. The individual terms are the absorbed radiation in the layer and the radiative and convective heat exchange to the adjacent panes, to the room, or to the exterior.

The absorption is dependent on several parameters. This absorption can be calculated by specific window analysis programs such as WINDOW,[5] using standardized data such as that provided by the program GLAD.[6] These programs calculate coefficients which are available to the users of building dynamics programs in the form of libraries. Data for the calculation of the heat transfer through the window frame are included in these libraries.

Solar Shading and Solar Protection Devices

Shading by massive, fixed elements on the facade such as overhangs or sunscreens are treated as shading by parts of the building. Any solar protection devices in front, in between, or behind a window need a more sophisticated model due to the interaction with the window glazing. It has to be noted that a device might give 100% shading to direct solar radiation while still transmitting diffuse radiation and thus light (diffuse light or beams reflected from the ground).

Simple models for louvers and other solar protection devices are based on a statement of constant reduction of the solar radiation flux on the window. A common assumption is that a louver is controlled so that no direct light can penetrate into the room.

Shading systems become an important factor for thermal behavior in cases of buildings with low internal loads. The analysis of energy-efficient buildings with advanced facade systems also require advanced models for the solar protection system. Basically the whole system—shading device, glazing, spacers, and window frame—must be integrally modeled, taking into account the direct and indirect transmission (including multiple reflections) of direct and diffuse solar radiation and the solar absorption in the individual panes or slats (considering conduction, convection, and infrared radiation exchange). CEN has issued a reference calculation method.[7] More advanced models also consider the effect of ventilation in the gap between individual glass panes or solar protection blinds.[8]

11.3.3.3 Room Models

In thermal building simulation, a thermal zone can be a part of a room, a room, or a combination of rooms defined as a part of the conditioned space, throughout which the internal temperature is assumed to have negligible spatial variations. The zone is enclosed by the surrounding walls (floor, ceiling, roof, wall elements) and windows.

For the numerical treatment, the energy exchange processes in a zone, as outlined earlier, are incorporated into a so-called room model.[9,10]

The room model consists of nodes, which are interconnected by heat exchange paths (Fig. 11.36). The nodes represent either surface temperatures of the individual walls or the zone air temperature. For each node, an energy balance is formulated. From the resulting set of equations, the temperatures and heat fluxes can be determined.

Most room models contain only one zone air node, thus assuming perfect mixing of the zone air and a homogenous temperature distribution in the space. Spatial temperature variations, such as vertical temperature gradients, are not considered. For specific applications such as displacement ventilation or atria, models with several zone air nodes in the vertical direction have been developed.[11]

The room models implemented in the codes can be distinguished further by how detailed the models of the energy exchange processes are. Simple models use a combined convective–radiative heat exchange. More complex models use separate paths for these effects. Mixed forms also exist. The different models can also be distinguished by how the problem is solved. The energy balance for the zone is calculated in each time step of the simulation.

Moisture Transport

Moisture-transport simulation includes transport as well as storage phenomena, quite similar to the thermal dynamic analysis, where heat transfer and heat storage in the building elements are modeled. The moisture content in the building construction can influence the thermal behavior, because material properties like conductance or specific heat depend on moisture content. In thermal building–dynamics simulation codes, however, these

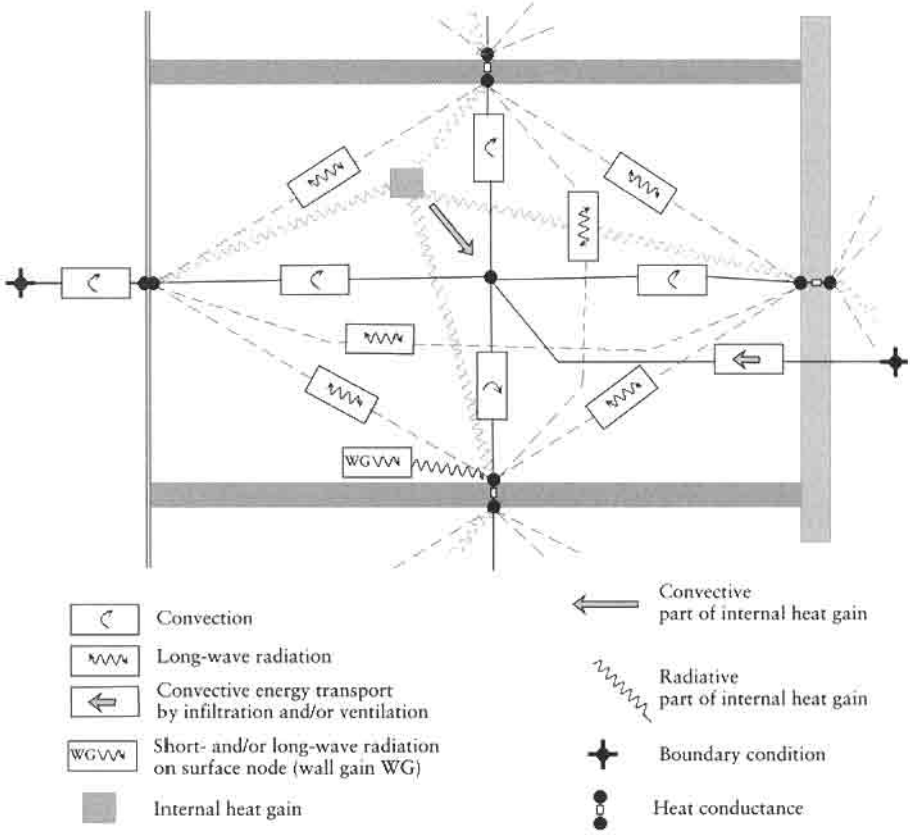

FIGURE 11.36 The room model characterizes the individual energy flux paths as thermal resistances, which are connected to the individual surfaces and to the room air node.

material properties are mostly constant input values. Therefore, variable material properties or even phase-change effects cannot readily be considered.

Moisture is also transported by ventilation airflows. This is dealt with in more detail in Section 11.4.

11.3.3.4 Modeling of HVAC Systems

Depending on the program, HVAC systems must be defined either by selecting individual components and defining their parameters and their connections or by choosing one of the systems available in the program.

Different modeling techniques are used, from empirical formulations using polynomial approximations, to process definition (e.g., on the basis of psychrometrics as depicted in the h-x or Mollier diagram), and finally to detailed physical modeling including all kinds of energy exchange and control processes. Directly related to the modeling used is the kind and amount of input data required. In principle, three application fields can be distinguished for the use of HVAC models:

- Development of HVAC components: design and optimization
- Selection of size of HVAC components in the planning process (dimensioning) and simulation of the behavior of the system under partial load
- Energy-demand calculations

For the first kind of application, the focus is on certain elements of the HVAC component under consideration. The simulation is used to study and optimize design-specific aspects such as the pipe size and spacing or wetted area and fin geometry in a heat exchanger. This kind of modeling requires detailed knowledge on many input parameters and the related physical processes.

The second kind of modeling is focused on the needs of the planner and HVAC engineer, who has to comply with certain criteria for heat delivery or removal for comfort and energy efficiency and from this has to select a certain type of component available on the market. Once the component is selected, only the performance of this component under variable load is of interest. This kind of modeling normally requires much less input, because actually only the change in performance from a given design point to a point for the actual load has to be determined.[12]

Systems and control configurations as required may not be available in the simulation code or may not be able to be described and modeled in the required detail. Depending on the application, an optional system extension or change can be defined using the existing model. Otherwise, a new model has to be developed and integrated into the code. In these cases, it is decisive for the selection of code used whether and how easily such an extension can be implemented.

11.3.3.5 Control

Temperature control

Thermal building–dynamics simulation can be run basically under two different conditions:

- Zone temperature control: In this case the indoor temperature is controlled to specified temperature levels. These levels can be according to temperature or other schedules, can depend on other parameters, or as the simplest case, can be constant.
- Free floating: In this case the indoor temperature is left free to fluctuate without any mechanical cooling device.

HVAC System Control

Many HVAC system engineering problems focus on the operation and the control of the system. In many cases, the optimization of the system's control and operation is the objective of the simulation. Therefore, the appropriate modeling of the controllers and the selected control strategies are of crucial importance in the simulation. Once the system is correctly set up, the use of simulation tools is very helpful when dealing with such problems. Dynamic system operation is often approximated by series of quasi-steady-state operating conditions, provided that the time step of the simulation is large compared to the dynamic response time of the HVAC equipment. However, for dynamic systems and plant simulation and, most important, for the realistic simulation

of control systems, the 1-h time step, normally required when dealing with thermal building-dynamics simulation, is much too large. In these cases, the HVAC system has to be modeled separately with a much smaller time step, using the results of the dynamic building simulation as boundary conditions.

11.3.3.6 Limitations

Several limitations stem from the methods just outlined. The most important ones are summarized below; others have already been mentioned in the text.

- Perfect mixing of the room air is assumed in the individual zone, except in room models with more than one air node (displacement ventilation model, atria model).
- Ventilation pattern (plumes, etc.) can be considered only in a very limited way.
- Conduction in walls is often modelled one-dimensionally.
- Most room models are nongeometric, with the radiation exchange between surfaces being calculated solely on an area-weighted basis. This has to be considered when splitting walls or floors into several elements, because in such models, these elements have a direct radiative exchange, while in reality there is no exchange or only an indirect one via opposite surfaces.
- Solar radiation is distributed in the first room and not transmitted into adjacent rooms through an internal window (more sophisticated modeling may allow for this).
- Radiation from internal heat sources is not directly considered in thermal comfort calculations.
- HVAC components are mostly modeled in a steady state. However, the normally used time step of 1-h in the simulation is too large for the simulation of control processes.

11.3.4 Required Input

11.3.4.1 Building Modelization

Building modelization is the process by which the program's user represents a building as a number of thermal zones, separated by walls. HVAC systems are connected to these zones. Abstraction is necessary for the definition of the zones and the buildup of walls, and those components available in the code which match the reality best must be selected.

The user must have experience in thermal analysis and HVAC dimensioning and be familiar with the theoretical principles and details upon which such analysis is based in the program used. Engineering judgment will have to be used for the definition of the input parameters.

The information required to run a thermal building-dynamics simulation can be classified on the base of the following items:

- Outdoor climate
- Building
- HVAC system
- Internal heat gains in conditioned spaces (casual gains)
- Operation and use of building

11.3.4.2 Outdoor Climate

In order to run a dynamic simulation, weather data files are needed, providing (usually hourly) data on the following quantities: air temperature, air humidity, ground temperature, global and diffuse irradiation on horizontal surfaces, and wind speed and direction.

11.3.4.3 Building

Location and Orientation

In order to specify the building location on the surface of the earth, the values of latitude, longitude, and altitude of the site are required. The orientation of the building can be specified as an azimuth angle between the main axis of the building and the north (or south) direction.

Neighbor Buildings and Shading Devices

Position, size, and orientation of external objects must be specified in order to take into account both the shade cast on the exterior of the building and the modification of wind conditions. External objects are nearby buildings, trees, hills, or attached objects, such as overhangs.

Identification of Zones

The identification of zones can be made in different degrees of detail, depending on the specific purpose of thermal building–dynamics simulation. In most cases a zone can include several rooms having the same thermal conditions. Sometimes it is necessary to split a very large room into two or more thermal zones in order to have more accurate results.

- The size (volume, floor area) of each zone has to be specified.
- The envelope characteristics of each zone are to be specified as described later.
- The thermal behavior of a zone is affected by the presence of internal heat sources and by HVAC operating features, which are dealt in the next sections.

Opaque Elements

The opaque elements of the building are exterior and interior walls, roofs, interior floors, exterior and interior doors, and underground walls and floors, which are all referred to as *walls* in this text.

Thermal characteristics of material layers for each type of wall must be specified, including thickness, conductivity, density, and specific heat. Moreover, the features of internal and external surfaces of each wall must be specified, including solar absorptance and roughness, which affect surface heat transfer coefficients.

For the individual wall, the wall element type, size, position, and connections to adjacent zones must be specified.

Windows

Both thermal and optical characteristics of each type of window must be specified, including the dependence on the incidence angle. These characteristics normally are precalculated using a specific code (see Section 11.3.3, "Heat

Transfer through Windows") and made available in the simulation code by means of a database.

For the individual window, the window type, size, and position must be specified. For natural ventilation analysis it may be necessary to specify also the air-tightness characteristics of the windows.

CABD and Databases

Links or interfaces to CABD (computer-aided building design) tools have become a common feature of many building simulation tools. Efforts to standardize the building model format significantly contribute to this trend. CABD can be used for the establishment of input data as well as for the checking of input data. Normally, the geometric information from CABD drawings must be reduced quite substantially for the thermal simulation input. On the other hand, besides geometric data, information such as material properties, etc., must be supplied. This information is normally not included in the CABD data set, but links to database entities may be established.

A graphic representation of the building input data by CABD offers an easy way of checking the geometric input data.

11.3.4.4 HVAC Systems

HVAC system parameters include information for the sizing of components. First of all, the type of HVAC system must be specified, and the thermal zones served by the system must be identified. Afterward, information must be specified on the following items:

- Airflow into and out of each zone and HVAC system (supply air, exhaust air, outside air)
- Zone temperature control characteristics (set point, type of thermostat, throttling range)
- Supply air conditions (set points, control strategy, limits)
- Characteristics of HVAC components

11.3.4.5 Internal Heat Gains (Casual Gains)

Maximum specific internal gains must be specified for each zone, including gains from people, lighting, machinery, equipment, and other sources. Some detailed models also require splitting sensible heat into convective and radiative fractions. This split is important when defining the loads from lighting or machinery. Data on this split between convective and radiative heat release for typical heat sources can also be found in the *ASHRAE Fundamentals Handbook*.[13] In Table 11.4, measured internal heat gains in industrial premises are presented.[14] Loads from electric motors can be established considering the power efficiency. For some heat sources (e.g., people), it is useful to distinguish between sensible and latent fractions of energy supplied. Data may be found in *Design Guide Book Fundamentals* Chapter 5, or in VDI Standard 2067.[15] For loads from lighting and machines, part load factors, use factors and, also in case of multiple sources, simultaneity factors have to be considered.

11.3.4.6 Operation and Use of Building

The use of the building is characterized by schedules for indoor environmental conditions, ventilation airflow rates, internal heat gains (casual gains),

TABLE 11.4 Internal Heat Gains for Different Types of Industrial Manufacturing

Industry	Internal heat gain, total effective [W/m² floor]
Manufacturing of dairy products	30–60
Manufacturing of bakery products	80–200
Textile, wearing apparel industries	70–230
Manufacturing of furniture	45
Printing and publishing	40–120
Manufacture of glass and glass products (furnace department)	500–1000
Manufacture of concrete and concrete products	20–40
Manufacture of metal fabricated products, machinery, and equipment	40–100

occupancy, and HVAC system operation. For the casual gains of lighting, machinery, and equipment, use factors and load factors have to be considered. In order to take into account temporal variations of building use, daily, weekly, and yearly schedules should be specified for occupancy, for different kinds of casual gains, and for temperature and humidity set points.

11.3.5 Expected and Available Results

The results of thermal building-dynamics simulation are generally referred to by zone level. They can be divided into instantaneous results and summary results.

The primary results of thermal building-dynamics simulations are hourly values of the following quantities:

- Zone air temperatures, wall surface temperatures, operative temperatures
- Space cooling or heating loads
- Building elements' heat gains or losses
- Supply airflow rates
- Supply air temperature and humidity
- Energy input to HVAC system components
- Zone humidity levels

The primary summary results of thermal building-dynamics simulations are peak values of these items and monthly or seasonal values of the following quantities:

- Building elements' heat gains or losses
- Cooling or heating energy demand
- HVAC energy demand

Results for the whole building can be obtained by considering the results for all zones.

11.3.6 Example

11.3.6.1 Building

The building is an industrial laundry with high thermal loads, ventilated naturally or by hybrid ventilation. The laundry cleans, among other things, hospital textiles; thus, high hygienic standards are required. Three different levels of internal thermal loads were assumed (60, 100, 160 W/m²) for the simulations.

11.3.6.2 Problem

For a representative summer case, the outdoor air exchange and the room air temperatures in various zones are to be determined.

11.3.6.3 Approach

For the calculations, several software tools were used. The natural ventilation and the thermal behavior were computed using the dynamic building and system simulation program TRNSYS.[16] In TRNSYS, the natural airflows were modeled as power-law functions, basically considering stack effects. These functions were established using the COMIS[17] model. Also, the influence of the design and the insect screens on the flow resistance of the openings was carefully considered. The example is documented in more detail in Breer and Dorer.[18]

Space Load Factor

Outside air entering the space through openings near the ground spreads over the floor and absorbs energy from the floor surface. The resulting air temperature increase leads to buoyancy and forces the air up into the upper hall zone. This results in a temperature stratification in the hall. Due to this vertical temperature gradient, the air in the occupied zone does not reach the exhaust air temperature $\theta_{exhaust}$ (see Fig. 11.37).

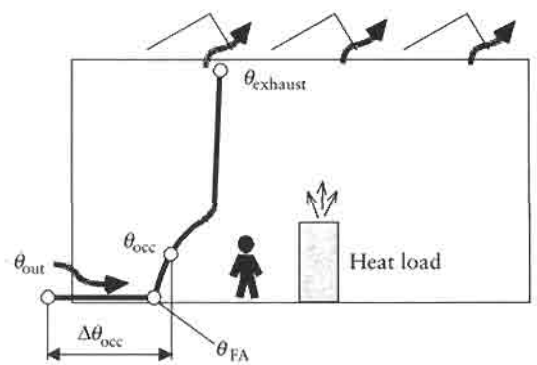

FIGURE 11.37 Temperature gradient related to the room height (schematic).

This has a positive effect on thermal comfort, particularly in the summer period. The thermal space load factor μ_t is used to quantitatively characterize this effect (θ_{out}, outside air temperature; θ_{occ}, air temperature at working space level; $\theta_{exhaust}$, exhaust air temperature):

$$\mu_t = \frac{\theta_{occ} - \theta_{out}}{\theta_{exhaust} - \theta_{out}} \tag{11.17}$$

Soil Temperature

In many industrial halls, conduction into the ground is a major factor for heat loss. Therefore, an adequate modeling of the floor slab and the underlying, thermally active, soil is very crucial for reliable simulation results. In this case, the soil model in the TRNSYS model was established using results from an additionally performed finite-element program analysis.

11.3.6.4 Results

Primary results of the simulation are the room air temperatures, the air change rates, and the space load factors (Figs. 11.38 to 11.40).

A space load factor $\mu_t \approx 0.75$ results for the important period of May–September. This corresponds very well with standard values given in VDI.[19]

During the summer period, high peak temperatures can be observed, which can be slightly reduced by using larger openings.

11.3.6.5 Conclusion

The study shows that in this particular case a natural ventilation system is a suitable and ecological possibility to remove the high internal thermal loads. Accurate information on the internal loads and the ventilation openings is crucial for the results of the thermal simulation.

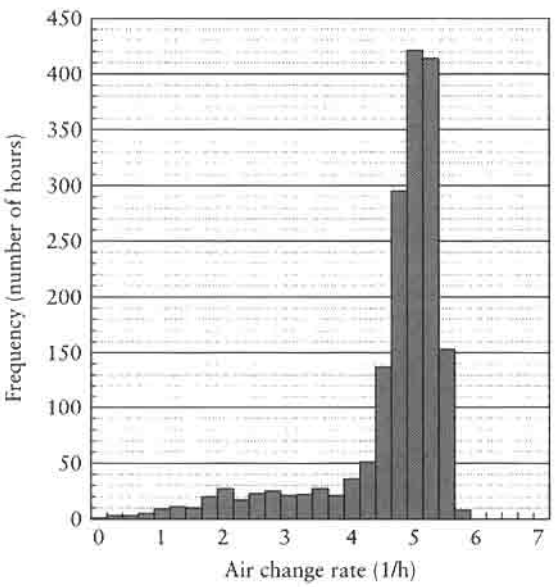

FIGURE 11.38 Air change rate during work time (7.30–17.30), for the period May–September.

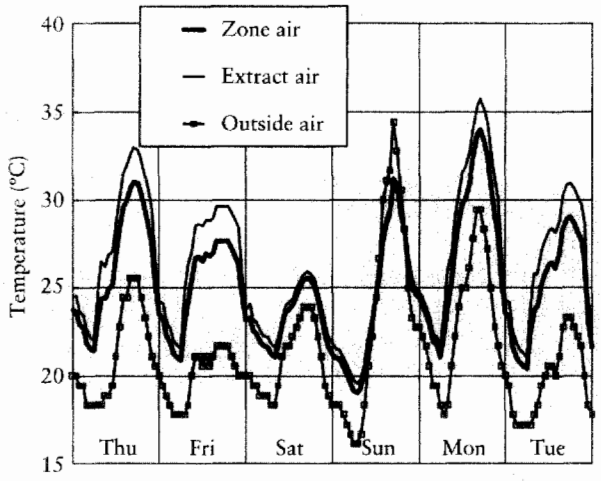

FIGURE 11.39 Temperature evolution over the period 11–16 August.

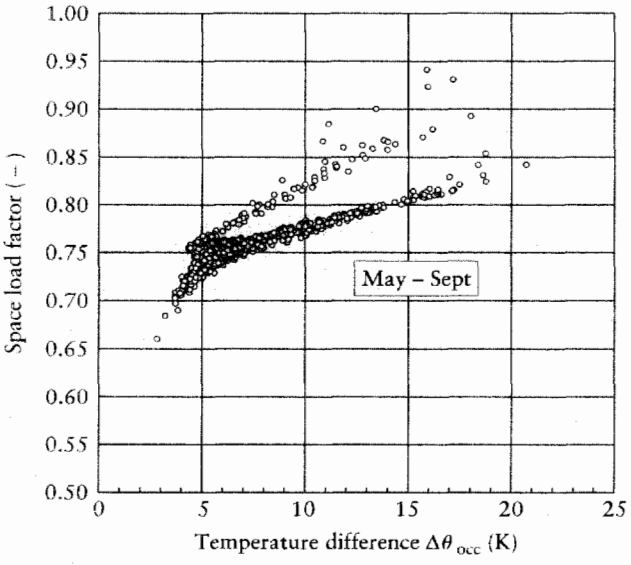

FIGURE 11.40 Space load factors $d\mu_t$ during work time.

11.3.7 Conclusions and Recommendations

11.3.7.1 Proper Use

For proper use of the simulation tools and to get reliable results, the following procedure is suggested:

- The purpose of the simulation is defined precisely and accurately (what do we want to know?). Parameters and requirements are specified for the performance assessment.

- Program and input are chosen according to the problem and the answers looked for.
- The problem resolution is gradually increased (e.g., from a single-zone to multizone approach, from design air change rate to thermally driven natural airflows, from simple energy-demand calculation to integrated performance assessment, considering energy, thermal and visual comfort, and indoor air quality).
- Building and systems are modeled in accordance with this purpose. Geometry input may be established via CAD, elements then linked to database entities for properties, etc.

Detailed knowledge about the code and the underlying physical phenomena is necessary for the definition of an appropriate building modelization and for the input definition.

- Results are extracted and prepared as appropriate.
- A log file is maintained which documents the assumptions and decisions made in the evolution of the project.
- Quality-assurance procedures have to be established for the checking of both input and results: checks of energy balances, plausibility tests, and comparison with steady-state calculations and with results from similar cases. These checks are demanding and time consuming and thus prone to be omitted but are mandatory for reliable simulations.
- Models and results are properly archived.

11.3.7.2 Difficulties

Usually, a precise definition of the input parameters in absolute terms is very difficult. Nevertheless, in many cases this does not cause crucial problems because relative results may be sufficient to compare different design options. The influence on the results of uncertainties in input should be evaluated whenever possible by using sensitivity analysis techniques.

11.3.7.3 Modeling and Dimensioning of HVAC System and Components

The HVAC system is quite often not simulated but dimensioned on the space load results of the simulation by using simpler tools. However, aspects of control and the related potential for optimization are then neglected.

11.3.7.4 Limitations

Thermal Comfort

For a person at a certain location in a room, direct radiation from internal heat sources may significantly affect the thermal comfort level. However, in the codes, room (or operative) temperatures are calculated on the basis of the room air and the wall surface temperatures only (both calculated considering the internal heat source, however).

Due to the methods and limitations outlined in Section 11.3.3, in thermal comfort analysis, draft risk evaluations cannot be performed using this type of room model. Analysis of air temperature stratification and thermal comfort for the occupant zone can be achieved only by using multi-air-node room models.

Room Airflow Pattern

Due to the assumption of well mixed air, detailed spacial zone air temperature distributions and ventilation efficiency studies cannot be performed. For this, CFD methods have to be applied (see Section 11.2).

However, with CFD, configurations with mostly known or at least steady-state boundary conditions and surface temperatures are calculated. In cases where the dynamic behavior of the building masses and the changing driving forces for the natural ventilation are of importance, thermal modeling and combined thermal and ventilation modeling must be applied (see Section 11.5).

References

1. Daskalaki E. Natural convection heat transfer coefficients from vertical and horizontal surfaces for building applications. *Energy and Buildings*, vol. 20, no. 3, 1994.
2. Gebhart B. Surface temperature calculations in radiant surroundings of arbitrary complexity—for gray, Diffuse Radiation. *Int. J. Heat Mass Transfer*, vol. 3, no. 4, 1961.
3. Stephenson D. G., and Mitalas G. P. *Calculation of heat conduction transfer functions for multi-layer slabs. ASHRAE Transactions*, vol. 77, part II, p. 117, 1971.
4. ISO/FDIS 13370:1998: *Thermal performance of buildings—heat transfer via the ground—calculation methods.* ISO, 1998.
5. *WINDOW: A PC program for analyzing window thermal performance.* Berkeley, CA: Lawrence Berkeley National Laboratory.
6. Frank T., Nussbaumer T., and Carl S. *Optical and thermal properties of glazing materials.* Final report BEW-project EF-REN(92) 081 "*Glasdatenbank GLAD-PC*" [in German]. Düebendorf: EMPA, 1996.
7. prEN 13363: *Solar protection devices combined with glazing—calculation of solar and light transmittance. Part 1: Simplified method, Part 2: Reference calculation method.* CEN, 1999.
8. Simmler H., and Manz H. *Measurement and modelling of solar façade components and shading systems.* CisBât 99. Lausanne: EPF, 1999.
9. Clarke J. A. *Energy simulation in building design.* Bristol and Boston: Adam Hilger, 1985.
10. Seem J. E. *Modelling of heat transfer in buildings.* Ph.D. thesis, University of Wisconsin, 1987.
11. Koschenz M. *Simulation of displacement ventilation in building energy codes* [in German]. *HLH*, No. 9, 1993.
12. Zweifel G., Dorer V., Koschenz M., and Weber A. *Building energy and systems simulation programs: Model development, coupling and integration.* IBPSA Fourth Internat. Conference, Madison, WI, Aug. 1995.
13. *ASHRAE fundamentals handbook*, 1997. *Non-residential cooling and heating load calculations*, ch. 28. Atlanta, GA: American Society of Heating, Refrigeration and Air-Conditioning Engineers.
14. Aro T., and Koivula K. *Learning from experience with industrial ventilation.* CADDET Analyses Series No. 10, 1993. Atlanta, GA: American Society of Heating, Refrigeration and Air-Conditioning Engineers.
15. VDI Standard 2067. Part 11: *Energy demand calculation procedure for heated and air-conditioned buildings.* VDI, 1998.
16. *TRNSYS: A transient system simulation program*, Version 14.2. Madison: Solar Energy Laboratory, University of Wisconsin, 1998.
17. Pelletret R. *COMIS V3.0: A new simulation environment for multi-zone air flow modelling.* RoomVent '96 conference, Tokyo, May 1996.
18. Breer D., and Dorer V. *Industrial buildings with high thermal loads: simulation of natural ventilation.* RoomVent '98 conference, Stockholm, 1998.
19. VDI. *Air-conditioning systems for factories* [in German]. Berlin: Beuth Verlag GmbH, 1997.

Bibliography

CIBSE Application Manual 11: Building and environmental modelling. London: Chartered Institute of Building Services Engineers (CIBSE), 1998.

Siegel R., and Howell J. R. *Thermal radiation heat transfer.* Washington, DC, Philadelphia, PA, London: Hemisphere Publishing, 1992.

Duffie J. A., and Beckmann W. A. *Solar engineering of thermal processes.* New York: John Wiley & Sons, 1991.

EN ISO 6946: *Building components and building elements—thermal resistance and thermal transmittance—calculation method.* 1998. Brussels: European Committee for Standardization

prEN ISO 13791: *Thermal performance of buildings, internal temperatures of a room in the warm period without mechanical cooling—general criteria and calculation procedures.* 1995. Brussels: European Committee for Standardization.

Feist W. *Thermal building simulation: Critical evaluation of different modelling approaches* [in German: *Thermische Gebäudesimulation: Kritische Prüfung verschiedener Modellansätze*]. Heidelberg: C. F. Müller Verlag, 1994.

Glück B. *Room model for heat transfer analysis* [in German: *Wärmetechnisches Raummodell*]. Heidelberg: C. F. Müller Verlag, 1997.

11.4 MULTIZONE AIRFLOW MODELS

11.4.1 Purpose

Multizone airflow models may be used to evaluate these items:

1. *Airflows:* Determination of airflow rates in buildings, including infiltration, exfiltration, room-to-room airflows in building systems driven by mechanical means, wind pressures acting on the exterior of the building, and buoyancy effects induced by temperature differences between the building and the outside; design of natural and hybrid (combined natural and mechanical) ventilation systems; determination and checks of pressure hierarchies between zones; influence of infiltration on performance of mechanical ventilation systems; interaction between natural and mechanical driving forces in hybrid ventilation systems.
2. *Contaminant concentrations:* Dispersal of airborne contaminants such as odors, fumes, smoke, VOCs, etc. transported by these airflows and transformed by a variety of processes including chemical and radiochemical transformation, adsorption, desorption to building materials, filtration, and deposition to surfaces; evolution of contaminant concentrations in the individual zones; air quality checks in terms of CO_2 levels; cross-contamination evaluation of zones; air quality evaluations in relation to perception as well as health. Methods are also applicable to smoke control design.
3. *Personal exposure:* Predictions of exposure of occupants to airborne contaminants for risk assessment, inhaled doses, or time-integrated concentration values.

Combined thermal and multizone models are needed for problems such as thermal comfort analysis in naturally ventilated buildings, determination of heat-removal capacity by natural ventilation, design and evaluation of free cooling by nighttime ventilation. This is outlined in more detail in Section 11.5.

11.4.2 Method

11.4.2.1 Summary

Multizone airflow models are used to calculate airflows between zones and the outside, driven by pressure forces induced by wind action, stack effects, and fans.

Multizone airflow models are based on a network approach. The building is subdivided into zones or nodes, representing spaces of perfectly mixed air. Each zone is characterized by its zone node temperature and pressure and possibly its contaminant concentrations. The zone nodes are linked by conductances (airflow elements), modeling the airflow paths (cracks, openings, ducts, etc.). Pressure coefficients, relating local wind pressure at the building façade to the reference wind pressure, can be attributed to external nodes. Not only wind effects but also buoyancy effects resulting from air density differences are taken into account. In addition, pressure and flows induced by components of a mechanical ventilation system (fans, ducts) are also considered. Using air mass conservation, a system of nonlinear equations is built and iteratively solved for the zone pressures, providing airflow rates through all conductances. From these, zone-related flows are determined.

With given contaminant source and sink schedules and outdoor concentrations, concentration evolutions over time can be determined for the individual zones on the basis of the calculated airflow rate values per time step. Further postprocessing allows the determination of accumulated values such as air change rate or concentration histograms (see the later example) or inhaled dose values.

Basic Equations

Considered are mass conservation of air and species (contaminants and humidity). Momentum equations are not considered on a global scale but have been used in some cases for the definition of the airflow-pressure relation of the individual links. Heat fluxes and thus energy conservation equations are not considered.

Multizone Models vs. Zonal Models

The terms *zonal model* and *flow element* are also used for the simplified characterization of the flow field in a single enclosure.[1] There, a zone represents a partial volume of air in the enclosure, whereas in the multizone models described here, a zone represents a specific enclosure which is connected to other enclosures by air conductances (see "The Airflow Network" later).

11.4.2.2 Driving Mechanisms

Infiltration and ventilation are driven by pressure differences across the building envelope, which are caused by

- Wind-induced pressures. The pressure at a location on the envelope depends on the shape of the building, the shielding of the building, the wind direction, and the wind speed. Air-exchange due to wind turbulence effects is normally not considered.
- Pressure differences due to the different densities of the air inside and outside the building (stack effect).

- Pressures induced by fans or by appliances such as combustion devices or forced-air heating systems.

11.4.2.3 Building Modelization

Building modelization is the process by which the user represents a building as a number of zones that exchange air with each other and the outdoor environment. A given building can be idealized in a number of ways, depending on the building layout, the ventilation system configuration, and, very important, the problem of interest.

The user must have experience in airflow and indoor air quality analysis and be familiar with the theoretical principles and details upon which indoor air quality analysis is based. Engineering judgment will have to be used for the setup of the building representation and the definition of the input parameters.

11.4.2.4 The Airflow Network

The airflow network (Fig. 11.41) is composed of nodes, interconnected by links, representing individual airflow paths. Internal nodes represent the individual zones of the building, and external nodes represent façade locations, related to a specific set of wind pressure coefficients. Each link represents a specific airflow conductance type.

Zones

A zone represents a volume in the building which can be characterized by a single value each for its air temperature, its pressure at zone reference level, and the concentration of the individual contaminants considered. Thus, a zone is considered as a volume of perfectly mixed air.

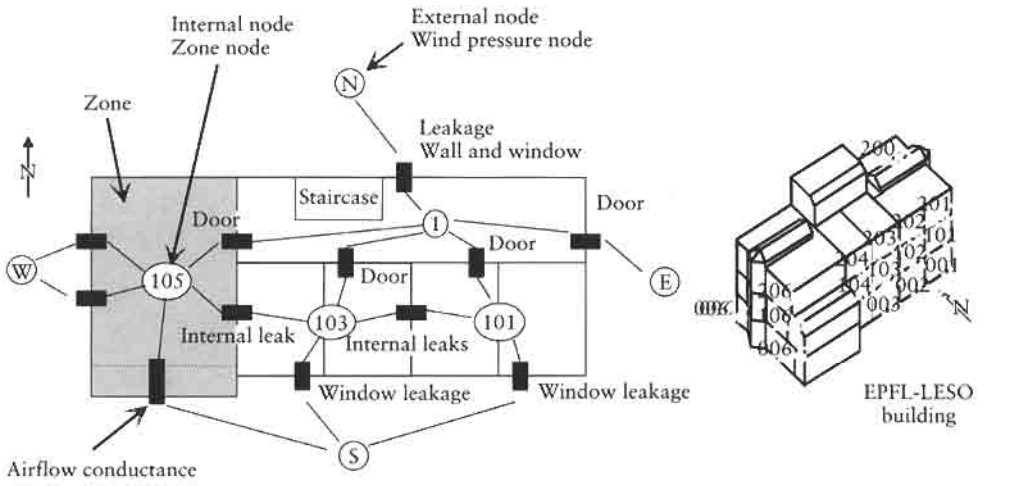

FIGURE 11.41 In multizone models, zones are represented by nodes which are interconnected by flow conductances. A typical network is given for the first floor of a multistory office building.

In certain computer models, a user-defined temperature, humidity, or contaminant concentration gradient can be considered. Nevertheless, this gradient is preset in the input and is not recalculated by the program on the basis of the results of the previous time step.

Airflow Conductances

Airflow conductances can be

- Leaks in the building envelope, due to cracks in walls or joints, gaps in window and door frames
- Purposely provided openings such as ventilators or passive stacks
- Large openings (windows and doors)
- Ducts, T-junctions, inlet and outlet grills
- Fans
- Flow controllers

Leak and opening-type airflow conductances normally are characterized by a power-law relation between the pressure difference across the conductance Δp and the resulting mass airflow q_m through the conductance (C, flow coefficient; n, flow exponent):

$$q_m = C(\Delta p)^n \tag{11.18}$$

For large openings, the vertical pressure profiles on both sides of the opening are considered, and the air exchange is determined by calculating the velocity profile in the opening. This is determined using Bernoulli equations for the individual horizontal stream lines. From this, two airflow rate values, one for each flow direction, are calculated for a given situation (Fig. 11.42). For pure convectional flow (no net flow through the opening) and homogeneous temperature distribution in the two zones, the air exchange volume flow through a rectangular opening (q_v) can be described by

$$q_v = c_d \cdot A \cdot 1/3\sqrt{\frac{\Delta T}{T} \cdot g \cdot H}, \tag{11.19}$$

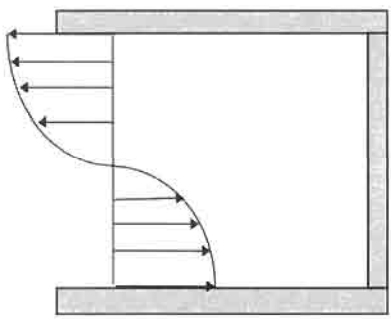

FIGURE 11.42 Vertical velocity profile in a large opening (warmer air inside, colder air outside, no influence of wind or other openings in the building).

where c_d is the discharge coefficient, A is the net cross-sectional area of opening, ΔT is the temperature difference between inside and outside [K], T is the mean temperature [K], g is gravity acceleration, and H is the height of opening.

The airflow rates depend on the selected discharge coefficient c_d, which is introduced to account for both friction and contraction effects.[3] Flow through large openings has been the subject of quite a number of recent research projects. Van der Maas[4] deals with flow through internal as well as external openings, Weber[5] gives discharge coefficient values for horizontally pivoted hinge window openings, and Dascalaki et al.[6] cover the relative influence of gravitational and inertia forces on the discharge coefficient in single-sided ventilation situations. For the interrelation between flow rates and thermal behavior of the room, see Section 11.5.

External Nodes

An external node represents a boundary node, i.e., a fixed pressure value or a location on the building façade which is linked to a specific set of wind pressure coefficients $c_{p,e}$ for this location (a set of values for different wind directions Θ_w). The pressure p_e at such a location e is then given by (v_{ref}, wind velocity at reference level; ρ, air density):

$$p_e = c_{p,e}(\Theta_w) \cdot \tfrac{1}{2} \cdot \rho \cdot v_{\text{ref}}^2 \tag{11.20}$$

11.4.2.5 Solution Process for Airflows

Airflows are determined basically by a steady-state calculation for each time step. At each time step, first, pressures at external nodes are calculated on the basis of the wind pressure coefficients and the actual wind speed and direction. Then, for all conductances, the local pressures at each side of the link are calculated. At internal links, this pressure is dependent on the (unknown) zone pressure p_i and the aerostatic pressure variation due to the height of the link with respect to the zone reference height. At external links, this pressure is dependent on the external node pressure and the aerostatic pressure variation due to the height of the link with respect to the stack reference height. For the aerostatic pressure, the air density is determined considering the temperature, the humidity, and (if relevant) the contaminant concentrations in the zone or in the outside air, respectively. From this, the pressure differences across each conductance can be calculated, and from this the mass airflow $q_{c,j}$ for each conductance j.

The mass flow total f_i for each zone i is set up ($q_{c,j}$, flows through the individual conductances connected with zone; nj, number of conductances connected with zone i), and the requirement of mass flow balance for each zone i leads to the iterative solution for the unknown zone pressures $\mathbf{p} = (p_1, p_2, \ldots, p_i)$.

$$f_i(\mathbf{p}) = \sum_{j=1}^{nj} q_{c,j} = 0 \tag{11.21}$$

Usually, modified Newton-Raphson methods with relaxation are applied.[7] Additional iteration loops are necessary for the determination of the dynamic pressure losses in ducts and duct fittings.

At the start of the iteration, an initial guess for the zone pressures can be found by using linearized pressure-airflow relations for the links, zero pressure values, or values from the previous time step.

11.4.2.6 Humidity and Contaminant Transport

The humidity and contaminant transport calculation is based on the previously calculated airflows, applying again the principle of mass conservation for the species under consideration. For each time step, the concentrations are calculated on the basis of the airflows, the source and sink strengths in the zones, and the concentration values at the previous time step. In contrast to the airflow calculation, which is a steady-state calculation at each time step, the contaminant transport calculation is dynamic. Therefore, the accuracy of the concentration results depends on the selected time-step interval.

11.4.2.7 Limitations

As previously outlined, perfect mixing is assumed in the individual zones. The spatial distribution of air velocities, contaminant concentrations, and air temperatures in a zone cannot be determined. Air exchange due to wind turbulence effects is not considered.

Many natural ventilation problems are related to the thermally driven air exchange in a building. Such cases must be most often treated using combined thermal and ventilation models or thermal models with an integrated natural ventilation model (see Section 11.5). For example, in COMIS,[8] a simple, single-zone thermal model is included for transient single-sided ventilation calculations.

In COMIS, source or sink strength can be defined as time dependent but not dependent on actual concentrations or temperatures. COMTAM96[9] includes more sophisticated models such as chemical reactions, adsorption and desorption to building materials, filtration, and deposition to surfaces.

Also, in the tools presented, possibilities for control functions, e.g., temperature-dependent window opening or demand-controlled fan operation, are very limited.

11.4.3 Required Input

11.4.3.1 Parameters

The following input parameters may be defined as time dependent in schedules:

- Outdoor climate and outdoor contaminant concentrations
- Zone temperature
- Zone humidity (if humidity is not considered as species in the contaminant transport calculation)
- Link operating factor (fan operation, window opening)
- Contaminant and humidity source and sink strengths
- Occupants: presence in each zone

11.4.3.2 Difficulties

Quite often it is difficult to define the input data needed for a multizone airflow simulation, especially for the following two input parameters.

Building	Location	Altitude, orientation
	Wind pressure distribution	Set of wind pressure coefficient data for each external node
Network	Zones	Height of zone reference level Volume Air temperature
	Links	Conductance type Zone connection (from/to) Height in relation to zone reference level Link factor (e.g., opening factor) Associated link schedules
Conductances (link types)	Crack	Flow coefficient, flow exponent
	Large opening	Type of opening (rectangular, horizontally pivoted) Width, height (position of hinge axis) Discharge coefficient Opening geometry as a function of opening factor
	Ducts and fittings	Diameter, length, specific data for pressure-loss calculation
	Fan	Fan characteristics (flow as a function of pressure)
Outdoor climate	Wind	Wind speed and direction
	Air	Outdoor air temperature and humidity
	Contaminants	Outdoor air contaminant concentrations
Contaminants	Characterization	Molar mass Source and sink models
	Time-dependent values	Source and sink strengths per zone Initial concentration per zone
Occupants	Characterization	Characteristics of smoking or other contaminant-releasing activities

Leakage Distribution of the Building

In some texts[10] guidance is given to estimate and evaluate the leakage of buildings and building components. The multizone airflow model can also be used to adjust the assumed conductances to an overall building leakage, measured by blower door technique, for example.

Wind Pressure Distribution on the Building Envelope

Data are available only for simple building geometries.[10] In Allard,[11] a tool for the calculation of wind pressure coefficients for simple geometries is made available, and another tool is described in Knoll et al.[12] Existing wind pressure data have to be examined carefully, because many data represent peak pressure values needed for static building analysis. Real cases with obstructions and buildings in the close surroundings are difficult to handle. Wind-tunnel tests on scale models or CFD analysis will be required.

Nevertheless, in many cases, mean wind velocities can be assumed. In ventilation-system reliability studies, e.g., where minimum ventilation rates are to be determined, a calm situation with little wind must be assumed anyhow, and the need for accurate wind pressure coefficient data is not so obvious.

11.4.4 Expected and Available Results

The primary results of multizone airflow calculations are the flows for each conductance. For large openings, the two flows in either direction through the opening are calculated. From this, the following results can be derived (per time step):

- Flows: Total flow per zone, total outdoor airflow rate per zone, air change value per zone, outdoor air change value per zone, total outdoor airflow for building, total air change value for building
- Pressures: Pressure loss across link, zone pressures
- Contaminants: Concentration in the zones, cross-contamination effects

With simulation in time, using weather file and schedules, these results can be obtained:

- Evolution of airflow, air change and concentration values
- Average flow and air change values, histograms of airflow rate or concentration values, number of hours with airflows too low or too high, or with contaminant concentrations too high
- Maximum concentrations, integrated exposure values, inhaled dose values

11.4.4.1 Limitations

Due to the methods and limitations outlined in Section 11.4.2, thermal comfort and draft risk evaluations cannot be performed using multizone airflow models. (From the flow across an opening, a rough estimate for the air velocity in the vicinity of the opening may be made.)

Due to the assumption of well-mixed air, room ventilation efficiency studies also cannot be performed. However, a multizone ventilation efficiency index for the whole building may be determined.

Without a thermal model, energy studies are also very limited (see Section 11.5).

11.4.5 Tools (Programs)

Quite a number of multizone airflow models have been developed and are available. An overview of available codes, physical models applied, and necessary input parameters is given in Orme.[13] An intermodel comparison of five models can be found in Allard.[11] Four typical and widely used codes are presented below.

11.4.5.1 COMIS

COMIS calculates the air and contaminant transport in multizone buildings. It includes a graphic user interface and database links. It was initially developed in a one year workshop at the Lawrence Berkeley National Lab[14] and further developed and extensively validated in the frame of the Annex 23 Multizone Airflow Modelling project of the IEA (International Energy Agency).[8,15] There exists an adapted version of the COMIS simulation engine to be used in the TRNSYS building and systems simulation code (see Section 11.5).

11.4.5.2 CONTAM96

CONTAM96 is based on earlier programs by NIST (National Institute of Standards and Technology), AIRNET (airflows), CONTAM (contaminant dispersal), and ASCOS (smoke transport).[9]

11.4.5.3 BREEZE

BREEZE is a software package for ventilation airflows in single and multicelled buildings, developed by the Building Research Establishment. BREEZE also includes a contaminant analysis routine.[16]

11.4.5.4 AIOLOS

This code originates from the University of Athens and has been further developed in the frame of an European project, the results of which are documented in Allard,[11] including a CD with the AIOLOS code.

11.4.6 Example

11.4.6.1 Building

A factory building (Fig. 11.43) consists of two spaces: a hall with mechanical extract ventilation for combined abrasive and chemical treatment and subsequent bonding and a naturally ventilated assembly hall.

VOCs are released during chemical cleaning of bonding surfaces. The extract system is designed on the basis of the steady-state concentration determined for maximum source strength and considering the mechanical extract ventilation only and no air-exchange with the assembly hall. This concentration must be kept below the threshold concentration (TVL) which is set to 300 mg/kg in this example.

11.4.6.2 Problem

The problem is to evaluate cross-contamination of the assembly hall by VOCs from the chemical cleaning and bonding process in the treatment hall.

11.4.6.3 Approach

Simulation Code Used

The simulations were made using COMIS 3.0.[8]

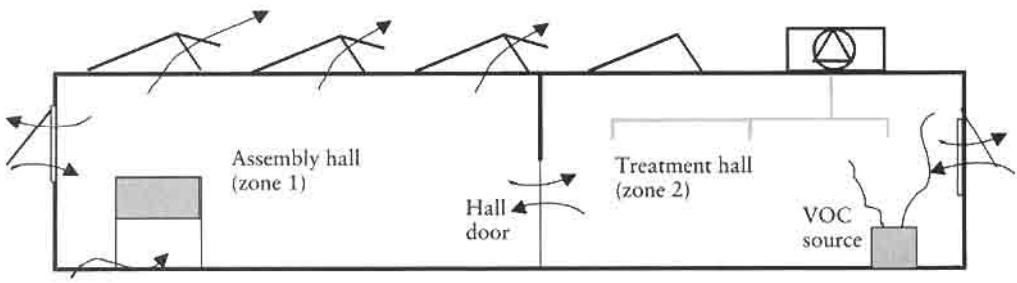

FIGURE 11.43 The factory building with the two halls, the ventilation openings, and the mechanical extract system.

Model

The factory is modeled as a two-zone network with door, horizontally pivoted windows, and roof shed windows as airflow elements. The extract fan and the duct and hood are modeled as additional airflow elements. Wind pressure coefficient data are taken from literature for a simple rectangular building shape surrounded by buildings of equal height.

Schedules

The simulation is made for one month (720 h) with a weather file for moderate climate conditions (April in Zurich, Switzerland), using a 1-h time step. Working hours are from 7 A.M. to 6 P.M. The fan is running during these working hours. Values for air temperatures are taken from simple thermal modeling estimates. Window opening and contaminant source strength schedules are fixed according to usual working operation, adapted to the 1-h simulation time step. See Figs. 11.44 and 11.45.

Results

Primary results of the simulation are air change rates and concentrations in the two zones per time step (Figs. 11.46 and 11.47). From this, a concentration histogram is derived for the two halls (Fig. 11.48). The results show that the TLV is never reached in the analyzed time period.

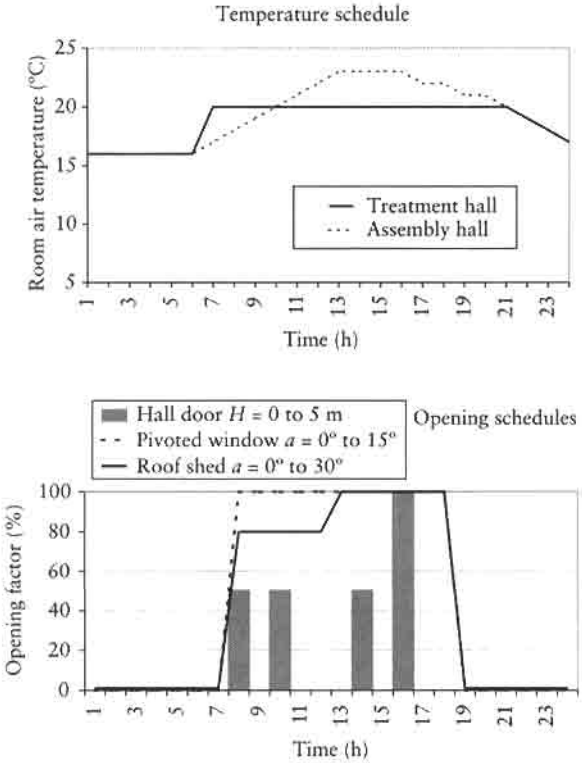

FIGURE 11.44 Schedule values for a 24 h time period for room air temperature and opening percentage of windows and roof sheds.

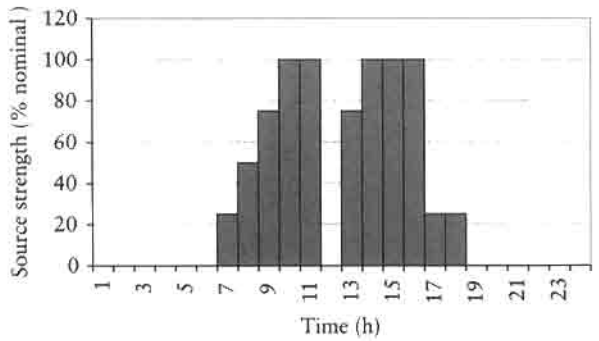

FIGURE 11.45 Schedule values for a 24 h time period for containment source strength (nominal value 0.6 kg/h).

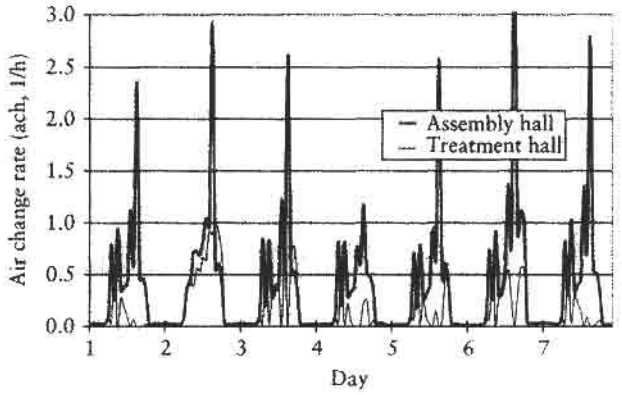

FIGURE 11.46 Air change rates for a 7 day period. The peaks stem from opening the hall door. At night, all openings are closed.

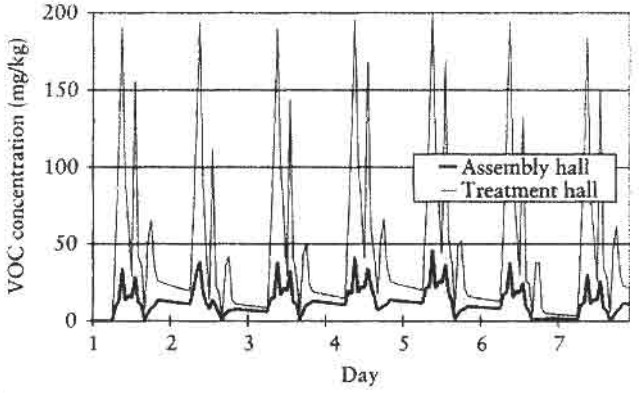

FIGURE 11.47 Concentrations for a 7 day period.

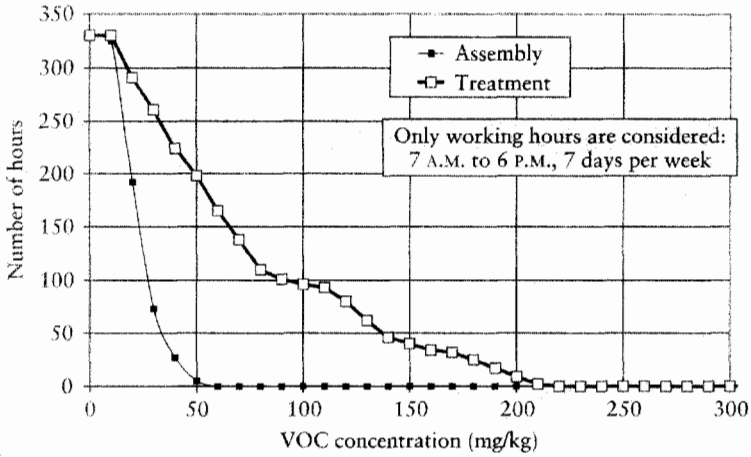

FIGURE 11.48 Concentration histogram for assembly and bonding hall for a one-month period. The figure shows the number of hours during which the concentration exceeds a certain level. Only working hours are considered.

11.4.7 Conclusions and Recommendations

11.4.7.1 Problem-Adapted Approach

Choice of program and input should be in accordance with the problem and the answers sought. For simple problems, adequate results may also be obtained with an adapted simple model. Many cases can be solved using a single-zone model; various models are available.[17–20] A single-zone model is also described in a CEN standard.[21]

11.4.7.2 Sensitivity Analysis and Comparative Studies

In certain cases, a precise definition of the input parameters in absolute terms may be difficult. Nevertheless, in many cases this does not cause crucial problems because relative results may be sufficient to compare different design options. The influence on the results of uncertainties in input should be evaluated whenever possible by using sensitivity analysis techniques.

11.4.7.3 Multizone Modeling vs. CFD

As outlined earlier, in multizone models, perfect mixing is assumed in the individual zone. The spatial distribution of velocities, contaminant concentrations, and air temperatures in a zone can be determined only by using CFD. On the other hand, wind effects are easily accounted for in multizone models, and unsteady-state simulation is normally performed. On the combined use of the two methods, see Schaelin et al.[22]

11.4.7.4 Multizone Modeling and Thermal Models

Many natural ventilation problems are related to the thermally driven air-exchange in a building. Such cases most often must be treated using combined thermal and ventilation models or thermal models with an integrated natural ventilation model. This is outlined in more detail in Section 11.5.

References

1. Inard C., Bouia H., Dalicieux P. Prediction of air temperature distribution in buildings with a zonal model. *Energy and Buildings*, vol. 24, 1996.
2. Dorer V., Fürbringer J.-M. Comparison of multizone airflow measurements and simulations of the LESO building including sensitivity analysis. 14th AIVC Conference, Copenhagen, Sept. 1993.
3. Andersen K. T. Inlet and outlet coefficients, a theoretical analysis. Proceedings of RoomVent '96, Japan, 1996.
4. Van der Maas J. (ed.). *Airflow through large openings in buildings*. IEA-ECBCS Annex 20 Technical Report. 1992.
5. Weber A. Model for natural ventilation through horizontally pivoted window openings [in German: Modell für natürliche Lüftung durch Kippfenster]. TRNSYS User Day, Stuttgart, Nov. 1997.
6. Dascalaki E., et al. Predicting single sided natural ventilation rates in buildings. *Int. J. Solar Energy*, vol. 55, no. 5, 1995.
7. Herrlin, M. K. *Airflow studies in multizone buildings, models and applications*. Bulletin No. 23. Stockholm: Royal Institute of Technology, Department of Building Services Engineering, 1992.
8. Pelletret R. COMIS V3.0: A new simulation environment for multizone airflow modeling. RoomVent '96 conference, Tokyo, May 1996.
9. Walton, G. N. CONTAM96 manual. NISTIR 6056. Gaithersburg, WA: National Institute of Standards and Technology, 1997.
10. Orme M., Liddament M., Wilson A. *Numerical data for air infiltration and natural ventilation calculations*. Coventry: Air infiltration and ventilation centre (AIVC), Feb. 1998.
11. Allard F. (ed.). *Natural ventilation in buildings*. London: James & James, 1998.
12. Knoll B., Phaff J. C., de Gids W. F. Pressure simulation program. 16th AIVC Conference, Palm Springs, FL, 1995.
13. Orme M. *Applicable models for air infiltration and ventilation calculations*. Coventry: Air Infiltration and Ventilation Centre (AIVC), 1998.
14. Allard F., et al. *Fundamentals of multizone airflow model—COMIS*. Coventry: Air Infiltration and Ventilation Centre (AIVC), 1990.
15. Fürbringer J.-M., Roulet C.-A., Borchiellini R. (eds.). Evaluation of COMIS, final report IEA-ECB&CS Annex 23 Multizone Airflow Modelling, LESO-PB, EPFL, 1015 Lausanne, Switzerland, 1995.
16. *BRE: Manual of BREEZE*. Garston, Watford: Building Research Establishment, 1997.
17. Liddament, M. W. *Air infiltration calculation techniques: An application guide*. Coventry: Air Infiltration and Ventilation Centre (AIVC), 1986.
18. Shaw, C. Y. *Methods for estimating air change rates and sizing mechanical ventilation systems for houses*. Ottawa: NRC, 1987.
19. Sherman, M. H. Air infiltration in buildings. Ph.D. thesis, Lawrence Berkeley Laboratory, Berkeley, CA, 1980.
20. Santamouris M. NORMA—*a method to calculate the thermal performance of passively cooled buildings. Cooling loads of buildings*, vol. 5. Dublin: School of Architecture, University College Dublin, 1994.
21. prEN 13465: Simplified calculation methods for the determination of airflow rates in dwellings. Brussles: European Standards Organisation, 1999.
22. Schaelin A., Dorer V., van der Maas J., Moser A. Improvement of multizone model predictions with detailed flow path values from CFD calculations. ASHRAE 93, Denver, 1993.

Bibliography

ASHRAE Fundamentals Handbook, ch. 25: Ventilation and Infiltration. Atlanta, GA: American Society of Heating, Refrigeration and Air-Conditioning Engineers, 1997.

Awbi H. B. *Ventilation of buildings*. London: E&FN Spon, 1991.

Etheridge D., Sandberg M. *Building ventilation: Theory and measurement*. Chichester: John Wiley & Sons, 1996.

Liddament M. W. *A guide to energy efficient ventilation*. Coventry: Air Infiltration and Ventilation Centre (AIVC), 1996.

11.5 INTEGRATED AIRFLOW AND THERMAL MODELING

11.5.1 Purpose

Integrated thermal and airflow modeling is needed for problems such as these:

- Determination of heat-removal capacity by natural ventilation
- Thermal comfort analysis in naturally ventilated buildings
- Design and evaluation of passive cooling potential by natural nighttime ventilation
- Design of innovative natural ventilation systems such as systems with solar towers, glazed double façades, façades with passive shaft ventilation or with some means of heat recovery

This section deals mainly with the interaction of thermal models as outlined in Section 11.3 and airflow models as described in Section 11.4 for the purpose of integrated modeling of thermally induced (stack-driven) natural ventilation, governed by the thermal behavior of the building. For the integrated analysis of air velocity fields and radiative and thermal effects in the building using CFD codes, see also Section 11.2 and Ott[1] and Schild.[2]

11.5.2 Method

In thermal models, the ventilation airflow rates normally are input parameters, to be defined by the user or to be calculated by the program on the basis of a nominal air exchange (or flow rate) and some control parameters (demand-controlled ventilation, variable air volume flow ventilation systems). In airflow models, on the other hand, room air temperatures must be defined in the input (see Fig. 11.49).

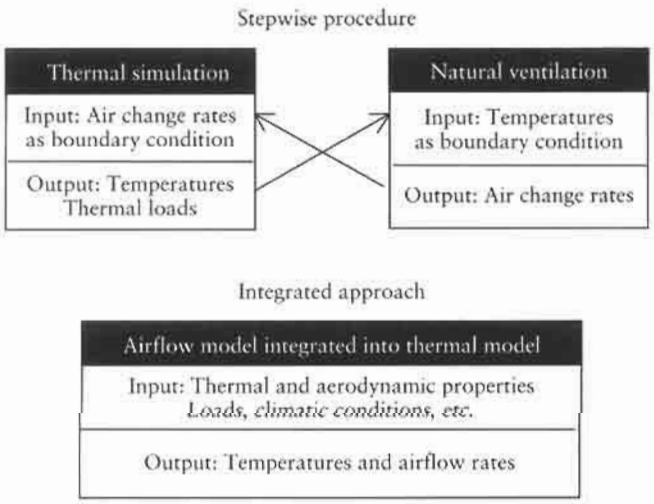

FIGURE 11.49 In thermal models, the ventilation airflow rates are input parameters. In airflow models, on the other hand, room air temperatures must be defined in the output. Since natural ventilation airflows and room air temperatures are interdependent, both parameters must be integrally considered in the solution process. This is possible only by an integration of the natural airflow model into the thermal model.

However, in thermally driven naturally ventilated enclosures, airflow rates and room air temperatures are interdependent and can be determined only simultaneously by using an integrated airflow and thermal model.[3,4]

For the data exchange between the airflow and the thermal model, several levels can be distinguished:

1. Sequential coupling. Here the link between one model and the other has to be established by the user, e.g., by defining specific input and output files for the airflow and the temperature results respectively and by proceeding in an iterative way toward a solution.
2. "Ping-pong" coupling. Here the results of one model for a certain time step are used in the other model for the calculation in the next time step. In the iterative solution process at a certain time step, however, there is no data exchange between the two models. This means that the calculated airflows and the room air temperatures physically do not fully comply. The ping-pong coupling may be established by the user or may be realized in an interoperable environment where the data exchange between the airflow and thermal models is automated.
3. Integration. Here, at a certain time step in the simulation, the airflow model is repeatedly called within the iterative solution process in the thermal model, and the airflow results are considered within this iterative solution process. Thus, the resulting airflows and room air temperatures fully comply in terms of the underlying physics.

Also, for this option, several levels can be observed concerning the integration of the airflow model. The lowest level of integration still requires separate input for the thermal and the airflow model respectively with a high degree of redundancy in the input parameters (e.g., zones must be input for both models), and the connectivity of the airflows and the zones in the thermal model must be established manually by the user. More sophisticated levels have reduced redundancy and automatic establishment of the link connectivity.

A higher level of integration is achieved when the airflow model is fully integrated in the thermal model and the input for the airflow part is just an addition to the input required for the thermal model.

The highest level of integration would be to establish one large set of equations and to apply one solution process to both thermal and airflow-related variables. Nevertheless, a very sparse matrix must be solved, and one cannot use the reliable and well-proven solvers of the present codes anymore. Therefore, a separate solution process for thermal and airflow parameters respectively remains the most promising approach. This seems to be appropriate also for the coupling of computational fluid dynamics (CFD) with a thermal model.[5]

11.5.2.1 Limitations

For the models described, the usual assumption for air nodes in regard to the room air distribution is still valid. This means that each air node represents a volume of perfectly mixed air. Thus, the same limitations as for thermal and airflow models apply: Local air temperatures and air velocities as well as local contaminant concentrations can be neither considered nor determined. This also means that thermal comfort evaluations in terms of draft risk cannot be performed.

If time-dependent spatial airflow and temperature distributions in a room are requested, the coupling of CFD with a thermal model has to be considered.[1,5]

11.5.3 Required Input

Input is required for both the thermal model and the airflow model. Input parameters are identical to the ones outlined for the thermal model in Section 11.3.3 and for the airflow model in Section 11.4.3. Depending on the data-exchange mode, additional information on the data links between thermal and airflow models must be given.

11.5.4 Expected and Available Results

Results may be obtained for thermal and for ventilation and indoor air quality aspects of the problem. The most frequently requested result parameters are

- For thermal comfort evaluations: room air and/or operative temperatures in the zones
- For indoor air quality evaluations: minimum (and mean) airflow rates, contaminant concentrations

11.5.5 Tools (Computer Programs)

Most of the dynamic building programs have some kind of simple model to consider natural ventilation, but very few allow full multizone airflow and contaminant transport calculations. However, updates of these codes as well as new developments include a multizone ventilation model. Also, a number of programs have been specifically developed for passive cooling applications. The following sections give examples of widely used programs for both the detailed multizone models and the simplified single-zone models.

11.5.5.1 Detailed Multizone Programs

ESP-r

ESP-r is a building and plant energy simulation environment based on a numerical approach in which building and plant energy flows and their interconnections are represented.[3,6] In particular, the system is able to integrate heat, air, moisture, daylighting, and power flows, while including special components such as photovoltaic cells, advanced glazings, and renewable technologies. For advanced lighting applications, ESP-r is able to pass (automatically) its building representation to the RADIANCE daylighting simulation code and receive back, for example, the internal illuminance distribution as an input to a user-specified lighting controller.

TRNSYS with COMIS

The multizone airflow model COMIS is adapted as a TRNSYS type, to be used in combination with the TRNSYS Type 56 thermal multizone building model.[7] Input is somewhat redundant. Separate input files are necessary for the thermal model and the ventilation model, but not for meteorological and link schedules.

EnergyPlus

EnergyPlus is a new-generation building energy simulation program that builds on the best features and capabilities of BLAST and DOE-2.[8] EnergyPlus includes innovative simulation capabilities including time steps of less than an hour, built-in template and external modular-systems simulation modules that are integrated with a heat balance–based zone simulation, and input and output data structures tailored to facilitate third-party interface development. Other planned simulation capabilities include multizone airflow and electric power simulation, including photovoltaic systems and fuel cells.

IDA–ICE

IDA Indoor Climate and Energy (ICE) is a new generation of building performance simulation tools.[9] The mathematical models are described in terms of equations in a formal language, NMF. Whenever appropriate, models recommended by ASHRAE have been used. Advanced database features support model reuse.

11.5.5.2 Single-Zone Models

LESOCOOL

LESOCOOL is an easy-to-use computer program for the determination of passive cooling potential by nighttime ventilation.[10,11] It is based on a simple combined airflow and thermal model, originally described in Van der Maas and Roulet.[12]

NATVENT

This code is a product of the pan-European EU-JOULE research project NatVent.[13,14] The program is intended to be used in an early stage of the building design process to predict airflow rates and indoor air temperatures. The code is an integrated single-zone model with an airflow model and a thermal model. Thermal analysis is made using a solar radiation model and a simple, single-zone room model with fixed geometry, heat transfer coefficients, and a user-defined active mass ratio. Overhangs and solar protection systems are considered.

11.5.6 COMIS and TRNSYS Application Example

11.5.6.1 Building

This example considers the thermal summer condition evaluation of a large, naturally ventilated test laboratory hall at EMPA (Fig. 11.50).

11.5.6.2 Purpose of the Study

The large, civil engineering test laboratory hall at EMPA is going to be refurbished. Large parts of the roof will be glazed for maximum daylight use. Solid walls will be better insulated.

The simulation study should give answers to the following questions:

1. Overheating risk under summer conditions
2. Temperature reduction potential using passive cooling by natural nighttime ventilation

FIGURE 11.50 The laboratory hall with the glazed roof during retrofit work.

3. Different ventilation-opening control strategies in terms of compliance with thermal comfort requirements
4. Risk of draft due to cold airstreams falling from the cold roof windows in the winter season

11.5.6.3 Approach

Due to the thermally driven air exchange and the large building masses involved, the problem must be studied using a dynamic thermal building model with an integrated ventilation model.

The study is performed for a representative section of the hall. A network model was established for COMIS, considering doors, openings at floor level, and the large openable ventilation hoods on the roof. Relationships are established for the air-exchange rate as a function of the temperature difference between inside and outside for different opening configurations. The effect of a temperature gradient in the hall is evaluated additionally. As a conservative approach, wind effects are neglected.

The relationships between air exchange rate and temperature difference were determined using COMIS (Fig. 11.51) and then integrated as the ventilation model in the thermal model. The thermal behavior is modeled with the TRNSYS multizone type, considering the hall and the room below the thick concrete test floor slab. For the hall, a room model with two air temperature nodes (one for the occupied zone and one for the rest of the hall) and geometrically detailed radiation exchange is used.

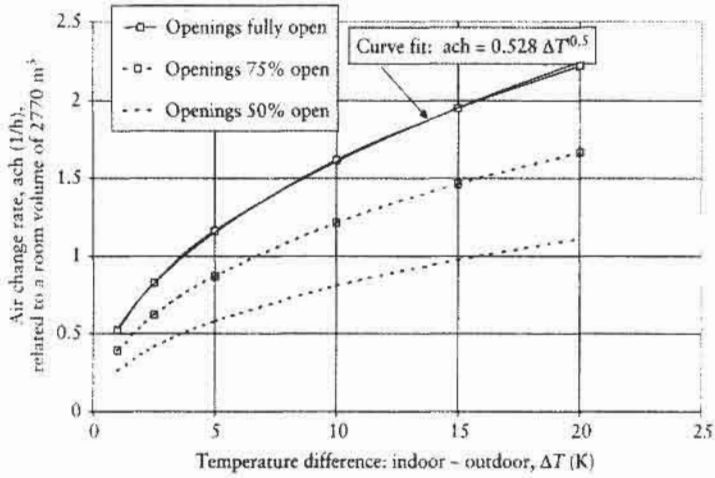

FIGURE 11.51 Characteristics of the natural air change rate in the hall as a function of the difference between indoor and outdoor air temperature, as calculated using COMIS. These characteristics were then integrated into the thermal model (TRNSYS).

For the determination of downdraft risk in the winter case, three-dimensional and transient CFD computations were performed using the TASC flow code. Boundary conditions were defined from the results of the thermal modeling.

Ventilation Model

The ventilation model is a simple flow network with one zone and the different openings modeled as airflow links from the hall to outside (Fig. 11.52). For the flow through the roof hood, two additional nodes were considered between the different cross-sections through which the air flows (Fig. 11.53).

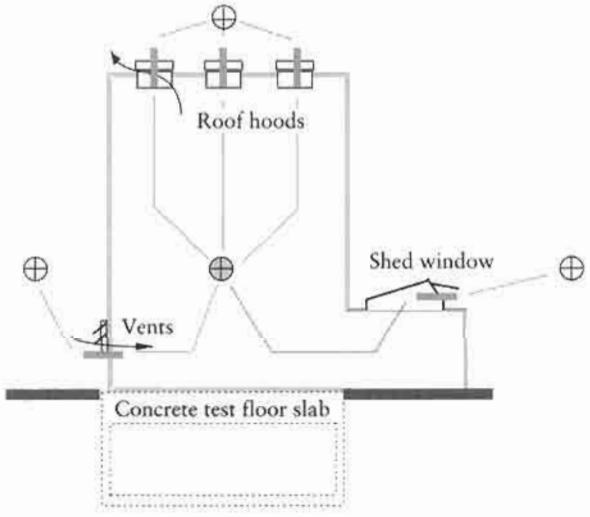

FIGURE 11.52 The ventilation model consists of one zone (the hall), which is connected to the external nodes by the different opening links.

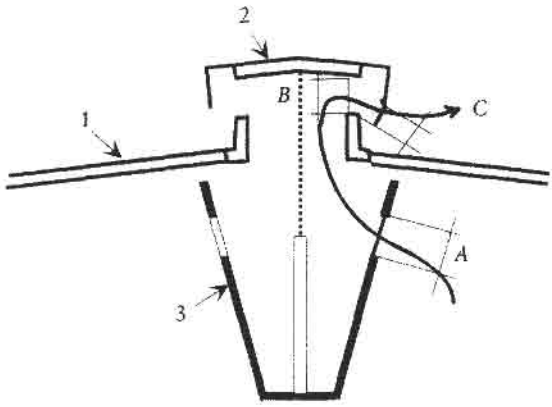

FIGURE 11.53 Section through the roof hood with the glazed roof (1), the movable hood (2), and the hood support (3). The individual ventilation-opening sections across the hood are labeled *A*, *B*, and *C*.

Thermal Model

The thermal model consists of two zones (Fig. 11.54). The hall is modeled with an air node for the occupied zone and another air node for the rest of the hall. The main heat source in the hall is the insulation through the glazed roof. Additional internal heat sources are rather marginal and therefore are not considered in the simulation.

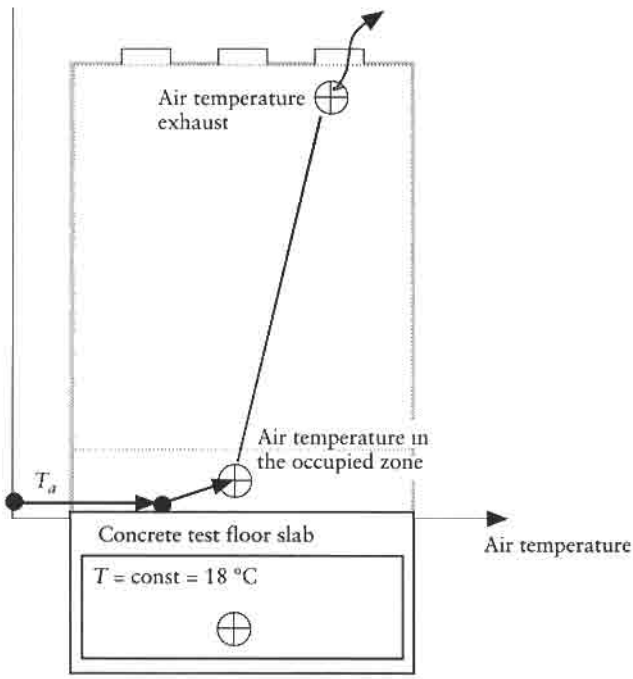

FIGURE 11.54 The two-zone thermal model. The hall is modeled with an air node for the occupied zone and another air node for the rest of the hall.

11.5.6.4 Simulation Results for the Summer Case

Thermal Comfort Evaluation

The thermal comfort was evaluated with hourly mean values of the air temperature in the occupied zone, plotted against the maximum 1 h mean outdoor temperature value of the day. Only the period from April 1 to October 30 and only working hours (7 A.M. to 6 P.M.) are considered. This evaluation method is based on the Swiss standard SIA V382/2.[15] The minimum and maximum allowable comfort temperatures are adapted to the usual activity and clothing levels of the workers in the hall (see Figs. 11.55 and 11.56).

Winter Case

The draft risk due to cold air pillows under the roof glazing dropping into the occupied zone was determined by transient CFD calculations. As can be seen from Fig. 11.57, velocities do not exceed 0.2 m/s. Therefore, the draft risk was assumed to be marginal.

11.5.6.5 Conclusions from the Example Case

Nighttime ventilation is necessary under summer conditions to keep temperatures in the comfort range. The ventilation openings should be closed if

- Outdoor air is warmer than inside temperature. This is, of course, possible only for such a hall where the air volume is very large in comparison to the required airflow rate.
- Outdoor temperature at night falls below a certain threshold, in order to prevent too low temperatures in the hall in the morning.

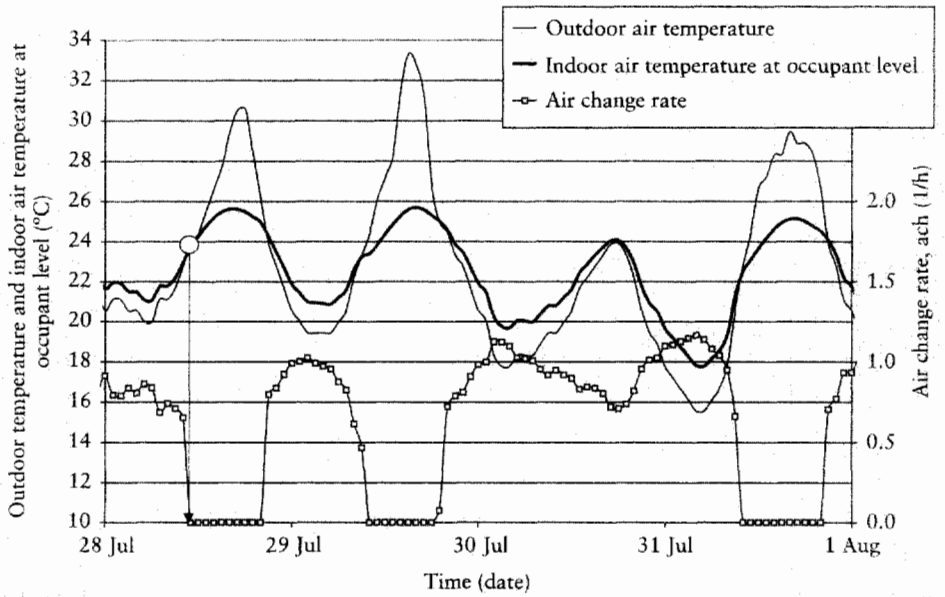

FIGURE 11.55 Air change rate, outdoor air temperature (T_a) and room air temperature in the occupied zone (T_i), for a four-day summer period. Ventilation openings are opened 0–24 hours if $T_i > T_a$. The moment when T_a becomes greater than T_i is highlighted on the first day, with the air exchange dropping to zero.

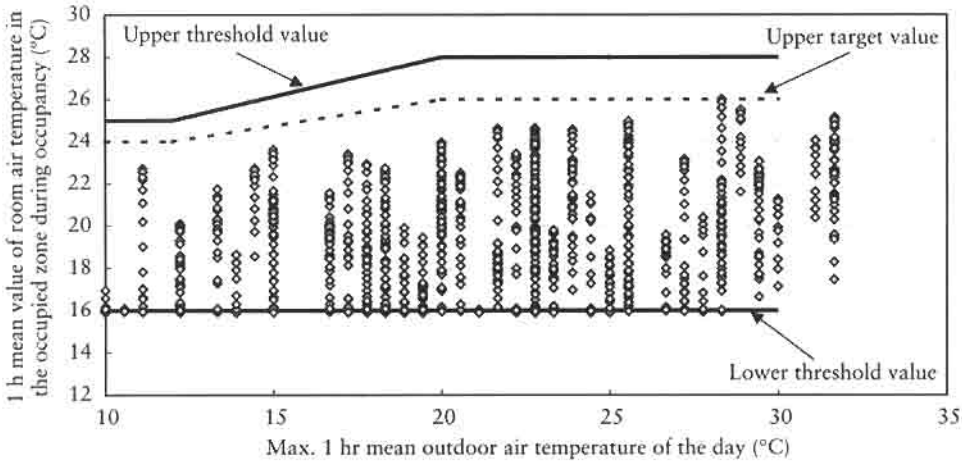

FIGURE 11.56 Hourly room air temperatures in the occupied zone (T_i) are plotted as a function of the daily 1-h maximum air temperature, according to Swiss standard SIA 382/2. Limit threshold temperatures are adopted to the working conditions in the hall. Ventilation openings are open 0–24 h, but only if $T_i > 16°C$ and $T_i > T_o$ (T_o = actual outdoor temperature).

The three-dimensional and dynamic CFD computations show a strong intermittent behavior of the cold-air downdrafts. Two-dimensional and steady-state models produce results which rarely reflect the real situation.

11.5.7 Conclusions and Recommendations

11.5.7.1 Integration Levels

The integration of the ventilation model into the thermal building model can be realized on different levels, from simple stack-flow equations to a full integration of a multizone airflow and contaminant transport model.

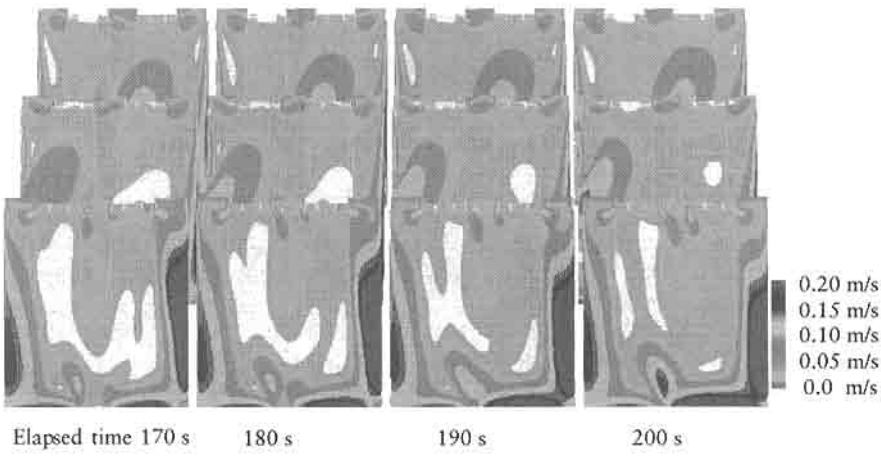

FIGURE 11.57 Airflow velocity fields for three cross-sections in the hall. Results of a transient CFD calculation over a prolonged time period. Scale 0–0.2 m/s.

11.5.7.2 From Simple to Complex Models

Simple, single-zone models are suitable for quick but rough estimates, e.g., of the cooling potential of nighttime ventilation. However, with such simulation tools, a detailed analysis of the thermal comfort and air quality situation in the working area of a room normally is not possible. If a specific configuration must be checked, e.g., against required design values, then only the combined modeling with both a detailed thermal and a detailed ventilation model may produce satisfying results. This is especially true in cases with several zones, more complex ventilation openings, and sophisticated glazing and solar protection systems.

11.5.7.3 CFD vs. Combined Thermal and Ventilation Modeling

CFD is appropriate in cases where the detailed flow field is of interest in a configuration with mostly known or at least steady-state boundary conditions (surface temperatures). Combined thermal and ventilation modeling is more suited to cases where the dynamic behavior of the building masses and the changing driving forces for the natural ventilation are of importance.

References

1. Ott F. *Numerical coupling of airflow, radiation and thermal behavior of the building* [in German]. Thesis No. 11805, Federal Institute of Technology, Zurich, 1996.
2. Schild P. Accurate prediction of indoor climate in glazed enclosures. Ph.D. thesis 1997:27, NTNU Trondheim, Norway, 1997.
3. Hensen J. L. M. *On the thermal interaction of building structure and heating and ventilating system.* Thesis, Technical University of Eindhoven, The Netherlands, 1991.
4. *Overview of combined modeling of heat transport and air movement*, AIVC Technical Note TN 40. Coventry: Air Infiltration and Ventilation Centre, 1993.
5. Negrão C. O. R. Integration of computational fluid dynamics with building thermal and mass flow simulation. *Energy and Buildings*, vol. 27, 2, April 1998.
6. *ESP-r: A building and plant energy simulation environment. User Guide Version 9 Series.* ESRU Publication. Glasgow: University of Strathclyde.
7. Dorer V., Weber A. Air, contaminant and heat transport models: Integration and application. *Energy and Buildings*, vol. 30, p. 97–104, 1999.
8. Crawley D., et. al. *EnergyPlus, a new-generation building energy simulation program.* Proceedings of Renewable and Advanced Energy Systems for the 21st Century, Hawaii, 1999.
9. Sahlin P. *Modeling and simulation methods for modular continuous systems in buildings.* Stockholm: Royal Institute of Technology, 1996.
10. Roulet C.-A., Van der Maas J., Flourentzou F. *A planning tool for passive cooling to buildings.* Indoor Air '96, Nagoya, Japan, 1996.
11. *LESOCOOL V 1.0 Manual.* Lausanne: EPFL-LESO, 1997.
12. Van der Maas J., Roulet C.-A. *Multizone cooling model for calculating the potential of night time ventilation.* 14th AIVC Conference, Copenhagen, 1993.
13. Svensson C. *A design tool for natural ventilation.* 18th AIVC Conference, Athens, 1997.
14. Svensson C. *The NatVent™ program: Fundamentals.* Malmö, Sweden: AB Jacobson & Widmark, 1998.
15. Standard SIA V 382/2: *Determination of the cooling load demand of buildings* [in German]. Zurich: SIA (Swiss Engineers and Architects Association), 1992.

Bibliography

Allard F. (ed.). *Natural ventilation in buildings.* London: James & James, 1998.

Santamouris M., Asimakopolous D. *Passive cooling of buildings.* London: James & James Science Publishers, 1996.

12 EXPERIMENTAL TECHNIQUES

KAI SIREN

Helsinki University of Technology, HVAC Laboratory, Espoo, Finland

GUNNAR ROSÉN

Arbetslivsinstitutet, National Institute for Working Life, Solna, Sweden

JÁNOS VAD

Technical University of Budapest, Department of Fluid Mechanics, Budapest, Hungary

PETER V. NIELSEN

Aalborg University, Department of Building Technology, Aalborg, Denmark

Industrial Ventilation Design Guidebook

12.1 INTRODUCTION

The use of experimental techniques is one method of designing, testing, and commissioning ventilation systems. A variety of complex problems are encountered in the wide field of industrial ventilation, the most common being the acceptability of airflow and temperature related to a new or rebuilt system. A complicated problem would be to experimentally investigate the influence of a hot oven on the airflow patterns in a large hall and how it influences the thermal conditions at the workplace. Ventilation engineers require answers to many difficult questions not only at the design stage, but at the commissioning and operating stage as well.

The carrying out of visualization techniques or measurements is one approach to obtain answers to these questions. Computer simulation is another method that is now becoming a more exact science. A third, essential approach is to depend on experience and good engineering judgment. All the above methods may eventually lead to success; however, the effort and cost of the work may differ considerably. This chapter describes the measurement and visualization techniques that can be applied in industrial ventilation problems.

In planning experimental work, the following approach can be used:

1. Set goals: What information is required as an output of the exercise?
2. Select an experimental approach: visualization, full-scale measurements, reduced-scale measurements
3. Select measurement methods
4. Ensure reliable analysis of results
5. Select instruments
6. Install and test the instrumentation
7. Carry out the measurements
8. Treat basic data to achieve the desired information

Careful planning of how the measurements are taken is essential, and is described in detail in the following chapters. First, however, the most effective approach for the specific case, experiment, or simulation has to be decided. Or should they be used side by side? Experience or good guidance is essential in making the correct decision. The following is given as an analysis and support for engineers dealing with problems of this nature.

Experiment or simulation? A decision may be based on the following considerations, but the final choice rests with the ventilation engineer:

Design or trouble shooting: During the design stage an on-site experiment with the actual equipment is not usually possible. Numerical prediction may then be simpler. However, for trouble shooting, field measurements are strongly recommended, ideally complemented by simulations techniques.

Available facilities and expertise: Are test facilities, instrumentation, and data acquisition systems available? Are simulation tools, hardware, and specialized staff for numerical simulation available? The final decision depends on answers to these important questions.

Scaling laws: If a full-scale test is not possible, reduced-scale experiments provide a good alternative. However, certain scaling laws must be observed (see Section 12.4). Correct scaling for isothermal flow is normally possible. Scaling of buoyant flows in large rooms may be difficult or impossible, so numerical simulation is the better choice.

Ventilation components of small geometric detail: It is difficult to model the geometry of diffusers that have complex geometry. Therefore, it is more reliable to measure airflow around such devices of the actual size.

Accident simulation: Large-scale accident situations cannot normally be staged for experimental purposes. It is impossible to set a building on fire, just to see how smoke spreads. In this case, numerical simulation is the only sensible approach.

Parameter variation and optimization: If parameter sensitivity is to be investigated, the simulation approach is cheaper and quicker than experiments. Trends are normally well predicted by the use of computer models.

Time available: It takes considerable time to set up a simulation case. After ensuring that a basic configuration has run successfully, it is easy and quick to carry out additional computer simulations with changed boundary conditions. Experiments, on the other hand, are generally more time-consuming.

Accuracy and reliability: If maximum quantitative accuracy and reliability are desired, full-scale measurements are the best approach. Simulations are recommended when meaningful trends are noted or to have a qualitative picture of the situation.

Cost: Whether measurement or a computation technique is cheaper depends on the situation in question. In small and simple problems, it is usually more profitable to use measurement techniques. In large and complex problems, where parametric/sensitivity study is the objective, computation may be a better alternative.

Ideally, experiments and simulations are carried out side by side and their results complement each other.

TABLE 12.1 Experimental Methods and Their Applicability

Approach	Applicability
Visualization (Section 12.2)	To determine the characteristics and qualitative nature of a phenomenon/problem, when no quantitative information (numbers) is needed.
Measurements (in general) (Section 12.3)	Any problem in which the framework to carry out the measurements exists.
Scale model experiments (Section 12.4)	In the case where there is no site to carry out full-scale measurements (planning phase), or it would be too expensive or space-demanding to construct a full-scale experiment (large facilities/rooms/buildings).

In case experiments have been selected, the next step is to decide on the method: visualization, full-scale measurements, or scale model experiments. Some features of these are listed in Table 12.1.

In most cases, visualization combined with measurements is the most effective method. Visualization is carried out first to obtain some idea what is happening and to select the source of relevant information. This approach assists in planning the measurement stage.

Scale model experiments are chosen for several reasons, the most obvious being that the intended building or space does not exist. For example, during the planning phase, it is possible to obtain measured information by building a scale model and carrying out measurements using the model. Another reason for selecting the scale model approach is that it is more practical, more convenient, and simpler to work with a reduced-scale model than with large full-scale objects. Reduced-scale models can also be positioned in the laboratory, where the conditions are under better control than in the field.

All three experimental approaches are presented in this chapter: visualization of airflow and contaminant dispersion (Section 12.2), measurement techniques including laser-based-techniques (Section 12.3), and scale model experiments (Section 12.4).

12.2 VISUALIZATION OF AIRFLOW AND CONTAMINANT DISPERSION

Clean air and many air contaminants are under normal conditions invisible. It is, however, often desired to actually see the movement of air or the emission and transport of contaminants in order to ensure good air quality. Methods aimed at the visualization of airflow, contaminants emission to the air, and their transportation out in the workplace and to the breathing zone of the worker are therefore important tools for designers of industrial ventilation systems.

The main purpose with flow visualization is to make the airflow field or the emission and transport of air contaminants visible and thereby possible to study. In technical terms, flow visualization gives possibilities to study airflow field and contaminant dispersion and changes in it depending on general changes in geometry, boundary conditions, inlet and exhaust airflow, etc. It is

also used to study airflow field and contaminant dispersion in the near field of a potentially exposed worker and how it changes depending on the behavior and position of the worker, or to collect an overview of airflow patterns before more detailed measurements are performed. In its simplest application it is used for checking that the ventilation system is working, e.g., that an airflow really is coming out of an inlet air unit.

The purpose of visualization of contaminant dispersion is to study the concentration of the substance of interest in a special point, area, or volume as a function of parameters of interest for the reduction of that concentration. One such point of special interest is in the breathing zone of a worker.

The reasons for using airflow or contaminant dispersion visualization techniques may be divided into purely technical and pedagogical, both with the purpose to give a base for the design and proper use of a contaminant control technology for workplaces with a good air quality.

The technical reasons for using visualization techniques are obvious. The designers of the ventilation have a great interest in studying how the airflow in a factory hall around a certain process or machine is distributed, to see if the design of a local ventilation unit is successful. The designer also needs to know in what way, in this context, disturbing factors such as heat sources, physical obstacles, or the presence and movements of a worker may affect the efficiency of the ventilation system.

The pedagogical background for using visualization methods is the fact that proper use and maintenance of industrial ventilation in most situations are dependent on persons without the deep knowledge about air and contaminant transport phenomena that can be expected from the designer of the systems. There are numerous examples of well designed industrial ventilation systems not fulfilling their original function due to a lack of knowledge regarding how to take advantage of and maintain the system in the most effective way. Knowledge of some basic qualities of the system and important air transport phenomena among the staff that is supposed to use and take advantage of the ventilation system is therefore fundamental to reach desired goals. This is of special importance when local ventilation systems are used, since the efficiency of the system very often is dependent on the behavior of the worker. Visualization techniques have thereby proved to be an effective tool to give basic knowledge of interest in this context.

To involve the staff in a change process, of which the installation or improvement of a ventilation system is one example, is also of vital importance for a successful result. Their knowledge of how the work is or may be done in an effective way, combined with the knowledge of the ventilation expert, increases the chance for an effective and durable solution of an air quality problem. Visualization methods have thereby proved to be effective both to communicate important knowledge and to motivate the staff to take part in the process.[1]

In this chapter the most common and/or well-evaluated techniques for the visualization of airflow and contaminant dispersion are described. The strategy for its use as a pedagogic tool is not included; this can be found elsewhere.[1] To separate the different methods according to either airflow or contaminant dispersion studies is meaningless and not always possible. For example, smoke may many times be used for both purposes. The emitted smoke acts like a substitute for the contaminant in question and visualizes its dispersion to, e.g., the

breathing zone of the worker at the same time as it enables the airflow patterns in the area to be studied. The two different purposes behind the use of the visualization methods have therefore not been explicitly separated.

To document by video or photography what is being visualized is often very useful. This makes it possible to analyze more carefully what has been documented. It is not possible to see all details the first time and the joint analysis of the results by all involved persons will many times be valuable.

There are of course a number of methods that can be classified as methods for the visualization of airflow and contaminant dispersion. This chapter describes some of these that are useful for designers of industrial ventilation. Methods that not are presented in more detail here are, for example, to fill small soap bubbles or ordinary balloons with helium in order to study the airflow field in large rooms. A large number of textbooks focus on flow visualization. The research in this area can also be followed in *The Journal of Flow Visualization and Image Processing*.[2]

12.2.1 Direct Observation of Aerosols Enhanced by Special Light

Air contaminants in solid or liquid state (aerosols), e.g., wood dust, welding smoke, or oil mist, are all in principle directly visible. The dispersion of those contaminants and the airflow patterns around the source may therefore be studied without any special tools. It is, however, not always possible to see the contaminant if, for example, the concentration in the air is low, the size of the particles is small, or the lighting is poor. The fact that the contaminant can't be seen may stem from the acceptable low level of the concentration but that can of course not be used to conclude that the control is acceptable. That conclusion depends not only on the contaminant's toxicological qualities but on how visible it is in air. The ability to see the particles directly is also, as said above, a function of their size. Small particles, able to be transported deep into the thinner airways of the lungs, are many times also difficult to see directly.

The lighting conditions are in many ways crucial to see an aerosol. A general increase in the intensity of light will to a certain degree increase the visibility of the particles. More important, however, is the quality of the light and the geometrical relations of the light source, the contaminated air volume, and the observer.

An ordinary photography spotlight, desk lamp, or electric torch will improve the visibility of the aerosol a lot if used in the best way. Figure 12.1 illustrates this with a smoke source with only general lighting (*a*), with the use of a spotlight close to the observer (*b*), and with the spotlight arranged opposite with a screen placed to avoid dazzling the observer (*c*). The effect of the extra light is obvious, especially when the geometry is optimal.

If a spotlight with a parabolic reflector is used, resulting in mainly parallel beams of light, the effect will be further improved. The effect is the same as when the sun (parallel light beams) is shining through the window, making all airborne particles visible. This effect is called the Tyndall effect and is utilized in special dust or Tyndall lamps.[3] The dust lamp is based on the effect that when parallel beams of light are directed to a cloud of fine particles, the most intensively scattered light is in the forward direction. The angle of this scattered light is small, and it is therefore of special importance that the anglelamp–dust cloud–observer be close to 180°. A devi-

(a) (b) (c)

FIGURE 12.1 Improved visibility of smoke by changed lighting.

ation between 5° and 15° is optimum. This implies that some kind of shield is necessary between the lamp and the observer.

This kind of spotlight enhances the visibility markedly and is very useful for the visualization of fine particles emitted from a relatively small source. Figure 12.2 illustrates the effect of a dust lamp used to visualize wood dust emission and exposure when sanding wood.

A drawback with the dust lamp compared to the photography spotlight is the limited volume of interest that will be illuminated. The cross-section of the light beam can never be wider than the diameter of the reflector in the lamp. A large reflector may certainly be used but will often be impractical for the purpose. With a lamp of the type in Fig. 12.2, it will therefore not normally be possible to see the emission of the contaminant at the same time as the exposure is visualized. This drawback, however, is many times compensated by the better capacity to visualize low concentrations of aerosols.

Typical examples where the use of extra light in general and the dust lamp in particular is very useful include checking that enclosures and local exhausts are effectively capturing emitted particles from, e.g., crushing, grinding, or sanding operations; checking for leakage from partly or totally enclosed

FIGURE 12.2 Use of dust lamp.

processes; or studying to what extent emitted particles reach the breathing zone. Another important use is to improve the visibility of smoke emitted to visualize airflow, etc. (see Section 12.2.2). The principles for the use of light for that purpose are the same as described above.

12.2.2 Smoke Generation

12.2.2.1 Principles

A common principle for the production of smoke for this purpose is to evaporate a mineral oil by electrically heating it and to mix the vapor into air. The oil will then condense and form a mist. Different such apparatus can be found on the market. Some of them are aimed for the visualization of airflow but others are intended for special effects in theaters, discotheques, etc. Figure 12.3 shows one such apparatus commonly used for this purpose.

The smoke generator shown in Fig. 12.3 allows the user to adjust the flow rate of the smoke and also to connect different types of spreaders through a several-meter-long tube. This makes it possible to simulate different types of sources, such as a point source with low or high momentum, a line source, a surface source, or any other source with any geometry. Some examples are illustrated in Fig. 12.4.

An application of the smoke generation principle described above is the "smoke wire." This simulates a line source and makes it possible to effectively study the airflow patterns in a layer, which is often desirable. A thin steel wire is

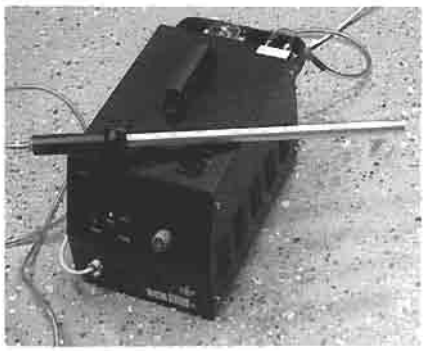

FIGURE 12.3 Smoke generators.

(*a*) (*b*) (*c*)

FIGURE 12.4 Three examples of smoke sources: line, surface, and three-dimensional.

wetted with the same type of oil used in the smoke generator described above. The wire is stretched and heated by passing an electric current through it, controlled by an adjustable transformer.[4] This technique has proved to be especially useful for studies of airflow patterns near obstacles in wind tunnel experiments.

Two other principles that have been made commercially available are (1) the reaction between pyrosulfuric acid ($H_2S_2O_7$) and water (water vapor in air) to form sulfuric acid aerosol and (2) the reaction between titanium tetrachloride ($TiCl_4$) and water to form titanium dioxide (TiO_2) and hydrogen chloride (HCl). Figure 12.5 shows two different hand-held, disposable smoke emitters.

These methods are the simplest, cheapest, and practically most accessible for airflow visualization. They are sold in the form of small glass tubes or plastic bottles through which air is pumped manually. Time for use of one unit is typically one hour or up to one day. One drawback of these two principles is the fact that the emitted smoke is strongly irritating if inhaled and also corrosive. Therefore, they must be used with some care, but this will normally not lead to any major restrictions. Another limitation is the low amount of smoke that is emitted.

Smoke emitters developed for fire exercises, pressure-testing of chimneys, etc. are sometime used for airflow studies. They normally take the form of big tablets that are put in fire and emit large amounts of smoke (Fig. 12.6). Also, smoke bombs giving different colors of smoke are available.

(*a*) (*b*)

FIGURE 12.5 Two types of hand-held smoke emitters.

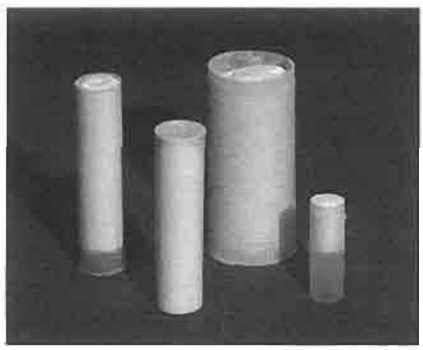

FIGURE 12.6 Smoke-emitting tablets.

Another method that has been used is heating/melting of tablets of metacetaldehyde, which then form a large number of particles that spread out from the source. By combining this with a photographic technique it is possible to determine both air velocity and airflow direction at single points.[5] The use of that principle is, however, limited since the generated smoke is harmful to persons. Magnesium carbonate ($MgCO_3$) powder has also been used combined with a laser light sheet.[6]

Dry ice (frozen carbon dioxide) can also be used to generate "smoke" for the same purpose.[7] By just letting air pass over a piece of dry ice, a mist is formed that is neither corrosive nor especially toxic if used in moderate amounts.

As said earlier in this chapter, the use of properly arranged illumination will improve the visibility of the smoke markedly. Extra light should be arranged so that the light beams are directed almost directly into the eyes of the observer or into the lens of a camera. Direct dazzling must be avoided with the help of some shield. The use of a laser beam expanded to a sheet makes it possible to visualize the airflow in a special layer in the room. This technique makes it possible to study the airflow in more detail, e.g., near an enclosure or around a machine.[8]

12.2.3 Flow Indicators

The most urgent and simplest question asked when a ventilation system is to be checked is, "Is the ventilation system on?" or "Is there any airflow passing through the system?" That the electric switch is on or that an operating lamp is shining does not always indicate that everything is alright. The airflow may, for many reasons, be reduced or stopped without any indication of malfunction. Nor is it always easy to determine whether the airflow rate from, e.g., an inlet air unit is as it is supposed to be. One common reason is that the unit is placed high above the floor, beyond the person's reach. A simple, inexpensive, and effective method to arrange for hourly or continuous checking is to place some string or a strip of light material so that it will flutter distinctly. A cotton string, paper or plastic strip, or any other suitable material glued, screwed, firmly tied, or fixed with tape to some part in the inlet airflow will serve perfectly well. A change in how the flow indicator behaves will give reason for a more accurate check of the ventilation system. This technique has also been used for surface flow visualization, especially for wind tunnel studies in the automotive and the aircraft industry.[8]

12.2.4 Thermocamera Methods

Many gases invisible in normal light absorb infrared radiation (IR) to a certain degree and may therefore be made visible with the help of an IR source and a video camera aimed for IR. Two different arrangements have been used: one with the IR source as a big screen behind the observed workplace seen from the IR camera,[9] and the other with the IR source close to the IR camera with a reflector screen behind the workplace.[10] The picture from the IR video camera will show the background (IR source or IR reflector) in one color and the workplace machinery and, if there, the worker as silhouettes in another color when no air contaminant is present (below the detection level). Emissions of a gas concentration high enough will be seen in the picture from the camera as a cloud spreading out from the source.

Figure 12.7 illustrates how leakage of nitrous oxide (anesthetic gas) spreads out from the patient during surgery in an operation theater.

(*a*)

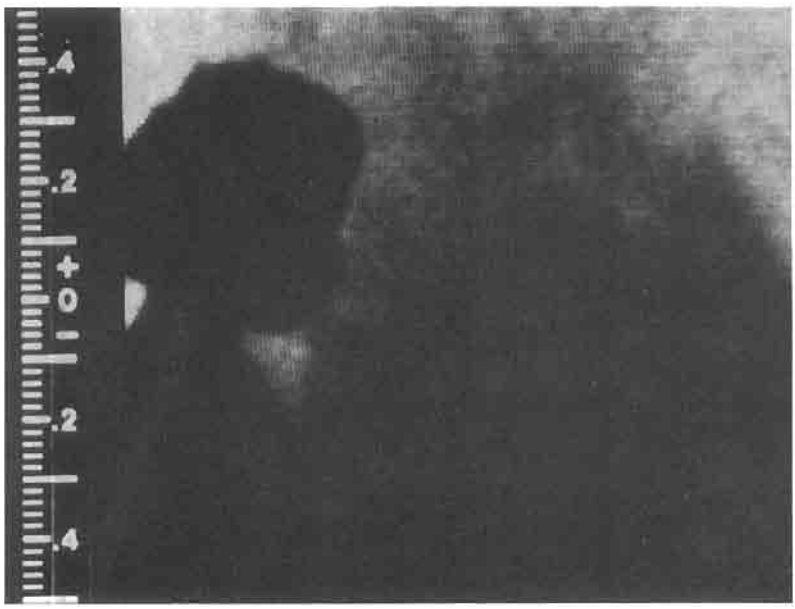

(*b*)

FIGURE 12.7 Thermocamera picture visualizing exposure to nitrous oxide during surgery: (*a*) without nitrous oxide in the breathing zone; (*b*) with nitrous oxide. (Picture from B. Ljungqvist.)

Applications that have been tested with good results are cases where nitrous oxide has been the air contaminant of current interest or used as a tracer gas. Other applications have been carbon disulfide in a rayon factory and styrene vapor, one of the volatile components from a surface-coating material.

The thermocamera method has the important advantage that it very effectively visualizes emission and air transport of, and workers' exposure to, the otherwise invisible gas. By using a system that gives a presentation where different colors represent different average concentrations between the camera and the IR source, it is also possible to clearly visualize concentration gradients in the studied area. Some of the limitations are the limited number of gases that may be studied with this method and the relatively complicated work to arrange the big monochrome IR source. The price level of the equipment used is another limitation. No ready product for this method has been presented on the market, but the needed components are largely available.

12.2.5 Graphical Presentation of Area Measurements

By measuring the concentration of an air contaminant at the same time in several points with the help of a real-time monitoring instrument it is possible to visualize its spatial distribution by making a graphical presentation of data. If the measurements for example are made at a constant distance from the floor and at regularly placed measuring points in a grid, it is easy to produce a 3D graph illustrating how the contaminant concentrations are distributed.[11] A grid with 3×3 points may be enough to give a rough view, but a slightly denser grid with 5×5 measuring points may be preferable. Experience shows that it is possible to collect data manually within a few minutes for a denser grid. By manual collection of data it is therefore possible to visualize the spatial distribution if the situation is mainly stable within the time limits for collection of data.

Many different standard software packages for computers may be used for the processing of data to a 3D graph. Figure 12.8 illustrates such a grid map produced from data from a 5×5 points measuring grid. By also superimposing the graph over a perspective drawing of the measured area, the result will very effectively visualize how, for example, contaminants are leaking out from a machine and in what direction the contaminants are transported. By making a series of such measurements and graphical presentations it is possible to visualize the effect of changes such as alterations in the ventilation system.

To produce this kind of grid map by quickly measuring the concentrations at some points for immediate processing and graphical presentation is a simple and often effective way to communicate the results to persons who are not trained to analyze primary results of measurements. The method must, however, be used with care since there is a risk that the sampling of data itself may affect the airflow in the studied area. The equipment needed is relatively expensive, and the method is therefore of interest when the prerequisites are already available for other reasons.

It is of course also possible to arrange so that the measurements are made at every point with a fixed instrument and the data transferred to a computer equipped with suitable software to produce the grid map, all in real time. If the graph is also superimposed on a video picture from the measured area, the result will be a video, visualizing the spatial distribution in real time.

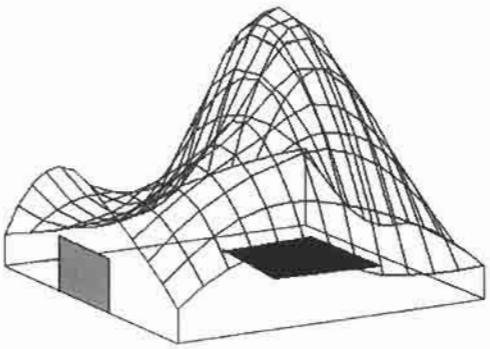

FIGURE 12.8 Grid map picture illustrating distribution of air contaminants on one level above the floor in a factory hall.

A similar graphical presentation of the spatial distribution of a tracer gas or a real contaminant and thereby to some extent the airflow in the studied area is based on the use of computed tomography and optical remote sensing.[12,13] IR beams are sent out horizontally and reflected back to an IR analytical instrument, analyzing the average concentration of the contaminant along the IR beam. By combining data from several measured lines it is possible to present data in a similar way to Fig. 12.8. Those methods presuppose access to an expensive and complicated sampling/data processing system.

12.2.6 Graphical Presentation of Measured Parameters in a Video

One of the most important goals for designers of industrial ventilation is to reduce the concentration of an air contaminant in the breathing zone of the workers. Smoke, dust lamps, and graphical presentations of area measurements are very important tools for the studies of airflow in the workplace and how the contaminant is dispersed out of the workplace. Those methods will, however, only give good indications of how much of the contaminant reaches the breathing zone. Strategies to visualize the concentration at the breathing zone may therefore serve as an important tool for the industrial ventilation expert.

One method for the visualization of workers' exposure to air contaminants is the PIMEX method.[1,14] The method is based on the simultaneous use of real-time monitoring instruments for the contaminant in question and video recording. The instrument is placed so that it samples in the breathing zone of the worker. The work is videotaped with the help of a video camera. The results from the measurements are presented as a graph, which is superimposed on the video picture. Many different technical solutions for this have been presented. Equipment that is available on the market uses telemetry to transfer the signal from the instrument to a laptop computer equipped with needed hardware and software for the task. The software makes it possible to present data as a bar graph or as a time-concentration graph, in both cases continuously updated. The software also facilitates a detailed analysis regarding the variation of concentrations in the breathing zone and their dependence on the situation in the workplace.[15,16] Figure 12.9 shows two examples of how data is presented in the video picture.

FIGURE 12.9 Pictures from a PIMEX video. To the left, a superimposed bar graph showing momentary contaminant exposure. To the right, a moving graph and digits showing the same.

This method has been used for a variety of applications to visualize the concentration of different air contaminants in the breathing zone and how it relates to factors like design of local ventilation, etc. Typical situations where it has been used are when the contaminant source is close to or handled by the worker, e.g., welding, painting, and woodworking.

The most important advantage with this visualization method is that it highlights the object of design effort, the concentration in the breathing zone of the exposed worker. There are many reasons to do so. One is that the presence and motions of the worker near the source or the ventilation units will have a considerable influence on the flow field around him or her and thus on the dispersion of the contaminant from the source to the breathing zone. If the designer of the ventilation system does not take this into consideration, there could be a big risk of failure in many situations. Another reason is that good communication between the expert, the industrial ventilation designer, and the subject of the work will facilitate solutions that not only function in technical terms, but also are accepted and in the best case also understood by the worker. A method that visualizes the concentration of the contaminant in the breathing zone is then an important pedagogic tool.

A disadvantage of this method, as with some of the methods described above, is that it presumes access to relatively complicated equipment that also implies basic training of the user.

References

1. G. Rosén. *Workplace Improvement Strategy by PIMEX: Final Report to European Commission.* SAFE Project no. 97 202356 05F05. National Institute for Working Life, Stockholm, Sweden, 1999.
2. *Journal of Flow Visualization and Image Processing*, Begell House, Inc., ISSN 1065-3090.
3. BOHS. *Controlling Airborne Contaminants in the Workplace.* British Occupational Hygiene Society Technical Guide no 7. Science Reviews Ltd., H & H Scientific Consultants Ltd., Leeds, 1987 (reprinted 1988).
4. A. Sreenath, G. Ramachandran, J.H. Vincent. Experimental investigations into the nature of airflows near bluff bodies with aspiration, with implications to aerosol sampling. *Atmospheric Environment* 31 (15), 1997.
5. Frank Scholzen. Bestimmung des dreidimensionalen geschwindigkeitsfeldes in räumen durch quantitative strömungsvisualisierung. Doctoral thesis. Diss. ETH Nr.11963. Eidgenössischen Technischen Hochschule, Zürich, 1997.

6. S. Murakami, S. Kato, S. Akabayashi. Visualization with laser light sheet applied to internal and external airflows in building environmental engineering. In *Fluid Control & Measurement*, vol. 2, Tokyo, 1985.
7. W.A. Heitbrink, D.R. Farwick. *Survey Report: Control Technology for Manual Powder Weigh-Out Operations at Merck and Company, Wilson, North Carolina.* Report no. CT-197-13a. Engineering Control Technology Branch, Division of Physical Sciences and Engineering, NIOSH, Cincinnati, OH, 1994.
8. Yang Wen-Jey. *Handbook of Flow Visualisation.* Hemisphere, New York, 1989.
9. C. Allander, B. Ljungqvist. *Air Movements—The Dispersion of Pollution. Exploratory Tests Using IR Techniques.* Document D16:1979. Swedish Council for Building Research, Stockholm, Sweden, 1979.
10. W.M. ter Kuile, B. Knoll, P.G.M. Hesselink. Measurement and imaging of gases in industrial environments with the infrared gas cloud scanner. *Appl. Occup. Environ. Hyg.* 8(1), 1993.
11. G. Rosén, I. -M. Andersson. GripMap: An aid in elimination of air contaminants in workplaces. *Appl. Ind. Hyg.* 2, 1989.
12. M.G. Yost, A.J. Gadgil, A.C. Drescher, Y. Zhou, M.A. Simonds, S.O. Levine, W.W. Nazaroff, P.A. Saisan. Imaging indoor tracer-gas consentrations with computed tomography: Experimental results with a remote sensing FTIR system. *Am. Ind. Hyg. Assoc. J.* 55, 1994.
13. L. Todd, G. Ramachandran. Evaluation of algorithms for tomographic reconstruction of chemical concentrations in indoor air. *Am. Ind. Hyg. Assoc. J.* 55, 1994.
14. G. Rosén. PIMEX. Combined use of air sampling instruments and video filming: Experience and results during six years of use. *Appl. Occup. Environ. Hyg.* 8(4), 1993.
15. W.A. Heitbrink, M.G. Gressel, T.C. Cooper. Video exposure monitoring—A means of studying sources of occupational air contaminant exposure. Part 2: Data interpretation. *Appl. Occup. Environ. Hyg.* 8(4), 1993.
16. I. Andersson, G. Rosén. Detailed work analysis for control of exposure to airborne contaminants in the workplace. *Appl. Occup. Environ. Hyg.* 10(6), 1995.

12.3 MEASUREMENT TECHNIQUES

12.3.1 Introduction

In the wide field of industrial ventilation many factors require measurements to be carried out. One of the most common is the commissioning of a new or a renovated ventilation system. In this case the client has to see that the system works according to the specifications made with the consulting engineer, manufacturer, and contractor. Many other situations require quantitative information on ventilation and related systems, like

The satisfactory functioning of a ventilation system,
Troubleshooting in existing facilities,
Testing the dynamics of subsystems, such as controls,
Determining reasons for complaints,
Checking on specified target values in a space,
Carrying out an energy audit,
Collecting data for renovation planning, and
Collecting boundary values for a computational approach.

The only method to determine the actual system performance is to carry out measurements. The questions to be answered are: What should be measured? How and when? How should the results be interpreted? Some of the answers to these questions are found in the following sections.

The most common quantities to be measured in the field of industrial ventilation are air temperature, humidity, airflow rate, velocity, pressure

difference, and the concentration of different contaminants. Besides these, some other quantities, such as temperatures of other media (water, solid surfaces), noise and vibration, some additional air quality parameters, and tracer concentrations may be required. From these many other quantities can be calculated, like energy use, the thermal environment, air quality, or ventilation efficiency.

On-site measurement is not the only approach to gain information on a system. In the case of a building/system at the planning stage, it is not possible. Measuring is also expensive, especially if carried out on a large scale for a long time. If quantitative information (numbers) is not absolutely necessary and qualitative information (visual observation, video, photographs, etc.) will do, visualization is an alternative in investigating flow patterns. Visualization can also be used to supplement the measurements or vice versa. If, however, numbers are required, reduced-scale measurements can be used. They can be carried out also during the planning stage by constructing a scale model. Finally, modelling techniques like CFD or thermal/zone models can be used in some cases as an alternative for measurements.

Careful consideration has to be given to all aspects of each approach—such as the reliability, the total cost, and the need for equipment and expertise—before making the final decision. The main advantage of measurements is the reliability of the results, the disadvantage being the need for often expensive equipment.

12.3.2 Measurement Planning

12.3.2.1 Setting the Goal

The planning of measurements is the first consideration to obtain information by the measurement approach. Why is it essential to make plans before any action is taken? Could one not just take the instruments and carry out the monitoring? In very simple situations this approach might provide a satisfactory result, but it could result in failure as well. In complicated situations failure, in terms of missing information, would be likely. Hence in order to obtain a sufficient quantity of high-quality information and to avoid the need to repeat any measurement or monitoring, and thus to save time and effort, the planning of measurements is essential.

When setting the goals of a measurement project, it has to be asked, What exactly has to be determined? What are the final quantities required and what is the inaccuracy that can be tolerated in these quantities? Only when these factors are known can an analysis be made, where the quantities to be measured and the measurement accuracy of each quantity are defined. This analysis is based on the measurement method selected, and on the computation of measurement uncertainties. Usually the analysis of measurement uncertainties is made after monitoring; however, making it beforehand is part of good planning practice. This approach ensures that the correct information with the desired accuracy is achieved.

12.3.2.2 Selection Methods

The measurement is always carried out according to a given method. The measurement of a single quantity may be simple, but complications may arise when measuring several quantities and the results require special consideration.

The goals and the final quantities to be obtained determine the method to be used. As a first approach, it is always worth checking if a documented and proven method exists. Standardized methods are often the best. They are developed by experts in the field and are usually of a high quality and are well documented. Frequently no standards can be applied and generally known methods have to be relied on. Sometimes situations occur when the whole of the measurement procedure has to be tailored for the specific situation. This is a very demanding task and considerable experience is required.

12.3.2.3 The Phenomena and the Quantities

The features of the phenomena to be investigated and the quantities to be measured should always be taken into account at the planning stage. Static phenomena, where the measured quantities do not change with time, are extremely rare in industrial ventilation applications. Usually everything moves and changes with time and from place to place. For this reason, it seldom is adequate to take only one sample of the measured quantity. An example would be mean air velocity measurements in an occupied space. The air velocity is changing all the time, and to obtain a value for a local mean velocity, several readings during a time interval have to be taken. Besides temporal variations, the velocity also has different values in different places. So local mean values should be measured in several places in the occupied zone in order to determine the mean value in the whole space.

Different kinds of disturbances, which distort the collected information, can also influence the measurements under examination. For example, opening a large door in an industrial hall will immediately influence the pressure distribution in the whole building, causing changes in airflows and indoor temperatures as well. If the person carrying out the measurement ignores this fact the wrong information may be obtained. Such a disturbance is called an external disturbance. An internal disturbance is due to the measurement itself, when the measured quantity is changed by the existence of the measurement arrangements. Reducing the supply or exhaust airflow with a flow meter or changing the surface temperature with the temperature probe are internal disturbances.

Most of the measured quantities, like temperatures, velocities, and concentrations, vary from place to place. Hence, it is important to consider in advance the correct measuring positions. The probe location is different depending on the application, such as to determine the thermal boundary conditions for CFD computations or to determine the reasons for complaints of thermal discomfort in the occupied zone. Another important factor to consider is the time when the measurements are taken, which can be critical in some cases. The timing normally relates to the state of the processes, the running mode of the HVAC systems, or the weather conditions. All these influence each other, the flow patterns, temperatures, energy use, and other measured quantities in the industrial environment. If the task is to determine the contaminant exposure of a worker, it might not be sufficient to monitor during the heating season, since the resulting flow pattern and associated concentration levels might be totally different during the cooling season.

12.3.2.4 Instrument Selection

The selection of instrumentation for a specific task is an important part of measurement planning. The instrumentation consists of measuring probes, the meters to convert the signals from the probes, and some intelligence to guide the

monitoring and auxiliary equipment. The performance of the instrumentation depends on the quality of the probes and meters; hence these components must be selected according to the information required. The instrument measuring range has to be consistent with the scale that is of interest. The inaccuracy of the probes and meters should fulfill the demand of the preliminary error analysis. The equipment drift must be known in order to make necessary calibrations during longer monitoring periods. The dynamics of the probes should be selected to allow rapid changes of the measured quantities to be followed, if necessary. If, e.g., the velocity probe is slow in following the fluctuations of the airflow, the resulting value of turbulence intensity could be highly erroneous.

Organizing the measurements is also one part of planning and is closely tied to instrument selection. In a simple case there is normally no problem with organizing the work. The measurement is carried out manually. However, in more complicated cases, such as determining the energy performance of a large industrial ventilation system, numerous monitoring points are required. Manual measurement would be time-consuming, unpractical, and even impossible to carry out due to the constantly changing parameters. In this instance automation of the measurements is essential. The arranging of automatic recording equipment is time-consuming. The level of automatic recording and control has to be optimized so that the required information is achieved with the minimum time, effort, and cost.

One aspect related to automatic measurements is how the automation is achieved: it may be either centralized or decentralized. The centralized method is based on a data acquisition system consisting of a selection of measurement cards or units connected to a computer. The probes are placed in the monitored process and connected to meters with measurement cables. Provided the distance between the farthest probes is not too long, this approach is suitable. However, if quantities are to be measured simultaneously in different zones of a large building, the centralized approach may be impractical due to the very long wiring distances. In this case the decentralized approach, where several smaller data acquisition units are used, would be better. A wide selection of small data acquisition units are available and some of them are very powerful and high-quality instruments.

12.3.2.5 Time Schedule and Other Aspects

It is essential to plan the time schedule of a measurement project—the more detailed, the more important it is to carry out the measurements in a specified time. The time schedule is achieved by dividing the whole project into smaller tasks and assessing the time required to carry out these subtasks. A rough division of a measurement project could contain the following elements:

Measurement planning,
Installing the instrumentation,
Testing of the instrumentation,
Taking measurements,
Analyzing results, and
Reporting and other documentation.

The testing stage of complicated situations can take a considerable time and, if underestimated, will delay the project. In simple routine measurements

or when past experience of a specific task exists, the time planning can be controlled. However, when a large measurement project containing new elements is planned, special attention is required in assessing the time allocation. Several problems may occur. The support of the companies delivering the instrumentation is essential in case of equipment failure or breakage. A good "rule of thumb" is to multiply the initial time estimate by a factor of 2.

12.3.2.6 Analyzing and Presenting Results

It is not good practice to carry out the measurement analysis at the end of a measuring session. Some source of error not detected during the instrument testing period may influence the results and require repeating all measurements. To avoid such a situation, the first results analysis should be carried out during the measurement period and, if problems are noted, necessary action can be taken immediately. In case of long-term monitoring, the preliminary analysis has to be continuous to check the data quality and the equipment condition.

The final treatment of the data is then carried out when all results are available. How this treatment and analysis is achieved depends on many factors. With regards to presenting the results, few general principles can be given. One should always consider the status of the reader of the report—the target group—and adjust the level of presentation accordingly. If large quantities of data are to be presented, a table is a poor choice. Graphs and figures are more illustrative than tables. The data can often be treated statistically with mean values and standard deviations shown to the reader. The use of nondimensional groups of quantities, like Reynolds number or Biot number, is an ideal way of presenting results. Error analysis should always accompany the general analysis and treatment of data, showing the reliability of the measurements.

12.3.2.7 Documentation

A report describing the measuring arrangements, instrumentation, and main results and findings is often the only information of the measurements carried out. With simple or routine measurements this is usually a sufficient level of documentation. In larger research and development activities or more scientific projects it is wise to expand the documentation to cover other material. Later on there may be a need to check some of the initial results, to treat the raw data according to a new idea, or give the data to somebody else for his or her own purposes. For this reason the raw data should be organized, labeled, and stored so that even after several years it can be reused. For the same reason, a sufficient amount of supplementary information like dates, places, persons, weather, running mode of ventilation and other systems, and status of doors and windows should be documented and stored. It often is wise to photograph some details of the measurement arrangements, for reference. All this documentation can be stored on some powerful storage device, such as a CD-ROM disk of adequate storage capacity.

12.3.3 Treatment of Measurement Uncertainties

12.3.3.1 Introduction

The probable largest inconsistency in all measurements is the fact that, regardless of the instruments used and the methods applied, we never find the true value of the quantity that is being measured. It is possible to improve the

estimate of the true value but still fall short of the ideal. This fact, which cannot be avoided, is the "First Law of Measurements." It is a consequence of the existence of measurement errors, and is not sufficiently understood among all those involved with measuring instruments and carrying out measurements. Before focusing on errors and their causes, it will be of benefit to define a few fundamental terms:[1,2]

True value of a quantity: This characterizes a perfectly defined quantity, in the conditions existing at the time the value was observed.

Result of a measurement: This is the value of the measured quantity obtained by measurement.

Error of measurement: This is the discrepancy between the result of measurement and the true value of the quantity.

12.3.3.2 Measurement Errors

The measurement errors are divided into two categories: systematic errors and random errors.[1]

Systematic error is an error which, in the course of a number of measurements carried out under the same conditions of a given value and quantity, either remains constant in absolute value and sign, or varies according to definite law with changing conditions.

Random error varies in an unpredictable manner in absolute value and in sign when a large number of measurements of the same value of a quantity are made under essentially identical conditions.

The origins of the above two errors are different in cause and nature. A simple example is, when the mass of a weight is less than its nominal value, a systematic error occurs, which is constant in absolute value and sign. This is a pure systematic error. A ventilation-related example is, when the instrument factor of a Pitot-static tube, which defines the relationship between the measured pressure difference and the velocity, is incorrect, a systematic error occurs. On the other hand, if a Pitot-static tube is positioned manually in a duct in such a way that the tube tip is randomly on either side of the intended measurement point, a random error occurs. This way, different phenomena create different types of error. The (total) error of measurement usually is a combination of the above two types.

The question may be asked, What is the reason in dividing the errors into two categories? The answer is the totally different way of dealing with these different types. Systematic error can be eliminated to a sufficient degree, whereas random error cannot. The following section shows how to deal with these errors.

12.3.3.3 Systematic Errors

Systematic error, as stated above, can be eliminated—not totally, but usually to a sufficient degree. This elimination process is called "calibration." Calibration is simply a procedure where the result of measurement recorded by an instrument is compared with the measurement result of a standard. A standard is a measuring device intended to define, to represent physically, to conserve, or to reproduce the unit of measurement in order to transmit it to other measuring instruments by comparison.[1] There are several categories of standards, but, simplifying a little, a standard is an instrument with a very high accuracy and can for that reason be

used as a reference for ordinary measuring instruments. The calibration itself is usually carried out by measuring the quantity over the whole range required and by defining either one correction factor for the whole range, for a constant systematic error, or a correction curve or equation for the whole range. Applying this correction to the measurement result eliminates, more or less, the systematic error and gives the corrected result of measurement.

A primary standard has the highest metrological quality in a given field. Hence, the primary standard is the most accurate way to measure or to reproduce the value of a quantity. Primary standards are usually complicated instruments, which are essentially laboratory instruments and unsuited for site measurement. They require skilled handling and can be expensive. For these reasons it is not practical to calibrate all ordinary meters against a primary standard. To utilize the solid metrological basis of the primary standard, a chain of secondary standards, reference standards, and working standards combine the primary standard and the ordinary instruments. The lower level standard in the chain is calibrated using the next higher level standard. This is called "traceability." In all calibrations traceability along the chain should exist, up to the instrument with the highest reliability, the primary standard.

The question is often asked, How often should calibration be carried out? Is it sufficient to do it once, or should it be repeated? The answer to this question depends on the instrument type. A very simple instrument that is robust and stable may require calibrating only once during its lifetime. Some fundamental meters do not need calibration at all. A Pitot-static tube or a liquid U-tube manometer are examples of such simple instruments. On the other hand, complicated instruments with many components or sensitive components may need calibration at short intervals. Also fouling and wearing are reasons not only for maintenance but also calibration. Thus the proper calibration interval depends on the instrument itself and its use. The manufacturers recommendations as well as past experience are often the only guidelines.

12.3.3.4 Estimation of Random Errors

Normal Distribution

Due to its nature, random error cannot be eliminated by calibration. Hence, the only way to deal with it is to assess its probable value and present this measurement inaccuracy with the measurement result. This requires a basic statistical manipulation of the normal distribution, as the random error is normally close to the normal distribution. Figure 12.10 shows a frequency histogram of a repeated measurement and the normal distribution $f(x)$ based on the sample mean and variance. The total area under the curve represents the probability of all possible measured results and thus has the value of unity.

The experimental sample on which the frequency histogram is based has an experimental mean m and an experimental variance s^2, which are

$$m = \sum_{i=1}^{n} x_i \tag{12.1}$$

and

$$s^2 = \frac{\sum_{i=1}^{n} (x_i - m)^2}{n-1}, \tag{12.2}$$

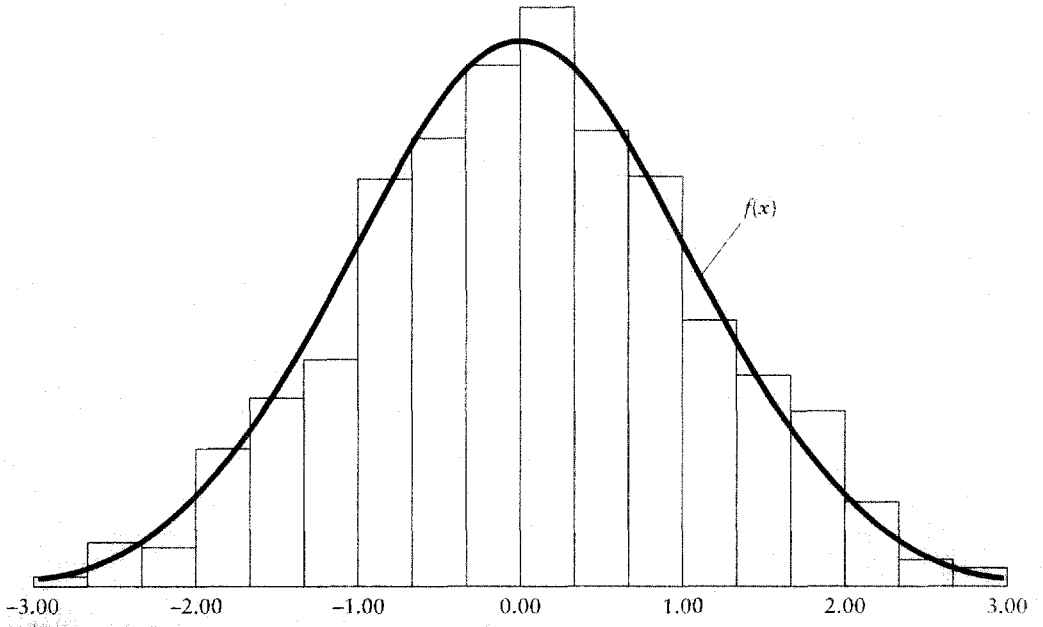

FIGURE 12.10 Frequency histogram and normal distribution.

where n is the sample size. When the sample approaches infinity, the experimental mean and the experimental variance approach the mean μ and the variance σ^2 of the $N(\mu, \sigma)$ normal distribution. Thus m is an estimate of μ and s^2 is an estimate of σ^2.

The probability density of the normal distribution $f(x)$ is not very useful in error analysis. It is better to use the integral of the probability density, which is the cumulative distribution function

$$F(a) = \int_{-\infty}^{a} f(x)dx = \frac{1}{\sigma\sqrt{2\pi}} \int_{-\infty}^{a} e^{-\frac{1}{2}\left(\frac{x-\mu}{\sigma}\right)^2} dx. \tag{12.3}$$

This function represents the area under the density curve of the normal distribution between $-\infty$ and a. This is the probability for the random variable X to obtain a value smaller or equal to a. Expressed mathematically,

$$P(X \leq a) = F(a) \tag{12.4}$$

The probability for the random, normally distributed variable X to obtain a value between some limits a and b is

$$P(a \leq X \leq b) = F(b) - F(a) \tag{12.5}$$

This is illustrated in Fig. 12.11. As the integral in Eq. (12.3) cannot be evaluated by elementary methods, the cumulative distribution function is determined from tables.

To deal with all kinds of normal distributions of different means and variances, the cumulative distribution is further normalized. This introduces a new variable $u = (x - \mu)/\sigma$. This operation changes a $N(\mu, \sigma)$ distribution to a $N(0, 1)$ distribution. From Eq. (12.3) the following is obtained:

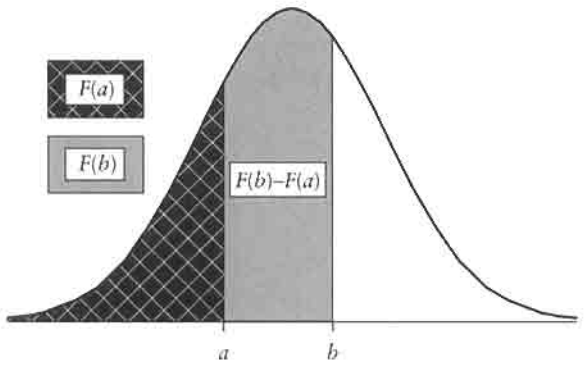

FIGURE 12.11 Normal distribution and probabilities.

$$F_N(u_1) = \frac{1}{\sqrt{2\pi}} \int_{-\infty}^{u_1} e^{-\frac{1}{2}u^2} du, \tag{12.6}$$

which is the cumulative distribution function of a normal distribution with mean 0 and variance 1 and where $u_1 = (x_1 - \mu)/\sigma$ is a fixed value of the variable u. As $F(x) = F_N[(x - \mu)/\sigma]$, the following is obtained:

$$P(a \le X \le b) = F(b) - F(a) = F_N\left(\frac{b-\mu}{\sigma}\right) - F_N\left(\frac{a-\mu}{\sigma}\right). \tag{12.7}$$

Having available the table (or function in a calculator or spreadsheet program) for the $F_N(0, 1)$ distribution, the probability of any $F(\mu, \sigma)$ distributed random variable required to obtain a value between the limits $[a, b]$ can be evaluated. Table 12.2 gives values for the $N(0, 1)$ distribution. As an example, the following probabilities can be evaluated from the table:

$$P(-1 \le u \le 1) = P(\mu - \sigma \le X \le \mu + \sigma) = 0.682,$$
$$P(-2 \le u \le 2) = P(\mu - 2\sigma \le X \le \mu + 2\sigma) = 0.954, \text{ and}$$
$$P(-3 \le u \le 3) = P(\mu - 3\sigma \le X \le \mu + 3\sigma) = 0.997$$

The precondition for the use of the normal distribution in estimating the random error is that adequate reliable estimates are available for the parameters μ and σ. In case of a repeated measurement, the estimates are calculated using Eqs. (12.1) and (12.3). When the sample size increases, the estimates m and s approach the parameters μ and σ. A rule of thumb is that when $n \ge 30$, the normal distribution can be used.

t-Distribution

If a measurement is repeated only a few times, the estimate for the distribution variance calculated from this sample is uncertain and the normal distribution cannot be applied. In this case another distribution is used. This distribution is Student's distribution or the t-distribution, and it has one more parameter: the number of degrees of freedom, ν. The t-distribution takes into account, through the ν parameter, the uncertainty of the variance. The values of the cumulative t-distribution function cannot be evaluated by elementary methods, and tabulated values or other calculation methods have to be used.

TABLE 12.2 Values for the Cumulative $N(0, 1)$ Distribution

a	$F_N(a)$	a	$F_N(a)$	a	$F_N(a)$	a	$F_N(a)$	a	$F_N(a)$	a	$F_N(a)$
0.00	0.5000	0.50	0.6915	1.00	0.8413	1.50	0.9332	2.00	0.9772	2.50	0.9938
0.01	0.5040	0.51	0.6950	1.01	0.8438	1.51	0.9345	2.01	0.9778	2.51	0.9940
0.02	0.5080	0.52	0.6985	1.02	0.8461	1.52	0.9357	2.02	0.9783	2.52	0.9941
0.03	0.5120	0.53	0.7019	1.03	0.8485	1.53	0.9370	2.03	0.9788	2.53	0.9943
0.04	0.5160	0.54	0.7054	1.04	0.8508	1.54	0.9382	2.04	0.9793	2.54	0.9945
0.05	0.5199	0.55	0.7088	1.05	0.8531	1.55	0.9394	2.05	0.9798	2.55	0.9946
0.06	0.5239	0.56	0.7123	1.06	0.8554	1.56	0.9406	2.06	0.9803	2.56	0.9948
0.07	0.5279	0.57	0.7157	1.07	0.8577	1.57	0.9418	2.07	0.9808	2.57	0.9949
0.08	0.5319	0.58	0.7190	1.08	0.8599	1.58	0.9429	2.08	0.9812	2.58	0.9951
0.09	0.5359	0.59	0.7224	1.09	0.8621	1.59	0.9441	2.09	0.9817	2.59	0.9952
0.10	0.5398	0.60	0.7257	1.10	0.8643	1.60	0.9452	2.10	0.9821	2.60	0.9953
0.11	0.5438	0.61	0.7291	1.11	0.8665	1.61	0.9463	2.11	0.9826	2.61	0.9955
0.12	0.5478	0.62	0.7324	1.12	0.8686	1.62	0.9474	2.12	0.9830	2.62	0.9956
0.13	0.5517	0.63	0.7357	1.13	0.8708	1.63	0.9484	2.13	0.9834	2.63	0.9957
0.14	0.5557	0.64	0.7389	1.14	0.8729	1.64	0.9495	2.14	0.9838	2.64	0.9959
0.15	0.5596	0.65	0.7422	1.15	0.8749	1.65	0.9505	2.15	0.9842	2.65	0.9960
0.16	0.5636	0.66	0.7454	1.16	0.8770	1.66	0.9515	2.16	0.9846	2.66	0.9961
0.17	0.5675	0.67	0.7486	1.17	0.8790	1.67	0.9525	2.17	0.9850	2.67	0.9962
0.18	0.5714	0.68	0.7517	1.18	0.8810	1.68	0.9535	2.18	0.9854	2.68	0.9963
0.19	0.5753	0.69	0.7549	1.19	0.8830	1.69	0.9545	2.19	0.9857	2.69	0.9964
0.20	0.5793	0.70	0.7580	1.20	0.8849	1.70	0.9554	2.20	0.9861	2.70	0.9965
0.21	0.5832	0.71	0.7611	1.21	0.8869	1.71	0.9564	2.21	0.9864	2.71	0.9966
0.22	0.5871	0.72	0.7642	1.22	0.8888	1.72	0.9573	2.22	0.9868	2.72	0.9967
0.23	0.5910	0.73	0.7673	1.23	0.8907	1.73	0.9582	2.23	0.9871	2.73	0.9968
0.24	0.5948	0.74	0.7704	1.24	0.8925	1.74	0.9591	2.24	0.9875	2.74	0.9969
0.25	0.5987	0.75	0.7734	1.25	0.8944	1.75	0.9599	2.25	0.9878	2.75	0.9970
0.26	0.6026	0.76	0.7764	1.26	0.8962	1.76	0.9608	2.26	0.9881	2.76	0.9971
0.27	0.6064	0.77	0.7794	1.27	0.8980	1.77	0.9616	2.27	0.9884	2.77	0.9972
0.28	0.6103	0.78	0.7823	1.28	0.8997	1.78	0.9625	2.28	0.9887	2.78	0.9973
0.29	0.6141	0.79	0.7852	1.29	0.9015	1.79	0.9633	2.29	0.9890	2.79	0.9974
0.30	0.6179	0.80	0.7881	1.30	0.9032	1.80	0.9641	2.30	0.9893	2.80	0.9974
0.31	0.6217	0.81	0.7910	1.31	0.9049	1.81	0.9649	2.31	0.9896	2.81	0.9975
0.32	0.6255	0.82	0.7939	1.32	0.9066	1.82	0.9656	2.32	0.9898	2.82	0.9976
0.33	0.6293	0.83	0.7967	1.33	0.9082	1.83	0.9664	2.33	0.9901	2.83	0.9977
0.34	0.6331	0.84	0.7995	1.34	0.9099	1.84	0.9671	2.34	0.9904	2.84	0.9977
0.35	0.6368	0.85	0.8023	1.35	0.9115	1.85	0.9678	2.35	0.9906	2.85	0.9978
0.36	0.6406	0.86	0.8051	1.36	0.9131	1.86	0.9686	2.36	0.9909	2.86	0.9979
0.37	0.6443	0.87	0.8078	1.37	0.9147	1.87	0.9693	2.37	0.9911	2.87	0.9979
0.38	0.6480	0.88	0.8106	1.38	0.9162	1.88	0.9699	2.38	0.9913	2.88	0.9980
0.39	0.6517	0.89	0.8133	1.39	0.9177	1.89	0.9706	2.39	0.9916	2.89	0.9981

(continues)

TABLE 12.2 *(continued)*

a	$F_N(a)$	a	$F_N(a)$	a	$F_N(a)$	a	$F_N(a)$	a	$F_N(a)$	a	$F_N(a)$
0.40	0.6554	0.90	0.8159	1.40	0.9192	1.90	0.9713	2.40	0.9918	2.90	0.9981
0.41	0.6591	0.91	0.8186	1.41	0.9207	1.91	0.9719	2.41	0.9920	2.91	0.9982
0.42	0.6628	0.92	0.8212	1.42	0.9222	1.92	0.9726	2.42	0.9922	2.92	0.9982
0.43	0.6664	0.93	0.8238	1.43	0.9236	1.93	0.9732	2.43	0.9925	2.93	0.9983
0.44	0.6700	0.94	0.8264	1.44	0.9251	1.94	0.9738	2.44	0.9927	2.94	0.9984
0.45	0.6736	0.95	0.8289	1.45	0.9265	1.95	0.9744	2.45	0.9929	2.95	0.9984
0.46	0.6772	0.96	0.8315	1.46	0.9279	1.96	0.9750	2.46	0.9931	2.96	0.9985
0.47	0.6808	0.97	0.8340	1.47	0.9292	1.97	0.9756	2.47	0.9932	2.97	0.9985
0.48	0.6844	0.98	0.8365	1.48	0.9306	1.98	0.9761	2.48	0.9934	2.98	0.9986
0.49	0.6879	0.99	0.8389	1.49	0.9319	1.99	0.9767	2.49	0.9936	2.99	0.9986

The probabilities for a t-distributed random variable are obtained in a similar way to those in the normal distribution:

$$P(t \leq a) = T(a, \nu) \tag{12.8}$$

$$P(a \leq t \leq b) = T(b, \nu) - T(a, \nu), \tag{12.9}$$

where t is a t-distributed random variable and $T(t, \nu)$ is the corresponding cumulative distribution. The only difference from the normal distribution is the use of the number of degrees of freedom, which in case of a repeated measurement is $\nu = n - 1$.

Confidence Limits of a Repeated Measurement

The confidence limits of a measurement are the limits between which the measurement error is with a probability P. The probability P is the confidence level and $\alpha = 1 - P$ is the risk level related to the confidence limits. The confidence level is chosen according to the application. A normal value in ventilation would be $P = 95\%$, which means that there is a risk of $\alpha = 5\%$ for the measurement error to be larger than the confidence limits. In applications such as nuclear power plants, where security is of prime importance, the risk level selected should be much lower. The confidence limits contain the random errors plus the "residual" of the systematic error after calibration, but not the actual systematic errors, which are assumed to have been eliminated.

Since the confidence limits of a repeated measurement are based on the dispersion of the measurement result, they usually are presented as symmetrical limits:

$$dx = \pm\tau(\alpha, \nu)s_x, \tag{12.10}$$

where $\kappa(\alpha, \nu)$ is a coefficient depending on the sample size (or number of degrees of freedom) and on the risk level chosen, and s_x is the experimental standard deviation of the measurement result. If the measurement is repeated several times ($n \geq 30$), the confidence limits for the experimental mean are

$$dx = \pm u(\alpha)\frac{s_x}{\sqrt{n}}, \tag{12.11}$$

where the coefficient $u(\alpha)$ is a value of the variable of the $N(0, 1)$ distribution. If the measurement is repeated only few times ($n < 30$) the confidence limits are evaluated using Student's distribution:

$$dx = \pm t(\alpha, \nu)\frac{s_x}{\sqrt{n}}, \tag{12.12}$$

where $t(\alpha, \nu)$ is a value of the variable of the t-distribution and $\nu = n - 1$ is the number of the repeated measurements minus 1.

Confidence Limits of a Single Measurement

Usually there is no opportunity to repeat the measurements to determine the experimental variance or standard deviation. This is the most common situation encountered in field measurements. Each measurement is carried out only once due to restricted resources, and because field-measured quantities are often unstable, repetition to determine the spread is not justified. In such cases prior knowledge gained in a laboratory with the same or a similar meter and measurement approach could be used. The second alternative is to rely on the specifications given by the instrument manufacturer, although instrument manufacturers do not normally specify the risk level related to the confidence limits they are giving.

Confidence Limits of Combined Measurements

Frequently the value of the quantity of interest has to be determined indirectly. For example, the determination of the efficiency of any system is based on the measurement of several quantities and some equation relating the measured quantities X_i and the "final" quantity Y under consideration. When the confidence limits of the different measured quantities are known, and the relationship $Y = f(X_i)$ is known, an estimate for the "cumulated" confidence limits $\pm dy$ of the "final" quantity can be determined from

$$dy = \pm\sqrt{\sum_{i=1}^{n}\left(\frac{\partial Y}{\partial X_i}\right)^2 dx_i^2}, \tag{12.13}$$

where n is the number of the measured quantities X_i, and dx_i are the confidence limits of these quantities. This equation is derived from the law of combination of standard errors. Hence, all the confidence limits should correspond to the same value of risk level.

12.3.3.5 Instrument Performance[1,2]

The performance of a measuring instrument can be expressed in several ways. The *precision* or *accuracy* describes the instrument performance in a general and qualitative sense. Thus, these expressions cannot be characterized using numbers.

The *bias error* is a quantity that gives the total systematic error of a measuring instrument under defined conditions. As mentioned earlier, the bias should be minimized by calibration. The *repeatability error* consists of the confidence limits of a single measurement under certain conditions. The *inaccuracy* or *error of indication* is the total error of the instrument, including the

systematic error (bias) as well as the random (repeatability) error. The measuring instrument *drift* is the variation in the metrological properties, including the bias error of an instrument during a long period of time. Because of drift, repeated calibration of an instrument is required; where the time interval between the calibration is the shorter, the larger the drift.

12.3.3.6 Target Values

In the case of measuring airflow, temperature, and other performance-related quantities of new or renovated air-handling systems, the commissioning engineer attempts to determine if the system target values are met. To meet a target value exactly is not the goal. The objective is to reach a value between some specified tolerances. The tolerances are often placed symmetrically on both sides of the nominal target value, but they may be nonsymmetrical or even single-sided. Single-sided tolerances are often used for efficiencies, contaminant concentrations, and other quantities where a maximum or minimum value is of concern. The usual procedure is to approve the value if the result of measurement is between the tolerances or on the correct side of a single-sided tolerance value. This, however, is not the correct procedure from the technical measurement aspect. Even if the measurement results seem to have a proper value, the true value of the quantity may be outside of the specified range. For this reason, the demand must be set in such a way, that the true value of the measured quantity fulfills the requirements. This can be achieved by demanding that the measurement result, with its confidence limits, is between or on the correct side of the tolerance values. A more precise expression for this demand is

$$\begin{aligned} x_t^+ &\geq x_m + dx \\ x_t^- &\leq x_m - dx, \end{aligned} \tag{12.14}$$

where x_t^+ and x_t^- are the upper and lower tolerance values, x_m is the measurement result, and dx is the confidence limit value (Fig. 12.12). Even if the condition (12.14) is fulfilled, the risk always exists that the true value is out of the range. This risk can, however, be limited at an appropriate level by choosing the confidence level (risk level) in a proper way.

Figure 12.12 demonstrates that the larger the confidence limits of measurement are, the closer to the target value the measurement result must be for symmetrical tolerances. A consequence of this is that if the confidence limits of the measurement are larger than the tolerance intervals $|x_m - x_t|$, it is impossible to ensure that the true value is inside the desired interval. In such a case, a more precise instrumentation must be chosen.

12.3.4 Dynamics of Measurements

12.3.4.1 Measurement Characteristics

If the measured quantity is constantly changing with time, the measurement result always follows the measured quantity with a time lag. This fact relates to all types of measurements, and can be called the "Second Law of Measurements." The reason for this Second Law is that any event requires a finite time in order for it to be executed. The event can be, for example, heat transfer from air to a temperature probe, the movement of a tracer sample to

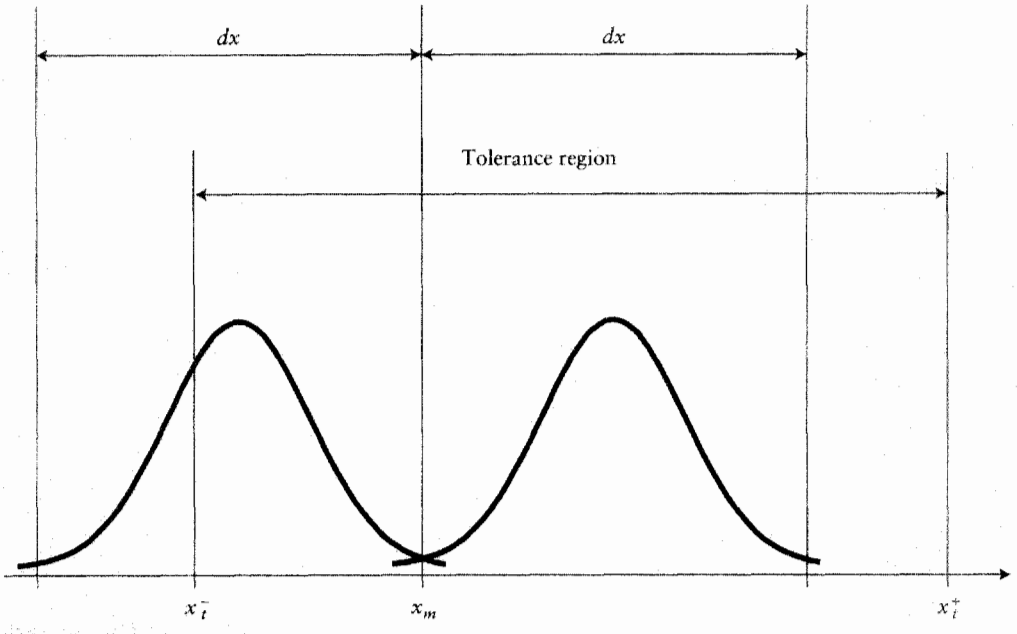

FIGURE 12.12 Quantities related to the target value fulfillment.

the analyzer, or light traveling from the measurement volume to a laser anemometer detector. Obviously these events all require very different times, from several seconds to approximately 10^{-9} seconds, but regardless of the time span no event can be executed in zero time. The important fact is the inertia of the instrument compared with the speed (frequency) of variations in the quantity value. If the instrument is slow, information regarding the behavior of the measured quantity is lost. If the mean value is of primary interest, this may not be critical. However, if there is a need to closely follow the changes of the measured quantity, it is essential that the instrument is selected in an approved manner.

The time difference (delay) between the measured quantity and the measurement result is called the *inertial error.* A definition[2] is the error due to inertia (mechanical, thermal, etc.) of the parts of a measuring instrument. In ventilation equipment the critical component in the measuring chain, from the dynamic point of view, is often the sensor or the measuring transducer (probe).

The sensor is the element of an instrument directly influenced by the measured quantity.[2] In temperature measurement the thermal mass (capacity) of the sensor usually determines the meter's dynamics. The same applies to thermal anemometers. In IR analyzers used for concentration measurement, the volume of the flow cell and the sample flow rate are the critical factors. Some instruments, like sound-level meters, respond very fast, and follow the pressure changes up to several kHz.

Depending on the sensor/probe construction, there may be from one to several capacities, each increasing the inertial error. The inertial error depends not only on the features of the instrument, but also on the character of the

change in the measured quantity. There are of course many types of variation the measured quantity can follow. To estimate the inertial error using a simple computational approach, the changes can roughly be classified as either a single step-type change; an exponential-type change; or a continuous up-and-down, oscillating, sine-type change.

The step change is close to the situation where the sensor is suddenly moved from one place to another having a different state of the measured quantity. The exponential change could, for example, be the temperature change of a heating coil or some other first-order system. Finally, the velocity fluctuations of room air can be approximated with a sine or cosine function.

12.3.4.2 Systems of First Order

Step Response

In an ideal first-order system, only one capacity causes a time lag between the measured quantity and the measurement result. Typically, an unshielded thermometer sensor behaves as a first-order system. If this sensor is rapidly moved from one place having temperature T_1 to another place of temperature T_2, the change in the measured quantity is close to an ideal step. In such cases, the sensor temperature indicated by the instrument has a time history as shown in Fig. 12.13.

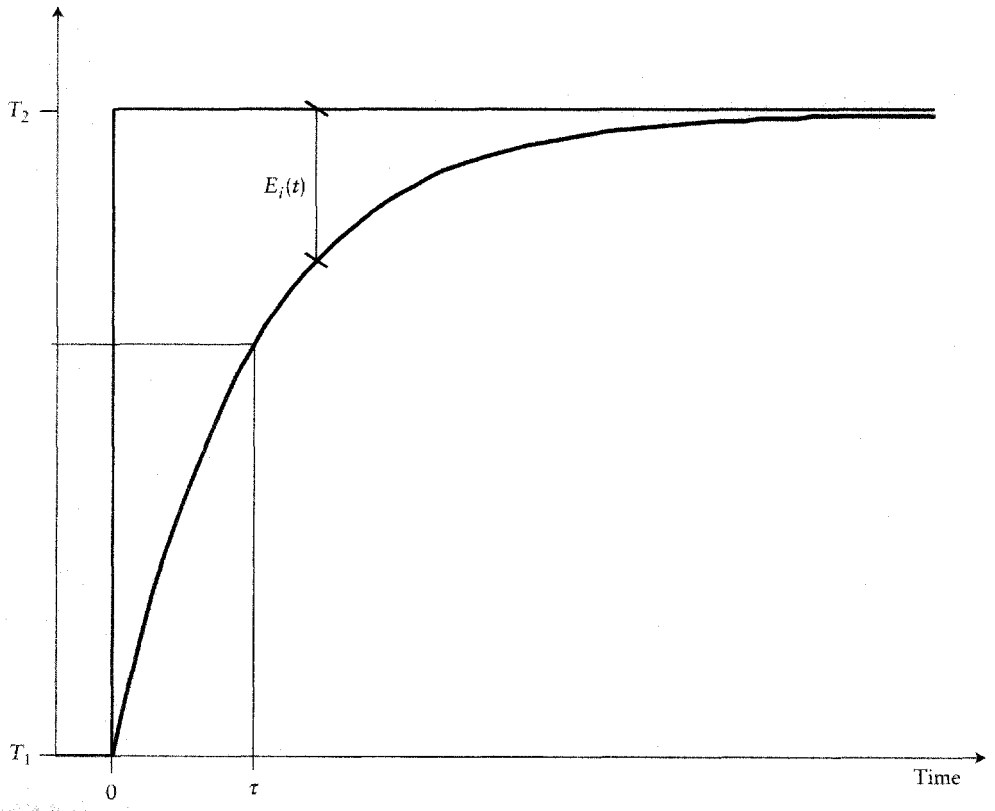

FIGURE 12.13 Step response of a first-order system.

The sensor temperature $T = T(t)$ as a function of time can easily be shown to be

$$T(t) = T_1 + (T_2 - T_1)(1 - e^{-t/\tau}) \quad , \tag{12.15}$$

where t is time and τ is the sensor time constant. From Eq. (12.15) the sensor temperature can be computed at any time instant, provided the initial temperature, the final temperature, and the time constant are known. In the above case the temperature measurement is used as an example, but the same principle and equation apply to any quantity, provided the system is first order.

Inertial Error

Continuing the above example, the inertial error obviously is the difference between the final temperature and the sensor temperature. From Eq. (12.15), the inertial error of a first-order system is

$$E_i(t) = (T_2 - T_1)(1 - e^{-t/\tau}) \quad . \tag{12.16}$$

The error has its maximum value $E_i = T_2 - T_1$ at $t = 0$ and decreases toward $E_i = 0$ when the time approaches infinity. From Eq. (12.16), the desired time for the inertial error to reach a certain value can be solved for.

Time Constant

The time constant in the previous equations is, in principle, the product of the sensor capacity and the resistance of the flow into the sensor,

$$\tau = RC. \tag{12.17}$$

In the case of a temperature probe, the capacity is a heat capacity $C = mc$, where m is the mass and c the material heat capacity, and the resistance is a thermal resistance $R = 1/(hA)$, where h is the heat transfer coefficient and A is the sensor surface area. Thus the time constant of a temperature probe is $\tau = mc/(hA)$. Note that the time constant depends not only on the probe, but also on the environment in which the probe is located. According to the same principle, the time constant, for example, of the flow cell of a gas analyzer is $\tau = V/q_v$, where V is the volume of the cell and q_v the sample flow rate.

Response Time

The time constant is one way of determining the dynamic features of a measurement system. Not all instrument manufacturers use the time constant; some use the response time instead. The response time is the time between a step change of the measured quantity and the instant when the instrument's response does not differ from its final value by more than a specified amount.[1,2] The response time is defined according to a deviation from the final value. Often response times for the relative deviation of 1%, 5%, 10%, or 37% are used. The corresponding response times are denoted by 99%, 95%, 90%, or 63% response time, respectively. The response time for a first-order system can be solved from Eq. (12.15). Note that the 63% response time of a first-order system is the same as the time constant τ of the system.

12.3.4.3 Systems of Higher Order

Not all instruments behave as a first-order system. If several capacities exist in a series connection and none dominates, i.e., is much larger than the others, then the response differs from a first-order system. The step response of a higher-order sys-

tem is shown in Fig. 12.14. The curve is typically S-shaped and deviates more from the first-order exponential curve, the higher the number of the active capacities.

For example, a temperature-measuring device, having its sensor placed in a protecting tube, is a system of second order. For such a system no single time constant exists in the same way as a first-order system. The behavior of such a system is often given by a response time. Another concept is to give the apparent time constant τ_a, which can be constructed by placing a line in the inflection point of the step response curve; see Fig. 12.14.

12.3.5 Temperature Measurement

12.3.5.1 Measurement Principles[3–6]

Temperature measurement is one of the most common applications in ventilation systems. The air temperature in several places in the ventilation system and in the ventilated space is usually of primary interest. The surface temperature of enclosures is also of interest in some cases. A rare application in connection with ventilation is the measurement of temperatures inside a structure. All these tasks can be solved by using the contact measurement principle. Surface temperatures can be measured using the noncontact principle as well.

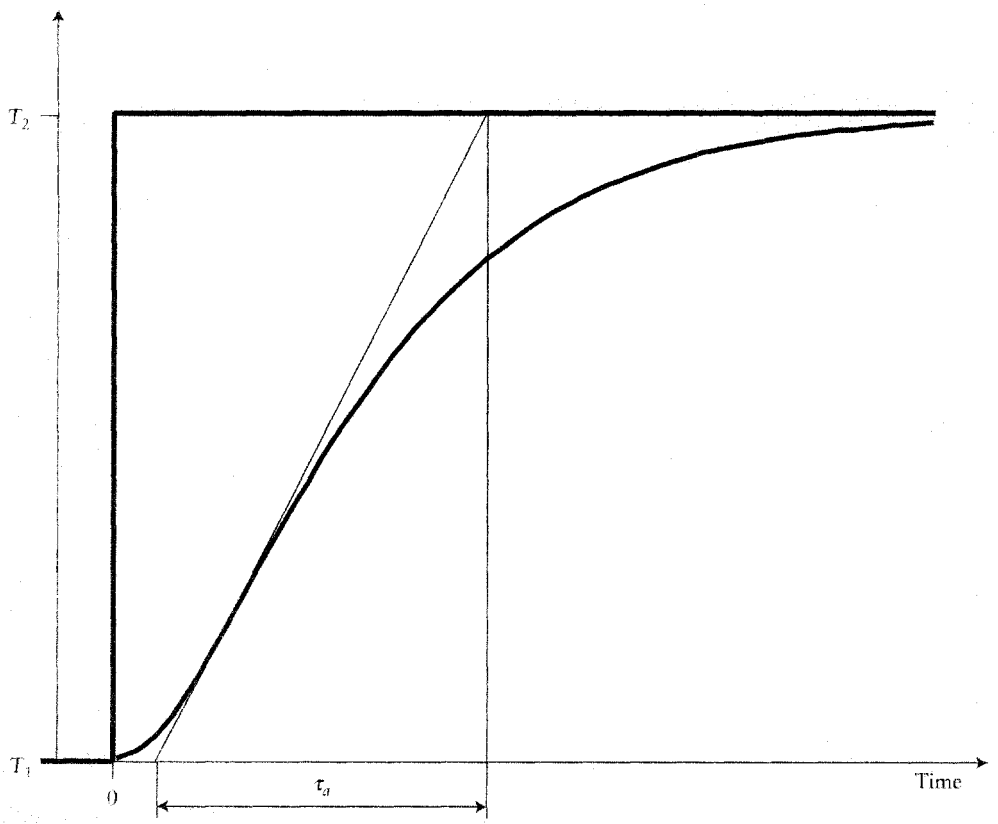

FIGURE 12.14 Step response of a higher-order system.

Contact temperature measurement is based on a sensor or a probe, which is in direct contact with the fluid or material. A basic factor to understand is that in using the contact measurement principle, the result of measurement is the temperature of the measurement sensor itself. In unfavorable situations, the sensor temperature is not necessarily close to the fluid or material temperature, which is the point of interest. The reason for this is that the sensor usually has a heat transfer connection with other surrounding temperatures by radiation, conduction, or convection, or a combination of these. As a consequence, heat flow to or from the sensor will influence the sensor temperature. The sensor temperature will stabilize to a level different from the measured medium temperature. The expressions "radiation error" and "conduction error" relate to the mode of heat transfer involved. Careful planning of the measurements will assist in avoiding these errors.

Instruments based on the contact principle can further be divided into two classes: mechanical thermometers and electrical thermometers. Mechanical thermometers are based on the thermal expansion of a gas, a liquid, or a solid material. They are simple, robust, and do not normally require power to operate. Electrical resistance thermometers utilize the connection between the electrical resistance and the sensor temperature. Thermocouples are based on the phenomenon, where a temperature-dependent voltage is created in a circuit of two different metals. Semiconductor thermometers have a diode or transistor probe, or a more advanced integrated circuit, where the voltage of the semiconductor junctions is temperature dependent. All electrical meters are easy to incorporate with modern data acquisition systems. A summary of contact thermometer properties is shown in Table 12.3.

The noncontact measurement principle, usually called optical or radiation temperature measurement, is based on detecting electromagnetic radiation emitted from an object. In ventilation applications this method of measurement is used to determine surface temperatures in the infrared region. The advantage is that the measurement can be carried out from a distance, without contact with the surface, which possibly influences the heat balance and the temperatures. The disadvantages are that neither air (or other fluid) temperature nor internal temperature of a material can be measured. Also the temper-

TABLE 12.3 Contact Thermometers and Useful Measuring Ranges

Type of thermometer	Temperature range (°C)	Accuracy	Speed of response
Liquid-in-glass	−60 to 510	Medium to high	Medium
Liquid-in-metal	−40 to 650	Medium	Slow
Vapor actuated	−40 to 320	Medium	Medium (bare bulb)
Gas actuated	−85 to 540	Medium to high	Fast (bare bulb)
Bimetallic	−40 to 540 (430 constant)	Low to medium	Medium to slow
RTD	−70 to 540	High	Medium to fast
Thermistor	−120 to 400	Medium to high	Fast (bare)
Electronic	−18 to 180	High	Fast

ature of a small area is difficult to measure, as the radiation thermometer is usually receiving the radiation from a larger area. Finally, the surface emissivity is often required as an input value to obtain a good result, even though some instruments are able to make some form of emissivity correction.

12.3.5.2 Mechanical Thermometers [3–6]

Liquid-in-Glass Thermometers

Liquid-in-glass thermometers measure the thermal expansion of a liquid, which is placed in a solid container, on a length scale. The mercury thermometer is one example of liquid thermometers. Alcohol is also used with this type of instrument. The temperature range is −80 to +330 °C depending on the liquid. The quality, stability, and accuracy vary considerably. The advantages are a simple construction and low price. A disadvantage is that they are not compatible for connection to monitoring systems.

Filled Thermometers

In filled thermometers the thermal expansion of a gas or a liquid is transmitted through a thin capillary tube to a bellows or helix, where the deformation indicates the temperature. The temperature range of filled thermometers is very wide, approximately −200 to +700 °C. They are extremely robust but are not very high in accuracy. The application is mainly for process instrumentation and as stand-alone control devices.

Bimetallic Thermometers

When two strips of different metals having different thermal expansion coefficients are rigidly attached to each other, the material will bend or straighten according to its temperature. This deformation is by means of cogs and levers converted to the movement of a pointer. The measurement range of bimetallic thermometers depends on the materials used. The range between −50 and +550 °C can be spanned with this type of instrument. The accuracy is low but the simplicity and low cost are an advantage.

12.3.5.3 Electrical Temperature Measurement

Resistance Thermometers

Resistance thermometers are made of a pure metal, such as platinum, nickel, or copper. The electrical resistance of such a material is almost linearly dependent on temperature. Resistance thermometers are stable, having a small drift. A widely used and the best-known resistance probe is the PT-100 probe, which is platinum, having a resistance of 100 ohms at the temperature of 0 °C. Other resistance values for PT probes are available. The resistance versus temperature values as well as tolerances for platinum probes are standardized.[7,8] The shape and size of a resistance probe can vary considerably, resulting in changes in probe dynamics.

The probe resistance can be measured either directly by passing a small constant current through the probe and measuring the voltage drop, or by connecting the probe to a bridge. In any case, the current should be low enough to avoid self-heating of the probe. To compensate for the resistance of the measuring wires, the resistance probe can be connected to the system by a three-wire

or a four-wire connection. If only two wires are used, the connecting wires must not be too long in order to keep the resistance as low as possible.

The measurement range for platinum is –200 to +800 °C, for nickel –50 to +250 °C, and for copper –50 to +200 °C. The advantages are good accuracy, almost linear characteristics, and stability. A disadvantage is the small change of resistance with temperature, which requires a high sensitivity from the rest of the measurement equipment.

Thermistors

Thermistors are temperature-dependent resistances, normally constructed from metal oxides. The resistance change with temperature is high compared with the metallic resistances, and is usually negative: the resistance decreases with temperature increase. The temperature characteristics are highly nonlinear. Such thermistors, having a negative temperature coefficient, are called NTC thermistors. Some thermistors have a positive temperature coefficient (PTC), but they are not in common use for temperature measurement.

The resistance of a thermistor is achieved in a similar manner to the measurement of metallic probes. The advantage of thermistors is that their resistance is usually high, and the compensation for the measurement wire resistance is not so critical.

The measurement range of a thermistor is dependent on the probe type, typically –100 to +300 °C. The stability is not as good as that of metallic resistances. Thermistors are not standardized like some of the metallic probes. The thermistor has the advantage of a high change of the resistance with temperature. A very wide variety of sizes and shapes and a low price makes them attractive in relation to the metrological performance.

Thermocouples[9]

Thermocouples are primarily based on the Seebeck effect: In an open circuit, consisting of two wires of different materials joined together at one end, an electromotive force (voltage) is generated between the free wire ends when subject to a temperature gradient. Because the voltage is dependent on the temperature difference between the wires (measurement) junction and the free (reference) ends, the system can be used for temperature measurement. Before modern electronic developments, a real reference temperature, for example, a water-ice bath, was used for the reference end of the thermocouple circuit. This is not necessary today, as the reference can be obtained electronically. Thermocouple material pairs, their temperature-electromotive forces, and tolerances are standardized.[10–13] The standards are close to each other but not identical. The most common base-metal pairs are iron-constantan (type J), chomel-alumel (type K), and copper-constantan (type T). Noble-metal thermocouples (types S, R, and B) are made of platinum and rhodium in different mixing ratios.

The measurement ranges for the base-metal thermocouples are –40 to +750 °C (type J), –200 to +1200 °C (type K), and –200 to +350 °C (type T). The noble-metal thermocouples can be used at higher temperatures up to 1700 °C. The dynamic response of sheathed thermocouples is not very fast; however, a probe made from bare, thin wires can have very fast dynamic properties. One of the best features of thermocouples is the simplicity of making new probes by soldering or welding the ends of two wires together.

12.3.5.4 Infrared Thermometers[14,15]

There are several types of optical thermometers: total radiation pyrometers, brightness pyrometers, two-color pyrometers, and infrared radiation thermometers. The measurement range and applications of these instruments differ from each other. The main principle is the same: The measurement is based on observing the electromagnetic radiation emitted by the surface or gas. As a consequence, the second common feature is the noncontact-type measurement, where the measurement is carried out at a distance from the object without touching it with a probe. Different pyrometer-type instruments are used for high temperatures, covering the range between 300 and 6000 °C. In ventilation applications the relevant temperatures are, however, considerably, lower. For this reason only the infrared radiation thermometer is of interest.

In the infrared thermometer, long-wave radiation is focused on the detector with a lens or mirror system. Lenses must be made of a glass capable of not absorbing too much radiation. The detector, which converts the radiation to an electrical signal, can be a thermal detector such as a thermopile, a photovoltaic detector, or a photomultiplier. The focusing system can be connected to the detector through an optical fiber, which gives flexibility in placing the different parts of the instrument. The detector signal is amplified and treated to give a proper output for the display.

The measurement range is dependent on the instrument but can cover the range −50 to +500 °C. The accuracy is not as high as the best contact thermometers. One reason for this is that the emissivity of the surface has an effect on the measurement result, and an emissivity correction is necessary for most instruments. The positive features are noncontact measurement and very fast dynamics, which enable a rapid scan of surface temperatures from a distance; this is convenient when carrying out, for example, thermal comfort measurements.

12.3.5.5 Measurement Errors

In temperature measurement there are always several factors that introduce errors into the results. Here the main focus is on the external or environmental factors outside the measuring instrument.

With contact temperature measurement, placing the measurement probe in contact with the object of measurement (duct, surface, etc.) produces an additional route for heat conduction to or from the object. This perturbation error[9] changes the initial temperature field in the vicinity of the contact point and creates measurement errors.

The fouling of the probe when inserted into a duct or pipe acts as an isolating layer and increases the measurement error. To avoid this conduction error, the probe should be a poor heat conductor. In measuring surface temperatures, the probe should not have an insulating effect, as this will change the temperature in the measuring point.

Also, the radiation exchange between the probe and surrounding surfaces can be a cause of measurement error. For example, measuring the air temperature near to a hot heating coil can produce errors if no radiation shield is used around the probe. In general, conduction and radiation errors can usually be eliminated to a sufficient degree. This just requires some knowledge of the different modes of heat transfer, and applying this knowledge to the problem.

Another error related to the use of resistance-type probes is the self-heating error. To carry out resistance measurement of the probe, a current must be introduced to the probe. The current generates electrical power in the probe, heating it up and causing a self-heating error. The magnitude of the self-heating error can be predicted using the heat balance of the probe. In stationary situations the heating power generated in the probe must equal the power dissipated from the probe to the environment. From this, the self-heating error is

$$\Delta T_{sh} = \frac{I^2 R}{hA}, \tag{12.18}$$

where I is the measurement current, R is the probe resistance, h is the heat transfer coefficient between the probe and the environment, and A is the probe surface area. If radiation effects are important, they can be taken into account by the linearization of the radiation term and introducing a radiation heat transfer coefficient. In this case the term h in the above equation also contains the radiation heat transfer coefficient.

12.3.5.6 Calibration[16]

The calibration of thermometers is based on the International Temperature Scale of 1990, ITS-90.[17] This scale became an internationally recognized standard on January 1, 1990. It defines temperatures between 0.65 K and 5 K in terms of the vapor-pressure temperature relations of 3 He and 4 He. Above 5 K, the ITS-90 assigns temperatures to 16 fixed points, which are triple-points, melting points, or points of solidification of chosen substances. In the low-temperature end, different gases such as hydrogen, noble gases, and oxygen are used. The range –38 to +156 °C is obtained using mercury, water, gallium, and indium. Tin, aluminium, silver, and other metals are utilized at the high end of the scale.

Between the fixed points, temperatures on the ITS-90 are obtained by interpolation using standard instruments and assigned formulae. These standard instruments are the helium gas thermometer (3 K to 24.5 K), the platinum resistance thermometer (13.8 K to 1235 K), and the optical thermometer (above 1235 K).

From the ventilation point of view, the fixed points –38.83 °C (triple-point of mercury), 0.010 °C (triple-point of water), 29.76 °C (melting point of gallium), and 156.60 °C (freezing point of indium) are of relevance. The triple-point of water is relatively simple to achieve and maintain with a triple-point apparatus.[18] Some freezing point cells are covered in standards.[19] In practical temperature calibration of measuring instruments, the ITS-90 fixed points are not used directly.

The so-called standard instrument is used for interpolation between the fixed points and for the calibration of other thermometers lower in the metrological hierarchy. The standard instrument in the moderate temperature range is a special platinum resistance probe, as it has to fulfill set requirements. It is important in all calibration that traceability to a primary normal, here the fixed-point ITS-90 scale, exists.

12.3.6 Air Humidity Measurement

12.3.6.1 Parameters of Moist Air

Several quantities are used to describe air humidity (see Section 4.2). The most common are humidity ratio and relative humidity, shown also on the psychrometric chart.

Some air humidity meters measure the relative humidity directly. Others measure either the wet-bulb temperature, the dewpoint temperature, or the absolute water vapor mass in a sample of air. The measured wet-bulb temperature is not the thermodynamic wet-bulb temperature, but an equilibrium temperature of a wet wick. In this equilibrium state the heat flow by convection (and conduction and radiation) is equal to the heat flow due to evaporation of the water from the wick.

The partial pressure of water vapor can be calculated as a function of the dry-bulb and wet-bulb temperatures, Eq. (12.23), and the relative humidity from its definition:

$$\varphi = \frac{p_w}{p_{ws} T_{db}}, \tag{12.19}$$

where p_w is the partial pressure of water vapor and p_{ws} is the saturation pressure of water vapor at the air dry-bulb temperature T_{db}. The saturation pressure as a function of the temperature can be determined from tables or equations;[20] see Table 12.4. Using the water vapor pressure, the humidity ratio is

$$W = 0.622 \frac{p_w}{p - p_w}, \tag{12.20}$$

where p is the total pressure of moist air. If, on the other hand, the dewpoint temperature T_d is measured, the saturation pressure of water vapor at the dewpoint temperature is equal to the partial pressure of water vapor $p_w = p_{ws}(T_d)$. By substituting this partial pressure into Eq. (12.19) or (12.20), the relative humidity or the humidity ratio can be calculated. Some fundamental instruments used as references for calibration measure the mass of water in a sample of air. In this case, the humidity ratio can easily be computed on the basis of its definition:

$$W = \frac{m_w}{m_a}, \tag{12.21}$$

where m_w and m_a are the masses of water and dry air, respectively. The relative humidity can further be determined using the equation

$$\varphi = \frac{p}{(1 + 0.622/W) p_{ws} T_{db}}. \tag{12.22}$$

12.3.6.2 Electrical Hygrometers

Capacitive Sensors

The majority of modern, compact air humidity meters are based on electrical measurement principles. The capacitive sensor is an electrical capacitor having a moisture-dependent capacitance. The probe contains electrodes with a hygroscopic insulation material in between. The insulation material is chosen to have a small dielectric constant, whereas the dielectric constant of water is high. As a consequence, the absorbed water has a strong influence on the sensor's capacitance. The electronics of the instrument determine the probe capacitance and convert it into a relative humidity reading. Because of the small sensor capacitance, electronic processing has to be completed close to the sensor. The capacitive sensors are usually manufactured using thin-film technology using polymers deposited on a glass or silicon substrate then coated with a porous metal electrode layer to protect the sensor as the insulating layer material.

Capacitive sensors are small and rapidly respond to changes in air humidity. The measurement range is 0–100% RH. Due to the electrical principle, they can

TABLE 12.4 Saturation Pressure (Pa) over Liquid Water for the Temperature Range 0–40 °C

Degrees C	Tenths of degrees C									
	0	0.1	0.2	0.3	0.4	0.5	0.6	0.7	0.8	0.9
0	611	616	620	625	629	634	638	643	648	652
1	657	662	667	671	676	681	686	691	696	701
2	706	711	716	721	726	732	737	742	747	753
3	758	763	769	774	780	785	791	796	802	808
4	813	819	825	831	837	843	848	854	860	866
5	872	879	885	891	897	903	910	916	922	929
6	935	942	948	955	961	968	975	982	988	995
7	1002	1009	1016	1023	1030	1037	1044	1051	1058	1066
8	1073	1080	1088	1095	1102	1110	1117	1125	1133	1140
9	1148	1156	1164	1172	1179	1187	1195	1204	1212	1220
10	1228	1236	1245	1253	1261	1270	1278	1287	1295	1304
11	1313	1321	1330	1339	1348	1357	1366	1375	1384	1393
12	1403	1412	1421	1431	1440	1450	1459	1469	1478	1488
13	1498	1508	1518	1527	1537	1548	1558	1568	1578	1588
14	1599	1609	1620	1630	1641	1651	1662	1673	1684	1694
15	1705	1716	1728	1739	1750	1761	1772	1784	1795	1807
16	1818	1830	1842	1854	1865	1877	1889	1901	1914	1926
17	1938	1950	1963	1975	1988	2000	2013	2026	2038	2051
18	2064	2077	2090	2104	2117	2130	2144	2157	2171	2184
19	2198	2212	2225	2239	2253	2267	2281	2296	2310	2324
20	2339	2353	2368	2383	2397	2412	2427	2442	2457	2472
21	2488	2503	2518	2534	2549	2565	2581	2597	2613	2629
22	2645	2661	2677	2694	2710	2726	2743	2760	2777	2763
23	2810	2827	2845	2862	2879	2897	2914	2932	2949	2967
24	2985	3003	3021	3039	3058	3076	3094	3113	3132	3150
25	3169	3188	3207	3226	3246	3265	3284	3304	3324	3343
26	3363	3383	3403	3423	3444	3464	3484	3505	3526	3546
27	3567	3588	3609	3631	3652	3673	3695	3717	3738	3760
28	3782	3804	3827	3849	3871	3894	3916	3939	3962	3985
29	4008	4032	4055	4078	4102	4126	4150	4173	4198	4222
30	4246	4270	4295	4320	4345	4369	4394	4420	4445	4470
31	4496	4522	4547	4573	4599	4626	4652	4678	4705	4732
32	4759	4786	4813	4840	4867	4895	4922	4950	4978	5006
33	5034	5063	5091	5120	5148	5177	5206	5236	5265	5294
34	5324	5354	5384	5414	5444	5474	5505	5535	5566	5597
35	5628	5659	5690	5722	5754	5785	5817	5849	5882	5914
36	5947	5979	6012	6045	6078	6112	6145	6179	6213	6247
37	6281	6315	6350	6384	6419	6454	6489	6525	6560	6596

(continues)

TABLE 12.4 *(continued)*

Degrees C	Tenths of degrees C									
	0	0.1	0.2	0.3	0.4	0.5	0.6	0.7	0.8	0.9
38	6631	6667	6704	6740	6776	6813	6850	6887	6924	6961
39	6999	7036	7074	7112	7150	7189	7227	7266	7305	7344
40	7383	7423	7463	7502	7542	7583	7623	7664	7704	7745

be applied to different control and automation systems. They suffer to some extent from drift and require repeated calibration to maintain good accuracy.

Resistive Sensors

The resistive measurement principle is based on a humidity-dependent electrical resistance. The early probes used lithium chloride as the hygroscopic resistive material. Such probes are still available under the name Dunmore sensors. The measurement range of such devices is quite narrow, and the resistance versus humidity relationship is extremely nonlinear.

Recent developments are leading toward other materials like silica gel or polymers. Certain types of semiconductors are also used as resistive probes. The measurement range of resistive sensors varies depending on materials used. It can be as wide as 0–99% RH. The dynamics are fast enough for normal ventilation applications and the stability of good resistive sensors is high. This does not reduce the need for calibration, but the intervals of successive calibrations can be extended.

12.3.6.3 Mechanical Hygrometers[21]

Mechanical hygrometers are the oldest type of humidity-measuring instruments. They are based on the change of length of a stretched strip, bundle, or membrane of some hygroscopic material such as natural hair or, for example, cellulose butyrate. The length of the material increases when water is absorbed from the surrounding moist air. On the other hand, the effect of temperature changes is small. As a consequence the instrument responds practically only to air humidity and is calibrated to indicate relative humidity. The change in the probe length is transmitted to the movement of a pointer or a pen. A strain gauge can be used to provide an electrical signal. The accuracy of mechanical hygrometers is low. They suffer from nonlinearity, hysteresis, and drift, which cause a need for frequent recalibration. However, they are relatively cheap instruments, often available with a simple mechanical continuous recording feature. Mechanical hygrometers have a slow response and should not be used in situations where the humidity is changing rapidly.

12.3.6.4 Psychrometers [21–24]

A psychrometer measures the dry-bulb and wet-bulb temperatures simultaneously. The measurement of the wet-bulb temperature is achieved by means of a wet wick placed over the thermometer bulb. The thermometer can be practically of any type. A cylindrically shaped sensor is preferred. The wet-bulb temperature-sensing element, covered with the wick, and the dry-bulb temperature sensor, are placed in the airstream to be measured. The stream, generated by a small fan, should have a velocity of 3–5 m s^{-1} and can be either transverse or axial. The

wick-covered sensor is cooled down by evaporation until it reaches a thermal equilibrium state where the (almost only) convective heat transfer is covering the heat required for water vaporization from the wick.

The humidity can be determined using either charts or equations provided by the psychrometer manufacturer. The partial pressure of water vapor provides a more general approach and can be calculated from the "psychrometer equation"

$$p_w = p_{ws}(T_{db}) - A(T_{db} - T_{wb})p \ , \tag{12.23}$$

where A is the psychrometer constant and T_{wb} is the wet-bulb temperature. The psychrometer constant has values between 5.4 and 6.9 $\times 10^{-4}$ L K^{-1},[22,23,25] depending on the airstream velocity and some other factors. To reduce the radiative exchange in hot environments, radiation shields should be fitted to both sensors. The thermometers must be adequately spaced from each other to avoid the wetting of the dry bulb. The dry-bulb sensor should not be in the wake of the wet-bulb sensor to ensure that the correct temperature is measured. The water used in the wick should be pure distilled water to stop lime scale buildup on the wick.

A psychrometer fitted with a fan is called an aspirated psychrometer or Assmann hygrometer. Another variant is the sling or whirling hygrometer. In this case the wet- and dry-bulb thermometers are attached to a frame with a handle. When measuring the temperatures, the frame is whirled around like a football rattle. The measurement range is dependent on the range of the thermometers but is usually wide enough for ventilation measurements. The response of the psychrometer is slow, taking a few minutes to reach the wet-bulb equilibrium state. Rapidly changing humidity cannot be monitored. The advantage of an instrument of this kind is that its construction and the fundamental nature of the measurement are simple. For this reason, if handled with care, it is a cheap but reliable instrument.

12.3.6.5 Dewpoint Hygrometers

The dewpoint hygrometer detects the dewpoint temperature of air by cooling a surface in contact with the air to the dewpoint temperature. There are several ways to achieve cooling and to observe the formation of condensate on the surface. The early dewpoint hygrometers were cooled simply by applying the vaporization of ether or some other suitable liquid. Condensate formation on the surface was determined visually. Other cooling methods are to use a refrigerant flow in direct or indirect contact with the back of the surface, or to use electricity with a (thermoelectric) Peltier element.

The observation may be by a lamp illuminating the surface and a photocell to detect the scattered light due to the water droplets on the surface. The accurate measurement of the surface temperature, which is the dewpoint temperature, is critical. If a coolant is used, a close approximation for the surface temperature is the fluid temperature; otherwise a small thermocouple or resistance sensor can be attached to or embedded into the surface.

The range of dewpoint hygrometers depends on the temperature range of the cooled surface. In principle a temperature range of air from -70 to $+100$ °C can be covered. The measurement of the frost point at low temperatures involves large measurement errors. Typical error sources are surface contamination, gases dissolving in the water, cold-spot errors, and pooling or flooding.[22] These factors considerably reduce the accuracy of the measurement. The dynamical response is slow and cannot handle rapid fluctuations of temperature or humidity.

The dewpoint hygrometer is claimed to be the most accurate instrument for measuring air humidity. When properly calibrated, the inaccuracy can be ±0.5% RH.[26] On the whole, the dewpoint hygrometer is a reliable fundamental instrument suitable for many ventilation applications, but is more expensive than other humidity instruments.

12.3.6.6 Calibration of Hygrometers

Most hygrometer types require constant calibration. Especially mechanical hygrometers may have a strong drift, causing a bias error during a short period of time. Electrical hygrometers also require constant calibration. The only type not requiring calibration is the psychrometer, if it is based on stable temperature measurement, such as high-quality liquid-in-glass thermometers. In fact, the psychrometer can be used as the reference meter in simple calibration procedures.

The simplest way to calibrate a hygrometer is to use ambient air. The humidity of ambient air is measured using both the calibrated meter and the reference meter. A simple psychrometer or an Assmann hygrometer can be used as a reference. Provided the air conditions are stable, this method is used to check hygrometers in field measurements and other not too demanding purposes.

If the one-point calibration in ambient air is not sufficient, the next best approach is to use the calibration box method.[21] The air state is created in a closed box made of nonhygroscopic material, like metal or plastic. A controlled state of humidity is maintained by exposing the air in the box to a liquid surface of a saturated salt solution. In practice, a dish containing the saturated water solution of a salt is placed on supports at the bottom of the box. The air in the box is circulated by means of a small fan. The box should be airtight and positioned in a constant temperature environment. The calibrated instruments are placed in the box. A dewpoint hygrometer can be used as a reference. A wide range of humidity can be created by using solutions of different salts. Table 12.5 shows a few examples of equilibrium humidities achieved with different salt solutions.

If high calibration accuracy is required, the simple box to create and maintain the state of air is not sufficient. In such a case equipment that keeps

TABLE 12.5 Relative Humidity of Air over Various Saturated Solutions of Salts[21]

	Temperature, °C						
Saturated salt solution	**0**	**10**	**20**	**30**	**40**	**50**	**60**
Potassium chloride	89	88	86	84	82	81	80
Sodium chloride	76	76	76	75	75	75	75
Ammonium nitrate	77	72	65	59	53	47	42
Magnesium nitrate	60	57	55	52	49	46	43
Potassium carbonate	—	47	44	43	42	—	—
Magnesium chloride	34	34	33	33	32	31	30
Potassium acetate	25	24	23	22	20	—	—
Lithium chloride	15	13	12	12	11	11	11

the partial pressure of water vapor constant by saturating the air with water at a specified temperature can be used.[27]

12.3.7 Pressure Difference Measurement

12.3.7.1 Introduction

The absolute, barometric pressure is not normally required in ventilation measurements. The air density determination is based on barometric pressure, but other applications are sufficiently rare. On the other hand, the measurement of pressure difference is a frequent requirement, as so many other quantities are based on pressure difference. In mass flow or volume flow measurement using orifice, nozzle, and venturi, the measured quantity is the pressure difference. Also, velocity measurement with the Pitot-static tube is basically a pressure difference measurement. Other applications for pressure difference measurement are the determination of the performance of fans and air and gas supply and exhaust devices, the measurement of ductwork tightness or building envelope leakage rate, as well as different types of ventilation control applications.

The measured pressure differences in ventilation applications are low or very low. The measurement range varies from a few pascals to several thousand pascals. At the lower end are typically building leakage and air movement–related measurements, where only a few pascals can cause a remarkably large airflow. The largest pressure differences probably occur in fan performance determination and similar applications. This wide range requires special demands on the measuring equipment and selection of the correct instrument for each application (Fig. 12.15).

12.3.7.2 Mechanical Manometers[4,28,29]

Mechanical manometers are the oldest, simplest, and most reliable pressure measurement instruments. They have some disadvantages, which is one reason the use of electrical manometers is expanding. Their simplicity and fundamental nature can, however, be an advantage.

Fluid Manometers

Fluid manometers are devices where the readout of the pressure differential is the length of a liquid column. The most fundamental implementation of this principle is the U-tube manometer. This is simply a tube of U shape filled with manometer fluid, as shown in Fig. 12.16. The pressure differential is applied at both ends of the tube, making the manometer fluid move downward in one limb and upward in the other, until the forces acting on the fluid are in balance.

In ventilation applications, where the density of the manometer fluid is much higher than the density of air, the pressure difference Δp can be expressed using the equation

$$\Delta p = \rho g h, \tag{12.24}$$

where ρ is the density of the manometer fluid, g is the acceleration due to gravity, and h is the height between the two columns of the manometer fluid. Because the density of the manometer fluids commonly used is quite high (800–1000 kg m^{-3}), the sensitivity of the U-tube manometer is low.

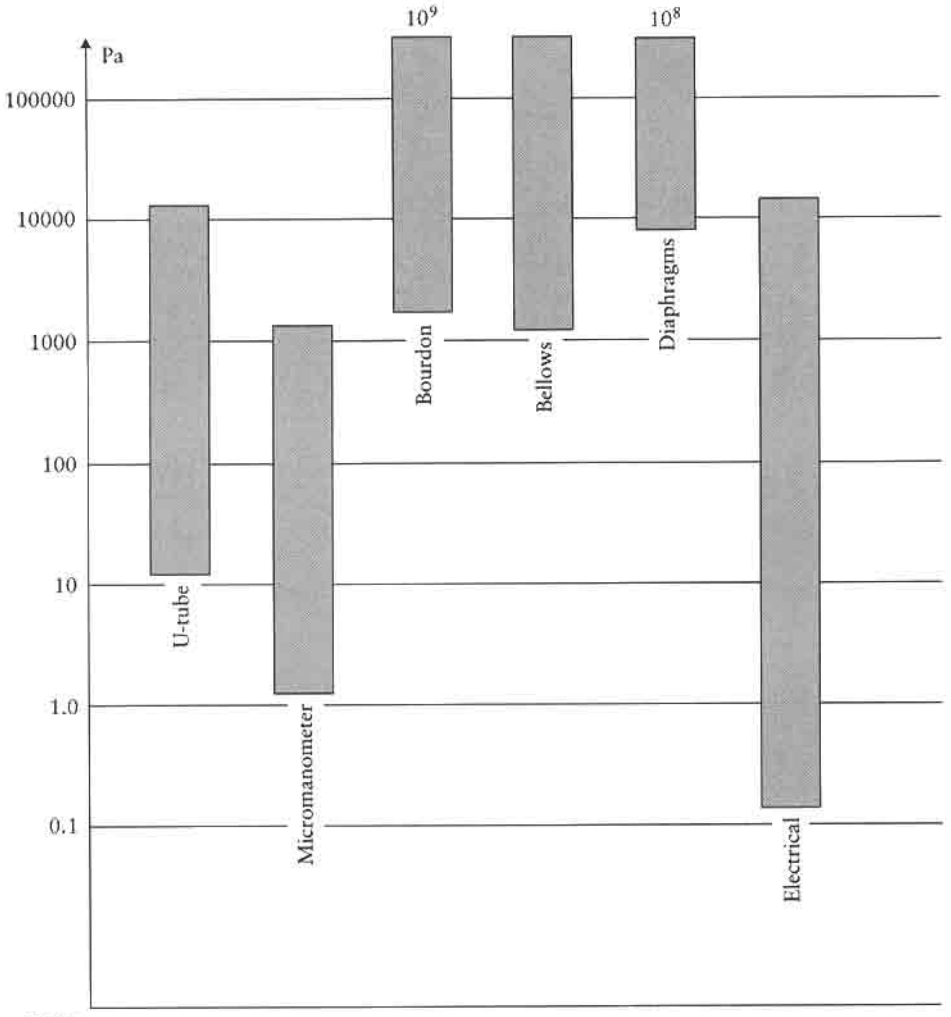

FIGURE 12.15 Measurement range of different types of manometers.

Several other variations of the fluid manometer provide a higher sensitivity. The inclined well–type manometer (Fig. 12.17) has a large-cross-section container for the manometer fluid connected to an inclined tube with a scale. The pressure difference becomes

$$\Delta p = \rho g l \sin\alpha, \tag{12.25}$$

where l is the length of the fluid column in the tube and α is the angle between the inclined tube and horizontal.

The sensitivity of the well manometer can be adjusted by changing the angle α and can be some 30 times that of the U-tube. This type is also often called a micromanometer due to its ability to measure very small pressure differences. Several other types of micromanometers and fluid manometers are also available.

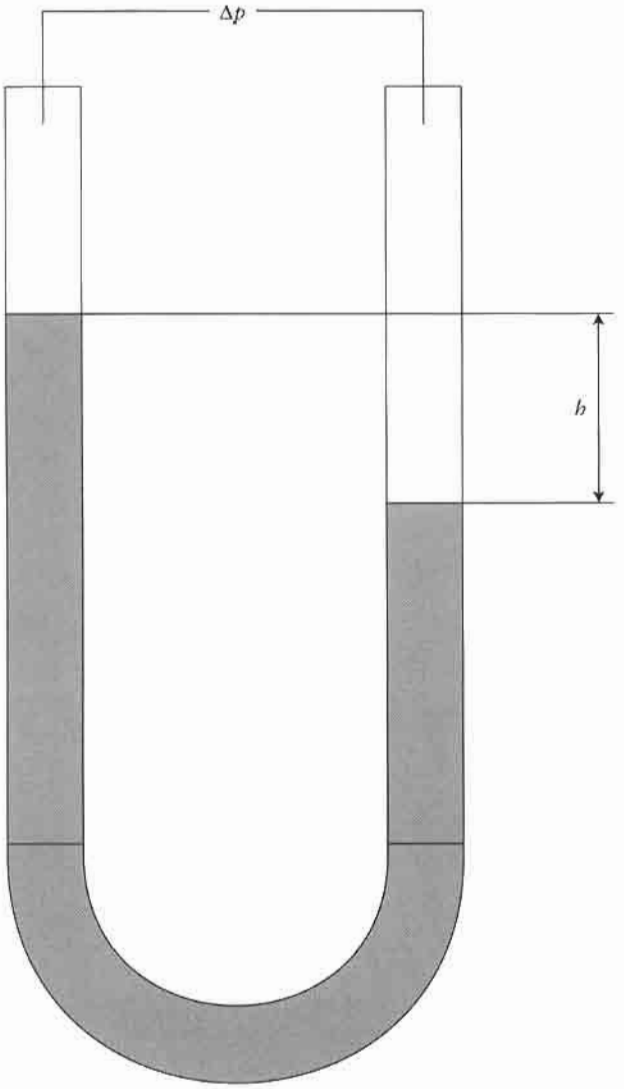

FIGURE 12.16 Principle of a U-tube manometer.

The most common manometer fluids are water, alcohol, and mercury. The density of water and alcohol are quite close to each other, whereas the density of mercury is much higher. Many factors have to be considered when selecting a fluid for a manometer, including

Density
Specific gravity
Surface tension
Corrosive properties
Coefficient of thermal expansion
Viscosity changes with temperature

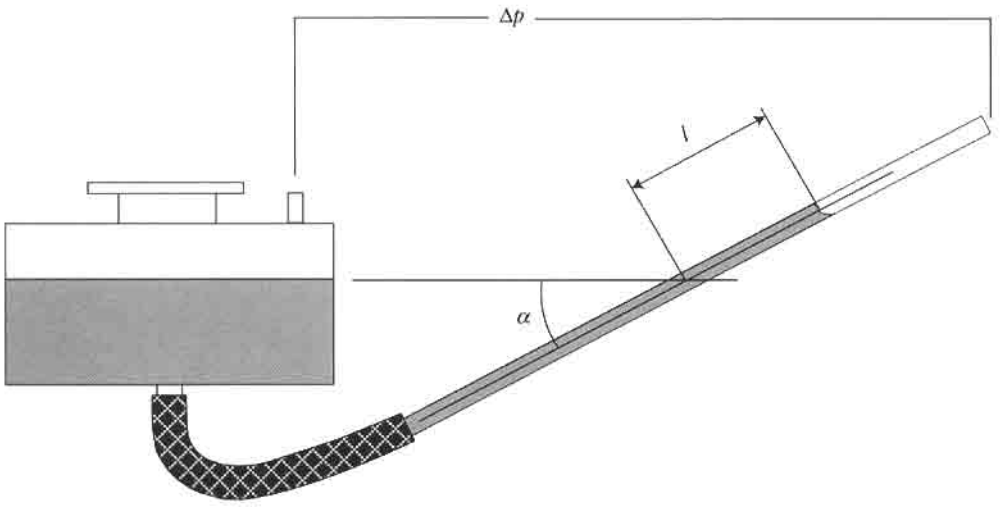

FIGURE 12.17 Principle of an inclined well-type manometer.

The effect of coloring dye added
The influence of the absorption of water vapor from the atmosphere into the fluid

The specific gravities of oils and alcohols are about 0.8, of water 1.0, and of mercury 13.6. Alcohol has a low surface tension; however, it tends to absorb water and evaporate, and its density varies considerably with temperature.

A very obvious way to change the measurement range and sensitivity of a fluid manometer is by using fluids of different densities. There are only a few suitable liquids with specific gravity between that of water and mercury. Ethylene bromide has a specific gravity of 2.2 and acetylene tetrabromide 3.0., but they are corrosive.

Other Mechanical Pressure Transducers

The most frequently applied mechanical manometers in ventilation applications are fluid manometers, but the following types are also used. The Bourdon tube is a small-volume tube with an elliptic cross-section bent to the shape of a circular arc, the C-type. One end is open to the applied pressure while the other end is closed. The pressure inside the tube causes an elastic deformation of the tube and displaces the closed end, which is then converted, by means of a linkage mechanism, into the movement of a pointer. The Bourdon tube may be of a spiral or helical design as well.

The metallic bellows is a series of circular parts, resembling the folds in an accordion. It is joined together in such a manner that it can freely expand or contract axially by changes in pressure. The metal used must be thin enough to be flexible, ductile enough for ease of fabrication, and have a high resistance to fatigue failure. This pressure is mechanically amplified and converted to the movement of a pointer. The bellows is the most sensitive of the nonfluid transducers and most suitable for small pressure differences.

A diaphragm is a flexible membrane used for pressure measurement, usually made of metal. A capsule consists of two diaphragms attached at their perimeters

to form a closed volume. A pressure difference applied over the membrane deforms the structure. This deformation can be converted into the movement of a pointer by means of attached linkages. The diaphragm surface can be of different shapes: dished, flat, or corrugated. The choice depends on the force and deflection needed. The diaphragm can be utilized as a pressure transducer. A capsule made of diaphragms offers a larger movement. The sensitivity can further be increased by attaching several capsules in series to form a stack.

12.3.7.3 Electrical Manometers[4,28,29]

Electrical manometers have developed during the last 30 years. Modern electrical manometers are well suited for ventilation applications, both in the laboratory and in the field. The advantage of this type of instrument is that they are sensitive enough to measure small pressure differences with electrical output, enabling monitoring. A convenient feature, especially in the field is that the instrument is hand-held and there is no need for leveling on a bench, as for fluid manometers. The conversion of the pressure difference into an electrical signal can be based on several different phenomena.

Position-to-Electrical Transducers

Position-to-electrical transducers cover all those mechanisms where the pressure difference is converted into mechanical movement, and this is further converted into an electrical signal. A mechanical structure can serve a coil, a diaphragm, a capsule, a stack of capsules, or a Bourdon tube. The coil movement is linked to an electrical device, such as a potentiometer, a capacitor, or a magnetic-coupled linear-variable differential transformer. Due to friction, potentiometers are not very sensitive devices. Usually they also need a large mechanical travel, which creates limitations. The advantages are simplicity and low cost. Magnetic transformers provide a friction-free, sensitive, linear output signal. They are widely used in instruments for midrange pressure differences. The capacitive transducer is the most sensitive and for this reason is the most used in low- and very-low-pressure differential instruments.

Capacitive Transducers[30,31]

Capacitive transducers measure the deflection of an elastic diaphragm. The simplest capacitive construction is made of two adjacent metallic plates with a dielectric material between them. When a pressure difference over one of the plates causes the plate to deflect, the capacitance changes as a function of the pressure difference. This relationship is nonlinear. To overcome the nonlinearity characteristic, a three-plate differential capacitive sensor can be used. When an alternating voltage and its antiphase voltage are applied to the two outer plates, the voltage amplitude of the center plate (diaphragm) is a linear function of the deflection. Using signal conditioning, the AC voltage amplitude is converted to a DC output signal. Modern manometers, based on a capacitive transducer, are able to measure from a few pascals up to many kilopascals, thus providing good sensitivity over a wide range.

Strain Gauge Transducers

Strain gauges operate on the resistance change of the gauge material with applied strain. The slight molecular structure deformation of a metallic wire causes a

change in resistance of a metallic strain gauge. The concentration and mobility changes of minority charge carriers influence the resistance of a semiconductor strain gauge. The strain gauge can be either bonded to a diaphragm that is exposed to the pressure difference, or the strain can be transferred to the gauge by mechanical linkage. The pressure difference–induced strain is measured using a Wheatstone bridge circuit. Strain gauges are widely applied in pressure measurement. The sensitivity of certain types is suitable also for ventilation applications.

12.3.7.4 Measurement Errors

As well as measurement errors due to the pressure measurement instrument itself, other errors related to pressure measurements must be considered. In ventilation applications a frequently measured quantity is the duct static pressure. This is determined by drilling in the duct a hole or holes in which a metal tube is secured. The rubber tube of the manometer is attached to the metal tube, and the pressure difference between the hole and the environment or some other pressure is measured.

It is essential to ensure that the following criteria are met; otherwise errors will result. First, the mouth of the hole inside the duct must be smooth and flush with the duct inner surface. No burrs or other irregularities must be on the surface in the vicinity of the hole. Second, the hole must be perpendicular to the tube axis. The size of the hole has an effect on the measured pressure as well. A general rule is, the smaller the hole the better. Very small holes do, however, slow down the response of the instrument. Usually the hole diameter is a few millimeters. Note also that the smaller the hole, the greater the risk of blockage. Further information on the effect of the hole size can be found, e.g., in Ower and Pankhurst.[32]

When working with fluid manometers, the following factors should be remembered to reduce errors. Manometer fluid may enter the connecting rubber hose, resulting in a faulty reading. Air bubbles in the manometer fluid must be removed. Dirt in the measuring tube or impure manometer fluid will influence the meniscus formation and thus the reading. In general, for all pressure difference measurement, the hoses transferring the pressure to the manometer should be absolutely tight, clean, and free of any internal obstructions.

12.3.7.5 Calibration

From the calibration point of view, manometers can be divided into two groups. The first, fluid manometers, are fundamental instruments, where the indication of the measured quantity is based on a simple physical factor: the hydrostatic pressure of a fluid column. In principle, such instruments do not require calibration. In practice they do, due to contamination of the manometer itself or the manometer fluid and different modifications from the basic principle, like the tilting of the manometer tube, which cause errors in the measurement result. The stability of high-quality fluid manometers is very good, and they tend to maintain their metrological properties for a long period.

The second, mechanical and electrical manometers, require more frequent calibration. Changes in the elastic properties of the pressure transducer, wearing in mechanical parts, and electronic circuitry drift influence the properties of the instruments, giving rise to repeated calibration.

The principle of calibration is to compare the measurement result of the manometer to be calibrated to that of the measurement result of the reference

instrument when both manometers are connected to the same reference pressure. The problem is providing a stable reference pressure, that is not sensitive to environmental temperature variations. Stabilizing the environment temperature is a complex matter and adds to the cost of the calibration equipment.

12.3.8 Velocity Measurement

12.3.8.1 Introduction

In industrial ventilation the majority of air velocity measurements are related to different means of controlling indoor conditions, like prediction of thermal comfort; contaminant dispersion analysis; adjustment of supply airflow patterns, and testing of local exhausts, air curtains, and other devices. In all these applications the nature of the flow is highly turbulent and the velocity has a wide range, from 0.1 m s^{-1} in the occupied zone to 5–15 m s^{-1} in supply jets and up to 30–40 m s^{-1} in air curtain devices. Furthermore, the flow velocity and direction as well as air temperature often have significant variations in time, which make measurement difficult.

In air ducts, the measurement of the local air velocity is used to determine the flow rate in the duct. The duct flow is usually more stable and the flow direction under better control than in the room space. Different types of disturbances in the ductwork, such as bends, tees, or dampers, will influence the nature of the flow and cause swirl and other problems in velocity measurement.

12.3.8.2 Thermal Anemometers

Thermal anemometers are a group of velocity measurement instruments that depend on the principle of electrically heating the sensor and measuring the velocity based on the cooling of the sensor: The higher the flow velocity is, the greater the cooling rate. Thermal anemometers are typically used for measuring in the low velocity range from 0.1 m s^{-1}, but many types are capable of measuring high velocities as well.

Hot-Wire Anemometers

The hot-wire anemometer sensor is a very fine wire with a diameter of few micrometers and length of few millimeters. This wire is connected to a measurement bridge and an electrical current is fed through the wire. The wire is heated to a temperature above the air temperature and the air velocity is determined by the cooling effect of the wire. The voltage over the wire, U_w, is a function not only of the velocity but also of the excess temperature and the fluid properties in the following way:[33]

$$U_w^2 = R_w(A + Bv^n)(T_w - T_a)\,, \tag{12.26}$$

where R_w is the wire resistance, A and B are coefficients dependent on the physical dimensions of the wire and properties of the fluid (air), v is the flow velocity, n is a constant (close to 0.5), T_w is the wire temperature, and T_a is the ambient air temperature.

The wire-type sensor (probe) can be a single-wire construction, or it may have two or three separate wires. With a three-wire sensor, all three velocity components can be determined. As well as wire-type sensors, there are hot-

film sensors, which are more robust but, due to a larger thermal inertia, are not as fast-responding as wires.

Modern hot-wire anemometers are normally used in the constant temperature (CT) mode, where the wire resistance and wire temperature are kept virtually constant. In the CT-mode the wire is one part of a Wheatstone bridge circuit, which has a feedback from the bridge offset voltage to the top of the bridge (see Fig. 12.18).

A hot-wire anemometer, working in the CT mode, is capable of measuring rapid velocity fluctuations. This is an advantage in the measurement of flow turbulence and is also the main area of application for the hot-wire anemometer. It is an instrument mainly for scientific purposes.

For various reasons, this type of anemometer is not a suitable instrument for practical measurements in the industrial environment. The thin wire probe is fragile and sensitive to contamination and is unsuited to rough industrial environments. The wire temperature is often too high for low-velocity measurements because a strong natural convection from the wire causes errors. Temperature compensation, to correct for ambient air temperature fluctuations may not be available or may not cover the desired operating range.

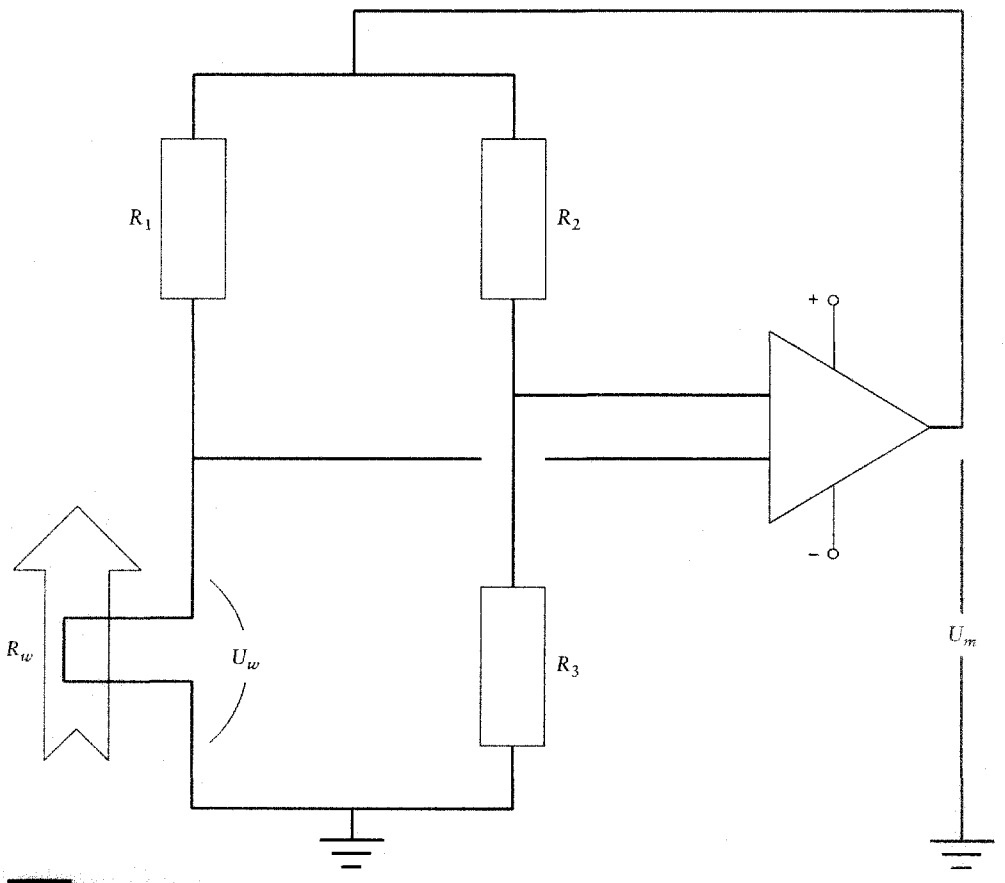

FIGURE 12.18 Principle of a CT hot-wire anemometer.

Other Thermal Anemometers

For measuring mean velocities in the low and moderate velocity range, there are other types of thermal anemometers, that are more robust, easier to use, and not as expensive as the "real" hot-wire anemometers. These anemometers use larger sensors, thermistors, and spherical and cylindrical sensors. The working mode often differs slightly from the hot-wire anemometer. Instead of keeping the sensor resistance/temperature constant as in the CT mode, the system tries to keep the excess sensor temperature constant. According to Eq. (12.26), this eliminates the main effect of ambient air temperature fluctuations and gives temperature compensation. The excess temperature is kept low to prevent the effect of natural convection at low velocities.

Usually this type of anemometer does not provide information on the flow direction. Vice versa, the sensors are made as independent of the flow direction as possible—omnidirectional. This is an advantage for free-space ventilation measurements, as the flow direction varies constantly and a direction-sensitive anemometer would be difficult to use. Naturally, no sensor is fully omnidirectional, but satisfactory constructions are available. Due to the high sensor thermal inertia, this type of anemometer is unsuitable for high-frequency flow fluctuation measurement. They can be used to monitor low-frequency turbulence up to a given cut-off frequency, which depends on the dynamic properties of the instrument.

The precision of a thermal anemometer is dependent on the instrument quality and the conditions of use. A general rule is, the lower the measured velocity, the higher the inaccuracy and vice versa. When measuring very low indoor velocities, around 0.1 m s^{-1}, the relative error can be as high as 100% and not much lower than 30%. Low velocities are extremely difficult to measure with accuracy.

12.3.8.3 Pitot-Static Tube

The Pitot-static tube is a basic instrument that predicts flow velocity based on Bernoulli's equation:

$$\tfrac{1}{2}\rho v^2 + p_s = p_t \,. \tag{12.27}$$

This states that the sum of the velocity pressure $0.5\rho v^2$ plus the static pressure p_s, the total pressure, is constant along a streamline. In the case of standard air density (1.2 kg m^{-3}), $0.5\rho v^2$ becomes $0.6v^2$. When a Pitot-static tube is immersed into the flow, as in Fig. 12.19, the velocity at the stagnation point at the tube nose is $v = 0$ and the local static pressure equals the total pressure p_t. The flow static pressure p_s is measured a short distance downstream from the surface of the tube. The flow velocity is obtained by applying Eq. (12.27):

$$v = K\sqrt{\frac{2\Delta p}{\rho}}, \tag{12.28}$$

where a constant K is added to take into account the deviations from the ideal (Bernoulli) case, $\Delta p = p_t - p_s$ is the pressure difference between the total (stagnation) pressure and the static pressure, and ρ is the fluid density. The factor K is dependent mainly on the tube construction and is close to ideal ($K = 1$) for properly

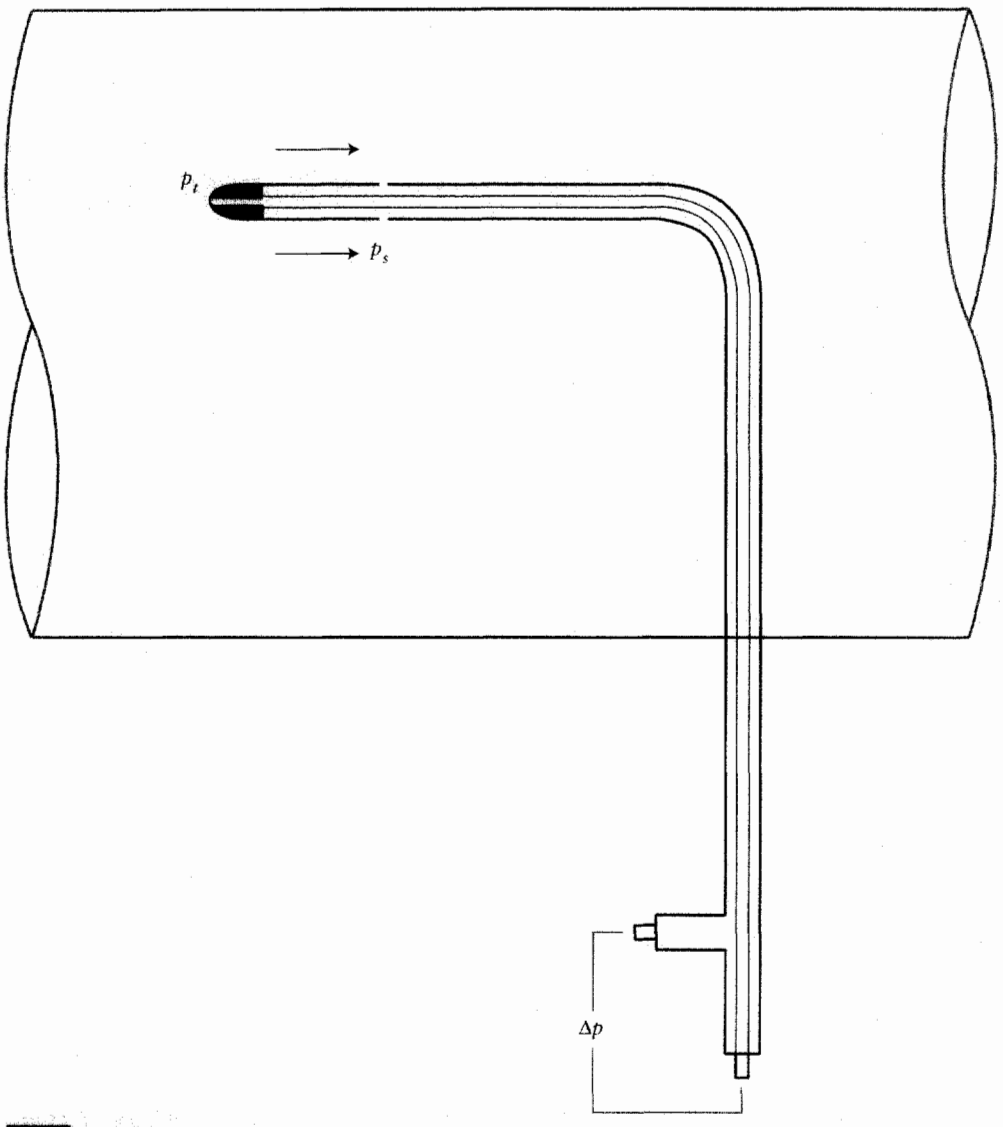

FIGURE 12.19 Principle of the Pitot-static tube.

constructed Pitot-static tubes. There are several standardized constructions,[34] which have different shapes of the tube nose (spherical, ellipsoidal, conical) and slightly different static pressure hole arrangements. A factor $K = 1.00$ for all these tubes can be applied in all practical ventilation measurements. In scientific work additional corrections for Reynolds number, fluid compressibility, turbulence, viscosity, and velocity gradient[32,34] can be applied.

By connecting manometer hoses to both output pressures given by the tube, the pressure difference Δp can be measured directly. The barometric pressure and the fluid temperature are required for the determination of the fluid density. The Pitot-static tube is not a suitable instrument for measuring low velocities. It can be applied in cases where the flow velocity is high

enough for the manometer to provide a reliable pressure difference reading. To have, for example, a pressure difference of 10 Pa in measuring airflow, the velocity has to be in the 4 m s^{-1} range. In practice this means measurements in air ducts, supply openings, jets, and similar cases where the velocity is sufficient.

When the axis of the Pitot-static tube is not aligned to the main flow direction, an error of inclination occurs known as yaw. It is not more than 1% for the measured pressure difference if standard tubes are used and the deviation from the flow direction is less than 11–13°.[32,34] When the yaw is further increasing, the error increases rapidly. Hence it is of prime importance to place and align the Pitot-static tube carefully in the direction of flow.

12.3.8.4 Vane Anemometer

The vane anemometer is an old invention. It can be likened to a small wind turbine with 4–10 rotating blades and a handle, as in Fig. 12.20. Earlier constructions were fully mechanical, where the spindle rotation was transmitted to a pointer through a series of gears. In modern vane anemometers, an electrical sensor records the spindle rotation and the signal is processed, giving the velocity on a digital display. Such an instrument usually is able to integrate the mean velocity over a time interval.

The vane anemometer's physical dimensions are often quite large (compared with other local velocity measurement instruments). It does not strictly measure a local velocity at all, but rather provides a spatially integrated mean value. This is an advantage in many cases where the air volume flow rate has to be predicted using "local" velocities and an integration principle.

The measurement range of a vane anemometer is typically between 0.3 and 30 m s^{-1}. It may start rotating with slightly lower velocities, but due to the characteristic curve having a small nonlinear part in the low-speed end, the useful range is narrower. The actual precision depends on the quality of the instrument; however, the inaccuracy may vary between 1% and 5% of the scale. The larger the vane, the higher the accuracy.

The vane anemometer is not seriously affected by small deviations in alignment in the main flow direction. However, care is necessary since over 20° misalignment causes significant errors. With regard to providing a correction for fluid density, slightly different opinions exist.[32,35] Based on measurements, it is recommended[35] that the following density correction procedure be applied:

$$v_c = v_m \sqrt{\frac{\rho_m}{\rho_c}}, \tag{12.29}$$

where v is velocity, ρ is density, and indices c and m refer to calibration conditions and actual measurement conditions, respectively.

12.3.8.5 Measurement Errors

Errors related to velocity measurement instruments have different origins depending on the measurement principle. The most important of these have been covered in previous sections. One common source of error for all instruments is the disturbance of the flow field by the sensor/meter or the person carrying out the measuring. The influence of the sensor in an open space is usually

FIGURE 12.20 The vane anemometer.

not critical. The effect of the measuring person, however, can be. In the case of hand-held instruments, the person carrying out the measurements must take care not to influence the flow at the measurement point with his or her body.

In measuring the local velocity in ducts, the sensor will obstruct a part of the duct cross-section. This results in accelerated flow by the sensor and an error occurs. In a Pitot-static tube, this is called stem blockage. If the ratio of the tube diameter to the duct diameter is smaller than 0.02, stem blockage can be neglected. Otherwise a correction has to be applied.[34]

The blocking effect does not apply to the Pitot-static tube alone. Any sensor/instrument immersed into a duct has a similar effect; the larger the sensor is, the greater the problem. For other types of instruments an analysis must be made, so as not to block large proportion of the duct cross-section with the meter. A good rule of thumb to avoid corrections is to keep the cross-section of the meter less than 5% of the duct cross-section.

12.3.8.6 Calibration

Constant calibration of most velocity instruments is necessary. Hot-wire or other thermal anemometers require frequent calibration due to their complex and sensitive nature. They usually have a significant time change in their metrological characteristics, a drift. Vane anemometers are not that sensitive but require checking at set intervals. The Pitot-static tube is the only exception. Due to its fundamental nature, it does not require calibrating. It also can be used as a reference for other meters. This applies to the tube itself, provided it maintains its original geometry unchanged. However, the manometer used in conjunction with the Pitot-static tube requires calibration.

A calibration facility must produce the desired velocity range for the meter to be calibrated. The air temperature should be kept constant over the test to ensure constant density. For thermal anemometers, velocity calibration only is not sufficient. They should also be checked for temperature compensation. In the case of omnidirectional probes, sensitivity to flow direction should be tested. In the case of low-speed (thermal) anemometers, their self-convection error should be measured, and, for instruments measuring flow fluctuation (turbulence), dynamic characteristics testing should be carried out as well.[36]

Manufacturers of thermal anemometers provide small rigs for their calibration. They typically consist of a nozzle, an air supply unit, and a regulating valve. The probe is placed into the nozzle jet. The reference velocity is calculated from the nozzle upstream pressure and nozzle characteristics. Due to its small size, this type of rig can be used only for hot-wire or other thermal anemometers.[33]

A good method for a simple calibration facility is a system where a constant airflow is produced by using two water containers and an arrangement of a virtually constant pressure head.[37] The constant water flow into the second container displaces an equal airflow out of the container (Fig. 12.21). With this arrangement the difficult measurement of a small airflow is changed into a much easier and accurate measurement of a small water flow.

The calibration air flows through a thin tube. The probe is placed at the exit of the tube. When the tube is long enough and the tube flow is laminar, the reference velocity for calibration can be calculated from the theoretical, fully developed laminar velocity profile.

To calibrate larger sensors/instruments such as vane anemometers, a wind tunnel is required. A calibration wind tunnel consists of an open or closed tunnel, a fan to deliver the air, a nozzle to shape the velocity profile, and a mesh arrangement to uniform and reduce the flow turbulence. It may be necessary to control the air temperature in the tunnel by means of a heating/cooling sys-

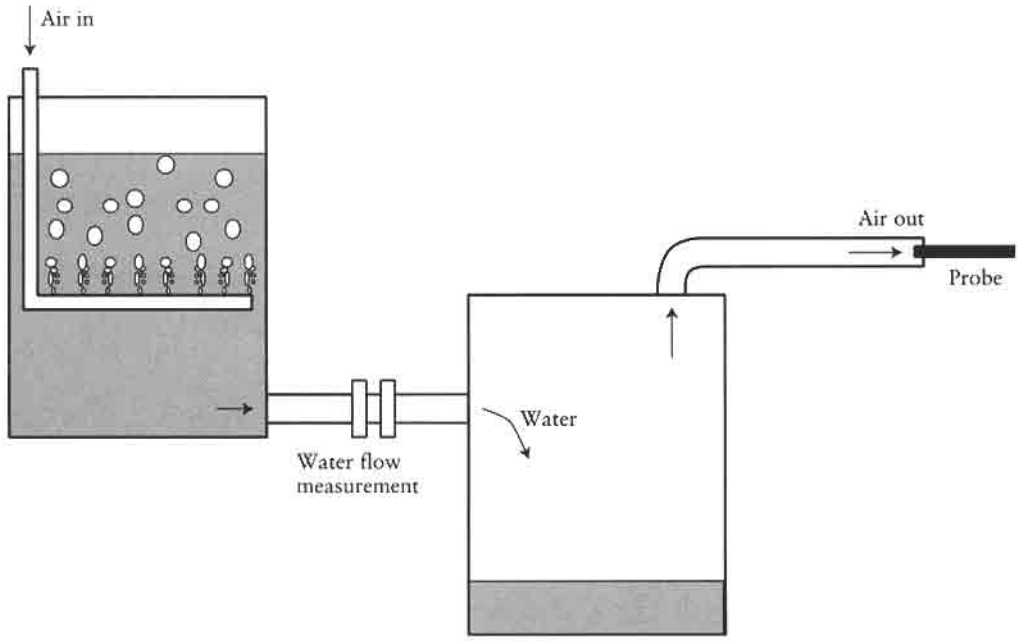

FIGURE 12.21 A simple calibration facility for small thermal probes.

tem. The instrument to be calibrated is placed downstream from the nozzle, where an almost flat velocity profile is formed. The reference velocity may be based on the measured flow rate and a known nozzle velocity profile, or it may be measured close to the calibrated sensor using a Pitot-static tube. High-quality calibration wind tunnels are expensive facilities requiring skilled personnel to carry out the calibrations.

Very low (below 0.5 m s^{-1}) velocities are difficult to achieve in normal wind tunnels. In this range a slide tunnel is a better alternative. In a slide tunnel the air stands still and the sensor moves with a constant velocity on a slide. The reference velocity is based on the calibration distance and the traveling time. As the length and time can be measured very accurately, the calculated reference velocity value is of good quality. Convective currents inside the slide tunnel restrict the lowest calibration velocities to around 0.05 m s^{-1}. On the other hand, high velocities are restricted by the length of a straight tunnel, because a certain length of the tunnel is required for acceleration and deceleration of the slide.

12.3.9 Flow Rate Measurement

12.3.9.1 Introduction

The air volume flow rate plays a major role in planning, commissioning, and running industrial ventilation systems. In the planning phase of a system, the supply, exhaust flows, and total flow rates are specified. When the system is built and running, the contractor and/or the client measures the airflows to determine if they agree with the specification. In such a situation, it is of interest to

all parties to have a sound foundation for the necessary measurements. Because of the importance of the measurement of flow rate in ventilation and many other fields, a comprehensive selection of standards covering different measurement methods and instruments is available.

The range of the airflow in ventilation systems is wide. The flow rate in an individual supply or exhaust terminal may only be a few liters per second, while the flow in a main duct or supply chamber of a large system may be in excess of 100 cubic meters per second. No general method to deal with the whole range exists. Each case requires individual consideration for the most suitable methods and instrumentation to be selected.

12.3.9.2 Orifice, Venturi, and Nozzle

The orifice, the venturi, and the nozzle are instruments for the measurement of duct or pipe flow rate. A constriction, throttling the flow, is placed in the duct, and the resulting differential pressure developed across the constriction is measured. It is the difference in the geometric shape that characterizes the three devices; see Fig. 12.22.

The orifice plate is simple to manufacture and has a relatively low cost. It does, however, create a quite large permanent pressure loss when installed in the ductwork. The venturi is smoothly shaped with a low permanent pressure loss but requires more space and is more expensive. The nozzle is a compromise between the orifice and the venturi. All three devices are standardized flow meters with very detailed descriptions of their geometry, material, manufacturing, installation, and use.[38–42]

Based on the measured pressure difference over the device, the throat diameter, and some other parameters, the flow rate can be determined. The equation for the volume flow rate is, in general,[38]

$$q_v = CE\epsilon\frac{\pi d^2}{4}\sqrt{\frac{2\Delta p}{\rho}}, \tag{12.30}$$

where C is the coefficient of discharge, E is the velocity approach factor, ϵ is an expansion factor, d is the diameter of the throat of the device, Δp is the measured pressure differential, and ρ is the fluid density at the upstream pressure tapping. Correspondingly, the mass flow rate is

$$q_m = CE\epsilon\frac{\pi d^2}{4}\sqrt{2\Delta p\rho}. \tag{12.31}$$

The product of the discharge coefficient and the velocity approach factor, $\alpha = CE$, is called the flow coefficient. For the orifice, the discharge coefficient is given by the equation[38]

$$\begin{aligned} C = {} & 0.5959 + 0.0312\beta^{2.1} - 0.184\beta^8 + 0.0029\beta^{2.5}\left[\frac{10^6}{\mathrm{Re}_D}\right]^{0.75} \\ & + 0.09L_1\frac{\beta^4}{1-\beta^4} - 0.0337L_2\beta^3, \end{aligned} \tag{12.32}$$

where $\beta = d/D$ is the diameter ratio of the throat and the duct diameters, Re_D is the duct Reynolds number, $L_1 = l_1/D$ is the distance of upstream pressure tapping from the upstream face of the orifice plate divided by the duct diameter, and $L_2 = l_2/D$ is the distance of the downstream pressure tapping

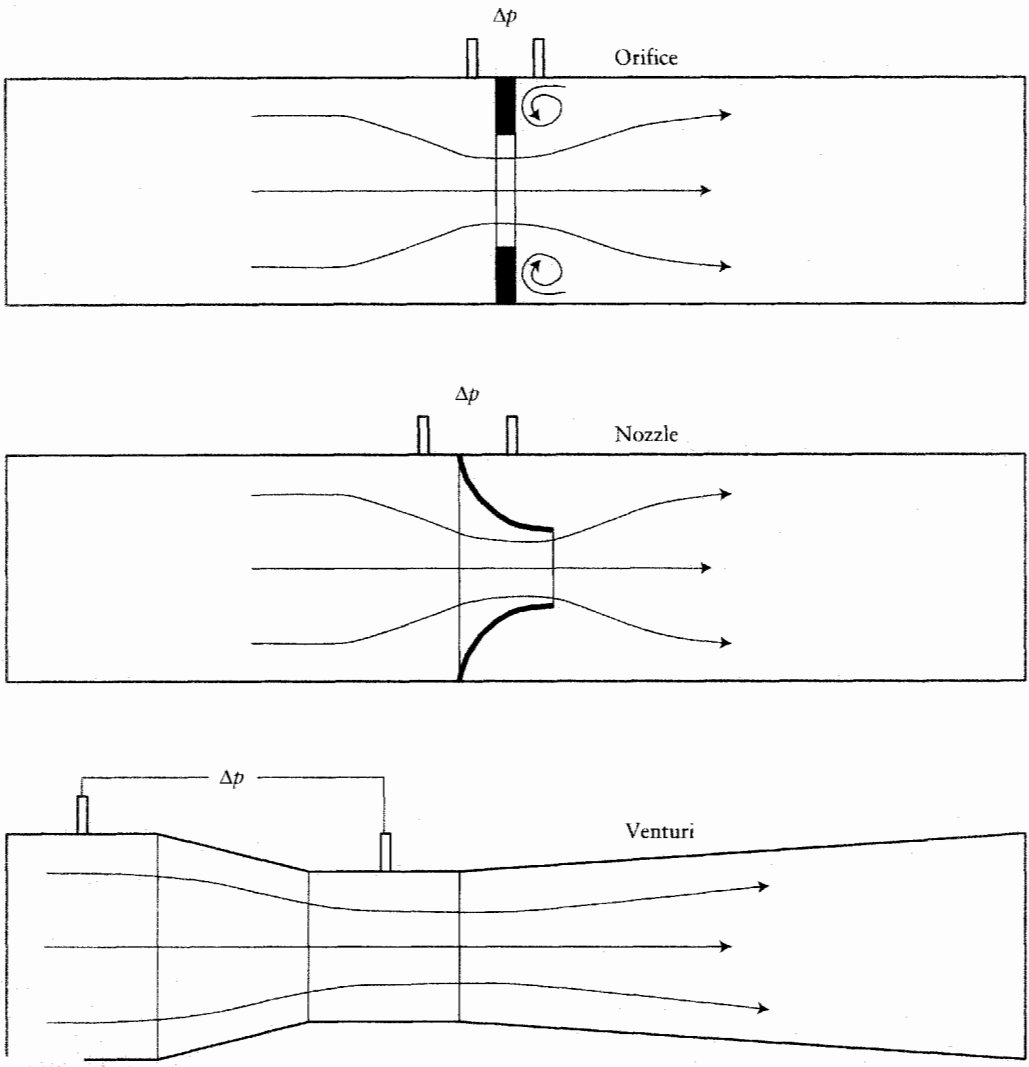

FIGURE 12.22 Schematic of three flow meters based on the obstruction principle.

from the downstream face of the plate divided by the duct diameter. From the above it can be noticed that the calculation of the discharge coefficient is an iterative process, as the duct Reynolds number is included in the equation. The discharge coefficient for a nozzle is given by a slightly simpler equation:

$$C = 0.99 + 0.2262\beta^{4.1} + [0.000215 - 0.001125\beta + 0.00249\beta^{4.7}]\left[\frac{10^6}{\mathrm{Re}_D}\right]^{1.15}. \tag{12.33}$$

The discharge coefficient of the venturi tube depends on the convergent of the venturi, but is given as a constant value for a specified device. The range is from 0.984 for a rough-cast convergent to 0.995 for a machined convergent.[38]

The velocity approach factor is dependent on the diameter ratio only:

$$E = \frac{1}{\sqrt{1-\beta^4}}. \tag{12.34}$$

The expansion factor ϵ takes into account the compressibility effects of the fluid. It is close to unity in most industrial ventilation applications.

For the above equations to be valid, the measurement devices must be manufactured according to standards and also must be installed according to given specifications. There are strict requirements concerning the minimum upstream and downstream straight lengths. These lengths depend mainly on the diameter ratio of the device and the type of the nearest upstream fitting causing a disturbance in the incoming flow velocity profile. Table 12.6 provides typical values of the required straight lengths for orifice plates and nozzles.

If the lower values in the brackets are applied, an additional ±0.5 uncertainty (error on 5% risk level) has to be added arithmetically to the flow coefficient confidence limits. The use of flow straighteners is recommended in cases when a nonstandard type of upstream fitting disturbs the flow velocity profile.

Every measured quantity or component in the main equations, Eqs. (12.30) and (12.31), influence the accuracy of the final flow rate. Usually a brief description of the estimation of the confidence limits is included in each standard. The principles more or less follow those presented earlier in *Treatment of Measurement Uncertainties*. There are also more comprehensive error estimation procedures available.[43–46] These usually include, beyond the estimation procedure itself, some basics and worked examples.

12.3.9.3 Other Flow Obstruction Meters

Any obstruction inserted into a duct or pipe that creates a measurable pressure difference can be used as a flow meter. The three basic standardized flow measurement devices presented above are perhaps more suitable for laboratory work than installation as permanent ductwork instruments in ventilation applications. They are sensitive to flow disturbances, relatively expensive, require considerable space, and have a narrow measurement range and a high permanent pressure loss. For these reasons, numerous attempts have been made to develop instruments without these drawbacks. Some of them, like the

TABLE 12.6 Some Required Straight Lengths (*L*/*D*) for Orifice Plates and Nozzles[38]

	Upstream side of the primary device			Downstream side
β	Single 90° bend or tee	Two or more 90° bends in different planes	Expander (0.5*D* to *D* over a length of 1*D* to 2*D*)	All fittings
<0.2	10 (6)	34 (17)	16 (8)	4 (2)
0.4	14 (7)	36 (18)	16 (8)	6 (3)
0.6	18 (9)	48 (24)	22 (11)	7 (3.5)
0.8	46 (23)	80 (40)	54 (27)	8 (4)

Dall tube,[47] which is a modification of the venturi, have even been standard instruments. Several other solutions based on plates, rings, or wing-type obstructions are commercially available. This wide variety of devices is not covered here. For further information, the reader should contact the manufacturers of such instruments.

12.3.9.4 Traversing Methods

The principle of the traversing method is to measure the local velocity at one or several points of the flow cross-section and then calculate the flow rate based on this information. Generally speaking, an integration of the local velocity over the flow cross-section is made. Mathematically, this is expressed as

$$q_v = \int_A v \, dA, \tag{12.35}$$

where q_v is the volume flow rate, v is the local velocity, and dA is a differential area of the flow cross-section. In practice the number of measured local velocities is finite, and the integration is carried out using different graphical or numerical methods. For duct flow, a standard is available describing the traversing methods where a Pitot-static tube for velocity measurement is used.[48] This document divides the determination of the flow rate into three categories: graphical integration, numerical integration, and arithmetical methods.

The graphical integration method is based on graphical presentation of the average flow profile. For a circular duct, the cross-section is virtually divided into several concentric ring elements. The spatial mean velocity v_m of such an element is determined as an arithmetical mean of local velocities along the circumference of the corresponding radius. For a circular cross-section the flow rate can be expressed as

$$q_v = \pi R^2 \int_0^1 v_m \, d\left(\frac{r}{R}\right)^2, \tag{12.36}$$

where R is the radius of the duct and r is the radial distance from the duct center point. For graphical integration the spatial mean velocities v_m are plotted against $(r/R)^2$. The area under this curve is then the integral term in Eq. (12.35) and has only to be multiplied by the duct cross-section area. For this method the measuring points may be located at any position in order to obtain satisfactory knowledge of the velocity profile.

In the numerical integration method, the graphical velocity profile is replaced by an algebraic curve, and the integration is carried out numerically. A procedure has been described[48] where the velocity profile is approximated using a third-degree curve between the successive pairs of mean velocity values. A simpler approach, though not included in standards, is the use of the general formulas for numerical integration. For example, Simpson's rule[49] for an even $(2n)$ number of equal subintervals between the velocity points along the radius gives

$$\begin{aligned} q_v = \pi R^2 \frac{1}{6n} \Bigg[& 4v_{m1}\left(\frac{r}{R}\right)_1 + 2v_{m2}\left(\frac{r}{R}\right)_2 + 4v_{m3}\left(\frac{r}{R}\right)_3 + \cdots \\ & + 2v_{m(2n-2)}\left(\frac{r}{R}\right)_{(2n-2)} + 4v_{m(2n-1)}\left(\frac{r}{R}\right)_{(2n-1)} \Bigg], \end{aligned} \tag{12.37}$$

where the number of velocity points is $2n - 1$ (the center point and the point at the duct wall cancel out of the sum) and the distance between successive points along the radius is $1/(2n)$. For a rectangular cross-section similar methods are available.

In the arithmetical methods[50,51] a circular flow cross-section is divided into concentric rings and a central element. The areas of the elements are equal except for the outermost ring, which has only half of that area. A hypothesis is made for the velocity profile for each element. For example the log-linear rule assumes a velocity profile of

$$v = A \log y + By + C \ , \tag{12.38}$$

where y is the distance from the duct wall and A, B, and C are constants. Based on the velocity profile assumption, measurement points for each element are located in places where the (measured) local velocity is equal to the mean velocity of the element. This approach allows certain measurement point locations, dependent on the number of the points and the assumed velocity profile, to be determined. Table 12.7 gives measuring points for the log-linear rule in a round duct.

The volume flow rate is calculated as the arithmetical mean of the measured velocities multiplied by the duct cross-sectional area. The number of diameters along which the traversing occurs is not defined. If a near-symmetrical velocity profile is expected, an even traverse along one diameter may be sufficient. In case of a more disturbed profile, traversing along two or more diameters is recommended.

In the case of a rectangular cross-section, a variety of methods and corresponding measurement point locations exist.[48,52] Table 12.8 shows the required measuring points for the log-Tchebycheff rule, where the velocity distribution in the wall-connected elements is logarithmic and in the central elements polynomial.

As an example, for the $5 \times 6 = 30$ points case, the principle for placing the measurement points is shown in Fig. 12.23.

There is also a standardized method based on the estimation of the flow rate on one measurement point only.[53] In this method the velocity probe is placed in the duct so that the measured local velocity is equal to the mean axial velocity. In fully developed turbulent duct flow, this distance from the wall

TABLE 12.7 Measuring Point Distances for the Log-linear Rule Circular Cross-Section[50]

Number of measurement points per diameter	Distance from wall in duct diameters									
4	0.043	0.290	0.710	0.957						
6	0.032	0.135	0.321	0.679	0.865	0.968				
8	0.021	0.117	0.234	0.345	0.655	0.816	0.883	0.979		
10	0.019	0.076	0.153	0.217	0.361	0.639	0.783	0.847	0.924	0.981

TABLE 12.8 Measuring Point Distances for the Log-Tchebycheff Rule, Rectangular Cross-Section[48,52]

Number of measurement points per traversing line	Distance from wall (l/L or h/H)									
5	0.074	0.288	0.500	0.712	0.926					
6	0.061	0.235	0.437	0.563	0.765	0.939				
8	0.046	0.175	0.342	0.400	0.600	0.658	0.825	0.954		
10	0.037	0.141	0.263	0.338	0.456	0.544	0.662	0.737	0.859	0.963

is $y = 0.242R$. This approach has severe restrictions, as the velocity profile in the measurement cross-section has to be very close to the fully developed profile, requiring minimum upstream straight lengths of about 30 to 80 duct diameters depending on the type of the nearest flow disturbance.

Apart from ducts, the traversing principle can be utilized in any cross-section where the flow rate has to be determined, such as supply or exhaust grills, the

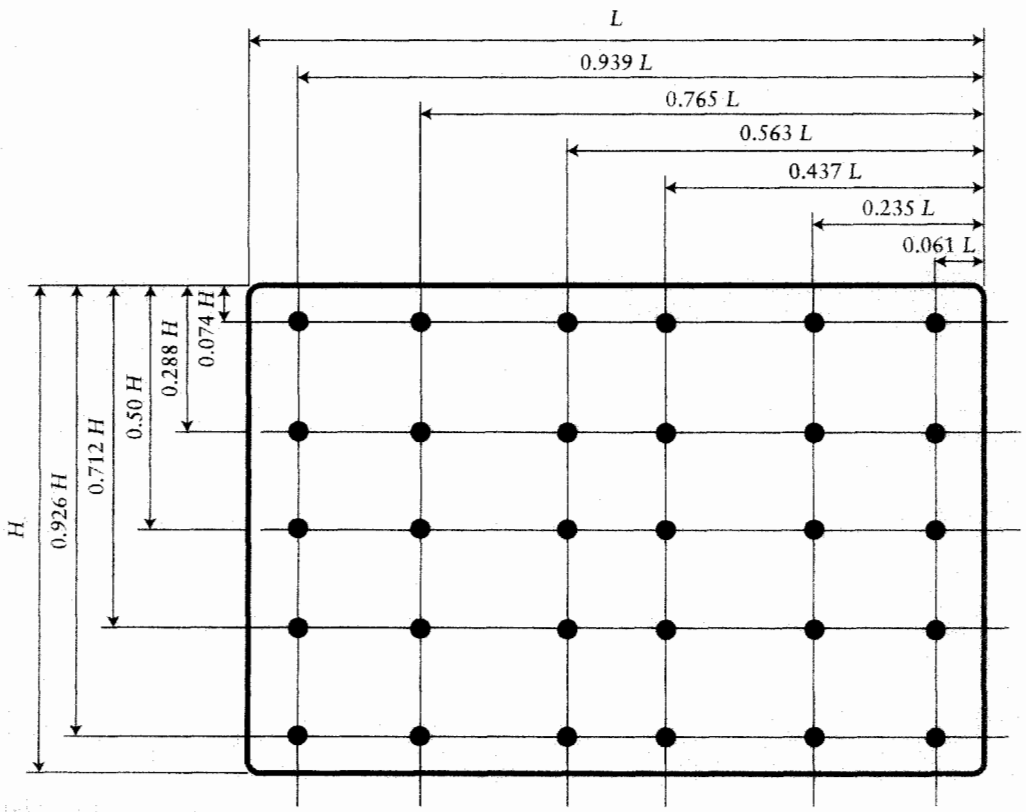

FIGURE 12.23 An example of measuring point locations for a rectangular cross-section.

surface of a large heating/cooling coil, or the intake opening of a fan. If the velocity is high enough, the Pitot-static tube may be used. On the other hand, the vane anemometer is a convenient instrument for traversing larger surfaces, as it has an integrating character due to its larger dimensions.

12.3.9.5 Tracer Method

The use of tracers for airflow measurement in ventilation ducts is not very common. There are several reasons for this. Compared to other flow measurement methods, tracers require more complicated equipment, skilled personnel, and are more expensive. There are, however, situations when conventional measurement methods are not applicable. For instance, if the space available is small, and hence the flow meter cannot be installed, or if no space is free to carry out traversing measurements, the use of a tracer might be an alternative.

Tracer methods are not as well standardized as some of the conventional methods. One standard[54] is available, but it comprises radioactive tracers only, which are perhaps not the best alternative for measurements in buildings. In principle, at least three different measurement methods are available:[55] the constant injection method, the pulse injection method, and the concentration decay method. Of these three, the first is the best approach for normal ventilation measurements. The other methods require special instrumentation and do not produce as reliable results.

Constant Injection Method

The tracer is injected into the duct at a constant rate and mixed with the flowing air. The concentration of the air-tracer mixture is measured further downstream. Assuming perfect mixing and that the air entering the test section has a zero concentration, the air volume flow rate q_{va} can be calculated based on the mass balance of the tracer

$$q_{va} = \frac{p_t T_a q_{vt}}{p_a T_t C_{vt}}, \tag{12.39}$$

where p_t and T_t are the pressure and (Kelvin) temperature of the injected tracer, p_a and T_a are the corresponding quantities for the air, q_{vt} is the volume flow rate of the injected tracer and C_{vt} is the downstream measured tracer (volume) concentration. Good mixing of the tracer and air between the injection point and the measurement cross-section is essential. Failure to achieve this will result in errors. The injection and the sampling should be carried out by a multipoint approach. A ring, cross, or rectangle formed tube with many small holes is a good injection device that will spread the tracer effectively. Similar solutions can be used for sampling. A fan is an ideal mixing device between the injection and the sampling sections. The error due to incomplete mixing using a fan has been shown to be only few percentage points.[56] In the case of a straight empty duct between the injection and sampling sections and a one-point injection/sampling, a distance of at least 80 duct diameters is required to keep the incomplete mixing error less than 5%. Adding a multipoint injection/sampling and some mixing elements can reduce the corresponding distance to 10–20 duct diameters;[57] see Table 12.9.

As a tracer, either a gas or particles can be used. In ventilation ductwork measurement, gas is recommended. Particles tend to adhere to the duct surface,

TABLE 12.9 Required Mixing Lengths (*L/D*) to Keep the Error due to Incomplete Mixing Smaller Than 5% or 10%[57]

Type of injection, sampling, and duct section	*L/D* Maximum error 5 %	*L/D* Maximum error 10 %
Straight duct without disturbance Injection at center, sampling at center	80	60
Straight duct without disturbance Injection through a ring whose diameter is 63% of the duct's (four holes in ring)		
(a) Sampling at center	25	20
(b) Sampling at four points in duct (situated as in injection)	15	10
Duct with two 90° bends Injection through a ring whose diameter is 63% of the duct's (four holes in ring)		
(a) Sampling at center	20	15
(b) Sampling at four points in the duct (situated as in injection)	10	5
Injection before a fan and sampling after the fan Injection through a ring whose diameter is 63% of the duct's (four holes in ring)	10	5

which will adversely influence the measurement and also hygiene. Widely used tracer gases are nitrous oxide (N_2O) and sulfur hexafluoride (SF_6), which are readily detectable using infrared analyzers or gas chromatographs. It is advisable to use a diluted tracer with a density close to air density. Otherwise mixing with air in the duct is difficult, and can lead to large measurement errors. Tracers having strong ozone-depleting features are not recommended.

12.3.9.6 Measurement of Supply or Exhaust Flows

The previous methods are mainly used to measure duct flow. When measuring flows on supply or exhaust terminals, different methods are used. The measurement on exhaust terminals is simple to carry out, as the velocity field near the terminal is relatively constant, with no steep gradients or swirls. In the case of a grill, traversing across the terminal surface using a suitable velocity instrument is a good alternative. A suitable instrument for most cases is the vane anemometer.

Different nozzle-shaped tubes are available, which are pressed onto the exhaust terminal. The air passes through the tube and a one-point velocity measurement is carried out in the throat of the device. The flow rate is determined from the calibration curve.

One of the best and most convenient methods of measuring the flow in the terminal is to use the terminal characteristic pressure difference. This requires that the manufacturer of the terminal provide calibration curves, where the flow rate is expressed as the function of the characteristic pressure difference. Some devices have integrated pressure measurement tappings, and the user has only to attach a manometer to measure the pressure difference.

Flow measurement on supply terminals is difficult, as each terminal creates its own velocity pattern, and a reliable correlation between a local velocity and

the flow rate is difficult to achieve. The balometer is a hood-shaped device that is pressed onto the terminal, and the airflow is passed through the instrument's throat. The local velocity is measured at several points in the throat using fixed thermal sensors. In modern balometers the flow rate is computed in an electronic module into which the calibration information has been fed.

The old, tedious, but quite reliable method is to measure the supply flow by the bag method. A tightly rolled plastic bag empty of air at the commencement of the test is pressed on the terminal with all the supply air passing into the bag. The filling time of the bag is measured and the flow rate calculated based on this information. The bag volume has to be determined in advance by a special measurement. Finally, the characteristic pressure difference method, mentioned above, can also be applied to supply terminals.

12.3.9.7 Measurement Errors

The measurement errors encountered in determining flow rate depend on the methods and instruments used. In conventional duct flow measurements, the greatest error-generating phenomenon is the irregularity and swirl of the duct flow itself. The duct flow velocity profile strongly influences the result of the measurement. The shape of the profile changes along the ductwork. At the end of a long straight duct (30 to 50 duct diameters) the profile is fully developed. Any other components such as tees, bends, or dampers reshape the velocity profile, after which it begins to move again toward the fully developed profile until it hits the next disturbance.

Because all measurement methods and instruments are sensitive to the velocity profile, the choice of the measurement cross-section is of vital importance. In most ventilation systems there is seldom enough straight duct to allow a fully developed velocity profile to develop, which is the most favorable for flow measurement. Thus, the principle in selecting the measurement cross-section is to find the place where the velocity profile is as near to the fully developed profile as possible. In practice the distance from the nearest source of disturbance upstream is maximized, ensuring that the distance to the nearest downstream disturbance is at least 3 to 5 duct diameters.

12.3.9.8 Calibration

Constriction measurement devices constructed to standards[42] do not necessarily require calibration. One idea of strict standardization is to define the manufacturing, tolerances, and other features in such a way that the instruments made according to these rules require no calibration. The properties are so well known that a certain accuracy can be guaranteed. If the accuracy specified in the standard is inadequate, additional calibration procedures are required. The same applies to Pitot-static tubes made according to standard specifications.[48]

The simplest calibration procedure for a gas flow–measuring device is to connect it in series with a reference meter and allow the same flow to pass through both instruments. This requires a reference instrument of better metrological quality than the calibrated instrument. One fact to consider when applying this method is that the mass flow rate in the system containing both instruments is constant (assuming no leakage), but the volume flow rate is not. The volume flow rate depends on the fluid density and the density depends on the pressure and the temperature. The correct way to calibrate is to compare either the measured mass

flow rates or the volume flow rates which have been converted to correspond to the identical state (pressure and temperature) of the fluid.

12.3.10 Laser-Based Techniques

12.3.10.1 Introduction

In addition to their widespread use in research and development in fluid dynamics, laser-based techniques[58–60] are also suited to experiments in industrial ventilation. The use of these advanced experimental methods is reasonable when their advantages in comparison with traditional measurement techniques counterbalance the significantly higher expenses of instrumentation.

Laser-based techniques are characterized as follows:

- Not a solid-state measurement device but an "optical probe" of high-intensity laser light is introduced into the fluid under investigation, avoiding disturbance on the flow field.
- With the use of appropriate transmission optics, high focusing of the laser light is carried out and the extension of the optical probe is considerably reduced. Accordingly, laser-based techniques offer the possibility of measurements of high spatial resolution.
- The optical flow measurement techniques are based on detection of light scattered by microscopic objects moving with the fluid. Since the light-scattering objects trace the flow, the scattered light provides relevant information on the flow properties. The flow information can be quickly obtained, according to the fast propagation of light, the applied fast-response optical detectors, and advanced electronic data acquisition and signal processing techniques. Hence, measurements of high temporal resolution and high data rate can be carried out.
- Depending on the structure of the optical probe, components of vector quantities (velocity field, displacement field) and their signs can be distinguished in measurements, ensuring directional sensitivity.
- Since the calibration factors for these techniques are known and relatively stable (depending on constant optical and geometrical parameters), the calibration process for laser-based measurements is simple or can be ignored.
- In certain cases, the optical probe can be used at a large distance from the experimental equipment. Hence, spatial zones can be probed that are normally accessible with difficulty or inaccessible for traditional measurement devices. This arrangement provides a means for remote measurements.

The use of laser-based techniques is ideal for practicing engineers in the field of industrial ventilation for the following on-site measurements and laboratory applications:

- Determination of high-resolution, accurate flow data providing a basis for boundary conditions used in CFD, for the verification of CFD results, and for improvement in CFD codes
- Fast, accurate, and convenient on-site calibration of traditional measurement devices

Comprehensive experiment-based preparation for the selection of special air-handling system elements
Convenient methods of studying flow characteristics related to structural elements that are accessible with difficulty for traditional measurement devices

For the investigation of airflow, air-particle and air-droplet systems (dusty and humid air), and the related technical equipment, laser-based techniques fulfill the following experimental demands:

Flow visualization
Velocity and turbulence measurements
Particle and droplet size distribution measurements
Particle and droplet concentration measurements
Simulation of transport and measurement of concentration distribution of air pollutants
Vibration and acoustic measurements

The corresponding laser-based experimental methods are covered below, with special regard to the laser Doppler anemometer technique, which offers the greatest application use in industrial ventilation at the lowest cost.

12.3.10.2 Laser Doppler Anemometry (LDA)

Even though the LDA principle is based on the optical Doppler effect, its lifelike interferometric interpretation is presented here.

In the intersection space (optical probe) of two coherent laser beams, planar interference fringes are formed. These are normal to the plane of beams, parallel to the beam bisector, and of a known uniform distance.

If the detected frequency of the flashing light scattered by a microscopic object when crossing the fringes is multiplied by the fringe distance, the velocity component of the scattering object normal to the beam bisector and parallel to the laser beam plane is determined.

The light-scattering objects must track the flow accurately, ensuring that their velocity represents the fluid velocity with a high accuracy. The light-scattering objects are either in the flow as a natural impurity such as dust, or are artificially introduced into the airflow at an optimum concentration ("seeding").

The complete LDA system includes the appropriate transmission and detection optoelectronics, traverse mechanisms, computer-controlled signal processing, and a data acquisition and evaluation system. The LDA equipment is a powerful tool for the measurement of flow velocity and velocity fluctuation, as well as the local concentration of particles or droplets transported in the airflow.

In industrial ventilation applications, LDA experiments fulfill the following needs:

The highly resolved velocity profile can be mapped in the vicinity of solid boundaries such as the walls of a room and in the entire enclosure, providing relevant data for CFD boundary conditions. These data form a basis for verification of CFD results and for improvement of CFD codes.
Very low air velocity can be measured; it is limited, however, by the sedimentation of the light-scattering objects.

Full use can be made for the on-site and off-site calibration of traditional anemometers such as thermal probes and propeller anemometers.
Velocity measurements in flow regions where other devices fail to operate suitably—boundary layers, stagnating air zones—are typical applications.
The local dust concentration in the airflow can be measured.

When the use of LDA is required in industrial ventilation, a single-component LDA system measuring one velocity component at a time is sufficient and provides a method of reasonable cost.

The layout recommended is a small-size, mobile, compact LDA probe that integrates the transmitting and back-scattering detection section and comprises a diode laser and fiber optics. Such LDA equipment is portable, together with a laptop data acquisition and evaluation computer. It is easy to install and reconfigure for measuring different velocity components in field experiments. The internal characteristics of the rugged LDA probe are unaffected by normal vibration, mechanical shock, and temperature change. Hence, no calibration or adjustment is required. To protect the LDA equipment from a humid or aggressive environment, special sealing is required.

Considering the possible contamination of the LDA front optics in field experiments as well as the reduced signal quality due to flaring noise from diffuse surfaces such as building surfaces, a sophisticated signal processor is used to clear up noisy signals. The LDA software controls the measurement, performs the signal processing, and presents the data in a comprehensive manner.

Some general quantitative characteristics (orders of magnitudes) of LDA systems are: velocity measurement range 1 mm s^{-1}–100 m s^{-1}; relative measurement uncertainty 0.1–1%; rate of accepted data 0.1–10 kHz; size of the optical probe 10 μm–1 mm for each dimension; measuring distance 0.1–1 m.

The LDA equipment must be installed so that the velocity component to be mapped is parallel to the beam plane, and normal to the beam bisector.

If the light-scattering objects originally present in the airflow are unsuitable for LDA measurements due to insufficient concentration or incorrect estimated flow-tracking capability, the air must be seeded with oil smoke, tobacco smoke, or titanium dioxide tracer particles or droplets. A simple smoke candle is generally suitable for seeding, even if the enclosure is large and the air path is not closed as in several cases of industrial ventilation.

Attention must be paid to the specific technical problems posed by measuring flow in industrial ventilating systems, such as high turbulence level and long time–variation of mean velocity. The LDA measurement conditions (statistically sufficient number of LDA data, suitably long duration of LDA measurements for recognition of long-term phenomena) must be carefully selected for an appropriate treatment of these problems.

12.3.10.3 Phase Doppler Anemometry (PDA)

Single-component PDA equipment is similar to LDA, but two detectors (not one) are installed with different detection angles. By means of simultaneous processing of signals supplied by the two detectors, information on the velocity and on the size of the scattering objects can be acquired. Therefore, velocity distribution, size distribution, and number density (local concentration)

distribution on the multitude of spherical scattering objects in the submicrometer to larger particulate matter range can be measured. Air-particle and air-droplet systems can be simultaneously mapped. Such experiments assist in the preparation or design of special dust or liquid separation equipment by field measurements of filter performance claims.

12.3.10.4 Laser Sheet (LS) Techniques

A thin laser "light sheet" of high intensity is produced with the use of appropriate optics, by means of which an entire "slice" of the fluid flow is illuminated (probed). If a sufficient concentration of light-scattering material such as oil smoke is ensured, the LS technique is a powerful tool for flow visualization. Beyond such qualitative studies, a quantitative, tomographic characterization of the flow field can be carried out by recording and digital processing of the scattered image.

Particle image velocimetry (PIV) supplies two-dimensional velocity data simultaneously in a planar flow section illuminated by the laser sheet. Another quantitative application of the LS method is the simulation of transport and measurement on the concentration distribution of gaseous or dusty air pollutants. If the dusty pollutant is present in the airflow at a high concentration, it appears as a "natural" multitude of light-scattering objects. Otherwise, the flow must be seeded, simulating the dusty or gaseous pollutants being transported. The seeding particles or droplets must be capable of tracing the turbulent flow with high accuracy. Based on the analogy of turbulent mixing of gases, the seeding particle or droplet distribution corresponds to the gaseous pollutants in the actual application. The grey-level distribution of the scattered image is determined and corrected by means of an image processing method, and corresponds to the pollutant concentration distribution.

12.3.10.5 Laser Optical Vibration and Acoustic Measurements

This aspect is not included here, but is related to optical flow diagnostics. It is based again on the principle of the optical Doppler effect. Multifunctional equipment is available for noncontact measurements of flow-induced vibration on surfaces of structural elements, for acoustic measurements, and for calibration of accelerometers and vibration transducers.

As the measuring distance for such equipment can be up to about 50 m, this technique is advantageous in cases when conventional acoustic or vibrometer devices are difficult or even impossible to use, such as high-frequency vibration measurements on the walls of high-level air ducts.

Nomenclature

A area
c material heat capacity
C capacity, coefficient of discharge, concentration
d diameter (throat)
D diameter (duct)
dA differential area

dx	confidence limits for the quantity X
dy	confidence limits for the quantity Y
E	velocity approach factor
E_i	inertial error
$F(a)$	cumulative distribution
$f(x)$	probability density
g	acceleration due to gravity
h	heat transfer coefficient, height
I	electrical current
l	length
L	relative length
m	experimental mean, mass
n	sample size
$N(\mu, \sigma)$	normal distribution
p	pressure
P	probability
q_m	mass flow rate
q_v	volume flow rate
r	radius
R	resistance, radius
Re	Reynolds number
s^2	experimental variance
s_x	experimental standard deviation of the variable X
t	random variable, time
T	temperature
$T(t, \nu)$	t-distribution
u	variable
$u(\alpha)$	a value of the $N(0, 1)$ distribution
U	voltage
v	velocity
V	volume
W	humidity ratio
x	value of the random variable (quantity) X
X	random variable (quantity)
Y	a quantity derived from measurement results
α	risk level, angle, flow coefficient
β	diameter ratio
ϵ	expansion factor
φ	relative humidity

κ coefficient
μ true mean
ν number of degrees of freedom
ρ density
σ^2 true variance
τ time constant

References

1. OIML. *Vocabulary of Legal Metrology: Fundamental Terms,* 2nd ed. International Organisation of Legal Metrology, 1978.
2. *International Vocabulary of basic and General Terms in Metrology,* 2nd ed. International Organisation for Standardisation, 1993.
3. T. D. McGee. *Principles and Methods of Temperature Measurement.* New York: John Wiley & Sons, 1988.
4. R. P. Benedict. *Fundamentals of Temperature, Pressure, and Flow Measurements.* New York: John Wiley & Sons, 1984.
5. F. Henning, H. Moser. *Temperaturmessung.* Berlin: Springer Verlag, 1977.
6. H. Breunig, F. Lieneweg. *Handbuch der technischen Temperaturmessung.* Vieweg, 1976.
7. IEC 60751 (1983-01). *Industrial Platinum Resistance Thermometer Sensors.* International Electrotechnical Commission, 1983.
8. ASTM E1137-97. *Standard Specification for Industrial Platinum Resistance Thermometers.* American Society for Testing and Materials, 1997.
9. *Manual on the Use of Thermocouples in Temperature Measurement.* ASTM Manual MNL 12. American Society for Testing and Materials, 1993.
10. IEC 60584-1 (1995-09). *Thermocouples—Part 1: Reference Tables.* International Electrotechnical Commission, 1995.
11. IEC 60584-2 (1982-01). *Thermocouples—Part 2: Tolerances.* International Electrotechnical Commission, 1982.
12. ASTM E230-96e1. *Standard Specification for Temperature-Electromotive Force (EMF) Tables for Standardized Thermocouples.* American Society for Testing and Materials, 1996.
13. ASTM E988-96. *Standard Temperature-Electromotive Force (EMF) Tables for Tungsten-Rhenium Thermocouples.* American Society for Testing and Materials, 1996.
14. D. P. DeWitt. *Theory and Practice of Radiation Thermometry.* New York: John Wiley & Sons, 1988.
15. J. C. Richmond. *Applications of Radiation Thermometry.* ASTM Special Technical Publication. American Society for Testing and Materials, 1984.
16. J. V. N. White. *Traceable Temperatures: An Introduction to Temperature Measurement and Calibration.* New York: John Wiley & Sons, 1994.
17. H. Preston-Thomas. The International Temperature Scale of 1990. *Metrologia,* 27, (1), 1990, pp. 3–10.
18. ASTM E1750-95. *Standard Guide for Use of Water Triple Point Cells.* American Society for Testing and Materials, 1995.
19. ASTM E1502-92. *Standard Guide for Use of Freezing-Point Cells for Reference Temperatures.* American Society for Testing and Materials, 1992.
20. *ASHRAE Handbook of Fundamentals.* American Society of Heating, Refrigerating, and Air-conditioning Engineers, Atlanta, 1997, Chapter 6.
21. M. J. Hickman. *Measurement of Humidity.* Notes on Applied Science, no 4. National Physical Laboratory, 1970.
22. ASHRAE Standard 41.6-1994. Measurement of Moist Air Properties. American Society of Heating, Refrigerating, and Air-conditioning Engineers, Atlanta, 1994.
23. ASTM E337-84(1996)e1. *Standard Test Method for Measuring Humidity with a Psychrometer.* American Society for Testing and Materials, 1996.
24. *Moisture and Humidity: International Symposium on Moisture and Humidity.* Washington, DC, 1985.
25. R. G., Wylie, T. Lalas. Accurate psychrometer coefficients for wet and ice-covered cylinders in laminar transverse air streams. In *Moisture and Humidity 1985: Measurement and Control in science and Industry,* pp. 37–56.

26. A. Carotenuto, M. Dell'Isola, L. Crovini, A. Actis. Accuracy of commercial dew-point hygrometers. *ASHRAE Transactions,* 101, (2), 1995.
27. J. L. Hales. The two-temperature generator in the UK humidity standard. In *Moisture and Humidity 1985: Measurement and Control in Science and Industry.*
28. J. P. Holman. *Experimental Methods for Engineers.* New York: McGraw-Hill, 1994.
29. H. L. Trietley. *Transducers in Mechanical and Electronic Design.* New York: Marcel Dekker, 1986.
30. P. G. Dargie, S. T. Hughes. A thick-film capacitive differential pressure transducer. *Measurement Science and Technology, 5,* 1994, pp. 1216–1220.
31. D. Marioli, E. Sardini, A. Taroni. High-accuracy measurement techniques for capacitance transducers. *Measurement Science and Technology,* 4, 1993, pp. 337–343.
32. E. Ower, R. C. Pankhurst. *The Measurement of Air Flow.* New York: Pergamon Press, 1977.
33. H. H. Bruun. *Hot-Wire Anemometry.* New York: Oxford University Press, 1995.
34. ISO Standard 3966. *Measurement of Fluid Flow in Closed Conduits—Velocity Area Method Using Pitot Static Tubes.* International Organisation for Standardisation, 1977.
35. F. Finaish, R. George, H. J. Sauer. Experimental study of temperature, pressure, humidity and/or density effects on vane anemometers. *ASHRAE Transactions,* 101 (2), 1995, pp. 240–251.
36. A. Melikov, ed. *Calibration and requirements for accuracy of Thermal Anemometers for Indoor Velocity Measurements.* Report ET-IE9701. Technical University of Denmark, Laboratory of Indoor Environment and Energy, 1997.
37. Z. Yue, T. G. Malmström. A simple method for low-speed hot-wire anemometer calibration. *Measurement Science and Technology,* 9, 1998, pp. 1506–1510.
38. ISO 5167-1:1991. *Measurement of Fluid Flow by Means of Pressure Differential Devices–Part 1: Orifice Plates, Nozzles and Venturi Tubes Inserted in Circular Cross-section Conduits Running Full.* International Organisation for Standardisation, 1991.
39. ISO/TR 9464:1998. *Guidelines for the Use of ISO 5167-1:1991.* International Organisation for Standardisation, 1998.
40. ASHRAE 41.2-1987. *Methods for Laboratory Air Flow Measurement.* American Society of Heating, Refrigerating, and Air-conditioning Engineers, Atlanta, 1987.
41. ASHRAE 41.7-1984. *Standard Method for Measurement of Flow of Gas.* American Society of Heating, Refrigerating, and Air-conditioning Engineers, Atlanta, 1984.
42. BS EN ISO 5167-1:1997. *Measurement of Fluid Flow by Means of Pressure Differential Devices: Orifice Plates, Nozzles and Venturi Tubes Inserted in Circular Cross-section Conduits Running Full.* British Standards Institution, 1997.
43. ISO/TR 5168:1998. *Measurement of Fluid Flow—Evaluation of Uncertainties.* International Organisation for Standardisation, 1998.
44. ASME MFC-2M-1983. *Measurement Uncertainty for Fluid Flow in Closed Conduits.* American Society of Mechanical Engineers, New York, 1983.
45. BS ISO TR 7066-1:1997. *Assessment of Uncertainty in Calibration and Use of Flow Measurement Devices: Linear Calibration Relationships.* British Standards Institution, 1997.
46. BS 7118: Part 2: 1989. *Measurement of fLuid Flow: Assessment of Uncertainty in the Calibration and Use of Flow Measurement Devices: Non-linear Calibration Relationships.* British Standards Institution, 1989.
47. I. O. Miner. The Dall flow tube. *Instrument Engineer,* April 1957, pp. 45–49.
48. ISO 3966:1977. *Measurement of Fluid Flow in Closed Conduits—Velocity Area Method Using Pitot Static Tubes.* International Organisation for Standardisation, 1977.
49. E. Kreyszig. *Advanced Engineering Mathematics.* New York: John Wiley & Sons, 1999.
50. A. L. Winternitz, C. F. Fischl. A simplified integration technique for pipe-flow measurement. *Water Power,* June 1957, pp. 225–234.
51. W. Richter. Log-linear-regel—ein einfaches verfahren zur volumenstrommessung in rohrleitungen. *Heiz. Lüft. Haustechnik,* 20, 1969, pp. 407–409.
52. W. Richter. Arithmetische methoden für netzmessungen des volumenstroms in leitungen mit rechteck-querscnitt. *Heiz. Lüft. Haustechnik,* 23, 1970, pp. 250–253.
53. ISO 7145:1982. *Determination of Flowrate of Fluids in Closed Conduits of Circular Cross Section—Method of Velocity Measurement at One Point of the Cross-section.* International Organisation for Standardisation, 1982.
54. ISO 4053-1:1977. *Measurement of Gas Flow in Conduits—Tracer Methods—Part 1: General.* International Organisation for Standardisation, 1977.
55. S. B. Riffat, M. Holmes. Measurement of airflow in HVAC systems using tracer-gas techniques. In *Proceedings of the 11th AIVC Conference,* vol. 1, 1990, pp. 195–214.

56. K. H. Presser, R. Becker. Mit lachgas dem luftstrom auf der spur. *Heizung, Lüftung/Klima, Haustechnik*, 39, January 1988, pp. 7–14.
57. A. Svensson. *Methods for Measurement of Air Flow Rates in Ventilation Systems*. National Swedish Institute for Building Research Bulletin M83:11, 1983.
58. F. Durst, A. Melling, J. H. Whitelaw. *Principles and Practice of Laser-Doppler Anemometry*. London: Academic Press, 1976.
59. L. E. Drain. *The Laser Doppler Technique*. London: John Wiley & Sons, 1988.
60. B. Ruck. *Lasermethoden in der Strömungsmesstechnik*. Stuttgart: AT-Fachverlag, 1990.

12.4 SCALE-MODEL EXPERIMENTS

12.4.1 Introduction

One of the methods used for the determination of airflow in large spaces is model experiments. This method is also useful in the study of local ventilation around a working area in the industrial environment.

Large ventilated air spaces—e.g., shopping arcades, industrial buildings, atria, and exhibition buildings—have for a decade been built in large numbers. It is not possible to use full-scale experiments in the design of air distribution systems due to the large dimensions of such buildings. It is also difficult to use simplified design methods like those based on throws of jets and penetration depths of nonisothermal jets because of the complicated geometry present in many situations. Several sources that produce air movements, such as diffusers, pressure difference around buildings, cold downdraft, and thermal plumes, also make the use of simplified methods difficult. Computational fluid dynamics (see Section 11.2) and scale-model experiments are two possible methods for the determination of mass transport, contaminant transport, and energy transport in large buildings.

The ventilation of a working area in an industrial environment is established by a combination of a general and a local ventilation system. The general ventilation ensures the air quality and comfort far away from the contaminants, whereas the local ventilation—often as exhaust hoods—ensures the contaminant transport close to the emission sources and protects the people working there. It is very important that the contaminant control system be efficient because it represents one of the first elements in a chain process that might bring the contaminant out into the room. A well-designed local ventilation system will reduce the energy consumption of the total system because it is an energy-saving method to remove the airborne pollution as close to the emission source as possible. A local ventilation system can be efficiently optimized by model or full-scale experiments.

Scale-model experiments have been used to study a variety of ventilation problems as air movement in a room, air movement around a building, energy flow in a building, contaminant distribution at an operator's workplace, and smoke movement in a building on fire. The theory is discussed at a general level in the references.[1–6]

12.4.2 Governing Equations and Dimensionless Numbers

Similarity principles for a physical process can either be derived from an assumption of the number of physical parameters involved (Buckingham's

π-theorem) or from the governing equations of the flow. The latter is to be preferred because this method will give a sufficient amount of dimensionless numbers. Furthermore, it will connect the numbers to the physical process via the equations and give important information in cases where it is necessary to make approximations.

The governing equations for mass flow, energy flow, and contaminant flow in a room will be the continuity equation, Navier-Stokes equations (one in each coordinate direction), the energy equation, and the mass transport equation, respectively.

The continuity equation for an incompressible flow is given by the following expression:

$$\frac{\partial \hat{u}}{\partial x} + \frac{\partial \hat{v}}{\partial y} + \frac{\partial \hat{w}}{\partial z} = 0, \tag{12.40}$$

where $\hat{u}$, $\hat{v}$, and $\hat{w}$ are the velocities in the three coordinate directions x, y, and z. The symbol ^ indicates that the variables are instantaneous values. For example, $\hat{u}$ is the sum of a mean value u and a turbulent fluctuation u'.

The Navier-Stokes equation in the direction of gravity (y-direction) is given by the expression

$$\rho_0\left(\frac{\partial \hat{v}}{\partial t} + \hat{u}\frac{\partial \hat{v}}{\partial x} + \hat{v}\frac{\partial \hat{v}}{\partial y} + \hat{w}\frac{\partial \hat{v}}{\partial z}\right) = -\rho_0\beta g(\hat{T}-T_0) - \frac{\partial \hat{p}}{\partial y} + \mu_0\left(\frac{\partial^2 \hat{v}}{\partial x^2} + \frac{\partial^2 \hat{v}}{\partial y^2} + \frac{\partial^2 \hat{v}}{\partial z^2}\right), \tag{12.41}$$

where $\hat{p}$, $\hat{T}$, and t are pressure, temperature, and time, respectively, and T_0 is a reference temperature (supply temperature). ρ_0, β, μ_0, and g are density, volume expansion coefficient, viscosity, and gravitational acceleration, respectively. The density and the viscosity are in principle functions of the instantaneous temperature $\hat{T}$, but except for the gravitational term the effect is ignored due to the level of temperature differences that occur in practice. $(\hat{T} - T_0)$expresses the influence of the temperature in the gravitational term in a formulation called the Boussinesq approximation.

The energy equation is given by the expression

$$\rho_0 c_p\left(\frac{\partial \hat{T}}{\partial t} + \hat{u}\frac{\partial \hat{T}}{\partial x} + \hat{v}\frac{\partial \hat{T}}{\partial y} + \hat{w}\frac{\partial \hat{T}}{\partial z}\right) = \lambda\left(\frac{\partial^2 \hat{T}}{\partial x^2} + \frac{\partial^2 \hat{T}}{\partial y^2} + \frac{\partial^2 \hat{T}}{\partial z^2}\right), \tag{12.42}$$

where c_p and λ are specific heat and thermal conductivity.

The mass transport equation for gas in air (binary mixture) has a similar structure:

$$\frac{\partial \hat{c}}{\partial t} + \hat{u}\frac{\partial \hat{c}}{\partial x} + \hat{v}\frac{\partial \hat{c}}{\partial y} + \hat{w}\frac{\partial \hat{c}}{\partial z} = D_{AB}\left(\frac{\partial^2 \hat{c}}{\partial x^2} + \frac{\partial^2 \hat{c}}{\partial y^2} + \frac{\partial^2 \hat{c}}{\partial z^2}\right), \tag{12.43}$$

where $\hat{c}$ is the instantaneous concentration and D_{AB} is the binary mass diffusion coefficient.

Equation (12.43) is called an Eulerian approach because the behavior of the species is described relative to a fixed coordinate system. The equation can also be considered to be a transport equation for particles when they are

small, without any influence from gravity. Flow of larger particles can be simulated by the following transport equation if the influence of gravity is introduced in the y convection term:[7,8]

$$\frac{\partial \hat{c}}{\partial t} + \hat{u}\frac{\partial \hat{c}}{\partial x} + (v_s + \hat{v})\frac{\partial \hat{c}}{\partial y} + \hat{w}\frac{\partial \hat{c}}{\partial z} = D_{AB}\left(\frac{\partial^2 \hat{c}}{\partial x^2} + \frac{\partial^2 \hat{c}}{\partial y^2} + \frac{\partial^2 \hat{c}}{\partial z^2}\right), \tag{12.44}$$

where v_s is the settling velocity in air. Settling velocity versus particle size is given by

$$v_s = 3 \times 10^{-5} d^2 \,(\mathrm{m\,s^{-1}}), \tag{12.45}$$

where d is the diameter in μm. The density of the particles is 1 g cm^{-3} and the particles are assumed to be of spherical shape in Eq. (12.45). Simulation of concentration distribution given by Eq. (12.44) is restricted to situations where initial particle velocity and particle inertia can be ignored.

It might be necessary to describe a particle contaminant source as a distribution of particle sizes with initial velocity different from the local air velocity. A typical example of this situation is the particle distribution and particle trajectory from a grinding wheel. The particle inertia is important in this situation, which makes it necessary to work with a model where the particles are treated individually through the solution of a particle motion equation. Reference 7 gives the simplified equations that govern the motion of a spherical particle (inertia equals friction and gravity forces) in a flow field. This approach, called the Lagrangian approach because the concentration changes are described relative to the moving fluid, will not be considered further.

Equations (12.40) to (12.45) describe the velocities u, v, w, the temperature distribution T, the concentration distribution c (mass of gas per unit mass of mixture, particles per volume, droplet number density, etc.) and pressure distribution p. These variables can also be used for the calculation of air volume flow, convective air movement, and contaminant transport.

It should be noted that radiant heat transfer, which can be an important part of the heat flow in a building, has not been considered.

The next step toward the similarity principles is to develop the governing equations in a nondimensional form. The equations are normalized by first defining the dimensionless, independent variables as

$$x^* = x/h_0, \quad y^* = y/h_0, \quad \text{and} \quad z^* = z/h_0, \tag{12.46}$$

where h_0 is a characteristic length of interest in the problem. A typical characteristic length in ventilation problems (general ventilation) is the height of the supply slot h_0 or the square root of the supply area $\sqrt{a_0}$. The height of a hot or a cold surface ℓ can also be used as characteristic length in situations where free convection is the most important problem as, for example, in the case of cold downdraft in an atrium at low outdoor temperatures.

The velocities

$$\hat{u}^* = \hat{u}/u_0, \quad \hat{v}^* = \hat{v}/u_0, \quad \text{and} \quad \hat{w}^* = \hat{w}/u_0 \tag{12.47}$$

are normalized by the supply velocity u_0 found from

$$u_0 = q_0/a_0, \tag{12.48}$$

where q_0 is the volume flow rate to the diffuser and a_0 is the supply area of the diffuser.

Temperature and concentration are normalized by the following expressions:

$$\hat{T}^* = \frac{\hat{T} - T_0}{T_R - T_0} \quad \text{and} \quad \hat{c}^* = \frac{\hat{c} - c_0}{c_R - c_0} \tag{12.49}$$

where T_0, T_R, c_0, and c_R are supply temperature, return temperature, supply concentration (if any), and return concentration, respectively.

Pressure $\hat{p}$ and the independent variable t time are normalized by the following expressions:

$$\hat{p}^* = \hat{p}/u_0^2\rho_0 \quad \text{and} \quad t^* = tu_0/h_0. \tag{12.50}$$

Equations (12.46), (12.47), (12.49), and (12.50) are substituted into Eqs. (12.40) to (12.44), and the following nondimensionalized governing equations are obtained:

$$\frac{\partial \hat{u}^*}{\partial x^*} + \frac{\partial \hat{v}^*}{\partial y^*} + \frac{\partial \hat{w}^*}{\partial z^*} = 0 \tag{12.51}$$

$$\frac{\partial \hat{v}^*}{\partial t^*} + \hat{u}^*\frac{\partial \hat{v}^*}{\partial x^*} + \hat{v}^*\frac{\partial \hat{v}^*}{\partial y^*} + \hat{w}^*\frac{\partial \hat{v}^*}{\partial z^*} = \frac{\beta g h_0 (T_R - T_0)}{u_0^2}\hat{T}^* - \frac{\partial \hat{p}^*}{\partial y^*} + \frac{\mu_0}{\rho_0 h_0 u_0}\left(\frac{\partial^2 \hat{v}^*}{\partial x^{*2}} + \frac{\partial^2 \hat{v}^*}{\partial y^{*2}} + \frac{\partial^2 \hat{v}^*}{\partial z^{*2}}\right) \tag{12.52}$$

$$\frac{\partial \hat{T}^*}{\partial t^*} + \hat{u}^*\frac{\partial \hat{T}^*}{\partial x^*} + \hat{v}^*\frac{\partial \hat{T}^*}{\partial y^*} + \hat{w}^*\frac{\partial \hat{T}^*}{\partial z^*} = \frac{\lambda}{c_p \rho_0 h_0 u_0}\left(\frac{\partial^2 \hat{T}^*}{\partial x^{*2}} + \frac{\partial^2 \hat{T}^*}{\partial y^{*2}} + \frac{\partial^2 \hat{T}^*}{\partial z^{*2}}\right) \tag{12.53}$$

$$\frac{\partial \hat{c}^*}{\partial t^*} + \hat{u}^*\frac{\partial \hat{c}^*}{\partial x^*} + \hat{v}^*\frac{\partial \hat{c}^*}{\partial y^*} + \hat{w}^*\frac{\partial \hat{c}^*}{\partial z^*} = \frac{D_{AB}}{h_0 u_0}\left(\frac{\partial^2 \hat{c}^*}{\partial x^{*2}} + \frac{\partial^2 \hat{c}^*}{\partial y^{*2}} + \frac{\partial^2 \hat{c}^*}{\partial z^{*2}}\right) \tag{12.54}$$

$$\frac{\partial \hat{c}^*}{\partial t^*} + \hat{u}^*\frac{\partial \hat{c}^*}{\partial x^*} + \left(\frac{v_s}{u_0} + \hat{v}^*\right)\frac{\partial \hat{c}^*}{\partial y^*} + \hat{w}^*\frac{\partial \hat{c}^*}{\partial z^*} = \frac{D_{AB}}{h_0 u_0}\left(\frac{\partial^2 \hat{c}^*}{\partial x^{*2}} + \frac{\partial^2 \hat{c}^*}{\partial y^{*2}} + \frac{\partial^2 \hat{c}^*}{\partial z^{*2}}\right) \tag{12.55}$$

It is observed that the following dimensionless numbers appear in the equations:

$$\text{Ar} = \frac{\beta g h_0 (T_R - T_0)}{u_0^2}, \tag{12.56}$$

$$\text{Re} = \frac{\rho_0 h_0 u_0}{\mu_0}, \tag{12.57}$$

$$\text{Pr} = \frac{\mu_0 c_p}{\lambda}, \tag{12.58}$$

$$\text{Sc} = \frac{\mu_0}{\rho_0 D_{AB}}, \tag{12.59}$$

$$v_s^* = \frac{v_s}{u_0}. \tag{12.60}$$

Ar, Re, Pr, Sc, and v_s^* are called the Archimedes number, Reynolds number, Prandtl number, Schmidt number, and the settling velocity ratio, respectively.

The Archimedes number may be considered as a ratio of thermal buoyancy force to inertial force, while the Reynolds number may be looked upon

as a ratio of inertial force to viscous force. The Prandtl number is the ratio of momentum diffusivity to thermal diffusivity, while the Schmidt number is the ratio of momentum diffusivity to mass diffusivity.

Ar and 1/Re appear in the Navier-Stokes equation (Eq. (12.52)) and 1/(Re Pr) in the energy equation (Eq. (12.53)). 1/(Re Sc) appears in the transport equations for contaminants (Eqs. (12.54) and (12.55)), and the settling velocity ratio v_s^* appears in the contaminant transport equation for large particles (Eq. (12.55)).

The dimensionless numbers are important elements in the performance of model experiments, and they are determined by the normalizing procedure of the independent variables. If, for example, free convection is considered in a room without ventilation, it is not possible to normalize the velocities by a supply velocity u_0. The normalized velocity can be defined by $\hat{u}^* = \hat{u}\ell\rho_0/\mu_0$ where ℓ, is the height of a cold or a hot surface. The Grashof number, Gr, will then appear in the buoyancy term in the Navier-Stokes equation (ΔT_s is the temperature difference between the hot and the cold surface):

$$\mathrm{Gr} = \frac{\beta g \rho_0^2 \ell^3 \Delta T_s}{\mu_0^2}. \tag{12.61}$$

The Grashof number can be expressed as

$$\mathrm{Gr} = \mathrm{Ar}\,\mathrm{Re}^2. \tag{12.62}$$

12.4.3 Similarity Principles and Conditions for Model Experiments

The general conditions for scale-model experiments with flow in a room are

1. Identical dimensionless sets of boundary conditions, including geometry, in the room and in the model;
2. Identical dimensionless numbers, Eqs. (12.56) to (12.60), in the governing equations for the flow in the room and in the model;
3. The constants ρ_0, β, μ_0, . . . in the governing equations (Eqs. (12.40) to (12.44)) should have only a small variation within the applied temperature and velocity levels.

The requirement of identical dimensionless boundary conditions is met when the model is geometrically similar to full scale in all details that are important for the volume flow, the energy flow and the contaminant flow; see Fig. 12.24.

The dimensionless supply profile from the diffuser in an experiment with general ventilation given by

$$\hat{u}^*, \hat{v}^*, \hat{w}^* = f(x, y, z, t) \tag{12.63}$$

must thus be identical for both room and model. This can be obtained by using a diffuser in the model that is geometrically similar to the expected diffuser in the room, but it is an expensive solution because it is difficult to reproduce all the details in the diffuser when the model, for example, is one-tenth of full scale. The problem can be simplified if it is possible to replace the diffuser by a simple opening able to generate a similar flow in the model. The problem is somewhat similar to the use of the inlet-box method or the prescribed velocity method in computational fluid dynamics; see Section 11.2.

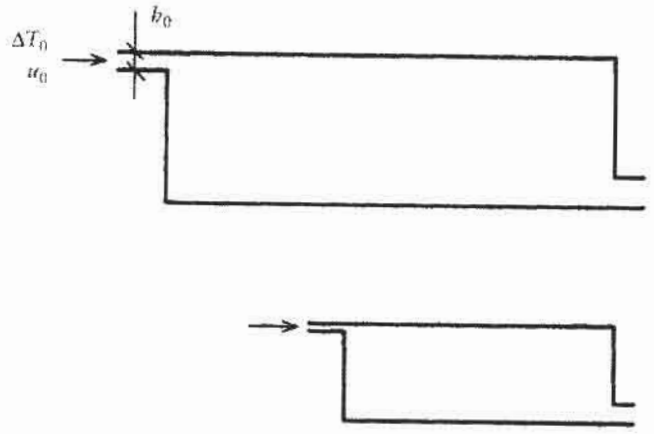

FIGURE 12.24 Full-scale room with slot inlet and a similar scale model.

Figure 12.25 shows an example of the use of a simplified supply opening in the model. The diffuser in the room is mounted on the end wall, and it supplies the air through a row of small openings at an angle of 45° toward the ceiling. This diffuser is simulated in a model experiment by a nozzle that supplies a jet in the same direction toward the ceiling; see Fig. 12.25. Figure 12.26 shows the velocity decay of centerline velocity u_x versus distance x in the two cases. The agreement between the velocity decay from the diffuser and the decay in the model seems to be fair.

It is difficult to obtain the correct temperature boundary conditions in a model. Radiation between surfaces in a room and conduction through the surfaces are important for the level of the surface temperature $T_s(x, y, z)$. It is difficult to establish the similarity principles based on radiation and conduction. A practical method is to estimate the influence of radiation and conduction and include this level in the boundary values of the model. In this way it

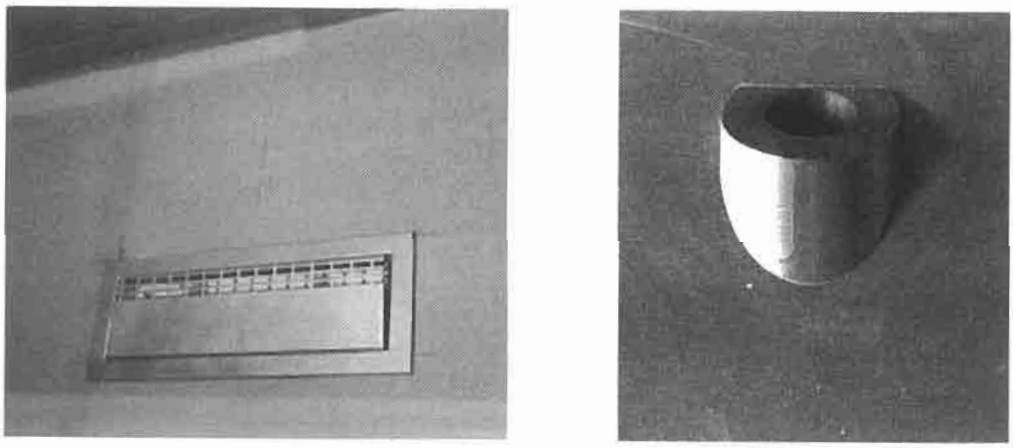

FIGURE 12.25 Wall-mounted diffuser in a full-scale test room and a nozzle in a model room.

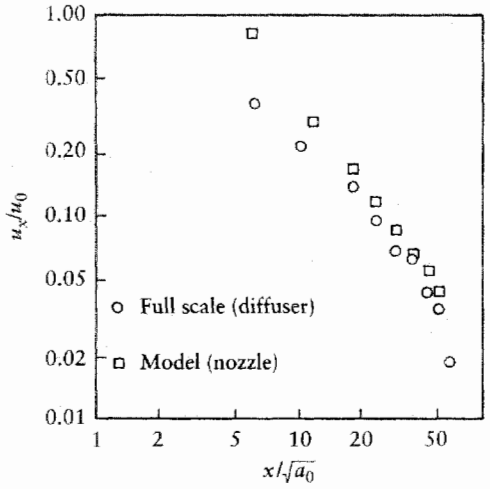

FIGURE 12.26 Velocity decay in a wall jet along the ceiling in a room and in a model.

is possible to obtain an identical dimensionless temperature distribution $T_s^*(x, y, z)$ in the full scale and in the model.

The conditions for model experiments can be explained in the following way. The governing equations are made nondimensional in the full scale and in the reduced scale used in the model experiments. For example, the velocity in the room is divided by the diffuser velocity in the room, and the velocity in the model is divided by the supply velocity in the model in order to normalize all velocities. The two sets of equations are identical and they describe the same solution provided that requirements 1, 2, and 3 mentioned at the beginning of this section have been met.

It is difficult to carry out a model experiment on a reduced scale if all the dimensionless numbers must be kept constant. If, for example, the scale is reduced by a factor of 10, then the velocity also has to be increased by a factor of 10 due to the Reynolds number, which will give an increase in the temperature difference by a factor of 1000 in order to keep the Archimedes number. The Prandtl number is, on the other hand, unchanged when air is used as the fluid in the model experiments. The problem with the temperature level can be slightly reduced when water is used as fluid in the model experiments and, as shown in the next section, the problem can also be reduced when the flow is a fully developed turbulent flow.

It is only possible to obtain similar solutions in situations where the governing equations (Eqs. (12.40) to (12.44)) are identical in the full scale and in the model. This requirement will be met in situations where the same dimensionless numbers are used in the full scale and in the model and when the constants $\rho_0, \beta, \mu_0, \ldots$ have only a small variation within the applied temperature and velocity level. A practical problem when water is used as fluid in the model is the variation of β, which is very different in air and in water; see Fig. 12.27. Therefore, it is necessary to restrict the temperature differences used in model experiments based on water.

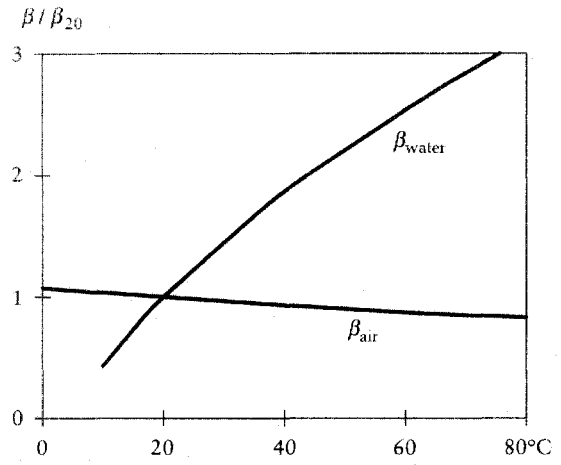

FIGURE 12.27 Relative change in the volume expansion coefficient for air and water.

12.4.4 Model Experiments in the Case of Fully Developed Turbulent Flow

The problems that arise when experiments are carried out in a greatly reduced scale can be overcome if the Reynolds number is high and the flow pattern is governed mainly by fully developed turbulence. It is possible to ignore the Reynolds number, the Schmidt number, and the Prandtl number because the structure of the turbulence and the flow pattern at a sufficiently high level of velocity will be similar at different supply velocities and therefore independent of the Reynolds number. The transport of thermal energy and mass by turbulent eddies will likewise dominate the molecular diffusion and will therefore also be independent of the Prandtl number and the Schmidt number.

Figure 12.28 shows as an example how the dimensionless maximum velocity in a room u_{rm}/u_0 is constant at different supply velocities, u_0, for Reynolds numbers larger than 45 000 in the case of isothermal flow. This value is called the critical Reynolds number, Re_c, or the threshold Reynolds number for the maximum velocity in the room. A model experiment in the room (Fig. 12.28) with the purpose of determining the maximum velocity in the occupied zone can therefore be carried out at any Reynolds number larger than Re_c if the full-scale flow has a Reynolds number larger than Re_c. It is also obvious that the Reynolds number must have the same value in the full scale and in the model for Reynolds numbers smaller than Re_c. It is not given that all quantities in the flow are Reynolds number–independent, although the dimensionless maximum velocity in the occupied zone has reached that level, but increasing velocity will of course make all quantities Reynolds number–independent at a given velocity level; see, e.g., ref. 9.

The similarity of velocity and of turbulence intensity is documented in Fig. 12.29. The figure shows a vertical dimensionless velocity profile and a turbulence intensity profile measured by isothermal model experiments at two different Reynolds numbers.[10] It is obvious that the shown dimensionless profiles of both the velocity distribution and the turbulence intensity distribution are similar, which implies that the Reynolds number of 4700 is above the threshold Reynolds number for those two parameters at the given location.

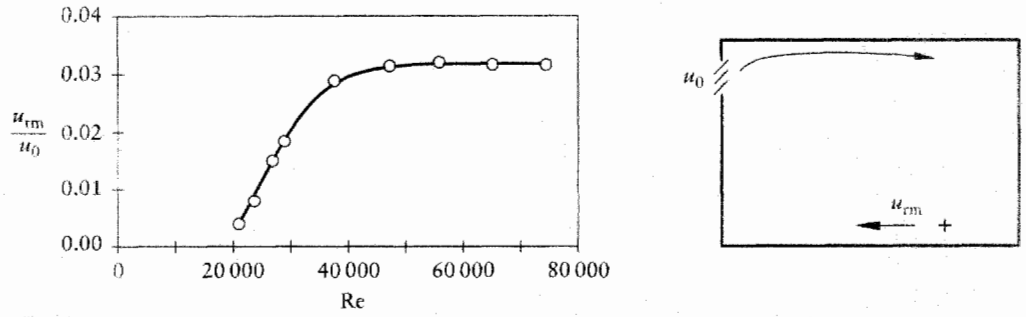

FIGURE 12.28 Normalized velocity versus Reynolds number in a ventilated room.[4]

It is necessary to study the Reynolds number independence in the full scale and in the model as part of a complete model experiment. The threshold or the critical Reynolds number, Re_c, for the problem considered should be found by the experiments, and measurements should be made at either the same Reynolds number as in the full scale or at a Reynolds number equal to or larger than Re_c if the Reynolds number in the full scale is larger than Re_c for the problem considered.

Fully developed nonisothermal flow may also be similar at different Reynolds numbers, Prandtl numbers, and Schmidt numbers. The Archimedes number will, on the other hand, always be an important parameter. Figure 12.30 shows a number of model experiments performed in three geometrically identical models with the heights 0.53 m, 1.60 m, and 4.75 m.[11] Sixteen experiments carried out in the rooms at different Archimedes numbers and Reynolds numbers show that the general flow pattern (jet trajectory of a cold jet from a circular opening in the wall) is a function of the Archimedes number but independent of the Reynolds number. The characteristic length and velocity in Fig. 12.30 are defined as $\ell = 4WH/(2W + 2H)$ and $u = q_0/WH$, where W is the width of the room and H is the height of the room.

The neglect of a low turbulence effect and a laminar flow is not justified in regions close to solid surfaces where the turbulent velocity fluctuations

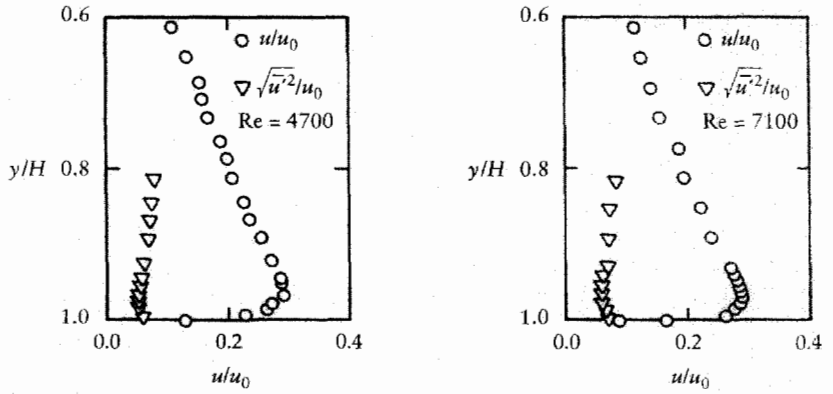

FIGURE 12.29 Velocity distribution and turbulence intensity in the occupied zone of a room at two different Reynolds numbers. H is the height of the room.

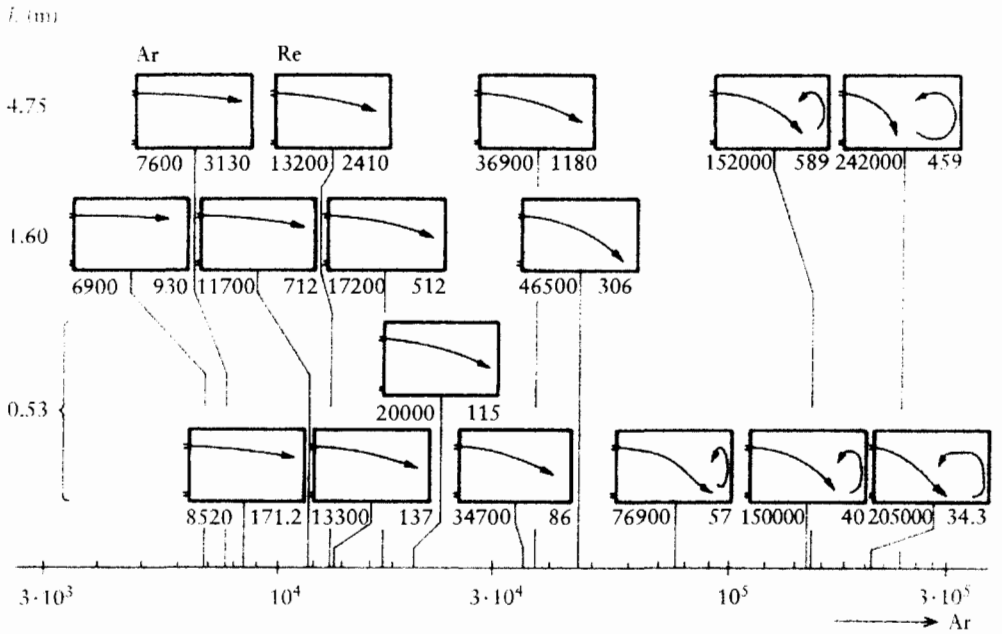

FIGURE 12.30 Model experiments with nonisothermal flow in three different models with ceiling heating.

must tend to zero. In experiments where the correct level of heat transfer and mass transfer through the boundary layer is important, it is necessary to take all dimensionless numbers involved into full consideration. It is possible to draw a parallel to the situation in computational fluid dynamics where a k-ϵ turbulence model describes the main flow clear of surfaces as a fully developed turbulent flow used together with wall functions, which take the low turbulent effect and laminar flow close to surfaces into consideration.

Model experiments where free convection is the important part of the flow are expressed by the Grashof number instead of the Archimedes number, as in Eq. (12.61). The general conditions for scale-model experiments are the use of identical Grashof number, Gr, Prandtl number, Pr, and Schmidt number, Sc, in the governing equations for the room and in the model.

A practical approach is to simulate cold or hot surfaces with replacement jets which match the airflow in the model to the flow in the full-size room. This method is described by Nevrala and Probert[12].

12.4.5 Model Experiments in Connection with Local Ventilation in the Industrial Environment

Experiments on the scale of 1 to 1 are often used to study the local ventilation around an operator's workplace. Tracer gas is used to simulate the contaminant transport, and a high concentration level of the model tracer gas makes it possible to work with a convenient level of concentration for the measurements. Figure 12.31 shows an enclosure with an emission source S and a laboratory setup with a model source S_l. The dimensionless concentration c/c_R is

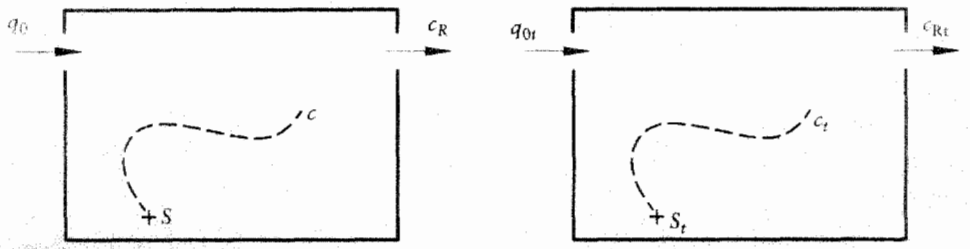

FIGURE 12.31 Enclosure with a containment source S and a laboratory model with a model source S_t.

identical with c/c_{Rt} in the laboratory model if the Archimedes numbers are identical in the full scale and in the model, and if the Reynolds numbers in both cases are identical or above the critical value for the concentration distribution.

The concentration at a given position close to an emission source can be calculated from

$$c = c_t \frac{c_R}{c_{Rt}}, \tag{12.64}$$

where c_t, c_{Rt} and c_R are tracer gas concentration at the corresponding position in the laboratory model, tracer gas concentration in the reference point in the laboratory model (return opening), and contaminant concentration in the reference point, respectively.

The emission source can be found from

$$S = S_t \frac{cq_0}{c_t q_{0t}}, \tag{12.65}$$

where q_0 is the volume flow around the local ventilation and q_{0t} is the volume flow around the model.

12.4.6 Laboratory Experiments with General and Local Ventilation

This section shows some examples of the use of model experiments. The examples cover the range from natural ventilation of buildings, comfort ventilation of an exhibition hall, to local ventilation in industrial areas.

12.4.6.1 The Danish Pavilion in Seville

The Danish Pavilion at the EXPO '92 World Exhibition is shown in Fig. 12.32. It has two main elements: a steel-framed structure, facing west, with a floor area of 45.0 m × 2.5 m and a height of 24 m, and a fiberglass construction, facing east, which leans against the steel structure. The large room formed between the fiberglass surface and the steel building is enclosed by glass walls to the north and to the south. This room is the exhibition hall and it was visited by more than 800000 people during EXPO '92.

The occupied zone design load of the exhibition hall is 48 kW, corresponding to 300 persons in the pavilion. The equipment for slides and video will generate another 130 kW, which is expected to move upward in convective flows, causing a high temperature in the upper part of the pavilion.

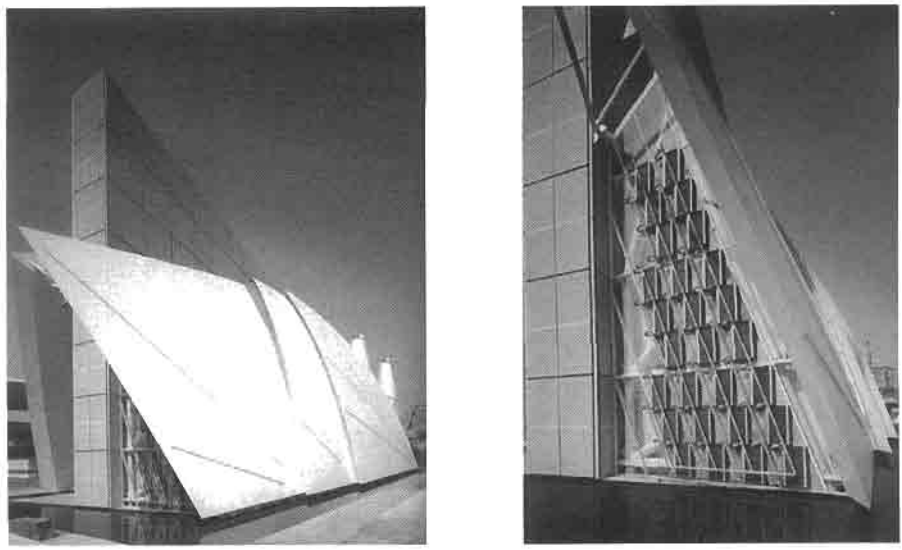

FIGURE 12.32 The Danish Pavilion at the World Exposition EXPO '92 in Seville and the cooling elements in the south gable.

The ventilation system is based on an extract fan in the north top of the exhibition hall (smoke ventilation) and on exposed cooling elements in the south gable; see Fig. 12.32. Air is drawn through the cooling elements, where it cools and falls to the floor. It is difficult to give an estimate of the downdraft from the 12 m high diffuser in the gable, and therefore it was decided to carry out scale-model experiments and CFD predictions of the flow.

The model experiments were carried out in a model on the scale of 1 to 10. Experience with measurements on flow from wall-mounted diffusers for displacement ventilation indicates that it is possible to ignore the level of the Reynolds number at the given dimensions, which will enable reasonable temperature differences in the model experiments.

Figure 12.33 shows the velocity distribution down through the full length of the exhibition hall. It is quite obvious that the flow is a stratified flow with the highest velocity in the occupied zone. Smoke measurements show that the cold air from the cooling device accelerates down into the occupied zone, due to gravity, and moves horizontally as a stratified flow along the floor in the restaurant and exhibition section.

Measurements show that the velocity has a fairly constant level in the occupied zone even far downstream from the wall with the cooling device. The flow is plane, and general experience indicates that the velocity in a plane stratified flow is constant and independent of the distance from the inlet device. Prediction of the flow by computational fluid dynamics shows a similar velocity level in the hall.[13] The full-scale measurements shown in Fig. 12.33 indicate a very low velocity in most of the hall due to the practical difficulties in obtaining a correct load during the full-scale experiment.

12.4.6.2 School Building

Experiments with natural ventilation of large constructions such as shopping arcades and atria necessitate a set of boundary conditions outside the

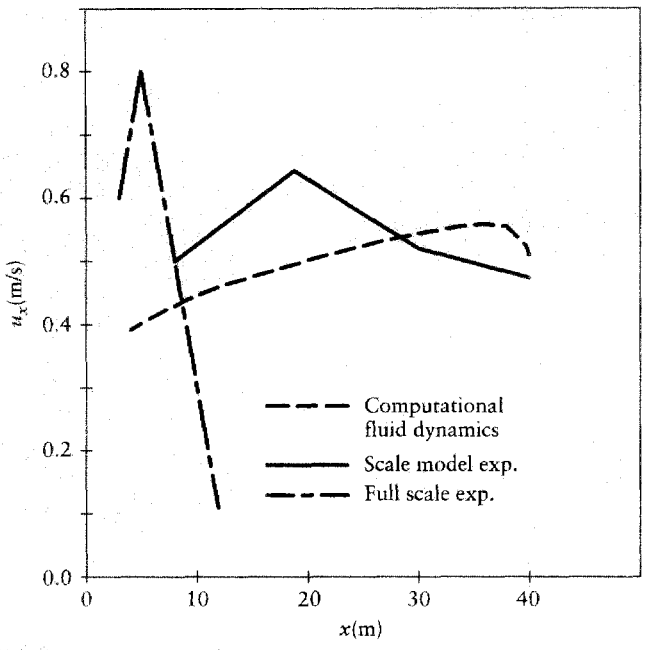

FIGURE 12.33 Velocity distribution in the restaurant and exhibition hall of the Danish Pavilion.

openings in the building because the pressure distribution (and flow) around a building are an important part of the problem.

These experiments have to be carried out in an environmental wind tunnel.[3,14] A roughness on the surface in such a wind tunnel generates a typically vertical profile, and the whole building and the neighboring buildings are exposed to the flow. Figure 12.34 illustrates an experiment. The flow around a model of a school building in Tanzania is shown by the streamlines of lightweight particles in the air. It is possible to study the flow in the double ceiling, the flow through the window openings, and the recirculating flow in the classroom.

12.4.6.3 Filling Machine

The contaminant source considered in this section is a filling machine for paint. Figure 12.35*a* shows the machine with a filling tube (to the left in the figure) and equipment for closing of the cans (to the right in the figure). The machine was originally delivered without exhaust equipment, but an exhaust opening has been mounted behind the filling tube. Measurements at the operator's workplace show an exhaust flow rate of 180 $m^3\ h^{-1}$ and an acceptable air quality in the operator's breathing zone.

Figure 12.35*b* shows a model of the machine on the scale of 1 to 1. Many details and surfaces are made in the correct size and location to achieve a good reproduction of the actual capturing zone. The capture efficiency α is used for the evaluation of the system and it is defined as the ratio between the flow rate of the contaminant S_E directly captured from the process and the total flow rate of the contaminant S released from the process:

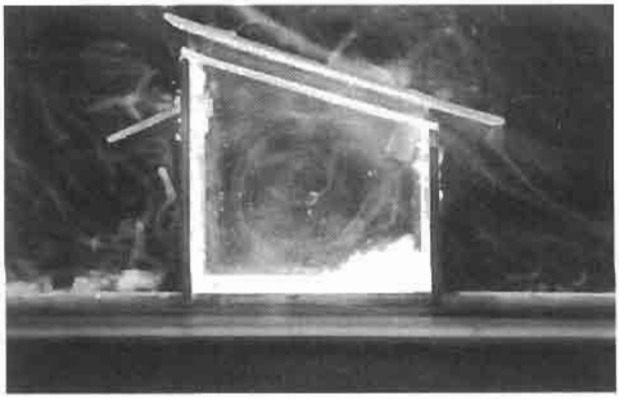

FIGURE 12.34 Scale-model experiment with natural ventilation of a school building.

$$\alpha = \frac{S_E}{S}. \tag{12.66}$$

Figure 12.36 shows the capture efficiency as a function of the exhaust flow rate q_E both with the emission source at the filling position and with the emission source at the closing position. The last position shows the lowest values in capture efficiency due to the distance to the exhaust opening. The shaded area in the figure corresponds to the position between the filling and the closing of the cans.

The exhaust air represents a high energy consumption and therefore it is important to have a design with a high capture efficiency at low flow rates. Figure 12.37 shows a new design of the exhaust opening where parts of the machine are integrated into the opening and in this way act as flanges for the

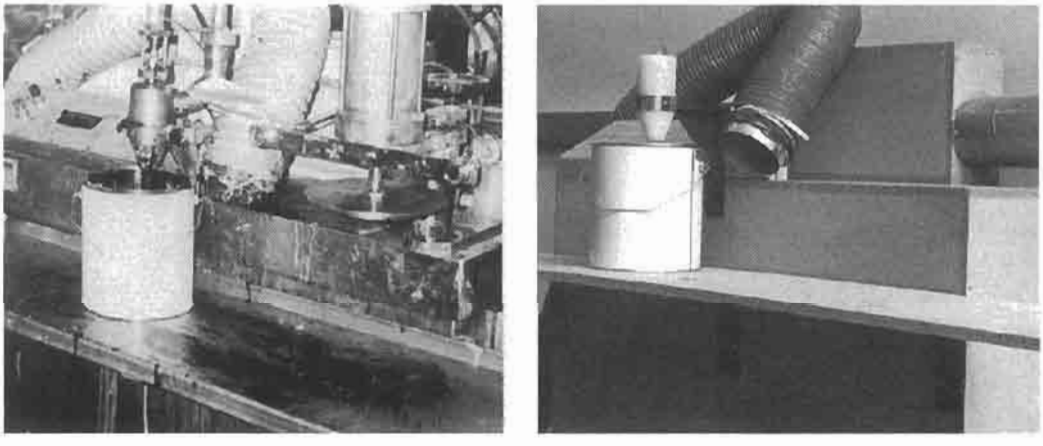

(*a*) (*b*)

FIGURE 12.35 (*a*) Filling machine from the paint industry and (*b*) full-scale model of the machine.

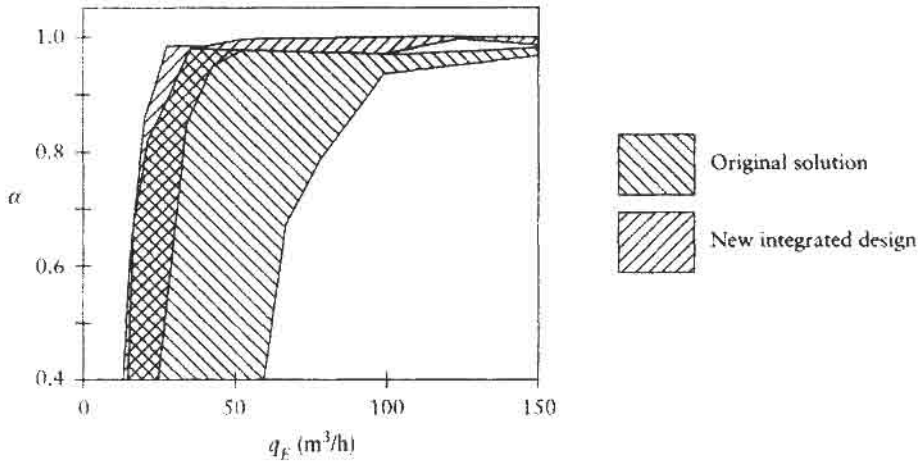

FIGURE 12.36 Capture efficiency versus flow rate for the original solution and for the new integrated design.

flow. It is shown in Fig. 12.36 that this solution makes it possible to decrease the flow substantially (by 65%) and still keep the high capture efficiency.[15]

Generally it must be concluded that the exhaust openings should be an integrated part of the machine or the equipment to obtain an optimal solution.

12.4.6.4 Film-Developing Machine

Figure 12.38 shows a film-developing machine and the corresponding model for laboratory experiments on the scale of 1 to 1. The machine consists of two sections, a developing section in the lower part and an air-drying

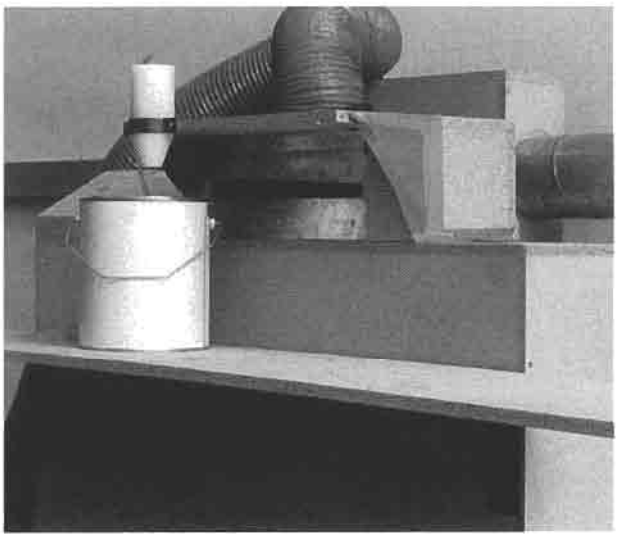

FIGURE 12.37 New design of an exhaust opening integrated into the can-filling machine.

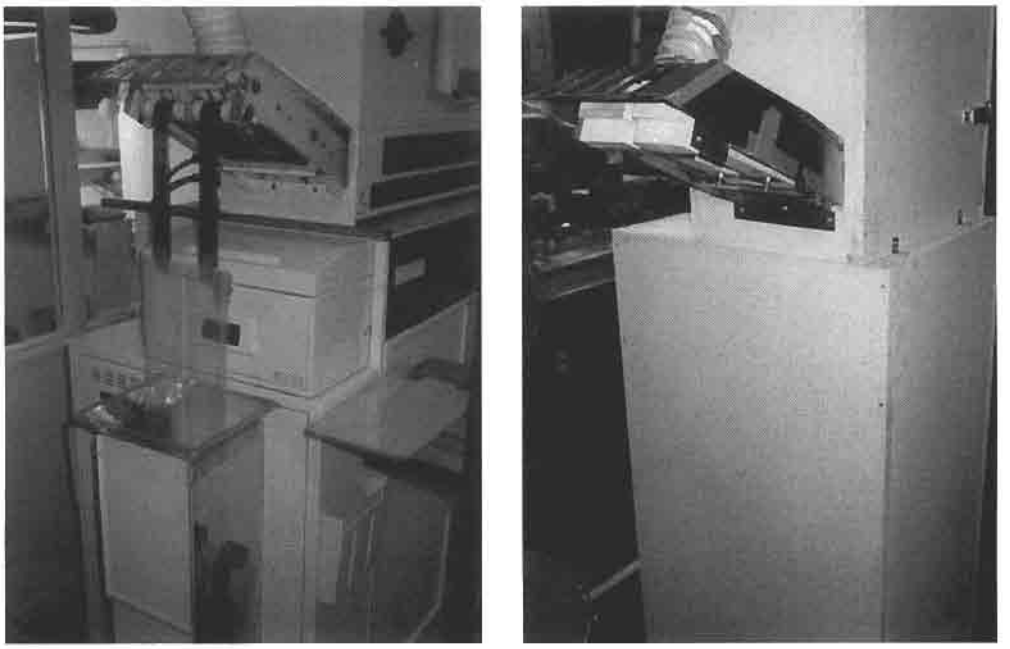

FIGURE 12.38 Film-developing machine and a laboratory model.

section in the upper part. The newly developed films leave the air-drying section through the opening shown in the upper part of the figure. Air is supplied to the drying section from ventilators and is blown out into the surroundings through the opening for the films and, consequently, causes low air quality in the room. In addition, the operator of the developing machine will be highly exposed when standing in front of the machine and changing the films.

The initial solution to this problem was to install an exhaust channel on the opening for the films, as in Fig. 12.38. Laboratory experiments show that the principle is inexpedient and it is possible only to obtain a capture efficiency of 70% at a flow rate of 100 $m^3\ h^{-1}$.

The experiments show that it is impossible to make a simple design of the opening to improve the air quality in the room. A proper solution should have been chosen in the design phase of the machine. It would, for example, be obvious to reverse the direction of the airflow and extract the air from the room through the machine.

12.4.6.5 Vortex Exhaust

The vortex exhaust has a geometry that generates a rotating flow behind the opening. It is suitable for installation in a narrow space and it is traditionally used with hand-held equipment producing jets of air and particles. This type of exhaust opening is also called a tornado exhaust or a cyclone exhaust.

Figure 12.39 shows an exhaust opening used for capture of concrete dust from a hand-held grinding machine. Figures 12.39*b* and 12.39*c* show two labo-

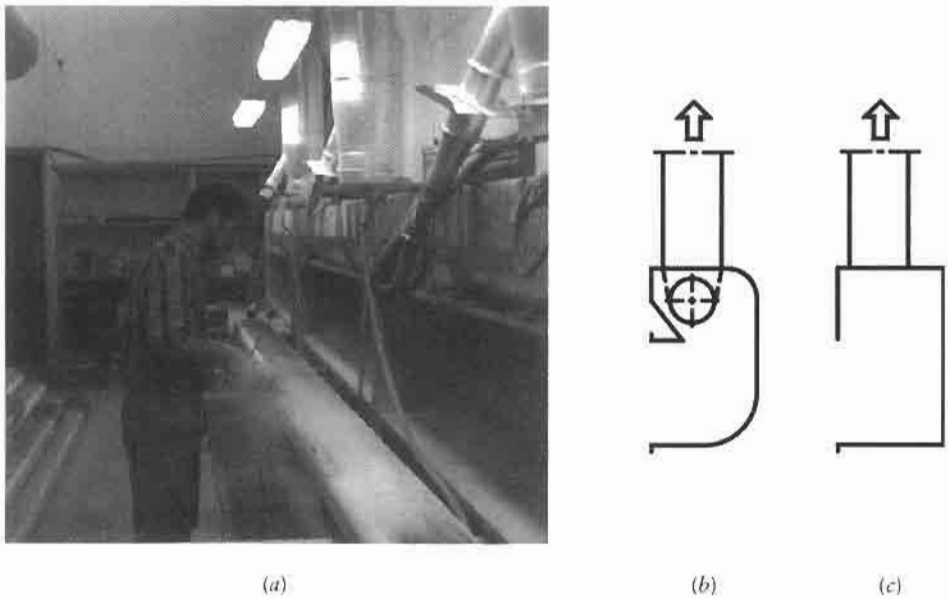

(*a*) (*b*) (*c*)

FIGURE 12.39 (*a*) Vortex exhaust at a concrete element factory, (*b*) laboratory model of the vortex exhaust, and (*c*) simplified model of the exhaust.

ratory models made on the scale of 1 to 2. The first model (Fig. 12.39*b*) is identical with the real opening, while the other model has a simplified geometry.

A reduced scale of the model requires an increased velocity level in the experiments to obtain the correct Reynolds number if $\mathrm{Re} < \mathrm{Re}_c$ for the problem considered, but the experiment can be carried out at any velocity if $\mathrm{Re} > \mathrm{Re}_c$. The influence of the turbulence level is shown in Fig. 12.40. A velocity u is measured at a location in front of the opening and divided by the exhaust flow rate q_E in order to obtain a normalized velocity. The figure shows that the normalized velocity is constant for Reynolds numbers larger than 10 000, which means that the flow around the measuring point has a fully developed turbulent structure at that velocity level. The flow may be described as a potential flow with a normalized velocity independent of the exhaust flow rate at large distances from the exhaust opening—and far away from surfaces.

Comparisons between measurements on the two geometries, Figs. 12.39*b* and 12.39*c* show that a rotating flow will be generated in both cases. The T-shaped exhaust opening in the middle of the rotating flow in the original design is not the only element that generates the vortex; the asymmetry is also important as a source of vortex flow. The T-connection will smooth the capture velocity in the horizontal direction compared with the velocity distribution obtained in the simplified design.

It is important that the vortex exhaust has a high capture efficiency in connection with blasts from high-pressure air-cleaning equipment. The geometry is designed to capture jets from different directions and experiments with two versions (Figs. 12.39*b* and 12.39*c*) indicate that both versions have high capture efficiency of concentrated jets.

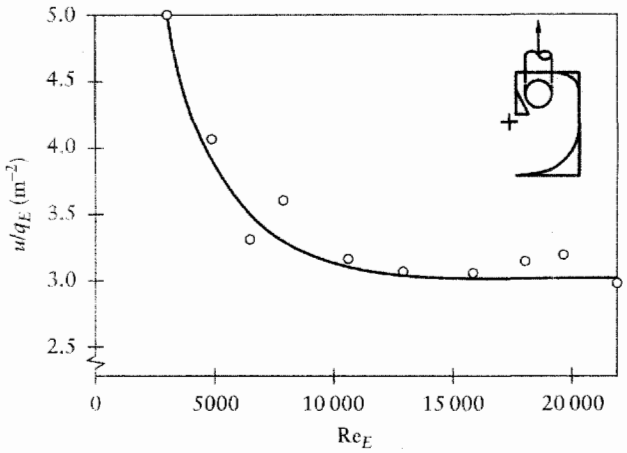

FIGURE 12.40 Normalized velocity versus Reynolds number for a vortex exhaust. The location of the measuring point is indicated in the figure.

The T-connection in the original vortex exhaust will increase the pressure loss and increase the consumption of energy. Measurements of the pressure difference in the two versions show a sevenfold higher pressure difference in the original version (Fig. 12.39*b*) compared with the pressure difference in the simplified version (Fig. 12.39*c*). This fact is very important in connection with selection of a given solution.

12.4.7 Using Similarity Principles in Planning Experiments

It is useful to take similarity principles and dimensionless numbers into consideration when planning experiments. Experiments may involve different levels of velocities and temperature differences. It is important to select values that give a large variation of Archimedes number (12.56) to obtain a high possibility of large physical effects in the measurements.

The assumption of a self-similar flow (Reynolds number–independent flow) simplifies full-scale experiments and is also a useful tool in the formulation of simple measuring procedures. This section will show two examples of self-similar flow where the Archimedes number is the only important parameter.

Figure 12.41 shows the results of three experiments with a similar Archimedes number and different Reynolds numbers. The figure shows vertical temperature profiles in a room ventilated by displacement ventilation. The dimensionless profiles are similar within the flow rates shown in the figure, although the profile may involve areas with a low turbulence level in the middle of the room. A test of this type could indicate that further experiments can be performed independently of the Reynolds numbers.

Figure 12.42 shows another example of the use of similarity principles in experiments. The temperature effectiveness ϵ_T is measured in a room ventilated by displacement ventilation. The measurements are made at different flow rates q_0 to the room, at different loads (from 100 W to 500 W) and by

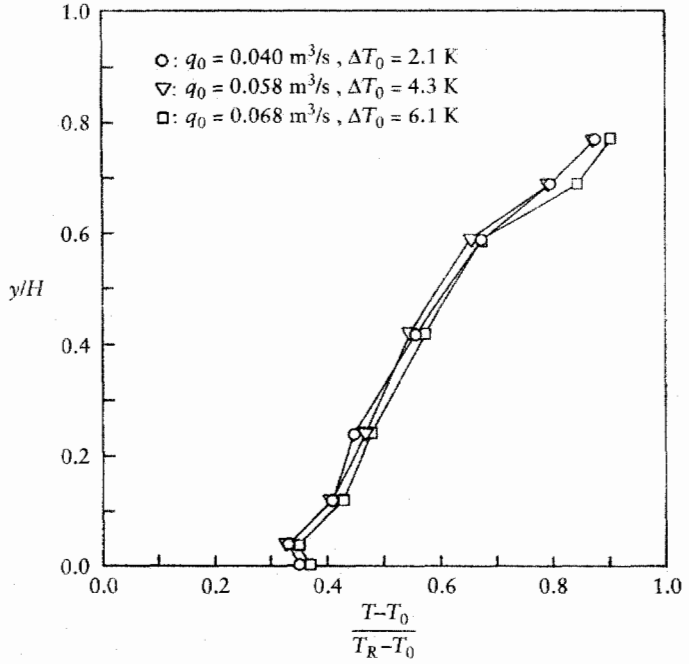

FIGURE 12.41 Vertical temperature profile in the room for three different experiments with identical Archimedes number.[16]

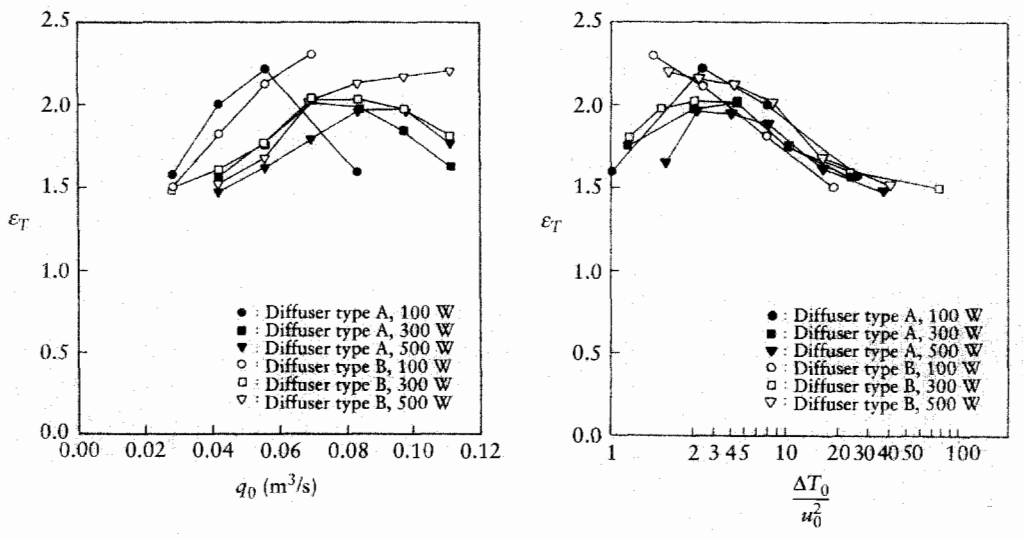

FIGURE 12.42 Temperature effectiveness versus airflow rate q_0 and Archimedes number $\Delta T_0/u_0^2$.[16]

two different wall-mounted diffusers. Figure 12.42*a* shows ϵ_T values between 1.5 and 2.3; however, it is difficult to reach other conclusions from this figure such as, for example, the importance of the two different diffusers.

Figure 12.42*b* shows the measurements given as a function of the Archimedes number $\mathrm{Ar} \sim \Delta T_0/u_0^2$. This figure is more informative than Fig.12.42*a*. The figure shows that the temperature effectiveness ϵ_T is a function of the Archimedes number. An identical level of ϵ_T for the two diffusers A and B at the same Archimedes number implies that the temperature effectiveness is rather independent of the diffuser design and the local induction close to the diffuser. The effectiveness is probably more dependent on other parameters that are constant in the experiments, such as heat source and heat source location.

References

1. S. Mierzwinski. Scale model experiments. In *Ventilation of Large Spaces in Buildings* (eds. P. Heiselberg, S. Murakami, C.-A. Roulet). Aalborg University, Aalborg, Denmark, 1998.
2. H. B. Awbi. *Ventilation of Buildings*. Chapman & Hall, London, 1991.
3. D. Etheridge, M. Sandberg. *Building Ventilation: Theory and Measurement*. John Wiley & Sons, Chichester, 1996.
4. P. V. Nielsen. Model experiments for the determination of airflow in large spaces. In *Indoor Air '93: Proceedings of the 6th International Conference on Indoor Air Quality and Climate*. Helsinki, Finland, 1993.
5. P. V. Nielsen. Design of local ventilation by full-scale and scale modelling techniques. In *Ventilation '97: Proceedings of the 5th International Symposium on Ventilation for Contaminant Control*, vol. 1, 47–57. Ottawa, Canada, 1997.
6. S. Kato, S. Murakami, C. N. Kong, H. Nakagawa. Model experiment on indoor climate and space air distribution in large-scale room. In *Proceedings of the International Symposium on Scale Modeling*. Japan Society of Mechanical Engineers, 1988.
7. P. V. Nielsen. Prospects for computational fluid dynamics in room air contaminant control. In *Ventilation '94: Proceedings of the 4th International Symposium on Ventilation for Contaminant Control*. Stockholm, Sweden, 1994.
8. S. Murakami, S. Kato, S. Nagano, Y. Tanaka. Diffusion characteristics of airborne particles with gravitational settling in a convective-dominant indoor flow field. *ASHRAE Transactions*. 98(1), 1992, 82–97.
9. Z. Popiolek, S. Mierzwinski, M. Hurnik, J. Wojciechowski. Air flow characteristic in scale models of room ventilation. In *Roomvent '98: Proceedings of the 6th International Conference on Air Distribution in Rooms*, vol. 1, pp. 287–293. Stockholm, Sweden, 1998.
10. P.V. Nielsen. Flow in air conditioned rooms. Ph.D. thesis. Technical University of Denmark, 1974.
11. H. Müllejans. Über die ähnlichkeit der nicht-isothermen strömung und den wärmeübergang in räumen mit strahllüftung. Ph.D. thesis. T. H. Aachen, 1963.
12. D. J. Nevrala, S. D. Probert. Modelling convective currents in rooms by means of wall jets. *Building Services Engineering Research & Technology*, 2(1), 1981.
13. P. V. Nielsen. Airflow in a world exposition pavilion studied by scale-model experiments and compurational fluid dynamics. *ASHRAE Transactions*, 101(2), 1118–1126, 1995.
14. T. V. Lawson. *Wind Effect on Buildings*. Applied Science Publishers, London, 1980.
15. P. V. Nielsen, U. Madsen, D. J. Tveit. Experiments on an exhaust hood for the paint industry. In *Ventilation '91: 3rd International Symposium on Ventilation for Contaminant Control* (eds. R. T. Hughes, H. D. Goodfellow, G. S. Rajhaus. Cincinnati, 1991.
16. P. V. Nielsen. Displacement ventilation in a room with low-level diffusers. *Kälte-Klima-Tagung*. Deutscher Kälte- und Klimatechnischer Verein e.V., 1988.

This page intentionally left blank

13 GAS-CLEANING TECHNOLOGY

PETRI SJÖHOLM

Laboratory of Energy Economics and Power Plant Engineering, Helsinki University of Technology, Espoo, Finland

DEREK B. INGHAM

Department of Applied Mathematics, University of Leeds, UK

MATTI LEHTIMÄKI

VTT Automation, Tampere, Finland

LEENA PERTTU-ROIHA

Fortum Oil and Gas Oy, Porvoo, Finland

HOWARD GOODFELLOW

University of Toronto, Department of Chemical Engineering and Applied Chemistry, Toronto, ON, Canada

HEIKKI TORVELA

Centre for Environmental Technology, Meri-Lappl Institute, University of Oulu

Industrial Ventilation Design Guidebook

13.1 GENERAL

This chapter deals with the fundamentals of gas-cleaning technology. Gas-cleaning technology deals with all types gases, from air to flue gases and process gases. In this section, due to the complex nature of the subject, only a simple approach to gas-cleaning technology is presented. The topics covered are of prime importance due to new international statutory requirements. The developing international market in this field is a very important one for designers and manufacturers.

Particle size distribution relating to gas cleaning is well understood in the industry. This section deals with general rules of thumb. Certain important issues not included in this section are flue gas desulfurization, flue gas denitrification, hazardous waste gas cleaning, waste incineration gas cleaning, and removal of CO_2 from flue gas. All these topics have special requirements, which must be considered separately in the design process.

Table 13.1 shows the physical and chemical nature of particles, from molecular level to 10 mm size. Table 13.1 can be divided into three sections:

1. Chemical
2. Physical
3. Human behavior and methods

These sections are related to the same table but also can be used separately when connecting the particle size axis from the end of the table.

Table 13.1 can be used only as a provisional rule of thumb in order to obtain a general picture of what the end result will be. In the actual design process, the problem must be solved by a proven design approach.

Table 13.1 covers general information for different particulates, liquids in gas, typical particles and gas dispersoids, behavior of particles in the human body, charging mechanisms, principles of particle size analysis, methods for particle size analysis, and an estimation of the general collection efficiency of available commercial particle removal equipment.

TABLE 13.1 The Physical and Chemical Nature of Particles, from Molecular Level to 10 mm Size

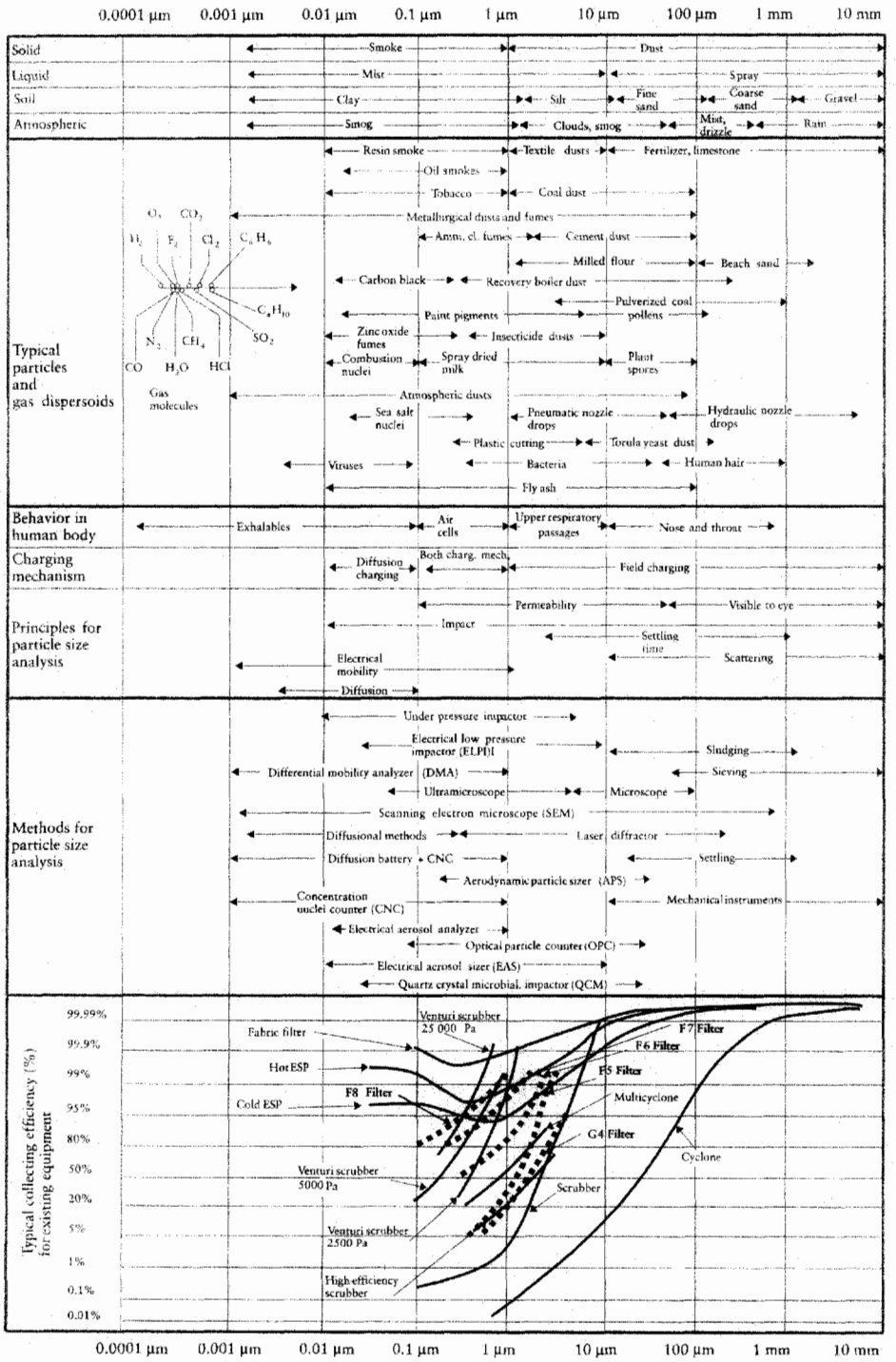

Note that the presented particle collection efficiencies cannot be assumed to be for the best available technology and are shown for equipment existing in industry. Dimensioning of particle removal equipment makes it possible to achieve better removal efficiencies in most cases presented in Table 13.1. All particulate and gas-cleaning equipment must be separately designed to meet specified local conditions.

All definitions used in Table 13.1 are covered in the Appendix.

13.2 PARTICLE REMOVAL

13.2.1 Cyclones in Industrial Ventilation

13.2.1.1 Working Principles of the Cyclone

Cyclone collectors are popularly used both for particle removal and for particle sampling (Fig. 13.1). The separation process of a cyclone relies on the centrifugal accelerations that are produced when particle-laden fluid experi-

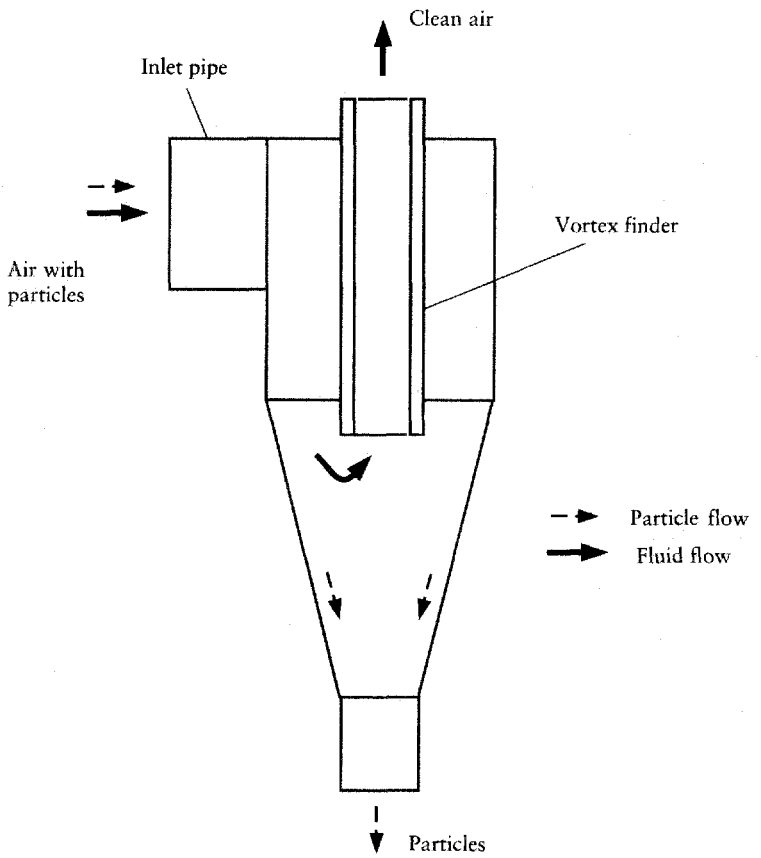

FIGURE 13.1 A schematic diagram of a classical reverse-flow cyclone.

ences a rapidly swirling motion in the cyclone. The larger the particle, the stronger the centripetal acceleration it acquires and, therefore, the easier it is for the particle to be collected. Figure 13.2 is a schematic diagram of the trajectories for a small and a large particles in a typical cyclone. A particle of small diameter penetrates the cyclone, whereas a particle of large diameter finds its way to the side wall of the cylindrical portion of the cyclone and is then collected at the apex of the cyclone via the boundary layer flow.

The collection efficiency curve is usually employed to demonstrate the performance of a cyclone. Figure 13.3 shows a typical collection efficiency curve for a cyclone at a particular airflow rate. The size of particles that have a collection efficiency of 50% is usually employed as a simple indication of the separation efficiency of the cyclone, and is known as the cut-off particle size d_{50}. Particles larger than the cut-off size d_{50} are more likely to be separated by the cyclone, and particles smaller than the cut-off size are more likely to penetrate the cyclone.

Pressure loss through the cyclone is also a key performance parameter, and this depends mainly on the design of the cyclone. In general, the pressure drop across the cyclone collector is small compared with most other dust collectors, but the higher the collection efficiency required, the larger the pressure drop and hence the energy consumption required.

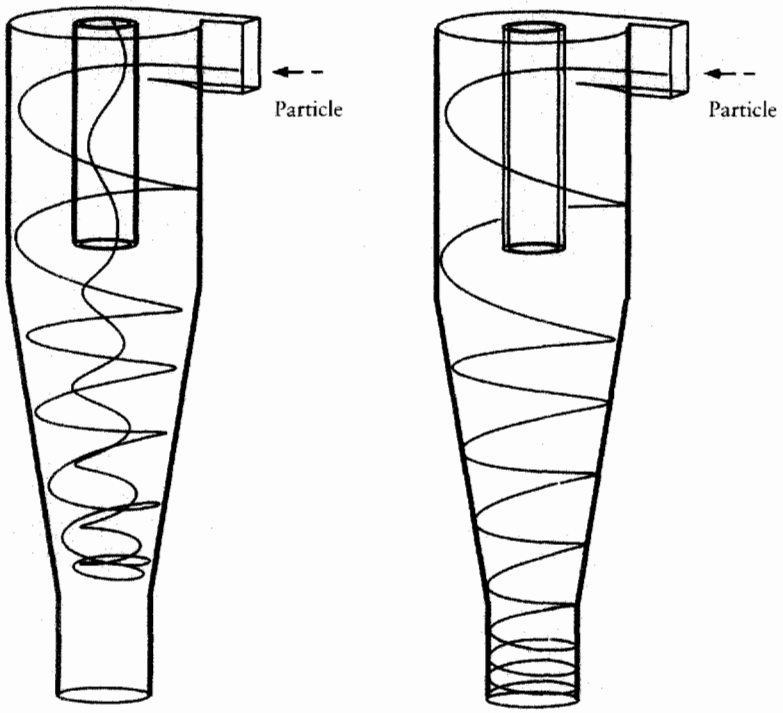

(*a*) Particle of small diameter (*b*) Particle of large diameter

FIGURE 13.2 A schematic diagram of the trajectories for two different sizes of particles in a typical cyclone.

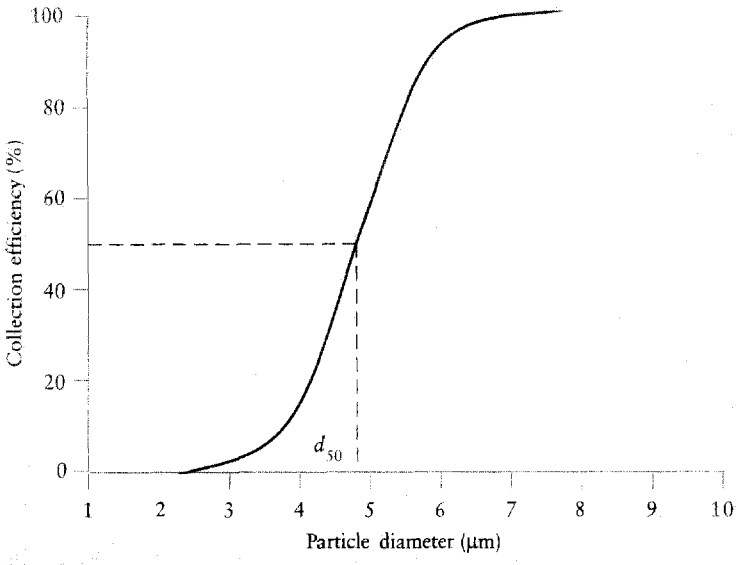

FIGURE 13.3 Typical collection efficiency curve of a cyclone.

13.2.1.2 Theoretical Analysis

A series of theoretical analyses of the fluid and particle collection efficiency of cyclones were performed in the 1970s by Bloor and Ingham[1–3] and they have been found to be in good agreement with the experimental data.

Fluid Flow Model

The steady, laminar, incompressible fluid flow in cyclone collectors is governed by the Navier-Stokes equations:

$$\nabla\left(\frac{p}{\rho}+\frac{V^2}{2}\right)-\mathbf{V}\times\Omega=\frac{\mu}{\rho}\nabla\times\Omega \tag{13.1}$$

$$\nabla\cdot\mathbf{V}=0, \tag{13.2}$$

where V is the fluid velocity; $\nabla\times\mathbf{V}$ is the vorticity; and p, ρ, and μ are the pressure, density, and viscosity of the fluid, respectively.

It is convenient to employ two sets of coordinate systems. Spherical polar coordinates (r, θ, λ) are defined with the origin at the vertex of the cone; the axis is $\theta = 0$, the surface of the conical portion of the cyclone is the cone $\theta = \alpha^*$, and the azimuthal coordinate is λ. Using the same origin, cylindrical polar coordinates (R, λ, Z) are defined, where $R = r \sin\theta$ and the Z-axis coincides with the axis $\theta = 0$.

Flow in the (r, θ) Plane The experimental data of Kelsall[4] gave strong evidence that fluid flow in the cyclone may be assumed to be axisymmetrical.

Therefore, a stream function Ψ may be introduced in the meridian plane of the cyclone, i.e., the (r, θ) plane in the spherical coordinate system:

$$\frac{\partial \Psi}{\partial r} = -V_\theta r \sin\theta, \quad \frac{\partial \Psi}{\partial \theta} = V_r r^2 \sin\theta , \tag{13.3}$$

where the subscripts denote the particular components of the fluid velocity V.

For fluid flow in the (r, θ) plane, it is reasonable to assume that the fluid is inviscid, as the Reynolds number of the fluid flow usually exceeds $O(10^5)$. Thus Eq. (13.1), with $\mu = 0$, may be integrated along the streamlines to give the Bernoulli equation as follows:

$$\frac{p}{\rho} + \frac{V^2}{2} = H(\Psi) . \tag{13.4}$$

Similarly, integrating the λ component of Eq. (13.1) along a streamline shows that the angular momentum of the fluid remains constant throughout every streamline as follows:

$$r \sin\theta V_\lambda = C(\Psi), \tag{13.5}$$

where $H(\Psi)$ and $C(\Psi)$ are arbitrary functions of the stream function. Therefore, the following differential equation for Ψ may be obtained from Eq. (13.1)

$$\frac{1}{r^2 \sin\theta}\left[\frac{1}{\sin\theta}\frac{\partial^2 \Psi}{\partial r^2} + \frac{\partial}{\partial \theta}\left(\frac{1}{r^2 \sin\theta}\frac{\partial \Psi}{\partial \theta}\right)\right] = f(\Psi) . \tag{13.6}$$

Subject to the boundary conditions that must be imposed at the axis, at the inlet, and on the wall boundaries of the cyclone, Bloor and Ingham[3] found that the solution for Ψ may be approximated by the expression

$$\Psi = B(r\theta)^{3/2}(\alpha^* - \theta) \quad \text{or} \quad \Psi = BR^{3/2}\left(\alpha^* - \frac{R}{Z}\right) , \tag{13.7}$$

where α^* is the semi-angle of the cone of the cyclone and B is a constant that may be determined by the volume flux of air through the cyclone as follows:

$$2\pi B c^{3/2}(\alpha^* - c/l) = Q , \tag{13.8}$$

where c is the outer radius of the vortex finder and l is the distance between the entrance plane of the vortex finder and the vertex of the cone.

Thus, the velocity components of the fluid may be determined, in cylindrical polar coordinates, as follows:

$$V_Z = \frac{1}{R}\frac{\partial \Psi}{\partial R} = \frac{B}{2\sqrt{R}}\left(3\alpha^* - 5\frac{R}{Z}\right) \tag{13.9}$$

$$V_R = -\frac{1}{R}\frac{\partial \Psi}{\partial Z} = -\frac{BR^{3/2}}{Z^2} . \tag{13.10}$$

The Spin Velocity Under the inviscid flow assumption, where all fluid that enters the cyclone does so with approximately the same amount of momentum, a free vortex may be predicted for the spin velocity distribution as

follows:

$$V_\lambda = A/R^n, \tag{13.11}$$

where A is a constant and $n = 1$. Due to the effects of viscosity, this expression actually overestimates the spin velocity. Therefore, Svarovsky[5] suggests that n takes a value in the region 0.2–0.9 and has to be determined experimentally.

However, more accurate predictions for the spin velocity may be obtained with allowance made for the effect of viscosity in the governing equation for the spin velocity. According to the experimental data of Kelsall,[4] which indicates that the spin velocity in a cyclone is a function of R only, the λ component of Eq. (13.1) in the cylindrical polar coordinate system may reduce to

$$\rho \frac{V_R}{R} \frac{\partial}{\partial R}(V_\lambda R) = \left(\frac{\partial}{\partial R} + \frac{2}{R}\right)\left[\mu\left(\frac{\partial V_\lambda}{\partial R} - \frac{V_\lambda}{R}\right)\right]. \tag{13.12}$$

A proper representation of the effective viscosity is often problematic. Based on the Prandtl mixing length model for turbulence, Bloor and Ingham[2] suggest that the variation in μ should be of the form

$$\mu = \frac{M}{Z^2}\left|\frac{dV_\lambda}{dR} - \frac{V_\lambda}{R} + K\right|, \tag{13.13}$$

where M is a constant related to the turbulence viscosity at the inlet of the cyclone and K is another constant that reflects the shear near the axis of the cyclone.

Since V_λ is independent of Z in Eq. (13.1), the boundary condition at the level of the inlet may be employed as follows:

$$V_\lambda = 0 \text{ at } R = 0 \tag{13.14}$$

$$V_\lambda = V_i \text{ at } R = R_c, \tag{13.15}$$

where V_i is the speed of the fluid at the inlet and Rc is the radius of the cyclone. If V_R can be regarded as known from Eq. (13.10), then Eq. (13.12) may be solved numerically to obtain V_λ.

Particle Collection Model

In most cyclone applications in industrial ventilation, the particle concentration in the cyclone is very low and it may be assumed that the particles have very little chance of colliding with each other in the main body of the cyclone. Hence, the fate of the particles, whether they are collected or they penetrate the cyclone, may be determined by tracking the motions of individual, isolated particles suspended in the fluid flow.

The motion of an isolated particle in a highly rotating cyclone airflow is normally determined based on the balance on the resulting centrifugal force acting on the particle and the drag exerted by the airflow. In industrial ventilation, cyclone collectors are often employed as precleaners and the particle to be separated is normally larger than about 10 mm. Therefore, the drag exerted on the particles may be considered the dominate force on the particle by the

air flow, and the effects of the turbulent diffusions may be ignored. For a spherical particle of diameter d placed in a fluid stream of speed V, the drag F is given by Stokes's law as follows:

$$\mathrm{F} = 3\pi\mu(\mathrm{V} - \mathrm{V}_p)d\,, \tag{13.16}$$

provided that the particle Reynolds number Re_p, which is defined by

$$\mathrm{Re}_p = \rho|\mathrm{V} - \mathrm{V}_p|d/\mu\,, \tag{13.17}$$

is less than $O(1)$. Fortunately, in most cases of interest, Re_p is very small and the use of Eq. (13.16) is adequate. In the case where the particle Reynolds number is not small, empirical formulas may be obtained for the drag as follows:

$$\mathrm{F} = 3C_D\pi\mu(\mathrm{V} - \mathrm{V}_p)d\,, \tag{13.18}$$

where C_D is the drag coefficient, often expressed as an empirical function of the particle Reynolds number

$$C_D = 1, \qquad 0 < \mathrm{Re}_p \leq 1 \tag{13.19}$$

$$C_D = \left(1 + \frac{3}{16}\mathrm{Re}_p\right), \qquad 1 < \mathrm{Re}_p \leq 4 \tag{13.20}$$

$$C_D = (0.324 + 21.9416/\mathrm{Re}_p^{0.718})\mathrm{Re}_p/24 \qquad 4 < \mathrm{Re}_p \leq 2000 \tag{13.21}$$

$$C_D = 0.4\mathrm{Re}_p/24 \qquad \mathrm{Re}_p > 2000 \tag{13.22}$$

Theoretically, for a particle of a given size that moves in the highly rotating fluid flow in a cyclone, a particular radial orbit position may be found in every horizontal plane of the cyclone where the outward centrifugal force is just balanced by the drag exerted on the particle by the radial inward fluid flow. If Stokes's law (13.16) is assumed, then the position of the equilibrium orbit on each horizontal plane of the cyclone may be obtained and is given by

$$\frac{BR^{3/2}}{Z^2} = (\rho_p - \rho)\frac{d^2V_\lambda^2}{18\mu R}\,. \tag{13.23}$$

See Bloor and Ingham[2] for more details.

In the vertical plane of the cyclone, two important lines may be obtained that determine the fate of the particle in the cyclone. One is the equilibrium line (Fig. 13.4), which may be obtained from Eq. (13.23), and the other is the line of zero vertical fluid velocity, which is obtained from Eq. (13.9) as follows:

$$R = 3\alpha^* Z/5\,. \tag{13.24}$$

Particles inside the equilibrium line penetrate the cyclone with the inward fluid flow, while the particles outside the equilibrium line, and cannot reach the equilibrium line, are collected by the downward fluid flow. When the particles do reach the equilibrium line, their fate is determined by the direction of the vertical fluid velocity at this point (i.e., whether it is upward or downward at the equilibrium line). If a particle is in equilibrium in an upward-moving stream, it will penetrate the cyclone; otherwise it will be collected. It is evident that small particles find their equilibrium orbit at small radii and therefore are more likely to join the upward

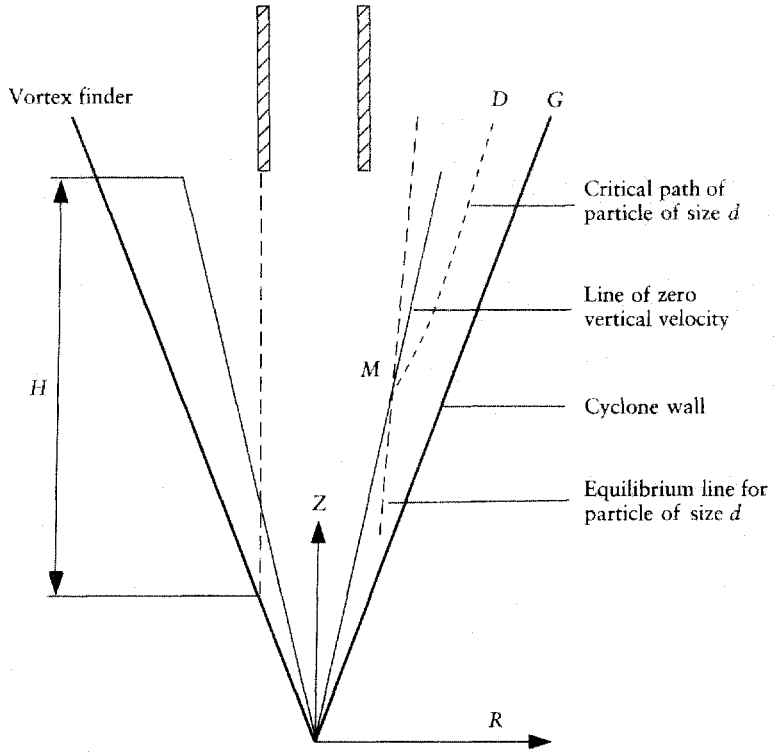

FIGURE 13.4 A schematic diagram of the critical trajectory of a particle of diameter

fluid flow and penetrate the cyclone, while the large particles find their equilibrium line in the region of the downward fluid flow and are collected.

For a given particle of size d, from the point M where the equilibrium line meets the line of zero vertical velocity (see Fig. 13.4), the critical path of the particle may be defined. All particles of this size between points D and G are entrained in the downward stream and are collected. The remaining particles of this size join in the upward-moving stream of fluid and penetrate the cyclone. The point D may be obtained by tracking back the particle trajectory from the point M using the equation of the particle trajectory, which is given by

$$\frac{dZ}{dR} = V_Z \Big/ \left[V_R + \frac{(\rho_p - \rho) d^2 V_\lambda^2}{18 \mu R} \right] . \tag{13.25}$$

Therefore, Bloor and Ingham[2] found that the collection efficiency of a cyclone for the particle size d may be estimated by the following formula:

$$E_m(d) = \frac{\alpha^* l / c^{3/2}}{1 - c/(\alpha^* l)} \left(\frac{R_D}{R_c} \right)^{3/2} \left(1 - \frac{R_D}{R_c} \right) , \tag{13.26}$$

where R_D is the value of R at point D, and R_c is the radius of the cyclone.

Estimation of the Pressure Losses through Cyclones

Conventionally, the pressure drop of a cyclone is expressed in terms of the fluid velocity head in the cyclone. If the head of the fluid velocity at the inlet of

the cyclone is employed, then the pressure loss of a cyclone may be expressed as follows:

$$\Delta p_c = C_f \frac{\rho}{2} V_{in}^2, \tag{13.27}$$

and we know from dimensional analysis that the total loss factor C_f is a function of the fluid Reynolds number, Re. However, under the normal operating conditions of cyclones, Re is usually larger than $\sim 10^5$, indicating that the inertial force dominates over the viscous force and thus C_f becomes practically a constant for the particular cyclone type.

A number of attempts to relate the geometric design parameters of a cyclone to the pressure drop have led to various empirical formulas for the loss factor C_f. One of the simplest formulas is an expression proposed by Sheperd and Lapple:[6]

$$C_f = \frac{\Delta p}{\rho V_\lambda^2/2} = 16ab/D_e^2, \tag{13.28}$$

where a is the width of the cyclone inlet orifice, b is the height of the cyclone inlet orifice, and D_e is the diameter of the outlet pipe of the cyclone.

A more sophisticated theory was given by Barth,[7] in which the pressure drop of a cyclone is defined as a function of the swirling velocity head of the fluid in the outlet pipe as follows:

$$\Delta p_c = C_f \frac{\rho}{2} V_{\lambda,e}^2, \tag{13.29}$$

where C_f is the total loss factor of the cyclone. The swirling component of the fluid velocity at the outlet pipe may be estimated using the balance between the angular momentum at the inlet and at the outlet of the cyclone, taking into consideration the wall friction of the cyclone:

$$\left(\frac{V_\lambda}{V_Z}\right)_e = \frac{\pi R_e R_i}{A_i \alpha + C_\lambda \pi H R_i}, \tag{13.30}$$

where A_i is the cross-sectional area of the inlet pipe, R_i is the radial distance from the axis of the cyclone to the axis of the inlet pipe, R_e is the radius of the outlet pipe, C_λ is a surface friction factor, and H is the length of the cyclone chamber below the outlet pipe at the diameter of the outlet of the pipe (see Fig. 13.4). The constant α takes values ranging from 0.5 to 1.0 depending on the design of the inlet pipe of the cyclone (see, for example, Klinzing et al.[8]).

Barth assumed that the pressure loss of a cyclone consists mainly of the pressure loss required to overcome the wall friction of the cyclone and the pressure drop to drive the fluid out of the cyclone outlet pipe. This leads to the following expression for the total loss factor C_f:

$$C_f = \frac{\Delta p_c}{\rho V_{\lambda,e}^2/2} = \frac{R_e}{R_i}\left\{\frac{1}{\left[1 - \left(\frac{V_\lambda}{V_Z}\right)_e \frac{HC_\lambda}{R_e}\right]^2} - 1\right\} + 1 + K\left(\frac{V_\lambda}{V_Z}\right)_e^{-2/3}, \tag{13.31}$$

where it is recommended that K take the value 4.4 for sharp-edged outlet pipes and 3.4 for rounded-edged pipes. An experimental value of $C_\lambda = 0.018$ was found to suit a wide range of applications, but a modified value may be obtained in situations where the mass load ratio of the solid particles is to be taken into account—for example, in a pneumatic conveying system. In this case, the following expression may be employed to determine the value of C_λ (see, for example, Klinzing et al.[8]):

$$C_\lambda = 0.005\left[1 + 3\left(\frac{m_s}{m_f}\right)^{1/2}\right], \tag{13.32}$$

where m_s and m_f are the mass flow rate of the solid and of the fluid, respectively.

It should be noted that most of these theories for the prediction of the pressure losses in cyclones ultimately require the assignment of certain experimentally determined quantities in order to produce reasonable agreement between theory and experiment. The involvement of these empirical constants almost certainly restrains the use of the theories to the limited group of cyclones that the experiment has covered in order to produce good predictions of pressure drops through the cyclone. Therefore, these empirical theories may be used only as a preliminary estimate of the energy consumption in cyclones. Prototype cyclone experiments may well be required in order to obtain an accurate value of the pressure loss for a newly designed cyclone.

13.2.1.3 Numerical Simulations of the Fluid and Particulate Flows in the Cyclone

The rapid development of high-speed digital computers has made it practically possible to fully simulate three-dimensional turbulent fluid flow and particle movement in cyclones by numerically solving the governing fluid and particulate flow equations. As a result of the numerical solution, a group of discrete values for the fluid velocity, pressure drop, particle trajectories, etc. can be obtained, and this may give a clear picture of what is going on in the cyclone being investigated.

Simulation of the Fluid Flow

Due to the very low volumetric concentration of the dispersed particles involved in the fluid flow for most cyclones, the presence of the particles does not have a significant effect on the fluid flow itself. In these circumstances, the fluid and the particle flows may be considered separately in the numerical simulation. A common approach is to first solve the fluid flow equations without considering the presence of particles, and then simulate the particle flow based on the solution of the fluid flow to compute the drag and other interactive forces that act on the particles.

For steady, incompressible fluid flow in a cyclone separator, the governing Navier-Stokes equations of motion are given, in a Cartesian coordinate system, by:

$$\rho u^j \frac{\partial u^i}{\partial x^j} = -\frac{\partial_p}{\partial x^i} + \frac{\partial}{\partial x^j}\left[\mu\left(\frac{\partial u^i}{\partial x^j} + \frac{\partial u^j}{\partial x^i}\right)\right] + \frac{\partial \tau^{ij}}{\partial x^j} \tag{13.33}$$

$$\frac{\partial u^i}{\partial x^j} = 0, \tag{13.34}$$

where u^i is the fluid velocity, with the superscripts $i, j = 1, 2, 3$ indicating the components in the Cartesian coordinate system, and τ^{ij} is known as the Reynolds stress tensor, which represents the effects of the turbulent fluctuations of the fluid flow.

An appropriate model of the Reynolds stress tensor is vital for an accurate prediction of the fluid flow in cyclones, and this also affects the particle flow simulations. This is because the highly rotating fluid flow produces a strong nonisotropy in the turbulent structure that causes some of the most popular turbulence models, such as the standard k-ϵ turbulence model, to produce inaccurate predictions of the fluid flow. The Reynolds stress models (RSMs) perform much better, but one of the major drawbacks of these methods is their very complex formulation, which often makes it difficult to both implement the method and obtain convergence. The renormalization group (RNG) turbulence model has been employed by some researchers for the fluid flow in cyclones, and some reasonably good predictions have been obtained for the fluid flow.

Simulation of the Particle Motion

In practice, particle tracking is usually performed in a Lagrangian frame of reference, and the motion of a particle is governed by

$$\frac{\rho_p \pi d^3}{6} \frac{du_p^i}{dt} = F^i, \tag{13.35}$$

where F^i is given by Eq. (13.18).

By integrating Eq. (13.35) step by step in time, the particle trajectory of the particle may be obtained. In the integration, the interaction between the particle and the wall may be approximated as being fully elastic; however, when the particle hits the sidewall of the cyclone, the particle may be treated as being collected and the computation for the particle may terminated in order to save the computational time that may be required to track the particle to the bottom of the cyclone. If the particle trajectories for a range of particle diameters at different rates of fluid flow through the cyclone are determined, then the particle efficiency curve and the cut-off particle diameter of the cyclone may be obtained.

13.2.1.4 General Recommendations

As a simple and efficient particle separation device, cyclone collectors can be used for anything from dust removal in a fluid stream to material collection in the fluid conveying system. However, the cyclone is not suitable or economical for the separation of extremely small particles (say, less than 1 μm), which frequently occur in industrial processes. It is recommended that the size of particles to be separated in an industrial ventilation cyclone be in the region of around 10 to 100 μm. However, for the purpose of aerosol sampling, the size of particles to be separated may be much less than 10 μm.

For a specific size of particle to be separated by the cyclone, a first rough estimate of the cyclone size may be obtained by estimating the particle drift velocity in the cyclone. A large cyclone may be used if the particle drift velocity is large. If n is the number of the revolutions that the particle travels with the fluid in the cylindrical part of the cyclone, then the smallest particle of diameter d that can be separated by the cyclone may be approximated by (see Baturin[9])

$$d = 3\sqrt{\frac{\mu}{\pi \rho_p n V_\lambda}(R_c - R_{iw})}, \tag{13.36}$$

where R_{in} is the radius of the inner wall of the inlet pipe of the cyclone. Baturin[9] suggested that three full revolutions of the fluid stream in the cylindrical portion of the cyclone are adequate, as an increase in the number of revolutions improves the efficiency slightly but makes the construction unduly long and complex.

For conventional cyclones, it is recommended that the inlet fluid velocity be around 10–20 m/s and the conical angle of the cyclone be usually made smaller than 25°. If a single cyclone cannot meet the large fluid throughput required, then the use of multiple cyclones in parallel should be considered.

In general, a cyclone with a smaller diameter, longer length, and small vertex angle usually possesses a higher collection efficiency. While small cyclones are usually more efficient than the larger cyclones, it should be stressed that as the size of the cyclone decreases the pressure drop increases.

For a fixed value of pressure drop, the fluid flow rate is approximately proportional to the size of the overflow diameter. A reduction in the overflow diameter leads to an increase in the pressure drop over the cyclone in order to keep the fluid flow rate unchanged. When the fluid flow rate is fixed, then, in general, the reduction in the size of the overflow diameter results in an increase in efficiency. This is simply because a small outlet opening makes it difficult for the particles to penetrate the cyclone.

Normally the vortex finder should extend down into the conical portion of the cyclone. It is thought that the vortex finder plays an important role in the maintenance of a stable spiraling fluid flow in the cyclone, and this makes it more difficult for the particles to leak through the boundary layer on the roof of the lid of the cyclone to the overflow tube.[2] Without a vortex finder, the efficiency may be reduced by 4–5%.[9] However, an excessive long vortex finder may hinder the high spin velocity in the fluid flow and thus reduce the efficiency of the cyclone.

For a cyclone of fixed dimensions, the collection efficiency may be improved by increasing the fluid flow rate through the cyclone. As a consequence of this, the pressure drop over the cyclone increases. It can be shown that the relationship between the cut-off diameter d_{50} and the fluid flow rate Q may be approximated as follows:[5]

$$d_{50} \sim \left(\frac{1}{Q}\right)^{1/2}. \tag{13.37}$$

In terms of the pressure drop Δp across the cyclone, we have

$$d_{50} \sim \left(\frac{1}{\Delta p}\right)^{1/4}, \tag{13.38}$$

and this implies the general rule that the higher the efficiency, the larger the pressure drop across the cyclone.

Once these first estimates for the geometric dimensions of the cyclone have been obtained, a full theoretical analysis of the fluid and particle motions in the cyclone may be performed using the theoretical models given in Section 13.2.1.2. A substantial use of the expression (13.26) for the collection efficiency should be employed so that an updated design of the geometry of the cyclone can be obtained.

Based on the theoretical estimates of the design and operating conditions of the cyclone, the computational fluid dynamics approaches described

in Section 13.2.1.3 should then be employed for a more detailed analysis of the fluid and particle flows and the performance characteristics of the cyclone.

Once a design of the cyclone has been estimated, a prototype of the cyclone should be made with sufficient flexibility left in its design so that as many quantities as possible can be easily adjusted. Experimental investigations should then be performed under realistic operating conditions. Using the observations made above on the adjustment of various operating conditions and geometric parameters, the cyclone should be modified in order to meet the needs of the particular application for which it is to be employed. Once this has been done, the bulk manufacture of the cyclone may be initiated.

13.2.2 Electrostatic Precipitators: Fundamentals

13.2.2.1 History of Electrostatic Precipitation

Electrostatic precipitation is one of the fundamental means of separating solid or liquid particles from gas streams. This technique has been utilized in numerous applications, including industrial gas-cleaning systems, air cleaning in general ventilation systems, and household room air cleaners.

The influence of the electrostatic forces on airborne particles has been known for centuries. The early discoveries are summarized in several books, including the classical book *Industrial Electrostatic Precipitation* by White[10] and many others.[11–14] An excellent historical review has been presented by White.[10] This review includes information about the early steps in the development of electrostatic gas cleaning.

The earliest information dealing with this phenomenon dates back to 600 B.C. It was found that a piece of amber after it had been rubbed was able to attract small fibers. More recent observations are from the 17th century, when William Gilbert noticed that amber, sulfur, and other dielectrics charged by friction could attract smoke. Similar observations were made by Boyle (1675) and Otto von Guericke (1672). Francis Hauksbee (1709) reported that he had discovered a phenomenon which is now called ionic wind or electric wind. Ionic wind and the glow from the corona discharge was discussed by Isaac Newton (1718).

The early pioneers also include Benjamin Franklin and Charles de Coulomb. Franklin studied the effect of point electrodes in drawing electric currents. Coulomb discovered that a charged object gradually loses its charge; i.e., he actually discovered the electrical conductivity of air. Coulomb's importance for the development of electrostatic air-cleaning methods is great, mainly because the present theories about electric charges and electric fields are based on his work.

The first experiment with the electrostatic gas cleaning was made in 1824, when Hohlfeld show that a fog was cleared from a glass jar which contained an electrically charged point electrode. Similar demonstrations were published in the 19th century, an example being the precipitation of tobacco smoke in a glass cylinder by Guitard (1850).

The commercial utilization of electrostatic precipitation started at the end of 19th century and the beginning of the 20th century. The first gas-cleaning

applications were realized by Lodge (in England), Cottrell (in the United States) and Möller (in Germany). Lodge made experiments with an electrostatic precipitator starting in 1880, and in 1883 he published a paper in which he indicated the commercial possibilities of electrostatic precipitation. Together with Walker and Hutchinsson, he installed the first commercial electrostatic precipitator at a lead smelter. This attempt failed, however, mainly because of the primitive high-voltage generator and the fact that particles from a lead smelter are very fine and their conductivity is low.

A person whose work has been of great importance for the development of electrostatic precipitators is F. G. Cottrell. He first aimed at collecting sulfuric acid mist with the aid of centrifuge, but after unsuccessful attempts he started experiments with electrostatic precipitation. Cottrell was able to utilize alternating current transformers and a mechanical rectifier to construct an efficient high-voltage supply. He also invented a new type of discharge electrode, so-called pubescent wire, which increased the stability of the corona discharge.

Many of the typical features found in present-day electrostatic precipitators are based on work by W. A. Schmidt. One of his most important applications is the electrostatic precipitator that was installed at the Riverside Portland Cement Company in 1912. This plant handled a gas flow of 470 m/s at the temperature of 400–500 °C. This was the first precipitator in which thin wire was used as discharge electrode.

The development of electrostatic precipitators was based mostly on empirical work, and it has produced more than 1000 patents covering all aspects of electrostatic air cleaning. From the theoretical point of view, important milestones were papers published by Deutsch[15] as well as White.[16] These papers deal with the collection efficiency of the electrostatic precipitator. The most important early papers dealing with the electrical charging of particles are the ones published by Arendt and Kallmann,[17] Pauthenier and Moreau-Hanot,[18] and White.[19]

The development of electrostatic precipitators soon led to new applications, including the separation of metal oxide fumes. This was followed by various metal manufacturing processes such as the lead blast furnace, ore roaster, and reverberatory furnace. Electrostatic gas cleaning was soon applied also in cement kilns and in several exotic applications, such as recovering valuable metals from exhaust gases.

The growth of the consumption of electric power led to the development of pulverized coal burning techniques, which were superior to earlier techniques. It was, however, discovered that the fly ash in the exhaust gas caused a significant environmental problem. It was also found that an electrostatic precipitator is relatively efficient for the removal of fly ash, and the first power station precipitator was started in 1923. In the first phase, it was difficult to reach 90% efficiency, but gradually significant progress was made, leading to efficiencies as high as 99.9%.

In general, electrostatic precipitators have been shown to best suit those applications where high gas flows must be handled and relatively high efficiency is required. It must also be emphasized that the use of electrostatic precipitators is limited to those applications where the explosion risks are minimal.

13.2.2.2 Basic Principles

Electrostatic gas cleaning is based on the electrostatic force which is applied directly to the particles. Thus, the separation energy is focused directly to

the particles and not to the entire gas flow. Therefore, the energy required to separate particles from a gas stream is normally lower than in those methods in which the separation energy must be applied primarily to the gas flow.

The operation of the electrostatic precipitator is based on three major factors:

- Particle charging
- Electrostatic collection of charged particles
- Removal of collected particles

The basic principle of single-stage electrostatic precipitation is shown in Fig. 13.5. Particle charging in an electrostatic precipitator is realized with a continuous flow of gas ions across the space between two electrodes. One of the electrodes is connected to a high-voltage power supply, while the other is connected to ground potential. Particles become charged when passing through this region. The electric field between the electrodes causes an electrostatic force on the charged particles, leading to particle drift toward grounded collection electrode.

Particle charging and collection can take place in different sections, as illustrated in Fig. 13.6. In this two-stage system, the collection of particles takes place in a region without gas ions, i.e., the electric field is generated by the high-voltage electrode only.

The electrostatic force is directly proportional to the net charge of an aerosol particle. Therefore, effective charging of the particles is of great importance. Airborne particles are normally charged either due to their birth processes or due to charge transfer from gas ions to particles. The natural charging of particles is normally so weak that it has no practical importance for electrostatic air cleaning.

Particle charging in electrostatic precipitators is caused by gas ions generated with high-voltage corona discharge. Corona discharge is utilized to create regions with a high concentration of unipolar gas ions. Ion concentration and electric field are the important parameters affecting the particle-charging process. Electrostatic force is proportional to the particle charge and the electric field. Thus, it is evident that a strong electric field is important for good performance of an electrostatic gas-cleaning system.

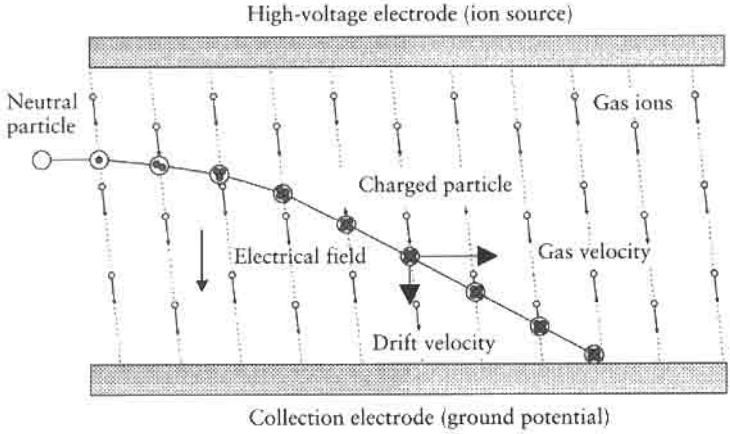

FIGURE 13.5 Principle of electrostatic precipitation.

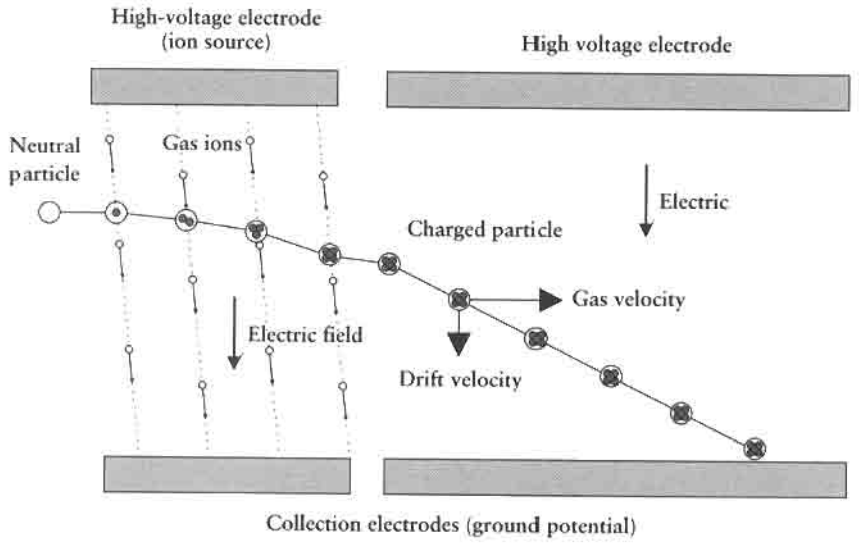

FIGURE 13.6 Principle of electrostatic precipitation utilizing separate charging and collection sections.

A very important part of the gas-cleaning process is the removal of the collected particles from the cleaning system. This should be as controlled as possible in order to avoid particle reentrainment to the gas flow. This can be accomplished in the case of liquid particles such as acid fume or tar or oil smoke. Solid particles are normally removed by periodic rapping of discharge and collection electrodes. Solid particles can also be removed with the aid of water, as is done in wet electrostatic precipitators.

Many types and configurations of precipitators are used, the most typical being duct and pipe types. The principle of the pipe-type precipitator is illustrated in Fig. 13.7. Almost all industrial applications are of the single-stage type (Fig. 13.8). As mentioned earlier, the typical feature of a single-stage precipitator is that particle charging and collection take place in the same region. This is normally accomplished with a system of several discharge electrodes between plate collection electrodes. In pipe- or tube-type precipitators, the high-voltage discharge electrode is placed inside a grounded tube or duct.

Two-stage precipitators consist of separate sections for particle charging and collection. Particle charging is realized with corona wires between grounded metal plates. The collection of particles takes place in a system of parallel plate electrodes of opposite polarities. Two-stage precipitators are typically used in indoor air cleaning and light industrial applications.

Electrostatic force can create particle migration velocities which are much larger than those caused by gravitational or inertial forces. Thus, typical features of the electrostatic technique are the relatively high efficiency and the negligible flow resistance. One of the advantages of the electrostatic method is the possibility of operating at high temperatures. Also, the operation costs can be kept at a reasonable level. The major drawback of the electrostatic precipitator is the high investment cost. Electrostatic precipitators are also relatively large in size, and in

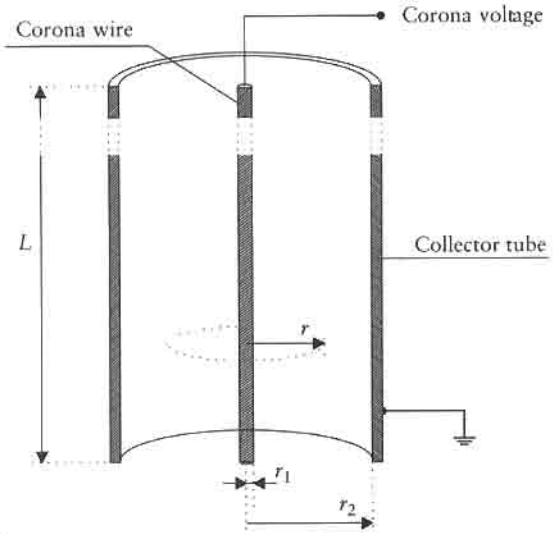

FIGURE 13.7 Principle of the tubular electrostatic precipitator.

many cases their flexibility to changes in operating conditions is limited. A significant drawback is the fact that the performance of electrostatic precipitators may be very poor for particles with either very low or very high electrical conductivity.

The next sections deal with the basic phenomena and factors which are of great importance for performance of the electrostatic gas cleaning. These topics include

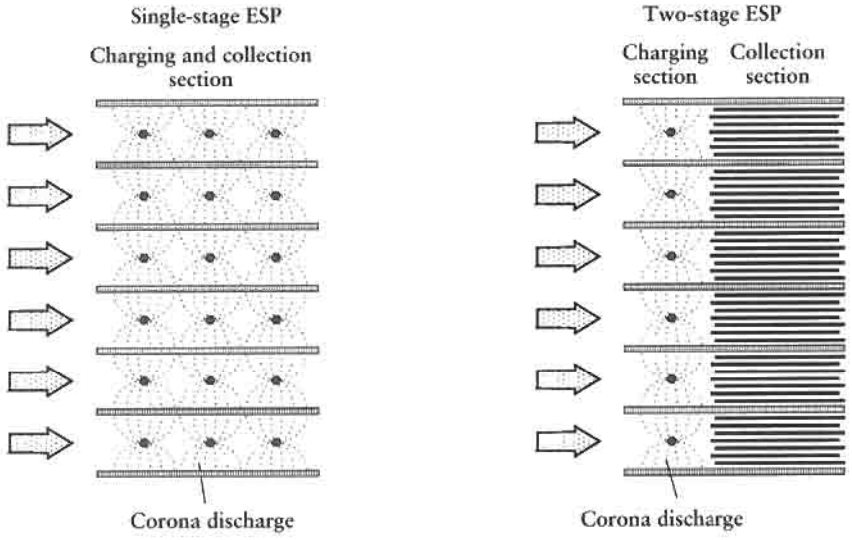

FIGURE 13.8 Principles of single-stage and two-stage electrostatic precipitators.

- corona discharge,
- properties of gas ions,
- electric field,
- particle charging, and
- collection of particles.

For simplicity, the basic theoretical considerations of electrostatic precipitation are given in terms of cylindrical geometry, i.e., pipe-type electrostatic precipitation. This makes it possible to show most of the basic principles without numerical modeling.

13.2.2.3 Corona Discharge

As mentioned earlier, gas ions are essential for the charging of particles. In addition, gas ions play a very important role for the formation of the electric field inside the electrostatic precipitator. Thus, the controlled generation of ions is of major importance for the performance of the electrostatic precipitator. The most effective and practical means of generating gas ions is controlled corona discharge. A controlled corona discharge requires a nonuniform electric field, which is typically formed near a discharge electrode with small dimensions (e.g., needle or wire) compared with the rest of the system. By applying a high voltage to the discharge electrode, a sufficient electric field for the controlled corona discharge near the electrode can be created.

The corona discharge generates a glow, the form and the brightness of which vary depending on the discharge conditions. The light from the corona discharge can be seen as bright spots, brushes, streamers, or a steady glow. Positive corona discharge forms a steady glow, while a negative corona tends to form localized discharges, bright spots, and streamers. A typical feature of the phenomenon is a steep growth of the electric current with increasing voltage.

A gas which contains only neutral molecules or atoms does not conduct electric current. The natural background radiation (e.g., gamma radiation and cosmic radiation), however, continuously generate free electrons and positive ions. Electrons are rapidly captured with electronegative gas molecules, forming negative ions. Electrons and ions move under the influence of the electric field. Thus, a weak electrical conductivity of the gas is produced. If the voltage is increased, the electric field on the surface of the discharge electrode becomes high enough to initiate corona discharge. The voltage corresponding the critical electric field is called the onset voltage of the corona discharge. The critical electric field required to initiate the discharge depends on

- gas composition,
- gas pressure and temperature, and
- diameter and roughness of the discharge electrode.

In a strong electric field, a free electron acquires enough kinetic energy to cause an impact ionization; i.e., an electron impacting on a neutral molecule causes an emission of a new electron, leading to the formation of new electron-ion pair. The new free electron is, in turn, accelerated to a velocity sufficient to cause further ionization. This leads to an avalanche-type generation of free electrons and ions. The electric field provides the necessary energy in such a way that the process can continue without the external radiation which was necessary for the onset of the process.

A negative discharge electrode attracts positive ions and forces them to impact on its surface. These impacts provide an additional source of electrons which contribute to the process. Ultraviolet light generated by the corona glow causes photoelectric emission of electrons from the electrode surfaces, which further enhances the formation of free electrons.

The lifetime of a free electron is normally very short; i.e., the electrons drifting toward the other electrode are captured by gas molecules, forming negative ions. As ions move toward the outer electrode, the electric field becomes so weak that corona discharge is not possible. Negative ions move in the electric field, but their velocity is much lower than the velocity of free electrons. Thus, a dense cloud of negative ions (order of magnitude: 10^7–10^8 ions/cm^3) is formed in the region between the electrodes, and it is in this zone that the particles become charged. Negative ions form a space charge, which is of great importance for the electric current and the electric field between the electrodes.

In some gases (e.g., nitrogen), the lifetime of free electrons can be very long; i.e., negative ions are not formed. Due to the high mobility of free electrons, the corona current rises very steeply with voltage, and therefore it is difficult to create a stable corona discharge. Thus, the presence of electronegative gases which effectively capture free electrons is necessary for the stable operation of negative corona discharge.

The corona discharge generated by positive voltage differs significantly from the negative corona. In a sufficiently strong electric field, the avalanche process takes place, but now the positive electrode attracts electrons, while positive ions drift toward the opposite electrode. Under these circumstances, new electron-ion pairs are not produced as effectively as in the case of negative corona discharge.

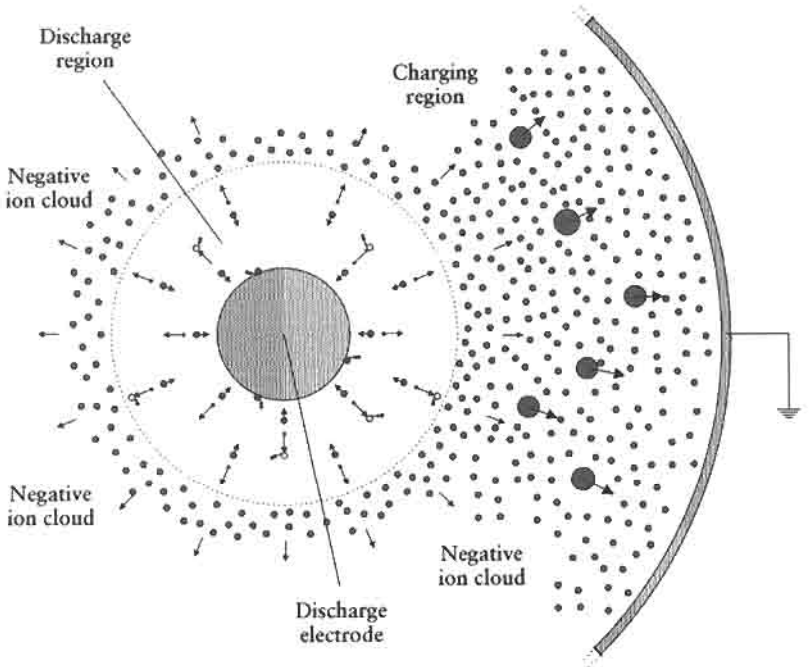

FIGURE 13.9 Principle of negative corona discharge.

There are, however, also similarities between the two discharge types. Positive ions drifting toward the opposite electrode form a space charge that affects the electric field and the corona current principally in the same way as in a negative corona discharge. Also, the charging of particles takes place almost in the same way for both types of corona discharge.

A characteristic feature of the positive discharge is that a stable discharge is formed even though the gas does not contain electronegative components. The operation range, however, is more limited than in the case of negative corona; i.e., increasing the corona voltage leads to a breakdown at a lower voltage level than in negative corona. In industrial applications, negative corona is normally used because it provides a higher collection efficiency.

The composition of the gas plays an important role in the electrical behavior of a corona discharge. The attachment of free electrons to gas molecules varies strongly, depending on the gas composition. Hydrogen, nitrogen, and argon have no electron affinity, and therefore negative ions are not formed. In most cases, however, electronegative gases (e.g., oxygen and sulfur dioxide) are present, and therefore negative ions are formed.

An increase in gas temperature normally means that sparking (from the grounded electrode) occurs at a lower voltage. Gas temperature and pressure affect both the onset voltage of the corona discharge and the mobility of ions. The mobility of a gas ion may change because of the change in gas density but also because of the change in the size of the ion. The decrease in gas density may cause an increase in the apparent ion mobility because of the longer free paths of electrons, which increase the velocity of the charge carriers. A high temperature may also cause thermal electron emission, which enhances the formation of free electrons.

The increase in the free path of electrons modifies the space charge between the electrodes. This produces a more unstable current-voltage relationship because the operation range of the negative corona becomes more limited; i.e., the breakdown voltage is closer to the onset voltage. This is especially important at high temperatures. The effect of gas density for a positive corona is less important because the electric current is transported by positive ions only. Thus, at high temperatures the positive corona discharge may produce more stable operation than a negative corona.

13.2.2.4 Properties of Gas Ions

The properties of gas ions are of great importance for the electrical performance of an electrostatic precipitator. They also are very important for particle-charging processes. The size of gas ions is normally such that they can be regarded as gas molecules carrying a single elementary charge. It can even be assumed that ions form a gas component with a very low partial pressure. Thus, the thermal motion of gas ions is assumed to be similar to that of gas molecules. The most important parameters describing the properties of gas ions are

- mobility Z_i,
- diffusion coefficient D_i,
- mean thermal speed c_i, and
- mean free path λ_i.

The mobility of a gas ion, Z_i, is defined as the ratio of ionic drift velocity v_i to the electric field E, i.e.,

$$v_i = Z_i E \,. \tag{13.39}$$

The relationship between the ion mobility and mass may be very complicated, mainly because the gas ions may form clusters, the size of which can vary depending on the gas composition and temperature. Empirical mobility values in standard conditions for several gases can be found in the literature.[20] Normally, the mobility of a gas ion can be assumed to be in the range of $1.0 \cdot 10^{-4}$ to $3.0 \cdot 10^{-4}$ ($m^2/V\,s$). According to Oglesby,[20] it is beneficial for the operation of an electrostatic precipitator if the gas contains components with high electron affinity and the ion mobility is low. These factors produce circumstances for high voltages and intense electric field.

The random thermal motion or the diffusion of gas ions is characterized by the diffusion coefficient D_i, which is related to the ion mobility Z_i by

$$D_i = \frac{kT}{e} Z_i \,, \tag{13.40}$$

where k is the Boltzmann constant ($k = 1.3807 \cdot 10^{-23}$ J/K), T is absolute temperature, and e is elementary charge ($e = 1.6021 \cdot 10^{-19}$ A s). Another factor which illustrates the random motion of gas ions is the mean thermal speed, c_i, which is given by

$$c_i = \frac{8kT}{(\pi m_i)^{1/2}} \,. \tag{13.41}$$

Besides these parameters, the properties of a gas ion are sometimes characterized with mean free path λ_i, which illustrates the mean distance between successive impacts with gas atoms or molecules. The mean free path of ions in air is in the range of 10^{-8} to $2 \cdot 10^{-8}$ m.

13.2.2.5 Electrical Properties

Electric Field

The electric field between the discharge electrode and the collection electrode is of great importance for the particle-charging and -collection processes. Besides the dimensions of the electrode system, the electric field depends on the voltage which is applied between the electrodes and the space charge which is formed by gas ions and charged particles. Electric field and ion concentration can be modeled relatively easily by assuming a simple tubular geometry, i.e., a thin corona wire on the center line of the cylindrical collection tube (Fig. 13.7).

At low voltages, i.e., below the onset of the corona discharge, the electric field $E(r)$ depends on the voltage and the geometry of the system only. The electric field is given by

$$E(r) = \left[\frac{U}{\ln(r_2/r_1)}\right]\left(\frac{1}{r}\right), \tag{13.42}$$

where U is the voltage of the corona wire electrode, r_1 is the radius of the corona wire, r_2 is the radius of the collector tube, and r is the radial distance

from the centerline. This equation is based on the assumption of zero space charge between the electrodes.

The effect of space charge can be taken into account by means of the Poisson equation, which in the case of a cylindrical geometry is expressed in the form

$$\left(\frac{1}{r}\right)\frac{\partial}{\partial r}[E(r)r] = \left(\frac{e}{\epsilon_0}\right)[n(r) + n_q(r)]\,, \tag{13.43}$$

where E is the electric field, n is the ion concentration, e is the elementary charge, n_q is the charge concentration due to the charged particles, and ϵ_0 is the vacuum dielectric constant.

Corona current per unit length of the discharge electrode, j_L, is given by

$$j_L = \frac{I}{L} = 2\pi e Z_i n(r) E(r) r\,, \tag{13.44}$$

where I is corona current and L is the length of the discharge region. In the case of a zero particle-space-charge concentration (i.e., $n_q = 0$), one obtains the following solution for the electric field:

$$E(r) = \left[E_c^2\left(\frac{r_1}{r}\right)^2 + \frac{j_L}{2\pi\epsilon_0 Z_i}\left[1 - \left(\frac{r_1}{r}\right)^2\right]\right]^{1/2}. \tag{13.45}$$

For high corona currents and for $r >> r_1$, electric field can be estimated by

$$E(r) \approx \left[\frac{j_L}{2\pi\epsilon_0 Z_i}\right]^{1/2}. \tag{13.46}$$

According to this equation, the electric field is constant in the region some distance from the corona wire.

A rough approximation for the relationship between corona current and voltage can be obtained from $E(r) = -\partial U/\partial r$. Solving this equation yields an approximation:

$$j_L \approx \frac{2\pi\epsilon_0 Z_i}{r_2^2} U^2\,. \tag{13.47}$$

According to this equation, corona current is proportional to the square of the corona voltage. The combination of Eqs. (13.46) and (13.47) produces a simple approximation for the electric field:

$$E \approx \frac{U}{r_2}\,. \tag{13.48}$$

According to Eq. (13.48), the electric field should be a function of voltage and tube radius alone. Thus, the polarity of the corona discharge should have no influence. It must, however, be emphasized that these results are quite rough approximations which are not necessarily valid if the geometry of the system differs significantly from the wire-in-pipe configuration. Also, it must be noticed that these rough approximations do not take into account the effect of the onset voltage of the corona discharge.

These equations are based on the assumption of zero particle space charge. In practice, however, charged particles can significantly affect the electric field

between the electrodes. The effect of charged particles on the performance of an electrostatic precipitator is a very complicated process. It can, however, be approximated relatively easily by assuming a constant particle- space-charge concentration, i.e., $dn_q/dr = 0$.

Figure 13.10 illustrates the relationship between electric field and radial distance in various space-charge conditions. In the case of zero space charge (i.e., without ions and charged particles), the electric field decreases steeply with radial distance. If the space charge due to gas ions is included, the electric field is practically independent of the radial distance. If the space charge due to ions and charged particles is included, the electric field increases with distance. It is worth noticing that, due to the particle space charge, the electric field at the surface of the collection electrode is higher than in the case of ionic space charge only. The particle space charge tends to decrease the electric field near the discharge electrode, leading to a decrease in the corona current.

Ion Concentration

The concentration of gas ions significantly influences the particle-charging process. The high ion concentration is essential for the effective charging of fine particles. The distribution of ion concentration in a pipe-type electrostatic precipitator can be approximated by using the equations presented in the previous section.

By combining Eqs. (13.44), (13.47), and (13.48), it is possible to give an expression for the ion concentration $n(r)$. In the case of a thin wire electrode inside a large tube, the ion concentration can be approximated with

$$n(r) \approx \frac{\epsilon_0 U}{e r_2} \frac{1}{r}. \tag{13.49}$$

According to these equations, ion concentration is directly proportional to the corona voltage and inversely proportional to the radial distance. Equation

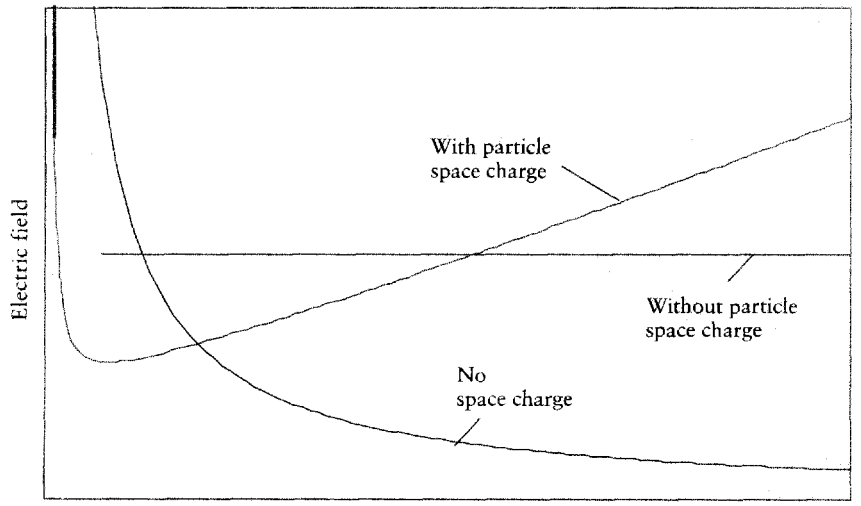

FIGURE 13.10 Electric field as a function of radial distance (tubular geometry).

(13.49) can also be used to estimate the mean ion concentration, n_{ave}, between the electrodes, i.e.,

$$n_{ave} \approx 2\frac{\epsilon_0 U}{e r_2^2}. \tag{13.50}$$

These solutions correspond to the idealized case; i.e., space charge due to aerosol particles is assumed to be zero.

13.2.2.6 Particle Charging

When the particles are exposed to either positive or negative gas ions, the unipolar particle-charging process causes the accumulation of electric charge on the particles. Due to the stochastic nature of the particle-charging process, the number of elementary charges carried by a particle is an integer. The probability that a particle carries a certain number of elementary charges depends on several factors, including particle size and dielectric constant, ion concentration, electric field, and charging time.

In most practical applications, especially in the case of large particles, it is not necessary to know the charge distribution. Thus, the particle charging can be modeled by means of the average charge number. There are two basic mechanisms responsible for the charging of aerosol particles. These are referred to as field and diffusion charging. Particle charging in an electric field is assumed to be due to ordered motion of ions under the influence of the electric field. This approach is applicable predominantly for large particles ($d_p > 0.5$ μm). Diffusion charging is due to ion attachment to particles caused by the random motion of the ions. The diffusion charging model must be utilized especially if the charging of fine particles ($d_p < 0.2$ μm) is considered. Particle charging in an electrostatic air-cleaning system takes place in a strong electric field and high ion concentration; i.e., both charging mechanisms must be taken into account.

Field Charging

Electrostatic air-cleaning systems are normally based on particle charging by means of corona discharge. Thus, the charging takes place in a relatively strong electric field, and therefore the classical field charging theory[10] can be successfully applied. The classical field charging theory assumes that the ions drift along the electric field lines as illustrated in Fig. 13.11.

According to the field charging theory, the external electric field drives ions to the aerosol particle until the repelling electric field prevents ions from reaching the surface of the particle. This condition corresponds to the saturation; i.e., the particle has reached a stable value which cannot be exceeded. The relationship between the net charge of the particle and charging time is given by

$$s(t) = s_0 \frac{t}{t + t_s}, \tag{13.51}$$

where the saturation charge number s_0 is given by

$$s_0 = \frac{3\pi\epsilon_0}{e} \frac{\epsilon_r}{\epsilon_r + 2} d_p^2 E_0 \tag{13.52}$$

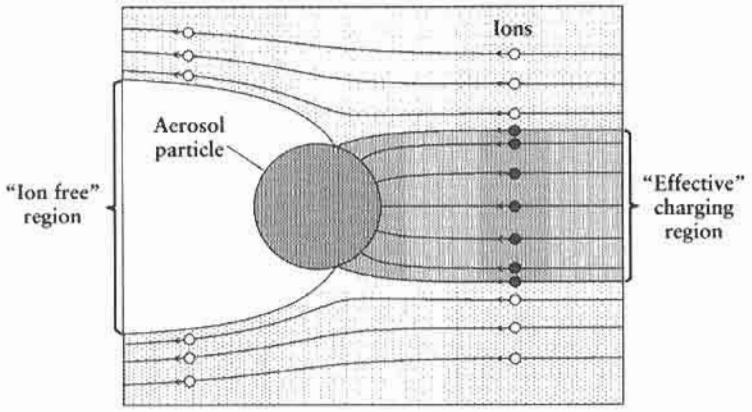

FIGURE 13.11 Field charging (ion paths in the vicinity of a charged particle in an electric field).

and the time constant t_s is given by

$$t_s = \frac{4\epsilon_0}{neZ_i}. \tag{13.53}$$

According to Eq. (13.52), saturation charge is directly proportional to the square of the particle diameter and the external electric field. Particle charging depends also on the composition of the particle, which is taken into account by the relative dielectric constant ϵ_r. It is worth noticing that the field charging model should not be applied for small particles ($d_p < 0.5$ μm).

Particle charging in a electrostatic gas-cleaning system should take place as quickly as possible. Therefore, the time constant t_s should be as low as possible. This requires that the ion concentration in the charging region be high.

Diffusion Charging

The direct effect of the external electric field on the particle charging decreases with particle size and electric field. Instead, the random thermal motion of ions starts to dominate the charging process; i.e., the ion attachment to aerosol particles is governed by the ion diffusion, as illustrated in Fig. 13.13. This charging process is called diffusion charging (see, e.g., Pui[21]), and it is a dominating process for small particle ($d_p < 0.2$ μm). It is worth noticing that in the case of low electric field, diffusion charging can play an important role in the charging of large particles as well. Due to diffusion charging, the saturation charge given by Eq. (13.52) is not an absolute maximum; i.e., the particle charge can slightly exceed the saturation charge due to the diffusion charging.

The traditional unipolar diffusion charging model is based on the kinetic theory of gases; i.e., ions are assumed to behave as an ideal gas, the properties of which can described by the kinetic gas theory. According to this theory, the particle-charging rate is a function of the square of the particle size d_p, particle charge numbers and mean thermal velocity of ions c_i. The relationship between particle charge and time according White's

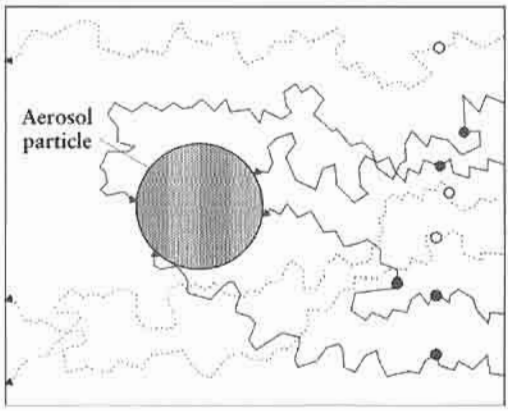

FIGURE 13.12 Diffusion charging (ion paths in the vicinity of the aerosol particle).

equation is

$$s(t) = \frac{d_p}{d_0} \ln\left[1 + \frac{\pi}{4} d_p d_0 c_i n t\right], \tag{13.54}$$

where c_i is the mean thermal velocity of the ions, n is ion concentration, and t is charging time. Coefficient d_0 is given by

$$d_0 = \frac{e^2}{2\pi\epsilon_0 kT}. \tag{13.55}$$

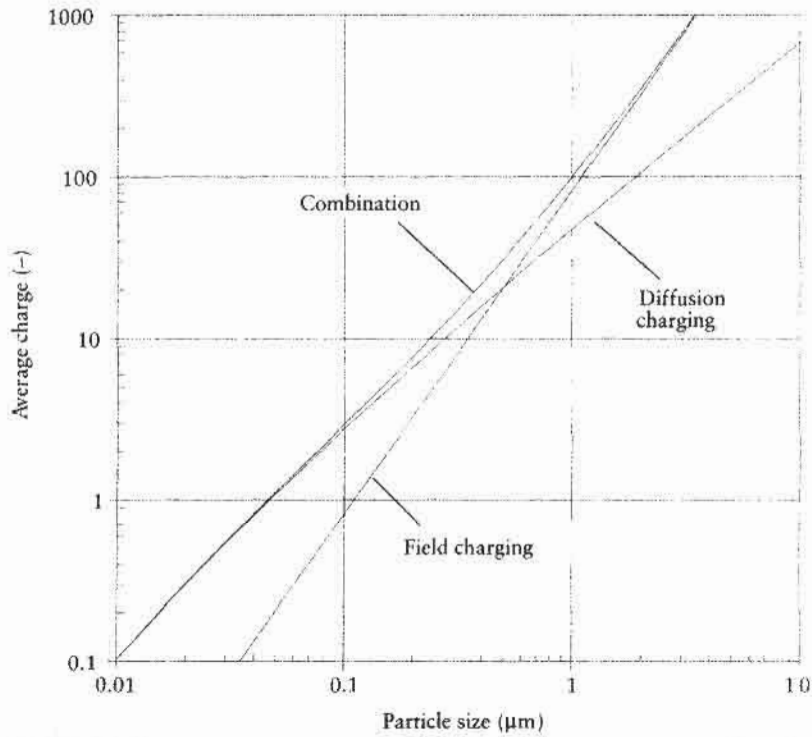

FIGURE 13.13 Combining diffusion and field charging (E = 2500 V/cm, $nt = 10^8$ s/cm^3).

White's equation is widely used mainly because it is easy to use and because it gives values which are in reasonable agreement with the experimental ones. However, because this model is based on the kinetic theory of gases, it should be used for small particles only. This model (as many others) assumes that particle charge can be described with a continuous function. Especially in the case of small particles, only the lowest charge numbers (0, 1, 2) are possible, and therefore the model—which does not take into account the discrete charge numbers—is somewhat questionable.

Combining Field and Diffusion Charging

Particle charging by corona discharge normally requires that both charging mechanisms be taken into account. Thus, a model which combines the field charging model with the diffusion charging model is necessary. The sophisticated theoretical models which combine both charging mechanisms are relatively complicated, and they hardly produce significant benefit for the calculation of particle charging in electrostatic gas-cleaning systems.

The most straightforward approach is to assume that the field charging and diffusion charging are independent processes; i.e., particle charge can be presented as a sum of charges due to field (s_f) and diffusion (s_d) charging. Another simple approach to estimating the combined effect is

$$s = s_f + s_d - \frac{s_f s_d}{s_f + s_d} \,. \tag{13.56}$$

It is easy to see that this solution asymptotically approaches s_f as particle size increases. On the other hand, this solution approaches s_d when particle size approaches zero.

13.2.2.7 Collection of Particles

Charged Particle in an Electric Field

The motion of a charged aerosol particle in a gas is governed by the electrostatic force and the aerodynamic forces. The theory dealing with the particle motion has been discussed in several books (see, e.g., Hinds[22]). The electrostatic force F caused by the electric field E is given by

$$F_E = seE, \tag{13.57}$$

where s is the particle charge number, e is the elementary charge ($e = 1.6021 \cdot 10^{-19}$ A s). This force causes a particle drift in the direction of the electric field. Electrostatic force is balanced by the gas resistance force or drag force. Normally, the particle drift velocity is low; i.e., the particle Reynolds number is small, and the drift velocity w due to the electrostatic force can be approximated by

$$w \approx \frac{se}{3\pi\mu d_p} E = Z_p E \,. \tag{13.58}$$

In this equation, Z_p is the electrical mobility of the particle. In the case of fine particles, the slip correction must be taken into account, and the mobility is given by

$$Z_p = \frac{se}{3\pi\mu d_p}\left[1 + \frac{\lambda}{d_p}\left(A + Be^{-C\frac{d_p}{\lambda}}\right)\right], \tag{13.59}$$

where λ is the mean free path of the gas molecules (for air, $\lambda = 6.53 \cdot 10^{-8}$ m). The values of the coefficients A, B, and C are: $A = 2.154$, $B = 0.8$, and $C = 0.55$.

These equations are valid for spherical particles. For nonspherical particles, a more detailed model must be used; i.e., the effect of the irregular shape of the particles must be taken into account by means of shape factors.[22]

Figure 13.14 shows examples of particle drift velocities calculated by different charging models. These curves clearly indicate that the drift velocity of large particles is almost totally due to field charging, while in the case of small particles, diffusion charging dominates. Figure 13.14 also illustrates that the minimum of the drift velocity is in the particle size range between 0.1 and 1 m.

If particle charging and collection take place in the same electric field E, the drift velocity of large particles can be estimated by

$$w \approx \frac{\epsilon_0}{\mu} \frac{\epsilon_r}{\epsilon_r + 2} d_p E^2 \tag{13.60}$$

According to this approximation, the drift velocity is proportional to the square of the electric field. This is a clear indication of the importance of the electric field inside an electrostatic precipitator. Equation (13.60) is a valid approximation for large particles ($d_p > 0.5$ m), provided that particle charge is close to the saturation level. In the case of small particles, the effect of diffusion charging must be taken into account.

Basic Collection Models

There are two basic approaches to handling the particle collection in an electrostatic gas-cleaning system. The first approach is based on the assump-

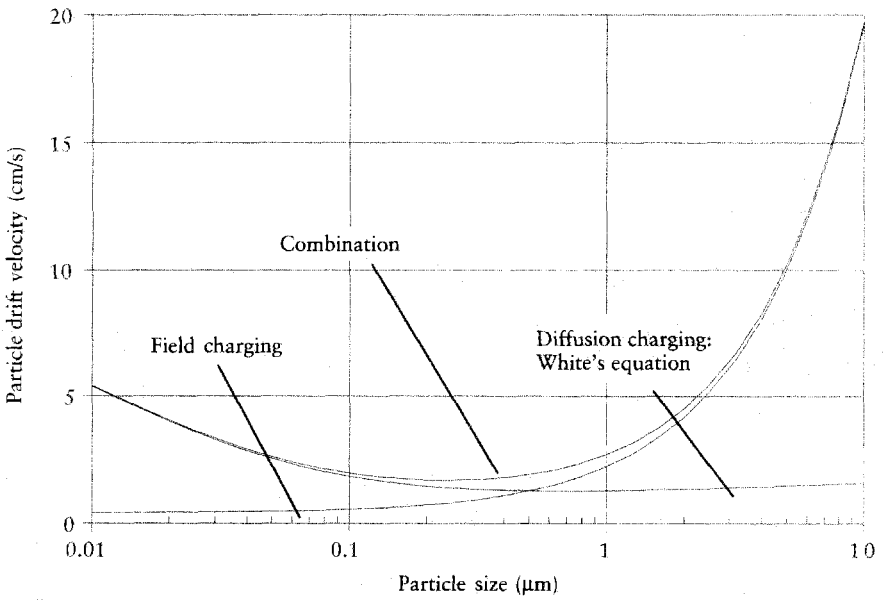

FIGURE 13.14 Particle velocities in an electric field based on different charging models (E = 2500 V/cm, $nt = 10^8$ s/cm^3).

tion of laminar gas flow, while the other assumes a turbulent flow. In the case of laminar airflow between two parallel plate electrodes, the particle collection efficiency η_L can be presented with a simple equation:

$$\eta_L = \frac{Z_p AE}{q} = \frac{wA}{q} \qquad (0 \le \eta_L \le 1.0), \tag{13.61}$$

where A is the area of the collection surface and q is the volumetric flow rate. According to this model, the collection efficiency is directly proportional to the drift velocity and the collection area and inversely proportional to the flow rate. In practice, laminar gas flow requires that the distance between the electrodes be short. A typical example is a two-stage electrostatic precipitator in which particle collection is realized with a large number of parallel plate electrodes. The right side of the equation represents the Deutsch number, $\mathrm{De} = wA/q$, which is frequently used when discussing the removal efficiency of an electrostatic precipitator.

In most cases, laminar gas flow is an unrealistic assumption. A more realistic alternative is to assume a complete mixing of air in the collection system. The collection efficiency in the case of turbulent flow η_T is given by

$$\eta_T = 1 - e^{wA/q} = 1 - e^{-\mathrm{De}} \ . \tag{13.62}$$

This equation, which is called the Deutsch equation, has been shown to be a useful tool for estimating the performance of electrostatic precipitators. An interesting detail in the Deutsch equation is the exponent, which is equal to the collection efficiency of a laminar flow system. The equations based on laminar flow and turbulent flow can be assumed to be the extreme conditions, and the true situation is somewhere in between these two cases (see Fig. 13.15).

These simple models are based on the assumption of constant drift velocity; i.e., particles are assumed to achieve their final charge instantaneously. This is a reasonable assumption in the case of large particles, the charging of which is governed by field-driven ion motion. The characteristic distance x_s corresponding to the time constant t_s in Eq. (13.53) is given by

$$x_s = vt_s = \frac{4\epsilon_0 v}{neZ_i} \ . \tag{13.63}$$

It is easy to see that, under normal circumstances, the characteristic distance is much shorter than the effective length of the precipitation system.

Advanced Modeling of Particle Collection

Particle collection in an electrostatic air-cleaning system can be modeled with more sophisticated methods, such as

- modifying the Deutsch equation,
- solving the particle trajectories in certain flow field and electric field conditions,
- solving the convective diffusion equation, or
- utilizing effective migration velocities.

A relatively simple modification of the Deutsch equation is obtained by assuming that the particle concentration near the collection surface is linearly

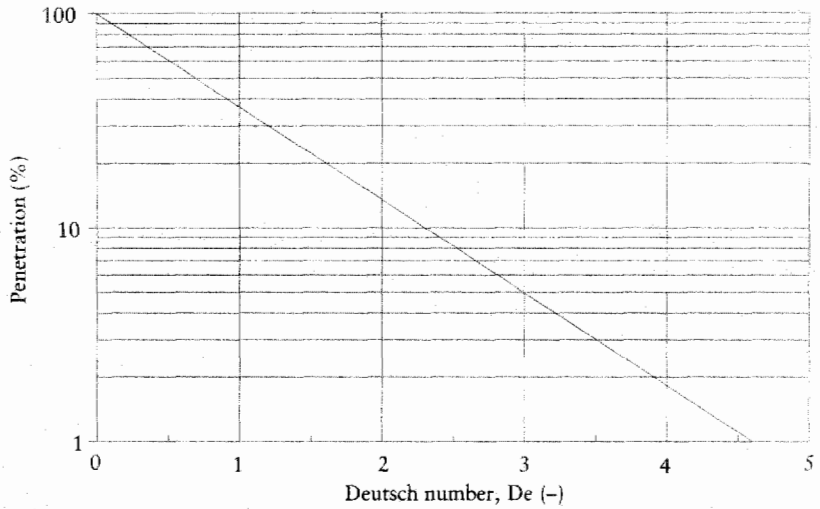

FIGURE 13.15 Particle penetration as a function of the Deutsch number.

dependent on the mean concentration at that location of the electrostatic precipitator. This leads to a modified Deutsch equation:

$$\eta_T = 1 - e^{-h\,\mathrm{De}}\,, \tag{13.64}$$

where h is the concentration ratio ($h = c_{\text{surface}}/c_{\text{ave}}$). Unfortunately, there is no good model for the coefficient h. It is reasonable to assume that its value depends on several factors, including the turbulent mixing inside the collection system as well as the electric field and particle size.

Particle trajectories can be calculated by utilizing the modern CFD (computational fluid dynamics) methods. In these calculations, the flow field is determined with numerical means, and particle motion is modeled by combining a deterministic component with a stochastic component caused by the air turbulence. This technique is probably an effective means for solving particle collection in complicated cleaning systems. Computers and computational techniques are being developed at a fast pace, and one can expect that practical computer programs for solving particle collection in electrostatic precipitators will become available in the future.

Another approach to modeling the particle-collection process is based on the convective diffusion equation

$$\frac{dc}{dt} = D\nabla^2 c - \nabla \cdot (vc) = 0\,, \tag{13.65}$$

where D is the diffusion coefficient, which takes into account the eddy diffusion. Velocity v is the combination of fluid velocity and the migration velocity due to the electrostatic force. The diffusion equation can be solved numerically, provided that the diffusion coefficient is known. Unfortunately, the turbulent mixing of air inside an electrostatic precipitator is a very complicated phenomenon which depends on the flow conditions, including the ionic wind, i.e., air movements caused by the repulsion of gas ions.

The efficiency of an electrostatic precipitator is influenced by several factors (e.g., reentrainment of collected particles and gas sneakage around precipitation sections) which are difficult to include in simple theories. Therefore, the performance of electrostatic precipitators is often characterized with effective migration velocities, which are often derived from field experiences. Thus, effective migration velocity can be regarded as a semiempirical parameter which characterizes the mass transfer in electrostatic precipitation. Effective migration velocity is a practical tool because it can used for estimating the total mass efficiencies. This is of great importance, because the total mass emission is a key parameter when designing and operating electrostatic precipitators today. A widely used equation which illustrates the relationship between mass efficiency η_m and effective migration velocity w_k is

$$\eta_m = 1 - e^{-[(A/q)w_k]^k}, \tag{13.66}$$

where k is a parameter having a value around ½.

13.2.2.8 Effects of Dust Layer

Most of the results presented in the previous chapters are based on idealized conditions. In practice, the performance of an electrostatic precipitator can be significantly influenced by the dust layers on discharge and collection electrodes; i.e., dust layers may alter the electrical properties of the system. It is also possible that dust layers are not stable; i.e., collected particles become loose, increasing the particle concentration in the outlet of the precipitator. These problems play a much smaller role if the surface collection electrode is continuously flushed with water. These wet electrostatic precipitators, however, cannot be used in all applications.

Electric Field and Voltage

A layer of high-resistivity dust on the collection surface may significantly affect the performance of the electrostatic gas-cleaning system. In practice, the effect of a dust layer affects the performance and operation of an electrostatic precipitator in a very complicated way. The corona current flowing through the dust layer generates a voltage which tends to decrease the effective voltage between the electrodes. The electric field E_d in the dust layer and the voltage U_d across the dust layer are given by

$$E_d = \frac{U_d}{\Delta x} = j_A \rho, \tag{13.67}$$

where j_A is the corona current density (I/A), ρ is the resistivity of the dust, and Δx is the thickness of the dust layer. Depending on the density of corona current and the resistivity of the collected dust, the electric field inside the dust layer may even grow so high that it initiates sparkover or back corona.

Back corona is caused by the electrical breakdown of gas in the dust layer. This breakdown produces positive ions, which drift toward the negative discharge electrode. The presence of ions with opposite polarity causes a reduction in the particle-charge and -collection efficiency. To avoid this problem, several methods are used. These include

- Good electrode geometry (i.e., even current-density distribution)
- Adjustment of corona current
- Utilization of pulsed high-voltage supplies
- Gas conditioning (i.e., injection of SO_3 or NH_3 into the flue gas)
- Temperature and humidity control (e.g., reducing resistivity with the aid of reduced gas temperature)

Thus, the corona voltage is normally adjusted to compensate for the adverse effects of a dust layer; i.e., the operating conditions of the electrostatic precipitator are kept as ideal as possible.

The stability of the collected dust is of great importance for the overall performance of the electrostatic precipitator. The behavior of the collected dust layer is governed by electrical, molecular, and mechanical forces. Molecular forces (e.g., van der Waals forces) tend to keep particles together. These forces depend on the properties of particle surfaces. Mechanical forces are due to the interlocking of particles and to interparticle friction. Electrostatic force that affects the dust layer depends on two components. The electric field between the discharge electrode and the surface of the dust layer creates a force F_c that tends to extract particles from the surface, while the electric field inside the dust layer creates a force F_d that tends to compress the dust layer and prevent particles from escaping.

The net electric force per unit area is given by

$$F = F_d - F_c = \frac{1}{2}\epsilon_0[(\epsilon_r j_A \rho)^2 - E^2] \,. \tag{13.68}$$

In this equation, ϵ_0 is the vacuum dielectric constant, ϵ_r is the dielectric constant of the dust and E is the electric field in the gas adjacent to the dust layer. According to Eq. (13.68), the electrostatic force due to the electric field in the dust layer increases with increasing dust resistivity. If the dust resistivity decreases below a certain limit, the total electrostatic force becomes negative, i.e., electrostatic force no longer holds the dust layer on the collection surface. Thus, the probability of dust reentrainment to the gas flow increases. The dust layer is, however, influenced by chemical and mechanical holding forces, which normally significantly diminish particle reentrainment. On the other hand, if the resistivity of the collected dust is very high, the electrostatic force may be so strong that the removal of dust may become very difficult.

13.2.2.9 Practical Aspects

Electrostatic precipitators have been used in various gas-cleaning applications almost for a century. During the past decades, a large number of modifications to electrostatic precipitators have been developed, the most common being duct and pipe types. The utilization of electrostatic precipitation extends from small household air cleaners up to huge industrial gas-cleaning systems.

The two-stage electrostatic precipitators used in light-industry applications are compact devices which can be fitted into the ventilation system. These air cleaners are normally used to clean air from dusts, smokes, and fumes in industrial workplaces. The basic features of these devices are the separate sections for particle charging and collection. The charging section consists of thin metal wires installed between grounded metal plates. The distance

between the discharge wire and grounded plate electrodes is typically in the range of 1.5–3 cm. The collection section consists of a set of parallel metal plates installed in a such way that every second plate is connected to the high voltage, while every second plate is connected to the ground potential. The separation between the plates is typically 5–10 mm.

Positive corona discharge is normally used, mainly because of lower ozone production than with negative corona discharge. The corona voltage is in the range of 9–13 kV. The collection voltage is typically half of the corona voltage. In some constructions the collection voltage equals the corona voltage. The length of the collection section is typically 10–30 cm, and the airflow velocities are in the range of 0.5–3 m/s.

The most important application of electrostatic precipitation is, however, the solving of environmental pollution problems caused by many heavy-industry processes. The dimensions, corona voltages, and currents of these gas-cleaning systems are much larger than for ventilation electrostatic precipitators. Typical applications of industrial electrostatic precipitators are

- collection of fly ash from electric power boilers,
- particle collection from furnace operations in metallurgical processes,
- particle collection from black-liquor recovery furnaces in paper mills,
- particle collection from cement and gypsum manufacturing processes, and
- cleaning of stack emissions in municipal incinerators.

Pipe-type electrostatic precipitators are used to collect liquid aerosols (e.g., mists and fogs). They are also used in applications which require water flushing of collection electrodes. The diameter of precipitator pipes is typically in the range of 15–40 cm, and the length is in the range of 3–6 m. The number of pipes depends on the total gas flow. The gas-flow rates in pipe-type electrostatic precipitators is normally much lower than in duct-type precipitators.

Duct-type electrostatic precipitators are the most important electrostatic gas-cleaning devices today. Duct-type electrostatic precipitators are made of vertically mounted collection plate electrodes, with discharge electrodes placed midway between plates. The width of the collection plates in a large electrostatic precipitator can be several meters and the height up to 15 m. An electrostatic precipitator system may include several sections energized from separate high-voltage supplies. The spacing between the plates is typically in the range of 20–40 cm. The gas-flow velocity is typically 0.5–2 m/s. The ratio of collection area to the volumetric gas flow is in the range of 20–150 $(m/s)^{-1}$. The corona voltages of large electrostatic precipitator systems are typically in the range of 40–100 kV, and the corresponding corona current densities (i.e., corona current divided by collection area) are in the range of 0.05–1 mA/m^2. It is worth noticing that the corona voltage is normally generated by means of a thyristor-controlled transformer/rectifier system. Thus, a cyclic corona voltage and current are applied to a precipitator section.

Electrostatic precipitators are operated near the sparking limit; i.e., corona voltage is continuously adjusted to maximize the collection efficiency. This is normally achieved at the sparking rate of 10–50 sparks per minute. Sparking occurs mostly in the front section(s) of an electrostatic precipitator. In the case of high-resistivity ($>10^{10}\ \Omega$ cm) dust, special techniques must be

used to avoid the formation of back corona. This requires sophisticated systems for controlling corona voltage and current. The formation of back corona can also be reduced with intermittent or low-frequency energization. This technique is based on the extension of the time period between corona current bursts. Thus, much higher current bursts can be used without causing back corona. Pulse energization is a more elaborate technique, which is based on current bursts of microsecond duration.

Besides optimal energization of an electrostatic precipitator, several other factors must be controlled to achieve a good performance. The gas velocity profile should be even to fully utilize the capacity of an electrostatic precipitator. Also, the gas flow outside the active collection sections (sneakage) should be minimized. Keeping the electrodes clean is also of great importance, especially when eliminating the harmful effects of high-resistivity dust. The collected dust is normally removed by rapping forces, which are generated by mechanical impacts or by vibration of electrodes. Collection plates are normally cleaned with either a magnetic-impulse rapper or a rotating-hammer rapper. Adjustment of the rapping frequency and intensity is of great importance for the controlled removal of collected dust without excessive particle reentrainment.

The design and operation of a large electrostatic precipitator requires lot of practical knowledge about the general properties of electrostatic particle separation. In addition, the properties of the dust must be known, and correct techniques (e.g., altering dust resistivity by means of gas conditioning) must be utilized. Depending on the application, the performance of an electrostatic precipitator can be affected by several factors in a rather complicated way. Therefore, practical work with electrostatic precipitators often requires empirical information about the separation process. Thus, the experimental results from existing installations are of great importance when designing new ones. Even though theoretical calculations provide less feasible information for design purposes, they still help to understand the basic factors influencing the overall performance of the electrostatic precipitator.

13.2.3 Fabric Filters

Design and application of fabric filters are covered in various references.[23–31]

The Industrial Gas Cleaning Institute Inc. (IGCI) defines a baghouse as follows: "A fabric filter is one in which the dust-bearing gas is passed unidirectionally through a fabric in such a manner that the dust particles are retained on the dirty gas side of the fabric, while the cleaned gas passes through the fabric to the clean gas side, where it is removed by natural and/or mechanical means." Simply, fabric filter collectors remove particulates from gas streams by impaction, impingement, and diffusion. Large particles will not pass through the weave of the filter and are sieved out. Medium-sized particles are caught by impingement on the filter fibers. Small particles diffuse and are caught by the filter fibers due to Brownian movement. The main mechanisms for fabric filters are impingement and diffusion. If large particles have not settled out ahead of the filter, it is common to add an inertial separator or cyclone to remove the coarse particles and reduce the dust loading to the filter.

The separation of dust from the gas stream consists of passing the dusty gas through a porous, flexible layer of textile material called a filter element. These filter elements, which are bag-shaped, are placed in structural enclo-

sures called baghouses or fabric filter collectors. In addition to supporting the filter elements, the baghouse contains baffle plates for directing airflow into or out of these hoppers, a type of cleaning mechanism to remove the particulate from the filters, and a dust hopper for the collection and drainage of the dust. As dust accumulates on the filter, the pressure drop across the filter increases. Dust buildup on the filter is removed periodically by vigorous cleaning of the filter to maintain the pressure drop in a satisfactory way.

This type of bag-cleaning method is a fundamental characteristic of this type of collector. Terminology in the fabric filter field is not totally consistent or comprehensive. Table 13.2 presents acceptable definitions for common fabric filter terminology.

Important technical features of fabric filter collectors are listed in Table 13.3. A brief description of each characteristic follows. Detailed descriptions of fabric filters are presented in the literature.[23–31,33]

Baghouses may operate under negative or positive pressures. Negative pressure baghouses operate upstream of the fan and must be designed to withstand the maximum head developed by the fan. This could correspond to the case in which all the inlet dampers are closed and the fan is operating under cold conditions. Although the pressure drop across the filter unit may only be 50–200 mm WG, the compartment walls may have to be designed to 1000 mm WG. The compartment must be designed to minimize in-leakage air so that the fan does not have to be oversized. If the dust–air mixture can become explosive, the unit must be designed to resist a positive pressure that is determined from dust-explosion tests. Venting requirements for the baghouse to limit pressure buildup can be determined from a publication by Schofield.[34] The allowable positive pressure for baghouse design must be specified.

Positive pressure baghouses are common for large structural units in the metallurgical industry. These units have to be designed only to withstand the pressure loss across the baghouse. They also have the advantage that an open grating can be used around the outside of the compartments, which allows ambient air to cool the exhaust gas.

Fabrication of baghouses can be of modular design, factory-welded subassemblies, or structural design. The selection of the type of fabrication depends on size of unit, transportation requirements, site location, physical location of unit at plant (e.g., on roof), and materials of construction.

Modular designs have become very popular because of the high-quality workmanship, which can be controlled in the manufacturing plant, and the ease of erection in the field. These units can be complete, factory-assembled units consisting of bolted or welded components. The units may include the dust hopper, timer, cleaning accessories, supporting legs, bags, and internal baffles. For some installations, the units can be lifted directly into a base and the legs bolted in place. Large volumes can be handled using a multiplicity of units connected in parallel. The dusty inlet duct and clean outlet ducts may be connected to a common internal plenum or to external ductwork manifolds with inlet and outlet connections on each.

Factory-welded subassemblies are based on separate fabrication of bag housing, dust hopper, inlet plenum, outlet plenums, etc., to form the largest subassemblies that can be shipped over the road. Connections are made to adjacent components by welding or bolting at the job site. Bags can be already

TABLE 13.2 Common Terminology for Fabric Filter Collectors

Cleaning
Cleaning method: The physical principle used to dislodge and remove the collected dust from the fabric.
Cleaning mechanism: The specific mechanical or pneumatic system used to clean the fabric.
Cleaning sections: The number of segments into which the cleaning mechanism is divided. (An intermittent baghouse would have a single section, while automatic or continuous baghouses would have two or more sections.)
Compartments: The number of rooms in a continuous baghouse that can be entered for maintenance while the remainder of the baghouse is operating (may contain one or more cleaning sections).
Cleaning methods
Intermittent: Periodic cleaning, with total flow interruption.
Automatic: "Continuous automatic" cleaning, without total flow interruption.
Continuous: "Continuous automatic" cleaning and maintenance possible, without total flow interruption.
Filtering fabric area
Gross fabric: The total effective area of filter fabric installed in the baghouse.
Net fabric: The gross fabric area less the area of fabric being continuously or periodically cleaned.
Filter-cleaning operations
Cleaning cycle: The total elapsed time from commencing to clean a section of the baghouse to commencing to clean that same section again.
Cleaning interval: The elapsed time from commencing to clean a section of the baghouse to beginning to clean the next section. (The cleaning interval times the number of sections equals the cleaning cycle.
Cleaning period: The total elapsed time that a section of the baghouse is off-stream for cleaning. (This time increment determines the total availability of section fabric for filtration use.)
Filter ratings
Air-to-cloth ratio: The unit capacity of a fabric filter, i.e., the total volume of gas in actual m^3/s divided by the gross or net fabric area in m^2.
Operational problems
Dusting: Dust passing through the fabric upon initial start-up or immediately following cleaning.
Bleeding: Dust continuously passing through the fabric during normal operation.
Blinding: A situation wherein fabric and dust cake permeability cannot be maintained. The collected dust so adheres to or is so embedded in the fabric substrate that it cannot be removed by the cleaning method employed. This is evidenced by continually increasing pressure drop.

Source: Smith and Lucas[32]

TABLE 13.3 Technical Features of Fabric Filter Collectors

Characteristic	Description
Operating conditions	Positive pressure/negative (section) pressure
Fabrication techniques	Modular design/factory-welded subassemblies/structural
Collector configuration	Single compartment/multicompartment
Type of cleaning	Mechanical shaking/reverse air/pulse jet
Cleaning requirements	Continuous/automatic/intermittent
Type of fabric	Woven/nonwoven
Filrer element	Bags or tubular/pocket or envelope/cartridge

installed in the bag housing with all cleaning accessories factory piped and factory wired. If the bags are factory installed, field welding is precluded.

Structural baghouses are limited to very large baghouses. All structural components are fabricated as separate panels with formed flanges. The panels are bolted or welded in the field. These flanged joints serve as stiffeners to the hoppers, plenum, tube sheets, and baghouse enclosures.

The collector configuration can be single compartment or multicompartment. Multicompartment designs are used where it is important to maintain a relatively constant pressure drop during collector operations. Multicompartment design allows compartments to be taken off-line for cleaning or maintenance with the collector system still in operation.

The three major types of filter cleaning are mechanical shaking, reverse air, and pulsejet. Mechanical shaking is used to clean woven fabrics because of their good resistance to vigorous shaking. The cloth may be fabricated into long tubes called bags or envelopes. Bags are hung vertically, with the closed end fastened at the top to a motor-driven shaker bar and the open end attached to the tube sheet for the entry of the dust-laden gas. The dirty gas passes through the fabric from inside to outside, with the dust deposited on the inside surface. The envelope type is mounted over a metal spacer or screen, with the open ends attached to a tube sheet at one side of the unit. The dirty gas passes from outside to inside and deposits the dust on the outside surface. For cleaning either of the preceding units, the airflow must be interrupted to permit the dislodged dust to fall to the hopper. The use of multicompartment design with enough capacity so that one unit can be shut down provides for continuous filtering operation.

Reverse airflow for filter cleaning was initially developed for delicate fabrics, such as glass cloth, that are used for their special chemical or heat-resisting properties. Reverse air is now applied to all types of fabrics for a wide range of applications. The prime advantage of reverse air is the long bag life that can be obtained for a well-operating system. The reverse-air system has a disadvantage of requiring another fan (reverse-air fan) and numerous air-regulating dampers. If the static pressure for the reverse-air fan is not selected correctly, the system can become inoperative since the bags cannot be cleaned because of high pressure drops.

Pulse-jet filters are commonly used for both dusts and fumes. These filters have the gas flow from outside to inside through internally supported bags of felted rather than woven fabric. Dust is deposited on the outside of the bag. The

clean gas flows up and out the top of the compartment. A tube sheet located at the top of the bag separates the dirty gas from the clean gas and prevents the dirty gas from escaping between the bags to the clean side. The felted fabric is used to keep the pressure drop at a reasonable level. Pulse-jet filters operate at higher air-to-cloth ratios than reverse-air or mechanical-shaking types (i.e., typically two to four times higher). This higher air-to-cloth ratio results in the dust particles' penetrating deeper into the material of the bag and necessitating a more effective method of bag cleaning. The cleaning technique used is a pulse-jet technique, which consists of a pulse of air introduced into the open top of the filter bag. The pulsejet expands the bag suddenly, and the dust which has accumulated on the outside of the bag is dislodged and collected in the hopper below. This pulse cleaning operation is carried out with the unit on-line or off-line, depending on such factors as filter bag material, application, and the basic design principles utilized. The pulse can be a traditional high-pressure type (650 kPa) or a newer development using a low-pressure pulse (250 kPa).

The cleaning requirements can be continuous, automatic, or intermittent. Continuous cleaning requires a multicompartment unit. A typical cleaning cycle is to take one compartment off-line to clean. For some applications, on-line cleaning can be used with pulse-jet filters. In steady-state operation, cleaning may be done on a timed cycle. Automatic controls can be installed so that the cleaning mechanism is activated only when the pressure drop across the collector exceeds a certain setpoint. This automatic control using pressure drop can result in significant improvements in bag life. An intermittent cleaning cycle is applicable when the process can be stopped for a few minutes to clean the bags. A typical application would be for a plant that operates only on a day shift, in which the collector could be cleaned at the end of the shift.

The properties of the filter fabrics must be understood and properly specified to ensure successful operation. Final selection should be made by test and by an economic analysis that examines original cost against maintenance expenses. Important fabric properties are permeability, mechanical strength, solids retention, corrosion resistance, heat resistance, cleanability, and dimensional stability.[28] Fabrics may be felted or woven. Felted fabrics are formed by compressing fibers under high pressure, and they are relatively thick. Woven fabrics are composed of twisted yarns that are woven into geometric patterns having various spacings between the yarns and having a specific surface finish. The permeability of these fabrics depends on the type of fiber, the tightness of the twist, the size of the yarn, the type and tightness of weave, and the type of surface finish.

The filter elements can be tubular bags, pocket filters, or cartridges. Bags are the most common filter elements and come in standard sizes and specified bag length-to-diameter ratios. Europe is the home of the "pocket" or envelope-type filter. This device is characterized by especially large filter areas per unit of installed collector space. This minimal space advantage has favored application in Europe. Cartridge-type filters, which are used primarily for low inlet dust loadings, employ pleated filter cartridges. These filters have a large filtering area per unit volume. They use a lower filter velocity, which improves air cleaner performance by lowering penetration and reducing differential pressure, thus resulting in lower operating energy requirements.[30,31] Figure 13.16 shows typical bag, pocket, and cartridge filter elements and units.

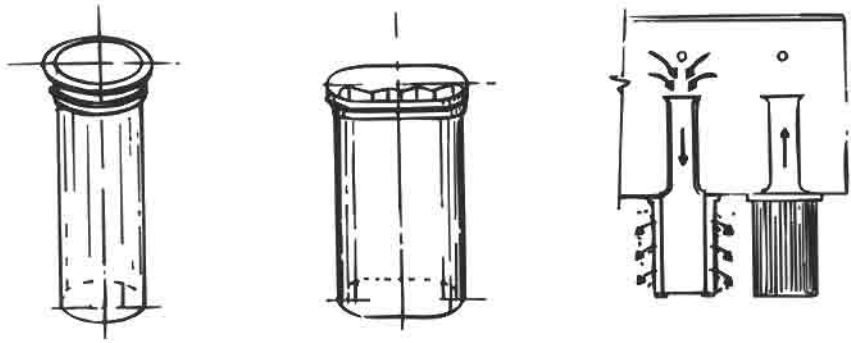

FIGURE 13.16 Typical bag, pocket, and cartridge filters.

Table 13.4 lists the physical and chemical properties of common filter media. Many other fabrics are available for special applications. These other fabrics are more expensive and should be considered only if the common types of fabric are clearly not suitable for the proposed service. These special applications should be discussed with specialists from filter media firms.

The electrostatic properties of both the dust and the collecting fabric have an important effect on the filtration and cleaning process. Frederick[35] has proposed that the optimal performance of collection by fabric media is dependent on relating the relative triboelectric properties of dusts and fabrics and then utilizing these data with other characteristics to specify filter fabrics. Table 13.5 presents the electrostatic charging order of filter fibers. Dusts may be classified in a similar triboelectric series. The charge polarity and magnitude developed on either the dust or the fiber are a function of the processing conditions and the materials themselves. In the dust-cleaning process, the charge dissipation rate is a very important property. Stainless steel fibers have been woven into filter cloth for dissipating the electrostatic charges and for protection from fires and dust explosions.[36] Penny[37] has examined the possibility of depositing the dust in a relatively porous layer or filter cake using charged particles. Some tests indicated a marked reduction in pressure drop. Another approach is to apply an electric field across the filter to enhance dust-collection efficiency. Further work is required to establish how these effects can be incorporated into a more efficient design of a dust collector.

A major market which has developed for fabric filters is for the control of flue-gas fly ash in the utility industry. This market is primarily at the expense of electrostatic precipitators. Fabric filters have the inherent advantage of operating at a high level of collection efficiency for a wide range of dust and gas conditions.

Pertinent literature on fabric filter applications covers topics from status reports to detailed descriptions of operation and maintenance problems and the use of a pulse-jet fabric filter. Leith, Gibson, and First[38] observed that filter resistance diminished by a factor of 4 and penetration by a factor of 2 when the gas inlet was moved from bottom to top, with all else remaining constant. It also appears that the top inlet design results in all bags operating at a constant face velocity, while the bottom inlet design results in the bag face velocity decreasing with time.

TABLE 13.4 Properties of Fiber Materials

	Physical characteristics				Relative resistance to attack by			
Fiber	Relative strength	Specific gravity	Normal moisture content (%)	Maximum usable temperature (°F)	Acid	Base	Organic solvent	Other attribute
Cotton	Strong	1.6	7	180	Poor	Medium	Good	Low cost
Wool	Medium	1.3	15	210	Medium	Poor	Good	—
Paper	Weak	1.5	10	180	Poor	Medium	Good	Low cost
Polyamide (nylon)	Strong	1.1	5	220	Medium	Good	Good[a]	Easy to clean
Polyester (Dacron)	Strong	1.4	0.4	280	Good	Medium	Good[b]	—
Acylonitrile (Orlon)	Medium	1.2	1	250	Good	Medium	Good[c]	—
Vinylidene chloride	Medium	1.7	10	210	Good	Medium	Good	—
Polyethylene	Strong	1.0	0	250	Medium	Medium	Medium	—
Tetrafluoro-ethylene	Medium	2.3	0	500	Good	Good	Good	Expensive
Polyvinyl acetate	Strong	1.3	5	250	Medium	Good	Poor	—
Glass	Strong	2.5	0	550	Medium	Medium	Good	Poor resistance to abrasion Expensive
Graphitized fiber	Weak	2.0	10	500	Medium	Good	Good	—
Asbestos	Weak	3.0	1	500	Medium[d]	Medium	Good	Poor resistance to moisture
"Nomex" nylon	Strong	1.4	5	450	Good	Medium	Good	

[a]Except phenol and formic acid
[b]Except phenol.
[c]Except heated acetone.
[d]Except SO_2.
Source: Stern[25]

In the late 1970s, early development work in the field of fabric filter technology involved the application of filters at high air-to-cloth ratios on metallurgical fume. Goodfellow, Geren, and Foord[39] reviewed the status of the development work in the field and presented pertinent operating data from full-scale installations. The conventional approach for this application has been to use shaker or reverse-air-type fabric filters at a filtration velocity of about 0.75–0.9 m/min. Early experience with pulse-cleaned fabric filters on metallurgical fume led to "blinding" and "bleeding" problems; as a consequence, there was very little activity for many years. In the 1970s, new synthetic fabrics and finishing techniques were developed; testing showed that mechanical shaking and reverse-air cleaning could be operated at ratios as

TABLE 13.5 Electrostatic Charging Order of Filter Fibers

Material	Relative charge of generation
Wool	+ 20
Silicon-treated glass (filament and spun)	+ 15
Woven wool felt	+ 11
Nylon (spun)	+ 7 to + 10
Cotton (sateen)	+ 6
Orlon (filament)	+ 4
Dacron (filament)	0
Dynel (spun)	− 4
Orlon (spun)	− 5 to − 14
Dacron (spun)	− 10
Steel	− 10
Polypropylene (filament)	− 13
Acetate	− 14
Saran	− 17
Polyethylene (filament and spun)	− 20

Source: Frederick[35]

high as 1.25–1.8 m/min for low grain loadings. Technology has also developed for the successful operation of pulse-jet units for fume applications. Advantages of the successful application of high-ratio technology include significant capital and operating cost savings and significant reductions in space layout requirements for the units. Pulse-jet units are now widely accepted by industry for metallurgical fumes.

The information supplied to the manufacturer should be as detailed as possible and cover the following factors:

1. Process description and operations
2. Emission sources to be controlled
3. Gas flow rate, moisture content, and temperature
4. Chemical and physical characteristics of the gas
5. Chemical and physical characteristics of the solids
6. Solids flow rate
7. Performance
8. Preliminary layout drawings

Figure 13.17 shows isometrics of mechanical shaking, reverse air, cartridge, and pulse-jet types of bag filter units.

The selection and sizing of fabric filters are complex issues because of the many variables and the range of applications. The selection depends primarily on judgment based on experience. It is common for the user or the engineer to size the fabric filter based on first-hand knowledge or indepth experience from similar operations. The equipment manufacturer may also size the equipment. If no good experience exists, it may be necessary to operate a pilot test filter to collect the necessary sizing data. Dennis, Cass, and Hall[40] have presented a quantitative

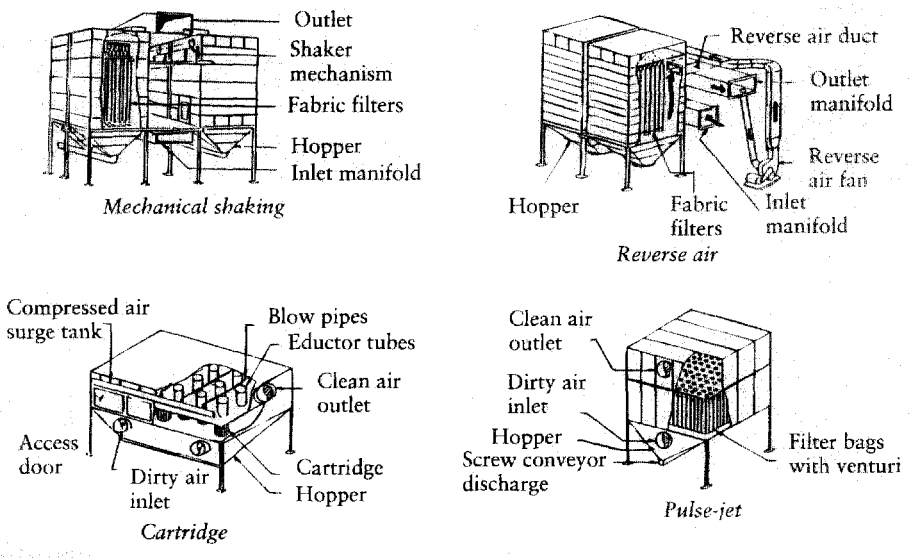

FIGURE 13.17 Isometrics of four types of bag filter units.

relationship between local filtration velocities and the distribution of fabric dust loadings. This relationship provides a rational basis for predicting filter system behavior. Comparison between predicted and experimental performance showed excellent agreement for glass fabric–fly ash systems. The developed equations are in metric units. Since no formal system exists for reporting fabric filtration parameters in the metric system, Table 13.6 presents filtration parameters in the common British units and metric equivalents.

The sizing parameter for fabric filters is the ratio of gas flow rate (m^3/s) to the area of filtering media (m^2). This ratio is termed the air-to-cloth ratio. The expression *filtration velocity* is used synonymously with air-to-cloth ratio for describing fabric filters. For example, an air-to-cloth ratio of 1.5:1 (1.5 m^3/s per m^2) is equivalent to a filtration velocity of 1.5 m/s. Data are available in the literature on filtration velocities for different industrial application.[23,33] Selection of a filter starts with a detailed specification. The bids, as prescribed by the vendors, should first be analyzed to ensure that they comply with the basic design criteria and that the proposed units are suitable for the dust-collection application. Unless first-hand knowledge is available, filter testing should be carried out either at the vendor's pilot plant or a field pilot plant. The procedure to establish cloth area from the testing program is outlined by Kraus.[29]

These are the three major performance criteria for a filter:

1. Collection efficiency
2. Total energy input requirements
3. Costs

Collection efficiency is the single most important parameter in the performance of a filter. Based on typical operational efficiencies for various gas-

TABLE 13.6 Filtration Parameters in Metric and British Units

Filtration parameter	Units		Equivalency
	Metric	British	
Filter resistance	N/m^2	in. H_2O	1 in. water $\equiv$ 250 N/m^2
Filter drag	(N min)/m^3	(in. H_2O min)/ft	(1 in. water min)/ft = 817 (N min/m^3)
Velocity	m/min	ft/min	1 ft/min = 0.305 m/min
Volume flow	m^3/min	ft^3/min	1 ft^3/min = 0.0283 m^3/min
Fabric area	m^2	ft^2	1 ft^2 = 0.093 m^2
Areal density	g/m^2	lb/ft^2	1 lb/ft^2 = 4882 g/m^2
Areal density	g/m^2	oz/yd^2	1 oz/yd^2 = 33.9 g/m^2
Specific resistance	(N min)/(g m)	(in. H_2O min ft)/lb	(1 in. water min ft)/lb = 0.167 N min/g m
Coefficient dust concentration	g/m^3	gr/ft^3	1 grain/ft^3 = 2.29 g/m^3

Source: Dennis, Cass, and Hall[40]

cleaning devices as a function of particle sizes below 2 microns in diameter, the fabric filter has the highest collection efficiency for particulates less than 0.1 micron in diameter.

For high-performance filters, it is common to use penetration (P) rather than efficiency (η), where penetration is defined as the outlet dust concentration divided by the inlet dust concentration. The efficiency (η) is defined as follows:

$$\eta = 1 - P = 1 - \left(\frac{\text{outlet dust concentration}}{\text{inlet dust concentration}} \right) \tag{13.69}$$

Penetration or efficiency may be determined for an operating filter by simultaneous measurements of inlet and outlet dust concentrations using appropriate stack sampling techniques. Efficiencies can be considered as instantaneous or cumulative since efficiencies change with the quantity of dust captured by the filter and the filtering time. Filtering ability is provided by the fabric initially, until a filter cake builds up and provides added filtering ability. A new, unused fabric filter has a collection efficiency in the range of 50–75% for submicron particulate. As the dust loading increases, the efficiency increases. After a short period of time, the efficiency increases up to 90%. Usually, after an hour or so, the overall collection efficiency will be at the 99% level. After a period of cyclic filtration and cleaning, the overall collection efficiency will exceed 99.9%.

Total energy input requirements are primarily a function of the operating pressure drop for the filter. The pressure drop relationship for a reverse-air or a mechanical shaker baghouse is given by the following equation.[40]

$$\Delta p = K'_2 C_i V^2 t, \tag{13.70}$$

where:

Δp = operating pressure drop across filter (mm WG)
K'_2 = specific dust/fabric filter resistance coefficient
C_i = inlet dust concentration (g/m^3)
V = average filtering velocity (cm/s)
t = operating time between cleaning cycles (s).

This equation shows that the operating pressure drop is proportional to the square of the filtering velocity. For a fixed set of operating conditions, increasing filtering velocity to reduce the size of the collector will result in increases in pressure drop, fan power costs, and penetration and probably reduction in bag life.

For pulse-jet filters, the operating pressure drop is given approximately by the following equation:[30]

$$\Delta p = 2 C_i^{1.4} p^{-2} R^{-0.5}, \tag{13.71}$$

where

Δp = operating pressure drop across filter (mm WG)
C_i = inlet dust concentration (g/m^3)
p = reservoir compressed air pressure (Pa)
R = reservoir pulse rate (pulses per bag per minute).

As with mechanical shaker and reverse-air baghouses, the operating pressure drop is approximately proportional to their square of the filtering velocity.

Costs for filters vary, depending on their size and the kind and arrangement of fabric and cleaning apparatus. Historically, the lowest purchase cost plus installation cost has been the determining factor for baghouse selection. A simple comparison shows that the present value of the operation and maintenance costs for the filter over 10 years is greater than the purchase plus installation cost. The cost of the filtering media is a major portion of the initial expense as well as of long-term operating costs. The life of fabrics on dry dusts is expected to be of the order of one to four years. Conway and Jacenty[41] have proposed that a careful economic evaluation should be carried out to examine the lifetime cost of a filter installation. The specifications should determine the purchase, installation, operation, and maintenance costs of the system. The best engineering and economic decision can be reached by properly identifying and evaluating all of the baghouse installation's life costs through use of the life-cycle costing technique.

Life-cycle costing is a method of optimizing equipment selection and minimizing cost for a project by measuring and comparing all of the costs of a project and translating them into today's dollars. Chapter 15 covers life-cycle costing in more detail. It provides a technique for comparing several feasible solution alternatives by putting all of the costs on a common basis, and it allows the designer to choose an optimum.

Life-cycle cost of a filter installation = total purchase cost
+ installation cost
+ operating cost
+ cost of capital
– salvage value
– depreciation value
– tax consideration

Each factor should be determined individually to determine its relevance and significance.

13.2.3.1 High-Efficiency Particulate Air (HEPA Filters)

By definition, a HEPA filter is a throw-away, extended-medium, dry-type filter having the following characteristics:

1. A minimum particle removal efficiency of 99.97% for 0.3 micron particles.
2. A maximum resistance, when clean, of 25 mm WG when operated at rated airflow capacity
3. A rigid casing extending the full depth of the medium

Common air filters used in conventional air-cleaning applications are unable to decontaminate air to the levels required to meet the maximum permissible concentration values that have been established for radioactive substances in air. The lowest threshold limit values specified for most chemical contaminants in air are at least two orders of magnitude higher than the maximum permissible concentration of any radioactive material. HEPA filters must be used to meet these very low levels. For these components to meet their specified performance, all the system components, such as ductwork, dampers, etc., must meet standards of design and installation substantially higher than those for the nonnuclear industry. Burchsted, Fuller, and Kahn[42] cover the design, construction, and testing of very high efficiency particulate air-cleaning systems.

HEPA filters consist of a filter pack sealed into a case. The filter pack or core is made by pleating a continuous web of fiberglass paper back and forth over corrugated separators. The filter pack is sealed into a full-depth wood or steel casing using a elastomeric sealant. Gasketing is a critical item to ensure that the filter passes the air leakage tests.

The decision to use prefilters must be determined for each application on the basis of total air-cleaning system costs and the risks associated with exposing HEPA filters to the environment without protection. The effect of installing prefilters may range from being insignificant to increasing the life of the HEPA filter by a factor of 2 or 3. As a guideline, prefilters should be used if particles are larger than 1 or 2 microns in diameter or if dust concentration is greater than 23 mg/m^3.

The primary factor in filter replacement is pressure drop. Typically, HEPA filters are replaced when the pressure drop exceeds 100 mm WG. By specification, HEPA filters must have sufficient structural pressure to withstand a continuously applied overpressure of 250 mm WG or higher for at least 15 minutes without visible damage or loss of efficiency.

HEPA filters are one of the components of the total air-cleaning system. Burchsted, Fuller, and Kahn[42] describes the design requirements in detail for

the complete air-cleaning system. Design considerations for the system include environmental factors (zoning, airborne particulates and gas, moisture, heat and hot air, corrosion, vibration), operational factors (operating mode, filter-change frequency, building supply filters, prefilters, underrating, uniformity of airflow), system considerations (components, type of system), and emergency factors (shock and overpressure, fire and hot air, power and equipment outage, air-cleaning system layout).

For HEPA filters, the major design parameter is the system airflow, which can be used to establish the size and number of HEPA filters required. The penetration, resistance, and airflow are determined by the manufacturer before the filter is shipped from the factory.[43] Table 13.7 gives the standard sizes for HEPA filters.

13.2.4 Scrubbers: Wet Cyclonic, Packed Tower, Impingement, and Venturi

Scrubbers are the most commonly used technique for separating particulates from gas streams. The field of scrubber technology is very mature, with literally hundreds of thousands of scrubbers in operation worldwide, some in operation for more than 50 years.

The basic principle of wet collectors is to wet the contaminant particles in order to remove them from the gas stream. There is a wide range in scrubber design, cost, and performance.[44–52] Because of this wide variability, scrubbers must be carefully matched to specific applications.

Many investigators have attempted to define the parameters which relate cleaning efficiency to scrubber design and operating conditions. The conclusion from their investigations is that scrubber efficiency depends on energy input per unit of gas flow, whether the energy is supplied to the air or the water (contact power theory). This conclusion applies only to well-designed equipment when the energy is expended in the gas–liquid contacting process. As a result, equivalent power requirements give comparable collection efficiencies for all different equipment manufacturers.

TABLE 13.7 Standard Parameters for HEPA Filters

		Design airflow capacity at clean filter resistance	
Face dimensions (in.)	**Depth, less gasket (in.)**	**1.0 in. WG (scfm)**	**25 4 mm WG (m^3/h)**
24 × 24	$11\frac{1}{2}$	1000	1607
24 × 24	$5\frac{7}{8}$	500	803
12 × 12	$5\frac{7}{8}$	125	200
8 × 8	$5\frac{7}{9}$	50	80
8 × 8	$3\frac{1}{16}$	25	40

Source: Burchsted, Fuller, and Kahn[42]

The principal requirements of an effective wet scrubber are these:

1. Bring liquid and particulates into intimate contact to promote high collection efficiency.
2. Prevent dust buildup and plugging at the wet inlet interface.
3. Provide a suitable method to prevent water carryover in the cleaned exhaust gas.
4. Provide an acceptable disposal system for the collected dust.

The three mechanisms by which dust particles are wetted and collected are impingement, diffusion, and condensation. The mechanism of impingement is making dust particles impinge and adhere to water droplets or a water film. Diffusion is the mechanism by which the smaller particles are collected by the larger particles. Condensation takes place if a liquid spray causes the gas to pass through its dew point, with the dust particles acting as condensation nuclei. This results in an increase in effective size of particles and simplifies their subsequent collection by mechanical means. This is important in cases where a high collection efficiency is required for relatively low concentrations of very fine dusts.

Wet scrubbers find a wide range of applications because of the following advantages:

1. Moisture-laden gases or sticky, adhesive particles can be handled without plugging.
2. Hot gases can be handled easily and economically. The hot gas is cooled at the collector inlet so that the collector can be sized to handle the smaller cooled gas volume.
3. Fire or explosion hazards are eliminated.
4. Collected material can be disposed of dust-free.

These are disadvantages of wet scrubbers:

1. Scrubbers often convert an air pollution problem into a water pollution problem. If regulations require 100% recycling, the scrubber water may require flocculants or neutralizing chemicals or both.
2. Corrosion can be a serious problem requiring high maintenance or special materials of construction.
3. Very high power consumptions are required to collect very fine particles.
4. Extensive freezing protection is required for the whole scrubber system in cold climates.
5. Loss of plume buoyancy can affect ground-level concentrations.
6. High fan maintenance costs.
7. High noise level.

Although there are numerous scrubber designs, typical characteristics of four of the more common types are listed in Table 13.8. Table 13.9 presents data on the features, operating principles and problem areas with these common scrubbers. A brief description of each scrubber type follows.

A wet cyclonic scrubber is a cyclone collector with centrally located, coarse water sprays. These water sprays are usually directed radially outward,

TABLE 13.8 Typical Characteristics of Gas-Cleaning Equipment

Equipment type		Typical dust loading (g/m^3)	Air velocity (m/s)	Approximate collection efficiency (wt%) 1 micron	1–5 microns	5–10 microns	Pressure loss (mm WG)	Power requirement (kW per m^3/s)	Remarks
Inertial separators	Settling chamber	20	0.1–0.4	10	10	10	5–15	0.2	Large space requirement, collects coarse dust only, precleaner.
	Baffled chamber	20	1–5	10	10	20–60	5–15	0.2	Potential for a compact layout, collects coarse dust only, precleaner.
	High-throughput cyclone	2–200	10–20	10	10	40–80	5–75	0.2–1.0	Good efficiency at 20–40 microns, cheap, any material of construction
	High-efficiency cyclone	0.2–20	10–20	10	10–40	80–95	50–125	0.8–2.0	Good efficiency at 5–10 microns, cheap, any material of construction, higher pressure drop.
Wet scrubbers	Wet cyclonic	0.2–20	10–20	10	20–80	90–95	50–150	0.8–2.0	Most common type, utilizes centrifugal forces, low water rates.
	Packed tower	0.2–20	1–1.5	N/A	N/A	N/A	40–100	0.7–1.5	Primarily used for gases, vapors, and mist removal; packing may plug with high dust loads.
	Impingements	0.2–20	15–25	10	20–80	90–95	100–150	1.7–2.5	Widely used for average to coarse dust, good for hot gas, low to medium energy requirements.
	Venturi	0.2–20	100	80–90	99	99	750–1000	13–17	Require high fan speed, imbalance and corrosion problems, good for fume collection.
Electrostatic precipitators	Dry	0.2–2	1–2.5	80–99	80–99	+99	5–20	0.4–1.2	Suitable for high temperature or corrosion; efficiency sensitive to variations in dust, gas, or process.
	Wet	0.2–2	1–2.5	80–99	90–99	+99	5–20	0.4–1.2	Suitable for high temperature or corrosion, reentrainment of fine dust is eliminated.
Fabric filters	Mechanical shaking	0.2–20	0.005–0.025	99	99.9	+99.9	50–125	0.8–2.0	Highest-efficiency cost ratio if can be applied, temperature max. of 300 °C, caution with sticky dusts and high-moisture gases.
	Reverse air	0.2–20	0.005–0.025	99	99.9	+99.9	50–125	0.8–2.0	Handles more difficult dusts, can obtain good bag life.
	Pulse jet	0.2–20	0.01–0.1	99	99.9	+99.9	100–200	1–2.5	More compact design, new applications on metallurgical fume, cleaning air must be dry.

(continues)

TABLE 13.8 *(continued)*

Equipment type		Approximate collection efficiency (wt%)							
		Typical dust loading (g/m^3)	Air velocity (m/s)	1 micron	1–5 microns	5–10 microns	Pressure loss (mm WG)	Power requirement (kW per m^3/s)	Remarks
	Cartridge	0.02–0.2	1.3	99.9	+99.9	+99.9	50–150	0.8–2.5	Newer development, very attractive for recirculation of plant air, can be used with limestone precoating for supply air.
HEPA	Throw-away pleated cartridge	0.02	1.3	+99.9	+99.9	+99.9	25–50	0.4–0.8	Highest efficiency, used in the nuclear industry for filtering radioactive dusts.

Source: Goodfellow.[33]

and their prime purpose is to cool the gas and prevent reentrainment. The dust collected on the walls is slurried and carried away by centrifugal force.

A packed-tower scrubber consists of a tower filled with packing to provide surface area for the liquid–gas contacting process. The scrubbing liquid is introduced at the top of the packing and trickles down through it. For a countercurrent design, the contaminated gas passes up through the wetted packing, while the liquid flows downward. As the gas stream rises, it loses some of its contaminant. The clean liquid being introduced at the top allows the remaining contaminant to be absorbed more easily. A suitably designed mist eliminator is critical for a successful installation.

An impingement scrubber is designed to make the dust particles impinge and adhere to water droplets. Gas is introduced at the bottom and passes up through water-covered perforated trays, where dust is removed by the scrubbing liquid.

A venturi scrubber is a venturi-shaped air passage with water introduced just ahead of or into the venturi throat. The liquid–gas contact is at a maximum in the venturi throat. The relative velocity between gas and liquid aerosol droplets is high, with the gas velocities in the range of 50–100 m/s. The particles are conditioned in the throat, and condensation is the important collection mechanism. After the particles in the gas have been deposited on droplets, a comparatively simple device such as a cyclone collector can be used to collect the wetted dust.

The collection efficiency of wet scrubbers is dependent on parameters such as the size and quantity of liquid droplets, the liquid/gas ratio, high water-to-particle relative velocity, wettability of dust, particle density, gas viscosity, etc. For any specific application, the design procedure is to review operating data available from the technical literature or from manufacturers for similar applications. If data are not available, it may be necessary to perform pilot scale tests, which can be used for scale-up purposes.

The key to a successful scrubber installation is the proper selection of a given scrubber method for a given application. Specific industrial applications are covered in subsequent volumes of the *Design Guidebook*.

TABLE 13.9 Characteristics of Common Scrubbers

Type	Features	Operating principles	Problem areas
Wet cyclonic	Individually controlled spray nozzles. Simple design. Low energy requirements. No baffles or impingement surfaces. minimum entrainment. Easy to service.	Gas introduced at bottom. Tangential inlet. Helical gas-flow pattern. Radially injected spray pattern, follows helical gas-flow pattern.	Spray or orifice wear, pattern ineffectiveness. Plugged orifice. Flow is critical-reduced, or increased flow causes functional problems, poor turndown or turnup. Shell wear, high dust concentration.
Counterflow packed tower	Low energy requirements. Easy maintenance. Good gas absorption. Large contact area. Can be fabricated from variety of materials. Inexpensive to operate.	Vertical gas flow. Gas introduced at bottom. Gas passes through bed of irrigated packing. Gas and liquid contact in lower bed. Dry upper, bed, mist eliminator, or demister pad.	Particulates blind bed. Plugged drain. Limited volume. Corrosion, unless proper material is selected.
Impingement	Low to medium energy requirements. Underspray system prevents wet-dry interface problems. Nonplugging weir. High efficiency-to-horsepower ratio. Can be used as heat-transfer unit for cooling gases. Variable number of trays.	Gas introduced at bottom. Flow passes through water zone consisting of spent liquor and water from nozzles under plates. Trays can be flooded to varying depths, depending on heat-transfer needs. Gas flows through perforated plates. Gas impinges on tabs, passes through water layer. Small drops help encapsulate dust, simplify removal. Spent liquor exists at bottom.	Plate flooding because of excessive gas volume. Bypassing seal pots because of high pressure drop. Plugged trays. Gases not sufficiently saturated. Spray failure, poor coverage. Improper weir setting. Incorrect water flow, improper pressure. Missing deflector plates on multiple-tray unit.
Venturi	Submicron particles can be removed efficiently. Free-flow liquid entry. Low maintenance needs.	Gases enter at top. Accelerated gas stream shatters scrubbing liquor, forming fine drops that wet and agglomerate particles. Scrubbing liquor and particles are separated by cyclonic action.	High or low gas and water flows. Venturi throat and cyclone erode and plug. Plugged drains. Inadequate coverage of inlet by scrubbing liquor.

Source: Adapted from Bloss[47]

References

1. Bloor, M.I.G., and D.B. Ingham. Theoretical Investigations of the Flow in a Conical Cyclone. *Trans. Inst. Chem. Engrs.* 51 (1973), pp. 36–41.
2. Bloor, M.I.G., and D.B. Ingham. Theoretical Aspects of Hydrocyclone Flow. In *Progress in Filtration and Separation*, vol. 3, New York: Elsevier (1983), pp. 57–148.
3. Bloor, M.I.G., and D.B. Ingham. The Flow in Industrial Hydrocyclones. *J. Fluid Mech.* 178 (1987), pp. 507–519.
4. Kelsall, D.F. A Study of the Motion of Solid Particles in a Hydraulic Cyclone. *Trans. Inst. Chem. Engrs.* 30 (1952), pp. 87–108.
5. Svarovsky, L. *Hydrocyclones*. New York: Holt, Rinehart & Winston (1984).
6. Sheperd, C.B, and C.E. Lapple. *Ind. Eng. Chem.* 32 (1940), p. 1246.
7. Barth, W. Berechnung und auslegung von Zyklonabscheidern auf Grundneuerer Untersuchungen. *Brennstoff Warme Kraft.* 8 (1956), pp. 1–9.
8. Klinzing, G.E., R.D. Marcus, F. Rizk, and L.S. Leung. *Pneumatic Conveying of Solids: A Theoretical and Practical Approach*. 2nd ed. New York: Chapman & Hall (1997).
9. Baturin, V.V. *Fundamentals of Industrial Ventilation*. New York: Pergamon Press (1972).
10. White, H. J. *Industrial Electrostatic Precipitation*. Reading, MA: Addison-Wesley (1963).
11. Moore, A. D. *Electrostatics and Its Applications*. New York: John Wiley & Sons (1973).
12. Strauss, W. *Industrial Gas Cleaning*. Oxford: Pergamon Press (1975).
13. Oglesby, S. and Nichols, G. B. *Electrostatic Precipitation*. New York: Marcel Dekker (1978).
14. Parker, K. R. *Applied Electrostatic Precipitation*. London: Blackie Academic & Professional (1997).
15. Deutsch, W. Bewegung und Ladung der Elektrzitatstrager Im Zylinderlondensator. *Ann. der Physik* 68 (1922), p. 335.
16. White, H. J. Modern Electrostatic Precipitation. *Ind. Eng. Chem.* 47 (1955), p. 932.
17. Arendt, P. and H. Kallmann. The Mechanism of Charging Mist Particles. *Z. Phys.* 35 (1926), p. 421.
18. Pauthenier, M. M., and M. Moreau-Hanot. La Charge des Particules Spheriques Dansun Champ Ionise. *Journal de Physique et le Radium.* 3 (1932), p. 590.
19. White, H. J. Particle Charging in Electrostatic Precipitation. *Trans. Am. Inst. Electr. Eng.* 70 (1951), p. 1189.
20. Oglesby, S. and G. B. Nichols. Electrostatic Precipitation. In *Air Pollution*, Vol 4: *Engineering Control of Air Pollution*, A. C. Stern, ed. New York: Academic Press (1977), pp. 189–256.
21. Pui, D. Y. H. Experimental Study of Diffusion Charging of Aerosols. Thesis, Particle Technology Laboratory, Mechanical Engineering Department, University of Minnesota (1976).
22. Hinds, W. C. Aerosol Technology: Properties, Behavior, and Measurement of Airborne Particles. New York: John Wiley & Sons. (1982).
23. Buonicore, A. J., and W. T. Davis. *Air Pollution Engineering Manual*. Air & Waste Management Association, New York: Van Nostrand Reinhold (1992).
24. Strauss, W. *Industrial Gas Cleaning*. London: Pergamon Press (1966).
25. Stern, A. C. *Air Pollution*, Vol. 3, 3rd ed. New York: Academic Press (1977).
26. Engineering Equipment Users Association. *Separation of Dust from Gases*. In *EEUA Handbook No. 19*. London: Constable (1968).
27. McIlvaine, R. W. *The Fabric Filter Manual*. Chicago: McIlvaine (1980).
28. Krauss, M. N. Baghouses: Separating and Collecting Industrial Dusts. *Chem. Eng.*, (Apr. 9, 1979), pp. 94–106.
29. Kraus, M. N., Baghouses: Selecting, Specifying, and Testing Industrial Dust Collectors. *Chem. Eng.*, (Apr. 23, 1979), pp. 133–142.
30. Billings, C. E. Fabric Filter Installation for Flue Gas Fly Ash Control—Status Report. *Powder Technol.* 18 (1977), pp. 79–110.
31. Holcomb, M. L., and R. C. Scholz. *Evaluation of Air Cleaning and Monitoring Equipment Used in Recirculation Systems*, NIOSH Technical Report, DHHS (NIOSH) Publication No. 81-133. Cincinnati: U.S. Department of Health and Human Services, (Apr. 1981).
32. Smith, E. M., and R. L. Lucas. Information Required for the Specification and Performance Evaluation of Industrial Baghouses (Fabric Filters). *J. Air Pollution Control Assoc.*, 25, no. 7, (July 1975), pp. 715–720.

33. Goodfellow, H. D. *Advanced Design of Ventilation Systems for Contaminant Control*, Amsterdam: Elsevier Science Publishers, 1985.
34. Schofield, C. *Guide to Duct Explosion Venting*. London: Institution of Chemical Engineering. (1984).
35. Frederick, E. R. How Duct Filter Selection Depends on Electrostatics. *Chem. Eng.* 68, no. 13, (1961), p. 107.
36. Vansteenkistle, P. Prevention of Static Charges in Dust Filter Fabrics with Stainless Steel Fibers. *Filtration Separation* (Mar./Apr. 1981), pp. 135–139.
37. Penny, G. W. Using Electrostatic Forces to Reduce Pressure Drop in Fabric Filters. *Powder Technol.* 18 (1977), pp. 111–116.
38. Leith, D., D. D. Gibson, and M. W. First. Performance of Top and Bottom Inlet Pulse-Jet Fabric Filters. *J. Air Pollution Control Assoc.* 28, no. 7, (July 1978), pp. 696–698.
39. Goodfellow, H. D., R. J. Geren, , and E. F. C. Foord. Applications of Fabric Filters at High Air-to-Cloth Ratios on Metallurgical Fumes. In *The User and Fabric Filtration Equipment III*, APCA Specialty Conference Proceedings, Buffalo, NY (Oct. 1–3, 1978).
40. Dennis, R., R. W. Cass, and R. S. Hall. Dust Dislodgement from Woven Fabrics Versus Filter Performance. *J. Air Pollution Control Assoc.* 28, no. 1 (Jan. 1978), pp. 47–52.
41. Conway, J. and J. Jacenty. Saving Money on Your Baghouse. *Plant Eng.* (Apr. 19, 1979), pp. 285–286.
42. Burchsted, C. A., A. B. Fuller, and J. E. Kahn. *Nuclear Air Cleaning Handbook—Design, Construction, and Testing of High-Efficiency Air Cleaning System for Nuclear Application*, ERDA 76-21, UC-11, 70 NTIS, Springfield, VA (1976).
43. Dorman, R. G. High Efficiency Air Filters Development, Installation and Testing. *Filtration Separation* (May/June, 1980), pp. 237–241.
44. Buonicore, A. J. and W. T. Davis. *Air Pollution Engineering Manual.* Air & Waste Management Association. New York: Van Nostrand Reinhold (1992).
45. Calvert, S. How to Choose a Particulate Scrubber. *Chem. Eng.* (Aug. 29, 1978), pp. 54–68.
46. Metallurgical Applications of Wet Scrubbers. *J. Air Pollution Control Assoc.* 27, no. 11 (Nov. 1977), pp. 1069–1085.
47. Bloss, H. E. A Basic Guide to Upgrading Scrubber Performance. *Plant Eng.* (Dec. 13, 1979), pp. 73–75.
48. Jones, D. G., O. W. Hargrove, and T. M. Morasky. Lime/Limestone Scrubber Operation and Control. *J. Air Pollution Control Assoc.* 29, no. 10 (Oct. 1979), pp. 1099–1105.
49. Calvert, S., J. Goldschmid, D. Leith, and D. Mehta. *Scrubber Handbook*, A.P.T. Report No. EPA-R2-118a, NTIS No. PB 213-016 (Aug. 1972).
50. McIlvaine, R. W. *The McIlvaine Scrubber Manual.* Chicago: McIlvaine, (1979).
51. Brady, J. D. Understanding Venturi Scrubbers for Air Pollution Control. *Plant Eng.* (Sepr. 30, 1982), pp. 53–55.
52. Hesketh, H. E. *Air Pollution Control for Traditional and Hazardous Pollutants.* Lancaster, Pa: Technomic Publisher (1991).

Bibliography

Böhm, J. *Electrostatic Precipitators.* Amsterdam: Elsevier. (1982).
Cooper, C. D., and F. C. Alley. *Air Pollution Control: A Design Approach.* Boston: PWS Publishers. (1986).
Cottrell, F. G. *Art of Separating Suspended Particles from Gaseous Bodies.* U.S. Patent No. 895 729. (1908).
Hewitt, G. W. The Charging of Small Particles for Electrostatic Precipitation. *Trans. Am. Inst. Electr. Engrs.* 76 (1957), pp. 300–306.
Licht, W. *Air Pollution Control Engineering.* New York: Marcel Dekker (1988).
Liu, B. Y. H., and A. Kapadia. Combined Field and Diffusion Charging of Aerosol Particles in the Continuum Regime. *J. of Aerosol Sci.* 9 (1978), pp. 227–242.
Pauthenier, M., and M. Moreau-Hanot. *J. Phys. Radium.* 3(1932), p. 590.
White, H. J. Control of Particulates by Electrostatic Precipitation. In *Handbook of Air Pollution Technology*, S. Calvert, and H. M. Englund eds. New York: John Wiley & Sons. (1984), pp. 283–317.
Zhibin, Z. and Guoquan, Z. Investigations of the Collection Efficiency of an Electrostatic Precipitator with Turbulent Effects. Aerosol Science and Technology. 20 (1994) 2, pp. 169–176.

13.3 GASEOUS COMPOUNDS

13.3.1 The Control of Organic Compound Emissions

13.3.1.1 Introduction

While process and equipment modification are generally the preferred alternatives for reducing emissions from a plant, some form of control is necessary before emissions are discharged into the environment. Technologies discussed in this section are applicable in preventing emissions from point sources such as process or tank vents. These technologies fall into two main categories:

1. Destruction methods, including incineration and biological gas purification
2. Recovery methods, including adsorption, absorption and condensation

The different technologies can be used separately or combined, such as gas adsorption followed by incineration. Depending on the system used and the organic compound content in the gas stream being treated, the resulting destruction efficiencies normally range between 90% and 99%.

Thermal and catalytic incinerators, condensers, and adsorbers are the most common methods of abatement used, due to their ability to deal with a wide variety of emissions of organic compounds. The selection between destruction and recovery equipment is normally based on the feasibility of recovery, which relates directly to the cost and the concentration of organic compounds in the gas stream. The selection of a suitable technology depends on environmental and economical aspects, energy demand, and ease of installation as well as considerations of operating and maintenance. The selection criteria may vary with companies or with individual process units; however, the fundamental approach is the same.

The aim of this section is to introduce the fundamentals of incineration, adsorption, absorption, condensation, and biological treatment in order to provide a basic knowledge for the selection of suitable equipment. The waste gas characteristics that play a major role in the selection of gas-cleaning equipment are also considered. A detailed presentation of the theory of combustion, adsorption, absorption, condensation, or biological decomposition required for a complete understanding of the subject is not covered in this section (the theory can be found in the handbooks such as Perry's *Chemical Engineers' Handbook*).

Emission abatement methods covered are suitable for the emission control of volatile organic compounds (VOCs). The VOCs include organic compounds existing in the gaseous phase in air at 293.15 K. However, organic compounds, which are not regarded as VOCs, can be treated by the methods covered in this section.

13.3.1.2. Factors Influencing Equipment Selection

General

The first task in selecting an abatement method is the preparation of an emission inventory. The inventory is the basis of planning and the selection of options. By the preparation of an inventory, all emission sources requiring treatment can be determined and recorded. The emission inventory

should cover the entire facility, source by source (Fig. 13.18); the following characteristics must be included in the inventory:

1. Pollutants emitted
2. Individual chemical species within each waste gas stream
3. Composition of waste gas (ranges of each component indicated)
4. Oxygen content of waste gas
5. Operating pressure
6. Operating temperature
7. Emission type (continuous/intermittent)
8. Emission rates (hourly, annual, and average rates and maximum rate at the worst conditions)
9. Condition of source or equipment
10. Availability of suitable control
11. Regulatory considerations, covering national and international standards with proposed future changes and developments

The characteristics of the downstream pollution discharge must be monitored (see Fig. 13.18). It is essential that the operation and maintenance of the pollution control equipment be included in a quality audit procedure, assisting in determining the operation efficiency of the equipment and the formation of unwanted and possibly toxic compounds in the pollution control steps. Unsuitable operation of an incinerator may result in partial oxidation and formation of unwanted combustion products or excessive formation of NO.

Effluent Stream Characteristics

Volumetric Flow Rate The equipment size is normally dictated by its capacity and is therefore directly related to investment costs. Incineration systems are capable of handling large amounts of waste gases and are often the most cost-effective method when handling large flows. Adsorption systems can handle large volumes of gases, provided that the gas stream is fairly dilute. Absorption will

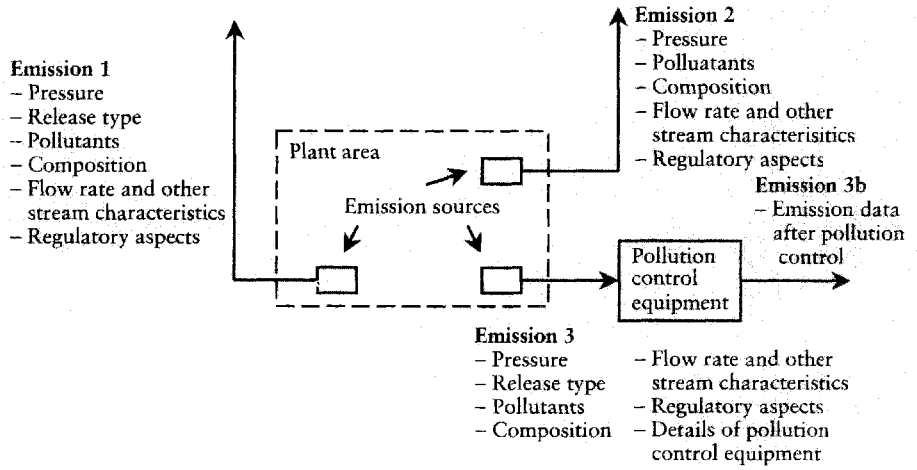

FIGURE 13.18 Emission inventory.

handle large gas volumes, but it is not a cost-effective method when very large columns are necessary. Condensation is used mainly for low gas flow rates.[1]

Concentration and Composition[2] The average concentration of organic compounds in a waste gas determines the applicability of the abatement method. Recovery methods usually require high inlet concentrations. They may need a concentrator prior to actual treatment, which increases the investment cost.

Lower and upper explosive limits (LEL, UEL) must be considered in order to avoid dangerous operation in the incinerators. Thermal incinerators are normally designed to operate with concentrations below 25% of the LEL. Typically, the LEL ranges from 2500 to 10 000 ppmv.[3]

When a mixture of compounds is to be treated, more limitations may be placed upon the selection of a suitable abatement method. There may be several compounds in the waste gas, some being unsuitable to one method, while others are unsuitable to another method. In such cases, thermal incineration may be the best solution. When recovering mixtures, additional separation equipment may be needed for recycling the reclaimed compounds.

Temperature and Humidity[1,2] When adsorption, absorption, or condensation is employed, the lowest inlet gas temperature is desirable. Adsorbent and absorbent capacities generally increase with the decreasing gas temperature. High waste-gas temperatures may preclude the use of adsorption or condensation due to the cost of chilling. Thermal and catalytic oxidation benefit from a hot effluent gas stream, as that reduces the supplementary fuel requirement. In biological treatment, a waste-gas temperature of near 37 °C is ideal.

The degree of humidity of the waste gases adds to the heat load on incineration options. Condensation of the moist gases produces an aqueous phase, which must be separated to prevent freezing of the condenser. When activated carbon is the adsorbent, 50% relative humidity should not be exceeded. Some zeolites can withstand a relative humidity in the 80–90% range.[4] Biological treatment is suitable for humid gases. Relative humidity over 90% is required in the incoming gas stream for compost biofilters.

Particulate Matter, Chlorinated Hydrocarbons, and Toxic Pollutants[1,2] Many compounds can cause problems in pollutant-control equipment. Particulate matter, liquids, or solids in the waste stream can plug the adsorber beds, heat-recovery beds in regenerative thermal incinerator systems and biofilters. Conventional filtration systems are used to remove particulate matter before or after the process.

As many emissions involve chlorinated compounds, corrosion is a major problem in many control methods. The corrosion of columns and surface condensers can be prevented or reduced by the correct material selection. However, corrosion remains a constant threat to the interior of incinerators. Additional pollution control equipment such as scrubbers may also be required to remove acidic compounds from treated gases before discharging into the atmosphere.

When toxic or hazardous pollutants are handled, special waste-disposal and material-handling requirements are essential. Adsorption, absorption, and

condensation processes all produce some liquid or solid waste. In catalytic incinerators the catalyst may become contaminated with toxic or hazardous pollutants and will require replacing. Thermal incineration normally removes all troublesome pollutants.

Removal Efficiency

Emissions can be managed by one of two methods:

1. Total concentration or mass of organics emitted is limited.
2. Resulting ambient concentration of each compound must be below an air quality standard.

Both these methods relate to the required removal efficiencies of the pollution control equipment. All abatement methods achieve high removal efficiencies when used in the correct applications (Fig. 13.19). The highest efficiency (with limitations) is in most cases achieved with incineration. When removal efficiencies of 99% or greater are required, incineration is usually recommended.[1]

Recovery of Pollutants

Recovering and recycling organic compounds make possible some cost savings in the pollution control equipment. Savings may be in raw material costs, which are normally the most significant item of a chemical plant. Solvent recovery is best suited for applications dealing with expensive or easily

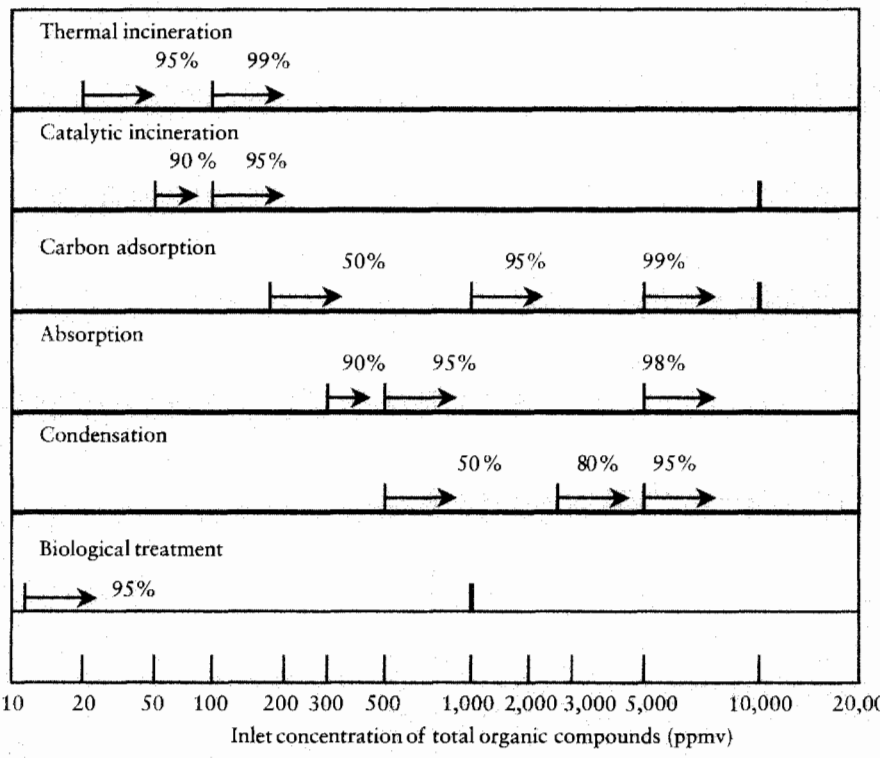

FIGURE 13.19 Typical removal efficiencies.

recoverable compounds. Recovery is economical if the recovered compounds can be reused in a process as a fuel or raw material or sold to another user. Waste minimization practices are important from the environmental regulatory viewpoint, encouraging the recovery of reusable organic pollutants.

Adsorption and condensation are the normal recovery options. If recycling is considered and is economically feasible, consideration of incinerators as destruction devices may be unnecessary. Generally, recovery units like adsorbers and absorbers result in higher total capital investment than modular, packaged incinerators.

Location

Many factors must be considered when selecting a location for the control unit, the actual position being partially dictated by the type of unit. Adsorption, absorption, condensation, and biotreatment units can usually be located near the existing process areas. Incinerators and carbon adsorbers cannot always be placed close to hazardous process areas due to the risk of fire and explosion. Positioning the unit remote from the waste gas source increases the cost of ducting and piping, which may be excessive when handling large waste-gas quantities.

Generally, adsorption, absorption, and biofilter units require more space than compact incinerators and condensers. If the plant room is restricted, a local roof-mounted system may be the best alternative. However, roof structural reinforcement may be required even for small and lightweight units. Consideration must be given to the effects of noise and vibration. Small adsorption systems, such as adsorption canisters, require an additional central regeneration unit on site, or they must be regenerated or disposed of off site. A central regeneration unit may require long runs of costly ductwork.[2]

Cost

The economic factors must be considered in every application. It is important to find a technique that will meet both the technical and economical requirements. In short, pollution control costs depend on the system characteristics and the application. Some cost equations that generalize the economics of the managing systems are available in the literature. Most of these equations give rough estimates and have an accuracy of only about 30% to 50%. For a comprehensive cost comparison of different units, a detailed cost analysis based on the equipment tender proposals and the special characteristics of the project is necessary.

13.3.1.3 Abatement Methods

Thermal Incineration

General Incineration (oxidation) is the best-known method for the removal of gaseous industrial waste. Combustible compounds containing carbon, hydrogen, and oxygen are converted to carbon dioxide and water by the overall exothermic reactions [Eq. (13.72)]. When chlorinated or sulfur-containing compounds are present in the effluent, the products of combustion include HCl/Cl_2 or SO_2/SO_3.[5]

$$C_xH_yO_z + (x + y/4 - z/2)\, O_2 \rightarrow x\, CO_2 + y/2\, H_2O \qquad (13.72)$$

Destruction efficiencies over 99% can be achieved when the inlet concentration of organic compounds of the waste gas is over 100 ppmv.[6] Thermal

oxidation units are most commonly used for streams consisting of dilute mixtures of organic compounds and air[7] and when the waste-gas concentration is over 15% of LEL (lower explosion limit). Thermal incineration is also suited if there is large variation in the inlet concentrations or if the waste gas contains compounds that could contaminate the catalyst.[8] For safety reasons the organic concentration of incoming gas should be limited to less than 25% of LEL.[2] If the organics content is over 25% of LEL, the waste gas is diluted prior to incineration by adding air, and the waste-gas composition is continuously monitored.[9]

The advantages of thermal incineration are that it is simple in concept, has a wide application, and results in almost complete destruction of pollutants with no liquid or solid residue. Thermal incineration provides an opportunity for heat recovery and has low maintenance requirements and low capital cost. Thermal incineration units for small or moderate exhaust streams are generally compact and light. Such units can be installed on a roof when the plant area is limited.[6] The main disadvantage is the auxiliary fuel cost, which is partly offset with an efficient heat-recovery system. The formation of nitric oxides during the combustion processes must be reduced by control of excess air temperature, fuel supply, and combustion air distribution at the burner inlet. The formation of thermal NO increases dramatically above 980 °C.[10] (see Table 13.10)

Types of Thermal Incinerators Three types of thermal oxidation systems are available:

1. Direct-flame incinerator
2. Recuperative incineration unit
3. Regenerative incineration unit

TABLE 13.10 Characteristics of Thermal Incineration

Equipment types	(a) Direct flame (b) Recuperative (c) Regenerative
Capacity range, m s^{-1}	over 0.5
Inlet gas concentration, ppmv	100–2500
Removal efficiency, %	95–99 +
Recovery	no
Unsuitable inlet gas characteristics	Compounds requiring high destruction temperatures
Advantages	(a) Can treat dilute streams and complex mixtures of organic compounds. (b) Can treat gases containing particulates, water, or catalyst poisons. (c) Simple operating concept. (d) Wide applicability (e) Compact, light units available.
Disadvantages	(a) Fuel costs. (b) Further treatment required when Cl- and S-containing gases are treated.

The difference between the units is mainly in their heat-recovery systems. A thermal incineration system generally consists of a refractory-lined chamber, burner(s), a temperature control system, fan(s), and heat-recovery equipment. In the incineration process, waste gas is introduced to the combustion chamber, where it is raised to the appropriate combustion temperature by burning an auxiliary fuel such as natural gas or fuel oil. In general, the concentration of organic compounds in industrial effluents is not high enough to provide self-sustaining combustion. Therefore, additional fuel is required. After heat recovery, the resulting flue gases are exhausted into the atmosphere.[9]

The direct-flame incinerator is the simplest type of thermal oxidation system. It comprises a combustion chamber and supplementary fuel-injection system with no energy-recovery equipment. Direct-flame incineration is suitable only for gases that support combustion without requirements for auxiliary fuel (concentrated streams) or for intermittent use.

In the recuperative incinerator (Fig. 13.20), the hot exhaust gases preheat the incoming gas in a shell-and-tube heat exchanger (preheater). The heat-recovery efficiency is normally between 50% and 70%. Regenerative oxidation systems offer heat-recovery efficiencies as high as 95% and are used for airstreams with low calorific values and large volumes.[8] In the regenerative system (Fig. 13.21), the inlet gas is heated while passing through the hot ceramic bed. After oxidation in the chamber, the hot gases pass through another cold ceramic bed and preheat it to the combustion chamber outlet temperature. The process flows are then reversed, so that the inlet stream can be fed to the hot bed.[5]

Catalytic Incineration

In catalytic incineration, organic contaminants are oxidized to carbon dioxide and water. A catalyst is used to initiate the combustion reaction, which occurs at a lower temperature than in thermal incineration. Catalytic incineration uses less fuel than the thermal method. Many commercial systems have removal efficiencies greater than 98%.

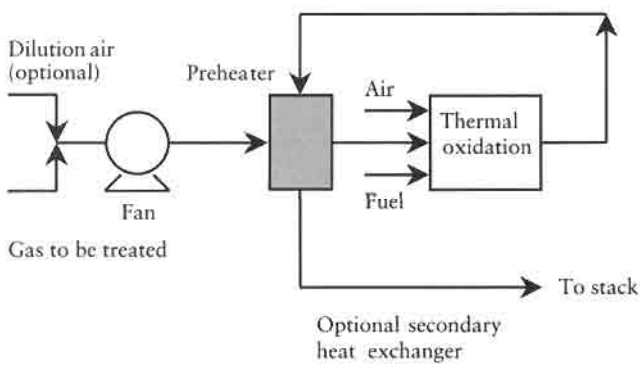

FIGURE 13.20 Recuperative thermal incineration unit.

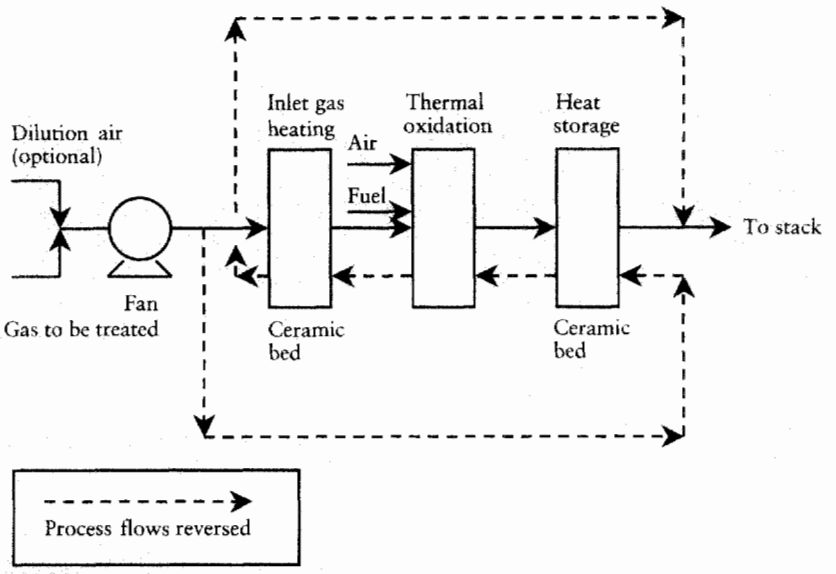

FIGURE 13.21 Regenerative thermal incineration unit.

The catalysts used in incinerator systems for gaseous organic compound control are usually precious or base metals or metal salts. The catalysts can be supported on inert materials such as alumina (Al_2O_3) or ceramics.[9] For the destruction of organic compound mixtures, a highly active but nonselective catalyst is required.[11]

In catalytic incineration, there are limitations concerning the effluent streams to be treated. Waste gases with organic compound contents higher than 20% of LEL (lower explosion limit) are not suitable, as the heat content released in the oxidation process increases the catalyst bed temperature above 650 °C. This is normally the maximum permissible temperature to which a catalyst bed can be continuously exposed. The problem is solved by dilution; this method increases the furnace volume and hence the investment and operation costs. Concentrations between 2% and 20% of LEL are optimal. The catalytic incinerator is not recommended without prefiltration for waste gases containing particulate matter or liquids which cannot be vaporized. The waste gas must not contain catalyst poisons, such as phosphorus, arsenic, antimony, lead, zinc, mercury, tin, sulfur, or iron oxide.[9,12] (see Table 13.11)

The operation of a catalytic incinerator is similar to that of a thermal unit. The preheated waste gas can be further heated in a preheat chamber before passing through the catalyst bed. The most common reactor design for reducing the organics-containing stream with a catalyst is the fixed-bed catalytic incinerator with the catalyst monolith (Fig. 13.22).[13] Other types are the packed-bed reactor with pelletized catalyst particles on shallow trays and the fluidized-bed reactor. Generally, all types of catalytic incinerators are equipped with recuperative or regenerative heat-recovery equipment. The recuperative exchangers are the most common, giving heat-recovery efficiencies between 50% and 70%.[8]

TABLE 13.11 Characteristics of Catalytic Incineration (Fixed-Bed Incinerator)

Equipment types	Fixed bed
Capacity range, $m^3 s^{-1}$	0.5–47.2
Inlet gas concentration, ppmv	100–2000
Removal efficiency, %	95–98+
Recovery	No
Unsuitable inlet gas characteristics	(a) Particulates and liquids that cannot be vaporized. (b) Catalyst poisons
Advantages	(a) Can treat compounds with high destruction temperatures. (b) Low fuel cost.
Disadvantages	(a) Catalyst deactivation. (b) Gas pretreatment usually required. (c) Further treatment if Cl-containing gases are treated.

Adsorption

General Adsorption is a physical process in which organic species are transferred onto the surface of a solid adsorbent. Adsorption is a particularly attractive control method as it can handle large volumes of gases of low pollutant concentrations. It is capable of removing contaminants down to very low levels.[1] Removal efficiency is typically greater than 95%. The most frequently used adsorbent in the organic compound applications is activated carbon, although zeolites and resins are also used.

Adsorption technologies focus on two applications:

1. The recovery of valuable industrial solvents
2. The removal of organic compounds such as toxic compounds

Adsorption is the most widely used solvent-recovery technique and is also used for odor control. The latter application is necessary to meet statutory air pollution control requirements. Depending on the application, adsorption can be used alone or with other techniques such as incineration.[14]

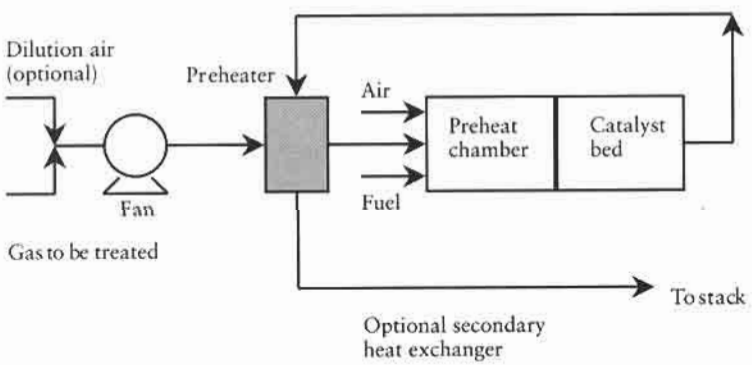

FIGURE 13.22 Catalytic incineration unit.

Solvent recovery with adsorption is most feasible when the reusable solvent is valuable and is readily separated from the regeneration agent. When steam-regenerated activated-carbon adsorption is employed, the solvent should be immiscible with water. If more than one compound is to be recycled, the compounds should be easily separated or reused as a mixture.[9] Only very large solvent users can afford the cost of solvent purification by distillation.[1]

The advantages include the availability of long-term operating data. In addition, adsorbers can handle varying flow rates or varying concentrations of organic compounds. The main disadvantage of adsorption is the formation of a secondary waste, such as the spent adsorbent, unusable recovered organic compounds, and organics in the waste water if steam is used for regeneration. Secondary waste may require off-site treatment or specialist disposal.[12] (see Table 13.12)

Types of Adsorbers Five types of adsorption equipment are used in collecting gases containing organic compounds:

1. Regenerable fixed-bed adsorbers
2. Disposable/rechargeable canisters
3. Moving-bed adsorbers
4. Fluidized-bed adsorbers
5. Chromatographic baghouses

Of these, the most commonly used for air pollution control are the fixed-bed and canister units. Fixed beds are also used in solvent-recovery applications. Major process steps include adsorption, regeneration, and further treatment of the desorbed organic compounds. Typically, further treatment includes condensation and separation.

TABLE 13.12 Characteristics of Adsorption (Fixed-Bed Adsorber)

Equipment types	Fixed bed
Capacity range, $m^3\ s^{-1}$	0.05–125
Inlet gas concentration, ppmv	Below 20–5000
Removal efficiency, %	Over 95 Over 99.5 with frequent regeneration
Recovery	Yes
Unsuitable inlet gas characteristics	(a) Complex mixtures (b) Particulates (c) Contaminants reacting with adsorbent (d) Compounds difficult to desorb (e) Compounds with molecular weight of over 130 g mol^{-1} or below 45 g mol^{-1}
Advantages	(a) Low outlet concentrations possible. (b) Dilute mixtures can be treated. (c) Lots of operating data available.
Disadvantages	(a) Energy-intensive regeneration. (b) Gas pretreatment usually required.

Fixed-bed adsorbers may be operated in either intermittent or semicontinuous mode. A typical removal system is a semicontinuously operated dual-bed system; one bed is in adsorption mode while the other is being regenerated (Fig. 13.23).[14] The adsorption performance of the bed can be monitored by analyzing the outlet gas. Once organic vapors are detected in the gas stream, the incoming gas stream is routed to the parallel adsorber, and the exhausted bed is regenerated. The adsorption and desorption cycles can also be fixed.

Canister-type adsorbers differ from fixed-bed units in that they are normally limited to the removal of low-volume, intermittent gas streams, such as storage-tank vent gases.[3] Process economics usually dictate whether regenerable or throw-away canisters are appropriate. Each canister unit consists of a vessel, adsorbent, fan (not always necessary), inlet connection and distributor, and an outlet connection for the purified gas. The disadvantage in using canisters is that poor operating efficiencies result if the adsorber becomes saturated. Because the adsorber will probably be disposed of, there is a temptation to operate it until the adsorber is saturated. Unlike fixed-bed units, the concentration of the outlet gases is not usually monitored.[3]

Absorption

The removal of one or more components from a gas mixture by absorption is probably the most important and familiar operation in the control of gaseous pollutant emissions. Though most often used for the control of inorganic gases, absorption can also be used for recovery of organic compounds. Absorption in-

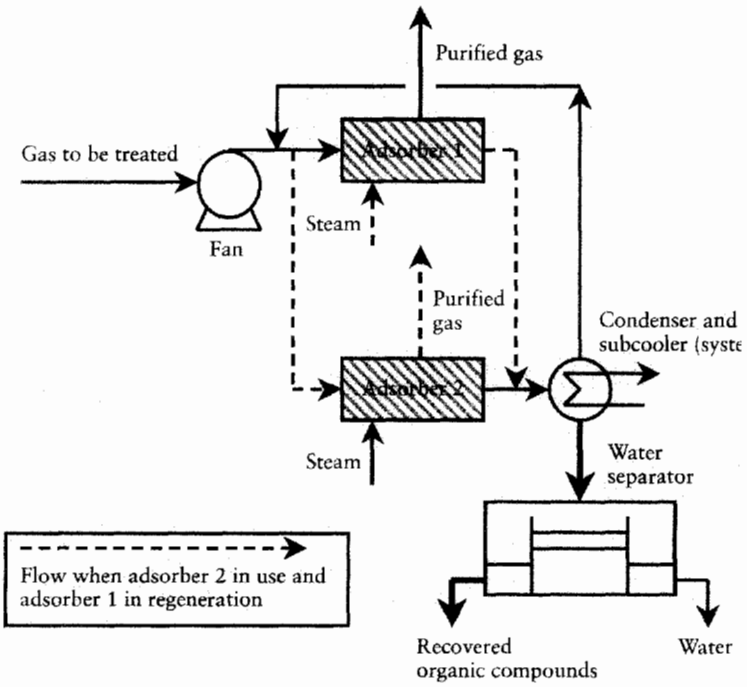

FIGURE 13.23 Simplified sketch of adsorption unit.

volves a mass transfer of one or more components from a gas stream into a nonvolatile liquid (solvent, absorbent). The absorption rate is enhanced by using low operating temperatures, high pressures, large mass-transfer surface areas, high liquid-to-gas ratios, and high organic concentration in the gas stream.[15]

The main advantage of absorption is its applicability to the control of pollutant gases present in large concentrations (several percent by volume).[1] In these applications, removal efficiencies of 98% or greater can be achieved. The main disadvantage is inflexibility; to achieve the best performance, the gas stream components are fixed once the column is designed. (see Table 13.13)

A typical absorption system (Fig. 13.24) consists of a counterflow absorption column. The regeneration is carried out in a desorption column at a reduced pressure and increased temperature. Regeneration is achieved by stripping, distillation, or extraction. Packed columns are most commonly used for the absorption of gaseous pollutants and have a high removal efficiency and a low pressure drop.[2] The most common absorbents are water, silicon oils, paraffins, high-boiling-point esters, and polyalkylglycolethers.[16]

Condensation

Condensation can be achieved by either increasing the pressure or reducing the temperature of the gas. Generally, condensation systems operate at a constant pressure (at the same pressure as the emission source).[12] A removal efficiency of 95% is attainable with high inlet gas concentrations. However, the minimum concentration of organic compounds obtained in the outlet gas effluent is equal to the saturation concentration at the operation temperature. Chilled water, brine, refrigerant propylene, and liquid nitrogen can be used as coolants.

Condensation is normally used for the recovery of organic compounds from process or tank vent gases or from releases during loading. Condensation is used to recover valuable compounds prior to incineration, or to reduce the organic load entering other control systems, such as adsorbers or absorbers.[7] Adsorption and absorption processes benefit from low condenser outlet temperatures.

TABLE 13.13 Characteristics of Absorption

Equipment types	Packed or plate columns
Capacity range, $m^3 s^{-1}$	4.7–52.8
Inlet gas concentration, ppmv	Over 800
Removal efficiency, %	Over 90
Recovery	Yes
Unsuitable inlet gas characteristics	(a) Concentration of organics below 300 ppmv (b) Mixtures of organic compounds when recycling is required
Advantages	(a) High organic concentrations can be treated. (b) Moist gases can be treated. (c) Effective when organic compounds are soluble in absorbent.
Disadvantages	(a) More complex than other methods. (b) Inflexible.

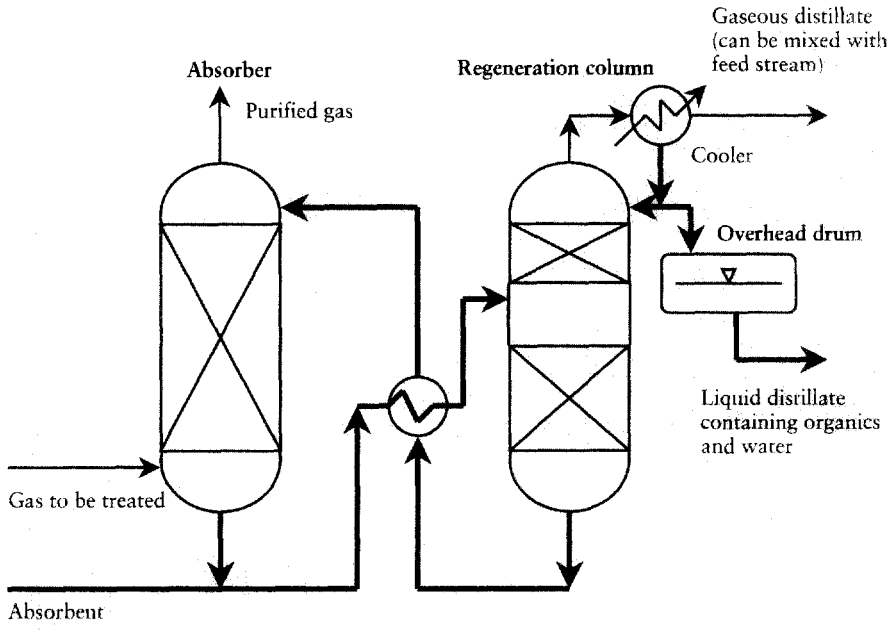

FIGURE 13.24 Absorption unit.

The advantages of indirect condensation are product recovery, modest space requirements, and no additional waste generated if the gas stream is dehumidified prior to the condenser.[6] The start-up and shutdown times of the unit are short.[17] Condensers can handle nearly any flow stream with adequate concentration of organic compounds (over 3000 ppmv).[12] Disadvantages include corrosion or ice formation if water is allowed to condense in the system. The incoming gas flow rate and its composition must be reasonably constant to avoid changes in the operating temperature.[12] One of the biggest problems in surface condensers is the accumulation of air or inert gases, which decrease the cooling capacity.[18] (see Table 13.14)

TABLE 13.14 Characteristics of Condensation

Equipment types	Surface condenser
Capacity range, $m^3 s^{-1}$	Below 1.4
Inlet gas concentration, ppmv	Over 3000
Removal efficiency, %	50–95+
Recovery	Yes
Unsuitable inlet gas characteristics	(a) Compounds that can polymerize, foul, or solidify in a condenser (b) Mixtures when recycling is required
Advantages	(a) High organic concentrations can be treated. (b) Modest space requirements. (c) Short start-up and shutdown times.
Disadvantages	(a) Explosion hazard. (b) Corrosion and ice formation. (c) Low operating temperatures normally required.

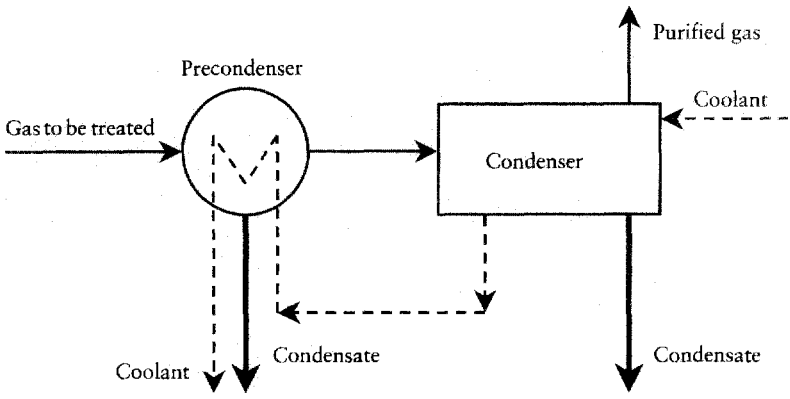

FIGURE 13.25 Condensation unit.

Surface condensers are typically shell-and-tube heat exchangers. A condensation unit (Fig. 13.25) generally consists of precondenser(s) for water removal, condenser, and demister.[17,18] The elimination of an explosion hazard when flammable vapors are condensed requires sophisticated control equipment and an inert operating environment of airtight construction.[9] Condensation of moisture and possible equipment freezing can be avoided by dessicant that dries the incoming gas stream. Precooling and separation of the organic compounds from water can be omitted by drying.

Biological Gas Purification

In biological gas purification, microorganisms oxidize organic compounds to carbon dioxide and water in a moist and oxygen-rich environment. The oxidation of sulfur or nitrogen-containing compounds and chlorinated organic compounds also generates inorganic acids. If undegradable compounds are not present, a control efficiency greater than 90% can be achieved with reasonable filter volumes and low investment and operation costs. Odors are often completely removed.[19]

Advantages of the biological gas purification include low operating temperatures and the possibility of treating gas streams with low organic loads. Due to the low operating costs, bio-filtration can provide significant advantages over other air pollution technologies when the waste gases contain low concentrations of readily biodegradable and water-soluble compounds.[12,19] Biotreatment is not recommended for gases containing organic sulfur compounds.[12] It is essential that dust, oil, and grease are removed from the waste gas stream before they enter the biological treatment zone.[20] (see Table 13.15)

Biofilters are used for the control of organic compounds, air toxics, and organic and inorganic odors. Most biofilters are built as open single-bed systems, the most common filter media being compost and soil.[19] In biofiltration, effluent gases are vented through a biologically active material, and with sufficient residence time, the contaminants diffuse into a wet, biologically active layer (biofilm) that surrounds the filter particles. Aerobic degradation of pollutants occurs while the microorganisms metabolize them. The system consists of an effluent gas blower, a gas humidifier,

TABLE 13.15 Characteristics of Biofiltration

Equipment types	Compost or soil filters
Capacity range, $m^3 s^{-1}$	0.3–41.7
Inlet gas concentration, ppmv	Below 100
Removal efficiency, %	Over 90
Recovery	No
Unsuitable inlet gas characteristics	(a) Water-insoluble compounds (b) Very high flow rates (c) High organic concentrations
Advantages	(a) Low organic concentrations can be treated. (b) Simple operating concept.
Disadvantages	(a) Process automation impossible. (b) Sensitivity to pH and moisture in a filter. (c) Excess biomass disposal. (d) Daily manual operation required. (e) Lots of space needed.

and a biofilter including an air-distribution system and filter material (Fig. 13.26). For biological purification, bioscrubbers such as fixed-bed bioreactors or trickle-bed bioreactors can also be used.

Membranes

Membrane technology is a new alternative for the treatment of gas-phase organic pollutants. It is commercially viable when combined with other control technologies such as condensation and incineration. Membranes used in the vapor separation processes are selectively permeable to organic compounds but relatively impermeable to air and inert gases such as nitrogen and carbon dioxide. Separation occurs as the different compounds transport across the membrane barrier at different rates. The pressure difference between the feed side of the membrane and the permeate side is the driving force of the separation process.[21] The pressure difference across the membrane can be maintained either by compressing the feed stream (Fig. 13.27) or by the use

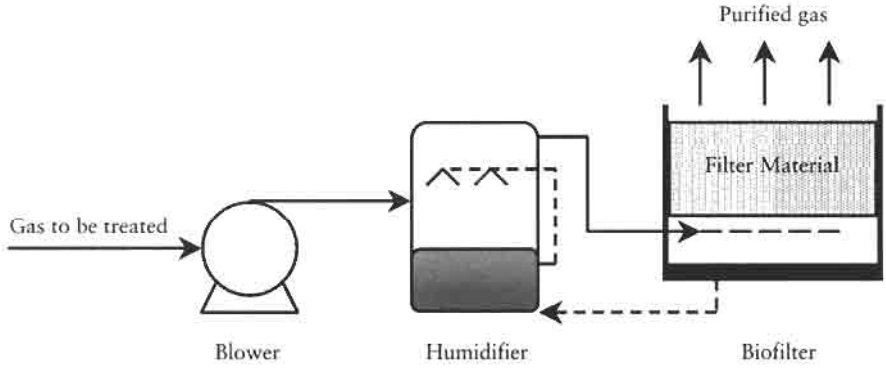

FIGURE 13.26 Biofilter.

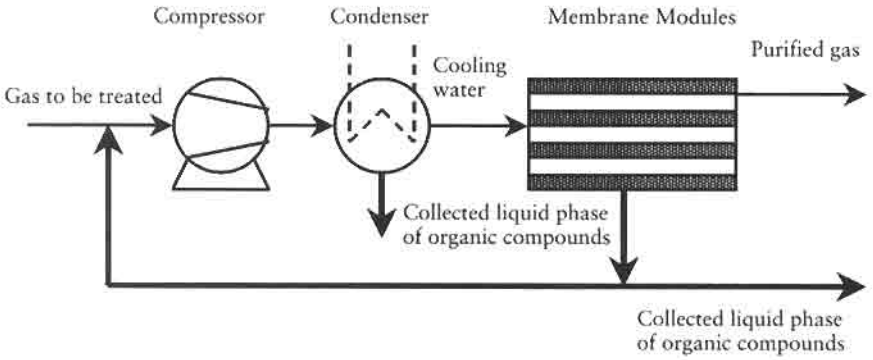

FIGURE 13.27 Membrane unit.

of a vacuum pump on the permeate side. Recovery efficiencies of 90–99.99% have been achieved with spiral-wound composite membranes.[22] The primary advantage of the membrane recovery system is that condensation occurs at temperatures above the freezing point of water, resulting in no predrying, multistage cooling, or refrigeration. Another advantage of this system is that secondary waste streams are not created.

13.3.1.4 Summary

The technologies used in the control of gaseous organic compound emissions include destruction methods such as thermal and catalytic incineration and biological gas treatment and recovery methods such as adsorption, absorption, condensation, and membrane separation. The most common control methods are incineration, adsorption, and condensation, as they deal with a wide variety of emissions of organic compounds. The most common types of control equipment are thermal and fixed-bed catalytic incinerators with recuperative heat recovery, fixed-bed adsorbers, and surface condensers. The control efficiencies normally range between 90% and 99%.

In the selection of control equipment, the most important waste-gas characteristics are volumetric flow rate, concentration and composition of organic compounds in the waste-gas, waste-gas temperature and humidity, and the content of particulate matter, chlorinated hydrocarbons, and toxic pollutants. Other factors influencing the equipment selection are the required removal efficiency, recovery requirements, investment and operating costs, ease of installation, and considerations of operation and maintenance. The selection of a suitable control method is based on the fundamental selection criteria presented as well as the special characteristics of the project.

References

1. Rinko, J., Jr., and M. Traister. Practical Considerations for the Selection of Pollution Control Equipment for VOC Emissions, 81st Annual Meeting of APCA, Dallas, June 19–24, 1988.

2. Ruddy, E. N., and L. A. Carroll. Select the Best VOC Control Strategy. *Chem. Eng. Prog.* 89 (1993) no. 7, pp. 28–35.
3. Vatavuk, W. M., W. L. Klotz, and R. L. Stallings. Carbon Adsorbers. In *OAQPS Control Cost Manual*, 4th ed. Research Triangle Park, NC: EPA (1990).
4. Otten, W., E. Gail, and T. Frey. Einsatzmöglichkeiten Hydrophober Zeolite in der Adsorptionstechnik. *Chem. Ing. Tech.* 64 (1992) no. 10, pp. 915–925.
5. van der Vaart, D. R., W. M. Vatavuk, and A. H. Wehe. Thermal and Catalytic Incinerators for the Control of VOCs. *J. Air Waste Manage. Assoc.* 41 (1991) no. 1, pp. 92–98.
6. McInnes, R., S. Jelinek, and V. Putche. Cutting Toxic Organics. *Chem. Eng.* 97 (1990) no. 9, pp. 108–113.
7. Kumar, K. S., R. L. Pennington, and J. T. Zmuda. Capture or Destroy. *Chem. Eng. (Environ. Eng.)* 100 (1993) no. 6, pp. 12–17.
8. Drohan, D. Different Routes to VOC Control. *Pollut. Eng.* 24 (1992) no. 16, pp. 30–33.
9. Katari, V. S., W. M. Vatavuk, and A. H. Wehe. Incineration Techniques for Control of Volatile Organic Compound Emissions. *JAPCA* 37 (1987) no. 1, pp. 91–99.
10. Marks, J. R., and R. F. Weston. Technical and Cost Comparison of VOC Emission Reduction Techniques, 1989 AIChE Summer National Meeting, Philadelphia, August 22, 1989.
11. Spivey, J. J. Complete Catalytic Oxidation of Volatile Organics. *Ind. Eng. Chem. Res.* 26 (1987), pp. 2165–2180.
12. Martin, A. M., et al. Control Odors from CPI Facilities. *Chem. Eng. Prog.* 88 (1992) no. 12, pp. 53–61.
13. Vatavuk, W. M., et al. Thermal and Catalytic Incinerators. In *OAQPS Control Cost Manual*, 4th ed. Research Triangle Park, NC: EPA (1990).
14. Shah, G. C. Improve Activated Carbon Bed Adsorber Operations. *Hydrocarbon Processing* 71 (1992) no. 11, pp. 61–63.
15. Nordén, H. V. Kemian laitetekniikka II course material, Helsinki University of Technology, Espoo.
16. Müller, G., and M. Ulrich. Abtrennung und Rückgewinnung von Stoffen aus Abluft- und Abgasströmen. *Chem. Ing. Tech.* 63 (1991) no. 8, pp. 819–830.
17. Hakala, E. Liuotinhöyryjen talteenotto kondensaatiotekniikalla. *Muovi* (1991) no. 5, pp. 28–29.
18. Järveläinen, M. Kemian laitetekniikka I course material, Helsinki University of Technology, Espoo.
19. Leson, G., and A. M. Winter. Biofiltration: An Innovative Air Pollution Control Technology for VOC Emissions. *J. Air Waste Manage. Assoc.* 41 (1991) no. 8, pp. 1045–1054.
20. Wittorf, F., et al. Biocatalytic Treatment of Waste Air. *Chem. Eng. Technol.* 16 no. 1, pp. 40–45.
21. Lahiere, R. J., et al. Membrane Vapor Separation: Recovery of Vinyl Chloride Monomer From PVC Reactor Vents. *Ind. Eng. Chem. Res.* 32 (1993), pp. 2236–2241.
22. Baker, R. W., et al. Membrane Systems for VOC Recovery from Air Streams. *Filtration and Separation* 31 (1994) no. 3, pp. 231–235.

13.4 FUME CONTROL TECHNOLOGY

13.4.1 Basic Principles

Fumes are defined as solid airborne particulates that have been produced by a change of state. Many industrial operations produce fumes which affect both the indoor environment and the outdoor environment. For many operations, fumes are generated by a high-temperature process. The gas stream containing the fume is usually of high temperature and contains combustibles. The combustibles may form an explosive mixture, thus necessitating specialized design inputs for most fume control ventilation systems. The major elements of a fume control system are pictured in Fig. 13.28.

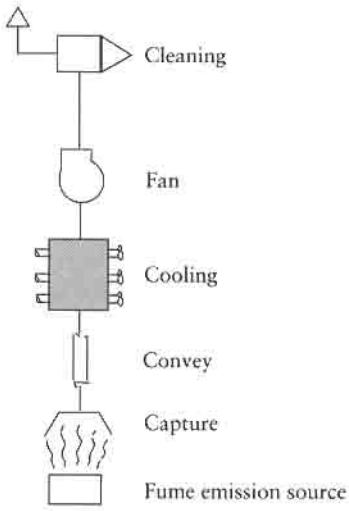

FIGURE 13.28 Elements of a fume control system.

For a fume control problem, the questions which should be asked, in order of priority, are as follows:

1. Can the fume generation process be eliminated?
2. Can the fume be captured or totally contained at the source?
3. Can the fume be captured at low level?
4. Can the fume be captured remotely?

To establish whether the fume generation process can be eliminated, the following types of questions must be asked:

1. Can the process be changed? (This should be pursued in depth at an early stage of the project.)
2. Can more material be handled at one time?
3. Can the material be handled less frequently?
4. Can the material be moved over shorter distances?
5. Can the material be handled with different equipment or systems?
6. Can the material composition be changed?
7. Can the material be handled at a temperature beneficial to fume suppression?

If the fume generation process cannot be eliminated, a fume control system must be designed. An overview of design methodology and design procedures for the different types of fume control systems follows.

Detailed designs for fume control systems and selection of specialized gas-cleaning equipment for specific industries are covered in published reference materials.[1–10]

13.4.2 Emission Source Characterization

13.4.2.1 Design Methodology

The first essential step in the design of a fume control system and selection of gas-cleaning equipment is the characterization of the fume emission source. Design procedures which can be used for new and existing industrial plants follow. The characterization of fume emission sources includes parameters such as plume flow rates (m^3/s), plume geometry (m), source heat flux (J/s), physical and chemical characteristics of particulates, fume loadings (mg/m^3), etc.

For a new process plant, calculations can be carried out using the heat release and plume flow rate equations outlined in Table 13.16 from a paper by Bender.[11] For the theory to be valid, the hood must be more than two source diameters (or widths for line sources) above the source, and the temperature difference must be less than 110 °C. Experimental results have also been obtained for the case of hood plume eccentricity. These results account for cross drafts which occur within most industrial buildings. The physical and chemical characteristics of the fume and the fume loadings are obtained from published or available data of similar installations or established through laboratory or pilot-plant scale tests.[12] If exhaust volume requirements must be established accurately, small-scale modeling can be used to augment and calibrate the analytical approach.

For an existing process plant, the designer has the opportunity to take measurements of the fume or plume flow rates in the field. There are two basic approaches which can be adopted. For the first approach, the fume source can be totally enclosed, and a temporary duct and fan system installed to capture the contaminant. For this approach, standard techniques can be used to measure gas flow rates, gas compositions, gas temperatures, and fume loadings. From the collected fume samples, the physical and chemical characteristics can be established using standard techniques. For most applications, this approach is not practical and not very cost effective. For the second approach, one of three field measurement techniques, described next, can be used to evaluate plume flow rates and source heat fluxes.

13.4.2.2 Propeller Anemometer Technique

Fume velocity can be measured at the roof truss level by using several propeller-type anemometers mounted on a grid. The output from the anemometers can be connected to a recorder located at the operating floor level. Experience has shown that six to eight anemometers are usually sufficient to give a good description of the plume velocity. This approach has the advantage of obtaining both a velocity profile and an average velocity for the plume. The combined information of velocity distribution and observed plume size provides the necessary design parameters to ensure a satisfactory performance for the designed hood. Figure 13.29 is a plot of average plume flow rates measured at roof truss level as a function of time for a typical tapping operation on an electric steelmaking furnace. To carry out such velocity measurements as a standard method is not recommended because fume and dust tend to harm the propeller bearings, making the anemometer inoperative after a number of tests.

TABLE 13.16 Jet and Plume Equations for Line and Point Sources

	Dimensions	Point jet	Line jet	Point plume	Line plume
Characterizing source quantity	v_s assumed uniform	"Massless" momentum flux $M = Q_s v_s$ (m^4/s^2)	"Massless" momentum flux $M = Q_s v_s$ (m^3/s^2)	Buoyancy flux = const. $F = Q_s \Delta_s$ (m^4/s^3)	Buoyancy flux = const. $F = Q_s \Delta_s$ (m^3/s^3)
Volume flow rate Q	$\frac{m^3}{s}$	$\left(\frac{8M}{\pi}\right)^{1/2} \pi \alpha z = u_{max} \pi b^2$	$4\left(\frac{\alpha M}{\sqrt{2}}\right)^{1/2} z^{1/2} = u_{max} \sqrt{\pi} b$	$\frac{6\pi\alpha}{5}\left(\frac{18F\alpha}{5\pi}\right)^{1/3} z^{1/3} = u_{max} \pi b^2$	$2\alpha\left(\frac{F}{\alpha}\right)^{1/3} z = u_{max} \sqrt{\pi} b$
Mass flux G	$\frac{g}{s}$	$Q\rho_0$	$Q\rho_0$	$Q\rho_0$	$Q\rho_0$
"Massless" momentum flux M	$\frac{m^4}{s^2}$	M = const.	M = const.	$\frac{\pi}{2}\left(\frac{18FQ}{5\pi}\right)^{2/3} z^{4/3} = \frac{u_{max}^2 \pi b^2}{2}$	$\sqrt{2}\alpha\left(\frac{F}{\alpha}\right)^{2/3} z = u_{max}^2 \sqrt{\pi/2}\, b$
Kin. energy flux (power) E	$\frac{g m^3}{s^3}$		$\rho_0\left(\frac{M^3\sqrt{2}}{\alpha}\right)^{1/2} z^{-1/2} = \rho_0 u_{max}^3 \sqrt{\pi}/3 \frac{b}{2}$	$\rho_0 F z = \rho_0 u_{max}^3 \frac{\pi b^2}{3}$	$\frac{\rho_0 F}{\sqrt{3}} z = \rho_0 u_{max}^3 \sqrt{\pi/3} \frac{b}{2}$
Centerline velocity u_{max}	$\frac{m}{s}$	$\left(\frac{M}{2\pi}\right)^{1/2} \frac{1}{\alpha} z^{-1}$	$\left(\frac{M}{\sqrt{2}\alpha}\right)^{1/2} z^{-1/2}$	$\frac{5}{6\alpha}\left(\frac{18\alpha F}{5\pi}\right)^{1/3} z^{-1/3}$	$\left(\frac{F}{\alpha}\right)^{1/3}$ = const.
Entrainment const. α	—	0.057	0.068	0.093	0.156
Length scale b	m	$2\alpha z$	$(4/\sqrt{\pi})\alpha z$	$(6/5)\alpha z$	$(2/\sqrt{\pi})\alpha z$

Relationship between buoyancy flux and pollutant flux:

Buoyancy $\Delta = g\frac{\rho_0 - \rho}{\rho_0} \approx g\frac{T - T_0}{T_0}$

Concentration of pollutant $C = g\frac{\text{grainloading}}{\rho_0}$

Buoyancy flux $F = (\Delta_{max}/2) \cdot Q$ = const.

Pollutant flux $(C_{max}/2) \cdot Q$ = const.

For pure plumes the distribution of velocity, buoyancy, and concentration is the same.

$$\frac{u_{max}}{u(r)} = \frac{\Delta_{max}}{\Delta(r)} = \frac{C_{max}}{C(r)}$$

From source heat flux q, the buoyancy flux F is

$$F = \int_0^\infty \Delta(r) u(r)\, dA = \frac{qg}{C_0 T_0 \rho_0}$$

C = local pollutant concentration, m/s^2, ft/s
C_{max} = plume centerline concentration, taken at hood face when used for nondimensionalizing, m/s^2, ft/s^2
C_p = specific heat of ambient fluid, J/g K, BTU/fb °R
Q = plume flow rate, m^3/s, ft^3/s
q = source heat flux, J/s, BTU/s
r = radial coordinate, m, ft
T = local plume temperature, K, °R
T_0 = temperature of ambient fluid, K, °R
u = local vertical plume velocity component, m/s, ft/s
Δ = local plume buoyancy, m/s^2, ft/s^2
ρ = local plume fluid density, g/m^3, lb/ft^3
ρ_1 = hood exhaust fluid density, g/m^3, lb/ft^3
ρ_0 = ambient fluid density, g/m^3, lb/ft^3

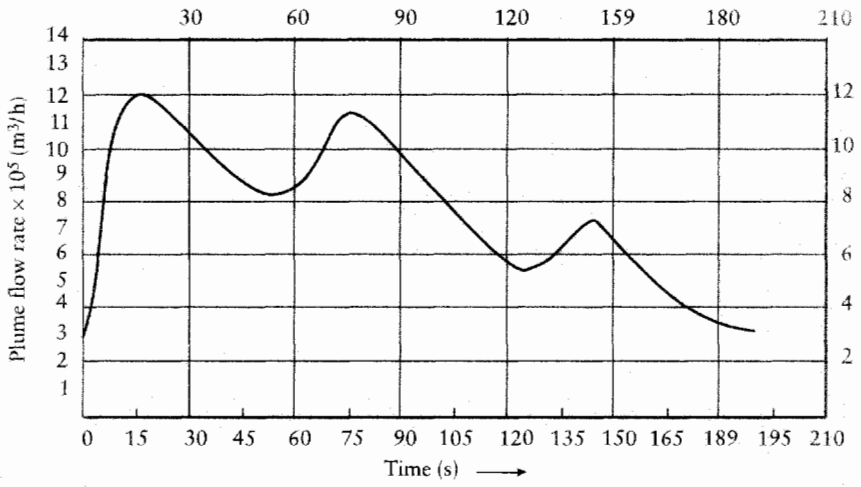

FIGURE 13.29 Average plume flow rate at roof truss level for a tapping operation.

13.4.2.3 Stopwatch Technique

The stopwatch technique for determining emission volume flow rate is based on measuring with a stopwatch the elapsed time for fume to rise between two known levels (e.g., Z_1, Z_2). For this test procedure to be valid, the test must be carried out in a region where the rising fume clearly exhibits buoyancy-dominated plume behavior. The calculation procedure depends on a good estimate of the location of the virtual origin of the plume and the heat release for the process.

At the Z_2 level, the plum volumetric flow rate is given by

$$Q_{Z_2} = 0.026\left(\frac{Z_2 - Z_1}{t}\right)\left(\frac{1-a}{1-a^{2/3}}\right), \tag{13.73}$$

where $a = (Z_2 - Z_1)/t$, the observed maximum plume velocity, is equal to

$$\frac{\int_{Z_1}^{Z_2} U_{\max} dZ}{Z_2 - Z_1}, \tag{13.74}$$

where Q_{Z_2} is obtained by substituting the formulas for Q from Eq. (13.73) and $U_{\max}$.

This technique permits estimation of the volumetric flow rate at any level above a source, provided that the result is matched to the gravitational fume acceleration terms applicable near the source. The result of such an analysis is shown in Fig. 13.30. The emission flow rate from an electric arc tapping process has been estimated at any level above the steel ladle using the stopwatch technique in conjunction with the plume theory.

The nature of the preceding analysis does not permit the application of the technique to design of local capture hoods but rather to the design of remote or canopy fume hoods. For this approach to be valid, the hoods must usually be at least two source diameters away from the emission source.

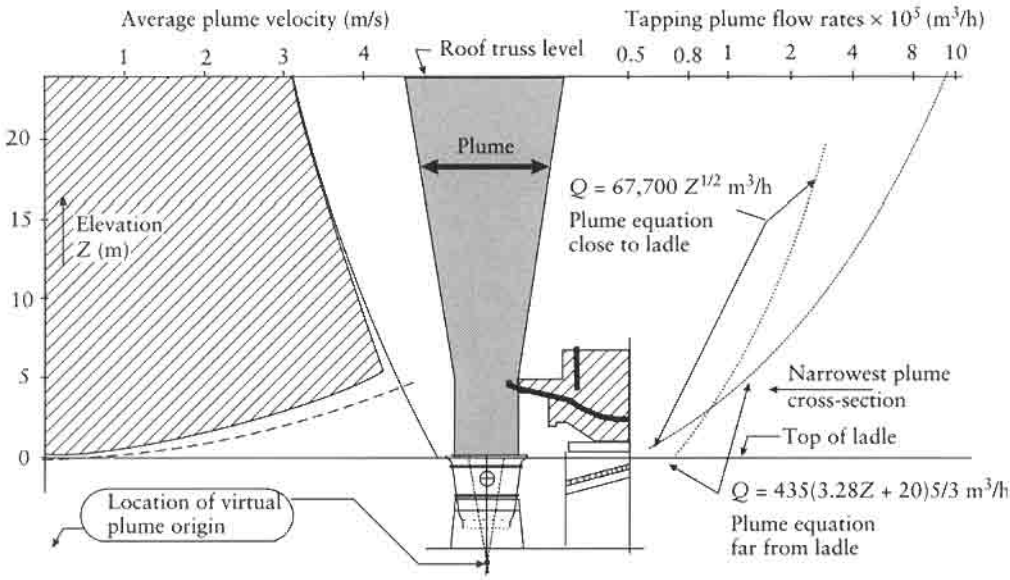

FIGURE 13.30 Average plume velocity and flow rate during an electric furnace tapping operation.

13.4.2.4 Plume Photographic Scaling Technique

For an existing industrial process plant, Goodfellow and Bender[13] have developed a simple, expedient, and low-cost technique for establishing the average plume flow rate and plume geometry. Once the flow rate is known, the heat flux for the source can be established easily through off-gas temperature measurements. This technique is called the plume photographic scaling technique or the movie scaling technique. This technique has been used successfully to solve numerous fume hood design problems in Canada, the United States, and elsewhere around the world.[2,3] This approach is preferred over the earlier two approaches because it is simple, cost effective, and accurate.

The plume photographic scaling technique is based on proper illumination of the fume (preferably by oblique-angle back lighting) and the inclusion in the scene of an object suitable for movie scaling. During the early development of this technique, an accurate average velocity of heavily contaminated turbulent flows was obtained by taking 8-mm or 16-mm color movies of the emission. The movie camera found most suitable for this purpose used a standard 18 frames per second. Although high-speed movie cameras have been used, it was concluded that they are unsuitable for this work.

Recent developments in the field-testing procedure have demonstrated that a motor-driven 35-mm camera at up to three frames per second produces superior results to a movie camera.[14,15] The analysis of the film is carried out by scaling the distance that fume advances from one consecutive photograph to the next. The diameter of the plume as a function of the distance above the source can be scaled directly off the photograph.

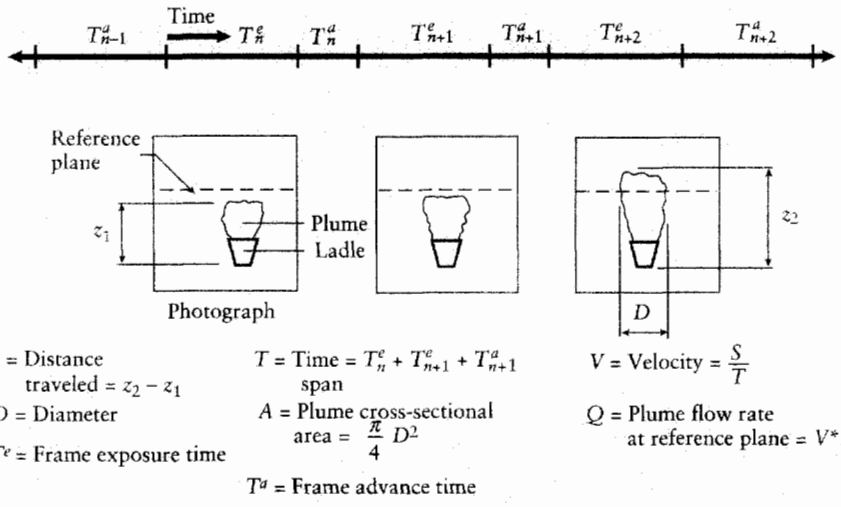

Note:
Frames are shot in sequence at up to three frames per second with a motor-driven 35mm camera.

FIGURE 13.31 Plume photographic scaling technique and calculation procedure.

Figure 13.31 is a pictorial representation of the scaling technique and the calculation procedure. Figure 13.32 shows a typical application of this technique to calculate a plume flow rate from an electric furnace scrap-charging process. Although the technique seems very simple and straightforward, its successful application requires experienced judgment and careful attention to detail during the critical data analysis stage.

13.4.3 Fume Capture Design Methodology

More stringent environmental regulations are requiring significant improvements in both air pollution and the workplace environment. As a result, fume control systems must be designed to operate efficiently. Equation (13.75) represents the general equation for overall system performance:

$$\eta_{\text{overall}} = \eta_{\text{capture}} - \eta_{\text{capture}}\left(1 - \frac{\eta_{\text{cleaning}}}{100}\right) = \frac{\eta_{\text{capture}} - \eta_{\text{cleaning}}}{100} \tag{13.75}$$

where

η_{overall} = overall fume control system performance
η_{capture} = percentage of total fume generated which is captured by control system
η_{cleaning} = percentage of fume collected by gas cleaning relative to total fume load to fume system

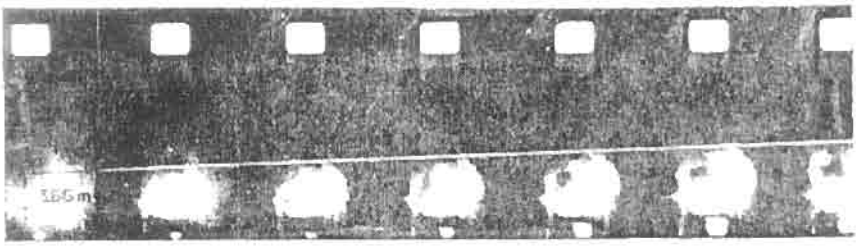

Flow rate = Velocity × Area = (Height/Time) × $(Dia)^2$ × 3.14/4
= (9.76 − 3.66)/(1/9 s × 13 frames) × $(9.45)^2$ × 3.14/4
= 296 m^3/s

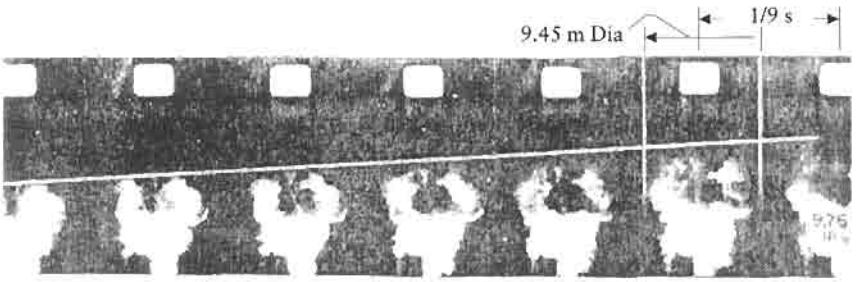

FIGURE 13.32 Application of plume photographic scaling technique to electric furnace scrap-charging process.

Sample Problem

Consider a fume control system with an overall hood fume capture efficiency of 60% and a fume cleaning efficiency of 99%. Calculate overall fume control system performance.

Solution The overall fume control system performance is

$$\frac{(60)(99)}{100} = 59.4\%.$$

The technology in the fume capture field is not well developed, and performances of many capture systems are low and typically may be in the 30% to 60% range. There is a paucity of fundamental research and development in the fume capture field. In contrast, hundreds of million of dollars have been spent on research and development activities in the gas-cleaning area, which is mature and well developed. It is not uncommon to specify and to measure gas-cleaning equipment performances of over 99.9% collection efficiency. As shown in Eq. (13.75), the overall fume control system performance is determined by the product of the capture efficiency and the gas-cleaning efficiency. This equation clearly shows the need to improve the efficiency of capture of the fume at the source in order to obtain significant improvements in the overall fume control system performance.

Fume capture techniques can be classified into three specific types as follows:

1. Source capture or direct evacuation
2. Low-level or close-capture hood
3. Canopy or remote-capture hood

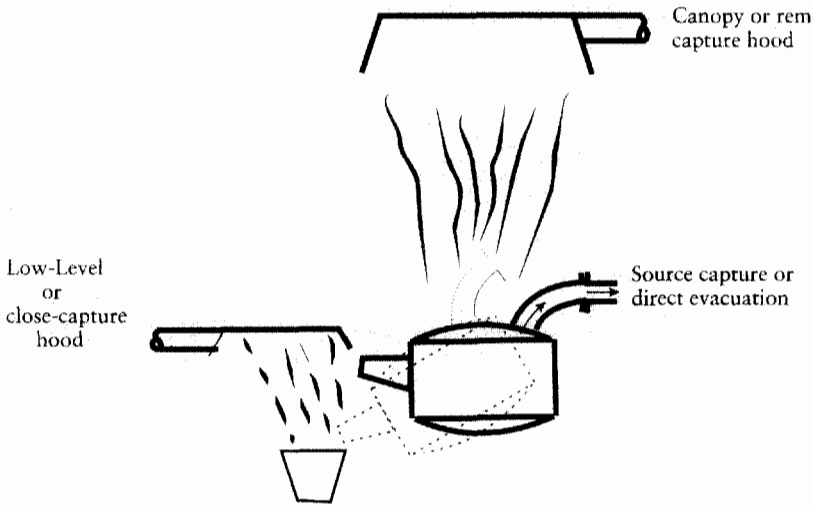

FIGURE 13.33 Classification of fume capture techniques.

A pictorial representation of the different fume capture techniques is shown in Fig. 13.33.

Table 13.17 lists some of the important considerations for the different fume capture techniques. From the point of view of cost effectiveness, the usual preference is source collection or a low-level hood, provided an acceptable scheme can be developed within the process, operating, and layout constraints. The cost of fume control systems is almost a direct function of the gas volume being handled. Hence, the lower volume requirements for the source capture or low-level hood approach often results in significant capital and operating cost savings for the fume control system.

The use of a source capture or a direct evacuation system is the most positive form of fume capture. A well-designed system can operate at high fume capture efficiencies. For many of these systems, the captured gas temperature for the processing operation is very high (1000–1500 °C), and gas cooling may be required

TABLE 13.17 Comparison of Fume Capture Techniques

	Source capture	Low-level hood	Canopy hood
Gas volume to be treated	Lowest	Low	Very high
Gas temperatures	Very high	Medium/low	Low
Fume loadings	Very high	High	Low
In-plant environment	Excellent	Good/excellent	Often poor (cross-drafts)
Process interference	May be significant	May be significant	Not significant
Layout constraints	May be significant	May be significant	Not significant
System costs	Lowest	Medium/high	Highest

ahead of the gas-cleaning equipment. Specific processing information, such as feed rates, chemical composition of feed, operating levels, etc., is required in order to define the necessary design parameters for the direct-evacuation fume system. A typical example of the processing information required for sizing the fume system for an electric steelmaking furnace is shown in Table 13.18. From a completed questionnaire, design calculations can be carried out to calculate gas flows, gas temperatures, and gas compositions. These calculations form the basis for the subsequent sizing of direct-evacuation fume systems.

TABLE 13.18 Canopy-Hood Design Equations

Sketch	Equations		Reference
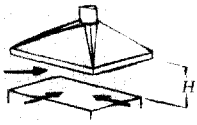	Open type		ACGIH[16]
	$Q = 1.4PHV$	Q = flow rate P = perimeter of tank H = height of hood above tank V = velocity (50–500 FPM)	
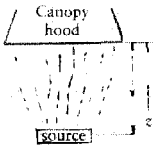	Two sides enclosed		ACGIH[16]
	$Q = (W + L)HV$	W, L = open sides of hood	
	Three sides enclosed		ACGIH[16]
	$Q = WHV$	W = open side of hood	
	Contained flow angle of air column = 12°–20°		Danielson[17]
	Typical design flow angle = 15°		
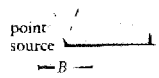			
	Face velocity hood = 150–200 FPM		
		v_z = velocity at distance z (ft)	
		Z = height above point source	Hemeon[18]
	$v_z = \frac{37}{z^{0.29}}\sqrt[3]{H'}$	= effective height (ft)	
	$q_z = 7.4z^{3/2}\sqrt[3]{H'}$	$= y + 2b$	
		y = distance from source to hood (ft)	
		B = width of source (ft)	
		H = rate sensible heat transfer to air column (BTU/min)	
		q_z = total airflow rate (ft^3/min)	
	$D = z^{0.98}/2$	D = diameter of air column (ft)	
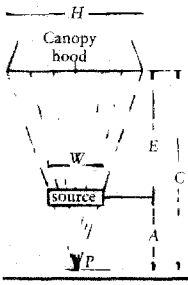	$H = 0.437\ C^{0.98}$	H = hood diameter (m) W = furnace diameter (m) P = theoretical point	Eisenbarth[19]
	$A = 2.58\ W^{1.38}$	Hood face velocity = 0.5–1.0 m/s	

The advantages of low-level hoods are listed in Table 13.17. The first step is to verify that the general principle of local capture of emissions is acceptable and feasible for the process. The next step is to establish the most efficient hood geometry. In most cases, this involves a balancing of the degree of process interference tolerable against the degree of emission source enclosure required.

The factors affecting the performance of a local exhaust system are well known.[18] For fume control, an added factor is the effect of heat release or buoyancy. Important design parameters are process heat release and the size and geometry of air-supply openings and their location relative to major surfaces of the enclosure. The location of the fume off-take is usually only of secondary importance.

Figure 13.34 gives an example of a local exhaust hood above a vessel holding a hot product. There are three different design approaches which can be used to establish the exhaust volume requirement for the low-level hood. These three approaches, in order of increasing accuracy, are as follows:

1. Rule of thumb
2. Analytical approach applying the three fluid mechanics equations
3. Small-scale modeling tests

For the rule-of-thumb approach, the control velocities required through A and A_2 to prevent fume emissions from the hood are obtained from standard references.[16,18] The exhaust required to control emissions from the opening A is greater when the pot is empty. The short-circuiting of flow Q_2 is not a serious problem as long as the clearance A_2 is small. These rule-of-thumb estimates can be improved by applying the three well-established fluid mechanics equations governing conservation of mass, energy, and momentum to the fume collection process.[20] These equations simply state that "flows in" must equal "flows out" and that all flow forces (pressures) must be balanced at all times. Unfortunately, a high degree of inaccuracy still exists in this approach because of the large number of assumptions regarding the expected flow field in the hood. For industrial applications in which complex hoods are needed, it

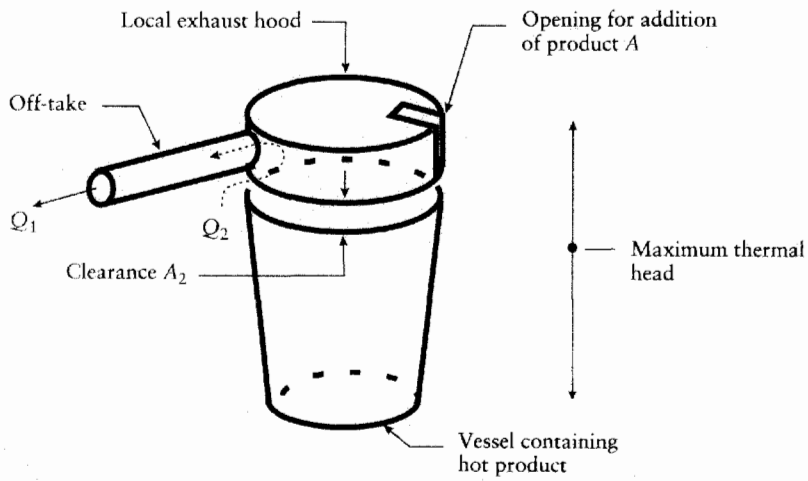

FIGURE 13.34 Example of a local exhaust hood above a vessel containing a hot product.

is essential to carry out a small-scale model study in order to establish the minimum exhaust volume required to control fume emissions.

For modeling, the similitude laws governing modeling must be followed. The topics of dynamic similitude and theory of models are discussed in most textbooks on fluid mechanics,[20] and only the resulting equations are discussed here.

In order to create dynamic physical models, it is necessary that the following criteria be met:

1. Exact geometric similitude between the model and the real-world prototype
2. An identical balance of forces between the model and the real-world prototype

In the set of conservation equations described earlier, the Reynolds number and the Froude number must be the same for the model and the prototype. Since most industrial operations involve turbulent flow for which the Reynolds number dependence is insignificant, part of the dynamic similarity criteria can be achieved simply by ensuring that the flow in the model is also turbulent. For processes involving hot gases (i.e., buoyancy driving forces), the Froude number similarity yields the required prototype exhaust rate as follows.

$$\text{Froude}_{\text{model}} = \text{Froude}_{\text{prototype}}$$

$$\left.\frac{V^2}{g_c\left(\frac{\rho_0-\rho}{\rho}\right)L}\right|_m = \left.\frac{V^2}{g_c\left(\frac{\rho_0-\rho}{\rho}\right)L}\right|_p \tag{13.76}$$

where

V = representative velocity (L/θ)
g_c = gravitational acceleration (L/θ)
ρ_0 = ambient fluid density (M/L^3)
ρ = representative fluid density (M/L^3)
L = representative dimension

All parameters must be in consistent units.

A representative velocity can be taken as the ratio of the hood off-take flow rate to the hood off-take cross-sectional area. For this basis, the prototype off-take flow rate is obtained from the following equation.

$$Q_p = Q_m \frac{[(\rho_0-\rho)/\rho)]_p^{1/2}}{[(\rho_0-\rho)\rho]_m^{1/2}} \times S^{5/2} \tag{13.77}$$

$$= Q_m \frac{[(T_0-T)/T]_p^{1/2}}{[(T_0-T)/T]_m^{1/2}} \times S^{5/2}, \tag{13.78}$$

where

Q = volumetric flow rate (L^3/θ)
S = model scale (e.g., for a model 1/100 the size of the prototype, $S = 100$)
T = representative gas temperature
T_0 = ambient gas temperature

This equation can be rewritten by substituting for the temperatures to give the following equation:

$$Q_p = Q_m \left(\frac{\rho_m q_p}{\rho_p q_m}\right)^{1/3} \left(\frac{D_p}{D_m}\right)^{5/3}, \tag{13.79}$$

where

q = heat flux rate (H/θ)
D = characteristic dimension (L)

If the model test uses the same fluid medium as the prototype at similar ambient temperatures, Eq. (13.79) can be simplified:

$$Q_p = Q_m \left(\frac{Q_p}{q_m}\right)^{1/3} \left(\frac{D_p}{D_m}\right)^{5/3}. \tag{13.80}$$

In this context, it is important to note that a model test simulating the operation of an air pollution control scheme can also be modeled in water. For some air pollution problems, an air model might become quite large in order to ensure modeling the turbulent nature of the prototype flow rate. For some applications, a water model can be used which will give a reasonable scale size.

Important conclusions can be drawn from the general modeling Eq. (13.79). The equation shows that the required prototype flow rates are directly proportional to the model flow rates. For scaling, the equation shows that the prototype flow rate has a strong dependence on the accuracy of the model scale (5/3 power). Both of these parameters are easy to establish accurately. The flow rate is rather insensitive (varies as the 1/3 power) to the changes in the model and prototype heat flow rates, densities, and temperatures. This is desirable because an inaccuracy in the estimate of the model variable will have a rather small effect on the resulting prototype flow rate.

The use of canopy hoods or remote capture of fume is usually considered only after the rejection of source or local hood capture concepts. The common reasons for rejecting source or local hood capture are usually operating interference problems or layout constraints. In almost all cases, a canopy hood system represents an expensive fume collection approach from both capital and operating cost considerations. Remote capture depends on buoyant air currents to carry the contaminated gas to a canopy hood. The rising fume on its way to the hood is often subjected to cross-drafts within the process buildings or deflected away from the hood by objects such as cranes. For many of these canopy systems, the capture efficiency of fume may be as low as 30–50%.

Canopy hoods have existed for a long time, and almost all industries have canopy-hood installations of some shape or size. Canopy design, until the mid-1970s, was an art based on rule of thumb and highly empirical approaches. Analytical work done to arrive at procedures for canopy-hood design is described in papers by Bender,[11] Goodfellow and Bender,[13] and Goodfellow.[3]

It is only recently that technology has developed so that canopy-hood efficiencies can be predicted and measured in a quantitative way. One of the difficulties in this area has been the use of different definitions for canopy-hood efficiency. Goodfellow and Bender[13] have proposed a standard

method for measuring canopy-hood performance which accounts for three parameters:

1. Ratio of spilled pollutant to total pollutant arriving at the hood
2. Ratio of hood suction to plume flow rate at the hood
3. Type of canopy hood

Hood types were classified into three groups.[13]

Type A—Ideal hood. Fume of the lowest concentration at the fringes of the plume spills first.
Type B—Actual hood. Falls in the intermediate range between type A and type C.
Type C—Worst hood. Spills fume of an average concentration.

The type C hood performance is due to turbulent mixing within the hood, which is caused by an inappropriate hood design or by objects below the hood face.

Figure 13.35 is a schematic of a canopy hood where

Q_I = hood suction flow rate (m^3/s)
Q_H = plume flow rate at the hood face level (m^3/s)
Q_S = spilled plume flow rate at the hood (m^3/s)
G_C = contaminant captured by hood (kg/s)
G_H = contaminant arriving at hood (kg/s)
G_S = contaminant spilled (kg/s)

An equation can be developed which expresses the ratio of spilled contaminant to total contaminant in terms of the ratio of hood suction to plume flow rate. This equation is as follows:

$$\left(\frac{G_S}{G_H}\right) = \left(1 - \frac{Q_I}{Q_H}\right)^X, \tag{13.81}$$

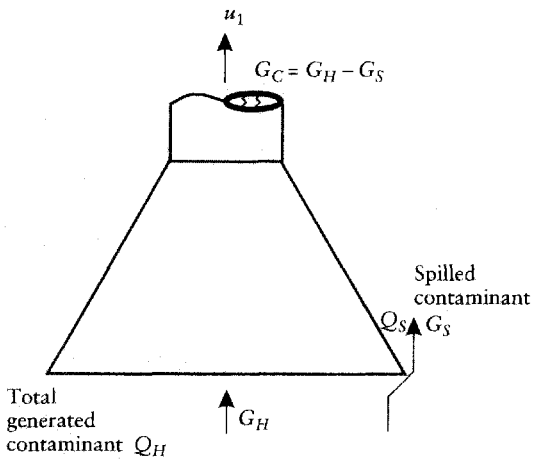

FIGURE 13.35 Canopy hood schematic.

where

$X = 2$ for type A—ideal hood
$1 < X < 2$ for type B—actual hood
$X = 1$ for type C—worst hood

Figure 13.36 is a plot of the preceding equation for the three types of hoods. The plot shows the curve for the actual and the worst hoods requiring a hood flow rate larger than the plume flow rate in order to get 99% fume capture.

The preceding results can be extended to relate canopy-hood performance to opacity. This is a significant step because air pollution legislation in many countries has a reference to opacity levels (i.e., a fume concentration level which must be met at the point of discharge of fume from a process building). Equations can be developed of this form:

$$OP = 1 - (1 - OP_{\max})^{(1-(Q_1/Q_H))^X}, \tag{13.82}$$

where

OP = observed opacity
$OP_{\max}$ = the maximum opacity observed for zero hood suction for an existing installation

Figure 13.37 is a plot of relative roof monitor opacity as a function of fume hood suction.

Following a similar approach to that used for low-level hoods, small-scale modeling is often pursued for the design of canopy hoods for a new facility or for modifications to an existing installation.[19,21–24] Bender[11] describes tests carried out

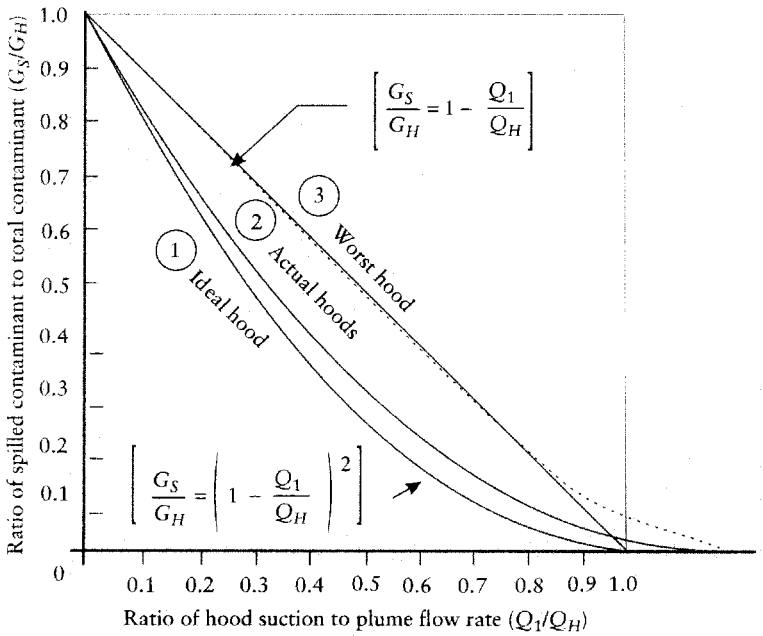

FIGURE 13.36 Contaminant spilled, G_S, as a function of contaminant arriving at hood.

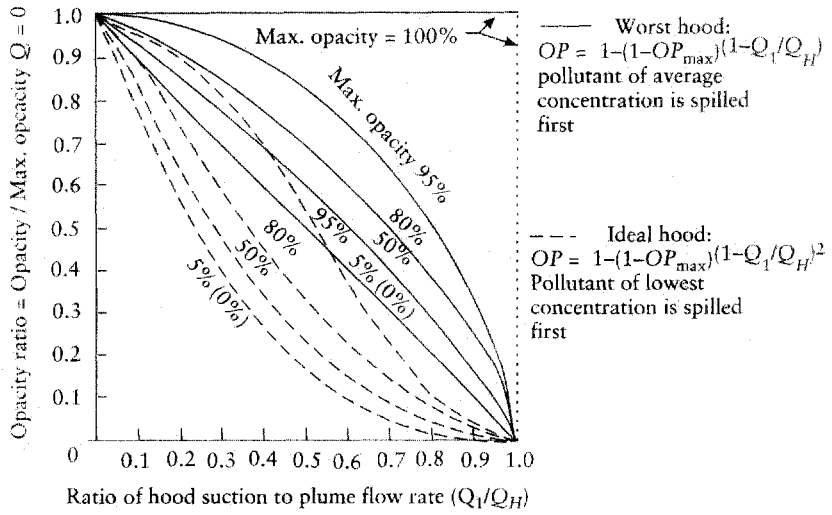

FIGURE 13.37 Relative roof monitor opacity as a function of fume hood suction.

to examine the design of canopy hoods and describes a technique for the development of a fume hood design for fluctuating plume flow. The problems of recirculation and temporary storage of fume in hoods have also been examined. Test results have shown that a baffle plate arrangement for fume hoods can significantly improve the performance of canopy hoods under specific plume flow conditions.

References

1. Davis, W. T. *Air Pollution Engineering Manual.* 2nd ed. New York: Air & Waste Management Association, Van Nostrand Reinhold (2000).
2. Goodfellow, H. D. *Advanced Design of Ventilation Systems for Contaminant Control.* Amsterdam: Elsevier Science (1985).
3. Goodfellow, H. D. *Fume Control for Electric Furnaces—Past, Present and Future.* Ventilation '94, Stockholm, September 5–9, 1994.
4. Goodfellow, H. D., et al. Hood System Design for Capture of Process Fugitive Particulate Emissions. *Heating/Piping/Air Conditioning* 58 (February 1986) no. 2, pp. 47–54.
5. Goodfellow, H. D., and P. Safe. Analysis of Remote Receptor Hoods Under the Influence of Cross Drafts. ASHRAE Winter Meeting, Chicago, IL, Jan. 28–Feb. 1, 1989.
6. Goodfellow, H. D., and P. Safe. Theoretical Analysis of Captor Hoods for Contaminant Control. *Ann. Occup. Hygiene* (October 1988).
7. Goodfellow, H. D. Hood Design for Ventilation Systems. *Heating/Piping/Air Conditioning* 59 (February 1987) no. 2, pp. 60–66.
8. Goodfellow, H. D. *Ventilation Systems for Fume Control.* Brussels: von Karmen Institute for Fluid Dynamics (May 1998).
9. Goodfellow, H. D. *Energy Savings and Cost Cutting in Ventilation.* Brussels: von Karmen Institute of Fluid Dynamics (May 1998).
10. Goodfellow, H. D. Future Trends in Design of EAF Fume Systems. 5th European Electric Steel Congress, Paris, June 19–23, 1995.
11. Bender, M. Fume Hoods, Open Canopy Types—Their Ability to Capture Pollutants in Various Environments. *Am. Industrial Hygiene Assoc. J.* 40 (1979), pp. 118–127.
12. United States Environmental Protection Agency. *Compilation of Emission Factors.* Publication No. AP-42. Washington, DC: U.S. Government Printing Office (Aug. 1982).
13. Goodfellow, H. D., and M. Bender. Design Considerations for Fume Hoods for Process Plants. *Am. Industrial Hygiene Assoc. J.* 41 (1980), pp. 473–484.

14. Goodfellow, H. D., and M. Bender. Movie Scaling of Plume Flowrates. *Pollution Eng.* (July 1980) no. 7, p. 30.
15. Goodfellow, H. D. Solving Air Pollution Control Problems in the Metallurgical Industry. Proceedings of 7th International Clean Air Conference, Adelaide, Australia, Aug. 1981.
16. American Conference of Governmental Industrial Hygienists, Committees on Industrial Ventilation. *Industrial Ventilation: A Manual of Recommended Practice*, 21st ed. Cincinnati: ACGIH (1992).
17. Danielson, J. A. *Air Pollution Engineering Manual*. U.S. Department of Health, Education and Welfare, Public Health Service Publication No. 999-AP-40. OH (1967).
18. Hemeon, W. C. L. *Plant and Process Ventilation*. New York: Industrial Press (1963).
19. Eisenbarth, M. J. Fume Extraction Hoods in the Iron and Steel Industry. In APCA Specialty Proceedings—Air Pollution Control in the Iron and Steel Industry, Chicago, IL, Apr. 1981, pp. 28–41.
20. Roberson, J. A., and C. T. Crow. *Engineering Fluid Mechanics*. Boston: Houghton Mifflin (1980).
21. Flux, J. H. Containment of Melting Shop Roof Emissions in Electric-Arc Furnace Practice. *Ironmaking Steelmaking* 1 (1974) no. 3, pp. 121–136.
22. Marchand, D. Waste Gas Collection on Electric Arc Furnaces: BFI Research and Development During the Last 20 Years. In APCA Specialty Proceedings–Air Pollution Control in the Iron and Steel Industry, Chicago, IL, Apr. 1981, pp. 42–57.
23. Bender, M., T. Cesta, and K. L. Minnick. Fluid Dynamic Modelling of Arc Furnace Charging and Tapping Emissions. In Proceedings of the Symposium on Iron and Steel Pollution Abatement Technology, Detroit, MI, Oct. 1983.
24. Flux, J.H. *Modelling Studies of Roof Extraction Systems for Arc Furnace Melting Shops*. Luxembourg: E.S.C. (Sept. 1974).

13.5 EMISSION MEASUREMENT TECHNOLOGY

13.5.1 Introduction

Emissions monitoring is essential in controlling industrial environments and processes to ensure good air quality standards are maintained. It is also required in order that the various regulations and guidelines related to air quality are met. In addition to gaseous emissions, such as sulfur dioxide, carbon monoxide, nitrogen oxides, hydrocarbons, and many others, the emissions of particulate material and heavy metals must also be controlled.

Guiding values for particulate material PM_{10} (aerodynamic diameter smaller than 10 μm) are given by the United States and the European Union. Major debates are in progress regarding the importance of introducing values for the size $PM_{2.5}$.

Air pollution control legislation is aimed at protecting human health and the overall environment. It also provides a means of reducing economic losses and a decline in environmental amenity as a consequence of air pollution.[1]

In industry, many process streams are involved in the gas phase.

The reasons for measuring these streams are process optimization, mandated regulatory information, analyzer application development, and identification of process or effluent abnormalities.[2]

13.5.1.1 Air Quality and Emissions

Basic Properties of Air

In practical calculations relating to air quality analysis, ideal gas laws can be applied with negligible error. The water vapor in air often varies from ideal conditions somewhat more than gases; however, the errors involved in using the

ideal gas laws for water vapor can be ignored.[3] In calculations, reference is made to standard conditions with the temperature of 273.15 K and the pressure of 101.325 kPa. The volume of one mole of gas at these conditions is 22.41 L.

In conversion calculations between the state functions temperature (T), pressure (p) and volume (V), the ideal gas law states that

$$pV = nRT$$

where

p = absolute pressure
V = volume
n = number of moles
R = universal gas constant, and
T = absolute temperature.

Thus, the volume of one mole of gas at a temperature T_1 is approximately $(T_1/273) \times 22.4$ L, if the pressure remains the same. The value of R is 8.314 J/(K mol). The units must be consistent.

Example

Particulate emission is sampled at a temperature of 70 °C by an isokinetic sampling nozzle, i.e., the sampling velocity is the same as the gas velocity around the nozzle in the duct.

Gas velocity is measured over an aperture in the heated zone of the sampling train, at a temperature of 110 °C, to remove the moisture by heating. Determine the gas velocity at the sampling nozzle if the measured velocity is 28 m s^{-1} for the sampling diameter used. The water concentration determined from the condensate is 75 g m^{-3}(n).

Solution The gas volume under the same pressure is greater by 383/343 at the higher temperature. When the sampling diameter remains the same, the gas velocity at the higher temperature is greater by the same factor. Water is assumed to be in vapor form, behaving as a gas, as the concentration is less than that in saturated air.

The gas velocity at the nozzle is thus $(343/383) \times 28$ m s^{-1} = 25.1 m s^{-1}.

Water in droplets: At 100 °C the droplets evaporate producing an additional volume of $m/18 \times 22.4 \times 383/273$ L at 110°C, where m is the mass (in grams) of the water droplets.

Air Composition

The main components of standard air are listed in Table 13.19.

Measurement of Atmospheric Emissions

The behavior of gases in air, as shown by studies in atmospheric physics and chemistry, depends on the physical and chemical properties of these gases, such as density and reactivity. Examples of gas and air densities are given in Table 13.20.

Emission measurements are required for many purposes. They can be used as the basis for emission and air quality studies, as well as for process control and specific technologies to reduce emissions. The reliability of the measured values is constantly improving with developments in monitoring techniques.

TABLE 13.19 Chemical Composition of Standard Air[3]

Substance	Percentage by volume in dry air
N_2	78.09
O_2	20.94
Ar	0.93
CO_2	0.03
Ne	0.0018
He	0.00052
CH_4	0.00022
Kr	0.00010
N_2O	0.00010
Xe	0.00008
H_2	0.00005

In many industrial gas measurements, water vapor is present in high concentrations. The sample cell of the measurement instrument and sample line can be heated up to 200 °C to remove water vapor. Sometimes, the sample gas is dried by condensation or by using Peltier gas dryers.

Particulate Matter

Particulate material consists of solid or liquid substances that may be visible or invisible.[3] The particles affect visibility and can be transported over long distances by wind. The small particles, less than PM_{10}, are particularly dangerous to human health as they can pass through nostril hairs (cilia) and enter the lungs.

Aerosols are small particles dispersed in gas. In aerosols, the particles are relatively large compared with the gaseous particles.

Aerosol dynamics are based on spherical particles, a premise which almost never exists in practice.[3] However, if there is consistency in handling the aerosol dynamics calculations, the aerodynamic diameter (see Section 13.5.2.2) that is measured gives fairly accurate predictions of aerodynamic behavior. As a result, the difference between the real shape and size of the particles and the aerodynamic shape and size is unimportant for most practical purposes.

TABLE 13.20 Densities of Air and Some Gases at 273 K, 101.3 kPa (kg m^{-3})[4]

Air	1.293	NH_3	0.771
CO	1.250	H_2S	1.539
CO_2	1.977	CH_4	0.717
NO_2	2.053	C_2H_6	1.357
NO	1.340	C_2H_4	1.260
N_2O	1.979	C_3H_8	2.010
SO_2	2.927	O_3	2.14

13.5.2 Basic Procedures for Emission Measurements

Basically, emission measurements are carried out by using either of two sampling methods:

- the extractive (or diluting) method, by which the sample gas from the exhaust channel is led to the analyzer (or taken to the laboratory) through a sampling tube line, or
- the *in situ* method, in which a sensor is placed in the outlet pipe or the measurement is performed across the pipe, in the case of optical methods.

Measurement principles are shown in Fig. 13.38.

For the analysis of total emissions, the volumetric flow of the emission gas must be measured in addition to its concentration. This is based on the gas velocity in the duct.

13.5.3 Particulate Material Emissions

13.5.3.1 Mass Concentration

Sampling Methods: Gravimetric Method

The gravimetric method depends on the sampling of flowing, particulate-laden gas from different positions across the exhaust gas duct and the determination of the mass of the particulate material. The sample is collected over a certain time period from each point. The volumetric gas flow is measured. The result is obtained by the following steps:[5]

- Determine the volumetric flow of the gas, based on the measurement of the gas velocity.
- Collect the particulate material sample (on filter).
- Adjust the sample gas flow extracted (isokinetic sampling).
- Determine the volume of the sample gas.
- Weigh the particulate material.
- Calculate the concentration and the mass flow.

The method is applicable for the determination of the concentration (and emission) of the particulate material from a mixture of gas and particulate material flowing through a known cross-sectional area of a duct.

Procedure A sharp-edged nozzle is positioned in the duct, facing into the moving gas stream, and a gas sample is extracted isokinetically (see later) for a measured period of time.[6] To allow for nonuniformity of particulate concentration in the duct, samples are taken at preselected positions in the duct cross-section. The particulate concentration is calculated from the weighed particulate mass and the gas sample volume. Figure 13.39 shows the measuring arrangement.

Isokinetic Sampling The sample gas partial volume flow must be extracted isokinetically to avoid aerodynamic separation effects and to ensure correct particle size distribution. Isokinetics means that the velocity and direction of the sample gas partial flow at the sample nozzle are the same as at the main gas stream.[7]

1. Manual method

- Sampling
- One-point result
- Analysis in the laboratory

Examples:

- Particulates
- Metals (bound on particles)
- Organic compounds (PAH and PCD compounds, PCDD, PCDF)

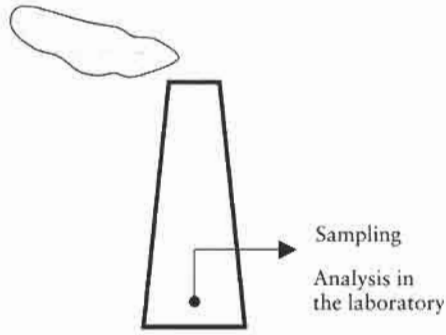

2. Continuous measurement

- Sampling gas led into the analyzer
- One-point result
- Registration at the measurement site

Examples:

- SO_2, NO_x, CO, CO_2, O_2, TRS (total reduced sulfer compounds), hydrocarbons

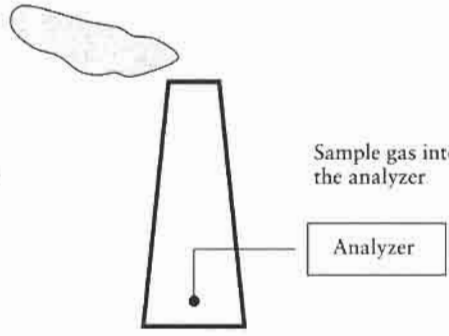

Methods requiring no sampling

3. In situ measurements

- No sampling
- One-point result or integrated result
- Registration at the measurement site

Examples:

- Gas sensors
- Optical measurements method

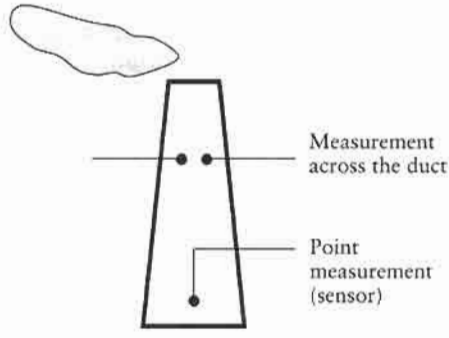

4. Remote measurement

- No sampling
- One-point result or integrated result
- Registration at the measurement site

Example:

- Optical measurements method

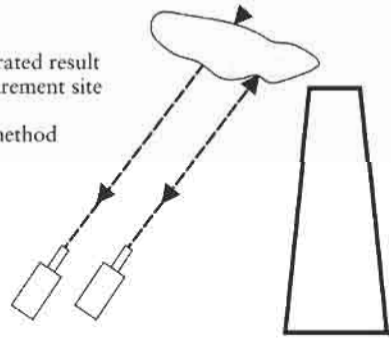

FIGURE 13.38 Basic procedures for emission measurements.

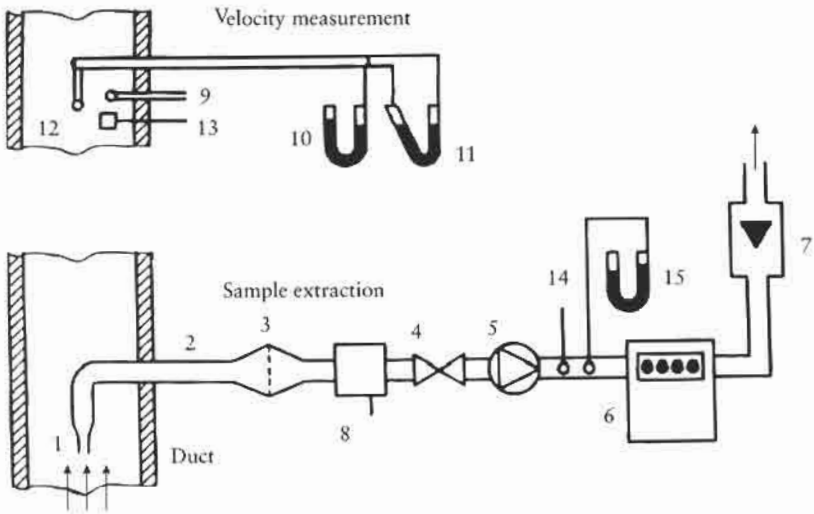

FIGURE 13.39 Example of a measuring-equipment arrangement with water removal upstream of the gas-metering device[6]

1. Entry nozzle
2. Probe tube
3. Particle separator
4. Sampling flow rate control device
5. Exhauster
6. Gas volume meter
7. Sampling flow rate measuring device
8. Water-removing device
9. Duct thermometer
10. Instrument for measuring effective static pressure in duct
11. Sensitive differential pressure instrument connected to Pitot tube
12. Gas velocity measuring device
13. Humidity measuring instrument
14. Thermometer at gas-metering device
15. Instrument for measuring effective static pressure at gas-metering device.

For isokinetic sampling, the duct sampling-point gas velocity has to be measured, and the corresponding sample gas flow calculated and adjusted.[6] Normally, a Pitot static tube is used for the measurement of duct gas velocity.

Particle Collection Particles in the extracted partial volume flow are retained in the collector filter. The particle mass emitted is determined by the weight difference of the filter before and after the collection. Factors crucial to the measuring precision and the smallest measuring range of particle concentration are[7]

- Correct configuration of the extraction and collection systems
- Correct preparation and subsequent handling of the measuring filter
- Resolution of the precision scales used

Sampling Points To obtain a representative result, the gas normally has to be sampled at more than one point in the sampling plane, depending on the sampling plane area. This plane is usually divided into equal areas at the centers at which gas is extracted.[6] To determine the particulate concentration in the plane, the nozzle is moved from one sampling point to the other,

extracting gas isokinetically at each point. Sampling periods should be equal for each sampling point, resulting in a composite sample.

The degree to which this sample represents the total gas flow depends on[6]

- Homogeneity of the gas velocity within the sampling plane
- Sufficient number of sampling points in the sampling plane
- True isokinetic extraction of the sample

Sampling Train The sample is extracted through a sampling train, which consists of

- sampling probe tube with entry nozzle,
- particle separator, in-stack or external,
- gas-metering system, in-stack or external, and
- suction system.

Tapered-Element Oscillating Microbalance Sampler

The tapered-element oscillating microbalance (TEOM) sensor, as described by Patashnick and Rupprecht,[8] consists of an oscillating tapered tube with a filter at its free end (Fig. 13.40).[9] The mass of the filter increases due to the collected aerosol and produces a shift in the oscillation frequency of the tapered tube that is directly related to mass.

The TEOM sampler draws air through a hollow tapered tube, the wide end of the tube being fixed, while the narrow end oscillates in response to an applied electric field. The narrow end of the tube contains the filter cartridge. The sampled air flows from the sampling inlet, through the filter and tube, to a flow controller. The tube–filter unit acts as a simple harmonic oscillator with[10]

$$\omega = (k/m)^{0.5}$$

where

ω = the angular frequency,
k = the restoring force constant, and
m = the oscillating mass.

As particles are collected on the filter, the oscillating mass changes, resulting in a change of the oscillating frequency. An electronic control system maintains the tapered tube in oscillation and continuously measures this oscillating frequency and its changes. The relationship between the changes in mass and frequency can be expressed as[11]

$$dm = k_0\left(\frac{1}{f_1^2} - \frac{1}{f_0^2}\right)$$

where

dm = change in mass,
k_0 = spring constant,
f_0 = initial frequency (Hz), and
f_1 = final frequency (Hz).

In the measurement of emission gas mass concentration at sources, a gas sample is extracted via an automatic isokinetic particulate-sampling instrument. The monitoring system generates a direct, real-time emission particulate mass

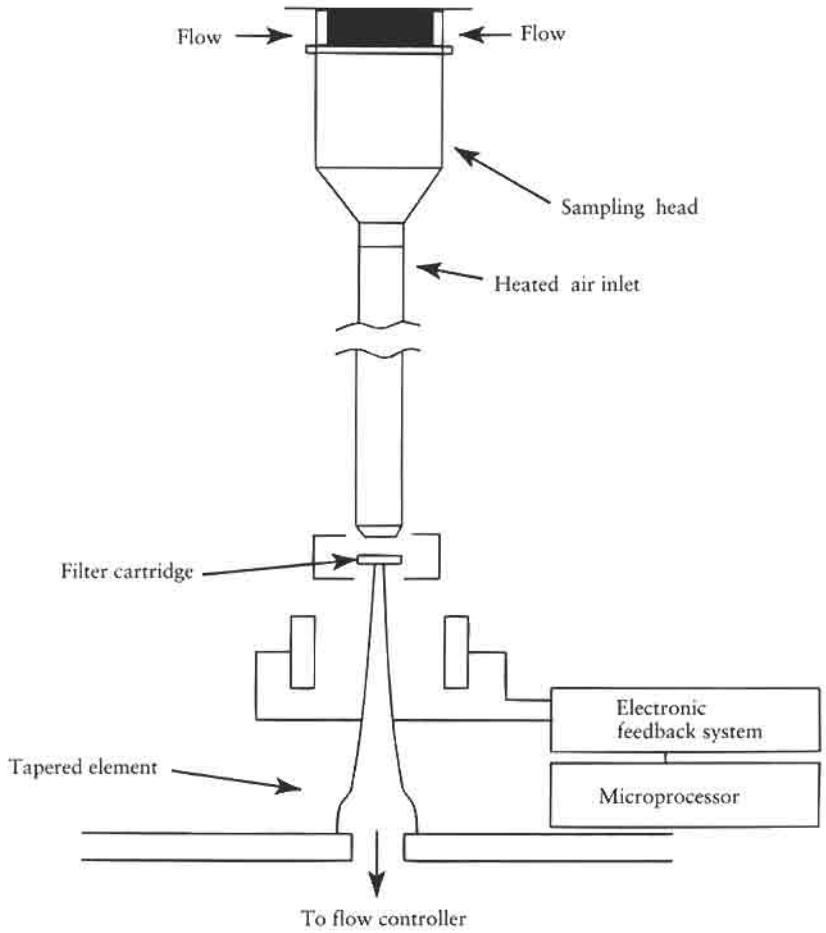

FIGURE 13.40 TEOM sampler.[10]

concentration signal (mg m^{-3}) using a mass transducer in the stack.[12] The mass transducer contains two sample inlets: the main flow is the low-flow sample that passes through the TEOM mass transducer and the manual sample flow is a high-flow sample directed through a manual filter holder mounted behind the mass transducer. The manual sample is intended as a verification tool. Mass concentration averaging times can range from a few seconds to 15 minutes.

The system can be used for continuous measurement of the mass concentration at a single point for up to 12 hours, for traverse measurements of stack particulate mass concentrations using sample probe extensions, with the mass transducer up to 6 m in the stack, or for intermittently measuring particulate mass concentrations of emission gases for long-term readings (e.g., 30-sec samples every 60 minutes).[12]

Beta Gauge

A beta attenuation sampler uses a 30-mCi Krypton-85 source (with energy of 0.74 MeV) and detector to determinate the attenuation caused by deposited aerosols on a moving filter.[9] To improve the stability over time, a reference reading is periodically made of a foil with attenuation similar to that of the filter and collected aerosol.

Quasi-continuous particulate monitors, based on the use of the isotope ^{14}C as the beta radiation source of low activity (12.5 to 100 μCi), are used for the emission control of different processes. Their minimum sampling cycle is approximately five minutes. They use Geiger-Müller counter tubes as detectors. The isotope ^{14}C emits electrons at a low energy (0.156 MeV), making the dependence of the absorption on the chemical composition of the particles lower.[13,14] It reduces the requirements for site-specific reference calibration. The gas sample is extracted isokinetically.

The main parts of these monitors are

- Sample probe, heated to constant temperature
- Measurement unit
- A heated sample line through which the sample is directed onto the filter tape in a gas-tight holder
- A step motor and tape reels to accomplish filter tape feed
- Pump and mass flow controller
- Beta-ray emission source and Geiger-Müller counter
- Microprocessor-based electronics and functions control

The concentrations monitored by these instruments range from a few milligrams to 4000 mg/m^3. A flow diagram of a beta gauge particulate monitor is shown in Fig. 13.41.

Elemental Analysis of Particulate Material

Interest in the elemental composition of aerosol particles arises from concerns about health effects and the value of these elements to trace the sources of suspended particles.[9] The following physical analysis methods have been applied for the elemental measurements of aerosol samples. A schematic drawing of an x-ray fluorescence system is presented in Fig. 13.42.

- Instrumental neutron activation analysis (INAA)
- Photon-induced x-ray fluorescence (XRF)
- Particle-induced x-ray emission (PIXE)
- Atomic absorption spectrophotometry (AAS)

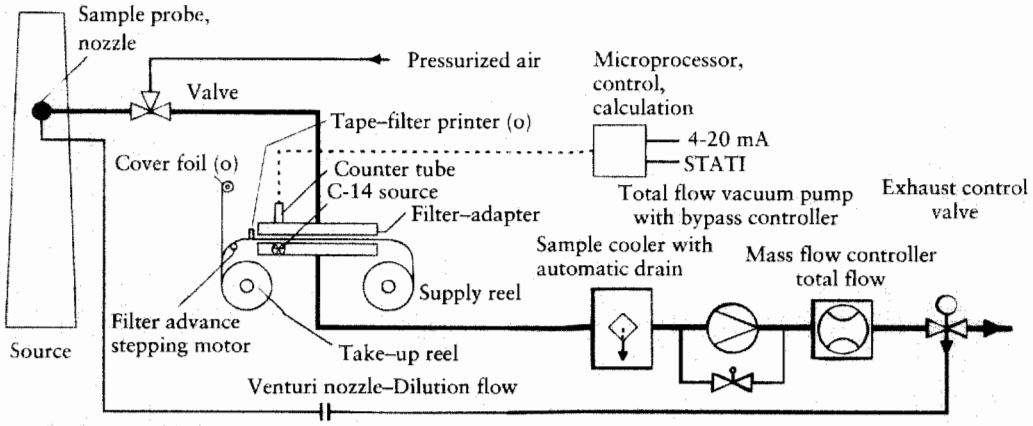

FIGURE 13.41 Flow diagram of beta gauge particulate monitor.[13]

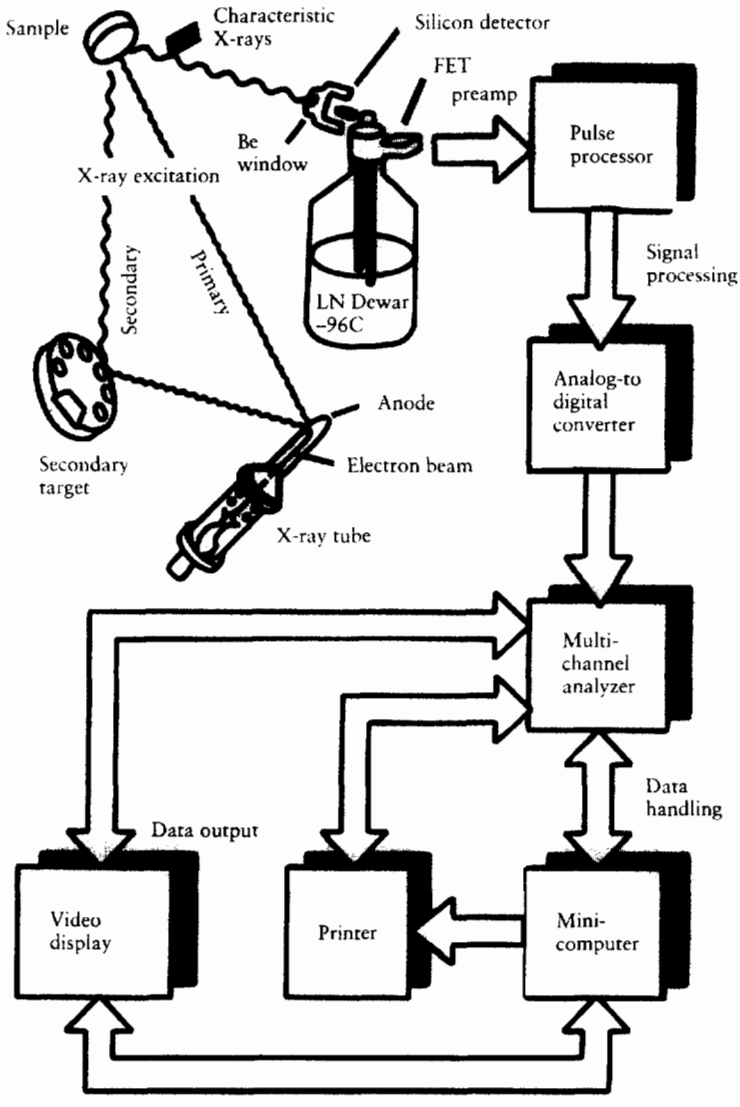

FIGURE 13.42 Schematic of a typical x-ray fluorescence system.[9]

- Inductively coupled plasma with atomic emission spectroscopy (ICP/AES)
- Scanning electron microscopy with x-ray fluorescence (SEM/XRF)

13.5.3.2 Particle Size Distribution

Aerodynamic Diameter The aerodynamic diameter of a particle is defined as that of a sphere, whose density is 1 g cm^{-3} (cf. density of water), which settles in still air at the same velocity as the particle in question.[15] This diameter is obtained from aerodynamic classifiers such as cascade impactors.

Impactor

Impactors utilize aerodynamic forces to separate the various particle size classes. This is consistent with the particles' aerodynamic diameter. The operation

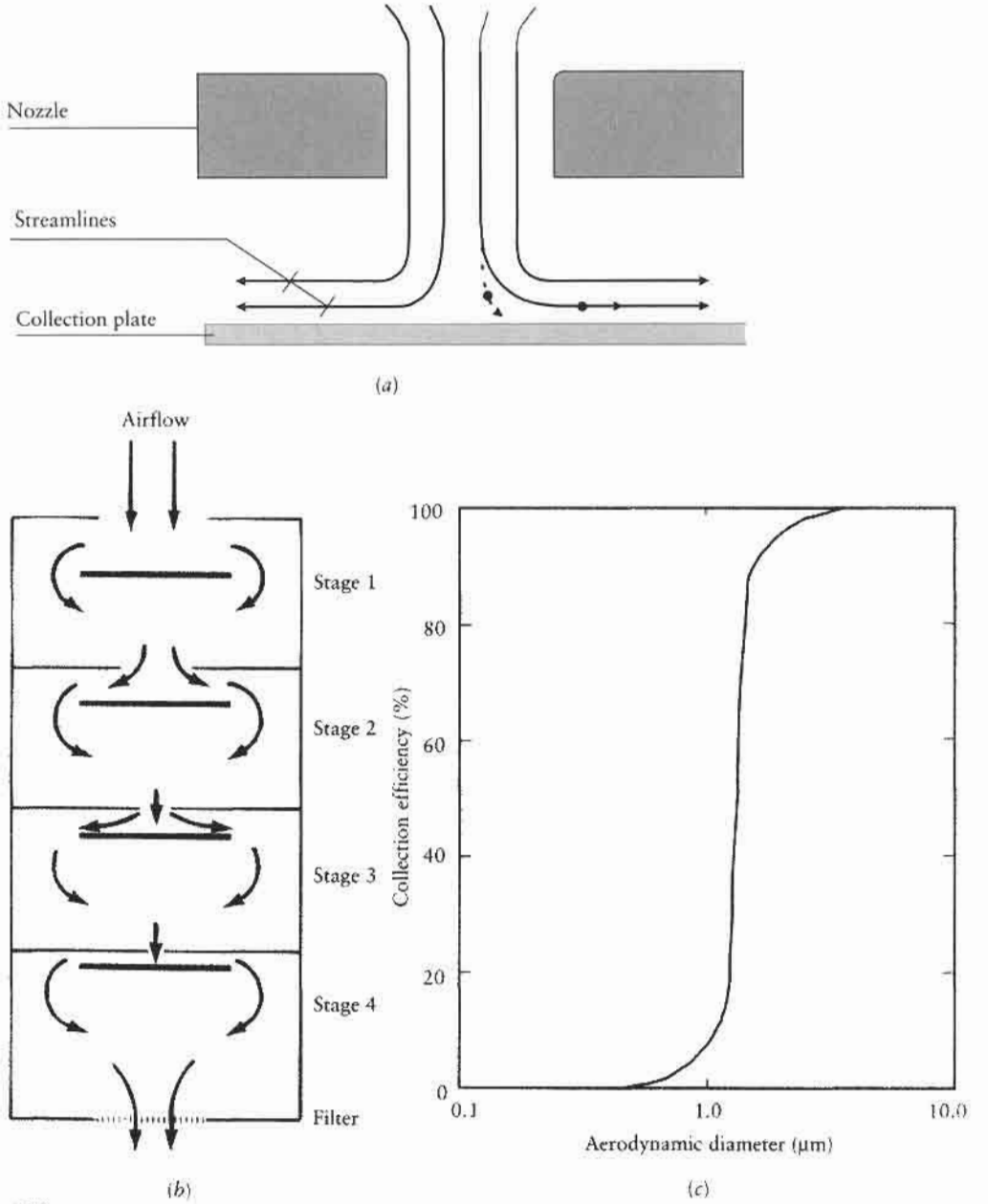

FIGURE 13.43 (*a*) Principle of the impactor, (*b*) cascade impactor,[15] and (*c*) impactor collection efficiency curve.

principle of an impactor is that the particle is carried through an orifice with a gas stream directed against a plate (Fig. 13.43*a*). This is the impaction or collection plate. It changes the flow into an abrupt 90° turn. Particles, which are too slow, are not capable of following the change in the direction and collide with the plate. The cross-section of the impactor is shown in Fig. 13.43*a*.

Cascade Impactor For particles to be classified into various sizes, individual impactors are connected together in series to form a cascade impactor (Figure 13.43*b*). The individual impactors, or stages of the cascade are arranged in order, with the largest cut diameter (cut diameter is the smallest aerodynamic diameter retained by the stage) being first and the smallest last. The cut diameter is reduced in stages by changing the orifice diameter or the number of orifices and the distance of the impaction plate from the orifice plate. The impaction plates are demountable, so that the collected particles can be weighed and analyzed. After the last stage, there is usually a filter to collect particles smaller than the last-stage cut diameter.

It is assumed that at each stage of a cascade impactor all the particles larger than its cut diameter are collected. A practical impactor collection efficiency curve is shown in Figure 13.43*c*). The cumulative mass of the particles is normally plotted on the particle size distribution graph as a function of the upper limit of the particle size range corresponding to each stage. Using a cascade impactor, emission gas particle samples can be classified into 12 fractions (aerodynamic diameter ranging from 0.15 to over 7 μm).

Electrical Low-Pressure Impactor

The electrical low-pressure impactor (ELPI) has been developed, using the Berner-type multijet low-pressure impactor stages.[16] The cut sizes of the seven-channel system range from 0.030 to 1.0 μm. Real-time measurements can be achieved due to the instrument's fast time response.[17] The schematic representation of the impactor construction is shown in Fig 13.44.

The electrical low-pressure impactor was used to measure the number concentrations of diesel exhaust particles. The particle size distribution ranges from 30 nm upward were then determined using the aerodynamic diameter as the characteristic dimension.[17]

Instrument Based on Fraunhofer Diffraction of Laser Light

The particle size distribution is determined from the diffraction pattern. For a simplified case of monosized spherical particles, for instance, the radius r_0 of the smallest dark ring is

$$r_0 = 1.22\lambda f/d$$

where

λ is the laser wavelength,
f is the focal length of the lens, and
d is the particle diameter.

The wavelength of 632.8 nm of the He-Ne laser is generally used in laser particle-size analyzers.

The particle size analyzer, based on laser light diffraction, consists of a laser source, beam expander, collector lens, and detector (Fig. 13.45). The detector contains light diodes arranged to form a radial diode-array detector. The particle sample to be measured can be blown across the laser beam (dry sample), or it can be circulated via a measurement cell in a liquid suspension. In the latter case, the beam is directed through the transparent cell.

A laser diffraction spectrometer can measure particles as small as 0.2 μm and up to about 1000 μm. Some instruments allow the operation of the analyzer for

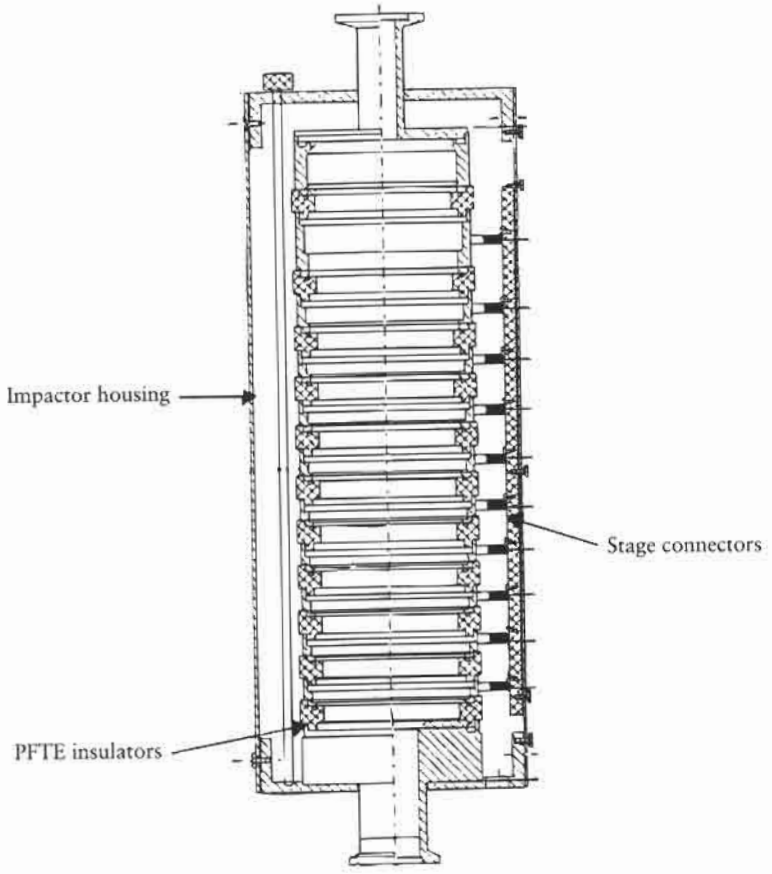

FIGURE 13.44 Construction of electrical low-pressure impactor.[16]

continuous monitoring and process control. In some instruments, laser source and receiver units can be used in high-temperature environments inside a water-cooled probe.[18] Particles flow through an access region of the probe, and the light signal is transferred to the detectors by fiber optics.

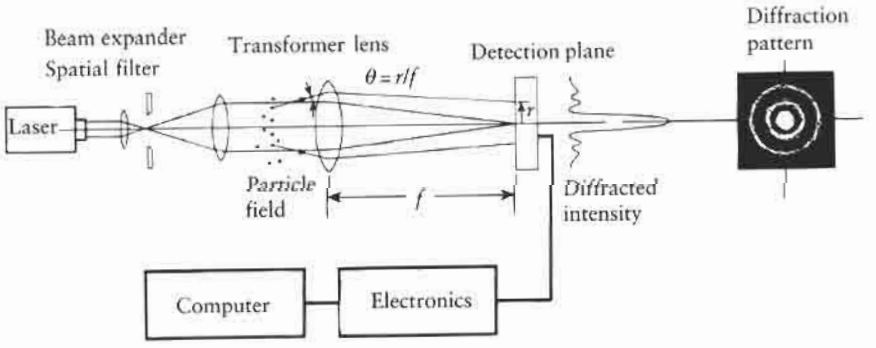

FIGURE 13.45 Schematic of particle size analysis based on the diffraction of forward-scattered laser light.

13.5.4 Gaseous Emissions

13.5.4.1 Carbon Monoxide and Carbon Dioxide

Nondispersive Infrared Analyzers

When measuring the concentrations of carbon monoxide and carbon dioxide from emission gases, the equipment frequently used is based on the absorption of infrared light. These instruments utilize the characteristic wavelength band of infrared light. The gas to be measured absorbs infrared light within the band. The wavelength band is selected by using an optical band-pass filter. This equipment is called a nondispersive infrared (NDIR) gas analyzer.

With *interference filters*, two narrow wavelength bands are selected.[19] These are the absorption (or measurement) and reference bands, within which the gas absorption is as high and as low as possible. The filters are mounted on a rotating disk, and the intensities are registered synchronously. The ratio of the intensities is used as the signal related to the gas concentration (Fig. 13.46).

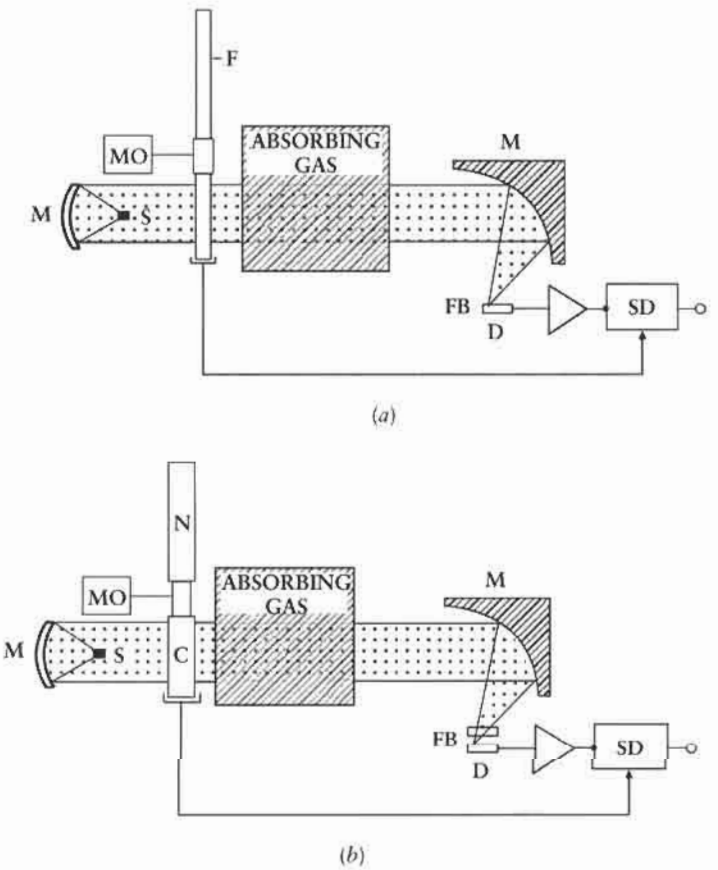

FIGURE 13.46 Nondispersive infrared analyzer based on (*a*) interference filters and (*b*) gas correlation techniques.[19] *M* = mirror, *D* = detector, *S* = source, *F* = filter disk, *MO* = motor, *FB* = band-pass filter, *SD* = synchronous detection, *C* = correlation cell, *N* = nitrogen filter.

The measurement principle, based on the ratio of the intensities, is insensitive to fluctuations in the source intensity. Changes associated with wavelength dependence can cause error in the measurement.

In the *gas correlation techniques*, gas-filled cells mounted on a rotating disk cross the analyzing infrared beam in turn. One correlation cell is filled with a gas that will not absorb infrared light, such as nitrogen (N_2). The other cell (or cells) are filled with a high concentration of the gas to be measured. The wavelength range is selected at the absorption band of the gas to be measured by an optical band-pass filter.

When measuring CO concentration, the reference signal is obtained when the beam is passed through the sample chamber and the CO cell. The absorption is then saturated due to the high CO concentration in the cell. Consequently, the reference signal is practically nondependent on the CO concentration in the sample gas. When the beam passes through the sample chamber and the N_2 filter, the absorption is dependent on the CO concentration in the sample chamber, as the N_2 filter does not absorb energy from the infrared beam.

In the gas correlation method, the measurement and reference signals are obtained from the same wavelength band. The temperature changes in the light source and other wavelength-related changes do not disturb the measurement.[19]

Figure 13.46 shows the operation principles and arrangements of nondispersive gas analyzers.

In nondispersive gas analyzers, interferences by other gases that possibly absorb at the measurement and reference bands should be taken into account. In the measurement of CO, interferences by overlapping in the measurement band can be caused by COS, N_2O, CO_2, and water vapor. Another source of uncertainty is interference in the reference band.

Other Techniques

Carbon monoxide and carbon dioxide can be measured using the FTIR techniques (Fourier transform infrared techniques; see the later section on the Fourier transform infrared analyzer). Electrochemical cells have also been used to measure CO, and miniaturized optical sensors are available for CO_2 monitoring.

13.5.4.2 Hydrocarbons and VOCs

Flame Ionization Detector

Volatile organic compounds (VOCs) include organic compounds with appreciable vapor pressure. They make up a major class of air pollutants.[15] This class includes not only pure hydrocarbons but also partially oxidized hydrocarbons (organic acids, aldehydes, ketones), as well as organics containing chlorine, sulfur, nitrogen, or other atoms in the molecule.

Some of the analytical methods utilize highly selective and sensitive detection techniques for specific functional groups of atoms in compounds, whereas others respond in a more universal manner, i.e., to the number of carbon atoms present in the organic molecule.[20]

By using a flame ionization detector (FID), most compounds having a bond of carbon and hydrogen can be measured. This detector was originally developed for gas chromatography and employs a sensitive electrometer that measures the change in ion intensity resulting from the combustion of air

containing organic compounds. The flame ionization detector can be considered an organic carbon analyzer.[20]

In a hydrocarbon analyzer using flame ionization, the sample gas is conducted along a heated sampling line to the detector, in the hydrogen flame of which the hydrocarbons are ionized into electrons and positive ions.

The operating principle of the flame ionization detector is shown in Fig. 13.47. The detector consists of a combustion chamber and a burner. Hydrogen passes through the burner nozzle and the combustion air through a hole around the nozzle into the combustion chamber. The collector electrode placed near the flame collects the ions and electrons. The combustion nozzle serves as one of the electrodes, and the current flowing between the electrodes is registered as the concentration signal.

A pure hydrogen flame produces a very low ion concentration. Instead, compounds brought into the flame, which contain bonds of carbon and hydrogen, produce carbon ions in the flame.[21] If the gas measured contains several hydrocarbons, the resulting response depends on the carbon number and inter-atomic bonding. Thus, aliphatic, aromatic, alkenic, and acetylenic compounds all respond similarly to give relative responses of 1.00 ± 0.10 for each carbon atom present in the molecule (e.g., 1 ppm hexane $\propto$ 6 ppm C; 1 ppm methane $\propto$ 1 ppm C; 1 ppm propane $\propto$ 3 ppm C). Carbon atoms bound to oxygen, nitrogen, or halogens give reduced relative responses.[20]

The flame ionization detector is capable of measuring only gaseous hydrocarbons, in other words, hydrocarbons that have a low boiling point. Emission gases can, however, also contain hydrocarbons in liquid form at ambient temperature and pressure. Therefore, analyzers based on flame ionization detection are generally equipped with heating elements to keep the sampling line and the detector at about 200 °C.

Variations in oxygen concentration may affect the response of the flame ionization analyzer. The oxygen concentration can vary considerably, for instance,

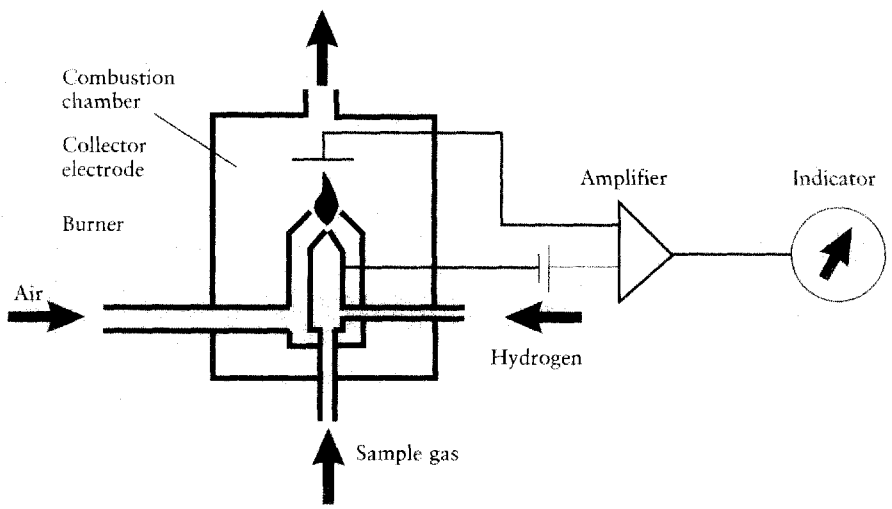

FIGURE 13.47 Diagram of flame ionization detector.[22]

when measuring hydrocarbon concentrations of gases from combustion processes. To minimize the error caused by this effect, the fuel used can be a mixture of hydrogen and helium, of which hydrogen accounts for 40% and helium 60%. The flow rate of the fuel has to be increased so that the hydrogen flow remains the same as without helium.[21]

A device based on flame ionization measures the total concentration of hydrocarbons. By using a catalyst, such as a heated platinum wire, hydrocarbons other than methane can be removed from the sample gas. With a platinum catalyst, these hydrocarbons are oxidized at a lower temperature than methane. Hence, the total concentration of hydrocarbons, methane, and hydrocarbons other than methane can be determined.

Other Techniques

Gas chromatographic techniques and FTIR techniques are also used for the monitoring of VOCs.

13.5.4.3 Sulfur Oxides

Ultraviolet Fluorescence Method

Molecular Fluorescence When a gas containing sulfur dioxide is irradiated by ultraviolet light of appropriate wavelength, sulfur dioxide molecules are excited to a higher energy level than the original. On returning to the lower energy level, excited molecules give up their extra energy, giving fluorescent radiation (also in the ultraviolet wavelength range), the intensity of which can be detected.

Molecular fluorescence is a more complicated phenomenon than atomic fluorescence (e.g., x-ray fluorescence). In molecular fluorescence, energy changes in the vibrational and rotational motions are involved, in addition to the electronic transitions.

Reactions Producing Fluorescent Radiation In the reaction chamber of the ultraviolet fluorescent analyzer reactions producing fluorescence are

$$SO_2 \xrightarrow{I_a} SO_2^* \qquad \text{(creation of an electronically excited state)}$$

$$SO_2^* \xrightarrow{k_f} SO_2 + h\nu \qquad \text{(de-excitation of the excited state causing fluorescence)}$$

Dissociation and quenching also occur, reducing the yield.

In the preceding formula, I_a denotes the intensity absorbed from the excitation radiation (intensity I_0). This absorbed intensity I_a generates fluorescent radiation and other reactions.

$$I_a = I_0(1 - e^{-\alpha_\lambda cl})$$

where c is the concentration of sulfur dioxide, and $e^{-\alpha_\lambda cl}$ describes the portion of the radiation transmitted through the sample gas according to the Lambert-Beer law. The intensity of the fluorescent radiation, I_f, is proportional to the intensity absorbed, I_a.

The proportion factors related to the reaction constants, together with the geometrical factors of the reaction chamber, can be included in one coefficient G, giving

$$I_{f,\lambda'} = GI_0(1 - e^{-\alpha_\lambda cl}),$$

where α_λ is the absorption coefficient of sulfur dioxide to the excitation radiation, the wavelength of which is λ; λ' denotes the fluorescent radiation, and l is the absorption length. With low sulfur dioxide concentration and short absorption length this gives:

$$I_{l,\lambda'} = k \cdot c$$

where k is a proportionality factor. In practice, a linear relationship is achieved at concentrations lower than 500 ppmv (parts per million by volume).[23]

Construction and Operation of Analyzer The construction principle of a sulfur dioxide analyzer based on the ultraviolet fluorescence principle is shown in Fig. 13.48. Undesired wavelengths are removed from the irradiating beam as far as possible using filters. The irradiating light (214 nm) is focused by a lens at the center of the reaction chamber.

The sulfur dioxide analyzer based on the ultraviolet principle is a sensitive instrument. Its detection limit can be less than one ppbv (parts per billion by volume). When used in emission measurements, the sample gas is normally diluted prior to the measurement using a diluting stack sampler.

Hydrogen Sulfide and Other Reduced-Sulfur Compounds

TRS Converter To measure hydrogen sulfide and reduced–organic sulfur compounds, the technique used is thermal oxidation, in which sulfur dioxide is produced. Hydrogen sulfide and other reduced-sulfur compounds are measured by using methods applicable to the measurement of sulfur dioxide concentrations. One method is a technique based on ultraviolet fluorescence.

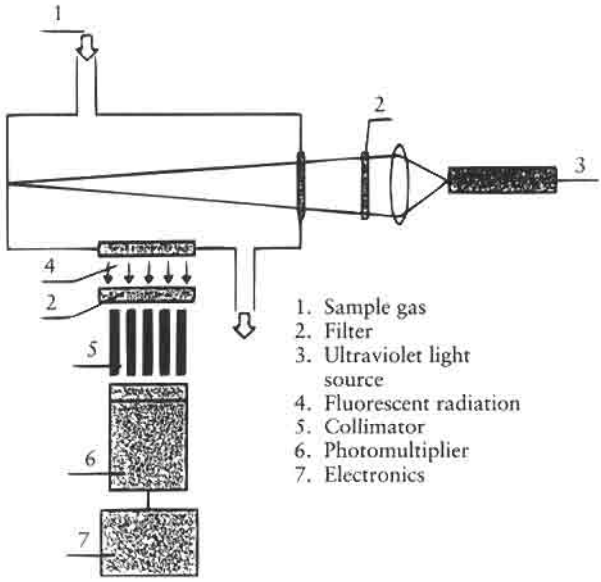

FIGURE 13.48 Schematic of sulfur dioxide analyzer based on the ultraviolet fluorescence principle.

By this method it is possible to determine the total concentration of reduced-sulfur compounds or the concentration of TRS compounds, as in a paper pulp plant. The oxidation temperature of the furnace is about 800 °C. The flue gas must contain a minimum of 1% oxygen to ensure that all TRS compounds are fully oxidized to sulfur dioxide.

If the gas to be measured contains sulfur dioxide, it has to be scrubbed from the gas before oxidation of the reduced compounds can occur. The gas is scrubbed using an SO_2 scrubber. This may contain citrate buffer solution (potassium citrate or sodium citrate). The collection efficiency of the sulfur dioxide may be as high as 99%.

Other Techniques Continuous methods for monitoring sulfur dioxide include electrochemical cells and infrared techniques. Sulfur trioxide can be measured by FTIR techniques. The main components of the reduced-sulfur compounds emitted, for example, from the pulp and paper industry, are hydrogen sulfide, methyl mercaptane, dimethyl sulfide and dimethyl disulfide. These can be determined separately using FTIR and gas chromatographic techniques.

13.5.4.4 Nitrogen Oxides

The measurement of NO_x concentration is based on chemiluminescence; this is light generation due to a chemical reaction. This occurs when nitrogen monoxide and ozone react with each other.

Chemiluminescence Method

In chemiluminescence, some of the chemical reaction products developed remain in an excited state and radiate light when the excitation is discharged. This is particularly so at low pressures, when the collision frequency is low; the excitation is discharged as light radiation. The extra energy bound to the excited molecule can discharge through impact or molecular dissociation.

The chemiluminescence reaction between nitrogen monoxide and ozone is formulated as:

$$NO + O_3 \longrightarrow NO_2^* + O_2$$
$$NO_2^* \longrightarrow NO_2 + h\nu.$$

NO_2^* refers to the excited nitrogen oxide molecule. These molecules can decay by emission of light of wavelengths longer than 600 nm.[24]

An instrument for measuring nitrogen oxides based on chemiluminescence is shown in Fig. 13.49. The ozone required for the reaction is produced in the ozone generator, which is part of the device. One of the reaction chamber walls is an optical filter through which a red-sensitive photomultiplier tube measures the chemiluminescence radiation intensity and converts it into a current signal.

The chemiluminescent method is very sensitive and is used in air quality monitoring.

The device for nitrogen oxides based on chemiluminescence measures the nitrogen monoxide concentration. The same equipment can be used to measure the concentration of nitrogen dioxide. Nitrogen dioxide is reduced to nitrogen monoxide in a converter by a molybdenum catalyst. In order to

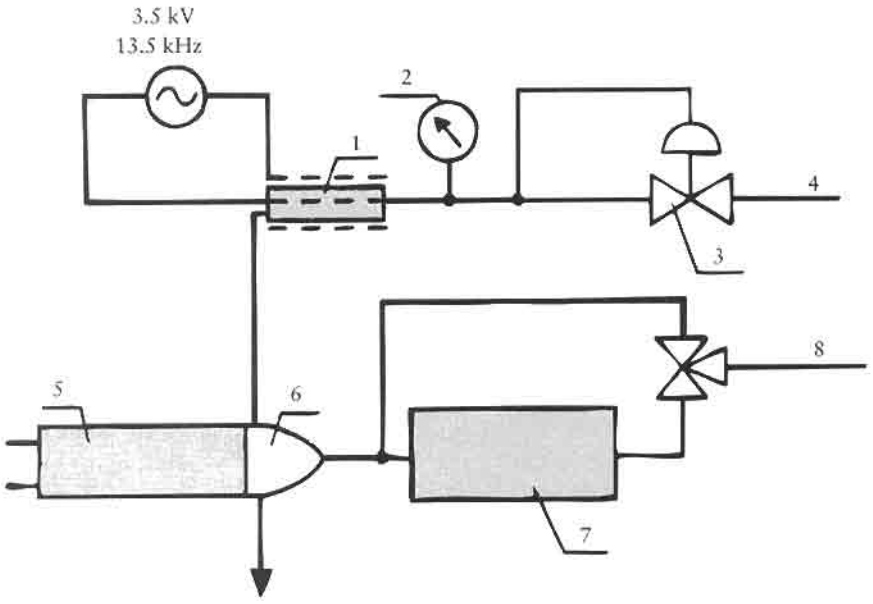

FIGURE 13.49 Schematic diagram of an instrument for the measurement of nitrogen oxides based on chemiluminescence. 1. ozone generator; 2. pressure gauge; 3. oxygen control; 4. air; 5. photomultiplier tube; 6. reaction chamber; 7. NO_x converter; 8. sample gas.

get reliable measurements, the converter must have a conversion efficiency of over 95%.

Other Techniques

Electrochemical cells are sometimes used to measure nitric oxide and nitrogen dioxide. These, together with nitrous oxide (N_2O), are measured using the FTIR techniques.

13.5.4.5 Optical Multigas Analysis Techniques

Differential Optical Absorption Spectrometer

The differential optical absorption spectrometer (DOAS) is based on the differential absorption of gaseous atoms or molecules.[25] The Lambert-Beer law gives the concentration

$$C = \log(I'_0/I)/(\epsilon L),$$

where

I'_0 = light intensity without differential absorption,
I = light intensity due to gas absorption,
ϵ = differential absorption coefficient of the gas, and
L = length of the absorption light path.

The wavelength-specific differential absorption coefficient ϵ is generally lower than the total absorption coefficient. The spectrometer and signal-processing system analyze UV and visible light intensities over a range of 200 to 1000 nm in determining the concentrations of the absorbing species.[25,26]

When evaluating gas concentrations in practical applications, a reference spectrum is least squares fitted to the received absorption spectrum. This improves the system accuracy, since the spectral fingerprint over the whole scanning range contributes to the result.[25]

Structure of Instrument The differential optical absorption spectrometer is composed of a light source, an optical light receiver, a fiber-optic cable, a spectrometer and a computer.[26] The light source is a high-pressure xenon arc lamp. The spectrometer and software signal-processing system rapidly analyze the UV and visible light intensities to determine the absorbing gas concentrations.

The light collected in the receiver is focused onto the entrance fitting coupled to a fiber-optic cable. The light transmitted by the fiber-optic cable enters the spectrometer and is reflected and collimated by a mirror before a grating reflects it. A step motor controls the grating position. A second mirror focuses the light onto an exit slit. Light detection is accomplished using a photomultiplier tube. In front of the entrance to the photomultiplier tube is a rotating disk with radially arranged slits. The slit width is about 0.2 mm, and the rotation speed is 600 rpm. In this configuration, a spectral range of 40 nm is scanned within 10 ms, which results in a resolution of 0.2 nm and channel overlapping of 80%.[26]

Unknown broadband influences due to atmospheric aerosols, lamp fluctuations, and dust on the mirrors are minimized by dividing the spectrum by a fitted fifth-order polynomial. The construction of the measuring instrumentation is shown in Fig. 13.50.

Applications The differential optical absorption spectrometer has been used to monitor concentrations of gases or intermediate compounds such as SO_2, NO_2, O_3, HCHO, HNO_2, CS_2, NO_3, and OH in the atmosphere.[25,26] In atmospheric measurements with open paths of 100 to 1000 m, a detection limit of about 1 ppb can be achieved. In the emission measurements, the path length across the duct or the plume can range in meters.

Fourier Transform Infrared Analyzer

Fourier transform infrared (FTIR) analyzers can be used for industrial applications and *in situ* measurements in addition to conventional laboratory use. Industrial instruments are transportable, rugged and relatively simple to calibrate and operate. They are capable of analyzing many gas components and determining their concentrations, practically continuously. FTIR analyzers are based on the spectra characterization of infrared light absorbed by transitions in vibrational and rotational energy levels of heteroatomic molecules.

The basic principle of a Fourier transform spectrometer can be visualized using the conventional Michelson interferometer. There is a coherence of two light components coinciding at the beam splitter, and the resulting interference spectrum is registered. The two beams originate from the same source, but the light is divided into two parts using a semitransparent ("half-silvered") mirror or a beam splitter. One part of the light is reflected from a fixed mirror, while the other part is reflected from a moving mirror, from which the interference is formed (Fig. 13.51). The interference spectrum (interferogram) is turned into

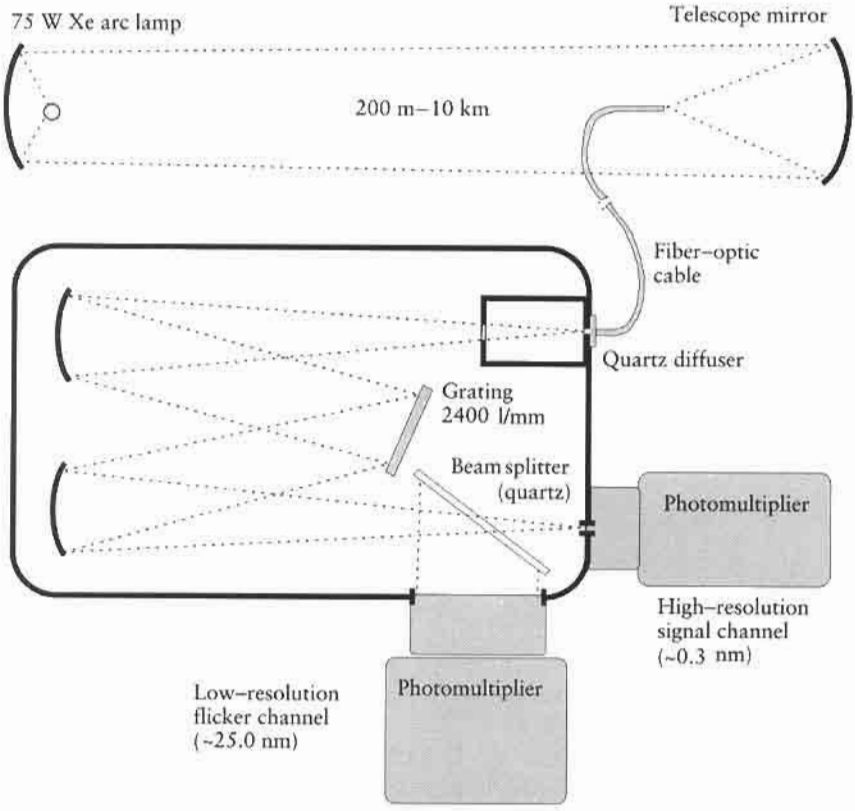

FIGURE 13.50 Operational scheme of a DOAS analyzer.[27]

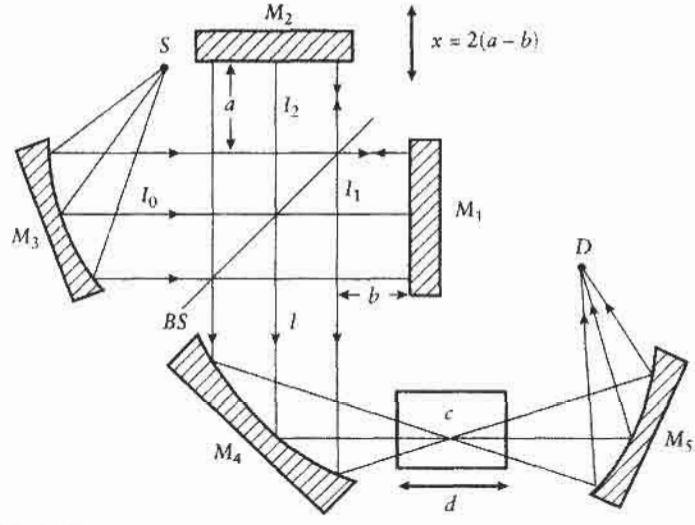

FIGURE 13.51 *Fourier* transform spectrometer, based on the Michelson interferometer.[28] S is the source, M_1–M_5 are mirrors, I, I_0–I_2 are intensities, BS is the beam splitter, c is the concentration of the gas to be analyzed by the IR spectrum, d is the absorption length, and D is the detector.

an energy spectrum using the Fourier transform performed by the instrument's computer.

The position of the moving mirror (M_2) determines the phase δ between the intensities I_1 and I_2 as follows:[28]

$$\delta = 2\pi 2(a-b)/\lambda = 2\pi\nu x$$

where $\nu = 1/\lambda$, $x = 2(a-b)$ is the optical path difference, λ is the wavelength, and ν is the wave number.

FTIR techniques offer a high signal-to-noise ratio. This is due to these factors:

1. High throughput; i.e., high light energy is utilized compared with dispersive instruments. An increase in the throughput results in an increased signal-to-noise ratio.[2]
2. All the wavelengths are observed simultaneously.

In an industrial-design FTIR spectrometer, a modified form of the Genzel interferometer is utilized.[29] A geometric displacement of the moving mirrors by one unit produces four units of optical path difference (compared with two units of optical difference for a Michelson type interferometer). The modified Genzel design reduces the time required to scan a spectrum and further reduces the noise effects associated with the longer mirror translation of most interferometers.

To make the actual analysis simple and fast, a large amount of precomputed information is utilized.[30] By using library spectra of pure molecular gases together with a special mathematical multicomponent analysis, it is possible to calculate the partial pressures of the gases in a gas mixture.[31]

Applications Transportable FTIR analyzers have been used in monitoring applications such as continuous emissions monitoring, process gas analysis, and car exhaust and industrial air hygiene.[32]

For industrial applications, low-resolution FTIR spectrometers of simple, rugged design can be used.[30] High signal-to-noise ratio spectra can be obtained without the use of the more traditional liquid nitrogen–cooled detectors. Due to low resolution, the spectral analysis speed is increased, and the data storage requirements are reduced. The dynamic range for quantitative analysis is greater for low- than for higher-resolution spectrometry, due to lower absorbance values and noise levels.

Gases analyzed include hydrocarbons, carbon monoxide, carbon dioxide, sulfur dioxide, sulfur trioxide, nitrogen oxides (also nitrous oxide, N_2O), hydrogen chloride, hydrogen cyanide, ammonia, etc.

Unanticipated gases can be determined. Table 13.21 shows the measuring ranges and detection limits of an FTIR analyzer. The detection limit depends on the optical path in the sample gas chamber; this can range from a few meters to about 10 m in industrial instruments.

13.5.4.6 Gas Sensors

Solid-State Gas Sensors

Voltage Cell Type Oxygen Sensor The operation of the zirconia oxygen sensor utilizes the conduction of oxygen ions by virtue of anion or oxygen ion vacancies in the crystalline lattice.[34] The anion vacancies are created when the

TABLE 13.21 Optional Factory Calibration for Motor Exhaust Gas: Typical Measuring Ranges[33]

Component	Range 1	Range 2	Typical detection limit, 1–s measuring time
1,3-Butadiene	0–500 ppm		<10 ppm
1-Butanol, C_4H_9OH	0–200 ppm	0–1000 ppm	<4 ppm
1-Propanol, C_3H_7OH	0–200 ppm	0–1000 ppm	<4 ppm
Acetaldehyde	0–500 ppm		<10 ppm
Acetic acid	0–500 ppm		<10 ppm
Acetylene	0–500 ppm		<10 ppm
Ammonia, NH_3	0–100 ppm	0–1000 ppm	<2 ppm
Benzene	0–500 ppm		<2 ppm
Butane, C_4H_{10}	0–200 ppm	0–1000 ppm	<4 ppm
Carbon dioxide, CO_2	0–1%	0–20%	
Carbon monoxide, CO	0–500 ppm	0–50 000 ppm	<4 ppm
Carbonyl sulfide, COS	0–500 ppm		<2 ppm
Ethane, C_2H_6	0–500 ppm	0–2000 ppm	<4 ppm
Ethylene, C_2H_4	0–500 ppm		<4 ppm
Ethanol, C_2H_5OH	0–500 ppm	0–10 000 ppm	<4 ppm
Formaldehyde	0–500 ppm		<4 ppm
Formic acid	0–500 ppm		<4 ppm
Hydrogen cyanide	0–100 ppm	0–1000 ppm	<2 ppm
Isooctane, C_8H_{18}	0–500 ppm	0–10 000 ppm	<4 ppm
Methane, CH_4	0–1000 ppm	0–10 000 ppm	<4 ppm
Methanol, CH_3OH	0–200 ppm	0–10 000 ppm	<4 ppm
MTBE, $(CH_3)_3COCH_3$	0–500 ppm		<4 ppm
Nitric oxide, NO	0–500 ppm	0–10 000 ppm	<10 ppm
Nitrogen dioxide, NO_2	0–100 ppm	0–5000 ppm	<4 ppm
Nitrous oxide, N_2O	0–100 ppm	0–1000 ppm	<2 ppm
Propane, C_3H_8	0–500 ppm	0–5000 ppm	<4 ppm
Propylene, C_3H_6	0–500 ppm		<4 ppm
Sulfur dioxide, SO_2	0–500 ppm	0–2000 ppm	<2 ppm
Toluene	0–500 ppm		<2 ppm
Water, H_2O	0–1%	0–20%	

lower-valent stabilizing ion such as Y^{+3} substitutes for a Zr^{+4} ion in the crystal lattice. The electronic conductivity of stabilized zirconia is almost zero. The operation temperature of the zirconia oxygen sensor is normally greater than 500 °C, as at these temperatures the ionic conductivity is adequate for practical applications.

The basic zirconia oxygen sensor design is illustrated in Fig. 13.52, which shows the principle of the zirconia solid oxygen-ion electrolyte. The sensor consists of a closed-end tube of ceramic zirconia (ZrO_2). The zirconia ceramic

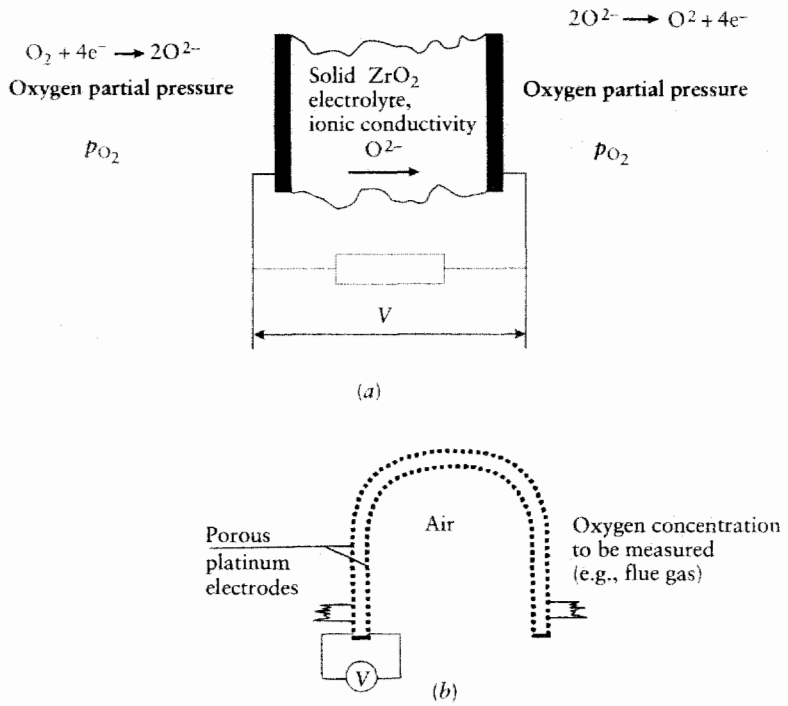

FIGURE 13.52 (*a*) Solid electrolyte and (*b*) arrangement of the zirconia sensor.

separates two gas atmospheres having oxygen partial pressures $p^1_{O_2}$ and $p^2_{O_2}$.[34] The inner and the outer tube surfaces are covered by catalytic porous platinum electrodes, which promote the electrochemical reaction:

$$O_2 + 4e^- \Leftrightarrow 2O^{2-}$$

where e^- represents an electron and O^{2-} represents an oxygen ion. The chemical potential of oxygen gas at each electrode, μ_1 and μ_2, is defined by the oxygen partial pressure over each electrode.

The galvanic potential E is related to the difference in chemical potential by the relation[34]

$$E = -(1/(ZF))\int_{\mu_1}^{\mu_2} t_{ion} d\mu$$

where Z is the valence of the oxygen ion ($Z = 2$), F is the Faraday constant ($F = 9.65 \times 10^4$ C mol^{-1}), and t_{ion} is the ionic transference number for oxygen ions (ratio of the ionic conductivity to the total conductivity, taken as being unity). The chemical potential is related to the oxygen partial pressure by the relation

$$\mu = \mu_0 + (RT/2) \ln p_{O_2}$$

where R is the gas constant [(8.314 J/(K mol)] and T is the absolute temperature. Combining these two equations gives

$$E = -(RT/4F)\int_{p^2_{O_1}}^{p^2_{O_2}} (t_{ion}/p_{O_2}) dp_{O_2}$$

Because the ionic transference number for zirconia material is taken as being unity, then this equation reduces to the Nernst equation[34]

$$E = (RT/4F)\ \ln(p_{O_2}^{1}/P_{O_2}^{2})$$

Air is normally the reference gas used in the exhaust gas sensor. If the oxygen partial pressure in the engine exhaust gas is known as a function of the engine air/fuel ratio, the theoretical galvanic potential of the sensor is easily determined by the Nernst equation.

Application The zirconia oxygen sensor is widely used for combustion control processes and for air/fuel ratio regulation in internal combustion engines. The closed-end portion of the electrode tube is inserted into the exhaust gas stream.[34] In the control of industrial combustion processes, no out-stack sampling system is required.

Other O_2 Measurement Techniques The oxygen concentration in the emission gases of combustion processes is often measured based on the strong paramagnetic character of oxygen. A sampling line with appropriate sample treatments is required with this method.

Semiconductor Gas Sensors Semiconductor gas sensors are used to indicate concentrations of gases such as CO and H_2S. The device responds to the change in the composition of the surrounding atmosphere with a change in conductance of a gas-sensitive semiconductor.[35] Oxide semiconductors with wide band gaps (SnO_2, ZnO, WO_3, In_2O_3) are typical sensing semiconductors, since the sensors operate at elevated temperatures up to around 500 °C. The chalcogenides SnO_2 and CdS, utilized as gas sensor materials, are n-type semiconductors with band gaps of 3.6 eV (SnO_2) and 2.5 eV (CdS). CdS is a typical II-VI compound semiconductor.[36] The semiconducting behavior arises in both structures from point defects, donors being related to oxygen vacancies in SnO_2 to cadmium interstitials, or to sulfur vacancies in CdS.

Theory for Operation of SnO_2-Based Semiconductor Gas Sensors The negative surface charge due to the ionosorbed oxygen species generates a depletion layer and a potential energy barrier on the surfaces of ionic n-type semiconductor grains of the gas sensors. For planar geometry, the height of this barrier eV_s is given by the Schottky equation:[37]

$$eV = \frac{e^2 N_t^2}{2\epsilon\epsilon_0 N_d}$$

where $N_t = [O^{2-}] + [O^-]$ is the surface density of ionosorbed oxygen species, $\epsilon\epsilon_0$ is the permittivity, and N_d is the volumetric density of the single electron donors. In tin dioxide material in gas sensors, the certain lack of oxygen at the surface can be expressed as SnO_{2-x}.[38]

In conduction models of semiconductor gas sensors, surface barriers of intergranular contacts dominate the resistance. Electrons must overcome this energy barrier, eV_s, in order to cross from one grain to another.[36] For these

models, the conductance activation energy is usually assumed to be eV_s, to a first approximation in the ohmic voltage range. Then the conductivity G at a temperature T is described by[39]

$$G = G_0 \exp(-eV_s/kT) ,$$

where kT is the thermal energy, and G_0 is a factor including the bulk intragranular conductivity and geometrical effects.

It is assumed that all the donors are ionized and that the voltage dependence of the current is ohmic. The temperature dependence of G_0 may be considered constant. A schematic diagram of a porous gas sensor sample together with its band structure is shown in Fig. 13.53.[40]

Response The conductance response of semiconductor gas sensors has been modeled by describing the barrier energy in terms of physisorption of oxygen molecules in the surface, the ionosorption of O_2 to O_2^- according to Fermi-Dirac statistics, and the catalytic reactions of reducing gases with physisorbed O_2 molecules.[41]

The model gives the nature of measured power law of the conductance response to oxygen:

$$G \propto p_{O_2}^{-\beta}$$

with $\beta = kT/E_0$. E_0 is an energy constant characteristic of the sensor.[42] The values of β vary between 0.25 and 0.5. When a reducing gas G_i removes physisorbed oxygen from the surface via a catalytic reaction,

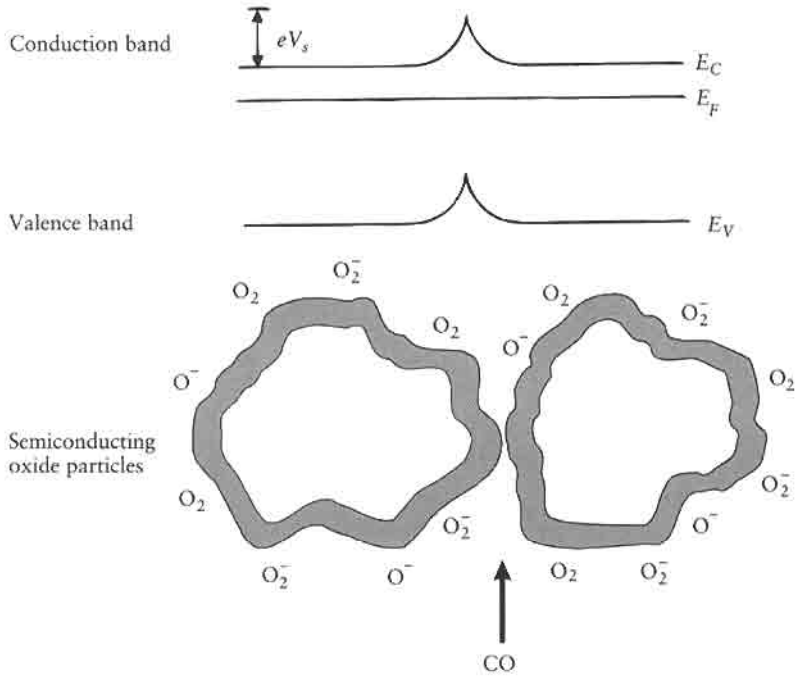

FIGURE 13.53 Formation of a Schottky potential energy barrier on the surface of the particles of the gas sensor material.[40] The negative surface charge due to ionosorbed oxygen species generates a depletion layer. E_F is the Fermi energy.

$$n_i G_i + O_{2\text{surf}} \longrightarrow G_{\text{prod}} ,$$

the conductance changes according to

$$G \propto p_{O_2}^{-\beta}(1 + K_i p_i n_i)^{\beta} ,$$

where p_{O_2} and p_i are the partial pressures of oxygen and reducing gas G_i, n_i is a reaction coefficient, and K_i is the sensitivity coefficient for gas G_i. The response time of the sensor is determined by the kinetics of electron transitions between the conduction band and the surface states. For a commercial sensor, the sensitivity coefficient factors (K_i) have been measured:[41] $K_{CH_4} \approx 5 \times 10^{-3}$ ppm^{-1}, $K_{H_2O} \approx 5 \times 10^{-3}$ ppm^{-1}, $K_{H_2} \approx 0.1$ ppm^{-2}, and $K_{CO} \approx 1 \times 10^{-3}$ ppm^{-2}. This sensor is very sensitive to the presence of hydrogen.

Construction In tin dioxide semiconductor sensors, the sensing material is small sintered particles. For the sensor current flow, particle boundaries form potential energy barriers, which act as a random barrier network. Different types of semiconductor gas sensors are shown in Fig. 13.54.

The gas-sensitive material in *thick-film* gas sensors has a sintered layer area of a few square millimeters, and about 30 μm in thickness, on a ceramic substrate (Fig. 13.54*b*). In other types of gas sensors, it is on the outer surface of a thin tube or as a sintered button (Fig. 13.54*a* and *c*). The sensor is heated to the operating temperature of 300–500 °C by means of a resistor.

Applicability of Semiconductor Gas Sensors Research into the applications of this type of sensor has mainly been concerned with measuring carbon monoxide concentration in flue gases. Tests show that sensors follow the concentration of carbon monoxide in the flue gas. Improvement in sensor performance has resulted with the introduction of a catalytic additive (palladium or platinum).[43,44]

In combustion processes tests, it has been noticed that Pd-catalyzed SnO_2 sensors follow the variations in the concentration of CO in the combustion gases, even in the case of solid fuels.[44]

Optical Gas Sensors

Electrically Tunable Micromachined Fabry-Pérot Interferometer The Fabry-Pérot interferometer is an optical resonator consisting of two parallel mirrors. Fabry-Pérot interferometers can be made by silicon bulk micromachining.[45,46] Silicon surface micromachining is also a suitable technique for making interferometers for infrared wavelengths.

The principle of a gas concentration measurement system operating on an electrically tunable micromachined Fabry-Pérot interferometer is NDIR (nondispersive infrared) single-beam dual-wavelength measurement.[46] The interferometer is tuned so that the pass band coincides with the absorption band of the measured gas. A detector records the signal strength after the measurement chamber. The pass band of the Fabry-Pérot interferometer then shifts to either side of the absorption band, and the signal now detected constitutes the reference signal (Fig. 13.55).

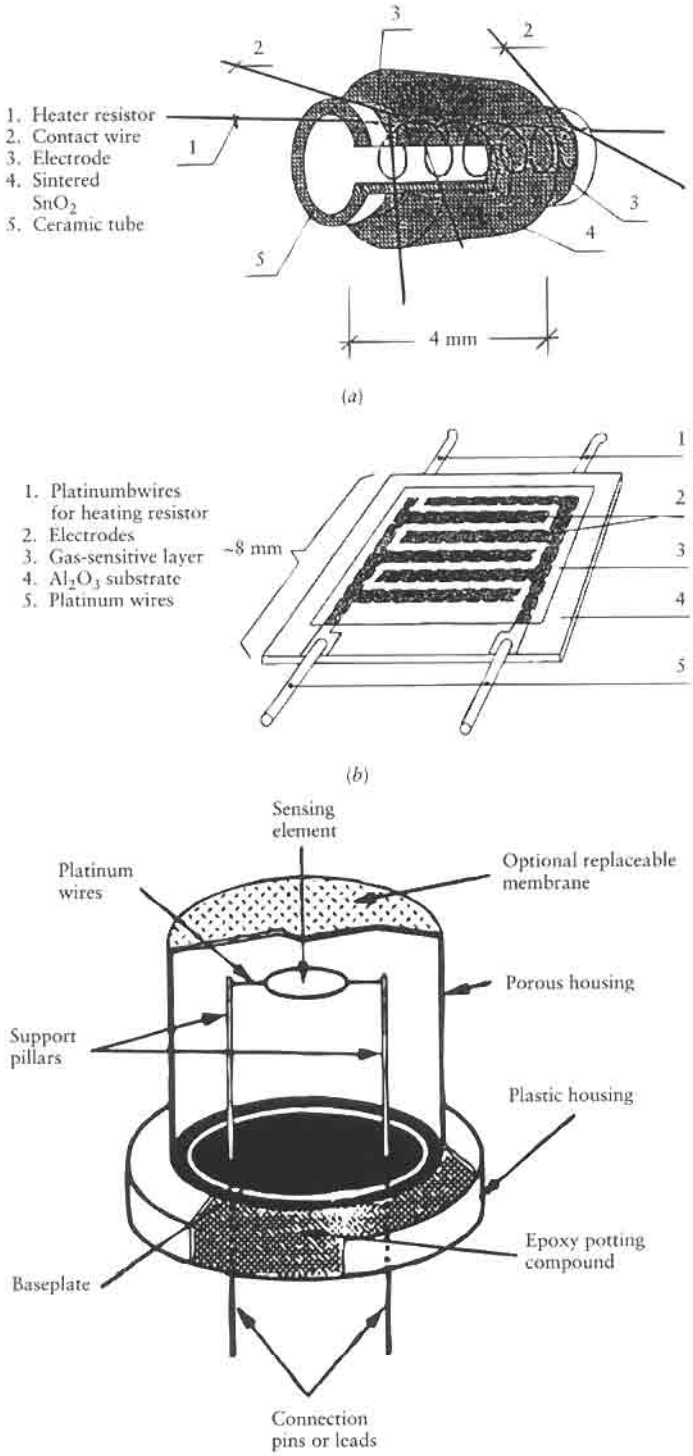

FIGURE 13.54 Semiconductor gas sensors: (*a*) tubular, (*b*) thick film, (*c*) bulk-type one-electrode sensor where a thin Pt wire spiral is embedded inside a sintered oxide semiconductor button.[35]

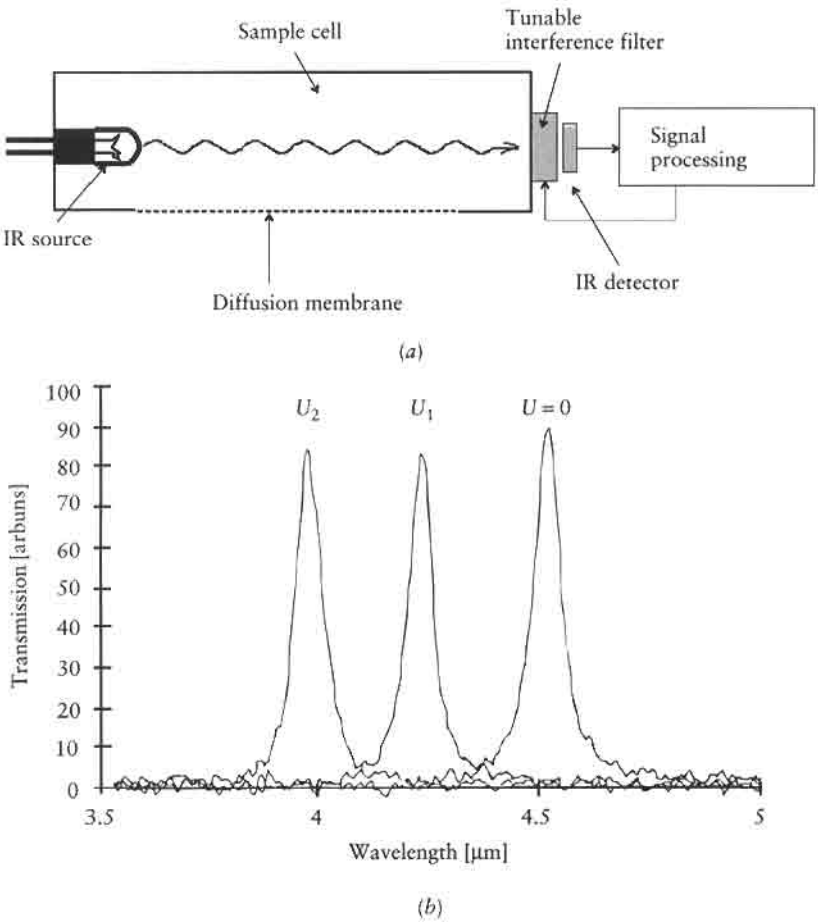

FIGURE 13.55 (*a*) Principle of gas sensor based on an electrically tunable micromachined Fabry-Perot interferometer[47] and (*b*) the shifting of the pass band controlled by the tuning voltage.[46]

The resonance condition of a Fabry-Pérot interferometer is $2L = n\lambda$, where L is the mirror spacing, λ is the wavelength, and n an integer. In the construction of Blomberg et al.,[46] $n = 1$ or $L = \lambda/2$. The aperture of this Fabry-Pérot interferometer is approximately 1 mm and the wavelength 4.3 μm (CO_2).

Tuning The interferometer is tuned by electrode voltage control. The band-pass center wavelength is displaced accordingly. The FWHM of the transmission pass band is approximately 70 nm at the 4.2 μm wavelength. The stable tuning range of L is

$$L_0 \geq L > \frac{2}{3}L_0,$$

where L_0 is the zero-voltage separation of the mirrors.[46]

Figure 13.55 shows the principle of a gas sensor based on an electrically tunable micromachined Fabry-Pérot interferometer, and the shifting of the pass band controlled by the tuning voltage.

Light-Emitting Diode Sensors Some gas detection sensors utilize light-emitting diodes (LEDs) or laser emitters together with photodetectors operating at appropriate wavelengths. The radiation is emitted at the wavelength of an absorption maximum of the gas to be measured. An example of an infrared CO_2 sensor is shown in Fig. 13.56.

The production of emitting sources requires further development in material technology, as the emitting wavelength is controlled by the compositions of alloy semiconductors to form heterostructures such as InGaAs/InAs[48,49] or III-V alloy systems.[50]

The composition must be controlled to give the required emission wavelength. Techniques utilized include molecular-beam epitaxy (MBE) and liquid-phase epitaxy (LPE).

Several LED chips have been mounted together on the same thermoelectric cooler shown in Fig. 13.56*b*.[51] This nondispersive IR analyzer utilizes sample and reference PbSe photoresistors as detecting elements. The LED emission (4.3 μm for CO_2 and 4.7 μm for CO detection) is focused onto a sample photodetector by a concave mirror.

13.5.5 Case Example

13.5.5.1 Monitoring of Emission Gases at Pulp and Paper Industry

In the pulp and paper industry, the main gas emissions are from the pulp production. The main sources of emission are in the soda recovery boiler, lime kiln, evaporation plant, and bark combustion boiler.

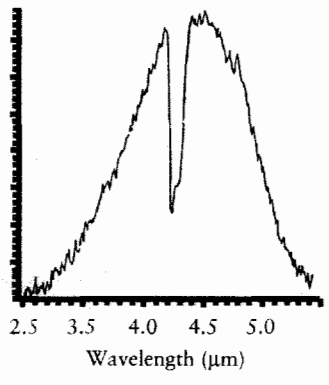

(*a*)

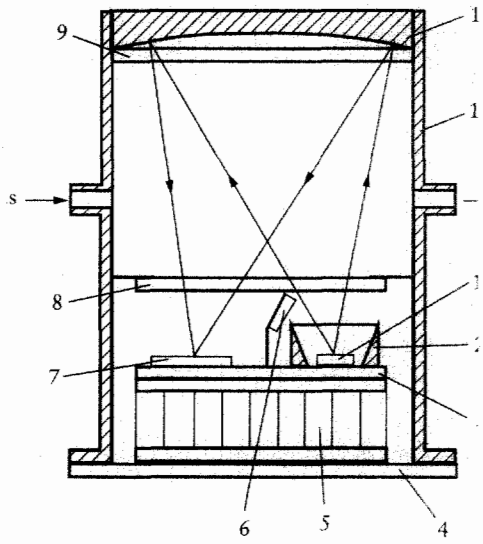

(*b*)

FIGURE 13.56 (*a*) The emission spectrum of an LED.[49] The 4.3-μm LED spectrum shows a dip at around 4.3 μm, which corresponds to background carbon dioxide absorption typically present at concentrations of the order of 300 ppmv. (*b*) IR gas sensor configuration utilizing several LED chips.[50,51] 1. IR LEDs; 2. microreflector; 3. thermosensor; 4. TO-3 header; 5. thermoelectric cooler; 6. reference photodetector; 7. sample photodetector; 8. sapphire window; 9. protection window; 10. spherical mirror; 11. gas chamber.

The gases normally monitored include:

oxides of sulfur and nitrogen (SO_2, NO_x),
malodorous (reduced) sulfur compounds, generally expressed as TRS,
particulates (PM), and
carbon monoxide (CO) and carbon dioxide (CO_2).

Continuous monitoring of emission gases is necessary to ascertain that the emissions from a production unit remain within the limit values.[52] The limit value for SO_2 in Finland is 4 kg or less per tonne of pulp produced. The authorities often require plants to continuously monitor the main emissions. Information on the environmental load generated by a production unit is available to customers upon request. This information is also used for the environmental management of the plant.

Special conditions in the paper pulp industry require reliable monitoring. Emission gases, including corrosive gases and particulates, are generally moisture laden. Fouling and blocking of the sampling system is a major problem in continuous monitoring. It is noted that stationary monitoring systems frequently show low values, even though the service and calibration have been properly performed.[52] This is due to partial blocking of the sampling line by moisture, leakages, etc.

References

1. Sarkkinen, Seppo. Air Pollution Control Legislation and Administration in Finland. *Finnish Air Pollution Prevention News* (1995) (no. 3), pp. 4–6.
2. Tate, J. D. and Petri Jaakkola. The Use of Portable Low-Resolution FT-IR for Industrial Gas Analysis. In Petri Jaakkola, Industrial Applications of Low Resolution FT-IR Gas Phase Spectrometry. *Annales Universitatis Turkuensis*, Ser. A I Tom. 222, Astronomica—Chemica—Physica—Mathematica, University of Turku (1997), pp. 93–115.
3. Ayers, Mike. Basic Air Pollution Theory. In E. Roberts Alley & Associates, Inc., *Air Quality Control Handbook*. New York: McGraw-Hill (1998), pp. 2.3–2.29.
4. Weast, Robert C., Melvin J. Astle, and William H. Beyer. *CRC Handbook of Chemistry and Physics*. Boca Raton, FL: CRC Press (1983).
5. SFS 3866. *Ilmansuojelu. Päästöt. Kiintoaineen määritys manuaalisella menetelmällä*. Helsinki: Suomen Standardisoimisliitto. (1990).
6. ISO 9096. Stationary Source Emissions—Determination of Concentration and Mass Flow Rate of Particulate Material in Gas-Carrying Ducts—Manual Gravimetric Method. (1992).
7. Gravimat SHC 502 Gravimetric Dust Concentration Measuring System. Operating instructions. SICK AG; Waldkirch, Germany: Erwin Sick Optic Electronic Ltd.
8. Patashnick, H. and E.G. Rupprecht. Continuous PM_{10} Measurements Using Tapered Element Oscillating Microbalance. *J. Air Waste Manage. Assoc.* 41 (1991), pp. 1079–1083.
9. EPA. *Air Quality Criteria for Particulate Matter. 4. Sampling and Analysis Methods for Particulate Matter and Acid Deposition*. Research Triangle Park, NC. http://www.epa.gov/nceawww1/pm_vol 1.htm.
10. EPA. *Guidance for Using Continuous Monitors in $PM_{2.5}$ Monitoring Networks*. Research Triangle Park, N.C. http://www.epa.gov/ttnamti1/files/ambient/pm25/r-98-012.pdf.
11. TEOM® series 1400a ambient particulate (PM-10) monitor. Operating manual. Revision B. Albany, NY: Rupprecht & Patashnick Co., Inc. (1996).
12. TEOM® series 7000 source particulate monitor. Albany, NY: Rupprecht & Patashnick Co., Inc. (1998).
13. Verewa F-904-K. Extractive Beta Gauge Particulate Monitor. Principle of Operation. Hamburg: Umwelt-und ProzeBmeBtechnile GmbH (1998).
14. Beta 5 M. Continuous Particulate Emissions Monitor by Beta Ray Attenuation. Poissy, France: Émission S. A. (1995).

15. Cooper, C. David, and F. C. Alley. *Air Pollution Control: A Design Approach*. Prospect Heights, IL: Waveland Press (1990).
16. Moisio, Mikko. Real Time Size Distribution Measurement of Combustion Aerosols. Doctor of technology thesis, Tampere University of Technology (1999).
17. Ahlvik, Peter, Leonidas Ntziachristos, Jorma Keskinen, and Annele Virtanen. Real Time Measurements of Diesel Particle Size Distribution with an Electrical Low Pressure Impactor. SAE Technical paper 980410. Reprinted from *General Emissions* (SP-1335). International Congress and Exposition, Detroit, February, 23–26 (1998).
18. GIV Produktinformation. Verfahrenstechnik. Meteorologie. Staubmesstechnik. Vakuumtechnik. Magnetik. Kryotechnik. Gesellschaft für Innovative Verfahrenstechnik MBH, Breuberg.
19. Malinen, Jouko, Markku Tapola, and Jyrki Uimonen. Teollisuuden tarpeenmukainen ilmanvaihdon ohjaus ja anturitekniikka. Espoo: Technical Research Centre of Finland, Research Notes 838, (1988).
20. Air Quality Criteria for Ozone and Related Photochemical Oxidants. Volume I.3. Tropospheric Ozone and Its Precursors. Research Triangle Park, NC: EPA (1996). http://www.epa.gov.ncea/ozone.htm.
21. Signal, Model 3000, Operation Manual. Santa Barbara: RC Electronics, Inc. (1988).
22. Vesterinen, R. Energiantuotannon päästöjen mittaaminen. Näytteenottomenetelmät, mittalaitteet, työtavat ja niiden kenttäkelpoisuus. Espoo: Technical Research Centre of Finland, Research Notes 887 (1988).
23. Okabe H., P. L. Splitstone, and J. J., Ball. Ambient and Source SO_2 Detector Based on a Fluorescence Method. *Air Pollution Control Assoc.* 23 (1973), pp. 514–516.
24. Air Quality Criteria for Ozone and Related Photochemical Oxidants. Volume I.3. Tropospheric Ozone and Its Precursors. Research Trangle Park, NC: EPA (1996). http://www.epa.gov.ncea/ozone.htm.
25. Edner, Hans, Anders Sunesson, Sune Svanberg, Leif Unéus, and Svante Wallin. Differential Optical Absorption Spectroscopy System Used for Atmospheric Mercury Monitoring. *Applied Optics* 25 (1986), pp. 403–409.
26. Stevens, R. K., R. J. Drago, and Y. Mamane. A Long Path Differential Optical Absorption Spectrometer and EPA-Approved Fixed-Point Methods Intercomparison. *Atmospheric Environment* 27B (1993), pp. 231–236.
27. Reisinger, Andreas R., Grahame J. Fraser, Paul V. Johnston, Richard L. McKenzie, and W. Andrew Matthews. Slow-Scanning DOAS System for Urban Air Pollution Monitoring. XVIII Quadrennial Ozone Symposium '96, University of L'Aquila, L'Aquila, Italy, September 12–21, 1996. http://www.aquila.infn.it:80/o3symp.html/main.html.
28. Kauppinen, Jyrki K. FTIR Spectrometers for Industrial Applications. Lecture notes, University of Turku, Department of Applied Physics (1993).
29. Räsänen, J., and J. Kauppinen. Focussing Interferometer. U.S. patent application #08-258,674 (1993).
30. Jaakkola, Petri, Industrial Applications of Low Resolution FT-IR Gas Phase Spectrometry. *Annales Universitatis Turkuensis*, Ser. A I Tom. 222, *Astronomica—Chemica—Physica—Mathematica*, Turku: (1997), pp. 5–13.
31. Saarinen, Pekka, and Jyrki Kauppinen. Multicomponent Analysis of FT-IR Spectra. *Applied Spectroscopy* 45 (1991), pp. 953–963.
32. Gasmet RT-IR analyzer. Helsinki: Temet Instruments. http://temet.fi/gasmet.html.
33. Motor exhaust gas. Helsinki: Temet Instruments. http://temet.fi/exhaust.htm.
34. Eddy, David S. Physical Principles of the Zirconia Exhaust Gas Sensor. *IEEE Trans. Vehicular Technol.* VT-23 (1974), pp. 125–128.
35. Golovanov, V., J. L. Solis, V. Lantto, and S. Leppävuori. Different Thick-Film Methods in Printing of one-Electrode Semiconductor Gas Sensors. *Sensors Actuators* B34 (1996), pp. 410–416.
36. Lantto, V., and V. Golovanov. A Comparison of Conductance Behaviour between SnO_2 and CdS Gas-Sensitive Films. *Sensors Actuators* B24-25 (1995), pp. 614–618.
37. Lantto, V., and P. Romppainen. Response of Some SnO_2 Gas Sensors to H_2S after Quick Cooling. *J. Electrochem. Soc.* 135 (1988), pp. 2550–2556.
38. Has, Uwe. Sensor Controlled Pyrolysis in Consumer Ovens. *Sensor Review* 18 (1998), pp. 188–192.

39. Morrison, S. R. Measurement of Surface State Energy Levels of One-Equivalent Adsorbates on ZnO. *Surface Sci.* 27 (1971) pp. 586–604.
40. Lantto, V. and P. Romppainen. Electrical Studies on the Reactions of CO with Different Oxygen Species on SnO_2 Surfaces. *Surface Sci.* 192 (1987), pp. 243–264.
41. Clifford, P. K. Mechanisms of Gas Detection by Metal Oxide Surfaces. Ph.D. Dissertation, Carnegie-Mellon University, (July 1981).
42. Lantto, V., P. Romppainen, and S. Leppävuori. Response Studies of Some Semiconductor Gas Sensors under Different Experimental Conditions. *Sensors Actuators* 15 (1988), pp. 347–357.
43. Torvela. H., Capteurs de gaz à semiconducteur céramic. Application *à l'étude* des combustion et au contrôle de la pollution atmosphérique. *Revue Générale de Thermique* XXIX (1990), no. 341, pp. 1–7.
44. Torvela. H., A. Harkoma-Mattila, and S. Leppävuori. Characterization of a Combustion Process Using Catalysed Tin Oxide Gas Sensors to Detect CO from Emission Gases. *Sensors Actuators* B1 (1990), pp. 83–86.
45. Jerman, J. H., and D. J. Clift. Miniature Fabry–Pérot Interferometers Micromachined in Silicon for the Use in Optical Fiber WDM Systems. Transducers '91 *Conference, Digest of Technical Papers* (1991), pp. 372–375.
46. Blomberg, M., A. Torkkeli, A. Lehto, C. Helenelund, M. Viitasalo. Electrically Tuneable Micromachined Fabry-Pérot Interferometer in Gas Analysis. *Physica Scripta* T69 (1997), pp. 119–121.
47. Vaisala. The new CARBOCAP® carbon dioxide sensor. Helsinki: Vaisala Oyj. http://www.vaisala.com/.
48. Malinen, J., T. Hannula, N. V. Zotova, S. A. Karandashov, I. I. Markov, B. A. Marveev, N. M. Stus, and G. N. Talalakin. Nondispersive and Multichannel Analyzers Based on Mid-IR LEDs and Arrays. SPIE Proceedings 2069 (September 1993), pp. 95–101.
49. Mabbit, Allen, and Andrew Parker. Methane and Carbon Dioxide Detection Using LED Sources. *Sensor Rev.* 16 (1996), pp. 38–41.
50. Matveev, B. A., G. A. Gavrilov, V. V. Evstropov, N. V. Zotova, S. A. Karandashov, G. Y. Sotnikova, N. M. Stus, G. N. Talalakin, and J. Malinen. Mid-infrared (3–5 μm) LEDs as Sources for Gas and Liquid Sensors. *Sensors Actuators* B38–39 (1997), pp. 339–343.
51. Matveev, Boris A. CO_2 *Infrared Sensor Head.* St. Petersburg: IOFFE Physical–Technical Institute (1996).
52. Pesari, Juha, Erja Monto, Jari Tamminen, Esa Marttila, Simo Hammo, and Ritva Käyhkö. Jatkuvatoiminen ilmapäästöjen mittaus sellutehtailla. *Paperi ja Puu* [Paper and Timber] 79 (1997), (no. 6), pp. 400–402.

14
PNEUMATIC CONVEYING

MARKKU J. LAMPINEN

Laboratory of Applied Thermodynamics, Helsinki University of Technology, Helsinki, Finland

LIST OF SYMBOLS

Roman Letters

A Cross-sectional area (m^2)
c Velocity of the conveyed material (m/s)
c_p Specific heat at constant pressure (J/kg K)
C_d *coefficient of drag*

Reprinted from M. Lampinen, "Calculation Methods for Determining the Pressure Loss of Two-Phase Pipe Flow and Ejectors in Pneumatic Conveying Systems," *Acta Polytechnica Scandinavica*, Mechanical Engineering Series No. 99, published by the Finnish Academy of Technology, Helsinki, 1991.

d_s diameter of particle (m)
D diameter of pipe (m)
f force (N/m^3)
F_d drag force (N)
Fr Froude number
g acceleration due to gravity, $\equiv$9.82 m/s^2
h specific enthalpy (J/kg)
i summation index
k coefficient in the formulas of free-falling velocity
l length of the pipe (m)
L linear momentum of falling particles (N)
m mass (kg)
$\dot{m}$ mass flow (kg/s)
$\dot{m}''$ mass flux (kg/m^2 s)
n exponent in the formulas of free-falling velocity
N number of particles
p pressure (N/m^2)
P''' power per unit volume (W/m^3)
Re Reynolds number
s integration variable; empty distance between particles
t time (s); integration variable
T temperature (K)
v velocity of gas (m/s)
V volume (m^3)
$\dot{V}$ volume flow (m^3/s)
w_{SO} free-falling velocity of particle (m/s)
w_s falling velocity of particles in a vertical pipe (m/s)
x coordinate, horizontal axis of probability size distribution, logarithm of particle diameter
y coordinate, vertical axis of probability size distribution

Greek Letters

α slope of the size distribution line
δ inclination angle of the pipe
Δ difference
ϕ volume fraction, of the gas or void fraction
γ exponent in Eq. (14.72), a function of Re
λ friction coefficient in the pressure loss equation
μ mixture ratio; mean diameter of particles in logarithmic scale
μ_f friction coefficient
ν kinematic viscosity (m^2/s)
ρ density (kg/m^3)
σ mean variance
ζ pressure drop coefficient

Subscripts

A reference state
o initial state

s	solid (partial density, etc.)
g	gas (partial density, etc.)
S	solid (real density, etc.)
G	gas (real density, etc.)
d	particle
v	vertical
h	horizontal
i	individual particle (identification index)
m	mean
w	wall
int	internal

14.1 INTRODUCTION

Conveying systems normally use air as the transport medium to convey granular, crushed, or pulverized materials. Modelling the flow of pneumatic conveying and calculating its pressure loss is a problematic task. The greatest problem arises from the fact that different mass flow ratios, solid flow rate divided by the gas flow rate, imply different flow types in pneumatic conveying. Each of these flow types, which can be classified in many different ways, requires its own specific model in order to provide a concrete calculation method.

At relatively high gas velocity, solids are conveyed in an apparently uniform suspension in a so-called lean or dilute-phase flow. Dilute-phase conveying systems are commonly used in so-called long-distance pneumatic conveying systems, where the transport distances may be one kilometer or even more. These systems operate effectively and reliably, even under rather dilute conditions. Well-known examples of these applications are the transportation of cement, fly ash, wood chips, and other products for building works and backfilling in mines. In Section 14.3 we derive a specific model for dilute phase flow from the general balance equations. The following considerations apply well to dry and non-sticky materials, and not so well to very fine materials. As an example of this model we show how it can be used for calculating the pneumatic conveying of wood chips. Finally, we compare the calculated results with measurements made in a pneumatic transport plant. The energy requirements for such systems are provided by a fan, blower, compressor, or injector. This topic is also presented in Section 14.3.

14.2 BASIC PRINCIPLES OF PNEUMATIC CONVEYING

14.2.1 Concepts and Notations

The mass flow ratio μ, sometimes also called mixture ratio, is defined as

$$\mu = \frac{\dot{m}_s}{\dot{m}_g}, \tag{14.1}$$

where $\dot{m}_s$ is the mass flow of solid particles (kg/s) and $\dot{m}_g$ is the mass flow of gas. In pneumatic conveying systems the gas is almost always air.

Let us then consider an arbitrarily selected point in a pipe in which gas and solid particles are flowing. The flow of the mixture of gas and solid particles need not be homogeneous, i.e., the concentration of particles may vary across the cross-section of the pipe. This means that the mixture ratio μ should generally be regarded as a function of position in the pipe, and therefore the definition, Eq. (14.1), should be replaced by

$$\mu = \frac{\dot{m}_s''}{\dot{m}_g''}, \tag{14.2}$$

where $\dot{m}_s''$ and $\dot{m}_g''$ are the mass flow densities (kg/m^2 s) of solids and gas, respectively, at a certain point in the pipe.

The flows of gas and solid particles are assumed to be parallel. This means that the velocity of gas v and the velocity of solid particles c are both in the direction of the pipeline. On the other hand, because we do not assume a homogeneous flow at this stage of the theory, the absolute values of v and c may vary across the cross-section of the pipe.

A differential volume element dV in the flow field contains a mass of gas dm_g and a mass of solids dm_s. The corresponding volumes taken by gas and solids are denoted by dV_g and dV_s. The sum of these partial volumes is the total volume of the mixture,

$$dV = dV_g + dV_s . \tag{14.3}$$

The real density of the gas at the point of the volume element dV is

$$\rho_G = \frac{dm_g}{dV_g} \tag{14.4}$$

and the corresponding apparent or partial density of the gas is

$$\rho_g = \frac{dm_g}{dV} . \tag{14.5}$$

The real density ρ_G is the mass of the gas divided by the volume occupied by the gas. The apparent density or partial density ρ_g is the mass of the gas divided by the total volume of the solid-gas mixture.

We define the corresponding densities for solid particles analogous to Eqs. (14.4) and (14.5),

$$\rho_S = \frac{dm_s}{dV_s} \tag{14.6}$$

and

$$\rho_s = \frac{dm_s}{dV} . \tag{14.7}$$

ρ_S is the real density of the solid particles and ρ_s is the partial density of particles in the mixture.

The volume fraction of the gas in the mixture, or void fraction or voidage, as it is also called, is defined as

$$\phi = \frac{dV_g}{dV} . \tag{14.8}$$

From Eqs. (14.4) and (14.5) it follows immediately that

$$\frac{\rho_g}{\rho_G} = \phi, \tag{14.9}$$

and from Eqs. (14.6), (14.7), and (14.3) it follows that

$$\frac{\rho_s}{\rho_S} = 1 - \phi. \tag{14.10}$$

On the other hand, if dl is a differential length in the direction of the flow, the differential volumes can be written as

$$\begin{aligned} dV &= dA\ dl \\ dV_g &= dA_g\ dl \\ dV_s &= dA_s\ dl \end{aligned} \tag{14.11}$$

where dA_g is the cross-sectional differential area through which the gas flows and correspondingly dA_s is the area for flowing solid particles. The sum of these two partial areas is

$$dA = dA_g + dA_s. \tag{14.12}$$

On the basis of Eqs. (14.11), the volume fraction of gas can also be written in the form

$$\phi = \frac{dA_g}{dA}. \tag{14.13}$$

This interpretation of ϕ we shall need in connection with linear momentum equations.

With the aid of the partial densities ρ_g and ρ_s, the mass flow densities can be expressed as follows:

$$\dot{m}_g'' = \rho_g v \tag{14.14}$$

$$\dot{m}_s'' = \rho_s c, \tag{14.15}$$

where v is the velocity of the gas and c is the velocity of the conveyed material. The total mass flow density is the sum of these two fluxes,

$$\dot{m}'' = \rho_g v + \rho_s c. \tag{14.16}$$

Substituting Eqs. (14.14) and (14.15) into Eq. (14.2), we obtain

$$\mu = \frac{c}{v} \cdot \frac{\rho_s}{\rho_g} = \frac{c}{v} \cdot \frac{1-\phi}{\phi} \cdot \frac{\rho_S}{\rho_G}, \tag{14.17}$$

where the last equality follows from Eqs. (14.9) and (14.10).

When the mixture ratio μ and the velocity ratio v/c are known, the void fraction ϕ can be determined from Eq. (14.17). As an example of this we have calculated $\phi = \phi(\mu, c/v)$ for the case $\rho_G = 1.2\ \text{kg/m}^3$ and $\rho_S = 1500\ \text{kg/m}^3$. Since mostly $c \leq v$ and $dV_g \leq dV$, it follows that $0 \leq c/v \leq 1$ and $0 \leq \phi \leq 1$. However, in some cases c can be greater than v, for instance in downward pneumatic conveying or after a pipestepping. The results of the calculations are shown in Fig. 14.1.

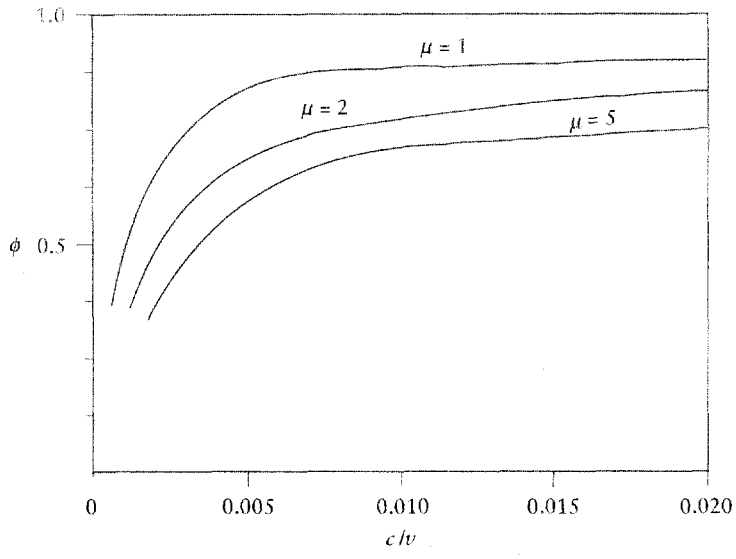

FIGURE 14.1 The void fraction $\phi = \phi(\mu, c/v)$ in the case where $\rho_G = 1.2$ kg/m^3 and $\rho_S = 1500$ kg/m^3.

The curves in Fig. 14.1 are not drawn down to zero, as the void fraction in a mixture with solid particles can not be zero. Equation (14.17) makes sense only in connection with equations of motion and particle size.

14.2.2 Classification of Different Types of Flow

Figure 14.1 shows that the void fraction ϕ comes close to zero as soon as the ratio c/v approaches zero, and, the smaller the mixture ratio μ, the greater the void fraction ϕ. In some cases, the void fraction ϕ alone may be a good characteristic number for classification of the type of flow in pneumatic conveying. But generally speaking, the void fraction ϕ is not the only criterion that determines the behavior of the flow.

Besides the void fraction ϕ, a very important parameter is the size of the particles. Using a simple cubic model for packing spherical balls, which represent the particles, we get the following expression for the void fraction

$$\phi = \frac{\pi}{6}\left(\frac{d}{d+s}\right)^3,$$

where d is the diameter of the balls and s is the empty distance between the balls, i.e., the distance between the centers of the balls is $d + s$. Solving for s in the equation above, we get

$$s = \left[\left(\frac{\pi}{6\phi}\right)^{1/3} - 1\right]d, \tag{14.18}$$

from which we see that for the same void fraction ϕ, the distance between particles is proportional to the size of the particle d.

Obviously, the closer the particles are to each other, the more likely it is that they will stick together and form larger clumps, which usually means that the flow is not uniform. This view combined with Eq. (14.18) is a greatly simplified explanation of why the mass flow ratio μ for dry wood chips can rise to five or even higher and still the flow of the mixture of air and large chip particles can be handled as a uniform suspension, a uniform dilute-phase flow, although it is not actually dilute. The mass flow ratio for fine coal powder, however, has to be much less than five in order for the flow to be handled as a uniform dilute flow.

Even the void fraction together with particle size distribution does not provide all of the necessary information on the kind of flow. The mutual forces between distinct particles depend not only on the distance between the particles but also on the surface properties of the particles. The strength of the attractive forces between particles depends on conditions. For instance, the moisture content of the solid is essential for determining the attractive forces between particles, especially for hydroscopic materials such as wood. Airflow between particles usually tends to separate particles, whereas the surface forces, adhesion forces, tend to bring them together.

One widely-used picture for illustrating the different types of flow in pneumatic conveying is the so-called state diagram,[1,2] in which the pressure drop is related to the air velocity.

As shown in Fig. 14.2, the material conveying region is bounded by the air-only curve and the stationary-plug curve, where the air merely percolates through or flows above a packed bed of stationary particles. Dense-phase conveying occurs when v, the velocity of air, is below the so-called saltation velocity.

The dense-phase regime can be further subdivided into three distinct regions,[3,4] which are shown in Fig. 14.3. In continuous dense-phase flow the material moves by saltation over a stable creeping bed, in discontinuous dense-phase flow particles move as groups, and in the solid dense-phase the solids are extruded through the pipe as a continuous slag.

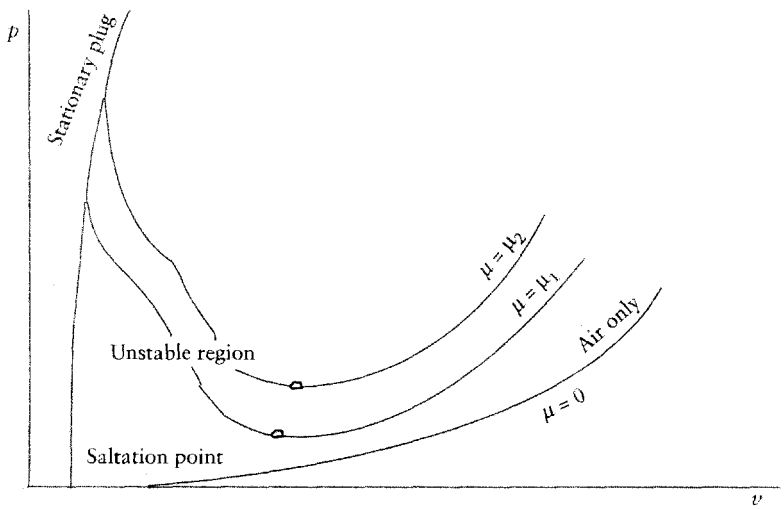

FIGURE 14.2 State diagram of pneumatic conveying.

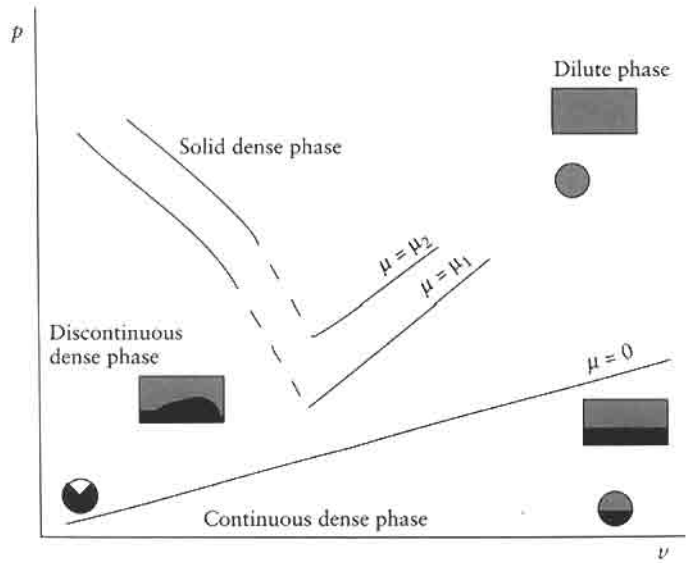

FIGURE 14.3 Distinct phases of pneumatic conveying.[3,4]

Dense-phase conveying offers some clear advantages over dilute-phase conveying. It has a lower power consumption, wear is reduced, and the gas/solids separators and the size of pipe required are smaller. The disadvantage is the greater pressure loss per unit length of the pipe, which limits the use of dense-phase conveying to shorter transport distances. The other factor is that many materials, mainly granular materials and materials with large particle size, simply do not flow as dense-phase flow. Granular materials (plastic pellets or seeds) that are more or less consistent in size, flow in stable plugs because the void fraction between grains is high enough. Only granular materials with "fines" have to be stabilized artificially.

Besides the conventional classification of flow shown in Fig. 14.3, there are also other possibilities, see, e.g., Leung.[5] Independent of the method of classification, the essential point is that there is no general method and there are no general simple parameters that reliably predict the behavior of the flow in a new application. For each case the type of flow has to be examined experimentally.

14.2.3 Mathematical Analysis of the Free-Falling Velocity

We start by considering the free-falling velocity of a single particle of diameter d_s. When the particle reaches the free falling-velocity, w_{SO}, the gravitational force and the drag force are in equilibrium, after which the falling velocity is constant.

The basic problem in determining the falling velocity lies in the evaluation of the drag force that a particle experiences as a result of motion relative to the surrounding gas. The gas flow and resulting drag force, F_d, have been characterized most thoroughly for the motion of a smooth nonrotating sphere moving at constant velocity through an otherwise undisturbed and un-

bounded gas. The result obtained under these highly idealized conditions is normally represented by a standard drag coefficient curve, which expresses the relationship between the coefficient of drag, C_d, defined by

$$C_d = \frac{F_d}{\frac{\pi d_s^2}{4} \cdot \rho_G \cdot \frac{w_{SO}^2}{2}}, \tag{14.19}$$

and the particle Reynolds number, defined by

$$\mathrm{Re}_d = \frac{w_{SO} d_s}{\nu}, \tag{14.20}$$

where ν is the kinematic viscosity of the gas. With the dimensionless parameters C_d and Re_d the problem is to find the correlation

$$C_d = f(\mathrm{Re}_d), \tag{14.21}$$

which then, together with the force equilibrium condition that the drag force F_d and the gravitational force minus hydrostatic force are equal, i.e.,

$$F_d = \frac{4}{3}\pi\left(\frac{d_s}{2}\right)^3 (\rho_S - \rho_G)g, \tag{14.22}$$

gives us the free-falling velocity w_{SO}. Here g is the acceleration due to gravity, 9.82 m/s^2.

Despite the long history of determinations of the standard drag curve, Eq. (14.21), values for the drag coefficient under idealized conditions are still a matter of dispute. A comprehensive review has been represented by R. Clift and W. H. Gauvin.[6]

Here we consider the problem from another point of view, namely how a set of particles of different sizes fall in a gas. In other words, we wish to find a simple way to calculate the free-falling velocity of a group of particles when we know the distribution of the size of the particles. But before we can do this, some basic widely-used formulas for calculating the free-falling velocity of a separate single particle are introduced.

The drag coefficient based on the theoretical analysis of Stokes is

$$C_d = f(\mathrm{Re}_d) = \frac{24}{\mathrm{Re}_d}, \tag{14.23}$$

Substituting this into Eq. (14.19) and then combining this with the definition of Re, Eq. (14.20), and the force equilibrium condition, Eq. (14.22), we obtain the following equation for the free-falling velocity:

$$w_{SO} = \frac{\rho_S - \rho_G}{\rho_G} \frac{d_s^2}{18\nu} g, \tag{14.24}$$

If the gas is air at atmospheric pressure ($p = 1.023$ bar) and at temperature 20 °C, then $\rho_G = 1.20$ kg/m^3 and $\nu = 15 \times 10^{-6}$ m^2/s. In the case that $\rho_S = 1500$ kg/m^3 we get from Eq. (14.24) the values shown in Table 14.1.

The greater the Reynolds number becomes, the more inaccurate Eq. (14.24) will be. For $\mathrm{Re}_d < 5 \times 10^{-2}$ the drag coefficient may be calculated with sufficient accuracy from Stokes's law (Eq. (14.23)) and in these cases Eq. (14.24) is adequate.

TABLE 14.1 The Free-Falling Velocity of a Spherical Particle in Air (20 °C, 1.023 bar) based on Stokes's Theory

d_s, μm	w_{SO}, m s^{-1}	Re_d	C_d
6	1.6×10^{-3}	6.5×10^{-4}	3.69×10^{4}
10	4.5×10^{-3}	3.0×10^{-3}	8.0×10^{3}
15	1.0×10^{-2}	1.0×10^{-2}	2.4×10^{3}

The density of the solid particle is 1500 kg/m^3.

Beard and Pruppacher have examined the free-falling velocity for small water droplets in saturated air.[7] These results could be correlated as follows

$$C_d = \begin{cases} 24\mathrm{Re}_d^{-1} + 2.4\mathrm{Re}_d^{-0.05}, & 0.001 \le \mathrm{Re}_d \le 2 \\ 24\mathrm{Re}_d^{-1} + 2.76\mathrm{Re}_d^{-0.20}, & 2 \le \mathrm{Re}_d \le 21 \\ 24\mathrm{Re}_d^{-1} + 2.45\mathrm{Re}_d^{-0.368}, & 21 \le \mathrm{Re}_d \le 200 \end{cases} \tag{14.25}$$

Combining this with Eqs. (14.19) and (14.22), the corresponding free-falling velocity w_{SO} can be determined.

The old empirical equation of Schiller and Nauman,[8]

$$C_d = 24\ \mathrm{Re}_d^{-1} + 3.60\ \mathrm{Re}_d^{-0.313}, \tag{14.26}$$

has been observed to fit the recent results, too, over a wide range of Reynolds number (approximately $1 \le \mathrm{Re}_d \le 1000$).

Clift and Gauvin[9] modified Schiller and Nauman's Eq. (14.26) to represent the drag force throughout the transitional and turbulent regimes:

$$C_d = 24\ \mathrm{Re}_d^{-1} + 3.60\ \mathrm{Re}_d^{-0.313} + \frac{0.42}{(1 + 4.25 \times 10^4\ \mathrm{Re}_d^{-1.16})}. \tag{14.27}$$

The region $1000 \le \mathrm{Re}_d \le 200\ 000$, sometimes called Newton's regime, is characterized by relatively constant drag coefficient, indicating that there are no major changes occurring in the flow pattern. The most significant change is the transition from laminar to turbulent flow in the detached boundary layer. From Eq. (14.27) we get

$$C_d = 0.47 \quad \text{for } \mathrm{Re}_d = 1000$$

and

$$C_d = 0.49 \quad \text{for } \mathrm{Re}_d = 200\,000.$$

Substituting

$$C_d = \text{const.} = 0.5 \tag{14.28}$$

into Eq. (14.19) and then using Eq. (14.22), we get the well-known Newton's formula for the free-falling velocity,

$$w_{SO} = \left[\frac{8}{3}\frac{\rho_S - \rho_G}{\rho_G} g d_s\right]^{1/2} \tag{14.29}$$

which is a good approximation in the region $1000 < \mathrm{Re}_d < 200\ 000$.

In the pneumatic conveying process the flow around the particle is not uniform, the particle is not in steady-state motion, and the flow contains turbulence which is not merely generated by the particles. Thus the use of Eqs. (14.23)–(14.29) is of course rather restricted. Despite these limitations we will now estimate the free-falling velocity of a set of different-sized particles based on the assumption that we know the free-falling velocity of each single particle.

Particles of different sizes fall at different velocities. When a set of different-sized particles falls in a group, the particles collide with each other and the faster ones tend to accelerate the slower ones. In all collisions the linear momentum is conserved, so that if all particles collide with each other sufficiently many times, the set of particles will achieve one mean free-falling velocity. Thus the mean free-falling velocity of the set of particles can be defined by

$$w_{SO} = \frac{\sum_{i=1}^{\infty} m_i w_{SOi}}{\sum_{i=1}^{\infty} m_i} \tag{14.30}$$

where m_i is the mass of a particle whose diameter is d_{si} and whose free-falling velocity is correspondingly w_{SOi}. Since

$$m = \sum_{i=1}^{\infty} m_i \tag{14.31}$$

is the total mass of falling particles, we see from Eq. (14.30) that mw_{SO} is equal to the total linear momentum of the particle set. The identification index i is allowed to take any large values without any limitations, i.e., the number of different particles can be infinite.

In order to use Eq. (14.30) we need to know the particle size distribution. In many cases it has been observed that the size distribution obeys normal probability distribution, or at least can be well approximated by it. In fact, the number of particles dN whose logarithm of diameter

$$x = \ln d_s \tag{14.32}$$

lies in the interval $x \ldots x + dx$ is

$$\frac{dN}{N(t)} = \frac{1}{\sqrt{2\pi}\sigma} e^{-\left(\frac{x-\mu}{2\sigma^2}\right)^2} dx, \tag{14.33}$$

where μ is the mean diameter of the particles (in logarithmic scale, Eq. (14.32)), σ is the mean variance, and $N(t)$ is the total number of the particles.

It will be useful to give a geometrical illustration of the concepts μ and σ included in Eq. (14.33). First, we will construct a special coordinate system.

The coordinates, x- and y-axes, are provided with nonuniform scales, denoted by u and v, as follows:

$$u(x) = e^x \tag{14.34}$$

$$v(y) = \frac{1}{\sqrt{2\pi}} \int_{-\infty}^{y} e^{-\frac{1}{2}s^2} ds. \tag{14.35}$$

Note that the u scale is precisely the same as the d_s scale (Eq. (14.32)).

We will now show that the distribution Eq. (14.33) will be a straight line in the coordinate system x-y, whose axes are provided with the nonuniform scales of Eqs. (14.34)–(14.35). To show this we first write Eq. (14.33) in the integrated form

$$\frac{N(x)}{N(t)} = \frac{1}{\sqrt{2\pi}\sigma} \int_{-\infty}^{x} e^{\frac{(t-\mu)}{2\sigma^2}} \, dt \,, \tag{14.36}$$

where $N(x)$ describes the number of those particles whose diameters are in the region

$$-\infty \leq \ln d_s \leq x, \text{ i.e., } 0 \leq d_s \leq e^x.$$

Changing the integration variable t to

$$s = \frac{t-\mu}{\sigma}, \tag{14.37}$$

we get from Eq. (14.36)

$$\frac{N(x)}{N(t)} = \frac{1}{\sqrt{2\pi}} \int_{-\infty}^{\frac{x-\mu}{\sigma}} e^{-\frac{1}{2}s^2} ds. \tag{14.38}$$

Comparing this with Eq. (14.35), we see that

$$\frac{N(x)}{N(t)} = v(y), \tag{14.39}$$

where the value of y is a linear function of x,

$$y = \frac{x-\mu}{\sigma}. \tag{14.40}$$

These results are illustrated in Fig. 14.4. The value of μ gives a mean diameter

$$d_m = e^{\mu}, \tag{14.41}$$

which divides the set of particles into two groups. Half of the particles are smaller than or equal to d_m and the other half are larger than d_m. The variance σ gives the slope of the line in Fig. 14.4, i.e.,

$$\tan\alpha = \frac{1}{\sigma}. \tag{14.42}$$

From Fig. 14.4 we may, as an example, read that 40% of the particles (measured in numbers) are smaller than 2.2 μm.

Before we go back to Eq. (14.30), we shall evaluate the mass distribution function for the particles whose size distribution is of the form (14.33), i.e., normal probability size distribution.

The mass of the particles dN is

$$dm = \frac{4}{3}\pi\left(\frac{d_s}{2}\right)^3 \rho_S \, dN, \tag{14.43}$$

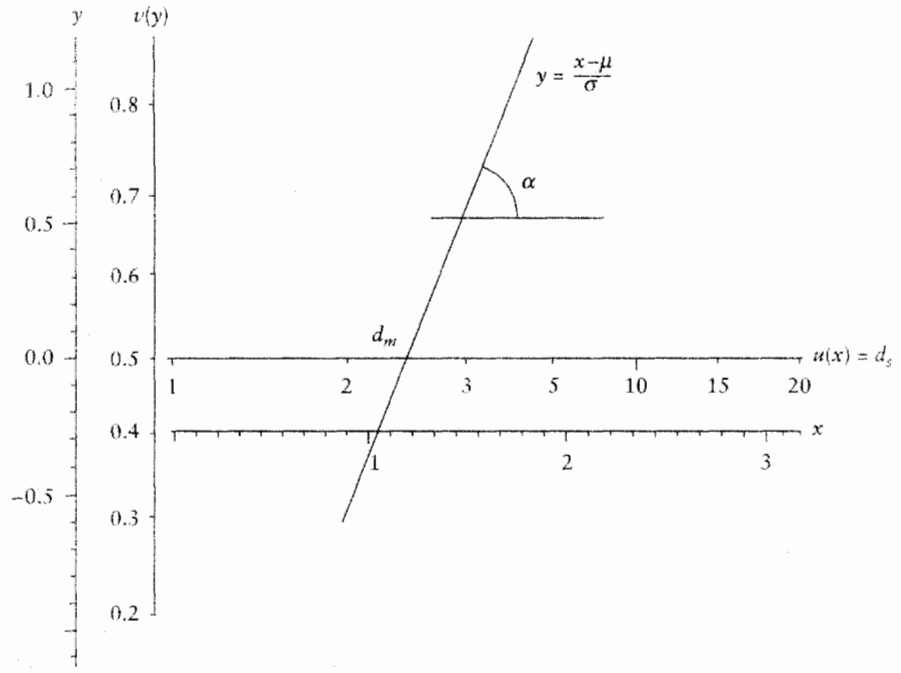

FIGURE 14.4 Log-normal probability size distribution.

which can, on the basis of Eq. (14.33), be written in the form

$$dm = \frac{\pi}{6} d_s^3 \rho_S \frac{N(t)}{\sqrt{2\pi}\sigma} e^{-\frac{(x-\mu)^2}{2\sigma^2}} dx. \tag{14.44}$$

Taking into account that $d_s = e^x$, Eq. (14.44) can be written as

$$dm = \rho_S \frac{\pi}{6} \frac{N(t)}{\sqrt{2\pi}\sigma} e^{-\frac{1}{2\sigma^2}(x-(\mu+3\sigma^2))^2} e^{-\frac{1}{2\sigma^2}(\mu^2-(\mu+3\sigma^2)^2)} dx. \tag{14.45}$$

We define the mass distribution function as follows:

$$\frac{m(x)}{m(t)} = \frac{1}{m(t)} \int_{-\infty}^{x} dm. \tag{14.46}$$

The function $m(x)$ gives the mass of all those particles whose diameter d_s satisfies the condition $d_s \leq e^x$. The total mass of the particles is denoted by $m(t)$.

Substituting Eq. (14.45) into Eq. (14.46) the function $m(x)$ can be evaluated. Note that the only x-dependent part of the integrand is

$$e^{-\frac{1}{2\sigma^2}(x-(\mu+3\sigma^2))^2},$$

all the other terms being constant. Since

$$\frac{1}{\sqrt{2\pi}\sigma} \int_{-\infty}^{\infty} e^{-\frac{1}{2\sigma^2}(x-(\mu+3\sigma^2))^2} dx = 1,$$

we get

$$m(t) = \rho_S \frac{\pi}{6} N(t)\, e^{-\frac{1}{2\sigma^2}(\mu^2 - (\mu + 3\sigma^2)^2)}$$

and hence

$$\frac{m(x)}{m(t)} = \frac{1}{\sqrt{2\pi}} \int_{-\infty}^{\frac{1}{\sigma}(x - (\mu + 3\sigma^2))} e^{-\frac{1}{2}s^2} ds \,. \tag{14.47}$$

Using the same reasoning as with the particle number distribution above, we observe that if the x- and y-axes are provided with the nonlinear scales, u and v, defined by Eqs. (14.34) and (14.35), the mass distribution $m(x)/m(t)$ can be described by a straight line

$$y = \frac{1}{\sigma}(x - (\mu + 3\sigma^2)) \,. \tag{14.48}$$

The only difference compared to the number distribution Eq. (14.40) is that the medium point is transferred to the right by the amount $3\sigma^2$. The slope of the line is the same. The result is illustrated in Fig. 14.5.

Now we go back to Eq. (14.30). The free-falling velocity (w_{SO}) of a single particle, with diameter d_s can be estimated as

$$w_{SO} = k\, d_s^n, \tag{14.49}$$

where, applying Stokes's law (Eq. (14.24)) for small particles,

$$n = 2 \tag{14.50}$$

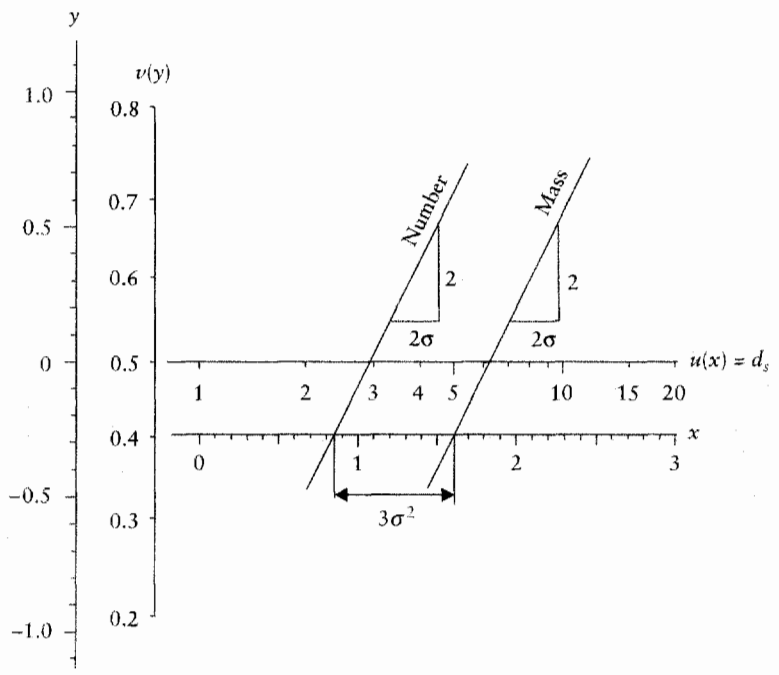

FIGURE 14.5 Log-normal probability size distributions, illustrating geometrical transposition between number and mass curves.

and

$$k = \frac{\rho_S - \rho_G}{\rho_G} \cdot \frac{g}{18\nu} . \tag{14.51}$$

Correspondingly, applying Newton's formula (Eq. (14.29)) for larger particles,

$$n = \frac{1}{2} \tag{14.52}$$

and

$$k = \left[\frac{8}{3} \cdot \frac{\rho_S - \rho_G}{\rho_G} \cdot g\right]^{1/2} . \tag{14.53}$$

All other cases are between the extreme limits of Stokes's and Newton's formulas. So we may say, that modeling the free-falling velocity of any single particle by the formula (14.49), the exponent n varies in the region $0.5 \leq n \leq 2$. In the following we shall assume that k and n are fixed, which means that we consider a certain size-class of particles.

The linear momentum dL of particles whose logarithm of diameter, $x = \ln d_s$, lies in the interval $x \ldots x + dx$ is

$$dL = dm\ k\ d_s^n, \tag{14.54}$$

where dm is given by Eq. (14.45). Since $d_s^n = e^{xn}$, we get on the basis of Eq. (14.45)

$$dL = \rho_S \frac{\pi}{6} \frac{N(t)k}{\sqrt{2\pi}\sigma} e^{-\frac{1}{2\sigma^2}(x-(\mu+(3+n)\sigma^2))^2} e^{-\frac{1}{2\sigma^2}(\mu^2-(\mu+(3+n)\sigma^2)^2)} dx \quad . \tag{14.55}$$

Equation (14.55) contains same kind of algebraic manipulation with the term e^{xn} as Eq. (14.45).

The linear momentum distribution function is

$$\frac{L(x)}{L(t)} = \frac{\int_{-\infty}^{x} dL}{\int_{-\infty}^{\infty} dL}, \tag{14.56}$$

where $L(x)$ gives the linear momentum of all the particles whose diameter d_s is $d_s \leq e^x$. The total linear momentum of all particles is denoted by $L(t)$.

Substituting Eq. (14.55) into (14.56) the function $L(x)$ can be evaluated. Since

$$\frac{1}{\sqrt{2\pi}\sigma} \int_{-\infty}^{\infty} e^{-\frac{1}{2\sigma^2}(x-(\mu+(3+n)\sigma^2))^2} dx = 1 \ ,$$

we get from Eq. (14.56)

$$\frac{L(x)}{L(t)} = \frac{1}{\sqrt{2\pi}} \int_{-\infty}^{\frac{1}{\sigma}(x-(\mu+(3+n))\sigma^2)} e^{-\frac{1}{2}s^2} ds. \tag{14.57}$$

Here we have changed the integration variable x to s, which is defined by

$$s = x - (\mu + (3+n)\sigma^2)/\sigma \ . \tag{14.58}$$

The result, Eq. (14.57), can be interpreted in a similar way to Eq. (14.47). If x- and y-axes are provided with nonlinear scales u and v, defined by Eqs. (14.34) and (14.35), the linear momentum distribution $L(x)/L(t)$ can be described by a straight line

$$y = \frac{1}{\sigma}(x - (\mu + (3+n)\sigma^2)) \tag{14.59}$$

and then

$$\frac{L(x)}{L(t)} = v(y). \tag{14.60}$$

On the other hand the total mass of the particles is

$$m(t) = \int_{-\infty}^{\infty} dm = \rho_s \frac{\pi}{6} N(t) e^{-\frac{1}{2\sigma^2}(\mu^2 - (\mu + 3\sigma^2)^2)} \tag{14.61}$$

and correspondingly the total linear momentum is

$$L(t) = \int_{-\infty}^{\infty} dL = k\rho_s \frac{\pi}{6} N(t) e^{-\frac{1}{2\sigma^2}(\mu^2 - (\mu + (3+n)\sigma^2)^2)} . \tag{14.62}$$

Replacing the infinite sums in Eq. (14.30) by the integrals in Eqs. (14.61) and (14.62), we get for the mean free-falling velocity of the set of particles

$$w_{SO} = \frac{L(t)}{m(t)} = k e^{n\left(\mu + \frac{6+n}{2}\sigma^2\right)} . \tag{14.63}$$

The corresponding diameter of a single particle with free-falling velocity w_{SO} is, according to Eq. (14.49),

$$w_{SO} = k d_{sm}^n . \tag{14.64}$$

Combining Eqs. (14.63) and (14.64), we obtain

$$d_{sm} = e^{\mu + \frac{6+n}{2}\sigma^2} . \tag{14.65}$$

This gives us a mean particle diameter, that has the same free-falling velocity as the set of particles of different sizes. Taking a logarithm of Eq. (14.65), we get

$$x_m = \mu + 3\sigma^2 + \frac{n}{2}\sigma , \tag{14.66}$$

where

$$x_m = \ln d_{sm} . \tag{14.67}$$

Comparing this result with Eq. (14.48) and Fig. 14.5, we see that the mean size of the particle in the sense of linear momentum, and therefore also in the sense of free-falling velocity, is always greater than the mean mass size

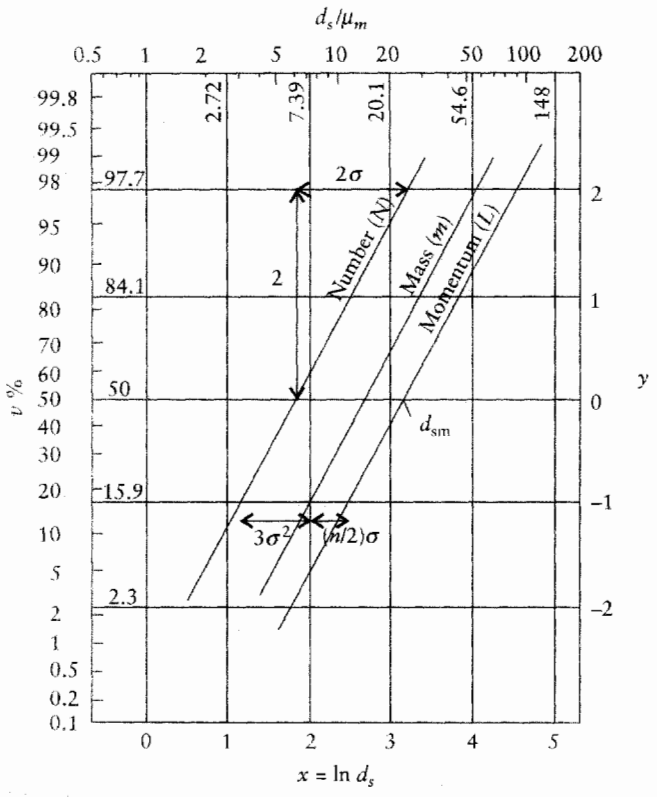

FIGURE 14.6 Log-normal probability size distributions, illustrating geometrical transposition between number, mass, and linear momentum curves and the mean size particle d_{sm}, which can be used in estimating the free-falling velocity of the particle group.

particle. The difference between these two values is $(n/2)\sigma$. The result is illustrated in Fig. 14.6.

14.2.4 Modeling of Falling Velocity in a Tube

In the previous section we determined the equivalent particle diameter d_{sm} of a set of particles of different sizes, with the aid of which we can treat the mixture as composed of one size of particles, namely d_{sm}. The mean free-falling velocity of the mixture is the same.

So far we have considered the free-falling velocity in air which is at rest. But the falling phenomenon in a tube differs from this because the falling of solid particles itself causes an airflow upwards (see Fig. 14.7). The modeling idea of Fig. 14.7 is from Weber.[2] The air volume replaced by the falling particle flows upward and this airflow rate is

$$v_m A_g = w_s A_s, \tag{14.68}$$

where w_s is the falling velocity of the particles in the tube, the quantity that we wish to determine, A_g is the cross-sectional area for airflow, and A_s is the

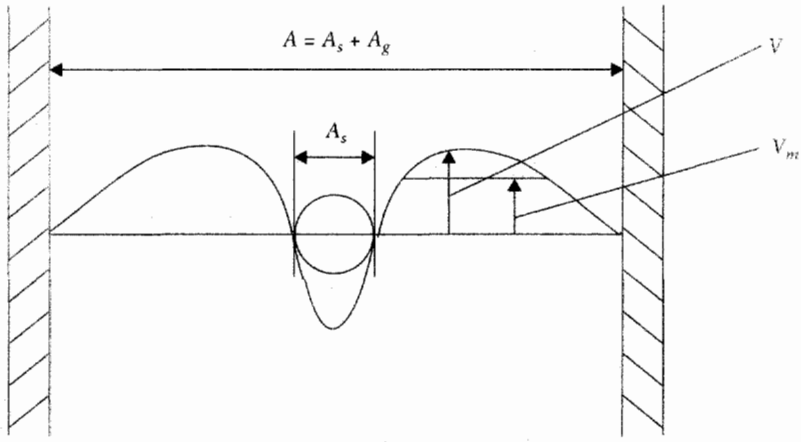

FIGURE 14.7 Falling of a solid particle in a tube.

cross-sectional area of the solid particle. Equation (14.68) assumes that the flow is incompressible.

In the coordinate system moving upward with velocity v_m, the particle is falling as if the air around it were at rest. In other words, the free-falling velocity is the sum of the two velocities

$$w_{SO} = w_s + v_m. \tag{14.69}$$

Solving for v_m from Eq. (14.68) we obtain

$$v_m = \frac{A_s}{A_g} w_s = \frac{A - A_g}{A_g} w_s = \left(\frac{1}{\phi} - 1 \right) w_s, \tag{14.70}$$

where we have used Eq. (14.13). Substituting Eq. (14.70) into Eq. (14.69), we get a very simple result for the falling velocity:

$$w_s = \phi w_{SO}. \tag{14.71}$$

Equation (14.30), whose analytical form was Eqs. (14.64) and (14.65), can be used for determining the free-falling velocity w_{SO} in the case that the particles behave like separate particles but due to the great number of random collisions have one free-falling velocity w_{SO}. Then Eq. (14.71) gives the correction to calculate the falling velocity in tube flow.

But, if the assumption of particles behaving separately is not adequate, i.e., the particles form large clumps which fall at different velocity, then neither Eq. (14.30) nor Eq. (14.71) is applicable. Then Eq. (14.71) has to be replaced by an empirical correlation.

In the following we will give some empirical formulas for the correlation between w_s and w_{SO}, where w_{SO} is to be understood as a proper mean free-falling velocity of the mixture, but is not necessarily given by the analysis based on Eq. (14.30).

Maude and Whitmore[10] have presented a correlation

$$\frac{w_s}{w_{SO}} = \phi^{\gamma}, \tag{14.72}$$

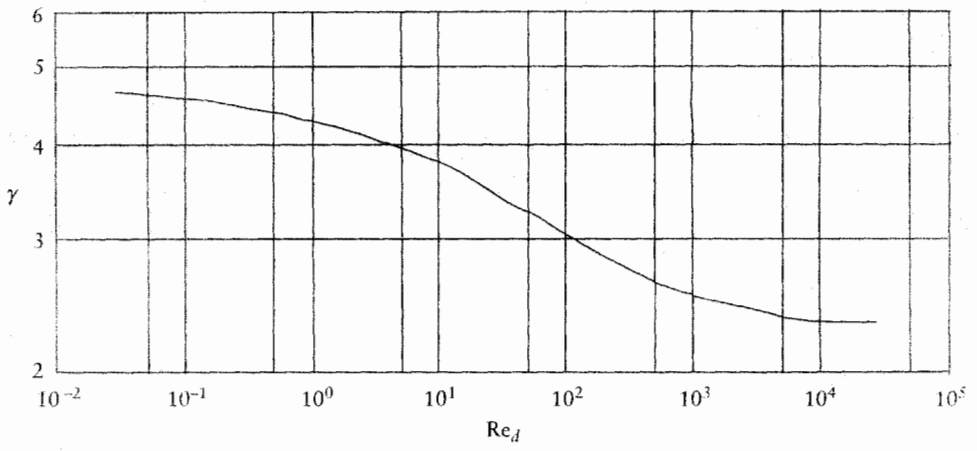

FIGURE 14.8 Exponent γ in Eq. (14.72).[10]

where γ is a function of Reynolds number Re_d defined by Eq. (14.20), i.e.,

$$\gamma = \gamma(\mathrm{Re}_d). \tag{14.73}$$

The function $\gamma(\mathrm{Re}_d)$ is graphically shown in Fig. 14.8.

However, the correlation between w_s and w_{SO} is essentially dependent on the flow pattern, and therefore the correlations, for example Eq. (14.72), are limited to distinctly specified cases. Figure 14.9 illustrates different types of vertical flow, each of which requires its own model for the correlation between w_s and w_{SO}.

To conclude this section we express Brauer's[11] correlation

$$\frac{w_s}{w_{SO}} = \frac{\phi}{\left(1 + \dfrac{1-\phi}{\phi^2}\right)\left(1 + \dfrac{1.2}{\sqrt{\dfrac{1}{2} + \dfrac{\pi/12}{1-\phi}}}\right)}. \tag{14.74}$$

If the volume fraction of air ϕ is close to 1, the correlations of Figs. (14.71) and (14.74) are close to each other. The more ϕ deviates from 1, the greater is the difference in the ratio w_s/w_{SO}. The comparison of these two formulas is shown in Fig. 14.10.

Because of the great uncertainty between w_s and w_{SO}, as Fig. 14.10 shows, we try to determine w_s directly on the basis of pressure loss measurements; this approach is presented in Section 14.3.3.

14.2.5 Estimation of Transportation Velocity of Solid Particles in Pipe Flow at Various Inclination Angles

The important factor in the pressure loss calculations will be c, the velocity of the conveyed material, and therefore it is important to know this term. It is clear that with the same gas velocity v, the velocity of the conveyed material will be different at various pipe inclination angles δ. In this section we

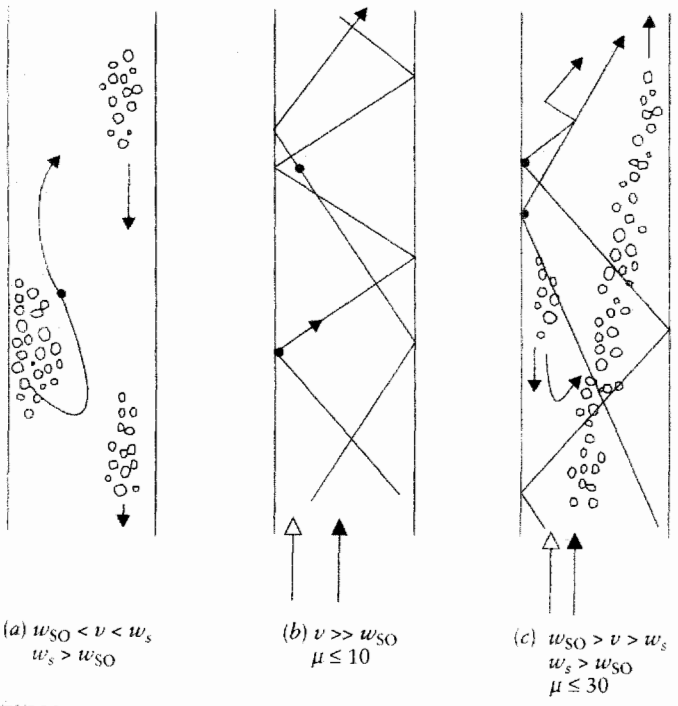

FIGURE 14.9 Different flow patterns in vertical transport.[2]

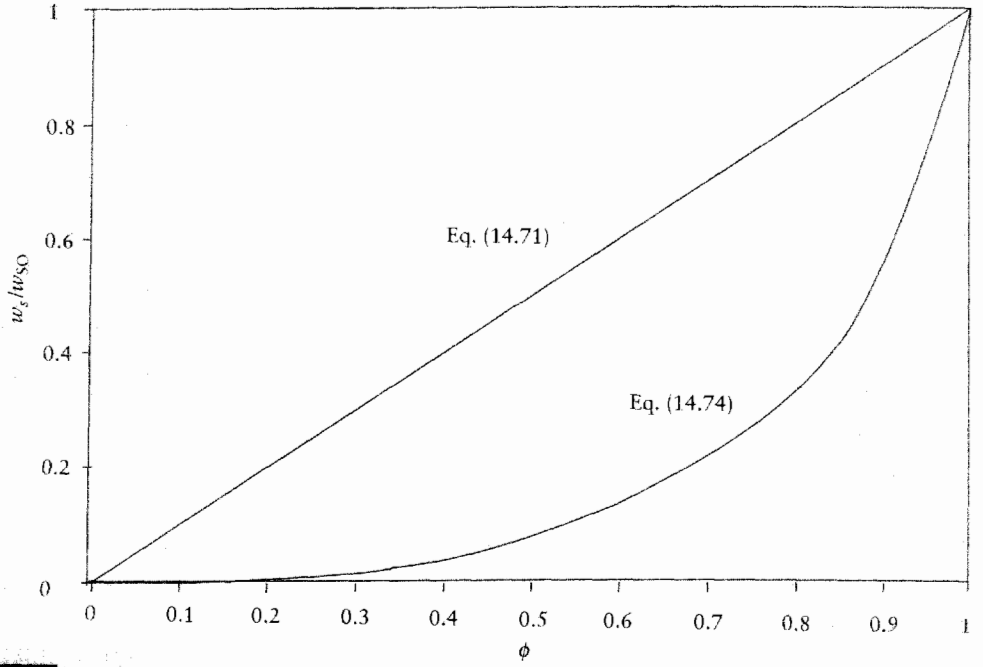

FIGURE 14.10 Comparison of formulas (14.71) and (14.74).

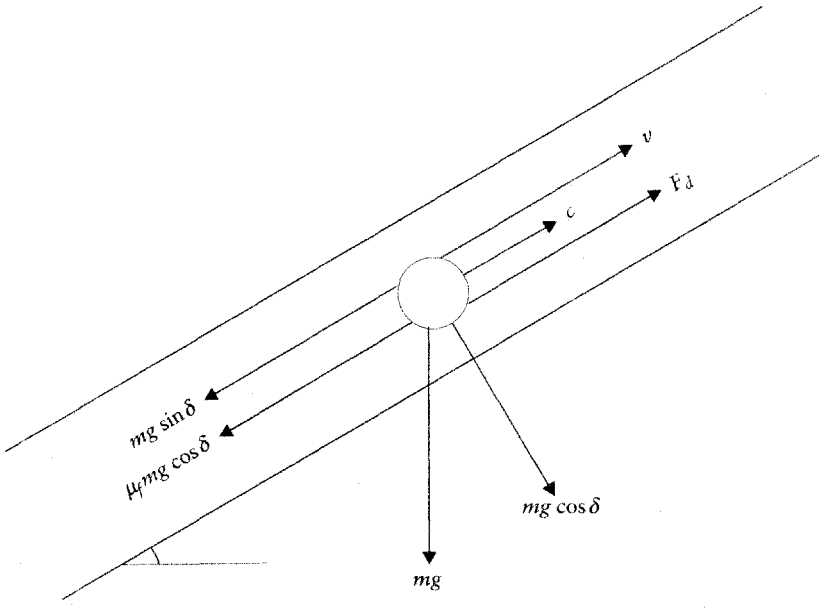

FIGURE 14.11 The force balance of a solid particle in pipe flow.

derive an equation for the velocity difference $v - c$ at various angles δ (see Fig. 14.11), when its value is known in horizontal and vertical pipes. We begin by considering the force balance of a solid particle in a pipeline as shown in Fig. 14.11.

The velocity difference $v - c$ causes a drag force F_d, which can be described according to Eq. (14.19):

$$F_d = C_d \frac{\pi d_s^2}{4} \frac{\rho_G}{2} (v - c)^2 . \tag{14.75}$$

The other forces affecting the particle are the gravitational force and friction; hence the force balance is

$$m \frac{dc}{dt} = C_d \frac{\pi d_s^2}{4} \frac{\rho_G}{2} (v - c)^2 - mg \sin\delta - \mu_f mg \cos\delta , \tag{14.76}$$

where

$$m = \rho_s \frac{4}{3} \pi \left(\frac{d_s}{s} \right)^3$$

and μ_f is the friction coefficient.

In a steady state the acceleration term vanishes, and then it follows from (14.76) that

$$\mu_f \cos\delta = A(v - c)^2 - \sin\delta , \tag{14.77}$$

where the constant A is

$$A = \frac{1}{mg} C_d \frac{\pi d_s^2}{4} \frac{\rho_G}{2} . \tag{14.78}$$

Substituting $\delta = 0$ into Eq. (14.77), we obtain

$$\mu_f = A(v - c_h)^2, \tag{14.79}$$

where we have denoted

$$c_h = c(\delta = 0), \tag{14.80}$$

i.e., c_h is the velocity of material in a horizontal line.

Then, substituting $\delta = \pi/2$ into Eq. (14.77) we get

$$A(v - c_v)^2 = 1, \tag{14.81}$$

where

$$c_v = c(\delta = \pi/2) \tag{14.82}$$

is the velocity of material in a vertical line. Now, from Eqs. (14.79) and (14.81) we can solve for the constants A and μ_f and then, substituting them into Eq. (14.77), we obtain

$$(v - c)^2 = (v - c_h)^2 \cos\delta + (v - c_v)^2 \sin\delta,$$

or

$$v - c = [(v - c_h)^2 \cos\delta + (v - c_v)^2 \sin\delta]^{1/2}. \tag{14.83}$$

Equation (14.83) gives us an estimate for the velocity c at various pipeline angles δ when the corresponding values for vertical and horizontal lines are known. It is an estimate, of course, because its derivation was based on the force balance of a single particle and not on the balance of the mixture of particles as a whole.

The velocity difference in the vertical line is usually greater than the falling velocity of the particles in the tube,

$$v - c_v \geq w_s, \tag{14.84}$$

and can be estimated by the method discussed in Section 14.3.1, where we also present how to determine the corresponding velocity difference in the horizontal line, $v - c_h$.

Assuming that $v - c_v \cong w_{SO}$, we get from Eq. (14.81)

$$A \cong \frac{1}{w_{SO}^2}. \tag{14.85}$$

Substituting this into Eq. (14.79) we get

$$\mu_f = \left(\frac{v - c_h}{w_{SO}}\right)^2, \tag{14.86}$$

which can be used for estimating c_h, provided that the friction coefficient μ_f is known.

To give an example of Eq. (14.83) we have calculated the velocity difference $v - c$ for wood chips, when $v - c_h = 8.0$ m/s and $v - c_v = 20.0$ m/s (see Section 14.3.3). The results are shown in Fig. 14.12.

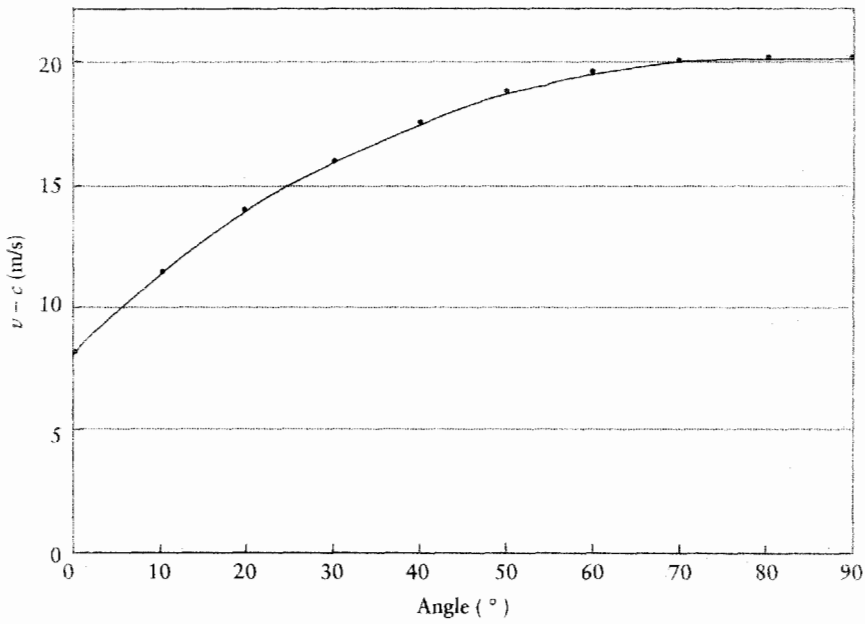

FIGURE 14.12 The velocity difference for wood chips at various pipeline angles based on Eq. (14.83).

14.2.6 An Empirical Approach for Calculating the Pressure Drop in Pneumatic Transport

The pressure loss for pure gas flow in a pipe of length dl is

$$dp = \frac{1}{D}\lambda_G \frac{\rho_G}{2} v^2 dl, \tag{14.87}$$

where D is the diameter of the pipe. The pipe friction coefficient λ_G can be calculated from

$$\lambda_G = 0.3164\ \mathrm{Re}^{-1/4} \tag{14.88}$$

for Reynolds numbers $2320 < \mathrm{Re} < 10^5$, or from

$$1/\sqrt{\lambda_G} = 2.0\ \log_{10}(\mathrm{Re}\sqrt{\lambda_G}) - 0.8, \tag{14.89}$$

which is valid for fully turbulent flow. The Reynolds number is defined by

$$\mathrm{Re} = \frac{vD}{\nu}, \tag{14.90}$$

where ν is the kinematic viscosity of the gas.

For calculating the pressure loss in pneumatic transport, the following simply modified version of Eq. (14.87) is often presented in the literature:

$$dp = \frac{1}{D}(\lambda_G + \mu\lambda_S)\frac{\rho_G}{2} v^2 dl. \tag{14.91}$$

Equation (14.91) contains only the mass flow ratio μ as a characteristic number of the mechanics of similitude of the mixture. All the other important factors, such as particle size, solid density, etc., are contained in the additional pressure-loss coefficient of the solid particles, λ_S, which is determined separately for each material.

But how can we estimate the pressure-loss coefficient λ_S? Stegmaier[12] has summarized horizontal transport for several fine-granular solids by a correlation which contains some characteristics of the material. The same idea has been used by Weber,[13] who has found a correlation of the pressure-loss coefficient for vertical pneumatic conveyance based on data measured by Flatow.[14] In order to express these models, we first introduce two dimensionless numbers

$$\mathrm{Fr} = \frac{v^2}{Dg} \tag{14.92}$$

and

$$\mathrm{Fr}_s = \frac{w_{SO}^2}{d_s g}, \tag{14.93}$$

where g is the acceleration due to gravity (9.82 m/s^2) and w_{SO} is the free-falling velocity of a solid particle of diameter d_s. The numbers Fr and Fr_s are called Froude numbers related to the pipe and solids, respectively.

The mathematical model developed by Stegmaier for horizontal transport is

$$\lambda_S = 2.1\,\mu^{-0.3}\mathrm{Fr}^{-1}\mathrm{Fr}_s^{0.25}\left(\frac{D}{d_s}\right)^{0.1}. \tag{14.94}$$

Equation (14.94) is an average value for the most solids. This has a rather high standard deviation, which can be seen from Fig. 14.13.

If the relatively high standard deviation is not acceptable, each type of solid can be correlated separately. This is a standard approach in the literature but we shall not repeat it here.

It is known from experience with vertical pneumatic transport that the influence of weight prevails at low velocities, but as the velocity increases friction gains importance. Therefore, in the calculation of the pressure loss one must find not only the weight of the solids, which could be set up theoretically, but also an empirical relationship for vertical transport from the measured data. A correlation of the pressure-loss coefficient for vertical pneumatic conveyance according to data measured by Flatow[14] has been developed by Weber,[13] and the result is

$$\lambda_S = \frac{v/c}{1200} + \frac{2v/c}{\mathrm{Fr}}. \tag{14.95}$$

The correlation of Eq. (14.95) with Flatow's measurements is rather good, as shown in Fig. 14.14. Its standard deviation is about 15%.

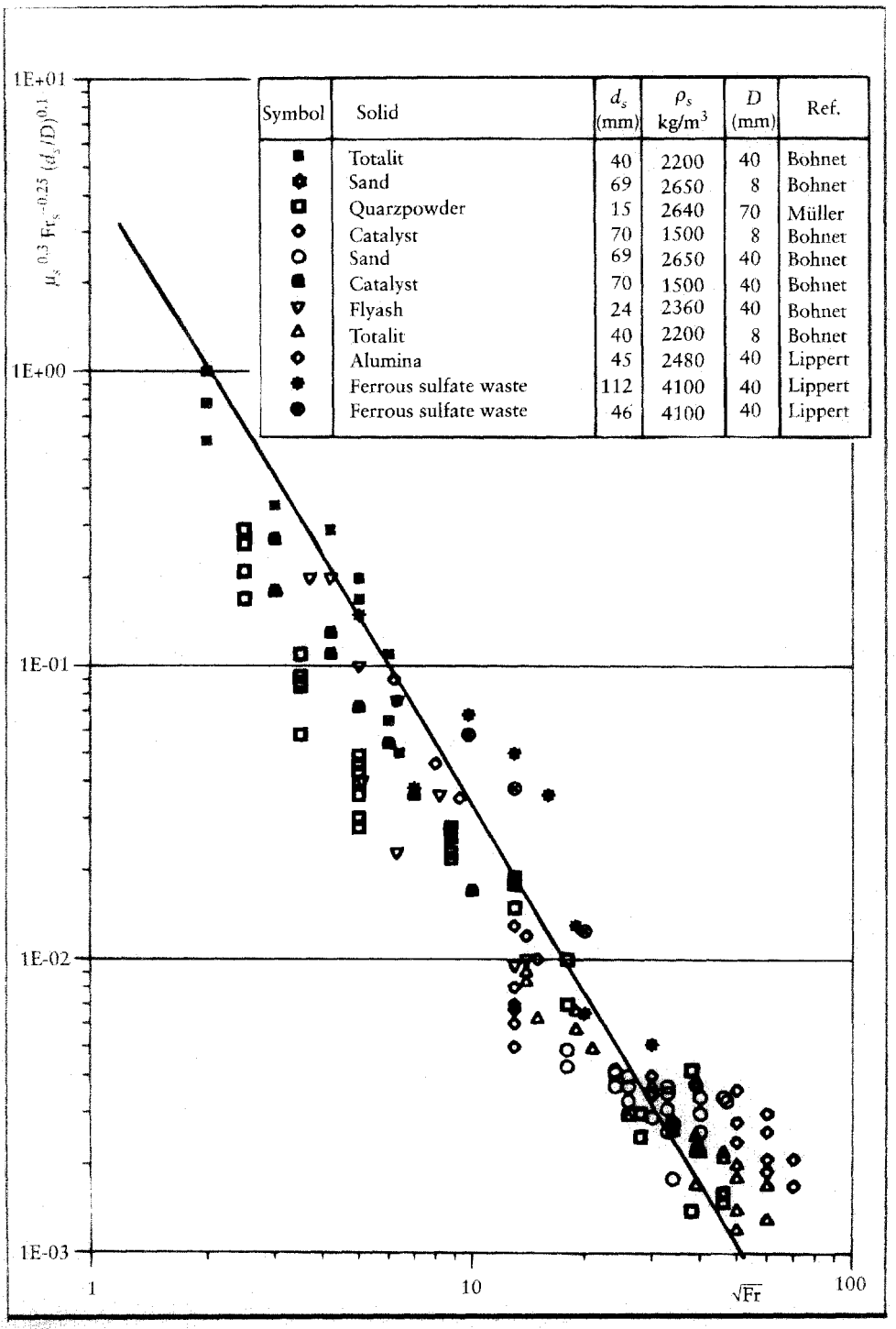

Symbol	Solid	d_s (mm)	ρ_s kg/m^3	D (mm)	Ref.
■	Totalit	40	2200	40	Bohnet
✱	Sand	69	2650	8	Bohnet
□	Quarzpowder	15	2640	70	Müller
◇	Catalyst	70	1500	8	Bohnet
○	Sand	69	2650	40	Bohnet
■	Catalyst	70	1500	40	Bohnet
▽	Flyash	24	2360	40	Bohnet
△	Totalit	40	2200	8	Bohnet
◇	Alumina	45	2480	40	Lippert
✱	Ferrous sulfate waste	112	4100	40	Lippert
●	Ferrous sulfate waste	46	4100	40	Lippert

FIGURE 14.13 Pressure-loss coefficient for horizontal transport according to Stegmaier.[12]

	d_s (mm)	D (mm)	μ
+ Polystrole	1/2.7	50/100/200	0.5/27
○ Glass spheres	1.21	50/100/200	0.5/19
● Steel spheres	1.13	50/100/200	0.5/12

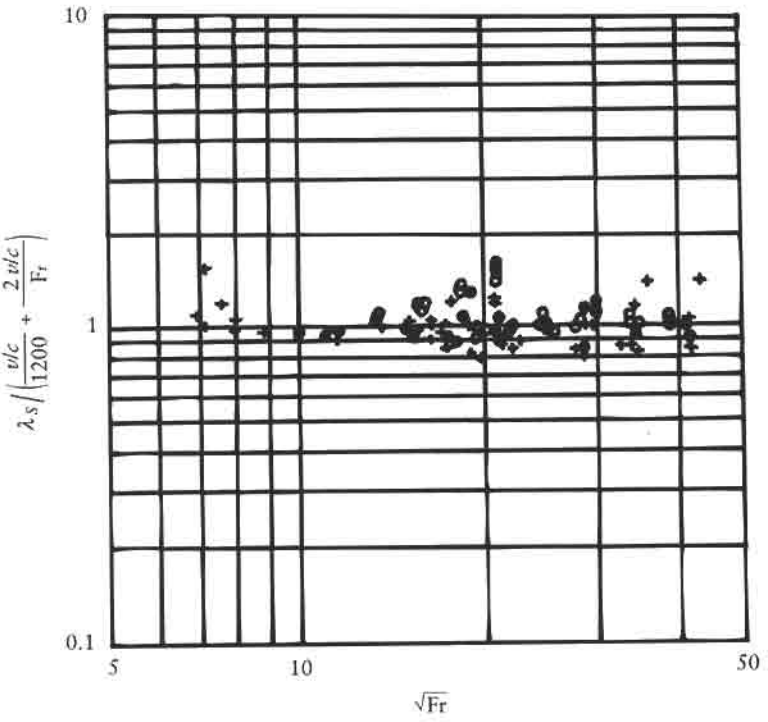

FIGURE 14.14 Correlation of the pressure loss coefficient for vertical pneumatic conveyance based on Flatow's data according to Weber.[13]

References

1. Krambrock, W., *German Chem. Eng.*, 6 (1963), pp. 199–210.
2. Weber, M., *Strömungs-Fördertechnik*, Krausskopf-Verlag GmbH, Mainz, 1974.
3. Jodlowski, C., Proc. of Pneumatech 2, Canterbury, U.K., 1984.
4. Klintworth, J., and Marcus, R. D., A review of low-velocity pneumatic conveying systems. *Bulk Solids Handl.*, 5 (1985), No. 4, pp. 747–753.
5. Leung, L. S., Vertical pneumatic conveying: A flow regime diagram and a review of choking versus non-choking systems. *Powder Technology*, 25 (1980), pp. 185–190.
6. Clift, R., and Gauvin, W. H., Motion of entrained particles in gas streams. *Can. J. Chem. Eng.*, 49 (1971), pp. 439–448.
7. Beard, K. V., and Pruppacher, H. R., *J. Atmos. Sci.*, 26 (1969), p. 1066.
8. Schiller, L., and Nauman, A., *Z. Ver. Deut. Ing.*, 77 (1933), p. 318.
9. Clift, R., and Gauvin, W. H., Proceedings of Chemeca '70. Vol. 1, Aug. 1970, pp. 14–28. Butterworths of Australia, Melbourne.
10. Maude, A. D., and Whitmore, R. L., A generalized theory of sedimentation. *B. J. Appl. Physics*, 9 Dec. (1958), p. 477.

11. Brauer, H., *Grundlagen der Einphasen- und Mehrphasenströmungen*, Verlag Sauerländer Aarau und Frankfurt, 1971.
12. Stegmaier, W., Zur Berechnung der horizontalen pneumatischen Förderung feinkörniger Stoffe, *Fördern and Heben*, 28 (1978), p. 363–366.
13. Weber, M., Correlation analysis in the design of pneumatic transport plant. *Bulk Solids Handl.*, 2 (1982), No. 2, pp. 231–233.
14. Flatow, J., Untersuchungen über die pneumatische Flugförderung in lotrechten Rohrleitungen. VDI-Forsungsheft 555, 1973.

14.3 A NEW PRESSURE LOSS EQUATION

14.3.1 A Theoretical Approach for Calculating the Pressure Drop in Pneumatic Transport

We consider the pipe inclined upward at an angle δ from the horizontal as shown in Fig. 14.15.

The mixture element shown in Fig. 14.15 contains the flowing gas and solid particles. The partial densities of these two elements are ρ_g and ρ_s, respectively. The void fraction is ϕ and this can be interpreted as the partial cross-sectional area for gas flow (see Eq. (14.13)). This means that if the pressure of the gas is p, then the pressure force per unit area of the total mixture affecting the flow of gas is ϕp and the pressure force affecting the flow of solids is $(1 - \phi)p$.

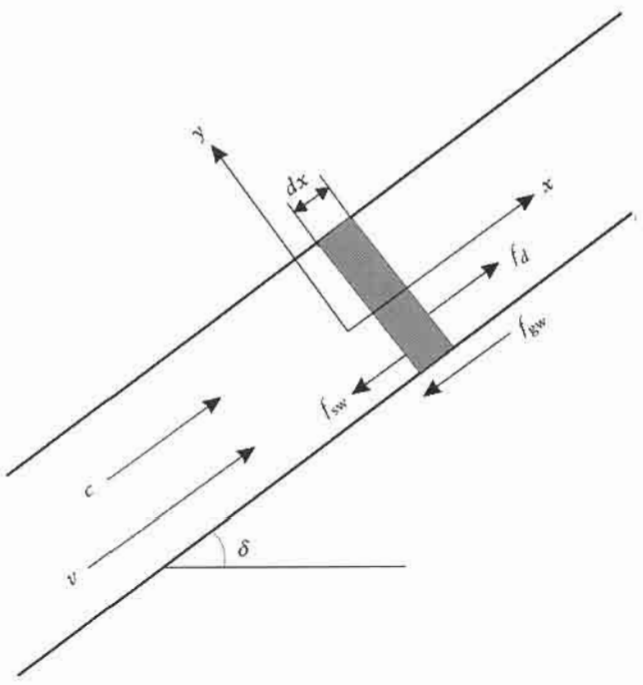

FIGURE 14.15 The friction forces affecting the flowing gas-solid mixture.

The momentum balance equation for the solid particles in the direction

$$\rho_s \frac{dc}{dt} = -\frac{d}{dx}((1-\phi)p) - \rho_s g \sin\delta - f_{sw} + f_d, \tag{14.96}$$

where f_{sw} contains the interactive force due to the different velocities of particles and the friction force caused by the walls. The force f_d is the drag force caused by the surrounding gas flow. The drag force f_d is an interactive force between gas and solids, this means that the opposite of the force, $-f_d$, is the force that affects the gas flow.

The momentum balance equation for the gas flow in the direction of x-axis is

$$\rho_g \frac{dv}{dt} = -\frac{d}{dx}(\phi p) - \rho_g g \sin\delta - f_{gw} - f_d, \tag{14.97}$$

where f_{gw} is the friction force caused by the walls and f_d is the same drag force as in Eq. (14.96).

The solid particles vibrating up and down along the y-axis, perpendicular to the x-axis, change the internal velocity profile of the gas, so that the friction force is not the same as in an empty tube. We may divide the friction force f_{gw} into two parts:

$$f_{gw} = \frac{\lambda_G \rho_g}{D} \frac{v^2}{2} + f_{int}, \tag{14.98}$$

where the first part is the normal friction due to the walls, assuming the absence of the particles. The force f_{int} arises from the fact that neither the velocity nor the pressure distribution is uniform along the y-axis and this creates a complicated internal fluid flow pattern, which also implies an additional friction force in the direction of the x-axis.

Due to the nonuniform velocity and pressure distribution along the y-axis, the particles remain separate and floating in the gas stream. In a vertical transportation the force f_{int} is obviously zero, because then the particles do not tend to fall and gather on the bottom of the tube. The force f_{int} cannot be included in the drag force f_d, because the drag force f_d pushes the particles forward in the direction of the x-axis, whereas f_{int} does not affect the particles but the gas itself.

The way in which the force f_{int} is modeled clearly determines the type of the pneumatic flow; this has been discussed earlier in Section 14.2.2, where we considered the classification of different types of flow. In the following we will give a detailed description for the force f_{int} in a way that suits a particular type of flow. This approach will be adequate for so-called dilute-phase flow or, more generally speaking, for homogeneous flow where the particles move separately.

We wish to solve the following problem: how to model the force f_{int} so that it implies the floating effect which prevents the particles from falling down to the bottom of the tube? The question itself already suggests the answer. The idea is based on the so-called virtual power method. An excellent review of this topic has been represented by G.A. Maugin.[1]

The power per unit volume (W/m^3) needed to keep the particles floating in the direction of the y-axis is

$$P''' = \rho_s g \cos\delta \cdot w_s \cos\delta. \tag{14.99}$$

On the other hand this power is, on the basis of the ideal of the virtual power method, the same as the force f_{int} multiplied by the velocity of the gas v, i.e.,

$$P''' = f_{int} v. \tag{14.100}$$

Combining Eqs. (14.99) and (14.100), we get a constitutive equation for the force f_{int}:

$$f_{int} = \rho_s g \frac{w_s}{v} \cos^2 \delta. \tag{14.101}$$

Equation (14.101) was first derived by Weber,[3] although it is formally represented in a different way.

Summing Eqs. (14.96) and (14.97), we get

$$\rho_g \frac{dv}{dt} + \rho_s \frac{dc}{dt} = -\frac{dp}{dx} - \frac{\lambda_G}{D} \frac{\rho_g}{2} v^2 - \rho_g g \cdot \sin\delta - \rho_s g \cdot \sin\delta - f_{int} - f_{sw}. \tag{14.102}$$

For the force f_{int} we have a model, Eq. (14.101), but we also need a formula for the force f_{sw}. The following model is based on our own idea and is not presented elsewhere. In Section 14.3.2 we will briefly discuss another way of modeling the force f_{sw}, but without any detailed mathematical analysis.

The friction force f_{sw} can formally be expressed with the aid of the friction coefficient

$$f_{sw} = \mu_f \rho_s g \cos\delta. \tag{14.103}$$

The friction coefficient μ_f is a complicated function of the flow conditions (i.e., of the velocities v and c) and of the angle δ. In a horizontal flow ($\delta = 0$) we get from substituting Eq. (14.86) into Eq. (14.103)

$$f_{sw}(\delta = 0) = \left(\frac{v - c(\delta = 0)}{w_s} \right)^2 \rho_s g, \tag{14.104}$$

where we have replaced w_{SO} by w_s, i.e., the falling velocity of the mixture of solid particles rather than the w_{SO} falling velocity of a single particle.

Next we make a very straightforward approximation. Equation (14.104) gives the force f_{sw} for the angle $\delta = 0$. To get the force at other angles, all we do is replace $c(\delta = 0)$ by the corresponding velocity $c = c(\delta)$, i.e., we write

$$f_{sw} = \left(\frac{v - c}{w_s} \right)^2 \rho_s g. \tag{14.105}$$

Substituting the specific constitutive Eqs. (14.101) and (14.105) into the general force balance Eq. (14.102) we get

$$\begin{aligned} \rho_g \frac{dv}{dt} + \rho_s \frac{dc}{dt} = &-\frac{dp}{dx} - \frac{\lambda_G \rho_g}{D} \frac{}{2} v^2 - \rho_g g \sin\delta \\ &-\rho_s g \sin\delta - \rho_s g \frac{w_s}{v} \cos^2\delta - \left(\frac{v - c}{w_s} \right)^2 \rho_s g. \end{aligned} \tag{14.106}$$

Next we develop further the left-hand side of Eq. (14.106). The total derivatives, also called material derivatives, are

$$\frac{dv}{dt} = \frac{\partial v}{\partial t} + v\frac{\partial v}{\partial x} \tag{14.107}$$

$$\frac{dc}{dt} = \frac{\partial c}{\partial t} + c\frac{\partial c}{\partial x}. \tag{14.108}$$

The derivation of Eqs. (14.107) and (14.108) can be found in any textbook of continuum mechanics, e.g., Mayer.[2]

In a stationary flow, the partial derivatives with respect to time vanish, i.e., $v = v(x)$ and $c = c(x)$, and

$$\frac{dv}{dt} = v\frac{dv}{dx} \tag{14.109}$$

$$\frac{dc}{dt} = c\frac{dc}{dx}. \tag{14.110}$$

On the other hand, in the steady state the mass balance for the gas in a tube with a constant cross-sectional area is simply

$$\rho_g v = \text{constant} = \dot{m}_g'', \tag{14.111}$$

and similarly the mass balance for the material flow is (see Eq. (14.17))

$$\rho_s c = \text{constant} = \mu\rho_g v = \mu\dot{m}_g''. \tag{14.112}$$

Substituting Eqs. (14.109)–(14.112) into Eq. (14.106) and using Eq. (14.17), we obtain

$$\begin{aligned} -\frac{dp}{dx} = {} & \rho_g v\left[\frac{dv}{dx} + \mu\frac{dc}{dx}\right] + \frac{\lambda_G \rho g}{D}\frac{v^2}{2} + \rho_g g \sin\delta\left[1 + \mu\frac{v}{c}\right] \\ & + \mu\rho_g g\left[\frac{w_s}{c}\cos^2\delta + \frac{v}{c}\left(\frac{v-c}{w_s}\right)^2\right]. \end{aligned} \tag{14.113}$$

With the aid of this equation the pressure loss in a pneumatic conveying system can be calculated. All we need to know are the velocity difference between gas and solid particles,

$$v - c = f(\rho_G, \delta), \tag{14.114}$$

and the falling velocity of solid particles in the vertical tube,

$$w_s = g(\rho_G). \tag{14.115}$$

Both of these functions f and g are specific for the solid material in question and to some extent also for the diameter of the tube and the mixture ratio μ. The great advantage of Eq. (14.113) is that no material or particle friction factors are needed.

Based on the models and discussions presented in Sections 14.2.3–14.2.5 we may now write Eqs. (14.114) and(14.115) in more concrete forms. Since $\rho_S >> \rho_G$, it follows from Eqs. (14.29), (14.63), and (14.71) that

$$w_s \sim \frac{1}{\sqrt{\rho_G}}, \tag{14.116}$$

which means that Eq. (14.115) can be written in the form

$$w_s = g(\rho_G) = w_{sA}\sqrt{\frac{\rho_{GA}}{\rho_G}} = w_{sA}\sqrt{\frac{p_A}{p}}. \tag{14.117}$$

Hence, using this approximation the only experimental data required is a falling velocity w_{sA} with a known gas density ρ_{GA}.

On the other hand, the velocity difference in the vertical pipe is the same as the falling velocity (see Eq. (14.84)), and hence

$$v - c_v = f\left(\rho_G, \delta = \frac{\pi}{2}\right) = (v - c_v)_A\sqrt{\frac{\rho_{GA}}{\rho_G}}, \tag{14.118}$$

where c_v is the velocity of solid particles in the vertical pipe.

Correspondingly for the horizontal pipe we may write

$$v - c_h = f(\rho_G, \delta = 0) = (v - c_h)_A\sqrt{\frac{\rho_{GA}}{\rho_G}}, \tag{14.119}$$

where c_h is the velocity of solid particles in the horizontal pipe. Note that v in Eq. (14.118) and in Eq. (14.119) is the velocity of gas in the vertical and in the horizontal pipe line, respectively.

Finally, the angle dependence can be estimated by Eq. (14.83), i.e.,

$$v - c = f(\rho_G, \delta) = \sqrt{\frac{\rho_{GA}}{\rho_G}}[(v - c_h)_A^2\cos\delta + (v - c_v)_A^2\sin\delta]^{1/2}, \tag{14.120}$$

which is, of course, as its derivation revealed, a very rough estimation and should only be used if no experimental data on the angle dependence are available.

14.3.2 Some Further Considerations and Development of the Pressure Loss Equation

The pressure loss equation (14.113) was derived from the general equation (14.102) by modeling the forces f_{int} and f_{sw}.

The force f_{int} was obtained with the aid of the virtual power method by assuming that the floating power arises only from the force f_{int}. This kind of approach has been used by Weber.[3]

Modeling of the force f_{sw} was actually based on the force balance of a single solid particle; extending the result to cover a larger set of solid particles, we obtained Eq. (14.105). This method of modeling is adequate for a homogeneous flow where the particles move separately, not as a new kind of solid-phase structure. Weber[3] has written the friction force in the form

$$f_{\text{sw}} = \frac{\lambda_z^*}{D}\frac{1}{2}\rho_s c^2, \tag{14.121}$$

where λ_z^* is a friction factor that is analogous to the friction factor λ_G. Equation (14.121) brings an additional parameter to the pressure-loss equation that has to be determined experimentally. The advantage of this approach is that it enables us to handle the different types of pneumatic flows discussed in Section 14.2.2, whereas the model of Eq. (14.105) is restricted to dilute flows.

The first term on the right-hand side of Eq. (14.113) comes from the inertial forces. Because of the pressure drop the density of gas decreases in the direction of the flow and therefore, on the basis of mass balance of gas flow, the velocity v increases along the flow. If the pipe is isolated, then the flow can be treated as adiabatic, which on the basis of energy balance implies that along the flow we have

$$h + \frac{1}{2}v^2 = \text{constant}, \tag{14.122}$$

where h is the specific enthalpy of the gas (J/kg).

On the other hand, when the gas is modeled as an ideal gas, then $h = h(T)$ (enthalpy does not depend on the pressure), and since the velocities are quite low, we deduce from Eq. (14.122) that

$$T \cong \text{const.}$$

along the flow. For instance, if the velocity of air changes from zero to 60 m/s, it decreases the temperature only by

$$\Delta T = -\frac{v^2/2}{c_p} = -\frac{60^2/2}{1000}\frac{\text{m}^2/\text{s}^2}{\text{J/kg °C}} = -1.8\ ^\circ\text{C}$$

so that the approximation of constant temperature is accurate. Hence the flow, can be treated as an isothermal process provided that the pipeline is isolated.

In the dilute flow, a good approximation is $\phi \cong 1$. For instance, if $c/v \geq 0.5$ (very common), $\rho_S/\rho_G \geq 1000$, and $\mu \leq 10$, we get from Eq. (14.17)

$$\phi = \frac{1}{1 + \mu \cdot \frac{v}{c} \cdot \frac{\rho_G}{\rho_s}} \geq \frac{1}{1 + 10 \cdot 2 \cdot 0.001} = 0.980\,.$$

The approximation $\phi \cong 1$ means that the partial density $\rho_g\,(= \phi\rho_G)$ can be replaced by ρ_G in Eq. (14.113). Using $\rho_g \cong \rho_G$ the mass balance of gas flow is

$$\rho_G v = \text{const.},$$

from which it follows that

$$\rho_G\frac{dv}{dx} = -v\frac{d\rho_G}{dx} = -v\frac{d}{dx}\left(\frac{pM}{Rt}\right) = -\frac{\rho_G v}{p}\frac{dp}{dx}, \tag{14.123}$$

where we have also used the ideal gas law and $T = \text{const}$. Since $dp/dx < 0$, we see from Eq. (14.124) that $dv/dx > 0$, as expected.

The velocity of material, c, also increases as a function of x. By differentiating the relation

$$\frac{v - c}{v_A - c_A} = \sqrt{\frac{\rho_{GA}}{\rho_A}} = \sqrt{\frac{p_A}{p}}, \tag{14.124}$$

which follows from Eqs. (14.118)–(14.119) and from the ideal gas law combined with Eq. (14.123), we obtain

$$\frac{d(v-c)}{dx} = (v_A - c_A)\sqrt{p_A}\left(-\frac{1}{2}\right)p^{-3/2}\frac{dp}{dx}.$$

Consequently, combining this with Eqs. (14.124) and (14.123) we obtain

$$\frac{dc}{dx} = -\frac{1}{2}\frac{v+c}{p}\frac{dp}{dx}, \tag{14.125}$$

which shows that $dc/dx > 0$ because the pressure drops ($dp/dx < 0$).

Substituting Eqs. (14.123) and (14.125) into Eq. (14.113) and replacing ρ_g by ρ_G (the approximation $\phi \cong 1$), we obtain

$$-\left[1 - \frac{\rho_G v^2}{p} - \frac{1}{2}\rho_G \mu \frac{v(v+c)}{p}\right]\frac{dp}{dx} = \frac{\lambda_G}{D}\frac{\rho_G}{2}v^2 + \rho_G g \sin\delta\left[1 + \mu\frac{v}{c}\right] + \mu\rho_G g\left[\frac{w_s}{c}\cos^2\delta + \frac{v}{c}\left(\frac{v-c}{w_s}\right)^2\right]. \tag{14.126}$$

Equation (14.126) is our final result; it can be used for calculating the pressure loss in the pipe flows.

In ejectors and tube bends the most important part of the pressure loss comes from the acceleration of solid particles. In a bend the velocity of the particles is reduced due to the friction and the pressure loss is caused by the reacceleration of the particles after the bend.

The pressure loss due to the acceleration of solids is obtained from Eq. (14.113):

$$-\frac{dp}{dx} = \rho_G v \mu \frac{dc}{dx}, \tag{14.127}$$

where we have replaced ρ_g by ρ_G ($\phi \cong 1$). Integrating Eq. (14.127), we get

$$p_2 - p_1 = -\rho_G v \mu (c_2 - c_1), \tag{14.128}$$

where c_1 is the initial and c_2 the final velocity of the solids.

Equation (14.128) can be used for calculating the pressure drop due to the acceleration of solid particles provided that the velocity change $c_2 - c_1$ can be estimated. In addition to the acceleration pressure loss we have the "normal" pressure drop

$$\Delta p = \zeta \frac{1}{2}\rho v^2, \tag{14.129}$$

where ζ is the pressure drop coefficient of the bend.

If the material ejector in the pipe is accelerated from a velocity of zero to c then the corresponding pressure drop is

$$\Delta p = -\rho_G v \mu c. \tag{14.130}$$

In the next two sections we present how these formulas are used in some applications.

14.3.3 Evaluation of the Pressure Loss Parameters on the Basis of Measured Data

We consider now a concrete example of pneumatic conveying in order to show how the parameters included in Eq. (14.126) are determined on the basis of pressure loss measurements. The two parameters, which are specific for

each material, are included in Eqs. (14.117) and (14.124):

$$v - c = (v_A - c_A)\sqrt{\frac{p_A}{p}} \tag{14.131}$$

$$w_s = w_{sA}\sqrt{\frac{p_A}{p}}, \tag{14.132}$$

i.e., the parameters to be determined are the velocity difference $v_A - c_A$ and the falling velocity w_{sA} at some specified pressure p_A and, of course, at a known inclination angle of the pipeline δ. Then using Eqs. (14.131)–(14.132), the velocities c and w_s can be calculated for each v and p. The effect of the inclination angle δ on the velocities can be estimated with Eq. (14.83).

In principle, the velocities c and w_s can be determined by taking a series of pictures at a very high frequency of the flow through a transparent plastic tube. Because of the particle size distribution, each particle moves at a different velocity, and this makes this method difficult to apply in practice. We have therefore used an indirect method, where we have measured the pressure losses of pneumatic conveying for two mixture ratios and then fit the parameters so that Eq. (14.126) coincides as accurately as possible with measured pressure losses.

We measured the pressure losses for two different mixture ratios in a horizontal pipeline with a length of 89.6 m:

$\mu = 2.45$	$\Delta p = 5.3$ kPa	$p_o = 117.5$ kPa	$v_o = 52.6$ m/s
$\mu = 1.577$	$\Delta p = 4.6$ kPa	$p_o = 115.2$ kPa	$v_o = 52.6$ m/s

The temperature was 293 K in both cases. The material conveyed was partially moist wood chips with about 25% sawdust and the cubic bulk weight was 370 – 380 kg/m^3. The inner diameter of the pipe was $D = 0.440$ m. The static pressure p_o and the corresponding velocity of air v_o are the values at the initial point ($x = 0$), and hence the pressures at the end of the tube ($x = 89.6$ m) in these two experiments were $p = 117.5 - 5.3 = 112.2$ kPa ($\mu = 2.45$) and $p = 110.6$ kPa ($\mu = 1.577$).

Equation (14.126) is solved numerically by Euler's method. Equation (14.126) is written in the form $-dp/dx = F(v(x), c(x), w_s(x), \rho_G(x)) = f(x)$ and the derivative is calculated at each point using the previous known values for v, c, w_s and p. Figure 14.16 shows the principle of the solution method.

We have data from two independent measurements and two parameters to be fitted with these data. The more data we have, the more reliable will be the parameter fitting. Changing the values c_A and w_{sA} and repeating the numerical calculation of the pressure loss by Eq. (14.126), we found that the best coincidence with the empirical data presented was obtained by

$$v_A - c_A = 8.0 \text{ m/s (horizontal line)} \tag{14.133}$$

$$w_{sA} = 18.0 \text{ m/s} \tag{14.134}$$

for air with $p_A = 1.0$ bar and $T_A = 293$ K. The values (14.133)–(14.134) are valid for pneumatic conveying of slightly moist wood chips by air.

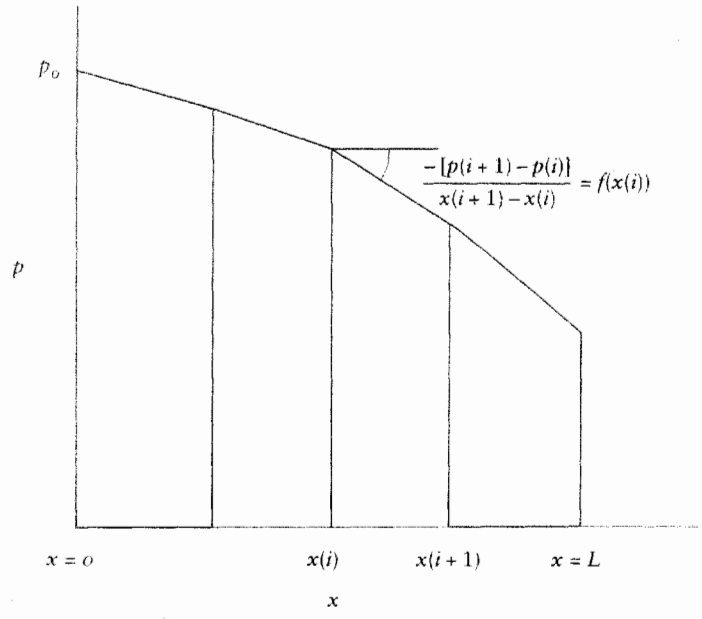

FIGURE 14.16 Numerical solution principle of Eq. (14.126).

Correspondingly, for the vertical pipeline we have made a pressure-loss measurement with the following results:

$\mu = 2.62$ $\Delta p = 4.3$ kPa $p_o = 116.5$ kPa $v_o = 40.7$m/s
$L = 14.1$ m $D = 0.319$ m

The temperature here was also 293 K. The parameter to be fitted with this data is the velocity difference $v_A - c_A$ in the vertical line. The material conveyed was wood chips as above. Making the same analysis as above with the horizontal line, the open parameter $v_A - c_A$ for the vertical line was fitted in Eq. (14.126) together with (14.134) so that the pressure loss measured was achieved. The best coincidence was obtained by

$$v_A - c_A = 23.0 \text{ m/s (vertical line)} \tag{14.135}$$

for air with $p_A = 1.0$ bar and $T_A = 293$ K.

Now, when these three parameters are known, Eq. (14.126) can be used for calculating the pressure losses in pneumatic conveying of wood chips in any other conditions. Also the pressure-loss curves for planning pneumatic conveying systems for wood chips can now be drawn. Figures 14.17 and 14.18 present examples of these. Similar curves can now be drawn for any pipe diameter D and for any air velocity v_A by solving Eq. (14.126) numerically according to Fig. 14.16.

Using the parameters (14.133)–(14.134) in Eq. (14.126), we can compute the pressure losses corresponding to the measured case, and we get for horizontal transport:

$\mu = 2.45$ Δp(computed) = 5.6 kPa Δp(measured) = 5.3 kPa
$\mu = 1.577$ Δp(computed) = 4.8 kPa Δp(measured) = 4.6 kPa

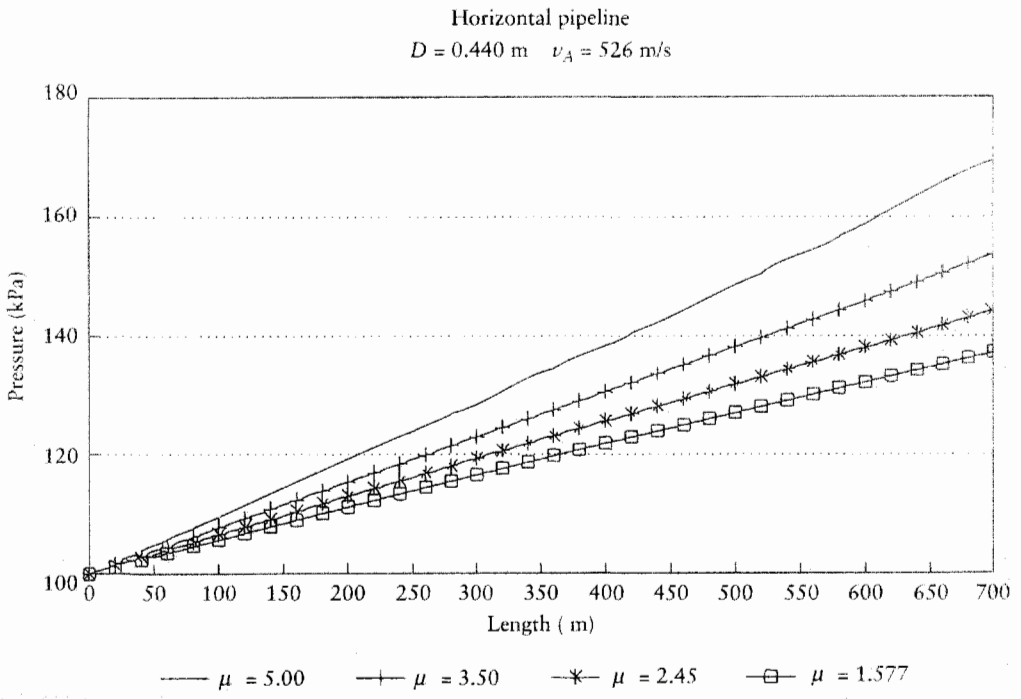

FIGURE 14.17 Pressure loss in a horizontal pipeline with parameters $v_A - c_A = 8.0$ m/s, $w_{sA} = 18.0$ m/s, $p_A = 1.0$ bar, and $T_A = 293$ K.

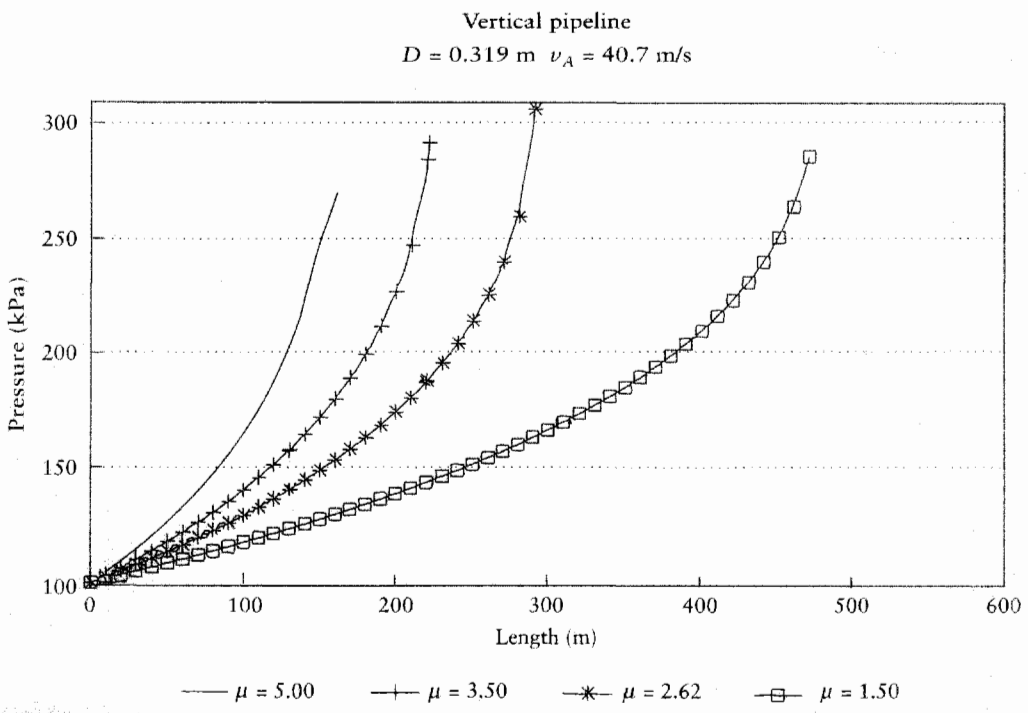

FIGURE 14.18 Pressure loss in a vertical pipeline with parameters: $v_A - c_A = 23.0$ m/s, $w_{sA} = 18.0$ m/s, $p_A = 1.0$ bar and $T_A = 293$ K.

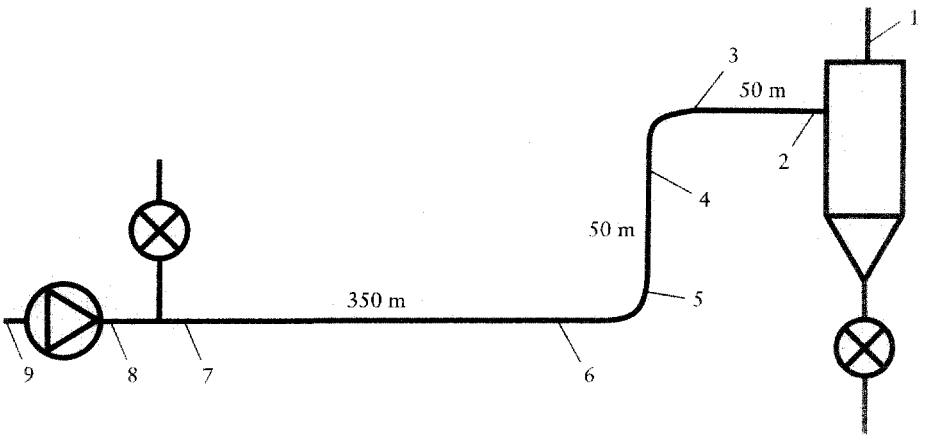

FIGURE 14.19 A pneumatic conveying system.

The corresponding result for vertical transport was

$\mu = 2.62$ Δp(computed) = 4.1 kPa Δp(measured) = 4.3 kPa

14.3.4 Example of Calculating the Pressure Losses in a Pneumatic Conveying System

We study a pneumatic conveying system shown in Fig. 14.19 for the conveying capacity $\dot{m}_s = 27.3$ kg/s. The material conveyed is wood chips, for which the parameters (14.133)–(14.135) are valid.

The first step in the dimensioning process is to choose the mixture ratio μ. For the compressor type, which is not considered here, we choose $\mu = 3.0$, i.e., $\dot{m}_i = 9.1$ kg/s. Next we have to decide D, the diameter of the tube, i.e., we need a criterion for the choice of velocity of air. A crucial aspect which affects the choice of velocity is the wearing of the tube; the higher the velocity is the greater is the wear. On the other hand, the velocity cannot be too low because of the risk of plugging (the velocity difference $v - c$ has to be positive in all parts of the piping). Here we choose $v_A = 50$ m/s with $\rho_A = 1.2$ kg/m^3. This gives $D = 0.44$ m.

The result of the calculations are shown in Table 14.2.

The compressor should give a pressure increase of $\Delta p = 51.8$ kPa and its volume flow at the suction side is $\dot{V} = (9.1/1.2)$ m^3/s = 7.6 m^3/s.

14.3.5 Calculating the Pressure Loss of an Ejector in a Pneumatic Conveying System

As another example of calculation and dimensioning of pneumatic conveying systems we consider an ejector shown in Fig. 14.20. In fluidized bed combustion systems a part of the ash is circulated with the hot flue gas. The task of the ejector, is to increase the pressure of the circulating gas to compensate the pressure losses of the circulation flow. The motivation for using an ejector, rather than a compressor, is the high temperature of the flue gas. The energy

TABLE 14.2 Computed Pressure Losses in the Pneumatic Conveying System Shown in Fig. 14.19

Position (i)	Pressure $p(i)$ (kPa)	Velocity of air $v(i)$ (m/s)	Velocity diff. $v(i) - c(i)$ (m/s)	Falling vel. $w_s(i)$ (m/s)	Density of air $\rho_G(i)$ (kg/m^3)	Equation used
1	100.0	50.0	——	——	1.200	——
2	102.0	49.0	7.9	17.8	1.224	Cyclone
3	105.4	47.4	7.8	17.5	1.265	Eq. (14.126)
4	108.8	46.0	22.1	17.3	1.306	Eqs. (14.128)–(14.129)*
5	122.5	40.8	20.8	16.3	1.470	Eq. (14.126)
6	123.1	40.6	7.2	16.2	1.477	Eqs. (14.128)–(14.129)†
7	146.8	34.1	6.6	14.9	1.762	Eq. (14.126)
8	151.8	32.9	——	——	1.822	Eq. (14.130)‡
9	100.0	50.0		——	1.200	——

$D = 0.44$ m, $\dot{m}_l = 9.1$ kg/s, $\dot{m}_s = 27.3$ kg/s, $\mu = 3.0$. Wood chips, $v_A - c_A = 23.0$ m/s (vertical), $v_A - c_A = 8.0$ m/s (horizontal), $w_{sA} = 18.0$ m/s and $p_A = 1.0$ bar.

*We have estimated $c_2 - c_1 \approx 15$ m/s, which is same as the difference of vertical and horizontal conveying velocities $c(4) - c(3)$. $\zeta = 0.5$.

† $c_2 - c_1 \approx 0$, because $c(6) = c_h \gg c_v = c(5)$. $\zeta = 0.5$

‡ $c = (34.1 - 6.6)$ m/s $= 27.5$ m/s

required to increase the pressure is taken from pressurized air, which of course, also cools the flue gas. Therefore the energy balance equation is also needed in this connection.

The mass, momentum and energy balances for the mixing zone are

$$\begin{aligned} \dot{m}_1 + \dot{m}_2 &= \dot{m}_3 \text{(gas flows)} \\ \dot{m}_{2s} + \dot{m}_{3s} &= \dot{m}_s \text{(ash)} \end{aligned} \tag{14.136}$$

$$[\dot{m}_1 v_1 + (\dot{m}_2 v_2 + \dot{m}_s c_2)] - [\dot{m}_3 v_3 + \dot{m}_3 c_3] = (p_3 - p_2) A_3 \tag{14.137}$$

$$\dot{m}_1 c_{p1} T_1 + \dot{m}_2 c_{p2} T_2 + \dot{m}_s c_{ps} T_2 = \dot{m}_3 c_{p3} T_3 + \dot{m}_s c_{ps} T_{3s}. \tag{14.138}$$

The pressure changes in the nozzle and in the diffusor, respectively, can be estimated by

$$p_5 - p_1 = (1 + \zeta_1)\frac{1}{2}\rho_1 v_1^2 \tag{14.139}$$

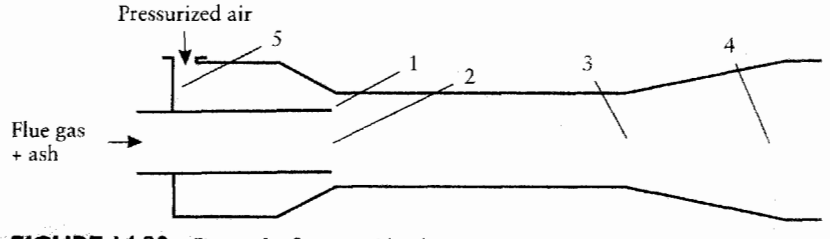

FIGURE 14.20 Ejector for flue gas with ash.

$$p_4 - p_3 = \frac{1}{2}(1 - \zeta_3)\rho_3 v_3^2 - \frac{1}{2}\rho_4 v_4^2 . \tag{14.140}$$

The velocities are

$$v_i = \frac{\dot{m}_i}{\rho_i A_i}, \quad i = 1, \ldots, 5 \tag{14.141}$$

and due to the geometry of Fig. 14.20 there are two important additional relations

$$p_1 = p_2 \tag{14.142}$$

$$A_1 + A_2 = A_3. \tag{14.143}$$

If we assume that $T_{3s} \approx T_3$, then on the basis of Eqs. (14.136) – (14.143) the ejector can be designed and the pressures calculated. An example of this is shown in Table 14.3.

The essential difference in dimensioning an ejector for pneumatic conveying systems comes from the acceleration term of the solids, Eq. (14.137).

TABLE 14.3. Calculations for an Ejector of a Pneumatic Conveying System, According to Fig. 14.20

Stage	Calculated/chosen	Equation used	Remarks
1	$v_2 = 20$ m/s	——	Chosen
2	$c_2 = v_2 - 5$ m/s	——	Estimated
3	$\rho_2 = 3.67$ kg/m^3	$\rho = Mp/(RT)$	Ideal gas
4	$A_2 = 1.771 \cdot 10^{-3}$m^2	Eq. (14.141)	$D_2 = 47.5$ mm
5	$\rho_1 = 13.7$ kg/m^3	$\rho = Mp/(RT)$	Ideal gas
6	$\dot{m}_1 = 0.13$ kg/s	$\dot{m}_1/\dot{m}_2 \approx \sqrt{\rho_1/\rho_2}$	
7	$\dot{m}_3 = 0.38$ kg/s	Eq. (14.136)	
8	$T_3 = 566$ K	Eq. (14.138)	Assumption $T_{3s} = T_3$
9	$p_3 = 12.0$ bar	Eq. (14.140)	$v_3 = 39.7$ m/s $\zeta_3 = 0.1$†
10	$c_3 = 34.7$ m/s	$c_3 = v_3 - 5$ m/s	Estimated
11	$v_1 = 492$ m/s, $A_1 = 3.70 \cdot 10^{-5}$ m^2	Eqs. (14.137), (14.142)–(14.143)	
12	$A_3 = 1.808 \cdot 10^{-3}$ m^2	Eq. (14.143)	
13	$v_3 = 39.7$ m/s	Eq. (14.141)	
14	$p_5 = 29.7$ bar	Eq. (14.139)	$\zeta_1 = 0.1$

$\dot{m}_2 = 0.13$ kg/s , $\dot{m}_s = 0.5$ kg/s
$p_1 = p_2 = 11.5$ bar, $p_4 = 12.1$ bar
$T_1 = 293$ K, $T_2 = 1093$ K
*Rough approximation for the optimum mass ratio $\dot{m}_1/\dot{m}_2$.
†A guess at this stage. The iteration cycle consists of stages 9–13.

References

1. Maugin, G. A., The method of virtual power in continuum mechanics: Application to coupled fields. *Acta Mechanica*, *35* (1980), pp. 1–70.
2. Meyer, R. E., *Introduction to Mathematical Fluid Dynamics*. Dover, New York, 1982.
3. Weber, M., *Strömungs-Fördertechnik*, Krausskopf-Verlag GmbH, Mainz, 1974.

14.4 CONCLUSIONS

In this chapter the pressure drop for pneumatic conveying pipe flow is studied. The conventional calculation method is based on the use of an additional pressure loss coefficient of the solid particles. The advantage of this classical method is that in principle it can be applied to any type of pneumatic flow. On the other hand, its great disadvantage is that the additional pressure loss coefficient is a complicated function of the density and the velocity of the conveying gas. Also, it is difficult to illustrate the additional pressure loss coefficient and this makes the theoretical study of it troublesome.

The new pressure loss equation presented here is based on determining two parameters: the velocity difference between gas and conveyed material and the falling velocity of the material. The advantage of this method is that no additional pressure loss coefficient is needed. The two parameters are physically clear and they are quite easily modeled for different cases by theoretical considerations, which makes the method reliable and applicable to various applications. The new calculation method presented here can be applied to cases where solids are conveyed in an apparently uniform suspension in a so-called lean or dilute-phase flow.

15 ENVIRONMENTAL ASSESSMENT TOOLS

BENGT STEEN

Department of Environmental Systems Analysis, Chalmers University of Technology, Gothenburg, Sweden

15.1 INTRODUCTION

Several tools can be used to evaluate the environmental consequences of an industrial ventilation project. Some of the most common methods used are covered in this chapter. The life cycle assessment tool is considered in detail, as it is a comprehensive and product-oriented approach that is covered by international standardization. Other tools, such as risk assessment, cost-benefit

Industrial Ventilation Design Guidebook

analysis, and environmental impact assessment, are also covered, but it must be mentioned that these methods are used and understood in various ways by different practitioners.

15.2 LIFE CYCLE ASSESSMENT

15.2.1 History of LCA

The first well-known LCA study was funded by Coca-Cola in 1969. Its purpose was to compare resource consumption and emissions associated with beverage containers. During the energy crisis, several studies were performed with an emphasis on energy. Before 1990, LCA studies dealt mainly with emissions and use of resources and were limited to technical systems.

During the early 1990s, several methods were developed to interpret the results of LCA studies in terms of environmental impacts. Some methods were also developed to weigh various impacts against each other. In the early 1990s, the practicing number of LCA experts increased considerably.

One reason for this expansion was the increase in computer software capable of handling the large amounts of LCA data. Another reason was the clear signal from governments to focus on products and initiate sustainable development.

15.2.2 The Role of LCA in Industry

LCA serves several purposes in industry. It is a good learning process and a method of systematically handling and processing environmental information related to products. The application of LCA to accounting may also be used for decision-making in various situations, such as purchasing, product development, or the development of a company's environmental strategy.

The use of LCA for communicating environmental achievements to interest groups is an important option. In many practical situations, LCA requires much time and effort, and more simple "rules of thumb" are needed. Some of these use Environmental Performance Indicators, the so-called EPIs. LCA can be used to full advantage to develop EPI-based "rules of thumb."

15.2.3 The LCA Framework[1]

International organizations, like SETAC and ISO, have worked on the harmonization of LCA methodology.

Life cycle assessment is defined by ISO 14040[1] as "compilation and evaluation of inputs, outputs and the potential environmental impacts of a product system throughout its life cycle." The ISO standards regulate the procedural aspects of LCA. They do not, however, provide all the information required for carrying out an LCA study. The main phases of LCA are goal and scope definition, inventory, impact assessment, and interpretation. The various applications of LCA are not regulated by the standard (Fig. 15.1).

There is no single method applicable for conducting all LCAs. As it depends on the goal and scope, the level of detail, system borders, and data

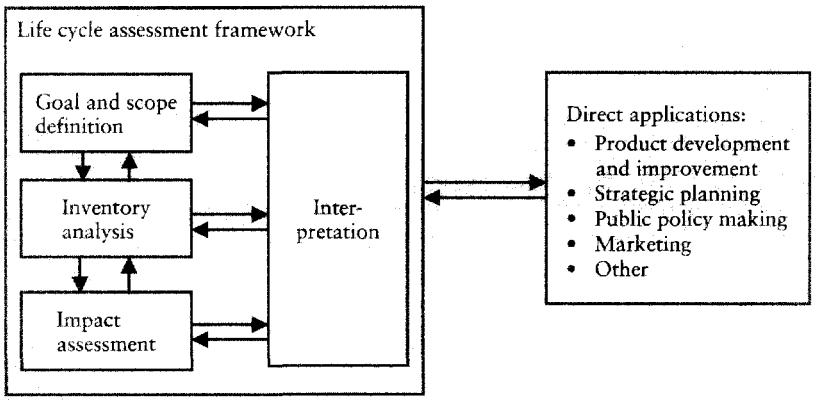

FIGURE 15.1 Phases of an LCA study.

sources, choice of focus can vary considerably. An LCA is in many ways an iterative procedure. The goal and scope may be redefined at any stage if motives arise from any of the phases. A complementary inventory may have to be carried out, if it is required by the findings in impact assessment or in the interpretation phases.

15.2.4 The Goal and Scope Phase[2]

The goal and scope definitions inform the reader of the intended use of the study, including

- system functions,
- the functional unit,
- system products,
- corresponding boundaries,
- how to handle allocation procedures, and
- what forms of environmental impacts will be considered.

It also specifies data requirements, assumptions, limitations, eventual type of critical review, and the report requirements. For example, a study could be done to select between one of two materials when developing a dust transport container for a baghouse filter. The intended audience may be the designers, the results being used to indicate which one of the two materials provides the lowest environmental impact. The system function may be to transport dust from the baghouse filter to a landfill site, and the functional unit may be one metric ton or m^3 of dust. The system boundaries may be described by considering which processes are included and which are outside the system limits.

15.2.5 The Inventory Phase[2]

The various steps of the inventory phase are shown in Fig. 15.2. The aim of the inventory phase is to comprehensively identify and quantify flows between the technical product system and the environment, i.e., emissions and resources. An example of an inventory of a product system is shown in Fig. 15.3 and Table 15.1.

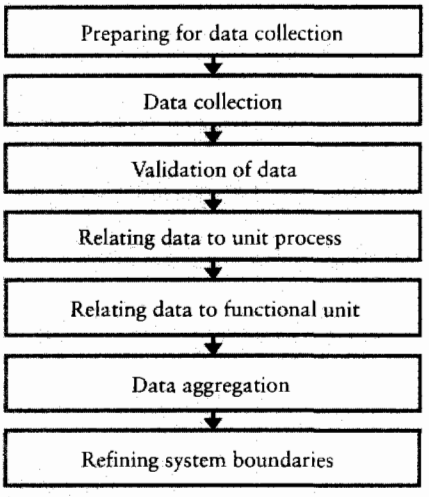

FIGURE 15.2 Steps of the inventory phase.

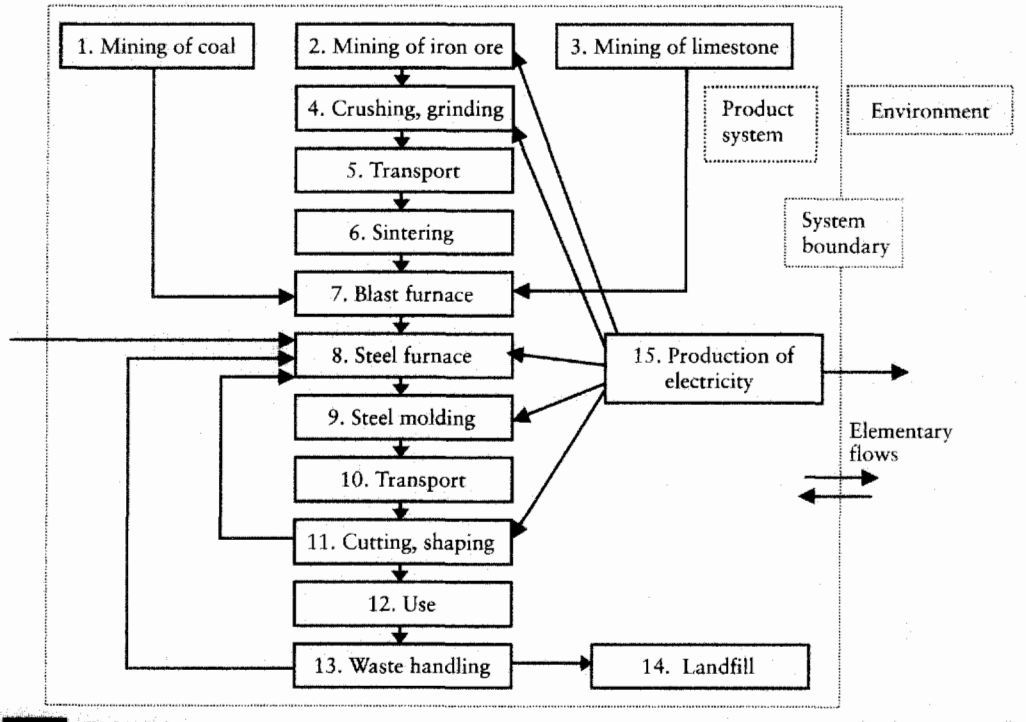

FIGURE 15.3 Example of a product system, production and use of steel sheet metal, for life cycle inventory analysis.

TABLE 15.1 Calculation of Total Elementary Flows from the Steel-Sheet Product System of Fig. 15.3

Unit process	Dust emission per unit process reference flow, D (kg/ton or kg/MJ)	Unit process reference flow per product system reference flow, F (ton/ton or MJ/ton)	Dust emission per product system reference flow, $D \times F$ (kg/ton steel-sheet)
1. Coke oven	0.25	0.50	0.125
2. Mining of iron ore	1.00	2.10	2.1
3. Mining of limestone	1.00	0.30	0.3
4. Crushing grinding	0.15	2.10	0.315
5. Transport	0.01	2.10	0.021
6. Sintering	5.31	2.10	11.151
7. Blast furnace	0.16	1.13	0.1808
8. Steel furnace	1.00	1.10	1.1
9. Steel molding	0.00	1.10	0
10. Transport	0.01	1.10	0.011
11. Cutting, shaping	0.00	1.0	0
12. Use	0.00	1.0	0
13. Waste handling	0.02	1.0	0.02
14. Landfill	0.03	1.0	0.03
15. Production of electricity	0.0002	2000 MJ/ton	0.4
The whole product system		Sum	15.75

Note: Figures are fictitious, but not unrealistic

The boxes in Fig. 15.3 represent so-called unit processes. Each one can consist of several actual processes, which for practical purposes are treated together as unit processes.

A unit process is defined as the smallest unit for which flows are specified. For each one of the unit processes, there may be mass and energy flows to and from

- other unit processes (intermediate product flows),
- the environment (elementary flows), and
- product systems outside the system boundaries (product flows).

For each unit process, a reference flow may be defined, and the inputs and outputs to the unit process calculated in relation to the reference flow. For instance, the reference flow for mining of iron ore is the mass of iron ore mined per year, and the emissions to the air may be expressed as kg dust per metric ton of ore.

Reference flow and the functional unit are defined for the entire product system, and the elementary flows are calculated in relation to these. The flow figures are normally aggregated, and the total flow of each substance recorded and used for impact assessment.

Inventory calculations can be made in several ways. An example of one method of calculating is shown in Table 15.1. The calculation process is similar for other emissions and resources.

In practical product design, a full LCA is seldom performed. The unit operations represent whole systems, which are used as building blocks. Typical examples include elementary flows determined for the "manufacture of 1 m^2 1-mm sheet metal of galvanized steel," "incineration of 1 kg of polyethylene," or "production and distribution of 1 MJ electricity."

15.2.6 The Impact Assessment Phase[3]

As shown in Fig. 15.4, there are several steps in a life cycle impact assessment.

Sometimes LCA stops at the end of the inventory step. There may be two explanations for this. One is that all emissions and resource depletion improve, when compared to a reference alternative. In this case an impact assessment is not required.

The other approach is of a more philosophical nature. The environment is regarded as starting at the end of the stack or wastewater pipe, and emissions are regarded as the environmental impacts.

Ecologists tend to define the environment in terms of physical, chemical, or biological properties within the environment. In LCIA, such definitions are called the category indicators, numerical entities belonging to impact categories. For example, the indicator "moles of H^+" belongs to the impact category "acidification."

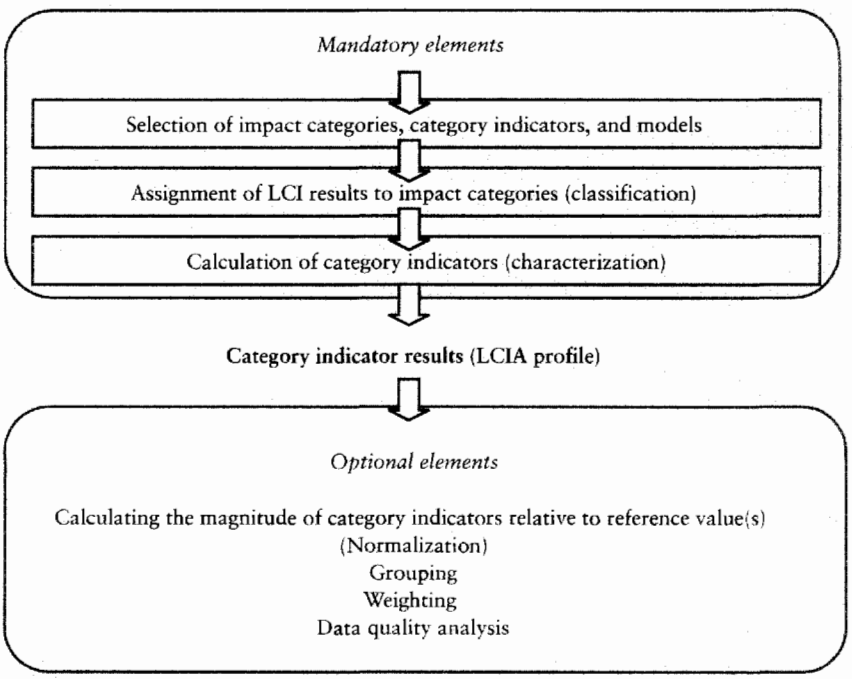

FIGURE 15.4 Elements of the life cycle impact assessment procedure.

Once the indicator is defined, a model can be developed that predicts the indicator value as a function of an emission. Such models are normally simple linear models defined by characterization factors. If an emission is multiplied by a characterization factor, an indicator value is obtained.

The sum of indicator values obtained when multiplying all emissions assigned to that impact category by their respective characterization factors is called the category indicator result. The indicator "moles of H^+" may, for instance, be the sum of contributions from sulfur dioxide, nitrogen oxides, and hydrogen chloride, and there is a characterization factor for each of them relative to the indicator.

The category indicator results may then be analyzed further by normalization, grouping, and weighting. These procedures are optional in the standard, as they are not as well known as the preceding steps and they contain more subjective elements. The aim of these steps is to clarify the results by comparing them to some reference.

An indicator result could, for instance, be compared to the total indicator value in an area, or to the average indicator value per inhabitant per year. Other common methods are to compare with national reduction targets and with damage costs from emissions and resource depletion. Sometimes these are weighed across impact categories made by expert panels. However, some studies using this technique would not meet the requirement of transparency for the weighting process set by ISO.

When making an LCA for a product or technical concept, all these steps are not determined from the start at each occasion. It is common to use ready-made lists of characterization and weighting factors. In this way, the impact assessment is speeded up. Examples from such lists are shown in Table 15.2.

The ecoscarcity method was developed by Ahbe et al.[4] It is essentially based on an "Ecofactor" which is calculated for each emission equal to $(F/F_k) \cdot 1/F_k \cdot K$, where F is the emission in the area, F_k is the emission target or the critical load in the area (country), and K is a constant used for practical purposes to obtain easy-to-handle magnitudes of the figures.

The effect category method[4] is similar to the ecoscarcity method, but it uses equivalent emissions for environmental themes, such as global warming and acidification. Instead of relating CO_2 alone to a critical load, all emissions of greenhouse gases are transformed to CO_2 equivalents, in terms of global warming potential and the total CO_2 equivalent emissions are compared to the critical load of greenhouse gases.

The EPS enviro-accounting method, version 96[4,5] and the previous version, estimates the willingness to pay (WTP) of OECD inhabitants in EURO for avoiding changes in five safeguard subjects:

- human health,
- biodiversity,
- ecosystem production capacity,
- natural resources, and
- aesthetic values.

The value 0.064 for CO_2 given in Table 15.2 represents the sum of all impacts on human health, biodiversity, etc.

TABLE 15.2 Combined Characterization and Weighting Factors Obtained with Different Methods and Different Evaluation Principles

Substance	Ecoscarcity—CH	Ecoscarcity—S	Tellus	Effect category	EPS-96
Oil from ground	40	40		5 5 6	0 5
Coal from ground	30	30		4 8	0 05
Al ore			12 9		0 42
Cr ore					5
Cu ore					57
Fe ore					0 68
CFC 11	273 000	3 340 000		1 580 000	217
CH_4			0 09	230	1 56
CO	36	16	0 009	11	0 064
Dust				42	0 037
SO_x	23 000	5700	13	2 400	0 055
NO	42 300	4700	8	3 900	0 39
N O				3 190	20 3
C H	14 300	10 500	5 5 5 5	3 100	0 7
C O	57	25	0 93	330	0 19
CO_2	3 830	400		400	0 006
N_{tot}	905			7 100	0 01
P_{tot}	756 000	42 032		71 000	0 075

Ecoscarcity: CH denotes that the calculation relates to Switzerland and S refers to Sweden.

The Tellus method[4] is also based on the willingness to pay, but in this case the WTP concerns cleaning equipment. The highest cleaning cost per mass unit of an emission is used to represent society's WTP for not emitting that substance.

The various weighting methods often give different results. This is natural as they express different weighting principles. The ecoscarcity and effect categories methods compare the LCI results with current emission policy in the area and give a high weighting to those substances that are subject to regulations. The EPS enviro-accounting method has a more global, long-term-damage-oriented approach, and puts a considerable weight on resources and greenhouse effects. The Tellus method provides some indication of what the cleaning cost could be. If weighting is done, it is recommended that several weighting methods be used.[4] Recent advances in weighting are described by Bengtsson.[6]

15.2.7 The Interpretation Phase[7]

The interpretation phase consists of three elements: identification of significant issues, evaluation by various checks and conclusions, and giving recommendations and reporting (Fig. 15.5).

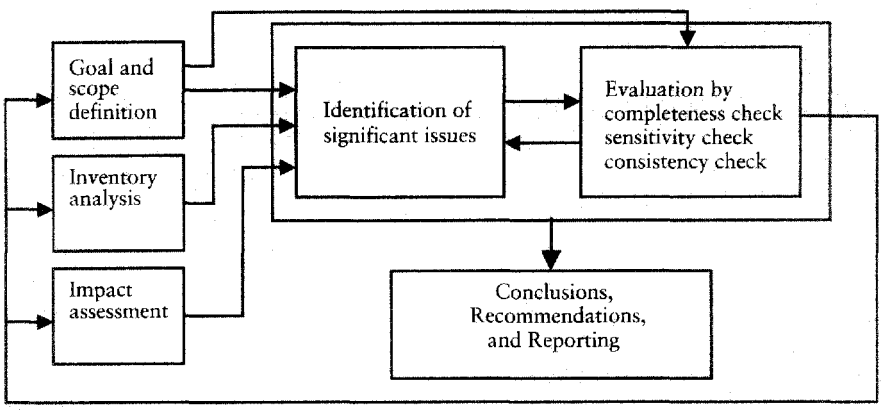

FIGURE 15.5 Elements of the interpretation phase of an LCA study.

15.2.8 Examples

In a study that compared an electrostatic precipitator with a fabric filter, LCI results according to Table 15.3 were obtained. The dust-cleaning capacity of the FF was higher than for the ESP, but the energy used for operating the FF was higher, leading to increased CO_2 emissions and depletion of fossil resources. The question then becomes, which method is preferable?

Using the factors from Table 15.2, all the methods recommend the electrostatic precipitator (Table 15.4). The priorities obtained by different methods do not always agree. The EPS method is more sensitive to resource depletion than the other methods.

The weighting methods are not used by many LCA practitioners today and the ISO standard specifically says that weighting must not be used for

TABLE 15.3 LCI Results from Comparison of an Electrostatic Precipitator and a Fabric Filter

Resource or emission		ESP (kg)	FF (kg)
Emission to air	CO_2	190.7	240
Emission to air	Carbon monoxide	0.0182	0.0323
Emission to air	NO_x	0.329	0.429
Emission to air	C_nH_m	0.0136	0.0246
Emission to air	SO_x	0.671	1
Emissions to air	Dust	0.132	0.1
Use of resource	Coal in ground	83.2	104.8
Use of resource	Oil in ground	2.85	5.3
Use of resource	Al ore	0.24	0.193
Use of resource	Cr ore	0.00012	0.00012
Use of resource	Cu ore	0.0115	0.0059
Use of resource	Fe ore	4.66	1.403

TABLE 15.4 Weighting Results Using Different Methods

	Results	
Combined characterization & weighting method	**ESP**	**FF**
Ecoscarcity—CH	39 000	53 500
Ecoscarcity—S	11 200	15 200
Env. themes, short-term, S	5 630	7 630
Env. themes, long-term, S	11 400	15 100
EPS	21.7	26.7
Tellus	13.2	18.8

comparative assertions (claims of overall superiority) disclosed to the public. It is, however, preferred by designers in companies for internal use. For optimization purposes, it is necessary to determine some weighting criteria.

15.2.9 Special Issues with Respect to Industrial Ventilation

It must be noted that LCA is a fairly new approach, at least for use in design contexts. There is a comparatively long tradition of compiling site-specific LCI data with reasonably good accuracy; however, these LCA methods are expensive and time-consuming.

Most LCA practitioners today see LCA as a tool based on natural science, and hesitate to do anything that does not give definite results. For designers, however, the quality of the product concept is the focus. Any information likely to give a better product may be used. Therefore, the willingness to include "soft" information that is important but not easy to quantify is greater among designers and others working with product development. For instance, the work environment is seldom included in LCA, although various methodologies have been suggested. When optimizing industrial ventilation, taking the work environment into account is critical.

A serious methodological debate has existed for a long time over the treatment of emissions and resources in electric power generation. There are two schools of thought; one that considers marginal effects and one that considers average figures. The problem becomes more complicated when considering the evolving free market for electricity. For instance, the inventory data in our example are based on an average European electricity production mix. If the electricity was bought from a hydroelectric power station, then the priority may be changed. However, in these discussions it is important to once again look at the goal and scope of the study.

When optimizing industrial ventilation, the real consequences for the environment due to decisions made are of interest. Therefore, the marginal effect on the whole energy system is what is required. This is of course difficult. Many practitioners use electricity produced from coal processes as marginal, but some use natural-gas-fired power plants. It depends mainly on the area and time frame that is being considered.

The implementation of environmental assessment tools is complicated at all levels, for many reasons. It must, however, be an essential part of all the processes.

For this reason many organizations use different calculation methods in practice, even if it is known that the situation may change in the near future. Organizations must get used to using these methods. Renewing an existing system is easier than starting a new system.

One example is Finland, where in 1999 the EPS system was chosen as the reference method in the area of building services, including industrial air technology.

15.2.10 Information Sources

There are several sources of information on LCA methodology and of LCA studies. There are a considerable number of cross-references in these information sources, so only a few of them need be considered here in order to provide a starting point for further studies.

The ISO 14040 standards[1] are now complete as far as the framework is concerned. However, work is being undertaken in preparing technical reports that give practical examples on the use of these standards.

SETAC, the Society for Eco-toxicology and Chemistry, has a special theme on LCA and has initiated working groups and conferences and produced several reports and guidelines on LCA methodology.[8] Information on SETAC's activities can be found at www.setac.org.

The EU has shown interest in LCA as a tool in product policies. An integrated product policy (IPP) is being developed in which LCA plays an important role. The EU has shown interest in LCA in its support for research in the EU framework programs, in directives where LCA is mentioned, and in LCA information by the European Environmental Agency, EEA.

There are a number of LCA databases and software available which simplify the tasks involved. Some are freeware, but most are commercial, with prices ranging from 100 EURO to about 10 000 EURO. The EEA publishes a list of LCA expertise and tools.

A few international journals are available that have LCA as a theme, including the International Journal of LCA and the Journal of Cleaner Production. The Journal of Industrial Ecology sometimes contains LCA articles.

References

1. ISO, "Environmental Management—Life Cycle Assessment—Principles and Framework" (ISO 14040:1997).
2. ISO, "Environmental Management—Life Cycle Assessment—Goal and Scope Definition and Inventory Analysis" (ISO 14041).
3. ISO, "Environmental Management—Life Cycle Assessment—Life Cycle Impact Assessment" (ISO/DIS 14042).
4. *Nordic Guidelines on Life-Cycle Assessment*, Nordic Council of Ministers, Report Nord 1995:20., Copenhagen, 1994.
5. B. Steen, "EPS—Default Valuation of Environmental Impacts from Emission and Use of Resources, Version 1996," Swedish Environmental Protection Agency, AFR, Report 111, April 1996.
6. M. Bengtsson and B. Steen, "Weighting in LCA: Approaches and Applications," *Environmental Progress* 19(2), 2000, 101–109.

7. ISO, "Environmental management—Life cycle assessment—Life cycle interpretation" (ISO/DIS 14043).
8. SETAC *Guidelines for Life-Cycle Assessment: A Code of Practice*, Proceedings from the SETAC workshop held in Sesimbra, Portugal, March 31–April 3, 1993.

15.3 RISK ASSESSMENT

Risk is often defined as the likelihood of a certain event times a measure of the severity of its consequences. Most risk assessment studies concentrate on estimating the likelihood of certain events. They often concern the release of chemicals, or accidents in engineering projects and the project outcome. In this section, the subject of accidents is not covered. Risk assessment (RA), as a technique, has been adopted by various national governments, by EU,[1] and by OECD.[2]

RA has four basic components.

1. The collection of problems at the "formulation stage," which identifies the compound or activity of concern, the persons or species to be protected, and the effect and end-point evaluation.
2. Hazard evaluation or the definition of the effects that may occur, including dose-response characteristics and other intrusive processes.

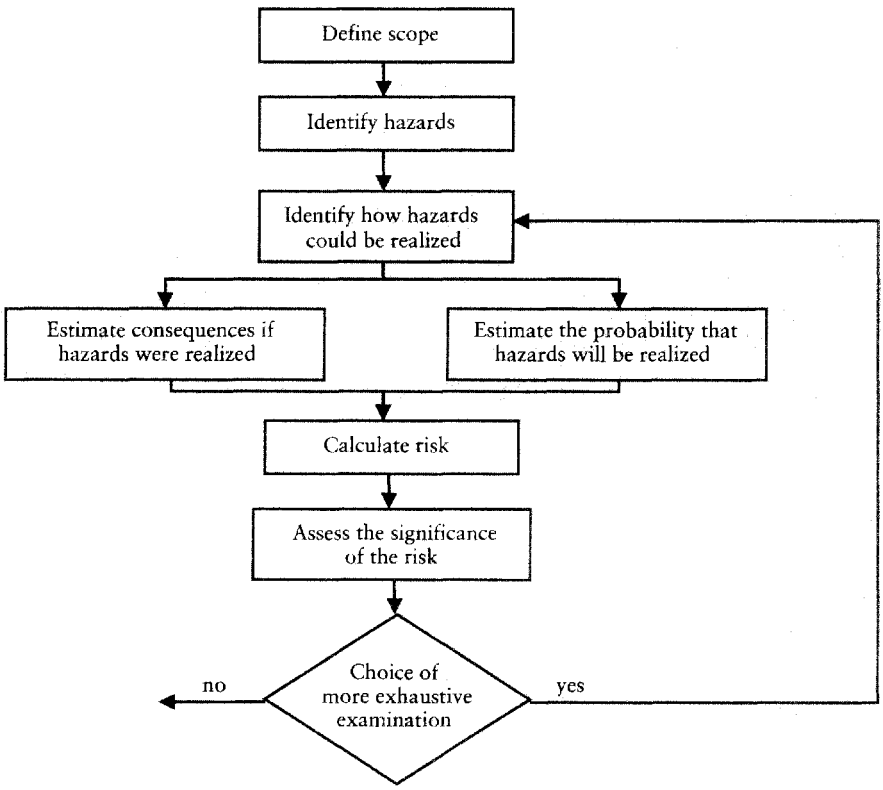

FIGURE 15.6 Steps in a risk assessment.

3. The evaluation of the actual exposure circumstances. The hazard evaluation and the exposure evaluation are then combined in a fourth component.
4. The risk characterization, where the likelihood of an exposure sufficient for an impact is estimated.

If no significant risks are found, no further evaluation is made. If a significant risk is found, the RA is refined with more comprehensive hazard evaluations, exposure assessments, and mitigation actions. The components of the RA process are detailed further in Fig. 15.6. Concepts such as "risk perception" and "risk management" often appear together with risk assessments. The risk perception by various population groups may be investigated as part of a risk management program.

Using formalized risk assessment techniques for industrial ventilation projects may complicate the issue more than necessary. The work environment and its exposure conditions are the focus. However, when evaluating new technology, including waste management, the risk assessment approach may be valuable.

References

1. Technical Guidance Document in Support of the Commission Directive 93/67/EEC on Risk Assessment for New Notified Substances and the Commission Regulation (EC) 1488/94 on Risk Assessment for Existing Substances, European Commission, 1996.
2. OECD, Environmental Health and Safety Documents, 1988–1999.

15.4 COST-BENEFIT ANALYSIS

In a cost-benefit analysis (CBA), the cost of a remedial measure is weighed against the environmental benefits it creates. Is it worth investing in a new scrubber for a plant if the impacts on its surroundings decrease by 10%?

CBA relies heavily on the costs of environmental impacts. Some impacts may be easily expressed in monetary values, like crop loss or even increased morbidity among people. Others, like impact on biodiversity and the depletion of natural resources, are more difficult to describe in terms of monetary values. Large time scales and global impacts also complicate the methodology and confuse the understanding of the results. Some of the environmental consequences of today's activities appear only after several hundred or thousand years. Even low interest rates tend to diminish these types of impact, even if they are very large.

A typical CBA involves a description of the expected decrease in emissions and a model of the impact pathways, such as an estimation of the average damage per emission unit. It involves a valuation of damage units such as "loss of 1 kg crop," "one person admission to hospital due to respiratory infections," etc. As an example, a part of a result table from a study in determining external environmental costs for the production of electricity from coal[1] is shown in Table 15.5.

The CBA technique is frequently used in the United States. It is relevant for evaluating industrial ventilation projects, but is possibly not feasible for

TABLE 15.5 Selected Results from ExternE

	Valuation estimate (mECU/kWh)			
Damage category	**West Burton**	**Lauffen**	**Range**	**Confidence**
Acute effects on mortality caused by particles	3.15	10.93	Regional	L
Chronic effects on mortality caused by particles	IQ	IQ	Regional	L
Respiratory hospital admission from particles	0.0012	0.0046	Regional	M
Restricted activity days	0.24	0.94	Regional	L
Shortness of breath in asthmatics	0.021	0.057	Regional	L
Bronchitis in children	0.0050	0.0155	Regional	M
Transport accidents, deaths	0.042	NQ	Local	H
Mining accidents, deaths	0.20	0.47	Local	H
Corrosion of galvanized steel, unpainted	0.44	0.19	Regional	L
Noise from rail traffic	0.02	NQ	Local	M

West Burton and Lauffen are two plant locations.

Range means the range for which impact has been estimated.

Confidence levels are high (H) if the impacts are quantified within an order of magnitude, medium (M) for order of magnitude level, and low (L) for other cases.

IQ means impacts are quantified but not valued, and NQ means that they are not quantified but discussed.

single projects unless software is used. The United States has produced this type of software.

Reference

1. ExternE, (1995) "Externalities of Energy" European Commission, DG-XII, Vol. 2, "Summary," Brussels-Luxembourg, 1995.

15.5 ENVIRONMENTAL IMPACT ASSESSMENT

Environmental impact assessment (EIA) is normally used to evaluate the possible environmental constraints for an industrial plant or project. In some cases it is used as part of a permit process for an industrial plant, road, or other project. The owner has to show that no major environmental impacts are caused by the plant or road, or if there are such impacts, to take remedial measures necessary to decrease and monitor the impacts or relevant indicators.

An EIA may be an extensive exercise, covering many topics, such as

- Project description and objectives
- Sources of emissions and activities causing impacts during construction and use phases

- The environmental state in the area, ecological as well as economic
- Relevant trends in the area
- Scope of the EIA
- Project alternatives
- Impacts studied and methods used
- Prediction of impacts with and without the project
- Definition of mitigation measures
- Monitoring recommendations.

Normally EIA is a major effort in itself, and is therefore mainly used in a systematic manner for large industrial plants or infrastructure projects.

Some elements of the EIA process may be relevant for evaluating industrial ventilation projects. Of particular interest are the requirements for industrial ventilation put forth by EIAs.

Such requirements could deal with the selection and performance of gas cleaning equipment, and with the design of the duct systems (including stacks).

Further information on the EIA can be found in *Environmental Impact Assessment* by P. Wathern.[1]

Reference

1. P. Wathern, *Environmental Impact Assessment.*, Routhledge, London and New York, 1988.

This page intentionally left blank

16 ECONOMIC ASPECTS

SAKARI SAINIO

Espoo-Vantaa Institute of Technology, Espoo, Finland

16.1 INTRODUCTION

The aim of life cycle cost calculations is to ensure that investment decisions are not made solely on the basis of a low purchase price, but that the life cycle operating costs are considered in the equation.

The subject of the study can be either a single energy-using device, such as a pump, or an entire ventilation system with all its components. A study focuses on the life cycle of the system or device, and normally is a comparison of two or more alternatives. The goal is to find the most economical solution on the basis of the total costs (investment and operation).

Considering the energy and maintenance costs during the life cycle, the cheapest investment is not always the best. It may, for instance, be profitable to buy a ventilation unit with a heat recovery system, which may increase the unit investment by 50%. The return on the investment in such a case may be in excess of 20%.

Another way to utilize LCC calculations is in support of a purchase. The supplier can offer both the purchase price and an estimate of the present value of the life cycle operating costs At the same time the supplier guarantees the operating cost for some period, for example, 3 years. If these target costs are exceeded, the supplier pays a penalty, and if the operating costs were overestimated, the supplier and the customer share the bonus.

Life cycle cost calculations are an application of investment calculations that have been used in planning and design in industry for several decades.[1–4]

Industrial Ventilation Design Guidebook

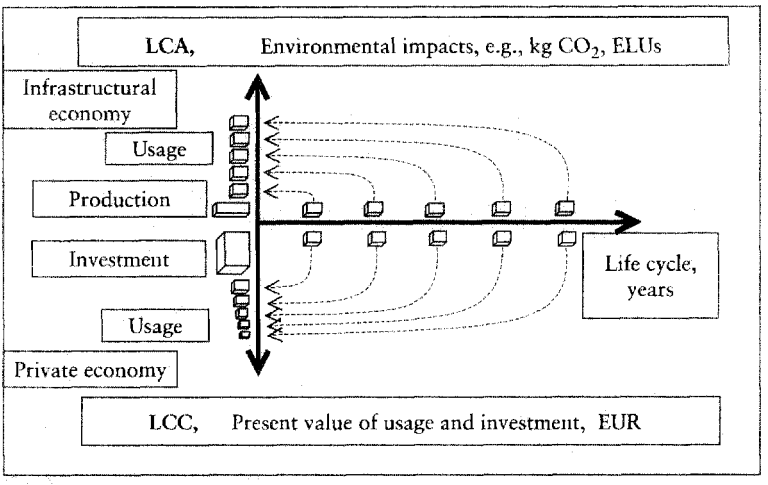

FIGURE 16.1 Comparison of life cycle assessment and life cycle cost calculations. The result of LCA is (weighted) emissions and the present value of investment and operating costs, e.g,. in Euros. Note that in LCA calculations the present value coefficient is 1, but the present value of LCC is always affected by interest rate and the length of the period.[5]

In ventilation design, these calculations are used routinely for equipment comparison. Plans are, however, to include life cycle cost calculations in the terms-of-tender contract.

LCC calculations frequently provide energy-efficient solutions. This gives reduced energy consumption and a reduction in environmental pollution. For example, the installation of a heat recovery system in a ventilation system may reduce the energy consumption and emissions by 50 to 80%. Figure 16.1 compares life cycle cost and life cycle assessment calculations.

References

1. A. Ashworth. *Cost Studies of Buildings.* Longman Group Limited, London, 1995.
2. I. H. Seeley. *Building Economics.* Macmillan Press LTD, London, 1996.
3. D. J. Ferry and P. S. Brandon. *Cost Planning of Buildings.* Blackwell Science LTD, Oxford, 1997.
4. S. L. Gruneberg. *Construction Economics.* Macmillan Press LTD, London, 1997.
5. S. Sainio. *LCA and LCC in Building Services.* Finnish Development Center for Building Services LTD, Helsinki, 1999.

16.2 BASIC CALCULATIONS AND SENSITIVITY ANALYSIS

Life cycle cost calculations are an application of investment calculations. Typically, the present value of total costs (investment and operation) are calculated. In this case, the equation is[6]

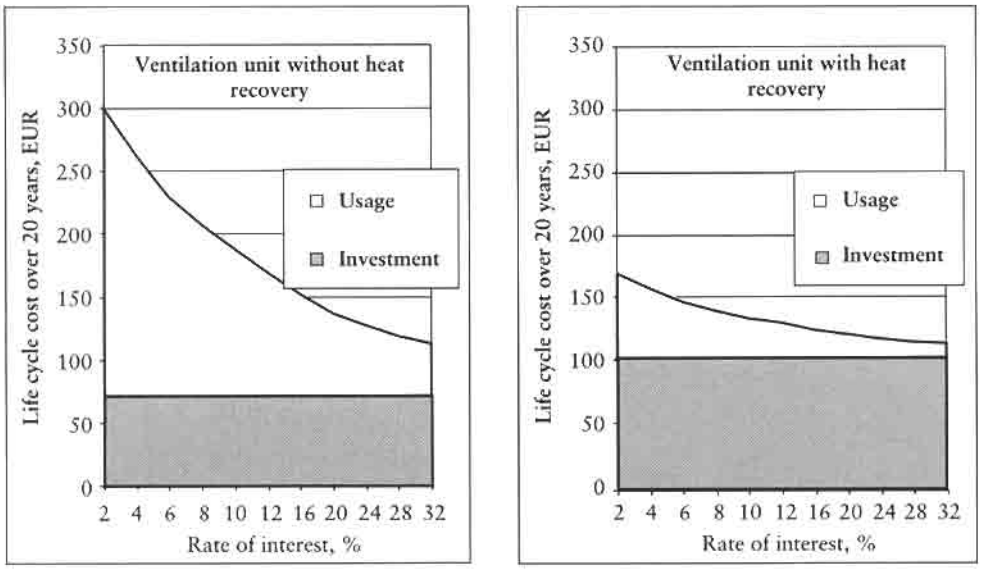

FIGURE 16.2 The proportion of operating costs can be rather small in the life cycle costs of energy-efficient investments; e.g., discounts in purchase price can be more significant than small variations in temperature efficiency of the heat recovery system. The higher the interest rate, the lower the operating costs are at the time of investment.

$$\begin{aligned} LCC_{TOT} &= \text{Investment} + \text{Energy cost (present value)} \\ &+ \text{Maintenance cost (present value)} + \text{Disposal cost (present value)} \end{aligned} \tag{16.1}$$

Calculations can be sensitive to the interest rate (Fig. 16.2) and the time of the calculation period (Fig. 16.3), which is the utilization time or the life cycle of the device. Thus, it is often advisable to consider sensitivity analysis for these factors. Elements of uncertainty can also be found in the estimation of energy consumption and investment (in design phase at the pre-tender stage).

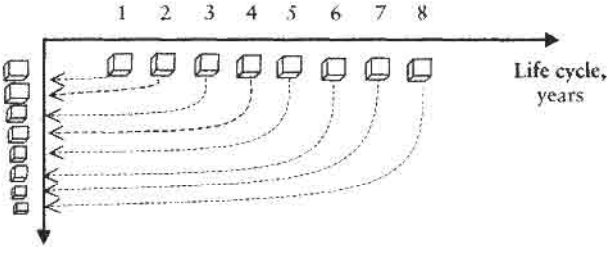

FIGURE 16.3 The present value of energy costs is smaller for higher interest rate and longer calculation period.

Reference

1. ENEU 94. *Guidelines for the Procurement of Energy Efficient Equipment and Machines in Industry.* Association of Swedish Engineering Industries, Stockholm, 1997.

16.3 INVESTMENT COSTS

The investment costs should be estimated as accurately as possible. As can be seen in Fig. 16.2, a small difference in investment costs can influence the ranking of two heat recovery systems.

When the present value of energy costs is 50% of the total costs, a discount of purchase price by 10% equals a 20% change in used energy (e.g., ventilation unit with heat recovery, interest rate 6%). This means that in this case a 10% more expensive unit will use 20% less energy than a less expensive unit.

16.4 ENERGY COST

Energy consumption for energy-using devices and systems is typically the same year after year, if heat exchanger surfaces, filters, pipelines, and other plant items are kept clean.

The present value of future energy costs (Fig. 16.3) can be calculated as

$$\mathrm{LCC}_E = Qq\frac{1}{(i-p)}\frac{[1+(i-p)]^n-1}{[1+(i-p)]^n} \tag{16.2}$$

where

LCC_E = present value of energy cost
Q = yearly energy consumption
q = present energy price
p = expected annual rise of energy price
n = calculation period in years
i = interest rate

16.5 OPERATING AND MAINTENANCE COSTS

The maintenance period of a device or system can be other than a full year or its multiples, e.g., 1.5 years. In accurate calculations, the present value of maintenance costs (Fig. 16.4) can be calculated separately

$$\mathrm{LCC}_M = E\sum_{m=1,3,\ldots,9}\frac{1}{[1+(i-p)]^m} \tag{16.3}$$

where

LCC_M = present value of maintenance cost
E = maintenance cost for one period
p = expected annual rise of maintenance cost

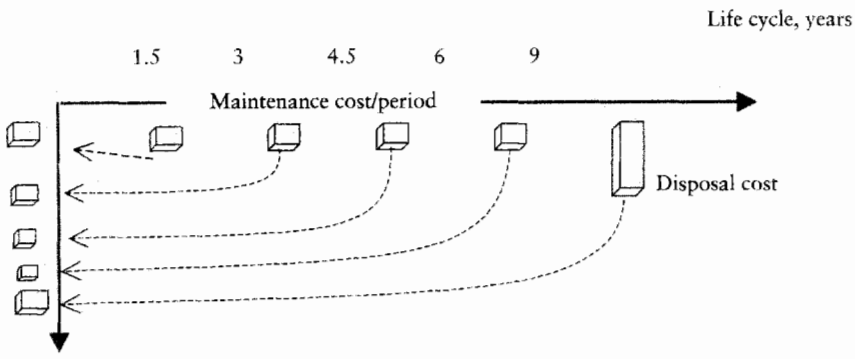

LCC_M and LCC_D, Maintenance and disposal cost (present value)

FIGURE 16.4 Disposal costs will be calculated separately and added to the present value of the investment. The same method applies to maintenance costs if they are not constant every year.

m = calculation period in years
i = interest rate.

16.6 DECOMMISSIONING COSTS

Decommissioning or disposal costs can be calculated in the same manner as maintenance costs, in Eq. (16.3) of Section 16.5. Decommissioning costs may be positive or negative. In some cases the equipment's depreciated value is greater than the disposal costs. The plant owner can sell the used equipment at a higher price than the cost of dismantling and transporting it.

As environmental protection and recycling become more important, dumping and recycling charges and taxes will be used to control environmental pollution in the future. For the plant owner, this means an increase in the decommissioning costs.

16.7 EXAMPLES

Design Phase LCC calculations can be either for a single device or a whole system. Comparison of different systems is a typical consideration for the design phase. In the tender phase, the supplier can use LCC calculations to show the improved economy of a single device. Figure 16.5 shows that the present value of investment and energy cost are the most significant. Typically, investment in a heat recovery system reduces the total cost. Maintenance costs in this case are not significant. The proportion of disposal costs is also small, but could be a more significant factor in the future.

Different filter areas and types are compared in Fig. 16.6. Due to the short annual operating time in this case, the optimum area was rather small. In the sensitivity analysis the variation of the interest rate did not significantly influence the ranking of the alternatives. An increase in operating time results in larger filter areas becoming more cost-effective.

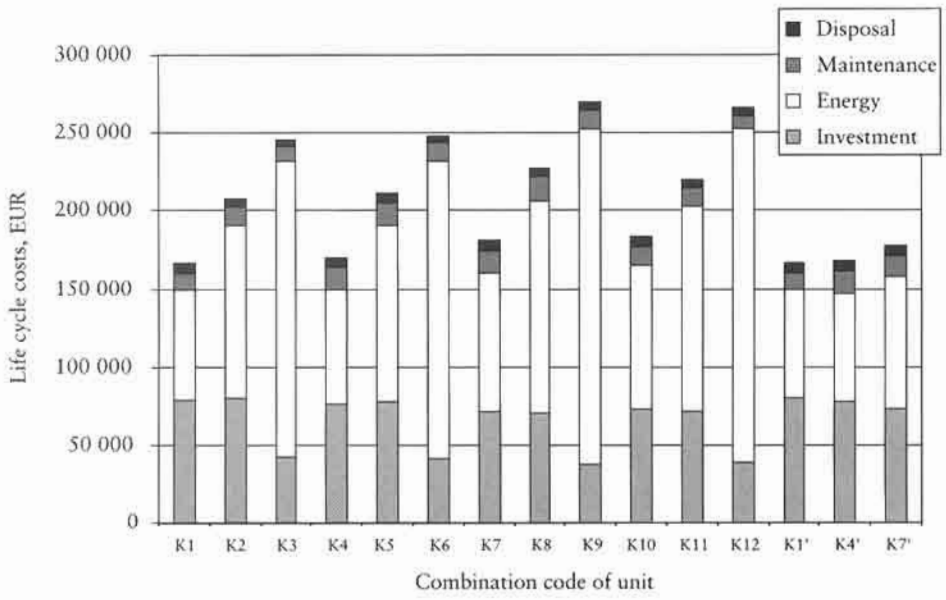

FIGURE 16.5 Comparison of different ventilation unit combinations. The life cycle is 20 years and the interest rate is 4%. In sensitivity analysis the variation of the interest rate did not change the order of different combinations significantly.

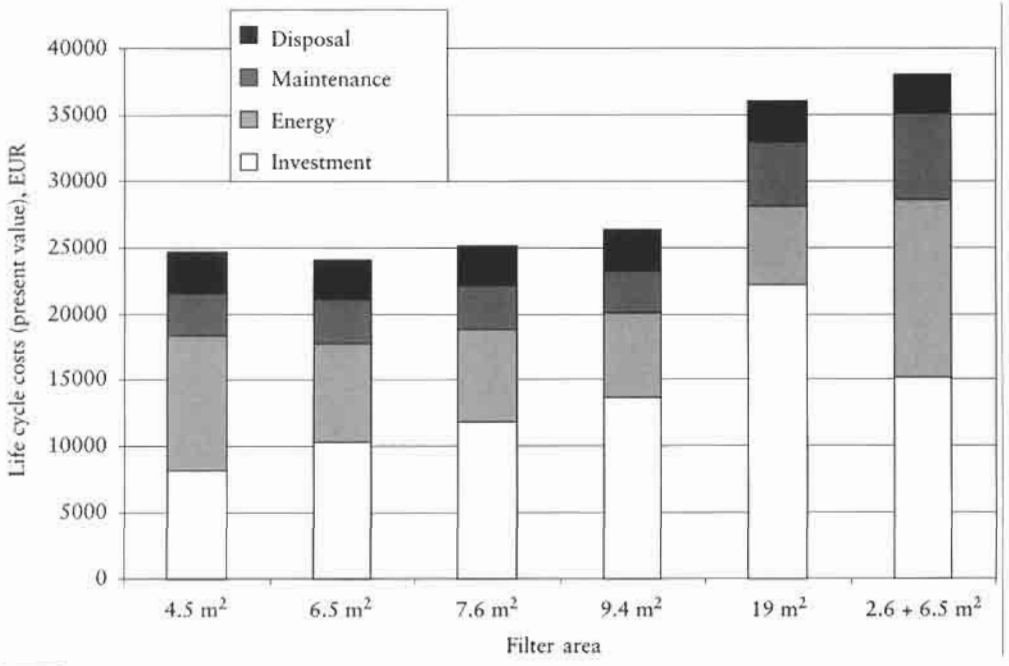

FIGURE 16.6 Optimizing the filter area of a ventilation unit. The calculation period is 20 years and the interest rate is 4%. The annual operating time of a ventilation unit is less than 2600 hours. The optimum filter area increases with increasing operating time.

TABLE 16.1 Example of a Spreadsheet for Calculating Energy and Maintenance Costs in the Procurement Process: a Liquid Cooling Unit

Cooling power dissapation per year, kW	Operating time at partial cooling power, h/y	Cooling energy, MWh/y	COP,* quoted estimate of supplier	Electric power, quoted estimate of supplier, kW	Electric energy, quoted estimate of supplier, MWh/y	Energy costs, quoted estimate of supplier, EUR/y	Estimated maintenance costs, quoted estimate of supplier, EUR/y
1 000	500	500	6.2	160	80	4 000	—
2 000	350	700	5.9	340	120	6 000	—
3 000	250	750	5.2	580	145	7 250	—
4 000	200	800	4.7	850	170	8 500	—
5 000	50	250	3.9	1 280	64	3 200	—
Total	1 350	3 000	—	—	579	28 950	5 200

COP, Coefficient of Performance, is equal to cooling power per needed electric power.

Procurement Phase In LCC calculations the energy consumption is of prime importance. Table 16.1 gives an example of the energy calculations for consumption guarantee in the procurement process. In this case, the designer has estimated the power dissipation for a liquid cooling unit and the supplier defines the performance of his equipment by means of COP and energy consumption. The maintenance costs and guaranteed costs are given.

The tender with the lowest total costs (sum of investment, energy and maintenance costs) is the best and the supplier guarantees energy, and maintenance costs for, say, a three-year period. If the target costs are exceeded, the supplier pays a penalty; if the operating costs are lowered, the supplier and the customer share the bonus.

This page intentionally left blank

APPENDIX

ERIC F. CURD

West Kirby Wirral, United Kingdom

BASIC SI UNITS

TABLE A.1 SI Basic Units

Term	Name	Symbol
Length	meter	m
Mass	kilogram	kg
Time	second	s
Electric current	ampere	A
Temperature	kelvin	K
Luminous intensity	candela	cd
Amount of substance	mole	mol

Industrial Ventilation Design Guidebook

TABLE A.2 Multiples

Magnitude	Term	Symbol
10^{-12}	pico	p
10^{-9}	nano	n
10^{-6}	micro	μm
10^{-3}	milli	m
10^{-2}	centi	c
10^{-1}	deci	d
1	——	——
10	deca	da
10^{2}	hecto	h
10^{3}	kilo	k
10^{6}	mega	M
10^{9}	giga	G
10^{12}	tera	T
10^{15}	peta	P
10^{18}	exa	E

SUPPLEMENTARY AND DERIVED SI UNITS

TABLE A.3 Heat

Quantity	Name	Symbol	Dimension
Heat, work, or energy	joule	J	N m
Heat flow rate, power	watt	W	$J\ s^{-1}$
Temperature (thermodynamic unit)	kelvin	K	K
Temperature (customary unit)	Celsius	θ	°C
Heat flow rate		φ	$W\ m^{-2}$
Thermal transmittance	transmittance coefficient	U	$W\ m^{-2}\ K^{-1}$
Thermal conductivity		λ	$W\ m^{-1}\ K^{-1}$

TABLE A.4 Force and Pressure

Quantity	Name	Symbol	Dimension
Force	newton	N	$kg\ m\ s^{-2}$
Pressure, stress	pascal	Pa	$N\ m^{-2}$

Note: 1 bar = 10^5 Pa.

TABLE A.5 Viscosity

Quantity	Name	Symbol	Dimension
Kinematic viscosity	stokes	St	$10^{-4}\ m^2\ s^{-1}$
Dynamic viscosity	poise	P	$10^{-1}\ N\ s\ m^{-2}$

TABLE A.6 Mass and Density

Quantity	Name	Symbol	Dimension
Mass	kilogram	m	kg
Density	——	ρ	$kg\ m^{-3}$

Note: 1 metric ton $= 10^3$ k

UNIT CONVERSION FACTORS

TABLE A.7 Electrical

Quantity	Name	Symbol	Dimension
Potential	volt	V	$W\ A^{-1}$
Resistance	ohm	Ω	$V\ A^{-1}$
Magnetomotive force	ampere	A	A
Charge	coulomb	C	A s
Capacitance	farad	F	$A\ s\ V^{-1}$
Inductance	henry	H	$V\ s\ A^{-1}$
Frequency	hertz	Hz	s^{-1}

TABLE A.8 Light

Quantity	Name	Symbol	Dimensions
Luminous flux	lumen	lm	cd sr
Illuminance	lux	lx	$lm\ m^{-2}$

TABLE A.9 Length (L)

	km	m	mm	mile	foot	inch	μm
km	1	10^3	10^6	6.214×10^{-1}	3.281×10^3	——	——
m	10^{-3}	1	10^3	6.214×10^{-4}	3.281	3.937×10	10^6
mm	10^{-6}	10^{-3}	1	——	3.281×10^{-3}	3.937×10^{-2}	10^3
mile	1.609	1.609×10^3	——	1	5.28×10^3	——	——
foot	3.048×10^{-4}	3.048×10^{-1}	3.048×10^2	——	1	1.2×10	——
inch	——	2.54×10^{-2}	2.54×10	——	——	1	2.54×10^4
μm	——	10^{-6}	10^{-3}	——	——	——	1

TABLE A.10 Area ($A = L^2$)

	m^2	ft^2	in^2
m^2	1	1.076×10	1.55×10^3
ft^2	9.29×10^{-2}	1	1.44×10^2

TABLE A.11 Volume ($V = L^3$)

	m^3	L	ft^3	gallon
m^3	1	10^3	3.531×10	2.200×10^2
L	10^{-3}	1	3.531×10^{-2}	2.200×10^{-1}
ft^3	2.832×10^{-2}	2.832×10	1	6.229
gallon	4.546×10^{-3}	4.546	1.605×10^{-1}	1

Note: The U.S. gallon is 3.785×10^{-3} m^3.

TABLE A.12 Mass (m)

	kg	g	lb	grains
kg	1	10^3	2.205	——
g	10^{-3}	1	——	1.543×10
lb	4.536×10^{-1}	4.536×10^2	1	7.0×10^3

TABLE A.13 Mass per Unit Length ($m\ L^{-1}$)

	$kg\ m^{-1}$	$lb\ ft^{-1}$
$kg\ m^{-1}$	1	6.720×10^{-1}
$lb\ ft^{-1}$	1.488	1

TABLE A.14 Mass per Unit Area ($m\ L^{-2}$)

	$kg\ m^{-2}$	$lb\ ft^{-2}$
$kg\ m^{-2}$	1	2.048×10^{-1}
$lb\ ft^{-2}$	4.882	1

TABLE A.15 Force ($N = kg\ m\ s^{-2}$)

	N ($kg\ m\ s^{-2}$)	kN	lb f
N	1	10^{-3}	2.248×10^{-1}
kN	10^3	1	2.248×10^2
lb f	4.448	4.448×10^{-3}	1

Note: 1 kg f = 9.807 N = 2.205 lb f.

TABLE A.16 Power (W = J s^{-1})

	W (J s^{-1})	Horsepower
W	1	1.341×10^{-3}
Horsepower	7.457×10^{2}	1

TABLE A.17 Quantity of Heat (W)

	MJ	kWh	Btu
MJ	1	2.778×10^{-1}	9.478×10^{2}
kWh	3.6	1	3.412×10^{3}
Btu	1.055×10^{-3}	——	1

Note: 1 kcal = 4.187 kJ = 3.968 Btu and 1000 kcal = 1 Thermie.

TABLE A.18 Specific Heat (c)

	kJ kg^{-1}	Btu lb^{-1} °F^{-1}
kJ kg^{-1}	1	2.388×10^{-1}
Btu lb^{-1} °F	4.187	1

TABLE A.19 Heat Flow Rate (ϕ)

	W	Btu h^{-1}	Refrigeration (Ton)
W	1	3.412	2.843×10^{-4}
Btu h^{-1}	2.931×10^{-1}	1	8.333×10^{-5}
Refrigeration (Ton)	3.517×10^{3}	1.200×10^{4}	1

Note: 1 kcal h^{-1} = 1.163 W = 3.96 Btu h^{-1}.

TABLE A.20 Heat Emission or Gain

	W m^{-2}	Btu ft^{-2} h^{-1}
W m^{-2}	1	3.170×10^{-1}
Btu ft^{-2} h^{-1}	3.155	1

TABLE A.21 Heat Transfer Coefficient, *U*

	$W\ m^{-2}\ K^{-1}$	$Btu\ ft^{-2}\ h^{-1}\ °F^{-1}$
$W\ m^{-2}\ K^{-1}$	1	1.761×10^{-1}
$Btu\ ft^{-2}\ h^{-1}\ °F^{-1}$	5.678	1

TABLE A.22 Heat Flow per Unit Volume

	$W\ m^{-3}$	$Btu\ ft^{-3}\ h^{-1}$
$W\ m^{-3}$	1	9.662×10^{-2}
$Btu\ ft^{-3}\ h^{-1}$	1.035×10	1

TABLE A.23 Heat Flow per Unit Length

	$W\ m^{-1}$	$kW\ m^{-1}$	$Btu\ ft^{-1}\ h^{-1}$
$W\ m^{-1}$	1	10^{-3}	1.040
$kW\ m^{-1}$	10^{3}	1	1.040×10^{3}
$Btu\ ft^{-1}\ h^{-1}$	9.615×10^{-1}	9.615×10^{-4}	1

TABLE A.24 Thermal Conductivity (λ)

	$W\ m^{-1}\ K^{-1}$	$Btu\ in\ ft^{-2}\ h^{-1}\ °F^{-1}$
$W\ m^{-1}\ K^{-1}$	1	6.933
$Btu\ in\ ft^{-2}\ h^{-1}\ °F^{-1}$	1.442×10^{-1}	1

TABLE A.25 Mass Calorific Value, Latent Heat

	$kJ\ kg^{-1}$	$Btu\ lb^{-1}$
$kJ\ kg^{-1}$	1	4.299×10^{-1}
$Btu\ lb^{-1}$	2.326	1

TABLE A.26 Volume Calorific Value

	$MJ\ m^{-3}$	$Btu\ ft^{-3}$
$MJ\ m^{-3}$	1	2.684×10
$Btu\ ft^{-3}$	3.726×10^{-2}	1

TABLE A.27 Pressure (p)

	kN m^{-2} (kPa)	MN m^{-2} (MPa)	b (bar)	lbf in^{-2}	atm	ft head
kN m^{-2} (kPa)	1	10^{-3}	10^{-2}	1.450×10^{-1}	9.869×10^{-3}	3.346×10^{-1}
MN m^{-2} (MPa)	10^{3}	1	10	1.450×10^{2}	9.869	3.346×10^{2}
b (bar)	10^{2}	10^{-1}	1	1.450×10	9.869×10^{-1}	3.346×10
lbf in^{-2}	6.895	6.895×10^{-3}	6.895×10^{-2}	1	6.805×10^{-2}	2.307
atm	1.013×10^{2}	1.013×10^{-1}	1.013	1.470×10	1	3.390×10
ft head	2.989	2.989×10^{-3}	2.989×10^{-2}	4.335×10^{-1}	2.950×10^{-2}	1

Note: 1 kg f/cm^2 = 98.07 kN/m^2 (kPa) = 14.22 lbf/in^2.

TABLE A.28 Pressure (p)

	N m^{-2} (Pa)	mb	in Hg	in H_2O
N m^{-2} (Pa)	1	10^{-2}	2.953×10^{-4}	4.015×10^{-3}
mb	10^{2}	1	2.953×10^{-2}	4.015×10^{-1}
in Hg	3.386×10^{3}	3.386×10	1	1.360×10
in H_2O	2.491×10^{2}	2.491	7.356×10^{-2}	1

TABLE A.29 Density (ρ)

	kg m^{-3} (g L^{-1})	kg L^{-1}	lb ft^{-3}	lb gal^{-1}
kg m^{-3}	1	10^{-3}	6.243×10^{-2}	1.002×10^{-2}
kg L^{-1}	10^{3}	1	6.243×10	1.002×10
lb ft^{-3}	1.602×10	1.602×10^{-2}	1	1.605×10^{-1}
lb gal^{-1}	9.978×10	9.978×10^{-2}	6.229	1

TABLE A.30 Specific Volume

	m^3 kg^{-1} (L g^{-1})	L kg^{-1}	ft^3 lb^{-1}	gal lb^{-1}
m^3 kg^{-1}	1	10^{3}	1.602×10	9.978×10
L kg^{-1}	10^{-3}	1	1.602×10^{-2}	9.978×10^{-2}
ft^3 lb^{-1}	6.243×10^{-2}	6.243×10	1	6.229
gal lb^{-1}	1.002×10^{-2}	1.002×10	1.605×10^{-1}	1

TABLE A.31 Concentration, Mass per Unit Volume

	g m^{-3}	grain ft^{-3}	oz gal^{-1}
g m^{-3}	1	4.370×10^{-1}	1.604×10^{-4}
grain ft^{-3}	2.229	1	3.670×10^{-4}
oz gal^{-1}	6.236×10^{3}	2.725×10^{3}	1

TABLE A.32 Concentration, Mass per Unit Mass

	kg kg^{-1}	g kg^{-1}	grain lb^{-1}
kg kg^{-1}	1	10^{3}	7000×10^{3}
g kg^{-1}	10^{-3}	1	7.0
grain lb^{-1}	1.429×10^{-4}	1.429×10^{-1}	1

TABLE A.33 Mass Fluid Flow (q_m)

	kg s^{-1}	kg h^{-1}	lb h^{-1}
kg s^{-1}	1	3.6×10^{3}	7.937×10^{3}
kg h^{-1}	2.778×10^{-4}	1	2.205
lb h^{-1}	1.260×10^{-4}	4.536×10^{-1}	1

TABLE A.34 Volumetric Flow of Fluids (q_v)

	m^3 s^{-1}	m^3 h^{-1}	ft^3 min^{-1}	L s^{-1}	L h^{-1}	gal min^{-1}	gal h^{-1}
m^3 s^{-1}	1	3.6×10^{3}	2.119×10^{3}	10^{3}	3.6×10^{6}	1.320×10^{4}	7.919×10^{5}
m^3 h^{-1}	2.778×10^{-4}	1	5.886×10^{-1}	2.778×10^{-1}	10^{3}	3.666	2.20×10^{2}
ft^3 min^{-1}	4.719×10^{-4}	1.699	1	4.719×10^{-1}	1.699×10^{3}	6.229	3.737×10^{2}
L s^{-1}	10^{-3}	3.6	2.119	1	3.6×10^{3}	1.320×10	7.919×10^{2}
L h^{-1}	2.778×10^{-7}	10^{-3}	5.886×10^{-4}	2.778×10^{-4}	1	3.666×10^{-3}	2.220×10^{-3}
gal min^{-1}	7.577×10^{-5}	2.728×10^{-1}	1.605×10^{-1}	7.577×10^{-2}	2.728×10^{2}	1	6.0×10
gal h^{-1}	1.263×10^{-6}	4.546×10^{-3}	2.676×10^{-3}	1.263×10^{-3}	4.546	1.667×10^{-2}	1

TABLE A.35 Velocity (v)

	m s^{-1}	ft s^{-1}	ft min^{-1}
m s^{-1}	1	3.21	1.968×10^{2}
ft s^{-1}	3.048×10^{-1}	1	6.0×10
ft min^{-1}	5.080×10^{-3}	1.667×10^{-2}	1

TABLE A.36 Pressure Drop per Unit Length

	Pa m^{-1}	mm H_2O m^{-1}	in H_2O ft^{-1}	in H_2O 100 ft^{-1}	lbf in^{-2} 100ft^{-1}
Pa m^{-1}	1	1.020×10^{-1}	1.224×10^{-3}	1.224×10^{-1}	4.421×10^{-3}
mm H_2O m^{-1}	9.807	1	1.200×10^{-2}	1.200	4.335×10^{-2}
in H_2O ft^{-1}	8.172×10^{2}	8.333×10	1	10^{2}	3.613
in H_2O 100 ft^{-1}	8.172	8.333×10^{-1}	10^{-2}	1	3.613×10^{-2}
lbf in^{-2} 100 ft^{-1}	2.262×10^{2}	2.307×10	2.768×10^{-1}	2.768×10	1

TABLE A.37 Absolute (Dynamic) Viscosity (μ)

	P (poise) = 10^{-1} N s m^{-2}	cP (centipoise)	lbf s ft^{-2}	lbf h ft^{-2}
P (poise)	1	10^{2}	2.089×10^{-3}	5.802×10^{-7}
cP	10^{-2}	1	2.089×10^{-5}	5.802×10^{-9}
lbf s ft^{-2}	4.788×10^{2}	4.788×10^{4}	1	2.778×10^{-4}
lbf h ft^{-2}	1.724×10	1.724×10^{8}	3.600×10^{3}	1

TABLE A.38 Kinematic Viscosity (v)

	St (stokes) = 10^{-4} m^2 s^{-1}	cSt (centistokes)	ft^2 s^{-1}	ft^2 h^{-1}
St	1	10^{2}	1.076×10^{-3}	3.875
cSt	10^{-2}	1	1.076×10^{-5}	3.875×10^{-2}
ft^2 s^{-1}	9.290×10^{2}	9.290×10^{4}	1	3.600×10^{3}
ft^2 h^{-1}	2.581×10^{-1}	2.581×10	2.778×10^{-4}	1

SYMBOLS, GREEK ALPHABET, AND ABBREVIATIONS

TABLE A.39 Symbols

Term	Units	Symbol
	A	
Absolute radiant heat flow	W m^{-2}	φ_{abs}
Absolute static pressure	Pa	p_{sa}
Absolute total pressure (stagnation pressure)	Pa	p_{ta}
Acceleration	m s^{-2}	a
Acceleration due to gravity	m s^{-2}	g
Air, gas, vapor, or fluid flow rate		
mass flow	kg s^{-1}	q_m
volume flow	m^3 s^{-1}	q_v

(continues)

TABLE A.39 *(continued)*

Term	Units	Symbol
Air leakage factor	$m^3\ s^{-1}\ m^{-2}$	F
Air leakage rate	$m^3\ s^{-1}$	q_{vl}
Air temperature	°C	θ_a
Air velocity	$m\ s^{-1}$	v_a
Air velocity at time t	$m\ s^{-1}$	v_t
Allowable exposure time	h	AET
Angle (plane)	Radian (rad) or degree (°)	α
Angle (solid)	Steradian (Sr)	Ω
Angular acceleration	$rad\ s^{-2}$	α_a
Angular velocity	$rad\ s^{-1}$	ω
Approach velocity	$m\ s^{-1}$	v_{app}
Area	m^2	ω
Area, actual (filter face)	m^2	ω_f
Area, duct cross section	m^2	A_{dcs}
Area (filter medium)	m^2	A_{fm}
Area (filter surface)	m^2	A_{fs}
Atmospheric pressure	Pa	p_a
	B	
Basal metabolic rate	$W\ m^{-2}$	BM
Blade (fan) tangential velocity	$m\ s^{-1}$	u
Body heat storage	$W\ m^{-2}$	S
Body height	m	h_b
Body mass	kg	m_b
Body surface area	m^2	A_{Du}
Body surface area covered with clothing	%	A_{cov}
Boundary layer insulation	Clo	I_a
Breadth	m	b
Bulge or sag of a duct or enclosure	m	s
	C	
Capacity (dust-holding)	$kg\ kg^{-1}$	C_{dh}
Carbon dioxide production	$L\ CO_2\ h^{-1}$	q_{v,CO_2}
Cartesian coordinates	——	x, y, z
Celsius temperature	°C	θ
Chilling temperature	°C	θ_{ch}
Coefficient of cubical expansion	K^{-1}	β

(continues)

TABLE A.39 *(continued)*

Term	Units	Symbol
Counting rate	s^{-1}	N
Clothing insulation	m^2 °C W^{-1}	Clo
Clothing mass variation	kg	Δm_{clo}
Clothing surface temperature	°C	θ_{clo}
Coefficient of thermal conductivity	W m^{-1} °C	λ
Component of air velocity along the x axis	m s^{-1}	v_x
Component of air velocity along the y axis	m s^{-1}	v_y
Component of air velocity along the z axis	m s^{-1}	v_z
Compressibility factor of a gas	——	Z
Conductive heat exchange	W m^{-2}	φ_{cond}
Convective heat exchange	W m^{-2}	φ_{conv}
Convective heat exchange (±) from globe thermometer to air	W m^{-2}	φ_g
Convective heat transfer coefficient	W m^{-2} K^{-1}	h_c
Core temperature	°C	θ_c
Cross section area	m^2	A_c
	D	
Darcy friction factor	——	λ
Deflection	m	δ
Density	kg m^{-3}	ρ
Dew point temperature	°C	θ_d
Diameter ratio of a flow measuring device	——	β
Diameter		
outer	——	D
inner	——	d
Differential pressure	Pa	Δp
Distance to v m s^{-1} isovelocity line	m	L_v
Draft rating	%	DR
Drop of air jet from its leaving center line	m	h_v
Dry heat loss	W m^{-2}	φ_{dry}
Dryness fraction, steam	%	X
Duration, limited exposure	h	D_{LE}

(continues)

TABLE A.39 *(continued)*

Term	Units	Symbol
Dynamic pressure	Pa	p_d
Dynamic viscosity	N s m^{-2}	μ
	E	
Effective area of a device	m^2	A_{eff}
Effective clothing insulation	m^2 ∘ C W^{-1}	I_{clo}
Effective length	m	l
Effective mechanical power	W m^{-2}	W
Effective radiant heat flow	W m^{-2}	$\varphi_{r\,eff}$
Effective radiating area of a body	m^2	A_r
Efficiency	——	η
Efficiency average	——	η_{av}
Emissivity of a surface or sensor	——	ϵ_s
Emissivity of black globe	——	ϵ_g
Energy	J	E
Energy loss per unit mass	J kg^{-1}	Δy
Enthalpy per unit mass	J kg^{-1}	h
Entropy per unit mass	J kg^{-1} K^{-1}	s
Equivalent diameter of a rectangular duct	m	d_e
Evaporative heat transfer coefficient	W m^{-2} Pa $^{-1}$	h_e
Exposed area	m^2	A_{exp}
	F	
Face loading (filter)	kg m^2	——
Fan air power	W	P_f
Fan or pump efficiency	——	η_r
Fan equivalent orifice	m^2	O_{fe}
Fan or pump head	m, Pa	H
Fan or pump impeller power	W	P_{fi}
Fan or pump work per unit mass	J kg^{-1}	Y
Fan pressure	Pa	P_f
Fan or pump shaft power	W	P_s
Flow coefficient of leakage	m^3 (s Pa^n)$^{-1}$	C_l
Flow coefficient of subsonic flow in an orifice	——	α
Flow mass	m^3 s^{-1}	q_m
Flow volumetric	m^3 s^{-1}	q_V

(continues)

TABLE A.39 *(continued)*

Term	Units	Symbol
Fluid density upstream of a measuring device	kg m^{-3}	ρ_u
Force	N	F
Frequency	s^{-1}	f
G		
Globe temperature	°C	θ_g
Gross body mass loss	kg	Δm_g
H		
Heat capacity	J K^{-1}	C
Heat flux	W	ϕ
Heat flux density	W m^{-2}	φ
Height	m	H
Height above datum	m	Z
Height of v m s^{-1} isovelocity line	m	h_v
Humidity ratio	kg water kg^{-1} dry air	W_a
Humidity ratio at saturation	kg water kg^{-1} dry air	W_{as}
Humidity ratio expired air	kg water kg^{-1} dry air	W_{ex}
Humidity ratio inhaled air	kg water kg^{-1} dry air	W_a
Hydraulic diameter	m	d_h
I		
Impeller tip diameter of a fan	m	D
Impeller tip radius of a fan	m	R
Increase in body core temperature	°C	$\Delta\theta_{co}$
Internal diameter of a pipe or duct	m	D
Insulation of clothing	m^2 K W^{-1}	I_{cl}
Internal energy per unit mass	J kg^{-1}	u
Isentropic exponent	——	k
J		
Jet angle	°	α, β
Jet drop	m	h_d
Jet rise	m	h_r
Jet spread	°	β
Jet temperature	°C	θ_j
Jet throw	m	L_j

(continues)

TABLE A.39 *(continued)*

Term	Units	Symbol
	K	
Kinematic viscosity	$m^2 s^{-1}$	ν
Kinetic energy (mass)	$J kg^{-1}$	e_K
	L	
Latent heat (mass)	$J kg^{-1}$	l
Length	m	L
Lewis relationship	$°C kPa^{-1}$	LR
Limit value for body heat gain or loss	$W h m^{-2}$	Q_{lim}
Local skin temperature	°C	θ_{sk}
	M	
Mach number	——	Ma
Mass	kg	m
Mass of dry air	kg	m_{da}
Mass flow rate (gas or fluid)	$kg s^{-1}$	q_m
Mass of water vapor	kg	m_{wv}
Maximum body heat storage	$W h m^{-2}$	Q_{max}
Maximum evaporative heat transfer from skin	$W m^{-2}$	E_{max}
Mean penetration (filter)	——	P_m
Mean pressure drop	Pa	Δp_m
Mean skin temperature	°C	θ_{sk}
Mean velocity of flow in a conduit	$m s^{-1}$	v_m
Metabolic rate	$W m^{-2}$	M (met)
Molar mass	$kg mol^{-1}$	MM
Momentum	$kg m s^{-1}$	p
Motor input power	W	P_E
Motor output fan efficiency	——	η_M
Motor power output	W	P_M
	N	
Natural wet bulb temperature	°C	θ_{wb}
Nominal volume air flow	L	$q_{v\,nom}$
	O	
Operative temperature	°C	θ_{op}
Overall fan efficiency	——	η_F

(continues)

TABLE A.39 *(continued)*

Term	Units	Symbol
Overall heat transfer coefficient	W m^{-2} K^{-1}	U
Overlap length (ductwork)	m	l_p
	P	
Partial pressure	Pa	p_v
Particle production rate	s^{-1}	Q_p
Particle size	μm	d_p
Percentage dissatisfied	%	PD
Periodic time	s	t
Permeability index for clothing layer	——	I_{clo}
Plane angle	Rad or °	α, β, γ
Plane radiant temperature	K	T_{pr}
Polytropic coefficient	——	n
Position of control setting	% or °	s
Power	W	P
Predicted mean vote	——	PMV
Predicted percentage dissatisfied	%	PPD
Pressure difference between points	Pa	Δp_t, Δp_s, etc.
Pressure loss coefficient	——	ξ
Pressure total	Pa	p_t
Primary air flow rate	m^3 s^{-1} or l s^{-1} or kg s^{-1}	q_{vp} or q_{mp}
	Q	
Quantity of heat	J	Q
	R	
Radiation heat transfer coefficient	W m^{-2} K^{-4}	h_r
Radiation temperature asymmetry	°C	T_{as}
Radiative heat exchange	W m^{-2}	φ_r
Radiative heat exchange between globe thermometer and surroundings	W m^{-2}	φ_g
Radiative heat transfer coefficient	W $m^{-2}K^{-1}$	h_r
Radius		
inner	m	r
outer	m	R

(continues)

TABLE A.39 *(continued)*

Term	Units	Symbol
Radius of curvature	m	r_m
Ratio of specific heat capacities	——	γ
Relative fluid velocity to an impeller	m s^{-1}	w
Relative humidity	——	ϕ
Reverberation time	s	t
Rotational speed	s^{-1}	n
	S	
Saturation pressure of a vapor	kPa	p_{sat}
Saturated water vapor pressure at skin temperature	kPa	p_{sks}
Saturated water vapor pressure at wet bulb temperature	kPa	$p_{as,w}$
Secondary air flow rate		
mass flow	kg s^{-1}	q_{vs}
volume flow	m^3 s^{-1} or l s^{-1}	q_{ms}
Shaft fan power efficiency	——	η_A
Solid angle	sr	Ω
Sound power level	dB	L_w
Sound pressure level	dB	L_p
Specific heat capacity	J kg^{-1} K^{-1}	c
Specific heat capacity at constant pressure	J kg^{-1} K^{-1}	c_p
Specific heat capacity at constant volume	J kg^{-1} K^{-1}	c_v
Spread of a jet	m	b_z
Stagnation pressure	Pa	p_{ta}
Static gauge pressure	Pa	p_s
Stefan-Boltzmann constant	W m^{-2} K^{-4}	σ
STPD reduction factor	——	F
Surface area	m^2	A_s
Surface heat transfer coefficient	W m^{-2} K^{-1}	h
Surface temperature	°C	θ_s
Surface tension	N m^{-2}	σ
	T	
Tangential component relating to a fan, or pump impeller, or fluid	m s^{-1}	c_u
Temperature difference	K or °C*	ΔT or $\Delta\,\theta$*
Thermal diffusivity	m^2 s^{-1}	A

(continues)

TABLE A.39 *(continued)*

Term	Units	Symbol
Thermodynamic (absolute) temperature	K*	T^*
Thickness	m	t or d
Thickness of dynamic boundary layer	m	δ
Thickness of thermal boundary layer	m	δ_T
Throw of a jet	m	L_J
Time	s	t
Time constant, exponential change	s	τ
Tip Reynolds number of a fan impeller	——	Re_u
Tip speed of a fan impeller	m s^{-1}	U
Torque	N m	T
Total gas or air flow rate		
mass flow	kg s^{-1}	q_{mt}
volume flow	m^3 s^{-1}; L s^{-1}	q_{vt}
Total gauge pressure	Pa	p_t
Total heat transfer coefficient	W m^{-2} °C^{-1}	H
Turbulence intensity	%	T_u
	U	
Universal gas constant	J kg^{-1} K^{-1}	R
	V	
Velocity	m s^{-1}	v
Velocity components in the x, y, z directions	m s^{-1}	u, v, w
Velocity of sound	m s^{-1}	c
Volume	m^3	V
Volume flow rate	m^3 s^{-1} or L s^{-1}	q_v
	W	
Water vapor latent heat of vaporization	W m^{-2}	φ_L
Water vapor partial pressure	kPa	P_a
Water vapor pressure at skin temperature	kPa	p_{sk}
Wave length	m	λ
Weight	N	G
Weighted sound pressure level	dB A	L_{pA}
	dB B	L_{pB}
	dB C	L_pC

(continues)

TABLE A.39 *(continued)*

Term	Units	Symbol
Wet bulb globe temperature	°C	θ_{wbg}
Wetted duct perimeter	m	χ
Width	m	b
Wind chill index	W m^{-2}	WCI
Work	J	W
	Y	
Young's modulus	N m^{-2}	E

*In normal work, °C is used in preference to the absolute temperature K. However, it is essential that K be used when working with the gas laws, radiation, and the coefficient of cubical expansion. The symbol for normal temperature is θ followed by a suffix, while T always denotes absolute temperature.

TABLE A.40 The Greek Alphabet

Name	Symbols	
Alpha	A	α
Beta	B	β
Gamma	Γ	γ
Delta	Δ	δ
Epsilon	E	ϵ
Zeta	Z	ζ
Eta	H	η
Theta	Θ	θ
Iota	I	ι
Kappa	K	κ
Lambda	Λ	λ
Mu	M	μ
Nu	N	ν
Xi	X	χ
Omicron	O	o
Pi	Π	π
Rho	P	ρ
Sigma	Σ	σ
Tau	T	τ
Upsilon	Y	υ
Phi	Φ	ϕ
Chi	X	χ
Psi	Ψ	ψ
Omega	Ω	ω

TABLE A.41 Symbols for Operations

Symbol	Definition
$\equiv$	is identical to
$\neq$	does not equal
$\cong$ or $\approx$	is approximately equal to
$\propto$	is directly proportional to
$\longrightarrow$	tends to
$<$	is less than
$>$	is greater than
$\leq$	is less than or equal to
$\geq$	is greater than or equal to
Δx	finite increase in x
δx	variation in x
dx	total differential in x
grad	gradient
div	divergence
curl	curl
∇^2	Laplacian
!	factorial
( )	parentheses
exp or e^x	exponential of x
$\ln x$	logarithm to base e of x
$\log_{10} x$	logarithm to base 10 of x
[ ]	brackets
[1]	one-dimensional
[3]	three-dimensional
$\sum$	summation

TABLE A.42 Abbreviations

Meaning	Abbreviation
About	ca.
Absolute	abs
Alternating current	a.c.
Apparatus dew point	Adp
Atomic weight	At.wt.
Boiling point	b.p.
Boundary layer	b.l.
Centerline	c.l.
Compare	cf.

(continues)

TABLE A.42 *(continued)*

Meaning	Abbreviation
Direct current	d.c.
Dry bulb temperature	d.b.t.
Electromotive force	emf
Equation	Eq.
For example	e.g.
High pressure	H.P.
Hydrogen ion concentration	pH
Liquid (specified)	L (followed by the appropriate chemical symbol)
Liquid oxygen	LOX
Liquefied petroleum gas	LPG
Melting point	m.p.
Molecular weight	mol.wt.
Namely	viz.
Note well	n.b.
Outside diameter	OD
Parts per million	ppm
Per cent	%
Relative humidity	RH
Research and development	R & D
Specific	Sp.
That is	i.e.
Latin terms	
In the place cited (reference to an earlier quote)	*loc. cit.*
In the work cited (a further reference to a book previously mentioned, but this time in a different passage)	*op. cit.*
In the same place (a reference to a topic covered in a preceding reference)	*ibid.*
And another or and others (e.g., Burgess et al. rather than Burgess, Ellenbecker, and Treitman)	et al.

PHYSICAL CONSTANTS

Mean molecular weight of dry air $M_a = 28.969$ kg kmol^{-1}
Mean molecular weight of water $M_v = 18.02$ kg kmol^{-1}
Density of dry air at 101.325 kPa and 0 °C = 1.293 kg m^{-3}
Density of water at 4 °C = 1000 kg m^{-3}
Density of water at 20 °C = 998.23 kg m^{-3}
Barometric pressure at standard temperature and pressure = 101.325 kPa
Standard temperature and pressure (STP) = 0 °C at 101.325 kPa (also known as normal temperature and pressure)

Universal gas constant $R_{gas} = MR = 8.3143$ J mol^{-1} K^{-1}
Volume of 1 mol of the permanent gases (at 101.325 kPa and 0 °C) = 22.4136 m^3
Characteristic gas constant for dry air $R_a = 287$ J kg^{-1} K^{-1}
Characteristic gas constant for steam $R_v = 462$ J kg^{-1} K^{-1}
Mean specific heat of air at constant pressure $c_{pa} = 1005$ J kg^{-1} K^{-1}
Mean specific heat of air at constant volume $c_{va} = 718$ J kg^{-1} K^{-1}
Mean specific heat of steam of air at constant pressure $c_{pv} = 4210$ J kg^{-1} K^{-1}
Mean specific heat of steam at constant volume $c_{vv} = 1810$ J kg^{-1} K^{-1}
Adiabatic index for air at room temperature and pressure = 1.4
Latent heat of steam at 0 °C = 2500 kJ kg^{-1} K^{-1}
Standard gravity ≡ 9.806 65 m s^{-2}
Velocity of sound in air at normal temperature and pressure c = 331.46 m s^{-1}
Stefan's Constant $\sigma = 5.67 \times 10^{-8}$ W m^{-2} K^4

DIMENSIONLESS NUMBERS

The following dimensionless numbers may be expressed in various forms due to the use of other relevant parameters.

Archimedes Number

$$\text{Ar} = \sqrt{\frac{\Delta\rho g L}{\rho v^2}} = \frac{\text{Buoyancy force}}{\text{Inertia force}}$$

The ratio $\Delta\rho/\rho$ can be replaced by $\Delta T/T$. Ar relates the influence of velocity and temperature of a jet when discharged into an environment of a different temperature. In some instances the Froude number, Galileo number, or Grashof number may replace the Archimedes number.

Colburn j-Factor

$$\text{Colburn j-factor} = \frac{\text{Nu}}{\text{Re Pr}^{0.33}} = \text{St} \cdot \text{Pr}^{0.66}$$

Used in heat-transfer applications.

$$\text{Colburn j-factor} = \frac{\text{N}}{\text{Re Se}}\text{Sc}^{0.66}$$

Used in mass-transfer applications.

Condensation Number

$$\text{Co} = h\left(\frac{\eta}{\rho^2 g \lambda^3}\right)^{0.33}$$

Euler number

$$\text{Eu} = \frac{p}{\rho v^2} = \frac{\text{Pressure force}}{\text{Inertia force}}$$

Froude number

$$\mathrm{Fr} = \frac{v^2}{gL} = \frac{\text{Inertia force}}{\text{Gravity force}}$$

See Archimedes number.

Graetz number

$$\mathrm{Gz} = \frac{q_m c}{\lambda l}$$

Same as Peclet number except $\frac{d_w}{L}$ considered (entrance region).

Grashof number

$$\mathrm{Gr} = \frac{\beta g \rho^2 l^3 \Delta\theta}{\eta^2} = \frac{(\text{Buoyancy forces})(\text{Inertia force})}{(\text{Viscous forces})^2}$$

Used for free convection.

Knudsen number

$$\mathrm{Kn} = \frac{l_1}{0.5d} = \frac{\text{Molecular mean free path}}{\text{Characteristic length}}$$

Used for particulate movement in a gas.

Lewis number

$$\mathrm{Le} = \frac{\mathrm{Sc}}{\mathrm{Pr}} = \frac{\kappa}{D}$$

where

$$\kappa \equiv \frac{\lambda}{c\rho} = \frac{\text{Thermal diffusivity}}{\text{Mass diffusivity}}$$

Used for calculations involving the vaporization of a fluid.

Mach number

$$\mathrm{Ma} = \frac{\rho l^2 v^2}{Kl^2} 2 = \frac{v}{\frac{K}{\rho}} \text{ or } \frac{v}{\sqrt{\frac{K}{\rho}}} = \frac{\text{Inertia force}}{\text{Compressibility force}}$$

Nusselt number

$$\mathrm{Nu} = \frac{\phi l}{\lambda \Delta\theta} = \frac{hl}{\lambda}$$

Ratio of temperature gradients, used for heat transfer taking place with fluid flow.

Peclet number

$$\mathrm{Pe} = \frac{vlC_p\rho}{\lambda} = \mathrm{Re} \cdot \mathrm{Pr} = \frac{\text{Heat convection}}{\text{Heat conduction}}$$

Used for convective flow in heat-transfer applications.

$$\text{Pe} = \frac{lv}{D} = \frac{\text{Mass transfer}}{\text{Mass diffusivity}}$$

Used in mass transfer applications involving aerosols.

Prandtl number

$$\text{Pr} = \frac{c\eta}{\lambda} = \frac{\nu}{\kappa} = \frac{\text{Molecular diffusivity of momentum}}{\text{Molecular diffusivity of heat}}$$

Used for heat transfer with fluid flow.

Reynolds number

$$\text{Re} = \frac{v\rho l}{\eta} = \frac{vl}{\nu} = \frac{\text{Inertia force}}{\text{Viscous force}}$$

Relates the nature of the fluid flow in and around bodies.

Richardson Number

$$\text{Ri} = \frac{-g\left(\dfrac{\partial T}{\partial z}\right) + G}{T\left(\dfrac{\partial v}{\partial z}\right)^2} = \frac{-g\left(\dfrac{\partial \theta}{\partial z}\right)}{\left(\dfrac{\partial v}{\partial z}\right)^2} = \frac{\text{Buoyancy}}{\text{Momentum gradient}}$$

Schmidt number

$$\text{Sc} = \frac{\nu}{D} = \frac{\text{Momentum diffusivity}}{\text{Mass diffusivity}}$$

Used for mass transfer = Pr number for mass transfer = Colburn number.

Sherwood number

$$\text{Sh} = \frac{\dfrac{\beta}{D}}{\dfrac{}{l}} = \frac{\beta l}{D} = \frac{(\text{Mass transfer coefficient})(\text{Length})}{\text{Diffusion coefficient}}$$

This is the Nusselt number for mass transfer.

Stanton number

$$\text{St} = \frac{\text{Nu}}{\text{Re} \cdot \text{Pr}} = \frac{\phi}{V\rho c\Delta\theta} = \frac{h}{V\rho c} = \frac{\text{Wall heat-transfer rate}}{\text{Heat transfer by convection}}$$

Used for convective heat transfer applications.

Stokes number

$$\text{Stk} = \frac{\rho d^2 v C_f}{18\eta L} = \frac{\text{Stopping distance}}{\text{Characteristic length}}$$

where C_f = Cunningham's factor. Used for particulate settling calculations.

GLOSSARY

A

A weighting scale, dBA The unit of sound intensity expressed as a logarithmic scale, related to a reference level of 10^{-12} W m^{-2}. The A weighting scale is the most commonly used scale, as it reduces the response of sound meters to very high and low frequencies and emphasize those within the range audible by the human ear.

Abatement The reduction in air or water pollution from all sources by preventive measures.

Abrasive blasting The process of product cleaning by the use of an abrasive material.

Abrasive dusts Dusts used for abrasive blasting, grinding, polishing, and buffing.

Absolute filters Strictly dry filters used in installations that require a very clean environment, classified according to efficiency.

Absolute humidity The mass of water vapor present in a unit mass of dry air.

Absolute pressure The pressure recorded relative to the absolute zero value of pressure.

Absolute radiant heat flow The radiant energy emitted per unit area in one direction.

Absolute roughness The roughness of a pipe or duct wall, normally expressed as a dimensionless ratio of the linear measure of the internal roughness k_s divided by the diameter.

Absolute total pressure Sometimes called stagnation pressure, the algebraic sum of the velocity and static pressure at a given location in a moving system, in Pa.

Absolute ventilation efficiency A value that provides a means of determining the actual ability of a ventilating system to reduce the concentration of a pollutant, compared to that theoretically possible.

Absolute zero The temperature at which a perfect gas kept at constant volume exerts no pressure; it is equal to –273.16 °C (0 K).

Absorber The material that is used in an absorption process.

Absorption

1. The process of diffusion in which molecules are transferred from the gas phase into a solid or liquid sorption medium.
2. The taking up of radiant energy by a material as it encounters the body, or as it passes through. A physical change or chemical change or both may accompany it.

Absorption coefficient Measure of the amount of sound or heat absorption provided by a material.

Absorption spectroscopy Analytical technique involving measuring the amount of energy absorbed by a compound.

Absorptivity The fraction of the energy incident on a body that is absorbed by that body (absorbance). Relating to thermal radiation and acoustics.

Acceleration loss The energy input necessary to accelerate air to a higher velocity.

Acceptable air quality When workspace air has no known harmful contaminants present which may influence the immediate or future health of the occupants.

Access door An opening providing access to some plant item or ductwork to allow for inspection, cleaning, or maintenance.

Accessibility Ease of access to a plant item.

Acclimatization The state of the human body becoming accustomed to a given thermal environment, either heat or cold.

Accuracy The degree of closeness of a measurement to the true reading of the value being measured.

Acid A substance that liberates hydrogen ions in solution.

Acid cleaning The use of acids to clean scale or other deposits from pipes or tanks.

Acid dew point The temperature at which a vapor containing an acid appears as condensate on a cool surface, causing corrosion.

Acid fumes Particles in the air generated by the condensation of acid vapors. They may also arise from sublimation, condensation, or chemical reaction.

Acid mists Mists resulting from a process in which an acid is produced or used.

Acidic smuts Solid and liquid conglomerates formed by the condensation of water vapor and sulfur trioxide on a cold surface. A typical case is combustion products in a flue, which come into contact with surfaces at temperatures below the flue gas dew point temperature. These products contain metallic sulfate and carbon aqueous particles approximately 1–3 mm in size.

Acoustics The science and understanding of the behavior of sound in the environment.

Acoustic environment The level of sound in an internal or external environment, related to a standard prescribed level.

Acoustic force An acoustic field used to enhance the evaporation, coagulation, or condensation of particulate matter.

Acoustic insulation A material that has the ability to absorb sound energy.

Acoustic leak detection A technique used to detect cracks in a building structure through which infiltration or exfiltration is taking place. A constant source of high frequency sound is produced within the building and a detector microphone positioned outside the building detects the weak spots by recording a volume increase.

Acoustic muff (muffler) Sound-absorbing material that is placed around a noisy item in a plant.

Acoustic pod Sound-absorbing material inserted in ductwork to absorb sound.

Action level A term describing the airborne concentration that triggers certain provisions of a regulation; generally, but not always, it is 50% of the PEL value.

Activated alumina Hydrated aluminum oxide, a granular desiccant activated at high temperature that absorbs moisture and gases.

Activated carbon or activated charcoal Carbon in the form of charcoal granules, which has an affinity to adsorb many gases and vapors and, in so doing, removes odors. It is manufactured by exposing coal, coconut shells, or peat to steam at 800 to 900 °C.

Activated carbon filter A canister filter containing activated carbon.

Active site The position on an adsorbate surface where adsorbate molecules are trapped.

Activity The nature of the work carried out by a person, measured in Met units. Also, the decay rate of radioactive particles.

Actuator An automatic device providing valve or damper control of fluid flow by means of an electrical, hydraulic, or pneumatic motor.

Acute The immediate influence of given concentrations of an air pollutant on the health of a person.

Acute effects Symptoms of injury or other physical manifestations that follow an acute exposure.

Acute exposure Exposure to a high level or concentration of a pollutant for a relatively short time.

Adhesion The phenomenon of particles sticking to the fiber surfaces in a filter.

Adhesion of particles Small particles experience adhesion forces, allowing them to attach to surfaces. These forces may be made up from surface tension of liquid films, or London (Van der Waals) forces.

Adiabatic A process that takes place without loss or gain of heat, e.g., when air rises it expands adiabatically in the atmosphere.

Adiabatic lapse rate The adiabatic temperature change that takes place with height of a rising (or falling) parcel of air, approximately –1 °C/100 m.

Adiabatic mixing A mixing process that takes place without the removal or addition of heat.

Adiabatic saturation temperature The temperature attained after an adiabatic process.

Adjustable flow rate A controlled state of flow that is achieved by means of a damper or valve.

Adjustable grill See grill.

Adjustable pattern air diffuser An air diffuser incorporating a device that allows the direction of the leaving air to be adjusted.

Adjustable pitch fan A fan in which the pitch angle can be set to provide the required airflow rate. The pitch angle may be preset or controlled with the fan running.

Administrative controls The working method that allows workers to be exposed to set exposures of contaminants in the workplace. Lower exposure levels are achieved by the use of work assignment, job rotation, with set periods working away from the hazard zone.

Adsorbate The contaminant collected by an adsorber.

Adsorbent A medium that traps vapor or gaseous contaminants on its surface by chemical and physical properties.

Adsorbent, regenerable An adsorber, which is treated when fully contaminated in order to restore its original collection properties.

Adsorber An adsorbent material used in the adsorption process.

Adsorption A physical process in which a molecule of a vapor or gas (adsorbate) is condensed on and taken up by the surface of a porous material (adsorbent) such as silica gel or activated carbon.

Adventitious opening Any unintended openings in a building structure, such as cracks through which infiltration or exfiltration can occur. The terms unintentional opening, fortuitous leakage, and crackage are also used.

Aerobic microbes Microbes used in a biofiltration process in which gaseous pollutants are removed from a process gas stream by aerobic digestion.

Aerodynamic diameter The diameter of a unit-density sphere that has the same settling velocity in air as the particle in question.

Aerosol A special class of particulate consisting of colloidal suspensions larger than molecular size, but not large enough to settle under gravity.

Aerosol, monodisperse An aerosol with a size-distribution function described by a geometrical standard deviation less than 1.15. If the deviation is between 1.15 and 1.5, it is classified as a quasi-monodisperse aerosol.

Aerosol, polydisperse An aerosol with a geometric standard of deviation of size-distribution greater than 1.5.

Aerosolize Mixing a gas and a liquid to form microscopic (0.5 to 10 μm) airborne droplets.

After filter A filter located in the flow stream after another filter to remove any particulate matter that may have passed the upstream unit.

After heater An air or water heater positioned in a long duct or pipe work run to remedy distribution heat losses.

Afterburner A unit installed after the main combustion zone in a process to further provide combustion to reduce the emission of certain pollutants. It may be

1. A direct-flame afterburner, in which an auxiliary fuel burner provides all the heat from a flame, or
2. A catalytic afterburner, in which the surface action of catalysts allows incineration to take place at a temperature lower than a direct flame, reducing the auxiliary heat required, or

3. A recuperative afterburner, a heat exchanger combined with a direct flame unit, that preheats the combustion gases.

Age of air A statistical measure of the air in a space.

Agglomeration The process of the clustering or adhering together of a number of small particles.

Aging Any chemical process that reduces the effectiveness of the properties of a material.

Agitator A device used to stir or agitate a fluid, reducing stagnation or stratification.

Air

Air The composition of gases that make up the earth's atmosphere, approximately 79% nitrogen and 21% oxygen. "Pure air" has no definite meaning regarding the proportion of these gases; this term is used to imply the absence of industrial particulate matter.

Air after-treatment Treatment of the supply air after the main treatment.

Air barrier A device that provides a jet barrier between two zones in a building. See Air curtain.

Air bleed-in Openings at the end of a branch duct that provide increased flow rates for the transportation of heavy particulate matter.

Air change coefficient The ratio of air volume flow rate and the volume of the space.

Air change efficiency The ratio of the nominal time constant and the time taken to change the air within a space.

Air change rate The ratio of the volume of air supplied or extracted to the volume of the space usually measured in air changes per hour (ach) and normally related to the fresh air change rate.

Air cleaner A device that removes airborne contaminants from air.

Air cleaning equipment Equipment that removes airborne contaminants, either

- Equipment to clean the ambient air, normally classified as air filters, or
- Equipment that will collect large concentrations of particulate matter from industrial processes, called dust collectors.

Air conditioning The process of air treatment in which the temperature, moisture content, purity, and distribution is controlled to set conditions. The resulting conditions may be chosen for human thermal comfort or to meet the requirements of a manufacturing process

Air conditioning installation Any plant assembly which can achieve the conditions outlined above.

Air conditioning, partial The process of air conditioning which is lacking one or more of the ideals, i.e., no moisture control, no heating, or no cooling.

Air contaminants Aerosols, gases, vapors or dusts which may cause adverse effects if discharged into the indoor or outdoor atmosphere.

Air core area The gross area of the openings of an air terminal device (ATD).

Air core velocity The air flow volume divided by the core area of an air terminal device (ATD).

Air current Air movement in a space produced by either thermal or mechanical means.

Air curtain A high-velocity air jet that provides an air barrier between two different building or work zones.

Air diffuser A circular, linear, rectangular or square device from which supply air is discharged in a controlled direction.

Air-diffusing ceiling The process of air distribution into a given space through a perforated ceiling.

Air diffusion The process of air distribution into a space by means of an air terminal unit. The components of air diffusion are

- **Air terminal devices (ATD),** components of the installation

which are designed for the purpose of achieving the predetermined movement of air into or from the treated space, e.g., grills, diffusers, etc.,

- **Complementary accessories for ATD** components of the installation which are used in conjunction with, and in several cases form an integral part of, the air terminal device for the purpose of achieving the predetermined profile or rate of flow into or from the air terminal device (e.g., air flow controllers, dampers, flow equalizers, baffles, etc.), and
- **Fixed accessories for ATD,** components of the installation which assist the fitting and fixing into place and/or maintenance of the air terminal devices and their complementary accessories (e.g., plaster frames, snap-in fasteners, etc.).

Air discharge velocity The average velocity of the air discharged from the opening of an ATD, $V_c/(C_d A_{rf})$.

Air distribution The mechanical or natural delivery of air into a space in a designed manner, or the transport of air in ductwork. The components of air distribution are

- **Elements of air distribution,** the components involved in ensuring air distribution from the plant room to the space, e.g., ductwork, damper, etc.,
- **Air terminal units (ATUs),** item at the end of a duct run to control velocity, pressure, flow rate, and/or temperature,
- **Accessories of distribution,** any components to keep the unit in place, or allow maintenance to be carried out.

Air douches Versions of fresh air jets in which air is discharged from a wide nozzle or plenum at a relatively low velocity close to the worker.

Air, dry A mixture of air with no moisture content present.

Air duct An enclosure that conveys air from one location to another.

Air ejectors (jet pumps) A device injecting high-velocity (pressurized) primary air into the secondary air. It allows air to be moved without passing through a fan, it may be a simple or Venturi-type ejector.

Air envelope The surface of a jet produced by an ATD with the same velocity.

Air excess Air provided to a combustion or ventilating process in excess of that theoretically required for the combustion process.

Air exfiltration The uncontrolled rate of air interchange from a space to outdoors due to density variations, or by space pressurization by means of a fan.

Air exhaust The volume or mass flow of air that is mechanically rejected to outdoors due to its unsuitability for further use within the space. See also Extract air (EA) classification.

Air extraction The removal of contaminated air from a space, either directly to outdoors or recirculated back to the space after suitable treatment. See also Extract air (ETA) classification.

Air extraction cooker hood A range hood positioned above kitchen cooking equipment, designed to collect without spillage the plume generated at the range.

Air filters

Air filter A device that removes particulate matter from a gas flowing through it. These are classified as

- **Absolute** A high-efficiency particulate air filter that is at least 99.79% efficient in the removal of thermally generated monodisperse dioctylphthalate smoke particles with a diameter of 0.3 μm, also known as a HEPA filter.

- **Activated carbon** An adsorption filter that makes use of an activated carbon bed to remove odors and various gases from a ventilating or gas cleaning system.
- **After** A filter that is positioned after a coarse filter, to ensure that the air entering a space is at the required degree of cleanliness.
- **Automatic roll** A motor-driven continuous roll of material, either viscous or fiber, which ensures a set pressure drop in the airflow. Its operation depends on sensors that record the pressure differential on either side of the filter.
- **Blow-off** A filter, such as a bag filter, that has the dust burden (cake) on the surface blown off by strong blasts of compressed air.
- **Cleanable** A filter that can be cleaned by manual or automatic washing.
- **Coarse** A filter fitted before a HEPA filter to remove the larger particulate matter to ensure the HEPA filter has a longer life without clogging up.
- **Dry** A filter manufactured from cotton wool, glass–fiber fabric, pleated paper, foamed polyurethane, cellular polythene, or other suitable materials. As the name suggests, the filter is dry in nature and has no oil coating.
- **Electrostatic** A filter in which a high voltage is used to collect the particulate matter onto earthed plates.
- **Fabric** A dry throwaway filter in panel or wedge form mounted in supporting frames.
- **Grease** A filter used in kitchen air extraction systems to prevent the contamination of the ductwork system with grease, which would be a fire hazard.
- **HEPA** See Absolute.
- **Impingement** The process by which particulate matter is stopped in its path by colliding with a surface, normally a surface coated with oil.
- **Panel** Any type of filter material mounted in a rigid frame. The frame must allow only the absolute minimum of particulates to pass between the frame and the sides of the filter material.
- **Pre** A prefilter is placed before the main filter to extend the life of the main filter.
- **Rotary viscous** A continuously rotating oil-coated roll of material. The filter resistance is kept low by a motor drive that ensures a clean surface is always presented to the airflow.
- **Self-cleaning** A filter similar to the rotary viscous in which the filter plates are passed through an oil bath to remove the collected dust.
- **Terminal** The ultimate filter at the end of a run, which ensures that the airflow entering the room is at the required design purity.
- **Throwaway** A filter which is thrown away after collecting its dust burden, no attempt being made to clean it.
- **Viscous** As the rotary viscous or fixed-cell type, in which the particulate matter sticks to the oil-coated material.
- **Wet** The various forms of washers and scrubbers.

Air filter cell The material that forms the active part of a filter.

Air filter dust-holding capacity The amount of dust, by weight, retained by a filter under a standard test such as EN779.

Air filter efficiency The ability of a filter to remove dust from the air, expressed in terms of the contaminant concentrations

upstream and downstream of the filter. It may be obtained by

a. Weight test (gravimetric),
b. Dust spot test,
c. Arrestance tests, or
d. Particle counting.

Air filter medium The material type from which the filter is constructed.

Air filter performance An overall assessment of the collection efficiency, pressure drop, flow rate, fire rating, health aspects, and behavior of a filter in the environment in which it is used.

Air filter resistance The pressure drop created between the upstream and downstream faces of a filter, increases as the dust burden.

Air filter resistance, final The maximum pressure drop allowed across a filter to ensure that the design airflow rate is achieved.

Air filter test Any test to determine filter efficiency, flow rates, or other characteristics by some preset method.

Air free area (A_F) The sum of the smallest areas of the cross section of the opening of an ATD.

Air free area ratio (A_{RF}) The ratio of free area to the core area.

Air grill An entry or exit in a duct consisting of a mesh or lattice opening; it may be fixed (unadjustable) or adjustable.

Air grill, adjustable An air grille with manual or automatic adjustable louvers.

Air handling function The ability of an air handling plant to perform a given type of air treatment.

Air handling unit A self-contained unit for the introduction or removal of air from a space. It consists of one or more of the following plant items: heating or cooling coils, filters, fans, damper provision for mixing and recirculation, humidification controls, and acoustic treatment.

Air heating and cooling coil As tube or plate heat exchanger in which air, the secondary fluid, is either heated or cooled with a primary medium.

Air humidity The moisture content of air. See Absolute humidity and Relative humidity.

Air infiltration The uncontrolled air interchange through structural imperfections and other openings into a space, due to natural convection, rising currents, or wind forces over a building.

Air infiltration, balanced Infiltration that takes place at a constant or balanced rate.

Air infiltration, unbalanced Infiltration that takes place at an unbalanced or variable rate.

Air inlet Any opening that provides air for any purpose, either from outside or inside the building.

Air leakage See Air infiltration.

Air leakage rate The leakage of air through an enclosure such as a building or ductwork, expressed as air loss in L/s per m run, or as a percentage loss of the total volume.

Air, make-up The air quantity necessary to replace air extracted from the space, this may be required for combustion or process work and may be obtained by mechanical or natural means.

Air mass flow rate The mass flow of air or any other fluid, expressed in kg s^{-1}.

Air monitoring The process of continuous sampling and measuring of the quantity of pollutants present in indoor or outdoor air.

Air movement The direction and velocity of air within an enclosure.

Air pollutant Any undesirable element present in indoor or outdoor air, such as air contaminants, moisture, etc.

Air pollution The presence of foreign matter (gaseous or particulate or combinations of both), bacteria, sound, or other undesirable elements in air, which is detrimental to the health or welfare of man, animals, plants, or materials.

Air pre-treatment See air treatment.

Air pressure Atmospheric air pressure or static, velocity or total pressure in a ventilating system, Pa.

Air, primary The actual quantity of air injected into a space before secondary air induction occurs.

Air-purifying respirator A respirator that removes airborne contaminants, such as particulates, gases, vapors and fumes, from ambient air through filtration, absorption, adsorption, or chemical reactions on the media contained in the cartridge or filter.

Air quality The concentration of one or more pollutants in the air, measured in either ppm or $\mu g\ m^{-3}$. It may be related to pollution sources inside an enclosure or outdoor air. Temperature and moisture conditions may also be considered.

Air quality standard (AQS) A standard providing a level beyond which air pollutants in the atmosphere can cause damage to plants, animals, or materials. The concentration and time factors have to be considered.

Air, recirculated Any air that is mechanically extracted from a space that, after suitable treatment, is returned to the space.

Air recirculation The process of returning exhaust air to the air-treatment plant and after treatment returning it to the space.

Air relief The release of air from a space, either by pressure difference or mechanical extraction.

Air resource management The enforcement of set standards to reduce contamination supported by control regulations, planning, and quality testing facilities.

Air, return The air returned from a space for processing (also called recirculated air).

Air, sample The air obtained for analytical testing.

Air sampling The process of collection of an air sample to determine its contamination level and dust concentration.

Air, secondary Air entrained in a primary airflow, or the additional air supplied to a combustion process.

Air sedimentation A measuring technique for particulate matter using a micromeorograph, to determine the Stokes number of fall.

Air space The gap between two surfaces containing either still or moving air.

Air spread The maximum horizontal distance between two vertical or horizontal planes of equal velocity in a jet, tangential to the supply envelope from the ATD.

Air stratification The layering of air within a space due to density differences.

Air stream A defined air current within an enclosure, resulting from natural thermal air movement or from mechanical air movement produced by a jet.

Air supply The quantity and condition of treated or untreated air discharged into a space.

Air terminal device (ATD) A specially designed component in an installation, which provides a predetermined air movement into or from a treated space. They are classified as

- Automatically controlled, if they have moving parts to change the local conditions of temperature, humidity, pressure difference, airflow rate, and levels of pollution,
- Fixed, if they are preset to achieve the desired results and have no moving parts, or
- Manually adjusted, if adjustments are made manually by the service engineer or the occupants.

Air terminal unit Air distribution equipment that provides set conditions by the mixing of primary and secondary air. The device may be fixed, having no control or means of manual adjustment, automatically controlled or manually controlled. If automatically controlled, a sensor is used to indicate any required

change in temperature, humidity, airflow rate, pressure, or CO_2 entering the room.

Air terminal unit assembly The air terminal unit, consisting of casing, mixing section, flow control, heating, cooling, filters, fans, sound attenuators, etc.

Air throw The maximum distance from the outlet of an ATD to a plane tangential to the jet envelope and perpendicular to the initial jet section where the velocity is reduced to a predetermined level.

Air transfer Air that is allowed to pass either mechanically or naturally from one zone to another. In the mechanical case, the transfer volume is controlled by means of suitable control valves.

Air transfer device A mechanical device that allows controlled flow of air from one room or zone to another.

Air treatment Any technique used to control the temperature, moisture content, or levels of dusts, gases, vapors, pollens, bacteria or viruses in air.

Air treatment, thermodynamic Relating to the various thermodynamic changes that occur in the specific volume, enthalpy, and wet and dry bulb temperatures of treated air.

Air turning vane A vane fitted in a ductwork bend to reduce pressure loss.

Air type Classification of air at a specific point in its passage through an air conditioning or ventilation system, either in the duct or the space, e.g., outdoor air, supply air, treated air, recirculated air, extract air, etc.

Air, vitiated Contaminated or polluted air unsuitable for a given application.

Air volume flow rate (q_v) The volume of air or gas moved per unit of time.

Air washer One of the following devices that adds water to an airstream to increase the moisture content of the leaving air.

- **Capillary cell** An arrangement of porous pads sprayed with water, through which the air to be treated is passed.
- **Saturation efficiency** Relating to air washers, the percentage of water added to the flowing air supply compared to that which must be added for the air to leave fully saturated.
- **Spinning disc** A rotating disc onto which a fine jet of water impinges, resulting in fine droplets that add moisture to the air supply.
- **Spray** Banks of water sprays that inject atomized water particles into the airstream.

Airflow Steady or unsteady air mass or volume movement past a fixed point, either in a duct or in a free space.

Airflow model A mathematical or computer model of the airflow path within an enclosure.

Airflow pattern The air distribution within a space resulting from discharges from a fan or ductwork.

Airflow rate The speed of volume or mass airflow that takes place in a duct or space.

Airflow rate controller Any mechanical, pneumatic, or electrical device that controls the air flow rate into or out of a space by increasing or decreasing the flow resistance. See Dampers and Valve.

Airflow straighteners Vanes in a ductwork section positioned to reduce turbulence after a change in section.

Airlock A two- or three-door enclosure providing access to a clean room that reduces the air leakage of external polluted air into the clean room.

Airlock, active An airlock connected to an air treatment device.

Airlock, passive An airlock that is not connected to the air conditioning system.

Airtightness ductwork class A description of the quality of a ductwork system and its ability to contain air with the minimum of air or gas leakage, classified

based on air leakage factor f, expressed in L s^{-1} m^{-2} or m^3 s^{-1} m^{-2}, a function of pressure p in Pa

Airtightness class	f (maximum)
A	$0.027\ p_s^{0.65}$
B	$0.009\ p_s^{0.65}$
C	$0.003\ p_s^{0.65}$
D	$0.001\ p_s^{0.65}$

Aitken nuclei Particles, generally with diameters less than 0.1 μm, that are true aerosols when they form the nucleus for condensation or ice formation.

Algorithm A method of calculation that produces a control output by operating on an error signal or a time series of error signals.

Alkali, alkaline A substance that neutralizes acids.

Allergens Pollutants that may cause an allergy, including pollens, dusts, animal dander, insect debris, mold and fungi spores.

Allergic alveolitis An allergic response to inhalation of organic particles that involves inflammation of the small terminal branches of the bronchioles. Symptoms include coughing, increased production of mucus, fever, fatigue, and muscle aches.

Allergic contact dermatitis Skin condition that occurs in response to exposure to sensitizing material. It is characterized by redness, swelling and cracking and, sometimes more severe reactions involving the entire immune system.

Allergic reaction A body reaction due to exposure to an allergen.

Allergic response The release of antibodies by the immune system in response to foreign molecules in the body.

Allergy A hypersensitivity reaction of the human body due to a particular substance.

Allowable exposure time (AET) The recommended maximum exposure time allowed for an operator in a workspace when subject to a physical or biological pollutant.

Alveolar fraction Particles with approximate aerodynamic diameters of 0.5–3 μm.

Alveoli The small terminal air sacs in the lungs, through which gas exchange between the blood and the inhaled air takes place.

Amber zone A ventilation containment zone used in the atomic energy industry.

Ambient air Air from the surroundings; used to describe the air pollution concentrations in the open air as compared to the point of generation within the workspace.

Amorphous silica The noncrystalline forms of silica or quartz.

Amplification The reflection of a greater amount of sound than originally impacted the surface.

Analog A continuously variable function in a control system ranging from off to full flow.

Analyte The components of an air sample to be measured directly or indirectly.

Anechoic A room that has a low degree of acoustic reverberation, such as an anechoic test chamber.

Anemometer An instrument used to measure the velocity of air or gas.

Aneroid gauge A gauge used for the measurement of static, velocity, or total pressure with a pitot tube.

Aneroid gauge, electronic An aneroid gauge with the advantage of being able to integrate the velocity pressure directly into velocity.

Anesthetic gases Narcotic gases which when inhaled give a feeling of well-being followed by unconsciousness.

Angle factor The geometrical shape factor used in calculating radiation exchange between surfaces i and j.

Angle of divergence The leaving angle of an air jet from an outlet, or the angle of change in a ductwork section.

Angle of transformation piece The angle between the opposite faces of a converging or diverging ductwork section.

Anisokinetic Not isokinetic; a sample collected at a velocity different from that of the airflow in the ventilation system.

Antibodies Specific substances within the human body formed in response to invasion by an antigen.

Anti-C Anti-contamination protective clothing used in the radiation industry.

Anti-sneakage baffles Baffles in an electrostatic precipitator that prevent untreated gas from bypassing the active treatment zone.

Antivibration mounting A designed support placed between a rotating or reciprocating machine and the building structure to reduce the transmission of vibration.

Antidegeneration clause A term used in the U.S. Clean Air Acts implying not only that air quality standards must be achieved, but also that nowhere should air quality be allowed to worsen, even if standards are exceeded.

Antoine's equation An equation used for calculating saturation vapor pressure.

Apparatus dew point For practical purposes, the average temperature of a cooling coil surface.

Appliance A functional device, such as a fan or a combination of package units.

Approach velocity The velocity of airflow into a filter bank or heat exchanger.

Approved codes of practice (ACOPs) Legislation in the United Kingdom dealing with the safety aspects of dangerous materials.

Arc A high-voltage discharge to ground.

Archimedes number A dimensionless number that relates the ratio of buoyancy forces to momentum forces, expressed in many forms depending on the nature of the Reynolds number.

Area, actual filter face The area of a filter perpendicular to the flow direction.

Area, body surface (A_{Du}) The total surface area of a nude person, determined by the Du Bois equation, $A_{Du} = 0.203 W^{0.425} H^{0.725}$

Area, duct cross-sectional The duct area perpendicular to the direction of gas flow.

Area, face The frontal face area of a filter or coil through which a gas passes.

Area, filter medium The total area of the filter medium that is available for gas flow.

Area, filter surface The area formed by the filter medium normal to the direction of flow.

Area, nominal filter face The frontal face area of a filter including the header frame.

Area samples Samples taken by placing the sampling train in a fixed location in the workplace.

Arrestance A measure of the ability of a filter to remove a standard test dust from the air under test conditions.

Arrestance, average The weighted percentage ratio of the total amount of standardized test dust retained by a filter to the total amount of dust fed into the filter in order to achieve a specified final pressure drop.

Arrestance, initial The arrestance value recorded during the first loading cycle in a filter test.

Arrestment The removal of a pollutant from a gas stream by an arrester or a cleaning device.

As low as reasonably achievable (ALARA) A standard for controlling and reducing worker exposure to pollutants.

Asbestos A natural fibrous form of several silicate minerals of the following types.

- Chrysotile (white)
- Amosite (brown)
- Crocidolite (blue)

Each of the above forms has different OEL requirements.

Asbestosis A disease caused by the inhalation of asbestos fibers.

Ash The nonvolatile inorganic residue left when a fuel is fully combusted.

Aspect ratio The ratio of the length of a grill or duct to the breadth.

Asphyxiant Simple asphyxiants are inert gases which deplete the oxygen supply in the breathing air to below the critical value of 18% by volume, such as gaseous fuels or nitrogen. Chemical asphyxiants, such as carbon monoxide and hydrogen cyanide, have a direct biological effect.

Assigned protection factor (APF) The minimum level of respiratory protection that a respirator can be expected to provide, assuming it is properly fitted, worn, and functioning. APFs are assigned by NIOSH.

Assmann psychrometer An apparatus which uses a clockwork or electrical fan located above wet and dry bulb thermometers, positioned in a cylinder to provide a set airflow rate over the thermometer bulbs for accurate temperature readings of both bulbs.

Asthma A diseased condition of the lungs caused by pollution and other factors.

Atmosphere The gaseous envelope of air that surrounds the earth, held together by gravitational attraction. It consists of 79.1% nitrogen and 20.9% oxygen by volume, with approximately 0.03% CO_2, traces of the noble gases (argon, krypton, xenon, neon, and helium), water vapor, organic matter, ammonia, ozone, various salts, and suspended solid particulates.

Atmospheric dust concentration The dust burden present in atmospheric air measured in mg m^{-3}.

Atmospheric dust spot efficiency A test to measure the extent to which a filter paper is soiled after dust-laden air has passed through it.

Atmospheric pressure The pressure due to the air column above sea level at 45° latitude at 0 °C is 101.325 kPa.

Atmospheric stability The state of the atmosphere in which vertical air movement is restricted.

Atom The smallest particle of an element that retains the characteristics of the element.

Atomic Absorption An analytical method in which the sample is converted into a vapor by passing it through a flame or other energy source and the absorbance at a particular wavelength is measured and compared with that of a reference substance. The absorbance measured is proportional to the concentration of that substance in the sample.

Atomic number The number of protons in the nucleus of an atom of an element. Also, the number of electrons in a neutral atom of the element.

Atomic weight The relative atomic mass of a substance.

Atomization The process by which a solid or liquid is reduced to very small particles or droplets, as in a fine spray.

Attenuation The reduction of sound or radiant energy.

Attenuator A unit fitted in air-handling or other noise-producing equipment to absorb sound.

Audiogram The report produced by an audiometry test, showing measured hearing threshold levels at frequencies of 500, 1000, 2000, 3000, 4000, and 6000 Hz.

Audiometry The assessment of damage to a person's hearing.

Automatic control system A control system that reacts to a change or imbalance of a variable. It controls the imbalance by adjusting other variables to restore the system to the set control condition.

Auxiliary fuel firing Combustion of an auxiliary fuel to provide additional heat to an incinerator in order to either dry or ignite the waste material and to maintain ignition, to ensure complete combustion of solids, liquids, and gases in the incinerator.

Averaging time The time period over which the measuring procedure provides a single value.

Avogadro's Hypothesis States that Equal volumes of different gases at the same pressure and temperature contain the same number of molecules. Hence, the volume occupied by any gas whose mass is numerically equal to its molecular weight is a constant quantity.

Axial-flow fan A fan positioned in a cylindrical casing in which the air enters and leaves the impeller in a direction parallel to the casing axis. The fan may have fixed-pitch blades or variable-pitch blades.

B

Bacharach smoke scale A scale of 10 shades of white to black for a smoke stain formed in a prescribed manner by a pumping action through a filter paper, used for the assessment of smoke from combustion appliances.

Back corona (back ionization) The discharge phenomenon that takes place from a particulate layer in an electrostatic precipitator.

Backdraft dampers Dampers installed in a system to prevent reversed flow of gases.

Backdrafting The action of extracted air or the products of combustion returning to a space due to adverse high pressures at the point of extraction.

Background level The concentration of a particular substance present in the air without any local source of the pollutant, or the concentration of the pollutant at some distance from its source.

Bacteria The collective name for cellular microorganisms.

Bacteria Count The count of bacteria collected on a slide within a duct run or in a space.

Bad air Air that contains any form of contamination.

Baffle A device fitted in equipment or ductwork runs that changes the flow direction.

Baffle chamber A chamber consisting of baffles (slats) which present an obstruction to the flow of dust-laden air. These obstructions slow down the heavy particulate matter, which then settles by gravity into an adjacent hopper.

Bag house An enclosure containing a series of frame-mounted bag filters and a hopper collection unit.

Balanced design method A method of duct sizing to ensure the correct airflow rate in all branches, also known as the static pressure balancing method.

Balancing The process of obtaining the design airflow in hoods and ductwork by the use of static pressure balancing or blast gates. In the case of a liquid it is achieved by means of balancing valves.

Bar The unit of pressure equal to 100 kPa, approximately one atmosphere. It is not strictly an SI unit due to its magnitude being 10^2 not 10^3 as is required.

Barograph An instrument for recording atmospheric pressure.

Barometer An instrument used to measure the barometric pressure at a given location in the earth's atmosphere.

Basal metabolic rate The rate of oxygen consumption by a person at rest.

Basic thermal insulation of a garment The thermal resistance provided by a given item of clothing.

Battery, heat exchange coil A device used to either heat or cool air in a duct run.

Bauxite lung See Shaver's disease.

Beaufort scale The scale used for estimating and reporting wind forces, in which 0 is calm (velocity less than 0.5 m s^{-1}) and 12 is a hurricane.

Bed depth The depth of adsorbent material through which the gas being treated passes.

BEI See Biological exposure index.

Bend A duct or pipe fitting which changes the direction of flow through a specified angle.

Benign Not associated with negative health effects, self-limiting.

Bernoulli effect At any point in a conduit through which a liquid is flowing, the sum of pressure energy, potential energy, and kinetic energy is constant.

Bias A consistent deviation from the true value in the results of a measurement.

Bifurcated fan An axial flow fan that directs the airstream around the motor, which is enclosed in a protective casing. It is used for handling corrosive, high-temperature, and explosive dusts, vapors and gases.

Bimetal thermometer A thermometer that uses two dissimilar bars of metals (with different rates of linear thermal expansion) riveted together. A variation in temperature produces a bending moment on the bar, which is magnified by a lever to record temperature on a dial.

Bio-aerosol A general term relating to airborne viruses, bacteria, pollen, and fungus spores.

Bioclean classes The various standards of contaminant control to which clean rooms are held.

Biofiltration The process by which gaseous pollutants are removed from a gas stream by aerobic digestion.

Biological agent Any of a range of microorganisms which have an adverse effect on human health, including those genetically modified cell cultures and endoparasites.

Biological exposure index (BEI) Reference values developed by ACGHI as guidelines for the evaluation of potential health hazards.

Biological half-life The time required for one-half of the material accumulated in a tissue to be removed.

Bioprocess The facility necessary in a biotechnology clean room to protect the worker, the product, and the environment.

Biosafety The safety requirements necessary in biotechnology clean rooms, fume cupboards, stores, etc.

Black body A hypothetical body that has an absorptance and an emissivity of unity, i.e., it absorbs all the radiation falling on it.

Blackness test A filter test for air or the products of combustion, in which a dust spot is formed on filter paper, the degree of reflection is determined by a light meter, and the result is related to a standard.

Blade shape Relating to the shape of a fan blade, either airfoil, solid, radial, forward-curved and backward-curved.

Blank-corrected Data that have had trace contamination amounts (detected in a nonexposed sample) deducted from the total amount of contaminant detected in the sampling media.

Blast gates Adjustable sliding gates (dampers) on extract ductwork used to balance the system.

Blender An enclosure in which two different fluid streams are mixed.

Blower A device producing air movement.

Blow-out panels Safety panels provided to some process, such as an oven, that will protect the structure in case of an explosion by releasing the force of the explosion.

Blow-through unit An air-handling unit downstream of the supply fan.

Body core temperature increase The increase in body core temperature that takes place due to the inability of the body to get rid of heat.

Body heat gain or loss The positive or negative change in the heat content of the human body caused by an imbalance between heat production and heat loss.

Body heat storage The heat stored in the body due to metabolism.

Body height The standing height of a human body, H_b, in m.

Body mass The mass of the unclothed human body in kg, which is a measure of its inertia, or resistance to any alteration in its motion. The mass of a given body is the same anywhere on the earth or in space.

Body mass loss, gross The reduction in body mass over a given period of time, Δm_g, in kg.

Body mass loss, respiration The loss of body mass due to respiratory evaporation, in kg.

Body mass loss, sweat The body mass loss due to sweating, Δm_{sw}, in kg.

Body mass variation for solids The variation in body mass due to food intake and subsequent excretion, Δm_{sol}, in kg.

Body mass variation for water The body mass variation due to intake of water and excretion of urine, Δm_{wat}, in kg.

Body surface area The total surface area of the human body, determined from the Du Bois Index.

Body surface area covered by clothing The percentage of the body surface area covered by clothing.

Body temperature The temperature of a human body, either the body core temperature, the mean temperature of the body, or the temperature at some point on the skin. Also, the temperature of a surface which is radiating, conducting, or convecting heat.

Body thermal sensation The response of the body to changes in the thermal environment, relating to moisture, air movement, or temperature.

Boiling point The temperature at which the vapor pressure of a liquid is equal to the external pressure, and the liquid changes phase into the vapor state.

Boundary conditions The actual environmental conditions within a controlled zone.

Boundary layer A layer of fluid, extending from the boundary into the bulk of the fluid, in which fluid motion is influenced by the frictional drag at the boundary.

Boundary layer insulation The thermal resistance at the boundary of the skin or clothing, I_a, in Clo $m^2 W^{-1}$.

Bourdon gauge A pressure gauge in which the sensing element is constructed from a coiled flattened tube closed at one end.

Boyle's law See Laws of perfect gases.

Bracket A support for any item of equipment either on the main building structure or on another item of equipment.

Branch duct entry The position at which a branch duct enters the main duct run.

Breakthrough A condition that exists when the backup section of a sorbent tube is found to contain 20–25 percent of the total amount of contaminant captured in the front section.

Breakthrough time In the context of chemical protective clothing, the time between initial contact of the chemical on the barrier material surface and the analytical detection of the chemical on the other side of the material.

Breathing zone The space around an operator in which breathing occurs, normally taken as being a hemisphere of radius 0.3 m circumscribing the ears, the top of the head and the larynx.

Breathing zone sample The sample of a contaminant or contaminants collected in the working operator's breathing zone.

BRI See Building-related illness.

Bronchi The larger air passages of the lungs (bronchus, singular).

Bronchioles The very small airways of the lungs that terminate in the alveoli.

Bronchitis Inflammation of the lining of the bronchi, which may be caused infection or by the effect of pollution.

Bronchogenic carcinoma A lung cancer associated with asbestos exposure.

Brownian diffusion (Brownian motion) The diffusion of particles due to the erratic random movement of microscopic particles in a disperse phase, such as smoke particles in air.

Bubble plate A plate or cap used in absorption equipment.

Buffer zone The zone of clean air in a room adjacent to a clean room; an air lock.

Building automation system Sometimes called building management system, a system that controls the mechanical

and electrical (M&E) services within a building.

Building related illness (BRI) Any health problem related to poor air quality, due to equipment malfunction or contaminants in buildings. See also Sick building syndrome (SBS).

Building Services All of the mechanical, air, water, electrical, and transport services required to provide satisfactory environmental conditions within a building, with due consideration of the health and safety of the occupants and energy conservation.

Bulging or caving of a duct The maximum deflection that occurs in the sides of a duct due to negative (caving) or positive (bulging) pressure differences. The reference plane is that existing with no pressure difference.

Bulk density Apparent density of bulk solids, kg m^{-3}.

Buoyancy The upward force exerted on any object immersed in a fluid of greater density. Hot pollutant gases rising in cooler air have positive buoyancy. A volume of gas denser than the surrounding air has negative buoyancy.

Buoyancy effect See Buoyancy.

Butt connection The interface between two pieces of metal that are joined together by welding.

Butterfly damper or valve See Dampers and Valve.

Bypass The provision for a secondary flow path from the main flow in duct or pipe flow.

Bypass damper A damper positioned in the airstream which allows a given quantity of air to be diverted to another run or rejected to outdoors.

Bypass factor The ratio of the secondary flow to the sum of the main flow and secondary flow.

Byssinosis Reactive airway disease associated with inhalation of organic textile fibers, such as cotton, flax, linen, and hemp.

C

Ca A notation used by NIOSH to indicate that a substance is considered a known or potential occupational carcinogen.

Calibration The adjustment of a measuring instrument to ensure that it is giving the correct readings.

Calm A meteorological term describing a wind speed of less than 0.5 m s^{-1}.

Calorific value The measure of the heating capacity of a fuel, usually expressed as the available heat resulting from the complete combustion of that fuel in kJ kg^{-1} or kJ m^{-3}. Gross calorific value includes the heat of condensation of the water vapor in a hydrogen fuel; net calorific value excludes this.

Canopy hoods A capture hood located above a process, designed to provide a suitable capture velocity to ensure the safe removal of the contaminant produced by the process.

Capacity The actual duty of a fan, heater battery, filter, or other item of equipment.

Capacity, total lung (TLC) The volume of gas contained in the lungs at full inhalation.

Capacity, vital The maximum gas volume that can be expired from the lungs following maximum inhalation.

Capture velocity The air velocity necessary at a point in order to capture and transport to the exhaust opening the contaminants being emitted from a process.

Carbon dioxide (CO_2) The gas formed by complete combustion of carbon-containing substances. Also a product of the metabolic process.

Carbon dioxide production The quantity of carbon dioxide exhaled from the human body, depends on the metabolic rate.

Carbon monoxide (CO) A colorless odorless gas formed by incomplete combustion. Highly toxic if allowed to accumulate in the blood.

Carboxyhemoglobin A molecule formed by the combination of carbon monoxide and hemoglobin.

Carcinogen Any substance that has been shown to cause cancer in animals or humans.

Carnot cycle The cycle of a perfect heat engine, in which the heat is and rejected at constant temperature and the whole cycle is perfectly reversible.

Carnot principle States that no engine can be more efficient than a reversible engine when both operate between the same temperature limits.

Carrier gas An inert gas that moves the sample through the column of a gas chromatograph.

Cartridge filters Filters normally consisting of nonwoven V-pleated filter paper made into flat panels or cylindrical cartridges.

Cascade impactor An instrument used to sample and separate particulates into a number of successive fractions of different sizes.

Casing An external cover of any plant item, covering the whole of the item or part of it.

Catalyst A substance used to speed up a chemical reaction, including the transformation of certain pollutants present in a combustion process.

Catalytic combustor A device used to remove various solid, liquid, or gaseous pollutants from air or another gas, in which the gas is heated by an open burner to between 250 and 500 °C and passed through a catalyst bed in which the organic contaminants are oxidized into harmless by-products.

Catalytic oxidizer Used to promote oxidization of a combustible pollutant.

Ceiling exposure limit The maximum allowed concentration of a contaminant to which a worker may be exposed, set by legislation.

Celsius A temperature scale that sets the freezing point of pure water at atmospheric pressure at 0 °C and the boiling point of pure water at atmospheric pressure at 100 °C.

Cenosphere Small, hollow, spherical ash particles formed from the combustion of liquid or solid fuels.

Central chambered system A combination of components in a dedicated chamber.

Central nervous system (CNS) The system of the body composed of the brain and spinal cord, which controls important body functions.

Central station A central ventilation or air-conditioning unit that provides treated air to various zones within a building.

Centrally recirculated Exhaust air from one or more treated spaces that is reintroduced through a central unit before air treatment occurs.

Centrifugal A driving force that causes a body to move in a circular path, for example, a centrifugal fan, centrifugal separator, or centrifugal pump.

Centrifugal collectors Separators for the removal of particulate matter from gas streams, classified as

- Straight-through cyclones with fixed impellers,
- Straight-through cyclones with moving impellers,
- Scroll collectors,
- Induced-draft fans combined with collectors,
- Reversed-flow cyclones, or
- Multiple cyclones.

See also Cyclone.

Centrifugal fan See Fan.

Chain of custody Documentation necessary to trace sample possession from the time of collection throughout the time of analysis.

Chamber A gas- or dust-tight enclosure.

Chambering Components contained in a chamber erected on-site.

Charcoal cloths A filter manufactured from pretreated woven cellulose fiber cloth.

Charged particles Particles that have a positive or negative electrical charge. The nature of this charge effects the collection of the particles in a precipitator.

Charles' law See Laws of perfect gases.

Chemical agent Any chemical element or compound.

Chemical asphyxiant A substance that interferes with the absorption or utilization of oxygen in the body, e.g., carbon monoxide.

Chemisorption An adsorption process in which the solute chemically reacts with the adsorbent to form a new compound.

Chilled water Water that is cooler than ambient temperature, obtained from a refrigeration plant, cooling tower, or a well.

Chiller A heat exchanger in which heat is removed from the warmer water or air.

Chilling temperature See Temperature, chilling.

Chimney A free-standing or built-in structure used to remove the products of combustion from a process or to provide natural ventilation.

Chimney effect See Stack effect.

Chlorinated hydrocarbons Hydrocarbons in which some or all of the hydrogen atoms are replaced by chlorine.

Chlorofluorocarbons (CFCs) Aliphatic carbon compounds containing both chlorine and fluorine atoms.

Chromatography A method of analysis using separation of mixtures based on selective adsorption.

Chronic exposure Long-term repeated exposure to low levels of pollutants, which may cause damage to the health of occupants.

Chrysotile One of the types of fibrous mineral asbestos.

Chute A device used for removing waste material or charging a furnace.

Cilia Fine hairlike structures found in the membranes that line the respiratory tract that assist in particulate removal.

Circulating fan See Fan.

Circulation time The time necessary for complete mixing of a tracer gas in a space.

Class I–III Cabinets Containment cabinets used for various requirements. In a high-risk area, a Class III cabinet would be used. Class I and II cabinets are used in low-risk areas.

Classes for clean rooms Many national standards are in use for the classification of clean rooms. It is recommended that the standard of the country in which they are to be installed be referred to.

Clean in place (CIP) A system used in clean rooms, consisting of tanks, piping, pumps, and associated controls for the distribution of wash and rinse solutions.

Clean-out door A door in an item of equipment or ductwork that provides access to the inside of the unit for cleaning purposes.

Clean room A room in which the environmental conditions of air purity, temperature, moisture content and air movement are maintained to high and accurate standards.

Clean tunnel A tunnel providing access of operators or production components from one clean area to another.

Clean zone Any area, such as a clean room, in which set standards of air purity and other environmental conditions are maintained.

Cleaning system A system or device that cleans a fluid or solid medium to a given standard.

Clearance samples Samples taken following a lead, asbestos, or other removal action, which must indicate the contaminant concentration to be at or below a specific level before the area can be cleared for normal occupation and work activities.

Cleat A device used to connect two or more items together.

Clo The SI unit of insulation value of clothing; 1 Clo = 0.155 m^2 K W^{-1}. The term tog may be seen in the literature

but tog is not an SI unit and should not be used.

Closed face sampling Sampling performed through a small hole in the top of a filter cassette.

Closed system The primary containment of a process in a biotechnology clean room.

Cloth-filter collectors A mechanical method of filtration of particulate matter from a gas stream by the use of a number of cloth bags. Its operation is similar to a vacuum cleaner method of removal.

Clothing area factor The ratio f_{cl} of the surface area of a clothed body to the surface area of a nude body.

Clothing insulation The resistance of a uniform layer of clothing covering the entire body that has the same effect as the actual clothing worn on the sensible heat flow under still-air conditions, I_{cl}, in Clo m^2 °C W^{-1}.

Clothing insulation, effective The increased body insulation due to clothing, compared to the nude state, the difference between the total insulation and the boundary layer insulation, I_{cle} in Clo m^2 °C W^{-1}.

Clothing insulation, minimum requirements The minimum clothing insulation required to maintain body thermal equilibrium at a subnormal level of mean temperature, $IREQ_{min}$, in Clo m^2 °C W^{-1}. This represents the highest admissible body cooling in occupational work.

Clothing insulation, neutral requirements The thermal insulation of clothing necessary to provide conditions of thermal neutrality $IREQ_{neutral}$ in Clo m^2 °C W^{-1}. It represents the state of no or absolute minimum cooling of the body.

Clothing insulation, required The required clothing insulation to ensure a given body thermal balance.

Clothing insulation, resultant The true level of thermal insulation provided by clothing under given conditions, I_{clr}, in Clo m^2 °C W^{-1}.

Clothing surface temperature The actual mean surface temperature of clothing.

Clouds A mass of droplets of water or other liquids remaining at a more or less constant height. Clouds are usually formed by condensation after warm moist air rises by convection into cooler regions and cools by expansion to below its dew point.

Coagulation The process of particulates sticking together on coming into contact. As the process continues, the particle size distribution becomes coarser and settles out.

Coalescence The merging of small drops of a liquid into a larger droplet.

Coanda effect When a jet becomes and remains attached to a surface due to static pressure differences, as in the case of a wall jet.

Coarse solid particles Any solid particle larger than 50 μm, and solid particles contained in or on any liquid particle.

Coated/treated filters Filters that have been coated with a chemical specific for the contaminant to be collected. The coatings enhance the collection by chemically reacting with the contaminant as the air is drawn through the filter.

Cochlea A snail-shaped fluid-filled organ of the inner ear, lined on its inner surface with specialized hair cells that convert sound pressure vibrations into nerve impulses.

Coefficient of discharge A coefficient describing the actual discharge of a fluid jet compared to the theoretical discharge.

Coefficient of hood entry The coefficient describing the pressure drop that occurs when gases flow through a collecting hood or other enclosure.

Coefficient of velocity The coefficient describing the actual velocity of a jet, compared to the theoretical value.

Cohort A group of individuals that share a particular statistical or demographic characteristic, e.g., exposure.

Coincident error An error due to the presence of more than one particle in the measurement volume of an optical particle counter.

Cold-generated DOP A cold-generated aerosol dioctylphthalate (DOP) test, used to measure the efficiencies of high-efficiency filters. A hot DOP test may also be used.

Cold stress Physiological stress on the body created by excessive loss of body heat.

Collar A connecting piece used to connect two components of duct or pipe.

Collecting surface area The actual surface area of a filter on which particulate matter is collected, normally greater than the filter face area.

Collection efficiency The efficiency of a collection process, expressed as a percent of theoretical (100%) collection.

Collectors Any device used to collect particulate matter, preventing it from entering the environment.

Combined section of air-handling plant A section of equipment that consists of two or more items of equipment necessary for its operation.

Combustion The chemical process that occurs when a given combination of fuel and oxygen is heated to a given temperature at which the combustible matter burns, with an increase in temperature.

Combustion air The air quantity that has to be supplied to a combustion process to ensure complete combustion. The air quantity may be either theoretical or excess.

Comfort conditions The environmental conditions in a space that will ensure statistically the majority of occupants are comfortable. Relates to thermal, acoustic, and visual conditions.

Comfort indices Relating to the many comfort scales, either empirical or calculated, that are in common use.

Comfort ventilation The minimum amount of air that must be provided to a worker to ensure

- Relative air velocity for comfort,
- Body heat removal, and
- Removal of body odor and cigarette smoke, etc.

Comfytest A measuring instrument used to predict thermal comfort in a space.

Commissioning The process of setting to work an HVAC system in order to meet the operating design requirements.

Compensating control The process of automatically adjusting the control point of a controller to compensate for changes in a second measured variable.

Component Any functional element of an HVAC system. See also Air diffusion and Air distribution.

Components of ventilating or air conditioning A single functional element forming a part of a ventilation or air conditioning system.

Compound hood An extraction hood that has two or more points of appreciable entry loss.

Compressed air Air at a pressure greater than the atmospheric pressure at that location. In the case of a fan, if the outlet pressure exceeds 30 kPa it is classified as a turbo compressor.

Computational fluid dynamics (CFD) The technique of using computers to provide an assessment of the flow of air and other fluids.

Concentration The amount of a substance present in a given volume of a gas or liquid, in parts per million (ppm) or $\mu g\ m^{-3}$. In the case of gases, the ppm is proportional to the molecular concentration, hence the relationship between ppm and $\mu g\ m^{-3}$ depends on the molecular weight of the gas concerned.

Condensate The liquid formed from condensation of a vapor generally on a cool surface.

Condensation Formation of a liquid from a gas, as when its temperature is lowered at constant pressure.

Conductive hearing loss Hearing loss that is caused by blockage or other interference in the path by which sound energy is transferred to the inner ear.

Conductive heat exchange Heat flow that takes place by thermal conduction between two surfaces in contact or along or across a solid body due to temperature difference, in W m^{-2}.

Confined space As defined by OSHA, any space that is large enough for an employee to enter and perform work that has limited or restricted means for entry or exit and is not designed for human occupancy.

Connector Any device that joins two or more components together.

Consensus standards Existing standards that are voluntarily being followed by industry, typically containing the minimum requirements for materials, procedures, and applications.

Constant dryness or constant quality lines Lines on a steam, gas, or psychrometric chart passing through all the "state points" of equal dryness fraction.

Constant volume lines Lines on a steam or psychrometric chart passing through the "state points" representing an equal volume of steam or air (dry or wet).

Containment The process of ensuring that all contaminants are contained in a room or cabinet.

Contaminant The same as pollutant, but usually used to describe indoor conditions.

Contamination Any unwanted material, such as radioactive material, present in a location. Also refers to loose radioactive materials that can be easily removed from surfaces.

Continuity relation The mass flow rate in unit time is the product of the density multiplied by the volume flow in unit time.

Continuous-flow mode The mode of air supply in which a regulated amount of air is supplied to the face-piece at all times.

Continuous sampling The uninterrupted sampling of air or pollutant from a space at a fixed rate.

Contra-rotating fan See Fan.

Contraction The size reduction of a duct allowing it to fit into tight spaces.

Control A manual or automatic device allowing the regulation of pressure, temperature, and moisture content of volume flow of a system.

Control agent The medium in which the manipulated variable exists. In a steam process, the control agent is steam and the manipulated agent is the flow of steam.

Control device A manual, mechanical, pneumatic, or electrical device that controls any component, e.g., fan, thermostat, etc.

Control point The actual value of the controlled variable (set point plus or minus offset).

Controlled medium The medium in which the controlled variable exists. In controlling space temperature the controlled variable is the space temperature and the controlled medium is the air in the space.

Controlled variable The quantity or condition that is measured and adjusted.

Controller Any device that senses changes in the controlled variable and provides the corrective output.

Convection The mechanism of heat transfer due to different temperatures, and hence different densities in fluids. It may be natural, dependent only on thermal forces, or forced, when use is made of a rotodynamic device to improve the rate of heat exchange.

Convective appliance A room-mounted device that transfers hot or cold air into the space mainly by convection.

Convective heat exchange The heat interchange by convection between the clothing surface or skin and the surrounding environment, C, in W m^{-2}.

Convective heat exchange coefficient A complicated factor involving the surface ge-

ometry, fluid velocity, and the various fluid properties. Its magnitude governs the rate of heat exchange.

Convective heat exchange, globe The convective heat exchange that takes place between the surface of a globe thermometer and the surrounding air, C_g, in W m^{-2}.

Convective heat exchange, respiratory The heat exchange that takes place by convection in the respiratory tract, C_{res}, in W m^{-2}.

Conveying system A system of ductwork used to convey powder, dust, or granular material from the point of generation to a collection chamber.

Cooker hood A device to collect cooking fumes from above a kitchen range and discharge them to the outside. It may incorporate a grease filter, fan, and fire damper or non-return flow damper.

Cooler See Chiller.

Cooling The removal of sensible or latent heat from a medium by means of a chiller.

Cooling coil A heat exchanger (battery) in which the chilling of a fluid occurs by means of a heat-transfer medium.

Cooling, direct A cooling system in which the medium to be cooled is not affected by another medium situated between it and the refrigerating apparatus.

Cooling effect Heat removed by a refrigerating appliance or heat exchanger.

Cooling, indirect A cooling system in which the medium to be cooled is affected by another medium situated between it and the refrigerating apparatus.

Cooling load The quantity of heat to be removed from a process or a space in order to meet the plant design or environmental conditions.

Cooling load, latent The quantity of heat to be extracted from a medium, without temperature change, in order to produce a given mass of fluid or condensate from the vapor.

Cooling load, sensible The quantity of heat to be removed from a fluid stream to maintain a desired fluid temperature.

Cooling tower A packed tower in which a warm liquid is allowed to fall by gravity, cooling it to within 1 °C of the wet bulb temperature of the entering air.

Cooling water Water used as the cooling medium in refrigerating plant condensers. It may be from a well or river or recooled.

Core area of air terminal device That part of an air terminal device located within a convex closed surface of the minimum area required to include all of the air terminal device openings inside the surface.

Core area of sand trap louver The product of minimum height h and minimum width b of the front opening in the sand trap louver assembly with the louver blades removed.

Core temperature The deep core temperature of a living body resulting from metabolism.

Corona The luminous discharge that appears at the surfaces of a conductor in an electrostatic precipitator due to air ionization.

Corrected effective temperature An empirical comfort index that uses the dry bulb, wet bulb, and globe temperatures and the relative air velocity in a space.

Corrective action A control action that provides a change in the manipulated variable.

Corrosion The process of a material being destroyed by chemical, electrochemical, or microbiological action.

COSHH (Control of Substances Hazardous to Health) UK legislation regulating toxic dusts, vapors, and gases.

Cotton filter cloths Woven cotton cloth stretched on a frame to produce a filter medium.

Counting rate The number of counting events per unit time.

Cowl A roof-mounted device designed to provide airflow out of a building with the minimum of flow reversal.

Crackage Cracks in the building structure through which infiltration or exfiltration

can occur by means of wind forces or temperature and pressure differences.

Criteria Set values used to establish guidelines for air or water quality standards.

Criterion level The 8-hour TWA limit for noise exposure, used for determining the noise dose.

Critical pressure The pressure at which the gas starts to liquefy at its critical temperature.

Critical temperature The temperature above which a given gas cannot be liquefied, regardless of the pressure.

Crocidolite See Asbestos.

Cross-drafts The unwanted or wanted movement of air within a space, which may be natural or mechanical. See Cross ventilation.

Cross-sectional area of a duct The area of a duct perpendicular to airflow, A_c. In the case of a circular duct,

$$A_c = \pi D^2/4 \approx 0.7854\, D^2,$$

and for a rectangular or square duct $A_c = a \cdot b$. For oval and other shapes of ductwork the appropriate equations are used.

Cross ventilation Ventilation that takes place by the circulation of air introduced at one side of the room and extracted at the other side.

Cumulative Additive.

Cumulative effect The building up of dangerous products within the body with successive or continuing exposures.

Cumulative errors Errors in a measuring process consistently in the same direction, either positive or negative.

Cumulative frequencies Accumulated sums of frequency values in a frequency distribution.

Cumulative sampling A system in which the sample is accumulated over the time, either by being taken continuously or for periods at regular intervals to a given single sample. Its composition is regarded as representative of the whole period of its accumulation.

Cunningham correction factor A factor used as a refinement to the Stokes equation for falling particles of small diameter. These tend to slip between the air molecules and, as a result, fall faster.

Cup anemometer A device used by meteorologists for the measurement of wind speed.

Curie (Ci) A unit of radioactivity, related to the emission from 1 g of radium, it is equal to 3.7×10^{10} disintegrations per gram per second. This unit has been replaced by the Becquerel (Bq); 1 Bq = 27.03 pCi.

Cuvette Small cylinder (test tube) used to hold a sample in a spectrophotometer.

Cycle The sequence of events in a heat engine, refrigerating machine, or any process where, during the performance of mechanical work, heat is supplied to and rejected from the working fluid, which is returned to its original condition.

Cycling A periodic change in the controlled variable from one value to another. If uncontrolled this is known as hunting.

Cyclone A device for the removal of particulate matter from gas streams by centrifugal force and a velocity reduction. There are three main patterns of operation

a. Descending spiral flow.
b. Ascending spiral flow.
c. Radial inward flow.

Cyclones may be subdivided into

- Dry dynamic precipitator,
- Gravity,
- High efficiency,
- Inertial separation, and
- Wet centrifugal.

See also Centrifugal collectors.

D

Daily noise dose (DND) The allowable noise exposure for an 8-hour workday.

Dalton's law of partial pressure States that the total pressure of a gas mixture is equal to the sum of the pressures which each component gas would exert if it occupied the same space alone.

Dampers Devices fitted in ductwork to provide a flow resistance to control the air supply. Dampers may be

- Butterfly: A plate which turns on a diametrical axis inside a duct, or a pair of flaps hinged to a common spindle to allow flow in one direction only.
- Plate (single blade): A hinged flap that, by virtue of its position relative to airflow, creates a flow variation. This simplest form of damper, only used on small duct sizes, does not provide accurate control.
- Horizontally-opposed: A multileaf damper in which adjacent blades rotate in opposite directions.
- Iris: A circular damper with moving leaves that forms a variable orifice.
- Parallel-blade: A damper that allows a gas to flow, in which the blades rotate in the same direction.

Damper control fan See Fan control methods.

Damper section A section of HVAC equipment containing a damper or valve.

Data Information collected in a given test.

Data acquisition The identification and collection of information relating to the performance of a particular piece of equipment.

DC pressurization A test of the air-tightness of a building in which a fan is used to pressurize the building to a uniform static pressure. The pressure differential between indoors and outdoors is measured to determine the air-tightness of the building structure.

DCV See Demand controlled ventilation.

Dead band A range of the controlled variable in which no corrective action is taken.

Decay The spontaneous disintegration of an unstable atomic nucleus to form another more stable element or isotope of a lower atomic mass.

Decay method The time from the liberation of a given concentration of a tracer gas into a space before its concentration decreases to a set value in the air.

Decay rate The rate at which the concentration of an air pollutant decreases with time, due to absorption or precipitation.

Decipol A unit derived in an attempt to quantify odor concentration by the perception of odor.

Decontamination factor A logarithmic scale used to measure the collection efficiency of a particulate collection device.

Decontamination index The logarithm to the base 10 of the decontamination factor.

DDC Direct digital control. See Digital control.

Deflection of a duct The largest deformation of a duct subjected to an imposed load, given as the measured difference in distance between a plane through the points of support and a plane through the lowest point of the duct under a load.

Deflection of a joint The largest deformation of a joint subjected to a positive or negative pressure, given by the measured difference in distance from a reference plane outside the joint to the joint with and without pressure.

Degasser A packed tower through which a fluid to be degassed flows. Air is forced through the fluid stream, stripping the gas from the liquid.

Degree-days Temperature data recorded over a 24-hour period as deviation from a certain base temperature used to determine the operating costs of a heating or air conditioning system depending on the external climatic conditions.

Degree of enclosure The actual protection offered by an enclosure in the containment of a generated contaminant.

Dehumidification The removal of water vapor from a gas.

Dehumidification load The mass of water vapor to be removed from a space or a process in order to meet design conditions.

Demand-controlled ventilation (DCV) A ventilation system in which the room airflow rate is governed by an automatic control that depends on the level of a given pollutant within the space. A typical example is allowing the CO_2 in a space to reach a certain level before the extract fans come into operation. However, in many industrial environments other pollutants control fan operation.

Demand mode The mode of air supply in which inhalation creates a negative pressure inside the face-piece, causing the regulator to release air into the face-piece. Respirators that operate in this mode are not recommended and have been largely replaced by respirators operated in the pressure-demand mode, in which the face-piece is maintained under a slight positive pressure at all times.

Demand ventilation A system that is capable of supplying varying amounts of fresh air in response to either manual or automatic control. See Demand controlled ventilation (DCV).

Density The measure of the amount of mass in a unit volume. The density of a gas is a function of its pressure and temperature. It can be determined by using the ideal gas laws.

Density Factor A factor used to correct the density of standard air or other gases for altitude, temperature, or moisture content.

Deposit gauge A collection device that records the deposition rate of solid or liquid particulate matter from the air.

Deposition Relating to either the dry or wet deposition of a particulate.

- Dry: The interception and retention by surfaces of gases or particulate matter by diffusion, gravitational settling, or thermal forces.
- Wet: The process of gas or particulate interception by sprays.

Depressurization A fan test used to determine the rate of air leakage from a building by creating a negative static pressure.

Depth loading The deposition of particles mainly within the filter interstices, rather than on the filter surface.

Desiccator A sealed container containing a water-absorbing substance such as silica gel or calcium chloride used to dry test materials in the laboratory.

Design standards The appropriate industrial, national, or international standards covering

- Air
- Air filters
- Clean rooms
- Comfort
- Contamination levels
- Fans
- Health
- Noise and vibration
- Pharmaceutical

Desorption The removal of adsorbed materials from a solid sorbent by the use of a solvent or the application of heat.

Desulfurization The removal of sulfur from flue or other sulfur–containing gases.

Detector tube A direct method for identifying airborne contaminants, also known as length-of-stain tube. It is a convenient tool for detecting and quantifying contaminants in field or emergency situations.

Determinant A chemical metabolic product of the change in the body's chemistry caused by exposure to a pollutant. The level of determinant is measured in a biological sample collected from the exposed worker, and compared to the biological exposure index (BEI).

Determination The analytical measurement of a pollutant.

Detoxification The process of decomposition of toxic substances in the body to produce harmless substances, which are duly eliminated from the body.

Deviation Difference between a set point and the controlled variable in a control device at any instant.

Dew point The temperature at which a particular gas starts to condense on a cool surface.

Dew point, acid The temperature at which acid vapor in a gas stream condenses out of the flow onto a cold surface or in a cold gas stream.

Dew point depression The difference in temperature between the wet and dry bulb readings.

Differential pressure The difference in pressure between two locations in a fluid.

Diffuser A device of variable cross-sectional area used to spread airflow into a space.

Diffusion The mixing of substances by molecular motion to equalize a concentration gradient. Applicable to gases, fine aerosols and vapors. (See Brownian diffusion.)

Diffusion effect The capture of particles due to Brownian motion.

Diffusion of particles The transfer of small particles and gas molecules into the surrounding air due to concentration difference.

Diffusiophoresis See Stephan flow.

Digital control A control loop in which a microprocessor-based controller directly controls equipment by means of sensors. Its operation depends on a series of on-off pulses arranged to convey information.

Dilution The reduction in concentration of a solute by the addition of solvent.

Dilution equations Mathematical equations that allow the determination of the decay rate of a pollutant in a space due to mechanical or natural ventilation.

Dilution ventilation or general exhaust ventilation A mixed airflow designed to dilute the contaminants within a space to required safe concentration limits. The air is extracted from the space as a whole rather than from the zone of pollution generation.

Direct-fired heater A heat generator that allows the combustion products to be mixed with the air to be heated.

Direct flame incineration A fume control device in which organic pollutants in the waste gas stream are oxidized to form nonpolluting by-products.

Direct interception Particle removal from a gas stream by a filter with geometry such that the particulate matter does not deviate from the fluid flow lines.

Direct reading A sampling approach that provides immediate or very fast feedback such as a meter or colorimetric method.

Directivity The characteristic associated with sound energy in the form of waves moving in a straight line from the source.

Discharge or entry loss of a louver The reduction in airflow caused by a louver. The discharge loss coefficient is equal to the actual airflow rate divided by the theoretical airflow rate at given pressure difference across the louver. If tested with the airflow in the reverse direction, the coefficient becomes the entry loss coefficient.

Discharge coefficient A dimensionless number describing the energy loss that occurs when a fluid is discharged from an orifice.

Discharge stack A stack that conveys combustion products or other pollutants from a space directly to outdoors. The pollutants may be removed before the remaining gas is allowed to discharge into the atmosphere.

Discharge system A system that discharges unwanted gaseous, solid, or liquid products.

Dispersion The manner in which a pollutant spreads from its point of generation, becoming diluted with distance from the source.

Dispersoid The particles involved in the act of dispersion.

Displacement air diffusion Air diffusion where the mixing of supply air and room air external to the air terminal device is at a minimum. See also Air diffusion and Air terminal devices.

Displacement flow, actual Actual flow pattern in an enclosure, resulting in uniform air distribution with virtually no mixing.

Displacement flow, ideal Ideal flow pattern in an enclosure, in which uniform air diffusion is provided without mixing.

Displacement ventilation Room ventilation created by room air displacement, by introducing air at a low level in a space at a lower temperature than the room air.

Disposal The action involved in the disposal of waste matter.

Distance to the v isovel (displacement air) The maximum horizontal distance L from the center of an air terminal device to the rectangle circumscribing the specific isovel. It is independent of the distance from the floor.

Distribution The act of conveying a medium from one point to another.

Distribution ducting The supply or extract air ductwork, which conveys air from the plant room to the conditioned space and vice versa.

DND See Daily noise dose.

Door and inspection panel Sealed openings in air-handling plant and ductwork providing access for cleaning or maintenance.

Door air leakage The leakage due to pressure differences through the crack around a door.

DOP (Dioctylphthalate) Generated particles of this chemical are used in filter efficiency tests.

Dose

a. The level or amount of exposure to a hazardous chemical or physical agent.
b. The level or amount of a chemical or ionizing radiation that has been absorbed, usually expressed as amount per weight of the exposed organism, e.g., mg kg^{-1}.

Dose rate The amount of a pollutant taken or received by an individual per unit of time.

Dose-response relationship The toxicological concept that the toxicity of a substance depends not only on its toxic properties, but also on the amount of exposure or dose.

Downdraft A natural or mechanical downward airstream, either that may, due to its temperature and/or velocity, cause thermal discomfort. In the case of a stack discharge, the term downwash may be used for the downward air current in the lee of the chimney that takes the smoke and other emissions below the emission discharge level causing ground-level pollution.

Downdraft hood A hood positioned under a process that receives gases, vapors or dusts from the source above.

Downstream Relating to a position after a filter has treated a gas, or some distance away from a measuring device.

Downwash See Downdraft.

Draft An airstream within an occupied zone that causes thermal discomfort of the occupants due to its temperature and/or velocity. Also, the thermal uplift caused by density differences required to provide adequate air both for the combustion process and the removal of the products of combustion.

Draft proofing The process of filling in air gaps around a structure to reduce the rate of air interchange.

Draft risk (DR) The percentage of people dissatisfied by a particular combination of air movement and temperature.

Draft risk rating The percentage of people predicted to be dissatisfied due to draft.

Drag anemometer An instrument used for the measurement of wind velocity by measuring the drag forces.

Drag coefficient The coefficient relating to the influence of drag over a surface in either laminar or turbulent flow.

Drain plug or cock A removable plug or valve that allows water, condensate, or other liquids to be drained from a system.

Drift velocity The velocity of the air as it drifts from a high-pressure zone to a low-pressure zone in a building.

Drop of jet The vertical distance between the lowest horizontal plane tangent to a specified isovel and the center of the core of an air jet.

Droplet A very small particle of a liquid suspended in a gas stream.

Dry bulb temperature See under Temperature.

Dry heat loss The sensible heat loss from the body that takes place by raising the temperature of the air around it.

Dry scrubber An absorption system which uses a dry solvent directly injected into the gas stream.

Drying The process of fluid removal from a medium, either by heat or vacuum.

Drying oven An oven or stove used for the drying of a product.

Drying time The time necessary under given ambient or artificial conditions to remove a required amount of water or solvent from a manufactured product.

Dryness fraction of wet steam The mass of pure saturated steam contained in unit mass of wet steam.

Dual-circuit heat exchanger Combined air heater and air cooler battery, with independent pipework or ductwork circuits for the heating and cooling media.

Dual duct unit An air terminal unit assembly consisting of two-ducted air inlets and a means of automatically adjusting the mixing ratio of the two air streams.

Du Bois area The total body surface area of a person,

$$A_{Du} = 0.203\ W^{0.425}\ H^{0.725}$$

See Area, body surface.

Duct A conduit to distribute supply air or to extract air from a space, or a boxed run in which pipework or electrical cables are carried.

Duct board A rigid board of insulation material with one or both sides faced with a finishing material. The outer face is normally a vapor barrier and air barrier.

Duct branch Used to subdivide the flow from one or more ducts into two or more ducts, or, conversely, to unite the flow from two or more ducts into one duct (T pieces, Y pieces, cross pieces, etc.) It may or may not include diverting elements. Note: Rigid components of ductwork allow sound and vibration transmission; the fixing of flexible sleeves on branches reduces the magnitude of this transmission.

Duct connection component Items intended to facilitate the joining of two components of ductwork, including

- Collars,
- Flanges,
- Connectors,
- Cleats, and
- Slip joints.

Duct design The process of sizing ductwork to ensure the optimum performance in initial costs, running costs, and the distribution of air in a duct distribution system. The design techniques may be

- Constant pressure drop,
- Constant velocity, or
- Static regain.

Duct fitting Component of ductwork incorporating a change in one or several of the following:

- The length of the duct.
- The orientation of the duct.
- The shape of the straight length of the duct.
- The area of the cross-section of the duct.
- The direction of the duct, e.g., bend, elbow, or tee.

Transformation affects a change of area and/or the form of the cross-section. If the transformation is continuous, then an area reduction is termed convergent and an area increase is termed divergent. If the transformation is abrupt, then an area reduction is termed an abrupt contraction and an area increase is termed an abrupt enlargement.

Duct sealing Measures taken to ensure that the air distribution system has an airtight seal.

Duct support The spacing of hangers or supports on a duct run to ensure that it is capable of self-support with any imposed load.

Duct transformation See Duct fitting.

Ducted fan See Fan.

Ductwork components Individual elements of ductwork, which are intended to be joined together at the time of installation. These components are of various types. See also Duct connection component and Duct fitting.

Duration limited exposure (DLE) The rec ommended maximum time of exposure, in h.

Dust The solid particulate matter formed by the breaking up of larger particulates by mechanical action. The particles range up to 75 μm in diameter; larger particles are classified as grit.

Dust cake The dust layer that builds up on a fabric filter, initially improving its collection efficiency.

Dust collection mechanisms The various means by which particulate matter is collected, which may be classified as

- Dynamic dry: The dust is collected under dry conditions.
- Dynamic wet: The dust stream is exposed to a liquid such as water to improve the collection efficiency.

Dust disposal The methods for safely disposing of the collected dust.

Dust explosion An explosion caused by the ignition of certain dusts allowed to exceed a given volume for volume concentration in air.

Dust fall The deposit rate of grits and dusts collected from the air in a measuring instrument.

Dust-holding capacity The weight of dust retained by a filter under specified test conditions.

Dust porosity The porosity of the dust cake, which has a direct influence on the filter pressure drop.

Dust suppression The preventive measures taken to eliminate or reduce the spread of dust generated by a process into surrounding areas.

Dwelling The portion of a building in which people live.

Dynamic pressure The pressure equivalent of a fluid velocity at a given point.

E

Ecology The interactions between living organisms and their environment.

Economic velocity The velocity at which gases or fluids are conveyed to ensure that running costs are kept at an economic minimum and that damage is not caused by erosion.

ED_{25} The dose of a toxic product which has an effect on 25% of the exposed population.

Eddy A current in a fluid that moves in a direction contrary to that of the main stream, often having a rotary motion.

Eddy diffusion The interchange of liquids, gases, or vapors that takes place in an eddy current.

Effective area, air terminal The net area determined aerodynamically from an A_k factor.

Effective drift velocity The velocity resulting from air flowing from one zone to another due to a pressure differential.

Effective length, duct The dimension that a straight duct contributes to the length of an air distribution installation.

Effective length, fitting The dimension that a duct fitting contributes to the length of an air distribution installation.

Effective mechanical power The energy spent in overcoming external mechanical forces on the body, in W, normally ignored for most activity.

Effective radiant heat flow The heat exchange by radiation between the walls of the enclosure and the human body, E_{eff}, in W m^{-2}.

Effective radiating area of a body The net effective radiating area of a body exposed to its surrounding.

Effective specific gravity The true specific gravity of an extract gas stream, as opposed to the specific gravity of the air alone.

Effective stack or Chimney height The sum of the stack height and the effective plume rise, determined for the buoyancy plume and its associated efflux velocity.

Effective temperature (ET) See Temperature, operative.

Efficiency The useful energy output of a device divided by the energy input into the system.

Efficiency average The efficiency of an item of equipment, such as a filter, boiler, or heating or cooling coil over its life cycle.

Efficiency, counting The proportion of particles in a volume or mass flow that are counted as they pass through the sensing element of an optical particle counter.

Efficiency, dust spot The capability of a filter to remove the staining portion of atmospheric dust from a gas under set test conditions, expressed as a percentage.

Efficiency, filter The ratio of the number of particles retained by a filter or other air cleaning device to the number of particles entering, expressed as a percentage.

Efficiency, fractional See Efficiency, particle size.

Efficiency, initial The efficiency determined prior to the first loading cycle in a filter test.

Efficiency integral See Efficiency, overall.

Efficiency, local The efficiency of a given point on a filter at set operating conditions.

Efficiency, minimum The minimum efficiency obtained during the performance classification of a filter.

Efficiency, overall The average efficiency of a filter or other item of equipment under set operating conditions.

Efficiency, particle size The ability of a collection device to remove particles of a specified size or size range.

Effluent Any unwanted material, such as water or exhaust gases, discharged into the environment.

Efflux velocity The discharge velocity of waste gases from the top of a stack.

Egg crate straighteners A lattice device inserted in a ductwork run to straighten the airflow vortex after a bend or other directional change.

Ejector A device used to provide a primary airstream into which the contaminated air is entrained for subsequent removal. Used when corrosive products, high temperatures, fan blockage by particulate matter, or fire or explosion risk make a fan unsuitable.

Electric control An electrical device that controls some mechanical function, such as a damper control.

Electrical properties Relating to the resistance, electrical capacity, and insulating characteristics of a conductor or electrical device.

Electromagnetic interference Interference created by rotating electrical equipment causing problems in areas such as microelectronics clean rooms.

Electronic air cleaner A device used to clean particulate matter from a gas stream, consisting of a fan and an electrostatic precipitator.

Electronic control A control system operating on low voltage, making use of solid-state components to amplify input signals from which the control functions are performed.

Electronic filter A filter incorporating an electrostatic precipitator. A fibrous filter that has its collection efficiency electrostatically enhanced.

Electrostatic The properties of electrically charged bodies, and the resulting associated electrical phenomena that occur in the immediate vicinity of these materials.

Electrostatic charging The creation of a different electrostatic charge between particulate matter and droplets. An increased efficiency in contact between the dust particle and the droplets is achieved.

Electrostatic filter See under Air filter.

Electrostatic force A field in which stationary electrically charged particles are subjected to a force of attraction or repulsion, as the result of another stationary electric charge.

Electrostatic precipitator A filtering system for the removal of particles from an air stream by giving them an electrical charge. The charged particles are attracted to plates of opposite polarity onto which they adhere. The precipitators are classified as

- Dry,
- Wet,
- Rapping,
- Low Voltage,
- Medium Voltage, or
- High Voltage.

Electrostatic shocks Electric shocks experienced by occupants due to a static discharge. Increasing the humidity and using non-static materials reduce the frequency of such events.

Element of distribution See Air distribution.

Eliminator plate A plate that mechanically separates droplets of moisture from a gas passing through it.

Elutriation The separation of particles in a fluid by gravity, which allows those with the greater falling speed settle as the fluid flows through an elutriator.

Emission The undesirable liberation of a dust, gas, or vapor from a process, either indoors or outdoors.

Emission factor A value representing the average amount of a pollutant that is emitted from a particular source in relation to the amount of product.

Emission generation The volume or mass of a pollutant liberated in unit time.

Emission limit The maximum design or statutory values of the given emission of a given pollutant in a work area.

Emission rate The rate of pollutant discharge into the surrounding atmosphere.

Emission standard The allowable quantity of a pollutant that can be discharged from a particular process. It may be expressed as

- Mass discharge over a given time period, kg h^{-1},
- Mass of pollutant per mass of processed material, g kg^{-1},
- Parts of the pollutant in a unit volume of air, ppm, or
- Mass of pollutant per unit volume of the gas in which it is discharged, mg m^{-3}.

Emissivity (ϵ) The ability of a surface to emit radiant heat transfer.

Emphysema, pulmonary The swelling and breaking down of the air sacs in the lungs. This reduces the area available for oxygen and carbon dioxide exchange within the lungs.

Enclosure A box, cupboard, or room in which a toxic process is carried out in safety.

Enclosing hood An extract hood, which partially or completely encloses the point of pollution generation.

End-of-service-life indicator (ESLI) A warning system that alerts a respirator user that the cartridge or canister is approaching the end of its usefulness.

Energy The capacity of a body for doing work. Mechanical energy may be either potential (by virtue of the body's position), or kinetic (by virtue of its motion).

Energy balance The arithmetic relationship between the energy input and output of a system.

Energy conservation Measures taken to reduce the use of energy.

Engineered control The removal or reduction of a hazard through implementation of an engineered solution, such as material substitution, process change, or installation of an exhaust ventilation system.

Enthalpy The total heat content of a gas.

Entrainment velocity The velocity in a jet stream that effectively entrains the dust or gas particles that surround it.

Entropy A function of the state of a substance related to order or disorder. The entropy increases as the substance receives heat.

Entry The breaking of the plane by any part of the body at the opening of a space that requires an entry permit.

Entry loss The loss of energy in the moving stream that takes place as a fluid enters an opening.

Environment Indoor or outdoor conditions, including pollutants, thermal conditions, moisture, noise, and light.

Environment impact statement (EIS) A document used in the United States that details the influence of proposed Federal legislation on the environment.

Environmental temperature A design value used by the CIBSE in heating and cooling calculations, equal to $0.33\ \theta_a + \theta_r$.

Epidemiology The study of the development and cause of diseases.

Epidermis The outermost skin of the body, through which some dangerous chemicals can be absorbed into the body.

Epigenetic carcinogen A substance that causes cancer through a mechanism other than interaction with the genetic material.

Equilibrium dust content The amount of dust held on a clean filter cloth, which after a period of time remains approximately constant.

Equivalent diameter of a duct The diameter d_e of a duct that will cause the same pressure drop at the same friction factor at equal flow as a given straight rectangular duct.

Equivalent diameter of a particle The diameter of a standard-density sphere whose motion would be similar to a given real particle, which may not be spherical.

Equivalent evaporation The evaporation that takes place in a boiler at or above 100 °C.

Equivalent exposure The exposure to a harmful product experienced by a worker. It is the sum of the exposure fraction of each component in a mixture.

Equivalent leakage area (ELA) The specified design pressure difference that allows a given air quantity to pass through a set orifice area.

Equivalent pressure The pressure corresponding to standard density,

$$p_e = p_a \left(\frac{1.2}{\rho_a} \right).$$

Equivalent temperature A synthetic comfort scale that takes into account the effects of dry bulb temperature, air movement, and mean radiant temperature.

Equivalent warmth An early UK thermal comfort scale devised by Bedford.

Ergonomics The science dealing with the application of information on physical and psychological characteristics to workplace design.

Erosion control The protection of the containing material, which stops the fluid flow, from gradual removal by particulates or gas bubbles.

Error An individual or cumulative mistake made in any experiment or test.

Eupatheoscope An early device used in the UK for the assessment of thermal comfort.

Evacuated container A sealed vacuum sampling container, which is opened for the collection of a given material.

Evaporation The process of conversion of a liquid to a vapor, without necessarily reaching the boiling point.

Evaporative cooling The cooling of a body by virtue of latent heat removal to the surrounding environment.

Evase An increase in the size of a ductwork section.

Excess air Air supplied to a combustion process over and above the air theoretically required for efficient combustion.

Exchange rate The doubling of sound energy for each increase of 3 dB.

Excursion limit A time-weighted average of pollutant exposure over a length of time specified by OSHA that cannot be exceeded during the working day. See Peak limit.

Exfiltration The uncontrolled leakage of air from a building, either by natural or mechanical means.

Exhausting The process of removing gases or vapors from a space or process and discharging them safely to outdoors.

Exhaust air See Air, exhaust.

Exhaust air (EHA) classification CEN/TC 156 classifies exhaust air (EHA) into four categories related to the extract air (ETA) classifications.

EHA Classification

Pollution Level	Description
EHA 1: Low pollution	ETA 1, or ETA 2 after cleaning.
EHA 2: Moderate pollution	ETA 2, or ETA 3 after cleaning.
EHA 3: High pollution	ETA 3, or ETA 4 after cleaning.
EHA 4: Very high pollution	ETA 4.

In industrial ventilation, the boundaries selected must be clearly stated for each application. See Extract air (ETA) classification.

Exhaust rate The controlled quantity of air, gases, vapors, and particulate matter that is removed from a space or process.

Exhaust ventilation The removal of polluted air from either a point source or a number of positions in a space direct to outdoors.

Expansion joint A flexible joint in a run of pipework or ductwork that allows expansion or contraction.

Experimental variance Permission granted by OSHA for the use of an alternative method of worker protection during an approved experiment to demonstrate or validate new safety and health techniques. The variance terminates upon study completion unless another type of variance is issued by OSHA.

Expired air temperature The air temperature of the breath on leaving the nose.

Explosion, dust See Dust explosion.

Explosive limits The maximum and minimum concentrations of a mixture of gas, dust, or vapor in air or another gas which will explode if ignited.

Explosiveness A measure of the liklihood of a material to explode. For example, aerosol particles provide a very large surface area, accelerating the oxidation reaction, resulting in a high explosion risk.

Exposed area The particle capture area of a filter medium free from obstructions, through which a gas flows.

Exposure The period of time an organism has been in contact with a certain concentration of a pollutant.

Exposure by inhalation The toxic exposure of the body due to breathing contaminated air.

Exposure limits Guidelines for worker exposure to physical agents and hazardous chemicals, usually expressed as an allowable time of exposure or an air concentration below which health hazards are unlikely to occur among most exposed workers.

Exterior hood A hood that is located close to but does not enclose the point of pollution generation.

External fan pressure difference The difference between the total gauge pressure at the outlet of an air handling unit and the total gauge pressure at the inlet.

External fan pressurization See DC pressurization.

External work Energy used in overcoming external mechanical forces on the

ETA Classification

Pollution Level	Description	Examples
ETA 1: Low pollution	Air of the same quality as outdoors, with respect to humidity. From rooms with pollutant sources from humans and building materials only.	Offices, storage rooms, public service places with no pollution sources, including smoking.
ETA 2: Moderate pollution	Air from occupied spaces that have impurities in addition to ETA 1.	Rooms with smoking, eating areas, etc.
ETA 3: High pollution	Spaces in which moisture, chemical processes, etc., substantially lower air quantity	Toilets, kitchens, garages, tunnels, car parks, solvent areas, laboratories, etc.
ETA 4: Very high pollution	Air containing impurities and odors detrimental to health in concentrations higher than regulations permit.	Industrial process areas, laboratories, etc.

body, or the fraction of metabolic energy related to mechanical efficiency.

Externally mounted air terminal device A unit such as a louver that prevents the ingress of rain, snow, birds, etc., into the ductwork.

Extinguishing system A system designed to extinguish fires by means of certain chemicals, gases, or water, either manual or automatic.

Extract air (ETA) classification Treated or untreated air that is removed from a space and discharged to outdoors. CEN/TC 156 classifies extract air into four categories. (See top of page.)

See also Exhaust air (EHA) classification.

Extract duct Any duct through which air or another gas is removed from a space and expelled to outdoors.

Extract temperature differential The increase or decrease in temperature between the supply air and the extract air.

Extract terminal device The grille or other device that is positioned in the main or branch duct that extracts air from a space.

Extract ventilation The mechanical ventilation arrangement to extract polluted air away from a space, either directly or by means of ductwork.

Extractor Any fan used for the extraction of air from a space.

F

Fabric arrester The collection of particulate matter by means of a suitable fabric material.

Fabric collector A filter manufactured from various fabrics expanded on a frame or formed into a bag or sock.

Fabric filter See Fabric collector.

Face loading The weight of dust collected by a filter divided by the effective filter medium area.

Face velocity The average velocity across an opening or item of equipment, such as a hood, fume cupboard, heating or cooling coil, or filter.

Fans

Fan A rotodynamic bladed device that conveys air at a given pressure and quantity in ductwork or a space by means of mechanical energy supplied.

Fan, abrasion-resistant A fan designed to minimize abrasion of the parts by the use of suitable materials.

Fan alignment The positioning of the fan shaft and its associated pulley in a line with the driving motor shaft and pulley.

Fan-assisted balanced ventilation Supply or extract ventilation within a space designed to provide the correct ratio of supply to extract air by means of one or more fans.

Fan control method	Description
Variable speed control	Speed change may be achieved by belts, pulleys, gear box sliding couplings, or a variable-speed motor.
Damper control	A damper positioned in the fan inlet or outlet will either increase or decrease the flow resistance and result in a variation in flow rate. This may be achieved either manually or automatically.
Vane control	Fan inlet vanes alter fan performance by controlling the swirl.
Variable blade pitch control	The impeller blade angle is varied when the fan is in operation, normally only for axial flow fans.
Adjustable pitch	The blade angle can be altered.
Fixed pitch	The blade angle cannot be altered from the manufacturer's setting.

Fan-assisted exhaust ventilation Extract ventilation of a space by means of a fan, with the supply air provided by induced leakage into the building.

Fan-assisted induction terminal unit CEN/TC 156 defines these as constant flow or variable flow.

- Constant flow: An assembly within which the primary airflow rate is modulated and mixed with air induced from the surroundings by means of a fan (also known as *series type*).
- Variable flow: An assembly within which the primary airflow rate is modulated and mixed with air induced from the surroundings by means of a noncontinuous running fan that provides a variable flow in response to thermal loads (also known as *parallel type*).

Fan-assisted supply The ventilation of a space achieved by means of powered air movement components in the supply air.

Fan, conveying A fan used for the conveying of particulate matter entrained in the air stream.

Fan, corrosion-resistant A fan constructed from materials designed to withstand the corrosive properties of the gases being carried.

Fan curve A curve relating the total pressure and airflow rate for a fan.

Fan, dust A purpose-designed fan that is capable of extracting a dust-laden gas.

Fan energy The energy required by a fan in order for it to provide a given airflow rate against a set resistance.

Fan, flameproof A fan with a flameproof motor and bearings.

Fan, gas-tight A fan with a casing that will provide a set air leakage rate at a given operating pressure.

Fan, general-purpose A fan used to handle air that will not affect its working life, i.e., with no special requirements for temperature, moisture, or corrosive, abrasive, or flammable properties.

Fan, hot gas A fan capable of handling hot gases of a given temperature for a set operating time, normally designed to be installed with its motor outside the gas stream.

Fan, impeller tip diameter The maximum diameter measured over the tips of the fan blades.

Fan inlet The opening through which the air enters the fan casing, either rectangular or circular.

Fan installation

Fan laws The equations that describe the relationship between fan flow rate, pressure, density, power, size, rotation speed, and noise levels.

Fan motor systems The methods by which an electric motor drives a fan or pump system.

Fan, non-clogging A fan with an impeller designed to reduce the clogging of the material being handled.

Fan outlet The opening through which air leaves the fan, either rectangular or circular.

Fan pressure

- **Static** The fan total pressure minus the dynamic pressure corresponding to the mean air velocity at the fan outlet. The fan static pressure is the bursting or collapsing pressure on the enclosure.
- **Total** The algebraic difference between the mean total pressure at the fan outlet and the mean total pressure at the fan inlet.
- **Velocity (or dynamic)** Pressure associated with the kinetic energy in the air stream in the fan exerted in the direction of flow.

Fan section of air handling unit A unit in which one or more fans are housed.

Fan, spark-resistant A fan designed to reduce the risk of spark generation from stationary or moving parts.

Fan, special-purpose Any fan selected to overcome the shortcomings of a general-purpose fan.

Fan types Classifications of fans based on specific properties.

Fan tables Data provided by the manufacturer that describes the relationship between the volumetric output of a fan, energy requirements, and noise level for a given fan operating at different static pressures.

Fanger's comfort equations The various equations devised by Professor Fanger relating to activity, clothing, vapor pressure, mean radiant temperature, air temperature, and air velocity.

Federal standards Standards laid down by federal governments covering certain control aspects.

Female connection A circular sleeve used to join two duct or pipe components together. The male ends of the two components are inserted into the female connection.

Fiber counting A microscopic technique which is of particular relevance to asbestos, where the fibers are counted on a filter paper.

Fiberglass A filler having a glass fiber medium.

Fibrous filter Any filter consisting of a mass of fibers as opposed to a mesh.

Type	Description
Centrifugal	A fan in which air enters the impeller with an axial direction substantially parallel to the radial plane. The impeller is defined as backward curved, inclined, radial, or forward curved depending on whether the outward direction of the blade at the periphery is backward, inclined, radial, or forward relative to the direction of the rotation.
Axial flow	A fan in which the air enters and leaves the impeller axial to the fan.
Contra-rotating	An axial flow fan which has two impellers arranged in series and rotating in opposite directions.
Reversible axial flow	An axial flow fan, specially designed to rotate in either direction.
Propeller	A fan with an impeller with a small number of broad blades of uniform material and thickness designed to operate in an orifice.
Plate-mounted	An axial flow fan mounted in an orifice or spigot.
Bifurcated	A fan in which the direct drive motor is separated from the airstream, reducing corrosion rate, allowing higher operating temperatures, and reducing wear and tear on bearings.

Fick's law States that the molecular diffusion of water vapor in a gas without appreciable displacement of the gas is analogous to the conduction of heat, and is governed by a similar type of law.

FID See Flame ionization detector.

Field blanks Sample media that are exposed to the same conditions as the media use for the actual sampling but are not connected to a sampling pump. See also Laboratory blanks.

Film badge A personal dosimeter containing photographic film that is darkened by ionizing radiation, used to evaluate the degree of ionizing radiation exposure in comparison to a control film.

Filters

Filter Any medium used for the separation of solid, gaseous, or liquid contaminants from a gas or fluid stream. The collection efficiency depends on the materials used. Some types of filters are listed here.

- **Activated carbon** A canister filter containing a porous form of pure carbon, which is capable of adsorbing gases and removing odors.
- **Automatic roll** A roll filter that constantly or intermittently provides a clean portion of filter in the air stream by means of a pressure switch activating an electric motor, which winds the filter from a clean spool to a dirty spool.
- **Bag** An extended surface filter in the form of a pocket or bag. A typical example of a bag filter is a mineral fiber bag made up of three layers, in which the first layer acts as a prefilter, the second is for fine filtration, and the third prevents fiber migration from the material used.
- **Brush** An air filter constructed from a medium of intermeshing brushes.
- **Cartridge** A replaceable in-line filter.
- **Cellular** Replacement filter elements, which may be installed in a multiple, bark, or wall structure.
- **Cleanable** A filter that, having collected a given amount of particulate matter, can be removed from the filter frame, cleaned, and reused.
- **Coarse** A filter positioned before a fine filter to remove the larger particulates in order to extend the operating time of the fine filter.
- **Cylindrical** A filter contained in a cylindrical form.
- **Disposable** The opposite of a cleanable filter, which after collecting a certain dust burden is thrown away.
- **Dry cell panel** A dry filter mounted in a rigid frame. In the past these were manufactured from woven fabrics and felts; however, synthetic fibers are replacing these. They have fiber diameters of 20 μm with average spacing of 300 μm and allow air velocity in the 2 m s–1 range.
- **Electret** A type of filter that does not require a power supply, and depends on the use of a filter medium with a permanent charge. Best performance is achieved with dry air.
- **Electronic** A fibrous filter that is electrostatically enhanced.
- **Electrostatic** The filter in an electrostatic precipitator.
- **Fabric** A filte made of either woven or felted textile.
- **Final** The last filter in a system of a multiple array of filters.
- **Fine** A filter made up of fibers about 1 μm in diameter, with spacings of about 10 μm, and air velocity in the 0.02 to 0.1 m s^{-1} range.
- **HEPA** A high-efficiency particulate air filter designed to deal with particles below 1 μm with efficiencies

of 99.95 or better. Air velocities are 0.03 m s^{-1} or less.

- **Insertable** A freely removable filter fitted in a frame.
- **Louver** A filter pleated in a louver form to increase the face surface area.
- **Membrane** A filter that incorporates a membrane as the collection medium.
- **Metal** A filter constructed from metal mesh, fibers, or sintered porous metal.
- **Panel** A shallow parallel-faced filter element or cell.
- **Passive electrostatic** A mechanical filter in which the medium is electrostatically charged without the aid of a continuous external power supply.
- **Pocket** An extended-surface filter in which the medium is formed into pockets or bags through which the dust-laden gas flows. They may be supported by the air pressure or self-supporting.
- **Primary** A filter that removes airborne particles 5 μm and larger, normally supplied in panel types.
- **Roll** A roll of filter medium on a drum that advances clean new material as the filter becomes clogged that may be manually or automatically driven.
- **Second-stage** Filters for particulate matter from 0.5 to 5 μm. They have an extended face area in order to reduce the through velocity.
- **Self-cleaning** An air-cleaning device that has the ability to be mechanically or chemically cleaned.
- **Sorption** A filter that removes gaseous or vapor contaminants from a gas stream by an adsorptive or absorptive process.
- **Ultra-low-penetration air filter (ULPA)** A filter that has a penetration of less than 0.0005%, measured under CEN test conditions.
- **Viscous** Filters constructed of a metal or synthetic mesh wetted with oil to retain dust particles.

Filter, air See Air filter.

Filter class A certain range of filter performance characteristics as specified by international standards.

Filter element The supporting housing of a filter medium.

Filter insert The replacement part of a filter medium that is inserted in the filter housing.

Filter medium A material used for filtering particulate matter from gases or liquids.

Filter medium face velocity The volume flow rate divided by the effective area of the filter element.

Filter pack A filter medium uniformly folded and interleaved with spacers.

Filter section of an AHU The section of an air-handling unit that contains a filter.

Filtration The process of removing particulate or gaseous matter from a fluid stream.

Final control element Any device that changes the value of a manipulated variable, such as a damper.

Fire damper See Fire and smoke damper.

Fire point The temperature at which a liquid gives off sufficient flammable vapor to produce sustained combustion.

Fire and smoke damper A device used to isolate one area of a building from fire or smoke in another, or one part of a duct run from fire or smoke in another. The device is mechanically or electrically operated in case of fire.

Fit test A method for evaluating how well a respirator seals against the wearer's face. OSHA requires that a respirator be found to have a satisfactory fit before it can be used.

Fixed air terminal device A component that has fixed (nonadjustable) parts.

Fixed contamination A term used in the context of radiation for nonremovable contamination.

Fixed-direction grill A grill in which the discharge direction of air velocity is nonadjustable.

Fixed non-directional grill A grill in which the discharge direction may be fixed to ensure the correct discharge pattern.

Fixing accessory of an ATD Any component that provides easy fitting and removal of air terminal devices.

Flame ionization detector (FID) A nonspecific air-sampling instrument used to identify the amount of a substance by measuring the absorption of electrons resulting from its ionization as it passes through a hydrogen flame. It is generally used for detecting organic compounds, specifically hydrocarbons.

Flame-retardant Any item in a HVAC system that will slow the passage of flames, should a fire occur.

Flammable atmosphere Any atmosphere that represents a fire or explosive hazard by virtue of gases, vapors, or dusts contained in it.

Flammable limits The minimum and maximum concentrations of a gas or vapor in air which can be ignited and sustain a self-propagating flame.

Flange A connection device that allows two sections of duct or pipe to be bolted together.

Flare A device used to burn rich mixtures of combustible waste gases containing pollutants.

Flash chamber A chamber provided to allow the burning of a flammable gas in a process. In a refrigeration system, it is the separating tank between the expansion valve and the evaporator.

Flash point The lowest temperature at which a heated liquid fuel will ignite.

Flexible duct A non-rigid duct that can be bent, expanded, or compressed within set limits without fracturing its cloth, metallic, or plastic covering.

Floor temperature dissatisfaction risk The degree of dissatisfaction experienced by occupants in a space due to the floor surface temperature.

Flow The movement of a vapor, fluid, sludge, or gas in a conduit. The flow may be forced or due to gravity.

Flow coefficient The constant K used in a typical flow equation, $V = K\ (\Delta P)^n$.

Flow equalizer A component used in a conduit to reduce turbulence or eddies in the flow.

Flow exponent The exponent n of the pressure difference in the flow equation. Its value ranges from 0.5 for turbulent flow to 1.0 for laminar flow.

Flow meter A device used to measure gravimetric or volumetric flow in a conduit.

Flow rate controller An item of equipment that will control the flow rate at a fixed value for a given pressure difference.

Method of control	Description
Mechanical, constant flow rate	Self-actuating and deriving its energy from the airstream to maintain the constant flow rate function.
Mechanical, variable flow rate	Self-actuating and deriving its energy from the airstream to maintain the constant flow rate function and having facilities for resetting the required value depending on an external system.
Pneumatic or electric	Deriving the energy for maintaining the constant flow rate function from an external source. It can be either of the constant or variable type.
System-powered	Deriving its energy from the dynamic pressure in the airstream to maintain its constant flow rate function and can be either a constant or variable type.

Flow rate pressure characteristic The relationship between the flow rate and a given pressure differential.

Flow reversal The backflow that occurs when a fluid changes its flow direction due to an imposed pressure gradient.

Flue A tube through which the gases generated during the combustion process are discharged to the external environment.

Flue gas The mixture of gases produced during the combustion process.

Fluidized bed A bed of solid particles floating on air or any other gas, on which combustible matter is burnt.

Fluorescence spectroscopy Analysis in which the intensity and wavelength of the energy that is emitted from excited atoms is used to indicate the presence of certain compounds.

Fly ash Fine ash particulate matter found in flue gases.

Foam scrubber A cleaning device that uses foam as a collecting medium for particulate matter in a gas stream.

Fog A naturally occurring aerosol of water vapor containing water droplets less than 100 μm in diameter, typically 15–35 μm.

Forced draft The forcing of air by means of a fan into a closed chamber for combustion or other purposes. The pressurization of the chamber forces the air and combustion products up a stack.

Form view factor A factor which describes the effects of the relative area of two surfaces, the geometry of the surfaces in relation to each other, and the two emissivities on radiation heat exchange between the surfaces.

Foul air Air that is unsuitable for respiration.

Fractional efficiency The efficiency of a device expressed for different fractions, e.g., the efficiency of a filter for particles of different sizes.

Free area velocity The velocity in a device where the flow is not influenced by changes in section.

Free delivery The actual volume flow from a fan outlet with no imposed system pressure.

Free-falling diameter Also known as sedimentation or Stokes diameter, the diameter of a sphere with the same terminal settling velocity and density as a nonspherical or irregular particle.

Freezing point The temperature at which a liquid solidifies. The same as melting point.

Freons The trade name for the series of chlorofluorocarbons (CFCs).

Fresh air Air taken directly from the external atmosphere, on the assumption that its purity is superior to that within the space to which it is being supplied.

Freshness Relating to the sensation of air entering the nose, creating a feeling of freshness rather than stuffiness.

Free area of an ATD The area available in an air terminal device for the discharge of air, as opposed to the actual area.

Free area ratio The ratio of an actual opening to the obstructed portion of that opening.

Friction The property possessed by two bodies in contact which prevents or reduces the motion of one body relative to the other.

Friction factor Describes the relationship between the wall roughness, Reynolds number, and pressure drop per unit length of duct or pipe run.

Friction loss The pressure energy loss that takes place in duct or pipe flow. It is related to the Reynolds number, boundary layer growth, and the velocity distribution.

Frictional resistance The resistance to fluid flow resulting from the friction between the fluid and the surrounding solid surface.

Frit A porous structure that breaks an airstream entering a solution into small bubbles, maximizing the surface area of air in contact with the solution and

increasing the amount of contaminant dissolved in the airstream.

Full-face respirator A respiratory protective device that covers the entire face from hairline to under the chin.

Fully adjustable air diffuser An air diffuser that has the provision of adjusting the discharge flow direction through a wide angle.

Fuel A substance suitable for the rapid and economic supply of heat by combustion.

Fume cupboard Cupboards of various efficiency classifications in which dangerous gases, dusts, and vapors are contained.

Fumes Small solid particulate matter normally spherical in shape and ranging in size from 0.001 to 1 μm.

Fumigation The result of a pollutant being trapped under or in an inversion layer, or the process of using poisonous gases to kill insects.

Functional check A check on the performance of an item of operating equipment.

Functional measurement Relating the check on the performance of an item of equipment to the design specification.

Fungus A simple organism that contains no chlorophyll, which may consist of one cell or of many cellular filaments called hyphae. If allowed to grow in HVAC equipment it may cause allergic reactions.

G

Galvanized steel A zinc-coated steel sheet or plate with good corrosion resistance properties used for ductwork and other applications.

Gamma ray The shortest wavelength and highest energy type of all electromagnetic radiation. It originates in the nucleus of radioactive isotopes along with alpha particle, beta particle, or neutron emissions.

Garment insulation The degree of resistance to heat flow to and from the human body that a particular clothing arrangement will provide.

Gas A state of matter in which a substance completely fills the region in which it is contained, no matter how small the amount. Or any fuel in a gaseous form for use in an atmospheric or forced-draft burner.

Gas absorption The process of absorption of gases that takes place in certain solids or liquids.

Gas adsorber A device for the removal of gaseous impurities from a gas or liquid phase, two methods are in use, physical adsorption and chemisorption.

Gas chromatograph (GC) An analytical instrument with an internal tube or column that contains a solid sorbent, which allows some components of an injected sample to pass more quickly than others, separating the substances in the sample.

Gas collectors A sampling bag used to collect a sample for analysis.

Gas constant The coefficient R used in the ideal gas law, 8.3143 J mol^{-1} K^{-1}.

Gas contaminants Any matter that contaminates a pure gas or air above a given concentration level.

Gas monitoring The use of measuring or recording instruments to determine the concentration of a given gas within a space.

Gas physics The study of the various laws relating to the behavior of air or other gases.

Gas sensors Electrical or chemical devices that record the presence or level of a certain gas.

Gas scrubber A device for the removal of particulate matter from a gas stream by scrubbing the gas with a liquid.

Gaseous ion diffusion A method of charging particles in an electrostatic precipitator.

Gasket A semirigid or flexible sealing material fitted in the connection between two surfaces.

Gauge (or gage) A measuring instrument used for the determination of pressure,

flow, temperature, moisture, or the thickness of materials.

Gauge, altitude A pressure gauge which displays the force per unit area in terms of the height of a column of a named liquid required to exert that force.

Gauge, Bourdon See Bourdon gauge.

Gauge, compound A device that allows pressures below and above atmospheric pressure to be measured.

Gauge pressure The pressure of a system over and above atmospheric pressure.

Gauge pressure of a space The positive or negative pressure in a space with respect to its surroundings, due to wind or thermal forces or the relationship of supply air to extract air.

General-duty clause A clause in the OSH act that requires the employer to provide a workplace that is free from recognized hazards likely to cause death or serious physical harm.

General exhaust ventilation (GEV) See Dilution ventilation.

Geometrical standard deviation A measure of the range of particulate sizes present in a collection of particles.

Globe temperature The temperature of the surroundings (mean radiant temperature) as recorded by a black globe thermometer.

Glove box A sealed enclosure used for handling toxic products by means of long impervious gloves sealed to form part of the enclosure.

Grab sample A sample of air collected over a short time period in the workspace.

Grade efficiency See Fractional efficiency.

Gravimetric analysis The chemical analysis of materials by the separation of the constituents and their measurement by weight. This describes the gas mixture by giving the percentage by weight of each component gas. See also Volumetric analysis.

Gravitational settling The fallout of particulate matter from a gas stream due to the gravity forces being predominant over the flow velocity forces.

Gravimetric efficiency The efficiency of a dust collector to remove a given weight of particulate matter related to the total weight present in the air stream.

Gravity settling device A chamber in which a change in velocity and/or direction of a dust-laden airstream allows the dust to settle into a collection hopper.

Grease absorption efficiency The ratio by weight of the quantity of grease retained by a grease filter to a reference quantity.

Green zone A compartment of secondary containment used in the atomic energy industry.

Greenhouse effect The retention of heat by the earth and the atmosphere due to certain gases being transparent to incoming solar radiation but opaque to the longer-wave radiation back from the earth.

Grill An air terminal device with designed outlets for airflow and distribution.

Grit Particulate matter with a diameter greater than 75 μm.

Ground level concentration The pollution concentration at ground level resulting from the emission of a pollutant from a stack or other extraction point.

Grill type	Description
Adjustable	Grill intended to vary the direction or directions of the air delivered to the treated space consisting of one or more series of adjustable parallel ribs.
Fixed directional	Grill intended to diffuse the air in one or more fixed directions, consisting of one or more series of fixed parallel ribs.
Fixed non directional	Grill not intended to change the direction of air, consisting of parallel lamina ribs, perforated metal grid, wired grid, etc.

Grounding requirements All components that handle flammable gases and dusts are electrically grounded to provide a safe path for an electrostatic charge to leak away.

Guards A cover to provide occupant safety from any exposed moving parts or live electrical parts.

Guideline, air quality Any guideline that indicates the level and duration of a substance above which it is assumed that the effects produced will adversely influence animal or vegetable life.

H

Half-face respirator See Half-mask respirator.

Half-life The time required for the concentration of a pollutant to decay to half its original value.

Half-mask respirator A respiratory protective device that covers roughly half of the face, from under the chin to the bridge of the nose.

Halocarbon (HCFC) A class of refrigerants that contain fluorine, chlorine, carbon, and hydrogen.

Halogenated compound A compound that contains one or more of the elements chlorine, bromine, fluorine, or iodine as a part of its structure.

Haze The presence of particulate matter in the air, reducing visibility.

Header An element of a ductwork or pipework run which circuit branches are taken from.

Hearing threshold level (HTL) The lowest level at which a person can detect a sound or tone. Test frequencies used to establish HTLs include 500, 1000, 2000, 3000, 4000, and 6000 Hz.

Heat balance The thermal balance that occurs in a building when the heat gains equal the heat losses. Also known as balance point or break-even point.

Heat cramps Muscle cramps, usually of the legs and abdomen, caused by heavy sweating that results in an imbalance in the salts and minerals in the muscles.

Heat drop The difference between the heat contained in a working fluid at any two points in a cycle.

Heat engine A machine that enables mechanical work to be done from heat energy, usually by changes in the volume of a working fluid.

Heat exchanger A device that transfers heat from one fluid to another without allowing the fluids to come into contact with each other.

Heat exchanger, cross flow A heat exchanger in which the fluid flow direction in the shell is perpendicular to the direction of flow in the tubes.

Heat exchanger, counter flow or counter current A heat exchanger in which the flow inlet of one fluid is adjacent to the outlet of the second fluid and vice versa; the fluids flow in opposite directions.

Heat exchanger, parallel flow A heat exchanger in which the fluids enter the same end of the heat exchanger and leave at the opposite end; the fluids flow in the same direction.

Heat exchanger, pipe A heat exchanger in which the transport medium changes between gaseous and liquid states.

Heat exchanger, plate A heat exchanger in which the fluids are separated by a thin plate as opposed to a tube.

Heat exchanger, unidirectional A heat exchanger that is used to provide a heat exchange in one direction only.

Heat exhaustion The physiological condition resulting from the body suffering heat stress and loss of body fluids.

Heat island Relating to an area where the average air temperature is higher than the surroundings.

Heat load The heat input necessary to ensure that a treated space provides the internal design temperature at a given external temperature.

Heat load, latent The heat input necessary to ensure that a treated space is

maintained at given moisture content. This process is assumed to take place at a constant temperature.

Heat load, sensible The heat input necessary to bring about a temperature change.

Heat loss, dry The heat exchange that takes place from the human body to the surroundings by convection, radiation, and conduction but not by evaporation.

Heat output The useful heat output from a heat generator or a heat exchanger.

Heat pump A "reversed" heat engine or refrigerator that takes in heat from a body at low temperature and by the expenditure of mechanical work rejects heat to a body at a higher temperature.

Heat rash A rash that appears as small red spots on hot, moist skin. The spots are inflamed sweat glands.

Heat recovery The process of collecting waste heat from a gas or liquid and utilizing it for space heating or a process.

Heat recovery section of an AHU The part of an AHU in which a sensible or latent heat gain or loss takes place by means of a heat-transfer medium.

Heat removal luminaire A light fitting provided with an extract duct from which the heat generated within the fitting, and a portion of that generated in the space, is extracted either directly to outside or for recirculation.

Heat, specific The amount of heat required to raise the temperature of a unit mass of a substance one Kelvin.

Heat storage, body The amount of heat that can be stored in a body due to its temperature, mass, and specific heat capacity.

Heat stress index An index devised by Belding and Hatch to determine the effect of extreme heat stress.

Heat stroke A serious acute condition caused by the elevation of the body temperature above the danger level. Symptoms can include redness of the face, reduced sweating, erratic behavior, confusion, dizziness, collapse, or unconsciousness.

Heat syncope Fainting that occurs in some people after standing for a long period of time.

Heat transfer coefficient A proportionality factor used in an equation for determining the rate of heat transfer.

Heating The process by which sensible heat is added to one medium from another.

Heating capacity The capacity of a heat emitter, heat generator, or heat exchanger.

Heating coil A heat exchange coil (battery) containing the primary heat transfer fluid positioned in a run of ductwork where it passes its heat to the secondary fluid.

Heating, direct Any heating system that does not have a heat-transfer medium, e.g., an electric fire or a gas fire.

Heating, indirect A heating system that makes use of a heat-transfer medium to convey heat from the heat generator to a heat emitter.

Heating water Water in a heat exchanger used for space and process heating. It can be low, medium or high temperature, from 30 °C to 160 °C.

Heavy metal A general term relating to a specific group of metals, which as suspended and deposited particulates can contaminate the environment.

HEG See Homogenous exposure group.

Height allowance A percentage added to heat loss calculations to compensate for the vertical temperature gradient.

Hemoglobin The protein in red blood cells that binds with and transports oxygen.

Henry's law States that the mass of a gas dissolved in a definite volume of liquid at constant temperature is proportional to the partial pressure of the gas.

HEPA (high-efficiency particulate air) filters Also known as absolute filters, the large collection filter surface area provides a high collection efficiency for particulate matter.

Hertz (Hz) The frequency with which sound pressure changes. One oscillation per second is equal to one Hertz.

High potential hazard The health, fire, or explosion risk resulting from the presence of certain materials in excess of a certain limit.

High-volume sampler A device used for extracting particulates from the air for analysis that requires a shorter sampling period than a low-volume sampler.

Histogram A diagram of the frequency of occurrences of values of a variable, grouped according to value in a number of separate ranges.

Hit and miss damper or valve A damper or valve consisting of two or more slotted slides operating in parallel.

Homogeneous exposure group A population or group of workers with similar exposure.

Hood A device that is located over a working area to collect any emissions generated at the source.

Hood, capturing A hood that has a sufficient flow rate to ensure that most contaminants are drawn into the hood.

Hood entry loss The pressure drop (energy loss) that occurs due to turbulence at the entrance to the extraction system.

Hood, receiving A hood intended to receive generated contaminants at some distance from the source.

Hood static pressure The negative static pressure available at a hood.

Hopper A collection bin for the supply or disposal of powdered or granular material

Hot air column A rising column of low-density air inside or outside a building.

Hot film anemometer An instrument for the measurement of fluid velocity similar to the hot wire anemometer, but more robust as it consists of a thin quartz rod covered with a film of platinum rather than a wire.

Hot grid anemometer An instrument for the measurement of fluid velocity similar to the hot wire anemometer, but with the heating and sensing elements are separated.

Hot wire anemometer An instrument for the measurement of fluid velocity by measuring the resistance of a fine platinum or nichrome wire, which may or may not be shielded by a silica tube. The wire resistance is proportional to the temperature and the fluid flow rate.

Hot wire microphone anemometer An instrument for the measurement of fluid flow.

Housing A device or enclosure that contains any item of HVAC equipment.

HTL See Hearing threshold level.

Human factors A term sometimes used synonymously with ergonomics, it may also refer to psychological and sociological aspects of ergonomic issues.

Humid air Air that is high in moisture content at a given temperature.

Humidification The process of adding moisture to air by spinning disk, ultrasonic, steam, direct water injection, or other methods.

Humidification efficiency The ratio of the actual mass of water evaporated by a humidifier to the theoretical mass of water needed to achieve saturation at a given temperature.

Humidification load The mass of water that must be added to the airsteam in order to ensure that the design conditions are met.

Humidifier fever An illness caused by the growth of microorganisms in air cooling coils. These microorganisms or their generated toxins may be carried in the airstream to the conditioned space, causing an allergic response in susceptible people.

Humidifier section of an AHU The part of an AHU in which water vapor is added to the air.

Humidistat A measuring and control device used to control the humidity of a space.

Humidity The water vapor content present in atmospheric air.

Humidity, absolute The actual mass of water vapor present in a unit mass of air.

Humidity ratio The ratio of the mass of water vapor present in air to the mass of dry air.

Humidity ratio, saturation The humidity ratio of a gas at saturation.

Humidity ratio, expired air The mass ratio of water vapor to dry air in expired air.

Humidity, relative The ratio of the mole fraction of water vapor in moist air to the mole fraction of water vapor in saturated air at the same temperature and pressure.

Humidity, specific The mass of water vapor per unit mass of dry air.

HVAC The heating, ventilation and air conditioning system that circulates and delivers filtered, humidified or dehumidified, and cooled or warmed air to the interior of a building.

Hybrid (mixed mode) ventilation A system that makes use of a mix of natural and mechanical ventilation. May be further subdivided into seasonal hybrid, e.g., natural ventilation in summer and mechanical ventilation in winter or spatial hybrid, e.g., mechanical ventilation in core areas and natural ventilation at the perimeter.

Hydraulic efficiency The ratio of the actual head to the ideal head.

Hydrocarbons Chemical compounds containing only hydrogen and carbon.

Hydrogen sulfide A highly toxic gas with the characteristic smell of rotten eggs.

Hydrograph An instrument that measures and records relative humidity.

Hydrophobic Water-resistant or having a lack of affinity for water, usually said of a substance or material that does not absorb moisture.

Hydrostatic pressure The pressure at a point of a fluid at rest, due to the weight of the fluid above.

Hygrometer An instrument used for measuring the moisture content of the air.

Hygroscopic The ability of a material to absorb moisture.

Hyperbolic expansion The expansion of a fluid according to the law $pV = c$.

Hypothalamus The temperature control center at the base of the brain, which regulates body temperature.

Hypothermia The physiological state resulting when the deep core body temperature drops below 35 °C. It results in vasoconstriction and shivering in an attempt to conserve body heat.

Hypoxia A condition characterized by a deficiency of oxygen reaching the tissue.

Hz See Hertz.

I

IAQ See Indoor air quality.

Ideal gas A gas that obeys the ideal gas law.

Ideal gas law This relates to the properties of a gas and can be represented in the form $pv = nRT$.

IDLH See Immediately dangerous to life and health.

Ignition source A source that is of a high enough temperature or has enough energy in a spark to cause the ignition of a gas or a material being conveyed.

Immediately dangerous to life and health (IDLH) A condition that poses a threat of exposure to airborne contamination likely to cause death or immediate or delayed permanent adverse health effects, or that prevents escape.

Immission The rate at which a receptor of pollution encounters a pollutant.

Impact damage Damage caused to lungs, surfaces of ductwork, or fans by particulate matter.

Impaction Collection mechanism where the contaminants collide with the surface of the filter by inertia, interception, or Brownian diffusion.

Impactor A general term for instruments that sample particles in the air by allowing them to impact on a retaining plate.

Impactor, cascade An instrument consisting of stages for producing successively increasing air velocities for collecting particles by size range.

Impeller tip diameter (fan or pump) The maximum diameter measured over the tips of the blades of the impeller.

Impingement The collision of a dust particle upon a surface, leaving the particle on, e.g., a filter fiber.

Impinger A sample collector that resembles a graduated cylinder with a long tube fitted into a stopper. The inlet tube extends nearly to the bottom of the outer tube, which holds the solution. The sampling pump is connected so that negative pressure is created inside the impinger, drawing air through the inlet tube into the solution, allowing the air to bubble up through the solution.

Implementation plan A plan that makes practical provision to ensure that set environmental standards are met.

Impulse noise Noise of short duration, i.e., three seconds or less. Also called impact noise.

Incineration The process of burning solid, liquid, or gaseous combustible wastes, leaving a sterile residue containing little or no combustible matter.

Inclined manometer A manometer in which the vertical movement of the liquid column is amplified by inclination of the U-shaped reading tube.

Index number A number that is used to indicate general trends in a quantity.

Indoor air (IOA) classification Categories defined by CEN 156 to classify the quality of indoor air.

Category	Description
IDA 1	Excellent air quality
IDA 2	Typical air quality
IDA 3	Low but acceptable air quality

Indoor air is also classified based on CO_2 concentration.

Classification	CO_2 (ppm)	Percentage dissatisfied (%)
IDA-C1	800	15
IDA-C2	1000	20
IDA-C3	1500	30

Indoor air quality can be controlled using several methods.

Classification	Description
No control	A constantly running system
Simple control	A system that only runs at the dictate of a sensor, such as an infrared sensor detecting movement
Direct control	A system controlled by a sensor that detects levels of indoor contaminants within the space

Indoor air quality The actual quality of air within a space compared with a given sample or standard, related to temperature, moisture, biological content, and contaminant levels.

Indoor climate The actual temperature, moisture content, and air velocity within a space.

Indoor pollution Pollution inside a building due to internally generated pollutants as well as external pollutants entering the building.

Induced air The quantity of secondary air entrained into a primary airstream.

Induced air temperature See Temperature.

Induced draft Air drawn through a fuel bed, a furnace, or a space by means of a fan situated beyond the item.

Induced leakage Leakage into an enclosure to equalize a pressure difference due to natural or mechanical ventilation.

Induction The process by which secondary air is entrained into the primary jet air. The mixing process is due to the momentum forces in the primary air jet.

Induction effect See Induction.

Induction ratio The ratio of entrained air to primary air.

Induction supply ATD An air terminal device in which the primary air from the duct induces secondary airflow from the treated space in such a way that a high rate of mixing between the air from these two sources takes place within the device.

Induction terminal unit An air terminal assembly which by virtue of the configuration of the primary air inlet(s) within the unit can induce secondary air from the surrounding atmosphere before being discharged to the treated space. The flow rate of the primary air may or may not be variable. The inlet aperture(s) for the secondary air may be fixed or adjustable by means of manual remote control.

Industrial hygiene The science and art devoted to the anticipation, recognition, evaluation, and control of those environmental factors or stresses arising from the workplace which cause sickness, impaired health and well-being, or significant discomfort and inefficiency among workers or among the citizens of the community.

Industrial hygienist A person qualified in the associated sciences dealing with the industrial environment.

Inert gas A gas that does not react with other substances under ordinary circumstances, e.g., nitrogen.

Inertia The resistance of a body to a change in its momentum or direction of motion.

Inertia bases Bases for the mounting of fans, pumps, or other rotating machines that are designed to eliminate the transfer of inertial forces to the structure.

Inertial deposition The deposition of particulate matter that occurs under the influence of an inertial force.

Inertial effects The force due to inertia equal in magnitude but opposite in direction to the accelerating force.

Inertial impaction This is the predominant mechanism used in all particle collection devices.

Inertial separator A device used for separating bodies from one another, or from a fluid in which they are contained, by virtue of inertial differences.

Infiltration The leakage of air through the imperfections in a building structure, due to thermal or wind forces.

Infiltration rate The rate at which outdoor air enters into a room through the imperfections in the building structure, expressed in air changes per hour or L s^{-1}.

Influx The rate at which a gas enters a space.

Influx velocity The velocity of a gas as it enters an opening.

Ingestion The absorption of substances into the gastrointestinal tract.

Inhalable fraction Particles with aerodynamic diameters up to 10 μm, which can enter the lungs.

Inhalation The process of breathing in, when the air enters the respiratory tract.

Inlet The opening that allows air or a contaminant into a system by either natural or mechanical forces.

Inlet bells or boxes Aerodynamically shaped inlet ducts for a fan.

Inlet vane dampers Dampers inserted in the airstream at the inlet of a fan.

Inlet vanes Specially-designed adjustable vanes inserted in the airstream entering a fan inlet to control fan performance by producing a swirl of the gas in the direction of the rotation of the impeller.

Insertion length See Overlap length.

Insertion loss, weather louver The difference in simulated rain penetration between the test specimen and the calibration plate at the same test conditions.

Inspection panels See Door and inspection panel.

In-stack filters A filter positioned in the discharge stack to remove pollutants before the waste gases are discharged to outdoors.

Installation The complete plant arrangement.

Instantaneous Relating to the measurement of a variable, it may be either a peak reading or a measure at any other time during sampling.

Instrumentation A sensor that either simply or automatically controls HVAC equipment or that records some particular function of the plant operation, such as temperature, pressure, or flow.

Insulation of clothing The resistance to sensible heat transfer provided by a clothing ensemble, reflecting the intrinsic insulation between the skin and the surface of the clothing, excluding the resistance provided by the layer of air surrounding the clothed body.

Integrated sampling Samples taken by drawing the air to be tested through the sampling medium, which is then analyzed by a laboratory to determine the amount of contaminant transferred.

Interception A special case of impingement, in which a particle is trapped on a fiber due to the effect of Van der Waals forces rather than inertia. The interception of a particle in a particle collection device occurs when the particle follows a gas streamline round a collector at a distance less than the radius of the particle.

Interferent Any undesirable component in a sample to be analyzed that will adversely influence the instrument reading.

Interim order An official statement issued by OSHA allowing an employer to continue operations under existing conditions while an application for a variance is being considered.

Intermittent sampling Any sampling process carried out for limited periods of time rather than continuously.

Internal energy The energy contained in a substance, which is its ability to do work.

Internal heating load Heat gains that occur in a space from process loads, lighting, solar gain, occupants, machines, etc.

Internal leakage The leakage that takes place into an enclosure or ductwork from outside.

Internal pressure The pressure inside a space or container, as opposed to the pressure outside.

Internal temperature The temperature inside a space, as opposed to the external temperature.

Internally induced airflow rate of an ATD Volume of air induced into the primary airflow inside the air terminal device in unit time.

Internally mounted air transfer device See Air transfer device.

Interstitial Situated between the cells of a structure or part.

Interstitial condensation Condensation that occurs within the interstices of a material when the dew point is reached.

Intoxication The general state of the body caused by the effects of a toxic substance.

Intrinsic clothing thermal efficiency Reduction of sensible heat exchange due to wearing clothes.

Intrinsically safe Instruments that can be safely operated in an explosive or corrosive atmosphere.

Intermittent duty The duty of a device when operating on a part-time basis, as opposed to continuous duty.

Inversion The condition that occurs when the lapse rate is positive, i.e., temperature rises with height at a rate greater than the adiabatic lapse rate 3 °C per 300 m. In these conditions stagnant air pollution builds up and is trapped under this layer.

Involute A geometrical curve as used in a centrifugal fan casing.

Ionization The critical voltage at which gas molecules are separated into positive and negative ions in an electrostatic precipitator.

Ionizing radiation Radiation that is capable of causing ionization to occur, either directly or indirectly through interaction with matter.

Iris damper or valve See Dampers and Valve.

Irradiance The radiant flux striking a unit area of a surface.

Irradiation The exposure to radiation of any kind.

Isentropic operation A change in conditions at constant entropy.

Isokinetic A process in which the velocity at the entrance to the sample probe in a gas stream is the same as the velocity at a given point in the duct or stack at a given time.

Isokinetic sampling The sampling of a gas such that the motion of the gas entering the sampling device is identical to that of the gas being sampled.

Isolation The process of disconnecting a supply, electricity, fuel, or air.

Isotherm A line in a flow system or on a graph connecting points of equal temperature, or a mathematical or graphical relationship between two variables at constant temperature. Or a display using lines on a drawing to show constant-temperature contour lines, as from thermal imaging with infrared techniques.

Isothermal change A process that takes place at constant temperature, such as the isothermal expansion of a gas.

Isotopes Atoms of the same element (having the same atomic number) that differ in mass number.

Isovel A line in a flow system or on a graph connecting points with constant velocity.

J

Jet A gaseous or liquid stream issuing from a slot, orifice, or nozzle.

Jet angle The angle at which a jet or array of jets diverges into a free space.

Jet, Coanda A jet attached to a surface.

Jet drop The downward change in the direction of a jet due to the difference between its velocity or temperature and that of the ambient air. Also called jet fall.

Jet, enclosed A jet that is allowed to expand within a channel or duct and then is constrained by the channel or duct walls.

Jet envelope The boundary between a jet and the surrounding air.

Jet fan See Fan functions.

Jet, free A jet which, on leaving an orifice, is allowed to expand freely without coming into contact with any surfaces.

Jet, isothermal An air jet of the same temperature as the space it is entering.

Jet, nonisothermal An air jet of a different temperature from that of the space it is entering.

Jet rise The upward change in direction of a jet due to the difference between its velocity and temperature and that of the surrounding air.

Jet spread The angle of divergence of a jet from its point of origin.

Jet, wall A jet that attaches itself to a surface. See also Coanda effect.

K

Kata cooling power The rate of cooling of a silvered or unsilvered kata thermometer due to the relationship between the air temperature and the air velocity over the bulb.

Kata thermometer A thermometer that allows the air velocity to be determined by its cooling power.

Katharometer A device that compares the thermal conductivity of two gases, used to detect the presence of impurities in air.

Kelvin effect The electrical potential gradient caused by a temperature gradient along a conducting wire. Also known as the Thomson Effect.

Kinematic coagulation The scavenging of small particles by large particles, which increases the speed of the larger particles by differential settlement, such as in rain drops or from spray nozzles.

Kinetic energy The energy a body possesses by virtue of its motion.

Kinetic theory A mathematical explanation of the behavior of gases on the assumption that gases consist of molecules in ceaseless motion in space. The molecular kinetic energy depends on the temperature of the gas.

Kirchhoff's law The relationship that exists between the absorptivity and emissivity of radiating bodies. It is the capacity of a body to absorb radiation, which varies with the wavelength of the incident radiation and the angle of incidence.

L

Laboratory blanks Sample media that is not sampled on, but is analyzed by the laboratory to detect contamination or other problems associated with preparation and analysis of the samples. See also Field blanks.

Lag A delay between a change in a condition at one point in a system and its effect.

Lambert-Beer law The mathematical description of the attenuation of a light beam by absorption and scattering by dust particles in the airstream.

Laminar flow Fluid flow in which the fluid particles move in straight lines parallel to the axis of the pipe or duct.

Land breeze The air movement that takes place after sunset, when the land cools and air currents flow from the land to the cooler sea.

Langmuir equations The mathematical expressions that describe vapor adsorption equilibria.

Lapse rate The rate of temperature increase with height.

Laser Light amplification by stimulated emission of radiation.

Laser anemometer See Laser Doppler anemometer.

Laser Doppler anemometer An instrument for determining fluid velocity by measuring the difference in frequency between the incident beam and that scattered from particles moving with the flow.

Latent heat The quantity of heat that is absorbed or released in an isothermal transformation of phase, in kJ kg^{-1} $°C^{-1}$.

Latent heat of vaporization The heat added during an isothermal change of phase from liquid to gas.

Laws of perfect gases

a. **Boyle's law** The volume of a gas is inversely proportional to its pressure, at constant temperature.
b. **Charles' law**
   a. The volume of a gas is proportional to its absolute temperature, at constant pressure.
   b. The pressure of a gas is proportional to its absolute temperature, at constant volume.
3. **Joule's law** The internal energy of a given quantity of gas depends only on its temperature and is independent of its pressure and volume.

Laws of thermodynamics

a. **First law** Heat and work are mutually convertible.
b. **Second law** Heat will not pass from a colder to a hotter body spontaneously.

LCL See Lower confidence limit.

LD_{50} (median lethal dose) A standard measure of toxicity indicating the dose of a substance that will kill 50% of a group of test organisms.

Lead dioxide candle A device for determining the amount of sulfur dioxide in the air. The SO_2 reacts with a film of lead dioxide to produce lead sulfate, which is measured to determine the concentration.

Leakage The rate of fluid loss from an enclosure due to a pressure difference between the inside and outside of the enclosure.

Leakage function The relationship of the leakage occurring in a building to

the pressure difference, measured in $m^3\ h^{-1}\ Pa^{-1}$.

Leakage path leeward Leakage of building air that takes place due to structural openings on the downwind or sheltered side of a building.

Legionella pneumophila (LD) Infections, particularly pneumonia, caused by inhaling *Legionella pneumophila* and other bacteria from the family *Legionellaceas* in water droplets drifting from cooling towers, showers, etc.

LEL See Lower explosive limit.

Length-of-stain tube See Detector tube.

LEV See Local exhaust ventilation.

Lewis relationship The ratio of the convective heat-transfer coefficient to the evaporative heat-transfer coefficient.

Lesion An injury to the body due to the intake of certain atmospheric pollutants.

LFL See Lower flammable limit.

LIDAR An instrument that uses a laser-radar to study the concentration and location of particulate matter by the reflection or absorption of a laser beam.

Life cycle The design of any combination of plant items that considers the owing and operating costs of the plant.

Life cycle assessment (LCA) An analysis defined by ISO 14040 as "compilation and evaluation of inputs and outputs and the potential environmental impacts of a production system throughout its life cycle."

Limestone scrubbing A process using a ground limestone and water mix to neutralize sulfur dioxide in waste gas products.

Limit, opening The maximum sash opening that can be allowed on a laboratory fume cupboard to ensure safe working conditions.

Limit of detection (LOD) The smallest amount of contaminant that can be reliably detected by a particular analytical method.

Limit of quantification (LOQ) The smallest amount of contaminant that can be reliably quantified using a particular analytical technique.

Limit value A reference figure giving the allowable concentration of a chemical or biological agent in the air.

Linear air diffuser An air terminal device with single or multiple slots, each of which has an aspect ratio not less than 10:1. Each slot may consist of a number of separate elements and may or may not have an adjustable member, which allows the directions of the air delivered to the treated space to be varied.

Linear grill grill with an aspect ratio not less than 10:1.

Liquefied natural gas (LNG) Natural gas cooled to −162 °C to achieve a significant volume reduction, then stored under pressure.

Liquefied petroleum gas (LPG) Paraffin hydrocarbon gases comprising propane, butane, and pentanes derived from natural gas wells and from the petroleum refining process that remain as liquids when stored under pressure in tanks and bottles.

Liquid entrainment separator Any device that removes and collects moisture present in an airstream.

Load In a ventilating or heating system, the magnitude of heat, airflow, or cooling the system must provide to meet the design conditions. The work the system must perform. The heating, ventilating, or cooling load requirement of a space or appliance.

Load, connected The sum of all the individual loads related to an HVAC system.

Load factor The ratio of the average demand to the maximum demand; may relate to electrical, heating, or cooling load.

Load pattern The load change over time.

Load utilization factor Ratio of the effective load in a given space to the load supplied.

Loading dust The selected synthetic dust used to determine the dust-holding capacity of a filter.

Local air velocity The air velocity in the zone in which the design conditions have to be met. Or, the air velocity recorded at a specific location in a space or in a jet stream.

Local exhaust ventilation (LEV) The removal of a contaminant at or near the point of its generation.

Local cooling The cooling of a given area in a space by means of chilled air jets or chilled water panels.

Local mean velocity The magnitude of the time-averaged vector of velocity at a point in an airstream.

Local response The response of an occupant or control device to changes in the local environment.

Local ventilation The transportation of air into or from a space near its point of use.

Long-term exposure limit (LTEL) An exposure limit requirement based on the assumption that the total body intake of a pollutant below this limit over an 8-hour working day will have no harmful effect on the worker over a working life. See also Maximum exposure limit (MEL), Occupational exposure limit (OEL), and Short-term exposure limit (STEL).

Louver An opening that allows air to enter or leave a space, which has inclined vanes to provide protection from the entry of rain, snow, and animals.

Low-leakage seal A seal on a fluid-handling device that ensures system leakage is at or below a given level.

Low potential hazard A concentration of pollutants within a space, which will present a very low hazard to the occupants or the plant.

Low-velocity ATD An air terminal device which is designed for thermally controlled ventilation, e.g., displacement flow applications. See also Air terminal device.

Low-volume high-velocity (LVHV) The method of local exhaust using small hoods, which exhaust contaminants from a process at velocities of 50–100 m s^{-1}.

Lower confidence limit (LCL) A statistical procedure to estimate whether the true value is lower than the measured value.

Lower explosive limit (LEL) The lowest concentration of a substance in air at ambient temperature that will explode if ignited, expressed as a percentage of the substance in the room air by volume. See also Upper explosive limit (UEL).

Lower flammable limit (LFL) The lowest concentration of a substance in air that will sustain combustion.

Lower limit of a duct The algebraic difference between the minimum limit of size and the corresponding nominal size.

Lubrication The use of oil or grease on moving parts in order to reduce the friction force.

Lung function Relating to the transfer of oxygen from air into the blood and the disposal of carbon dioxide from the blood to the air.

M

Macropores Pores of diameter greater than 0.005 mm in the structure of an adsorbent medium.

Magnehelic dial gauges A measuring device recording the static pressure of a fluid.

Make-up air Air introduced into a space to replace air that is being extracted.

Main air treatment The part of the treatment of air that, by virtue of the number of air handling functions involved or of the effect achieved, is considered the principal treatment.

Male connector A short circular sleeve to join two pieces of spiral duct together. The ends of the male connectors are inserted into the spiral tube ends.

Manifold A section in the exhaust air ductwork of an air treatment system into which exhaust air enters from a number of orifices or ducts, or a header pipe in a fluid flow system that has branches.

Manometer An instrument that measures pressure by fluid displacement in a U-shaped tube.

Manometer pressure The pressure recorded on a manometer, measured in Pa or mm water gauge.

Manual damper or valve A metal or plastic flap used to control the rate of airflow in a duct manually.

Manually adjusted ATD See Air terminal device.

Marginal irritant A material that is capable of causing an irritation response after repeated exposures.

Masking Relating to an additive introduced into the air supply in an attempt to neutralize or conceal an odor.

Masks A protective device complete with an approved filter designed to keep dangerous chemicals from being inhaled into the lungs.

Mass flow rate Mass of matter, which crosses a given surface, divided by time.

Mass spectrometer (MS) An instrument that identifies substances by causing them to be ionized and subjecting the resulting ions to a strong electromagnetic field.

Mass transfer The transfer of mass across a boundary, similar to heat transfer.

Maximum allowable concentration (MAC) An old American definition used before the term TLV came into use (the term is still used in Germany). See Threshold limit value (TLV).

Maximum body heat storage (Q_{max}) The maximum value of the body heat gain achievable by the subject such that the resulting increase in body core temperature does not induce pathological effect, in W h m^{-2}.

Maximum exposure limit (MEL) The maximum concentration of an airborne substance, averaged out over a reference period to which employees may be exposed by inhalation.

Maximum penetrating particle size The particulate size for which a filter has minimum removal efficiency under test conditions.

Maximum-risk employees Workers who are most likely to be exposed to the highest levels of hazardous agents.

Maximum use concentration (MUC) The maximum atmospheric concentration of contaminants in which a respirator cartridge or filter is recommended for use. Can be approximated by multiplying the PEL for the contaminant of concern by the assigned protection factor.

Mean, arithmetic The sum of a set of n numbers divided by n, often called the average.

Mean air temperature See Temperature.

Mean diameter The geometric mean diameter of the size range.

Mean free length The mean free length of a particle (μm) used in particle scrubbing equations.

Mean free path The average distance travelled by a particle between collisions. In a gas it is inversely proportional to the pressure.

Mean, geometric The nth root of the product of n terms.

Mean particle diameter The mean value of the particle size distribution of the test aerosol.

Mean radiant temperature The average temperature of the six surfaces of a cubicle enclosure, used in thermal comfort work and in other heat-transfer applications. It is the sum of all the surface areas multiplied by the temperature of the surface divided by the total surface area.

Mean skin temperature The average temperature of the skin exposed to a given environment.

Means, best The best practical means for preventing the escape of noxious or offensive gases, smoke, grit, and dust from a process into the atmosphere. (U.K. Alkali Regulations.)

Measured variable A variable that is measured, and may be controlled.

Measurement station Element inserted in ductwork or pipework to facilitate the determination of temperature, humidity, flow rate, and/or pressure.

Measuring procedure Procedure for sampling and analyzing one or more chemical agents in the air, including the storage and transportation of the sample to the laboratory.

Mechanical constant flow rate controller See Flow rate controller.

Mechanical diffusion Eddy diffusion caused by mechanically-produced turbulence.

Mechanical efficiency The actual work possible by a machine, related to the work put into that machine.

Mechanical variable flow rate controller See Flow rate controller.

Mechanical rapping The mechanism that vibrates electrostatic precipitators or bag filters in order to remove the dust burden.

Mechanical shakers A table that vibrates at a given frequency in order to remove particulate matter from a casting.

Mechanical turbulence Any turbulence produced by means other than natural, such as fans. The term is also used incorrectly to define wind currents set up in and around buildings.

Mechanical ventilation Ventilation created by fans or other air-moving devices within a building, which can be divided into the following classifications:

- Mechanical extract—induced inlet.
- Mechanical inlet—forced outlet.
- Mechanical inlet—mechanical outlet.

Mechanism An arrangement that allows rotary movement to be converted to linear movement or vice versa. A linkage for dampers, etc.

Media filters Filters that collect particulate matter on individual filter elements.

Median The central value of a series of observations ranked in order of magnitude.

Medical surveillance program The evaluation of an employee's health status, performed on a regular periodic basis by a health professional, to detect problems associated with exposure to health hazards, so that appropriate steps can be taken to prevent permanent or debilitating injury. Medical surveillance programs may also be used to ensure that an employee's health status will allow the continued safe use of protection equipment, or the continued safe performance of work.

Membrane A film used for collection of particulates in which the size of the microscopic pores is controlled.

Mesopores Pores of diameters from 0.00005 mm to 0.005 mm that form the internal structure of an adsorbent material.

MEL See Maximum exposure limit.

Melanoma A skin tumor containing dark pigment.

Melting point The temperature at which a solid liquefies. The same as freezing point.

Mercaptans Organic compounds containing sulfur, which have an unpleasant odor.

Mesh A metal fiber or other material formed into a woven lattice, used to strain or filter out particulate matter from a fluid or gas.

Met unit The metabolic rate of a sedentary person at rest, 1 met = 58.2 W m^{-2}.

Metabolic energy transformation Metabolic rate.

Metabolic heat production The production of body heat due to the intake of oxygen and carbohydrates.

Metabolic rate *(M)* The rate of transformation of chemical energy into heat and mechanical work by aerobic and anaerobic metabolic activities within an organism, usually expressed per unit area of the total body surface, in met or W m^{-2}.

Metabolic rate, basal *(BM)* Metabolic energy transformation calculated from measurements of heat production or oxygen consumption in an organism in a rested, awake, fasting, and thermoneutral state, in W m^{-2}.

Metabolic rate, seated (M_s) The heat liberated from a body when the occupant is seated at rest, in met or W m^{-2}.

Metal fume fever A fever suffered by workers who inhale metal fumes from a process.

Metal poisons Certain metals that cause illness or death when inhaled or ingested.

Methods of air distribution Can be classified into the following groups.

- **Crosswise** Airflow that takes place from one side of a space to the other. This may be achieved by one or more jets or by allowing the air to enter the whole of one side surface and extracting the air by the whole area of the opposite side. The latter arrangement provides a piston effect, ensuring good air and contaminant transport.
- **Downward** The supply air enters at ceiling level or high wall level and is extracted at low level. A perforated ceiling may be used to provide a piston effect. Good air mixing is achieved if cool air enters at high level at the correct temperature and velocity.
- **Mixed upward and downward** Downward supply with a small proportion of high-level extraction. The largest proportion of the extraction occurs at low level. This arrangement provides good mixing of the room air, if care is taken to ensure that short-circuiting of the high-level input and extraction does not take place.
- **Upward** Air enters the space at low level and is extracted at high level, ideally suited for warm air supply.

Microclimate The distinctive pattern of temperature, humidity, air movement, and purity within a relatively small zone either inside or outside a building.

Microclimate suit A suit worn to protect an operator who is working in adverse conditions of either heat or cold.

Micrometer (μm) The SI unit of measurement of particulate matter, equal to 1×10^{-6} meter. The non-SI term is the micron (μ).

Microorganisms Organisms that can only be seen with the aid of a microscope, such as bacteria, viruses, and some fungi.

Micropores Pores of diameter less than 0.0005 mm that form the internal structure of an adsorbent material.

Migration The movement of dust collected in a filter in the direction of flow.

Migration velocity The electrophoretic velocity of a charged particle in an electric field.

Millibar (mbar) A unit of pressure equal to 100 Pa.

Minimum air change rate The lowest possible air change rate that can be used in a space in order to attain the recommended air purity standards.

Minimum filter efficiency The value of a filter's efficiency relating to its performance classification under specified operating conditions. See also Maximum penetrating particle size.

Minimum ventilation requirements The lowest possible airflow rates that will ensure all obnoxious products are removed from the air by the introduction of fresh air.

Mist The suspension in air of small droplets of materials that are liquids at normal pressure and temperature.

Mist elimination The removal of a mist from a gas stream either by condensation or by the use of baffles.

Mitered elbows A bend in pipe or ductwork formed by a series of flat sections.

Mixed flow, actual An actual flow pattern in an enclosure resulting in the air being mixed to such an extent that conditions are almost the same at every point in the occupied zone.

Mixed flow, ideal The flow pattern in an enclosure in which the air is completely mixed and has the same conditions at every point.

Mixed air Air that contains two or more streams of air.

Mixing The process by which fluids of different density are combined naturally or by some mechanical device. One or more of the following mechanisms may produce the mixing process:

- Displacement.
- Piston flow.
- Spot (local).
- Laminar flow.
- Layering.

Mixing actuator Component designed to mix two airflows without controlling the volume.

Mixing air diffusion Air diffusion where the mixing of supply air and room air is intended.

Mixing controller Component designed to mix two airflows while controlling the volume flow.

Mixing factor A factor used in air distribution relating to the actual degree of mixing that takes place between the room air and a contaminant generated in that room.

Mixing height The height above an internal or external pollutant source within which emitted pollutants are dispersed and mixed with the surrounding atmosphere. In meteorological terms, this is the area below the inversion layer.

Mixing section of an ATD A section in which two air streams of different temperatures or moisture content are damper controlled to provide a given flow rate before mixing occurs.

Mixing section of an AHU A section where outdoor airflow and the recirculation airflow are mixed in a controlled manner.

Mixture rule A mathematical expression applying to workers simultaneously exposed to chemicals that act on the same organ or organ system. The exposure level for each chemical must remain at a fraction of the permissible exposure level (PEL) so that the sum of the fractional exposures does not exceed unity.

$$\mathrm{PEL}_{\mathrm{mix}} = \frac{C_1}{\mathrm{PEL}_1} + \frac{C_2}{\mathrm{PEL}_2} + \frac{C_n}{\mathrm{PEL}_n}$$

Model A model of a particular flow problem, which may be either

- **Mathematical** A mathematical simulation of the emission, dispersion, and chemical process relating to the concentration of pollutants.
- **Physical** A model system in which tests are carried out on the emission and dispersion of a pollutant, e.g., a wind tunnel.

Modulating The control action of minute increments and decrements of adjustment in a system, such as in automatic control valves.

Moisture content The mass of water vapor present in a unit mass of dry air.

Moisture recovery Measures taken to prevent the moisture present in the air from leaving the treated space.

Molar diagram A plot of the thermodynamic properties of a substance that has specific enthalpy as one of its coordinates.

Mold diseases Diseases produced by the concentration of mold or fungi spores within a space.

Mole The SI unit of quantity; the amount of a pure element or chemical compound that contains the same number of atoms or molecules. It is often simpler to use moles rather than volume or mass when working with gases. Moles are given by

$$n = \frac{m}{\mathrm{MM}}.$$

For example 32 kg of O_2 = 1 mole of oxygen and 16 kg of O_2 = 0.5 mole of oxygen.

Molecular diameter of air Air at atmospheric pressure is 0.00037 μm at 20 °C.

Molecular sieve Zeolites used for ion exchange in water treatment.

Monitoring The continuous or regular observation of a fixed or variable parameter.

Morbidity The incidence of disease in a community or a working group.

Multiple-leaf damper or valve An air damper or valve that has more than one damper, arranged to provide low flow loss.

N

Narcotic gases Gases that produce sleep, stupor, or insensibility when inhaled in certain concentrations.

Natural atmospheric dispersoids The American Meteorological Society classifies natural dispersoids by size:

- Haze 1.0 μm
- Mist 1–5 μm
- Cloud or fog 5–200 μm
- Drizzle 200–500 μm
- Rain 500–8000 μm

Natural circulation Circulation occurring in a fluid due to temperature changes.

Natural ventilation Ventilation achieved by means of wind forces or density differences or a combination of the two, as opposed to mechanical ventilation, which depends on a rotodynamic device.

Natural ventilation system Ventilation of a space by the influence of thermal forces and wind forces over and around a building. Under certain conditions only one of these applies, however, in the majority of cases it is assumed that both apply.

Necrosis The death of any cell tissue by the action of pollutants.

Negative pressure A pressure less than the ambient pressure, which may be created due to stack effect or by mechanical means.

Negative rated operating pressure The tested maximum negative pressure at which a duct is rated.

Nephelometer A device used to determine the suspended particulate size and concentration by the scattering of light.

Neutral clothing insulation See Clothing insulation, neutral requirements.

Neutral solution A chemical solution that is neither acidic nor alkaline.

Neutral zone The physical state within a building where no pressure difference exists between inside and outside the building. Also used in relation to the effect of a chimney in removing the products of combustion.

Nitrogen oxides A number of different compounds of nitrogen and oxygen, normally referred to as NO_x.

Noise An unwanted sound that causes annoyance or distraction.

Nominal length, flexible duct The actual length of a flexible duct after decompression in an unstressed state.

Nominal length, rigid duct The actual length of a rigid duct without fittings or components.

Nominal size of an ATD The nominal value of dimensions of the prepared opening (duct) into which the air terminal device is to be fitted. For an air diffuser, the nominal size is generally defined as the duct size into which the neck of the device is fitted.

Nominal size of a duct or fitting The reference dimension used for the designation, calculation, and application of ducts and fittings.

Nomogram A chart consisting of variables, and provided two of these are known others can be determined.

Non-overloading fan A fan with backward-curved blades, which has power characteristics that tend to flatten with increasing flow rates, so that as the maximum volume flow rate is approached the power consumed may become constant or even decrease. The

power characteristics of a fan with forward-curved blades steepens at high volume flow rates, and so such fans are overloading.

Nonspecific When an instrument responds to more than one contaminant that is known to be present in the air.

Normal temperature and pressure (NTP) See Standard temperature and pressure (STP).

Nosocusis Hearing loss resulting from causes other than noise, such as disease, heredity, etc.

Noxious A term relating to any chemical that is harmful to the occupants of the space in which it exists.

Nozzle An air terminal device used to obtain the maximum conversion of static pressure to dynamic energy with minimum entrainment.

NTP Normal temperature and pressure. See Standard temperature and pressure (STP).

Nucleation A cleaning process using a humidification and cooling cycle, causing water or another fluid to condense on sub-micrometer particles. This process increases particle size until impingement on packing is possible.

Null point The distance from a generated pollution source at which the initial energy or velocity of the contaminants is dissipated, and collection by a hood is possible.

Nuisance dusts Any dust that creates a nuisance, rather than being a health risk, such as dusts that cause sneezing, coughing, eye irritation, etc.

O

O Ring A device used to seal a shaft of a device or a pipeline that is conveying a fluid.

Obscuration The concealing from sight; lack of visibility due to dust, fumes, or smokes.

Occupied zone The volume of air confined by horizontal and vertical planes defined to include space occupied by persons.

Occupational exposure limits (OEL) The maximum time a person can work in a given polluted environment.

Occupational exposure standards (OES) U.K. standards relating to the concentration of an airborne substance that can be tolerated without harmful effects on workers over a reference period. See Long term exposure limit (LTEL) and Short term exposure limit (STEL).

Octave band frequency The band in frequency scale that is split into bands, each assigned a sound power level, that is twice the power level of the lower limit.

Odor Relating to the sense of smell, a substance that stimulates the olfactory organ, allowing us to detect if a smell is pleasant or unpleasant.

	Distance from the inner surface of the elements, m	
Element	**Typical range**	**Default value**
External windows, doors, and radiators	0.5–1.5	1.0
External and internal walls	0.25–0.75	0.5
Floor (lower boundary)	0.00–0.2	0.1
Floor (upper boundary)	1.30*–2.0**	1.8

*Mainly seated occupants

**Mainly standing occupants.

It will be appreciated that in the industrial environment, each case will have to be considered in its own rights. Except when agreed otherwise, the default values shall be applied.

Odor control The elimination of odor in a space by the use of masking chemicals or special filters.

Odor dispersion time Time taken to reduce an odor to a defined level from a given concentration in a standard test.

Odor reduction factor The efficiency of odor reduction by a medium capable of removing odors.

Odor threshold The minimum concentration of an odorous gas which 50% of a panel of trained sniffers can detect.

Off-gassing of materials The liberation of volatile organic compounds (VOC) and other gases from building products or from a manufacturing process.

Offset A sustained deviation between the control points and the set point of a proportional control system.

Oil slant gauge An inclined manometer tube using oil as the measuring fluid to record the pressure.

Olfaction The sense of smell or the act of smelling.

Online Relating to either

- The measurement of a variable in a process that is in operation, or
- A computer arrangement to process input data without delay and to present an output result.

On/off control A simple two-position control system that is only capable of performing these two functions (on and off).

Once-through scrubber system A system seldom used due to the problem of using large quantities of fresh water and the resulting discharge of a large volume of polluted water.

Opacity The degree to which a plume of exhaust gases obscures the view of an observer, measured in terms of percentage obscuration, with 100% meaning that the plume completely obscures the line of sight through the plume.

Open face Sampling with the top portion of a filter holder or cassette removed to ensure the full filter surface is exposed.

Open rotor An open air lock with open ends between the rotor blades and the blade seal.

Operating point The static pressure and volumetric airflow that a fan is capable of producing.

Operative temperature See Temperature.

Opposed-blade damper A damper in which the adjacent blades rotate in opposite directions, so that the leading edges seal against each other and the trailing edges seal against each other.

Optical anemometer An instrument for measuring gas flow rate using a laser, in which small frequency shifts are visualized as interference fringes.

Optical particle counter An optical-electronic instrument for measuring the number of airborne particles in different size ranges.

Optimum droplet size The ideal size of a water droplet in a centrifugal spray scrubber or spray tower to ensure the highest possible cleaning efficiency.

Oral temperature The temperature in the mouth recorded by a thermometer or thermocouple.

Organic Relating to or derived from living matter that has organs or an organized physical structure. Organic chemistry is the study of carbon compounds.

Organic contamination The contamination of products by organic matter, particularly in clean room applications.

Organic material A material from an organic source.

Organic solvents An organic liquid capable of dissolving an organic material or compound.

Organoleptic A material that influences a sensory organ, as in the perception of odor by the human nose.

Orifice meter See Orifice plate.

Orifice plate A metal plate with a hole of diameter smaller than the pipe or duct run in which it is fitted. The pressure drop that takes place across the plate is used to calculate the fluid velocity.

Category	Description
ODA 1	Pure air, which may be temporarily dusty (e.g., pollen).
ODA 2	Air with significant concentration of dust.
ODA 3	Air with significant concentrations of gaseous pollutants.
ODA 4	Air with significant concentrations of gaseous pollutants and dust.
ODA 5	Air with very high concentrations of gaseous pollutants or dust.

Orifice venturi A measuring device used to determine the flow rate of a fluid by means of the pressure drop across the device.

Outdoor air Air introduced into a building from a source external to the building.

Outdoor air (ODA) classification This classification covers five categories of air quality from ODA 1 to ODA 5 as shown at the top of the next page.

Outdoor pollution Natural or man-made pollution produced by sources external to a building.

Outlet An opening through which air or effluent is discharged, either by natural or mechanical means.

Outlet damper A device fitted in a duct that will allow the flow of gas to be controlled either manually or automatically.

Overall heat-transfer coefficient The heat flow per unit area for a given construction for an overall temperature difference of 1 K.

Overall uncertainty of a measuring procedure or of an instrument The quantity used to characterize the uncertainty of results given by an apparatus or a measuring procedure, expressed on a relative basis by a combination of bias and precision, according to a formula.

Overbreath In using a respirator, when the wearer's breathing rate exceeds the ability of the respirator to provide a volume of air sufficient to ensure that a positive pressure is maintained inside the face piece.

Overlap length The length by which a fitting or duct overlaps a connecting duct.

Oxidants Substances present in air, such as nitrogen dioxide, ozone, etc., that are capable of oxidizing other chemicals or elements in oxidation-reduction type chemical reactions.

Oxygen consumption The rate at which the lungs take up oxygen.

Oxygen-deficient An atmosphere consisting of less than 19.5% oxygen.

Oxygen-enriched An atmosphere containing more than 23% oxygen.

P

P4SR Predicted 4-hour sweat rate. A scale used to predict the evaporation rate from a body under hot conditions.

Package units Air-handling equipment containing all the components together in a common casing.

Packed beds An absorption separator that employs a fluidized bed of plastic spheres constrained between horizontal screens.

Packed-tower wet scrubber A gas scrubber that removes gases and vapors, by using either water or a chemical liquid method. Efficient pollutant removal depends on the contact time between the entering gas stream and the wetted surface of the pack in the tower. This type of scrubber can be classified as

a. Concurrent flow,
b. Cross-flow, or
c. Countercurrent flow.

Paddle wheel impellers A radial blade impeller on a fan, used for dust conveying due to its self-cleansing properties.

Panel fans A simple form of axial fan with its impeller mounted in a ring or diaphragm; it discharges air both axially and radially.

PAP See Photochemical air pollution.

Parallel flow Referring to the operation of two or more fans or pumps connected in parallel with each other. May also relate to a standby fan in a system.

Parameter A quantity that serves to determine a measurable or quantitative characteristic, or the variable feature of a measurement.

Partial air treatment Treatment that involves one or more of the possible methods of treatment but is not complete.

Partial enclosure An enclosure used for work with toxic dusts, gases, or vapors in which one or more of the sides may be open to the remainder of the work area.

Partial pressures See Dalton's law of partial pressures.

Partial ventilation system A local exhaust system designed to provide an airflow less than that required for all the hoods that form part of the system. The application is to provide system diversity.

Particle The nature of an aerosol or other pollutant.

Particle aerodynamic diameter The diameter of a sphere of density 1 g cm^{-3} that has the same terminal velocity due to gravitational force in still air at set conditions of temperature, pressure, and relative humidity as the particle in question.

Particle counters A manual or automatic device used to determine the particulate concentration of a given gas sample.

Particle migration velocity The velocity at which a charged particle moves in a given direction in an electric field.

Particle scrubbing A gas-cleaning device that generates large particles that can be easily collected by combining them with liquid droplets issued from fine jets.

Particle size distribution A method of relating the size or weight of particulate matter, e.g., 50% with diameters in the 0.1–1.0 μm range, 25% in the 1–5 μm range, etc.

Particulate concentration The concentration of one or more particulates in a given quantity of a gas.

Particulate matter Matter consisting of particulate liquid and solid substances ranging in size from 0.0002 μm to 500 μm in diameter.

Parts per billion (ppb) Parts of a contaminant in a billion parts of air or water. Care has to be taken in ensuring the term billion is the correct one. In the past in the UK, a billion was 10^{-12}, but in the U.S. a billion is 10^{-9}. It is now assumed that current practice relates to the latter. Other terms encountered are parts per hundred million (pphm) and parts per million (ppm).

Parts per million (ppm) The number of parts of a contaminant by volume in a million total parts. Volume ratio = −mole ratio = pressure ratio in the case of ideal gases.

Partition fan See Fan.

Passive sampling Sampling that depends on the diffusion of the contaminant into a solid sorbent.

Pathogen A material that is capable of producing disease in living organisms.

Pathology The study of the causes and results of disease.

Peak-above-ceiling exposure limit The short-term exposure peak permitted above the OSHA standard ceiling exposure level.

Peak limit A pollutant or noise level that exceeds the ceiling exposure limit, but is allowed for a specific limited time during the work shift.

Penetration The distance particles of a particular size will travel into a given filter before coming to rest.

Per capita air rate Volume intake of outdoor air per occupant.

Percentage saturation The ratio of the moisture content of moist air at a given temperature to the moisture content of saturated air at the same temperature. Also known as degree of saturation.

Perforated plate See Flow equalizer.

Performance The operating characteristics of a device, as compared with those of the original design. Or the performance of an item of plant as stated by a manufacturer.

Peripheral nervous system Nerve tissues lying outside the brain and spinal cord, functions include the transmittal of sensory information such as touch, heat, cold, and pain, and the motor impulses for limb movement.

Permeation efficiency Reduction factor for latent heat exchange through clothing.

Permissible exposure limit (PEL) The maximum exposure level allowed by OSHA, expressed as an 8-hour time-weighted average. These are legally enforceable in the U.S.

Permissible range The range of a physical quantity that satisfies the different parameters for each of the categories of the specified environment.

Permit space As defined by OSHA, a confined space that contains a hazardous atmosphere, a material that could engulf an occupant, a configuration that could trap an occupant, or any other recognized safety or health hazard.

Personal protective equipment (PPE) Devices and apparel worn by employees to prevent or reduce exposure to health and safety hazards in any adverse environment. Examples include respirators, gloves, chemical-resistant overalls, earplugs, and safety glasses.

Personal sample The result obtained from the products collected during the process of personal sampling.

Personal sampler A collection device attached to a person that obtains samples of air to be tested for radioactive, chemical, or biological agents.

Petri dish A shallow dish used to culture bacteria.

pH The unit used to relate the acidity or alkalinity of a liquid. Pure water is neutral and has a pH of 7.0, values below this denote acidity, and those above this denote alkalinity.

Phase equilibria The relationship between contaminant solubility in the gas and liquid phases at equilibrium, which must be known for absorption separator design.

Photoallergic A reaction similar to other allergic reactions of the skin.

Photochemical Relating to a chemical reaction brought about when sunlight encounters certain gaseous mixtures.

Photochemical air pollution (PAP) Pollutants such as nitrogen oxide and certain hydrocarbons that cause photochemical reactions in the air.

Photometer An analytical instrument containing a light source on one side and a light detector on the opposite side that measures the amount of light that passes through the sample.

Photophoresis Particle motion that takes place in the direction of radiation, due to the absorbed radiation warming one side of the particle more than the other.

Physical absorption The process of collecting a gas in water or another fluid.

Physical adsorption An exothermic physical process that gives off less heat than chemisorption.

Physical testing Any process involving an actual test in order to obtain results.

Physiology Study of the function of the human body.

Piezometer tube An open-ended calibrated glass or plastic tube that measures the pressure in a pipe or vessel full of a fluid.

Piping A metallic, plastic, glass, etc. enclosure, for the conveying of a fluid, vapor, or gas.

Piston effect The ideal method of air distribution, in which uniform airflow occurs over the whole of a room, such as when the air is injected into the room over the whole surface area of one wall and extracted from the opposite wall.

Pitch The spacing of holes in a flange, or the angle of fan blades. That attribute of auditory sensation depending primarily on the frequency of the sound in terms of which sounds may be ordered on a scale extending from low to high.

Pitot-static traverse The set positions of a Prandtl tube in a duct run required to provide a statistically valid set of readings. A series of measurements of the total and static pressure taken across an area of a duct to determine the air velocity at that point. The sampling distance should be at least 7.5 times the diameter of the duct away from any disturbances of air flow.

Pitot-static tube A measuring device consisting of two concentric tubes used to measure the total and static pressures in a duct run, known as a Prandtl tube.

Plane radiant temperature See Temperature.

Plaster frame See Fixing accessory of an ATD.

Plate-mounted axial flow fan See Fan types.

Plate-type design (space heaters) Type of heat exchanger characterized by a substantial proportion of its heat output being by way of radiant energy.

Plenum box A component forming an interface between ductwork and one or more air terminal devices. By virtue of its design or by the inclusion of accessories, it can also be used to equalize the pressure/velocity across air terminal devices.

Plenum chamber Any air compartment connected to one or more ducts or to a slot in an air distribution hood.

Plenum system A ventilation system that holds a space at positive pressure.

Plume Effluent discharged from a chimney or exhaust duct, composed of gases alone or gases and particulate matter. The plume shape depends on temperature difference and turbulence. The flow of visible hot gases or vapor from an outlet.

Pneumatic Any device operated by or filled with compressed air or a liquid.

Pneumatic control A control system that operates on compressed air as the operating medium for the control of valves and dampers, etc.

Pneumatic conveying The conveying of dusts, powders, or granular materials in ducts or pipes by means of a difference in air pressure.

Pneumoconiosis A lung disease experienced by miners caused by industrial dust.

Pollen Small particles of the male fertilizing seeds of plant life, which may cause various allergic reactions especially of the respiratory tract, known as hay fever.

Pollutant Any unwanted liquid, solid, or gaseous product, resulting from the activity of man. It can be further divided in the case of air into

- **Primary** A pollutant that is discharged into the ambient air.
- **Secondary** A pollutant formed in the air as a result of reactions of primary pollutants.

Polluter pays principle (PPP) The term that relates to either the industry or the individual being responsible for the cost of all pollution-control measures.

Pollution Relating to any environmental constituent present in air or water to such an extent that it presents a hazard to the present or future health of humans or any ecosystem.

Polonium chamber Any air compartment connected to two or more ducts, or a slot in an air distribution hood.

Polychlorinated biphenyls (PCBs) Highly toxic organic compounds used in the electrical industry, use of which is now restricted.

Polydisperse aerosol See Aerosol, polydisperse.

Pore diffusivity The ability of a material to diffuse gas through its pores, trapping the contaminants.

Porosity The presence of spaces within a material that can absorb gases or moisture.

Positive rated operating pressure The tested maximum positive pressure at which the duct is rated.

Potential temperature The temperature an air envelope would acquire if brought adiabatically from its initial or actual pressure to a standard pressure of 1000 mb.

Powder A substance or combination of substances in the form of fine dry particles.

ppb See Parts per billion.

Powered air-purifying respirator (PAPR) A type of air-purifying respirator that utilizes a battery-powered fan to draw contaminated air through the cartridge or filter into the facepiece.

Prandtl tube See Pitot static tube.

Precipitator, electrostatic A device for collecting particulate matter from a gas stream by using electric forces to impart a negative charge to the particulate matter in the gas stream. These charged particulates are attracted to collecting surfaces which have the opposite polarity.

Precipitation When a solid is formed from a solution, or the separation of particles from a fluid by the process of precipitation.

Precursor A substance involved in the formation of new air pollutants, i.e., a hydrocarbon is the precursor to the formation of ozone.

Precleaners A device to remove a contaminant from a liquid or gas stream before the main cleaner.

Precision The degree of agreement between independent test results obtained under the same conditions.

Predicted mean vote index (PMV) An index used to predict the mean value of thermal sensation votes of a large group of persons, expressed on a 7-point scale.

Predicted percentage dissatisfied An index that predicts the percentage of a large group of people who are likely to feel thermally dissatisfied, i.e., feel either too warm or too cold.

Prefilter A rough filter positioned before a fine filter to reduce clogging of the fine filter.

Preheat coil A heating coil in a ductwork run sized either to temper the air or to stop the filter from freezing.

Pressure The force per unit of area exerted in all directions by a gas or liquid on the walls of its container.

Pressure, atmospheric The pressure of the atmosphere as indicated by a barometer, in kPa.

Pressure blowers Variations of radial-bladed fans with narrow housings and impellers, developing pressures in excess of 25 kPa at low volumes.

Pressure burst A failure in a filter, ductwork, or an air handling unit due to high differential pressure.

Pressure depressions The differences in air pressure between zones necessary to stop contaminant drift.

Pressure drop The static pressure difference due to friction or turbulence between two locations in a ventilation system.

Pressure drop, final The value to which the filtration performance is measured in order to classify the filter

Pressure drop, final recommended The manufacture recommended operating pressure drop of a filter at rated flow conditions.

Pressure drop, initial The pressure drop obtained on a test on a clean filter.

Pressure factor The test ratio between the suction effect and air velocity passing over a cowl or roof outlet, represented by

$$-\xi = \frac{\Delta p_s}{p_d}$$

Pressure gradient The rate of change in the pressure in a fluid at any given time.

Pressure loss See Pressure drop.

Pressure maintenance Maintenance of specified (differential) pressures in spaces or pipe/duct systems.

Pressure sensor A recording or measuring device that corrects the pressure of a fluid when it varies by a given amount from its design set point.

Pressure, static The potential pressure that is exerted in all directions by a fluid at rest.

Pressure, total The algebraic sum of the velocity pressure and static pressure.

Pressure, velocity The kinetic pressure exerted in the direction of flow that is necessary to cause a fluid at rest to flow at a given velocity.

Pressure ventilation The ventilation of a space by providing air movement from a high-pressure region to a low-pressure region.

Pressure, water vapor partial The pressure that the water vapor in air would exert if it alone occupied the volume of the humid air at the same temperature, in kPa.

Pressurization The process by which a space is held at a pressure greater than the surrounding areas.

Prevailing wind direction The direction from which the wind is most frequent for a given period.

Primary air The air provided to a combustion process to ensure efficient combustion, or the air leaving an outlet, forming a jet.

Primary airflow rate The mass or volume of air entering a supply air terminal device in unit time from an upstream duct or a plenum box. Or the air leaving through an opening and entering a space.

Primary air induction system Air introduced via an air duct to the induction unit, generally in the form of treated outdoor air.

Primary air temperature See Temperature.

Primary calibration standard A calibration standard based on direct measure of a reference value.

Primary collector An air-cleaning device that removes the larger particulate matter before a HEPA filter.

Primary containment The enclosing structure around a red zone used in the atomic energy industry, which has a specific leak tightness.

Priming The carryover of particles of water or other fluid in gas flow, mainly in steam boilers.

Probability A quantitative measure having values between 0 and 1 inclusive.

Process The general term that describes a method of manufacture or control.

Process requirements The conditions, for a given process, including the boiler or cooling.

Process ventilation Ventilation provided primarily for process purposes, the requirements of the occupants being secondary.

Product recovery The recovery of the waste products from a process reducing pollution, saving energy or materials.

Promoter A chemical substance or specific set of conditions that is favorable to, or triggers the development of, cancer.

Propeller anemometer A device used for measuring airflow in which the air velocity revolves a propeller, the shaft of which is connected to a gearbox and measuring dial.

Propeller fan See Fan types.

Proportional band In a proportional controller, the control point range through which the controlled variable must pass in order to move the final control element through its full operating range.

Proportional control A control algorithm in which the final control element moves to a position proportional to the deviation of the value of the controlled variable from the set point.

Proportional integral (PI) control A control algorithm that combines the proportional response and integral response control algorithms.

Proportional integral derivative (PID) control A control algorithm that enhances the PI control algorithm by adding a component that is proportional to the rate of change of the deviation of the controlled variables.

Protective equipment, personal See Personal protective equipment (PPE).

Psychrometric chart A chart constructed so that knowing any two air properties the remaining thermodynamic properties of air at that condition can be determined.

Psychrometric coefficient The coefficient in the equation for the determination of the water vapor partial pressure from the wet bulb depression.

Psychometrics The study of the properties of moist air.

Pulse The regular beating of the blood in the main blood vessel, a pulse of electricity, the vibrating of a mechanical or electrical device.

Pulsed hot wire anemometer A device used for gas flow measurement, similar to the hot grid anemometer, in which measurement, are made by pulses of hot air at a downstream sensor.

Pump A device that moves a fluid by mechanical or electrical means. The movement being created by a pressure differential between the inlet and outlet.

Pumping The act of forcing a fluid along a conduit by overcoming frictional resistance.

Push nozzle A push jet, located either on a working surface or above a process.

Push-pull exhaust See Push-pull hood.

Push-pull hood A protecting hood around a process with the air supply on one side of the contaminant source and the extract on the other side.

PVC Polyvinyl chloride, a polymeric plastic material.

Pyrolysis The chemical decomposition of a material caused by the application of heat.

Q

Quartile If a set of observations are ranked in order of magnitude, then the quartiles are those three values which divide the observations into four equal parts, i.e., the lower quartile is that value below which one quarter of the observations lie, and the upper quartile is that value below which three quarters of the observations lie.

Quenching Heat removal from a solid by means of a fluid, either oils or water.

Quick disconnecting ducts Ductwork provided with a quick-release mechanism for disconnection providing easy access for cleaning the ductwork.

Quick-release access doors Doors located in strategic areas of a plant to allow access for maintenance or cleaning.

R

Radial Arranged like a wheel with lines (spokes) radiating from a center point.

Radial acceleration Rate of velocity change with respect to time in a radial direction.

Radial-bladed fan See Paddle wheel impellers.

Radiant cooling The cooling of a human body or other surface by means of a radiant panel.

Radiant heating The heating of a human body or other surface by means of a radiant panel.

Radiant temperature The temperature of a surface emitting heat to surrounding bodies by means of electromagnetic radiation.

Radiant temperature asymmetry The difference between the plane radiant temperature and the temperatures at the sides of an element.

Radiation Energy provided to a body by electromagnetic waves.

Radiation shape factor The angle factor representing the fraction of the angular field of view from which energy exchange is trading places.

Radiative heat exchange The heat exchange by radiation between the clothing surface, including uncovered skin, and the environment, in $W\ m^{-2}$.

Radiative heat exchange, globe The heat exchange by radiation that takes place

from a black globe thermometer, in W m^{-2}.

Radiative heat transfer coefficient The heat-transfer coefficient wholly attributed to radiative heat transfer.

Radiator A body warmer than its surroundings that emits its heat to the cooler surroundings.

Radioactive materials Elements that have unstable nuclei that spontaneously disintegrate, releasing radiation in the form of subatomic particles and energy.

Radioactivity The property of spontaneous disintegration possessed by certain unstable nucelides.

Radiometer A sensitive instrument for the measurement of heat radiation.

Radiometric forces Weak forces that cause the motion of particulate matter, including diffusiophoresis, thermophoresis, and photophoresis.

Radon A radioactive element, the heaviest of the noble gases, formed by the radioactive decay of radium.

Radon daughters The series of unstable isotopes that are formed as radon atoms undergo radioactive decay.

Rain louver or weather louver A fresh air inlet to a duct designed to reduce the ingress of driving rain.

Random particle motion See Brownian diffusion.

Range The interval defined by the largest and smallest values in a set of observations.

Range hood An extraction hood positioned above a cooking range to provide the best possible capture velocity of the fumes.

Raoult's law States that at equilibrium, the partial pressure of a solute vapor over a liquid mixture is equal to the vapor pressure of the pure solute at the given temperature times the mole fraction of the solute liquid component in the mixture.

Rapping A method used on bag or other filters to dislodge the dust cake from the fabric when the airflow resistance exceeds a certain value.

Rated airflow The flow rate specified by the manufacturer for an item of equipment.

Rating conditions A set of operating conditions over which specified performance will result.

Rating plate The plate fitted to an item of equipment showing the operating characteristics.

Raynaud's syndrome Diminished blood flow or loss of blood to the fingers, caused by vibration, also known as white or dead finger.

Reactive metal A metal that readily enters into a chemical reaction.

Receiving hood An extract hood in the immediate vicinity of a process that extracts the generated pollutants in an effective manner.

Receptor A body (e.g., a person or animal) that absorbs a pollutant from the air, which may suffer some adverse effects.

Receptor system A system which contaminants enter without inducement.

Recirculated air Exhaust air returned as supply air to the air treatment system from which it originated.

Recirculation The process of returning air to the space from which it has been removed, with or without treatment.

Recovery The collection of the products of a process for reuse.

Recycling The reuse of scrap material for pollution control and conservation purposes.

Red zone The primary air containment zone in ventilating systems in the atomic energy industry.

Re-entrainment The induction of air that has been discharged back into a jet, at a position upstream from the discharge.

Reference method A method of analysis to which other methods of analysis are compared.

Reference period A specified time period allowed for human exposure to a specific concentration of a biological agent or chemical.

Refractories A special heat-resistant heat-retaining brick used in furnaces, chimneys, and boilers.

Reflectance A measure of the extent to which a surface is capable of reflecting radiation, defined as the ratio of the intensity of reflected radiant flux to the intensity of the incident flux.

Refrigeration The controlled removal of heat from a substance.

Regenerable adsorbers See Adsorbent, regenerable.

Regenerative blowers A fan that generates pressure by centrifugal force, in which, in contrast to a centrifugal fan, the airflow is around the circumference of the impeller.

Regenerative thermal oxidizers A series of beds made from heat-resistant material which alternately store heat from the combustion chamber exhaust gases and release heat into the cooler gases entering the combustion chamber.

Register A combined grille and damper assembly.

Regression A statistical method used to investigate the dependence of one variable on one or more other variables.

Regulations Any legislation or statutes enforced by law.

Relative humidity The ratio of the partial pressure of the water vapor in moist air at a given temperature to the partial pressure of water vapor in saturated air at the same temperature.

Relative ventilation efficiency A quantity describing how the collection efficiency of a ventilation system varies between different parts of an enclosure.

Relaxation time The time necessary for a moving particle to adjust from one given steady state velocity to another, e.g., the time for a falling particle to reach its terminal velocity. It is independent of the nature of the force applied to the particle.

Rem (Röntgen equivalent man) The unit of measure of the radiation dose to the internal tissues.

Replacement The process of air entering a space to fill the void created by either natural or mechanical extraction.

Replacement air Air supplied to a space to replace the air removed by a combustion process or by natural or mechanical ventilation.

Reproducibility The extent to which any measurements taken during tests performed under the same conditions will provide statistically similar results.

Residence time The time a pollutant remains in a space after it is released.

Resistance The opposition to flow caused by friction as air passes through a ductwork or pipework system.

Resistivity A property of a material equal to the reciprocal of its conductivity.

Resistivity of dust The electrical resistivity of a dust, which is one of the factors that influences the practical efficiency of an electrostatic precipitator.

Resonant frequency The sound frequency for which a particular system provides the maximum absorption. The amount of sound absorption in a system depends on the degree of damping achieved; this depends on the mass and the associated air space.

Respirable particles Particulate matter of such a size that it can pass through the body defences and into the lungs, where, depending on its nature, it will either deposit itself or be exhaled.

Respiratory protection The use of face masks, respirators, or separate air supply to reduce the intake of pollutants into the lungs.

Response A reaction of a living organism caused by a pollutant. Also, the reaction time of a measuring instrument or control device to perform an action.

Respirable particulates Particulates in the size range that can pass through the defence mechanisms in the human body and enter the lungs during inhalation.

Resultant temperature See under Temperature.

Return air Air that has been removed from a space that is returned to the space either mechanically or naturally with or without treatment.

Reverberation The continuation and enhancement of a sound caused by rapid multiple reflections between the surrounding surfaces.

Reverberation time The time required for a sound to fall to a given level in an enclosure.

Reverse air cleaning filters Filters that become self-cleaning by dislodging the impacted dust when the gas flow is reversed.

Reverse pulse The use of jets of high-pressure air to dislodge material from the exterior of a bag filter.

Reversible heat engine A heat engine, which will convert a certain quantity of heat into an amount of work (W), that will produce the original quantity of heat if the same amount of work is expended in driving the engine backwards.

Reversible process A process that may be performed in the opposite direction to return to the initial state of the working fluid.

Reynolds number A dimensionless parameter that represents the ratio of the inertia forces to the viscous forces in a flow. Its magnitude denotes the actual flow regime, such as streamline (laminar), transitional, or turbulent.

Ringelmann chart A method for the visual comparison of smoke from a chimney. The estimation is made by the comparison of the shade of smoke against shade cards.

Riser A vertical section of duct or pipe in a distribution system.

Risk assessment The sequence of events necessary to ensure that a system is designed to provide the safest possible working arrangement.

Röntgen The amount of x-ray or gamma radiation that produces one unit of charge in 1 cc of dry air.

Roof ventilator A natural or mechanical unit positioned in the roof to provide air extraction from the space.

Room air conditioner A package air-conditioning unit for the air treatment of the space in which it is located.

Room air conditioner (self-contained) A room air conditioner complete with a direct expansion (dx) system condenser and evaporator fans, filtration, and thermostatic control.

Room air distribution system The method by which air is distributed within a space.

Rotating anemometer An instrument used to measure gas flow that depends on the rotation of vanes mounted on a spindle.

Rotation The angular displacement of a body about a specified axis in a specified direction in unit time.

Rotor The rotating portion of an electric motor; the stator is the stationary part.

Route of entry Path by which toxins and other substances may enter the human body. These include inhalation, ingestion, and absorption through the skin. Less common routes include injection and absorption through moist surfaces surrounding the eyes and ear canal.

Runaround coils The coils in a heat recovery system that collect heat from the hot waste steam and supply it to the cold incoming stream via heat exchangers.

S

Safety cabinets A protective air enclosure (workstation) used in microbiological laboratories.

Safety factor An uncertainty factor that is used in combination with the no-adverse-effect level data to estimate the safe human dose.

Safety guards Devices to protect operators from moving machine parts.

Sample badge A small clip-on device that contains solid sorbent and is used for

the collection of a variety of airborne materials. It is a passive sampler that is typically clipped to the worker's lapel and worn throughout a shift.

Sample bag A bag made from an inert polymer such as Teflon, complete with a fitting for connecting to an air-sampling pump.

Sampling The action of selecting a set of items for measurement of a given parameter.

Sampling and analytical error (SAE) A numerical factor used in analytical methods to account for uncontrollable errors. Its value is taken into consideration in the determination of whether the exposures are within acceptable limits.

Sampling box An enclosed chamber in which sampling is carried out or samples are protected after collection for dispatch to the testing laboratory.

Sampling duration The period of time that sampling takes place at a specified sampling rate.

Sampling medium The device or material through which contaminated fluids are drawn in order to collect the contaminants for analysis.

Sampling train The assembly of sample medium in its holder, with connecting tubing and sample pump.

Sampling volume flow rate The induced flow rate into a sampling system.

Saturated steam Steam that has the same temperature and pressure as the water from which it is formed.

Saturated vapor A vapor that can exist in equilibrium with its liquid.

Saturated vapor pressure The pressure exerted by a saturated vapor. This pressure is a function of the temperature.

Saturation efficiency A measure of the performance of an air washer. It is the amount of water added to the air leaving the washer expressed as a percentage of the amount of water that would have been added if the air had left the washer in a fully saturated condition.

Saturation tables Tables that relate the dryness properties of a gas to its temperature and pressure.

Saturation vapor density The density of a saturated vapor.

Sauter mean diameter The average ratio of the volume to the surface area used in the determination of the pressure drop in a scrubber.

Scales of sensation A simple numerical scale used to report the response of a person to temperature, humidity, air velocity, air purity, noise, light, taste, etc.

Scan test A test used to determine the local efficiency of an air filter.

Scatter diagram A graph in which values of one variable are plotted against the corresponding values of another property.

Scavenging The removal of an unwanted product.

Screening The separation of particulate matter by the use of filters, mesh screens, or other devices. Also, the covering of a plant item to improve the visual impact.

Screw conveyor A conveyor that uses an Archimedes screw to convey granular material from a hopper to point of use.

Scroll collectors A centrifugal collector in which a scroll imparts a centrifugal motion to the dust stream, concentrating the dust in the peripheral layer, from where it is passed to a secondary collector, and then to exhaust.

Scrubbers and absorbers Wet systems used for the removal of aerosols and other gaseous pollutants from an airstream.

Scrubbing The process of cleaning contaminated gas by passing it through a water spray or cascade.

Seals A device on a container or conduit run that ensures that the internal products do not escape from any joints.

Secondary air Air that is introduced above a combustion process in addition to the primary air in an attempt to obtain complete combustion.

Secondary containment The enclosing structure around a green zone in the atomic energy industry.

Secondary filter A filter to provide final cleaning of the air after the main filter in a system.

Sedimentation The process of settling solid particulates out of suspension in a fluid or a gas.

Selectivity The degree of independence from interference.

Sensible heat The portion of heat supplied to a substance that produces a change in temperature without changing the state of the substance.

Sensing element A component that measures of the value of a variable and provides the input for control devices.

Sensitization The development of an adverse immune response following more than one exposure to a substance.

Sensitizer A substance that stimulates a response from the immune system.

Sensitivity The ability of a chemical analysis to detect low levels of the analyte. Also, any abnormal reaction of the human body to chemical substances.

Sensor A device used to measure flow, temperature, pressure, or another property of a medium.

Sensory hearing loss Irreversible hearing loss resulting from damage to the inner ear tissue that translates sound pressure into nerve impulses.

Series operation The connection of two fans or pumps in succession in order to increase the available pressure in a system.

Serpentine An asbestos mineral with a wavy appearance, such as chrysotile.

Set point The value on the scale of a controller at which the design conditions are set.

Settling The process of particulate matter falling out of a gas stream or a fluid.

Settling chamber A chamber in which large particulate matter settles out of the air due to gravity. By increasing the cross sectional area of this chamber the air velocity decreases, allowing settling to take place.

Settling velocity The velocity that has to be attained to ensure that particles of a particular size settle at a given distance from the generation source due to the influence of gravity.

Shaver's disease A disease of the lungs found in workers exposed to fumes or dusts containing aluminium oxide. It is a type of pneumoconiosis and results in interstitial fibrosis and decreased lung function.

Shedding The loss of fibers from a filter.

Shivering The process of metabolic regulation against cold by muscular action.

Shock losses The energy loss in a moving fluid stream due to one or more of the following:

- Violent mixing producing eddy formation.
- Separation occurring due to contractions or expansions in duct flow.

Shock ventilation The purging of a space prior to or after a process or occupancy.

Shock wave A pressure wave resulting from the rapid closure of a valve or damper in a pipeline or ductwork system, or from an explosion.

Short circuiting The process in which air from an inlet is extracted from the space before it has chance to mix, caused by the extract being positioned too near the input grille.

Shot blasting room A ventilated room devoted to the cleaning of castings by the use of various grades of shot.

Short term exposure limit (STEL) The permissible exposure limit for a given contaminant averaged out over any 10-minute period during an 8-hour working shift. See also Occupational exposure limit (OEL) and Long-term exposure limit (LTEL).

Sick building syndrome (SBS) The group of symptoms related to poor air quality,

including headaches, irritation of mucous membranes of the eyes and nose, breathing difficulties, etc., experienced by occupants in poorly ventilated buildings. See also Building-related illness (BRI).

Siderosis A benign reddish discoloration resulting from deposits of iron oxide in the lungs.

Sieving The use of sieves for the collecting of particulate matter or for the grading by size of particulate matter for classification purposes.

Significance A statistical term relating to tests made to ascertain the probability of an effect or correlation.

Silicates Chemicals used as adsorbents.

Silicosis Pneumoconiosis resulting from inhalation of crystalline silica (quartz).

Simple asphyxiant Substance that displaces air, producing an oxygen-deficient atmosphere.

Sink A storage device for a fluid or heat.

Sintered filters A self-supporting sintered element used in gas cleaning systems.

Size-selective sampling Industrial hygiene sampling methods that collect particles with a specific range of aerodynamic diameters.

Skew distribution Any set of values measured during a test that is not symmetrically distributed.

Skin notation The word skin included as part of an exposure limit. It is used for those substances for which absorption through the skin is considered to be a significant route of entry into the body.

Slant gauge An inclined calibrated manometer tube.

Sling psychrometer An instrument used to measure the dry-bulb and wet-bulb temperatures of the air, from which the humidity of the air can be determined by means of calculations, tables, or charts.

Slip (Cunningham factor) A factor used in particle physics to predict the behavior of small particles.

Slot venturi A device used to adjust the pressure drop in a scrubber.

Sludge The waste product formed by a wet cleaning process.

Smell See Odor.

Smog A mixture of smoke and fog, that arises from nitrogen oxides and hydrocarbons and the photochemical action of sunlight.

Smoke Aerosols formed from minute solid or liquid particles, most less than 1 μm in diameter, generated by the incomplete combustion of a fuel or by sublimation.

Smoke bomb A firework type of device that produces smoke used for the observation of airflow within a space.

Smoke damper A damper installed in a ductwork system designed to close in case of fire by means of a fusible link and electrical or magnetic device to stop the spread of smoke.

Smoke extraction A mechanical or natural means by which smoke generated during a process or a fire is removed from the space to outdoors.

Smoke generator A device that electrically heats oil-producing smoke. The smoke is liberated from a nozzle by either thermal forces or by means of a fan and used to observe airflow patterns within a space or to observe leakage from ductwork, etc.

Smoke stain When a certain quantity of dirty air is passed through a filter paper, the degree of staining on the paper is measured and expressed as a concentration of equivalent standard smoke by means of an optical reflectometer.

Smoke tube A tube or a canister containing a smoke-generating chemical used to observe air movements within a room.

Smuts Unburned carbon emitted from chimneys. If sulfur is present in the fuel these smuts will be acidic.

Sociocusis Hearing loss that results from exposure to the noises of everyday life.

Sodium flame test A test of HEPA filter efficiency using small particles generated from NaCl.

Solid phase The condition of a body being a solid, such as ice.

Soiling index The degree of soiling of a filter paper fitted in a sampling device through which a contaminated gas has been passed.

Soot The aggregates leaving a combustion chamber due to incomplete combustion of a carbonaceous fuel.

Sorbent Any agent that is used in a sorption process.

Sorbent tubes Small glass tubes that contain sampling media such as silica gel or activated charcoal.

Sorption Adsorption (a surface process) or absorption (a volume process).

Sound A physiological sensation received by the ear, which may or may not cause annoyance.

Sound intensity The sound power distributed over unit area, in units of W m^{-2}.

Sound power The rate at which sound energy is produced at the source, given in watts.

Sound pressure The average variation in atmospheric pressure caused by a sound, given in pascals.

Sound rating The manufacturer's rating of the noise level produced by an item of rotating or reciprocating plant.

Source Where any form of pollution is generated.

Source sampling The testing and measurement of an emission at its point of generation.

Space requirements The footprint (m^2) or volume for a given item of equipment.

Sparking The production of sparks; occurs under certain conditions on electrostatic precipitators.

Speciation The process of determining the different species present in a chemical agent.

Species The different forms in which a biological or chemical agent may be present.

Specific flow The volumetric air change rate within a space, denoted by n, the flow volume rate into and out of the space divided by the volume of the space.

Specific gravity The weight of a material in kg that would occupy one cubic meter under a definite state of conditions.

Specific heat The amount of heat (or mechanical work) required to raise the temperature of a unit mass of a substance one degree Celsius. In the case of gases there are two specific heats, according as to whether the heating takes place at constant pressure or at constant volume.

Specific humidity The mass of water vapor that is present in a unit mass of moist air.

Specific leakage Relating to the leakage that takes place from an enclosure due to a pressure difference created either mechanically or naturally. It is the ratio of leakage area in m^2 divided by the floor area in m^2.

Specific measuring range The range of concentration values for which the overall uncertainty of a measurement procedure is intended to lie within specific limits.

Spectrophotometry A photometer for comparing two light radiations, wavelength by wavelength.

Spirometry A test method used to evaluate lung function that measures volume of exhaled air passing through a tube during a given time.

Splitters Turning vanes inserted in a fluid flow system to reduce frictional losses.

Spontaneous combustion Any combustion that takes place without a source of ignition due to the nature of the material and its packing arrangements.

Spread The angle of divergence of a jet or plume from its origin.

Squirrel cage fan A fan with a squirrel cage rotor, which has the advantages of low cost, low maintenance, and sturdiness.

Stability The state of being stable.

Stable Relating to a chemical that is not readily decomposed, or a stable condition in a working environment.

Stack effect The pressure forces set up in space due to the density differences between the hot and cold columns.

Stack solids The solid content of a gas stream leaving a chimney or exhaust duct.

Stagnation A situation in which flow is assumed not to occur.

Standby fan A fan or fans included in a system to provide a backup in case of failure, and/or to provide a rapid air change in the case of a chemical spill.

Standard The maximum level of an air contaminant allowed in workplace or external air as defined by a legal authority. Or any national or international standard relating to a product or code of practice.

Standard air Air at standard temperature and pressure (STP) which is the same as normal temperature and pressure (NTP) 0 °C and 101.325 kPa, with the force due to gravity 9.80665 N kg^{-1}.

Standard conditions Relating to normal conditions such as standard temperature and pressure (STP), which is the same as normal temperature and pressure (NTP).

Standard deviation A statistical measure of the scatter of a series of numbers or measurements about their mean value.

Standard temperature and pressure (STP) This is the same as normal temperature and pressure (NTP), 0 °C and 101.325 Pa.

Standard threshold shift (STS) An increase of 10 dB or more in a person's HTL in the 2000 to 4000 Hz range, significant because it represents loss of a significant proportion of hearing.

Static efficiency The ratio of fan static pressure to fan total pressure.

Static electricity Phenomena associated with electric charges at rest, due purely to the electrostatic field produced by the charge.

Static head The difference between the total fluid pressure and the dynamic pressure.

Static pressure curve A graphical representation of the static pressure and volume flow of a fan at a set speed.

Static pressure regain The increase in static pressure that takes place due to a decrease in the air velocity causing the velocity pressure to be converted into static pressure.

Static sample The result of the process of static sampling.

Static sampler A device not attached to a person that samples air in a particular location.

Static sampling The use of a static sampler to determine a particular property.

Stator The stationary portion of an electric motor.

Steam Water in gaseous state above its boiling point.

Steam tables Tables containing the thermodynamic properties of steam over a range of pressures and superheat.

STEL See Short-term exposure limit.

Step control A control method in which a multiple switch assembly sequentially switches on or off various stages of a device, such as a heater battery.

Stephan flow The flow of molecules towards or away from the surface of a volatile liquid due to either evaporation or condensation.

Stokes diameter The equivalent spherical diameter of the particle being considered.

Stokes law This relates to the factors that control the passage of a spherical particle through a fluid. The Stokes diameter of a particle is the diameter of a sphere of unit density, which would move in a fluid in a similar manner to the particle in question, which may not be spherical.

Stoichiometric The exact quantity of reactants required to completely react according to a particular chemical equation. If

the reaction were complete only products and no reactants would remain.

Stopping distance The maximum distance a moving particle will travel in still air after all the external forces are removed. In the Stokes region it is the velocity of the particle times the relaxation time.

STP See Standard temperature and pressure.

Straighteners Vanes fitted in ductwork or air handling units before or after a change in section to produce a reduction in pressure drop.

Stuffing box A box that provides a seal for a fan shaft.

Subcutaneous The deepest layer of skin, containing fatty and connective tissue that provides a cushion and insulative base for the skin and also binds the skin to the underlying tissues.

Superheated steam Steam that has a temperature above that corresponding to boiling temperature, corresponding to the pressure at which it exists.

Superheated vapor See Superheated Steam.

Supersaturation An unstable condition in which the concentration of a solution or a vapor is greater than that corresponding to saturation.

Supply air Treated or untreated air entering the space. For the purpose of drawings it is color-coded to show the various thermodynamic treatments.

Number of thermodynamic treatments	Color code for drawings
None	Green
1	Red
2 or 3	Blue
4	Violet

Supply air (SUP) classification

Category	Description
SUP 1	Supply air containing only outdoor air
SUP 2	Supply air containing a mixture of outdoor and recirculated air

Supply system An arrangement that provides the distribution of a fluid, vapor, gas, electricity, or another medium.

Surface contaminant Any contaminant that adheres to a surface in a clean room.

Surface tension A characteristic of a liquid surface, with effects at liquid-gas or liquid-liquid interfaces.

Suspended matter (particulates) Particles that remain in suspension in a gas or a fluid for a sufficient time in to be detected by physical means.

Sutherland's equation An equation that allows the effect of temperature on the viscosity of a gas to be determined.

Swirl nozzles Nozzles used to distribute primary air into a space by creating a swirl. This arrangement provides good entrainment and mixing of the air.

Synergism The phenomenon in which the effect produced by two causes together is greater than the sum of the effects that would be produced by the causes separately.

System curves The graphical representation of the resistance (static pressure) that occurs in a ventilation or pump system at different flow rates.

System effect The effect that system components and/or the room have on the air quantity and pressure delivered to the space.

System life The duration of the life cycle of an item of equipment or a complete system.

System specification The engineering specification produced by the manufacturer of the equipment, or by the system designer for the plant as a whole, stating what the system is capable of achieving.

System toxin A substance that affects target organs or entire organ systems.

T

Table exhaust Mechanical extractions of pollutants generated on a worktable during a process. The extraction takes

place through a perforated workbench or from the sides or back of the table.

Tachometer An instrument used to determine the speed of rotation of a shaft, normally in revolutions per second (rps).

Tackifier A substance applied to a particulate collection device to increase its efficiency in dust retention.

Take-off Any pipework or ductwork branch taken from a main run.

Target A desirable air quality or temperature to aim for. Also items affected by pollutants.

Tangential acceleration Acceleration of a fluid tangentially to a vane or impeller due to rotary motion.

Target level The predetermined concentration of a dominant contaminant to be achieved by air technology using chemical or other control methods. It may relate to an entire room volume or a building zone.

Target organ A specific organ where the toxic effect of a substance is manifested.

Teflon filter A chemical-resistant hydrophobic filter composed of polytetrafluouroethylene (PTFE) used for industrial hygiene sampling.

Telemetering Signal transmission from a measuring instrument by telephone or radio to a distant point for recording or display.

Temperature

Temperature The degree of molecular activity in a body; high activity gives a high temperature, low activity a low temperature. The degree of activity is based on the assumption that absolute zero has no molecular movement at all. The following are some specific temperatures:

- **Absolute** The temperature relative to absolute zero, expressed in Kelvin. Also called thermodynamic temperature.
- **Asymmetry (radiant)** The difference between the plane radiant temperatures of the two opposite sides of a small plane element.
- **Dew point** The temperature of a mixture of air and water vapor at which further cooling or the addition of more water vapor will cause moisture to condense from the air.
- **Difference (vertical air)** The difference in air temperature measured at 1.1 m and 0.1 m above the floor.
- **Differential in occupied zone** The largest value of the difference between the measured air temperatures in the occupied zone.
- **Dry bulb** The air temperature recorded by a dry bulb thermometer, a sensory device excluding any effects of moisture or radiation.
- **Effective** See Operative
- **Environmental** The sum of two-thirds of the mean radiant temperature and one-third of the air temperature.
- **Equivalent** The temperature as recorded by an Eupatheoscope, taking into consideration air temperature, air velocity, and thermal radiation.
- **Globe** The temperature recorded by a 100 mm black bulb (globe) thermometer.
- **Gradient risk** The percentage of people predicted to be dissatisfied due to a difference in air temperature between the ankle and the head.
- **Induced** The temperature of the internally induced air flow.
- **Jet** The leaving temperature of a jet from an opening or the average jet temperature at a given cross-sectional area of a jet.
- **Mean in occupied zone** The arithmetic average of the measured values of air temperature in the occupied zone.

- **Mean radiant** The theoretical uniform surface temperature of an enclosure in which an occupant would exchange the same amount of radiant heat as in the actual nonuniform enclosure.
- **Operative** The theoretical uniform temperature of an enclosure in which an occupant would exchange the same amount of heat by radiation and convection as in the actual nonuniform space.
- **Optimum operative** The temperature that satisfies the greatest possible number of people at a given clothing and activity level.
- **Plane radiant** The uniform temperature of an enclosure where the radiance on one side of a small plane element is the same as in the non-uniform actual environment.
- **Primary** The temperature of the primary airflow.
- **Primary difference** The difference between the primary air temperature and the reference air temperature in the reference zone.
- **Resultant** The temperature recorded by a thermometer in the center of a 100 mm diameter blackened globe, corrections for the air velocity.
- **Resultant temperature** For air velocities less than 0.1 m s^{-1}, it is given by

$$\theta_{res} = 0.5\theta_r + 0.5\theta_a$$

and if the air velocity is above 0.1 m s^{-1},

$$\theta_{res} = \frac{\theta_r + \theta_a\sqrt{10v}}{1 + \sqrt{10v}}$$

where θ_{res} = dry resultant temperature, θ_r = mean radiant temperature, θ_a = air temperature and v = velocity in m · s^{-1}

- **Room reference** The average of at least five measurements of the air temperature at a height of 1.1 m from the floor and outside the area directly influenced by the device.
- **Thermodynamic** A Kelvin is 1/273.16 of the triple point of water.
- **Total** The air temperature of a total flow from an ATD.
- **Wet Bulb** The temperature as recorded by a thermometer bulb covered by a wet wick.

Tempering The process of heating or cooling make-up air being supplied to a space in order to provide the required temperature limits.

Temporary threshold shift (TTS) A temporary shift in hearing threshold level that goes away after the person has been in a quiet environment for a few hours. It is confirmed by an audiogram retest following a suspected standard threshold shift (STS) after at least 14 hours away from high levels of noise.

Temporary variance An OSHA variance issued to an employer who is unable to comply with a standard by its effective date for reasons beyond their control. The employer must demonstrate a plan for coming into compliance within a period not to exceed one year and provide all available measures to protect the employees in the interim.

Teratogens Toxins that cause abnormal development or birth defects.

Terminology Relating to current word usage of technical terms.

Terminal Falling Velocity See Terminal settling velocity.

Terminal Settling Velocity The maximum velocity attained by falling particulate matter, at which the gravitational force is balanced by the viscous drag created by the fluid in which it is falling. Terminal free-fall velocity of a sphere moving through a fluid, derived by using Stokes' law, Newton's drag coefficient, and Reynolds number, is proportional to the radius of the sphere squared and to the density, and is inversely proportional to the fluid viscosity.

Test aerosols Aerosols for testing the efficiency of filters generated from various grades of dusts.

Test airflow rate The rated airflow in equipment testing.

Test dust Various grades of dust used to test the collection efficiency of filters.

Test procedures The arrangements of the various sequences of events necessary for carrying out a test on a system during commissioning or for any other testing.

Test volume flow rate See Test airflow rate.

Theoretical air quantity The stoichiometric quantity of air required for complete combustion of a given quantity of a specific fuel.

Thermal anemometer An anemometer that employs the principle that the quantity of heat removed by a gas stream passing a heated element has a direct relationship to the velocity of the gas stream.

Thermal coagulation The process by which Brownian movement causes particulate matter to collide and adhere.

Thermal comfort That state in which the human body is in a state of thermal equilibrium, also called thermal neutrality.

Thermal currents Natural convection currents set up in a fluid due to density differences.

Thermal discomfort Discomfort experienced due to excessive heat loss or gain from or to the human body due to radiation, convection, conduction, evaporation, or air movement.

Thermal ignition sources A source that will cause the ignition of a flammable gas, vapor, or dust, such as an electric spark, flame, or hot surface.

Thermal load The heating or cooling requirements of a space due to structural gains or losses and the air infiltration and mechanical ventilation. The load produced by a process in a working environment.

Thermal oxidizers Devices used for the destruction of hazardous or toxic gases by oxidation at elevated gas temperature, producing primarily carbon dioxide and water.

Thermal pollution The effect of the emission of high emission temperature waste products into the environment, creating significant temperature change.

Thermal updraft The air movement that is created by a thermal plume.

Thermocouple An instrument for the measurement of temperature consisting of two wires of different metals joined at each end. An electrical electromotive force is generated, the magnitude of which allows the temperature to be measured.

Thermodynamics The branch of engineering that deals with the relationship between heat, power, and gases

Thermograph A device for measuring and recording air temperature.

Thermography The use of a tube or IR film to determine surface temperatures

Thermohydrograph A mechanical or electrical device that records simultaneously the relative humidity and temperature of the air throughout the day.

Thermometer A device used to determine the temperature of a medium.

Thermometer anemometer An instrument that measures the heat removed by an air stream passing over a heated element or bulb to determine the air velocity. See Kata thermometer.

Thermophoresis The motion of particulate matter in the direction of a cooler gas or surface due to the hot side of the particles exerting more force than the cool side.

Thermostat An instrument used to detect temperature changes and provide corrective output.

Thoracic fraction Particles with aerodynamic diameters of 5–10 μm, which enter the lungs but not the alveoli.

Threshold A level or dose of a pollutant below which it is assumed to have no effect on life.

Threshold dose A dosage or exposure level below which the adverse effects of a substance are not realized or expressed by the exposed population.

Threshold limit concentration (TLC) The concentration of an air pollutant allowed in the work space.

Threshold limit value (TLV) The limits of airborne concentration of chemical substances that are allowed in workplaces published by the American Conference of Governmental and Industrial Hygienists (ACGIH). Also known as MAC.

Threshold limit value-ceiling (TLV-C) The concentration that should not be exceeded during any part of the working exposure.

Throttling The expansion of a fluid through a constricted passage (across which there is a pressure difference), during which no external work is done. The initial and final velocities of the fluid are equal, and there is no heat exchange with external sources. A change in entropy will, however, take place.

Throttling range In a proportional controller, the control point range through which the controlled variable must pass to move the final control element through its full operating range.

Through ventilation Ventilation that takes place through a space due to wind forces, normally resulting in poor mixing of the room air due to short circuiting.

Throw The distance a fluid stream travels on leaving an outlet before its velocity is reduced to a specific value.

Tidal volume The volume of gas inhaled or exhaled during each cycle of breathing.

Tight building syndrome See Sick building syndrome (SBS).

Time constant The time required for a dynamic component, such as a sensor, to reach 63.2% of the total response to a change in its input.

Time-weighted average (TWA) exposure The average exposure to contaminant that an operator is exposed to over a work period.

Tinnitus The perception of high-pitched noises in the ears, such as ringing, roaring, or hissing caused by a bodily condition rather than an eternal source.

Tip speed The velocity of the tip of a fan or pump impeller.

Titration An analytical method involving the quantitative addition of reagents to a solution until an endpoint is reached as indicated by a color change or a precipitate.

TLC See Capacity, total lung or threshold limit concentration.

Tolerance The ability of a person to withstand adverse conditions of air quality, infectious agents, noise, vibration, or light without showing signs of infection or disease.

Total airborne particles All the particles surrounded by air in a given volume of air.

Total efficiency The ratio of the power added to the airstream to the power put into the fan or other device at the shaft.

Total energy The sum of the internal energy, pressure energy, and kinetic energy of a fluid or substance.

Total lung capacity (TLC) See Capacity, total lung.

Total pressure The algebraic sum of the velocity and static pressure, recorded at a set position within the system.

Toxicity The ability of a substance to be poisonous or injurious to living organisms.

Toxicology The study of the body's responses to toxic substances.

Tracer gases Gases used with an instrument to determine the air change rate within a space.

Tracer technique The use of a tracer gas in air for the study of air movement within a space.

Tracheobronchial region The middle region of the respiratory system, comprised of the trachea and the bronchi.

Trajectory The actual path taken by air or particulate matter due to its velocity and density when allowed to enter a space either naturally or mechanically.

Transition A change in a duct from square or rectangular to round or vice versa.

Transitional flow The nature of flow in the zone between laminar and turbulent flow.

Transport velocity The air velocity required in an extract duct conveying dust to ensure that the particulate matter remains in suspension and does not settle.

Traversing The process of moving across a grid line in a duct or on a hood with a Pitot tube in order to determine the velocity or pressure distribution.

Trickle valves Manual or automatic valves or openings that allow a given quantity of air or other gas to pass from one space to another.

Trigger finger An industrial injury caused by a constriction of the tendon characterized by the inability to bend or straighten a finger.

Troubleshooting The sequence of events carried out by a service engineer to determine the reason for faulty operation of a system.

True value A theoretical value that exactly relates a quantity for specific conditions.

Tube-axial fans An axial flow impeller mounted in a tubular housing, which contains the rotational velocity.

Turbulence Fluid motion made up of random eddies as opposed to streamline flow.

Turbulence loss The energy loss that takes place in a ventilation system through air turbulence.

Turbulent ventilated rooms The method of air distribution within a space that ensures the maximum amount of air mixing.

Turn-down ratio The lowest percentage of capacity at which a fluid flow device can be set in order to obtain suitable design flow conditions.

Turning vanes Curved vanes added to ductwork elbows in an attempt to ensure streamline flow and, by so doing, reduce turbulent losses.

Tyndall lamp A parallel light beam projected onto a cloud of dust particles generated from a process to produce scattering of the light, allowing an assessment of the magnitude and path of the cloud.

U

U-Tube manometer An instrument used for measuring pressure differences in a fluid or a gas by means of a U-shaped tube containing a fluid such as mercury or oil.

Ultraviolet (UV) analyzer An instrument using the wavelength of UV light to determine the properties of a gas or vapor.

UV Radiation Electromagnetic radiation in the wavelength range of approximately 4×10^{-7} to 5×10^{-9} m, i.e., between visible light waves and X-rays.

UV sterilization Sterilization of air or water by means of UV rays.

U value The overall heat-transfer coefficient, in W m^{-2} °C.

Ultraclean room A high-efficiency clean room used in surgical operations.

Uniform mixing The mixing of two or more fluids that ensures complete uniformity of the mix.

Unit A quantity or dimension adopted as a standard of measurement.

Unit collector A particulate-collection device that is self-contained with fans, filters, etc.

Unidirectional flow See Laminar flow.

Unidirectional jet Airflow in one direction only. It is essential that the temperature differential between the jet air and the ambient air is small and the leaving air velocity is high.

Unstable Relating to a fluid in a state that is not stable. See Stable.

Upstream The location of a fluid before entering a process.

Upper confidence limit (UCL) A statistical procedure used to estimate whether the true value is higher than the measured value.

volume of air entering or leaving the lungs in one respiratory cycle.

Ventilation, dilution See Dilution ventilation.

Ventilation effectiveness The ability of a ventilation system to remove the pollution generated within a space.

Ventilation efficiency Indices that provide a method of assessing the mixing characteristics of incoming air with the room air. It presents a means of determining the pollutant distribution within the space.

Ventilation heat loss or gain The quantity of sensible and latent heat lost or gained from an enclosure due to natural or mechanical ventilation.

Ventilation, local exhaust See Local exhaust ventilation.

Ventilation, mechanical Air movement created in a space by a fan or other air-moving device.

Ventilation, natural Air movement created by wind forces, thermal forces, or a combination of both.

Ventilation rate The actual mechanical or natural air change rate within a space, expressed in L/s or air changes per hour. The supply air may be all fresh air, or a mixture of fresh and recirculated air.

Ventilation strategy The method of planning to ensure that the best method of ventilation is provided to a space.

Ventilation system Any natural or mechanical system that provides some form of ventilation.

Ventilation thermal load The heating or cooling load required to compensate for thermal losses resulting from natural or mechanical ventilation.

Venturi A tube that is constricted and then opens out again, used to either measure the flow of a fluid or to assist the scrubbing of a gas by a liquid.

Venturi meter A measuring instrument used to determine the fluid velocity, achieved by the comparison of pressure differentials across its throat.

Venturi Scrubber A scrubber with water velocities of between 60 and 100 m s^{-1} or higher, which create shear stresses, breaking up a gaseous air stream to provide effective particulate removal.

Vibration The rapid oscillating movement of a solid body due to an alternating force, for example, a rotating piece of machinery that is out of balance.

Vibration isolator A flexible cloth or plastic connection placed between the source of a vibration, such as a fan housing, and a potential conductor of the vibration, such as ductwork.

Viruses The causative agent of many infectious diseases.

Viscosity The resistance to fluid flow caused by the shear forces between layers in the fluid.

Viscosity, dynamic Sometimes called absolute viscosity, the shear stress in a fluid divided by the velocity gradient.

Viscous flow See Laminar flow.

Viscosity, kinematic The ratio of dynamic viscosity to density.

Visibility The measure of the clearness of air.

Vital capacity (VC) The volume of air that can be taken in and pushed out of the lungs.

Vitiated air Bad or polluted air.

Volatile organic compounds (VOC) A varied group of pollutants that are liberated from certain synthetic building materials and fabrics. They are assumed to be responsible for some of the aspects of sick building syndrome.

Volumetric analysis The determination of the amount of a particular gas in a mixture of gases, as the percentage of the total volume. See Gravimetric analysis.

Volumetric efficiency The ratio of the net volume flow rate handled by the machine to the volume flow rate handled by the impeller.

Volumetric heat The heat required to raise the temperature of a unit volume of a gas one degree Celsius.

Volumetric flow rate The flow of a fluid expressed in $m^3 s^{-1}$ or $L s^{-1}$.

Vorticity Rotary motion, such as in a tornado.

Vortex Fluid flow that takes place with rotary motion, such as that observed in the wakes of buildings.

Vortex breakers 1. A device used to straighten out rotary flow in a duct a short distance after a fan. 2. A device found in a cyclone discharge fitted to reduce shell erosion by particulate abrasion.

Vortex gas cleaners A gas pollutant separator that makes full use of a vortex for the separation of particulate matter.

Vortex shedding anemometer A device for measuring air velocity by placing an obstruction in a gas flow and measuring the frequency of vortex is formation downstream of the obstruction.

W

Walk-in fume cupboard A fume cupboard that has the sash opening from the floor of the laboratory.

Walk-through survey An examination or inspection of a workplace involving a review of hazardous materials present and/or used, observation of work practices, and consversations with individuals to identify all of the actual or potential chemical, physical, biological, and ergonomic hazards.

Wall function See Boundary conditions.

Wall ventilator A wall air outlet or inlet with a weatherproof cover to provide air exchange between inside and outside by natural forces.

Warning properties The physical and chemical characteristics of a substance that allow it to be tasted or smelled at unsafe concentration levels.

Warmth The state or quality of the body being warm; it is not necessarily a state of thermal equilibrium.

Washing See Scrubbing.

Washer, air A device for adding moisture to an air stream by means of spray or capillary action. This term should not be used to relate to any wet cleaning process of a gas or other air stream.

Washout Equipment attached to dust collectors, that allows the collected particulate matter to be washed away.

Waste energy Any waste liquid, solid, or gas that contains useful energy after a process.

Waste heat Heat from a process that is surplus to requirement; this heat may be supplied to a heat recovery device for use in another part of the plant or process.

Water chiller A water-cooling device operating either by the direct expansion of a refrigerant by an absorption system or by evaporative cooling.

Water hardness The hardness of a water sample due to the salt content.

Water make-up The extra treated or untreated water required to replace water lost by evaporation or absorption into dust particulates.

Water purification The treatment necessary to ensure that water used for a process or discharged from a process is of an approved standard.

Water raw Water as supplied from a source before any treatment.

Water, softening A chemical process used to change the chemical composition of water by the removal of hardness salts.

Water, vapor Water in the gaseous state that can be liquefied by increasing the pressure without altering the temperature.

Weather strip A purpose-made strip fitted around doors and windows to reduce infiltration.

Weight, arrestance Tests carried out with synthetic dusts to determine the weight of dust collected on a filter during testing.

Weighting A The frequency-selective device on a sound level meter used to measure the A frequency network.

Weighting scale The A, B, or C weighting scales, used to approximate the response

of the human ear at different ranges of sound pressure levels.

Weld fumes The fine fumes that are produced and liberated into the room air during the welding process.

Wet air filter Any filter that depends on water or another fluid to improve the efficiency of collection of contaminants in a gas stream.

Wet bulb globe temperature (WBGT) A heat stress index, which provides information on comfort conditions.

Wet bulb temperature See under Temperature.

Wet centrifugal A dust collector that uses water or other fluid in a centrifugal action in order to improve the particulate collection efficiency.

Wet collector A gas-cleaning device that uses a fluid for the removal of a pollutant from an air or gas stream.

Wet chemical processes A gas-cleaning process that uses certain chemicals to ensure the maximum retention of a given pollutant in the cleaning fluid.

Wetted wall column An experimental apparatus used to determine the mass transfer that takes place through laminar boundary layers.

White zone A ventilation containment zone used in the atomic energy industry.

Wide-open volume The maximum flow volume a fan is capable of delivering with no resistance on the outlet side.

Wind Air motion relative to the earth's surface caused by thermal forces and the earth's rotation.

Windbreak A natural or artificial barrier that protects a building from the prevailing winds.

Wind chill index An empirical scale that correlates well with the sensation of bare dry skin due to the chilling effect of the outdoor air temperature and wind speed.

Wind infiltration Infiltration of outdoor air into a building caused by the pressure difference across the faces of the building.

Wind pressures The resulting positive or negative pressures due to the wind velocity set up on the walls and roof of a structure.

Wind rose A graphical method of showing the direction, velocity, and frequency of wind for a given location over set time periods.

Wind shear The change in the wind velocity and direction with height above some reference plane.

Wind speed The wind velocity measured at a point in open undisturbed country 10 m from the ground. Corrections have to be made for other locations, and for heights above 250 m.

Wind stop A flat plate or a cone fitted over an outlet or inlet duct in order to reduce the possibility of flow reversal due to wind pressure.

Wind tunnel A fan-assisted test rig used to determine the air forces and flow patterns acting on model buildings or components.

Wind vane A revolving instrument used to indicate the direction in which the wind is blowing.

Windward The side of a building or duct opening on which the wind is blowing, also known as upwind.

Work benches A bench on which a process is carried out.

Work field analysis The actual analysis of a given task or the determination of the concentration of pollutants within a work region.

Work region Any area in which an allotted work task is carried out.

Work room A room in which an operator carries out some allotted process.

Work pattern The sequence of activities carried out by the worker over a given work period.

Workplace The defined working area or areas in which work is carried out.

Work platform A platform provided around a plant item for safe maintenance of the unit.

Work space The area or volume of a space in which work on a given process is carried out. The term is also used for the clearance area provided around equipment for maintenance.

Work station Any area in which some aspect of work activity is carried out.

Working level (WL) The allowable level of exposure of a person to an atmosphere that contains any combination of Radon daughters.

Working level month (WLM) An exposure of 1WLM can be taken to be received by a person working in a Radon daughter concentration of 1WL for 170 hours.

Working procedures Set requirements on how an industrial work process is carried out.

X

X-rays Short-wavelength electromagnetic energy that originate outside the nucleus as electrons suddenly move from higher to lower energy levels, giving up energy.

Y

Yield point The point at which material extension is no longer proportional to tension applied. Up to this limit, elastic deformation occurs; after this limit, plastic deformation occurs.

Z

Zeolite Pellets or granules of aluminum silicate, used in water treatment or air-cleaning applications.

Zero count rate The number of counts recorded in unit time by an optical particle counter when a particle-free gas is passed through the measuring chamber.

Zero exposure standards Relating to carcinogens, which have essentially zero allowable exposure levels.

Zone A set area or volume, either indoors or outdoors, in which work may or may not be carried out, depending on pollutant levels.

Zone, capture The area or volume in which a capturing device contains the generated emissions around a process. The capture velocity in this zone must be high enough to ensure the efficient collection of pollutants.

Zone, comfort The area or volume of a space that has its thermal and acoustic environment held at a set standard for the comfort of occupants.

Zone, control The area or volume of a space that has its acoustic, visual, thermal, and air purity conditions controlled to specified levels.

Zone, dead The part of an environment in which the influence of air interchange can be considered negligible.

Zone, exterior Any area or volume outside a building or process.

Zone, interior The most central portion inside a building or process.

Zone, local The area or volume in which the air is controlled locally. The control requirements may be for

- Worker protection and comfort,
- Process control, or
- Product protection.

Zone, main Normally the largest area, often the same as the occupied zone, in which the specified pollutant levels must be maintained.

Zone, multi Any area or volume within a building that may have more than one requirement for the set environmental conditions.

Zone, occupied The zone of a building in which humans or animals are housed.

Zone, perimeter The inside portion of a building or process that is nearest to the outside environment.

Zone, pressure A zone within a building or a process that is held at a given positive, negative, or neutral pressure in order to contain process contaminants.

Zone, protection The area or volume in a working space in which protection of

the process or occupants is maintained to set conditions.

Zone, trapped air Any area in the working environment in which the air movement is inadequate to remove the pollutants generated within the space.

Zone, uncontrolled Any area in which the space conditions are not specified or controlled.

Zone, working The volume or area of a building in which a given activity is being carried out.

Zoning The practice of dividing a building into sections for heating and cooling control, in order to ensure that one controller is capable of dealing with the requirements of one zone alone.

NATIONAL BODIES

AAIH
American Academy of Industrial Hygiene
ABIH
American Board of Industrial Hygiene
ABOK
Association of Engineers in Heating, Ventilation, Air Conditioning, Heat Supply, and Building Thermal Physics (Russia)
ACCA
Air Conditioning Contractors of America
ACGIH
American Conference of Governmental Industrial Hygienists
ADC
Air Diffusion Council (USA)
AGA
American Gas Association
AENOR
The National Standards of Spain
AFNOR
Association Francaise de Normalisation (French Standards Association)
AIHA
American Industrial Hygiene Association
AMCA
Air Movement and Control Association, Inc. (USA)
ANSI
American National Standards Institute
ASHRAE
American Society of Heating, Refrigeration and Air Conditioning Engineers
ASTM
American Society for the Testing of Materials
BSI
British Standards Institution
BSRIA
The Building Services Research & Information Association (UK)
CEC
Commission of the European Communities

CEN
European Committee for Standardization
CIBSE
Chartered Institute of Building Services Engineers (UK)
COSMT
The National Standards of the Czech Republic
COSTIC
Comite Scientifique et Technique des Industries de Chauffage (French Heating Research Organization)
CSA
Canadian Standards Association
CSTB
Centre Scientifique et Technique des Batiment (French Building Research Organization)
CSM
The National Standards of Bulgaria
CYS
The National Standards of Cyprus
DIN
Deutsche Institut fur Normung (The German Standardization Institute)
DS
The National Standards of Denmark
DSC
The National Standards of Albania
DZMN
The National Standards of Croatia
ELOT
The National Standards of Greece
EPA
Environmental Protection Agency (USA)
EU
European Union
EUROVENT/CECOMAF
The European Committee of Air Handling, Air Conditioning and Refrigeration Equipment Manufacturers
EVS
The National Standards of Estonia
FIMET
Federation of Finnish Metal, Engineering and Electrotechnical Industries
FIOH
Finnish Institute of Occupational Health
GOSTR
Russian National Standards
HEVAC
Heating, Ventilating and Air Conditioning Manufacturers Association (UK)
HSE
Health and Safety Executive (UK)
IBN/BIN
The National Standards of Belgium
IEA

International Energy Agency
IEC
International Electrochemical Commission
I Chem. E
Institute of Chemical Engineers (UK)
I of E
Institute of Energy (UK)
ILO
International Labor Organization
I Mech. E.
Institute of Mechanical Engineers (UK)
INRS
Institute National de Recherché et de Securie (The French Research Organization dealing with the Prevention of Occupational Accidents and Diseases)
INVENT
The Program covering Industrial Ventilation Financed by Various Organizations in Finland
IQP
The National Standards of Portugal
IRS
The National Standards of Romania
ISO
International Organization for Standardization
JISC
The National Standards of Japan
LVS
The National Standards of Latvia
LST
The National Standards of Lithuania
MSZT
The National Standards of Hungary
NAPCA
National American Pollution Control Administration
NBFU
National Board of Fire Underwriters (USA)
NFPA
National Fire Protection Association (USA)
NIOSH
National Institute for Occupational Safety and Health (USA)
NIWL
National Institute of Working Life (Sweden)
NNI
The National Standards of the Netherlands
NSF
The National Standards of Norway
NSIA
The National Standards of Ireland
ON
The National Standards of Austria

OSHA
Occupational Safety and Health Administration (USA)
PKN
The National Standards of Poland
REHVA
Federation of European Heating and Air Conditioning Associations
SEE
The National Standards of Luxembourg
SFS
The National Standards of Finland
SHASE
The Society of Heating, Air Conditioning and Sanitary Engineers (Japan)
SIS
The National Standards of Sweden
SMIS
The National Standards of Slovenia
SNV
The National Standards of Switzerland
STRI
The National Standards of Iceland
TSE
The National Standards of Turkey
UMNS
The National Standards of Slovakia
UNI
The National Standards of Italy
VDI
Verein Deutscher Ingenieure (The Association of German Engineers)
VDMA
German Machinery and Plant Manufacturers Association
WHO
World Health Organization (The United Nations Agency that deals with the Relationship between Human Health and Pollution)
WMO
World Meteorological Organization (The United Nations Agency concerned with the Atmospheric Composition

BIBLIOGRAPHY

ISO 13349:1999, Industrial fans—Vocabulary and definitions of categories.
ISO 3258:1976, Air distribution and air diffusion—Vocabulary.
ISO 3649:1980, Cleaning equipment for air or other gases—Vocabulary.
ISO 31, Parts 0-13, Quantities and units.
ISO 1000: 1992, SI units and recommendations for the use of their multiples and certain other units relative to the air.
CR 12792:1996, Ventilation for buildings—symbols, units and terminology.
EN 689:1995, Workplace atmospheres—Guidance for the assessment of exposure by inhalation to chemical agents for comparison with limit values and measurement strategy.
EN 1540:1998, Workplace atmospheres—Terminology.
CEN/TC 195 N 94, Air filters for general cleaning—Terminology.

This page intentionally left blank

INDEX